Ultrastructural Pathology
The Comparative Cellular Basis of Disease

Second Edition

Ultrastructural Pathology The Comparative Cellular Basis of Disease
Second Edition Norman F. Cheville
© 2009 Wiley-Blackwell. ISBN: 978-0-813-80330-2

Ultrastructural Pathology
The Comparative Cellular Basis of Disease

SECOND EDITION

Norman F. Cheville, DVM, PhD, DHC

WILEY-BLACKWELL
A John Wiley & Sons, Inc., Publication

Norman F. Cheville, DVM, PhD, DHC, is Professor Emeritus of Veterinary Pathology, Iowa State University, Ames, Iowa. Previously he was Chair of the Department of Veterinary Pathology and Dean of the College of Veterinary Medicine at Iowa State University, and Chief of Pathology for the National Animal Disease Center.

First Edition first published 1994
Second Edition first published 2009
© 1994 Iowa State University Press
© 2009 Wiley-Blackwell

Blackwell Publishing was acquired by John Wiley & Sons in February 2007. Blackwell's publishing program has been merged with Wiley's global Scientific, Technical, and Medical business to form Wiley-Blackwell.

Editorial Office
2121 State Avenue, Ames, Iowa 50014-8300, USA

For details of our global editorial offices, for customer services, and for information about how to apply for permission to reuse the copyright material in this book, please see our website at www.wiley.com/wiley-blackwell.

Authorization to photocopy items for internal or personal use, or the internal or personal use of specific clients, is granted by Blackwell Publishing, provided that the base fee is paid directly to the Copyright Clearance Center, 222 Rosewood Drive, Danvers, MA 01923. For those organizations that have been granted a photocopy license by CCC, a separate system of payments has been arranged. The fee code for users of the Transactional Reporting Service is ISBN-13: 978-0-8138-0330-2/2009.

Designations used by companies to distinguish their products are often claimed as trademarks. All brand names and product names used in this book are trade names, service marks, trademarks or registered trademarks of their respective owners. The publisher is not associated with any product or vendor mentioned in this book. This publication is designed to provide accurate and authoritative information in regard to the subject matter covered. It is sold on the understanding that the publisher is not engaged in rendering professional services. If professional advice or other expert assistance is required, the services of a competent professional should be sought.

Library of Congress Cataloging-in-Publication Data

A catalog record for this book is available from the U.S. Library of Congress.

Cheville, Norman F., 1934–
Ultrastructural pathology : the comparative cellular basis of disease / Norman F. Cheville. – 2nd ed.
p. ; cm.
Includes bibliographical references and index.
ISBN-13: 978-0-8138-0330-2 (alk. paper)
ISBN-10: 0-8138-0330-6 (alk. paper)
1. Diagnosis, Electron microscopic. 2. Pathology, Cellular. 3. Veterinary pathology. I. Title.
[DNLM: 1. Cells–pathology. 2. Animal Diseases–pathology. 3. Cells–ultrastructure. 4. Microscopy, Electron–methods. QZ 4 C528u 2009]

RB46.7.C48 2009
616.07'5–dc22

2008054079

Set in 10 on 12 pt Palatino by SNP Best-set Typesetter Ltd., Hong Kong
Printed and Bound in Singapore.

Disclaimer
The contents of this work are intended to further general scientific research, understanding, and discussion only and are not intended and should not be relied upon as recommending or promoting a specific method, diagnosis, or treatment by practitioners for any particular patient. The publisher and the author make no representations or warranties with respect to the accuracy or completeness of the contents of this work and specifically disclaim all warranties, including without limitation any implied warranties of fitness for a particular purpose. In view of ongoing research, equipment modifications, changes in governmental regulations, and the constant flow of information relating to the use of medicines, equipment, and devices, the reader is urged to review and evaluate the information provided in the package insert or instructions for each medicine, equipment, or device for, among other things, any changes in the instructions or indication of usage and for added warnings and precautions. Readers should consult with a specialist where appropriate. The fact that an organization or Website is referred to in this work as a citation and/or a potential source of further information does not mean that the author or the publisher endorses the information the organization or Website may provide or recommendations it may make. Further, readers should be aware that Internet Websites listed in this work may have changed or disappeared between when this work was written and when it is read. No warranty may be created or extended by any promotional statements for this work. Neither the publisher nor the author shall be liable for any damages arising herefrom.

1 2009

Dedication

To five scientists who had great impact on my scientific development:

George Christensen—Anatomist, Iowa State University
Barney Easterday—Virologist, Army Biological Laboratories
Harley Moon—Pathologist, National Animal Disease Center
Carl Olson Jr.—Pathologist, University of Wisconsin
Gabriele Zu Rhein—Neuropathologist, University of Wisconsin

. . . and to the many graduate students and visiting scientists in my laboratory from 1963 to 2004 who contributed electron micrographs, ideas, and new concepts in science:

Mark Ackermann
Timothy Anderson
Lawrence Arp
Juan Badiola
Dean Barnett
Jeanne Barnett
Timothy Bertram
Carole Bolin
Arliss Boothe
Dominique Brees
Freddy Coignoul
Randall Cutlip
Phillipe Detilleux
Mark Dominick
Paul Estes
Olaf Hedstrom
Johnny Hoskins
John Kluge
Vince Meador
James Meehan
Eichii Momotani
Yoshiharo Odagiri
Mitchell Palmer
Darryl Patrick
Michael Pedin
Joachim Pohlenz
James Proctor
Ingrid Pruimboom-Brees
Deng Puhui
Douglas Rogers
S. Sato
Ronald Sharp
Paul Smith
Jay Tappe
Daryl Thake
Bruce Thomsen
Catherine Wilhelmsen
Gian Winkler

Contents

Preface xi
Contributors xiii
Prologue xv

Part I: Structural Basis of Cell Injury 3

1 Response to Cellular Injury 5
Acute Cell Swelling 5
Adaptive Responses to Persistent Injury 21

2 Cell Death 33
Necrosis 35
Programmed Cell Death 40
Interplay of Necrosis and PCD 49
Getting Rid of the Dead Cell 52
Endothelial Cell Death 54

3 Cellular Defense and Recovery 61
Plasma Membrane in Recovery 61
Detoxification: Smooth Endoplasmic Reticulum and Peroxisomes 62
Mitochondria in Recovery 63
Nucleoli, DNA, and the Genome in Recovery 64
Proteostasis 67
Autophagy: Removal of Debris 69

Part II: Organelle Pathology 75

4 The Cell Surface 77
The Plasma Membrane 77
Cytoskeleton 86
Intercellular Junctions 97
Surface Structures 101

5 Intracellular Trafficking 109
Endocytosis 109
Phagocytosis 115
Lysosomes and Cytoplasmic Trafficking 116
Exocytosis 118

6 Nucleus, Ribosomes, the Golgi Complex, and Secretion 125
Nucleus 125
Ribosomes 136
Rough Endoplasmic Reticulum 138
Golgi Complex 139
Secretion 142

7 Peroxisomes, Smooth Endoplasmic Reticulum, and Lipids 153
Peroxisomes 153
Smooth Endoplasmic Reticulum 156
Glycogen 161
Lipids 164
Lipoproteins 169
Lipid Metabolism Disorders 173

8 Mitochondria 181
The Normal Mitochondrion 181
Mitochondrial Swelling: Response to Acute Injury 184
Mitochondriopathy of Metabolic and Chronic Diseases 188
Mitochondrial DNA-Based Disorders 193

Vet-ebooks.com

Part III: Inflammation and Hemostasis 199

9 Endothelium 201

Endothelial Interface with Blood and Perivascular Space 201
Endothelial Thromboresistance vs. Procoagulation 206
Endothelial Response to Hypoxia and Circulatory Dysfunction 208
Inflammation 209
Mast Cell and Basophil Interface with Endothelium 217
Angiogenesis 223

10 Leukocytes and Platelets 231

The Neutrophil 231
Eosinophils 243
Platelets 246
Thrombosis 257

11 The Mononuclear Phagocyte System and Lymphocytes 269

The Monocyte-Macrophage System 269
Dendritic Cells 274
Lymphocytes 283

12 The Extracellular Matrix 295

Collagen Fibers 297
Microfibrils 303
Extracellular Ground Substance 304
Basement Membranes 307
Mucins and Other Barriers 310

Part IV: Infectious Diseases 317

13 Cytopathology of Viral Diseases 319

Family *Poxviridae* 319
Family *Herpesviridae* 327
Family *Adenoviridae* 338
Family *Papillomaviridae* 343
Family *Polyomaviridae* 347
Family *Parvoviridae* 349
Family *Iridoviridae* 353
Family *Asfarviridae* 353
Family *Hepadnaviridae* 354
Family *Circoviridae* 355
Family *Orthomyxoviridae* 356
Family *Paramyxoviridae* 358
Family *Rhabdoviridae* 366
Family *Filoviridae* 369
Family *Coronaviridae* 370
Family *Reoviridae* 373
Family *Arenaviridae* 379
Family *Togaviridae* 381
Family *Arteriviridae* 384
Family *Bornaviridae* 386
Family *Flaviviridae* 386
Family *Bunyaviridae* 391
Family *Birnaviridae* 392
Family *Nadoviridae* 394
Family *Picornaviridae* 394
Family *Caliciviridae* 399
Family *Astroviridae* 401
Family *Retroviridae* 401

14 Cytopathology of Pathogenic Prokaryotes 425

Structure of the Bacterial Cell 425
Phylum Tenericutes, Order Mycoplasmatales 442
Order Entomoplasmatales 447
Order Incertae Sedis 447
Phylum Proteobacteriae, Order Rickettsiales 448
Order Rhizobiales 453
Order Burkholderiales 457
Order Neisseriales 459
Order Campylobacterales 461
Order Aeromonadales 466
Order Enterobacteriales 466
Order Legionellales 476
Order Pasteurellales 477
Order Pseudomonadales 482
Order Thiotricales 484
Order Vibrionales 484
Phylum Chlamydiae, Order Chlamydiales 485
Order Actinomycetales 487
Phylum Firmicutes, Order Bacillales 496
Order Lactobacillales 500
Order Clostridiales 502
Order Spriochaetales 505
Order Bacteroidales 509
Order Fusobacteriales 510
Other Bacteria 510

15 Pathogenic Protozoa 525

Amoebas 526
Ciliates 528
Flagellates 529
Hemosporidians 538
The Malarial Organisms 543
The Coccidia 549
The Microsporans 560
Protozoa of Uncertain Taxonomy 563

16 Algae, Fungi, and Other Eukaryotes 573

Algae 573
Fungi 576

Vet-ebooks.com

The Myxozoans 595
Intracelllar Metazoan Parasites 597

Part V: Toxicologic Diseases 605

17 Toxicologic Pathology 607

Lysosomotropic Hepatotoxins 609
Rough Endoplasmic Reticulum Hepatotoxins 613
Hepatotoxins and the Golgi Complex 619
Smooth Endoplasmic Reticulum and Hepatotoxicity 619
Mitochondrial Hepatotoxins 623
Steatosis and Hepatotoxicity 626
Hepatic Toxins That Act on the Nucleus 626
Hepatocyte Toxins That Act on the Cytoskeleton 627
Particulate Hepatotoxins 627

18 Myotoxins 635

Cardiotoxicity 635
Myocardial Toxins 643
Skeletal Muscle 651
Smooth Muscle Toxicity 658

19 Neurotoxins and Neurodegeneration 667

Introduction 667
Neuronopathies 668
Myelin Toxins: Myelinopathies 678
Neuropathies: The Peripheral Nerves 681
Neurotoxins That Act at Nerve Termini and Synapses 683
Glial Toxins 687
Vascular Neurotoxins and the Blood-Brain Barrier 688

20 Nephrotoxins 695

Glomerular Toxins 695
Proximal Convoluted Tubule Toxins 697
Distal Tubule Toxins 705
Toxins in the Medulla 705
The Juxtaglomerular Apparatus 708
Crystal Nephropathy 710
Confounding Lesions in Nephrotoxicity 711

21 Toxicity of Respiratory Systems 717

The Normal Mammalian Lung 717
Reaction to Pulmonary Toxins 719
Substances Damaging to Lung 723
Acute Toxic Pulmonary Injury 726
Chronic Inhalant Injury 728
Chronic Exhalant Toxicity 734
Comparative Respiratory Systems 736

Part VI: Pathologic Growth 741

22 The Cell Cycle: Dysfunction in Aging, Senescence, and Hibernation 743

The Cell Cycle 743
Regeneration 747
Aging and Senescence 750
Hibernation 751
Cell Senescence 752

23 The Neoplastic Cell 757

The Genomic Landscape 758
Benign or Malignant 761
Neoplastic Cell Structure 761
Neoplastic Cell Surfaces 763
The Nucleus of the Neoplastic Cell 766
Cytoplasm 769
The Tumor Microenvironment 775
Metastasis 780
Neoplastic Cell Death 785

Part VII: Diagnostic Pathology 795

24 Calcification 797

Intracellular Calcification 797
Extracellular Calcification 798
Microliths 802

25 Pigments 811

Melanin 811
Chromatophores 815
Hemoglobin-Derived Pigments 815
Erythrophagocytosis 817
Copper-Containing Pigments 822
Exogenous Pigments 824

26 Amyloid, Protein Misfolding Defects, and Inclusions 829

Amyloid 829
Tauopathies 839
Synucleinopathies 840
Misfolded Proteins and Inspissated Inclusions 842

27 Metabolic and Storage Diseases 857

Lipid Storage Diseases 857
Neuronal Ceroid Lipofuscinoses 862
Glycoproteinoses 863
Mucopolysaccharidoses 864
Mucolipidoses 866
Glycogen Storage Diseases 866

Vet-ebooks.com

Amino Acid Transport Storage Diseases 869
Other Storage Diseases 870

28 Arteriopathy 875

Responses of the Artery to Injury 875
Atherosclerosis 881

29 The Renal Glomerulopathies 891

Membranous Glomerulonephritis 891
Proliferative Glomerulonephritis 898
Minimal Change Disease 900
Glomerulonephritis Associated with Systemic Disease 900
Diabetes 903

30 Prions 911

Prions Defined 911
The Transmissible Spongiform Encephalopathies 912

Index 917

Vet-ebooks.com

Preface

Ultrastructural Pathology was originally designed for pathologists who interpret cellular changes in lesions encountered in the postmortem room. This edition has shifted to an **atlas format**, reducing text and grouping and labeling electron micrographs for easier identification of organelles. **Comparative pathology** is again emphasized, and has been strengthened by using diseases that extend through different vertebrate species. Ontogeny and phylogeny are basic concerns in comparative medicine, particularly the tendency of closely related animal species to suffer similar metabolic, neoplastic, and infectious diseases. A section on **diagnostic electron microscopy** has been added for those who work day to day on disciplines that demand specialized technologies for electron microscopy. **Invertebrate pathology** is also included; although spontaneous diseases of invertebrate species are not mirrors of their counterparts in vertebrate animals, the biologic processes are similar and at the level of the cell may even be identical. One of the most exciting eras of pathology was begun by observations on the inflammatory response of the water flea. Lastly, **basic elements of description**—size, structure, and location in the cell—are emphasized throughout the book.

Ultrastructural Pathology contains electron micrographs acquired from my 40 years in the discipline at four different institutions. Over 75 micrographs have been contributed by electron microscopists working in comparative or medical pathology—all micrographs of exceptional quality.

To my many colleagues who have contributed to this book, I am deeply grateful. I acknowledge in particular the graduate students in veterinary pathology who have contributed ideas and micrographs (see dedication). The quality of electron micrographs is due in no small way to the technical staff of the National Animal Disease Center, particularly Judy Stasko, Karen Schlueter, Doris Buck, and James Heminover. Gene Hedberg has done outstanding work on many of the line drawings, and preparation of micrographs has been done by Wayne Romp and Tom Glasson. I am also grateful to the staff of Wiley-Blackwell, who have done a patient job of managing and editing the manuscript.

Vet-ebooks.com

Contributors

Chapter Authors

Mark R. Ackermann, DVM, PhD
Department of Veterinary Pathology
Iowa State University

Kim A. Brogden, PhD
College of Dentistry
University of Iowa

Vincent P. Meador, DVM, PhD
Amgen, Inc.

James A. Meehan, DVM, PhD
Wyeth Research Laboratories

Randy E. Sacco, PhD
National Animal Disease Center
U.S. Department of Agriculture

Reviewers

Joseph Alroy, DVM, PhD
School of Veterinary Medicine
Tufts University

Randall Cutlip, DVM, PhD
National Animal Disease Center
U.S. Department of Agriculture

Bernard Jortner, DVM, PhD
College of Veterinary Medicine
North Carolina State University

Howard Lehmkuhl, PhD
National Animal Disease Center
U.S. Department of Agriculture

Mitch Palmer, DVM, PhD
National Animal Disease Center
U.S. Department of Agriculture

Vet-ebooks.com

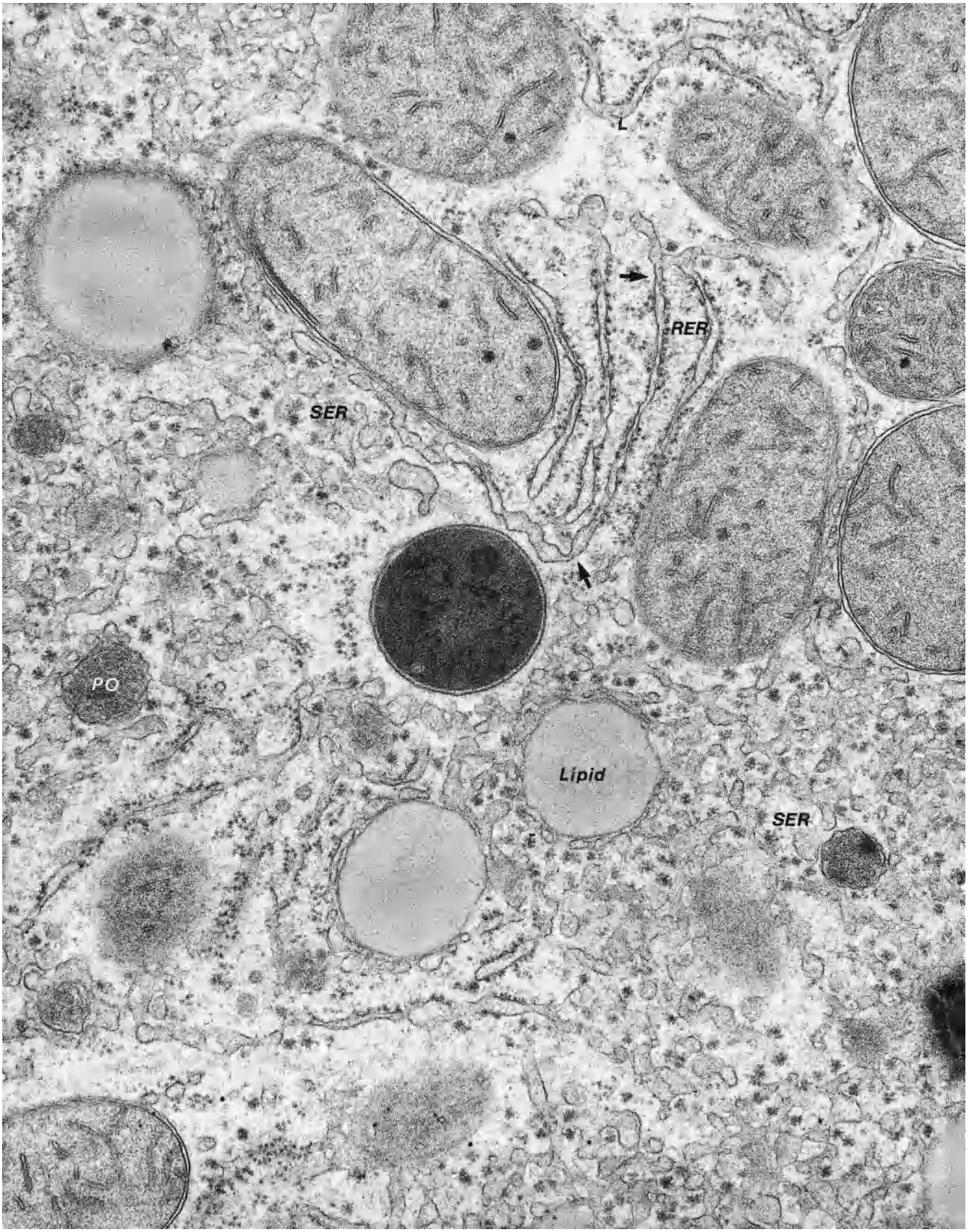


Fig. P.1 Normal hepatocyte. Relationships of rough endoplasmic reticulum (*RER*), smooth endoplasmic reticulum (*SER*), peroxisomes (*PO*), mitochondria, and lipids in the cytoplasm, hepatocyte, dog. Cisternae of SER and RER communicate (*arrows*). Glycogen and lipid globules are associated with SER. Dense calcium-sequestering bodies are present in mitochondria.

Vet-ebooks.com

Prologue

In eukaryotic cells, control of function and development resides chiefly in the nucleus; metabolic and synthetic processes occur in the cytoplasm. The gel substance of the cytoplasm, the **cytosol**, is composed of a system of tiny filaments and various organelles and inclusions. **Organelles** are considered the internal functioning organs. **Inclusions** are sequestered accumulations of metabolites (lipid globules, glycogen, protein crystals, and pigments) that are not required to maintain cell life (Fig. P.1). To correctly describe or interpret a cellular structure in an electron micrograph, three important determinations are required:

- **Size**
- **Structure**
- **Location** in the cell

Injured cells develop changes in movement, density, and size. Cellular electrolytes are altered, metabolic pathways are interrupted or shifted, and structural changes develop in organelles. In the classic sequence of degeneration and death, the affected cells become pale and swollen, suffer irreversible injury from both direct and secondary effects, and collapse into shrunken, dark amorphous masses.

Site of injury is the critical factor in determining early cellular responses. Damage may be directed to cell surfaces, to mechanisms of nuclear control, to sites of energy formation in mitochondria, or to production of organelles in the cytoplasm. Nearly all injurious substances cause damage at multiple sites in the cells, and artificial emphasis on early dominant sites of injury must not obscure the complexity of cell degeneration.

Ultrastructural interpretation of pathologic change requires a systematic analysis of all components of the cell. Changes must be compared with the normal cell, including differences in location of the cell within the tissue and alterations that the normal cell undergoes in the process of diurnal or cyclical variation. For example, the normal hepatocyte is controlled and modified by hormones, cytokines, and stimuli of feeding and changes structurally during different stages of function.

Pathologic changes that develop in response to injury also depend upon (1) **duration of effect** and **concentration in tissue** of the injurious agent, (2) **metabolic characteristics of the cell**, and (3) tissue **vascular supply** and blood flow to the cell, including the amount of oxygen, the pH, and the temperature of circulating blood. Metabolically active cells are, in general, most susceptible to injury. Factors that increase metabolism predispose cells to injury. In liver, increased circulating thyroid hormones or increased dietary protein increase metabolism and oxygen consumption and augment cellular degeneration.

Injured tissues are typically composed of cells in various stages of **degeneration**, **necrosis**, or **recovery**. On one hand, injury may be so lethal that some cells are killed outright and appear within minutes as necrotic masses; conversely, other cells, because of their protected location or inactive metabolic state, appear to escape or to suffer only slight damage. Their manifestations of injury are not swelling and collapse, but a more slowly developing accumulation of molecules that the injured cell cannot process.

Pitfalls in the correct interpretation of electron micrographs are a lack of knowledge of conditions under which tissue was processed, especially the method of fixation. Osmium fixatives cause leaching of chromatin and other nuclear proteins, while glutaraldehyde is harsh on membranes. Different buffers and temperatures will also affect how cells appear.

Vet-ebooks.com

Mitochondria are extremely labile, and even with careful fixation techniques, artifacts are common. Often there is artifactual change, accentuated because of pathologic swelling of the mitochondrion. All of these pitfalls are superimposed upon the dietary and environmental influences that affect the living animal.

Descriptions of structure must be clear and free of equivocal terms, especially inexact labels such as "fuzzy" or "almond-shaped." Size, too often ignored, is the foundation of accuracy. The ribosome is approximately 22 nm in diameter and, since it is in nearly every cell, can be used for crude comparisons with unknown structures.

Because the sample size in electron microscopy is small, the most valid ultrastructural studies depend on quantitative or **morphometric analyses** to give a clear picture of change. The number and volume of organelles in cells from different mammalian species are relatively uniform. For example, livers of dogs and rats have similar amounts of endoplasmic reticulum, although dogs have slightly smoother and rats rougher endoplasmic reticulum. Dogs have double the volume of peroxisomes as rats, and rats have nearly twice as much neutral fat. Both are subject to cyclical nutritional variances.

In examination of any organ, one must systematically analyze **blood and lymph vessels**, **nerves**, and **interstitial tissue** that surround sites of injury. This includes mast cells, fibroblasts, and other cells. The vascular system should not be excluded from the descriptive process. Acute swelling in endothelial cells impedes blood flow mechanically and by binding surfaces of blood cells as they pass along injured endothelium. In either case there will be secondary effects on parenchymal cell populations.

Precise and accurate quantification of cellular changes in electron micrographs has traditionally used stereological tools to measure numbers of organelles as well as the surfaces, lengths, and volumes. **Immunoelectron microscopy** using gold labels in intracellular compartments expanded the use of morphology in cellular pathology, and quantitative analysis of gold labels in intracellular compartments added precision (see Mayhew, *Histochem Cell Biol* 119:332, 2003; Lucocq, *J Hist Cyt* 52:991, 2004).

The introduction of **cryoelectron microscopy** in the early 1980s allowed improved images and extension of resolution for determining viral structure from electron micrographs. In electron cryomicroscopy, unfixed sections are frozen in a thin (100 nm) layer of ice and a series of micrographs are taken at different angles. Fourier analysis is used to produce a three-dimensional (3-D) reconstruction.

The 3-D reconstruction begins with one or more electron micrographs in which each particle is a 2-D projection of a specimen. The relative orientation of each specimen, denoted by polar and azimuthal angle pair, defines the angle or view of the corresponding projection.

Electron microscopic tomography provides 3-D constructs of organelles (Figs. P.2–P.4). Individual tomograms are calculated from data on images obtained from samples on grids mounted on high tilt holders; final combined tomograms are viewed with specific software programs.

The coupling of **stereology** with electron tomography produces stacks of slices from electron microscopic sections—so-called quantitative 3-D electron microscopy. These parallel optical slices allow direct stereological analysis including number estimation with optical dissector methods and volume estimation based on the Cavalien principle.

Aberration-corrected electron lenses in transmission electron microscopy (TEM) allow structural studies at atomic-scale resolution. Use of aberration-corrected TEM determines the occupancies of atom sites and permits atomic-scale imaging of chemical composition and bonding (Uran, *Science* 321:506, 2008). This technology will be critical for explaining changes in nuclear structure and function in disease (Figs. P.5–P.7). Other new technology for ultrastructural analysis can be found on the following websites:

Microscopical Society of America: www.microscopy.org

Microbeam Analysis Society (instrumentation): www.microprobe.org

Whatever the method, one is cognizant that in vitro studies of ultrastructural change are artificial relative to changes in vivo and in ovo. Cellular organelles and pathways in vitro must alter to meet the demands of growth in the culture tube. For example, many of the alterations in cytoplasmic vacuoles based upon research in cell culture systems lack correlates for vacuolar changes of cells in the living animal. It is important that the microscopist does not become overly specific in identification of cytoplasmic vacuoles—specificity unjustified by the technique used for identification.

Vet-ebooks.com

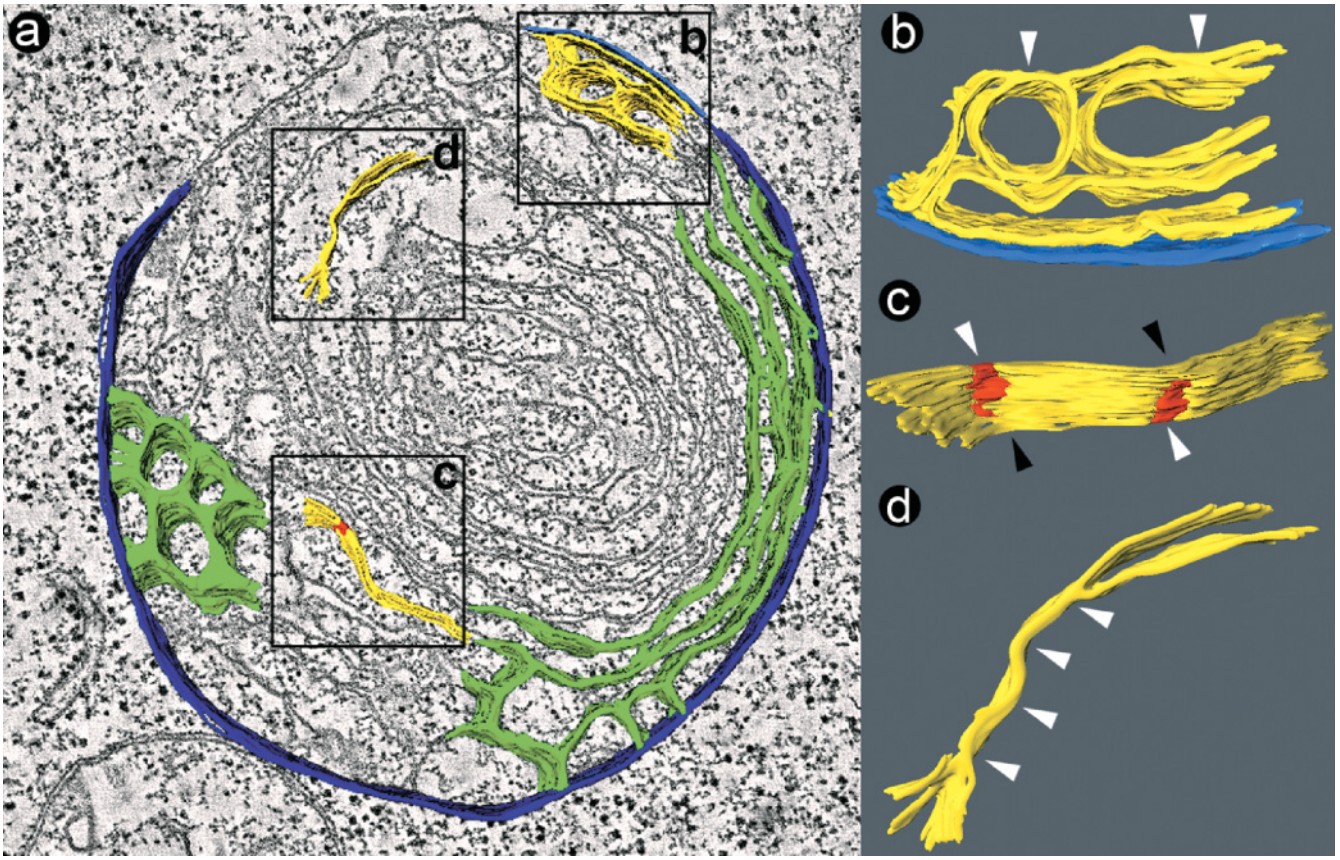


Fig. P.2 Tomogram of giant mitochondrion: lymphoblast, human Barth syndrome. **A**. **Tomogram slice**: surface-rendered depiction of a 3-D model, showing cristae in green and peripheral compartments (outer membrane + intermembrane space + inner membrane) in dark blue. Cristae are in honeycomb and concentric patterns. Boxes mark three segmented details, in which the outer membrane is bright blue and inner membrane is yellow. **B–D**. 3-D models of membranes in corresponding boxes: zones of inner membrane adhesion (*white arrowheads*), adhesions of inner membranes (*red*), and areas with open intracrista spaces (*black arrowheads*). (Micrographs: Devrin Acehan and Michael Schlame, *Laboratory Investigation* 87:40, 2007.)

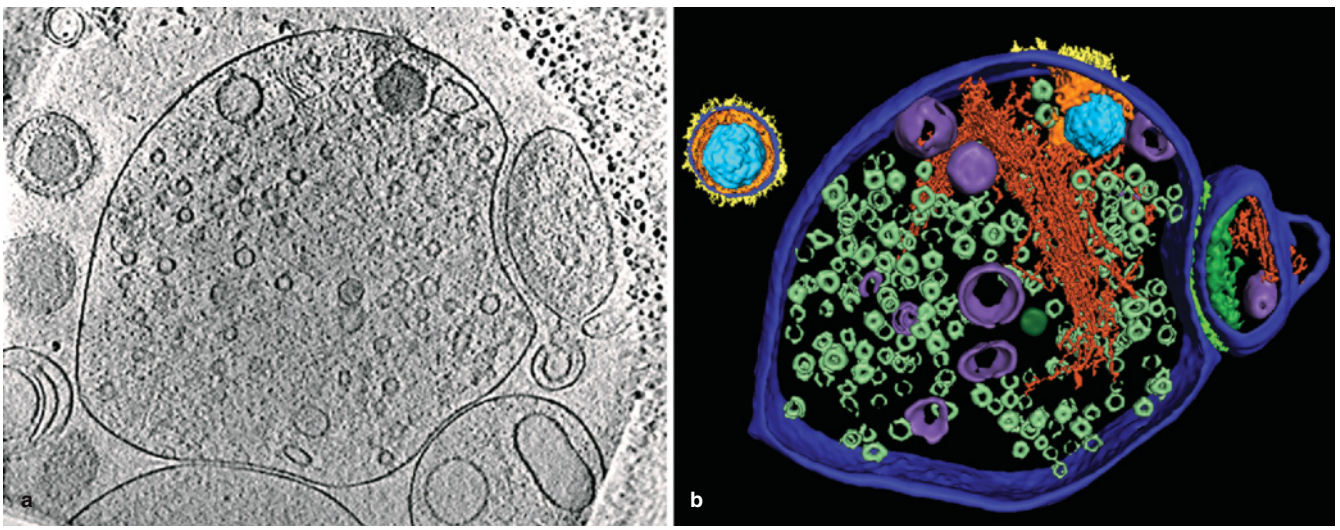


Fig. P.3 Cryo electron microscopic tomography: Herpes simplex virus-1 entering a synaptosome. **A. Capsid is inside the presynaptic element** (left). Glycoprotein spikes are on the outer phase; tegument proteins correspond to local densities near the cytoplasmic area of the plasma membrane. **B. Surface rendering of one virion and in synaptosome** from the tomogram in A: capsid (light blue), **tegument** (orange), **glycoproteins** (yellow), **cell membrane/viral membrane** (dark blue), **actin** (dark red), **vesicles** (purple), synaptic vesicles (only partially segmented—metallic green), **synaptic cleft** (light green), and **postsynaptic density** (green). Scale bars, 100 nm. Micrographs: Ulrike E. Maurer, Beate Sodeik, and Kay Gruunwald, *Proc Nat Acad Sci USA* 105:10559, 2008).

Vet-ebooks.com

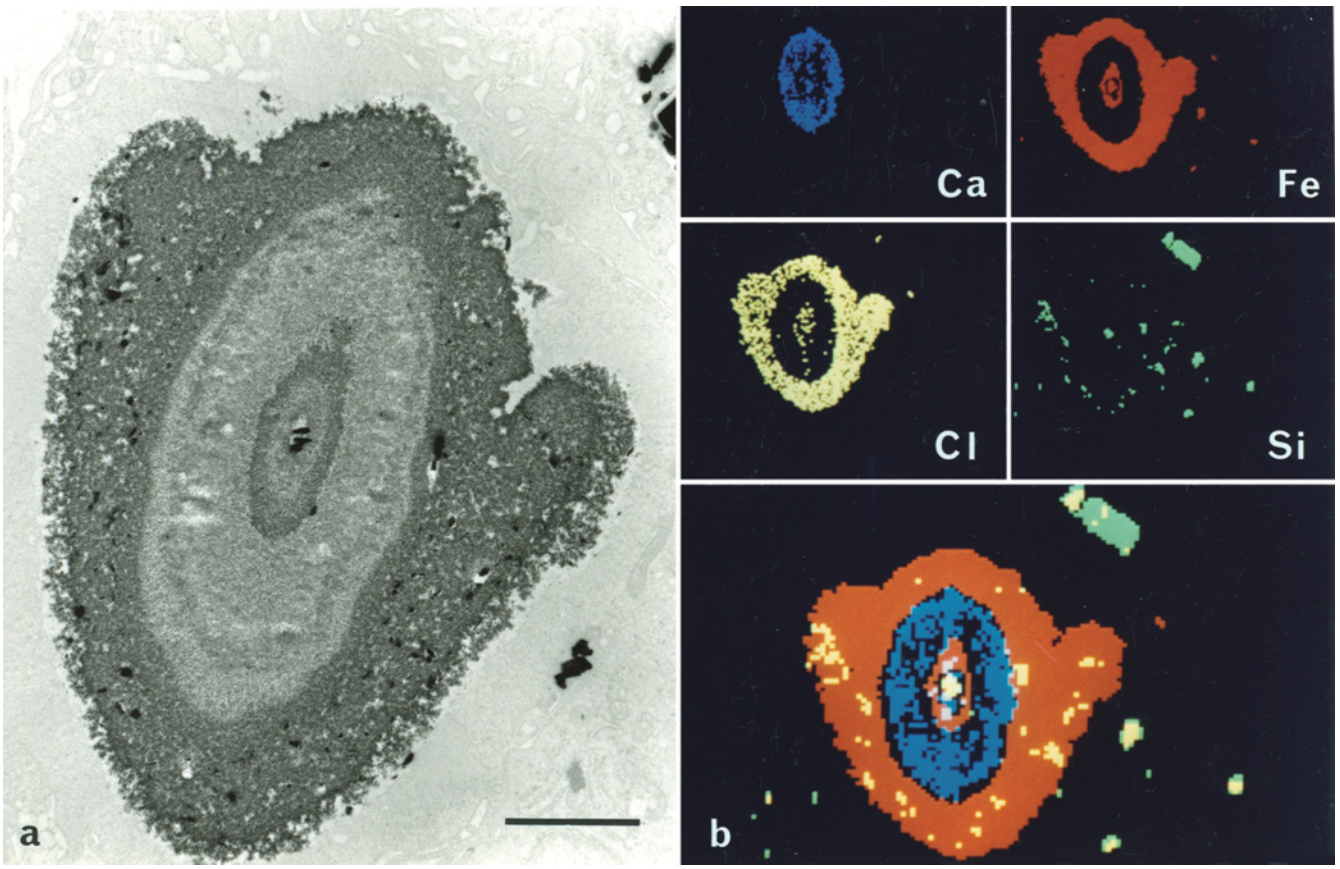


Fig. P.4 Asbestos body: x-ray microanalysis spectra. **A**. **Asbestos body TEM**: characteristic annular morphology. Asbestos fragments are in the dark peripheral zone; bar = 2 µm. **B**. **X-ray microanalysis map of asbestos body in *A***: localization of individual chemical elements in the coat of the body characterized by a silicon (*Si*) signal. Co-localization of iron (*Fe*) and chlorine (*Cl*); distinct distribution of iron (*Fe*) and calcium (*Ca*). Composition and localization of elements are shown (*bottom*). (Micrograph: H. K. Koerten, *Am J Pathol* 136:141, 1990.)

Vet-ebooks.com

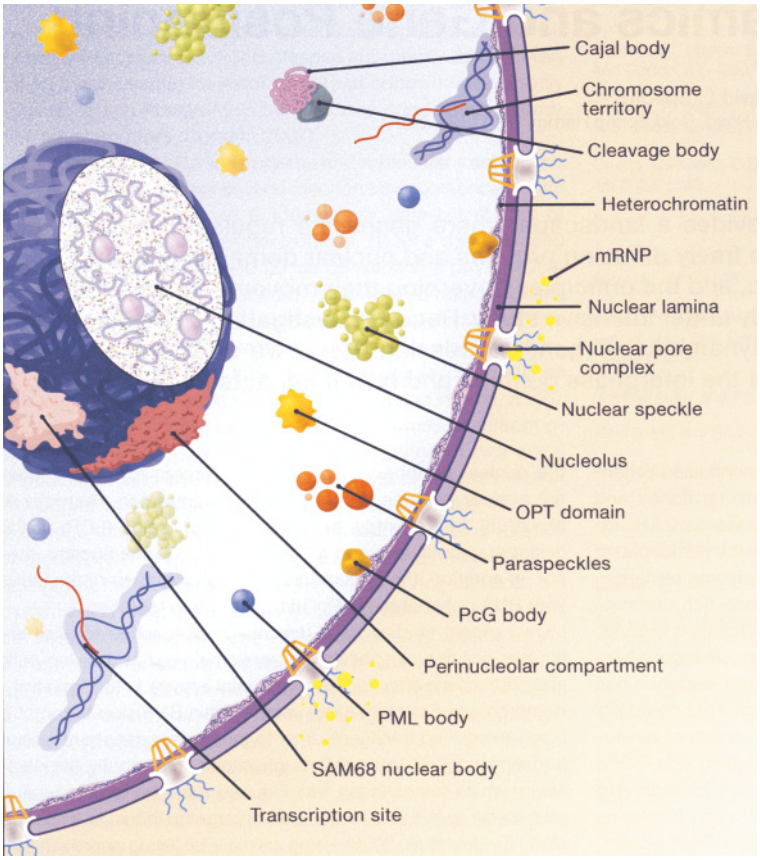


Fig. P.5 Nucleus: chromosome territories and nuclear bodies. (Drawing: R. Kumaran and David L. Spector, *Cell* 132:929, 2008.)

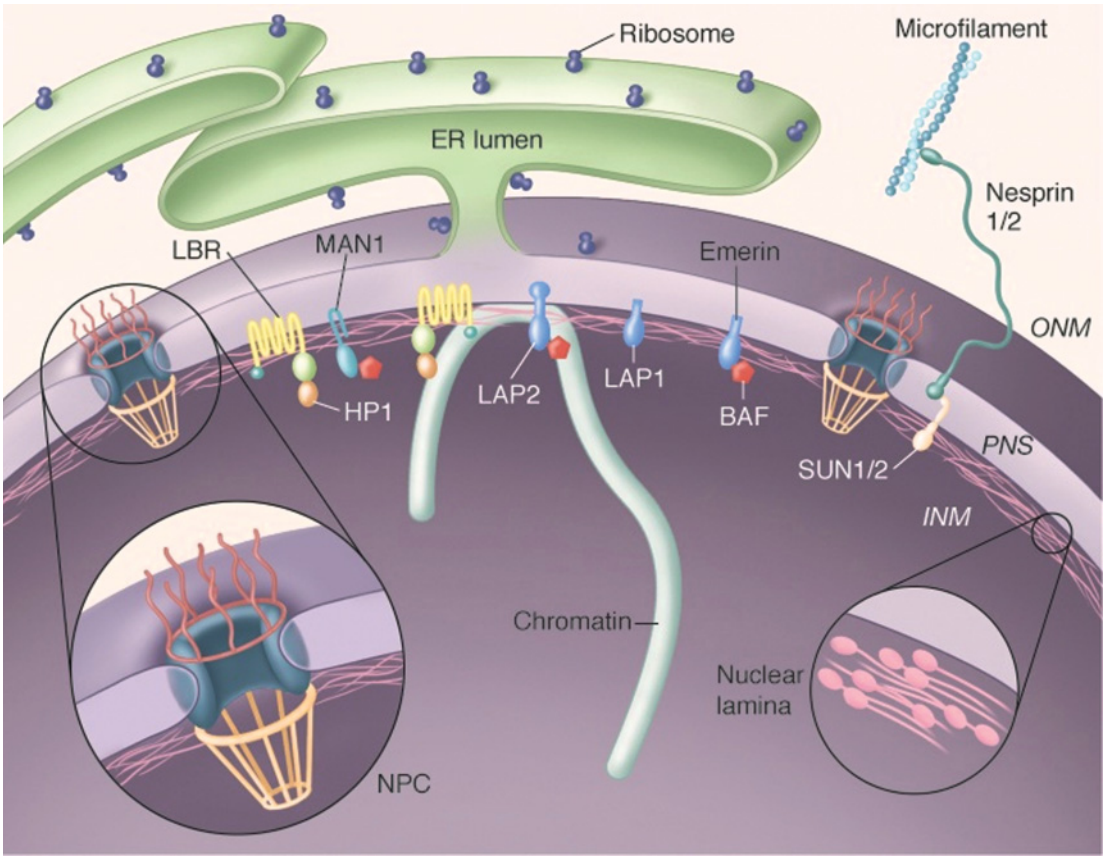


Fig. P.6 Nuclear envelope: inner nuclear membrane (*INM*) proteins, including lamina-associated polypeptides 1 and 2 (*LAP1 and LAP2*) and lamin B receptor (*LBR*), interact with HP1 and barrier-to-autointegration factor (*BAF*) and provide links to chromatin. Lamin filaments form the nuclear lamina. The outer nuclear membrane (*ONM*) cytoskeleton-associated nesprin proteins are tethered by Sun1 and Sun2 in the *INM*; the *ONM* is continuous with the *ER*. (Drawing: Colin L. Stewart, Brian Burke, *Science* 318:1408, 2007.)

Vet-ebooks.com

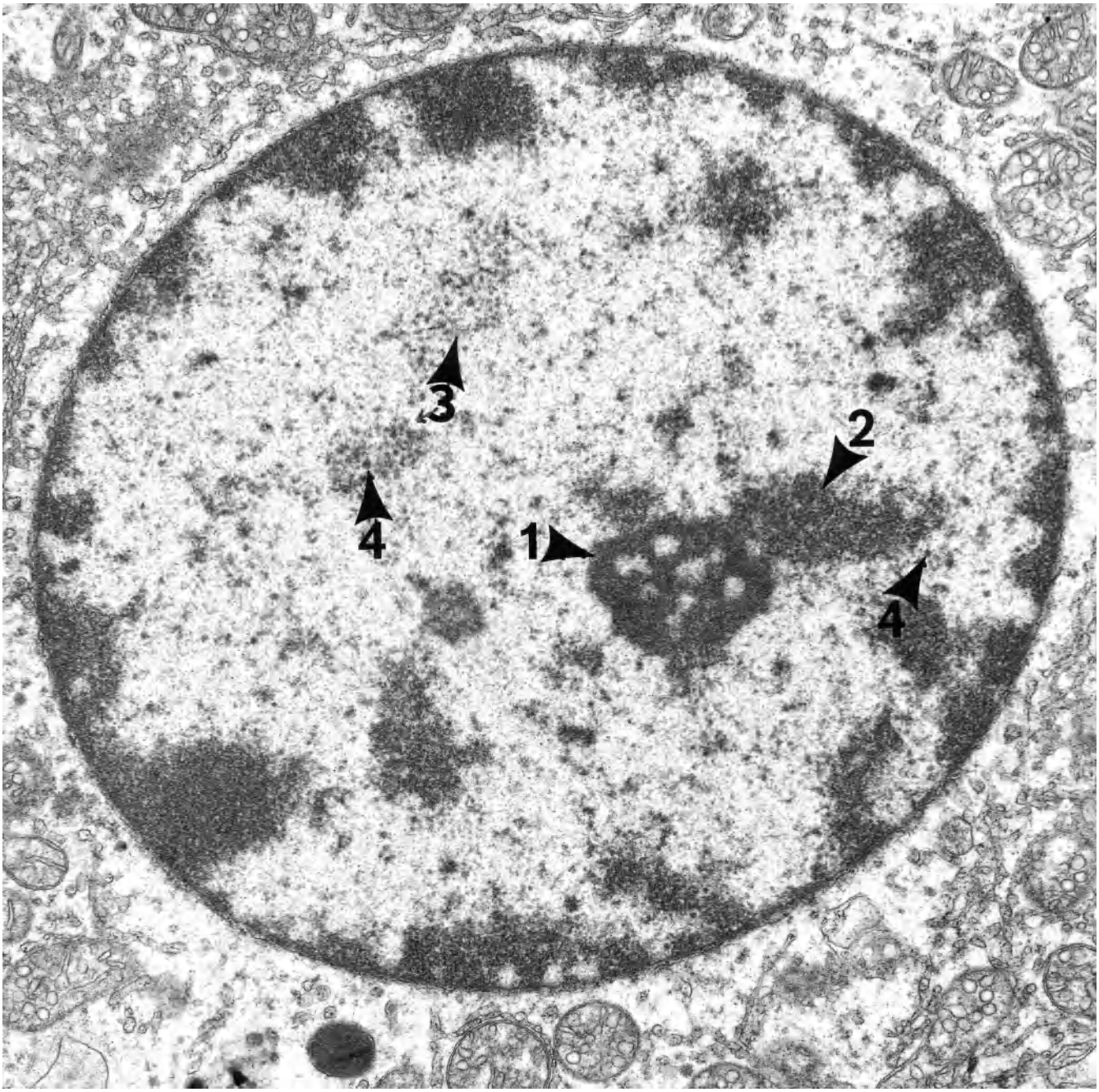


Fig. P.7 **Nuclear activation**: nucleus of a secretory cell of the adrenal cortex sampled after marked anaphylaxis with associated massive stimulation for secretion corticosteroids. **Nucleolus** is large with a clearly defined nucleolus and much **perinucleolar chromatin**. Nuclear structures are (*1*) nucleolus, fibrillar part; (*2*) nucleolus, granular part; (*3* and *4*) interchromatin granule clusters (nuclear speckles).

Vet-ebooks.com

Part I

Structural Basis of Cell Injury

Ultrastructural Pathology The Comparative Cellular Basis of Disease
Second Edition Norman F. Cheville
© 2009 Wiley-Blackwell. ISBN: 978-0-813-80330-2

Vet-ebooks.com

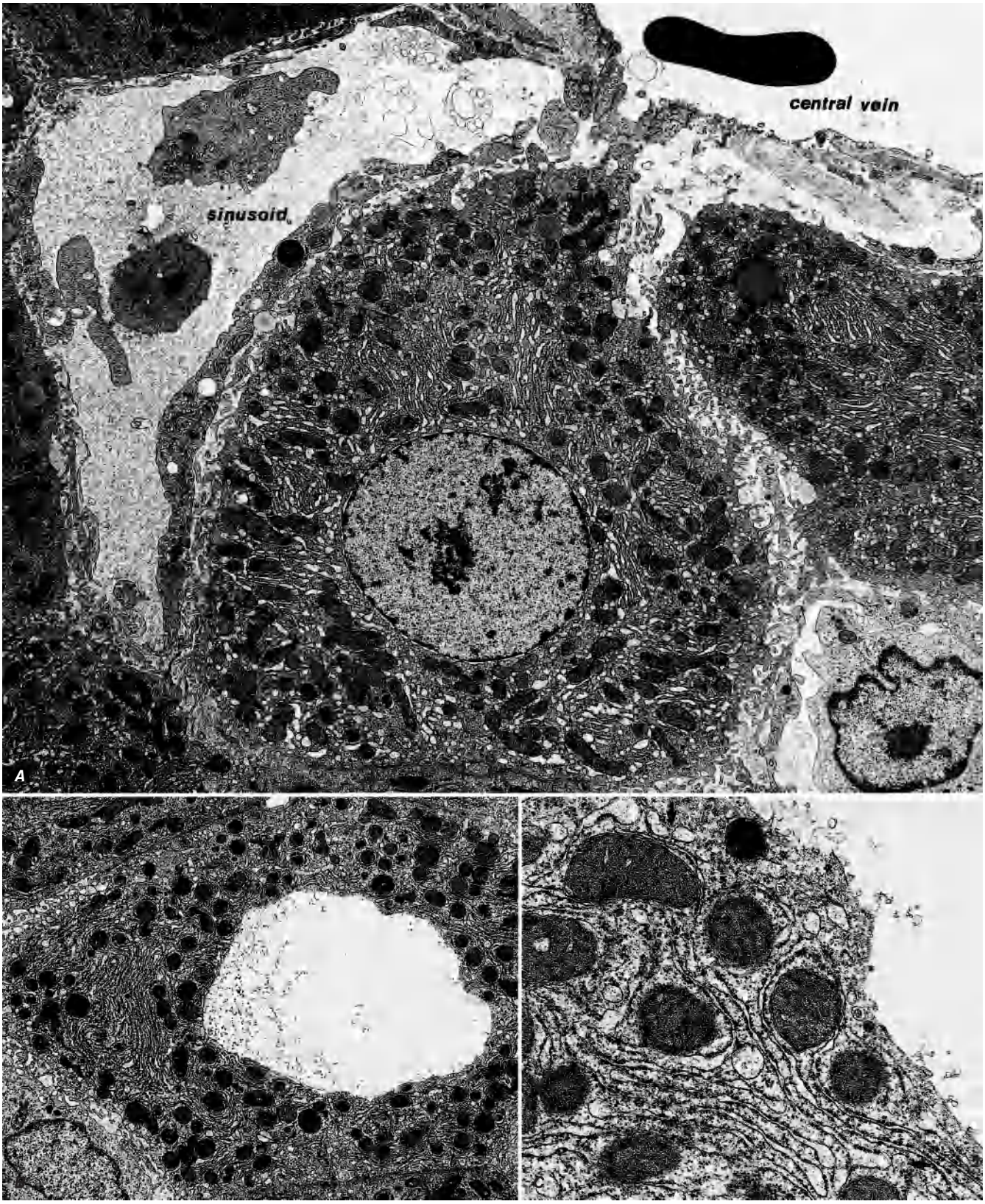


Fig. 1.1 **Acute cell swelling**: hepatocyte, rat, *Pasteurella* type D toxin. There is increased cell volume, dilatation of the cisternae of the nuclear envelope and rough endoplasmic reticulum (RER), and dilatation of hepatic sinusoids (*top right*) and central vein. Note: endothelial cell degeneration in central vein. **B**. **Focal cytoplasmic vacuolation**: RER. **C**. **Vacuole margin**: dilatation of termini of RER sacculi (*arrow*) and vesiculation of membranes of the vacuole.

© 2009 Wiley-Blackwell. ISBN: 978-0-813-80330-2

Vet-ebooks.com

1 Response to Cellular Injury

Acute Cell Swelling

Acute cell swelling is expansion of cell volume due to loss of control of water intake. It is a fundamental expression of acute injury, and is to the dying cell what electrolyte imbalance is to the dying animal, a basic killing mechanism over which are superimposed many other degenerative phenomena. With time, acute cell swelling progresses to a spectrum of changes that begin with clarification of the cytoplasm and extend to diffuse disintegration of intracellular proteins.

Dilatation of Cytocavitary Network Cisternae

The first evidence of acute cell swelling is dilatation in cisternae of the cytocavitary network: **endoplasmic reticulum (ER)**, **nuclear envelope**, and **Golgi complex** (Fig. 1.1). Early changes are due to excess water uptake, which dilutes the cytoplasmic matrix and causes the cell to appear pale and relatively structureless. Membranes of cytoplasmic organelles pump ions between the cytosol and organelles to maintain water balance and, if injured, water accumulates in cisternae of the **rough endoplasmic reticulum (RER)**. Cisternal spaces are wider than normal and the apposing membranes are less straight than in normal cells. With time, membranes of the RER become disoriented, so that the regular arrangement of saccules of the RER and Golgi complex become tortuous and bulbous. Diffuse dilatation of RER is one of the earliest signs of injury in most cells. If uncertain as to proper interpretation, examine the ends of the sheets of RER; it is here that water first accumulates.

Hydropic degeneration is a form of severe acute cell swelling characterized by water free in the cytosol and proteolysis arising from proteases activated by injury. In ultrastructural analysis, hydropic degeneration is used to indicate massive expansion of the cell by excess water and disappearance of proteins in the cytosol. In epithelium, hydropic degeneration is characterized by massive expansion of the cell and lysis of keratin fibrils. Referred to as ballooning degeneration, this pattern is common in vesicular disease.

Fragmentation of Cytocavitary Network Membranes

Rupture and fragmentation of membranes are invariable in acute cell swelling. As membranes of the endoplasmic reticulum and Golgi complex begin to fragment, water may accumulate in vesicles, cytoplasmic lakes, or vacuoles (Fig. 1.2).

Cytoplasmic Vesiculation

As membranes of the ER begin to fragment, many fragments reorient and reseal to form small vesicles. Continued function of membrane pumps causes water to accumulate in and to expand the vesicle. **Cytoplasmic vesiculation** is one hallmark of early acute swelling. Vesicles are formed from fragments of both RER and Golgi complex, and slightly later in **smooth endoplasmic reticulum (SER)**. As swelling progresses, large numbers of vesicles replace areas normally occupied by components of the ER.

Cytoplasmic Lakes

Cytoplasmic lakes develop as gels of protein and water that are free in the cytoplasm. Histologically,

Vet-ebooks.com

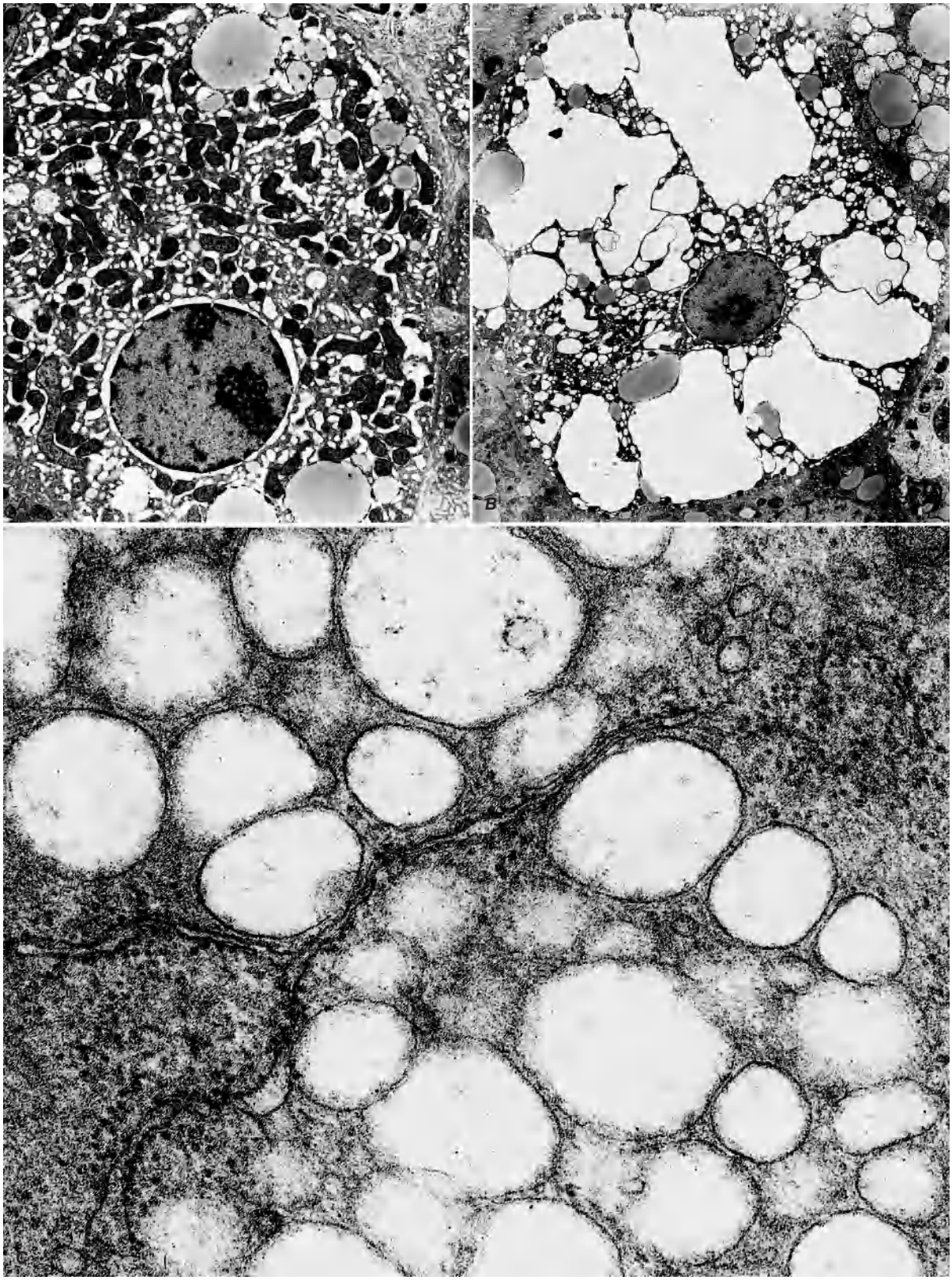


Fig. 1.2 **Vacuolation**: hepatocyte, rat, acute cell swelling of carbon tetrachlorine (CCl_4) toxicity. **A. Hydropic degeneration (vesicular)**: cisternae of the cytocavitary network (endoplasmic reticulum, Golgi complex, and nuclear envelope) are distended with water. Note: stretched nuclear pores, lipid globules, and edema of pericellular space. **B. Hydropic degeneration (vacuolar)**: vacuoles are distended with water, there is marked fragmentation of the cytocavitary network. Remnants of cytoplasm persist only around the nucleus and areas adjacent to the plasma membrane. The nucleus is small and has moved to an eccentric position in the cell. **C. Cytoplasm at high magnification**: note **vesiculation** and membrane fragmentation of rough endoplasmic reticulum (RER), **ribosomal degranulation** from RER membranes with accumulation of ribosomal fragments in the cytosol, and **membrane vesiculation** (vesical formation) of RER membranes that form large vacuoles.

Vet-ebooks.com

lakes appear as eosinophilic inclusions; ultrastructurally they are opaque, non-membrane bound foci of delicate fibrils (Figs. 1.1B and 1.1C). Lakes are bordered by intact and fragmenting RER.

Cytoplasmic Vacuoles

Cytoplasmic vacuoles are filled with ions and water. Perisinusoidal vacuolation of hepatocytes is common in toxic disease, and in systemic diseases such as burns and heatstroke.[1] **Diffuse vacuolar degeneration** is most common in parenchymal cells of liver, kidney, and other organs whose parenchymal cells bear large amounts of internal membranes that actively pump ions. Water moves rapidly into and distorts the endoplasmic reticulum and Golgi complex.[2] In severe peracute injury, there is massive accumulation of water in large, and often coalesced vacuoles. This severe injury leads to lysis of the cell with liberation of cell fluids and proteins into tissue spaces. In liver, **focal vacuolation** develops in sublethal toxicities, typically first seen along sinusoidal margins of centrilobular hepatocytes, appears to originate by **endocytosis** at cell surfaces, and vacuoles often contain remnants of microvilli, the disintegration of which is also an early degenerative change.[3]

Cytoplasmic Edema

Cytoplasmic edema, also called cytoplasmic rarefaction, is the hallmark of early cell swelling. As cell volume increases, the cytoplasm is diluted without an associated increase in cytoplasmic organelles. **Cytoplasmic palor** is seen as organelles and inclusions are separated by electron-lucent areas of cytoplasmic matrix, and there is the appearance of a loss of free ribosomes, endoplasmic reticulum, and glycogen. Tissue architecture is maintained, but the pale, enlarged cells press upon one another and normal tissue arrangements are distorted.

Cytoplasmic edema is most clearly evident in cells normally equipped to transport ions rapidly, for example, endothelium, renal tubular epithelium, and lining cells of the lungs, brain ventricles, and bladder. Acute cell swelling is especially significant in blood vessels, where endothelial cells are forced into the lumen and they impede blood flow by compressing intercellular junctions.

Ribosomal Degradation

Detachment of ribosomes from membranes of the RER results when protein synthesis is inhibited or redirected. In foci of **ribosomal degranulation**, detached ribosomes rapidly disintegrate, leaving the area filled with irregular ribosomal fragments that are smaller than the 22 nm diameter of normal ribosomes. With time, the detached ribosomes disappear, leaving a diffuse, finely granular background in the affected area. Ribosomal detachment is a manifestation of direct injury to ribosomal polymerases or to RER membranes, or occurs indirectly after primary injury to nucleolar structure on which ribosomes depend for their formation.[4–6] Whatever the cause, detached ribosomes are blocked from their normal function of mRNA translation into peptide chains.

Cytoplasmic Proteolysis

As ribosomes disappear, proteases that degrade ribonucleoproteins in the cytoplasmic matrix are activated. As proteolysis progresses, the cytoplasm becomes cleared, at first in foci and then in large segments (Fig. 1.3). Acute swelling, in cells that contain large amounts of ribosomes or protein filaments, leads to **cytoplasmic proteolysis**, the progressive clearing and lysis of cytoplasmic proteins. Lysis of membranes and filaments leaves in its wake only an opaque background of protein debris. In skin and other keratinized epithelia, keratin fibrils are lysed, leaving a massive fluid-filled, turgid cell with only delicate fibrils remaining where solid keratin fibrils should be. **Neuronal chromatolysis** is lysis of rough RER that accompanies cell swelling and leads to large, pale neurons devoid of Nissl substance. Neuronal chromatolysis (not to be confused with chromatolysis related to disintegration of nuclear chromatin) is characteristic of injury caused by neurotropic viruses and of traumatic injury.

Peptide Fragment Accumulation

In severe acute cell swelling, protein synthesis is stopped. If the various phases of transcription, translation, and post-translational modification are not affected uniformly, excess peptides will accumulate and polymerize as aberrant fibrils or granules. These proteins may be free in the cytoplasmic matrix or nuclear matrix, or develop within cisternae of the cytocavitary network. Cells that secrete continuously, such as hepatocytes, commonly have combinations of fluids and proteins in secretory vacuoles. Water that accumulates in vesicles and vacuoles is mixed with secretory proteins and glycoproteins that are released into the fluids of the vacuole. Enzymes that cleave large macromolecules into active fragments (such as proinsulin to insulin) may act at the wrong site to cause the accumulation of abnormal cleavage products. Instead of being directed to the proper secretory granule, the abnormal peptides are shunted into the lysosomal pathway.

Vet-ebooks.com

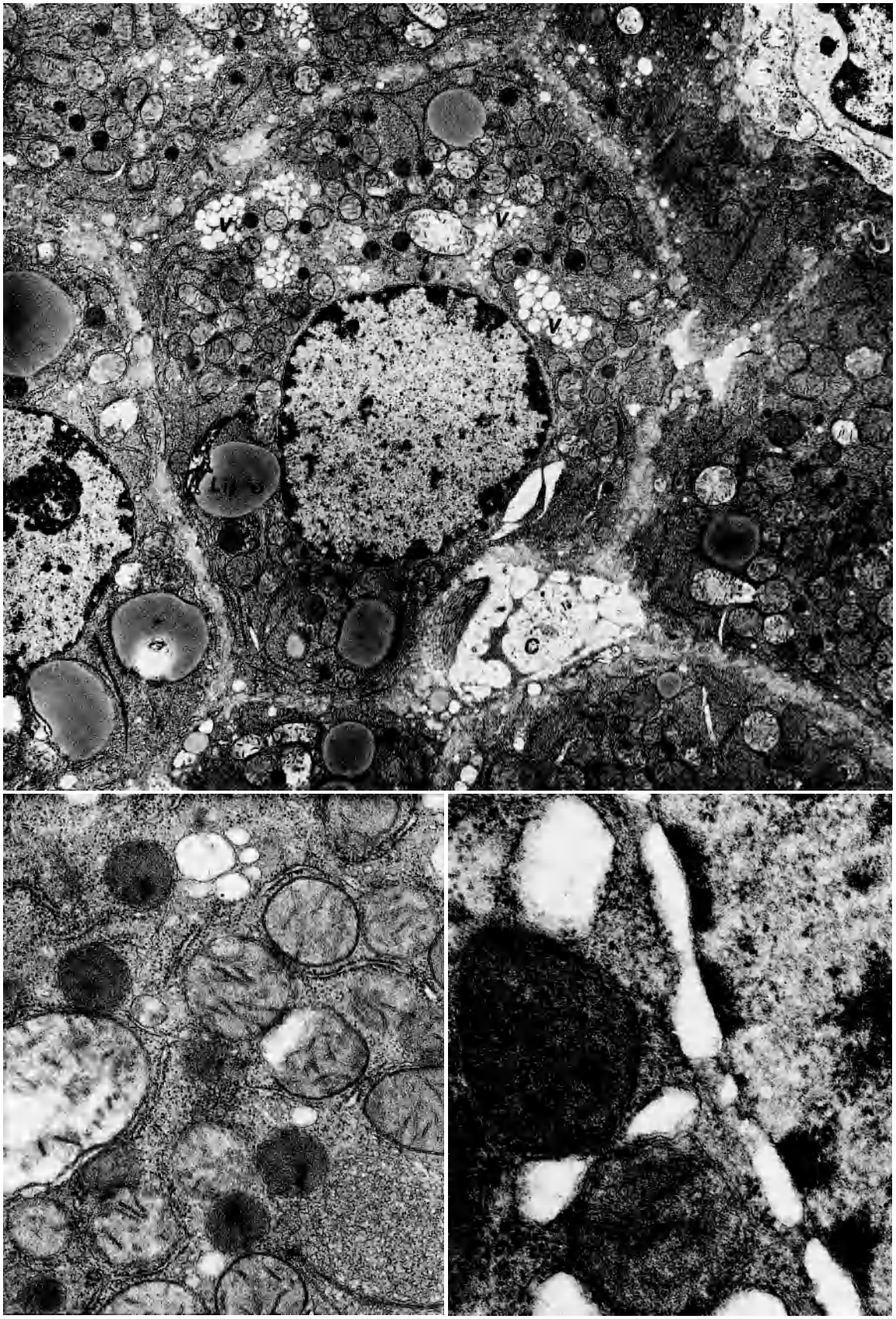


Fig. 1.3 **Acute cell swelling**, hepatocyte, rat, CCl_4 toxicity. **A**. **General view**: vacuolation (*V*), accumulation of smooth endoplasmic reticulum, swelling of mitochondria (*arrow*), areas of degranulation and breakage of membranes of rough endoplasmic reticulum with accumulation of ribosomes. Capillary endothelium (*C*) is swollen, and there is debris in intercellular spaces. **B**. **Peroxisomes**: note association with damaged membranes. **C**. **Dilatation of nuclear envelope**: acute cell swelling. Nuclear pores are stretched and distorted.

Vet-ebooks.com

Golgi Complex Vesiculation

Golgi complex injury causes formation of abnormal Golgi vesicles and retrograde changes in rough endoplasmic reticulum. **Golgi vacuolation** is invariable in acute swelling. Fragmentation and vesiculation of Golgi membranes contribute to the cytoplasmic vesicles of early cell swelling. The products of inhibited protein synthesis may accumulate in cisternae of the Golgi complex. Glycosylation of proteins and lipids is impaired in injured cells and abnormal peptides and lipoproteins accumulate within the Golgi vesicles.[7,8]

Intracisternal granules of protein and lipids in Golgi saccules are common findings in diseases involving metabolic dysfunction. In hepatocytes and renal tubule cells, large spherical membrane-bounded inclusion bodies form within cisternae of the endoplasmic reticulum in Golgi vacuoles that develop in acute cell swelling. Within these structures, abnormal proteins (as well as normal cellular proteins) may polymerize into fibrils that interact to form crystalline lattices, a development that is enhanced by delays in fixation.

Glycogen-Lipid Droplet Ratio Reversal

Aerobic metabolism is suppressed in acute swelling and anaerobic glycolysis is activated to produce energy. There is a rapid **disappearance of glycogen**; simultaneously there is an **accumulation of lipid globules** in the cytoplasm. Neutral lipid accumulation results from suppressed protein synthesis, which blocks utilization of lipids for lipid-protein conjugation. Initially, the excess neutral lipids accumulate in small lipid globules (microglobular fatty degeneration) but in advanced degeneration the hepatocyte is distended with large globules of lipid (macroglobular fatty degeneration). Marked fatty degeneration, manifest as a massive increase of lipid globules, is most often a sign of subacute sublethal injury, rather than of severe acute cell swelling that leads to lysis. Most lipid globules develop in the cytoplasmic matrix (free, not membrane bound) adjacent to smooth endoplasmic reticulum. In severe peroxidative injury such as CCl_4 toxicity, lipid globules also form within the cytocavitary network; the site depends largely upon the type of toxin involved.[9]

Smooth Endoplasmic Reticulum Proliferation and Aggregation

In sublethal toxic injury, the SER persists and proliferates; this is the structural manifestation of detoxification. The first evidence of SER alteration occurs discretely, in parts of the organelle located between mitochondria, and, in time, these areas develop large aggregates of SER membranes. Duplication of the SER is the expected change in the early stages of acute poisoning, which develops while other organelles degenerate in the early stages of acute cell swelling. In injury that develops within the SER, membranes fragment and form vesicles similar to those in injured RER.

Calcisomes are calcium pumping vesicles (similar to SER) that regulate intracellular Ca^{++} flow in nonmuscle cells. Calcisomes remain functional even in cells with severe swelling. In neurons, for example, disintegration of rough endoplasmic reticulum involves loss of most cytoplasmic structures, yet the calcisomes, those parts of the endoplasmic reticulum bearing calcium pumps, remain intact.

Mitochondrial Swelling

Mitochondria behave as osmometers, and the swelling that develops after injury reflects entry of solutes and water into the mitochondrial matrix. In severe swelling, excess water uptake leads to large, opaque mitochondria with broken cristae (Fig. 1.4). When primary injury to mitochondria is the cause of swelling, these organelles may be massively enlarged. Some toxins accumulate in or damage mitochondria selectively; for example, toxins that interfere with oxidative phosphorylation or electron transport in mitochondrial cristae will rapidly lead to ATP depletion and swelling. In lethal cell injury, the shut-down of ATP production is manifest as

- **Mitochondrial swelling**: water uptake from cytosol
- **Cristolysis**: breakup of cristae
- **Matrix lysis**: degradation of proteins in the matrix
- **Calcium-sequestering granule formation** in the matrix
- **Ballooned cristae**: water uptake plus electrolyte imbalance

Mitochondria take up Ca^{++} from the cytosol and store it as hydroxyapatite when its concentration rises above normal; the rising cytoplasmic Ca^{++} in degeneration typically causes an increase in size and number of calcium-sequestering granules. In lethal toxicity the Ca^{++} imbalance may be so severe that foci of mineral develop within mitochondria to form crystalline arrangements.

Mitochondria are exquisitely sensitive to changes in many factors that control metabolism, for example, oxygen tension, water and electrolyte balance, pH, temperature, and glycolytic products that feed into the mitochondrial pathways. Degeneration thus occurs

Vet-ebooks.com

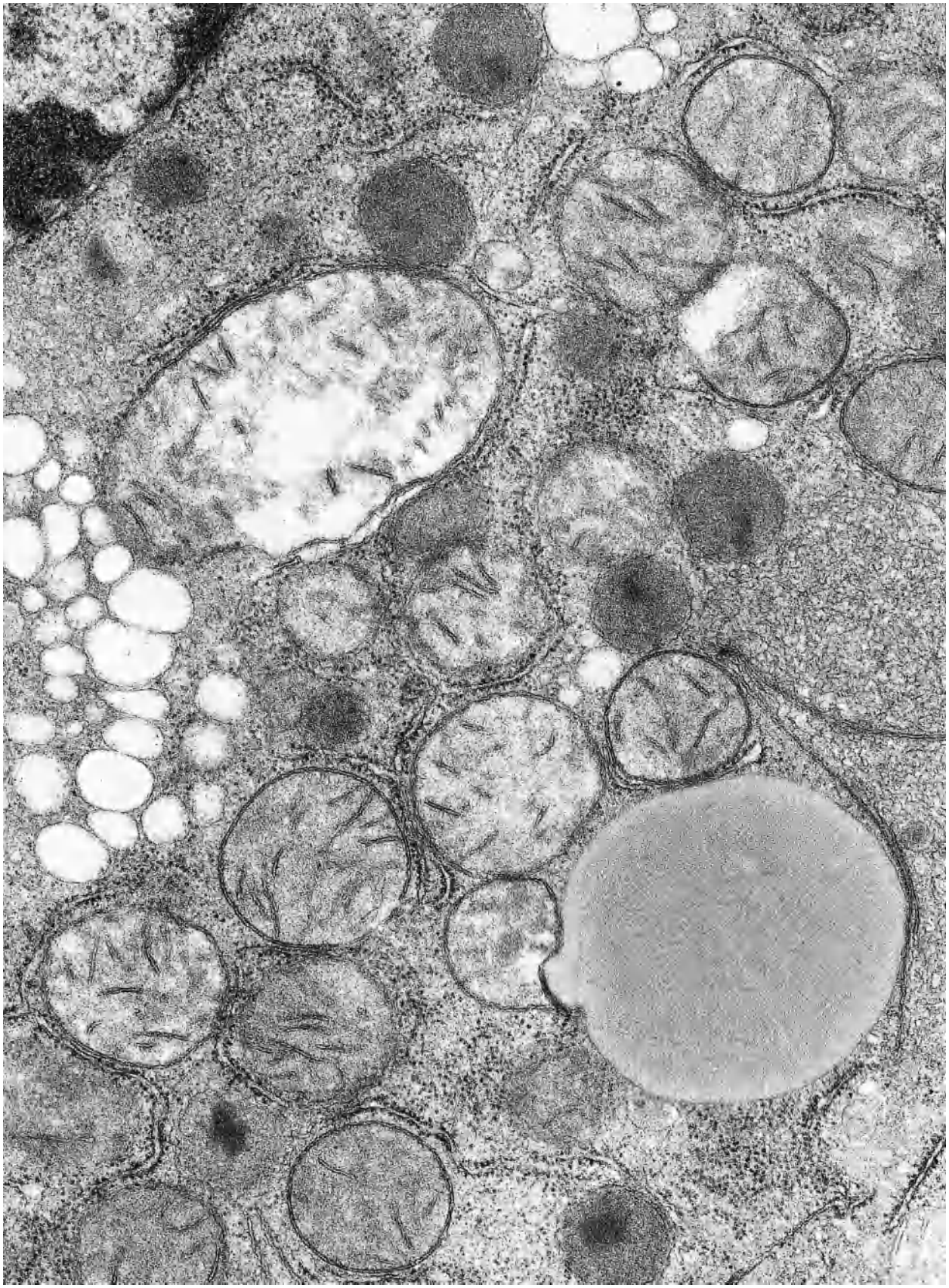


Fig. 1.4 Acute cell swelling, hepatocyte, rat, carbon tetrachloride toxicity.

Vet-ebooks.com

secondary to almost every systemic insult to tissue and is widespread in conditions such a hypoxia, fever, acidosis, and toxemia.[10]

Mitochondrial Oxygen Deficit

Anoxia is rapidly translated into damage of mitochondrial cristae.[11] Oxygen is required at the end of the electron transport chain to accept electrons and to form water, and anoxia suppresses oxidative phosphorylation. The effects of abolishing oxidative phosphorylation are magnified by its tight coupling with the citric acid cycle. NADH accumulates and exerts a powerful effect to inhibit dehydrogenases of the cycle; for example, pyruvate dehydrogenase no longer will catalyze the flux of pyruvate to CoA. In acute **anoxia**, damage to mitochondrial membranes in electron micrographs suggests that shifts in ion balance are responsible for early damage (see the section in chapter 8 on oxidative stress).

Lysosome Activation and Autophagosome Formation

Autophagy is a general manifestation of injury. Sequestration of damaged organelles and abnormal proteins in **autophagosomes** is a mechanism of cellular repair and follows all types of sublethal injury. The fusion of autophagosomes with enzyme-bearing lysosomes forms the **autophagolysosomes** that degrade cellular debris. Internalization of damaged organelles such as cilia, microfilaments, microtubules, and cell junctions causes these structures to appear deep within the cytoplasm.

If cellular injury is severe, the cell may not be able to process debris adequately because of overload or exhaustion of lysosomal enzymes. Degradation of membranous cellular components may lead to accumulation of membranes that rearrange in **membranous whorls** or of proteins that aggregate into **lattice arrangements** within autophagosomes (Fig. 1.5). Cells then become swollen and foamy due to masses of large phagolysosomes or autophagolysosomes filled with inspissated granular debris, membranes, and lipids—a change sometimes referred to as **granulovacuolar degeneration** by light microscopists. Cells with high rates of membrane activity, such as steroid-producing cells of the adrenal cortex or interstitial cells of the testes, form large membranous whorls when they degenerate.

Membrane Fragment Accumulation

As these membranes fragment and degrade, membrane remnants accumulate as parallel strands or **concentric lamellar arrangements** that persist free in the cytoplasmic matrix. Membrane fragments are also taken into autophagic vacuoles, where they also form concentric lamellae. When the **endoplasmic reticulum** degenerates, many of the membranes collapse into long irregular fragments that aggregate and reorient into laminar arrangements. These membrane "bodies" are called **myelin figures** and are commonly found free in the cytosol. Myelin figures are especially frequent in cells with much endoplasmic reticulum; for example, in skeletal muscle cell injury, large myelin figures are found in the interfibrillar spaces. Membrane fragments are also taken into autophagosomes. Autophagosomes bearing myelin figures are referred to as **myeloid bodies**.

Secretory Granule Degradration

As secretory cells degenerate, secretory granules become pleomorphic and irregular, and are distributed in unusual sites in the cytoplasm. **Crinophagy**, the autophagic uptake of secretory granules, is increased as the cell attempts to rid itself of the damaged granules. In goblet cells, granular pneumocytes, and other cells bearing granules important in protection of injured surfaces, there may be a hyperplastic response with increased granule production and crinophagy.[12]

Tubulation

Tubular projections from organelles of the endoplasmic reticulum and the other components of the cytoplasmic vacuolar system (transport vesicles, endosomes, lysosomes, Golgi complex) develop as an early manifestation of acute cellular injury. Tubular projections extending from the membrane of Golgi saccules appear as long, thin 90 nm tubules. Tubulation is associated with damage to the coating process that guides the various forms of transport vesicles to the proper destination. As these coat proteins fail to function, large areas of the Golgi complex form these tubules, which move peripherally into the cytoplasm, dispersing enzymes of the Golgi backward into the endoplasmic reticulum.[13,14]

Increase in Peroxisomes

Peroxisomal duplication occurs in nearly all injuries to rapidly metabolizing cells. Pleomorphic peroxisomes are typically massed in groups at sites of cellular injury. If mitochondria are the primary site of damage, newly formed peroxisomes will accumulate adjacent to them, often with membranes of the two in close apposition. In liver, centrolobular hepatocytes

Vet-ebooks.com

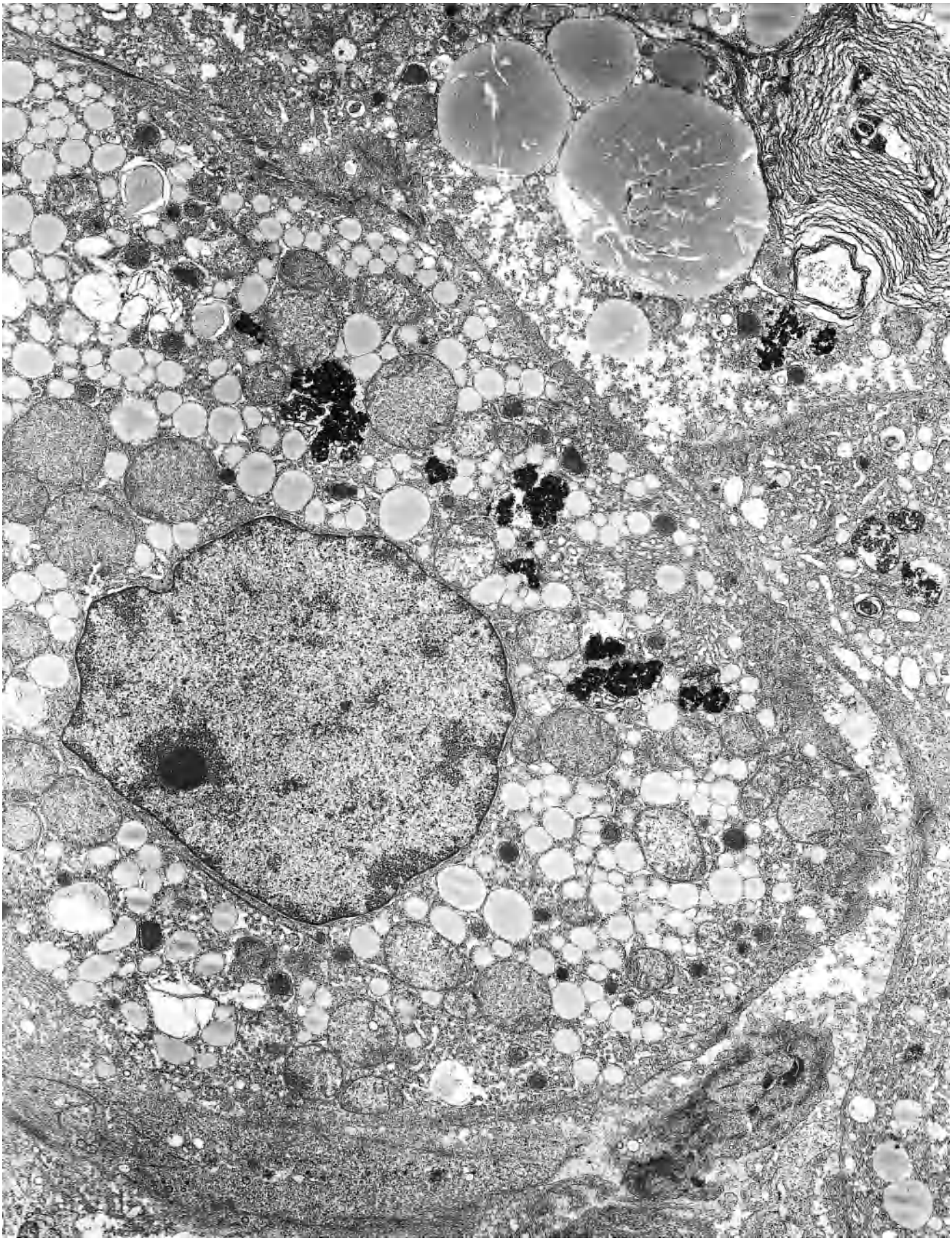


Fig. 1.5 Autophagy and steatosis: hepatocyte, dog, subacute toxic hepatic necrosis. Increased numbers of lipid globules reflect a marked production of triglycerides. Autophagic vacuoles are present throughout the cell. Note: myelin figures (*top right*), mitochondrial cristolysis, and accumulations of matrix proteins and debris in interstitial spaces.

Vet-ebooks.com

are most sensitive to peroxisomal proliferation; abnormal peroxisomes with matrix tubules are apt to occur in more peripheral areas.

The Nucleus in Acute Cell Swelling

Nuclear Pores Disintegrate

The **nuclear envelope** undergoes major changes in acute cell swelling. It becomes turgid and the perinuclear space dilates. **Nuclear pores**, which are avenues for exchange of water, ions, and proteins between nucleus and cytoplasm, become stretched, lose their **septae** (diaphragms), and disintegrate. The network of delicate **fibrils** that connect adjacent pores and radiate inward from the pores into the nucleoplasm is affected early, especially those fibrils that connect adjacent pores. At the cytoplasmic face of the nuclear envelope, the cytoskeleton collapses around the nucleus. This collapse may reinforce the closure of nuclear pores that protect the nucleus from toxins in the cytoplasm.

Nucleoli Become Eccentric and Disintegrate

Nucleoli move to the periphery of the nucleus. **Nucleolar margination** is an attempt to facilitate nuclear-cytoplasmic interchange in early cell injury. As injury progresses however, this is ineffective and the nucleolus begins to degenerate. When severely injured, nucleoli disintegrate in the following progression:

- **Disassembly of fibrillar centers** and surrounding **dense fibrillar components**, a change caused by diminished transcription of rRNA genes by RNA polymerase I and leading to aggregation and disappearance of fibrillarin and small nuclear RNAs
- **Disassembly of the granular component**, which is brought about by the diminished assembly of preribosomal particles
- **Dissociation of components**, the fibrillar component, granular cortex, and intranucleolar chromatin
- **Segregation of fibrillar and granular components** into distinct zones
- **Disappearance of fibrillar and granular areas**

Nucleolar damage is most obvious when DNA or its polymerases are specifically injured.[15,16] For example, aminonucleoside antibiotics selectively inhibit the nucleolar enzyme RNA polymerase I and block production of preribosomal RNA, the product of this enzyme; affected nuclei segregate, form microspherules, and fragment, and the remaining nucleolar components condense.[17]

Chromatin and Nuclear Proteins Aggregate

Clumping of chromatin accompanies cell injury. Granules of chromatin disappear from the central karyoplasm as chromatin increases in areas adjacent to the inner side of the nuclear envelope. Attributed, in part, to the lowered pH of acute cell swelling, this change reverses upon recovery. **Perichromatin granules**, electron-dense solitary 30–35 nm granules with a surrounding halo, accumulate around nucleoli in some toxic reactions, a change associated with decreased protein synthesis.[18,19]

In sublethal injury, chromatin may be depleted or there can be massive deposits. In severe injury,

- **Small fragments of chromatin are randomly formed in the karyoplasm**: a change caused by indiscriminant breaking of chromatin strands (Fig. 1.6)
- **Chromatin segments are small and uniformly dispersed** throughout the karyoplasm: chromatin segments have been cleaved evenly
- **Massive crescent-shaped deposits** of chromatin adjacent to the nuclear envelope: a change caused by minimal breaks of single strands of DNA by specific endonucleases without further proteolytic breakdown (see apoptosis, chapter 2)

Excessive production of protein (or failure to degrade protein) leads to deposition of proteinaceous granules or filaments, most often from inappropriate aggregation of nucleoproteins. Massive aggregates of proteins or protein-membrane complexes appear as **intranuclear inclusions**, and are common in diseases caused by the DNA viruses, and by toxicity of heavy metals such as lead and bismuth. **Nuclear pseudoinclusions** (formed from invaginations of the nuclear envelope back into the nucleoplasm) must be differentiated from true nuclear aggregates.

DNA Damage

DNA damage is a common sequela of injury, particularly in neurons of the traumatized brain. Experimental studies in the traumatized rat brain reveal single- and double-strand DNA breaks and suggest that there are several pathways in the evolution of DNA damage after trauma.[20] Cytochemical techniques for in situ identification of DNA damage include DNA polymerase I-mediated biotin-dATP nick-translation (PANT, for single-strand DNA breaks), terminal deoxynucleotidyl transferase-mediated dUTP nick-end labeling (TUNEL, for double-strand DNA breaks), and the Klenow fragment of DNA polymerase I-mediated biotin-dATP nick-end labeling (for single and double breaks).

Vet-ebooks.com

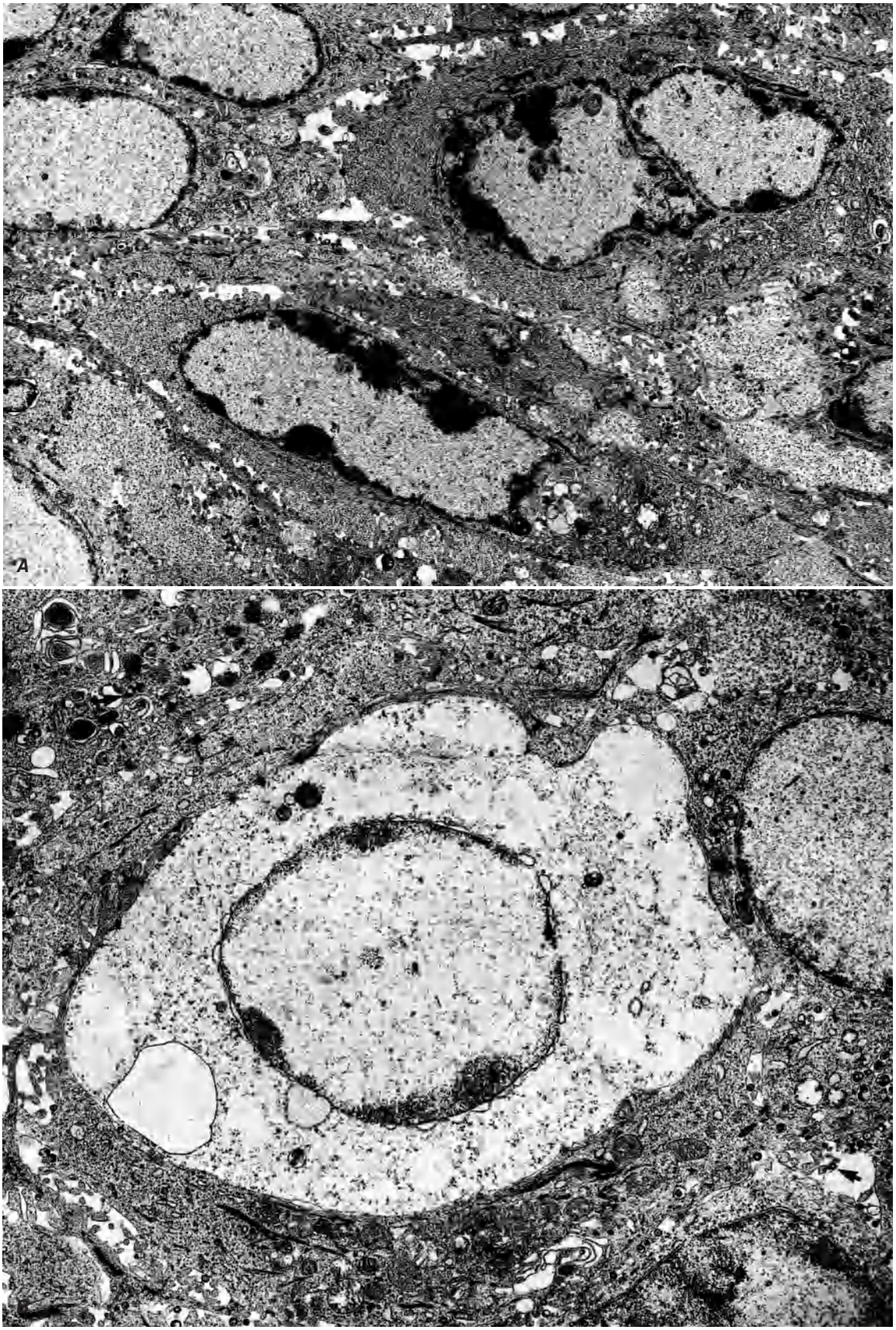


Fig. 1.6 Nuclear and cytoplasmic proteolysis: keratinocyte, cow, acute cell swelling, herpesvirus infection (infectious bovine rhinotracheitis). **A**. **Nuclear inclusions**: peripheralization of chromatin and nucleoli, and lysis of nuclear matrix. **B**. **Nuclear membrane breakdown**: there are lysis of cytoplasmic components, vacuoles and lysis of nucleoplasm with viral nucleocapsids in nucleoplasm and virions outside the cell (*arrow*). Note the disintegration of the nuclear envelope with liberation of nucleocapsids into the cytoplasm.

Vet-ebooks.com

Rarefaction of Nucleoplasm

Nucleoplasmic rarefaction is a hallmark of acute swelling. After injury, enzymes are activated that degrade and lyse proteins and nucleic acids. Rarefaction of nucleoplasm is accompanied by clumping, or **peripheralization of chromatin** along the inner surface of the nuclear envelope. Chromatin clumping is most frequently a consequence of decreased cellular pH that occurs with accumulation of lactate. **Focal nucleoplasmic rarefaction** is uncommon but does occur in cellular injury that is slight and prolonged, typically where discrete metabolic pathways are specifically blocked.

Nuclear Envelope Collapse and Invagination

In severe injury, the nuclear surface becomes highly irregular and may invaginate on itself. Duplication of membranes of the envelope results in blebs that protrude into the cytoplasm. More commonly, the pressure of swelling causes invagination into the nucleus of focal areas of the cytoplasm, which, in cross section, appear as membrane-bound inclusions called **pseudoinclusions**. **Evagination** or **blebbing** of portions of the nucleus into the cytoplasm has been reported, but many of these types of inclusions are fixation artifacts. The outer membrane of the nuclear envelope does, however, bulge into cytoplasmic areas, usually in association with annulate lamellae formation.

Nucleus Contracts

Contraction of the nucleus with precipitation of chromatin into dense masses is the hallmark of lethal injury. Rupture of the nuclear membrane with fragmentation and release of nuclear contents, called **karyorrhexis**, terminates as **karyoklasis**. This total breakdown of the nucleus leaves only dense chromatin aggregates in the necrotic cell.

Plasma Membrane Is Irregular or Discontinuous

Structural defects in the **plasma membrane** and its **glycocalyx** and in the **cytoskeleton** below the membrane reflect a progressive loss of cellular architecture in acute swelling. Massive changes in the distribution of integrins, receptors, and adhesion molecules occur at the cell surface, and enhance the process of swelling and segregation of the cell from its neighbors.

Morphometeric studies of acute swelling clearly show a marked increase in cell volume. Swollen epithelial cells bulge from the normal limits of the epithelium. Extending outward into the surrounding cavity or lumen, the cell surface is irregular or bulbous, and by scanning electron microscopy can be seen to contain waves and pits. Epithelial surfaces develop a cobblestone appearance as open pits appear where cells have desquamated. Normal cells adjacent to swollen cells flatten and become dome-shaped as they move laterally to cover the basal area after the bulging degenerate cell is squeezed from the epithelium.[21]

As the cell surface is injured, integral proteins embedded in the plasma membrane move laterally in the membrane, away from the site of injury. Although not detectable by routine microscopy, this change in membrane protein distribution can be readily seen by freeze-fracture techniques. The protein knobs that are usually regularly distributed over the surface are missing at sites of injury. In some cases, lacerations of the membrane can be detected in these areas.[21]

Transmembrane proteins, which have random distributions in the plasma membrane, become aggregated or disappear.[22,23] By scanning electron microscopy, changes in membrane particles can be assessed and quantified. During acute cell swelling, integrins and other adhesion receptors are internalized by endocytosis, and this leads to disassociation, detachment, and exfoliation.[24]

Cell Surfaces Are Pitted

Surface pitting associated with accelerated endocytosis occurs in acute cell swelling of some cell types, especially in motile cells such as lymphocytes and erythrocytes. Surface pitting is a characteristic degenerative response, and scanning electron micrographs of cells injured by various membrane poisons reveal surface pits and craters. In experimental studies in vitro on cellular degeneration of thymocytes caused by corticosteroids, surface pitting was a result of exocytosis involving vesicles aggregated at the cell surface.[25]

Focal Lysis of Plasma Membrane

In discrete injury, focal discontinuities may be present in the lipid bilayers of the cell membrane (Fig. 1.7). This change should not be reported unless fixation of the specimen is rigidly controlled and accompanied by appropriate controls. Even then, it is best to have evidence that the agent involved is located at the site of injury. If a specific toxin, enzyme, or porin can be identified by immunolabels attached to the membrane, a discrete defect can be confirmed.

Vet-ebooks.com

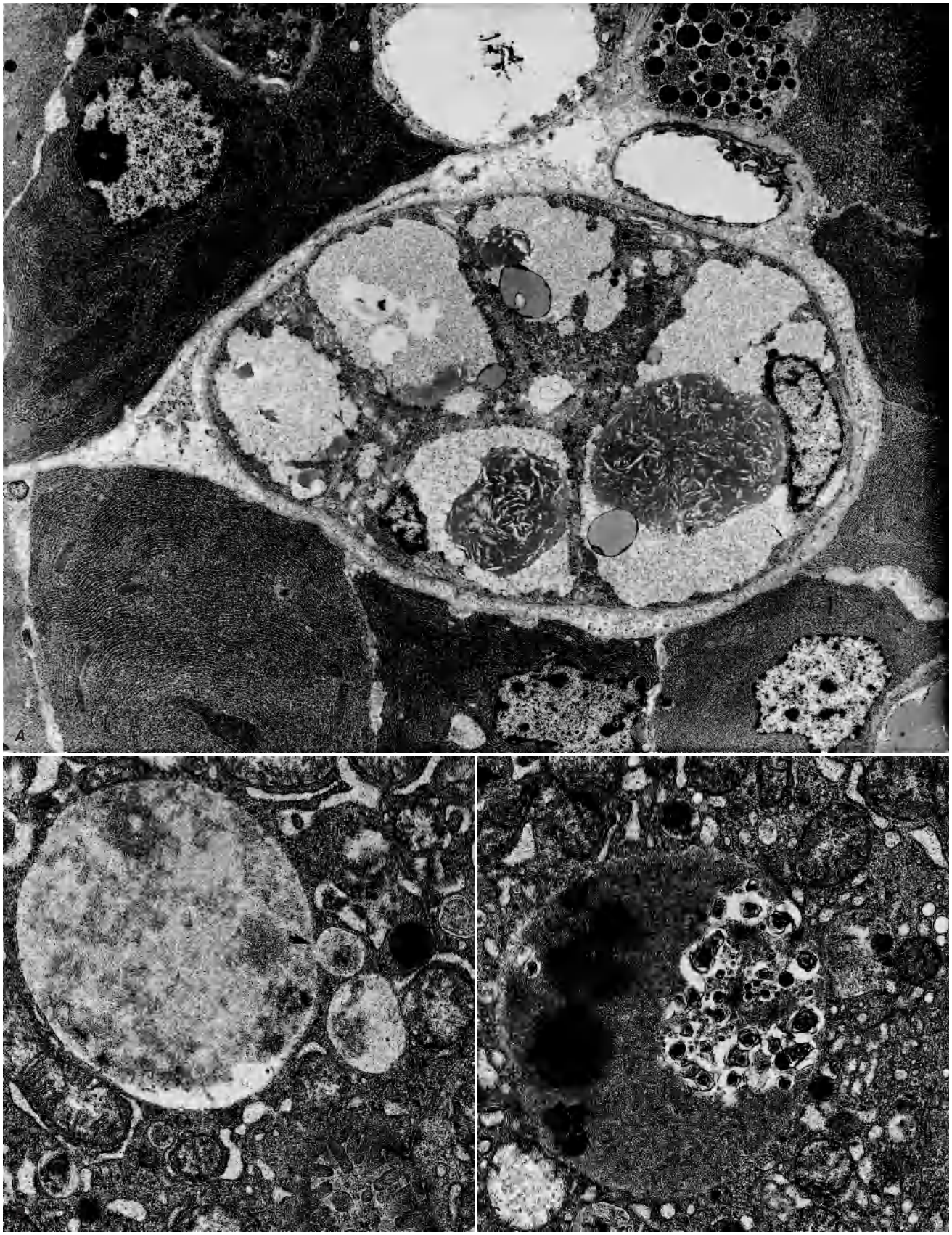


Fig. 1.7 Cytoplasmic lesions. **A**. **Acute cell swelling with glycogen and lipid**: pancreatic ductule, dog, acute pancreatic necrosis. Escape of enzymes into interstitial tissues causes necrosis in all components of tissue including capillary (*top right*), acinar cells, and ductal epithelium. **B–C**. **Proteinaceous vacuoles (hyalin globules)**, liver. **B**. **Early stage**: multiple granular inclusions formed by fusion of small protein-bearing vacuoles (*arrow*). **C**. **Late stage**: large dense proteinaceous inclusion bearing myelin figures and protein debris.

Vet-ebooks.com

Granulovesicular Debris Accumulates in Intercellular Spaces

As acute swelling progresses, tiny granules of protein debris accumulate, and the cytoplasm becomes blurred and disorganized. Membranes, because they become undulant, irregular, and twisted, are less distinct. At cell surfaces, accumulation of debris in interstitial spaces masks alterations that have occurred in the plasma membrane, microvilli, and intercellular junctions, and makes the interpretation of change difficult. The filling of intercellular spaces with granular debris and vesicles is a hallmark of advanced acute cell swelling. In low-power electron micrographs these spaces are clear and cells are closely apposed in most normal tissues; in acute cell swelling the membranes are indistinct and spaces are electron dense because of the debris.

Cell-to-Cell Contact Is Disrupted

The normal close apposition of parenchymal or epithelial cells is disrupted as cells are injured and acute swelling progresses. Cell junctions disintegrate and cells lose their normal cohesiveness with neighboring cells. Production of adhesion molecules and counterreceptors is suppressed, and this leads to separation of cells from their neighbors and sloughing from the surface. Internalization of persisting adhesion molecules by endocytosis enhances cell-to-cell detachment. Sloughing of epithelium results from loss of cell-to-basal lamina contacts; that is, the connections formed by hemidesmosomes and adhesion plaques with the extracellular matrix and basement membrane. In human renal biopsies from patients with acute tubular necrosis, there is focal epithelial loss in the nephron. Some single cells or arrays of cells are detached from the underlying basement membrane but are held in place by a few remaining junctional attachments to neighboring cells.[26]

Gap Junctions Close

One of the first events to occur in acute swelling, the separation and shut-down of gap junctions, is brought about by decreasing pH (cellular acidosis) and increasing calcium concentrations.[27] Gap junctions function in intercellular communication to transmit small molecules (just under the size of glucose) from cell to cell. The closing of gap junctions inhibits the spread of injurious agents and lethal amounts of cytokines. Gap junction loss may be a subtle change in micrographs taken by standard transmission electron microscopy. When hepatocytes affected by acute swelling are examined by freeze-fracture techniques, **connexons** (the large protein complexes that make up the channels in gap junctions) are decreased. Connexon proteins separate, disintegrate, and are dispersed within the plasma membrane and, in severe injury, are removed by internalization and autophagy. Gap junctions rapidly become disordered in swollen ischemic cardiac myocytes in human myocardial infarcts. When examined by immunolabeling techniques, gap junctional proteins, instead of being discretely aggregated at the intercalated disk, are widely diffused over the cell surface.[28]

Tight Junctions Disassociate

As cytoplasmic ionic balances shift, the plasma membrane becomes leaky and fluid accumulates in the cell. Because capillary endothelium is also affected at sites of injury, fluid tends to leak into and accumulate in interstitial spaces, isolating cells from one another and accentuating cellular "individualization." As this process proceeds, **tight junctions** disintegrate and cells tend to remain attached only at desmosomes.

Hemidesmosomes Detach

Hemidesmosomes maintain the attachment of basal surfaces of epithelial cells to the underlying basement membrane. After injury, hemidesmosomes are irregular and frayed. With special techniques, the anchoring fibrils can be shown to be missing from the subbasal lamina lucida. In the process of acute cell swelling, hemidesmosomal proteins disintegrate and the link between epithelial cell and basement membrane is severed.

Desmosomes Disintegrate

Desmosomes, the intercellular junctions that connect adjacent cells by strong mechanical coupling, are remarkably resistant to injury. They are the last cell junctions to disintegrate in severe acute cell swelling. As swelling progresses, however, desmosomes disintegrate. The dense desmosomal components separate from the plasma membrane, evaginate into the cytoplasm, are endocytosed, and are transported to lysosomes for degradation. **Intermediate filaments**, which are anchored in the desmosomal plaque, are released and aggregate in the cytoplasm.[29]

Cytoskeleton Disassembles

Disassembly of components of the subsurface cytoskeleton may be a direct effect of toxins, or may be secondary to degenerative effect elsewhere in the cell. In either case, there is disintegration of **microfilaments**

Vet-ebooks.com

(and the linker proteins that connect them to the plasma membrane), and of **intermediate filaments** that stabilize on intracellular junctions. This disruption of the peripheral cytoskeleton causes the cell to become rounded and to separate from its neighbors, a process referred to as **individualization**.

As a general response to acute cell swelling, microfilaments disintegrate into irregular globular aggregates of actin.[30] This change is difficult to assess in routine preparations but can be demonstrated by special immunolabeling techniques. Some toxins cause microfilaments to accumulate; actin polymerization is excessive and actin is assembled into large bundles of microfilaments. As with microfilament loss, the functional connections of actin with the plasma membrane and its surface structures are inefficient.

Other components of the cytoskeleton may be abnormal. **Intermediate filaments** thin or thicken with different types of injury.[31,32] Specific injury is directed to **microtubules** by colchicine[33,34] and by halothane and other volatile anesthetics, which cause **dissociation of microtubules** into component filaments with aberrant reassembly into twisted ribbons.[35,36]

When the cytoskeleton is damaged diffusely, cells rapidly change shape, becoming rounded. Loss of cortical structural support is associated with degradation of surface structures and shedding of massive areas of cytoplasm into interstitial areas, desquamation from lumenal surfaces, or embolization of large cell fragments.

Surface Structures Are Disorganized or Missing

Filopodia Are Altered

Injured cells typically have surfaces that are irregular and undulant, with **filopodia** of increased length and number. Filopodia are important in establishing connections with other cells, and are critical for the binding of macrophages and inflammatory leukocytes to each other, and to endothelial cells of blood vessels. Filopodia have binding properties that exceed other areas of the cell surface because their plasma membranes are rich in integrins and other adhesion molecules. Filopodia not only bind to other cells but also attach to bacteria and other microorganisms.[37]

Microvilli Are Distorted

With progressive acute cell swelling, the cell surface becomes disorganized and microvilli become irregular and are lost from the cell. Microvilli that remain are generally shorter than normal but, in some types of injury, as some microvilli disappear, others become longer. In acute toxic injury the actin core of the microvillus disintegrates, core microfilaments lose connections with the plasma membrane covering the microvillus, and the microfilament bundle disintegrates, causing the microvillus to shorten. In the kidney, microvilli of the proximal convoluted tubule are highly susceptible and rapidly disappear after injury. This is also characteristic of injured biliary canaliculi and of epithelium of the intestine where the remaining stubby microvilli often fuse together[38] (Fig. 1.8). In the small intestine, microvilli disintegrate into tiny vesicles, often in such large numbers that they may be confused with virions.

Cilia Disappear

Cilia become deformed, shortened, and disappear. Microtubular components retract and disassociate from other filaments in the cilium. Affected cilia may break or may retract with loss of internal components to the cytoplasmic matrix of the underlying cytoplasm. **Deciliation**, a common response of the respiratory tract, is typical of viral diseases such as influenza and paramyxovirus infections. Degeneration of the basal body that anchors cilia in the cell body usually precedes loss of cilia. Loss of cilia may be part of an active controlled process in the injured cell (rather than direct destruction by toxins). Some protozoa and algae cast off flagellae and other microtubule-containing components in response to injury. **Flagellar excision** involves severing of microtubules at specific sites near transition zones, special regions between flagellar axoneme and basal body, and is initiated by an increase in calcium in the cell.

Damaged Cytoplasm Is Shed by Exocytosis

Cytoplasmic Shedding

Cytoplasmic shedding is the exocytotic release of cellular material into the environment, either into interstitium or into lumens and ducts. Shed structures include:

- **Exosomes** (originating in microvesicles)
- **Membrane fragments**
- **Cytoplasmic blebs**

Cytosplasmic shedding is particularly active in surfaces bearing microvilli; for example, circulating leukocytes release procoagulant materials into the circulation by blebbing and cytoplasmic shedding. Cytoplasmic shedding is markedly increased in acute cellular injury, but also operates in normal cells in which it acts as a mechanism for release of small

Vet-ebooks.com

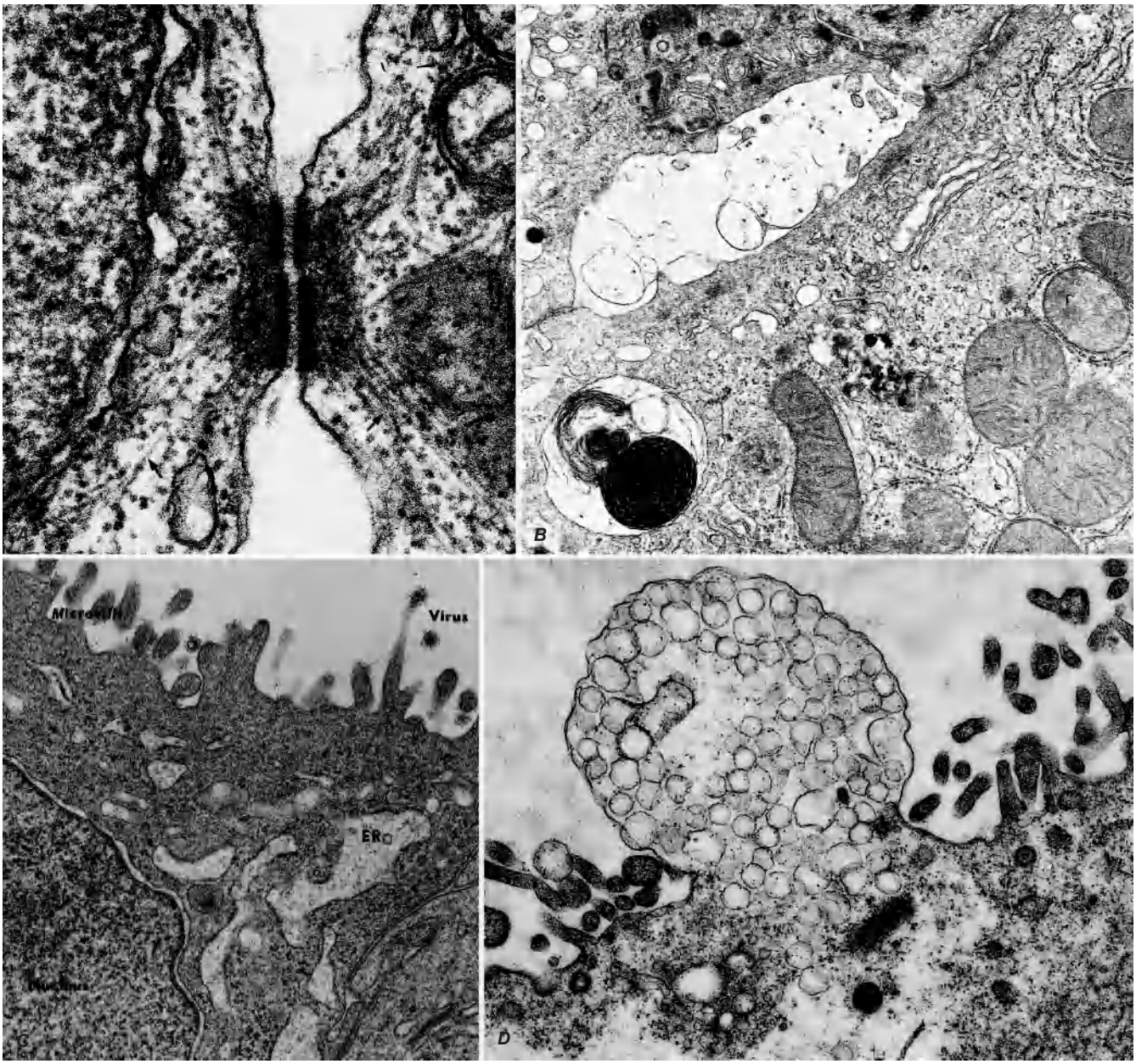


Fig. 1.8 Cell Surface pathology. A. Intercellular edema, persistence of desmosome: epidermis, fish. Intercellular filaments (*arrow*) radiate into the cytoplasm from submembrane plates of the desmosome. **B. Intercellular space expansion**: biliary canaliculus, liver, rat. Note increased thickness of intercellular junctions and loss of microvilli. **C. Surface structure degradation**: acute cell swelling, tracheal epithelium, paramyxovirus infection. Cisternae of the endoplasmic reticulum (*ER*) and nuclear envelope are dilated. Cilia are absent, and the cortical cytoplasm is devoid of basal bodies and microfilaments. Surface microvilli are irregular. Virions at the cell surface are labeled with ferritin (*Virus*). **D. Surface blebbing**: blebs, or bullae, on the surface of a pulmonary type I cell, lung, measles pneumonitis, monkey.

packets of damaged cellular components (see the section in chapter 5 on exocytosis).

Microvesicular Exocytosis

Small membrane fragments released as tiny **microvesicles** typically remain attached to the cell surface. In the kidney, microvesicles containing procoagulant material bleb from glomerular epithelial cells. Microvesicles are released into the lumen of the nephron and appear in urine;[39] an increase in microvesicles in urine is an index of renal injury.[40] Microvesicular shedding increases rapidly in injured renal tubules. Electron micrographs of renal tubular epithelium of rats poisoned with gentamicin reveal **membrane fragments** and dense **myelin figures** at the lumenal surfaces; micrographs of centrifuged urine show the same structures.[41]

Vet-ebooks.com

Surface Blebs Sequester Cytoplasm

Cytoplasmic blebs, also called **bullae**, are bulbous bubble-like evaginations of the plasma membrane that contain amorphous cytoplasmic debris mingled with fragments of endoplasmic reticulum, ribosomes, and vesicles. Rarely glycogen may be present, but larger organelles such as mitochondria, Golgi complex, and lysosomes are usually excluded. Blebs vary greatly in size and content. In acute cell swelling, they are typically small, spherical, and pale, with fine granules and small vesicles. Where the plasma membrane has been directly injured, as by phospholipases or lecithinases, blebs may be large and contain larger cytoplasmic organelles.

During **blebbing**, cytoplasmic material in the bleb is lost either by rupture of the bleb, or by release of the intact bleb. If the bleb is lysed, the underlying plasma membrane rapidly seals and the cell surface is repaired. In contrast, the entire bleb may be released as a vesicle; for example, as the bleb enlarges and protrudes away from the surface, the attachment to the cell becomes constricted. As these regions become pinched off, the bleb is released into the surrounding spaces of the cell.

Loss of integrity of the cytoskeleton near the cell surface is responsible for blebbing. Blebs develop as parts of the cytoplasm pass through focal defects in the cortical cytoskeleton. As acute cell swelling proceeds and surface microvilli and cilia fragment, the cytoskeletal network of microfilaments and microtubules that underlies the plasma membrane begins to disintegrate. As actin in microfilaments depolymerizes, focal areas of weakening appear under the cell surface. The supportive cytoskeletal network disappears in spotty areas so that the overlying plasma membrane bulges outward, creating foci of weakness in the cytoplasmic matrix, and leading to formation of blebs on the surface. Like a hernia in the abdominal wall, the cytoskeletal defect permits components of the cytoplasm to push outward from the cell surface.

Blebbing is a remarkably uniform process in different types of cells. The site where blebbing occurs is dependent upon the site and type of injury. In the polarized hepatocytes of the liver, bleb formation develops on canalicular surfaces when the biliary tract has been specifically damaged. In contrast, in hypoxic or toxic injury, blebs first appear on sinusoidal and basolateral surfaces, often protruding through endothelial fenestrations into the hepatic sinusoid.

The mechanism of bleb formation most commonly is caused by **ATP depletion**. Because polymerization of monomeric G actin to filamentous F actin requires ATP, **actin depolymerization** occurs when ATP is no longer available. Changes in cellular Ca^{++}, pH, and cell volume can enhance blebbing, but generally are subservient to loss of ATP in the formation of blebs.[42] Oxidative stress induced by formation of toxic oxygen radicals (O_2^+, H_2O_2, OH•) causes blebbing (unrelated to ATP loss); thiol depletion and calcium accumulation related to inhibition of calcium transport systems may be involved in this mechanism. The plasma membranes of blebs have disturbed phospholipid distributions, and the **phosphatidylserine scramble** that follows membrane injury is a signal for macrophage uptake.

Hypoxia is a common cause of blebbing. In the liver, centrolobular hepatocytes are prone to this type of injury and develop blebs that project into the sinusoidal lumens. Experimentally, in rat livers made hypoxic, the blebs have been shown to arise from preexisting microvilli. An early change produced by bacterial **enterotoxins** on intestinal epithelial cells is marked formation of surface blebs, most of which, like blebs of the hepatic canaliculus, arise from damaged microvilli.[43]

In cell cultures, blebbing can be reversed by processes that remove or stop the injurious process or that correct the calcium level of the cell. In cultured hepatocytes, as Ca^{++} rises in the cell, surface blebbing rapidly progresses; correction of the ionic balance prevents blebbing.[44,45] Blebbing arising from focal lipid peroxidation within the plasma membrane can be prevented if peroxidation is controlled by antioxidants such as tocopherol.[46]

Irregular, pleomorphic, club-shaped processes on the surface, referred to as **pseudopod formation**, are common in cells of severely ill individuals. Foci of pseudopodia or blebs are particularly common on erythrocytes in uremia, heat stroke, plasma electrolyte imbalance, chemical toxicity, and generalized maligant neoplasms.

Pericellular Environment Is Altered

Cells Are Missing

As cells degenerate and die they are either phagocytized in situ or are released into lumens or interstitial spaces. As cell loss increases, these areas appear as denuded surfaces or empty foci in the tissue. In place of cells, there are tissue debris, inflammatory cells, and precipitates of plasma proteins. Within the vascular system, degenerate leukocytes may fragment and appear as pseudoplatelets. Endothelial cells are commonly sloughed from vascular lumenal surfaces and circulate in the bloodstream.

Vet-ebooks.com

Adaptive Responses to Persistent Injury

Hypertrophy

Hypertrophy is an increase in size or volume of the cell. Hypertrophic cells have a decrease in the nucleus to cell volume ratio, and there is marked expansion of the cytoplasm with striking changes in shape of the soma and nucleus. Changes in cell shape and nuclear shape are closely coupled; desmin and lamin B are anchored to each other at the nuclear pore through anchorage proteins so that expansion of the cytoplasm pulls the nuclear envelope peripherally.[47] Organelles and inclusions of hypertrophied cells are larger than normal, and their size is increased in proportion to their increased function.

In hypertrophic cells, increased metabolic activity is first seen as expansion of **rough endoplasmic reticulum** and enlargement of **mitochondria** (Fig. 1.9). Amplification of RER, both in volume and density of attached ribosomes, is the most striking change in hypertrophy.[48] The **Golgi complex** is enlarged[49] and, like the RER, may contain aggregates of cisternal proteins. Adjacent to the Golgi complex are many vesicles and "prosecretory granules."

The most common examples of hypertrophy arise from increased workload, especially from persistent endocrine or neural stimulation.[50] Hypertrophy is manifest as an increase in protein synthesis, especially for proteins that are involved in cellular growth. In kidney there is an increase in **transport vesicles** associated with ion transport, in endocrine and exocrine gland epithelial cells there is an increase in **secretory granules**, and in muscle there is an increase in **myofilaments**.

Hyperplasia

Hyperplasia is an increase in the number of cells in a tissue. As in hypertrophy, the hyperplastic cell and its organelles are not qualitatively abnormal; they are simply present in greater numbers. The significant changes in cell ultrastructure resemble those of hypertrophy; for example, increase in the amount of **RER**,

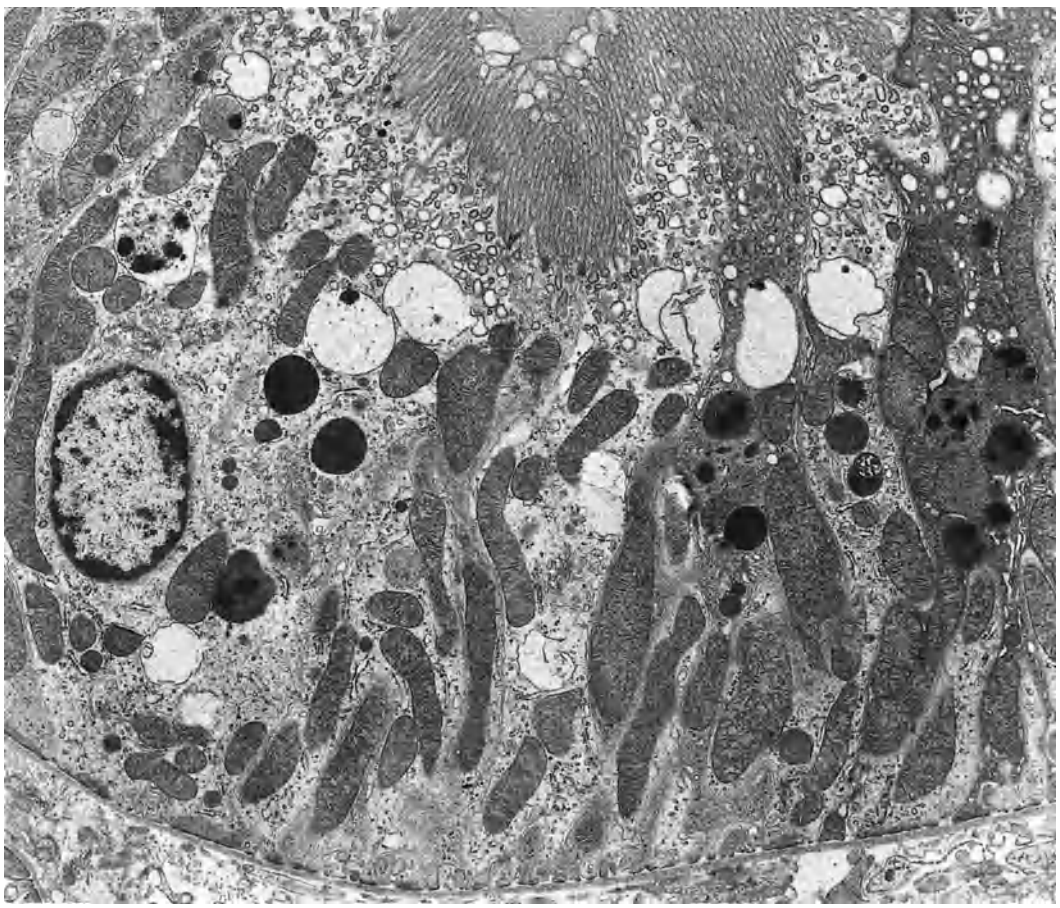


Fig. 1.9 Hypertrophy: right kidney, dog, compensatory hypertrophy. Kidney sample was taken 2 weeks after unilateral nephrectomy of the left kidney. Marked enlargement of mitochondria.

Vet-ebooks.com

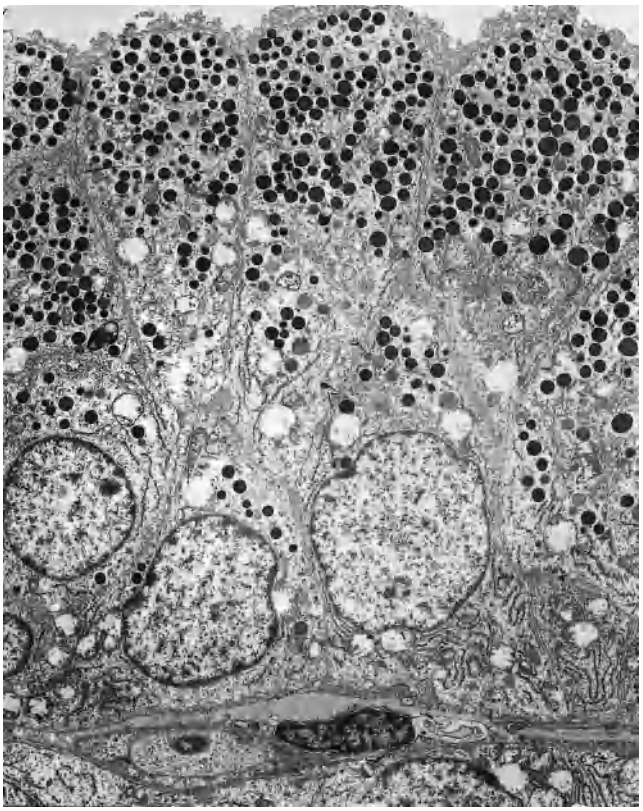


Fig. 1.10 Hyperplasia—chronic: prostate, dog, prostate hyperplasia. Epithelial cells are enlarged, polar, and filled with masses of secretory granules.

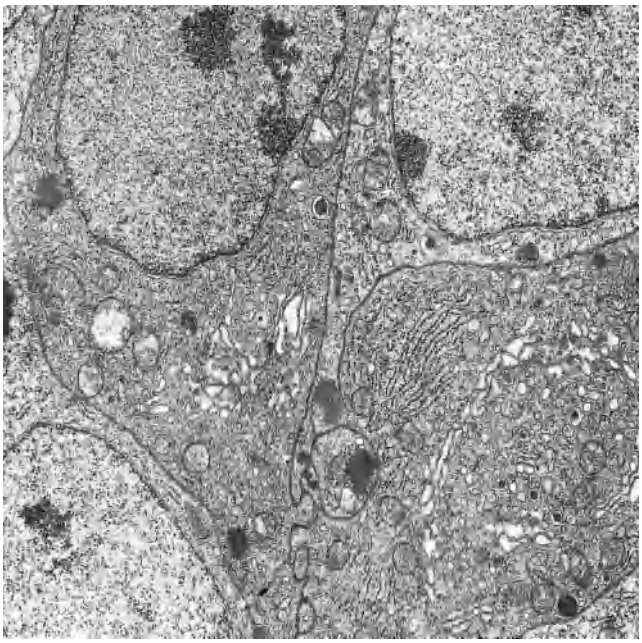


Fig. 1.11 Hyperplasia—active chronic: parathyroid gland, turkey, vitamin D deficiency. Hyperplastic pale chief cells have large Golgi complexes with many vesicles and irregular plasma membrane infoldings. Cytoplasm is vacuolated.

in size of **Golgi complexes**, and in length of the **plasma membrane**. Hyperplastic cells of endocrine glands under continual stimulation have strikingly prominent RER and there are multiple Golgi complexes with many Golgi vesicles, especially in the trans Golgi network (Fig. 1.10). **Nuclei**, because of active transcription, have very large nucleoli and large numbers of perichromatin granules and small ribonucleoprotein (RNP) particles.

In long-term hyperplasia of secretory cells under low-grade stimulation, **secretory granules** accumulate (Fig. 1.11). There are also marked changes in **glycogen** and **lipid globules**. In human **parathyroid glands** obtained from patients with primary hyperparathyroidism, a significant criterion for hypertrophy is a decrease in the amount of cytoplasmic lipid.[51]

Common causes of hyperplasia are stimulation by hormones, cytokines, and certain viruses. Chronic microbial infection and trauma induce hyperplasia in epithelia; for example, a callus in the skin arises from hyperplastic keratinocytes. Parasite infestation of the skin, gut, respiratory tract, or urogenital system is noted for inducing epithelial hyperplasia, mediated by cytokines or parasite products that have cytokine-like activity.

Hyperplasia of Endocrine Cells Endocrine cells in **late stages** of hypertrophy and hyperplasia have few secretory granules. After prolonged stimulation, the cell is no longer responsive to stimulation and develops vacuoles and fat globules. **Endoplasmic reticulum** becomes fragmented and vesicular, contributing to vacuolation. Those **secretory granules** that remain are often irregular in size and density. Endoplasmic reticulum commonly forms abnormal arrangements or whorls. The large amounts of ribonucleoproteins produced from intense stimulation may result in nuclear inclusion bodies, especially in rodent tissues.[52] **Chronic hyperplasia** in endocrine tissue typically leads to nodular islands of hyperplastic cells. In certain strains of animals, nodular hyperplasia is characterized by neoplastic change.[53]

Hypertrophy and hyperplasia of the **adrenal cortex** occurs in diseases that demand increased aldosterone or glucocorticoid secretion. When adrenocortical cells are stimulated by ACTH to secrete, there are progressive decreases in cytoplasmic steroid lipid bodies, increases in smooth endoplasmic reticulum, and reduplication of mitochondrial cristae.[54,55] Rough endoplasmic reticulum transforms into smooth in response to ACTH. **Mitochondria** are actively engaged in synthesis of steroid hormones and exhibit striking changes when stimulated. Cristae become bulbous and appear as small rings within the mitochondrion when they are cut in cross section. The inner membrane of cristae shows most rapid change since this is the site

Vet-ebooks.com

where hydroxylases required for steroid synthesis are located. Stimulation of rats with corticotropin releasing hormone leads to increase in serum corticosterone and rapid changes in the mitochondrial inner membrane (membrane increases in a biphasic time course with peaks at 2 and 8 hr after stimulation); an increase in mitochondrial volume occurs later, at 24 hr.[56]

After a single intense stimulus, target endocrine cells undergo an explosive secretion that produces ultrastructural characteristics of **secretion exhaustion** (Fig. 1.12). Nuclei have large activated nucleoli and the cytoplasm lacks the normal number of secretory granules and is filled with vacuolated secretory vesicles and larger vacuoles, which are remnants of aberrant secretory vacuoles. During rapid secretion, the endocrine cell cytoplasm may evert into blebs that project into sinusoidal lumens through fenestrae in endothelial cells.

Cytomegaly

Cytomegaly is pathologic enlargment of cells. Cytomegalic cells are expanded in both nuclear and cytoplasmic volume. Specific pathways of metabolism are blocked in cytomegaly, while others remain productive. The cell continues to grow but does not divide or stop its synthetic activity accordingly (cytomegaly is the reverse of neoplasia; the cell grows but does not reproduce). Cytomegaly associated with chronic infection is characteristic of certain viruses, intracellular fungi and nematodes, drug toxicity, and excessive endocrine stimulation.[57]

Cell volume in cytomegaly can be expanded up to 1,000 times that of the normal cell. Specific organelles may be preferentially increased, but in most cases the dominant growth change occurs in nuclei and in **ribosomes**, **RER**, and other protein synthesizing structures (Fig. 1.13). The **nucleus** enlarges at a rate consistent with that of the cytoplasm. Nucleoli are expanded and are often increased in number. Multiple nuclei develop in some types of cytomegaly, and this is most common in rodents. In toxic cytomegaly, **smooth endoplasmic reticulum** may be involved. The large pale homogeneous "ground glass" cytoplasm of hepatocytes that is seen in livers of human toxicity is associated with massive reduplication of smooth endoplasmic reticulum. Striking increases in nuclei per hepatocyte have been recorded in the cytomegaly of **aflatoxicosis**.

Cytomegaloviruses produce marked cytomegaly in various types of cells in several organs. The mechanism of development involves a marked stimulation of the mechanisms of protein synthesis with increases in DNA, RNA, and ribosomes. The nucleus and cytoplasm enlarge simultaneously, and in final stages may become 10 times the diameter of normal cells (and 100 times normal cell volume). Avian and ovine **adenoviruses** induce striking cytomegaly; for example, in splenic macrophages in "marble spleen disease" and in pulmonary macrophages in adenoviral pneumonia of sheep. The most striking example of viral cytomegaly is in lymphocystic disease of fish; the causal **iridoviruses** induce large DNA-containing inclusions that produce giant cells up to 1 mm in diameter.

Multinucleate Giant Cells

Multinuclear giant cells (syncytia, polykaryons) develop in two ways: by **fusion** of two or more cells to form one large cell with multiple nuclei, or by **nuclear division** with failure of subsequent cell division.

Nuclear Division

Giant cells that form by division of nuclei without cytoplasmic division occur in congential dysplasias and neoplasms. One of the most studied giant cells is the **Reed-Sternberg cell** of Hodgkin's disease. Giant cells that form in toxic or dysplastic conditions lack the surface interdigitations of inflammatory giant cells and instead contain characteristic changes in nuclei. Giant cells formed in the atrophic and dysplastic testis of rats treated with pasteurella toxin show striking formations of giant cells.

Cell-to-Cell Fusion

In inflammation and reactions to foreign bodies, fusion of monocytes and macrophages can give rise to giant cells. Ultrastructurally, there are extensive interdigitations in the **plasma membranes** of fusing macrophages. Cell fusion occurs in these closely apposed membranes, the result being large cells with multiple nuclei. Nuclei may be clustered in the center of the cell or arranged in ring form around the periphery.

Giant Cells Caused by Bacteria and Fungi Multinucleated giant cells may be induced directly by microbial products or indirectly by antigen-induced release of cytokines.[58,59] When stimulated by specific antigens, T lymphocytes produce a soluble protein that causes circulating monocytes to fuse and form multinucleated cells.[60] The fungal metabolite **cytochalasin** produced by some aspergilli affects cell movement by altering microtubules of macrophages. Cell membranes are also affected, and fusion results in large, multinuclear giant cells.[61] Cytochalasin inhibits cytokinesis (cytoplasmic division), without affecting karyokinesis (nuclear division), by drug-induced

Vet-ebooks.com

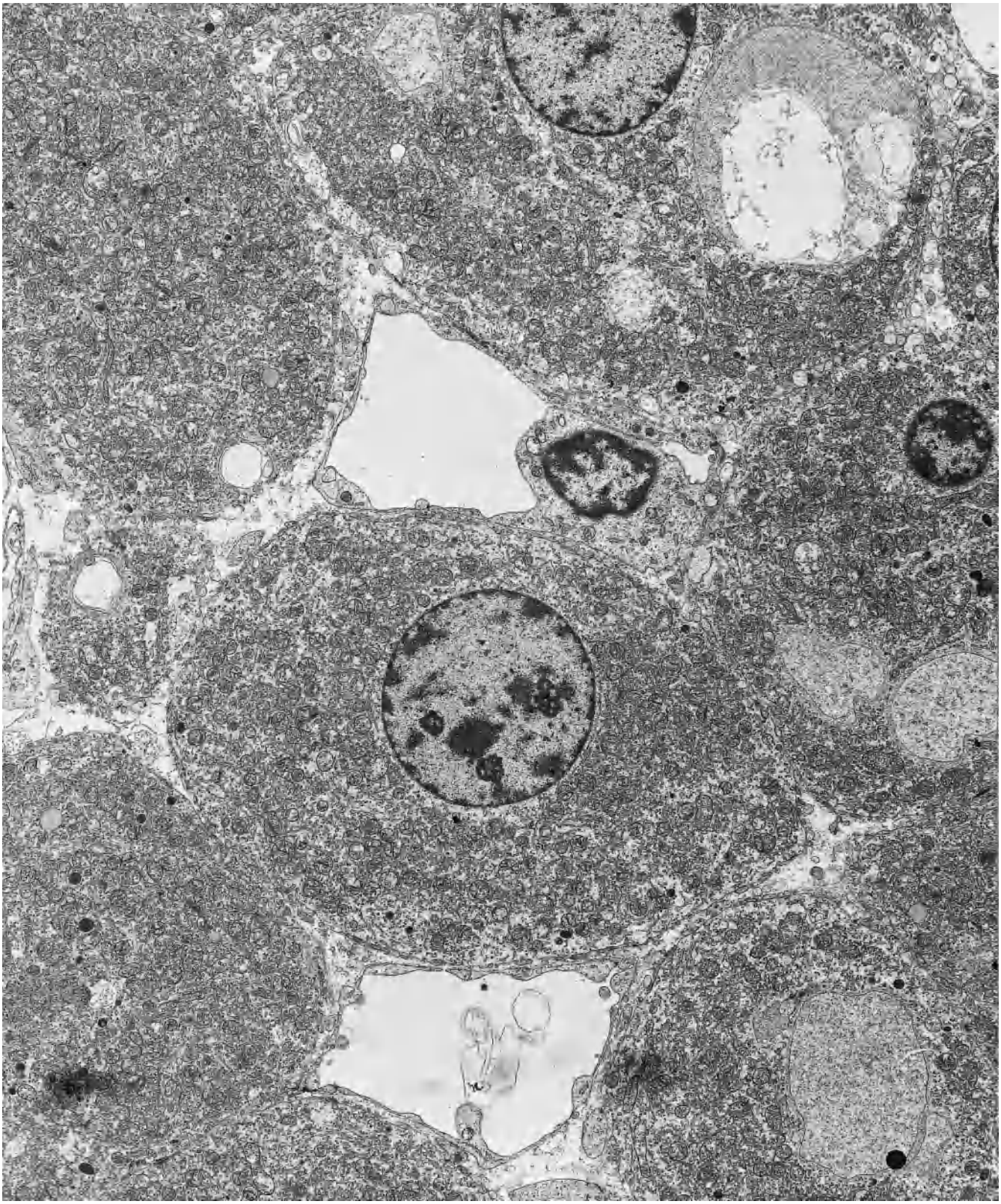


Fig. 1.12 Hyperplasia—peracute: adrenal medulla, sheep, massive secretory release during acute anaphylaxis. Cells are vacuolated and depleted of secretory granules. Nuclei have multiple nucleoli. Parenchymal cells are closely related to capillaries, the endothelium of which contains membrane blebs and other defects.

Vet-ebooks.com

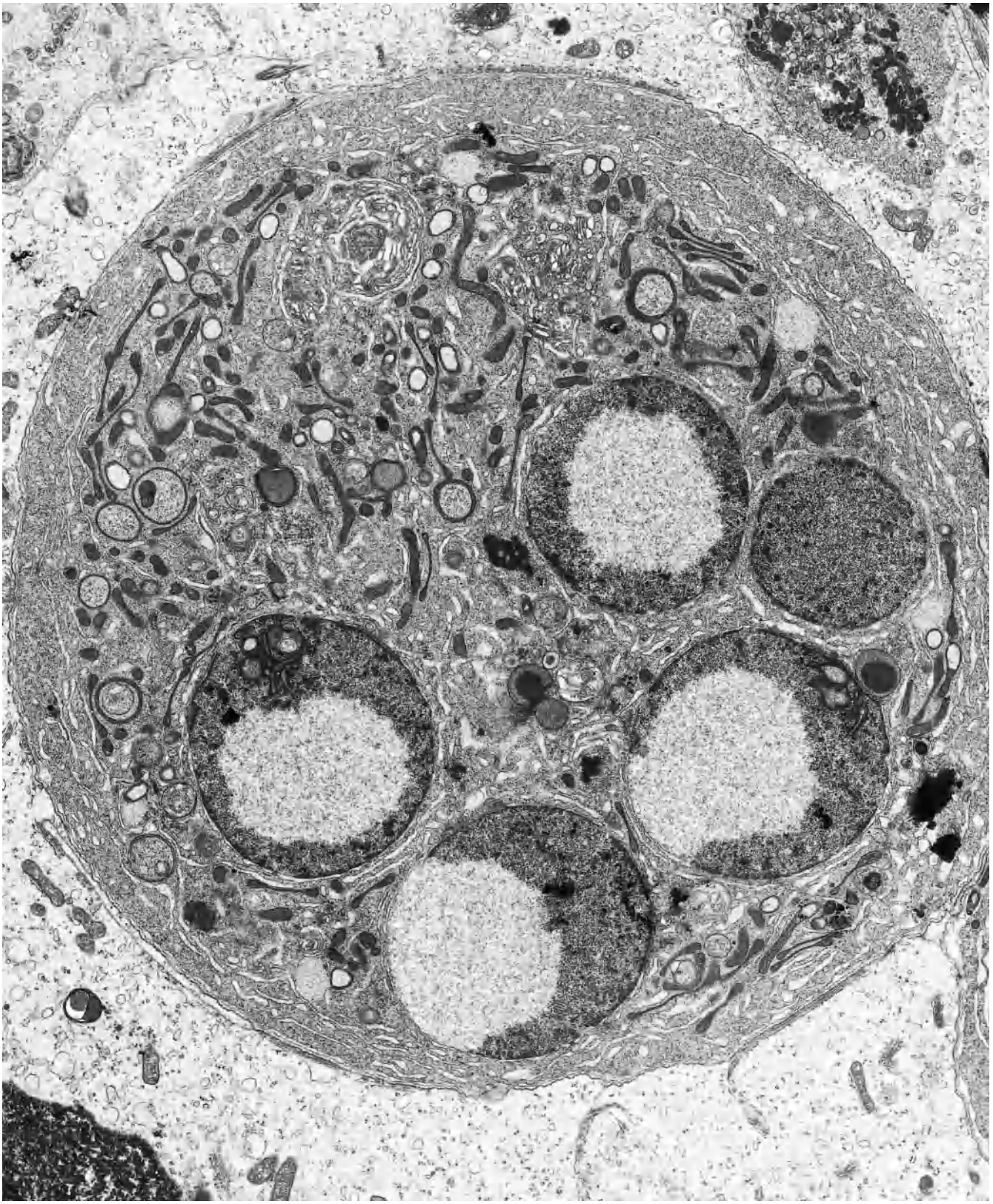


Fig. 1.13 Cytomegaly: multinucleate giant spermatid: testicle, rat given pasteurella toxin. Cytoplasm is markedly changed, and nuclei of phagocytized spermatogonia have electron-lucent zones. (Micrograph: Mark Ackermann, *J Toxic Pathol* 20:103, 1992.)

Vet-ebooks.com

changes in microfilaments. Cell movement and granule secretion are also inhibited by the same mechanism.

Virus-Induced Giant Cells Viruses typically produce giant cells through massive production of viral proteins that requires viral intervention in the control of protein synthesis (Fig. 1.14). Viruses that contain fusion proteins on the virion surface (paramyxoviruses, togaviruses, and the viruses of measles and canine distemper) produce giant cells by inducing fusion of plasma membranes of adjacent infected cells. Virions of paramyxoviruses have surface spikes of hemagglutinin and fusion protein. Membrane fusion requires the viral agglutinin, which brings membranes together, and the fusion protein, which promotes rearrangements for membrane fusion. Clustered at sites where release of virions is to occur, these glycoproteins initiate fusion with adjacent cells.

Metaplasia

Metaplasia is substitution by one type of fully differentiated adult cell in a tissue for another adult cell type normally found there. Also called **transdifferentiation**, it represents replacement of vulnerable cells by cells that are more resistant to an inciting injurious agent. Metaplasia develops over a long period of persistent low-level injury. For example, bile duct epithelium exposed to ductal foreign bodies, stones, or parasites develops degenerative changes; during incomplete attempts at recovery there are marked changes in metaplastic epithelial cells that show striking changes in intercellular junctions, increased mitotic rates, and variability in number and form of mucous granules.[62]

Metaplasia typically arises from a direct effect on stem cell populations. The defect involves divergence from normal paths of differentiation in these totipotential cells. For example, hepatocytes can develop from ductal epithelium of the pancreas.[63,64] In **salivary gland hyperplasia**, there is gradual dedifferentiation of acinar cells and hyperplasia of acinar, ductal, and myoepithelial cells.[65]

Squamous metaplasia of epithelia of respiratory, urinary, and alimentary tracts often occurs when these tissues are chronically irritated or inflamed. Lesions in lungs of smokers are especially prominent at tracheal bifurcations—sites where particles of smoke are deposited.[66,67]

Mucous metaplasia is a response of squamous epithelia to chronic inflammation. Mucous metaplasia caused by chronic gastroesophageal reflux in the human esophagus is composed of a wide spectrum of mucus producing cell types, all of which may arise from primordial gastric mucous neck cells of the stomach.[68,69]

Atrophy

Atrophy is the decrease in size of cells that have gained full development. Atrophy represents adaptation to a changed cellular environment. Cells shrink when their level of work is diminished or when their source of nutrition or stimulation is removed. Skeletal myocytes wasted away in muscle disuse, prostate epithelium atrophic after castration, the regressing mammary gland epithelial cell shrunken in old age,[70] neurons of the cardiac ganglia atrophic after vagotomy[71]—all are examples of atrophy.

Atrophic cells are small and, except for lysosomes, their cytoplasmic organelles are fewer in number and size (Fig. 1.15 and 1.16). **Nuclei** are small and in an eccentric position. Striking nuclear changes are the loss of nucleoli and disappearance of chromatin and RNP granules. In the cytoplasm, the loss of ribosomes, endoplasmic reticulum, and secretory granules reflects the lack of stimuli for transcription, translation, and conjugation of secretory proteins. In secretory cells, secretory granules are degraded, and there is loss of membrane integrity, fusions of adjacent granules, and disintegration of granule content from periphery inward.[72,73]

Autophagy (autophagocytosis) is the process responsible for the end-stage appearance of lysosome-rich atrophic cells.[74–76] **Autophagic vacuoles**, which develop from the RER and Golgi complex, engulf degenerate cellular organelles for degradation and removal. As atrophic cells die, autophagic vacuoles fill the cell and are excreted into the surrounding extracellular environment.[77]

Interstitial fibrosis accompanies atrophy in most organs. Even minimal regressive changes in parenchyma are associated with production of collagen and basement membrane material and, in some cases, by development of fat cells. Morphometric analysis of testicular tissue of human males after **vasectomy** showed focal interstitial fibrosis as well as reduced Sertoli cells and spermatocytes per tubule cross section.[78]

Atrophy of Starvation and Cachexia

Restriction of food intake below the daily caloric requirement results in atrophy in adipose tissue, liver, pancreas, salivary glands, and gastrointestinal tract.[79] In this slowly progressive atrophy, parenchymal cells decrease in volume. In intestinal epithelium, microvilli regress, nuclei shrink, and lysosomes change into autophagosomes that degrade the cellular proteins.

Vet-ebooks.com



Fig. 1.14 Adenoviral cytomegaly: splenic reticular cell, avian adenovirus infection, chicken. Massive enlargement of nucleus and cytoplasm (compare to adjacent lymphocytes and reticular cells). Necrotic cells (*bottom left*) have undergone karyorrhexis, and have been phagocytized by other splenic reticular cells. Nuclear virions are preserved in necrotic cell (*bottom center*).

Vet-ebooks.com

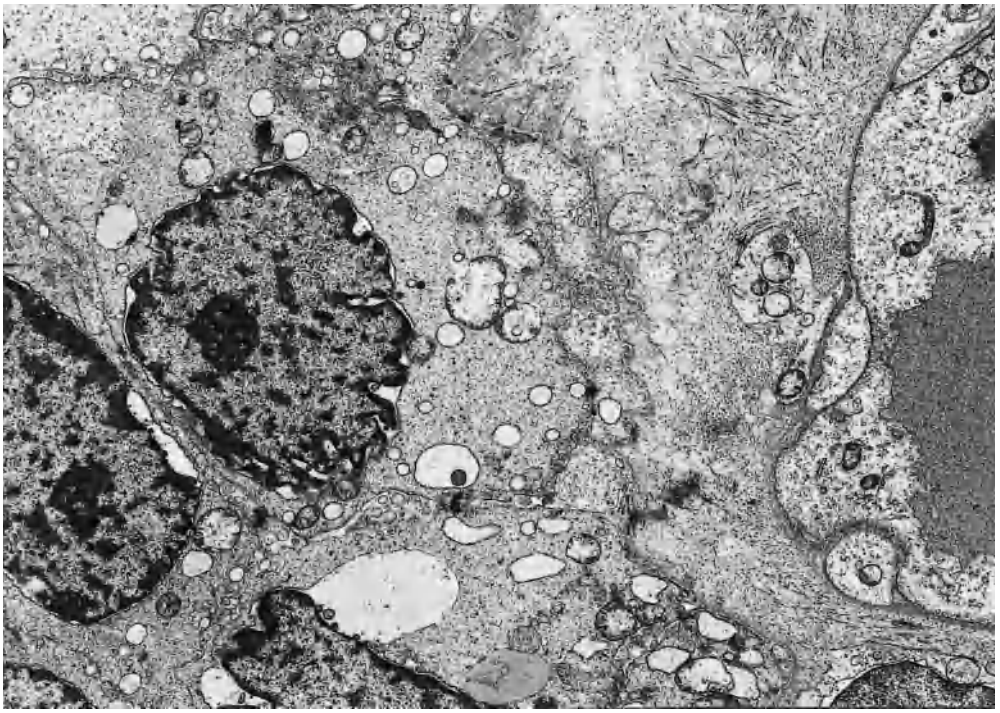


Fig. 1.15 Atrophy. Prostate epithelium, castrated dog. Epithelial cells are small: cytoplasm is markedly reduced, secretory granules are vacuolated, nuclei are shrunken, and the nuclear membrane is irregular. Basement membranes are thick and mesenchymal tissue is dense.

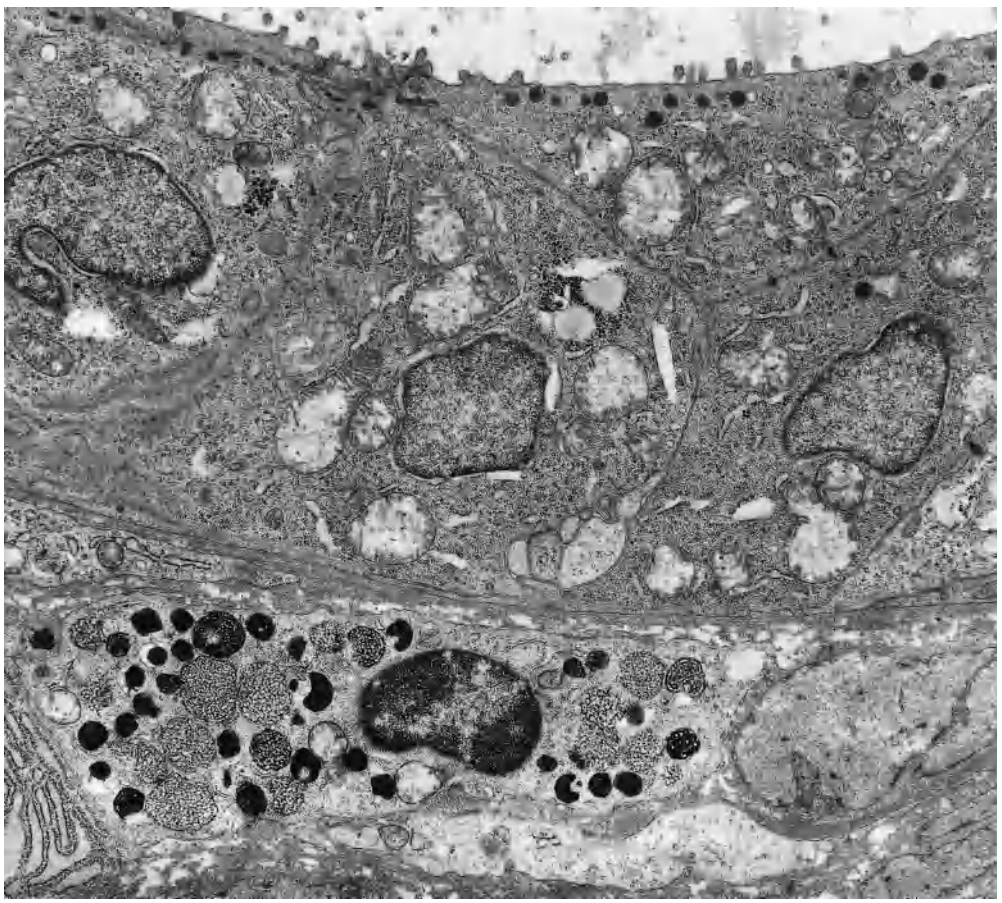


Fig. 1.16 Gastric chief cell, uremia: cell is long and narrow, secretory granules are small and irregular, and surface microvilli are small and diminished in number.

Vet-ebooks.com

Muscle wasting syndromes that result from aging, nutritional deficiencies, and prolonged chronic infections often result in diffuse atrophy of **skeletal muscle**. In cachectic atrophy, myofibers vary considerably in size, and shrunken atrophic fibers are intermingled with normal fibers. As the myofiber diminishes in size, nuclei become pyknotic and persist in linear arrangement in the destroyed myofiber. Destruction of myoglobin incites lysosomes to develop in perivascular spaces and along sarcolemmal sheaths.

The **liver** of starved animals is smaller than normal. **Hepatocyte** volume is reduced up to 50% and both smooth and rough endoplasmic reticulum are reduced. The number of mitochondria may remain unchanged, but individual mitochondria are increased in size by excessive matrix material.[80,81] These regressive changes result from loss of glycogen and shutdown of cell enzyme systems and synthesis of protein and lipids, brought about in part by the lowering of the serum thyroid hormone T_3 (with concomitant increase in noncalorigenic T_3 metabolites). Within 24 hr of food deprivation, blood glucose and hepatic glycogen are markedly decreased. There are simultaneous increases in glycogen phosphorylase (for glycogen degradation) and decreases of glycogen synthetase (for synthesis). As fasting continues, there are profound alterations in other enzyme systems relating to utilization for glucose and fatty acids.

Denervation Atrophy

Atrophy of skeletal myofibers is a direct consequence of denervation. Ultrastructural studies in rodents reveal the cellular changes to be present in the second month after denervation, a time when type II fiber atrophy is greater than that in type I fibers.[82] Myofilaments disappear in a variable and spotty manner. Mitochondria are rounded and small. Sarcoplasmic reticulum is duplicated and disorganized. Glycogen, lipid globules, and autophagic vacuoles are present in the cytoplasm. Muscle spindles persist. In addition to myocyte atrophy, long-term denervated muscle has evidence of myofiber and capillary death.[83] Microvascularization changes strikingly in atrophic muscle with loss of capillaries and medial hyperplasia in arterioles.[84] Myogenesis is abortive in attempts at repair.[85]

References

1. Kew MC, et al. 1978. Ultrastructural changes in the liver in heatstroke. *Am J Pathol* 90:609.
2. Peterlik M, Kerjaschki D. 1979. Interference of tris (hydroxymethyl)aminomethane with structure and function of Golgi membranes. *Lab Invest* 40:313.
3. Walker RM, et al. 1983. Scanning electron microscopic examination of acetominophen-induced hepatotoxicity and congestion in mice. *Am J Pathol* 113:321.
4. Farber E, et al. 1971. Dissociation of effects on protein synthesis and ribosomes from membrane change induced by carbon tetrachloride. *Am J Pathol* 64:601.
5. Kisilevsky R, et al. 1973. Ribosomal alterations following ethionine intoxication. *Lab Invest* 28:8.
6. Leduc EH. 1973. Sulfaguanidine protection of mouse liver from carbon tetrachloride-induced necrosis. *Lab Invest* 29:186.
7. Petito CK, Lapinskyi RL. 1986. Postischemic alterations in ultrastructural cytochemistry of neuronal Golgi apparatus. *Lab Invest* 55:696.
8. Verbin RS, et al. 1969. The biochemical pathology of inhibition of protein in vivo. *Lab Invest* 20:529.
9. Novikoff PM, Edelstein D. 1977. Reversal of orotic acid-induced fatty liver in rats by clofibrate. *Lab Invest* 36:215.
10. Sasaki S, et al. 2004. Ultrastructural study of mitochondria in the spinal cord of transgenic mice with a G93A mutant SOD1 gene. *Acta Neuropathol* 107:461.
11. Ades IZ, Cascarano J. 1979. Mitochondrial alterations in heart, kidney and liver of rats subjected to anemia hypoxia. *Exp Molec Pathol* 30:94.
12. Balis JE, et al. 1988. Ozone-induced lamellar body responses in rat model for alveolar injury and repair. *Am J Pathol* 132:330.
13. Hobman TC, et al. 1992. The rubella virus E1 glycoprotein is arrested in a novel post-ER, pre-Golgi compartment. *J Cell Biol* 118:795.
14. Klausner RD, et al. 1992. Brefeldin A: Insight into the control of membrane traffic and organelle structure. *J Cell Biol* 116:1071.
15. Lombardi B. 1976. Relation between nucleolar microspherule formation by urethan and inhibition of RNA and protein synthesis. *Cancer Res* 36:2210.
16. Merski JA, et al. 1979. Acute ultrastructural effects of the antitumor antibiotic carminomycin on nucleoli of rat tissue. *Cancer Res* 39:1239.
17. Studzinski GP, Albanese EA. 1980. Nascent RNA chain termination and ultrastructural changes in nucleoli isolated from SV40-transformed fibroblasts treated with aminonucleoside of puromycin. *Lab Invest* 43:427.
18. Derenzini M, Boyne G. 1978. The nucleolar origin of certain perichromatin granules: A study with α-amantin. *J Ultrastruct Res* 62:213.
19. Jacob M, et al. 2007. Chromatin breakdown by deoxyribonuclease 1 promotes acetaminophen-induced liver necrosis: An ultrastructural and histochemical study on male CD-1 mice. *Histochem Cell Biol* 128:19.
20. Clark RSB, et al. 2001. Detection of single- and double-strand DNA breaks after traumatic brain injury in rats. *J Neurotrauma* 18:675.
21. Henrikson CK, et al. 1989. Morphologic and functional effects of bile salt on the porcine colon during injury and repair. *Lab Invest* 60:72.
22. Coleman SE, et al. 1976. Plasma membrane changes in freeze-fracture rat kidney cortex following renal ischemia. *Lab Invest* 35:63.

Vet-ebooks.com

23. Van Deurs B, Behnke O. 1980. Membrane structure of nonactivated and activated human blood platelets as revealed by freeze fracture. *J Cell Biol* 87:208.
24. Racusen L. 1992. Alterations in tubular epithelial cell adhesion and mechanisms of acute renal failure. *Lab Invest* 67:158.
25. Morris RG, et al. 1984. Hormone-induced cell death. *Am J Pathol* 115:426.
26. Olson TS, Hansen HE. 1990. Ultrastructure of medullary tubules in ischemic acute tubular necrosis and interstitial nephritis in man. *APMIS* 98:1139.
27. James JL, et al. 1986. Alterations in hepatocyte plasma membrane in carbon tetrachloride poisoning. *Lab Invest* 54:268.
28. Smith JH, et al. 1991. Altered patterns of gap junction distribution in ischemic heart disease: An immunohistochemical study of human myocardium using laser scanning confocal microscopy. *Am J Pathol* 139:801.
29. Schenk P. 1975. Desmosomale Strukturen im Cytoplasma normaler und pathologischen Keratinocyten. *Arch Dermatol Res* 253:23.
30. Gabbiani G, et al. 1975. Phalloidin-induced hyperplasia of actin filaments in rat hepatocyte. *Lab Invest* 33:562.
31. Ohta M, et al. 1988. Pathologic changes in the cytoskeleton pericanalicular sheath in experimental cholestasis and alcoholic fatty liver. *Lab Invest* 59:60.
32. Rungger-Brandle E, Gabbiani G. 1983. The role of cytoskeletal and cytocontractile elements in pathologic processes. *Am J Pathol* 110:361.
33. Magalhaes MC, et al. 1985. Effects of vinblastine and colchicine on the rat adrenal cortex. *J Ultrastruc Res* 91:149.
34. Pavelka M, Ellinger A. 1983. Effect of cochicine on the Golgi complex of rat pancreatic acinar cells. *J Cell Biol* 97:737.
35. Hinkley RE Jr. 1976. Microtubule-macrotubule transformations induced by volatile anesthetics. *J Ultrastruc Res* 57:237.
36. Nicolson GL, et al. 1976. Effects of local anesthetics on cell morphology and membrane associated cytoskeletal organization in Balb/3T3 cells. *J Cell Biol* 68:395.
37. Young VB, et al. 1990. The invasion protein of *Yersinia enterocolitica*: Internalization of invasin-bearing bacteria by eukaryotic cells is associated with reorganization of the cytoskeleton. *J Cell Biol* 116:197.
38. Hirokawa N, et al. 1983. Mechanism of brush border contractility studied by the quick-freeze, deep-etch method. *J Cell Biol* 96:1325.
39. Wiggins R, et al. 1987. Lipid microvesicles and their association with procoagulant activity in urine and glomeruli of rabbits with nephrotoxic nephritis. *Lab Invest* 56:264.
40. Birk H-W, et al. 1992. Analysis of Na^+-D-glucose cotransporter and other renal brush border proteins in human urine. *Kidney Int* 40:825.
41. Josepovitz C, et al. 1985. Contrasting effects of gentamicin and mercuric chloride on urinary excretion of enzymes and phospholipids in the rat. *Lab Invest* 52:375.
42. Gores GJ, et al. 1990. Plasma membrane bleb formation and rupture: A common feature of hepatocellular injury. *Hepatology* 11:690.
43. McDonel JL, et al. 1978. The effects of *Clostridium perfringens* enterotoxin on rat and rabbit ileum. *Lab Invest* 39:210.
44. Jewell SA, et al. 1982. Bleb formation in hepatocytes during drug metabolism is caused by disturbances in thiol and calcium ion homeostasis. *Science* 217:1257.
45. Russo MA, et al. 1982. Ultrastructural pathology of phalloidin-intoxicated hepatocytes in the presence and absence of extracellular calcium. *Am J Pathol* 109:133.
46. Noronha-Dutra AA, et al. 1988. Epinephrine-induced cytotoxicity of rat plasma. *Lab Invest* 59:817.
47. Lockard VG, Bloom S. 1993. Trans-cellular desmin-lamin B intermediate filament network in cardiac myoctes. *J Mol Cell Cardiol* 25:303.
48. Wiest DL, et al. 1990. Membrane biogenesis during B cell differentiation: Most endoplasmic reticulum proteins are expressed coordinately. *J Cell Biol* 110:1501.
49. Inoue K, Kurusumi K. 1989. Ultrastructural observation of the trans-Golgi associated plate-like cisternae in the secretory cells of the rat anterior pituitary gland with special reference to the intracisternal skeleton. *Anat Rec* 225:272.
50. Barron KD, et al. 1982. Fine structure of neurons of the hypertrophied human inferior olive. *J Neuropathol Exp Neurol* 41:186.
51. Cinti S, et al. 1992. Parathyroid glands in primary hyperparathyroidism: An ultrastructural morphometric study of 25 cases. *J Pathol* 167:283.
52. Nickerson PA. 1973. Induction of intranuclear inclusions by estrogen in mammotrophs of the Mongolian gerbil. *J Ultrastruc Res* 44:41.
53. Tischler AS, et al. 1985. Spontaneous proliferative lesions of the adrenal medulla in aging Long-Evans rats. *Lab Invest* 53:486.
54. Finegold MJ, Green LE. 1970. Mitochondrial damage in experimental and congenital adrenal hyperplasia. *J Cell Biol* 45:455.
55. Giacomelli F, et al. 1965. Cytological alterations related to stimulation of the zona glomerulosa of the adrenal gland. *J Cell Biol* 26:499.
56. Bornstein SR, et al. 1992. Structure and dynamics of adrenal mitochondria following stimulation with corticotropin releasing hormone. *Anat Rec* 234:255.
57. Sigg C, Hedinger C. 1983. The frequency and morphology of "giant spermatogonia" in the human testis. *Virch Arch B* 44:115.
58. Kreipe H, et al. 1988. Multinucleated giant cells generated in vitro. *Am J Pathol* 130:232.
59. Sone S, et al. 1981. Kinetics and ultrastructural studies of the induction of rat alveolar macrophage fusion by mediators released from mitogen-stimulated lymphocytes. *Am J Pathol* 103:234.
60. Postlethwaite AE, et al. 1982. Formation of multinucleated giant cells from human monocyte precursors. *J Exp Med* 155:168.
61. Krishan A. 1971. Fine structure of cytochalasin-induced multinucleated cells. *J Ultrastruct Res* 36:191.
62. Eng F, Youson JH. 1992. Morphology of the bile ducts of the brook lamprey, *Lampetra lamottenii* (Le Sueur) before and during infection with the nematode, *Truttaedacnitis*

Vet-ebooks.com

stelmioides (Vessichelli, 1910) (Nematoda: Cucullanidae). *Anat Rec* 234:201.
63. Makino T, et al. 1990. Transdifferentiation of ductular cells into hepatocytes in regenerating hamster pancreas. *Lab Invest* 62:552.
64. Rao MS, et al. 1989. Role of periductal and ductular epithelial cells of the adult rat pancreas in pancreatic hepatocyte lineage. *Am J Pathol* 134:1069.
65. Dardick I, et al. 1985. Salivary gland components involved in the formation of squamous metaplasia. *Am J Pathol* 119:33.
66. Boucher RC, et al. 1980. The effect of cigarette smoke on the permeability of guinea pig airways. *Lab Invest* 43:94.
67. Woodworth CD, et al. 1983. Squamous metaplasia of the respiratory tract. *Lab Invest* 48:578.
68. Levine DS, et al. 1989. Specialized metaplastic columnar epithelium in Barrett's esophagus. *Lab Invest* 60:418.
69. Zwas F, et al. 1986. Scanning electron microscopy of Barrett's epithelium and its correlation with light microscopy and mucin stains. *Gastroenterology* 90:1932.
70. Gas N, Noailliac-Depeyre J. 1976. Studies on intestinal epithelium involution during prolonged fasting. *J Ultrastruc Res* 56:137.
71. Wong WC, et al. 1987. Effects of bilateral vagotomy on the ultrastructure of the cardiac ganglia in the monkey (*Macaca fascicularis*). *J Anat* 150:75.
72. Donath K, et al. 1973. Zur Pathogenese der Parotisatrophie nach experimentelle Gangunterbindung. *J Anat* 359:31.
73. Eppig JJ, Leiter EH. 1977. Exocrine pancreatic insufficiency syndrome in CBA/J mice. *Am J Pathol* 86:17.
74. Cole S, et al. 1971. Autophagic vacuoles in experimental atrophy. *Exp Mol Pathol* 14:158.
75. Glauman H, et al. 1975. Lysosomal degradation of cell organelles. *Lab Invest* 33:239.
76. Pfeifer U. 1970. Cellulare Autophagie: Glykogensegregation im Fruhstadium einer partielle Leberatrophie. *Virch Arch B* 5:242.
77. Gobe GC, Axelsen RA. 1987. Genesis of renal tubular atrophy in experimental hydronephrosis in the rat. *Lab Invest* 56:273.
78. Jarow JP, et al. 1985. Quantitative pathologic change in the human testis after vasectomy. *New Engl J Med* 313:1252.
79. Nevalainen TJ, Janigan DT. 1974. Degeneration of mouse pancreatic acinar cells during fasting. *Virch Arch B* 15:107.
80. Reid IM. 1973. An ultrastructural and morphometric study of the liver of the lactating cow in starvation ketosis. *Exp Molec Pathol* 18:316.
81. Riede UN, et al. 1973. Einfluss des Hunger auf die quantitativ Cytoarchitektur der Rattenleberzelle. *Beitr Pathol* 150:246.
82. Lu DX, et al. 1997. Electron microscopic study of long-term denervated rat skeletal muscle. *Anat Rec* 248:355.
83. Ashley Z, et al. 2007. Atrophy, but not necrosis, in rabbit skeletal muscle denervated for periods up to one year. *Am J Physiol Cell Physiol* 292:C440.
84. Borisov AB, et al. 2000. Remodeling of the vascular bed and progressive loss of capillaries in denervated skeletal muscle. *Anat Rec* 258:292.
85. Borisov AB, et al. 2005. Abortive myogenesis in denervated skeletal muscle. *Anat Embryol (Berl)* 209:269.

Vet-ebooks.com

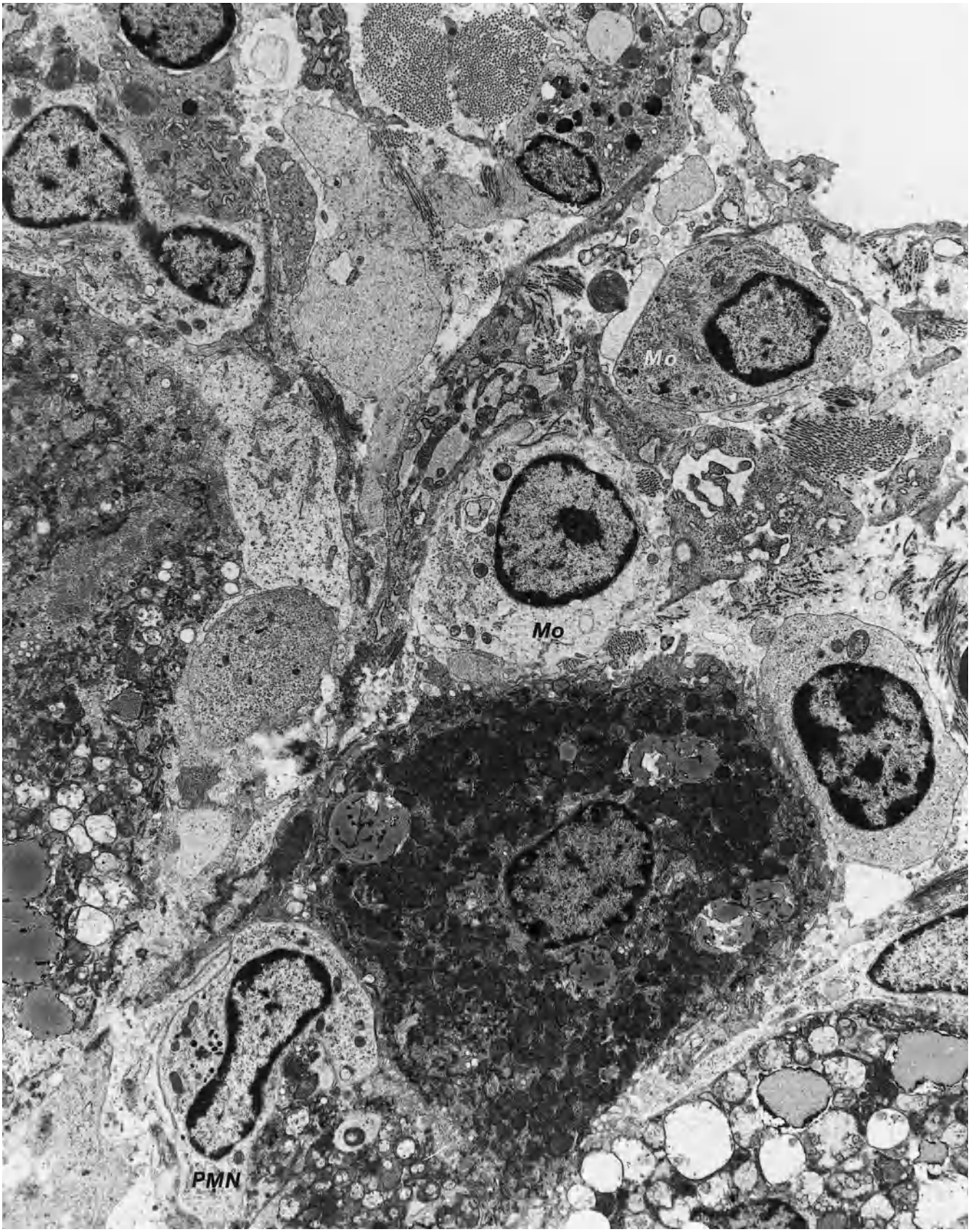


Fig. 2.1 Coagulation necrosis: hepatocytes, liver, carbon tetrachloride toxicity, rat. There is activation of endothelial cells, infiltration by monocytes (*Mo*) and a neutrophil (*PMN*), and debris and collagen in interstitial areas.

© 2009 Wiley-Blackwell. ISBN: 978-0-813-80330-2

Vet-ebooks.com

2 Cell Death

The two major pathways to cell death are cytonecrosis and programmed cell death. **Cytonecrosis** arises from massive, direct cellular injury and leads to release of cellular components. In contrast, **programmed cell death (PCD)** is initiated by activation of genetic or intracellular signaling pathways that ends in death of single cells without release of cellular components or soluble products.

Cytonecrosis and PCD are not mutually exclusive. They can both contribute to death of individual cells and in any given tissue can develop concurrently.[1] In injured tissue, necrosis and PCD often coexist, since PCD develops after tissue injury to eliminate damaged cells that cause biological mischief. The characteristics of these patterns of cell death include the following:

- **Cytonecrosis:** arises from direct or indirect injury from external sources that leads to uncontrolled degradative events; necrotic cells alter the tissue environment, releasing cytokines that alter vascular tissue and incite inflammation and healing. Necrosis is manifest in a spectrum of cellular changes, the extremes of which are:
  - **Shrinkage cytonecrosis:** cell components collapse and condense into an electron-dense, amorphous mass (Fig. 2.1); denatured proteins, cytoplasmic debris, and degraded cytoplasmic organelles collapse into a shrunken, dark, amorphous mass.[2] If the **nucleus** is lysed, the remaining cytoplasmic mass appears as a darkly staining anucleate globule, sometimes referred to as a Councilman body.
  - **Lytic cytonecrosis:** intake of water, degradation of cytoplasmic proteins, and rupture of membranes produce an expanded cell ghost with internal contents spewed into interstitial spaces (Fig. 2.2). Cells are large, pale, and relatively transparent, characteristics brought about by proteolysis, membrane fragmentation, and massive swelling.
- **Programmed cell death (apoptosis)** is initiated by specific regulatory signals that lead to loss of mitochondrial transmembrane potential, chromatin condensation, and membrane phosphatidylserine externalization; PCD progresses with precise and controlled changes in organelles. Apoptotic cells do not release external signals and do not incite inflammation.
  - **Caspase-induced apoptosis:** death signaling events both internal (from genes in embryogenesis and cancer) and external (from atrophy and injury-induced cell surface signals) activate the lethal caspase cascade that systematically shuts down mitochondria (called the intrinsic or mitochondrial pathway).
  - **Non-caspase-induced apoptosis:** cell death pathways not dependent on caspase activation induce apoptotic death from proteolysis that is induced by calcium, free radicals, halogens, and serine and aspartyl proteases (called the extrinisc pathway).

In modern pathology, the term **cytonecrosis** is shortened to simply necrosis. Note however, that **necrosis** (Gr. *nekrosis*, deadness) is defined as death of tissues and cells in the living animal; it has been used classically as a basic descriptor of gross pathology and histology. In this text, the use of necrosis infers cellular necrosis or cytonecrosis.

How a cell responds to external injury or external signals depends on the etiologic agent, and is influenced by the cell's metabolic profile and the adequacy of blood flow bringing oxygen and nutrients. In acute toxic injury of the liver, hepatocytes of centrolobular

Vet-ebooks.com

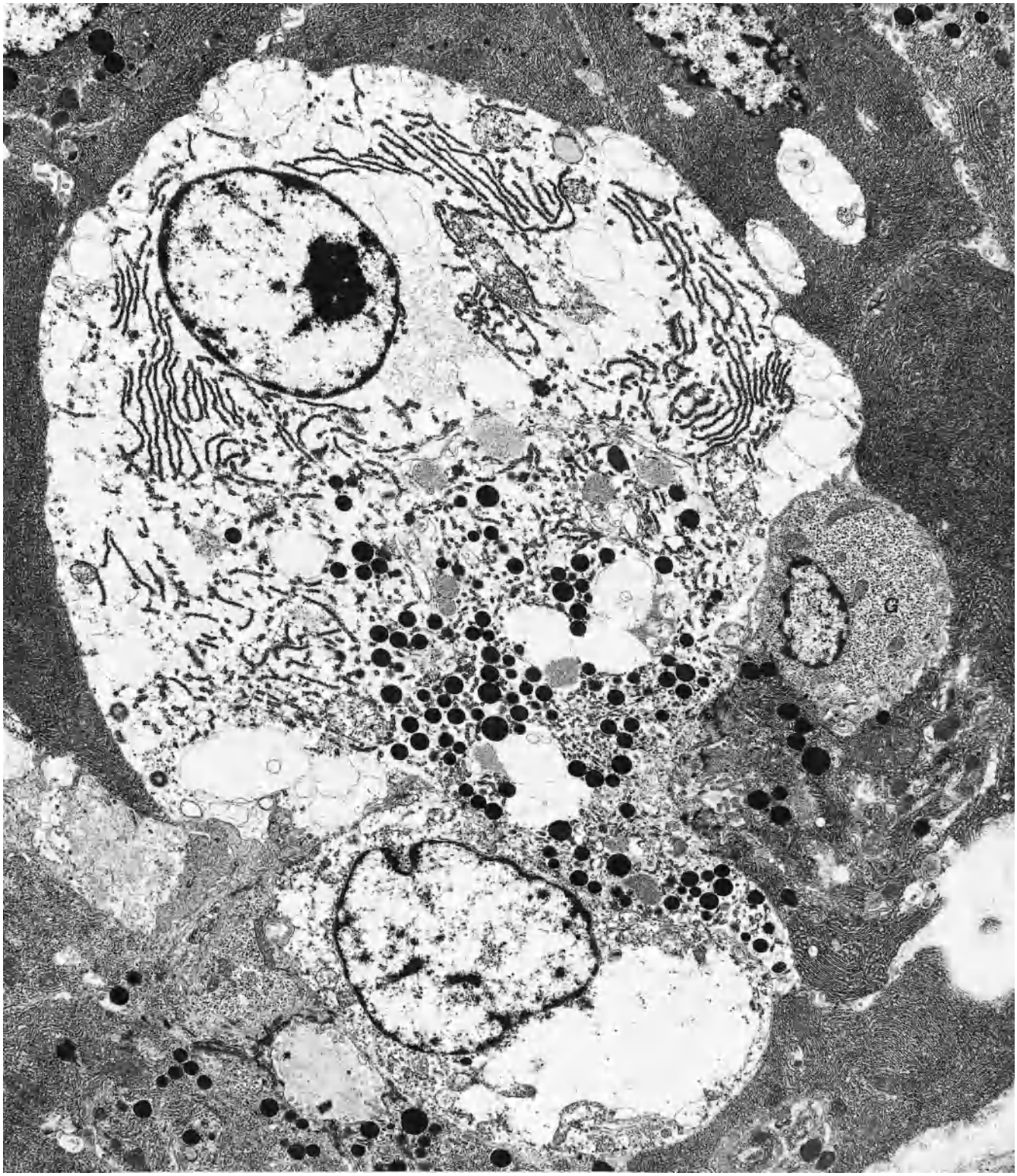


Fig. 2.2 Lytic necrosis: pancreatic acinar cells, acute pancreatic necrosis, dog. There is necrosis of capillary endothelium (*bottom*) and accumulation of large amounts of glycogen (*G*) in a mononuclear cell.

Vet-ebooks.com

zones typically die by coagulation cell death, yet cells immediately surrounding the centrolobular vein often die by lysis. These differences relate to blood flow through the hepatic lobule.

Necrosis

The site of **primary injury** determines the spectrum of ultrastructural changes in necrosis. Dying cells end in a final death pathway, the processes of which are centered on mitochondria. **Mitochondriopathy** in injured cells may be reversible but, if uncontrolled, rapidly causes cell death. In both necrosis and programmed cell death, mitochondria regulate death pathways via mitochondrial permeability transition, an event induced by high levels of matrix calcium, and characterized by unregulated opening of the mitochondrial permeability transition pore.[3] When loss of ATP, drop in pH, and rise in Ca^{++} continue, cells reach a state of irreversible injury in which critical organelles are damaged and their shutdown makes recovery impossible. In the end, ATP depletion halts all energy-requiring processes, and degeneration becomes necrosis.

Degenerating cells suffer **secondary injury** because of the interdependency of cell structures and functions. Secondary factors that amplify the cascade of degeneration into death include **pressure** changes of swelling, **lower pH** as lactate accumulates (acidosis), **increased metabolic rates** due to fever-induced temperature elevation, and **hypoxia**, which often results from decreased blood flow and directly affects mitochondria and energy production.

Plasma Membrane Is Leaky

Agents that cause lysis are generally powerful lysins—enzymes that destroy phospholipids in lipid bilayer of the plasma membrane; for example, clostridial enzymes, snake venoms, and endogenous toxins such as those that cause pancreatic necrosis.[4] Strong membrane lysins dissect through tissue having marked effects on capillaries and lymphatics. Plasma membrane lesions causing leakage are also produced by porins that insert into the membrane, creating channels.

Unrestricted Entry of Ca^{++} Kills the Cell

When plasma membrane permeability is altered, **Ca^{++}** rushes into the cytosol from higher amounts present in interstitial fluids. Biochemical analysis of necrotic cells reveals increased Ca^{++} and Na^{+}, and decreased K^{+}. These changes contribute to cell death. It is the increased Ca^{++} that is most responsible for necrosis, largely because of the role of Ca^{++} as a signal molecule that initiates many cellular processes. As Ca^{++} accumulates in the cytosol, it acts in four major ways:

- **Uncoupling of gap junctions:** isolating the injured cell from its neighbors, an attempt to prevent the spread of injury or infection
- **Depolymerization of cytoskeletal microfilaments:** microfilaments and microtubules in the cell periphery disappear and cannot function in cell movement, phagocytosis, and secretion
- **Fragmentation of DNA**[5]
- **Activation of endogenous phospholipases** within membranes.

The Ca^{++} content of normal cells, which is low relative to that in interstitial fluid, is maintained by cyclical activity of **calcium channels** that admit Ca^{++} and **calcium pumps** that remove Ca^{++} from the cell. In acute cell swelling the plasma membrane pumps are less efficient and Ca^{++} entering through the leaky membrane cannot be removed. Once inside the cell, Ca^{++} is bound by one of a family of **calcium-binding proteins** that fix Ca^{++} to various parts of the cell. **Calmodulin** plays a crucial protective role in acute cell swelling. Any factor that suppresses calmodulin will enhance cell degeneration and necrosis.

Because the cytosol is highly sensitive to change, the calcium-loaded cell sequesters Ca^{++} internally by moving it across membranes of mitochondria, endoplasmic reticulum, and Ca^{++}-containing vesicles (calcisomes). In lethal acute cell swelling, the membranes of these organelles are damaged so that Ca^{++} is released back into the cytosol. Mitochondria do not normally sequester large amounts of calcium so that it is the endoplasmic reticulum and its vesicles that are chiefly involved in the internal elevation of cytosolic calcium. Ca^{++} entering leaky **mitochondria** in large amounts causes lethal effects on electron transport and oxidative phosphorylation.

Calcium accumulates in massive amounts in most dying cells.[6,7] In prolonged ionic imbalance, calcium precipitates within the cell. Calcium salts are deposited diffusely throughout the cell, causing it to be granular and electron dense, especially in cells located in tissues undergoing marked changes in interstitial pH and electrolyte levels; for example, cardiac and skeletal myocytes, gastric parietal cells, renal tubular epithelium, and neurons.

Endogenous Phospholipases Are Activated

Release of phospholipases within the plasma membrane leads to a cascade of reactions that degrade membranes in the cell. Specific phospholipid molecules are present in membranes in an asymmetric pattern and are maintained by an aminophospholipid

Vet-ebooks.com

translocase, which moves specific phospholipids between the lipid bilayer leaflets. Loss of energy causes phospholipids to become symmetric, and this signals processes for cell death. Membrane phospholipid degradation releases **phospholipid catabolites**. As cellular membranes disintegrate, phospholipids are broken down to release lysophosphatides, arachidonic acid, and other catabolites. Hydrophobic lipid breakdown products are important signal molecules that often exacerbate the process of necrosis (see chapter 4).

Plasma Proteins Enter the Cell

As the plasma membrane is injured in the process of necrosis, large protein molecules from plasma and interstitial fluid enter the cell. When cardiac myocytes are killed by anoxia, as in myocardial infarction, heart muscle can be shown to contain large amounts of albumin, globulin, and fibrinogen by using immunolabeling techniques. Similarly, in the brain, neurons take up plasma proteins. Diagnostic radiographic techniques based on altered plasma membrane permeability and protein entry used in myocardial infarction include I^{131}-labeled antibodies against cardiac myosin enter and concentrate in ischemic myocytes; radiographic imaging then reveals the site and extent of myocardial injury.

Protein Exits the Cell

Plasma membrane injury causes intracellular proteins, enzymes, and other large molecules to escape from the cell cytoplasm into interstitial spaces during acute swelling. In severe, irreversible injury, cellular enzymes can be detected in circulating blood, and the increase in plasma enzymes is a marker of injury. Massive injury to liver and cardiac or skeletal muscle leads to progressively increased concentrations of cellular enzymes in plasma.

Cytoskeleton Depolymerizes

Damage to the **cytoskeleton** appears coincident with cell swelling. In experimental ischemic injury to myocardium, actin filaments separate from Z lines and intercalated disks and this leads to zonal lesions at the ends of the myofiber.[8–10] Even minor cytoskeletal changes predispose the myocyte to mechanical injury induced by contracture of myofilaments in the swollen cell.[11] In ischemic myocardium, the subplasmalemmal cytoskeletal network of periodic densities with linking microfilaments (called **leptomeres** or **leptofibrils**) appears as dense bars spaced at regular intervals of 150–200 nm and linked by thin microfilaments. Desmin, the major **intermediate filament** protein subclass in cardiac muscle, occurs largely at Z bands and intercalated disks, but is also distributed along the sarcolemma. During ischemia, this protein and its linker participate in the subplasmalemmal densities. In the ischemic heart, concentrations of **lysophosphatides** (lysophosphatidyl choline and lysophosphatidyl ethanolamine) increase rapidly after onset of ischemia. Detectable adjacent to the sarcolemma by electron microscopic autoradiography of myocardium,[12] lysophosphatides increase in venous outflow from the ischemic myocardium and are associated with early myocardial electrophysiologic abnormalities.

Cell Surfaces Are Deformed

Surfaces of cells dead of necrosis are irregular, rippled, and pitted.[13] The plasma membrane is discontinuous, and surface structures such as cilia and microvilli are broken or missing.

Cytoskeleton-Plasma Membrane Connections Are Broken Detachment of the cytoskeleton from the plasma membrane is a hallmark of the transition from reversible to lethal degeneration. Subplasmalemmal densities that link filaments to the plasma membrane become irregular, and the important linking proteins (alpha actinin, myosin, F-actin, desmin, talin, and vinculin) precipitate into small dense material. This change is especially important in muscle where the linker proteins of Z lines (that provide attachment for contractile filaments) aggregate. These events cause the **cytoskeleton** to disintegrate and the loss of stability causes the normal shape to be distorted and the cell more round, dark, and dense. **Intercellular junctions** are broken and, as the cell becomes isolated from adjacent cells, it is dislodged from its normal position.

Surface Blebs Remnants of **surface blebs** project outward, especially over surfaces that are exposed to lumens. On surfaces of cells made uniform by thick basal laminae, blebbing may be inverted; for example, **submembrane blebs** develop into the cytoplasm, giving the surface a washboard effect. Focal plasma membrane damage is often manifest as vacuolation of peripheral areas of cytoplasm. In **lytic necrosis** caused by potent lysins, the plasma membrane and underlying organelles are destroyed (Fig. 2.3).

Mitochondriopathy: Loss of Mitochondrial Structural Integrity

In necrosis, **mitochondrial cristae** and **matrix proteins** disintegrate, and large **dense granules** accumulate in the matrix, a hallmark of oxygen deficit and death.[14,15]

Vet-ebooks.com

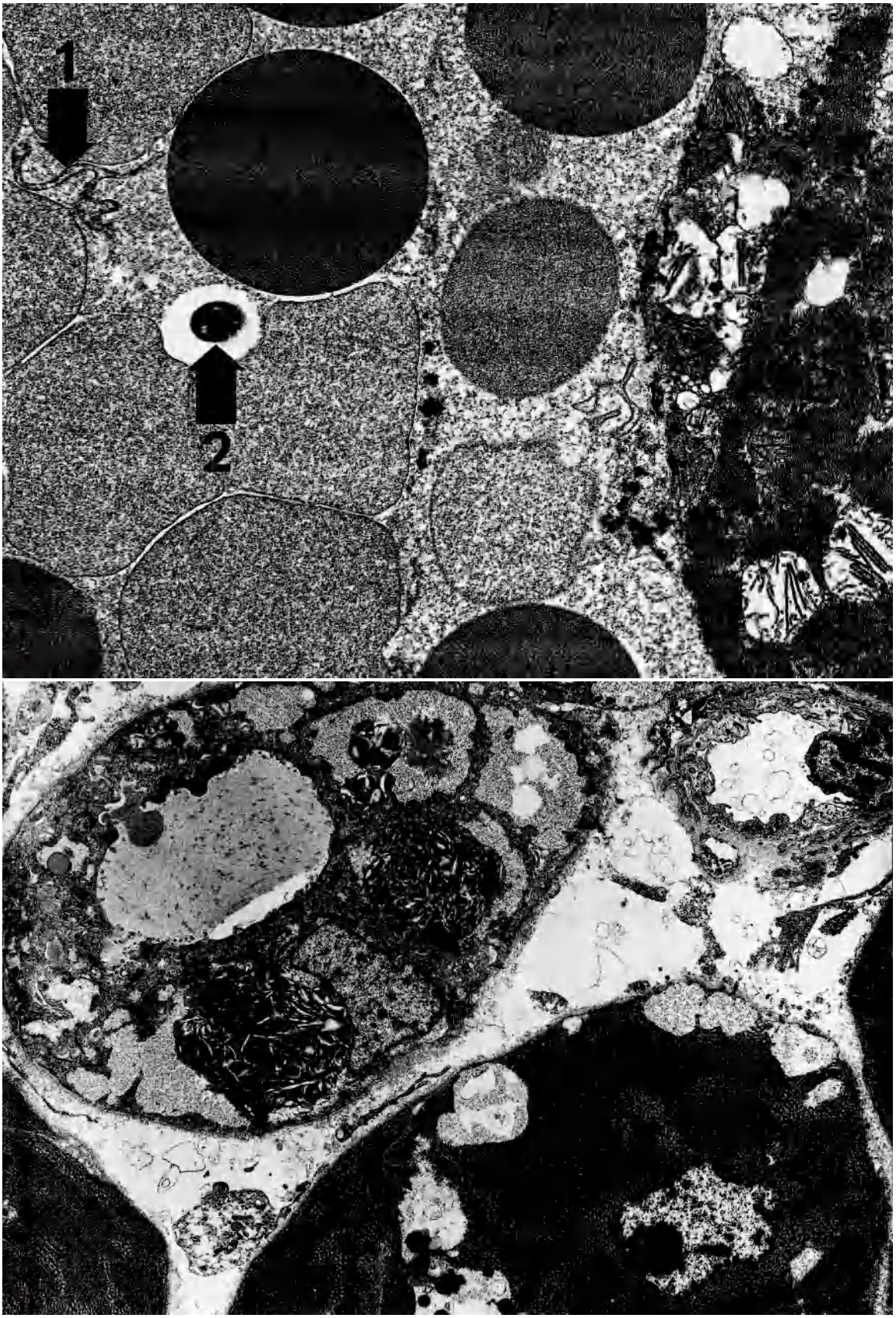


Fig. 2.3 **Lytic necrosis**: acute, diffuse. **A**. **Bacterial toxin**: *Clostridia septicum* α-toxin causes global lysis throughout hemorrhagic, necrotic skeletal muscle. Necrotic skeletal myocyte (*right*). Erythrocytes are in various stages of lysis in the lumen of a necrotic capillary. Erythrocytes are rounded, swollen, and pale because of loss of hemoglobin, precipitates of which are in the vascular lumen. Note the erythrocyte ghost (*arrow 1*) and the halo around a bacterium (*arrow 2*). **B**. **Endogenous toxin**: acute pancreatitis, dog. Severe damage to pancreatic acinar cell, duct, and capillary. Duct has much glycogen and many large lipid globules. Ductal lumen is filled with inspissated secretions.

Vet-ebooks.com

Anoxia, the total oxygen deficit, rapidly induces **mitochondrial swelling** by paralyzing energy production; within seconds of anoxia, ATP values fall to 0, mitochondrial cristae disappear, and membranes disintegrate. **Mitochondriopathy** is associated with

- **Depletion of ATP**
- **Dumping of mitochondrial proteins into the cytosol**
- **Rise in cytoplasmic Ca^{++}**
- **Activation of intrinsic lytic enzymes** in mitochondrial membranes
- **Acidification** of the cytoplasm

ATPase Complex Dysfunction

Loss of the **mitochondrial ATPase complex** from the inner mitochondrial membrane is an early critical step to irreversibility in necrosis. Inactivation of the inner membrane ATPase complex is related to loss of essential ions at these specific enzyme sites. In rat kidney slices in vitro, inner membrane spheres, which are normally present on cristae, began to disappear after 2 hr of ischemia.[16]

Permeability Transition Pores Open

Mitochondrial leakiness, called mitochondrial permeability transition, begins with the opening of **permeability transition pores** that cause loss of ionic homeostasis, matrix swelling, and outer membrane rupture. Osmotic imbalance results from toxins that specifically attack mitochondria. In chronic ethanol toxicity in rats, abnormalities of the mitochondrial transition pore have been demonstrated ultrastructurally.[17] Cell death initiated by pathways of both necrosis and programmed cell death converges on the uncontrolled opening of mitochondrial transition pores.

Inner Membrane Degradation

A significant step in irreversible mitochondrial injury is alteration of **inner membrane** structure. Liberation of free fatty acids from the damaged phospholipid bilayers brings about the point of no return, since fatty acids act as respiratory uncouplers by separating the electron transport chain from oxidative phosphorylation (see chapter 8).

Reactive Oxygen Species Cause Oxidative Stress

Superoxide anions (O_2^-) are formed nonenzymatically in all aerobic cells from autooxidation of components of the mitochondrial electron transport chain, and also from enzymatic reactions by xanthine oxidase and other oxidases in the cytosol. In mitochondria, the electron transport system produces water as the sole product of oxygen reduction. Large-scale production of O_2^-, hydrogen peroxide, and hydroxyl radicals (OH•) are thereby avoided. Collectively, these radicals are referred to as **reactive oxygen species (ROS)**, and the damage they do is referred to as **oxidative stress**. Inside the cell, O_2^- reacts with mitochondria, as well as proteins, DNA, and lipids. A consequence of many toxins is the interaction of toxic O_2^- with amino acids, a cause of significant damage to cell proteins.

Dysfunctional mitochondria generate ROS that, when uncontrolled, lead directly to abnormal mitochondrial permeability.[18] Membranes, DNA strands, and proteins are the cellular structures most affected by free radical–induced injury. The major damage is from

- Lipid peroxidation of **membrane** damage throughout the cell
- Random breakage of **DNA strands** in the nucleus
- Oxidation and cross-linking of **proteins**

Protection against ROS-induced injury is afforded by **superoxide dismutase (SOD)**. Mitochondria use SOD to control **oxidative stress**, the balance between generation and inactivation of **ROS** that is generated in ATP production. Necrosis is enhanced by any depletion or defectiveness of SOD. A unique mechanism of **mutant superoxide dismutase toxicity** to motor neurons has been reported in **amyotrophic lateral sclerosis**. Motor neurons of transgenic mice bearing a defective mutant superoxide dismutase undergo slow degeneration characterized by mitochondrial swelling, DNA strand breakage, and aggregation of dysfunctional Na,K-ATPases. Affected neurons accumulate mitochondria and high levels of superoxide, nitric oxide, and peroxynitrite. Death appears to be related to oxidative stress, protein nitration and aggregation, and excitotoxicity; cell death is unrelated to the caspase cascade or to apoptosis.

Iron is especially important in injury caused by ROS. Superoxide reduces ferric iron (Fe^{3+}) to ferrous iron (Fe^{2+}), which is required for iron to participate in the formation of hydroxyl radicals that enhance tissue injury ($H_2O_2 + Fe^{2+} \rightarrow Fe^{3+} + OH$).

Nitric Oxide Causes Nitrosative Stress

Perturbation of mitochondrial membranes releases signals for a mitochondrial nitric oxide–dependent pathway of mitochondrial destruction. **12(S)-Hydroxyeicosatetraenoic acid (12-HETE)**, a metabolite of arachidonic acid involved in mitochondria and oxidative stress, increases **intramitochondrial calcium**.

Vet-ebooks.com

Elevation of calcium stimulates **mitochondrial NO synthase (mtNOS)** activity, which produces **nitric oxide (NO)**. The mtNOS-derived NO causes mitochondrial dysfunction by decreasing respiratory and transmembrane poteniation. NO binds to **cytochrome C oxidase**, the terminal acceptor in the mitochondrial electron transport chain, in competition with oxygen. This can elicit the injurious intramitochondrial signaling events, including the diversion of oxygen to nonrespiratory substrates. This diversion reactivates prolyl hydroxylases and the destablization of hypoxia-inducible transcription factor.

In some situations, NO can interact with superoxide anion to produce **peroxynitrite**. Peroxynitrite induces several damaging events including cytochrome c release, increased mitochondrial lipid peroxidation, increased protein tyrosine nitration of mitochondrial proteins, and aggregation of mitochondria—all events that lead to apoptosis.

Mitochondrial Calcification

Calcium metabolism is disturbed in severe cellular injury[19] and as necrosis develops, mitochondria accumulate calcium in a process energetically coupled to electron transport. Accumulation is accompanied by uptake of equivalent amounts of phosphate, which results in enlargement of mitochondrial **dense granular bodies** in the mitochondrial matrix. Continued deposition of $CaPO_4$ results in large, distinctly abnormal **granular matrix inclusions** (Fig. 2.4). For every pair of electrons passing from NADH to O_2, approximately six Ca^{++} accumulate from the cytoplasmic matrix. When Ca^{++} accumulates in this manner, no oxidative phosphorylation of ADP occurs; that is, electron transport energy can be used to accumulate Ca^{++} or to form ATP but not both.

In late necrosis, calcium may form salts that precipitate as **spicules** around degenerate mitochondria; these dense structures with peripheral spicules have been characterized by x-ray energy dispersive analysis.[20] Calcification occurs by initial formation of soluble species of $CaPO_4$, with subsequent change to less soluble forms with a higher Ca:P ratio. In ischemia, mitochondrial granular inclusions are composed of soluble calcium phosphates. The elements Mg, S, Si, K, and Cl are also detectable in finely spicular inclusions of very large masses.[21]

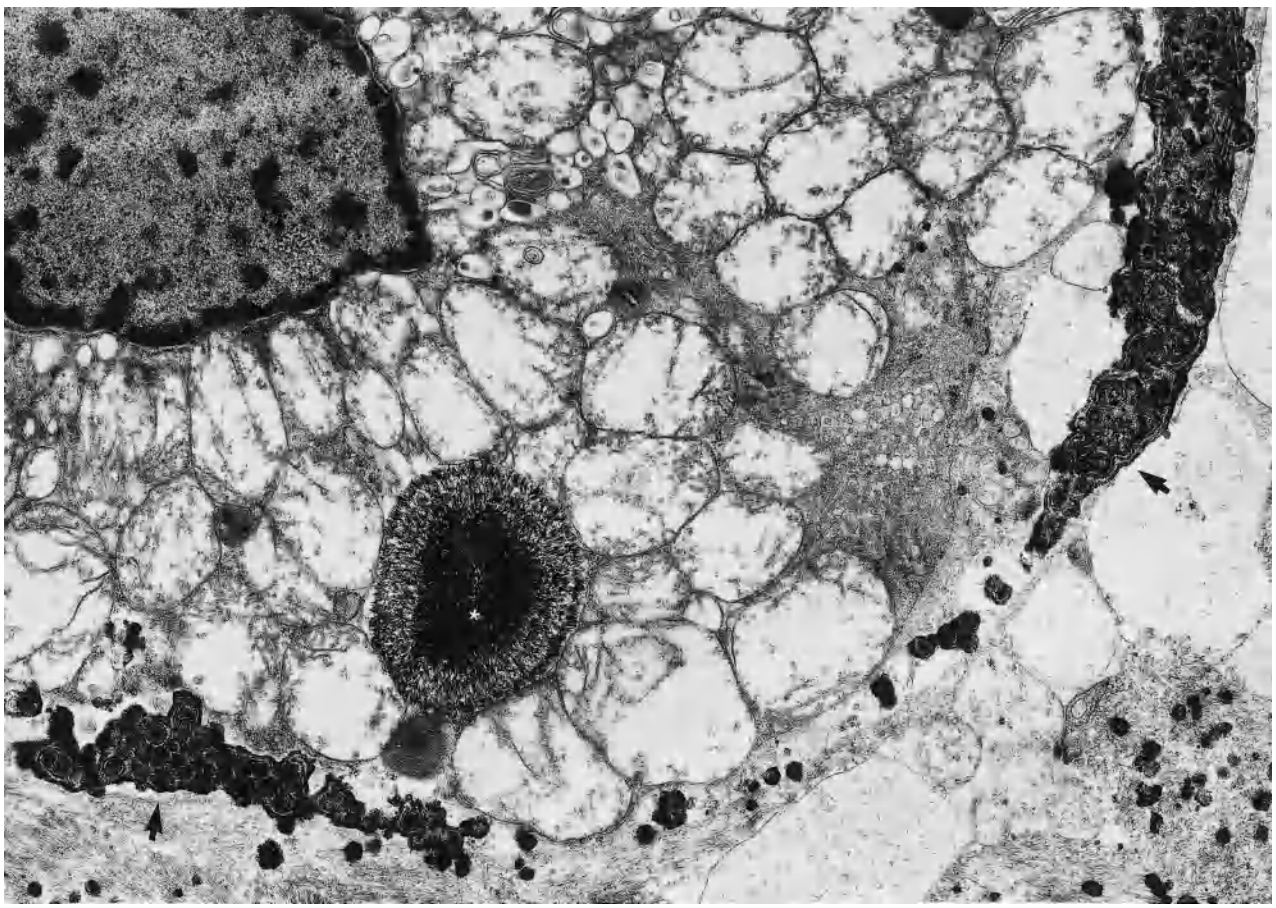


Fig. 2.4 Mitochondrial swelling and calcification: necrosis of gastric parietal cell, uremia. There is calcification of one mitochondrion (*) inside the cell and extensive extracellular laminar calcification at the periphery of the cell (*arrows*).

Vet-ebooks.com

Mitochondrial permeability transition induced by high levels of **matrix calcium** is implicated in both necrosis and apoptosis of neurons. Brain infarcts in mice, after occlusion of the middle cerebral artery and reperfusion, are reduced in size if apoptosis is active. Cyclophilin D, a regulator of the cell cycle and a component of mitochondrial permeability transition, mediates this protective effect on neuronal death after focal cerebral ischemia.[22]

Endoplasmic Reticulum and Golgi Complex Are Contracted

Ribosomes, which are detached from membranes of the rough endoplasmic reticulum early in degeneration, accumulate as the cell is killed. Together with remnants of the cytoskeleton and other cytoplasmic proteins, they aggregate into dense amorphous masses. As ribosomes disintegrate, the peptide chains associated with them are degraded. Ribosomal function and protein synthesis may persist during necrotic cell death.[23]

An obligatory step in the process of protein breakdown is the binding of the denatured protein to **ubiquitin**; this is the first step in proteolysis.[24] When the ubiquitin system is overloaded or insufficient, peptides accumulate in cisternae of the endoplasmic reticulum and Golgi complex.

Studies of the **Golgi complex** using thiamine pyrophosphate to mark the trans cisternae have shown that glycosylation of proteins and lipids is impaired.[25] Similarly, secretion is prevented and, in necrotic secretory cells, there are accumulations of large and irregular **secretion granules**.

Nuclei Shrink and Chromatin Aggregates

Chromatin clumping is a consequence of both protease activity and a decrease in cellular pH that occurs as lactate builds up in the degenerating cell. Injuries directed to the nucleus lead to unique patterns of chromatin aggregation and to characteristic changes in nucleoli and other nuclear structures. In most necrotic cells, dense deposits of chromatin are aggregated along the nuclear envelope. The persistence of chromatin and the manner in which it aggregates are determined by the type of necrosis. **Karyolysis** is the lysis of nuclear chromatin and disappearance of nuclear remnants. It occurs when proteases leak into the nucleoplasm—proteolysis results in a pale structureless nucleus. In some cases of marked swelling and lysis, little chromatin can be seen. In some tissue, disintegration of nucleoproteins is accompanied by reformation of these substances into strands and tubules, particularly when aldehyde fixatives are used, or when tissues have been pre-fixed in formalin.[26] As the cell dies, nuclei are shrunken, and chromatin is condensed to solid, structureless masses, a condition called **pyknosis**.

DNAase initiates chromatin breakdown. Necrosis in toxic injury may be enhanced by chromatin degradation by DNAase; for example, DNAase knockout mice are protected against **acetominophen**-induced liver necrosis.[27]

Intracellular Trafficking Is Suppressed

Lethal levels of calcium coupled with disturbed water balance interrupt intracellular signaling, which, in turn, suppresses movement of cytoplasmic vesicles. Cytoplasmic vacuolar systems are rapidly shifted to autophagy (see chapter 3). In early phases of the necrotic process, lysosomes are activated. In late stages, if membranes are damaged, endogenous lysosomal enzymes leak into the cytosol to drive the necrotic process to irreversibility. Multiple causal agents converge on a peptidase-driven core stress response pathway that, in the absence of serpin regulation, triggers a lysosome-dependent necrotic cell death.[28]

Programmed Cell Death

Programmed cell death or **apoptosis** is a regulated, homeostatic mechanism that deletes cells that are no longer needed, or that in some way would be damaging to the animal. PCD is regulated and driven by "death genes" and by "death signal pathways" that activate **death proteins** that flow through the cytoplasm to collectively bring about cell death. These proteins direct other executioner molecules to break chromosomes, depolymerize the cytoskeleton, and cause mitochondria to dump proteins—all events that kill and fragment the cell in a controlled manner.[29,30]

PCD plays an essential role in gene-directed cell deletion in embryogenesis, removal of neoplastic cells with lethal mutations, and cell loss in remodeling and involution of atrophy. There are intracellular processes in which the initiating signal arises from within the cell; that is, "death genes" that encode for proteins that activate PCD are turned on, directing their products to the appropriate sites in the cell. Signals that initiate PCD may also arise extracellularly, a common pathway in drug toxicity and in the death of cells from microbes during inflammation. These signals from outside the cell initiate PCD by binding to specific cell surface receptors.

Vet-ebooks.com

PCD occurs without clinical sequelae because the dying cell's function has been fulfilled. In contrast to other forms of cell death, cells dying in PCD do not release panic signals of impending death. There is no increase in surface molecules or release of cytokines that attract leukocytes or activate endothelial cells to initiate inflammation or repair. PCD is not accompanied by concomitant vascular injury, the major cause of inflammation in necrosis of other types.

In normal adult animals, PCD occurs as a part of normal cell turnover; for example, in normal squamous epithelium, **epithelial cells** in the basal layer change into squamous cells, cornify, and die. Nuclei shrink, desmosomes disintegrate, and cornified keratinocytes desquamate from the skin or lumenal surface. Death of erythrocytes and leukocytes is largely through PCD.

Cellular changes in PCD evolve in orderly and reproducible sequences because genetic codes and signaling pathways contain specific instructions for death. PCD leads to cell shrinkage with progressive rounding and pyknosis of nuclei. The cytoplasm contracts, chromatin condenses, nuclear envelopes disintegrate, and autophagosomes form that contain membranous whorls. Dead cells are engulfed by macrophages, and in some tissues by neighboring cells, which sequester components of the dead cells within secondary lysosomes.[31] Cellular changes characteristic of PCD (Fig. 2.5) are collectively referred to as the lesions of apoptosis; they include:

- **Pro-apoptotic cytosolic proteins** translocate into mitochondria
- **Mitochondria** become dysfunctional and leaky
- **Nuclear chromatin** depolymerizes and re-aggregates
- **Nuclear lamins** disconnent, undergo proteolysis
- **Cytoskeleton** is degraded
- **Cell junctions** disengage and cells become round
- **Cytoplasmic blebs and pyknotic nuclei** are shed from cell

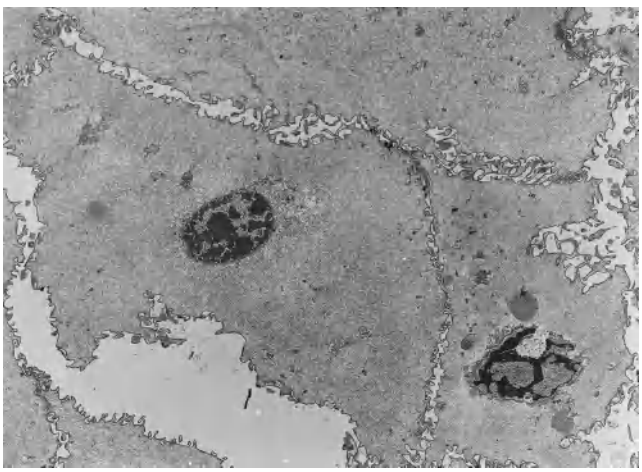


Fig. 2.5 Programmed cell death: stratified squamous cells, esophagus. Nuclei are degenerate, cell junctions are separated, and cytoplasm is homogenous and lacks organelles.

Apoptosis is executed by caspases and regulated by the opposing factions of the Bcl-2 protein family. The **caspase cascade** is the major death signaling pathway in PCD. **Caspases**, a family of protein-cleaving cysteine proteases, initiate cellular change in PCD. Caspases cleave their substrates at specific aspartic acids segments, and play the critical roles in two phases of programmed cell **death signaling** and **execution:**

- **Initiator caspases** (caspases 8 and 10) respond to death signals and activate execution.
- **Executioner caspases** (caspases 3, 6, 7, and 9), make specific cuts in key proteins that are required for cell survival.[32]

Procaspases begin the caspase cascade when they are activated by binding to adaptor proteins. **Procaspase 8** is located primarily in mitochondria, where it is co-localized with cytochrome c, both identified by immunogold techniques in the intermembrane space, inner membrane, and matrix.[33] **Procaspase activation** in intrinsic pathways is initiated by death genes. Intrinsic pathways of PCD can activate procaspase from genetic signals. In contrast, extrinsic procaspase activation can be triggered from outside the cell by activation of death receptors on the cell surface.

In summary, the detection of PCD in cells is confirmed by the increase of apoptotic-related substances in the cell. This includes increased levels of procaspase 8, cytochrome c, and Bak. Note that cell death pathways that induce patterns of apoptotic death but that are not dependent on caspase activation include the following:

- Calcium-dependent proteolysis
- Proteolysis by serine and aspartyl proteases
- Halogenation
- Reactive oxygen species via free radical induced proteolysis
- Nitric oxide synthase deficiency
- Amyloid Aβ in Alzheimer's disease
- PolyQ in Huntington's disease

In **genotoxicity**, damage to DNA activates gene *p53*. The ***p53* gene** encodes the **protein p53**, which plays critical roles in recovery by blocking the cell cycle and stimulating DNA repair; if injury is severe, protein p53

Vet-ebooks.com

also triggers programmed cell death. In cells with DNA damage and *p53* expression, levels of protein p53 rise. In mitochondria, p53 is involved in mtDNA repair as a first response in cardiomyocytes poisoned with adriamycin in mice.[34] In mitochondria, p53 levels correlated with mtDNA oxidative damage.

Dysfunctional mitochondria generate ROS that, when uncontrolled, lead directly to abnormal mitochondrial permeability. ROS critically damage DNA, both nuclear and mitochondrial; it thereby activates the genomic guardian, p53. In heart failure, ROS are a major cause of mtDNA damage and causes both necrosis and apoptosis in the cardiac myocyte.

ROS → DNA Strand Breaks → p53 Activation → Apoptosis

Mitochondriopathy

Mitochondria are the critical effector organelles. Mitochondria control PCD through four connected events: increased outer membrane permeability, cytochrome c release, apoptotic protease activation factor-1 induction, and caspase 9 activation. Mitochondrial ultrastructural changes that develop during these events include compartmentalization of the inner mitochondrial membrane, a process that segregates different compositional areas. Analysis of this change using three-dimensional electron microscopic tomography (which gives a composite time-course overview of morphologic change) reveals swelling and vesiculation of the inner mitochondrial membrane. These changes were associated with release of proteins from intermembrane and intercristal spaces.[35]

Mitochondrial Permeability Transition

The initial event in the mitochondrial pathway of apoptosis is **mitochondrial permeability transition**, an increased permeability of the mitochondrial outer membrane. Collapse of the normal mitochondrial membrane permeability barrier is due to abnormal opening of **mitochondrial transition pores**, which, in turn, leads to a spectrum of changes that include uncoupling of the respiratory chain, depletion of reduced glutathione, generation of superoxide anion, cessation of ATP synthesis, outflow of matrix Ca^{++}, and dumping of cytochrome c and other membrane proteins into the cytosol—all events that are associated with cell death.

Dumping of Mitochondrial Proteins Creates Apoptosomes

Apoptosomes are large caspase-activating complexes that are assembled from the scaffold protein **protease-activating factor-1 (Apaf-1)** and caspase-9 when cytochrome c is released during mitochondrial-dependent cell death.[36–39] Pro-apoptotic proteins released from mitochondria regulate the protein composition of apoptosomes. The **caspase 9-Apaf-1 complex** is a caspase-activating structure. **Cytochrome c** released from mitochondria binds to a critical protein, **Apaf-1**, which binds to and activates **caspase 9**. Caspase 9 then activates **caspase 3**, which causes many of the effects of PCD. Apaf-1 detected by immunogold labeling has a cytosolic distribution.

Cells respond to apoptotic signals according to their individual spectrum of caspases. In some cells, caspase 7 can be incorporated into apoptosomes, but its apoptotic effects appear to be blunted by an inhibitory molecule, **X-linked inhibitor of apoptosis (XIAP)**.

Dumping of cytochrome c (and other proteins) from mitochondria is suppressed by the proteins **Bcl-2** and **Bcl-xL**, which regulate the apoptotic program independently from the apoptosome (see chapter 3). The complex role of Bcl-2 and Bcl-xL in regulating apoptosis in vitro, particularly via interactions with pro-apoptotic growth factors such as TGF-β, is evolving.

Translocation of Cytosolic Pro-apoptotic Proteins to Mitochondria

Pro-apoptotic Genes Activation of the pro-apoptotic gene ***Bax*** (which encodes the protein **Bax**) and a related gene, ***Bak*** (which encodes **Bak**),[40,41] leads to cell death. **Bax**, **Bak**, and **PUMA** (p53 upregulated modulator of apoptosis) are proteins that lead to cell death, and are pro-apoptotic targets of p53. The Bax protein is located in the cytosol. Under the appropriate pro-apoptotic signal, Bax oligomerizes and is translocated into the mitochondrion, where it initiates apoptosis. One of the major pathways (as determined in cells in vitro) involves signaling of caspases via the **TNF-α-related apoptosis-inducing ligand (TRAIL):**

Bax/Bak → TRAIL → caspase 3 → apoptosis

Bax-dependent **pro-apoptotic drugs**, such as actinomycin D and staurosporein, activate Bax by causing **intracellular alkalinization**. The rise in cytosolic pH causes translocation of Bax into mitochondria. Chloride channel inhibition by furosimide prevents intracellular alkalinization, and consequent cytochrome c release and apoptosis. Release of procaspase 8 is blocked by **cyclosporine**, an inhibitor of the mitochondrial permeability transition pore. Caspase inhibitors do not affect the cytosolic translocaton of cytochrome c (but prevent that of Bax).

Reactive Oxygen Species and Cell Death

Dysfunctional mitochondria can generate damaging amounts of **reactive oxygen species**. ROS critically

Vet-ebooks.com

damage DNA, both nuclear and mitochondrial. Damage to mtDNA activates the gene ***p53***, and the **p53 protein** induces apoptosis.[42] ROS-induced apoptosis evolves as follows:

ROS → DNA strand breaks → p53 activation → apoptosis

Protein Nitrosylation-Initiated Apoptosis

Protein S-nitrosylation/denitrosylation serves as a regulatory process in apoptosis and in other signal transduction pathways. In normal cells, **nitric oxide** inhibits apoptosis by S-nitrosylation of active-site caspases.[43,44] Endogenous production of NO by endothelial cells and some lymphocytes protects against activation-induced apoptosis. The anticancer drug tamoxifan induces oxidative stress and apoptosis via this mitochondrial NO-dependent pathway.[45]

Pro-apoptotic Proteins: DAP3 and Bid

Death-associated protein 3 (DAP3) is a GTP-binding protein involved in intra-mitochondrial protein synthesis and respiration; it is localized in the small unit of the **mitochondrial ribosome**, and is encoded by mtDNA. **DAP3** has dual functions and can initiate apoptosis by the extrinsic cell death pathways of TNF-α and IFN-γ.[46] During apoptosis, DAP3 induces mitochondrial fragmentation. It functions downstream from other signaling pathways.[47]

Bid, a pro-apoptotic cytosolic protein, is cleaved by caspase 8 during apoptosis, and the truncated Bid **(tBid)** translocates to **mitochondria** by targeting **cardiolipin**, a mitochondrial phospholipid critical for oxidative phosphorylation.[48,49] Once in the mitochondrion, tBid destabilizes membranes and uncouples respiration.[50] Bid triggers oligomerization of Bak and Bax, and release of mitochondrial proteins (such as cytochrome c, endonuclease G, and smac) into the cytosol. Bid reorganizes mitochondrial cristae and enhances cytochrome c release from mitochondrial intermembranous spaces (by a mechanism independent of the mitochondrial permeability transition pore).[51] Bid (activated by ligated death receptors) is a primary signal molecule for generation of ROS by targeting to mitochondria—most ROS production is dependent on Bid.[52]

Apoptosis-Inducing Factor

Mitochondrial damage can initiate PCD without caspase activation. **Apoptosis-inducing factor (AIF)**, a free-radical scavenger oxidoreductase, normally confined to the mitochondrion, is released on mitochondrial injury.[53] AIF functions downstream of cytochrome c and does not induce its activation. Pro-apoptotic proteins such as Bax cause release of cytochrome c, but not of AIF.

Mitochondrial Kinase Signaling Pathways

Major **kinase signaling pathways** can be stimulated to target the mitochondrion; these include protein kinase A, protein kinase B/Akt, protein kinase C, extracellular signal-regulation protein kinase, c-Jun N-terminal kinase, and p38 mitogen-activated protein kinase. Given the sensitivity of these signaling pathways to ROS and RNS, the activation of mitochondrial kinases is a signaling mechanism for communication of mitochondria with other parts of the cell.

Signal Transduction in Oxidative Stress Although ROS-induced oxidative stress leads directly to cell death, cells are equipped with signal transduction systems that initiate adaptations to oxidative stress. These systems center on important transducing enzymes that are involved in many facets of cell regulation including gene expression, cell proliferation, and PCD. These are enzymes that are activated by diverse stimuli and lead to varied and seemingly contradictory cell responses. These opposing roles arise from signal activation by different stimuli, cell types, and temporal environments.[54]

- **P38 mitogen-activated protein kinase (MAPK):** activation induces these scaffold proteins to develop into multienzyme complexes that upregulate antioxidant defense systems and relay oxidative stress signals to the gene expression apparatus.
- **c-Jun NH(2)-terminal kinase (JNK1):** sustained JNK/c-Jun/AP-1 activation promotes apoptosis; in contrast, JNK is a target in the prevention of apoptosis.
- **Apoptosis signal-regulating kinase 1 (ASK1):** ASK-1 is an upstream regulator of the stress-activated MAPK cascades and plays a critical role in ROS-mediated cellular responses.
- **Extracellular signal-regulated kinase 1/2 (ERK 1/2):** activation confers hepatocyte resistance to death; ERK 1/2 acts as a protective response to chronic oxidative stress; enhanced activation of this kinase sensitizes hepatocytes to death from free fatty acids.

These signal transduction systems are targets for prevention of apoptosis. For example, metallothionein inhibits MAPK in order to exert its powerful preventative effects on doxorubin-induced cardiomyopathy (see chapter 18).

Vet-ebooks.com

Nuclear Changes in PCD

Chromatin aggregation into dense masses along the inner surface of the nuclear membrane is a hallmark of PCD. Massive deposits of chromatin line the nuclear faces of the nuclear envelope and commonly appear as characteristic dense crescents (Fig. 2.6). Later, nuclei become convoluted so that the **nuclear membrane** is indented or invaginated into the nucleoplasm. The **nuclear envelope** remains intact until late in the process so that, when cells are lysed, nuclei are liberated into the environment. Early in PCD, these intact nuclei are shed from the cell and taken up by adjacent cells, a pattern of cytophagocytosis that gives a characteristic appearance to PCD.

Nuclei, which tend to be preserved in early phases of PCD, either undergo karyorrhexis (rupture of the nuclear envelope with release of nuclear fragments) or are ejected from the cell. The round, homogenous, anuclear remnants of the dead cell that remain are called **apoptotic bodies**. Early hallmarks of PCD are **DNA fragmentation** and **chromatin condensation**. Although sequential, these two processes develop via independent pathways.[55]

Nucleoli are fragmented, and other structures of the nucleus are lost in the areas of dense chromatin. Within the nucleolus, fibrillar and granular parts are segregated, but fibrillar centers tend to be preserved due to the cleavage of transcriptionally active ribosomal genes. The characteristic pattern of chromatin condensation is due to conservation of the inactive ribosomal DNA protected within the nucleolin-rich fibrillar center.

In caspase-dependent pathways, the **inhibitor of caspase-activated DNase/DNA fragmentation factor of 45** kDA (DFF45) is cleaved by activation of caspase-3, releasing the coupled caspase-activated DNase/DFF-40 to digest chromatin DNA into nucleosomal fragments. In the caspase-independent pathways, endonuclease G is activated to substitute caspase-activation DNase/DFF40.

Endonuclease Activation and DNA Cleavage

One of the early events in PCD is the cleavage of DNA into uniform nucleosomal fragments that aggregate into dense clumps of chromatin.[56] Masses of dense, crescentric chromatin aggregate along the inner nuclear envelope. A unique ladder of nucleosomal DNA fragments appears on gel electrophoresis of pooled DNA extracts. Histochemical studies with in situ labeling of DNA breaks in nuclei in tissue sections reveal that chromatin cleavage is initiated at the periphery of the nucleus, is relatively short, and that cell death occurs in clusters. Intermediate filaments control cellular distribution of caspases in apoptosis.[57]

Nuclear Lamins Disappear

Internucleosomal DNA fragmentation involves nuclear **lamins**, substrates for members of the **IL-1β converting enzyme (ICE) family** of cysteine proteases that are activated during PCD and function downstream of *Bcl-2*. **Lamin cleavage** during PCD correlates with ICE-related cell death.[58,59]

Genotoxicity: DNA Damage Triggers PCD

Any injury to DNA induces the expression of p53 and the product of p53 rises in cells with DNA damage. The **gene *p53*** produces a protein that initiates apoptosis as part of its function of controlling the cell cycle and stopping for DNA repair when injured. Studies detecting p53 using immunogold techniques show that mitochondrial p53 is involved in mtDNA repair as a first response to cardiomyocytes poisoned with adriamycin in mice.[60]

The final death event centers on the ratio of the protein products of two genes: (1) pro-apoptotic ***Bax*** (and a related gene, ***Bak***), genes that lead to cell death, and (2) pro-survival (apoptosis inhibitor) ***Bcl-2***. It is the ratio of agonist to antagonist that determines whether or not the cell will respond to signals for PCD.[61] The Bcl-2 protein family members may be pro-apoptotic or pro-survival in their regulatory control. **Bim** (Bcl-2-interacting mediator of cell death) is a pro-apoptotic protein that promotes cell death—either by binding to and inactivating pro-survival Bcl-2, or by binding to and activating pro-apoptotic Bax and Bak proteins.

In the rat spinal cord, in which neuronal death was produced by avulsion of the sciatic nerve, lumbar motor neuron apoptosis developed in 7–14 days. Immunogold labeling of injured motor neurons destined to undergo apoptosis detected single-strand DNA breaks, increased p53, BAX translocation to mitochondria, and cytosolic cytochrome c.[62] Thus, apoptosis was DNA damage-induced, and p53- and Bax-dependent. Data also suggested that apoptosis was mediated by upstream NO and ONOO- genotoxicity and downstream p53 and Fas activation;[63] that is, neuronal apoptosis was **Fas death receptor-dependent** when triggered by DNA damage caused by nitric oxide and superoxide. Motor neurons in mice lacking functional Fas receptor and Fas ligand were protected from apoptosis. Apoptosis was shifted to necrosis by mutant SOD1.

Cytoskeletal Degradation: Blebbing and Cell Rounding

Loss of the peripheral cytoskeleton leads to rounding of the cell. This change, when accompanied by

Vet-ebooks.com

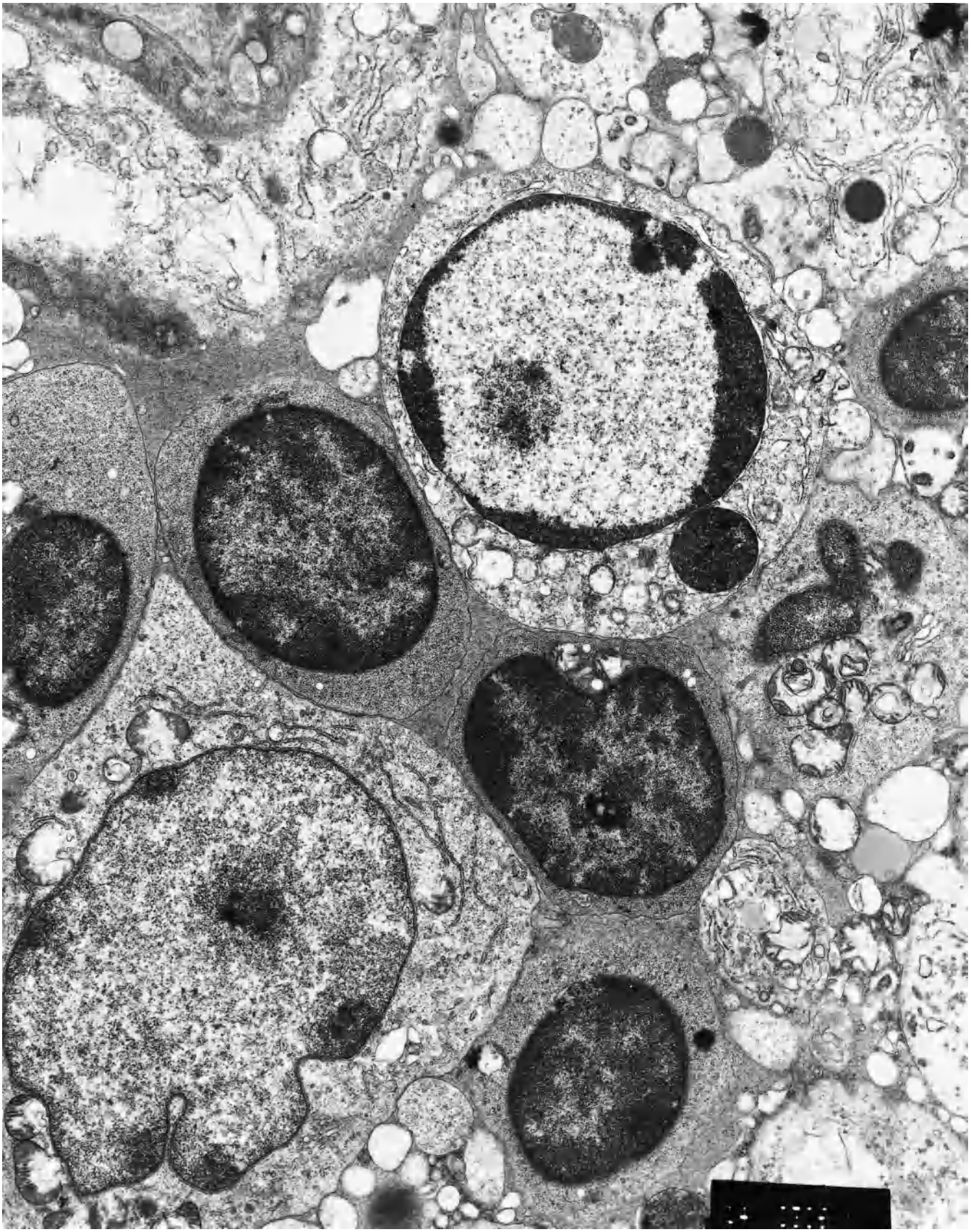


Fig. 2.6 Programmed cell death: lymphocytes, lymph node draining site of vaccination with modified live *Brucella mellitensis*, goat. Aggregates of chromatin have formed crescent-shaped masses along the nuclear membrane.

Vet-ebooks.com

karyorrhexis and loss of internal structure, is called **single cell necrosis**, and is a prototypic manifestation of PCD. Cell rounding is due to multiple breaks in the cytoskeleton, particularly the depolymerization of actin microfilaments and loss of their connections to the plasma membrane. Like small hernias, the loss of cytoskeletal support allows formation of cytoplasmic blebs at the cell surface. An intact cytoskeleton is required for movement of ***src*** from its site of production to the site of action in **adhesion plaques** along the plasma membrane. Small G proteins of the *Rho* family specify the peripheral localization in focal adhesions or along the membrane.

Blebbing is exaggerated so that the surface of cells undergoing PCD has blebs and protuberances that pinch off to form extracellular membrane-bounded bodies.[64] These pieces, sometimes referred to as apoptotic bodies, are phagocytized by resident cells and macrophages.

Endoplasmic Reticulum

Cytoplasmic vacuoles and autophagic vacuoles are reported in the rough endoplasmic reticulum (RER) in apoptotic cells. Autophagy has been presented as causal in apoptosis by some investigators, but is most likely a reparative phenomenon in the cell attempting to recover.

In addition to its function in protein synthesis, the RER regulates protein folding, cellular calcium levels, and intracellular trafficking. Dysfunction in these processes leads to **ER stress**, which, if severe, causes PCD. Lethal ER stress caused by misfolded proteins or cytotoxic drugs induces PCD through phosphorylation of the pro-apoptotic protein Bim, preventing its ubiquitinization and proteosomal degradation.[65]

Inositol 1,4,5-triphosphate (IP3) acts on the **IP3 receptor (IP3r)**, an IP3-activated **Ca^{++} channel** on the ER. The IP3r discharges Ca^{++} from ER stores in response to agonist stimulation, and delivers Ca^{++} to the mitochondrion.[66] Caspase-3-induced truncation of IP3r accelerates apoptosis. IP3r agonists inhibit PCD, and antagonists induce PCD via pathways that require Beclin-1, and Atg 5, 10, and 12.

Extrinsic Pathways of PCD

Sublethal **cellular injury** can trigger the terminal pathway of PCD as a means to remove dead cells and repair injured tissue. Events that activate extrinsic PCD are activation of cell surface death receptors such as the Fas-Fas ligand pathway, and other pathways initiated by non-caspase-inducing factors. Toxins, drugs, cytokines, and steroid hormones can all initiate PCD via specific signaling events, many of which occur at the cell surface. When a PCD-inducing toxin attaches to a critical receptor molecule embedded in the plasma membrane, a specific signal is conveyed to the nucleus to activate death genes. The two main pathways of PCD, the death receptor (extrinsic) and the mitochondrial (intrinsic) pathways, are activated by caspase 8- and 9, respectively, both of which are found in the cytosol.

The absence of functional extrinsic pathways of PCD is associated with disease; for example, in humans and mice, deficits in Fas-Fas ligand signaling systems are associated with lymphoproliferative disorders and accelerated autoimmune disease.

Cell Surface-Induced PCD: Fas Signaling

Fas-Fas ligand signaling initiates an extrinsic pathway to PCD via activation of caspase 8. Binding of Fas on one cell to Fas ligand (FasL) of another cell initiates stimulus for PCD. When FasL binds to Fas (its receptor), it induces death in the Fas-bearing cell. Fas-FasL signaling controls the killing of target cells in overproduction of cells in the immune system and suppresses unwanted reactions of T cell-mediated cytotoxicity. Many cells express Fas, whereas only **activated T cells** express FasL. When Fas binding to FasL is completed at the cell surface, the first signal is **caspase 8 activation**, at the site where the Fas extends through the plasma membrane into the cytoplasm. Both Fas and TNF-α can initiate PCD through caspase 8 activation and cleavage of Bid.

Cytotoxic lymphocytes kill target cells via Fas signaling-induced PCD. FasL on the lymphocyte surface binds to the Fas protein on the target cell, causing Fas molecules to form surface clusters. The **adapter protein** called **FADD** (for Fas-associated death domain) then binds to the clustered Fas-FasL molecules. Because FADD also contains a caspase-binding domain, it recruits inactive **procaspase 8** molecules, which then autoactivate to initiate the caspase cascade. Fas also activates **caspase-3** by inducing cleavage of its active subunits, and by stimulation of denitrosylation of its active-site thiol.[67] Different subsets of memory T cells have differing sensitivities to apoptotic pathways. Primed T cells are more resistant to Fas-mediated activation-induced PCD than naive T cells. The cytokines IL-2 and IL-7 differentially regulate the balance between proliferation and Fas-mediated apoptosis.[68]

Cytotoxic T lymphocytes and **NK cells** can kill target cells by different mechanisms: (1) membrane destruction by release of channel-forming porins; (2) granzyme-induced PCD; or (3) Fas-Fas ligand killing[69–72] (Fig. 2.7). Specific **cell surface death receptors** may shunt injury into PCD; for example, **mannose-6-phosphate/insulin-like growth factor II receptor** is a

Vet-ebooks.com

death receptor for granzyme B in cytotoxic T cell-induced apoptosis.[73]

Erythrocytes express both the death receptor Fas and its ligand, FasL, which are used in contact-initiated cell death in developing erythrocytes on nurse cell macrophages to prevent overproduction. During stress, erythropoietin receptor signaling downregulates erythroblast Fas and FasL, consequently increasing erythroiesis.[74]

Pathogenic microorganisms have genes that can promote and suppress apoptosis (Fig. 2.7). **Viruses** commonly encode proteins that block cell death to allow for completion of the viral cycle. Viral FLICE-inhibitory proteins (v-FLIPs) encoded by poxviruses, herpesviruses, and other viruses share the ability to inhibit PCD after engagement of death receptors. In contrast, several viruses do induce apoptosis in host cells by initiating Fas ligand expression.[75] Caspases 3 and 7 have been shown to mediate apoptosis in viral infections.[76]

Cytokine-Induced Apoptosis: TNF-α

Potent cytokines such as **tumor necrosis factor-α (TNF-α)** can trigger PCD in target cells by activating PCD. TNF-α-induced apoptosis is commonly encountered in endothelium and in lymphoid tissues, where it is associated with severe inflammation. **TNF-α** binds to its specific death receptor to initiate caspase-independent PCD. The **TNF-α-related apoptosis-inducing ligand** induces a necrosis-like cell death pathway that depends both on caspases and RIP kinase activity.[77] Ceramide acts as a mediator of caspase-independent PCD caused by death receptors such as TRAIL and TNF-R55. The following pathway of progressive activation is based on studies in vitro:

TNFα → Bax/Bak → TRAIL → caspase 3/ceramide → apoptosis

TRAIL is an antiviral protein against some viruses. TRAIL appears to induce apoptosis in cancer cells but not most normal cells. TRAIL-induced apoptosis is mediated by its receptors DR4 (TRAIL-R1) and DR5 (TRAIL-R2) and the **adapter protein Fas-associated death domain protein** (**FADD**). **TNF-like weak inducer of apoptosis (TWEAK)** binds to cell surface receptor FGF-inducible 14 (**Fn14**) to regulate cell responses including vascular permeability and apoptosis. In the brain, the TWEAK-Fn14 pathway protects neurovascular units during cerebral ischemia.

Other cytokines that have been shown to induce apoptosis include **interleukin-1 (IL-1) and interferon-gamma (IFN-γ)**.[78] **IL-1** and IL-1 receptors are involved in progressive neurodegeneration in ischemia injury.[79]

TNF-α triggers Bid-dependent **lysosomal permeabilization** with release of cathepsin B into the cytosol and activation of caspase 2.

During TNF-α-mediated hepatocyte toxicity, cathepsin B is released from lysosomes and contributes to PCD by promoting mitochondrial dysfunction.

Lysosomal executioner caspases cause caspase-independent PCD. Cysteine cathepsins released from the lysosome into the cytosol can trigger PCD that does not require caspase executioner proteases, but instead is mediated by toxic ROS. Neutrophil constitutive death involves caspase, calpain, ROS, cell death signaling pathways, mitochondria, and BCL-2 family members.[80]

Phagocytosis-Induced Cell Death: Mac-1

Phagocytosis-induced cell death (PICD) is common in neutrophils as they take up complement-opsonized targets at sites of inflammation. The process typically begins with **mac-1-mediated phagocytosis** and the release of large amounts of ROS, TRAIL, and chemokines by phagocytizing neutrophils. PICD requires a sustained oxidative burst that generates large amounts of ROS. **ROS** cause focal degradation of the **lysosomal membrane**, allowing leakage of **cathepsin D**, which triggers **caspase 8 and 3**, the key players in most pathways of extrinsic, death receptor-mediated PCD.[81] TNF-α synergizes with this pathway to enhance apoptosis.

PICD also triggers the competing **MARK/ERK-dependent survival pathway**. MARK/ERK suppresses PCD through granulocyte-macrophage colony stimulating factor (GM/CSF), which, although it enhances ROS generation in phagocytosis, suppresses PICD by increasing ERK activation and depressing caspase 8 activation.

Programmed Cell Death in Development and Injury

Embryogenesis

In **embryogenesis**, PCD deletes lineages of cells that are no longer required by the developing embryo, or that might in some way be destructive.[82] In human ontogenesis, embryonic **muscle** degenerates and dies in defined patterns of PCD.[83] **Dysfunctional PCD** during embryogenesis results in fetal defects; for example, aberrant PCD in the developing kidney leads to renal **hypoplasia**.[84]

Embryogenesis in the **brain** involves PCD of approximately half of the **neurons** before adulthood. In the developing chick embryo, there is massive cell death in the spinal cord at 4–5 days of incubation. Affected

Vet-ebooks.com

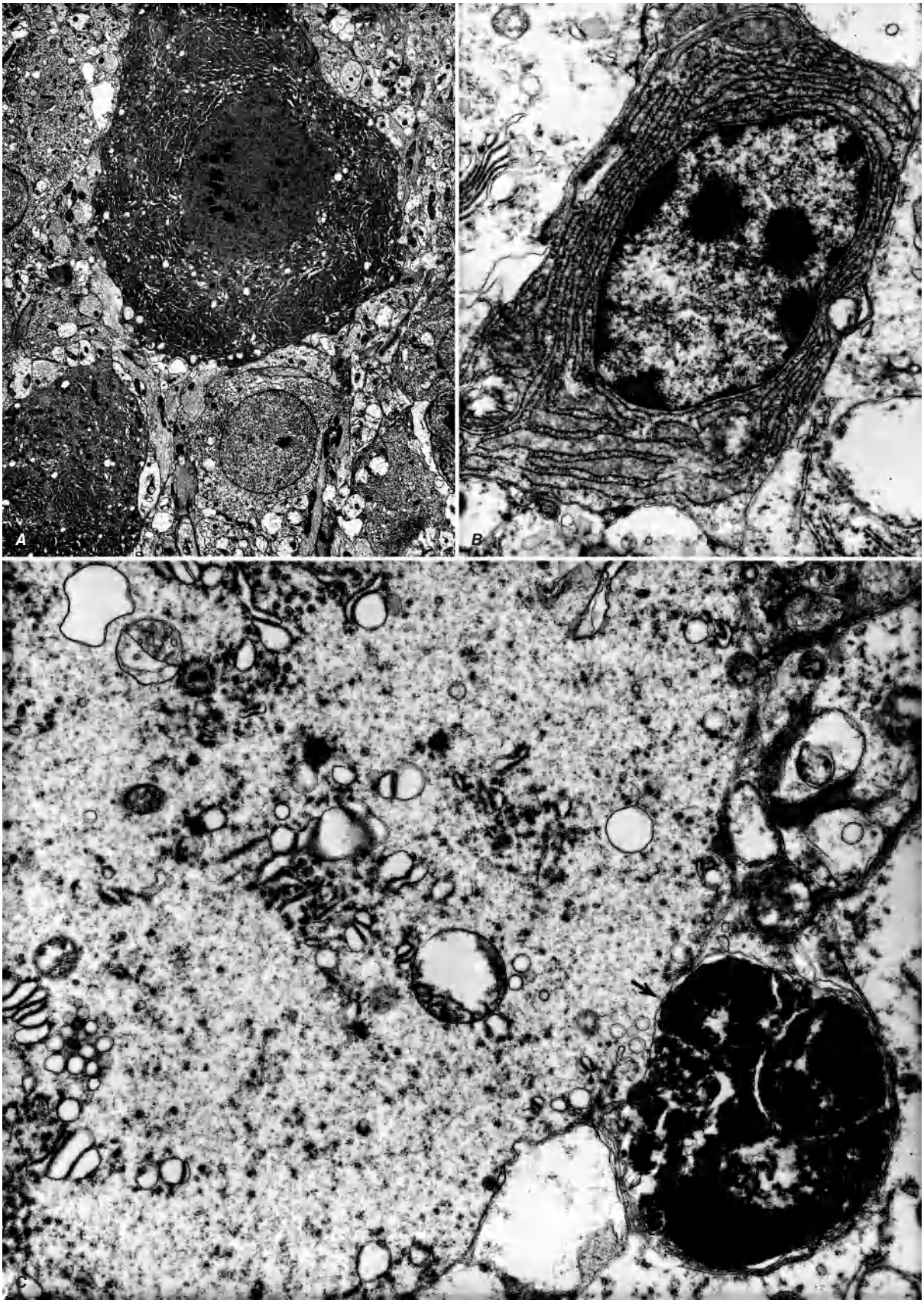


Fig. 2.7 **Programmed cell death**: brain. **A**. **Cerebellum**, **necrotic neuron (Purkinje cell)**: enteroviral infection, chicken. Neuron is dense and contracted. **B**. **Plasmacyte-neuron interface**. Neuronal endoplasmic reticulum communicates directly with plasmacyte cytosol. **C**. **Cerebellum**: **necrotic plasmacyte** apposed to intact Purkinje cell. Plasmacyte has undergone PCD after attachment to the surface of a picornavirus-infected neuron (avian encephalomyelitis virus).

Vet-ebooks.com

cells show decreased nuclear size, clumping of chromatin beneath the nuclear envelope, increased electron opacity, disappearance of the Golgi complex, and disintegration of polyribosomes; there is progressive loss of the nuclear envelope and most of the endoplasmic reticulum. As these events occur, bundles of filaments appear and crystals of ribosomes form in the cytoplasm.

Autophagy, a critical process for PCD during embryogenesis, is characterized by autophagic vacuolation, organelle autophagy, and punctate distribution of RER-autophagosomal membrane proteins.[85,86] **Residual bodies** are present in large numbers in some dying cells. Some investigators thus view this as a unique pattern of PCD and refer to it as **nonapoptotic PCD** ("autophagic cell death," type II cell death); that is, the designation of these vacuoles as autophagosomes implies that autophagy triggers cell death (or is induced to resist ongoing death), and so is more than a scavenger process that clears cellular damaged organelles and debris.

Metamorphosis

Tadpole tail breakdown in amphibians during metamorphosis results from thyroxin-dependent autolysis initiated in the myocyte. Early cytoplasmic changes include folding of myofibrils and loss of striation. Degeneration of mitochondria is also an early change and is followed by disorganization and disintegration of sarcoplasmic reticulum and the development of lysosomes. Macrophages replace and destroy myocytes as lysosomes release hydrolases into the tissue that degrade cell protein fragments.[87]

Atrophy

PCD is critical in atrophy such as involution of the uterus (after birth), mammary gland, and other organs in which previously functioning cells must be deleted without inciting other host cellular responses. In **thymic atrophy**, a large percentage of newly formed thymocytes die by PCD with ultrastructural changes of membrane-bound cytoplasmic bodies and nuclear fragments taken up by resident phagocytic cells including dendritic cells and macrophages. These cells progressively develop large cytoplasmic phagolysosomes. Viral-induced lymphocyte death in **thymic atrophy** of young animals may follow a similar type of PCD. In lymphoid tissues, B cells destined for PCD express a unique CD77 glycolipid on their surfaces that is the signal for cell death.[88] **Erythropoiesis** in bone marrow involves apoptosis of erythroblasts by FasL- and TRAIL-sensitive pathways.[89]

Sublethal Injury

In **acute cell injury**, cellular signals are generated when specific molecules bind to receptors at the cell surface, activating signal molecules that flow to the cytoplasm to activate apoptotic pathways or to the nucleus to activate death genes.[90] PCD is an essential component of the healing response. For example, in the eye, keratocyte and stromal apoptosis is an early, initiating event in corneal wound repair.[91,92] PCD plays critical roles in blood vessel regression and angiogenesis.[93] In endothelial cells, activation of apoptotic signaling pathways mediates PCD.

PCD is a critical process for deletion of cells infected and damaged by viruses, bacteria, and parasites. PCD is an important mechanism to remove parasitized cells. Protozoan parasites can initiate their own PCD, but can also inhibit PCD in host cells as a mechanism of survival.[94]

Interplay of Necrosis and PCD

In injured tissues, necrosis and apoptosis can both contribute to death of cells and, in any given tissue, can develop concurrently. In each individual injured cell, the processes of necrosis and programmed cell death often coexist, since apoptosis develops after tissue injury to eliminate damaged cells that cause biological mischief. **Necroptosis** and **necraptosis**, terms proposed for pathways involving necrosis/apoptosis or necrosis/apoptosis/autophagy, respectively, are inadequately defined and are not used in this text. When apoptotic pathways are activated in injured cells, the process of necrosis can be diverted to apoptosis.

Ischemia

Ischemia is a local deficiency of blood in tissue due to obstruction or constriction of a blood vessel. It is a major cause of cell death. Failure of blood to circulate through tissue leads to **anoxia** and a progressive, cascading series of events that ends in necrosis (Table 2.1). In hypoxic tissue, necrotic and apoptotic cell death mechanisms are both operational. The dominant cell death pathway is determined by the cell phenotype for pro-apoptotic proteins and the rapidity of the process.

The earliest cellular change in ischemia is **mitochondrial dysfunction**, which includes shutdown of oxidative phosphorylation, shutdown of ATP production, production of reactive oxygen species, and calcium overload in the matrix. The latter two events activate mitochondrial permeability transition pores

Vet-ebooks.com

Table 2.1 Events in necrosis caused by anoxia.

Change	*Manifest by*	*Reference to ultrastructural pathology*
Mitochondrial enzyme dysfunction	Loss of ATP. Shift in Ca^{++}. Depletion of critical enzymes leads to mitochondrial degradation	**Ades**, *Exp Mole Pathol* 30:94, 1979; **Fidzianska**, *Acta Neuropathol* 81:572, 1991 (fetal muscle); **Garcia**, *Virch Arch* 25:191, 1977 (brain); **Gobe**, *Lab Invest* 63:770, 1990 (kidney); **Hanzlikova**, *J Ultrastruct Res* 60:121, 1977 (skeletal muscle); **Jennings**, *Am J Pathol* 92:187, 1978 (dog, heart); **Jones**, *Arch Pathol* 99:634, 1975 (pancreas, shock); **Kalimo**, *Virch Arch B* 25:207, 1977 (brain); **Kreisberg**, *Virch Arch B* 22:121, 1976 (rat, kidney, hypotension)
Mitochondrial phospholipase activation	Activation within mitochondrial membranes arises (from disturbed Ca^{++} homeostasis), leads to degradation of phosphlipids	**Saffitz**, *Lab Invest* 50:278, 1984 (lysophosphaglycerides)*
Mitochondrial ATP: anaerobic shift	Glycolytic production of ATP replaces aerobic production by oxidative phosphorylation increase in glycolysis; inhibition of lipid metabolism	**Colell**, *Cell* 129:983, 2007
β-oxidation of fatty acids is inhibited	Acyl-CoA esters accumulate and have detergent effect on membranes	**Lamhonwah**, *Biochem Biopys Res Commun* 345:1315, 2006
Cytoskeletal degradation	Depolymerization of microtubules and microfilaments	**Frenzel**, *Virch Arch B* 21:79, 1976 (liver, endothelium)
Ion shifts	Entry of Na^{+} and additional Ca^{++} into cytosol; loss of K^{+}	**Jewell**, *Science* 217:1257, 1982;* **Shen**, *Am J Pathol* 67:417, 1972 (heart)
Ca^{++} increases to critical levels	Cytoskeleton contracts. Mitochondria mineralize. High calcium levels cause cell death	**Balantine**, *J Neuropathol Exp Neurol* 43:500, 1979 (nerve); **Elz**, *Am J Pathol* 117:131, 1984; **Farber**, *Lab Invest* 47:114, 1982; **Ganote**, *Am J Pathol* 116:94, 1984; **Ganote**, *Am J Pathol* 129:327, 1987; **Lockhard**, *Am J Pathol* 1139:565, 1991 (human muscle calcium); **Myagkaya**, *Virch Arch B* 49:61, 1985 (rat liver);† **Sage**, *Am J Pathol* 133:327, 1987 (dog heart)†
Membrane lysis	Loss of electrolytes and water; liberation of lysosomal enzymes	**Boutet**, *Lab Invest* 34:482, 1976 (muscle, catecholamines)
Entry of proteins into the cell	Plasma proteins (and tracer molecules) detected in the ischemic cell	**Fahimi**, *Am J Pathol* 62:143, 1971 (muscle, lanthanum tracer)
Loss of proteins	Cellular enzymes appear in interstitium and bloodstream	**Hoffstein**, *Am J Pathol* 79:207, 1975 (heart);† **Kent**, *Lab Invest* 46:265, 1982 (heart); **Lemasters**, *J Cell Biol* 97:778, 1983 (liver)*
Autophagy	Formation of autophagosomes in response to cell injury	**Glaumann**, *Lab Invest* 45:479, 1981 (Kupffer cells); **Iamura**, *Acta Neuropathol* 75:131, 1988 (rat, brain)

*In vitro study.
†Animal model.

(PTP). Persisting loss of energy leads to plasma membrane damage, which permits entry of water, electrolytes, and plasma proteins into the cells, all of which are associated with swelling and disintegration of mitochondria. **Superoxide radical production** (and production of other reactive oxygen species) from leaky sites in the mitochondrial electron transport chain is a major damaging event causing ischemia.[95]

Calcium overload leads to irreversible cytopathic changes and necrosis. After vascular reflow, damage caused by **calcium repletion** (after a calcium-free interval) is called the "calcium paradox" and is attributed to calcium overload due to uncontrolled entry of Ca^{++} into the cell. Calcium overload in the mitochondrial matrix activates PTP and is linked to the induction of apoptosis.[96]

Glycogen is depleted in most necrotic cells. As mitochondria disintegrate and ATP levels fall, metabolism is briefly shifted to anaerobic glycolysis for energy production. This shift augments glycolysis and contributes to cell viability and continued function. In myocardial anoxia caused by ischemia, there is a burst

Vet-ebooks.com

of accelerated glycolysis, but it is brief. Because blood flow is stopped, the glycolytic rate falls rapidly and intracellular lactic acid increases. Accumulation of lactate and hydrogen ions causes a drop in pH within ischemic cells and inhibits glycolysis by suppressing enzymes of glycolytic pathways involved in glucose utilization and glycogenolysis. Accumulation of lactate also enhances degenerative changes within the mitochondria. Paradoxically, **monoparticulate glycogen** may develop in mitochondria during ischemia, especially in the myocardium. Solubilization of enzymes of glycogen synthesis in the cytosol coupled with altered permeability of mitochondrial membranes may allow these enzymes to seep into the mitochondrial matrix and produce glycogen.[97]

Ischemic injury occurs in an **anoxic** phase, during which blood flow is shut down, and in a **postischemic** phase, as blood flow begins again (the reflow-injury phenomenon). In clinical situations in which animals survive an ischemic event, much of the tissue injury occurs during this reflow period and is based on damage by reactive oxygen species. Release of enzymes from hypoxia-injured cells occurs only after blood flow resumes.

Myocardial Ischemia

Myocardiocyte death in ischemia arises from the effects of high matrix Ca^{++} in the mitochondrial matrix and the mitochondrial permeability transition pore opening—both of which incorporate apoptotic pathways.[98] Although apoptosis plays a minor role in myocardiocyte death during infarction,[99–101] it plays a major role in the removal of inflammatory cells during healing.[102] A major factor in ischemic myocardial death is the strong contracture of myofilaments, which causes sarcolemmal membrane defects.[103] After reoxygenation, **cell contraction** occurs, associated with increased plasma membrane permeability and release of cytoplasmic enzymes. Oxygen-induced resumption of ATP production by mitochondria provides energy for contraction and enzyme release. As hypoxic cells become energy depleted, Na^{+} and Ca^{++} levels rise and activate contractile proteins. With reoxygenation, the sudden increase in ATP induces cell contraction before ionic pumps can reestablish ionic equilibrium.

Persistent ischemia causes **hydroxyapatite crystals** to develop free in the sarcoplasm. A magnesium-poor environment favors conversion of amorphous $CaPO_4$ into the needle-like crystals of hydroxyapatite. Examination of human heart tissue using electron probe microanalysis has revealed heavy crystalline deposits in Z band regions and nuclear chromatin with fine calcium deposits throughout the sarcoplasm.[104,105]

Chronic ischemic myocardiocytes may protect themselves by initiating **autophagy**, the degradation process for turnover of dysfunctional organelles and proteins. Repetitive myocardial ischemia produced in pigs suggests that ischemia-induced autophagy is an efficient protective mechanism.[106]

Hepatocytes in Ischemia

In the **liver** in which portal venous and hepatic arterial blood supplies are occluded for greater than 3 hr, all hepatocytes are damaged. Hepatocytes, when examined histologically, do not appear necrotic and there is no increase in total liver calcium. However, when blood flow is reestablished, hepatocytes rapidly develop coagulation necrosis and calcium is markedly increased.[107] Experimental hepatic ischemia in rats provides evidence that apoptosis plays a signicant role in reflow injury. Apoptosis occurs early and is more prominent in sinusoidal endothelial cells than in hepatocytes.[108]

Ischemia induces xanthine oxidase-dependent hydrogen peroxide production in hepatocytes of midzonal areas and apoptosis of sinusoidal endothelial cells.[109] Circulating erythrocytes appear to scavenge hydrogen peroxide produced by the xanthine oxidase pathway.[109,110]

Neurons in Ischemia

Ischemia of the brain leads to widespread necrosis of neurons. In studies of brains of fetal lambs made ischemic by clamping of the umbilical cord, necrotic neurons were found in the mesencephalon, pons, and deep cerebellar nuclei; in contrast, apoptotic neurons were found in both white and gray matter, not limited to these regions.[111] Ischemia probably underlies the patterns of apoptosis and necrosis in neurons in the edematous brain.[112]

Normal protein synthesis requires a functional translation initiation complex, a key element of which is **eukaryotic initiation factor 2 (eIF2)**, which in a complex with GTP introduces the met-tRNA. During postischemic brain reperfusion, reduced protein synthesis in neurons is due to phosphorylation of eIF2. There is a marked increase of a variant eIF2 that induces apoptosis. Localized by immunogold electron microscopy, eIF2 was found in the nucleus with nucleoli and associated with strands of heterochomatin and nuclear filaments.[113]

Denervation Atrophy

Denervation of **skeletal muscle** is followed by progressive myocyte atrophy with death that is slow to develop and lacks inflammation. The mechanism of cell death in post-denervation atrophy resembles PCD. Ultrastructural analysis of denervated rodent skeletal muscle revealed nuclei with hypercondensed chroma-

Vet-ebooks.com

tin and fragmented nuclei typical of apoptosis.[114] However, the large discrepancy between morphologic markers of apoptosis and histochemical staining for DNA fragmentation suggested that fragmentation of genomic DNA is not an obligatory step in atrophy and death of myocytes.

In the **brain**, neuron apoptosis is **Fas death receptor-dependent** when triggered by DNA damage caused by nitric oxide and superoxide. Motor neurons in mice lacking functional Fas receptor and Fas ligand are protected from apoptosis. For example, spinal motoneurons of mice with experimental unilateral sciatic nerve avulsion undergo apoptosis that is mediated by upstream NO and ONOO+ genotoxicity and downstream p53 and Fas activation, and is shifted to necrosis by mutant SOD1.[115] After injury, levels of Fas protein and cleaved caspase 8 increased; Fas upregulation was p53 dependent; NO and peroxynitrite (ONOO+) increased; DNA single strands (breaks) increased. Motorneurons lacking Fas and Fas ligand were protected from injury; those lacking nNOS and iNOS resisted apoptosis.

Getting Rid of the Dead Cell

The dying cell emits signals to the body that it must be removed. These are "eat me" signals that spew out to neighboring cells and into the circulating blood. Here they stimulate phagocytosis—either by sluggish neighboring parenchymal cells or by highly efficient monocytes that, when activated, move into tissue and transform into macrophages (Fig. 2.8). The complement component **C1q** marks cells for phagocytic

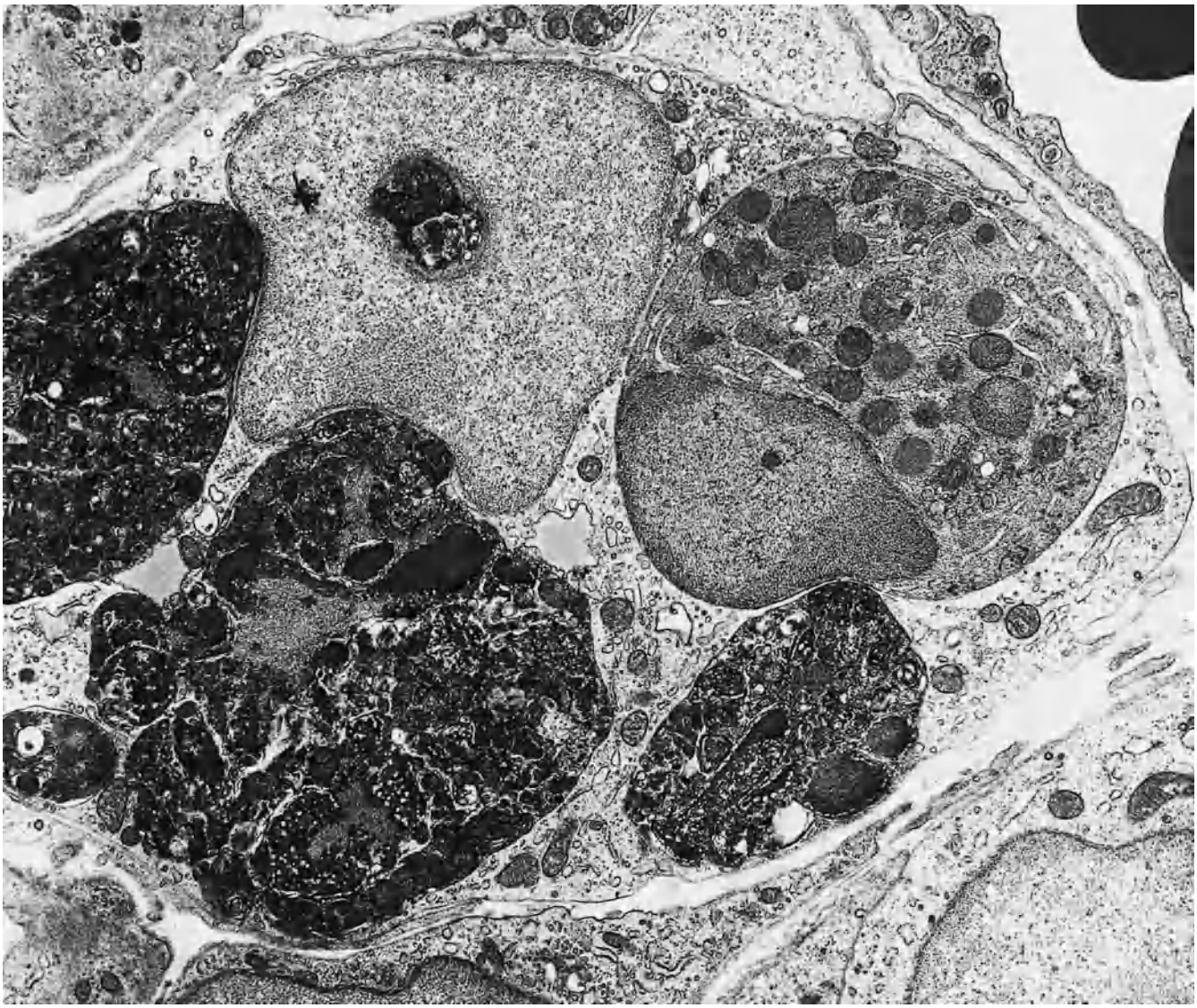


Fig. 2.8 Phagocytosis: macrophage in the lamina propria of an intestinal villus has taken up entire granulocytes, which are in various stages of degeneration within giant lysosomes.

Vet-ebooks.com

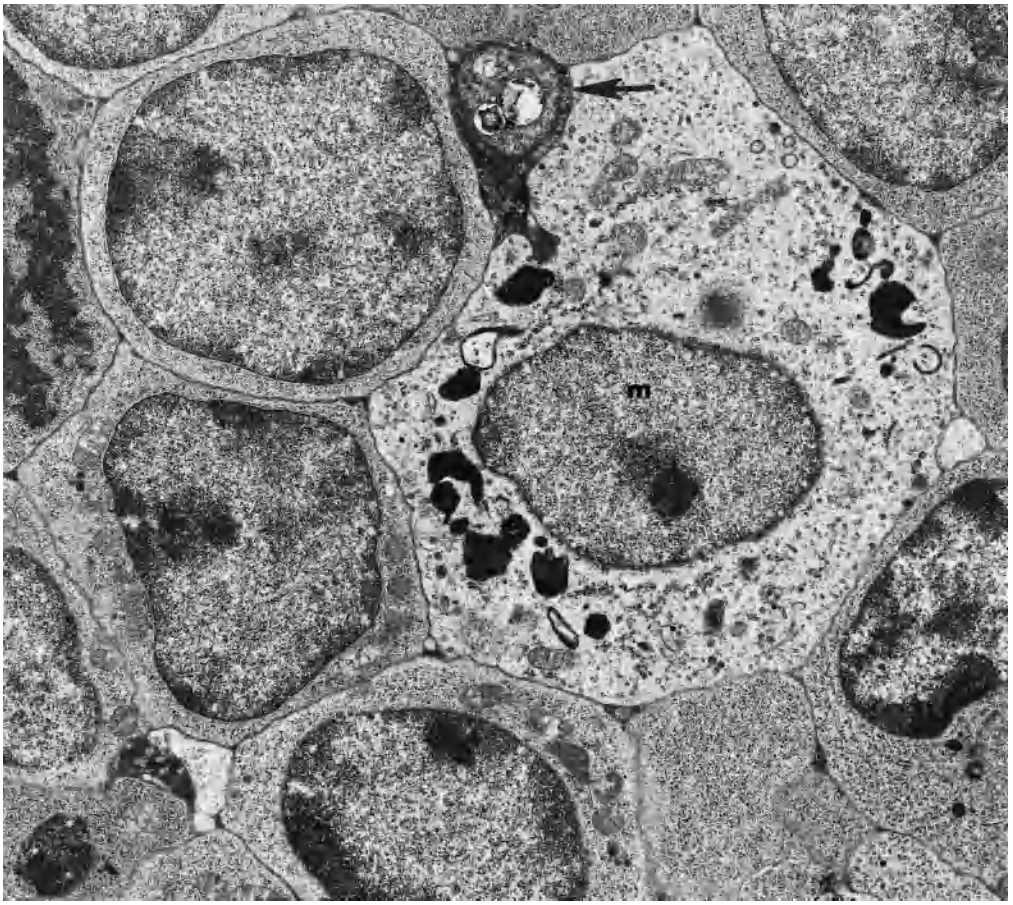


Fig. 2.9 Phagocytosis: thymic atrophy, systemic viral infection (hog cholera), pig. Pale, lysosome-bearing macrophage contains phagolysosomes filled with dense debris that originated in necrotic lymphocytes (*arrow*).

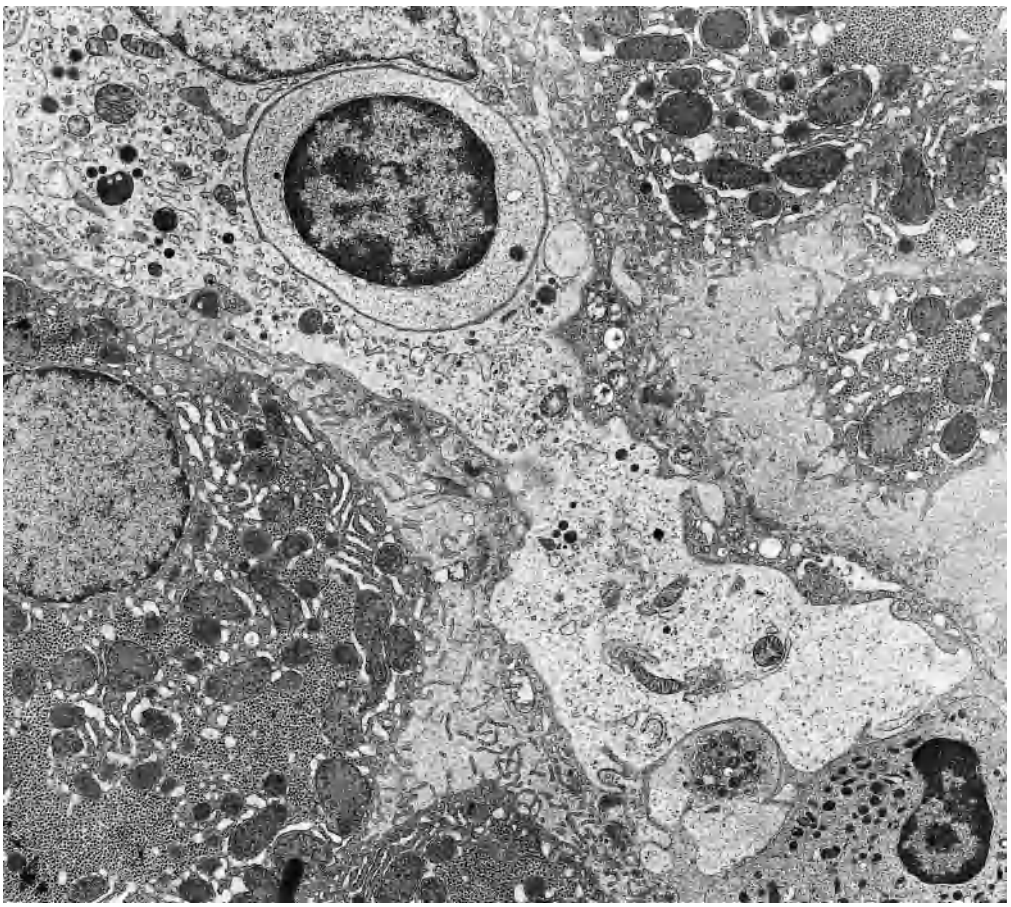


Fig. 2.10 Cytophagocytosis: lymphocyte (*top*) within a large, tortuous macrophage, hepatic sinusoid, liver, dog.

Vet-ebooks.com

uptake. Complement system activation via C1q on the dead cell surface is the bait for complement receptors on macrophage surfaces.[116–120] C1q and other collectins (such as pulmonary surfactant proteins) are powerful apoptotic cell clearance molecules that work through the calcium-binding protein calreticulin.

Complement is a powerful system so that an inhibitory factor is required to prevent overzealous phagocytosis and stimulation of unwanted inflammation. The **C4b-binding protein (C4Bb)** is the key inhibitor for classic and lectin pathways of complement. In the brain, another complement protein (which blocks the complement system) is protective; ischemic neurons express C1q, a signal to destroy the neuron. However, a soluble form of the complement receptor protein CR1 binds to C1q on the neuron's surface, protecting it from leukocytes and platelets that would cause excessive destruction of tissue.

As phagocytosis progresses, the **interstitium** surrounding necrotic cells is infiltrated by inflammatory cells, largely **monocytes**, but also neutrophilic, eosinophilic, and basophilic leukocytes. The type of etiologic agent and the pattern of necrosis determine which cell dominates. **Monocytes** and **neutrophils** attracted to necrotic tissue release potent lytic enzymes that can cause necrosis directly.[121]

Removal of Extracellular Debris

Macrophage Phagocytosis of Cell Debris

In early stages of cell death, blebs of cytoplasm bearing small granules of protein and lipid debris are released into the interstitium. These extruded components of the damaged cell are taken up by macrophages (Fig 2.9). The exofacial display of phosphatidylserine on the cell surface—the **phosphatidylserine scramble**—that develops in apoptosis is a potent signal for macropinocytosis and phagocytosis.

Tissues that remain viable despite necrosis of individual parenchymal cells are invaded by large numbers of monocytes that rapidly develop into macrophages and phagocytize the debris of necrotic cells. In necrosis that is associated with inflammation, especially reactions involving massive cytokine release, large numbers of neutrophils also invade areas of degeneration and necrosis.

There are striking alterations in **extracellular spaces** in necrotic tissue. Plasma proteins and cellular debris accumulate and distend spaces between cells. Capillaries are abnormal with endothelium that is usually swollen. **Basal membranes**, which play important roles in maintaining cell structure and polarization, often survive injuries that are lethal to parenchymal cells and serve in recovery as scaffolds for migration and attachment of new cells.[122,123]

Cytophagocytosis

The entire dead cell may be phagocytized by a macrophage, a process called **cytophagocytosis**. In these macrophages, the dead cell is present within a giant phagolysosome with its architecture preserved. With time, these cells are degraded by a progressive transfer of debris to newly developed autolysosomes. In slowly developing necrosis, marked bleb formation occurs at the surface of the dying cell. Large fragments of the cytoplasm may be released. This type of blebbing and cytophagocytosis is typical of programmed cell death, especially that which occurs in embryogenesis. Phagocytosis of dead cells renders macrophages dysfunctional, even in apoptotic cells.[124]

Empiripolesis is the active penetration of one cell by another that remains intact;[125] that is, empiripolesis involves the presence of an intact living cell within the cytoplasm of another cell (Fig. 2.10). Granulocytes, monocytes, and lymphocytes that develop close appositions to dying target cells commonly bind to and enter these cells by invasion. In degenerative lesions of the central nervous system, astrocytes may contain oligodendrogliocytes. Astrocytic empiripolesis is most common in various types of acute demyelinating lesions.[126] It is typical of the acute lesions of multiple sclerosis where it represents phagocytosis of new oligodendroliocytes by reactive astrocytes. The process may be responsible for the failure of remyelination that typifies multiple sclerosis.

The term **entosis** has been coined for the active invasion of one cancer cell into another. The invading cell is the active partner in entosis, and becomes completely enclosed by pulling the host cell around itself using cadherins and other adhesins. In human breast carcinomas, the invading cell is typically destroyed, but can not only survive but pop out of the host cell to survive extracellularly.[127]

Endothelial Cell Death

Vascular Damage

Analysis of **endothelial cells** in necrotic tissues is critical since a major decision is to determine if parenchymal cell damage is primary, or if it has been preceded by vascular damage. For example, apoptotic death of endothelial cells precedes myocyte death in experimental ischemia/reperfusion injury.[128] Endothelial cells, pericytes, and basal laminae are typically damaged during tissue necrosis.

Necrotic cell death of endothelial cell death follows the spectrum of change between cell shrinkage and cell lysis (Fig. 2.11). All components of the endothelium are affected similarly. Perivascular components

Vet-ebooks.com

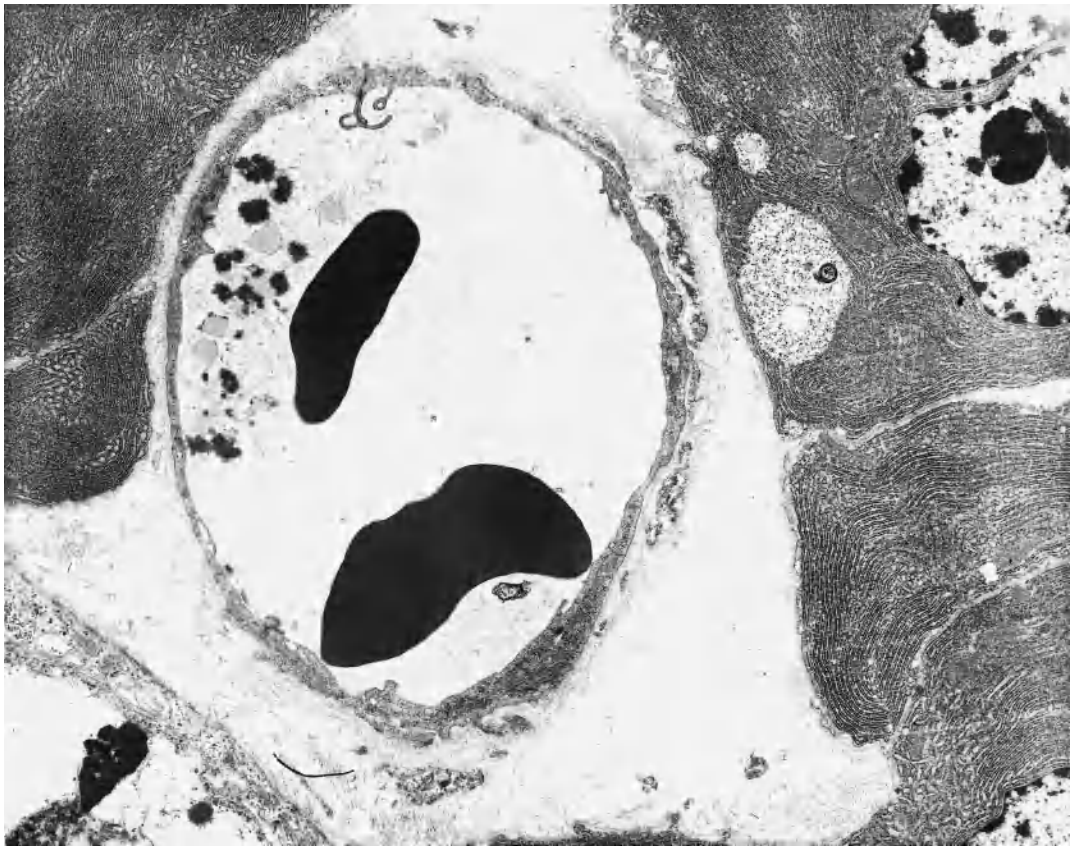


Fig. 2.11 Endothelial cell death. Necrosis: Diffuse necrosis in all components of the capillary, clostridial myositis, cow. Pericapillary space contains plasma proteins and cellular debris.

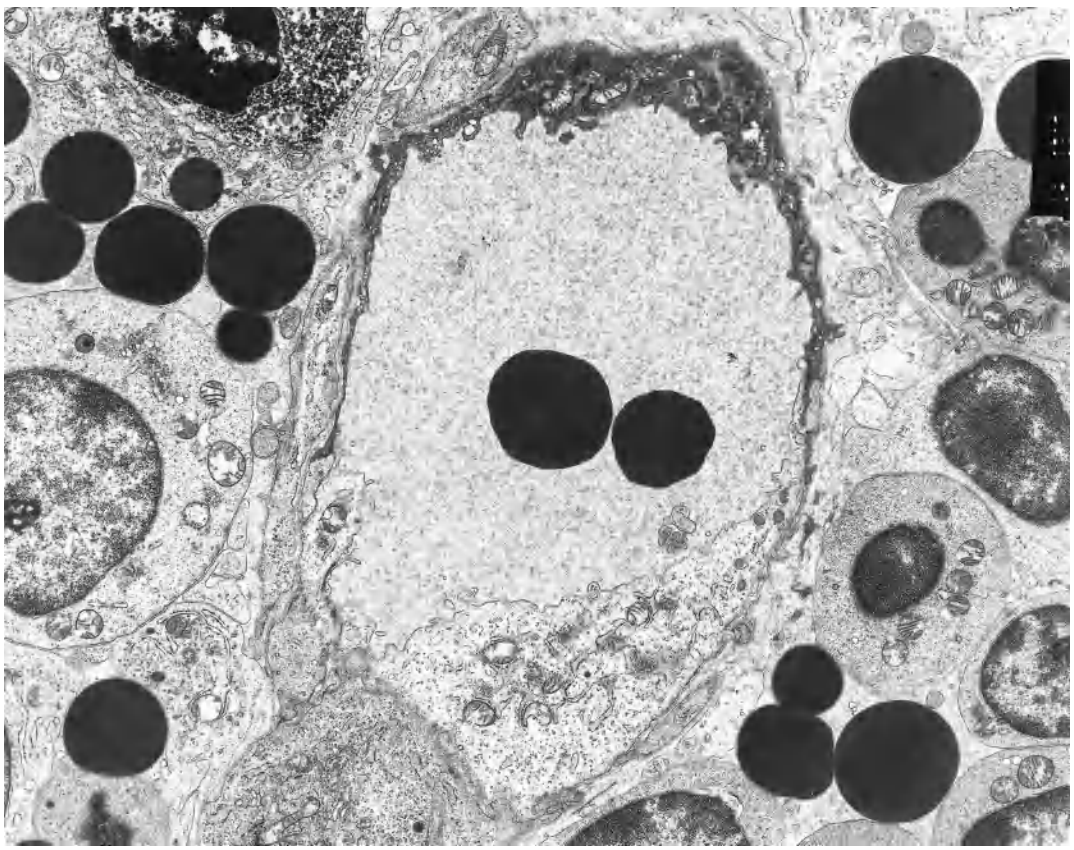


Fig. 2.12 Endothelial cell death. Programmed cell death: lymphadenitis, brucellosis, goat. Death of an individual endothelial cell, capillary.

Vet-ebooks.com

of the vascular wall are directly and indirectly affected by death of endothelial cells. If the basal lamina persists in necrosis it provides the scaffold for migration, positioning, and attachment of new cells during recovery. If destroyed, regeneration can be delayed or prevented. Endothelial cell necrosis in injured tissue is complicated by vascular damage that is secondary to edema, hemorrhage, and acute inflammation. In turn, the extent of endothelial cell death directly influences the response of the parenchymal cell. Cytokines released by the injured endothelium have a direct impact on the manner and appearance of necrosis of parenchymal cells.

In **programmed cell death**, endothelial cells are affected differentially. Early signs of endothelial cell PCD include cell retraction and shrinkage, protrusion into the capillary lumen, and formation of adherens junctions (Fig. 2.12). Nucleus and cytoplasm condense uniformly. Dead endothelial cells are sloughed into the flowing blood of the lumen, or are phagocytized by adjacent endothelial cells that have remained viable.[129]

References

1. Yellon DM, Hausenloy DJ. 2007. Myocardial reperfusion injury. *New Engl J Med* 357:1121.
2. Zeligs JB, et al. 1975. The course and nature of acinar cell death following pancreatic ligation in the guinea pig. *Am J Pathol* 80:203.
3. Javadov S, Karmazyn M. 2007. Mitochondrial permeability transition pore opening as an endpoint to initiate cell death and as a putative target for cardioprotection. *Cell Physiol Biochem* 20:1.
4. Lerch MM, et al. 1992. Acute necrotizing pancreatitis in the oppossum: earliest morphological changes involve acinar cells. *Gastroenterology* 103:205.
5. Ray SD, et al. 1993. Ca^{++} antagonists inhibit DNA fragmentation and toxic cell death induced by acetaminophen. *FASEB J* 7:453.
6. Boskey AL, et al. 1989. Calcium-acidic phospholipid-phosphate complexes in human hydroxyapatite-containing pathologic deposits. *Am J Pathol* 133:22.
7. Farber JL. 1982. Membrane injury and calcium homeostasis in the pathogenesis of coagulative necrosis. *Lab Invest* 47:114.
8. Cuenoud HF, et al. 1978. Ultrastructure of the myocardium after pulmonary embolism. *Am J Pathol* 92:421.
9. Guillemin K, Krasnow M. 1997. The hypoxic response. *Cell* 89:9.
10. Ratliff NB, et al. 1975. Formation of myocardial zonal lesions. *Am J Pathol* 79:321.
11. Ganote CE, Vander Heide RS. 1987. Cytoskeletal lesions in anoxic myocardial injury. *Am J Pathol* 129:327.
12. Saffitz JE, et al. 1984. Pathophysiologic concentrations of lysophosphaglycerides quanitified by electron microscopic autoradiogrpahy. *Lab Invest* 50:278.
13. Morris RG, et al. 1984. Hormone-induced cell death. 2. Surface changes in thymocytes undergoing apoptosis. *Am J Pathol* 115:426.
14. Blair OM, et al. 1968. Hepatocellular ultrastructure in dogs with hypovolemic shock. *Lab Invest* 18:172.
15. Myagkaya GL, et al. 1985. Quantitative analysis of mitochondrial flocculent densities in rat hepatocytes during normothermic and hyperthermic ischemia *in vitro*. *Virch Arch B* 49:61.
16. Mergner WJ, et al. 1979. Studies on the pathogenesis of ischemic cell injury. VIII. ATPase of rat kidney mitochondria. *Lab Invest* 40:686.
17. Yan M, et al. 2007. Ethanol induced mitochondria injury and permeability transition pore opening. *World J Gastroenterol* 13:2352.
18. Nieminen A-L, et al. 1997. Mitochondrial permeability transition in hepatocytes induced by *t*-BuOOH: NAD(P)H and reactive oxygen species. *Am J Physiol* 272:C1286.
19. Bonucci E, et al. 1973. The organic-inorganic relationship in calcified mitochondria. *J Cell Biol* 59:185.
20. Ballantine JD, Greene WB. 1984. Ultrastructural pathology of nerve fibers in calcium-induced myelopathy. *J Neuropathol Exp Neurol* 43:500.
21. Hagler KH, et al. 1981. Quantitative x-ray microanalysis of mitochondrial calcification in damaged myocardium. *Lab Invest* 45:241.
22. Schinzel AC, et al. 2005. Cyclophilin D is a component of mitochondrial permeability transition and mediates neuronal cell death after focal cerebral ischemia. *Proc Natl Acad Sci USA* 102:12005.
23. Saelens X, et al. 2005. Protein synthesis persists during necrotic cell death. *J Cell Biol* 168:545.
24. Hershko A. 1983. Ubiquitin: roles in protein modification and breakdown. *Cell* 34:11.
25. Petito CK, Lapinsi RL. 1986. Postischemic alterations in ultrastructural cytochemistry of neuronal Golgi apparatus. *Lab Invest* 55:696.
26. Kawanami O, et al. 1979. Nuclear inclusions in alveolar epithelium of patients with fibrotic lungs disease. *Am J Pathol* 94:301.
27. Jacob M, et al. 2007. Chromatin breakdown by deoxyribonuclease 1 promotes acetaminophen-induced necrosis: an ultrastructural and histochemical study on male CD-1 mice. *Histochem Cell Biol* 128:19.
28. Luke CJ, et al. 2007. An intracellular serpin regulates necrosis by inhibiting the induction and sequelae of lyosomal injury. *Cell* 130:1108.
29. Reed JC. 2004. Mechanisms of apoptosis. *Am J Pathol* 157:1415.
30. Zeiss CJ. 2003. The apoptosis-necrosis continuum. *Vet Pathol* 40:481.
31. Ellis RE, et al. 1991. Mechanism and functions of cell death. *Ann Rev Cell Biol* 7:663.
32. Friedlander RM. 2003. Apoptosis and caspases in neurodegenerative diseases. *New Engl J Med* 348:1365.
33. Qin ZH, et al. 2001. Pro-caspase-8 is predominantly localized in mitochondria and released into cytoplasm upon apoptotic stimulation. *J Biol Chem* 276:8079.
34. Nithipongvanitch R, et al. 2007. Evidence for p53 as guardian of the cardiomyocyte mitochondrial genome

Vet-ebooks.com

following acute adriamycin treatment. *J Hist Cyt* 55:629.
35. Sun MG. et al. 2007. Correlated three-dimensional light and electron microscopy reveals transformation of mitochondria during apoptosis. *Nat Cell Biol* 9:1057.
36. Schafer Z, Kornbluth S. 2006. The apoptosome. *Devel Cell* 10:549.
37. Moreno S, et al. 2006. Apoptosome impairment during development results in activation of an autophagy program in cerebral cortex. *Apoptosis* 11:1595.
38. Twiddy D, et al. 2004. Pro-apoptotic proteins released from the mitochondria regulate the protein composition of caspase-processing activity of the native Apaf-1/caspase 9 apoptosome complex. *J Biol Chem* 279:19665.
39. Hausmann G, et al. 2001. Pro-apoptotic apoptosis protease-activating factor 1 (Apaf-1) has a cytoplasmic localization distinct from Bcl-2 or Bcl-x(L). *J Cell Biol* 149:623.
40. Gajkowska B, et al. 2001. Expression of BAX in cell nucleus after experimentally induced apoptosis revealed by immunogold and embedment-free electron microscopy. *Cell Biol Int* 25:725.
41. He L, et al. 2003. Bcl-X_L overexpression blocks bax-mediated mitochondrial contact site formation and apoptosis in rod photoreceptors of lead-exposed mice. *Proc Natl Acad Sci USA* 100:1022.
42. Martin LJ, Liu Z. 2002. Injury-induced spinal motor neuron apoptosis is preceded by DNA single-strand breaks and is p53- and Bax-dependent. *J Neurobiol* 50:181.
43. Carreras MC, Poderoso JJ. 2007. Mitochondrial nitric acid in the signaling of cell integrated responses. *Am J Physiol Cell Physiol* 292:C1569.
44. Mannick JB. 2007. Regulation of apoptosis by protein S-nitrosylation. *Amino Acids* 32:523.
45. Nazarewicz RR, et al. 2007. Tamoxifen induced oxidative stress and mitochondrial apoptosis via stimulating mitochondria nitric oxide synthase. *Cancer Res* 67:1282.
46. Kim H-R, et al. 2007. Mammalian *dap3* is an essential gene required for mitochondrial homeostasis *in vivo* and contributing to the extrinsic pathway for apoptosis. *FASEB J* 21:188.
47. Mukamel Z, Kimchi A. 2004. Death-associated protein 3 localizes to the mitochondria and is involved in the process of mitochondrial fragmentation during cell death. *J Biol Chem* 279:36732.
48. Liu J, et al. 2004. The cardiolipin-binding domain of Bid affects mitochondrial respiration and enhances cytochrome c release. *Apoptosis* 9:533.
49. Lutter M, et al. 2001. The pro-apoptotic Bcl-2 family member tBid localizes to mitochondrial contact sites. *BMC Cell Biol* 2:22.
50. Gonzalvez F, et al. 2005. tBid interaction with cardiolipin primarily orchestrates mitohchondrial dysfunctions and subsequentlty activates Bax and Bak. *Cell Death Differ* 12:614.
51. Kim TH, et al. 2004. Bid-cardiolipin interaction of mitochondrial contact site contributes to mitochondrial cristae reorganization and cytochrome C release. *Mol Biol Cell* 15:3061.
52. Ding WX, et al. 2004. Bid-dependent generation of oxygen radicals promotes death receptor activated-induced apoptosis in murine hepatocytes. *Hepatology* 40:408.
53. Nhan TQ, et al. 2006. Physiological functions of caspases beyond cell death. *Am J Pathol* 169:729.
54. Singh R, Czaja MJ. 2007. Regulation of hepatocyte apoptosis by oxidative stress. *J Gastroenterol Hepatol* Suppl 1:S45.
55. Lu Z, et al. 2005. Nucleoplasmin regulates chromatin condensation during apoptosis. *Proc NAS* 102:2778.
56. Gavrieli Y, et al. 1992. Identification of programmed cell death in situ via specific labeling of nuclear DNA fragmentation. *J Cell Biol* 119:493.
57. Dinsdale D, et al. 2004. Intermediate filaments control the intracellular distribution of caspases during apoptosis. *Am J Pathol* 164:395–407.
58. Rao L, et al. 1996. Lamin proteolysis facilitates nuclear events during apoptosis. *J Cell Biol* 135:1441.
59. Zakeri ZF, et al. 1993. Delayed internucleosomal DNA fragmentation in programmed cell death. *FASEB J* 7:470.
60. Nithipongvanitch R, et al. 2007. Evidence for p53 as guardian of the cardiomyocyte mitochondrial genome following acute adriamycin treatment. *J Hist Cyt* 55:629.
61. Hayakawa Y, et al. 1999. Apoptosis and overexpression of bax protein and bax mRNA in smooth muscle cells within intimal hyperplasia of human radial arteries. *Arterioscler Thromb Vasc Biol* 19:2066.
62. Martin LJ, Liu Z. 2002. Injury-induced spinal motor neuron apoptosis is preceded by DNA single-strand breaks and is p53- and Bax-dependent. *J Neurobiol* 50:181.
63. Martin LJ, et al. 2005. Adult motor neuron apoptosis is mediated by nitric oxide and Fas death receptor linked by DNA damage and p53 activation. *J Neurosci* 25:6449.
64. Pretorius E, et al. 2006. Ultrastructural effects of low dosage endocrine disrupter chemicals on neural cells of the chicken embryo model. *Horm Metab Res* 38:639.
65. Puthalakath H, et al. 2007. ER stress triggers apoptosis by activating BH3-only protein Bin. *Cell* 129:1337.
66. Joseph SK, Hajńczky G. 2007. IP3 receptors in cell survival and apoptosis: Ca^{2+} release and beyond. *Apoptosis* 12:951.
67. Mannick JB, et al. 1999. Fas-induced caspase denitrosylation. *Science* 284:651.
68. Gupta S, Gollapudi S. 2007. Susceptibility of naive and subsets of memory T cells to apoptosis via multiple signaling pathways. *Autoimmun Rev* 6:476.
69. Calderon B, et al. 2006. In CD4+ T-cell-induced diabetes, macrophages are the final effector cells that mediate islet β-cell killing. *Am J Pathol* 169:2137.
70. Wesche-Soldato DE, et al. 2007. $CD8^+$ T cells promote inflammation and apoptosis in the liver after sepsis. Role of Fas-FasL. *Am J Pathol* 170:87.

Vet-ebooks.com

71. Hickey WF, et al. 1992. Exogenously-induced natural killer cell-mediated neuronal killing: A novel pathogenetic mechanism. *J Exp Med* 76:811.
72. Meyaard L, et al. 1992. Programmed death of T cells in HIV infection. *Science* 257:217.
73. Motyke B, et al. 2000. Mannose 6-phosphate/insulin-like growth factor II receptor is a death receptor for granzyme B during cytotoxic T cell-induced apoptosis. *Cell* 103:491.
74. Socolovsky M. 2007. Molecular insights into stress erythropoiesis. *Curr Opin Hematol* 14:215.
75. Chen LC, et al. 2006. Enterovirus71 infection induces Fas ligand expression and apoptosis of Jurkat cells. *J Med Virol* 78:780.
76. Blondel B, et al. 2005. Poliovirus, pathogenesis of poliomyelitis, and apoptosis. *Curr Top Microbiol Immunol* 289:25.
77. Meurette O, et al. 2007. TRAIL induces receptor-interacting protein 1-dependent and caspase-dependent necrosis-like cell death under acidic extracellular conditions. *Cancer Res* 67:218.
78. McCullough CT, et al. 2007. c-Myc partially mediates IFN-γ-induced apoptosis in the primary hepatocytes. *Int J Exp Pathol* 88:129.
79. Basu A, et al. 2005. Interleukin-1 and the interleukin-1 type 1 receptor are essential for the progressive neurodegeneration that ensues subsequent to a mild hypoxia/ischemic injury. *J Cereb Blood Flow Metab* 25:17.
80. Luo HR, Loison F. 2007. Constitutive neutrophil apoptosis. *Am J Hematol* 83:288.
81. Conus S, et al. 2008. Caspase-8 is activated by cathepsin D initiating neutrophil apoptosis during the resolution of inflammation. *J Exp Med* 205:685.
82. Domingos PM, Steller H. 2007. Pathways regulating apoptosis during patterning and development. *Curr Opin Genet Dev* 17:294.
83. Lauzon RJ, et al. 1992. A morphological and immunohistochemical study of programmed cell death in *Botryllus schlosseri* (Tunicata, Ascidiaceae). *Cell Tiss Res* 272:115.
84. Nagata M, et al. 1996. Apoptosis during an early stage of nephrogenesis induces renal hypoplasia in *bcl-2*-deficient mice. *Am J Pathol* 148:1601.
85. Wang L, et al. 2007. TMEM166, a novel transmembrane protein, regulates cell autophagy and apoptosis. *Apoptosis* 12:1489.
86. Gonzalez-Polo RA, et al. 2005. The apoptosis/autophagy paradox: autophagic vacuolization before apoptotic death. *J Cell Sci* 118:3091.
87. Fox H. 1973. Degeneration of the tail notochord of *Rana temporaria* at metamorphic climax. *Z Zellforsch Mikrosk Anat* 138:371.
88. Mangeney M, et al. 1991. CD77: An antigen of germinal center B cells entering apoptosis. *Eur J Immunol* 21:1131.
89. Zamai L, et al. 2006. In vitro apoptotic cell death during erythroid differentiation. *Apoptosis* 9:235.
90. Ledda-Columbano GM, et al. 1992. Rapid induction of apoptosis in rat liver by cyclohexamide. *Am J Pathol* 140:545.
91. Wilson SE, et al. 2007. Apoptosis in the initiation, modulation and termination of the corneal wound healing response. *Exp Eye Res* 85:305.
92. Mohan RR, et al. 2007. Apoptosis, necrosis, proliferation, and myofibroblast generation in the stroma following LASIK and PRK. *Exp Eye Res* 76:71.
93. Sakamaki K. 2004. Regulation of endothelial cell death and its role in angiogenesis and vascular regression. *Curr Neurovasc Res* 1:305.
94. Bruchhaus I, et al. 2007. Protozoan parasites: Programmed cell death as a mechanism of parasitism. *Trends Parasitol* 23:376.
95. Li C, Jackson RM. 2002. Reactive species mechanisms of cellular hypoxia-reoxygenation injury. *Am J Physiol Cell Physiol* 282:C227.
96. Orrenius S, et al. 2003. Regulation of cell death: calcium-apoptosis link. *Nat Rev Mol Cell Biol* 4:552.
97. Buja LM, et al. 1972. Occurrence of intramitochondrial glycogen in canine myocardium after prolonged anoxic cardiac arrest. *J Mol Cell Cardiol* 4:237.
98. Abbate A, et al. 2007. Electron microscopy characterization of cardiomyocyte apoptosis in ischemic heart disease. *Int J Cardiol* 114:118.
99. Takemura G, Fujiwara H. 2006. Morphological aspects of apoptosis in heart diseases. *J Cell Mol Med* 10:56.
100. Ohno M, et al. 1998. "Apoptotic" myocytes in infarct area in rabbit hearts may be oncotic myocytes with DNA fragmentation: analysis by immunogold electron microscopy combined with in situ nick end-labeling. *Circulation* 98:1355.
101. Freude B, et al. 2000. Apoptosis is initiated by myocardial ischemia and executed during reperfusion. *J Mol Cell Cardiol* 32:197.
102. Takemura G, et al. 1998. Role of apoptosis in the disappearance of infiltrated and proliferated interstitial cells after myocardial infarction. *Circ Res* 82:1230.
103. Elz JS, Nayler WG. 1984. Ultrastructural damage associated with the Ca^{++} paradox. *Am J Pathol* 117:131.
104. Lockard VG, Bloom S. 1991. Morphologic features and nuclide composition of infarction-associated cardiac myocyte mineralization in humans. *Am J Pathol* 139:565.
105. Kalantari F, et al. 2007. Cellular and molecular mechanisms of abnormal calcification following ischemia-reperfusion injury in human liver transplantation. *Mod Pathol* 20:357.
106. Yan L, et al. 2005. Autophagy in chronically ischemic myocardium. *Proc Natl Acad Sci USA* 102:13807.
107. Chien KR, et al. 1979. Ischemic myocardial cell injury. *Am J Pathol* 97:505.
108. Kohli V, et al. 1999. Endothelial cell and hepatocyte deaths occur by apoptosis after ischemia-reperfusion injury in rat liver. *Transplantation* 67:1099.
109. Motoyama S, et al. 2003. Hydrogen peroxide-dependent declines in Bcl-2 induces apoptosis in hypoxic liver. *J Surg Res* 110:211.
110. Motoyama S, et al. 2000. Red blood cells attenuate sinusoidal endothelial cell injury by scavenging xanthine oxidase-dependent hydrogen peroxide in hyperoxic perfused rat liver. *Liver* 20:200.

Vet-ebooks.com

111. Goni-de-Cerio F, et al. 2007. Nearly cell death in the brain of fetal preterm lambs after hypoxic-ischemic injury. *Brain Res* 1151:161.
112. Castejon OJ, Arismendi GJ. 2006. Nerve cell death types in the edematous human ceebral cortex. *J Submicrosc Cytol Pathol* 38:21.
113. Goldstein EN, et al. 1999. Ultrastructural localization of phosphorylated elF2-alpha [elF2alpha(P)] in rat dorsal hippocampus during reperfusion. *Acta Neuropathol* 98:493.
114. Borisov AB, Carlson BM. 2000. Cell death in denervated skeletal muscle is distinct from classical apoptosis. *Anat Rec* 258:305.
115. Martin LJ, et al. 2007. Motor neuron degeneration in amyotrophic lateral sclerosis mutant superoxide dismutase-1 transgenic mice: Mechanisms of mitochondriopathy and cell death. *J Comp Neurol* 500:20.
116. Ravichandran KS. 2003. "Recruitment signals" from apoptotic cells. C*ell* 113:817.
117. Thiele J, et al. 1984. Empiripolesis—a peculiar feature of megakaryocytes as evaluated in chronic myeloproliferative diseases by morphometry and ultrastructure. *Virch Arch* B 46:256.
118. Hack CE, et al. 1997. A role for secretory phospholipase A2 and C-reactive protein in the removal of injured cells. *Immunol Today* 18:111.
119. Riedemann NC, Ward PA. 2003. Complement in ischemia reperfusion injury. *Am J Pathol* 162:363.
120. Trouw LA, et al. 2005. C4b-binding protein binds to necrotic cells and DNA limiting DNA release and inhibiting complement activity. *J Exp Med* 201:1937.
121. Szabo S, et al. 1980. Pathogenesis of experimental adrenal hemorrhagic necrosis ("apoplexy"). *Lab Invest* 42:533.
122. Vracko R, et al. 1988. Basal lamina of rat myocardium. Its fate after death of cardiac myocytes. *Lab Invest* 58:77.
123. Vracko R, et al. 1988. Myocyte reactions at the borders of injured and healing rat myocardium. *Lab Invest* 59:104.
124. Erwig L-P, Henson PM. 2007. Immunological consequences of apoptotic cell phagocytosis. *Am J Pathol* 170:2.
125. Lee KP. 1989. Empiripolesis of hematopoietic cells within megakaryocytes in bone marrow of the rat. *Vet Pathol* 26:473.
126. Ghatak NR. 1992. Occurrence of oligodendrocytes within astrocytes in demyelinating lesions. *J Neuropathol Exp Neurol* 51:40.
127. Overholtzer M, et al. 2007. A nonapoptotic cell death process, entosis, that occurs by cell-in-cell invasion. C*ell* 131:966.
128. Scarabelli T, et al. 2001. Apoptosis of endothelial cells precedes myocyte cell apoptosis in ischemia/reperfusion injury. *Circulation* 104:253.
129. Azmi TI, O'Shea JD. 1984. Mechanism of deletion of endothelial cells during regression of the corpus luteum. *Lab Invest* 51:206.

Vet-ebooks.com

3 Cellular Defense and Recovery

Sublethal injury is associated with striking changes in the recovering cell. Cytoplasmic changes include increases in smooth endoplasmic reticulum, peroxisomes, and autophagolysosomes (Fig. 3.1), all associated with detoxification of injurious compounds that have entered the cell and the removal of damaged organelles. Expansion of nuclear components, especially nucleoli and chromatin, reflects the extensive reprogramming of genetic transcription required for recovery. The cell must synthesize unique regulatory proteins, shift metabolic pathways, and alter the spectrum of receptors and ion channels on the cell surface. Immediate recovery depends on how rapidly genetic reprogramming can be shifted to insert new proteins into the plasma membrane—molecules that regulate and preserve membrane permeability, as well as control ions and proteins that move across a damaged plasma membrane barrier.

Plasma Membrane in Recovery

Maintenance of the normal plasma membrane requires that small bits of the membrane be continuously repaired. Loss of surface membrane patches must be balanced by membrane pieces imported and patched into place by fusion of vesicles at the surface. In repair of plasma membranes of skeletal muscle, the repair complex fusogen **dysferlin** permits rapid resealing of plasma membranes disrupted by the mechanical stress of exercise.[1] Dysferlinopathy has been applied to myodystrophy arising from mutations in the dysferlin gene.[2]

Mechanical injury to the plasma membrane is typically lethal and leads to acute lytic necrosis. In small rupture wounds where the cytoplasm is not lost, however, the membrane can heal by reorientation. Molecules of the **lipid bilayer** move toward one another to seal the hole. The physicochemical nature of the membrane makes it self-sealing since a hole is energetically unfavorable. With time, cells repair membrane defects by routing membranous vesicles to the cell surface. The vesicles fuse with and become patched into the plasma membrane at sites where injury has occurred.

Calcium-Facilitated Membrane Repair

Cells require extracellular **calcium** to undergo rapid plasma membrane repair seconds after mechanical damage. **Calpains**, proteases required for calcium-facilitated repair, act by remodeling the cortical cytoskeleton at the site of injury.[3] Calpains also initiate autophagy and, when activated by membrane-localized epidermal growth factor, increase motility. At sites of injury, calpain substrates talin and vimentin exposed at the cell surface are involved in autoproteolytic activation of calpain. Cytokines such as IFN-γ and integrin-linked kinases such as ILK are essential molecules in supporting repair.

Lysosomal Membrane Repair After Infection

A lysosome-mediated repair process has been reported in intracellular infections. Plasma membranes altered by entry of bacteria required reconstruction. In chlamydial infections, the appearance of LAMP-1 at the infected cell surface implicated lysosomes in membrane repair.[4]

© 2009 Wiley-Blackwell. ISBN: 978-0-813-80330-2
Vet-ebooks.com

Membrane Ion Channels Increase in Acute Swelling

Increasing the numbers of ion pumps and channels on the cell surface is a strategy for survival in acute swelling. As more **ion pumps** are placed in the plasma membrane, more cytoplasmic fluid is moved out of the cell. Cells increase ion transport by increasing the number of Na-K-ATPase pumps and by expanding pump-bearing surface membranes. In the colon of animals deprived of sodium, epithelial cells show marked expansion of basolateral surfaces and increased ATPase activity. The new membrane surfaces are a response to move more Na^+ into the body from gut fluids. Increasing plasma membrane channels that expel toxins from the cell is a major protective mechanism. One of the most important membrane channel proteins, **P-glycoprotein**, functions as a "hydrophobic vacuum cleaner" to excrete hydrophobic drugs, anesthetics, and toxins. P-glycoprotein is especially important in secretory cells of the renal tubular epithelium.

Membranes Condense in Hypothermia

Plasma membrane remodeling is critical in hibernation. The plasma membrane condenses in hypothermia or torpor and expands on arousal.[5] This change is especially critical in the brain, where it protects cortical neuronal networks from prolonged hypothermia.

Detoxification: Smooth Endoplasmic Reticulum and Peroxisomes

SER Proliferation

Proliferation of membranes of the **smooth endoplasmic reticulum (SER)** is a detoxification response in acute injury. It is a hallmark of sublethal toxic injury. Many toxins induce large masses of SER, the membranes of which bear mixed-function oxidases that are the important detoxification enzyme complex. Duplication of the SER is the expected change in early phases of acute toxicity; it develops while other organelles degenerate in the early stages of acute cell swelling. Chronic toxicity is typically accompanied by massive development of the SER. For example, in chronic ethanol toxicity, hepatocytes have extensive proliferation of SER.

Cells in late stages of acute swelling show persistence of SER; this is evidence of a failed attempt to detoxify a lethal compound. Commonly, there is marked **whorling of membranes** in laminar arrangements; these membranes often surround lipid globules and mitochondria.[6] SER membrane whorling may occur in areas of glycogen formation; for example, in human hepatotoxicity from halothane anesthesia.[7]

Proliferation, also called **duplication**, is induced by sublethal doses of drugs and toxins. Because the cell survives, SER membranes and enzymes involved in detoxification are increased. For example, sublethal doses of phenobarbitol, the glycolytic poison galactosamine, and the nucleolar poison aflatoxin all induce large masses of SER.[8] SER has a close spatial relationship with mitochondria and peroxisomes (Fig. 3.2).

Ultrastructurally, **SER reduplication** often is manifest as straight tubules bundled together like a handful of pencils; in cross section tubules appear as packed in hexagonal arrays, often designated as **crystalloid endoplasmic reticulum**. When SER reduplication is induced in vitro by inhibiting HMG CoA reductase, an enzyme of the SER, with the drug compactin, crystalloid forms of SER develop that contain large amounts of HMG CoA reductase. Treatment with LDL (cholesterol) leads to increased cholesterol content of SER membranes (as detected by filipin labeling) and this, in turn, to a decrease in the amount of SER.[9]

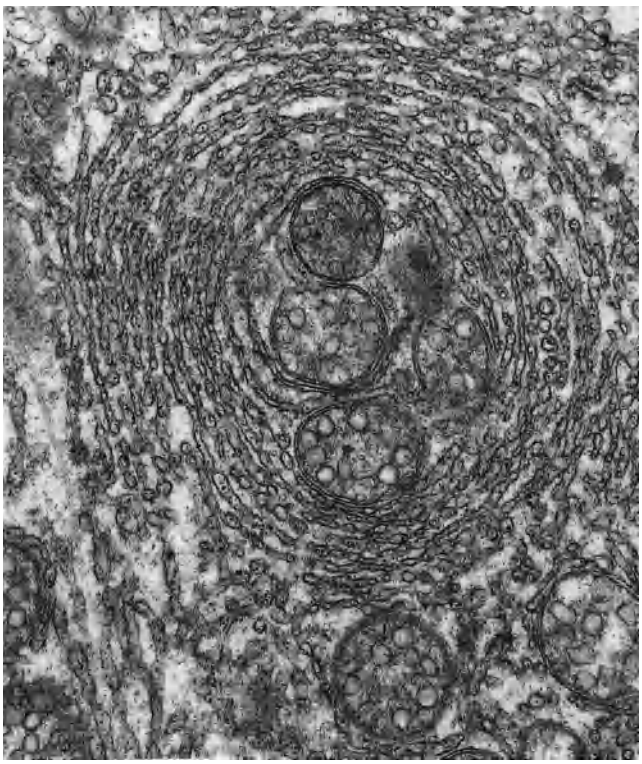


Fig. 3.2 Smooth endoplasmic reticulum–mitochondrion interface: adrenal cortical cell after massive stimulation for secretion of corticosteroids. Saccules of SER form whorled patterns around a mitochondrion.

Vet-ebooks.com

Proliferation of SER interspersed with large amounts of **glycogen** results from the toxic action of many drugs. The progressive accumulation of glycogen leads to large irregular cytoplasmic membrane-glycogen inclusions; for example, hepatocyte lesions in livers of alcoholics on aversion therapy with cyanamide.[10]

SER Degradation

Degradation of the SER is a response to lethal doses of toxins that act directly on membranes or, in contrast, to poisons that are not directly toxic but are converted into toxic intermediate molecules within the SER (the intermediate then acts directly on the membrane, often by causing lipid peroxidation). In sublethal injury, it is common to find the ultrastructural effects of both proliferation and degradation; that is, the cell, although having survived long enough for SER to proliferate, finally succumbs to the combined effects of the drug and other secondary phenomena. Typically, increased SER is accompanied by an increase in peroxisomes and lipid globules.

Peroxisomes in Recovery

Peroxisomal duplication occurs in nearly all injuries to rapidly metabolizing cells. Their potent oxidases and catalases are essential for recovery. In acute cell swelling, peroxisomes are not only increased in number and size but have moved to establish an interface with damaged membranes throughout the cell, particularly to mitochondria. Pleomorphic peroxisomes are typically massed in groups at sites of cellular injury. If mitochondria are the primary site of damage, newly formed peroxisomes will accumulate adjacent to them, often with membranes of the two in close apposition. In liver, centrolobular hepatocytes are most sensitive to peroxisomal proliferation; abnormal peroxisomes with matrix tubules are apt to occur in more peripheral areas.[11,12]

Mitochondria in Recovery

Anaerobic Shift to Glycolysis

When a cell is deprived of oxygen, ATP production in mitochondria is shifted from aerobic to anaerobic metabolism. ATP-utilizing processes such as membrane transport, filament contraction, and signaling continue for a short time, but accumulation of ADP and inorganic phosphate lead to the **anaerobic shift** to glycolysis, a hallmark of the hypoxic cell. Glycogen is rapidly broken down, and calcium accumulates and is redistributed. The shift from aerobic respiration in mitochondria to the more transient, inefficient anaerobic glycolysis prevents irreversible damage. Increased demand results in marked enlargement of mitochondria. When mitochondria in metabolically active cells are damaged, the glycolytic enzyme GAPDH translocates to the nucleus, where it induces gene expressions that drive autophagy to degrade damaged mitochondria.[13]

Antioxidant Factors Are Increased

To neutralize an increase in O_2^-, and other ROS, the cell shifts to production of antioxidants (see chapter 2). For example, the mitochondriopathy produced by **adriamycin cardiotoxicity** results in excessive ROS production, which is counteracted by superoxide dismutase and nitric oxide.[14] The important protectants of ROS injury are the following:

- **Superoxide dismutase (SOD):** SODs protect against toxic $\mathbf{O_2^-}$ and are found in mitochondrial matrix and cytosol—sites where most $\mathbf{O_2^-}$ is generated. SODs catalyze conversion of harmful superoxide-free radicals to hydrogen peroxide and oxygen.[15,16]
- **Metallothionein (MT):** MT is a metal-binding protein that protects against toxicity of heavy metals and, because it can scavenge hydroxyl radicals, against oxidative injury. Hepatocytic MT synthesis is increased by several hepatotoxic drugs; MTs are present in fetal and neonatal tissues in very high concentrations and appear to function in storage of metals, especially zinc, that are used for rapid growth in young animals.
- **Glutathione peroxidase:** Cyclic oxidation and reduction of glutathione is a major antioxidation phenomenon. Glutathione peroxidase catalyzes the oxidation phase: glutathione + H_2O_2 → glutathione disulfide + H_2O (selenium participates as a cofactor of glutathione peroxidase). Peroxides are destroyed by this reaction immediately after they are generated during the interaction of membranes with free radical groups (produced during cell catabolism). Glutathione peroxidase is especially important in myocardium, which has less SOD and catalase than does liver and other tissues.

Glutathionylation

In many injuries, the redox state of mitochondrial glutathione pool drives the mitochondrial response

Vet-ebooks.com

to oxidative damage. **Protein glutathionylation** is a response to oxidative stress. The mitochondrial thiol transferase **glutaredoxin 2** is a key player in oxidative stress since it catalyzes both glutathionylation and **protein disulfide formation** (many mitochondrial proteins contain reactive thiols and form disulfides with glutathione); thus, an increase in oxidized glutathione also modifies mitochondrial proteins by thiol disulfide exchange. Immunogold electron microscopy has been used to localize **glutathione *S*-transferase**.[17] Biopsies of livers of children with steatohepatitis, when examined by immunogold electron microscopy, had evidence of oxidative damage and marked increases in protein glutathionylation.[18]

Nitrosylation

In normal cells, **nitric oxide (NO)** inhibits apoptosis by S-nitrosylation of active-site caspases. **NO synthase** activity can suppress this action (see chapter 2).

Mitochondrial Cytoprotective Enzymes Are Activated

Several mitochondrial enzymes are activated to suppress oxidant injury at specific sites. **Heme oxygenase-1 (HO-1)** is cytoprotective against oxidative stress; for example, HO-1 is active in the chronic pulmonary disease of cigarette smoking. Mitochondrial localization of HO-1, as determined by immunogold labeling, increases in human bronchial epithelial cells exposed to cigarette smoke.[19]

GADPH Protects against Cell Death

Glyceraldehyde-3-phosphate dehydrogenase (GAPDH), a glycolytic enzyme, is a potent inhibitor of **caspase-independent cell death (CICD)**. In the mitochondrion, GAPDH increases **glycolysis** that generates ATP; in the nucleus, GAPDH induces ATG12 expression, which initiates **autophagy** of damaged mitochondria—both events that protect cells from cell death. These activities are associated with increase in mitochondrial mass.[20] GAPDH is overexpressed in many types of cell injury. In large amounts, it accumulates in mitochondria and induces pro-apoptotic mitochondrial permeabilization, the critical event in the intrinsic pathway of apoptosis. Detected by immunogold labeling in isolated mitochondria, GADPH was shown to be imported and to interact with voltage-dependent anion channels.[21] Affected mitochondria had matrix swelling, permeabilization of the inner membrane, and release of cytochrome c and apoptosis-inducing factor.

Nucleoli, DNA, and the Genome in Recovery

Nucleoli and Polysomes Reform

Resumption of protein synthesis in recovering cells is manifest by the reappearance of the nucleolus in the nucleus and polyribosomes in the cytoplasm. **Nucleoli** are often larger than normal and have evidence of large amounts of the precursors of ribosomal proteins (Fig. 3.3). During degeneration, abnormal peptides may be produced or there is a genomic shift to produce other proteins such as collagen. In recovery, these proteins disappear and normal proteins are again produced.

Nuclear DNA Is Repaired

DNA molecules are not permanent but slowly undergo decay. This requires mechanisms of repair that maintain cellular genomes from normal "wear-and-tear" damage. The procedures to protect the DNA molecule against mutagenesis include two major pathways: **repair in situ**, and **excision repair** (or "cut-and-patch" repair), in which a damaged segment of DNA is replaced with newly synthesized DNA units. The latter process involves endonucleases (for incision of damaged DNA segments), exonucleases (for subsequent degradation), polymerases (initiation of DNA replication for repair), and ligases (for rejoining of the new segment into the DNA molecule).

After toxic or radiation injury to the genome, cells either repair DNA or are eliminated through the homeostatic control mechanisms of p53-driven apoptosis. Cells have a complex **DNA-damage response** to ensure that DNA breaks are repaired with minimal impact on genome stability. This includes the spatial reorganization of double-strand break repair and moving proteins into nuclear structures that surround the site of injury. For example, **radiation** leads to development of "ionizing radiation-induced foci" that encompass the site of DNA breakage; these sites are recruitment areas for damage control proteins—the DNA-damaged mediator protein (**MDC1**), the p53-binding protein-1 (**p53BP1**), and the breast cancer susceptibility protein (**BRCA1**)—that recruit ubiquitin ligases that activate G2/M DNA damage checkpoints for resistance to ionizing radiation.

Protective Genes Are Activated

Protein p53 Blocks the Cell Cycle for Repair

The ***p53* gene** encodes the **protein p53**, which plays critical roles in recovery by blocking the cell cycle and

Vet-ebooks.com

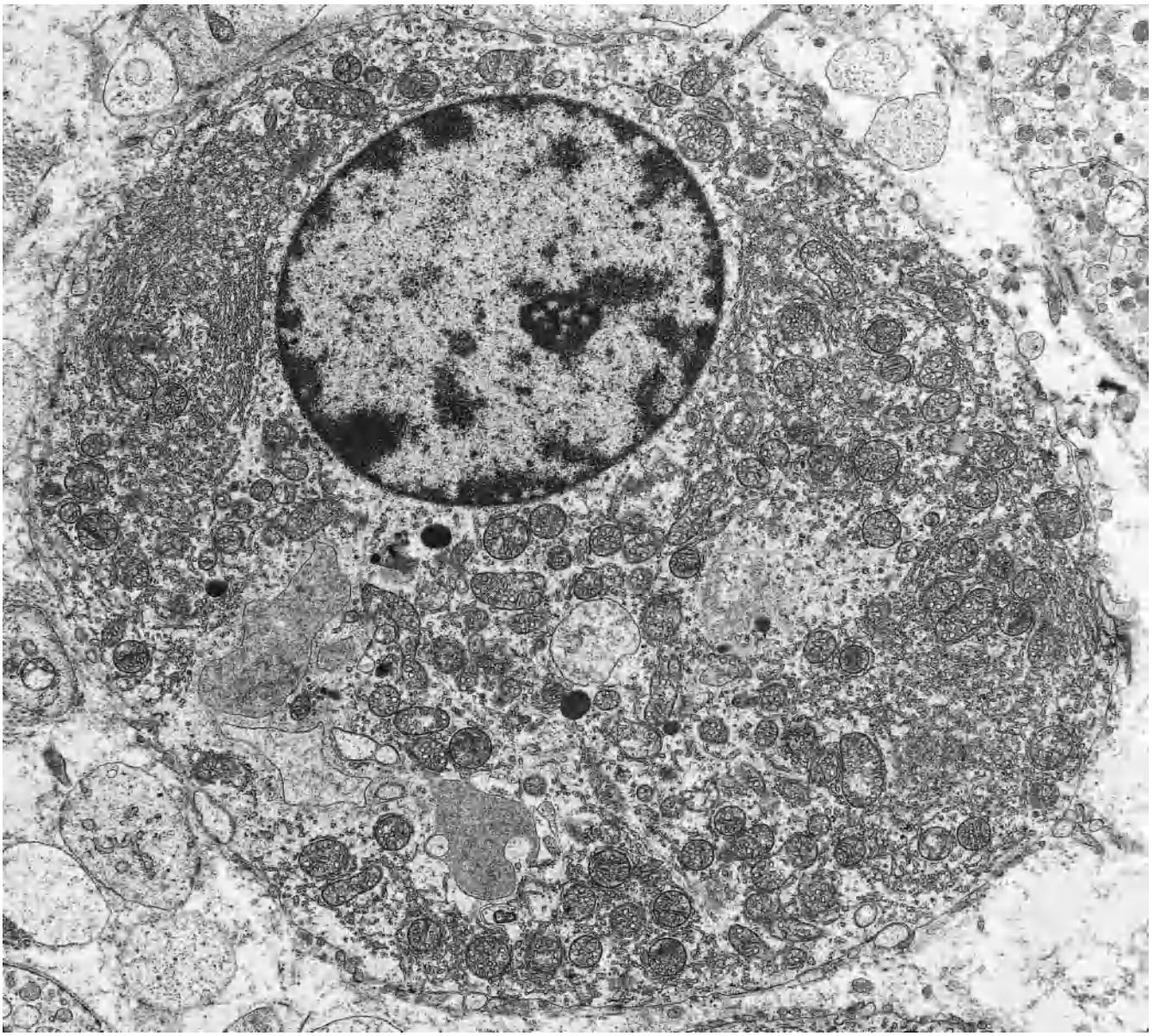


Fig. 3.3 Nuclear activation: nucleus of a secretory cell of the adrenal cortex after massive stimulation for secretion corticosteroids. **Nucleolus** is large with a clearly defined nucleolus and much **perinucleolar chromatin**.

stimulating DNA repair. Protein **p53** holds cells in the G1 phase of the cell cycle for repair. Acting as a transcription factor, p53 binds to and controls other genes. Acting as a "guardian of the genome," p53 blocks the cell cycle to provide time for DNA repair, and if injury is too severe, to trigger **programmed cell death**. Any injury to DNA induces the expression of p53 and the product of p53 rises in cells with DNA damage. Studies detecting p53 using immunogold techniques show that mitochondrial p53 is involved in mtDNA repair as a first response in cardiomyocytes poisoned with adriamycin in mice.[22]

Gene *Bcl-2* Encodes a Death Repressor Molecule

The gene ***Bcl-2*** encodes for a 25-kd integral membrane protein found in mitochondria, the nuclear envelope, and endoplasmic reticulum. **Bcl-2 protein** prevents PCD. Immunogold techniques used on mouse liver report that Bcl-2 protein is located predominantly in the inner membrane and cristae of mitochondria.[23] If *Bcl-2* is inactivated or deleted from a cell, PCD is initiated.

Bcl-2 family proteins block effects on mitochondria by inserting ion channel pores into the outer mitochondrial membrane. Thus, Bcl-2 proteins block the

Vet-ebooks.com

release of cytochrome c from mitochondria, possibly by preventing ionic imbalances that lead to mitochondrial swelling. Bcl proteins also appear to directly bind to the pro-apoptotic **apoptosis protease-activating factor-1 (Apaf-1)** to prevent caspase activation.[24] ***Bcl*** genes are particularly important in neoplasia, where excess *Bcl-2* makes cells unresponsive to death signals.[25]

The final death event in most cells centers on the ratio of pro-survival genes such as ***Bcl-2*** and the protein products of death genes (such as the mitochondrial guardians ***BAX, Bak***, and **PUMA**). It is this ratio of agonist to antagonist that determines whether or not the cell will respond to signals that block PDC.

Nuclear Factor-κB Induces Protection

Nuclear factor-κB (NF-κB) is a transcription factor that plays a key role in cellular protection and recovery. It induces cytokines, reactive oxygen species scavengers, and apoptosis inhibitors—all factors that regulate recovery from toxins, infection, and radiation. **Superoxide dismutase** is a major NF-κB-responsive factor that protects against the excessive ROS generated by radiation. Mice with a genetic defect in NF-κB signaling have enhanced sensitivity to radiation injury. Toll-like receptor (TLR) signaling is an important inducer of NF-κB, and TLR 5, acting through NF-κB, has radioprotective activity in animals.

Survivin

Survivin is a subunit of the **chromosomal passenger complex** and is essential for proper chromosome segregation and cytokinesis; it is also an apoptosis inhibitor. Survivin directly interacts with **nuclear export receptor** Crm1 to tether the chromosomal passenger complex to the centromere.[26] In ischemic necrosis, expression of survivin is associated with survival of infarcted tissue; for example, survivin can be localized to surviving myocytes at the periphery of myocardial infarcts.[27] In neoplasia, the survivin-Crm1 interaction is required for the cytoprotective activity of survivin; this function is exploited in chemotherapy, and the nuclear localization of survivin is a favorable prognostic factor in cancer patients.

Hypoxia Is a Strong Signal for Energy Conservation

Hypoxic cells sense diminished oxygen levels well before their ATP pools are depleted, and respond with a program to curb energy use by shutdown of nonessential cellular functions. Hypoxia triggers expression of genes involved in the protective response, including isoforms of glycolytic enzymes and glucose transporters that function best in a low oxygen environment. Many of these responses arise through hypoxia-induced production of the transcription factor **hypoxia inducible factor-1 (HIF-1)**. Oxygen-sensing enzymes (such as prolyl hydroxylase-1) regulate the stability of HIF-1, allowing it to activate "hypoxic" genes that reprogram basal metabolism—selectively decreasing glucose oxidation and switching to more anaerobic glycolysis.

Mitochondrial Hypoxic Stress Response

The ***HIF-1*** gene is the pivotal regulator of hypoxic gene expression. **Cardiomyocytes** responding to hypoxia adapt to consume less oxygen by shifting ATP production from mitochondrial fatty acid beta-oxidation to glycolysis. Transcriptional activation of glucose transporters and glycolytic enzymes by hypoxia is mediated by HIF-1. In addition to adaptation to anaerobic metabolism, other responses to hypoxia initiated by HIF-1 include stimulation of erythropoiesis, vasodilation, and angiogenesis. The means to these ends involve HIF-induced activation of genes for the following products:

- **Erythropoietin (EPO)**[28]
- **Vascular endothelial growth factor (VEGF)**[29]
- **Plasminogen activator inhibitor-1 (PAI-i)**[30]
- **Hepatocyte growth factor receptor (c-met)**[31]
- **Insulin-like growth factor binding protein-1 (IGFBP-1)**[32]
- **Nitric oxide synthase (iNOS)**[33]

Activity of the pro-apoptotic cytokine **C-Jun N-terminal kinase (JNK)**, a major mediator of PCD in acute hepatitis, is antagonized by the AP-1 transcription factor **c-Jun/AP-1**. A target of JNK, c-Jun/AP-1 is a key regulator of hepatocyte proliferation and is hepatoprotective through regulation of **nos2/NO**.

Shift in Protein Synthesis to Stress Proteins

A major response to injury is a shift to production of **stress proteins**, unique molecules that protect the cell by binding to abnormally folded or denatured proteins. Stress proteins appear rapidly in the cytoplasm of injured cells,[34] and cells that efficiently produce stress proteins survive an otherwise lethal amount of injury. The prototype stress protein **BiP** binds transiently to normal peptides (but permanently to misfolded peptides) to control assembly into protein chains. Stress proteins are classified into at least two families:

- **Heat shock proteins** are distinct because they protect the cell by binding to abnormally folded or denatured proteins.[35]

Vet-ebooks.com

- **Glucose-regulated proteins (GRPs)** are induced by drugs, glycosylation inhibitors, and calcium ionophores.

Although cells respond to injury by shutting down synthesis of most proteins, sublethal injury is characterized by redirection of proteins synthesis to the production of stress proteins. Stress proteins are synthesized in the nucleus and accumulate in the cytoplasm near ribosomes, so that the endoplasmic reticulum of injured cells contains a high concentration. In recovering cells, **stress granules** composed of aggregates of stress proteins appear as dense, membrane-less cytoplasmic bodies. **Hemoxygenase I** (**HO-1**, or HSP32) is a part of a potent protective system, particularly in the brain.

In the **kidney**, hypoxic activation of HIF-1 and its target gene EPO is closely regulated by the oxidant/antioxidant equilibrium involving superoxide dismutase. Extracellular SOD (referred to as SOD-3) is released at the apical surfaces of proximal convoluted tubular epithelial cells and acts as the primary enzymatic scavenger of superoxide.

In all of the responses to hypoxia, mitochondria are the important organelles for oxygen sensing. Mitochondria in the chronically hypoxic skeletal myocytes of Sherpas and of mountaineers returned from the Himalayas have activated glycolytic pathways, reduced lipids, and accumulations of lipofuscin, a mitochondrial degradation product.

Proteostasis

Proteostasis is the maintenance of the cellular **proteome** (the complete set of proteins produced from information encoded in the genome) by reforming protein synthesis through transcription and translation.[36] Proteostasis, or "protein homeostasis," centers on the balance between protein folding and degradation, and controls whether a protein folds normally or is misfolded and aggregates. Pathways of proteostasis involve several classes of chaperones, folding enzymes, and stablizing ligands that work in concert to minimize protein aggregation. **Chaperones** maintain the stability of the proteome by facilitating the corrective folding of misfolded and aggregation-prone proteins.

Increased Activity of the Proteasome-Ubiquitin System

Ubiquitinization is the proteolytic process used in normal cells to selectively recognize unwanted endogenous proteins and shunt them to proteasomes for degradation and to autophagic pathways.[37,38] The **proteasome** (from *protease* + *some*, body) is a hollow cylinder with multiple catalytic sites that is the structural form of the proteolytic complex [Note: the **proteasome** is the cluster of genes that encodes components of the cell's proteolytic complex]. The ubiquinization process involves (1) attachment of **ubiquitin** to abnormal peptides to form a **ubiquitin-peptide complex;** (2) movement of the ubiquitin-peptide complex to a **proteasome;** and (3) recognition by the proteasomal **proteolytic complex** of the ubiquitin component, and degradation of the substrate peptide. The process is controlled by the specificity of ubiquitin.

In post-translational modifications, misfolded proteins are conjugated to ubiquitin through ubiquitin ligase (E3 enzymes). The extent of ubiquitinization determines intracellular traffic. **Polyubiquitination**, in which a chain of ubiquitins is attached, moves the ubiquinated target protein to the proteolytic degradation pathway. **Mono-ubiquitination**, wherein a single ubiquitin moiety is appended, is a signaling device that directs the peptide to other intracellular proteins that harbor ubiquitin-binding domains.

Ubiquitin levels rise in degenerating cells. In the brain, ubiquitin is increased in degenerating neurons.[39,40] **Chaperones** participate in peptide degradation by binding other peptides that facilitate protein folding, oligomer formation, and localization of proteins; they have the ability to recognize many unrelated ligands.[41] Chaperones stabilize protein folding pathways, and prevent polypeptides from collapsing into compacted molten globules.

Aggresomes

Aggresomes are pericentrosomal cytoplasmic structures that contain polyubiquinated misfolded proteins, chaperones, and proteasomes (Figs. 3.4 and 3.5). Aggresome formation is a cytoprotective mechanism whereby these misfolded protein complexes are shrouded in intermediate filaments and shunted to juxtanuclear locations. Aggresome presence near the centrosome, like that of other organelles, requires active, microtubule-dependent transport, and the presence of γ-tubulin is their distinctive feature.[42,43] Linker proteins such as Hook2 that associate with the motor protein dynein contribute to aggresome movement. Aggresomes are associated with neurodegenerative diseases, and are associated with a malfunction of the ubiquitin-proteasome system (UPS).[44] In the brain, aggresomes are particularly common in ischemia and neurodegenerative disorders.[45] Lewy bodies of Parkinson's disease begin as aggresomes,[46] Mallory bodies in the hepatocyte are cytokeratin aggresomes, and Lafora bodies in the neuron are tubulin aggresomes.

Vet-ebooks.com

The MAPK/ERK Pathway

Mitogen-activated protein kinases (MAPK) and **eukaryotic protein kinase (ERK)** pathways play crucial roles in most cellular processes. In experimental lung transplantation in rats, **carbon monoxide (CO)** inhalation by donor and recipient is cytoprotective to pulmonary endothelium through activation of the MAPK pathway.[47] The carcinogen lindane inhibits autophagolysosomes in target cells,[48] a defect associated with activation of MAPK/ERK pathways—sustained activation of the ERK pathway appears to be sufficient to commit cells to autophagy.

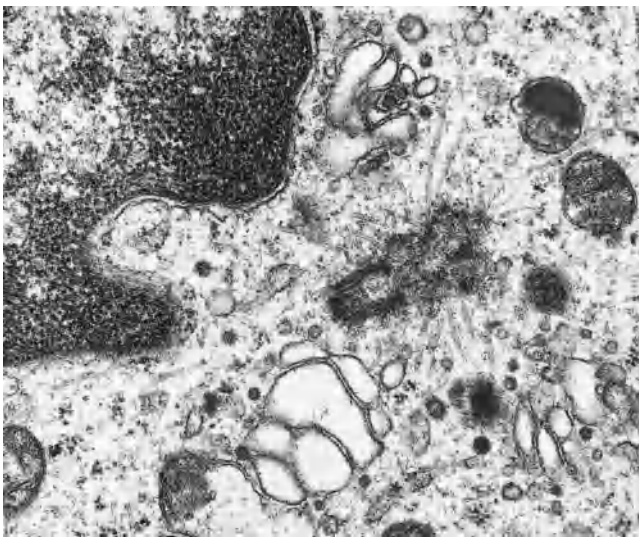


Fig. 3.4 Aggresomes: pericentriolar cytoplasmic granular inclusions for ubiquitinization. Centriole (center) has radiating microtubules and is surrounded by granular aggresomes.

Signalosomes: Intracellular Signal Transduction Networks

Signalosomes are multimolecular aggregates of ribosome-sized protein complexes that are involved in signal transduction; they mediate crosstalk between different signaling pathways.[49,50] Signalosomes are asymmetric and heterogenous, and cannot be identified in electron micrographs without specific labeling of their components. Signalosomes integrate upstream signals and control downstream effectors. Major signalosomes include:

- **COP9 signalosomes** regulate ubiquitin by activating ubiquitin ligases and other proteins; they bind p53, targeting it to the ubiquitin-proteasome pathway.[51–53]

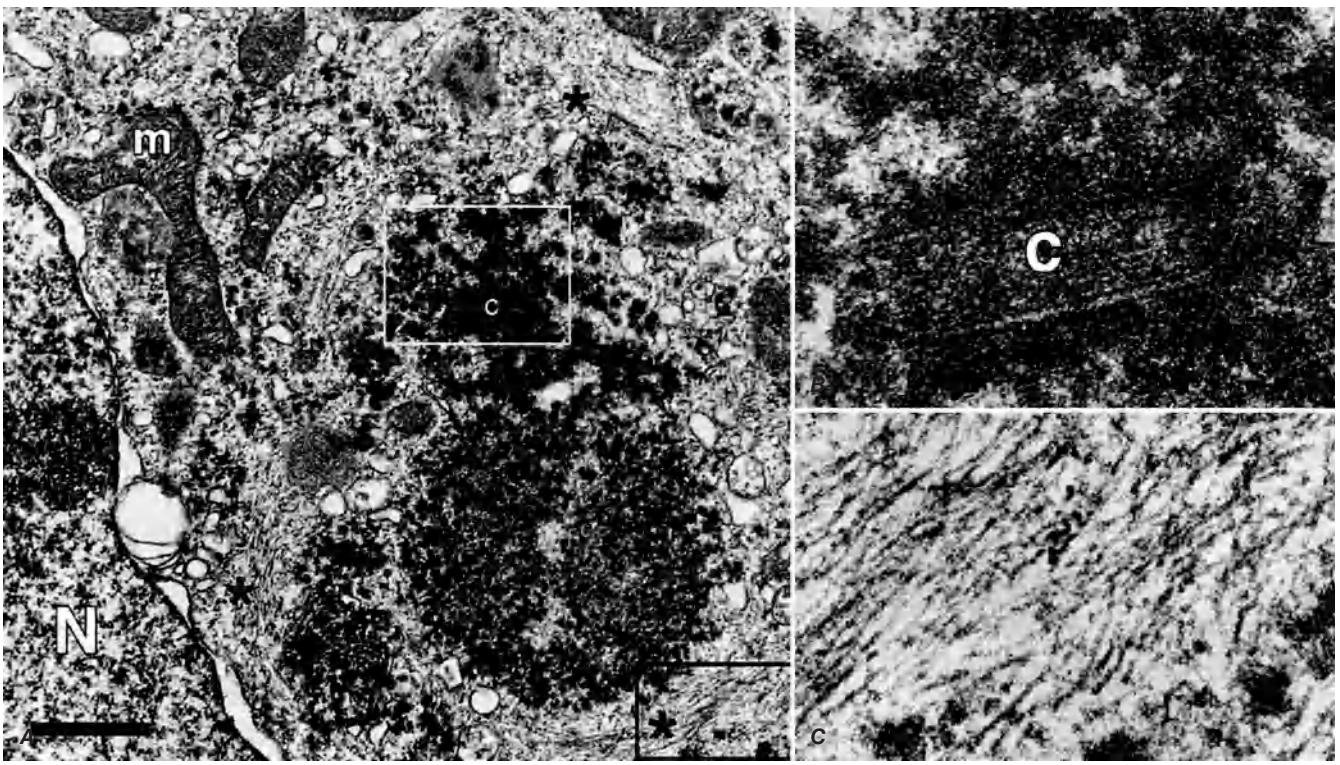


Fig. 3.5 Aggresomes: pericentriolar membrane-free, cytoplasmic inclusions containing misfolded, ubiquitinated proteins ensheathed in a cage of intermediate filaments; HEK cell overexpressing ΔF508 and treated with A/LNN. **A**. **Aggresomes**: mitochondia (*m*), intermediate filaments (*), nucleus (*N*). **B** (centrosome) and **C** (intermediate filaments) are high magnifications of white and black boxes in A. (Micrographs: Jennifer A. Johnston and Ron R. Kapto, *J Cell Biol* 143:1883, 1998.)

Vet-ebooks.com

- **Low-density lipoprotein receptor-related protein 6 (Lrp6)** signalosomes are induced by attachment of Wnt growth factors to Wnt ligands; Lrp6 aggregates contain Wnt-pathway components as well as co-clustering of receptors and scaffold proteins, which in turn trigger Lrp6 phosphorylation that promotes Axin recruitment and β-catenin stabilization.[54]
- **mAKAPbeta** serves as a scaffold for a large signalosome (responsive to upstream cAMP, Ca^{++}, and protein kinase signaling) that controls and induces cardiac myocyte hypertrophy.

Endoplasmic Reticulum Stress Response

The **endoplasmic reticulum stress response** leads to dysfunctional protein folding, and damaged proteins are retained and degraded within the endoplasmic reticulum.[55] As this process becomes unbalanced, misfolded and aberrantly glycosylated proteins accumulate and aggregate in RER cisternae. As recovery proceeds, ribosomes are differentially activated so that synthesis of proteins is skewed toward those proteins required for recovery. Peptide sequences contain new information that directs the proteins to organelles involved in recovery. Transforming growth factor-β and other growth factors play major roles in regeneration in late phases of the ER stress response.

Autophagy: Removal of Debris

Autophagy ("self-eating") is the uptake and degradation of damaged cellular components in autophagic vacuoles. Autophagy is a major biologic process for elimination of unneeded organelles, aggregate-prone proteins, and persistent intracellular pathogenic microorganisms.[56] Using the proteolytic functions of the **ubiquitin-proteasome system**, autophagy is a potent process for recovery. The presence of abnormal proteins in the cisternae of the RER can initiate autophagy.[57]

Autophagosomes

Autophagosomes, the initial autophagic vacuole, are formed by budding from membranes of the endoplasmic reticulum. Once free in the cytosol, they move to, bind, and sequester damaged cellular proteins and organelles. Microtubules facilitate autophagosome movement and fusion with endosomes.[58] Fusion with endosomes causes the autophagosome to become more acidic.[59] In the degradative phase of autophagy, autophagosomes fuse with enzyme-bearing lysosomes, the merger forming the degradative **autophagolysosome** (Fig. 3.6).[60] In summary, definitions of names applied to vacuoles of the autophagic, endosomal, lysosomal, and phagocytic pathways include:

- **Autophagosome:** vacuole formed by budding of membranes from the rough endoplasmic reticulum; autophagosome-forming sequestering membranes are referred to as **phagophores**.
- **Autophagolysosome:** autophagosome that has fused with a lysosome to acquire acid phosphatase and other enzymes used to degrade cellular debris.
- **Amphisome:** vacuole formed by fusion of autophagosome and endosome.
- **Residual bodies:** an enlarging autophagolysosome that is filled with degradation products of proteins, membranes, and lipids that have polymerized.

In sequestering degenerate cytoplasmic structures, the damaged parts are encircled by the thin, cup-shaped cisternae budding from the endoplasmic reticulum that seal at their rims, forming the **autophagosome**. Within the enlarging **residual body**, the fragments of degraded membrane polymerize into large membranous whorls referred to as **myeloid bodies**.

If the cell is unable to adequately process debris because of overload or exhaustion of lysosomal enzymes, the excessive degradation of membranes leads to accumulation of membranes that rearrange in **membranous whorls** or of proteins that aggregate into **lattice arrangements** within autophagosomes. Cells then become swollen and foamy due to masses of large phagolysosomes or autophagolysosomes filled with inspissated granular debris, membranes, and lipids—a change sometimes referred to as **granulovacuolar degeneration**. Cells with high rates of membrane activity, such as steroid-producing cells of the adrenal cortex or interstitial cells of the testes, typically form large membranous whorls when they degenerate.

Autophagosomal membranes have few **intramembrane particles** by freeze-fracture electron microscopy.[61] However, endogenous proteins embedded in autophagosomal membranes guide and control autophagy. **Calpain** is a regulator of autophagosome formation.[62] Maturation of **autophagic vacuoles** is associated with loss of proteins from the inner leaflet of the membrane. Most normal cellular processes are suppressed during injury. In slowly developing necrosis, intracellular movement is stopped and the block of exocytosis leads to accumulation of secretory granules.[63] In recovery, autophagosomes develop to degrade these granules.

Vet-ebooks.com

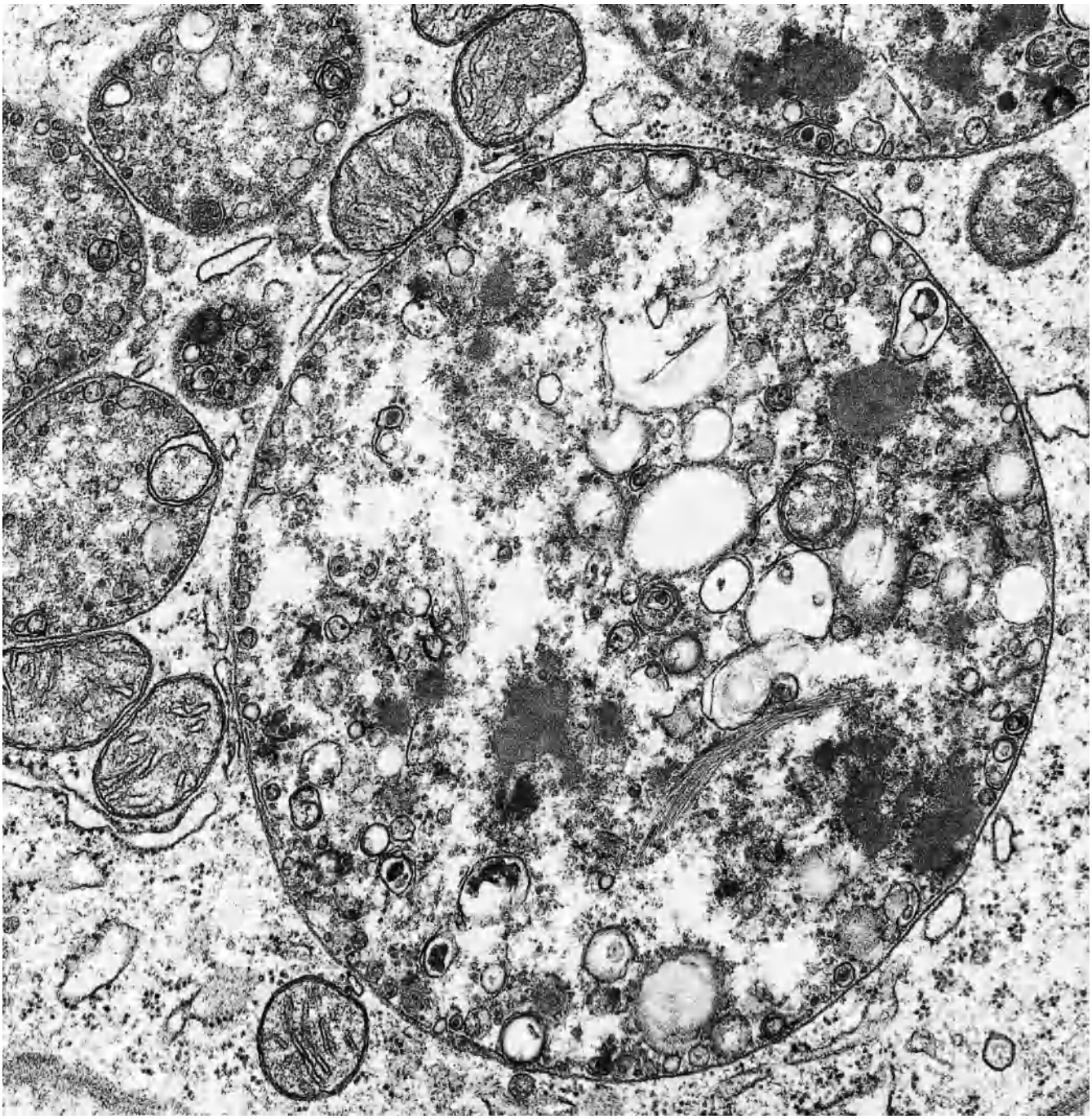


Fig. 3.6 Autophagic vacuole: single, large **autophagolysosome** is filled with vesicles, protein debris, and phospholipid membrane fragments, many of which have formed parallel arrangements. Surrounding mitochondria are degenerate.

Functions of Autophagy

Autophagy promotes cell survival during stress, starvation, and microbial infection. Although its major function is intracellular housekeeping, autophagy plays major roles in the following processes:

- Removal of abnormal degraded proteins
- Triggering cell death
- Presentation of antigens of MHC II
- Microbial killing
- Development and anti-aging processes
- ATP production during metabolic depletion

Autophagy in Disease

Autophagy is a general manifestation of cellular injury, and the sequestration of damaged organelles and

Vet-ebooks.com

abnormal proteins in autophagosomes is a mechanism of cellular repair that accompanies sublethal injury. Conversely, autophagy can trigger apoptosis. In severe anoxic injury in the brain, the inhibition of autophagy suppresses cell death—experimentally, ischemic neuronal death can be rescued by a deficit of **Atg7**, a gene essential for autophagy induction.[64]

Autophagy in Toxic Injury

In cells injured sublethally by toxins, damaged organelles are removed by autophagy.[64,65] Damaged **mitochondria** that produce harmful reactive oxygen species are removed by autophagy. Membranes of **smooth endoplasmic reticulum** that develop in response to toxicity are rapidly broken down by autophagy. Acinar cells of the parotid salivary glands of rats fed the metabolic analogue ethionine develop large autophagic vacuoles that contain **ribosomes, rough endoplasmic reticulum**, and **secretory granules;** as vacuoles enlarge the denatured proteins reassemble as large crystalloids.[66]

In recovery stages of hepatocytes of rats given phenobarbitol, marked increases in lysosomes and autophagolysosomes occur. Hepatocytes release damaged cellular organelles and proteins by blebbing. **Heterophagy** by Kupffer cells also occurs; Kupffer cells develop villous projections that surround fragments released by the hepatocytes.

Autophagy in Neuromuscular Disease

Abnormal autophagocytosisis is the basis for several neuromuscular degenerative diseases such as Alzheimer's disease, Parkinson's disease, and distal type myopathy. In **Danon disease cardiomyopathy**, autophagic vacuoles accumulate in cardiomyocytes as a result of autophagic dysfunction involving deficiency of the lysosomal protein Lamp-2. Studies on autophagocytosis in a hamster cardiomyopathy model have shown that granulocyte colony-stimulating factor (G-CSF) alleviates the disease through an anti-autophagic effect.[67]

Autophagy is an established neuropathologic feature of **Alzheimer's disease (AD)**. Using immunogold techniques with compartmental markers on biopsies of AD brains, autophagosomes and autophagolysosomes were identified in neurons affected with neurofibrillary change; they are also present in dystrophic neurites, particularly in neuritic processes including synaptic terminals.[68] Neuronal autophagy is also a hallmark of the presenilin 1/APP mouse model of beta amyloidosis, a model in which autophagosomes are associated with both beta-amyloidogenic and cell survival pathways.[69]

Autophagic vacuoles, prominent features of many neuromuscular disorders, are also pathognomonic for an emerging group of conditions called **autophagic vacuolar myopathies**.[70] These diseases include rimmed vacuolar myopathy, maltase deficiency, X-linked myopathy, and Danon disease (which is due to mutation in the gene for the transmembrane lysosomal protein LAMP-2).

Autophagy in Microbial Disease

Autophagy, in cells infected with most species of intracellular bacteria, is a mechanism of protection and recovery. In contrast, certain pathogens usurp the autophagic pathway to support their life cycle in the infected cell; for example, *Mycobacteria* spp.,[71] *Chlamydia* spp.,[72] and *Vibrio* spp.[73] all divert autophagolysosomes to **bacteriophorous vacuoles** as part of the infectious cycle. The autophagosome marker LC3 applied in immunostaining studies shows punctate staining at sites of autophagosome formation.

Autophagy in Development

Autophagy is subject to diurnal variation and in normal cells is inhibited by insulin.[74,75] Autophagy plays important roles in normal embryonic processes of **differentiation, metamorphosis**, and **apoptosis**. In apoptosis, an ATP-driven shift in membrane phosphatidylserine (from inner to outer leaf of the lipid bilayer) presents this phosphopholipid signal on the apoptotic cell to ensure its clearance.[76]

References

1. Glover L, Brown RH Jr. 2007. Dysferlin in membrane trafficking and patch repair. *Traffic* 8:785.
2. Inoue M, et al. 2006. Expression of myoferlin in skeletal muscle of patients with dysferlinopathy. *Tohoku J Exp Med* 209:109.
3. Mellgren RL, et al. 2007. Calpain is required for the rapid, calcium-dependent repair of wounded plasma membrane. *J Biol Chem* 282:2567.
4. Beatty WL. 2007. Lysosome repair enables host cell survival and bacterial persistence following *Chlamydia trachomatis* infection. *Cell Microbiol* 9:2141.
5. Ruedigier J, et al. 2007. Dynamics in the ultrastructure of asymmetric axospinous synapses in the frontal cortex of hibernating European ground squirrels (*Spermophilus citellus*). *Synapse* 61:343.
6. Gorgas K, Krisans SK. 1989. Zonal heterogeneity of peroxisome proliferation and morphology in rat liver after gemfibrozil treatment. *J Lipid Res* 30:1859.
7. Wills EJ, Walton B. 1978. A morphologic study of unexplained hepatitis following halothane anesthesia. *Am J Pathol* 91:11.
8. van Bezooigen CFA. 1990. Morphology, ultrastructure and function of hepatocytes during liver drug metabolism. *J Elec Microsc Tech* 14:152.

Vet-ebooks.com

9. Orci L, et al. 1984. Increase in membrane cholesterol. *Cell* 36:835.
10. Guillen FJ, Vazquez JJ. 1984. Cyanamide-induced liver cell injury. *Lab Invest* 50:385.
11. Baumgart E, et al. 1987. Proliferation of peroxisomes in pericentral hepatocytes of rat liver after administration of a new hypocholesterolemic agents (BM 15766). *Lab Invest* 56:554.
12. Eguchi M, et al. 1979. Peroxisomes of rat peritoneal macrophages during phagocytosis. *Am J Pathol* 95:281.
13. Colell A, et al. 2007. GAPDH and autophagy preserve survival after apoptotic cytochrome-c release in the absence of caspase activation. *Cell* 129:983.
14. Cole MP, et al. 2006. The protective roles of nitric oxide and superoxide dismutase in adriamycin-induced toxicity. *Cardiovasc Res* 69:186.
15. Chaiswing L, et al. 2005. Manganese superoxide dismutase and inducible nitric oxide synthase modify early oxidative events in acute adriamycin-induced mitochondrial toxicity. *Mol Cancer Ther* 4:1056.
16. Chang L-Y, et al. 1988. Molecular immunocytochemistry of the CuZn superoxide dismutase in rat hepatocytes. *J Cell Biol* 107:2169.
17. Daggett DA, et al. 1998. Effects of lead on rat kidney and liver: GST expression and oxidative stress. *Toxicology* 128:191.
18. Piemonte F, et al. 2007. Protein glutathionylation increases in the liver of patients with non-alcoholic fatty liver disease. *J Gastroenterol Hepatol* 6 Aug [E-pub].
19. Slebos DJ, et al. 2007. Mitochondrial localization and function of heme oxygenase-1 in cigarette smoke-induced cell death. *Am J Respir Cell Mol Biol* 36:409.
20. Colell A, et al. 2007. GAPDH and autophagy preserve survival after apoptotic cytochrome-c release in the absence of caspase activation. *Cell* 129:983.
21. Tarze A, et al. 2007. GAPDH, a novel regulator of the pro-apoptotic mitochondrial membrane permeabilization. *Oncogene* 26:2606.
22. Nithipongvanitch R, et al. 2007. Evidence for p53 as guardian of the cardiomyocyte mitochondrial genome following acute adriamycin treatment. *J Hist Cyt* 55:629.
23. Motoyama S, et al. 1998. Bcl-2 is located predominantly in the inner membrane and crista of mitochondria in rat liver. *Biochem Biophys Res Commun* 249:628.
24. Hausman G, et al. 2000. Pro-apoptotic apoptosis protease-activating factor 1 (Apaf-1) has a cytoplasmic localization distinct from Bcl-2 or Bcl-x(L). *J Cell Biol* 149:623.
25. Soini Y, et al. 2005. Activation and relocalization of caspase 3 during the apoptotic cascade of human mesothelioma cells. *APMIS* 113:426.
26. Stauber RH, et al. 2007. Nuclear and cytoplasmic survivin: molecular mechanism, prognostic, and therapeutic potential. *Cancer Res* 67:5999.
27. Santini D, et al. 2004. Surviving acute myocardial infarction: survivin expression in viable cardiomyocytes after infarction. *J Clin Pathol* 57:1321.
28. Suliman HB, et al. 2004. Superoxide dismutase-2 promotes full expression of the EPO response to hypoxia. *Blood* 104:43.
29. Hoppeler H, et al. 2003. Response of skeletal muscle mitochondria to hypoxia. *Exp Physiol* 88:109.
30. Fink T, et al. 2002. Identification of a tightly regulated hypoxia-response element in the promoter of human plasminogen activator inhibitor-1. *Blood* 99:2077.
31. Hara S, et al. 2006. Hypoxia enhances c-Met/HGF receptor expression and signaling by activating HIF-1alpha in human salivary gland cancer cells. *Oral Oncol* 42:593.
32. Lofqvist C, et al. 2007. IGFBP3 suppresses retinopathy through suppression of oxygen-induced vessel loss and promotion of vascular regrowth. *Proc Natl Acad Sci USA* 104:10589.
33. Hasselblatt P, et al. 2007. Hepatocyte survival in acute hepatitis is due to c-Jun/AP-1-dependent expression of inducible nitric oxide synthase. *Proc Natl Acad Sci USA* 104:17105.
34. Dickson DW, et al. 1990. Ubiquitin immunoreactive structures in normal human brains. *Lab Invest* 63:87.
35. Sadacharan SK, et al. 2001. Immunoelectron microscopy provides evidence for the presence of mitochondrial heat shock 10-kDa protein (chaperonin 10) in red blood cells and a variety of secretory granules. *Histochem Cell Biol* 116:507.
36. Balch WE, et al. 2008. Adapting proteostasis for disease intervention. *Science* 319:916.
37. Glickman MH, Ciechanover A. 2002. The ubiquitin-proteasome proteolytic pathway. *Physiol Rev* 82:373.
38. Schwartz AL, et al. 1992. Immunoelectron microscope localization of the ubiquitin-activating enzyme E1 in HepG2 cells. *Proc Nat Acad Sci USA* 89:5542.
39. Huang J, et al. 1999. Neuronal protection in stroke by an sLex-glycosylated complement inhibitory protein. *Science* 285:595.
40. Jortner BS, et al. 1996. Ubiquitin expression in degenerating axons of equine cervical compressive myelopathy. *Vet Pathol* 33:356.
41. Hartl FU, Hayer-Hartl M. 2002. Molecular chaperones in the cytosol. *Science* 295:1852.
42. Johnson JA, et al. 1998. Aggresomes: A cellular response to misfolded proteins. *J Cell Biol* 143:1883.
43. Johnson JA, et al. 2002. Cytoplasmic dynein/dynactin mediates the assembly of aggresomes. *Cell Motil Cytoskeleton* 53:26.
44. Ardley HC, et al. 2004. UCH-L1 aggresome formation in response to proteasome impairment indicates a role in inclusion formation in Parkinson's disease. *J Neurochem* 90:379.
45. Hu BR, et al. 2000. Protein aggregation after transient cerebral ischemia. *J Neurosci* 20:3191.
46. McNaught KS, et al. 2002. Aggresome-related biogenesis of Lewy bodies. *Eur J Neurosci* 16:2136.
47. Kohmoto J, et al. 2007. Carbon monoxide protects rat lung transplants from ischemia-reperfusion injury via a mechanism involving p38 MAPK pathway. *Am J Transplant* 7:2279.
48. Corcelle E, et al. 2006. Disruption of autophagy at the maturation step by the carcinogen lindane is associated with the sustained mitogen-activation protein kinase/extracellular signal-regulated kinase activity. *Cancer Res* 66:6861.

Vet-ebooks.com

49. Bosu DR, Kipreos ET. 2008. Cullin-RING ubiquitin ligases. *Cell Div* 3:7.
50. Hetfeld BK, et al. 2008. The COP9 signalosome-mediated deneddylation is stimulated by caspases during apoptosis. *Apoptosis* 13:187.
51. Kapelari B, et al. 2000. Electron microscopy and subunit-subunit interaction studies reveal a first architecture of COP9 signalosome. *J Mol Biol* 300:1169.
52. Uhle S, et al. 2003. Protein kinase CK2 and protein kinase D are associated with the COP9 signalosome. *EMBO J* 22:1302.
53. Bilic J et al. 2007. Wmt induces LRP6 signalosomes and promotes dishevelled-dependent LRP6 phosporylation. *Science* 316:1619.
54. Bech-Otschir D, et al. 2001. COP9 signalosome-specific phosphorylation targets p53 to degradation by the ubiquitin system. *EMBO J* 20:1630.
55. Ding W-X, et al. 2007. Linking of autophagy to ubiquitin-proteasome system is important for the regulation of endoplasmic reticulum stress and cell viability. *Am J Pathol* 170:513.
56. Levine B, Kroemer G. 2008. Autophagy in the pathogenesis of disease. *Cell* 132:27.
57. Kamimoto T, et al. 2006. Intracellular inclusions containing mutant alpha1-antitrypsin Z are propagated in the absence of autophagic activity. *J Biol Chem* 281:4467.
58. Köchl R, et al. 2006. Microtubules facilitate autophagosome formation and fusion of autophagosomes with endosomes. *Traffic* 7:129.
59. Lucocq J, Walker D. 1997. Evidence for fusion between multilamellar endosomes and autophagosomes in HeLa cells. *Eur J Cell Biol* 72:307.
60. Wattiaux R, Wattiaux-de Coninck S. 1984. Effects of ischemia on lysosomes. *Int Rev Exp Pathol* 26:85.
61. Fensrud M, et al. 2000. Ultrastructural characterization of the delimiting membranes of isolated autophagosomes and amphisomes by freeze-fracture electron microscopy. *Eur J Cell Biol* 79:871.
62. Demarchi F, et al. 2007. Calpain as a novel regulator of autophagosome formation. *Autophagy* 3:235.
63. Koike H et al. 1982. Pancreatic effects of ethionine blockade of exocytosis and appearance of crinophagy and autophagy precede cellular necrosis. *Am J Physiol* 242: G297.
64. Koike M, et al. 2008. Inhibition of autophagy prevents hippocampal pyramidal neuron death after hypoxic-ischemic injury. *Am J Pathol* 172:454.
65. Papadopoulos T, Pfeifer U. 1986. Regression of rat liver autophagic vacuoles by locally applied cyclohexamide. *Lab Invest* 54:100.
66. Oliver C, et al. 1979. Formation and fate of ethionine-induced cytoplasmic crystalloids in rat parotid acinar cells. *Am J Anat* 155:185.
67. Miyata S, et al. 2006. Autophagic cardiomyocyte death in cardiomyopathic hamsters and its prevention by granulocyte colony-stimulating factor. *Am J Pathol* 168:386.
68. Nixon RA, et al. 2005. Extensive involvement of autophagy in Alzheimer disease: An immuno-electron microscopy study. *J Neuropathol Exp Neurol* 64:113.
69. Yu WH, et al. 2005. Macroautophagy—a novel beta-amyloid peptide generating pathway activated in Alzheimer's disease. *J Cell Biol* 171:15.
70. Holton JL, et al. 2006. Autophagic vacuolar myopathy in twin girls. *Neuropathol Appl Neurobiol* 32:253.
71. Alonso S, et al. 2007. Lysosomal killing of Mycobacterium mediated by ubiquitin-derived peptides is enhanced by autophagy. *Proc Natl Acad Sci USA* 104:6031.
72. Al-Younes HM, et al. 2004. Interaction of *Chlamydia trachomatis* serovar L2 with the host autophagic pathway. *Infect Immun* 72:4751.
73. Gutierrez MG, et al. 2007. Protective role of autophagy against *Vibrio cholerae* cytolysin, a pore-forming toxin from *V. cholerae*. *Proc Natl Acad Sci USA* 104: 1829.
74. Pfeifer U. 1984. Application of test substances to the surface of rat liver *in situ*: opposite effects of insulin and isoproteronal on cellular autophagy. *Lab Invest* 50:348.
75. Pfeifer U. 1978. Inhibition by insulin of the formation of autophagic vacuoles in rat liver. *J Cell Biol* 78: 152.
76. Yoshimori T. 2007. Autophagy: Paying Charon's toll. *Cell* 128:833.

Vet-ebooks.com

Part II

Organelle Pathology

Ultrastructural Pathology The Comparative Cellular Basis of Disease
Second Edition Norman F. Cheville
© 2009 Wiley-Blackwell. ISBN: 978-0-813-80330-2

Vet-ebooks.com

4 The Cell Surface

The Plasma Membrane

The **plasma membrane (cell membrane, plasmalemma)** with its external glycocalyx and the subsurface cytoskeleton controls the barrier, adhesion, and transport functions of the cell surface. The plasma membrane is a lipid bilayer (appearing in micrographs as a bilayer 8.5–10 nm thick) with exofacial (outer) and cytoplasmic (inner) membranes. The unique negative surface charge of the inner leaflet is attributed to unique phospholipids that target and localize polycationic proteins (such as K-Ras) to the plasma membrane.

Phospholipids, the backbone of the membrane, are distributed asymmetrically between inner and outer layers in normal cells. **Phosphatidylserine (PS)** and the **polyphosphoinositides** (PIP_2, PIP_3, and other derivatives of phosphatidylinositol) are essential for transmembrane signaling. These individual phospholipids freely diffuse laterally and, when stimulated by certain signals, change their structure and flip-flop from inner to outer parts of the lipid bilayer.[1] In healthy cells, phosphatidylserine is found only in the inner leaflet, where it serves as a molecular beacon for proteins that have a C-2 domain. After injury, a **phosphatidylserine scramble** occurs as PS is translocated to the outer membrane. The presence of exofacial PS is a hallmark of apoptosis, and is a strong signal for macropinocytosis and phagocytosis. Defective phosphatidylserine metabolism is associated with serious diseases.

Glycolipids resemble phospholipids except that they are derived from sphingosin, not glycerol. The simplest glycosphingolipid is cerebroside, which has only one sugar residue, either glucose or galactose. Gangliosides are more complex and contain branched chains of several oligosaccharides. Cytochemical and immunolabels label localize glycolipids ultrastructurally.[2]

Cell surface **glycosphingolipids**, which have a ceramide anchored in the membrane and saccharide chains projecting outward, function as differentiation antigens, tumor antigens, blood group antigens, and as receptors for microbes. Orientation of saccharide moieties of glycosphingolipids on plasma membranes influences receptor function; that is, changes in position that expose or mask different epitopes on the saccharide molecule determine binding to the cell.[3]

Ceramide, released by activity of sphingomyelinases, is critically involved in cell responses to receptor-dependent stimuli; for example, in signaling cascades that mediate apoptosis after death receptor stimulation.[4,5] Ceramide forms distinct membrane domains, named ceramide-enriched membrane platforms, that support the clustering of receptor molecules.

Cholesterol and other sterols are embedded in the lipid bilayer and impose immobility on lipid molecules nearest the membrane surface but increase freedom of motion deeper within the hydrophobic core. That is, the ratio of cholesterol : phospholipid determines molecular fluidity within the membrane. **Abnormal ratios** of cholesterol-phospholipid or phospholipid-sphingomyelin are responsible for abnormal plasma membrane rigidity. Movement of transmembrane proteins in the increased fluidity of membranes plays a critical role in membrane metabolism. Cholesterol has been identified ultrastructurally in membranes by labeling it with filipin; filipin-cholesterol complexes appear as unique protuberances on the cell membrane.[6]

The glycocalyx is composed of oligosaccharide chains that are attached to membrane proteins or

© 2009 Wiley-Blackwell. ISBN: 978-0-813-80330-2

Vet-ebooks.com

lipids and project outward from the cell surface. Oligosaccharide chains originate from integral proteins (as glycoproteins) or to phospholipids (as glycolipids).[7,8] Oligosaccharide moieties provide specificity for attachment; for example, neuraminic acid imparts a special reactivity to lymphocytes where it is a receptor for attachment of certain viruses.

Membrane Proteins and Glycoproteins

Transmembrane proteins embedded in the membrane traverse the bilayer to expose segments to interact with substances at both the cell surface and in the cytoplasm. Although membrane proteins may be **integral** (embedded within the membrane) or **peripheral** (loosely associated with the cytoplasmic face), most are **transmembrane proteins** and function as structural proteins, receptors, enzymes, and ion-transporting channels.[9,10]

Location of plasma membrane proteins is demonstrated by the **freeze fracture technique** (Fig. 4.1). Plasma membranes are rapidly frozen to the temperature of liquid nitrogen (rapid freezing prevents formation of ice crystals). In this state the membrane, when given a gentle tap, falls apart along the plane of least resistance, the central plane of the lipid bilayer; that is, it comes apart between the lipid tails. This exposes the two half-membranes, each containing half the bilayer. One side of each half-membrane is the true membrane surface; the other is a view of the interior of the membrane, termed the **fracture face**. The background lipid is smooth, so the large protein molecules stand out as particles or depressions.[11] In freeze fracture studies, membrane proteins are seen to be missing or abnormally aggregated in response to several types of injury.[12,13]

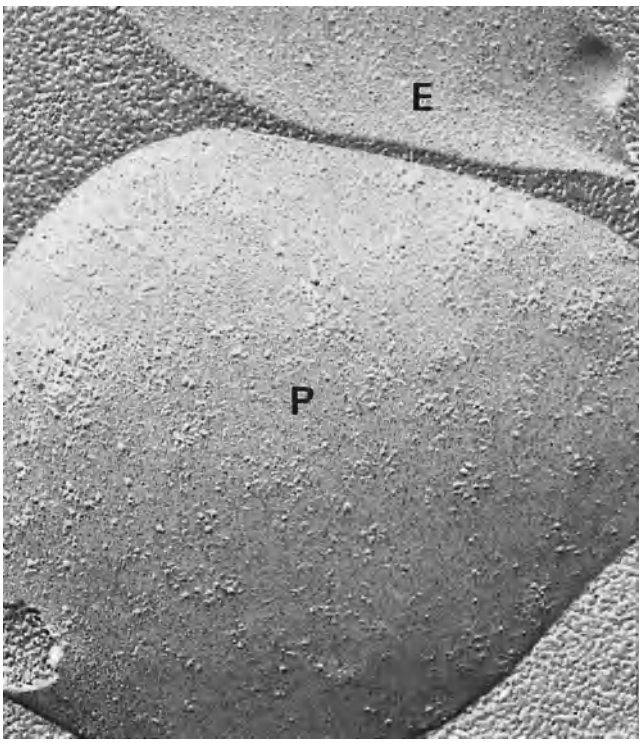


Fig. 4.1 Plasma membrane: freeze fracture preparation of human platelet. External (***E***) and internal (***P***) faces of the lipid bilayer. Membrane proteins appears as surface particles. (Micrograph: B. van Deurs, *J Cell Biol* 87:208, 1980.)

Membrane Microdomains

Membrane microdomains (also called **lipid rafts**, or **protein clusters**) are specialized microdomains in the plasma membrane that increase the efficiency of membrane activities. Plasmalemmal proteins move to and organize within these submicrometer-sized, sterol-enriched lipid rafts. Clustering of membrane proteins in lipid rafts, which are visible by electron microscopy, conformationally constrains these intramembrane molecules.[14] Several integral membrane protein isoforms segregate in non-overlapping clusters, including receptors, anion transporters, phosphatases, and attachment proteins. Syntaxins are members of the SNARE family of proteins that mediate membrane fusion in intracellular trafficking; on the appropriate signal, syntaxin monomers freely diffuse through the plasma membrane and aggregate into **syntaxin clusters** that facilitate vesicle secretion.[15]

Membrane microdomains are critical for compartmentalization of signaling. For example, **caveolae** in adipocytes are required for insulin metabolic signal transduction. In adipocytes in a state of TNFα-induced insulin resistance, the inhibition of insulin signaling and elimination of insulin receptors from caveolae microdomains are associated with accumulation of ganglioside GM3.

Detection of Transmembrane Proteins

Detection of specific transmembrane proteins by immunolabeling techniques reveals a wide spectrum of functions. Typically, cells are mosaics—they have membrane proteins with several different functions. A single protein may have multiple functions. The main functions of proteins in the plasma membrane include the following:

- **Transport proteins:** hydrophilic channels transport solutes
- **Signal transduction:** receptors bind signaling ligands causing a conformation change that sends a message into the cell

Vet-ebooks.com

- **Enzymatic activity:** enzyme has active sites exposed to extracellular matrix (ECM)
- **Cell-cell recognition:** glycoproteins with moieties specific for other cells
- **Cell-cell adhesion:** binds to like protein on other cells to form intercellular junctions
- **Attachment to cytoskeleton:** binds to microfilaments and other cytoskeletal structures to maintain cell shape and stability
- **Attachment ECM:** coordinates intra- and extracellular activities

Cell-cell adhesion, maintained by multiprotein assemblies that cluster at cell contacts and link to the cytoskeleton, is controlled by protein tyrosine phosphatases (PTPs) and kinases (Fig. 4.2). PTPs combine cell adhesive and catalytic activities in one molecule and act as sensors in phosphorylation-based signaling events.[16] Many cell surface complexes are components of important intercellular signal pathways. For example, receptor tyrosine kinases of the Eph family bind to cell surface-associated ephrin ligands on neighboring cells; **Eph-Ephrin signals** are bidirectional pathways that are major communication pathways between cells.[17]

Membrane Transport

The plasma membrane is a highly selective semipermeable barrier between the cell and the extracellular environment. To maintain a constant internal environment, molecules and ions are selectively transported across the membrane by several different mechanisms. A few small molecules such as oxygen, carbon dioxide, and ethanol pass the plasma membrane by **simple diffusion**, that is, by dissolving into the hydrophobic phase of the lipid bilayer and then back into the aqueous phase as it enters the cell.

Larger molecules, unable to diffuse, require **facilitated diffusion** through a specialized integral membrane protein called a **permease**—a protein that is specific for the uptake of a particular substance. Some permeases occur on nearly every cell type, while others are restricted to specialized cells. The plasma membrane of each type has its own battery of permease proteins, tailored to the needs of the cell. For example, glucose enters the erythrocyte via a **glucose transporter** (or glucose permease). As glucose enters the erythrocyte it is rapidly phosphorylated to glucose-6-phosphase, a reaction that prevents it from exiting the cell.

The Membrane Water Channel: Regulation of Intracellular Water

Water slowly crosses plasma membranes by diffusion through the lipid bilayer; movement occurs passively by diffusion equilibrium. In certain cell types, passage of water occurs through specialized water-selective channels. In erythrocytes, the glucose transporter and anion exchanger permit small amounts of transmembrane water movement, but neither is a water channel.

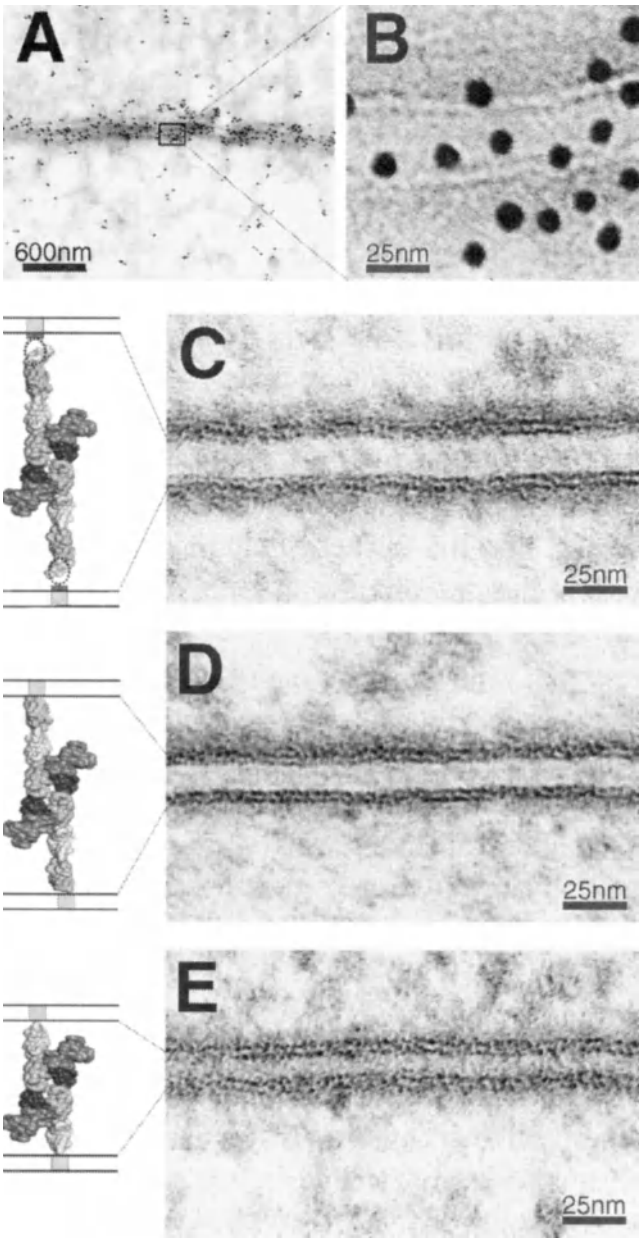


Fig. 4.2 Plasma membrane cadherins control intercellular spaces: ectodomain length of type IIB receptor protein tyrosine phosphatases (RPTPs) varies at adhesive interfaces. **A**. **RPTP accumulation** at adhesive interfaces: immune-EM. **B**. Enlargement of A. **C**–**E**. Transmembrane RPTPs induce complex cell contact regions with aligned plasma membranes. Intermembrane distances shorten progressively as RPTP domains are deleted. Phosphatases regulate adhesion by dephosphorylating components of cadherin-catenin complexes. (Micrograph: A. Radu Aricescu, E. Yvonne Jones, *Science* 317:1217, 2007.)

Vet-ebooks.com

Aquaporins are a family of tetrameric channel membrane proteins that transport water and/or small, uncharged solutes across lipid membranes according to prevailing osmotic or chemical gradients. They function as water-selective channels in plasma membranes. Open aquaporin channels permit water permeation but exclude protons.[18–20] At least eight aquaporins are expressed at distinct sites in the kidney. CHIP-28 (AQP-CHIP) is the major water channel of the erythrocyte plasma membranes and is heavily expressed at sites of rapid water transport in the proximal tubule and descending limb of the kidney; AQP-CD is the vasopressin-regulated water channel of the renal CD. Chemically, aquaporins have a unique hourglass structure that forms a pore that allows both selective water transport and solute rejection.[21]

P-glycoproteins Regulate Drug Transport

P-glycoprotein is an ATP-dependent, membrane-bound transport protein that regulates drug transport at cellular and subcellular levels. Intracellularly, P-glycoprotein is distributed in caveoli, cytoplasmic vesicles, Golgi complex, RER, and along the nuclear envelope. In the blood-brain barrier, P-glycoprotein localizes to both luminal and abluminal membranes of capillary endothelial cells, as well as adjacent pericytes and astroglia.[22]

Plasma Membrane ATPases Increase During Injury

In **active membrane transport**, critical movement of cations is accomplished by reactions that require energy. The integral membrane protein that transports the ion is an **ATPase**. As ATPase splits ATP into ADP, it uses the energy released to move ions up a concentration gradient. Ions transported in and out of cells directly coupled to ATP hydrolysis are Na^+, K^+, Ca^{++}, and H^+. Cells expand their ability to excrete ions by increasing the number of ion pumping ATPases and by expanding cell surfaces bearing pumps. Actions of Na-K-ATPase are called the **sodium-potassium pump** because the movement of these ions is linked in actively pumping Na^+ out of and K^+ into the cell. Immunolabeling of Na-K-ATPases in the **intestine** has been done using antibodies against either whole enzyme or its subunits.[23] In **kidney**, the enzyme is detected in the pumping areas of the ascending and descending limbs of the nephron. In **liver**, Na-K-ATPase is distributed heavily on the sinusoidal and lateral surfaces, but not on bile canaliculi; when hepatocytes are separated in vitro, the enzyme appears to then move into canalicular areas.[24] Epithelial cells of the **colon** expand basolateral surfaces and increase ATPase activity when an animal is deprived of Na^+ (or given excess K^+). Colonic epithelial cells of K^+-loaded animals have enlarged **mitochondria**, presumably due to an increased demand for ATP production to drive the basolateral pumps.[25] Increases in Na-K-ATPase in the plasma membrane occur in

- **Hyperkalemia:** expansion of basolateral pumps moves large amounts of K^+ into the cytosol, where it is then released into the gut lumen at the microvillous surface.
- **Thyroid hormone** increases pumps to enhance metabolism.
- **Catecholamines** increase the Na-K-ATPase pumps by a direct regulatory action.
- **Epinephrine** plays a significant role in regulating cell swelling in acute injury by influencing ion pumps at the cell surface.

Adhesion Glycoproteins

Several families of special receptor molecules on the cell surface cause cells to adhere to one another, or to the extracellular matrix. Leukocytes, endothelial cells, and other mobile cells alter their activities by changing production and removal of surface adhesion molecules. The major families of adhesion molecules include:

- **Selectins**, receptors bearing lectin-like domains that mediate leukocyte-endothelial adhesion: L-selectin (LECAM-1), P-selectin (PADGEM or GMP140), and E-selectin (ELAM-1).
- **Cadherins**, calcium-dependent hemophilic cell-to-cell adhesion proteins.
- **Immunglobulin superfamily adhesins**, receptors for cell-to-cell adhesion in embryogenesis, inflammation, and wound healing.
- **Integrins**, transmembrane proteins connected to the cytoskeleton that project out from the cell surface to bind ligands for adherence to other cells or to the extracellular matrix.

By binding to ligands or counterreceptor molecules on other cells, adhesion glycoproteins control movement and stability of cells. Adhesion molecules may be increased when cells are activated; for example, when neutrophils are stimulated, they develop hyperadhesive surfaces and bind to endothelium. All integrins are αβ heterodimers, both subunits of which are transmembrane glycoproteins, each with a single hydrophobic transmembrane segment. For most integrins the cytoplasmic domain is short; the larger extracellular domain combines to form the αβ dimer. Electron micrographs of the fibronectin receptor show a globular head formed by both α and β subunits and two stalks extending into the lipid bilayer.[26]

Vet-ebooks.com

Receptor Glycoproteins

Receptor proteins recognize and cause specific molecules to attach to the cell surface.[27] Receptors have binding sites with great specificity, and the protein stud exposed to the cytoplasm below the membrane provides communication for cellular events. Pathogenic viruses use cell surface receptors to bind and infect cells; for example, the canine parvovirus binds to the transferring receptor.[28] Typically, membrane receptor proteins are **glycoproteins**, which are complexes of α and β subunits that associate and disassociate to become active or inactive. The **β unit** is often the receptor and the **α unit** an action molecule that moves within the membrane to transmit the appropriate signal. Substances that attach to glycoprotein receptor molecules on the cell surface by binding to oligosaccharide chains are called **ligands**. Ligand binding triggers changes in the viscosity of the plasma membrane by causing phospholipid molecules to change position and even to flip-flop in the membrane. As a result, phospholipids are pushed aside, and **ligand-receptor complexes** move to sites of further interaction with other membrane proteins.

The largest family of integral membrane proteins is that of the **G protein-coupled receptors**, which communicate signals across plasma membranes to a wide spectrum of extracellular stimuli including photons and cations as well as peptides. Once activated, G protein-coupled receptors trigger a cascade of responses inside the cell via interaction with their G protein partners, regulators that are switched on and off by binding GTP. This astonishing network of signals is exquisitely coordinated. Among the most studied are rhodopsin (the light-sensitive receptor in the mammalian eye), the β_2-adrenergic G protein-coupled receptor, and receptors for diffusable hormones and neurotransmitters.[29]

Intramembrane Lysis and Transmembrane Signaling

Regulated Intramembrane Proteolysis

Regulated intramembrane proteolysis (RIP) is a critical signaling pathway initiated by different families of intramembrane proteins. RIP is initiated outside the membrane in response to ligand binding, which provokes a conformational change that triggers a second intramembrane cleavage event that, in turn, releases an active cytoplasmic fragment. Some of the RIP initiating signals are Notch, the amyloid precursor proteins (APP), and the LDL receptor-related protein (LRP). In ischemic tissue, **LRP** mediates a signal transduction that causes cell death. LRP, cleaved of its cytoplasmic site by a γ-secretase, releases its intramembrane domain into the cytoplasm to move the death signal.

Regulated Intramembrane Phospholipid Degradation

Membrane degradation releases phospholipid catabolites such as lysophosphatides, arachidonic acid, and other catabolites. Hydrophobic lipid breakdown products are important signal molecules that often exacerbate cellular injury.

- Soluble head-group molecules of phosphoinositides, **1,4,5-triphosphate (IP_3)**, interact with Ca^{++} channels to enhance Ca^{++} release; at the plasma membrane **diacyl glycerol** activates **protein kinase C**, a signal molecule with widespread effects.[30]
- **Sphingosine**, a sphingolipid breakdown molecule, is an inhibitor of protein kinase C and opposes the activity of diacylglycerol.
- **Arachidonic acid** is the precursor for **eicosanoids**, the messenger molecules (prostaglandins, leukotrienes) that influence many cellular activities.
- **Phosphoinositide 3-kinase (PI3K) signaling pathways** begin with cell surface-induced activation of cytoplasmic PI3K to localize PI3K at the plasma membrane, where it phosphorylates the membrane lipid PIP_2 to produce phosphatidylinositol 3,4,5-triphosphate, PIP_3—all leading to downstream signaling pathways that control cell growth and survival.

PI3K is activated upon binding of phosporylated **receptor tyrosine kinases (RTKs)** and/or adaptor proteins at the plasma membrane and signals to multiple downstream effects such as **Akt**. Aberrant activation of PI3K pathway components is universal in neoplasia. Drugs targeted to inhibit RTKs and the downstream PI3K signaling pathway show anticancer activity.

Inositol pyrophosphates have a prominent role in the signal transduction and regulation of a wide range of cell responses including vesicle trafficking, DNA repair, telomere maintenance, and cell signaling. Inositol pyrophosphates are derivatives of the second messenger IP_3—the second messenger involved in calcium release—which is a precursor to more highly phosphorylated inositol phosphate molecules such as inositol tetrakis (IP_4), pentakis (IP_5), and hexakis (IP_6) phosphates. IP_6 activates voltage-dependent calcium channels, exocytosis, and endocytosis. Additional phosphorylation of IP_6 produces IP_7 and IP_8. Inositol pyrophosphates contain high-energy pyrophosphate bonds, with free energy of hydrolysis similar to that of ATP. Thus, IP_7 can directly phosphorylate proteins in an ATP- and enzyme-independent manner.[31]

Vet-ebooks.com

Intramembrane phospholipases are components of the normal plasma membrane and are activated nonspecifically during plasma membrane stimulation and injury. In acute cell swelling, intramembrane phospholipases are activated by the rising levels of intracellular Ca^{++}. Degradation of membrane phospholipids produces several important signals molecules that play important roles in driving critical molecular rearrangements in the plasma membrane. Some of the early events in the general response of membranes to injury are

- **Degradation of membrane phospholipids with release of breakdown products**, chiefly phosphoinositides and arachidonic acid metabolites that modulate cellular activities.
- **Alteration of plasma membrane viscosity** caused by changes in or movement of cholesterol and phospholipid molecules, and that leads to suppressed or enhanced action of membrane receptors and other transmembrane proteins.
- **Suppression of membrane proteins**, including a wide variety of receptor molecules, ion transport proteins, and adenyl cyclase.

In this last category are most of the critical ion and molecule transporting proteins that control intracellular glucose, calcium, and pH. Their shutdown has ramifications that extend throughout the cell and may involve such diverse changes as abnormal movement, cell adhesion, and secretion.

Exogenous Phospholipases

Enzymatic attack directed to phospholipids within the plasma membrane is a major cause of lethal injury. **Exogenous phospholipases** in chemical solvents and in venoms, bacterial lysins, and other biologic toxins hydrolyze phospholipids to cause membrane leakage and cellular lysis. All **snake venoms** contain a phospholipase A_2 that destroys membrane phospholipids to release unsaturated fatty acids and lysophosphatides.

Microbial Lysins Many bacteria produce **phospholipases** (lecithinases) that directly attack membrane phospholipids. *Clostridium* spp. produce potent phospholipases that degrade membranes and cause extensive lytic necrosis of target cells (Fig. 4.3). The highly lethal **α-toxin** of *Clostridium perfringens* converts membrane lecithin moieties to phosphoryl choline and a diglyceride. Released into muscle, the toxin produces rapid and indiscriminant lysis that destroys myocytes, erythrocytes, and endothelial cells.

Bacterial phospholipases produce a wide spectrum of membrane damage that varies from small discrete holes to large cavities and pits (Fig. 4.4). The marine bacterium *Vibrio damsela*, growing on fish spines that puncture human skin, release a **phospholipase D** that lyses phospholipids, a reaction that causes cellulitis and gangrene.

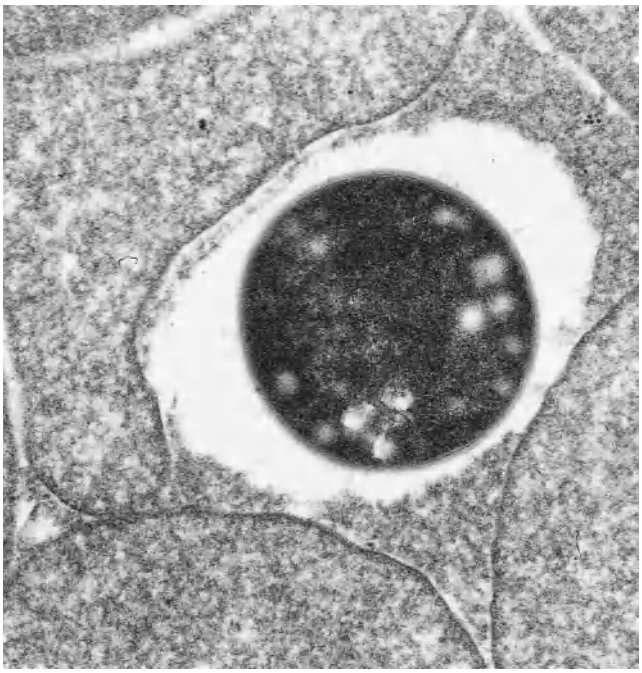


Fig. 4.3 Plasma membrane lysis: erythrocytes, phospholipase-induced lysis, site of hemorrhage caused by *Clostridium septicum*, skeletal muscle, sheep. Hemoglobin is depleted from erythrocytes and occupies extracellular spaces. The bacterium has fine surface filaments and is surrounded by a halo of lysis.

Plasma membrane lysis results from activation of normal **endogenous phospholipases** of the body at ectopic sites. For example, acute pancreatic necrosis results from the premature activation of the potent pancreatic enzyme **phospholipase A_2** (normally confined to the pancreatic duct) in ductules bordering acinar cells. There is widespread and indiscriminant lysis of all cell types.

Membrane Internalization

Membrane internalization, a response to focal injury, is manifest as focal irregular invaginations of the plasma membrane. Invaginations develop into small submembranous vacuoles by endocytosis. Membrane internalization commonly occurs in diseases where abnormal intracellular metabolism alters the plasma membrane, and is also a usual pathway of injury in aging and toxic hemolysis. Membrane internalization is induced by several drugs, including primaquine, hydrocortisone, vinblastine, and chlorpormazine, and it occurs in relation to the dose administered and is dependent upon ATP-energized states of the membrane.

Vet-ebooks.com

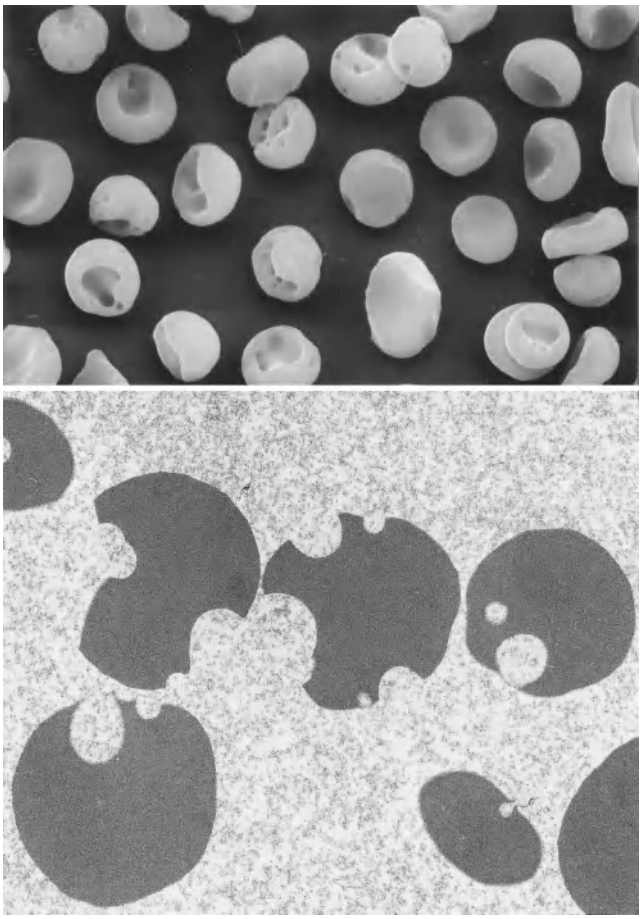


Fig. 4.4 Pitting of cell surface: *Corynebacterium pseudotuberculosis* toxin, erythrocytes, scanning (*top*) and transmission (*bottom*) electron microscopy. (Micrographs: Kim A. Brogden, *Am J Vet Res* 51:874, 1990.)

Porin-Induced Membrane Damage

Cells are lysed when exogenous proteins bind to and aggregate on the plasma membrane to form protein complexes called **porins**. These channel-forming proteins cause the cell to become leaky, allowing K^+ to leak from, and Ca^{++} and water to enter, the cell. Protein complexes that assemble on plasma membranes to create pores include the **complement attack sequence** and **lymphocyte porins**, which are released onto membranes of bacteria (Table 4.1), and some **bacterial toxins**, which are secreted directly onto target cell surfaces.

Complement Attack Sequence

Complement kills microbes and causes cell injury by insertion into the plasma membrane. In late stages of microbial disease, antibodies appear in the bloodstream and attack infected cells, which contain the specific microbial antigens on their surfaces. The reaction of the antibody molecule with plasma membrane antigen attracts components of the complement system, which form protein complexes on the cell surface. Complement **membrane attack sequences**, the last five components of complement (C5 through C9), act together to lyse bacterial cells (Fig. 4.5). The **membrane attack complex** (**MAC**, C5b-9 complex) is initiated when complement protein C5 is proteolytically activated into two fragments, C5a and C5b, in the complement cascade. C5b sequentially binds C6, C7, C8, and multiple copies of C9 to form the MAC. The process begins when C7 binds to the membrane surface. C8α then penetrates the lipid bilayer to cause loss of membrane integrity. C8 is a trimer of proteins C8α and C8β, each of which contain a MACPF domain for membrane insertion, and a lipocalin protein, C8γ, that is covalently linked to C8α.[32] After C5b-8 assembly, multiple C9 molecules bind and oligomerize into pores of 12–18 C9 monomers that are ~100 Å wide and 160 Å high. The complement pore has been detected on cell surfaces by special techniques.[33,34] Host cells are protected from MAC attack by CD59, which prevents pore formation by binding to C8α and C8β during MAC assembly.

Complement plays a role in development, tagging unwanted synapses in the brain for removal. Astrocytes induce neurons to secrete C1q, which tags unwanted synapses for removal by microglia.

Perforin-Induced Cell Death

Cytotoxic T cells (CTL) and certain **natural killer (NK) cells** destroy microorganisms and infected host cells by releasing **perforin**, a peptide that aggregates and polymerizes on target cell surfaces. Perforin multimerizes to form pores of ~20 monomers; it does not use accessory proteins for membrane binding.

During infection, protein antigens embedded in the target cell surface attract CTL and NK cells. After a CTL binds to an infected target cell, perforin molecules are released, aggregate as polyperforin, and embed in the plasma membrane, producing pores that cause the cell to become leaky. Polyperforin molecules aggregating on the infected cell produce ring-shaped structures with a central channel that moves ions from the cytosol, causing the cell to become leaky.[35,36]

Attacking lymphocytes also inject a serine protease, **granzyme B**, through the perforin pore into the cell to block specific metabolic pathways in order to kill the target cell. Granzyme B from T cells also kills target cells by inducing apoptosis.

Killing of host cells via **NK cells** has been reported in guanethidine toxicity. **Guanethidine** is an adrenergic neuron-blocking agent that induces destruction of sympathetic neurons in superior cervical ganglia. Given experimentally to rats, it causes neurons in the

Vet-ebooks.com

Table 4.1 Transmembrane proteins.

Protein	*Functon*	*Eference to ultrastructure*
	Adhesion Glycoproteins	
Cadherins	Intercellular junction adherence	**D'Amico**, *Arch Oral Biol* 52:161, 2007 **Vorbrodt**, *J Mol Histol* 37:27, 2006
Integrins	Epithelial adherence	**Underwood**, *J Histochem Cytochem* 57:123, 2009
Selectins	Endothelial cell adherence	**Easton**, *Microvasc Res* 62:335, 2001
	Transport Proteins: Ion Channels (Permeases); ATPase uses metabolic energy to move molecules and ions against an electrochemical gradient	
Na-K-ATPase	Sodium pump	**Ernst**, *J Cell Biol* 91:803, 1981 (nephron); **Kyte**, *J Cell Biol* 68:287, 1976 (nephron); **Marxer**, *J Cell Biol* 109:1057, 1989 (intestine); **Sztul**, *J Cell Biol* 104:1239, 1987 (hepatocyte); **Takemura**, *J Cell Biol* 99:1502, 1984 (hepatocyte, dog)
	Inhibition	**Wolburg**, *Acta Neuropathol* 34:255, 1976 (oubain)
	Enhancement	**Kashgarian**, *Lab Invest* 42:581, 1980 (colon, hyperkalemia)
Ca-Mg-ATPase	Calcium transport	**Jorgensen**, *J Cell Biol* 93:883, 1982
Proton pump	Proton transport	**Blair**, *Science* 245:855, 1989 (osteoclast); **Brown**, *J Cell Biol* 105:1637, 1987, **Nielsen**, *J Cell Biol* 120:371, 1993 (nephron)
Bicarbonate	Band 3 protein	**Satlin**, *J Cell Biol* 109:1279,1989 (kidney, collecting duct)
	Endogenous Porins	
Complement	Cell lysis, inflammation, et al.	**Biesecker**, *Lab Invest* 49:237, 1983; **Dourmashkin**, *Immunology* 35:205, 1978; **Podack**, *Proc Natl Acad Sci* 79:574, 1982; **Tranum-Jensen**, *J Cell Biol* 97:618, 1983; **Tranum-Jensen**, *Scand J Immunol* 7:45, 1978
Perforin	Cell lysis and killing	**Dennert**, *J Exp Med* 157:1483, 1988; **Podack**, *J Exp Med* 160:695, 1984
	Exogenous Porins	
Microbial porins	Staphylococcus α-toxin	**Bhakdi**, *Proc Natl Acad Sci* 78:5475, 1981; **Bhakdi**, *Prog Allergy* 40:1, 1988; **Fussle**, *J Cell Biol* 91:83, 1988
	Entamoeba histolytica	**Young**, *J Exp Med* 156:1677, 1982
	Toxoplasma gondii	**Nichols**, *J Ultrastruct Res* 83:85, 1983
Ionophores	Na^+: Monensin	**Smith**, *J Parasitol* 69:666, 1983
Toxins	Gramicidin	**Wallace**, *Science* 241:182, 1988
	Defective Channels	
Cystic fibrosis	CFTR protein	**Crawford**, *Proc Nat Acad Sci USA* 88:9262, 1991
	Chloride channel	**Welsh**, *Cell* 73:1251, 1993

ganglia to express certain proteins on their surfaces that inadvertently target them for NK cell killing.[37,38]

Drugs That Insert As Ion Channels

Gramicidin is one of the simplest molecules that forms ion channels through lipid membranes. An antibiotic derived from *Bacillus brevis*, it provides a fixed transmembrane ion channel by forming a 2.6 nm long tube composed of two polypeptide chains wrapped in a helical coil. The polypeptide backbone forms the interior of a hydrophilic pore. The outer channel surfaces rest among the long chain lipid molecules of the membrane and protruding tryptophan regions constrain the helical twisting and deformation of the channel. Gramicidin-type ion pores act very differently from ion carrier molecules such as valinomycin, which are not fixed but must diffuse through the membrane to act.

Ionophores are compounds that carry ions across membranes. They form lipid soluble complexes with cations and become embedded in the plasma mem-

Vet-ebooks.com

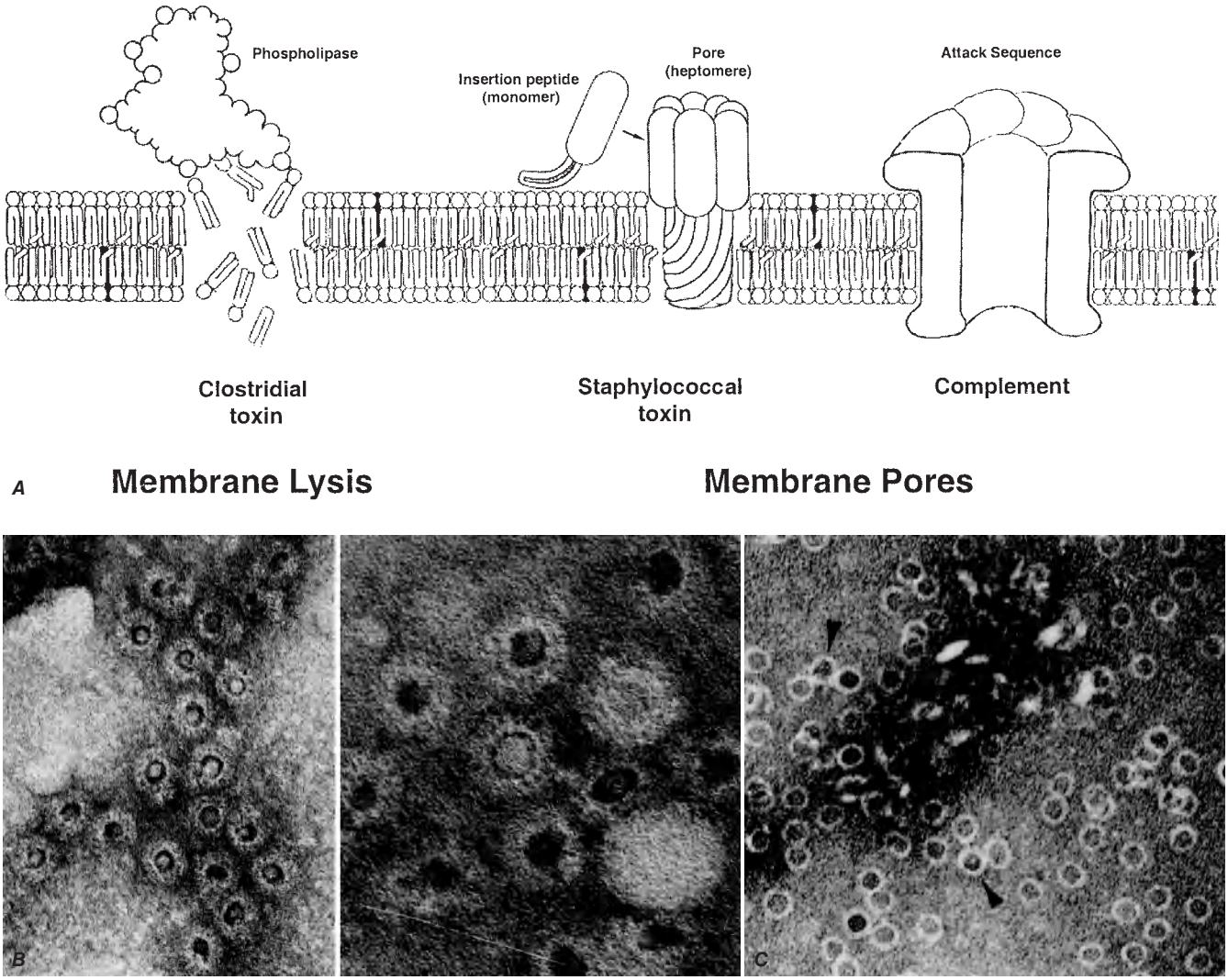


Fig. 4.5 Porin membrane lysins. **A**. **Comparison of membrane injury**. Direct phospholipid degradation by phospholipases (*left*) differs from that by the pore-forming staphylococcal toxin and the channel-forming complement attack sequence (*right*). **B**. **Pore complexes: complement attack sequence:** holes in the plasma membrane formed by complement complexes (seen en face) on the lysed membrane. Negative staining outlines rings or annuli that represent molecules of complement fragments C5–C9, the membrane attack sequence. (Micrograph: J. Tranum-Jensen, *Scand J Immunol* 7:45, 1978.) **C**. **Pore complexes: perforin**. Pore complexes (*arrowheads*) created by membrane-bound polyperforin molecules that were embedded in the plasma membrane of a host cell after being released by lymphoid cells. Pore diameters are approximately 16 nm. (Micrograph: Gunther Dennert, *J Exp Med* 157:1483, 1983.)

brane to function as channel molecules. These diverse compounds have in common a central ring of liganding oxygens that form a critical cavity in which a particular ion can fit. Several naturally occurring antibiotics function as ionophores; for example, there are ionophores with relative specificity for H^+ (dinitrophenol), K^+ (valinomycin), Ca^{++} (the drug A23187), and Na^+ (monensin).[39,40]

Microbial Porin-Induced Lysis

Microbial porins are major mechanisms of virulence in bacterial and protozoal diseases and include **perfringolysin** of clostridial myositis, **leishporin** of leishmaniasis, **α-toxin** of staphylococcal infection, and **α-hemolysin** and **enterohemolysin** of infections caused by *E. coli*. Secreted directly onto target cell surfaces, these potent porins cause lysis of host cells. Perfringolysin O is a thiol-activated cytolysin and the toxin receptor in the membrane, cholesterol, plays critical roles in attachment, oligomerization, and stablization of the membrane pore. Studies of ion conductance during pore formation suggest that, with the appearance of each new pore, a discrete amount of current crosses the membrane. This current change reflects the progressive incorporation of single channels into the lipid bilayer that makes up the plasma membrane.

Vet-ebooks.com

Some strains of *Streptococcus* and *Staphylococcus* also kill cells by secreting porin-like molecules.[41–44] Because of their small size, bacterial porins are difficult to detect by electron microscopy. *Toxoplasma gondii*, a protozoan that replicates in lymphoid tissues of many species, secretes protein components into target host cells that cause injury.[45] *Entamoeba histolytica*, an enteric human protozoan parasite, produces extensive necrosis by secreting a polypeptide that inserts into the plasma membrane of target cells and functions as an aqueous pore.[46] *Trypanosoma cruzi* secretes a protein related to C9.[47] **Mellitin**, the cytolytic peptide of bee venom, appears to be an insertion protein pore.

Defective Plasma Membrane Channels

Cystic fibrosis, a common lethal hereditary disease, is caused by an **abnormal chloride selective channel** in the apical membrane of epithelial cells. Normal efflux of Cl^+ is disrupted; activation of protein kinase by cyclic AMP occurs normally in cystic fibrosis cells, but the kinase fails to activate chloride conductance. Sweat is excessively salty (caused by decreased reabsorption by duct cells after normal sodium secretion by acinar cells).

Concentrations of sodium and Cl^+ secreted into sweat glands are normal; unlike most epithelium, cells of the sweat ducts are relatively impermeable to Cl^+. Thus as sweat moves to the surface, the reabsorption of Cl^+ and the accompanying sodium does not occur. The dehydrated airway surface results in thick mucus in which *Pseudomonas aeruginosa* thrives. The cystic fibrosis gene on human chromosome 7 produces a messenger RNA transcript that encodes for a protein designated the **CF transmembrane conductance regulator** or CFTR; the mutant gene produces a CFTR that lacks phenylalanine at codon 508. Embedded in the plasma membrane, immunostaining for CFTR reveals its distribution to be restricted to the apical plasma membrane of epithelial cells.[48,49] CFTR acts as a receptor for the outer core oligosaccharide of the LPS of *P. aeruginosa*, the cause of lethal infections in CF. In normal humans, binding to *P. aeruginosa* initiates an innate immune response that includes phagocytosis, nuclear factor κB activation, and cytokine secretion—all processes absent in CF patients—all responses that contribute to resistance to infection.

Cytoskeleton

The major components of the cytoskeleton—**microtubules, microfilaments, intermediate filaments**, and **subsurface matrix**—provide the structural framework of the cell (Fig. 4.6).[50] Ramifying throughout the cell, they constantly shift in position and structure to adapt to such diverse activities as phagocytosis, granule secretion, exocytosis, and migration. These four components are connected to each other and to the plasma membrane by linker proteins, which provide both a system for movement and for attachment and stability of cytoplasmic organelles. The analogy has been made that microtubules and microfilaments act as bone and muscle.

The force that provides for movement of the cytoskeleton is produced from the energy of ATP hydrolysis. ATP is used to power the sliding of filaments against one another. This ATP-driven motion is generated by two distinct groups of proteins: in microfilaments, by actin (and its coupling ATPase, myosin); and in microtubules, by tubulin (and its ATPase, dynein) (Table 4.2).

Microtubules

Microtubules maintain cell shape, and are responsible for orienting microfilament-induced movement along a particular axis. Ultrastructurally, microtubules are long, well-defined, and relatively rigid. In transmission electron micrographs, they are typically seen in short segments since they pass into and out of the plane of section. Examined in cross section, microtubules are tiny circles, 20–25 nm in diameter with walls 5–7 nm thick. At high magnification it is clear that the circles are composed of round subunits that are dimers (double molecules) of proteins called α- and β-tubulin.[51]

Microtubules form when **tubulin** subunits are assembled into rings and then into stacks of rings. The developing tubules become elongated as additional dimers assemble at one end. Assembly and disassembly of microtubules are constantly in progress in living cells.[52] Small changes in intracellular Ca^{++} affect tubulin assembly and calmodulin, a Ca^{++}-regulating protein, mediates assembly and disassembly of microtubules. In cells undergoing mitosis, centriolar satellite bodies serve as nucleation sites for tubulin polymerization and microtubules (which guide chromosomal movement in metaphase) radiate around these dense irregular foci.

Microtubule-associated proteins (or MAPs) project from the surface of microtubules.[53,54] They act as connecting devices between different microtubules and microfilaments. By controlling cytoskeletal interaction MAPs play a crucial role in assembly and disassembly of the cytoskeleton.

At cell surfaces microtubules operate in movement and shape change by cooperating with microfilaments. This interaction has been most studied in platelets and

Vet-ebooks.com

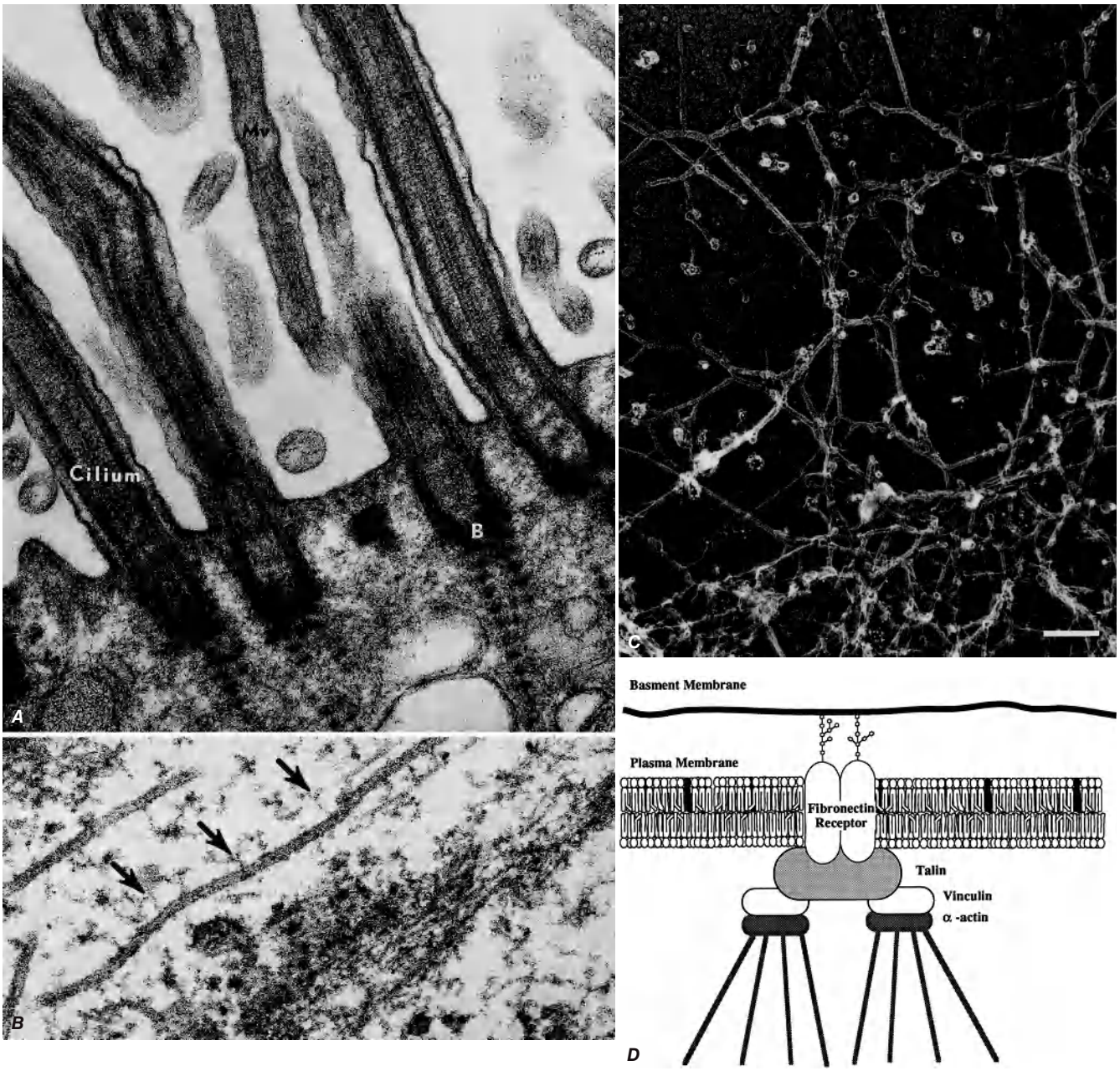


Fig. 4.6 Cytoskeleton. **A**. **Microtubules**: rigid microtubules within the shaft of cilia originate in basal bodies (*B*); microvillus (*Mv*). **B**. **Microtubule-associated filaments**: small filaments composed of microtubule-associated proteins are attached to the microtubule (*arrows*). **C**. **Microfilaments**: negatively stained preparation of microfilaments. Gelsolin (stained with gold-labeled antibodies) is located on the ends of short filaments. Viewed in stereo, gold particles are located at filament-membrane interfaces where filaments intersect the cytoplasmic side of the membrane. (Micrograph: John Hartwig, *J Cell Biol* 108:467, 1989.) **D**. **Cytoskeleton-plasma membrane complex**: actin microfilaments are anchored to membrane adhesion proteins via the adhesion plaque complex, which is composed of α-actinin, vinculin, and talin.

leukocytes, which, when activated by external stimuli, change their shape by retracting and elongating their cytoplasm. Microtubules also act spectacularly in cilia, spermatozoa, and some other cells to achieve motion.[55] In enterocytes of the small intestine microtubules interact with actin filaments to shorten surface microvilli.[56]

Microtubular Transport

Microtubules play essential roles in the movement of chromosomes during cell division, motility of cell surface cilia, and direction for endo- and exocytotic vesicles through the cytoplasm. Membranes of vesicles and organelles that move along microtubular

Vet-ebooks.com

Table 4.2 Cytoskeletal toxins

Component	*Toxin*	*Reference to ultrastructure*
	Microtubules: 20 nm diameter	
Tubulin	Colchicine	**Pavelka**, *J Cell Biol* 97:737, 1983 (pancreas); **Wild**, *Am J Anat* 170:531, 1984 (secretion); **Wisniewski**, *Lab Invest* 17:577, 1967 (brain)
	Vinblastine	**Magalhaes**, *J Ultrastr Res* 91:149, 1985 (adrenal); **Nanci**, *Anat Rec* 219:113, 1987 (tooth)
	Taxol	**Hausmann**, *J Ultrastr Res* 82:212, 1983*
	Microfilaments: 7 nm diameter	
Actin	Botulism CS toxin	**Reuner**, *Eur J Cell Biol* 43:134, 1987*
	Cytochalasin D	**Prentki**, *J Cell Biol* 81:592, 1979 (liver)
	Phalloidin	**Russo**, *Am J Pathol* 109:133, 1982 (liver); **Watanabe**, *Am J Pathol* 122:101, 1986 (liver)
	Intermediate filaments: 10 nm diameter	
Keratin, type I	Acidic	**Miller**, *J Cell Biol* 122:123, 1993
Keratin, type II	Basic	**Blouin**, *Exp Cell Res* 187:234, 1990
Type III	Vimentin: Cytochalasin	**Pagan**, *Exp Cell Res* 222:333, 1995; **Berg**, *Histochem Cell Biol* 131:103, 2009
	Desmin (muscle): cholera toxin	**Shinde**, *Neuromuscul Disord* 18:215, 2008#
	Glial fibrillary protein (astrocyte): Shiga toxin	**Boccoli**, *Brain Res* 1230:320, 2008
	Peripherin	**Eriksson**, *BMC Neurosci* 9:26, 2008
Type IV	Neurofilament protein: bacterial exotoxin	**Ohlsson**, *Restor Neurol Neurosci* 22:33, 2004
Type V	Nuclear lamins (karyoskeleton): α-amanitin	**Kumaran**, *J Cell Biol* 159:783, 2002; **Spann**, *J Cell Biol* 156:603, 2002
Type VI	Nestin (neuron): botulinum toxin	**Kang**, *J Neurosci* 27:5948, 2007§
	Subsurface Cytoskeleton	
Spectrin	Calpain	Glantz, Biochemistry 46:502, 2007

*In vitro study.
#Tissue from patients with myofibrillar myopathy caused by mutation of desmin genes.
§Calpain-catalyzed spectrin proteolysis.

guides are endowed with receptors for the ATP motor protein attached to the microtubular surface.

Active transport of cytoplasmic organelles uses the molecular motor proteins dynein and kinesin-1, which transport cargo toward the cell center (the minus end of the microtubule) and cell periphery (the plus end), respectively. **Dynein** has a large, complex motor domain that moves along the microtubular surface in steps; movement requires an accessory complex, dynactin. How dynein and its complex with microtubules function has been clarified by cryoelectron microscopy, including how a conformational change in the dynein domain generates movement along the microtubule.[57]

For **secretion**, microtubules guide the secretory granule to the cell surface, where contact with the cell membrane permits exocytosis of granule contents; that is, they act as stable guidelines, or tracks, along which particles are drawn by microfilaments or other contractile proteins. In **neurosecretion**, microtubules move large secretory granules along the nerve axon. Microtubles are indispensible for **mitosis** because, as spindle fibers, they guide the movement of chromosomes. In endocrine secretion, microtubules guide **secretory granules** of the salivary gland, pancreas, thyroid, and other exocrine glands from the Golgi complex to the plasma membrane for exocytosis.

Centrosomes and Centrioles

Microtubules grow out from a **centrosome**, a region located near the nucleus that is a microtubule-organizing center. Microtubules radiate from the centrosome, providing girders that resist compression of the cell. Within the centrosome are a pair of **centrioles**, each composed of nine sets of triplet microtubules arranged in a ring. Prior to mitosis, the centrioles replicate (see the section on cilia).

Vet-ebooks.com

Microtubule Poisons

Colchicine, a toxic alkaloid from the meadow saffron *Colchicum autumnale*, has been used to treat gout and in the lab to stop cells in mitosis. Colchicine binds to specific sites on the tubulin dimer and stops cell division in prometaphase by destroying the microtubules that make up the spindle apparatus. Colchicine-poisoned humans and animals develop defective intracellular transport and exocytosis of secretory granules. Colchicine causes an increase in **annulate lamellae** because they are involved in transfer of RNA from nucleus to cytoplasm. Failure to transport secretory proteins is evident in exocrine glands where, in treated animals, **secretory granules** decrease in lumens and apical vesicles, but accumulate in the Golgi complex. Rats given 0.5 mg/100 g body weight show disorganization of the **Golgi complex** in pancreatic cells including pleomorphic zymogen granules, vacuoles, and shortened cilated Golgi saccules.[58] Damage to microtubules by antitubulin drugs leads to alterations in other components of the cytoskeleton, for example, accumulation of excessive microfilaments or intermediate filaments.

Other microtubular poisons include vinblastine,[59–62] vincristine,[63] podophyllin, and taxol.[64] **Vinca alkaloids** bind to tubulin to block spindle formation and mitosis. In poisoned cells, vinblastine-tubulin complexes can form paracrystalline inclusions. Open coils and ring-like fragments can form from the ends of microtubules. Coils are composed of two protofilaments and result in striking helices in negatively stained preparations. Taxol is a plant-derived antitumor drug that binds polymerized tubulin at sites different from colchicine to inhibit polymerization of tubulin.

Microtubular aggregates have been documented in neurons of humans and animals with neurologic disease.[65–69] When injected into the subarachnoid space of rats, vinblastine causes a pattern of degeneration that mimics the neuronal degeneration of aging. There is microtubule (neurotubule) loss accompanied by proliferation of microfilaments and accumulation of abnormal neurofilaments. The block in the process of forming neurotubules is associated with accumulation of these other components of the cytoskeleton.

Hereditary Defects in Microtubules

Defects in cytoskeletal components are associated with defects in structures and cells whose function depends upon the cytoskeleton, for example, cilia and spermatozoa.[70–73] **Immotile cilia syndromes** (see the section on cilia) are a heterogenous group of human ciliary dysfunction diseases (Fig. 4.7).[74,75]

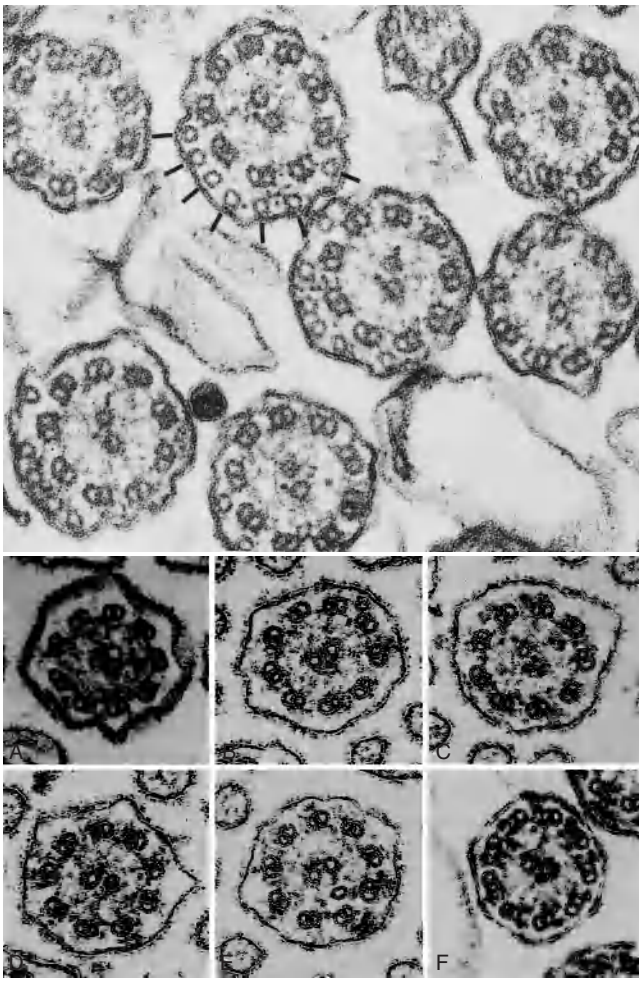


Fig. 4.7 Immotile cilia syndrome. A. Human: cilia, cross section. Five cilia have three to seven supernumerary outer single microtubules (*small lines*). (Micrograph: Eveline E. Schneeberger, *J Ultrastruct Res* 73:34, 1980.) **B. Rat**: cross sections of respiratory cilia of WIC-Hyd rats (*A–E*) and a control WIC rat (*F*). Most cilia are 9 + 2 axonemal configuration, but an abnormal 9 + 3 is shown in *E*. Both inner and outer dynein arms are absent. The nexin link and radial spokes are clearly demonstrated in some sections. Thirteen protofilaments in singlets and A-rings, and 10 in B-rings, are seen in *B–F*. A cilium from a control WIC rat shows prominent dynein arms in *F*. (Micrograph: Chikao Torikata, *Am J Pathol* 138:341, 1991.)

Microfilaments

These 7 nm diameter **actin filaments** occur throughout the cytoplasm but typically are aggregated into bundles near the cell surface. Microfilaments control cell surface activities such as movement, shape change, and microvillus formation—all of which are mediated by the polymerization of **monomeric actin** (globular actin, G-actin) into a double helix of bead-like units (called F-actin) that form the microfilament. This process is reversed in depolymerization as filaments

Vet-ebooks.com

are degraded and actin returns to globular form. Polymerization and disassembly of actin generates the microfilament network that causes the cell's shape to change. Monomeric actin also shuttles into and out of the nucleus, where it regulates chromatin structure and transcription.[76]

Microfilaments function through connections with both plasma membrane and the larger, more rigid microtubules. They are anchored to the plasma membrane via connections with the actin-binding protein **α-actinin** (in skeletal muscle, microfilaments are anchored to **α-actinin** of the Z line). Microfilaments combine with **myosin** to form **actomyosin complexes** that function in cell movement translocation of plasma membrane proteins (just as muscle action is achieved by sliding of actin and myosin filaments across one another).

Other **actin-binding proteins** bind microfilaments to other structures. Their different designations reflect their role in the cell: **tropomyosin** binds in grooves on actin helices to regulate actin binding to myosin; **vinculin** binds ends of actin microfilaments to membranes; and **filamin** also links adjacent microfilaments and myosin.

Gelsolin and **profilin**, together with the **formins**, are cytosolic proteins that bind to actin in a way that controls polymerization.[77–79] Formins remodel actin and microtubule cytoskeletons; they are a widely expressed family of proteins that govern adhesion, cell shape, cytokineses, and morphogenesis.

Gelsolin, an actin-severing protein, causes disassembly of actin networks. It binds to the actin microfilaments and remains attached to one of the new segments. Acting on actin filaments that are in a gel network, gelsolin converts a gel to a sol (thus the name "gel-solin"). Gelsolin is related to villin, the actin-binding protein of intestinal villi. As cells change shape (as in the explosive actin polymerization of platelet activation), gelsolin moves from the cytosol to associate with the plasma membrane.

In the resting cell, **profilin** binds to actin monomers, preventing polymerization into microfilaments. When the appropriate signal is received by the action of ligand-receptor binding at the platelet surface, the profilin-actin complexes dissociate. Experimentally, this signal can be transmitted by contact with phosphoinositides released from the plasma membrane during binding of ligand and membrane receptor molecules.[80]

Actin microfilaments are especially important in healing tissues, where large numbers help to bind fibroblasts and myofibroblasts to substrata. **Stress fibers** is a term applied to bundles of actin microfilaments that are common in cells in vitro; their increase is associated with a shift from globular (G) to F-actin.

When these cells begin to move, filament bundles come apart to form a diffuse mesh that organizes in the cortical cytoplasm. Microfilaments are inserted into the plasma membrane at **adhesion plaques**, where cells attach to glass or other inert materials. As the cell moves, microfilament action causes the two major types of pseudopodia to move; for example, **lamellipodia**, which are broad, ruffled protrusions that slowly wave back and forth, and are the main locomotory organ, and **filopodia**, long thin, rod-like extensions that wave freely in the medium, provide guides for the direction of cell movement.

Microfilament Poisons

Cytochalasin D destabilizes microfilaments and is used experimentally to inhibit actin polymerization. Cells in culture treated with cytochalasin have reduced microfilaments and develop marked surface blebbing. Plasma membrane protein receptors are inhibited and phagocytosis and granule secretion, which depend on microfilament contraction, are suppressed. Not all types of secretion are affected; for example, in hepatocytes, secretion of lipoproteins is altered but not that of albumin. Exocytosis, which involves microtubular movement, is not inhibited and may even be enhanced.

Phalloidin, one of the toxins of the amanita mushroom, binds to actin, preventing microfilament depolymerization. It causes blebbing in cell culture by stabilizing microfilaments. Treatment leads to accumulation of microfilament networks at the base of each bleb or protrusion.[79] Cultured hepatocytes incubated with phalloidin have disruption of microfilaments that is reflected in and around biliary canaliculi, for example, pericanalicular vacuoles, abnormal microvilli, and blebs.[81,82]

Some microbial toxins act through effects on microfilaments. Bacteria of the genus *Clostridium* produce toxins which ADP ribosylate monomeric G actin thereby blocking **actin polymerization** and preventing microfilament formation. ADP-ribosylated actin acts as a capping protein that binds to the growing barbed ends of polymerizing F actin to further inhibit polymerization of remaining normal actin. In vitro *Clostridium perfringens* iota toxin and *C. botulinum* C2 toxin induce destruction of the microfilaments network, causing cells to become necrotic. Stress fibers disappear and large amounts of amorphous material are present in the cytoplasm.[83]

Linkage Protein Defects

Defects in proteins that link the cytoskeleton to the plasma membrane (or internal membranes) have been reported. Muscular dystrophy of the Duchenne type

Vet-ebooks.com

is caused by a defective gene, *dmd*, on the X chromosome. **Dystrophin**, the protein product of the *dmd* gene, is located on the sarcolemmal membranes of normal skeletal muscle but is absent from the skeletal muscle of humans with muscular dystrophy and from muscles of animals that have models of this disease;[84] for example, *xmd* dogs and *mdx* mice.

Dystrophin is a cytoskeletal linker protein located on the cytoplasmic face of the plasma membrane, where it anchors sarcolemmal proteins to the underlying cytoskeleton. Its absence is accompanied by loss of other important liner glycoproteins that are required for normal muscle functions. Ultrastructurally, degenerating muscle is characterized by separation of the cytoskeleton from membranes of the myocyte and disintegration of myocyte Z lines.

In *xmd* dogs the early change is dilatation of the sarcoplasmic reticulum. Although there are focal subsarcolemmal changes there is no significant sarcolemmal defect.[85] Later, as myocytes degenerate there are Z-band streaming and nemalin rods followed by necrosis of individual muscle cells.

X-linked muscular dystrophy of *mdx* mice is a mutation in the dystrophin gene similar to human Duchenne and Becker muscular dystrophies. Mutants show progressive skeletal muscle degeneration and regeneration, and have persistently increased levels of plasma creatine kinase and decreased dystrophin staining in skeletal muscle.[86]

Intermediate Filaments

These are 10 nm filaments (range: 8–10 nm), a diameter that distinguishes them from microfilaments (6 nm) and microtubules (23 nm). More than 30 different proteins are known to be capable of forming intermediate filaments (IFs); these form nearly identical 10 nm filaments by virtue of having a common α-helical rod domain with varying head and tailpieces.[87] Although IFs are structurally similar in different cells,[88] the proteins from which they are made fall into several distinct classes, each with specific biochemical reactivity: **keratin** in cells of epithelial origin, **vimentin** in mesenchymal cells, **desmin** in muscle cells, astrocyte **glial fibrillary protein**, and neuronal **neurofilament protein** (Table 4.2). Using specific antibodies against them, these different proteins can be localized in different cell types,[89,90] and are used to diagnose and classify highly malignant tumors whose histologic source is not obvious on routine microscopic examination.

Most IFs are formed from homopolymers of the appropriate protein. The keratins, however, are a group of over 20 proteins. In tissue development and growth these different proteins are switched on and off. Differentiation of keratinocytes in skin begins in basal cells that produce keratin types K5 and K14, which assemble into filaments. As differentiation and migration into the spinous layer begin, keratinocytes switch to production of differentiation-specific keratins K1 and K10, and intermediate filaments containing K1 and K10 replace those containing K5 and K14 as major intermediate filaments in the spinous layer. In the granular layer, non-intermediate filament proteins (filaggrin, loricrin) that promote keratin aggregation are produced.[91] Transglutaminases that catalyze formation of lysine cross-links in keratin are activated to induce the insoluble cornified keratin of the stratum corneum.

Plectin is a versatile cytoskeletal linker protein that preferentially localizes at interfaces between intermediate filaments and the plasma membrane. It is concentrated at sites of mechanical stress, such as hemidesmosomes in skin, sarcolemma and Z disk in skeletal muscle, and intercatalated disks in cardiac muscle. In muscle, plectin and desmin play vital roles in stabilzing the subsarcolemmal cytoskeleton.[92]

Hereditary Disorders Involving Intermediate Filaments

Intermediate filament defects have been found in keratin and in neurofilaments. In epidermis, intermediate filaments are composed of keratin. Two sequence types of keratins co-assemble into parallel, coiled-coil heterodimers, which then align as antiparallel tetramers. The assembled 10 nm intermediate filament is composed of four intertwined protofibrils.

Pathogenic mutations in **plectin** lead to simplex variety of epidermolysis bullosa, progressive myopathy, and myasthenic syndromes. Ultrastructural changes in muscle include myofibrial disarray, thick-filament loss, intranuclear nemaline rods, and vacuolar changes.[93]

Keratin Keratin intermediate filaments are ubiquitous constituents of cytoskeletons of epithelial cells. Over 30 different types of keratin chains have been grouped into two distinct sequence types: acidic type I and neutral-basic type II keratins. Keratin filaments are heteropolymers and require one chain of each sequence type. Each epithelial cell type typically expresses a defined pair of chains; for example, basal epithelial cells express keratin 5 (type II) and 14 (type I) chains. Suprabasal cells committed to terminal differentiation diminish expression of this pair and begin to express the keratin 1 (type II) and 10 (type I) pair of chains.

The hallmark of this heterogeneous group of cutaneous disorders known as **epidermolysis bullosa (EB)** is blister formation at sites of rubbing or trauma. EB is subclassified, based upon electron microscopic

Vet-ebooks.com

appearance of lesions, into simplex, junctional, and dystrophic types. In **dystrophic type EB**, blisters develop beneath the lamina lucida; the lesion is caused by defects in anchoring fibrils that arise from a mutation in the gene encoding type VII collagen, the major component of anchoring fibrils.

Simplex type EB results from fragile epidermal cells that arise from mutations of genes encoding keratin intermediate filaments proteins. Analysis of genes K5 and K14 from human simplex EB have revealed point mutations in the severest form of the disease (Dowling-Meara disease) and in the Koebner form. The mutation in one family of patients with the disease was mapped to chromosome 17, where the K14 gene is located. Blisters arise from degeneration of basal epithelium. Clumping of keratin intermediate filaments is the characteristic ultrastructural change in this form of EB.[94,95]

Point mutations in keratin 10 occur in **epidermalytic hyperkeratosis**, a skin disease characterized by keratin filaments clumping and degeneration of terminally differentiating suprabasal epidermal cells.[96,97] Other tissues are affected with defects in proteins of intermediate filaments. Cellular fragility of EB simplex basal keratinocytes closely resembles several syndromes of fragile erythrocytes, including hereditary spherocytosis, elliptocytosis, and pyropoikilocytosis, all of which involve fragile, misshapen cells.

Pemphigus vulgaris antigens have been localized ultrastructurally on keratinocytes of dogs.[98] Other rare genetic defects are known that involve abnormal intermediate filaments in skin. **Congenital icthyosis**, an inborn error of epidermal keratinization, is characterized by massive acanthosis that is present at birth. The defect involves depletion of keratohyalin granules, and ultrastructural analysis shows that normal keratin is diminished in affected individuals.[99,100] **Familial acantholysis** of Angus calves is characterized by shedding of epidermis due to an anomalous development of **tonofilaments** of the desmosome-tonofilament complexes. This allows detachment of intercellular junctions.[101] Accumulations of spherical particles in interstitial spaces, seen in rapidly growing tissues, are probably due to excess material shed in the remodeling of desmosomes and other junctions.

Nerve Cell Defects Large swollen neurons filled with neurofilament bundles and inclusions are typical of several toxic diseases of the central nervous system. Intoxication with **iminodipropionitrile** impairs slow axonal transport and causes segregation of neurofilaments from microtubules and other axoplasmic components.[102,103] Neurofibrillary abnormalities also occur in intoxication with aluminum chloride.[104]

Several hereditary diseases of the brain and spinal cord are associated with degeneration of neurons that develop aggregates of neurotubules and neurofilaments in the perikaryon or axons and dendrites, for example, **amyotrophic lateral sclerosis, Werdnig-Hoffmann disease**,[105] **familial motor neuron disease**,[106] and others.[107] In hereditary canine spinal muscular atrophy, chromolytic perikarya of motor neurons of the brainstem and ventral spinal cord show chromatolysis and accumulation of neurofibrils in dendrites and axons that appears to be a primary defect in the perikaryal cytoskeleton (Fig. 4.8).[108]

Defects in the Intestine Infants with **microvillous inclusion disease** have severe, intractable diarrhea associated with a congenital defective Na^+-K^+ exchange in the jejunal brush border. Ultrastructural examination of jejunal biopsies reveals that the intestine has markedly hypoplastic villi. Enterocytes have smooth apical surfaces and contain cytoplasmic inclusions.[109–111] There are few inflammatory cells in the lamina propria. The disease appears to be autosomal and recessive with high mortality.

Subsurface Cytoskeleton

A complex matrix system of filamentous and globular proteins is associated with the cytoplasmic face of the plasma membrane, where it forms a stabilizing structural meshwork to support the plasma membrane and link it to the cytoskeleton. In erythrocytes, which are used as a model to study skeletal proteins, a subsurface network made from the protein **spectrin** maintains the discoid shape of the cell[112,113] and is linked to transmembrane proteins in the plasma membrane. Electron microscopy of en face preparations of erythrocyte ghosts has clearly shown the spectrin meshwork and its stabilization by other linker proteins.

A family of spectrin-like molecules does the same in other cells.[114] Many of these proteins have been identified near the plasma membrane by immunogold staining.[115] In leukocytes, spectrin proteins control shape change and movement. They are stored in discrete groups in the trans-Golgi region that act as a reservoir for rapid distribution to the surface when the leukocyte is activated; that is, activation induces a rapid reorganization of spectrin and other linker proteins.

The submembrane cytoskeletal spectrin system is closely connected to actin molecules to form a **spectrin-actin complex**. Spectrin is a rod-shaped protein that associates with F-actin at each end. Spectrin and actin, together with accessory proteins, form a polygonal network. **Adducin** is a membrane-skeletal protein that promotes association of spectrin with actin, an interaction that is regulated by calcium/calmodulin.[116]

Vet-ebooks.com

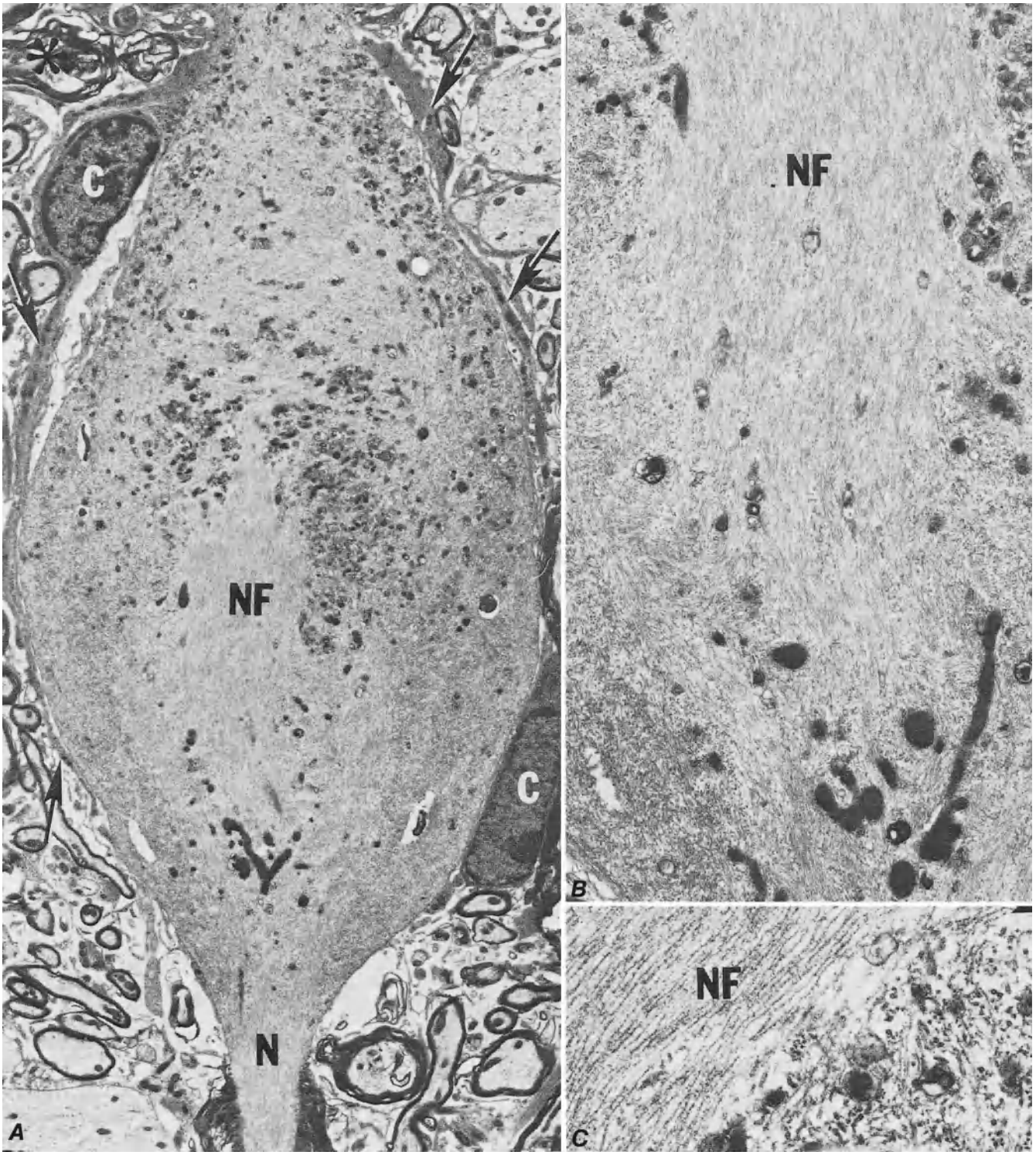


Fig. 4.8 Microfilament bundling, neuron: axonal swelling, internodal segment, canine spinal muscular atrophy. **A**. The myelinated axon is distended with massive accumulations of neurofilaments (*NF*). Mitochondria, vesicular material, and dense bodies are trapped in neurofilament masses; node of Ranvier (*N*), ensheathing cells (*C*), myelin debris (*), processes at margins of axonal swelling (*arrows*). Swollen zone is devoid of myelin. **B** and **C**. High magnification of neurofilaments (*NF*). (Micrographs: Linda C. Cork, *Lab Invest* 46:89, 1982.)

Vet-ebooks.com

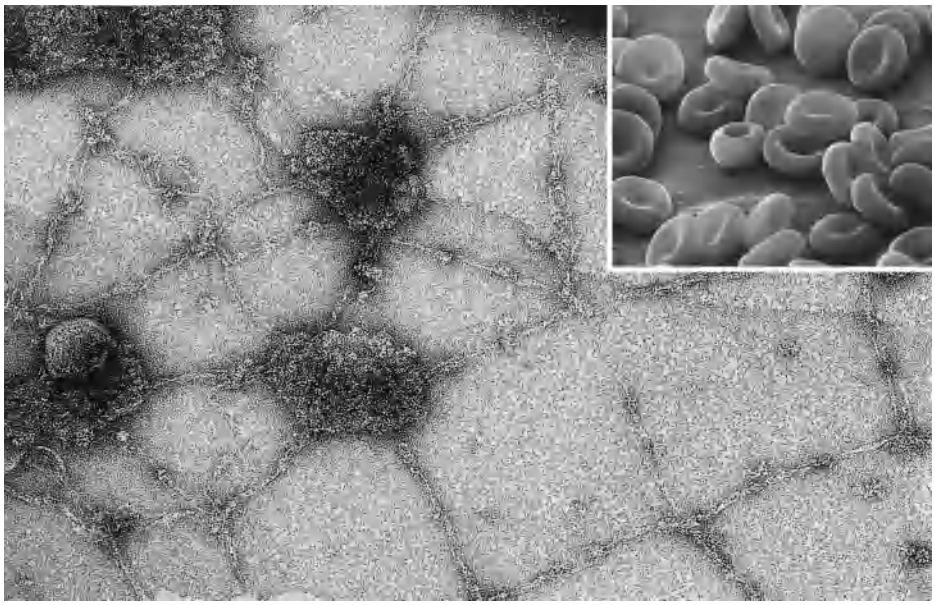


Fig. 4.9 Subsurface cytoskeleton: spectrin and associated proteins. (Micrograph: S-C Liu, *J Cell Biol* 104:527, 1987.) *Inset*: Normal mammalian discocytes.

The Spectrin-Actin Subcortical Cytoskeleton of Erythrocytes

The simplicity of the anucleate mammalian erythrocyte provides a model for plasma membrane structural change. Circulating erythrocytes have highly negative surface charges that prevent contact with endothelium, leukocytes, and platelets. The net negative charge is due to anionic sites such as neuraminic acid termini on glycoprotein carbohydrate moieties. The surface charge is altered by absorption of globins and other circulating macromolecules into the erythrocyte surface. Swelling and shrinking responses of mammalian erythrocytes to injury occur through change in the **plasma membrane** and its connections to the **subsurface cytoskeleton** (Fig. 4.9). Ultrastructural studies of the erythrocyte cytoskeleton show five or six extended spectrin molecules attached to each actin filament, together making up the structural form of the hexagonal spectrin-actin network.[117–119]

Spectrin-actin complexes form a highly specialized part of the cortical cytoskeleton that, because they are attached to the plasma membrane, endows the erythrocyte with both stability and flexibility (Fig. 4.10). It is the anastomosing network of spectrin that makes the erythrocyte sufficiently pliant to pass splenic and capillary channels less than half its diameter yet sufficiently durable to withstand turbulent passage through the heart.[120–123]

Spectrin-actin complexes are attached to transmembrane proteins in the lipid bilayer by specialized binding proteins, including ankyrin and band 4.1 protein. **Ankyrin** links spectrin to the cytoplasmic domain of the transmembrane anion exchange (band 3) protein. Ankyrins have been detected in many other cell types; for example, ankyrin purified from brain links spectrin-like proteins to transmembrane Na-K-ATPases. **Band 4.1 protein** is a second major attachment protein for spectrin. It binds spectrin to glycophorin A or to glycophorin C. Protein 4.1 is also widely distributed in nucleated cells, and is critical for nuclear assembly.[124] **Adducin** is a calcium/calmodulin-dependent binding protein in the erythrocyte that is part of the cytoskeleton. It forms stable complexes with spectrin-actin complexes and promotes binding of additional spectrin tetramers. Many other proteins have been identified that associate in some as yet unidentified way with the spectrin-actin meshwork.

Subsurface spectrin polymers determine the surface appearance of abnormal erythrocytes. If spectrin becomes highly polymerized and forms a rigid network, the cell will become a **spiculocyte**. At the other extreme, if spectrin tetramers disaggregate and become detached from the cytoplasmic face of the plasma membrane, the erythrocyte will lose its discoid shape and become a **spherocyte** (Fig. 4.11). **Spherocytes** have fragile membranes and **spiculocytes** (echinocytes) have exceptionally rigid, knobby membranes. Forces that change erythrocyte shape are related to ATP content and to intramembrane energy-requiring biochemical reactions that alter the cytoskeleton, transmembrane proteins, and phospholipid molecules of the plasma membrane; that is, the organelles that maintain the discoid shape of the cell.

Vet-ebooks.com

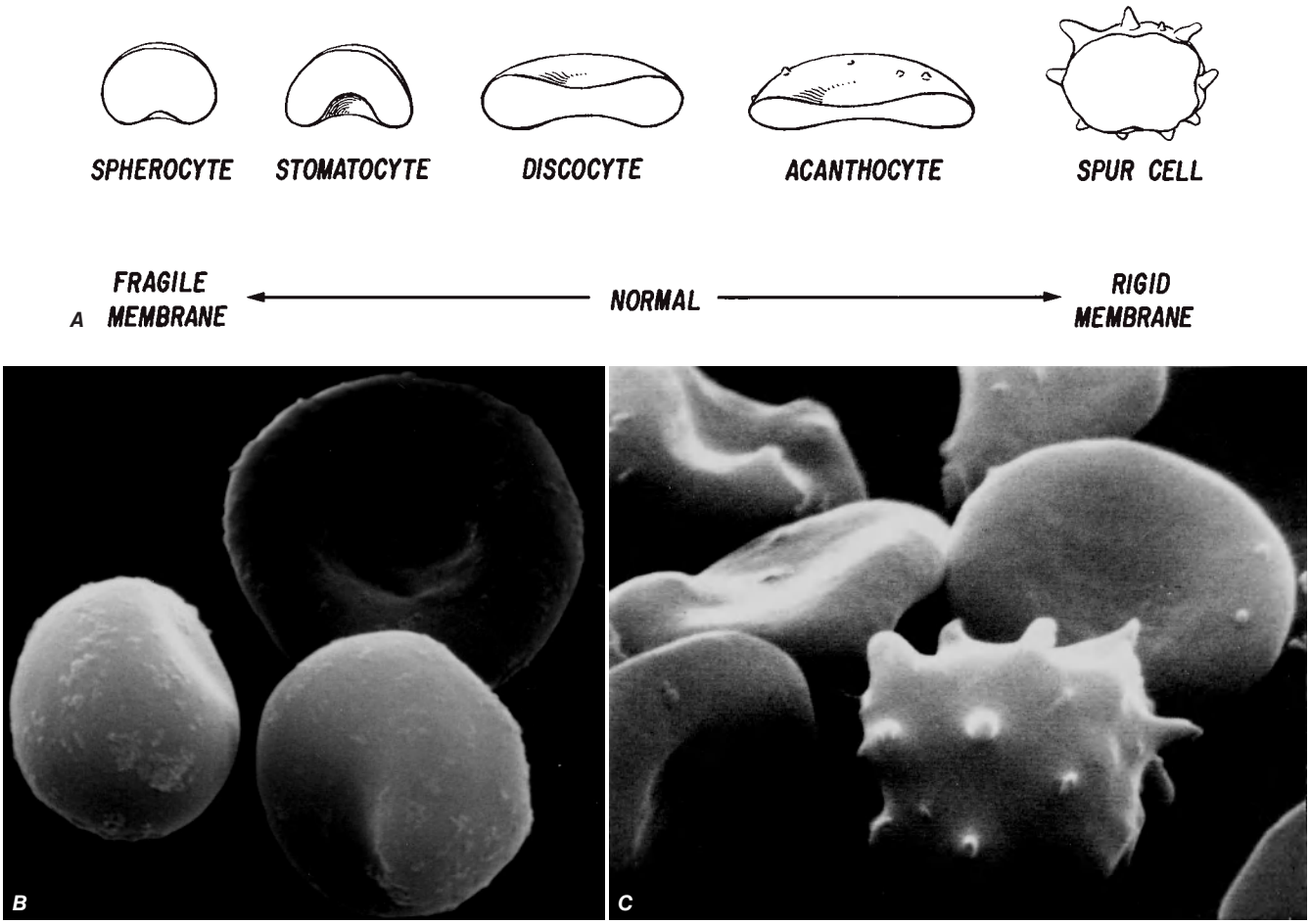


Fig. 4.10 Cell shape change: erythrocytes. **A**. **Spectrum of shape change**: based on alterations in plasma membrane rigidity. **B**. **Erythrocyte swelling**, scanning electron micrographs: relatively normal discocyte (*upper right*), spherocyte (*left*), and stomatocyte (lower right). **C**. **Spiculocytosis** (echinocytosis): spiculocyte (*bottom center*); other affected erythrocytes have surface knobs.

When an erythrocyte swells, it loses the discoid shape and becomes round (with less total diameter). If swelling is limited, the central depression of the normal discocyte remains visible on stained blood smears as a small slit and the cell is called a **stomatocyte**. Stomatocytes most often result from discrete abnormalities in the plasma membrane. Although spherocytosis can be seen in severe trauma (especially burns), it is most common in toxicity and in specific genetic diseases.

Congenital erythrocyte membrane defects may be associated with stomatocytosis. **Spectrin deficiency** with increased erythrocyte osmotic fragility is a hallmark of hereditary spherocytosis, a congenital hemolytic anemia in humans and animals.[125]

Drug-induced spherocyotisis or stomatocytosis results when drugs affect the inner and outer leaflets of the lipid bilayer differently. There is an asymmetric distribution of anionic phospholipids in the inner and outer parts of the lipid bilayer of the plasma membrane. Cationic drugs produce stomatocytosis, while anionic drugs cause crenation. Because the inner, cytoplasmic layer of the membrane is most negative, cationic compounds will locate there preferentially and expand the membrane to cause stomatocytosis. Venoms and bacterial toxins tend to produce erythrocyte **lysis** rather than changes in shape. Nevertheless, in small amounts, the **phospholipases** A_2, C, and D, and sphingomyelinase C that are common in biological toxins can produce stomatocytes (although hydrolysis with phospholipase A_2 typically causes crenation).[126]

Cytoskeleton-Plasma Membrane Linkage

Cytoskeletal filaments are linked to the plasma membrane by a specialized group of linkage molecules.[127] These molecules bind both to cytoskeletal proteins such as actin and spectrin and to proteins of the plasma membrane. By forming and breaking these bonds, the linker proteins control cell shape, stabilize

Vet-ebooks.com

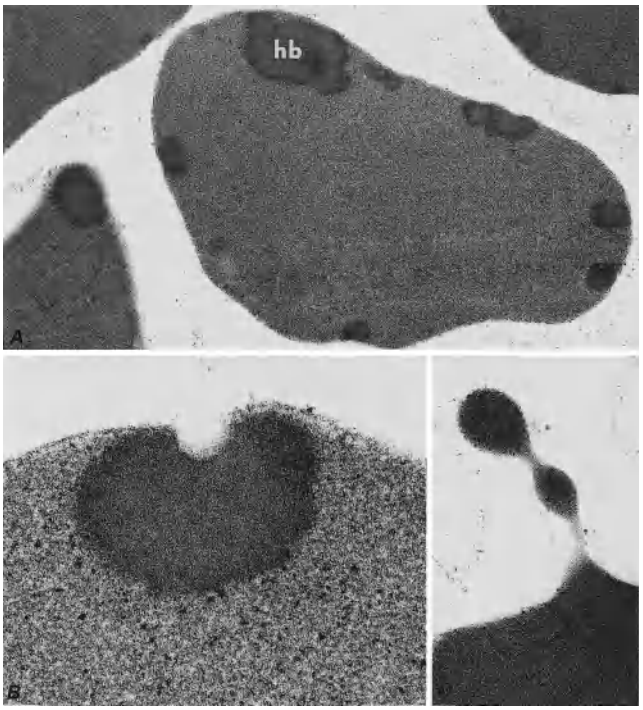


Fig. 4.11 Erythrocyte surface pathology. A. Precipitates of hemoglobin (*hb*), Heinz bodies. **B. Pitting of erythrocytes**. **C. Pseudopodium** (filopodium) at erythrocyte surface, uremia, dog.

attachments to other cells, and regulate cell movement and other cytoplasmic responses.[128] Identified by methods of protein chemistry, the precise cellular localization of linker proteins has been defined using immunogold techniques. Many linker proteins are found in tight junctions, desmosomes, and other intercellular junctions, structures that are readily identifiable ultrastructurally. Elsewhere, the extent and strength of the connections of filaments to the plasma membrane vary from the delicate "spot-welds" (such as those mediated by spectrin-band 4.1-ankyrin complexes) to the concentrated clusters of focal adhesion plaques.

Focal Adhesion Plaques

Adhesion plaques maintain cell-to-cell or cell-to-matrix adhesion. They appear as electron-dense foci on the cytoplasmic face of the plasma membrane. Most adhesion plaques are sites where termini of cytoplasmic microfilaments are bound to plasma membrane proteins called **integrins**. Within the plaque, actin of the microfilament binds to the cytoplasmic part of the integrin β subunit. The integrin-microfilament link is strengthened by special actin-binding proteins such as talin, vinculin, and α actinin.

Embedded in the plasma membrane, integrin molecules project outward from the cell, where they bind either to adjacent cells or to extracellular matrix proteins such as collagen and fibronectin.

The **integrin-adhesion complex** forms on another cell or to certain amino acid sequences on collagen, fibronectin, or other extracellular matrix proteins. Assembly and disassembly of focal adhesion plaques coordinate adhesion, migration, proliferation, and survival.[129] Adhesion kinases control focal adhesion plaque processes. They have unique functions in different tissues; for example, in epidermal barriers, they regulate plasma membrane localization of the actin-directed Na^+/H^+ exchanger 1.[130]

Epithelial cells form plaques to enhance tissue stability. A unique plaque on luminal cell surfaces of bladder epithelium stabilizes epithelium during bladder distention. Adhesion proteins that form these plaques, when identified by immunogold techniques, are composed of hexagonal arrays of 12 nm particles.[131]

Adhesion plaques are often transient. During migration, motile cells such as leukocytes develop focal adhesion plaques to temporarily stabilize binding to endothelial or epithelial cells or to components of the extracellular matrix. Cell adhesion molecules (CAMs) mediate events that form and maintain adhesion plaques, especially in their functions in tissue differentiation and development.[132]

Integrins Integrins are a large family of cell surface transmembrane receptors that mediate both cell-to-cell or cell-to-matrix interactions ("integrin" is coined from their role in **integrating** the cytoskeleton with the extracellular matrix). Integrins are heterodimeric glycoproteins composed of large α and small β chains. For example, the $\alpha_5\beta_1$ **integrin** is a fibronectin receptor that binds directly to cytoskeletal proteins. Three known families of integrins exist. The β chain is shared in common by all members of a family, but each has a different α chain. Extracellularly, the part of the integrin molecule that projects from the cell surface acts as a receptor to specifically bind its ligand. Inside the cell, the cytoplasmic part associates with talin, and other actin binding proteins complete the connection with the cytoskeleton.

The ligands for integrins are the **adhesion molecules**. Binding of integrin and ligand activates the cytoskeleton, a crucial event in phagocytosis and movement. Integrins bind to their ligands with varying specificity. The VLA glycoproteins, a subgroup of the integrin family, are receptors with monospecificity to individual connective tissue components. One member is multispecific; it promiscuously binds to collagen I and VI, fibronectin, and laminin.[133]

Cell-to-cell adhesion is highly regulated by adhesion molecules that act as nucleation points for multi-

Vet-ebooks.com

protein assemblies that cluster at cell contacts and link to the cytoskeleton. Opposing actions of protein tyrosine kinases and protein tyrosine phosphatases tune the level of tyrosine phosphorylation that controls the integrity of each assembly. The ectodomains of these molecules act as distance gauges that regulate the diameter of the intercellular space and thus control aspects of receptor signaling.[134]

Intercellular Junctions

Intercellular junctions play important coupling and regulatory roles in epithelium. The structure of the three major categories of junctions is closely related to their function (Fig. 4.12).

- **Tight junctions** are composed of two plasma membranes held together by interlinked rows of integral membrane proteins creating an impermeable seal.
- **Gap junctions** are circular foci of closely apposed plasma membranes that are spanned by integral membrane proteins organized into tubules that provide channels for intercellular communication.
- **Desmosomes** contain peripheral and integral membrane proteins that bridge the plasma membranes and connect internal cytoskeletons of adjacent cells.

Tight Junctions (Zonula Occludens)

Tight junctions (intercellular occluding junctions) appear in electron micrographs as a series of fusions of the external leaflets of plasma membranes of adjacent cells. Between epithelial cells, tight junctions prevent free passage of molecules across the epithelial barrier; that is, they control diffusion of ions and other small molecules through the intercellular spaces.[135,136] Specific proteins that form the tight junction have been localized in various tissues by use of immunogold techniques.[137] Cadherins and other cytoplasmic proteins are bound to termini of the cadherin cytoplasmic domain and regulate their function.[138]

In freeze fracture replicas, tight junctions appear as a net-like mesh of strands or grooves. In intestinal epithelia, tight junctions form a circular belt or gasket that prevents leaks and separates the plasma membranes of adjacent cells into two zones: apical and basolateral. This controls flow through the **paracellular pathway**, from lumen to intercellular spaces.[139] When the lumenal area of an epithelial surface is exposed experimentally to a solution of some marker material (such as the protein ferritin), the marker readily penetrates the intercellular space but is stopped by the intimate contact with the tight junction (Fig. 4.13).

The two plasma membranes of the tight junction are not simply adhered together but are actually fused at a series of points. Tight junction ridges are composed of two rows of tightly packed particles made of integral membrane proteins. Each row is contributed to by one of the adjacent plasma membranes. The rows of particles make head-to-head contact, like a zipper. Because these membrane proteins are interlocked the integral proteins embedded within the membrane cannot migrate; for example, membrane proteins of the lumenal surface membrane cannot migrate to the lateral surface.

Tight junctions maintain tissue integrity during extrusion of cells from epithelial surfaces. Villus tip extrusions zones on intestinal epithelium do not become leaky during loss of cells. Newly formed junctional areas form in zipper-type arrangements that are closed as extrusion occurs, and this prevents transepithelial leakage during extrusion.[140] In damaged epithelium, tight junction repair occurs rapidly so as to prevent fluid loss.[141]

Gap Junctions

Gap junctions (nexus, communicating junction) consist of two apposed plasma membranes (with a 2–3 nm gap) of neighboring cells that contain a closely packed array of cell-to-cell channels. These channels form aqueous pores (1.5–2 nm through the center) that permit the direct transfer of chemical messages between cells by allowing exchange of ions and small molecules. Gap junctions disappear and reform according to changes in cellular metabolism. They also increase on demands for increased function; for example, uterine smooth muscle gap junctions increase markedly immediately before parturition and decline rapidly thereafter. Assembly of gap junctions is closely related to changes in the cytoskeleton. Different tissues have different specific **gap junction proteins**, some in related families, others unrelated biochemically. The cell modulates the sieving nature of its gap junctions by closing or opening sets of channels with specific reactivity and diameters (rather than being simply composed of fixed dimension conduits).

Each gap junction channel is composed of two **connexons**, one from each membrane, aligned head to head across the gap. The connexon is shaped as a cylinder 7.5 nm in height and 7 nm in diameter. Each connexon has sixfold symmetry and consists of six identical protein subunits.[142,143] In effect, the subunit proteins of the connexon, which are arranged into hexamers, form intercellular pipes that bridge the spaces

Vet-ebooks.com

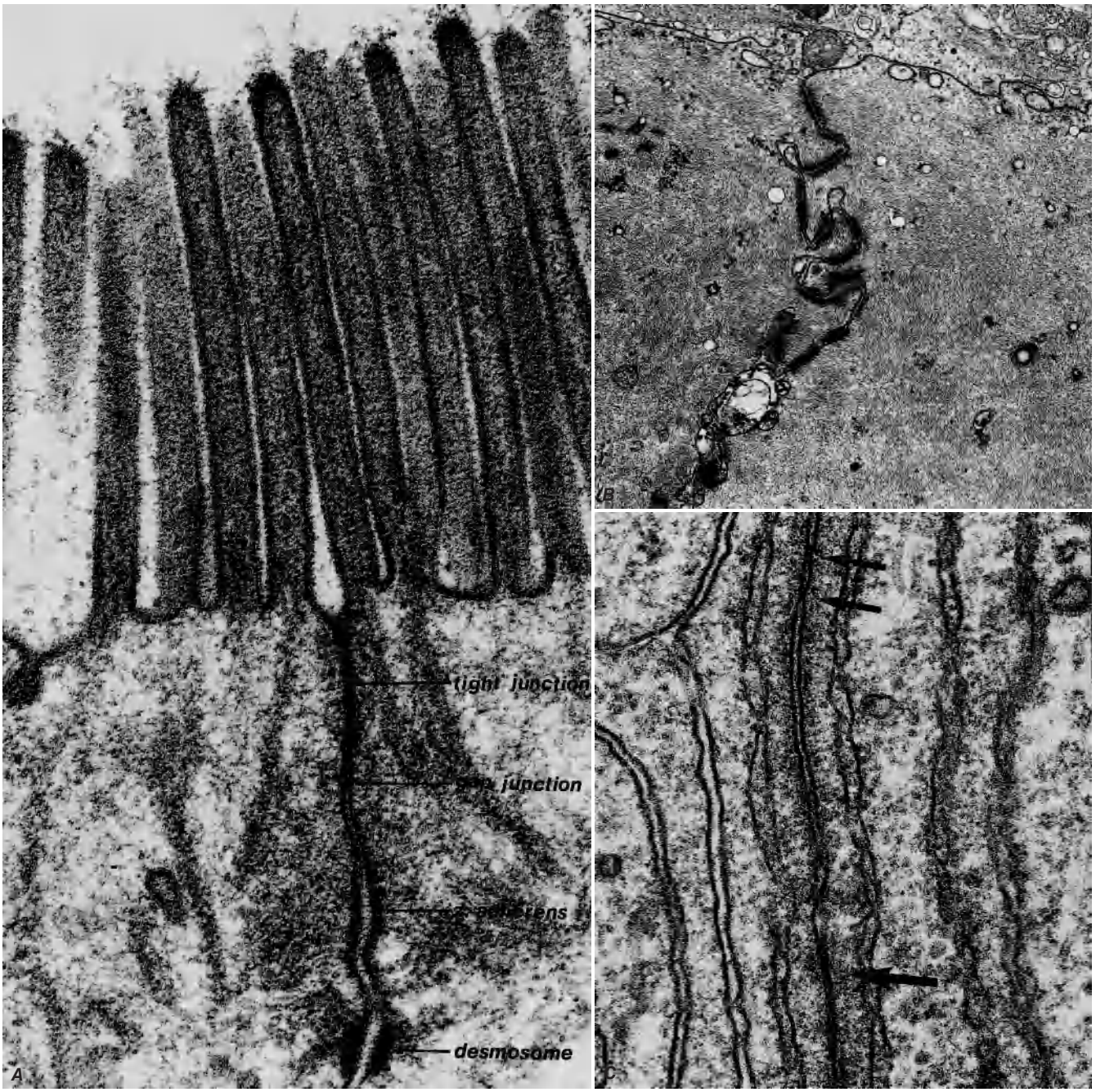


Fig. 4.12 Intercellular junctions. **A**. **Intercellular junction types** between intestinal epithelial cells. There is a close contact zone between two cells at the tight junction. Microvilli (with glycocalyx) at top. **B**. **Desmosomes**: disintegration and endocytosis of desmosomes, proliferative response in epithelium of oral mucosa, vesicular stomatitis, cow. **C**. **Gap and tight junctions**: gap junctions (*large arrow*) and tight junctions (*small arrows*), normal Sertoli cell plasma membrane (adjacent to a migrating spermatocyte), adult mink. Subsurface filaments and RER cisternae are present. (Micrograph: R.-Marc Pelletier, *Am J Anat* 183:68, 1988.)

between cells.[144] These models of gap junctions have been constructed with data from electron microscopy, x-ray diffraction, and Fourier-based three-dimensional reconstruction techniques. Gap junctions from hepatocytes, when analyzed using an atomic force microscope, have a thickness of 14.4 nm.[145]

Use of tracer molecules has shown that molecules up to 1,000 MW can pass from one cell to another through gap junctions. In this range are most sugars, amino acids, steroid hormones, and messenger molecules such as cyclic AMP. Groups of endocrine cells use gap junctions to coordinate release of hormones;

Vet-ebooks.com

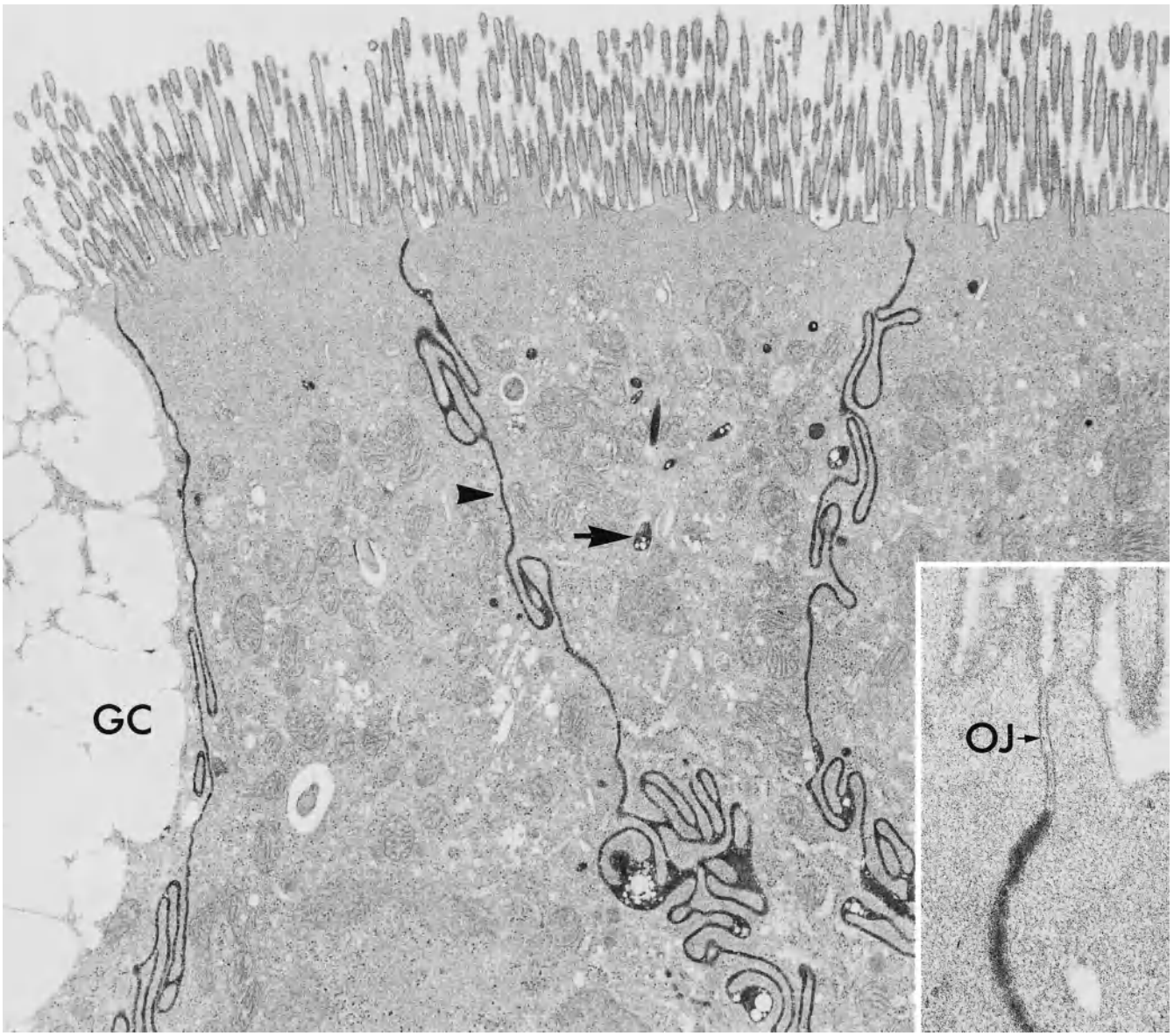


Fig. 4.13 Permeability of interepithelial spaces: intestine labeled with stain for horseradish peroxidase (HRP) used as a tracer molecule. The intercellular occluding (tight) junction separates the intestinal lumen from the paracellular space, serving as a barrier that restricts passive paracellular flow of ions. HRP is excluded from the paracellular space at the level of the occluding junction (*OJ*); goblet cell (*GC*), paracellular spaces (*arrowhead*), pinocytotic vesicles (*arrow*). (Micrograph: Manual Marcial and James Madera, *Lab Invest* 56:424, 1987.)

in pancreatic islets, there is an increased development of junctions between β-cells as insulin is released.[137] Intercellular communication via gap junctions enables cells to coordinate their activities and to respond uniformly to stimuli.

In the nervous system, axoaxonic gap junctions contribute to the generation of very fast network oscillations and hypersynchronous electrical activity of epilepsy.[146] In the eye, defects in genes for gap junction proteins in the cochlea are associated with deafness in humans and mice due to degeneration of the organ of Corti and impaired endocochlear potential, a K^+ diffusion electric potential generated across the apical membrane of the stria vascularis intermediate cells.[147]

Desmosomes

Desmosomes (macula adherens) are specialized intercellular junctions of polarized epithelial cells that provide strong intercellular mechanical coupling and anchoring sites for cytoskeletal intermediate filaments. The **cytoplasmic face** of the desmosome contains a dense plate containing the specialized adherence molecules that cause strong cell-to-cell cou-

Vet-ebooks.com

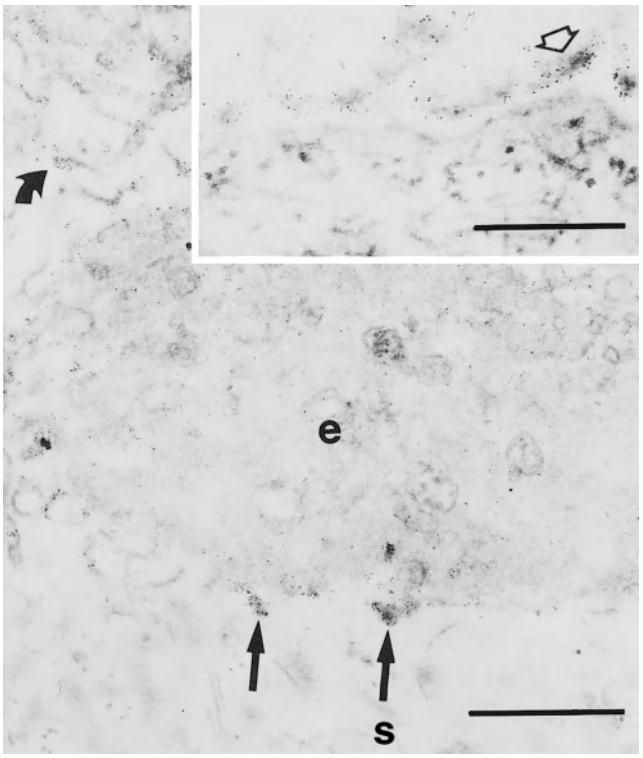


Fig. 4.14 Transmembrane extracellular matrix receptor: receptor is of the integrin family of $\alpha_6\beta_4$ localized with immunogold techniques to the hemidesmosome; antiserum was against the β_4 subunit. Gold particles are grouped in patches along the region of epithleial cell-connective tissue interaction (*straight arrows*). Gold particles also occur along the convoluted apical and lateral surfaces (*curved arrow*); bar = 1.0 μm. *Inset*: Intact hemidesmosomes labeled with gold particles (*open arrow*); bar = 0.5 μm. (Micrograph: Michelle A. Kurpakus, *J Cell Biol* 115:1737, 1991.)

pling (Fig. 4.14). In epidermis, proteins antigenically related to nuclear lamins (that bind intermediate filaments to the nuclear envelope) have epitopes that bind to vimentin.[148–150] The **intercellular space** in the desmosome contains central, dense lamellae composed of neuraminidase-resistant glycoproteins. Ultrastructurally, the space contains central, dense lamellae composed of glycoproteins. At high magnifications, it can be seen as a zigzag structure with lateral extensions to the outer surface of the plasma membrane. Polypeptides of desmosomes include **plakoglobin**, the common plaque protein of intercellular adhering junctions; **desmoplakins** I and II, which are restricted to desmosomal plaques; **desmoglein**; **desmocollins** I and II, which are located in viscous collagenous glue of the desmoglea; and a calcium-binding protein.[151,152]

Variants of desmosomal arrangements that form cytoskeletal filament-anchoring junctions in epithelia include the following:

- **Belt desmosomes** (zonula adherens) form a band of 7 nm filaments that link adjacent epithelial cells just below tight junctions; the filaments contain actin, and the area containing belt desmosomes contracts in the presence of ATP.
- **Spot desmosomes** are button-like points of contact between plasma membranes; their filaments, unlike those of belt desmosomes, contain larger, 10 nm tonofilaments, which do not contract, but offer tensile strength and structural frameworks for the cytoplasm.
- **Focal adhesions** link the cell and the extracellular matrix, and act in anchorage, migration, and detection of physical cues in the environment. In normal cells, integrins drive much of the activity of focal adhesions, and many integrin-regulated linkages exist to active FAK or Src, both of which function to promote cell cycle progression and motility.
- **Focal adhesion kinase** (FAK), a component of focal adhesion structures, controls the epidermal permeability barrier by the post-transcriptional regulation of acidification.[153] Acidification, in turn, regulates important functions. FAK alters barrier homeostasis by regulation of actin-directed Na^+/H^+ exchanger 1 plasma membrane localization. FAK plays critical roles in resealing interendothelial junctions after the transient openings of liquid flux from blood to tissue.[154] The FAK promoter contains p53-binding sites allowing FAK to play a major role in mitosis, and thus in cancer.[155]

Hemidesmosomes

Hemidesmosomes (half-desmosomes) are plaques along basal plasma membranes that link epithelial cells to underlying connective tissue. Intermediate filaments attach to the periphery of the plaque and extend into the cytoplasm. Anchoring fibrils traverse from the plaque's outer membrane to the lamina densa of the basement membrane.[156]

Hemidesmosomes have protein components that differ from desmosomes. Immunoelectron microscopy has topographically identified three proteins to cutaneous hemidesmosomes: **bullous pemphigoid antigen 1**, a noncollagenous protein within the keratinocyte (and an autoantigen in the blistering disease bullous pemphigoid); **bullous pemphigoid antigen 2**, a transmembrane collagenous protein that is also an autoantigen; and $\alpha_6\beta_4$ **integrin**, which is in the extracellular space, polarized to the underside of epidermal keratinocytes on the surface adjacent to the basement membrane.

The dense plaque area of the hemidesmosome contains other integrins, all of which have adhesive functions for the keratinoctye. In stratified squamous cell hemidesomsomes, the $\alpha_6\beta_4$ complex is a major compo-

Vet-ebooks.com

nent, playing a critical role in assembly and adhesive functions of this junction.[157–159]

Surface Structures

Cilia

Cilia are cellular projections whose beating generates fluid flow in the respiratory and genital tracts. In the respriatory tract, **motile cilia** operate in a seromucous environment working like oars, with alternating power and recovery strokes generating force that moves fluid and particular material in the direction perpendicular to the cilium's axis.

Primary cilia, nonmotile cilia present as a single copy on surfaces of most cell types, lack both the central microtubule pair and dynein arms. They function as antenna-like structures to probe the extracellular environment for molecules that are recognized by the receptors that these cilia bear. This sensory function coordinates intercellular signaling pathways that control growth and differentiation. Primary cilia regulate (and are required for) the **sonic hedgehog** (Shh), the protein of a fundamental signaling system throughout vertebrate development.[160] Mutations in genes encoding proteins essential for cilia assembly (such as the intraflagellar transport proteins) lead to dysfunctional Shh signaling and severe developmental disorders.[161] The basal body that assembles primary cilia is derived from the mature centriole, a component of the centrosome, and centriole-associated proteins.[162]

Mutations in genes for components of cilia underlie some diseases. Cilia in brains of human patients with Bardet-Bidel syndrome have a mutation in one of the BBS genes that underlies cilia abnormalities and related retinal degeneration.[163]

Immotile Cilia Syndromes

Immotile cilia syndromes are a heterogenous group of human ciliary dysfunction diseases. Patients have recurrent respiratory tract infections, abnormal sperm, and **situs inversus totalis**, defects that are all related to abnormal cilia. In the respiratory tract the accumulation of mucus, cellular debris, and inhaled particles that occurs because of failure in the coordinated beat of cilia leads to rhinitis, bronchitis, and sinusitis. Otitis media results from obstruction of the ciliated eustachian tube. Defects in cilia identified ultrastructually in human immotile cilia syndrome include deficiencies in the dynein arms, radial spokes, the nexins, and radial spoke defect, transposition of microtubules, and supernumerary microtubules (see Fig. 4.7). Ciliary destruction is produced by severe inflammatory disease of any cause, and the finding of one well-preserved normal cilium is sufficient to exclude the diagnosis of complete dynein arm defect. **Ciliary aplasia** may be found in lesions of severe inflammation, especially if squamous metaplasia is present.

Typical immotile cilia have outer dynein arm defects, whereas other lesions are associated with asynchronous ciliary beating. Dyneins, a family of ATPases that cause the microtubule sliding in cilia and flagellar axonemes, are critical to normal function. The **dynein arm defect** is the most prevalent defect. In the complete dynein defect, cilia lack the inner and outer dynein arms. A partial dynein defect may be a lack of outer or inner dynein arm.

In the **radial spoke defect** there is disorganization of the spoke linkage and disorientation of the central core of cilia. This defect can be identified by the eccentric position of the central core and there may be displacement of one of the outer microtubular doublets toward the center of the cilium. It is difficult to establish since radial spokes cannot be reliably seen even when present in normal tissues.

In the **microtubular transposition defect**, the central core above the axosomal region is abnormal or missing, and one of the outer doublet tubules is transposed to the central regions. This defect is commonly found in inflammation, and the diagnosis of the primary defect must be carefully confirmed. Immotile cilia syndromes have been reported in animals, especially in dogs[164] and a mutant strain of rats, WIC-Hyd (see Fig. 4.7).

Microvilli

Microvilli line the lumenal surfaces of epithelial cells of the gastrointestinal tract, tubular parts of the genital tracts, and free surfaces of proximal convoluted tubules of the kidney (as the brush border). The brush border surface also consists of **membrane invaginations** between microvilli, the only part of the apical surface sterically accessible for membrane fusion and budding events; many of these invaginations appear as pleiomorphic, deep apical tubules that extend up to 0.5–1 μm into the terminal web region of the cell.

Actin filamentous webs form the center of the microvillus. Driven by their motor myosin and connections to the cell cytoplasm, actin filaments cause microvillous retraction and expansion. In hypertension (and other vascular pressure changes) and inflammation, these membrane components and actin filament retract and move with striking rapidity.[165]

Because of their high throughput of absorptive functions, membranes of microvilli are organized in cholesterol/sphingolipid-rich microdomains commonly referred to as lipid rafts. Plasma membranes of the microvillus contain specific receptor, ion pump, and transport proteins that have been identified ultra-

Vet-ebooks.com

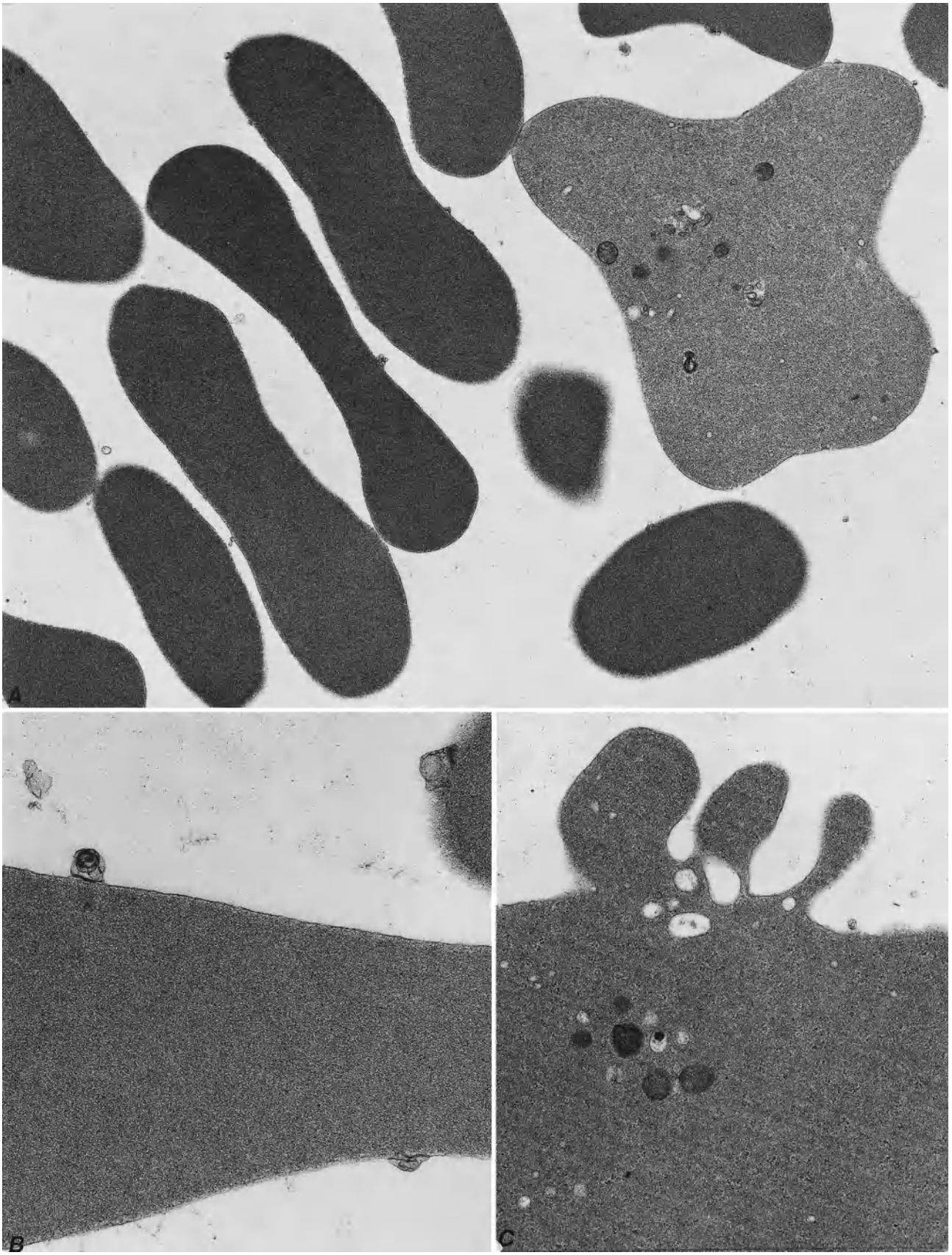


Fig. 4.15 Erythrocyte surface pathology. **A** and **B**. **Surface membrane remnants**: pyruvate kinase deficiency, Basenji dog. **C**. **Pseudopod formation**: vesicles and internalization, cortisone therapy for lymphosarcoma, cat.

Vet-ebooks.com

structurally with immunogold techniques. **Intelectin** is a D-galactosyl-specific lipid raft lectin that acts as an organizer and stabilizer of the brush border membranes to prevent loss of digestive enzymes in the gut lumen and to protect glycolipid microdomains from pathogens.[166] **Antiglycosyl antibodies**, major group of proteins associated with the enterocyte brush border membrane, have been identified by immunogold techniques; they too, protect the lipid raft microdomains against pathogens; for example, cholera toxin entry into pig enterocytes occurs via a lipid raft- and clathrin-dependent mechanism.[167,168]

Filopodia and Lamellipodia

The leading edge of migrating cells is formed from two types of actin cytoskeletal projections, lamellipodia and filopodia. **Filopodia** are slender, filamentous pseudopodia with pointed ends that are often branched. Filopodia are actin-rich finger-like protrusions at the leading edge of migrating cells that provide directional sensing for movement. Myosin-X (myoX), the N-terminal domain of which functions as a motor, promotes formation of filopodia.[169] MyoX moves toward the tips of filopodia and transports cargo molecules. **Lamellipodia** are broad, sheet-like extensions of cytoplasm that form transient adhesions with the cell substrate and move, allowing migration along the substrate. In abnormal cells, aberrant surface changes markedly distort these appendages (Fig. 4.15).

References

1. Daleke DL, Huestis WH. 1989. Erythrocyte morphology reflects the transbilayer distribution of incorporated phospholipids. *J Cell Biol* 108:1375.
2. van Genderen IL, et al. 1991. Subcellular localization of Forssman glycolipid in epithelial MDCK cells by immuno-electronmicroscopy after freeze-substitution. *J Cell Biol* 115:1009.
3. Stromberg N, et al. 1991. Saccharide orientation at the cell surface affects glycolipid receptor function. *Proc Natl Acad Sci USA* 88:9340.
4. Grassmé H, et al. 2007. Biological aspects of ceramide-enriched membrane domains. *Prog Lipid Res* 46:161.
5. Gulbins E. 2003. Regulation of death receptor signaling and apoptosis by ceramide. *Pharmacol Res* 47:393.
6. Robenek H, et al. 1982. The topography of filipin-cholesterol complexes in the plasma membrane of cultured hepatocytes and their relation to cell junction formation. *J Ultrastruc Res* 78:95.
7. Kunz A, et al. 1985. Ultrastructural localization of glycocalyx domains in human kidney podocytes using the lectin-gold technique. *Lab Invest* 53:413.
8. Roth J, et al. 1983. Regional distribution of N-acetyl-D-galactosamine residues in the glycocalyx of glomerular podocytes. *J Cell Biol* 96:1189.
9. Coleman RA, et al. 2006. Use of anti-fluorophore antibody to achieve high-sensitivity immunolocalization of transporters and ion channels. *J Hist Cyt* 54:817.
10. Pollanen J, et al. 1988. Ultrastructural localization of plasma membrane-associated urokinase-type plasminogen activator at focal contacts. *J Cell Biol* 106:87.
11. van Deurs B, Behnke O. 1980. Membrane structure of nonactivated and activated human blood platelets as revealed by freeze fracture: evidence for particle redistribution during platelet contraction. *J Cell Biol* 87:209.
12. Coleman SE, et al. 1976. Plasma membrane changes in freeze-fractured rat kidney cortex following renal ischemia. *Lab Invest* 35:63.
13. Marcial MA, Madara JL. 1987. Analysis of absorptive cell occluding junction: Structure-function relationships in a state of enhanced junctional permeability. *Lab Invest* 56:424.
14. Sieber JJ, et al. 2007. Anatomy and dynamics of a supermolecular membrane protein cluster. *Science* 317:1072.
15. White SH. 2007. Crowds of syntaxins. *Science* 317:1045.
16. Aricescu AR, et al. 2007. Structure of a tyrosine phosphatase adhesive interaction reveals a spacer-clamp mechanism. *Science* 317:1217.
17. Pasquale EB. 2008. Eph-Ephrin bidirectional signaling in physiology and disease. *Cell* 133:38.
18. Fu D, Lu M. 2007. The structural basis of water permeation and proton exclusion in aquaporins (Review). *Mol Membr Biol* 24:366.
19. Kawedia JD, et al. 2007. Interaction between transcellular and paracellular water tranport pathways through aquaporin 5 and the tight junction complex. *Proc Natl Acad Sci USA* 104:3621.
20. Shields SD, et al. 2007. Anatomical and functional analysis of aquaporin 1, a water channel in primary afferent neurons. *Pain* 131:8.
21. Kumar M, et al. 2007. Highly permeable polymeric membranes based on the incorporation of the functional water channel protein aquaporin Z. *Proc Natl Acad Sci USA* 104:20719.
22. Bendayan R, et al. 2006. In situ localization of P-glycoprotein (ABC1S1) in human and rat brain. *J Hist Cyt* 54:1159.
23. Marxer A, et al. 1989. (Na^+ + K^+)-ATPase and plasma membrane polarity of intestinal epithelial cells. *J Cell Biol* 109:1057.
24. Sztul ES, et al. 1987. Localization of the Na^+,K^+-ATPase α-subunit to the sinusoidal and lateral but not canalicular membrane of rat hepatocytes. *J Cell Biol* 104:1239.
25. Kashgarian M, et al. 1980. Amplification of cell membrane surface in potassium adaptation. *Lab Invest* 42:581.
26. Nermut MV et al. 1988. Electron microscopy and structural model of human fibronectin receptor. *EMBO J* 7:4093.

Vet-ebooks.com

27. Kawai T, Akira S. 2007. SnapShot: Pattern-recognition receptors. *Cell* 129:1024.
28. Hafenstein S, et al. 2007. Asymmetric binding of transferrin receptor to parvovirus capside. *Proc Natl Acad Sci USA* 104:6585.
29. Ranganathan Rl 2007. Signaling across the cell membrane. *Science* 318:1253.
30. Oyasu M, et al. 2007. Immunogold electron microscopic demonstration of distinct submembranous localization of the activated (gamma)PKC depending on the stimulation. *J Hist Cyt* 56:253.
31. Nagamatsu S, Ohara-Imaizumi M. 2007. IP7 debut in insulin release. *Science* 318:1249.
32. Hadders MA, et al. 2007. Structure of C8α-MACPF reveals mechanism of membrane attack in complement immune defence. *Science* 317:1552.
33. Biesecker G. 1983. Membrane attack complex of complement as a pathologic mediator. *Lab Invest* 49:237.
34. Tranum-Jensen J, Bhakdi S. 1983. Freeze-fracture analysis of the membrane lesions of human complement. *J Cell Biol* 97:618.
35. Podack ER, Konigsberg PJ. 1984. Cytotoxic T-cell granules. *J Exp Med* 160:695.
36. Dennert G, Podack ER. 1988. Cytolysis by H-2-specific T killer cells. *J Exp Med* 157:1483.
37. Hickey WF, et al. 1992. Exogenously induced natural killer cell-mediated neuronal killing. *J Exp Med* 76:811.
38. Schmidt RE, et al. 1990. Ultrastructural and immunohistochemical characterization of guanethidine induced destruction of peripheral sympathetic neurons. *J Neuropathol Exp Neurol* 49:150.
39. Melhorn HG, et al. 1983. The action of polyether ionophorous antibiotics (monensin, salinomycin, lasolacid) on developmental stages of *Eimeria tenella*. *Zt Parasitenkunde* 69:457.
40. Smith CK, GAlloway RB. 1983. Influence of monensin on cation influx and glycolysis of *Eimeria tenella* sporozoites in vitro. *J Parasit* 69:666.
41. Ward RJ, Leonard K. 1992. The *Staphylococcus aureus* α-toxin channel complex and the effect of Ca^{2+} ions on its interaction with lipid layers. *J Struct Biol* 109:129.
42. Bhakdi S, et al. 1981. Staphylococcal α-toxin. *Proc Nat Acad Sci USA* 78:5475.
43. Bhakdi S, Tranum-Jensen J. 1988. Damage to cell membranes by pore-forming bacterial cytolysins. *Prog Allergy* 40:1–43.
44. Fussle R, et al. 1988. On the mechanisms of membrane damage by *Staphylococcus aureus* α toxin. *J Cell Biol* 91:83.
45. Nichols BA, et al. 1983. Secretion from the rhoptries of *Toxoplasma gondii* during host-cell invasion. *J Ultrastruc Res* 83:85.
46. Young J, et al. 1982. Characterization of a membrane pore-forming protein from *Entamoeba histolytica*. *J Exp Med* 156:1677.
47. Andrews NW, et al. 1990. A *T. cruzi* secreted protein immunologically related to the complement component C9. *Cell* 61:1277.
48. Crawford I, et al. 1991. Immunocytochemical localization of the cystic fibrosis gene product CFTR. *Proc Natl Acad Sci USA* 88:9262.
49. Welsh MJ, Smith AE. 1993. Molecular mechanisms of CFTR chloride channel dysfunction in cystic fibrosis. *Cell* 73:1251.
50. Heuser JE, Kirchner MW. 1980. Filament organization revealed in platinum replicas of freeze dried cytoskeleton. *J Cell Biol* 86:212.
51. Wehland J, et al. 1983. A rat monoclonal antibody reacting specifically with the tyrosylated form of a-tubulin. *J Cell Biol* 97:1467.
52. Mandelkow E-M, et al. 1991. Microtubule dynamics and microtubule caps: a time-resolved cryo-electron microscopy study. *J Cell Biol* 114:977.
53. Jensen CG, Smaill BH. 1986. Analysis of the spatial organization of microtubule-associated proteins. *J Cell Biol* 103:559.
54. Wille H, et al. 1992. Domain structure and antiparallel dimers of microtubule-associated protein 2 (MAP2). *J Struct Biol* 108:49.
55. Reaven E, et al. 1983. Unique microtubules in luteal cells from superovulated rats. *J Ultrastruc Res* 83:284.
56. Hirokawa N, et al. 1983. Mechanism of brush border contractility studied by the quick-freeze, deep-etch method. *J Cell Biol* 96:1325.
57. Mizuno N, et al. 2007. Three-dimentional structure of cytoplasmic dyenin bound to microtubules. *Proc Natl Acad Sci USA* 104:20832.
58. Pavelka M, Ellinger A. 1983. Effect of colchicine on the Golgi complex of rat pancreatic acinar cells. *J Cell Biol* 97:737.
59. Nanci A, et al. 1987. The effects of vinblastine on the secretory ameloblasts. *Anat Rec* 219:113.
60. Magalhaes MC, et al. 1985. Effects of vinblastine and cochicine on the rat adrenal cortex. Morphometric and cytochemical studies. *J Ultrastruc Res* 91:149.
61. Nevalainen TJ. 1975. Cytotoxicity of vinblastine and vincristine to pancreatic acinar cells. *Virch Arch* 18:119.
62. Hodgkinson JL, et al. 1992. X-ray solution scattering studies on vinblastine-induced polymers of microtubule protein: structural characterisation and effects of temperature. *J Struct Biol* 109:28.
63. Schochet SS Jr, et al. 1968. Neuronal changes induced by intrathecal vincristine sulfate. *J Neuropathol Exp Neurol* 27:645.
64. Hausmann K, et al. 1983. The effects of taxol on microtubular arrays. In vivo effects on heliozoan axonemes. *J Ultrastr Res* 82:212.
65. Schochet SS JR, et al. 1969. Intraneuronal conglomerates in sporadic motor neuron disease: A light and electron microscopic study. *Arch Neurol* 20:548.
66. Terry RD, Pena C. 1965. Experimental production of neurofibrillary degeneration. 2. Electron microscopy, phosphatase histochemistry and electron probe analysis. *J Neuropathol Exp Neurol* 24:200.
67. Wisniewski H, et al. 1968. Effects of mitotic spindle inhibitors on neurotubules and neurofilaments of anterior horn cells. *J Cell Biol* 38:224.
68. Wisniewski H, Terry RD. 1967. Experimental colchicine encephalopathy. I. Induction of neurofibrillary degeneration. *Lab Invest* 17:577.

Vet-ebooks.com

69. Janota I. 1972. Ultrastructural studies of an hereditary sensory neuropathy in mice (dystonia musculorum). *Brain* 95:529.
70. Heath E, et al. 1985. Microtubular mass defect of spermatozoa in the stallion. *Am J Vet Res* 46: 1121.
71. Mierau GW, et al. 1992. The role of electron microscopy in evaluating ciliary dysfunction: report of a workshop. *Ultrastr Pathol* 16:245.
72. Torikata C, et al. 1991. Ultrastructure of respiratory cilia of WIC-Hyd male rats. *Am J Pathol* 138:341.
73. Afzelius BA, et al. 1975. Lack of dynein arms in immotile human spermatozoa. *J Cell Biol* 66:225.
74. Afzelius BA, Eliasson R. 1979. Flagellar mutants in man: on the heterogenetity of the immotile-cilia syndrome. *J Ultrastruc Res* 69:43.
75. Sturgess Jm, et al. 1980. Transposition of ciliary microtubules. Another cause of impaired ciliary motility. *New Engl J Med* 303:318, 1980.
76. Wu JI, Crabtree GR. 2007. Nuclear actin as choreographer of cell morphology and transcription. *Science* 316:1710.
77. Ono S. 2007. Mechanism of depolymerization and severing of actin filaments and its significance in cytoskeletal dynamics. *Int Rev Cytol* 258:1.
78. Romero S, et al. 2007. How ATP hydrolysis controls filament assembly from profilin-actin. *J Biol Chem* 282:8435.
79. Hartwig JH, et al. 1989. Association of profilin with filament free regions of human leukocyte and platelet membranes and reverse membrane-binding during platelet activation. *J Cell Biol* 109:1571.
80. Prentki M, et al. 1979. Actin microfilament, cell shape, and secretory processes in isolated rat hepatocytes. Effect of phalloidin and cytochalasin D. *J Cell Biol* 81:592.

81 Russo MA, et al. 1982. Ultrastructural pathology of phalloidin-intoxicated hepatocytes in the presence and absence of extracellular calcium. *Am J Pathol* 109:133.

82. Watanabe S, Phillips MJ. 1986. Acute phalloidin toxicity in living hepatocytes. *Am J Pathol* 122:101.
83. Reuner KH, et al. 1987. Botulinum C2 toxin ADP-ribosylates actin and disorganizes the microfilament network in intact cells. *Eur J Cell Biol* 43:134.
84. Bonilla E, et al. 1988. Duchenne muscular dystrophy: deficiency of dystrophin of the muscle cell surface. *Cell* 54:447.
85. Valentine BA, et al. 1990. Canine X-linked muscular dystrophy: morphologic lesions. *J Neurol Sci* 97:1.
86. Wakayama Y, Shibuya S. 1990. Observations on the muscle plasma membrane-associated cytoskeleton of mdx mice by quick-freeze, deep-etch, rotary-shadow replica method. *Acta Neuropathol* 80:618.
87. Birkenberger L, Wallace I. 1990. Properties of desmin tail domain. *J Cell Biol* 111:2063.
88. Steinert PM, et al. The molecular biology of intermediate filaments. *Cell* 42:411, 1985.
89. Rappersberger K, et al. 1990. Immunogold staining of intermediate-sized filaments of vimentin type in human skin. *J Invest Derm* 94:700.
90. Tokuyasu KT, et al. 1983. Immunoelectron microscopic studies of desmin (skeletin) localization and intermediate filaments organization in chicken skeletal muscle. *J Cell Biol* 96:1727.
91. Mehrel T, et al. 1990. Identification of a major keratinocyte cell envelope protein, loricrin. *Cell* 61:1103.
92. Hijikata T, et al. 2003. Plectin tethers desmin intermediate filaments onto subsarcolemmal dense plaques containing dystrophin and vinculin. *Histochem Cell Biol* 119:109.
93. Banwell BL, et al. 1999. Myopathy, myasthenic syndrome, and epidermolysis bullosa simplex due to plectin deficiency. *J Neuropathol Exp Neurol* 58:832.
94. Coulombe PA, et al. 1991. A function for keratins and a common thread among different types of epidermolysis bullosa simplex diseases. *J Cell Biol* 115:1661.
95. Epstein EH Jr. 1992. Molecular genetics of epidermolysis bullosa. *Science* 256:799.
96. Cheng J, et al. 1992. The genetic basis of epidermolytic hyperkeratosis: a disorder of differentiation-specific epidermal keratin genes. *Cell* 70:811.
97. Chipev CC, et al. 1992. A leucine → proline mutation in the H1 subdomain of keratin 1 causes epidermolytic hyperkeratosis. *Cell* 70:821.
98. Suter MM, et al. 1990. Ultrastructural localization of pemphigus vulgaris antigen on canine keratinocytes in vivo and in vitro. *Am J Vet Res* 51:507.
99. Arnold M-L, et al. 1988. Icthyosis congenita type III. Clinical and ultrastructural charactersitics and distinction within the heterogeneous icthyosis congenita group. *Arch Dermatol Res* 280:268.
100. Dale BA, et al. 1990. Heterogeneity in Harlequine icthyosis, an inborn error of epidermal keratinization. *J Invest Derm* 94:6.
101. Jolly RD, et al. 1973. Familial acantholysis of Angus calves. *Vet Pathol* 10:473.
102. Chou SM, Hartmann HA. 1965. Electron microscopy of focal neuroaxonal lesions produced by B,B' iminodipropionitrile (IDPN) in rats. *Acta Neuropathol* 4:590.
103. Clark AW, et al. 1980. The axonal pathology in chronic IDPN intoxication. *J Neuropathol Exp Neurol* 39:42.
104. Terry RD, Pena C. 1965. Experimental production of neurofibrillary degeneration. *J Neuropathol Exp Neurol* 24:200.
105. Chou SM, Fakadej AV. 1971. Ultrastructure of chromatolytic motoneurons and anterior spinal roots in a case of Werdnig-Hoffmann disease. *J Neuropathol Exp Neurol* 30:368.
106. Schocet SS Jr, et al. 1969. Intraneuronal conglomerates in sporadic motor neuron disease. *Arch Neurol* 20:548.
107. Hughes JT, Jerrome D. 1971. Ultrastructure of anterior horn motor neurons in the Hirano-Kurland-Sayre type of combined neurological system degeneration. *J Neurol Sci* 13:389.
108. Cork LC, et al. 1982. Pathology of motor neurons in accelerated hereditary canine spinal muscular atrophy. *Lab Invest* 46:89.
109. Cutz E, et al. 1989. Microvillus inclusion disease: An inherited defect of brush-border assembly and differentiation. *New Engl J Med* 320:646.

Vet-ebooks.com

110. Rhoads JM, et al. 1991. Microvillus inclusion disease. *Gastroenterology* 100:811.
111. Schofield DE, et al. 1992. Gastrointestinal microvillus inclusion disease. *Am J Clin Pathol* 98:119.
112. Elgsaeter A, et al. 1986. The molecular basis of erythrocyte shape. *Science* 234:1217.
113. Liu S-C, et al. 1987. Visualization of the hexagonal lattice in the erythrocyte membrane skeleton. *J Cell Biol* 104:527.
114. Drenckhahn D, et al. 1985. Colocalization of band 3 with ankyrin and spectrin at the basal membrane of intercalated cells in the rat kidney. *Science* 230: 1287.
115. Fujimoto T, Ogawa K. 1989. Immunoelectron microscopy of fodrin, the rat uriniferous and collecting tubular epithelium. *J Hist Cyt* 37:1345.
116. Joshi R, et al. 1991. Primary structure and domain organization of human alpha and beta adducin. *J Cell Biol* 115:665.
117. Byers TJ, Branton D. 1985. Visualization of the protein associations in the erythroctye membrane skeleton. *Proc Nat Acad Sci USA* 82:6153.
118. Liu SC, et al. 1987. Visualization of the hexagonal lattice in the erythrocyte membrane skeleton. *J Cell Biol* 104:527.
119. Shen BW, et al. 1986. Ultrastructure of the intact skeleton of the human erythrocyte membrane. *J Cell Biol* 102:997.
120. Lux SE. 1979. Spectrin-actin membrane skeleton of normal and abnormal red blood cells. *Semin Hematol* 16:21.
121. Marchesi VT. 1983. The red cell membrane skeleton. *Blood* 61:1.
122. Nicholson GL, et al. 1971. The localization of spectrin on the inner surface of human red blood cell membranes by ferritin-conjugated antibody. *J Cell Biol* 51:265.
123. Schmid-Schonbein H, et al. 1986. Spectrin red cell shapes and deformability. *Blut* 52:149.
124. Krauss SW, et al. 2003. Nuclear actin and protein 4.1. *Proc Natl Acad Sci USA* 100:10752.
125. Slappendel RJ, et al. 2005. Hereditary spectrin deficiency in Golden Retriever dogs. *J Vet Intern Med* 19:187.
126. Christiansson A, et al. 1985. Lipid molecular shape affects erythrocyte morphology. *J Cell Biol* 101:1455.
127. Beckerle MC, et al. 1989. Activation-dependent redistribution of the adhesion plaque protein, talin, in intact human platelets. *J Cell Biol* 109:3333.
128. Luna EJ, Hitt AL. 1992. Cytoskeleton-plasma membrane interactions. *Science* 258:955.
129. Lietha D, et al. 2007. Structural basis for autoinhibition of focal adhesion kinase. *Cell* 129:177.
130. Ilie D, et al. 2007. Focal adhesion kinase controls pH-dependent epidermal barrier hemostasis by regulating actin-directed Na+/H+ exhanger 1 plasma membrane localization. *Am J Pathol* 170:1807.
131. Yu J, et al. 1990. Uroplakin I: a 27kD protein associated with the asymmetric unit membrane of mammalian urothelium. *J Cell Biol* 111:1207.
132. Matsuzaki F, et al. 1990. cDNAs of cell adhesion molecules of different specificity induce changes in cell shape and border formation in cultured S180 cells. *J Cell Biol* 110:1239.
133. Kaufmann R, et al. 1989. Integrin VLA-3: Ultrastructural localization at cell-cell contact sites of human cell cultures. *J Cell Biol* 109:1807.
134. Aricescu AR, et al. 2007. Structure of a tyrosine phosphatase adhesive interaction reveals a spacer-clamp mechanism. *Science* 317:1217.
135. Mazariegos MR, et al. 1984. Alteration of tight junctional permeability in the rat parotid gland after isoproterenol stimulation. *J Cell Biol* 98:1865.
136. Miller RB, Baldridge WH. 1985. The tight junction as a barrier to cholesterol in canine epithelial cells. *J Ultrastruc Res* 90:275.
137. Schnabel E, et al. 1990. The tight junction protein ZD-1 is concentrated along slit diaphragms of the glomerular epithelium. *J Cell Biol* 111:1255.
138. Itoh M, et al. 1993. The 220-kD protein colocalizing with cadherins in non-epithelial cells is identical to ZO-1, a tight junction-associated protein in epithelial cells. *J Cell Biol* 121:491.
139. Gumbiner B. 1987. Structure, biochemistry, and assembly of epithelial tight junctions. *Am J Physiol* 253:C749.
140. Madera JL. 1990. Maintenance of the macromolecular barrier at cell extrusion sites in intestinal epithelium. Physiological rearrangement of tight junctions. *J Memb Biol* 116:177.
141. Hudspeth AJ. 1975. Establishment of tight junctions between epithelial cells. *Proc Nat Acad Sci USA* 72:2711.
142. Lowenstein WR. 1987. The cell-to-cell channel of gap junctions. *Cell* 48:725.
143. Stauffer KA, et al. 1991. Isolation and purification of gap junction channels. *J Cell Biol* 115:141.
144. Rash JE, et al. 2005. Ultrastructural localization of connexions (Cx36, Cx43, Cx45), glutamate receptors and aquaporin-4 in rodent olfactory mucosa, olfactory nerve and olfactory bulb. *J Neurocytol* 34:307.
145. Hoh JH, et al. 1991. Atomic force microscopy and dissection of gap junctions. *Science* 253:1405.
146. Hamzei-Sichani F, et al. 2007. Gap junctions on hippocampal mossy fiber axons demonstrated by thin-section electron microscopy and freeze fracture replica immunogold labeling. *Proc Natl Acad Sci USA* 104:12548.
147. Cohen-Salmon M, et al. 2007. Connexin30 deficiency causes intrastrial fluid-blood barrier disruption within the cochlea stria vascularis. *Proc Natl Acad Sci USA* 104:6229.
148. Holthöfer B, et al. 2007. Structure and function of desmosomes. *Int Rev Cytol* 264:65.
149. Cartaud A, et al. 1990. A protein antigenically related to nuclear lamin B mediates the association of intermediate filaments with desmosomes. *J Cell Biol* 111:581.
150. Jones JCR, Goldman RD. 1985. Intermediate filaments and the initiation of desmosome assembly. *J Cell Biol* 101:506.
151. Cowin P, et al. 1985. The complement of desmosomal plaque proteins in different cell types. *J Cell Biol* 101:1442.

Vet-ebooks.com

152. Schwarz MA, et al. 1990. Desmosomes and hemidesmosomes: constitutive molecular components. *Ann Rev Cell Biol* 6:46.
153. Ilic D, et al. 2007. Focal adhesion kinase controls pH-dependent epidermal barrier homeostasis by regulating actin-directed Na^+/H^+ exchanger 1 plasma membrane localization. *Am J Pathol* 170:2055.
154. Quadri SK, Bhattacharya J. 2007. Resealing of endothelial junctions by focal adhesion kinase. *Am J Physiol Lung Cell Mol Physiol* 292:L334.
155. Golubovskaya VM, Cance WG. 2007. Focal adhesion kianse and p53 signaling in cancer cells. *Int Rev Cytol* 263:103.
156. Heida Y, et al. 1992. Identification of a new hemidesmosomal protein, HDI. *J Cell Biol* 116:1497.
157. McMillan JR, et al. 2006. Colocalization of multiple laminin isoforms predominantly beneath hemidesmosomes in the upper lamina densa of the epidermal basement membrane. *J Hist Cyt* 54:109.
158. Sonnenberg A, et al. 1991. Integrin $\alpha_6\beta_4$ complex is located in hemidesmosomes, suggesting a major role in epidermal cell-basement membrane adhesion. *J Cell Biol* 113:907.
159. Stepp MA, et al. 1990. $\alpha_6\beta_4$ integrin heterodimer is a component of hemidesmosomes. *Proc Nat Acad Sci USA* 87:8970.
160. Christensen ST, Mott CM. 2007. A ciliary signaling switch. *Science* 317:330.
161. Scholey JM, Anderson KV. 2006. Intraflagellar transport and cilium-based signaling. *Cell* 125:439.
162. Graser S, et al. 2007. Cep164, a novel centriole appendage protein acquired for primary cilium formation. *J Cell Biol* 179:321.
163. Davis RE, et al. 2007. A knockin mouse model of the Bardet-Bidel syndrome 1 M390R mutation has cilia defects, ventriculomegaly, retinopathy, and obesity. *Proc Natl Acad Sci USA* 104:19422.
164. Edwards DF, et al. 1983. Immotile cilia syndrome in three dogs from a litter. *J Am Vet Med Ass* 183:667.
165. Yang LE, et al. 2005. Redistribution of myosin VI from top to base of proximal tubule microvilli during acute hypertension. *J Am Soc Nephrol* 16:2890.
166. Wrackmeyer U, et al. 2007. Intelectin: A novel lipid raft-associated protein in the enterocyte brush border. *Biochemistry* 45:9188.
167. Hansen GH, et al. 2005. Anti-glycosyl antibodies in lipid rafts of the enterocyte brush border. *Am J Physiol* 289:G1100.
168. Hansen GH, et al. 2005. Cholera toxin entry into pig enterocytes occurs via a lipid rat- and clathrin-dependent mechanism. *Biochemistry* 44:873.
169. Tokuo H, et al. 2007. The motor activity of myosin-X promotes actin fiber convergence at the cell periphery to initiate filopodia formation. *J Cell Biol* 179:229.

Vet-ebooks.com

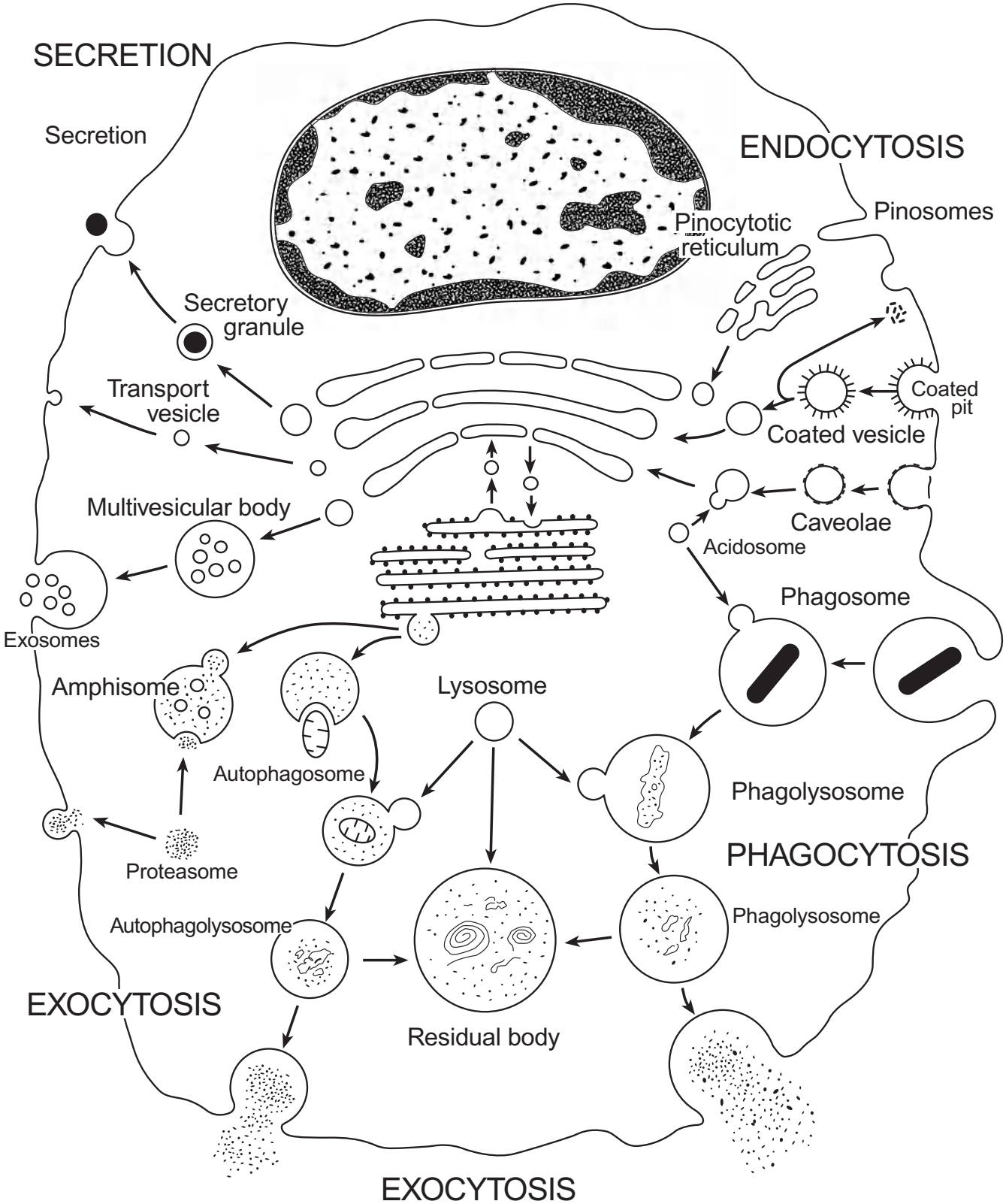


Fig. 5.1 Organelles of intracellular trafficking. Lysosomes are central to trafficking in injured tissues. **Phagosome** and **autophagosome** pathways merge at various points with other cellular traffic. Vesicles bearing proton pumps acidify several different vesicles.

© 2009 Wiley-Blackwell. ISBN: 978-0-813-80330-2
Vet-ebooks.com

5 Intracellular Trafficking

The **cytoplasmic transport system** moves fluids, proteins, and other macromolecules between organelles, and between organelles and the plasma membrane (Fig. 5.1). The flow of transport may involve endocytosis (uptake) and exocytosis (release).[1,2] Shunting of transport vacuoles through the cytoplasm occurs both by directed and nondirected mechanisms. In directed movement, cargo-bearing organelles are targeted to the appropriate pathway by specific receptors and signal transduction molecules. Migration is achieved by motor proteins, and is guided through the cytoplasm by microtubules and other components of the cytoskeleton.

Endocytosis

Endocytosis is the uptake of fluids, macromolecules, and particulate matter into pits formed by inward invagination of the plasma membrane. On the appropriate signal, noninvolved membrane proteins move to the periphery of the point of contact, the membrane changes viscosity, and a vesicle dents into the cytosol. The pit so formed surrounds the cargo, separates from the cell surface, and moves deeply into the cytoplasm carrying its cargo in this vesicle, the **endosome.**

Transcytosis, the passage of fluids and macromolecules **through** the cell, is a common reflection of hyperactive endocytosis, and involves massive endocytosis at one surface, coalescing vesicular transport across the cell, and exocytosis on the opposite surface. Endosomal transcytosis is common in activated endothelial cells, intestinal epithelia, and endocrine glands (Fig. 5.2).[3]

Endocytosis occurs by two major, distinct mechanisms: **absorptive endocytosis**, or low-affinity endocytosis, by which materials are nonspecifically taken into the cell, and **receptor-mediated endocytosis**, or high-affinity endocytosis, a specific mechanism for acquiring material from the environment. Endosomal membranes that lack domains with specific sorting signals move by adsorptive endocytosis; that is, by slow, fluid-phase bulk flow. **Fluid phase transport** is sometimes used to indicate this type of vesicular transport when large amounts of fluid move into and through cells.[4]

Directional movement of trafficking vesicles, typically to and from plasma membrane to RER or Golgi complex, is determined by proteins embedded in the vesicle membrane and coat. In animal tissue, the major endocytic pathways and their endosomal vesicles are

- **Pinocytosis** by smooth plasmalemmal vesicles and pinosomes
- **Caveolar endocytosis** by caveolae and caveosomes
- **Clathrin-mediated endocytosis** by clathrin-coated pits and vesicles
- **Phagocytosis** by phagocytic cups and phagosomes

Structural definitions of the plasmalemmal pits and cytoplasmic vesicles that carry out endocytic functions are reasonably clear, but the receptors and signal transduction molecules that direct traffic for these organelles are continually being refined. Most research on intracellular trafficking is done in cell cultures, and these in vitro studies suggest that endomembranes are differentiated in early (sorting) endosomes, late endosomes, and the endocytic recycling compartment (ERC).[5–7] However, there are clear distinctions between the demands of culture systems on fluid transport and similar trafficking pathways in vivo—pathways that

Vet-ebooks.com

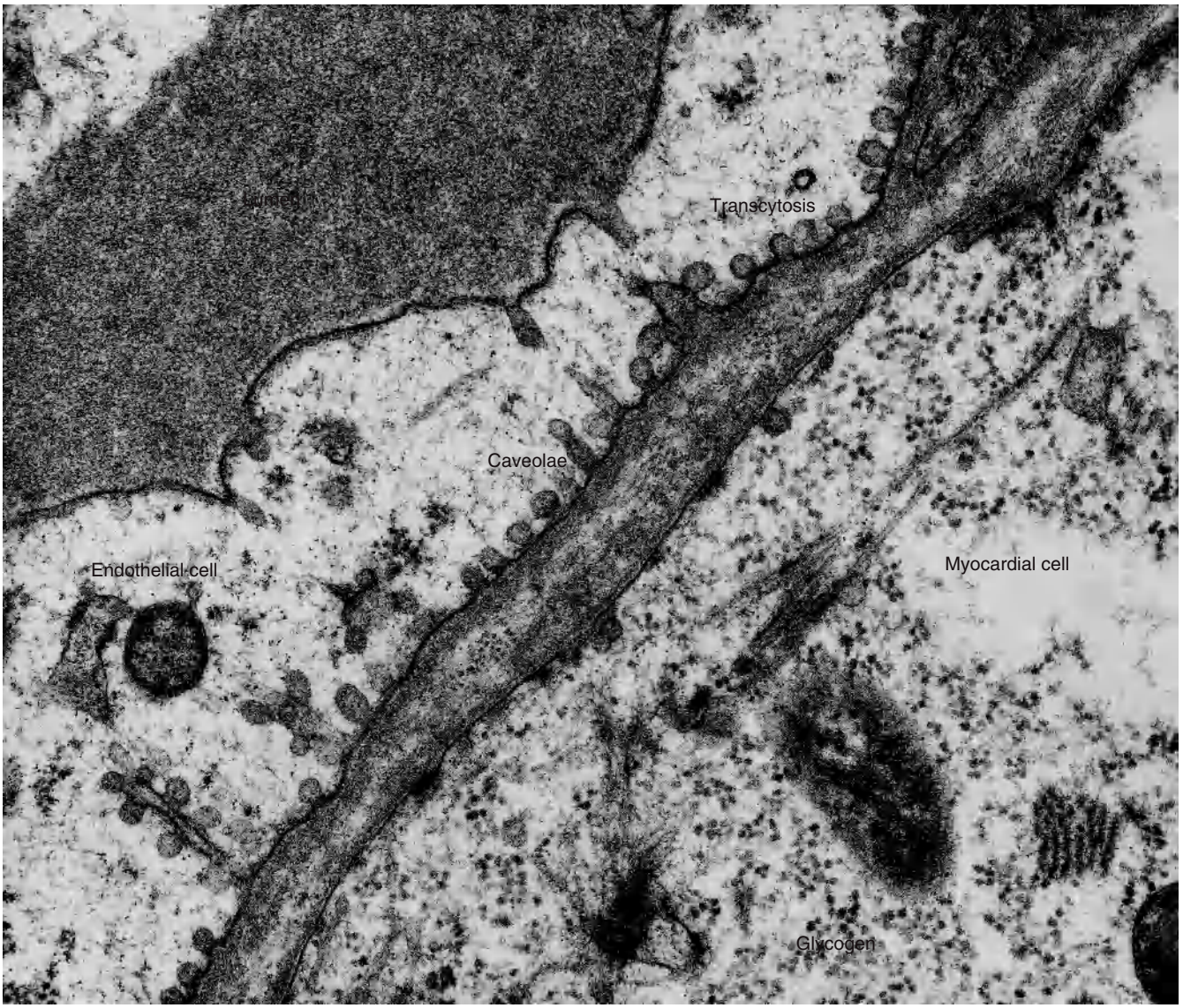


Fig. 5.2 **Transcytosis**: pathways of endo- and exocytosis.

are highly influenced by the extracellular matrix and the vascular system.

Pinosomes

Pinocytosis, or **absorptive endocytosis**, is the uptake of small amounts of fluid into **pinosomes** (**pinocytotic vesicles**, or **smooth endosomes**). Pinosomes begin as smooth plasmalemmal vesicles that are tiny incuppings or invaginations that pinch off from the plasma membrane to become endocytotic vesicles. These virgin **pre-endosomal vesicles** have not yet fused with acidified endosomes, and are the earliest compartment of the endocytic route. Rapid fixation, for example, labeling cell surfaces with marked lectins such as ConA gold at 4°C and warming cells to 37°C for 30 sec with rapid fixation, may be required for detection of pre-endosomal vesicles.[8]

The internal mileu of the pinosome varies with time, and "early" and "late" endosomes are distinguished by the nature of their membranes and matrices. Early pinosomes are devoid of acid hydrolases, coats of clathrin or caveolin, and complex cargo. Early endosomes become acidic soon after formation by fusing with **acidosomes**—tiny vesicles whose membranes are enriched with proton (H^+) pumps—with large multisubunit complexes that function as ATP-driven **vacuolar proton ATPases.**[9] Acidification confers the name **intermediate endosomes.** The low pH within the endosome activates enzyme activity, generation of chemical gradients, and ligand-receptor binding. Acidity in the vacuole also causes dissociation of ligands (which go to lysosomes) and receptors (which

Vet-ebooks.com

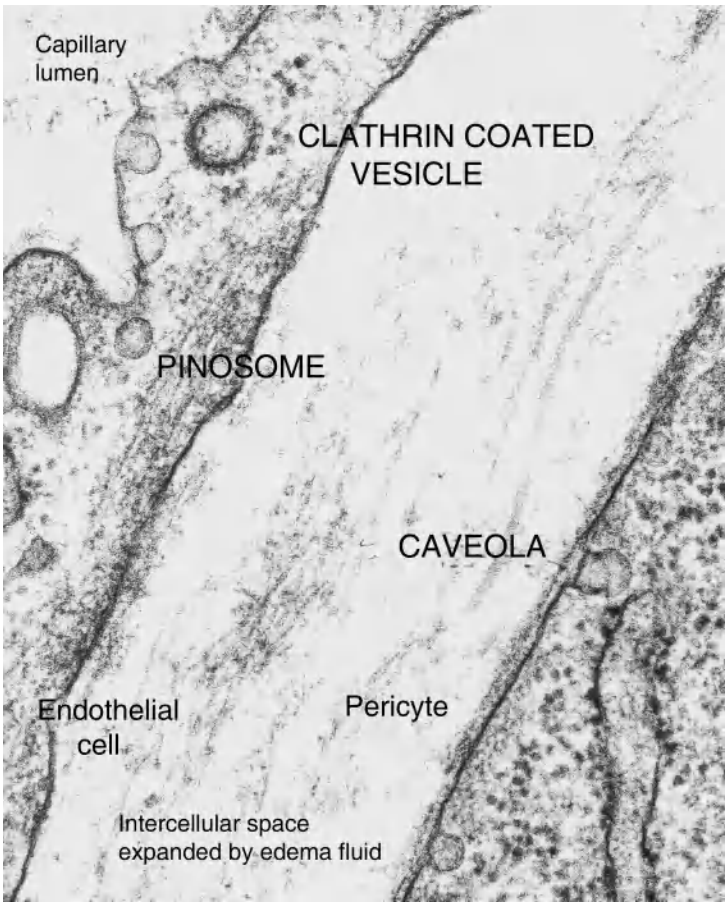


Fig. 5.3 Endocytosis: **caveolae** (plasmalemmal vesicles) on surface of endothelial cell and pericyte.

recycle to the plasma membrane).[10,11] Drugs that neutralize vacuolar pH thus can inhibit endocytosis or exocytosis. Vacuolar acidity has been analyzed using labeled weak bases such as chloroquine, primaquine and 2,4-dinitroanilino-3′-amino-N-methyldipropylamine (DAMP).[12]

In some tissues, tubular pinosomes, or **pinocytotic tubules**, align on plasma membranes, and rapidly take up solutes. They transform into pinocytotic vesicles and pass material to intermediate endosomes. Use of horseradish peroxidase (HRP) as a fluid-phase endocytic tracer has revealed tubular endosomes that form focal multibranching networks (but do not fuse with the endoplasmic reticulum).[13,14]

Caveolae

Caveolae are invaginated vesicles of uniform diameter of 50–100 nm that are formed at the plasma membrane (Fig. 5.3). They are prominent in endothelial cells, smooth muscle cells, and fibroblasts, and participate in endocytosis, cell signaling, and lipid recycling. Orifices of caveolae at the cell surface contain a diaphragm that represents unique **peristomal rings** that develop at the point of invagination from the plasma membrane. Caveolae have inner surface coats of caveolin—filaments arranged in concentric patterns that tend to form scrolls.[15–17]

Caveolins are a family of integral membrane proteins that oligomerize to coat flask-shaped caveola; they confer the invagination function on caveolae. Caveolin types include Cav-1α, -1β, -2, and -3; all regulate signaling proteins that initiate caveolae formation in the plasma membrane. Within the membrane, coordination of signaling and movement is achieved by the development of **lipid rafts**, the microdomains that compartmentalize proteins and lipids.[18] Lipid rafts are key regulators of caveolar-raft endocytosis and trafficking integrins.[19]

Integrin signal transduction phosphorylates caveolin-1. Translocation of phosphorylated caveolin-1 from focal adhesions to caveolae (an event that occurs after cell detachment) induces **cholesterol-enriched membrane microdomains (CEMMs)** in the vesicle membrane. Internalization of vesicles with CEMMs is mediated by dynamin-2, a regulator of caveolin-1 and caveolae dynamics. The global cellular impact of this is that integrins prevent downregulation of Erk, PI3K, and Rac-dependent pathways by

Vet-ebooks.com

inhibiting caveolin-1-dependent endocytosis; that is, this pathway regulates integrin-mediated **Rac membrane targeting**, allowing coupling of Rac to downstream mediators.

Caveolae use receptor-mediated uptake, referred to as **potocytosis**, to take in ligands. Receptors, exposed when caveolae are open, are located adjacent to protein channels or transporters. After dissociation of ligand and receptor, the ligand passes into the cytoplasm. Thereafter, caveolae can (but usually do not) detach from the plasma membrane, and can reutilize the receptor molecules for added ligand uptake. Internalization initiated by ligand-receptor interactions in caveolae includes that for albumin,[20] cholera toxin, cholesterol, lipoproteins, tetanus toxin, and folate, all of which have glycosylphosphatidylinositol (GPI)-linked receptors.

Folate binds to its receptor, an integral membrane protein anchored in the membrane by GPI. **Folate receptors** occur in dense clusters in the surface membrane near caveolae. They concentrate the vitamin 5-CH_3FH_4 at the cell surface so that it can be transferred into the cell cytoplasm. After binding, the **folate-receptor complex** aggregates near caveolae, but following uptake is not found to be associated with coated vesicles or endosomes.[21]

Some ligands are transported by both caveolin and clathrin-mediated endocytosis. **IFN-γ** bound to its cell surface receptor (which activates the Jak-STAT pathway) is internalized by both caveolin and clathrin pathways, perhaps for different target cell components.[22]

Clathrin-Coated Pits and Vesicles

Clathrin-coated pits form in the plasma membrane and bud into the cytoplasm as **coated vesicles.** They are unique because of their exterior surface coat of fibrillar clathrin. Coated pits develop in response to specific ligand-receptor interactions. Binding of ligands to membrane receptors initiates the invaginations of the plasma membrane and attraction of clathrin (Fig. 5.4).

As clathrin inserts into and coats a focal spot on the plasma membrane, it causes the coated area to indent, pulling the membrane into the cytoplasm to form a coated pit. The pit converts into a coated vesicle as it separates from the plasma membrane. Thus, the attached ligand-receptor material on the plasma membrane exterior comes to lie on the inside of this new vesicle, and the clathrin coat on the outside. Clathrin coats also form along membranes of the trans-Golgi network (see Golgi complex, chapter 7). In the cytoplasm, coated vesicles rapidly release their clathrin coats and fuse with other membrane compartments

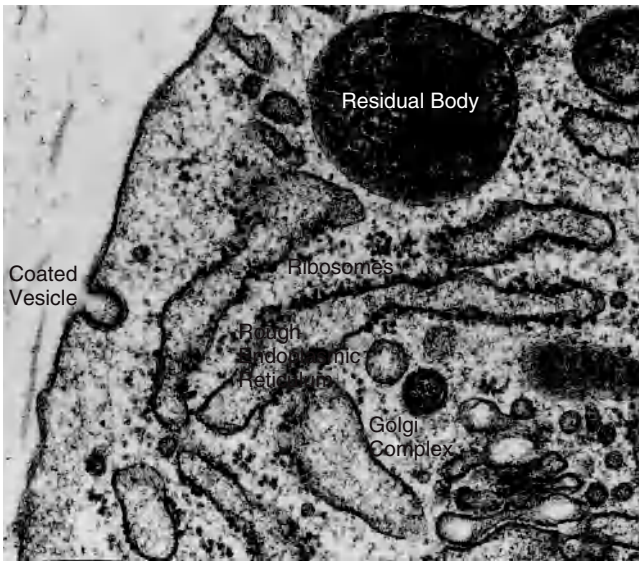


Fig. 5.4 Endocytosis: clathrin-coated pit and vesicles.



Fig. 5.5 Clathrin-coated vesicles: cytoplasmic face of the plasma membrane, fibroblasts in culture. En face image used quick-freeze, deep-etch method. (Micrograph: John Heuser, *J Cell Biol* 108:389, 1989.)

to form specialized endosomes, vesicles that lack digestive enzymes and that are destined to become transport vacuoles that carry molecules to specific destinations.[23–27]

Clathrin

As coated pits develop at sites of ligand-receptor binding, clathrin aggregates on the cytoplasmic side of the plasma membrane (Fig. 5.5).

Vet-ebooks.com

Clathrin coats are composed of two subunits: the triskelion and the clathrin adaptor protein complex. The characteristic three-legged clathrin molecule, called a **triskelion**, forms a polyhedral lattice when it polymerizes on membranes to form the clathrin coat.[28] The **adaptor protein subunit** is a multi-protein complex of α and β adaptins and other proteins.[29]

Four members of the **adaptor protein** (AP-1 to AP-4) family are heterotetrameric cytosolic complexes in intracellular trafficking of cargo proteins between organelles. AP-4 is in clathrin-coat machinery of the Golgi complex, endosomes, and transport vesicles.[30] Differences in pathways and morphology depend on how AP-4 co-localizes in the cytosol; typically it co-localizes with a cation-independent mannose-6-phosphate receptor (CI-MPR), but not with LAMP-2 or the transferrin receptor.

Receptor-Mediated Endocytosis in Clathrin-Coated Pits

Receptor-mediated endocytosis (RME) occurs when substances outside the cell bind tightly (with high affinity) to specific receptor molecules on the cell surface. RME is designed to move large bulk cargos rapidly across the plasma membrane. In cargo overload, plasma membrane receptors can be endocytosed through clathrin-dependent and clathrin-independent pathways. For example, **the epidermal growth factor receptor (EGFr)**, when stimulated by EGF, is internalized exclusively via the clathrin pathway (and is not ubiquinated); however, at high concentrations, EGFr is also internalized by non-clathrin pathways.[31]

The classic model for RME is that of plasma **low-density lipoproteins** and their receptor located on surfaces of cells that take up and degrade these atherogenic lipids.[32] LDL ligands are endocytosed into coated pits. LDL ligand-bearing vesicles fuse with lysosomes, the ligand-receptor complexes are degraded, and receptors are recycled back to the cell surface. Ligands with similar pathways for ligand-receptor binding are transferrin,[33] ricin,[34] growth factors,[35] and other ligands.[36–39]

Vesicular pH determines ligand binding avidity. Receptors bind ligands tightly at neutral pH, but ligands rapidly dissociate when pH goes below 5.5. When the receptor-ligand complex enters an acidic endosome, the ligand is separated and becomes soluble in the vesicles lumen; the receptor remains bound to the membrane and is recycled.[40]

In the specific direct cell-to-cell transfer of cytoplasmic material from one cell to filopodia of another, receptor-mediated endocytosis is effected. For example, Leydig cells in the testis form long tentacular filopodia and lamellipodia that join with coated pits of macrophages to transfer refuse of steroid metabolism for degradation.[41]

Intermediate Endosomes: The Endosomal Pool

Pinocytotic Reticulum

The **pinocytotic reticulum** (or "pinocytotic channel") is a cytoplasmic, subsurface system of pleomorphic pinocytotic vesicles and tubules in cells with high rates of metabolism. Areas of pinosomal fusion into complex vesicles are also referred to as the **endosomal tubuloreticular compartment**, "late endosomes", or late endosomal vacuoles. Endosomes of this compartment fuse with lysosomes, multivesicular bodies, or saccules of the Golgi complex. They also fuse with the plasma membrane for exocytosis.[42]

Micropinocytosis vermiformis is the name given to pinocytosis that involves marked folding and lamellar arrangements of the plasma membrane, usually of 80–125 nm widths, that invaginate into the cell cytoplasm. Lamellae have a delicate "line" of basolaminar material through the middle of the lamellae. Micropinocytosis vermiformis is typically found in phagocytic cells, for example, Kupffer cells in liver, intravascular macrophages of the lung, and in splenic macrophages.[43]

Pinocytotic Reticulum in the Liver In hepatocytes, the pinocytotic reticulum is a system of thin, 20 nm anastomosing smooth surfaced tubules with associated vesicles at the sinusoidal surface that are receptor enriched and function actively in endocytosis. It is here that receptors and ligands are uncoupled and this region was once referred to as **CURL** (for compartment of uncoupling of receptor and ligand).

During active transfer of blood-borne macromolecules to hepatocytes, proteins pass through endothelial cells into spaces of Disse and from there into the hepatocyte. In the hepatocyte, endosomes leave the pinocytotic reticulum and pass directly to biliary canaliculi, or are diverted to cytoplasmic lysosomal systems. Immediately after the intraportal injection of tracer-marked ligands, the tracer appears in the pinocytotic reticulum that lies close to the sinusoidal surface of the hepatocyte.[44–47]

Asialoglycoproteins (ASGPs) are glycoproteins that circulate in the bloodstream, where they undergo desialylation, a process that makes them recognizable to specific ASGP receptors on the hepatocyte plasma membrane. Asialylation is a mechanism for targeting glycoproteins for clearance and destruction by the liver.[48–50] Special receptors for transferrin, growth factors, lipoproteins, and other substances provide

Vet-ebooks.com

similar instructions for endocytosis. Lactoferrin, a cationic iron-binding protein secreted by specific granules of neutrophils, is rapidly taken up by sinusoidal cells of the liver by endocytosis.[51]

Immunglobulin A (IgA) is transported from the bloodstream through hepatocytes to the bile. In rat hepatocytes, IgA is taken up by endosomes that do not fuse with other vacuoles but move directly to the plasma membrane of the biliary canaliculus.[52] The receptor, called **secretory piece**, is proteolytically removed from the membrane and the IGA-receptor complex enters the bile.

Macroendosomes

Macroendosomes are giant endosomes filled with endocytosed proteins. They are typically found in hepatocytes and renal epithelial cells exposed to large amounts of protein; for example, the proximal convoluted tubule cell during protein-losing nephropathy. Seen histologically as PAS-positive hyalin droplets, these large membrane-bound structures are pale, homogenous, and granular, but lack evidence of acid hydrolases or intracellular digestion.

Macropinocytosis is a form of bulk uptake of fluid and solid cargo into cytoplasmic vacuoles. It requires extensive plasma membrane reorganization or ruffling to form an external macropinocytotic structure that is then enclosed and internalized. Macropinosomes are distinguished from other forms of pinocytotic vesicles by their large size, lack of coat structures, and structural heterogeneity.[53–54] They do not simply funnel cargo into endocytic pathways, but have competence for regulated exocytosis and other membrane properties.

Directing Traffic in the Endosomal Pool

In the plasma membrane, specific membrane proteins direct endosomal pathways. Cells of different organ systems have their own unique signaling proteins that use specialized targeting signals. In neurons, the cytoplasmic protein **phocein** is involved in **clathrin-** and **dynamin-dependent pathways.** The endosomal protein **flotillin** induces a specific subpopulation of intermediate endosomes that are distinct from both **caveolin-** and **clathrin-dependent endosomes.** The pathways of these proteins are defined in vitro; for example, flotillin-driven endosomes are defined by their capacity to move cholera toxin and GPI-anchored proteins.

Microtubule Guidance for Endocytosis Microtubules guide the movement of endosomes to their designated targets. Movement is regulated by interaction of membrane adhesins of the cargo-bearing vesicle with cytoplasmic motor proteins. The motor protein **dynein** and its cofactor, dynactin, move endosomes to microtubules, the vesicle-microtubule connection being made through microtubule-associated proteins. Other motor proteins are responsible for movement. In the skin, melanosomes in dendrites of the melanocyte are transported to the cell body by **kinesin** and kinectin.[55] Many transport processes are dependent on the protein **dynamin**, a large GTPase that constricts lipid bilayers.[56]

Lipid Raft-Mediated Endocytosis Endosomes that bear signal molecules that band and cluster onto lipid rafts are endocytosed in clathrin-independent pathways. They are a discrete population of endosomes en route to the Golgi.[57] Caveolae are "raft- and dynamin-dependent" while dynamin-independent raft pathways are mediated by non-caveolar intermediates.[58] Two distinct caveolae-mediated (clathrin-independent) endocytic pathways exist: (1) caveolin-1 regulated caveolae-mediated pathway to the **Golgi complex**, and (2) calveolar endocytosis via caveosomes from plasma membrane to **RER**.

Caveolae and pinosomes use lipid rafts for clustering of proteins in the membrane (and CEMMs) that drive intermediate endosomes in the plasma membrane–Golgi complex pathway. In experimental studies, markers used to define clathrin-independent endocytosis have been cholera toxin B subunit and GPI-anchored proteins. Ultrastructurally, the carriers for cholera toxin appear as uncoated, tubular or ring-shaped structures with GPI-anchored proteins and fluid-phase markers.[59]

Endosomal Receptors in Tissue In the **intestine**, receptors move cargo across microvilli of polarized epithelial cells.[60] Immunogold labeling studies have followed **megalin**, an endocytic receptor of the low-density lipoprotein receptor family that is expressed on absorptive epithelial cells. Megalin is an endocytic receptor that binds several specific ligands, and cooperates with the **sonic hedgehog** in the control of development and growth.[61]

In the **kidney**, brush borders of proximal convoluted tubules contain endocytic receptors that initiate renal clearance of hemoglobin, albumin, and other proteins from the glomerular filtrate. In vasopressin-driven **water transport** by renal collecting tubules, endocytic receptors translocate membranous vesicles bearing **aquaporins** to the apical plasma membrane.[62]

Ion channels play a role in regulating endocytosis. For example, the loss of **chloride channels** impairs endocytosis by causing defective trafficking of the endocytic receptors megalin and cubilin. In **Dent's disease**, a loss of renal endosome-associated chloride

Vet-ebooks.com

channels and defective trafficking of megalin and cubilin strongly inhibit endocytosis by the proximal tubule.[63]

Ligand-receptor initiated signals for vesicular movement are mediated by **GTP-binding proteins (GTPases):** ***ras*-GTPases** ensure specificity of budding vesicles by coupling the reaction to hydrolases of bound GTP; ***rab*-GTPases** mediate specificity of interaction between molecules in donor and acceptor membranes; rab-4 and 5 have been localized to early endosomes, rab-7 to late endosomes. Rab-5 and rab-7 are the rate-limiting endocytic catalysts in these bulk protein transporting cells. Although most of the materials moved by this system are trapped in the interior of the vacuole, the membrane of the vacuole functions to shuttle membrane proteins from vacuolar membrane to the plasma membrane and back again.

Phagocytosis

Phagocytosis is the process of uptake of particulate material by the massive deformation of the cell surface in order to surround the cargo. The first phase of phagocytosis is **attachment**, either by nonspecific chemicoadsorption to the cell surface or by fusion with specific receptor molecules. The second phase is **uptake**, which arises from plasma membrane movement initiated by the contraction of microfilaments. **Pseudopodia** (or **podosomes**) develop at the cell surface to form a **phagocytic cup** that moves outward to surround the entering particle (Fig. 5.6). After attachment of target surface to the plasma membrane, phagocytic cups use a zipper mechanism to move the target into a **phagosome.** Strongly phagocytic cells have surfaces specialized for uptake—urothelial umbrella cells of the bladder have apical surfaces covered with rigid concave urothelial plaques that are critical in uptake of uropathogenic *E. coli*.[64] **Pseudopodia** contain a meshwork of contracting actin microfilaments complexed to myosin. These microfilament complexes can be seen around the neck of the invaginating phagosome. Phagocytosis of dead cells by macrophages and other phagocytic cells is part of normal tissue remodeling.

Phagosomes

Phagosomes are vacuoles formed by the phagocytic uptake of particulate material. Phagosomes do not stain for hydrolytic enzymes, but move to and fuse with other organelles of intracellular trafficking. Domains within the plasma membrane of cells taking up bacteria play an essential role in phagocytosis.

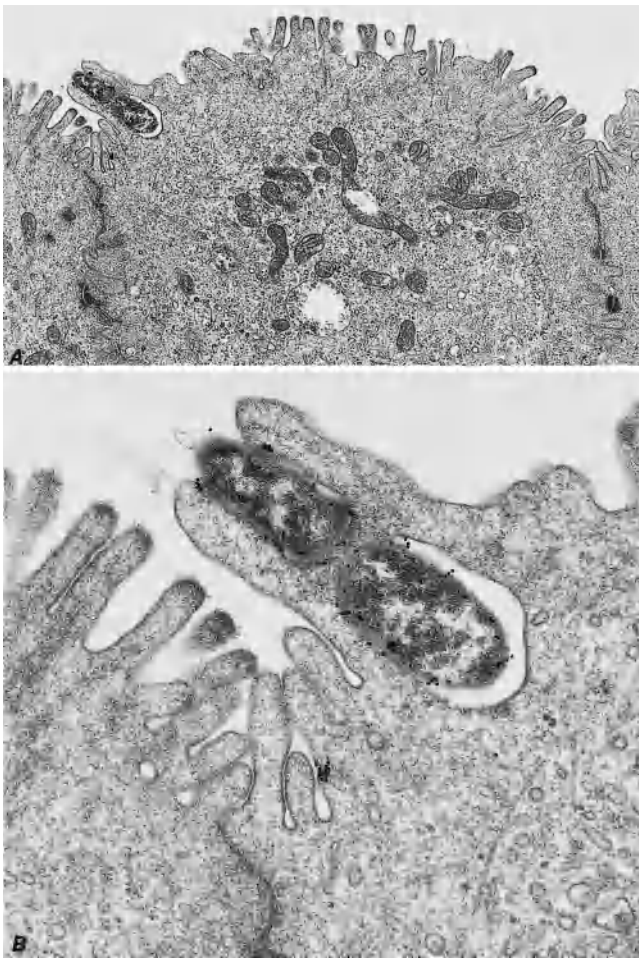


Fig. 5.6 Phagocytosis of bacteria by M cells: epithelium overlying intestinal Peyer's patch, calf. **A**. **M cell filopodia**: extend outward to surround the bacterial cell. **B**. **Bacterium surface stained with gold particles**: immunogold technique using antibodies against *Brucella. abortus*. (Micrograph: Mark Ackermann, *Vet Pathol* 28:267, 1991.)

Phagosomal biogenesis is critical for microbial killing and antigen presentation. Fusion of phagosomes with other endocytic organelles is regulated, in part, by rab-5. **Rab-5** activates both PI3 kinase-dependent and independent effectors that promote phagosomal maturation.[65,66] Rab-5 appears to restrict fusion, allowing transient "kiss-and-run" contact that transfers solutes but restricts complete fusion.

Membranes required for formation of new phagosomes are contributed by the endoplasmic reticulum. ER fuses with the plasma membrane at the cytoplasmic sites of phagosomal cup formation, patching new segments of membrane into the developing phagosome. There is also concurrent translocation of ER-localized SNARE proteins (syntaxins) into the new phagosome.[67–69] This process allows the developing phagosome access to the most abundant endogenous membrane source in the cell.

Vet-ebooks.com

Specificity in Phagocytosis

The nature and specificity of attachment determine speed of phagocytic uptake. Phagocytosis of bacteria usually occurs slowly if attachment is nonspecific. In contrast, when there is interaction of ligands such as **immunoglobulins** or **complement** with specific plasma membrane receptors on the cell, phagocytosis is much quicker. This opsonin-dependent phagocytosis is energy requiring, and it is suppressed by drugs that inhibit glycolysis and ATP formation; however, nonspecific phagocytosis is not inhibited.

Inflammasomes

Potentially lethal cargo within phagosomes is monitored by granular cytoplasmic foci referred to as inflammasomes, a cell mechanism to divert the phagosome and trigger protective cytokines. The **inflammasome** is a multiprotein aggregate of caspase-activating complexes that is the reactive site for production of IL-1 and other proinflammatory cytokines (it contains caspases 1 and 5, Pycard/Asc, and NOD-like receptors).[70] Many cellular receptors sense danger signals for the cell in the cargo of the phagosome, notably the **toll-like receptors (TLRs)** and the **NOD-like receptors (NLRs)**, nucleotide-binding and oligomerization domain-like receptors. Both TLRs and NLRs recognize damaged cellular components and microbes (by their surface muramyldipeptides). When activated, these receptors move to and interact with the inflammasome.

Frustrated Phagocytosis

The NOD-like receptor **Nalp3** (cryopyrin) senses components of microorganisms and large particulates. Large particulates and crystals such as silica, asbestos, and urates of gout, too large and inert to be adequately phagocytized, trigger macrophages to enter a "frustrated" state that is characterized by activation of NADPH oxidase and the generation of reactive oxygen species (ROS). Diffusing to the **Nalp3 inflammasome** is the protein complex that stimulates caspase-1 activation to promote the processing and secretion of proinflammatory cytokines. ROS initiates the production of the potent proinflammatory cytokine **interleukin1β.**[71]

NADPH oxidase → ROS → Nalp3 + ASC + caspase 1 → IL-1

Thioredoxin, a protein that detoxifies ROS, acts as a brake on this reaction. Low K^+ in the cytosol also triggers inflammasome formation.

Lysosomes and Cytoplasmic Trafficking

Lysosomes

Lysosomes are membrane-bound vesicles that bear acid phosphatase, β-glucuronidase, and other digestive enzymes. They degrade macromolecules from the secretory, endocytic, autophagic, and phagocytic membrane-trafficking pathways.[72,73] The **primary lysosome** is a small, dense granule with its enzymes in an inactive state (Fig. 5.7). It is identified with specific techniques for acid phosphatase or other hydrolases. Enzymes and other protein components of lysosomes are synthesized in ribosomes, transported into the rough endoplasmic reticulum, glycosylated, put in proper order, and packaged within the Golgi complex. As the new **prelysosomal vesicle** emerges from the trans face of the **Golgi complex**, its hydrolytic enzymes, structural proteins, and glycosaminoglycans are complexed in an inactive state, awaiting the appropriate stimulus for activation. The interior of lysosomes is acidified by an H^+ translocating ATPase that generates a transmembrane H^+ gradient and a membrane potential.[74]

Lysosomes are differentiated from other vacuoles by specific markers: **lysosome-associated membrane protein-1** and **-2** (**LAMP-1** and **LAMP-2**) (lysosomal markers), the Atg8 homologue **LC3** (autophagolysosomal marker), and the small GTPases **rab-5** and **7** (late endocytotic pathway markers).[75] **Rab-7** functions in late endocytic pathways and lysosome biogenesis, and participates in the final maturation of autophagic vacuoles. Recruitment of rab-7 to autophagic vacuoles is retarded in cells deficient in the lysosomal membrane proteins LAMP-1 and LAMP-2.[76] In **Danon disease**, an X-linked cardioskeletal myopathy caused by primary deficiency of LAMP-2, LAMP-2 is absent in histochemical staining.[77]

In lysosomes, biologically active proteases are held in check by a family of intracellular peptidase inhibitors, the **serpins.** Although most serpins are secreted, a unique family of serpins protects the lysosome, and the loss of serpin activity can lead to necrotic cell death.[78]

In the kidney, endocytosis provides an alternative pathway for lysosome biogenesis in the renal tubule. Epithelial cells of the proximal tubule reabsorb lysosome enzymes from the glomerular filtrate by megalin-mediated endoytosis and transfer these enzymes to lysosomes.[79]

Phagolysosomes

Phagolysosome is the name given to phagosomes after they fuse with lysosomes. These are the dominant

Vet-ebooks.com

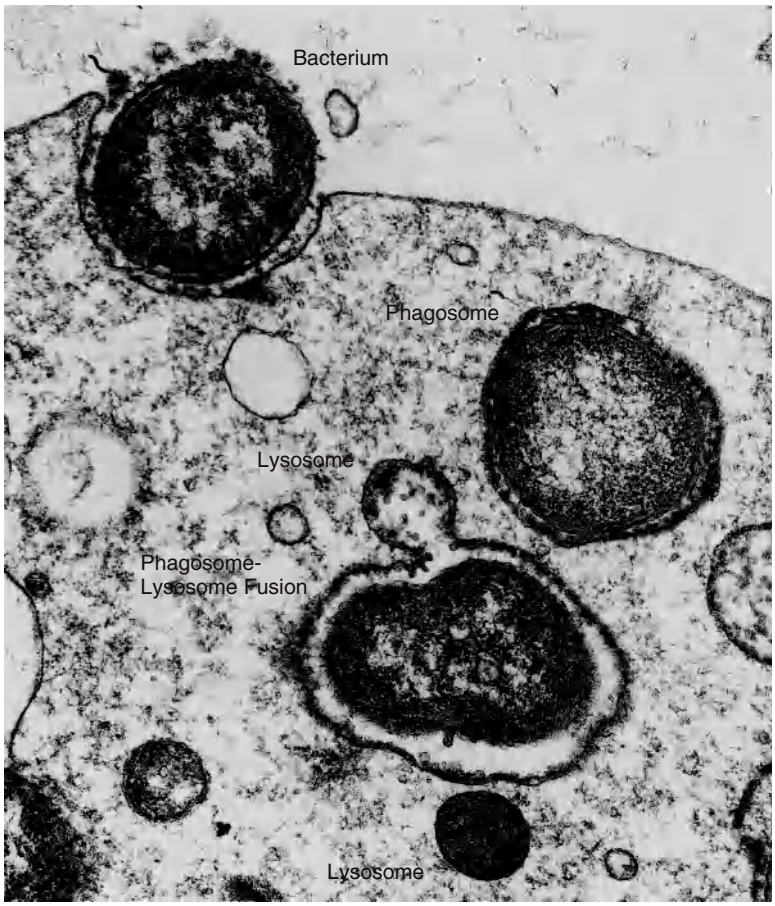


Fig. 5.7 Phagosome-lysosome fusion: Uptake of *Salmonella* spp. into a leukocyte, pig. Bacterium indents into the cell surface (*top left*) and is connected by tiny surface strands to the plasma membrane of the leukocyte. Within the cytoplasm are primary lysosomes, a phagosome containing a bacterium and vesicles, and a bacterium-bearing phagosome in the process of fusion. In the developing phagolysosome, note small vesicles in the lysosomal part and adjacent to membranes of newly formed phagolysosome.

organelle for intracellular degradation of microbes and exogenous particular material. **Phagosome-lysosome fusion** is a major trafficking pathway, and is disrupted by many toxins and microbial virulence factors. As lysosomes fuse with phagosomes, they release potent acid hydrolases that are activated in the phagolysosomal environment and begin to enzymatically degrade phagolysosomal contents.

Tubular lysosomes may rarely be seen in cells stimulated to increased endocytosis. Narrow but very long (to 220 nm), they are prominent adjacent to infoldings in the plasma membrane and may fuse to form small foci of anastomosing networks.[80]

Abnormal Lysosomal Degradation in Metabolic Disease

In normal cells, autophagosomes filled with remnants of membranes and senescent proteins are continually produced. Cellular membranes are continually recycled—tiny portions of membrane are sequestered into autophagolysosomes so that specific enzymes can degrade membrane phospholipids, glycolipids, and glycoproteins for reuse. When this membrane repair process is driven to excess, phospholipid membrane fragments accumulate in lysosomes. Drugs of low toxicity that increase cellular metabolism generally cause an increase in lysosomes and in activity of acid hydrolases.[81,82] In certain genetic defects that involve loss of lysosomal enzymes, autophagolysosomes cannot degrade the proteins and membranes taken up by autophagy.

Acquired defects in phospholipid metabolism lead to production of abnormal membrane fragments that accumulate as whorled masses of disconnected membranes within giant autophagolysosomes. Mechanisms involved in membrane injury may arise either by stimulated uptake of phospholipids (which is rare), or by toxin-induced inhibition of phospholipid degradation. The latter occurs by direct enzymatic inactivation (gentamicin) or by binding of drugs to lysosomal membrane phospholipids, rendering them resistant to degradation (chloroquine). Intralysosomal concentric lamellar bodies, which are aggregates of phospholipid membranes, are associated with many cationic amphophilic drugs that alter metabolism of phospholipids and saccharides. Histologically, affected cells appear foamy, like those of triglyceride fatty degeneration. However, the cytoplasmic lipids do not stain for neutral lipids, but rather with phospholipid stains

Vet-ebooks.com

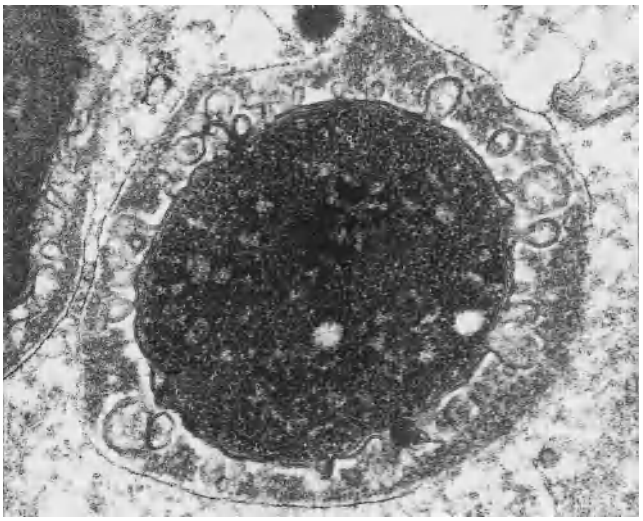


Fig. 5.8 Phagolysosomes: residual body, macrophage, spleen. Blebbing of the outer membrane of *Escherichia coli* is associated with release of endotoxin. (Micrograph: Lawrence Arp, National Animal Disease Center, Ames, Iowa.)

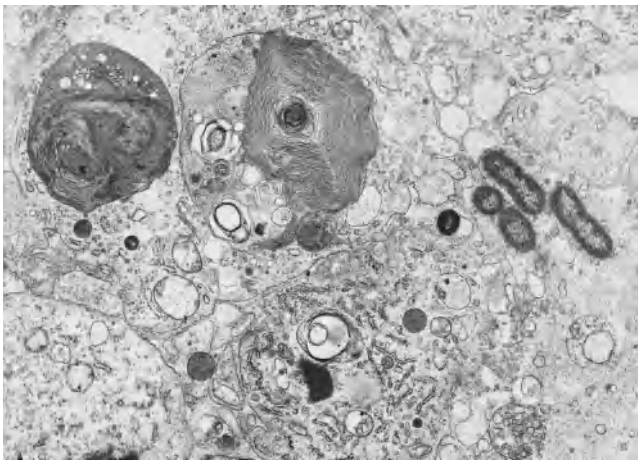


Fig. 5.9 Phagolysosomes: residual body (myeloid body), macrophage, granulomatous peritonitis caused by *Actinomyces* sp., dog. Residual bodies contain whorls of membranes called myelin figures. Bacteria are located extracellularly and within phagosomes inside macrophages.

and with the PAS technique for glycolipids and glycoproteins.

Ultrastructurally, lysosomes enlarged during excessive membrane degradation appear first as large granules filled with small vesicles and granular debris. These change rapidly to giant autophagosomes containing dense cellular debris and masses of membrane fragments. As the process progresses, membranes reform into laminar arrangements called **myelin figures;** myelin figure-bearing lysosomes are referred to as **myeloid bodies** (Fig. 5.8). When specific enzymes are missing, glycoproteins may polymerize in a more defined manner to form characteristic tubules and twisted fibrils.

Residual Bodies

Residual bodies are large, end-stage phagolysosomes or autophagolysosomes that have acquired massive amounts of partially degraded cellular material (Fig. 5.9). Residual bodies must have evidence of the residue of digestion, and typically they contain dense granular debris, fragments of membranes, and small lipid globules.[83] Membrane phospholipids are particularly difficult to digest and accumulate because appropriate lipases are not present. When large amounts of membrane are present, these structures become arranged in laminated, concentric **myelin figures.**[84] Some intracellular lipids become oxidized to pigmented autofluorescent **lipofuscin** (aging pigment). Lipofuscin can be discharged from phagocytic cells or, as in the case of neurons and cardiac myocytes, remain within the residual body.

Exocytosis

Exocytosis is the excretion or externalization of cellular materials through the release of membrane-bound vesicles. Normally, cells release materials via cargo-bearing vesicles and secretory granules (see the section in chapter 6 on secretion). In injured cells, mass movement of cargo material also occurs by excretion of exocytotic bodies and blebbing.

Exosomes

Exosomes are small vesicles whose membranes contain degraded proteins no longer needed by the cell. They originate in two ways: (1) budding of vesicles from the membrane into the matrix of **multivesicular bodies**, which then move to the plasma membrane to release the exosomes into the extracellular space, and (2) surface budding of the plasma membrane directly into extracellular spaces (these are sometimes referred to as **exocytotic vesicles** and bear surface antigens expressed on the plasma membrane). In both pathways, exosomes are released from the cell surface.

Exosomes can be found in organ lumens and in interstitial areas. Exocytotic vesicles are shed from dendritic cells and other cells that carry integral membrane proteins into extracellular spaces.[85] When a multivesicular body fuses with the plasma membrane, its exosome packet is released into the extracellular space. In this way, exosomes present antigens, send signals, and even transfer nucleic acids to other cells. For example, mast cells transfer exosomal RNA efficiently

Vet-ebooks.com

to other mast cells (but not to other cells).[86] Terms used for special exovesicles include:

- **Acidosomes:** ion-secreting exosomes released by acidic vesicles
- **Iccosomes:** immune complex-coated bodies produced by follicular dendritic cells
- **Argosomes:** exosomes that carry membrane-bound morphogens in embryos
- **Amphisomes:** large complex bodies, arising from the merger of MVBs and autophagosomes, that fuse with lysosomes to form autophagolysosomes

Secretory Vesicles

Secretory vesicles, also called **transport vesicles**, move in an unregulated (constitutive) manner to pass material quickly, without storage, to the cell surface. They are small and have a short half-time, and are difficult to find in electron micrographs. During acid secretion, gastric parietal cells accumulate proton-producing vesicles in the cytoplasm near the apical surface (Fig. 5.10). In the resting state, these secretory vesicles and their tubular connections form a tubulovesicular system that, in the activated state, rapidly reorganizes to form massive secretory canaliculi (see the section in chapter 6 on secretion).

Renal Excretion of Exosomes in Urine

Excretion of exosomes is a major pathway by which proximal convoluted tubular epithelium removes degraded cellular membranes. The identification and proteomic profiling of exosomes in urine is an efficient means of biomarker identification. Aquaporin-2, fetuin A, and other apical transporters reach urine through secretion of exosomes (membrane vesicles that originate as internal vesicles in multivesicular bodies [MVBs]). Chromatographic analysis of urine has revealed nearly 300 different proteins in human urine, some of which are protein products of genes associated with disease; for example, polycystic kidneys, **Batten's disease**, and other genetic disorders.[87] Proximal convoluted tubule cells also eliminate cellular debris by secreting acid hydrolases and other lysosomal constituents into the urinary filtrate; in some metabolic diseases, myelin figures can be found in urine.



Fig. 5.10 Exocytosis: acidosomes. Vesicles fixed in the process of being released into a lumenal cellular canaliculus of a gastric parietal cell. Microvilli are short and thick, and the cell has released microvesicles into the lumen of the canaliculus.

Exosome Defects

Tubulin disruptors such as colchicine lead to **exocytotic constipation**, a consequence of defective tubulin/lysosomal interaction. Microtubules play a critical role in lysosomal degradation in normal skeletal myocytes, and the vacuolar myopathy in colchicine toxicity results directly from impaired trafficking of exosomes.[88]

Multivesicular Bodies

MVBs are large pale spherical vacuoles that contain **exosomes** (Fig. 5.11). Exosomes arise by inward budding of the MVB membrane. They also arise, but only rarely, from other vesicles within the MVB, from large blebs that indent into the vacuole, or by autophagy-like engulfment of preexisting vesicles in the cytoplasm. Exosomal membranes, like those of the MVBs, have high cholesterol : phospholipid ratios (relative to Golgi membranes). MVBs can be light or dark depending on variations in density of the matrix.

Movement of the MVB membrane into its intralumenal vesicles is regulated by the membrane proteins' **endosomal sorting complexes required for transport (ESCRTs).** ESCRT complexes recognize membrane proteins that are modified with ubiquitin (and thus marked for sorting to lysosomes).[89] ESCRT complexes sort these cargoes to specific domains of endosomes and regulate both invagination and scission of invaginated membrane buds to form intralumenal vesicles. Cells depleted of ESCRTs have suppressed autophagy and accumulate protein aggregates containing ubiquinated proteins.[90]

Mutations in ESCRT subunits are associated with neurodegenerative diseases such as ALS and frontotemporal dementia.

Vet-ebooks.com



Fig. 5.11 **Multivesicular body**: epithelium, trachea.

MVBs in Intracellular Trafficking

Interposed between endosomes and plasma membrane in the cytoplasmic traffic system, MVBs receive, store, and transmit membrane proteins (as component exosome membranes). In hepatocytes, MVBs are an intermediate vesicular compartment in the receptor-mediated catabolic pathway for low-density lipoproteins.[91] It has also been suggested that the MVB is a proton-sequestering compartment that is responsible for cytoplasmic alkalinization.[92]

MVB traffic also goes from plasma membrane to endosomes. **Cytokine receptors** taken into cells by specific receptor-mediated endocytosis are sent to MBVs, where they are either shunted to lysosomes for degradation or are moved back into endosomes for recycling to the cell surface.[93]

Large complex MVBs may merge with lysosomes (and stain for acid phosphatase), and are considered lysosomes because of their involvement with the lysosomal system and their tendency to transform into autophagosomes.

MVBs Provide Rapid Excretion

The excretory function of MVBs, in which transmembrane proteins no longer needed by the cell are moved outside the cell, is efficient in cells that are rapidly growing and dividing. **Hemopoietic stem cell** maturation involves loss of surface proteins that had been used as receptors (those that are typical of the undifferentiated stem cell but not of the mature cell) but are no longer needed. For example, as reticulocytes mature to erythrocytes, they lose plasma membrane **transferrin receptors**, which are no longer needed to transfer iron. Reticulocytes, whose plasma membranes are rich in transferrin receptors, mature into erythrocytes whose plasma membranes are not enriched. During maturation, receptors are sequestered in vesicles the inner membranes of which are lined by receptor molecules. These transform into MVBs as vesicles bud internally; that is, the MVB contains round bodies of about 50 nm diameter that bear receptors on their external surfaces (the limiting membrane of the MVB is free of receptors).[94]

Enlargeosomes

Enlargeosome is a name applied to small cytoplasmic vesicles that are discharged by regulated exocytosis. They are small vesicles in the vicinity of the plasma membrane, and are identified by their membrane marker, desmoyokin/Ahnak. On stimulation, enlargeosomes begin exocytosis by forming flat patches in the plasma membrane.[95]

Cytoplasmic Blebs

Cells release masses of damaged cytoplasm by **cytoplasmic shedding** (or blebbing). Shedding occurs when **bullae** form at the cell surface and portions of the cytoplasm pinch off and are lost to the extracellular space. Bullae contain cytoplasmic components and vesicles (that are fragments of endoplasmic reticulum). Blebs are clear relative to adjacent cytoplasm and of low viscosity as indicated by increased Brownian movement. In contrast to **vesicular exocytosis**, however, cytoplasmic shedding, although common, is not a major excretory process in the normal cell.

Microvesicular shedding is a variant of blebbing that typically occurs in epithelia lining lumens and in leukocytes. Many different membrane-bound spherical particles have also been described that cover cell surfaces and come to lie in interstitial spaces. **Microvesicles** in the acinar lumens of exocrine glands are common during active secretion. Devoid of membrane proteins and cholesterol, they contain only one major

Vet-ebooks.com

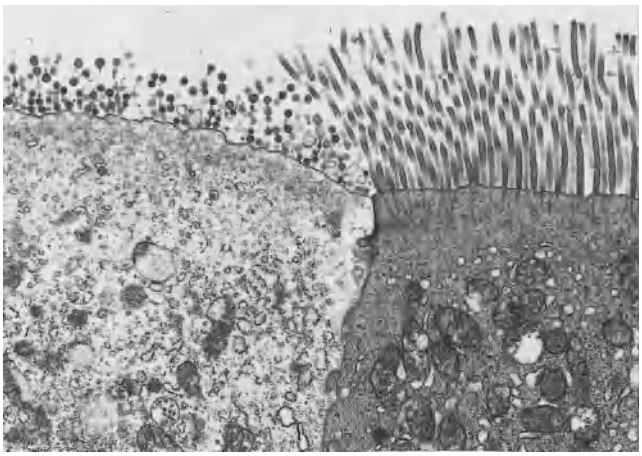


Fig. 5.12 Glycocalcyceal bodies: spherical bodies on the surface of an intestinal absorptive cell (*left*). Cell at right has relatively normal microvilli.

protein and represent a mechanism for release of membrane material.[96] Similar surface microvesicles have been given other names in different tissues, for example, the **spherical microparticles** of cardiac muscle and **glycocalyceal bodies** of cells bearing microvillous surfaces, especially those of the respiratory and intestinal tracts (Fig. 5.12).[97] Microvesicular blebbing of platelets is an important mechanism for release of procoagulant factors. In the activated platelet, dissociation of focal areas of the plasma membrane from the underlying cytoskeleton leads to blebbing and release of vesicles bearing procoagulant factors.[98]

References

1. Evergren E, et al. 2006. Differential efficiency of the endocytic machinery in tonic and phasic synapses. *Neuroscience* 141:123.
2. Polo S, Di Fiore PP. 2006. Endocytosis conducts the cell signaling orchestra. *Cell* 124:897.
3. Cloutier M, et al. 2006. Internalization and transcytosis of pancreatic enzymes by the intestinal mucosa. *J Hist Cyt* 54:781.
4. Gonnella PA, Neutra MR. 1984. Membrane-bound and fluid-phase macromolecules enter separate prelysosomal compartments in absorptive cells of suckling rat ileum. *J Cell Biol* 99:909.
5. Grant BD, Sato M. 2007. Intracellular trafficking. *WormBook*.
6. Saraste J, Goud B. 2007. Functional symmetry of endomembranes. *Mol Biol Cell* 18:1430.
7. Mukhopadhyay D, Riezman H. 2007. Proteasome-independent functions of ubiquitin in endocytosis and signaling. *Science* 315:201.
8. Hansen SH, et al. 1991. The preendosomal compartment comprises distinct coated and noncoated endocytic vesicle populations. *J Cell Biol* 113:731.
9. Forgac M. 2007. Vacuolar ATPases: rotary protein pumps in physiology and pathophysiology. *Nat Rev Mol Cell Biol* 8:917.
10. Clapp WL, et al. 1988. Axial heterogeneity in the handling of albumin by the rabbit proximal tubule. *Lab Invest* 58:549.
11. Madsen KM, Tisher CC. 1984. Response of intercalated cells of rat outer medullary collecting duct to chronic metabolic acidosis. *Lab Invest* 51:268.
12. Anderson RGW, Orci L. 1988. A view of acidic intracellular compartments. *J Cell Biol* 106:539.
13. Rabinowitz S, et al. 1992. Immunocytochemical characterization of the endocytic and phagolysosomal compartments in peritoneal macrophages. *J Cell Biol* 116:95.
14. Tooze J, Hollinshead M. 1991. Tubular early endosomal networks in AtT20 and other cells. *J Cell Biol* 115:635.
15. Anderson RGW, et al. 1992. Potocytosis: sequestration and transport of small molecules by caveolae. *Science* 255:410.
16. Peters K-R, et al. 1985. Endothelial plasmalemmal vesicles have a characteristic striped bipolar surface structure. *J Cell Biol* 101:2233.
17. Aoki T, et al. 2007 Internalization of caveolae and their relationship with endosomes in cultured human and mouse endothelial cells. *Anat Sci Int* 82:82.
18. Echarri A, et al. 2007. Intracellular trafficking of raft/caveolae domains: insights from integrin signaling. *Semin Cell Dev Biol* 18:627.
19. Dvorak AM, Feng D. 2001. The vesiculo-vacuolar organelle (VVO): A new endothelial cell permeability organelle. *J Hist Cyt* 49:419.
20. Ghitescu L, et al. 1986. Specific binding sites for albumin restricted to plasmalemmal vesicles of continuous capillary endothelium: Receptor-mediated transcytosis. *J Cell Biol* 102:1304.
21. Rothberg KG, et al. 1992. Caveolin, a protein component of caveolae membrane coats. *Cell* 68:673.
22. Sadir R, et al. 2001. Caveolae and clathrin-coated vesicles: two possible internalization pathways for IFN-gamma and IFN-gamma receptor. *Cytokine* 14:19.
23. Heuser JE, et al. 1989. Effects of cytoplasmic acidification on clathrin lattice morphology. *J Cell Biol* 108:401.
24. Schmid SL, Smythe E. 1991. Stage-specific assays for coated pit formation and coated vesicle budding in vitro. *J Cell Biol* 114:869.
25. Dickson RB, et al. 1981. α_2-Macroglobulin absorbed to colloidal gold: a new probe in the study of receptor-mediated endocytosis. *J Cell Biol* 89:29.
26. Michaely P, et al. 2007. Identification of a VLDL-induced FDNPVY-independent internalization mechanisms for the LDLR. *EMBO J* 26:3273.
27. Yamashira DT, et al. 1984. Segregation of transferrin to a mildly acidic (pH 6.5) para-Golgi compartment in the recycling pathway. *Cell* 37:789.
28. Nathke IS, et al. 1992. Folding and trimerization of clathrin subunits at the triskelion hub. *Cell* 68:899.
29. Peeler JS, et al. 1993. The appendage domain of the AP-2 subunit is not required for assembly or invagination of clathrin-coated pits. *J Cell Biol* 120:47.

Vet-ebooks.com

30. Barois N, et al. 2005. The adaptor protein AP-4 is a component of the clathrin coat machinery: a morphological study. *Biochem J* 385:503.
31. Sigismund S, et al. 2005. Clathrin-independent endocytosis of ubiquinated cargos. *Proc Natl Acad Sci USA* 102:2760.
32. Anderson RGW, et al. 1982. Surface distribution and recycling of the low density lipoprotein receptor as visualized with anti-receptor antibodies. *J Cell Biol* 93:523.
33. Yamashiro DT, et al. 1984. Segregation of transferrin to a mildly acidic (pH 6.5) para-Golgi compartment in the recycling pathway. *Cell* 37:789.
34. van Deurs B, et al. 1986. Routing of internalized ricin and ricin comjugates to the Golgi complex. *J Cell Biol* 102:37.
35. Dunn WA, et al. 1986. Receptor-mediated endocytosis of epidermal growth factor by rat hepatocytes: Receptor pathway. *J Cell Biol* 102:24.
36. Nair P, et al. 2005. Characterization of the TGN exit signal of the human mannose 6-phosphate uncovering enzymes. *J Cell Sci* 118:2949.
37. Hansen GH, et al. 1999. Transcytosis of immunoglobulin A in the mouse enterocyte occurs through glycolipid raft- and rab 17-containing compartments. *Gastroenterology* 116:610.
38. Czekay RP, et al. 1997. Endocytic trafficking of megalin/RAP complexes dissociation of the complexes in late endosomes. *Mol Biol Cell* 8:517.
39. Kostrouch Z, et al. 1991. Thyroglobulin internalized by thyrocytes passes through early and late endosomes. *Endocrinology* 129:2202.
40. Larkin JM, et al. 1986. Potassium-dependent assembly of coated pits. *J Cell Biol* 103:2619.
41. Miller SC, et al. 1983. Structure, cytochemistry, endocytotic activity, and immunoglobulin receptors of rat testicular interstitial tissue macrophages. *Am J Anat* 168:1.
42. Bomsel M, et al. 1990. Microtubule- and motor-dependent fusion in vitro between apical and basolateral endocytoic vesicles from MDCK cells. *Cell* 62:719.
43. Winkler GC, Cheville NF. 1987. Postnatal colonization of porcine lung capillaries by intravascular macrophages. *Microvasc Res* 33:224.
44. Creemers J, Jacques PJ. 1971. Endocytic uptake and vesicular transport of injected horseradish peroxidase in the vacuolar apparatus of rat liver cells. *Exp Cell Res* 67:188.
45. Goldfischer S, et al. 1970. Hemoglobin uptake by rat hepatocytes and its breakdown within lysosomes. *J Cell Biol* 44:513.
46. Graham RC Jr, et al. 1968. The uptake and transport of exogenous proteins in mouse liver. *Lab Invest* 20:298.
47. Mori M, Novikoff AB. 1977. Induction of pinocytosis in rat hepatocytes by partial hepatectomy. *J Cell Biol* 72:695.
48. Burwen SJ, Jones AL. 1990. Hepatocellular processing of endocytosed proteins. *J Elec Microsc Tech* 14:140.
49. Geuze HJ, et al. 1984. Ultrastructural localization of the mannose 6-phosphate receptor in rat liver. *J Cell Biol* 98:2047.
50. Hubbard AL, et al. 1979. An electron microscope autoradiographic study of the carbohydrate recognition systems in rat liver. *J Cell Biol* 83:47.
51. Courtoy PJ, et al. 1984. Uptake of lactoferrin by the liver. II. Endocytosis by sinusoidal cells. *Lab Invest* 50:329.
52. Hoppe CA, et al. 1985. Transcellular transport of polymeric IgA in the rat hepatocyte. *J Cell Biol* 101:2113.
53. Jones AT. 2007. Macropinocytosis. *J Cell Mol Med* 11:670.
54. Falcone S, et al. 2006. Macropinocytosis: regulated coordination of endocytic and exocytic membrane traffic events. *J Cell Sci* 119:4758.
55. Vancoillie G, et al. 2002. Kinesin and kinectin can associate with melanosomal surfaces to form a link with microtubules in normal human melanocytes. *J Invest Derm* 114:421.
56. Mears JA, et al. 2007. A corkscrew model for dynamin constriction. *Structure* 15:1190.
57. Glebov OO, et al. 2006. Flotillin-1 defines a clathrin-independent endocytic pathway in mammalian cells. *Nat Cell Biol* 8:46.
58. Echarri A, Del Pozo AA. 2006. Caveolae internalization regulates integrin-dependent signaling pathways. *Cell Cycle* 5:2179.
59. Kirkham M, et al. 2005. Ultrastructural identification of uncoated caveolin-independent early endocytic vesicles. *J Cell Biol* 168:465.
60. Ishii M, et al. 1990. Morphologic demonstration of receptor-mediated endocytosis of epidermal growth factor by isolated bile duct epithelial cells. *Gastroenterology* 98:1284.
61. Morales DR, et al. 2006. Epithelial trafficking of sonic hedgehog by megalin. *J Hist Cyt* 54:115.
62. Barile M, et al. 2005. Large scale protein identification in intracellular aquaporin-2 vesicles from renal inner medullary collecting duct. *Mol Cell Proteomics* 4:1095.
63. Christensen EI, et al. 2003. Loss of chloride channel CIC-5 impairs endocytosis by defective trafficking of megalin and cubilin in kidney proximal convoluted tubules. *Proc Natl Acad Sci USA* 100:8472.
64. Wang H, et al. 2008. Characteristics of the phagocytic cup induced by uropathogenic *Escherichia coli*. *J Hist Cyt* 56:597.
65. Vieira OV, et al. 2003. Modulation of Rab5 and Rab7 recruitment to phagosomes by phosphatidylinositol 3-kinase. *Mol Cell Biol* 23:2501.
66. Duclos S, et al. 2000. Rab5 regulates the kiss and run fusion between phagosomes and endosomes and the acquisition of phagosome leishmanicidal properties in RAW 264.7 macrophages. *J Cell Sci* 19:3531.
67. Gagnon E, et al. 2002. Endoplasmic reticulum-mediated phagocytosis is a mechanism of entry into macrophages. *Cell* 110:119.
68. Becker T, et al. 2005. Differential use of endoplasmic retciulum membrane for phagocytosis in J774 macrophages. *Proc Natl Acad Sci USA* 102:4022.
69. Hatsuzawa K, et al. 2006. Involvement of syntaxin 18, an endoplasmic reticulum (ER)-localized SNARE protein, in ER-mediated phagocytosis. *Mol Biol Cell* 17:3964.

Vet-ebooks.com

70. Martinon F, et al. 2002. The inflammasome: A molecular platform triggering activation of inflammatory caspases and processing of proIL-beta. *Mol Cell* 10:417.
71. Dostert C, et al. 2008. Innate immune activation through Nalp3 inflammasome sensing of asbestos and silica. *Science* 320:675.
72. Luzio JP, et al. 2007. Lysosomes: Fusion and function. *Nat Rev Mol Cell Biol* 8:622.
73. Ly KT, Casanova JF. 2007. Mechanisms of Salmonella entry into host cells. *Cell Microbiol* 9:2103.
74. Ludwig T, et al. 1991. Distribution of newly synthesized lysosomal enzymes in the endocytic pathway of normal rat kidney cells. *J Cell Biol* 115:1561.
75. Huynh KK, et al. 2007. LAMP proteins are required for fusion of lysosomes with phagosomes. *EMBO J* 26:313.
76. Jager S, et al. 2004. Role for Rab7 in maturation of late autophagic vacuoles. *J Cell Sci* 117:4837.
77. Bertini E, et al. 2005. Phenotypic heterogenetity in two unrelated Danon patients associated with the same LAMP-2 gene mutaton. *Neuropediatrics* 36:309.
78. Scott FL, et al. 1999. The intracellular serpin proteinase inhibitor 6 is expressed in monocytes and granulocytes and is a potent inhibitor of the azurophilic granule protease, cathepsin G. *Blood* 93:2089.
79. Nielsen R, et al. 2007. Endocytosis provides a major alternative pathway for lyososmal biogenesis in kidney proximal tubular cells. *Proc Natl Acad Sci USA* 104:5407.
80. Robinson JM, et al. 1986. Unusual lysosomes in aortic smooth muscle cells. *J Cell Biol* 102:1615.
81. Decker RS, Wildenthal K. 1981. Lysosomal laterations in heart, skeletal muscle and liver of hyperthyroid rabbits. *Lab Invest* 44:455.
82. Mezey E, et al. 1980. Effect of ethanol feeding on hepatic lysosomes in the monkey. *Lab Invest* 43:88.
83. Novikoff AB, Shin W-Y. 1978. Endoplasmic reticulum and autophagy in rat hepatocytes. *Proc Nat Acad Sci USA* 75:5039.
84. Hruban Z, et al. 1963. Focal cytoplasmic degradation. *Am J Pathol* 42:657.
85. Obregon C. et al. 2006. Exovesicles from human activated dendritic cells fuse with resting dendritic cells, allowing them to present alloantigens. *Am J Pathol* 169:2127.
86. Valadi H, et al. 2007. Exosome-mediated transfer of mRNAs and microRNAs is a novel mechanism of genetic exchange between cells. *Nat Cell Biol* 9:654.
87. Pisitkun T, et al. 2004. Identification and proteomic profiling of exosomes in human urine. *Proc Natl Acad Sci USA* 101:13368.
88. Kuncl RW, et al. 2003. Exocytotic "constipation" is a mechanism of tubulin/lysosomal interaction in colchicine myopathy. *Exp Cell Res* 285:196.
89. Marsh M, van Meer G. 2008. No ESCRTs for exosomes. *Science* 319:1191.
90. Filimonenko M, et al. 2007. Functional multivesicular bodies are required for autophagic clearance of protein aggregates associated with neurodegenerative disease. *J Cell Biol* 179:485.
91. Hornick CA, et al. 1985. Isolation and characterization of multivesicular bodies from rat hepatocytes: an organelle distinct from vesicules of the Golgi apparatus. *J Cell Biol* 100:1558.
92. Nilsson M, et al. 1989. Increased endocytosis and formation of multivesicular bodies in phorbol ester-stimulated human monoblastic U-937 cells. *Exp Cell Res* 181:551.
93. Felder S, et al. 1990. Kinase activity controls the sorting of the epidermal growth factor receptor within the multivesicular body. *Cell* 61:623.
94. Pan B-T, et al. 1985. Electron microscopic evidence for externalization of the transferrin receptor in vesicular form in sheep reticulocytes. *J Cell Biol* 101:942.
95. Cocucci E, et al. 2007. Enlargeosome traffic: exocytosis triggered by various signals is followed by endocytosis, membrane shedding or both. *Traffic* 8:742.
96. Beaudoin AR, et al. 1986. Detection and characterization of microvesicles in the acinar lumen and in joice of unstimulated rat pancreas. *J Hist Cyt* 34:1079.
97. Afzelius BA. 1984. Glycocalyx and glycocalyceal bodies in the respiratory epithelium of nose and bronchi. *Ultrastr Pathol* 7:1.
98. Fox JEB, et al. 1990. Role of the membrane skeleton in preventing the shedding of procoagulant-rich microvesicles from the platelet plasma membrane. *J Cell Biol* 111:483.

Vet-ebooks.com

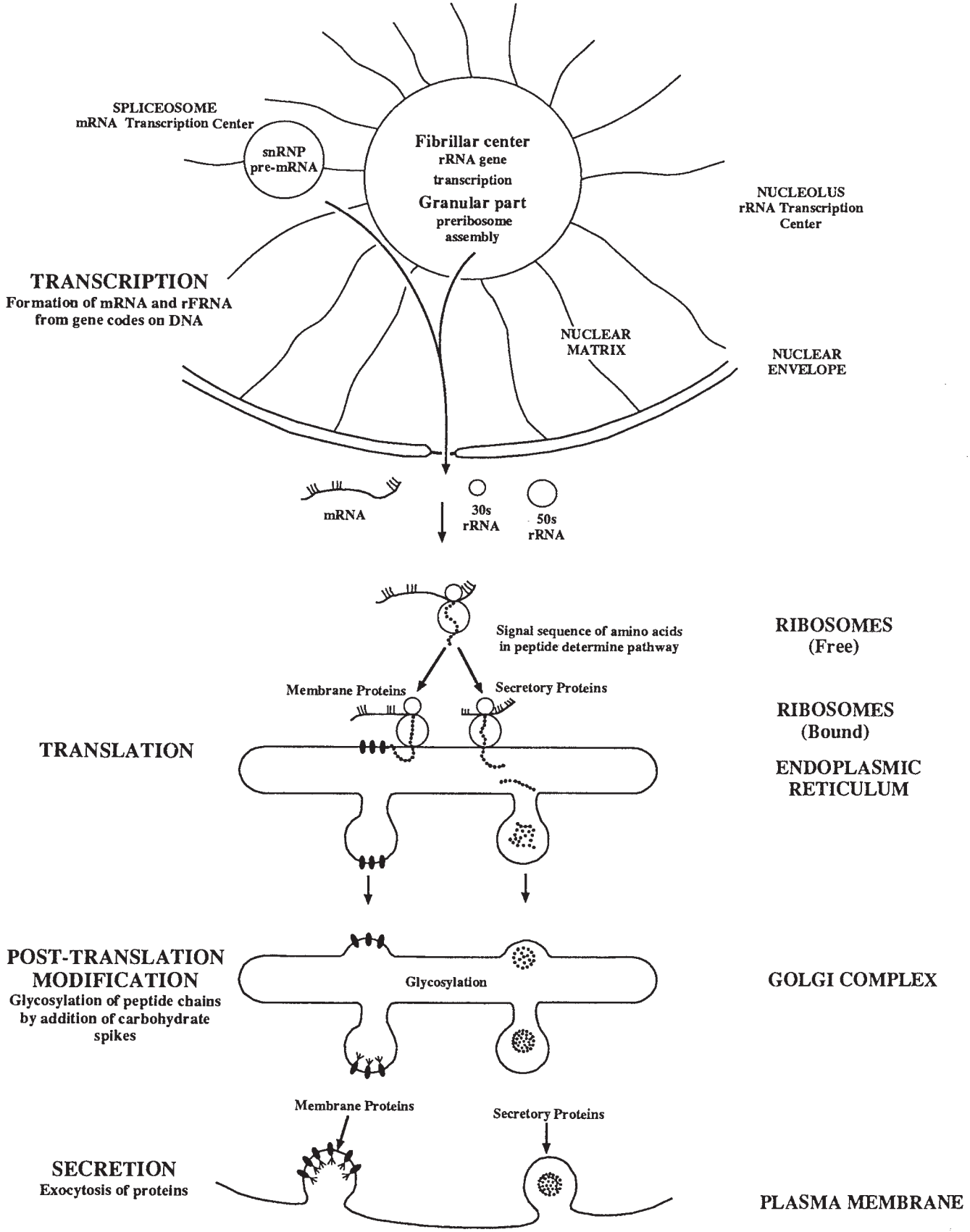


Fig. 6.1 Protein synthesis: pathways of transcription, translation, and post-translational modifications. Transcription occurs within the nucleus (to form ribosomal RNA, or rRNA) and in nucleoplasm (for mRNA). During translation, peptides may be secreted into the cytosol by free ribosomes or directly into cisternae of the endoplasmic reticulum by rough endoplasmic reticulum-bound ribosomes.

© 2009 Wiley-Blackwell. ISBN: 978-0-813-80330-2

Vet-ebooks.com

6 Nucleus, Ribosomes, the Golgi Complex, and Secretion

Nucleus

The **nucleus** is the control center for the cell. Genes, located on the chromosomes, provide the template from which RNA messenger molecules are transcribed. These RNAs pass to the cytoplasm to control protein synthesis in ribosomes. The great variance in size and conformation of nuclei (Fig. 6.1) is a reflection of the activity of transcription. The cyclical flow of specific messenger molecules and receptor-ligand complexes that activate genes alters nuclear size. The nucleus expands and increased undulation of the nuclear envelope allows increased contact between nucleus and cytoplasm.

Three sequential phases connect the reading of genes to the final release of protein chains into the cytocavitary network. First, **transcription** of DNA codes onto templates of messenger RNA (mRNA) occurs on chromosomes in the nucleus; second, **translation** of the mRNA into the desired peptide chains occurs in ribosomes; finally, the **folding** and **conjugation** of new peptides into the final protein product occur in the rough endoplasmic reticulum and Golgi complex.

Much of the gene activity occurs in nucleoproteins of the nucleolus and, when the cell's activities demand increased protein, the nucleolus enlarges and moves to the nuclear membrane to facilitate nuclear cytoplasmic exchange. The location of the nucleus in the cell is controlled by communication between the nuclear envelope and the cytoskeleton.[1]

Nuclear Envelope

The **nuclear envelope (NE)** separates the major activities of gene expression: transcription and maturation of mRNA in the nucleus from translation of mRNA into protein in the cytoplasm.[2,3] The nuclear envelope in cells with high levels of nuclear-cytoplasmic transport is often undulated to increase the area available for activity (Fig. 6.2).

The NE is formed of **inner** and **outer membranes** separated by a **perinuclear space**, a regular gap of 30–50 nm. Inner and outer nuclear membranes are distinct; the inner membrane bears a unique array of integral membrane proteins, whereas the outer membrane shares its structure and functions with membranes of the endoplasmic reticulum to which it is connected. The perinuclear space enters into cisternae of the endoplasmic reticulum at multiple sites in the NE.

The nuclear envelope, and its nuclear pores and nuclear lamina, modulate gene expression, cell differentiation, and other nuclear functions. Lamins associate with gene regulatory proteins such as histones, c-Fos, and the tumor suppressor pRB. Furthermore, integral membrane proteins of the inner nuclear membrane (lamin B, emerin, Lap2β (lamina-associated polypeptide 2β) interact with transcriptional repressors. The inner nuclear membrane signaling protein MAN1 is linked with TGF-β, which in turn is tied to a bone morphogenic protein; this pathway when aberrant is causal in disorders of increased bone density; for example, osteopoikilosis, Buschke-Ollendorff syndrome, and melorheostosis.

Nuclear Lamina

The nuclear face of the inner membrane of the nuclear envelope is lined with a fibrous protein meshwork, the **nuclear lamina** (fibrous lamina), a network of

Vet-ebooks.com

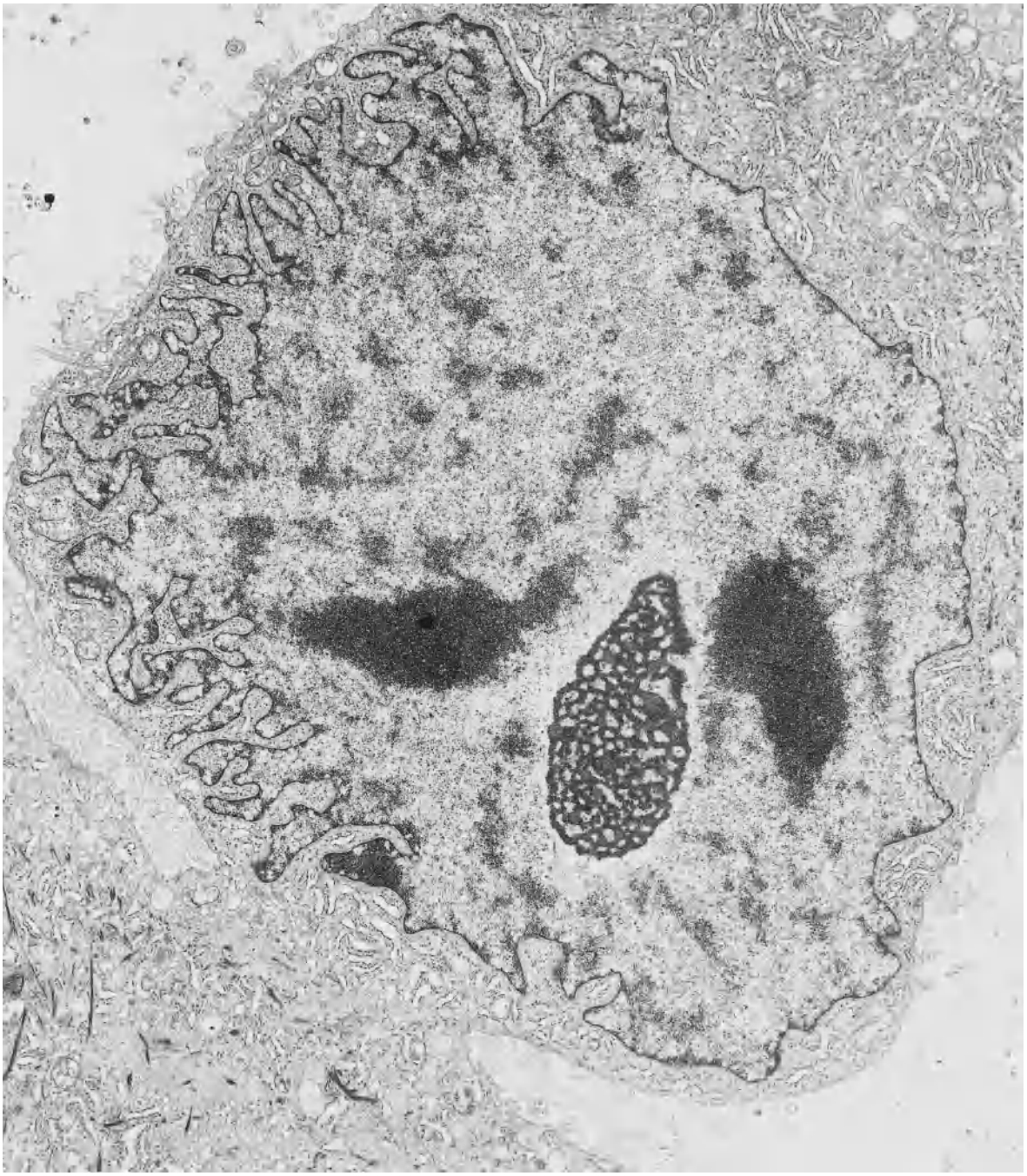


Fig. 6.2 **Hypertrophy**: trophoblast, normal placenta, horse. Note marked increase in nuclear volume, nuclear membrane undulation, and nucleolar size.

Vet-ebooks.com

10–20 nm thick filaments made of polypeptides called **lamins**. Lamins are attachment sites for cytoskeletal filaments (lamin B is the major receptor for intermediate filaments in the nuclear envelope). Somatic cells in vertebrates may contain as many as five different lamins.

The A- and B-type lamins, members of the type V intermediate filament superfamily, are closely related to intermediate filaments of the cytoplasm.[4] **Nesprin-3**, a novel outer nuclear membrane protein, associates with the cytoskeletal linker protein **plectin**.[5] Because of these connections, lamins play critical roles in gene expression, protein degradation, and formation of chromatin; they are anchoring sites for interphase chromosomes. Laminotoxic drugs and some toxins disrupt lamin assembly, the consequences of which lead to deficits in the following functions of lamins:

- Decline in mechanical integrity of the nucleus and cytoplasm, including reduced cytoplasmic elasticity and viscosity
- Loss of centrosome from its paranuclear position
- Abnormal distribution of heterochromatin
- Abnormal nuclear pore complexes with retention of membrane products
- Disrupted participation of nuclear pores in signaling for nucleocytoplasmic transport

Laminopathies Systemic disease can disrupt lamin assembly; for example, changes in pH will cause chromatin to aggregate on the lamin scaffold. Viruses use a wide variety of strategies for subverting or bypassing nuclear transport pathways in host cells (see chapter 13). Influenza A and adenoviruses encode adaptor proteins that import their genomes into the nucleus.

Laminopathies that result from mutations within lamin genes are rare disorders that disrupt lamin assembly. At least eight human syndromes that arise from mutation of the lamin A (*LMNA*) gene are known. ***LMNA* mutations** include metabolic disorders of the myocyte and adipocyte, as well as the progerias (premature aging syndromes). Laminopathies have been grouped into three categories:

- Striated muscle (cardiac and skeletal) and peripheral nerves
- Skeletal and fat development and homeostasis
- Premature aging: the progerias (see chapter 22)

Only one disease, autosomal dominant leukodystrophy, is linked to the *LMNB1* gene. Mutations in lamin A genes cause muscle laminopathies such as dilated cardiomyopathy and Emery-Dreifuss muscular dystrophy (the X-linked form of which is linked to mutations in the emerin gene). However, some who are diagnosed with these disorders do not carry mutations in lamin genes; it may be that nonmuscle laminopathy may arise from defect in other proteins that are dependent on the nuclear lamina.

Hutchinson-Gilford progeria syndrome (HGPS) is a fatal genetic disorder characterized by segmental, accelerated aging. The major causal mutation triggers abnormal mRNA splicing of the lamin A gene. The resultant changes in nuclear architecture trigger apoptosis. Mice strains deficient in various lamins have been developed.[6,7]

Nuclear Pores

Nuclear pores, spherical channels for molecular exchange between nucleus and cytoplasm, are embedded in the nuclear envelope (Fig. 6.3). Nuclear pores function as an aqueous channel, allowing passive diffusion of ions and small molecules (sucrose migrates by passive diffusion from cytoplasm to nucleus). Translocation of cargoes larger than ~40 kD requires specific transport receptors. Hijacking of nuclear entry and exit pathways is associated with several diseases.[8]

The **nuclear pore complex (NPC)** has three substructures: (1) rings (annuli) on both inner nuclear and outer nuclear membranes, (2) a central granule or plug, and (3) eight central spokes or projecting tips.[9,10] The NPC core consists of globular subunits sandwiched between two coaxial ring-like structures of which the ring facing the nuclear interior is capped by the nuclear basket. Individual NPC proteins have been localized to the NPC core and its associated basket with immunogold techniques; for example, Nup98 in the core region, and Nup153 in the coaxial ring.[11]

Viewed en face in negatively stained preparations, eight spokes are arranged in octagonal symmetry (Fig. 6.4). Electron microscopy coupled with image analysis to calculate three-dimensional maps of detergent-released nuclear pore complexes reveals that each of the eight spokes is built from four closely related subunits.[12]

Use of high resolution scanning electron microscopy reveals the nucleoplasmic face of the NPC to be a basketlike structure attached to the nucleoplasmic coaxial ring. In amphibian oocytes, a highly regular flat sheet of fibers termed the **nuclear envelope lattice** (distinct from the nuclear lamina) is found attached to the distal ring of the basket.[13]

Fibrils are connected to the pore and extend outward into both nucleoplasm and cytoplasm. Those that extend into the nucleoplasm have been shown to form basketlike structures. Some of these connect to other pore complexes to provide stability. Freeze dry/rotary shadow preparations of isolated nuclear pore complexes show that filaments associated with

Vet-ebooks.com

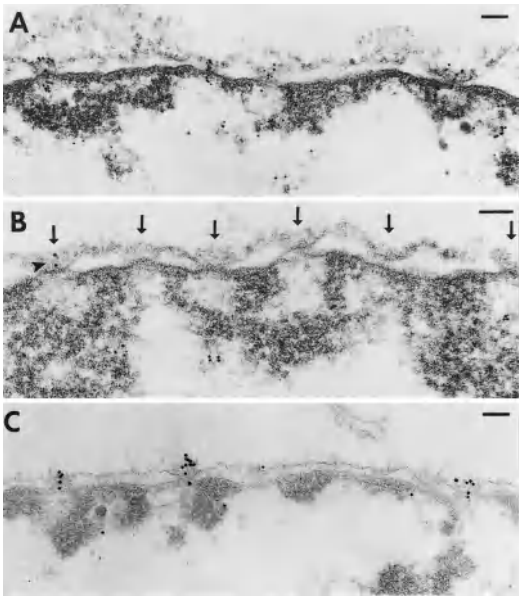


Fig. 6.3 **Nuclear pores**: movement of proteins through nuclear pores. **A**. Colloidal gold particles coated with anti-HAS; **B**. with mutant HSA; and **C**. with nucleoplasmin. Nucleoplasmin-coated gold particles are translocated through nuclear pores in A, but mutant-HSA-coated gold particles are not. (Micrograph: Donald D. Newmeyer, *Cell* 52:641, 1988.)

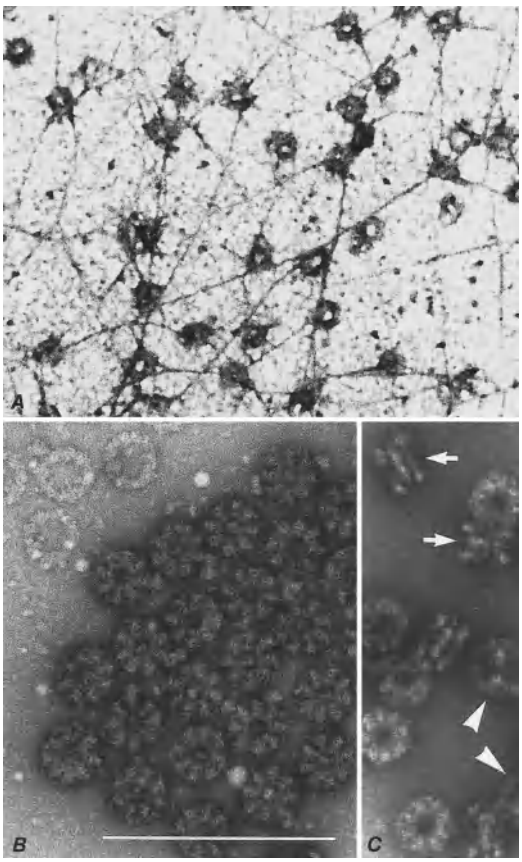


Fig. 6.4 **Nuclear pores**. **A**. **Inter-pore fibers**: en face view of nuclear envelope; fibrils connect pores. (Micrograph: Ulrich Scheer, University of Wurzburg and *J Cell Biol* 69:1, 1970.) **B** and **C**. **Nuclear pore complexes**: released onto the microscope grid and negatively stained. **B**. **En face view** of nuclear pore complexes (*lower right*) and rings (*upper left*). **C**. **Oblique** (*arrowheads*) and edge (*arrows*) **views:** nuclear pore components. (Micrograph: Jenny E. Hinshaw, *Cell* 69:1133, 1992.)

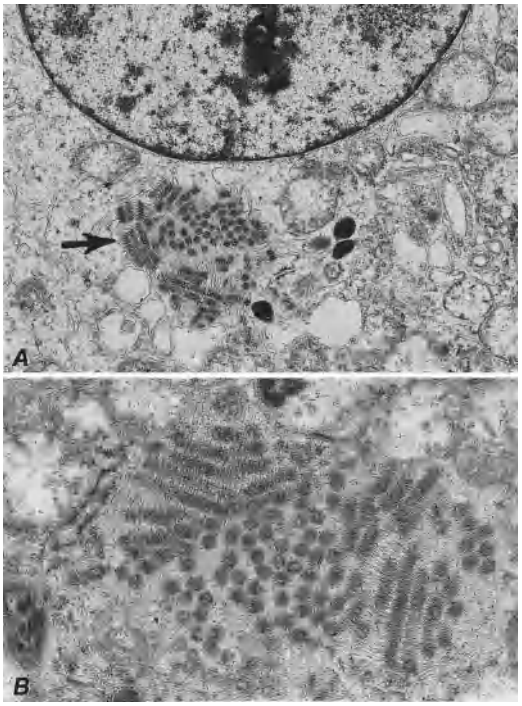


Fig. 6.5 **Annulate lamellae**: cytoplasm of testicular neoplastic cells (interstitial cell tumor). Low (*top*) and high power (*bottom*).

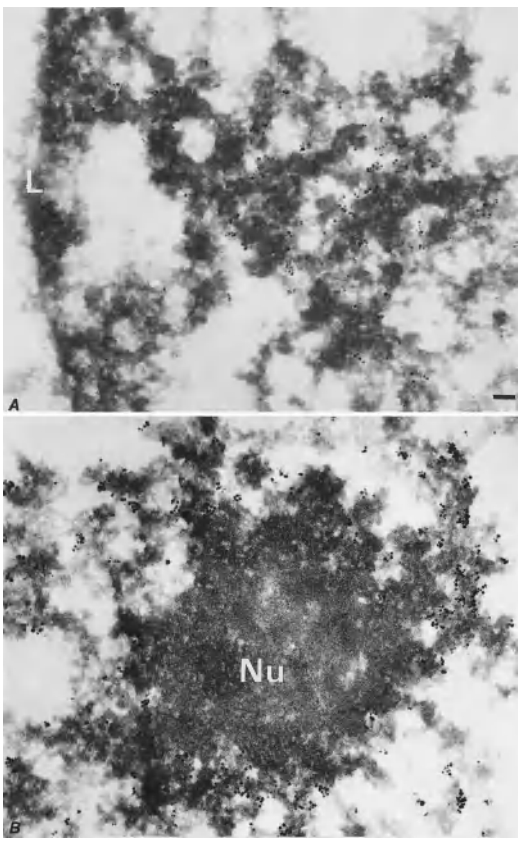


Fig. 6.6 **Nuclear matrix proteins**: localization in HeLa cell nuclei using a silver-enhanced immunogold probe for P125. **A**. **Nuclear matrix structures** associated with the lamina-pore complex (*L*). **B**. **Nuclear matrix structures** associated with nucleolus (*Nu*). Bar = 0.1 µm. (Micrograph: Arjan de Graff, *J Hist Cyt* 39:1035, 1991.)

Vet-ebooks.com

cytoplasmic and nuclear rings differ in structure and function.[14,15]

Nucleocytoplasmic Transport Nucleocytoplasmic protein transport across the nuclear envelope is regulated by **NPCs**.[16] Each vertebrate NPC is a supramolecular assembly of ~30 different proteins that surround a central pore ~40 nm in diameter. **Nucleoporins (Nups)**, the constituent proteins of the NPC, are located near the nuclear and cytoplasmic peripheries of the NPC. Nups drive nucleocytoplasmic transport by binding to transport receptors known as **karyopherins (Kaps)**; Kaps (also called importins and exportins) are required for proteins greater than 40 kD in size (but smaller than the pore diameter).[17] Export of mature mRNA to the cytoplasm is the culmination of the nuclear part of gene expression. As transport-competent, mature **mRNP export complexes** are formed in the nucleus, they pass through NPC.[18]

Nups have been identified using immunogold labeling. Use of dextran tracers has shown a controlled migration of cytoplasmic peptides through pore complexes.[19–21] Importation into the nucleus can be separated into two distinct steps: nuclear pore binding and translocation.[22,23] Nuclear pores increase in number with increasing metabolic activity; for example, in cells stimulated to undergo mitosis the numbers of pores double.[24]

Control of bidirectional nucleocytoplasmic transport involves interplay of the nuclear pore transport channels, transport receptors and the cargo molecule. Receptor mediated transport requires a transport receptor to recognize a signal-bearing cargo to form a cargo-receptor complex, which promptly docks on the side of the nuclear pore complex where it engages sequential interactions with nucleoproteins during translocation. Nuclear localization of transport signals uses NF-κB and p53 signaling. The cell cycle regulator p53 shuttles between nucleus and cytoplasm, its location varying with the stage of the cell cycle. In response to injury, p53 is retained in the nucleus by a masking mechanism that blocks the interaction with the nuclear pore.

Annulate Lamellae

Annulate lamellae are aggregates of membranes that contain nuclear pore complexes, typically arranged in stacks and parallel arrays in the cytoplasm. Pore diameters vary from 60 to 100 nm, but in individual cells pores are of the same size. In rapidly proliferating cells, uncontrolled duplication of pores may lead to large aggregates of pore complexes in the cytoplasm adjacent to the nucleus (Fig. 6.5), a common finding in embryonic and neoplastic cells. Cytoplasmic annulate lamellae arise from the nuclear envelope by blebbing; the vesicles released fuse and flatten to form membranous saccules.[25,26] Chromatin plays an instructive role in the development of the nuclear envelope and the absence of chromatin is associated with formation of annulate lamellae.[27] Annulate lamellae may also, though rarely, be seen in nuclei, that is, blebbing of the inner membrane of the nuclear envelope will give rise to these structures in the nucleus.

Nuclear Compartments

The interphase nucleus is compartmentalized so that chromosomes occupy discrete territories and regulatory proteins are localized in specific nuclear bodies.[28,29] **Chromosome territories** are segregated into gene-rich chromosomes that occupy a central position and gene-poor chromosomes that are closer to the periphery. The nuclear periphery contains silent chromatin. **Interchromatin regions** between chromosomal territories contain regulatory nuclear bodies that include (see Fig. P.2):

- **Interchromatin granule clusters (nuclear speckles):** enriched with pre-mRNA splicing factors and proteins involved in gene regulation (anti-SC35 is a speckle marker protein)[30]
- **Cajal bodies:** sites for biogenesis of spliceosomal small nuclear ribonucleoproteins (snRNPs)
- **Paraspeckles:** mRNA processing sites that contain factors required for initiation of pre-mRNA 3′ end activities[31]
- **Perinucleolar compartment:** include perinucleolar chromatin and other components

Proteins identified in **interchromatin granule clusters** include transcription factors, the large subunit of RNA polymerase II, and cdk8 (the kinase partner of cyclin c, and a component of the mediator complex).[32]

Nucleoproteins are embedded in a **nuclear matrix**, a filamentous network that remains after treatment of cells with nucleases and other procedures that remove membranes and chromatin. Receptors, ligands and other proteins that drive nuclear function have been localized using immunogold techniques (Figs. 6.6 and 6.7). These include **small nuclear ribonucleoprotein particles (snRNPs)** and **heterologous nuclear RNA (hnRNA)**, a precursor of mRNA that complexes with protein to form **heterologus nuclear ribonucleoprotein (hnRNP)**.

Chromatin

Chromatin fibers are complexes of DNA and protein. The inactive chromatin visible by electron microscopy

Vet-ebooks.com

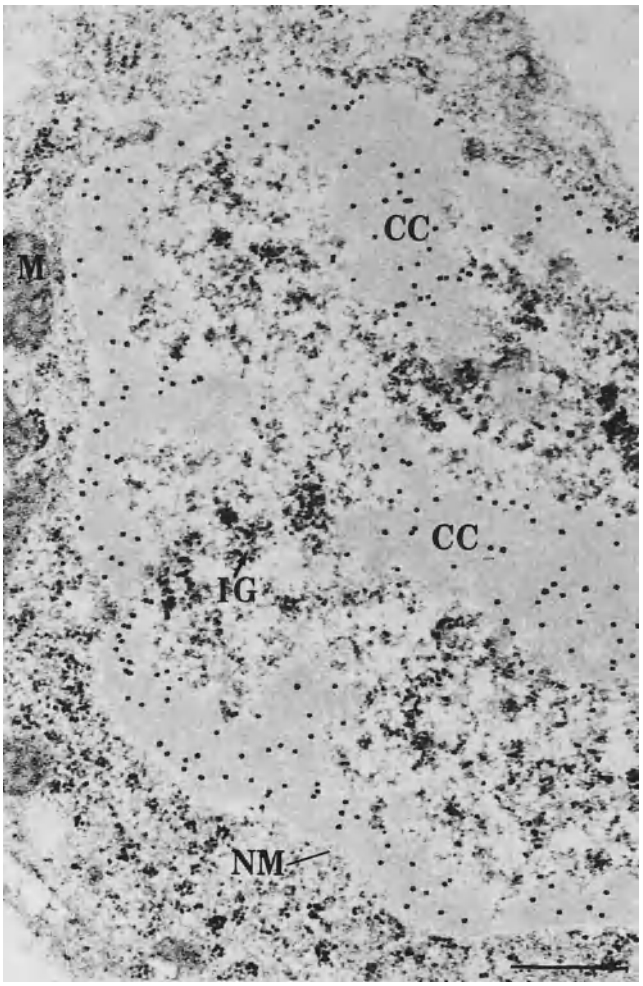


Fig. 6.7 Nuclear receptors: localization of progesterone receptors in uterine stromal cell nuclei. Thin sections were incubated with gold-labeled antireceptor antibodies and chromatin bleached with EDTA. Labeled progesterone receptors are associated with bleached condensed chromatin (*CC*). Ribonucleoprotein structures in the nucleoplasm are not bleached; e.g., interchromatin granules (*IG*). Nuclear membrane (*NM*). Bar = 0.5 µm. (Micrograph: Martine Perrot-Applanat, *J Cell Biol* 102:1101, 1986.)

is referred to as **heterochromatin; euchromatin**, which cannot be seen ultrastructurally, is the active synthesizing part of chromatin. The functional units of chromatin are the **chromosomes**, which become physically distinct only during mitosis; that is, chromosomes condense during mitosis and decondense during interphase.

The precise helical structure of the **condensed chromatin fiber** is not known although scanning electron microscopy studies support a double helical, cross-linked model.[32] Chromatin fibers, when experimentally stretched, have the appearance of beads on a string; the beads represent nucleosomes and the strand the DNA. In the long threadlike DNA molecule, purine and pyrimidine bases carry genes, and sugar and phosphate groups have a structural role.

Telomeres, the DNA-protein complexes located at the end of linear eukaryotic chromosomes, function in chromosome stability during mitosis and meiosis, and they equip normal somatic cells with a cellular clock that deterimines their replicative lifespan. The double-stranded part of the telomere is bound to a multiprotein complex known as shelterin, which prevents telomeres from being recognized and processed as double-stranded breaks. Telomeres are in a gene-less, heterochromatic state; they are transcriptionally silent and have the ability to silence transcription.[33] Immunogold techniques have been applied to localize some proteins in telomeres of cells in vitro.[34]

The **centromere** is the specific locus on each chromosome that directs formation of the **kinetochore**, the multiprotein complex that interacts with the spindle microtubules to promote proper chromosomal alignment and segregation during mitosis. Centromeres are organized into a specialized chromatin structure by incorporation of the centromere-specific histone H3 variant (**CenH3**).[35,36]

DNA

DNA is packaged in nuclei by complexing with histone proteins (H2A, H2B, H3 and H4), which form chromosomal regions that are either permissive or repressive for gene expression. Methylation of histones controls transcription by allowing chromsosomal regions to toggle between on and off states.[37] DNA is coiled up in chromosomes and is uncoiled for gene activity. The complex process of DNA coiling occurs through several stages to reach the highest degree of condensation found in transcriptionally inactive chromatin. At the first level, DNA is wrapped around a set of histones in the **nucleosome**, the structural subunit of the chromatin fiber. A chain of nucleosomes, or 10 nm fibers, is coiled in a 30 nm fiber, which is further coiled or folded. DNA, in its various locations, has been localized ultrastructurally using immunogold techniques,[38,39] and by techinques that extract RNAs and phosphoproteins that mask DNA.[40]

The structure of the **histone octomer**, as determined by electron microscopic crystallography at 22 A resolution and confirmed by x-ray structural determination at 3.1 A resolution, is a unit of four core histones complexed in an octamer, each wrapped in two turns of the DNA helix.[41]

Gene expression begins with selective unfolding of chromosomes. During inactivity, histones bind DNA, which, by constraining it physically, prevents transcription. In this way, the **nucleosome** is the universal

Vet-ebooks.com

repressor of transcription initiation. Critical regions of the genome are embedded within the nucleosome, unavailable to the enzymes that start the transcription process. Conversion of genes from a repressed state to a transcriptionally active stage is accompanied by changes in chromatin. Under the proper stimulus, enhancer regions with nuclease hypersensitive sites are rearranged and move away from the nucleosome. The DNA strand unwinds, allowing transcription to begin.[42]

RNA Polymerases

RNA polymerases initiate gene reading. A gene is transcribed when the massive enzyme RNA polymerase binds to DNA and moves along the length of the molecule copying the sequence of nucleotide bases into their RNA equivalent. The first step in the process is the binding of the enzyme to the beginning or 5′ end of the gene, the **promoter** region. As transcription proceeds a new **RNA transcript** is completed. A **cap** is added to the 5′ end, and a string of 200 adenine molecules (the poly-A tail) is added to the back (3′) end. The RNA transcript then associates with other proteins and exits from the nucleus through the nuclear pore, carrying its codon copies to the ribosomes, where they direct the assembly of amino acids into peptide chains.

All eukaryotic cells contain three different **RNA polymerases**, designated I, II, and III. Each catalyzes transcription of genes encoding different classes of RNA. Polymerase I is found in the nucleolus and initiates synthesis of ribosomal precursor RNAs. Polymerase II catalyzes transcription of all the protein-coding genes or mRNAs. Polymerase III acts outside the nucleolus to transcribe genes for tRNA, 5S rRNA, and for various small RNAs, many of which function in RNA processing.

Gene Regulation by Transcription Factors and MicroRNAs

Transcription factors (TFs) and **microRNAs (miRNAs)** are the largest families of transacting, gene regulatory molecules in eukaryotic cells. By binding to discrete regulatory elements, TFs and miRNAs control dozens of target genes. In fact, most genes are controlled by a combination of transacting factors.[43]

Transcription Factors In the interaction of eukaryotic RNA polymerase subunits and DNA, different proteins help the polymerase to locate the appropriate initiation site to begin transcription. These **transcription factors** can be classified into three types: those that are required for initiation of transcription, those acting later in elongation of the RNA transcript, and those that help in forming an active preinitiation complex (but may not be required after transcription is begun). Specificity resides in the third type, which helps regulate transcription of particular genes.

MicroRNAs **MicroRNAs** are small RNA molecules encoded by the genome that are not translated into proteins; instead, they regulate gene expression. Genomic regions that encode miRNAs are transcribed in the nucleus, and the new miRNAs are then incorporated into RNA-induced silencing complexes (RISC) which suppress translation or promote degradation of target messenger RNAs. In the brain, miRNAs are abundant and disruption of miRNA networks underlies some neurodegenerative disease; for example, the gradual loss of dopamine neurons in Parkinson's disease.[44] New miRNA-based therapeutic strategies include suppression of those that contribute to disease and delivery of drugs that mimic those that promote health. In some diseases microRNAs are overexpressed, and the goal is to inject a complementary RNA sequence (called **antagomirs**, because they antagonize microRNA) that binds to and disables the target microRNA.

Non-Protein-Coding RNAs **Non-coding RNAs (ncRNAs)** are expressed by eukaryotic cells—miRNAs are an integral component of chromosomal structure where RNA-directed processes recruit histone-modifying complexes and DNA methyltransferases that are used in changes that involve epigenetic memory.[45] **Long ncRNAs** direct chromosome silencing, regulate gene expression, or maintain chromosome integrity.

Some of the large viruses express ncRNAs that allow infected cells to evade innate immune responses.[46] For example, **herpesviruses** encode long ncRNAs that inhibit interferon responses, and miRNAs that block expression of proteins that trigger apoptosis, stabilize mitochondrial energy production, and block recognition of infected cells by natural killer cells.

Cyclic AMP Mediates Regulatory Signals

Polymerases that transcribe genes are activated by different messenger molecules. **Cyclic AMP** (cAMP) is a mediator of the regulatory signal of several polypeptides. It modulates nuclear events such as specific regulation of transcription of cAMP-induced enzymes and proteins, phosphorylation of histones and nonhistone chromsomal proteins, and nuclear mechanisms that are involved in cAMP regulation of cell proliferation. It does so via cAMP-dependent protein kinases

Vet-ebooks.com

that are important links with the nuclear events. These enzymes contain a regulatory subunit dimer and two catalytic subunits that have been localized using immunocolloidal gold electron microscopy in heterochromatin and the nucleolus.[47]

Ultrastructure of Transcription

Ultrastructural analysis has aided in characterization of the **primary transcripts** that arise from gene transcription.[48] The first transcripts to be seen in electron micrographs were ribosomal DNA from nucleoli of frog oocytes. Oocytes have very large amounts of rDNA and large numbers of nucleoli that make pre-rRNA. When lysed, nuclear contents spread on a grid and when dried and shadowed, the ribosomal DNA transcription unit can be seen. It appears as a feather-like structure centered on a spine of nucleolar DNA. The nascent pre-rRNA molecules project out from the spine and elongate as transcription proceeds (Fig. 6.8).

Ribosomal RNA (rRNA) Ribosomal RNA is the precursor material for cytoplasmic ribomes. A single pre-rRNA gene is sufficient to be a **nucleolar organizer**, and all other components of the ribosome diffuse to the newly formed pre-rRNA. The structure of the induced nucleolus appears to be the same as a normal nucleolus with several hundred rRNA genes.[49]

Messenger RNA (mRNA) Synthesized in the nucleus as large precursors (pre-mRNAs), mRNAs direct protein synthesis. The protein coding sequences in pre-mRNA molecules are arranged in discontinuous segments called **exons**, which are interspersed with noncoding sequences called **introns**. The production of mature mRNAs requires precise removal of introns and joining of exons by RNA splicing. Among the components necessary for these reactions are the **small nuclear RNAs (snRNAs)**.[46] The complex of snRNAs and its associated protein (with which it exists in cells) is referred to as **small nuclear ribonucleoproteins**.

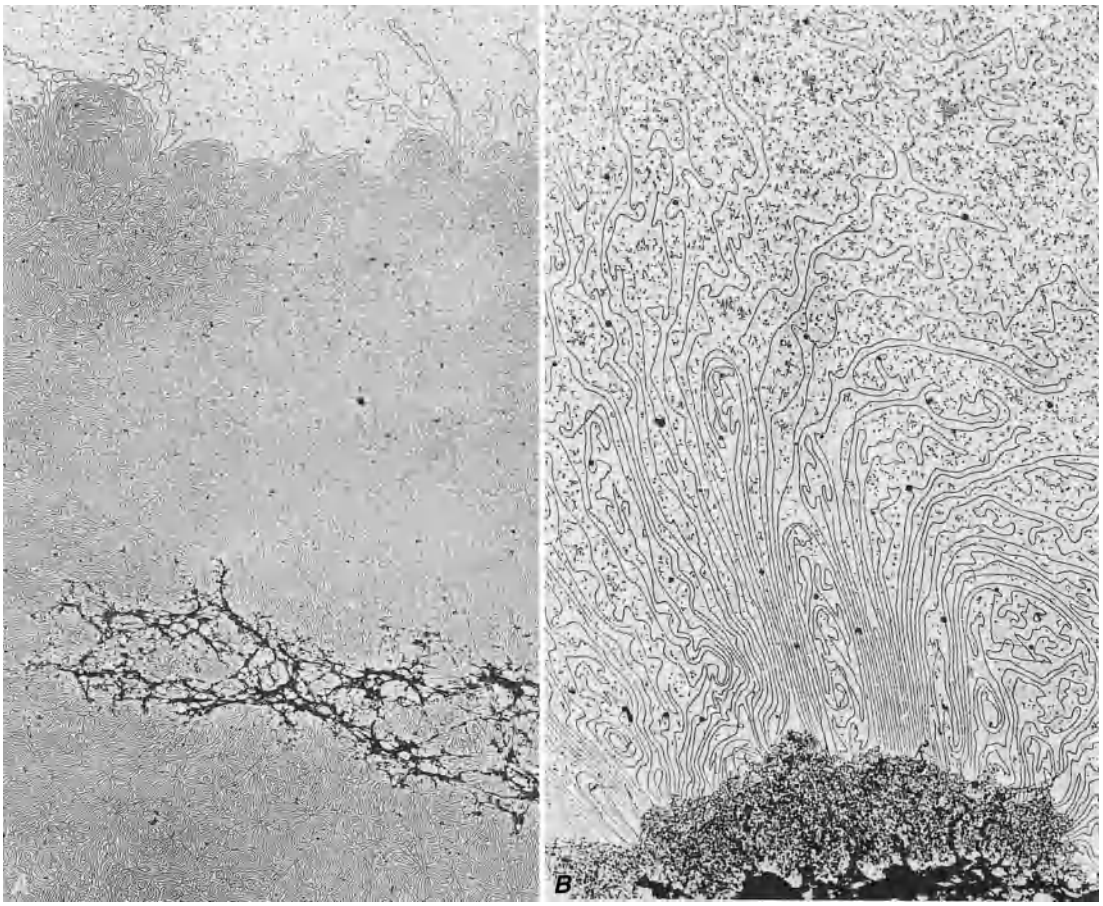


Fig. 6.8 Chromosome metaphase: histone-depleted metaphase chromosome of HeLa cell. Dark fibrous scaffold in the center is surrounded by DNA, which is attached to the scaffold in loops. Low power (*left*); high power (*right*). (Micrograph: James R. Paulson and U. K. Laemmli, *Cell* 12:817, 1977.)

Vet-ebooks.com

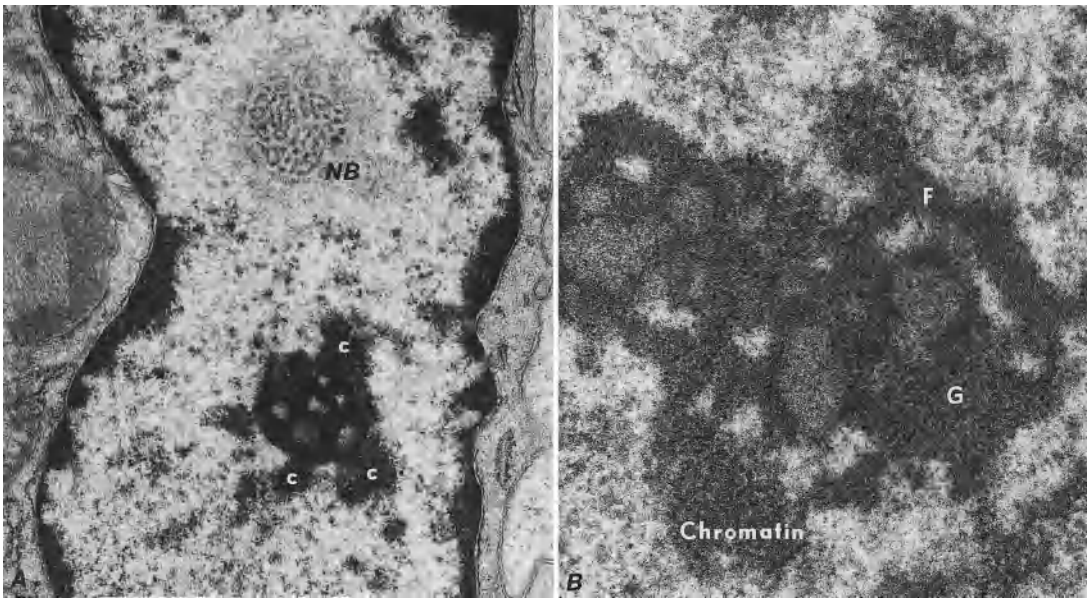


Fig. 6.9 Nuclear body (*NB*) and nucleolus: **A,** perinucleolar chromatin (*c*). **B,** fibrous part (*F*), and granular part (*G*), keratinocyte. Note perichromatin granules and interchromatin granules.

Nuclear regions rich in snRNPs and another non-snRNP pre-mRNA splicing factor are organized in interphase nuclei in the form of a reticular network that extends between the nucleolar surface and the nuclear envelope.[50]

Spliceosomes

During splicing reactions the snRNPs, the pre-mRNA, and other protein factors form a macromolecular complex, the **spliceosome**. Under the electron microscope spliceosomes appear as 40–60 nm particles with distinct morphology.[51] Data indicates that splicing begins before the completion of transcription in active RNA synthesis from chromosomes. Genes have bowed regions on individual nascent transcripts that correspond in size and position to known introns.

RNA editing is a posttranscriptional process that changes the nucleotide sequence of RNA relative to that of the encoding DNA. RNA molecules can also act as enzymes (ribozymes); self-cleaving RNAs have been found in hepatitis D virus, plants, and mitochondria of fungi.

The Nucleolus

Nucleoli are sites where ribosomal RNA (rRNA) synthesis is transcribed and processed and where preribosomes are assembled. Composed of fibrillar and granular parts, they contain various types of ribonucleoproteins in association with and surrounded by chromatin (Fig. 6.9).[52–56]

Nucleoli are largest in metabolically active cells and are prominent at sites where new cells are being formed and in neoplasms. In rapidly metabolizing cells, large, active nucleoli reside at the periphery of the nucleus, probably an attempt to facilitate nuclear cytoplasmic exchange.

Within each component of the nucleolus there are distinct structural and functional domains.[57] Transcription of rRNA genes by RNA-polymerase I takes place in the **fibrillar centers**. Subsequent preribosome formation occurs in the **dense fibrillar component** surrounding the fibrillar centers. Further assembly of preribosomal particles occurs in the **granular compartment**.

Different nucleolar proteins have been identified, each localized to a different nucleolar component. **Fibrillarin**, a protein associated with small nucleolar RNA (snRNA) in the dense fibrillar component, has a key role in ribosomal biogenesis.[58] The ultrastructural location of ribosomal genes in nucleoli has been detected using a silver staining technique for nucleolar organizing regions (rDNA).[59] Some nucleolar proteins have been shown to shuttle back and forth from nucleus to cytoplasm. **Nucleolin**, a protein that localizes primarily to nucleoli with RNA polymerase I (with which it interacts during transcription), also functions as a receptor that shuttles among the nucleus, cytoplasm, and plasma membrane. Immunogold

Vet-ebooks.com

labeling techniques to track the nucleolar localization signal **nuclear phosphoprotein 140 (Nopp140)** have shown that it moves along tracks that extend from the dense fibrillar component across the nucleoplasm to the nuclear pore complex.[60]

The normal interphase nucleolus is bipartite; that is, it consists of a **fibrillar core** of 5 nm diameter fibrils in a loose reticulum and a **granular cortex** composed of spongelike aggregates of dense RNA granules 10–15 nm in diameter. RNA, produced in the fibrillar components, is the precursor for that of the granular regions. Actively transcribing rRNA genes are at the periphery of the **fibrillar centers;** transcription causes progressive accumulation of ribosomal transcripts, giving rise to a **dense fibrillar component**. Fibrillar parts of the nucleolus are composed of two types of fibrillar material: dense and light (also called the fibrillar center). In some studies, five structural components of the nucleolus (the first three of which are sites of silver staining) are listed as: fibrillar center (NOR); dense fibrillar component; nucleolar interstices; condensed associate chromatin; and granular component.

Dense **perichromatin granules** occur in the nucleoplasm at the margins of chromatin and are the storage or transport forms of mRNA. These electron-dense, solitary, spherical granules are 30–35 nm in diameter and are separated from surrounding chromatin by a halo of about 7.4 nm. Nonnucleolar RNA synthesis occurs at the border of condensed chromatin in ribonucleoprotein (RNP) containing **perichromatin fibrils**, structures that require special fixation and staining techniques.

Nucleolar segregation is the major response to toxic injury (Figs. 6.10 and 6.11) (see chapter 1). Nucleolar segregation and up-regulation of nucleolin in hepatocyte nuclei are reported to be a feature of cold-acclimatized fresh water fish; these nucleolar changes are thought to be due to changes in temperature and photoperiod of fish habitats.[61]

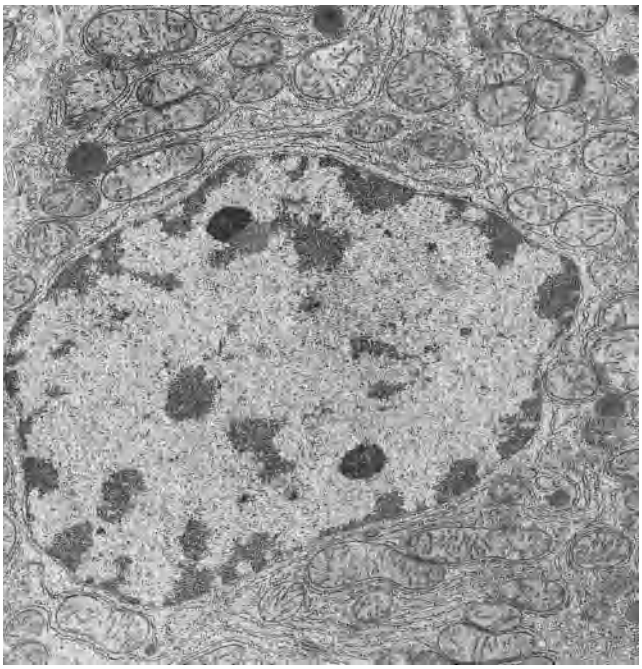


Fig. 6.10 Nucleolar separation: fibrillar and granular parts of the nucleolus have aggregated separately with fibrillar material, reforming in a large nuclear inclusion; cyclophosphamide toxicity, liver, rat.

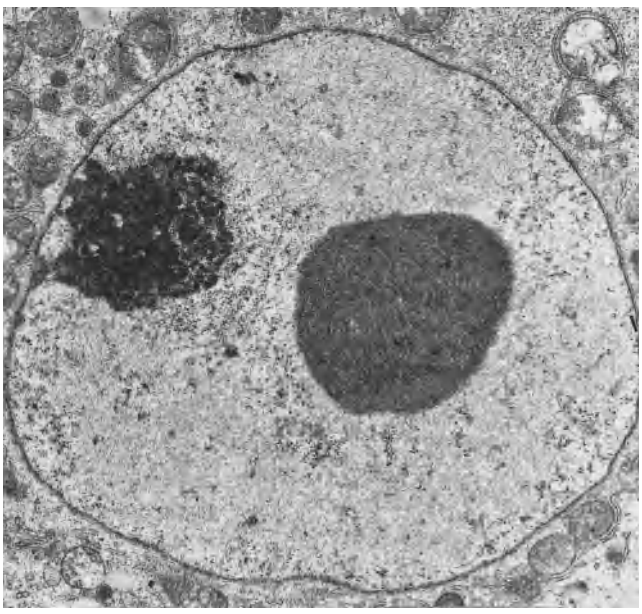


Fig. 6.11 Nucleolar degeneration: actinomycin toxicity, liver, rat. Fragmentation and disintegration of nucleoli, lysis of chromatin, and peroxisomes at sites of degranulation of rough endoplasmic reticulm. (Micrograph: Tim Bertram and Freddy Coignoul, National Animal Disease Center.)

Other Nuclear Structures

Nuclear Body

Nuclear bodies are spherical heterogeneous aggregates of granules in nuclei. Typically they contain central dense particulate material and peripheral zones of fibrils. They are prominent in cells with high metabolic activity and are common in hypertrophic and neoplastic cells, but are rare in degenerate cells. Nuclear bodies originate by segregation of ribonucleoprotein fibrils and granules from nucleoli and contain ribosomal or rRNA, which they store or transport.

Vet-ebooks.com

Experimentally, nuclear bodies develop in cells stimulated by trophic hormones, cyclic AMP, and prostaglandins.[62]

Polymorphic Interphase Karyosomal Association Region

In addition to the nucleolus and nuclear body, the nucleoplasm is organized into minor domains that include some recently identified regions. A subnuclear domain visible by phase contrast as a region of decreased density has been referred to as the **polymorphic interphase karyosomal association region** (PIKA). PIKA proteins, which have been localized with immunogold techniques, are associated with chromatin but their function is not known.[63]

Cajal Bodies

The **Cajal body**, or **coiled body**, is a round to oval, 0.5–0.8 μm diameter body of coiled and fibrillar strands that is associated with the nucleolar periphery. It can be found in interchromatin spaces at variable distances between the nucleolus and the nuclear envelope. Identified originally in neurons as the "accessory body of Cajal," Cajal bodies are argyrophilic, Feulgen-negative, and nonbasophilic,[64,65] and represent a specific nuclear area that can be identified ultrastructurally and that contains specific proteins.[66]

Cajal bodies are associated with biogenesis of spliceosomal small nuclear ribonucleoproteins (snRNPs).[67] Cajal bodies participate in the processing of pre-mRNA. Primary transcripts in mRNA formation require extensive processing, including both splicing and polyadenation, to yield mature mRNA. **snRNPs** are major subunits for splicing complexes, and are required for spliceosome assembly. They locate pre-mRNAs, assemble into functional complexes and, when splicing is complete, are recycled.

Ultrastructural studies using immunogold labeling reveal that Cajal bodies contain aggregates of splicing snRNPs and several nucleolar antigens, including **fibrillarin** and **Nopp140**. In addition, autoimmune patient sera have identified a coiled body-specific protein, called **p80 coilin**, which plays a role in nuclear organization. Coiled bodies in coilin knockout mice fail to recruit snRNPs. Nopp140 shuttles between nucleoli and coiled bodies to chaperone protein transport.

Nucleolar Channel System

A nucleolar channel system, reported in few cells, consists of endoplasmic reticulum harboring the marker glucose-6-phosphatase. Similar membrane systems, termed R-rings, are induced in nuclei in cell cultures by overexpression of the central repeat domain of the nucleolar protein Nopp140. R-ring formation begins at the nuclear envelope through a calcium-mediated Nopp140-membrane interaction.[68]

Metabolic Defects in DNA and Nucleoli

Agents that act on DNA, or on polymerases that transcribe its genetic code, tend to produce the most rapid and widespread changes. When DNA is disrupted, structural evidence of injury occurs in **nucleoli**, in **ribosomes** (from abnormal translation and peptide formation), and in the **Golgi complex** and its vesicles (where conjugation and packaging of proteins are affected).[69] DNA double-strand breaks are highly cytotoxic, and affected cells are killed if they are unable to repair the injury before they enter mitosis. These defects are particularly important in the developing fetus, where the deletion of specific progenitor populations leads to gross defects.[70] Specific sites of damage are produced by the following toxins:

- **Alkylation of DNA nucleotides** causes necrosis in cells with high mitotic rates: **cyclophosphamide** intensely alkylates guanosine molecule.
- **Intercalation of DNA: actinomycin D** interferes with DNA transcription by binding tightly to the double helix of DNA, thereby inhibiting the enzyme RNA polymerase from progressing along the chromatin to build RNA chains (the molecular symmetry of actinomycin matches the symmetry of DNA).
- **Blockade of DNA by DNA analogues: 6MP and 5FU** are substituted for DNA molecules during DNA synthesis (in the mitotic cycle), and cannot function in cell metabolism during mitosis.
- **Folate blockers: trimetroxate** inhibits DNA metabolism by blocking enzymes for synthesis of folates used to produce nucleotides; drugs prevent the enzyme from interacting with para-aminobenzoic acid, a component in folate synthesis.
- **Block of RNA polymerase:** aberrant perichromatin granules accumulate as forms of abnormally processed or synthesized pre-rRNP granules.
  - **Aminonucleoside antibiotics** inhibit the nucleolar enzyme RNA polymerase I and interfere with processing of its product, 45S preribosomal RNA; they terminate elongation of nascent RNA chains through attachment of

Vet-ebooks.com

an aminonucleoside metabolite to the growing point of the RNA chain. Large pronase-sensitive granules, **microspherules**, are commonly found in the segregated nucleoli of toxic cells.

- **Rifampicin:** this synthetic analog of rifamycin specifically inhibits initiation of RNA synthesis by interfering with the first phosphodiester bond in the RNA chains of the B subunit of RNA polymerase.
- **Aflatoxins** cause liver necrosis by degrading RNA polymerase and impairing emergence of ribosomal subunits; the major effect in nucleoli.
- **Amantin:** binds to RNA polymerase, which suppresses activity of the enzyme and interferes with extranucleolar transcription.

Urinary bladder epithelium is highly susceptible, for it receives toxins both hematogenously and via toxic metabolites in stored urine. Lesions produced by alkylation of DNA are followed by a wave of regenerative activity characterized by increased production of DNA, nucleolar fibrillar protein, and RNA. Because these products are abnormal, they segregate, and distinct large nuclear inclusions of granular, fibrillar and chromatin components develop in the nucleus.

The Transcription Stress Response

Cells have a complex **DNA-damage response** to ensure that DNA breaks are repaired with minimal impact on genome stability (see chapter 3). DNA damage-induced responses including DNA repair, transcriptional reprogramming, and delay of cell cycle progression; genotoxicity can also end in apoptosis. **DNA damage sensors** that initiate these responses include **RNA polymerase II**, which when in contact with a damaged DNA base, activates **p53** to stop actions at cell cycle checkpoints.[71] The RNA polymerase II transcription machinery acts as a molecular motor that traverses the genome sensing DNA damage and activates DNA repair when it becomes stalled at blocking lesions.

Ribosomes

Ribosomes are 20–25 nm ribonucleoprotein (RNP) granules that are sites of protein synthesis. They are composed of two subunits, each consisting of several proteins associated with a long rRNA molecule. Within the ribosome, amino acids are assembled into polypeptide chains as the genetic message borne from the chromosome by the mRNA molecule is translated. A **polysome** (or polyribosome) is a series of ribosomes (engaged in translation) associated with a single mRNA strand. Polysomes are stabilized by the microtubular lattice, usually near the nucleus. In contrast, a **monomeric ribosome** is free to diffuse throughout the cytoplasm. Polyribosome formation accelerates as protein synthesis increases.

Ribosomes synthesize different proteins by interacting with different **messenger RNAs** (mRNA), which contain the templates or codes for protein production. Ribosomes provide an environment that controls interaction between mRNA codons and tRNA anticodons. Amino acids are brought to the ribosome by tRNA. Protein synthesis begins when an **initiation complex** is formed by joining of a 40S subunit and a binding site on mRNA. Several small proteins called **initiation factors** bind to a special tRNA and bind it to the small RNA subunit.

Bacteria Use Ribosomes for Replication

Ribosomes are subverted by pathogenic microorganisms and reprogramed to produce specific microbial proteins. Many viruses produce their progeny by using protein synthesis on host cell ribosomes. Intracellular bacteria such as *Brucella* spp. and *Legionella* spp. replicate within cisternae of the rough endoplasmic reticulum and appear to use peptides to produce the ribosome of the host cell (Fig. 6.12).

Toxins Affecting Ribosomal Translation

Toxic injury to components of the ribosome results in failure of ribosomes to develop or, if formed, to disintegrate and detach from the membranes of the RER. Failure of ribosomes to produce enzymes and structural proteins required for cell maintenance has consequences for the plasma membrane, mitochondria, and other organelles. Ultrastructural changes include dilatation of the RER and Golgi complex, and degranulation of RER with aggregates of ribosomes in the cytoplasm. Lipoprotein particles develop in Golgi saccules. Chromatin decondenses or uncoils, and nucleoli become less spherical and develope irregular shaggy edges, a change related to facilitation of transcription of genes that specify new rRNA and ribosomal protein. Ribosomal pathways affected by toxins include:

- **Cyclohexamide** interferes with translation by binding to the large 60S subunit of ribosomes. Binding excludes subsequent binding of guanosine triphosphate (GTP), the energy source for

Vet-ebooks.com

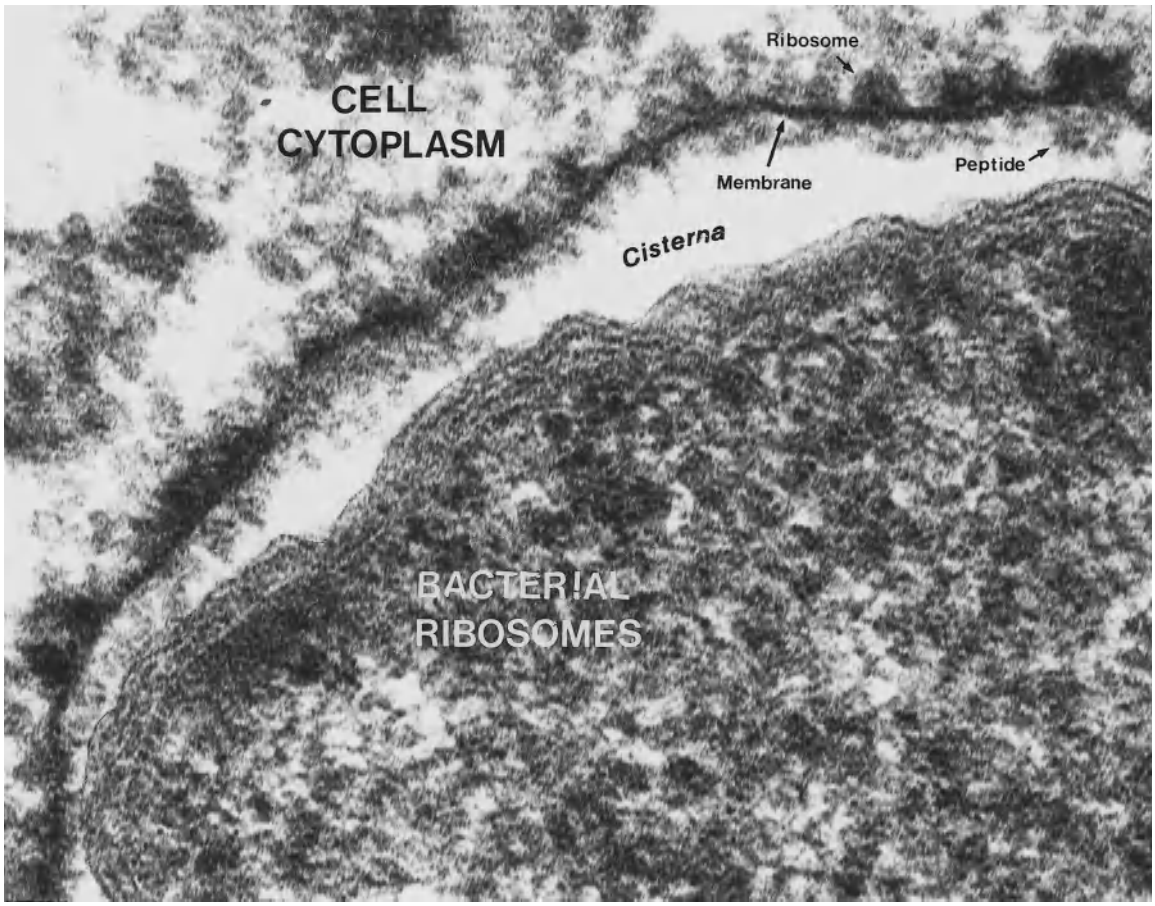


Fig. 6.12 Rough endoplasmic reticulum: ribosomes of RER. Cisterna of RER contains *Brucella abortus*, an intracellular bacterium. Ribosomes on cytoplasmic face of the RER membrane release peptides that protrude into the cisterna.

translation, so that ribosomal protein synthesis is blocked.[72]

- **Diphtheria toxin** is an ADP-ribosyltransferase that cleaves NAD^+ and transfers its ADP-ribose moiety to a specific substrate protein; the critical cellular target proteins are GTPases and target cells are killed by ADP-ribosylation of elongation factor-2, which blocks protein synthesis.
- **Ethionine**, an analog of methionine, reduces ATP by trapping adenine as S-adenosylethionine. Energy cannot be produced, and synthesis of protein and RNA are affected; hepatocytes and pancreatic acinar cells degenerate with loss of membrane-bound ribosomes, destruction of nucleoli, and accumulation of triglycerides within RER.[73,74]

Other models for toxic effects on ribosomal protein synthesis in the liver are vinblastine, ethanol, vinyl chloride, and halothane (see chapter 17). Rifampicin and streptomycin are potent inhibitors of the initiation of RNA synthesis; the latter interferes with binding of formylmethionyl tRNA to ribosomes and thereby prevents protein synthesis.

Genetic Defects in Ribosomal Translation

Genetic mutations may produce abnormal proteins that are trapped in the ribosome, or that accumulate at some post-translational site. If newly synthesized proteins fail to obtain the correct tertiary or quaternary structure they are retained in the cisternae of the rough endoplasmic reticulum and are degraded.

Mutations of human genes bearing codes for α_1-**antitrypsin** and **LDL receptors** cause the production of abnormal proteins that become trapped in the endoplasmic reticulum. The lack of the normal gene results in a genetic disease. In **familial hypercholesterolemia** the receptor is synthesized and glycosylated but does not reach the cell surface.[75]

Vet-ebooks.com

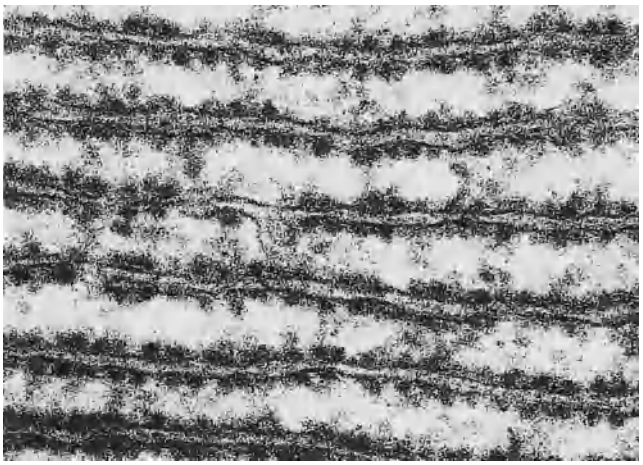


Fig. 6.13 Ribosomes: attached to rough endoplasmic reticulum; pancreatic acinar cell.

α_1-Antitrypsin Deficiency

Livers of **α_1-antitrypsin deficiency** patients produce an abnormal antitrypsin and this leads to accumulation of amorphous material surrounded by irregular, undulant membranes of endoplasmic reticulum in the cisternae of the SER. Large inclusions develop that are composed of a central osmophilic core surrounded by an electron-lucent halo.[76–79]

Rough Endoplasmic Reticulum

Rough endoplasmic reticulum (RER) is a closed membrane-bound system of anastomosing canaliculi and saccules that ramify throughout the cytoplasm. **Ribosomes** are attached to the peripheral membrane (Fig. 6.13) and secrete new peptide chains through the membrane and into the **RER cisternae**. The extent of the RER varies greatly with cellular metabolic activity.[80,81]

Transport of peptides through the membrane of the RER occurs by activation of discrete regions in the peptide chain termed **signal** and **stop-transfer sequences**, which initiate and terminate translocation, respectively. A specific receptor or "transport site" on the membrane binds the newly formed polypeptide signal sequence, which dangles from ribosomes lying free in the cytoplasmic matrix; this binding attaches the ribosome to the membrane and allows its newly formed polypeptide to pass through the membrane into the cisternae. Once in the lumen of the RER, the polypeptide folds spontaneously and achieves a configuration that prevents it from passing back into the cytosol. After translation is complete, ribosomes detach and move back into the cytoplasmic matrix.

Post-translational Modification in the RER

Folding, glycosylation, cross-linking, and sorting of peptides into appropriate conformations are called **post-translational modifications**. They begin in cisternae of the RER, even though most are completed in the Golgi complex.[82] Complete proteins can be detected in the RER cisternae by cytochemical methods; for example, albumin is detected in the RER of hepatocytes.[83] **Glycosylation** adds covalently linked oligosaccharides to the proteins to form glycoproteins, a process also completed in the Golgi complex.[84] Oligosaccharide-processing enzymes, resident in the RER membrane, remove and add terminal sugar molecules, for example, glucosidases that remove glucose units. Glucose-6-phosphatase, a marker for the RER, heavily labels this organelle in hepatocytes and other cells that metabolize glucose.[85] Some of these enzymes are also found in membranes of the Golgi complex and cytoplasmic vacuolar transport system.[86]

Chaperones are high molecular weight complexes with ATPase activity that control the folding and assembly of proteins. Chaperones recognize and stabiize partially folded polypeptides during assembly and disassembly. **RER chaperones** for newly synthesized proteins including BiP, calnexin (CNX), calreticulin (CRT), GRP94, protein disulfide isomerase (PDI), ERp57, and ERp72. Protein disulfide isomerase catalyzes thiol or disulfide reactions that influence peptide folding. Binding to any one of these RER proteins seems to be sufficient to prevent forward transport.

Members of the Hsp60 family of **stress proteins** mediate the folding of many different proteins. Electron micrographs of negatively stained chaperonin complexes show structures that appear as double doughnuts with a central channel of 6 nm that may bind substrates.[87] The quaternary structure of chaperonin oligomers from bacteria has been revealed by electron microscopy.

Properly folded proteins leave the RER at membrane exit sites where components of the COPII coat associate with the cytosolic surface of the RER membrane. These complexes bud off as COPII vesicles and tubular saccules to begin export to the Golgi complex.[88] After detaching from the RER membrane, COPII vesicles form **vesiculotubular clusters**.

Vet-ebooks.com

Protein Degradation in the RER: Ubiquitinization

Abnormal proteins of various origins accumulate in the cisternae of the endoplasmic reticulum if there are defects in the primary or secondary structure of the molecule. Proteins that fail to fold or assemble correctly are not released from the endoplasmic reticulum but are retained in the cisternae and removed by ubiquitinization. This proteolytic system in the pre-Golgi endoplasmic reticulum is rapid and highly selective.

Misfolded Proteins and Proteosomes

In the RER cisternae, persistently misfolded proteins are retrotranslocated to the cytosol and degraded by the **proteasome**. In the injured cell, similar unique transitional vesicles transport abnormal proteins from RER to proteosomes via a pathway that does not use the same coat proteins and exit mechanisms as normal transitional vesicles. This pathway uses an **ER degradation-enhancing α-mannosidase-like protein-1 (EDEM 1)** that targets misfolded glycoproteins for proteosomal degradation, removing them from the calnexin/calreticulin cycle.[89]

Golgi Complex

The Golgi complex is a series of stacks of membranous saccules surrounded by tubules and vesicles. In metabolically active cells, Golgi saccules form a broad, continuous perinuclear network composed of three separate compartments, each identified by unique cytochemical reactivity according to the different functions (Fig. 6.14).[90]

The Golgi complex is a maturation site where newly synthesized proteins are glycosylated, concentrated, and packaged into granules. Cytochemical localization of enzymes and their products have established that the construction of N-linked oligosaccharides in the Golgi is a three stage process: (1) trimming of mannose residues started in the RER is continues in the *cis* Golgi network, (2) addition of N-acetylglucosamine and removal of additional mannose residues occur in the *medial* cisternae, and (3) addition of galactose followed by sialic acid is done in the *trans*-cisternae.[91]

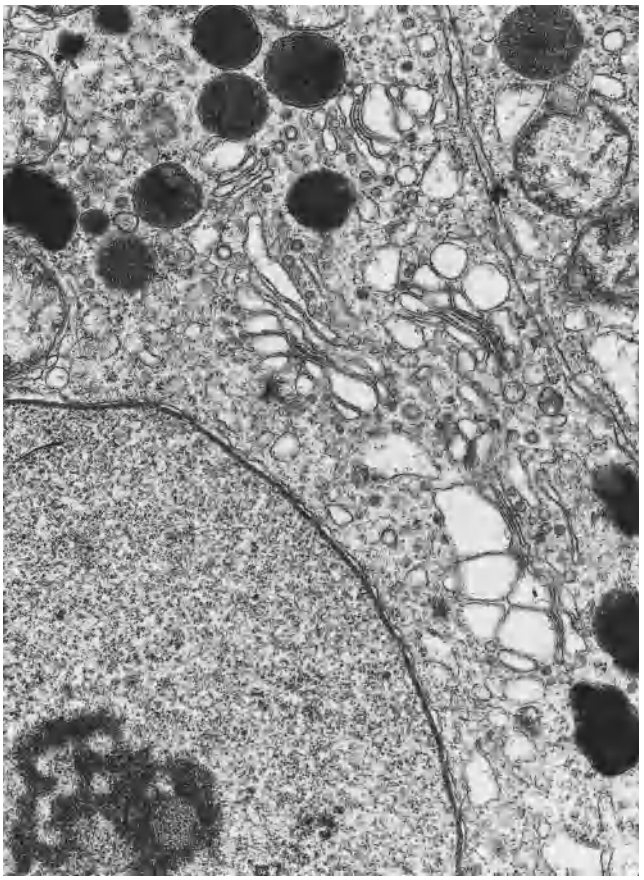


Fig. 6.14 Golgi complex: adrenal cortex, zona fasciculata. Golgi complex is vacuolated and surrounded by vesicles and dense granules.

Golgi cis Face: Transitional Vesicles from RER to Golgi

Small **transitional vesicles** move cargo from the RER to the cis face (or forming face) of the Golgi complex. Transitional vesicles form by budding into the cytosol from RER membranes. During transport to the cis face, peptides are glycosylated and folded into the proper configuration. Specificity comes from membranes **receptors** the bind the cargo proteins, and cytosolic **coat proteins** that complex to membrane sites where the receptor-cargo protein complex is fixed. These coat proteins cover the cytoplasmic surfaces of transitional vesicles and control their destination; coat proteins have been identified by immunogold techniques.[92]

Golgi saccules also receive material from **endosomes;** for example, proteins that attach to the cell surfaces can be shown to be transported by endosomal vesicles directly to the Golgi complex.[93]

Retrograde Transport: Golgi to RER

Transitional vesicles also return peptides from the Golgi to the RER, a process called **retrograde trans-**

Vet-ebooks.com

port.[94] A recycling pathway from the **cis** face to the endoplasmic reticulum moves MHC class I molecules.[95] Called the "cis-Golgi network," it allegedly is used as a sorting organelle to select proteins for return to the endoplasmic reticulum. Retrograde transport back to the RER occurs by replacement of membrane COPII coats with a COPI coat; COPI vesicles mediate the return back to the ER.

Medial Face: Intra-Golgi Vesicles

Vesicular transport systems of smooth and coated vesicles (of 75 nm diameter) shuttle newly synthesized proteins through successive compartments of the Golgi complex. Many cytosolic and membrane-associated proteins are involved in Golgi membrane trafficking. Other membrane-associated coat proteins are important in budding of vesicles.

Two major classes of vesicles are associated with the Golgi complex: (1) **clathrin-coated vesicles** transport in the endocytic pathway, and to and from the trans Golgi network (TGN); the coats of these vesicles consist of heavy and light chains of clathrin, and α, β, or v adaptin complexes. (2) **nonclathrin-coated vesicles** are involved in transport within the Golgi, and between Golgi and endoplasmic reticulum; these vesicles have a transiently attached coat of **adaptin complexes** formed of α, β, γ, and δ **coatamer proteins (COP)**. **Adaptins** (proteins that provide binding sites for the sorting signals) on membranes of TGN vesicles act in sorting M6P receptors into different sites.

Nonclathrin-coated vesicles bud from membranes of the cis Golgi area. They rapidly transform to smooth vesicles by shedding their coat.[98] Coat material is not clathrin (clathrin-coated vesicles are restricted to the **trans** Golgi network). **ADF ribosylation factors** are a family of low molecular weight GTP-binding proteins that are a component of Golgi-derived nonclathrin-coated transport vesicles. They function to modulate vesicle budding and uncoating through controlled GTP hydrolysis.[96]

Maturing Component: The Trans Face

The **trans face** of the Golgi complex (also called the concave or maturing face) contains long saccules with dilated ends, and a variety of associated vesicles, tubules and granules (Fig. 6.15). Grouped together these structures are also called the **trans Golgi network** (TGN, trans Golgi reticulum).[97–99] Glycosylated proteins in the trans face move to the dilated periphery of the saccule and are released as product-bearing vacuoles; for example, in the pancreatic β cell, proinsulin, abundant in Golgi stacks, is transferred to clathrin-coated granules, where conversion to insulin occurs.[100] As maturation proceeds, clathrin disappears and vesicles appear as smooth-surfaced mature secretory granules.[101]

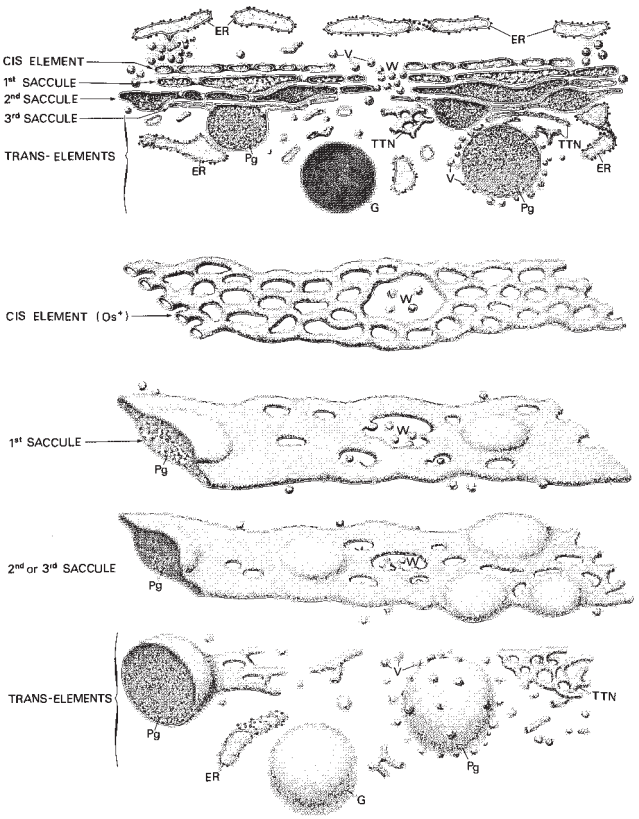


Fig. 6.15 Golgi saccules: coated and smooth vesicles transport material from the *cis* to the *trans* face. (Drawing: A. Rambourg, *Am J Anat* 183:187, 1988.)

Directing Traffic in the Trans Face

Carbohydrate moieties of glycoprotein receptors in membranes of the Golgi complex direct intracellular traffic. In effect, these sugars are address markers, comparable to postal zip codes, directing proteins to appropriate destinations. For example, acid hydrolases are directed to lysosomes by terminal **mannose-6-phosphate (M6P)** residues on oligosaccharide chains of the enzyme molecule. The M6P is a recognition marker by which these enzymes are sorted for delivery. The presence of M6P enables the enzyme to bind to **M6P-receptors** on membranes of vesicles in the trans Golgi network. The receptor-ligand complexes are then carried in clathrin-coated vesicles to prelysosomes. The acidic interior of the prelysosome triggers separation of enzyme from the M6P-receptor (which

Vet-ebooks.com

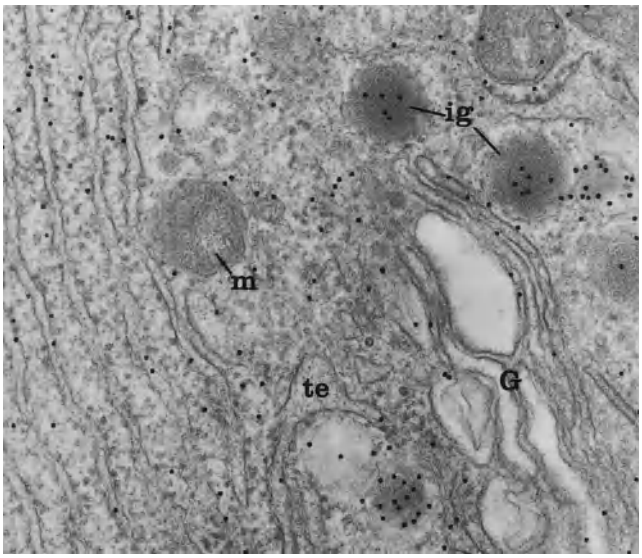


Fig. 6.16 Golgi complex: pancreatic B cell labeled for insulin by the protein A-gold technique. Gold particles are over secretory granules (*ig*) and over cisternae of rough endoplasmic reticulum and transitional elements (*te*) of the endoplasmic reticulum at the *cis* side of the Golgi complex (*G*); mitochondria (*m*). (Micrograph: M. Bendayan, *Am J Anat* 185:205, 1989.)

is then carried back to the trans Golgi network in noncoated vesicles to complete the transport cycle).[102,103]

Trans Golgi sorting of newly synthesized lysosomal enzymes uses the M6P signal, which directs cargos to clathrin-coated vesicles that fuse with endosomes to reach lysosomes. Lysosomal enzymes are efficiently, but not fully, segregated from secretory proteins.

Redistribution of **membrane cholesterol** occurs as membranes progress through the Golgi complex. Membranes gradually incorporate cholesterol as they move through the complex; that is, there is a gradient from ER-like cholesterol distribution at the cis face to plasma-membrane-like at the trans face. Using filipin probes, membrane cholesterol increases progressively from ER to Golgi cis, to Golgi trans, to nascent secretory granules, to plasma membrane.[104]

Acidification occurs in the trans face where membranes contain integral proteins that control pH. Trans face vesicles are acidified by the electrogenic proton pump, and by a band 3-type anion exchanger (which exchanges bicarbonate for chloride at neutral pH, and cotransports sulfate and protons at slightly acid pH).[105]

Secretory granules originate in the Golgi (Fig. 6.16), and upon appropriate stimulation, product-bearing vesicles pinch off from the concave maturing face and are either stored in the cytoplasm or move to the cell surface where their contents are expelled.[106,107]

Golgi Complex in Disease

Inhibited Protein Synthesis Leads to Golgi Vacuolation

Degeneration of the Golgi complex occurs secondary to any disruption of the protein synthetic pathway. The Golgi complex becomes vacuolated, and its membranes fragment into vesicules. In early cell swelling, abnormal proteins and lipoprotein particles may develop in cisternae of the Golgi complex. Glycosylation of proteins and lipids is impaired in injured cells and these substances accumulate within the vesicles. Fragmentation of the Golgi can be induced by depolymerization of microtubules and by alteration of trafficking of vesicles between ER and GA.[108,109]

Drugs That Poison the Golgi

Enzymes that catalyze reactions within each part of the Golgi complex modify proteins to create specific "signatures" that send proteins in a particular destination. Blockage of these pathways selectively stops the flow of peptides through the Golgi stack and, in some cases, even reverse their flow.[110] All drugs that affect protein synthesis or protein secretion produce a secondary effect on the Golgi complex, and changes in the Golgi complex have important secondary effects on secretory granules.[111]

Protein Synthesis Blockade Brefeldin, ricin, abrin, modecin, Shiga toxin, and diphtheria toxin all inhibit protein synthesis, and are used experimentally to poison the Golgi complex. **Brefeldin A**, a fungal metabolite, causes disassembly of the Golgi complex and redistribution of medial and cis Golgi proteins to the endoplasmic reticulum. It causes the Golgi complex to swell and to extend tubular processes out to the cellular periphery. Tubules rapidly fragment, and merge with the endoplasmic reticulum.[112–114] Brefeldin A specifically blocks movement of protein from the RER to Golgi cis areas. It does not block backward movement from Golgi to endoplasmic reticulum. Treatment of Brefeldin A is a specific inhibitor of vesicular movement and exocytosis because it binds to the vesicle coat protein β-COP.

Disruption of Golgi Membranes **Monensin**, an ionophore that causes membranes to become leaky, affects post-translational glycosylation of glycoproteins by disrupting membrane permeability to protons thus making cisternae alkaline and inhibiting receptor

Vet-ebooks.com

recycling. Monensin has a predilection for cardiac and skeletal muscle cells in which the intake of Na^+ and loss of H^+ are accompanied by entry of Ca^{++} and degeneration and necrosis. Monensin impairs processing beyond the high-mannose stages, while N-linked oligosaccharides are being processed from high-mannose precursors to mature complex forms (during passage of molecules from the endoplasmic reticulum through the Golgi cis, medial, and trans areas). By this action it has widespread effects and causes defective cleavage and processing of proteins, reducing secretion, and inhibiting internalization. Human bone marrow neutrophil precursor cells incubated with monensin produce granules that lack peroxidases and other Golgi-contributed enzymes.[115] An increase in cytosolic Ca^{++} leads to exocytosis.

Viral Usurpation of the Golgi Complex

The secretory pathway in the ER and Golgi complex provides the environment for replication of several pathogenic viruses. Immature dengue virions bud into the ER of an infected cell and pass to the TGN where the low pH causes them to undergo a reversible conformational change. Acidification renders them accessible to cleavage by furin, a protease primarily localized in the TGN.[116]

Cytoskeleton Disruption: Colchicine

Normal Golgi complex function requires an intact cytoskeleton. Microtubule toxins such as colchicine or vinblastine causes loss of enzymes in the Golgi saccules and formation of foci of transport vesicles and small pleomorphic secretion granules.[117] In treated cells, Golgi stacks fragment into vesicles that lack appropriate enzyme activities. The Golgi region of hepatocytes of rats treated with colchicine is diminished and contains large vacuoles that contain globules of very low-density lipoproteins.[118,119]

Secretion

Secretory granules contain cargos as diverse as enzymes, hormones, plasma membranes and bile. The spectrum of contents runs from protons and water to the complex conjugates of proteins and lipids that are secreted as milk and yolk. Secretion of these diverse products occurs, in most cells, by one of two major pathways: constitutive or regulated.

- **Constitutive secretion** occurs via **secretory transport vesicles** that leave the Golgi complex and rapidly and continuously migrate to and fuse with the plasma membrane; secretions are released by **exocytosis** immediately after they are produced.
- **Regulated secretion** occurs via large, protein-bearing secretory granules or small secretory vesicles.

In general, **secretory granules** contain large well-defined proteins in large bulk amounts; for example, the granules of cells of the pancreas and salivary glands. After their cargo has been synthesized in the RER and matured in the Golgi complex, secretory granules are shunted to the cytoplasm for storage. Secretion occurs when the cell receives an external stimulus.

Secretory Transport Vesicles

Secretory vesicles, also called **transport vesicles**, move in an unregulated (constitutive) manner to pass proteins quickly, without storage, from the Golgi complex to cell surface. **Secretory vesicles** release ions and other small molecules, for example, the acid-secreting vesicles of gastric parietal cells. At the plasma membrane, secretory vesicles dock and fuse at specialized structures in the plasma membrane referred to as **porosomes**.[120] After docking, vesicles swell allowing expulsion of intravesicular contents. Secretory vesicles are smaller and do not have the dense cores of secretory granules. Since they have a short half-time, secretory vesicles may be difficult to find in electron micrographs.

Vesicles similar to transport vesicles provide new phospholipid bilayers as replacement for damaged segments of membranes. The vesicle fuses with the plasma membrane so that patches of new membrane are inserted into the old plasma membrane. The Golgi complex is, in a sense, a membrane factory that provides a continual source of new membranes for the cell. Old membrane segments, like most of the discharging secretory vesicle, are removed by apical endocytotic vesicles and degraded.

Secretory Canaliculi

In the resting state secretory vesicles and their tubular connections form a **tubulovesicular system**.[121,122] In the stimulated, activated state the tubulovesicular system is rapidly reorganized to form massive **secretory canaliculi** ("intracellular canaliculi") (see figure 5.10). During transformation there is mobilization of actin and spectrin as secretory vesicles are moved to the cell surface.[123] Mitochondria-rich cells in the renal

Vet-ebooks.com

collecting duct acidify urine through similar acid release mechanisms.[124]

In the **secretory pathway**, bioactive materials are first stored in **secretory vesicles** and are released only when cells are stimulated by an external secretagogue. The pathway involves movement of secretory vesicle to the subplasmalemmal region, tethering, and docking at release sites on the plasma membrane. Docking triggers membrane fusion with release of vesicle contents and retrieval of vesicle membranes. Exocytosis is typically regulated at the docking stage, and is critical for release of hormones such as insulin. **Granuphilin**, specifically expressed in the pancreatic β cell, is essential for docking and of imposition of a braking effect on exocytosis.[125]

Secretory Granules

Secretory granules are composed of dense matrices of secretory products bounded by a membrane. For ultrastructural analysis the secretory peptide or glycoprotein can be specifically labeled using the immunogold technique. Antibodies against the protein are tagged with colloidal gold and this reagent is incubated with tissue sections.[126–128] Although secretory granules of endocrine and exocrine glands generally are committed to specific products, they can contain different peptides and, under appropriate stimuli, secretion can be converted from one peptide to another.[129]

Secretory granules remain inactive until affected by the appropriate stimulus. Secretagogues, agents that stimulate secretion, cause rapid and massive expulsion of granules.[130] In polarized epithelial cells, secretory granules are released at lumenal surfaces. However, in massive secretagogue-induced stimulation, there may be a shift to granule release at intercellular spaces.[131] In addition, there can be granule fusion to form irregularly shaped giant granules.

Secretory Exocytosis

The process of granule exocytosis, once initiated, is a continuous one.[132,133] It can be conceptually divided into four distinct phases:

- **Movement** of the granules to the cell surface
- **Fusion** of the granule membrane to the plasma membrane
- **Fusion pore** formation in granule membranes with entry of water into the matrix and dispersal of granule components
- **Degranulation:** expulsion of granules leaving empty **exocytotic pockets**

Explosive secretion involves granule swelling with unwinding of proteins and glycoproteins (Fig. 6.17). The water channel **aquaporin-1**, present in the secretory granule membrane, acts in rapid GTP-induced granule swelling.[134]

As secretion is initiated, actin microfilaments aggregate adjacent to the secretory granule and the granule is moved to the cell surface. At the precise site where contact is to occur, proteins within the membrane are moved aside and the two membranes (plasma membrane and granule membrane) touch, interact, and fuse.[135] Freeze-fracture micrographs at this stage have revealed a fusion rosette on the membrane and a corresponding annulus on the secretory vesicle.[136] Annexins (synexin, calpactin, et al.) are a family of proteins that bind membrane phospholipids to cause vesicules to move, and their membranes to fuse.[137]

Membrane fusion is a basic cellular process that is involved in both exo- and endocytosis, and to cytoplasmic vesicular traffic of all types. Electrophysiologic analaysis of mast cell exocytosis and other model systems suggests that the initial fusion pore is 2–2.5 nm in diameter.[138,139]

The plasma membrane changes as the granule bulges from the surface. It is free of protein particles, which have accumulated at the edges of the bulge. The lipids in the membranes are removed, the secretory vesicle discharges its contents, and the remaining vesicle membrane fuses with the plasma membrane. As the secretion process is completed, sites of granule release at the cell surface are distorted. In endocrine tissue, parenchymal cells form close associations with adjacent capillaries and may project lamellipodia into sinusoidal lumens.

Calcium in Secretion

Exocytosis of granules in most secretory cells requires and is stimulated by an increase in Ca^{++} in the cytosol. Intracellular calcium exists in three physico-chemical forms: free in cytosol, calmodulin-bound in cytosol, and sequestered in cytoplasmic organelles. Ligands that bind to surface receptors cause Ca^{++} to enter as the free form. For example, bridging of mast cell-bound IgE by antigen induces not only Ca^{++} influx into the cell, but a redistribution of intracellular Ca^{++}.[140]

During Ca^{++}-dependent secretion, the calcium-binding protein **calmodulin** associates with granule surfaces. Calmodulin can be labeled with a protein A-gold technique and anti-calmodulin antibodies on the surface of lamellar bodies.[141]

The role of calcium is markedly affected by pH. The pH inside secretory granules is regulated by ion

Vet-ebooks.com

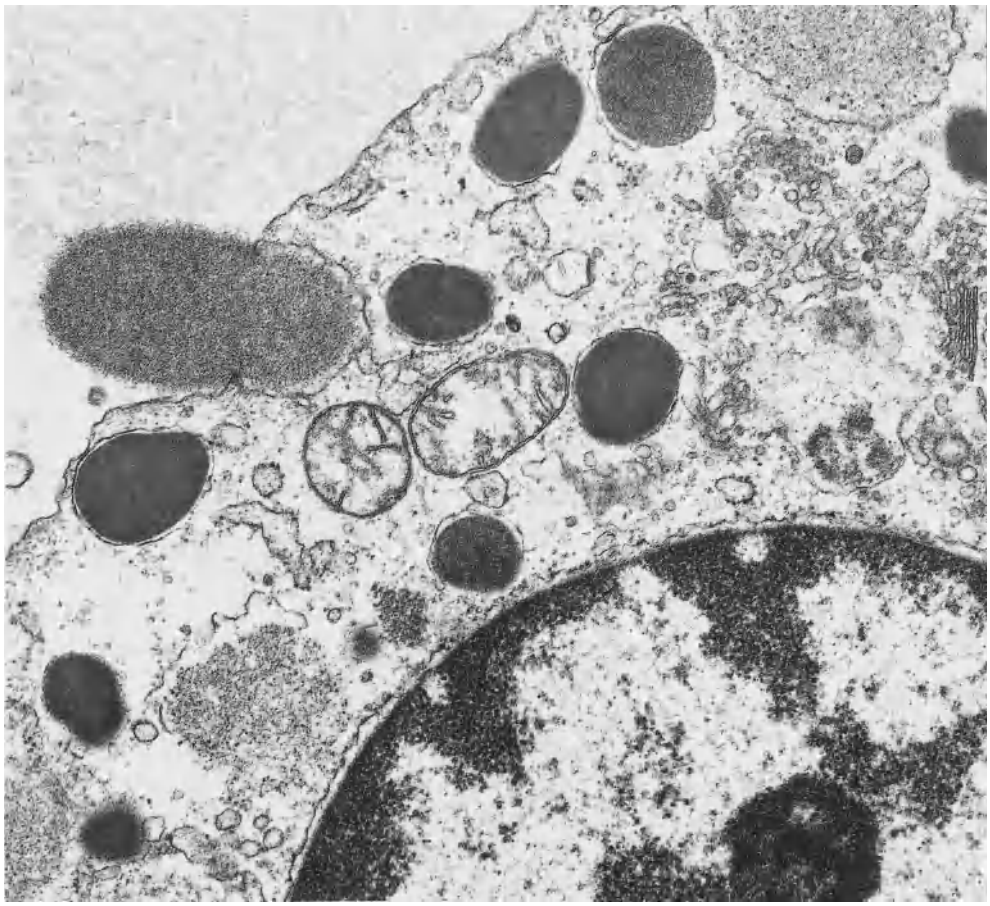


Fig. 6.17 Degranulate mast cell: skin, rat given pateurella toxin intradermally. Mast cell granules are swollen, and granule matrix is expanded. One granule has been released by exocytosis.

pumps in the membrane; for example, in most endocrine cells, secretory granules are acidified by opening of chloride channels.[142]

End-Stage Secretory Granules

After extended periods of stimulation and secretion, large exhaustion vacuoles develop in the cytoplasm. Secretory granules have largely disappeared leaving many Golgi vesicles and a few large pale vacuoles. These vacuoles form coincident with a rise in Ca^{++} that accompanies activation of receptors involved in the stimulation of secretion.[143] Effete secretory granules are degraded **crinophagy**, the fusion of secretory granules with lysosomes. This is a process whereby secretory cells eliminate excess secretions. Fusion of corresponding limiting membranes occurs and contents of the granule are discharged into the enlarged secondary lysosome. In goblet cells, granular pneumocytes, and other cells bearing granules that are important in protecting organ surfaces, there may be a hyperplastic response with increased granule production and crinophagy.[144]

One cell may secrete two different proteins, one by each mechanism; for example, macrophages secrete some proteins directly yet isolate other protein in lysosomes. Similarly, an endocrine cell can secrete two different hormones by different mechanisms. On the other hand, the same enzyme may be secreted in different pathways by dissimilar cell types. Macrophages store hydrolytic enzymes in primary lysosomes, whereas osteoclasts secrete them directly into the environment for use in resorption of bone mineral and organic matter.[145]

In the Golgi complex, the sequestration of proteins for lysosomes and secretory granules may be incomplete so that, in disease, small amounts of lysosomal peptides may contaminate the secretory granule matrix.

Vet-ebooks.com

Special Pathways for Secretion

Secretion pathways vary greatly according to differences in tissue function and the cargos they bear. For example, in epithelial cell glycocalyces in the gastrointestinal and respiratory tracts, glycocalyces contain adhesion proteins such as **osteopontin** that accelerate secretion and phagocytosis.[146]

Acid Secretion: The Gastric Model

Gastric parietal cells use the proton pump, H^+-K^+-ATPase, to secret acid into the lumen of the stomach. Specialized H^+-K^+-ATPase-enriched, ion-secreting transport vesicles called **acidosomes** aggregate at lumenal surfaces of cells that secrete large amounts of acid (see Fig. 5.10). When stimualted, parietal cells accumulate proton-producing vesicles in the cytoplasm near the surface.[147–150] During reversion from active to resting state, there is a progressive translocation of H^+-K^+-ATPases from apical to cytoplasmic regions. The intercellular canaliculi disappear and membranes form multilamellar autophagosomes that label intensely for H^+-K^+-ATPases.[151]

Secretory Granules: The Insulin Model

Nutrient-induced increases in intracellular free calcium concentrations are the key trigger for insulin release from pancreatic islet β cells. Release of insulin by the stimulated pancreatic β cell occurs in two phases: first, a rapid (and transient) phase from a subset of granules that have previously docked at the plasma membrane; second, a sustained phase from a reserved group of granules located in the cytoplasm. This biphasic release of insulin-bearing granules from the β cell is controlled by phosphorylated inositol compounds.[152–154] Imaging studies of live pancreatic β cells reveal that the first phase docked granules localize with syntaxin 1A, a membrane protein involved in docking and fusion of granules in many secretory cell types. Granules, in the second phase of insulin release, move to fusion without syntaxin 1A association.

Interruption of the insulin secretory pathway typically occurs in the Golgi complex; for example, mutations in insulin genes that cause misfolding of proinsulin lead to accumulation of proinsulin in pre-Golgi intermediate vesicles.[155]

Mammary Epithelial Secretion of Lipids

In exocrine tissues, such as the mammary gland, the complex secretory process is enhanced by contraction of myoepithelial cells that lie at the basal surface of the secretory cell and enhance the release of secretory granules (Fig. 6.18). Milk fat globules originate as small triacylglycerol-rich droplets formed in the endoplasmic reticuum. Droplets are moved from the ER into the cytosol as microlipid droplets coated by proteins and polar lipids. Droplets fuse so that there are lipid droplets of all sizes. Secretion at the plasma membrane has not been defined.[156,157]

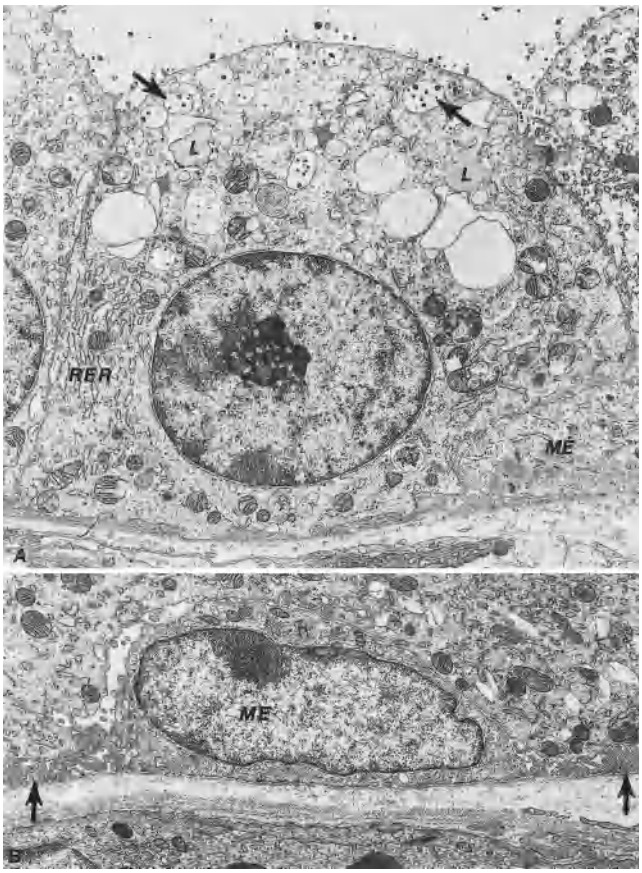


Fig. 6.18 Secretory granules: epithelial cell, mammary gland, cow. **A**. **Complex secretory vacuoles**: small dense lipid globules in secretory vacuoles (*arrows*) contain casein; lipid (*L*), rough endoplasmic reticulum (*RER*). **B**. **Myoepithelial cell** (*ME*): basal area of mammary acinus; basal filopodia (*arrows*).

Yolk Epithelial Secretion of Lipids in Birds

Throughout avian embryogenesis, endodermal cells of yolk sac epithelium take up and process yolk substances, which are then transported to the liver via the vitelline circulation. Yolk lipids are taken up by different pathways; for example, yolk granules are phagocytized and small lipid globules are internalized by receptor-mediated endocytosis (Fig. 6.19).[158,159]

Secretory Exhaustion: Epinephrine Release

Massive release of granules by the adrenal medulla is a stress response to demands for epinephrine. In

Vet-ebooks.com

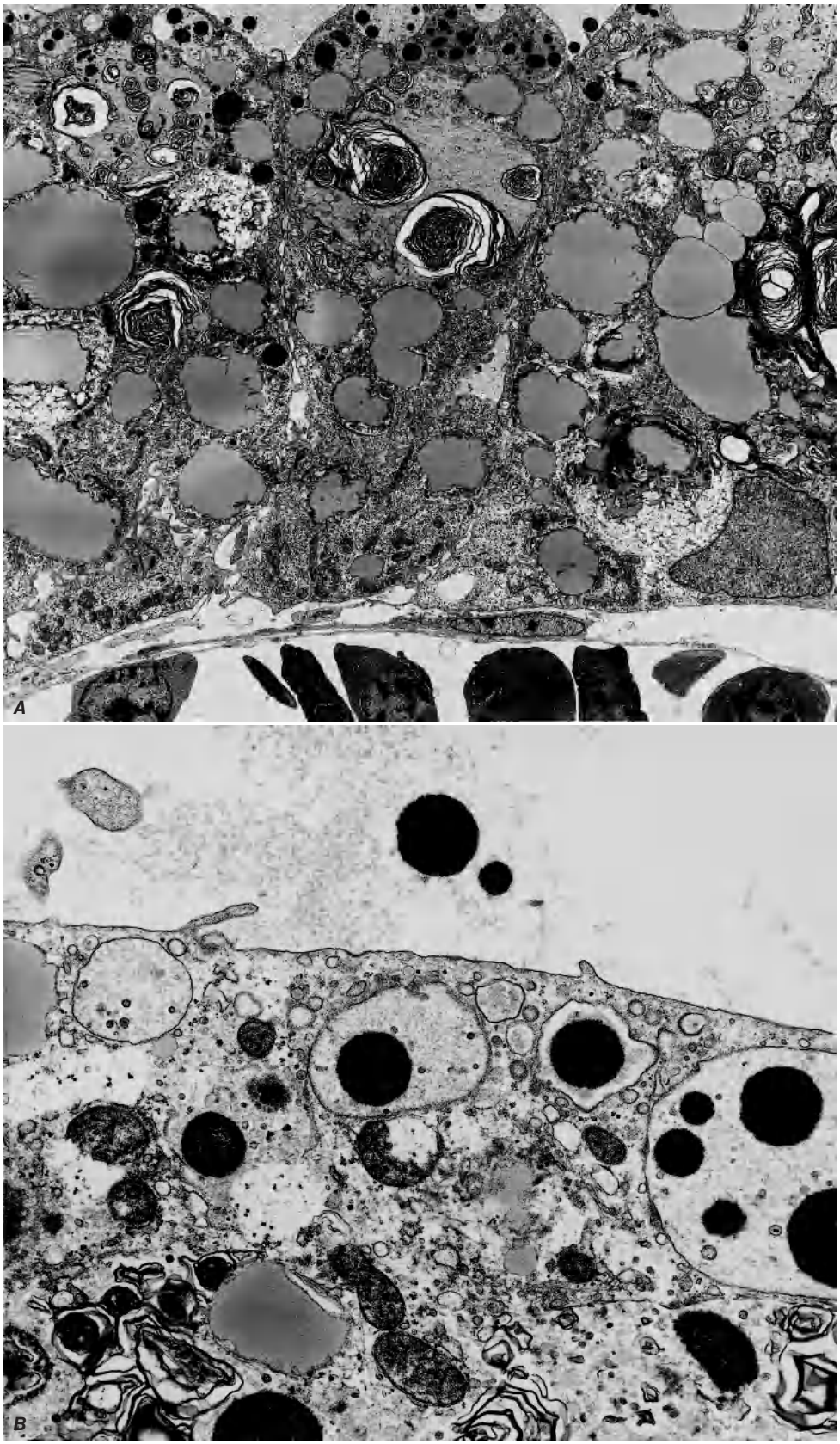


Fig. 6.19 Secretory granules: yolk sac epithelium, chick embryo at 16 days incubation. **A**. **Epithelium**: Polarity of endodermal cells is characterized by basal nuclei, glycogen, and mitochondria; midregion contains lipid globules and lysosomes bearing myeloid bodies; luminal zone of intact yolk granules with phagosomes. **B**. **Yolk granules** in yolk (*top*) and within phagosomes in endodermal cell cytoplasm. Granules in yolk are associated with small vesicles.

Vet-ebooks.com

massive release, granules are depleted, granules are distorted, and the cells become vacuolated. Within the stimulated cells, massive release of calcium triggers the activation of syntaxins and SNAP complexes (synaptosome-associated protein) in chromaffin vesicles. Exocytosis via this pathway has been followed using immunogold techniques.[160,161]

References

1. Starr DA. 2007. Communication between the cytoskeleton and the nuclear envelope to position the nucleus. *Mol Biosyst* 3:583.
2. Stewart CL, et al. 2007. Blurring the boundary: The nuclear envelope extends its reach. *Science* 318: 1408.
3. Maraldi NM, et al. 2007. The nuclear envelope, human genetic diseases and ageing. *Eur J Histochem* 51 (Suppl 1):17.
4. Heitlinger E, et al. 1992. The role of the head and tail domain in lamin structure and assembly. *J Struct Biol* 108:74.
5. Wilhelmsen K, et al. 2005. Nesprin-3, a novel outer nuclear membrane protein, associated with the cytoskeletal linker protein plectin. *J Cell Biol* 171:799.
6. Stewart CL, et al. 2007. Mouse models of the laminopathies. *Exp Cell Res* 313:2144.
7. Halaschek-Wiener J, Brooks-Wilson A. 2007. Progeria of stem cells. *J Gerontol A Biol Sci Med Sci* 62:3.
8. Terry LJ, et al. 2007. Crossing the nuclear envelope: Hierarchical regulation of nucleocytoplasmic transport. *Science* 318:1412.
9. Liu Q, et al. 2007. Functional association of Sun 1 with nuclear pore complexes. *J Cell Biol* 178:785.
10. Weis K. 2007. The nuclear pore complex. *Cell* 130:405.
11. Krull S, et al. 2007. Nucleoporins as components of the nuclear pore complex core structure and Tpr as the architectural element of the nuclear basket. *Mol Biol Cell* 15:4261.
12. Hinshaw JE, et al. 1992. Architecture and design of the nuclear pore complex. *Cell* 69:1133.
13. Goldberg MW, Allen TD. 1992. High resolution scanning electron microscopy of the nuclear envelope: Demonstration of a new, regular, fibrous lattice attached to the baskets of the nucleoplasmic face of the nuclear pores. *J Cell Biol* 119:1429.
14. Jarnik M, Aebi U. 1991. Toward a more complete 3-D structure of the nuclear pore complex. *J Struct Biol* 107:291.
15. Zhang Q, et al. 2005. Nesprin-2 is a multi-isomeric protein that binds lamin and emerin at the nuclear envelope and forms a subcellular network in skeletal muscles. *J Cell Sci* 118:673.
16. Dingwall C, Laskey R. 1992. The nuclear membrane. *Science* 258:943.
17. Lim RYH, et al. 2007. Nanomechanical basis of selective gating by the nuclear pore complex. *Science* 318:640.
18. Stewart M. 2007. Ratcheting mRNA out of the nucleus. *Mol Cell* 25:327.
19. Dworetzky SI, Feldherr CM. 1988. Translocation of RNA-coated gold particles through the nuclear pores of oocytes. *J Cell Biol* 106:575.
20. Feldherr CM, Akin D. 1990. The permeability of the nuclear envelope in dividing and non-dividing cell cultures. *J Cell Biol* 111:1.
21. Lang I, et al. 1986. Molecular mobility and nucleocytoplasmic flux in hepatoma cells. *J Cell Biol* 102: 1183.
22. Newmeyer DD, Forbes DJ. 1988. Nuclear import can be separated into distinct steps in vitro: Nuclear pore binding and translocation. *Cell* 52:641.
23. Richardson WD, et al. 1988. Nuclear protein migration involves two steps: Rapid binding at the nuclear envelope followed by slower translocation through nuclear pores. *Cell* 52:655.
24. Stewart M. 2007. Molecular mechanism of the nuclear protein import cycle. *Nat Rev Mol Cell Biol* 8:195.
25. Kessel RG, et al. 1985. Freeze-fracture studies of annulate lamellae in zebrafish oocytes. *Cell Tiss Res* 240:293.
26. Scheer U, Franke WW. 1969. Negative staining and adenosine triphophatase activity of annulate lamellae of newt oocytes. *J Cell Biol* 42:519.
27. Dabauvalle M-C, et al. 1991. Spontaneous assembly of pore complex-containing membranes ("annulate lamellae") in *Xenopus* egg extracts in the absence of chromatin. *J Cell Biol* 112:1073.
28. Li B. 2007. The role of chromatin during transcription. *Cell* 128:707.
29. He D, et al. 1991. Localization of heterogeneous nuclear ribonucleoprotein in the interphase nuclear matrix core filaments and on perichromosomal filaments at mitosis. *Proc Nat Acad Sci USA* 88:7469.
30. Lamond AI, Spector DL. 2003. Nuclear speckles: A model for nuclear organelles. *Nat Rev Mol Cell Biol* 4:605.
31. Cardinale S, et al. 2007. Subnuclear localization and dynamics of the pre-mRNA 3" end processing factor mammalian cleavage factor 1 68 kDa subunit. *Mol Biol Cell* 18:1282.
32. Kumaran RI, et al. 2008. Chromatin dynamics and gene positioning. *Cell* 132:929.
33. Azzalin CM, et al. 2007. Telomeric repeat-containing RNA and RNA surveillance factors at mammalian chromosome ends. *Science* 318:798.
34. Dolnik AV, et al. 2003. Telomere-binding TRF2/ MTBP localization during mouse spermatogenesis and cell cycle of the mouse cells L929. *J Anti Aging Med* 6:107.
35. Dalal Y, et al. 2007. Structure, dynamics, and evolution of centromeric nucleosomes. *Proc Natl Acad Sci USA* 104:15974.
36. Morris CA, Moazed D. 2007. Centromere assembly and propagation. *Cell* 128:647.

Vet-ebooks.com

37. Quintana C. 1991. X-ray microanalysis of cell nuclei. *J Elec Microsc Tech* 18:411.
38. Bendayan M. 1981. Ultrastructural localization of nuclei acids by the use of enzyme-gold complexes. *J Hist Cyt* 29:531.
39. Scheer U, et al. 1987. High sensitivity immunolocalization of double and single-stranded DNA by a monoclonal antibody. *Eur J Cell Biol* 43:358.
40. Testillano PS, et al. 1991. A specific ultrastructural method to reveal DNA. *J Hist Cyt* 39:1427.
41. Burlingame RW, et al. 1985. Crystallographic structure of the octameric histone core of the nucleosome at a resolution of 3.3 Å. *Science* 228:546.
42. Miller OL. 1981. The nucleolus, chromosome, and visualization of genetic activity. *J Mol Biol* 91:15s.
43. Hobert O. 2008. Gene regulation by transcription factors and microRNAs. *Science* 319:1785.
44. Hébert SS, De Strooper B. 2007. miRNAs in neurodegeneraton. *Science* 317:1179.
45. Amaral PP, et al. 2008. The eukaryotic genome as an RNA machine. *Science* 319:1787.
46. Cullen BR. 2007. Outwitted by viral RNAs. *Science* 317:329.
47. Kuettel MR, et al. 1985. Localization of nuclear subunits of cyclic AMP-dependent protein kinase by the immunocolloidal gold method. *J Cell Biol* 101:965.
48. Kornberg RD. 2007. The molecular basis of eukaryotic transcription. *Proc Natl Acad Sci USA* 1l04:12955.
49. Derenzini M, et al. 2006. Structural and functional organization of ribosomal genes within the mammalian cell nucleolus. *J Hist Cyt* 54:131.
50. Carmo-Fonseca M, et al. 1993. Assembly of snRNP-containing coiled bodies is regulated in interphase and mitosis: Evidence that the coiled body is a kinetic nuclear structure. *J Cell Biol* 120:841.
51. Stark H, Luhmann R. 2006. Cryo-electron microsocpy of spliceosome components. *Ann Rev Biophys Biomed Struct* 35:435.
52. Raska I, et al. 2006. New insights into nucleolar architecture and activity. *Int Rev Cytol* 255:177.
53. Hernandez-Verdun D. 2006. The nucleolus: A model for the organization of nuclear functions. *Histochem Cell Biol* 126:135.
54. Boisvert FM, et al. 2007. The multifunctional nucleolus. *Nat Rev Mol Cell Biol* 8:574.
55. Baran V, et al. 2002. Nucleolar changes in bovine nucleotransferred embryos. *Biol Reprod* 66:534.
56. Hamilton HM, et al. 2004. Ovine ooplasm directs initial nucleolar assembly in embryos cloved from ovine, bovine and porcine cells. *Mol Reprod Dev* 69:117.
57. Geraud G, et al. 1991. Computer reconstruction of nucleolar architecture by interactive three-dimensional color display. *J Elec Microsc Tech* 18:354.
58. Jansen RP, et al. 1991. Evolutionary conservation of the human nucleolar protein fibrillarin and its functional expression in yeast. *J Cell Biol* 113:715.
59. Derenzini M, et al. 1990. Ultrastructural cytochemistry of the mammalian cell nucleolus. *J Hist Cyt* 381237.
60. Meier UT, Blobel G. 1992. Nopp140 shuttles on tracks between nucleolus and cytoplasm. *Cell* 70:127.
61. Puvion-Dutilleul F. 1984. Morphology of transcription at cellular and molecular levels. *Int Rev Cytol* 84:57.
62. Yunis EJ, et al. 1984. Studies on the nature of fibrilar nuclei. *Am J Pathol* 15:84.
63. Alvarez M, et al. 2006. Ultrastructural changes of the carp (*Cyprinus carpio*) hepatocyte nucleolus during seasonal acclimatization. *Biol Cell* 98:457.
64. Hardin JH, et al. 1969. The paranucleolar structure, accessory body of Cajal, sex chromatin, and related structures in nuclei of rat trigeminal neurons. A cytochemical and ultrastructural study. *Anat Rec* 164:403.
65. Schultz MC. 1989. Ultrastructural study of the coiled body and a new inclusion, the "mykaryon," in the nucleus of the adult rat Sertoli cell. *Anat Rec* 225:21.
66. Andrade LEC, et al. 1991. Human autoantibody to a novel protein of the nuclear coiled body. *J Exp Med* 173:1407.
67. Stanek D, Neugebauer KM. 2006. The Cajal body: A meeting place for spliceosomal snRNPs in the nuclear maze. *Chromosoma* 115:343.
68. Kittur N, et al. 2007. The nucleolar channel system of human endometrium is related to endoplasmic reticulum and R-rings. *Mol Biol Cell* 18:2296.
69. Brasch K. 1990. Drug and metabolite-induced perturbations in nuclear structure and function. *Biochem Cell Biol* 68:408.
70. Shah RM, et al. 1991. Pathogenesis of bromodeoxyuridine-induced cleft palate in hamster. *Am J Anat* 190:219.
71. Lindsey-Bolz LA, Sancar A. 2007. RNA polymerase: The most specific damage recognition protein in cellular responses to DNA damage. *Proc Nat Acad Sci USA* 104:13213.
72. Verbin RS, et al. 1969. The biochemical pathology of inhibition of protein synthesis *in vivo*. The effects of cyclohexamide on hepatic parenchymal cell ultrastructure. *Lab Invest* 20529.
73. Arstila AV, Trump BF. 1972. Ethionine-induced alteration in the Golgi apparatus and in the endoplasmic reticulum. *Virch Arch B* 10:344.
74. Kisilevsky R, et al. 1973. Ribosomal alterations following ethionine intoxication. *Lab Invest* 28:8.
75. Pathak RK, et al. 1988. Immunocytochemical localization of mutant low density lipoprotein receptors that fail to reach the Golgi complex. *J Cell Biol* 106:1831.
76. Berg NO, Eriksson S. 1972. Liver disease in adults with alpha 1-antitrypsin deficiency. *New Engl J Med* 287:1264.
77. Palmer PE, et al. 1973. Hepatic changes in adult α_1-antitrypsin deficiency. *Gastroenterology* 65:284.
78. Németh A, et al. 1983. Alpha-1-antitrypsin deficiency and juvenile liver disease. *Virch Arch B* 44:15.
79. Yunis EJ, et al. 1976. Fine structural observations of the liver in alpha-1-antitrypsin deficiency. *Am J Pathol* 82:265.
80. McLeese J, Bergeron M. 1990. Fasting induces modifications of the endoplasmic reticulum in intestinal cells. *J Elec Microsc Tech* 16:56.

Vet-ebooks.com

81. Sato S. 2004. Ultrastructural morphometric studies of normal rat hepatocytes. *J Submicrosc Cytol Pathol* 36:131.
82. Tooze J, et al. 1989. Condensation-sorting events in the rough endoplasmic reticulum of exocrine pancreatic cells. *J Cell Biol* 109:35.
83. Courtoy PJ, et al. 1981. Plasma protein synthesis in experimental cirrhosis. *Lab Invest* 45:67.
84. Baenziger, J. O. 1985. The role of glycosylation in protein recognition. *Am J Pathol* 121:382.
85. Kanai K, et al. 1986. High and testosterone-dependent glucose-6-phosphatase activity in epithelium of mouse seminal vesicles. *J Hist Cyt* 34:1207.
86. Brada D, et al. 1990. Cell type-specific post-Golgi apparatus localization of a "resident" endoplasmic reticulum glycoprotein, glucosidase II. *J Cell Biol* 110:309.
87. Langer T, et al. 1992. Chaperonin-mediated protein folding: GroES binds to one end of the GroEL cylinder, which accommodates the protein substrate within its central cavity. *EMBO J* 11:4757.
88. Zeuschner D, et al. 2006. Immuno-electron tomography of ER exit sites reveals the existence of free COPII-coated tranport carriers. *Nat Cell Biol* 8:377.
89. Zuber C, et al. 2007. EDEM1 reveals a quality control vesicle transport pathway out of the endoplasmic reticulum not involving the COPII exit sites. *Proc Natl Acad Sci USA* 104:4407.
90. Pavelka M, Ellinger A. 1991. Cytochemical characteristics of the Golgi apparatus. *J Elec Microsc Tech* 1735.
91. Nilsson T, et al. 1993. Overlapping distribution of two glycosyltransferases in the Golgi apparatus of HeLa cells. *J Cell Biol* 120:5.
92. Orci L, et al. 1991. Mammalian Sec23p homologue is restricted to the endoplasmic reticulum transitional cytoplasm. *Proc Nat Acad Sci USA* 88:8611.
93. Van Deurs B, et al. 1986. Routing of internalized ricin and ricin conjugates to the Golgi complex. *J Cell Biol* 102:37.
94. Tanaka K, Fukudome H. 1991. Three-dimensional organization of the Golgi complex observed by scanning electron microscopy. *J Elec Microsc Tech* 17:15.
95. Hsu VW, et al. 1991. A recycling pathway between the endoplasmic reticulum and the Golgi apparatus for retention of unassembled MHC class 1 molecules. *Nature* 352:441.
96. Serafini T, et al. 1991. ADP-ribosylation factor is a subunit of the coat of Golgi-derived COP-coated vesicles: A novel role for a GTP binding protein. *Cell* 67:239.
97. Chanat E, Huttner WB. 1991. Milieu-induced, selective aggregation or regulated secretory proteins in the *trans*-Golgi network. *J Cell Biol* 115:1505.
98. Geuze HJ, Morre D. 1991. Trans-Golgi reticulum. *J Elec Microsc Tech* 17:24.
99. Nilsson T, et al. 1991. The membrane spanning domain of β-1,4-galactosyltransferase specifies *trans* Golgi localization. *EMBO J* 10:3567.
100. Orci L, et al. 1985. Conversion of proinsulin to insulin occurs coordinately with acidification of maturing secretory vesicles. *J Cell Biol* 103:2273.
101. Tooze J, Tooze SA. 1986. Clathrin-coated vesicular transport of secretory proteins during the formation of ACTH-containing secretory granules in AtT20 cells. *J Cell Biol* 103:839.
102. Brown WJ, et al. 1986. Mannose-6-phosphate receptors for lysosomal enzymes cycle between the Golgi complex and endosomes. *J Cell Biol* 103:1235.
103. Waguri S, et al. 2007. The luminal domain participates in the endosomal trafficking of the cation-independent mannose 6-phosphate receptor. *Exp Cell Res* 312: 4090.
104. Trier JS, Madara JL. 1984. Distribution of filipin-sterol complexes in villus goblet cell membranes of rat small intestine. *Lab Invest* 50:673.
105. Kellokumpu S, et al. 1988. A 115-kD polypeptide immunologically related to erythrocyte band 3 is present in Golgi membranes. *Science* 242:130.
106. Rothman JE, Orci L. 1990. Movement of protein through the Golgi stack. *FASEB J* 4:1460.
107. Griffiths G, et al. 1989. The dynamic nature of the Golgi complex. *J Cell Biol* 108:277.
108. Cole NB, et al. 1996. Golgi dispersal during microtubule disruption: Regeneration of Golgi stacks at peripheral endoplasmic reticulum exit sites. *Mol Biol Cell* 7:631.
109. James Morré D, Mollenhauer HH. 2007. Microscopic morphology and the origins of the membrane maturation model of Golgi apparatus function. *Int Rev Cytol* 262:191.
110. Lippincott-Schwartz J, et al. 1989. Rapid redistribution of Golgi proteins into the endoplasmic reticulum in cells treated with brefeldin A. *Cell* 56:801.
111. Yorde DE, Kalkhoff RK. 1986. Quantitative morphometric studies of pancreatic islets obtained from tolbutamide-treated rats. *J Hist Cyt* 34:1195.
112. Lippincott-Schwartz J, et al. 1990. Microtubule-dependent retrograde transport of proteins into the ER in the presence of brefeldin A suggests an ER recylcing pathway. *Cell* 60:821.
113. Orci L, et al. 1991. Brefeldin A, a drug that blocks secretion, prevents the assembly of non-clathrin-coated buds on Golgi cisternae. *Cell* 64:1183.
114. Sandvig K, et al. 1991. Ricin transport in brefeldin A-treated cells: Correlation between Golgi structure and toxic effect. *J Cell Biol* 115:971.
115. Parmely RT, et al. 1988. Monensin disruption of neutrophil granule genesis. *Am J Pathol* 133:537.
116. Yu I-M, et al. 2008. Structure of the immature dengue virus at low pH primes proteolytic maturation. *Science* 319:1834.
117. Busson-Mabillot S, et al. 1982. Microtubules and protein secretion in rat lacrimal gland: Localization of short-term effects of colchicine on the secretory process. *J Cell Biol* 95:105.
118. Pavelka M, Ellinger A. 1983. Effect of colchicine on the Golgi complex of rat pancreatic acinar cells. *J Cell Biol* 97:737.
119. Lu Z, et al. 2001. Golgi complex reorganization during muscle differentiation: Visualization in living cells and mechanism. *Mol Biol Cell* 12:795.

Vet-ebooks.com

120. Jena BP. 2006. Porosome: The fusion pore revealed by multiple imaging modalities. *Methods Mol Biol* 319:295.
121. Heuser JE, Anderson RGW. 1989. Hypertonic media inhibit receptor-mediated endocytosis by blocking clathrin-coated pit formation. *J Cell Biol* 108:389.
122. Hanzel D, et al. 1991. The secretion-stimulated 80K phosphoprotein of parietal cells is ezrin, and has properties of a membrane cytoskeletal linker in the induced apical microvilli. *EMBO J* 10:2363.
123. Mercier F, et al. 1989. Membrane-cytoskeleton dynamics of rat parietal cells. *J Cell Biol* 108:441.
124. Madson KM, Tisher CC. 1984. Response of intercalated cells of rat outer medullary collecting duct to chronic metabolic acidosis. *Lab Invest* 51:268.
125. Gomi H, et al. 2005. Granuphilin molecularly docks insulin granules to the fusion machinery. *J Cell Biol* 171:99.
126. Beaudoin AR, Grondin G. 1991. Secretory pathways in animal cells. *J Elec Microsc Tech* 17:51.
127. Bendayan M, et al. 1989. Ultrastructural localization of insulin and C-peptide antigenic sites in rat pancreatic B cells obtained by applying the quantitative high-resolution protein A-gold approach. *Am J Anat* 185:205.
128. Childs GV, et al. 1989. Localization and quantification of hormones, ligands, and mRNA with affinity-gold probes. *Am J Anat* 185:223.
129. Horvath E, et al. 1990. Propylthiouracil-induced hypothyroidism results in reversible transdifferentiation of somatotrophs into thyroidectomy cells. *Lab Invest* 63:511.
130. Ichikawa M, et al. 1989. Immunocytochemical localization of amylase in gerbil salivary gland acinar cells processed by rapid freezing and freeze-substitution fixation. *J Hist Cyt* 37:185.
131. Scheele G, et al. 1987. Exocytosis occurs at the lateral plasma membrane of the pancreatic acinar cell during supramaximal secretagogue stimulation. *Gastroenterology* 92:345.
132. Rothman JE, Orci L. 1992. Molecular dissection of the secretory pathway. *Nature* 355:409.
133. von Zastrow M, Castle JD. 1987. Protein sorting among two distinct export pathways occurs from the content of maturing exocrine storage granules. *J Cell Biol* 105:2675.
134. Cho SJ, Jena BP. 2006. Secretory vesicle swelling by atomic force microscopy. *Methods Mol Biol* 319:317.
135. Franke WW, et al. 1976. Involvement of vesicle coat material in casein secretion and surface regeneration. *J Cell Biol* 69:173.
136. Heuser J, et al. 1979. Synaptic vesicle exocytosis captured by quick-freezing and correlated with quantal transmitter release. *J Cell Biol* 81:275.
137. Nakata T, et al. 1990. Conformational change and localization of calpactin I complex involved in exocytosis as revealed by quick-freeze deep-etch microscopy and immunocytochemistry. *J Cell Biol* 110:13.
138. Knoll G, et al. 1988. Fusion of liposomes and the plasma membrane of epithelial cells. *J Cell Biol* 107:2511.
139. White JM. 1992. Membrane fusion. *Science* 258:917.
140. Horoyan M, et al. 1991. Localization of calcium changes in stimulated rat mast cells. *J Hist Cyt* 40:51.
141. Hill DJ, et al. 1984. Localization of calmodulin in differentiating pulmonary type II epithelial cells. *Lab Invest* 51:297.
142. Barasch J, et al. 1988. Thyrotropin induces the acidification of the secretory granules of parafollicular cells by increasing the chloride conductance of the granular membrane. *J Cell Biol* 107:2137.
143. Leslie BA, Putney JW. 1983. Ionic mechanisms in secretagogue-induced morphological changes in rat parotid gland. *J Cell Biol* 97:1119.
144. Balis JE, et al. 1988. Ozone-induced lamellar body responses in rat model for alveolar injury and repair. *Am J Pathol* 132:330.
145. Baron R. 1988. Polarized secretion of lysosomal enzymes. *J Cell Biol* 106:1863.
146. Qu-Hong, Dvorak AM. 1997. Ultrastructural localization of osteopontin immunoreactivity in phagolysosomes and secretory granules of cells in human intestine. *Histochem J* 29:801.
147. Forte TM et al. 1977. Ultrastructural changes in oxyntic cells associated with secretory function: A membrane-recycling hypothesis. *Gastroenterology* 73:9841.
148. Ito S, Schofield GS. 1974. Studies on the depletion and accumulation of microvilli and changes in the tubulovesicular compartment of mouse parietal cells in relation to gastric acid secretion. *J Cell Biol* 63:364.
149. Brown D, et al. 1987. Structure of the novel membrane-coating material in proton-secreting epithelial cells and identification as an H^+-ATPase. *J Cell Biol* 105:1637.
150. Nguyen NV, et al. 2004. Gastric parietal cell acid secretion in mice can be regulated independently of H/K-ATPase endocytosis. *Gastroenterology* 127:145.
151. Sawaguchi A, et al. 2006. Ultrastructural transformation of gastric parietal cells reverting from the active to the resting state of acid secretion revealed in isolated rat gastric mucosa model processed by high-pressure freezing. *J Electron Microsc (Tokyo)* 55:97.
152. Orci L, et al. 1984. A clathrin-coated, Golgi-related compartment of the insulin secreting cell accumulates proinsulin in the presence of monensin. *Cell* 39:39.
153. Orci L, et al. 1986. Conversion of proinsulin to insulin occurs coordinately with acidification of maturing secretory vesicles. *J Cell Biol* 103:2273.
154. Rutter GA, et al. 2006. Ca^{2+} microdomains and the control of insulin secretion. *Cell Calcium* 40:539.
155. Zuber C, et al. 2004. Misfolded proinsulin accumulates in expanded pre-Golgi intermediates and endoplasmic reticulum subdomains in pancreatic beta cells of Akita mice. *FASEB J* 18:917.
156. Heid HW, Keenan TW. 2005. Intracellular origin and secretion of milk fat globules. *Eur J Cell Biol* 84:245.
157. Nickerson S, et al. 1980. Role of microtubules in milk secretion—action of colchicine on microtubules and exocytosis of secretory vesicles in rat mammary epithelial cells. *Cell Tiss Res* 207:361.
158. Cheville NF, Coignoul F. 1984. Calcium in the turkey yolk sac during late development and postembryonic involution. *Am J Vet Res* 445:2458.

Vet-ebooks.com

159. Chandler DE, et al. 1989. High molecular weight polymers block cortical granules exocytosis in sea urchin eggs at the level of granule matrix disassembly. *J Cell Biol* 109:1269.
160. Höhne-Zell B, Gratzl M. 1996. Adrenal chromaffin cells contain functionally different SNAP-25 monomers and SNAP 25/syntaxins heterodimers. *FEBS Lett* 394: 109.
161. Lawrence GW, Dolly JO. 2002. Multiple forms of SNARE complexes in exocytosis from chromaffin cells. *J Cell Sci* 115:667.

Vet-ebooks.com

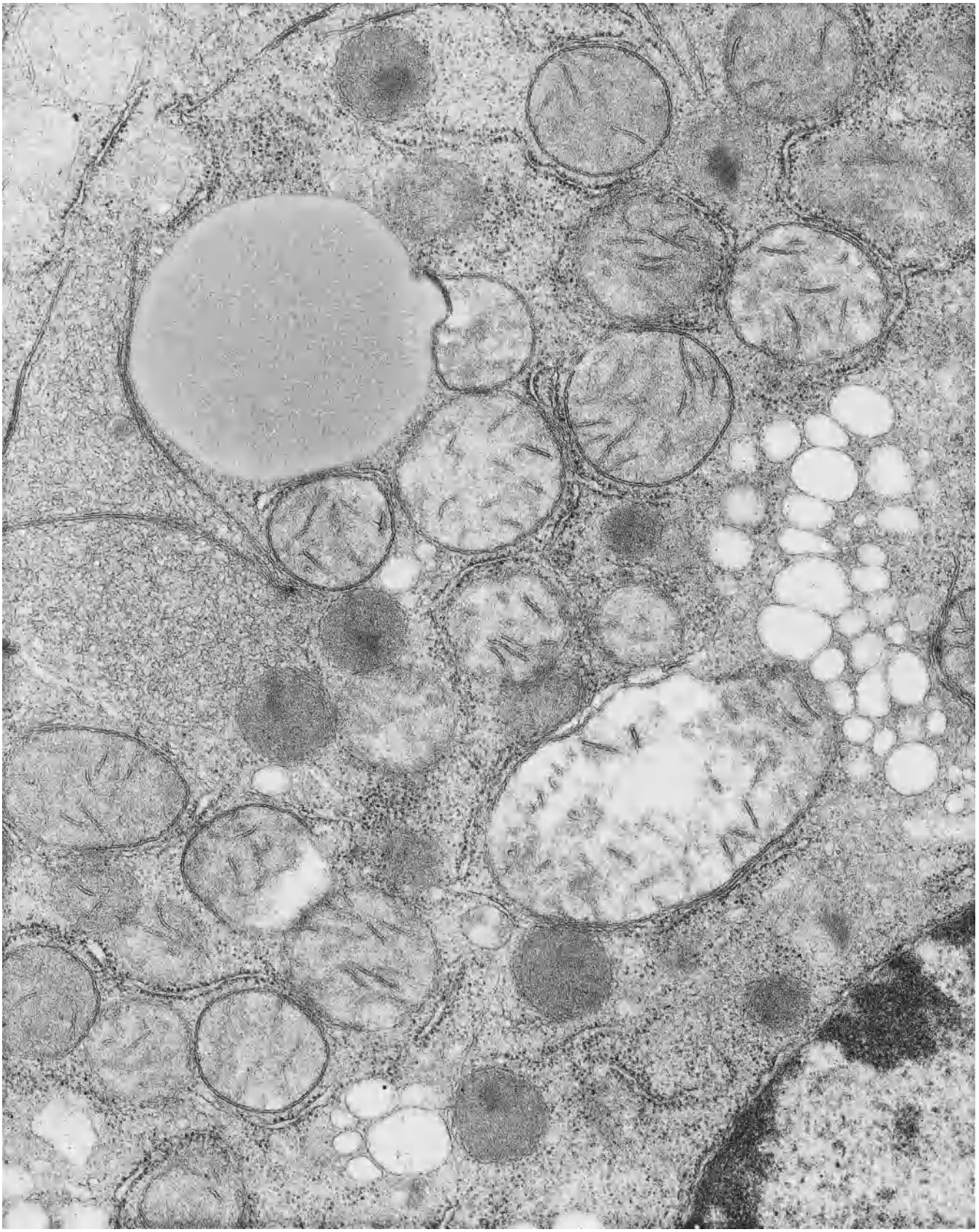


Fig. 7.1 Peroxisomes and smooth endoplasmic reticulum (*top right*), and relationships to rough endoplasmic reticulum and other organelles.

© 2009 Wiley-Blackwell. ISBN: 978-0-813-80330-2
Vet-ebooks.com

7 Peroxisomes, Smooth Endoplasmic Reticulum, and Lipids

Peroxisomes

Peroxisomes play critical roles in oxidation and detoxification reactions—their enzymes are largely peroxidative, hence the designation peroxisomes.[1] They contain **catalase** (which converts hydrogen peroxide to water),[2] hydrogen peroxide-generating **oxidases**, and enzymes that facilitate α-, β-, and ω-oxidation of complex fatty acids. Peroxisomes contain superoxide dismutase, which maintains balance in the peroxisomal redox states; using immunogold techniques, MnSOD is found in the core and limiting membrane.[3]

Peroxisomes measure 0.1–1.5 μm in diameter,[4] and are composed of a granular matrix surrounded by a single membrane (Fig. 7.1). The limiting membrane is thinner than that of lysosomes and lacks the electron-lucent zone between the matrix and membrane.[5,6] Crystalline inclusions of different types are common in the peroxisomal matrix; for example, the central polytubular core inclusions of urate oxidase of hepatic peroxisomes, and the marginal plates of hydroxyacid oxidase in renal peroxisomes.[7] Peroxisomes are prominent in hepatocytes, renal tubular cells, and steroid-synthesizing cells. In hepatocytes there may be 1,000 peroxisomes per cell, all in close relation to endoplasmic reticulum.

Peroxisomal Biology

Proteins of the peroxisomal matrix are synthesized on free ribosomes and are transported posttranslationally into the peroxisome. Proteins destined for translocation into the peroxisomal matrix are recognized by import vectors, two of them being named Pex5p and Pex7p. **Peroxisomal proliferator-activated receptors** (PPARs) are lipid-activated transcription factors that regulate metabolism, and play a critical role in induction of peroxisomal duplication. Candidates for ligands that are able to modulate PPARs are important in drug development. For example, in skeletal muscle PPARδ agonists are involved in fatty acid burning and adaptive responses of skeletal muscle to environmental changes. Treatment of obese animals with PPARδ agonists results in normalization of lipid metabolism.

There are large differences in content of various oxidases in peroxisomes of different species and even of different tissues; for example, the dense, central **core** (sometimes called the nucleoid) of urate oxidase crystals present in many species are absent in peroxisomes of humans and birds.[8,9] In rat liver, there is a difference in the reaction of peroxisomes in different zones. Centrolobular hepatocytes are most sensitive to peroxisomal proliferation while abnormal peroxisomes with matrix tubules are apt to occur in more peripheral areas. Lamellar arrangements of protein in the **core** may appear as fine or coarse polytubular crystals. These form from parallel bundles of dense hollow tubules, which in cross section have a honeycomb appearance.

Peroxisomes develop de novo in the cytoplasm, and have a close association with **smooth endoplasmic reticulum**. In rapidly regenerating cells, or cells treated to increase peroxisomes, wisps of membranes or tail-like extensions are common on peroxisomal membranes—these have been shown to form in tubules that connect to other peroxisomes in a network referred to as the **peroxisomal reticulum**, a membrane reservoir for proliferation of peroxisomes.[10,11] In activated macrophages, there is evidence for fusion of

Vet-ebooks.com

peroxisomes with phagosomes and subsequent release of catalase.

Peroxisomes in Lipid Metabolism

The close metabolic and structural association of peroxisomes with smooth endoplasmic reticulum and mitochondria facilitates the shuttle of lipid molecules between these organelles during synthesis of complex lipids.[31,32] **Carnitine**, essential for the beta-oxidation of fatty acids, maintains homeostasis in the acyl-CoA pools of the cell, keeping acyl-CoA/CoA pool constant during high turnover and providing a constant source of CoA. Carnitine derivatives are shuttled back and forth between peroxisomes, mitochondria and the SER. The **carnitine transporter** and catalase have been demonstrated in peroxisomes using immunogold techniques.[12]

Peroxisomes are critical sites of **cholesterol metabolism** because they contain oxidases that affect intermediates of cholesterol metabolism, and can convert cholesterol to proprionic acids. 3-Hydroxy-3-methylglutaryl coenzyme A reductase, a rate-limiting enzyme of sterol biosynthesis, and proteins that carry cholesterol intermediates have been localized immunocytochemically to peroxisomes.[13,14]

Peroxisomal Responses to Injury

Peroxisomes are sensitive to **hypoxia**. In hepatocytes, **hypoxia-inducible factor**, arise from hypoxic tissue environments and move to nuclei to activate HIF-inducible genes. Using gold-labeled catalase and HIF-hydroxylases, HIF was shown to localize in peroxisomes and plays a role in the endogenous HIF pathway.[15]

Microbodies

The term **microbodies**, although used synonymously with peroxisomes in liver, is a more general term that encompases several subcategories including peroxisomes, glyoxysomes, and other organelles.

Glyoxysomes, found in certain microorganisms, contain fatty acid β-oxidation enzymes and enzymes of the glyoxylate cycle, a Krebs cycle variant for conversion of lipids into carbohydrates. The glyoxylate cycle is catalyzed by two unique enzymes, isocitrate lyase and malate synthase, and allows the decarboxylation steps of the tricarboxylic acid cycle to be bypassed and the carbons derived from fatty acid oxidation to be converted to glucose. Glyoxylate cycle enzymes have recently been identified in the human liver.[16]

Glycosomes, present only in kinetoplastida, contain the first nine enzymes of glyolysis and glycerol metabolism as well as fatty acid β-oxidation pathways.

Hydrogenosomes, found solely in amitochondrial ciliated protozoa, differ from other microbodies in that they are enclosed by a double membrane and lack both catalase and β-oxidation enzymes.[17]

Peroxisomes in Metabolic Disease

Deficits in peroxisomes or their oxidases or catalases will result in metabolic abnormalities. Morphologic evidence of these defects may involve decreased numbers or sizes of peroxisomes. In species having catalase cores, these will be irregular or missing. Hepatic peroxisomes have dark central zones that have been related to uricase storage.[18] Dalmatian dogs, which have a hereditary **uricase deficiency**, have fewer of these dark centers than do other dogs.

Peroxisomal Hypertrophy from Hypolipidemic Drugs

Livers of patients treated with peroxosomal proliferating drugs (to reduce hyperlipidemia) have hepatocytes with marked increases in peroxisomes.[19,20] Peroxisomes are pleomorphic and are usually massed in groups at sites of cellular injury. If mitochondria are the primary site of damage, peroxisomes will accumulate adjacent to them, often with membranes of the two in close apposition.

An association between catalase-producing peroxisomes and serum lipids exists. Agents that inactivate **catalase** or block its synthesis produce hyperlipemia (catalase given IV has a hypercholesteremic effect). Reduplication of peroxisomes is induced by hypolipidemic drugs such as clofibrate, which is widely used for treatment of hyperlipidemia in humans.[21–24] Other drugs that induce peroxisome formation in rats include: aryloxyalkanoic acids plus amide analogues, and thio, benzimidazole, phenyl piperaxine, and oxazole derivatives.[25]

Peroxisome proliferation induced by hypolipidemic drugs is associated with increases in catalase activity and changes in peroxisome structure; that is, absence of matrix tubules or striations and elongated profiles (Fig. 7.2). There are cavitations and compartmentalization with extensions of canaliculi from the peroxisome periphery.[26]

Congenital Peroxisome Defects

In humans, Zellweger's syndrome, neonatal adrenoleukodystrophy, and infantile Refsum's disease are

Vet-ebooks.com

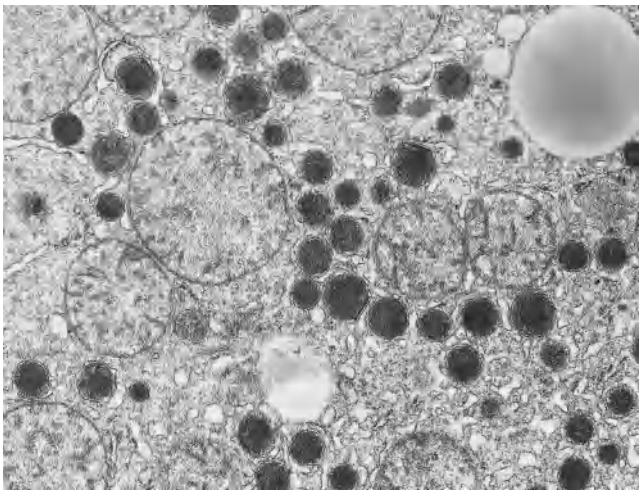


Fig. 7.2 Peroxisome proliferation: clofibrate toxicity, rat. Marked increase in peroxisome number and size, with close apposition of membranes of endoplasmic reticulum and peroxisomes.

genetic disorders characterized by absence of catalase-positive peroxisomes and a general impairment of peroxisomal functions. In many cases there is ultrastructural evidence of peroxisomal membrane ghosts that contain membrane proteins but that lack matrix enzymes.

Cerebrohepatorenal Syndrome of Zellweger

Based on the absence of peroxisomes, this human disease is lethal within several months of birth. There is defective peroxisomal fatty acid oxidation and this leads to accumulation of very long-chain fatty acids.[27] In the brain, both neurons and glia contain pleomorphic granules and lipid globules.[28] Malformations of the cerebrum, inferior olive, and cerebellum include reduced neurons and subcortical heterotopic neurons; this suggests that neuronal migration is widely disrupted during development. Visceral anomalies include hepatic fibrosis, renal cortical microcysts, and mitochondrial myopathy.[29]

Fibroblasts from Zellweger syndrome lack peroxisomes; integral membrane proteins are present but located in large empty membrane structures.[30] This defect involves mechanisms for **import matrix proteins**, which are rapidly degraded if not used. Catalase is present in normal amounts in Zellweger patients' cells but is free in the cytosol, not in peroxisomes. Peroxisomal proteins are synthesized on free ribosomes and assembled post-translationally into preexisting peroxisomes; when peroxisomes are absent the proteins are degraded.

Lesions of **hyperpipecolic acidemia** closely resemble those of the Zellweger syndrome. The finding of high level of serum pipecolic acid is accompanied by retarded development, and neurologic and hepatorenal failure. Ultrastructural examination of liver biopsies and brain tissues shows vesiculation of smooth endoplasmic reticulum with development of cytoplasmic vacuoles.[31] Lesions in peroxisomes have not been reported and the role of pipecolic acid in vacuolation is not known.

Adrenoleukodystrophy

Deficiency of peroxisomal oxidation is the basis for the human central nervous syndrome diseases called **adrenoleukodystrophy**[32] and its X-linked juvenile form, **Schilder's disease**. Long-chain fatty acids accumulate in peroxisomes, which are diminished in size and numbers.[33–35] Fibroblasts from these patients are deficient in their ability to oxidize long-chain fatty acids, and there is progressive destruction of cerebral white matter and adrenal cortex.

Hyperoxaluria

Primary hyperoxaluria type 1 is an autosomal recessive disease caused by a deficiency, either partial or complete, of the hepatic peroxisomal enzyme alanine/glyoxylate aminotransferase (AGT).[36] In man, hepatic AGT is entirely peroxisomal (in cats AGT is entirely mitochondrial, and in rats is both peroxisomal and mitochondrial). In hyperoxaluria patients that have residual AGT activity, the enzyme has been localized by protein A-gold immunolabeling to mitochondria.[37] The deficit appeared to be in uptake of AGT into the peroxisome (distribution of catalase was not altered). An abnormal distribution of peroxisomal protein, as occurs in **Zellweger's syndrome**, is unlikely since peroxisomal structure was relatively normal in these patients.

Other Hereditary Peroxisomal Diseases

Other hereditary diseases in which peroxisomes are altered include glycinuria, cerebrotendinous xanthomatosis, and testicular feminization of humans, and acatalasemia of mice. **Congenital total lipodystrophy** (lipotrophic diabetes mellitus; Berardinelli-Seip syndrome) is characterized by diabetes mellitus, a paucity of fat in adipose tissue, and increased fat in liver and blood.[38] Patients exhibit enhanced growth with muscle hypertrophy. Hepatocytes have an increase in number and irregularity of peroxisomes, accumulation of lipid droplets, and lamellar structures in cup-shaped mitochondria.[39]

In **Refsum's disease** (hereditary motor sensory neuropathy type IV) of human infants, liver contains cytosolic catalase but no catalase-positive peroxisomes. Oxidation of pipecolic and phytanic acids is impaired,

Vet-ebooks.com

but oxidation of very-long-chain fatty acids is only partially decreased; the three peroxisomal beta-oxidation enzymes (acyl-CoA oxidase, enoyl-CoA hydratase/3-hydroxyacyl-CoA dehydrogenase, and 3-ketoacyl-CoA thiolase) are detectable in liver tissue.[40] **Rhizomelic chondrodysplasia** and **alpha-methyl-acyl-CoA raemase deficiency** are peroxisomal diseases associated with β-oxidation deficits.

Smooth Endoplasmic Reticulum

Smooth endoplasmic reticulum (SER) is the site of synthesis and metabolism of fatty acids, phospholipids, and steroids (Fig. 7.3). Most prominent in actively secreting cells, it increases and decreases with the metabolic demands of the cell. SER is especially prominent in steroid-secreting cells in which membranes form arrays and interweaving tubules[41] and extensive lamellar arrangements.[42,43] Striking specialization of ER develops in different species: hypertrophy of chloride cells in gills of freshwater fish that adapt to seawater[44] and novel heat-producing mitochondria-rich muscle cells that warm the eyes and brain of oceanic fish.[45]

At certain sites, the SER is connected to the RER. Lipids developing in SER cisternae are conveyed to junctions with RER where they are conjugated with

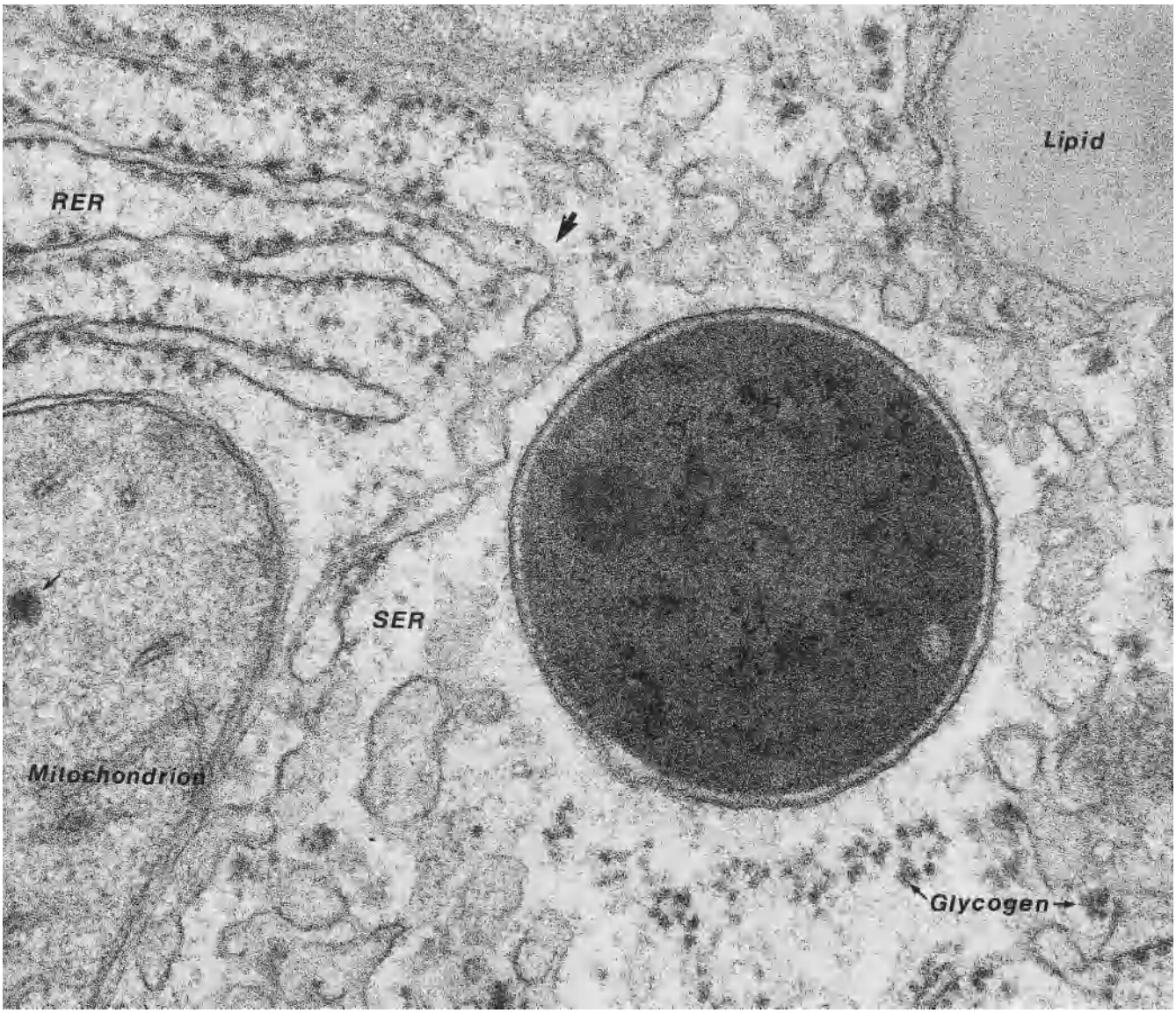


Fig. 7.3 Smooth endoplasmic reticulum (*SER*): site of communication of rough endoplasmic reticulum (*RER*) with SER (*large arrow*), centrolobular hepatocyte. Large dense lysosome at *center right*. Dense calcium-sequestering bodies are present in mitochondria (*small arrow, left*). Note glycogen and lipid in areas of SER.

Vet-ebooks.com

peptides to form lipoproteins. The SER also contains enzymes that modify and detoxify chemicals such as carcinogens and pesticides by conjugating them and converting them to water soluble products that can be easily secreted.

Drug-Induced Injury

Smooth endoplasmic reticulum of the **hepatocyte** is the dominant detoxification organelle for most drugs and toxins. Most of these agents act most strikingly in centrolobular areas of the liver and centrolobular hepatocytes contain more SER than do periportal hepatocytes (Figs. 7.4 and 7.5).[46,47]

SER Proliferation

In the liver, most lipophilic drugs and steroids are metabolized in the mixed function oxidase system, a chain of enzymes that includes cytochrome P450. These enzymes, located primarily in centrolobular hepatocytes, are associated with drug-induced SER proliferation.

The Phenobarbital Model In hepatocytes, phenobarbital is metabolized and causes marked **SER proliferation**, which leads to hypertrophy of hepatocytes and, in chronic therapy, to liver enlargement. Ultrastructurally, hepatocytes are hypertrophic and there are increases in both SER and RER, but few other changes at doses typical of clinical treatment. Experimentally, after intravenous injection there are parallel increase in hepatocyte SER and drug-metabolizing enzymes. Hepatocytes enlarge, the greater cell volume due to increased surface areas and volume of SER. Cell recovery occurs after withdrawal of the drug and SER returns to normal within 15 days.[48] Morphometric ultrastructural analysis reveals a predilection of phenobarbital for centrolobular zones.[49–51] After 1 day of phenobarbital treatment, centrilobular hepatocytes contained an increased amounts of SER. In chronic therapy in drinking water, SER increased 317% in centrilobular hepatocytes but only 176% in peripherolobular hepatocytes.

SER Degeneration

Acute damage to membranes of the SER leads to fragmentation with reformation as vesicles. In global damage, vesicles are distributed throughout the cell (Fig. 7.6).

The Carbon Tetrachloride Model In the liver, carbon tetrachloride is converted in the SER to highly toxic free metabolites. The trichloromethyl radical is the major destructive product and its covalent binding to membrane phospholipids is the basis for SER destruction.[52] SER, one of the first organelles to degenerate, fragments into tiny vesicles. Carbon tetrachloride also affects protein synthesis. One of the earliest structural changes is the disintegration of ribosomes and their detachment from membranes of the rough endoplasmic reticulum. The effect on protein synthesis involves defective incorporation of amino acids into peptide chains. Membranes of the RER fragment into tiny vesicles—first in focal areas and then involving the entire cytoplasm. Within a few hours after injection, cisternae of the RER and nuclear envelope are markedly dilated, and irregular fragments of membrane are frayed into the adjacent cytoplasm.[53,54] There are accompanying alterations in lipoprotein synthesis that lead to accumulation and inspissation of liposomes (lipoprotein droplets) with the RER cisternae. The chief protein suppressive effect is an inhibition of proteins that bind to triglycerides so that triglycerides accumulate as small intracisternal liposomes and large fat globules free in the cytoplasmic matrix.

Toxicologic Enhancement in SER

Single large doses of several drugs will suppress detoxification. Inhibition of detoxifying enzymes by one poison will strikingly lower the lethal dose of a second poison that acts directly on the cell.

- **Heavy metals** such as lead and methyl mercury inhibit the mixed-function oxidases and lead to increased susceptibility to other toxins.
- **Phenobarbital** enhances CCl_4 toxicity by increasing free radical formation (chloramphenicol protects against toxicity, possibly by acting as a free radical-sequestering agent)
- **Ethanol** inhibits drug-metabolizing enzymes and produces a markedly enhanced susceptibility to barbiturates.[55] Like many other toxins, ethanol has different effects on the SER at different doses or exposure times.

Structures Associated with Smooth Endoplasmic Reticulum

Tubulocisternal Endoplasmic Reticulum

Tubulocisternal endoplasmic reticulum (TER) is a network of cisternae adjacent to the lumenal plasma membrane of epithelia that transport large amounts of electrolytes and water. Together with tight junctions,

Vet-ebooks.com

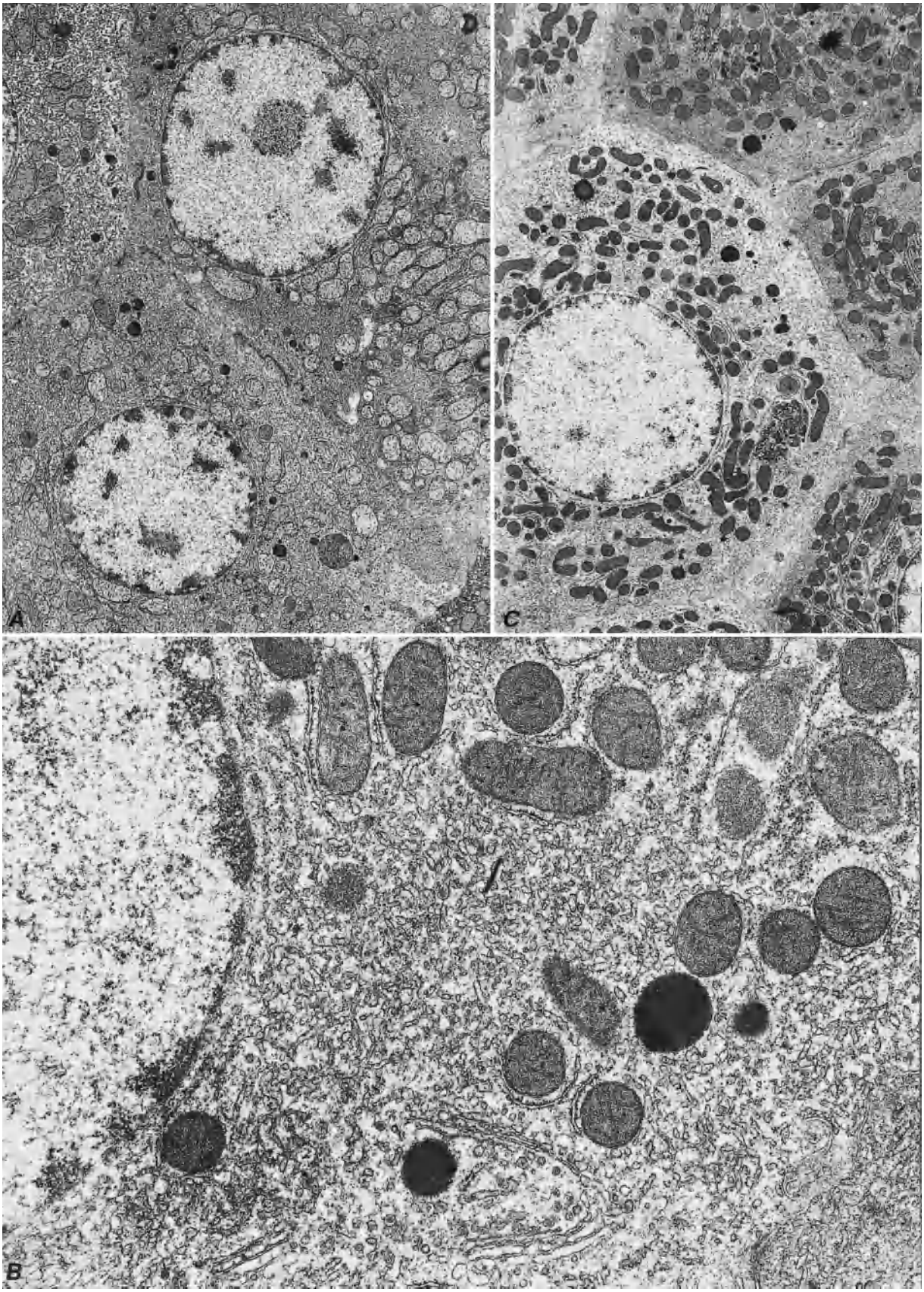


Fig. 7.4 Smooth endoplasmic reticulum duplication, galactosamine toxicity, hepatocyte, rat. **A**. **Early changes**: multiple foci SER duplication, mitochondrial enlargement, and segregation of nucleoli. **B**. **Focus of SER duplication**: Golgi complex (*bottom center*). **C**. **Late changes**: disappearance of nucleoli and chromatin, accumulation of debris in lysosomes, and mitochondrial swelling.

Vet-ebooks.com

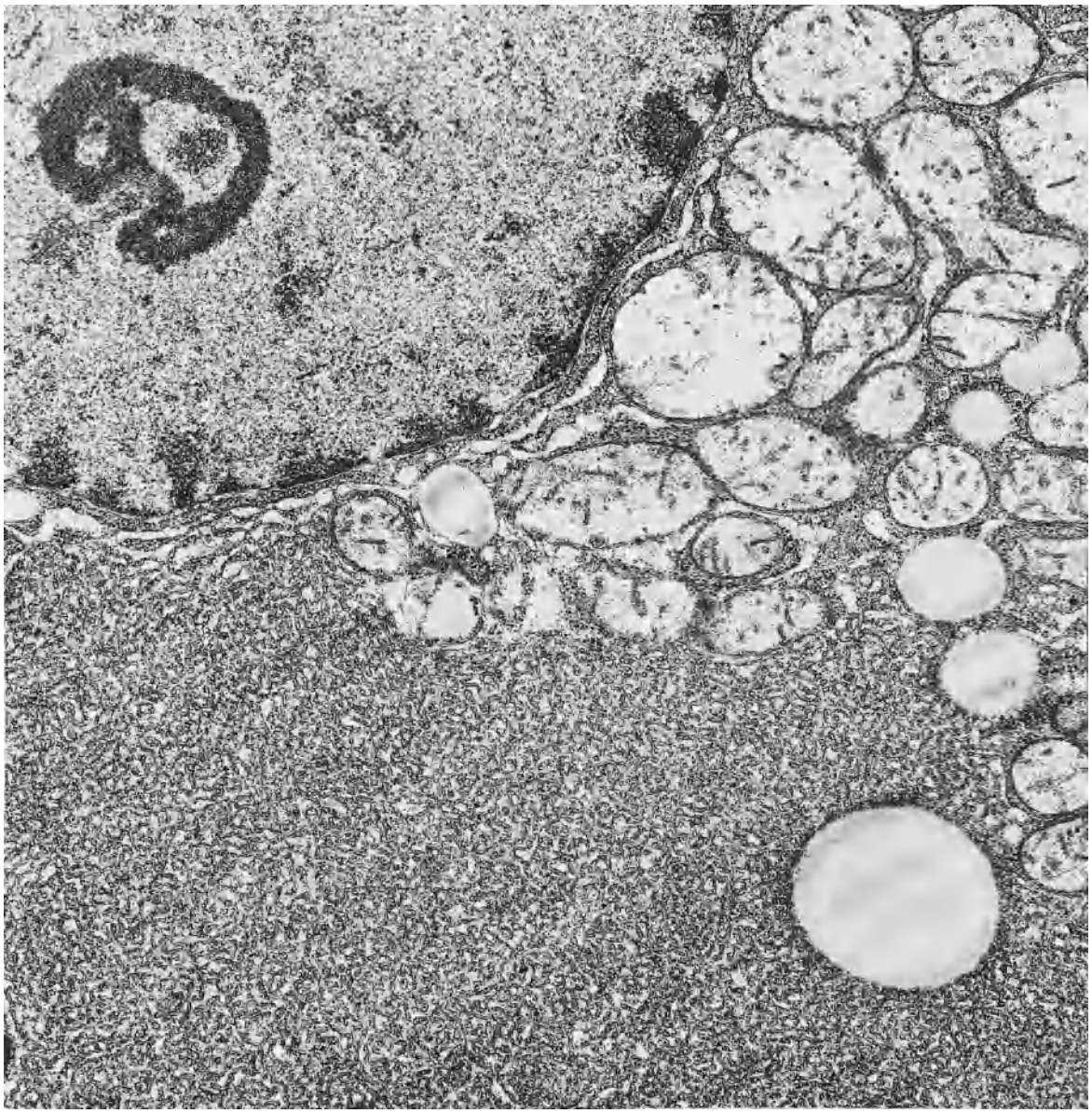


Fig. 7.5 Smooth endoplasmic reticulum duplication: galactosamine toxicity, rat. Note masses of compact SER (*bottom*), mitochondrial swelling (*top right*), lysis of chromatin, and nucleolar segregation and disintegration.

they regulate secretion and absorption in glands. For example, in human eccrine sweat glands, the secretory coil produces the isotonic precursors of sweat; the **sweat duct** absorbs Na^+ against a gradient, producing a hypertonic absorbate (and hypotonic sweat).[56] Tubulovesicular membranes of intercalated cells of renal collecting ducts respond to acidosis by increasing surface areas of apical plasma membranes (as the TER disappears).[57] Acidification is regulated by insertion of H^+ pumps into lumenal membranes of these mitochondria-rich cells.

Calcisomes in Non-muscle Cells

Calcisomes are small, heterogenous, calcium pumping vesicles that regulate intracellular flow of Ca^{++} in non-muscle cells. Calcisomes contain membrane Ca^{++}-ATPase molecules and calreticulin, a protein similar to calsequestrin. Although they appear as part of the endoplasmic reticulum in routinely processed electron micrographs, immunogold labeling for specific protein distinguishes them by their reactivity for Ca^{++}-ATPases and calcium binding protein.[58,59] In Purkinje cells of

Vet-ebooks.com

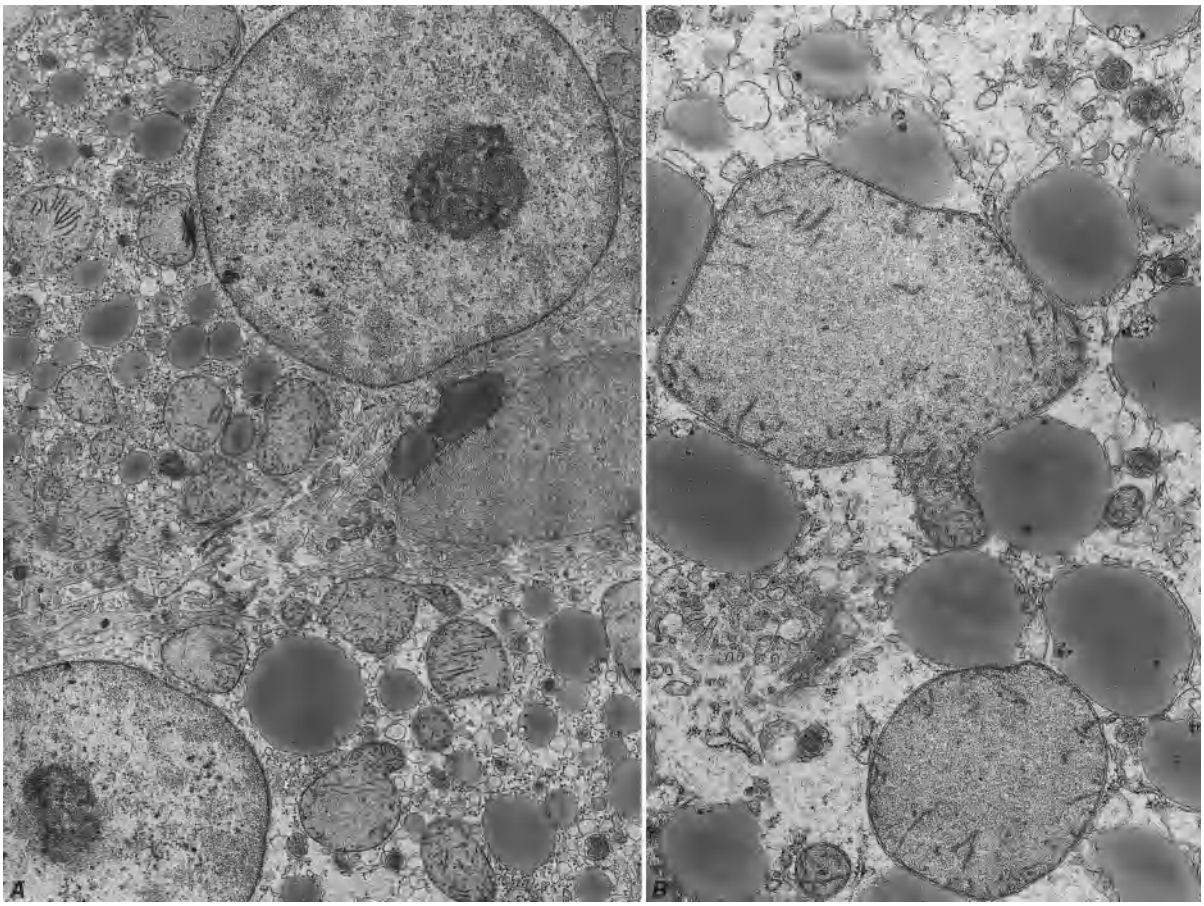


Fig. 7.6 **Steatosis**: microglobular type, liver, diabetes mellitus, dog. *Left*: mitochondria are swollen and distorted. Kupffer cells contain lipid globules; nuclei are normal, globules dominate in cytoplasm, and glycogen is absent. Smooth endoplasmic reticulum is fragmented and vesicular. The cytoplamsic matrix is rarefied. *Right*: mitochondrial enlargement, cristolysis, and pleomorphism. Lipid globules are closely apposed to mitochondria.

the cerebellum for example, smooth segments of endoplasmic reticulum, although cisternae are connected, differ from adjacent rough endoplasmic reticulum in having characteristics of calcisomes.[60]

Calcium Retention Defects

Calcium channel blockers (calcium antagonists) such as verapamil, nifedipine, and diltiazem protect myocardial cells from the Ca^{++} accumulation brought on by ischemia. Changes in myocardial infarction include sarcolemmal disruption, smudging of Z lines, and mitochondrial swelling with inclusion of dense granules and membrane fragments along cristae. These changes are exaggerated by treatment with calcium and are diminished with calcium channel blockers.[61]

Calcium Retention in Sarcoplasmic Reticulum

Sarcoplasmic reticulum (SR) of muscle cells (an analogue of SER in other cell types) is a calcium sequestering organelle. Because shifts in Ca^{++} are crucial to muscle contraction, defects in Ca^{++} pumps cause disease. Acquired and hereditary defects in Ca^{++} transport produce serious and often lethal myopathy or cardiomyopathy. Calcium in the sarcoplasmic reticulum lumen regulates Ca^{++} entry, release, and Ca^{++} stress-induced apoptosis.[62–65]

Vesicles of SR from cardiac and skeletal muscle contain the complete chain of glycolytic enzymes from aldolase to pyruvate kinase. ATP generated by SR-associated glycolytic enzymes is coupled to SR Ca^{++} active transport.[66]

Mutations in human cardiac **calsequestrin** (CASQ2), a high-capacity calcium-binding protein that regulates calcium release channels in the sarcoplasmic reticulum, have been linked to effort-induced vetricular arrhythmia and sudden death. Cardiac calsequestrin-null mice exhibit catecholaminoergic ventricular tachycardia.[67] Expression of canine CASQ2 protein carrying the ventricular tachycardia-linked mutation on calcium signaling in myocytes in vitro

Vet-ebooks.com

confirmed a link between CASQ2 mutation and arrhythmia.

Glycogen

Glycogen, the storage form of glucose, is a branched polymer of glucose molecules. It occurs free in the cytoplasmic matrix, as dense granules of 10–30 nm diameter, a range that reflects the varying size of glycogen polymers. **Monoparticular glycogen** (β-particles) is typical of most tissues, including muscle. In hepatocytes of normal well-fed animals, glycogen is produced in large amounts and occurs as **glycogen rosettes** (α-particles), aggregates of monoparticular glycogen, which are 150 (50–200) nm in diameter.[68–70]

Glycogenesis

The key enzymes of glycogen synthesis are muscle glycogen synthase and liver glycogen synthase, which are encoded by the glycogen synthase 1 gene). Liver enzyme expression is restricted to the liver (hepatic glycogen pools maintain blood glucose during fasting), whereas the muscle enzyme is ubiquitously expressed. In the cell, newly synthesized **glycogen particles** first appear among the labyrinth of the **smooth endoplasmic reticulum**.[71–73] In hepatocytes, glycogen granules develop betweem rows of saccules in foci of SER, the site where activation of glycogen synthase occurs.[74] Starved animals show loss of liver glycogen, and upon refeeding, rapid reduplication of SER occurs, chiefly in centrolobular hepatocytes.

Glycogen-SER Inclusion Bodies

Cytoplasmic masses of SER and glycogen are found incidentally in liver, kidney, muscle, and genital tissues. **Glycogen-membrane complexes** formed by whorled membranes interrupted by glycogen particles are common in glycogenesis of muscle and some other tissues.[75] In certain metabolic disorders, large cytoplasmic inclusions referred to as **glycogen bodies** are found in hepatocytes. Glycogen bodies are composed of single rows of α-rosettes interspersed with smooth-surfaced, parallel arrays of membranes of the smooth endoplasmic reticulum, typically in fingerprint patterns.[76] When large, these lightly eosinophilic, homogenous inclusions may occupy the entire cytoplasm giving rise to the name hyaline lakes or, in the liver, as "ground glass" hepatocytes.

Galactogen A polymer of galactose units, galactogen also assembles into rosettes that resemble glycogen particles. Galactogen rosettes are larger than glycogen, are resistant to diastase, and fail to stain with iodine.[77] Galactogen is common in invertebrates; for example, secretions of gastropod albumen glands that coat the fertilized eggshell and are metabolized by the embryo contain galactogen.

Glycogenolysis

Degradation of glycogen to glucose occurs in the cytosol where, as molecules are broken, monoparticulate glycogen disintegrates. Glycogenolysis is initiated when ATP becomes depleted in the cell; that is, ATP deficit leads to increased cyclic-3′5′-adenosine monophosphate (cyclic AMP) formation from breakdown production of ATP. Cyclic AMP activates the glycogen-splitting enzyme, glycogen phosphorylase.

A striking example of glycogenolysis occurs in livers of neonates. The fetus accumulates large hepatic glycogen stores in the last few days of gestation and glycogen is rapidly mobilized immediately after birth. **Glucagon** treatment to newborns accelerates glycogen breakdown and increases differentiation (glucose and insulin prevent both).[78]

Cells with long-standing glycogen overload may show evidence of glycogenolysis. In normal cells, granules disintegrate as glycogen is slowly degraded in the cytosol. In massive deposition, glycogen is also degraded within lysosomes. This occurs when glycogen is present in large amounts and when the glycogenolytic stimulus is intense. **Glycogenosomes**, the large, glycogen-filled autophagosomes, stain for acid phosphatase.[79,80]

In **ketosis** (whether from starvation, diabetes, or alcohol), insulin levels are low; glucagon levels are high relative to insulin. A consequence of this high glucose-low insulin mixture is **hepatic glycogen depletion** (the hepatocyte requires glycogen for its large ketogenic capacity).

Glycogen Overload

Massive accumulation of glycogen in the cytoplasm distorts the cell and causes other organelle systems to disappear (Fig. 7.7). Conditions where glycogen overload is prominent include (1) drug-induced metabolic disease with disturbed carbohydrate metabolism; (2) enzymatic deficiencies associated with the hereditary glycogen storage disease; (3) hyperglycemia of any cause, commonly that of early diabetes mellitus; and (4) glycogen-storing tumor cells.

Vet-ebooks.com

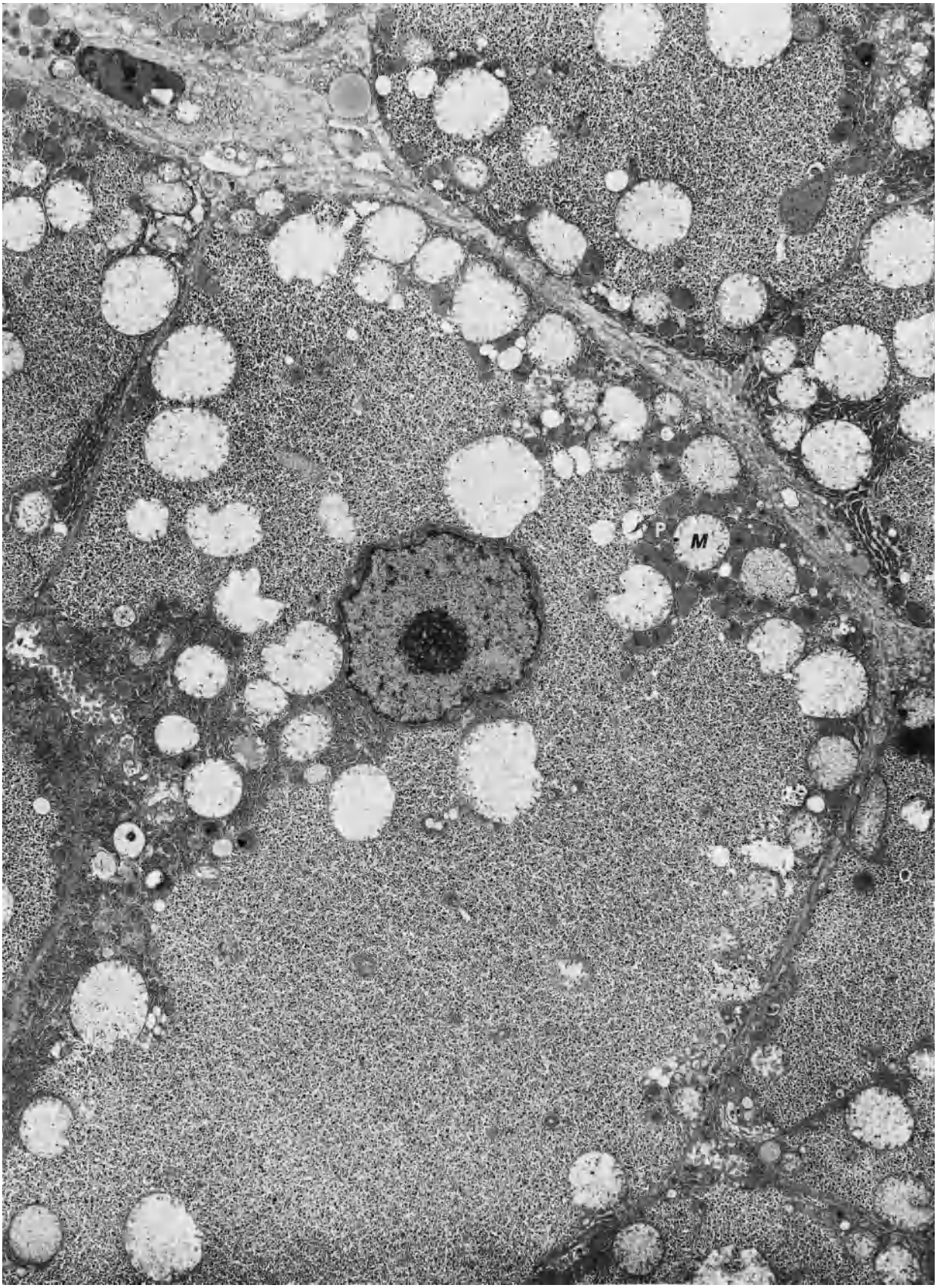


Fig. 7.7 Glycogenosis: hepatocyte, cortisol treatment, rat. Cell is enlarged by massive accumulation of glycogen particles. Rough endoplasmic reticulum is fragmented with remnants around nuclear and plasma membranes. Mitochondria (*M*) are swollen; peroxisome (*P*).

Vet-ebooks.com

Drug-Induced Glycogen Overload

Powerful hormonal influences control carbohydrate metabolism and usually underlies glycogen overload. Large doses of adrenal corticosteroids cause massive accumulation of glycogen in the liver, kidney, and skeletal and cardiac muscle. Hepatocytes double in size, the nucleus moves to the periphery, and the cytoplasm becomes packed with glycogen. Endoplasmic reticulum and other organelles disappear with only remnants persisting adjacent to the nuclear envelope and plasma membrane. If severe, osmotic changes lead directly to mitochondrial swelling and cristolysis.[81,82]

Adrenal corticosteroids stimulate glycogen synthesis in muscle and one of the deleterious effects of prolonged glucocorticoid therapy is glycogen overload in skeletal myocytes, primarily in type 2 glycolytic fibers.[83] Glucocorticoids also affect the cardiac muscle and humans on long-term therapy seem to suffer an increased incidence of heart disease. Experimentally, hearts of rats placed on high doses for one week show no major degenerative effects[84] while high doses for two weeks have led to cardiomyopathy characterized by glycogen accumulation, cytoplasmic vacuolation, deposition of fibrillogranular material, and myolysis.[85]

Nuclear Glycogen Nuclei bearing glycogen are enlarged and have large electron-lucent central areas. Intranuclear glycogen is synthesized in interchromatin regions. Large aggregates of monoparticular glycogen form nuclear inclusions (Fig. 7.8). Intranuclear glycogen is a common finding in hepatocytes of patients with diabetes mellitus, transplantation and other metabolic disorders.[86,87] Nuclear glycogen is common in the livers of aged ruminant species. It is also is seen in neoplastic cells whose nuclei contain glycogen synthetase.

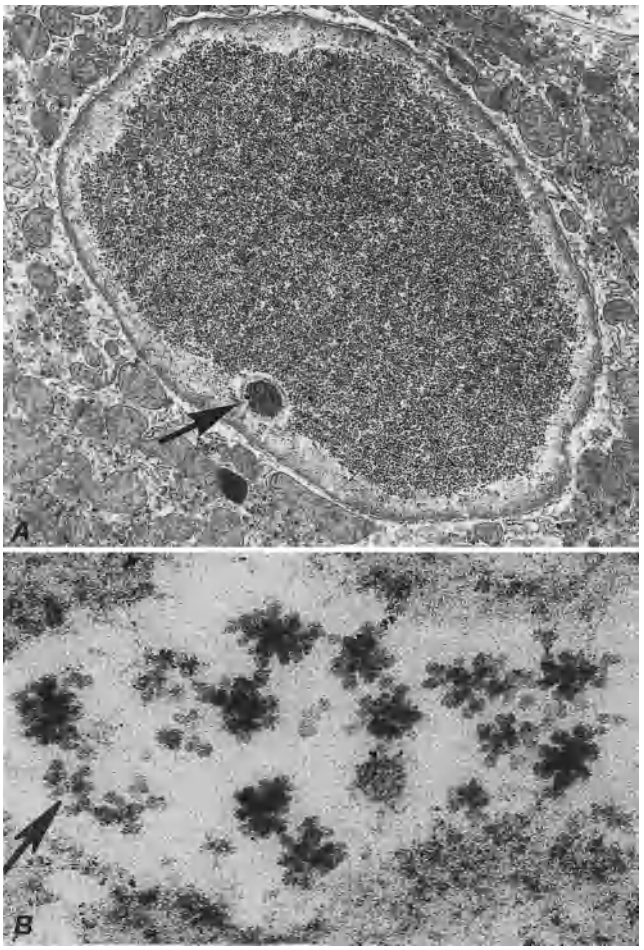


Fig. 7.8 Glycogen. **A**. **Nuclear glycogen**: nucleus is expanded by glycogen particles; glycogen body that is glycogen accumulated within a nuclear body (*arrow*). **B**. **Glycogen α-rosettes** (*arrow*).

Diabetes Mellitus: Hyperglycemia and Glycogen Overload

Diabetes mellitus is a systemic metabolic disorder that arises from defects in insulin action and the resultant loss of capacity to oxidize carbohydrates. Hyperglycemia, and its attendant effects upon cells, underlies the pathologic lesions of diabetes mellitus. Defects include excessive glycosylation of proteins, osmotic lysis of cells, and inactivation of ATPases.

Glycosylation of Proteins in Diabetes Excessive glycosylation of proteins underlies the most serious defects. Cell surfaces, especially of circulating erythrocytes, platelets and leukocytes, are excessively glycosylated. Extracellular proteins are cross-linked by glucose-derived metabolites (especially the long-lived proteins such as collagen and lens crystallin), and this leads to thickening of basement membranes. The novel monosaccharide fructose-3-phosphate has been identified in lens tissue of diabetic rats where it and its breakdown products appear to be important glycosylating agents.

Hepatocytes in diabetes mellitus do not accumulate glycogen but develop large amounts of lipids and fragmentation of endoplasmic reticulum. Lipid metabolism is defective and, in the fatty degeneration of uncontrolled diabetes, there is fragmentation of the smooth endoplasmic reticulum.[88]

Renal tubules accumulate glycogen from the urinary filtrate in diabetes. Hyperglycemia results in spill of glucose into the glomerular filtrate and glycosuria. Proximal convoluted tubules, the nephron segments involved in glucose absorption, accumulate glucose and large glycogenosomes develop in tubular

Vet-ebooks.com

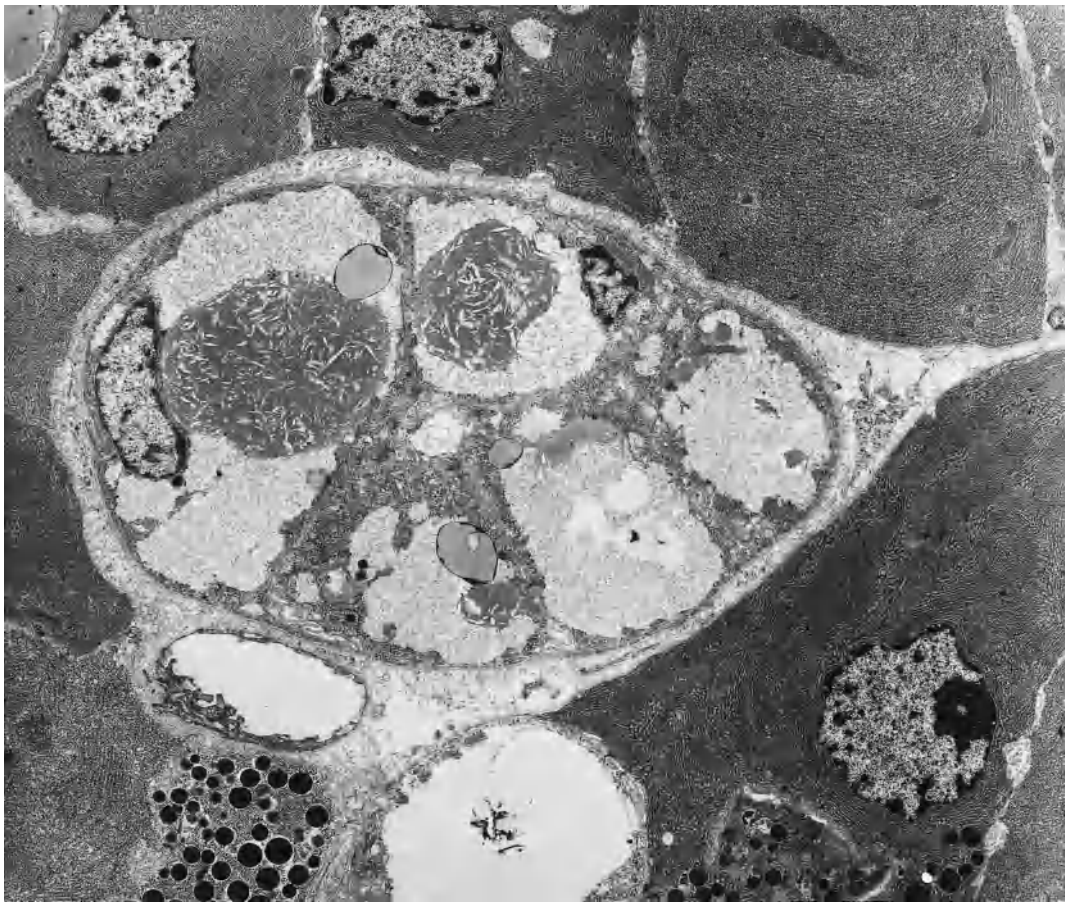


Fig. 7.9 Glycogen and cell swelling: pancreatic duct, acute pancreatitis, dog. Ductal epithelial cells are markedly increased in size and contain large amounts of cytoplasmic glycogen (pale areas) and lipids.

cells.[89,90] Similarly, ductal epithelium in other glands will accumulate glycogen and lipid. Human diabetic patients have increase amounts of glycogen in their kidneys; severity is related to the degree of hyperglycemia. Increased glycogen is throughout the nephron but is most striking in the distal convoluted tubules and in arteriolar smooth muscle cells.[91] In islet cell destruction-induced hyperglycemia associated with acute pancreatitis, glycogen accumulates in swollen epithelial cells of the pancreatic ducts (Fig. 7.9).

Insulin and Glucose Transporters

Glucose is tranported into cells by **glucose transporters** (GluT) which are embedded in the plasma membrane to create a pore that, when in proper position, permits the passage of glucose. Each GlutT consists of a polypeptide chain of about 500 amino acids that is folded to create 12 membrane-spanning segments. Recruitment of GluTs to the cell surface has been followed by immunogold techniques. When tagged by gold only 1% were found on cell surfaces before insulin stimulation; after insulin about 40% of the gold-labeled GluTs were on the cell surface.[92]

Lipids

Lipid globules (lipid droplets) are composed of neutral lipids that exist free within the cytoplasmic matrix due to high surface tension of the external phospholipid monolayer surrounding the globule.[93] They are surrounded, not by a typical lipid bilayer, but by a monolayer of phospholipids. In adipocytes and steriodogenic cells, lipid droplets store and metabolize triglycerides, fatty acids and cholesterol. Membrane-bound lipids have been reported in metabolic diseases but the interpretation of these structures suggests they are intralysosomal lipids with the lysosomal membrane closely apposed to the lipid.[94]

Ultrastructurally, triglyceride **lipid globules** are spherical, non-membrane-bound, and homogeneous

Vet-ebooks.com

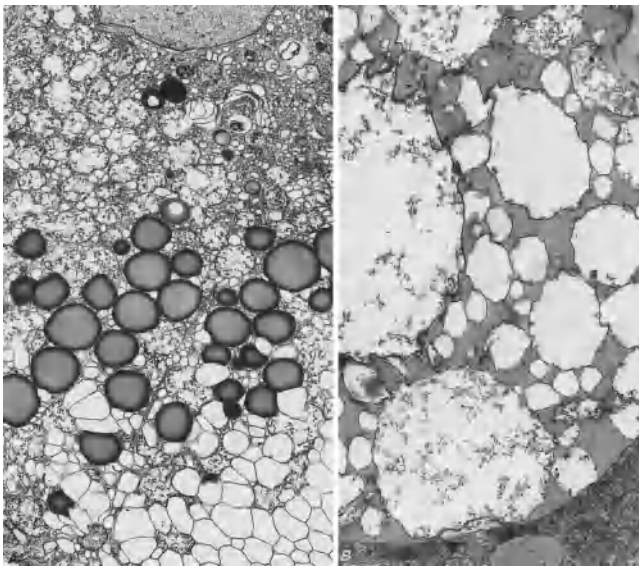


Fig. 7.10 Lipid globules: **steatosis,** adrenal cortex. **A**. **Lipid globules**: zone of small dark-staining lipid in midcytoplasm separates markedly vacuolated peripheral areas from perinuclear zones. **B**. **Lipid locule**: vacuolation. Multiple small vacuoles have blebbed into the lipid locule during lipolysis.

(Fig. 7.10). Although of varying size, the typical lipid globule of normal hepatocytes is approximately 500 nm in diameter and this increases 4–10 times in fatty degeneration. In the abnormal lipid accumulations of steatosis, lipid droplets shift to production of abnormal profiles of **lipid globule-associated proteins** such as perilipins, adipophilin, and others. The lipid body-endoplasmic reticulum interface is a metabolically active site where ribosomes, endoplasmic reticular membranes, and ribosomal proteins contribute to lipid droplet structure.[95]

Steatosis (fatty degeneration) is the excessive accumulation of **lipid globules** in the cytoplasm of non-fat cells (Fig. 7.11). Although most cells produce cytoplasmic lipids upon injury, few develop the large amounts of lipids that characterize fatty degeneration in hepatocytes, cardiac myocytes, and renal tubular epithelial cells. In severe steatosis, neutral lipids pass into the nucleus, probably through connections between the cytocavity network and nuclear pores.[96]

Injury may result in the accumulation of complex **cytoplasmic lipid inclusions**, especially in

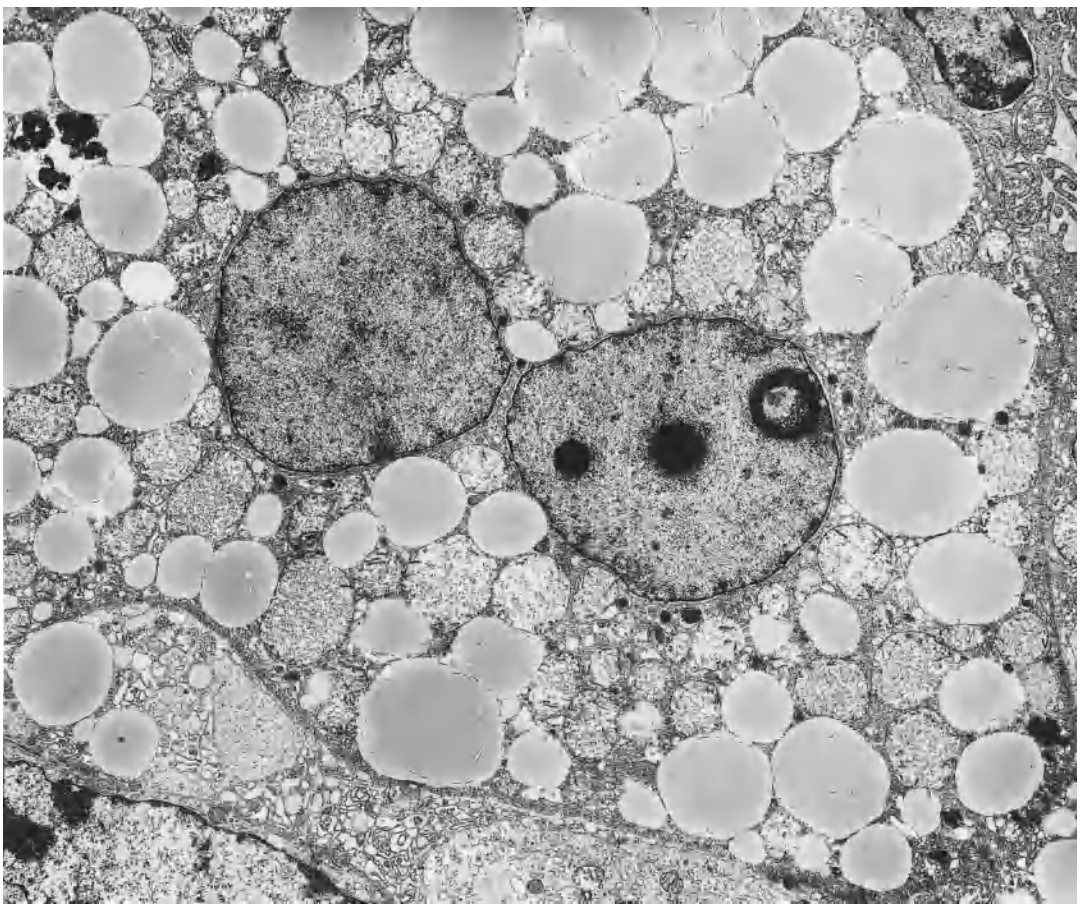


Fig. 7.11 Lipid globules: aflatoxicosis, hepatocyte, horse. Large globules of neutral lipids fill the cytoplasm. Hepatocyte contains two nuclei, one with separation of nucleolar components.

Vet-ebooks.com

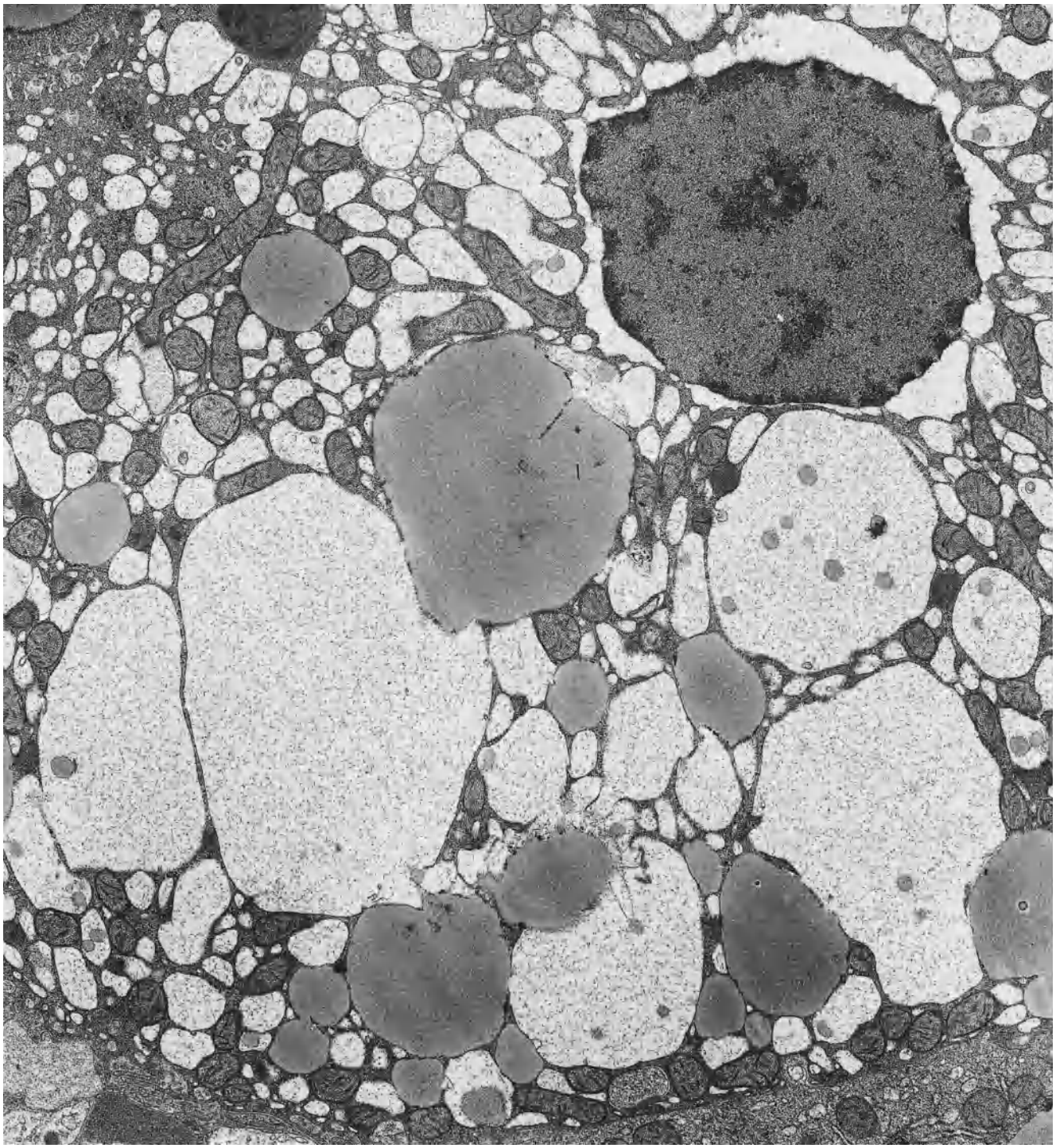


Fig. 7.12 Liposomes: liposomes of neutral lipid within vacuoles and dilated cisternae of endoplasmic reticulum, acute cell swelling, carbon tetrachloride poisoning, liver, dog. Note marked dilatation of cisternae of the nuclear envelope.

parenchymal cells of the liver, adrenal cortex, kidney and gastric mucosa (Fig. 7.12). These are large, spherical membrane-bound bodies composed of a homogeneous lipid matrix filled with small electron-lucent vesicles. Because of their high content of membranes they contain large amounts of phospholipids. When transported to the cell surface, the phospholipids are released by exocytosis and form a protective hydrophobic layer; for example, over the epithelium of the gastrointestinal lumen.

Vet-ebooks.com

Adipocytes

Normal adult fat cells (adipocytes) contain a single large triglyceride-containing lipid droplet, or **lipid locule**, that is homogeneous and of varying electron density.[97,98] Triglycerides are formed from free fatty acids that enter the fat cell from the bloodstream. Adipocyte caveolae are sites of insulin action, and insulin receptors and insulin receptor substrate-1 have been identified by immunogold techniques.[99]

Lipogenesis

During lipogenesis, complex lipoprotein particles such as chylomicrons are hydrolyzed at endothelial surfaces of capillaries that supply fat tissue, and the fatty acids that are released are transferred across the endothelial cell and through the interstitial space to the fat cell. In moving from endothelium to fat cell the fatty acids may pass within membranes liberated from cell surfaces. The complex filopodia that project from fat cell surfaces to interact with endothelium enhance fatty acid transfer.[100] Insulin receptors and other surface molecules that drive adipocyte metabolism have been detected with immunogold techniques.[101]

Lipolysis

During **lipolysis,** triglycerides are again converted to fatty acids, which leave the cell. Ultrastructurally, fat cells undergoing lipolysis develop several changes: (1) lipid locules become irregular and heterogeneous, (2) frond-like cytoplasmic processes project from the cell surface, (3) plasmalemmal vesicles develop and fuse forming characteristic **microvesicular rosettes,** especially close to the fat cell surface, and (4) basement membranes become folded, irregular and duplicated.[102] With appropriate fixatives, lipid globules are encased by arrays of filaments, perhaps a reflection of the role played by the cytoskeleton in lipid movement.

Triglycerides and cholesterol, released during adipocyte lipolysis, circulate in the bloodstream. In plasma they do not exist free but are packaged into lipoprotein particles. Lipids form a hydrophobic core that is surrounded by a coat of apoprotein, phospholipid, and small amounts of free cholesterol. Apoproteins direct the lipoprotein particles to their proper sites for metabolism by binding to enzymes or receptor molecules on cell surfaces.

Adipocyte Defects

Adipocytes have altered rates of metabolism in **obesity.** Adipocytes of the obese (ob/ob) strain of mouse are larger than normal and have a diminished content of plasma membrane protein particles.[103] In humans and most mammalian species, adipocyte sizes occur in a bimodal pattern with populations of very small cells and large mature fat cells, and these patterns are altered in human obesity.[104]

The lesions of **multiple systemic lipomatosis (Launois-Bensaude's disease)**, a human syndrome of enlarging symmetric fat deposits, are composed of adipocytes that resemble brown fat cells. Preadipocytes in these lesions have mitochondria that are large and have long parallel cristae, and multivacuolar lipid deposits.[105] This syndrome occurs in alcoholics and may be associated with liver disease. Adipocytes have defective lipolysis and catabolism of triglycerides differs from that of normal white adipocytes.

Brown Fat Cells

These large mitochondria-rich cells generate heat in fetuses, neonates, and hibernating and cold-acclimated adults.[106] The thermogenic mechanism, an uncoupling of oxidative phosphorylation from ATP generation, results in heat production. This role of brown fat is an important protective mechanism, and these cells are increased in hypothermia and hypothyroidism. In some types of obesity, brown fat cells are defective and do not produce heat in response to epinephrine.[107] **Uncoupling protein 1** (UCP1), the mammalian thermogenic mitochondrial protein, is found only in brown adipocytes.[108] Morphometric analysis of immunogold staining for UCP1 reveals a nonhomogeneous pattern of immunostaining (the Harlequin phenomenon), and co-localization with the heat shock protein heme oxygenase-1.[109]

Fat Atrophy

The watery and translucent appearance of atrophic fat in starving animals is responsible for the term **serous atrophy of fat**. Lipid locules of the adipose cell break up and decrease in size when fat undergoes atrophy. Ultrastructural changes in adipose cells during starvation include marked irregularities in cell surface with increases in pseudopodial projections and pinocytotic vesicles. There is an increase in the basement membrane material of the surface lamina, which becomes irregular and evaginated (Fig. 7.13). Increase in smooth endoplasmic reticulum and development of autophagosomes also occur. Significant changes occur in the **interstitium** of adipose tissue of starving animals. Large mesenchymal cells appear that actively synthesize and release large amounts of collagen and basement membrane material. Acid mucopolysaccharides

Vet-ebooks.com

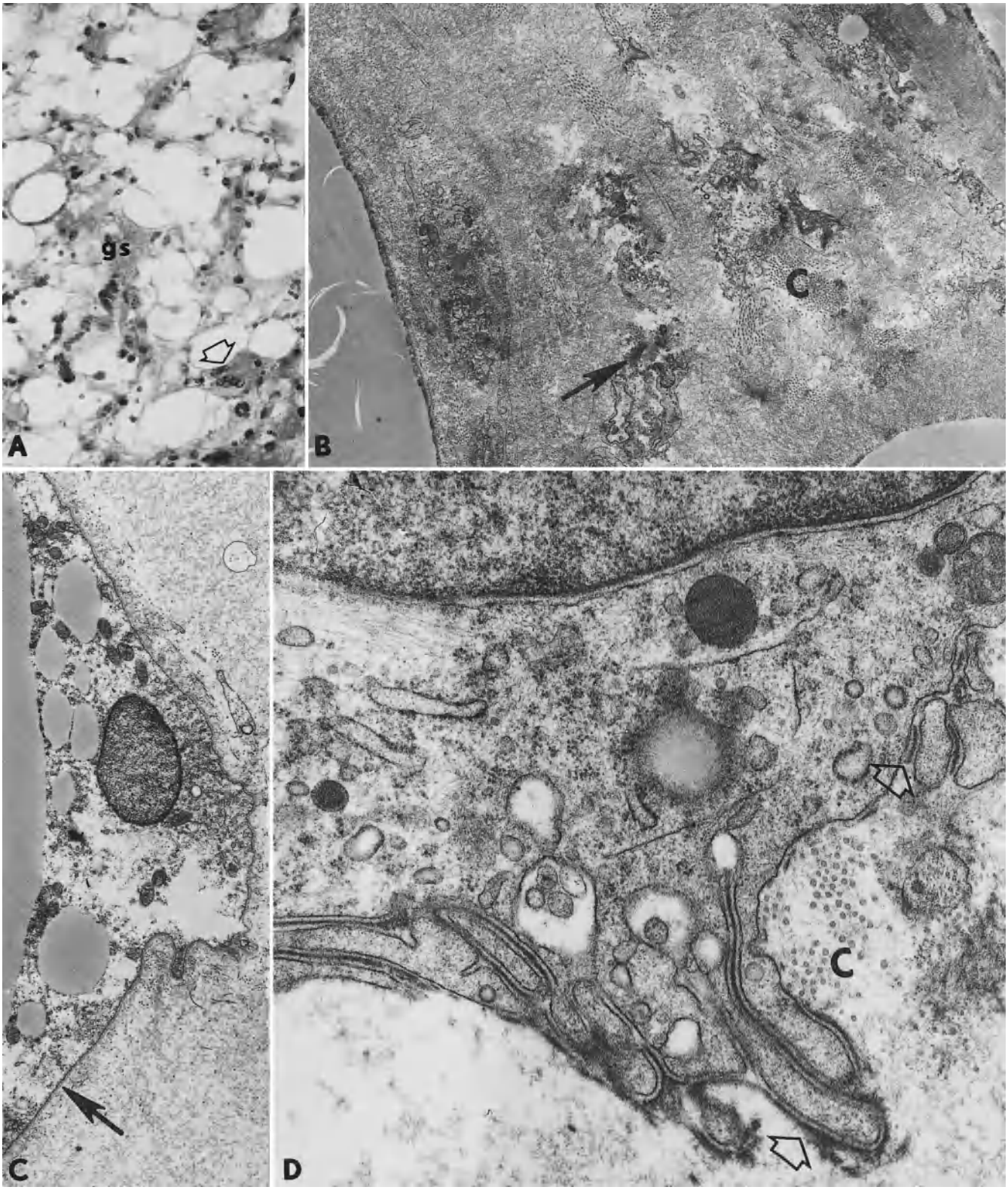


Fig. 7.13 **Atrophy of fat**: pericardial fat, malnutrition, dog. **A. Atrophic adipose cells** are irregular and embedded in deposits of ground substance (*gs*) and protein precipitates; multinuclear cell (*arrow*). **B. Ground substance** between adipocytes contains collagen (*C*) and proteolgycans (*arrow*). **C. Adipocyte margin** with fat locule breakdown into cytoplasmic globules; cell surface is surrounded by basement membrane (*arrow*). **D. Convoluted plasma membrane** and duplicated basement membrane in mesenchymal cell; collagen (*C*).

Vet-ebooks.com

are deposited, and the interstitium stains intensely with techniques that detect glycosaminoglycans. In extensive delipidation, there a major reduction in adipogenic transcription factors and other components the support lipogenesis.[110]

Mitochondria are central to lipid metabolism in adipocytes, and toxic injury to mitochondria may lead to cachexia. Depletion of mtDNA (accompanied by mitochondrial proliferation) underlies the subcutaneous wasting and adipocyte loss in AIDS patients treated with nucleoside reverse transcriptase inhibitors.[111]

Lipids in the Hepatocyte

Fatty acids are taken up by hepatocytes from circulating blood. In the cytoplasmic matrix they may be shunted into three major pathways: (1) To **mitochondria** for energy production. Fatty acids are activated to acetyl coenzyme A (CoA) by enzymes in the outer mitochondrial membrane, transported across the inner membrane, and degraded in the matrix by oxidation. Derivatives contribute electrons to the respiratory chains and carbon units to oxaloacetate of the citric acid cycle. Fatty acid oxidation is the major energy-yielding process in severe exercise and in starvation. (2) To **triglyceride globules** for storage as fuel molecules for later use. Fatty acids are complexed with glycerol in a series of acylations catalyzed by membrane-bound triacylglycerol-synthetase complexes. Resulting triglycerides are stored free in the cytosol as neutral lipids. (3) To **smooth endoplasmic reticulum** for use as building blocks of phospholipids and sphingolipids of membranes and other structures.

Triglycerides arising within **cisternae of SER** and apoprotein moieties formed in **RER** are combined at sites where these organelles are connected. The new lipoprotein molecules are transported in vesicles to the **Golgi complex**, where cholesterol and phospholipids are incorporated to form **very low-density lipoproteins (VLDLs)**, which are then packaged into secretory granules and released from the hepatocyte.[112–114] VLDL can reach sizes approaching 100 nm.

The main protein component in secreted VLDLs is **apolipoprotein B (apoB)**. ApoB is concentrated around lipid globules and may appear ultrastructurally in lipid crescents. In one study, apoB was localized to a cluster of electron-lucent particles 50–100 nm in diameter adhering to cytoplasmic **lipid globules**.[115] In the mammalian hepatocyte, lipid esters stored in cytoplasmic lipid globules are used to synthesize VLDL into which apoB is integrated cotranslationally. Once formed, apoB-containing lipoproteins exit the ER as dense lipid-protein complexes; this exit uses the COPII pathway. Further expansion of the VLDL particle occurs via post-ER lipidation. VLDLs mature in the Golgi complex by apoB conformational changes and expansion of lipoproteins, changes that favor apoE binding.[116]

In hepatocytes, an increase in lipid globules suggests one of the following mechanisms:

- Long-standing **elevation of blood lipids**
- **Chronic hypoxia** with inhibition of lipid metabolizing enzymes
- **Acute sublethal toxic injury** that suppresses lipid pathways
- **Chronic progressive metabolic disease** arising from defective cellular enzymes

Lipoproteins

Complex lipoprotein globules circulate in the **bloodstream** carrying cholesterol, phospholipids, and other molecules between the intestine, liver, adipose tissue, and the organs that use lipids for energy. These circulating lipoproteins are spherical microemulsions that vary widely in size. The particles contain a central core of nonpolar lipids (primarily triglycerides and cholesteryl esters) and a surface monolayer of polar lipids (largely of phospholipids). Unesterified cholesterol is present on the surface monolayers, and with increasing particle size it becomes incorporated progressively into the core. The proteins of the monolayer, like the phospholipids, have amphipathic or detergentlike properties due to polar and nonpolar amino acids. The density of lipoprotein particles in inversely related to their size, a reflection of the relative amounts of low-density, nonpolar core lipids and high-density, surface proteins.

Abnormal serum lipoproteins have been characterized in serum from patients with hyperlipidemias and other lipid metabolism disorders. Serum from patients with **abetalipoproteinemia** lacks all the lipoproteins that contain B apolipoproteins, those carrying most of the cholesterol and triglycerides in plasma. Electron microscopic studies on sera of these patients fail to demonstrate apoB by immunocytochemical means.[117–119] LDL and VLDL density intervals have a distinct cuboidal, square-packing appearance with and 8–9 nm periodicity.[120] Like the abundant high-density lipoprotein (HDL) particles, the lipoproteins of the LDL density interval show a decreased ratio of lecithin to sphingomyelin. About one-half of the cholesterol is unesterified, compared with less than one-third in normal LDL.

Vet-ebooks.com

Lipoprotein Metabolism: The Chylomicron Pathway

Enterocytes

In the intestinal lumen, dietary fats are cleaved by pancreatic lipase into fatty acids and monoglycerides. In the presence of bile acids, these form water-soluble micelles that attach to and are taken up by intestinal absorptive cells by passive diffusion.[121–123] Molecules composed of short-chain fatty acids are released into the portal circulation. Long-chain fatty acids are converted to triglycerides surrounded by a protein coat to form **chylomicrons**. Soon after a fatty meal, fats are resynthesized as triglycerides in the **Golgi complex** and **smooth membrane vesicles**.[124] Chylomicrons incorporate apolipoproteins in the **Golgi complex** and are secreted by exocytosis from the basolateral plasma membrane of the enterocyte.[125] During fasting, entocytes release apolipoproteins from the apical surface.

Bloodstream

As chylomicrons are formed they are secreted into lacteals of intestinal villi and enter the general circulation via the thoracic duct. Within lacteals and circulating blood, apoproteins synthesized in the enterocyte are augmented by transfer of apoproteins from HDLs. The high levels of chylomicrons in circulating blood (**chylomicronemia**) that occur after feeding are transient because the pathways of chylomicron metabolism are efficient and rapid.

Endothelium

Too large to pass endothelial barriers (80–500 nm), **chylomicrons** are metabolized at endothelial surfaces of capillaries in muscle and adipose tissue. Chylomicrons bind to the enzyme **lipoprotein lipase** that is embedded in the plasma membranes of endothelial cells. A special apoprotein component of the chylomicron molecule activates lipoprotein lipase, which in turn acts on triglycerides to liberate free fatty acids and monoglycerides. Fatty acids then enter **muscle** for use in energy production, or **adipocytes** for reesterification and storage.[126,127]

Lipoprotein lipase activity on endothelial surfaces, which determines the rate of uptake of fatty acids, varies with nutritional status. Normally, lipase activity is high in adipose tissue capillaries but low in heart and skeletal muscle; thus free fatty acids tend to be taken up by adipocytes. During fasting, enzyme activity falls in adipose tissue but rises in muscle, so fats are diverted to muscle cells for energy. As triglycerides are hydrolyzed by lipoprotein lipase, chylomicron particles shrink. The triglyceride core is depleted and the remaining surface phospholipids and cholesterol are released from the endothelial surface, reentering the circulation as chylomicron remnants. **Chylomicron remnants** (30–80 nm) are carried to the liver, where they bind to receptors on the hepatocyte surface. They are taken up by receptor-mediated endocytosis and degraded in hepatocyte lysosomes. Their cholesterol is liberated to be used by the heaptocyte to produce new lipoproteins, chiefly very low-density lipoproteins. Thus, the liver rapidly takes up dietary cholesterol in the form of chylomicron remnants. Much cholesterol is disposed of in the bile and may be reabsorbed in the intestine and again delivered to the liver (enterohepatic circulation).

Lipoprotein Metabolism: VLDL-LDL Pathways

Hepatocytes

Triglycerides produced in the liver are mobilized by lipolysis followed by reesterification to reassemble triacylglycerol before incorporation into **very low-density lipoprotein** particles. Triacylglyerol hydrolase (localized on the endoplasmic reticulum by immunogold techniques) participates in VLDL assembly without using VLDL lipids as substrates.[128] The VLDL package is released into the bloodstream for transport to adipose tissue. **VLDLs** (30–80 nm) are assembled in the hepatocyte cytoplasm by combination of triglycerides from **smooth endoplasmic reticulum**, and apoprotein from **rough endoplasmic reticulum**.[129] Cholesterol (which is derived from chylomicron remnants if dietary cholesterol is available and synthesized if it is not) is also incorporated into the VLDL molecule. VLDLs are packaged in the hepatocyte **Golgi complex** and secreted into the sinusoids. VLDL formation thus allows the liver to remove excess fatty acids from plasma and mobilize them for storage in fat.[130] Triglycerides and cholesteryl esters are extremely hydrophobic and when they accumulate in hepatocytes will form long, irregularly shaped, electron-lucent crystals.[131,132]

Blood

In the bloodstream, VLDLs interact with endothelial lipoprotein lipase and release their triglycerides. VLDL remnants are formed as their triglycerides are removed. VLDL-lipase interaction is less efficient than chylomicron-lipase interaction, so VLDLs persist in the circulation much longer. As more triglycerides are removed, the particles diminish in size (and increase in density) and lose apoE as they are converted to **intermediate-density lipoproteins (IDLs)**. Excess

Vet-ebooks.com

surface material, like that of chylomicrons, is transferred to HDL particles. IDL particles are released into the circulation.

In **hepatic sinusoids**, the remaining triglycerides of the IDL are removed and most apoproteins are lost. The remaining particle of cholesterol ester and one specific apoprotein are called **low-density lipoprotein (LDLs)**, the major cholesterol-carrying paritcle in human blood. The cholesterol in the tiny LDL particle (22 nm) constitutes most of the plasma cholesterol in carnivores. The LDL particle consists of about 2,000 molecules of cholesterol, 1,000 molecules of phopholipid and one large protein on the surface, apolipoprotein B-100.

A variant molecule **lipoprotein(a)** in human plasma is identical to LDL except that it has an additional surface piece called **apolipoprotein(a)**, a molecule that closely resemble plasminogen. Humans with high levels of lipoprotein(a) have an increased risk of coronary heart disease, and this molecule is found within **atherosclerotic plaques**. Apolipoprotein(a), although it cannot dissolve fibrin, competes with plasminogen for access to fibrin, to receptors on cell surfaces, and for plasminogen activators. These activities, while having a positive effect in wound healing, may enhance the growth of atherosclerotic plaques.

LDLs deliver cholesterol to all cells. They are removed from circulation only by cells that contain specific receptor molecules on their surfaces. LDLs may be also removed from circulation and degraded by macrophages via a less efficient, nonreceptor mechanism. This occurs when LDL levels are very high, as in familial hyperlipidemias, and the expanding macrophages appear as foam cells.

Uptake of Low-Density Lipoprotein

The tiny LDL particle (20–25 nm) contains most of the cholesterol of plasma. The outer surface of the sphere is a phospholipid monolayer membrane in which is embedded a single type of hydrophobic protein, **apoB**. Inside is a highly apolar core of cholesterol esterified to a long-chain fatty acid. LDLs are removed from circulation only by cells containing specific receptors in their plasma membranes.[133]

LDL receptors on hepatocyte surfaces binds to and internalizes lipoproteins that contain apolipoproteins B100 (apoB100) or apolipoprotein E (apoE).[134] Taken into coated vesicles and delivered to lysosomes, the LDLs are degraded as their proteins and cholesterol are hydrolyzed. Unesterified cholesterol so liberated enters the cytosol where it is used in membrane synthesis and suppresses further de novo cholesterol synthesis.[135]

In vivo, most circulating LDL is taken up by the liver, by both hepatocytes and nonparenchymal cells. Studies in human fibroblast cultures have shown that **receptors** for LDL particles are located in coated pits, even in unstimulated cells. Taken into **clathrin-coated vesicles** by receptor-mediated endocytosis, LDL particles move through endosomes, including **uncoating vesicles** (pH 7.0), where apoB separates from the receptors, and **uncoupling vesicles** (pH 5.0, CURL), in which LDL separates from receptors and passes into secondary lysosomes, where components are degraded.

In rats, studies using immunogold-labeled apolipoprotein B revealed marked uptake by Kupffer cells. Treatment with estrogens, which enhances LDL receptor production, increased LDL uptake, especially by hepatocytes.[136] Labeled LDLs were found attached to microvilli and later to microvesicles; eventually, LDLs were transported to biliary canaliculi.

Cholesterol derived from LDL enters the hepatocyte via receptor-mediated endocytosis. To deliver their cholesterol, circulating LDLs bind to specific receptor glycoproteins embedded in **coated pits** on the surface of hepatocytes and other cells and are taken into the cell where they are hydrolyzed within lysosomes by acid lipases. Unique **microvillar channels** for uptake of large amounts of lipoproteins have been demonstrated on adrenal cortical cells.[137] Plasma lipoproteins become concentrated on these specialized structures formed by closely associated plasma membranes of sinusoidal microvilli of zona fasciculata cells.

High-Density Lipoproteins

High-density lipoproteins remove excess cholesterol from cells. Lipid-free HDL apolipoproteins remove cholesterol and phospholipids.[138] Apoproteins A (apoA) are the major proteins of HDL; apoA-I is the main HDL constituent. HDL is internalized through cubilin-mediated endocytosis and is transported to lysosomes. **Cubilin** is a high affinity endocytic receptor for HDL holoparticles. Double immunogold labeling studies show that, in endocytic vesicles, cubilin and HDL exist in distinct sites. In early endosomes both are localized in the membrane; in late ensomes, HDL were in the matrix.[139] Cubilin is present in large amounts in the embryonic yolk sac where it is a receptor for acquisition of maternal HDL.

Caveolae are the major organelles that facilitate transport of excess cholesterol to HDL on the surface of endothelial cells.[140] Immunogold studies on rat aorta showed that caveolin-1 and ATP-binding cassette transporter A1 (ABCA1) are involved in HDL-mediated cellular cholesterol efflux in endothelial cells.[141] In cholesteryl ester uptake, surface-associated

Vet-ebooks.com

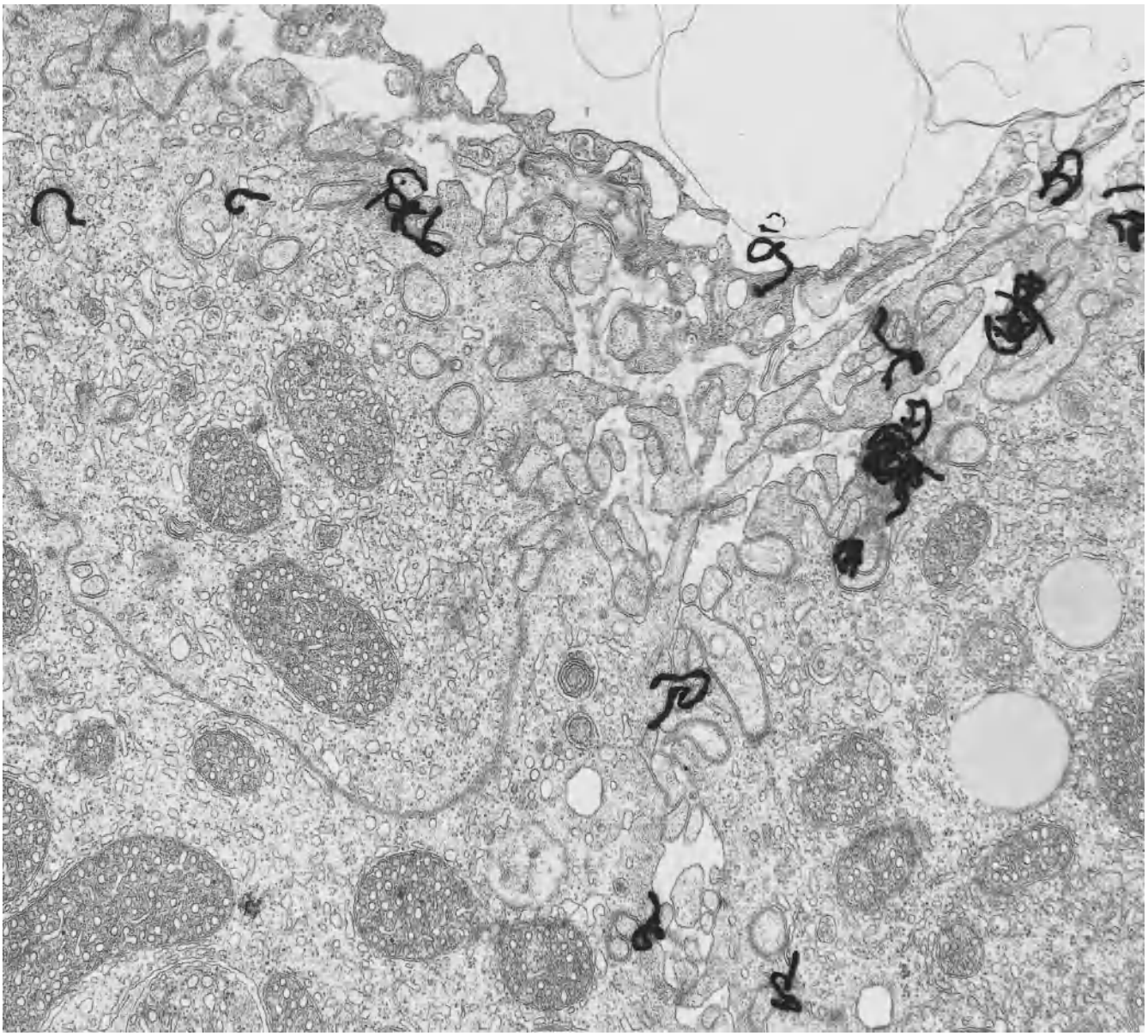


Fig. 7.14 HDL apoprotein: adrenal. Autoradiogram, sinusoidal surface, adrenal cortical cell. Exposed grains represent the distribution of ^{125}I-labeled rHDL apoprotein and are on microvilli with preference of microvillar channels. (Micrograph: Eve Reaven, *J Lipid Res* 30:1551, 1989.)

lipoproteins (HDL and LDL) are trapped in the space formed between closely apposed surface microvilli; they enter specialized microvillar channels, a complex channel system for selective HDL-cholesteryl ester uptake. Microchannel formation is promoted by the expression of scavenger receptor B1 (SC-B1).[142] SR-B1 is also responsible for most LDL-CE uptake.

In **plasma**, surface components of triglyceride-rich lipoproteins are transferred to HDL during lipolysis. Phosphatidyl choline and cholesterol in some HDLs are acted on by the enzyme **lecithin-cholesterol acyltransferase (LCAT)** to yield lysolecithin and cholesteryl ester; the former is transferred to albumin and removed from the blood, and the latter is transferred to other lipoprotein particles. The esterification of cholesterol by LCAT and removal of lipoproteins by the liver is a reverse cholesterol transport pathway, where -by cholesterol in extrahepatic cells is delivered to the liver (Fig. 7.14).

Vet-ebooks.com

Lipid Metabolism Disorders

Defective Lipid Transport

Human primary hyperlipidemia can be due to the following defects: (1) **Lipoprotein lipase deficiency** (type I or exogenous hyperlipidemia), in which the enzyme for hydrolysis of triglycerides carried on chylomicrons and VLDLs prior to entry into adipocytes is missing, resulting in marked hypertriglyceridemia (plasma VLDLs may be normal). The severity of cutaneous xanthomatosis, hepatosplenomegaly, pancreatitis, and other clinical signs (there is no direct association with atherosclerotic disease) correlates with the severity of chylomicronemia, which in turn relates to dietary fat intake. A very rare familial deficiency of apolipoprotein C-II, a cofactor of lipoprotein lipase, causes a similar syndrome.

(2) **Deficit of LDL receptors on cell surfaces** is a type of familial hypercholesterolemia, in which the LDL receptor (LDLr) is missing or defective, and there is loss of feedback control, unchecked production of LDL by the hepatocyte, and elevated levels of **cholesterol** that induce premature atherosclerosis, even in fetuses,[143] and cutaneous xanthomas.

(3) **Defective catabolism of protein remnants** results in defective apolipoproteins, so LDL remnants are not degraded. As in lipoprotein lipase deficiency, the chylomicrons and remnants are atherogenic and are deposited in vascular walls.

(4) **Apoprotein synthesis defect** results from abnormal synthesis of apoprotein moieties and leads to decreased serum cholesterol and triglycerides, with deposition of cholesterol esters in tissues. In **abetalipoproteinemia**, caused by congenital absence of apolipoprotein B (required for chylomicron formation) in serum, triglycerides are stored in cells in the liver and intestine because they cannot be moved into lymphatics. This underlies the hypolipidemia. Hepatocyte peroxisomes may be abnormally pleomorphic and large.

Familial Combined Hyperlipidemia

Familial combined hyperlipidemia is an autosomal dominant trait with high penetrance that leads to elevated levels of VLDL, LDL, of both in plasma. It is the most prevalent genetically determined lipoprotein disorder of humans, and carries a significant risk of coronary arteriosclerosis.

Familial Lecithin:Cholesterol Acyltransferase Deficiency

Familial lecithin:cholesterol acyltransferase deficiency results in a failure of LCAT to esterify cholesterol in plasma, and leads to clinical abnormalities that may include corneal opacities, glomerulopathy, abnormal erythrocytes, and unique plasma lipoprotein particles rich in unesterified cholesterol and phosphatidyl choline. Renal lesions have foam cells in glomeruli and arteriosclerotic changes with subendothelial deposits of lipids. Ultrastructurally, capillary lumens are obstructed with meshworks of membranes and amorphous particles. Sea-blue histiocytes, macrophages filled with membranes of unesterified cholesterol and phosphatidyl choline arranged in lamellae, are large foam cells present in the spleen and bone marrow of these patients.[144]

Acid Lipase Deficiency

Cholesteryl ester storage disease is an inborn error of metabolism that results from accumulation of cholesteryl esters and triglycerides in most tissue of the body.[145] The defect is in lysosomal acid lipase (acid cholesteryl ester hydrolase) activity. In the liver there is accumulation of fat in hepatocytes, bile duct epithelium, and Kupffer cells. The Kupffer cells are markedly hypertrophic with PAS-staining granules and cholesterol crystals. **Wolman's disease** is a more severe form of acid lipase deficiency with death in infancy from hepatosplenomegaly, steatorrhea, and adrenal cortical calcification. Cholesteryl esters accumulate in tissues in which they are normally synthesized, for example, adrenal cortex, liver, intestine, spleen, and abdominal lymph nodes. Cholesterol clefts are common in Kupffer cells.[146]

Chylomicron Retention Disease

A rare familial disorder characterized by hypobetalipoproteinemia with selective deletion of apoB-48 is referred to as **chylomicron retention disease**. In affected infants, chylomicrons are absent in plasma after meals and both LDL and HDL levels in plasma are low. Biopsies of the small intestine reveal that enterocytes are packed with lipid globules that cluster in the supranuclear region (Fig. 7.15).[147,148]

Deficiency of Lipoprotein Lipase

In humans, deficiency of lipoprotein lipase is a rare familial trait in which hypertriglyceridemia is expressed as a buildup of chylomicrons after consumption of a fatty meal. **Combined lipase deficiency (*cld*)** is a recessive mutant in the T/t complex of chromosome 17 of mice; it causes deficits of both lipoprotein lipase and hepatic lipase, enzymes necessary for uptake of triacylglycerol from chylomicrons and VLDL in blood, and for conversion of VLDL to LDLs.

Vet-ebooks.com



Fig. 7.15 Fat absorption: human jejunal absorptive cell obtained 60 min after a fatty meal. Cells are filled with lipid globules within smooth endoplasmic reticulum cisternae and are in supranuclear regions; basement membrane (*bm*). (Micrograph: Claude C. Roy, *Gastroenterology* 92:390, 1987.)

Mice homozygous for this defect (*cld/cld*) do not metabolize plasma lipoproteins at normal rates and die within 3 days if they suckle; that is, they develop lethal hyperchylomicronemia as a consequence of nursing. Large amounts of chylomicrons are found in capillaries.[149]

Macrophage Uptake in Hyperlipidemia

The consequence of severe, long-term elevation in blood lipids is deposition of triglycerides, cholesterol or phospholipids in tissue. In some diseases, macrophages in lymphoid tissues are affected, with minor deposits in phagocytic cells elsewhere.[150,151] In others, the vascular wall is involved (see atherosclerosis). In addition to the systemic deposition of circulating lipids in macrophages, curious local deposits, referred to as xanthomatosis, occur in normolipidemic animals.[152]

Macrophages, essential for removal of lipids from tissue, rapidly internalize and process exogenous cholesterol, low-density lipoproteins, and other lipids. Because enzymes for synthesis are balanced with cell surface receptors, cholesterol does not accumulate in large amounts. When cholesterol does accumulate in excess of need, it is stored as cholesteryl esters in lipid globules, just as it is in steroid-secreting cells.[153,154]

Xanthomatosis

Sitosterolemia, or xanthomatosis, is a human inherited lipid storage disease. Accelerated atherosclerosis and arthritis are due to reduced cholesterol synthesis and a deficit of **HMG-CoA reductase**, the rate controlling enzyme of cholesterol biosynthesis (but offset by enhanced expression of tissue LDL receptor). Intestinal absorption of dietary plant sterols, normally restricted, is markedly increased, so that sterols accumulate in blood, and are metabolized to unusual intermediates in the liver. Liver cells are normal ultrastructurally.[155]

Increased HDLs and Tangier Disease

HDLs, which are reservoirs for lipids and apolipoproteins, are altered in several rare inborn errors of metabolism. **Tangier disease**, characterized by accumulation of cholesteryl esters in foam cells in many tissues, arises from a severe deficiency or absence of normal HDL. Plasma cholesterol concentrations are low. Triglyceride levels are normal. Clinically manifestations include hyperplastic orange tonsils, splenomegaly, and relapsing neuropathy. Foam cells are found in tonsils, bone marrow, jejunal submucosa, myenteric plexus, nonvascular smooth muscle cells, and nerves (in Schwann cells). Ultrastructurally, foam cells are characterized by relatively uniform small electron-lucent lipid globules of cholesteryl esters. Deposits are spherical, electron-dense, and birefringent. In some cells these deposits are within lysosomes and may be in crystalline shapes.[156,157]

The cellular defect in Tangier disease is associated with abnormal lysosomes and Golgi saccules of monocytes and other phagocytes. Dysfunction of lipid metabolism leads to overproduction of triglycerides and esterified cholesterol and to increased synthesis and catabolism of phospholipids. Macrophages fail to respond normally to HDL with a coordinated regulation of lipids, and they accumulate cholesteryl esters.[158]

Vet-ebooks.com

References

1. Schrader M, Fahimi HD. 2006. Growth and division of peroxisomes. *Int Rev Cytol* 255:237.
2. Zhou Z, Kang YJ. 2000. Cellular and subcellular localization of catalase in the heart of transgenic mice. *J Hist Cyt* 48:585.
3. Singh AK, et al. 1999. Manganese superoxide dismutase in rat liver peroxisomes. *Mol Cell Biochem* 197:7.
4. Tolbert NE, Essner E. 1981. Microbodies: Peroxisomes and glyoxysomes. *J Cell Biol* 91:271s.
5. Litwin JA, et al. 1987. Immunocytochemical localization of peroxisomal enzymes in human liver biopsies. *Am J Pathol* 128:141.
6. Sternlieb I, Quintana N. 1977. The peroxisomes of human hepatocytes. *Lab Invest* 36:140.
7. Zaar K, et al. 1991. Purification of marginal plates from bovine renal peroxisomes: Identification with L-α-hydroxyacid oxidase B. *J Cell Biol* 113:113.
8. Usuda N, et al. 1988. Tissue specificity and species differences in the distribution of urate oxidase in peroxisomes. *Lab Invest* 58:100.
9. Usuda N, et al. 1991. Immunoelectron microscopic evidence of organ differences in the composition of peroxisome-specific membrane polypeptides among three rat organs: Liver, kidney, and small intestine. *J Hist Cyt* 39:1357.
10. Baumgart E, et al. 1989. Biogenesis of peroxisomes: Immunocytochemical investigation of peroxisomal membrane proteins in proliferating rat liver peroxisomes and in catalase-negative membrane loops. *J Cell Biol* 108:2221.
11. Lazarow PB, Fukiki Y. 1985. Biogenesis of peroxisomes. *Ann Rev Cell Biol* 1:489.
12. Lamhonwah AM, et al. 2005. OCTN3 is a mammalian peroxisomal membrane carnitine transporter. *Biochem Biophys Res Commun* 338:1966.
13. Keller G-A, et al. 1986. 3-Hydroxy-3-methylglutaryl coenzyme A reductase localization in rat liver peroxisomes and microsomes of control and cholestyramine-treated animals: Quantitative biochemical and immunoelectron microscopical analyses. *J Cell Biol* 103:875.
14. Keller GA, et al.1989. Subcellular localization of sterol carrier protein-2 in rat hepatocytes: Its primary localization to peroxisomes. *J Cell Biol* 108:1353.
15. Kahn Z, et al. 2006. Peroxisomal localization of hypoxia-inducible factors and hypoxia-inducible factor regulatory hydroxylases in primary rat hepatocytes exposed to hypoxia-reoxygenation. *Am J Pathol* 169:1251.
16. Davis WL, Goodman DBP. 1992. Evidence for the glyoxylate cycle in human liver. *Anat Rec* 234:461.
17. Keller G-A, et al. 1991. Evolutionary conservation of a microbody targeting signal that targets proteins to peroxisomes, glyoxysomes, and glycosomes. *J Cell Biol* 114:893.
18. Goldfischer S, Reddy KJ. 1984. Peroxisomes (microbodies) in cell pathology. *Int Rev Exp Pathol* 26:45.
19. Hruban A, et al. 1974. Effects of some hypocholesteremic agents on hepatic ultrastructure and microbody enzymes. *Lab Invest* 30:474.
20. Baumgart E, et al. 1987. Proliferation of peroxisomes in pericentral hepatocytes of rat liver after administration of a new hypocholesterolemic agent (BM 15766). Sex-dependent ultrastructural differences. *Lab Invest* 56:554.
21. Rao MS, et al. 1986. Induction of peroxisome proliferation in hepatocytes transplanted into the anterior chamber of the eye. *Am J Pathol* 124:519.
22. Reddy JK, Ohno S. 1981. Testicular feminization of the mouse. Paucity of peroxisomes in Leydig cells of the testis. *Am J Pathol* 103:96.
23. Reddy JK, et al. 1984. Induction of hepatic peroxisome proliferation in nonrodent species, including primates. *Am J Pathol* 114:171.
24. Yarrington JT, et al. 1981. Effect of the hypolipidemic drug RM1 14,514 on hepatic ultrastructure of rats. *Exp Molec Pathol* 34:307.
25. McGuire EJ, et al. 1991. Peroxisome induction potential and lipid regulating activity in rats. *Am J Pathol* 139:217.
26. Svoboda DJ. 1978. Unusual responses of rat hepatic and renal peroxisomes to RMI 14,514, a new hypolipidemic agents. *J Cell Biol* 78:810.
27. Goldfischer S, et al. 1973. Peroxisomal and mitochondrial defects in cerebro-hepato-renal syndrome. *Science* 182:62.
28. Powers JM, et al. 1989. Structural and chemical alterations in the cerebral maldevelopment of fetal cerbro-hepato-renal (Zellweger) syndrome. *J Neuropathol Exp Neurol* 48:270.
29. Muller-Hocker J, et al. 1984. Mitochondrial myopathy with loosely coupled oxidative phosphorylation in a case of Zellweger syndrome. *Virch Arch B* 45:125.
30. Santos MJ, et al. 1985. Peroxisomal organization in normal and cerebrohepatorenal (Zellweger) syndrome fibroblasts. *Proc Nat Acad Sci USA* 82:6556.
31. Challa VR, et al. 1983. Pathologic alterations in the brain and liver in hyperpipecolic acidemia. *J Neuropathol Exp Neurol* 42:627.
32. Takeda S, et al. 1989. Adrenoleukodystrophy—early ultrastructural changes in the brain. *Acta Neuropathol* 78:124.
33. Goldfischer S, et al. 1985. Peroxisomal defects in neonatal-onset and X-linked adrenoleukodystrophies. *Science* 227:67.
34. Powers JM, Schaumburg HH. 1981. The testis in adrenoleukodystrohy. *Am J Pathol* 102:90.
35. Ulrich J, et al. 1978. Adrenoleukodystrophy. *Acta Neuropathol* 43:77.
36. Purdue E, et al. 1990. Identification of mutations associated with peroxisome-to-mitochondrion mistargeting of alanine/glyoxylate aminotransferase in primary hyperoxaluria type 1. *J Cell Biol* 111:2341.
37. Danpure CJ, et al. 1989. An enzyme trafficking defect in two patients with primary hyperoxaluria type 1: Peroxisomal alanine/glyoxylate aminotransferase rerouted to mitochondria. *J Cell Biol* 108: 1345.
38. Collins JC, et al. 1989. Hepatic peroxisomal abnormalities in abetalipoproteinemia. *Gastroenterology* 97: 766.

Vet-ebooks.com

39. De Craemer D, et al. 1992. Hepatic ultrastructure in congenital totoal lipodystrophy with special reference to peroxisomes. *Ultrastr Pathol* 16:307.
40. Aubourg P, et al. 1993. Pseudo infantile Refsum's disease: Catalase deficient peroxisomal particles with partial deficiency of plasmalogen synthesis and oxidation of fatty acids. *Pediatr Res* 34:270.
41. Black VH. 1972. The development of smooth-surfaced endoplasmic reticulum in adrenal cortical cells of fetal guina pigs. *Am J Anat* 135:381.
42. Hrudka F. 1988. Nodulous corpuscles and mitochondrial inclusions in Sertoli cells of deer hybrids. *J Ultrastruc Molec Struc Res* 100:107.
43. Nagato T, et al. 1984. Unusual smooth endoplasmic reticulum in submandibular acinar cells of the male round-eared bat, *Tonatia sylvicola*. *J Ultrastruct Res* 87:275.
44. Pisam M, et al. 1988. Ultrastructural features of chloride cells in the gill epithelium of the Atlantic salmon, *Salmo salar*, and their modifications during smoltification. *Am J Anat* 183:235.
45. Block BA, Franzini-Armstrong C. 1988. The structure of the membrane systems in a novel muscle cell modified for heat production. *J Cell Biol* 107:1099.
46. Chedid A, Nair V. 1972. Diurnal rhythm in endoplasmic reticulum of rat liver: Electron microscopy study. *Science* 175:176.
47. Jones AL, et al. 1978. A quantitative analysis of hepatic ultrastructure in rats during enhanced bile secretion. *Anat Rec* 192:227.
48. Bolender RP, Weibel ER. 1973. A morphometric study of the removal of phenobarbital-induced membrane from hepatocytes after cessation of treatment. *J Cell Biol* 56:746.
49. Burger PC, Herdson PD. 1966. Phenobarbital induced fine structural changes in rat liver. *Am J Pathol* 48:793.
50. Massey ED, Butler WH. 1979. Zonal changes in the rat liver after chronic administration of phenobarbitone. *Chem Biol Interact* 24:329.
51. Staubli W, et al. 1969. Correlated morphometric and biochemical studies on the liver cell. II. Effects of phenobarbital on rat hepatocytes. *J Cell Biol* 42:92.
52. Trudell JR, et al. 1982. Reductive metabolism of carbon tetrachloride by human cytochrome P-450 reconstituted in phospholipid vesicles. *Proc Natl Acad Sci USA* 79:2678.
53. Leduc EH. 1973. Sulfaguanidine protection of mouse liver from carbon tetrachloride-induced necrosis. *Lab Invest* 29:186.
54. Pasquali-Ronchetti I, et al. 1980. Ultrastructural and biochemical changes induced by progressive lipid peroxidation on isolated microsomes and rat liver endoplasmic reticulum. *Lab Invest* 42:457.
55. Lieber CS. 1988. Biochemical and molecular basis of alcohol-induced injury to liver and other tissues. *New Engl J Med* 319:1639.
56. Baron DA, et al. 1984. Tubulocisternal endoplasmic reticulum in human sweat glands. *Lab Invest* 51:233.
57. Madsen KM, Tischer CC. 1984. Response of intercalated cells from the rat outer medullary collecting duct to chronic metabolic acidosis. *Lab Invest* 51:268.
58. Hashimoto S, et al. 1988. Immunocytochemistry of calciosomes in liver and pancreas. *J Cell Biol* 107:2524.
59. Volpe P, et al. 1988. "Calcisome," a cytoplasmic organelle. *Proc Natl Acad Sci USA* 85:1091.
60. Villa A, et al. 1991. Intracellular Ca^{2+} stores in chicken Purkinje neurons. *J Cell Biol* 113:779.
61. Saito A, et al. 1988. Ultrastructure of the calcium-release channel of sarcoplasmic reticulum. *J Cell Biol* 107:211.
62. Brochet DXP, et al. 2005. Ca^{2+} blinks: Rapid nanoscopic store calcium signaling. *Proc Natl Acad Sci USA* 102:3099.
63. Gathercole DV, et al. 2000. Immunogold-labeled L-type calcium channels are clustered in the surface plasma membrane overlying junctional sarcoplasmic receticulum in guinea pig myocytes. *J Mol Cell Cardiol* 32:1981.
64. Krenács T, Dux L. 1994. Silver-enhanced immunogold labeling of calcium-ATPase in sarcoplasmic reticulum of skeletal muscle. *J Hist Cyt* 42:967.
65. Nixon GF, et al. 1994. Immunogold localization of inositol 1,4,5-triphosphate receptors and characterization of ultrastructural features of the sarcoplasmic reticulum. *J Muscle Res Cell Motil* 15:682.
66. Xu KY, Becker LC. 1998. Ultrastructural localization of glycolytic enzymes on sarcoplasmic reticulum vesicles. *J Hist Cyt* 46:419.
67. Chopra N, et al. 2007. Modest reductions of cardiac calsequestrin increase sarcoplasmic reticulum Ca^{2+} leak independent of luminal Ca^{2+} and trigger ventricular arrhythmias in mice. *Circ Res* 101:617.
68. Babcock MB, Cardell RR. 1975, Fine structure of hepatocytes from fasted and fed rats. *Am J Anat* 143:399.
69. Sakaida M, et al. 1987. Physiological role of skeletal muscle glycogen in starved mice. *Anat Rec* 218:l267.
70. Zang X, et al. 1990. Scanning tunneling microscopic images show a laminated structure for glycogen molecules. *FASEB J* 4:3140.
71. Cardell RR, et al. 1985. SERGE, the subcellular site of initial hepatic glycogen depostion in the rat. *J Cell Biol* 101:201.
72. Garfield SA, et al. 1984. The effects of insulin replacement and withdrawal on hepatic ultrastructure and biochemistry. *Am J Anat* 170:127.
73. Michaels JE, et al. 1984. Lobular and cellular patterns of early hepatic glycogen deposition in the rat as observed by light and electron micrscopic radioautography after injection of ^{3}H-galactose. *Am J Anat* 170:23.
74. Cardell RR, Cardell EL. 1990. Heterogeneity of glycogen distribution in hepatocytes. *J Elec Microsc Tech* 14:126.
75. Davidowitz J, et al. 1983. Membrane-glycogen complexes in rabbit extraocular muscle. *J Ultrastruct Res* 82:64.
76. Wills EJ. 1992. Ground glasslike hepatocytes produced by glycogen-membrane complexes ("glycogen bodies"). *Ultrastr Pathol* 16:491.
77. Nieland ML, Goudsmit EM. 1969. Ultrastructure of galactogen in the albumen gland of *Helix pomatia*. *J Ultrastruct Res* 29:119.

Vet-ebooks.com

78. Chiu HF, Phillips MJ. 1974. Glucagon induces premature structural differentiation of fetal hepatocytes. *Lab Invest* 30:305.
79. Pfeifer U. 1972. Zur Stellung des lysosomalen Glykogenabbaues im hepato-cellularen Glykogentoffwechsel. *Virch Arch B* 10:108.
80. Becker FF, Cornwall CC. 1971. Phlorizin-induced autophagocytosis during hepatic glycogenolysis. *Exp Molec Pathol* 14:103.
81. Wiener J, et al. 1968. A quantitative description of cortisone-induced alterations in the ultrastructrue of rat liver parenchymal cells. *J Cell Biol* 37:47.
82. Badylak SF, Van Vleet JF. 1982. Tissue-γ-glutamyl transpeptidase activity and hepatic ultrastructural alterations in dogs with experimentally-induced glucocorticoid hepatopathy. *Am J Vet Res* 43:649.
83. Stern LZ, et al. 1972. The fine structure of cortisone-induced myopathy. *Exp Neurol* 36:530.
84. Mall G, et al. 1980. Morphometric observations on the rat heart after high-dose treatment with cortisol. *Virch Arch A* 385:169.
85. Clark AF, et al. 1982. Glucocorticoid-induced alterations in the rabbit heart. *Lab Invest* 47:603.
86. Bejarano PA, et al. 2006. Liver glycogen bodies: Ground-glass hepatocytes in transplanted patients. *Virch Arch* 449:539.
87. Wisell J, et al. 2006. Glycogen pseudoground glass change in hepatocytes. *Am J Surg Pathol* 30:1085.
88. Reaven EP, et al. 1973. The effect of experimental diabetes mellitus and insulin replacement on hepatic ultrastructure and protein synthesis. *J Clin Invest* 52:248.
89. Orci L, Stauffacher W. 1971. Glycogenesomes in renal tubular cells of diabetic animals. *J Ultrastruct Res* 36:499.
90. Powell HC, et al. 1979. Glycogen accumulation in the nerve and kidney of chronically diabetic rats. *J Neuropathol Exp Neurol* 38:114.
91. Biava C, et al. 1966. Ultrastructural on renal glycogen in normal and pathologic human kidneys. *Lab Invest* 15:330.
92. Slot JW, et al. 1991. Immuno-localization of the insulin regulatable glucose transporter in brown adipose tissue of the rat. *J Cell Biol* 113:123.
93. Novikoff PM, Edelstine D. 1977. Reversal of orotic acid-induced fatty liver in rats by clofibrate. *Lab Invest* 36:215.
94. Hayashi H, Sternlieb I. 1975. Lipolysosomes in human hepatocytes. Ultrastructural and cytochemical studies of patients with Wilson's disease. *Lab Invest* 33:1.
95. Wan H-C, et al. 2007. Role and origins of leukocyte lipid bodies: Proteomic and ultrastructural studies. *FASEB J* 21:167.
96. Karasaki S. 1973. Passage of cytoplasmic lipid into interphase nuclei in preneoplastic rat liver. *J Ultrastruct Res* 42:463.
97. Cushman SW. 1970. Structure-function relationships in the adipose cell. *J Cell Biol* 46:326.
98. Gustavsson J, et al. 1999. Localization of the insulin receptor in cavevolae of adipocyte plasma membrane. *FASEB J* 13:1961.
99. Karlsson M, et al. 2004. Colocalization of insulin receptor and insulin receptor substrate-1 to caveolae in primary human adipocytes. *Eur J Biochem* 271:2471.
100. Blanchette-Mackie EJ, Scow RO. 1981. Lipolysis and lamellar structures in white adipose tissue of young rats. *J Ultrastruct Res* 77:295.
101. Jarett L, Smith RM. 1975. Ultrastructural localization of insulin receptors on adipocytes. *Proc Natl Acad Sci USA* 72:3526.
102. Blanchette-Mackie EJ, et al. 1989. Cytochemical studies of lipid metabolism: Immunogold probes for lipoprotein lipase and cholesterol. *Am J Anat* 185:255.
103. Carpentier J-L, et al. 1977. Perturbation of the adipose cell plasma membrane in obese (ob/ob) mice. *Lab Invest* 37:260.
104. Julien P, et al. 1989. Scanning electron microscopy of very small fat cells and mature fat cells in human obesity. *J Lipid Res* 30:293.
105. Zancanaro C, et al. 1990. Multiple symmetric lipomatosis. *Lab Invest* 63:253.
106. Geloen A, et al. 1990. In vivo differentiation of brown adipocytes in adult mice. *Am J Anat* 188:366.
107. Assimacopoulos-Jeannet F, et al. 1976. Alteration of brown adipose tissue in genetically obese (ob/ob) mice. *Endocrinology* 110:439.
108. Bing C, et al. 2000. Increased gene expressison of brown fat uncoupling protein (UCP)1 and skeletal muscle UCP2 and UCP3 in MAC16-induced cancer cachexia. *Cancer Res* 60:2405.
109. Cinti S, et al. 2002. CL3136,243 and cold stress induce heterogeneous expression of UCP1 mRNA and protein in rodent brown adipocytes. *J Hist Cyt* 50:21.
110. Bing C, et al. 2006. Adipose atrophy in cancer cachexia: Morphologic and molecular analysis of adipose tissue in tumour-bearing mice. *Br J Cancer* 95:1028.
111. Nolan D, et al. 2003. Mitochondrial DNA depletion and morphologic changes in adipocytes associated with nucleoside reverse transcriptase inhibitor therapy. *AIDS* 17:1329.
112. Alexander CA, et al. 1976. Subcellular localization of B apoprotein of plasma lipoproteins in rat liver. *J Cell Biol* 69:241.
113. Hamilton RL, et al. 1967. Lipid transport in liver. I. Electron microscopic identification of very low density lipoprotein in perfused rat liver. *Lab Invest* 16:305.
114. Schlunk RR, Lombardi BC. 1971. Liver liposomes. *Lab Invest* 17:30.
115. Gusarova V, et al. 2007. Golgi-associated maturation of very low density lipoproteins involves conformational changes in apolipoprotein B, but is not dependent on apolipoprotein E. *J Biol Chem* 282:19453.
116. Ohsaki Y, et al. 2006. Cytoplasmic lipid droplets are sites of convergence of proteasomal and autophagic degradation of apolipoprotein B. *Mol Biol Cell* 17: 2674.
117. Forte T, Nichols AV. 1972. Application of electron microscopy to the study of plasma lipoprotein structure. *Adv Lipid Res* 10:1.
118. Gotto AM, et al. 1971. On the nature of the protein defect in abetalipoproteinemia. *New Engl J Med* 284: 813.

Vet-ebooks.com

119. Scanu AM, et al. 1974. A study of the abnormal lipoproteins in abetalipoproteinemia. *J Clin Invest* 53:440.
120. Forte TM, et al. 1985. Formation of phospholipid-rich HDL: A model for square-packing lipoprotein particles found in interstitial fluid and in abetalipoproteinemia plasma. *Biochim Biophys Acta* 834:386.
121. Montoudis A, et al. 2006. Intestinal fatty acid binding protein and lipid transport in human intestinal epithelial cells. *Biochem Biophys Res Commun* 339:248.
122. Hansen GH, et al. 2003. Scavenger receptor class B type I (SR-BI) in pig enterocytes: Trafficking from the brush border to lipid droplets during fat absorption. *Gut* 52:1424.
123. Levy E, et al. 2002. Localization of microsomal triglyceride transfer protein in the Golgi: Possible role in the assembly of chylomicrons. *J Biol Chem* 277:16470.
124. Marenus KD, Sjöstrand FS. 1982. Sequence of structural changes in columnar epithelium of small intestine during early stages of fat absorption. *J Ultrastruct Res* 79:92.
125. Danielsen EM, et al. 1993. Apical secretion of apolipoproteins from enterocytes. *J Cell Biol* 120:1347.
126. Blanchette-Mackie EJ, et al. 1986. Effect of the combined lipase deficiency mutation (*cld/cld*) of ultrastructure of tissues in mice. *Lab Invest* 55:347.
127. Blanchette-Mackie EJ, et al. 1989. Cytochemical studies of lipid metabolism immunogold probes for lipoprotein lipase and cholesterol. *Am J Anat* 185:255.
128. Gilham D, et al. 2005. Triacylglycerol hydrolase is localized to the endoplasmic reticulum by an unusual retrieval sequence where it participates in VLDL assembly without utilizing VLDL lipids as substrates. *Mol Biol Cell* 16:984.
129. Reaven EP, Reaven GM. 1974. Mechanisms for development of diabetic hypertriglyceridemia in streptozotocin-treated rats. *J Clin Invest* 54:1167.
130. Glaumann H, et al. 1975. Study on the synthesis, intracellular transport of lipoprotein particles in rat liver. *J Cell Biol* 64:356.
131. Handley DA, et al. 1983. Ultrastructure of hepatic cholesterol crystals in the hypercholesterolemic diabetic rat. *Pathol Res Pract* 177:13.
132. Ontko JA, et al. Formation of crystalline tripalmitin-rich spicules in isolated hepatocytes. *J Lipid Res* 30:1375, 1989
133. Handley DA, et al. 1983. Ultrastructural visualization of low-density lipoproteins during receptor binding and cellular endocytosis. *J Ultrastruct Res* 83:43, 1983
134. Michaely P, et al. 2007. Identification of a VLDL-induced, FDNPVY-independent internalization mechanism for the LDLR. *EMBO J* 26:3273.
135. Iozzo RV, et al. 1982. Cellular and subcellular distribution of ^{125}I-labelled very low density lipoproteins in the liver of normal and estrogen-treated rabbits. *Am J Pathol* 107:6.
136. Kleinherenbrink-Stins MF, et al. 1990, Light- and immunoelectron microscopic visualization of *in vivo* endocytosis of low density lipoproteins by hepatocytes and Kupffer cells in rat liver. *Lab Invest* 63:73.
137. Reaven E, et al. 1989. Microvillar channels: A unique plasma membrane compartment for concentrating lipoproteins on the surface of rat adrenal cortical cells. *J Lipid Res* 30:1551.
138. Lin G, Oram JF. Apolipoprotein binding to protruding membrane domains during removal of excess cellular cholesterol. *Atherosclerosis* 149:359.
139. Ishida T, et al. 204. Immunocytochemical analysis of cubilin-mediated endocytosis of high density lipoproteins (HDL) in epithelial cells of the rat visceral yolk sac. *Cell Tiss Res* 318:533.
140. Chao WT, et al. 2003. Visualizing caveolin-1 and HDL in cholesterol-loaded aortic endothelial cells. *J Lipid Res* 44:1094.
141. Lin YC, et al. 2007. Molecular interaction between caveolin and ABCA1 on high density lipoprotein-mediated cholesterol efflux in aortic endothelial cells. *Cardiovasc Res* 75:575.
142. Reaven E, et al. 2001. Expression of scavenger receptor class B type 1 (SR-B1) promotes microvillar channel formation and selective cholesteryl ester transport in a heterologous reconstituted system. *Proc Nat Acad Sci USA* 98:1613.
143. Zeng Y, et al. 2003. Endocytosis of oxidized low density lipoprotein through scavenger receptor CD36 utilizes a lipid raft pathway that does not require caveolin-1. *J Biol Chem* 278:45931.
144. Jacobsen CD, et al. 1972. Sea-blue histiocytes in familial lecithin:cholesterol acyltransferase deficiency. *Scand J Haematol* 9:106.
145. Di Bisceglie AM, et al. 1990. Cholesterol ester storage disease: Hepatopathology and effect of therapy with lovastatin. *Hepatology* 11:764.
146. Lough J, et al. 1978. Wolman's disease. *Arch Pathol* 89:103.
147. Powell HC, et al. 1983. Peripheral neuropathy in the twitcher mutant. *Lab Invest* 49:19.
148. Roy CC, et al. 1987. Malabsorption, hypocholesterolemia, fat-filled enterocytes with increased intestinal apoprotein B: Chylomicron retention disease. *Gastroenterology* 92:390.
149. Blanchette-Mackie EJ, et al. 1986. Effect of the combined lipase deficiency mutation (*cld/cld*) on ultrastructure of tissues in mice. *Lab Invest* 55:347.
150. Schmalbruch H, et al. 1987. Abnormalities in spinal neurons and dorsal root ganglion cells in Tangier disease presenting with a syringomyelia-like syndrome. *J Neuropathol Exp Neurol* 46:533.
151. Thompson JC, et al. 1989. The ultrastructural pathology of five lipoprotein lipase-deficient cats. *J Comp Pathol* 101:251.
152. Ferrando J, Bombi JA. 1979. Ultrastructural aspects of normolipidemic xanthomatosis. *Arch Dermatol* 216:143.
153. McGookey DJ, Anderson RGW. 1983. Morphologic characterization of the cholesteryl ester cycle in cultured mouse macrophage foam cells. *J Cell Biol* 97:1156.
154. Takahashi K, et al. 1989. Endocytic pathway of high density lipoprotein via trans-Golgi system in rat resident peritoneal macrophages. *Lab Invest* 61:270.

Vet-ebooks.com

155. Nguyen LB, et al. 1990. A molecular defect in hepatic cholesterol biosynthesis in sitosterolemia with xanthomatosis. *J Clin Invest* 86:923.
156. Ferrans VJ, Fredrickson DS. 1975. The pathology of Tangier disease: A light and electron microscopic study. *Am J Pathol* 78:101.
157. Schmitz G, et al. 1985. Tangier disease: A disorder of intracellular membrane traffic. *Proc Nat Acad Sci USA* 82:6305.
158. Robinek H, Schmitz G. 1991. Abnormal processing of Golgi elements and lysosomes in Tangier disease. *Arterioscler Thromb* 11:1007.

Vet-ebooks.com

8 Mitochondria

The Normal Mitochondrion

Mitochondria provide the enzymes and structural framework for generation of ATP by the citric acid cycle, and by the coupled reactions of electron transport and oxidative phosphorylation. During phosphorylation, ATP is formed from ADP at the surface of the inner membrane and is released into the mitochondrial matrix. It is then transferred to the cytosol, where it is used to power most of the energy-requiring processes of the cell. Uncoupling of electron transport and oxidative phosphorylation diverts energy away from production of ATP into heat.

Mitochondria are preferentially located close to the smooth endoplasmic reticulum (which metabolizes glycogen and lipids for energy production) and to sites of energy utilization (Fig. 8.1). In myocardiocytes, mitochondria are aligned end to end along myofibrils; in spermatozoa, they are wrapped around the tailpiece to provide energy for motility.

Mitochondria critically regulate **calcium homeostasis**, an important consideration in any interpretation of the mitochondrion in acute injury. In the swelling brain, for example, mitochondria are transported along neuronal processes to synapses to support the high metabolic demand for calcium.[1]

Ultrastructurally, mitochondria have a close relationship with lipid globules (Fig. 8.2), and in metabolic disease the **mitochondria-lipid globule interface** is critical for evaluation. A major mitochondrial function is **β-oxidation of fatty acids**, and dysfunctional fatty acid metabolism leads to uncoupling of electron transport from oxidative phosphorylation.

Outer Mitochondrial Membrane

The **outer membrane** maintains mitochondrial shape and structure. It is porous and freely permeable to ions, and is separated from the inner membrane by the **intermembrane space**. Peptides produced in the cytosol enter mitochondria at sites of apposition of outer and inner membranes.[2] Membrane lipid rafts are critical for signaling events with the cytosol.[3] During intense signaling, mitochondria responding to calcium and other signals may be enlarged, and have evidence of deformation of cristae and membrane fusion (Fig. 8.3).

Mitochondrial permeability transition, although regulated by inner membranes, requires the opening of outermembrane pores,[4] voltage-dependent anion channels (VDACs) that mediate trafficking of small molecules and ions across the outer membrane; electron microscopic data show that VDAC-1 is a cylindrical channel with a diameter of 20–30 Å (see Hiller, *Science* 321:1206, 2008). Fusion driven by intermembrane GTPases appears to be a critical event in mitochondrial pore transition.[5] In hepatocytes, the mitochondrial outer membrane contains glycerol 3-phosphate acyltransferase, carnitine-palmitoltransferase, and other enzymes that catalyze the early steps in phospholipid and triacylglycerol synthesis.

Inner Mitochondrial Membrane

The inner membrane is closely apposed to the outer membrane. The non-cristae part of the membrane bears integral membrane proteins that are dedicated

© 2009 Wiley-Blackwell. ISBN: 978-0-813-80330-2
Vet-ebooks.com

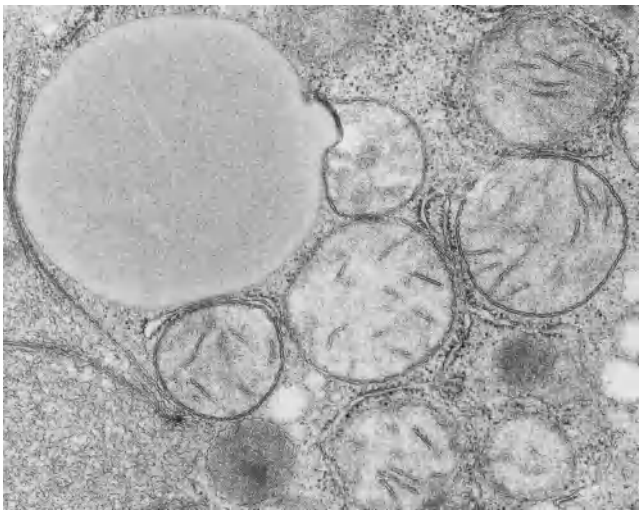


Fig. 8.2 Mitochondrion-lipid interface: close association of lipid globules with mitochondria, carbon tetrachloride toxicity, rat.

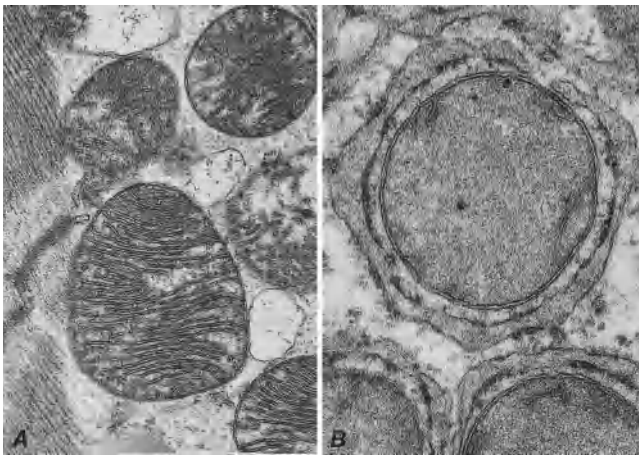


Fig. 8.4 Mitochondria from cells with high and low rates of oxidative phosphorylation. **A**. **Large mitochondria with many cristae**: myocardium, cardiac hypertrophy. **B**. **Short stubby cristae:** hepatocellular carcinoma; most tumor cells obtain energy from glycolysis and do not produce large amounts of ATP in mitochondria.

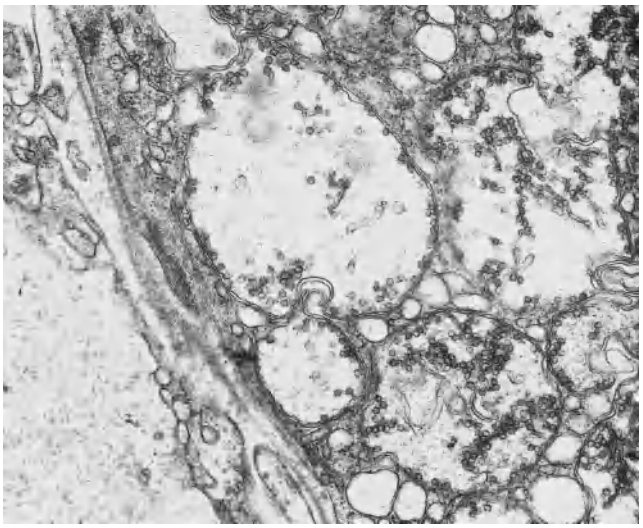


Fig. 8.3 Mitochondrial hyperactivity and fusion: adrenal medulla, anaphylaxis-stimulated secretion. Note mitochondrial enlargement, focal fusion of adjacent mitochondria, dispersal and rounding of cristae, and matrix lysis.

to mitochondrial-cytosol transport. Osmotic balance is maintained by water transporting aquaporins. In hepatocytes, the aquaporin-8 channel is permeable to water and ammonia, and is regulated by the thyroid hormone T3.[6]

Mitochondrial Transition Pores

Mitochondrial permeability is regulated by opening and closing of **permeability transition pores (PTP)**, structures that maintain osmotic imbalance. The PTP consists of the adenine nucleotide translocator, a voltage-dependent anion channel, and cyclophilin D, a prolyl isomerase located within the mitochondrial matrix. Uncontrolled opening of mitochondrial transition pores causes cell death (see chapter 2). Misfolded proteins associated with mitochondria have been shown to clog the permeability transition pore; for example, lodgment in and obstruction of transport pores by amyloid precursor protein lead to mitochondrial dysfunction.[7]

Mitochondrial Cristae

The inner mitochondrial membrane is extensively folded into ridges called **cristae**.[8,9] Cristae are highly reactive and nonporous, and contain the proton- and electron-carrier proteins of the electron transport chain. In most cells, there is a correlation between number of cristae and rate of mitochondrial respiration (Fig. 8.4).

Within the cristae membranes, complexes I to IV are the **electron transport chain**, a series of sequentially acting electron carriers, most of which are integral membrane proteins.[10] Energy released is used to pump protons out of the inner membrane through complexes I, III, and IV. **Oxidative phosphorylation** generates mitochondrial ATP by means of five multiple subunit enzyme complexes (I–V), plus the adenine nucleotide translocator, which shuttles ATP and ADP across the membrane.

The mitochondrial **ATPase complex**, which catalyzes formation of ATP, consists of spherical, 8.5 nm ATP synthase particles linked with components in the membrane; in negatively stained preparations of

Vet-ebooks.com

membrane, these appear as surface knobs that dot the matrix side of the inner membrane and include a **headpiece**, **stalk** and **membrane fragment**. Loss of the **mitochondrial ATPase complex** from the inner mitochondrial membrane is an early critical step to irreversibility in necrosis.

Uncoupling of Electron Transport and Oxidative Phosphorylation Uncoupling of electron transport and oxidative phosphorylation at any point along this pathway diverts energy away from ATP production and into production of heat. This occurs normally in mitochondria of brown fat cells where heat is required for survival of neonatal and hibernating animals.[11] A unique mammalian thermogenic mitochondrial protein, **uncoupling protein 1 (UCP1)**, is found only in brown adipocytes. UCP1 expression, identified in mitochondria by immunogold morphometry, increases markedly in cold stress and declines after heating.[12] The heat shock protein **heme oxygenase-1** (HO-1) is expressed in adrenergically stimulated brown adipose tissue in cells that are expressing UCP1.

Mitochondrial Matrix

Within the **matrix** are the complicated series of chemical transformations of the citric acid cycle (carbohydrates undergo glycolysis to pyruvate, fatty acids are degraded by β-oxidation to carnitine, and amino acids are deaminated by several reactions) that lead to acetyl CoA and other intermediates. Under aerobic conditions, pyruvate (the end product of glycolysis) enters the mitochondrion and is oxidatively decarboxylated to acetyl coenzyme A (CoA). **Glycogen** may develop in the mitochondrial matrix during ischemia, especially in the myocardium. Solubilization of enzymes of glycogen synthesis in the cytosol coupled with altered permeability of mitochondrial membranes allows these enzymes to seep into the mitochondrial matrix and produce glycogen.

Calcium-Sequestering Granules

Mitochondrial calcium is stored as hydroxyapatite in **calcium-sequestering granules** in the matrix. In acute cell swelling, the rising calcium level in the cytosol causes mitochondria to take up calcium and there is an increase in size and number of mitochondrial calcium-sequestering granules. In lethal toxicity the calcium imbalance may be so severe that foci of mineral develop within mitochondria to form crystalline arrangements.

Mitochondrial accumulation of **calcium** is energetically coupled to electron transport, and calcium accumulation is accompanied by uptake of equivalent amounts of phosphate, which results in deposition of calcium phosphates in calcium-sequestering granules. For every pair of electrons passing from NADH to oxygen, approximately six calcium ions accumulate from the cytosol. When calcium accumulates in this manner, no oxidative phosphorylation of ADP occurs; that is, electron transport energy can be used to accumulate calcium or to from ATP but not both.

Mitochondrial DNA

Mitochondrial DNA (mtDNA) is in the matrix. The mammalian mitochondrial genome is a circular DNA molecule that encodes 13 of the proteins required for oxidative metabolism, as well as 22 tRNAs and 2 rRNAs required for their translation. With aldehyde fixation and standard TEM processing, DNA appears in electron-lucent areas as aggregates of tiny filaments. MtDNA has a limited coding capacity and is insufficient to provide genomic independence; it determines the mRNA of a few cytochromes and the rRNA of the mitochondrial ribosomes (nuclear DNA codes for all other structures of the mitochondrion). Coordination of nuclear and mitochondrial **transcriptional activation** is coordinated by trans-acting elements in the two genomes. Mitochondrial receptors that act on transcription include those for glucocorticoids, thyroid hormones, estrogens, and androgens, and all have been localized with immunogold techniques.[13]

Damage to mtDNA is a consequence of several drugs and toxins. **Mitochondrial p53** participates in mtDNA repair, and an increase in mitochondrial p53 has been detected by immunogold labeling in cardiomyocytes poisoned with adriamycin.[14]

Base excision repair (BER) is the main pathway for removal of small DNA base modifications, such as alkylation, deamination, and oxidation, all of which are generated as by-products of normal mitochondrial metabolism.[15,16] Defective BER processing promotes neuronal cell death. Hepatotoxicity of the anti-retroviral drug **stavudine** results from inhibition of mtDNA. The resulting decrease in the NAD/NADH ratio reduces oxidative phosphorylation and fatty acid β-oxidation, changes that result in mitochondrial proliferation.[17]

The mitochondrial genome is transmitted asexually from mother to offspring, and thus does not benefit from genetic recombination. Maternally inherited mtDNA has a high mutation rate, but avoids the accumulation of severe mutations in its protein-coding genes by selecting against them during oocyte maturation. Oocytes bearing less severe mutations may survive to later produce degenerative diseases including myopathy, cardiomyopathy, and neurologic and endocrine disorders.[18]

Vet-ebooks.com

Mitochondrial Ribosomes

Protein synthesis occurs in **mitochondrial ribosomes**, which occur as 10–12 nm granules in the matrix. Mitochondrial ribosomes translate essential components of the oxidative phosphorylation system as well as the GTP-binding protein DAP3. Like protein synthesis in bacteria, mitochondrial protein synthesis is inhibited by some antibiotics that do not inhibit DNA elsewhere in the cell. Most mitochondrial proteins, however, originate in cytoplasmic ribosomes and bear signals that direct them to mitochondria where they are translocated across inner and outer membranes to the matrix. Many mitochondrial proteins have been localized by immunogold electron microscopy including cytochrome c, fumarase, Hsp60, Hsp10, and tumor necrosis factor receptor-associated protein 1 (TRAP 1).[19–21]

Evaluation of Mitochondrial Ultrastructure

Mitochondria responding to injury tend to follow three general pathways, and the interpretation of ultrastructural change requires consideration of the following lesions and the etiologic agents that cause them.

- **Mitochondrial swelling**
  - Hypoxia
  - Toxicity of mitochondrial respiration/citric acid cycle
  - Metabolic stress: acidosis, hyperkalemia
  - Systemic inflammatory disease
- **Mitochondrial enlargement**
  - Hypertrophy
  - Vitamin-deficit hypertrophy
  - mtDNA mutation-based mitochondriopathy
  - Neoplasia (rare)
- **Mitochondrial reduction in size and mass**
  - Atrophy
  - Pre-apoptotic change
  - Neoplastic cells

In evaluating mitochondrial lesions, there are two important exogenous situations that affect any interpretation of ultrastructural change: (1) The **dual localization of mitochondrial proteins in extramitochondrial locations**; for example, mitochondrial aspartate aminotransferase (mAspAT), a major enzyme in amino acid metabolism, is both a mitochondrial and cell surface enzyme; it has been localized to mitochondria and plasma membranes (where it is identical to a fatty acid-binding protein).[22] **P32 protein**, a receptor for the complement component C1q, is a binding protein for nuclear pre-mRNA splicing factors and other nuclear and cell surface proteins, yet it is also present in the mitochondrial matrix.[23] Many of these proteins, such as TRAP-1, are primarily mitochondrial matrix proteins that localize in extramitochondrial sites.[24] (2) Mitochondria are sensitive to **metabolic shifts** in cellular oxygen tension, pH, temperature, water and electrolyte balance, and glycolytic products that feed into the mitochondrial pathways (Fig. 8.5). Mitochondria are also influenced by dietary change, especially to ketogenic diets.[25,26]

Mitochondrial Swelling: Response to Acute Injury

Mitochondria behave as osmometers, and the swelling that develops after injury reflects entry of solutes and water into the mitochondrial matrix. **Mitochondrial swelling** occurs secondary to almost every systemic toxic insult to the cell, and is widespread in conditions such a hypoxia, fever, acidosis, and toxemia. Calcium levels determine the swelling response of the injured cell. In severe swelling, excess water uptake transforms mitochondria into structure-less **mitochondrial vacuoles** that contribute to the vacuolated appearance of swollen cells. When primary injury to mitochondria is the cause of swelling, these organelles may be massively enlarged.

Cristolyis is the lysis and breakage of mitochondrial cristae; it is the hallmark of mitochondrial injury (Fig. 8.6). Some toxins accumulate in or damage mitochondria selectively; for example, toxins that interfere with oxidative phosphorylation or electron transport in mitochondrial cristae will rapidly lead to ATP depletion and swelling.

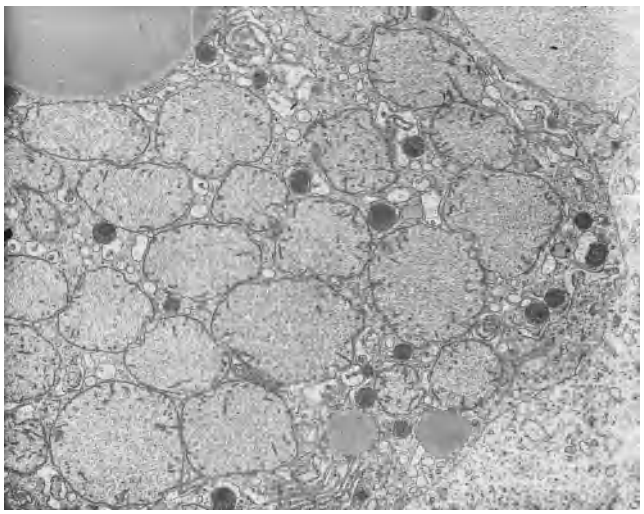


Fig. 8.5 Mitochondrial enlargement: mitochondria are uniformly large, cristae are rudimentary, and matrices are homogenous. No dense granules are present.

Vet-ebooks.com

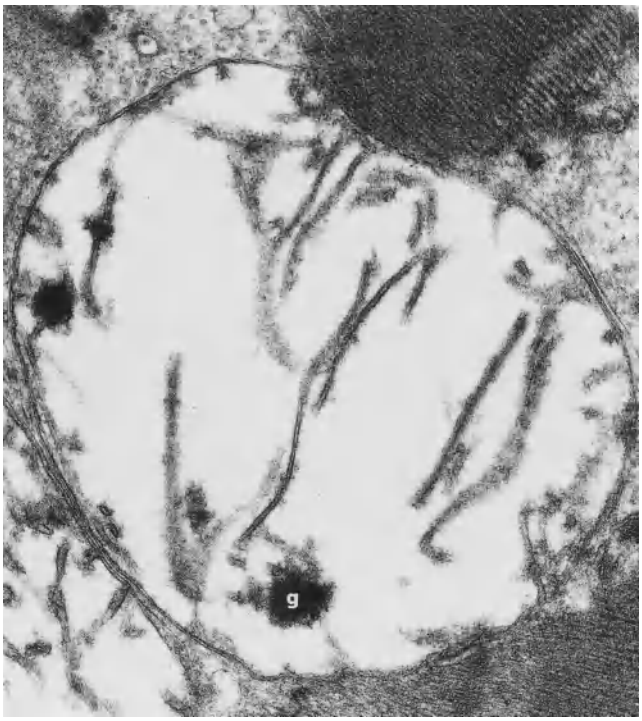


Fig. 8.6 Mitochondrial swelling: cristolysis and matrix lysis; accumulation of dense granules (*g*). Necrosis of skeletal muscle, clostridial myositis.

Oxidative Stress

Oxidative stress occurs when generation of **reactive oxygen species (ROS)**, the free radicals that are generated in ATP production, exceeds their inactivation. The highly oxidizing ROS are superoxides (O_2^-), hydroxyl radicals (OH^-), and hydrogen peroxide (H_2O_2). By-products of mitochondrial metabolism, ROS produce lethal cellular damage—they corrode molecules by snatching their electrons (see chapter 2).

Within the electron transport chain of hyperactive mitochondria, the main free radical generators are complex I and III (Fig. 8.7). Once generated in excess, ROS attack lipids, carbohydrates, protein and DNA. The products of lipid peroxidation are highly reactive molecules that can enhance lipoxidative damage to mitochondrial DNA and proteins. For example, peroxidized cardiolipin in mitochondrial membranes inactivates cytochrome oxidase by mechanisms similar to that of H_2O_2. The end result is loss of ATP, drop in pH, and rise in Ca^{++}, all of which cause cells to reach a state of irreversible injury. These events secondarily suppress mitochondrial function and lead to irreversible damage (see chapter 3).

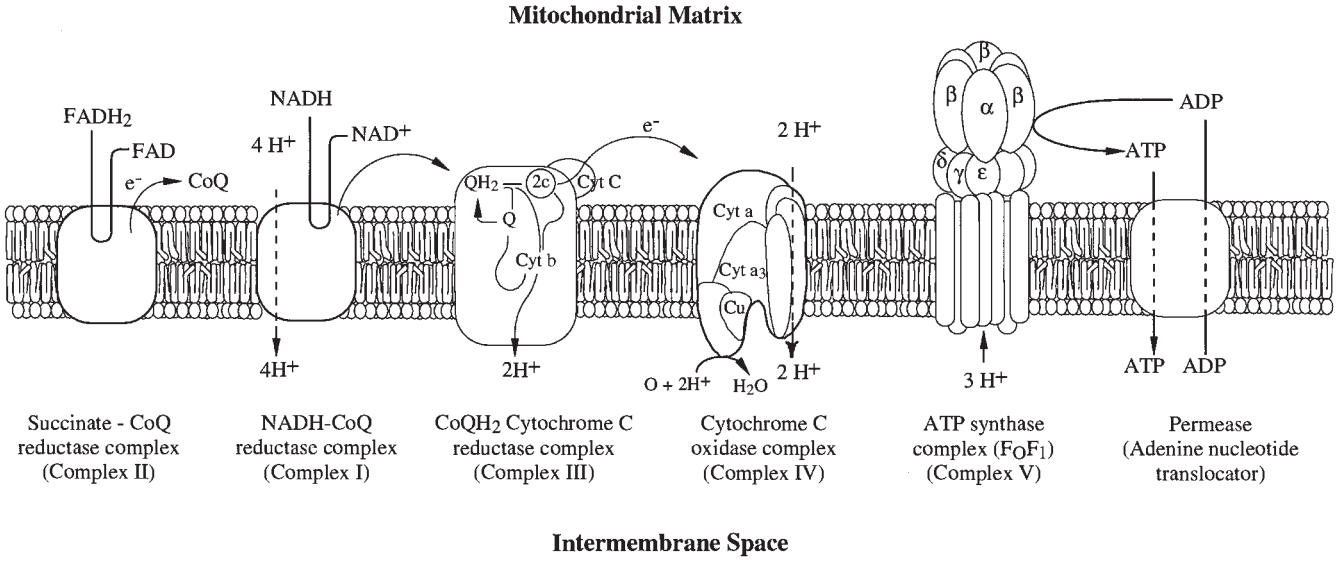


Fig. 8.7 Mitochondrial respiratory chain: provides electrons for acceptance of oxygen to form water and protons (H^+) to drive oxidative phosphorylation. Phosphorylation couples energy released by oxidation to synthesis of ATP. NADH donates its two electrons and one proton to a carrier molecule, **flavin mononucleotide** (FMN), embedded in mitochondrial membranes. FMN transfers two protons to the inner compartment. In the sequence of oxidation-reduction, pairs of electrons make three trips crossing the membrane and export six protons. The proton circuit is completed by the **ATP synthase complex** (F_0F_1), where two protons drive inward, causing synthesis of ATP. **Cytochrome c oxidase (CO)**, the terminal enzyme in the respiratory chain, conserves energy—it is a proton pump that uses redox reactions to drive protons from the mitochondrial matrix across the membrane to the intermembrane space. Electron transfer into CO is initiated by binding of cytochrome c to subunit II on the external side of the membrane. Free radicals that induce lipid peroxidation and lipoxidative damage to mitochondria are generated mainly by mitochondrial complexes I and III. (Data: Saraste, *Science* 283:1488, 1999, and Hulbert, *Physiol Rev* 87:1175, 2007.)

Vet-ebooks.com

Normal mitochondria control the balance between generation and inactivation of ROS. The mitochondrial enzyme **superoxide dismutase (SOD)** controls oxidative stress, but is rapidly depleted in severe injury. In these conditions, active **proteosomes** are required for suppression protection; proteosome inhibition increases cell vulnerability to normally subtoxic levels of free radicals, and amplifies mitochondrial damage.

Peroxynitrite Adds to Oxidative Stress

Nitric oxide (NO)-induced events lead to a broad spectrum of deleterious impacts on mitochondrial respiration. **Mitochondrial membrane injury**, one pathway for NO generation, releases 12(S)-hydroxyeicosatetraenoic acid (12-HETE), a metabolite of arachidonic acid. 12-HETE increases intramitochondrial **calcium**, and elevated calcium stimulates mitochondrial **NO synthase (mtNOS)** activity. Immunogold techniques have localized mtNOS in the mitochondrion.[27] NO derived from mtNOS causes mitochondrial dysfunction by decreasing respiratory and transmembrane potential. In some circumstances, NO produces **peroxynitrite** that induces cytochrome c release, increases mitochondrial lipid peroxidation, increases protein tyrosine nitrations of certain mitochondrial proteins, and stimulates aggregation of mitochondria—all events that can lead to apoptosis.

Calcium in Mitochondrial Oxidative Stress

Mitochondria contain the two Ca^{++}-dependent proteinases (**mu-calpain** for micromolar Ca^{++}-requiring proteinase, and **m-calpain** for the millimolar Ca^{++}-requiring proteinase), and their proteinase inhibitor (**calpastatin**). Studies in vitro suggest that these proteinases regulate the interplay of Ca^{++} with ROS, NO, and hypoxia-inducing factor (HIF-1α). Co-formation of superoxide and nitric oxide induces a massive calcium release, which, in turn, activates **calpain** to degrade **HIF-1α**. Insufficient access of certain enzymes to calcium-calmodulin leads to their reduced activation and mislocalization; for example, dysfunctional localization of endothelial nitric oxide synthase (eNOS) to mitochondria leads to reduced mitochondrial nitric oxide (NO) release.

Hydrogen Sulfide May Be Protective

Hydrogen sulfide (H_2S), potentially lethal at 500 ppm in inhaled air, is naturally produced by the body. It has recently been shown to have a protective effect in ischemic neurons and myocytes of mice. Myocardial mitochondria of H_2S-treated mice did not suffer the damage found in untreated control mice; the mechanism proposed was an H_2S-induced increase in the natural antioxidant glutathione. Any clinical benefit from this event may be trumped by the widespread system damage that can result from H_2S.

Carbon-Directed Free Radical Injury

Carbon-directed free radical injury to mitochondrial membranes is important in toxic injury, and is exemplified by conversion of carbon tetrachloride to its toxic intermediate: $CCl_4 \rightarrow CCl_3^{\bullet} + Cl^{\bullet}$. This reaction is driven by the P-450 mixed-function oxidases in the smooth endoplasmic reticulum (SER). Destruction of mitochondrial membranes occurs when $CCl_3^{\bullet}$ causes auto-oxidation of fatty acids of phospholipid molecules (lipid peroxidation) that make up mitochondrial membranes.

Toxins That Block Mitochondrial Pathways

Mitochondria are selectively poisoned by drugs and toxins that specifically interrupt intramitochondrial biochemical pathways (see chapter 17). Segments of these pathways are pyruvate to acetyl CoA conversion, citric acid cycle reactions, and electron transport and oxidative phosphorylation. When mitochondrial pathways are blocked, electrons are not passed to oxygen for formation of water, and proton electrochemical energy is not generated to drive phosphorylation to produced ATP—the loss of ATP shuts down all cell processes. Prototype toxins that cause mitochondriopathy by blocking specific sites along these pathways are

- Mitochondrial protein synthesis: chloramphenicol
- Citric acid cycle: fluoroacetate
- Respiratory chain:
  - Complex I: rotenone
  - Complex II: antimycin A
  - Complex III: cyanide, azide, carbon monoxide
- Oxidative phosphorylation (uncoupling): arsenate, dinitrophenol

Complex I is the target of many drugs and poisons. Rotenone and other herbicides are **complex I inhibitors** that induce lethal oxidative stress. Annonacin, a plant toxin, is a complex I inhibitor that causes tauopathy (see neurodegeneration, chapter 19).

Hypoxia

Mitochondrial swelling and **crystolysis** are the lesions of oxygen deficit, and are especially prominent in cells with high rates of metabolism. As acute cell swelling

Vet-ebooks.com

progresses, mitochondria become increasingly swollen, cristae and matrix proteins disintegrate, and the large dense granules that accumulate in the matrix are a hallmark of necrosis. Within seconds of **anoxia**, ATP values fall to 0, mitochondrial cristae disappear, and membranes disintegrate. **Oxygen** is required at the end of the electron transport chain to accept electrons and to form water. Its absence suppresses oxidative phosphorylation and these interruptions are rapidly translated as damage to mitochondrial cristae. The effect of abolishing oxidative phosphorylation is magnified by its tight coupling with the citric acid cycle. **NADH** accumulates and exerts a powerful effect to inhibit dehydrogenases of the cycle; for example, pyruvate dehydrogenase can no longer catalyze the flux of pyruvate to CoA.

Ischemia

In **ischemia**, there is mitochondrial uncoupling with inhibition of electron transport between complex I and ubiquinone, and accelerated production of hydrogen peroxide (from NADH and NADH oxidase activity). Hydrogen peroxide can be localized ultracytochemistry in mitochondrial cristae in ischemic tissue.[28] In **chronic ischemia** that is of low level and prolonged, **mitochondrial enlargement** may be striking; for example, the myocardium of patients with severe anemia coupled with poor myocardial perfusion may have increased mitochondrial mass and volume (Fig. 8.8).

Radiation

Acute lethal irradiation causes mitochondrial swelling, cristolysis, and matrix clearing.[29] In x-irradiated tissue, there is typically an increase in the total cellular mitochondrial mass. Over time, there is loss of parenchymal cell populations with significant collagen production.

X-Radiation Kills by Genotoxicity and Free Radical Injury

An accepted paradigm for radiation is that direct DNA damage via energy deposition triggers the downstream consequences of DNA double-strand breaks.

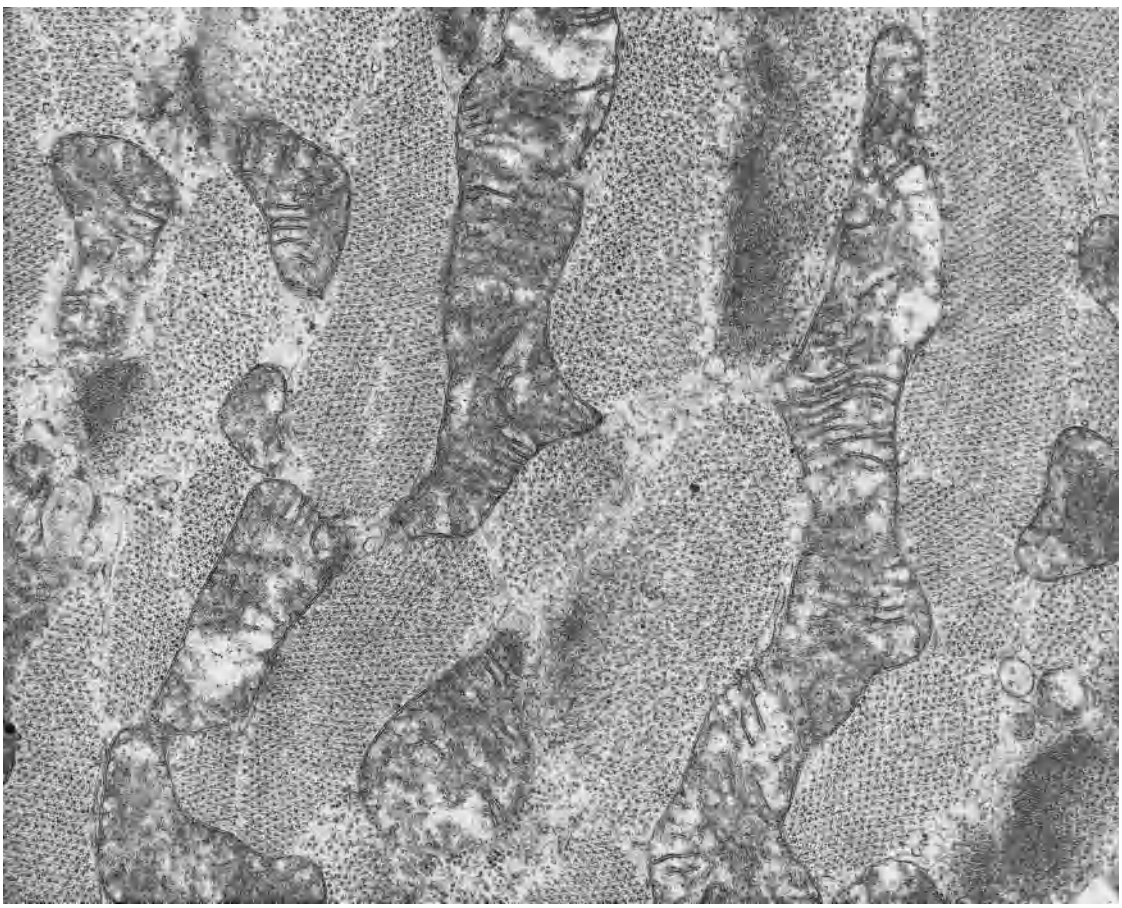


Fig. 8.8 Mitochondrial hypertrophy: myocardiocyte, newborn kitten with severe anemia, edema, and heart failure. Increased mitochondrial volume is associated with irregular surfaces, elongated cristae, and granular matrices.

Vet-ebooks.com

P53 binding protein 1 forms foci at DNA break sites and is the important sensor of genotoxicity.

Lethal ionizing radiation also induces formation of free radicals, either by direct ionization or indirectly by action of radiolytic products. In acute radiation injury, radiolysis of water in the cell leads to formation of highly toxic hydroxyl radicals, superoxide anions, and hydrogen peroxide. All of these react with mitochondrial membrane phospholipids to cause lipid peroxidation and striking mitochondrial change.[30] Selective accumulation of hydroperoxides in cardiolipin is related to cytochrome c content in the mitochondrial matrix; caspase 3/7 activation and phosphatidylserine externalization are proportional to the cytochrome c content in irradiated cells.[31]

The "bystander effect" is radiation-like damage in nonirradiated cells in the vicinity of irradiation injury; that is, the ability of directly irradiated cells to interact with their nonirradiated neighbors, which then develop responses similar to those of targeted cells.

Radiation-induced apoptosis is a major consequence in radiation damage to mitochondria. Mitochondria are the critical effector organelles in the intrinsic pathways of apoptosis. They control apoptosis through four connected events: increased outer-membrane permeability, cytochrome c release, apoptotic protease activation factor-1 induction, and caspase 9 activation. Cytochrome c is an important catalyst of cardiolipin peroxidation, and is required for radiation-induced apoptosis. The gene dap3 is required for mitochondrial homeostasis, and contributes to an extrinsic pathway of apoptosis.[32] Mitochondrial ultrastructural changes that develop during these events include compartmentalization of the inner mitochondrial membrane, a process that segregates different compositional areas. Analysis of this change has been done using three-dimensional electron microscopic tomography (see chapter 2).

Ultraviolet and Infrared Radiation

UV radiation causes photodamage to epidermal cells by activating **Nox1-based NADPH oxidase** to produce ROS that stimulate PGE_2 synthesis. Apoptosis appears to be driven by photodynamically oxidized cytochrome c and activation of apoptosis. **Infrared A radiation** is a major component of sunlight and induced gene transcription.

Nitrogen Gas

Mitochondrial swelling results from nitrogen gas bubble uptake. Coalescence of bubbles fills intramitochondrial spaces during anoxia. This leads to the inability of mitochondria to take up oxygen and, in turn, to cell death.[33]

Mitochondriopathy of Metabolic and Chronic Diseases

Dysfunctional metabolic pathways can lead to structural change in the mitochondrion.[34,35] Pathways that are associated with metabolic mitochondrial disease and ATP deficiency include:

- **Electron transport chain** dysfunction
- **Respiratory uncoupling** of electron transport and oxidative phosphorylation
- **Permeability transition pore** instability
- **Oxidative inhibition** of matrix dehydrogenases and adenine nucleotide transport
- **Nitrosylation**: nitric oxide inhibition of cytochrome c
- **Deficit of NAD** for dehydrogenase reactions that maintain NAD/NADH ratios
- **Fatty acid β-oxidation dysfunction**: fatty acids uncouple electron transport from oxidative phosphorylation

Mitochondrial Hypertrophy

Increased size and number of mitochondria are hallmarks of metabolic deficits that directly or indirectly increase mitochondrial metabolism. Most metabolic toxins cause accumulation of enzymes or substrates in the mitochondrial matrix. In certain deficiencies there is a close association of mitochondrial surfaces with endoplasmic reticulum, apparently as a result to increased access to newly formed proteins. These mitochondria typically have elongated and curved ends that are covered by membranes of the endoplasmic reticulum and are referred to as **hooded mitochondria**.[36,37]

Mitochondrial filaments appear in dysfunctional mitochondria as filamentous strands of proteins arranged in groups of fibrils (usually 6–10 nm in diameter). **Filamentous laminae** in the matrix are common in biopsy and necropsy material from patients with metabolic disease, uremia or other severe terminal illness (Fig. 8.9). Intramitochondrial fibrils are especially common in skeletal muscle.[38] Ischemia, acidosis, and other systemic changes are common causes of filamentous laminae in the mitochondrial matrix.[39–42]

Intramitochondrial protein crystals develop when protein production and degradation are unbalanced so that mitochondrial proteins precipitate to form filaments that polymerize in laminar arrangements. These laminar fibrils appear as irregular aggregates or as

Vet-ebooks.com

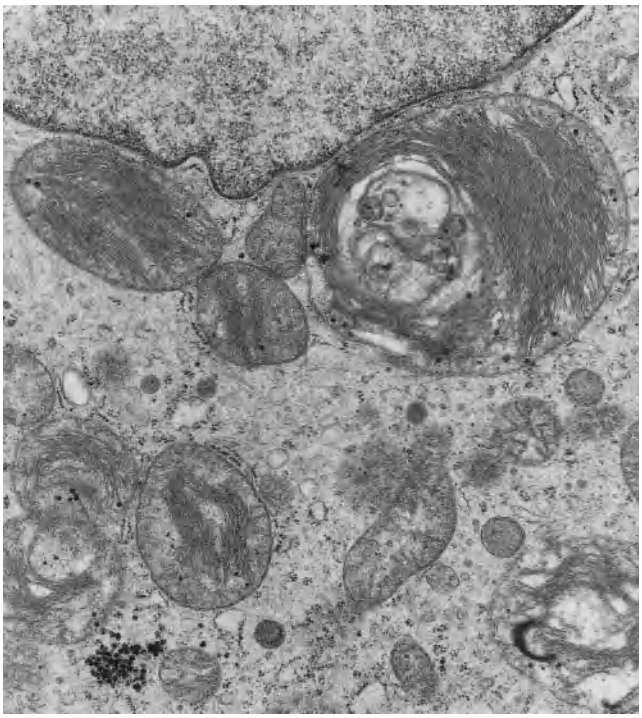


Fig. 8.9 Mitochondrial gigantism: duplication of cristae, stomach, uremic gastropathy, dog.

crystalloids, often in large, bizarre-shaped mitochondria (Fig. 8.10).[43,44] Intramitochondrial crystalloids of fibrils were found in 8 of 52 random human liver biopsies with no common etiologic association.[45] In a study of proximal convoluted tubules in human renal disease, giant mitochondria with dense matrices and various forms of filaments were found in 36% of 100 biopsies.[46]

Intramitochondrial protein crystals are especially common in metabolic defects of skeletal muscle in the human mitochondrial myopathies, and are also common in tissues of equidae and some other species.[47] **Giant mitochondria** containing paracrystalline inclusions have been reported in liver tissue from human patients that take oral contraceptives and drugs that cause cholestasis,[48] and in lymphomas of horses (Fig. 8.10).[49] Rapid shutdown of cells that are in active protein synthesis leads to inspissation of proteins in mitochondria. Cristae in these regressing mitochondria develop into parallel, closely apposed membranes. **Intramitochondrial tubules** are common in hypertrophy, especially in steroid secretory cells.

Megamitochondria

Megamitochondria (also called macromitochondria) are enormous mitochondria with markedly enlarged matrix areas, reduced numbers of cristae and reduced function. They are typical of muscular dystrophies, certain chemical toxicities, the vitamin deficiencies, and some rare neoplasms.[50,51] Formation of megamitochondria results either from fusion of adjacent mitochondria or from suppression of mitochondrial division. Experimentally, cuprizone, ethidium bromide, isoniazid, and chloramphenicol have been used to induce megamitochondria in hepatocytes by inhibiting protein synthesis. In these experiments megamitochondria form by fusion since there are fewer numbers per cell and the suppressed synthesis would not favor mitochondrial division.

Megamitochondria are found in **Luft's disease**, a nonthyroidal hypermetabolic disease due to a respiratory control defect that causes mitochondria to be very large, to increase in number, and to have densely packed cristae.[52]

Thiamine Deficiency

Most water-soluble **B vitamins** are components of coenzymes that function in mitochondrial metabolism. Lesions of deficiency are initially mitochondrial hypertrophy but give way to degeneration in prolonged deficiency.[53,54] **Thiamine** is a component of thiamine pyrophosphate (TPP), the prosthetic group of three important enzymes that transfer activated aldehyde units: pyruvate dehydrogenase, α-ketoglutarate dehydrogenase, and transketolase. As a component of the pyruvate dehydrogenase complex, TPP serves as the initial catalytic cofactor in the oxidative decarboxylation of pyruvate. Thiamine deficiency affects the metabolically active cells of the brain and myocardium; for example, in **Wenicke's encephalopathy** (due to thiamine deficiency) this is reflected in clinical signs of ataxia. In the brains of rodents with experimental thiamine deficiency, astrocytes and oligodendrogliocytes develop swelling as the initial change;[55] mitochondria were not adequately examined in these studies.

Vitamin B_{12}

Vitamin B_{12} (cobalamin) catalyzes conversion of methylmalonyl CoA into succinyl CoA. Deficiency of vitamin B_{12} in the rat leads to methyl malonic aciduria, hepatocyte accumulation of methylmalonyl CoA, and mitochondrial hypertrophy.[56] In hepatocytes there is an increased number of mitochondria and an increase in the association of mitochondria with rough endoplasmic reticulum. **Hooded mitochondria**, mitochondria that are enlarged at one end and small and curved at the other where the endoplasmic reticulum covers the mitochondrial surface, are common in these lesions.

Vet-ebooks.com

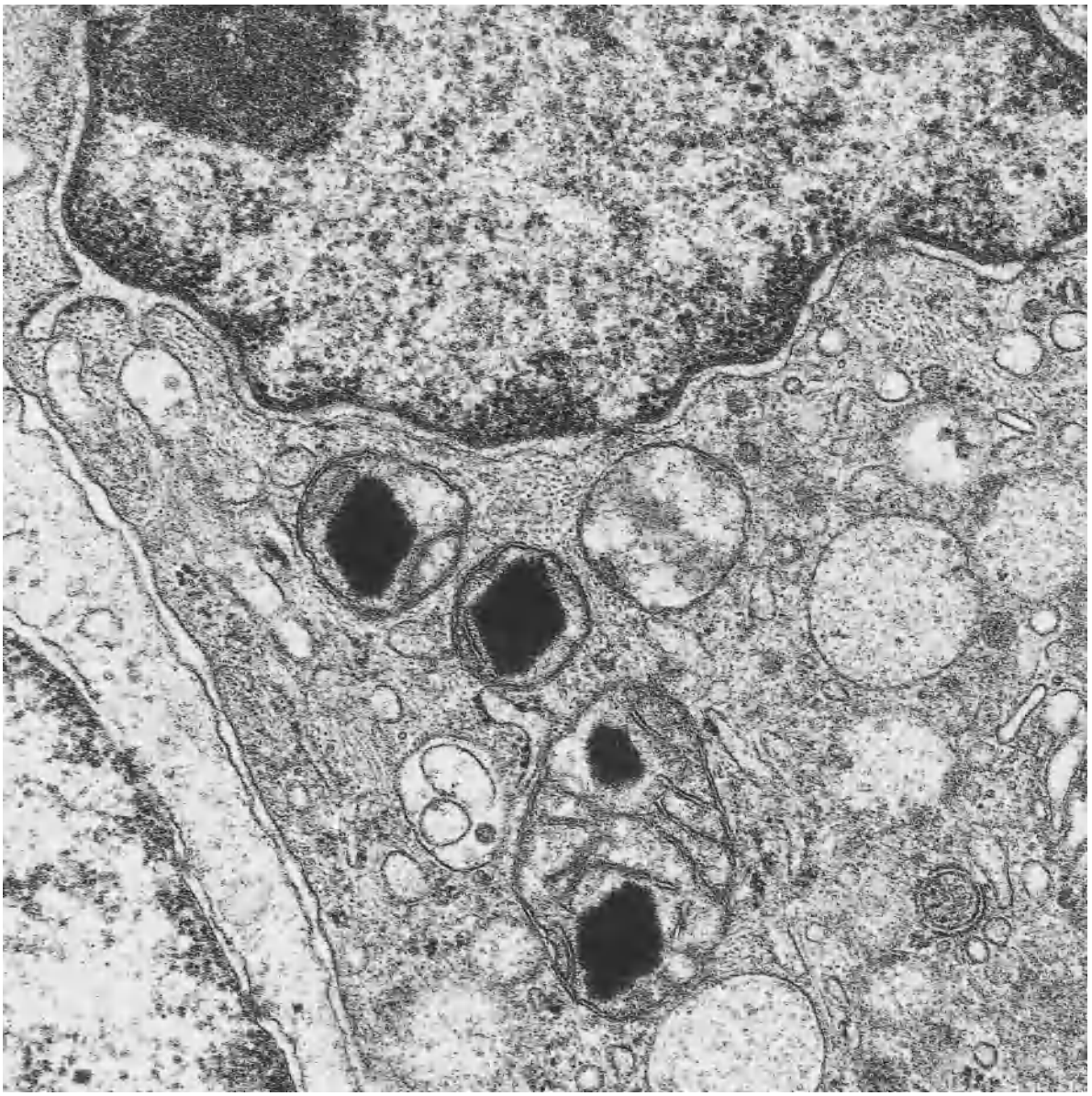


Fig. 8.10 Mitochondrial crystals: intramitochondrial lamellar arrangement of protein filaments; macrophage, histocytic lymphoma, horse.

Riboflavin

Morphometric studies of livers of rats deprived of riboflavin for over 10 wk have shown a decrease of mitochondrial fractional volume and cristae surface, an increase in hepatocyte size, and an increase in peroxisomes, glycogen and smooth endoplasmic reticulum.[57] Mice placed on riboflavin-free diets develop massive enlargements of hepatic mitochondria, most of which are not distorted or disorganized, although they are rich in matrix and poor in cristae. If riboflavin is given to affected mice, mitochondria return to normal via division.[58]

Vitamin E

Skeletal muscle dystrophy develops when vitamin E is deficient in the diet of pigs and calves. Lesions are exacerbated by diets low in selenium and high in polyunsaturated fatty acids. In early phases, mitochondria of affected cells are enormously enlarged by the lack of antioxidant effect of vitamin E on mitochondrial membranes (Fig. 8.11). Vitamin E may be involved in **Keshan disease**, a selenium-responsive human cardiomyopathy in China. Skeletal muscles of pigs and calves with nutritional myopathy have myofibers that are enlarged and in various stages of myocytolysis

Vet-ebooks.com

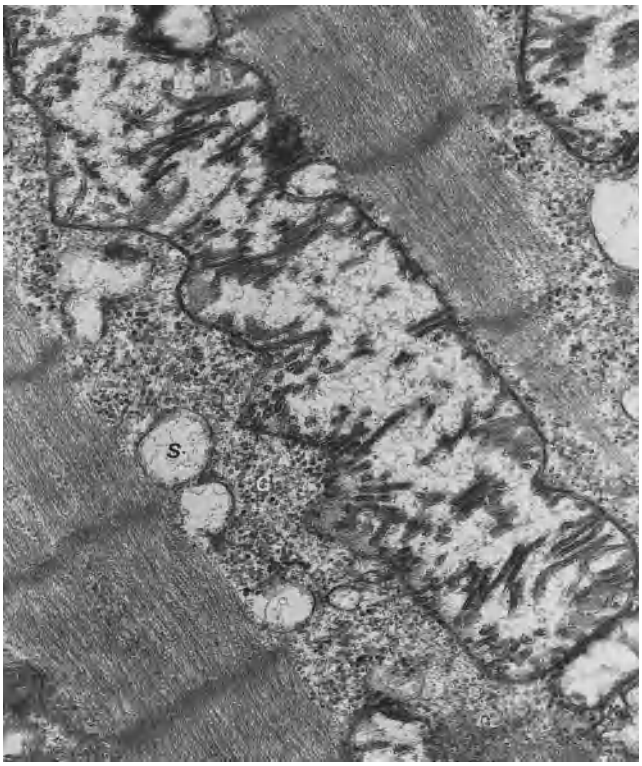


Fig. 8.11 Mitochondrial gigantism: vitamin E deficiency, skeletal muscle, chick. Marked expansion of mitochondrial volume. Note myofibrillar degeneration beginning at Z lines, glycogen, and dilated sarcoplasmic tubules (*S*).

and coagulation necrosis. Myofibrils become markedly disorganized and lyse. Ultrastructurally, there is vesiculation of the sarcoplasmic reticulum, and lysosomes bearing myelin figures and lipofuscin are common.[59] Lesions of the cardiac conduction system occur in cattle.

Metabolic Defects in Mitochondria

Steatosis and Defects in β-oxidation of Fatty Acids

Mitochondrial **β-oxidation of fatty acids** is critical for energy production during periods of fasting and metabolic stress. Consistency and homeostasis of the **acyl-CoA pools** are provided by the **carnitine system**, which gives cells a constant, critical source of free CoA. Carnitine derivatives pass organelle barriers to provide a shuttle mechanism between mitochondria, peroxisomes, and endoplasmic reticulum.[60] Inherited disorders exist for many steps in this pathway. Mouse models have been developed for deficiencies in mitochondrial trifunctional protein-alpha, medium-/short-chain hydroxyacyl-CoA dehydrogenase, carnitine palmitoyltransferase-1a, and the very long-chain-, long-chain-, and short-chain-acyl-CoA dehydrogenase deficiencies.

Human **non-alcoholic steatohepatitis** is characterized by mitochondrial dysfunction, insulin resistance, and fatty liver. Liver biopsies of human patients reveal hepatocyte enlargement, macrosteatosis and microsteatosis, dilated endoplasmic reticulum and Mallory bodies; it is also associated with mitochondrial crystalline inclusions (not seen in animal models).[61] The leptin-deficient ob/ob mouse has been used as a model for this condition.[62] Biopsies of livers of children with steatohepatitis, when examined by immunogold electron microscopy, had evidence of oxidative damage and marked increases in protein glutathionylation.[63]

Malignant Hyperthermia

Mice with a **malignant hyperthermia** mutation (Y522S) in the ryanodine receptor (RyR1) display muscle contractures, rhabdomyolysis, and death in response to elevated temperatures. The RyR1 mutation causes Ca^{2+} leak, which drives increased generation of **reactive nitrogen species** (RNS). Subsequent S-nitrosylation of the mutant RyR1 increases its temperature sensitivity for action, producing muscle contractures. The Y522S mutation in humans is associated with central core disease. Mitochondria in muscle of heterozygous mice are swollen and misshapen; mitochondrial lesions show increased lipid peroxidation with aging.[64]

Familial hyperinsulinemia hypoglycemia of infancy, or medium- and short-chain 1–3-hydroxyacyl-CoA dehydrogenase deficiency (M-SCHAD), is a rare recessively inherited disorder of fatty acid oxidation characterized by hyperglycemia and hyperinsulinism. Mutations in the SCHAD gene leads to abnormal mitochondrial fatty acid oxidation that increases insulin secretion by pancreatic beta cells even in the face of hypoglycemia.

Hepatic Encephalopathy

In patients dying of **hepatic encephalopathy**, proliferation of cerebrocortical protoplasmic **astrocytes** (Alzheimer type II astrocytes) is the principal neuropathic change. Astrocytes first enlarge by reduplication of mitochondria and endoplasmic reticulum and then undergo acute cell swelling. Ultrastructurally, there is mitochondriopathy, distinct nuclear enlargement, pallor, chromatin margination, large nucleoli and nuclear glycogen inclusions.[65] The cytoplasm is swollen, particularly at the end feet as they abut the cerebral capillaries. Initial hypertrophy is probably associated with ammonia detoxification (by reductive

Vet-ebooks.com

amination of α-ketoglutarate) and later degenerative changes with ammonia toxicity.

Reye's Syndrome

Reye's syndrome appears as encephalopathy coupled with fatty degeneration of viscera and **hyperammonemia**. It is an important cause of death in human infants. Antecedent viral illness, often influenza, is a precipitating factor. Mitochondrial abnormalities distinguish RS from other clinically similar diseases.

In the **liver**, the primary lesion is associated with reversible damage to hepatocyte mitochondria and an ensuing deficit of certain mitochondrial enzymes. Ultrastructural analysis of liver biopsies from children with Reye's syndrome reveal that mitochondria are very large and distorted, and are decreased in numbers.[66] Mitochondrial size correlates with clinical neurologic disease although abnormalities are difficult to detect in some patients.[67] There are other metabolic defects in hepatocytes including glycogen depletion, peripheral lipolysis and protein synthesis defects. In plasma there is a decrease of pre-β lipoproteins, clotting factors and complement, and there may be a selective impairment of mitochondrial biogenesis tied to fatty acidemia.

Isolated liver mitochondria, when exposed to serum of Reye's syndrome patients, expand, lose cristae, and become less dense and irregular. **Salicylate** abolishes aerobic synthesis of ATP at 1–2 mM amounts. Normally it is converted to a nontoxic intermediate in the liver. If salicylate metabolism is blocked, mitochondria may suffer from uncoupling.[68]

Brain lesions (due to ammonia) involve swelling of Alzheimer type II cells.[69] There are peculiar unraveling and bleb forms reminiscent of lesions produced by hexachlorophene. There is a decrease in activity of mitochondrial enzymes while enzymes of the cytosol are normal.

Rodent models of Reye's syndrome have been produced,[70–72] including several produced with viruses that cause enteritis. Reye's-related drug toxicity appears to involve a progression of opened mitochondrial transition pores, uncoupling of the respiratory chain, inhibited oxidative phosphorylation, and cell death.[73]

Defects in Urea Cycle Enzymes

Citrullinemia

Citrullinemia is a rare inborn error of metabolism. An enzymopathy of the urea cycle, citrullinemia is characterized by marked elevations of citrulline in plasma due to deficiency of arginosuccinate synthetase, and an inability to dispose of ammonia. Human infants and calves with severe disease develop neurologic signs in the first week of life; a progressive metabolic instability leads to hepatic steatosis with giant mitochondria.[74] In one study of human biopsies, 20% of mitochondria were enlarged with paracrystalline inclusions and electron-dense bodies in the matrix.[75] Brain lesions of diffuse astroglial edema in calves, which are associated with high levels of ammonia, are consistent with hyperammonemic encephalopathy.[76]

Hyperornithinemia

Ornithine, in addition to its place in the urea cycle, is involved in the synthesis of creatine and polyamines, and in the ornithine-δ-aminotransferase reaction. Enzymes that control these metabolic pathways are expressed differently in different tissues (and in different species for the same tissue). For example, ornithine transcarbamoylase is expressed mainly in the liver, and to a lesser extent in epithelial cells of intestine and kidney. Two distinct human disorders are associated with significant increases in plasma ornithine concentrations: gyrate atrophy of the choroid and retina and the **hyperornithinemia-hyperammonemia-homocitrullinemia (HHH)** syndrome. In the HHH syndrome, the histology of liver biopsies is normal but, ultrastructurally, hepatocyte mitochondria are elongated and of bizarre shape, often with crystalloid structures representing elongate cristae.[77,78] Deficiency of ornithine carbamyl transferase (the second enzyme of the urea cycle) has been reported in human infants with HHH syndrome that died in the first few weeks of life with an acute hyperammonemic coma. Ammonia is the cause of the neurologic syndrome.

The **X-linked sparse fur mouse** is a model for this disease. The enzyme defect limits its capacity to catalyze formation of citrulline from carbamyl phosphate and ornithine. Excess mitochondrial carbamylphosphate volatilizes to ammonia or shifts to the cytoplasm to form orotic acid (via the pyrimidine pathway).[79]

Human patients with **gyrate atrophy** are typically normal except for visual disturbances that arise from damage to the pigmented layers of the eye. Deficiency of ornithine-δ-aminotransferase explains most of the lesions, but how chorioretinal degeneration occurs is unexplained. Intravitreal injection of ornithine causes degeneration of pigment epithelial cells in both rats and monkeys.[80] Gyrate atrophy has been reported in a cat with marked retinal degeneration and involvment of pigment epithelium, neuroretina, and choriocapillaries.[81]

Skeletal muscle weakness develops in gyrate atrophy due to dystrophy of type 2 myocytes (fast twitch fibers). These cells are small and contain aggre-

Vet-ebooks.com

gates of parallel-oriented tubules formed by concentric membranes.[82] These tubular aggregates are not specific for gyrate atrophy and have been reported in hyperthyroidism, myasthenia gravis, and other dystrophic lesions.[83,84]

Toxic Injury to mtDNA

Toxins that act on **mtDNA** or on the polymerases that transcribe its genetic code tend to produce the most rapid and widespread changes. Cells are killed if they are unable to repair the injury before they enter mitosis. Cyclophosphamide, which is used clinically to treat cancer, causes necrosis in tissues with high mitotic rates by alkylating DNA nucleotides (guanosine is most markedly alkylated). Zudovidine (AZT) and other antiretroviral nucleoside analogues terminate DNA chains by inhibiting the DNA polymerase for mtDNA synthesis. The anti-hepatitis drug 1-(deoxyfluoroarabinofluranoxyl 5-iodo) uracil is incorporated into mtDNA and has caused a lethal mitochondrial hepatopathy in patients being treated experimentally (see chapter 17).

Mitochondrial DNA-Based Disorders

Genes for mitochondrial proteins are in both **nuclear DNA** and **mitochondrial DNA (mtDNA)**. Respiratory complex I consists of over 30 polypeptides, 7 of which are encoded by the mtDNA. The inheritance of mtDNA is maternal, and is unique in other ways. Cells can contain mixtures of mutant and normal mtDNA, and when they divide, the mutant and normal DNA segregate randomly in the daughter cells so that the mtDNA genotype fluctuates from one cell division to the next. After multiple cell divisions, the amount of mutant mtDNA may drift to either predominantly mutant or normal.

Mutations in mtDNA

Mutations in mtDNA lead to striking ultrastructural changes in mitochondria. Human mitochondrial **oxidative phosphorylation (OXPHOS)** diseases due to mtDNA mutations with large scale rearrangements include the following:

- Kearns-Sayre syndrome
- Pearson's syndrome
- Progressive external ophthalmolgia
- Mitochondrial OXPHOS disease due to point mutations include:
  - Mitochondrial encephalomyelopathy, lactic acidosis, and stroke-like episodes (MELAS)
  - Myoclonus epilepsy and ragged red fiber disease (MERRF)
  - Neurologic weakness, ataxia, and retinitis pigmentosa (NARP)
  - Hearing loss, ataxia, and myoclonus (HAM)
  - Leber's hereditary neuropathy (LHON)
  - Nonsyndromic and aminoglycoside-induced sensorineural hearing loss (SNHL)

Congenital syndromes that involve impaired oxidative metabolism are most often manifest as a disturbance of **skeletal muscle**. In humans, these defects appear clinically as muscle fatigue and exercise intolerance, often with episodes of muscle swelling and myoglobinuria. Defects of respiratory chain complexes I, III, and IV have been widely reported as causes of human muscle disease.[85,86] Defects of complex II or the citric acid cycle are rare and involve impaired succinate oxidation (normal glutamate oxidation) and mitochondrial crystals, dense granular inclusions, and deposition of iron in mitochondria.

Kearns-Sayre Syndrome

Mutation of mtDNA is responsible for several rare human neuromuscular syndromes in which genetic control of one or more components of electron transport and oxidative phosphorylation is abnormal. The **Kearns-Sayre syndrome** is a multisystem disorder in which nearly half the mtDNA genome is lost. Signs of disease include opthalmoplegia, mitochondrial myopathy, encephalopathy, heart block and pigmentary degeneration of the retina. As a result of the genetic mutation in mtDNA, cytochrome c oxidase (the terminal enzyme in the respiratory chain) and other mitochondrial enzymes are deficient.[87] Ultrastructural abnormalities of mitochondria in muscle and basal ganglia are constant, and underlie the myoclonic epilepsy and myopathy (ragged red fiber disease) of these diseases.[88,89] Affected mitochondria are enlarged, lack cristae and usually have paracrystalline inclusions in the matrix (Fig. 8.12).

Neural lesions of Kearns-Sayre syndrome involve widespread spongy change in the brain, especially in white matter and basal ganglia.[90] Basal ganglia show prominent neuronal degeneration and gliosis. Basal ganglia are rich in iron, which is alleged to result from a high content of respiratory chain enzymes, and accumulations of iron-containing pigments are seen in these areas.

Wilson's Disease

Hepatocyte mitochondria in the human copper-loading disorder **Wilson's disease** are abnormal. Mitochondria in chronically affected patients have

Vet-ebooks.com

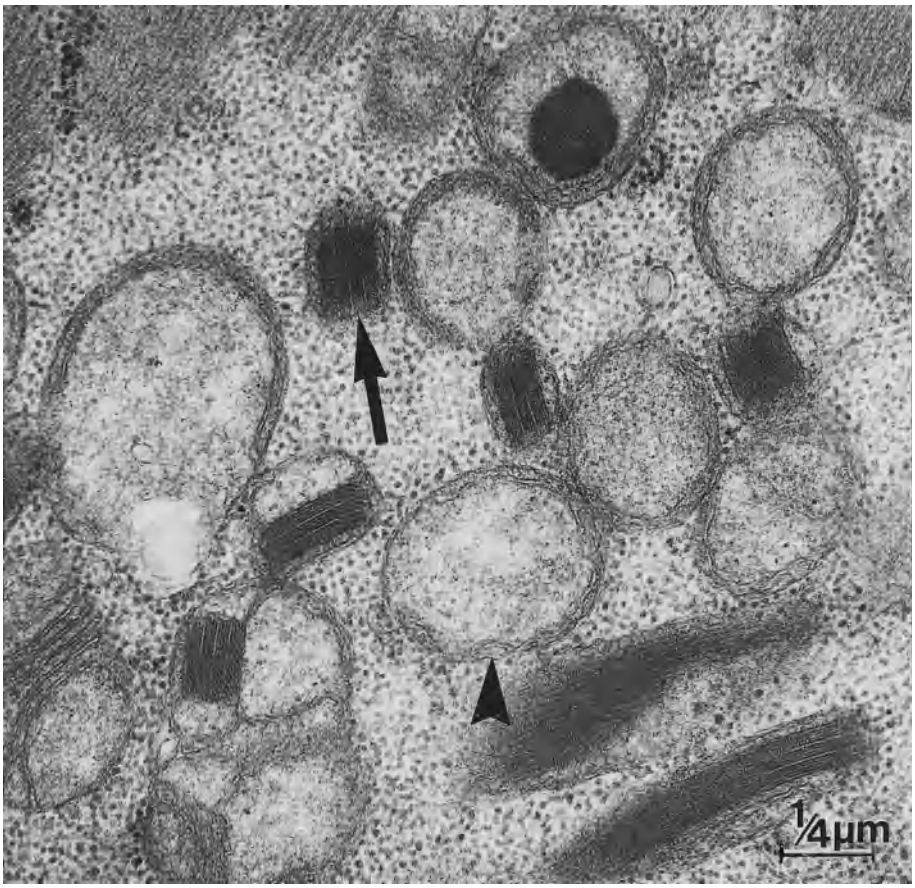


Fig. 8.12 Mitochondrial inclusions: abnormal cristae (*long arrow*) and paracrystalline inclusions (*short arrow*), Kearns-Sayre syndrome. (Micrograph: A. Oldfors, *Acta Neuropathol* 80:541, 1990.)

dense matrices, discrete inclusions, and cystic dilatations in cristae. The same lesions occur in the **toxic milk mutant mouse (tx-j)**, a model of Wilson's disease that develops clinical signs of liver injury at 6 months of age. **Mitochondrial complex IV** declines markedly beginning at 5 mo of age, and expression of mitochondrial transfer factor (TFAM) mRNA declines progressively. Levels of antioxidant proteins capable of binding copper (thioredoxin-2 and peroxiredoxin-3) rise in the first 6 months of life.[91]

Other Mitochondrial Syndromes

Less massive deletions of **mtDNA** are associated with syndromes of less severity. Like Kearns-Sayre syndrome, they appear to arise spontaneously (and are not hereditary). All of the patients with minor deletions of mtDNA have ophthalmoplegia and paralysis of the extraocular muscles (muscles that contain many mitochondria). **Progressive ophthalmoplegia** may be accompanied by minor skeletal muscles weakness. Abnormal mitochondria associated with deficits of mitochondrial **cytochrome c oxidase** have been reported in human infants with myopathy. These infants have heterogeneous populations of normal and abnormal mitochondria in muscles.[92,93]

Leber's hereditary optic neuropathy, a point mutation involving a single base substitution, is a maternally inherited form of central optic nerve death and blindness.[94]

Glutaric Acidemia

Glutaric acidemia type II (multiple acyl-CoA dehydrogenase deficiency) is a lethal inborn error in human infants that leads to accumulation and excretion of oxidation products of all substrates normally oxidized by mitochondrial flavin-containing acyl-CoA dehydrogenases. It is characterized by nonketotic hypoglycemia and metabolic acidosis with steatosis of liver, renal tubules and myocardium. Ultrastructurally, there is marked accumulation of small lipid globules in hepatocytes and parenchymal cells of other viscera. Renal anomalies and focal dysplasia of the brain are common. Electron-dense, membrane-bound cytoplasmic bodies have been reported in the brain.[95,96]

Vet-ebooks.com

Myocardiopathy from Dysfunctional β-Oxidation of Fatty Acids

The main source of energy for the heart is β-oxidation of fatty acids. Hereditary defects in enzymes or transport proteins involved in **β-oxidation of fatty acids** are responsible for cardiomyopathy; for example, carnitine transport defect, carnitine-acylcarnitine translocase and carnitine palmitoyltransferase II defects, and defects in several mitochondrial enzymes (acyl-CoA dehydrogenase and 3-hydroxyacyl-CoA dehydrogenase deficiencies).[97]

Congenital Cardiolipid Disorders

Barth syndrome is an X-linked multisystemic disease caused by a defect in metabolism of the mitochondrial phospholipid **cardiolipin**. Mitochondrial lesions result from mutations in the **taffazzin gene**, which encodes for a putative phospholipid acyltransferase that affects phospholipid composition. Phospholipid abnormalities in mitochondria lead to partial uncoupling of oxidative phosphorylation and destabilization of respiratory chain supercomplexes. Affected cells compensate by expanding the mitochondrion. Mitochondrial lesions involve adhesions of the inner membranes and collapse of the intracristae space, and are responsible for the clinical signs of cardiomyopathy, skeletal muscle weakness, and growth retardation.[98]

Mitochondriopathy in Neurologic Disease

Mitochondria are directly involved in aging, and in several neurodegenerative disorders. During normal **aging**, mitochondrial metabolism becomes less efficient, especially in specialized neural cells of the ear and eye. Retinal photoreceptors undergo structural changes. In humans, mitochondriopathy with accumulation of electron-dense globules has been documented from the fifth decade of life onwards.[99] Mitochondrial dysfunction is implicated in several age-related diseases in the eye; in **macular degeneration**, alterations in mitochondrial DNA and membranes play a role in the pathogenesis of disease.[100]

Superoxide Dismutase and Amyotrophic Lateral Sclerosis

Deficits in **superoxide dismutase (SOD)** associated with mitochondriopathy and motor neuron death are caused by unique mechanisms arising from oxidative stress. In human **amyotrophic lateral sclerosis** (and in the murine mutant SOD1 model) a sequential recruitment of molecular elements of the mitochondria-dependent apoptotic pathway causes neuron death.[101] The proapoptotic protein Bax translocates from the cytosol to mitochondria, and cytochrome c translocates from mitochondria to the cytosol.

Analysis of brains of transgenic mice bearing human mutant SOD suggests that motoneuron degeneration is caused by the effects of the SOD mutation including oxidative stress, excitotoxicity, and protein nitration and aggegation.[102,103] In mSOD-1 transgenic mice, motor neurons (MNs) undergo slow degeneration characterized by somal and mitochondrial swelling and formation of DNA single-strand breaks prior to double-strand breaks that occur in nuclear and mitochondrial DNA. Mitochondria accumulate NADPH diaphorae and inducible nitric oxide synthase (NOS), and iNOS gene deletion extends significantly the life span of the affected mouse. Cell swelling is associated with Na/K-ATPase aggregation and dysfunction. p53 and p73 are activated in degenerating MNs, but without nuclear import. MN death lacks similarity to apoptosis and is independent of caspase activation.

Alpha-synuclein and Parkinson's Disease

Mutations in the synaptic protein alpha-synuclein (alpha-Syn) cause Parkinson's disease (PD). Transgenic mice expressing human mutant alpha-Syn develop profound and fatal neurologic disease characterized by progressive motor deficits, paralysis and neurodegeneration with marked mitochondrial abnormalities. Studies similar to those in mutant ALS of mice reveal the mitochondrial nitrative stress and dysfunction of mitochondrial trafficking are antecedents of motor neuron cell death.[104]

Frataxin and Friedreich's Ataxia

Frataxin, a mitochondrial matrix protein, is an inducer of oxidative phosphorylation. It increases mitochondrial membrane potential, oxygen consumption and ATP synthesis. Frataxin directs mitochondrial synthesis of **iron-sulfur clusters** (Fe/S) essential for several mitochondrial enzymes in the respiratory chain. It is encoded in the nucleus but moves post-translationally into the mitochondrial matrix. Frataxin deficits are associated with human **Friedreich's ataxia**.[105]

Confounding Mitochondrial Lesions in Neurologic Disease

Mitochondrial change due to oxidative injury, acidosis, and other systemic shifts can cause mistaken interpretations during ultrastructural analysis. In humans, **mitochondriopathy of chronic hypertension**, which is common in long-standing hypertension and other

Vet-ebooks.com

hemodynamic disorders,[106] has lesions that include enlargement and accumulation of crystalloid matrix arrays. In the rare disorder **mitochondrial encephalomyopathy**, mitochondria are enlarged with aberrant cristae and large paracrystalline inclusions in intracristal spaces.[107]

References

1. Chang DT, Reynolds IJ. 2006. Mitochondrial trafficking and morphology in healthy and injured neurons. *Prog Neurobiol* 80:241.
2. Schwaiger M, et al. 1987. Characterization of translocation contact sites involved in the import of mitochondrial proteins. *J Cell Biol* 105:235.
3. Garofalo T, et al. 2007. Lipid microdomains contribute to apoptosis-associated modifications of mitochondria in T cells. *Cell Death Differ* 12:1378.
4. Gazaryan IG, Brown AM. 2007. Intersection between mitochondrial permeability pores and mitochondrial fusion fission. *Neurochem Res* 32:917.
5. Meeusen S, et al. 2006. Mitochondrial inner-membrane fusion and crista maintenance requires the dynamin-related GTPase Mgm1. *Cell* 127:383.
6. Calamita G, et al. 2007. Triiodothyronine modules the expression aquaporin-8 in rat liver mitochondria. *J Endocrinol* 192:111.
7. Devi L, et al. 2006. Accumulation of amyloid precursor protein in the mitochondrial-import channels of human Alzheimer's disease brain is associated with mitochondrial dysfunction. *J Neurosci* 26:9057.
8. Perkins GA, et al. 1997. Electron tomography of neuronal mitochondria. *J Struct Biol* 119:260.
9. Prince FP, Buttle KE. 2004. Mitochondrial structure in steroid-producing cells. *Anat Rec* 278:454.
10. Dudkina NV, et al. 2005. Structure of a mitochondrial supercomplex formed by respiratory chain complexes I and III. *Proc Natl Acad Sci USA* 102:3225.
11. Psarra AM, Sekeris CE. 2008. Steroid and thyroid hormone receptors in mitochondria. *IUBMB Life* 60:210.
12. Perkins GA, et al. 1998. Electron tomography of mitochondria from brown adipocytes reveals crista junctions. *J Bioenerg Biomembr* 30:431.
13. Clinti S, et al. 2007. CL316,243 and cold stress induces heterogeneous expression of UCP1 mRNA and protein in rodent brown adipocytes. *J Hist Cyt* 50:21.
14. Nithipongvanitch R, et al. 2007. Evidence for p53 as guardian of the cardiomyocyte mitochondrial genome following acute adriamycin treatment. *J Hist Cyt* 55:629.
15. Weissman L, et al. 2007. DNA repair, mitochondria, and neurodegeneration. *Neuroscience* 145:1318.
16. Wilson DM 3rd, McNiell DR. 2007. Base excision repair and the central nervous system. *Neuroscience* 145:1187.
17. Kamal MA, French SW. 2004. Drug-induced increased mitochondrial biogenesis in a liver biopsy. *Exp Molec Pathol* 77:201.
18. Fan W, et al. 2008. A mouse model of mitochondrial disease reveals germline selection against severe mtDNA mutations. *Science* 319:958.
19. Sadacharan SK, et al. 2005. Localization of mitochondrial DNA encoded cytochrome c oxidase subunits I and II in rat pancreatic zymogen granules and pituitary growth hormone granules. *Histochem Cell Biol* 124:409.
20. Sadacharan SK, et al. 2001. Immunoelectron microscopy provides evidence for the presence of mitochondrial heat shock 10-kDa protein (chaperonin 10) in red blood cells and a variety of secretory granules. *Histochem Cell Biol* 116:507.
21. Bowes T, et al. 2007. Subcellular localization of fumarase in mammalian cells and tissue. *Histochem Cell Biol* 127:335.
22. Cachetto JD, et al. 2002. Immunogold localization of mitochondrial aspartate aminotransferase in mitochondria and on the cell surface in normal rat tissues. *Histol Histopathol* 17:353.
23. Soltys BJ, et al. 2000. Localization of P32 protein (gC1q-R) in mitochondria and at specific extramitochondrial locations in normal tissues. *Histochem Cell Biol* 114:245.
24. Cechetto JD, Gupta RS. 2000. Immunoelectron microscopy provides evidence that tumor necrosis factor receptor-associated protein 1 (TRAP-1) is a mitochondrial protein which also localizes at specific extramitochondrial sites. *Exp Cell Res* 260:30.
25. Eagles DA, Chapman GB. 2007. A light- and electron-microscope study of hepatocytes of rats fed different diets. *C R Biol* 330:62.
26. Soane L, et al. 2007. Mechanisms of impaired mitochondrial energy metabolism in acute and chronic neurodegenerative disorders. *J Neurosci Res* 85:3407.
27. Gan S, et al. 2004. Docking of endothelial nitric oxide synthase (eNOS) to the mitochondrial outer membrane: A pentabasic amino acid sequence in the autoinhibitory domain of eNOS targets a proteinase K-cleavable peptide on the cytoplasmic face of mitochondria. *J Biol Chem* 279:15968.
28. Maxwell MH, et al. 1996. Evidence of ultracytochemical mitochondria-derived hydrogen peroxide activity in myocardial cells from broiler chickens with an ascites syndrome. *Res Vet Sci* 61:7.
29. Kïratlï H, et al. 2007. Ultrastructural alterations in extraocular muscles following iodine-125 brachytherapy for uveal melanoma. *Strabismus* 15:103.
30. Saibara T, et al. 1994. Acute hepatic failure with swollen mitochondria and microvesicular fatty degeneration of hepatocytes triggered by free radical initiator. *Lab Invest* 70:517.
31. Belikova NA, et al. 2007. Cardiolipin-specific peroxidase reactions of cytochrome C in mitochondria during irradiation-induced apoptosis. *Int J Radiat Oncol Biol Phys* 69:176.
32. Kim H-R, et al. 2007. Mammalian *dap3* is an essential gene required for mitochondrial homeostasis *in vivo* and contributing to the extrinsic pathway for apoptosis. *FASEB J* 21:188.

Vet-ebooks.com

33. VanDeripe DR. 2004. The swelling of mitochondria from nitrogen gas; a possible cause of reperfusion damage. *Med Hypotheses* 62:294.
34. Bardosi A, et al. 1990. Myopathy with altered mitochondria due to a triosephosphate isomerase (TPI) deficiency. *Acta Neuropathol* 79:387.
35. Dominick MA, et al. 1993. Morphogenesis of a zone-specific adrenocortical cytotoxicity in guinea pigs administered PD 132301-2, an inhibitor of acyl-CoA:cholesterol acyltransferase. *Toxicol Pathol* 21:54.
36. Daugherty CC, et al. 1987. A morphometric study of Reye's syndrome. *Am J Pathol* 129:313.
37. Egger J, Wilson J. 1983. Mitochondrial inheritance in a mitochondrially mediated disease. *New Engl J Med* 309:142.
38. Heiner H, Schaeg G. 1979. Origin and function of "rod-like structure" in mitochondria. *Acta Anat* 103:1.
39. Hagler HK, et al. 1979. Effect of different methods of tissue preparation on mitochondrial inclusions of ischemic and infarcted canine myocardium. *Lab Invest* 40:529.
40. Thyberg J, et al. 1982. Mitochondrial distribution and ATP levels in *Chironomus* salivary gland cells as related to growth, metabolic activity, and atmospheric oxygen tensions. *Devel Biol* 90:31.
41. Fujioka T, et al. 1978. Unusual mitochondrial ultrastructure in the pig adrenal cortex. *Cell Tiss Res* 187:129.
42. Minio F, Gautier A. 1967. L'Ultrastructure du foie humain lors d'icteres idopathiques chroniques. *Z Zellforsch Mikrosk Anat* 78:267.
43. Mugnaini E. 1964. Filamentous inclusions in the matrix of mitochondria from human livers. *J Ultrastruct Res* 11:525.
44. Schaff A, et al. 1974. Study of the tridimensional structure of intramitochondrial crystalline inclusions. *J Microscopie* 20:259.
45. Spycher MA, Ruttner JR. Kristalloide Einschlusse in menschlichen Lebermitochondrien. *Virch Arch B* 1:211, 1968.
46. Suzuki T, et al. 1975. Giant mitochondria in the epithelial cells of the proximal convoluted tubules of diseased human kidneys. *Lab Invest* 33:578.
47. Sasaki H, Suzuki T. 1989. Intramitochondrial helical filaments in medullary tubules of the rat kidney. *J Ultrastruc Molec Struc Res* 102:229.
48. Schaff A, et al. 1974. Study of the tridimensional structure of intramitochondrial crystalline inclusions. *J Microsc* 20:259.
49. Detilleux P, et al. 1989. Ultrastructure and lectin histochemistry of equine cutaneous histiolymphocytic lymphosarcomas. *Vet Pathol* 26:409.
50. Lindal S, et al. 1992. Mitochondrial diseases and myopathies. *Ultrastr Pathol* 16:263.
51. Volk TL, Scarpelli DG. 1966. Mitochondrial gigantism in the adrenal cortex following hypophysectomy. *Lab Invest* 15:707.
52. Bonilla E, et al. 1977. Luft's disease. *J Ultrastruct Res* 58:1.
53. Maltin CA, et al. 1983. Mitochondrial abnormalities in muscle from vitamin B_{12}-deficient sheep. *J Comp Pathol* 93:429.
54. Wu BC, et al. 1971. Mitochondrial ultrastructure and energy transduction in rat heart during progressive thiamine deficiency. *Virch Arch B* 9:97.
55. Aikawa H, et al. 1984. Low energy levels in thiamine-deficient encephalopathy. *J Neuropathol Exp Neurol* 43:276.
56. Tandler B, et al. 1991. Unusual mitochondria in the hepatocytes of rats treated with a vitamin B_{12} analogue. *Anat Rec* 231:1.
57. Reith A. 1973. The influence of triiodothyronine and riboflavin deficiency on the rat liver with special reference to mitochondria. *Lab Invest* 29:216.
58. Tandler B, Hoppel CL. 1980. Ultrastructural effects of riboflavin deficiency on rat hepatic mitochondria. *Anat Rec* 196:183.
59. Kennedy S, Rice DA. 1992. Histopathologic and ultrastructural myocardial alterations in calves deficient in vitamin E and selenium and fed polyunsaturated fatty acids. *Vet Pathol* 29:129.
60. Lamhonwah AM, Tain I. 2006. Novel localization of OCTN1, an organic cation/carnitine transporter, to mammalian mitochondria. *Biochem Biophys Res Commun* 345:1315.
61. Caldwell SH, et al. 2007. The effects of 48 weeks of rosiglitazone on hepatocyte mitochondria in human nonalcoholic steatohepatitis. *Hepatology* 46: 1101.
62. García-Ruiz I, et al. 2007. Effects of rosiglitazone on the liver histology and mitochondrial function in ob/ob mice. *Hepatology* 46:414.
63. Piemonte F, et al. 2007. Protein glutathionylation increases in the liver of patients with non-alcoholic fatty liver disease. *J Gastroenterol Hepatol* 6 Aug [Epub].
64. Durham WJ, et al. 2008. RyR1 S-nitrosylation underlies environmental heat stroke and sudden death in Y522S RyR1 knockin mice. *Cell* 133:53.
65. Norenberg MD. 1977. A light and electron microscopic study of experimental portal-systemic (ammonia) encephalopathy. *Lab Invest* 36:618.
66. Daugherty CC, et al. 1987. A morphometric study of Reye's syndrome. *Am J Pathol* 129:313.
67. Svoboda DJ, Reddy JK. 1975. Pathology of liver in Reye's syndrome. *Lab Invest* 32:571.
68. You K. 1983. Salicylate and mitochondrial injury in Reye's syndrome. *Science* 221:163.
69. Partin JS, et al. 1978. Brain ultrastructure in Reye's syndrome. *J Neuropathol Exp Neurol* 37:796.
70. Crocker JFS, et al. 1986. Biochemical and morphologic characteristics of a mouse model of Reye's syndrome induced by the interaction of influenza B virus and a chemical emulsifier. *Lab Invest* 54:32.
71. Hug G, et al. 1981. Reye's syndrome simulacra in liver of mice after treatment with chemical agents and encephalomyocarditis virus. *Lab Invest* 45:89.
72. Rarey KE, et al. 1987. Response of epithelial cells of the choroid plexus in the ferret model for Reye's syndrome. *Lab Invest* 56:249.

Vet-ebooks.com

73. Lemasters JJ, et al. 2003. Role of mitochondrial inner membrane permeabilization in necrotic cell death, apoptosis, and autophagy. *Antioxid Redox Signal* 4:769.
74. Mihatsch MJ, et al. 1974. Liver morphology in a case of citrullinemia (a light and electron microscopic study). *Beitr Pathol* 151:200.
75. Zamora SA, et al. 1997. Mitochondrial abnormalities of liver in two children with citrullinaemia. *J Inherit Metab Dis* 20:509.
76. Harper PAW, et al. 1988. Ultrastructural findings in citrullinemia in Holstein-Friesian calves. *Acta Neuropathol* 76:306.
77. Haust MD, et al. 1981. Ultrastructure of hepatocyte mitochondria in a child with hyperornithaemia, hyperammonaemia, and homocitrullinaemia. *Human Pathol* 12:212.
78. Zimmer KP, et al. 1995. Ultrastructural, immunocytochemical and stereological investigation of hepatocytes in a patient with the mutation of the ornithine transcarbamylase gene. *Eur J Cell Biol* 67:73.
79. Qureshi IA, et al. 1979. Ornithine transcarbamylase deficiency in mutant mice. *Pediatr Res* 13:807.
80. Kuwabara T, et al. 1981. Experimental model of gyrate atrophy in animals. *Ophthalmology* 88:331.
81. Valle DL, et al. 1981. Gyrate atrophy of the choroid and retina in a cat. *Invest Ophthalmol Vis Sci* 20:251.
82. Sipila I, et al. 1979. Gyrate atrophy of the choroid and retina with hyperornithinemia: Tubular aggregates and type 2 fibers atrophy in muscle. *Neurology* 29:996.
83. Niakin E, et al. 1985. Tubular aggregates: Their association with myalgia. *J Neurol Neurosurg Psychiatry* 48:882.
84. Rosenberg NL, et al. 1985. Tubular aggregates: Their association with neuromuscular diseases, including the syndrome of myalgias/cramps. *Arch Neurol* 42:973.
85. Di Mauro S, Schon EA. 2003. Mitochondrial respiratory-chain diseases. *New Engl J Med* 348:2656.
86. Moreadith RW, et al. 1984. Deficiency of the iron-sulfur clusters of mitochondrial reduced nicotinamide-adenine dinucleotide-ubiquinone oxidoreductase (complex I) in an infant with congenital lactic acidosis. *J Clin Invest* 74:685.
87. Egger J, Wilson J. 1983. Mitochondrial inheritance in a mitochondrially mediated disease. *New Engl J Med* 309:142.
88. Oldfors A, et al. 1990. Neuropathology in Kearns-Sayre syndrome. *Acta Neuropathol* 80:541.
89. Takeda S, et al. 1990. Involvement of extraocular muscle in mitochondrial encephalomyopathy. *Acta Neuropathol* 80:118.
90. Schneck L, et al. 1973. Ophthalmoplegia plus with morphological and chemical studies of cerebellar and muscle tissue. *J Neurol Sci* 19:37.
91. Roberts EA, et al. 2008. Mitochondrial stress and function in the untreated Jackson toxic milk (tx-j) mouse, a model for Wilson's disease. *Mol Genet Metab* 93:54.
92. Haginoya K, et al. 1990. Mosaicism of mitochondria in mitochondrial myopathy: An electron microscopic analysis of cytochrome *c* oxidase. *Acta Neuropathol* 80:642.
93. Muller-Hocker J. 1989. Cytochrome-c-oxidase deficient cardiomyocytes in the human heart—an age-related phenomenon. *Am J Pathol* 134:1167.
94. Wallace DC, et al. 1988. Familial mitochondrial encephalomyopathy. *Cell* 55:601.
95. Harkin JC, et al. 1986. Glutaric acidemia type II: Phenotypic findings and ultrastructural studies of brain and kidney. *Arch Pathol Lab Med* 110:399.
96. Peluchetti D, et al. 1991. Riboflavin responsive multiple acyl-CoA dehydrogenase deficiency. *J Neurol Sci* 105:93.
97. Kelly DP, Strauss AW. 1994. Inherited cardiomyopathies. *New Engl J Med* 330:913.
98. Acehan D, et al. 2007. Comparison of lymphoblast mitochondria from normal subjects and patients with Barth syndrome using electron microscopic tomography. *Lab Invest* 87.40.
99. Nag TC et al. 2006. The occurrence of cone inclusions in the ageing human retina and their possible effect on vision: An electron microscope study. *Brain Res Bull* 71:224.
100. Feher J, et al. 2006. Mitochondrial alterations of retinal pigment epithelium in age-related macular degeneration. *Neurobiol Aging* 27:983.
101. Martin LJ. 2007. Transgenic mice with human mutant genes causing Parkinson's disease and amyotrophic lateral sclerosis provide common insight into mechanisms of motor neuron selective vulnerability to degeneration. *Rev Neurosci* 18:115.
102. Martin LJ, et al. 2007. Motor neuron degeneration in amyotrophic lateral sclerosis mutant superoxide dismutase-1 transgenic mice: Mechanisms of mitochondriopathy and cell death. *J Comp Neurol* 500:20.
103. Guégan C, et al. 2001. Recruitment of the mitochondrial-dependent apoptotic pathway in amyotrophic lateral sclerosis. *J Neurosci* 21:6569.
104. Martin LJ, et al. 2006. Parkinson's disease alpha-synuclein transgenic mice develop neuronal mitochondrial degeneration and cell death. *J Neurosci* 26:41.
105. Baron M, et al. 2007. Mitochondrial dysfunction in neurodegenerative disorders. *Biochem Soc Trans* 35:1228.
106. Daugherty CC, et al. 1996. Mitochondrial enlargement and crystalloid matrix arrays: Distinctive finding in childhood portal hypertension due to cavernous transformation of the portal vein. *Pediatr Pathol Lab Med* 16:263.
107. Lewandowska E, et al. 2006. Ultrastructural study of mother and daughter muscle changes with mitochondrial encephalomyopathy. *Folia Neuropathol* 39:271.

Vet-ebooks.com

Part III

Inflammation and Hemostasis

Ultrastructural Pathology The Comparative Cellular Basis of Disease
Second Edition Norman F. Cheville
© 2009 Wiley-Blackwell. ISBN: 978-0-813-80330-2

Vet-ebooks.com

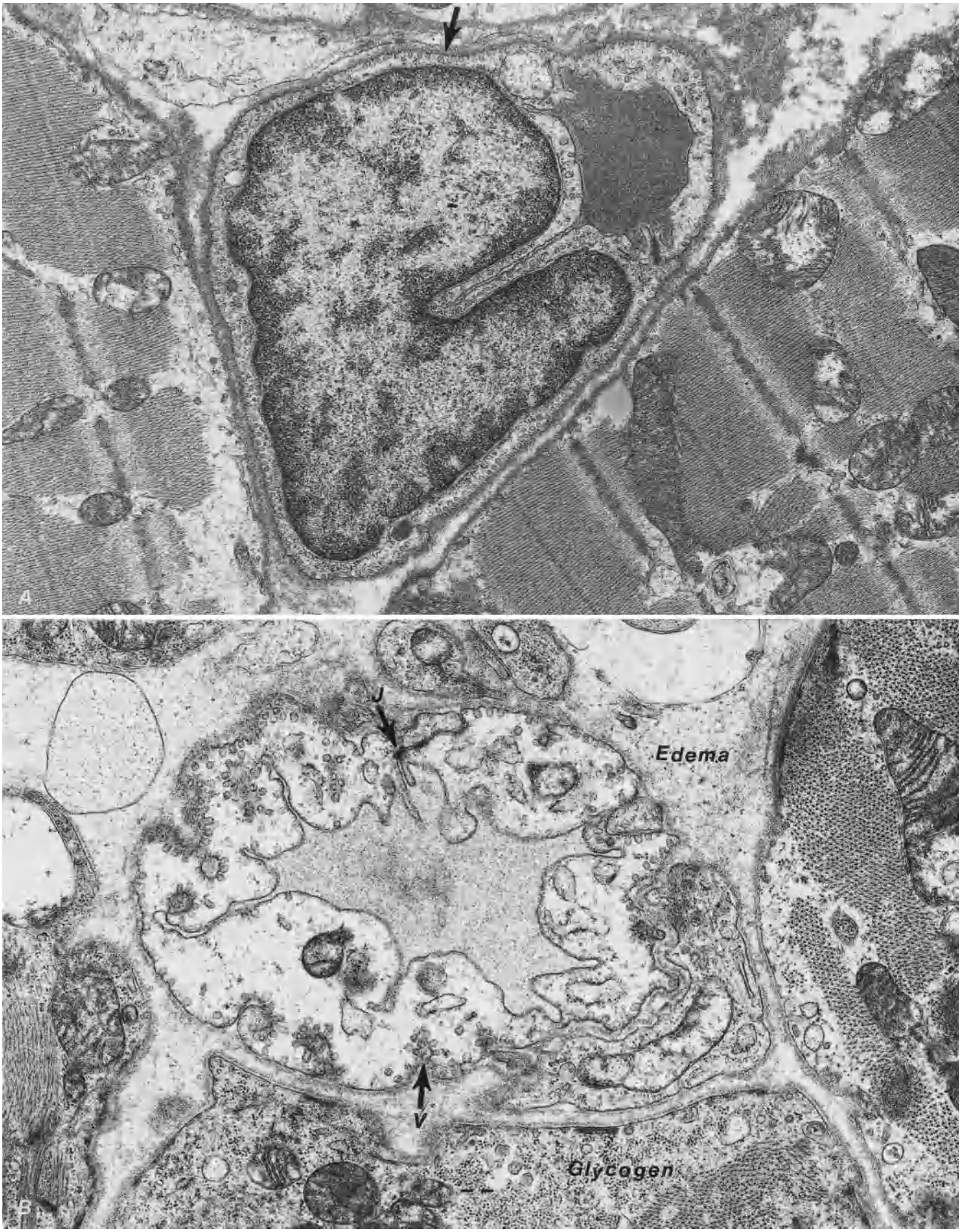


Fig. 9.1 Capillary endothelial cells in cardiac hypertrophy and failure: ventricular myocardium. **A**. **Hypertrophy**: myocardial enlargement, aged dog. Basal membrane (*arrow*) is lined with plasmalemmal vesicles (caveolae) that are organized and uniform in size. **B**. **Cardiac failure:** marked dilatation of heart, anemia, and edema. Endothelial cell swelling and edema of perivascular spaces, cat. Plasmalemmal vesicles (*V*) at plasma membrane are enlarged and disoriented. Cytoplasm is swollen, and numerous infoldings are in the lumenal plasma membrane. Increased density of intercellular junctions (*J*) is evident.

© 2009 Wiley-Blackwell. ISBN: 978-0-813-80330-2

Vet-ebooks.com

9 Endothelium

Endothelial Interface with Blood and Perivascular Spaces

Endothelial cell (EC) surfaces are highly reactive. They define pathologic lesions by maintaining blood-tissue barriers, and react to injury by responding to endogenous stimuli as well as to the impact of such diverse events as trauma, hypoxia, microbial attachment, or bacterial endotoxin,[1] all of which are associated with **endothelial cell activation**. By increasing surface adhesion molecules, undergoing increased oxidative burst activity, and releasing granules, the activated endothelial cell moves into a hyperfunction mode characterized by enhanced transport, resistance to hypoxia, and altered anticoagulant surface properties. The endothelial cell protein Gas6 amplifies EC activation, and plays critical roles in endothelial-inflammatory cell interfaces in inflammation.[2] Activation responses enhance the interaction of ECs with circulating leukocytes and platelets.

Organelles of Endothelial Transport

Endothelial cells have a highly developed system of plasmalemmal vesicles that transport ions and macromolecules from bloodstream to tissue spaces. The well-developed subsurface **cytoskeleton** allows the activated endothelial cell to rapidly move its organelles to adapt to changes in blood flow and to the damage of injury.[3,4]

Caveolae

Caveolae (plasmalemmal vesicles) are a distinguishing feature of capillary endothelium (Fig. 9.1). During transport, they pass large molecules into and out of endothelial cells. These unique vesicles, which line luminal and basal surfaces, have annuli or peritoneal rings that line the union between plasma membrane and vesicle.[5–7] Membranes of these vesicles contain specific glycoprotein receptors and enzymes associated with ATP production. In capillaries of the heart, endothelial caveolae are increased in hypertrophy, and become progressively disorganized as cardiac failure develops.

Transport by caveolae has been clarified by experiments with tracer particles. Two minutes after intravenous injection of ferritin, particles appear in caveolae near the plasma membrane. Subsequently, they progressively occur in all vesicles, in microvesicular bodies, in the basement lamina, and in pericapillary spaces. These experiments clearly demonstrate the capacity to transport macromolecules.[8,9]

Albumin, in its role of transporting fatty acids, steroids, hormones and bilirubin between plasma and interstitium, is transported across endothelium by caveolae. After experimental infusion, albumin binds with low affinity to endothelial surfaces, is transported via caveolae, and appears in pericapillary spaces within 15 sec after beginning perfusion.[10] Tracers of albumin-gold complexes, when injected intravenously into mice, appear in endothelial plasmalemmal vesicles in 5 min (Fig. 9.2). Gold complexed with **fibrinogen** or **fibronectin** does not label caveolae comparable

Vet-ebooks.com

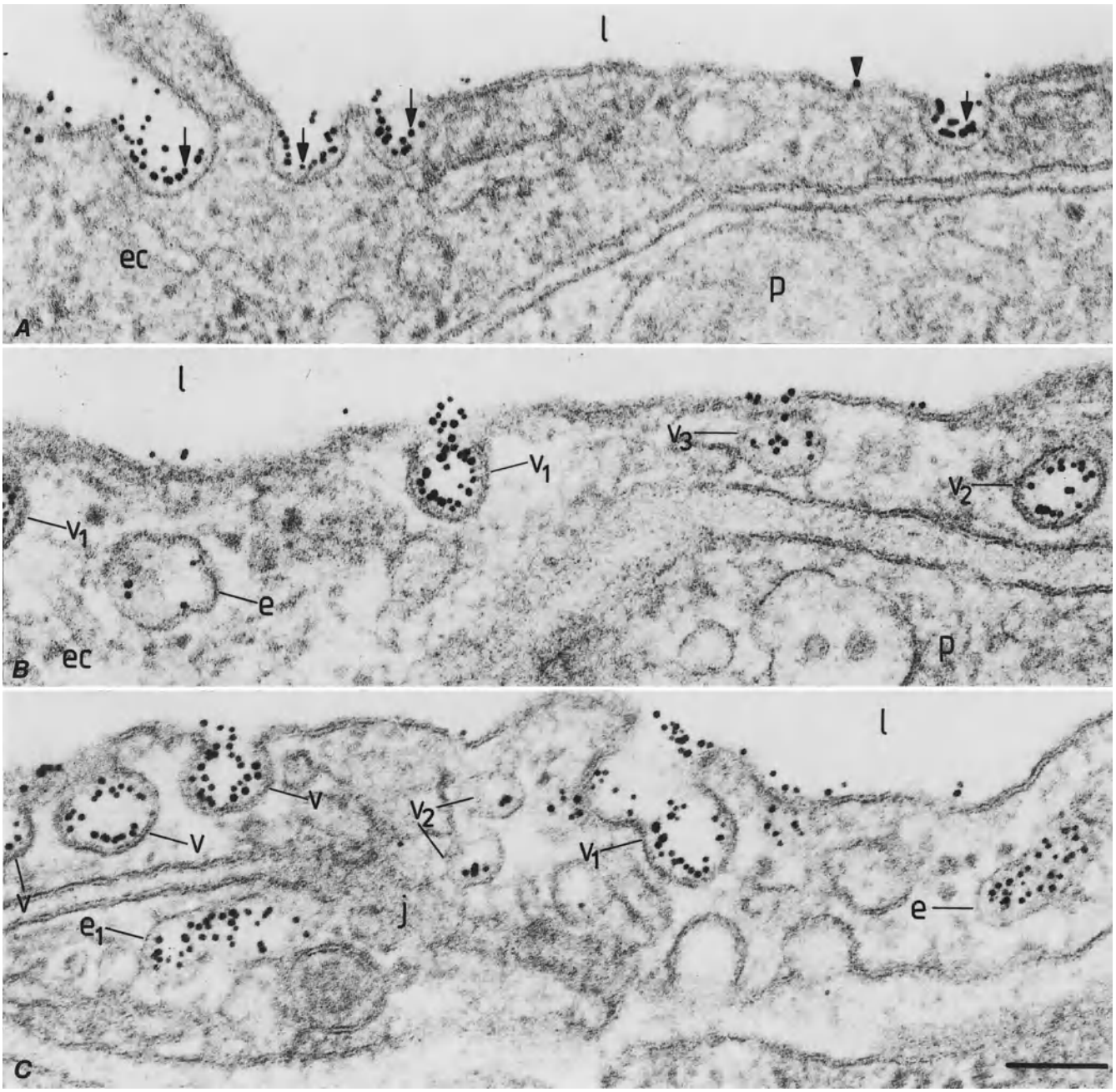


Fig. 9.2 Endothelial cell endocytosis: uptake of albumin-gold complexes, endothelial cells (*ec*), alveolar capillary endothelium, mouse lung. Structures: endosomes (e), caveolae (*v*), junction (*j*), lumen (*l*), and pericyte (*p*). **A–B**. Gold-albumin complexes are in coated pits (*arrows*) with rare complexes at the lumenal surface (*arrowhead*); 3 min after IV injection of complexes. **C**. Complexes are in caveolae: fused caveolae (v_1) and tubuloreticular structures identified as endosomes (e and e_1). Bar = 1 µm. (Micrograph: Maya Simionescu, Lucien Ghitescu, *J Cell Biol* 102:1304, 1986.)

to that of albumin.[11] Albumin is an important regulator of osmotic pressure of plasma and influences capillary transport and permeability by forming a fiber matrix on endothelial surfaces via interaction with other proteins.

Transendothelial Channels

In activated endothelial cells—especially in hypoxia, edema, and inflammation—**transendothelial channels** form by fusion of plasmalemmal vesicles. This results in invaginations from both sides of the capillary wall that connect to form large pores for the rapid flow of material across endothelium.[12] There is agreement between the number of PVs and the biological activity of the endothelial cell. In endothelial hypertrophy, which occurs in capillaries of the heart during cardiac hypertrophy, there are marked increases in vesicles associated with the plasma membrane. In explosive activation, the entire transport compartment

Vet-ebooks.com

of the endothelial cell is strikingly expanded (Fig. 9.3). **Vesiculo-vacuolar organelle (VVO)** was coined to define the transendothelial-caveolar transport organelle that functions in regulated transendothelial cell passage of soluble macromolecules.[13]

Coated Pits and Vesicles

Receptor-mediated endocytosis via **coated pits** occurs in endothelium although coated pits and vesicles are not commonly seen in endothelium in most tissues.

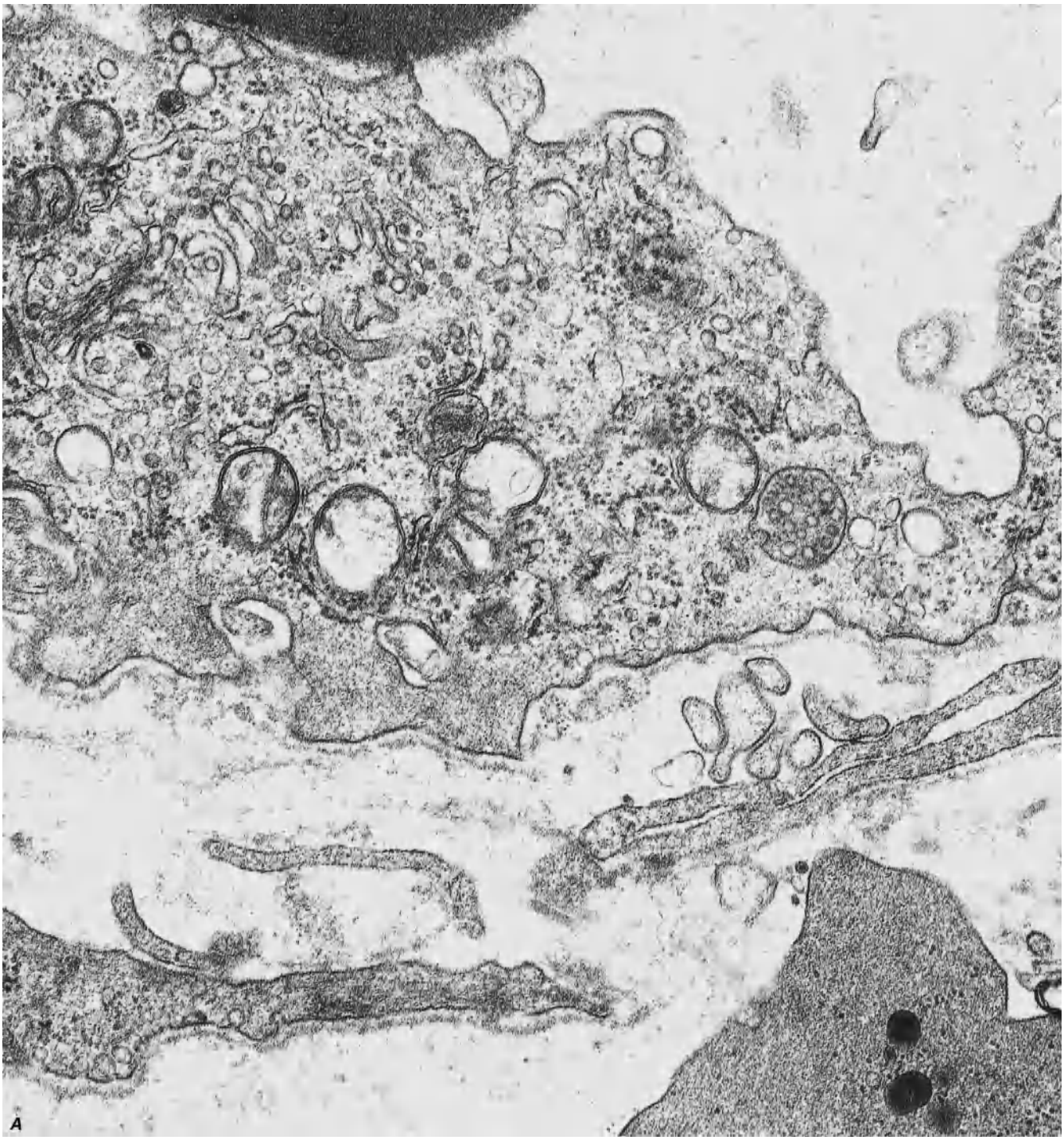


Fig. 9.3 Endothelial cell activation, acute inflammation, rat. A. Swollen endothelium: endothelial cell lumenal surface is undulant and cytoplasm is markedly increased in volume and has many vesicles, multivesicular bodies, and tubules. Interstitial spaces are enlarged with edema fluid, subendothelial basement membrane is discontinuous, and pericyte processes (*bottom*) are not connected.

Vet-ebooks.com

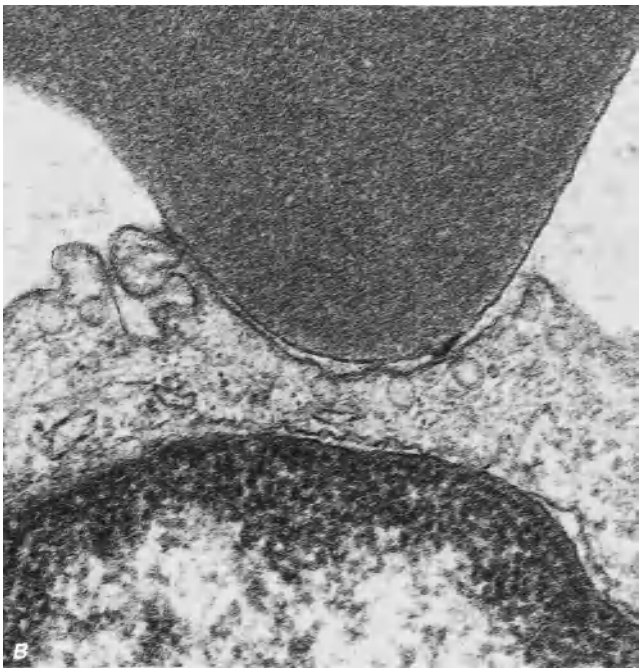


Fig. 9.3 B. Endothelial cell-erythrocyte binding: sites of binding occur at the periphery of the indentation of the erythrocyte into the surface of an endothelial cell.

This pathway is more prominent endothelium of some tissues than in others, and is especially important in the transport of low-density lipoproteins (LDL) via specific LDL receptors on endothelial surfaces.

Phagosomes

Endothelial cells are phagocytic although this function is slight and varies greatly in different tissues.[14] Bone marrow sinusoidal endothelial cells are unique among postcapillary venules in that they remove particulate material from the circulation by both intracellular and transcellular processes; that is, phagocytic uptake and transmural passage of particles to extracellular spaces.[15]

Plasmalemmal Microparticles **Plasmalemmal microparticles** derived from endothelium orignate from blebbing and shedding from endothelial cell plasma membranes. They are present in normal plasma in low numbers, but are markedly increased after direct endothelial injury and by other events on the lumenal surface (thrombin activation, C5b-9 attack, and PF4-antibody interactions).[16] Plasmalemmal microparticles are common in sepsis, thrombotic thrombocytopenic purpura, and hemoglobinuria, where they are also derived from platelets and monocytes. The severe bleeding disorder in humans known as **Scott syndrome** is associated with a defect in the ability to form microparticles.

Interendothelial Junctions

In capillaries, endothelial cells are joined by specialized **tight junctions** that have macula occludens with 4 nm gaps. Luminal sides adhere tightly but junctions are looser at outer surfaces.[17] At intercellular junctions a thin cytoplasmic lamella, the **marginal ridge**, projects outwards into the capillary lumen. Lumenal surfaces may contain microvilli. Endothelial cells may contain centrioles; these appear to vary in structure according to the cell cycle.[18] Interendothelial cell junctions contain proteoglycans of the fused external layers of endothelial cell membranes. **Fenestrae** are present in capillaries of the liver, intestinal mucosae, endocrine glands, and renal glomeruli, and in these organs are important in regulation of permeability.

Endothelial cells respond to injury by altering intercellular junctions. One of the first changes is a decrease in the size and density of **gap junctions**, the important sites of interendothelial communication. Freeze fracture studies show a loss of gap junctions in early phases of repair and endothelial proliferation.[19,20]

Normally, some macromolecules are transported directly through **intercellular junctions** between endothelial cells. Horseradish peroxidase (40,000 MW), when used as a tracer, permeates intercellular clefts.[21] In inflammation, injury to the endothelial cell loosens its intercellular attachments, and transportation of fluids through altered cell junctions is a markedly increased. In toxic injury, the first discrete evidence of capillary injury is seen as separation of endothelial cells and development of small cavities in intercellular spaces.[22]

Junctional Adhesion Molecules

Junctional adhesion molecules (JAM), composed of JAM-A, -B, -C, -4, and ESAM and CAR, are enriched at tight junctions of cell-to-cell contacts. JAM-C is a component of endothelial tight junctions; it is also a component of the autotypic junctional attachment of Schwann cells where it maintains function of myelinated peripheral nerves.[23]

Vascular endothelial-cadherin (VE-cadherin) is an endothelial-specific adhesion molecule that maintains junctions between endothelial cells. Mechanisms that regulate VE-cadherin-mediated adhesion control vascular permeability, especially during leukocyte extravasation and angiogenesis.

The Perivascular Environment

Capillaries are formed of a single endothelial layer. They have luminal diameters of 5–10 μm, are not innervated, and do not have encircling muscular

Vet-ebooks.com

layers. Two major capillary types are distinguished: continuous and fenestrated. **Fenestrae** are present in capillaries of the liver, pancreas, intestinal mucosa, endocrine glands and renal glomeruli, and are important in regulation of permeability.[24]

Sinusoids are large irregular blood vessels that are lined by a single layer of endothelial cells that follows the shape of the underlying parenchymal tissue. These endothelial cells are more actively endocytotic and have a more developed cytoplasmic vesicular transport system than to other endothelial cells. The prototype sinusoidal system occurs in the liver; sinusoids also are in spleen, bone marrow, adrenal cortex, and other endocrine organs. Sinusoidal endothelial cells express a set of surface molecules that differs from endothelium at other sites. Unique proteins from human sinusoidal endothelium serves as an anchoring molecule.[25]

Pre- and postcapillary blood vessels are those small arterioles and venules that connect with capillary endothelium, are surrounded by perivascular cells and, in contrast to capillaries, are always embedded in tissue parenchyma. **Precapillary arterioles** contain a small myocyte sheath and end in the capillary network, having a diameter of about 14 μm. **Precapillary sphincters** are a group of small muscular cells that encircle the capillary at its origin from the arteriole. **Postcapillary venules** range from 10 to 100 μm in diameter and have walls that are thinner than those of precapillary arterioles.

Basement Membrane

The **basement membrane** (or basal lamina) of the capillary is a fibrillary layer approximately 50 nm thick synthesized by endothelial cells.[26] It contains molecules of collagen IV meshed with glycoproteins such as **laminin** and **fibronectin** (Fig. 9.4), molecules released in small amounts that are incorporated into the underlying matrix. Anionic groups (primarily on heparin sulfate) along the edges of the lamina densa of the basal lamina are the major charge barriers to passage of circulating anionic macromolecules in capillaries of the intestine, pancreas, and other organs. Anionic domains are especially prominent on fenestral diaphragms but almost absent on luminal vesicles.[27]

The basal lamina, especially its collagenous components, functions as a filter, allowing passage of water and small molecules of less than 10 nm but not colloids. It also serves as a skeleton for endothelial regeneration following injury to the capillary. Proper maintenance of endothelial cell-basal lamina connections is regulated by integrins, which, if dysfunctional, can induce endothelial apoptosis.[28] Capillary basement membranes in edematous tissues are dispersed and degraded by the fluids in perivascular spaces (Fig. 9.5).

Morphometric analysis of capillary basement membranes is widely used in research.[29] **Basement membrane area** (BMA) can be determined in electron micrographs using the formula BMA = T − (M + E + Lu), where T is the total cross sectional area, M is pericyte area, E is endothelial cell area, and Lu is

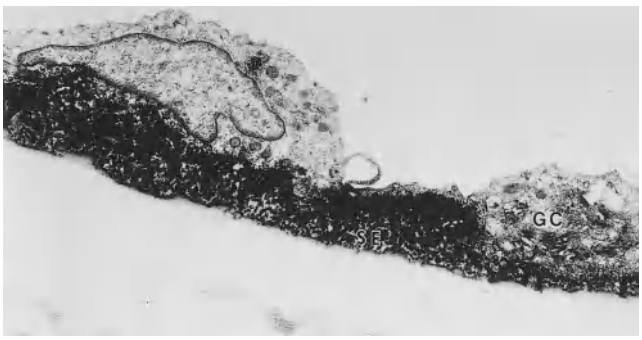


Fig. 9.4 Blood vessels. **Fibronectin**: cytochemical localization in aortic endothelium; rat, 48 hr after endotoxin treatment. There is heavy staining of subendothelial basement membranes. Within the endothelial cell, the Golgi complex (*GC*) is stained. (Micrograph: Yuan-Hsu Kang, *Anat Rec* 229:86, 1991.)



Fig. 9.5 Transendothelial channels: capillary endothelium in acute inflammation, skin, rat. Caveolae (plasmalemmal vesicles) are large, are separated from endothelial surfaces, and have fused to form channels. Basement membranes are discontinuous and irregular.

Vet-ebooks.com

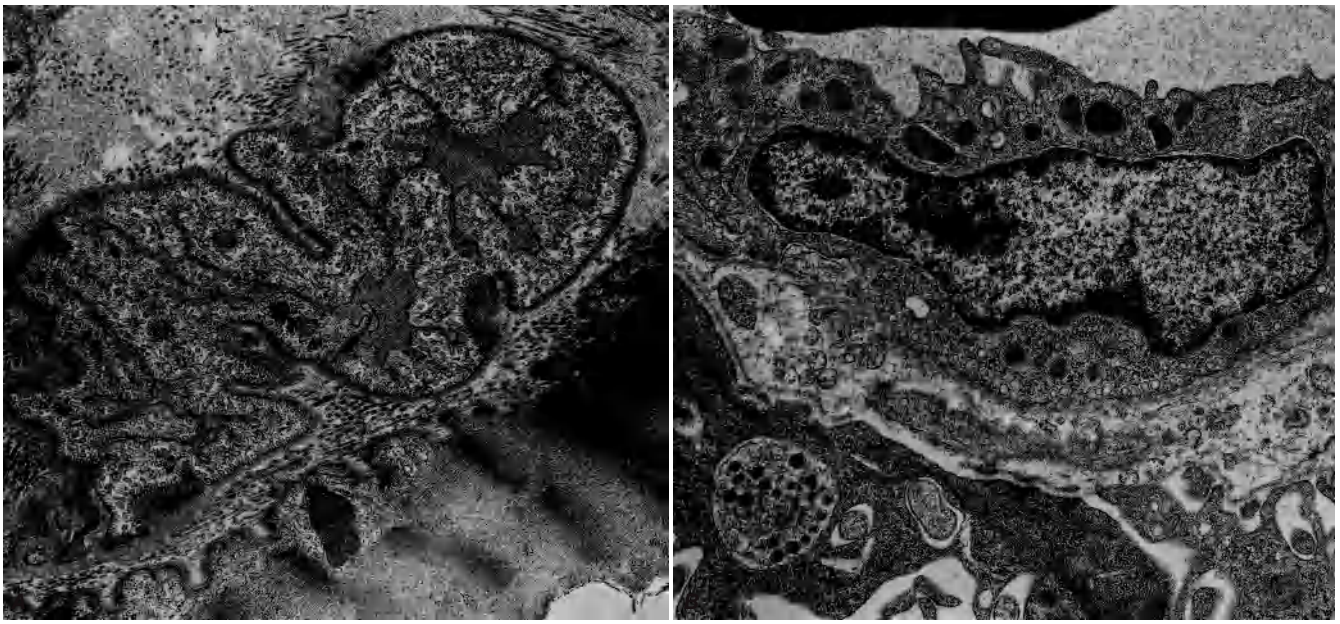


Fig. 9.6 Endothelial cells. A. Basement membrane expansion: retraction and collapse of capillary, congenital muscular dystrophy, dog. The primary defect is in the A lines of the myofibril (*lower right*). Interstitial space is filled with collagen fibrils and proteoglycan granules. Capillary endothelium is tortuous and filled with plasmalemmal vesicles. **B**. **Endothelial cell dense granules**: capillary, tracheal submucosa, influenza, chicken. Epithelial cell indentations are formed by nerve endings.

luminal area. **Basement membrane length** (BML) can be determined by dividing the length of lines delimiting BMA by 2. Relative data expressed in terms of basement membrane per unit length are thus BMA/BML.

In tissues undergoing **atrophy**, basement membranes surrounding capillary endothelium are markedly thickened (Fig. 9.6); these processes, common in atrophic mammary glands and prostates deprived of endocrine stimulation, are also found in dystrophies of muscle and bone.

Pericytes

Pericytes are modified smooth muscle cells that surround venules and capillaries of continuous and fenestrated types. They contain both muscle and nonmuscle actin microfilaments. The branching stellate processes grasp the capillary and may extend to other vessels. Monoclonal antibodies against glycoproteins and ganglioside antigens have been developed that are specific markers for pericytes.[30] Pericytes function in angiogenesis, microcontractility, and phagocytosis. They may become phagocytic in the processes of edema and inflammation. Transitional forms between pericytes and smooth muscle cells occur and are difficult to differentiate.[31]

Endothelial Thromboresistance vs. Procoagulation

Endothelial cells synthesize and release many different proteins and glycoproteins that remain on the luminal surface in order to regulate the endothelial environment. Molecules secreted onto luminal surfaces typically remain attached to the endothelial cell and contribute to the highly reactive coat of proteins, proteoglycans, and anionic sialoproteins that maintain the balance of thromboresistance and coagulation. A major function is the control of excessive coagulation.[32–36] Secretion pores, reported on lumenal plasma membranes of endothelial cells, are remnants of endothelial exocytosis of dense bodies in response to hypoxia.[37]

Three potent mechanisms of resistance to thrombosis prevent excessive coagulation in the vascular system: (1) **thromboresistance** of endothelial surfaces, (2) **lysis of fibrin** by the fibrinolytic system in circulating blood, and (3) **thrombin inhibition** by antithrombin III (which inactivates thrombin by irreversibly complexing with it), heparin, and plasma anticoagulation protein S (Gas6, growth arrest-specific gene 6). Endothelial thromboresistance is the primary line of defense against excessive coagulation.

Vet-ebooks.com

Thromboresistance of Endothelium

Normal endothelium is resistant to thrombosis because of several different but overlapping mechanisms: (1) **α_2-macroglobulins** in the glycocalyx coat the lumenal surfaces of endothelial cells and inhibit proteases of coagulation, (2) enzymes within endothelial cells convert endoperoxides to **prostaglandins** (particularly PGI_2 and PGE_1), which prevent or reverse platelet aggregation, and (3) activation of endothelial cell **thrombomodulin**, which inhibits thrombin and activates the anticoagulant protein C. These powerful surveillance systems cooperate to prevent thrombosis at endothelial surfaces during normal body functioning. In addition, powerful anticoagulant mechanisms operate in the extracellular matrix; for example, heparan sulfate proteoglycans with glycosaminoglycan chains are active anticoagulants for the coagulation factors that seep into the vascular wall.[38]

Thrombomodulin

Thrombomodulin is an integral protein on the surface of endothelial cells; it arises in the Golgi complex and is transported to the surface where it remains. Thrombomodulin is a receptor for and binds to thrombin. It binds in such a way that the fibrinogen-cleaving activity of thrombin is abolished, but its protein C-cleaving ability is markedly increased.

Protein C (PC) circulates in plasma as a zymogen, and is activated by thrombin bound to its endothelial receptor, thrombomodulin. The endothelial PC receptor (EPCR) binds protein C, and further enhances its activation by the thrombin/thrombomodulin complex. **Activated protein C (ACP)**, a serine protease, is a major anticoagulant that proteolytically inactivates clotting factors Va and VIIIa. ACP also has potent anti-inflammatory and cytoprotective capabilities.[39]

Plasma Proteins Absorbed to Endothelial Surfaces from Blood

In addition to the glycoproteins that are synthesized by the cell, other proteins are absorbed from circulating blood. **Coagulation factors** IX and X, when activated, bind to endothelial surfaces. As coagulation is initiated many more of these proteins attach to the endothelial surface and require that the endothelial cells be able to prevent uncontrolled coagulation.

α_2-Macroglobulins in the glycocalyx coat the lumenal surfaces of endothelial cells and inhibit proteases of coagulation.[40] α_2-Macroglobulin circulating in plasma specifically localizes on endothelial surfaces and protects the vascular system by inhibiting various protease-generating reactions; for example, this protein inhibits the intravascular proteolytic enzymes of coagulation, fibrinolysis, and kinin generation triggered by inflammation.

Procoagulant Activity of Endothelium

In tissue wounds, endothelium is transformed from antithrombotic into prothrombotic status. When endothelium is eroded, circulating platelets and coagulation factors are exposed to a complex milieu of subendothelial ground substances that includes collagen, fibronectin, and laminin. The injured endothelial cell releases von Willebrand factor, which initiates the binding of platelets to these substances.

Von Willebrand Factor

Endothelial cells store the adhesive glycoprotein **von Willebrand factor (vWF)** in elongate **dense granules**, commonly referred to as **Weibel-Palade bodies**. Dense granules are a key marker in the identification of endothelial cells. Their characteristic shape is determined by the molecular configuration of vWF.[41] Patients having inborn deficits of vWF have abnormal Weibel-Palade bodies.

At sites of endothelial injury, platelet aggregation is promoted by vWF throughout the phylogenetic scale. Dense granules are more common in lower vertebrates where they are known to store other clotting factors. There are regional differences in the prevalence of dense granules in endothelium. A study of the vascular system of the pig has shown that they are present in endothelium of the myocardium and numerous in the vena cava and pulmonary artery, but are lacking in the thoracic aorta and rare in the abdominal aorta.[42] In all species, dense granules tend to be more common in pathologic states involving increased transportation of macromolecules across the endothelial cell (Fig. 9.6).

Factor VIII-related antigen has been localized in dense granules with protein A-gold techniques. Cisternae of the endoplasmic reticulum and cytoplasmic vacuoles are also labeled, suggesting that endothelial cells synthesize vWF and store it in dense granules to be released by exocytosis.[43]

Procoagulant Microparticles

Procoagulant microparticles are released by endothelial cells in response to injury, and their presence is a hallmark of damage to the endothelium. Procoagulant microparticles convey tissue factor, two procoagulant factors, and exposed membrane phosphatidylserine.[44] They provide added procoagulant

Vet-ebooks.com

surfaces for assembly of clotting enzymes and thrombin generation.

Endothelial Response to Hypoxia and Circulatory Dysfunction

Hypoxia

Hypoxia incites marked change in the endothelium.[45,46] Endothelial cells are highly glycolytic and consume relatively low amounts of oxygen compared with other cells; that is, oxidative phosphorylation is not the main source of ATP. The **heme oxygenase** (HO) and **nitric oxide synthase** (NOS) enzymes generate the gaseous signaling molecules CO and NO, respectively, that are key regulators in hypoxia. These enzymes localize to caveolae, and their activity is modulated by caveolin-1.[47]

At low levels of oxygen, endogenous **nitric oxide (NO)** plays a key role in preventing accumulation of **hypoxia-inducible factor-1**. At higher oxygen concentrations, NO facilitates production of mitochondrial reactive oxygen species, which, in turn, activates AMP-activated protein kinase.[48]

Hypoxia and Edema of Circulatory Failure

Endothelial cells involved in stasis are swollen and organelles are disoriented. Fluid and protein precipitates disrupt the basement membranes and pericapillary spaces. In the end stage of **cardiac failure**, myocardial capillaries have caveolae that accumulate at both sides of the endothelial cell in attempts to increase the flow of fluid from interstitium to blood vessel (Fig. 9.7).

Hypotension

Hypotension is associated with marked endothelial damage in capillaries of the intestine, lung, and kidney; these are changes that can be ameliorated by infusions of endothelin-1, superoxide dismutase and other protective agents.[49]

Endothelins

When activated, endothelial cells release several important vasoactive substances. **Endothelins** are potent, long-acting vasoconstrictors. They are a family of peptides that are synthesized as a propeptide,

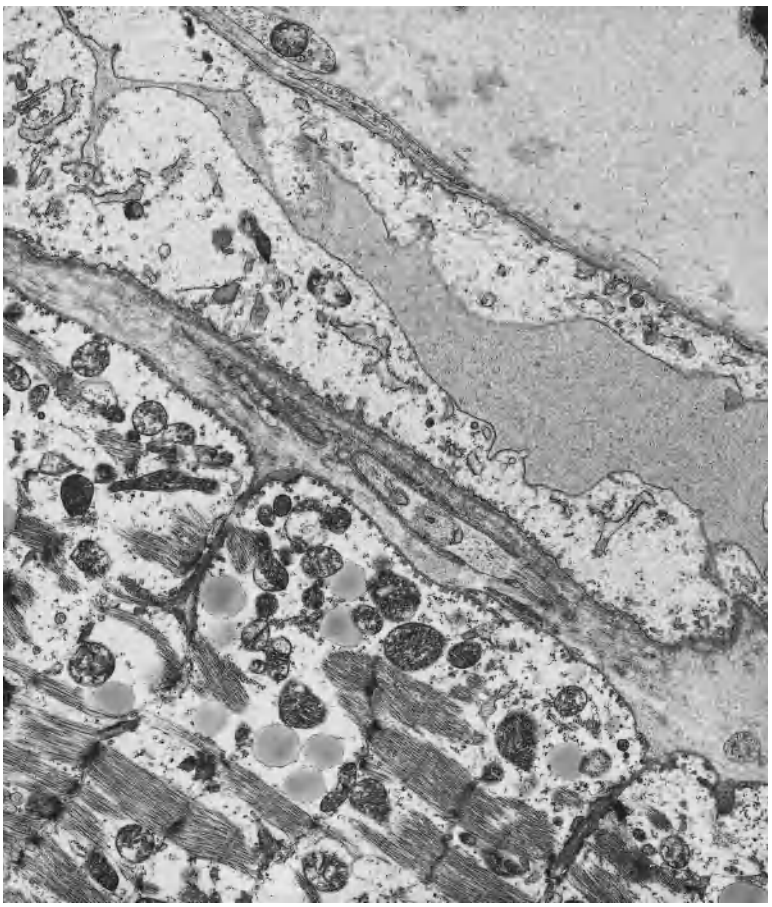


Fig. 9.7 **Hypoxia**: cardiac failure, capillary of the left ventricular myocardium of an aged dog with massive myocardial dilatation. **Endothelial cell** is swollen, obstructs the lumen, and contains vesicles, irregular organelles, and remnants of transendothelial channels. **Myocardial cell** (*bottom*) has evidence of myofibrillar lysis with Z line destruction, fragmented tubular systems, and lipid globules. Perivascular space contains plasma protein aggregates (*top*).

Vet-ebooks.com

cleaved to form big endothelin and then further cleaved by **endothelin-converting enzymes** to form the active peptide.[50] Endothelin-1 is produced by vascular endothelium and endothelin-3 by nervous tissue (the existence of endothelin-2 is debated). Other endothelins are found in epithelial cells of lungs, kidney, liver, and brain. Injected intravenously, endothelins produce vascular leaks and capillary endothelial cell damage. Endothelin is the prototype of a family of vasoactive peptides that includes "vasoactive intestinal contractor" and others.

Nitric Oxide

The vasodilatory agent **nitric oxide (NO)** is formed in endothelial cells, produced from arginine via catalysis by the **NO synthase** isoform, **eNOS** (the isoform specific for endothelial cells). NO is a potent signaling molecule in mammals (among nonmammalian species, endothelial cell NO release occurs in amphibians, but fishes tend to produce vasodilating prostanoids rather than NO). **Low levels of NO** produced by constitutive NOS enzymes are anti-inflammatory; **high sustained levels of NO** produced by inducible NOS are proinflammatory. NOS inhibitors (inhibited NO) increase the numbers of neutrophils that migrate toward IL-8.[51]

NO production is increased by many toxins and drugs. For example, the lipid-lowering **statins** (3-hydroxy-3-methylglutaryl-coenzyme A [HMG-CoA] reductase inhibitors), in addition to lowering cholesterol, enhance endothelial functions via activation of eNOS and increase in endothelium-derived NO. The mechanism involves **Rho/Rho-kinase (ROCK)**-mediated change in the actin cytoskeleton.

Angiotensin

Endothelial cells produce soluble factors that control blood pressure. The powerful vasoconstrictor, angiotensin II, induces widespread structural change in both endothelium and its major target, vascular smooth muscle. In endothelial cells, there are increases in caveolae and widening of intercellular junctions. **Angiotensin-converting enzyme**, a dipeptidyl carboxypeptidase that cleaves the C-terminal dipeptide histidine-leucine from angiotensin I to make vasoactive **angiotensin II**, has been localized by immunocytochemical methods.[52]

Hypertension

Blunted nitric oxide activity and reduced NOS synthesis are associated with **pulmonary hypertension**. In humans, arterial pulmonary hypertension is a fatal disease of unknown etiology characterized by impaired vascular maintenance and growth. It is associated with low levels of pulmonary NO.

Inflammation

The major events of inflammation are centered on the microvasculature; these include altered surface properties of endothelial cells, increased permeability of capillaries and venules, and exudation of fluids and inflammatory cells (Table 9.1).[53–55] Whether injured directly by trauma or toxins, or affected secondarily by hypoxia or by endogenous mediators such as histamine, leukotrienes, or cytokines, endothelial cell alterations determine the extent and character of protein-rich fluid movement from vascular lumen into extravascular spaces (Fig. 9.8). If inflammation is accompanied by lethal damage to cells, the endothelium becomes necrotic. Loss of tone leads to marked expansion of the blood vessel and packing of the lumen with erythrocytes. Stasis of blood flow occurs, and platelets, attracted by damaged to vascular surfaces, adhere to endothelium (Table 9.2).

Classic studies on inflammation in the 1960s showed that when histamine is injected subcutaneously, followed by intravenous trypan blue, the dye complex begins to leak, allowing the site of histamine injection to become blue. It does so in relation to the extent of

Table 9.1 Vascular change in acute inflammation.

Capillaries and postcapillary venules become abnormally permeable: tissue damage, microbial virulence factors, and other substances produce a direct effect at the primary site of injury.

Endothelium becomes leaky peripheral to the site of injury; albumin molecules leak into perivascular spaces.

Endothelial cells are activated peripheral to injured site and release
- prostaglandins → vasodilation
- cytokines (IL-1, TNF, TGF-β) → chemotaxis of leukocytes
- procoagulant factors → coagulation

Arterioles dilate due to nerve stimuli from axonal reflex arcs.

Blood flow stasis arises from capillary filling, endothelial swelling.

Margination of leukocytes in flowing blood—cells move to periphery.

Erythrocytes develop sticky surfaces.
- **move to periphery** and pass through capillary walls
- **bind to endothelial cells** and pass the capillary wall
- **hemoconcentration**, as fluid escapes, → further slows blood flow

Leukocytes are activated—become sticky as surface ligands increase.

Lymphatic vessels become discontinuous, increasing lymph flow.

Vet-ebooks.com



Fig. 9.8 Acute inflammation, **postcapillary venule**, **skin**: endothelial cells are swollen and have irregular surfaces, vesicular cytoplasm, and expanded interendothelial junctions. Perviascular spaces are expanded by finely granular precipitates of albumin (edema) and contain inflammatory cells. Neutrophils and monocytes are in the venular lumen and perivascular space. Erythrocytes are deformed and adhered to endothelial surfaces; one flattened erythrocyte (*arrow*) lies between the endothelium and subendothelial pericytic processes.

Vet-ebooks.com

Table 9.2 Perivascular change in acute inflammation.

Fluids move into perivascular spaces
- **Plasma proteins** exude into interstitium
- **Lymph flow** is increased early (is suppressed in late stages)
- **Fibrin** polymerizes from fibrinogen

Perivascular mast cells degranulate and release:
- histamine → ↑ postcapillary permeability
- heparin → ↓ coagulation and stimulates angiogenesis
- serotonin → ↑ capillary permeability
- leukotrienes → pain

Neutrophils and monocytes emigrate—pass vascular walls
- **Endothelial surfaces** become sticky, then attract and bind neutrophils and monocytes
- **Neutrophils** pass between endothelial cells and pseudopodia reach out and surround the cells
- **Neutrophils** bound to vascular walls release factors that increase vascular permeability
- **Monocytes** pass capillary walls and transform into macrophages
- **Macrophages** are activated, release cytokines
  IL-1 and **TNF** act on endothelial cell to increase permeability
  TGF-β induces chemotaxis of monocytes and fibroblasts, enhances extracellular matrix deposition, and promotes angiogenesis

Nerves stimulated to release neuropeptides
- **substance P** causes vasodilation
- **neuropeptides** induce mast cell degranulation

histamine-induced endothelial injury. Ultrastructural examination of lesions produced by histamine followed by carbon intravenously shows that carbon leaks through intercellular spaces with fluid and is trapped by basement membranes, which allows exudation of plasma but not particulate material. Histamine exerts its effect on postcapillary venules. Similar tracer studies have used ferritin (10 nm diameter) and horseradish peroxidase (4 nm); both substances exude through intercellular spaces and fenestrae. Peroxidase, because of its smaller size, shows earlier and more extensive localization.

Ultrastructural Evidence of Inflammation

When the capillary bed in early preclinical stages of inflammation is examined by electron microscopy, subtle changes of endothelial activation are found in capillaries and postcapillary venules. Endothelial cells are swollen. Cytoplasmic volume is expanded so that cells protrude into and often block the vessel lumen. The increase in cell volume typical of acute cell swelling may be masked by the dilatation of the capillary, which spreads the cell, making it appear thinner than normal.

Endothelial cells that are injured directly at the **site of injury** will show acute cell swelling and other changes according to the specific agent of injury, typically changes that lead to desquamation and necrosis. Peripheral to the primary site of injury, endothelial cells are activated by cytokines and other vasoactive substances, which are released by mast cells, monocytes, and macrophages—inflammatory cells that enter the site of injury to activate and sustain the inflammatory response.[56] Around the inflamed blood vessels, perivascular spaces are expanded by exuding fluids and plasma proteins, which appear ultrastructurally as delicate, granular material (Fig. 9.9).

The **cytoplasm** of inflamed endothelial cells has increased electron opacity and disorganized organelles. Cisternae of the endoplasmic reticulum are dilated and small **vacuoles** are dispersed throughout the cytoplasm. Multivesicular bodies are usually present in greater numbers. In subacute inflammatory lesions, there is apt to be an increase in cytoplasmic volume, especially in the content of free ribosomes, but this change is rarely seen in acute lesions.

Endothelial Cell Fluid Transport

Immediately after injury, **plasmalemmal vesicles** (caveolae) are increased in size and number on luminal and basal surfaces of the endothelial cell. **Fenestrae**, when present, are enlarged (in vessels that contain them). As they move across the endothelial cell, they may coalesce to form direct channels that traverse endothelium.

Although plasmalemmal vesicles transport fluid into the interstitium early, the massive amounts of fluid that exude do so mostly through **intercellular junctions**, in the gaps and cavities that form between endothelial cells. Loose-type junctions are enlarged. **Tight junctions** have increased densities due to increased amounts of glycosaminoglycans and other surface glycoproteins.

Ultrastructurally, **intercellular junctions** are irregular and often thickened (Fig. 9.10). Although involved in transport of inflammatory fluid, they are paradoxically longer, tortuous, and denser than normal. At the lumenal surface, activated endothelial cells develop a highly undulant plasma membrane with increases in **microvilli** and irregular convolutions of the surface. **Blebs** of cytoplasm bulge into tissue spaces through breaks in the basement membranes.

Endothelial Cell Activation in Inflammation

At the site of injury, **endothelial cells are activated** and begin to express adhesion molecules on their surface membranes that bind to ligands on circulating leukocytes. These changes cause endothelial surfaces

Vet-ebooks.com

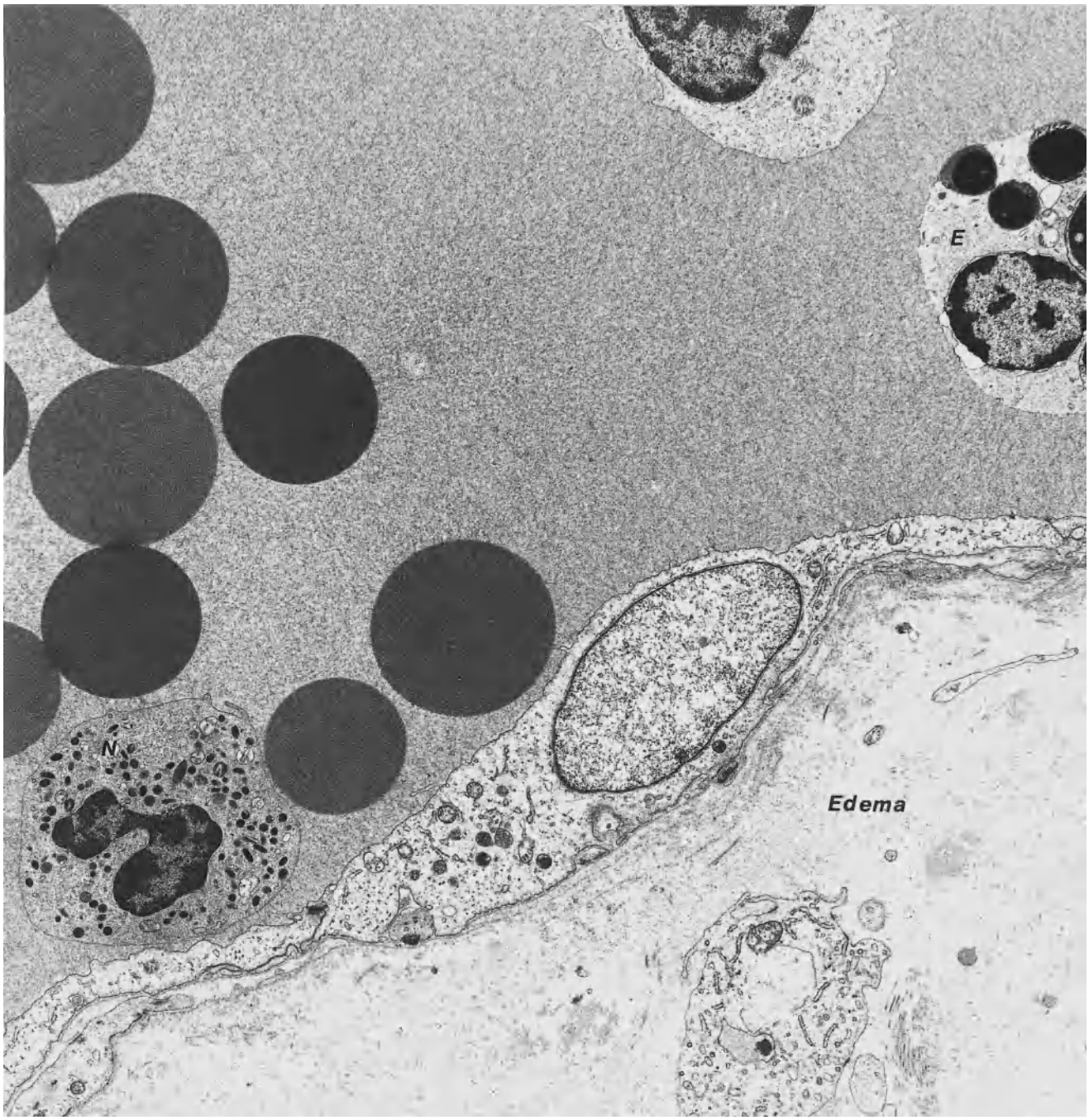


Fig. 9.9 Inflammation: hyperemia and edema, capillary, adipose tissue, dog. Vascular lumen is expanded with dense, granular, albuminous precipitates, erythrocytes, and inflammatory cells including a neutrophil (*N*) and eosinophil (*E*). Perivascular space is markedly expanded by granular precipitates of exuded plasma proteins (from edema fluid). Endothelial cell contains large dense granules and has basement membranes that are discontinuous and expanded by edema fluid.

to become sticky and permeable, and lead directly to attachment of leukocytes. Subsequently there is exudation of both leukocytes and plasma proteins from the blood vessel lumina into the interstitium.

The **cell surface** of the activated endothelial cell is irregular and shows increases in number and length of **filopodia**, and in the spectrum of glycoproteins displayed on plasma membrane. Activated endothelial cells show loss of some surface glycoproteins with an increase in others. Ion pumps are shifted in relation to the injury; for example, calcium-activate ATPases are altered. Frond-like extensions from the endothelial cell surface project into the lumen providing contact sites for inflammatory cells, particularly neutrophils.

Vet-ebooks.com

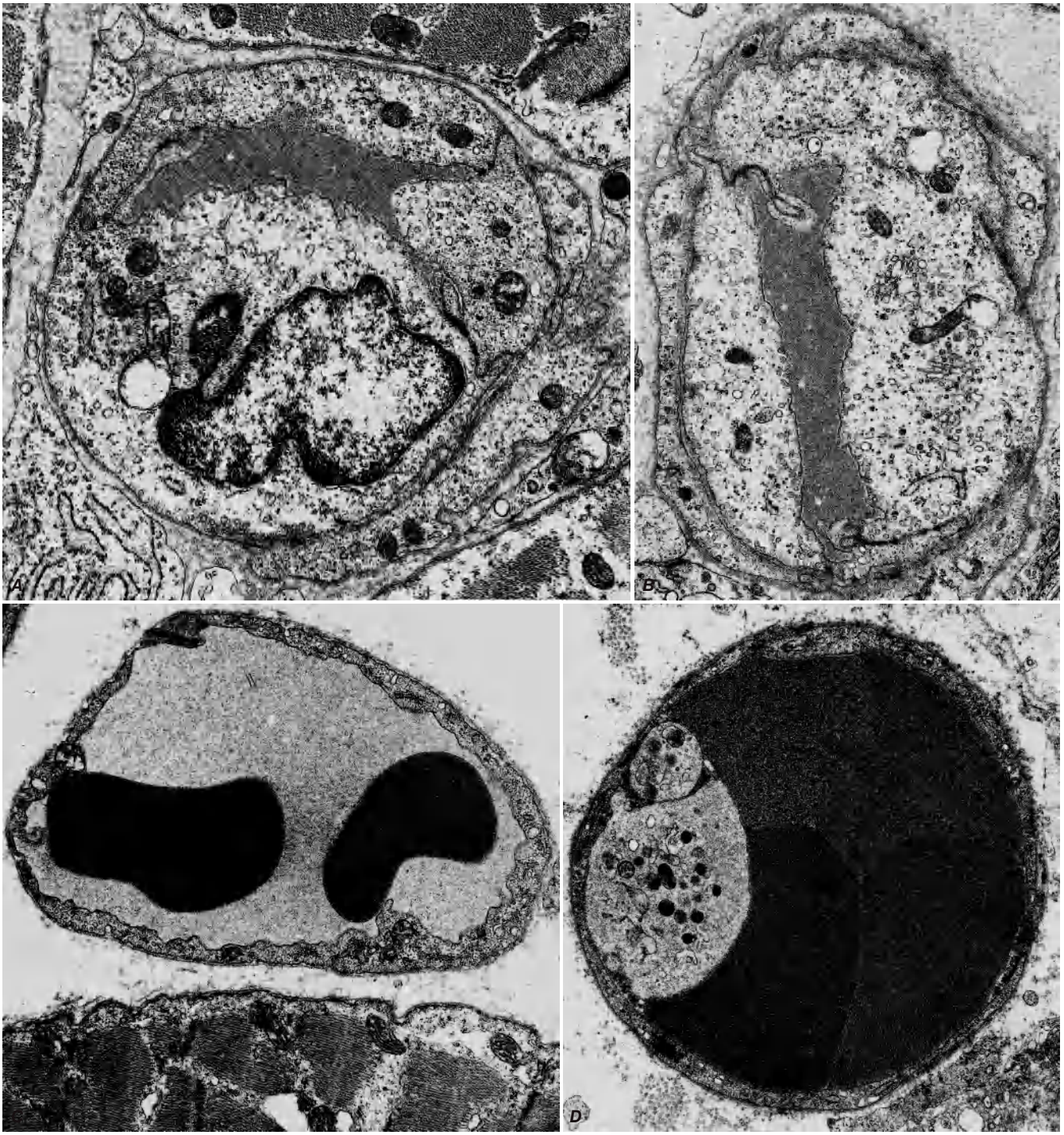


Fig. 9.10 Endothelial cells in acute inflammation: skeletal muscle, rat. **A. Acute cell swelling**: endothelial cells protrude into the capillary lumen. Cytoplasm is pale with little increase in organelles. Mitochondria are vesicular. Interendothelial junctions are lengthened and increased in density. Perivascular spaces are expanded. **B**. **Endothelial cell activation**: postcapillary venule. Cytoplasmic organelles are dispersed; endoplasmic reticulum is diminished and tiny vesicles are dispersed throughout the cytoplasm. Intercellular junctions are irregular and thick, and marginal folds of intraendothelial cell junctions are long and expanded. The basal lamina is frayed and irregular. **C**. **Dilatation of hyperemia**: capillary is dilated and lumen contains erythrocytes; intercellular junctions are thick and long, and marginal folds are obliterated. **D**. **Markedly dilated capillary:** necrotic endothelium, erythrocytes fill dilated lumen, and platelets cover defects in endothelium; capillary basement membrane is discontinuous and infiltrated with granular precipitates of fibrin and albumin. Perivascular spaces are expanded.

Vet-ebooks.com

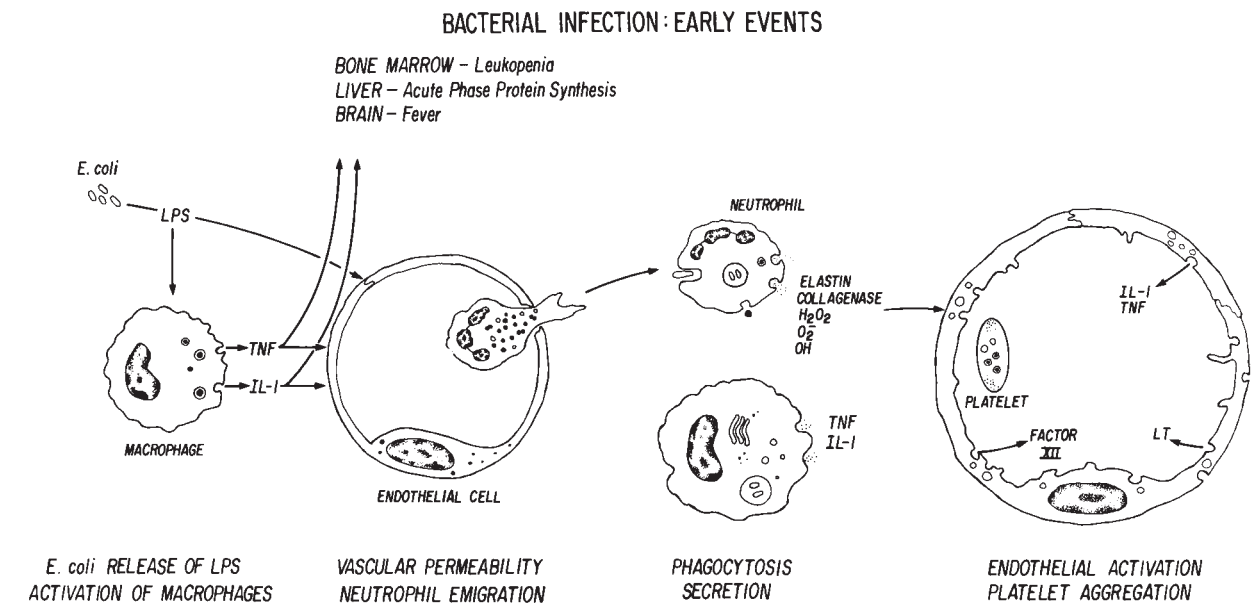


Fig. 9.11 Interaction of endothelium and inflammatory cells. Release of cytokines from inflammatory cells during the early events in inflammation caused by gram-negative bacteria. Release of bacterial lipopolysaccharide (*LPS*) initiates release of cytokines tumor necrosis factor (*TNF*), interleukin-1 (*IL-1*) and leukotriene (*LT*).

Studies of the cerebral vascular system show that these endothelial filopodia are important in movement of neutrophils, but not of lymphocytes, across endothelium.[57] Activated endothelial cells also take up and process material from perivascular spaces such as mast cell granules.[58]

The **cytoskeleton**, affected through its links with the luminal plasma membrane, is activated in inflammation. The **Rho family GTPases** (RhoA, Rac1, and Cdc42 are best characterized members) are regulatory molecules that link surface receptors to the actin cytoskeleton. They regulate endothelial barrier functions including leukotaxis, and platelet activation.[59]

Endothelial Transmembrane Receptors

Swollen endothelial cells protruding into the vessel lumen develop increased stickiness because of changes in surface **glycocalyx**. Two transmembrane glycoproteins that appear on the endothelial surface that function as adhesion molecules are **endothelial-leukocyte adhesion molecule-1** (ELAM-1) and **intercellular adhesion molecule-1** (*ICAM-1*). ELAM-1 is a glycoprotein embedded in the endothelial cell surface that promotes attachment of circulating neutrophils. In some, ELAM is stored in granules and released onto endothelial surfaces when the cell is activated (platelets contain similar materials that are stimulated by thrombi).

Components of other glycoproteins affect coagulation and act as receptors for various plasma proteins. Von Willebrand factor suddenly appears in the rough endoplasmic reticulum of activated endothelial cells.[60] Formation of **plasma protein-receptor complexes** plus the marked changes in the cell surface combine to markedly retard blood flow in capillaries and to cause stasis in smaller vessels. **Cytokine-activated endothelial cells** are prone to extravasation of leukocytes, which emigrate in large numbers through the vascular wall (Fig. 9.11).

Other endothelial surface adhesion proteins function in lymphocyte **trafficking** to the different lymphoid organs—cell surface adhesion proteins that act as homing receptors and counterreceptors (high endothelial venule ligands, vascular addressins). Adhesive interaction between circulating lymphocytes and the high endothelial venules of lymph nodes is mediated by lymphocyte L-selectin, the receptor for which is a molecule on the endothelial cell surface that functions as a scaffold for presentation of carbohydrates to the L-selectin lectin domain.[61]

Cytokine Activation of Endothelium

Stimulation of endothelial cells by cytokines and other factors that lead to activation causes a distinct growth of changes that characterize **activated endothelial cells**. Increase in cytoplasmic volume and surface area are invariably present. There are increased numbers of plasmalemmal vesicles and, in marked cases, there are vacuoles of varied size in the cytoplasm.[62,63]

In early phases of inflammation, potent cytokines are released by endothelial cells, and seep from the damaged cell to activate endothelium peripheral to

Vet-ebooks.com

the site of injury.[64,65] Endothelial cytokines also travel in the bloodstream to act at sites of hematopoiesis (bone marrow), lymphopoiesis (lymph nodes and spleen), and plasma protein synthesis (liver). As a result of this stimulation, leukocytes are released from the liver and bone marrow.

Endothelium both releases and responds to regulatory cytokines. Endothelial cells are specifically activated by cytokines of monocytes and macrophages; for example, tumor necrosis factor (TNF) and interleukin 1 (IL-1) cause rapid and marked endothelial cell activation. As a result, expression of **adhesion molecules** at endothelial surfaces is increased, and there is release of **tissue factor**, a procoagulant protein. TNF-α and IL-1 also decrease the binding and surface activation of **protein C** (as a result of rapid internalization and degradation of cell surface-associated **thrombomodulin**). Cytokines act synergistically and TNF in combination with interferon-gamma will cause a greater range of endothelial activation.[66]

TNF

Tumor necrosis factor (TNF) is a pleiotropic inflammatory mediator produced chiefly in activated macrophages and T lymphocytes. Vascular endothelial cells are an important TNF target, and respond to TNF by promoting recruitment and activation of leukocytes. Immunogold techniques have localized two distinct TNF receptors in cultured ECs, designated TNFR1 and TNFR2, which are differentially expressed on cells and initiate both distinct and overlapping signal transduction pathways. TNF receptors are on cell surfaces and in endocytic and transport vacuoles, and were shown to cluster in response to TNF.[67]

TNF-α also stimulates production and secretion of type 1 **plasminogen activator inhibitor**, [68] a change that promotes maintenance of the fibrin clot. Increased plasminogen activator inhibitors on endothelial surfaces promote intravascular thrombosis. Injected subcutaneously in primates they cause the morphologic characteristics of activation in endothelium, and the adhesion molecules ELAM-1 and ICAM-1 to appear on endothelial surfaces.

TNF and IL-1 are the mediators of endothelial changes caused by several toxins; for example, they will induce the priming phase of the Shwartzman reaction, which is classically produced by endotoxin,[69] the lipopolysaccharide complex in the outer wall of gram-negative bacteria. Given systemically, it causes severe injury to endothelium of pulmonary capillaries, especially in the lung, liver,[70] and large arteries.[71] Ultrastructural studies of pulmonary capillaries show that there is endothelial cell activation and degeneration followed by increased vascular permeability and pulmonary edema.[72,73] Leukopenia results from trapping of neutrophils in the pulmonary capillary bed, where their degranulation leads to severe tissue injury.

Although several chemotactic factors stimulate leukocytes to migrate to endothelium, activated endothelial cells also secrete surface proteins that cause neutrophils to adhere, trapping them in localized areas of tissue injury. Other leukocytes and even erythrocytes may be found adherent to activated endothelial cells. When the **complement fragment C5a** is infused into mesenteric veins of rats, granulocytes rapidly adhere to endothelium and plasma leaks soon thereafter.[74]

Complement Damages Endothelium

Stimulatory proteins, called **acute phase proteins**, pour into the bloodstream from the liver and travel back to the inflammatory site. Here they enter the tissue to provide stimulation to keep the inflammatory process going by chemoattraction and vasoactivity. **Complement components** interact to form a cascade of vasoactive peptides that attach to damaged endothelial cells. Attachment is designed to insert tiny peptide fragments into membranes and to form pores that cause cells and bacteria to become leaky and lyse. Although beneficial, complement can cause widespread destruction of endothelium.[75,76]

Specialized Endothelium

Regional differences in the permeability of capillaries to inflammatory signals are based on structural variations in the vascular wall. Three major capillary types are distinguished: continuous, fenestrated, and discontinuous; the ultrastructural distinction is based on completeness of their three layers. Transport kinetics indicate that permeability to macromolecules increases in tissues in the following order: limbs, intestine, liver sinusoids, brain. Superimposed on anatomical differences are systemic factors that alter permeability.

Lymph Vessel Endothelium

Endothelial cells of lymph vessels closely resemble those of blood vessels except that they tend to have fewer organelles and are less responsive to hypertension and to most cytokines. Special **stomata** or pores that aid in drainage of lymph into the lymphatic vessels have been documented on serosal surfaces of the diaphragm. Fluids and neutrophils in bacteria-induced exudates move to and enter the lymphatics via these pores.[77,78]

Vet-ebooks.com

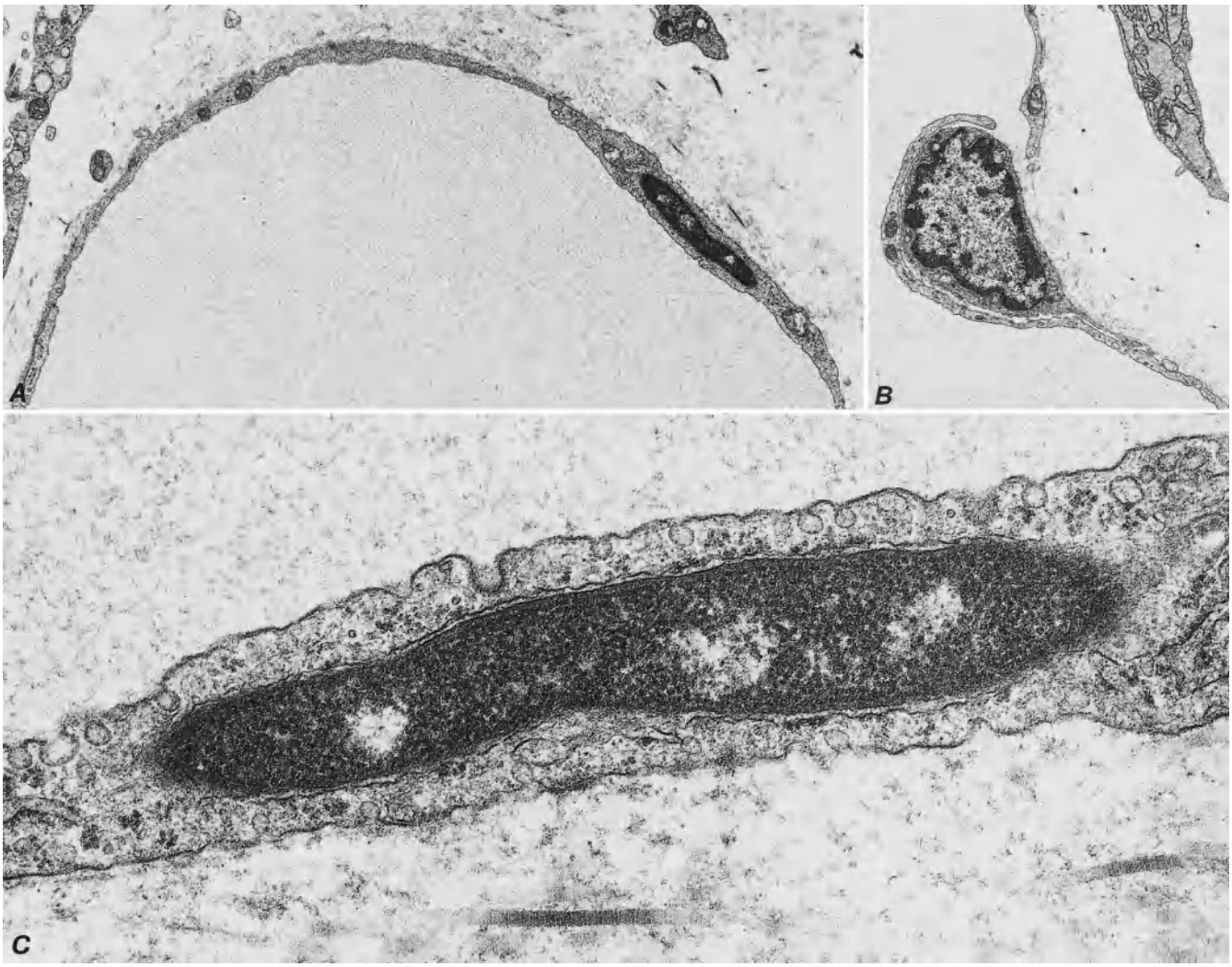


Fig. 9.12 Lymph vessels in acute inflammation: pasteurella toxin, skin, rat. **A**. **Dilated lymph vessel:** accumulation of plasma protein precipitates in the lumen and interstitium. **B**. **Apposition of cytoplasmic fronds** of lymphatic endothelial cells. **C**. **Lymphatic endothelial cell**: lumenal surface contains many caveolae and pinocytotic vesicles; perivascular surface has densities that represent small sites where connective tissue fibers are attached. Note collagen fibrils in perivascular space (*bottom*).

Injured endothelial cells of lymph vessels show changes similar to those of blood vessels.[79–81] In edematous tissue, interendothelial junctions are open wide and communicate directly with the edematous interstitial spaces. Fluid transfer is from interstitium to lymph vessel lumen. Anchoring filaments that surround lymphatic vessels play a major role in opening cell junctions and they disappear in inflammation. Lymph vessel endothelial cells become markedly expanded (Fig. 9.12). Ultrastructural localization of integrins α5 and αv have been localized in pathologic lymphatic vessels; blockade of these integrins inhibits lymphangiogenesis associated with inflammation.[82]

In endothelial cells of the dog, paracrystalline inclusions of closely packed hexagons (18 nm diameter), 24 nm diameter tubules in cisternae of the endoplasmic reticulum, and membranous whorls (10 nm thick, often in lamellae) have been reported.[83]

Long-standing **lymphangitis** progresses to fibrosis and swelling of the area being drained by the lymph vessels. The superimposition of active inflammation on these obstructed lymph vessels leads to severe inflammatory edema and fibrosis.[84]

Fenestrated Endothelium of the Liver

In the liver, the phenotypic features of sinusoidal endothelial cells (open fenestrae in sieve plates and lack of basement membranes) are lost with capillarization. In hepatic sinusoids, surface expression of **CD31** is a marker of dedifferentiated nonfenestrated sinus endothelial cells. The **VEGF**-mediated paracrine effect

Vet-ebooks.com

of hepatocytes of maintenance of sinus endothelial phenotypes requires autocrine production of nitric oxide by the endothelium.[85]

Blood-Tissue Barriers

Specialized capillary endothelial types form barriers to protect tissue: for example, the **blood-brain barrier** rigorously isolates the brain from circulating blood by its unique structure: (1) a continuous arrangement of tight junctions between endothelial cells, (2) lack of plasmalemmal vesicles (and transendothelial channels) that traverse endothelia of other organs, (3) lack of fenestrae, and (4) a corona of astrocytic foot processes that surround the capillary. Other blood-tissue barriers are the **blood-testis barrier**, the **perineural barrier**,[86] and the **blood-retinal barrier**.[87] Breaks in the blood-retinal barrier are detected by fluorescein dyes injected intravenously; dye seeps through retinal capillary walls at foci where inflammation has altered avascular permeability.

Mast Cell and Basophil Interfaces with Endothelium

Mast Cells

Located in perivascular locations throughout the mammalian body, mast cells are positioned to liberate the potent vasoactive factors stored in their cytoplasmic granules (Fig. 9.13). Degranulation is explosive, and strikingly alters the ultrastructural appearance of the mast cell surface, cytosol, and granule (Fig. 9.14). Mast cells have dendritic extensions that ramify through interstitial tissues (Fig. 9.15). Apposition to nerves indicates that mast cells can influence the nervous system.[88] In vitro, activated mast cells can induce apoptosis of endothelial cells through the combined action of TNF-α and chymase release.[89]

Mast cell size increases with progressive maturity. The Golgi complex is large but endoplasmic reticulum small. Intermediate filaments are common and one or more lipid globules may be present, especially in activated mast cells. Species differences in basophil and mast cell numbers and in granule size are important to differences in the inflammatory response. Granules are numerous in the dog, cat, cow, and hamster but are few in the rabbit and guinea pig.[90]

Mast cell populations have been differentiated morphologically into **type I mast cells** (elongate, ovoid, densely staining, and embedded in adventitia close to small blood vessels) and **type II mast cells** (large, more regular in shape, and loosely scattered along and around capillaries and in interstices away from blood vessels). Another scheme, based on protease composition, divides human mast cells into (1) **T cells** (tryptase +, chymase –), which dominate in the gut mucosa and lung and which have granules with well-defined scrolls and electron-spheres, and (2) **TC cells** (tryptase +, chymase –), which occur in skin and gut submucosa that are scroll poor but may have lattice structures.[91,92]

Mast Cell Granules

Mast cell granules are round, membrane-bound, and heterogeneous. The most mature granules are homogeneous, amorphous, and dense. Granules with scrolls or concentrically arranged cords are less mature. In some species, compound granules have crystalloids of protein. When granules are artificially ruptured, ultrastructural examination reveals small beaded filaments interpreted as heparin-protein complexes. Components of mammalian mast cell granules include

- **Heparin** is stored in heparin-protein complexes; content varies greatly in mast cells at different locations.[93]
- **Histamine** is stored in ionic linkage to heparin complexes and is released via a simple ion exchange between histamine in the granule and cations in the extracellular fluid.
- **Serotonin** (5-hydroxytryptamine)
- **Platelet activating factor (PAF)**, an acetylated alkyl phosphocholine, activates platelets, stimulates neutrophils, contracts smooth muscle, and increases capillary permeability.[94]

Mast cell granules are the source of the following substances. Granules also contain small amounts of other peptides, including **eosinophilic chemotactic factor**, **prostaglandins**, **leukotrienes**, **and TNF-α**.[95,96] Granules of some species contain major mediators of allergic disease including leukotriene C4, IL-4, and IL-13; these are preformed and are released in large quantities on activation. Mammalian mast cells and basophils have granules that contain **granzyme B**, the protease associated with cytoxic lymphocytes.[97,98]

In acute inflammatory lesions, mast cells may appear to be diminished in number because of degranulation and lysis. Those that remain have fewer and less dense granules. With time, injured mast cells can regranulate.

Effects of Mast Cell Degranulation

Degranulation of mast cells, an immediate reaction in tissue injury, leads directly to dilation and disunion of endothelial cells of postcapillary venules (Fig. 9.16). Leakage of plasma is limited to small and medium-sized (20–30 nm) venules rather than the capillary bed

Vet-ebooks.com

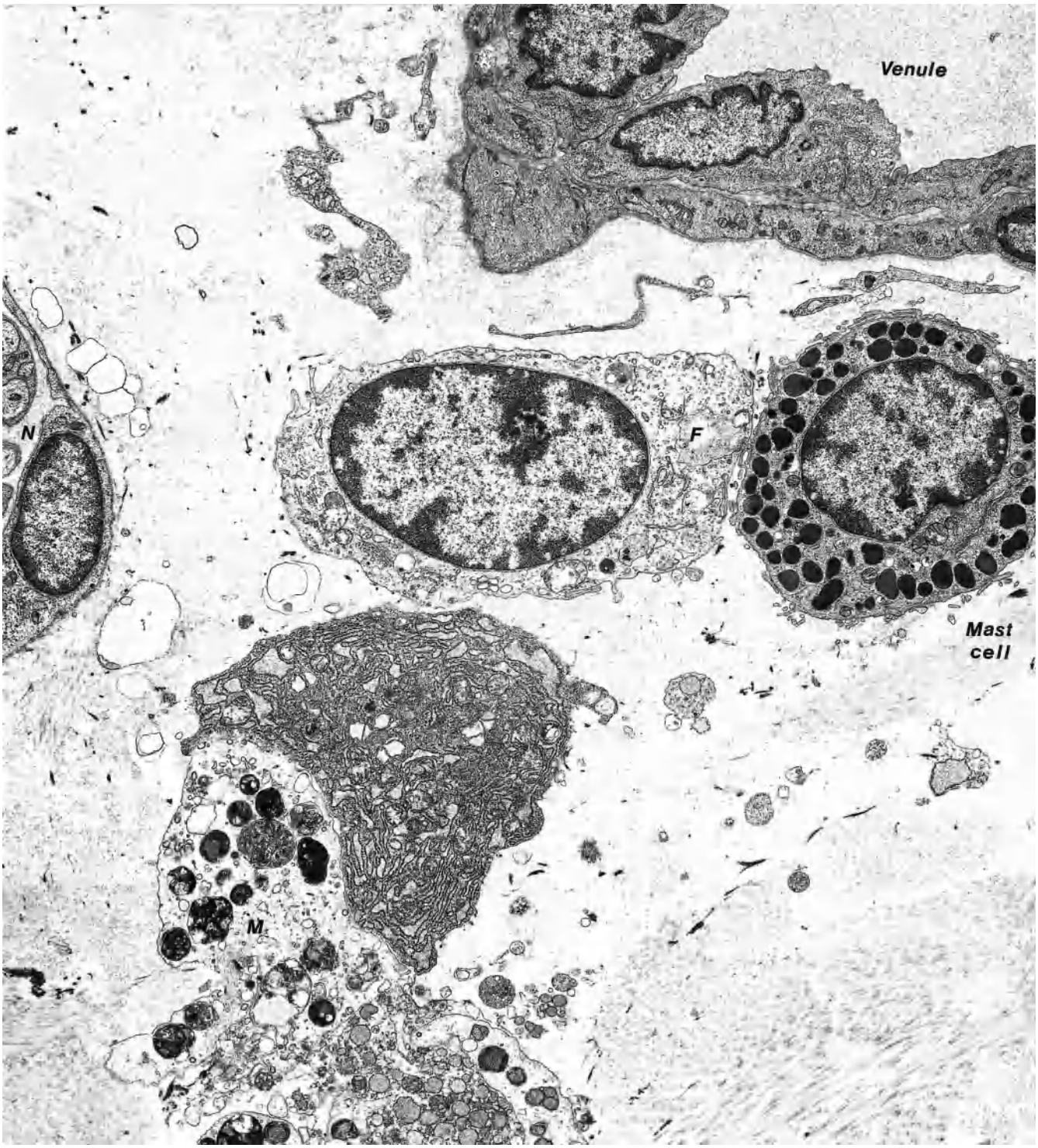


Fig. 9.13 Mast cell in early inflammation: skin, rat, pasteurella toxin. Interstitial edema and inflammatory cells surround postcapillary venule (*top right*); fibroblast (*F*), nerve (*N*), and macrophage (*M*). Small flecks of fibrin occur throughout areas of edema.

proper. Histamine, serotonin, and bradykinin cause intercellular gaps in vascular endothelium, due in part to endothelial cell contraction (Table 9.3). The anticoagulant effect of heparin prevents polymerization of fibrin from the exuding fibrinogen, thereby sustaining exudation. After the initial injury, mast cell degranulation is sustained by products secreted by activated leukocytes, for example, cationic polypeptides from neutrophils, eosinophil peroxidase,[99] and complement components C3a and C5a.

Degranulation involves structural changes in the plasma membrane including development of

Vet-ebooks.com

Fig. 9.14 Mast cell degranulation: inflammation, skin, rat, pasteurella toxin. Granules are mixture of dense and electron-opaque forms (in which proteoglycans are unwinding in preparation for exocytosis). Note secretion pore (*upper left*) and granule fusion (*lower right*).

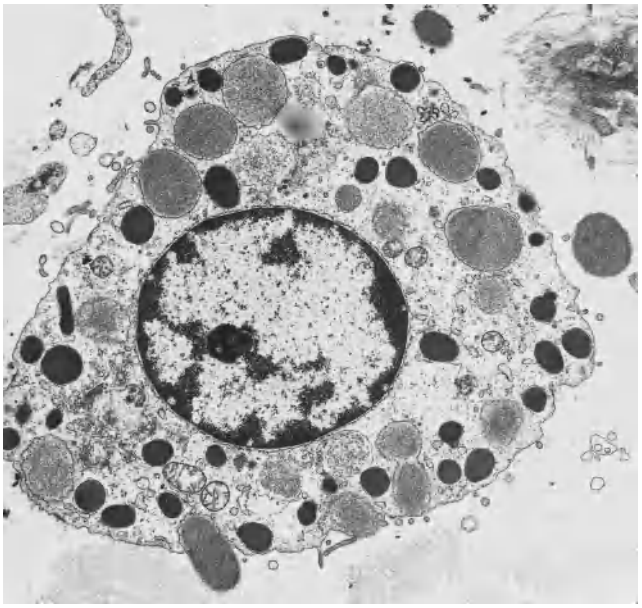


Table 9.3 Mast cells and basophil ultrastructure in tissue lesions.

Tissue lesion	*Change*	*Reference to ultrastructural pathology*
	Normal Structure	
Mast cells and basophils	In review	**Criag**, *Lab Invest* 60:147, 1989; **Galli**, *Prog Allergy* 34:1, 1984; **Yong**, *Pathology* 7:307, 1975
Mast cell granules	Heparin-protein macromolecule	**Serafini-Fracassini**, *J Ultrastruct Res* 28:141, 1969
Mast cell precursors	Rat blood	**Zucker-Franklin**, *Blood* 56:534, 1980; **Zucker-Franklin**, *Blood* 58:544, 1981
Respiratory system	Trachea (human)	**Caulfield**, *J Cell Biol* 85:299, 1980; **Pearsall**, *Am J Anat* 170:83, 1984
Gastrointestinal tract	Perineural mast cells	**Criag**, *Am J Pathol* 124:427, 1986 (human); **Stead**, *Gastroenterology* 97:575, 1989
Urinary tract	Magnesium deficiency	**Cantin**, *Lab Invest* 27:495, 1972
	Inflammation	
Degranulation	Phospholipase A_2-induced	**Chi**, *Lab Invest* 47:579, 1982 (rat)
	IgE-mediated	**Dvorak**, *Lab Invest* 53:45, 1985 (human); **Dvorak**, *Lab Invest* 43:126, 1980 (human basophils)
	Phorbol ester-induced	**Dvorak**, *Am J Pathol* 141:1309, 1992 (human)
	F-met peptide-induced	**Dvorak**, *Lab Invest* 64:234, 1991 (human basophils)
	Anaphylactic	**Dvorak**, *Lab Invest* 46:461, 1982 (guinea pig basophils)
	Peroxidase-induced	**Henderson**, *J Exp Med* 152:265, 1980
	Compound 48/80-induced	**Rohlich**, *J Cell Biol* 51:455, 1971
Regranulation	Human mast cells	**Dvorak**, *Lab Invest* 54:663, 1986
Chemotaxis	Lymphocyte-induced	**Ward**, *J Immunol* 114:1523, 1975 (basophils)
Phagocytosis	*Schistosoma mansoni*	**Caulfield**, *J Parasitol* 67:776, 1981 (rat)
	Particulates	**Padawer**, *Lab Invest* 35:320, 1971
	Bacteria	**Sher**, *Lab Invest* 41:490, 1979 (rat)
Lung	Anaphylactic shock	**Borgers**, *Lab Invest* 37:1, 1977 (guinea pig)
	Secretion (human)	**Caulfield**, *J Cell Biol* 85:299, 1980
	Fibrotic lung disease	**Kawanami**, *Lab Invest* 40:717, 1979
	Abnormal Mast Cells	
Mastocytosis	Cutaneous mastocytosis *(Urticaria pigmentosa)*	**Mirowski**, *Lab Invest* 63:52, 1990; **Naveh**, *Acta Dermatovenerol* 55:443, 1975
	Systemic mastocytosis (human)	**Sauer**, *Z Kinderheilkd* 119:59, 1975; **Weidner**, *Am J Pathol* 140:847, 1992
	Equine cutaneous	**Cheville**, *Vet Pathol* 9:394, 1972
Charcot-Leyden crystals	Human blood	**Dvorak**, *Lab Invest* 60:557, 1989 (human)

Vet-ebooks.com

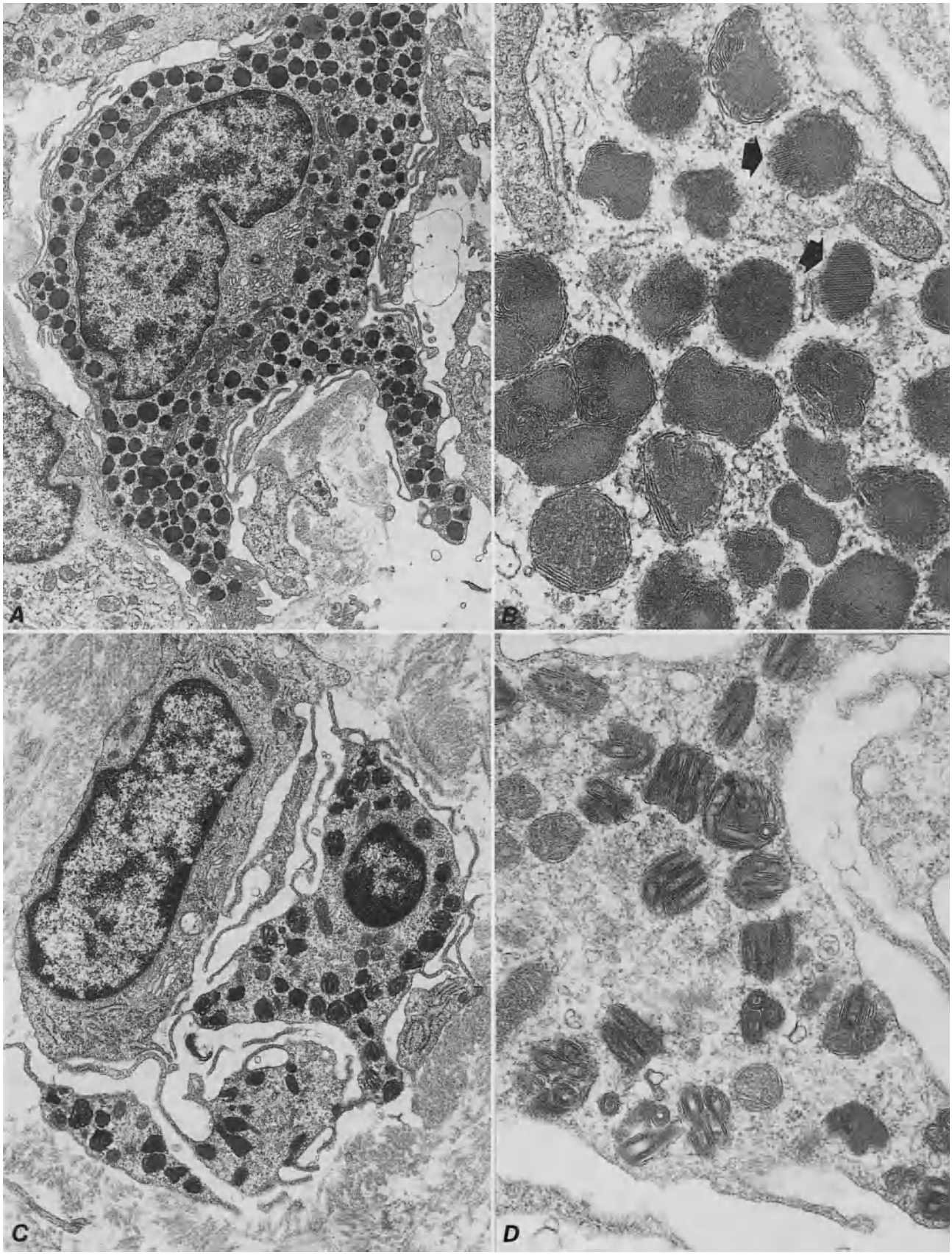


Fig. 9.15 Mast cells in human disease. **A–B**. **Dermatitis**: mast cell morphology. Numerous scroll-poor granules are characteristic of mast cells in dermatitis; laminar arrangements of proteins (*arrows*). **C–D**. **Mastocytosis**: scroll-rich mast cells. **C**. **Mast cells adjacent to monocyte**. **D**. **Scroll-rich granules**. (Micrograph: Noel Weidner, *Am J Pathol* 140:847, 1992.)

Vet-ebooks.com

undulations and filopodia that increase surface area.[100] Actin filaments polymerize in the subcortical cytoplasm, and granules show decreased density due to "unwinding" of heparin-histamine layers. Surfaces of degranulating mast cells become irregular.[101,102]

Immunologic Degranulation

Explosive immunologic degranulation occurs when appropriate antibodies bind to mast cell surfaces and are complexed with specific antigens. Both mast cells and basophils have surface receptors (FcR) that bind the Fc part of IgE with high affinity.[103] Exposure of these FcR bearing cells to the appropriate antigen initiates activation and secretion (Fig. 9.16).

In the rapid degranulation of human allergic disease, granules swell and the granule membrane and plasma membrane join, fuse, and lyse with extrusion of intact granules into the extracellular spaces.[104] Upon exit from the cell, the granule loses its density and becomes pale and granular. In exposive degranulation, granules are joined in a common membrane lined cisterna that opens at the cell surface. In the final stages of degranulation the mast cell is filled with anastomosing cavities (representing coalescing granule membranes), and the plasma membrane is shredded by release of many granules.

Basophils

Basophils originate in bone marrow from a precursor cell. Released into the bloodstream, they migrate to connective tissues where they emigrate through endothelium. In connactive tissue, basophils are distinguished from connective tissue mast cells by their smaller, multilobed nuclei that have denser peripheral chromatin, less numerous and larger granules, and less complex cell surfaces that lack granule-containing dendritic processes. Basophile granules resemble those of mast cells (Fig. 9.17). Charcot-Leyden crystals, typical of eosinophils, have been reported in basophils.[95]

Basophils localize in perivascular sites where degranulation has a maximal effect on vascular permeability (Fig. 9.18). Although mast cells are most important in inflammation, basophils migrating peri-

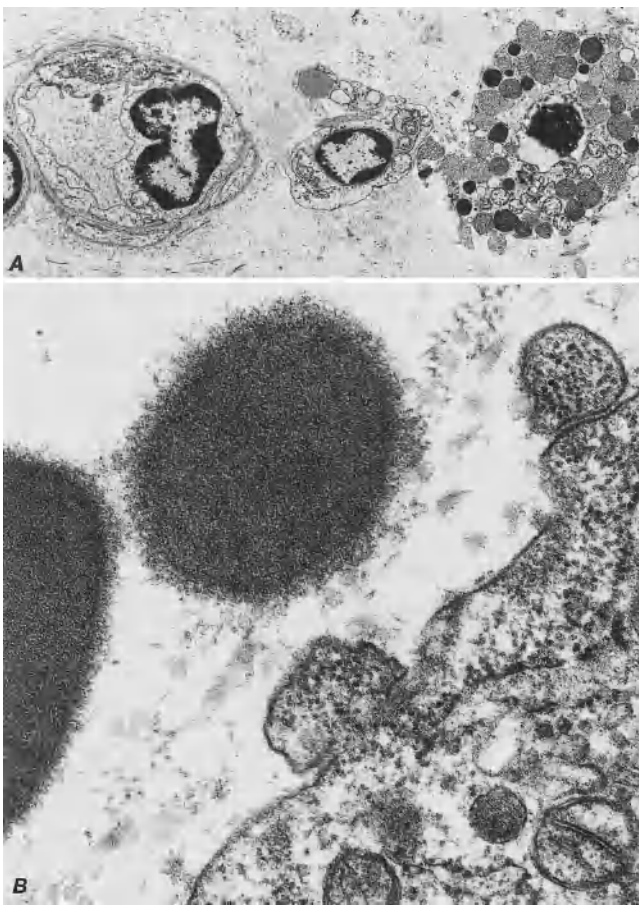


Fig. 9.16 Mast cell degranulation: myocarditis, cow.

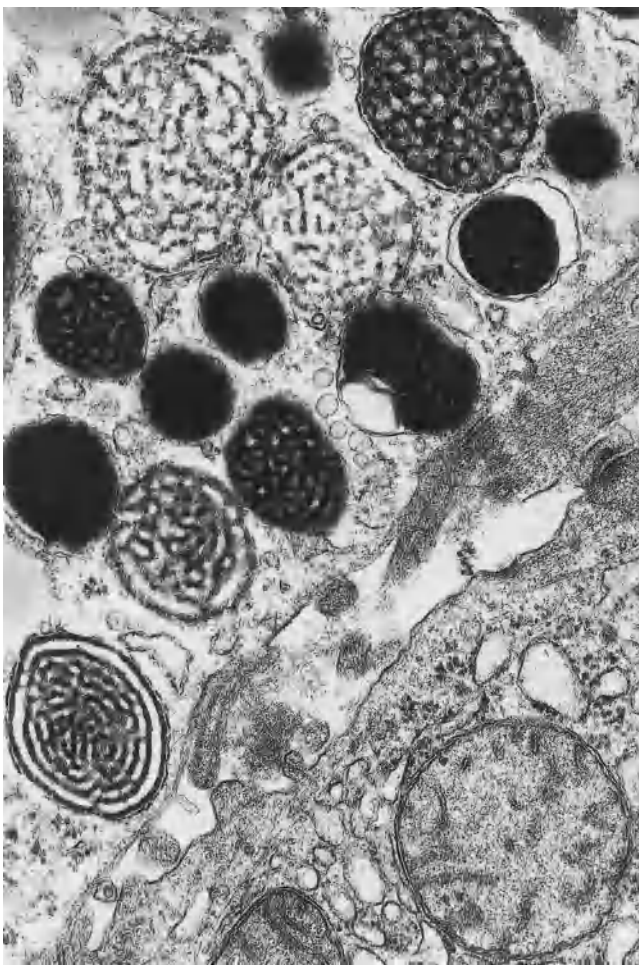


Fig. 9.17 Basophil granules: acute hepatitis, rat.

Vet-ebooks.com

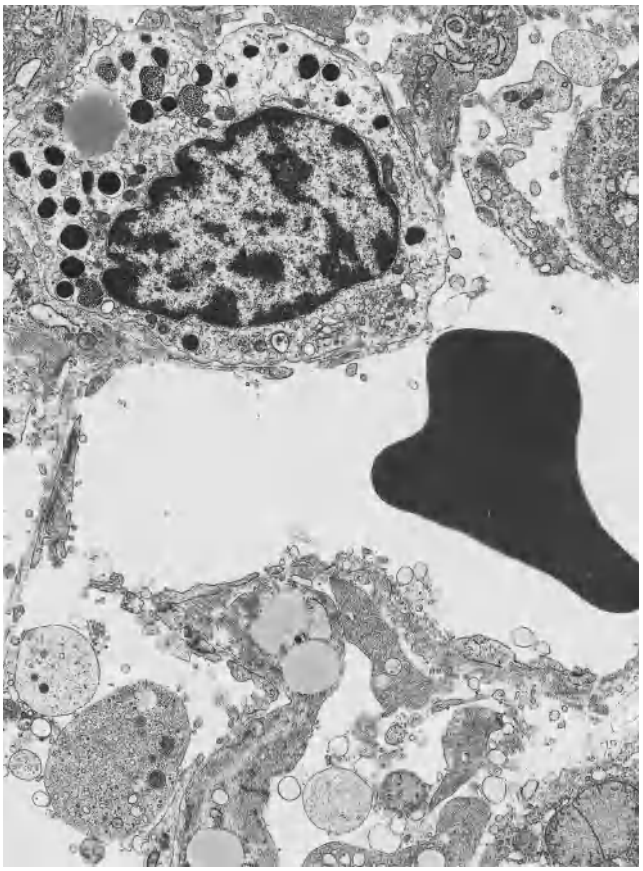


Fig. 9.18 Basophil: lodged in spaces of Disse, liver, acute hepatitis, dog. Hepatic sinusoid is expanded, and sinusoidal endothelium is degenerate and irregular.

vascularly are more important in chronic inflammation. In allergic reactions, IgE-sensitized basophils, when contacted by the appropriate antigen, release potent vasoactive materials; for example, platelet-activating factor has a unique spectrum of effects including smooth muscle contraction, chemotaxis, and increased capillary permeability.

Degranulation of basophils occurs directly when individual mast cell granules fuse with the plasma membrane and granule contents are extruded through pores in the membrane that are open to the exterior.[101] After marked stimulus, degranulation may be explosive. Individual granules are moved into large **degranulation vacuoles** in the cytoplasm. These vacuoles move to the cell surface and exocytotically release multiple granules. As studied ultrastructurally in human basophils stimulated by F-Met peptides, the intense forms of degranulation are characterized by large pale vacuoles that lack granules but have tiny membranous vesicles and remnants of granule matrix.

Basophils are often a component of chronic lesions arising from immune reactions, and they are attracted by lymphocyte secretions.[94] Having surface receptors of the complement fragment C3, they are phagocytic.



Fig. 9.19 Cutaneous mastocytosis: horse. Granules of mast cells are of various densities. Note filopodia on plasma membranes; degranulate eosinophil (*lower right*).

C3 receptors underlie the ability of basophils and mast cells to adhere to parasites that have become coated with complement.[91]

Granule release reactions in vitro are reported to involve two major pathways: **anaphylactic degranulation**, which involves extrusion of membrane-free granules through plasma membrane pores, and **piecemeal degranulation**, which is characterized by partially to completely empty, nonfused granules. Basophils in the latter group do not have a decreased number of granules and have large number of cytoplasmic vesicles.[95]

Cutaneous and Systemic Mastocyosis

Human mastocytosis occurs in two forms: **cutaneous mastocytosis** (urticaria pigmentosa), characterized by foci of mast cells and maculopapular eruptions related to release of histamine, serotonin and heparin; and **systemic mastocytosis**, a rare generalized variant in which mast cell aggregates develop in lymph nodes, bone marrow, spleen, and liver. In cutaneous mastocytosis, lesions range from bandlike infiltrates of the papillary dermis to large nodular aggregates extending throughout the dermis and subcutaneous fat. Mast cells, which may be heavily granulated or relatively nongranular, have irregular shapes, granules in various stages of maturity, and long interdigitating surface villi. Eosinophils occur among the mast cells and edema may be pominant.[105,106]

In generalized **equine cutaneous mastocytosis**, cutaneous nodules of mast cells grow progressively and then regress. Cells have characteristics of both basophils and mast cells (Fig. 9.19), and in regressing

Vet-ebooks.com

lesions, are elongate. Eosinophils progressively infiltrate the lesions but disappear in regressing lesions.[107] The pathobiology of mast cells in limiting tissue growth is unresolved.[108]

Angiogenesis

Angiogenesis is the formation of new blood vessels (like its synonym, **neovascularization**, it is generally not applied to embryonic development). In angiogenesis, endothelial cell mitosis and proliferation are due to direct injury and are most intense in areas lacking epithelium. Angiogenesis follows distinct phases of development (Fig. 9.20).[109,110] Newly formed endothelial cells that develop in angiogenesis are characterized by the typical endothelial markers (such as expression of vWF, CD31, CD105).

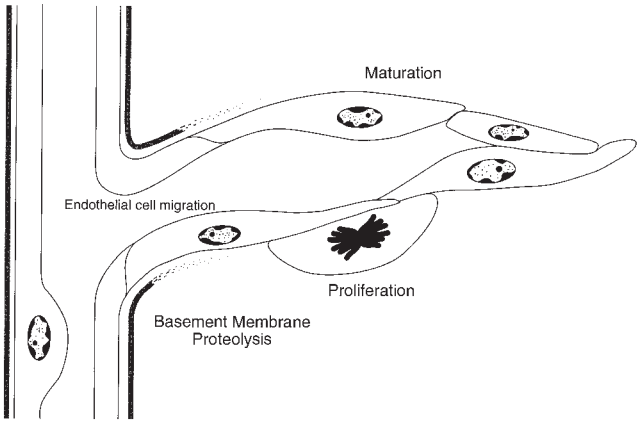


Fig. 9.20 Angiogenesis: granulation tissue. Steps include proteolytic degradation of basement membranes in the parent vessel, migration of endothelial cells toward angiogenic stimuli (VEGF, FGF), endothelial cell mitosis with proliferation behind the leading front of migrating cells, and endothelial cell maturation and remodeling into tubes and mature capillaries.

Two Sources of Angiogenesis

Activated endothelial cells move and migrate by lamellipodial extrusion, a process regulated by actin microfilaments.[111] Endothelial **lamellipodia** (ablumenal endothelial microprocesses) form and project into the interstitium. Membranes of lamellipodia contain and preferentially express glycoproteins that are important endothelial cell markers, for example, the antigen CD34.[112]

Angiogenesis from Surviving Blood Vessels

At the surviving borders of injured tissue, remodeling of vasculature is initiated by viable endothelial cells that remain. As endothelial cell sprouts arise from surviving capillaries, secretions digest the surrounding basement membrane and the extracellular matrix to facilitate invasion and migration into the site of injury. The advancing endothelial cell sprout must invade and migrate through the clot matrix of the wound (Fig. 9.20). The new vascular sprouts and syncytia fuse and canalize, and gradually establish a network of patent capillaries.[113–115]

Angiogenesis from Bone Marrow Stem Cells

Angiogenesis in mature animals can also invoke recruitment of **endothelial progenitor cells** in bone marrow that are directed, through surface receptors, to the needy sites of angiogenesis in healing tissue.[116] In embryonic development, the progenitor hemangioblast gives rise to hematopoietic stem cells and to angioblasts. During **fetal vasculogenesis**, endothelial progenitor cells in bone marrow give rise to angioblasts that move into and through the primordial vascular system to peripheral sites where they mature into endothelial cells of the arteries, veins and lymphatics. Angioblasts are pluripotential and can mature to pericytes and myocytes that surround these blood vessels.

Pathogenesis of Angiogenesis

Vascular endothelial growth factors (VEGF) and **angiopoietins** have the dominant effects on angiogenesis, even though many other peptides and growth factors have angiogenic activity. In cutaneous wound healing, the initial angiogenic stimulus is supplied by **fibroblast growth factor** (FGF) and is followed by the subsequent and more prolonged angiogenic stimulus provided by VEGF. VEGF is secreted by many mesenchymal cells and homes to **VEGF receptors** (*flk-1* and *flt-1*) that are found only on endothelial cells. **FGF** binds to heparin and is released by heparin (and its precursors), that is, endothelial mitogen is sequestered in basement membrane and released on injury.[117,118]

Tissue Hypoxia Stimulates Angiogenesis

In addition to cytokines, other physiologic stimulants to vascular growth include hypoxia, products from injured tissue, blood pressure differentials, and changes in the connective tissue stroma. The combination of these stimuli causes vascular syncytia (cords of cells) to form, to rapidly differentiate, and to form channels for blood flow. **Hypoxia** stimulates endothelial expression of **integrin αVβ3**. Multifunctional in angiogenesis, integrin αVβ3 binds to and regulates VEGF-R

Vet-ebooks.com

(receptor) and facilitates receptor-ligand bindings of fibronectin, thrombospondin, and osteopontin. The **VEGF/VEGF-R** system, induced by hypoxia, leads to growth of new blood vessels and is a mechanism to increase the oxygenation of hypoxic tissue.[119]

Extracellular Regulators of Angiogenesis

The mesenchymal stroma regulates angiogenesis by enhancing endothelial growth and maturation. **Angiopoietins** (Ang1 and Ang2) bind to an endothelial receptor Tie2 forming complexes that either stabilize (promoting maturity) or loosen (prolonging maturity) the vascular wall.[120–122]

- **Ang1** binds to endothelial cell receptor Tie2 to recruit pericyte and smooth muscle progenitors causing maturation of the new blood vessel.
- **Ang2** also binds to Tie2 but has the opposing effect, blocking its activity by disconnecting endothelial cells making them unable to form new blood vessels.

Angiopoietins regulate angiogensis by working through complex interactions at cell surfaces, activating the semiphorin family of transmembrane glycosylphosphatidylinositial(GPI)-anchored proteins.

Chemoattractants for Endothelial Cells

In support of angiogenesis, certain genes in endothelial cells are expressed to produce protein domains that are chemoattractants to other endothelial cells. For example, **epidermal growth factor-like domain 7 (EGLF7)** is a endothelial cell chemoattractant that is up-regulated in vascular injury and angiogenesis to recruit new endothelial cells.[123] EGLF7 is protective for endothelium against hypoxia and hypoxia-induced mitochondrial apoptosis.

Ancillary Growth Factors in Angiogenesis

Other growth factors help stabilize the developing blood vessels within the connective tissue matrix. **Platelet derived growth factor** (PDGF) recruits smooth muscle cells and **TGF-β** enhances production of glycoproteins of the extracellular matrix. Proteins that also influence the directed migration and motility of angiogenesis are the following:

- **Integrins** αVβ3 and αVβ5 are heavily expressed on activated endothelial cell surfaces and have a broad range and can attach to receptor sites on fibronectin, vitronectin, and other components of the clot matrix.
- **Heparin** (from mast cells) stimulates capillary endothelial proliferation.
- **Thrombospondin 1**, **tenascin C**, and other matricellular proteins degrade cell-matrix connections.
- **Matrix degrading proteases** (plasminogen activators, metalloproteinases) release FGF-2 and VEGF; endothelial cells shed matrix metalloproteinases in vesicles for focal proteolytic activity that precedes invasion.[124]
- **CD44** (cell surface receptor for hyaluronan) stabilizes developing endothelial tubular networks.[125]

Coagulation Factors and Platelets Regulate Healing

Fibrin provides a scaffold for vascularization. In the healing wound, new endothelial buds move into the wounded tissue along strands of fibrin. Fibrin is absorbed during vascular ingrowth but persists beyond the disappearance of neutrophils and is not entirely removed until vascular invasion is accomplished. Newly formed endothelial cells contain an activator of plasminogen and are fibrinolytic. Removal of fibrin polymers is necessary as capillary buds migrate into the wound. In this phase of healing, both fibroplasia and vascularization can be retarded by some nutritional deficits or severe systemic disease.

Platelet-derived growth factor (PDGF) is a mitogenic peptide secreted by platelets trapped at sites of thrombus formation. It stimulates angiogenesis and proliferation of fibroblasts and smooth muscle cells. **Platelet-activating factor (PAF)** is a potent phophatidylcholine autocoid whose activity occurs through a specific receptor, a member of the G-protein-coupled receptor superfamily, that activates several signaling pathways of angiogenesis. PAF influences capillary permeability by increasing VE-cadherin tyrosine phosphorylation in endothelial cells. In acute pancreatitis, elevated PAF levels develop in the pancreas, and PAF receptors are localized to microvascular endothelial cells.

Maturation of Angiogenesis

Matrix ligation, the connection of endothelial cells to underlying fibronectin, vitronectin, tenascin, and osteopontin, is essential for angiogenesis to be completed. Growth factors that suppress the expression of integrins αVβ3 and αVβ5 induce apoptosis and suppress angiogenesis.

Terminating Angiogenesis

As angiogenesis is completed, proteases are critical for remodeling of connective tissue, and cause release

Vet-ebooks.com

of **endostatin**, a fragment of collagen that inhibits angiogenesis.

Angiogenesis in Repair of Inflammation

Focal injury to endothelial surfaces leads to the following sequence of events: (1) plateletes adhere to the sites of injury and pavement of the exposed intima (but do not form thrombi), (2) this temporary "false" endothelium forms from modified smooth muscle cells, which are like endothelial cells in that platelets do not adhere to them, and (3) a continuous layer of true endothelial cells forms within 2 months.[126] Reendothelialization is approximately 6 times faster in axial directions of the blood vessels than in the circumferential direction.[127]

As endothelium regenerates, new endothelial cells are characterized by having tight junctions and gap junctions with increased widths.[128,129] Regenerating endothelium is started and stopped in defined times. In the model of liver regeneration in rats, new vascular buds form in portal areas and rapidly invade the hepatic parenchyma. Microfilaments (stress fibers) increase and the plasma membrane has increased cholesterol.

Vascular endothelium heals rapidly after injury. Experimental injury denuded areas can be totally repopulated with new endothelial cells within a few hours. Endothelial cells undergo mitosis in response to several growth factors that are associated with tissue regeneration.[130] When wounds become covered with epithelial surfaces, endothelial mitotic activity decreases.

References

1. Simionescu M, Antohe F. 2006. Functional ultrastructure of the vascular endothelium. *Handb Exp Pharmacol* 176 (Pt 1):1.
2. Tjwa M, et al. 2007. GAS6 promotes inflammation by enhancing interactions between endothelial cells, platelets and leukocytes. *Blood* 111:4096.
3. Gottlieb AI, et al. 1991. Structure and function of the endothelial cytoskeleton. *Lab Invest* 65:123.
4. White GE, Fujiwara K. 1986. Expression and intracellular distribution of stress fibers in aortic endothelium. *J Cell Biol* 103:63.
5. Gratton MP, et al. 2004. Caveolae and caveolins in the cardiovascular system. *Circ Res* 94:1408.
6. Pietra GG, et al. 1988. Inhibition of adsorptive endocytosis and transcytosis in pulmonary microvessels. *Lab Invest* 59:683.
7. Simionescu N, et al. 1983. Rings of membrane sterols surround the openings of vesicles and fenestrae, in capillary endothelium. *J Cell Biol* 97:1592.
8. Ghitescu L, et al. 1986. Specific binding sites for albumin restricted to plasmalemmal vesicles of continuous capillary endothelium: Receptor-mediated transcytosis. *J Cell Biol* 102:1304.
9. Simionescu N, et al. 1978. Structural basis of permeability in sequential segments of the microvasculature of the diaphragm. *Microvasc Res* 15:1.
10. DeBryn PP, et al. 1985. In-vivo endocytosis by bristle-coated pits and intracellular transport of endogenous albumin in the endothelium of the sinuses of liver and bone marrow. *Cell Tiss Res* 240:1.
11. Ghitescu L, Bendayan M. 1992. Transendothelial transport of serum albumin: A quantitative immunocytochemical study. *J Cell Biol* 117:745.
12. Frokjaer-Jensen J. 1980. Three-dimensional organization of plasmalemmal vesicles in endothelial cells. *J Ultrastruct Res* 73:9.
13. Feng D, et al. 2002. Ultrastructural studies define soluble macromolecular, particulate, and cellular transendothelial cell pathways in venules, lymphatic vessels, and tumor-associated microvessels in man and animals. *Microsc Res Tech* 57:289.
14. Geoffroy JS, Becker RP. 1984. Endocytosis by endothelial phagocytes. *J Ultrastruct Res* 89:223.
15. De Bruyn PPH, et al. 1975. Endocytosis, transfer tubules, and lysosomal activity in myeloid sinusoidal endothelium. *J Ultrastruct Res* 53:133.
16. Piccin A, et al. 2007. Circulating microparticles. *Blood Rev* 21:157.
17. Bundgaard M. 1984. The three-dimensional organization of tight junctions in a capillary endothelium revealed by serial-section electron microscopy. *J Ultrastruct Res* 88:1.
18. Bystrevskaya VB, et al. 1992. Centriole modification in human aortic endothelial cells. *J Struct Biol* 109:1.
19. Schwartz SM, et al. 1975. The aortic intima. *Am J Pathol* 81:15.
20. Spagnoli LG, et al. 1982. Morphometric analysis of gap junctions in regenerating arterial endothelium. *Lab Invest* 46:139.
21. Huang A-L, et al. 1992. Role of intercellular junctions in the passage of horseradish peroxidase across aortic endothelium. *Lab Invest* 67:201.
22. Gabbiani G, et al. 1974. Acute cadmium intoxication. *Lab Invest* 30:686.
23. Scheiermann C, et al. 2007. Expression and function of junctional adhesion molecule-C in myelinated peripheral nerves. *Science* 318:1472.
24. Hart TK, Pino RM. 1988. Pseudoislet vascularization. Induction of diaphragm-fenestrated endothelia from the hepatic sinusoid. *Lab Invest* 54:304.
25. Walsh LJ, et al. 1991. MS-1 sinusoidal endothelial antigen is expressed by factor XIIIa$^+$, HLA-DR$^+$ dermal perivascular dendritic cells. *Lab Invest* 65:732.
26. Jaffe EA, et al. 1976. Synthesis of basement membrane collagen by cultured human endothelial cells. *J Exp Med* 144:209.
27. Pietra GG, et al. 1983. Transcapillary movement of cationized ferritin in the isolated perfused rat lung. *Lab Invest* 49:54.

Vet-ebooks.com

28. Erdreich-Epstein A, et al. 2005. Endothelial apoptosis induced by inhibition of integrins αVβ3 and αVβ5 involves ceramide metabolic pathways. *Blood* 105: 4353.
29. Robison WG Jr et al. 1983. Retinal capillaries: Basement membrane thickening by galactosemia prevented with aldose reductase inhibitor. *Science* 222:1177.
30. Schlingemann RO, et al. 1990. Leukocyte antigen CD34 is expressed by a subset of cultured endothelial cells and on endothelial abluminal microprocesses in the tumor stroma. *Lab Invest* 62:690.
31. Sims DE. 1986. The pericyte—a review. *Tissue Cell* 18:153.
32. Fujimoto T, Singer SS. 1986. Immunocytochemical studies of endothelial cells in vivo. *J Cell Biol* 103:2775.
33. Ghitescu L, Fixman A. 1984. Surface charge distribution on the endothelial cell of liver sinusoids. *J Cell Biol* 99:639.
34. Simionescu M, et al. 1985. Differentiated microdomains of the luminal plasmalemma of murine muscle capillaries: Segmented variations in young and old animals. *J Cell Biol* 100:1396.
35. Simionescu M, Simionescu N. 1986. Functions of the endothelial cell surface. *Ann Rev Physiol* 48:279.
36. Horvat R, et al. 1986. Endothelial cell membranes contain podocalyxin—the major sialoprotein of visceral glomerular epithelial cells. *J Cell Biol* 102:484.
37. Goerge T, et al. 2002. Secretion pores in human endothelial cells during acute hypoxia. *J Memb Biol* 187:203.
38. de Agostini AI, et al. 1990. Localization of anticoagulantly active heparan sulfate proteoglycans in vascular endothelium. *J Cell Biol* 111:1293.
39. Geiger M. 2008. Soluble protein C receptor. *Blood* 111:3301.
40. Becker CG, Harpel PC. 1976. α_2-macroglobulin on human vascular endothelium. *J Exp Med* 144:1.
41. Wagner DD, et al. 1991. Induction of specific storage organelles by von Willebrand factor propolypeptide. *Cell* 64:403.
42. Gerbraine-Younes J, et al. 1991. Heterogeneous distribution of Weibel-Palade bodies and von Willebrand factor along the porcine vascular tree. *Am J Pathol* 139:1471.
43. Warhol MJ, Sweet JM. 1984. The ultrastructural localization of von Willebrand factor in endothelial cells. *Am J Pathol* 117:310.
44. Morel O, et al. 2006. Procoagulant microparticles. *Arterioscler Thromb Vasc Biol* 26:2594.
45. Meyrick B, Reid L. 1980. Endothelial and subintimal changes in rat hilar pulmonary artery during recovery from hypoxia: A quantitative ultrastructural study. *Lab Invest* 42:603.
46. Rabinovitch M, et al. 1986. Pulmonary artery endothelial abnormalities in patients with congenital heart defects and pulmonary hypertension. *Lab Invest* 55:632.
47. Kim HP, et al. 2004. Caveolae compartmentalization of heme oxygenase-1 in endothelial cells. *FASEB J* 18:1080.
48. Quintero M, et al. 2006. Mitochondria as signaling organelles in the vascular endothelium. *Proc Natl Acad Sci USA* 103:5379.
49. Korzonek-Szlacheta I, et al. 2007. Effects of endothelin-1 on prevention of microvascular endothelium injuries in hemorrhagic shock in rats. *Pharmacol Rep* 59:98.
50. Barnes K, et al. 1998. Endothelin-converting enzyme: Ultrastructural localization and its recycling form the cell surface. *Hypertension* 31:3.
51. Nolan S, et al. 2008. Nitric oxide regulates neutrophil migration through microparticle formation. *Am J Pathol* 172:265.
52. Laliberte F, et al. 1987. Cellular and subcellular immunohistochemical localization of angiotensin-converting enzyme in the rat adrenal gland. *Lab Invest* 56:364.
53. Movat HZ, Fernando NVP. 1963. Acute inflammation. The earliest fine structural changes at the blood tissue barrier. *Lab Invest* 12:895.
54. Cotran RS. 1987. New roles for the endothelium in inflammation and immunity. *Am J Pathol* 129:407.
55. Humphrey DM, et al. 1984. Morphologic basis of increased vascular permeability induced by acetyl glyceryl ether phosphorylcholine. *Lab Invest* 50:16.
56. Cotran RS. 1967. Delayed and prolonged vascular leakage in inflammation. *Exp Molec Pathol* 6:143.
57. Cross AH, Raine CS. 1991. Central nervous system endothelial cell-polymorphonuclear cell interactions during autoimmune demyelination. *Am J Pathol* 139:1401.
58. Atkins E, et al. 1964. Endogenous pyrogen release from rabbit blood cells incubated in vitro with parainfluenza virus. *Science* 146:1469.
59. Rolfe BE, et al. 2005. Rho and vascular disease. *Atherosclerosis* 183:1.
60. Reidy MA, et al. 1989. Injury induces increase of von Willebrand factor in rat endothelial cells. *Am J Pathol* 134:857.
61. Lasky LA, et al. 1992. An endothelial ligand for L-selectin is a novel mucin-like molecule. *Cell* 69:927.
62. Boogaerts MA, et al. 1982. Enhancement of granulocyte-endothelial cell adherence and granulocyte-induced cytotoxicity by platelet release products. *Proc Nat Acad Sci USA* 79:7019.
63. Pober JS, et al. 1983. Ia expression by vascular endothelium is inducible by activated T cells and by human γ interferon. *J Exp Med* 157:1339.
64. Pober JS. 1988. Cytokine-mediated activation of vascular endothelium. *Am J Pathol* 133:426.
65. Pober JS, Cotran RS. 1990. Cytokines and endothelial biology. *Physiol Rev* 70:427.
66. Munro JM, et al. 1989. Tumor necrosis factor and interferon-v induce distinct patterns of endothelial activation and associated leukocyte accumulation in skin of *Papio anubis*. *Am J Pathol* 135:121.
67. Bradley JR, et al. 1995. Disparate localization of 55-kd and 75-kd tumor necrosis factor receptors in human endothelial cells. *Am J Pathol* 146:27.
68. Schleef RR, et al. 1991. Immunoelectron microscopic localization of type 1 plasminogen activator inhibitor on the surface of activated endothelial cells. *J Cell Biol* 113:1413.

Vet-ebooks.com

69. Movat HZ, et al. 1989. Acute inflammation and a Shwartzman-like reaction induced by interleukin-1 and tumor necrosis factor. *Am J Pathol* 129:463.
70. Hirata K, et al. 1980. Effect of endotoxin on rat liver. *Lab Invest* 43:165.
71. Kang Y-H, Williams R. 1991. Endotoxin-induced endothelial injury and subendothelial accumulation of fibronectin in rat aorta. *Anat Rec* 229:86.
72. Meyrick B, Reid L. 1980. Ultrastructural findings in lung biopsy material from children with congenital heart defects. *Am J Pathol* 101:527.
73. Nagato N, et al. 1991. Anatomic pathology of pulmonary fluid leakage in endotoxemia. *Am J Pathol* 138:183.
74. Hammerschmidt DE, et al. 1981. Complement-induced aggregation in vivo. *Am J Pathol* 102:146.
75. Forbes RDC, Guttmann LD. 1982. Evidence for complement-induced endothelial injury in vivo. *Am J Pathol* 106:378.
76. Shaw JO, et al. 1980. Lung inflammation induced by complement-derived chemotactic fragments in the alveolus. *Lab Invest* 42:547.
77. Leak LV. 1983. Interaction of mesothelium to intraperitoneal stimulation. *Lab Invest* 48:479.
78. Tsilibary EC, Wissig SL. 1987. Light and electron microscope observations of the lymphatic drainage units of the peritoneal cavity of rodents. *Am J Anat* 180:195.
79. Casley-Smith JR. 1964. An electron microscope study of injured and abnormally permeable lymphatics. *Ann N Y Acad Sci* 116:810.
80. Leak LV, Kato F. 1972. Electron microscopic studies of lymphatic capillaries during inflammation. *Lab Invest* 26:572.
81. Schmid-Schoenbein GW. 1990. Microlymphatics and lymph flow. *Physiol Rev* 70:987.
82. Dietrich T, et al. 2007. Inhibition of inflammatory lymphangiogenesis by integrin α5 blockade. *Am J Pathol* 170:361.
83. Albertine KH, et al. 1980. Lymphatic endothelial cell inclusion bodies. *J Ultrastruct Res* 73:199.
84. Ewart A, Folse D. 1984. Lymphatic filariasis. *Am J Pathol* 115:135.
85. DeLeve LD, et al. 2004. Rat liver sinusoidal endothelial cell phenotype is maintained by paracrine and autocrine regulation. *Am J Physiol Gastrointest Liver Physiol* 287:G757.
86. Oldfors A, Sourander P. 1978. Barriers of peripheral nerve towards exogenous peroxidase in normal and protein deprived rats. *Acta Neuropathol* 43:129.
87. Essner E. 1987. Role of vesicular transport in breakdown of the blood-retinal barrier. *Lab Invest* 56:457.
88. Stead RH, et al. 1989. Mast cells are closely apposed to nerves in the human gastrointestinal mucosa. *Gastroenterology* 97:575.
89. Friend DS, et al. 1996. Mast cells that reside at different locations in the jejunuem of mice infected with *Trichinella spiralis* exhibit sequential changes in the granule ultrastructure and chymase pheotype. *J Cell Biol* 135:279.
90. Heikkilä HM, et al. 2007. Activated mast cells induce endothelial cell apoptosis by a combined action of chymase and tumor necrosis factor-α. *Arterioscler Thromb Vasc Biol* 28:309.
91. Caulfield JP, et al. 1981. Light and electron microscopic appearance of rat peritoneal mast cells adhering to shistosomula of *Schistosoma mansoni* by means of complement or antibody. *J Parasit* 67:776.
92. Craig SS, et al. 1993. Ultrastructural localization of heparin to human mast cells of the MC_{TC} and MC_{T} types by labeling with antithrombin III-gold. *Lab Invest* 69:552.
93. Oliani SM, et al. 1997. Immunocytochemical localization of heparin in secretory granules of rat peritoneal mast cells using a monoclonal anti-heparin antibody (ST-1). *J Hist Cyt* 45:231.
94. Camussi G, et al. 1981. Release of platelet-activating factor in human pathology. I. Evidence for the occurrence of basophil degranulation and release of platelet-activating factor in systemic lupus erythematosus. *Lab Invest* 44:241.
95. Dvorak AM. 2005. Immunogold ultrastructural techniques identify subcellular sites of chymase, Charcot-Leyden crystal protein, and histamine in basophils and mast cells. *Chem Immunol Allergy* 85:89.
96. Belloni AS, et al. 2006. Identification and localization of adrenomedullin-storing cardiac mast cells. *Int J Mol Med* 17:708.
97. Tschopp CM, et al. 2006. Granzyme B, a novel mediator of allergic inflammation. *Blood* 108:2290.
98. Strik MC, et al. 2007. Human mast cells produce and release the cytotoxic lymphocyte-associated protease granzyme B upon activation. *Mol Immunol* 44:3462.
99. Henderson WR, et al. 1980. Eosinophil peroxidase-induced mast cell secretion. *J Exp Med* 152:265.
100. Kops SK, et al. 1984. Mast cell activation and vascular alterations in immediate hypersensitivity-like reactions induced by a T cell-derived antigen binding factor. *Lab Invest* 50:421.
101. Hastie R, et al. 1977. The antigen-induced degranulation of basophil leukocytes from atopic subjects studied by electron microscopy. *Lab Invest* 36:173.
102. Ko L, Lagunoff D. 1976. Depletion of mast cell ATP inhibits complement-dependent cytotoxic histamine release. *Exp Cell Res* 100:313.
103. Nishigaki T. 1988. Mast cell degranulation and its inhibition by an antiallergic agent tranilast. *Virch Arch B* 55:311.
104. Dvorak AM, et al. 1985. Immunoglobulin E-mediated degranulation of isolated human lung mast cells. *Lab Invest* 53:45.
105. Mirowski G, et al. 1990. Characterization of cellular dermal infiltrates in human cutaneous mastocytosis. *Lab Invest* 63:52.
106. Weidner N, et al. 1992. Mast-cell phenotype in indolent forms of mastocytosis. *Am J Pathol* 140:847.
107. Cheville NF, et al. 1972. Generalized equine cutaneous mastocytosis. *Vet Pathol* 9:394.
108. Metz M, et al. 2007. Mast cells in the promotion and limitation of chronic inflammation. *Immunol Rev* 217:304.

Vet-ebooks.com

109. McCracken JS, et al. 1979. Morphologic observations on experimental corneal vascularization in the rat. *Lab Invest* 41:519.
110. Jost M, et al. 2007. Tumoral and choroidal vascularization. *Am J Pathol* 171:1369.
111. Wong MKK, Gotleib AI. 1984. In vitro reendothelialization of a single cell wound. *Lab Invest* 51:75.
112. Schlingemann RO, et al. 1990. Expression of the high molecular weight melanoma-associated antigen by pericytes during angiogenesis in tumors and healing wound. *Am J Pathol* 136:1393.
113. Stan RV. 2007. Endothelial stomatal and fenestral diaphragms in normal vessels and angiogenesis. *J Cell Mol Med* 11:621.
114. Hill JM, et al. 2003. Circulating endothelial progenitor cells, vascular function and cardiovascular risk. *New Engl J Med* 348:593.
115. Kubo H, Alitalo K. 2003. The bloody fate of endothelial stem cells. *Genes Dev* 17:322.
116. Sholley MM, et al. 1984. Mechanisms of neovascularization. Vascular sprouting can occur without proliferation of endothelial cells. *Lab Invest* 51:624.
117. Folkman J, et al. 1988. A heparin-binding angiogenic protein-basic fibroblast growth factor is stored within basement membranes. *Am J Pathol* 130:393.
118. Wakai S. 1988. Two- and three-dimensional ultrastructural observation of two cell angiogenesis in human granulation tissue. *Virch Arch* 56:127.
119. Ferrara N, et al. 2003. The biology of VEGF and its receptors. *Nat Med* 9:669.
120. Wakui S, et al. 2006. Localization of Ang-1, -2, Tie-2, and VEGF expression at endothelial-pericyte interdigitation in rat angiogenesis. *Lab Invest* 86:1172.
121. Tammela T, et al. 2005. Angiopoietin-1 promotes lymphatic sprouting and hyperplasia. *Blood* 105:4642.
122. Thurston G, et al. 1999. Leakage-resistant blood vessels in mice transgenically overexpressing angiopoietin-1. *Science* 286:2511.
123. Campagnolo L, et al. 2005. EGFL7 is a chemoattractant for endothelial cells and is up-regulated in angiogenesis and arterial injury. *Am J Pathol* 167:275.
124. Taraboletti G, et al. 2002. Shedding of the matrix metalloproteinases MMP-2, MMP-9, and MT1-MMP as membrane vesicle-associated components by endothelial cells. *Am J Pathol* 160:673.
125. Cao G, et al. 2006. Involvement of endothelial CD44 during in vivo angiogenesis. *Am J Pathol* 169:325.
126. Schwartz SM, et al. 1978. Endothelial regeneration. *Lab Invest* 38:568.
127. Haudenschild CC, Schwartz SM. 1979. Endothelial regeneration. II. Restitution of endothelial continuity. *Lab Invest* 41:407.
128. Reidy MA, et al. 1983. Endothelial regeneration. V. Inhibition of endothelial regrowth in arteries of rat and rabbit. *Lab Invest* 49:569.
129. Reidy MA. 1988. Endothelial regeneration. VIII: Interaction of smooth muscle cells with endothelial regrowth. *Lab Invest* 59:36.
130. Ausprunk DH, et al. 1975. Vascularization of normal and neoplastic tissue grafted to the chick chorioallantois. *Am J Pathol* 79:597.

Vet-ebooks.com

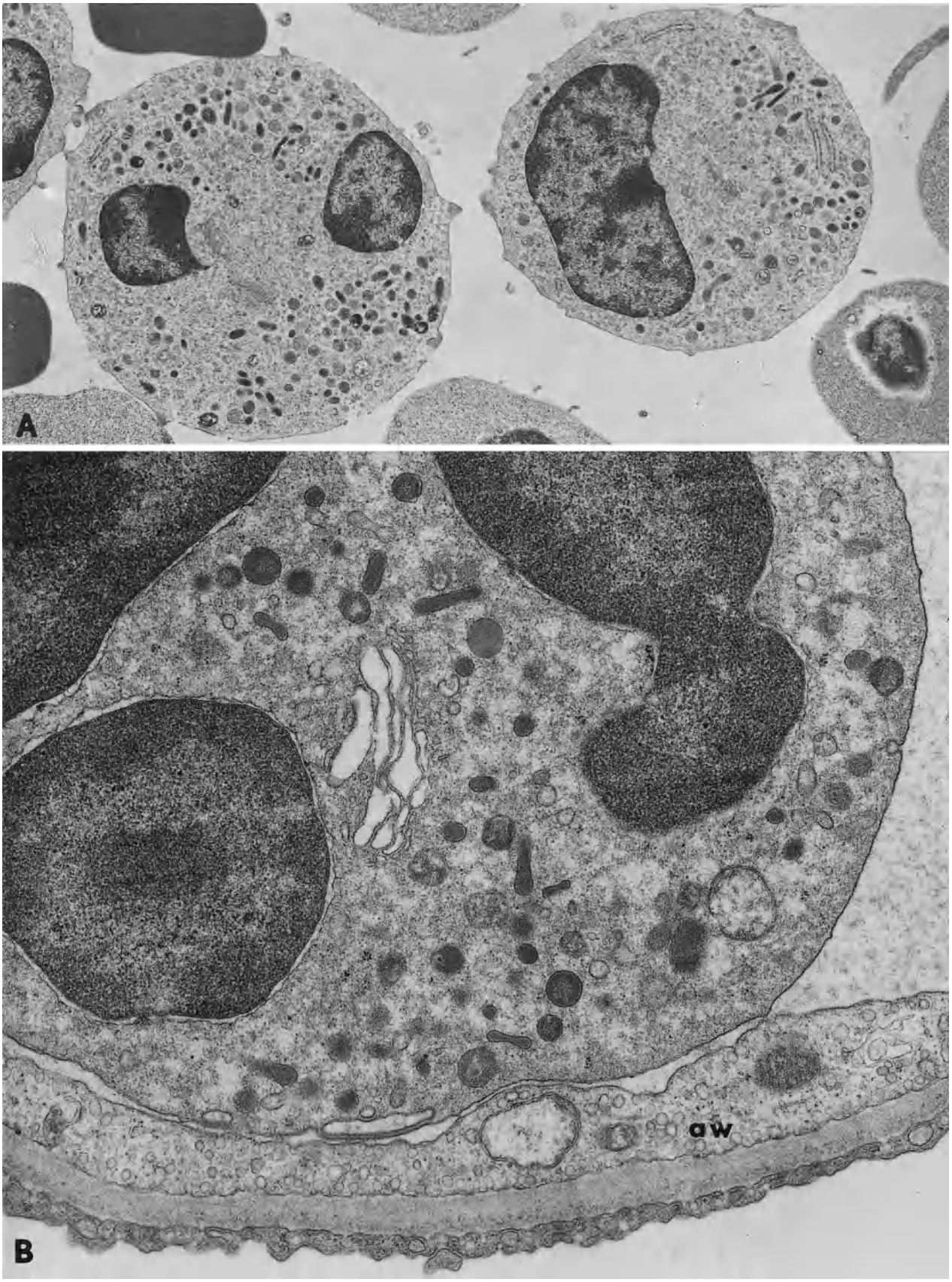


Fig. 10.1 Immature neutrophil: leukocytes, dog. **A. Bone marrow**: granules are peripheral and large Golgi complexes are central; cell at right is more immature—note large nucleus. **B. Pulmonary capillary**: pneumonic lung; alveolar wall (*aw*) at bottom; neutrophil adjacent to capillary endothelial cell.

© 2009 Wiley-Blackwell. ISBN: 978-0-813-80330-2

Vet-ebooks.com

10 Leukocytes and Platelets

The Neutrophil

Neutrophils are aggressively phagocytic cells, the first line of defense against invading microorganisms. They are capable of rapid ameboid movement, intense phagocytic activity, and production of potent lysosomal granules that digest particulate material. Neutrophils have the ability to degranulate and spew enzyme-laden granules into tissue at local sites of inflammation. Although highly mobile, they lack stability and cannot withstand the low pH and high temperature of severe inflammatory lesions. They are terminally differentiated, and have low levels of gene expression and short life spans.[1] Gene expression profiling has shown that circulating neutrophils have two major bursts of transcriptional activity; the first occurs in the bone marrow, where the innate defense armory is packaged into different granule subsets, and the second during emigration through the vascular wall, during which cytokines and chemokines are spewed into the perivascular spaces.

Neutrophil Granules

Primary Granules

Azurophil granules (primary granules) are lysosomes that appear early in the development of the neutrophil. They are fewer, larger, and denser than secondary granules (Fig. 10.1), and are identified by their staining for myeloperoxidase.[2,3] In human neutrophils, azurophil granules contain lysosomal enzymes (including acid phosphatase and β-glucuronidase), lysozyme, and myeloperoxidase, a neutrophil peroxidase that functions at pH optima in the acid range (Table 10.1). About one-third of human azurophil granules contain the proteolytic enzyme elastase.[4,5] The major inhibitor of elastase in serum is **α_1-antitrypsin,** a molecule synthesized primarily in the liver but also in the neutrophil primary granule (the enzyme and its inhibitor reside in the same granule).[6] **Granulophysin (CD63)** is a lysosomal protein present in many cell types and is an activation marker in neutrophils; it is found in azurophil granules.[7]

Azurophil granules also contain antimicrobial proteins. **Defensins**, which account for about 30% of the total protein in human azurophil granules, are small cationic, disulfide cross-linked proteins that cause lethal damage to plasma membranes of microorganisms.[8] Bacterial cells are killed only when metabolically active since defensins appear to form voltage-dependent channels in the lipid bilayer. For example, human **defensin alpha-1** destroys *Trypanosoma cruzi* by inducing membrane pore formation in its flagellar and plasma membranes; ultrastructural changes in the trypanosome include blebbing, cytoplasmic vacuolation, and induction of nuclear and mitochondrial DNA fragmentation.[9]

In humans and most mammals, there is structural heterogeneity in the two major granules types; for example, a subpopulation of myeloperoxidase-staining microgranules are different from other primary granules.[10] Peroxidase activity varies with some endocrine functions;[11] activity in neutrophils of the human uterus occurs and disappears with phases of the reproductive cycle.[12] Primary granules have also been subdivided into two classes on the basis of presence or absence of a fibrillar or crystalline core in their matrix.

Vet-ebooks.com

Table 10.1 Neutrophil granule contents.

Category	*Identity*	*Function*	*Reference to ultrastructural pathology*
		Azurophil (primary) Granules	
Acid phosphatase	APtase	Lysosomal enzyme	**Farquhar**, *J Cell Biol* 54:141,1972
α_1-antitrypsin	**α_1AT**	Inhibits elastase*	
Defensins	α–1 (human)		**Rice**, *Blood* 70:757, 1987
Elastase	Neutral elastase	Degrades elastin*	**Damiano**, *Am J Pathol* 131:235, 1988
Granulophysin	CD63	Inserts as pore-forming channel into membranes	**Cham**, *Am J Pathol* 144:1369, 1994
Lysosomal enzymes	Acid phosphatase	Lysosomal enzyme	**Farquar**, *J Cell Biol* 54:141, 1972 (rabbit)
	β-glucuronidase	Lysosomal enzyme	**Farquar**, *J Cell Biol* 54:141, 1972 (rabbit)
Lysozyme	Lysozyme	Degrades proteins	**Mutasa**, *Cell Tissue Res* 258:111, 1989
Myeloperoxidase§	MPO	Multiple	**Cramer**, *Blood* 65:423, 1985 (human); **Parmley**, *Blood* 70:1630, 1987 (human); **Takizawa**, *J Hist Cyt* 48:481, 2000
	Peroxidase	Oxidation	**Bentfield**, *Anat Rec* 187:219, 1977
Phosphodiesterase	PDE4A	Down-regulates cAMP signaling at plasma membrane	**Pryzwansky**, *Cell Tissue Res* 312:301, 2003
Plasminogen activator	PA urokinase type	Activates plasminogen	**Pedersen**, *J Ultrastr Pathol* 24:175, 2000
Presenilin	PS1	Co-localizes with myeloperoxidase and CD63	**Mirinics**, *Blood Cells Mol Dis* 28:28, 2002
Sialyl Lewis X	sLe(x)	Adhesive ligand for selectins; moves to PM on activation	**Suzuki**, *J Electron Microsc (Tokyo)* 49:359, 2000
		Specific (secondary) Granules	
Alkaline phosphatase	AP	Plasma membrane marker	**Pellmé**, *J Immunol Meth* 325:88, 2007
Collagenase	Collagenase	Degrades collagen	**Lazarus**, *Am J Pathol* 68:565, 1972
Elastase	Elastase	Degrades elastin	**Janoff**, *Am J Pathol* 68:579, 1972
Fibronectin	FN	Adhesions to ECM	**Salcedo**, *Exp Cell Res* 233:25, 1997
Peptidoglycan recognition protein (PGRP)	Bovine PGRP protein S	Secreted; binds and kills bacteria	**Tydell**, *J Immunol* 176:1154, 2006
	Human PGRP protein S	Co-localizes and is synergistic with lysozyme	**Cho**, *Blood* 106:2551, 2005
	Fish PGRP	Secreted; binds and kills bacteria	**Chang**, *Mol Immunol* 44:3005, 2007
Lactoferrin§	Lactoferrin	Iron transport	**Cramer**, *Blood* 65:423, 1985
Lysozyme	Lysozyme	Degrades protein	**Fröhlich**, *J Cutan Pathol* 20:54, 1993
		Tertiary Granules	
Gelatinase§	Matrix metalloproteinases	Degrades extracellular matrix	**Sawicki**, *Thromb Haemost* 80:836, 1998
	MMP-9	Degrades extracellular matrix	**Khandoga**, *J Leukoc Biol* 79:1295, 2006
NRAMP	NRAMP1#	Recruited to phagosome on activation	**Canonne-Hergaux**, *Blood* 100:268, 2002 (human)

*The major inhibitor of elastase in serum is **α_1-antitrypsin**, a molecule synthesized primarily in the liver but also in the neutrophil primary granule (the enzyme and its inhibitor reside in the same granule); about one-third of human azurophil granules contain elastase.
NRAMP1: natural resistance-associated macrophage protein 1 controls innate resistance to infection by moving from endosomes to phagosomes during activation (or to bacteriophorous or parasitophorous vacuoles).
§ Considered an experimental marker for this granule type.

Vet-ebooks.com

Secondary Granules

Specific granules (secondary granules) are peroxidase-negative dense granules that contain alkaline phosphatase, cationic proteins, lactoferrin, and most of the leukocyte's lysozyme. Specific granules do not contain acid phosphatase or other acid hydrolases and are, by definition, not lysosomes. Specific granules contain proteolytic enzymes that act on collagen, elastin, and some lipases that are lacking in macrophages. Specific granules contain **peptidoglycan recognition proteins (PGRPs)** that recognize peptidoglycan, a ubiquitous component of bacterial cell walls (Table 10.1).[13,14] PGRP-S is best known, but PGRPs L (liver), Iα, and Iβ have been reported for humans. PGRPs are highly conserved in evolution, and are present in invertebrates including insects.

Tertiary Granules

Gelatinase granules are small, peroxidase-negative granules.

NRAMP1 is recruited from tertiary granules (which are gelatinase) to the phagosomal membrane.[15] Mutations in NRAMP1 cause increased susceptibility to infection with intracellular pathogens.

Other Granule Types

A tubulovesicular compartment involved in exocytosis of substances contained in cytoplasmic granules has been demonstrated in human neutrophils using alkaline phosphatase as a marker. This canaliculus-like system consists of short tubules and long tubulosaccular structures that were shown to transport alkaline phosphatase to the surface when neutrophils are activated. Short rod-shaped organelles in the resting neutrophils, these organelles rapidly elongate and develop nodose cisternae after stimulation.[16]

Other populations of neutrophil granules have been reported in human and other species. **Bovine neutrophils,** which lack lysozyme and have a large capacity for oxygen-independent bacterial killing, have a third type of granules that are larger, denser, and more numerous, and which discharge by true secretion.[17,18]

Neutrophil Activation

Neutrophil activation is an early response in inflammation. It is also a response in chronic systemic disease such as septicemia, uremia, and neoplastic disease.[19] In these scenarios, neutrophils respond to stimuli from cytokines or soluble factors from bacteria (such as bacterial endotoxin) by developing oxidative burst activity, initiating exocytosis of granules, and increasing surface adhesion molecules (especially for adhesion-promoting receptors such as selectins and integrins).[20] Interactions of these molecules lead to chemotaxis, phagocytosis, and diapedesis.

Within the plasma membrane, activation of endogenous phospholipases initiates signaling cascades; for example, phopholipases liberate arachidonate, which is metabolized in neutrophils to **leukotriene B_4** via the 5-lipoxygenase pathway. Hydrolysis of other phospholipids yields **platelet-activating factor.** These pathways result in plasma membrane ruffling followed by polarization of cells and formation of broad agranular lamellipodia.[21]

Neutrophil Migration

In blood flowing through arterioles and capillaries of foci of acute inflammation, circulating neutrophils leave the flow in the middle of vessels and move to the periphery. In the normal bloodstream of arterioles, blood cells are concentrated in the central **axial zone** as opposed to the peripheral cell-free **plasmatic zone.** With slowing and stasis of blood, neutrophils marginate, attach to endothelial cells, and begin to emigrate through the vascular wall. Increased stickiness of the neutrophil is associated with increased amounts of glycoproteins secreted onto the cell surface during chemotactic stimulation.[22] Endothelium, activated by bacterial products and potent cytokines released from both neutrophils and monocytes, also changes the nature of its glycocalyx. At the site where the neutrophil sticks to the endothelium, actin polymerizes to interact with membrane proteins that stabilize attachment (Fig. 10.2).

Chemotaxis

Chemotaxis is the reaction by which the direction of locomotion of cells is determined by a substance in the environment (**chemokinesis** is the reaction by which the speed or frequency of locomotion of cells moving at random is determined).

Chemotactic signals generated at the neutrophil surface are transmitted to the **cytoskeleton,** where actin is critical for the movement of chemotaxis. Inherited disorders of dysfunctional actin are manifest by decreased neutrophil motility.[23] Overexpression of the actin-binding protein **lymphocyte-specific protein 1** (which, despite its name, is found on all hematopoietic cells) is associated with a rare disorder neutrophil motility called **neutrophil actin dysfuncton,** which arises from defective actin polymerization; hairlike F-actin-rich projections have been found on surfaces of affected cells.[24]

Vet-ebooks.com



Fig. 10.2 Neutrophil-endothelial cell contact: acute inflammation, dog. Cytoskeletal reformation: granular material at point of contact of neutrophil with endothelium (*arrows*) is polymerized actin.

Chemotactic factors react with receptor proteins on the cell surface, causing metabolic activation and ion fluxes. This leads to focal swellings, seen as ruffling and swelling of the advancing edge of the neutrophil. Depolymerization of actin filaments pushes cell contents into the "relaxed" swollen submembrane areas by continued contraction in the unswollen areas.[25] The rapid increase in intracellular calcium that accompanies chemotactic factor stimulation results from both displacement of calcium from cytoplasmic stores and increased plasma membrane permeability. The increased cytosolic calcium has a direct role in stimulating actin contraction.

Neutrophils respond to and move toward many chemoattractants. Fragments cleaved from normal plasma proteins or tissue proteins in foci of injury are strong, direct chemoattractants for neutrophils: **complement fragments** (C5a), **fibrinopeptides,** and **collagenolytic products.**[26] Inflammatory cells release strong chemoattractants including **leukotriene B4, IL-8, platelet activating factor,** and other chemoattractant peptides. **Platelet factor 4,** a potent heparin-binding protein released from α-granules when platelets adhere at sites of vascular injury, is also a strong chemoattractant.[27] **Transforming growth factor-β** has also been shown to recruit neutrophils into tissues.[28] The synthetic tetrapeptide N-formyl-methionyl-leucyl-phenylalanine (F-Met-Leu-Phe) is used experimentally to induce chemotaxis in vitro.[29,30]

Complement and Neutrophil Chemotaxis Complement plays a dominant role in chemotaxis and mediates activities caused by most microorganisms.[31,32] Initiation of the complement cascade, with attendant

Vet-ebooks.com

liberation of chemotactically active fragments C3 and C5, will strongly attract neutrophils. Enzymes capable of producing complement fragments include bacterial proteases, plasmin, trypsin, thrombin, and other tissue proteases. The complement system is especially potent for microbes. During infection, chemotaxis is markedly accelerated when complement adsorbs to microbial surfaces, a reaction most efficiently activated via the classic pathway by antibody. Complement is highly effective because it liberates its fragments into tissue fluids and because the mature neutrophil has specific surface glycoprotein **receptors** for the remnant C4b-C3b complex (which are called immune adherence receptors) that cause the migrating neutrophil to attach to the complement-coated microbe. Distribution and endocytosis of C3b receptors into coated pits on human neutrophils and monocytes have been shown by electron microscopy.[33]

Cytokines and Neutrophil Chemotaxis Cytokines such as **interleukin-1 (IL-1)** and **tumor necrosis factor (TNF)** that are released by antigen-stimulated macrophages modulate neutrophil movement. Neutrophil surfaces have IL-1 receptors, and the binding of IL-1 augments the effects of chemotactic peptides and other neutrophil activators. Activated neutrophils, although terminally differentiated with limited capacity for protein synthesis, can release a variety of cytokines in small amounts, for example, TNF, IL-1, IL-6, IL-8, G-CSF, M-CSF and IFN-α. Production of these cytokines at sites of inflammation plays a significant role in the evolution of acute inflammation and in directing healing and repair.

Activated neutrophils synthesize and release cytokines of the TNF family, including **B-lymphocyte stimulator** (BLyS) and **TNF-related apoptosis-inducing ligand** (TRAIL/APO2 ligand), a molecule that exerts selective apoptosis on tumor and virus-infected cells, and immunoregulatory functions on activated T lymphocytes.[34]

Leukotrienes Synthesis of leukotrienes from substrate arachidonic acid is initiated by 5-lipoxygenase in concert with 5-lipoxygenase-activating protein (FLAP). The capacity to generate large amounts of leukotrienes from arachidonate is largely confined to leukocytes.[35] Some nonleukocytes, although they lack sufficient 5-lipoxygenase and FLAP to synthesize appreciable amounts of leukotriene, cells that express LTA_4-metabolizing enzymes can take up leukocyte-derived LTA_4 and metabolize it into bioactive leukotrienes, a process called transcellular biosynthesis.

Binding to Endothelium

Specific receptors on neutrophils initiate and control responses of neutrophils in inflammation (Fig. 10.3). The classes of receptor molecules include those designed for adherence, chemotaxis, and phagocytosis of microbes.

- **Chemoattractant receptors** bind molecules such as complement C5a, formylmethionyl leucyl phenylalanine (fMLP), and LTB4; they are coupled to phosphoinositide hydrolysis, which leads to an increase in cytosolic free calcium and activation of protein kinase C, a signal cascade essential for triggering locomotion and secretion.[36,37]
- **Phagocytic receptors** are those for Fc components of antibodies and complement receptors for C3b (CR1) and C3bi (CR3). After CR1 binds its appropriate ligand it clusters on the neutrophil surface and is internalized in large flat vacuoles.[38]
- **Kininogen receptors** on the neutrophil surface interact with the plasma kinin system; kinins are vasoactive molecules, and facilitate neutrophil diapedesis and transudation of plasma during acute inflammation. Kininogen receptors bind plasma kallikrein (which drives kinin formation). Clusters of kininogen molecules have been demonstrated on the surfaces of human neutrophils by immunogold techniques.[39]
- **Annexin 1** exerts antimigratory actions in inflammation (annexins are Ca^{++} and phospholipid-binding proteins that function in membrane traffic); annexin A5 is a powerful anthithrombotic molecule.[40,41]
- **Galectins** and other β-galactoside-binding proteins are expressed by endothelium and inhibit neutrophil rolling and extravasation.[42]
- **Dectin 1** is a β-glucan receptor that originates in azurophile granules; it is also a major receptor on macrophages and is critical in fungal infections.[43]

Diapedesis

Diapedesis is the process by which neutrophils emigrate through vascular walls. As a prelude to diapedesis, neutrophils bind focally to endothelial cells, which become activated. Activated endothelial cells send villous projections into the lumen to stablize the neutrophil as it sticks to and penetrates the vessel wall (Fig. 10.4).[44] Neutrophils exert contractile stresses in the uropod, the rear of the cell (in contrast to the strongly adherent, slow moving fibroblasts in which the leading edge pulls the cell forward).[45] During diapedesis, the neutrophil moves directly through intact endothelium without its disruption, chiefly by way of expansion of intercellular junctions. As neutrophils migrate across endothelium they enhance the capillary permeability and hyperemia begun by histamine, probably by releasing prostaglandins and leukotrienes, into the vascular wall.[46,47]

Vet-ebooks.com

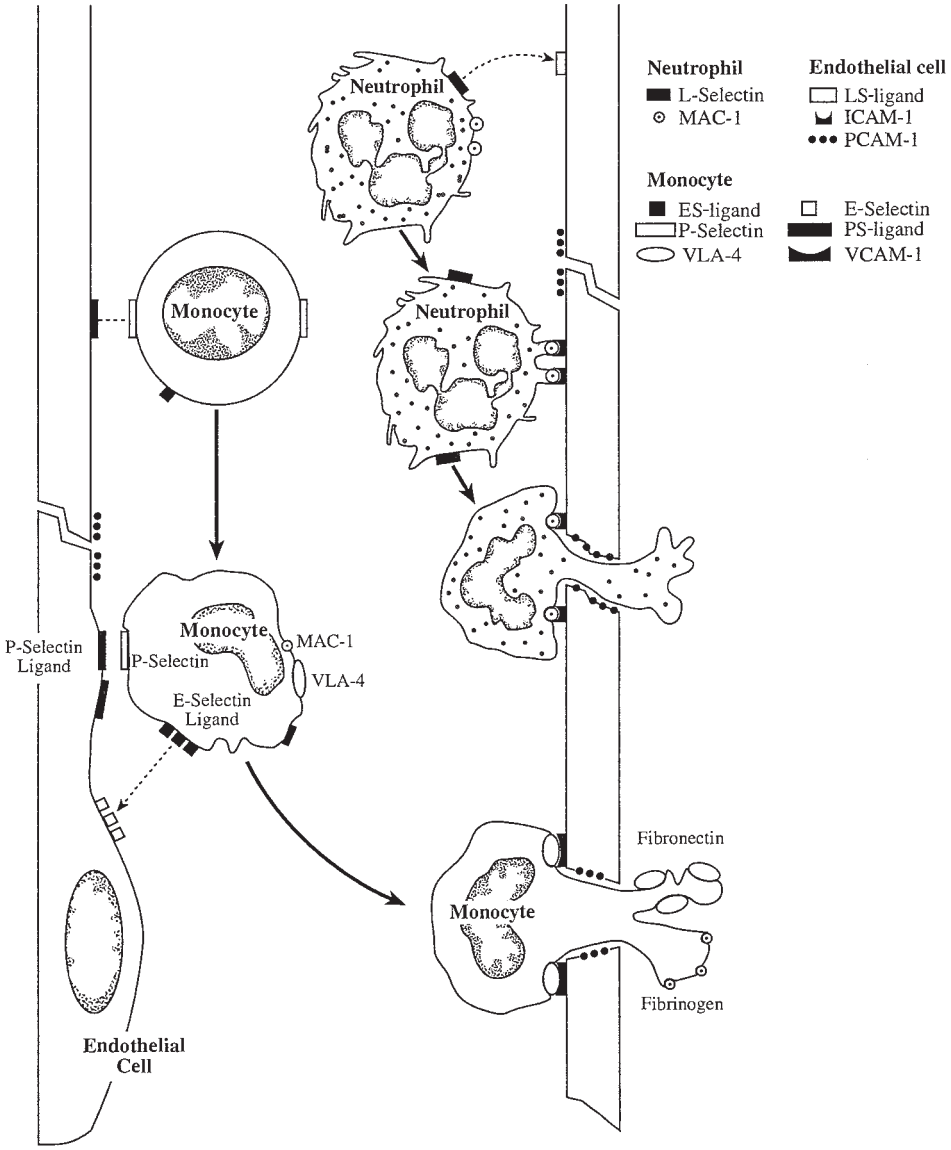


Fig. 10.3 Leukocyte emigration: binding of selectins and integrins, which promote leuykocyte emigration through capillary walls. Inflammatory stimuli to neutrophils initiate expression of **selectins**, which bind to selectin ligand on endothelial surfaces. Transient selectin binding of circulating neutrophils causes them to bounce and roll along endothelial surfaces. Subsequent binding of **integrins** (neutrophil MAC-1 to endothelial cell ICAM-1) causes adherence sufficient for transmigration. As the neutrophil moves through the vascular wall, MAC-1 and other extracellular matrix ligands bind to connective tissue fibronectin, pulling the neutrophil into the interstitial space. Monocytes follow a similar pattern of transient selectin and firm integrin binding to endothelium.

Diapedesis is controlled by specific surface adhesion molecules. **Selectins** that mediate leukocyte-endothelial adhesion and leukocyte emigration from blood vessel to interstitium include:

- **L-selectin,** the leukocyte selectin, enhances neutrophil-endothelial adhesion in early stages of acute inflammation.
- **E-selectin,** the vascular selectin, is induced on endothelial cells by inflammatory stimuli such as TNF and IL1, and facilitates movement of neutrophils, monocytes, and lymphocytes via recognition of sialylated derivatives of the sialo-Lewis X oligosaccharides (SLe^x).
- **P-selectin,** the platelet selection, is in platelet granule membranes and endothelial cells. It is rapidly mobilized to the cell surface after activation and recognizes oligosaccharides on monocytes and neutrophils.

L-selectin, concentrated on the filopodia of activated neutrophils, presents its oligosaccharide ligands to the inducible vascular selectins **E-** and **P-selectin.**[48] L-selectin recognizes carbohydrate determinants on neutrophil **addressin**, an antigen present on high endothelial venules of lymph nodes. The role of L-selectin is clearly different from that of β_2 integrins (CD11a, Cd11b/Cd18), the major integrin adhesion molecules involved in later extravasation of neutrophils. L-selectin and β_2 integrin mediate sequential adhesion events in neutrophil extravasation.

L-selectin (LECAM-1) on neutrophil surfaces binds to inflamed endothelium causing neutrophils to shed L-selectin and engage a second set of adhesion mole-

Vet-ebooks.com



Fig. 10.4 Neutrophil diapedesis: entrapment of circulating neutrophils by lamellipodia (*arrows*) of endothelial cell, postcapillary venule, skin, rat.

cules, the leukocyte β_2 **integrins.** The adhering neutrophil then penetrates the blood vessel wall by moving between interendothlelial junctions and then through the basement membrane into the interstitium. Stimulated endothelial cells actively promote neutrophil migration by synthesizing and releasing the cytokine IL-8, which acts to regulate transvenular traffic in acute inflammation.

As the neutrophil begins to move along tissue surfaces it becomes polarized and elongated with development of a broad **lamellipodium** anteriorly and a thin **uropod** posteriorly. This is associated with reorganization of plasma membrane receptor proteins and with polarization of actin microfilaments that concentrate in the lamellipodium and uropod. Whereas coated pits and vesicles are distributed diffusely in unstimulated neutrophils, they are found largely in the uropods of polarized migrating neutrophils that are responding to a chemotactic stimulus. Granules move to the leading lamellipodium and it is here that degranulation occurs. Neutrophils migrate across epithelium during inflammation. In the intestine, transmigration occurs via interepithelial tight junctions. Transient junction formation between neutrophil and epithelial cell (with cytoskeletal rearrangements at the site of junction) precedes actual migration.[49]

Phagocytosis

In neutrophils, intracellular traffic—including exocytosis, endocytosis, and phagocytosis—is highly efficient.[50,51] As **phagocytosis** begins, particles contact and bind to the surface of the neutrophil. **Binding filaments** develop that attach the particle to the cell surface. Striking surface projections develop and rapidly surround the target particle (Fig. 10.5). An invagination in the plasma membrane, the **phagocytic cup** appears.[52] As the phagocytic cup envelops the particle, a vacuole—the phagosome—is formed. The cytoplasmic matrix underlying the vacuole contains tiny particles of polymerized actin that are used in phagocytosis.

In **accelerated phagocytosis** (mediated by complement fragments, antibodies, bacterial components, and other opsonins), there is an increased affinity of the cell surface for particles. Uptake of bacteria into the neutrophil is mediated through **C3 receptors** embedded in the plasma membrane that tightly bind the complement, which covers the bacterial surface. Long tentacles form at a polar position in the neutrophil and provide increased surface area for phagocytosis.[53–55]

As **phagosomes** form at the cell surface, they become acidified. Embedded in the inner leaflet of the inverting plasma membrane that forms the inner lining of the phagosome are proton pumps and oxidases; they begin immediately to acidify the phagosome and to catalyze formation of superoxide anions and hydrogen peroxide.[56,57] Molecules of NADPH oxidase assemble at the phagosomal membrane and initiate formation of reactive oxygen species.

Phagolysosomes, formed as cytoplasmic granules fuse with the bacteria-containing phagosomes, initiate intracellular digestion. **Specific granules** are immediately reactive, while the lysosomal **azurophil granules** discharge more slowly. The rapid drop in pH that occurs in phagosomes containing bacteria is responsible for the sequential discharge of granules.[58,59] The initial alkaline environment favors specific granule activity, while the later acid pH allows lysosomal enzymes to be more effective.

The **IgG Fc receptor** (FcRIII or CD16), specific for the Fc domain of the immunoglobulin molecule, is on surfaces of neutrophils, and plays a vital role in phagocytosis by binding IgG1 and IgG3 with low affinity. In neutrophils, CD16 is anchored to the plasma membrane through a phosphatidylinositol glycan moiety; in NK cells and macrophages it has a peptide transmembrane anchor. The type of membrane anchor

Vet-ebooks.com

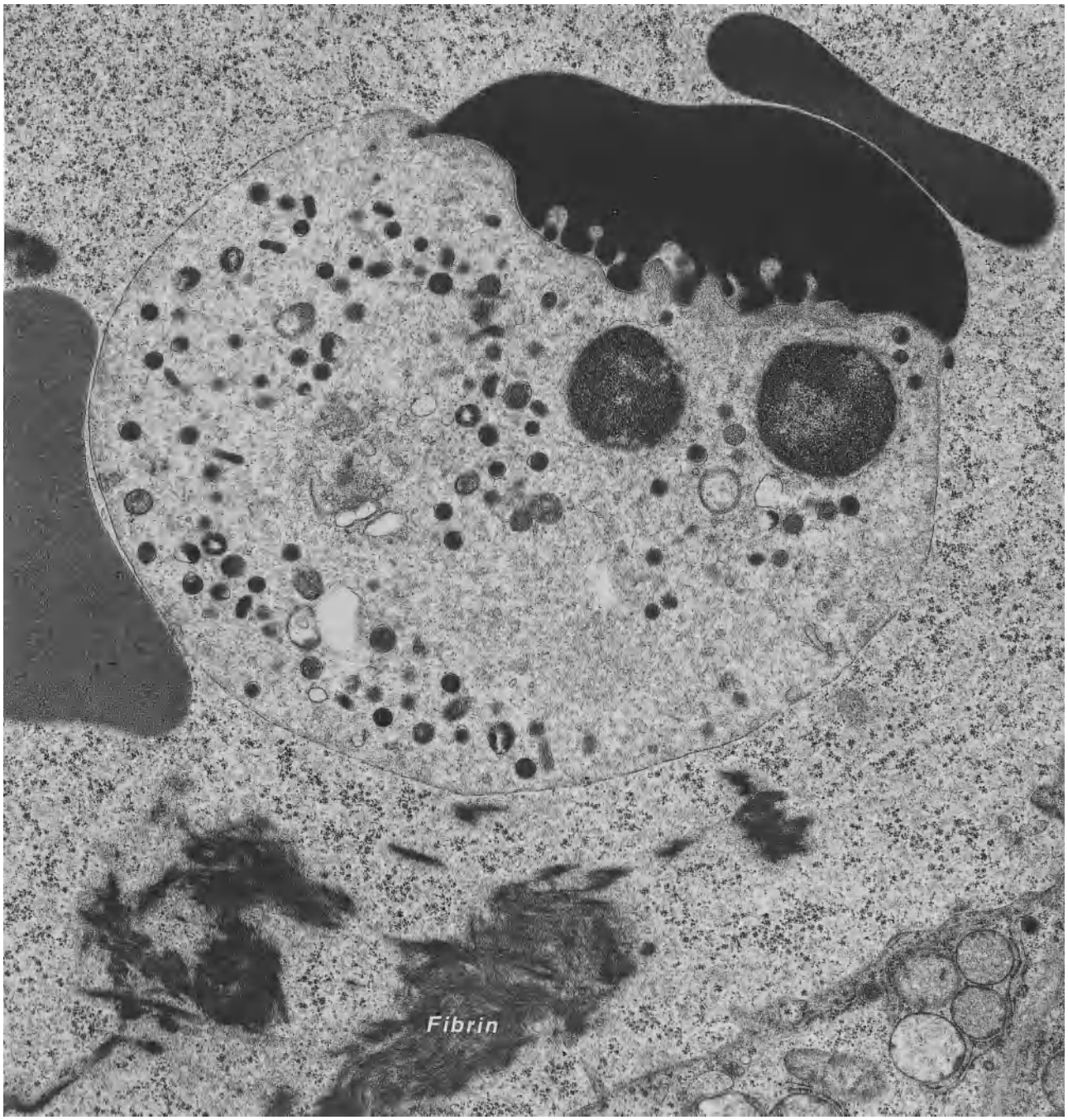


Fig. 10.5 Neutrophil erythrophagocytosis: blood stasis, hepatocellular carcinoma, dog. Marked undulation of the erythrocyte surface in contact with the neutrophil. Neutrophil is partially degranulate.

determines its function as a receptor. NK lymphocyte CD16 can trigger killing, cytokine secretion, and IL-2 receptor expression. Neutrophil CD16 is unable to do so; it functions as a simple binding site of IgG.

Microbial Killing

Neutrophils kill microorganisms by different mechanisms. Some of these mechanisms act independently, but most interact to form complex antibacterial systems. For example, **hydrogen peroxide** is microbicidal in the absence of a catalyst, but only in high concentration. It is most effective in association with neutrophil peroxidase (myeloperoxidase), with which it combines to form an enzyme-substrate complex with strong oxidative capacity. **Superoxide**, **hydroxyl radicals** and **singlet oxygen** are also antibacterial. These systems depend on oxygen for activity. Oxygen-independent microbicidal agents include lysozyme,

Vet-ebooks.com

lactoferrin, phospholipase, and the granule-associated cationic proteins. Chymotrypsin-like cationic proteins of the primary granules are most effective on gram-positive bacteria.

The Respiratory Burst

Contact of neutrophils with stimuli that initiate phagocytosis results in activation of an oxygen-consuming metabolic pathway, which is dormant in the unstimulated cell. The manifestations of this pathway include increased oxygen uptake, glucose consumption by way of the hexose-monophosphate shunt, and production of oxygen-related toxic agents: **superoxide anion (O_2^-), hydroxyl radical (OH·),** and **singlet oxygen (O_2).** This group of events are together the **respiratory burst** a consequence of activation of the particulate enzyme **NADPH oxidase** that catalyzes the reduction of oxygen to superoxide anion. NADPH oxidase is located in the lipid bilayers of membranes with a portion exposed to the cytoplasm, which uses NADPH (produced by the hexose-monophosphate shunt) as a substrate. Reaction between superoxide anions and hydrogen peroxide produces the bactericidal hydroxyl radical.

Superoxide anion (O_2^-), a free radical form of oxygen, is generated in the early autooxidative processes in the **phagosome.**[60] Superoxide has been localized cytochemically in the plasma membrane and phagocytic vacuoles of leukocytes in inflamed tissue.[61] Superoxide dismutase (SOD) protects the cell from superoxide anion toxicity but may also inhibit bactericidal activity. Superoxide anion and hydrogen peroxide accumulate in the phagosome where they interact with bacteria and also generate other oxidants such as OH· and O_2. Within the vacuole they are not interfered with by SOD or catalase, yet these enzymes protect other organelles of the cell from destruction.

Nitric oxide (NO) production is enhanced as the neutrophil is activated. Inflammation-induced extravasation of neutrophils upregulates the transcription and translation of iNOS, which can be detected by immunogold labeling.[62] Low levels of NO produced by constitutive NOS enzymes are anti-inflammatory; higher, sustained levels produced by inducible NOS are proinflammatory. NOS inhibitors (inhibited NO) increase the numbers of neutrophils that migrate toward IL-8.[63]

Calprotectin, a calcium-binding protein that makes up to 40% of the soluble cytoplasmic proteins of the neutrophil, sends signal molecules to other inflammatory cells and chelates Mn^{2+} to inhibit bacteria; Mn^{2+} is an essential component of bacterial superoxide dismutase.[64]

Degranulation

Neutrophils have the capacity to release granules by **exocytosis** in the absence of phagocytotic activity. In human neutrophils, specific and tertiary granules are readily exocytosed upon cell activation, whereas azurophil granules are directed to the phagosome.[65] Exocytosis of neutrophil granules requires calcium and energy, and uses actin microfilaments to move both granule and plasma membrane.

Exocytosis of granules is especially important when the neutrophil is in contact with large particles coated with antibodies or other opsonins. When complement activation is limited and the target particle is very large, lysosomal enzymes and granules are released without altering neutrophil viability.[66] Ultrastructurally, affected neutrophils exhibit transient aggregation of microfilaments, lysosomal fusion, and degranulation.[67,68] After degranulation, the neutrophil appears more dense.

Neutrophil Extracellular Traps After marked stimulation and activation, the massive generation of reactive oxygen species by NADPH oxidase causes neutrophil nuclei to lose their shape and the eu- and heterochromatin to homogenize. As the nuclear envelope and granule membranes disintegrate, mixtures of chromatin and granule proteins are released from the dying cell. Called **neutrophil extracellular traps (NETs),** the aggregates of chromatin and granule proteins bind and kill microorganisms.[69,70] Cell death and development of NETs follow neutrophil activation by the TNFα pathway:

$$\text{TNF}\alpha \rightarrow \text{NADPH oxidase} \rightarrow \text{ROS} \rightarrow \text{apoptosis} \rightarrow \text{NET release}$$

Human patients with chronic granulomatous disease are susceptible to bacterial infections because they carry mutations in genes for NADPH oxidase and cannot activate the NET pathway.

Tissue Injury and Repair

The microbe-killing activities of neutrophils may also damage normal cells. Acute inflammation may damage the hepatocytes in hepatitis, the renal tubular epithelium in nephritis, or alveoli of the lung in pneumonia. Oxygen radicals are especially important in inducing direct injury.[71] **Endothelium** is especially vulnerable in inflammation yet in some way is protected from neutrophil-induced injury.[72] First, neutrophils migrating through endothelium disrupt the monolayer integrity by less damaging oxygen radical-independent mechanisms.[73] Second, neutrophils attached to endothelial cells release less superoxide anion and

Vet-ebooks.com



Fig. 10.6 Degranulate neutrophil: fixed during phagocytosis of fibrin (*F*). Note polar position of neutrophil granules.

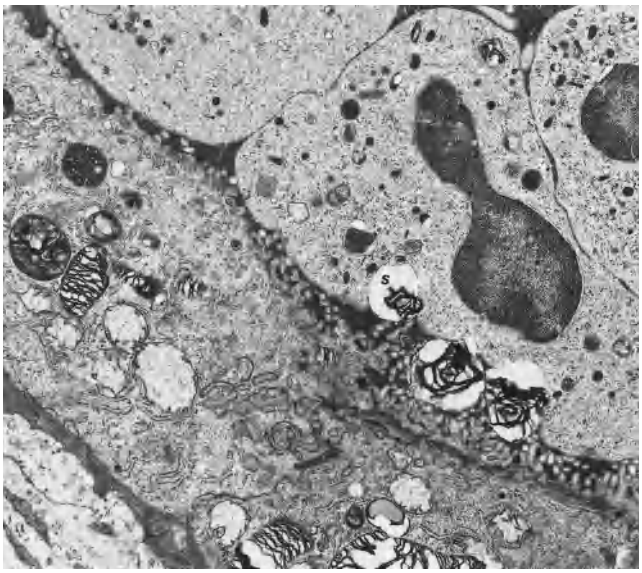


Fig. 10.7 Neutrophil phagocytosis: granular pneumocytes of the pulmonary alveolar wall (*upper right*) have released surfactant onto the alveolar wall. Neutrophils are degranulate and have attached to surfactant (*s*).

hydrogen peroxide than when in contact with foreign bodies or other cells; surface contact inhibits superoxide generation in the neutrophil.[74] Third, by its content of superoxide dismutase, endothelium can suppress the action of any superoxide released from neutrophils.[75]

Prolonged **elastase** release from degenerating neutrophils in chronic inflammation may cause irreversible tissue destruction. In lungs, elastase will gradually destroy elastic fibers in the alveolar wall, activity that underlies human emphysema. The circulating enzyme **α1-antitrypsin** suppresses the effects of neutrophil elastase. Humans deficient in this enzyme are especially prone to emphysema.

Tissue Repair

In healing and wound repair, neutrophils play important roles in clearing proteins and particulate debris from exudates. They avidly take up **fibrin** (Fig. 10.6) and degrade it. Phagocytosis is the mechanism through which neutrophils remove excessive amounts of soluble and fibrillar proteins such as fibrin, proteoglycans, and pulmonary surfactant (Fig. 10.7).

Toxic Neutrophils

Toxic neutrophils develop in severe systemic diseases, especially in septicemia and severe burns. Toxic neutrophils have markedly diminished chemotactic responsiveness a few days after burning and this promotes the septicemia common in burns. Elevations of free fatty acids in plasma occur in septicemia, toxemia, and other systemic diseases, and because of the effects of long-chain fatty acids on membranes, cause defective neutrophil chemotaxis.

The cytoplasm of toxic neutrophils contains **vacuoles** of varying sizes and several abnormal "toxic" granules. **Toxic granules** are dense, heavy-staining azurophil granules.[76] Vacuolated neutrophils are especially common in fever and septicemia. Vacuole formation is associated with disturbed fluid balance and changes in membrane ionic pumps (Fig. 10.8). Monensin, a monovalent ionophore that disrupts the electrolyte gradient required for the respiratory burst, causes neutrophil vacuolation, which begins in the Golgi complex.[77] **Döhle bodies**, which are light blue amorphous regions in the cytoplasm of toxic neutrophils, appear ultrastructurally as lamellar aggregates of rough endoplasmic reticulum.[78]

Glycogen is common, especially in neutrophils in oxygen-deficient tissue (Fig. 10.9). Glycogen is also common in circulating leukocytes in several metabolic diseases, for example, hepatic encephalopathy.[79] **Lipid globules** accumulate in toxic neutrophils, especially in tissue containing lipids and in the presence of hyperlipidemia.[80] Cytoplasmic lipid globules arise from defects in pathways of fatty acid metabolism.[81]

Vet-ebooks.com

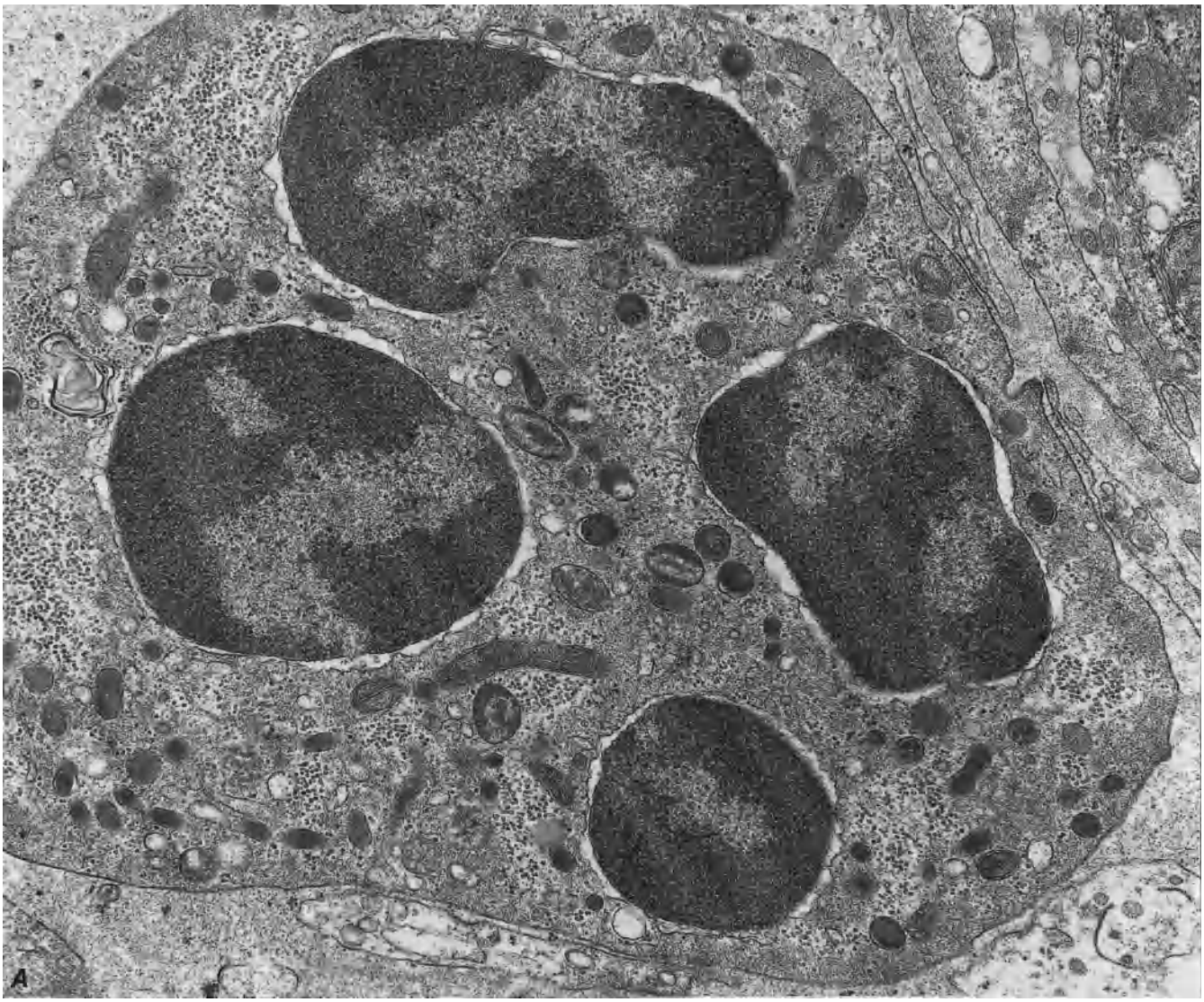


Fig. 10.8 Toxic neutrophil: cell is degranulate and contains large amounts of glycogen (shift to anaerobic metabolism).

Congential Abnormalities in Neutrophils

Chédiak-Higashi Syndrome

Chédiak-Higashi syndrome is characterized by anomalous giant granules in all granule-containing cells, increased susceptibility to infections, and defective pigmentation. The primary granules of the neutrophil are defective, and although phagocytosis occurs normally, bactericidal activity is diminished. Giant cytoplasmic inclusions occur in many types of granule-forming cells, including melanocytes, mast cells, neurons,[82] and pulmonary granular pneumocytes.[83] The giant granules in neutrophils arise from abnormal fusion of primary granules during myelopoiesis.[84,85] Neutrophils have abnormal chemotaxis because of defects in microtubule assembly and surface receptor functions.[86]

Animal models for the Chédiak-Higashi syndrome occur in mink, partially albino Hereford cattle, killer whales, and beige mice.[87,88] Similar syndromes have been reported in bison, white mutant tigers, and Persian cats.[89] In cattle, the defect involves abnormal bactericidal activity associated with the hexose-monophosphate shunt and delayed degranulation. The mechanism in beige mice is a failure of neutrophil granules to migrate to phagosomes.[90] The Chédiak-Higashi trait in the Aleutian mutant strain of mink is the basis for the remarkable susceptibility of these mink to the chronic, virus-induced plasmacytosis known as Aleutian disease.

Vet-ebooks.com

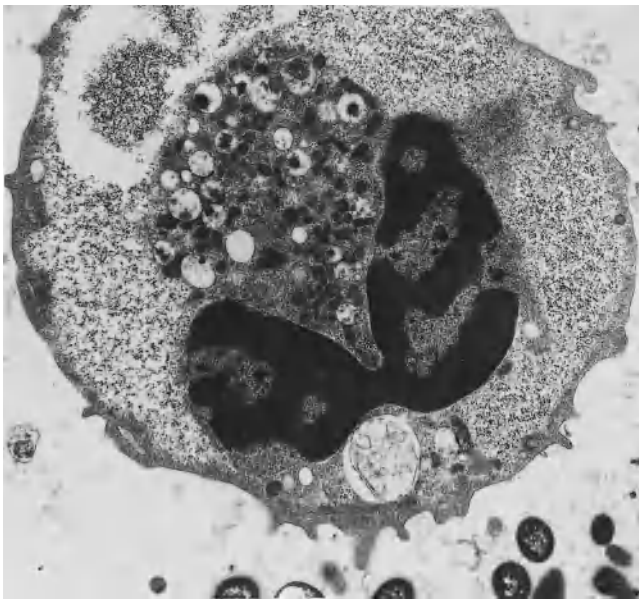


Fig. 10.9 Effete neutrophil: vacuolated, much glycogen, and central distribution of cytoplasmic granules; dental calculus, dog.

Cyclic Hematopoiesis

Cyclic hematopoiesis (cyclic neutropenia) involves cyclic depressions of neutrophil maturation in the bone marrow of infants, with consequential disappearance of mature neutrophils from the bloodsteam every 28 days caused by insufficient stem-cell production. Infants with cyclic neutropenia develop periodic bacterial infections that coincide with phases of neutropenia. Promyelocytes show defective primary granules and evidence of autophagy in nonneutropenic phases that precede neutropenia.[91] Bone marrow macrophages filled with huge autophagosomes containing many dense granules suggest that abnormal promyelocytes and neutrophils are taken up and destroyed by bone marrow macrophages. Pathologic changes occur in neutrophils, although these are indicative of toxin-induced degeneration, and probably represent secondary damage in a chronically ill patient.

Canine cyclic hematopoiesis (gray collie syndrome) has cycles of neutropenia at 11-day intervals.[92] Dogs bear a striking gray haircoat from the pigmentary defect and have ocular lesions (microophthalmia and sleral ectasia). Untreated dogs die with several weeks. With antibiotic therapy they survive only to succumb in early adulthood to enteritis, pneumonia, and amyloidosis.

Chronic Granulomatous Disease

Children affected with chronic granulomatous disease suffer severe recurrent bacterial infection due to impaired bactericidal activity of the neutrophil lysosomes.[93,94] Monocytes are similarly deficient. Despite vigorous neutrophil responses, normal degranulation, and adequate antibody formation, neutrophils are unable to kill bacteria.[95,96] The major metabolic defect is an absence of activity of the membrane-associated enzyme that generates O_2^-. Leukocytes have a variety of defects.[97] They do not exhibit a respiratory burst, and they cannot kill bacteria that lack catalase (which degrades H_2O_2) and do not produce hydrogen peroxide. Bacteria such as staphylococci that produce catalase but not H_2O_2 are not killed and proliferate to cause disease; streptococccci and other bacteria that excrete H_2O_2 are killed by defective leukocytes.

Lactoferrin Deficiency

Neutrophils of patients with lactoferrin deficiency show dysfunctions in killing, chemotaxis, and aggregation. Patients have an increased susceptibility to bacterial infection. Normal specific granules are absent from neutrophils while azurophil granules may be normal or increased in number.[98] Small vesicle-like granules are present and probably are abnormal secondary granules; that is, secondary granules may be present in normal numbers but unrecognized due to abnormal size (small), shape (elongate), and density (pale).[99]

Transmembrane Protein Defects

Leukocyte adhesion deficiency (LAD) is a heritable autosomal recessive disorder caused by a lack of production of leukocyte integrins. The leukocyte β_2 integrins are $\alpha\beta$ dimers and are classified as CD11/CD18, according to their α (CD11) and β (CD18) subunits. The β subunits are identical; the α subunits vary and are designated as LFA-1 (CD11a), Mac-1 (CD11b), and p150,95 (CD11c). The unique α subunits are noncovalently linked with a common β subunit; the β subunit is missing or defective in human LAD.[100]

Patients with LAD suffer recurrent life-threatening bacterial infections characterized by leukocytosis but lack of pus formation. Granulocytes, monocytes, and lymphocytes from these patients are defective in adhesion-related functions such as binding to endothelial cells, phagocytosis, and cytolysis.[100] Lesions are characterized by intravascular accumulation of neutrophils that fail to pass through endothelium into interstitial spaces. Ultrastructurally, affected neutrophils appear relatively normal but are not found attached to endothelium or within tissue spaces.

The syndrome in calves, called **BLAD,** appears with recurrent pneumonia, diarrhea, granulomatous stomatitis, periodontitis, and delayed wound healing.[101,102]

Vet-ebooks.com

Neutrophils in affected calves are consistantly elevated and cannot adhere to and pass vascular walls, but have normal ultrastructure. Neutrophil lysates have been shown to lack α subunits of Mac-1. Ultrastructurally, blood vessels throughout the body contain many neutrophils, even though few neutrophils are found in interstitial areas in inflammed tissues.

Pelger-Huet Anomaly

The **Pelger-Huet anomaly (PHA)** is manifest by incomplete segmentation of the nucleus of neutrophils and eosinophils, which causes nuclei to be round or bean-shaped. Affected neutrophils have condensed nuclear chromatin and large cytoplasmic granules.[103] PHA has been reported in other species, including Arabian horses, cats, and dogs (especially in foxhounds).[104]

Other Neutrophil Defects

Other congenital deficits in neutrophils include the following:

- **Myeloperoxidade deficiency,** in which peroxidase, located entirely in azurophil granules, is diminished[105]
- **Acatalasemia**[106]
- **Fechtner's syndrome** has leukocyte inclusions of endoplasmic reticulum, and thrombocytopenia.
- **May-Hegglin defect**
- **Intracellular deficiency of NADPH,** a defect associated with several different congenital deficiencies[107]
- **Endosomal adaptor protein p14 deficit** is a rare human primary immunodeficiency syndrome caused by deficiencies in p14 and MAPK signaling in late endosomes of neutrophils and other granules containing cells.[108]

Fetchtner's syndrome patients have nephritis, deafness, cataracts, macrocytothrombocytopenia, and leukocyte inclusions. **Fechtner's inclusions** are composed of clusters of ribosomes and fragments of rough endoplasmic reticulum, but lack the bundles of 10 nm filaments that are characteristic of the May-Hegglin granulocyte. Although they resemble Döhle bodies of septicemia, they are present in nearly every cell and lack parallel arrays of endoplasmic reticulum.[109]

Neutrophil Pseudoplatelets

Platelet-like fragments of neutrophils accumulate in the blood, especially in patients with septicemia and cancer. **Pseudoplatelets** are identified as neutrophils by myeloperoxidase staining of granules (which is absent in platelets) and nuclear fragments in the cytoplasm. Blood of patients with neutrophil pseudoplatelet will also have intact neutrophils that have large bulbous cytoplasmic extensions. Fragmentation of leukemic leukocytes to form platelet-size particles may cause spurious platelet counts.[110]

Neutrophils in Body Fluids

Neutrophils in body fluids have different characteristics than those in serum or blood. Components of saliva, urine, semen and milk all influence the behavior of the neutrophil. In **colostrum,** neutrophils have surface-adherent lipids, are deficient in the respiratory burst (relative to circulating neutrophils) and do not phagocytize staphylococci as readily; whole mature milk does not have this defect.[111]

Eosinophils

Eosinophils are large, sluggishly ameboid, bone marrow-derived phagocytic cells that have unique granules (Fig. 10.10). They generate and store a battery of proteins, including cationic proteins, growth factors, cytokines and chemokines. Secretory granules are released by vesicular transport after the appropriate stimulation of the eosinophil.[112] Eosinophils are prominant in mammalian parasitic diseases, and play important roles in human asthma, interstitial pulmonary disease, myocardiopathy, and Crohn's disease.

Eosinophil Granules

Eosinophil granules consist of a limiting membrane surrounding a cortical zone with high enzyme content. As granules fuse with phagosomes to initiate phagocytosis, changes in granule structure and refractive index suggest the extent to which enzymes have infiltrated and destroyed phagocytosed particles.[113] The primary constituent of the granule is **eosinophil major basic protein** (MBP), a protein that forms central crystalline lattices in the eosinophil granules of most species.[114,115] MBP has been localized in eosinophil granules using immunogold labeling.[116,117] MBP has a variety of toxic effects on tissue and induces noncytolytic release of histamine from basophils, prolonging the release of basophil-mediated events in immediate hypersensitivity.[118]

Other molecules identified in eosinophil granules by immunogold labeling include **matrix metalloproteinase-9,** which is implicated in parasitic eosinophilic meningitis;[119] **plasminogen activator inhibitor-2** (PAI-2);[120] **cAMP-specific phosphodiesterase;**[121] **cysteine-rich secretory protein 3** (CRISP-3);[122] the CC chemokine **RANTES;**[123] **urokinase;**[124] **tissue factor;**[125] **eosinophil**

Vet-ebooks.com

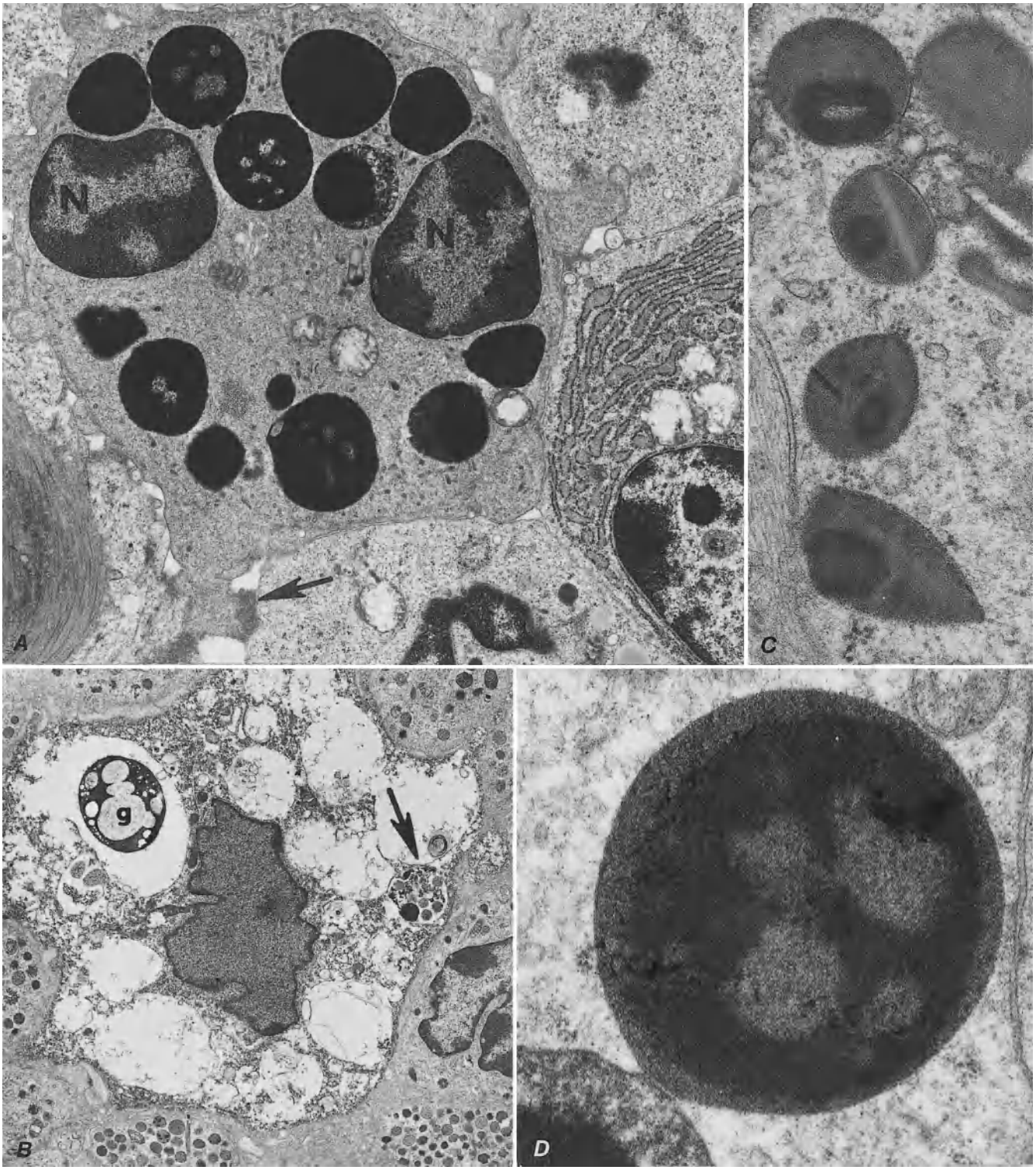


Fig. 10.10 Eosinophils. **A. Chronic parasitic enteritis**: intestinal mucosa, horse; granules are large, dense, and heterogeneous. Note granular deposits at ends of filopodia (*arrow*), which indicate affinity of eosinophil for parasite antigens. Mature plasmacyte at right; nucleus (*N*). **B. Degenerate eosinophil**: skin, horse, equine cutaneous mastocytosis; degenerate eosinophil surrounded by mast cells with one large pleomorphic granule present. Phagosome (*arrow*) contains mast cell granules. **C. Eosinophil granules**: sheep. **D. Eosinophil granule**: horse.

Vet-ebooks.com

cationic protein;[126] and **interleukin-2, -4, and -5.**[127–129] Cytoplasmic **lipid globules** are sites of localization of prostaglandin endoperoxide synthase (cyclooxygenase) production in eosinophils.[130]

Eosinophils are rich in **peroxidase,** which is released into vacuoles that open to the cell surface through surface pores.[131] In inflammation, peroxidase released by eosinophils can be taken up by neutrophils.[132] Eosinophil granules also contain several **acid hydrolases**. Acid phosphatase is associated with crystal-containing specific granules and is held in an inactive state prior to degranulation,[133] probably by complex carbohydrates of the granules.[134] **Charcot-Leyden crystals** are hexagonal bipyramidal structures found in eosinophils and basophils.[135] Using immunogold techniques for electron microscopy, Charcot-Leyden protein has been localized to a distinctive crystalloid-free granule in mature human eosinophils.[136]

Charcot-Leyden crystals are hexagonal bipyramidal crystals in tissues and secretions from sites of eosinophil-associated inflammation, and have been localized ultrastructurally by immunogold techniques.[137] Eosinophil granules are abnormal in the **Chédiak-Higashi syndrome,** and in other disease of leukocytes.[138]

Eosinophil Degranulation

Piecemeal degranulation is a term used for the differential release of eosinophil granule proteins, a mechanism that underlies the variability of plasma levels of eosinsophil granule proteins in disease. For example, allergen exposure causes piecemeal degranulation of peripheral blood eosinophils of allergic humans, and the degree of degranulation is reflected in the density of granules.[139]

Chemotaxis

In general, eosinophils are less responsive to chemotactic factors including complement components and tetrapeptides that are so effective for neutrophils.[140] However, eosinophils are highly attracted to immune complexes, which generate complement components that are strongly chemotactic.[140–144] Histamine is a specific chemoattractant for eosinophils, and mast cells are often associated with eosinophil exudates. Mast cell tumors and cutaneous mast cell lesions usually have large numbers of eosinophils.[145] Cytokines released by lymphocytes activated in immune responses are chemotactic for eosinophils.[146]

Tissue Eosinophilia

Eosinophils accumulate in tissue in reponse to stimuli as varied as gonadal hormones to parasite infestation.[147] In certain types of inflammation, they become the dominant inflammatory cell type (Fig. 10.11). In tissue, eosinophils often contain lipid bodies.[148] Metazoan parasites produce the most marked tissue and blood eosinophilia, especially in invasive and migratory phases of infection. Eosinophilic activity is generated both by release of chemoattractants by the parasite and by chemotactic activity resulting from the host's inflammatory response.

Cytokines from T lymphocytes often underlie eosinophilia. Human IL-2 cancer chemotherapy leads to marked eosinophilia. IL-2 injected into the patient causes an increase in IL-5, which in turn causes eosinophils to increase in the blood. In tissue there is degranulation of eosinophils and capillary leak syndrome.

The role of T lymphocytes in tissue eosinophilia is seen in athymic nude mice, which, lacking a functioning thymus, develop little or no eosinophilia after infection with **ascarid larvae.**[149] Defective eosinophils have been reported in some heritable disease, for example, the beige mouse.[150]

Eosinophils and Parasites

In schistosomiasis, larvae of *Schistosoma mansoni* transform from cercariae to schistosomula in the skin. Neutrophils adhere to, and fuse their plasma membranes with, the outer tegument of the larvae. Despite this attack, neutrophils do not discharge granules and do not kill the parasite. Eosinophils, in contrast, do kill larve of *S. mansoni*. They discharge granules onto the parasite surface and adhere to the discharged material.[151,152] **Mast cells** adhere to larvae via their receptors for C3 when the alterante pathway of complement is activated at the parasite surface.[153,154]

In immune animals, migrating schistosomes are damaged as they penetrate skin by aggregates of eosinophils that adhere to the antibody-coated parasite. Eosinophils contains specific receptors for complement and immunoglobulins on their surfaces.[155] After attachment, they secrete peroxidase onto the worm's surface. Focal lesions are produced in the parasitic tegument, causing it to separate from the body of the worm. Damage also results from activation of the alternate complement pathway (eosinophils adhere through their C3 receptors). In late stages of the reaction, eosinophils degenerate and are replaced by macrophages.[156]

Eosinopenic animals are more susceptible to parasitic infection. When animals cannot respond with eosinophils, there is no effect on expulsion of *Trichinella spiralis* from the intestine, but the number of larvae invading muscles is almost doubled.[157]

Vet-ebooks.com

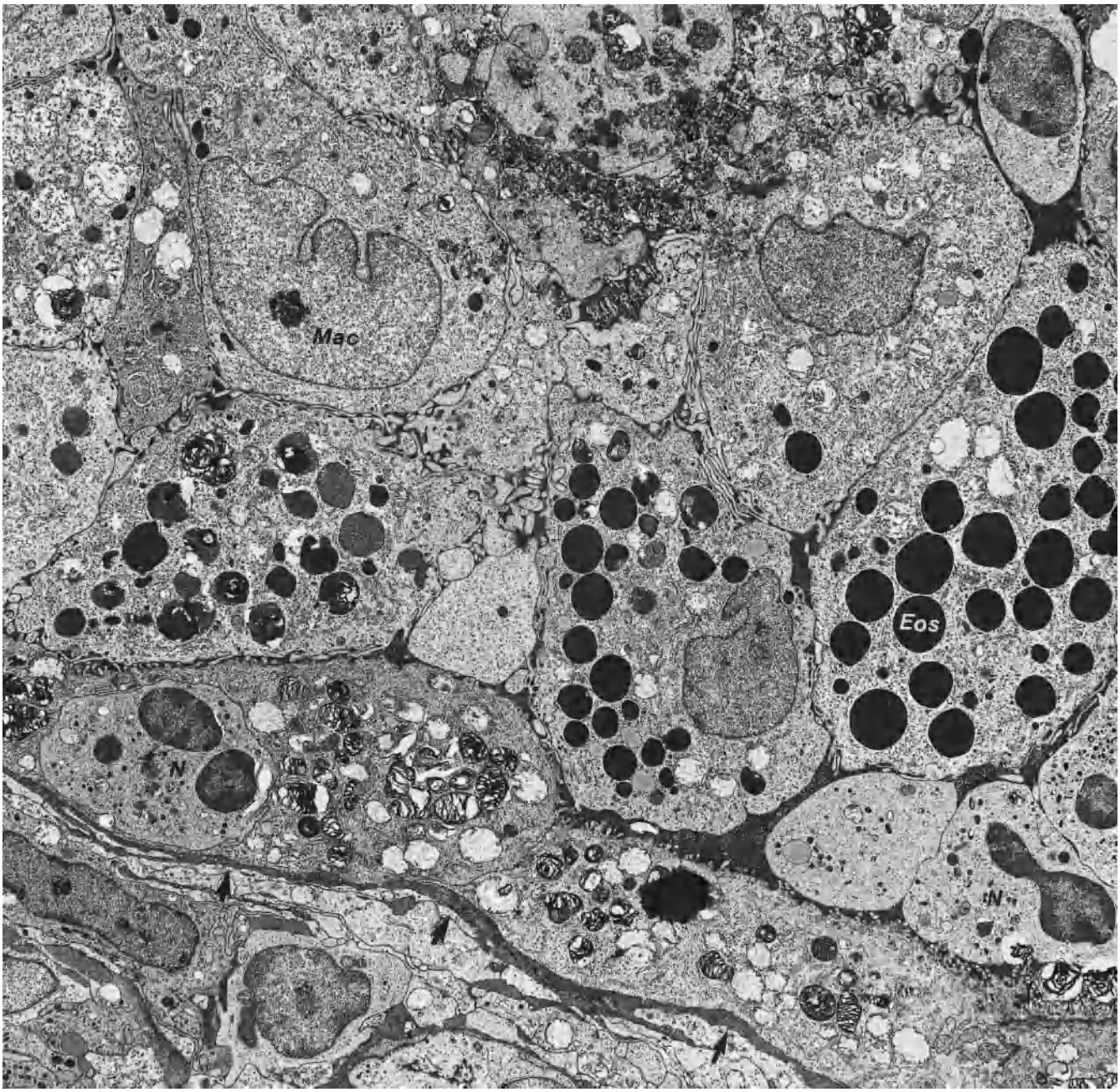


Fig. 10.11 Eosinophil exudate: inflammatory exudate, lung, pig with verminous pneumonia. Neutrophils (*N*), macrophage (*Mac*), eosinophil (*Eos*), and basement membrane of alveolar wall lined with granular (type II) pneumocytes (*arrows*).

Hypereosinophilic Syndromes

Human **hypereosinophilic syndromes** include food-allergy eosinophilic hyperplasia, eosinophilic gastroenteritis, eosinophilic lung disease (Loeffler's syndrome), and subcutanous angioblastic lymphoid hyperplasia with eosinophilia (Kimura's disease). Glucocorticoids, used in treatment of these syndromes, cause degeneration and disappearance of eosinophils. After steroid treatment, human blood eosinophils show degenerative ultrastructural changes.[158] In experiments in rats with intestinal parasites, corticosteroid treatment causes pyknosis and uptake of necrotic eosinophils by macrophages; within 3 hr of treatment nuclear chromatin condenses and granule matrix is altered.[159]

Platelets

Circulating platelets, or thrombocytes, are necessary for maintenance of normal endothelial integrity. As endothelial cells age and detach, platelets bind to

Vet-ebooks.com

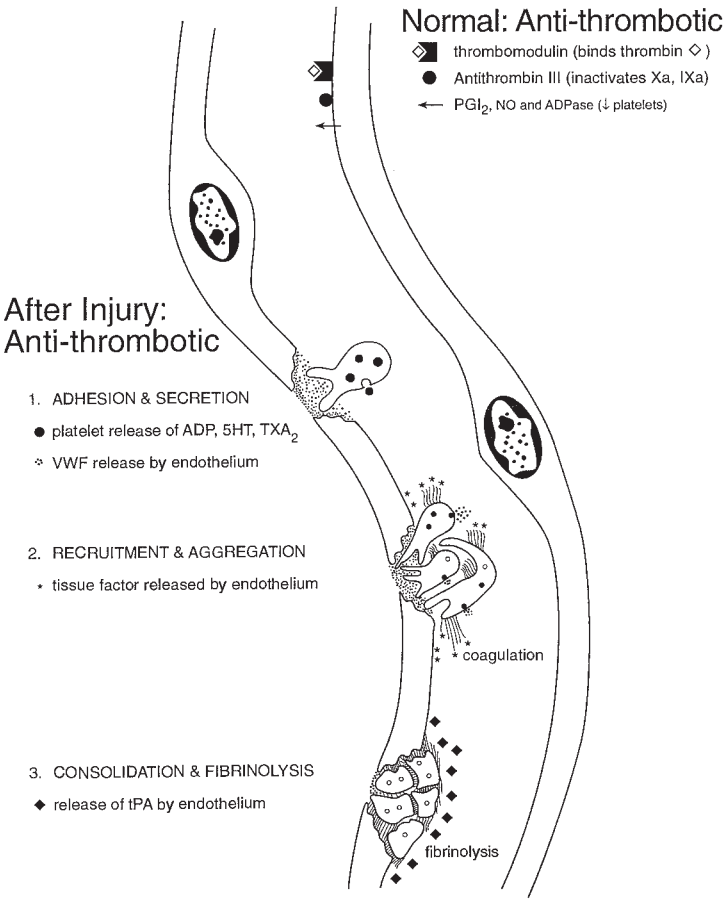


Fig. 10.12 Phases of hemostatic plug formation. 1. **Adhesion and secretion.** Immediate platelet adherence to basement membrane fragments and collagen (binding incorporates von Willebrand factor); release of ADP, serotonin (5-HT), and thromboxane A2 (TXA2)—all of which attract and activate circulating platelets; release of prostaglandins and nitric oxide, which limit thrombus expansion. 2. **Aggregation.** As platelets aggregate, they undergo the platelet release reaction, which is characterized by secretion of clot-promoting substances into the environment of the platelet mass. Phospholipoproteins on platelet surfaces attract thrombin, which initiates fibrin formation. 3. **Consolidation.** Neutrophils and erythrocytes contact the wound site and are incorporated into the developing thrombus, and the clot retracts. Fibrinolysis is initiated by release of tissue plasminogen activator (tPA) from endothelium. Thrombosis is contained by endothelial release of thrombomodulin (thrombomodulin binds thrombin, which activates protein C; protein C in turn cleaves factors Va and VIIIa) and heparin-like molecules that complex with antithrombin III to inactivate thrombin and coagulation factors Xa and IXa.

exposed subendothelial areas and extend long pseudopods that attach to subendothelial collagen to cover the defect. Surfaces of activated platelets serve as an assembly area for an enzyme cascade of coagulation factors that produce the protein-cleaving enzyme **thrombin** (Fig. 10.12). The target of thrombin is **fibrinogen,** a large protein circulating in plasma. When attached by platelet-bound thrombin, fibrinogen molecules polymerize to form **fibrin,** a large threadlike polymer. Fibrin strands form a network in the vicinity of platelets (because that is where thrombin is generated), giving the newly formed blood clot stability.

Normal Platelets

Megakaryocytes

Mammalian platelets are formed in the bone marrow by **megakaryocytes,** large, endoplasmic reticulum-rich, polyploid cells that develop under the influence of the cytokine **thrombopoietin.**[1–3] To produce platelets, megakaryocytes in the bone marrow move to sinusoidal blood vessels, attach, and extend long **proplatelet processes** through the vascular wall into the lumen. Imaging with multiphoton intravital microscopy has revealed that tips of the proplatelet processes are sheared by flowing blood releasing **proplatelet fragments** into the bloodstream.[160] Proplatelet fragments undergo further processing as they circulate, especially in the capillary bed of the lung (the platelet count in the pulmonary artery is lower than in the pulmonary vein).

Thrombopoietin (TPO) is a major regulator of platelet production.[161] Immunogold studies show that platelets contain thrombopoietin in the open canalicular system, but not in granules, and that is it released upon thrombin stimulation. In dogs, erythropoietin and IL-6 increase thrombocytopoeisis and responsiveness of platelets to thrombin.

During **thrombocytopenia,** when platelets are decreased in circulating blood, thrombopoietin is stimulated and megakaryocytes undergo hypertrophy.[162] Megakaryocytes may be spewed into the circulation prematurely. Megakaryocytes are rarely found in venous blood, however, because they are trapped in the lung and do not circulate.

Vet-ebooks.com

Platelet Ultrastructure

The fibrillar glycocalyx covering the plasma membrane is responsible for the intense activity and highly negative charge of the platelet surface (Fig. 10.13). Membrane glycoproteins with their oligosaccharide moeities radiating out into the blood readily absorb clotting factors and fibrinogen, giving platelets an extreme tendency to aggregate when in contact with rough surfaces. Platelets shed tiny procoagulant-rich vesicles from their surfaces that enhance coagulation.[163]

The **plasma membrane** of the platelet contains glycoproteins that function as ion channels, structural molecules, and receptors. Many of these molecules act as receptors to receive messages of vascular damage and to initiate platelet action. Endothelium damaged by hypoxia, toxins, or viral infections is prone to trapping of activated platelets (Fig. 10.14).

The Fibrinogen Receptor Glycoproteins IIb and IIIa combine to form the **GPIIb/IIIa complex,** which functions as a fibrinogen receptor. The GPIIb/IIIa complex ($\alpha_{IIB}\beta_3$ in the integrin nomenclature), binds fibrinogen as a co-factor in platelet aggregation. It is embedded in membranes at platelet surfaces and in α-granules.[164,165] The complex is cleared from the surface by lateral diffusion and entry into membranes of the open canalicular system. The GPIIb/IIIa complex/fibrinogen receptor is mobile; in activated platelets, clustering and patching of GPIIb/IIIa-fibrinogen complexes preceeding capping and endocytosis have been demonstrated using immunogold techniques.[166,167]

Collagen Receptors **Glycoprotein VI** (**GPVI**, CD36), a major receptor for collagen, is distributed over the entire surface of the platelet.[168] GPVI is also present on microparticles generated from activated platelets. Striking elevations in GPVI production occur when the platelet contacts collagen.

Open Canalicular System

The plasma membrane is connected to an internal system of channels called the **open canalicular system (OCS).** This system of channels is formed by invaginations of the plasma membrane of the platelet and functions as a pathway for the rapid release of granules and other materials. Platelets of cattle and some other species lack the OCS of human platelets and release granules solely by exocytosis via the plasma membrane.[169,170] Ligands that bind to platelet surfaces are transported into the OCS.[171,172] Conversely, membranes of the OCS can move to the platelet surface and serve as a reservoir for membranes that can be evaginated on platelet surfaces during aggregation.

Platelet Subsurface Cytoskeleton

Platelets have an extensive cytoskeleton on the cytoplasmic face of the plasma membrane. The lentiform shape of the platelet is maintained by this **marginal band,** bundles of microtubules and microfilaments at the periphery. **Microtubules,** which polymerize and depolymerize under various stimuli, are important in the formation of pseudopods, movement, and release of granules. The peripheral layer of actin **microfilaments** is linked to the acting-binding glycoprotein GPIb on the plasma membrane. As in erythrocytes, the actin filament network is complexed with spectrin that links it with the membrane.[173–175] The electron-dense subplasmalemmal region is a spectrin-rich network whose interstices contain glycoprotein Ib/IX-actin binding protein complexes.[176]

In cross sections on electron micrographs, 9 nm thick filaments can be identified that represent actin and its association with specific cytoplasmic proteins.[177] **Actin** is kept in its unpolymerized state by two actin-binding proteins: **profilin** forms binary complexes with actin monomers and prevents polymerization; **gelsolin** attaches to fast growing ends of actin filaments to prevent growth of filaments.

Platelet Granules

Platelets contain four types of granules: α-granules, dense granules, peroxisomes, and lysosomes. The first two of these are released in response to vascular injury and initiate and sustain platelet aggregation. In response to extracellular stimuli, intraplatelet granules or their components are released into the extracellular milieu by exocytosis. The fusion of granule and membrane, as analyzed ultrastructurally, involves formation of a 10–50 nm pore that connects the interior of the granules with the extracellular space. Small fibrils appear to connect the membrane with the unfused granule and as stimulation occurs, these are activated to promote secretion.

Dense Granules Dense granules of human platelets are heterogeneous in content and morphology. They contain serotonin, calcium, ADP, and the glycoprotein IIb/IIIa complex.[178] Most of these contents are absorbed from the circulation. ATP and ADP are packaged for secretion and, as the platelet circulates, may be released. Dense granules lie close to the plasma membrane in resting platelets, where they are anchored to the membrane by a bridge-like structure that is important in Ca^{++}-regulated granule secretion.[179] Rab GTPases control dense granule traffic; that is, secretion of platelet dense granules is regulated by Rab27b and other proteins.[180]

Vet-ebooks.com

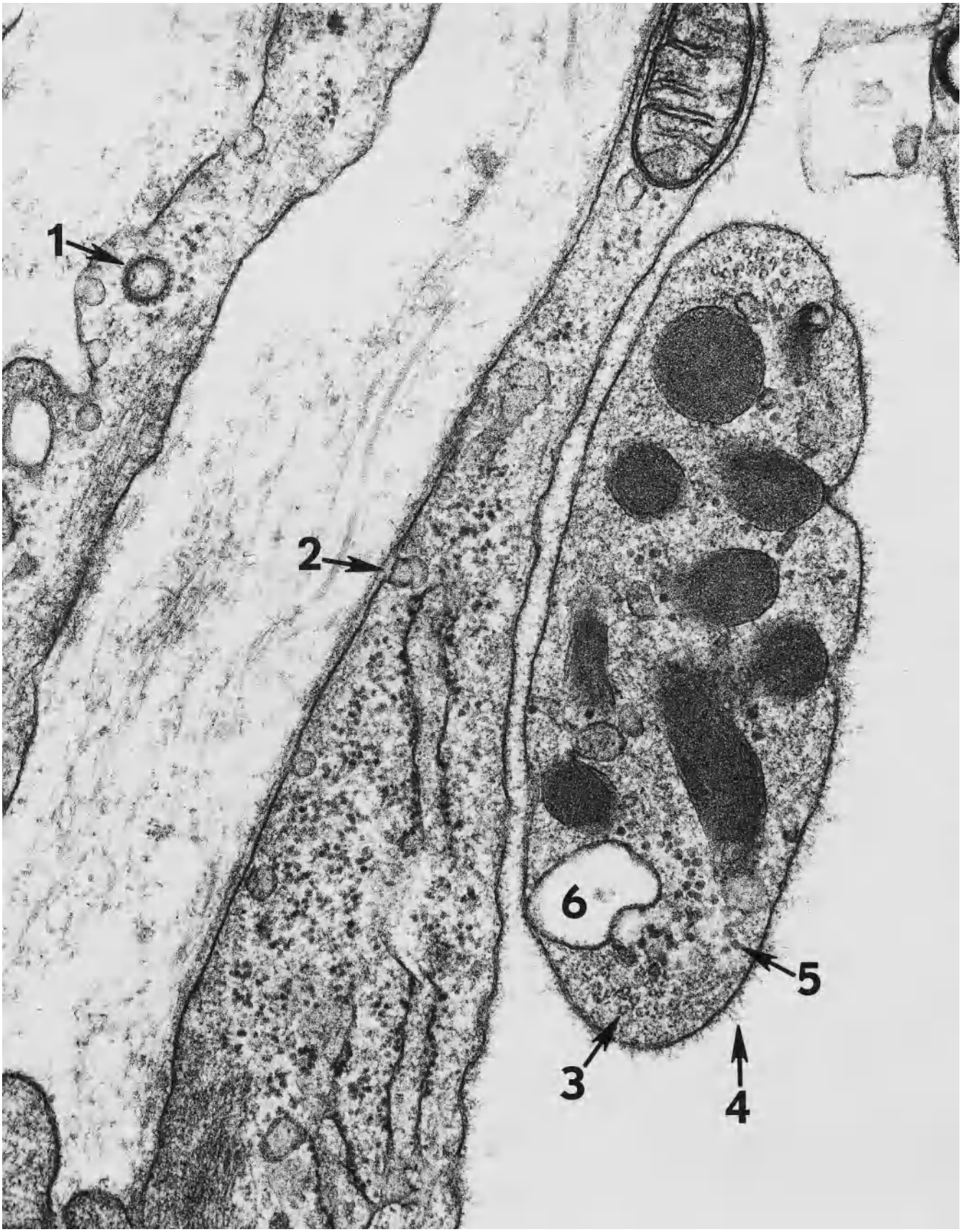


Fig. 10.13 Platelet attached to endothelium: capillary, intestinal villus. Coated vesicle (*1*), plasmalemmal vesicle with diaphragm and overlying basement membrane (*2*), microtubules (*3*), glycocalyx (*4*), glycogen (*5*), empty dense granule (*6*).

Vet-ebooks.com

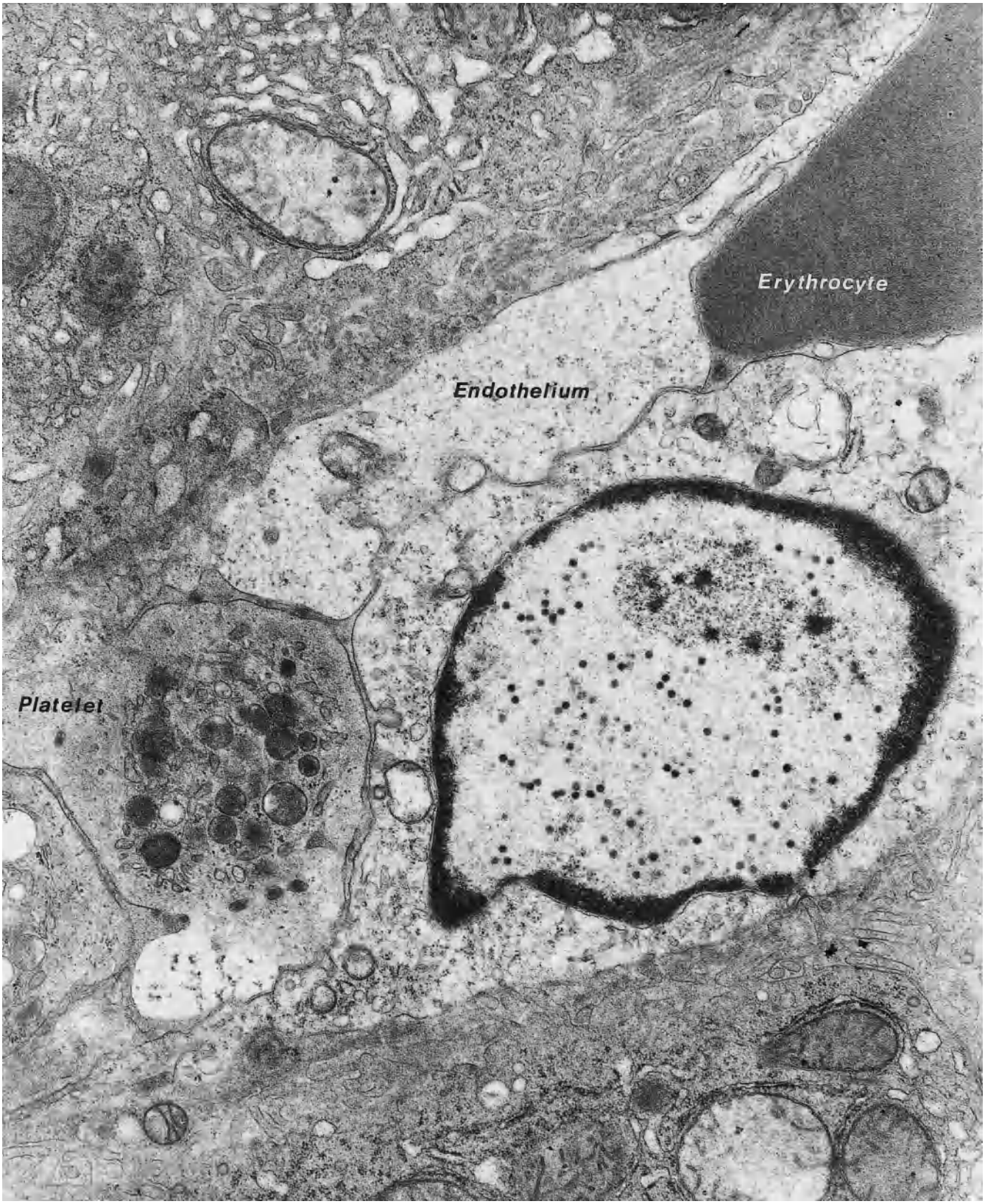


Fig. 10.14 Platelet trapping: hepatic sinusoid, infectious canine hepatitis. Endothelium is markedly swollen and obliterates the sinus lumen; the endothelial cell nucleus contains virions diffusely throughout the nucleoplasm, and there is lysis of chromatin and degeneration of the nucleolus. Platelet in the sinus lumen (*left*) has undergone the platelet release reaction, and has vesicles and granules located centrally.

Vet-ebooks.com

Alpha Granules Alpha granules are light and more numerous than dense granules. The adhesive glycoprotein **thrombospondin (TSP)** is the most abundant protein in platelet α-granules. It is synthesized by megakaryocytes (and a variety of cells including endothelial cells and macrophage; and is a component of the connective tissue matrix). TSP has been localized by immunogold techniques to connective tissue microfibrils; at these sites it is associated with subendothelial basement membranes of arteries and is important in thrombogenicity.

Platelet α-granules contain a variety of platelet-specific proteins including **β-thromboglobulin**, **platelet factor 4** (which counteracts the anticoagulant effect of heparin), **platelet osteonectin,** and **platelet-derived growth factor,** a potent mitogen.[181–183] Immunogold labeling has revealed that membranes of α-granules contain intrinsic glycoproteins such as GP IIb/IIIa (integrin $\alpha_{IIB}\beta_3$), granule membrane protein-140 (GMP140), and the multimeric platelet protein p155. These glycoproteins are transferred to the surface of activated platelets during fusion of α-granules with the plasma membrane during the platelet release reaction. In addition, several circulating proteins that are taken up by megakaryocytes are incorporated into developing α-granules.[184] α-granules contain **osteonectin**, a glycoprotein that complexes with TSP.[185]

α-granules of some species contain 200 nm tubules, which stain with gold labeled antibodies to von Willebrand factor (vWF). Tubules are smaller than microtubules (250 nm) and occupy a polar position, parallel to the long axis of elangated granules. They resemble Weibel-Palade bodies. Platelets of pigs with von Willebrand disease lack these tubules and do not stain for vWF.[186]

In platelets, the membrane protein **GMP-140,** a selectin, is unique to α-granules (although it is also present in endothelial cells). Also called PADGEM (platelet activation-dependent granule-external membrane protein), GMP-140 is an α-granule membrane protein in the resting platelet that acts as a leukocyte receptor for activated platelets that mediate adhesion to neutrophils and monocytes. GMP-140 is translocated to the plasma membrane during platelet activation and secretion;[187] it is part of the surface in activated platelets but is not so in resting platelets. GMP-140 is also redistributed into the open canalicular system when platelets are stimulated.

In response to certain substances, platelets under **receptor-mediated patching, capping,** and **endocytosis,** which may involve distinct pathways of entry for components of plasma, for example, α-granules, may acquire albumen and fibrinogen from plasma by endocytosis.[188]

The Platelet Release Reaction

Platelets undergo a remarkable transformation when they adhere to collagen at sites of endothelial damage (Fig. 10.15). They change shape from disks to swollen spheres, secrete their granules, extend spikelike pseudopods, and progress through a series of changes that collectively are called the **platelet release reaction.** In studies using stereologic electron microscopic methods on human platelets, a 45% increase in platelet circumference was found 3 min after activation, nearly all of which was due to a 13-fold increase in membranes of the newly formed pseudopods.[189]

Platelet Activation

Activation leads to a rapid and extensive polymerization of actin to form microfilaments in the cortical areas of the platelet. Bundles of actin microfilaments terminate at **adhesion plaques**—where fibronectin receptors, talin, fibrulin, and vinculin are concentrated. Adhesion plaques facilitate movement of the cell surface during activation.[190–195]

During activation, two distinct actin structures appear: bundles of long filaments within **filopodia** that end at the filopodial tips and a circumferential zone of orthogonally arrayed short filaments within **lamellipodia.** Immunogold labeling with antibodies against gelsolin reveals gelsolin molecules at the ends of some filaments in lamellipodia and filopodia. This suggests that gelsolin caps the barbed ends of the filaments in the resting platelet, and that uncapping of these filaments after activation leads to filopodila bundles.[196]

The **marginal band** of microtubules contracts forcing organelles to the cell center. The contents of dense bodies and α-granules are forced into the open canalicular system and extruded from the platelet to promote aggregation of other platelets. Granules disappear from the cell interior, fibrous substances resembling fibrin appear in the cisternae,[197] surface proteoglycans are depleted,[198] and transmembrane proteins of the plasma membrane are markedly altered (Fig. 10.16).[199,200] The platelet surface becomes remarkably sticky because of the adherence of secreted proteins and glycoproteins on the surface.[201,202]

The platelet release reaction begins when platelets contact connective tissues of the damaged vascular wall, thereby initiating **platelet aggregation** (Fig. 10.17). **Collagen** and its breakdown products are the most common initiators of platelet aggregation, although noncollagen microfibrils and basement membrane materials are also effective.[203] Adhesion of platelet and tissue is mediated by formation of an enzyme-substrate complex between galactosyl hydroxyllysine groups of collagen and transferase of

Vet-ebooks.com

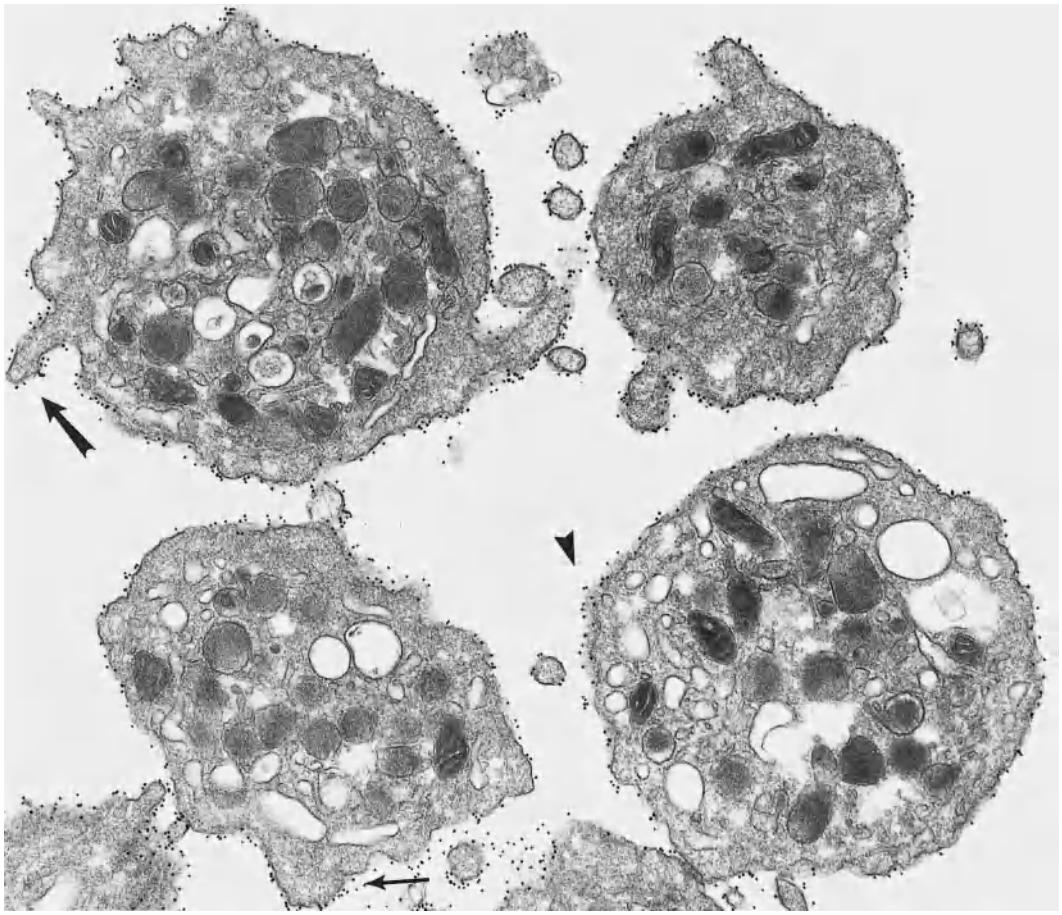


Fig. 10.15 Platelet release reaction: ADP-stimulated human platelets. Immunogold localization of GPIIb/IIIa shows uniform distribution over cell bodies (*arrowhead*), blunt projections (*thin arrow*), and pseudopods (*thick arrow*). (Micrograph: Mary E Hensler, *Am J Pathol* 141:707, 1992.)

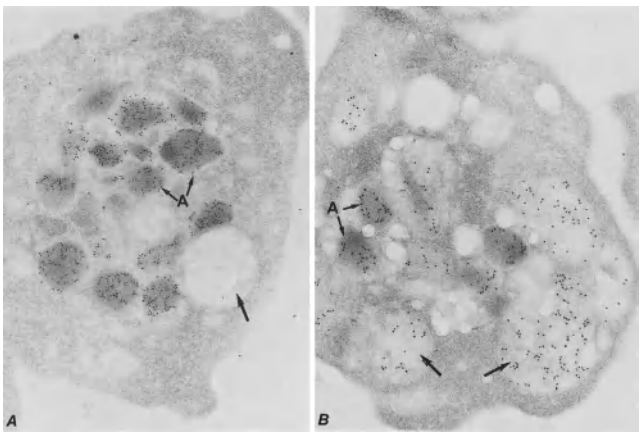


Fig. 10.16 Platelet granule dispersion: human platelets. Immunogold staining for fibrinogen in platelets before and after treatment with plasmin. **A. Before plasmin**: at 3ºC, fibrinogen is localized in α-granules (*A*); empty cytoplasmic vacuole (*arrow*). **B. After plasmin treatment**: labeling of fibrinogen is mainly in large cisternae of the canalicular system; few α-granules remain in the cytoplasm. (Micrograph: He-Lu, *Blood* 77:996, 1991.)

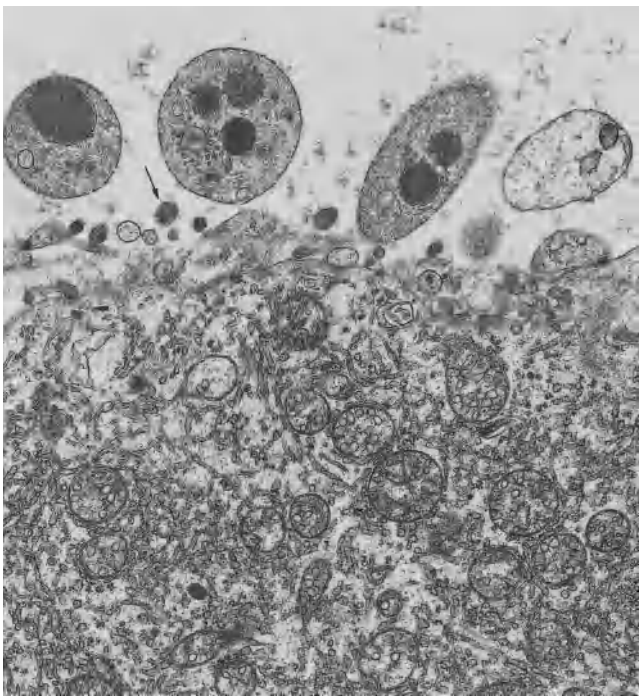


Fig. 10.17 Platelets bind to endothelial defect: anaphylaxis, capillary, adrenal cortex, sheep. Note discontinuities in endothelium; cross section of platelet processes (*arrow*) that have infiltrated the endothelial defect.

Vet-ebooks.com

the platelet plasma membrane. Particulate collagen is one of the most potent inducements of platelet aggregation. When parasitized animals are treated with parasitides, parasitic collagen is released and causes a massive local platelet aggregation.[204]

Plasma Membrane Alterations

On activation, **transmembrane proteins** in the plasma membrane redistribute. The receptor proteins that interact with extracellular materials such as fibrinogen are translocated to the surface of the platelet to enhance the ligand-receptor reactions that sustain the release reaction.[205] Connections between extracellular fibrin and the platelet cytoskeleton via these transmembrane proteins underlie platelet contraction and aggregation.[206] **Ligand-receptor clustering,** patching, and capping develop for fibrinogen, thrombospondin, vWF, and fibronectin, all of which coexist in the same granule.

The major integrin on platelet surfaces, the GPIIb-IIIa complex,[207] promotes binding of platelets to one another via soluble, multivalent mediator molecules. Fibrinogen and von Willebrand factor are the primary ligands for the GPIIb/IIIb during platelet aggregation.

As a **fibrinogen receptor,** GPIIb/IIIa has a major role in platelet aggregation. Dispersed randomly in the resting platelet, GPIIb/IIIa clusters on the membrane surface on activation. Clustering occurs primarily over the granulomere.[208] After binding, **fibrinogen-GPIIb-IIIa complexes** are rapidly mobilized.[209–211] Morphometric analysis of platelets with immunogold localization has shown that availability of the fibrinogen receptor increases during activation[212] and that fibrinogen bound to activated platelets causes patching and capping of the platelet surface.[213–215] Colocalization studies with labeled monoclonal antibodies show that fibrinogen is bound in close proximity to GPIIb/IIIa on pseudopods.

Platelet activation causes redistribution of proteins in the cytoplasmic matrix. Adhesion plaque proteins such as **talin** are moved into a position to facilitate platelet-to-platelet adherence. Other changes in the plasma membrane during platelet activation are marked lipid packing, lateral distribution of cholesterol, and transbilayer asymmetry of anionic phospholipids.[216] Small apertures, connections between channels of the **OCS,** are found in the cell surface, usually in clusters spread throughout the platelet.

Adsorption of vWF to thrombogenic surface induces conformational changes in tertiary structure that expose prothrombotic functional epitopes that then interact with platelets to cause platelet adhesion and thrombosis, interactions that involve adsorption of the vWF GPIb binding domain of collagen (Fig. 10.18).[217]

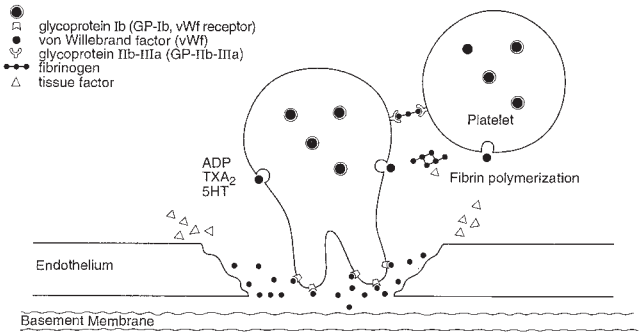


Fig. 10.18 Platelet attachment at a site of endothelial injury: Von Willebrand factor, released by damaged endothelial cells, binds to GP-Ib receptors on platelet surfaces. Circulating fibrinogen binds to $\alpha_{IIB}\beta_3$ (GP-IIb-IIIa) receptors to link platelets together.

Platelet Secretion

The platelet release reaction involves secretion of lysosomal enzymes, serotonin, fibrinogen, calcium, and adenine nucleotides into the surrounding environment. **Thrombospondin** released from α-granules is secreted and also binds to the platelet surface, and to the surfaces of adjacent platelets.[218] TSP thus serves as an endogenous lectin that is released by platelets when they are activated by thrombin. TSP has binding sites for fibrinogen and heparin (fibrinogen is probably the platelet-bound receptor for thrombospondin).[219]

Other proteins that circulate in the bloodstream can bind to the platelet surface and have an effect in aggregation. **Fibronectin** binds specifically to thrombin-induced receptors, such as the GPIIa molecules on platelet surfaces.[220] **Von Willebrand factor,** which is stored in both platelet and endothelial cell secretory granules, is released during coagulation and promotes platelet aggregation at sites of tissue injury.[221] Multimeres of VWf are stored as tubular structures by endothelial cells in specific granules, the Weibel-Palade bodies. The curled arrangement of the tubules suggests a high degree of protein folding within the Weibel-Palade body.[222]

Platelet activating factor (PAF) is a lipid released on antigenic challenge of **basophils** that have been sensitized with specific IgE antibody. PAF initiates aggregation and secretion of dense body constituents of platelets. PAF (acetyl glyceryl ether phosphorylcholine) is also a lipid mediator of inflammation. Released from IgE sensitized basophils, it induces platelet aggregation and secretion in various species. In acute serum sickness it increases vascular permeability

Vet-ebooks.com

and plays a crucial role in localization of immune complexes.[223]

Platelet-collagen interaction causes generation of **eicosanoids.** Arachidonic acid, freed from membrane phospholipids, is converted to prostaglandin endoperoxides PGG_2 and PGH_2 and to thromboxane A_2. The released ADP enhances aggregation and the endoperoxides and thromboxane cause both aggregation and further granule release.[224–226]

Platelets are the most concentrated source of **transforming growth factor-β** (TGF-β) in man. Released from α-granules, TGF-β starts a repair cascade in connective tissue. It is a potent chemotactic factor for macrophages, which it attracts, to activate them to synthesize other growth factors and to deactivate production of hydrogen peroxide (which would destroy nascent fibroblasts). It also stimulates production of matrix molecules such as collagen and fibronectin.

Platelet Aggregation

Platelet aggregation is characterized by close apposition of platelets and binding of platelet surfaces. Ultrastructural studies of clotting have shown characteristic bridging structures between plasma membranes of adjacent platelets.[227] Canalicular systems remain open and, by releasing platelet products, contribute to maintenance of platelet stickiness.

Platelet Phagocytosis

Platelets are phagocytic and, in septicemia and some local microbial infections, phagosomes develop in the cytoplasm. Normal mammalian platelets are activated by contact with most pathogenic bacteria. During aggregation, bacteria are trapped deep in the platelet aggregate and lie between platelets. Fibrinogen is an important factor in the platelet response to *Staphylococcus aureus*. Platelets from patients with **congenital afibrinogenemia** tend to avidly take up bacteria (Fig. 10.19).[228,229]

Platelets have been reported to phagocytize certain virions.[230] By causing a release of sialic acid from platelet surfaces, viruses can enhance clearance of the platelets from the blood.[231] By fusing to platelet membranes, virions can enter the platelet in vacuoles.

Thrombocytes of amphibians, birds and reptiles are nucleated. During activation, they behave as megakaryocytes and resemble the mammalian platelet. The nucleus disintegrates and cells break into small fragments.[232]

Platelets and Endothelial Injury

Activation of platelets can cause injury to endothelium. Contact of activated platelets with endothelium causes loosening of cells and foci of plasma membrane damage. Ultrastructurally, plasma membrane have focal defects associated with cytoskeletal abnormalities and extrusion of cytoplasmic vesicles.[233]

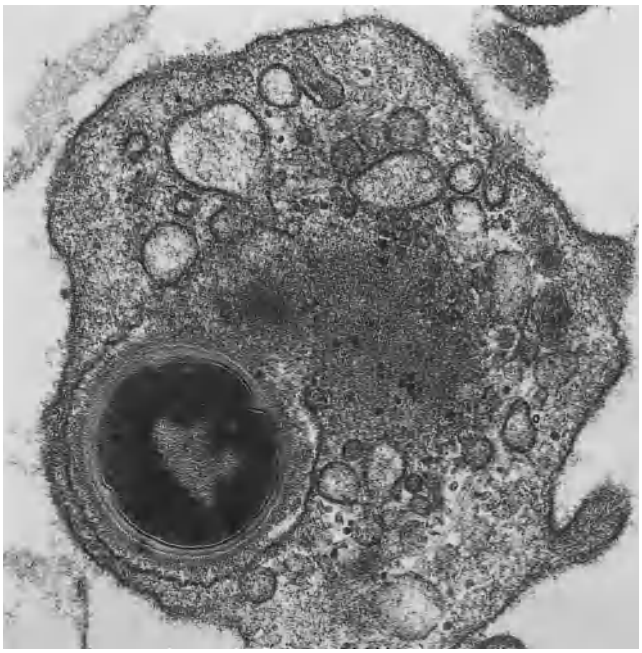


Fig. 10.19 Platelet phagosome: phagosome contains dense bacterial cell *(Staphylococcus)*; human platelet. (Micrograph: C. C. Clawson, *Am J Pathol* 98:197, 1980.)

Platelet Defects: Thrombocytopenia

Thrombocytopenia, a drop below normal in the number of circulating platelets, is a prominant feature in trauma, shock, septicemia, disseminated intravascular coagulation, thrombotic thrombocytopenic purpura, and the hemolytic-uremic syndrome. Some thrombocytopenic states result from intravascular platelet aggregation with subsequent sequestration as platelet or platelet-fibrin thrombi in various organs. The mechanisms of thrombocytopenia include (1) defects in formation of platelets, (2) excess utilization, and (3) premature destruction, either by intravascular lysis or by removal by macrophages.

Acquired thrombocytopenia occurs in systemic infectious diseases, acute radiation disease, drug toxicity, and in immunologic diseases involving antiplatelet antibodies. Viruses cause thrombocytopenia by destroying endothelium, which increases platelet consumption, and by replicating within platelets, causing lysis and altering platelet surfaces so that they are removed during circulation in the spleen. Both mechanisms operate in viral hemorrhagic diseases that show petechial and ecchymotic hemorrhages in

Vet-ebooks.com

Table 10.2 Hereditary defects of platelets.

Syndrome	*Platelet defect*	*Reference to ultrastructural pathology*
Bernard-Soulier syndrome	α-Actinin	**Maldonado**, *Mayo Clinic Proc* 50:402, 1975
Chédiak-Higashi sydrome	Human	**Bell**, *Blood* 48:175, 1976; **Gallin**, *Blood* 45:863, 1975 (also: mink, cow); **Rendu**, *Am J Pathol* 111:307, 1983
	Cat	**Kramer**, *Lab Invest* 36:554, 1977 (Persian)
	Cow	**Meyers**, *Am J Pathol* 106:364, 1982
	Mink	**Lutzner**, *Lab Invest* 14:2063, 1965
Fechtner's syndrome	Giant platelets	**Peterson**, *Blood* 65:397, 1985
Glanzmann's thrombasthenia	GPIIb/IIIa formed but transport from ER is impaired	**McNichol**, *Thromb Res* 103:25, 2001; **Nelson**, *J Thromb Haemost* 3:2773, 2005; **Rosenberg**, *Blood* 101:4808, 2003; **Smith**, *J Lab Clin Med* 128:601, 1996 (rat)#
Gray platelet syndrome	α-granule	**Breton-Gorius**, *Am J Pathol* 102:10, 1981; **Cramer**, *Blood* 66:1309, 1985; **Rosa**, *J Clin Invest* 80:1138, 1987; **White**, *Am J Pathol* 95:445, 1979
Hermansky-Pudlak syndrome	Dense granule	**White**, *Am J Pathol* 63:319, 1971
Idiopathic scoliosis	Ca^{++} transport	**Yarom**, *Lab Invest* 43:208, 1980
May-Hegglin anomaly		**Hamilton**, *Am J Clin Pathol* 74:663, 1980
Sebastian platelet syndrome (Macrothrombocytopenia)	Giant platelets with nuclear inclusions	**Greinacher**, *Blut* 61:282, 1990
Thrombasthenia	α-Actinin	**Gerard**, *Am J Pathol* 94:509, 1979
Wiskott-Aldrich syndrome	Cytoskeleton	**Moline**, *J Exp Med* 176:867, 1992*

*Studies in vitro.
#Animal model.

skin and mucosal surfaces. When platelets are depleted and sites of endothelial injury cannot be covered, hemorrhage occurs. A third mechanism, antibody-mediated platelet destruction, may cause thrombocytopenia in late stages of some viral diseases.

Platelet Defects: Thrombocytopathy

Defective platelets arise from many genetic deficits. Mutations in the anti-apoptotic Bcl-x_L gene cause accelerated death of platelets and platelet deficiency (Table 10.2).[234]

Acquired Thrombocytopathy

Defective platelet function is common as a side effect of therapy with aspirin, phenylbutazone, and other drugs. In aspirin toxicity, the enzyme cyclooxygenase is reversibly acetylated and inactivated thus inhibiting secretion mediated by prostaglandins and thromboxanes. Aspirin-like hereditary storage pool disease has also been reported.[235] Ristocetin induces platelet aggregation and is used to demonstrated defects in platelets.

Botrocetin, a toxic protein component in *Bothrops* snake venom, induces a von Willebrand-like syndrome and thrombocytopenia, when injected intravenously. Botrocetin interacts with vWF multimers and induces them to bind, via a domain that lies between valine and lysine, to receptors on platelet surfaces.[236] Thrombi, formed of discrete platelets that are not depleted of granules, lodge in capillaries of the lungs and spleen (not in liver or renal glomeruli). The attachment of vWF multimeres to platelets leads to platelet agglutination without stimulating platelet granule release of thromboxane production.

Immune (idiopathic) thrombocytopenic purpura (ITP) involves accelerated platelet destruction mediated by antiplatelet autoantibodies directed against platelet surface glycoproteins (IIb/IIIa or Ib/IX/V), and by increased phagocytic capacity (using Fc receptors) of cells of the macrophage-monocyte system. No structural abnormalities have been observed in ITP platelets but there is an increased immunogold labeling of IgG within α-granules.[237] Foam cells in spleens of patients with idiopathic thrombocytopenic purpura arise from phospholipid membranes that accumulate after platelet phagocytosis. Foam cells can be induced in mice by the subcutaneous injection of platelets.[238]

Vet-ebooks.com

Hereditary Thrombocytopathy

Human **platelet storage pool deficiencies** comprise a range of disorders that include varying degrees of reduced numbers and contents of platelet granules. Disorders of dense granules (**storage pool diseases**) are common. Defects in α-granules occur in only two storage pool diseases: **αδ-storage pool disease** and **α-storage pool disease** (gray platelet syndrome). There is marked pheotypic heterogeneity of α-granule defects in human platelets, especially in granule membrane proteins.[239–241]

Gray Platelet Syndrome The **gray platelet syndrome (GPS)** involves a defect in the α-granule. Because GPS platelets lack normal α-granules, they appear gray after routine staining of blood smears. Affected platelets are large and vacuolated, and either lack α-granules or have α-granules that are small (and may be confused with lysosomes or peroxisomes). Granule content of fibrinogen and von Willebrand factor are abnormal,[242,243] but α-granule content of the integral membrane protein GMP-140 (PADGEM) is near normal.[244] Despite normal numbers of other types of granules, GPS patients develop thrombocytopenia and bleeding. The α-granule defect occurs during development of megakaryocytes in bone marrow, and this suggests that precursors of α-granules are produced but that their contents are then lost due to Golgi packaging failure.[245] A GPS disorder in which a severe deficiency in the platelet collagen receptor GPVI accompanied the α-granule defect has been reported.[246]

Thrombasthenia Rare congenital platelet defects are termed **thrombasthenia** (weak platelets). In **Glanzmann's thrombasthenia,** there is a deficiency of the receptor molecule GPIIb/IIIa; in some cases, GPIIb/IIIa is formed but does not exit from the endoplasmic reticulum. Platelets from patients with this trait have a rudimental cytoskeleton and fail to aggregate in response to activation.

Ultrastructural studies in thrombocytopathy often reveal specific defects such as the α-actinin[247] or the defects in the **Bernard-Soulier syndrome.**[248] A wide variety of very rare and unusual hereditary platelet defects has been reported.

Giant Platelet Syndromes **Macrothrombocytopenia** includes a variety of hereditary defects in which affected platelets are very large and have a high density of central organelles and disorganized peripheral microtubules (Fig. 10.20).[249–251] Most also involve abnormal granulocytes with characteristic inclusions, for example, Alport's syndrome and Fechtner's syndrome. Similar thrombocytopenic disorders have been reported in patients whose megakaryocytes had normal dense bodies but abnormal, giant lysosomes.[252] Giant platelets similar to those in giant platelet syndromes have been reported in human patients with type 2B von Willebrand disease (characterized by an increased affinity of vWF for its platelet receptor, glycoprotein Ib).[253]

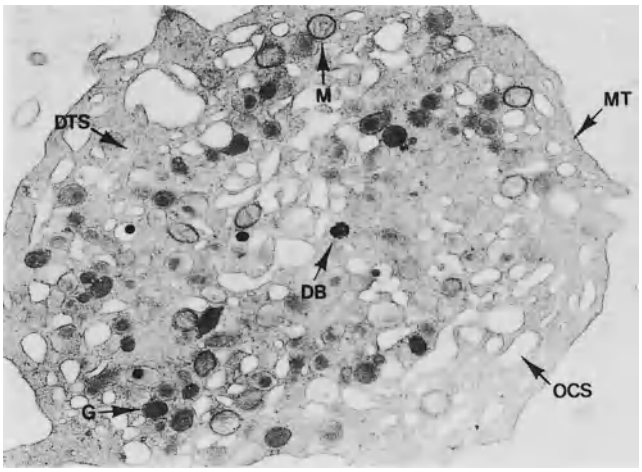


Fig. 10.20 Giant platelet syndrome: human. Dense body (*DB*), mitochondrion (*M*), dense tubular system (*DTS*), open canalicular system (OCS), granule (*G*), and microtubules (*MT*). (Micrograph: LoAnn C. Peterson, *Blood* 65:397, 1985.)

Other Platelet Disorders

Fechtner's syndrome is a rare hereditary disorder with the unusual combination of giant platelets with inclusions of leukocytes, nephritis, deafness, and cataracts.[254] Ultrastructurallly, affected platelets, despite the large size, do not differ significantly from normal platelets. Open canaliculus system channels are very prominent. Fechtner's syndrome leukocyte inclusions are composed of clusters of ribosomes and fragments of rough endoplasmic reticulum.

The **Wiskott-Aldrich syndrome** is an X-linked disorder with severe deficiency of leukocyte and platelet function. The product of the defective gene is unknown although the number of abnormalities is large, including marked decrease size and number of circulating platelets. Defective T lymphocytes have abnormal surfaces with fewer microvilli and abnormal surface glycoproteins. Recent studies suggest that the defect is in a gene that regulates the cytoskeleton.[255]

Platelets of human patients with **Hermansky-Pudlak syndrome** lack **dense granules.** This congenital disorder involves albinism and a tendency to hemorrhage.[256] Defective platelets in the **Chédiak-**

Vet-ebooks.com

Higashi syndrome, a familial disease of man and many species of animals (there are anomalous giant granules in all granule-forming cells), lack **dense granules;** α-granules, microtubules, and mitochondria are normal. Giant granules, typical of other cells in this syndrome, have not been seen in platelets.[257–259]

Abnormal platelets have been described in syndromes of which the pathogenetic bases are not clearly known, for example, in **idiopathic scoliosis**[260] and **congenital bleeding syndromes.** The **May-Hegglin anomaly** is a rare autosomal, dominant platelet disorder characterized by moderate thrombocytopenia and large, bizarre, cigar-shaped platelets with large, irregular granules and Döhle bodies.[261] Abnormal platelet granules are associated with several lysosomal storage diseases in both humans and animals.

Platelets, Factor VIII Complex, and von Willebrand Factor

Factor VIII is produced in the liver. After activation by trace amounts of thrombin, it accelerates coagulation by increasing the rate of factor X activation by factor IX. Structural models for factor VIII complex have been developed based upon scanning electron microscopy.[262]

In circulating blood, factor VIII is carried by the large adhesive glycoprotein, **von Willebrand factor,** a series of multimers with sizes that range into the millions of daltons. **Factor VIII complex** thus has two components: VIII (antihemophilic factor) and vWF. It plays roles in both clot formation and platelet adhesion, and two of the most common bleeding disorders are results of a deficiency in the activity of one or the other of these components. vWF was discovered in the platelet α-granule and endothelial cell Weibel-Palade body shortly after it was found that exercise and adrenal injury caused a rapid rise of blood levels.

vWF is synthesized by endothelial cells and megakaryocytes. By binding to platelet surfaces and to subendothelial collagen, it promotes shearing-dependent **platelet adhesion** to blood vessel walls.[263] Shear-induced binding of vWF to the platelet GPIb/V/IX complex plays a key role in initiating platelet adhesion and aggregation at sites of vascular injury. Ultrastructural immunogold techniques have localized vWF in platelet α-granules and in Weibel-Palade bodies of endothelial cells. vWF in platelets, endothelium, extracellular matrix, and plasma all contribute to hemostasis. In plasma, vWF is a huge multimere of several molecules. vWF is involved in thrombus growth and can substitute to some extent for fibrinogen in the aggregations of activated platelets in hypofibrinogenemic states.

von Willebrand Disease In von Willebrand disease, this endothelial component is deficient. Ultrastructural analysis of incision wounds in patients with von Willebrand disease show defects in platelet plugs.[264,265] The primary interactions of vWF that have functional clinical significance are interactions with: (1) factor VIII, which is stabilized by vWF; (2) platelets, especially the membrane protein GPIIb/IIIa; and (3) vascular basement membranes. In the later, the major binding agent is collagen IV, although other molecules bind vWF. The amount of vWF in basement membranes is regulated by the endothelial cell and is used to enhance endothelial attachment to vitronectin receptors.

Thrombosis

Thrombosis is the formation within a vascular lumen of a thrombus, an aggregate of coagulated blood containing platelets, fibrin, and entrapped cells (Fig. 10.21). Thrombosis is a pathologic process that forms a blood clot within the uninterrupted vascular blood system.

Coagulation

Blood coagulation proceeds through a series of reactions in which plasma zymogens of serine proteases are sequentially activated by limited proteolysis, culminating in the generation of thrombin. A clot is formed by this enzymatic cascade in which an activated form of one coagulation factor catalyzes the activation of the next. **Coagulation,** the formation of **fibrin,**[266] is initated when activated factor X (Xa) cleaves the circulating protein **prothrombin** into a nonfunctional fragment that is dissipated into blood, and **thrombin,** the proteolytic enzyme that converts plasma fibrinogen to fibrin (Fig. 10.22).[267] Coagulation exists in all vertebrate species; for example, fish possess all major proteins of coagulation, and thrombocytes that are analgous to platelets in adherence, secretion, and aggregation.[268]

Fibrinogen is a soluble plasma protein of nearly 340,000 MW.[269] The molecule is nodose and consists of three beads (6.5 nm diameter) held together by a thin strand of protein. Running throughout the molecule are three different chains (α, β, γ) interconnected by disulfide bonds. The triggering event in fibrin formation is the thrombin-catalyzed removal of small polar peptides (fibrinopeptides A and B) from the central regions of the α and β chains. Cleavage of fibrinopeptides reduces the marked negative charge on the central region, so that fibrin monomer assumes an overall positive charge. Since the terminal regions

Vet-ebooks.com

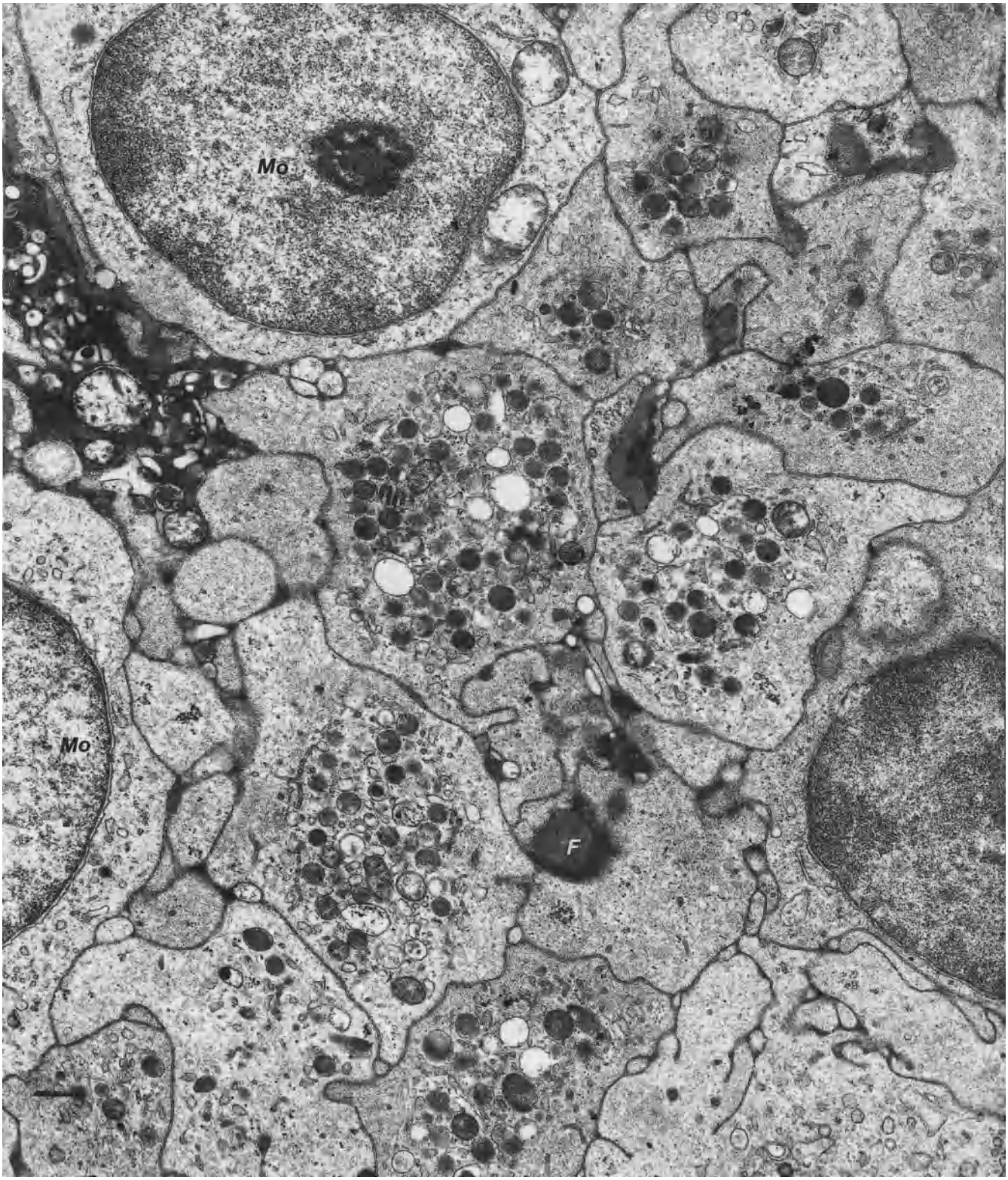


Fig. 10.21 Thrombus: artery, spleen, cat. Platelets have aggregated and plasma membranes are in close contact. Fibrin (*F*) is interspersed among platelet surfaces; monocyte (*Mo*).

Vet-ebooks.com

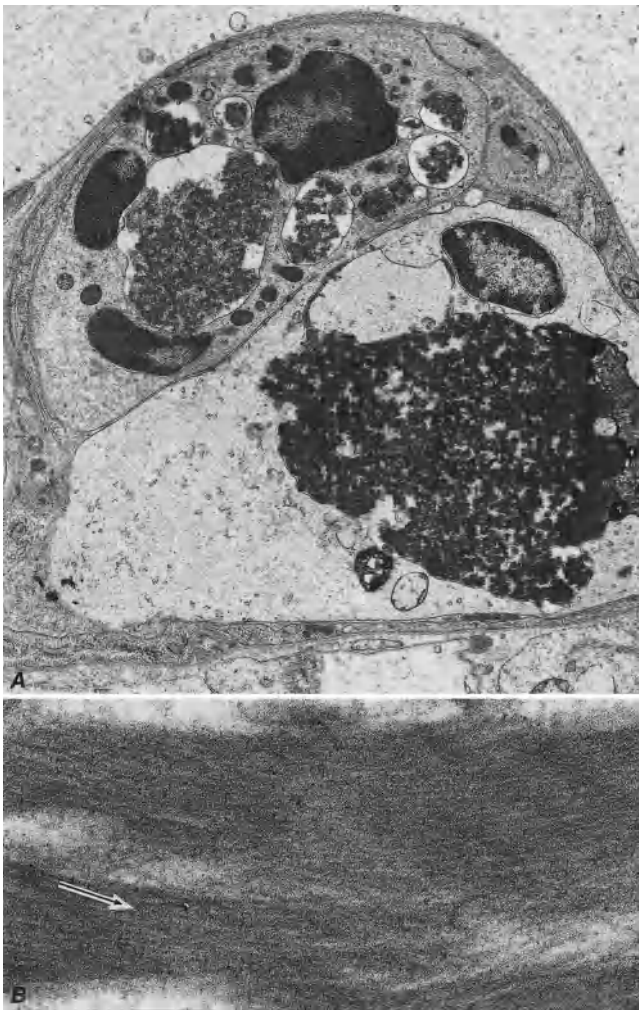


Fig. 10.22 Fibrin: anaphylaxis, pulmonary capillary bed, sheep. **A. Neutrophil uptake**: fibrin is present in large phagosomes of partially (*top*) and totally (*bottom*) degranulated neutrophils. **B. Periodicity of fibrin**: note striations (*arrow*).

Table 10.3 Ultrastructural characteristics of proteins in coagulation.

Protein	*Reference to ultrastructural pathology*
α_2-Macroglobulin	**Schroeter**, *J Struct Biol* 109:235, 1992
Complement	**Svehag**, *Nature* 238:117, 1972 (C1q)
Conglutinin	**Andersen**, *J Struct Biol* 109:201, 1992*
Fibrinogen	**Furie**, *Cell* 53:505, 1988
Fibrin	**Weisel**, *J Ultrastruct Res* 96:176, 1986
IgG (Cryoglobulin)	**Podell**, *Blood* 69:677, 1987
Matrix metalloproteinase-2	**Sawicki**, *Thromb Haemost* 80:836, 1998#

* **Bovine conglutinin** is a plasma lectin that binds to nonreducing terminal mannose, fucose, and N-acetyl-D-glucosamine residues. The antibacterial effect of conglutinin is based on its binding to N-linked glycan in C3 after C3 activation and generation of the C3b fragment.
# **Matrix metalloproteinase-2** (detected by immunogold) was randomly distributed throughout the cytosol in resting human platelets; activation causes translocation to extracellular spaces.

retain a negative charge, the fibrin monomers spontaneously polymerize into overlapping, staggered patterns that give the typical periodicity to fibrin in electron micrographs. Defects in fibrin α or β peptides lead to abnormal fibrin.[270]

Fibrin is stabilized by **factor XIII** (fibrinoligase). Establishment of covalent bonds between fibrin monomers by factor XIII strengthens fibrin strands and stabilizes the fibrin gel. Factor XIII is activated by thrombin from a precursor in plasma and in platelets, and it stitches neighboring fibrin monomers together by forming a peptide bond between side chains to form cross-links. In addition to fibrin-fibrin links, factor XIII also cross links fibrin-fibronectin and fibronectin-collagen thus forming a more stable thrombus. The nature of the fibrin polymer is a major factor in the interaction of fibrin with cells such as leukocytes and macrophages.[271]

α-Macroglobulin, a major proteinase inhibitor in plasma of vertebrates, is a proteinase scavenger that reacts rapidly and irreversible with endoproteinases to protect blood and tissue proteins from degradation during coagulation, fibrinolysis, and complement activation (Table 10.3).

Occuring outside vessels walls when shed blood contacts tissue, extrinsic coagulation is triggered by **tissue factor,** a glycoprotein embedded in membranes of most cells.[272] Also called **thromboplastin** and **coagulation factor III,** tissue factor modifies the enzyme proconvertin (factor VII), which in turn acts on factor X to initiate the common pathway of fibrin formation. In inflammatory lesions, RNA liberated from necrotic cells binds to clotting cascade cofactors and promote clotting.

Platelets in Menorrhagia

One of the best ultrastructural studies of human thrombosis comes from uteri of human patients with **essential menorrhagia.** Endometrial hemostasis during normal menstruation is inhibited (relative to hemostasis in other body parts); vessel lesions with-out any hemostatic reaction occur, hemostatic plugs are small and nonocclusive, and extravascular plugs are not present.[273] Uterine endothelium from patients with essential menorrhagia contains large hemostatic plugs that protrude into extravascular spaces. Ultrastructural analysis showed that thrombi

Vet-ebooks.com

were composed of poorly degranulated platelets with few fibrin fibers. The lack of fibrin is associated with enhanced fibrinolysis and a shift to prostaglandin release (PGI_2 and PGE_2) which inhibits platelet aggregation and promotes vasodilation.[274]

Variability of Thrombi

The heterogeneity of **thrombi** is a reflection of the sites where they are formed, the age of the thrombotic process, and the cells that contribute to thrombus formation. When the **fibrin** around a platelet thrombus becomes fully polymerized, circulating platelets no longer adhere to it easily.

Neutrophils stick to the fibrin-platelet mass by virtue of chemotactic factors produced by plasma-fibrin interaction and the release of platelet factors that interact with complement. Invading neutrophils play an important role in dissolution of the thrombus.[275,276] Neutrophils can also play a major role in the formative stages of thrombosis, particularly in trauma such as infected wounds and postoperative deep vein thrombosis. In studies of the jugular vein of cats after injury by stasis, the first evidence of injury was found to be the accumulation of neutrophils on the surface of endothelium. This was followed closely by adherence of platelets and erythrocytes.[277] Membrane-to-membrane contact has been shown to involve release of neutrophil enzymes onto platelet surfaces.

As thrombi age, **contraction** occurs. The contractile property of platelets resides in microtubules that contain a contractile protein called **thrombosthenin.**[278] Organization proceeds as condensed bands of fibrin and platelets attach to the vascular wall and become overgrown by endothelium.[279] If significant occlusion of the vessel has taken place, **recanalization** occurs by invasion with newly formed capillaries.

Sequential ultrastructural analysis of hemostasis in human skin wounds revealed thrombi at the ends of transected blood vessels. Platelets were enlarged and degranulate, and had pseudopods that interdigitated with adjacent platelets. Fibrin fibers were found at 30 sec both at the periphery of the hemostatic plug and more peripheral along the wound margin.[280,281] In patients treated with **acetylsalicylic acid,** platelets were less degranulate, with fewer pseudopods, and platelets were less interdigitated.

References

1. Zarbock A, Ley K. 2007. Mechanisms and consequences of neutrophil interaction with the endothelium. *Am J Pathol* 172:1.
2. Takizawa T, Robinson JM. 2000. FluoroNanogold is a bifunctional immunoprobe for correlative fluorescence and electron microscopy. *J Hist Cyt* 48:481.
3. Parmley RT, et al. 1987. Peroxidase-containing microgranules in human neutrophils. *Blood* 70:1630.
4. Damiano VV, et al. 1988. Ultrastructural quantitation of peroxidase- and elastase-containing granules in human neutrophils. *Am J Pathol* 131:235.
5. Parmley RT, et al. 1986. Ultrastructural morphology and cytochemistry of iron-deficient polymorphonuclear leukocytes. *Exp Molec Pathol* 44:57.
6. Mason DY, et al. 1991. $Alpha_1$-antitrypsin is present within the primary granules of human polymorphonuclear leukocytes. *Am J Pathol* 139:623.
7. Cham BP, et al. 1994. Granulophysin is located in the membrane of azurophilic granules in human neutrophils and mobilizes to the plasma membrane following cell stimulation. *Am J Pathol* 144:1369.
8. Rice WG, et al. 1987. Defensin-rich granules of human neutrophils. *Blood* 70:757.
9. Madison MN, et al. 2007. Human defensin alpha-1 causes *Trypanosoma cruzi* membrane pore formation and induced DNA fragmentation, which leads to trypanosome destruction. *Infect Immun* 75:4780.
10. Pryzwansky KB, Breton-Gorius J. 1985. Identification of a subpopulation of primary granules in human neutrophils based upon maturation and distribution. *Lab Invest* 53:664.
11. Bentfield ME, et al. 1977. Ultrastructural localization of peroxidase in leukocytes of rat bone marrow and blood. *Anat Rec* 187:219.
12. Press MF, King WJ. 1986. Distribution of peroxidase and granulocytes in the human uterus. *Lab Invest* 54:188.
13. Tydell CC, et al. 2006. Bovine peptidoglycan recognition protein-S antimicrobial activity, localization, secretin, and binding properties. *J Immunol* 176:1154.
14. Cho JH, et al. 2005. Human peptidoglycan recognition protein S is an effector of neutrophil-mediated innate immunity. *Blood* 106:2551.
15. Canonne-Hergaux F, et al. 2002. Expression and subcellular localization of NRAMP1 in human neutrophil granules. *Blood* 100:268.
16. Kobayashi T, Robinson JM. 1991. A novel intracellular compartment with unusual secretory properties in human neutrophils. *J Cell Biol* 113:743.
17. Baggiolini M, et al. 1985. Identification of three types of granules in neutrophils of ruminants. *Lab Invest* 52:151.
18. Gennaro R, et al. 1983. A novel type of cytoplasmic granule in bovine neutrophils. *J Cell Biol* 96:1651.
19. Adachi A, et al. 2007. Electron microscopic studies on the occurance of activated neutrophils in peripheral blood of children with acute leukemias. *J Submicrosc Cytol Pathol* 37:13.
20. Wright SD, et al. 1991. Activation of the adhesive capacity of CR3 in neutrophils by endotoxin. *J Exp Med* 173:1281.
21. Rossi AG, et al. 1993. Stimulation of human polymorphonuclear leukocytes by leukotriene B_4 and platelet-activation factor: An ultrastructural and pharmacological study. *J Leuk Biol* 53:117, 1993.

Vet-ebooks.com

22. Jones DB. 1970. The morphology of acid mucosubstances in leukocytic sticking to endothelium in acute inflammation. *Lab Invest* 23:606.
23. Coates TD, et al. 1991. An inherited defect of neutrophil motility and microfilamentous cytoskeleton associated with abnormality in 47-kD and 89-kD proteins. *Blood* 78:1338.
24. Howard TH, et al. 1998. Lymphocyte-specific protein 1 expression in eukarotic cells reproduces the morphologic and motile abnormality of NAD 47/89 neutrophiles. *Blood* 91:4786.
25. Mukherjee C, Lynn WS. 1978. Role of ions and extracellular protein in leukocyte motility and membrane ruffling. *Am J Pathol* 93:369.
26. Markiewski MM, Lambaris JD. 2007. The role of complement in inflammatory diseases from behind the scenes into the spotlight. *Am J Pathol* 170:715.
27. Devel TF, et al. 1981. Platelet factor 4 is chemotactic for neutrophils and monocytes. *Proc Natl Acad Sci USA* 78:4584.
28. Fava RA, et al. 1991. Transforming growth factor-β1 (TGF-β1) induced neutrophil recruitment to synovial tissues: Implication for TGF-β-driven synovial inflammation and hyperplasia. *J Exp Med* 173:1121.
29. Davis BH, et al. 1982. Membrane activity and topography of F-Met-Leu-Phe-treated polymorphonuclear leukocytes. *Am J Pathol* 108:206.
30. Issekutz AC. 1981. Vascular responses during acute neutrophilic inflammation. *Lab Invest* 45:435.
31. Johnson KJ, et al. 1986. Mediation of IgA induced lung injury in the rat. *Lab Invest* 54:499.
32. Morganroth ML, et al. 1986. Complement and neutrophil-mediated injury of perfused rat lungs. *Lab Invest* 54:507.
33. Abrahamson DR, Fearon DT. 1983. Endocytosis of the C3b receptor of complement within coated pits in human polymorphonuclear leukocytes and monocytes. *Lab Invest* 48:162.
34. Scapini P, et al. 2006. Proinflammatory modulators elicit secretion of the intracellular B-lymphocyte stimulator pool (BLyS) that is stored in activated neutrophils. *Blood* 105:830.
35. Peters-Golden M, Henderson WR. 2007. Leukotrienes. *New Engl J Med* 357:18.
36. Detmers PA, et al. 1987. Aggregation of complement receptors on human neutrophils in the absence of ligand. *J Cell Biol* 105:1137.
37. Ross GD, et al. 1978. The sequential appearance of Ia-like antigens and two different complement receptors during the maturation of human neutrophils. *J Exp Med* 147:730.
38. Carpentier J-L, et al. 1991. Internalization pathway of C3b receptors in human neutrophils and its transmodulation by chemoattractant receptors stimulation. *Cell Regulation* 2:41.
39. Figueroa CD, et al. 1992. Immunovisualization of high (HK) and low (LK) molecular weight kininogens on isolated human neutrophils. *Blood* 79:754.
40. Oliani SM, et al. 2001. Neutrophil interaction with inflamed postcapillary venule endothelium alters annexin 1 expression. *Am J Pathol* 158:603.
41. Gil CD, et al. 2006. Interaction of human neutrophils with endothelial cells regulates the expression of endogenous proteins annexin 1, galectin-1 and galectin-3. *Cell Biol Int* 30:338.
42. La M, et al. 2003. A novel biological activity for galectin-1: Inhibition of leukocyte-endothelial cell interactions in experimental inflammation. *Am J Pathol* 163:1505.
43. Kennedy AD, et al. 2007. Dectin-1 promotes fungicidal activity of human neutrophils. *Eur J Immunol* 37:467.
44. Guerry-Force ML, et al. 1988. Morphology of noncardiogenic pulmonary edema induced by perilla ketone in sheep. *Am J Pathol* 133:285.
45. Smith LA, et al. 2007. Neutrophil traction stresses are concentrated in the uropod during migration. *Biophys J* 92:L58.
46. O'Flaherty JT, et al. 1979. A possible role of arachidonic acid in human neutrophil aggregation and degranulation. *Am J Pathol* 96:799.
47. O'Flaherty JT, et al. 1981. Neutrophil-aggregating activities of monohydroxyeicosatetraenoic acid. *Am J Pathol* 104:55.
48. Picker LJ, et al. 1991. The neutrophil selectin LECAM-1 presents carbohydrate ligands to the vascular selectins ELAM-1 and GMP-140. *Cell* 66:921.
49. Nash S, et al. 1988. The selective and superoxide-independent disruption of intestinal epithelial tight junctions during luekocyte transmigration. *Lab Invest* 59:531.
50. Daukas G, Zigmond SH. 1985. Inhibition of receptor-mediated but not fluid-phase endocytosis in polymorphonuclear leukocytes. *J Cell Biol* 101:1673.
51. Fleit HB, et al. 1987. Fc-mediated endocytosis by human neutrophils. *Lab Invest* 57:699.
52. Weissman G, et al. 1971. Mechanisms of lysosome enzyme release from leukocytes exposed to immune complexes and other particles. *J Exp Med* 134:149s.
53. Zucker-Franklin D, et al. 1971. The effect of the morphine analog levorphanol on phagocytizing leukocytes. *Lab Invest* 25:415.
54. Weissman G, et al. 1972. Leukocyte proteases and the immunologic release of lysosomal enzymes. *Am J Pathol* 68:539.
55. Moore PL, et al. 1978. Phagocytosis of bacteria by polymorphonuclear leukocytes. *J Cell Biol* 76:158.
56. Robinson JM, et al. 1985. Release of superoxide and change in morphology by neutrophils in response to phorbol esters: Antagonism by inhibitors of calcium-binding proteins. *J Cell Biol* 101:1052.
57. Robinson JM, et al. 1987. Cell surface dynamics of neutrophil stimulated with phorbol esters or retinoids. *J Cell Biol* 105:417.
58. Bainton DF. 1973. Sequential degranulation of two types of polymorphonuclear leukocyte granules during phagocytosis of microorganisms. *J Cell Biol* 58:249.
59. Jacques YV, Bainton DF. 1978. Changes in pH within the phagocytic vacuoles of human neutrophils and monocytes. *Lab Invest* 39:179.
60. Becker EL, et al. 1979. Superoxide production induced in rabbit polymorphonuclear leukocytes by synthetic chemotactic peptides and A23187. *Am J Pathol* 95:81.

Vet-ebooks.com

61. Kontos CD, et al. 1992. Cytochemical detection of superoxide in cerebral inflammation and ischemia in vivo. *Am J Physiol* 263:H1234.
62. Saini R, et al. 2006. Nitric oxide synthase localization in the rat neutrophil. *J Leuk Biol* 79:519.
63. Nolan S, et al. 2008. Nitric oxide regulates neutrophil migration through microparticle formation. *Am J Pathol* 172:265.
64. Corbin BD, et al. 2008. Metal chelation and inhibition of bacterial growth in tissue abscesses. *Science* 319:962.
65. Mollineda F, et al. 2006. Combinatorial SNARE complexes modulate the secretion of cytoplasmic granules in human neutrophils. *J Immunol* 177:1831.
66. Henson PM. 1971. The immunologic release of constituents from neutrophil leukocytes. *J Immunol* 107: 1547.
67. Goldstein I, et al. 1973. Mechanisms of lysosomal enzyme release from human leukocytes. *Proc Natl Acad Sci USA* 70:2916.
68. Hoffstein S, Weissmann G. 1978. Microfilaments and microtubules in calcium ionophore-induced secretion of lysosomal enzymes from human polymorphonuclear leukocytes. *J Cell Biol* 78:769.
69. Brinkmann Y, et al. 2004. Neutrophil extracellular traps kill bacteria. *Science* 303:1532.
70. Fuchs TA, et al. 2007. Novel cell death program leads to neutrophil extracellular traps. *J Cell Biol* 176:231.
71. Guigui B, et al. 1988. Toxicity of phorbol myristate acetate-stimulated polymorphonuclear neutrophils against rat hepatocytes. *Lab Invest* 59:831.
72. Varani J, et al. 1985. Pulmonary endothelial cell killing by human neutrophils. *Lab Invest* 53:656.
73. Harlan JM, et al. 1985. Activated neutrophils disrupt endothelial monolayer integrity by an oxygen radical-independent mechanism. *Lab Invest* 52:141.
74. Hoffstein ST, et al. 1985. Surface contact inhibits neutrophil superoxide generation induced by soluble stimuli. *Lab Invest* 52:515.
75. Hoover RL, et al. 1987. Adhesion of polymorphonuclear leukocytes to endothelium enhances the efficiency of detoxification of oxygen-free radicals. *Am J Pathol* 126:258.
76. Gossett KA, MacWilliams PS. 1982. Ultrastructure of canine toxic neutrophiles. *Am J Vet Res* 43:1634.
77. Parmley PT, et al. 1988. Monensin disruption of neutrophil granule genesis. *Am J Pathol* 133:537.
78. McCall CE. 1969. Lysosomal and ultrastructural changes in human toxic neutrophils during bacterial infection. *J Exp Med* 129:267.
79. Yokoi S, Amano N. 1984. Glycogen in leukocytes from patients with hepatic encephalopathy. *Acta Neuropathol* 62:284.
80. Lutas EM, Zucker-Franklin D. 1977. Formation of lipid inclusions in normal human leukocytes. *Blood* 49:309.
81. Weller PF, et al. 1991. Cytoplasmic lipid bodies of neutrophils: Formation induced by *cis*-unsaturated fatty acids and mediated by protein kinase C. *J Cell Biol* 113:137.
82. Sung JH, Okada K. 1971. Neuropathological changes in mink with Chédiak-Higashi disease. *J Neuropathol Exp Neurol* 30:33.
83. Chi EY, et al. 1976. Abnormally large lamellar bodies in type II pneumocytes in Chédiak-Higashi syndrome in beige mice. *Lab Invest* 34:166.
84. Davis WC, et al. 1971. Ultrastructure of bone marrow granulocytes in normal mink and mink with the homolog of the Chédiak-Higashi trait of humans. *Lab Invest* 24:303.
85. Kjeldsen L, et al. 1998. Giant granules of neutrophils in Chédiak-Higashi syndrome are derived from azurophil granules but not from specific and gelatinase granules. *J Leuk Biol* 64:72.
86. Oliver JM. 1978. Cell biology of leukocyte abnormalities. *Am J Pathol* 93:219.
87. Lutzner MA, et al. 1965. Giant granules and widespread cytoplasmic inclusions in a genetic syndrome of Aleutian mink. *Lab Invest* 14:2063.
88. White JG. 1967. The Chédiak-Higashi syndrome. *Blood* 29:435.
89. Kramer JW, et al. 1977. The Chédiak-Higashi syndrome of cats. *Lab Invest* 36:554.
90. Gallin JI, et al. 1975. Defective mononuclear leukocyte chemotaxis in the Chédiak-Higashi syndrome of humans, mink and cattle. *Blood* 45:863.
91. Parmley RT, et al. 1984. Cyclic ultrastructural abnormalities in human cyclic neutropenia. *Am J Pathol* 116:279.
92. Scott RE, et al. 1973. Cyclic neutropenia in grey collie dogs. *Lab Invest* 28:514.
93. Quie PG, et al. 1967. In vitro bactericidal capacity of human polymorphonuclear leukocytes. *J Clin Invest* 46:668.
94. Eschenbach C, Seebach G. 1971. Anomalie der Lysosomenmembran von neutrophilen Granulocyten als Ursache der progressiven septischen Granulomatose. *Virch Arch B* 7:16.
95. Kauder E, et al. 1968. Leukocyte degranulation and vacuole formation in patients with chronic granulomatous disease of childhood. *J Clin Invest* 47:1753.
96. Mandel GL, et al. 1970. The effect of an NADH oxidase inhibitor (hydrocortisone) on polymorphonuclear leukocyte bactericidal activity. *J Clin Invest* 49:1381.
97. Oliver JM, et al. 1977. Mechanisms of microtubule disassembly in vivo. Studies in normal and chronic granulomatous disease leukocytes. *Br J Haematol* 37: 311.
98. Breton-Gorious J, et al. 1980. Lactoferrin deficiency as a consequence of a lack of a specific granule in neutrophils from a patient with recurrent infections. *Am J Pathol* 99:413.
99. Parmely RT, et al. 1983. Abnormal distribution of complex carbohydrates in neutrophils of a patient with lactoferrin deficiency. *Blood* 62:538.
100. Anderson DC, et al. 1985. The severe and moderate phenotypes of heritable Mac-1, LFA-1 deficiency. *J Infect Dis* 152:668.
101. Kehrli ME Jr, et al. 1992. Bovine leukocyte adhesion deficiency. β_2 integrin deficiency in young Holstein cattle. *Am J Pathol* 140:1489.

Vet-ebooks.com

102. Takahashi K, et al. 1987. Bovine granulocytopathy syndrome of Holstein-Friesian calves and heifers. *Jap J Vet Sci* 49:733.
103. Djaldetti M, et al. 1976. Ultrastructural features of the blood cells in a patient with Pelger-Huet anomaly. *Am J Clin Pathol* 65:942.
104. Bowles CA, et al. 1979. Studies of the Pelger-Huet anomaly in foxhounds. *Am J Pathol* 96:237.
105. Breton-Gorius J, et al. 1978. Cytochemical distinction between azurophils and catalase-containing granules in leukocytes. *Lab Invest* 38:21.
106. Nishimura ET, et al. 1976. Ultrastructural localization of peroxidatic catalase in human peripheral blood leukocytes. *Lab Invest* 34:60.
107. Griffin JD. 1983. Impaired superoxide production and prolongation of the respiratory burst due to a low-affinity NADPH-dependent oxidase. *Blood* 62:564.
108. Bohn G, et al. 2007. A novel human primary immunodeficiency syndrome caused by deficiency of the endosomal adaptor protein p14. *Nat Med* 13:38.
109. Peterson LC, et al. 1985. Fechtner syndrome—a variant of Alport's syndrome—with leukocyte inclusions and thrombocytopenia. *Blood* 65:397.
110. Hanker K, et al. 1983. Neutrophil pseudoplatelets. *Science* 220:415.
111. Pickering LK, et al. 1983. Inhibition of human polymorphonuclear leukocyte function by components of human colostrum and mature milk. *Infect Immun* 40:8.
112. Melo RC, et al. 2007. Mechanisms of eosinophil secretion. *J Leuk Biol* 83:229.
113. Weller PF, et al. 1991. Cytoplasmic lipid bodies of human eosinophils. *Am J Pathol* 138:141.
114. Gleich GJ, Adophson CR. 1986. The eosinophilic leukocyte: Structure and function. *Adv Immunol* 39:177.
115. Calafat J, et al. 1998. The bactericidal/permeability-increasing protein (BPI) is present in specific granules of human eosinophils. *Blood* 91:4770.
116. Egesten A, et al. 1986. Localization of eosinophil cationic protein, major basic protein, and eosinophil peroxiase in human eosinophils by immunoelectron microscopic technique. *J Hist Cyt* 34:1399.
117. Peters MS, et al. 1986. Localization of human eosinophil granule major basic protein, eosinophil cationic protein, and eosinophil-derived neurotoxin by immunoelectron microscopy. *Lab Invest* 54:656.
118. Frigas E, et al. 1980. Cytotoxic effects of the guinea pig eosinophil major basic protein on tracheal epithelium. *Lab Invest* 42:35.
119. Tseng YK, et al. 2004. Ultrastructural localization of matrix metalloproteinase-9 in eosinophils from the cerebrospinal fluid of mice with eosinophilic meningitis caused by *Angiostrongylus cantonensis*. *An Trop Med Parasitol* 98:831.
120. Swartz JM, et al. 2004. Plasminogen activator inhibitor-2 (PAI-2) in eosinophilic leukocytes. *J Leuk Biol* 76:812.
121. Pryzwansky KB, Madden YJ. 2003. Type 4A cAMP-specific phosphodiesterase is stored in granules of human neutrophils and eosinophils. *Cell Tiss Res* 312:301.
122. Udby L, et al. 2002. Identification of human cysteine-rich secretory protein (CRISP-3) as a matrix protein in a subset of peroxidase-negative granules of neutrophils and in the granules of eosinophils. *J Leuk Biol* 72:462.
123. Lacy P, et al. 1999. Rapid mobilization of intracellularly stored RANTES in response to interferon-gamma in human eosinophils. *Blood* 94:23.
124. Mabilat-Pragnon C, et al. 1997. Urokinase localization and activity in isolated eosinophils. *Thromb Res* 88:373.
125. Moosbauer C, et al. 2007. Eosinophils are a major intravascular location for tissue factor storage and exposure. *Blood* 109:995.
126. Sur S, et al. 1998. Localization of eosinophil-derived neurotoxin and eosinophil cationic proteins in neutrophilic leukocytes. *J Leuk Biol* 63:715.
127. Levi-Schaffer F, et al. 1996. Identification of interleukin-2 in human peripheral blood eosinophils. *Immunology* 87:155.
128. Moqbel R, et al. 1995. Identification of messenger RNA for IL-4 in human eosinophiles with granule localization and release of the translated product. *J Immunol* 155:4939.
129. Möller GM, et al. 1996. Ultrastructural immunogold localization of interleukin 5 to the crystalloid core compartment of eosinophil secondary granules in patients with atopic astham. *J Hist Cyt* 44:67.
130. Dvoràk AM, et al. 1994. Prostaglandin endoperoxide synthase (cyclooxygenase): Ultrastructural localization to nonmembrane-bound cytoplasmic lipid bodies in human eosinophils and 3T3 fibroblasts. *Int Arch Allergy Immunol* 105:245.
131. Henderson WR, et al. 1983. Horse eosinophil degranulation induced by the ionophore A23187. *Am J Pathol* 111:341.
132. Zabucchi G, et al. 1986. Uptake of human eosinophil peroxidase by human neutrophils. *Am J Pathol* 124:510.
133. Bass DA, et al. 1981. Activation of lysosomal acid phosphatase of eosinophil leukocytes. *Lab Invest* 44:403.
134. Parmley RT. 1982. Ultrastructural visualization of complex carbohydrates in eosinophilic leukocytes. *Am J Anat* 165:53.
135. El-Hashimi W. 1971. Charcot-Leyden crystals. *Am J Pathol* 65:311.
136. Dvorak AM, et al. 1988. Ultrastructural localization of the Charcot-Leyden crystal protein (lysophospholipase) to a distinct crystalloid-free granule population in mature eosinophils. *Blood* 72:150.
137. Zhou Z, et al. 1992. The gene for human eosinophil Charcot-Leyden crystal protein directs expression of lysophospholipase activity and spontaneous crystallization in transiently transfected COS cells. *J Leuk Biol* 52:588.
138. Hamanaka SC, et al. 1993. Ultrastructural morphology, cytochemistry, and morphometry of eosinophil granules in Chédiak-Higashi syndrome. *Am J Pathol* 143:618.
139. Karawajczyk M, et al. 2000. Piecemeal degranulation of peripheral blood eosinophils: A study of allergic subjects during and out of the pollen season. *Am J Respir Cell Mol Biol* 23:521.

Vet-ebooks.com

140. Ogawa H, et al. 1981. Comparative study of eosinophil and neutrophil chemotaxis and enzyme release. *Am J Pathol* 105:149.
141. Litt M. 1963. Studies in experimental eosinophilia. *Am J Pathol* 42:529.
142. Litt M. 1973. Studies in experimental eosinophilia. *J Reticuloendothel Soc* 103:158.
143. Walls RS, et al. 1971. Mechanism for eosinophilic and neutrophile leukocytosis. *Br Med J* 3:157.
144. Ward PA. 1969. Chemotaxis of human eosinophils. *Am J Pathol* 54:121.
145. Mann PR. 1969. An electron microscope study of the relation between mast cells and eosinophil leukocytes. *J Pathol* 98:183.
146. Colley DG. 1973. Eosinophils and immune mechanisms. *J Immunol* 110:1417.
147. Luque EH, Montes GS. 1989. Progesterone promotes a massive infiltration of the rat uterine cervix by the eosinophile polymorphonuclear leukocytes. *Anat Rec* 223:256.
148. Weller PF, et al. 1991. Cytoplasmic lipid bodies of human eosinophils. *Am J Pathol* 138:141.
149. Tsuda S, et al. 1980. Induction of T cell-independent eosinophilia in mice with polymyxin B and schistosome infection. *Lab Invest* 43:495.
150. Jungery M, et al. 1983. Functional abnormalities in the beige mouse eosinophil assessed using *T. spiralis* as a target. *J Pathol* 139:323.
151. Caulfield JP, et al. 1985. Ultrastructure of the attack of eosinophils stimulated by blood mononuclear cells produced on schistosomula of *Schistosoma mansoni*. *Am J Pathol* 120:380.
152. Eversole R, et al. 1999. Changes in the morphology and the distribution of rat intestinal eosinophils during infection with the nematode *Nippostrongylus Brasiliensis*. *Lab Invest* 79:785.
153. Caulfield JP, et al. 1980. The adherence of human neutrophils and eosinophils to schistosomula. *J Cell Biol* 86:46.
154. Caulfield JP, et al. 1980. Partial and complete detachment of neutrophils and eosinophils from schistosomula. Evidence for the establishment of continuity between a fused and normal parasite membrane. *J Cell Biol* 86:64.
155. James SL, Colley DG. 1978. Eosinophil-mediated destruction of *Schistosoma mansoni* eggs in vitro. *Cell Immunol* 38:35.
156. McLaren DJ, et al. 1978. Ultrastructural evidence for complement and antibody-dependent damage to schistosomula of *Schistosoma mansoni* by rat eosinophils in vitro. *Parasitology* 77:313.
157. Grove DI, et al. 1977. Eosinophils and resistance to *Trichinella spiralis*. *J Exp Med* 145:755.
158. Kelenyi G, et al. 1973. Effect of corticosteroids on eosinophil leukcoytes in hypereosinophlic syndromes. *Acta Haematol* (Basel) 49:235.
159. Kawabori S, et al. 1991. The dynamics of intestinal eosinophil depletion in rats treated with dexamethasone. *Lab Invest* 64:224.
160. Junt T, et al. 2007. Dynamic visualization of thrombopoiesis within bone marrow. *Science* 317:1767.
161. Klinger MH, Jelkmann W. 2001. Subcellular localization of thrombopoietin in human blood platelets and its release upon thrombin stimulation. *Br J Haematol* 115:421.
162. Bentfeld-Barker ME, Bainton DF. 1977. Ultrastructure of rat megakaryocytes after prolonged thrombocytopenia. *J Ultrastruct Res* 61:201.
163. Fox JEB, et al. 1990. Role of the membrane skeleton in preventing the shedding of procoagulant-rich microvesicles from the platelet plasma membrane. *J Cell Biol* 111:483.
164. Isenberg WM, et al. 1990. Monoclonal antibodies bound to subunits of the integrin GPIIb-IIIa are internalized and interfere with filopodia formation and platelet aggregation. *Blood* 76:1564.
165. Wencel-Drake JD. 1990. Plasma membrane GPIIb/IIIa. Evidence for a cycling receptor pool. *Am J Pathol* 136:61.
166. Santoso S, et al. 1986. Receptor patching and capping of platelet membranes induced by monoclonal antibodies. *Blood* 67:343.
167. White JG. 1990. Separate and combined interactions of fibrinogen-gold and latex with surface-activated platelets. *Am J Pathol* 137:989.
168. Suzuki H, et al. 2003. Intracellular localization of glycoprotein VI in human platelets and its surface expression upon activation. *Br J Haematol* 121:904.
169. White JG. 1987. The secretory pathway of bovine platelets. *Blood* 69:878.
170. Zucker-Franklin D, et al. 1985. Absence of surface-connected canalicular system in bovine platelets. *Blood* 65:241.
171. Nurden P, et al. 2003. Immunolocalization of P2Y1 and TOPalpha receptors in platelets showed a major pool associated with the membrane of alpha-granules and the open canalicular system. *Blood* 101: 1400.
172. Escolar G, et al. 1989. The fate of the open canalicular system in surface and suspension-activated platelets. *Blood* 74:1983.
173. Boyles J, et al. 1985. Organization of the cytoskeleton in resting, discoid platelets. *J Cell Biol* 101:1463.
174. Tanaka K, et al. 1984. Reorganization of contractile elements in the platelet during clot retraction. *J Ultrastruct Res* 89:98.
175. White JG, Rao GHR. 1983. Influence of a microtubule stabilizing agent on platelet structural physiology. *Am J Pathol* 112:207.
176. Hartwig JH, DeSisto M. 1991. The cytoskeleton of the resting human blood platelet: Structure of the membrane skeleton and its attachment to actin filaments. *J Cell Biol* 112:407.
177. Bearer EL. 1990. Platelet membrane skeleton revealed by quick-freeze deep-etch. *Anat Rec* 227:1.
178. Youssefian T, et al. 1997. Platelet and megakaryocyte dense granules contain glycoprotein Ib and IIb-IIIa. *Blood* 89:4047
179. Morimoto T, et al. 1990. Anchorage of secretion-competent dense granules on the plasma membrane of bovine platelets in the absence of secretory stimulation. *J Cell Biol* 111:79.

Vet-ebooks.com

180. Tolmachova T, et al. 2007. Rab27b regulates number and secretion of platelet dense granules. *Proc Natl Acad Sci USA* 104:5872.
181. Beckstead JH, et al. 1986. Immunohistochemical localization of membrane and α-granule proteins in human megakaryocytes. *Blood* 67:285.
182. Sander HJ, et al. 1984. Immunocytochemical localization of fibrinogen, platelet factor 4, and beta thromboglobulin in thin frozen sections of human blood platelets. *J Clin Invest* 72:1277.
183. Breton-Gorius J, et al. 1992. Localization of platelet osteonectin at the internal face of the alpha-granule membranes in platelets and megakaryocytes. *Blood* 79:936.
184. Handagama PJ, et al. 1987. Incorporation of a circulating protein into megakaryocyte and platelet granule. *Proc Nat Acad Sci USA* 84:861.
185. Breton-Gorius J, et al. 1992. Localization of platelet osteonectin at the internal face of the α-granule membranes in platelets and megakaryocytes. *Blood* 79:936.
186. Cramer EM, et al. 1986. Absence of tubular structure and immunolabeling for von Willebrand factor in the platelet α-granules from porcine von Willebrand disease. *Blood* 68:774.
187. Larson E, et al. 1990. PADGEM-dependent adhesion of platelets of monocytes and neutrophils is mediated by a lineage-specific carbohydrate, LNF III (CD15). *Cell* 63:467.
188. Santoso S, et al. 1986. Receptor patching and capping of platelet membranes induced by monoclonal antibodies. *Blood* 67:343.
189. Hensler ME, et al. 1992. Platelet morphologic changes and fibrinogen receptor localization. *Am J Pathol* 141:707.
190. Escolar G, et al. 1988. Ristocetin induces platelet aggregation: A morphological demonstration. *Br J Haematol* 69:379.
191. Hourdille P, et al. 1990. Thrombin induces a rapid redistribution of glycoprotein Ib-Ix complexes within the membrane system of activate human platelets. *Blood* 76:1503.
192. Kawaguchi Y. 1982. Ultrastructural study on the release reaction of the platelet. *Acta Pathol Jpn* 32:961 and 981.
193. Nakata T, Hirokawa N. 1987. Cytoskeletal reorganization of human platelets after stimulation revealed by the quick-freeze deep-etch technique. *J Cell Biol* 105:1771.
194. White JG, et al. 1988. Platelet membrane ultrastructure and its changes during platelet activation. *Progr Clin Biol Res* 283:1.
195. Wurzinger LJ, et al. 1987. Ultrastructural investigations on the question of mechanical activation of blood platelets. *Blut* 54:97.
196. Hartwig JH. 1992. Mechanisms of actin rearrangements mediating platelet activation. *J Cell Biol* 118:1421.
197. Droller MJ. 1974. An electron microscope study of the time course of platelet nucleotide, calcium, and acid phosphatase secretion. *Lab Invest* 31:197.
198. Ward JV, et al. 1976. Loss of sulfated proteoglycan from the surface of rabbit platelets during adenosine 5′-diphosphonate-induced aggregation. *Lab Invest* 35: 337.
199. Lupu F, et al. 1986. Changes in the organization of membrane lipids during human platelet activation. *Lab Invest* 54:136.
200. Stenberg PE, et al. 1984. Optimal techniques for the immunocytochemical demonstration of β-thromboglobulin, platelet factor 4 and fibrinogen in the alpha-granules of unstimulated platelets. *Histochem J* 16:983.
201. Wencel-Drake JD, et al. 1986. Localization of internal pools of membrane glycoproteins involved in platelet adhesive responses. *Am J Pathol* 124:324.
202. Wencel-Drake JD, et al.1986. Ultrastructural localization of coagulation factor V in human platelets. *Blood* 68:244.
203. Legrand YJ, et al. 1986. Activation of platelets by microfibrils and collagen. *Lab Invest* 54:566.
204. Kolwalski KA, et al. 1983. Modulation of equine platelet function by diethylcarbamazine (DEC). *Am J Pathol* 113:1.
205. Albrecht RM, et al. 1989. Distribution and movement of membrane-associated platelet glycoproteins. *Am J Anat* 185:149.
206. van Deurs B, Behnke O. 1980. Membrane structure of nonactivated and activated human blood platelets as revealed by freeze-fracture. *J Cell Biol* 87:208.
207. Polley MJ, et al. 1981. Thrombin-induced platelet membrane glcyoprotein IIb and IIIa complex formation. *J Exp Med* 154:1058.
208. Lewis JC, et al. 1990. Fibrinogen and glycoprotein IIB/IIIa localization during platelet adhesion. *Am J Pathol* 136:239.
209. Asch AS, et al. 1985. Platelet membrane topography: Colocalization of thrombospondin and fibrinogen with the glycoprotein IIb-IIIa complex. *Blood* 66:926.
210. Isenberg WM, et al. 1987. The platelet fibrinogen receptor: An immunogold-surface replica study of agonist-induced ligand binding and receptor clustering. *J Cell Biol* 104:1655.
211. Suzuki H, et al. 1989. Association of fibrinogen with human platelets pretreated with chymotrypsin or aggregated with ADP or thrombin: An immunocytochemical study. *Br J Exp Pathol* 70:479.
212. Hensler ME, et al. 1992. Platelet morphologic changes and fibrinogen receptor localization. *Am J Pathol* 141:707.
213. Behnke O. 1987. Surface membrane clearing of receptor ligand complexes in human blood platelets. *J Cell Sci* 87:465.
214. Hourdille P, et al. 1985. Distribution of glycoprotein IIb-IIIa complexes in the surface membrane of human platelets and megakaryocytes. *Br J Haematol* 59:171.
215. Loftus JC, Albrecht RM. 1984. Redistribution of the fibrinogen receptor of human platelets after surface activation. *J Cell Biol* 99:822.
216. Beaver E, Friend DS. 1986. Lipids of platelet membrane. *Lab Invest* 54:119.
217. Kang I, et al. 2007. Surface-dependent expression in the platelet GPIb binding domain within human von Willebrand factor studied by atomic force microscopy. *Thromb Res* 119:731.

Vet-ebooks.com

218. Wencel-Drake JD, et al. 1985. Ultrastructural localization of human platelet thrombospondin. *Blood* 65:929.
219. Galvin NJ, et al. 1985. Mapping of epitopes for monoclonal antibodies against human platelet thrombospondin with electron microscopy and high sensitivity amino acid analysis. *J Cell Biol* 101:1434.
220. Gardner JM, Hynes RO. 1985. Interaction of fibronectin with its receptor on platelets. *Cell* 42:439.
221. Rand JH, et al. 1987. Localization of surface vWF on resting and stimulated platelets. *Blood* 70:1297.
222. Valentijn KM et al. 2007. A new look at Weibel-Palade body structure in endothelial cells using electron tomography. *J Struct Biol* 161:447.
223. Macconi D, et al. 1985. Acetyl glycerylphosphorylcholine aggregates human platelets through two distinct pathways, both dependent on arachidonic acid metabolism. *Lab Invest* 52:159.
224. Friesen LL, Gerrard JM. 1985. The effects of 1-oleoyl-2-acetylglycerol on platelet protein phosphorylation and platelet ultrastructure. *Am J Pathol* 121:79.
225. Gerrard JM, et al. 1977. The influence of prostaglandin G_2 on platelet ultrastructure and platelet secretion. *Am J Pathol* 86:99.
226. Gerrard JM, et al. 1989. A role for protein kinase C in the membrane fusion necessary for platelet granule secretion. *Blood* 74:2405.
227. Morgenstern E, Reimers H-J. 1984. The platelet contacts during aggregation. *Blut* 48:81.
228. Clawson CC, White JG. 1980. Platelet interaction with bacteria. V. Ultrastructure of congenital afibrinogenemic platelets. *Am J Pathol* 98:197.
229. Youssefian T, et al. 2002. Host defense role of platelets: Engulfment of HIV and *Staphylococcus aureus* occurs in a specific subcellular compartment and is enhanced by platelet activation. *Blood* 99:4021.
230. Sottnek HM, et al. 1975. The pathogenesis of vaccinia virus toxicity. II. An electron microscopic study. *Lab Invest* 33:22.
231. Larke RPB, et al. 1977. Paramyxovirus-induced platelet aggregation. *Lab Invest* 37:150.
232. Shepro D, et al. 1969. Changes in thrombocyte ultrastructure during clot retraction. *J Cell Sci* 4:763.
233. Jorgensen L. 1986. Injury to cultured endothelial cells by thrombin-stimulated platelets. *Lab Invest* 54: 408.
234. Qi B, Hardwick JM. 2007. A Bcl-x_L timer sets platelet life span. *Cell* 128:1035.
235. Weiss HJ, Ames RP. 1973. Ultrastructural finding in storage pool disease and aspirin-like defect of platelets. *Am J Pathol* 71:447.
236. Sanders WE, et al. 1988. Thrombotic thrombocytopenia with von Willebrand factor deficiency induced by botrocetin. *Lab Invest* 59:443.
237. Hughes M, et al. 2000. The use of electron microscopy in the investigation of the ultrastructural morphology of immune thrombocytopenic purpura platelets. *Semin Hematol* 37:222.
238. Ishihara T, et al. 1984. Foamy cells associated with platelet phagocytosis. *Am J Pathol* 114:104.
239. Daniels TM, et al. 1986. Platelet storage pool deficiency in swine. *Blood* 67:1043.
240. Lages B, et al. 1991. Decreased content and surface expression of α-granule membrane protein GMP-140 in one of two types of platelet αδ storage pool deficiency. *J Clin Invest* 87:919.
241. Xu Z, et al. 1988. Ultrastructure and function of thrombocytes in a family with congenital bleeding tendency. *J Ultrastruc Molec Struc Res* 100:126.
242. Cramer EM, et al. 1985. Eccentric localization of von Willebrand factor in an internal structure of platelet α-granules resembling that of Weibel-Palade bodies. *Blood* 66:710.
243. White JG. 1979. Ultrastructural studies of the gray platelet syndrome. *Am J Pathol* 95:445.
244. Rosa J-P, et al. 1987. Gray platelet syndrome: Demonstration of alpha granule membranes that can fuse with the cell surface. *J Clin Invest* 80:1138.
245. Breton-Gorius J, et al. 1981. Defective alpha-granule production in megakaryocytes from gray platelet syndrome. *Am J Pathol* 102:10.
246. Nurden P, et al. 2004. Severe deficiency of glycoprotein VI in a patient with gray platelet syndrome. *Blood* 104:107.
247. Gerrard JM, et al. 1979. α-actinin deficiency in thrombasthenia. *Am J Pathol* 94:509.
248. Maldonado JE, et al. 1975. Ultrastructure of platelets in Bernard-Soulier syndrome. *Mayo Clinic Proc* 50:402.
249. Greinacher A, et al. 1990. Sebastian platelet syndrome: A new variant of hereditary macrothrombocytopenia with leukocyte inclusions. *Blut* 61:282.
250. Heynen MJ, et al. 1988. Congenital macrothrombocytopenia, leukocyte inclusions, deafness, and proteinuria: Functional and electron microscopic observations on platelets and megakaryocytes. *Br J Haematol* 70:441.
251. Wu S, et al. 2006. An inherited macrothrombocytopenic disorder with abnormal large granules. *Platelets* 17:259.
252. White JG, Ahlstrand GG. 2003. Giant electron dense chains, clusters and granules in megakaryocytes and platelets with normal dense bodies: An inherited thrombocytopenic disorder IV. Ultrastructural cytochemistry and analytical electron microscopy. *Platelets* 14:313.
253. Nurden P, et al. 2000. Platelet ultrastructural abnormalities in three patients with type 2B von Willebrand disease. *Br J Haematol* 110:704.
254. Peterson LC, et al. 1985. Fechtner syndrome—a variant of Alport's syndrome with leukocyte inclusions and macrothrombocytopenia. *Blood* 65:397.
255. Molina IJ, et al. 1992. T cell lines characterize events in the pathogenesis of the Wiskott-Aldrich syndrome. *J Exp Med* 176:867.
256. White JG, et al. 1971. Studies of platelets in a variant of the Hermansky-Pudlak syndrome. *Am J Pathol* 63:319.
257. Bell TG, et al. 1976. Decreased nucleotide and serotonin storage associated with defective function in Chédiak-Higashi syndrome in cattle and human platelets. *Blood* 48:175.
258. Meyers KM, et al. 1982. Ultrastructure of resting and activated storage pool deficient platelets from animals with the Chédiak-Higashi syndrome. *Am J Pathol* 106:364.

Vet-ebooks.com

259. Rendu F, et al. 1983. Evidence that abnormal platelet functions in human Chédiak-Higashi syndrome are the result of a lack of dense bodies. *Am J Pathol* 111:307.
260. Yarom R, et al. 1980. Platelet pathology in patients with idiopathic scoliosis. *Lab Invest* 43:208.
261. Hamilton RW, et al. 1980. Platelet function, ultrastructure, and survival in the May-Hegglin anomaly. *Am J Clin Pathol* 74:663.
262. Mosesson MW, et al. 1987. Studies on the ultrastructure of fibrin lacking fibrinopeptide B (β-fibrin). *Blood* 69:1073.
263. Mistry N, et al. 2000. Cytoskeletal regulation of the platelet glycoprotein Ib/V/IX-von Willebrand factor interaction. *Blood* 96:3480.
264. Hovig T, Stormorken H. 1974. Ultrastructural studies on the platelet plug formation in bleeding time wounds from normal individuals and patients with von Willebrand disease. *Acta Pathol Microbiol Scand A* 248:105 (Suppl).
265. Sawada Y, et al. 1986. Hemostatic plug formation in normal and von Willebrand pigs. *Blood* 67:1227.
266. Weisel JW. 1986. The electron microscope banding pattern of human fibrin. *J Ultrastruct Res* 96:176.
267. Furie B, Furie BC. 1988. The molecular basis of blood coagulation. *Cell* 53:505.
268. Carradice D, Lieschke GJ. 2008. Zebrafish in hematology. *Blood* 111:3331.
269. Podell DN, et al. 1987. Characterization of monoclonal IgG cryoglobulins: Fine-structural and morphological analysis. *Blood* 69:677.
270. Mosesson MW, et al. 1990. Structural model of porcine factor VIII and factor VIIIa molecules based on scanning transmission electron microscope (STEM) images and STEM mass analysis. *J Clin Invest* 85:1983.
271. Ciano PS, et al. 1991. Macrophage migration in fibrin gel matrix. *Lab Invest* 54:62.
272. Drake TA, et al. 1989. Functional tissue factor is entirely cell surface expressed on lipolysaccharide-stimulated human blood monoyctes and a constitutively tissue-factor-producing neoplastic cell line. *J Cell Biol* 109:389.
273. Sheppard BL, et al. 1983. An ultrastructural study of menstrual blood in normal menstruation and dysfunctional uterine bleeding. *Br J Obstet Gynaecol* 90:259.
274. Van Eijkeren MA, et al. 1991. Morphology of menstrual hemostasis in essential menorrhagia. *Lab Invest* 64:284.
275. Cybulsky MI, et al. 1988. Acute inflammation and microthrombosis induced by endotoxin, interleukin-1, and tumor necrosis factor and their implication in gram-negative infection. *Lab Invest* 58:365.
276. Ratliff NB, et al. 1979. Platelet-leukocyte interactions following arterial endothelial injury. *Am J Pathol* 96:567.
277. Schaub RG, et al. 1984. Early events in the formation of a venous thrombus following local trauma and stasis. *Lab Invest* 51:218.
278. Zucker-Franklin D, et al. 1967. Ultrastructure of thrombosthenin. *Science* 157:945.
279. Prathap K. 1972. Surface lining cells of healing thrombi in rat femoral veins. An electron-microscope study. *J Pathol* 107:1.
280. Wester J, et al. 1979. Morphology of the hemostatic plug in human skin wounds. *Lab Invest* 41:182.
281. Wester J, et al. 1978. Morphology of the early hemostasis in human skin wounds. *Lab Invest* 39:298.

Vet-ebooks.com

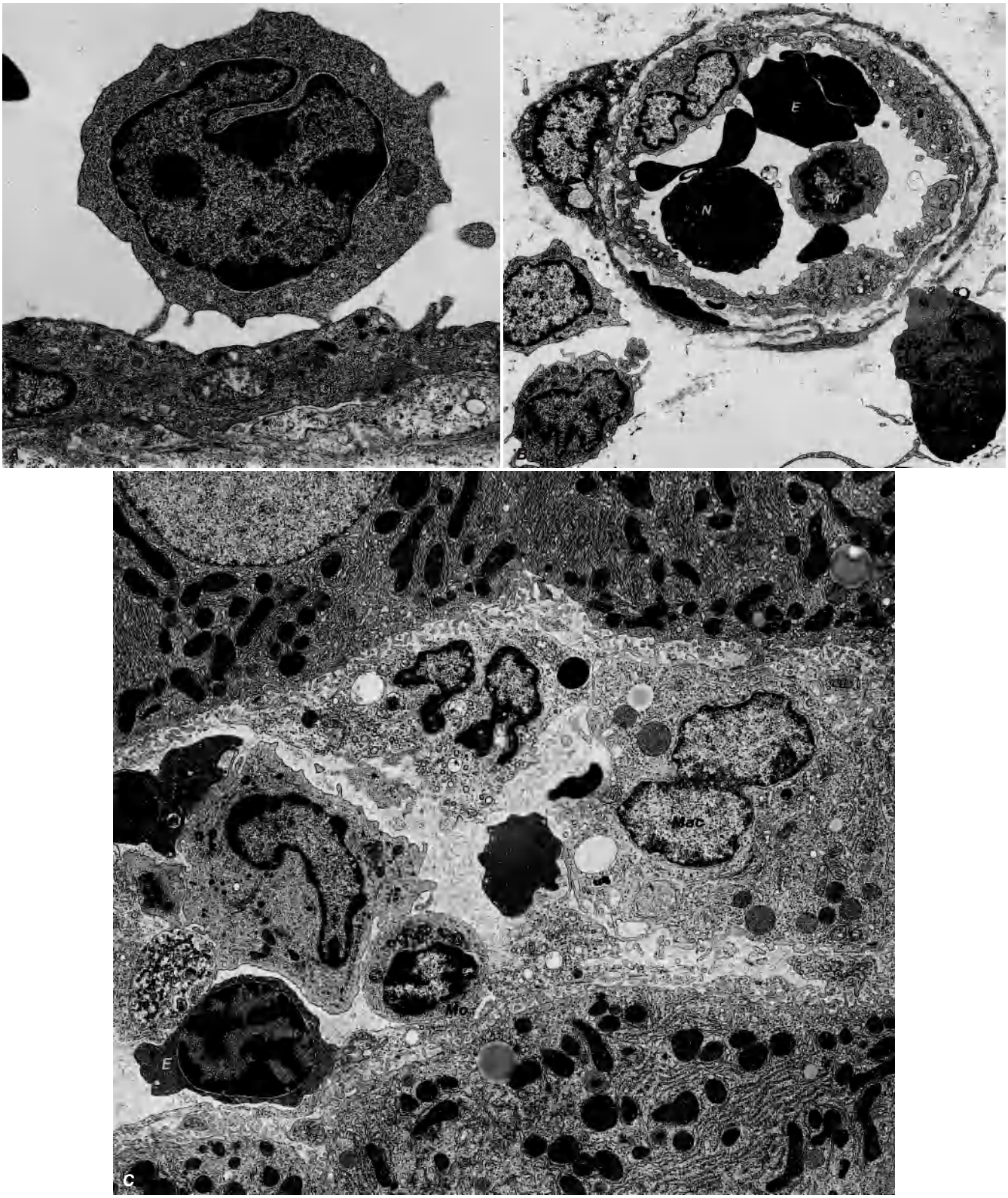


Fig. 11.1 Monocytes. **A. Monocyte**: attached to endothelium. **B. Inflammatory cells**: in lumen and surrounding a postcapillary venule in inflamed skin of a rat. Monocyte (*M*), neutrophil (*N*), erythrocyte (*E*). Endothelial cells are swollen with irregular surfaces. One monocyte (*lower left*) has passed through the vascular wall. **C. Large activated macrophages**: sinusoids of liver in a rat with hepatitis induced by pasteurella toxin. Endothelium of sinusoid is degenerate and irregular. Monocyte (*Mo*), macrophage (*Mac*), erythroblast (*E*).

© 2009 Wiley-Blackwell. ISBN: 978-0-813-80330-2

Vet-ebooks.com

11 The Mononuclear Phagocyte System and Lymphocytes

Randy E. Sacco

Cellular processes that are activated and interact during host immune responses include: (1) phagocytosis and antigen presentation by cells of the **mononuclear phagocyte system (monocytes, macrophages, and dendritic cells),** and (2) cell-mediated and humoral immunity by **lymphocytes** (B, T, and NK cells).

The Monocyte-Macrophage System

Monocytes

Blood monocytes are short-lived, immature members of the monocyte-macrophage system. They are destined to pass endothelial barriers and become one of the major types of phagocytic cells that populate the body. Monocytes are small cells with a large nucleus:cytoplasm ratio. Ultrastructurally, they have large Golgi zones and several Golgi-associated granules but few other organelles (Fig. 11.1). Monocytes are differentiated from large lymphocytes with specific staining techniques. In general, the cytoplasm of monocytes is more abundant, and the larger nucleus is eccentric and bean-shaped. The plasma membrane imparts special functions to these cells. It is thrown into many surface filopodia, which, in the process of migration through vascular walls, is important in contact with endothelial cells.

Monocyte activation, which occurs via a variety of cytokines and other stimuli, causes monocytes to transform into macrophages and to participate in the continual scavenging of microbes and tissue debris. **Interferon-γ** (IFN-γ) is a potent monocyte activator and causes increased expression of Fc receptors and class II MHC antigens on monocyte surfaces. Monocytes activated by IFN-γ have increased cytoplasmic volumes with increases in free ribosomes, rough endoplasmic reticulum, and Golgi saccules.[1] Coupling of IFN molecules with colloidal gold or ferritin and following movement by electron microscopy showed that IFN binds to cell surface IFNγR and clusters into coated pits. More recently, it was shown that the **IFNγ-IFNγ receptor complex** can be taken up via caveolae or clathrin-coated pits.[2] It was suggested that these two pathways could result in IFNγ-IFNγR accumulating in different subcellular compartments.

Monocytosis is a response to bacterial infection, both in acute disease and in recovery phases. In severe bacteremia and septicemia, monocytes phagocytize while in the bloodstream to become circulating macrophages. Monocytes emigrate into inflammatory lesions and promptly transform into macrophages. Evidence of synthesis of new lysosomal enzymes appears first in endoplasmic reticulum and can be detected as the monocyte adheres to endothelium. Monocytes enter acute inflammatory exudates simultaneously with neutrophils; they do not appear in large numbers in early stages because (1) substances chemotactic for neutrophils have little effect on monocytes, (2) monocytes are not as aggressively ameboid as neutrophils, (3) fewer monocytes circulate in blood, and (4) their reproduction is stimulated at a slower rate.

Macrophages

Macrophages, in the unstimulated state, are large, pale cells with highly developed Golgi complexes and many small primary lysosomes. Lysosomes contain potent acid hydrolases, lysozyme, and other enzymes.

Vet-ebooks.com

Ultrastructurally, resting macrophages have large elongate nuclei and a large volume of cytoplasm. Once activated, there is great variation in ultrastructure. Their appearance is a reflection of varible differentiation pathways, stages of maturation, and states of activation. Macrophages differentiate and mature in response to cytokines that direct the developing macrophage into appropriate pathways of the monocyte/macrophage lineage. Macrophages are involved in uptake and processing of antigens for the immune response. Antigens are taken up by endocytosis, shunted to lysosomes, processed and transported to appropriate pathways.

Activated Macrophages

Activation of macrophages occurs in the presence of particulate material and strong microbial antigens, and is mediated through interactions with cell surface receptors and in response to cytokines elaborated by cells in the local microenvironment. Activated (or stimulated) macrophages are distinguished from nonactive, or resting, forms by striking changes in the cell surface molecules expressed as well as changes in ultrastructure. **Activated macrophages** have increased numbers of lysosomes, mitochondria, and pinocytotic vesicles. The Golgi complex is enlarged, and there are various-sized granules throughout the cytoplasm. The rate of activation is influenced by increased body temperature, the protein microenvironment around the macrophage, and other factors.

Surface Receptors Macrophages have specific receptors on their surfaces designed for recognition and uptake of microbial structures as well as an array of endogenous molecules. For example:

- **Scavenger receptors (Class A–H)** mediate endocytosis of diverse groups of molecules, one of the most important being low-density lipoproteins that are involved in deposition of cholesterol in atherogenesis.
- **Receptors that contain scavenger receptor cysteine repeat (SRCR) domains** (e.g., CD163 binds hemoglobin : haptoglobin complexes).
- **CD11/CD18 family receptors** (CD11a (LFA-1), CD11b (CR3), CD11c (CR4 p150, 95)) of macrophage surface receptors have lectin-like sites that bind molecules such as bacterial cell surface molecules, complement components, and fibrinogen. The complexes that result have strong stimuli for endocytosis in resting macrophages.
- **CD14** binds to bacterial lipopolysaccharide (LPS)/lipopolysaccharide binding protein.
- **CD16, CD32, and CD64** have low and high affinity FcγR.
- **Receptors for various glycosylated proteins** (e.g., CD206, a mannose receptor).
- **Toll-like receptors (TLRs)** transduce signals in response to pathogen-associated molecule patterns (PAMPs) such as LPS, lipoticoeic acid, lipoarabinomannan (LAM).
- **Chemokine/cytokine receptors.**

Macrophage Cytokine Secretion Activated macrophages secrete two potent proinflammatory cytokines: **tumor necrosis factor-α** (TNF-α) and **interleukin 1β (IL-1β)**; they also release PGE_2, IL-6, IL-8, and other cytokines as well as complement components, plasminogen activators, chemokines, and several other substances. Cytokines have a marked effect at local sites of secretion; they also enter the bloodstream where they are rapidly cleared by binding to other proteins; in the bloodstream, **α_2-macroglobulin**, a proteinase inhibiter in plasma, binds several cytokines and inhibits their effects (e.g., **α_2-macroglobulin-TNF complexes** are rapidly cleared from the bloodstream).

Monocytes and macrophages secrete soluble mediators that are major contributors to the regulation of the cytokine/chemokine network. In addition to modifying the function of other cell types, monocyte/macrophage lineage cell function is also regulated by these immune mediators. **IL-1β** released by activated macrophages stimulates lymphocytes, endothelial cells, and other macrophages; it initiates chemotaxis and promotes adhesion of these cells to endothelium.[3] Macrophage-derived IL-1 and TNF can act in an autocrine manner to amplify immune complex responses by other macrophages. For example, production of reactive oxygen species by alveolar macrophages is significantly increased by IL-1.[4] The **CXC chemokine IL-8 (CXCL8)** secreted by activated macrophages is a key neutrophil chemotactic peptide. Macrophage secretion of **CC chemokines** (e.g., MCP-1 (CCL2), MIP-1α(CCL3), MIP-1β (CCL4), and MDC (CCL22)) is important for the timely recruitment of other leukocyte subpopulations (monocytes and lymphocytes) during inflammatory responses.[5]

Macrophages in Inflammation

In **acute inflammation**, macrophages are a critical line of defense. They phagocytize bacteria, fibrin, and other particulate material and digest it intracellularly. Fibrin is particularly important, since the manner in which it polymerizes will determine the extent to which macrophage processing and migration are inhibited.[6]

Macrophages are not rapidly attracted by the chemotactic molecules that attract neutrophils and they are less discriminating in the material they

Vet-ebooks.com

phagocytose. Bacteria are phagocytized, and the phagosomal membrane is tightly apposed to the bacterial surface. Phagocytosis is slower and degradation is less complete. In contrast to neutrophils, a large part of macrophage uptake occurs by pinocytosis. Digested debris accumulates in large membrane-bound residual bodies (secondary lysosomes), which may, by exocytosis, deposit their contents outside the cell.

Intracellular Microbial Killing **Activated macrophages** undergo a rapid and immediate respiratory burst with production of toxic oxygen intermediates. The reaction is microbiocidal and organisms are killed in a manner similar to that in activated neutrophils. A second system of toxic nitrogen intermediate production operates in macrophages that occurs later and that kills a different spectrum of organisms.

Nitric oxide (NO) is a short-lived intermediate derived in macrophages in a reaction catalyzed by nitric oxide synthase. LPS, interferon-γ, and other cytokines induce NO synthase (NOS) in macrophages. NO inhibits several metabolic pathways in the cell including the citric acid cycle, complexes I and II of mitochondria, and enzymes of iron release. NOS can play a role in normal physiological processes or in inflammation, these distinct roles being due to the differential expression of two major isoforms of NOS, constitutive (cNOS) and inducible (iNOS).

Phagolysosomes are the site of killing and degradation of microorganisms (Fig. 11.2). As degradation

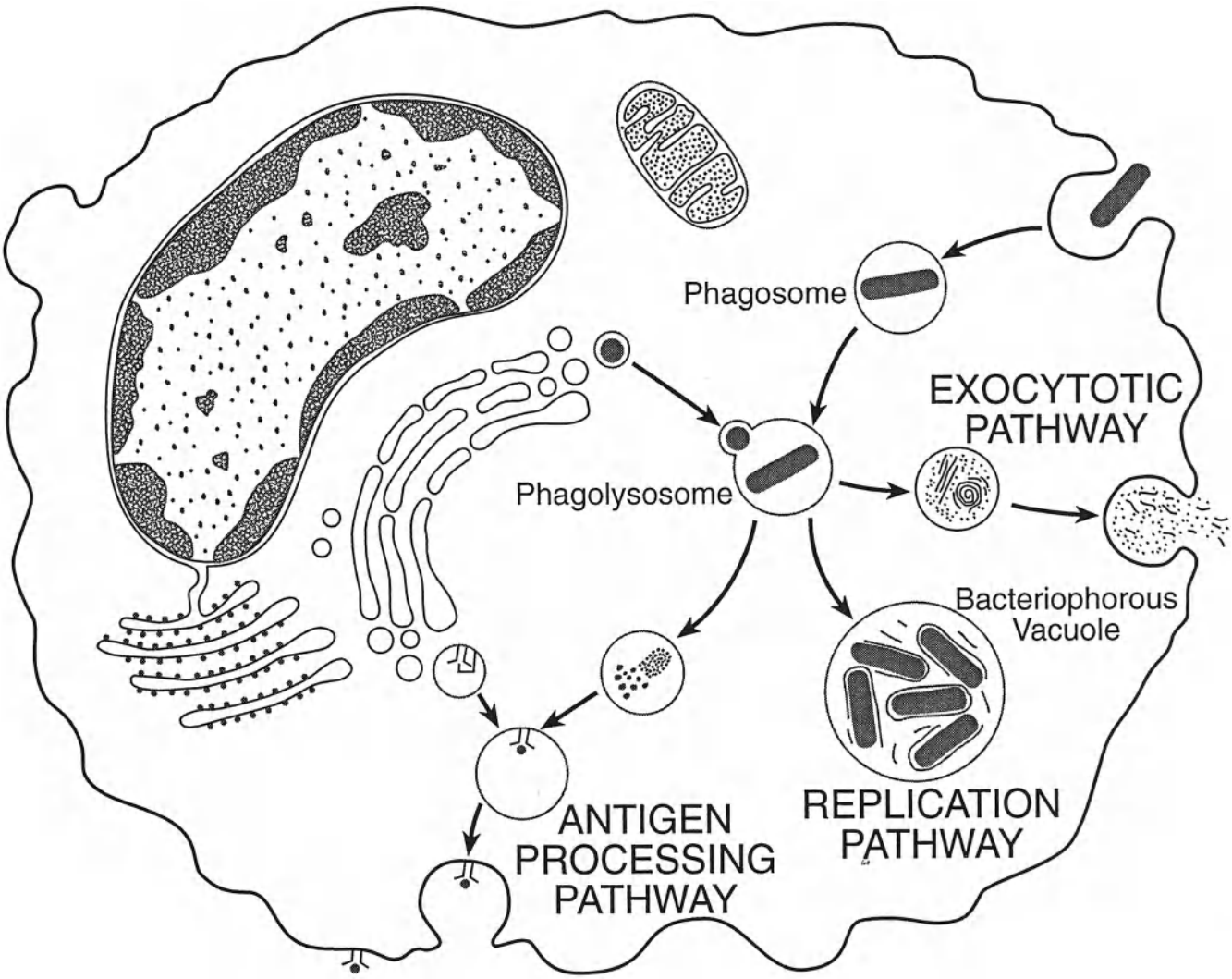


Fig. 11.2 Macrophages. Intracellular trafficking pathways for bacteria: (1) **uptake of bacillus** into endosome at the cell surface; (2) **phagosome** moves into the cytosol, and acidification occurs; (3) **phagolysosome** results from merger of bacteria-bearing phagosome with enzyme-bearing lysosome—three alternative routes are then taken; (4) **exocytotic pathway**: degradation and release of bacterial products from the cell; (5) **bacteriophorous vacuole pathway:** the phagolysosome is transformed by bacteria to assist bacterial replication; (6) **antigen processing pathway**: bacterial protein degraded to antigenic peptides, combined with carrier molecules and present at the cell surface.

Vet-ebooks.com

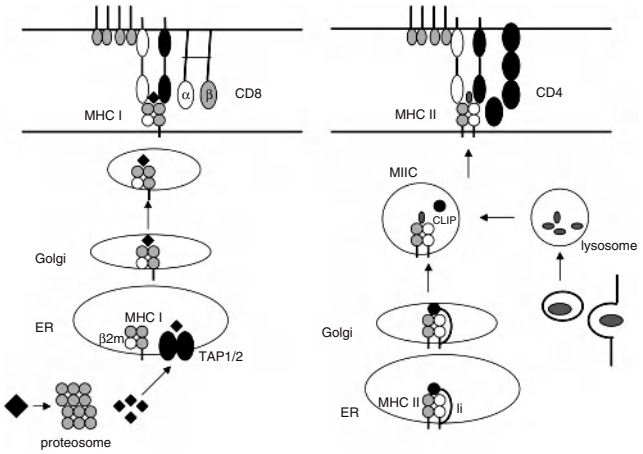


Fig. 11.3 Antigen processing pathways for presentation via **MHC class I** or **MHC class II molecules**. **Exogenous molecules** are degraded by lysosomal or endosomal enzymes. MHC class II molecules are assembled with chaparone invariant chain (Ii). **CLIP (class II-associated invariant peptide)** is degraded and antigenic peptides captured. Class II/antigenic peptide is expressed on the cell surface for presentation to CD4 T cells. **Endogenous antigens** are degraded by proteases and transported to the ER by **transporter-associated antigen processing (TAP)**, where they bind to MHC class I. MHC class I/antigenic peptide is expressed on the cell surface for presentation to CD8 T cells.

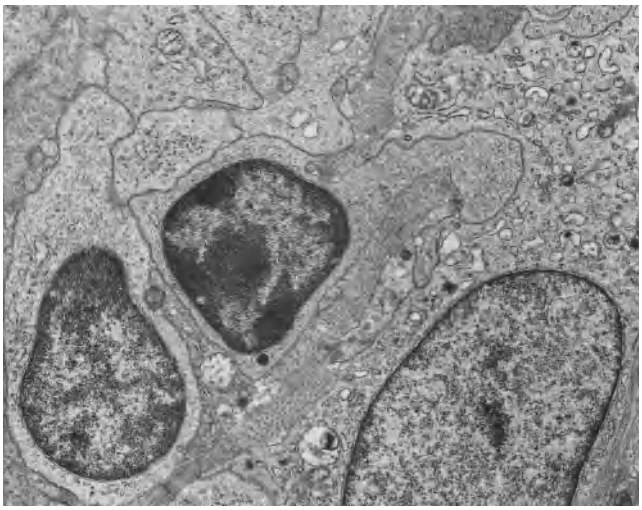


Fig. 11.4 Macrophages. **Interaction of macrophage** (*right*) with small lymphocyte (*center*).

proceeds, bacterial structure is effaced and the bacterial cell is increasingly difficult to identify. Bacterial antigens remain, however, and can be specifically labeled long after degradation is complete. There is typically a progressive accumulation of membranes in lysosomes degrading bacteria. Difficult to degrade, the membranes tend to realign in laminar or whorled arrangements.

The inner face of the **plasma membrane,** smooth in the resting macrophage, is spotted with clathrin as the process of phagocytosis progresses.[7] Cytoplasmic vacuoles and Golgi saccules move toward the reactive surface of the macrophage.[8] **Golgi complexes,** normally clustered near centrioles, are dispersed into vesicles and reorganized near basal surfaces. Cisternae of the Golgi complex swell, become fragmented, and decrease in number.

Antigen Presentation

Antigens are presented to lymphocytes by macrophages, dendritic cells, and B cells by mechanisms that operate at the cell surface (Figs. 11.3 and 11.4). The **MHC class II molecules** consist of two nonidentical glycoproteins, α and β chains that function at the surface of antigen presenting cells. During intracellular transport, MHC class II molecules are inserted into membranes of the **endoplasmic reticulum,** associated with the invariant chain Ii, a chaperone that inserts its CLIP region into the peptide binding cleft. The oligomeric complex of class II and CLIP is transported to an **endocytic compartment** where they dissociate, and class II molecules are then transported to the **plasma membrane**.[9] MHC class I molecules are composed of three alpha chains (α1, α2, and α3). These molecules present shorter peptides (8–10 mers) to CD8 T cells. Peptides are cleaved in the cytosol by various proteases (including the proteosome) and are transported to pre-Golgi where they participate in assembly of class I heavy chains with β2 microglobulin.[10]

Macrophages in Chronic Inflammation

Two patterns of tissue response occur in chronic inflammation; they form a spectrum, the extremes of which are

- **Persistent acute inflammation** is a continuing, unresolved acute process of neutrophils and exudates that slowly becomes dominated by macrophages, fibrous tissue, and blood vessels. The etiologic agents involved in this **active inflammation** are typically bacteria and fungi.
- **Evolving chronic inflammation** progresses slowly from the start in a process that is dominated by the **monocyte-macrophage lineage** cells that deal with persistent injury.

Macrophages and Granulomatous Inflammation
Granulomatous inflammation is dominated by activated monocytes and macrophages. Hypertrophied, vacuolar, and foamy macrophages are called **epithelioid cells**. Granulomatous inflammation is associated with substances that macrophage lysosomes cannot adequately degrade such as infections with mycobac-

Vet-ebooks.com

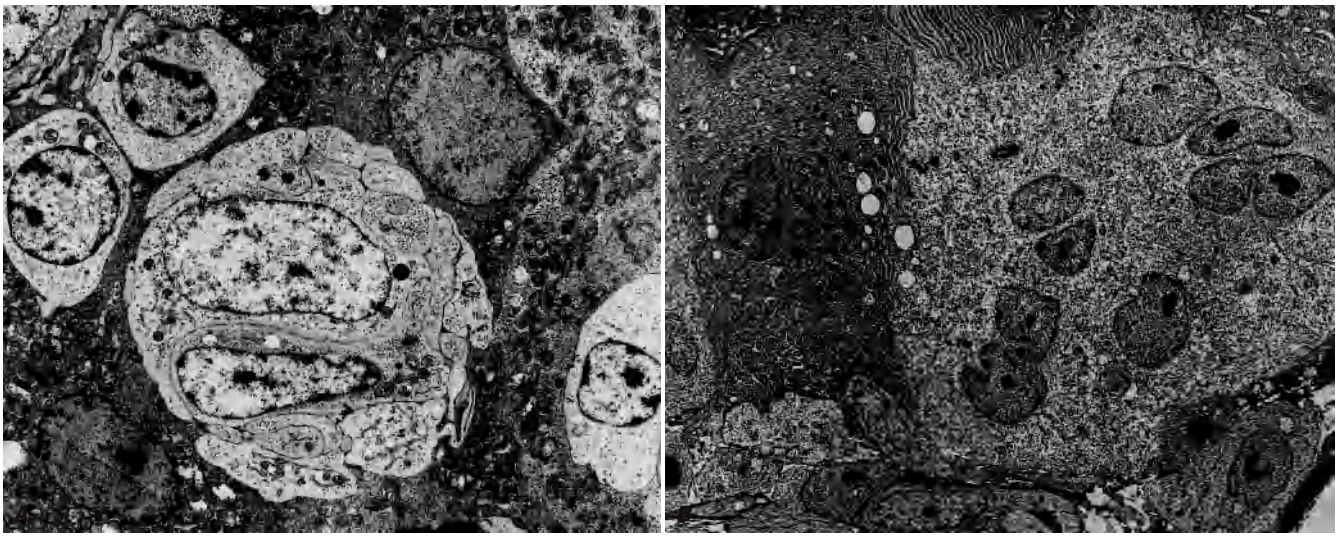


Fig. 11.5 Macrophage in chronic disease. A. Microgranuloma: macrophages are closely apposed and surrounded by monocytes, liver. **B. Giant cell**: lung, aspergillosis. Marked undulation and interdigitation of filopodia of giant cell with adjacent macrophages.

teria, fungi, aberrant parasites, and bacteria, and inert particles such as asbestos and silica. Phagocytosis of the inciting material is followed by failure of lysosomes to kill or digest the material, and degeneration and death of the macrophage. Blood monocytes and new macrophages collect in progressively enlarging foci called **granulomas** (Fig. 11.5). Granulomas provide effective means of localizing causal agents and allowing other inflammatory and immunologic mechanisms to act for longer periods of time.

Ultrastructurally, macrophages in progressively expanding granulomas have enlarged and developed increases in lysosomes, Golgi complexes, and vesicles. Lipids accumulate and, in some granulomas, give the macrophage a foamy appearance.[11] Striking undulations and pseudopods characterize the plasma membrane. Specific organisms and protein crystals can often be seen within phagosomes and phagolysosomes, but most often this material appears as amorphous debris and membrane fragments. As a result of degenerative processes initiated by phagocytized materials, autophagy is conspicuous.

Granulomas are chronic inflammatory lesions produced in response to a persistent nidus. For example, streptococcal cell wall polysaccharides induce granulomas with no specific T cell basis; neither antibodies nor lymphocytes play a role in the evolution or resolution of the lesions. Macrophage cytokines, released locally in the infected environment, amplify granuloma development in an autocrine or paracrine way; for example, TNF enhances its own synthesis and release. Macrophages (and fibroblasts) express embryonic fibonectins and other matrix components that are important in wound healing.[12]

As the infectious granuloma expands, it becomes increasingly complex. Although the dominant cell type remains the macrophage, many other cells invade the granuloma. Dendritic cells loaded with antigen migrate to draining lymph nodes where they interact with naive $CD4^+$ T cells. In response to antigen and IL-12, these cells differentiate into activated $CD4^+$ T_{H1} cells. **Antigen-specific lymphocytes** preferentially traffic to granulomas and lymphocyte cytokines released in the reaction induce not only the rapid infiltration of monocytes and macrophages but accelerate the activation of macrophages within the granuloma. Various other cell types, including B cells and neutrophils, can be found in the mature granuloma.

Pathologic Proliferation of Macrophages

Giant Cells

Fusion of monocytes and macrophages can give rise to **giant cells**. Giant cells have extensive undulation of plasma membranes and interdigitate with adjacent monocytes and macrophages (Fig. 11.5). Membrane fusion occurs in regions of extensive plasma membrane interdigitation, resulting in cells with multiple nuclei. Nuclei may be clustered in the center of the cell or arranged in ring form around the periphery.

Giant cells can be induced directly by microbial products or indirectly by antigen-induced release of cytokines by T lymphocytes. When stimulated by specific antigens, T lymphoyctes produce a soluble protein that causes circulating monocytes to fuse and form multinucleated cells. The fungal metabolite

Vet-ebooks.com

cytochalasin, produced by some aspergilli, affects cell movement by altering **microtubules** of macrophages; plasma membranes are affected, and fusion results in large, multinuclear giant cells. **Cytokinesis** (cytoplasmic division) is inhibited but **karyokinesis** (nuclear division) is not. Cell movement and granule secretion are also inhibited, and this may affect giant cell formation. Certain viruses also induce giant cells by causing cell fusion; for example, paramyxoviruses and other viruses that bud from plasma membranes. Human immunodeficiency virus-1 (HIV-1) interacts with the CD4 antigen and co-receptors (primarily CCR5 or CXCR4) on the surface of T lymphocytes and macrophages; these receptors interact with viral envelope glycoproteins (e.g., gp120). Fusion is mediated via the trimeric transmembrane glycoprotein gp41. Multinucleated giant cells form when envelope glycoproteins expressed on infected cells interact with CD4 and co-receptors on adjacent cells.[13]

Sarcoidosis

Sarcoidosis is an idiopathic disease with noncaseating granulomas in varying tissues. Granulomas are composed of closely apposed epitheliod cells, $CD4^+$ T lymphocytes and often Langerhans'-type giant cells in the center, and $CD8^+$ T cells and B lymphocytes in the periphery.[14] The more chronic lesions of sarcoidosis have fibrosis, hyalin scars, laminated concretions of calcium (Schaumann bodies, and stellate inclusions within giant cells (asteroid bodies).[15] These stellate inclusions can be observed by electron microscopy to be composed of microfilaments, microtubules, mature centrioles, and paracentrioles embedded in an amorphous matrix.[14] Recent data suggests that a T_{H1}-mediated immune mechanism is involved in sarcoidosis, in which T cells are activated, and secreted cytokines such as IL-2, IFN-γ, and TNF-α are involved in disease pathogenesis.[16]

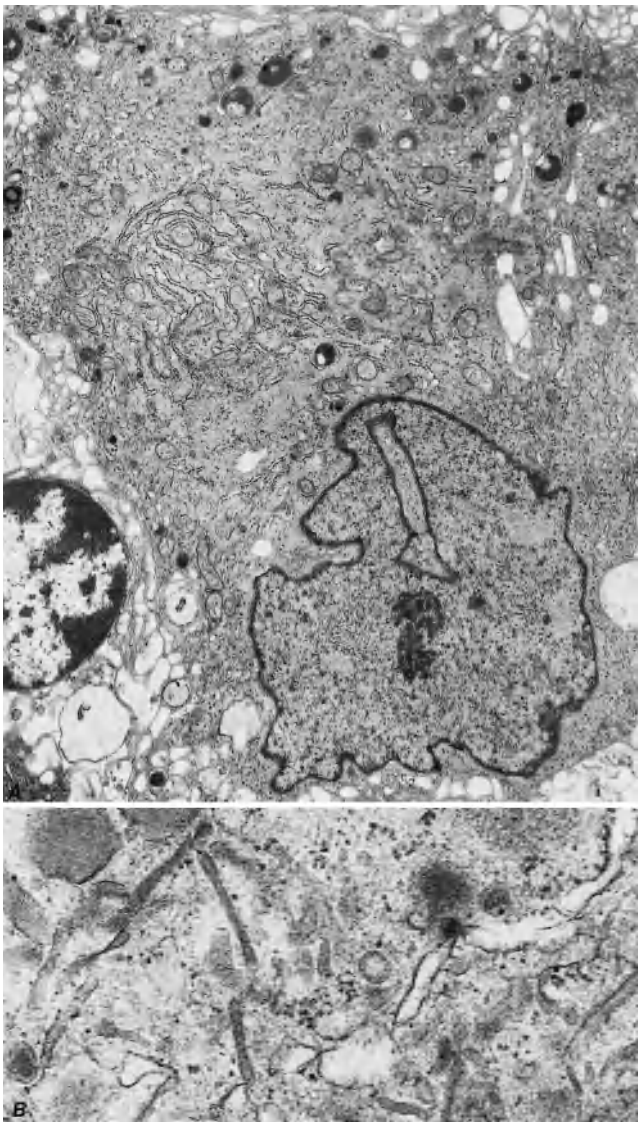


Fig. 11.6 Histiocytosis X: Histiocyte with abundant cytoplasm, many interdigitating projections, and indented nucleus. Birbeck granules are barely visible (*A*). Cluster of Birbeck granules (*B*). (Micrograph: M. Iwafuchi, *Am J Surg Pathol* 14:489, 1990.)

Langerhans' Cell Histiocytosis

Langerhans' cell histocytosis (LCH; formerly known as histiocytosis X) is a rare disease of unknown etiology in which there is an accumulation of cells with Langerhans' cell appearance.[17,18] LCH lesions are further characterized by infiltration of other cells, including T cells, macrophages, giant cells, and eosinophils. The majority of cases of LCH are seen in children between 1 and 15 years of age. The characteristic LCH cell closely resembles the epidermal Langerhans' cell ultrastructurally. It has abundant cytoplasm, abundant cytoplasmic granules, many interdigitating projections, and an indented nucleus (Fig. 11.6).[19] The granules are similar to Langerhans' cells and cisternae have peroxidase activity. LCH cells express CD1a, S-100, and CD207 (Langerin).[20] The majority of LCH cells express CD68, a sialomucin family member expressed in lysosomes. Langerhans' cells in normal skin do not express CD68, but express CD1a and S-100. Phenotypic differences that have been observed in LCH cells may be reflective of the stage of disease.

Dendritic Cells

The dendritic cell system is composed of a heterogeneous population of stellate dendritic cells that trap, process and present antigens. In addition to their

Vet-ebooks.com

critical role in regulation and initiation of adaptive immunity, DCs play a role in establishment of central tolerance in the thymus and in maintenance of peripheral tolerance. Phenotype, function, and stage of maturation can be used to distinguish various subpopulations of DCs. Studies have indicated that mature dendritic cells may develop from either myeloid or lymphoid pathways, though conventional DCs are mainly of myeloid origin.

Dendritic cells (DCs), as antigen-presenting cells, have the ability to induce primary immune responses. They are present in small number in most tissues, but are abundant and act as sentinels in organs that provide an environmental interface such as skin and mucosae of the respiratory and gastrointestinal tracts. Here, pathogens activate immature DCs triggering their maturation and an enhanced expression of co-stimulatory molecules. DCs act by secreting soluble messenger molecules and by releasing **exosomes** (vesicles formed of and released by the plasma membrane) that bear surface antigens (expressed on the plasma membrane).[21] **Antigen-antibody complexes** are quickly immobilized in lymphoid tissues by attachment to macrophages and dendritic cells (Fig. 11.7).

Specific Dendritic Cell Subsets

Conventional tissue dendritic cells are found in the epithelium and interstitial spaces of most non-lymphoid organs (e.g., heart, kidney, liver, lungs). Typically, characterized by long, slender cytoplasmic processes, nucleus with two or three nucleoli, and relatively scant cytoplasm (Fig. 11.7A). Immature DCs have abundant MHC class II molecules present in compartments (MIIC) containing multilaminar sheets (Fig. 11.7B). Following activation, MHC class II molecules in DCs are relocated from an intracellular pool to the cell surface.[22] Mature DCs have high levels of MHC class II and co-stimulatory molecule (e.g., CD80 and CD86) surface expression.

Interdigitating dendritic cells are accessory cells responsible for presenting antigen to T cells. In lymph nodes, they occur in the T cell-rich interfollicular areas. They are also present in the T cell-dependent areas of the tonsil, thymic medulla, and periarterial lymphoid sheath of the spleen. Interdigitating dendritic cells originate from bone marrow, have potent T lymphocyte stimulating activity, and bear a spectrum of cell surface markers that differ from those of the follicular dendritic cell.[23,24]

Follicular dendritic cells (FDCs) possess long cytoplasmic extensions and form a three-dimensional reticular network between B lymphocytes in the lymphoid follicle. In the cortical areas of the lymph node they retain antigen-antibody complexes so that they may interact with B lymphocytes in the germinal center over a long period of time. Follicular dendritic cells express adhesion molecules, receptors for complement (CD21, CD35) and FcRs (CD16, CD23, CD32) that facilitate the interaction with B cells expressing cognate ligands. FDC subsets localized in the light zone and dark zone of the germinal center can be distinguished phenotypically and morphologically.[25,26]

Ultrastructural studies show that dendrites of the follicular dendritic cell form a spectrum of changes that develop in response to antigens. **Filiform** dendrites are the normal, nonreactive form, and **beaded** dendrites have **nodose** enlargments that trap antigen-antibody complexes. A spherical structure composed of antigen-antibody complexes sandwiched between filiform and beaded dendrites called the **iccosome** (immune-complex coated body) of 0.3–0.4 μm is produced in developed germinal centers by FDC 1–3 days after a secondary antigenic challenge. Iccosome-derived antigens are processed by germinal center B cells by endocytosis, transit through the Golgi complex, and embed in the B cell surface membrane.[27] FDCs have been reported to display MHC class II-containing microvesicles (**exosomes**) that may play a role in T_H cell recruitment to the germinal center.[28]

In peripheral blood, dendritic cells are reported to be a minor subset of circulating leukocytes (0.1% or less in humans). In lymph, **circulating dendritic cells** have been termed veiled cells. Ultrastructurally, circulating dendritic cells are larger than monocytes, and have bluntly lobulated nuclei, clear cytoplasm, and dendritic processes. In human blood, several populations of dendritic cells have been identified.

Plasmacytoid dendritic cells found in blood and lymphoid tissues have a plasma cell-like morphology and are known producers of high levels of type I interferons in response to viral infections or TLR ligation. These cells evidently differ from other DC subsets with respect to expression of MHC class II transactivator (CIITA), a transcriptional factor that regulates MHC class II genes.[29]

Lymph Nodes

The mammalian lymph node can be divided into three distinct layers: cortex, paracortex, and medulla. The outer cortex contains primary follicles of B lymphocytes, macrophages and FDCs. Following antigenic challenge, secondary follicles containing germinal centers develop. Germinal centers are sites of intense B cell activation and differentiation. The paracortex is composed predominantly of helper T lymphocytes mixed with interdigitating reticulum cells. The medulla is populated mostly with antibody-secreting plasma cells.

Vet-ebooks.com

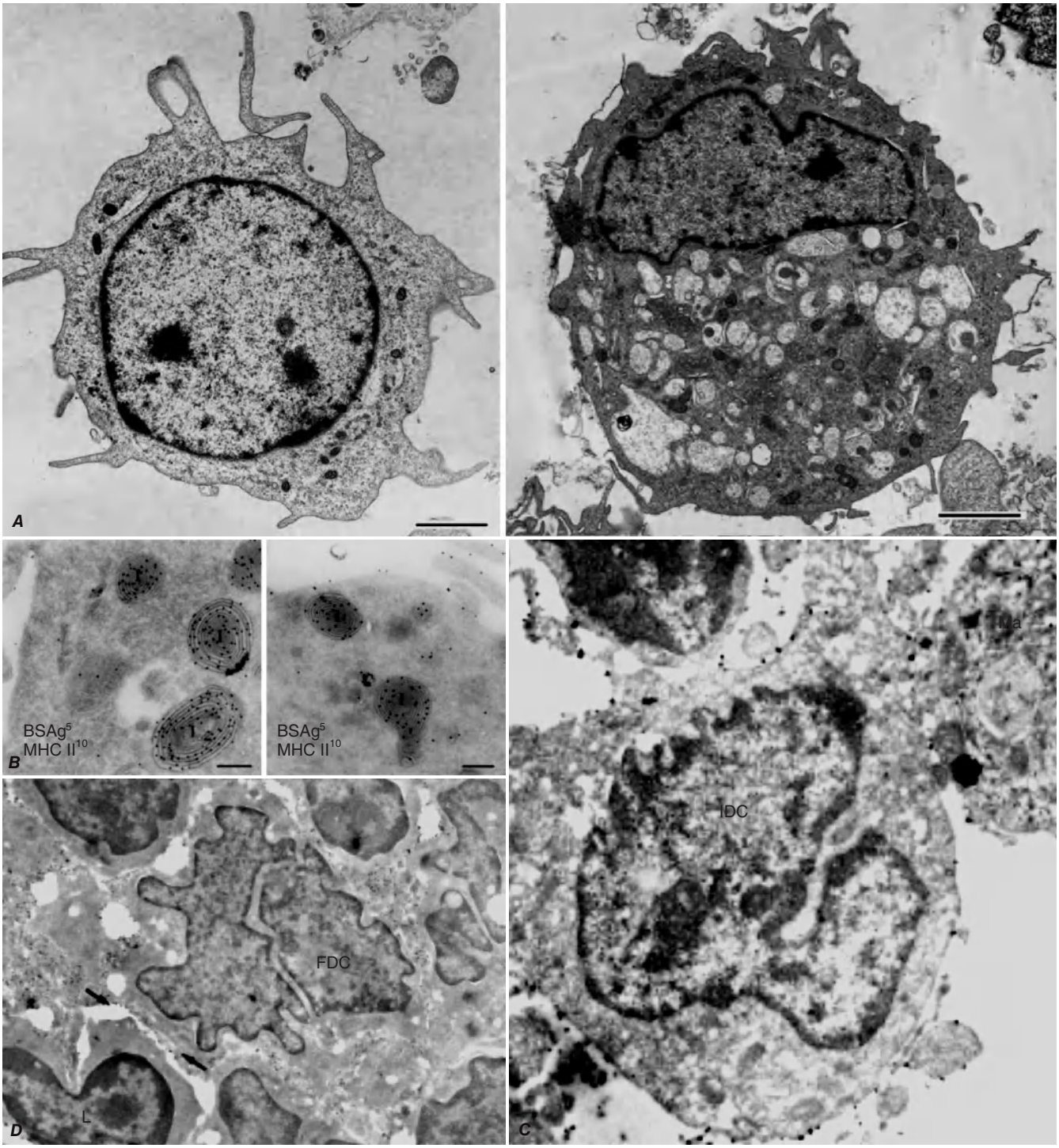


Fig. 11.7 Dendritic cells. A. Lung dendritic cell. Note ultrastructural differences between ovine lung DC and an in vitro monocyte-derived DC (MDDC). Lung dendritic cells typically have a large nucleus with scant cytoplasm (*left panel*). These cells have few cytoplasmic organelles. MDDCs typically have a larger, more complex cytoplasm compared to tissue DCs (*right panel*). **B. Activated dendritic cells.** Abundant MHC class II labeling in multilaminar MHC class II compartments (MIIC) of an unstimulated human MDDC (*left panel*). Following LPS treatment, MHC class II molecule expression is increased on DC cell surface and decreased in MIIC (*right panel*). (Micrograph: Hans J. Geuze, *Traffic* 3:894, 2002.) **C. Interdigitating DC.** Interdigitating cell (*IDC*) in the medulla of human thymus. Note an adjacent macrophage (*Ma*). Immunogold labeling with an antithymic cell monoclonal antibody. (Micrograph: Mary A. Ritter, *Microsc Res Tech* 38:237, 1997.) **D. Follicular DC.** Binucleated FDC surrounded by several B lymphocytes (*L*). Arrows indicate immunogold labeling of MHC class II and CD82-containing exosomes. (Micrograph: Hans J. Geuze, *J Immunol* 165:1259, 2000.)

Vet-ebooks.com

Reticular Cells of the Sinuses The antigen-retaining reticulum antigens, which arrive in efferent lymphatics, percolate through the loose reticular-cell networks of the subcapsular (cortical) sinuses, through the paracortical sinuses and cortical zones, and into the medulla of the lymph node. The reticular network spanning the sinuses is thinner and more delicate. This network pro-vides a three-dimensional scaffold for interactions between lymphocytes and antigen-presenting cells.[30]

Antigens are retained extracellularly on the **cytoplasmic processes** of nonphagocytic cells of the antigen-retaining reticulum. Nonphagocytic **antigen-transporting cells** adjacent to the subcapsular sinus take up antigen-antibody complexes and transport them through gaps in the lining of the subcapsular sinus.[27] Processes of these cells extend through the lining of the sinus into the lumen of the subcapsular sinus, forming a dendritic complex that can become coated with antigen-antibody complexes.[30]

Germinal Center Formation Germinal centers in the cortex provide the most efficient sites for affinity maturation and selection of high affinity clones of B cells. The primary follicle is seeded by naive B cells and FDCs. Active secondary follicles consist of a germinal center with B cell blasts, antigen-specific T cells and FDCs.

During the primary immune response the vascular structures of the node expand in association with lymphoid proliferation, and the medullary cords become filled with proliferating plasmablasts. Following exposure to antigen, activated B cells are subjected to the process of somatic hypermutation of immunoglobulin genes (becoming large basophilic centroblasts). These cells develop into lymphocytes with pale cytoplasm (centrocytes) on the outer periphery of the basophilic focus to create the germinal center; that is, a dark zone of centroblasts with an upper light zone of centrocytes. In the light zone, centrocytes with mutated B cell receptors undergo high affinity selection, isotype switching and differentiation into memory or plasma cells. The follicle is surrounded by small lymphocytes that form an eccentric corona (mantle zone). The follicular mantle contains naive B cells that are $CD62L^{+}CD21^{+}$.[25]

In the presence of antibody, the uptake of antigens becomes extremely efficient, and there is marked retention of antigens at sites surrounding the germinal centers. In highly reactive lymph nodes there is marked expansion of marginal zones at the sinus-medullary interface (and, in spleen, in marginal zones at the white-red pulp interface). In the sinus, histocytosis associated with toxoplasma and other chronic infections causes the accumulation of medium-sized lymphocytes in clusters inside and around intermediary sinuses, adjacent to subcapsular sinuses, and forming parafollicular rims.[31] Ultrastructurally these are B lymphocytes with irregular nuclei and abundant pale cytoplasm. These B cells have been referred to as monocytoid B cells. A relationship to marginal zone B cells has been suggested based on localization, cytology, phenotype and mutational analysis, but has not been fully proven.[31]

Antigen-Presenting Cells in Other Lymphoid Tissues

Skin: Langerhans' Cells In the mononuclear phagocyte system, Langerhans' cells in the suprabasal epidermis are dendritic antigen-presenting cells. These immature dendritic cells transport cutaneous antigens to local lymph nodes for presentation to helper T lymphocytes. Antigen-induced migration results in a maturation that is accompanied by increased expression in molecules involved in antigen presentation, such as MHC molecules, co-stimulatory molecules, and adhesion molecules.[32]

Of bone marrow origin, Langerhans' cells are identified ultrastructurally by the presence of specific cytoplasmic granules.[33] These Birbeck granules are rod- or racquet-shaped granules approximately 45 nm in thickness that contain central layers of electron-dense material with periodic substructure that appears as striations or in lattice arrangements. CD207 (Langerin), a Ca^{2+}-dependent C-type lectin, plays a role in the formation of Birbeck granules.[34] Resident APCs in the dermis of skin include interstitial dendritic cells and dermal macrophages.

Langerhans' cells are most prominent in the skin although the have been characterized in gingiva and oral mucosa, epithelia of the alimentary canal, uterine cervix, and lymphoid tissues including lymph nodes, thymus and tonsils.

Brain: Microglia **Microglial cells** form a regularly spaced network of resident phagocytic cells in the mammalian central nervous system. Resting microglia respond to pathologic stimuli by becoming activated. This leads to a rapid change that involves proliferation and alteration of phenotype and structure. Microglia play a key role in immunity. They present antigen to T lymphocytes, have marked cytotoxic properties, and respond to cytokines. **Astrocytes** are a subtype of glial cell characterized by their star-shaped appearance. These cells can present antigen and stimulate T cell proliferation. Astrocytes play an important role in inflammatory diseases of the central nervous system, such as multiple sclerosis.

Spleen Interposed in the bloodstream, the spleen traps and interacts with circulating antigens. Injected

Vet-ebooks.com

intravenously, antigens are rapidly taken up by avid macrophages in the red pulp adjacent to the white pulp areas. This **marginal zone** is the point where sheathed arterioles disperse into red pulp sinuses and cords. Within minutes, antigens become localized in the lymphoid sheaths where they linger on dendrites of reticular cells. Classic interdigitating dendritic cells occupy the central periarterial lymphoid sheath (PALS).

In the mouse spleen, follicular dendritic cells are in both germinal centers and adjacent mantles of secondary follicles. They are stellate with long thin sheets of cytoplasmic processes coated with extracellular amorphous electron-dense matter. Their nuclei are large and irregularly shaped with little chromatin.

After an immune response, large **plasmablasts** progressively develop in the lymphoid sheath. They appear within 24 hr of antigen injection and migrate to the periphery of the sheath. They enter the red pulp and leave the spleen in the circulating blood. Antigens become localized in **germinal centers** in the white pulp as antibody appears in the circulation.

Multiple populations of splenic dendritic cells have been described in laboratory mice including conventional and plasmacytoid subsets.[35] $CD4^-/CD8^+$, $CD4^+/CD8^-$, and $CD4^-/CD8^-$. CD8 DCs are found mainly in the T cell areas and $CD8^-$ DCs in the marginal zones. Upon antigenic stimulation, the $CD8^+$ DCs migrate into the T cell areas. Functional heterogeneity of $CD4^+$ and $CD8^+$ DCs has been shown.[36]

Mucosa-Associated Lymphoid Tissue Lymphocytes acquire the capacity to transform into immunoglobulin-secreting plasma cells or effector T cells in lymphoid follicles of the intestine, lung, and other peripheral tissues. Lymphoid follicles serve as the afferent limb of the immune system. These sites function to confer immunocompetence on undifferentiated lymphocytes.

Gut-associated lymphoid tissue (GALT) has been characterized in normal humans,[37] as well as in many species of domestic animals[38] and laboratory rodents.[39,40] GALT plays a dominant role in the development of immunity acquired through the intestine, but can also be a source of bacterial and viral infection, either by passing bacteria across the gut barrier or by permitting intracellular microbial replication.

Follicle-associated epithelium contains specialized **M cells** that have electron-lucent cytoplasm, short, thick microvilli (with few microfilaments), and many apical vesicles (Fig. 11.8). M cells are associated with intraepithelial mononuclear cells, even in normal animals. In crypt areas of some species, fungiform epithelial cells with tufts of long microvilli are seen. **Peyer's patches** are aggregates of lymphoid follicles in the small intestine. The colon and appendix contain similar lymphoid follicles.

Conjunctiva-associated lymphoid tissue (CALT) and **bronchus-associated lymphoid tissue** (BALT) resemble other mucosa-associated lymphoid tissues (MALT). The CALT follicle-associated epithelium contains clusters of lymphoid cells but is devoid of goblet cells.[41] As with other MALT, secretions are sampled for antigen and there is local generation of effector cells in response to antigen. Lymphoid follicles in CALT are not generally present at birth but rapidly develop, and become hyperplastic in chronic infections of the eye and conjunctivae. The prominence of BALT depends on species, age, and disease status.[42]

Tonsils Human pharyngeal lymphoid tissue is composed of nasopharyngeal tonsil (adenoids), and palantine, tubal, and linguinal tonsils. Together with smaller lymphoid collections, these tissues form the circular structure known as Waldeyer's ring. Highly penetrable epithelium of the tonsil receives antigens from the oropharynx. M cells, which have been described in tonsilar tissues of some species, have the ability to transport antigens to the subepithelium. The subepithelial, lymphoid compartments contain follicles (B cells, FDCs), surrounded by interfollicular areas (T cells, IDCs).[43] There are no afferent lymphatics in tonsils or adenoids, but DCs in the crypt epithelium transport antigens to B cell follicles or T cell areas.[44] Waldeyer's ring in humans seems to be functionally similar to nasopharynx-associated lymphoid tissue (NALT) in rodents.

Lungs Recent evidence from studies in several species indicates that pulmonary dendritic cells are an important antigen-presenting population in the lungs. In epithelial surfaces within the respiratory system, class II MHC antigen-bearing dendritic cells have been shown to form a tightly meshed network comparable to that of epidermal Langerhans' cells. Within alveoli, dendritic cells are located near alveolar septal junctions where they contact and partially surround one or more capillaries (Fig. 11.9). Continuously exposed to airborne antigens from the environment, these cells initiate immunological processes for protection. **Alveolar macrophages** are predominant resident cells in the alveolar spaces and conducting airways of the lung. These cells have key immunoregulatory functions in the host response to microbial pathogens.

Cloacal Bursa of Birds The avian **bursa of Fabricius** is the critical site of B cell transformation. Each of its lymphoid follicles contains a cortical zone filled with small dense lymphocytes, separated from a reticular medullary by a single layer of undifferentiated endodermal epithelial cells.[45] The epithelial cells

Vet-ebooks.com

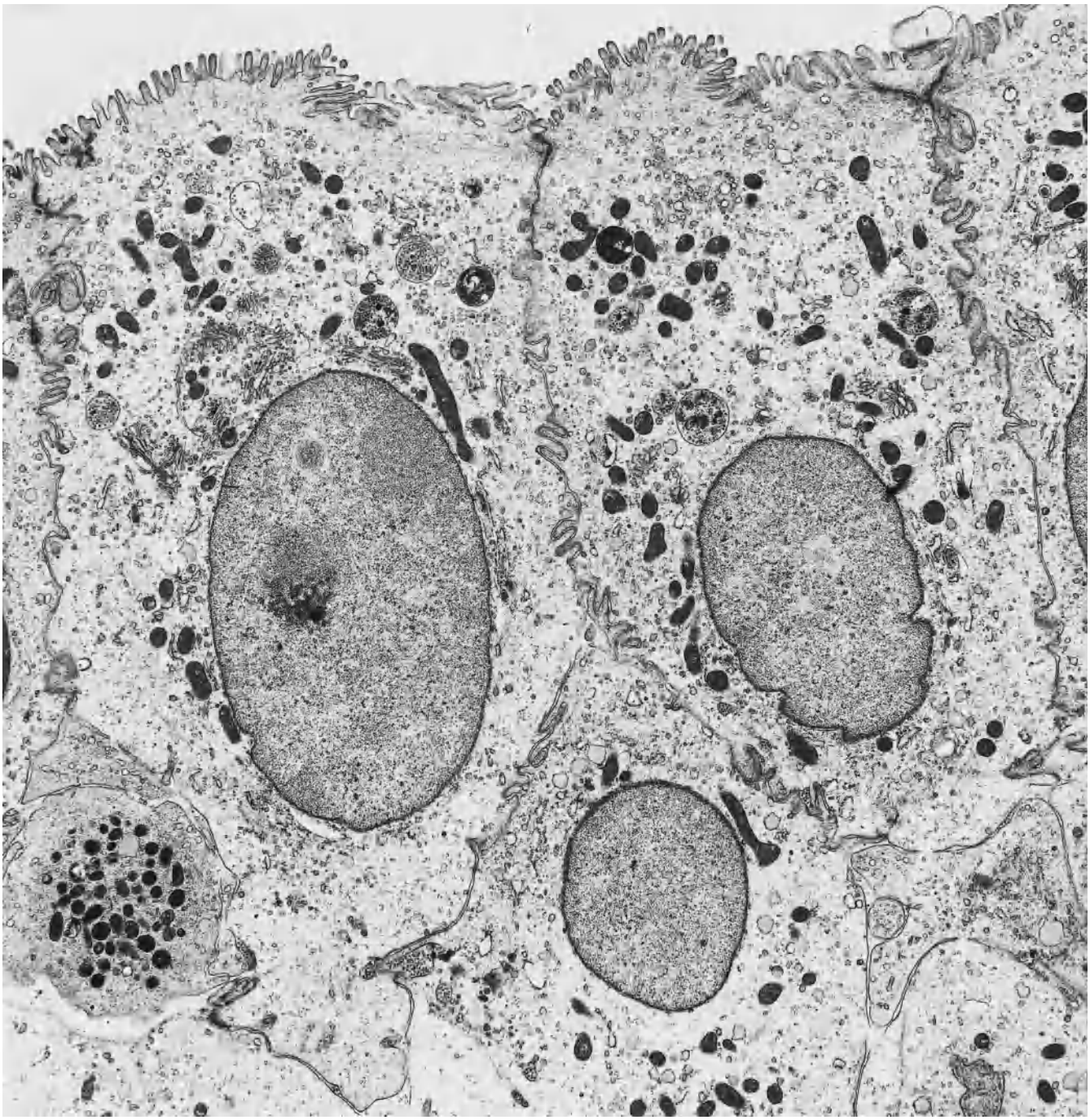


Fig. 11.8 M cells: intestinal lymphoid tissue in a calf infected with torovirus. M cells are cuboidal with short microvilli and active cytoplasmic vacuolar systems.

become prominent during age-related atrophy and may form mucus-secreting glandular epithelium (Fig. 11.10). Obliteration of the capacity to form B cells can be done by treatment of developing embryos with estrogens or by surgical removal of the bursa at hatching (accompanied by radiation to kill lymphocytes seeded peripherally before this time). Near the end of embryonic development stem cells, arriving from the yolk sac, liver, or bone marrow, are induced to undergo a switch in genetic commitment to become B lymphocytes.

Thymus The thymus is the primary lymphoid organ where differentiation from bone marrow-derived prothymocytes to immunocompetent T cells occurs. Differentiation involves intercellular communication

Vet-ebooks.com

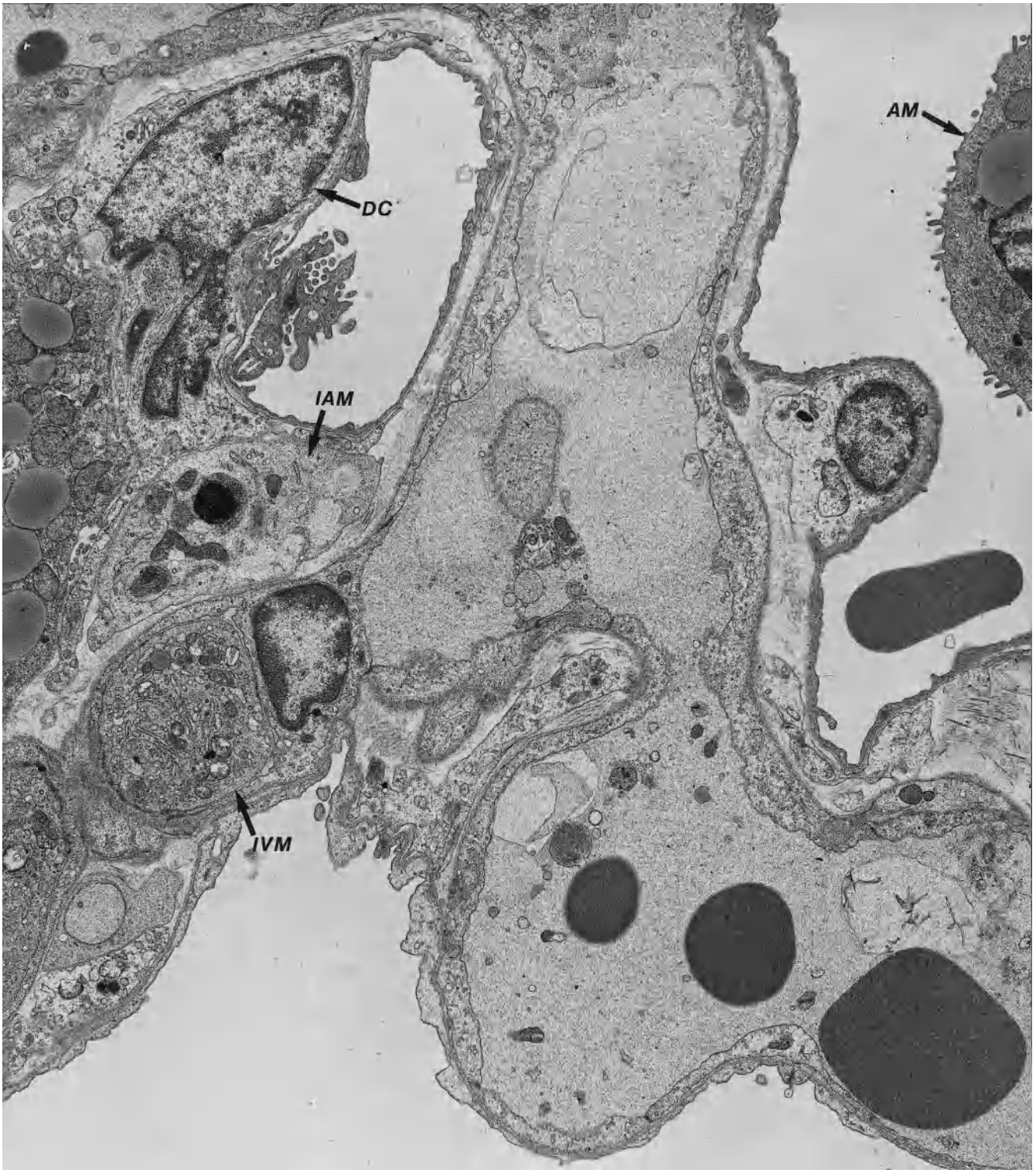


Fig. 11.9 Lung antigen-presenting cells. Macrophages and dendritic cells in ovine lung during acute inflammation. Marked dilatation of capillaries, expansion of interstitium, and cellular fragments within the capillary lumen. **Dendritic cell** (*DC*) partially surrounds a capillary in the alveolar wall, **intra-alveolar macrophage** (*IAM*) is in interstitial space of an alveolar wall, **intravascular macrophage** (*IVM*) is within a capillary lumen, and **alveolar macrophage** (*AM*) is in an alveolus.

Vet-ebooks.com

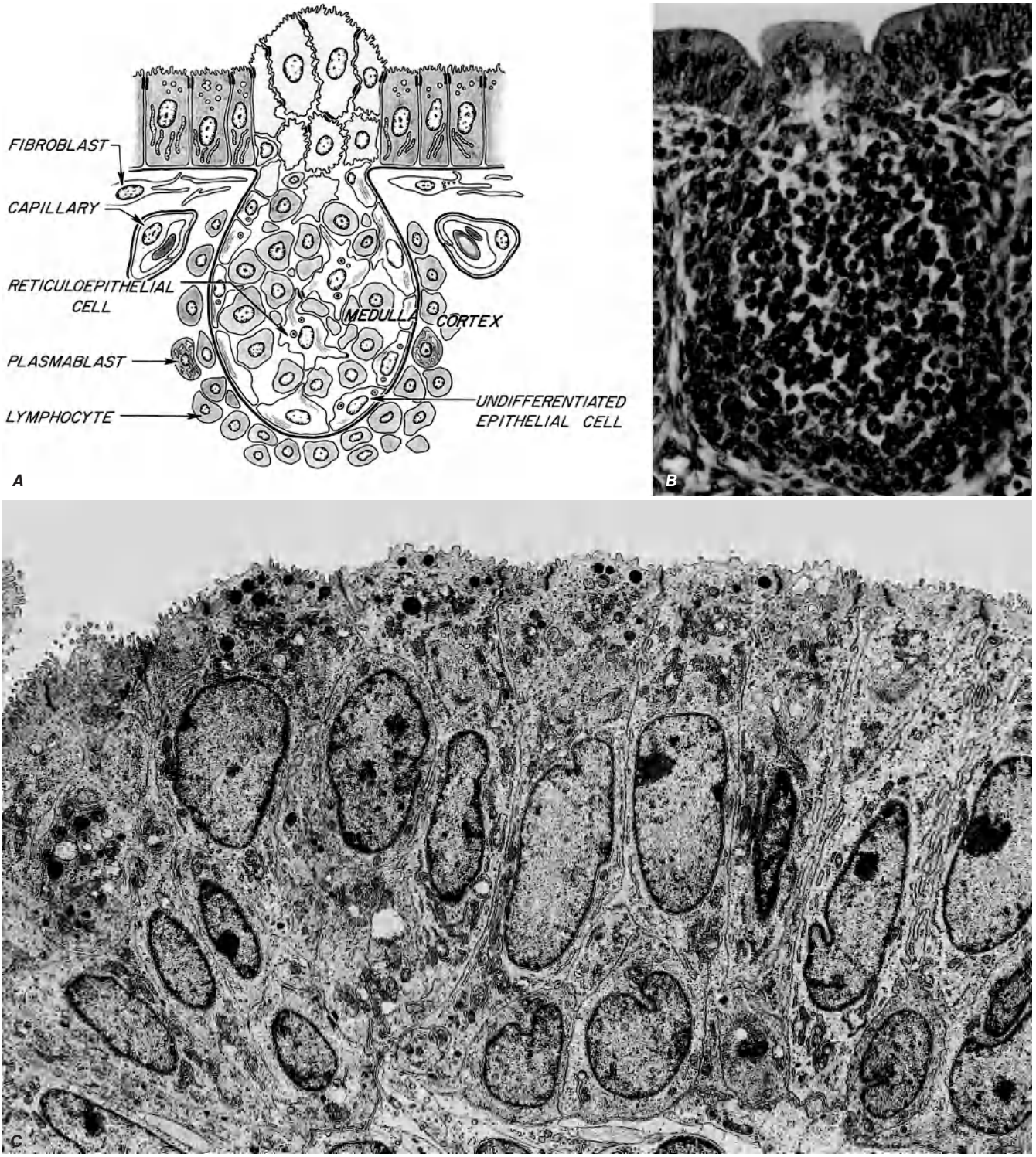


Fig. 11.10 Cloacal bursa (bursa of Fabricius): chicken. **A.** Tissue architecture. **B. Bursal lymphoid follicle:** specialized epithelial cells form a reactive pad at lumen of bursa, and connect in basal areas to the medulla of the lymphoid follicle. **C. Epithelium**: bursal follicular pad. These cells are comparable to mammalian M cells. Microvilli are short and have plasma membranes that bear specialized plaques for uptake of bacteria and other particles.

Vet-ebooks.com

between developing lymphoblasts and thymic epithelial and macrophage populations (Fig. 11.11). The thymic reticulum contains three major cell types (two are bone marrow-derived): **thymic epithelial** cells, **macrophages,** which have cytoplasmic lysosomes and are phagocytic, and **interdigitating cells**.[46–48] Interestingly, six types of thymic epithelial cells have been described based on ultrastructural analysis: type 1 cells line the capsule and surround perivascular spaces; types 2–4 range from electron-

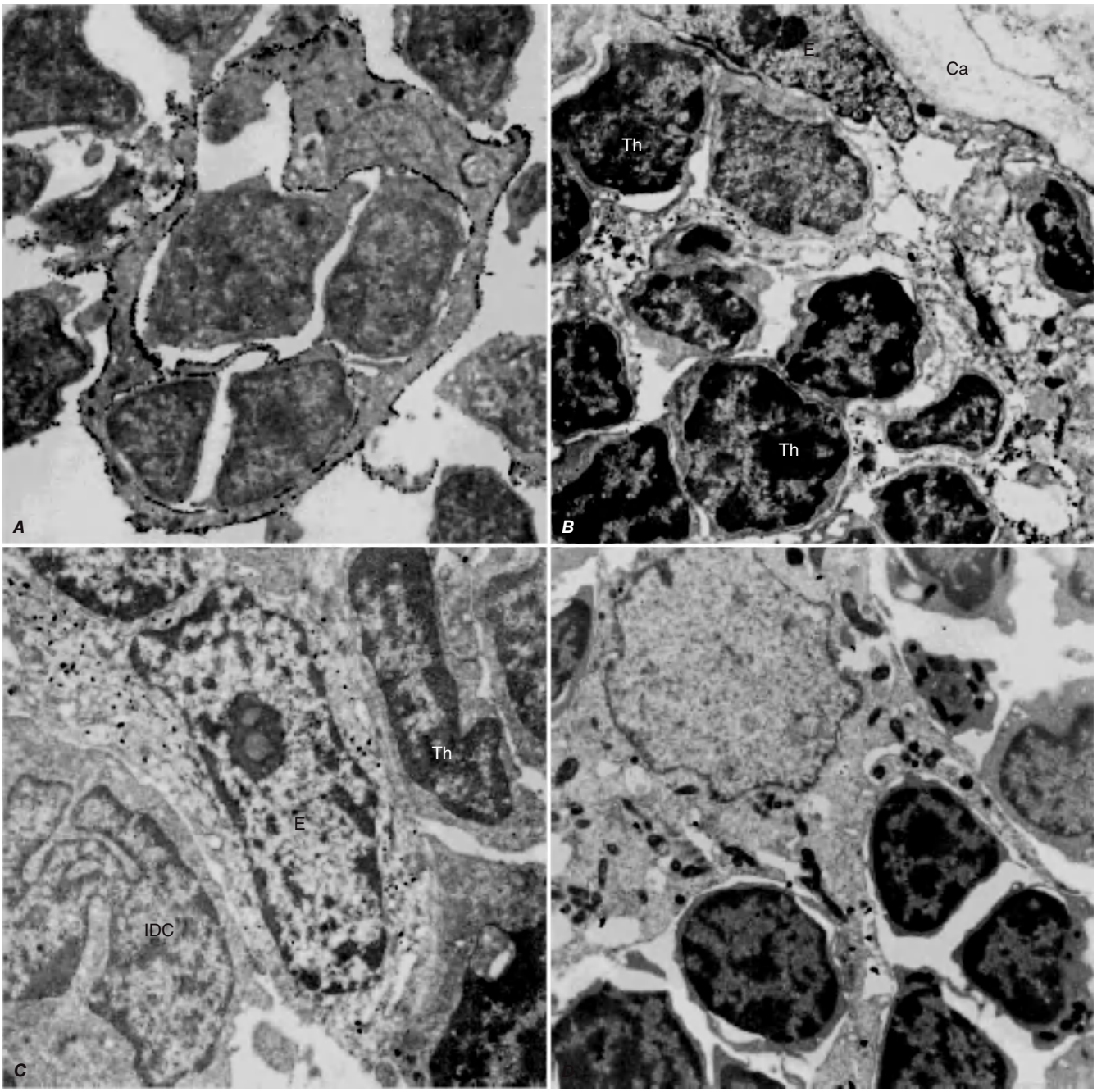


Fig. 11.11 Thymus. A. Cortical lymphoepithelial cell complex in human pediatric thymus. Monoclonal antibody (mAb) MR6 (cluster of epithelial staining (CTES) III) immunogold labeling shows a strongly reacting thymic nurse cell surrounding weakly labeled thymocytes. **B. Subcapsular type 1 epithelial cell (*E*)** with intracytoplasmic staining with MR19 (CTES II mAb). Note MR19-positive cytoplasmic processes surrounding thymocytes (*Th*). *Ca*, thymic capsules. **C. Medullary epithelial cell (*E*):** intracytoplasmic labeling with mAb MR10 (CTES II). Thymocyte (*Th*) and interdigitating dendritic cell (*IDC*) are negative. **D. Subcapsular epithelial cell** with numerous mitochondria, granules, and vacuoles. Note cytoplasmic processes of this epithelial cell surround cortical thymocytes. Immunogold labeling with antithymulin mAb. (Micrographs: Mary A. Ritter, *Microsc Res Tech* 38:237, 1997.)

Vet-ebooks.com

lucent to electron-dense cells in the cortex; type 5 are undifferentiated cortico-medullary cells; type 6 are medullary epithelial cells that contribute to Hassal's corpuscles.[49,50] **Thymic nurse cells** are MHC positive thymic epithelial cells in the outer cortex that have long cytoplasmic processes that can surround up to 50 intact actively dividing thymocytes. In fact, there is data to suggest that nurse cells are capable of internalizing thymocytes.[51]

During development, the thymic rudiment is seeded with bone marrow-derived stem cells. As thymic cells mature, each assembles the genes that encode a T cell receptor heterodimer through recombination of individual variable, diversity and joining germline elements for each chain (assembly is termed VDJ recombination). Mature T cells express only a single T cell receptor (TCR), the specificity of which determines the fate of the thymocyte as it undergoes selection.

Lymphocytes

Differentiation

During hematopoeisis, pluripotent stem cells differentiate in an ordered fashion through a stepwise loss of lineage potentials into mature blood cells. Self-renewing hematopoietic stem cells give rise to multipotent progenitors (MPP), which have lost the capacity for self-renewal. Further identifiable progenitors in bone marrow include the **common myeloid progenitor (CMP)** and **common lymphoid progenitor (CLP)**. From the CLP stage, lymphoid cell differentiation continues toward the B or T cell lineage. T cell development and selection occur predominately in the thymus, whereas early B cell development occurs in the bone marrow. Further stages of mammalian B cell development and differentiation occur in the periphery (Fig. 11.12).

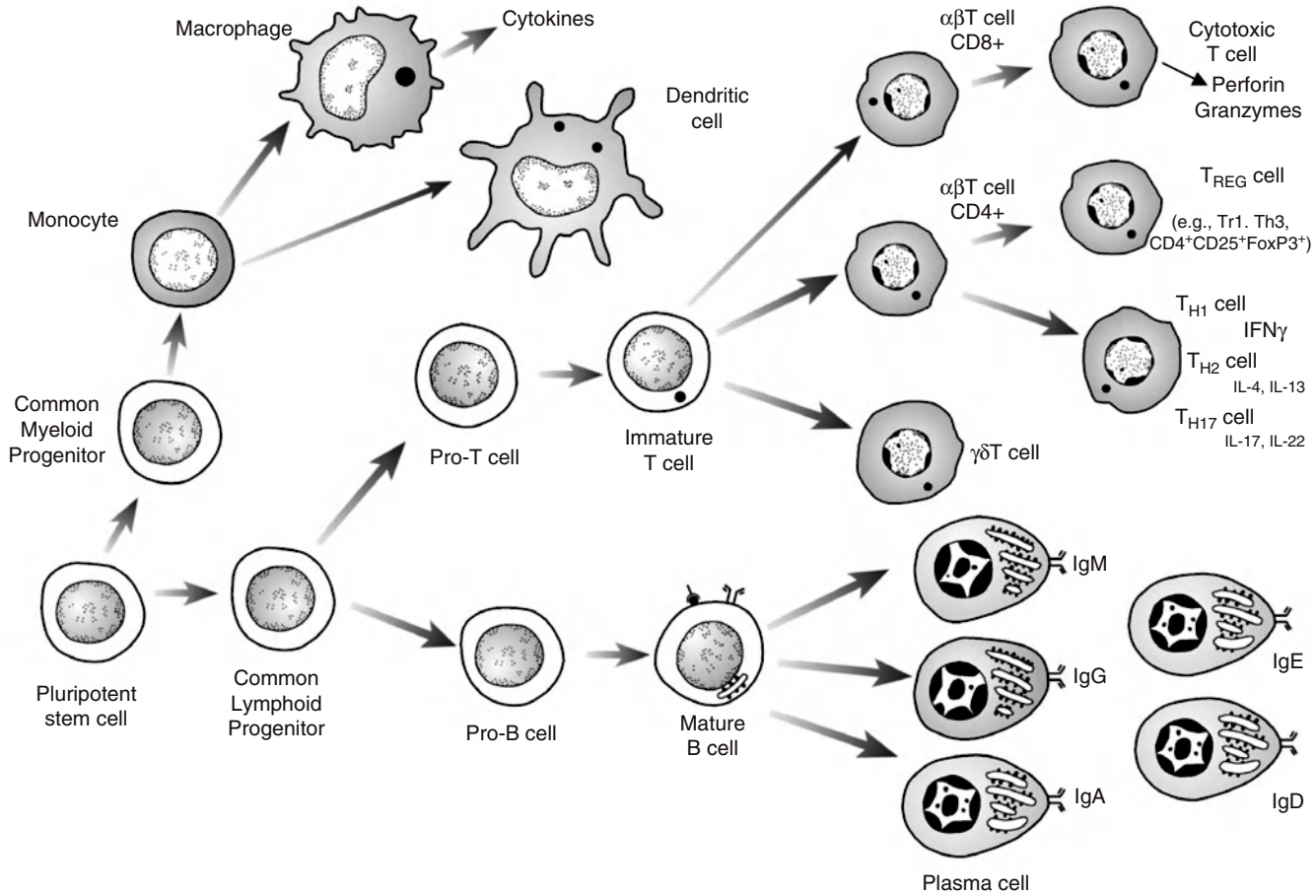


Fig. 11.12 Immunocyte differentiation: pluripotent stem cell differentiating along either myeloid or lymphoid pathways of development. Common lymphoid progenitor cells give rise to T or B lymphocyte precursor cells. Precursor cells differentiate further into naive resting lymphocytes. Small resting lymphocytes progress through the cell cycle to become blast cells. Lymphoblasts differentiate into effector or memory cells. In the B cell lineage, plasma cells are the effector population secreting antibodies of one of several classes (IgM, IgA, IgD, IgG, or IgE). Effector cells of the T cell lineage include cyotkine-secreting T helper (T_H) cells or cytotoxic T cells that recognize and eliminate altered self-cells. At least three subsets of T_H cells exist and are critical in the response to intracellular pathogens (T_{H1}), extracellular bacteria (T_{H17}), or parasitic worms (T_{H2}). Recently, subsets of regulatory T cells (T_{REG}) have been identified that provide counterregulation.

Vet-ebooks.com

Plasmacytes

B Cells and Plasmablasts

B cells are precursors of the plasma cells. Following contact with the appropriate antigen, B cells transform into large blast cells, termed **plasmablasts**. Ultrastructurally, B cells undergoing this transformation have evidence of a rapidly developing system of endoplasmic reticulum, the source of immunglobulins with antibody activity (Fig. 11.13A). In newly developing plasmablasts, antibodies first appear in the perinuclear spaces, then in cisternae of the endoplasmic reticulum.[52] Plasmablasts are short-lived, highly proliferative precursors of plasma cells. Plasma cells can be longer-lived and are a nondividing population.

Plasma Cells

Plasma cells are large relative to other lymphoid cells. The nucleus has characteristic aggregates of chromatin spaced along the nuclear surface of the nuclear envelope. The cytoplasm is composed largely of rough endoplasmic reticulum, the cisternae of which contain large amounts of globulins with antibody activity. Light and heavy chains of the immunoglobulin (Ig) molecule are assembled here and secreted from the cell.

In the terminal plasma cell, abnormal immunoglobulins are unable to be properly secreted and accumulate in large amounts, markedly dilating the cisternae of the rough endoplasmic reticulum. Present in massive aggregates, these are known as **Russell bodies**.[53]

Plasma cells are distinguished on the basis of Ig class that they produce. After antigenic exposure, large numbers of IgM-containing plasma cells appear in peripheral lymphoid tissues, including the medullary cord of lymph nodes and red pulp of spleen. This is followed by a progressive increase in IgG-containing cells expressing highly mutated Ig-variable regions. In oral immunization, IgA antibody-containing plasma cells are abundant throughout the intestine.

Plasma cells in tissue form large aggregates. These are end-stage cells that are filled with antibody molecules (Figs. 11.13B and C), but are not in an active state of production as are plasmablasts. Plasma cells have the capacity for long-term survival given the appropriate microenvironmental niche.[54] The ultrastructure of plasma cells and abnormal B lymphocytes in defects of differentiation has been described.[55]

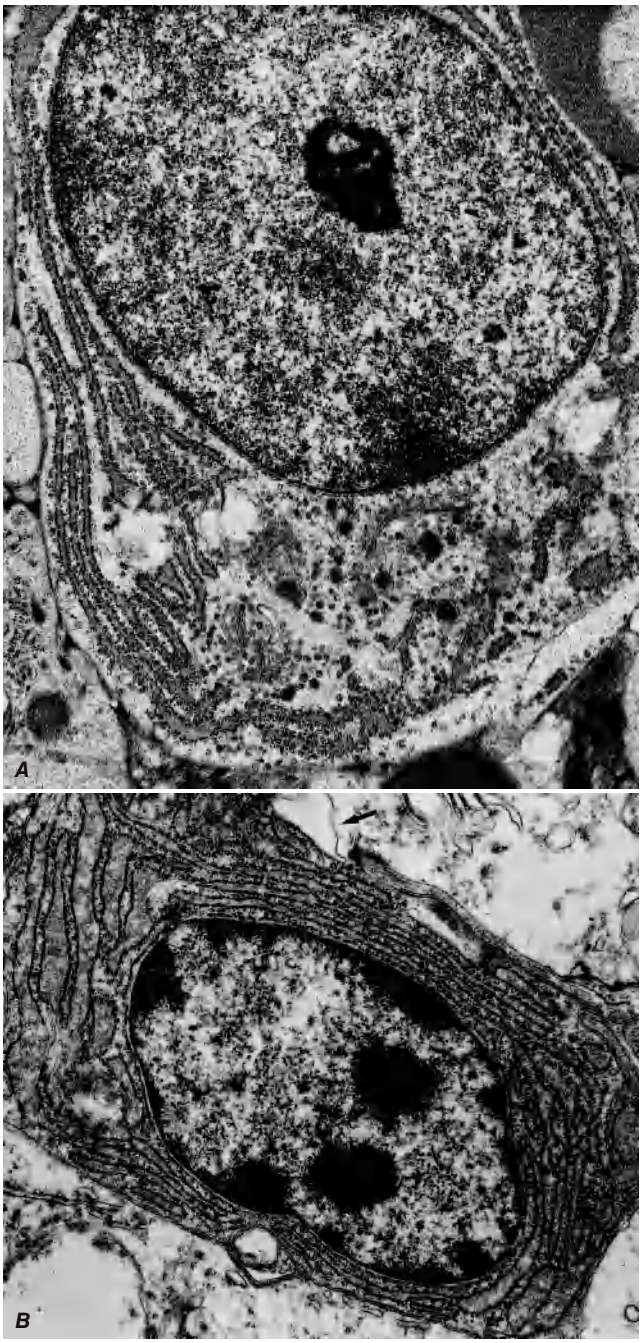


Fig. 11.13 Plasma cells. A. Plasmablast in the brain, picornaviral encephalitis. Cytoplasm contains large Golgi complex with many vesicles and large amounts of rough endoplasmic reticulum (ER). **B. Plasmacyte** interposed between two neurons. The plasma membranes of the cells are in close apposition. Large amounts of rough ER present in the plasmacyte. **C. Plasmacytes** in uterine lamina propria. Large amounts of rough ER, with cisternae that are filled with globulin precipitates. Nuclei of plasmacytes have characteristic cartwheel appearance, with large nucleoli.

Vet-ebooks.com

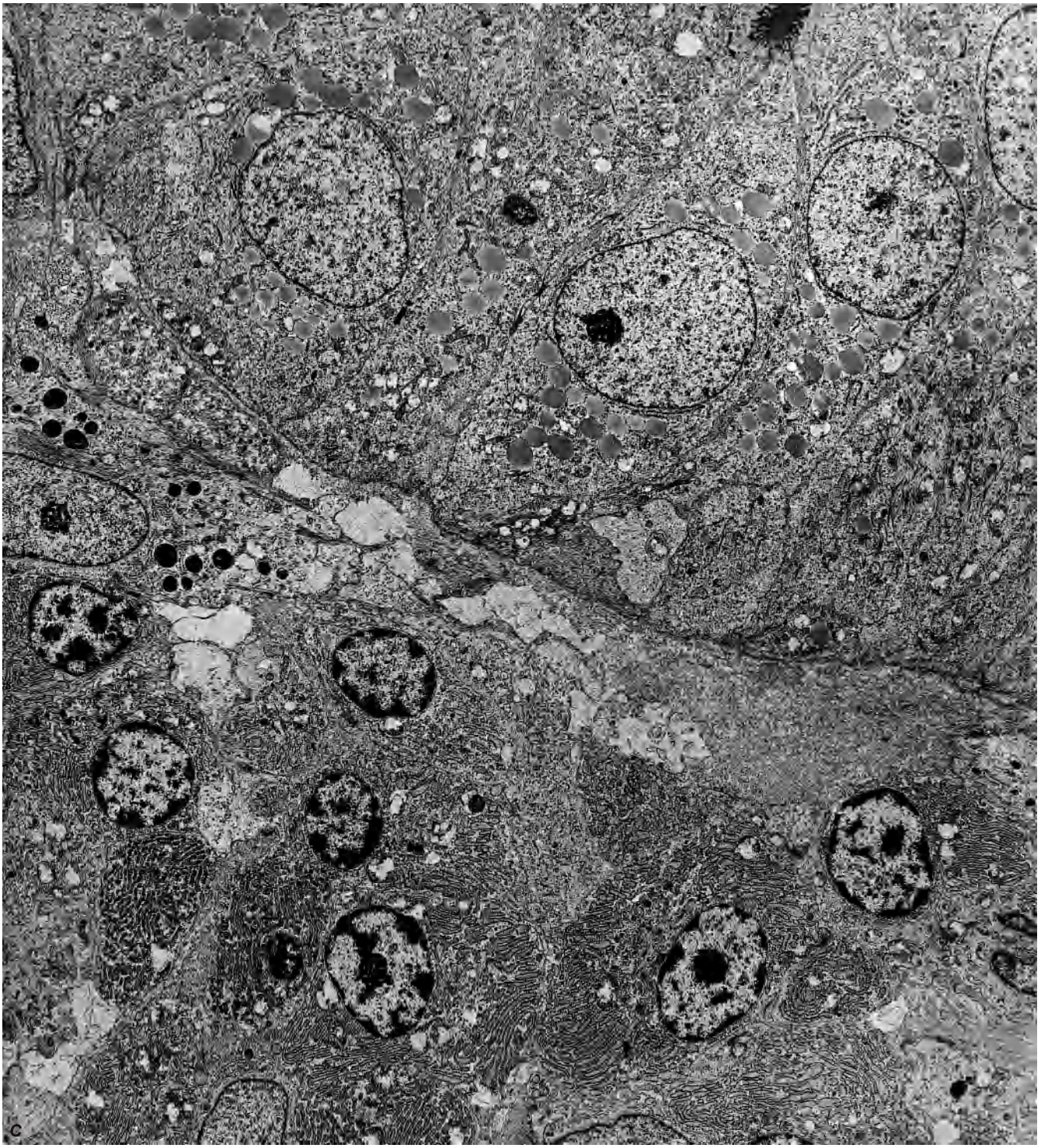


Fig. 11.13 *Continued*

Vet-ebooks.com

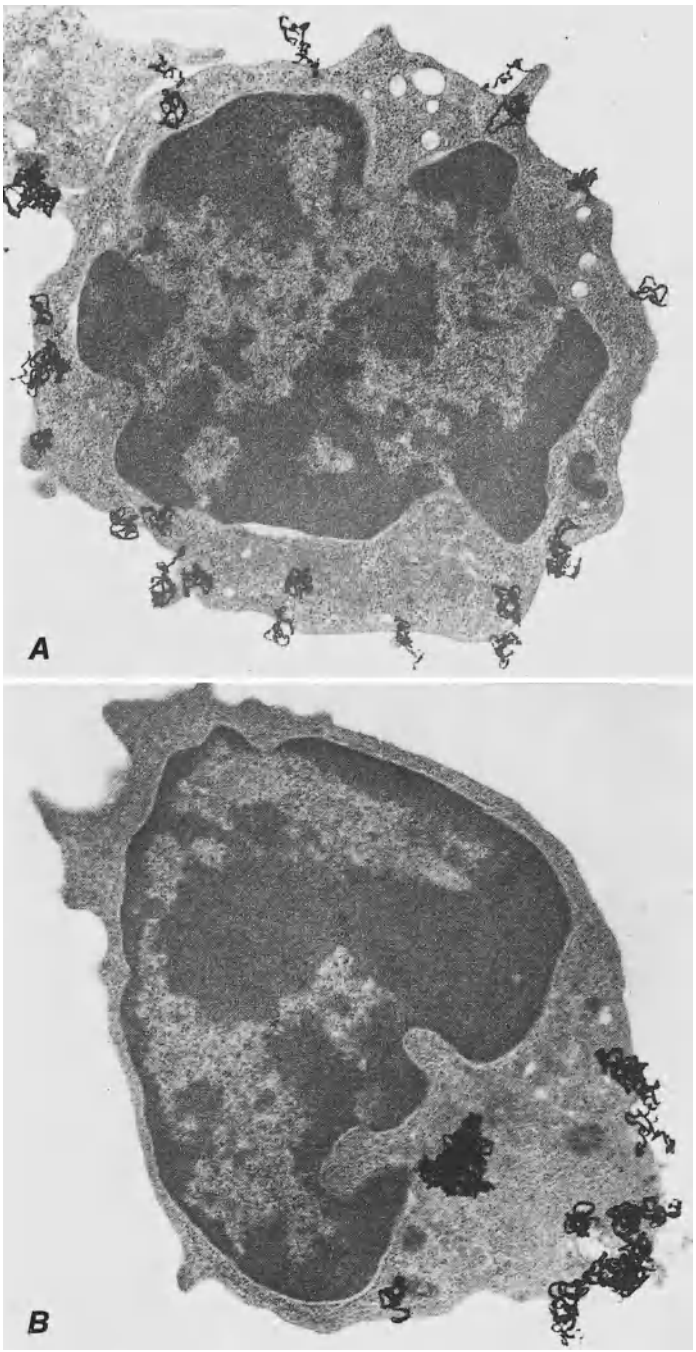


Fig. 11.14 Lymphocytes. A. Immunoglobulin metabolism: electron microscopic autoradiographs of mouse splenic lymphocytes incubated with ^{125}I-labeled anti-Ig. Random distribution of molecules on cell surface after 1 min. **B.** Polar and intracellular distribution, several minutes after incubation. (Micrograph: Emil R. Unanue, *J Exp Med* 136:885, 1972.)

Lymphocytes

Small Lymphocytes

Small lymphocytes are tiny round cells with a narrow rim of cytoplasm that contains largely free ribosomes. Their Golgi zones are small and only rarely are lysosomes seen. Dense azurophil granules (5–15 per cell) and clear vacuoles are commonly present. Nuclear chromatin is densely packed, particularly at the periphery of the nucleus. In the small lymphocytes, ameboid movement, phagocytosis, and chemotactic response are weak or absent. When stimulated, small lymphocytes change to a more activated appearance—increases in cell volume and in free ribosomes.

Small lymphocytes that circulate in the blood or that lodge in tissues represent several different populations of lymphoid cells, even though they cannot be distinguished ultrastructurally. These cells are differentiated on the basis of surface glycoprotein receptors (e.g., sIg on B cells) (Fig. 11.14), life span, their response

Vet-ebooks.com

to mitosis-inducing drugs, and their reactivity in immunologic assays.

The specialized, lineage-committed small lymphocytes originate from stem cells in bone marrow. Lymphocyte populations acquire their special characteristics by development in the thymus (to become T cells) or bone marrow or gut-associated lymphoid tissues (to become B cells). The primary B cell repertoire in mice and humans is generated by V, D, J gene rearrangements in the bone marrow. However, in other species (e.g., rabbits, chickens) only limited rearrangement (V genes) occurs in primary lymphoid tissue with further diversification in GALT.

Lymphocyte Recirculation

Lymphocytes recirculate through blood and lymph fluid to various lymphoid and non-lymphoid tissues. This complex process is critical for immune surveillance and for development of an inflammatory response. Lymphocytes shed into the **lymphatic circulation** enter the **bloodstream** via the thoracic duct. In **thoracic duct lymph,** over 90% of the cells are lymphocytes. Lymphocytes can be shown to enter the lymph nodes from the bloodstream, migrating through **postcapillary venules with high endothelium (HEV)** (Fig. 11.15) by extravasation. High endothelial venules express a variety of adhesion molecules, including tissue-specific molecules known as **vascular addressins**. Addressins direct the extravasation of recirculating lymphocytes to specific lymphoid organs.

Lymphocyte Activities

Capping is the movement and aggregation of integral proteins within the lipid bilayer of the plasma membrane in response to specific attachment of ligands on the cell surface.[56] In quiescent lymphocytes, surface proteins and glycoproteins freely diffuse within the lipid bilayer, assuming a random distribution. When appropriate messenger molecules act as ligands and attach to glycoprotein receptors on the cell surface, the distribution of the ligand-receptor complex becomes nonrandom; that is, the ligand-bearing receptor aggregates into patches and migrates to form polar caps (Fig. 11.16).

Capping is manifest by a microvilli-free ruffled edge with the ligand-receptor complexes redistributed in a microvilli-rich polar cap.[57] Movement of ligand-receptor complexes requires microfilament contraction. Ultrastructurally, there can be endocytosis of ligand-receptor complexes via small-walled micropinocytotic invaginations or by coated pits/vesicles.[58] Capping is accompanied by a transient loss or reduction in receptor-binding sites, and the plasma membrane over the surface blebs is nonreactive relative to adjacent cell surfaces. In addition to endocytosis, shedding may be another possible mechanism for membrane turnover.[58]

Lymphocytes have the capacity to kill target cells such as infected cells or neoplastic cells by releasing molecules such as **perforin** (pore-forming protein), **granzymes** (a family of serine esterases) or **granulysin** (a member of the saposin-like family). Ultrastructural studies reveal that the microtubule organizing center and Golgi complex of the cytotoxic T cell reorient towards the contact site of the two cells (Fig. 11.17). Effector CD8 cytotoxic T cells form an immunological synapse with the target cell. The synapse is likely important for both the lethal hit and facilitating the transfer of target cell membrane to the CTL.[59] Within the synapse, there is a secretory domain and membrane bridges.[60] After being released by the CTL, perforin binds to the target cell, inserts itself into the plasma membrane, and assembles into multimeric complexes that form pores[61,62] (Fig. 4.5C). The presence of perforins and other cytotoxic mediators in CTL cells are important in the pathogenesis of immune diseases such as rheumatoid arthritis.[63]

NK Cells (Large Granular Lymphocytes)

The term **null cell** is applied to lymphocytes that are unreactive in laboratory tests for B cell- or T cell-specific surface receptors. Some null cells have **natural killer** (NK) activity; they are effective in killing cells and microbes without any previous exposure to antigens. In viral diseases, NK cells appear early after infection and wane at about 6 days as lymphocytes with specific killing activity appear.

The NK cell has been identified in tissue as a **large granular lymphocyte (LGL)**. These cells are common in lymph nodes and visceral organs.[64–67] Human NK cell granules contain perforin, granulysin (not found in rodent cells), and granzymes. In addition, lysosomal enzymes (cathepsins) with roles in granzyme processing or cellular protection are found in lymphocyte cytotoxic granules.[68]

NK cells bind to target cells forming an immunological synapse. Once in contact with target cells, the NK cell changes ultrastructurally. Plasma membranes form interdigitations with target cell plasma membranes (Fig. 11.18). As the zone of interdigitation expands peripherally, the plasma membranes in the center separate leaving a central area where NK granules are secreted and where the released perforins attack the target cell plasma membrane. To facilitate this process, secretory granules, Golgi complexes, and cytoskeleton of the NK cell reorient towards the contact sites of the two cells. NK cells reacting with target cells develop long filopodia that indent into the cytoplasm

Vet-ebooks.com

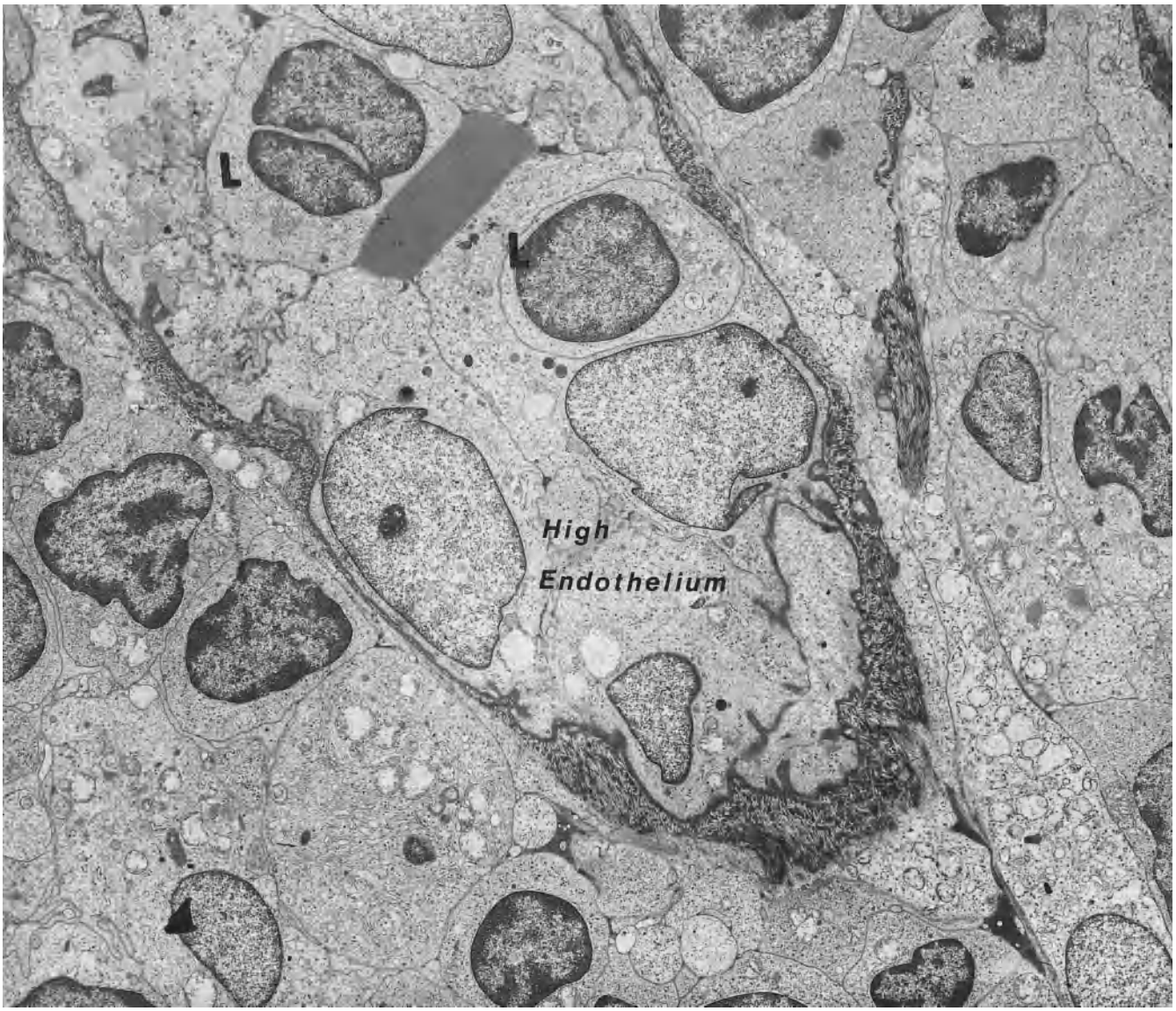


Fig. 11.15 Lymphocyte recirculation. High endothelium: postcapillary venule in a lymph node. Specific regions of vascular endothelium in postcapillary venules contain plump, cuboidal high endothelial cells. Circulating lymphocytes (*L*) extravasate through high endothelial cells into the lymph node.

of the target cell. Accompanying this interaction of NK cells and target cells, there is an exchange of cell surface proteins between the NK and target cell,[69] including inhibitory and activating NK receptors and their cognate ligands.

T Cells

T lymphocytes have specific reactivity designed to promote cell mediated immunity. Thymic differentiation of T cells involves rearrangement of T cell genes that encode plasma membrane glycoprotein receptors. This leads to the production of new membrane proteins that confer either helper, regulatory or cytotoxic functions to the T lymphocyte. Small lymphocytes, when harvested from blood or lymphoid tissue, fall into three major categories:

- **Helper T cells** (T_H cells), which enhance the actions of other T cells and provide cytokines important for B cell production of antibody responses; T_{H1}, T_{H2}, and T_{H17} cells have been described in the literature. T_{H1} cells are critical for responses against intracellular pathogens; T_{H2}

Vet-ebooks.com

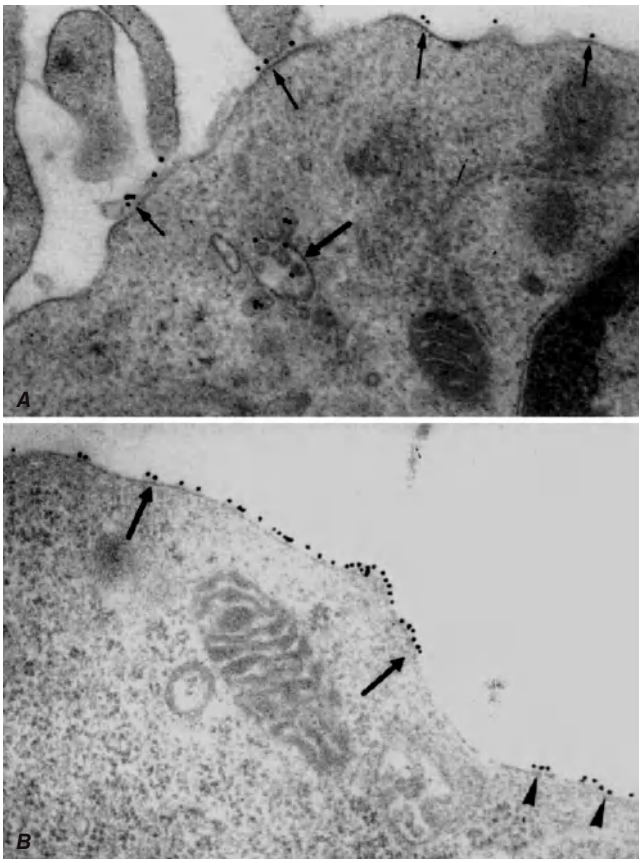


Fig. 11.16 Lymphocyte capping. A. Resting human lymphocyte. Characteristic distribution of CD8 on the surface of the lymphocyte (*arrows*). Note staining for CD8 in a cytoplasmic vesicle (*thick arrow*). **B. Activated human lymphocyte**. Receptor-ligand interaction results in aggregation into patches and polar capping (*arrows*). In the vicinity of the capping are smaller aggregates (*arrowheads*). Staining with anti-CD8 gold-labeled antibody. (Micrographs: Olaf Burkhardt, *Ann Anat* 184:45–53, 2002.)

cells against parasitic worms; T_{H17} cells against extracellular bacteria.

- **Regulatory T cells** (Treg cells), which provide counter-regulatory activities to other leukocytes, for example, TR1 ($CD4^+$, IL-10^+), $CD4^+CD25^+FoxP3^+$, and T_{H3} cells (TGF-β).
- **Cytotoxic T cells** (CTL or T_C cells), which directly kill target cells that are tumorigenic or infected (target cell contains antigens to which the CTL is sensitized).

T Lymphocyte Surface Receptors

T cell receptors expressed on the surfaces of T lymphocytes function to recognize microbial antigens and other foreign proteins presented in the context of MHC molecules. Immunologic responses are initiated by these receptor/ligand interactions. The recognition event, in which surface receptors on the immune T lymphocyte interact with antigen, triggers activation and the differentiation of the resting small T lymphocyte to an effector cell that produces cytokines.

Surface receptors on T cells interact with antigens in the peptide-binding groove of the MHC on

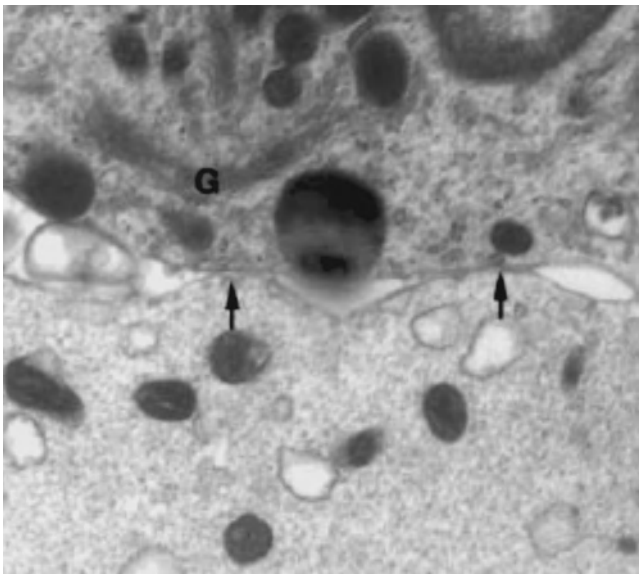


Fig. 11.17 Lymphocyte killing of target cells. A. Cytotoxic T lymphocyte (CTL) contacting a P815 target cell. Lytic granules can be seen at the immunological synapse. Gaps between otherwise tightly apposed cell membranes (*arrows*) appear to contain released granular content. CTL Golgi stacks (*G*) are arching toward the site of contact (Micrograph: Gillian Griffiths, *Immunity* 15:751–761, 2002.)

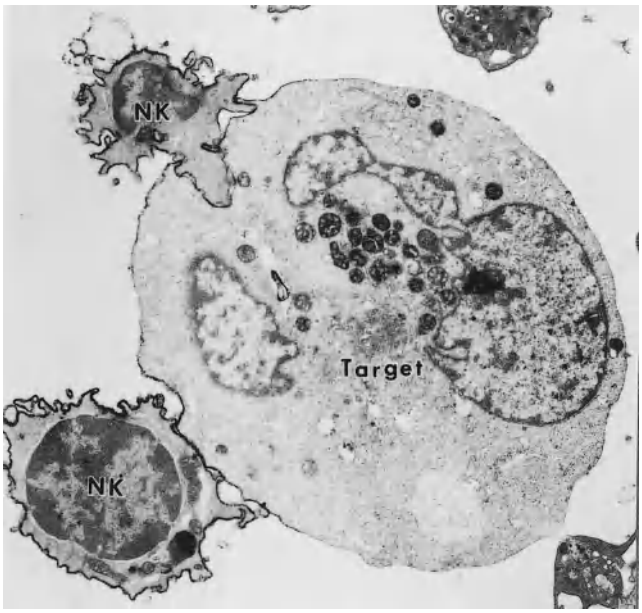


Fig. 11.18 Natural killer cells (*NK*) bound to target cell in culture; cytoplasmic filopodia project into the cytoplasm of the target cell. (Micrograph: Y-H. Kang, *Anat Rec* 217:290, 1987.)

Vet-ebooks.com

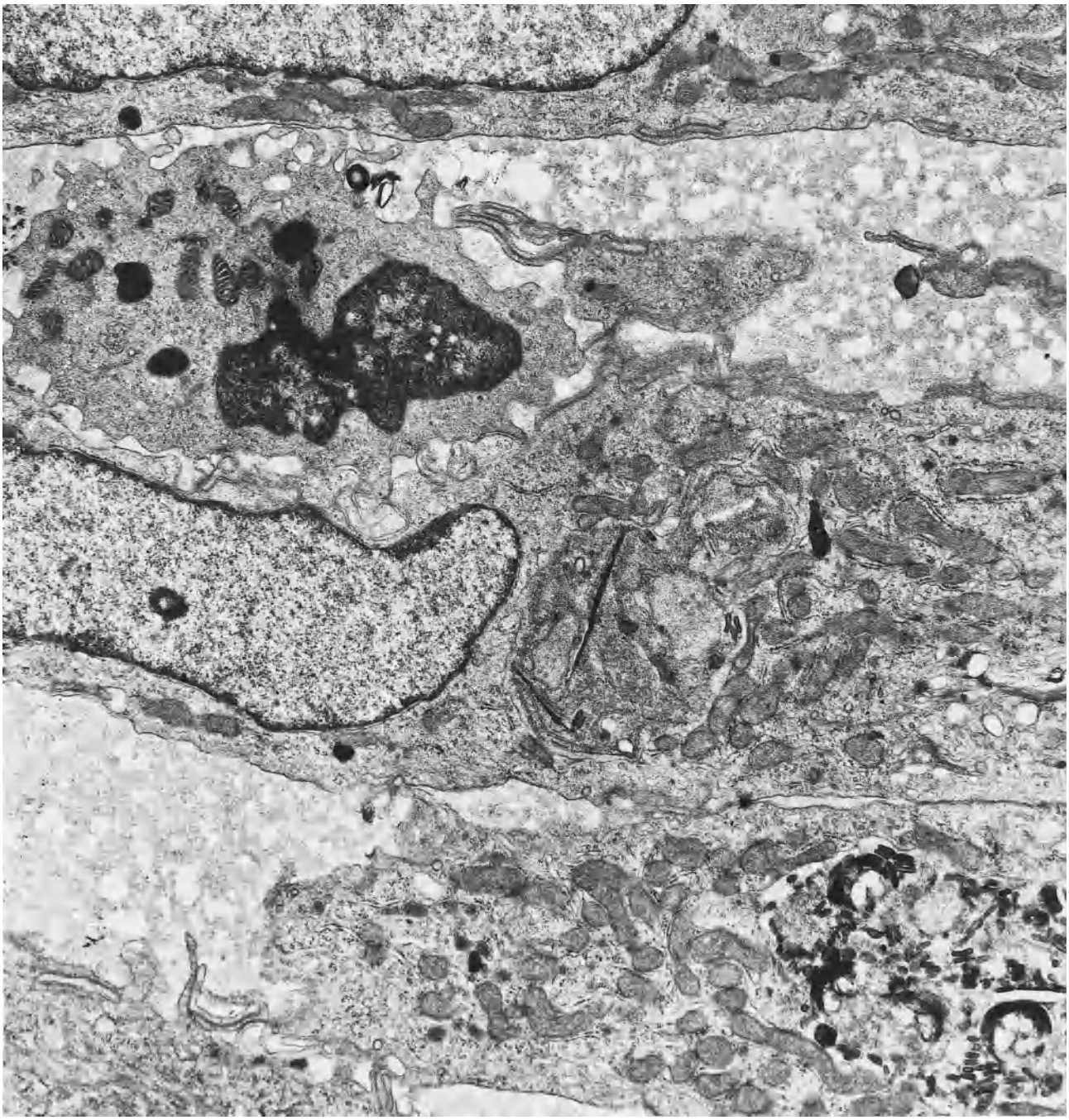


Fig. 11.19 Activated intraepithelial lymphocyte: intestinal biopsy from a human patient with AIDS and microsporidiosis; lymphocyte is adjacent to epithelial cells invaded by microsporidia. Note numerous cytoplasmic projections, mitochondria, and three large dense granules. (Micrograph: John R. Webber, Jr., and William O. Dobbins III, *Am J Surg Pathol* 10:627, 1986.)

antigen-presenting cells. The **T cell receptor (TCR)** is a disulfide-linked heterodimer, which is encoded by sets of rearranging gene segments. The initial intrathymic development, when most of the thymocyte proliferation occurs, involves rearrangement of these genes and production of mRNAs to produce the αβTCR that embeds in the plasma membrane.

The **αβTCR** heterodimer is associated with the membrane complex CD3 (θ, ε, δ, and γ), which is involved in signal transduction after TCR and antigen-MHC complex interact. A second type of TCR heterodimer described later consists of γ and δ chains. TCR with αβ or γδ heterodimers has been localized in cells by immunocytochemical or flow cytometric

Vet-ebooks.com

techniques. In most species, αβTCR cells predominate. However, in young ruminants and swine, a higher percentage of γδTCR T cells have been observed.

Triggering of the **TCR/CD3 complex** results in secretory granule movement, exocytosis, and delivery of the lytic granule contents to target cells. CTL cells can kill multiple target cells in a process referred to as serial killing.[59] Lymphocyte killing is a major cause of tissue damage in some diseases.[70]

T Lymphocytes in Tissue

T lymphocytes residing in different tissues have unique characteristics (Fig. 11.19). Mucosal lymphoid systems including the GALT, BALT, and others named for specific anatomic locations contain different subsets of T lymphocytes. For example, in the small intestinal wall, lymphocytes are found in the lamina propria (LPL) and epithelium (IEL). LPL subsets consist of $CD4^+$ and $CD8^+$ cells in nearly equal proportions.[71] On the other hand, IEL subsets are primarily CD8 T cells that express either CD8αβ heterodimers or CD8αα homodimers. The CD8αβ are αβTCR whereas CD8αα IEL cells express either αβTCR or γδTCR.[71] Similarly, the majority of IEL T cells in the lung express CD8 and those in the underlying lamina propria generally express CD4.[42]

References

1. Steiniger B, et al. 1990. Gamma interferon treatment in vivo provokes accumulation of activated monocytes in the venous circulation of rats. *Am J Pathol* 136:967.
2. Sadir R, et al. 2001. Caveolae and clathrin-coated vesicles: Two possible internalization pathways for IFN-gamma and IFN-gamma receptor. *Cytokine* 14:19.
3. Chensue SW, et al. 1991. In vivo biologic and immunohistochemical analysis of interleukin-1 alpha, beta, and tumor necrotic factor during experimental endotoxemia. *Am J Pathol* 138:395.
4. Warren JS, et al. 1988. Macrophage-derived cytokines amplify immune complex-triggered 0_2^- responses by rat alveolar macrophages. *Am J Pathol* 130:489.
5. Fantuzzi L, et al. 2003. Monocyte/macrophage-derived CC chemokines and their modulation by HIV-1 and cytokines: A complex network of interactions influencing viral replication and AIDS pathogenesis. *J Leuk Biol* 74:719.
6. Lanir N, et al. 1988. Macrophage migration in fibrin gel matrices. II. Effects of clotting factor XIII, fibronectin, and glycosaminoglycan content on cell migration. *J Immunol* 140:2340.
7. Aggeler J, Web Z. 1982. Initial events during phagocytosis by macrophages viewed from outside and inside the cell: membrane-particle interactions and clathrin. *J Cell Biol* 94:613.
8. Bainton DF, et al. 1989. Rapid fragmentation and reorganization of Golgi membranes during frustrated phagocytosis of immobile immune complexes by macrophages. *Am J Pathol* 134:15.
9. Li P, et al. 2005. Compartmentalization of class II antigen presentation: Contribution of cytoplasmic and endosomal processing. *Immunol Rev* 207:206.
10. Villadangos JA, Ploegh HL. 2000. Proteolysis in MHC class II antigen presentation: Who's in charge? *Immunity* 12:233.
11. Kelly JL, et al. 1985. Evolution of foam cells in subcutaneous rabbit carrageenan granulomas. II. Tissue and macrophage lipid composition. *Am J Pathol* 120: 391.
12. Brown LF, et al. 1993. Macrophages and fibroblasts express embryonic fibronectins during cutaneous wound healing. *Am J Pathol* 142:1990.
13. Johnston ER, et al. 2003. High frequency of syncytium-inducing and CXCR4-tropic viruses among human immunodeficiency virus type 1 subtype C-infected patients receiving antiretroviral treatment. *J Virol* 77:7682.
14. Ma YL, et al. 2007. The pathology of pulmonary sarcoidosis: Update. *Sem Diag Pathol* 24:150.
15. Papadimitriou JC, Drachenberg CB. 1992. Ultrastructural analysis of asteroid bodies. *Ultrastr Pathol* 16:413.
16. Noor A, Knox KS. 2007. Immunopathogenesis of sarcoidosis. *Clin Dermatol* 25:250.
17. Bechan GI, et al. 2006. Biology of Langerhans cells and Langerhans cells histiocytosis. *Int Rev Cytol* 254:1.
18. Geismann F, et al. 2001. Differentiation of Langerhans cells in Langerhans cell histiocytosis. *Blood* 97:1241.
19. Iwafuchi M, et al. 1990. Primary benign histiocytosis X of the stomach. *Am J Surg Pathol* 14:489.
20. Hage C, et al. 1993. Langerhans' cell histiocytosis (histiocytosis X): Immunophenotype and growth function. *Human Pathol* 24:840.
21. Obregon C, et al. 2006. Exovesicles from human activated dendritic cells fuse with resting dendritic cells, allowing them to present alloantigens. *Am J Pathol* 169:2127.
22. Barois N, et al. 2002. MHC class II compartments in human dendritic cells undergo profound structural changes upon activation. *Traffic* 3:894.
23. Schriever F, Nadler LM. 1992. The central role of follicular dendritic cells in lymphoid tissues. *Adv Immunol* 51:243.
24. Wacker HH, et al. 1990. Accessory cells in normal human and rodent lymph nodes: Morphology, phenotype and functional implications. *Curr Top Pathol* 84(Pt 1):193.
25. Lefevre EA, et al. 2007. Fibrinogen is localized on dark zone dendritic cells in vivo and enhances the proliferation and survival of a centroblastic cell line in vitro. *J Leuk Biol* 82:1.
26. Yoshida K, et al. 1993. Two functionally distinct follicular dendritic cells in secondary lymphoid follicles of mouse spleen, as revealed by CR1/2 and FcRγII-mediated immune-complex trapping. *Immunology* 80: 34.

Vet-ebooks.com

27. Szakal AK. 1989. Microanatomy of lymphoid tissue during humoral immune responses. *Ann Rev Immunol* 7:91.
28. Denzer K, et al. 2000. Follicular dendritic cells carry MHC class II-expressing microvesicles at their surface. *J Immunol* 165:1259.
29. LeibundGut-Landmann S, et al. 2004. MHC class II expression is differentially regulated in plasmacytoid and conventional dendritic cells. *Nat Immunol* 5:899.
30. Willard-Mack CL. 2006. Normal structure, function, and histology of lymph nodes. *Toxicol Pathol* 34:409.
31. Camacho FI, et al. 2001. Unique phenotypic profile of monocytoid B cells. Differences in comparison with the phenotypic profile observed in marginal zone B cells and so-called monocytoid B cell lymphoma. *Am J Pathol* 158:1363.
32. Cella M, et al. 1997. Origin, maturation and antigen presenting function of dendritic cells. *Curr Opin Immunol* 9:10.
33. Birbeck MS, et al. 1961. An electron microscopic study of basal melanocytes and high level clear cells (Langerhans cells) in vitiligo. *J Invest Derm* 37:51.
34. Valladeau J, et al. 2000. Langerin, a novel C-type lectin specific to Langerhans cells, is an endocytic receptor that induces the formation of Birbeck granules. *Immunity* 12:71.
35. Shortman K, Liu YJ. 2002. Mouse and human dendritic cell subtypes. *Nat Rev Immunol* 2:151.
36. Askew D, Harding CY. 2008. Antigen processing and CD24 expression determine antigen presentation by splenic $CD4^+$ and $CD8^+$ dendritic cells. *Immunology* 123:447.
37. Owen RL, Jones AL. 1974. Epithelial cell specialization within human Peyer's patches: An ultrastructural study of intestinal lymphoid follicles. *Gastroenterology* 66:189.
38. Liebler EM, et al. 1988. Gut-associated lymphoid tissue in the large intestine of calves. II. Electron microscopy. *Vet Pathol* 25:509.
39. McGhee JR et al. 1984. Mucosal immunoregulation: Environmental lipopolysaccharide and GALT T lymphocytes regulate the IgA response. *Microbiol Immunol* 28:261.
40. Woloshack GE, Tomasi TB. 1983. The immunology and molecular biology of the gut-associated immune system. *Crit Rev Immunol* 4:1.
41. Knop N, Knop E. 2005. Ultrastructural anatomy of CALT follicles in the rabbit reveals characteristics of M-cells, germinal centres, and high endothelial venules. *J Anat* 207:409.
42. Holt PG, et al. 2008. Regulation of immunological homeostasis in the respiratory tract. *Nat Rev Immunol* 8:142.
43. Perry M, Whyte A. 1998. Immunology of the tonsils. *Immunol Today* 19:414.
44. Brandtzaeg P. 2003. Immunology of tonsils and adenoids: Everything the ENT surgeon needs to know. *Int J Pediatr Otorhinolaryngol* 67 Suppl 1:S69.
45. Olay I, Glick B. 1992. Follicle-associated epithelium and medullary epithelial tissues of the bursa of Fabricius are two different compartments. *Anat Rec* 233:577.
46. Haynes BF, et al. 1984. Phenotypic characterization and ontogeny of mesodermal-derived and endocrine epithelial components of the human thymic microenvironment. *J Exp Med* 159:1149.
47. Kaneshima H, et al. 1987. Thymic epithelial reticular cell subpopulations in mice defined by monoclonal antibodies. *Lab Invest* 56:372.
48. Nabarra B, Papiernik M. 1988. Phenotype of thymic stromal cells. An immunoelectron microscopic study with anti-Ia, anti-MAC-1, and anti-MAC-2 antibodies. *Lab Invest* 58:524.
49. van de Wijngaert FP, et al. 1984. Heterogeneity of epithelial cells in the human thymus. An ultrastructural study. *Cell Tiss Res* 237:227.
50. Von Gaudecker B, et al. 1997. Immuno-electron microscopy of the thymic epithelial microenvironment. *Microsc Res Tech* 38:237.
51. Pezzano M et al. 2001. Questionable thymic nurse cell. *Microbiol Mol Biol Rev* 65:390.
52. Leduc EH, et al. 1968. Ultrastructural localization of antibody in differentiating plasma cells. *J Exp Med* 127:109.
53. Valetti C, et al. 1991. Russell bodies: A general response of secretory cells to synthesis of a mutant immunoglobulin which can neither exit from, nor be degraded in, the endoplasmic reticulum. *J Cell Biol* 115:983.
54. Manz RA, Radbruch A. 2002. Plasma cells for a lifetime? *Eur J Immunol* 32:923.
55. Bockman DE, et al. 1974. Altered fine structure of B lymphocytes correlated with defective terminal differentiation. *Am J Anat* 140:551.
56. Taylor RB, et al. 1971. Redistribution and pinocytosis of lymphocyte surface immunoglobulin molecules induced by anti-immunoglobulin antibody. *Nat New Biol* 233:225.
57. Bhalla DK, et al. 1979. Lymphocyte surface and cytoplasmic changes associated with translational motility and spontaneous capping of Ig. *J Cell Sci* 39:137.
58. Burkhardt O, Merker H-J. 2002. Immunoelectron microscopic investigations of patching, capping, endocytic and shedding processes in T and B lymphocytes. *Ann Anat* 184:45.
59. Bossi G, et al. 2002. The secretory synapse: The secrets of a serial killer. *Immunol Rev* 189:152.
60. Stinchcombe JK, et al. 2001. The immunological synapse of CTL contains secretory domain and membrane bridges. *Immunity* 15:751.
61. Criado M, et al. 1985. Cytotoxic granules from natural killer cells: Specificity of granules and insertion of channels of defined size into target membranes. *J Immunol* 135:4245.
62. Ojcius DM, et al. 1991. Cytolytic and ion channel-forming properties of the N terminus of lymphocyte perforins. *Proc Nat Acad Sci USA* 88:4621.
63. Young LHY, et al. 1992. Expression of cytolytic mediators by synovial fluid lymphocytes in rheumatoid arthritis. *Am J Pathol 140:1261.*
64. Abo T, et al. 1984. Characterization of human granular lymphocyte subpopulations expressing HNK-1 (Leu 7) and Leu-11 in blood and lymphoid tissues from fetuses, neonates and adults. *Eur J Immunol* 14:616.

Vet-ebooks.com

65. Dvorak AM, et al. 1983. Cloned mouse cells with natural killer function and cloned suppressor T cells express ultrastructural and biochemical features not shared by cloned inducer cells. *J Exp Med* 157:843.
66. Huhn D, et al. 1982. Large granular lymphocytes: Morphological studies. *Eur J Immunol* 12:985.
67. Luini W, et al. 1981. Morphological characterization of a cell population responsible for natural killer activity. *Immunology* 43:663.
68. Leiberman J. 2003. The ABCs of granule-mediated cytotoxicity: New weapons in the arsenal. *Nat Rev Immunol* 3:361.
69. Williams GS, et al. 2007. Membranous structures transfer cell surface proteins across NK cell immune synapses. *Traffic* 8:1190.
70. Sunagawa, et al. 2001. HLA class I-restricted and colon-specific cytotoxic T cells from lamina propria lymphocytes of patients with ulcerative colitis. *J Clin Immunol* 21:381.
71. Johansson-Lindbom B, Agace WW. 2007. Generation of gut-homing T cells and their localization to the small intestinal mucosa. *Immunol Rev* 215:226.

Vet-ebooks.com

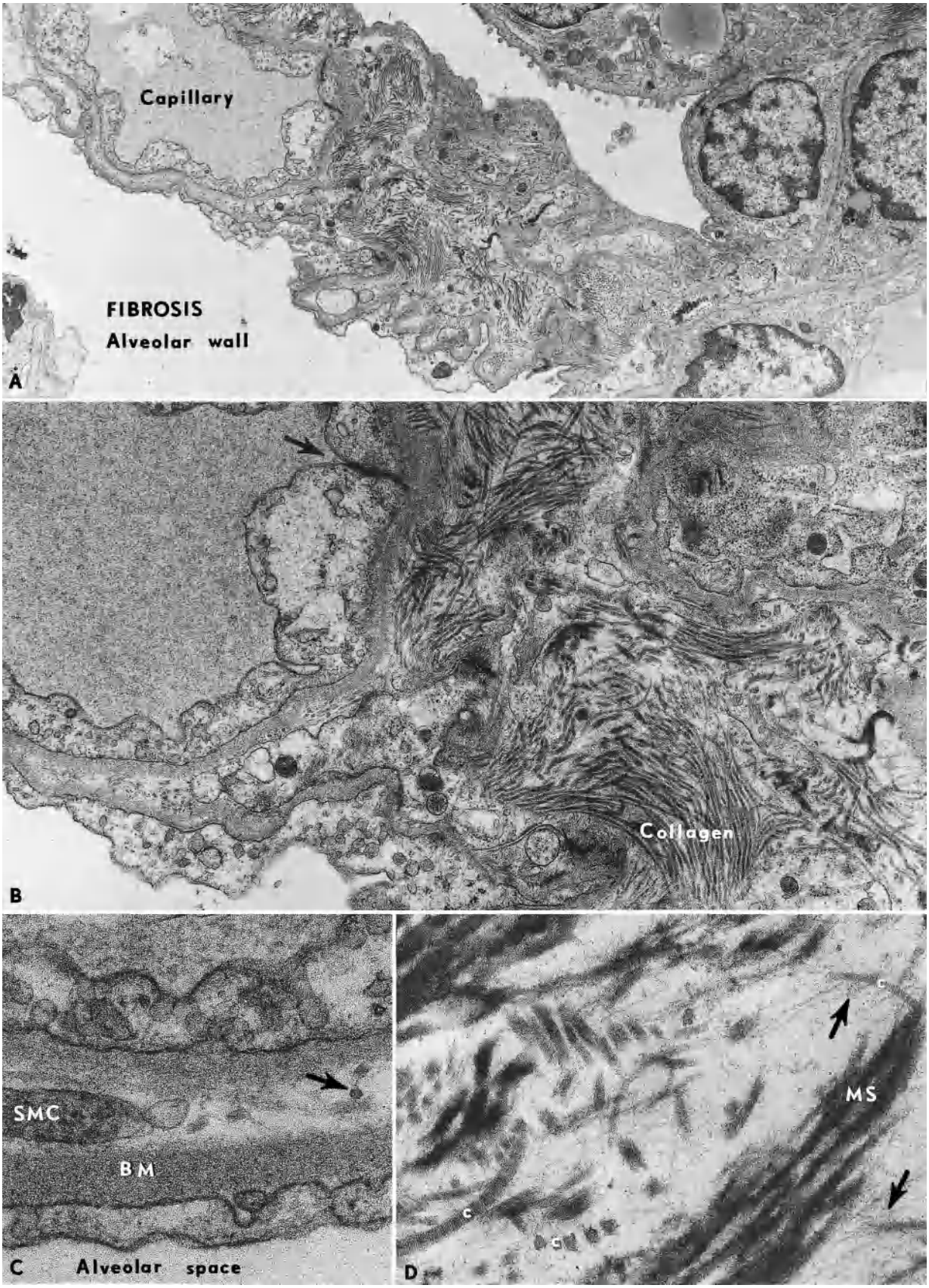


Fig. 12.1 **Fibrosis**: lung, chronic heart failure, dog. **A** and **B. Pulmonary alveolar walls**: markedly thickened with dilated capillaries. Interstitial deposits of collagen and other filaments. Basement membranes of both capillary endothelium and pneumocytes are thickened. **C. Basement membranes** (*BM*) are thickened. Smooth muscle cell (*SMC*); collagen fibrils, in cross section (*arrow*), are linked to basement membrane. **D.** Enlargement of interstitial collagen fibrils (*c*), mucosubstances (*MS*), and connective tissue filaments (*arrows*).

© 2009 Wiley-Blackwell. ISBN: 978-0-813-80330-2
Vet-ebooks.com

12 The Extracellular Matrix

Fibroblasts (fibrocyte, desmocyte, collagenoblast) are flat, elongated cells with oval nuclei and cytoplasmic processes at each end. Fibroblasts are differentiated into subpopulations based upon cytoskeletal differentiation markers.[1–3] Subepithelial fibroblasts in some tissues form contractile cellular networks by forming gap junctions that connect to epithelium, and neural and capillary networks—connections that allow for rapid changes in cell shape, contractile ability, and expression of receptors for vasoactive and neuroactive substances.[4]

Fibrosis (fibroplasia), the formation of fibrous tissue, arises from enhanced collagen production or from suppressed degradation of normal collagen when collagenases and elastases are missing or abnormal.[5–7] Fibroplasia occurs in such diverse conditions as atrophy, ischemia, and healing after injury. It is initiated and driven by signals created when **fibroblast growth factor (FGF)** binds its receptor (**FGFr**), and from supportive signals from **transforming growth factor-β (TGF-β)** in the connective tissue matrix. Mast cell granules are a potent source of these cytokines. The pathogenesis of fibrosis and collagen deposition have been documented in

- **Cutaneous fibrosis:** hypertrophic scars have fine, randomly organized collagen fibers and α-SM actin in myofibroblasts;[8] **keloids** contain large, thick collagen fibers composed of closely packed fibrils and amorphous extracellular material that surrounds fibroblasts, but lack myofibroblasts; **granulation tissue** surrounding silicone breast implants contains dense collagen, fibroblasts, and macrophages, and an associated network of endothelial cell-lined spaces.[9]
- **Hepatic fibrosis:** collagen I and III make up to 95% of the collagen in the fibrotic liver, and collagens IV and V are also synthesized; [10–12] both hepatocytes and fat-storing cells produce procollagen in cirrhotic livers.[13]
- **Pulmonary fibrosis:** fibrosis in alveolar walls, whether from circulatory failure or inflammation, is associated with fibrin and procoagulant factors that enhance development of fibrotic buds and myofibroblasts (Fig. 12.1).[14]
- **Synovial fibrosis.**[15]
- **Endocardial fibrosis** in rheumatic fever.[16]
- **Myocardial fibrosis.**[17]
- **Corneal fibrosis.**[18]

Existing fibrocytes are the major source of new fibroblasts in healing wounds, although the pluripotentiality of vascular endothelium, pericytes, and monocytes indicates that these cells may provide other types of matrix proteins. Fibroblasts are differentiated from their mature counterparts by large amounts of rough endoplasmic reticulum, dilated cisternae containing proteins, and prominent nucleoli, all evidence of active protein synthesis. The cytokines PDGF and TRF-β play roles in healing by preferentially triggering collagen and matrix synthesis.[19]

In uninfected, uncomplicated skin wounds, fibroblasts multiply and collagen is laid down until the wound is completely bridged at about 5–7 days (Fig. 12.2). In the subsequent 2–3 wk, when collagenization is largely completed, short dense elastic fibers begin to appear. They consist of linearly arranged amorphous globules of elastin complexes with a hydrated proteoglycan. Elastin components are interconnected, surrounded, and penetrated by bundles of microfibrils. The fibrillar-globular elastic fibers weave among collagen fibers, giving the newly formed connective tissue stretchability and elasticity.

Vet-ebooks.com

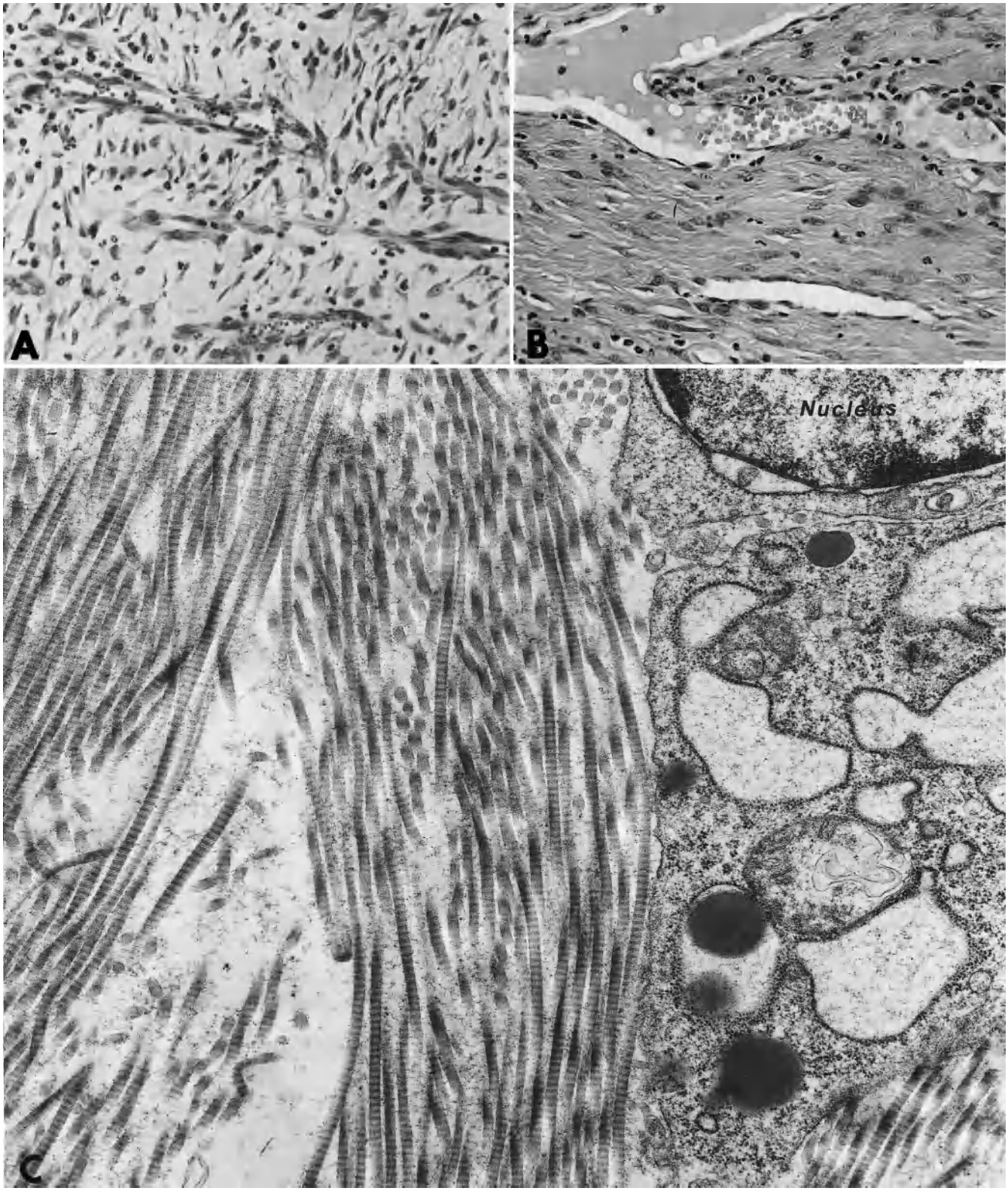


Fig. 12.2 Fibroplasia: healing wound, cat. **A. Endothelial cell invasion:** extension of fibroblasts parallel to endothelial cell buds (1 wk after surgical incision). **B. Advanced fibroplasias:** scar (4 wk after incision). **C. Collagen-producing fibroblast** (*right*) with large group of collagen fibrils at the surface. Bundle of fibrils makes up the collagen fiber (*center*). Fibroblast contains ribosomes and dilated RER, some of which contain procollagens.

Vet-ebooks.com

Myofibroblasts, specialized types of fibroblasts, are responsible for wound contraction.[20] These cells have irregular nuclear membranes, specialized surface attachment sites, and bundles of cytoplasmic actin microfilaments.[21–23] Myofibroblasts are similar to fibroblasts but have bundles of filaments called **stress fibers** that are oriented longitudinally and contain dense areas. Myofibroblasts are derived fibroblasts (and perhaps from pericytes) by the selective activation of genes for the production of actin and other smooth muscle-associated genes (such as desmin and vimentin). In wound healing fibroblasts are stimulated to temporarily express markers for smooth muscle differentiation.[24,25] Myofibroblasts are responsible for contraction of postinflammatory stricture in wounds.[26] To strengthen the connective tissue wound, actin microfilaments within the fibroblast are connected to filaments of polymerized fibronectin in extracellular spaces. These intra- and extracellular microfilaments are bridged on the plasma membrane by the **fibronectin receptor** to form a **fibronexus**.[27]

Chronic fibrosis is characterized by the enhanced collagen fibrillogenesis and concomitant increases in ground substance, connective tissue microfibrils, and basement membranes. The latter are attached to underlying collagen by specialized anchoring fibrils[28] and to the plasma membrane of overlying epithelium by hemidesmosomes. Glycosaminoglycans in the ground substance and bone marrow play crucial roles in how collagen is deposited.[29] Growth factors FGF and TGF-β are assisted in persistent fibrosis by VEGF and PDGF.

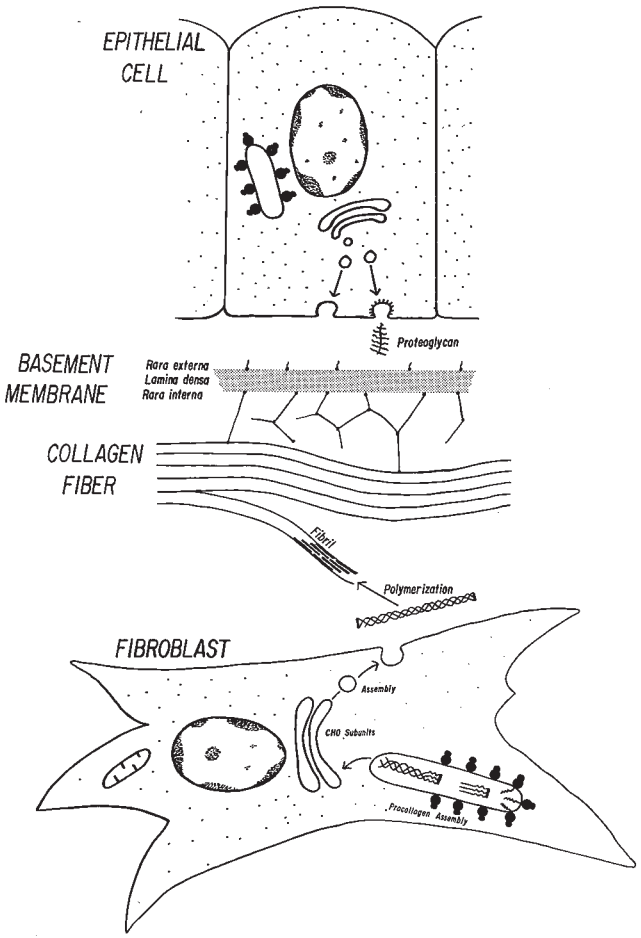


Fig. 12.3 Collagens and proteoglycans: relation to the basement membrane.

Collagen Fibers

Collagen molecules form the building blocks for connective tissue fibers, and for nonfibrous structures such as cartilage and basement membranes.[30] Mammalian fibroblasts produce at least 14 different collagen molecules, each with a gene that controls its synthesis. Each collagen is designed for a different structural form outside the cell.[31]

The first five genetically distinct collagen types (I–V) comprise at least nine separate gene products. Within each type, heterogeneity occurs since variations in hydroxylation, glycosylation, and cross-linking of the molecule are dependent on tissue type, age, and hormonal status. For example, collagen in type I in the Achilles tendon is highly cross-linked, whereas that of the tail tendons is much less so.

Collagen Fibrils

Collagen fibrils are composed of staggered arrays of fibrillar collagen molecules (types I, II, III, V, and XI). The structural form of the collagen fibril is an ordered polymer visible by electron microscopy as a banded structure in the extracellular matrix of connective tissue (Fig. 12.3). Collagen fibrils provide support scaffolds for the extracellular matrix of connective tissue. **Nonfibrillar collagen** molecules, less abundant, serve as bridges for stability of the extracellular matrix. A subgroup of collagens—types IX, XII, and XIV—are not secreted as procollagen, but associate as tiny filaments with the fibrillar collagens to stabilize the collagen fibers.

Fibrillogenesis, the formation of these banded fibers, often involves different collagens; that is, fibrils of skin may be types I and III, those of chick cornea of types I and V. Cartilage of developing chick embryos contains mixed fibrils of collagen types II, IX, and XI. Synovial membranes have collagen I, III, IV, V, and a peculiar collagenase-resistant collagen VI.[32] Collagen XII fibrils align to collagen fibrils in a way that suggests that they stabilize fibers to matrix.[33]

Fibrils of collagen I are approximately 50 nm in diameter, and aggregated side-by-side in parallel

Vet-ebooks.com

bundles to form the **collagen fibers,** the ordered aggregates of fibrils seen by light microscopy. **Tropocollagen,** the basic structural unit of the collagen I fibril, is a rod 300 nm long, one of the longest protein molecules known. Its peculiar amino acid composition allows for a stable conformation. Hydroxylysine and hydroxyproline, rarely found in other tissue proteins, permit extensive cross-linking; and glycine, which makes up one-third of the tropocollagen molecule, allows a wide range of folding in the peptide chain.

Collagen I accounts for about 90% of total body collagen. It is this collagen that forms large, well-organized fibrils and is the molecule present where tensile strength is important. Fibers containing only collagen I vary greatly in diameter and weave, depending on the strength required. Collagen I of tendon forms thick, uniform fibrils packed in parallel bundles, whereas type I collagen of bone is in contorted waves of finer fibrils. In many collagen I fibrils, extracellular filaments and fibrils of type IV collagen (with 100 nm periodic cross-banding) intertwine among regular collagen I fibrils (Table 12.1).

Collagen Synthesis

Fibroblasts are the major producer of collagen I. Synthesis begins with production of polypeptide chains on the ribosome. Peptides are transported to the Golgi complex where carbohydrate subunits are assembled. **Procollagen,** the large precursor of tropocollagen, has additional peptide chains at its amino and carboxy termini that prevent fibrillogenesis before the molecule is released from the cell. As procollagen is released from the fibroblast, it is acted upon by the enzyme procollagen peptidase, which cleaves away the peptide chains at either end of the molecule to form **tropocollagen**. While still near the cell surface, tropocollagen spontaneously assembles by linking together in an overlapping pattern to form the collagen fibril.[34]

Table 12.1 Collagen molecules.

Type	*Form*	*Found in*	*Reference to ultrastructural pathology*
I	Fibril[a]	Bone, tendon, dentin, skin, connective tissue	**Vogel**, *Lab Invest* 40:201, 1979; **Oh**, *J Orthop Res* 23:1226, 2005
II	Fibril	Cartilage, nucleus pulposus, eye (vitreous)	**Mizuta**, *Neurosci Lett* 434:104, 2008; **Sawhney**, *Cell Biol Int* 29:133, 2005
III	Fibril	Reticulin, arteries, granulation tissue	**Uhlig**, *Microsc Res Tech* 70:18, 2007; **Young**, *J Histochem Cytochem* 48:423, 2000
IV[b]	Granule	Basement membrane, lens capsule	**Bruggink**, *Lab Invest* [E-pub] 2007; **Bruns**, *J Cell Biol* 103:393, 1986
V	Microfibril	Basement membranes of muscle, fibroblasts	**Uhlig**, *Microsc Res Tech* 70:18, 2007; **Oh**, *J Orthop Res* 23:1226, 2005
VI	Microfibril	Intima	**Engvall**, *J Cell Biol* 102:703 1986; **Keene**, *J Cell Biol* 107:1995, 1988; **Okada**, *Lab Invest* 63:647, 1990
VII	Dimer	Anchoring fibril, "long-chain collagen"	**Keene**, *J Cell Biol* 104:611, 1987; **Sakai**, *J Cell Biol* 103:1577, 1986
VIII	Microfibril	Arteries, eye	**Sage**, *Lab Invest* 50:219, 1984
IX	Amorphous	Cartilage, vitreous body	**Wotton**, *FEBS Lett* 234:79, 1988
X	Amorphous	Cartilage, vitreous body[c]	**Poole**, *J Cell Biol* 109:2547, 1989
XI	Fibril	Cartilage, vitreous body[d]	**Petit**, *Histochemistry* 100:231, 1993
XII	Amorphous	Connective tissue	**Veit**, *J Biol Chem* 281:27461, 2006
XV	Collagen-PG complex	Basement membranes	**Amenta**, *J Hist Cyt* 53:165, 2005
XVIII	Globular	Basement membranes[e]	**Miosqe**, *J Hist Cyt* 51:285, 2003
XIX	Globular	Basement membranes, sarcoma	**Myers**, *Am J Pathol* 151:1729, 1997

[a] Collagen fibril has periodicity of 67 nm.
[b] Unlike other types, type IV is assembled into tetrameres before secretion from the cell; it has a unique extracellular aggregation mechanism (Engvall et al. 1986).
[c] Proteoglycan (single glycosaminoglycan attached to one of its three alpha chains) may be cross-linked to collagen II; function unknown.
[d] Collagen XI is made by hypertrophic growth plate chondrocytes; it is associated with collagen II and may direct calcification by inhibiting it.
[e] C-terminal endostatin from collagen XVIII is anti-angiogenic; perlecan is an adaptor molecule for the endostatin domain in basement membranes.

Vet-ebooks.com

Once linked, tropocollagen molecules are stabilized by cross-links between lysine side chains. Lysyl oxidase is the enzyme involved in cross-linking of collagen. Present at the periphery of developing fibers,[35] it catalyses the oxidative deamination of an amino group in lysine and hydrolyzes residues of collagen. Cross-linking confers mechanical strength, an event that is missing in some inherited diseases. **Lathyrism,** a disease caused by ingestion of seeds of *Lathyris odoratus*, the sweet pea, has been used as a model to study defects in collagen cross-linking, especially as a model for human dissecting aneurysms of the aorta.[36] The toxic agent in *L. odoratus* is β-aminopropionitrile, which inhibits the transformation of lysyl side chains into aldehydes. Collagen in affected animals is extremely fragile.

Anchoring Fibrils

Anchoring fibrils are fibrous structures within the subbasal lamina. They project perpendicularly from the basement membrane, one end inserting into the lamina densa and the other terminating in an amorphous electron-dense plaque.[37] The centrosymmetric banding pattern of anchoring fibrils indicates that they are aligned as lateral aggregates of antiparallel fibrous subunits.[38] Immunogold studies to localize collagen VII show that gold attached to regions where anchoring fibrils intersect with amorphous patches in the dermis.[39] Collagen VII of human cutaneous anchoring fibrils and plaques is secreted by keratinocytes and traverses the epidermal basal lamina to localize in the dermis.

Reticular Fibers

Reticular fibers are composed of units of collagen III, are smaller (0.5–2.0 μm in diameter) than collagen fibers, and form delicate networks instead of thick bundles of fibers. Loose networks of reticular fibers are interwoven and bound together by proteoglycans. Not apparent in routine histologic examination, reticular fibers stain with silver stains. Ultrastructurally, reticular fibers are composed of unit fibrils each with a 67 nm periodicity typical of collagen.

Dysfunctional Collagen Fibers

Long spacing fibers are unusual collagen polymers (periodicity up to 200 nm) which occur in connective tissue matrices with active fibrillogenesis, especially in neoplasms. They are also seen in pathologic fibroplasia, for example, in Dupuytren's contracture.[40] Long spacing fibers arise when there are increased levels of proteoglycans and collagenase during active collagen fibril remodeling.[41]

Amianthoid fibers are pathologic fibrils containing thick nodose enlargements that, when cut in cross section, seem to represent giant fibrils. Typically interspersed with normal collagen, they appear to arise by fusion of existing collagen fibrils.[42]

Globular Collagen Mutations

Mutations in a collagen VIII gene are associated with progressive deposition of collagen, laminin and fibronectin within Descemet's membrane in eyes of patients with a familial form of Fuchs corneal dystrophy.[43]

Collagen Degradation

Collagen degradation, a normal part of connective tissue metabolism, is enhanced in inflammation and necrosis. **Macrophages** produce collagenase, elastase, and plasminogen activator, all of which hydrolyze connective tissue proteins. These substances act together to facilitate degradation; for example, plasmin, when converted from plasminogen, allows macrophage elastase easier access to its substrate elastin and accelerates the rate of hydrolysis and matrix degradation.[44] Collagen can also be degraded by **fibroblasts**[45] and **epithelial cells,**[46] although these cells are less efficient than macrophages. After limited hydrolysis, macrophages then endocytose the protein matrix fragments, which are completely degraded within lysosomes.

Microbial Collagen Degradation

Migrating **parasites** move through the interstitium by causing degradation of extracellular matrix material. Larvae of *Schistosoma* spp. penetrate the skin and transform into a second larval form, the schistosomulum; this form losses some of its surface glycocalyx and secretes proteolytic substances from its glands that degrade the matrix and facilitate entry of parasites through the skin.[47] Pathogenic **bacteria** and other microbes also degrade collagen and ground substance as part of their infectious cycles. By degrading collagen, bacteria produce a better environment in which to replicate and destroy a barrier for their movement within tissue.

Intracellular Collagen Degradation

Phagocytosis of extracellular collagen occurs in stroma where large amounts of collagen are broken down, especially in chronic tissue destructive disease. Small

Vet-ebooks.com



Fig. 12.4 **Fibrosis**: skeletal muscle, muscular dystrophy, dog. Lesions include marked disintegration of myofilaments, accumulation of glycogen, and deposits of collagen, connective tissue filaments, and ground substance.

fragments of collagen fibrils are interspersed with granular debris. Macrophages and giant cells in chronic granulomas frequently contain intracellular collagen, for example, asteroid bodies in giant cells in sarcoidosis.[48]

Collagen Fiber Diseases

Defects in the production of the different chains of collagen may lead to defective collagen at specific tissue sites (Fig. 12.4). Defective genes for production of collagen I cause defects in collagen fibers (Table 12.2). Defective genes for collagen IV cause defect in basement membranes, for example, patchy thickening and thinning of glomerular basement membranes in Alport syndrome, which involves defects in the gene for α5(V) collagen chain.[49]

Dermatosparaxis

Dermatosparaxis is an inherited disease characterized by loose fragile skin easily torn during minor trauma. It results from a deficiency of **procollagen peptidase,** the enzyme that cleaves the amino terminal nonhelical extension from the precursor procollagen molecules. Removal of the N-propeptides of both α1 and α2 chains in type I collagen is deficient. Although procollagen has both carboxy and amino terminal extensions that are cleaved to yield collagen, procollagen with the amino terminus is the only precursor that accumulates in dermatosparaxis.[50]

The degree of enzyme deficit is a major species difference. Affected sheep have almost no collagen chains in skin and generally die at birth or within a few weeks. The defects are less severe in cats and calves, which have significant amounts of normal collagen chains.[51] Newborn calves with dermatosparaxis have extremely fragile skin with large numbers of flat, twisted, unbanded collagen fibrils in disordered patterns. The striking deficiency of mature collagen fibers is demonstrable by their lack of birefringence under polarized light[52] and abnormal X-ray diffraction patterns.[53]

Dermatosparactic collagen fibers vary greatly in size and shape. Instead of the normal weaving of fibers, dermal collagen has tangled organization of fibrils within the fiber and abnormal weaving patterns (Fig. 12.5). The aberrant collagen molecules alter the structure of individual fibrils, the assembly of fibrils into fiber bundles, and the woven network in the reticular dermis of skin. In calves, the abnormal fibrils are embedded in excess ground substance, which is responsible for the jelly-like touch of the skin.

Ehlers-Danlos Syndrome

Human syndromes of generalized dermal fragility due to defective collagen metabolism are termed collectively Ehlers-Danlos syndrome (EDS). These have in common the clinical signs of joint hypermobility, skin hyperextensibility, and easy bruising or laceration during trauma. There are at least seven forms of EDS: three are dominant (types I, II, and III), and four are recessive. The latter are due to specific enzyme defects, but mechanisms are not known for those inherited by dominant genes. Type IV, the most severe form, is characterized by rupture of large arteries, especially in soft tissues of the colon, uterus, and lung. Decreased amounts of collagen III in tissue may arise by production of abnormal collagen III, or by normal collagen synthesis but impaired secretion.

Ultrastructural studies on skin of human patients with Ehlers-Danlos syndrome have shown changes in connective tissue architecture and in collagen and elastic fiber morphology. Fiber bundles are poorly integrated in the dermis in types I, II, V, VI, and VII, and collagen fibril diameters are enlarged. Fibrils may be irregular and lobulated in many forms. Even though periodicity is normal, fibers are irregular, spiraled, or fragmented.[54] In nine cases of type I Ehlers-Danlos syndrome, collagen fibers had an increased mean diameter and an increased variance in width and shape.[55] Severe natural animal models for EDS exist, especially in the cat.

Ultrastructural aspects of poorly characterized hereditary defects in collagen synthesis or fiber fibrillogenesis (other than dermatosparaxis of cattle and

Vet-ebooks.com

Table 12.2 Steps in normal and defective collagen fiber formation.

Activity and location	*Defect*	*Reference to ultrastructural pathology*
Translation of mRNA amino acid assembly into polypeptides (pro-α-chains) on ribosomes of fibroblasts	**Protein deficiency:** Starvation	 **Gross**, *J Exp Med* 107:265, 1958
Hydroxylation of proline (and other amino acids) by proline hydroxylase on ribosomes of RER	**Inhibition of proline hydroxylation:** Ascorbic acid deficit (scurvy) Corticosteroid therapy Dilantin therapy[a]	 **Bates**, *Biochim Biophys Acta* 278:610, 1972 **Manthrope,** *Acta Endocrinol* 77:310, 1974 **Liu**, *Proc Soc Exp Biol Med* 142:253, 1973
Helix formation: aggregation of pro-α-chains into triple helix of procollagen in ER cisternae and Golgi complex by disulfide bonding	Toxins that disrupt the Gly-x-y amino acid sequence	**Brodsky**, *Biopolymers* 89:345, 2008
Release of soluble procollagen by secretory granules at the cell surface	**Inhibition of cell release:** Monensin (ionophore) Ehlers-Danlos (type IV) disease	**Uchida**, *Proc Natl Acad Sci USA* 76:1868, 1979 **Byers**, *Hum Genet* 47:141, 1979; **Holbrook**, *Lab Invest* 44:342, 1981
Extracellular alignment of tropocollagen from procollagen (pro-α-chains converted to α-chains by procollagen peptidase, which cleaves away amino and carboxy terminal peptides)	**Procollagen peptidase deficiency (failure in procollagen to collagen conversion):** Dermatosparaxis Ehlers-Danlos (type VII) disease	 **O'Hara**, *Lab Invest* 23:307, 1970 (calf); **Fjolsted**, *J Pathol* 112:183, 1974 (sheep); **Counts**, *J Invest Dermatol* 74:96, 1980 (cat) **Lichtenstein**, *Science* 182:298, 1973
Cross-linking of amino acids: formation of aldehyde end groups in tropocollagen Lysyl oxidase converts peptidyl lysine to allysine (aldehyde) Lysyl hydroxylase converts hydroxy lysine to hydroxyallysin	**Lysyl oxidase deficit:** β-aminopropionitrile poisoning (inhibits lysyl oxidase) Copper deficit[b] (dietary) Menke's kinky hair sydrome Enzyme deficiency in mottle (blotchy) mice **Lysyl hydroxylase deficiency:** Ehlers-Danlos (type VI) disease **Blockade of aldehyde groups:** D-Penicillamine toxicity Homocystinuria[a] Marfan's syndrome	 **Bjornstein**, *Am J Med* 49:429, 1970 **Shields**, *Am J Pathol* 41:603, 1962 **Oakes**, *Exp Mol Pathol* 25:82, 1976 **Andrews**, *Am J Pathol* 78:199, 1975; **Yajima**, *Acta Neuropathol* 48:133, 1979 **Pinnell**, *New Engl J Med* 286:1013, 1972 **Deshmukh**, *J Biol Chem* 244:1787, 1969 **Kang**, *J Clin Invest* 52:2571, 1973 **Sabatier**, *Mol Biol Cell* 2008 [E-pub]
Collagen fibril formation	**Defective fibrillogenesis:** Ehlers-Danlos (human: types I, II, III) Cutaneous asthenia (dog, mink) Fibrillogenesis defect	 **Vogel**, *Lab Invest* 40:201, 1979 **Hegreberg**, *Arch Pathol* 90:159, 1970; **Patterson**, *Lab Invest* 37:171, 1977

[a] Reported only in humans.
[b] Copper is an essential component of lysyl oxidase.

sheep) have been reported in dogs, cats, horses, and mink.[56,57]

Other Familial Collagen Diseases

Scleroderma

Ultrastructural analysis of skin in **systemic scleroderma** show heterogeneity of collagen fiber size. Thin collagen fibrils retain at their surface the aminopropeptide of type III procollagen.[58] **Microfibrils,** the 10 nm hollow-cored, fibrillin-containing structures that are associated with elastin and collagen in normal skin, are massively increased and are randomly arranged and intermingled with collagen fibrils (Fig. 12.6).[59,60]

Progeria

Progeria (Hutchinson-Gilform syndrome) is a heritable disorder of scleroderma-like skin, bone hypoplasia and resorption, short stature with nasal deformation, and cardiovascular abnormalities. Patients typically die in the second or third decade of myocardial infarction secondary to coronary thrombosis and

Vet-ebooks.com

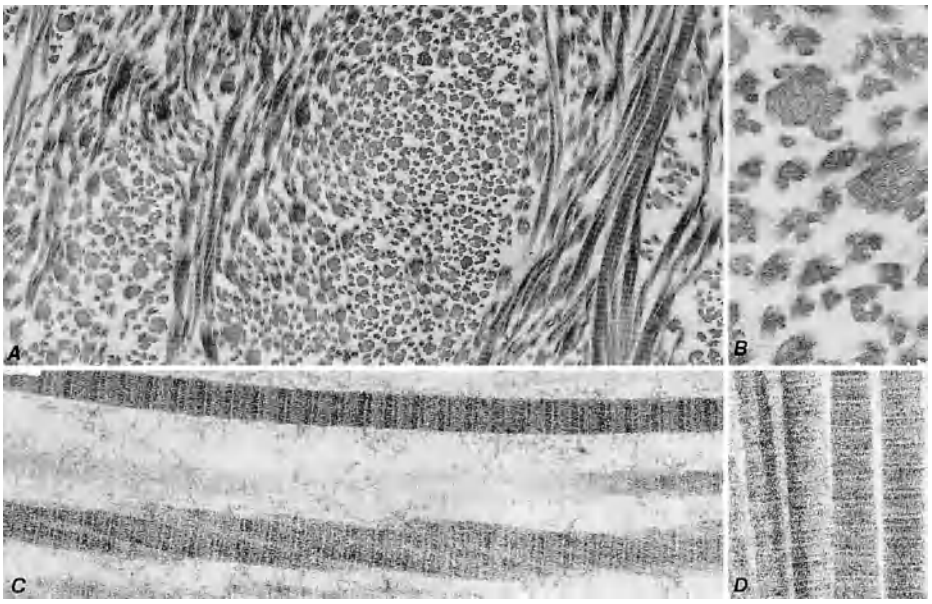


Fig. 12.5 Collagen fibrils, dermatosparaxis, cat. A. Abnormal collagen fibers: individual fibrils in various planes of section. **B. Collagen fibrils** (cross section)**:** bizarre shapes**. C. Collagen fibrils** (longitudinal section): loosely woven bundles of filaments spiral around one another (*bottom fibril*). **D. Collagen fibrils:** normal cat**.** (Micrographs: Karen A. Holbrook, *J Invest Dermatol* 74:100, 1980.)

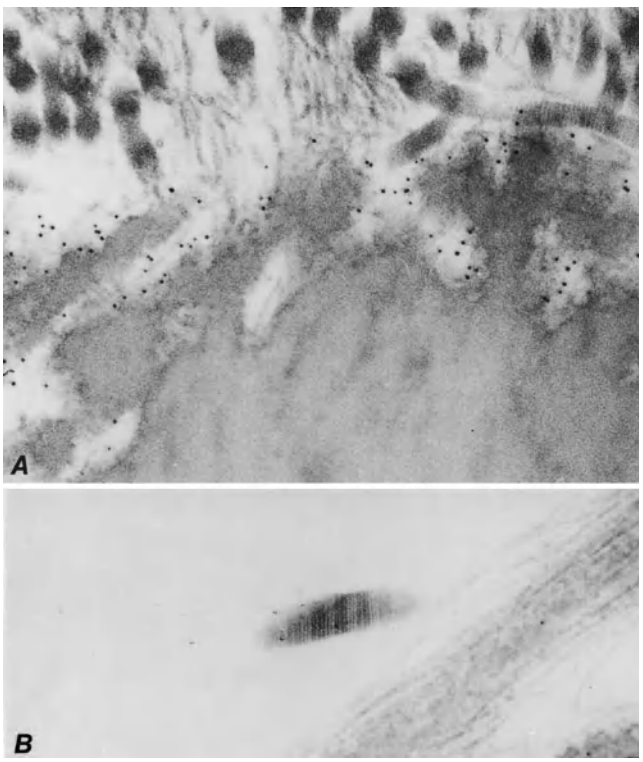


Fig. 12.6 Elastic fibril, human systemic scleroderma. **A**. **Immunogold labeling:** amorphous substance stains but microfibrils do not. **B**. **Microfibrils**: do not stain with elastin antibodies. (Micrograph: R. Fleischmajer, *Lab Invest* 64:791, 1991.)

atherosclerosis. The clinical picture of premature aging has been shown to involve specific increases in amounts of type IV collagen and superabundant networks of abnormal elastic fibers and thickened basement membranes in the skin.[61]

Chondrodysgenesis

Collagen synthesis may be abnormal in chondrogenesis. Disturbed extracellular matrix in articular cartilage caused by quinolones (such as the antibacterial compound difloxacin) is caused by degeneration of chondrocytes,[62] a change that begins in mitochondria.

Defective chondrogenesis is more often due to familial diseases. More than 70 mutations in the two structural genes for type I procollagen have been found in human patients with osteogenesis imperfecta. These include deletions, insertions, RNA splicing mutations, and single base substitutions that convert a codon for glycine to a codon for an amino acid with a bulkier side chain. The resulting structurally defective pro-α chains of procollagen I interfere with the folding of the triple helix or with self-assembly of collagen into fibrils.[63]

Abnormal chondrocytes of dwarf Alaskan malamutes (chondrodysplasia) have irregular distributions of rough endoplasmic reticulum and many vesicles with lack of condensation of extracellular matrix granules. Dwarf type II collagen has increased hexosamine and is abnormally soluble.[64] The cartilage matrix is thus abnormal and there are altered proteoglycan polymers in the matrix of most types of chondrodysplasia.[65]

Aminoaciduria

Rare, and often poorly defined, hereditary defects in connective tissue metabolism have been described in humans with **aspartylglycosaminuria,** a lysosomal disorder of glycoprotein degradation. Abnormal

Vet-ebooks.com

collagen fibrils with marked variations in fibril diameters are due to altered fibril formation.[66]

Scurvy

In vitamin C (ascorbic acid) deficiency fibroplasia is markedly retarded because this vitamin is required as a cofactor for proline hydroxylase. Fibroblasts of human scurvy patients and animals with vitamin C deficiency show deficiency of collagen production. Similar changes occur in fibroblasts in culture.[67] Characteristics of scurvy include extensive formation of fibroblasts and synthesis of ground substance but very little deposition of collagen. Fibroblasts do not form in parallel arrays, and the resulting signs of disease are related to delayed wound healing and abnormalities of bone.

Odontogenesis

Odontogenesis begins with a series of cell-cell and cell-matrix interactions that result in differentiation of odontoblasts and ameloblasts, which form dentin and enamel, respectively. Once the mantle of dentin is formed, ameloblasts differentiate and secrete various enamel proteins that assemble into an extracellular enamel matrix that controls the growth of mineral crystallites. **Amelogenins,** which make up over 90% of enamel proteins in the developing enamel matrix, have been identified ultrastructurally.[68,69]

Microfibrils

Throughout connective tissue, **microfibrils** are found as slender extracellular filaments of approximately 10 nm diameter and of indefinate length. In cross section, they appear to be hollow and have a periodic structure. Microfibrils are located on elastic fiber surfaces and zonular fibers in the posterior chamber of the eye.[70] **Fibrillin,** a large glycoprotein, is the major component of microfibrils.[71] Immunogold techniques have shown that microfibrils in subendothelial basement membranes contain thrombogenic proteins. The proteoglycan **perlecan** is an associated component of microfibrils close to basement membranes.[72]

Ultrastructural analysis has shown that microfibrils consist of **tubules** composed of stacked 8 nm diameter pentagonal segments (that react with amyloid P component) and **surface bands**. Microfilaments contain globular structures connected by ordered arrangements of fibrillin molecules, the periodicity of which is influenced by mechanical tension.[33]

Microfibrillopathies

Marfan Syndrome

Marfan syndrome is caused by a defect in **fibrillin** synthesis that leads to cardiovascular defects and excessive longitudinal growth of tubular conges in limbs, fingers and ribs. The Marfan patient has long thin limbs (colichostenomelia), spider fingers (arachnodactyly), and pectus excavatum. Death is caused by aortic dissection, abdominal aortic aneurysms, and other cardiovascular lesions. Defective or deficient fibrillin can be demonstrated to varying degrees. There is a reduction in microfibril production in fibroblasts taken from Marfan syndrome.[73]

Point mutations have been found in the **fibrillin gene** in patients with sporadic Marfan syndrome. Polymorphism in the fibrillin gene is tightly linked (no recombinants) to the Marfan phenotype in family linkage studies. The defective Marfan gene resides in the long arm of chromosome 15 (15q), and a probe from the cloned fibrillin gene (FBN1) has been mapped to the same region (15q21.1) by in situ hybridization techniques. A similar autosomal dominant disorder, **congenital contractural arachnodactyly,** is caused by mutations in a second fibrillin gene (FBN2) located on chromosome 5. A **bovine Marfan syndrome** associated with defective fibrillin has been reported.[74]

Elastic Fibers

Elastic fibers ramify and interconnect to form meshworks in loose connective tissue. Identified histologically only by special stains, they are composed of two structures: an amorphous component **elastin,** and **microfibrils,** small 10 nm diameter fibrils that aggregate around the amorphous component.

Elastin is made of hydrophobic amino acids and is rich in valine. It also contains desmosine and isodesmosine, two unique amino acids. Tropoelastin is synthesized and released at the periphery of fibroblasts where it aggregates and assembles into elastic fibers.[75,76] Extracellularly, lysyl oxidase catalyzes the formation of aldehyde groups on lysines just as in collagen synthesis.

Hereditary diseases suspected of bearing defective genes for elastin synthesis include the Marfan syndrome, **pseudoxanthoma elasticum,** and the **Buschke-Ollendorf syndrome**.[77] The role of elastin in acquired disease is even more unclear, although elastin degradation is very important in emphysema, pulmonary fibrosis, and atherosclerosis.

Mutations in the microfibrillar protein **fibulin**[78] lead to impaired dermal elastic fiber formation in **recessive cutis laxa**. The basic mechanism is a failure of elastin

Vet-ebooks.com

globules to fuse into a continuous elastic fiber core.[79] Studies in vitro revealed that the failure of mutant fibulin-5 to integrate with fibrillin induces an endoplasmic reticulum stress response.

The high concentration of calcium and phosphate in the extracellular space would cause calcification if it were not efficiently inhibited by matrix γ-carboxyglutamic acid and other glycoproteins that prevent calcium precipitation. Deficiencies of MCG lead to widespread elastic fiber calcification.[80]

Marfan Syndrome is an Elastic Fiber Disorder

Marfan syndrome is an autosomal dominant disorder of elastin. The underlying defect is a mutation in the fibrillin gene, and fibrillin, which makes up the 8–10 nm microfibrils that are associated with elastic fibers, is abnormal. In cattle, the lens disorder arises from defects in the ciliary zonular fibers of the suspensory ligament of the lens.[81] Human disease has musculoskeletal, cardiovascular and ocular manifestations including tall stature, aortic dilatation and rupture, and ectopia lentis.

Extracellular Ground Substance

Connective tissue ground substance is the extracellular gel of mucosubstances and fluid in which connective tissue fibers and cells are embedded. Its viscosity and gel nature are due to **proteoglycans** both free and attached to collagen and elastic fibers (Fig. 12.7). **Glycosaminoglycans** (GAGs) are those polysaccharides containing amino sugars (glucosamin, galactosamine) on their chains. Nearly all vertebrate GAGs also contain sugar groups with carboxylic acid units (glucuronic acid, galacturonic acid); they are referred to as acidic mucopolysaccharides with strongly acid sulfate groups on GAGs bound to protein.

Interstitial ground substances are mixtures of GAGs. **Chondroitin sulfates** dominate in cornea and cartilage. **Dermatan sulfate** is the most common molecule in skin, tendon, and gastric mucus. **Hyaluronic acid** is prevalent in synovial fluid, umbilical cord, connective and vascular walls. Enhanced synthesis or reduced degradation of the complexes may produce excesses in metabolic, inflammatory and neoplastic disease. Their deposition and degradation are markedly influenced by the anabolic steroid hormones.

Keratan sulphate proteoglycans in the cornea are key molecules for stromal transparency. **Macular corneal dystrophy** is a rare autosomal recessive disease of mutations in a gene encoding the enzyme responsible for keratan sulphate sulphation; it leads to disturbed keratan sulphate expression and diminished immunogold labeling for keratin sulphate proteoglycans.[82–84]

GAG units of the **proteoglycan molecule** aggregate during fixation for electron microscopy as small dense granules of 20–50 nm that have fine projections that interconnect to form a meshwork. Similar but smaller GAG granules are associated with basement membranes. When GAG molecules are purified and examined by electron microscopy, they appear as large, fern-shaped arrays with a stem of hyaluronic acid from which leaflets of protein-GAG complexes radiate (Fig. 12.8).

Cutaneous Proteoglycan Accumulation

In **myxedema,** the accumulation of GAGs, albumin, water, and mast cells in subcutis is a manifestation of **hypothyroidism**. Primarily a disease of adult humans, myxedema also occurs in dogs and other animals. GAGs accumulate around capillaries and veins.[85,86] Accumulation of fluid and albumin is due partly to the great capacity of hyaluronic acid to bind to water and to the subsequent suppression of lymphatic drainage. Deposits of GAGs in skeletal and cardiac muscle cells predispose to muscle weakness and cardiac failure. Affected renal glomeruli alter plasma filtration and enhance fluid and electrolyte defects.[87]

Striking accumulation of GAGs in ground substance follows stimulation by **sex hormones**, for example, growth of the cock's comb under the influence of testosterone and swelling of the vulva in primates due to progesterone. **Sex skin** in female nonhuman primates is a striking accumulation of proteoglycans that is attractant to males. The edematous, red, moist skin is caused by subepidermal capillary dilation, accumulation of fluid, and massive deposition of GAGs. These phenomena are associated with specific cell receptors, since GAGs are not increased in other tissues.

Adrenal **corticosteroids** have a promoting effect on GAGs in ground substance. Given in massive doses they act on capillaries to decrease permeability and edema, thereby playing a significant role in suppressing acute inflammation.

Tissue Injury and Inflammation

GAGs accumulate at sites of inflammation as a prelude to collagen fibrillogenesis and healing. In inflammation, hyaluronic acid imparts high viscosity to ground substance and is important in restricting the spread of bacteria through fascial planes. Some of the most invasive bacteria produce **hyaluronidases** that degrade hyaluronic acid and facilitate bacterial spread.

Vet-ebooks.com

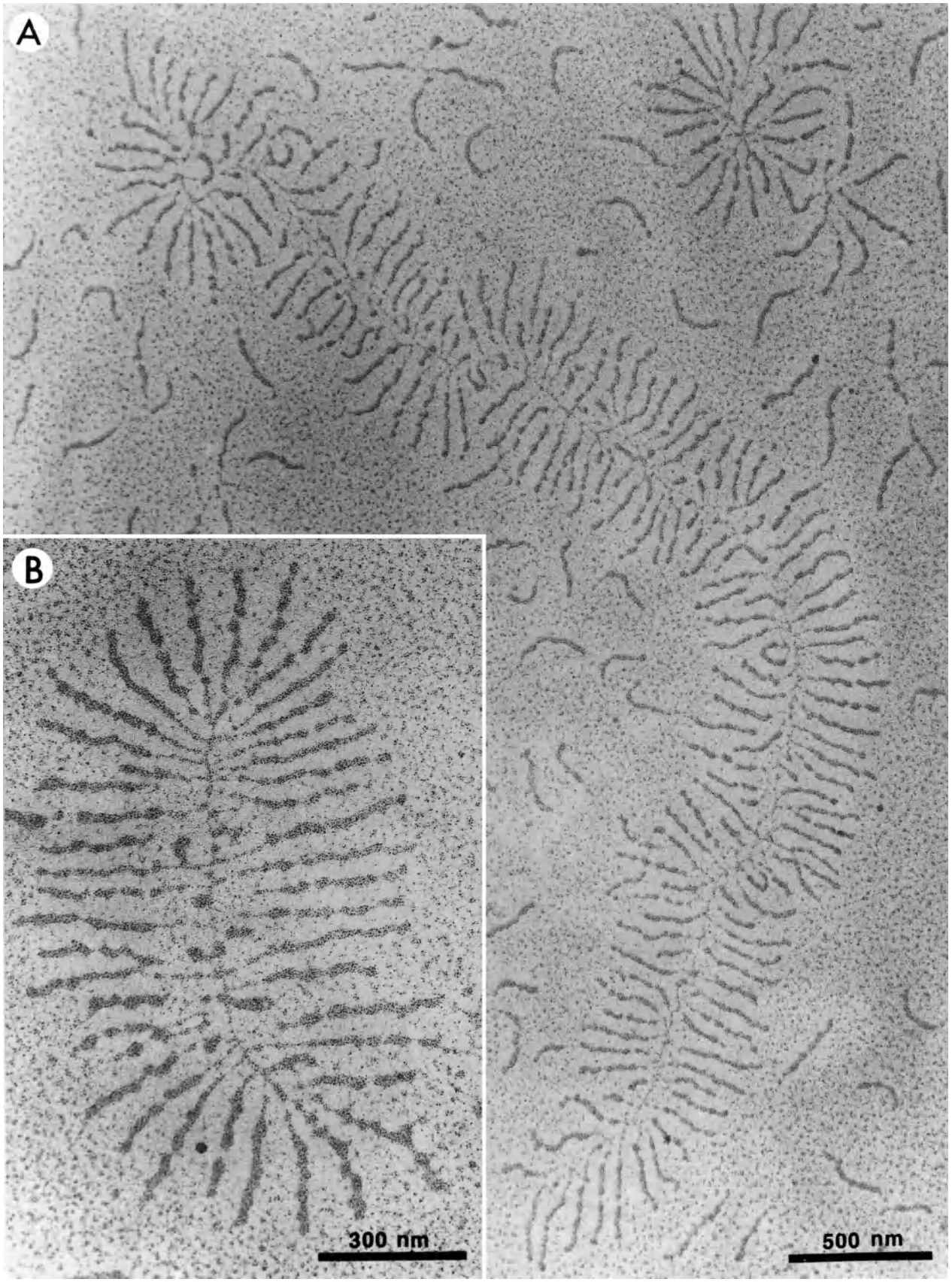


Fig. 12.7 Proteoglycan molecules: negatively stained preparation of purified proteoglycans. (Micrograph: J. A. Buchwalter, *Collagen Relat Res* 3:489, 1983.)

Vet-ebooks.com

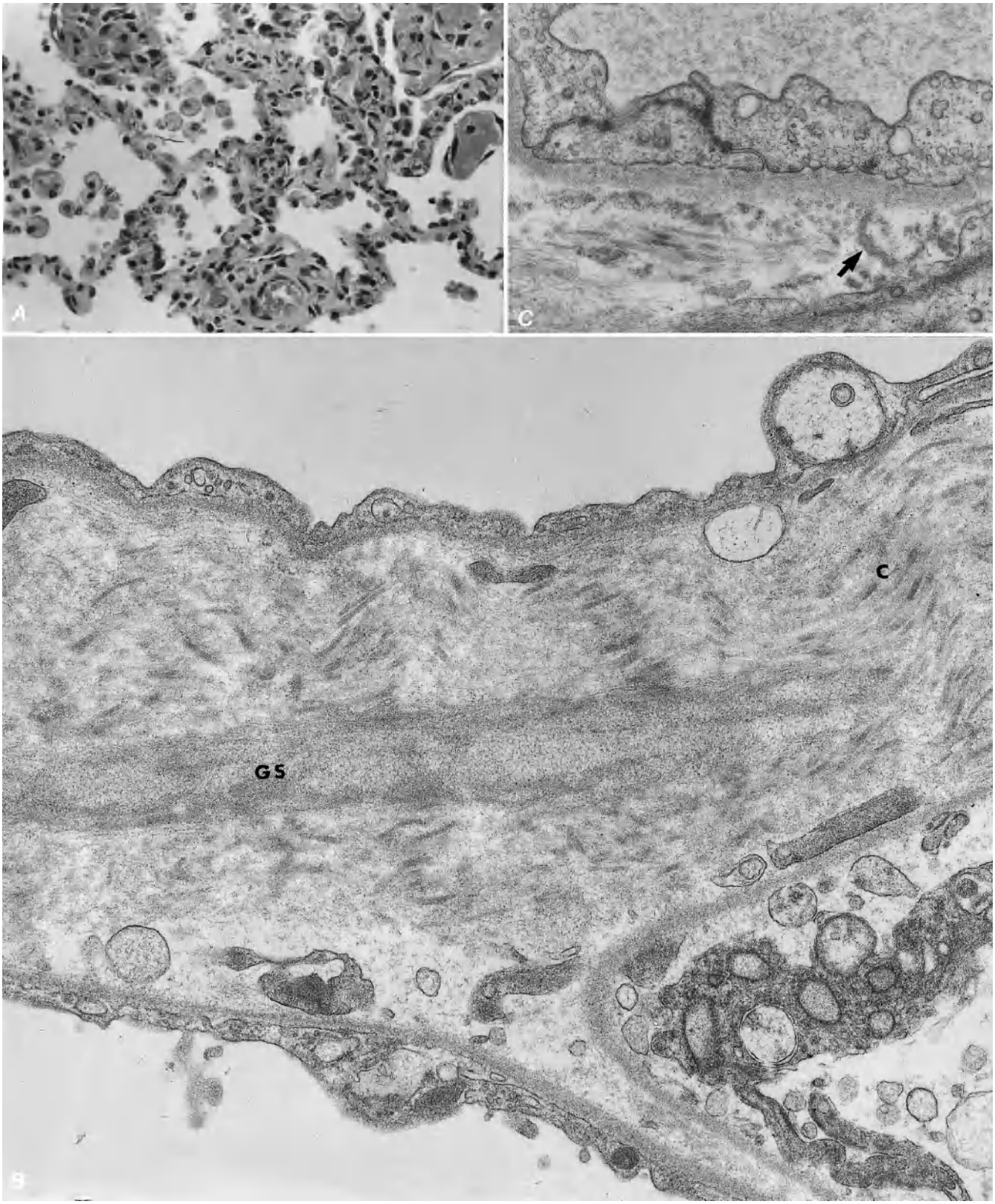


Fig. 12.8 Ground substance: fibrosis, alveolar wall, dog with severe dyspnea, hypoxia, and chronic lung disease (chronic heart failure). **A**. **Thick alveolar walls** and **"heart failure cells"** in alveoli (histology). **B**. **Deposits of granular ground substance** (*GS*) and collagen (*C*) in interstitium. Mitochondria are degenerate and protrude into alveolus (a manifestation of severe hypoxia); capillary (*lower right*) is degenerate. **C**. **Basal lamina is thickened**: elastin (*arrow*) is present outside the capillary wall.

Vet-ebooks.com

Embryonic Development

Fetal mesenchyme is rich in proteoglycans. During embryonal growth, extracellular collagen and proteoglycans direct mesenchymal and epithelial cell shape, motility, and differentation. Most epithelia will not grow and differentiate if separated from its underlying matrix; when matrix material is added, epithelial growth resumes. This stimulation of cell activity occurs via connections of collagen-fibronectin complexes with specific receptor molecules in the plasma membrane and extension of those connections from the receptor to submembrane actin filaments.[88,89]

Congenital Disease of Proteoglycan Synthesis

The rare familial **mucopolysaccharidoses** arise from defective enzymes in lysosomes. Storage of incompletely degraded glycosaminoglycans in cells that normally degrade these substances results from diminished activity of specific lysosomal hydrolases (see chapter 27, lysosomal diseases). The **chondrodysplasia** gene (*cho*) of mice acts on chondrocytes so that normal mucopolysaccharides are not released into cartilage matrix. Cho mice have a collagen-production defect that involves cartilage. Affected mice die of asphyxia shortly after birth due to collapse of the trachea. Cartilage matrix shows less basophilia and metachromasia than normal. Ultrastructurally the matrix has fewer fine fibrils and more large collagen fibrils. Chondrocytes show large Golgi zones, vacuoles and an absence of normal scalloped surfaces.

Basement Membranes

Basement membranes are composed of a scaffold of **collagen IV** molecules, which are complexed with **proteoglycans, laminin,** and other noncollagenous proteins such as **fibronectin**, **entactin**, and the glycoprotein **bullous pemphigoid antigen**. Heparin sulfate is prominent in most basement membranes and imparts a filter action largely because it is a strong polyanion. Most basement membranes are thin, measuring across approximately 100 nm or less. Basement membrane synthesis occurs in epithelial, endothelial, and myoepithelial cells.[90–92]

Collagen IV α chains contain long stretches of gly-x-y repeats that form triple helical trimers that join to form a three-dimensional lattice. Collagen IV linked to **laminin** forms the other major basal laminin a network by bridging with the glycoprotein **entactin**. Together, collagen IV and laminin networks make up the **basal lamina,** and interact with integrins to bring about adhesion. Collagen IV molecules remain granular and do not polymerize into fibrils due to glycosylation of its hydroxylysine residues. Specific monomers that make up collagen IV have been localized by immunogold techniques to certain basement membranes.[93]

Proteoglycans in basement membranes are localized in basement membranes with immunogold techniques using antibodies directed to the core protein or with cationic dyes (alcian blue, cuprolinic blue, ruthenium red) which react with GAG side chains of the proteoglycan molecule. These methods reveal that the core protein is within the lamina densa and that GAGs project above and below this layer.[94]

Ultrastructural examination of basement membranes reveals a meshwork of fibrils of 4 nm diameter arranged randomly in a granular matrix.[95] In conventional processing, basement membranes are composed of three layers:

- **Lamina lucida** (or **rara**), a 10–50 nm thick layer directly adjacent to overlying cells
- **Lamina densa** (or **basal lamina**), 20–300 nm thick
- **Lamina** (or **pars**) **fibroreticularis,** a poorly defined layer that makes up the transition with connective tissue

Cryofixation reveals that the lamina densa is in direct contact with epithelial cells, whereas in conventional fixation, it is separated from epithelium by the pale lamina lucida.[96] Immunoelectron microscopic analysis reveals that collagen is present in the lamina densa, and laminin and bullous pemphigoid antigen are in the lamina lucida. Some complex basement membranes, such as Reichert's membrane of the embryonic yolk sac, contain unbranched straight 7–10 nm tubules termed basotubules that run parallel to the surface of the basement membrane.[97]

Anchoring fibrils, the fibrous collagen VII structures within the subbasal lamina, connect basement membranes and adjacent structures. Immunogold studies to localize collagen VII show that gold attached to regions where anchoring fibrils intersect with amorphous patches in the dermis.

Components of the basement membrane are normally removed by phagocytosis and intracellular degradation of macrophages. In **involution** of organs such as uterus and mammary gland, large amounts of basement membrane material are processed and removed efficiently.[98] In contrast, tissue atrophy of **starvation** is characterized by widespread increased thickness of basement membranes in several organs, as well as excessive deposits of collagen and ground substance proteoglycans (see fat atrophy of starvation). The mechanism involves continued synthesis in the face of inhibited degradation and removal.

Vet-ebooks.com

Extracellular Matrix Glycoproteins

The glycoproteins of basement membranes, although poorly characterized chemically, are named for their location and action. **Fibronectin** (from the Latin: *fibra*, fiber, and *nectere*, to tie) promotes attachment of fibroblasts to collagen. It binds collagen and other fibrils of the stroma together. Similarly named are **laminin,** a specific attachment factor for epithelial cells to collagen IV, and **chondronectin,** which promotes attachment of cartilage cells to collagen.[99–101]

Fibronectin

Fibronectin is a noncollagenous glycoprotein secreted by fibroblasts that links connective tissue cells to the matrix.[102] In the extracellular matrix, fibronectin has specific binding sites for collagen, cell membranes, and proteoglycans. Fibronectin can cross-link with fibrin and to collagen by specific action of a plasma transglutaminase, factor XIII of the clotting cascade. Fibronectin is present in plasma as a dimer and in basement membranes and loose connective tissue as a multimer.[103]

Plasma fibronectin plays important roles in cell migration and adhesion, particlarly of platelets to collagen. Both plasma and cellular fibronectin are incorporated into fibrils of basement membranes.[104] Fibronectin is chemotactic for fibroblasts and stimulates phagocytosis by macrophages. Specialized granules termed "**adhesomes**" containing receptors for fibronectin, and laminin, as well as fibrinogen and complement, have been identified in human leukocytes.[105]

Fibronectin appears in large amounts in acutely inflammed tissues. Normally absent in dense connective tissue, it appears coincident with invading fibroblasts and disappears as collagen matures.[106] It functions as a matrix for organization of new collagen and promotes cell migration and adhesion.[107] Fibonectin also attaches to surfaces of invading bacteria to cause them to clump together.

Ultrastructural studies using antifibronectin antibody-horseradish peroxidase conjugates on sections of human lungs showed that alveolar basal lamina of normal lungs had little staining, while that of fibrotic lungs stained intensely for fibronectin.[108] In injured liver, fibronectin is released into spaces of Disse where the basement membrane is interposed between plasma and hepatocytes.[109]

Laminin

Laminin, a large, multidomain, three-peptide chain glycoprotein, is a major constituent of basement membranes. Laminin interacts with both cells and matrix. It is present in differing amounts in basement membranes in other connective tissues.[110–112] Within the basement membrane, laminin molecules bind to themselves to polymerize into long molecules. **Entactin,** a glycoprotein linker molecule, binds to laminin, causing it to bridge with collagen IV. Laminin can be detected at sites of synthesis in cells that produce basement membranes. Intracellular laminin develops in cisternae of the rough endoplasmic reticulum and Golgi complex and in secretory granules.[113]

Other Matrix Proteins

Other extracellular matrix glycoproteins are more restricted than fibronectin or laminin. **Tenascin** is a large oligomeric glycoprotein of the extracellular matrix. In the papillary dermis of the skin it is located beneath the basal lamina, in small amorphous patches located amongst collagen fibrils.[114] Common in embryos and in tumor stroma, it is very restricted in adult tissue. Tenascin (cytotactin, hexabrachion) is a large extracellular matrix glycoprotein associated with many tissues during cellular proliferation of embryonic development and pathologic processes. For example, increased focal tenascin expression occurs in vascular smooth muscle cells during prolonged hypertension. Other matrix glycoproteins in normal stroma are **entactin, fibrillin,** and **thrombospondin**.

Basement Membranes in Disease

Basement membranes are altered when epithelial or parenchymal cells to which they adhere are damaged. Acute epithelial injury is accompanied by discontinuity and irregularities of the underlying basement membrane.[115] Persistent injury, in contrast, is typically associated with basement membrane thickening. In degenerative lesions the basement membrane duplicates and thickened laminae are infiltrated with dense granules of glycoproteins and calcium salts. Glycoproteins such as fibronectin increase markedly.

Basement Membranes in Inflammation

Edema and **acute inflammation** are generally accompanied by leakiness or breaks in the basement membrane. When fluid accumulates in these processes, the basement membrane shows ultrastructural evidence of irregular lamination, breaks, and abnormal aggregation of granular components. Loss of the basement membrane barrier inflammation enhances the capacity of fluids and cells to move into damaged tissue.

Vet-ebooks.com

Fibronectin and fibrinogen are deposited in the areas of the basement membrane during inflammation as part of the provisional matrix of healing and play crucial roles in attachment of newly developing epithelial cells to the base of the wound.[116]

Chronic Inflammation commonly is accompanied by basement membrane thickening. As plasma proteins such as albumin and fibrinogen pass through the basement membrane filter in large amounts, parts of these molecules are retained, for example, protein overload of renal glomerular filtration. Any cause of **plasma protein overload** will cause basement membrane thickening.[117]

Mutations in Collagen IV: Alport Syndrome

In the renal glomerular basal lamina of the mammalian kidney, α1 and α2(IV) are present in the embryo and are replaced by α3–5(IV) chains as development proceeds. In humans, dogs, and mice, mutations of collagen α3, 4α, and 5α(IV) chain genes results in a delayed onset renal disease called **Alport syndrome**, a membraneous glomerulopathy with retention of α1 and 2(IV) collagens. In humans, mutation of the gene for the α5 chain of collagen IV is the primary defect in X-linked Alport syndrome. Ultrastructurally, the glomerular basement membrane is markedly thickened with a characteristic "basket-weave" appearance.[118] Localization of α5(IV) in the normal human glomerular basement membrane with colloidal gold conjugates shows that labeling is present throughout the thickness of the GBM. Male patients with X-lined Alport syndrome do not show this labeling.[119]

Epidermolysis Bullosa

Loss of basement membrane proteins leads to dysfunctional cell-to-cell adhesion. In skin, loss of basement membrane function is associated with blister formation. **Epidermolysis bullosa** is a heterogeneous group of human conditions characterized by the formation of blisters and erosions of the skin and mucous membranes in response to trauma. Classification, based upon diagnostic electron microscopy, reveals three categories: (1) **simplex**, nonscarring forms wherein blister formation occurs intraepidermally, within the keratinocytes; (2) **junctional,** in which tissue separation occurs within the dermal-epidermal basement membrane at the level of the lamina lucida; and (3) **dystrophic,** scarring forms characterized by tissue separation that occurs below the basement membrane in the upper dermis within the zone of anchoring fibrils.

In **junctional epidermolysis bullosa** there is widespread blistering with erosions of skin and mucous membranes. Skin blisters arise in the basement membrane that separates epidermis and dermis at the lamina lucida. Intact epidermis forms the roof of the blister and the lamina densa of the basement membrane remains as its base. Malformations of hemidesmosomes are associated with lesions.[120] A specific 600 kd glycoprotein of the epidermal basement membrane has been shown to be missing in these patients.

In **dystrophic epidermolysis bullosa,** blisters develop beneath the lamina lucida, and lesions are caused by defects in achoring fibrils that arise from a mutation in the gene encoding type VII collagen, the major component of anchoring fibrils. Ultrastructurally, cleavage occurs below the lamina densa, and there is absence of anchoring fibrils below the epidermis.[121]

Acquired types of epidermal bullosa, although they are clinically similar to the heritable forms, are typically an autoimmune disease in which the patient's serum contains autoantibodies directed against collagen VII. In several different blistering skin diseases, an autoimmune pathogenesis is reported with circulating autoantibodies the recognize cutaneous epitopes; for example, bullous pemphigoid and pemphigus vulgaris. Ultrastructural studies have localized **bullous pemphigoid antigen** to the lamina lucida, the electron-lucent region just below the basal cell plasma membrane in skin. Attachment of antibodies and cells to this areas cause the destruction that is manifest by blister formation.

Trapping of Immune Complexes

Immune complex diseases are due to inflammatory and degenerative changes induced in tissue by antigen-antibody-complement complexes. Trapping of microbial and self antigens in basement membranes is followed by complexing of antibodies as globulins pass through the membrane. Complement binds to the antigen-antibody complexes and attracts neutrophils, which release tissue damaging enzymes. The kidney is the organ most seriously affected. Other organs in which immune complex deposits are associated with clinical disease include the lung, testes, and thyroid.[122] **Glomerulonephritis** can result from deposition of circulating immune complexes, from attachment of circulating antibodies to antigens trapped in the glomerular filtration barrier, or from antibodies that cross-react with normal glomerular basement membrane,[123,124] multiple myeloma kidney,[125] lupus erythematosus,[126] and other renal diseases.[127]

- **Thyroids** of thyroidectomy patients manifest the same spectrum of changes that occur in the renal glomerulus (Fig. 12.9).[128]

Vet-ebooks.com

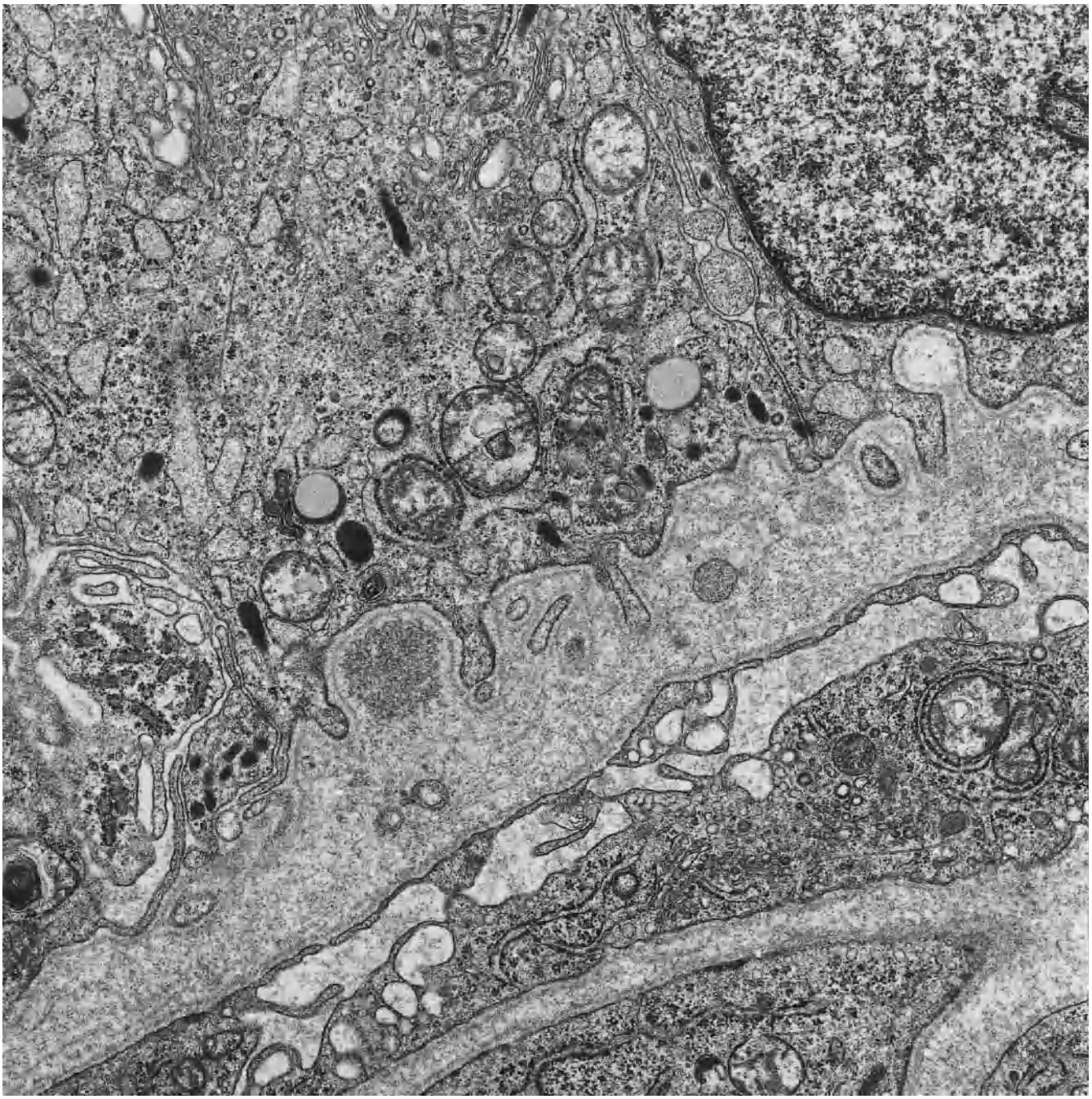


Fig. 12.9 Basement membrane, dense granular deposits: thyroid follicular epithelium, autoimmune thyroiditis, human with mild focal thyroiditis. Thyroid follicular epithelium at top. (Micrograph: Madeleine Pfaltz, *Lab Invest* 55:531, 1986.)

- **Immune complex orchitis** of men with infertility is characterized by thickened basement membranes around seminiferous tubules (Fig. 12.10).[129]
- **Atretic ovarian follicles** of mice with lupus-like syndrome, granular deposits of immune complexes develop in the zona pellucida.[130]
- **Nerves** in diabetes mellitus (Fig. 12.11).

Mucins and Other Barriers

Mucins

Mucins are high-molecular-weight glycoproteins produced by epithelial cells (and in some cases, by endothelial cells). Their properties are determined by the nature of their glycosylation. N-acetylgalactosamine is

Vet-ebooks.com



Fig. 12.10 Basement membrane, thickening and invagination: immune complex orchitis, human male. Large amounts of collagen occupy interstitial spaces (*bottom*). (Micrograph: Franco Salomon, *Lab Invest* 47:543, 1982.)

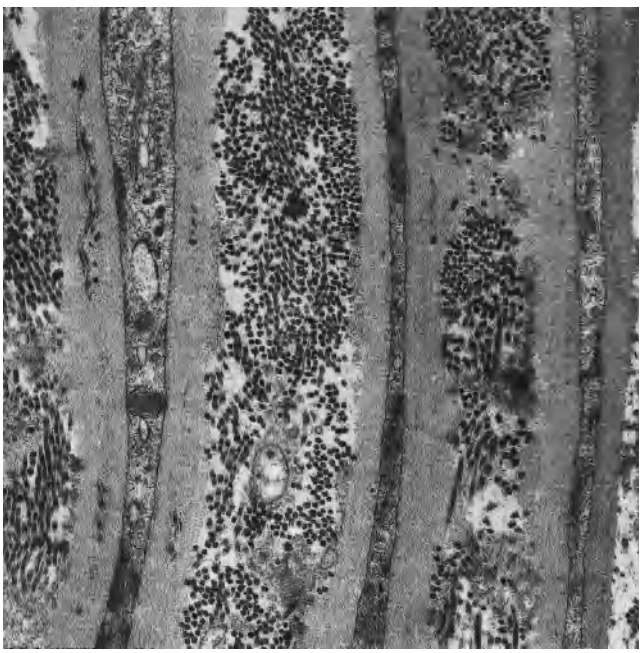


Fig. 12.11 Basement membrane, thickening: perineurial cell, sural nerve perineurium, diabetes mellitus, 58-year-old diabetic male. (Micrograph: Peter C. Johnson, *Lab Invest* 44:265, 1981.)

linked to a serine or threonine residue and is present in all mucins. On the basis of their structural properties, mucins are classified into three categories: the gel-forming/secreted mucins (produced by epithlelial cells), the soluble mucins, and the membrane-bound mucins.[131]

The Cutaneous Permeability Barrier

Formation of the **stratum corneum permeability barrier** in terrestrial animals involves two parallel processes, corneocyte formation and deposition of hydrophobic ECM. During final epidermal differentiation, granular cells transform into anucleate corneocytes, with highly resilient cornified envelopes. Immediately before cornification, large amounts of polar lipids are secretion from epidermal lamellar bodies into the extracellular spaces and are metabolized and organized into unique systems of parallel lamellar membrane arrays.[132]

Corneocytes lack a plasma membrane but are encased in a **cornified envelope** that consists of highly insoluble, cross-linked proteins with covalently

Vet-ebooks.com

attached lipids essential for water impermeability of skin. CE assembly is triggered by a rise in intracellular Ca^{2+}, which activates membrane-associated transglutaminase 1, which in turn catalyzes formation of CE precursor proteins. Proteins incorporated into the CE include involucrin, envoplakin, and periplakin. Loss of all three impairs the epidermal barrier.[133]

References

1. Muscariello L, et al. 2008. Cell surface protein detection with immunogold labelling in ESEM. *J Cell Physiol* 214:769.
2. Arntz Y, et al. 2006. Immunogold detection of type I and II chondrocyte collagen fibrils: An in situ atomic force microscopic investigation. *Microsc Res Tech* 69:283.
3. Sappino AP, et al. 1990. Differentiation repertoire of fibroblastic cells. *Lab Invest* 63:144.
4. Furuya S, Furuya K. 2007. Subepithelial fibroblasts in intestinal villi: Roles in communication. *Int Rev Cytol* 264:165.
5. Bellini A, Mattoli S. 2007. The role of the fibrocyte, a bone marrow-derived mesenchymal progenitor, in reactive and reparative fibroses. *Lab Invest* 87:858.
6. Faulkner JL, et al. 2005. Origin of interstitial fibroblasts in an accelerated model of angiotensin II-induced renal fibrosis. *Am J Pathol* 167:1193.
7. Wynn T. 2007. Cellular and molecular mechanisms of fibrosis. *J Pathol* 214:199.
8. Ehrlich HP, et al. 1994. Morphological and immunochemical differences between keloid and hypertrophic scar. *Am J Pathol* 145:105.
9. Emery JA, et al. 1994. The synovial structure of breast-implant-associated bursae. *Mod Pathol* 7:728.
10. Ijzer J, et al. 2006. Morphological characterization of portal myofibroblasts and hepatic stellate cells in normal dog liver. *Comp Hepatol* 16:5.
11. Miao S, et al. 1990. Two rat models of hepatic fibrosis. *Lab Invest* 63:467.
12. Nakatsukasa H, et al. 1990. Cellular distribution of transforming growth factor-β1 and procollagen types I, III, and IV transcripts in carbon tetrachloride-induced rat liver fibrosis. *J Clin Invest* 85:1833.
13. Takahara T, et al. 1988. Collagen production in fat-storing cells after carbon tetrachloride intoxication in the rat. *Lab Invest* 59:509.
14. Kuhn C, McDonald JA. 1991. The roles of the myofibroblast in idiopathic pulmonary fibrosis. *Am J Pathol* 138:1257.
15. Okada Y, et al. 1990. Localization of type VI collagen in the lining cell layer of normal and rheumatoid synovium. *Lab Invest* 63:647.
16. Fenoglio JJ, Wagner BM. 1973. Studies on rheumatic fever. VI. Ultrastructure of chronic rheumatic heart disease. *Am J Pathol* 73:623.
17. Bruggink AH, et al. 2007. Type IV collagen degradation in the myocardial basement membrane after unloading of the failing heart by a left ventricular assist device. *Lab Invest* 87:1125.
18. Zhang C, et al. 2006. Immunohistochemistry and electron microscopy of early onset Fuchs corneal dystrophy in three cases with the same L450W COL8A2 mutation. *Trans Am Ophthalmol Soc* 104:85.
19. Pierce GF, et al. 1994. Tissue repair processes in healing chronic pressure ulcers treated with recombinant platelet-derived growth factor BB. *Am J Pathol* 145:1399.
20. Hinz B, et al. 2007. The myofibroblast. *Am J Pathol* 170:1807.
21. Gabbiani G, et al. 1976. Collagen and myofibroblasts of granulation tissue. *Virch Arch B* 21:133.
22. Pourreau-Schneider N, et al. 1990. Helium-neon laser treatment transforms fibroblasts into myofibroblasts. *Am J Pathol* 137:171.
23. Squier CA, Kremenak CR. 1980. Myofibroblasts in healing palatal wound of the beagle dog. *J Anat* 130:585.
24. Darby I, et al. 1990. α-smooth muscle actin is transiently expressed by myofibroblasts during experimental wound healing. *Lab Invest* 63:21.
25. Kuhn C, McDonald JA. 1991. The roles of the myofibroblast in idiopathic pulmonary fibrosis. *Am J Pathol* 138:1257.
26. Ryan GB, et al. 1973. Myofibroblasts in an avascular fibrous tissue. *Lab Invest* 29:197.
27. Welch MP, et al. 1990. Temporal relationships of F-actin bundle formation, collagen, and fibronectin matrix assembly, and fibronectin receptor expression to wound contraction. *J Cell Biol* 110:133.
28. Kawanami O, et al. 1978. Anchoring fibrils. *Am J Pathol* 52:389.
29. Martinez-Hernandez A. 1985. The hepatic extracellular matrix. II. Electron histochemical studies on rats with CCl_4-induced cirrhosis. *Lab Invest* 51:57.
30. Leblond CP. 1989. Synthesis and secretion of collagen by cells of connective tissue, bone, and dentin. *Anat Rec* 224:123.
31. Exposito J-Y, et al. 2002. Evolution of collagens. *Anat Rec* 268:3l02.
32. Okada Y, et al. 1990. Localization of type VI collagen in the lining cell layer of normal and rheumatoid synovium. *Lab Invest* 63:647.
33. Keene DR, et al. 1991. Extraction of extendable beaded structures and their identification as fibrillar-containing extracellular matrix microfibrils. *J Hist Cyt* 39:441, 1991
34. Gerstenfeld LC, et al. 1988. Collagen expression, ultrastructural assembly, and mineralization in cultures of chicken embryo osteoblasts. *J Cell Biol* 106:979.
35. Kagan HM, et al. 1986. Ultrastructural immunolocalization of lysyl oxidase in vascular connective tissue. *J Cell Biol* 103:1121.
36. Nakashima Y, Sueishi K. 1992. Alteration of elastic architecture in the lathyritic rat implies the pathogenesis of aortic dissecting aneurysm. *Am J Pathol* 140:959.
37. Keene DR, et al. 1987. Type VII collagen forms and extended network of anchoring fibrils. *J Cell Biol* 104:611.
38. Sakai LY, et al. 1986. Fibrillin, a new 350-kD glycoprotein, is a component of extracellular microfibrils. *J Cell Biol* 103:2499.

Vet-ebooks.com

39. Regauer S, et al. 1990. Epithelial origin of cutaneous anchoring fibrils. *J Cell Biol* 111:2109.
40. Gokel JM, Hubner G. 1977. Intracellular fibrous long spacing collagen in morbus Dupuytren (Dupuytren's contracture). *Beitr Pathol* 161:176.
41. Kajikawa K, et al. 1980. The effect of collagenase on the formation of fibrous long spacing collagen aggregates. *Lab Invest* 43:410.
42. El-Labban NG, et al. 1986. Amianthoid fibres in muscle tissue associated with temporomandibular joint ankylosis. *Ultrastr Pathol* 10:571.
43. Zhang C, et al. 2006. Immunohistochemistry and electron microscopy of early-onset Fuchs corneal dystrophy in three cases with the same L450W COL8A2 mutation. *Trans Am Ophthalmol Soc* 104:85.
44. Werb Z, et al. 1980. Degradation of connective tissue matrices by macrophages. *J Exp Med* 152:1537.
45. Riede VN, Staubesand J. 1977. Die Rolle der Matrixvesikel und Lysosomen bei Erkrankungen des Bindegewebes und der Blutgefasse. *Beitr Pathol* 160:3.
46. Birek P, et al. 1980. Epithelial rests of Malassez *in vitro*. Phagocytosis of collagen and the possible role of their lysosomal enzymes in collagen degradation. *Lab Invest* 43:61.
47. Keene WE, et al. 1983. Degradation of extracellular matrix by larvae of *Schistosoma mansoni*. *Lab Invest* 49:201.
48. Azar HA, Lunardelli C. 1969. Collagen nature of asteroid bodies of giant cells in sarcoidosis. *Am J Pathol* 57:81.
49. Barker DF, et al. 1990. Identification of mutations in the COL4A5 collagen gene in Alport syndrome. *Science* 248:1224.
50. Wick G, et al. 1978. Immunohistologic analysis of fetal and dermatosparactic calf and sheep skin with antisera to procollagen and collagen type I. *Lab Invest* 39:151.
51. Holbrook KA, et al. 1980. Dermatosparaxis in a Himalayan cat. II. Ultrastructural studies of dermal collagen. *J Invest Derm* 74:100.
52. O'Hara PJ, et al. 1970. A collagenous tissue dysplasia of calves. *Lab Invest* 23:307.
53. Cassidy K, et al. 1980. X-ray diffraction investigations of collagen fibril structure in dermatosparactic lamb tissue. *Lab Invest* 43:542.
54. Black CM, et al. 1980. The Ehlers-Danlos syndrome: An analysis of the structure of the collagen fibres of the skin. *Br J Dermatol* 102:85.
55. Holbrook KA, Byers PH. 1981. Ultrastructural characteristics of the skin in a form of the Ehlers-Danlos syndrome type IV. *Lab Invest* 44:342.
56. Hardy MH, et al.1988. An inherited connective tissue disease in the horse. *Lab Invest* 59:253.
57. Patterson DF, Minor RR. 1977. Hereditary fragility and hyperextensibility of the skin of cats. A defect in collagen fibrillogenesis. *Lab Invest* 37:17.
58. Perlish JS, et al. 1988. Identification of collagen fibrils in scleroderma skin. *J Invest Derm* 90:48.
59. Fleischmajer R, et al. 1991. Extracellular microfibrils are increased in localized and systemic scleroderma skin. *Lab Invest* 64:791.
60. Hayes RL, Rodnan GP. 1971. The ultrastructure of skin in progressive systemic sclerosis (scleroderma). I: Dermal collagen fibers. *Am J Pathol* 63:433.
61. Colige A, et al. 1991. Abnormal gene expression in skin fibroblasts from a Hutchinson-Gilford patient. *Lab Invest* 64:799.
62. Burkhardt JE, et al. 1992. Ultrastructural changes in articular cartilage of immature beagle dogs dosed with difloxacin, a fluoroquinolone. *Vet Pathol* 29:230.
63. Kiuvaniemi H, et al. 1991. Mutations in collagen genes: Causes of rare and some common diseases in humans. *FASEB J* 5:2052.
64. Bingel SA, et al. 1983. Dwarfism in the Alaskan malamute: Ultrastructural features of dwarf growth plate chondrocytes. *Calcif Tiss Int* 35:216.
65. Rittenhause E, et al. 1978. Cartilage matrix deficiency (cmd). *J Embryol Exp Morphol* 43:71.
66. Nanto-Salonen K, et al. 1984. Abnormal collagen fibrils in aspartylglycosaminuria. Altered dermal ultrastructure in a glycoprotein storage disorder. *Lab Invest* 51:464.
67. Levene CI, et al. 1977. Scurvy; a comparison between ultrastructural and biochemical changes observed in cultured fibroblasts and the collagen they synthesize. *Virch Arch B* 23:325.
68. Massa LF, et al. 2006. Immunocytochemical study of amelogenin deposition during the early odontogenesis of molars in alendronate-treated newborn rats. *J Hist Cyt* 54:713.
69. Shiotani A, et al. 2002. Regulation of osteoclast differentiation and function by receptor activator of NFkB ligand and osteoprotegrin. *Anat Rec* 268:137.
70. Inoue S, et al. 1986. The microfibrils of connective tissue. *Am J Anat* 176:139.
71. Sakai LY, et al. 1986. Type VII collagen is a major structural component of anchoring fibrils. *J Cell Biol* 103:1577.
72. Tiedemann K, et al. 2005. Microfibrils at basement membrane zones interact with perlecan via fibrillin-1. *J Biol Chem* 280:11404.
73. Godfrey M, et al. 1990. Unilateral microfibrillar abnormalities in a case of asymmetric Marfan syndrome. *Am J Hum Genet* 46:661.
74. Parsons JC, et al. 1992. Normal elastin content of aorta in bovine Marfan syndrome. *Exp Molec Pathol* 57:145.
75. Bressan GM, et al. 1986. Relevance of aggregation properties of tropoelastin to the assembly and structure of elastic fibers. *J Ultrastruct Res* 94:209.
76. Campagnone R, et al. 1987. Pulmonary fibroblasts: A model system for studying elastin synthesis. *Lab Invest* 56:224.
77. Rosenbloom J. 1984. Elastin: Relation of protein and gene structure to disease. *Lab Invest* 51:605.
78. Miosge N, et al. 1999. Ultrastructural localization of microfibrillar fibulin-1 and fibulin-2 during heart development indicates a switch in molecular associations. *Cell Mol Life Sci* 54:606.
79. Hu Q, et al. 2006. Fibulin-5 mutations: Mechanisms of impaired elastic fiber formation in recessive cutis laxa. *Hum Mol Genet* 15:3379.

Vet-ebooks.com

80. Gheduzzi D, et al. 2007. Matrix G1a protein is involved in elastic fiber calcification in the dermis of pseudoxanthoma elasticum patients. *Lab Invest* 87:998.
81. Pessier AP, Potter KA. 1996. Ocular pathology in bovine Marfan's syndrome with demonstration of altered fibrillin immunoreactivity in explanted ciliary body cells. *Lab Invest* 75:67.
82. Young RD, et al. 2007. Differential immunogold localization of sulphated and unsulphated keratan sulphate proteoglycans in normal and macular dystrophy cornea using sulphation motif-specific antibodies. *Histochem Cell Biol* 127:115.
83. Lewis D, et al. 2000. Ultrastructural localization of sulfated and unsulfated keratan sulfate in normal and macular corneal dystrophy type 1. *Glycobiology* 10:305.
84. Bairaktaris G, et al. 1998. An ultrastructural investigation into proteoglycan distrubtion in human corneas. *Cornea* 17:396.
85. Kobayashi T, et al. 1976. Ultrastructure of localized myxedema. *Arch Dermatol Venereol* 56:173.
86. Parving H-H, et al. 1979. Mechanisms of edema formation in myxedema-increased protein extravasation and relatively slow lymphatic drainage. *New Engl J Med* 301:460.
87. Naeye RL. 1963. Capillary and venous lesions in myxedema. *Lab Invest* 12:465.
88. Hay ED. 1982. Interaction of embryonic cell surface and cytoskeleton with extracellular matrix. *Am J Anat* 165:1.
89. Montesano R, et al. 1991. Induction of epithelial tubular morphogenesis in vitro by fibroblast-derived soluble factors. *Cell* 66:697.
90. Inoue S, LeBlond CP. 1985. The basement membrane-like matrix of the mouse EHS tumor. *Am J Anat* 174:399.
91. Orkin RE, et al. 1977. A murine tumor producing a matrix of basement membrane. *J Exp Med* 145:204.
92. Timple R, Dziadek M. 1986. Structure, development, and molecular pathology of basement membranes. *Int Rev Exp Pathol* 29:1.
93. Desjardins M, et al. 1990. Heterogeneous distribution of monomeric elements from the globular domain (NCI) of type IV collagen in renal basement membranes as revealed by high resolution quantitative immunocytochemistry. *Lab Invest* 63:637.
94. Chan FL, et al. 1992. Localization of heparan sulfate proteoglycan in basement membrane by side chain staining with cuprolinic blue as compared with core protein labeling with immunogold. *J Hist Cyt* 40:1559.
95. Kefalides NA, et al. 1979. Biochemistry and metabolism of basement membranes. *Int Rev Cytol* 61:167.
96. Chan FL, et al. 1993. Cryofixation of basement membranes followed by freeze substitution or freeze drying demonstrates that they are composed of a tridimensional network of irregular cords. *Anat Rec* 235:205.
97. Inoue S, et al. 1983. Ultrastructure of Reichert's membrane, a multilayered basement membrane in the parietal wall of the rat yolk sac. *J Cell Biol* 97:1524.
98. Martinez-Hernandez A, et al. 1976. Removal of basement membrane in the involuting breast. *Lab Invest* 34:455.
99. Bender BL, et al. 1981. Immunolocalization of entactin, a sulfated basement membrane component, in rodent tissues and comparison with GP-2 (laminin). *Am J Pathol* 103:419.
100. Laurie GW, et al. 1982. Localization of type IV collagen, laminin, heparin sulfate proteoglycan, and fibronectin to the basal lamina of basement membranes. *J Cell Biol* 95:340.
101. Madri JA, et al. 1980. Ultrastructural localization of fibronectin and laminin in the basement membrane of the murine kidney. *J Cell Biol* 86:682.
102. Stenman S, Vaheri A. 1978. Distribution of a major connective tissue protein, fibronectin, in normal human tissue. *J Exp Med* 147:1054.
103. Courtoy PJ, Boyles J. 1983. Fibronectin in the microvasculature. *J Ultrastruct Res* 83:258.
104. Pesciotta Peters DM, et al. 1990. Co-assembly of plasma and cellular fibronectins into fibrils in human fibroblast cultures. *J Cell Biol* 111:249.
105. Singer II, et al. 1989. Adhesomes: Specific granules containing receptors for laminin, C3bi/fibrinogen, fibronectin, and vitronectin in human polymorphonuclear leukocytes and monocytes. *J Cell Biol* 109:3169.
106. Kurkinen M, et al. 1980. Sequential appearance of fibronectin and collagen in experimental granulation tissue. *Lab Invest* 43:47.
107. Fujikawa LS, et al. 1981. Fibronectin in healing rabbit corneal wounds. *Lab Invest* 45:120.
108. Torikata C, et al. 1985. Ultrastructural distribution of fibronectin in normal and fibrotic human lung. *Lab Invest* 52:399.
109. Martinez-Hernandez A. 1985 The hepatic extracellular matrix. II. Electron histochemical studies in rats with CCl_4-mediated cirrhosis. *Lab Invest* 53:167.
110. Abrahamson DR, Caulfield JP. 1985. Distribution of laminin within rat and mouse renal, splenic, intestinal, and hepatic basement membranes identified after the intravenous injection of heterologous antilaminin IgG. *Lab Invest* 52:169.
111. Abrahamson DR, et al. 1989. Selective immunoreactivities of kidney basement membranes to monoclonal antibodies against laminin. *J Cell Biol* 109:3477.
112. Schittney JC, Yurchenco PD. 1990. Terminal short arm domains of basement membrane laminin are critical for self assembly. *J Cell Biol* 110:825.
113. Holck S, et al. 1987. Laminin in the anterior pituitary gland of the rat. *Lab Invest* 56:481.
114. Lightner VA, et al. 1989. Tenascin/hexabrachion in human skin. *J Cell Biol* 108:2483.
115. Gas N, Noailliac-Depeyre J. 1976. Studies on intestinal epithelium involution during prolonged fasting. *J Ultrastruct Res* 56:137.
116. Fujikawa LS, et al. 1984. Basement membrane components in healing rabbit corneal epithelial wounds: Immunofluorescence and ultrastructural studies. *J Cell Biol* 98:128.
117. Mori H, et al. 1986. Proteinuria induced by transplantable rat pituitary tumor MtT SA5. Model for homologous protein-overload proteinuria. *Lab Invest* 54:636.

Vet-ebooks.com

118. Miner JH, Sanes JR. 1996. Molecular and functional defects in kidney of mice lacking collagen α3(IV): Implication for Alport syndrome. *J Cell Biol* 135:1403.
119. Yoshioka K, et al. 1994. Type IV collagen of α5 chain. *Am J Pathol* 144:986.
120. Tidman MJ, Eady RAJ. 1986. Hemidesmosome heterogeneity in junctional epidermolysis bullosa revealed by morphometric analysis. *J Invest Derm* 86:51.
121. Hovnanian A, et al. 1992. Genetic linkage of recessive dystrophic epidermolysis bullosa to the type VII collagen gene. *J Clin Invest* 90:1032.
122. Kalderon AE, et al. 1977. Electron-dense deposits in the follicular basal lamina of obese strain chickens with spontaneous hereditary autoimmune thyroiditis. *Lab Invest* 37:487.
123. Bohman S-O, et al. 1979. Evaluation of a process for systematic semiquantitative analysis of glomerular ultrastructure in human renal biopsies. *Lab Invest* 40:433.
124. Kashgarian M, et al. 1977. Renal disease. *Am J Pathol* 89:187.
125. Picken MM, et al. 1989. Light chain deposition disease derived from the K_1 light chain subgroup. *Am J Pathol* 134:749.
126. Weidner, N, Lorentz WB Jr. 1986. Scanning electron microscopy of the acellular glomerulus and tubular basement membrane in lupus nephritis. *Am J Clin Pathol* 85:135.
127. Shigematsu H, et al. 1979. Arthus-type nephritis. *Lab Invest* 40:492.
128. Pfaltz M, Hedinger CE. 1986. Abnormal basement membrane structures in autoimmune thyroid disease. *Lab Invest* 55:531.
129. Salomon F, Hedinger CE. 1982. Abnormal basement membrane structures of seminiferous tubules in infertile men. *Lab Invest* 47:543.
130. Accinni L, et al. 1980. Deposition of immune conplexes in ovarian follicles of mice with lupus-like syndrome. *Am J Pathol* 99:589.
131. Chaturvedi P, et al. 2008. Structure, evolution, and biology of the MUC4 mucin. *FASEB J* 22:966.
132. Demerjian M, et al. 2008. Acute modulations in permeability barrier function regulate epidermal cornification. *Am J Pathol* 172:86.
133. Sevilla LM, et al. 2008. Mice deficient in involucrin, envoplakin, and periplakin have a defective epidermal barrier. *J Cell Biol* 179:1599.

Vet-ebooks.com

Part IV

Infectious Diseases

Ultrastructural Pathology The Comparative Cellular Basis of Disease
Second Edition Norman F. Cheville
© 2009 Wiley-Blackwell. ISBN: 978-0-813-80330-2

Vet-ebooks.com

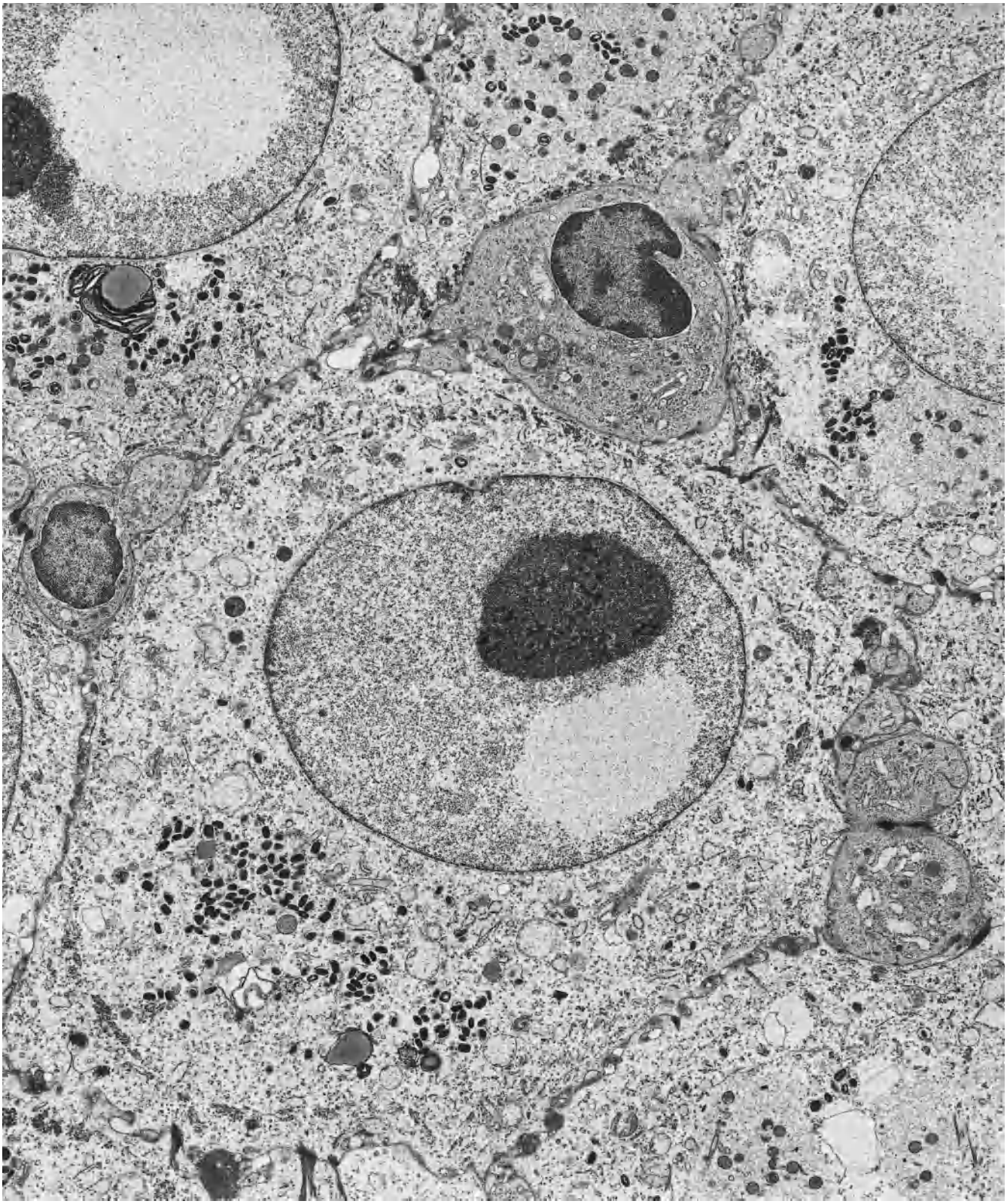


Fig. 13.1 Cytopathology of poxvirus infection: cytoplasmic inclusion bodies are composed of virions, viral ribosomes, and degenerate organelles. In nuclei, there are central foci of chromatin lysis, expansion and aggregation of nucleoli, and disappearance and dispersal of chromatin adjacent to the nuclear membrane. The Golgi complex is vesicular. Monocytes are between infected keratinocytes.

© 2009 Wiley-Blackwell. ISBN: 978-0-813-80330-2
Vet-ebooks.com

13 Cytopathology of Viral Diseases

Norman F. Cheville and Howard Lehmkuhl

Viruses produce disease by replicating inside cells to cause degeneration. To be pathogenic, viruses must be capable of specifically attaching to the surfaces of target cells. Attachment must alter the cell membrane so that a specific signal for uptake of virions occurs. After entering the cell, viruses must contain enzymes (or genomic codes to produce enzymes) that alter cell metabolism in favor of viral replication (Fig. 13.1). Viruses shut down host cell synthesis and subvert it toward replication of new virus-induced nucleic acids and proteins. This causes an **acute lytic infection** of cells that, if uncontrolled, leads directly to cellular destruction and systemic signs of illness.

Virions, the intact infectious particles, do not have ribosomes to synthesize protein and must use cellular organelles to reproduce. As they replicate, organelles in the host cell disappear and are replaced by viral proteins and other structures that are used to form new virions. Virions vary considerably in size and complexity (Fig. 13.2) and thus in how they replicate and are released from cells. Most virions are released when the host cell dies and disintegrates.

Introduction of cryoelectron microscopy in the early 1980s allowed improved images and extension of resolution for determining viral structure. The 3-D reconstruction of viruses begins with one or more electron micrographs in which each particle is a 2-D projection of a virus capsid specimen. The relative orientation of each specimen, denoted by polar and azimuthal angle pair, defines the angle or view of the corresponding projection.[1]

Family *Poxviridae*

The complex DNA-containing poxviruses (Table 13.1) have an affinity for epithelium, particularly epidermis. Most of them produce local epidermal proliferative lesions that form vesicles and then pustules that erode to leave a scab-covered ulcer. Within infected keratinocytes, large aggregates of virions develop that appear histologically as irregular, acidophilic, cytoplasmic inclusion bodies. Inclusions stain poorly with stains for DNA such as the Feulgen technique because of masking by other proteins. Poxviruses have a common nucleoprotein antigen and are arranged into subgroups according to antigenic and other relationships; for example, the orthopoxviruses (vaccinia subgroup) are related serologically and structurally, and produce similar cytopathology in vivo.

When scarified into skin, poxviruses enter the epidermis and dermal mesenchyme. Small, focal, nonelevated areas of erythema (the **macule**) appear. Proliferation of keratinocytes and subepidermal edema produces an elevation of the lesion above the level of normal skin, the **papule**. Infected epidermal keratinocytes progressively enlarge, develop hydropic degeneration and huge cytoplasmic inclusions. In the more cytopathic pox diseases, infected keratinocytes undergo lysis and serous fluid accumulates in tiny cystic spaces (microvesicles) that expand and coalesce to form **vesicles**. As a vesicle fills with neutrophils and fibrin it becomes a **pustule**. Pustules erode to circumscribed ulcers, but barring complications these lesions heal, leaving a small hyaline connective tissue scar.

Poxviruses commonly cause **viremia** and virus spread hematogenously to skin. **Systemic disease** is rare, except for those poxviruses that cause major plagues—human smallpox, myxomatosis of rabbits, and sheeppox. In these diseases, virus is transmitted via the respiratory tract; there is local replication in the pharyngeal lymphoid tissues followed by secondary viremia with virus localization in the skin.

Vet-ebooks.com

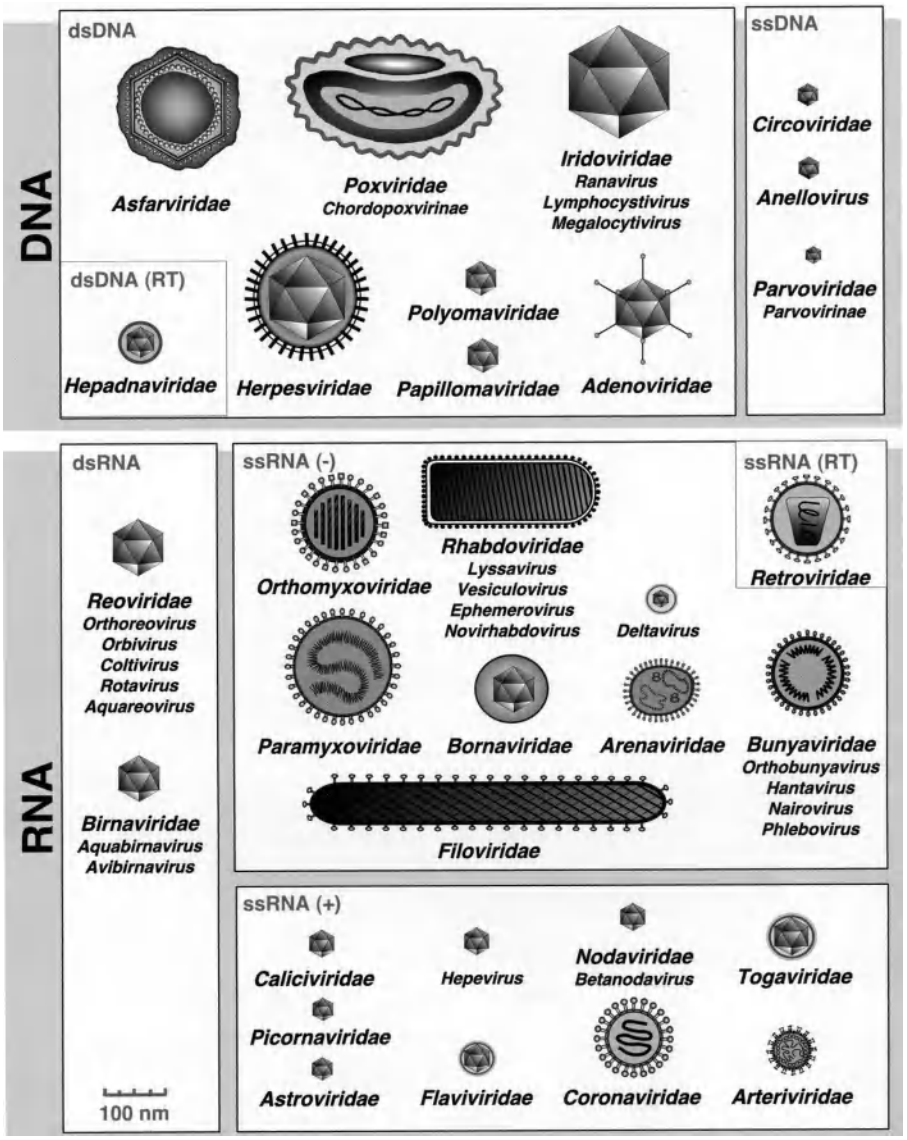


Fig. 13.2 Families and genera of viruses infecting vertebrates. (Drawing: C. M. Fauquet, *Virus Taxonomy*, Academic Press, 2007.)

Table 13.1 Family *Poxviridae*.

Virus	*Disease in*	*Reference to ultrastructural pathology*
		Subfamily *Cordopoxvirinae*
		Genus *Orthopoxvirus*
Variola virus (smallpox)	Human	**Avakyan**, *J Cell Biol* 24:337, 1965; **Bras**, *Doc Med Geogr Trop* 41, 1952; **Cruickshank**, *Lancet* 2:527, 1966 (diagnostic)*
	Monkey	**Cheville**, *J Infect Dis* 111:163, 1962;† **Mack**, *Lancet* 2:752, 1970
Cowpox virus	Cow	**Downie**, *J Pathol Bact* 48:361, 1939
	Cat	**Schulz**, *Zoonoses Public Hlth* 34:31, 2007 (skin, lung)
	Human	**Baxby**, *Br Med J* 1:1379, 1977; **Leroy**, *Semin Hop Paris* 29:1182, 1953
	Mouse	**Mims**, *Br J Exp Pathol* 49:24, 1968†
Vaccinia virus	Human	**Boughton**, *Med J Aust* 1:143, 1969 (necrotizing); **Chandra**, *Lancet* 1:687, 1969 (generalized); **Green**, *Lancet* 1:1296, 1966 (generalized); **Morgan**, *Virology* 73:43, 1976;* **Sodiek**, *J Cell Biol* 121:521,1993;* **Sottnek**, *Lab Invest* 33:522, 1975;* **Turkel**, *Cancer* 40:226, 1977 (necrotizing); **Wentworth**, *J Clin Pathol* 19:328, 1966 (placenta, fetus)
	Mouse	**Blinzinger**, *Acta Neuropathol* 40:193, 1977;† **Montasir**, *Am J Pathol* 48:877, 1966 (lung)
	Pig	**Danes**, *Acta Virol* 12:361, 1968;† **Moriguchi**, *Arch Virol* 54:353, 1977 (skin)†
	Rabbit	**Greer**, *Infect Immun* 9:452, 1974†

Vet-ebooks.com

Table 13.1 *Continued*

Virus	*Disease in*	*Reference to ultrastructural pathology*
Monkeypox virus	Monkey Chimpanzee Human Prairie dog	**Wenner**, *Arch Ges Virusforsch* 27:179, 1969 **McConnell**, *Am J Vet Res* 29:1675, 1968 **Jezek**, *Monogr Virol* 17:1, 1988; **Marennikova**, *Bull W H O* 46:599, 1972 **Langohr**, *Vet Pathol* 41:702, 2004
Camelpox virus	Camel	**Mahnel**, *Zbl Vet Med [B]* 20:572, 1973
Ectromelia virus	Mouse	**Berger**, *J Neuropathol Exp Neurol* 41:18, 1982 (meningitis); **Blandon**, *J Exp Med* 132:1035, 1970; **Leduc**, *J Ultrastruct Res* 64:66, 1962 (liver)
Raccoonpox virus	Raccoon Cat	**Thomas**, *Arch Virol* 49:217, 1975 **Yager**, *Vet Dermatol* 17:443, 2006
Skunkpox§	Skunk	**Meyer**, *J Virol Methods* 64:217, 1997
Taterapox virus#	African gerbil	**Piskurek**, *Proc Nat Acad Sci USA* 104:12046, 2007
Volepox virus	Vole, pinon mouse	**Knight**, *Virology* 190:423, 1992
		Genus *Parapoxvirus*
Orf virus (contagious ecthyma)	Sheep Human	**Abdussalam**, *J Comp Pathol* 67:217, 1957; **Büttner**, *Arch Ges Virusforsch* 14:657, 1964; **Kluge**, *Am J Vet Res* 33:1191, 1972 **Leavell**, *J Am Med Ass* 204:657, 1968; **Sanchez**, *Arch Pathol* 109, 166:1985
Bovine papular stomatitis virus	Cow	**Castrucci**, *Arch Ges Virusforsch* 29:315, 1970; **Griesemer**, *Am J Vet Res* 22:482, 1961; **Naggington**, *Vet Rec* 81:306, 1967; **Reczko**, *Zentralbl Bakt Parasit Infekt Hyg* 160:425, 1957
Pseudocowpox virus		**Cheville**, *J Am Vet Med Ass* 150:855, 1967; **Cohen**, *Virology* 23:56, 1964
		Genus Avipoxvirus§
Fowlpox virus	Chicken	**Grégoire**, *Compt Rend Sci* 254:4369, 1962; **Gruber**, *Avian Dis* 51:623, 2007 (great tit); **Hyde**, *J Ultrastruct Res* 35:626, 1971; **Kulich**, *Avian Pathol* 37:101, 2008 (blackcaps)
Falconpox virus	Falcon	**Thiele**, *Arch Virol* 62:77, 1979
Juncopox virus	Junco	**Beaver**, *Am J Pathol* 42:23, 1963
Pigeonpox virus	Pigeon	**Mayr**, *Arch Ges Virusf* 17:42, 1965
Sparrowpox virus	Sparrow	**Kato**, *Nat Inst An Hlth Qt* 5:130, 1965
Turkeypox virus	Turkey	**Cheville**, *Am J Pathol* 49:723, 1966
		Genus *Capripoxirus*
Sheeppox virus	Sheep	**Murray**, *Res Vet Sci* 15:201, 1973; **Plowright**, *J Comp Pathol* 69:400, 1959
Goatpox virus	Goat	
Lumpy skin disease virus	Cow	**Davies**, *Res Vet Sci* 12:123, 1971; **Prozesky**, *Onderstepoort J Vet Res* 49:167, 1982; **Weiss**, *Virol Monogr* 3:111, 1968;
		Genus *Leporipoxvirus*
Myxoma virus	Rabbit	**Marcato**, *J Submicrosc Cytol* 9:67, 1977 (skin); **Purcell**, *Arch Ges Virusforsch* 39:369, 1972; **Sprunt**, *J Exp Med* 56:601, 1932
Rabbit fibroma virus	Rabbit	**Allison**, *J Nat Cancer Inst* 36:859, 1966; **Kilham**, *Am J Hyg* 59:104, 1954; **Prose**, *Am J Pathol* 64:467, 1971; **Scherrer**, *Pathol Microbiol* 31:129, 1968;
Squirrel fibroma virus	Squirrel	**Kilham**, *Am J Hyg* 61:55, 1955; **Shively**, *J Natl Cancer* Inst 49:919, 1972
Rabbitpox	Rabbit	**Bedson**, *J Pathol Bact* 85:1, 1963; **Christensen**, *Lab Anim Care* 17:281, 1967
		Genus *Suipoxvirus*
Swinepox	Pig	**Borst**, *Vet Rec* 127:61, 1990 (congenital); **Cheville**, *Am J Pathol* 49:339, 1966; **Smid**, *Zbl Vet Med [B]* 20:603, 1973

Vet-ebooks.com

Table 13.1 *Continued*

Virus	*Disease in*	*Reference to ultrastructural pathology*
		Genus *Molluscipoxvirus*
Molluscum contagiosum virus	Human	**Bierwolf**, *Arch Geschwulstforsch* 331:97, 1968; **Dourmashkin**, *C R Acad Sci* 246:3133, 1958; **Epstein**, *J Invest Derm* 60:73, 1973; **Goodpasture**, *Am J Pathol* 3:385, 1927; **Nelson**, *Pediatrc Ann* 36:814, 2007; **Sutton**, *J Ultrastruct Res* 26:177, 1969; **Vreeswijk**, *J Ultrastruct Res* 54:37, 1976
	Primate	**Douglas**, *J Am Vet Med* Ass 151:901, 1967
	Horse	**Lange**, *J S Afr Vet Assoc* 62:72, 1991; **Rahaley**, *Vet Pathol* 20:247, 1983
		Genus *Yatapoxvirus*
Yaba monkey tumor virus	Monkey	**Niven**, *J Pathol Bact* 81:1, 1961; **Wolfe**, *J Natl Cancer Inst* 41:1197, 1968
Tanapox virus	Monkey	**Casey**, *Am J Pathol* 51:431, 1967; **Downie**, *Br Med J* 1:363, 1971; **Espana**, *Exp Mol Pathol* 15:34, 1971
	Human	**McNulty**, *Arch Dermatol* 97:286, 1968

*Studies in vitro.
†Animal model.
§Skunkpox, volepox, and racoonpox are grouped as New World orthopoxivures; this is in contrast to Old World orthopoxviruses of cowpox, variola, monkeypox, camelpox, ectromelia, and vaccinia.
#Taterapox was isolated from West African rodents, but is closely related to camelpox virus and to variola virus; it contains sequences related to the snakes.

Pox virions are brick-shaped and can be as large as 300–400 nm in diameter.[2] They are composed of (1) a **core** (nucleocapsid), a shell of inner and outer membranes containing viral DNA (in the form of linear 200,000 base pair duplex DNA molecule with hairpin loops connecting the two strands at each end); (2) an **intermediate coat**, an outer membrane and inner shell that expands into two **lateral bodies**; and (3) the lipoprotein **envelope**. A **dense body** is adjacent to the inner shell (Fig. 13.3).

The **core** of vaccinia, the prototype virion, contains virus-encoded enzymes, including a DNA-dependent RNA polymerase, a transcription factor, capping and methylating enzymes, and a poly (A) polymerase, all of which form a complete mechanism for synthesis of mRNA. Initially about 100 early genes are transcribed by the viral RNA polymerase. Replicated DNA provides the templates for the successive expression of later genes.

Poxviruses enter host cells by fusion with the plasma membrane and by endosomal uptake.[3]

At cytoplasmic sites of replication, immature naked viral forms appear that have dense eccentric bodies (nucleoids), a granular less dense matrix of viroplasm, and are enclosed by a membrane with surface projections or spicules. Surface spicules account for the rigidity of the membrane. The nucleoprotein is inserted into the immature forms just before closure of the envelope. Foci of assembly lack polyribosomes and endoplasmic reticulum, which suggests that late proteins are synthesized elsewhere in the cytoplasm and

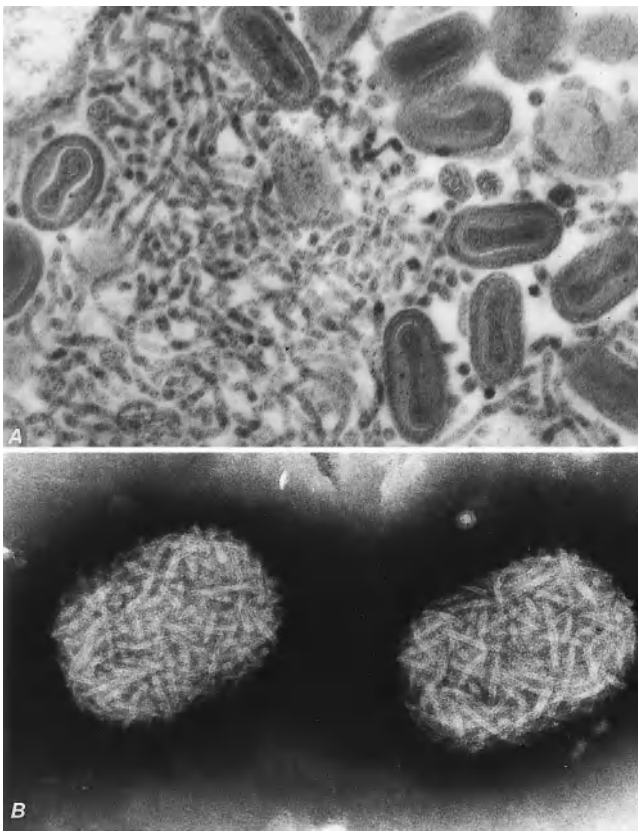


Fig. 13.3 Pox virions. A. Immature viral particles and virions enmeshed with outer coat tubules in a cytoplasmic inclusion body; fowlpox virus. **B. Virions**: negative stain preparation revealing outer coat of tubules.

Vet-ebooks.com

transported to assembly foci. The nucleoid becomes central and transforms into the biconcave disk of the virion. In vitro, virions are packaged by Golgi membranes and transported to cell surfaces where they are released by exocytosis.

Poxviruses encode several proteins that affect the host; for example, **vaccinia virus growth factor** (VGF). VGF uses cell receptors for epidermal growth factor to attach to and stimulate keratinocytes in foci of infection. By increasing metabolism in keratinocytes surrounding foci of infection the susceptibility of these cells to poxvirus infection is increased. Other proteins produced by poxviruses that act as virulence markers include proteins that modulate the complement pathway and inhibit complement-mediated cell lysis, serpin analogues (K2 B13, B24) that inhibit certain components of the inflammatory response to retard immune clearance, and analogues of tumor necrosis factor and superoxide dismutase. Vaccinia virus uses both actin and microtubules to migrate to the cell surface. Microtubules transport virions to the cell surface and actin tails form beneath cell-associated enveloped virus particles at the cell surface.[4]

Subfamily *Chordopoxivirinae*

Genus *Orthopoxvirus* (Vaccinia Virus Group)

Vaccinia **Vaccinia virus**[5] is scarified onto primate skin to prevent monkeypox. Strains used for vaccination are stable laboratory viruses that have evolved from field isolates of cowpox virus by passage for generation on calf skin and are genetic recombinants that differ both from cowpox and variola.

Dermal lesions of vaccinia show vasculitis, perivascular monocytes and lymphocytes, and necrotic fibrinopurulent exudates. Cell-mediated hypersensitivity contributes to the primary vaccination lesion. **Postvaccinial lymphadenitis** of draining lymph nodes involves many reticular and lymphoblastic cells interspersed in hyperplastic lymphoid tissue.

Systemic vaccinial disease can occur in vaccinated monkeys; in humans, it was a serious consequence of vaccination in immunologically deficient patients.[6] Systemic vaccinia occurs in two patterns:

- **Generalized vaccinia** occurs as widespread pox lesions that typically resolve with recovery; generalized vaccinia of the **fetus** occurs after infection of the placenta.
- **Progressive vaccinia** is the progression of the cutaneous vaccination lesion to involve the lungs and other viscera; epithelial lesions are also reported in bronchioles and pancreatic ducts; cessation of viral multiplication does not occur and the vesicles continue to enlarge forming a sloughing ulcer whose advancing edge is associated with large satellite lesions ("vaccinia necrosum"). Metastatic lesions appear at distant cutaneous and visceral sites and most cases are lethal.

Postvaccinial encephalitis is characterized by edema and perivascular cuffing of lymphocytes and monocytes, especially of meninges, choroid plexus and ependyma. In a study of five Japanese cases, viral antigens were found in only one brain by immunofluorescence. Deposition of Ig suggested deposits of antigen-antibody complexes. Dissociation of the complexes revealed viral antigens in two of the four remaining cases.[7]

Experimentally, **vaccinial pneumonitis** develops after nasal instillation or aerosolization in rabbits,[8] mice, and pigs. Virus occurs in lungs in high titer and is disseminated through lymphatic pathways where it interacts with platelets and may be associated with intravascular coagulation.[9] There is marked thickening of alveolar walls with edema and accumulation of macrophages. Virions are in both types of pneumocytes, capillary endothelium, and macrophages. Endothelial necrosis leads to hemorrhage. Neutrophils are prominent only if there is bacterial contamination. Vaccinia virus also infects the myocardium[10] and brain.[11] In experimental systemic infection of mice, vaccinia infects the CNS and vaccinial meningoencephalitis has been used as a model for viral infections of the brain.

Mousepox Natural **mousepox** (ectromelia) can take several forms: (1) mild infection with failure to thrive but without acute disease or skin lesions; (2) classic subacute or chronic mousepox, characterized by necrotic and ulcerating lesions of skin and extremities, with amputation of the limbs due to gangrenous necrosis (hence "ectromelia"); and (3) a rapidly fatal syndrome in which mice die in a few days because of necrosis of liver, spleen, pancreas, and other viscera, and severe pneumonitis and serous effusions. A primary viremia leads to infection of the regional lymph nodes, liver, and spleen. Virus replicates at these sites, producing a secondary viremia, with infection of viscera, brain and skin. Virus replicates in the liver. Infected hepatocytes show an early loss of glycogen, dilatation of cisternae of endoplasmic reticulum, mitochondrial swelling, and fatty degeneration. Nuclear changes are fragmentation of nucleoli and development of dense bodies within the nucleolus. In both hepatocytes and Kupffer cells, poxviruses develop within diffuse pale zones. Changes specific for viral infection include spherical, intermediate, and mature virions. Microtubules are seen associated with lipid vacuoles, and there are protein lamellar structures of alternating dense layers.

Vet-ebooks.com

Genus *Parapoxvirus*

Virions of the genus *Parapoxvirus* (orf virus group) differ from the vaccinia subgroup in being smaller (160–190 nm in diameter; 250–300 nm in length), and in having regular spiral filaments that give rise to a cross-hatch on the surface of the virion. Lesions of parapoxviruses are markedly proliferative. Macules appear 5–6 days after infection. Changes occur early in proliferating keratinocytes and include nucleolar enlargement, focal lysis of keratin fibrils, and peripheralization of keratin. Epithelial cell swelling results in characteristic ballooning degeneration, which, accompanied by cytoplasmic inclusions and nuclear shrinkage, is pathognomonic for orf (Fig. 13.4). Widening of intercellular spaces by edema fluid may initiate the formation of intraepidermal microvesicles, although this is not common in the paravaccinia lesions. Intense keratinocyte proliferation leads to marked acanthosis. Dermal infiltration by monocytes and lymphocytes is prominent around hyperemic capillaries and venules, especially late in the disease. Endothelial proliferation occurs and is due to direct infection with the virus. Edema may be sufficient to produce subepidermal vesicles with separation of dermis and epidermis. The spherical, pale, eosinophilic inclusions are aggregates of virions in varying stages of development and embedded in granular matrix. The virus is highly keratinoytic and inclusions appear to be floating in the fluid remains of the cytoplasm. Virions average 320 × 125 nm in length. All stages are present including early spheroids and intermediate forms. Small cytoplasmic inclusions must be differentiated from deeply basophilic keratohyalin granules and moderately eosinophilic larger intracellular keratin bodies.

Contagious ecthyma (orf) of sheep and **bovine papular stomatitis** of cattle are common proliferative pox diseases that affect hairless areas around the mouth and gums. Natural transmission to humans is also common but lesions are circumscribed and solitary, being largely confined to the hands of farmers or veterinarians. **Pseudocowpox** virus causes the most common pox lesions on teats of cattle and is the agent of milker's nodules in humans.

Genus *Avipoxvirus*

There are large numbers of poxviral isolates from birds, most of which are designated by host species names, for example, turkeypox, canarypox, pigeonpox, sparrowpox, and so forth. Transmission and cross-immunity experiments indicate that most are not antigenically identical to fowlpox virus. **Fowlpox** of chickens and turkeys is characterized by multiple papules in the comb, wattles and oral cavity. Papules rarely form vesicles or pustules but are apt to become confluent in a large scabby mass. Lesions of the feet and legs are common and, in severe cases, infection extends into the pharynx and esophagus ("wetpox"). Infected epithelial cells are greatly distended by immense cytoplasmic inclusion bodies that stain intensely for neutral lipids (Fig. 13.5).[12] Inclusions consist of large lipid molecules filled with mature virions and dense rodlets. Immature virions develop by formation of dense foci of viroplasm, which are sequestered by cup-shaped membranes. The final stages of maturation, however, involve the attachment of these virions to small lipid globules. Virions induce, enter, and then use **lipid globules** for massive production of surface rodlets, which then form the outer coat.

Genus *Capripoxvirus*

Sheeppox is a cutaneous proliferative disease that is accompanied by a severe systemic reaction characterized by fever and ocular and oronasal discharges. Lesions are composed of hyperplastic epithelial cells that undergo severe hydropic degeneration and lyse to form coalescing microvesicles that progress through pustular stages. Large eosinophilic inclusions are aggregates of virions and cellular debris. In nuclei, the central, electron-lucent, fibril-filled karyolytic regions resemble those seen in swinepox. Dermal macrophages also contain inclusions. Infections of endothelial cells lead to necrotizing vasculitis, thrombosis, and necrosis. Viremia occurs during the cutaneous phases and may result in lesions in the upper respiratory tract, lungs, and esophagus. Renal lesions have also been attributed to the virus.

Genus *Leporipoxvirus*

Rabbitpox is an epidemic exanthematous disease that occurs in rabbit colonies with high mortality. Vesiculopustular rash is accompanied by fever, viremia, and nasal and conjunctival discharges. Death occurs in 6–12 days. In severe cases, skin lesions are rare, but foci of necrosis occur in liver, adrenal gland, lung, and intestine. The primary site of infection is the upper and lower respiratory tract, where virus replication occurs prior to dissemination. Virus in blood is associated with leukocytes and is present when fever. Lesions arising from these viruses have intense proliferation of mesenchymal cells in the subcutis.

Infectious myxomatosis is a highly contagious disease of rabbits that is transmitted through wounds or insect bites, or via the respiratory tract. Within a few days the virus gives rise first to erythema at the site of infection, then to soft hemorrhagic gelatinous swellings. Severe systemic disease, purulent oculonasal discharges, fever, anorexia, and edema of the

Vet-ebooks.com

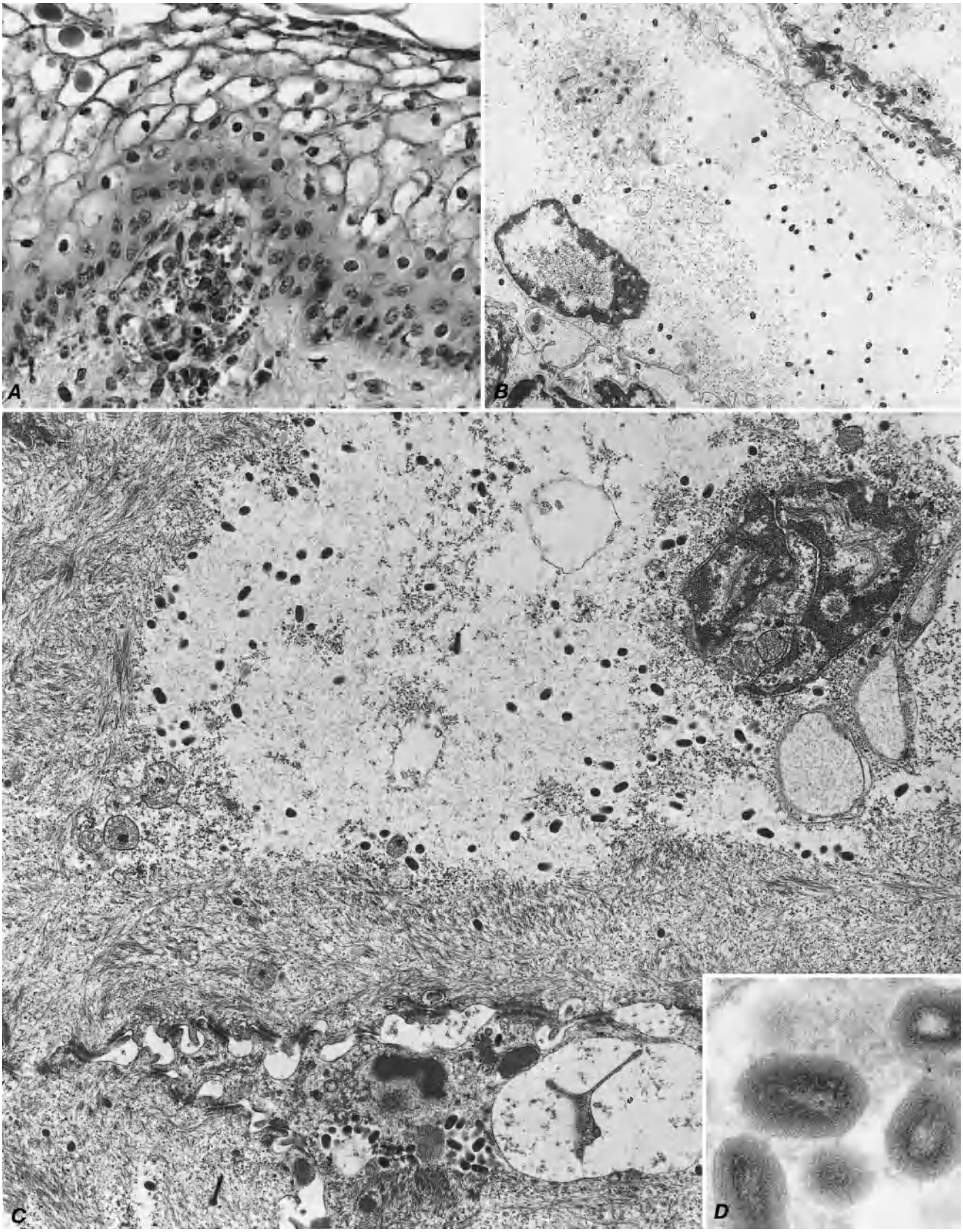


Fig. 13.4 **Parapoxviruses**: contagious ecthyma. **A**. **Cytoplasmic inclusions**, skin: ballooning degeneration of keratinocytes and hyperemia of dermal capillaries, histology. **B–C**. **Infected keratinocytes**: cytoplasmic proteolysis with pox virions in lysed areas of the cytoplasm. Note detachment of intercellular junctions and nuclear pyknosis. **D**. Virions. (Micrographs: A, B, and D: John P. Kluge, *Am J Vet Res* 33:1191, 1972.)

Vet-ebooks.com

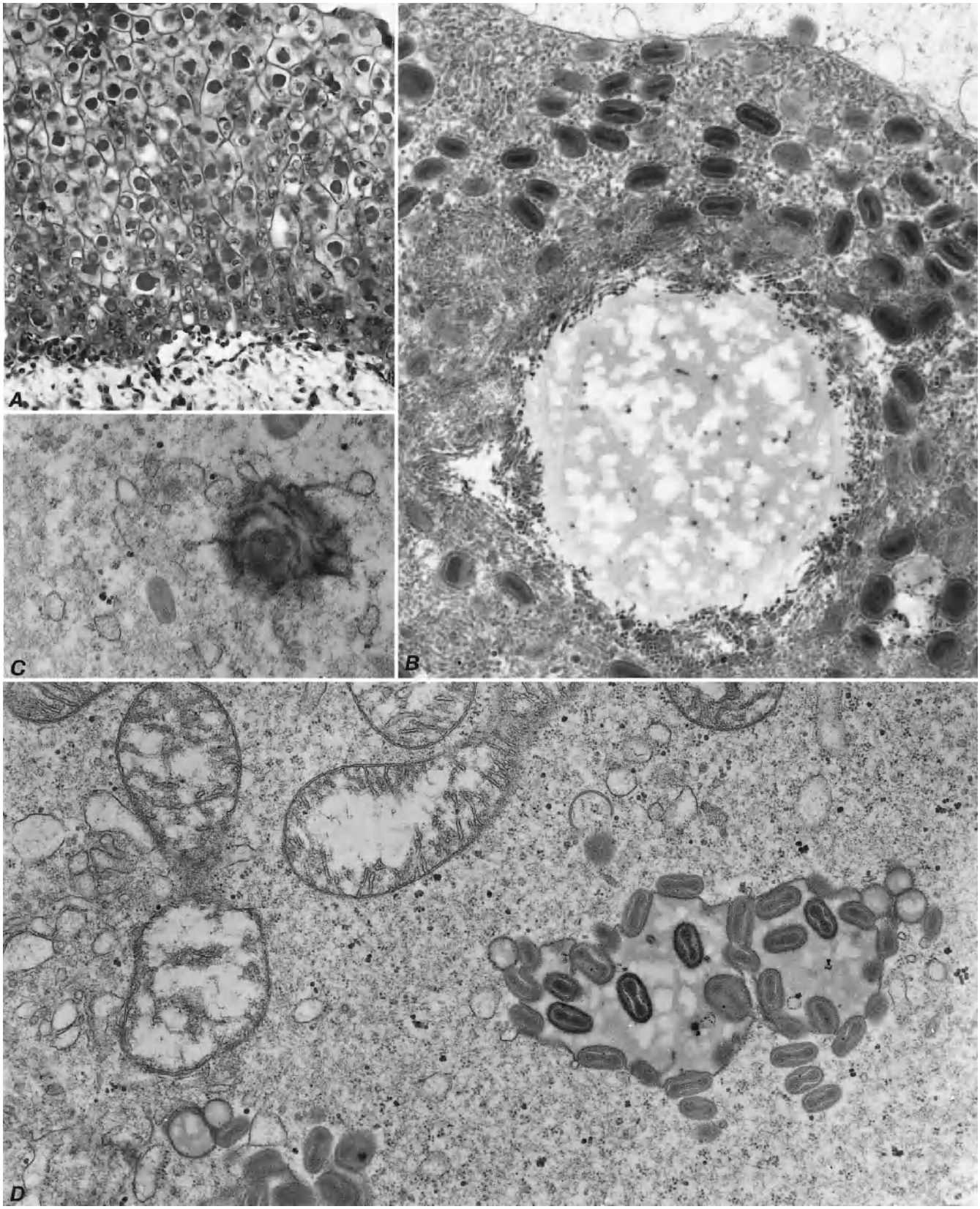


Fig. 13.5 **Avipoxvirus**: fowlpox virus. **A**. **Large dense lipid inclusions** in the cytoplasm, skin (histology). **B**. **Lipid inclusion**: filled with virions and excess coat tubules. **C**. **Initial focus of tubule formation**. **D**. **Immature viral particles** surround lipid globules during early inclusion formation. Virions within the inclusion have gained an additional outer coat. Note degenerate mitochondria, cytoplasmic vesicles, and many viral ribosomes.

Vet-ebooks.com

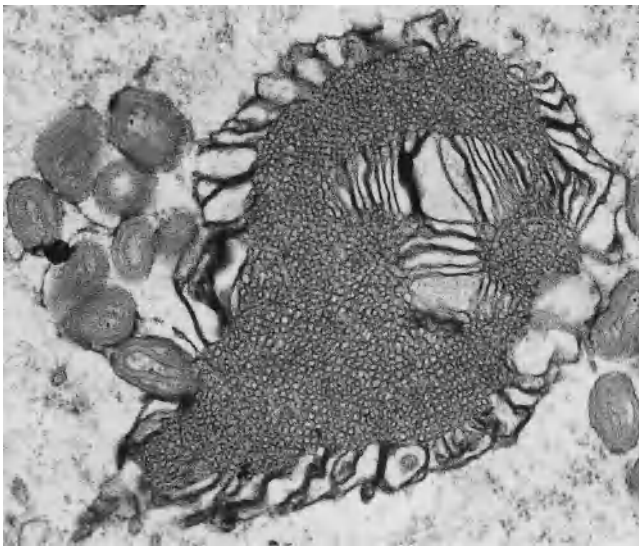


Fig. 13.6 **Swinepox**: lamellar membrane formation, keratinocyte, pig skin.

mucous membranes characterize the general dissemination of the virus. Death occurs between 5 and 15 days. Lesions of myxomatosis consist of masses of bizarre, spindle-shaped mesenchymal cells lying in edematous connective tissue. Poxviruses and granular viroplasm make up the large cytoplasmic inclusion bodies.[13] In the epidermis, there are large swollen inclusion-containing keratinocytes that lack normal keratin. Lucent areas containing delicate fibrils are present in nuclei. Marked endothelial cell lesions in dermal capillaries are responsible for edema of the lesions, which markedly expands the ground substance.[14]

Genus *Suipoxvirus*

Swinepox is a contagious pustular skin disease of young pigs, usually associated with infestations of the porcine suckling louse, *Haematopinus suis*, which serves as a mechanical vector. Skin lesions consist of immense, swollen keratinocytes filled with large cytoplasmic eosinophilic inclusion bodies (Fig. 13.6). Virions develop in association with lamellar arrays of membranes and closely resemble the other pox viruses. Swinepox virus growth is typically limited to the skin. Swinepox virus, when it infects pregnant sows, passes the placenta to infect the developing fetus. The **fetus**, infected in utero, is born covered with large cutaneous pox.

Genus *Molluscipoxvirus*

Lesions of **molluscum contagiosum** in humans are singular (although multiple lesions occur) and consist of pink, umbilicated nodules of massive epidermal proliferation and verrucous hyperplasia located typically on the trunk or anogenital areas. The immense eosinophilic cytoplasmic inclusions are pathognomonic. They are composed of virions (320 × 250 nm in diameter) and viral-induced. The virus is antigenically distinct from other chordopoxviruses. The circumscribed infection does not spread and except for the local lesions the disease is not serious. Molluscum contagiosum has been reported in chimpanzees and horses.

Genus *Yatapoxvirus*

Yaba Monkey Tumor Virus **Yabapox** was first repoted as subcutaneous nodules of spindle-shaped cells in rhesus monkeys in a colony in Yaba, Nigeria. Lesions are composed of rapidly proliferating histiocytes, and the nodular foci have been referred to as histiocytomas. Neoplastic transformation does not occur, and lesions regress in association with appearance of antibodies and cell-mediated immunity. Ultrastructural examination of these cells reveals large numbers of pox virions with many intermediate and immature forms in the cytoplasm. Large masses of viral-induced proteins and membranes are strewn through the cytoplasm. Lipid globules are common. Nuclei are swollen and may contain filaments, but they show no evidence of viral particles. Yabapox lesions also occurred in a baboon, and subsequent accidental transmission to humans has been reported. In monkeys, intravenous inoculation results in the development of nodules in the lungs, and lung lesions also occur after aerosol transmission.

Family *Herpesviridae*

Viruses in the *Herpesviridae* group tend to be epitheliotropic and to produce acute disease with much tissue damage (Table 13.2); most infections begin in epithelial cells of the oropharynx, upper respiratory tract, or skin. The **herpes virion** is large (~180 nm in diameter), and consists of a DNA-containing **core**; a **capsid** that is 100–110 nm in diameter and has 162 capsomeres arranged as an icosahedron; an amorphous layer referred to as the **tegument**; and an **envelope**, which is a lipid bilayer or membrane surrounding the tegument. Virions measure 120–200 nm in diameter. The envelope has surface projections that contain glycoproteins, which react with neutralizing antibodies. More than 30 peptides have been identified as structural by their presence in the prototype herpesvirus, **herpes simplex**.

The immature or naked **nucleocapsids** are the particles that appear in the nucleus early in development.[15] The nucleocapsid consists of a core and three

Vet-ebooks.com

Table 13.2 Family *Herpesviridae*.

Virus	*Host*	*Reference to ultrastructural pathology*
		Subfamily *Alphaherpesvirinae*
		Genus *Simplexvirus*
Human herpesvirus 1 (HHV-1)	Human	**Arsenio-Nunes**, *Acta Neuropathol* 33:245, 1975 (brain);† **Boddingius**, *J Med Microbiol* 24:93, 1987 (genital); **Chase**, *Rev Infect Dis* 9;329, 1987 (liver); **Croen**, *New Engl J Med* 137:1427, 1987 (ganglia); **Cunningham**, *J Clin Invest* 75:226, 1985 (recurrent); **Daniels**, *Am J Pathol* 91:119, 1978 (phagocytes);* **Flewett**, *J Clin Pathol* 22:60, 1969 (liver); **Johnson**, *J Exp Med* 119:343, 1964 (brain); **Lach**, *Acta Neuropathol* 75:354, 1988 (brainstem); **Macarak**, *Lab Invest* 53:280, 1985 (endothelium); **Marrie**, *Gastroenterology* 82:71, 1982 (liver); **Patrizzi**, *Am J Clin Pathol* 49:325, 1968 (liver, adrenal); **Roy**, *J Clin Pathol* 22:51, 1969 (brain); **Schuller**, *Am J Med* 94:29, 1993 (respiratory tract); **Sobel**, *Am J Pathol* 125:332, 1986 (immune response); **Swanson**, *Lab Invest* 15:1966, 1966; **Witmer**, *Arch Opthalmol* 79:331, 1968 (eye)
	Mouse model	**Murphy**, *Arch Ges Virusforsch* 21:463, 1967;† **Kristensson**, *Virch Arch B* 4:335, 1970 (neuron); **Kristensson**, *Acta Neuropathol* 17:44, 1971 (nerve); **Rabin**, *Science* 162:126, 1968 (nerve);† **Schwartz**, *J Neuropathol Exp Neurol* 34:359, 1975 (neonate);† **Stroop**, *Lab Invest* 50:27, 1984 (brain); **Stroop**, *J Infect Dis* 153:721, 1986 (nerve); **Townsend**, *Lab Invest* 40:178, 1979 (brain); **Yura**, *Arch Virol* 92:41, 1987*
	Rabbit	**Weissenböck**, Vet Pathol 34:44, 1997; **Schlitt**, *J Infect Dis* 153:732, 1986†
	Experimental study†	**Baringer**, *Prog Med Virol* 20:1, 1975 (review); **Baringer**, *J Neuropathol Exp Neurol* 29:89, 1970; **Schirmacher**, *Virch Arch B* 56:351, 1989 (liver)
Human herpesvirus 2 (HHV-2)	Human	**Martin**, *J Neuropathol Exp Neurol* 41:253, 1982 (spinal cord, optic nerve)
	Mouse model†	**Georgsson**, *Acta Neuropathol* 72:377, 1987 (brain); **Martin**, *Lba Invest* 51:656, 1984 (brain); **Schwartz**, *Am J Pathol* 79:509, 1975 (thymus); **Smith**, *Lab Invest* 43:278, 1980 (glomerulonephritis)
	Rabbit	**Hudson**, *J Infect Dis* 133:367, 1976 (cornea)†
	Monkey	**Fierer**, *Ann Int Med* 79:225, 1973 (eye); **Kaplan**, *J Infect Dis* 157:1090, 1988
Herpes B	Monkey	**Anderson**, *Lab An Sci* 44:526, 1994 (infants)
		Genus *Varicellovirus*
Human herpesvirus 3 (HSV-3)	Human	**Bastian**, *Arch Pathol* 97:331, 1974; **Charles**, *Am J Clin Pathol* 85:522, 1986 (zoster); **Esiri**, *J Neurol Sci* 15:35, 1972 (zoster); **Feusner**, *Am J Haemotol* 7:255, 1979 (platelet); **Hook**, *J Am Med Ass* 206:305, 1968; **Lutzner**, *J Ultrastruct Res* 7:409, 1962 (zoster, skin); **McCormick**, *Arch Neurol* 21:559, 1969 (zoster); **Minkowitz**, *Am J Med* 44:489, 1968 (glomerulonephritis); **Nagashima**, *Acta Neuropathol* 33:105, 1975 (spinal ganglia)
	Monkey	**Dueland**, *Lab Invest* 66:762, 1992;
Bovine herpesvirus 1	Cow	**Bowen**, *Am J Vet Res* 46:1095, 1985 (embryo); **Miller**, *Am J Vet Res* 47:223, 1986 (pregnancy); **Owen**, *Am J Vet Res* 29:1959, 1968
Canid herpesvirus 1	Dog	**Hashimoto**, *Am J Vet Res* 43:844, 1982 (placenta); **Strandberg**, *J Bact* 90:1790, 1965; **Yamamura**, *Jap Vet Med Sci* 54:779, 1992 (artery)
Equid herpesvirus 1 (equine abortion virus)	Horse	**Arhelger**, *Am J Pathol* 42:703, 1963 (hamster liver);† **Carman**, *J Vet Diagn Invest* 5:261, 1993 (brain, gut); **Charlton**, *Vet Pathol* 13:59, 1976 (brain); **Edington**, *Arch Virol* 90:111, 1986 (endothelium); **Jackson**, *Am J Vet Res* 38:709, 1977
	Experimental studies	**Darlington**, *J Bact* 92:250, 1966;* **Tajima**, *Am J Vet Res* 22:250, 1961*
Equid herpesvirus 4 (rhinopneumonitis)	Horse	**Reczko**, *Arch Ges Virusforsch* 17:231, 1965*
Felid herpesvirus 1 (rhinotracheitis)	Cat	**Hoover**, *Am J Pathol* 65:173, 1971; **Hoover**, *Am J Pathol* 58:269, 1970
Suid herpesvirus 1 (pseudorabies)	Pig	**Baskerville**, *Res Vet Sci* 13:127, 1972 (lung); **Ducatelle**, *Am J Vet Res* 45:1913, 1984; **McCraken**, *Acta Neuropathol* 25:207, 1973; **Narita**, *Am J Vet Res* 45:247, 1984 (tonsil); **Pol**, *Intervirology* 32:327, 1991 (nose)

Vet-ebooks.com

Table 13.2 *Continued*

Virus	*Host*	*Reference to ultrastructural pathology*
		Genus *Mardivirus*
Gallid herpesvirus 2 (Marek's disease virus)	Chicken	**Ahmed**, *Cancer Res* 32:187, 1972; **Calnek**, *J Natl Cancer Inst* 45:341, 1970; **Cauchy**, *Ann Rech Veter* 2:5, 1971; **Cho**, *Vet Pathol* 36:314, 1999 (skin); **Epstein**, *J Natl Cancer Inst* 41:805, 1968; **Kornegay**, *Acta Neuropathol* 75:597, 1988 (nerve); **Lampert**, *Acta Neuropathol* 40:103, 1977 (neuritis); **Okada**, *Jap J Vet Res* 19:64, 1971; **Prineas**, *Lab Invest* 26:258, 1978 (nerve); **Wight**, *J Comp Pathol* 79:563, 1969 (nerve)
Melegrid herpesvirus 1	Turkey	**Prasad**, *J Comp Pathol* 90:47, 1980
		Genus *Iltovirus*
Gallid herpesvirus 1 (infectious laryngotracheitis virus)	Chicken	**Richardson**, *Lab Invest* 44:144, 1981
	Finch	**Paulman**, *Vet Pathol* 43:963, 2006 (trachea)
		Subfamily *Betaherpesvirinae*
		Genus *Cytomegalovirus*
Human herpesvirus 5 (HHV 5)	Human	**Boldogh**, *Int J Cancer* 28:469, 1981 (Kaposi's sarcoma); **Martin**, *Am J Pathol* 145:440, 1994 (chronic fatigue syndrome isolates); **Ruebner**, *Am J Pathol* 48:987, 1966; **Stagno**, *J Clin Invest* 60:838, 1977 (immune complexes)
Monkey cytomegalovirus	Monkey	**Powers**, *Med Microbiol Immunol* 197:109, 2008
Porcine cytomegalovirus	Pig	**Duncan**, *Am J Vet Res* 26:939, 1965 (nose); **Valicek**, *Arch Ges Virusforsch* 414:344, 1973
		Genus Muromegalovirus
Murid herpesvirus 1 (mouse cytomegalovirus)	Mouse	**Brody**, *Lab Invest* 39:281, 1978 (lung); **Gang**, *Am J Pathol* 124:207, 1986 (heart); **Henson**, *Am J Pathol* 51:1001, 1967 (cortisone); **Johnson**, *J Infect Dis* 120:445, 1969 (placenta); **Ruebner**, *Am J Pathol* 44:799, 1964; **Tsutsui**, *Am J Pathol* 127:262, 1987 (embryo);* **van Bruggen**, *J Leuk Biol* 46:508, 1989 (macrophage)†
Guinea pig cytomegalovirus	Guinea pig	**Fong**, *Arch Virol* 64:97, 1980 (salivary gland); **Griffith**, *Am J Pathol* 122:112, 1986 (uterus); **Patrizzi**, *Am J Pathol* 50:779, 1967*
		Genus *Roseovirus*
Human herpesvirus 6	Human Chimpanzee	**Biberfeld**, *J Natl Cancer Inst* 79:933, 1987 **Lusso**, *J Virol* 64:2751, 1990 (T cells)*
		Subfamily *Gammaherpesvirinae*
		Genus *Lymphocryptovirus*
Human herpesvirus-4 (Epstein-Barr virus)	Human	**Achong**, *J Natl Cancer Inst* 36:877, 1966; **McGuire**, *Am J Pathol* 131:385, 1988 (thymoma); **Miller**, *Prog Med Virol* 20:84, 1975 (mononucleosis); **Payne**, *Am J Pathol* 106:71, 1982 (lymphocytes); **Purtillo**, *Lab Invest* 67:5, 1992 (lymphoproliferation); **Rabanus**, *Am J Pathol* 139:185, 1991 (keratinocyte); **zur Hausen**, *J Virol* 1:830, 1967 (tumor cells)*
	Marmoset	**Miller**, *J Exp Med* 145:948, 1977 (lymphoma)†
	Monkey	**Epstein**, *Int J Cancer* 12:309, 1973
	Mouse	**Sunil-Chandra**, *Am J Pathol* 145:818, 1994; **Weck**, *Nature Med* 3:1346, 1997 (arteritis)†
		Genus *Rhadinovirus*
Alcelaphine herpesvirus 1	Wildebeest	**Whitaker**, *Vet Rec* 161:692, 2007 (cow)
Alcelaphine herpesvirus 2	Hartebeest	
Bovine herpesvirus 4	Cow	**Miyano**, *J Vet Med Sci* 66:457, 2004 (mammae)
Caprine herpesvirus	Goat	**Piper**, *Aust Vet J* 86:136, 2008 (vaginitis)
Equine herpesvirus 2	Horse	**Vengust**, *J Vet Diagn Invest* 20:811, 2008
Human herpesvirus 8	Human	**Orenstein**, *Ultrastr Pathol* 32:211, 2008
Mouse herpesvirus 68	Mouse	**Nash**, *Philos Trans R Soc London B* 356:595, 2001
Ovine herpesvirus-2	Sheep	**O'Toole**, *Vet Pathol* 44:655, 2007 (bison)

Vet-ebooks.com

Table 13.2 *Continued*

Virus	*Host*	*Reference to ultrastructural pathology*
Saimiriine herpesvirus 2	Marmoset Monkey	**King**, Lab Invest 26:682, 1972 (lymphoma) **Giddens**, *Lab Invest* 32:492, 1975;* **Hunt**, *Vet Pathol* 3:1, 1966 (herpes T); **Hunt**, *J Med Primatol* 1:114, 1972 (lymphoma)
		Unclassified Herpesviruses
Duck herpesvirus	Duck	**Wojcinski**, *J Wildlife Dis* 27:129, 1991 (skin)
Elephant herpesvirus	Elephant#	**Richman**, *Science* 283:1171, 1999
Lizard herpesvirus	Lizard	**Watson**, *J Vet Diag Invest* 5:444, 1993
Owl herpesvirus	Owl	**Gomez-Villamandos**, *Vet Rec* 136:614, 1995
Seal herpesvirus	Harbor seal	**Gulland**, *J Wildlife Dis* 33:450, 1997

*Studies in vitro.
†Animal model.
#An endotheliotropic herpesvirus lethal for neonatal elephants; Asian elephant deaths were caused by cross-species infection of the herpesvirus naturally latent in African elephants.
§Members of the malignant catarrhal fever virus group include highly related but distinct ruminant rhadinoviruses: **ovine herpesvirus 2** (OvHV-2) causes sheep-associated malignant catarrhal fever; **alcelaphine herpesvirus 1** (AlHV-1) causes wildebeest-associated malignant catarrhal; there are also isolates from musk ox, Nubian ibex, and gemsbok.

concentric shells—inner, middle, and outer capsids. The enveloped nucleocapsid is the infectious particle but the unenveloped nucleocapsid may also be infectious when passed from cell to cell during fusion and syncytia formation. In situ hybridization techniques have defined sequences of viral RNA and DNA in herpesvirus-infected cells.[16] Cytokines such as interferon influence maturation of virions; for example, interferon treatment in vitro allows nucleocapsids to form but blocks production of extracellular virions. The ratio of virions to nucleocapsids and other viral components can also be altered by treatment with complement and cytokines.

Herpesviruses bind to surfaces of specific target cells and enter them by a modified form of phagocytosis. **Viral receptors** have been shown to be heparan sulfate moieties of proteoglycans attached to the host cell surface. Fibroblast growth factor has also been shown to specifically bind herpesviruses.[17,18] Microtubules are used to move incoming HSV-1 capsids to the nucleus. Keratinocytes use endocytosis for HSV-1 entry; in contrast, neurons are infected by direct fusion at the plasma membrane and release of the capsid into the cytosol—processes revealed by extraordinary analyses using cryoelectron tomography.[19]

Herpesviruses replicate initially in the **nucleus** where naked (nonenveloped) viral particles accumulate. Nuclear changes are rapid and severe (Fig. 13.7). The initial nuclear swelling during the viral replication phase is followed by nuclear contraction and dissolution and peripheralization of chromatin. Absence of chromatin gives the karyoplasm a finely granular homogenous appearance. In late stages of replication, aggregates of viral particles and granular protein inspissate into large dense inclusion bodies. Assembly of virions is inefficient and excess protein filaments aggregate in laminar arrays. **Immature viral particles** from the nucleus enter the **cytoplasm** and obtain an outer envelope (triple layered with 8–10 nm long projections) in passage through the nuclear membrane.[20] Virions are free in the cytoplasmic matrix, in vacuoles and extracellularly (Fig. 13.7). Cytoplasmic organelles in infected cells are degenerate and disorganized and there is an accumulation of lipid globules and precipitated proteins.

Characteristic epithelial lesions of acute cytolytic herpesviruses consist of progressively enlarging foci of necrosis. Cells of the epithelial germinal layer are first affected and spread of virus to neighboring cells quickly involves the entire thickness of the epithelium. Central areas of the lesion become necrotic, slough and leave in their place an ulcer filled at the base with cell debris, fibrin and necrotic mesenchymal tissue. The small lesion expands circumferentially, and necrosis obliterates many of the finite cell changes which are required for a diagnosis.

Subfamily *Alphaherpesvirinae*

Genus *Simplexvirus*

Herpes Simplex **Herpes simplex virus** (HSV) has a predilection for human tissues derived from embryonic ectoderm. Primary lesions affect the peroral skin and mucous membranes (cold sores). Genital vesicles,

Vet-ebooks.com

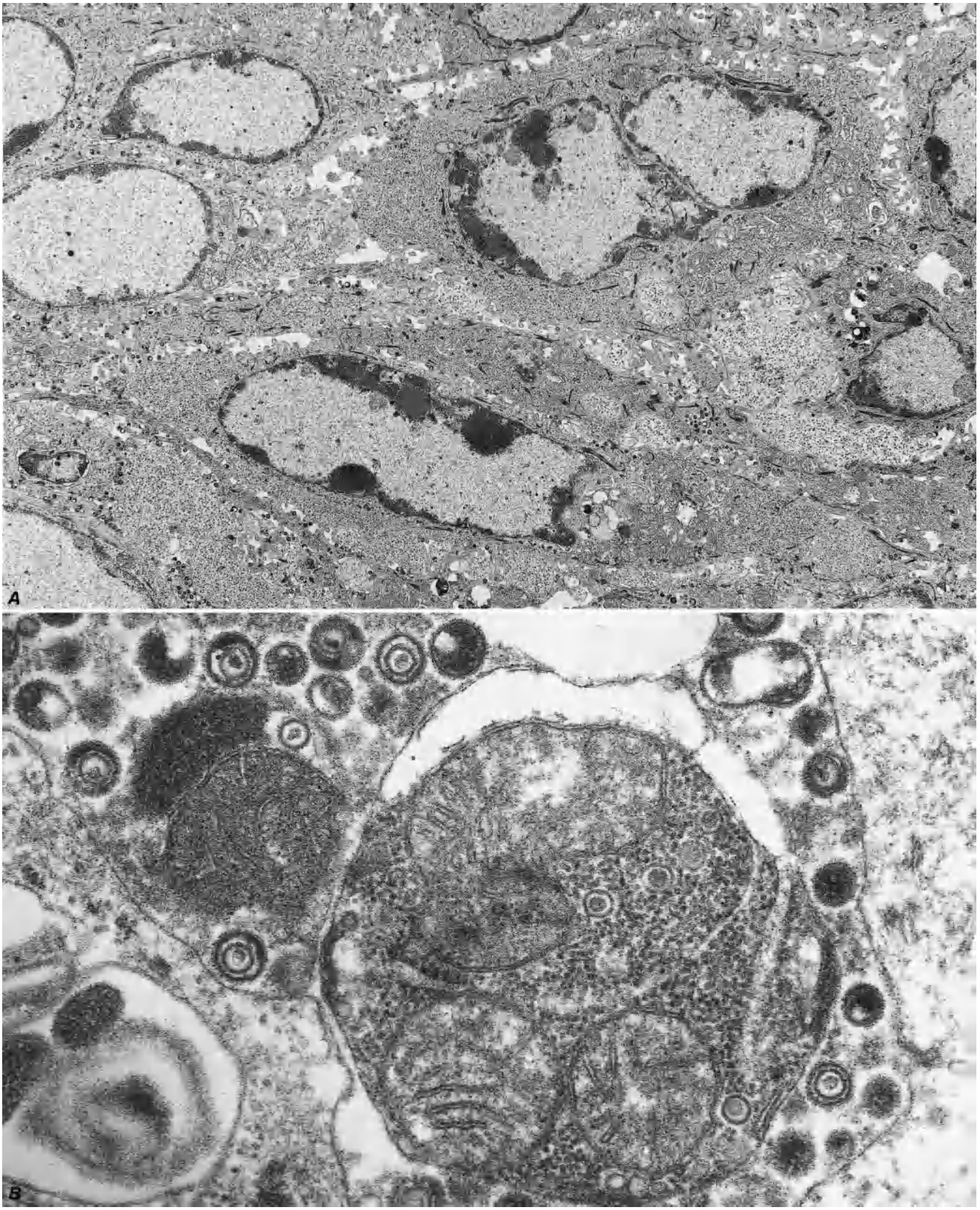


Fig. 13.7 Cytopathology of herpesvirus infection: bovine herpesvirus 1. **A**. **Degenerative keratinocytes** with large areas of nucleoplasmic proteolysis ("ground glass" nuclei), peripheralization of chromatin and nucleoli, and expansion of intercellular spaces. **B**. **Viral particles**: intercellular space between keratinocytes that is filled with virions, cellular debris, and a large autophagic vacuole that contains mitochondria, viral ribosomes, and nucleocapsids.

Vet-ebooks.com

keratoconjunctivitis, and lesions at other cutaneous sites are less common. Tracheobronchitis has been reported in immunosuppressed patients. Although HSV types 1 and 2 were first associated with oral and genital lesions respectively, these two viruses now infect both tissue sites.

The primary herpes lip lesion progresses through stages of erythema, vesiculation, pustules, and scab formation. In vesicular stages, the acute cell swelling of keratinocytes is characterized by keratinolysis and disintegration of most cellular organelles. Nuclear chromatin is rapidly lysed, leading to large pale nuclei that histologically have a "ground glass" appearance. As basal keratinocytes die, the subepithelial inflammatory reaction moves into the epidermis to create microvesicles and purulent epidermitis. In epithelium, there is a close association of HSV-1 expression with cellular differentiation. Connective tissue at the base of the lesion develops a severe vascular reaction. HSV replicates in endothelial cells and this influences connective tissue damage, reducing the production of matrix proteins, for example, collagen, fibronectin, and others.[21] Fluid from hyperemic capillaries progresses outward to expand the intraepidermal vesicle and expands laterally separating epidermis from dermis. Inflammatory cells, dominated by neutrophils early, become predominantly T lymphocytes, monocytes, and macrophages; NK and B cells are rare. T_H lymphocytes dominate in subepithelial and perivascular regions.

Ultrastructurally, HSV lesions have masses of virions in extracellular spaces and in the remnants of cytoplasm of necrotic keratinocytes (Fig. 13.8). Nuclei of dead cells are preserved, but structureless except for wisps of protein filaments and a few nucleocapsids. Spread of virus to neighboring cells quickly involves the entire thickness of the epithelium. The major DNA-binding protein forms a filamentous network in the nucleus of infected cells.[22] Filaments form spontaneously because of the high concentration of this protein in the nucleus during viral DNA synthesis.

HSV localizes in occult form in the **trigeminal ganglion**. Under a variety of stimuli, it will again induce vesicular lesions at the site of primary infection. Stress (including fever, malnutrition, immunologic deficiency, sunburn, and menstruation) will cause the virus to migrate down the sensory root of the trigeminal nerve and induce herpetic lesions of the lips. There are inflammatory changes present in the ganglia during facial herpetic lesions. Latent virus in the trigeminal ganglion can be shown with in situ hybridization techniques.

Recurrent episodes of **epidermal eruption** are not associated with significant changes in serum antibodies. Virus cannot be demonstrated in keratinocytes by fluorescent antibody techniques, by inoculating scrapings from former sites into rabbits or cell cultures, or by iontophoresis at the site of previous infection. Furthermore, recurrent skin sites autografted to nonrecurrent areas fails to develop lesions following stimulation with pyrogen, while lesions do occur at the original site. In experiments in mice, inoculation of the cornea with HSV is followed by spread of the virus through the root and into sensory parts of the trigeminal system in the brain stem and cerebral cortex. HSV ascends to the cortex from the olfactory bulb and establishes latency in olfactory system neurons via the primary olfactory cortex.[23] The replication cycle of the latent virus is restricted or blocked at some early point. Virus-encoded proteins are detectable in latently infected cells, some of which play a role in maintaining the latent infection,[24] and are important in recovery, at least in mice.[25] As parenchymal cells die they attract a few neutrophils, but lesions lack the purulent character of bacterial abscesses. Inclusion body-bearing cells are found only in degenerate cells at the periphery of the necrotic focus.

In addition to the common epidermal vesicular disease, HSV causes **generalized disseminated infection** with localization to viscera in neonates and immunosuppressed adults exposed to large amounts of virus. Infants with disseminated HSV typically develop focal necrosis in the liver, adrenals, and other

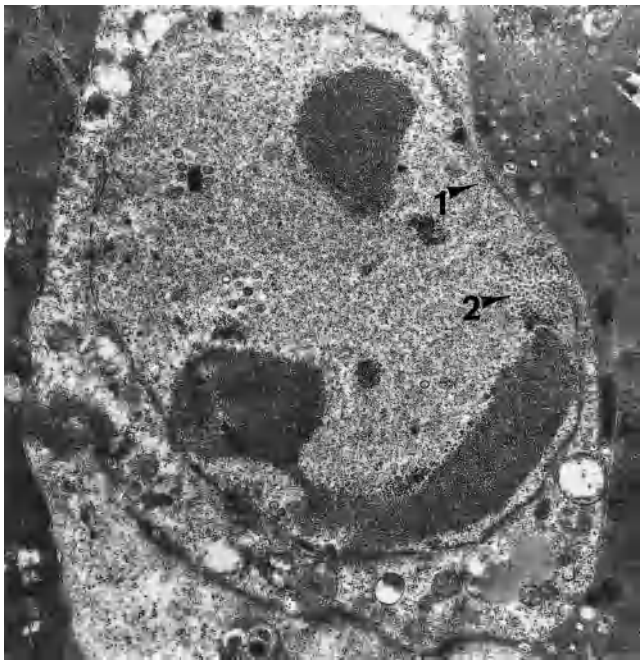


Fig. 13.8 Herpes simplex: human lip. Degenerate keratinocyte contains herpes nucleocapsids (*1*) and small empty virus particles (*2*). Virions are in dense cornified tissue.

Vet-ebooks.com

viscera.[26] T lymphocytes invade these lesions. Herpes B infection of infant macaques is a model for neonatal HSV-1 disease.[27] **Herpes simplex tracheobronchitis** is a rare but highly fatal illness that occurs largely in immunocompromised patients.[28] Neutrophils are attracted to sites of herpesvirus infection, especially to foci of necrosis (Fig. 13.9), but macrophages play the crucial role in resistance to dissemination of herpesviruses.

Acute necrotizing and inflammatory brain lesions of **herpes simplex encephalitis** involve the limbic system and adjacent areas of the temporal and frontal lobes of the cerebral cortex. In rare cases, lesions are restricted to the brain stem. Necrosis, perivascular lymphoid cuffing, and hemorrhage are typical; T4+ and T8+ lymphocytes are present in about equal numbers.[29] Gliosis and reactive astrocytosis surround areas of necrosis. Large, intranuclear eosinophilic inclusions occur in oligodendroglia and, less often, in nerve cells. Virions are best seen in biopsy specimens; inclusions present at the height of infection are often absent at necropsy. HSV invasion of the **eye** may result in severe keratitis, iridocyclitis, or uveitis. Virus replicates in all cells and there are large numbers of virions in all cell types of the iris. Acute herpetic encephalitis has been experimentally produced in rodents and rabbits. Inoculated into the forepaw, virus spreads along peripheral nerves, and block of the nerve suppresses the spread of infection. Progress of HSV from skin to brains may be hematologic, via perineural lymphatics, or neural. Scarification onto the cornea is followed by lesions in the fifth nerve and progression to the trigeminal ganglion, the fifth nucleus and cerebral cortex.

HSV-2 is transmitted by sexual contact or during birth. Although HSV-2 is responsible for most genital herpes infections, HSV-1 has become a more frequent isolate from the lesions.[30] The transient vesicles on the genital mucous membranes and external genitalia rapidly transform into superficial ulcers, and the subacute inflammatory lesions are accompanied by lymphadenitis of regional lymph nodes. HSV-2 is also associated with some neurologic infections and a murine model of encephalomyelitis has been developed.

Genus *Varicellovirus*

Chickenpox is the cutaneous disease caused by primary infection with **varicella virus** (human herpesvirus 3). Usually a benign disease of childhood, the vesicular cutaneous lesions heal quickly and children recover without sequelae.[31] In cutaneous lesions, infection begins in the basal stratum and spreads to the spinous layers. Infected epithelial cells swell, degenerate, lose their intercellular attachments, become round, and separate. Infected keratinocytes are markedly swollen. Nuclei are enlarged and pale due to chromatolysis with peripheralization of remaining chromatin. Viral nucleocapsids are in the nucleus and can often be found budding through the nuclear envelope. Virions, although commonly in cytoplasmic vacuoles, occur in large numbers in extracellular spaces. Fluid exudes into the degenerating areas of epidermis, and microvesicles form and coalesce. The end result is a large vesicle bounded on top by remnants of stratum corneum. Fibrin exudes into the lesion, it forms a scab, and healing occurs. In patients with disease of the lymphoreticular system or who are immunodeficient, varicella virus may cause severe disease and death involving viral pneumonia with necrosis, encephalitis, and liver. In these cases, platelet destruction is marked and thrombocytopenia may result from immune mechanisms. Pulmonary calcification is a consistent lesion.[32]

Herpes zoster (shingles) is a manifestation of cutaneous reinfection with varicella virus. It is characterized by erythematous and vesicular eruptions along the course of sensory nerves—most often on the face and trunk, the common sites of chickenpox rash. Cutaneous lesions resemble those of chickenpox. The virus produced, however, is less, and more closely cell-associated. In zoster, varicella virus persists after acute childhood infection. Virus or viral genome persists in neural ganglia and viral antigens have been demonstrated by immunofluorescent microscopy in Schwann cells of a patient with acute zoster. Neurons have a low DNA turnover and offer fewer opportunities for the viral genome to segregate and reestablish productive virogenic infection. **Varicella embryopathy** is a rare consequence of early fetal infection (late infection may produce only a varicellaform rash that develops within 8–10 days of birth). There are growth retardation, cystic formations in ducts of several organs, and CNS defects, often with retinitis.

Naturally occurring epizootics of **simian varicella** have been reported and the disease in primates closely resembles human varicella. Experimental simian varicella following intratracheal inoculation of virus leads to systemic disease with focal necrosis in viscera and infection of ganglia.

Genus *Mardivirus*

Marek's Disease **Marek's disease (MD)** virus causes two forms of disease in chickens: classic, neurotropic MD in which nerves are the chief site of lymphocyte proliferation; and lymphoma, largely of viscera. MD virus replicates in epithelium of the feather follicles and is transmitted by skin flakes in dust aerosols.

Vet-ebooks.com

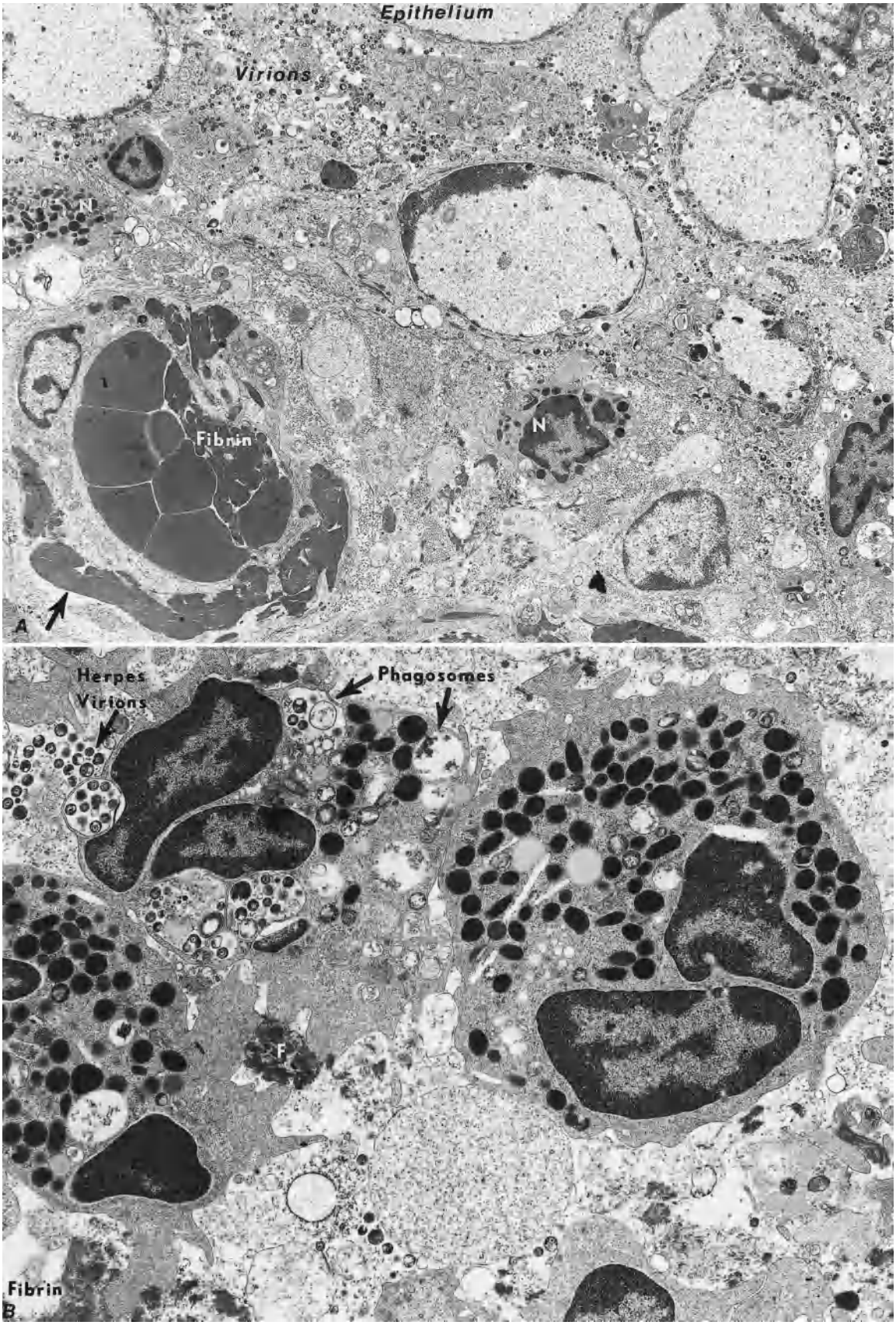


Fig. 13.9 Herpesviral vasculitis: fibrinopurulent inflammation below herpesvirus-infected epithelium, infectious bovine rhinotracheitis. **A**. **Perivascular fibrin** (*arrow*) and intravascular fibrin below infected epithelial surface; basement membrane; neutrophils (*N*). Epithelial cell nuclei have chromatin lysis and few immature viral particles. Fibrin is in interendothelial spaces and outside the capillary. **B**. **Neutrophils** have phagocytized fibrin and herpes virions.

Vet-ebooks.com

Feather follicle epithelium is hyperplastic with swollen cells that contain intranuclear inclusions. Nuclei contain nucleocapsids and virions are common in the cytoplasm. Virions are typical of the herpesvirus group (Fig. 13.10).

Three different host-virus relationships exist in MD: (1) productive infection in which both virions and viral antigens are present, and extracellular virus can be isolated, for example, in feather follicle epithelium; (2) viral antigens are present but virions are not, for example, nerve and visceral tumors; and (3) virions cannot be detected, but the viral genome present.[33]

Experimental inoculation of chickens with MD virus leads to acute cytolytic infection of lymphoid tissues and subacute inflammatory responses. Lymphocytolysis is marked in the thymic cortex where necrotic lymphocytes are taken by reticulum cells and macrophages. Cortical lymphocytes disappear and the medulla is expanded by reticuloendothelial hyperplasia. Reticulum cells become large and pale and may contain nuclear inclusions and cytoplasmic viral antigens. Syncytia may develop reflecting the predisposition of MD virus to spread from cell to cell by fusions of dendritic processes. These events may be followed by different syndromes. Some form small lesions in the nervous system that regress into an inflammatory-like condition dominated by edema with plasmacytes throughout the spongy nervous tissue. Birds given large doses of virus develop acute MD characterized by progressive, massive infiltration of peripheral nerves, particularly the sciatic nerve, by proliferating lymphocytes. Cells include lymphoblasts, small and medium lymphocytes, and dark-staining, basophilic cells with vacuolated cytoplasm ("MD" cells). Schwann cell activation, axonal degeneration, and demyelination and remyelination are present. The lymphocyte attack of myelin is viewed as a primary demyelination of the autoimmune type, and has been used as a model for the idiopathic polyneuritis/Guillain-Barre syndrome.[34]

Subfamily *Betaherpesvirinae*

Genus *Cytomegalovirus*

Cytomegaloviruses (CMVs) are large species-specific, double-stranded DNA viruses. CMVs preferentially infect cells of the monocyte-macrophage system, but can infect many cell types, even in neoplastic cells. The extent of intracellular replication is related to alterations in the immune statues of the host. Cells infected with CMV are markedly increased in size with large, pleomorphic nuclei bearing inclusions. CMV inclusions consist of dense granular viroplasm interspersed with nucleocapsids. Large virions occur free and in cytoplasmic vacuoles (Fig. 13.11). Hybridized sequences have been localized by immunogold techniques and viral DNA is found at the periphery of nuclear inclusions, associated with 70 nm nuclear dense bodies.[35]

Cytomegalic Inclusion Disease Cytomegaloviruses infect humans, monkeys, and pigs (inclusion body rhinitis). **Human cytomegaloviruses** (human herpesvirus 5) are transmitted in many ways: in utero from mother to fetus, perinatally as the fetus passes an infected birth canal, aerosol droplets among children, blood transfusion, transplantation of infected tissue grafts, venereally via semen or vaginal fluids, and from infected mother's milk. In humans, as in most animals, CMVs are associated with latent infection and lesions are found at necropsy. Primary infection is typically followed by transient excretion of CMV in the throat or urine. In immunosuppressed patients, systemic disease develops with large amounts of virus in spleen, lungs and other viscera. Infection in immunoincompetent infants, children and adults can lead to pneumonia, hepatitis, infectious mononucleosis (heterophil-negative), chorioretinitis, or encephalitis. The infectious mononucleosis syndrome occurs after blood transfusion from highly infected donors. Primary infection of the pregnant female will result in prolonged excretion of virus usually throughout pregnancy and subsequent infection of the fetus. The most significant disease associated with human CMV is congenital infection of the newborn. Human CMV is also commonly found incidentally in other disease. In Kaposi's tissue, involvement may be as widespread as in classic congenital CID, except for lesions in the brain. Using P^{32}-labeled human CMV DNA probes, CMV RNA was identified in 5 of 10 Kaposi's sarcomas.[36,37]

Genus *Roseolovirus*

Human herpesivirus 6 (HHV-6) is a major cause of febrile illness in children. Viremia is associated with the presence of the viral genome in circulating monocytes. In normal adults, infection is life-long, and HHV-6 DNA is present in saliva and blood leukocytes. Reactivation is associated with immunosuppression and may lead to pneumonitis. HHV-6 is the causative agent for human exanthema subitum (roseola infantum). HHV-6 is isolated from the syndrome of massive but painless cervical lymphadenopathy that occurs largely in children and young adults; HHV-6 persists in the host after recovery with intermittent shedding of virus from the oropharynx. Electron micrographs of chimpanzee lymphocytes infected with HHV-6 show virions in cytoplasmic vacuoles that originate from perinuclear cisternae.

Vet-ebooks.com

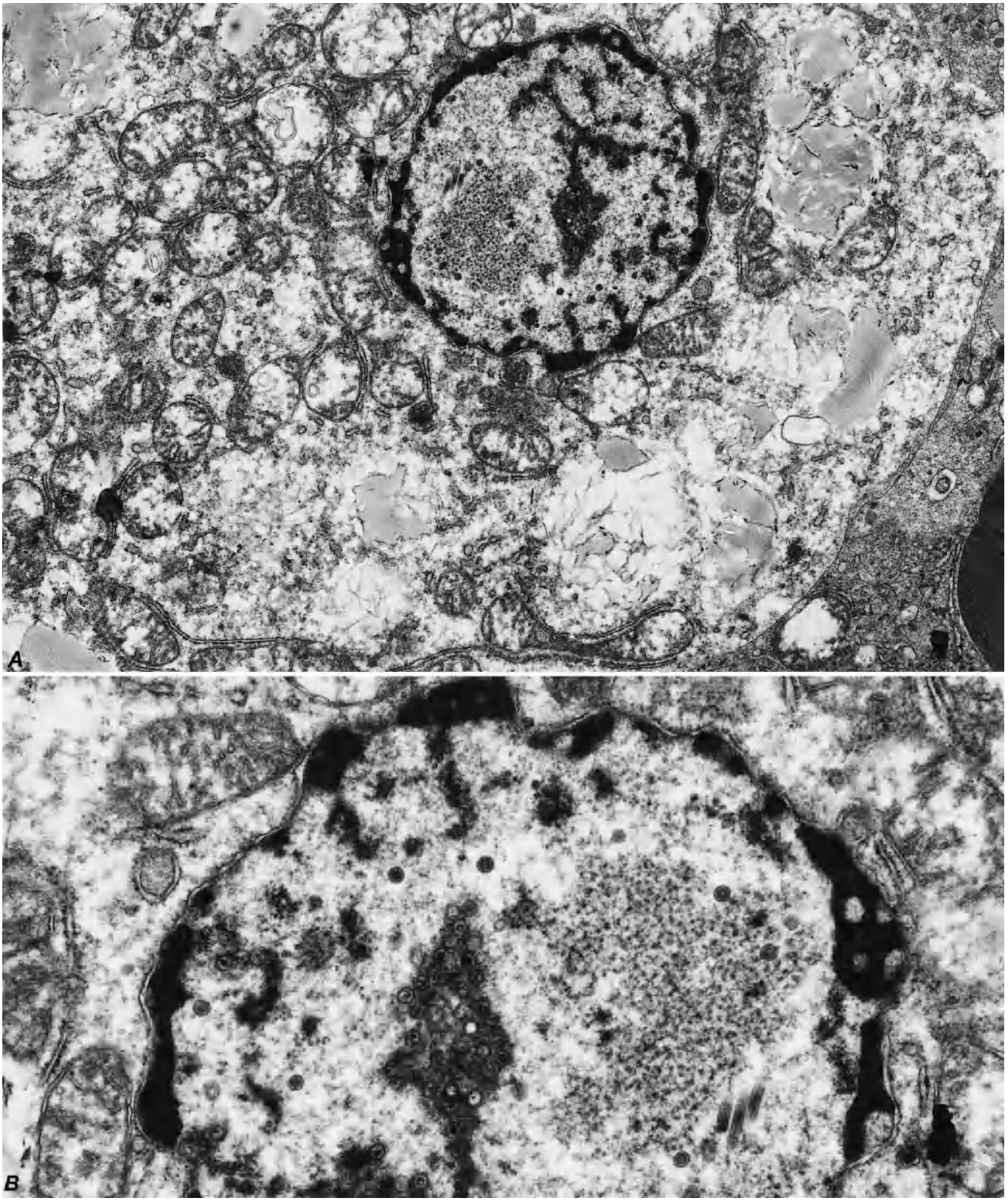


Fig. 13.10 Herpesviral hepatitis: duck plague. **A**. **Degenerate hepatocyte**, acute cell swelling, nuclear degeneration, and steatosis (note lipid globules). **B**. **Viral particles** in a degenerate nucleus. (Micrograph: S. James Proctor, *Vet Pathol* 12:349, 1975.)

Vet-ebooks.com

Subfamily *Gammaherpesvirinae*

Genus *Lymphocryptovirus*

Diseases of Epstein-Barr Virus **Epstein-Barr virus** (**EBV**, herpesvirus 4) is a ubiquitous herpesvirus with strict B lymphocyte tropism; it causes polyclonal immortalization of B cells. Ultrastructural changes of infected human B lymphocytes include enlargement, pleomorphism of nuclei and cytoplasm, and the presence of parallel tubular arrays in cisternae of the endoplasmic reticulum. EBV has a linear double-stranded DNA genome that persists within latently infected cells as multiple covalently closed circular episomes. In latently infected cells, viral gene expression is restricted to a few viral products, the EBV nuclear antigens, a membrane protein, terminal proteins, and EBV-encoded small RNAs. The host cell receptor for EBV is the **complement receptor type 2** (CR2, also CD21) to which EBV binds by its major envelope glycoprotein, gp 350/220. Infection occurs when oropharyngeal epithelial cells expressing CR2 become infected. B lymphocytes that bear surface CR2 are infected as they pass through foci of infection in epithelium. The CR2 receptor-EBV complex, together with surface immunoglobulins on B cells, transduces activation that leads to B cell proliferation.

Infectious Mononucleosis EBV replicates at low rates in healthy humans unless immunodeficiency and immunologic disequilibrium permit complete replication of the virus. In early childhood, inapparaent EBV infection is the rule. In adolescence, infectious mononucleosis is associated with primary infection. Oral excretion and leukocyte-associated viremia occur in the presence of high serum antibody titers to EBV. The blood in mononucleosis shows an absolute lymphocytosis. Many lymphocytes are atypical with up to 16 μm diameters, pleomorphic nuclei, and voluminous basophilic, granular cytoplasm that is vacuolated. Perivascular mononuclear infiltrates occur in liver, spleen, brain and other organs. Enlarged lymph nodes show marked proliferation of T cells in paracortical zones, prominent germinal centers, and distortion of normal architecture. Some nodes will contain Reed-Sternberg type giant cells which must be differentiated from Hodgkin's disease.

Burkitt's Lymphoma EBV was discovered by electron microscopy of cell cultures derived from a case of Burkitt's lymphoma of an African child. This tumor involves multifocal solid lymphomas of the viscera and occurs in epidemiologic patterns reminiscent of an infectious disease. EBV induced a proliferative lymphoreticular disease when inoculated experimentally into monkeys.[38]

EBV-Related Lymphoproliferative Disorders In the body, EBV is ubiquitous and replicates in the mucosal epithelium of the parotid gland, oropharynx, tongue, and uterine cervix. At these sites it can cause a wide variety of lesions and clinical syndromes. The discovery of the X-linked lymphoproliferative disease in 1975 suggested that EBV was the cause of infectious mononucleosis, acquired agammaglobulinemia, and non-Hodgkin's lymphoma in maternally related males with an inherited defect in the X chromosome. Recently EBV has been associated with a wide variety of post-transplant disorders.[39]

Hairy leukoplakia, a lesion that is most common on the lateral borders of the tongue of HIV-infected patients, is associated with productive EBV infection.[40,41] Keratinocytes in the upper two-thirds of these lesions, when stained with appropriate monoclonal antibody reagents, show diffuse staining components of the EBV early antigen complex, EBV 150-kd capsid antigen, EBV membrane antigen, and double-stranded DNA.[42,43]

Virions have not been reported in tumor tissue, but have been described during growth in vitro. The EBV genome is detectable in **nasopharyngeal carcinomas** by nucleic acid hybridization and antigen detection.[44] These methods are limited for carcinoma specimens by the highly restricted expression of the EBV genome. Only two viral proteins, EB nuclear antigen (EBNA-1) and the latent membrane protein (LMP), can effectively be detected in frozen sections of nasopharyngeal carcinoma. In EBV-transformed lymphocytes, very short nonprotein coding EBV transcripts (EBERs) are highly expressed and are detected by a riboprobe in formalin-fixed sections.[45]

Animal Models of EBV EBV induces a proliferative lymphoreticular disease when inoculated experimentally into monkeys. Inoculation of EBV into marmosets and owl monkeys may induce lymphomas. The demonstration that EBV is responsible for the lymphoma is based upon (1) demonstration of EBV nuclear antigen in the majority of lymphoma cells in imprints of tumor, and (2) EBV genome identified directly in tumor cell DNA by molecular hybridization techniques.[46] The cotton-top marmoset is exquisitely susceptible to EBV-induced lymphoproliferative disease; after inoculation, a lethal disorder develops in a few weeks. EBV-associated lymphoproliferative disease can also be induced in SCID mice.

Genus *Rhadinovirus*

The genus *Rhadinovirus* (ateline herpesvirus group) has a variable host range. It is common in New World monkeys. Members include ateline herpesvirus 2, saimiriine herpesvirus 2, and others. *Herpesvirus ateles*,

Vet-ebooks.com

isolated from inapparent infections in spider monkeys, can induce malignant lymphoma with leukemia in marmosets with 100% mortality in 4–6 wk.

Saimiriine herpesvirus 2 (*Herpesvirus saimiri*), an indigenous and noncytopathic virus in squirrel monkeys (*Saimiri sciureus*), produces rapidly progressing fatal malignant lymphoma of the reticulum cell type in marmosets (*Saguinus*. sp.), owl monkeys (*Aotus* sp.), spider monkeys (*Ateles* sp.) and several other simian species. Rabbits infected experimentally also develop neoplastic changes. In marmosets, the disease has a rapid course of 13–28 days, and there is extensive invasion of viscera by neoplastic reticulum cells. Tissue responses are both proliferative and necrotizing. Ultrastructurally, cells are mixtures of lymphoblasts and undifferentiated reticulum cells. In some animals lymphoblasts are the dominant cell types.

Malignant Catarrhal Fever **Malignant catarrhal fever (MCF)** is an acute lymphoproliferative disease of cattle and other ungulates. Two forms of the disease occur. In one, alcelaphine herpesvirus 1 and 2 infects wildebeest and hartebeest inapparently and induces MCF when it infects cattle. In the other form, ovine herpesvirus 2 has been identified where sheep act as inapparent carriers of infection. Injection of large amounts of blood or tissue into normal cattle from cattle with the second form will reproduce the disease.

Herpesviral Disease of Uncertain Classification

Frog Renal Carcinoma Large multilobular metastasizing renal adenocarcinomas occur in 2–5% of many frog populations in North America. Nuclei of tumor cells contain large inclusions filled with herpes virions. The renal carcinoma herpesvirus infects frog eggs when they are developing the water in spring and carcinomas appear in the frog's liver in the third or fourth summer. These "summer tumors" do not produce virus but do contain viral genomes. During the summer months the tumor grows and may expand to kill the frog. If it does not, tumor growth ceases at hibernation in the autumn. As tumor cells cease their growth cycles, they become virogenic. That is, they produce infectious virions which lyse the tumor cell. Virus is excreted into the urine, and, with the end of hibernation, is expelled into the pond water where it infects the eggs and tadpoles during the spring season.[47] The growth of frog herpesvirus is temperature-dependent and in the laboratory tumors cells can be converted from a virus-free summer state, in which the viral genome is present but unexpressed, to a viral state by merely lowering the environmental temperature of the host frog.

Duck Plague **Duck plague** occurs in many species of ducks, geese, and other wild waterfowl. It is characterized by severe diarrhea, dehydration, prostration, and high mortality. Although duck plague herpesvirus can cause sporadic deaths at any time, the disease tends to occur in explosive outbreaks, when excessive numbers of birds (per area of feeding ground) congregate for long periods. Lesions relate to the capacity of the virus to replicate in endodermal epithelium, the monocyte-macropahge system, and hepatocytes. Necrosis of spleen, thymus, bursa and other lymphoid structures is especially severe. Nucleocapsids are present in the nucleus, and virions are found throughout the cytoplasm and at cell surfaces. In affected organs, virions occur in hepatocytes and other parenchymal cells (Fig. 13.10), endothelial cells, macrophages and infiltrating lymphocytes, monocytes, and heterophiles. Other avian herpesvirus-induced systemic diseases with visceral necrosis include pigeon herpesviral hepatitis, owl hepatitis, and falcon hepatitis.

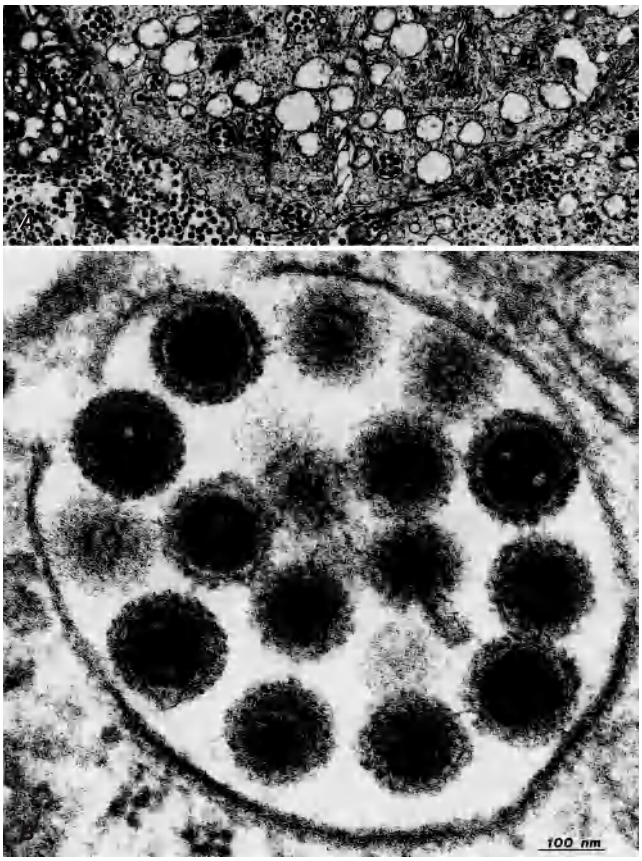


Fig. 13.11 **Cytomegalovirus**: lung, pig. **A**. **Extracellular and cytoplasmic virions**. **B**. **Virions**: enlargement of A. (Micrograph: Gian Winkler, National Animal Disease Center.)

Family *Adenoviridae*

Adenoviruses are DNA viruses with a capsid of 252 capsomeres arranged in an icosahedral structure with

Vet-ebooks.com

20 sides and 12 vertices. **Hexons** comprise 240 of the capsomeres while the vertices are occupied by **pentons**. The penton consists of a **base** that is locked in the capsid and a **fiber** that has a knob at the end. The penton has hemagglutinin activity and is the ligand for receptors of the host cell. The ion etching technique has revealed that the interior of the adenovirus virion contains 12 large spheres, one directly beneath each of the 12 vertices of the icosahedron that is the capsid. Called adenosomes, these spheres are condensed viral DNA, resembling nucleosomes coiled around a core of histones. Cryoelectron microscopy and image reconstruction techniques have shown the 3-dimensional structure of adenoviral virions.

Adenoviruses commonly infect the respiratory and enteric tracts and, in rare cases, the liver and pancreas (Table 13.3).[48,49] Although infection is common, overt disease is rare. Different adenoviruses can have three different interactions with host cells: **lytic** infection which involves the complete viral replicative cycle, latent or chronic infection of lymphoid tissues such as the tonsil, and **oncogenic transformation**. In the later, viral DNA is integrated into and replicated with the host cell DNA but no infectious virions are produced.

Table 13.3 Family *Adenoviridae*.

Virus	*Disease in*	*Reference to ultrastructural pathology*
		Genus *Mastadenovirus*
Bovine adenovirus	Cattle	**Darbyshire**, *Res Vet Sci* 7:81, 1966
Canine adenovirus	Dogs	**Davies**, *Virology* 15:87, 1961 (virion);* **Ducatelle**, *Res Vet Sci* 31:207, 1981 (pneumonia); **Gerhold**, *J Wildlife Dis* 43:734:2007 (fox); **Givan**, *Lab Invest* 20:36, 1969; **Lindblad,** *Acta Pathol Microbiol Scand* 62:155, 1964 (endothelium); **Tajima**, *Am J Vet Res* 19:666, 1958; **Yamamoto**, *J Gen Virol* 4:397, 1969
	Experimental	**Wright**, *Br J Exp Pathol* 62:183, 1981 and 64:312, 1983 (glomerulonephritis)†
Chimpanzee adenovirus	Chimpanzee	**Davis**, *Vet Pathol* 29:547, 1992
Equine adenovirus	Horse	**Ardans**, *Am J Vet Res* 35:431, 1974; **Edington**, *Res Vet Sci* 37:252, 1984 (neuritis)
Goat adenovirus	Goats	**Lehmkuhl**, *J Vet Diag Invest* 13:195, 2001
Human adenovirus	Human	**Becroft**, *J Clin Pathol* 20:561, 1967; **Carmichael**, *Am J Clin Pathol* 71:352, 1979 (hepatitis); **Chou** SM, *J Neuropathol Exp Neurol* 32:34, 1973 (encephalitis); **Pinkerton**, *Am J Pathol* 65:543, 1971 (pneumonia, infants); **Wigger**, *New Engl J Med* 275:870, 1966; **Yunis**, *Lab Invest* 33:347, 1975 (enteropathy)
	Experimental	**Kaup**, *Vet Pathol* 21:521, 1984 (pneumonia, guinea pig); **Mukai**, *Am J Pathol* 69:331, 1972 (neoplasia)
Murine adenovirus	Mouse	**Blailock**, *Exp Mol Pathol* 9:84, 1968 (myocarditis); **Takeuchi**, *Infect Immun* 13:568, 1976 (enteritis)
Otter adenovirus	Otter	**Park**, *Vet Path* 44:56, 2007
Ovine adenovirus	Sheep	**Cutlip**, *Am J Vet Res* 44:2395, 1983; **Lehmkuhl**, *Arch Virol* 48:39, 1975
Porcine adenovirus	Swine	**Chandler**, *J R Microsc Soc* 84:133, 1964; **Ducatelle**, *Arch Virol* 69:219, 1981 (intestine); **Koestner**, *Am J Pathol* 53:651, 1968
Rat adenovirus	Rat	**Ward**, *J Am Vet Med Ass* 169:952, 1976; **Worthington**, *Anat Rec* 175:37, 1975 (ileum)
Simian adenovirus	Primates	**Martin**, *Lab An Sci* 41:382, 1991 (pancreatitis); **McClure**, *Arch Pathol Lab Med* 102:150, 1978
	Experimental	**Merkow**, *Int J Cancer* 4:455, 1969 (neoplasia);† **Slifkin**, *Exp Mol Pathol* 11:285, 1969 (SV30, neoplasia)†
		Genus *Aviadenovirus*
Avian adenovirus	Chicken	**McFerran**, *Am J Vet Res* 36:527, 1975; **Dutta**, *Am J Vet Res* 28:296, 1967
		Genus *Atadenovirus*
Bovine adenovirus 4–8	Cattle	**Lehmkuhl**, *Arch Virol* 153: 891–897, 2008
Ovine adenovirus 7	Sheep	**Lehmkuhl**, *Arch Virol* 153: 891–897, 2008
Goat adenovirus 1	Goats	**Lehmkuhl**, *Arch Virol* 144: 1611–1618, 1999
Cervine adenovirus 1	Deer/Moose	**Lehmkuhl**, *Arch Virol* 146: 1187–1196, 2001

*In vitro study.
†Experimental model.

Vet-ebooks.com

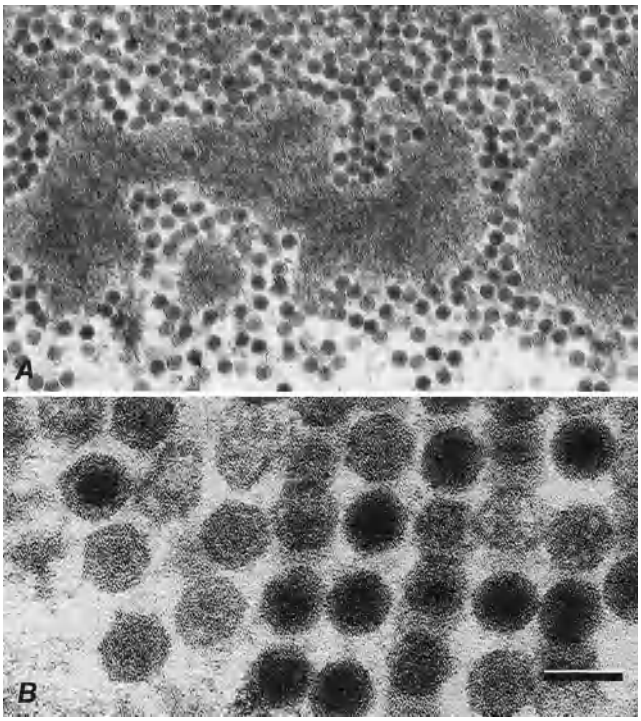


Fig. 13.12 Cytopathology of adenoviral infection. **A**. **Virions** within nucleolus, early inclusion body. **B**. **Virions**, bar = 100 nm.

As in lytic and chronic infection, T antigens are produced providing evidence of infection.

Large **nuclear inclusions** of virions develop in adenovirus-infected tissues (Fig. 13.12). Granular aggregates in nuclei of adenoviral infected cells are composed of various viral-induced proteins.[50] Compact fibrogranular masses with medium electron-dense granules label for DNA polymerase and terminal proteins, while filamentous masses of low electron density labeled for single-stranded DNA-binding protein and single-stranded DNA. Marked **cytomegaly** with enormous eosinophilic nuclear inclusions is typical of avian adenoviruses and respiratory mucosa and placenta of sheep infected with ovine adenovirus.

Genus *Mastadenovirus*

Human Adenoviral Disease Adenoviruses are associated with transient upper respiratory diseases that appear as minor flulike syndromes. Human clinical disease syndromes include a wide range of respiratory infections that arise from mild to moderate pharyngitis and tracheitis. Adenovirus type 7 has caused fulminant necrotizing bronchiolitis and pneumonia in infants and several types can cause severe acute respiratory disease in adults. Rare syndromes caused by adenoviruses include epidemic keratoconjunctivitis, infantile diarrhea, hemorrhagic cystitis, and meningoencephalitis. Adenoviral infection has been implicated in hepatic necrosis and in intestinal intussusceptions.

Pulmonary Adenoviral Disease in Animals In animals, immunosuppression and stress are often associated with outbreaks of adenoviral disease. In horses, adenoviral pneumonia occurs chiefly in young foals with combined immunodeficiency disease. Adenoviruses isolated from different animals are similar in structure, and are related (except for avian types) by a common protein antigen in the virion.

Canine adenovirus 2 (CAV-2), a natural respiratory pathogen for dogs, replicates in nonciliated epithelial cells to produce bronchitis and bronchiolitis within the lung. Progressing into lung parenchyma CAV-2 replicates in granular pneumocytes. Eventually, many cell types are infected and accumulation of debris produces obstruction in lower airways.[51] Other models of pulmonary adenovirus disease include those of the guinea pig and monkey. Infection of rhesus monkey fetuses at various gestational ages caused bronchiolar necrosis, a lesion prevented by immunization of the pregnant mother. Adenoviral pneumonia of sheep replicates in massively enlarged nuclei of epithelial cells in the terminal airways (but not in alveolar epithelium). Severe cytomegaly and hyperplasia of epithelial cells cause distinctive lesions in bronchioles that mimic lesions of cytomegaloviruses.

Enteric Adenoviruses Adenoviruses of several species replicate in enterocytes of the small intestine; for example, monkey, cow, pig, rat, and mouse (see Table 13.3). Most enteric adenoviruses are found by negative staining in feces from animals with diarrhea. Disease is difficult to reproduce although certain adenoviral types will consistently cause disease in pathogen-free pigs. Porcine adenoviruses infect only enterocytes, which contrast with bovine enteric adenoviruses, which also infect capillary endothelium. Infected enterocyte nuclei bear large numbers of virions and aggregates of viral protein, as well as highly distorted nucleoli.

Adenoviral Hepatitis **Infectious canine hepatitis (ICH)** is an acute febrile systemic disease of *Canidae* (dogs, coyotes, foxes, and wolves), *Ursidae* (black and polar bears), *Procyonidae* (raccoons) and *Mustelidae* (skunks) and is caused by **canine adenovirus type 1 (CAV-1)**. Infection occurs orally with early infection of the tonsil, and subsequent dissemination of the virus. Extensive liver necrosis with large nuclear adenoviral inclusions is diagnostic. Viral antigens and virion-filled inclusions develop in circulating monocytes and these cells spread the virus throughout the body. Virus enters the liver hematogenously and infects endothelium of the hepatic sinusoids. Endothelial cells are

Vet-ebooks.com

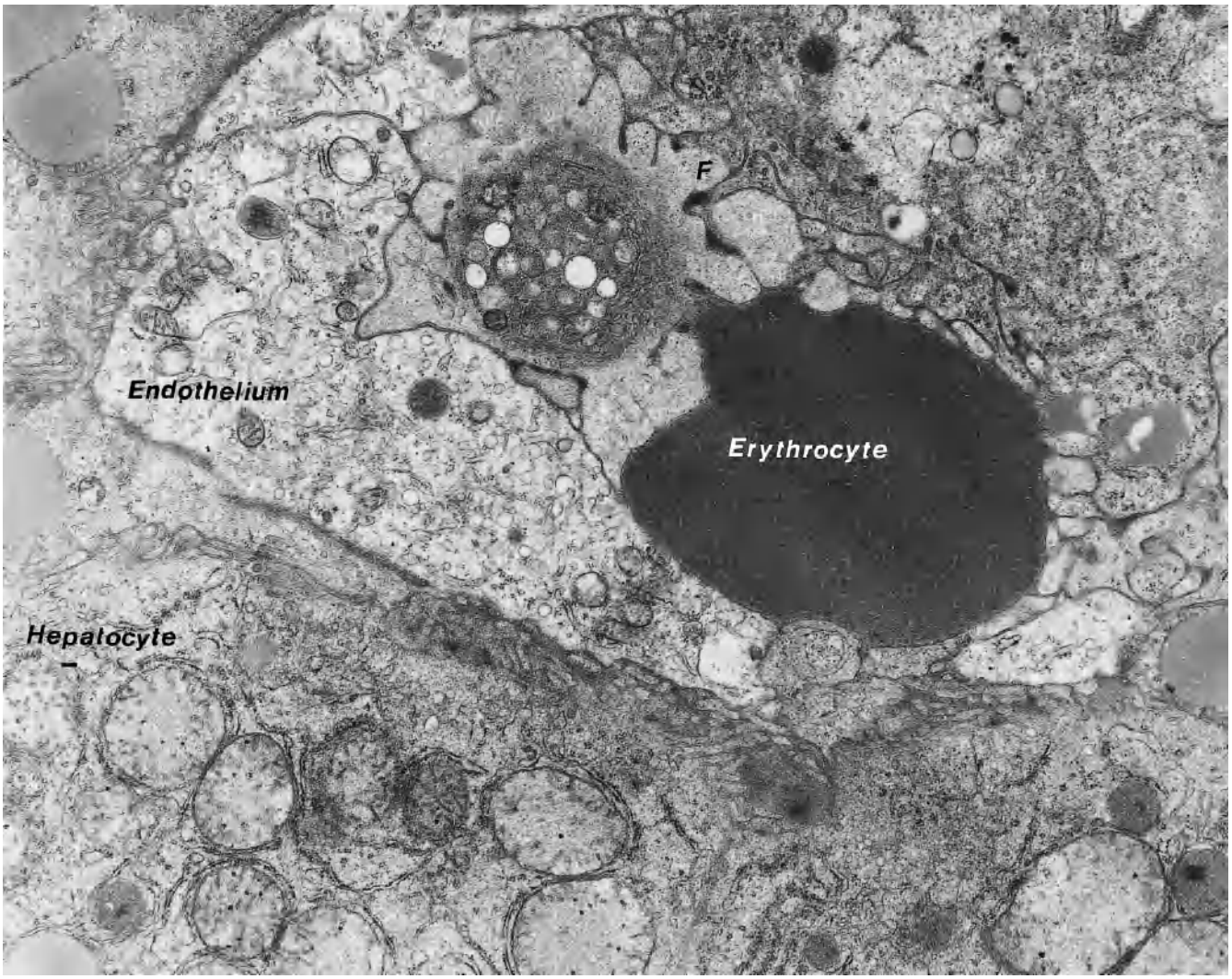


Fig. 13.13 Adenoviral hepatitis: infectious canine hepatitis, dog. Endothelial cells are markedly swollen. Undulations in hepatocyte surfaces fill subendothelial spaces. Hepatic sinusoid is blocked by swollen endothelium, erythrocytes, and an activated platelet that has many filopodia and centralized granules.

damaged and platelets are trapped in the sinusoids. Virus rapidly spreads to and destroys hepatocytes. In late ICH, both platelets and coagulation factors are inhibited so that bleeding is common. CAV-1 replicates in the kidney, and is a significant cause of glomerulonephritis.

In infected **hepatocytes**, nuclear inclusions are diagnostic. Nonspecific degenerative changes in the cytoplasm include mitochondrial disruption, excessive lipid, residual bodies, and dense tubules within the cisternae of the endoplasmic reticulum. Decrease of glycogen of affected hepatocytes appears to be related to the systemic effects of fever and anorexia. **Kupffer cells** contain nuclear inclusions early in the disease which reflect their capacity to phagocytize circulating virions and in turn to infect hepatocytes (Fig. 13.13). In subacute infection, proliferation of Kupffer cells is seen. Nuclear inclusions may be found in reticular and endothelial cells of the liver and, reflecting the systemic nature of the disease, in renal glomeruli and epithlium of the lower nephron, lymph nodes and spleen. Nuclear inclusions are also seen in capillaries and veins of the brain. In the **brain**, affected blood vessels may rupture and cause hemorrhages. During recovery, vascular hyperplasia may be seen and demyelination may occur in areas of severe edema and hemorrhage. **Hemorrhages**, which are so characteristic of severe ICH, are due both to viral-induced damage to the endothelium and to increased bleeding time. Bleeding is caused chiefly by thrombocytopenia, a consequence of viral damage to bone marrow megakaryocytes. In terminal disease, bleeding may be

Vet-ebooks.com



Fig. 13.14 Adenoviral cytomegaly: splenic reticular cell, avian adenovirus infection, chicken. Massive enlargement of nucleus and cytoplasm (compared to adjacent lymphocytes and reticular cells). Necrotic cells at bottom have undergone karyorrhexis, but nuclear virions are preserved.

Vet-ebooks.com

exaggerated by coagulation defects associated with the severe liver disease.

In the **eye**, corneal opacities and anterior uveitis often follow or accompany ICH. Early, uveitis is due to viral growth in reticular cells and vascular endothelium. Later, iridocyclitis with corneal opacity is due to an Arthus-type immunologic reaction. Viremia with localization of virus in the eye results in a primary iridocyclitis. Resolution without sequelae may occur if virus persists in the anterior uvea. Antibody production, including local formation in the iris and limbus, may react with cell-associated antigen producing the focal, Arthus-type hypersensitivity. Plasma exudes through damaged vessels into the cornea producing the corneal edema and secondary iridocyclitis.

Respiratory disease can develop, suggesting that aerosol spread can also occur. Pups with CAV-1 infection of the respiratory tract have episodes of coughing with mild dyspnea. At autopsy, their lungs are mottled with grey foci which represent thickened alveolar walls and lymphocyte/monocyte infiltrates. Necrotizing bronchiolitis is typical of severe disease.

CAV-1 may persist for up to 30 days in the **kidney**, and be excreted in urine. Lymphocytic interstitial nephritis, a rare sequel to CAV-1 infection, develops in the recovery phase. A second, immune complex renal disease with glomerulopathy may lead to chronic renal failure.[52]

Oncogenicity of Adenoviruses Some adenoviruses of human origin produce sarcomas in hamsters, a fact that has aroused suspicion but no evidence that similar oncogenic potential exists for humans.[53,54] Oncogenic adenoviruses induce tumors in rodents and transform cells in culture. The E1 region genes encode proteins responsible for oncogenic properties of the virus. There is complexing of viral oncoproteins with normal host cell proteins that regulate the cell cycle. The ultrastructural pathology of tumors produced in hamsters by simian adenoviruses are similar to those produced by human adenoviruses.[55,56]

Genus *Aviadenovirus*

Adenoviral Disease of Birds Widely distributed in the domestic poultry populations, avian adenoviruses are usually isolated in the absence of overt disease. The established pathogens are the adenoviruses of inclusion body hepatitis of chickens, marble spleen disease of pheasants, quail bronchitis, and hemorrhagic enteritis of turkeys. Oral inoculation of pathogenic adenoviruses is followed by replication in intestinal epithelium. Immunolabeling techniques reveal viral replication in cells in the mucosa and lamina propria of the terminal ileum and large intestine. Infected cells become markedly enlarged with massive inclusions in the nucleus and markedly increased nuclear:cytoplasmic ratios (Fig. 13.14). Some avian adenoviruses have a tropism for the spleen and infected macrophages and reticulum cells in marginal zones of the red pulp. Focal necrosis of the liver, kidney and respiratory tract occur in experimental infections but are rare in natural disease. Avian adenoviruses have been shown to be oncogenic for hamsters.[57] When given in very large doses they cause sarcomas; hepatomas have been reported.

Family *Papillomaviridae*

Papilloma virions are noneveloped particles of icosahedral symmetry and 55–60 nm that encapsulate a single copy of the double-stranded, circular DNA genome in the form of a chromatin-like complex with cellular histones. The viral capsid consists of 72 capsomeres, 12 of which contact 5 neighbors.[58] The adenovirus family contains over 20 genera (Table 13.4). Viral papillomas occur in skin, genital mucosa, and oral mucosa of many animal species. These focal proliferative lesions are characterized by **hyperkeratosis** (thickening of the stratum corneum), **parakeratosis** (extension of intact keratinoctyes into the stratum corneum), and **acanthosis** (thickening of the stratum spinosum). Large **papilloma cells** occur in the granular layer of the skin, at the junction of the spinous and cornified layers. These keratinocytes undergo lytic infection with production of virions. They are ballooned, with pale, structureless cytoplasm, marginated nuclear chromatin, and small clumps of basophilic material around degenerate nucleoli. Althrough rare, squamous cell carcinomas arise within viral papillomas of some species.

In keratinocytes, papillomaviruses elicit two different processes. In some cells there is increased activity, mitosis, and proliferation, a hyperplastic reaction responsible for the increased keratin. In other cells there is no mitotic activity but instead the cell degenerates with production of large numbers of virions in the nucleus. The papillomavirus life cycle is tightly coupled to the program of differentiation of the keratinocyte, and virion production is limited to differentiating suprabasal cells. The processes of hyperplasia and virus production are mutually exclusive. Factors which determine whether the virus will induce cell proliferation or cell death involve how the viral genome is inserted into that of the host cell and the particular stage of the host cell cycle.

When scarified into the skin of the appropriate host, no overt tissue reaction occurs for several weeks. At about 30 days after inoculation of most papillomaviruses, a small focus of basophilic and highly mitotic basal cell proliferation appears in the epidermis at the

Vet-ebooks.com

Table 13.4 Family *Papillomaviridae*.

Virus	*Disease in*	*Reference to ultrastructural pathology*
Bovine papillomavirus	Cow	**Brobst**, *Vet Pathol* 3:196, 1966
Canine oral papillomavirus	Dog	**Cheville**, *Am J Pathol* 445:849, 1964
Canine cutaneous papilloma	Dog	**Watrach**, *J Nat Cancer Inst* 45:915, 1970; **Le Net**, *Vet Pathol* 34:8, 1997
Chaffinch papillomavirus		**Osterhaus**, *Intervirology* 8:351, 1977
Deer cutaneous fibroma	Deer	**Sundberg**, *Am J Vet Res* 46:1150, 1985
Equine papillomavirus	Horse	**Fulton**, *J Ultrastruct Res* 30:328, 1970; **Garma-Avina**, *Equine Vet J* 13:59, 1981; **Hamada**, *Vet Pathol* 29:152, 1992 (Langerhans' cells); **Junge**, *J Am Vet Med Ass* 185:656, 1984
	Horse (aural)	**Fairly**, *Vet Pathol* 29:79, 1992
Giraffe papillomavirus	Giraffe	**Karstad**, *J Wildlife Dis* 14:309, 1978
Goat papillomavirus	Goat	**Moulton**, *N Am Vet* 35:29, 1954
Hamster papillomavirus	Hamster	**Barthold**, *Lab Anim Sci* 37:283, 1987 (lymphoma); **Coggin**, *J Nat Cancer Inst* 75:91, 1985; **Graffi**, *Proc Nat Acad Sci USA* 64:1172, 1967
Human cutaneous papillomavirus	Human	**Gissman**, *Virology* 76:569, 1977; **Jenson**, *Lab Invest* 47:491, 1982; **Viac**, *J Invest Dermatol* 70:263, 1978
	Human (epidermodysplasia verruciformis)	**Lutzner**, *Bull Cancer* 65:169, 1978; **Orth**, *Proc Nat Acad Sci USA* 75:1537, 1978
Human oral papillomavirus		**Frithiof**, *Arch Ges Virusforsch* 21:31, 1967
Impala fibroma	Impala#	**Karstad**, *J Wildlife Dis* 14:309, 1978
Lizard papilloma		**Raynaud**, *C R Hebd Seances Acad Sci* 283:845, 1976
Murine papilloma	European harvest mouse	**O'Banion**, *J Virol* 62:226, 1988
Ovine papilloma	Sheep	**Hayward**, *Vet Rec* 132:86, 1993
Parrot papillomavirus	Parrot	**O'Banion**, *Intervirology* 33:91, 1992
Porcine papillomavirus	Swine	**Parish**, *J Pathol Bact* 81:331, 1961; **Rieke**, *Dtsch Tieraerztl Wschr* 87:412, 1980
Rabbit cutaneous papillomavirus (Shope)	Rabbit	**De The**, *Bull Ass Etude Cancer* 47:569, 1960; **Stone**, *J Exp Med* 110:543, 1959 (skin)
Rabbit oral papillomavirus	Rabbit	**Rdzok**, *Cancer Res* 26:160, 1966;† **Sundberg**, *Am J Vet Res* 46:664, 1985
Turtle papillomavirus	Turtle	**Jacobson**, *J Am Vet Med Ass* 181:1325, 1982#

*Studies in vitro.
†Animal model.
#Viral etiology not clearly established.

point of scarification (Fig. 13.15). These rapidly dividing (but normal-appearing) keratinocytes begin the massive production of keratin which, in the early stages, markedly increases the width of the spinous cell layer. Virions or viral antigens are not detected histochemically in these early lesions although the viral genome can be shown by in situ hybridization techniques. Keratinocytes progress through normal processes of keratiniziation results in large numbers of deeply basophilic keratohyalin granules embedded in masses of keratin. Large eosinophilic globules of partially polymerized keratin are present and rapidly growing.

As papilloma cells move into the keratin, their cytoplasm disintegrates leaving arrays of virions encysted by degenerate nuclear membranes and keratin fibrils, materials that protect the virions when these materials are desquamated from the wart. As they mature, papillomas become progressively infiltrated with T lymphocytes. Langerhans' cells also play a role in the recovery phase. Hypofunctional and diminished in number in the early proliferative phase of papilloma

Vet-ebooks.com

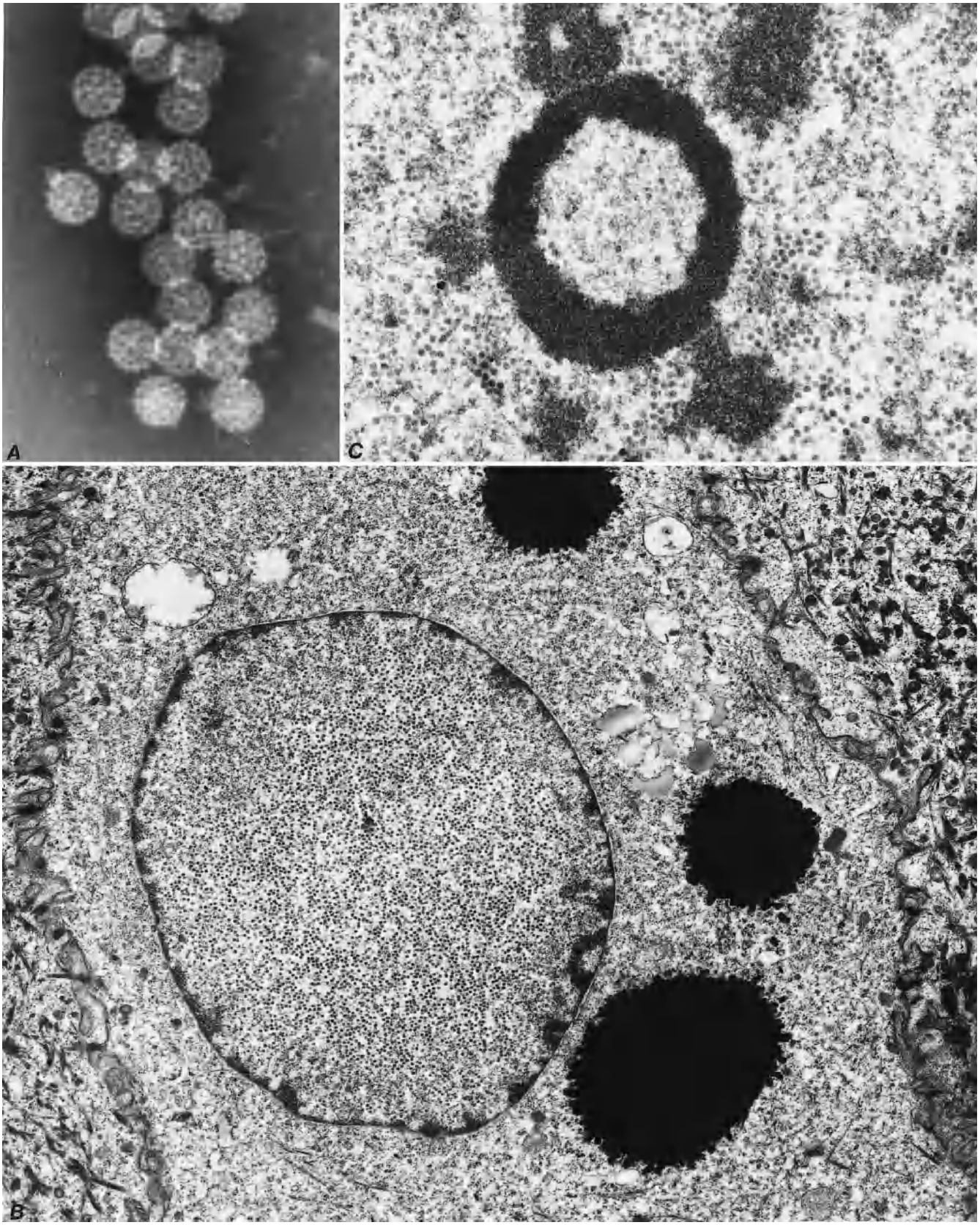


Fig. 13.15 Cytopathology of papillomaviral infection. **A**. **Papilloma virions** (negative stain preparation), bovine papillomavirus. **B–C**. **Infected keratinocyte**: skin, equine papilloma. Nucleus is filled with virions (nuclear inclusion). Large, dense cytoplasmic granules are keratohyalin granules. **C**. **Virions in nucleolus**: segregation of granular and fibrillar components with accumulation of virions in perinucleolar areas.

Vet-ebooks.com

growth, they increase as the papilloma matures and enhance cell-mediated immunity.

Human Papillomatosis

The common infectious **warts** on the hands of humans (verrucae vulgaris, verruca plana) are caused by **human papilloma virus (HPV)**. HPV is also associated with several less common conditions: (1) **condyloma accuminatum** are large warty lesions of the vulva or penis that are sexually transmitted; (2) **laryngeal papillomas** are also associated with HPV; (3) **epidermodysplasia verruciformis** involves warty papules, plaques, or scaly macules that become progressively generalized; and (4) **squamous cell carcinomas**—the role of HPV in human cancer is clearly established including carcinomas of the uterine cervix, vulva, penis, anus, and tonsil.

Genetic heterogeneity has been demonstrated for HPV strains causing common warts, genital warts, and laryngeal papillomas; that is, implying that different strains are involved in these conditions, and different strains induce papillomas with markedly different rates of virus production. Restriction enzyme analysis has revealed different strains of HPV in human cutaneous warts; HPV-1 and 2 are common. Although viral replication is somewhat sequestered from immune cells and antibody, the host's immune response with time does eliminate the lesion and infection. HPVs that infect the anogenital area can be separated on the basis of their clinical associations into low- and high-risk groups: HPV-6 and 11 are generally associated with benign anogenital warts that infrequently progress to cancer; lesions caused by HPV-16 and 18 have a high incidence of malignant progression, the common manifestation being cervical carcinomas.

HPV encodes 3 late proteins which are produced only in terminally differentiating keratinocytes: two are structural proteins of the virion; the third, E1–E4, causes destruction of the cytokeratin matrix. Accumulation of E1–E4 in cytoplasmic masses within keratinocytes correlates with disappearance of cytokeratins concerned with differentiation; tubulin and actin networks are not affected.

HPVs exert some of their oncogenic effects through binding to cellular proteins. HPV-16 Ey protein, like SV40 large T antigen and adenovirus E1 A, binds to the retinoblastoma tumor suppressor gene product, pRB. The E6 proteins of several HPVs bind to the cellular protein p53. The oncogenic potential of human papillomaviruses is reflected in vitro by their ability to alter the differentiation pattern of keratinocytes. The E6 and E7 genes of HPV-16 are both required for these changes, but appear to transform cells by different mechanisms.[59]

Genital Carcinoma

HPV infection of the uterine cervix is common and 5–10% of infected young women show mild dysplasia of cervical epithelium. Most dysplastic lesions regress but some may progress to cervical carcinoma. HPV particles or structural antigens have been identified in 40–50% of mild dysplasias of the uterine cervix.[60–62] HPV DNA sequences are consistently found by histochemistry in precancerous lesions of the uterine cervix. HPV DNA has also been defined using ultrastructural probes.[63] The combination of molecular hybridization and histologic analysis has shown that there is an association of specific HPV strains with certain lesions: HPV types 6 and 11 are present primarily in benign genital warts (condylomata); HPV-16 occurs almost exclusively in invasive carcinomas and precancerous lesions;[64,65] and HPV-18 occurs in both. Using biotinylated probes to several HPV types on paraffin-embedded sections of anal carcinomas, HPV antigens have been detected. Using in situ hybridization tests, HPV type 16 DNA was found in 82% of positive cases.[66] Types 31, 33, 35, and 51 have been associated with malignant lesions of the anogenital area.

Epidermodysplasia Verruciformis

These lesions are most commonly associated with HPV-3 and 4. They may be localized to the hands or disseminated to the shoulders, head, and limbs. Autoinoculation occurs, and basal and squamous cell carcinomas are complicating lesions. Neither virions nor viral antigens are demonstrable in the neoplastic cells. In familial cases there are lifelong eruptions with malignant transformation in about 25% of patients, usually in sun-exposed areas.

Bovine Cutaneous Fibropapillomatosis

Bovine papillomavirus (BPV) type 1 causes cutaneous fibropapillomatosis of the skin and teats of cattle. Papilloma cells develop at the junction of the spinous and cornified strata, but these swollen cells are not as obvious as in other papillomas, and nuclear inclusions are rare. Proliferating fibroblasts are large and produce moderate amounts of collagen, but they do not contain viral antigens, virions, or other overt evidence of virus.

BPV type 1 causes genital fibropapillomas on the penis of breeding bulls. In situ hybridization of fibropapillomas using an in vitro ^{3}H-labeled BPV-1 DNA probe reveals large amounts of BPV DNA in nuclei in epidermal lesions, indicating that vegetative viral DNA synthesis occurs. Transformed cells are not productively infected with the virus. The viral genome in cells transformed by BPV-1 is extrachromosomal; that

Vet-ebooks.com

is, integration is not necessary for transformation. BPV will induce extensive fibroplasia when placed experimentally in mesenchymal tissues of cattle, horses, or hamsters. When BPV is scarified intradermally in calves, an intense fibroblastic reaction is the earliest manifestation of infection, and if the virus is placed on the bladder mucosa or meninges, fibroblastic proliferation occurs at these sites.[67] In hamsters, nodules of similar tissue develop wherever inoculation has occurred; similar nodules may be found in the lungs.[68]

In horses, BPV is associated with equine sarcoid, a common connective tissue tumor on the legs of the horse. It does not metastasize but recurs readily after excision of the primary lesion. Naturally occurring equine sarcoids contain BPV DNA sequences as assayed by DNA-DNA hybridization.[69] When scarified onto horse skin, BPV reproduces the sarcoid lesions.[70]

Family *Polyomaviridae*

Polyoma virions are 40–55 nm in diameter, lack an envelope, and contain circular double-stranded DNA (Table 13.5). The viral genomes consist of early and late coding regions, and noncoding regulatory regions. The early region encodes DNA binding proteins known as large or small T (tumor) antigens, which bind to the regulatory region of the genome to facilitate the replication of late region viral DNA. Most of these viruses cause tumors when inoculated into hamsters.

Genus *Polyomavirus*

Progressive Multifocal Leukoencephalopathy **Progressive multifocal leukoencephalopathy (PML),** caused by **JC polyomavirus**, is a neurologic disease of human adults afflicted with immunosuppressive,

Table 13.5 Family *Polyomaviridae*.

Virus	*Disease in*	*Reference to ultrastructural pathology*
		Genus *Polyomavirus*
Bovine polyomavirus	Cow	**Nairn**, *Biologicals* 31:303, 2003 (culture contaminant)*
Human polyomavirus (BK)	Human (PML)	**Gardener**, *Lancet* 1:1253, 1971; **Mazlo**, *Acta Neuropathol* 49:133, 1980 (brain)
	Hamster	**Greenlee**, *Lab Invest* 36:636, 1977 (brain)†
Human polyomavirus (JC virus)	Human	**Aksamit**, *J Neuropathol Exp Neurol* 46:556, 1987 (brain biopsy); **Albert**, *Int Arch Allergy Appl Immun* 46:405, 1974; **Padgett**, *Lancet* 1:1257, 1971; **Watanabe**, *Acta Neuropathol* 36:101, 1976 (PML, glia)
	Monkey	**Miller**, *J Virol* 49:848, 1984 (brain); **Nagashima**, *Am J Pathol* 116:455, 1984 (brain)
	Hamster	**Zu Rhein**, *Prog Clin Biol Res* 105:205, 1983;† **Small**, et al. *Proc Nat Acad Sci USA* 83:8288, 1986 (oncogenicity);† **Varakis**, *Acta Neuropathol* 35:243, 1976 (pinealoma)†
Macaque polyomavirus	Monkey	**Gribble**, *Nature* 254:602, 1975 (PML); **Reissig**, *Infect Immun* 14:225, 1976 (stumptailed macaque virus); **Shah**, *Science* 195:404, 1977 (congenital transmission)
Simian virus 40	Monkey	**Granboulan**, *J Cell Biol* 17:423, 1963
	Human	**Weiss**, *Acta Neuropathol* 34:171, 1976 (meningioma)
	Mastomys	**Rabson**, *J Nat Cancer Inst* 29:765, 1962
	Mouse	**Biczyska**, *J Nat Cancer Inst* 51:1945, 1973 (embryo)
	Experimental	**Kartenbeck**, *J Cell Biol* 109:2721, 1989 (endocytosis)
Polyoma muris **(murine pneumotropic virus, K virus)**	Mouse	**Baron-Van Evercooren**, *Lab Invest* 66:39, 1992 (astrocytes); **Compans**, *J Exp Med* 126:267, 1967;* **Jordan**, *Exp Molec Pathol* 11:1, 1969 (lung); **MacKay**, *J Virol* 19:620, 1976; **Margolis**, *Am Rev Resp Dis* 114:45, 1976 (pulmonary endothelium); **Szomolanyi-Tsuda**, *Am J Pathol* 144:559, 1994 (myeloproliferative disease, SCID mouse)
Rabbit kidney vacuolating virus	Rabbit	
Hamster polyomavirus	Hamster	**Foster**, *Vet Rec* 151:13, 2002
Budgerigar fledgling disease polyomavirus	Parakeet	**Lehn**, *Virology* 151:362, 1986

*Studies in vitro.
†Animal model.

Vet-ebooks.com

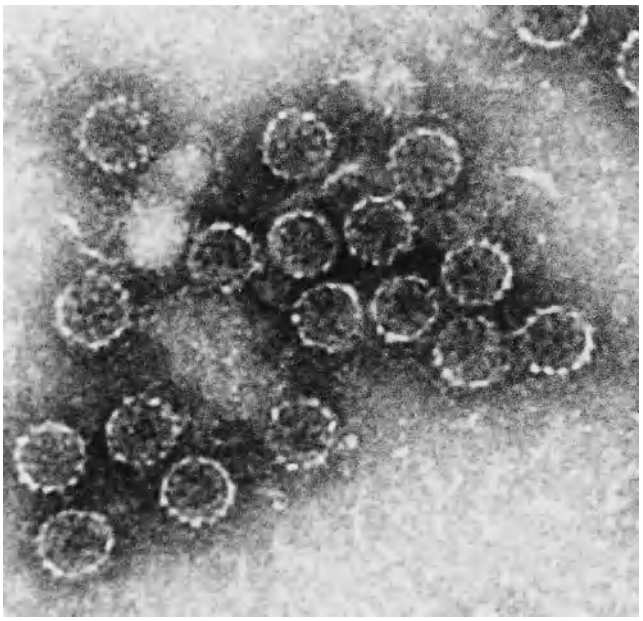


Fig. 13.16 Human polyomavirus. Negative stain of virions isolated from human patient with progressive multifocal leukoencephalopathy. (Micrograph: Gabrielle M. Zu Rhein, *Acta Neuropathol* 8:57, 1967.)

systemic, malignant disease.[71] Brain lesions are associated with a polyomavirus that develops in the late stages of profound immunosuppression. In an analysis of 93 AIDS patients, 27 had evidence of viral encephalitis and 3 of these had PML lesions. It was proposed that the papova virions not only damaged oligodendroglia but enhanced AIDS lesions by attracting HIV-infected monocytes to the brain.[72] The focal lesions of PML are characterized by degenerate oligodendroglia and immense cells with pleomorphic, hyperchromatic nuclei which closely resemble malignant astrocytes. PML virions are demonstrable ultrastructurally in nuclei and are seen almost exclusively in oligodendrogliocytes. Virions are pleomorphic and filamentous forms have been reported (Fig. 13.16).

The JC polyomavirus produces a high rate of unapparent infection and over 60% of children less than 16 years have serologic evidence of infection in some areas. JC virus produces sarcomas after subcutaneous inoculation, and medulloblastomas, glioblastomas and pinealomas on intracerebral inoculation. **Brain tumors** are produced in monkeys with human JC polyomavirus.[73] In one study, JC, BK, and SV40 viruses were inoculated intracerebrally in owl monkeys to produce PML. Held for months, none developed PML, but glial tumors were present in about 25% of monkeys inoculated with JC virus (but not the other viruses). The JC virus genome is present in tumor tissue.

Polyoma BK Viral Disease **Polyoma BK virus** (first isolated from urine) has antigenic characteristics distinct from JC virus and from SV40. BK virus causes hemorrhagic cystitis and nephritis in renal transplant patients and other immunosuppressed patients.[74] In hamsters, BK virus causes malignant islet-cell tumors of the pancreas; tumor cells are poorly granulated and involve all four islet cell types. BK is less oncogenic in hamsters than polyomas JC, although choroid plexus tumors have been induced.

Cynomolgus Polyomavirus **Cynomolgus polyomavirus** has been found in 12 of 57 cynomolgus monkeys after immunosuppression. The virus caused interstitial nephritis in six renal allografts. Lesions were tubulointerstitial nephritis with nuclear inclusions, apoptosis, and progressive destruction of collecting ducts, and were similar to those caused by BK polyoma virus in renal failure of humans.[75]

Mouse Polyoma Disease *Polyoma muris* exists as latent infection in wild and laboratory mice but is not associated with naturally occurring disease. Disease can be produced with large amounts of virus in neonatal mice or in mice which are immunologically deficient. In young mice, one of three possible results is obtained: immunity with or without latent infection, acute fatal polyoma disease, or chronic disease with tumor formation. Mice with experimentally induced fatal disease show viral antigens in the kidney, salivary glands, thyroid and other viscera. Polyomavirus muris produces tumors only under very specific circumstances: it must be inoculated into newborn mice during the first 24–48 hr of extrauterine life. Carcinomas or sarcomas that develop in mice inoculated with polyomavirus occur in salivary glands, kidney, and thymus.

Simian Polyoma **Simian virus 40** (simian vacuolating agent 40, SV40) was first isolated from cultures of monkey kidney cells and, later, from both live and inactivated polio cell culture vaccines to which millions of people had been exposed. Melnick demonstrated in 1964 that after ingestion of live vaccine, children had excreted SV40 virus in their feces for as long as 5 wk after vaccination. SV40 has been reported in rhesus monkeys with simian AIDS (SAIDS). Large nuclear inclusions contained polyoma virions and were found in renal tubular epithelium and oligodendrogliocytes in the brain.[76] Areas of inflammation and demyelination in the brain contained $CD8^+$ lymphocytes and numerous gemistocytic astrocytes that labeled for glial fibrillary acidic protein. When SV40 is inoculated into newborn hamsters, it produces fibrosarcomas and ependymomas.[77] Implantation of cells that have been transformed in culture induces a wide variety of tumors in the hamsters and the nude mice.[78] Early mouse embryos infected with SV40 and

Vet-ebooks.com

polyoma exhibit replication of the viruses in endodermal cells, yolk sac cells, and blood islands. Newly synthesized virus is taken up by the neural tube.

Mouse Pneumonitis **Mouse pneumonitis virus** (Murine pneumotropic virus, K virus) causes fatal interstitial pneumonitis in suckling mice, but no disease results from inoculation of older mice or other rodents. Nuclei of infected pulmonary endothelial cells contain large numbers of virions. The disease is systemic, and virions are also present in macrophages of the spleen and lungs and in Kupffer cells of the liver. Large membrane-bound aggregates of virions develop in the cytoplasm. Virus replicates exclusively in pulmonary endothelium, indicating a need for an oxygen-rich environment, although increasing oxygen tension does not influence viral replication.

Family *Parvoviridae*

Parvoviruses are 18–26 nm in diameter, nonenveloped, and have icosahedral symmetry. The small single-stranded DNA genome of the parvoviruses requires that many cellular functions be involved in the replication cycle. Active cellular DNA synthesis is required before replication can occur, and these viruses have affinity for dividing cells; thus they are especially tropic for tissues of fetal and neonatal animals. Rapidly dividing cells of the bone marrow, intestine, and placenta are markedly susceptible to parvoviruses, and most parvoviruses are associated with enteritis, leukopenia, and fetal defects (Table 13.6).

Parvoviruses cause infected cells to become ballooned by acute cell swelling. Virions develop in nuclei and capsid proteins are formed at different sites.

Table 13.6 *Parvoviridae*.

Virus	*Disease in*	*Reference to ultrastructural pathology*
		Subfamily *Parvovirinae*
		Genus *Parvovirus*
Canine parvovirus	Dog	**Hayes**, *J Am Vet Med Ass* 174:1197, 1979; **Matsui**, *Vet Pathol* 30:303, 1993
Feline panleukopenia virus	Cat	**Herndon**, *J Neuropathol Exp Neurol* 30:196, 1971 (fetal cerebellum); **Kilham**, *Lab Invest* 17:465, 1967
	Ferret	**Kilham**, *Lab Invest* 17:465, 1967
Mink enteritis virus	Mink	**Krunajevic**, *Acta Vet Scand* (Suppl) 30:1, 1970†
Lapine parvovirus	Rabbit	**Alexandrov**, *Arch Virol* 127:355, 1992
Porcine parvovirus	Swine	**Cutlip**, *Am J Vet Res* 36:1751, 1975; **Joo**, *J Comp Pathol* 87:383, 1977; **Mengeling**, *Am J Vet Res* 37:1393, 1976 (genital)
Rat parvovirus	Rat	**Baringer**, *Lab Invest* 27:514, 1972 (hemorrhagic encephalopathy); **Kilham**, *Am J Pathol* 49:457, 1966; **Ruffolo**, *Am J Pathol* 49:795, 1966 (hepatitis)
	Cat	**Kilham**, *Science* 148:244, 1965
	Hamster	**Lipton**, *Lab Invest* 27:508, 1972
		Genus *Erythrovirus*
Human parvovirus B19	Human	**Al-Lami**, *J Gen Virol* 5:485, 1969 (H-1 virus); **Anderson**, *J Infect Dis* 152:257, 1985; **Brown**, *Lancet* 2:1033, 1984 (uterus); **Caul**, *J Med Virol* 24:55, 1988 (uterus); **Ozawa**, *Science* 233:883, 1986*
		Genus *Bocavirus*
Human bocavirus	Human	**Brieu**, *J Clin Microbiol* 45:3419, 2007
		Genus *Dependovirus*
Adeno-associated virus, mammalian	Many	**Walters**, *J Virol* 78:361, 2004
Avian adeno-associated virus	Chicken	**Yates**, *Infect Immun* 7:973, 1973
	Goose	**Brown**, *Virology* 210:283, 1995
Bovine parvovirus	Cow	**Durham**, *Res Vet Sci* 38:209, 1985
		Genus *Amdovirus*
Aleutian mink disease virus	Mink	**Bloom**, *J Virol* 75:1116, 2001

*Studies in vitro.
†Animal model.

Vet-ebooks.com

Ultrastructurally, nuclear changes include nucleolar enlargement and disintegration, lysis of chromatin, aggregation of proteins into small granules, and large nuclear inclusion bodies (Fig. 13.17). Chromatin in nucleolar fibrous centers is condensed, converting these centers into vacuoles. The first inclusions to develop are pale and lightly eosinophilic. Large numbers of virions constitute most inclusions and virions may occur in lattice arrangements. Advanced inclusions are dense, basophilic, and stain intensely by immunofluorescence techniques. Inclusions usually are not present in late stages of disease; markedly enlarged nucleoli, which are evidence of repair of epithelial cells, may be mistaken for viral inclusions. As affected cells desquamate or are lysed, the nuclear inclusions disappear and are usually not present when the host dies.

Genus *Parvovirus*

Feline Panleukopenia **Feline panleukopenia**, a highly contagious, fatal, systemic disease of domestic cats and other Felidae, runs a rapid course marked by diarrhea, vomiting, and severe dehydration. Leukopenia is severe and involves all white blood cells (panleukopenia). Neutrophils are most rapidly destroyed. Anemia may be masked by the hemoconcentration, which is a manifestation of dehydration. Specific pathogen-free cats infected with FP virus develop profound leukopenia, but do not die as field cats do.

The tropism for highly mitotic cells leads to effects of FP virus for cells of the bone marrow, lymphoid tissue, and epithelium of the intestine. Bone marrow, as in irradiation toxicity, is largely devoid of cells in severe cases. Destruction and atrophy of the thymus is striking as lymphocytes in critical areas are destroyed and replaced by reticular cells. Thymic corpuscles enlarge and are filled with macrophages, cell debris, keratin, and deposits of calcium. Nuclear inclusions are common in reticular cells by do not occur in degenerate lymphocytes.

In intestine, FP virus replicates in epithelial cells. Crypts are lined by shrunken, thin, degenerate epithelium dilate and become filled with mucopurulent exudate, cell debris, and erythrocytes.[79] These "crypt abscessing" lesions are characteristic of large segments of the ileum. Large, irregular, pleomorphic, hyperplastic crypt cells are the rule as the intestinal epithelium begins to recover in the late stages of disease. The immense nucleoli of these cells can be mistaken for nuclear inclusions.

Infection of the central nervous system of the fetus (or very young kitten) results in **cerebellar hypoplasia** and ataxia in the neonate. The actively mitotic cells of the external germinal layer of the cerebellum are specifically attached by the virus, and they fail to migrate to form the definitive internal granular layer. Ultrastructural analysis of the organization of cerebellar glomeruli in the granuloprival cerebellum of infected ferrets revealed a marked depletion of granule cell dendrites and decrease in the number of mossy-fiber granule dendrite and Golgi axon-granule dendrite synapses.

Canine Paroviral Enteritis **Canine parvoviral enteritis** was described in 1978 as the cause of two syndromes: myocarditis and enteritis. In the **intestine**, virions replicate in enterocytes, leading to degeneration and necrosis of cells at the tips of villi. In the **heart**, nuclear inclusions develop in myocytes and are specifically labeled by anti–canine parvovirus antibodies. Parvovirus virions have been demonstrated ultrastructurally in the inclusions.[80] Since 1978, the virus has been widely disseminated and is now found worldwide. Viruses circulating after 1980 differ from those of 1978 and appear to have been derived from a variant virus that replaced the original strain. Five-day-old pups infected experimentally with canine parvovirus develop myocarditis even though infection may be clinically inapparent. Myocardial lesions at periods after inoculation are as follows: 23 hours, myocyte degeneration and nuclear inclusions; 51 hours, heavy lymphocytic infiltrates; and 108 hours, fibrosis with regressed inflammatory lesions. Ultrastructural analysis has revealed virions within cardiac myofibers in association with myocarditis.[81]

Genus *Erythrovirus*

Human parvovirus was discovered in the sera of normal blood donors and subsequently shown to be the causal virus of a transient febrile disease involving **bone marrow aplasia** and hemolysis, of the common childhood exanthem called **fifth disease**, and of a **polyarthralgia syndrome** of adults. Childhood infections involve fever, maculopapular rash, and erythema of the cheeks, the "slapped cheek syndrome." There are transient anemia and bone marrow hypoplasia. In bone marrow, the effect is on erythropoetic stem cells; there is little or no effect on myelopoiesis.[82] Human parvoviral virions develop in crystalline lattices and have been found in ultrastructural studies of erythroid progenitor cells from human bone marrow; erythrocyte precursors have nuclear inclusions.[83] Infections during pregnancy may allow passage of virus across the placenta and infection of the fetus. Abortion and hydrops fetalis have been reported. Human parvovirus B19 causes abortion, stillbirth and hydrops fetalis. Transplacental infection in hydrops fetalis occurs with virion in nuclei of erythropoietic cells.[84] B19 has a unique tropism for the differentiated human erythroid progentor cell, the P antigen (globoside) of which is the receptor for the virion.

Vet-ebooks.com

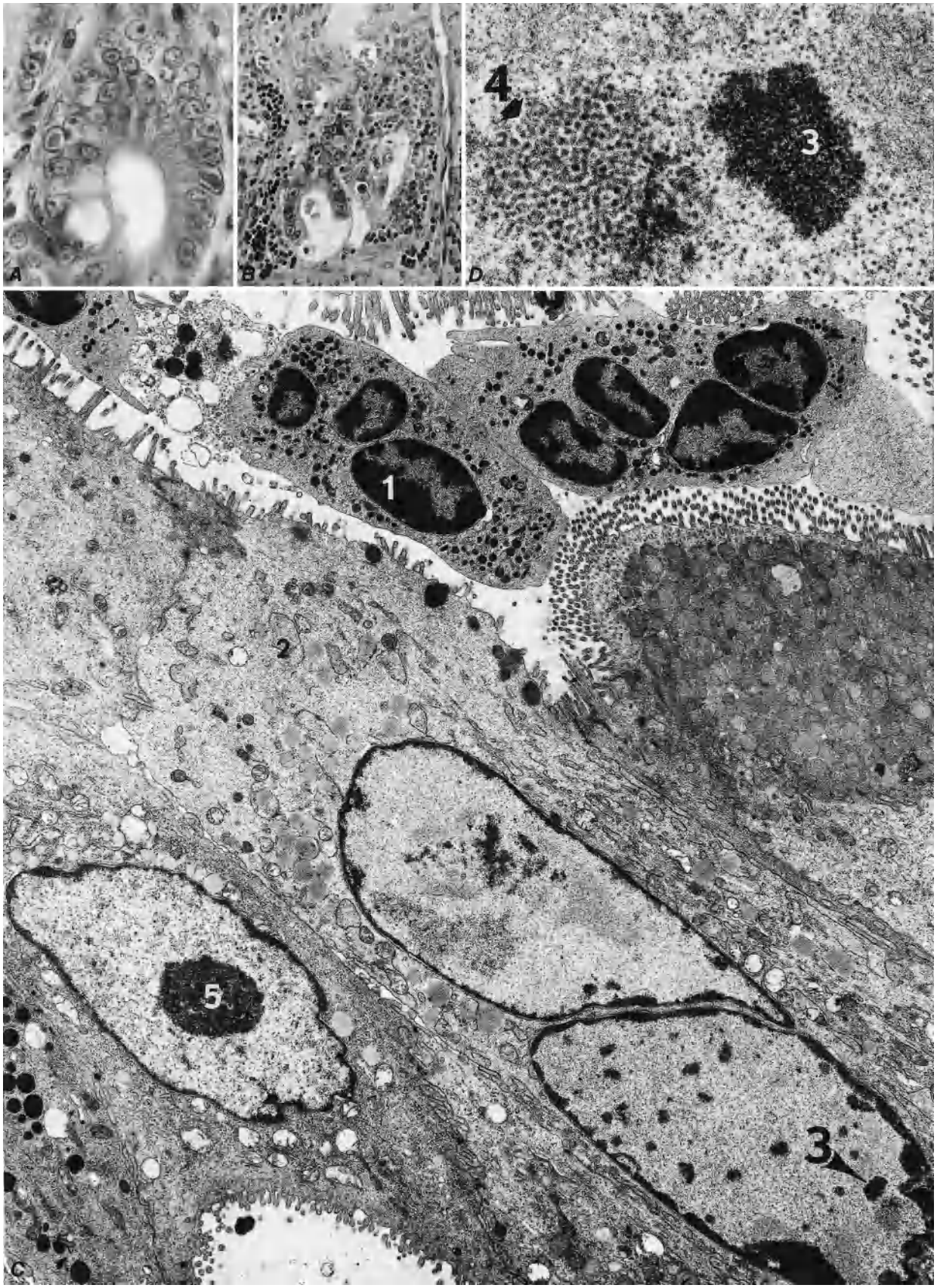


Fig. 13.17 Cytopathology of parvovirus infection. **A–B**. **Feline panleukopenia**: intestine, cat. **A**. **Nuclear inclusions** in swollen crypt cells, small intestine, early phase of infection. **B**. **Epithelial cell necrosis** and sloughing, late phase of infection; epithelium contains large nucleoli but no inclusions. **C–D**. **Mink enteritis**. **C**. **Nuclear inclusions**: neutrophils in intestinal lumen (*1*); degenerate mucous cell (*2*); nuclei of swollen crypt cells contain segregated nucleoli with virions associated with some remnants (*3*); and regenerating epithelial cells with large nucleolus (*5*). **D**. **Nucleolar remnant** (*3*) and virions (*4*).

Vet-ebooks.com

Table 13.7 Pathogens of the families *Iridoviridae* and *Asfarviridae*.

Virus	*Disease in*	*Reference to ultrastructural pathology*
		Family *Iridoviridae*
		Genus *Ranavirus*
Frog virus 3	Frog	**Darlington**, *Virology* 29:149, 1966 (renal carcinoma); **Lunger**, *Virology* 30:116, 1966 (virions); **Murti**, *Curr Topics Microbiol Immunol* 116:107, 1985 (cytoskeleton); **Tripier**, *J Ultrastruct Res* 56:249, 1976
Salamander iridovirus	Salamander	**Bollinger**, *J Wildlife Dis* 35:413, 1999; **Docherty**, *J Wildlife Dis* 39:556, 2003
Tadpole edema virus	Frog	**Wolf**, *J Infect Dis* 118:253, 1968
Iridovirus of *Bufo* spp.	Toads	**Speare**, *J Wildlife Dis* 27:457, 1991
Snake erythrocyte virus	Snake	**Smith**, *J Wildlife Dis* 30:169, 1994
		Family *Iridoviridae*
		Genus *Lymphocystivirus*¤
Lymphocystis disease virus	Fish	**Dunbar**, *J Infect Dis* 116:466, 1966 (bluegill);† **Howse**, *Virology* 44:211, 1971; **Walker**, *Ann N Y Acad Sci* 126:375, 1965
Japanese flounder lymphocystivirus	Flounder	**Kitamura**, *J Microbiol* 44:248, 2006
		Family *Iridoviridae*§
		Genus *Megalocystis*
Sea bass iridovirus#	Fish	**Mahardika**, *Dis Aquat Org* 79:163, 2008#
Turbot iridovirus¶	Turbot	**Kim,** *Dis Aquat Organ* 18:175, 2005
Epizootic haematopoietic necrosis virus	Fish	**Eaton**, *J Fish Dis* 14:157, 1991
Iridovirus of fish	Fish	**Fraser**, *J Vet Diagn Invest* 5:120, 1993 (gouramis)
		Family *Asfarviridae*
African swine fever	Pig	**Fernandez**, *Am J Vet Res* 53:1462, 1992; **Krauthausen**, *Dtsch Tierarztl Wschr* 99:49, 1992 (intestine); **Quintero**, *Am J Vet Res* 47:1125, 1986 (erythrocytes); **Wardley**, *Arch Virol* 55:327, 1977 (blood)
	Experimental	**Almeida**, *Arch Ges Virusforsch* 20:392, 1967;* **Breese,** *Virology* 31:508, 1967 (virions);* **Breese**, *Am J Pathol* 55:69, 1969*

*In vitro study.
†Experimental model.
¤**Lymphocystiviruses** have been divided into three genotypes: I, LCDV-1; II, Japanese flounder isolates; and III, rockfish isolates.
§*The family* ***Iridoviridae*** contains pathogens of insects and nematodes (see: Hess RT, Poinar GO. 1985. Iridoviruses infecting terrestrial isopods and nematodes. *Curr Topics Microbiol Immunol* 116:49).
#The family ***Iridoviridae***, genus *Megalocystivirus* includes fish viruses that are genetically similar: grouper sleepy disease iridovirus, African lampeye iridovirus, dwarf gouramii iridovirus, Taiwan grouper iridovirus, infectious spleen and kidney necrosis iridovirus, and others.
¶A genus *Tropivirus* has been proposed to include many of these as well as turbot iridovirus, sea bass iridovirus, and red sea bream iridovirus.

Nonhuman primates may carry parvoviruses that are markedly similar to human parvovirus B19, and which are also associated with anemia. Monkeys with severe anemia have nuclear inclusions in cells of the bone marrow that contain viral arrays of parvoviruses.[85]

Genus *Dependovirus*

Adeno-associated viruses (AAVs) are defective parvoviruses not associated with disease. Their progeny virus is produced only in cells coinfected with helper adenoviruses. Mature virions contain either positive or negative DNA strands. All AAVs share a common antigen. AAVs lack an early protein that is replaced by factors induced by the adenoviral infection. Mature virions contain either positive or negative DNA strands. All share a common antigen. In infected cells, AAVs appear as tiny virions, individually or in clusters that resemble other parvoviruses.

Genus *Amdovirus*

Aleutian mink disease virus infection in newborn mink kits results in acute disease with viral replication in type II pneumoncytes. Infection of adult Aleutian mink results in chronic disease known as Aleutian disease; there is viral replication in lymph node

Vet-ebooks.com

macrophages and persistent infection, hypergammaglobulinemia, and immune complex-mediated renal and arterial lesions.[86] Chronically infected mink die of terminal glomerulonephritis after a subclinical course of disease lasting several months or years. Viral proteins are degraded during infection, and many of them are involved in immune-complex development.

Family *Iridoviridae*

Iridoviruses are icosahedral, enveloped, DNA viruses that develop in the cytoplasm. They are the largest of the isometric viruses, with diameters from 160 to 350 nm. The genera found in vertebrates are associated with diverse diseases (Table 13.7). On cross section, iridoviruses have distinctive shapes but cytopathic changes in various iridoviral diseases do not resemble each other and there is no common basis in their manner of cell damage.

Genus *Ranavirus*

Tadpole edema virus is the cause of a fatal systemic disease of tadpoles with hemorrhage and necrosis in the kidney and stomach. **Frog virus 3** and the other frog cytoplasmic ranaviruses were isolated during experiments on the frog renal adenocarcinoma but are not associated with naturally occurring disease in frogs. Inoculated into rats and mice at high doses, frog virus 3 produces a rapidly fatal liver necrosis. Endothelial and Kupffer cell degeneration precedes that of hepatocytes and the mechanism appears to be viral toxicity.[87,88]

Genus *Lymphocystivirus*

Piscine iridoviruses are causal agents of serious systemic disease and have been identified in over 20 species of fish.[89] **Lymphocystis disease** is a common viral infection of bony fishes leading to large fleshy growths in connective tissue of muscle and subcutis. The virus induces fibroblasts to enlarge enormously. The striking characteristics of the lymphocystis cell are extreme cytomegaly, cytoplasmic basophilia, and large Fuelgen-staining (for DNA) cytoplasmic inclusion bodies. Ultrastructurally, cells contain enveloped hexagonal virions. An acidic mucopolysaccharide capsule that stains with the PAS technique develops around lymphocystis cells. When fish are experimentally infected, growths appear in 10–12 days and are associated with increasing amounts of infectious virus. Lesions persist for several weeks and regress when lymphocystis cells degenerate.

Family *Asfarviridae*

African swine fever virus was previously listed as a member of the family I*ridoviridae*. The new family name was derived from **A**frican **s**wine **f**ever **a**nd **r**elated viruses. Virions (200–300 nm in diameter) consist of an envelope, a capsid, and a nucleoprotein complex. Capsid/nucleoprotein exhibits icosahedral symmetry and has a diameter of 170–190 nm (Fig. 13.18).

Genus *Asfavirus*

African Swine Fever **African swine fever (ASF)** is a severe, systemic, febrile disease. There is marked edema, inflammation, and necrosis of lymphoid and vascular tissues. Virus initially infects the tonsils and pharyngeal lymph nodes, then spreads through regional lymphatics and into the vascular system. ASF virus infects monocytes and macrophages which transports virus throughout the pig. Virions are found in the cytoplasm of macrophages, including pulmonary intravascular macrophages.[90] The characteristic virus is enveloped by a two-membrane structure derived from the endoplasmic reticulum.[91] On exit from the cell, ASF virus induces filopodia-like projections of the plasma membrane directly beneath the virion.[92] Destruction of blood vessels is responsible for severe edema, hemorrhage, and infarction. Endothelial vacuolation and necrosis are prominent, and there is fibrin within vascular lumens. Virions can readily

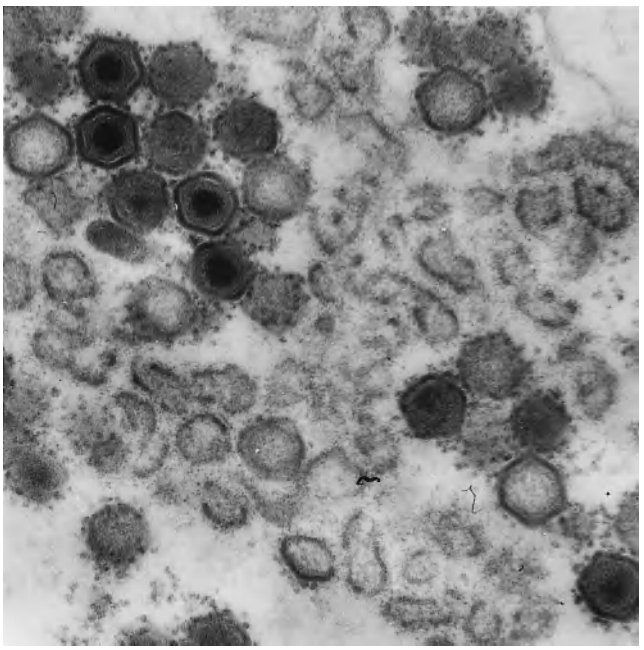


Fig. 13.18 **Asfarvirus**: African swine fever virus, cell culture. (Micrograph: Sydney Breese, *Am J Pathol* 55:69, 1969.)

Vet-ebooks.com

be found in the lumens of capillaries, often in groups associated with erythrocyte and endothelial surfaces; they also have been seen in intraerythrocytic vacuoles.[93]

Family *Hepadnaviridae*

These small (40–48 nm) enveloped, hepatotropic DNA viruses have an icosahedral nucleocapsid 30–35 nm in diameter. The coat of the virion is composed of S-, M-, and L-proteins. Hepadnaviruses cause acute and chronic liver disease and have been reported from man, woodchucks, ground squirrels, and ducks (Table 13.8). Their replication cycle involves open circular RNA genomes produced by reverse transcription of RNA intermediates. Hepadnaviruses share several biologic characteristics: frequent persistent infection, high concentrations of incomplete viral particles (as surface antigens) in the blood, and an association with hepatocellular carcinoma.

Genus *Orthohepadnavirus*

Hepatitis B **Hepatitis B virus (HBV)** of humans is the prototype virus of the Hepadnaviridae. Virions are demonstrable in hepatocytes and in serum. The virion contains an envelope (HBsAg) 7 nm wide, a nucleocapsid or inner core of 27 nm diameter (HBcAg/HBeAg), and an internal genome containing a DNA polymerase. Hepatocyte injury occurs as a consequence of free, episomal viral replication and the virus is either eliminated or integrated into the genome.

In affected hepatocytes, HBV virions and HBV-associated antigen have been identified by electron microscopy. Small (20–28 nm) nucleocapsids in the hepatocyte nucleus represent the viral core; they can fill the nuclear matrix to form a clear, ground glass inclusion (Fig. 13.19). The HBc antigen, produced on cytoplasmic ribosomes, migrates into the nucleus via nuclear pores and is assembled into core particles.[94,95] In infected humans, 16–25 mm spheres and filaments which are nucleic acid-free **defective particles** (with excess viral coat protein) accumulate in large concentrations (up to 10^{14} particles/ml blood). Although viral components are typically found in plasma, in some patients they occur in mononuclear and polymorphonuclear leukocytes.

HBV causes a spectrum of acute disease ranging from inapparent infection to fatal hepatocellular necrosis. About 10 % of acutely infected patients continue to carry the virus, half of which are healthy carriers. Those with severe liver disease typically progress to cirrhosis, and after 30 years or more, to primary

Table 13.8 Family *Hepadnaviridae*.

Virus	*Disease in*	*Reference to ultrastructural pathology*
		Genus *Orthohepadnavirus*
Hepatitis B virus	Humans	**Aoki**, *Lab Invest* 47:465, 1982 (virion);* **Bernauau**, *Lab Invest* 51:667, 1984 (macrophages); **Bianchi**, *Lab Invest* 35:1 1976 (nuclear inclusions); **Blum**, *Proc Natl Acad Sci USA* 80:6685, 1983 (DNA); **Dienes**, *Gastroenterology* 98:1017, 1990; **Gerber**, *Lab Invest* 52:572, 1985; **Huang**, *Lab Invest* 40:1, 1979 (viral antigen); **Roingeard**, *Hepatology* 11:277, 1990 (HBV antigen); **Sakamoto**, *Lab Invest* 48:678, 1983 (virions); **Si**, *Lab Invest* 50:341, 1984 (liver allografts); **Stein**, *Lab Invest* 26:262, 1972 (virions); **Weiss**, *Am J Med* 64:269, 1978 (skin); **Yamada**, *Hepatology* 12:133, 1990 (HbeAg)
	Chimpanzee	**Thung**, *Am J Pathol* 105:328, 1981†
	Mouse	**Schaff**, *Virch Arch B* 40:249, 1982;† **Summers**, *Hepatology* 1:179, 1981†
Prairie dog virus	Prairie dog	**Une**, *J Vet Med Sci* 58:933, 1996 (carcinoma)
Ground squirrel hepatitis virus	Ground squirrel	**Marian**, *Proc Natl Acad Sci USA* 83:4543, 1986; **Ranck**, *Vet Pathol* 45:388, 2008 (Harderian gland carcinoma)
Woodchuck hepatitis virus	Woodchuck	**Frommel**, Am J Pathol 115:125, 1984 (immunopathology); **Peters**, *Am J Pathol* 141:143, 1992 (kidney); **Ponzetto**, *J Virol* 52:70, 1984 (core antigen); **Popper**, *Proc Natl Acad Sci USA* 84:866, 1987 (carcinogenicity)
Woolly monkey hepatitis B virus	Woolly monkey	Lanford, *J Virol* 77:7814, 2003
		Genus *Avihepadnavirus*
Duck hepatitis B virus	Duck	**Halpern**, *Virus Res* 1:213, 1984; **Marion**, *Proc Natl Acad Sci USA* 81:898, 1984; **Yokosuka**, *Proc Natl Acad Sci USA* 82:5180, 1985
Heron hepatitis B virus	Heron	**Lin**, *J Gen Virol* 86:1335, 2005

*Studies in vitro.
†Animal model.

Vet-ebooks.com

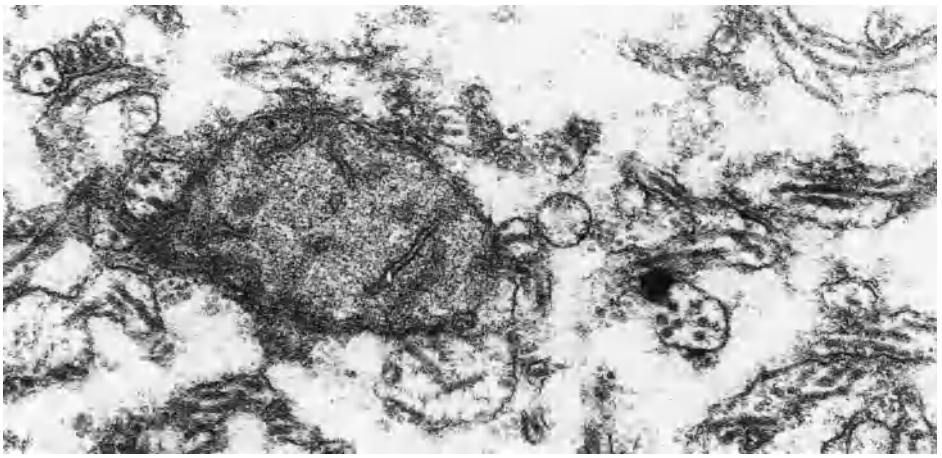


Fig. 13.19 Hepadnavirus: human hepatitis B, hepatocyte. Spherical and filamentous HBsAg particles, 20 nm in diameter, in dilated smooth endoplasmic reticulum. (Micrograph: Michael Gerber, *Lab Invest* 52:572, 1985.)

hepatocellular carcinoma. Skin rashes in which HBsAg can be localized have been reported in 5% of patients with hepatitis.

For attachment and penetration of the hepatocyte, HBV uses specific membrane receptors and passes the host cell membrane by endocytosis with fusion of virion with host membrane. Although infecting genomes are converted in the nucleus to double-stranded "proviral" DNA, most of the viral replication occurs in the cytoplasm. Core particles migrate from nucleus to cytoplasm through nuclear pores and protruding into the cisternae of the endoplasmic reticulum. HBV carries receptors for polymerized human serum albumin (polyalbumin) (there are also similar receptors on hepatocytes and albumin polymerizes on aging and is removed by liver cells).

Normal donor livers transplanted into patient with HBV-induced liver failure commonly develop severe HBV infection with massive nuclear HBV core antigen (HBcAg) and cytoplasmic HBV surface antigen (HBsAg). Ultrastructural analyses of these lesions estimate that there may be as much as 10^{18} HBV core particles in the liver.[96]

HBV-Associated Carcinoma HBV is causally related to hepatocellular carcinoma (HCC) of humans. There is a correlation to the presence of HBV carriers and the incidence of HCC. HBV antigens have been demonstrated in tumor cells and cultured cells derived from HCC, and integration of HBV DNA into the genome of HCC cells has been established. Carcinoma cells obtained from viral carriers contain viral DNA integrations and a large genomic DNA deletion is associated with HBV integration.[97,98]

Woodchuck Hepatitis **Woodchuck hepatitis virus** infection leads to mild transient hepatitis, or to severe chronic persistent hepatitis and an extraordinary high rate (up to one-third) of hepatocellular carcinoma. The woodchuck hepatitis virus primarily infects hepatocytes, but lymphoid cells are important in maintaining chronic infection and serve as reservoirs of latent viruses. Peripheral blood lymphocytes, in chronic infection, carry nonreplicateing hepadnaviral DNA and treatment of these lymphocytes in vitro with LPS has been shown to activate the lymphocyte to produce core particles and virions.[99] Like chronic hepatitis B virus infection in humans, woodchuck hepatitis has an association with membranous glomerulonephritis. Lesions appear as thickening of capillary loop basement membranes with subepithelial electron-dense deposits. Woodchuck hepatitis core antigen (WHcAg) has been detected along capillary loops in affected glomeruli. Immune-mediated glomerular lesions are rare, occurring in only 6 of 705 necropsies of woodchucks.[100]

Genus *Avihepadnavirus*

Duck Hepatitis **Duck hepatitis virus (DHV)** occurs sporadically and is responsible for high mortality in newly hatched Pekin ducklings. In the United States up to 10% of Pekin ducks are persistently infected with DHV; in China, nearly half the ducks carry DHV. Ducks with chronic infection occasionally develop cirrhosis and hepatocellular carcinoma. Integration of DHV DNA into hepatocellular carcinoma cells has been established. Unlike HBV, core and surface antigens of the duck and woodchuck hepatitis viruses are seen only in the hepatocyte cytoplasm with immunofluorescence studies. Replication-specific forms of viral DNA have been shown in liver, and also in kidney and pancreas (both acinar and islet cells).[101,102]

Family *Circoviridae*

The circoviruses are very small nonenveloped icosahedral viruses with single-stranded circular DNA genomes. The family includes several viruses that are

Vet-ebooks.com

pathogenic for birds, the **psittacine beak and feather disease, pigeon circovirus**, and **chick anemia viruses**.[102] The last two viruses cause lymphoid necrosis and atrophy of the thymus and bursae. A **porcine circovirus** has been associated with post weaning multisystemic wasting syndrome.[103]

Psittacine beak and feather disease has been isolated from feather follicle tracts of birds. It is icosahedral, nonenveloped, and 17–24 nm in diameter. Histopathologic section of lesions in feathers and follicular epithelium reveals nuclear and cytoplasmic basophilic inclusions. Ultrastructural analysis shows that crystalline arrays of virions are present in nuclei of feather epithelial cells and cytoplasmic inclusions are found in macrophages (Fig. 13.20). Virions stain specifically by immunogold techniques.[104]

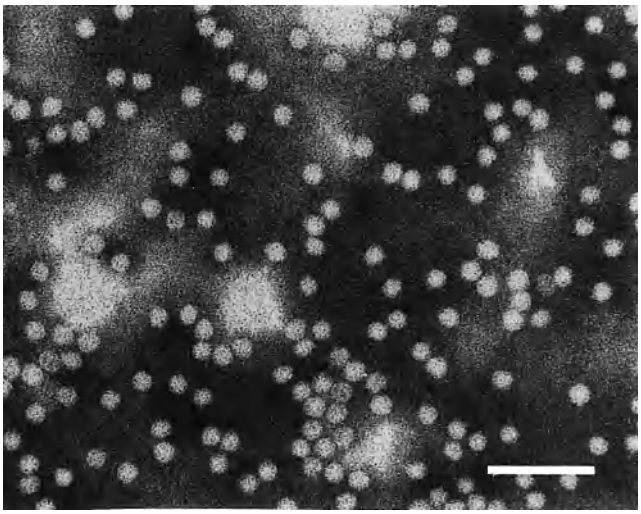


Fig. 13.20 **Circovirus**: psittacine beak and feather disease virus. Virions recovered from diseased cutaneous tissue, negatively stained with phosphotungstic acid. Bar = 0.1 µm. (Micrograph: K. S. Latimer, *Vet Pathol* 28:300, 1991.)

Family *Orthomyxoviridae*

Genera *Influenza virus A, B,* and *C*

Influenza **Influenza viruses** occur in birds, and in at least five species of mammals: swine, horses, seals, dogs, and humans (Table 13.9). All produce disease by destroying epithelial cells of the respiratory tract. Soon after initial foci of infection begins in epithelia of the nasal turbinates, virus spreads to involve the entire upper respiratory tract. An acute, intense, inflammatory response (rhinitis, tracheitis, and pneumonitis) is accompanied by coughing, fever, myalgia, and respiratory distress. In the lung, epithelium of the terminal bronchioles is especially vulnerable to infection. Affected epithelial cells swell and develop cytoplasmic basophilia. Disease results from destruction of bronchiolar tissue and from the massive, aberrant production and release of proinflammatory cytokines and chemokines.[105] These lead to the destructive upregulation of TRAIL (one of many death receptor ligands), apoptosis, and the reduced cytotoxicity of $CD8^+$ lymphocytes.

Upper respiratory infection is initiated by attachment of influenza virions to plasma membranes of

Table 13.9 *Orthomyxoviridae*.

Virus	*Disease in*	*Reference to ultrastructural pathology*
		Genera *Influenzavirus A/B/C*
Influenza A virus	Avian	**Blaskovic**, *Arch Ges Virusforsch* 38:250, 1972 (embryo); **Narayan**, *J Comp Pathol* 82:139, 1972 (turkey brain); **Rouse**, *J Comp Pathol* 78:525, 1968 (turkey); **Sterz**, *Ztbl Vet Med* 20:613, 1973(thrombocytes, chicken)
	Cat	**Kuiken**, *Science* 306:241, 2004 (avian); **Songserm**, *Emerg Infect Dis* 12:681, 2006 (avian)
	Dog	**Songserm**, *Emerg Infect Dis* 12:1744, 2006 (avian)
	Equine	**Van Maanen**, *Vet Q* 24:79, 2002
	Ferret†	**Rushton**, *J Pathol* 140:181, 1983 (fetus); **Tom**, *Br J Exp Pathol* 58:444, 1977 (nose)
	Human	**Jakab**, *Am Rev Resp Dis* 128:730, 1983 (lung)
	Pig	**Brown**, *Vet Pathol* 17:455, 1980 (fetus); **Nayak**, *Am J Vet Res* 26:1271, 1965 (respiratory); **Winkler**, *Am J Pathol* 122:541, 1986
	Mouse†	**Arnheiter**, *Exp Cell Biol* 44:95, 1976 (hepatitis); **Duffy**, *J Neuropathol Exp Neurol* 32:72, 1973 (encephalomyelitis); **Gamboa**, *Acta Neuropathol* 34:157, 1976 (encephalomyelitis); **Lemercier**, *Arch Ges Virusforsch* 44:337, 1974 (lung); **Plummer**, *Am J Pathol* 45:95, 1964 (pneumonia); **Ramphal**, *Am Rev Resp Dis* 120:1313, 1979 (trachea); **Reinacher**, *Lab Invest* 49:686, 1983 (brain)
Influenza B virus	Mouse†	**Chen**, *J Mol Evol* [E-pub] 2008 (virion); **Blisard**, *J Neuropathol Exp Neurol* 49:498, 1990 (brain, liver)
Influenza C virus	In vitro	**Stein**, *Microbios* 15:135, 1976

†Animal model.

Vet-ebooks.com

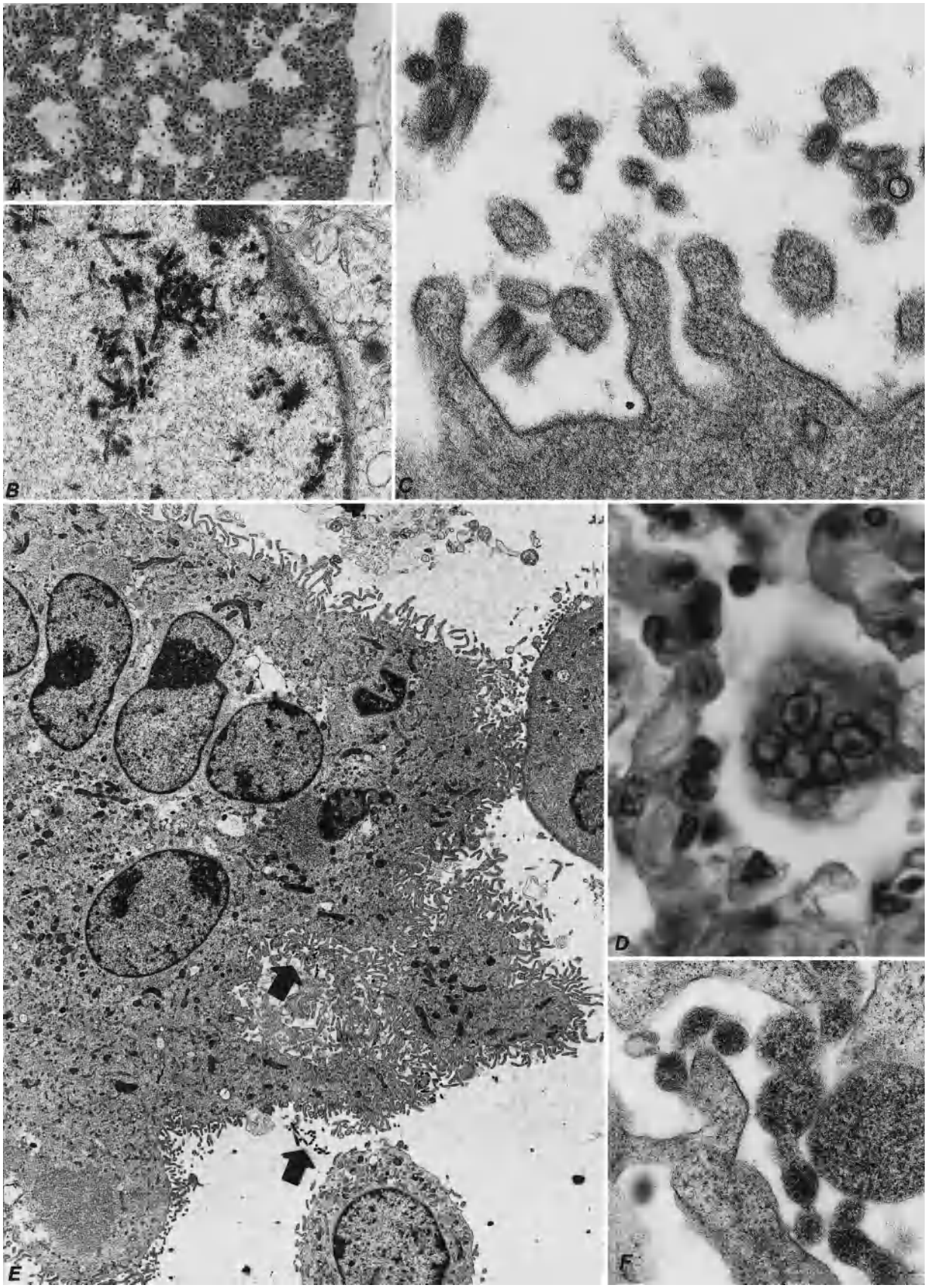


Fig. 13.21 Cytopathology of orthomyxoviruses and paramyxoviruses. A–C. **Porcine influenza. A**. **Alveolitis**: severe hyperemia and edema of alveolar walls with accumulation of fluid in alveoli and interlobular areas (histology). **B**. **Viral tubules** in nucleus of influenza-infected cell in vitro. **C**. **Spherical and tubular influenza virions** budded from cell surface; microvilli are irregular. **D–F**. **Measles pneumonitis**: lung, monkey. **D**. **Giant cell** bearing nuclei with viral inclusions (histology). **E**. **Giant cell** with marked irregularities of microvillous surface (*arrows*). **F**. **Virions** from surface of cell in E.

Vet-ebooks.com

cilia in the nasal turbinates. Cilia swell and become irregular. During attachment, the **ligand-receptor complex** that initiates cell entry is formed when viral hemagglutinin spikes attach to sialic acid residues on the host cell plasma membrane. Binding initiates endosomal uptake, and the acidic environment within the newly formed endosome starts the uncoating process. Disintegration of virus after entry into the host cell is followed by release of viral nucleic acids into the cytosol and their movement to the nucleus where viral reproduction begins. Export of new viral components from nucleus to cytoplasm depends on the viral matrix protein M1. M1 acts with new viral RNPs in the nucleus and escorts them to the cytoplasm. Immunogold labeling of M1 shows that exit from the nucleus occurs through nuclear pores.[106] Viral proteins are produced and routed through the cytoplasmic transport systems.[107] Long microvilli appear and are associated with exit of new virions from the cell (Fig. 13.21). Viral neuraminidase plays a role in release of virions. Ultrastructural changes during viral replication include increased density of nucleoli, followed by dispersion, and formation of discrete granular masses throughout the nucleus. Hemagglutinin proteins develop in the cytoplasm. Here ultrastructural changes include dense protein lattices. Aggregates of long protein fibers are also present and represent excess hemagglutinin. Assembly of complete virions occurs at the cell membrane by budding. The viral envelope arises from the host cell plasma membrane. Vesicles of 50–150 nm diameter and fibrils are associated with the plasma membrane at sites where virions have emerged. The host cell plasma membrane is altered in large areas.

Influenza viruses cause diffuse or multifocal **pneumonitis** with marked thickening of alveolar walls due to accumulation of fluid. There is marked involvement of bronchiolar epithelium with scattered infected cells in the lung parenchyma.[108] Recovery involves granular pneumocyte hyperplasia and filling of alveoli with macrophages. Purulent bronchopneumonia caused by *Haemophilus* spp., staphylococci, or other bacteria is the serious complication of influenza. Experimentally, previous infection of monkeys with influenza markedly increases the severity of respiratory infection with *Streptococcus pneumonia*.[109] Influenza predisposes the lung to bacterial pneumonia by (1) destruction of the mucociliary clearance function of the bronchioles, (2) production of pulmonary edema with lymphatic overload, and (3) direct inhibition of phagocytic activity of alveolar macrophages.

Human patients develop lymphopenia during acute influenza and circulating lymphocytes remain low for up to 4 wk. Both B and T lymphocytes are low. There is depressed chemotaxis of monocytes and inhibition of phagocytosis. Hemagglutin on virion surfaces causes an affinity for erythrocytic plasma membranes (in vitro, this reaction causes hemagglutination). After attachment, fusion occurs with liberation of viroplasm into the erythrocyte. Virions are also taken in by phagocytosis and can be seen within phagosomes embedded in hemoglobin.[110] Virions also absorb into and infect leukocytes and platelets.

Influenza viruses have been implicated as a cause of fetal malformation, but without adequate proof. Experiments in ferrets and pigs have shown that malformations of the lungs and other tissues can be produced at very precise stages of gestation by influenza virus.

Avian Influenza Influenza viruses isolated from birds differ widely in virulence. Some produce fulminating systemic disease; others cause only subclinical infection. Neurotropism, rare in mammalian influenza viruses, is common in avian influenza. Recombinants of human and avian strains can result in remarkable neurovirulence in mice.

After inhalation and attachment of virions to cilia, virulent strains of avian influenza replicate in the upper respiratory tract epithelium and are disseminated rapidly throughout the viscera and central nervous system. Lesions are edema, necrosis, and hemorrhage and are disseminated throughout lymphoid organs, liver, lungs, kidney, heart, and other viscera. Brain is infected hematogenously and there are disseminated focal encephalomalacic lesions with neuronal degeneration and glial proliferations. Virus replicates in choroid plexus epithelium and in random neurons, in which immunolabeling has detected antigens. Skeletal muscle becomes infected but virions are difficult to locate.[111]

Family *Paramyxoviridae*

Virions of *Paramyxoviridae* are spherical or pleomorphic including filamentous forms that range from 150 to 200 nm in diameter and 1,000 to 10,000 nm in length. They differ from orthomyxoviruses in that they form syncytia in epithelium, induce hemolysis (in addition to hemagglutination), synthesize ribonucleoprotein antigens in cytoplasm instead of nucleus, and tend to form eosinophilic cytoplasmic inclusions. The family *Paramyxoviridae* contains two subfamilies: *Paramyxovirinae* with five genera and *Pneumovirinae* with two genera (Table 13.10).

Paramyxoviruses contain two types of surface spikes: one with combined hemagglutinin/neuraminidase activity and the other a fusion factor. Activation of both involves specific cleavage by a host protease. Hemagglutinin is used for attachment and entry of

Vet-ebooks.com

Table 13.10 *Paramyxoviridae*.

Virus	*Disease in*	*Reference to ultrastructural pathology*
		Subfamily *Paramyxovirinae*
		Genus *Respirovirus*
Sendai virus	Mouse	**Bachi**, *Virology* 106:41, 1980 (virion);* **Tucker**, *Infect Immun* 14:1191, 1976; **Schwendemann**, *Acta Neuropathol* 46:85, 1979 (brain);† **Ward**, *Vet Pathol* 13:36, 1976
	Rat	**Castleman**, *Am J Pathol* 114:322, 1984 (lung); **Castleman**, *Am J Pathol* 129:277, 1987 (bronchiolitis)
Human parainfluenza virus 1 and 3	Human	
Bovine parainfluenza virus 3	Cow	**Allan**, *Res Vet Sci* 24:339, 1978; **Tsai**, *Infect Immun* 11:783, 1975
		Genus *Morbillibirus*
Measles virus	Human	**Bouteille**, *Revue Neurol* 113:454, 1968 (brain); **Breitfeld**, *Lab Invest* 28:279, 1973 (children); **Joliat**, *Virch Arch A* 358:215, 1973 (lung); **Kimura**, *Tohoku J Exp Med* 117:245, 1975 (skin); **Liebert**, *J Gen Virol* 67:2435, 1986 (brain); **Oyanagi**, *Acta Neuropathol* 18:58, 1971 (brain); **Tellez-Nagel**, *Science* 154:899, 1966 (brain); **Toga**, *Acta Neuropathol* 14:1, 1969 (brain)
	Animal models	**Baringer**, *Lab Invest* 23:335, 1970 (brain); **Fournier**, *J Ultrastruct Res* 77:319, 1981 (brain explants);* **Parhad**, *Lab Invest* 43:52, 1980 (eye); **Pottelsberghe**, *Lab Invest* 40:99, 1979 (brain, mouse); **Raine**, *Lab Invest* 33:108, 1975 (brain, hamster); **Tajima**, *Acta Pathol Jap* 26:367, 1976 (lung, monkey);
Canine distemper virus	Dog	**Bestetti**, *Acta Neuropathol* 43:69, 1978 (brain); **Confer**, *Am J Vet Res* 36:741, 1975; **Higgins**, *Acta Neuropathol* 58:1, 1982 (brain);† **Richter**, *Vet Pathol* 7:346, 1970 (bladder); **Summers**, *J Comp Pathol* 94:575, 1984 (brain);† **Vandevelde**, *Acta Neuropathol* 40:233, 1977 (brain); **Watson**, *Res Vet Sci* 17:188, 1974 (lymphocytes); **Wisniewski**, *Lab Invest* 26:589, 1972 (brain)
	Animal models	**Koestner**, *Lab Invest* 23:196, 1970 (brain explants);* **McCullough**, *Am J Pathol* 74:155, 1973 (lymphoid tissue); **Oglesbee**, *Lab Invest* 68:109, 1993;* **Oglesbee**, *Acta Neuropathol* 84:407, 1992;* **Tajima**, *Am J Vet Res* 32:913, 1971 (lymph node, mink)
Peste-des-petits-ruminants virus	Sheep, goat	
Phocine distemper virus	Seal	
Rinderpest virus	Cow	**Tajima**, *Am J Pathol* 62:221, 1971 (lymph node);
		Genus *Rubulavirus*
Mumps virus	Human Hamster†	**Johnson**, *J Neuropathol Exp Neurol* 27:80, 1968 (brain); **Johnson**, *J Neuropathol Exp Neurol* 27:591, 1968 (brain); **Wolinsky**, *Lab Invest* 31:403, 1974 (brain, hamster); **Wolinsky**, *Lab Invest* 37:229,1977 (brain, hamster)
Human parainfluenza 2, 4	Human	
		Genus *Henipavirus*
Hendra virus	Horse, human Guinea pig†	**Barclay**, *Vet J* 160:169, 2000 **Williamson**, *J Comp Pathol* 124:273, 2001
Nipa virus	Human	**Tan**, *Ann Neurol* 51:703, 2002 (encephalitis); **Wong**, *Am J Pathol* 161:2153, 2002 (vasculitis)
	In vitro	**Goldsmith**, *Virus Res* 92:89, 2003*
		Genus *Avulavirus*
Newcastle disease virus	Chicken	**Cheville**, *Lab Invest* 27:129, 1972; **Mast**, *Vet Pathol* 42:559, 2005 (vaccine, trachea)
	Chick embryo	**Donnelly**, *Am J Pathol* 62:87, 1971; **Yunis**, *Virology* 39:353, 1969
		Subfamily *Pneumovirinae*
		Genus *Pneumovirus*
Human respiratory syncytial virus	Human	**Bachi**, *J Virol* 12:1173, 1973 (virion);* **Mills**, *Proc Nat Acad Sci USA* 78:1209, 1981 (bone)
	Animal models†	**Liu**, *Kidney Int* 71:388, 2007 (kidney); **Prince**, *Am J Pathol* 82:339, 1976 (ferret)
Bovine respiratory syncytial virus	Cow	**Bryson**, *Vet Pathol* 28:293, 1991; **Castleman**, *Am J Vet Res* 46:554, 1985
Murine pneumonia virus	Mouse	**Rosenberg**, *Immunol Lett* 118:6, 2008
		Genus *Metapneumovirus*
Avian metapneumovirus	Chicken Turkey	**Aung**, *Avian Pathol* 37:65, 2008 (sinusitis)
Human metapneumovirus	Human	**Nicholls**, *Lancet* 361:1773, 2003 (fatal pneumonia); **Vargas**, *Pediatr Dev Pathol* 7:478, 2008 (children)

*In vitro study.
†Animal model.

Vet-ebooks.com

virus and neuraminidase to facilitate spreading of the virus over the cell and for release of new viruses by budding from the cell surface (Fig. 13.22). Cell fusion activity makes possible the spread of infection from cell to cell by fusion of adjacent plasma membranes and formation of syncytia.[112] Paramyxoviruses produce cytoplasmic inclusions and giant cells.

Paramyxovirus virions attach to and fuse with the plasma membranes of respiratory epithelial cells: hemagglutinin on the virion surface is complexed to receptors (membrane glycoproteins) on the cell surface. The reaction of virus and erythrocyte membrane has been a model for this fusion. Giant cells are characteristic of paramyxovirus infections. In human and simian measles, giant cells develop in the epidermis and hair follicular epithelium. Persistence of measles virus at these sites is related to poor immune responses by the host and in moderate immunosuppressed monkeys, **giant cell pneumonia** is the expected finding.

Subfamily Paramyxovirinae

Genus *Respirovirus*

The respirovirsues include human parainfluenza virus 1 and 3, bovine parainfluenza virus 3, and Sendai virus. In animals, these viruses are important causes of rhinitis, tracheobronchitis, and pneumonitis.

Human Parainfluenza Viruses **Human parainfluenza (PI) viruses** are responsible for a variety of human syndromes involving the upper respiratory tract. Infection is widespread in the general population but little is known about cytopathologic changes. Parainfluenza viruses isolated from human brains affected by multiple sclerosis have been shown to be neuropathic for monkeys and mice. In mice, these viruses replicated in ependymal epithelium and neurons (the accompanying lymphoid infiltrates were typical of viral encephalitis).[113] In **chimpanzees**, they produce severe respiratory disease and limited neuropathic changes when inoculated intranasally. When given intracerebrally, subacute encephalitis with extensive cortical and subcortial degeneration with vascular sclerosis and axonal dystrophy were observed.[114]

Sendai Virus **Sendai** is a ubiquitous virus that causes epizootics of pneumonitis, usually following shipping. The disease is characterized by mild respiratory signs, low mortality, and rapid recovery. In immunosuppressed mice, Sendai virus may cause a chronic debilitating disease with nuclear inclusions in respiratory epithelial and pulmonary pneumocytes. After intranasal inoculation, Sendai virus replicates in epithelium of the upper respiratory tract and in the larger bronchioles of the lungs. Given intracerebrally, virus replicates in epithelium of the leptomeninges, ependyma, and choroid plexus of the brain where it causes vacuolation and nucleocapsid inclusions. When given intravenously to pregnant mice, the virus can be reisolated from the fetus and, after birth, from the neonate. Viral antigens are widely distributed in fetal tissues, including the brain. Given intravenously in immunized mice, Sendai virus causes an IgA nephropathy with deposits of IgA in the glomerulus.

Genus *Morbillivirus*

Measles **Measles** is an acute febrile systemic disease, largely of children. High fever, lymphadenopathy, and a discrete papular rash appear at about the 14th day of infection and are the hallmarks of the disease. Stages of infection include: (1) infection—development of local lesions in the respiratory tract, transient primary viremia, and (in some cases) fleeting signs of disease; (2) asymptomatic phase—virus replicates in lymph nodes draining the respiratory tract; (3) secondary viremia—dissemination of large amounts of virus throughout the body; (4) virus replication throughout epithelial and the reticuloendothelial system; (5) anergy—a phase of viral-suppressed immunologic function due to exhaustion of T lymphocytes; and (6) either recovery or postinfectious syndromes. Although most children recover, sequelae from acute encephalitis and pneumonia may persist. Recovery is due chiefly to cell-mediated immunity. Newborn infants escape measles, in part, because of diminished viral receptors on their cells.

After primary dissemination, measles virus replicates in the cytoplasm of epithelial, lymphoid, and endothelial cells. Nuclear and cytoplasmic inclusion bodies contain viral antigens and tangled aggregates of internal components of the measles virion. Virions are rarely seen in tissue. The virus induces syncytial (giant) cell formation by induction of plasma membrane changes and cell fusion. Measles virus replicates in leukocytes and large inclusions composed of nucleocapsids are found in T and B lymphocytes and monocytes, especially those in an activated state.

Measles virus produces punctate lesions on mucosal surfaces (the enanthem) and a striking rash on skin (exanthem). Localization of viral antigens and immune T lymphocytes, and subsequent attraction of monocytes into sites of infection in skin, represents an immune phenomenon, probably dominated by cell-mediated reaction. At the peak of rash, multinucleate giant cells are found adjacent to cornified layers of the skin. No viral antigen or nucleocapsids have been found in epidermis but occur in endothelial cells of dermal capillaries—suggesting that the edema and

Vet-ebooks.com

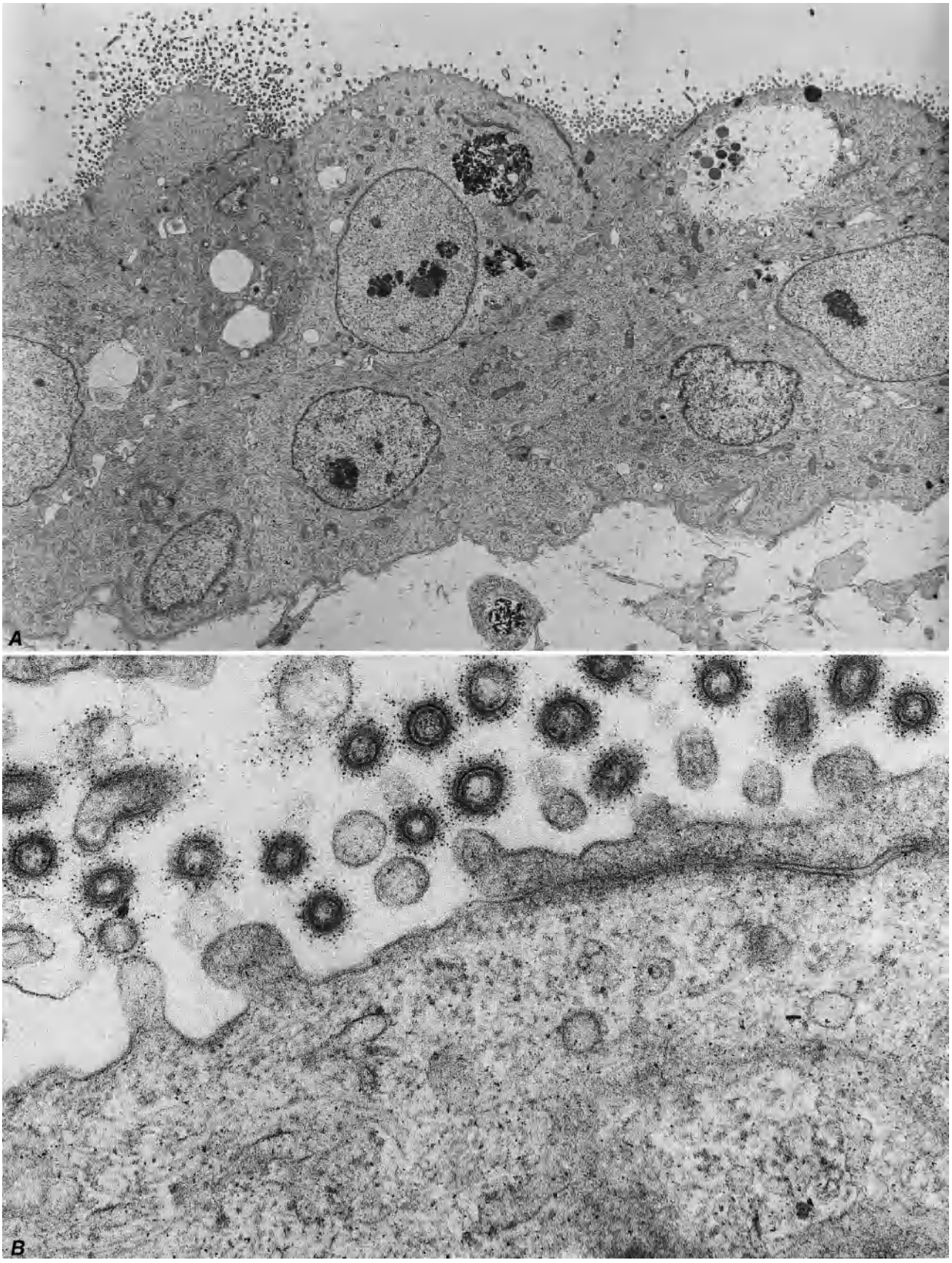


Fig. 13.22 **Paramyxovirus**: growth in ovo, Newcastle disease virus. **A**. **Virions**: budding from chorioallantoic epithelium. **B**. **Virions**: surface of chorioallantoic membrane. Virions are labeled with antibody-ferritin conjugates.

Vet-ebooks.com

perivascular inflammation may also involve Arthus reactivity.

In human cutaneous lesions, viral antigens are found in clusters of cells in the epithelium, corium, and hair follicles.[115] Syncytial cells with up to 60 nuclei can be found beneath the hypertrophic horny layer. Viral nucleocapsids develop in capillary endothelium. Giant cells in lymphoid tissue (Warthin-Finkeldy cells) are large and develop in the tonsils, Peyer's patches, spleen and lymph nodes.

Monkeys develop naturally occurring measles that can mimic any of the human disease syndromes, but which most typically takes the form of **giant cell pneumonia** (see Fig. 13.21). Monkeys, which are free of measles in their natural habitat, acquire the virus in contact with humans. Giant cells, which arise from virus-mediated fusion, are filled with viral nucleoprotein containing cytoplasmic and nuclear. They develop in lymphoid and reticular cells of the germinal centers of lymph nodes.

Subacute Sclerosing Panencephalitis Acute measles encephalitis usually occurs several days after recovery from acute systemic disease—changes are perivascular cuffing by inflammatory cells and demyelination. Injury is due to direct viral damage although there are few direct signs of the presence of virus in the CNS. In a very small number of children who have measles, virus persists in the brain and, slowly spreading by cell to cell contact, provokes a chronic glial and plasmacyte response called **subacute sclerosing panencephalitis (SSPE)**. The syndrome appears 5–7 yr after acute measles. It is a slowly progressive disease with unremitting mental deterioration and physical disability that is distinguished by intranuclear inclusions of measles nucleocapsids. In SSPE, measles virus is not present as a fully infectious virion but as asynchronous synthesis of viral subunits with defective incomplete virion assembly; only a portion of the viral genome is expressed.

Measles virus isolated from brains of children with SSPE will cause progressive fatal encephalitis in nonhuman primates. An SSPE-like disease has been reported in a baboon. Measles cervicitis and endometritis develop in pregnant females and may cause infertility. **Mice** are a widely used model for measles virus. Some neurotropic strains of virus produce fatal encephalitis in suckling mice with production of infectious virus and numerous cytoplasmic inclusions. In weanling mice the same strain will produce much less mortality with production of little infectious virus—perhaps because of maturation of host cells. Measles viruses inoculated into suckling and weanling **hamsters** spread immediately via the bloodstream.

Canine Distemper Dogs with acute canine distemper enter the clinic with fever, anorexia, lethargy, and seropurulent discharges from the eyes and nose. Dyspnea, diarrhea, and dehydration are common, and there are often cutaneous vesicles and pustules that contain streptococci or staphylococci. After infection of the upper respiratory tract, **canine distemper virus (CDV)** replicates in the oropharyngeal lymphoid tissues, and CDV is disseminated throughout the animal by lymphocytes. CDV causes widespread lymphoid tissue destruction and suppression of immune function.

CDV replication occurs in nearly all tissues (Fig. 13.23). Epithelial cells of the respiratory tract, urinary bladder, stomach (but rarely intestine), and other organs contain multiple, round eosinophilic cytoplasmic inclusion bodies. Cytoplasmic inclusions are composed of masses of viral nucleocapsids that aggregate. In neonates, CDV replication in the heart produces foci of necrosis and **myocarditis** that can be lethal. Infection of the nervous system can result in the following disease patterns:

- **Acute encephalitis** arises from infection of the choroid plexus, dissemination of CDV via cerebrospinal fluid, and nonsuppurative inflammation of the brain.
- **Subacute encephalitis** (or postinfectious encephalitis) in dogs that survive for 2–3 wk; lesions include nuclear inclusion in neurons and astrocytes, perivascular lymphocyte cuffs, and demyelination caused by selective destruction of the ensheathing myelin envelope (primary myelin loss with preservation of the axon fiber).
- **Chronic encephalitis** (old dog encephalitis) appears with ataxia and episodes of convulsions. There are widespread foci of viral antigens in white and gray matter, perivascular cuffs, gliosis, and demyelination. In the face of immune response, CDV persists within neurons for months. Demyelination is due to secondary, indirect damage to oligodendroglia.

Genus *Henipavirus*

Two related zoonotic and highly pathogenic paramyxoviruses form this genus. Natural hosts for both are species of fruit bats, genus *Pteropus*.

Hendra Virus **Hendra virus** (equine morbillivirus) causes fatal interstitial pneumonitis in horses and humans. In horses, the most distinct gross lesions are pulmonary edema with distension of subpleural lymphatics. Microscopically, there are marked alveolar edema with hemorrhage, dilated lymphatics, thrombosis in alveolar walls, and necrosis of small blood vessels. Syncytial giant cells form in endothelium and blood vessels walls in capillaries of the lungs, and also in the spleen, lymph nodes, brain, stomach, heart and kidneys. Viral antigens are found in endothelial and

Vet-ebooks.com

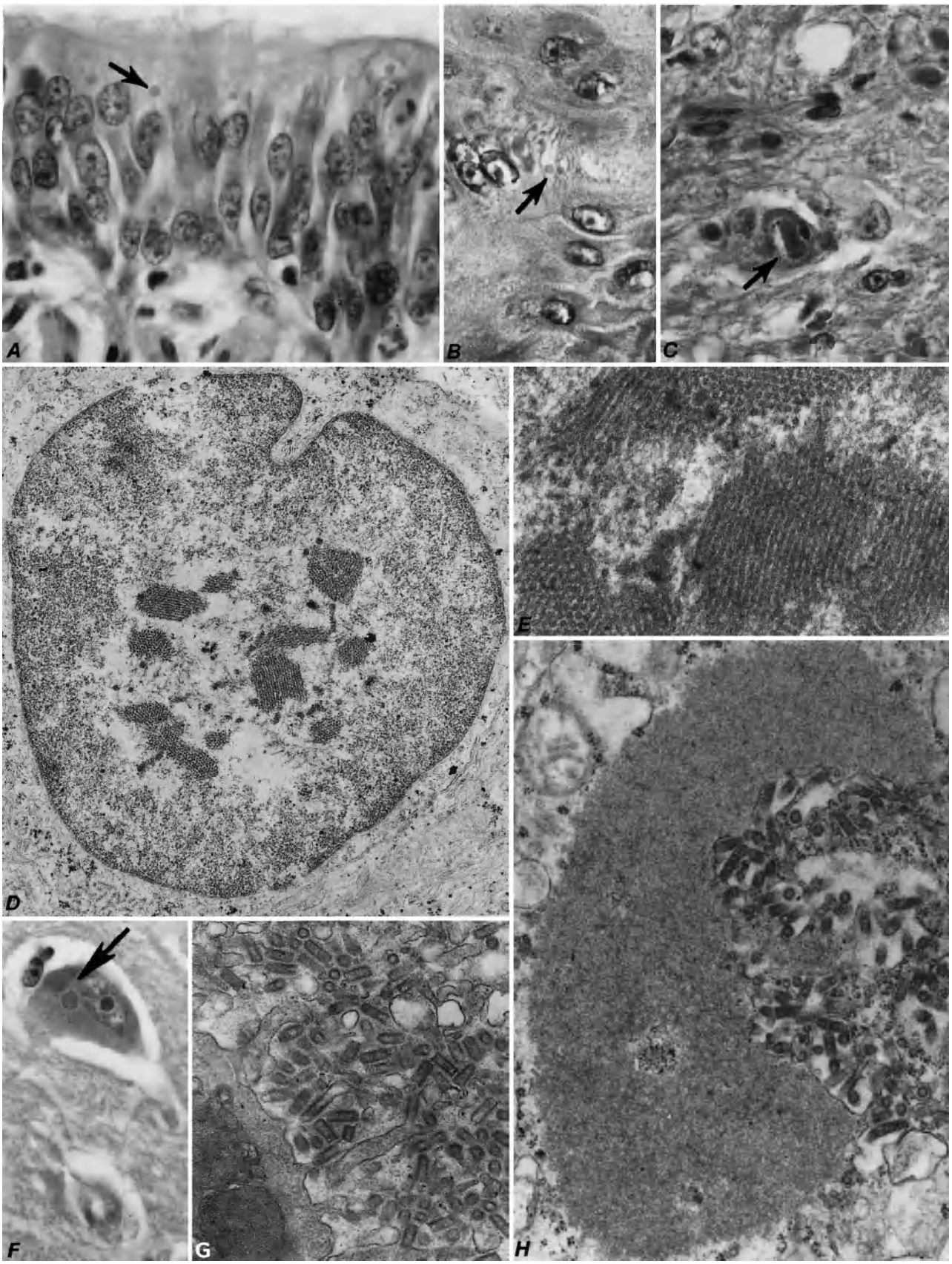


Fig. 13.23 A–E. Paramyxovirus: canine distemper, dog. **A**. **Viral cytoplasmic inclusions** (*arrow*), tracheal epithelium (histology). **B**. **Cytoplasmic inclusions** (*arrow*), skin of footpad. **C**. **Nuclear inclusions** (*arrow*), neuron. **D**. Intranuclear viral nucleocapsids. **E**. Nucleocapsids enlarged. (Micrographs D and E: Adalbert Koestner, *Lab Invest* 23:196, 1970.) **F–H**. **Rabies**. **F**. **Cytoplasmic inclusions**, brain (Negri body, *arrow*) (histology). **G**. **Rabies virions**: surface of mucigenic salivary gland cell, fox. **H**. **Rabies Negri body**: neuron, hippocampus, fox. Spherical and tubular virions are associated with granular, amorphous inclusion material. (Micrographs G and H: Richard Dierks, *Am J Pathol* 54:251, 1969.)

Vet-ebooks.com

syncytial cells, and less often in bronchial epithelium. Cytoplasmic inclusions of nucleocapsids typical of the *Paramyxoviridae* are found in endothelial cells and giant cells.[116] By negative staining, virions are pleomorphic, 38–600 nm in diameter and enveloped. The envelope is covered with 10 and 18 nm surface projections giving a double-fringed appearance in contrast to the single fringe of other *Paramyxoviridae*.[117]

Nipah Virus **Nipah virus** is the etiologic agent of a respiratory disease of pigs characterized by giant cell pneumonia with multinucleated syncytial cells and, in severe cases, with meningitis and evidence of viral infection in liver, kidney and other organs. Nipah virus is transmissible to and causes fatal acute vasculitis and encephalitis in humans, pigs, cats, and other animals. Endothlelial cells showed massive amounts of viral antigens. Necrotic endothelial cells were sloughed into the vascular lumens, although some endothelial cells developed syncytia. Less intense immunostaining was present in lung, heart, spleen, and kidney. In the initial human outbreaks in 1988–1989 in Malaysia, the central nervous system was characterized by diffuse vasculitis of the cerebral cortex and brain stem, and there was a late-onset pattern of encephalopathy.[118] Cells infected in vitro with Nipah virus have filamentous nucleocapsides within cytoplasmic inclusions and virions budded from plasma membranes. Nucleocapsids are 1.67 µm long with an average diameter of 500 nm. Extracellular virions are pleomorphic, with an average diameter of 500 nm.[119]

Genus *Rubulavirus*

Mumps **Mumps virus** is the cause of epidemic parotitis in humans. It replicates in parenchymal cells, buds from lumenal plasma membranes and is secreted into saliva. Complications include orchitis and oophoritis in adults and aseptic meningoencephalitis in children. In infected cells, ribonucleoprotein strands develop within 36 hr and are seen along the plasma membrane at sites of budding. Ferritin-conjugated antibody specifically tags the strands. Virions are roughly spherical and vary from 100 to 800 nm in diameter. Experimentally mumps virus infection can be produced in monkeys which develop foci of degeneration and necrosis in acinar epithelium of salivary glands. In hamsters and mice,[120] mumps viral encephalitis is a model for the pathogenesis of congenital, viral-induced disease. Neuroadapted strains of virus spread from ependyma and choroid to neurons in which they induce reduplication of smooth endoplasmic reticulum, cytoplasmic inclusions of viral nucleocapids, and budding of virions from the host cell plasma.

Genus *Avulavirus*

Newcastle Disease **Newcastle disease virus (NDV)** virions are pleomorphic and are spherical or tubular. NDV attaches to respiratory epithelial cells by the complexing of viral hemagglutinin to cell membrane glycoproteins. Engulfment of attached virions occurs by pseudopod formation and degenerate virions are seen in cytoplasmic vacuoles. Ribonucleoprotein strands form in the cytoplasm and viral antigens are distributed throughout the cytoplasm.[121] In the respiratory tract, NDV first attaches to cilia to infect respiratory epithelium. Infected cells undergo cell swelling, loss of cilia, and virions bud from the lumenal plasma membrane (see Fig. 1.8C). Although cilia are destroyed, infected cells remain intact, allowing excretion of virus. Virulent viruses produce widespread systemic damage that includes focal necrosis of lymphoid tissues. NDV replicates in cells of the endothelial, monocyte-macrophage, and reticular systems. NDV can infect erythrocytes, and the intravascular agglutination and lysis of erythrocytes lead to splenic erythrophagocytosis. In all tissues, virions are difficult to find because of the necrosis they produce—they are obscured by cellular debris. In late stages of disease, marked infiltration of plasmacytes, macrophages and lymphocytes occurs at sites of infection. The wide spectrum of NDV viruses of varying tropism, those causing major disease, include respirotropic NDV, neurotropic NDV, enterotropic NDV, and pantropic (viscerotropic) NDV. Neurotropic NDV first replicates in endothelial cells in capillaries of the brain and then spreads to neurons and glia (Fig. 13.24).

Subfamily *Pneumovirinae*

Genus *Pneumovirus*

Pneumovirus virions are spherical to pleomorphic and consist of an envelope and a nucleocapsid. Filamentous forms are common. Virions measure 150–250 (60–300) nm in diameter and can be 1,000–10,000 nm in length. Surface projections are hemagglutinin (H) and fusion (F) glycoproteins.

Respiratory Syncytial Viruses First isolated from an outbreak of "colds" in chimpanzees, the **respiratory syncytial viruses (RSVs)** are common, widespread, and recurring etiologic agents of respiratory disease in humans, cattle, sheep and goats. In normal human adults, RSV causes limited respiratory disease. Lung parenchyma is affected by bronchiolitis and patchy interstitial pneumonitis. Cytopathic changes are not documented but it is inferred from studies in vitro that

Vet-ebooks.com

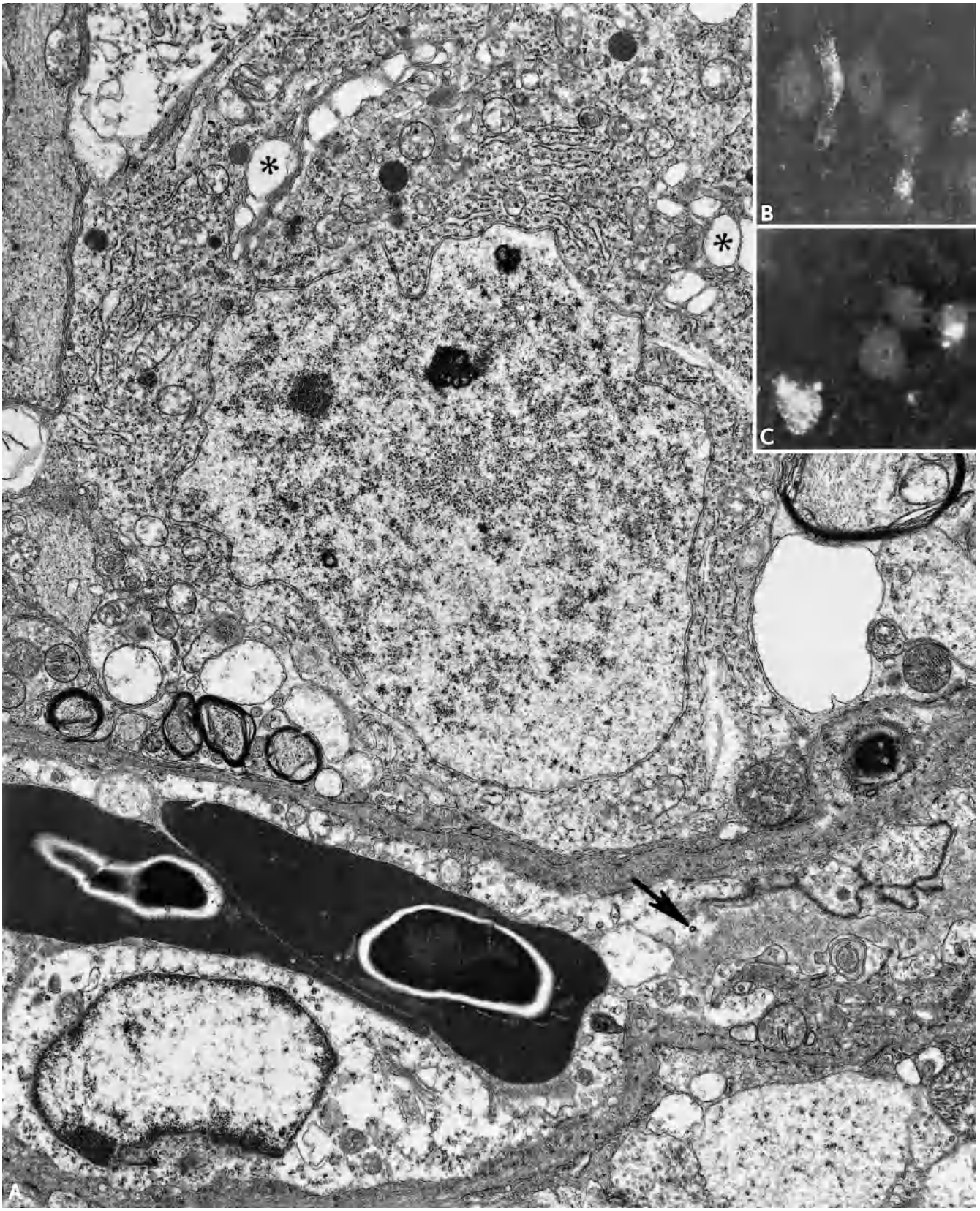


Fig. 13.24 Parmyxovirus: neuron and endothelium: Newcastle disease, chicken. **A**. **Endothelial cells** (*bottom*) are swollen and contain small, dense virions (*arrow*). Dilated Golgi complexes (*) of neuron reflect early cell swelling. **B** and **C**. **Viral antigens**: detected by fluorescent antibody test in endothelial cells in early disease (**B**) and in neurons in later phase (**C**).

Vet-ebooks.com

severe cell swelling is accompanied by cytoplasmic accumulation of nucleocapsid material and budding of virions from the plasma membrane. RSV infection in infant **ferrets** has been used as a model for human infection; infection of nasal epithelium occurs readily, and infection of the lungs relates to age with older animals being resistant.

Bovine RSV is a major pathogen of the lower respiratory tract of young cattle, in which viral replication occurs in bronchiolar epithelium and, in pneumonia, in alveolar walls. In experimental infections, type I pneumocytes undergo degeneration and necrosis whereas type II pneumoncytes show hyperplasia and syncytia formation.[122] Cytopathic changes resemble those of **pneumonia virus of mice**, another pneumovirus.

Genus *Metapneumovirus*

Human metapneumoviruses cause a spectrum of respiratory diseases that range from trivial coryzal signs to fatal pneumonia in immunocompromised children.[123]

Avian metapneumovirus virus causes disease in turkeys and chickens. The virus replicates in the respiratory tract producing respiratory disease, and may infect the reproductive tract resulting in a reduced ovum production.

Family *Rhabdoviridae*

Rhabdoviruses (Table 13.11) are grouped together according to morphology of virions and pathways of

Table 13.11 *Rhabdoviridae*.

Virus	*Host*	*Reference to ultrastructural pathology*
		Genus *Vesiculovirus*
Vesicular stomatitis virus	Cow	**Proctor**, *Vet Pathol* 12:362, 1975 (tongue)
	Mouse	**Dal Canto,** *Lab Invest* 35:515, 1976; **Dal Canto**, *J Infect Dis* 139:36, 1979 (brain); **Greenstein**, *Lab Invest* 44:487, 1981 (brain); **Grodums,** *Arch Virol* 51:75, 1976 (choroid plexus)
		Genus *Lyssavirus*
Rabies virus	Bat	**Fekadu**, *Arch Virol* 99:187, 1988 (salivary gland)
	Cat	**Murphy**, *Lab Invest* 43:231, 1980†
	Dog	**Fekadu**, *Arch Virol* 71:109, 1982†
	Human	**Burton**, *Arch Neurol* 62:873, 2005 (transplant patients); **Dupont**, *Neurology* 15:1023, 1966 (brain); **Iwasaki**, *J Neuropathol Exp Neurol* 44:185, 1985 (brain); **Srinivasan**, *New Engl J Med* 352:1103, 2005; **Jenson**, *J Virol* 3:265, 1969 (neuron); **Suja,** *Clin Neuropathol* 23:271, 2004 (fox bite); **Sung,** *J Neuropath Exp Neurol* 35:541, 1976 (Negri body)
	Fox	**Charlton**, *Lab Invest* 57:634, 1987; **Dierks**, *Am J Path* 54:251, 1969 (salivary gland)†
	Mouse	**Iwasaki**, *Lab Invest* 33:391, 1975 (brain); **Matsumoto,** *J Cell Biol* 19:565, 1963 (brain); **Murphy,** *Intervirology* 3:256, 1974 (muscle, brain)
	Rat	**Gille**, *J Neuropathol Exp Neurol* 45:619, 1986 (brain)
	Skunk	**Balachandran**, *Vet Pathol* 31:83, 1993 (salivary gland);† **Charlton**, *Lab Invest* 57:634, 1987 (brain); **Charlton**, *Lab Invest* 41:36, 1979
Australian bat lyssavirus	Human	**Warrilow**, *Curr Top Microbiol Immunol* 292:25, 2005
Lagos bat virus		**Shope**, *J Virol* 6:690, 1970 (virion)*
Mokola virus		**Harrison**, *Arch Virol* 57:167, 1978 (motor end plate)
Oita virus#	Mouse	**Iwasaki**, *Arch Virol* 49:1139, 2004 (bat isolate)
		Genus *Ephemerovirus*
Bovine ephemeral fever virus	Cow	**Murphy**, *Arch Ges Virusforsch* 38:234, 1972;* **Young**, *J Infect Dis* 142:50, 1980 (neutrophils)
		Genus *Novirhabdovirus*
Viral hemorrhagic septicemia virus	Fish	**Baroni**, *J Fish Dis* 5:439, 1982; **Olberding**, *J Gen Virol* 27:305, 1975 (trout)
Infectious hematopoietic necrosis virus	Fish	**Brudeseth**, *Vet Pathol* 39:180, 2002; **MacKenzie**, *BMC Genomics* 9:141, 2008
Unclassified	Crab	**Jahromi**, *J Gen Virol* 36:485, 1977 (blue crab)

*In vitro study.
†Animal model.
Natural host: wild horseshoe bat.

Vet-ebooks.com

intracellular replication; they show no serologic cross-reactivity. Virions are bullet shaped (i.e., planar at one end and hemispherical at the other). They contain a 15 nm internal component that is coiled helically and an outer membrane with glycoprotein projections 10 nm long. Several rhabdoviruses are important pathogens. Rabies and vesicular stomatitis viruses are the two important pathogens in this group. During cellular infection, virions are engulfed, phagocytized in vesicles and end in phagosomes where degradation occurs. Fusion of the envelope with the vacuolar membrane allows entry of ribonucleoprotein material into the cytoplasmic matrix. Foci of tiny filaments or viroplasmic factories develop which are sites of new ribonucleoprotein synthesis. Assembly of viral particles begins in these areas and new virions bud from membranes within the cytoplasm or at cell surfaces. The G glycoprotein of VS virus has been widely used as a cellular marker to follow traffic from the ribosome through intermediate compartments and Golgi complex to the plasma membrane.[124]

Genus *Vesiculovirus*

Vesicular Stomatitis **Vesicular stomatitis virus (VSV)** causes disease in horses, cattle, and swine as vesicular lesions in epithelium of the tongue, gingiva, snout, teats, and coronary bands and interdigital areas of the feet. Initial infection is followed by viremia, during which monocytes support the growth of virus. Papules appear initially but rapidly transform into large vesicles that coalesce into bullae. Microscopically, epithelial cells in the developing vesicle retract, become rounded, and are separated by intercellular fluids. Microvesicles form in the epidermis in which keratinocytes and inflammatory cells float freely. Fluid disseminates through the epidermis and subepidermis to form larger, multilocular vesicles that erode leaving shallow ulcers on the mucosa. Ultrastructurally, virions are formed on the surfaces of keratinocytes and bud into intercellular spaces. Sites of virion formation are characterized by submembranous vacuolation, focal separation of the closely apposed cell surfaces, and lysis of desmosomes (Fig. 13.25).[125] Alterations induced in the plasma membrane cause infected epithelial cells to become more spherical and less spinous. VSV grows in mice and this model has been widely used to differentiate mutant strains of virus.[126]

Genus *Lyssavirus*

Rabies **Rabies virus** persists in nature because of its unique duality of host infection. First, in skunks, foxes, bats, and other wild carnivores, virus replicates to high titer in salivary glands and is excreted in saliva.



Fig. 13.25 Rhabdovirus. A and **B**. **Vesicular stomatitis virus**: epithelial cells, tongue, cow. Virions have budded into intercellular spaces. Desmosomes persist.

Second, the encephalitis induces a change in the normal fearful attitude of the host to one of aggressive behavior in which the hosts will attack other potential host animals. After deposition of virus in subcutis by an animal bite, rabies virus invades skeletal muscle cells. Rabies antigens are initially found in single **skeletal muscle** cells; later, antigens are found in clusters of infected myocytes. Virions bud from myocyte plasma membranes, and from membranes of the sarcoplasmic reticulum.

Virus is disseminated systemically by invasion of local nerves in which it moves. Deep in the muscle of the wound, the peripheral nerves are exposed at neuromuscular spindles. After replication, virions are found in extracellular spaces of **neuromuscular junctions**. Neurotendinal spindles, the sensory stretch receptors deep in tendons, are also infected. The nerve cell receptor for rabies virus is the acetylcholine (AchR) receptor at neural synapses. Rabies virus has been localized in the trigeminal ganglia.[127] Invasion of the central nervous system occurs via nerve pathways (Fig. 13.26). Centrifugal passage of virus via peripheral nerves results in infection of salivary glands, eyes, dermal nerve endings, and viscera.[128]

Rabies virus has a predilection for neurons of the **brain stem**, where it causes acute lymphocytic leuko- and polioencephalomyelitis. Lesions include focal gliosis, mononuclear perivascular cuffs, and spherical

Vet-ebooks.com

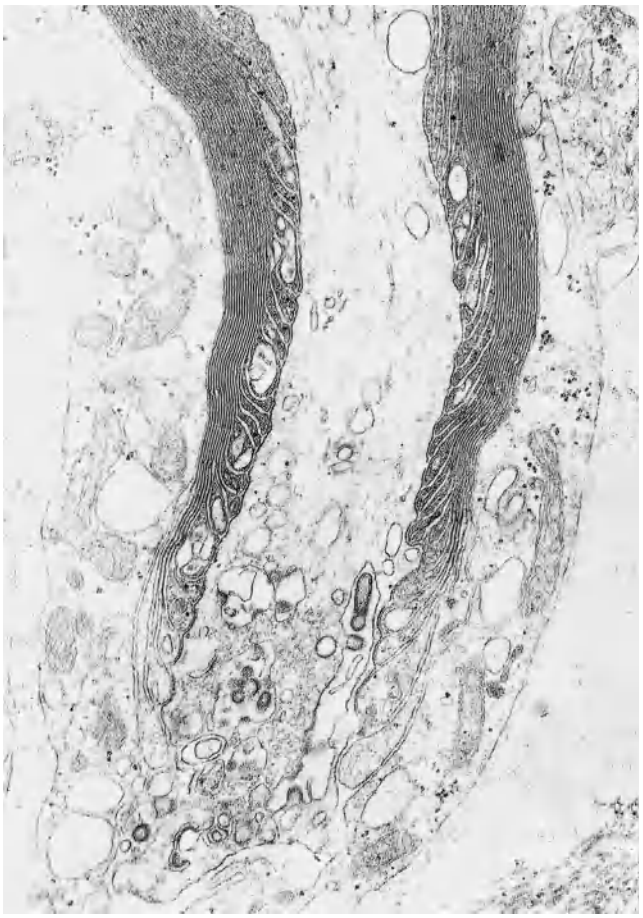


Fig. 13.26 Rhabdovirus, Mokola virus: node of Ranvier. Route of passive centripetal passage of rhabdovirus to central nervous system via peripheral nerve axoplasm, from invasion of unmyelinated distal end organ to progeny release at synaptic junctions of the spinal cord. (Micrograph: Fred Murphy, *Lab Invest* 28:361, 1973.)

cytoplasmic inclusions (Negri bodies). Spongiform lesions in the neuropil of the gray matter occur in rabies of skunks and foxes. Small vacuoles develop in dendrites and other cell processes and enlarge to compress adjacent nervous tissue and to rupture into extracellular spaces. Virus is concentrated in the limbic system with relative sparing of the neocortex—a basis for the fury of rabid animals. Viral replication and inclusion body formation are greatest in the larger neurons, for example, pyramidal cells of the hippocampus, ganglionic neurons of pontine nuclei, and cerebellar Purkinje cells. In human rabies, infection of the medulla, cerebellum basal ganglia, spinal cord, and dorsal root ganglia is reflected clinically in ascending paralysis.

Neurons infected with virulent virus undergo acute cell selling (chromatolysis) but the severity of cytopathic changes, compared to infected epithelial cells in the salivary gland, is minimal. Cell bodies may be strikingly well preserved despite the presence of large aggregates of dense granular viroplasm, which develop in the cytoplasm and which are seen by light microscopy as large, eosinophilic **Negri bodies** (Fig. 13.23F–H). **Cytoplasmic inclusions** in neurons are composed of mixtures of virions and viroplasmic granules. The bullet-shaped, 120 nm rabies virions bud from membranes of the endoplasmic reticulum in direct association with these foci of granular matrix material. Virions also bud from the plasma membrane of neuronal cells and processes and there is neuron-to-neuron transmission. Neuronal degeneration is accompanied by perivascular lymphoid infiltrates and gliosis with glial nodule formation. Infected neurons are surrounded by one or two lymphoid cells. The accumulation of rabies virus nucleocapsids in cells indicates defective coordination of assembly—a loss of balance between synthesis of precursor materials and assembly of virions, and Negri bodies are evidence of this defective assembly.

In carnivores, large numbers of virions are produced in infected **salivary glands**. There is acute degeneration of acinar epithelium (especially mucous cells) and the interstitium is infiltrated with lymphocytes and plasmacytes.[129] Masses of viral antigens develop in acini and in granular and striated ducts. Virions bud from lumenal plasma membranes of these cells and are released extracellularly into the lumen. Virions also accumulate in vacuoles within infected cells.

Rabies virions can also be found in chromaffin cells of the adrenal medulla, basal epithelial cells of the nasal mucosa and cornea, and in the basal cells of the epidermis and external root sheath cells of hair follicles.[130] These sites are frequently infected via peripheral nerves. Replication in these tissues is associated with large amounts of viral matrix and anomalous structures and small amounts of virus.

Genus *Ephemerovirus*

Bovine ephemeral fever, an arthropod-borne disease of African cattle, involves rapidly appearing fever, lachrymation, stomatitis, stiffness, lameness, and recovery. Microscopic lesions occur in epithelia, muscles, and vascular structures, including leukocytes. Rare fatalities have edema of the lymph nodes and subcutis and hemorrhages in the myocardium and upper respiratory tract. A CNS syndrome of ataxia and paralysis has been reported. Congenital deformities occur in calves born of cows that develop ephemeral fever during pregnancy. The causal rhabdovirus matures by budding from vacuoles in the cytoplasm or from plasma membranes.[131]

Vet-ebooks.com

Table 13.12 *Filoviridae*.

Virus	*Disease in*	*Reference to ultrastructural pathology*
		Genus *Marburgvirus*
Lake Victoria marburgvirus (Marburg virus)	Human	**Kolesnikova**, *Cell Microbiol* 9:939, 2007 (filopodia);* **Kolesnikova**, *J Virol* 78:12277, 2004 (Multivesicular bodies)*
	Guinea pig	**Ryabchikova**, *Arch Virol* 141:2177, 1996 (lung)
	Monkey	**Geisbert**, *Am J Pathol* 163:2347, 2003 (dendritic cells); **Geisbert**, *Am J Pathol* 163:2371, 2003 (endothelial cells); **Murphy**, *Lab Invest* 24:279, 1971
		Genus *Ebolavirus*
Zaire virus (Zaire Ebolavirus)	Human	**Zaki**, *J Infect Dis* 179:S36, 1999 (skin)
	Guinea pig	**Connolly**, *J Infect Dis* 179:S203, 1999†
	Monkey	**Baskerville**, *J Pathol* 147:199, 1985;† **Ellis**, *Brit J Exp Pathol* 59:584, 1979 (Sudan, Azire strains); **Geisbert**, *J Comp Pathol* 106:137, 1992 (Reston strain); **Fisher-Hoch**, *J Infect Dis* 166:753, 1992

*In vitro study.
†Animal model.

Family *Filoviridae*

Viruses in the family *Filoviridae* have been isolated from outbreaks of fatal hemorrhagic fevers of man in Africa, and subsequent fatal human laboratory infections (Table 13.12). They are large filamentous viruses that produce widespread necrosis with cytoplasmic inclusions in liver, lungs, and spleen. The hemorrhagic diatheses that occur in skin, mucous membranes, viscera and gut lumen in terminal stages of disease reflect generalized endothelial damage, thrombocytopenia, and depletion of coagulation factors. These, together with loss of plasma volume, dehydration, and hypoproteinemia, cause fatal shock and renal failure. Filoviruses have a uniform diameter of 80 nm but are of varying length up to 1,400 nm, some being filamentous and others U-shaped. They are composed of a helical nucleocapsid (50 nm in diameter) covered by a membrane envelope bearing a 10 nm–thick surface projection layer (derived from the host cell plasma membrane). These structures are used for attachment and entry into the host cell.[132] To mature, new virions bud from the surface of infected cells and foci of nucleocapsids accumulate in the cytoplasm.[133,134]

Genus *Marburgvirus*

Hemorrhagic diatheses into skin, mucous membranes, viscera, and gastrointestinal lumens characterize terminal phases of Marburg hemorrhagic fever. Foci of necrosis occur in liver, lymph nodes, kidneys and gonads. Hepatocytes contain large cytoplasmic inclusions. Necrotic cells collapse into Councilman-type inclusions but there are only sparse infiltrates of inflammatory cells. Interstitial pneumonitis, pancreatitis and iridocyclitis are common and virus can be isolated from fluids of the eye and from semen.

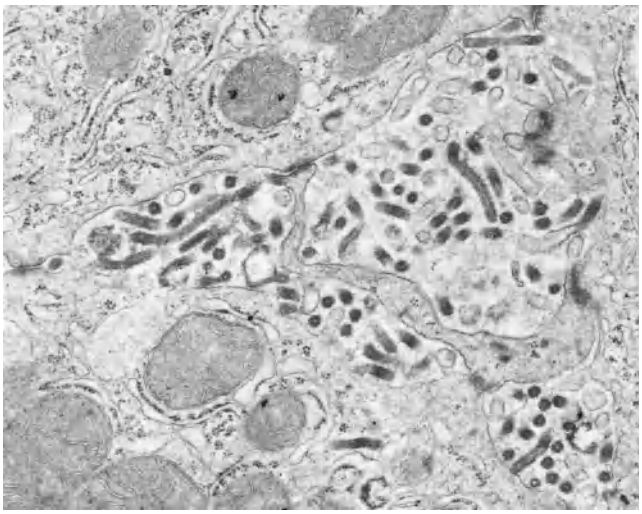


Fig. 13.27 **Filovirus**: *Marburg virus*, monkey. Bile canaliculus at day 7 postinoculation. Cylindrical forms of virus particles are in the canalicular lumen. (Micrograph: Frederick Murphy, *Lab Invest* 24:279, 1971.)

Monkeys inoculated intraperitoneally with Marburgvirus develop marked neutrophilia, depletion of lymphocytes and early failure of platelet aggregation. Later consumption coagulopathy develops with microangiopathic hemolytic anemia, thrombocytopenia and failure of prostacyclin production by vascular endothelium.[135] These are followed by liver dysfunction, dehydration, hypoalbuminemia, and, terminally, renal failure and shock. Changes in liver begin as widely scattered foci of infected hepatocytes that progress to widespread necrosis. Virions bud from plasma membranes, especially into biliary canaliculi (Fig. 13.27).[136,137] Excess production of core material produces cytoplasmic inclusions of viroplasm and closely aggregated viral tubular structures. Large

Vet-ebooks.com

aggregates of virions and necrotic cellular debris are found throughout the liver. Splenic changes develop later and have fewer virions.

Genus *Ebolavirus*

Ebolavirus causes a fatal disease in humans. Liver is a major site of damage. In monkeys, Ebolaviruses replicate throughout the body, producing virions and viral antigens in most tissues. Fibrin-platelet thrombi are common. Virions are prominent in the plasma and circulating monocytes and macrophages but are less common in lymphocytes.[138–140] Zairean strains produce more extensive lesions than do Sudanese strains and thus mimic disease in humans.[134] Zairean strains produce large numbers of virions in liver, lung, and spleen and necrosis of the spleen. In simian disease caused by Sudanese strains, virions are found only in liver, and there only in small numbers. The recently reported Reston strain of Ebolavirus is highly pathogenic for monkeys, but less so for humans.

Family *Coronaviridae*

Coronaviruses are associated with diarrheal disease caused by viral replication in enterocytes, degeneration and sloughing of affected cells into the lumen, and atrophy of intestinal villi. Several coronaviruses cause pneumonitis or encephalitis, especially in young animals (Table 13.13). Coronaviruses are pleomorphic and, by negatively stained images, vary from 80 to 160 nm in diameter. They have a distinctive fringe of petal-shaped peplomers or spikes that resemble a crown (or corona). Their peplomers are about 20 nm long and are 7 nm wide at the tip. There are about 200 peplomers per virion in mouse hepatitis virus. Nucleocapsids are 9–11 nm in diameter. Discrete holes in the virion surface can be produced by incubation of virus with antibodies.[141]

The coronavirus replicative cycle occurs in the cytoplasm. In intestinal enterocytes, virions appear in lumens of vacuoles and in markedly dilated cisternae of endoplasmic reticulum, abnormal membranes derived from rough endoplasmic reticulum, and Golgi complex.[142] Virions first penetrate enterocytes between microvilli, probably by phagocytosis. Virions are rarely found in the nuclear envelope and even more rarely, budded from the plasma membrane. Coronaviruses utilize lysosomes for intracellular replication and virions are found within and budding into these organelles.[143,144] Virions are typically released from the cell during exocytosis of virion-filled vesicles, and accumulate in large numbers in extracellular spaces (Fig. 13.28).

Genus *Coronavirus*

Severe Acute Respiratory Syndrome The **severe acute respiratory syndrome (SARS)** coronavirus replicates in pneumocytes and pulmonary macrophages to cause diffuse damage to the alveolar wall.[145] Lesions include pneumocyte desquamation, monocyte infiltration, and hyalin membrane formation. Pneumocyte cytomegaly and foamy macrophages have been reported in affected lungs. SARS in rhesus monkeys is a faithful model for the human disease.[146]

The SARS virion is pleomorphic and bears characteristic surface spikes.[147] In vivo the SARS virion has a mean diameter of 78 nm.[148] Infection begins when the virion spike binds to its receptor, angiotensin converting enzyme 2 (ACE2), an event that initiates conformational changes in the spike protein that drives virus-host membrane fusion.[149] Inside the cell, replication begins in **viral RNA replication complexes**, features of all mammalian positive-stranded RAN viruses.[150] SARS coronavirus-induced cytoplasmic aggregates within areas of enoplasmic reticulum are composed of membrane vesicles and tubules that contain viral RNA, viral nucleocapsid protein, and the nonstructural protein nsp3.[151] These viral replication sites are close to Golgi areas where spikes are fromed. Budding of virions occur within the ER-Golgi intermediate compartment.

Other Human Coronaviral Diseases Numerous reports identified coronaviruses from human feces and pharyngeal washings and these viruses have been implicated in both enteric and respiratory disease. Human coronaviruses cause colds in adults, the transmission and clinical signs of which closely mimic colds caused by rhinoviruses. Most isolates from the human respiratory tract are related antigenically to strain 229E or OC43, two distinct coronaviruses. Only rarely does serious infection of the lower respiratory tract occur, although cases of pneumonia have been described in infants. The correlation of diarrhea and coronaviruses in stools is far from absolute, but it is clear that enteric disease does result in infection, and that in rare cases in newborns, necrotizing entercolitis can result. Coronaviruses found by negative staining in stools of infants with necrotizing entercolitis show no cross reaction with other coronaviral strains.[152]

Coronavirus Disease of Animals **Murine hepatitis virus (MHV)** produces a febrile, systemic disease in young mice that is characterized by random foci of necrosis in the liver, lymphoid organs, and bone marrow. Large acidophilic, cytoplasmic bodies in hepatocytes arise from autophagy and are composed of aggregates of ribosomes, reduplicated endoplasmic reticulum, and autophagosomes. Virions are present

Vet-ebooks.com

Table 13.13 *Coronaviridae*.

Virus	*Disease in*	*Reference to ultrastructural pathology*
		Genus *Coronavirus*
Infectious bronchitis virus	Chicken Turkey	**Chong**, *J Comp Pathol* 92:199, 1982 (kidney); **Ducatelle**, *Zentralbl Vet Med B* 31:151, 1984 (trachea)
Bovine coronavirus	Cow	**Doughri**, *Exp Mol Pathol* 25:355, 1976; **Mebus,** *Vet Pathol* 10:45, 1973; **Mebus**, *Am J Vet Res* 36:1719, 1975; **Stair**, *Am J Vet Res* 33:1147, 1972
Canine coronavirus	Dog	**Evermann**, *J Vet Diagn Invest* 17:610, 2005; **Larson**, *Am J Vet Res* 40:477, 1979; **Takeuchi**, *Lab Invest* 34:539, 1976
Feline coronavirus	Cat	**Kipar**, *Vet Pathol* 42:321, 2005 (vasculitis); **Ward**, *Virology* 41:191, 1970 (virion)
		Evermann, *Vet Pathol* 18:256, 1981
Human coronavirus	Human	**Shieh**, *Hum Pathol* 36:303, 2005 (lung); **Neuman**, *J Virol* 80:7918, 2006 (lung); **Shi**, *Am J Gastroenterol* 100:169, 2005; **Snijder**, *J Virol* 80:5927, 2007 (cytopathology)
	Monkey	**Oin**, *J Pathol* 206:251, 2006†
	In vitro	**Beniac**, *PLoS ONE* 2:e1082, 2007; **Goldsmith**, *Emerging Infect Dis* 10:320, 2004 (virion); **Stertz**, *Virology* 361:304, 2007 (virion)
Human enteric coronavirus	Human	**Resta**, *Science* 229:978, 1985
Murine hepatitis virus	Mouse	**Fishman**, *Science* 229:877, 1985 (brain); **Fleury**, *Neuropathol Appl Neurobiol* 6:165, 1980 (brain); **Goto**, *Jap J Vet Sci* 47:971, 1985 (liver, nude mouse); **Hirano**, *Lab Invest* 15:270, 1966 (lymphoid tissue); **Knobler**, *Am J Pathol* 109:157, 1982 (brain); **Lampert**, *Acta Neuropathol* 24:76, 1973 (encephalitis); **Miyai**, *Exp Molec Pathol* 2:464, 1963 (liver); **Ruebner**, *Am J Pathol* 51:163, 1967 (cortisone); **Svoboda**, *Am J Pathol* 41:205, 1963 (liver); **Virelizier**, *Infect Immun* 12:1127, 1975 (brain); **Wang**, *Lab Invest* 66:744, 1992 (brain)
	Rat	**Watanabe**, *Lab Invest* 57:375, 1987
Murine coronavirus	Mouse	**Lavi**, *Lab Invest* 58:31, 1988 (encephalitis)
Porcine epidemic diarrhea virus	Pig	**Ducatelle**, *Arch Virol* 79:1, 1984; **Sun**, *Vet Microbiol* [E-pub] 2008
Porcine hemagglutinating encephalomyelitis virus	Pig	**Greig**, *Res Vet Sci* 12:304, 1971 (encephalitis); **Phillip**, *Vet Rec* 88:311, 1971
Rabbit coronavirus	Rabbit	**Edwards**, *J Infect Dis* 165:134, 1992 (myocarditis); **Fennestad**, *J Gen Virol* 67:993, 1986 (pleural effusion virus)†
Rat coronavirus		**Nagashima**, *Acta Neuropathol* 45:205, 1979 (brain)
Sialodacryoadenitis virus	Rat	**Percy**, *Vet Pathol* 26:238, 1989
Transmissible gastroenteritis virus	Pig	**Mengeling**, *Am J Vet Res* 33:297, 1972; **Moon** HW, *Vet Pathol* 12:434, 1975; **Olson**, *Am J Vet Res* 34:1239, 1973; **Pensaert**, *Arch Ges Virusforsch* 31:321 and 335, 1970; **Pospischil**, *Zbl Vet Med* 28:564, 1981; **Thake,** *Am J Pathol* 53:149, 1968; **Wagner**, *Can J Comp Med* 37:177, 1973
Turkey coronavirus (bluecomb)		**Gonder**, *Am J Vet Res* 37:1425, 1976 (enteritis); **Pomeroy**, *Am J Vet Res* 39:1348, 1978; **Ritchie**, *Avian Dis* 17:546, 1973 (virion)*
		Genus *Torovirus*
Bovine torovirus (Breda virus)	Cattle	**Fagerland**, *J Gen Virol* 67:1293, 1986 (virion); **Pohlenz**, *Vet Pathol* 21:407, 1984
Equine torovirus (Berne virus)	Horse	**Weiss**, *Arch Virol* 92:1, 1987
Human torovirus	Human	**Beards**, *J Med Virol* 20:67, 1986

*In vitro study.
†Animal model.

in cytoplasmic vacuoles. They are approximately 80–100 nm in diameter with 60 nm–wide nucleoids of dense particles. The inner core is enveloped by an outer membrane bearing filamentous projections. MHV also causes enteric disease, and lethal diarrhea has been reported. Cytopathic changes in infected cells in vitro are characterized by more extensive membrane damage. Clinical disease is induced by immunosuppression; nude mice are markedly susceptible to MHV.[153]

The JHM strain of MHV replicates in oligodendrogliocytes and produces an acute demyelinating

Vet-ebooks.com

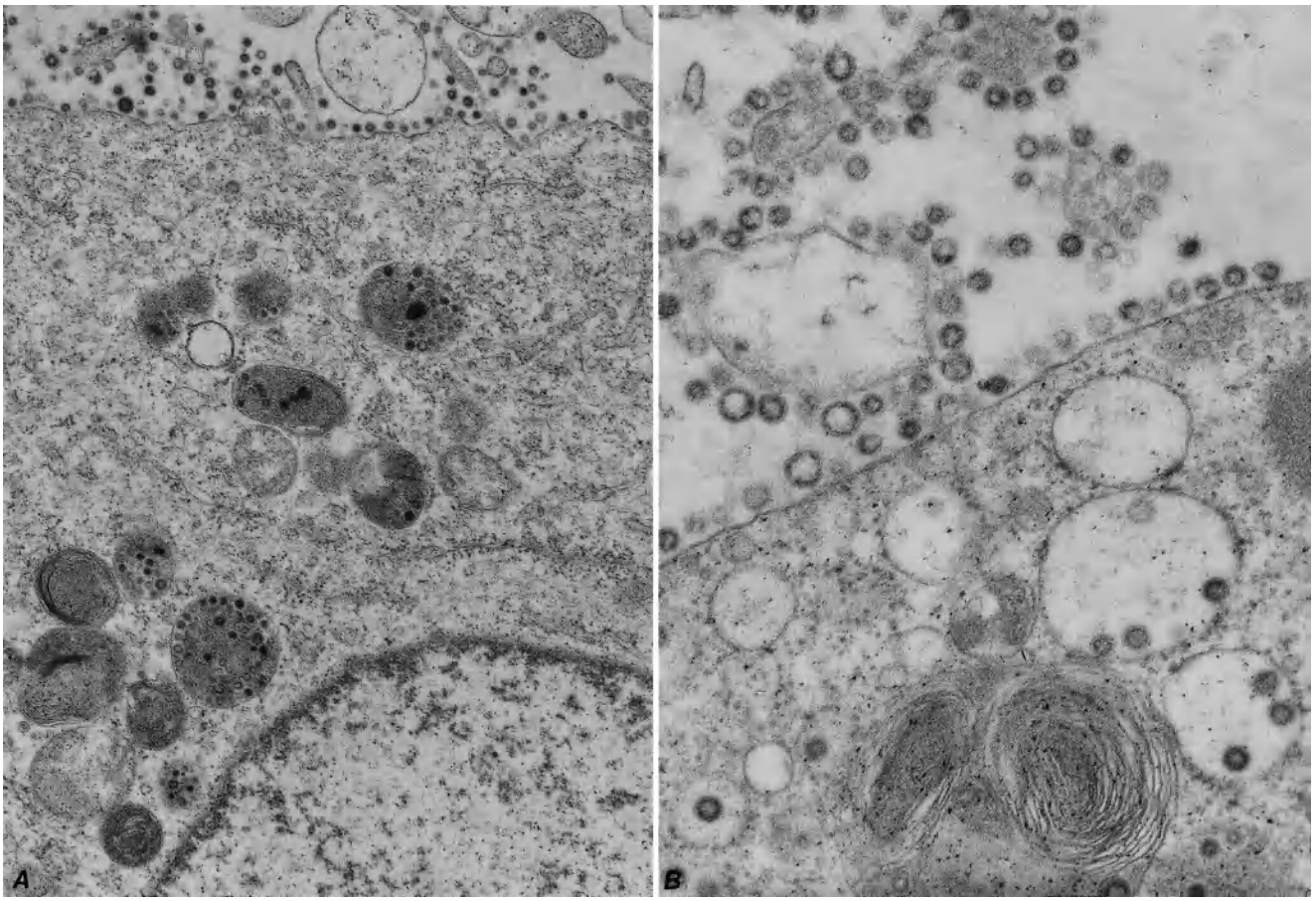


Fig. 13.28 Cytopathology of coronavirus infection: transmissible gastroenteritis, pig. **A**. **Virions** are at the cell surface and in cytoplasmic vacuoles. **B**. **Virions** are highly pleomorphic.

encephalomyelitis when inoculated into the brain and spinal cord of rat and monkeys. Inoculated intranasally, the JHM strain of MHV causes necrosis of nasal mucosal epithelium and high titers of virus in nasal exudates, spleen, and brain (but not liver). Neuronal degeneration in the olfactory tract and anterior commissure is followed by meningoencephalitis. Infected brains develop degenerate oligodendrogliocytes with acute cell swelling, vacuolation, and increases in microtubules, filaments, and aggregates of dense particles. Myelin figures are present in the cytoplasm and show connections with myelin lamellae. Virions are found with glial cell cytoplasmic vacuoles.[154] Astrocytes and macrophages are infected; giant cells form in suckling mice.

Sialodacryoadenitis of Rats Sialodacryoadenitis (SDA) is a naturally occurring coronavirus infection of the laboratory rat. Lesions include sialoadenitis of the submandibular and parotid salivary glands and necrotizing dacryoadenitis of exorbital and harderian lacrimal glands.[155]

Coronaviral Diseases of Swine **Transmissible gastroenteritis (TGE)** is an acute, rapidly spreading enteric disease of young pigs that is characterized by vomiting, diarrhea, dehydration and high mortality in neonates. The causal coronavirus is excreted in the milk of infected sows and infects sucklings. It replicates in and destroys absorptive cells on small intestinal villi. Degenerate cells are sloughed but are replaced by new cells migrating from the intestinal crypts, which are not directly affected by TGE virus. Affected villi become shorter because the core of the villus contracts and because new cells are flattened as they attempt to cover the naked villous surfaces. As villous atrophy becomes severe, the villi, which are normally long and slender, become small, distorted stubs over the basal surface of the intestine. The functional defect that results from atrophic villi is malabsorption.

Cell changes include degeneration and loss of the microvillous border, degranulation of endoplasmic reticulum, and cell shrinkage. Newly produced virions, which are 75–88 nm in diameter, bud from cytoplasmic membranes, particularly from those

Vet-ebooks.com

associated with the Golgi complex. Virions are also seen free in the cytoplasmic matrix and extracellularly between microvilli. Degenerate cells lose surface enzymatic activity, and viral antigens are present throughout the cytoplasm. Viral replication is limited to the absorptive cells on the villi, and crypt epithelium is sparse. In recovery, proliferation of crypt cells permits rapid replacement on the villi of short, cuboidal, newly regenerating epithelial cells. These cells have incomplete microvillous borders, narrow terminal webs, and numerous free ribosomes.

Hemagglutinating encephalomyelitis virus (HEV) of swine is associated with a "vomiting and wasting" disease of piglets and is spread from the nasal cavity of healthy swine. Cells infected with HEV vacuolated in vitro form syncytia, and develop granular cytoplasmic inclusions. Virions average 90 nm in thin section and have surface projections approximately 15 nm long. Virions are present within cytoplasmic vesicles and along cell surfaces in close apposition to the plasma.

Bovine Coronaviral Disease Bovine coronavirus diarrhea was first reported in the early 1970s as coronaviral enteritis in newborns. With fluorescent antibody techniques, viral antigens are seen in epithelial cells of the small intestinal villi and surface of the colon. Large amounts of virus are produced in the feces of infected calves and can be detected by electron microscopy. Virions are typically 90 nm by negative staining. In thin sections, cores (50–60 nm) are electron dense, with lucent centers; virions are 70–80 nm in diameter. Cellular uptake occurs via fusion of virions with plasma membranes covering microvilli or via fusion with lateral plasma membranes. Granular viral factories develop in the apical cytoplasm of intestinal absorptive cells, and membrane-bound dense granular matrices contain dense virions.

Feline Infectious Peritonitis Feline infectious peritonitis (FIP) is a lethal disease involving ascites and diffuse fibrinous peritonitis. Kittens with antibody in their serum develop more serious disease than do kittens that have never been exposed to the virus.[156] FIP virus is present in macrophages in lesions in the liver, spleen, and omentum where it incites a granulomatous vasculitis.[157] Virions, spherical and highly pleomorphic, appear in dilatations of the endoplasmic reticulum and in the matrix of large vacuoles, which also contain granular material. Surface spikes are apparent. Virions have a nucleoid that is 50–55 μm in diameter with a central lucent area of 20–30 μm.

Infectious Bronchitis of Chickens Infectious bronchitis virus (IBV) of chickens begins as a serous tracheobronchitis and progresses to catarrhal and fibrinous inflammation, with exudates in the sinuses, air sacs, and peribronchial areas of the lungs. In young chicks, infectious bronchitis virus also replicates in the ovary and epithelium of the oviduct (where it causes hypoplasia). Infection of renal tubules leads to nephrosis, with accumulation of urates.[158] Infected chicken embryos show runting and have lesions in the respiratory tract. Ultrastructural examination of infected tracheal epithelium reveals early acute cell swelling and marked intercellular edema.[159] Fluid disperses through the intercellular spaces separating epithelial cells. Degeneration involves vacuolar degeneration and accumulation of lipids. Necrosis with desquamation develops rapidly. Virions are seen confined within vacuoles in the cytoplasm and embedded in exudate at the luminal cell surface. As infection proceeds, mucous cell hyperplasia obliterates the early changes.

Bluecomb of Turkeys Transmissible enteritis (bluecomb) of turkeys is a highly infectious acute diarrheal disease involving anorexia and emaciation. Dehydration is often severe and is associated with urate deposits in the kidney. The causal coronaviruses vary from 50 to 150 nm in diameter and bear typical coronavirus projections on their surfaces. Epithelial degeneration and villous atrophy are constant.[160]

Genus *Torovirus*

Toroviruses have been isolated from neonatal horses (Berne virus) and cattle (Breda virus) with diarrhea.[161] Toro-like viruses have been reported from cats with a syndrome of diarrhea and protrusion of nictitating membrane virus is found in the feces in early stages of infection. Torovirus-like particles have also been found by negative staining in the feces of humans with diarrhea.[162] In infected cattle, large numbers of bean-shaped virions are excreted into feces but their role in disease is not clear. Diarrhea results from the experimental inoculation of newborn germ-free calves found vacuolated enterocytes containing virions and viral antigens 48–60 hr after infection.[163,164] Virions mature in the cytoplasm in membrane vacuoles interpreted to be lysosomes (Fig. 13.29).

Family *Reoviridae*

Reoviruses (from **r**espiratory-**e**nteric-**o**rphan virus) replicate in the cytoplasm, and many of them produce irregular, cytoplasmic inclusion bodies. Reoviruses have been found in feces of healthy and sick mammals, and isolates are grouped serologically into three types. Natural infections are common in birds and many mammals (Table 13.14). Except for the avian and

Vet-ebooks.com

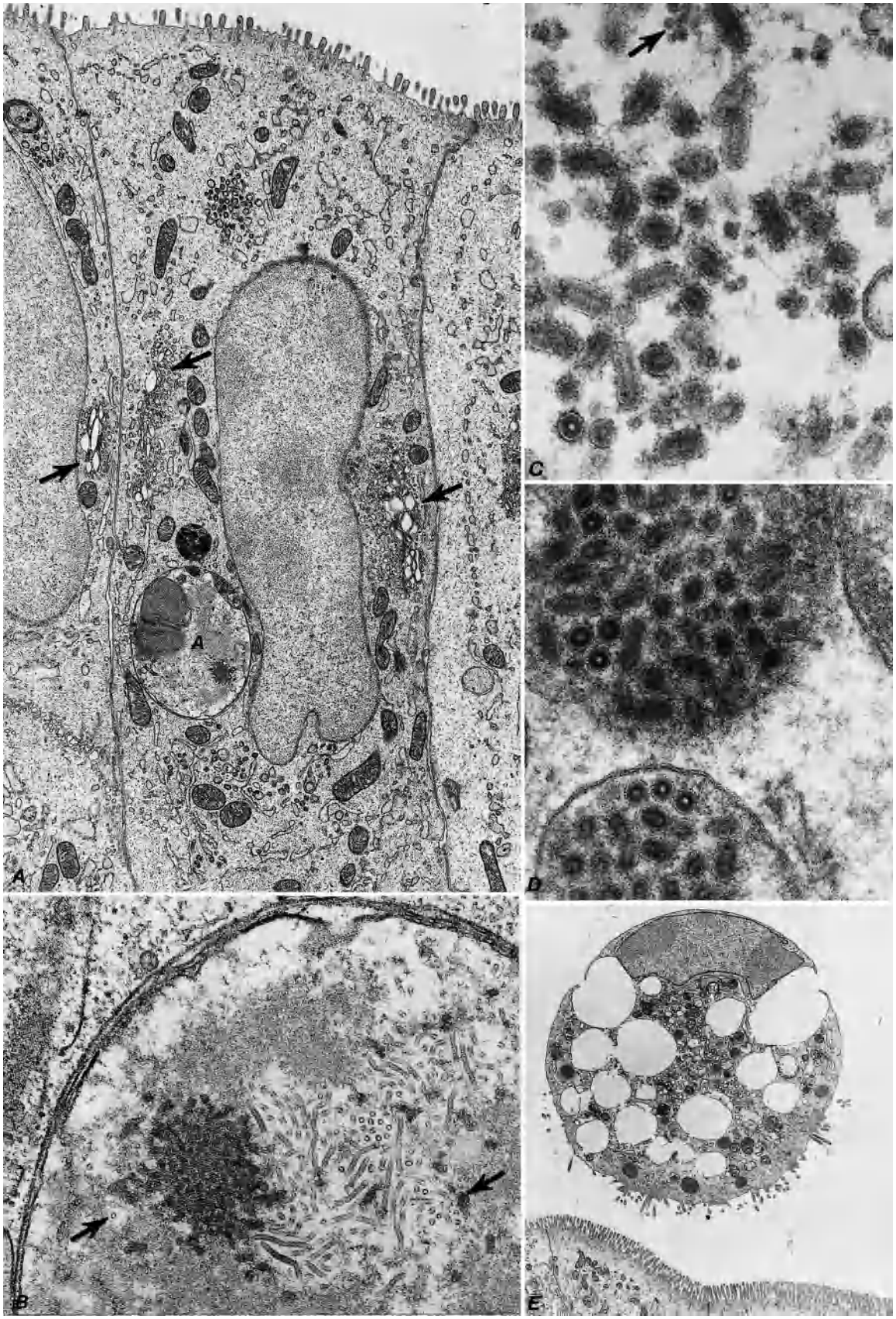


Fig. 13.29 **Torovirus**: intestine, calf infected with Breda virus. **A**. **Infected M cell** overlying intestinal lymphoid tissue. Golgi complex is vacuolar (*arrows*). Cytoplasm contains many vesicles and a large autophagosome (*A*) containing viral components. **B**. **Autophagosome**: matrix is filled with viral tubules and nucleocapsids (*arrows*). **C**. **Virions in cytoplasm**: extravacuolar. **D**. **Virions in cytoplasmic vacuoles**. **E**. **Vacuolated enterocyte**: cell has sloughed into the intestinal lumen.

Vet-ebooks.com

Table 13.14 *Reoviridae*.

Virus	*Disease in*	*Reference to ultrastructural pathology*
		Genus *Orthoreovirus*
Mammalian orthoreovirus 1,2,3	Human	**Wolf**, *Science* 212:471, 1980
	Ferret	**Margolis**, *Lab Invest* 21:189, 1969 (hydrocephalus)
	Mouse†	**Bass**, *Lab Invest* 58:226, 1988 (M cells, intestine); **Gonatas**, *Lab Invest* 24:101, 1971 (brain); **Hassan**, *Am J Pathol* 55:147, 1969 (embryo); **Hassan**, *Exp Mol Pathol* 4:66, 1969 (myocarditis); **Jenson**, *Am J Pathol* 49:1171, 1966; **Joske**, *Br J Exp Pathol* 44:337, 1966; **Margolis**, *J Neuropath Exp Neurol* 33:178, 1974 (eye); **Onodera**, *Science* 201:529, 1978 (pancreas); **Papadimitriou**, *Pathology* 11:447, 1979 (peritoneum)
Avian orthoreovirus	Chicken	**Walker**, *J Ultrastruct Res* 41:67, 1972 (arthritis)
		Genus *Orbivirus*
Bluetongue virus	Cow	**Bowne**, *J Am Vet Med Ass* 153:662, 1968
	Deer	**Howerth**, *Am J Vet Res* 49:1914, 1988; **Stair**, *Vet Pathol* 5:164, 1968
	In vitro	**Eaton**, **Virology** 157:107, 1987 (cytoskeleton);* **Eaton**, *J Struct Biol* 109:61, 1992 (virion);* **Lecatsas**, *Onderstepoort J Vet Res* 35:139, 1968;* **Owen**, *Onderstepoort J Vet Res* 33:9, 1966*
	Mosquito	**Bowne**, *Virology* 30:127, 1966
	Sheep	**Osburn**, *Lab Invest* 25:197, 1971 (brain)
African horse sickness virus	Horse	**Breese**, *J Am Vet Med Ass* 155:391, 1969;* **Newsholme**, *Onderstepoort J Vet Res* 50:7, 1983
Epizootic hemorrhagic disease virus	Deer	**Thomas**, *Can J Comp Med* 35:22, 1971;* **Tsai**, *Am J Pathol* 70:379, 1973; **Tsai**, *Can J Microbiol* 16:427, 1970
Equine encephalosis virus	Horse	**Van Niekerk**, *J Gen Virol* 84:581, 2003 (virion)
		Genus *Rotavirus*
Rotavirus	Human	**Poruchynsky**, *J Cell Biol* 114:651, 1991 (endoplasmic reticulum);* **Quan**, *Intervirology* 20:223, 1983 (endosomes);* **Woode**, *Inf Immun* 14:804, 1976 (comparative study); **Yeager**, *J Cell Biol* 110:2133, 1990 (virion)*
	Cow	**Mebus**, *Am J Vet Res* 38:553, 1977; **Stair**, *Vet Pathol* 10:155, 1973
	Monkey†	**Wyatt**, *Arch Virol* 50:17, 1976 (human viruses)
	Mouse	**Adams**, *Am J Pathol* 51:39, l967; **Banfield**, *Virology* 36:411, 1968; **Starkey**, *J Gen Virol* 67:2625, 1986: **Uhnoo**, *J Virol* 64:361, 1990 (hepatitis, monkey isolates)
	Pig	**Hall**, *Vet Pathol* 13:197, 1976; **Leece**, *Inf Immun* 14:816, 1976; **McAdaragh**, *Am J Vet Res* 41:1572, 1980; **Narita**, *J Comp Pathol* 92:589, 1982; **Pearson**, *Arch Virol* 59:127, 1979
	Rat	**Huber**, *Vet Pathol* 26:376, 1989; **Vonderfecht**, *J Virol* 52:94, 1984
	Sheep	**McNulty**, *Inf Immun* 14:1332 (1976); **Snodgrass**, *Arch Virol* 55:263, 1977
	Turkey	**McNulty**, *Arch Virol* 61:13, 1979
		Genus *Coltivirus*
Colorado tick fever virus	Human	**Emmons**, *J Gen Virol* 17:185, 1972 (erythrocyte); **Murphy**, *Virology* 35:28, 1968
	Monkey	**Gerloff,** *Am J Pathol* 35:1043, 1959
		Genus *Aquareovirus*#
American grass carp virus	Carp	**Mohd**, Virology 373:310, 2008; **Winton**, *J Gen Virol* 68:353, 1987 (virion)
Snakehead reovirus	Snakehead fish	**John**, *Dis Aquat Organ* 46:83,
Striped bass reovirus	Bass	**Attoui**, *J Gen Virol* 83:1941, 2003

*Studies in vitro.
†Animal model.
Aquareoviruses isolated from aquatic animals include a wide variety of named isolates: Chinook salmon reovirus, Coho salmon reovirus, Atlantic salmon reovirus, and striped bass reovirus.

Vet-ebooks.com

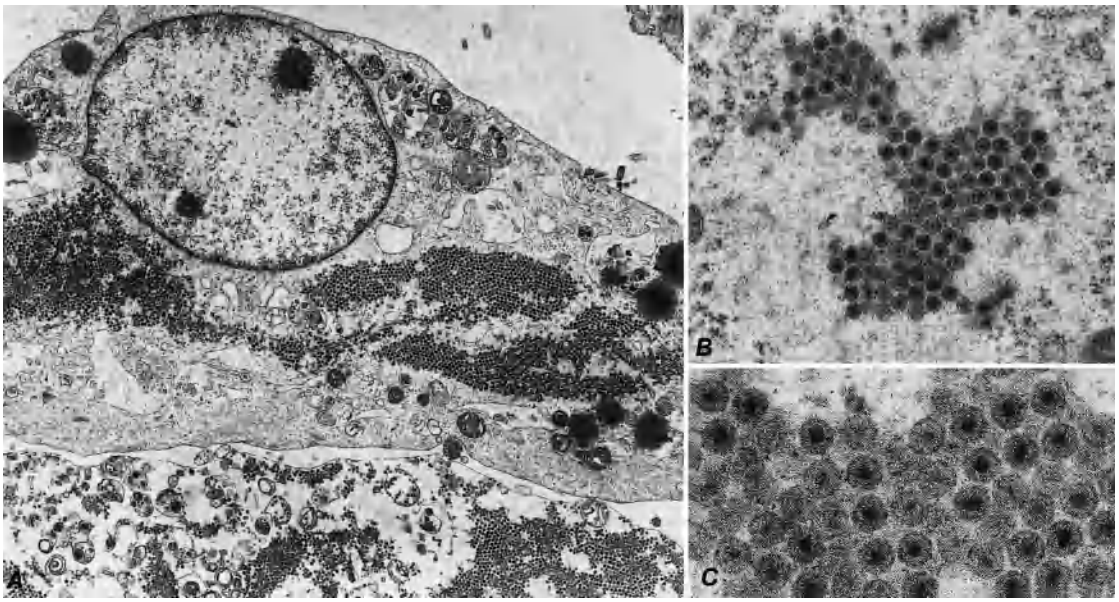


Fig. 13.30 Reovirus. A. Virions: free in the cytoplasm; cells in culture. **B** and **C. Virions in cytoplasm**.

murine isolates, the relation of these viruses to natural disease is vague.

Genus *Orthoreovirus*

Reoviruses are associated with natural infections in birds and many species of mammals. Reoviruses replicate in the cytoplasm producing large irregular eosinophilic inclusions of densely packed virions (Fig. 13.30). The reovirus genome is of double-stranded RNA. In the intestine, reoviruses enter the body through M cells of epithelium covering the intestinal lymphoid tissue. Experimentally, when closed ileal loops are infected with reoviruses, virions can be shown ultrastructurally to be attached to M cell surfaces within 30 min; by 60 min, virions are present in the cytoplasmic phagosomes as well as in coated pits and vesicles.[165] Virus is taken into cells via phagosomes which are rapidly transformed to lysosomes where the genome is uncoated. Virions develop within the lysosome, and later in foci of lysis in the cytoplasmic matrix. Virions in the cytosol are icosahedral, are nonencapsulated, and are approximately 75 nm in diameter, and have an inner electron-dense core of 45 nm surrounded by an inner shell. In foci of replication in the cytoplasm, virions are surrounded by a zone of lysis containing tiny filaments 5–8 nm in diameter.

Human Reoviral Disease Reoviruses are rarely implicated in human disease. Enteritis in infants and upper respiratory infection with fever, pharyngitis, rhinitis, headache, and rash have been reported. Types 1, 2, and 3 have all been isolated from humans. Reovirus type 3 has been reported in associated with hepatitis and bilary atresia in a neonate. The actual causal role of these viruses in the disease process is vague and adequate pathologic and ultrastructural studies have not been done.

Animal Reoviral Disease In young **mice**, acute reovirus infections occur naturally and are characterized by nervous signs, oily hair, and jaundice. Lesions include degeneration and necrosis of cells in visceral organs. Infection in neonates is especially severe. Pneumonia and myocarditis dominate with reovirus types 1 and 2; encephalitis is more marked with type 3. Congenital infection may result in persistent viremia. Virus replication leads to formation of large cytoplasmic inclusions and degeneration and necrosis in brain, retina, liver, intestine, myocardium, and peritoneum. Crystalline arrays of virions comprise the inclusions and also occur in membrane-bound vacuoles filled with necrotic debris. In the degenerate pancreas, virions have been seen in endocrine tissue and in duct cells of the exocrine tissue; it has been postulated that much of the acinar cell necrosis may be due to ductal obstruction.

In the brain, reoviruses are found in neurons and ependymal and glial cells where they are free in the cytoplasm, often in lattice or crystalline arrangements. Virions are surrounded by tiny irregular filaments 5–6.5 nm in diameter. In dendrites and some other parts of the cell, virions are associated with large filamentous forms that appear to be modified neurotubules. Macrophages surround degenerating neurons and contain virions in cytoplasmic autophagic vacuoles. **Hydrocephalus** has been induced experimentally by inoculation of murine reoviruses into various hosts.

Vet-ebooks.com

In reovirus type 1, CNS infection, viral antigens, and inclusions develop in ependymal cells of the choroid plexus from 3 to 10 days after inoculation, during which time there is progressive necrosis, lysis, and sloughing of infected cells into the ventricular cavities. Spared islands of ependyma on the denuded surfaces of the ventricles undergo abortive and inadequate regeneration, forming epithelial rosettes and buried ependyma-lined tubular structures. Proliferation of gliovascular granulation tissue results in overgrowth of residual ependyma and leads to adhesions of apposing ventricular walls.

Avian reoviruses have been isolated from two diseases: arthritis of chickens and a diarrheal disease of turkeys. In the chorioallantoic membrane of chick embryos, avian reoviruses replicate in and cause proliferation of mesenchymal cells. Large prominent cytoplasmic inclusions seen by light microscopy are composed of masses of lattice arrangements of reoviruses. Virions measure 75 nm in diameter, with inner cores of 45 nm.

Genus *Orbivirus*

Orbiviruses (from Latin *orbis*, ring or circle) have similar morphology and other properties but no common antigen. **Bluetongue virus (BTV)** is the prototype of the genus. The core particle consists of two major inner proteins plus the dsDNA genome. The two major (VP3 and VP7) and three minor proteins (VP1, VP4, and VP6) are surrounded by an outer capsid of two major proteins (VP2 and VP5). In infected cells three nonstructural proteins (NS1, 2, and 3) are formed, at least one of which appears to be a chaperonin and prevents core particles from assembling before the correct minor core proteins. BTV structure, as determined by cryoelectron microscopy, has an inner shell of icosahedral form with 260 triangular spikes of VP7 trimers arranged on a T+13,1 lattice. The outer shell consists of 120 globular regions.[166,167] The outer shell of the viral capsid is removed after the virion enters the target cell. Tubular forms of virus develop in vitro.

Orbiviruses are distinguished from other members in the family *Reoviridae* in that they multiply in insects and invertebrates. Orbiviruses that infect humans include bluetongue virus and several orbiviruses associated with human disease in tropical regions of Africa and South America.

Bluetongue **Bluetongue** is an arthropod-borne disease affecting ruminant animals. Virus replication occurs in the parenchymal cell cytoplasm in salivary glands of *Culicoides* mosquitos. Fever, ulcers of the oral cavity and lameness due to lesions in the coronary bands characterize this disease of sheep. The essential lesion in epithelium is a small focus of necrosis of keratinocytes which progresses to an ulcer. Intense hyperemia, edema and hemorrhage suggest a vascular disease and viral antigens have been found in vascular cells. During viremic stages BTV has been shown to bind and enter erythrocytes.[168] In the animal, subtle lesions may be present in the viscera, particularly in myocardium and skeletal muscle. **Hydroencephaly** and porencephaly are localized in white matter. Acute necrotizing encephalitis occurred in fetuses affected in early gestation; chronic inflammation in later stages.

African Horse Sickness **African horse sickness (AHS)**, a peracute, highly febrile, systemic disease of horses, donkeys, and mules, is transmitted by biting midges of the genus *Culicoides* (AHS is noncontagious). Death occurs a few hours after signs of disease appear and is due to terminal right heart failure. Horses have disseminated vascular lesions with edema and hemorrhage. Striking subcutaneous edema dissects through fascial planes and aponeuroses of underlying musculature, and extends to peripheral lymph nodes. Severe pulmonary edema contributes to death and edema is also present in the body cavities. There is marked lymphoid depletion and necrosis of germinal centers in lymphoid organs. Virions develop in endothelial cells, especially in the lungs.[169] Capillaries of the pulmonary bed are filled with microthrombi and fibrin. Affected endothelium has acute cell swelling with increased caveolae and accumulations of cytoplasmic viroplasm bearing virions.[170]

Epizootic Hemorrhagic Disease **Epizootic hemorrhagic disease (EHD)** is a highly lethal systemic disease of deer characterized by widespread vascular damage which is seen as hyperemia, edema, and hemorrhage. Hemorrhage occurs from viral replication in and damage to endothelial cells. Affected capillaries show marked endothelial damage with fibrin and platelets in the lumens. The terminal syndrome involves loss of plasma volume, hemoconcentration and shock, and the coagulation system is deranged. Virions of 60 nm diameter have been found in the cytoplasm of endothelial cells of infected deer. There is acute cell swelling with formation of large spherical cytoplasmic inclusions of viral granular material. Inclusions have ragged granular edges and viral particles develop within the interior. Tubular aggregates are associated with inclusions in cell infected in vitro.

Genus *Rotavirus*

Rotaviruses are a major cause of diarrheal disease. They are the agents of neonatal diarrhea in man and in many animal species including calves, pigs, lambs,

Vet-ebooks.com

foals, deer, and mice. Feces contain large amounts of virus and virions are easily found ultrastructurally by negative staining. In intestinal tissue, virions are clearly demonstrable ultrastructurally in the lumen of the intestine and in epithelial cells.[171,172]

Rotaviruses have been classified into 7 groups (A to G) based on antigenic relatedness and on migration patterns of RNA in gel electrophoresis. Group A rotaviruses are most widespread and are found in most mammalian species. Viruses of group B are found in humans and rats, and groups D, F and G are the avian rotaviruses. There is a serologic relationship between rotaviruses of different species that is mediated by antigens of the inner capsid; that is, calf virus can be used as a diagnostic antigen for human rotavirus and so forth.

Lesions caused by rotaviruses that produce acute enteritis are chiefly acute cell swelling with degeneration and necrosis of enterocytes. Virions are found in vacuoles in the cytoplasm. The cellular damage leads both to atrophy of intestinal villi and to fluid loss into the gut lumen. The virus infects and destroys villous epithelial cells, especially of the middle and posterior parts of the small intestine. Taken into cells by endocytosis,[173] virions are uncoated and replicate in the cytoplasm. Viral progeny acquire a temporary envelope by budding into cisternae of the rough endoplasmic reticulum. Evidence of viral infection occurs within 12 hours of infection and includes vacuolation and then loss of enterocytes.

During maturation, rotavirus cores form in the viroplasm and acquire the inner capsid proteins to form single-shelled particles. The rotavirus structural glycoprotein NSP4 is an intracellular receptor that mediates the acquisition of a transient membrane envelope as subviral particles bud into the endoplasmic reticulum. NSP4 also mediates diarrhea by potentiated chloride secretion by triggering a signal transduction pathway.

NS28, a transmembrane glycoprotein, modifies the endoplasmic reticulum and is the receptor for subsequent budding of single-shelled particles from the membrane into the endoplasmic reticulum cisternae. Budding is the process that forms the transient membrane-enveloped particle. During maturation, the membrane envelope is lost (uncoating) forming the virion. Glycosylation (and calcium) within the endoplasmic reticulum controls the final assembly process; for example, depletion of calcium and use of the glycosylation inhibitor tunicamycin both block maturation and lead to accumulation of enveloped intermediate particles.[174]

Enteric disease in most neonates is self-limiting, and epithelial regeneration begins within a few hours of injury. Many other mammalian species have rotaviruses that cause diarrhea in neonates. Oral inoculation of mice with **murine rotavirus** leads to infection of the small intestine but not of the colon. Diarrhea is maximal at 72 hr after inoculation. Only enterocytes in the upper two-thirds of the intestinal villus are infected.[175] **Simian rotavirus** causes an acute self-limiting disease in mice. Replication is limited to terminally differentiated inactive enterocytes on villi of the small intestine. Extramucosal spread and development of hepatitis occur in immunosuppressed mice.[176] Scanning electron microscopical studies of surfaces of rotavirus-infected intestinal epithelial cells reveal the striking changes of surface microvilli and sloughing of enterocytes into the lumen; for example, dogs infected with **canine rotavirus** develop swollen epithelial cells on villi, denuded foci, and villous atrophy.

Rotaviral Gastroenteritis: Group A Rotaviruses **Human rotaviral enteric disease** with severe diarrhea is a common disease of humans. The rotavirus of human infantile gastroenteritis induces diarrheal disease in 2–5 days when inoculated into newborn rhesus monkeys. Lesions occur in the small intestine where viral antigens are demonstrable by immunofluorescence on villous absorptive cells. Virions occur in cytoplasmic amorphous membrane-bound vacuoles.

Porcine rotaviruses infect differentiated columnar epithelial cells on villi of the posterior small intestine and induce transient diarrhea and malabsorption. Detectable 24 hr after infection, atrophy of villi is an early and consistent lesion. Viral antigens appear in small intestinal epithelium and persist up to 96 hr. They also occur in macrophages in the lamina propria and mesenteric lymph nodes, probably as antigens liberated from infected epithelium. Sporadic infected epithelial cells are also found in the colon. Viral antigens are detectable in fecal debris up to one week after infection. The initial response to infection is acute cell swelling; infected epithelial cells rapidly shrink, become cuboidal, develop cytoplasmic lipid globules, lose microvilli, and develop dense cytoplasmic inclusions formed of protein lattices. Virions are present in lucid areas of the cell and covering the stunted microvilli. Cells rapidly become necrotic and desquamate from the villi. Similar phenomena have been reported in epithelium of stomach and respiratory tract. Intranuclear tubules, similar to those in the mouse rotaviral infections, have been seen during early infection in pigs. The diameter of nuclear tubules is similar to that of tubule in the cytoplasm that represents viral capsid protein. Pigs are susceptible to infection with the bovine rotaviruses and experimentally become anorectic and depressed with profuse diarrhea.

Bovine rotaviral diarrhea develops when rotaviruses replicate in the cytoplasm of epithelial cells of the posterior small intestine. Villous tips are chiefly affected in contrast to the bovine coronavirus, which

Vet-ebooks.com

damages both crypts and villous epithelium. Viral-induced epithelial destruction results in blunting of intestinal villi, malabsorption, and dehydration. **Respiratory disease** in calves has also been associated with rotavirus infection; minimal lesions in the lungs and upper respiratory tract are produced upon experimental infection. Ultrastructural lesions of rotaviral disease of lambs are similar to those in cattle.

Epizootic diarrhea of infant mice (EDIM) is frequently severe in suckling and weanling mice. EDIM is often seasonally enzootic with peak morbidity in winter. Lesions occur in tips of villi in the small intestine. Infected epithelial cells are swollen, vacuolated, and foamy. Severe hyperemia and dilatation of lymphatics are present below the epidermis. Virions are present in membrane-bound vacuoles in the cytoplasm.

Infectious diarrhea of infant rats (IDIR) is caused by group B rotaviruses. Ultrastructural changes in the intestine of suckling rats closely resemble those found in group A infections, for example, vacuolation of enterocytes with virions within vacuoles.[177] Two distinct changes are present: formation of epithelial syncytia, and a highly transient presence of viral antigen. By immunolabeling, viral antigens are found only up to 48 hr after infection.[178]

Non-A Non-B Rotaviruses Viruses found associated with enteritis of several species including humans have been called pararotaviruses and are isolated with low frequency (1 in 200 cases of rotavirus infection) from stools of human infants with acute gastroenteritis. Pararotaviruses differ from rotaviruses antigenically but are similar in genomic structure. Ultrastructurally, pararotaviruses are double-shelled.[179]

Genus *Coltivirus*

Coltiviruses are spherical 80 nm diameter virions with two outer capsid sheaths. The central core has no projections. Surface capsomere structure of the core particles differ from the genus *Orbivirus*.

Colorado Tick Fever **Colorado tick fever (CTF)** is a tick-borne febrile disease of humans and other primates, characterized by chills, fever, somnolence, headache, and muscle pain. Convalescence is without sequelae and recovery is complete. In rare severe cases, a 2–3 day remission may be followed by a second febrile period with leukopenia; nervous signs, abortion, and disseminated intravascular coagulation have been reported. CTF virus is associated with erythrocytes in which it replicates. Experimental infection induced in rhesus monkeys is largely asymptomatic. Viremia occurs and may persist for several weeks. CTF virus has been adapted to mice by serial passage and these isolates are typically neurotropic. Lesions include destruction of neurons in the cerebellum and basal ganglia with hemorrhage and vascular engorgement. Cytoplasmic inclusions may be present in neurons. Virus can be propagated in chicken embryos, where it is found chiefly in the central nervous system.

Genus *Aquareovirus*

The genus *Aquareovirus* was created to group several viruses of fish and shell fish (see Table 13.14). Piscine aquareoviruses have been reported worldwide and cause a spectrum of diseases that include epizootic ulcerative syndrome (snakehead reovirus) and the American grass carp reovirus.[180]

Family *Arenaviridae*

Genus *Arenavirus*

Arenavirus (*Arenosus*, Latin, "sandy") virions are spherical to pleomorphic measuring 50–300 nm in diameter and consist of an envelope and a nucleocapsid. Distinctive club-shaped surface projections (peplomers), 8–10 nm long, are found on the surface. Small 20–30 nm granules are ribosomes formed of methylated 28S and 18S host cell rRNA. During replication, virions mature at the cell. Most arenaviruses are parasites of rodents (Table 13.15). In their rodent hosts the arenaviruses are associated with asymptomatic infection and persistent viral carriage and shedding. The tropism of rodent arenaviruses for the lymphoreticular tissues, although associated with an effective immune response, generally leads to lymphoid destruction, especially in the spleen. When disease does result, it is in newborns or young and, although there is a direct cytopathic effect of the virus, the disease is most often associated with an immunopathic mechanism.

Lymphocytic Choriomeningitis **Lymphocytic choriomeningitis (LCM)** is an acute disease of young field and laboratory mice characterized by wasting and CNS signs. Infection rates are high but disease is rare. LCM virus causes two syndromes: acute disease and asymptomatic persistent infection. Human infection with LCM virus, which occurs in laboratory workers and in owners of pet rodents, usually leads to an influenza-like syndrome with headache. Meningoencephalitic signs are seen in some cases but deaths are not recorded.

In **acute disease** in adult mice, LCM infection leads to death or recovery with immunity. There is systemic

Vet-ebooks.com

Table 13.15 Family *Arenaviridae*.

Virus	*Disease in*	*Reference to ultrastructural pathology*
		Genus *Arenavirus*
		LCM-Lassa Complex
Lymphocytic choriomeningitis virus	Human	**Cole**, *Fed Proc* 30:1831, 1971; **Dalton**, *J Virol* 2:1465, 1968;* **Walker**, *Exp Molec Pathol* 23:245, 1975; **Warkel**, *Neurology* 23:198, 1973
	Mouse	**Ronco**, *Lab Invest* 43:37, 1980 (glomerulonephritis)
	Rat	**Del Cerro**, *Lab Invest* 33:608, 1975(cerebral hypoplasia); **Monjan**, *J Neuropathol Exp Neurol* 32:110, 1973 (cerebellar hypoplasia)
Lassa virus	Human	**Buckley**, *Int Rev Exp Pathol* 18:97, 1978; **Walker**, *Am J Pathol* 107:349, 1977
		Genus *Arenavirus*
		Tacaribe Complex
Argentine hemorrhagic fever (Junin virus)	Human	**Cossio**, *Virch Arch A* 368:1, 1975 (kidney); **Elsner**, *Am J Trop Med Hyg* 22:229, 1973; **Gonzalez**, *Arch Pathol Lab Med* 104:250, 1980 (lymphoid tissue); **Maiztegui,** *J Infect Dis* 132:35, 1975; **Molinas**, *J Infect Dis* 143:1, 1981 (coagulation)
	Guinea pig	**Carballal**, *J Infect Dis* 135:367, 1977 (bone marrow)
Bolivian hemorrhagic fever (Machupo virus)	Human Monkey†	**Child**, *Arch Pathol* 83:434, 1967; **Stinebaugh,** *Am J Med* 40:217, 1966 **Kastello**, *J Infect Dis* 133:57, 1976; **McLoed**, *Am J Pathol* 84:211, 1976; **Terrel**, *Am J Pathol* 73:477, 1973

*In vitro study.
†Animal model.

infection and viral antigens can be detected in many tissues. Lymphocytes, macrophages, platelets, megakaryocytes, and epithelial cells at various sites are infected. Virus in the brain is largely limited to the meninges and choroid plexus.[181,182] In mice, LCM virus persistently infected pancreatic β-cells and leads to hyperglycemia and other evidence of diabetes mellitus.[183] Viral antigens can be demonstrated in granulosa cells and even though they appear to be lacking in the ovum, transmission of virus occurs.

The coupling of LCM persistence and systemic immunodeficiency is linked to viral targeting of fibroblastic reticular cells (**FRCs**) in lymphoid tissue.[184] When infected with LCM, the FRC stomal network upregulates expression of the inhibitory **programmed cell death ligand 1** (PD-1), and this pathway, by preventing excessive immunopathology, supports viral persistence.[184]

Death of mice is due to the anti-LCM immune lymphocyte responses. Immunosuppression will prevent fatal disease, and the effectiveness of thymectomy, antilymphocyte serum, cortisone and irradiation to suppress disease indicates that lesions are caused by the immune response. LCM virus forms new antigens on host cell plasma membranes, and T lymphocytes attack these antigens causing cellular lysis. The outcome of this process determines the status of the host: death, if too extensive; immunity, if successful; and tolerance, if the attack is incomplete. Failure of the immune response may be total (as with congenital carrier infections) or partial—resulting in "split tolerance," chronic persistent and slow wasting disease with glomerulonephritis. LCM virus is passed from pregnant female to offspring in utero by infection of the ovary.

Neonatal infection with persistent viremia is a distinct pattern of disease in mice with LCM. These mice survive with high titers of circulating virus that persist, often for the life of the mouse. This carrier state was originally thought to represent tolerance to infection but mice do produce both humoral and cellular immune responses. The absence of circulating antibody is due do the combination of circulating virus with newly formed antibody molecules. Persistently infected mice develop a chronic wasting disease with trapping of antigen-antibody complexes in renal glomeruli and chronic glomerulopathy.

Hemorrhagic Fevers Viruses associated with these outbreaks in human populations in Central and South America are named for the geographic site or causal virus; for example, Machupo virus is the cause of **Bolivian hemorrhagic fever** and Junin virus is the cause of **Argentine hemorrhagic fever** (Table 13.15). Disease consists of an early febrile phase followed by a hypotensive phase and a terminal shock syndrome. The intense erythema is due to vasodilation of small peripheral vessels and is followed by abrupt leakage of plasma from capillaries. Endothelial injury and thrombocytopenia are marked in severe disease and factor VIII-related antigens are elevated throughout the illness. The low arterial pressure of shock causes decreased renal blood flow. When combined with the direct vascular injury to the kidney, renal failure may

Vet-ebooks.com

ensue.[185,186] Viral-induced damage to platelets occurs and enhances hemorrhaging caused by the preceding vascular injury. Viral antigens can by found in hepatocytes, renal tubular epithelium, macrophages and dendritic cells of spleen and lymph node. Ultrastructural studies on bone marrow revealed cytoplasmic lysis and virions in megakaryocytes, probably the cause of thrombocytopenia during acute infection.[187]

In fatal cases, hepatic necrosis, both focal and diffuse, is typical. In hepatocytes, large masses of necrotic cytoplasm ball up into Councilman-type inclusions. The **rhesus monkey** is a model for these fevers and the lesions of the human disease are reproduced but foci of necrosis may be more extensive in the intestine, skin and adrenal gland.

Family *Togaviridae*

Most togaviruses were previously classified as **arboviruses** (for **ar**thropod **bo**rne) because they are maintained in nature by cyclical transmission between susceptible vertebrate hosts and blood-sucking arthropods, with viral replication in both. Togaviruses are important causes of encephalitis and hemorrhagic fevers in animals and humans (Table 13.16). Transmission by arthropods requires that the virus infect cells of the midgut and pass into the hemocoel in order to infect the salivary glands. Failure of viruses to cross the gut wall limits viral transmission; for example, failure of western equine encephalitis virus to disseminate across the gut wall in *Culex tarsalis* limits this species as a vector. Conversely, any factor that allows virus to directly enter the hemocoel leads to increased transmission. Endemic filariasis may promote togovirus transmission since microfilareae ingested in a blood meal rapidly penetrate the mosquito midgut and facilitate viral infection and dissemination.[188]

Genus *Alphavirus*

Alphavirus virions are spherical to pleomorphic, measure 70 nm in diameter, and consist of an envelope and a nucleocapsid. The nucleocapsid is an isometric spherical particle composed of a single-stranded RNA molecule and 240 copies of a single capsid protein. Inoculated subcutaneously during mosquito bites, they replicate locally in macrophages. Viremia follows,

Table 13.16 *Togaviridae*.

Virus	*Disease in*	*Reference to ultrastructural pathology*
	Genus *Alphavirus*	
Eastern equine encephalitis virus	Horse, human	**Kim**, *Am J Clin Pathol* 84:223, 1985 (brain biopsy)
	Experimental studies	**Murphy**, *Exp Mol Pathol* 13:131, 1970 (mouse brain);† **Nathanson**, *J Comp Pathol Ther* 79:109, 1969
Semliki Forest virus		**Acheson**, *Virology* 32:128, 1967;* **Barrett**, *J Gen Virol* 49:141, 1980;* **Erlandson**, *J Virol* 1:996, 1967;* **Grimley**, *Exp Mol Pathol* 12:1, 1970 (mouse brain);† **Helenius**, *J Cell Biol* 84:404, 1980;* **Kaluza**, *Arch Virol* 93:97, 1989 (mouse brain); **Kondor-Koch**, *J Cell Biol* 97:644, 1983;* **McGee-Russell**, *Nature* 214:1204, 1967 (brain)
Sindbis virus		**Jackson**, *Lab Invest* 58:503, 1988 (mouse brain);† **Jackson**, *Lab Invest* 56:418, 1987 (spinal cord)†
Venezuelan equine encephalitis virus	Horse, human	**Gorelkin**, *Am J Pathol* 73:425, 1973
	Experimental studies	**Garcia-Tamayo**, *Arch Pathol* 96:294, 1973 (mouse heart); **Jahrling**, *J Infect Dis* 132:667, 1975 (hamster); **Jelinková**, *Acta Virol* 18:154, 1974 (monkey olfactory mucosa);† **London**, *Teratology* 16:285, 1977 (monkey brain, eye);† **Ryzhikov**, *Arch Virol* 140:2243, 1995 (mouse, olfactory tract); **Walker**, *Am J Pathol* 84:351, 1976 (hamster brain)
Western equine encephalitis virus	Horse, human	**Houk**, *Virus Res* 2123, 1985 (mosquito); **Morgan**, *J Exp Med* 113:219, 1961*
	Genus *Rubivirus*	
Rubella virus	Human	**Esterly**, *Arch Pathol* 87:380, 1969 (congenital); **Weil**, *New Engl J Med* 292:994, 1975 (chronic disease)
	Experimental studies	**Cotlier**, *Nature* 217:38, 1968 (rat embryo);† **Murphy**, *J Virol* 2:1223, 1968*

*In vitro study.
†Animal model.

Vet-ebooks.com

and if of sufficient titer, results in infection of endothelial cells (thereby passing the blood-brain barrier) and neurons in the brain. The olfactory pathway is a major route to the CNS for some togaviruses.

Alphaviruses enter cells by receptor-mediated endocytosis via coated pits. Viruses attach to the plasma membrane, are trapped into coated pits, move into coated vesicles, and are sequestered into vacuoles and eventually into lysosomes. Within endosomes, acid-activated membrane fusion occurs. Endosomal acid triggers both release of nucleocapsid into the vacuole and conformation changes in viral glycoproteins, in a way that promotes fusion of membranes of host cell and virus. Penetration of the nucleocapsids containing the viral genome into the cytoplasmic matrix occurs through fusion between vacuolar membrane and viral membrane. Subsequent replication of alphavirus RNA occurs entirely within the cytoplasm, in vacuoles that develop and are used for viral RNA synthesis, translation of structural proteins, and assembly of new nucleocapsids.

Cytoplasmic vacuoles are sites of viral RNA synthesis and translation of structural protein, and assembly of new nucleocapsids. Synthesis of proteins occurs on complex ribonucleoprotein structures associated with the cytoplasmic surface of modified secondary lysosomes and endosomes.[189] New glycoproteins form a dimer in the rough endoplasmic reticulum and are transported to the plasma membrane of the cell via Golgi vesicles. Viral glycoproteins are clustered at the plasma membrane, in association with areas of viral budding.

Neurons are infected early and virions can be detected in the cytoplasm. The earliest degenerative changes occur in the endoplasmic reticulum and involve reduplication of membranes and widening of cisternae. Spherical virions consist of a 28–30 nm nucleoid closely wrapped in a membrane covered by projections. Nucleoids appear to migrate to membranes where they mature by budding, either into cytoplasmic vacuoles or at the plasma membrane (Fig. 13.31).[190] In brain, virion maturation occurs largely in cytoplasmic vacuoles and virions are expelled to the exterior of the cell. Thus they do not acquire antigenic components of the plasma membrane of the neuron. Neuronal degeneration and necrosis are accompanied by gliosis and infiltration of affected foci by plasmacytes, small lymphocytes, and neutrophils.

Alphaviral Encephalitides **Eastern** and **western equine encephalitis** are transmitted to humans, horses, and other animals by insects. Both viruses replicate in insect tissue. The viral reservoirs for insects are wild birds in which virus reaches very high titers in blood. In horses, a highly transient viremia occurs and the virus localizes in the brain. Human infections with eastern equine encephalitis virus involve extensive perivascular lymphoid cuffing and replication of virus in neurons.[191]

In horses dead of encephalitis, lesions are most common in the cerebral cortex, basal ganglia, hippocampus, and medullary nuclei; cerebellum and spinal cord are relatively spared. In the brain there are neuronal degeneration, neuronophagia, perivascular cuffs of lymphoid cells and a diffuse accumulation of glial and inflammatory cells. Foci of necrosis of gray and white matter develop in severe cases. Degenerative vascular lesions with thrombi and extravasated erythrocytes are common. Neuronal degeneration and necrosis are accompanied by gliosis and infiltration of affected foci by plasmacytes, small lymphocytes, and a few neutrophils. Lesions in mice closely resemble those in natural.

Immune lymphocytes and antibodies attack infected cells. Clearance of virus results from MHC class I-restricted lysis of virally infected cells by $CD8^+$ T lymphocytes. Neurons, which are not induced and express class I molecules by viral infection, may escape $CD8^+$ lymphocyte-mediated damage. Plasmacytes move to and attack neurons at sites of infection. Experiments with Sindbis virus in SCID mice have shown that antibody clears virus by restricting viral gene expression.[192]

Venezuelan equine encephalitis (VEE) infection in the horse differs from those of the eastern and western equine encephalitis infections. First, the viremia is longer and of greater quantity, sufficient to make possible the mechanical transmission by insects to other species. Second, virus is excreted into the saliva and urine of horses making horse-to-horse contact transmission possible. Third, the virus has a distinct tropism for lymphoid tissue and this is manifest in horses as severe leukopenia and necrosis of lymph nodes and spleen (in laboratory rodents, lymphoid necrosis is extensive). Fourth, the central nervous system lesions are chiefly vascular. The heavy infiltrations of inflammatory cells seen in eastern and western equine encephalitides are not present. Human VEE infections are rarely severe and less often fatal, although virions replicate in bone marrow reticulum cells, megakaryocytes and erythrocyte precursors and cause massive necrosis.

In experimental murine VEE, virions are first seen ultrastructurally in the brain at postinoculation day 5. They are best sought in endothelial cells but also occur in glia, allegedly due to phagocytosis. VEE virus during pregnancy is associated with congenital defects and both cerebral and ocular malformations have been induced in monkeys. In hamsters, the earliest lesions in the thymus and other lymphoid tissues are seen as clear foci containing dense necrotic debris. The predilection of VEE virus for the pancreatic islet β-cells has

Vet-ebooks.com

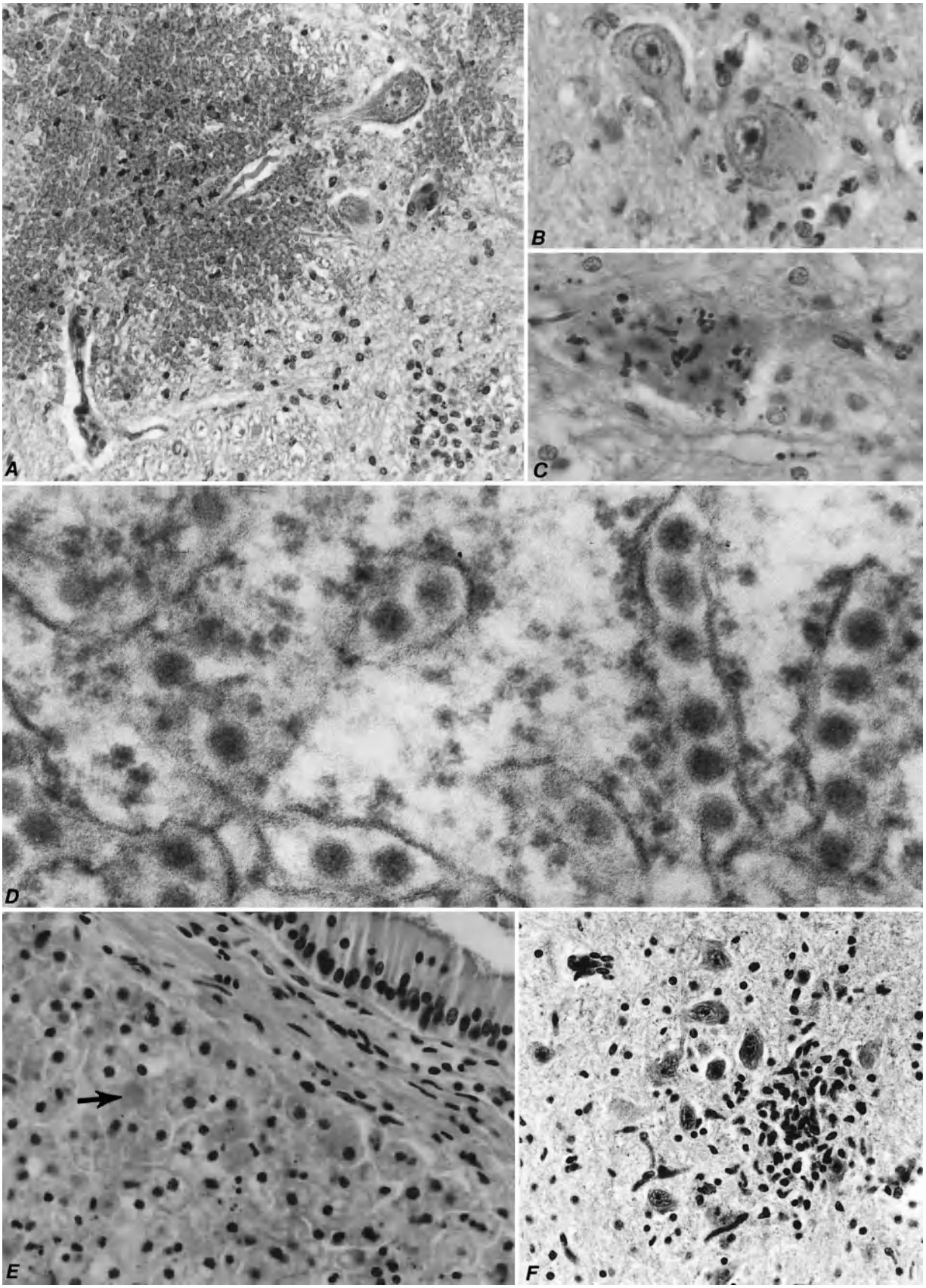


Fig. 13.31 Eastern equine encephalitis: brain, horse. **A–C**. **Histology**. **A**. **Necrosis** of neurons and capillaries. Glial nodule (*lower right*); focus of hemorrhage (*upper left*). **B**. **Neurons**: early phase of acute swelling; neurons surrounded by neutrophils and glial cells. **C**. **Neurons**: late phase of degeneration; neutrophils within cytoplasm of neurons. **D**. **St. Louis encephalitis**: neuron, mouse brain. Virions in cisternae of endoplasmic reticulum. (Micrograph: Fred Murphy, *Lab Invest* 19:652, 1968.). **E–F**. **Yellow fever**: rhesus monkey, experimental. **E**. **Hepatocyte necrosis**: rounded mass of necrosis is referred to as a Councilman body (*arrow*). Biliary epithelium is intact. **F**. **Necrosis of neurons**: inflammatory cells have invaded the infected area, brain.

Vet-ebooks.com

been used as a model for the study of viral-induced diabetes mellitus.

Genus *Rubivirus*

Intracellular development in vitro involves use of normal cellular organelles; for example, the E1 glycoprotein migrates through the endoplasmic reticulum and Golgi complex. Viral glycoproteins are assembled as they leave the rough endoplasmic reticulum and are complexed to form immature viral particles.[193]

Rubella Acute rubella (German measles) in children is a febrile systemic infection characterized by a rash that appears a few days after a primary viremia. In most cases, recovery is prompt although serious sequelae occur.[194] Rubella virus infects and causes limited damage in reticuloendothelial tissues. It replicates in the cytoplasm and release occurs after cellular lysis. Maternal viremia is accompanied by localization of rubella virus in the **placenta** with subsequent lymphocytic villous placentitis and progressive sclerosing inflammation. Angiopathy is common in both placenta and fetus. Cytopathologic changes in the **fetus** that follows viral infection in utero lead to **cardiovascular defects**, **cataracts**, and **ear damage** (to the organ of Corti and stria vascularis, with deafness). There may also be microcephaly, encephalitis (with mental retardation), bone defects, and general growth retardation. The fetus affected by rubella contains virus in tissues throughout the body. Infection may be focal or disseminated, and may occur via direct infection and through embolization. Lymphoid tissue is affected and cell-mediated immunity is impaired. **Eye** lesions include inflammation of the iris and ciliary body and necrosis of the lens. In mouse models, rubella antigens have been detected in the developing lens epithelium. Newborns with congenital rubella, despite the presence of serum antibodies, continue to excrete virus. At 15 months after birth, 20% are still excreting virus in the nasopharynx.

Family *Arteriviridae*

Genus *Arterivirus*

Virions consist of an envelope and a nucleocapsid and measure 60 nm in diameter. The nucleocapsid is isometric with a diameter of 35 nm. The *Arterivirus* genus contains four species: equine arteritis virus, lactate dehydrogenase-elevating virus, porcine reproductive and respiratory syndrome virus (type I European and type II American) and simian hemorrhagic fever virus (Table 13.17).

Equine Viral Arteritis **Equine arteritis viral (EAV)** typically appears as a flu-like disease of horses housed together. Clinical signs are fever, mucopurulent rhinitis, myalgia, and edema of the legs. Virus is excreted from the nasal cavity during and shortly after fever; because of renal infection, viremia may persist. In severe outbreaks it may cause "abortion storms" with serious losses of fetuses and death of mares. Placentitis is severe. In these horses EAV virus causes marked panleukopenia, vasculitis, and striking, widespread medial necrosis of small muscular arteries.

The essential lesion is replication of virus in endothelial cells of capillaries.[195] Endothelial cells swell, develop hydropic degeneration, and virions are present within cytoplasmic vacuoles (Fig. 13.32). Large aggregates of ribosomes and aberrant tubules develop. Capillary damage allows extensive loss of fluid into tissue spaces and terminal disease resembles the hemorrhagic fevers. The fatal sequence of capillary necrosis, increased vascular permeability, contraction of intravascular plasma volume, hemoconcentration, and hypotension are responsible for collapse and death. Virions are found largely in small vesicles in the cytoplasm and are difficult to identify without specific labeling procedures. EVA virus replicates in myocytes of the vascular wall and damage is exacerbated by viral-induced destruction of the vasovasorum and by superimposition of ischemia upon terminal shock

Table 13.17 *Arteriviridae*.

Virus	*Host*	*Reference to ultrastructural pathology*
		Genus *Arterivirus*
Equine arteritis virus	Horse	**Breese**, *Arch Ges Virusforsch* 35:2, 1971;* **Coignoul**, *Vet Pathol* 21:333, 1984 (placenta, fetus); **Estes**, *Am J Pathol* 58:235, 1970
Lactic dehydrogenase virus	Mouse	**Du Buy**, *J Exp Med* 123:985, 1966; **Martinez**, *Infect Immun* 27:979, 1980
Porcine reproductive and respiratory syndrome virus	Pig	**Dea**, *Can Vet J* 33:801, 1992; **Scruggs**, *Vet Path*ol 38:339, 2001 (vasculopathy); **Magar**, *Can J Vet Res* 57:300, 1993
Simian hemorrhagic fever virus	Monkey	**Allen**, *Am J Trop Med Hyg* 17:413, 1968 (pathology); **Wood**, *J Gen Virol* 7:129, 1970*

*In vitro study.

Vet-ebooks.com

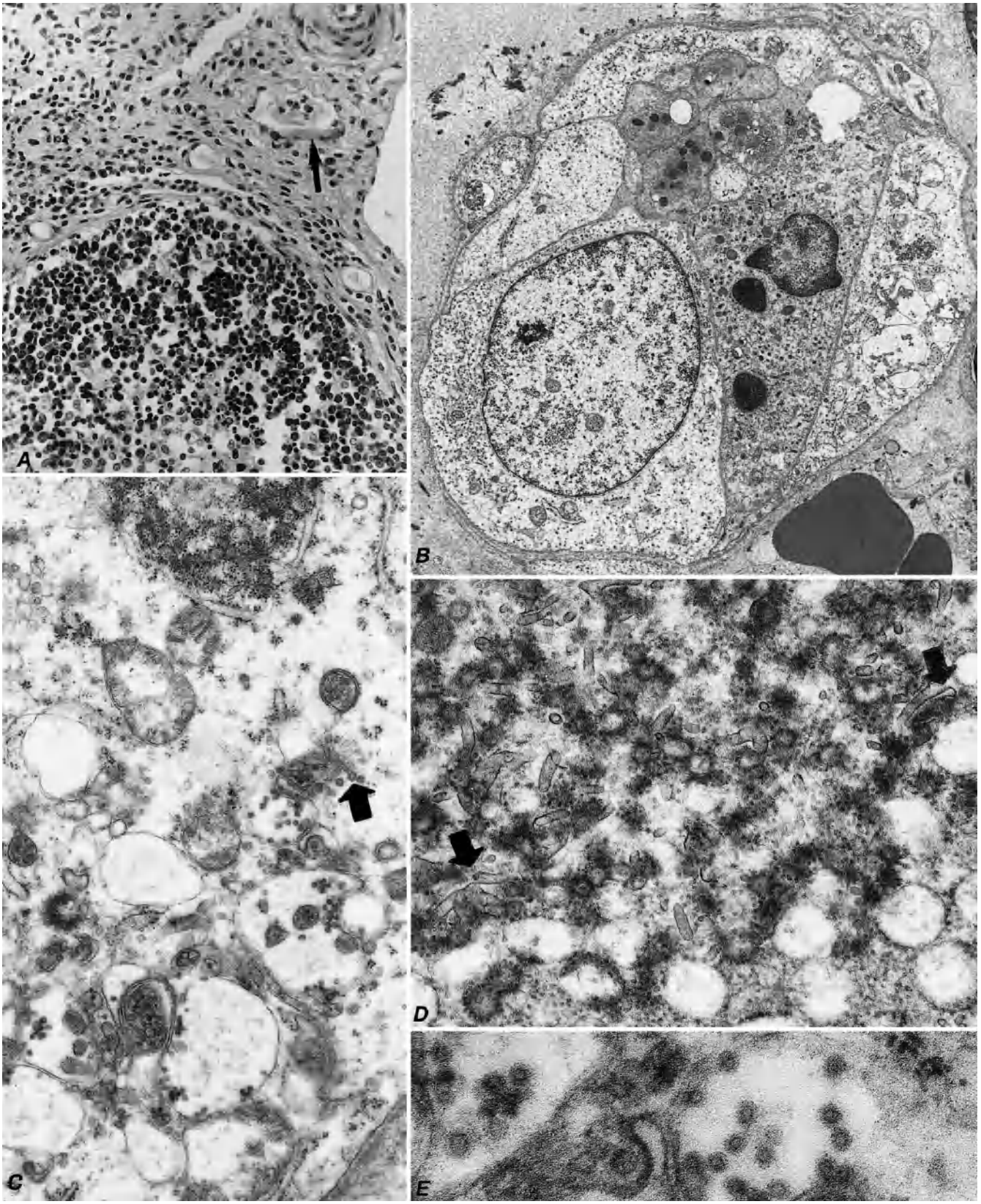


Fig. 13.32 ***Arterivirus:*** equine arteritis, viral, lymph node. **A**. **Vasculopathy** (*arrow*), lymphoid necrosis. **B**. **Degenerate capillary endothelium**: acute cell swelling; capillary lumen is obstructed by platelets and a neutrophil. Perivascular spaces contain erythrocytes, fibrin, and plasma protein precipitates. **C**. **Cytopathology in endothelial cell** (enlargement of B); cells are vacuolated. Note: virions (*arrow*), aberrant ribosomes (*top*), and vacuoles. **D**. **Viral tubules and ribosomes**. **E**. **Virions** in cytoplasmic vacuoles.

Vet-ebooks.com

syndrome. Viral replication also occurs in smooth muscle cells of the pregnant uterus and this, rather than viral infection of the fetus, is the basis for most abortion.

LDH Virus **Lactate dehydrogenase-elevating (LDH) virus** causes a natural infection of mice, with high plasma viral titers within 24 hr after infection. No disease is known to be caused by LDH virus.

Chronic viremia is accompanied by persistent elevation of several enzymes in plasma. Ultrastructural studies of infected lymph nodes show the presence of small virions of approximately 50 μm in diameter within cytoplasmic vacuoles.[196,197]

Porcine Reproductive and Respiratory Syndrome **Porcine reproductive and respiratory syndrome (PRRS)** is an important disease that causes reproductive failure in breeding stock and respiratory tract illness in young pigs. PRRS virus has an affinity for alveolar macrophages in which it is found in lumens of the ER and Golgi complex.[198] Late-term abortions, excessive stillbirths, and mummified fetuses are seen in sows affected with PRRS. Live born piglets can often show respiratory distress. Interstitial pneumonia in neonatal pigs with respiratory distress is a hallmark.[199,200] Aborted fetuses and stillborn piglets have had cutaneous hemorrhages and subcutaneous capillary angioplasia with proliferative vasculopathy.[201]

Simian Hemorrhagic Fever Viral zoonoses causing hemorrhagic fever are caused by three major viral families: *Arenaviridae, Bunaviridae*, and *Filoviridae*. **Simian hemorrhagic fever virus (SHV)** causes persistent infection without overt clinical signs of disease in most Old World monekys, but causes a fatal hemorrhagic fever in macaques. SHV was isolated from an epizootic of severe febrile hemorrhagic disease in a primate quarantine colony at the National Institutes of Health that killed 223 of 1,050 macaque monkeys. Sudden fever, facial edema, erythema, proteinuria, and epistaxis were characteristic. There was 100% mortality and death was due to shock from extensive disease of the capillary bed. Transmissibility was limited to simian primates, a differential factor from Kyasanur Forest disease. Lesions of simian hemorrhagic fever involved widespread necrosis in the monocyte-macrophage system and lymphoid organs. In spleen, the periarterial lymphoid sheaths contain necrotic cells, extravasated erythrocytes, and fibrin. Fibrin deposits are present in splenic venous sinuses, in capillaries in many organs, and in the renal glomerulus. In the kidney, the fibrin-plugged glomeruli and cortical necrosis suggest a Shwartzman reaction.[202]

Family *Bornaviridae*

Genus *Bornavirus*

Borna disease virus (BDV) is the cause of an infectious neurological disease that occurs sporadically in horses and sheep in central Europe. Lesions of natural Borna disease are lymphomonocytic encephalomyelitis, chiefly in gray matter. Although neuronal degeneration is uncharacteristic, nuclear inclusions occur in large neurons.[203] Ultrastructurally, there are decreased numbers of ribosomes in affected neurons.[204] Virions have not been identified ultrastructurally, but Borna virus cDNA encodes a protein recognized by antibodies in humans with behavioral diseases.[205] The virus is probably 85–125 nm in diameter. In immunofluorescence tests for Borna disease virus, antigen is in the nucleus and cytoplasm of neurons[206,207] throughout the central nervous system and retina.

Family *Flaviviridae*

Flaviviruses constitute a large diverse group of viruses, most of which are transmitted by invertebrates. During the life cycle, virus infects both arthropod and vertebrate hosts. Although smaller than the *Togaviridae*, the cytopathology and pathway of virion production in infected cells do not differ greatly. During the life cycle, virus infects both arthropod and vertebrate hosts. Virions are spherical to pleomorphic measuring 40–60 nm in diameter. The capsid/nucleocapsid has polyhedral symmetry and has a diameter of 25–30 nm. Flaviviruses develop in the cytoplasm, and virions bud from membranes of the endoplasmic reticulum and vacuolar system (Table 13.18). The cell's secretory pathway provides the environment for replication of flaviviruses. For example, immature dengue virions bud into the ER of an infected cell and pass to the TGN where the low pH causes them to undergo a reversible conformational change that renders them accessible to furin cleavage. Furin is a protease primarily localized in the TGN. The acidic environment of the trans Golgi network prevents membrane fusion.[208]

Experimental infection of monkeys[209] and mice[210] has clearly shown that cytoplasmic vacuoles are the site of viral maturation.

Genus *Flavivirus*

Yellow Fever In humans, following an incubation period of a few days, **yellow fever (YF)** virus may produce an asymptomatic infection or a peracute fatal syndrome with high fever, leukopenia, albuminuria, icterus, and petechiation. At autopsy, findings include

Vet-ebooks.com

Table 13.18 *Flaviviridae*.

Virus	*Disease in*	*Reference to ultrastructural pathology*
		GENUS FLAVIVIRUS
		Mosquito-borne Viruses
Dengue virus	Human	**Halstead**, *Yale J Biol Med* 42:350, 1970 (human)
	Experimental studies	**Ng**, *Arch Virol* 104:197, 1989 (antigens);* **Pokidysheva**, *Cell* 124:485, 2006 (virion);* **Sriurairatan**, *Infect Immun* 8:1017, 1973 (mouse);† **Sriurairatna**, *Am J Trop Med* 26:1199, 1977* (mosquito)
Yellow fever virus	Monkey	**Baruch**, *Exp Cell Res* 29:50, 1963 (monkey); **Bearcroft**, *J Pathol Bact* 83:59, 1962 (monkey); **Bergold**, *Virology* 17:554, 1962 (virions);* **McGavran**, *Am J Pathol* 45:501, 1964 (monkey)†
Wesselsbron virus		**Lecatsas**, *Arch Ges Virusforsch* 27:332, 1969*
		Japanese Encephalitis Subgroup
Japanese encephalitis virus	Monkey	**Hase**, *Virch Arch B* 63:25, 1992;* **Nathanson**, *Clin Exp Immun* 6:161, 1970 (monkey)†
	Mouse	**Oyanagi**, *Acta Neuropathol* 13:169, 1969 (mouse)
Murray Valley encephalitis virus	Human	
	Mouse	**Matthews**, *Int J Exp Pathol* 81:31, 2000 (brain)
St. Louis encephalitis virus	Mouse	**Monath**, *Lab Invest* 48:399, 1983; **Murphy**, *Lab Invest* 19:652, 1968
		Tick-borne Viruses
Kyasanur Forest disease virus	Monkey	**Webb**, *Trans R Soc Trop Med Hyg* 60:325, 1966
Louping ill virus	Sheep	***Doherty***, *J Comp Pathol* 83:481, 1973 (brain)
		GENUS PESTIVIRUS
Classical swine fever virus (hog cholera)	Swine	**Cheville**, *Lab Invest* 20:261, 1969 (chronic); **Sánchez-Cordón**, *Vet Pathol* 42:477, 2005 (spleen)
Bovine viral diarrhea virus 1 and 2	Cattle	**Peter**, *Am J Vet Res* 29:939, 1968
Border disease virus	Sheep	**Anderson**, *Lab Invest* 57:168, 1987; **Barlow**, *J Comp Pathol* 93:451, 1983; **Cancilla**, *Res Vet Sci* 9:88, 1968 (spinal cord)
		GENUS HEPACIVIRUS
Hepatitis C virus	Human	**Panda**, *Hepatol* 10:466, 1989
	Experimental studies	**Burk**, *J Med Virol* 7:1, 1981 (chimp, liver); **Feinstone**, *J Infect Dis* 144:588, 1981 (primates); **Jacob**, *J Infect Dis* 161:1121, 1990;* **Shimizu**, *Science* 205:197, 1979 (chimpanzee)

*In vitro study.
†Animal model.

severe, diffuse fatty degeneration of parenchymal cells of the liver, heart, and kidney. Cytolytic effects on hematopoietic and lymphoid tissues are extensive, including marked destruction of lymphocytes, endothelial cells, and bone marrow stem cells. Hemorrhages occur in many tissues, particularly the endocardium and gastric mucosa. Necrosis of hepatocytes causes prothrombinemia which exaggerates the hemorrhages caused by viral damage to thrombocytes (thrombocytopenia). Ultrastructural changes in hepatocytes include loss of glycogen, aggregation of ribosomes, and disorganization of cytoplasmic membranes. Virions develop in large cytoplasmic vacuoles, but because of rapid onset of necrosis, virions may be difficult to detect. YF virus replicates in neurons and encephalitis is often a component of the disease humans.

The experimental disease in monkeys is remarkably similar to that in humans. Injected subcutaneously, YF virus is removed by and replicates in phagocytes of the reticuloendothelial system (inhibition of macrophage function enhances dissemination of virus). In preclinical incubation stages, viremia occurs and viral antigens can be detected by immunolabeling in Kupffer cells of the liver. Necrosis of Kupffer cells is followed by diffuse fatty degeneration of hepatocytes. Large lipid globules accumulate in the cytoplasm and pale irregular eosinophilic intranuclear inclusions (Torres bodies) develop in the nucleus. Nucleoli disappear and chromatin marginates. Nuclei become

Vet-ebooks.com

increasingly pyknotic and remain only as small basophilic debris as the cytoplasm of the cell becomes a homogenous, hyaline, necrotic mass, the **Councilman body** (Fig. 13.31E–F). Changes are more conspicuous in midzonal areas of the liver, but this is not obvious in peracute disease.

Dengue **Dengue fever** is a benign febrile disease of humans in tropical Asia characterized by headache, rash, and lymphadenopathy. Dengue virus replicates in mosquitos and is injected during feeding upon human skin. After replication at the site of arthropod bites and in regional lymph nodes, virus disseminates and produces damage to vascular endothelium of liver, lymphoid organs, bone marrow and skin. The late-occurring maculopapular rash may involve cell-mediated immunity, that is, sensitized lymphocytes attach on viral-bearing cells of the dermis. Within the nervous system, virus replicates in neurons and glia. Early cytopathic changes include degranulation and dilatation of the endoplasmic reticulum, segregation of the fibrous and granular parts of the nucleolus, and development of fibrogranular structures. Virions develop in cisternae of the endoplasmic reticulum, especially in perinuclear areas.[211] In **dengue hemorrhagic fever**, a second syndrome associated with dengue virus, signs appear after a few days of classic dengue fever. Damage is due to severe direct viral-induced injury to capillaries and platelets, which combine to produce thrombocytopenia and hemorrhage.

The **dengue shock syndrome** occurs from the sequence of leakage of serum proteins into extravascular spaces, to cause hypoalbuminemia, hemoconcentration, and shock. The shock syndrome, a manifestation of an immune reaction, occurs in children or adults experiencing their second dengue infection. Virus is isolated with difficulty and drop in levels of complement; the severity of shock depends upon the sequence of viral types and the interval between eliciting and sensitizing infections which can be a minimum of 3 months and maximum of 5 years. IgG appears to mediate immunologic injury. One mechanism of damage may be due to the complexing of IgG to free virus, attraction of complement, and the subsequent aggregation of platelets resulting in thrombocytopenia.

Other Flaviviral Encephalitides The most prominent changes in **St. Louis encephalitis (SLE)** are neuronal degeneration, perineuronal and perivascular microglial proliferation, and perivascular infiltration of lymphoid cells and monocytes. In experimental infections in mice, SLE virions accumulate in cisternae of the endoplasmic reticulum. They are round, 38 nm in diameter and have electron-dense cores. Reduplication and convolution of pathologic endoplasmic reticulum lead to lattice and tubular structures in affected cytoplasm. Studies in hamsters indicate that the olfactory route is the principal pathway of infection of the brain. Viral antigens were detected in bipolar neurons of the olfactory epithelium, their dendrites, and axon bundles of submucosal olfactory nerves. Sequential analysis reveals infection of the olfactory neuroepithelium 4 days after inoculation, of olfactory bulbs at 5 days, and of the brain at 6 days postinoculation.[212] **Japanese B encephalitis**[213] causes cytopathic changes in natural and experimental hosts that are similar to those of St. Louis encephalitis.[214,215]

Tick-Borne Flaviviruses The tick-borne flaviviruses are set apart epidemiologically from the mosquito-borne viruses. Ticks become infected by feeding on animals during the viremic phase. Viral transmission in the tick is usually transovarial, that is, it is passed from female ticks to offspring through the ovary. The diseases tend to occur in forested regions.

The **Russian spring-summer encephalitis (RSSE)** complex causes human meningoencephalitis in Eastern Europe. Disease may be asymptomatic, a mild febrile syndrome, or a severe neurologic death with mortality about 30%. Brain lesions involve the gray matter and include necrosis of neurons, glial proliferation and inflammatory cells.[216] Virions are found in the thalamus, substantia nigra, and cerebellum. Electron micrographs reveal 42 nm diameter particles that are poorly defined.[217]

Louping Ill An encephalomyelitis of sheep that occurs in the spring in Scotland and northern England, louping ill causes a peculiar leaping (louping) gait. Transmission occurs via the tick *Ixodes ricinus*. Extensive necrosis of neurons, particularly of Purkinje cells of the cerebellum, occurs. Infected cells are surrounded by plasmacytes. Vascular necrosis develops.

Kyasanur Forest Disease **Kyasanur Forest disease**, a tick-borne vascular disease, caused widespread deaths in monkeys in India in 1956. It was characterized by diarrhea and severe vascular lesions and ended in shock, brachycardia, and death. Necrosis of vessels and portions of lymph nodes and spleen were found. In a few monkeys the virus replicated in neurons and glia, producing inflammation and necrosis in both gray and white matter. Humans infected with the virus developed hemorrhages, and lesions are limited to the hematopoietic system.

Genus *Pestivirus*

Hog Cholera **Hog cholera** (classical swine fever) is an acute febrile disease characterized by severe

Vet-ebooks.com

generalized vasculitis and necrosis. Pigs that die have widespread petechiation, thrombosis, splenic infarction, intestinal ulceration and encephalitis. Large amounts of virus are present throughout the reticuloendothelial, lymphoid and epithelial tissues.[218] The virus is highly destructive to lymphoid tissue, in which is causes necrosis of lymphocytes, reticular cell hyperplasia, and plasmacytosis. Late in disease there is thymic atrophy, absence of lymph node germinal centers, disappearance of splenic lymphoid tissue, all with marked histiocyte hyperplasia. Virions, measuring 53 nm in diameter, can be found among lysosomal debris and cytoplasmic vacuoles in macrophages, endothelium, and epithelium of the alimentary, respiratory and urinary tracts (Fig. 13.33). They are best sought in tonsil epithelial cells although even here they are difficult to identify due to the severity of cytopathic changes.

Chronically infected swine continue to excrete virus and viral antigens are limited to epithelium of the salivary gland, lower ileum and renal collecting ducts. **Glomerulonephritis** develops in the terminal stages of disease by several complex interrelated factors: direct viral-induced damage to the glomerular endothelium, inhibition in the processing of mesangial macromolecules such as fibrin polymers and clotting intermediates, reactions involving viral antigens in the glomerulus with circulating antibodies, and generalized failures in the coagulation mechanisms. Transplacental infection with hog cholera virus results in embryonic death, fetal anomalies and stillbirths. Cerebellar dysgenesis and hypoplasia, and defective CNS myelination occur in developing fetuses.

Bovine Viral Diarrhea **Bovine viral diarrhea (BVD)** is most often an acute systemic disease in which severe diarrhea is the dominant sign. Severe oral lesions, gastrointestinal hemorrhage, lymphoid tissue destruction, blunting of oral papillae, and interdigital erosions are seen at necropsy. Systemic lymphoid destruction is associated with immune dysfunction. Infected foci of the intestine begin with acute cell swelling of epithelium deep in the crypts and progress to intraepithelial microvesicles, foci of necrosis, and ulceration. Vasculitis is prominent in these lesions. Virions are associated with cytoplasmic vacuoles. Chronic BVD (mucosal disease) is manifest as severe destruction of lymphoid and vascular tissues. Affected cattle progress to death with a febrile systemic affliction involving leukopenia, diarrhea, oronasal discharge, anorexia, and circulatory collapse. Viral antigens are distributed throughout the epithelial and mesenchymal tissues of the host, including neurons, nasal mucosa, renal glomerulus, and corneal epithelium. BVD antigens are especially prominent in blood vessels, including perivascular reticulocytes and myocytes of the media of muscular arteries. Antigen-antibody complexes have been demonstrated in renal glomeruli. Infection of pregnant cows may result in cerebellar hypoplasia in the fetus, a process involving necrosis of the external granular layer, meningitis, edema, and hemorrhage.

Border Disease of Sheep Congenital infection of sheep and goats with certain variant strains of BDV virus is characterized by embryonic or fetal death with or without abortion, mummification, stillbirth, or birth of weak lambs with nervous signs and abnormal hairy birth coats. Lambs that are clinically normal may be persistently infected with BDV virus. Experimental infection of ewes is followed by dissemination of virus to maternal placenta. Virus replicates to high titer in the placentome and crosses to the fetus to cause necrosis of endothelium, thrombosis, and focal hemorrhages. Infection destroys rapidly dividing cells in the fetus. In utero infection leads to death and dysmorphogenesis, and the outcome depends upon the stage of gestation and the dose of virus.[219]

A wide range of congenital defects and malformations includes hydranencephaly, dysplasia/hypoplasia of the cerebellum, dilatation of ventricles, malacia, and cyst formation. Microencephaly and reduced spinal cord diameters are seen. Histologically, demyelination is the most consistent lesion; it occurs throughout the central nervous system, with prominence in the spinal cord; hypomyelination is associated with decreased thyroid hormone levels secondary to infection of the thyroid.[220] In the skin, there is enlargement of primary hair follicles, with reduction of the number of secondary follicles.

Genus *Hepacivirus*

Hepatitis C virus is the classic non-A, non-B hepatitis virus that causes a form of serum hepatitis. Spherical virions are estimated to be 50 nm in diameter and consist of an envelope and a nucleocapsid. Disease progresses to chronicity in up to 70% of infections and is the major cause of cirrhosis and liver transplantation in man.[221] Biopsies of hepatitis C patients closely resemble those of hepatitis B. In acute stages, the entire liver is involved. Hepatocyte necrosis is most marked in centers of lobules. Cell debris and inflammatory cells remain in areas of parenchymal cell damage. Affected hepatocytes are large and swollen with eosinophilic changes in the cytoplasm. Portal tracts are expanded with inflammatory cells. Fatty changes are absent and reticulin is preserved. In recovery, there are spotty areas of necrosis and mild portal tract inflammation with increases in reticuloendothelial activity and foci of iron-staining debris. In fulminent hepatitis, there may be fatty changes and formation of large hepatocytes with central nuclei (called morula).

Vet-ebooks.com

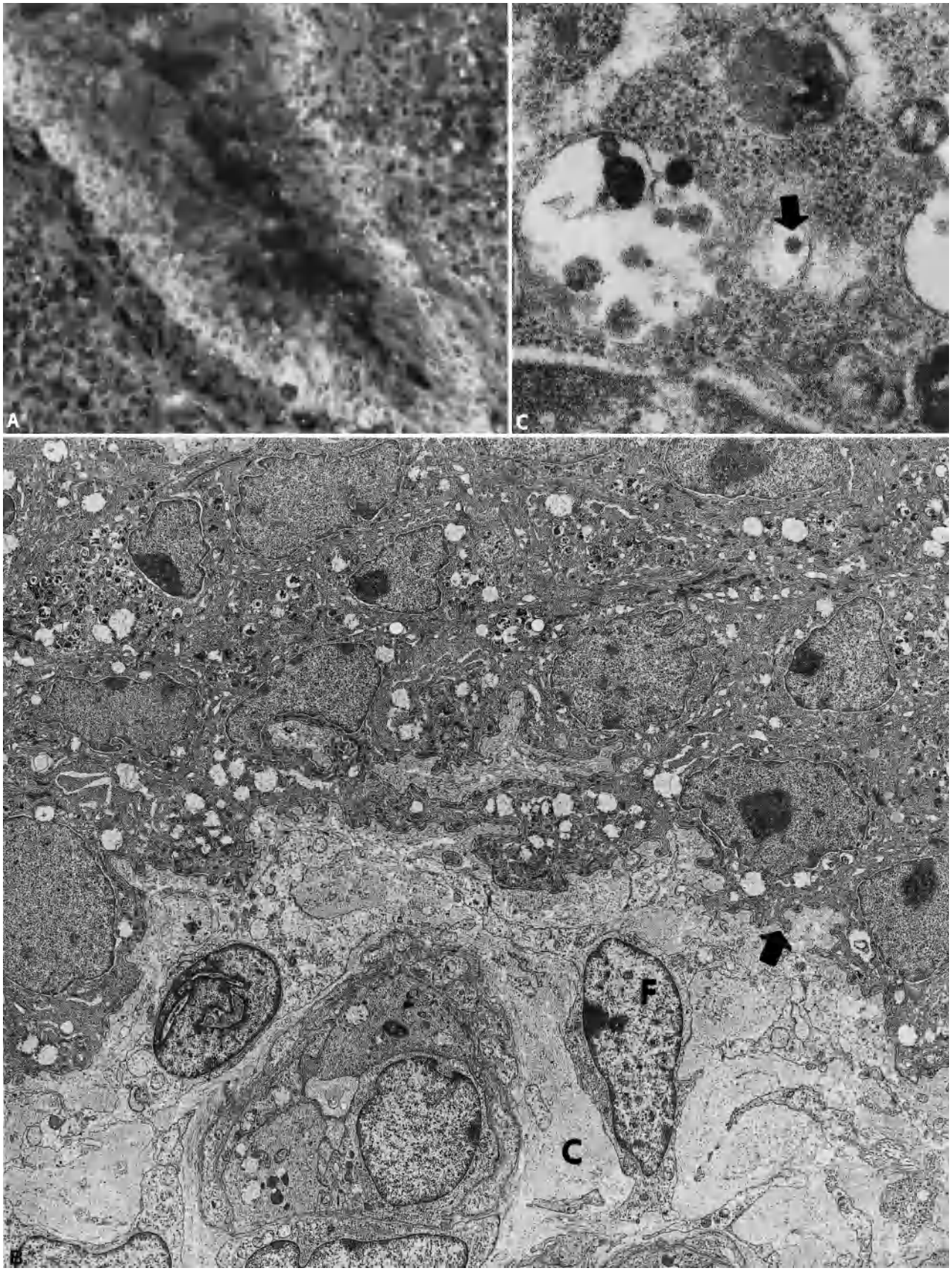


Fig. 13.33 **Pestivirus**: hog cholera (classical swine fever), tonsil epithelium, pig. **A**. **Viral antigens**: epithelium (fluorescent antibody stain). **B**. Infected epithelium: cells are vacuolated and contain autophagosomes. Subepithelial capillary has swollen endothelium and its lumen is blocked by monocytes. Basement membrane (*arrow*), fibroblast (*F*), collagen (*C*). **C**. **Autophagosomes** in epithelial cell contain virus particles (*arrow*).

Vet-ebooks.com

In **chronic infection**, there are mononuclear infiltrates and a presence of viral antigens in affected hepatocytes. Liver cell cytoplasmic tubules are diagnostic for non-A, non-B hepatitis. Particles are 39–46 nm in diameter and enveloped.[222,223]

Hepatitis C has been successfully transmitted to chimpanzees by inoculating them with plasma from infected patients.[224] Cytopathologic changes in hepatocytes of chimpanzees closely resemble those seen in human hepatitis C infection. At 5 wk after inoculation (1 wk before signs of disease) there are intranuclear aggregates of 20–27 nm viral particles. Affected nuclei have chromatin loss, irregular shapes, and abnormal nucleoli. At 12 wk there is unique fusion of membranes arranged in tubules and in circular profiles resembling bacteria. Livers of some animals examined in acute infection show tubular structures.[225]

Family *Bunyaviridae*

The family includes four genera, *Orthobunyavirus*, *Hantavirus*, *Nairovirus*, and *Phlebovirus*, that affect vertebrates (Table 13.19). In their vertebrate host, most replicate locally, often in skeletal muscle, then become viremic, pass the blood-brain barrier, and infect the brain to cause encephalitis.[226] Bunyaviruses are spherical, often pleomorphic, enveloped particles that are 80–100 nm in diameter and have glycoprotein surface projections. Replication occurs in the cytoplasm. Bunyamwera virus was isolated in 1943 by mouse inoculation from *Aedes* mosquitoes in Uganda. It produces lethal encephalitis in mice and other rodents and may spread to humans. Ultrastructural examination of mouse brain shows that virions develop by budding from cytoplasmic vacuoles.

Genus *Orthobunyavirus*

California Encephalitis The California complex of viruses are common causes of encephalitis in children. Viral isolates vary in virulence for mice and there is limited evidence that this correlates with similar variance in humans.[227] Cytopathic changes in the brain of infected mice are manifest by severe cerebral edema and inflammation. They include cell swelling, vacuolation, and reduplication and deformation of the cytocavitary network. Virions averaging 98 nm in diameter

Table 13.19 *Bunyaviridae*.

Virus	*Disease in*	*Reference to ultrastructural pathology*
	Genus *Orthobunyavirus*	
Akabane virus	Cow#	**Ito**, *Acta Virol* 23:198, 1979;* **Kurogi**, *Arch Virol* 51:67, 1976
	Sheep	**Parsonson**, *Infect Immun* 15:254, 1977; **Parsonson**, *J Comp Pathol* 99:215, 1988 (fetus)
Bunyamwera virus	Human	**Murphy**, *J Virol* 2:1315, 1968
Bwamba virus		
Cache Valley virus	Cattle, sheep, human	**Sexton**, *New Engl J Med* 336:547, 1997 (human)
California encephalitis virus	Human	**Johnson**, *J Neuropathol Exp Neurol* 27:390, 1968
	Genus *Hantavirus*	
Hantaan virus	Human	**Tao**, I*ntervirology* 23:97, 1985; **Wang**, *Ultrastr Pathol* 21:281, 1997 (skin)
	In vitro	**Lee**, *Lancet* 1:1070, 1981 (virion);* **Schmaljohn**, *J Infect Dis* 48:1005, 1983 (virion)
	Genus *Nairovirus*	
Crimean-Congo hemorrhagic fever virus	Human	**Booth**, *Virus Res* 21:199, 1991*
Nairobi sheep disease virus	Sheep	**Markzinke**, *Virology* 303:146, 2002
	Genus *Phlebovirus*	
Rift Valley fever virus	Sheep	**McGavran**, *Am J Pathol* 42:587, 1963
	Mosquito	**Lerdthusnee**, *Am J Trop Med Hyg* 53:331, 1995
	Experimental	**Ellis**, *J Med Virol* 24:161, 1988*
Sandfly fever group	Human	**Chen**, *J Virol* 65:1427, 1991 (Punta toro virus)*
	Mouse	**Cusi**, *Viriology* 333:66, 2005 (Toscana virus)†

*In vitro study.
Epizootic congenital arthrogryposis-hydranencephaly syndrome.
† Experimental model.

Vet-ebooks.com

are found in the spaces of the Golgi complex and in the cisternae of the endoplasmic reticulum. Nucleocapsids bud through the membranes retaining them as close fitting envelopes.[228] In mice, subcutaneous inoculation is followed by replication in the reticuloendothelial system, viremia of high titer, and infection of the CNS. CE virus replicates in endothelial cells of small cerebral blood vessels and subsequently infects adjacent neurons and glia.

Akabane Disease Akabane virus is associated with epizootics of congenital deformities in sheep, cattle, and goats. Experimentally, when ewes are infected at 30–36 days of gestation, about one-third of lambs born show deformities. Arthrogryposis, kyphosis, hydranencepahly, scoliosis, brachygnathia, and microencephaly are reported. In severe affliction, CNS lesions include decreased numbers of neurons in the spinal cord ventral horn, hypomyelination, skeletal muscle atrophy, and lymphoid hypoplasia.

Genus *Hantavirus*

Hantaviruses cause **hemorrhagic fever with renal syndrome (HFRS)** in humans. Viral isolates (and their principal reservoir) include Hantaan (striped field mice), Seoul (rats), Belgrade (yellow-necked mice), and Puumala (bank voles). First described in the 1950s as Korean hemorrhagic fever, hantaviruses cause widespread hemorrhages that may end in renal failure and death. **HFRS** affects humans who inhale contaminated feces.[229] **Hantavirus pulmonary syndrome** is a severe pulmonary disease in the southwestern United States. The virus was isolated from its reservoir, the deer mouse, *Peromyscus maniculatus*, and named Sin Nombre virus.[230] Lung lesions consisted of mononuclear cell infiltrates, edema, and focal hyaline membranes. Hantaviral antigens develop in endothelium and follicular dendritic cells, macrophages and lymphocytes. Ultrastructurally, hantaviral inclusions of granulofilamentous material were found in pulmonary endothelium. The identity of antigens and virions was confirmed by immunogold labeling. In cell cultures, virions have mean diameters of 112 nm with surface projections 7 nm long.[231]

Genus *Nairovirus*

Tick-borne hemorrhagic disease (**Crimean-Congo hemorrhagic fever**) has occurred in central Asia and the Balkans since the 12th century. Reported during clearing of forests in the Crimea after World War II, the disease was identified and the virus shown to be related to that of **Nairobi sheep disease**. Lesions in humans include vasculitis, edema, and necrosis in many organs but especially in brain, heart, and liver. Viral antigens are found in cells of monocytes/macrophages, Kupffer cells, and leukocytes. There is no animal model for this disease, although the virus is passed in baby mice via intracerebral inoculation.

Genus *Phlebovirus*

Rift Valley Fever **Rift Valley fever (RVF)** virus causes mosquito-borne enzootics at periodic intervals in the grassy coastal and plateau regions of east Africa. *Aedes* mosquitos transmit the virus among sheep and cattle which develop a febrile, systemic disease with viral replication in liver, lymphoid tissues and other organs. Pregnant females will suffer abortion. Newborn lambs are highly susceptible and develop fulminant, fatal hepatic necrosis. Hepatocytes undergo rapid shrinkage necrosis and contain delicate acidophilic inclusions. Livers of experimentally infected mice have virions in the endoplasmic reticulum and in large numbers in spaces of Disse. Aggregates of viral material and intranuclear fibrillar rods develop in the cytoplasm. Viral nucleocapsids bud into vacuoles. The outer membrane of the virion contains 350–375 surface spikes whose inner ends are within the nucleocapsid. RVF virus is spread to humans during episodes of animal disease. Humans are infected by aerosol exposure to blood or placental fluids and by mosquito bites. Shepherds and veterinarians are at greatest risk. Lesions are remarkably like those of yellow fever; that is, they are those of a hemorrhagic fever and include acute hepatic necrosis with jaundice, necrotic foci in lymphoid tissue, encephalitis, and retinitis.

Family *Birnaviridae*

Birnaviruses (Table 13.20) are dsRNA viruses with a icosahedral, nonenveloped virion approximately 60 nm in diameter with 92 subunits. The **capsid** is a single protein layer in T = 13 lattice form whose only subunits are VP2 trimers. VP2 is glycosylated and contains the viral neutralizing epitopes.[232,233] VP3, the other major structural protein, functions as a scaffold in the virion. The virion lacks surface projections. Viral cores are 45 nm in diameter in thin sections. The genus, *Entomobirnavirus*, contains *Drosophila* X virus and other insect viruses.

Genus *Aquabirnavirus*

Viruses in the genus *Aquabirnavirus* infect fish and produce a wide variety of systemic diseases, many of which are called by local names.

Infectious Pancreatic Necrosis **Infectious pancreatic necrosis (IPN)** is an acute contagious disease with high mortality in young salmonid fishes, especially hatchery-reared trout. IPN virus replicates in pancreatic parenchymal cells causing degeneration and

Vet-ebooks.com

Table 13.20 *Birnaviridae*.

Disease	*Disease in*	*Reference to ultrastructural pathology*
		Genus *Aquabirnavirus*
Infectious pancreatic necrosis virus	Fish	**McKnight**, *Brit Vet J* 132:81, 1976; **Moss**, *J Virol* 3:52, 1969; **Wolf**, *Arch Ges Virusforsch* 34:144, 1971
		Genus *Avibirnavirus*
Infectious bursal disease virus	Chicken	**Cheville**, *Am J Pathol* 51:527, 1967; **Inoue**, *Vet Pathol* 36:146, 1999 (bone marrow); **Lam**, *J Comp Pathol* 116:367, 1997 (apoptosis)

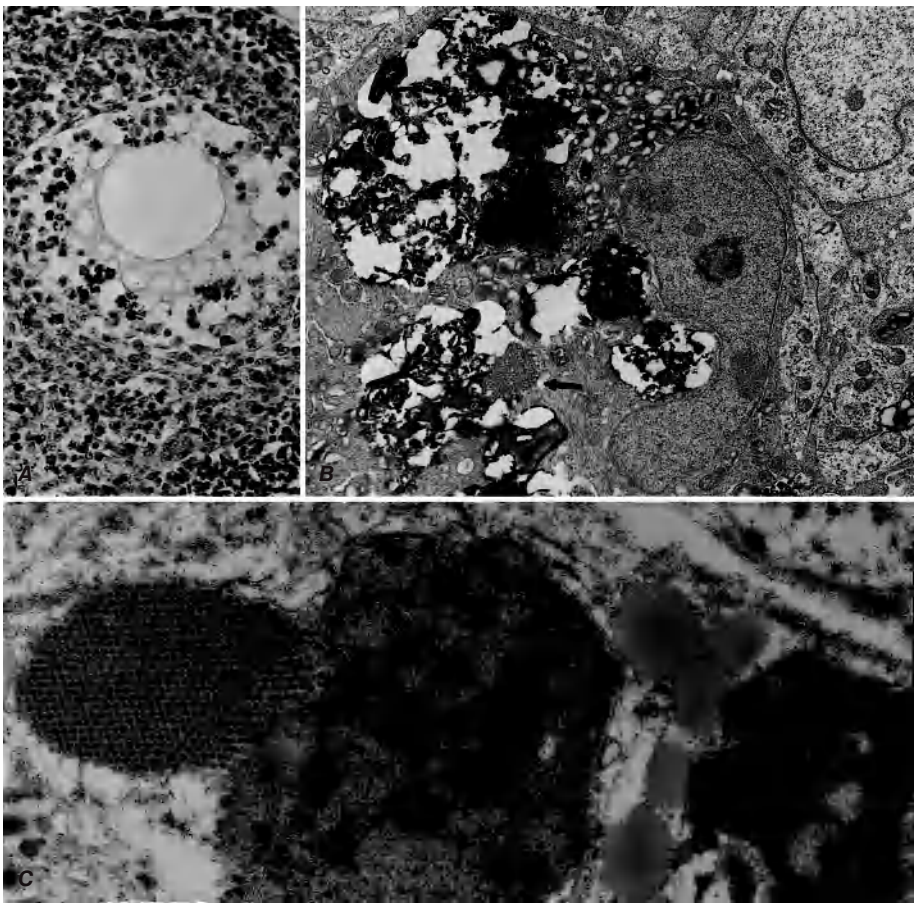


Fig. 13.34 **Birnavirus**: infectious bursal disease virus (IBDV). **A**. **Lymphocyte necrosis**: IBDV, cloacal bursa, chicken. **B**. **IBDV-infected macrophage** with large lysosomes and aggregate of virions (*arrow*). **C**. **IBDV virions** in a lysosome.

necrosis and attendant pancreatitis. Mortality wanes with increasing age.[234]

Genus *Avibirnavirus*

Infectious Bursal Disease **Infectious bursal disease** (IBD, Gumboro disease) of chickens is characterized by diarrhea, weight loss and destruction of lymphoid tissues with attendant immunosuppression. Virus is transmitted via the intestinal tract and chiefly affects lymphocytes in the bursa of Fabricius. In early stages, the bursa is markedly enlarged by edema but as this regresses, bursal atrophy ensues and lymphoid follicles are converted to mucus-producing epithelium.[235] The virus replicates in macrophages, lymphocytes, endothelial cells and reticuloepithelial cells in the thymus and spleen, and there is rapid depletion of these cells by apoptosis (Fig. 13.34).[236,237]

Picobirnaviruses **Picobirnaviruses** (PBVs) are small, nonenveloped viruses with a bisegmental dsRNA genome. They have a diameter of 33–35 nm, and a triangulation number of 3 (T = 3). They are widespread among mammalian and avian species, which are asymptomatic carriers. PBVs have been reported from watery stools of humans. They are also reported in feces of asymptomatic humans,[238] pigs, rats, and rabbits.[239]

Vet-ebooks.com

Family *Nadoviridae*

Genus *Betanodavirus*

The genus *Betanodavirus* contains noneveloped virions with icosahedral symmetry, approximately 25 nm in diameter with a viral genome of 2 single-stranded (ssRNA) segments. Betanodaviruses cause nerve and eye disease in fish and white tail disease of farmed prawn.

Viral Encephalopathy and Retinopathy **Viral encephalopathy and retinopathy** (viral nervous necrosis) is a disease of larvae and marine fish characterized by spongiform vacuolation of nervous tissue. Paracrystalline arrays and pieces of membrane-associated nonenveloped virions measuring ~30 nm in diameter are found in brain and retina of affected fish.[240–242]

Family *Picornaviridae*

Small, omnipresent picornaviruses are grouped into nine genera (Table 13.21). Virions consist of nonenveloped round capsids (formed of 60 copies of each of four viral proteins VP1, 2, 3, and 4) that form an icosahedral shell ~30 nm in diameter that is filled with a positive-sense, ssRNA genome. A feature of the capsid surface is a depression called the canyon, the site of receptor binding.

Genus *Enterovirus*

Enteroviruses are common infections of the gut that, in rare infections, extend into the circulation and infect the brain. In the typical asymptomatic infection, viruses replicate in enterocytes of the intestine and are shed in feces. Although large amounts of virus are produced, there is little significant cytopathic effect in the intestinal mucosa. Most animals acquire immunity as neonates when they still have maternal antibody and are thus protected from systemic disease.

Primary viremia in neonates that lack antibodies or in immunosuppressed adults will lead to infection of the nervous system. Within the brain, infection of neurons is preceded by involvement of vascular endothelium. Subsequent infection of neurons induces cell swelling, chromatolysis, and cell death (Fig. 13.35). Cell loss is a direct cause of the paralysis observed clinically. While different strains of enteroviruses show striking differences in virulence and neurotoprism, tissue invasion also depends markedly on stresses or immaturity of immune mechanisms in the host. Pregnancy, immunosuppression, corticosteroid therapy, and surgical procedures markedly increase the risk of paralytic disease.

Poliomyelitis **Poliovirus** replicates in the intestinal mucosa and is shed in large amounts in feces. In acute infection, viremia peaks rapidly and declines due to rapid development of serum antibodies. In neonates and other immunodeficient patients that lack serum antibodies, virus is disseminated systemically. Within the brain, infection of neurons is usually preceded by involvement of vascular endothelium.[243] Subsequent infection of neurons induces cell swelling, chromatolysis, and cell death. Cell loss is a direct cause of the paralysis observed clinically. The disintegration of neurons attracts neutrophils into infected areas. During the viremia phases, viruses replicate within the cytoplasm of circulating leukocytes and this helps to spread infection. In experimental studies on monkeys administered poliovirus into the brain, virions develop cytoplasmic in lattice forms;[244] although crystalloids of virions have not been reported in human tissue.

Coxsackieviral Disease **Coxsackieviruses** are enteroviruses that cause systemic infection with varied manifestations, including enteric, respiratory, meningeal, and epidermal lesions. Cellular cytopathic changes closely resemble those of poliovirus. Cardiac and skeletal muscle may be involved, but severe, acute cardiac disease is generally limited to infants and immunosuppressed children. Viral myositis has been a widely studied model in mice, including augmentation of disease by environmental stress.[245]

Echoviral Disease **Echoviruses** (the name is derived from the acronym for "enteric cytopathic human orphan" viruses), are frequently responsible for febrile illness and viral meningitis. In newborn infants, they can cause fatal disseminated infection.[246] Disease is variable and commonly subclinical. The pathogenesis and cytopathic effects closely resemble those of poliovirus. The specific receptor for echovirus type 1 is an integrin known as VLA-2 ($\alpha 2\ \beta 1$), a receptor for collagen and laminin.

Genus *Rhinovirus*

An immense number of serologically different **rhinoviruses** have been isolated from the human nasal cavity. Human rhinoviruses are divided into two groups. The major serotypes bind to intercellular adhesion molecule-1 (ICAM-1) as a receptor.[247] Rhinoviruses cause the common cold in humans, and many isolates produce this syndrome when inoculated by aerosol into human volunteers. Rhinoviruses differ from the enteroviruses in rarely being present in feces. The ribosome-size virions are found in crystalloids in the cytoplasm of infected cell. The adhesion molecule ICAM-1 is a receptor for human rhinoviruses. The

Vet-ebooks.com

Table 13.21 *Picornaviridae*.

Virus	*Disease in*	*Reference to ultrastructural pathology*
		Genus *Enterovirus*
Poliovirus	Human Monkey	**Anzai**, *Exp Molec Pathol* 10:176, 1969; **Dales**, *Virology* 26:379, 1965* **Mannweiler**, *Z Naturforsch* 16B:705, 1961 (brain)
Coxsackie A	Human Mouse	**Gjøen**, *Clin Diagn Virol* 8:183, 1997; **Madeley**, *Lancet* 1:1013, 1982 (intestine) **Bientz**, *Br J Exp Pathol* 50:471, 1969 (muscle); **Harrison**, *Exp Molec Pathol* 14:30, 1971 (muscle)
Coxsackie B	Human Monkey† Mouse†	**Haas**, *Lab Invest* 23:442, 1970 (myocarditis) **Sun**, *Br J Exp Pathol* 48:655, 1967 (pancarditis) **Klingel**, *Lab Invest* 78:1227, 1998 (myocarditis); **Harb,** *Beitr Pathol* 156:122, 1975 (pancreas); **Meyer**, *Pathol Microbiol* 32:139, 1968 (fetus); **Rabin**, *Am J Pathol* 44:775, 1964 (myocarditis); **Soike**, *J Infect Dis* 117:203, 1967 (pregnancy); **Sun**, *Proc Soc Exp Biol Med* 126:882, 1967 (nephritis)
ECHO	Human Mouse†	**Skinner**, *Virology* 36:241, 1968* **Bultmann**, *Virch Arch B* 35:177, 1981 (polymyositis)
Avian enterovirus (avian encephalomyelitis)	Bird	**Cheville**, *Am J Pathol* 58:105, 1970 (brain); **Kraus**, *Tierarzt Wschr* 79:480, 1966; **Yamagiwa**, *Jap J Vet Sci* 31:173, 1969 (neurons)
Avian nephritis	Bird	**Maeda**, *Avian Dis* 23:589, 1979; **Smyth**, *Avian Pathol* 36:119, 2007
Bovine enterovirus	Cattle	**Blas-Machado**, *Vet Pathol* 44:110, 2007 (intestine); *Yilma*, *J Gen Virol* 49:225, 1980
Duck picornavirus	Duck	**Tseng**, *Virus Res* 129:104, 2007
Mouse poliovirus	Mouse	**Nelson**, *Am J Pathol* 44:29, 1964 (MM strain, leukocytes)
Porcine enterovirus	Pig	**Dauber**, *Vet Microbiol* 67:1, 1999*
Simian enterovirus	Monkey	**Oberste**, *J Gen Virol* 88:3360, 2007*
Swine vesicular disease	Pig	**Fry**, *J Virol* 77:5475, 2003*
		Genus *Rhinovirus*
Human rhinovirus	Human	**Gaunt**, *Arch Ges Virusforsch* 41:382, 1973;* **Kawana**, *Jap J Microbiol* 15:207, 1971)*
Bovine rhinovirus	Cow	**Mattson**, *Am J Vet Res* 335:1337, 1974*
Equine rhinovirus	Horse	**O'Niell**, *Am J Vet Res* 45:1953, 1984*
		Genus *Cardiovirus*
Encephalomyocarditis virus	Baboon Human Mouse† Pig	**Hubbard**, *Lab Anim Sci* 42:233, 1992 **Dales**, *J Cell Biol* 14:281, 1962* **Adachi**, *Acta Neuropathol* 37:89, 1977 (nude mice); **Burch**, *Lab Invest* 26:163, 1972 (kidney) **Yoon**, *J Gen Virol* 37:225, 1977 (mouse, diabetes)†
Theilovirus (Theiler's virus)	Human Mouse	 **Blakemore,** *Acta Neuropathol* 76:581, 1988; **Dal Canto**, *Am J Pathol* 88:497, 1977 (brain); **Penney,** *Lab Invest* 40:324, 1979 (brain); **Rodriguez**, *Lab Invest* 49:672, 1982 (neonate); **Wrobleska**, *Lab Invest* 37:595, 1977 (brain)
		Genus *Aphthovirus*
Foot-and-mouth disease	Cattle, et al.	**Breese**, *Science* 150:1303, 1965*
Equine rhinitis A	Horse Camel	**Dynon**, *Aust Vet J* 85:46, 2007* **Wernery**, *J Gen Virol* 89:660, 2008 (abortion)
		Genus *Hepatovirus*
Hepatitis A	Human Marmoset Monkey	**Dienstag**, *Int Rev Exp Pathol* 120:1, 1979; **Cromeans**, *Am J Anat* 185:314, 1989 (antigens); **Shimizu**, *Infect Immun* 36:320, 1982 (liver); **Vallbracht**, *J Infect Dis* 160:209, 1989 (T cells) **Huang**, *Lab Invest* 41:63, 1979 (liver) **Keenan**, *Am J Pathol* 115:1, 1984

*In vitro study.
†Animal model.

Vet-ebooks.com

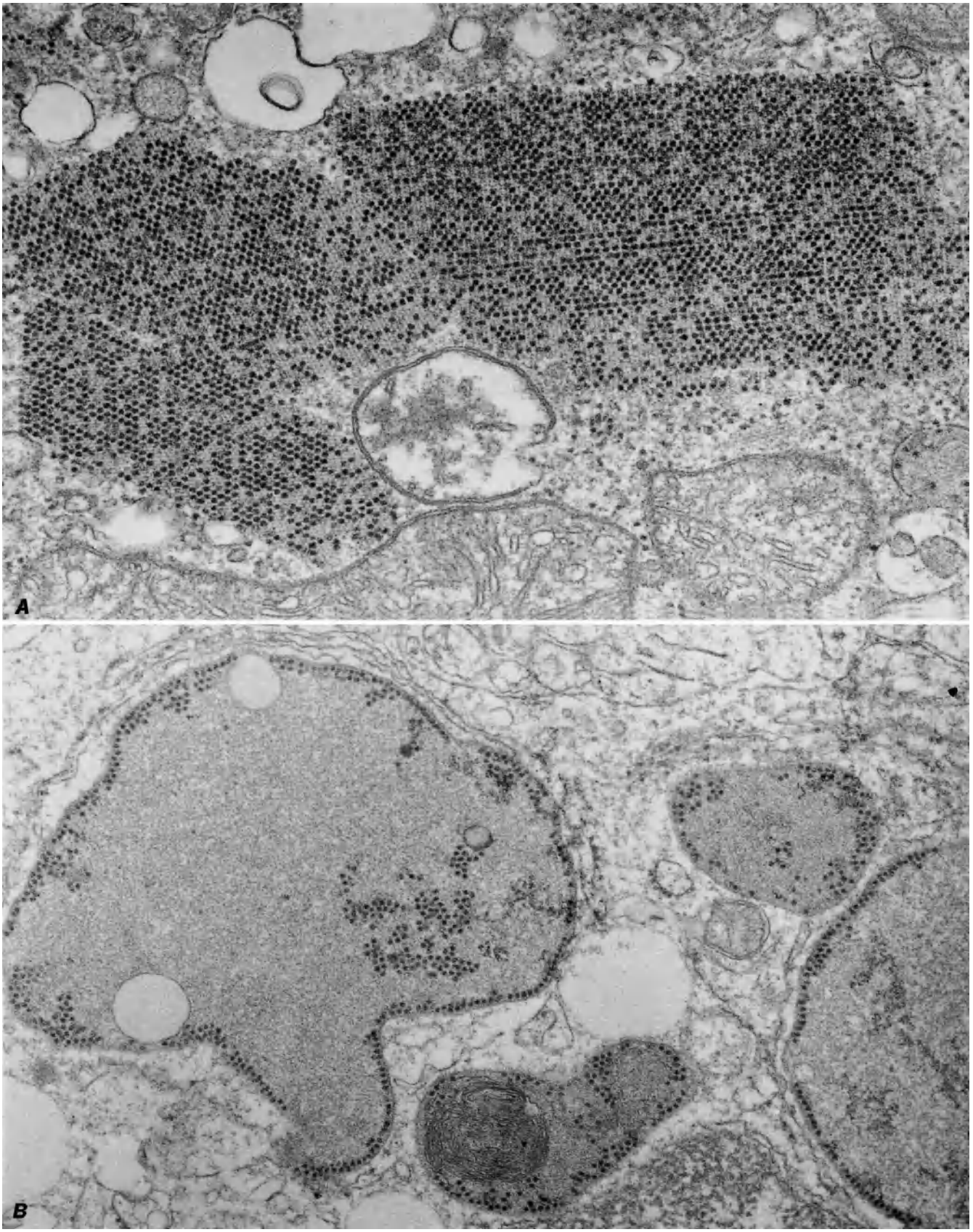


Fig. 13.35 Picornavirus: Theiler's murine encephalomyelitis virus, mouse brain. **A**. **Viral arrays**: virions free in the cytoplasm. **B**. **Membrane-bound virions**. (Micrograph: Moses Rodriquez, *Lab Invest* 49:672, 1983.)

Vet-ebooks.com

viral region that interacts with the receptor is an antibody-accessible canyon that circumscribes the virion. Rhinoviruses from cattle and horses have been isolated but their relation to respiratory disease in these species has not been clarified.

Genus *Cardiovirus*

Cardioviruses replicate in the cytoplasm. They are approximately 30 nm in diameter and are found free in the cytoplasm and within cisternae of the endoplasmic reticulum, usually as virions arranged in lattice formations. Viral genomes are single-stranded DNA, and the viruses are ether-resistant.

Encephalomyocarditis **Encephalomyocarditis (EMC)** viruses are ubiquitous agents which infect a variety of wild and domestic animals naturally. EMC virus is associated with a mild febrile illness in man. In swine, EMC virus causes fetal death and acute myocarditis. Rare, sporadic, fatal myocarditis can be caused in baboons, chimpanzees, several species of monkeys, and swine. Systemic lesions, which are largely restricted to the myocardium, are severe myocarditis and necrosis. Mice and rats are natural carriers of EMC virus. Infected rats excrete the virus persistently, and infect swine through feces-contaminated food. Experimentally, myocarditis is reproducible in mice.[248] Porcine strains, shown to replicate in pancreatic islet cells to cause diabetes mellitus, have been found to be strongly diabetogenic.

Ultrastructurally, EMC virions are found in myocytes, endothelial cells, and leukocytes.[249] Infected laboratory animals have been used as models of viral **myocarditis** and **encephalitis**. T cell deficient nude mice have significantly lower mortality and neural lesions of perivascular lymphocytic cuffing when inoculated with a dose of EMC virus that is lethal to normal mice. EMC Mengo, MM, and Columbia-SK viruses are antigenically identical strains of murine cardiovirus. The M variant replicates in pancreatic islet cells of mice and produces diabetes mellitus.

Murine Polioencephalomyelitis **Murine polioencephalomyelitis virus** (Theiler's virus) is a prevalent cause of asymptomatic enteric infection in young adult mice. The incidence of CNS disease is rare. As in human poliomyelitis, the clinical and pathologic manifestations of infection are age related. Mice infected during the first week of life die with fulminant encephalitis. By 2 wk of age they are less susceptible and develop persistent CNS infection with chronic relapsing demyelination. Encephalomyelitis may be biphasic: an early disease in which virus replicates in and causes pathology of the gray matter, leading to flaccid paralysis, and a late disease.[250]

Virions are difficult to detect ultrastructurally in brain tissue but are found in neurons and in macrophages. The best electron micrographs show virions both as membrane-bound virions studding the interior aspect of vacuoles and free (nonmembrane-bound) paracrystalline arrays in the cytoplasm.[251,252] Immunoperoxidase studies show viral antigens primarily within neurons of the cerebral cortex, basal ganglia, hippocampus, and anterior horn cells. The presence of viral antigens within apical dendrites and axonal projections of hippocampal pyramidal cells indicates that the virus travels intraaxonally.

Survivors of neonatal infection may develop persistent infection with marked infiltration of lymphocytes, monocytes, and plasmacytes in leptomeninges and white matter, and demyelination, particularly in the spinal cord, where macrophages filled with myelin debris are common. Viral antigens and virions are rarely found in these patchy areas of demyelination. Because the myelin lamellae appear to be stripped off by invading monocytes, an immune mechanism is suspected.[253] Elimination of the immune response by cyclophosphamide prevents demyelination. Lysis of oligodendroglia during acute infection may provide the stimulus for the late autoimmune demyelination.

Genus *Aphthovirus*

Foot-and-Mouth Disease Naturally infecting only cloven hoofed animals (cattle, sheep, goats, and swine), **foot-and-mouth disease (FMD)** appears with fever, anorexia, drooling, and lameness. FMD is highly contagious and there are high titers of virus in blood and body secretions. Transmitted by aerosol, FMD enters the oropharynx, rapidly penetrates the body, causes and primary viremia, and is disseminated throughout the host. Epithelial lesions include vacuolar degeneration and necrosis with marked intercellular hyperemia and edema. Vesicles, the hallmark of disease, rapidly break leaving ulcers. Tissues affected are all structures of the oropharynx, teats, interdigital spaces, and base of the horn. Lesions are found in viscera, especially pancreas, cardiac and skeletal muscle, mammary glands, and placenta (but rarely in fetus). FMD virus is slightly smaller than other picornaviruses), and replicates in the cytoplasm where it may occur in lattice arrangements.

Genus *Hepatovirus*

Hepatitis A **Hepatitis A** is an acute, self-limiting hepatitis that is highly contagious and spreads rapidly by the fecal-oral route. It appears with influenza-like signs of fever, headache, and myalgia. Infection does not lead to chronic hepatitis or a carrier state, although

Vet-ebooks.com

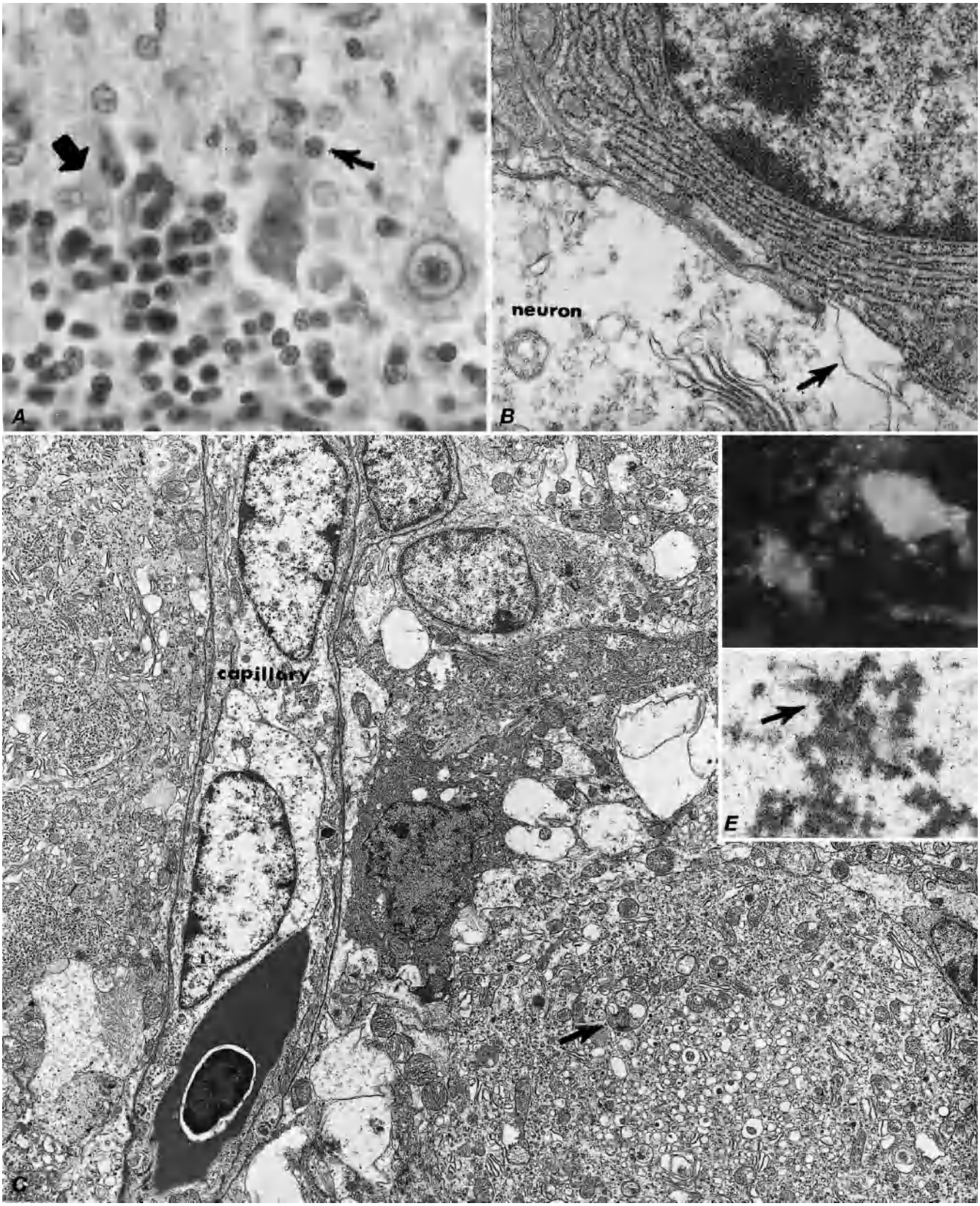


Fig. 13.36 Picornavirus: avian encephalomyelitis, brain, chicken. **A**. **Histology**: necrosis of neurons (*thick arrow*) and infiltrates of lymphoid cells (*thin arrow*), many of which are plasmacytes. **B**. **Fusion of plasma membranes**: plasmacyte (*top*) and neuron. **C**. **Degenerate neurons**: vesiculation of endoplasmic reticulum (*bottom right*) with myelin figures (*arrow*). Neuron (*left*) in early phase of swelling. Necrotic glial cell at center. **D**. Viral antigens: neuron, fluorescent antibody stain. **E**. **Virions**.

Vet-ebooks.com

a relapsing form is common. Cholestasis appears late in the acute phase of the disease. Viral antigens, detected by immunogold techniques, are found in hepatocytes.[254] Hepatocyte injury in acute hepatitis A virus infection is mediated by HAV-specific $CD8^+$ T lymphocytes, with less damage by viral cytopathic effects.

Avian Encephalomyelitis A small (23 nm) nonenveloped enterovirus causes avian encephalomyelitis, a sporadic, severe disease of newly hatched chickens manifested clinically by tremor, ataxia, paresis, paralysis, and death. Asymptomatic infections are common, and virus may be passed through the egg to progeny by carrier hens. Age is inversely related to susceptibility; infected older chicks may remain normal clinically or develop only transient paralysis. Immunosuppressed adults react to infection as though they were newly hatched chicks.[255] **Avian encephalomyelitis virus** replicates in neurons of the central nervous system and spreads to involve adjacent glia. Viral antigens fill affected cells, but virions are identified with difficulty (Fig. 13.36). Older chicks, which develop only mild clinical signs or are asymptomatic, may show marked perivascular plasmacytic infiltrates and vascular and glial proliferation. Similar infiltrates occur in the myocardium and other viscera and indicate the systemic nature of the infection. Plasmacytes infiltrate infected foci of the brain and fuse with infected neurons. This mechanism prevents spread of virus in the nervous system, and the effects of inhibiting viral replication surpass the deleterious effect of inflammation in causing clinical signs.

Family *Caliciviridae*

Caliciviruses are 27–39 nm in diameter and have a single major structural protein. In negatively stained preparations, virions have scalloped borders with 32 cup-shaped surface indentations (from which is derived the name "chalice" or "calyx") arranged in icosahedral symmetry (Fig. 13.37).[256] Virions are spherical with 60 surface spikes when examined by electron cryomicroscopy. Caliciviruses cause disease in several mammalian species (Table 13.22). **Human caliciviruses**, members of the genera ***Norovirus*** and ***Sapovirus***, replicate in the intestinal mucosa and produces severe diarrhea.

Genus *Norovirus*

The **Norwalk virus** was discovered in negatively stained filtrates of stools from children in Norwalk, Ohio, involved in an outbreak of vomiting. Virions isolated from feces are 26–34 nm in diameter with cubic symmetry. They lack an envelope, and are acid-stable and ether-resistant replicate in enterocytes. In human norovirus infections in gnotobiotic pigs, virions are found in cytoplasmic vesicles of vacuolated epithelial cells.[257]

Genus *Sapovirus*

Sapoviruses (SaV) are causal agents of gastroenteritis in humans and pigs (Sapporo virus is the prototype member). There are five genogroups, none of which cross-react with other viruses that cause gastroenteritis (norovirus, rotavirus, astrovirus, and adenovirus). Genogroups I, II, IV, and V cause human disease, and genogroup III is a pathogen of pigs.

Genus *Vesivirus*

Feline Calicivirus **Feline calicivirus (FCV)**, a common cause of upper respiratory disease in cats, replicates in epithelium of conjunctiva, oral mucosa, and tongue to produce vesicles, ulcers, and acute inflammation. Viral antigens are present in epithelial and endothelial cells of affected tissues.[258] Virulent mutants of FCV cause severe acute systemic disease characterized by jaundice, edema and hepatic necrosis. FCV virus replicates in both hepatocytes and Kupffer cells.[259]

Swine Vesicular Disease **Swine vesicular disease** (vesicular exanthema) is an acute febrile disease manifest by vesicle formation on the snout, lips, tongue, oral cavity, and feet. Viral replication occurs in squamous cells of the epidermis and leads to marked acute cell swelling and virions in the cytoplasm.[260,261]

Genus *Lagovirus*

Pathogens in the genus *Lagovirus* cause serious diseases of rabbit: **rabbit hemorrhagic disease (RHD)** and **European brown hare syndrome (EBHS)**. RHD is characterized by widespread hemorrhages and necrotizing hepatitis. RHD virus replicates in and kills endothelial cells to cause hemorrhage.[262,263]

Genus *Hepevirus*

Hepatitis E virus (HEV, non-A, non-B hepatitis virus) is a small (32–34 nm), icosahedral nonenveloped particle that is similar to members of the family *Caliciviridae* in its structural morphology. Epidemics of enterically transmitted **hepatitis E** (epidemic or enteric-transmitted non-A, non-B hepatitis) have been reported in Asia, Africa, and North America. HEV replicates in the enterocyte where it has been localized to the rough endoplasmic reticulum.[264] Responsible for sporadic cases of hepatitis in endemic areas, HEV is also the cause of a fulminant hepatitis of pregnancy. The cynomolgus monkey is susceptible to infection and develops hepatitis when given

Vet-ebooks.com

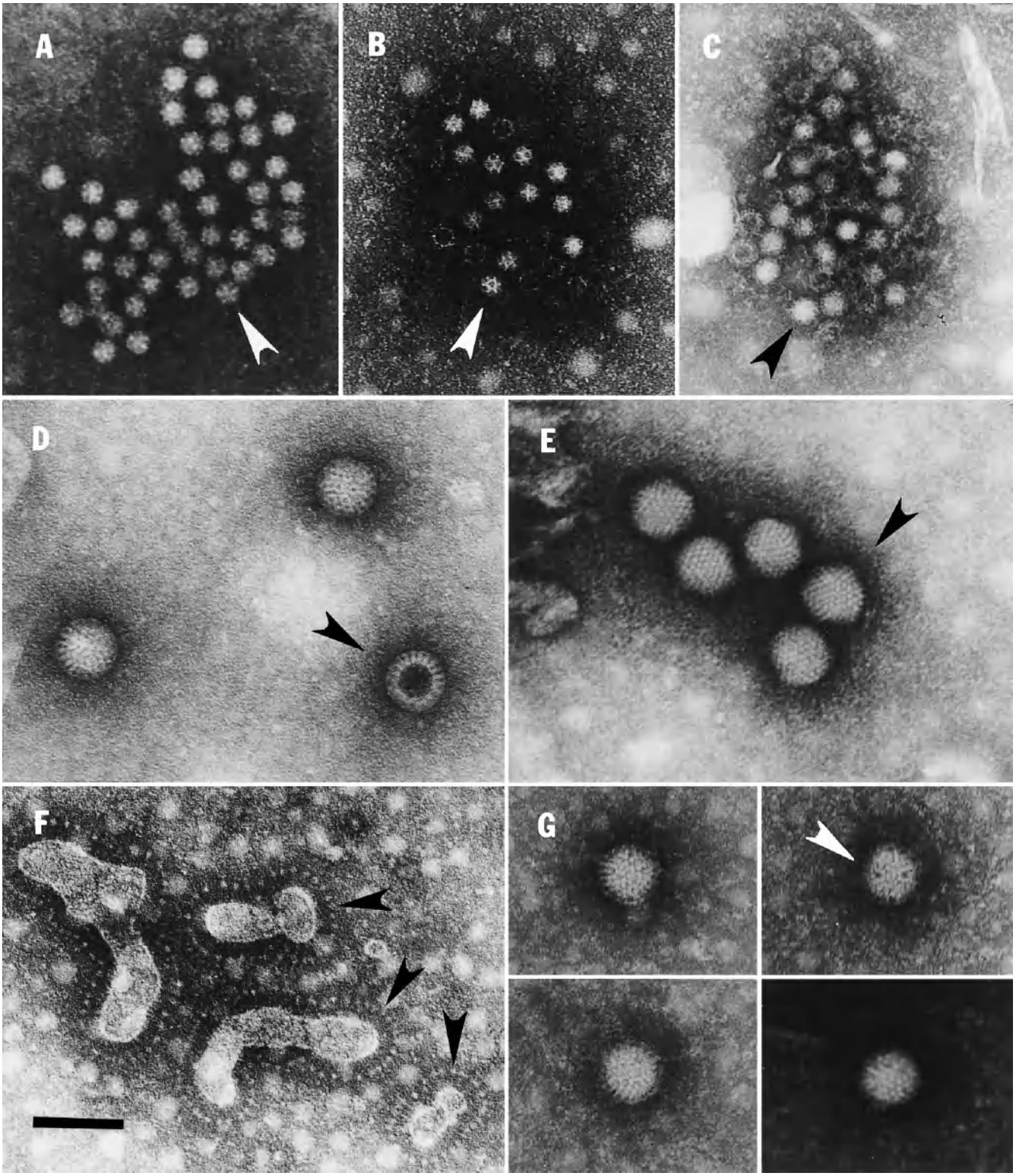


Fig. 13.37 Human fecal stools: electron micrographs of negatively stained specimens stored at –70ºC. Different surface characteristics are indicated with arrows. **A**. **Astrovirus. B**. **Calicivirus. C**. **Norovirus. D**. **Rota virus. E**. **Adenovirus. F**. **Coronavirus-like particles. G**. **T = 19 virus-like particles:** characteristic particles (*arrowhead*). Bar = 100 nm. (Micrographs: Fred P. Williams, Jr., *J Med Virol* 29:192, 1989.)

Vet-ebooks.com

Table 13.22 *Caliciviridae*.

Virus	*Disease in*	*Reference to ultrastructural pathology*
		Genus *Lagovirus*
European brown hare syndrome virus	Rabbit	**Frölich**, *J Wildl Dis* 32:280, 1996; **Lavazza**, *Zentralbl Veterinaermed B* 43:401, 1996
Rabbit hemorrhagic disease virus	Rabbit	**Ferreira**, *Vet Res Commun* 30:393, 2006
		Genus *Norovirus*
Norwalk virus	Human	**Dolin**, *J Infect Dis* 155:365, 1987;* **Dolin**, *Am J Med* 59:768, 1975
	Pig†	**Cheetham**, *J Virol* 80:10372, 2006
		Genus *Sapovirus*
Sapporo virus	Human	**Hansman**, *Arch Virol* 150:2529, 2005 (virion)
	Pig	**Yu**, *Arch Virol* 153:739, 2008
Swine calicivirus	Pig	**Chang**, *J Virol* 79:1409, 2005*
		Genus *Vesivirus*
Vesicular exanthema of swine virus	Swine	**Gelberg**, *Vet Pathol* 19:424, 1992;† **Zee**, *Am J Vet Res* 29:1025, 1968*
Feline calicivirus	Cat	**Coyne**, *Vet Rec* 158:544, 2006; **Pedersen**, *Vet Microbiol* 73:281, 2000; **Pesavento**, *Vet Pathol* 41:257, 2004
Canine calicivirus	Dog	**Evermann**, *Am J Vet Res* 46:218, 1985; **Pratelli**, *New Microbiol* 23:257, 2000
Porcine enteritc calicivirus	Pig	**Flynn**, *Am J Vet Res* 49:819, 1988
Mink calicivirus	Mink	**Evermann**, *Arch Virol* 76:257, 1983; **Guo**, *Arch Virol* 146:479, 2001
San Miguel sea lion virus	Sea lion	**Smith**, *Nature* 244:108, 1973
	Pig	**Gelberg**, *Vet Pathol* 19:424, 1992†
Skunk calicivirus	Skunk	**Seal**, *Virus Res* 37:1, 1995
Primate calicivirus	Chimpanzee	**Smith**, *Science* 221:79, 1983*
		Genus *Hepevirus* (family not assigned)
Hepatitis E virus	Human	**Bradley**, *J Gen Virol* 69:731, 1988;* **Bradley**, *Proc Natl Acad Sci USA* 84:6277, 1987; **Tsarev**, *Proc Natl Acad Sci USA* 89:559, 1992
	Monkey	**Gupta**, *Indian J Med Res* 91:87, 1990; **Van Cuyck-Gaudré**, *J Med Virol* 55:197, 1998
	Pig	**Usmanov**, *Vopr Virusol* 36:212, 1991
Avian hepatitis E virus	Chicken	**Hagshenas**, *J Gen Virol* 82:2449, 2001; **Huang**, *J Clin Microbiol* 40:4197, 2002
Swine hepatitis E virus	Pig	**Lee**, *Vet J* [E-pub] 2008†

*In vitro study.
†Animal model.

feces of infected human patients; ultrastructurally, virions were identified in bile by immunoelectron microscopy.[265]

Family *Astroviridae*

The family *Astroviridae* contains two genera: *Mamastrovirus* and *Avastrovirus*. **Astroviruses**, tiny viruses of 27–30 nm diameter, resemble five- or six-pointed stars. They have cubic symmetry, round and smooth edges, and triangular electron-lucent areas with an electron-dense center. Astroviruses have been identified in feces and in enterocytes of the intestine of lambs,[266] calves.[267] mice,[268] turkeys,[269] and humans. The mean diameter of virion found in lamb feces is nearly 30 nm (see Fig. 13.37). Virions appear in the cytoplasm of mature columnar epithelial cells over the apical two-thirds of the intestinal villus 14 hr after experimental infection. Crystalline arrays of virions have center-to-center distances of 29 nm. In vitro, endocytosis is the mechanism of entry into host cells.[270]

Family *Retroviridae*

Retrovirus virions consist of an envelope, a nucleocapsid, and either a concentric or eccentric nucleoid.

Vet-ebooks.com

Virions are spherical to pleomorphic measuring 80–100 nm in diameter. Retroviruses are the etiologic agents of lymphoproliferative, ranuloproliferative, and neoplastic diseases in many species. Their life cycles involve both nucleus and cytoplasm. The virions of most are difficult to locate in tissue but are present in large numbers in productive infections in vitro. Retroviruses cause neoplastic disease by several different mechanisms. **Insertional mutagenesis**, discovered in avian leukemia, involves activation of a cellular oncogene by a provirus being integrated in its vicinity. **Gene capture** is the capture of a cell gene (oncogene), which when reinserted into the host DNA leads rapidly to neoplastic change. In capturing the oncogene, viral genetic codes for replication may be lost but this mechanism is rare.

Retroviruses encode genetic information in RNA and use the unique viral polymerase **reverse transcriptase** to copy the genome into DNA, which is then integrated into the host cell genome as a **provirus**. Most retroviruses contain three genes: a gene for the internal core proteins called *gag*, the polymerase called *pol*, and the gene for the surface envelope protein, *env*. Signals for initiation of transcription lie within the long terminal repeat (LTR) sequences that flank the integrated provirus. Virions develop in the cytoplasm of infected cells and bud from the cell surface (Table 13.23). A common feature of human retroviruses is the transacting gene called *tat* that encodes a regulatory protein product which acts on the viral long terminal repeat (LTR) elements leading to abundant viral production. Certain viral genes are sometimes replaced by a cell-derived DNA sequence known as an *onc* gene, which enables the retrovirus to transform targets cells. Most natural pathogenic retroviruses of animals do not carry known *onc* genes. **Cell surface glycoproteins** on cells act as receptors for retroviruses and thus play a crucial role in pathogenesis of disease. The

Table 13.23 Family *Retroviridae*.

Virus	*Disease in*	*Reference to ultrastructural pathology*
		Subfamily *Orthoretrovirinae*
		Genus *Alpharetrovirus*
Avian leukosis virus	Chicken	**Di Stefano**, *J Nat Cancer Inst* 37:869, 1966 (congenital transmission); **Dougherty,** *Cancer Res* 27:322, 1967; **Heine**, *J Natl Cancer Inst* 29:41, 1962a (Wilms' tumor); **Simpson**, *Cancer Res* 26:590, 1966 (osteopetrosis); **Simpson**, *Cancer Res* 29:33, 1969 (ocular leukosis)
Rous sarcoma virus	Chicken	**Bucciarelli**, *J Nat Cancer Inst* 38:359, 1967 (meningiomas); **Heine**, *J Nat Cancer Inst* 29:211, 1962; **Morgan**, *J Virol* 2:1133, 1968
		Genus *Betaretrovirus*
Mouse mammary tumor virus	Mouse	**Bevilacqua**, *Gastroenterology* 96:139, 1989; **Brooks**, *Cancer Res* 30:2156, 1970 (lung); **Dmochowski**, *J Nat Cancer Inst* 40:1339, 1968 (milk); **Feldman**, *J Nat Cancer Inst* 30:477, 1963; **Imai**, *Cancer Res* 26:443, 1966 (carcinoma); **Moore**, *J Nat Cancer Inst* 44:965, 1970 (blood); **Tanaka**, *Virology* 33:197, 1967
Mason-Pfizer monkey virus	Monkey	**Chopra**, *Cancer Res* 30:2081, 1970 (monkey mammary tumor); **Feldman**, *Cancer Res* 39:1772, 1979 (placenta); **Payne**, *Onderstepoort J Vet Res* 53:87, 1986*
Jaagsiekte sheep retrovirus	Goat	**De las Herase**, *Vet Pathol* 32:19, 1995;† **Vitellozzi**, *J Vet Med* 40:459, 1993 (tumor); **Payne**, *J Vet Res* 50:317, 1983*
	Sheep	**Perk,** *J Natl Cancer Inst* 46:525, 1971 (tumor); **Nisbet**, *J Pathol* 103:157, 1971 (tumor)
Unclassified	Lemming	**Hiraki**, *Cancer Res* 33:3159, 1973 (mammary tumors)
		Genus *Gammaretrovirus*
Murine leukemia virus	Mouse	**Aoki**, *Proc Natl Acad Sci USA* 65:569, 1970*; **Barrett**, *Calcif Tissue Res* 19:295, 1976 (bone); **Baszler**, *Lab Invest* 63:612, 1990 (neuron); **Feldman**, *Cancer Res* 27:1513, 1967; **Hanna**, *Cancer Res* 30:1748, 1970 (Rauscher); **Leiter**, *Am J Pathol* 119:22, 1985 (pancreatic β cells); **Murray**, *Am J Pathol* 124:319, 1986 (osteopetrosis); **Oldstone,** *Am J Pathol* 88:193, 1977 (brain); **Park**, *Lab Invest* 71:78, 1994 (brain); **Schmidt**, *Am J Pathol* 129:503, 1987 (osteopetrosis)
Murine sarcoma virus	Mouse	**Pitts**, *Lab Invest* 49:171, 1983 (brain, vascular tumors); **Pitts**, *Lab Invest* 56:401, 1987 (brain)
Feline leukemia virus	Cat	**Feldman**, *Cancer Res* 31:1261, 1971 (mammary gland tumors); **Hoover**, *J Nat Cancer Inst* 53:1271 and 1277, 1974; **Laird**, *J Nat Cancer Inst* 41:867 and 879, 1968

Vet-ebooks.com

Table 13.23 *Continued*

Virus	*Disease in*	*Reference to ultrastructural pathology*
Feline sarcoma virus	Cat	**Herz**, *J Nat Cancer Inst* 44:339, 1970 (myeloproliferative disease); **McKissick**, *J Virol* 5:247, 1970 (virion);* **Snyder**, *J Natl Cancer Inst* 47:1079, 1971 (sarcoma)
Porcine retrovirus	Pig	**Dieckhoff**, *Vet Microbiol* 123:53, 2007; **Marcucci**, *Virology* 375:637, 2008*
Gibbon ape leukemia virus	Gibbon Ape	**Snyder**, *J Natl Cancer Inst* 51:89, 1973 (lymphoma)
Koala retrovirus	Koala	**Hanger**, *J Virol* 74:4264, 2000 (virion)*
Avian reticuloendotheliosis virus	Avian Partridge	**Perk**, *J Natl Cancer Inst* 62483, 1979 **Trampel**, *J Wildl Dis* 38:438, 2002
Turkey lymphoproliferative disease	Turkey	**Patel**, *Arch Virol* 95:159, 1987; **Paul**, *J Nat Cancer Inst* 58:1819, 1977 (reticuloendotheliosis)
Simian sarcoma virus	Monkey	**Robbins**, *Proc Natl Acad Sci USA* 78:2918, 1981 (virion)*
		Genus *Deltaretrovirus*
Bovine leukemia virus	Cattle Sheep	**Miller**, *J Nat Cancer Inst* 43:1297, 1969 **Olson**, *Cancer Res* 36:2365, 1976 (lymphosarcoma)
Human T-lymphotropic virus 1 and 2	Human	**Majorovits**, *PLoS ONE* 3:e2251, 2008 (virion);* **Matsuura**, *J Neuropathol Exp Neurol* 67:41, 2008 (inclusion body myositis)
	Monkey† Rat†	**Heraud**, *Virology* 361:402, 2007; **Kazanji**, *J Virol* 74:4860, 2000 **Kikuchi**, *Int J Exp Pathol* 83:247, 2002 (thymoma)
Simian T-lymphotropic virus 1, 2 and 3	Monkey	**Chevalier**, *J Virol* 81:6276, 2007 (virion)*
		Genus *Lentivirus*
Human immunodeficiency virus	Human	**Baccetti**, *J Cell Biol* 127:903, 1994 (sperm); **Nuovo**, *Am J Pathol* 144:1142, 1994 (sperm); **Levy**, *Science* 225:840, 1984; **Marche**, *Arch Anat Cytol Pathol* 32:120, 1984 (AIDS pathology); **Tenner-Racz**, *Am J Pathol* 123:9, 1986 (AIDS, lymph node)
Simian immunodeficiency viruses	Monkey Ape	**Giddens**, *Am J Pathol* 119:253, 1985 (retropeitoneal fibromatosis); **Lackner**, *Am J Pathol* 139:609, 1991 (brain); **Munn**, et al. *Lab Invest* 53:194, 1985; **Ward**, *Am J Pathol* 127:199, 1987
Bovine immunodeficiency virus	Cattle	**Boothe**, *J Virol* 13:197, 1974*
Equine infectious anemia virus	Horse	**Gonda**, *Am J Vet Res* 39:731, 1978; **Tajima**, *J Virol* 4:521, 1969 (virions);* **Weiland**, *Arch Virol* 55:335, 1977
Feline immunodeficiency virus	Cat	**Poli**, *J Comp Pathol* 110:319, 1994 (lymphoma); **Stefan**, *Hepatology* 23:964, 1996;* **Yamamoto**, *Am J Vet Res* 49:1246, 1988
Caprine arthritis-encephalitis virus	Goat	**Cheevers**, *Lab Invest* 58:510, 1988; **Cork**, Science 207:997, 1980; **Perk**, *Res Vet Sci* 49:367, 1990 (nerve)
Visna/maedi virus (ovine progressive pneumonia virus)	Sheep	**Lairmore**, *Am J Pathol* 125:173, 1986 (pneumonia); **Lairmore**, *J Virol* 61:4038, 1987 (alveolar macrophages); **Lee**, *Vet Microbiol* 49:93, 1996;* **Rosadio**, *Vet Pathol* 25:58, 1988; **Thormar**, *Virology* 14:463, 1961;* **Thormar**, *Virology* 25:145, 1965*
		Subfamily *Spumaretrovirinae*
		Genus *Spumavirus*
Simian foamy virus	Monkey	**Mergia**, *J Virol* 72:817, 1998
Human foamy virus	Human Mouse	**Aguzzi**, *Am J Pathol* 142:1061, 1993 (brain)†
Bovine foamy virus	Cattle	**Boothe**, *Arch Ges Virusforsch* 31:373, 1970*; **Bouillant**, *J Nat Cancer Inst* 72:1075, 1984
Equine foamy virus	Horse	**Lecellier**, *J Virol* 76:7220, 2002
Feline foamy virus	Cat	**McKissick**, *J Virol* 5:247, 1970
Rabbit spumavirus	Rabbit	**Brown**, *Proc Soc Exp Biol Med* 133:587, 1970 (rabbit syncytium virus)

*In vitro study.
†Animal model.

Vet-ebooks.com

receptor for HIV is the CD4 complex on lymphocyte surfaces. Murine retroviruses have been reported to use plasma membrane permease proteins similar to the transporter proteins for arginase, histidine and other amino acids.

Subfamily *Orthoretrovirinae*

Genus *Alpharetrovirus*

Avian Leukemia **Avian leukemia virus (ALV)** causes lymphomas in chickens. The primary site of development is the **cloacal bursa**, and there is spread to liver, spleen and other organs. Lesions are massive enlargement of the bursa, hepatosplenomegaly, anemia and muscle atrophy. Neoplastic transformation occurs in **B lymphocytes** and requires the presence of an intact bursa. The type of neoplasm that arises depends upon the strain of virus and the availability of target cells.[271] Expression of oncogenicity may involve myeloblasts, erythroblasts, embryonic kidney cells (embryonal nephromas), osteoblasts (osteopetrosis),[272] mesotheliomas,[273] angiosarcomas,[274] and lesions of the brain.[275]

When newly hatched chickens of a susceptible strain are inoculated with an oncogenic isolate of ALV, transformation of lymphoid cells in the bursa occurs at 6–8 wk of age. By 10–16 wk, transformed bursal follicles are visible grossly in nearly all birds and metastasis from the bursa to viscera occurs around the time of sexual maturity at 10 wk. The initial change is the development of isolated giant follicles within the bursa that progressively expand to compress and distort other follicles, and eventually spread to involve the entire bursa. Neoplastic B lymphocytes are large stem cells with large nucleoli and few cytoplasmic organelles. Endoplasmic reticulum is sparse and is not an efficient source for globulin production even though large amounts of IgM may be produced. Virions bud from the cell surface but are not common in natural tumors.

ALV is naturally transmitted from hen to chick via the egg. In the hen, virions are demonstrable in the ovary and oviduct and are most prevalent in the albumen-secreting glands of the oviduct. In the egg, ALV is concentrated in albumen (leaving in some cases, the embryo free from infection). Virions bud from the plasma membrane of cells in direct contact with oogonia and germinal epithelium. They bud from surface microvilli into the lumen and the zygote is exposed to high concentrations of virus in the magnum while it is still a single cell.

When the chicken embryo is infected, the chick appears tolerant to ALV and does not develop antibodies. At hatching, most chicks are viremic although a variable percentage will not have virus. Virions are demonstrable in most tissues, especially the liver and kidney. In infected flocks, maternal antibody is present in newly hatched chicks but gradually disappears and is gone in 4–6 wk.

Rous Sarcoma **Rous sarcoma virus (RSV)**-induced fibrosarcomas of the chicken were shown to be transmissible by Rous in 1910, and led to the discovery of the virion and the *src* gene. Development of tumors in the chicken depends upon host factors; for example, traumatic tissue wounding enhances development of sarcomas, by releasing PDGF or other growth factors during healing. RSV causes mesenchymal neoplasms in a wide variety of hosts by many different routes. Given intracerebrally to 11 dogs, RSV induced both meningeal sarcomas and meningiomas, and virions develop in the tumors.

Genus *Betaretrovirus*

Mouse Mammary Tumors **Mouse mammary tumor virus (MMTV)** causes adenocarcinomas of the parenchyma of the mammary gland. MMTV virions are classified as type A (50–70 nm, cytoplasmic) and B (110–120 nm, extracellular). Mature **B virions** have an eccentric electron-dense nucleoid. The immature virions have an electron-lucent nucleoid.[276] The immature cores, called **A particles**, are found in the cytoplasm of infected cells. They are directed to the plasma membrane where a myristilated matrix protein plays a key role in maturation. Intracytoplasmic A particles contain the unprocessed precursor polypeptides derived from translation of the viral genes *gag*, *gag-pro*, and *gag-pro-pol* which, after proteolytic cleavage, form the mature proteins of the virus. Immunogold labeling of viral proteins and negative staining for electron microscopy have demonstrated the radial organization of the polypeptide precursors that form the A particles.[277]

Natural mammary gland tumors are common in old females in mice. Most of the tumors are adenocarcinomas, but tumors of the ductal system also occur. Adenocarcinomas are typically well-differentiated neoplasms composed of masses of disoriented glandular acini (Fig. 13.38). Malignant mammary tumors in mice metastasize to the lungs where they grow nodules in which they provoke granular pneumocyte hyperplasia. Distinct basement membrane and connective tissue capsules are formed. Tumor cells contain secretory granules and glandular lumens are filled with proteinaceous material. The Golgi complex of tumor cells is large but has defects in protein production. Virions are invariable present in the cytoplasm of tumor cells and extracellularly in the centers of acini. In 1936 Bittner showed than MMTV was transmitted in mother's milk. Mice of low mammary tumor strains nursed by mothers of high cancer strains developed a

Vet-ebooks.com

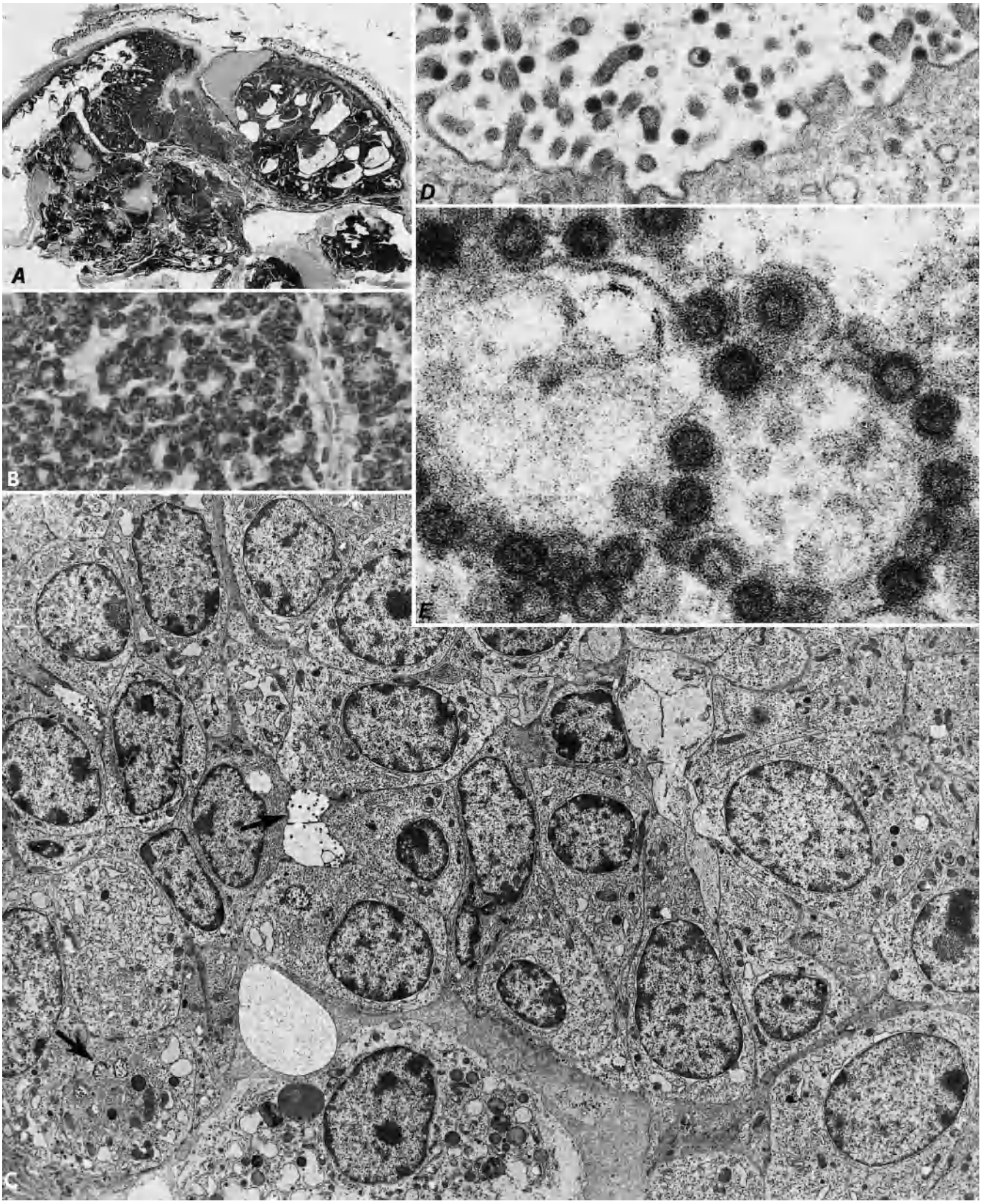


Fig. 13.38 Murine mammary gland tumor (spontaneous). **A**. **Cystic, highly vascular tumor:** histology. **B**. **Neoplastic cells**: acinar growth (histology). **C**. **Tumor acini**: virions bud from acinar lumens and cytoplasmic vacuoles (*arrows*). Pleomorphic neoplastic cells contain secretory granules; tumor acini are surrounded by basement membranes. **D**. **Budding virions**: lumenal plasma membrane. **E**. **Virions**: A particles surrounding and within cytoplasmic vacuole. (Micrographs C–E: Randall C. Cutlip, National Animal Disease Center.)

Vet-ebooks.com

high incidence of mammary tumors. Conversely, mice of high cancer strains suckled by foster mothers of low cancer strains developed only a few mammary tumors. When MTV is ingested, it is disseminated hematogenously and virions are found in blood. Virus infects the immature mammary gland and can be demonstrated within normal acinar cells.

Mammary tumors of other species have been associated with viruses. Virions have been reported in mammary tumor tissue of monkeys, baboons, cats and dogs, lemmings, and rats; however, their causal role in these species remains elusive, and they may be passenger viruses with no causal effect on the tumor.

Jaagsiekte **Jaagsiekte** is the Afrikaans' name of a natural contagious pulmonary bronchioalveolar papillary adenocarcinoma of the lungs of sheep (and to less extent, goats) that is sporadic and endemic worldwide. Tumors progressively expand to cause intra- and extrathoracic metastases. Neoplastic cells are derived from granular (type II) pneumocytes transformed by **jaagsiekte sheep retrovirus (JSRV)**, a virus that has antigens that cross-react with those of this group.[278] JSRV commonly coinfects the lung with an ovine lentivirus. JSRV virions are present in tumor tissue.

Genus *Gammaretrovirus*

Feline Leukemia **Feline leukemia virus (FeLV)** causes lymphoproliferative and lymphosuppressive diseases in cats. FeLV envelope glycoproteins gp70 and transmembrane protein p15e bear sites that bind virus to the FeLV cell receptor. Subgroup specificity is according to *env* gene sequences that code for N-terminal regions of the surface glycoprotein. Variant FeLV genomes may be replication-competent or replication-defective. In tissue, FeLV exists as mixtures of closely related viral genotypes and minor variations among FeLV strains can cause major differences in pathogenicity. The gene coding regions responsible for targeting infection to specific hemic or lymphoid tissue types have been mapped to the viral surface glycoprotein and long terminal repeat regions of the virus.

After initial **oral infection**, virus replicates locally in oropharyngeal lymphoid tissues, and in a few circulating lymphocytes. Macrophages, B and T lymphocytes, and then myeloid and erythroid hematopoietic progenitor cells become infected. Many cats are able to effectively inhibit and to terminate viral replication. Infection in some cats leads to persistent viremia and replication of FeLV in bone marrow and lymphoid tissues. Cats that fail to suppress viral replication and viremia develop infection of mucosal and glandular epithelium of the pharynx, nose, trachea, esophagus, urinary bladder, intestine, salivary glands and pancreas. This leads to enteropathy and diarrhea, infertility, and neurologic syndromes. FeLV *gag* antigens and infectious virus circulate continuously in plasma, leukocytes, and platelets (little or no neutralizing antibody is produced).

Continual FeLV replication over months to years leads to multiple proviral integrations within DNA of infected cells. This in turn leads to neoplastic transformation into lymphoma or leukemia. Simultaneously, the progressive lymphoid and myeloid depletion translates into **immunosuppression**, which leads not only to enhanced replication of FeLV but also to superinfections with other pathogenic microbes. Mutation or recombination of replicating viral genomes results in new and more pathogenic viral variants, the survival of which is favored by the immunosuppression.

FeLV-induced lymphoma occurs in four variants: **alimentary**, in which Peyer's patches and lymph node germinal centers are initially involved; **multicentric**, which begins in paracortical areas of lymph nodes; **thymic**, which also affects paracortical areas; and **leukemia**, which chiefly affects the bone marrow, splenic red pulp, and medullary areas of peripheral lymph nodes. The neoplastic cell types affected represent both B and T cells that have been transformed. In individual cats, the malignant cells may be predominantly lymphoblastic, prolymphocytic, histocytic or lymphohistiocytic. There is little correlation between cell type and clinical course of the disease.

Ultrastructural analysis of tumor tissue reveals that virions occur extracellularly, within cytoplasmic vacuoles, and budding from the plasma membrane;[279] and they are most prevalent in bone marrow, thymus, lymph node and spleen. In cells of the circulating blood, virions are most frequent within and budding from the surface of platelets. Megakaryocytes serve as a reservoir of virus and viral oncogenes. When young kittens are first infected, thrombocytopenia occurs as a direct effect of the virus in preleukemia phases.

Immunosuppression precedes development of lymphoma, and increases progressively throughout lymphomagenesis. Defects in T and B cell function, numbers of circulating CD4 T cell subsets, and thymic lymphoid populations appear in preneoplastic periods and gradually increase. In the preneoplastic phases of experimental disease, significant depression of cell-mediated immunity occurs and thymic atrophy is prominent. Experimentally, radiation increases the percent of animals which develop lymphosarcoma. Cats that have recovered from severe anemia induced by *Hemobartonella felis* have a higher incidence of lymphoma than do nonanemic cats. In natural disease, feline immunosuppressive virus (FIV) enhances lymphosarcoma production.

Preneoplastic **myeloproliferative diseases** involving proliferation of abnormal growth and differentiation of hematopoietic cells in the bone marrow are

Vet-ebooks.com

associated with FeLV. Most are seen as nonregenerative, often macrocytic anemias. In myelogenous leukemia proliferating marrow cells seed the body with immature-appearing, malignant progranulocytes. These large cells contain small dense granules typical of progranulocytes. Virions are best sought in bone marrow. The less differentiated cells are often associated with virions. In the spleen, cells infiltrate the pulp cords, sparing germinal centers until late in disease. In liver, periportal areas are first infiltrated (Fig. 13.39).

Erythremic myelosis (transformation of the erythrocyte series) and **erythroleukemia** (a mixture of neoplastic granulocytes and erythocytes) may occur in FeLV infection.[280] **Megakaryocytic myelosis** is characterized by megakaryocyte proliferation in bone marrow, and severe anemia is rare. The number of circulating platelets increases markedly and bizarre forms are deposited in the liver and spleen.

Fibrosarcomas in cats have been shown to be transmissible via a C-type virus similar to FeLV; virions are demonstrable in both natural and experimental tumors. After inoculation of virus into kittens, tumors arise in over three-fourths of the animals. Rapidly growing masses tend to have loose, myxomatous patterns of stellate cells with vacuolation and pleomorphic nuclei. The more slowly growing tumors are compact with fusiform-shaped cells and elongate nuclei. Virions of 115 nm diameter bud from the plasma membrane and can also be seen extracellularly and within cytoplasmic vacuoles.[281]

Murine Leukemia **Murine leukemia viruses (MLVs)** include a large spectrum of natural and laboratory viruses that cause leukemia and other disorders in mice. The natural lymphosarcoma of mice caused by MLV reported by Gross in 1951 was a T cell lymphosarcoma that originated in the thymus. MLV was widely distributed throughout the thymus of preleukemic mice where they occurred both in lymphocytes and thymic epithelial cells.

The mouse carries genomic information for producing three endogenous retroviruses distinguishable on ultrastructural, serologic, and biochemical criteria: **type C particles**, associated with leukemogenesis and autoimmune disease; **type B particles** (and their immature precursors, the cytoplasmic type A particle), associated with mammary carcinogenesis; and **intracisternal type A particles**, which are typically expressed in early embryogenesis. Unlike B and C viruses these are not shed from the cell surface but remain in cisternae of endoplasmic reticulum and do not bud from the plasma membrane (see Fig. 13.39A and B).[282]

Thymic changes, which initiate oncogenesis, begin unilaterally in one lobe. Lymphocytolysis is followed by narrowing of the cortex and loss of small lymphocytes. The medulla is expanded by histiocytosis and aggregation of small lymphocytes. Phagocytic reticulum cells, which become activated and hyperplastic, are an important factor in degradation of dying neoplastic cells.[283] Virions are seen free in the cytoplasm and budding from the plasma membrane of the cell. Budding occurs at sites on the plasma membrane which are free of the G (Gross) cell-surface antigen and of the major H-2 histocompatability antigen.[284] Large amounts of MLV are found in spleen. Massive accumulations of virions have been found in cisternae of the endoplasmic reticulum of splenic megakaryocytes and play a role in the systemic dissemination of the virus (Fig. 13.40).[285]

Malignant lymphocytes spread from thymic foci to involve the viscera. Lymphocytes injected intravenously are trapped chiefly in lungs and livers. In liver, they rapidly emigrate via pseudopods through sinusoids, but are not phagocytized by Kupffer cells. In very young mice, virions are most obvious in hematopoietic tissue from which they seed other lymphoid organs. Later, they are prominent in germinal centers of spleen and lymph nodes where they reside in close approximation to the dendritic webs of reticular cells.

Natural transmission of murine lymphosarcoma is through the embryo. In the **ovary**, virions bud from cells of the follicular theca and corpus luteum. They occur throughout the female genital tract and in spermatozoa and ductal system of the male genital tract. In utero infection induced tolerance against at least some of the antigen in the virion, and high levels of virus are present in the mouse throughout its life span. Some anti-MLV antibodies are produced and are responsible for membrane glomerulopathy which develops in aged infected mice.

MLV-induced motoneuronal paralysis occurs in infected wild mice.[286,287] Ecotropic type C retroviruses isolated from brains of paralyzed wild mice have been shown to be neurotropic in susceptible mice causing viremia and spongiform lesions in the brain. MLVs capable of causing neurodegenerative disease in mice include molecularly cloned wild mouse ecotropic viruses, temperature-sensitive mutants of laboratory MuLVs, and genetically engineered recombinants of these ecotropic MuLVs.[288] **Spongiform myeloencephalopathy** causes neurologic signs. Microglia and macrophages are important reservoir of MuLV in the brain. Spongiosis originates from both neuronal and oligodendroglial degeneration. There is degeneration of neurons in the anterior horn of the lower spinal cord, dentate nuclei of the cerebellum, and in some nuclei of the brain stem. Spongiform lesions may first appear as swelling of perivascular astrocyte processes.[289] Reactive gliosis and spongiosis are intense but an inflammatory response is lacking. Damage is due to a direct effect

Vet-ebooks.com

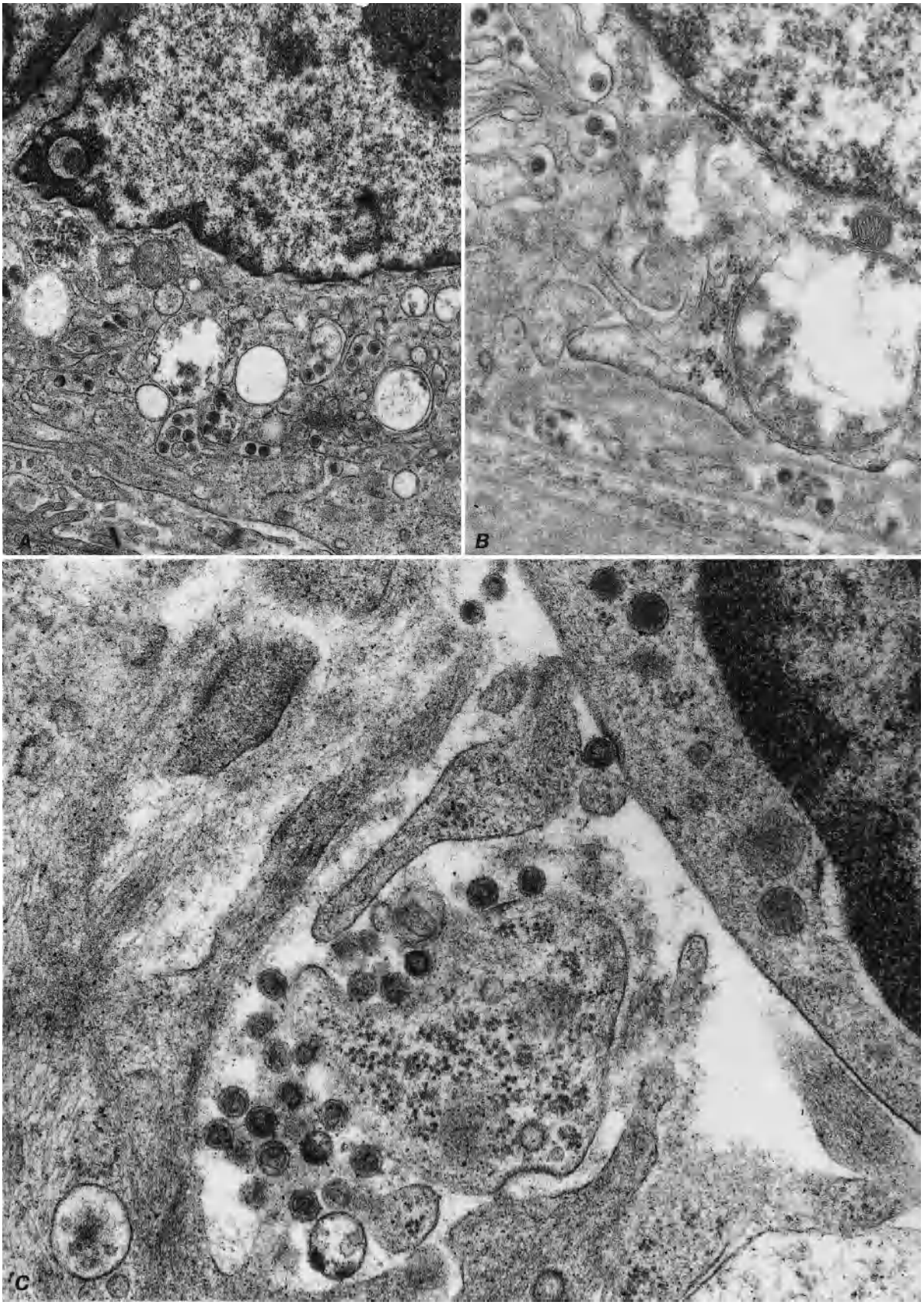


Fig. 13.39 **Animal retroviruses** associated with leukemia. **A** and **B**. **Murine leukemia virus:** kidney, NZB mouse. **C**. **Feline leukemia virus:** liver, cat with myelogenous leukemia.

Vet-ebooks.com

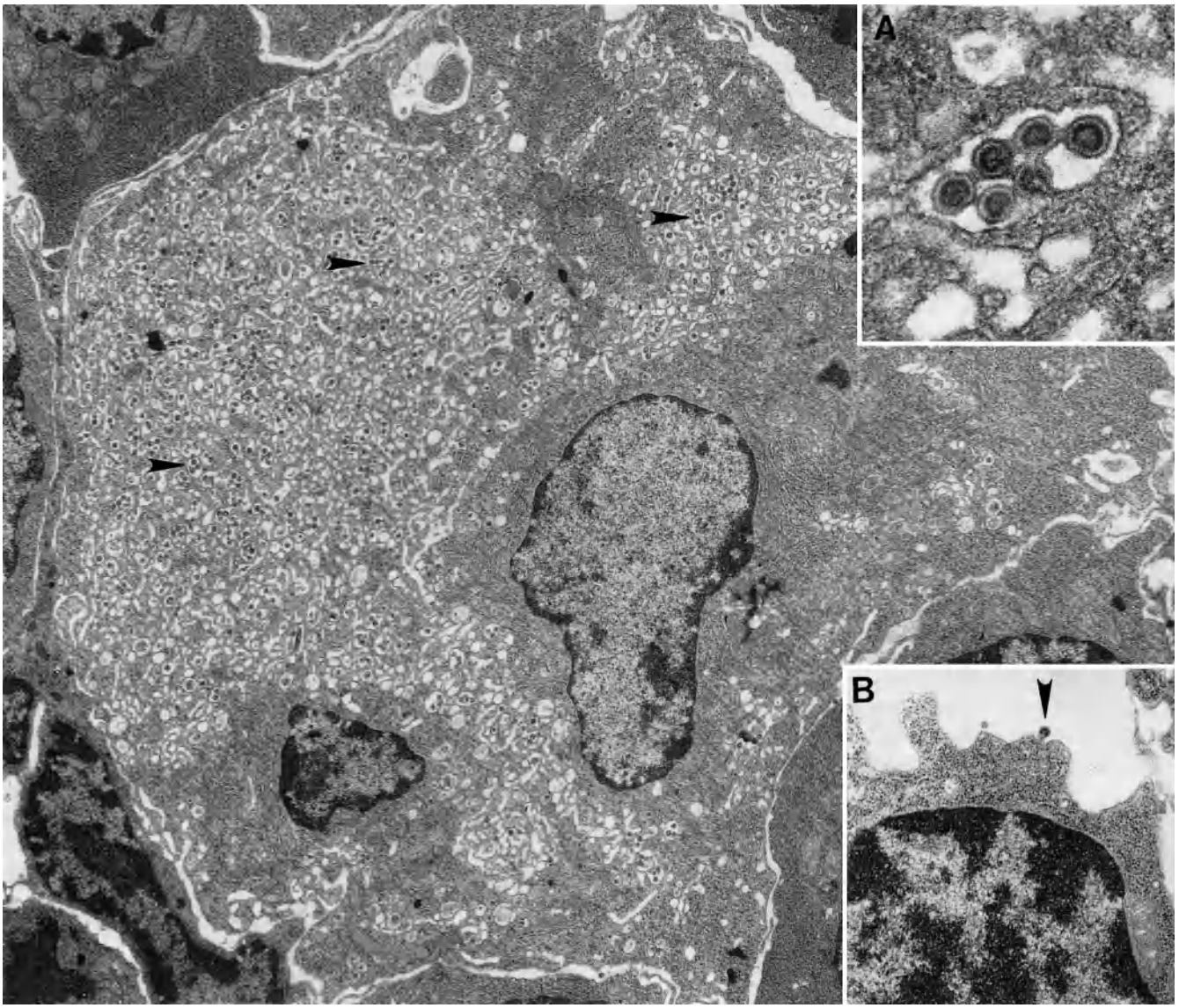


Fig. 13.40 Murine leukemia virus: megakaryocyte filled with virions, spleen, rat, 10 days after inoculation with MLV. Intracytoplasmic vacuoles contain many virions (*arrowheads*). *Inset A*: megakaryocytic vacuole: budding immature spheroid type C virions that have bilayered outer envelope and central nucleoids. *Inset B*: splenic lymphocyte with single virion (*arrowhead*). (Micrograph: Timothy V. Baszler, *Lab Invest* 63:612, 1990.)

of the virus and the attendant demyelination is due to infection and degeneration of oligodendrogliocytes. Cytopathic alterations in infected cells include swelling, vacuolation, autophagy, and disappearance of rough endoplasmic reticulum. **Virions** bud from the plasma membrane and from membranes of cytoplasmic vacuoles. Virions consist of cores composed of granule spheroids or hexagonal electron-dense centers surrounded by an outer envelope. Cylindrical and spherical particles develop in vacuoles and in large autophagic residual bodies.

One strain of MLV replicates in **endothelial cells** causing expansion of the cytoplasm and Golgi complex. Endothelial damage underlies the unique hemorrhages and thrombi seen in infected mice.[290]

The **thymic phase** of lymphoma development is necessary for full-blown neurologic lesions.[291] An MLV isolate from murine embryos reproduces chronic CNS disease when injected into neonatal or adult mice; a disease markedly resembling **amyotrophic lateral sclerosis**. The virus spreads hematogenously to infected endothelium and then spreads to nervous tissue. Virions bud from the basal part of the endothelial plasma membrane into the underlying basement membrane.

MLV causes lesions in many other tissues including **bone** and **liver**. Type A and C MLVs have been found ultrastructurally in pancreatic β-cells. In the islets of strain *db* mice, they may be involved in production of diabetes by enhancing an autoimmune process.[292]

Vet-ebooks.com

Noninflammatory spongiform neurodegeneration, resembling lesions of the TSEs, are caused by MLV that is maintained in feral mouse populations as exogenous viruses transmitted to neonates in maternal milk. Life-long viremia leads to neurologic disease if virus enters the brain. Oligodendrocytes are the primary target for the virus, and the receptor is the ubiquitous cationic amino acid transporter CAT1.[293]

Avian Reticuloendotheliosis **Avian reticuloendotheliosis virus** (ARV) was isolated from a turkey where it was associated with a rare fatal type of leukosis. ARV produces a rapidly fatal disease with splenomegaly and hepatomegaly in chickens and other birds. Disease is characterized by proliferation of mesenchymal cells, especially around vascular structures. Other viruses in this group are duck infectious anemia virus, spleen necrosis virus, and chick syncytial virus.

Genus *Deltaretrovirus*

Human T-lymphotropic Virus The prototype **human T-lymphotropic virus 1 (HTLV-1)** was isolated in 1978 from humans with mycosis fungoides/Sézary syndrome, and was found to be endemic to southwestern Japan, the Caribbean, and parts of Africa. It is associated with a variety of clinical manifestation including the rare but rapidly fatal lymphoproliferative syndrome, **adult T-cell leukemia**. The neoplastic cells are $CD4^+$ since HTLV has an affinity for T helper lymphocytes. There is a long latent period of infection and the disease terminates with generalized lymphadenopathy, hepatosplenomegaly, hypercalcemia, and skin lesions.

HTLV-1 is also associated with neurologic disorders termed **tropical spastic paralysis** and **HTLV-1-associated myelopathy**. In the latter, the spinal cord is preferentially affected by chronic diffuse infiltrates of lymphocytes and monocyte-lineage cells. Both gray and white matter are affected, and lesions subside, leaving gliomesenchymal foci, especially in corticospinal tracts.[294,295]

HTLV infects human T lymphocytes to produce a variety of cytokines, for example, osteoclast-activating factor (which probably causes hypercalcemia in patients with T-cell leukemia). HTLV contains antigens that cross-react with certain tissues. The viral p19 gag protein cross-reacts with a determinant found in the neuroendocrine thymic epithelium and with syncytiotrophoblasts of the placenta.

HTLV-1 can integrate into different chromosomal loci but each tumor cell in a single patient has the viral sequence integrated into the same site. Since the virus infects individuals before neoplastic transformation of T lymphocytes, it appears that a trans-acting transcriptional activation occurs. A regulatory factor stimulates transcription from a retroviral promoter and leads to increased viral replication rates (via a positive feedback loop). This factor may also increase transcription of cellular genes (important in mitosis) and be at least one factor important in neoplasia.

Viruses very similar to HTLV-1 occur in several Old World monkeys (without disease), and are distinguished from human retroviruses by molecular analyses. Ultrastructurally the virions are similar to those of HTLV.

Genus *Lentivirus*

Five groups of **lentiviruses** have been clustered on the basis of the hosts (primates, sheep and goats, horses, cats, and cattle) they infect. Lentiviruses are nononcogenic retroviruses that produce a variety of chronic progressive diseases with unusually long incubation periods. Most replicate in lymphoid tissues and cause immunosuppression. Several animal models for HIV infection of man have been developed including feline immunosuppressive virus (FIV) in cats.[296,297] The virion has a dense cylindrical core whose structural elements are encoded by the viral *gag* gene and which encase two molecules of the viral RNA genome. The core is surrounded by a lipid-bilayer envelope acquired as the virions buds from the host cell surface.

Acquired Immunodeficiency Syndrome **Human immunodeficiency viruses (HIVs)** are the cause of human acquired immunodeficiency syndrome (AIDS). HIV selectively infects monocytes and macrophages (which act as a reservoir for virus) and helper T lymphocytes bearing CD4 molecules on their surfaces (which are destroyed by the infection). Infection creates an immune defect that is progressive. HIV enters the body in any break in a dermal or mucosal barrier. HIV antigens have been found in Langerhans' cells in the epidermis, cells that bear T4 receptors. Binding of viral glycoprotein 120 to Langerhans' surfaces is via CD4, but may also occur through other molecules.[298] HIV **virions** can be seen in electron micrographs budding from the surfaces of lymphocytes of infected patients. Ultrastructural analysis reveals that virions released from lymphocytes are 105–115 nm in diameter with a characteristics central core[299–301] (Fig. 13.41). Variants of the original HIV isolates (called HIV-2) have been obtained from African patients and are similar in structure; it is reported that surface spikes are more readily observed on these viruses.[302]

T helper lymphocytes are selectively infected by HIV.[303] The **CD4 molecule** on the T4 lymphocytes is the high-affinity receptor for HIV. After binding, there is fusion of the gp41 of the viral envelope and the plasma membrane of the host cells. The virion is internalized and then uncoated.[304] Genomic RNA is transcribed to DNA by the reverse transcriptase. The proviral DNA is integrated into host chromosomal

Vet-ebooks.com

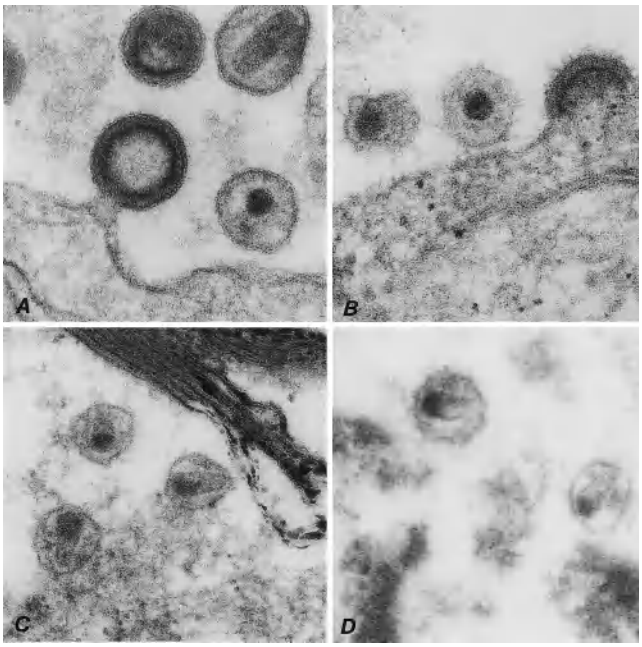


Fig. 13.41 Lentivirus: human immunodeficiency virus, human AIDS patient. **A**. **Mature viral particles**: half particle budded from cell surface. **B**. **Particles in cytoplasmic vacuole:** in vitro. **C**. **Virions**: conical nucleoids, CNS tissue. **D**. **Mature virions**: formalin fixation. (Micrograph: Jan Marc Orenstein, *Ultrastruct Pathol* 16:179, 1992.)

DNA through an endonuclease encoded by the viral *pol* gene. After integration of provirus, infection becomes latent; that is, the replication cycle is restricted until the cell becomes activated. When activation occurs, the proviral DNA transcribes viral genomic RNA and mRNA. Protein synthesis, processing, and virion assembly occur with budding of the mature virions from the cell surface. Large amounts of unintegrated proviral DNA accumulate in the host cell, and along with CD4-viral glycoprotein interactions, may cause cell degeneration and death.

The **host lymphocyte** is killed when active viral replication occurs. The mechanism of death may be related to the accumulation of viral DNA. **Dendritic cells** in lymphoid tissues carry HIV to uninfected T cells, enhancing the infectious cycles. The dendritic cells and responding T cells form discrete aggregates that efficiently transmit HIV, and may facilitate the lysis of antigen-specific $CD4^+$ T cells.[305] High levels of HIV *env* gene expression in CD4 cells leads to fusion with neighboring uninfected CD4 cells, and formation of multinucleated giant cells. Cytolysis of the fused cells then occurs, and this may enhance spread of HIV.[306]

In the **bloodstream**, HIV is carried by monocytes and T4 lymphocytes. Virions are not readily demonstrable ultrastructurally in leukocytes of infected patients but there is evidence of abnormal cell structure: 5–15% of mononuclear cells in the blood of male homosexuals with AIDS had tubuloreticular inclusions (none in controls) and there were cylindrical confronting lamellae in many sections.[307] Male AIDS patients invariably have atrophic testes and abnormal spermatogenesis, and HIV-1 nucleic acids have been localized to spermatogonia.[308]

In the **lymphoid system**, HIV replicates in lymph nodes to cause a generalized lymphadenopathy. Early there is a nonspecific change in B cell areas: follicular hyperplasia with depletion of mantle zone lymphocytes and marked plasmacytosis in medullary zones. This condition progresses in AIDS to marked follicular involution with lymphoid depletion and histiocytic lesions caused by opportunistic pathogens. Virions develop in the cytoplasm of monocytes and macrophages. They are also regularly associated with dendrites of follicular dendritic cells.[309–311] In these cells, virus-containing vacuoles arise from the Golgi complex. Two modifications of the endoplasmic reticulum are useful markers of infection: **tubuloreticular inclusions** are footprints of interferon production and also found in lupus and some viral infections, and **cylindrical confronting cisternae**, which are cylinders composed of apposed cisternae of rough endoplasmic reticulum with electron-dense material between them (these are also found in hepatitis C and HTLV-1).

Aggressive B cell lymphomas occur in HIV-infected humans. Both HIV and Epstein-Barr virus are implicated in pathogenesis. Serial lymph node biopsies of HIV-positive patients reveals progression from B cell proliferation to lymphoma, with both cell types frequently carrying EBV genomes and exhibiting c-*myc* deregulation. EBV can immortalize B lymphocytes (but not transform them) in vitro; c-*myc* activation has similar properties. Introduction of activated c-*myc* into EBV transformed B cell may lead to oncogenicity.

AIDS is complicated in late stages by **subacute encephalopathy**, a neurologic syndrome induced directly by HIV and characterized by progressive dementia with abnormalities in cognition, motor performance, and behavior. The main histologic changes occur in subcortical areas, notably in the central white matter, basal ganglia, thalamus, brain stem, and spinal cord. There is diffuse white matter pallor with central and periventricular astrocytic reactions. Monocyte/macrophage cells, microglia, and the giant cells derived from them, are infected with HIV in the brain. Astrocytes, oligodendrogliocytes, and neurons do not develop cytolytic infection, although vacuolar changes often are present in these cells.[312] Massive HIV-1 release and development within giant cell vacuoles suggest that excessive viral budding is related to the large surface area (compared to the more restricted membrane access of macrophages).[313] Using in situ hybridization with HIV RNA-specific probes on brain tissue it can be shown that HIV mRNA is expressed

Vet-ebooks.com

selectively in multinucleated giant cells in AIDS encephalopathy.[314,315] Most infected cells from areas of demyelination are macrophages and have evidence of phagocytosis, especially of lipid vacuoles and lysosomes bearing myelin debris.

Brain lesions have immature viral particles and virions in macrophages. Free, immature particles measure 105–115 nm in diameter and have a clear 70 nm central zone surrounded by a dense ring and separated from the outer double membrane by a less electron-dense zone. Mature particles have an enlarged and distorted outer membrane and typically contain an eccentric, spherical electron-dense core of approximately 40 nm diameter.[316] Similar changes have been reported in the retina.[317] CNS lesions of HIV encephalopathy are commonly complicated by the various opportunistic CNS infections that occur in AIDS, for example, the papovavirus of progressive multifocal leukoencephalopathy, herpes simplex, and other viruses.

Liver lesions in AIDS are a consequence of hepatic involvement by disseminated opportunistic infectious agents or by tumors, including Kaposi's sarcoma and lymphomas. Hepatic sinusoidal abnormalities that range from dilatation to **peliosis hepatis** (and that are independent from the above lesions) have been reported, for example, in 8 of 29 patients with HIV infection and liver abnormalities.[318] Ultrastructural lesions of the sinusoidal barrier were typical of peliosis hepatis. There is marked dilatation of the spaces of Disse, disruption of the endothelial lining, extravasation of erythrocytes, and layering of the sinusoidal endothelium. In addition there were many hyperplastic macrophages in the affected sinuses. The pathogenesis of the lesion is hypothesized to be a direct lesion of the sinusoidal barrier.

In the **lungs**, alveolar macrophages play a role in the interstitial pneumonitis of AIDS patients. Monocytes and macrophages in the lungs like those in the circulation have abnormal chemotaxis and microbial killing. Lesions in the **heart** of a small percentage of AIDS patients suggest that cardiomyopathy can be directly induced by HIV infection.[319] Other defects in AIDS patients have been reported in **salivary glands**[320] and **skeletal muscle** (Fig. 13.42) although the precise relation to HIV infection is not established.[321]

Simian AIDS **Simian immunodeficiency virus (SIV)** causes a natural infectious disease of the genus *Macaca*. **Simian AIDS (SAIDS)** can be caused by two groups of simian retroviruses: the **type D viruses**, and **simian lentiviruses** such as SIV. SIV is related morphologically and genetically to HIV-1 and 2, and the fatal disease in rhesus monkeys includes opportunistic infections with *Pneumocystis carinii* and *Mycobacterium* spp.

SAIDS can be induced by inoculating monkeys with blood, plasma, saliva, urine, or cell products containing SIV. SIV can be transmitted to female rhesus macaques by placing viral suspensions in the **vagina**. SIV-infected cells are found in the vaginal epithelium and in the submucosa of the vagina and cervix. Infected cells are more common in sites of inflammation than in normal areas of tissue.[322] **Lymph nodes** progressively develop follicular hyperplasia, involution, and lymphocyte depletion (with normal or expanded paracortical areas).[323] Viral proteins are preferentially localized in T4 lymphocytes, macrophages and dendritic cells in spleen and lymph node. The p27 gag protein is predominantly in follicular dendritic cells during hyperplastic stages; affected dendritic cells have swollen dendritic processes containing electron-dense material but virions are rarely seen in these cells. Later, macrophages and giant cells bearing viral antigens are predominant in lymphoid tissues.[324]

SIV is immunosuppressive, lethal to its host, and neurovirulent. In the **brain**, SIV is associated with giant cell encephalitis. SIV can be detected in neurons (Fig. 13.43), and by in situ hybridization techniques.[325,326] Macrophage and giant cells contain viral RNA and antigen and are the only sites were viral particles are detected ultrastructurally. SIV antigen and RNA are also associated with small blood vessels, the choroid plexus, and meninges. The infiltrating cells are largely monocyte/macrophages with occasional CD8-positive T cells.

There is an increased incidence of arteriopathy in monkeys with SAIDS that appears to be secondary to primary endothelial injury.[327] SIV-infected monkeys also develop cutaneous exanthemas,[328] enteropathy,[329] and testicular degeneration.[330]

Visna **Visna** is an insidious, chronic, progressive, paralytic, demyelinating CNS disease of sheep. After an incubation period of 2 years or more, lesions of patchy demyelination and encephalomyelitis begin, and there is progressive deterioration of the sheep's general condition. Gliosis and destruction of the neuropil are striking in affected brains. The major features are periventricular infiltrates of monocytes, lymphocytes, and plasmacytes that spread as perivascular cuffs into adjacent white and gray matter, sometimes accompanied by necrotic lesions. Demyelination is secondary; there is no evidence of humoral and cell-mediated immune processes against myelin antigens.[331]

Replication of visna virus in vitro includes mature virions, crescent-shaped buds at plasma membranes, and immature viral particles along the cell surface that lack dense cores of the mature, extracellular virion (Fig. 13.44). All of these—the buds, immature particles, and extracellular virions—are tagged by

Vet-ebooks.com

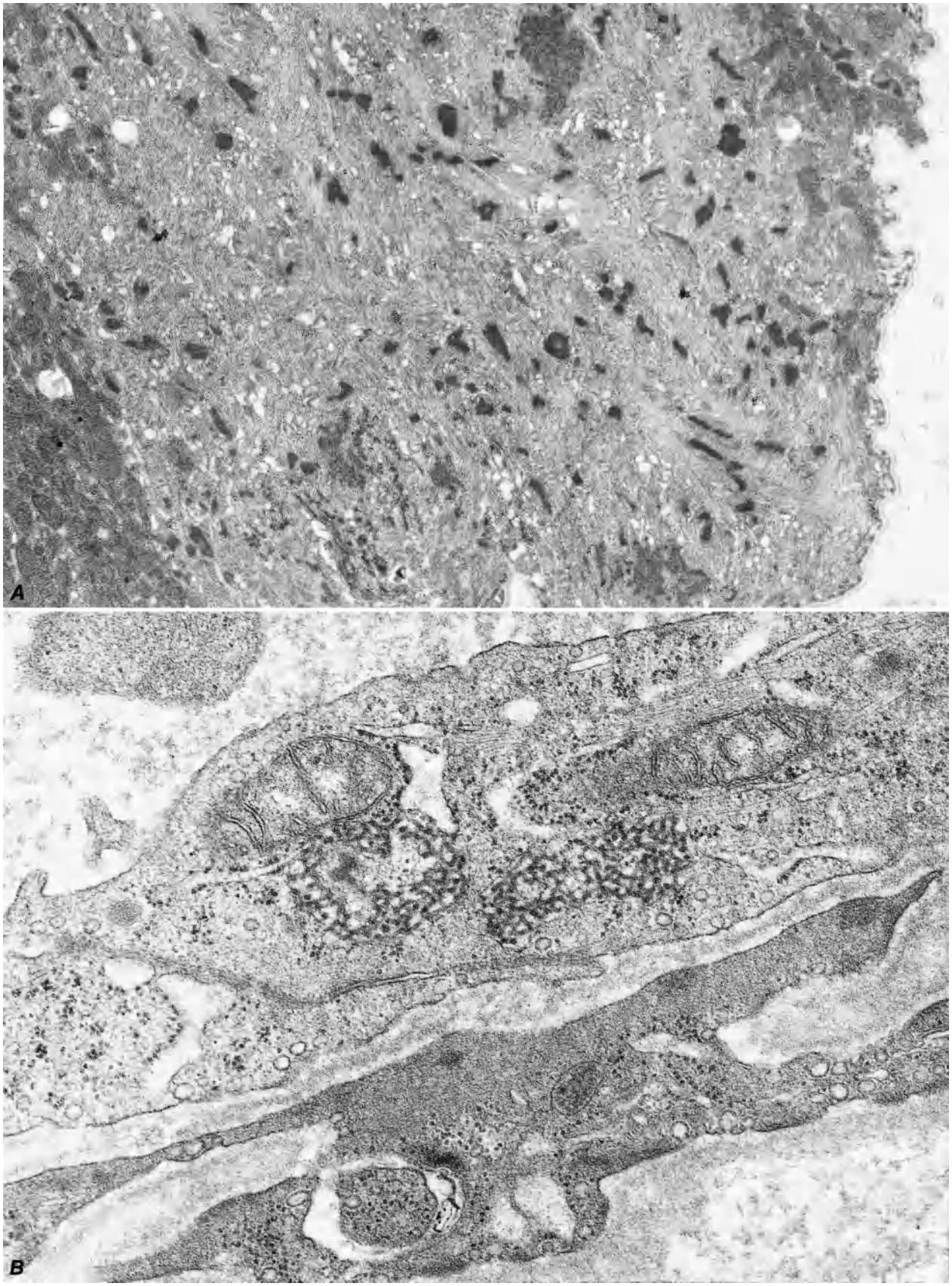


Fig. 13.42 Lentivirus: human immunodeficiency virus, skeletal muscle, human AIDS. **A**. **Myofibrillary disorganization:** dense rod-like structure in skeletal muscle cell. **B**. **Tubuloreticular inclusion:** muscle, capillary endothelial cell. (Micrograph: D. Hantai, *Acta Neuropathol* 81:496, 1991.)

Vet-ebooks.com

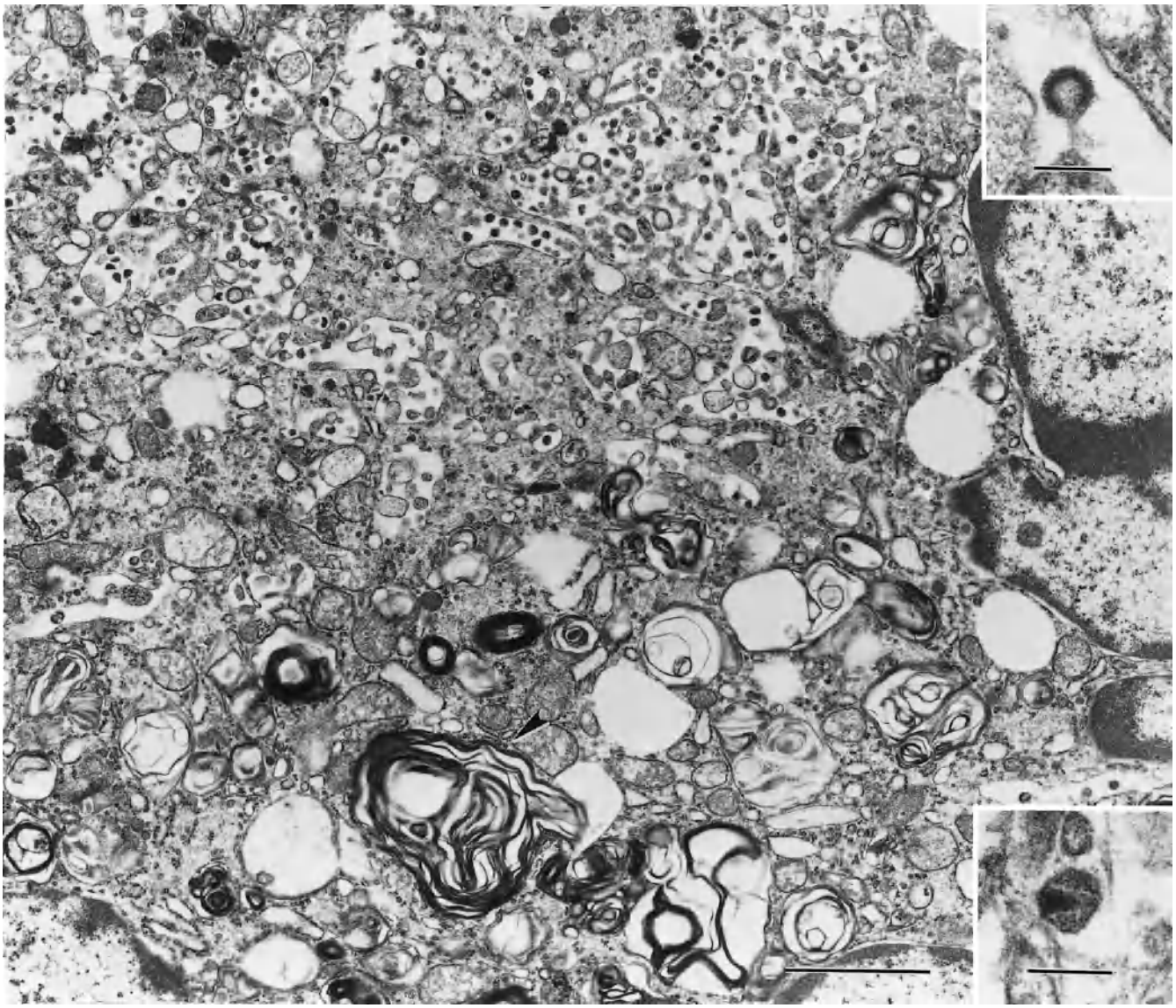


Fig. 13.43 Lentivirus: simian immunodeficiency virus. Multinuclear giant cell in the brain contains viral particles within dilated endoplasmic reticulum and small vacuoles; rhesus monkey. Nucleus (*right*); myelin inclusions (*arrowhead*). Bar = 2 µm. *Insets*: lentiviral bud (*upper right*); lentiviral particle with conical core and eccentric nucleoid (*lower right*); bars = 0.2 µm. (Micrograph: Andrew A. Lackner, *Am J Pathol* 139:609, 1991.)

ferritin-labeled antisera.[332] The mature virion is small (65–110 nm diameter) and has a dense 20–30 nm core. The immature particle as it buds from the plasma membrane is larger (100–140 nm) and coreless. Negatively stained virions are 90–100 nm particles with surface projections of 10 nm length.

Variants of visna virus cause other chronic diseases of sheep. **Ovine progressive pneumonia**, first recognized as maedi in Iceland, involves chronic multifocal lymphocytic and monocytic interstitial pneumonia with fibrosis and smooth muscle hyperplasia in alveolar walls, perivascular and peribronchiolar lymphoid hyperplasia, and epithelization of terminal respiratory passages. Virions are rare in lung tissue.[333,334] **Caprine arthritis encephalitis virus** was first recognized in the late 1970s in sheep with chronic progressive arthritis, encephalitis and mastitis. Ultrastructural studies of brain and ganglia reveal cytoplasmic A type retroviruses but no budding forms.[335,336]

Equine Infectious Anemia **Equine infectious anemia (EIA)** involves recurring episodes of fever, anemia, hemorrhages, and lymphoid proliferation. EIA virus is transmitted from mare to foal through insect vectors. Viremia is persistent despite host immune responses. Virus replicates in macrophages, and induces hyperplasia of the lymphoid and monocyte macrophage system.[337] Anemia is caused by depression of erythropoiesis and by decreased erythrocyte life span mediated by complement that covers erythrocyte surfaces.

Vet-ebooks.com

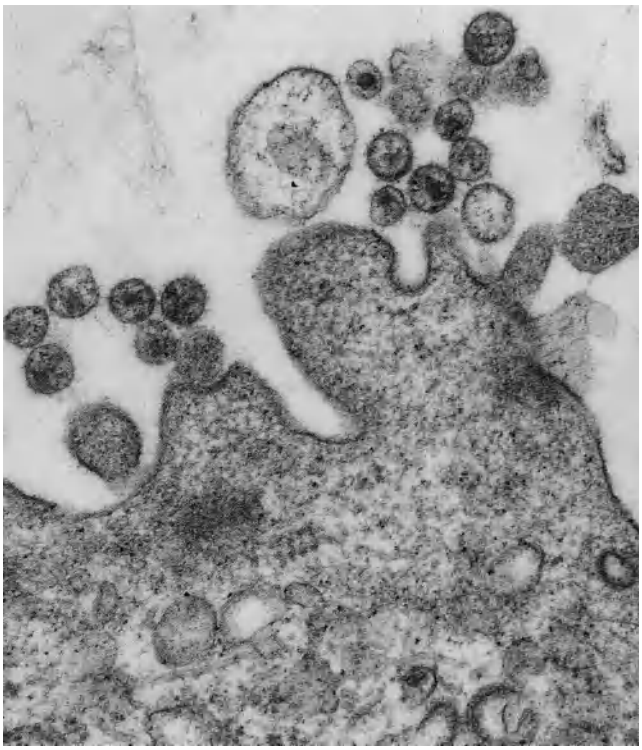


Fig. 13.44 Lentivirus: bovine immunodeficiency virus (BIV). Virions budding from surface of an infected cell. (Micrograph: Arliss D. Boothe, *J Virol* 13:197, 1974.)

The EIA virion is 80–120 nm in diameter with a dense nucleoid of 40–60 nm. It matures by budding from plasma membranes extracellularly or into cytoplasmic. In subacute and chronic phases, there are weight loss, anemia, and edema during recurring cycles of illness, often at biweekly intervals. Immune-complex glomerulopathy develops in 85% of chronic cases; IgG and C3 are in granular deposits along the glomerular basement membrane and in the mesangium.

Subfamily *Spumaretrovirinae*

Genus *Spumavirus*

Foamy viruses are spherical to pleomorphic, 80–100 nm in diameter with dense cores, and envelopes containing prominent radiating spikes 5–15 nm long (Fig. 13.45). Maturation involves budding from plasma membranes and into cytoplasmic vacuoles. In vitro, cytopathic reactions are formation of multinuclear giant cells and vacuolation ("foamy"). In vivo, foamy viruses cause latent, persistent infections in the presence of antibody, but none have been identified as causal in animal or human disease. Transgenic mice carrying the *bel* region of HFV (under transcriptional control of its own long terminal repeat) develop progressive degenerative disease of the brain and skeletal muscle, suggesting that these viruses may be involved in chronic disease of the central nervous system.[338]

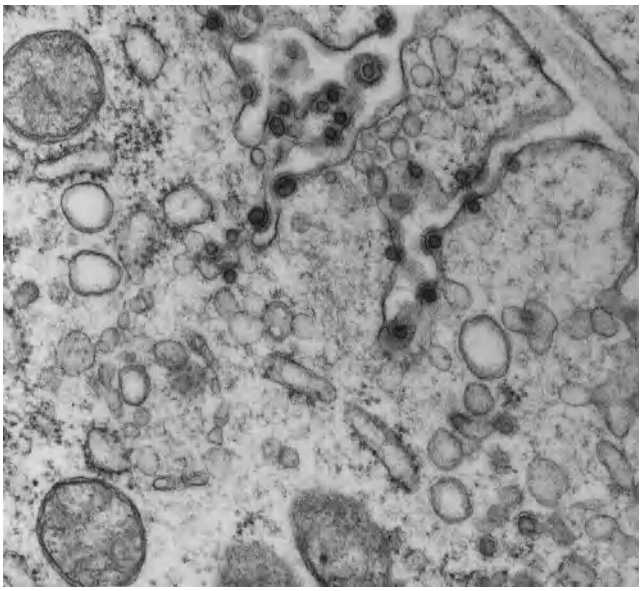


Fig. 13.45 Spumavirus: bovine syncytial virus. Virions with long surface spikes bud from the cell surface. (Micrograph: Arliss D. Boothe, *Arch Ges Virusforsch* 31:373, 1970.)

References

1. Martino RL, et al. 1994. Parallel computing in biomedical research. *Science* 265:902.
2. Sodiek B, et al. 1993. Assembly of vaccinia virus. *J Cell Biol* 121:521.
3. Townsley AC, Moss B. 2006. Two distinct low-pH steps promote entry of vaccinia virus. *J Virol* 81:8613.
4. Hollinshead M, et al. 2001. Vaccinia virus utilizes microtubules for movement to the cell surface. *J Cell Biol* 154:389.
5. Roos N, et al. 1996. A novel immunogold cryoelectron microscopic approach to investigate the structure of the intracellular and extracellular forms of vaccinia virus. *EMBO J* 15:2343.
6. Kurata T, et al. 1977. Demonstration of vaccinia virus antigen in brains of postvaccinal encephalitis cases. *Jap J Med Sci Biol* 30:137.
7. Lane JM, et al. 1968. Complications of smallpox vaccination. *New Engl J Med* 281:1201.
8. Lancaster MC, et al. 1966. Experimental respiratory infection with poxviruses. *Br J Exp Pathol* 47:466.
9. Sottnek HM et al. 1975. The pathogenesis of vaccinia virus toxicity. II. An electron microscopic study. *Lab Invest* 33:522.
10. Rabin ER, et al. 1965. Vaccinia virus myocarditis in mice. *Exp Mol Pathol* 4:98.
11. Kristensson K, Sourander P. 1969. Changes in vascular permeability of the CNS by experimental herpes simplex and vaccinia virus infection. *Acta Neuropathol* 14:38.

Vet-ebooks.com

12. Cheville NF. 1966. Cytopathologic changes in fowlpox (turkey origin) inclusion body formation. *Am J Pathol* 49:723.
13. Purcell DA, Clarke JK. 1972. Some aspects of the morphogenesis of myxoma virus in vivo. *Arch Ges Virusforsch* 39:369.
14. Duteyrat JL, et al. 2006. Ultrastructural study of myxoma virus morphogenesis. *Arch Virol* 151:2161.
15. Schrag JD, et al. 1989. Three-dimensional structure of the HSV1 nucleocapsid. *Cell* 56:651.
16. Puvion-Dutilleul F, Puvion E. 1991. Ultrastructural localization of defined sequences of viral RNA and DNA by in situ hybridization of biotinylated DNA probes on sections of Herpes simplex virus type 1 infected cells. *J Elec Microsc Tech* 18:336.
17. Jensen HL, Norrild B. 2005. Herpes simplex virus-cell interactions studied by immunogold cryosection electron microscopy. *Methods Mol Biol* 292:143.
18. Granzow H, et al. 2005. Entry of pseudorabies virus: An immunogold-labeling study. *J Virol* 79:3200.
19. Maurer UE, et al. 2008. Native 3D intermediates of membrane fusion in herpes simplex virus 1 entry. *Proc Natl Acad Sci USA* 105:10559.
20. Baines JE, et al. 2007. Glycoprotein M of herpes simplex virus 1 is incorporated into virions during budding at the inner nuclear membrane. *J Virol* 81:800.
21. Macarak EJ, et al. 1985. Herpes simplex virus type 1 infection of endothelium reduces collagen and fibronectin synthesis. *Lab Invest* 53:280.
22. Rose DSC, et al. 1986. A filamentous distribution for the Herpes simplex virus type-2 encoded major DNA-binding protein. *J Gen Virol* 67:1315.
23. Stroop WG, Schaefer DC. 1986. Production of encephalitis restricted to the temporal lobes by experimental reactivation of herpes simplex virus. *J Infect Dis* 153:721.
24. Stevens JG, et al. 1987. RNA complementary to a herpesvirus α gene mRNA is prominent in latently infected neurons. *Science* 235:1056.
25. Schirmacher P, et al. 1989. HSV hepatitis in the mouse: A light and electron microscopic study with immunohistology and in situ hybridization. *Virch Arch B* 56:351.
26. Tomita T, et al. 1992. Herpes simplex hepatitis before and after acyclovir treatment. *Arch Pathol Lab Med* 116:173.
27. Anderson DC, et al. Primary herpesvirus simiae (B-virus) infection in infant macaques. Lab An Sci 44:526, 1994.
28. Schuler D, et al. 1993. Herpes simplex virus from respiratory tract secretions. *Am J Med* 94:29, 1993.
29. Sobel RA, et al. 1986. The *in situ* cellular immune response in acute herpes simplex encephalitis. *Am J Pathol* 125:332.
30. Boddingius J, et al. 1987. Replication characteristics and core size of intranuclear herpes simplex virus (HSV-1) in genital skin lesions. *J Med Microbiol* 24:93.
31. Meier JL, Straus SE. 1992. Comparative biology of latent varicella zoster virus and herpes simplex virus. *J Infect Dis* 166:S13.
32. Jones EL, Cameron AH. 1969. Pulmonary calcification in viral pneumonia. J Clin Pathol 22:361.
33. Kornegay JN, Gorgacz EJ. 1988. Marek's disease virus-induced transient paralysis in chickens: Electron microscopic lesions. *Acta Neuropathol* 75:597.
34. Lampert P, et al. 1977. Demyelination in allergic and Marek's disease virus induced neuritis. Comparative electron microscopic studies. *Acta Neuropathol* 40:103.
35. Wolber RA, et al. 1988. Ultrastructural localization of viral nucleic acids by in situ hybridization. *Lab Invest* 59:144.
36. Boldogh I, et al. 1981. Kaposi's sarcoma. IV. Detection of cytomegalovirus DNA, cytomegalovirus RNA and CMNA in tumor biopsies. *Int J Cancer* 28:469.
37. Keh WC, Gerber MA. 1988. *In situ* hybridization for cytomegalovirus DNA in AIDS patients. *Am J Pathol* 131:490.
38. Epstein MA, et al. 1973. Pilot experiments with EB virus in owl monkeys (*Aortus trivirgatus*). *Int J Cancer* 12:309.
39. Purtillo DT, et al. 1992. Epstein-Barr virus-associated lymphoproliferative disorders. *Lab Invest* 67:5.
40. Belton CM, Eversole LR. 1986. Oral hairy leukoplakia: Ultrastructural features. *J Oral Pathol* 15:493.
41. El-Labban N, et al. 1988. Crystalline inclusions in epithelial cells of hairy leukoplia: A new ultrastructural finding. *Scand J Dent Res* 96:353.
42. Becker J, et al. 1991. Expression of proteins encoded by Epstein-Barr virus trans-activator gene depends on the differentiation of epithelial cells in oral hairy leukoplakia. *Proc Nat Acad Sci* 88:8332.
43. Rabanus J-P, et al. 1991. Subcellular distribution and life cycle of Epstein-Barr virus in keratinocytes of oral hairy leukoplakia. *Am J Pathol* 139:185.
44. McGuire LJ, et al. 1988. Epstein-Barr virus genome in thymoma and thymic lymphoid hyperplasia. *Am J Pathol* 131:385.
45. Wu T-C, et al. 1991. Abundant expression of EBER1 small nuclear RNA in nasopharyngeal carcinoma. *Am J Pathol* 138:1461.
46. Miller G, et al. 1977. Lymphoma in cotton-top marmosets after inoculation with Epstein-Barr virus. *J Exp Med* 145:948.
47. Skinner MS, Mizell M. 1972. The effect of different temperatures on herpesvirus induction and replication in Lucké tumor explants. *Lab Invest* 26:671.
48. Adeyemia OA, et al. 2008. Fatal adenovirus pneumonia in a person with AIDS and Burkitt lymphoma. *AIDS Read* 18:196.
49. Martin BJ, et al. 1991. Pancreatitis associated with simian adenovirus 23 in a rhesus monkey. *Lab An Sci* 41:382.
50. Murti KG, et al. 1990. Localization of adenovirus-encoded DNA replication proteins in the nucleus by immunogold electron microscopy. *J Gen Virol* 71:2847.
51. Castleman WL. 1985. Bronchiolitis obliterans and pneumonia induced in young dogs by experimental adenovirus infection. *Am J Pathol* 119:495.
52. Hervás J, et al. 1997. Focal mesangial-sclerosing glomerlonephritis and acute spontaneous infectious canine hepatitis. *Vet Immunol Immunopathol* 57:25.
53. Berman LK. 1967. Comparative morphologic study of the virus-induced solid tumors of Syrian hamsters. *J Natl Cancer Inst* 39:561.

Vet-ebooks.com

54. Mukai N, Kobayashi S. 1972. Undifferentiated intraperitoneal tumors induced by adenovirus type 12 in hamsters. *Am J Pathol* 69:331.
55. Merkow L, et al. 1969. Pathogenesis of oncogenic simian adenoviruses. IV. The histopathology and ultrastructure of intraperitoenal neoplasms induced by SA7. *Int J Cancer* 4:455.
56. Slifkin M, et al. 1969. Pathogenesis of oncogenic simian adneoviruses. VI. An ultrastructural investigation of SV30 replication. *Exp Mol Pathol* 11:285.
57. Bober FJ, et al. 1987. Expression of varying portions of the adenovirus 12 early region 1 in transformed cells affects tumorigenicity and interaction with extracellular matrix components. *Lab Invest* 56:37.
58. Baker TS, et al. 1991. Structures of bovine and human papillomaviruses. Biophys J 60:1445.
59. Iftner T, et al. 1992. Transcription of the E6 and E7 genes of human papillomavirus type 6 in anogenital condylomata is restricted to undifferentiated cell layers of the epithelium. *J Virol* 66:4639.
60. Gupta J, et al. 1987. Association of human papillomavirus type 16 with neoplastic lesions of the vulva and other genital sites by *in situ* hybridization. *Am J Pathol* 127:206.
61. Lancaster WD, et al. 1983. Human papillomavirus: Detection of viral DNA sequences and evidence for molecular heterogeneity in metaplasias and dysplasias of the uterine cervix. *Intervirology* 20:202.
62. Vallegjos H, et al. 1987. Characterization of human papilloma virus types in condylomata acuminata in children by *in situ* hybridization. *Lab Invest* 56:611.
63. Multhaupt HB, et al. 1992. Ultrastructural localization of human papilloma virus by nonradioactive *in situ* hybridization on tissue of human cervical intraepithelial neoplasia. Lab Invest 67:512.
64. Crum CP, et al. 1985. Cervical papillomaviruses segregate within morphological distinct precancerous lesions. J Virol 54:675.
65. Walboomers JMM, et al. 1988. Sensitivity of *in situ* detection with biotinylated probes of human papilloma virus type 16 DNA in frozen tissue sections of squamous cell carcinomas of the cervix. *Am J Pathol* 131:587.
66. Taxy JB, et al. 1989. Anal cancer. Microscopic condylomas and tissue demonstration of human papillomavirus capsid antigen and viral DNA. *Arch Path* Lab Med 113:1127.
67. Gordon DE, Olson C. 1968. Meningiomas and fibroblastic neoplasia in calves induced with bovine papilloma virus. *Cancer Res* 28:2423.
68. Cheville NF. 1966. Studies on connective tissue tumors in the hamster produced by bovine papilloma virus. *Cancer Res* 26:2334.
69. Lancaster WD, et al. 1977. Bovine papilloma virus. *Proc Nat Acad Sci* 74:524.
70. England JJ, et al. 1973. Virus-like particles in an equine sarcoid cell line. Am J Vet Res 34:1601.
71. Zu Rhein GM. 1967. Polyoma-like virions in a human demyelinating disease. *Acta Neuropathol* 8:5.
72. Wiley CA, et al. 1988. Human immunodeficiency virus (HIV) and JC virus in acquired immune deficiency syndrome (AIDS) patients with progressive multifocal leukodystrophy. *Acta Neuropathol* 76:338.
73. London WT, et al. 1978. Brain tumors in owl monkeys inoculated with a human polyomavirus (JC virus). *Science* 201:1246.
74. Bergsagel OJ, et al. 1992. DNA sequences similar to those of simian virus 40 in ependymomas and choroid plexus tumors of childhood. *New Engl J Med* 326:988.
75. van Gorder MA, et al. 1999. Cynomolgus polyoma virus infection. *Am J Pathol* 154:1273.
76. Horvath CJ, et al. 1992. Simian virus 40-induced disease in rhesus monkeys with simian acquired immunodeficiency syndrome. *Am J Pathol* 140:1431.
77. Rachlin J, et al. 1988. Inoculation of simian virus 40 into pregnant hamsters can induce tumors in offspring. *Lab Invest* 58:26.
78. Brooks SE, et al. 1988. Induction of lymphomas and fibrosarcomas in nude mice after implantation of simian virus 40-transformed human meningioma. *Lab Invest* 58:518.
79. Okaniwa A, et al. 1976. Fine structure of epithelial cells of Lieberkühns crypts in feline panleukopenia. *Natl Inst Anim Health Q* 16:167.
80. Matsui T, et al. 1993. Intranuclear inclusions in the stratified squamous epithelium of the tongue in dogs and cats with parvovirus infection. *Vet Pathol* 30:303.
81. Hayes MA, et al. 1979. Sudden death in young dogs with myocarditis caused by parvovirus. *J Am Vet Med Assoc* 174:1197.
82. Anderson MJ, et al. 1985. Experimental parvovirus infections in humans. *J Infect Dis* 152:257.
83. Krause JR, et al. 1992. Morphological diagnosis of parvovirus B29 infection. *Arch Pathol Lab Med* 116:178.
84. Caul EO, et al. 1988. Intrauterine infection with human parvovirus B19. *J Med Virol* 24:55.
85. O'Sullivan MG, et al. 1997. Experimental infection of cynomolgus monkeys with simian parvovirus. *J Virol* 71:4517.
86. Best SM, Bloom ME. 2005. Pathogenesis of Aleutian mink disease parvovirus and similarities in B19 infection. *J Vet Med B Infect Dis Vet Public Health* 52:331.
87. Bingen A, Kirn A. 1977. Hepatocellular necrosis during frog virus 3-induced hepatitis of mice. *Exp Mol Pathol* 27:68.
88. Gut JP, et al. 1981. Frog virus 3 induces a fatal hepatitis in rats. *Lab Invest* 45:218.
89. Oin OW, et al. 2002. Antigenic characterization of a marine fish iridovirus from grouper, *Epinephelus* spp. *J Virol Methods* 106:89.
90. Fernandez A, et al. 1992. Detection of African swine fever viral antigens in paraffin-embedded tissues by use of immuno-histologic methods and polyclonal antibodies. *Am J Vet Res* 53:1462.
91. Andrés G, et al. 1998. African swine fever virus is enveloped by a two-membrane collapsed cisternae derived from the endoplasmic reticulum. *J Virol* 72:8988.
92. Jouvenet N, et al. 2006. African swine fever virus induced filopodia-like projections at the plasma membrane. *Cell Microbiol* 8:1803.
93. Krauthausen E, et al. 1992. Licht-und elektronenmikroskopische Befunde am Darm bei spontäner und experimentell erzeugter Afrikanischer Schweinepest (ASP). *Dtsch Tieraerztl Wochenschr* 99:49.

Vet-ebooks.com

94. Sakamoto Y, et al. 1983. Full and empty particles of hepatitis B virus in hepatocytes from patients with HBsAg-positive chronic active hepatitis. *Lab Invest* 48:678.
95. Yamada G, et al. 1977. Hepatitis B core and surface antigen in liver tissue: Light and electron microscopic localization by the peroxidase-labeled antibody methods. *Lab Invest* 36:649.
96. Phillips MJ, et al. 1992. Post-transplant recurrent hepatitis B viral liver disease. *Am J Pathol* 140:1295.
97. Seitz S, et al. 2007. Cryo-electron microscopy of hepatitis B virions reveals variability in envelope capsid interactions. *EMBO J* 26:4160.
98. Konishi M, et al. 2007. Ultrastructural demonstration of hepatitis B virus production in a mouse model produced by hydrodynamic transfection. *Int J Mol Med* 20:31.
99. Popper H, et al. 1987. Hepatocarcinogenicity of the woodchuck hepatitis virus. *Proc Nat Acad Sci* 84:866.
100. Peters DN, et al. 1992. Immunopathology of glomerulonephritis associated with chronic woodchuck hepatitis virus infection in woodchucks (*Marmota monas*). *Am J Pathol* 141:143.
101. Marion PL, et al. 1984. Liver disease associated with duck hepatitis B virus infection of domestic ducks. *Proc Natl Acad Sci USA* 81:898.
102. Imai K, et al. 1991. Immunoelectron microscopy of chicken anemia agent. *J Vet Med Sci* 53:1065.
103. Kiupel M, et al. 1998. Circovirus-like viral associated disease in weaned pigs in Indiana. *Vet Pathol* 35:303.
104. Latimer KS, et al. 1991. A novel DNA virus associated with feather inclusions in psittacine beak and feather disease. *Vet Pathol* 28:300.
105. Korteweg C, Gu J. 2008. Pathology, molecular biology, and pathogenesis of avian influenza A (H5N1) in humans. *Am J Pathol* 172:1155.
106. Martin K, Helenius A. 1991. Nuclear transport of influenza virus ribonucleoproteins. *Cell* 67:117.
107. Kanaseki T, et al. 1997. Structural features of membrane fusion between influenza virus and liposome as revealed by quick-freezing electron microscopy. *J Cell Biol* 137:1041.
108. Winkler GC, Cheville NF. 1986. Ultrastructural morphometric investigation of early lesions in the pulmonary alveolar region of pigs during experimental swine influenza infection. *Am J Pathol* 122:541.
109. Berendt RF, et al. 1975. Influenza alone and in sequence with pneumonia due to *Streptococcus pneumoniae* in the squirrel monkey. *J Infect Dis* 132:689.
110. Bossart W, et al. 1973. Electron microscopic study on influenza hemagglutinin: Pinocytosis of virions by red cells. *Virology* 55:295.
111. McKenzie BE, et al. 1972. Light and electron microscopic changes in the myocardium of influenza-infected turkeys. *Am J Pathol* 69:239.
112. Merz DC, et al. 1980. Importance of antibodies to the fusion glycoprotein of paramyxoviruses in the prevention and spread of infection. *J Exp Med* 151:275.
113. Wolinsky JS, et al. 1976. Experimental panencephalitis induced in suckling mice by parainfluenza-1 (6-94) virus. *J Neuropathol Exp Neurol* 35:271.
114. Lief FS, et al. 1976. Infection and disease induced in chimpanzees with 6/94, a parainfluenza type 1 virus isolated from human multiple sclerosis brain. *J Neuropathol Exp Neurol* 35:644.
115. Olding-Stenkvist E, Bjorvatn B. 1976. Rapid detection of measles virus in skin rashes by immunofluorescence. *J Infect Dis* 134:463.
116. Hooper PT, et al. 1997. Lesions of experimental equine morbillivirus pneumonia in horses. *Vet Pathol* 34:12.
117. Murray K, et al. 1995. A Morbillivirus that caused fatal disease in horses and humans. *Science* 268:94.
118. Wong KT, et al. 2002. Nipah virus infection: Pathology and pathogenesis of an emerging paramyxoviral zoonosis. *Am J Pathol* 161:2153.
119. Tan CT, et al. 2002. Relapsed and late-onset Nipah encephalitis. *Ann Neurol* 51:703.
120. Kristensson K, et al. 1984. Mumps virus infection of the developing mouse brain. *J Neuropathol Exp Neurol* 43:131.
121. Cheville NF, Beard CW. 1972. Cytopathology of Newcastle disease. *Lab Invest* 27:129.
122. Bryson DG, et al. 1991. Ultrastructural features of alveolar lesions in induced respiratory syncytial virus pneumonia of calves. *Vet Pathol* 28:286.
123. Vargas SO, et al. 2008. Pathology of human metapneumovirus infection. *Pediatr Dev Pathol* 7:478.
124. Lotti LV, et al. 1992. Immunocytochemical analysis of the transfer of vesicular stomatitis virus G glycoprotein from the intermediate compartment to the Golgi complex. *J Cell Biol* 118:43.
125. Proctor SJ, Sherman KC. 1975. Ultrastructural changes in bovine lingual epithelium infected with vesicular stomatitis virus. *Vet Pathol* 12:362.
126. Dal Canto MC, Rabinowitz SG. 1981. Murine central nervous system infection by a viral temperature-sensitive mutant. *Am J Pathol* 102:412.
127. Yamamoto T, Ohtani S. 1978. Ultrastructural localization of rabies virus antigens in infected trigeminal ganglion of hamsters. *Acta Neuropathol* 43:229.
128. Murphy FA, et al. 1973. Comparative pathogenesis of rabies and rabies-like viruses. *Lab Invest* 28:361 and 29:151.
129. Charlton KM, Casey GA. 1979. Experimental rabies in skunks. Immunofluorescence, light, and electron microscopic studies. *Lab Invest* 41:36.
130. Balachandran A, Charlton K. 1993. Experimental rabies in skunks (*Mephitis mephitis*) and foxes (*Vulpes vulpes*). *Vet Pathol* 31:93.
131. Murphy FA, et al. 1972. Bovine ephemeral fever virus in cell culture and mice. *Arch Ges Virusforsch* 38: 234.
132. Bavari S, et al. 2002. Lipid raft microdomains: A gateway compartmentalized trafficking of Ebola and Marburg viruses. *J Exp Med* 195:593.
133. Mavrakis M, et al. 2002. Morphology of Marburg virus NP-RNA. *Virology* 296:300.
134. Ellis DS, et al. 1979. Ebola virus: A comparison, at ultrastructural level, of the behaviour of the Sudan and Zaire strains in monkeys. *Br J Exp Pathol* 59:584.
135. Fisher-Hoch SP, et al. 1992. Pathogenic potential of filoviruses. *J Infect Dis* 166:753.

Vet-ebooks.com

136. Murphy, FA, et al. 1971. Marburg virus infection in monkeys. *Lab. Invest* 24:279.
137. Geisbert TW, Jaax NK. 1998. Marburg hemorrhagic fever: Report of a case studied by immunohistochemistry and electron micrisocpy. *Ultrastr Pathol* 22:3.
138. Baskerville A, et al. 1985. Ultrastructural pathology of experimental Ebola haemorrhagic fever virus infection. *J Pathol* 147:199.
139. Geisbert TW, et al. 1992. Association of Ebola-related Reston virus particles and antigen with tissue lesions of monkeys imported to the United States. *J Comp Pathol* 106:137.
140. Fisher-Hoch SP, et al. 1983. Haemotological and biochemical monitoring of Ebola infection in rhesus monkeys. *Lancet* 5:1055.
141. Neuman BW, et al. 2006. Ultrastructure of SARS-CoV, FIPV, and MHV revealed by electron cryomicroscopy. *Adv Exp Med Biol* 581:181.
142. Krijnse-Locker J, et al. 1994. Characterization of the budding compartment of mouse hepatitis virus: Evidence that transport from the RER to the Golgi complex requires only one vesicular transport step. *J Cell Biol* 124:55.
143. Doughri Am, et al. 1976. Morphology and morphogenesis of a coronavirus infecting intestinal epithelial cells of newborn calves. *Exp Mol Pathol* 25:355.
144. Ducatelle R, Hoorens J. 1984. Significance of lysosomes in the morphogenesis of coronaviruses. *Arch Virol* 79:1.
145. Shieh WJ, et al. 2005. Immunohistochemical, in situ hybridization, and ultrastructural localization of SARS-associated coronavirus in lung of a fatal case of severe acute respiratory syndrome in Taiwan. *Hum Pathol* 36:303.
146. Oin C, et al. 2006. An animal model of SARS produced by infection of *Macaca mulatta* with SARS coronavirus. *J Pathol* 206:251.
147. Neuman BW, et al. 2006. Supramolecular architecture of severe acute respiratory syndrome coronavirus revealed by electron cryomicroscopy. *J Virol* 80:7918.
148. Goldsmith CS, et al. 2004. Ultrastructural characteristics of SARS coronovirus. *Emerging Infect Dis* 10:320.
149. Beniac DR, et al. 2007. Conformational reorganization of the SARS coronavirus spike following receptor binding. *PLoS ONE* 2:e1082.
150. Snijder EJ, et al. 2006. Ultrastructure and origin of membrane vesicles associated with the severe acute respiratory syndrome-coronavirus replication complex. *J Virol* 80:5927.
151. Stertz S, et al. 2007. The intracellular sites of early replication and budding of SARS-coronavirus. *Virology* 361:304.
152. Resta S, et al. 1985. Isolation and propagation of a human enteric coronavirus. *Science* 229:978.
153. Goto N, et al. 1977. Nasoencephalopathy of mice infected intranasally with a mouse hepatitis virus, JHM strain. *Jap J Exp Med* 47:59.
154. Powell HC, Pampert PW. 1975. Oligodendrogliocytes and their myelin plasma membrane connections in JHM mouse hepatitis virus encephalomyelitis. *Lab Invest* 33:440.
155. Percy DH, et al. 1989. Sequential changes in the Harderian and exorbital lacrimal glands in Wistar rats infected with sialodacryoadenitis virus. *Vet Pathol* 26:238.
156. Pedersen NC, Boyle JF. 1980. Immunologic phenomena in the effusive form of feline infectious peritonitis. *Am J Vet Res* 41:868.
157. Kipar A, et al. 2005. Morphologic features and development of granulomatous vasculitis in feline infectious peritonitis. Vet Pathol 42P:321.
158. Chong KT, Apostolov K. 1982. The pathogenesis of nephritis in chickens induced by infectious bronchitis virus. *J Comp Pathol* 92:199.
159. Ducatelle R, et al. 1984. Aetio-pathology of the fowl trachea early after inoculation with H52 infectious bronchitis virus. *Zbl Vet Med B* 31:151.
160. Dea S, et al. 1989. Intracellular synthesis and processing of the structural glycoproteins of turkey enteric coronavirus. *Arch Virol* 106:239.
161. Weiss M, Horzinek MC. 1987. The proposed family Toroviridae. *Arch Virol* 92:1.
162. Beards GM, et al. 1986. Preliminary characterization of torovirus-like particles of humans. J Med Virol 20:67.
163. Fagerland JA, et al. 1986. A morphological study of the replication of Breda virus (proposed family *Toroviridae*) in bovine intestinal cells. *J Gen Virol* 67:1293.
164. Pohlenz JFL, et al. 1984. Cellular lesions in intestinal mucosa of gnotobiotic calves experimentally infected with a new unclassified bovine virus (Breda virus). *Vet Pathol* 31:407.
165. Wolf JL, et al. 1980. Intestinal M cells: A pathway for entry of reovirus into the host. *Science* 212:471.
166. Hewat EA, et al. 1992. 3-D reconstruction of bluetongue virus tubules using cryoelectron microscopy. *J Struct Biol* 108:35.
167. Stuart DI, Grimes JM. 2006. Structural studies on orbivirus proteins and particles. *Curr Top Microbiol Immunol* 309:221.
168. Brewer AW, MacLachlan NJ. 1992. Ultrastructural characterization of the interaction of bluetongue virus with bovine erythrocytes. *Vet Pathol* 29:356.
169. Laegreid WW, et al. 1992. Electron microscopic evidence for endothelial infection by African horsesickness virus. *Vet Pathol* 29:554.
170. Gómez-Villamandos JC, et al. 1999. Pathogenesis of African horse sickness: Ultrastructural study of the capillaries in experimental infection. *J Comp Pathol* 121:101.
171. Bellamy AR, Both GW. 1990. Molecular biology of rotaviruses. *Adv Virus Res* 38:1.
172. Yeager M, et al. 1990. Three-dimensional structure of rhesus rotavirus by cryoelectron microscopy and image reconstruction. *J Cell Biol* 110:2133.
173. Quan CM, Doane FW. 1983. Ultrastructural evidence for the cellular uptake of rotavirus by endocytosis. *Intervirology* 20:223.
174. Poruchynsky MS, et al. 1991. Calcium depletion blocks the maturation of rotavirus by altering the oligomerization of virus-encoded proteins in the ER. *J Cell Biol* 114:651.
175. Starkey WG, et al. 1986. Kinetics, tissue specificity, and pathological changes in murine rotavirus infection of mice. *J Gen Virol* 67:2625.

Vet-ebooks.com

176. Uhnoo I, et al. 1990. Extramucosal spread and development of hepatitis in immunosuppressed and normal mice infected with rhesus rotavirus. *J Virol* 64:361.
177. Vonderfecht SL, et al. 1984. Infectious diarrhea of infant rats produced by a rotavirus-like agent. *J Virol* 52:94.
178. Huber AC, et al. 1989. Pathology of infectious diarrhea of infant rats (IDIR) induced by an antigenically distinct rotavirus. *Vet Pathol* 26:376.
179. Jashes M, et al. 1986. In vitro transcription of human pararotavirus. *J Virol* 57:183.
180. Mohd JF, et al. 2008. Complete characterization of the American grass carp reovirus genome (genus *Aquareovirus*: family Reoviridae) reveals an evolutionary link between aquareoviruses and coltiviruses. *Virology* 373:310.
181. Rodriguez M, et al. 1983. Ultrastructural localization of viral antigens in the CNS of mice persistently infected with lymphocytic choriomeningitis virus (LCM). *Am J Pathol* 110:95.
182. Walker DH, et al. 1975. Experimental Lassa virus infection in the squirrel monkey. *Am J Pathol* 80:261, 1975.
183. Oldstone MBA. 1984. Virus persists in β cells of islets of Langerhans and is associated with chemical manifestations of diabetes. *Science* 224:1440.
184. Mueller SN, et al. 2007. Viral targeting of fibroblastic reticular cells contributes to immunosuppression and persistence during chronic infection. *Proc Natl Acad Sci USA* 104:15430.
185. Elsner B, et al. 1973. Pathology of 12 fatal cases of Argentine hemorrhagic fever. *Am J Trop Med Hyg* 22:229.
186. Tao H, et al. 1987. Morphology and morphogenesis of viruses of hemorrhagic fever with renal syndrome. *Intervirology* 27:45.
187. Carballal G, et al. 1977. Junin virus infection of guinea pigs. Electron microscopic studies of peripheral blood and bone marrow. *J Infect Dis* 135:367.
188. Turell TG, et al. 1973. Pathology of Bolivian hemorrhagic fever in the rhesus monkey. *Am J Pathol* 73:477.
189. Froshauer S, et al. 1988. Alphavirus RNA replicase is located on the cytoplasmic surface of endosomes and lysosomes. *J Cell Biol* 107:2075.
190. Kail M, et al. 1991. The cytoplasmic domain of alphavirus E2 glycoprotein contains a short linear recognition signal required for viral budding. *EMBO J* 10:234.
191. Kim JH, et al. 1985. Human eastern equine encephalitis. *Am J Clin Pathol* 84:223.
192. Levine B, et al. 1991. Antibody-mediated clearance of alphavirus infection from neurons. *Science* 254:856.
193. Hobman TC, et al. 1992. The rubella virus E1 glycoprotein is arrested in a novel post-ER, pre-Golgi compartment. *J Cell Biol* 118:795.
194. Weil ML, et al. 1975. Chronic progressive panencephalitis due to rubella virus simulating subacute sclerosing panencephalitis. *N Engl J Med* 292:994.
195. Estes PC, Cheville NF. 1970. The ultrastructure of vascular lesions in equine viral arteritis. *Am J Pathol* 58:235.
196. du Buy HG, Johnson ML. 1966. Studies on the in vivo and in vitro multiplication of the LDH virus of mice. *J Exp Med* 123:985.
197. Stroop WG, Brinton MA. 1983. Mouse strain-specific central nervous system lesions associated with lactate dehydrogenase-elevating virus infection. *Lab Invest* 49:334.
198. Dea S, et al. 1989. Intracellular synthesis and processing of the structural glycoproteins of turkey enteric coronavirus. *Arch Virol* 106:239.
199. Sur JH, et al. 1998. Apoptosis induced in vivo during acute infected by porcine reproductive and respiratory syndrome virus. *Vet Pathol* 35:506.
200. Sirinarumitr T, et al. 1998. A pneumo-virulent United States isolate of procine reproductive and respiratory syndrome virus induces apoptosis in bystander cells both in vitro and in vivo. *J Gen Virol* 79:2989.
201. Scruggs DW, Sorden SD. 2001. Proliferative vasculopathy and cutaneous hemorrhages in porcine neonates infected with the porcine reproductive and respiratory syndrome virus. *Vet Pathol* 38:339.
202. Allen AM, et al. 1968. Simian hemorrhagic fever. *Am J Trop Med Hyg* 17:413.
203. Blinzinger K, Anzil AP. 1973. Large granular nuclear bodies (karyosphaeridia) in experimental borna virus infection. *J Comp Pathol* 83:589.
204. Bestetti G. 1976. Mikroskopische und ultrastrukturelle Untersuchungen am Joest-Degen'schen Eischlüsskorperchen bei spontaner Borna-Krankheit des Pferdes. *Schweiz Arch Tierheilkd* 118:493.
205. VandeWoude S, et al. 1990. A Borna virus cDNA encoding a protein recognized by antibodies in humans with behavioral diseases. *Science* 250:1278.
206. Ludwig H, et al. 1988. Borna disease. *Prog Med Virol* 35:107.
207. Roggendorf W, et al. 1983. Light microscopy and immunohistologic investigations of the brain of Borna disease virus infected rabbits. *Neuropathol Appl Neurobiol* 9:287.
208. Yu I-M, et al. 2008. Structure of the immature dengue virus at low pH primes proteolytic maturation. *Science* 319:1834.
209. Zlotnick I, et al. 1976. Experimental infection of monkeys with virus of the tick-borne encephalitis complex. *Br J Exp Pathol* 57:200.
210. Walker DH, et al. 1979. Ultrastructural and virological aspects of Langat virus-induced SSPE in suckling hamsters. *Br J Exp Pathol* 60:604.
211. Ng ML, Corner LC. 1989. Detection of some dengue-2 virus antigen in infected cells using immune-microscopy. *Arch Virol* 104:197.
212. Monath TIP, et al. 1983. Mode of entry of a neurotropic arbo-virus into the central nervous system. *Lab Invest* 48:399.
213. Hase T, et al. 1992. Cytopathology of PC12 cells infected with Japanese encephalitis virus. *Virch Arch B* 63:25.
214. Rosen L. 1986. The natural history of Japanese encephalitis virus. *Ann Rev Microbiol* 40:395.
215. Nathanson N, Cole GA. 1970. Fatal Japanese encephalitis virus infection in immunosuppressed spider monkeys. *Clin Exp Immunol* 6:161.
216. Shestopalova NM, et al. 1972. Electronmicroscopic study of the central nervous system in mice infected with Omsk hemorrhagic fever (OHF) virus. *J Ultrastruct Res* 40:458.

Vet-ebooks.com

217. Mazlo M, Szanto J. 1978. Morphological demonstration of the virus of tick-borne encephalitis in the human brain. *Acta Neuropathol* 43:251.
218. Cheville NF, Mengeling WL. 1969. The pathogenesis of chronic hog cholera (swine fever). *Lab Invest* 20:261.
219. Barlow RM. 1983. The pathology of spontaneous and experimental mucosal disease-like syndrome in sheep recovered from clinical border disease. *J Comp Pathol* 93:451.
220. Anderson CA, et al. 1987. Border disease virus-induced decrease in thyroid hormone levels with associated hypomyelination. *Lab Invest* 57:168.
221. Panda SK, et al. 1989. Enterically transmitted non-A, non-B hepatitis. *Hepatology* 10:466.
222. Burk KH, et al. 1981. Ultrastructural changes and virus-like particles localized in liver hepatocytes of chimpanzees infected with non-A, non-B hepatitis. *J Med Virol* 7:1.
223. Jacob JR, et al. 1990. Expression of infectious viral particles by primary chimpanzee hepatocytes isolated during the acute phase of non-A, non-B hepatitis. J Infect Dis 161:1121, 1990.
224. Feinstone SM, et al. 1981. Non-A, non-B hepatitis in chimpanzees and marmosets. *J Infect Dis* 144:588.
225. Shimizu YK, et al. 1979. Non-A, non-B hepatitis: Ultrastructural evidence for two agents in experimentally infected chimpanzees. *Science* 205:197.
226. Janssen R, et al. 1984. Mechanisms of bunyavirus virulence. *Lab Invest* 50:447.
227. Johnson KP, et al. 1974. Multiple fetal malformations due to persistent viral infection. *Lab Invest* 30:608.
228. Murphy FS, et al. 1968. St. Louis encephalitis virus infection of mice. Electron microscopic studies of central nervous system. *Lab Invest* 19:652.
229. Lyubskky S, et al. 1996. Histopathology of *Peromyscus leucopus* naturally infected with pathogens NY-1 Hantavirus pathologic marker of HPS viral infection in mice. *Lab Invest* 74:627.
230. Zaki SR, et al. 1995. Hantavirus pulmonary syndrome. *Am J Pathol* 146:552.
231. Goldsmith CS, et al. 1995. Ultrastructural characterization of Sin Nombre virus, causative agents of hantavirus pulmonary syndrome. *Arch Virol* 140:2107.
232. Luque D, et al. 2007. Infectious bursal disease virus capsid assembly and maturation by structural rearrangement of a transient molecular switch. *J Virol* 81:6869.
233. Pous J, et al. 2005. Structure of birnavirus-like particles determined by combined electron cryomicroscopy and x-ray crystallography. *J Gen Virol* 86:2339.
234. Moss LH, Gravell M. 1969. Ultrastructure and sequential development of infectious pancreatic necrosis virus. *J Virol* 3:52.
235. Cheville NF. 1967. Studies on the pathogenesis of Gumboro disease in the bursa of Fabricius, spleen, and thymus of the chicken. *Am J Pathol* 51:527.
236. Inoue M, et al. 1999. Lysis of myelocytes in chickens infected with infectious bursal disease virus. *Vet Pathol* 36:146.
237. Lam KM. 1997. Morphological evidence of apoptosis in chickens infected with infectious bursal disease virus. *J Comp Pathol* 116:367.
238. Pereira HG, et al. 1988. Novel viruses in human faeces. *Lancet II:*103.
239. Ludert JE, et al. 1995. Identification of picobirnavirus, viruses with bisegmented double stranded RNA, in rabbit faeces. *Res Vet Sci* 59:222.
240. Johans R, et al. 2002. Pathological changes in juvenile Atlantic halibut *Hippoglossus hippoglossus* persistently infected with nodavirus. *Dis Aquat Organ* 50:161.
241. Ucko M, et al. 2004. Nodavirus infections in Israeli mariculture. *J Fish Dis* 27:459.
242. Azad IS, et al. 2006. Viral nerve necrosis in hatchery-produced fry of Asian seabrass *Lates calcarfier*: Sequential microscopic analysis of histopathology. *Dis Aquat Organ* 14:73.
243. Sohal RS, et al. 1968. Ultrastructural changes in cardiac capillaries of coxsackievirus B4-infected mice. *Lab Invest* 19:399.
244. Hashimoto I, et al. 1984. Ultrastructural studies on the pathogenesis of poliomyelitis in monkeys infected with poliovirus. *Acta Neuropathol* 64:53.
245. Ukimura A, et al. 1997. Intracellular viral localization in murine coxsackievirus-B3 myocarditis. Ultrastructural study by electron microscopic in situ hybridization. *Am J Pathol* 150:2061.
246. Huang TW, Wiegenstein LM. 1977. Mesangiolytic glomerulonephritis in an infant with immune deficiency and echovirus infection. *Arch Pathol Lab Med* 101:125.
247. Olson NH, et al. 1993. Structure of a human rhinovirus complexes with its receptor molecule. *Proc Nat Acad Sci* 90:507.
248. Hirasawa K, et al. 1992. Encephalomyocarditis (EMC) virus-induced myocarditis by different virus variants and mouse strains. *J Vet Med Sci* 54:1125.
249. Hubbard GB, et al. 1992. An encephalomyocarditis virus epizootic in a baboon colony. *Lab An Sci* 42:233.
250. Blakemore WF, et al. 1988. Observations on demyelinating lesions induced by Theiler's virus in CBA mice. *Acta Neuropathol* 76:581.
251. Rodriguez M, et al. 1983. Neonatal infection with the Daniels strain of Theiler's murine encephalomyelitis virus. *Lab Invest* 49:672.
252. Wroblewska Z, et al. 1977. Virus-specific intracytoplasmic inclusions in mouse brain produced by a newly isolated strain of Theiler's virus. *Lab Invest* 37:595.
253. Patick AK, et al. 1991. Persistence of Theiler's virus infection following promotion of central nervous system remyelination. *J Neuropathol Exp Neurol* 50:523.
254. Cromeans T, et al. 1989. Use of immunogold preembdding technique to detect hepatitis A viral antigens in infected cells. *Am J Anat* 185:314.
255. Cheville NF. 1970. The influence of thymic and bursal lymphoid systems in the pathogenesis of avian encephalomyelitis. *Am J Pathol* 58:105.
256. Smith AW, et al. 1978. Immunoelectron microscopic comparison of caliciviruses. *Am J Vet Res* 39:1531.
257. Dolin R, et al. 1987. Novel agents of viral enteritis in humans. *J Infect Dis* 155:365.
258. Cheetham S, et al. 2006. Pathogenesis of a genogroup II human nororvirus in gnotobiotic pigs. *J Virol* 80: 10372.

Vet-ebooks.com

259. Pesavento PA, et al. 2004. Pathologic, immunohistochemical, and electron microscopic findings in naturally occurring virulent systemic feline calicivirus infection in cats. *Vet Pathol* 41:257.
260. Coyne KP, et al. 2006. Lethal outbreak of disease associated with feline calicivirus infection in cats. *Vet Rec* 158:544.
261. Flynn WT, et al. 1988. Pathogenesis of porcine enteric calicivirus-like virus in four-day-old gnotobiotic pigs. *Am J Vet Res* 49:819.
262. Ferreira RB, et al. 2006. Liver enzymes and ultrastructure in rabit hemorrhagic disease (RHD). *Vet Res Commun* 30:393.
263. Granzow H, et al. 1996. Rabbit hemorrhagic disease virus (RHDV). *Virus Res* 41:163.
264. Rehman S, et al. 2008. Subcellular localization of hepatitis E virus (HEV) replicase. *Virology* 370:77.
265. Tsarev SA, et al. 1992. Charcterization of a prototype strain of hepatitis E virus. *Proc Natl Acad Sci USA* 89:559.
266. Gray EW, et al. 1980. Ultrastructure of the small intestine in astrovirus-infected lambs. *J Gen Virol* 49:71.
267. Woode GN, et al. 1984. Astrovirus and Breda virus infections of dome cell epithelium of bovine ileum. J Clin Microbiol 19:623.
268. Kjeldsberg E, Hem A. 1985. Detection of astroviruses in gut contents of nude and normal mice. *Arch Virol* 84:135.
269. Thouvenelle ML, et al. 1995. Astrovirus infection in hatchling turkeys: Histologic, morphometric, and ultrastructural findings. *Avian Dis* 39:328.
270. Donelli G, et al. 1992. Mechanism of astrovirus entry into Graham 293 cells. *J Med Virol* 38:271.
271. Mladenov Z, et al. 1967. Strain MC29 avian leukosis virus. Myelocytoma, endothelioma and renal growths: Pathomorphological and ultrastructural aspects. *J Nat Cancer Inst* 38:251.
272. Frank RM, Franklin RM. 1983. Electron microscopy of avian osteopetrosis induced by retrovirus MAV.2-0. *Calcified Tiss Int* 34:382.
273. Chabot JF, et al. 1979. Mesotheliomas of peritoneum, epicardium, and pericardium induced by strain MC29 avian leukosis virus. *Cancer Res* 30:1287.
274. Carter JK, et al. 1983. Induction of angiosarcomas by ring-necked pheasant virus. *Infect Immun* 40:310.
275. Ewert DL, et al. 1990. *In ovo* infection with the avian retrovirus RAV-1 leads to persistant infection of the central nervous system. *Lab Invest* 62:156.
276. Bevilacqua G, et al. 1989. Ultrastructural features of the intestinal absorption of mouse mammary tumor virus in newborn BALB/cf RIII mice. *Gastroenterology* 96:139.
277. Menendez-Arias L, et al. 1992. Purification of immature cores of mouse mammary tumor virus and immunolocalization of protein domains. *J Virol* 66:5615.
278. Payne A, et al. 1986. Isolation and identification of a South African lentivirus from jaagsiekte lungs. *Onderstepoort J Vet Res* 53:55.
279. Laird HM, et al. 1968. An electron microscopic study of virus particles in spontaneous leukemia in the cat. *J Nat Cancer Inst* 41:867.
280. Hoover EA, et al. 1974. Erythroid hyperplasia in cats inoculated with feline leukemia virus. *J Nat Cancer Inst* 53:1271.
281. Snyder SP. 1971. Spontaneous feline fibrosarcomas. *J Nat Cancer Inst* 47:1079.
282. Leiter EH, Kufe EL. 1984. Intracisternal type A particles in murine pancreatic B cells. *Am J Pathol* 114:46.
283. Izard J, De Harven E. 1968. Increased numbers of a characteristic type of reticular cell in the thymus and lymph nodes of leukemia mice: An electron microscopic study. *Cancer Res* 28:421.
284. Aoki T,et al. 1970. G(Gross) and H-2 cell-surface antigens: Location on Gross leukemia cells by electron microscopy with visually labeled antibody. *Proc Nat Acad Sci* 65:569.
285. Baszler TV, Zachary JF. 1990. Murine retroviral-induced spongiform neuronal degeneration parallels resident microglial cell infection. *Lab Invest* 63:612.
286. Gardner MB, et al. 1973. A spontaneous lower motor neuron disease apparently caused by indigenous type C RNA virus in wild mice. *J Nat Cancer Inst* 51: 1243.
287. Portis JL. 1990. Wild mouse retrovirus: Pathogenesis. *Curr Topics Microbiol Immunol* 160:11.
288. Hoffman PM, et al. 1992. Cellular tropism and localization in the rodent nervous system of a neuropathogenic variant of Friend murine leukemia virus. *Lab Invest* 67:314.
289. Nagra RM, et al. 1992. Development of spongiform encephalomyopathy in retroviral infected mice. *Lab Invest* 66:292.
290. Park BH, et al. 1994. Pathogenesis of cerebral infarction and hemorrhage induced by a murine leuekemia virus. *Lab Invest* 71:78.
291. Stoica G, et al. 1992. Temporal lymphoreticular changes caused by ts1U, a paralytogenic mutant of Moloney murine leukemia virus TB. *Lab Invest* 66:427.
292. Leiter EH. 1985. Type C retrovirus production by pancreatic beta cells. *Am J Pathol* 119:22.
293. Clase AC, et al. 2006. Oligodendrocytes are a major target of the toxicity of spongiogenic murine retroviruses. *Am J Pathol* 169:1026.
294. McKhann G II, et al. 1989. Isolation and characterization of HTLV-1 from symptomatic family members with tropical spastic paraparesis (HTLV-1 encephalomyeloneuropathy). *J Infect Dis* 160:371.
295. Sarin PS, et al. 1989. Comparison of a human T-cell lymphotropic virus type I strain from cerebrospinal fluid of a Jamaican patient with tropical spastic paraparesis with a prototype R T-cell lymphotropic virus type I. *Proc Nat Acad Sci* 86:2021.
296. Pedersen NC, et al. 1987. A new feline T-lymphotropic lentivirus isolated from cats with immunodeficiency syndrome. *Science* 235:790.
297. Yamamoto JK, et al. 1988. Pathogenesis of experimentally induced feline immunodeficiency virus infection in cats. *Am J Vet Res* 49:1246.
298. Dezutter-Dambuyant C, et al. 1991. Trypsin-resistant glycoprotein 120 receptors are upregulated on short-term cultured human epidermal Langerhans cells. *Res Virol* 142:129.

Vet-ebooks.com

299. Gelderbloom HR, et al. 1989. Morphogenesis and morphology of HIV structure-function relationships. *Arch Virol* 106:1.
300. Gonda MA, et al. 1985. Sequence homology and morphologic similarity of HTLV-III and visna virus, a pathogenic lentivirus. *Science* 227:173.
301. Marx PA, et al. 1988. Computer emulation of thin section electron microscopy predicts an envelope-associated icosadeltahedral capsid for human immunodeficiency virus. *Lab Invest* 58:112.
302. Clavel F, et al. 1986. Isolation of a new human retrovirus from West African patients with AIDS. *Science* 233:343.
303. Klatzmann D, et al. 1984. Selective tropism of lymphadenopathy associated virus (LAV) for helper-induced T lymphocytes. *Science* 225:59.
304. Pauza CD, Price TM. 1988. Human immunodeficiency virus infection of T cells and monocytes proceeds via receptor-mediated endocytosis. *J Cell Biol* 107:959.
305. Cameron PU, et al. 1992. Dendritic cells exposed to human immunodeficiency virus type-1 transmit a vigorous cytopathic infection to CD4+ cells. *Science* 257:383.
306. Lifson JD, et al. 1986. AIDS retrovirus induced cytopathology: Giant cell formation and involvement of CD4 antigen. *Science* 232:1123.
307. Yoffe B, et al. 1989. *In vivo* and *in vitro* ultrastructural alterations induced by human immunodeficiency virus in human lymphoid cells. *Lab Invest* 61:303.
308. Nuovo GJ, et al. 1994. HIV-1 nucleic acids localize to the spermatogonia and their progeny. *Am J Pathol* 144:1142.
309. Orenstein JM. 1992. Ultrastructural pathology of human immunosuppressive virus infection. *Ultrastr Pathol* 16:179.
310. Sunila I, et al. 1997. Activated cytotoxic lymphocytes in lymph nodes from human immunodeficiency virus (HIV) 1-infected patients: A light and electron microscopy study. *Histopathology* 30:31.
311. Goto T, et al. 1998. The life-cycle of human immunodeficiency virus type 1. *Micron* 29:123.
312. Maier H, et al. 1989. Vacuolar myelopathy with multinucleated giant cells in the acquired immune deficiency syndrome (AIDS). *Acta Neuropathol* 78:497.
313. Harris JR, et al. 1989. Viral release from HIV-I-induced syncytia of CD4+ C8166 cells. *J Med Virol* 28:81.
314. Meyenhofer MF, et al. 1987. Ultrastructural morphology and intarcellular production of human immunodeficiency virus (HIV) in brain. *J Neuropathol Exp Neurol* 46:474.
315. Price RW, et al. 1988. The brain in AIDS. *Science* 239:586.
316. Koenig S, et al. 1986. Detection of AIDS virus in macrophages in brain tissue from AIDS patients with encephalopathy. *Science* 233:1089.
317. Pomerantz RJ, et al. 1987. Infection of the retina by human immunodeficieny virus type 1. *New Engl J Med* 317:1643.
318. Scoazec J-Y, et al. 1988. Peliosis hepatis and sinusoidal dilatation during infection by the human immunodeficiency virus (HIV). *Am J Pathol* 131:38.
319. Grody WW, et al. 1990. Infection of the heart by human immunodeficiency virus. *Am J Cardiol* 66:203.
320. Garry RF, et al. 1990. Detection of a human intracisternal A-type retroviral particle antigenically related to HIV. *Science* 250:1127.
321. Hantai D, et al. 1991. Skeletal muscle involvement in the immunodeficiency virus infection. *Acta Neuropathol* 81:496.
322. Miller CJ, et al. 1992. Localization of SIV in the genital tract of chronically infected female rhesus macaques. *Am J Pathol* 141:655.
323. Chalifoux LV, et al. 1987. Lymphadenopathy in macaques experimentally infected with the simian immunodeficiency virus (SIV). *Am J Pathol* 128: 104.
324. Ringler DJ, et al. 1989. Cellular localization of simian immunodeficiency virus in lymphoid tissues. *Am J Pathol* 134:373.
325. Lackner AA, et al. 1991. Localization of simian immunodeficiency virus in the central nervous system of rhesus monkeys. *Am J Pathol* 139:609.
326. Xing HQ, et al. 2003. Simian immunodeficiency virus encephalitis in the white matter and degeneration of the cererbral cortex occur independently in simian immunodeficiency virus-infected monkey. *J Neurovirol* 9:508.
327. Chalifoux LV, et al. 1992. Arteriopathy in macaques infected with simian immunodeficiency virus. *Lab Invest* 67:338.
328. Ringler DJ, et al. 1987. Immunophenotypic characterization of the cutaneous exanthem of SIV-infected rhesus monkeys. *Am J Pathol* 126:19.
329. Kuhn EM, et al. 1997. Intestinal manifestation of experimental SIV-infection in rhesus monkeys (*Macacca mulatta*). *Zentralbl Veterinaermed* 44:501.
330. Shehu-Xhilaga M, et al. 2007. The testes and epididymis are productively infected by SIV and SHIV in juvenile macaques during the post-acute stage of infection. *Retrovirology* 31:4.
331. Nathanson N, et al. 1976. Pathogenesis of visna. *Lab Invest* 35:444.
332. Coward JE, et al. 1972. Ferritin-conjugated antibody labeling of visna virus. *Virology* 50:925.
333. Cutlip RC, et al. 1988. Ovine progressive pneumonia (maedi-visna) in sheep. *Vet Microbiol* 17:237.
334. Weiland F, Bruns M. 1980. Ultrastructural studies on maedi-visna virus. *Arch Virol* 64:277.
335. Cork LC, Davis WC. 1975. Ultrastructural features of viral leukoencephalomyelitis of foals. *Lab Invest* 32:35.
336. Perk K. 1990. Presence of virus particles in neural cells of goats with caprine arthritis encephalitis. *Res Vet Sci* 49:367.
337. Gonda MA, et al. 1978. Squirrel monkey retrovirus: Electron microscopy of a virus from new world monkeys and comparison with Mason-Pfizer monkey virus. *Arch Virol* 56:29.
338. Aguzzi A. 1993. Human foamy virus proteins accumulate in neurons and induce multinucleated giant cells in brain of transgenic mice. *Am J Pathol* 142:1061.

Vet-ebooks.com

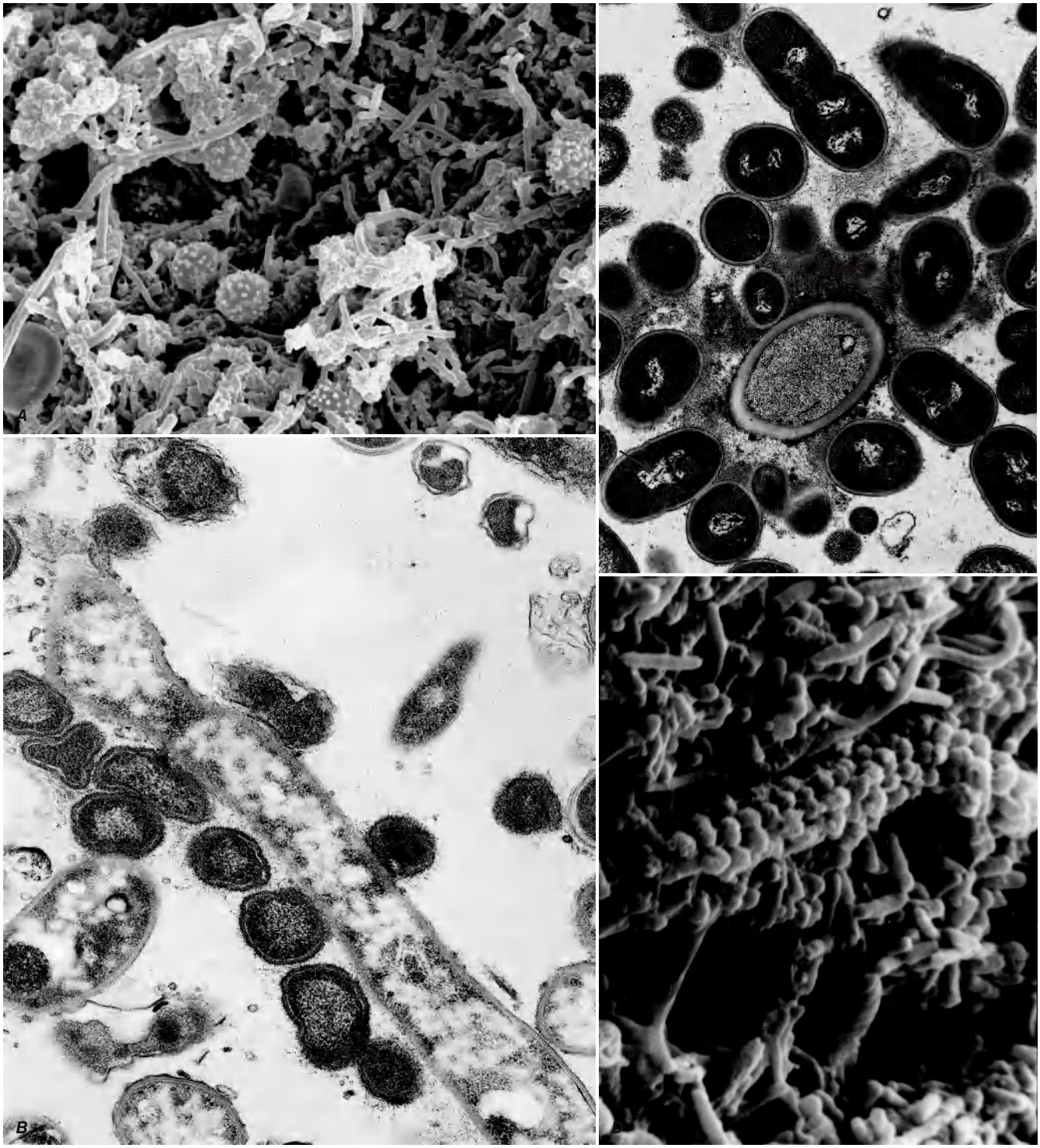


Fig. 14.1 Polymicrobial infections in the oral cavity: A. **Human gingival plaque:** mixed biofilm of rods and cocci with erythrocytes and leukocytes. (Micrograph: Janet M. Guthmiller, John E. Laffoon, *ASM Press*). **B**. **Canine Plaque:** large central filamentous bacterium (in longitudinal section) surrounded by gram-positive coccobacilli. **C**. **Canine plaque**: large central filamentous bacterium (in cross section) surrounded by gram-positive coccobacilli (arrow). Acidic glycosaminoglycans (aMPS) cover bacterial surfaces. **D**. **Canine plaque**: large filamentous bacterium with adhered coccoid bacteria ("corn-cob").

© 2009 Wiley-Blackwell. ISBN: 978-0-813-80330-2

Vet-ebooks.com

14 Cytopathology of Pathogenic Prokaryotes

Kim A. Brogden

Procaryotic microorganisms occur in two domains, the Archaea (*Archaeobacteria*) and bacteria (*Eubacteria*). *Archaeobacteria* are asocciated with extreme environments;[1] recent isolates from the oral cavity, human colon, and vagina may be associated with chronic disease. *Methanobrevibacter oralis*, a methanogen archaeal species, may be syntropic with other bacteria in subgingival crevices and promote colonization by secondary fermenters during periodontitis.[2]

Eubacteria contain more than 26 phyla that contain pathogens found in host-associated natural ecologies.[3] Genome sizes of *Eubacteria* generally correlate with the complexity of their morphology and their degree of dependence upon the host physiologic systems. Genomic sizes range from 580 kb for cell wall-less microorganisms like *Mycoplasma genitalium* to greater than 6 Mb for pathogens and opportunistic pathogens like *Pseudomonas* species.

Metagenomic analysis reveals an enormous diversity of microorganisms in the ecosystem. Analysis of 16S ribosomal DNA sequences from terrestrial and aquatic environments shows that known microbial species comprise less than 1% of that found in nature. Analysis of 16S ribosomal DNA sequences from host-associated natural ecologies is more definitive. The mammalian intestinal microbiota is composed of 10^{13} to 10^{14} microorganisms, whose collective genome ("microbiome") contains at least 100 times as many genes as the mammalian genome.[4]

Eubacteria induce disease in a variety of forms. Pathogens like *Pasteurella multocida* induce rapid, acute, and often lethal infections of poultry in the planktonic state. Other microorganisms persist and induce disease as either a single species biofilm or a mixed community biofilm.[5] Infection and colonization of the oral cavity is an example (Fig. 14.1). Yet, some microorganisms and viruses combine with *Eubacteria* to induce disease in polymicrobial infections.[6]

Structure of the Bacterial Cell

Eubacteria have well defined sizes ranging from approximately 0.2–0.8 μm wide × 0.3 to >10 μm long, with characteristic morphologic shapes and arrangements. These morphologies have diagnostic value when seen by light or electron microscopy in infected mucous secretions, blood, and tissues. *Eubacteria* have well developed, complex surfaces containing a variety of capsules, fimbriae, and flagella. Surface structures are related to pathogenicity allowing bacteria to avoid host defenses and attach, colonize, and persist in host tissues.[7–9] Many of these same bacteria produce virulence factors, including toxins and destructive enzymes (e.g., coagulase, hyaluronidase, etc.), which increase virulence (Table 14.1) and allow them to resist the opsonic and lytic effects of antibody and complement.[10]

Cell Envelope

The **cell envelope** is the outermost part of the *Eubacteria* surface (Fig. 14.2). Some species have an envelope containing a cell membrane and a thick cell wall, which retains a crystal violet-iodine complex and stains the microorganism blue (gram-positive bacteria) by the Gram stain procedure. Other species have a cell membrane, thinner cell wall, and an outer membrane that does not retain a crystal violet-iodine complex and counterstains red (gram-negative bacteria).

Vet-ebooks.com

Table 14.1 General categories of factors used by pathogenic bacteria to attach, infect, colonize, and cause disease in susceptible hosts.

Bacterial component	*Activity and examples*	*References to ultrastructural pathology*
	Attachment	
Fimbrial adhesins	Attachment of gram-negative and gram-positive bacteria to surfaces and host cells	**Telford**, *Nat Rev Microbiol* 4:509, 2006; **Scott**, *Mol Microbiol* 62:320, 2006; **Jonson**, *Contrib Microbiol* 12:67, 2005; **Craig**, *Nat Rev Microbiol 2:363, 2004*
Nonfimbrial adhesins	Surface components that mediate adherence of bacteria to surfaces and host cells	**Talay**, *Contrib Microbiol* 12:90, 2005; **Weiss**, *Microbe* 2:489, 2007; **Koretke**, *J Struct Biol* 155:154, 2006; **Ries**, *JEM* 200:1267, 2004; **Pizarro-Cerda**, *Cell* 124:715, 2006
	Colonization	
Capsule	Capsules of polysaccharide or protein provide resistance to desiccation and promote adherence to surfaces and host cells	**Taylor**, *Contrib Microbiol* 12:55, 2005; **Kasper**, *J Infect Dis* 153:407, 1986; **Whitfield**, *Can J Microbiol* 34:415, 1988; **Garcia**, *Res Microbiol* 151:429, 2000; **Llull**, *Curr Mol Med* 1:475, 2001; **O'Riordan**, *Clin Microbiol Rev* 17:218, 2004; **Mckenney**, *J Biotechnol* 83:37, 2000; **Bayer**, *Curr Topics Microbiol Immunol* 150:129, 1990; **Cross**, *Curr Topics Microbiol Immunol* 150:87, 1990; **Moxon**, *Curr Topics Microbiol Immunol* 150:65, 1990; **Comstock**, *Cell* 126:847, 2006; **Candela**, *Mol Microbiol* 60:1091, 2006; **Glomski**, *Infect Immun* 75:4754, 2007; **Kirby**, *Biophys J* 68:360, 1995; **Whitfield**, *Ann Rev Biochem* 75:39, 2006; **Roche,** *Trend Microbiol* 3:304, 1995
Surface proteins	Protect bacteria from environmental challenges, allow bacteria to use nutrients from their environment, allow bacteria to attach to specific environmental components, facilitate competition with other bacteria for specific niches, and assist in bacterial growth and division	**Scott**, *Ann Rev Microbiol* 60:397, 2006
	Tissue Damage	
Secretion systems	**Type I, Type II, Type III, Type IV, Type V, Type VI,** and **Type VII secretion systems** translocate virulence determinants from microbial cells to host cells	**Andersen**, *Rev Physiol Biochem Pharmacol* 147:122, 2003; **Andersen**, *EMBO Rep* 1:313, 2000; **Cescau**, *J Bacteriol* 189:1496, 2007; **Sandkvist**, *Infect Immun* 69:3523, 2001; **Ball**, *Mol Microbiol* 43:475, 2002; **Cianciotto**, *Trends Microbiol* 13:581,2005; **Lee**, *Infect Immun* 73:1695, 2005; **Mota**, *Ann Med* 37:234, 2005; **Mattick**, *Ann Rev Microbiol* 56:289, 2002; **Cristie**, *Mol Membr Biol* 22:51, 2005; **Henderson**, *Microbiol Mol Biol Rev* 68:692, 2004; **Zheng**, *Mol Microbiol* 66:1192, 2007; **Abdallah**, *Nat Rev Microbiol* 5:883, 2007
Lipopolysaccharides	Induce mediators that lead to fever, shock, and disseminated intravascular coagulation	**Jakway**, *Science* 234:743, 1986; **Morrison**, *Ann Rev Med* 38:417, 1987; **Hirata**, *Lab Invest* 43:165, 1980; **Kang**, *Anat Rec* 229:86, 1991; **Meyrick**, *Lab Invest* 55:164, 1986; **Nagato**, *Am J Pathol* 138:183, 1991
Cell wall fractions	Peptidoglycan is a proinflammatory molecule inducing symptoms of infectious illness, endotoxemia, and organ failure in animal models	**Moreillon**, *Scand J Infect Dis* 35:632, 2003; **Myjre**, *Shock* 25:227, 2006
Toxins	**Pore-forming toxins** include repeats-in-toxin (RTX) toxins, multifunctional auto-processing repeats-in-toxin (MARTX) toxins, and *Serratia marcescens* hemolysin. **Cytolethal distending toxins** initiate a eucaryotic cell cycle block at the G2 stage prior to mitosis. **ADP-ribosyltransferase toxins** include diphtheria toxin and *P. aeruginosa* exotoxin A. **Rho GTPase targeted cytotoxins** inactivate actin cytoskeletal pathways	**Satchell**, *Infect Immun* 75:5079, 2007; **Smith**, *Crit Rev Microbiol* 32;227, 2006; **Hertle**, *Curr Protein Pept Sci* 6:313, 2005; **Romer**, Nature 450:670, 2007; **Aktories**, *Nat Rev Microbiol* 3:397, 2005; **Kamal**, *Infect Immun* 75:6008, 2007; **Crosby**, *Gene* 388:83, 2006; **Yates**, *Trends Biochem Sci* 31:123, 2006; **Holbourn**, *FEBS J* 273:4579, 2006; **Voth**, *Clin Microbiol Review* 18:247, 2005

Vet-ebooks.com

Table 14.1 *Continued*

Bacterial component	*Activity and examples*	*References to ultrastructural pathology*
Enzymes	**Phospholipases** degrade cellular lipids and phospholipids; **hyaluronidases** degrade proteoglycans and promote the spread of bacteria; **coagulases** degrade fibrin and enhance accumulation of edema fluid; **IgA proteases** cleave IgA, facilitating the colonization of bacteria on mucosal surfaces	**Cotran**, *Am J Pathol* 129:407, 1987
	Persistence in the Host	
Inhibition of endocytic maturation and bacterial escape into the cytoplasm	Inhibition of phagosome and lysosome fusion promotes intracellular survival; actin polymerization permits intracellular bacteria to move through the intracellular and intercellular environments	**Santic**, *Trends Microbiol* 14:37, 2006
L-forms	Cell-wall deficient bacteria persist and are involved in chronic infections	**Astrauskiene**, *Clin Exp Rheumatol* 25:470, 2007
Evasion of host defenses	Capsules provide resistance to nonspecific and specific host immunity; sialylation of surface lipopolysaccharide induces resistance to killing by serum	**Taylor**, *Contrib Microbiol* 12:55, 2005; **Fox**, *Micro Pathog* 11:199, 1991; **Smith**, *FEMS Microbiol Lett* 100:287, 1992

The gram-positive bacterial envelope has a 20–80 nm multilayer peptidoglycan sheath with embedded teichoic and lipoteichoic acids just outside the **cytoplasmic membrane**.[11] A polysaccharide **capsule**, attached via covalent linkage to phospholipid or lipid A, may be on the outermost surface. Extracellular polysaccharide, with no visible means of attachment, may also be on the outermost surface and released as slime. Using cryo-transmission electron microscopy, *Bacillus subtilis* has an inner zone representing a periplasmic space confined between the plasma membrane and the wall matrix. The outer wall zone is the peptidoglycan-teichoic acid polymeric network of the wall.[12] Using cryo-transmission electron microscopy, *Staphylococcus aureus* has a wall above the plasma membrane consisting of a 16 nm low-density inner wall zone representing a periplasmic space,[13] followed by a 19 nm high-density outer wall zone. With cryo-electron microscopy, *B. subtilis* and *S. aureus* have a granular layer adjacent to the plasma membrane in the periplasmic space. This represents the sites of cell wall production.[14]

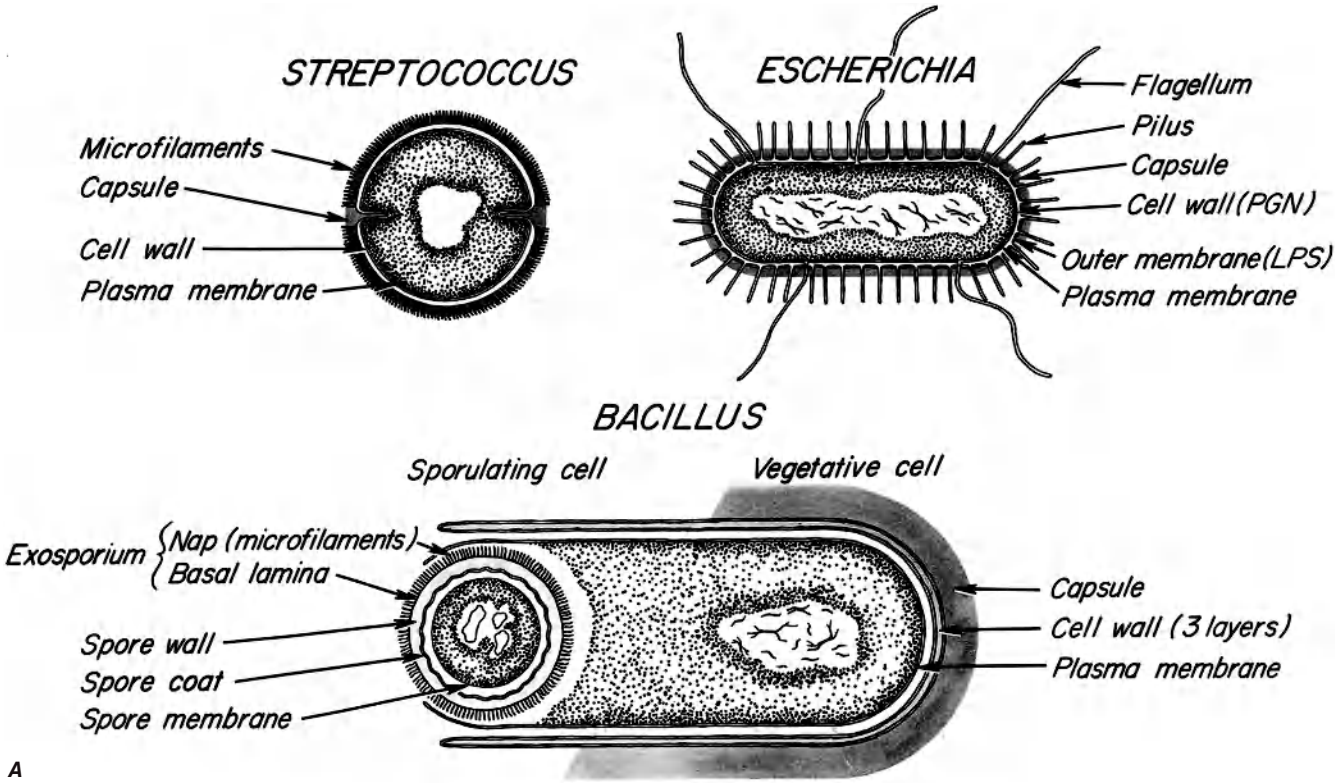
The gram-negative bacterial envelope has a 1–7 nm peptidoglycan layer, which lies near a **periplasmic space** between both an **outer membrane** and **inner membrane**[11](Fig. 14.3). The outer membrane has lipopolysaccharide on the outer leaflet and phospholipids on the inner leaflet. Nutrients and other small hydrophilic molecules (<600 Da) enter the cell by passive diffusion through porins in the outer membrane. Membranous **vesicles** bleb from the surface of the outer membrane, and serve as secretory vehicles carrying and transmitting virulence factors into host cells.

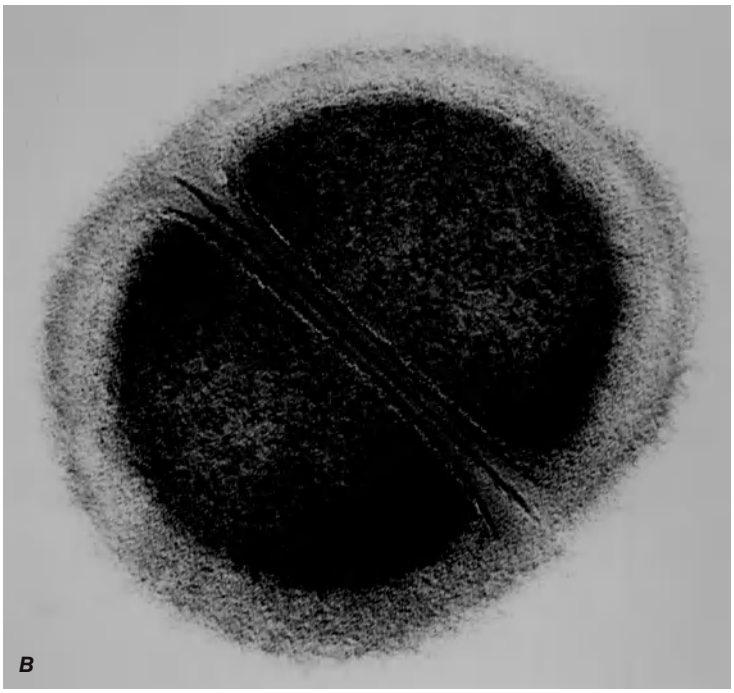
The surfaces of gram-negative bacteria also have attached **capsules** composed of complex glycoconjugates.[15] Capsular architectures are very diverse and their compositions are complex; they often consist of repeating units of extracellular polysaccharides. When carefully dehydrated during ultrastructural processing to reduce artifactual collapse, these capsules appear as a loose gel or fibrillar material. As virulence factors, they promote adhesion to mucosal surfaces or other microorganisms in biofilms; serve as a surface permeability barrier; and prevent phagocytosis.

The mycobacterial envelope contains large amounts of C60-C90 fatty acids and mycolic acids covalently linked to arabinogalactan.[16] As a result, this surface is of unusually low permeability.

Bacterial cell shape is determined by peptidoglycan and bacterial cytoskeletal proteins. The peptidoglycan layer, also called the **cell wall**, is a macromolecular structure of glycan chains cross-linked by flexible peptide bridges. Also present are homologues of the eukaryotic cytoskeletal elements for tubulin-like and actin-like proteins: FtsZ, MreB, and Mbl.[11] Together these maintain the shape of the bacterial cell and protect it from damage by changes in osmotic pressure. Projections from the surface include fimbriae and flagella. **Fimbriae** are composite fibers composed mainly of PapA with lesser PapE, PapF, PapK, and

Vet-ebooks.com





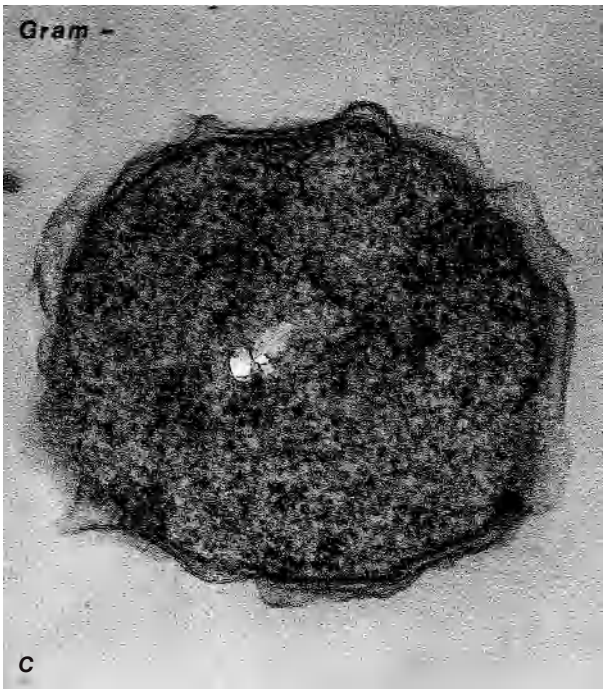


Fig. 14.2 **Bacterial cell structure: A**. Model of *Streptococcus*, *Escherichia*, and *Bacillus*. **B**. Dividing gram-positive coccus. **C**. Gram-negative bacillus.

PapG proteins.[17] They also bind plasma proteins; activate calcium influx; initiate proteolytic and signal transduction cascades; and facilitate motility. They are classified into functional groups. **Flagella** are composed of flagellin protein monomers and facilitate bacterial motility, participate in adherence, and initiate proinflammatory host responses.[17]

The septum of *S. aureus* consists of two high-density regions sandwiched between three low-density zones. The two zones adjacent to the membrane appear as an

Vet-ebooks.com

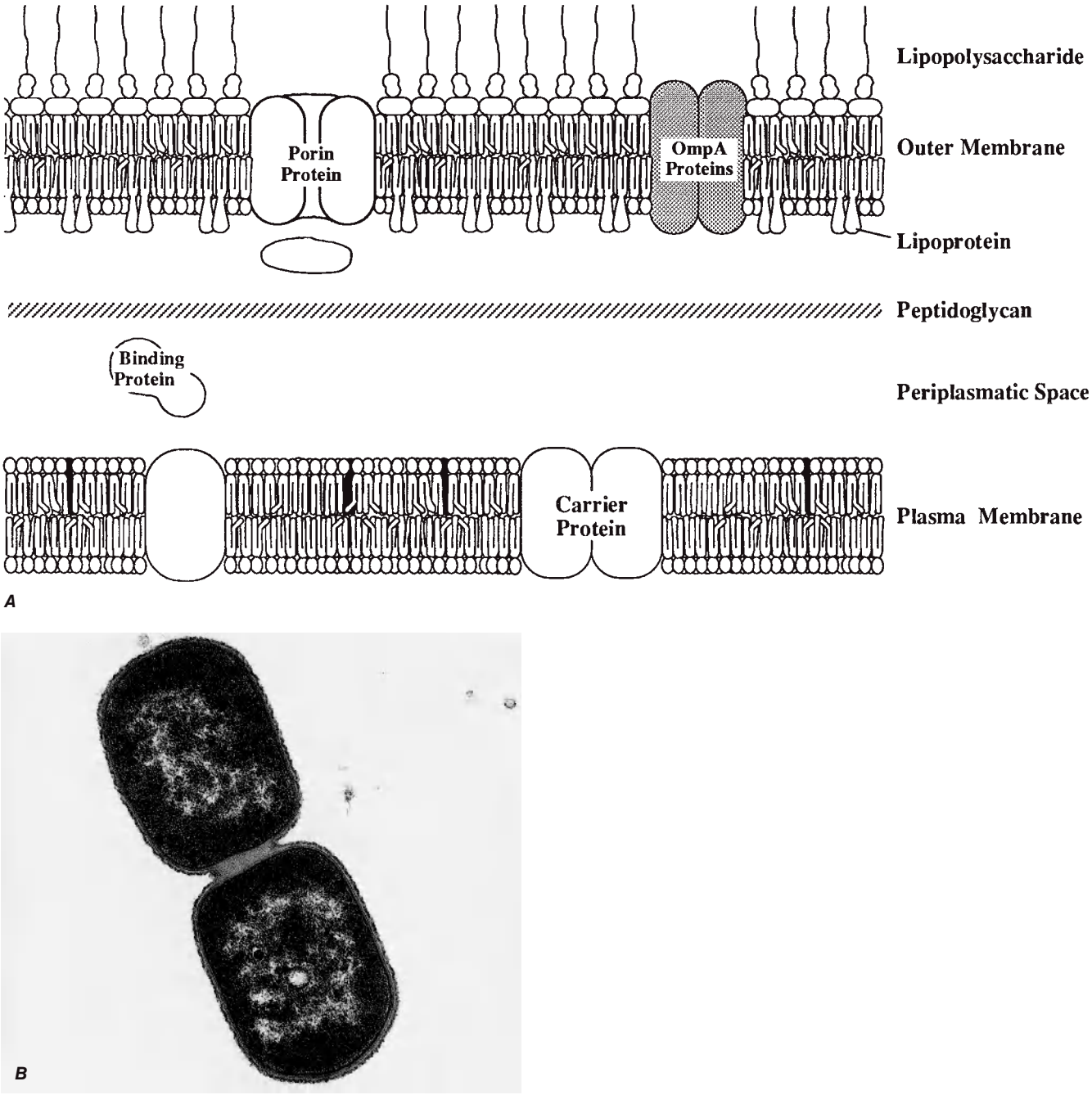


Fig. 14.3 Bacterial cell envelope: A. Model of the gram-negative bacterial envelope. **B.** Ultrastructure of a gram-negative bacterium.

extension of the periplasmic space seen in this organism's cell envelope and show no distinguishing structures within them.[18]

Cell Membrane

The **cell membrane** (also called the cytoplasmic membrane or the inner membrane of gram-negative bacteria) is an enclosed lipid bilayer surrounding the cytoplasm that serves as a permeability barrier. It contains enzyme and transporter proteins for protein export and DNA replication. Depending upon the bacterial species, the cell membrane can contain phosphatidylglycerol, phosphatidylethanolamine, lyso-cardiolipin, and cardiolipin. In freeze-fracture studies, *Veillonella* species contain high levels of phosphatidylserine.[19] Proteins in the outer leaflet, the inner leaflet or spanning the membrane function in transport of metabolites (**permeases**, or **transporters**), energy production, biosynthesis, or export of cellular products. These include, but not limited to, families of proteins for lipopolysaccharide biogenesis (SecYEG

Vet-ebooks.com

complex, β-barrel proteins, and lipoproteins), capsular polysaccharide biogenesis, oxidative phosphorylation, flagellar biogenesis, and nutrient transport. Novel membrane protein structures in specific types of membranes can be identified using single particle electron microscopy and mass spectrometry.[20]

Hydrophobic α-helical proteins generally span the cell membrane. The cell membrane also contains lipoproteins attached via an N-terminal N-acyl-diacylglycerylcysteine.[21]

The shape of the cell membrane conforms, via osmotic pressure, to that of the adjacent cell wall and cytoskeletal proteins. In mildly hypotonic or isotonic solutions, the cell membrane presses tightly against the cell wall. In hypertonic solutions, plasmolysis occurs. There is loss of water and cytoplasmic volume and the membrane shrivels away from the cell wall.[22] Damage to cell walls and plasma membranes can be extreme.[23] Altering the structure of the cell wall with metabolic inhibitors or the enzyme lysozyme often results in lysis of the bacterial cell. Sublethal amounts of lysozyme, like that encountered by *Pasteurella multocida* growing in vivo in avian blood, may actually facilitate the release of outer membrane blebs containing endotoxin.[24] Under controlled conditions in an isotonic solution, digestion of the cell wall forms **protoplasts** from gram-positive bacteria or **spheroplasts** from gram-negative bacteria. Spheroplasts or protoplasts serve as models to study the mechanisms of cationic antimicrobial peptide activity (e.g., attraction, attachment, insertion, and pore formation) with microbial membranes. In *Mycoplasma* species, lipid domains in the cell membrane correlate with resistance to osmotic lysis.[25]

Cell Wall

The cell walls of gram-negative bacteria are thin and relatively rigid, separating the outer and inner membranes. The cell walls of gram-positive bacteria, when stained with osmium, appear in transmission electron micrographs as an electron-dense layer 20–50 nm thick surrounding the plasma membrane (Fig. 14.2). This wall is a repeating disaccharide of N-acetylmuramic acid (MurNAc) linked to N-acetyl glucosamine (GluNAc) by a β 1–4 glycosidic bond. MurNAc and GluNAc strands are cross-linked together through their terminal D-alanine residues via a tetrapeptide. Cell wall associated teichoic acids may attach to peptidoglycan via a direct linkage. Teichoic acids may also attach to lipoteichoic acids associated with the cell membrane. This complex physically protects the cell from environmental pressures, is involved in trafficking ions and nutrients, and serves as a scaffold for surface proteins.[26] During growth, some bacteria give rise to wall-less progeny called **L-forms**, which may be involved in chronic diseases like reactive arthritis.

Peptidoglycan fragments are pyrogenic, somnogenic, and arthritogenic. A fragment of peptidoglycan called muramyl dipeptide (N-acetlmuramyl-L-alanyl-D-isoglutamine) stimulates nonspecific host resistance to infection, likely by the nucleotide-binding oligomerization domain protein 2 (NOD2/CARD15) pathways. NOD2 is an intracellular pattern recognition receptor that enhances host defense by inducing the production of antimicrobial peptides.[27]

Outer Membranes of Gram-Negative Bacteria The outer membrane of gram-negative bacteria is a permeability and asymmetric barrier.[21,28] The outer leaflet is composed entirely of lipopolysaccharide and the inner leaflet is composed of phospholipids (Fig. 14.3). The outer membrane is not energized by a proton gradient and adenosine triphosphate is not available in the underlying periplasm. **Outermembrane vesicles** extrude from this layer and are released from both pathogenic and nonpathogenic gram-negative bacteria.[29] These vesicles or "proteoliposomes" are spherical, 50–250 nm particles of outer membrane phospholipids and lipopolysaccharide. The lumens are electron dense and contain periplasmic proteins. They generally bud from sites where the links between the peptidoglycan and outer membrane are infrequent, absent, or broken.[30] Vesicles fuse with host cells, transmitting the virulence factors contained within them. Vesicles also fuse with other bacteria (1) releasing autolysins that kill competitive bacteria, (2) transferring antibiotic resistance enzymes, (3) transferring chromosomal DNA, plasmids, or phage DNA, or (4) inducing microbial aggregation.

Proteins in the outer membrane are typically amphipathic and fold into a β-barrel with a hydrophobic interior channel and a hydrophobic surface adjoining surrounding phospholipids and lipopolysaccharide. The outer membrane also contains lipoproteins attached via an N-terminal N-acyl-diacylglycerylcysteine.[21] Outer membrane proteins are synthesized in the cytoplasm as precursors with a short 25 amino acid, amino-terminal signal sequence required for transport across the cell membrane via the Sec pathway. In the periplasm, these proteins attach to chaperones, like Skp, escorting them to Omp85 for insertion into the outer membrane. For porins, oligomerization occurs after insertion.

The **periplasmic space** between the plasma membrane and the outer membrane of gram-negative bacteria is an aqueous compartment densely packed with binding proteins for nutrient transport, proteins for transport of materials to the outer membrane, and degradative enzymes (alkaline phosphatase). Measuring 11–15 nm in fixed tissue, it is large when examined

Vet-ebooks.com

by freeze-substitution methods.[31] Alkaline phosphatase, a virulence factor of periodontal pathogen *Porphyromonas gingivalis*, is labeled diffusely throughout the space[32] and cytochromes and nitrate reductases used by denitrifying bacteria have been localized to the periplasmic space.[33] After high-pressure freezing, *E. coli* and *P. aeruginosa* in cryosections have a diffuse dispersion of ribosomes and genetic material in the cytoplasm. However, the periplasmic space is compressed, suggesting it is filled with a compressible gel.[34]

Lipopolysaccharide (LPS), a complex and toxic glycolipid found in the outer leaflet of the outer membrane, forms a tight matrix along the surface of the cell, contributing to the decreased permeability of this layer. Structurally, LPS is an amphipathic molecule composed of a lipid A domain, a core oligosaccharide domain, and a O-specific antigen domain. Lipid A has a high degree of heterogeneity among bacteria but generally has a β1,6-linked D-glucosamine disaccharide backbone with seven long-chain fatty acyl residues attached. Addition of ethanolamine, 4-aminoarabinose, palmitate, or replacing myristate with 2-OH myristate on lipid A, increases resistance of bacteria to killing by cationic antimicrobial peptides. Lipid A is linked to the highly variable core heteropolysaccharide via 2-keto-3-deoxy-D-manno-octonate or KDO.

In *Escherichia coli*, the core domain contains four heptose, three glucose, and one galactose residues. Bacteria can contain rough forms of LPS, which are devoid of parts of the core domain. Attached to the core domain is a hypervariable polysaccharide O-antigen domain. This is the most variable part of LPS and even varies among different strains of the same microbial species.[21]

LPS is synthesized on the inner leaflet of the inner membrane. It is then flipped to the outer leaflet of the inner membrane by MsbA, an inner membrane protein belonging to the ABC-transporter family of proteins. Lipopolysaccharide is then transported across the periplasm, either at membrane adhesion sites (Bayer's bridges), or escorted through the periplasm by dedicated chaperone components and delivered to the outer membrane assembly site containing a large β-barrel protein called Imp and a small lipoprotein called RlpB. Here, Imp and RlpB function to receive LPS at the inner leaflet of the outer membrane and "flip" it to the outer leaflet of the outer membrane.[35]

Modifications in LPS increase virulence of some bacteria. Transfer of sialyl groups of cytidine 5′-monophospho-N-acetyl neuraminic acid (CMP-NANA) to surface lipopolysaccharide sites confers resistance of *Neisseria gonorrhoeae* to bactericidal antibody in human serum.[36] The surface structure seen on gonococci after treatment with CMP-NANA is due to sialylation of surface LPS previously described as a "capsule."[37]

Morphologically, purified LPS appears as spherical disks or long tubular complexes in negatively stained preparations.[38,39] **Endotoxin** is a suspension of **outer membrane vesicles** released from living bacterial cells by **blebbing** (Fig. 14.4). Blebbing is the process of releasing spherical, membranous vesicles of outer membranous material containing LPS and protein (endotoxin) from the bacterial cell surface.[40] Endotoxin contains LPS, protein, and phospholipids; LPS is not synonymous with endotoxin but is its most active component. Endotoxin is responsible for much of the toxicity of gram-negative bacteria[41,42] and is responsible for sepsis and shock. LPS interacts with hemoglobin, which enhances the binding of endotoxins to endothelial cells.

Ultrastructurally, hemoglobin is able to incorporate into LPS with the longitudinal direction parallel to the lipid A double-layer,[43,44] which may mediate the increase in LPS endotoxicity.

Porins Porins are transmembrane proteins embedded in the outer membrane that allow for diffusion of small hydrophilic solutes with masses up to 600 Da. Electron microscopy, atomic force microscopy, x-ray crystallography and molecular modeling clearly show that porins consist of three subunits. Each subunit is a polypeptide of 200–420 amino acids folded into 26- or 18-stranded antiparallel β-barrels. Three such barrels form a stable trimeric molecule. Porins divide into nonspecific porins (*E. coli* porins, OmpC, OmpF, and PhoE) that allow for solute concentration-dependent gradient diffusion, and specific porins (maltoporin, LamB; sucrose specific porin, SrcY) that exhibit Michaelis-Menten kinetics for selective transport.[45] Atomic models of the OmpF porin molecule within the outer membrane have been constructed based on data from atomic force microscopy.[46]

Membrane Pumps Five families of efflux-pump proteins are associated with multidrug antibiotic resistance: the ATP-binding cassette (ABC) superfamily, the major facilitator superfamily (MFS), the multidrug and toxic-compound extrusion (MATE) family, the small multidrug resistance (SMR) family, and the resistance nodulation division (RND) family.[47] These efflux pumps also confer resistance to the effects of bile, hormones, and cationic host-defense molecules contributing to the persistence of bacteria in the host.

Chemoreceptors Chemotaxis enables bacteria to find favorable growth conditions by migrating towards select attractants, yet it allows them to avoid potentially harmful environments. A sensory complex mediates chemotaxis; receptors are dimeric transmembrane proteins coupled with a cytoplasmic sensing domain

Vet-ebooks.com

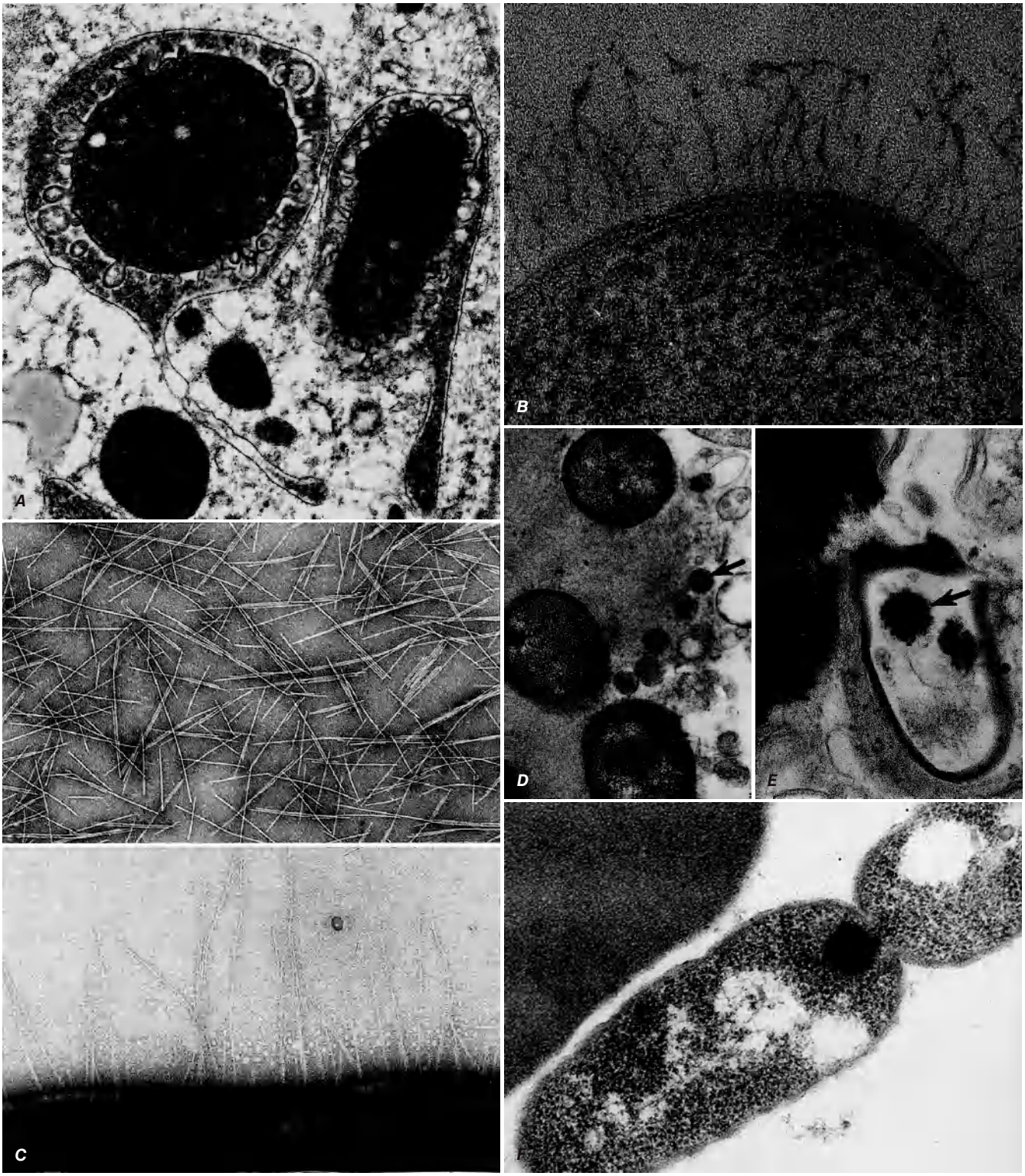


Fig. 14.4 Bacterial structure: A. Cell wall blebs, *Escherichia coli* showing the release of endotoxin. (Micrograph: Lawrence Arp.) **B. Surface filaments** of *Streptococcus*. (Micrograph: L. Graham and T. Beveridge, *J Bact* 173:1623, 1991.) **C. Fimbriae**, negative stain of purified *Escherichia coli* fimbriae (*top*) and fimbriae on the bacterial surface (*bottom*). (Micrograph: Lawrence Arp.) **D. Bacterial mucosubstances** (arrow) on bacteria embedded in granular mucopeptides in gingival plaque. **E. Calcification**, dead, calcified bacterium with intracellular apatite crystals (*arrow*). F. **Inclusion**, intracellular inclusion in *P. multocida* isolated from infected turkey blood.

Vet-ebooks.com

and cytoplasmic signaling domain.[48] Polar or lateral chemoreceptors on bacterial cells sense chemicals in their environment, particularly those in the ribose, glucose, peptide, maltose, and galactose uptake systems. Here, increased ligand binding causes a conformational change on the periplasmic domain and this signal moves through the transmembrane domain to the cytoplasmic domain.[49] A cascade involving proteins CheA, CheW, CheY, and CheB activates the flagellar motor and biases it towards clockwise rotation. As a result, cells swimming up a gradient have an increased occupancy of their receptors by ligand, have decreased tumbling motion, and increased zigzag directional trajectory.

Appendages and Adhesins

Bacteria use specialized surface appendages and adhesins for microbial attachment and motility. The expression of **fimbriae** and pili correlates with bacteria-to-cell and bacteria-to-bacteria adhesion, initial events necessary for colonization on mucosal tissue and organ surfaces. **Adhesins** are bacterial surface components that mediate adherence,[50,51] and may be structural subunits of fimbriae. Even flagella, the main appendages of bacterial motility, have roles in bacterial adherence. However, the majority of adhesins, called non-fimbrial adhesins, are only monomers or simple oligomers that are not detectable by standard electron microscopy. Examples include non-fimbrial, mannose-resistant hemagglutinins (NFA-1 and NFA-2) from *E. coli* O83:K1:H4 and O14:K?:H11; hemagglutinins A, B, C, and D of *P. gingivalis*; non-fimbrial adhesin YadA from *Yersinia* species; UspA1 and A2 from *Moraxella* species; Hia and Hsf from *Haemophilus* species; and BadA from *Bartonella henselae*.

Fimbriae

Pili are appendages for transfer of genetic material during bacterial conjugation. **Fimbriae** are filamentous surface structures for attachment of gram-negative and gram-positive bacteria to surfaces (Fig. 14.4). Both have clear roles in microbial pathogenicity; for example, many bacteria with pili and fimbriae are virulent and their mutant counterparts are avirulent. Yet, in addition to their ability to attach, fimbriae can (1) bind plasma proteins and initiate intrinsic proteolytic cascades, (2) activate calcium influx and signal transduction cascades, and (3) act as invasion factors and participate in the formation of intracellular and extracellular biofilms.[17]

Pili and fimbriae were once thought to be exclusive to gram-negative bacteria, but recent evidence indicates pili occur in gram-positive bacteria, too.[52,53]

Early classification schemes of fimbriae in gram-negative bacteria divided their differences into binding specificities (e.g., receptor specificity), antigenicity, and morphology. However, more recent classification schemes now divide fimbriae into families based on differences in fimbrial biosynthesis and assembly pathways and then divide them into groups based on receptor specificity or antigenic variation.[17]

The Chaperone-Usher Pathway Fimbrial Family

Classical **"common" Type 1 fimbriae** and P-blood-group-antigen-binding **P-fimbriae** are produced through the chaperone-usher pathway. The pathway includes gene clusters for fimbrial subunits, protein chaperones, outer membrane anchors for fimbrial shaft, and fimbrial regulatory genes. Generally, fimbrial subunits are translocated via the Sec system from the cytoplasm to the periplasm, are coupled to fimbrial chaperones and appropriate ushers, and are translocated and polymerized across the outer membrane.

Type 1 fimbriae are composite fibers containing a FimH homopolymer with minor components scattered throughout the filament, possibly as enhancers of polymerization or binding sites for receptors. Type 1 fimbriae on Enterobacteriaceae bind to D-mannose residues on eukaryotic cells. Typically, enterobacteria may have 50–400 or more Type 1 fimbriae projecting from its surface. Type 1 fimbriae are "mannose sensitive" because when added to suspensions of host cells (such as erythrocytes), mannose competes for binding sites with fimbriae. FimH activates host signal transduction events. Type 1 fimbriae initiate proinflammatory responses, mediate adherence, assist in invasion, and participate in the formation of intracellular biofilms.[17]

P fimbriae are composite fibers containing the major fimbrial subunit PapA and several minor subunits PapE, PapF, PapK, and PapG. PapA forms the fimbrial shaft and the other components are involved in PapA polymerization. Studies using freeze-etch electron microscopy show that the PapA fimbrial rod is a hollow cylinder. These rods are embedded in the outer membrane, extend outward from the surface, and are joined at the distal end to flexible adhesive fibrillae. Tip fibrillae are repeating subunits of PapE proteins in an open helical structure. **PapG**, localized in the distal end of the tip, recognize and bind to glycolipid receptors on mammalian cells. PapG recognizes Galα1–4Galβ components in receptor blood group antigen carrying globoseries glycolipids. To function, the rigid PapA rod projects the adhesin out and away from the interfering lipopolysaccharide molecules at the bacterial surface, whereas the flexible fibrillae allow PapG to move and find digalactoside moieties on the host cell.[54,55]

Vet-ebooks.com

The CS1 Fimbrial Family **CFA/I fimbriae** of enterotoxigenic *E. coli* and **Type II pili** of *Burkholderia cepacia* are assembled similar to the "chaperone-usher" pathway, although no homology exists among the CS1 fimbrial family components and the P fimbriae chaperone-usher components. The CS1 subunits (CooA) are translocated via the Sec system from the cytoplasm to the periplasm and assisted by protein CooB with a fimbrial chaperone-like function. CooA then interacts with CooC and CooD to polymerize. CooD is an initiator and lectin subunit.

Expression of F17 fimbriae allows *E. coli* K12 to cause diarrhea and septicemia in calves after binding to intestinal epithelium. It utilizes four genes for its expression and binds to N-acetyl-D-glucosamine, plasminogen, and the extracellular matrix protein laminin.

The Type IV Pili Pathway Family **Type IV pili** are multifunctional adhesive appendages found on a large variety of bacteria including *Neisseria*, *Pseudomonas*, *Dichelobacter*, *Moraxella*, and *Vibrio* species. The family also includes **bundle-forming pili** of enteropathogenic *E. coli*.[56] These pili are 5–7 nm in size, up to several millimeters in length, arranged in a helical confirmation of five subunits/turn, and can be glycosylated and/or phosphorylated. Up to 40 genes are required (e.g., *P. aeruginosa*) for production and regulation of the major pilin gene product and minor pilin-like proteins. Type IV pili are assembled in the cytoplasmic membrane or periplasm. A nucleotide-binding protein, a pre-pilin peptidase, and a multimeric outer membrane protein that forms a pore in the outer membrane for pilus protrusion are required.

Type IV pili bind to a variety of inert nonbiological surfaces: other bacteria, eucaryotic cells, and to connective tissue, plasma, and serum proteins. In eucaryotic cells, binding occurs at the distal tip to specific asialo-GM1 and asialo-GM2 glycosphingolipids receptors[17] via the carboxy-terminal disulfide bonded region of the pilin protein.

Type IV pili initiate a multistep adhesion cascade that involves production of pilin, extension of the pili, tethering to an appropriate surface/receptor, and retraction of the pili. For example, *Neisseria* pili bind to host cell CD46 and release calcium. This triggers lysosomal exocytosis and Lamp-1 to the cell surface. Pili retraction stress triggers polymerization accompanied by accumulation of phosphotyrosine containing proteins. Bacteria then disperse from microcolonies, pili disappear, and the diplococci become directly attached to the host cell plasma membrane.[17] A three-dimensional (3-D) electron microscopy structure of the *N. meningitidis* PilG multimer reveals an asymmetric bilobed structure approximately 125 A in length and 80 A in width. The larger lobe within the structure was identified as the N terminus by location of Ni-nitrilotriacetic acid nanogold particles to the N-terminal polyhistidine tag. We propose that the smaller lobe corresponds to the periplasmic domain of the protein, with the narrower "waist" region being the transmembrane section.[57]

Type IV pili are also responsible for twitching motility; flagella-independent spasmodic movement of *N. gonorrhoeae*, *P. aeruginosa*, and *M. xanthus* on solid, wet surfaces. Here, extension, tethering, and retraction of pili slowly propel the bacterial cell across the surface.

The Extracellular Nucleator Pathway Fimbrial Family AgfA fimbrial fibers or **"curli" fimbriae** are produced by *E. coli* and *S. enterica* serovar Typhimurium via the *cfg* gene cluster containing *csgABC* and *csgDEFG* genes. CsgA and CsgB secreted from the bacterium interact and polymerize into a unique twisted morphology. These fimbriae have a diverse spectrum of receptor targets including intestinal cells, plasma proteins, and extracellular matrix proteins.[17] Curli fimbriae activate the coagulation system. Factor XI, XII, prekallikrein, and H-kininogen all absorb to *E. coli* and *S. enterica* serovar Typhimurium producing curli fimbriae, but not to isogenic mutants not producing curli fimbriae.

Current classification schemes of pili on gram-positive bacteria divide their differences by morphology. However, this may change as more information becomes available. Fibrils are present on oral pathogens like *Streptococcus gordonii* and *Streptococcus oralis*. They are 1–2 nm wide and 0.07–0.5 μm long and are involved in adhesion and biofilm formation.[52] Pili are found on *Corynebacterium diphtheriae*, *Streptococcus* species, including *Streptococcus pneumoniae*. They are 0.3–3 μm wide and 3–10 nm long. They are rod-like pili containing three covalently linked subunits with a LPXTG amino acid motif. Sortases covalently attach pilin subunits to each other and to the peptidoglycan cell wall, and some are connected by non-disulfide covalent linkages.[52]

Unique Pili *Shewanella oneidensis*, *Synechocystis* species, and *Pelotomaculum thermopropionicum* produce electrically conductive pilus-like appendages called bacterial nanowires in direct response to electron-acceptor limitations.[58] Ultrastructurally these appendages contain bundles of electrically conductive filaments, each 10–20 nm in diameter.

Adhesins

Gram-positive bacteria commonly use non-fimbrial adhesins to attach to a wide variety of proteins (colla-

Vet-ebooks.com

gen, fibronectin, and elastin), glycoproteins (laminin, vitronectin, and fibrinogen), and glycosaminoglycans of the extracellular matrix.[50] *Streptococcus pyogenes* uses SfbI/F1, F2/PFBP, FBP54, Fba, FbaB, Protein H, M proteins, LTA, Cpa, HA capsule, Lbp, SpeB, R28, SClA/Scl1, and SClB/Scl2 to attach to host fibronectin, collagen, M proteins, surface CD molecules, laminin, and glycoproteins. *Streptococcus agalactiae* uses ScpB Lmb and alpha C protein to attach to host fibronectin and laminin. *Streptococcus pneumoniae* uses SpsA/CbpA/PspC, phosphorylcholine, and PavA to attach to PAF receptor, sIgA, and fibronectin. *Staphylococcus* species and *Listeria monocytogenes* have similar lists of adhesions to attach to host molecules found on mucosal surfaces, skin, and wounds.

Gram-negative bacteria also use non-fimbrial adhesins to attach to a wide variety of host surfaces. Tir (translocated intimin receptor) is the cellular receptor for enteropathogenic *E. coli* and enterohemorrhagic *E. coli*. Tir, injected via a Type III secretion system into host cells, inserts into the host cell membrane where it functions as a receptor for the outer membrane protein intimin. Invasin of *Yersinia* species binds with high affinity to the β1 chain integrin family; internalin of *Listeria monocytogenes* binds E-cadherin initiating events leading to cellular entry; hemagglutinin B of *P. gingivalis* binds to human coronary artery endothelial cells; and pertactin of *Bordetella pertussis* binds to ciliated cells of the upper respiratory tract.

Flagella

Bacterial flagella vary in structure, number, and arrangement among bacterial species. Flagella are present only at one pole of the bacterial cell (monotrichous, lophotrichous), present at both poles (amphitrichous), or distributed over the entire bacterium (peritrichous). In *Vibrio* species and *Helicobacter* species, a sheath covers the extracellular flagella. *Treponema* species and *Borrelia* species have flagella in the periplasmic space. Spirochetes have flagella, called endoflagella or periplasmic flagella, also in the periplasmic space.

Bacterial flagella are motility organelles. They rotate and the patterns of motility depend upon the direction of rotation and the handedness of the helical filament. Counterclockwise rotation of the flagella bundle causes the helical waveform to travel outward from the cell generating a directed, pushing motion. Clockwise rotation unravels the bundle and results in a more chaotic, nondirected tumbling motion.[49]

Flagella have an intricate structure composed of a basal body, a flagellar motor, a switch, a hook, a filament, capping proteins, junction proteins, and an export apparatus.[49] The basal body contains rings that traverse the inner membrane (MS ring), periplasmic space (P ring and rod), and the outer membrane (L ring). The stator component of the flagellar motor is attached to the peptidoglycan layer and is made from 2 proteins, MotA and MotB. The rotor component of the flagellar motor is made of PliG protein attached to the MS ring.

Activation of motility is under the control of the chemotactic sensory complex containing transmembrane proteins coupled with a cytoplasmic sensing domain and cytoplasmic signaling domain.[48] Activation involves switch proteins FliG, FliM, and FliN. FliG fuses with the MS ring protein FliF inducing torque and FliM and FliN form the cytoplasmic ring C. Attached is the hook, which functions as a universal joint and the flagellar filament. The filament is helical in shape, acting as an Archimedes screw to propel the bacterium. The filament contains 11 fibrils that form the cylinder. The flagellar filament consists of self-assembling subunits of **flagellin** monomers arranged in a helix and forming a hollow tube that assumes a macrohelical or corkscrew form.[59] There are Cap proteins at the tip of the filament. Flagella on organisms like *P. aeruginosa* and *Helicobacter pylori* are glycosylated.

Salmonella flagellin is a microbial target of the innate and adaptive immune system. It activates toll-like receptor 5 (TLR5), induces a proinflammatory response, and activates dendritic cells.[60] Flagellin is recognized by antibody and CD4 T cell responses during *Salmonella* infection.

Bacterial flagella are also organelles for secretion of virulence factors. The flagellar assembly pathway is related to the type III protein secretion pathway for translocation of bacterial virulence proteins into host cells.

Capsules

Capsules on the surfaces of many pathogenic and nonpathogenic bacteria are composed of complex glycans. They occur as microcapsules, large capsules (*E. coli*), or slimy amorphous capsules, **slime layers**, of complex chemical and antigenic structure (e.g., alginate containing capsules of *P. aeruginosa*). Capsules contain homopolymers or heteropolymers of single monosaccharides joined by glycosidic linkages. Variations in polymer branching or substitution of organic acetyl groups or inorganic phosphate groups adds to capsule diversity and complexity.[61] Capsules protect bacteria from the harmful effects of desiccation, mediate adhesion to biotic and abiotic surfaces, and confer resistance to innate and adaptive host immunity.[61] They allow some bacteria to attach to mucosal or tissue surfaces, inhibit phagocytosis, and resist antibody and complement killing. The glycocalyces on *Klebsiella*

Vet-ebooks.com

pneumoniae and *Enterococcus faecalis* biofilms are seen using polycationic dyes but the morphology varies depending upon the type of dye used.[62]

As a matrix, capsules contain a high proportion of water. If capsules are not properly stabilized using antibodies, ferritin, or lectins prior to dehydration for transmission electron microscopy, they collapse into blebs on the cell surface causing morphologic artifacts. Ultrastructural analysis with transmission electron microscopy together with freeze-fracture, freeze-etch, and immunolabeling techniques show that bacterial capsular polysaccharides appear as electron-dense fibers that radiate outward perpendicular to the cell surface.[63] Atomic force microscopy shows that bacterial polysaccharide strands, like that from the anionic heteropolysaccharide acetan of *Acetobacter xylinum*, are 2–10 nm wide. They align in a periodic helical structure that is characteristic of acetin, a cellulosic backbone substituted on every second glucose residue with a pentasaccharide side chain.[64]

The extracellular matrix of biofilms can contain the polysaccharides of several bacterial species simultaneously. In biofilms, the extracellular polymers produced by different organisms are seen using lectin or antibody-based marker systems prior to electron microscopy.[65] On an ultrastructural level, *Streptococcus sobrinus*, *Streptococcus oralis*, *Veillonella dispar*, *Fusobacterium nucleatum*, *Actinomyces naeslundii*, and *Candida albicans* are distinguished. Fibrillar polysaccharides are evident around microcolonies of *S. sobrinus*, and fluffy polysaccharides are detected near S. *oralis* microcolonies.[66]

The diversity of capsular polysaccharides is vast. For example, *E. coli* has more than 80 different capsular types and *Streptococcus pneumoniae* has over 90 different capsular types. In other bacteria, the diversity is less; for example, *Haemophilus influenzae* has six different capsular types. Capsule gene clusters in *E. coli* are considered as the paradigm for capsule gene clusters in gram-negative bacteria.[15,61] Genes cluster at a single locus and each of the four capsule groups is represented in *E. coli.* Capsules in Group 1, represented by *E. coli* K30, are similar to capsules in *Klebsiella* and *Erwinia*. Capsules in Group 2, represented by *E. coli* K1 and K5, are similar to alpha 2, 8-linked N-acetylneuraminic acid Group B capsules in *Neisseria meningitidis* and glucuronic acid linked N-acetylglucosamine capsules in *Pasteurella multocida* type D, respectively. Capsules in Group 3, represented by *E. coli* K10 and K54, are similar to capsules in *Neisseria* and *Haemophilus*. Capsules in Group 4, represented by *E. coli* K40 and 0111, are similar to capsules of many genera. Using lectin-gold labeling and negative staining, *E. coli* exopolysaccharide filaments, lipooligosaccharide, and colanic acid all serve as lectin-binding epitopes at the cell surface.[67]

Capsules on some gram-positive bacteria are composed of protein polymers like poly-gamma-glutamate.[68] In *Bacillus anthracis*, a poly-gamma-D-glutamic acid capsule confers anti-phagocytic properties and is essential for virulence.

Bacterial Cell Cytoplasm

The **cytoplasm** is rich in enzymes, especially those concerned in glycolysis of carbohydrates. Cytochromes, ferredoxins, and flavodoxins are also found in the cytoplasm. Components in the cytoplasm, when resolved by two-dimensional gels and identified by MALDI-TOF PMF and/or microLC-ESI-IT-MS/MS, have a large diversity of expression products corresponding to more than 458 different genes.[69] These include proteins and enzymes involved in carbohydrate, fatty acid, amino acid and nucleotide metabolism, replication, transcription, translation, cell wall synthesis, nutrient transport proteins affecting sugar import, and exopolysaccharide biosynthesis.

The cytoplasm of the bacterial cell also contains large numbers of dense, closely packed **ribosomes**, the sites of DNA translation. Ribosomes are nucleoproteins of definite size (210 angstroms), shape, and density. They sediment at 70S and contain two 30S and 50S subunits.[70] The 70S particle contains two-thirds RNA and one-third protein. The 30S subunit contains 16S rRNA and 21 ribosomal proteins; initiates the interaction of the ribosome with mRNA during translation; and decodes the message. The 50S subunit contains 23S rRNA, 5S rRNA, and 33 ribosomal proteins; serves as the site for peptide bond formation; and allows for passage of formed peptides into the cytoplasm. 70S ribosome architecture is derived from x-ray crystallographic and cryo-electron microscopic analysis and shows the relatedness of the subunits at the 50S/30S interface.[71] Recently, cryoscanning transmission electron microscopy has mapped the *E. coli* signal recognition particle; a structure important for binding between the ribosome and the signal sequence on the nascent polypeptide chain emerging from the ribosome.[72]

Protein enzymes and toxins are produced on ribosomes and pass through the inner and outer membranes to be secreted from the bacterial cell (Table 14.2). These include enzymes that destroy proteins (proteases), carbohydrates (glycohydrolases), nucleic acid (nucleases), connective tissue (hyaluronidase and collagenase), fibrin (streptokinase and staphylokinase), neuraminic acid (neuraminidase), and lipids and phospholipids (lipases, lecithinases, and phospholipases).

Extracellular bacterial proteins and protein toxins are classified into **exotoxins**, **membrane-acting toxins**

Vet-ebooks.com

Table 14.2 Bacterial virulence factors.

Bacterial species	*Virulence factors*	*Reference to ultrastructural pathology*
Pseudomonas species	**Fimbrial adhesins, nonfimbrial adhesins** (capsule and alginate slime), **enzymes** (elastase, alkaline protease, phospholipase, lecithinase), **toxins** (Exoenzyme S, Exotoxin A, lipopolysaccharide, leukocidin), and **other factors** (flagella, siderophores, and a siderophore uptake system)	**Farinha**, *Infect Immun* 62:4118, 1994; **FitzGerald**, *J Clin Invest* 74:966, 1984; **Hazlett**, *Scan Electron Microsc* Pt 3:1379, 1984; **Kadurugamuwa**, *J Bacteriol* 177:3998, 1995; **Klinger**, *Infect Immun* 43:912, 1984; **Paranchych**, *Clin Invest Med* 9:113, 1986; **Parkins**, *Mol Microbiol* 40:1215, 2001; **Plotkowski**, *Infect Immun* 62:5456, 1994; **Sobel**, *J Urol* 128:414, 1982; **Tummier**, *Infection* 15:311, 1987; **Valente**, *Microb Pathog* 29:345, 2000; **Woods**, *J Med Microbiol* 26:133, 1988
Streptococcal species	**Fimbrial adhesins**, **nonfimbrial adhesins** (capsule, secreted fibronectin binding protein, muramidase-released protein and extracellular protein factor), **enzymes** (fibrinolysin and streptokinase-like activity, hyaluronidase, proteases, streptokinase, superoxide dismutase), **toxins** (hemolysin and pyrogenic exotoxins), and **other factors** (bacteriocins, CAMP-factor, M-like protein)	**Almeida**, *Zentralbl Veterinarmed B* 40:707, 1993; **Bolotin**, *FEMS Immunol Med Microbiol* 50:366, 2007; **Charland**, *FEMS Immunol Med Microbiol* 14:195, 1996; **Fujita**, *Oral Microbiol Immunol* 22:289, 2007; **Hament**, *Pediatr Res* 55:872, 2004; **Jedrzejas**, *Front Biosci* 9:891, 2004; **Lalonde**, *Microbiol* 146:1913, 2000; **Lamy**, *Mol Microbiol* 54:1250, 2004; **Laur**, *Science* 309:105, 2005; **Mammerschmidt**, *Infect Immun* 73:4653, 2005; **Manetti**, *Mol Microbiol* 64:968, 2007; **Nizet**, *Adv Exp Med Biol* 418:627, 1997; **Rubins**, *Infect Immun* 61:1352, 1993; **Schubert**, *Infect Immun* 72:6197, 2004; **Segura**, *Frontiers in Biosci* 9:1157, 2004; **Sellin**, *Microb Pathog* 18:401, 1995; **Stinson**, *Infect Immun* 71:2365, 2003; **Vanier**, *Infect Immun* 72;1441, 2004; **Vanrobaeys**, *Microbiol* 145:335, 1999; **Wessels**, *PNAS* 86:8983, 1989
Porphyromonas species	**Fimbrial adhesins** (FimA)**, nonfimbrial adhesins** (hemagglutinins), **enzymes** (gingipains), **toxins** (lipopolysaccharide), **other factors** (capsular polysaccharide)	**Amorncha**t, *J Int Acad Periodontol* 5:98, 2003; **Andrian**, *Infect Immun* 72;4689, 2004; **Dorn**, *FEMS Microbiol Lett* 187:139, 2000; **Dorn**, *Infect Immun* 69:5698, 2001; **Dorn**, *Int Endod J* 35:366, 2002; **Du**, *Infect Immun* 65:3875, 1997; **Haapasalo**, *Scand J Dent Res* 97:355, 1989; **Hongo**, *J Periodontal Res* 42:114, 2007; **Kato**, *FEMS Microbiol Lett* 273:96, 2007; **Lamont**, *Infect Immun* 63:3878, 1995; **Njoroge**, *Infect Immun* 65:1980, 1997; **Noiri**, *J Dent Res* 83:941, 2004; **Sandros**, *J Periodontal Res* 28:219, 1993; **Sundqvist**, *Scand J Dent Res* 99:117, 1991; **Takii**, *Infect Immun* 73:883, 2005; **Tokuda**, *Infect Immun* 66:1159, 1998; **Yuan**, *FEMS Immunol Med Microbiol* 51:388, 2007
Staphylococcal species	**Fimbrial adhesins** (pili-like structures), **nonfimbrial adhesins** (ClfA, ClfB, FnbA, FnbB, IsdA, SdrC, SdrD, and SdrE bind to fibronectin and fibrogen; fibrinogen binding protein Efb; and protein A Spa), **enzymes** (hyaluronidase HysA; lipases Geh and Lip; nucleases Nuc; and coagulase Coa), **toxins** (hemolysins Hla, Hld, and HlgA-C; leukocidins and leukotoxins LukD, LukE, LukF, and LukS; exotoxins SEA to SEG; exfoliative toxin Eta and Etb; and toxic shock syndrome toxin TSST-1), **other factors** (capsular polysaccharide biosynthesis protein CapA-P; surface proteins for clumping factor ClfA and ClfB; proteins BlaZ and MecA encoding methicillin resistance; and protein VanA encoding vancomycin resistance)	**Abus**, *Infect Immun* 59:1008, 1991; **Aleida**, *Microb Pathog* 31:205, 2001; **Braga**, *J Chemother* 15:543:2003; **Bronner**, *FEMS Microbiol Rev* 28:183, 2004; **Brouillette**, *Microb Pathog* 35:159, 2003; **Burriel**, *New Microbiol* 21:49, 1998; **Evans**, *Clin Orthop Relat Res* 347:243, 1998; **Fujita**, *Urol Res* 20:399, 1992; **Gatermann**, *Zentralbl Bakteriol* 278:258, 1993; **Guzel**, *Neuro Endocrinol Lett* 28:52, 2007; **Kamaras**, *Pathology* 33:197, 2001; **Katsuyama**, *J Dermatol Sci* 38:197, 2005; **Mani**, *Infect Immun* 62:1506, 1994; **Massey**, *Infect Immun* 70:5339, 2002; **Mempel**, *Br J Dermatol* 146:943, 2002; **Merkel**, *Med Microbiol Immunol* 189:217, 2001; **Nayak**, *Indian J Med Res* 125:767,2007; **Olofsson**, *J Ultrastruct Mol Struct Res* 100:194, 1988; **Rollof**, *Eur J Clin Microbiol Infect Dis* 7:505, 1988; **Rupp**, *Infect Immun* 67:2627, 1999; **Schmitt**, *Arch Surg* 121:89, 1986; **Stoitsova**, *Folia Microbiol* (Praha) 45:359, 2000; **Tucker**, *FEMS Microbiol Lett* 186:151, 2000; **Yun**, *Laryngoscope* 109:2021, 1999

Vet-ebooks.com

(e.g., pore-forming toxins, heat-stable enterotoxins, and superantigens), and **Type III secreted cytotoxins**.[73] Genes encoding exotoxins are located on the bacterial chromosome (exotoxin A of *P. aeruginosa*), a bacteriophage (diphtheria toxin and cholera toxin), or a plasmid (heat-labile enterotoxin of *E. coli*) and are secreted as soluble proteins, where they enter eucaryotic cells through a receptor mediated process.[73] They generally have an AB structure. The A subunit comprises the catalytic domain and the B subunit comprises the receptor-binding domain.

Pore-forming toxins lack a catalytic A domain and only form lethal ion-conduction channels in eucaryotic membranes. These are the alpha toxin of *S. aureus*,[74] the aerolysin of *Aeromonas hydrophila*,[75] and RTX hemolysins of *E. coli*, *Mannheimia haemolytica*, and *Actinobacillus pleuropneumoniae*.[76–78] The heat-stable *E. coli* enterotoxin binds to susceptible cells and stimulates a signal cascade, which increases the guanylate cyclase activity inside the cell.[73] Superantigens of *S. pyrogenes* and *S. aureus* bind to the major histocompatibility complex on T lymphocytes.[73]

Yersinia species, *Shigella* species, *Bordetella* species, *Salmonella* species, *P. aeruginosa*, and *E. coli* all produce Type III secreted cytotoxins. They are delivered directly into eucaryotic cells via the Type III secretion system where they have various catalytic activities. The ExoS of *P. aeruginosa* is an ADP-ribosyltransferase; the ExoS of *P. aeruginosa* is a GTPase activating protein for Rho GTPase; the ExoY of *P. aeruginosa* is an adenylate cyclase; the SopE of *Salmonella* is a guanine nucleotide exchange factor; and the YopH of *Yersinia* is a protein phosphatase.[73]

Protein Enzyme and Toxin Secretion Systems

Secretion systems play a central role in bacterial-host interactions. These include proteins secreted by the signal sequence independent Type I pathway, the two-step Type II pathway, the contact-dependent "injectisome" Type III pathway, the protein and nucleoprotein Type IV pathway, the autotransporter Type V pathway, the Type VI pathway, and the Type VII pathway.[79–82]

Type I secretion systems of gram-negative bacteria are multidrug efflux pumps. In *E. coli*, the TolC protein forms an alpha-helical trans-periplasmic cylinder embedded in the outer membrane by a contiguous beta-barrel for toxin export and drug efflux to the outside environment.[83] TolC-like outer membrane proteins help to export hemophores from *Serratia marcescens*, RTX FrpC toxin from *Neisseria meningitidis*, alpha-hemolysin from *Escherichia coli*, and leukotoxin (LtxA) from *Aggregatibacter actinomycetemcomitans*.

Type II secretion systems are also widely distributed among bacteria and mediate the secretion of many toxins and degradative enzymes into the surrounding environment. The system is composed of at least 12 proteins. *Yersinia enterocolitica* uses a gene cluster designated Yts1; *Pseudomonas aeruginosa* uses an Xcp secretion to secrete elastase, lipase, phospholipase, and exotoxin A; and *Vibrio cholerae* uses this pathway to secrete cholera toxin, hemagglutinin-protease, and chitinase.

Type III secretion systems deliver protein effectors directly into the cytoplasm of the host cell. *Yersinia* species, *Salmonella* species, *Shigella* species, and enteropathogenic *E. coli* all use Type III secretion systems to modify guanosine triphosphate binding proteins, mitogen-activated protein kinases, nuclear factor-kappa B, and phosphoinositides to downregulate or promote proinflammatory responses, induce apoptosis, prevent autophagy, or to modulate intracellular trafficking.[80]

Type IV secretion systems are widely distributed among gram-negative and gram-positive bacteria and are ancestrally related to bacterial conjugation to translocate protein molecules from one bacterium to another or from one bacterium to a host cell.[79] The components appear to be homologous in sequence and structure to those of conjugative transfer systems (**sex pili**) of naturally occurring plasmids. The VirB/D4 transfer system of *Agrobacterium tumefaciens*, the pertussis toxin system of *B. pertussis*, and the dot/Icm system of *Legionella pneumophila* are good examples.

Type V secretion systems use the autotransporter system (Type Va or AT-1), the two-partner secretion pathway (Type Vb), and the Type Vc (AT-2) systems.[79] AlpA of *H. pylori*, SphBi of *B. pertussis*, and Aspa/Nalp of *N. meningitidis* are autotransporter proteins.

Type VI secretion systems resemble components of Type IV systems. These genes, called "VAS" (virulence-associated secretion), are required for cytotoxicity of *Vibrio cholerae* via hemolysin-coregulated protein and VgrG for amoebae and mammalian macrophages by a contact-dependent mechanism. Type VI secretion systems also occur in *Edwardsiella tarda* and *Burkholderia mallei*.[84]

A new **Type VII secretion system** is proposed for a mycobacterial secretion system to transport extracellular proteins across their hydrophobic, and highly impermeable, cell walls. Here mycobacterial genomes encode up to five of these transport systems. Two of these systems, ESX-1 and ESX-5, are involved in virulence and both affect the cell to cell migration of pathogenic mycobacteria.[85]

Prokaryotes contain a wide variety of **inclusions and microcompartments** of varying shapes and compositions.[86]

- **Volutin granules** are intracellular organelles in *Corynebacterium diphtheriae*, *C. xerosis*, and *C. glu-*

Vet-ebooks.com

tamicum for storing inorganic polyphosphate. Polyphosphate has a vital role in the stress response and stationary-phase adaptation.[87] Polyphosphate granules stained with toluidine blue or Neisser stains are called metachromatic granules and have diagnostic value for confirming the identity of *C. diphtheriae* in clinical specimens.

- **Poly (3-hydroxybutyrate) granules** or PHB are a class of bacterial storage products within the poly (3-hydroxyalkanoates). PHBs are osmotic neutral reservoirs of carbon and energy and are synthesized when more carbon sources are available than can be used by the bacteria.[88] Granules, 0.2–0.5 μm in size, are synthesized close to the cell membrane of *Ralstonia eutropha, Caryophanon latum,* and *Beijerinckia indica*.
- **Polyhedral bodies** include the carboxysomes, 1,2-propanediol (1,2-PD) utilization organelles, and the B_{12}-dependent ethanolamine degradation organelles.[89] Polyhedral bodies are large (100–150 nm) macromolecular complexes containing enzymes within a 3–4 nm protein shell.[90] Carboxysomes contain ribulose bisphosphate carboxylase/oxygenase (RuBisCO) and are found in chemoautotrophic bacteria. RuBisCO catalyzes the carboxylation of ribulose bisphosphate to two molecules of 3-phosphoglycerate, thus improving carbon fixation via the Calvin cycle at low CO_2 concentrations. 1,2-PD is a major product of the fermentation of rhamnose and fucose commonly found in plant cell walls, bacterial capsules, and glycoconjugates of eukaryotic cells. 1,2-PD utilization organelles are used by *Salmonella*, *Klebsiella*, *Shigella*, *Yersinia*, and *Escherichia* species to support the coenzyme B_{12}-dependent degradation of 1,2-PD as a carbon and energy source. B_{12}-dependent ethanolamine degradation organelles concentrate metabolic enzymes. Their substrates are used by *Salmonella enterica* to enhance and optimize ethanolamine and 1,2-PD degradation by multiple mechanisms.
- **Glycogen granules** occur in *Chromatium* species and granules are seen in the bacterial cells harvested at different stages of growth.[91]
- **Magnetosomes** are magnetic crystals 30–50 nm in size found in the α-Proteobacteria, δ-Proteobacteria, γ-Proteobacteria, and *Nitrospira* species.[92] They contain iron oxide magnetite (Fe_3O_4), or iron sulfide greigite (Fe_3S_4), surrounded by a lipid bilayer and held in long chains by an intracellular cytoskeleton. Magnetosomes align these organisms in magnetic fields as they move along oxygen or redox gradients to search for optimum microaerophilic environments in a process called magneto-aerotaxis. Thin connections between magnetosome chains may transfer the torque from the magnetosome during the orientation of magnetotactic bacteria to magnetic field lines.[93]
- Magnetotactic bacteria may also have **phosphorus-containing granules**, **sulfur globules**, or **poly 3-hydroxyalkanoates** inclusions. In uncultured magnetotactic bacteria there are two types of granules. Phosphorus-containing granules contain primarily P, O, and Mg. Phosphorus-sulfur-iron granules contain P, O, S, Na, Mg, Ca, and Fe.[94]
- **Crystalline protein inclusions** are produced by *Bacillus thuringiensis*. They contain proteins (delta-endotoxin) with insecticidal or nematocidal properties.[95] Ingestion of the inclusions by insect larvae leads to protoxin solubilization and conversion to toxins that form cation-selective channels in the membrane of cells lining the larval midgut with subsequent lethality.[96] Apatite crystals are also found.
- **Cellulosomes** of *Clostridium thermocellum* are huge extracellular multipolypeptide bacterial enzyme complexes engaged in degradation of cellulose. Ultrastructurally, they are spherical with multiple fibrillar structures, likely the fibrillar protein Cip A ("scaffoldin"). This architecture allows the catalytic domains of the enzymatic subunits to be exposed to the environment, to the substrate, and to the cellulose fibrils.[97]
- **Miscellaneous inclusions** consist of **R Bodies** of highly insoluble protein ribbons in bacteria that are obligate endosymbionts of protozoa;[98] **protein crystalloids** that are laminar arrangements of peptide chains; **gas vacuoles** in cyanobacteria organized into ribs 5 nm wide;[99,100] **lipid globules** produced in *Mycobacterium* species; and inclusions in *P. multocida* grown in vivo.[101]

Iron Inclusions

Bacteria require iron for metabolism and more than 100 metabolic enzymes utilize iron-containing cofactors.[102] In host environments, iron is sequestered as Fe(III) by families of iron-binding proteins: ferritin, hemosiderin, hemoglobin, transferrin, lactoferrin, and ovotransferrin. In inflamed tissues, iron also exists in **hemin**, which is present in hemoglobin, myoglobin, hemopexin and cytochromes.

Effective pathogens procure and take up iron from complex host environments using **hemophore** and **siderophore** systems.[103] Low iron concentrations induce planktonic forms and motility, both in *P. aeruginosa* and *B. cenocepacia*, while high iron concentrations stimulate aggregation and biofilm formation.[104] Siderophores are iron-chelating compounds produced by bacteria to acquire iron from the Fe(III)-

Vet-ebooks.com

glycoprotein complex and deliver it to the bacterial cell. Siderophore-dependent iron acquisition systems include catecholate, phenolate, hydroxamate, and carboxylate systems and multiple catecholate-hydroxamate, phenolate-hydroxamate, citrate-catecholate, and citrate-hydroxamate systems. Once iron is captured by a siderophore system, it is then available for uptake at the bacterial cell surface. Iron can be released from the siderophore and taken up as free iron across the membrane, or the whole Fe(III)–siderophore complex can be taken up.[102] In some cases, receptors for human transferrin have been localized by immunogold labeling on bacterial surfaces.[105] **Hemin storage** in the bacterial cell, although rare in prokaryotes, has been reported in *Escherichia*, *Pseudomonas*, and *Yersinia* species.[106]

Membranous Inclusions

Internal membranes form in prokaryotic cells and are connected to the plasma membrane. **Mesosomes** may be small and single (vesicular mesosomes) or large and complex (lamellar mesosomes) (Fig. 14.5). Mesosomes, infoldings into the cytoplasm of the plasma membrane, occur in microbial cells exposed to host-derived antimicrobial peptides. Transmission electron microscopy of *S. aureus* and *Staphylococcus epidermidis* treated with a derivative of indolicidin, CP10A, developed mesosome-like structures in the cytoplasm.[107] Whether mesosomes have a role in resistance is yet to be determined.

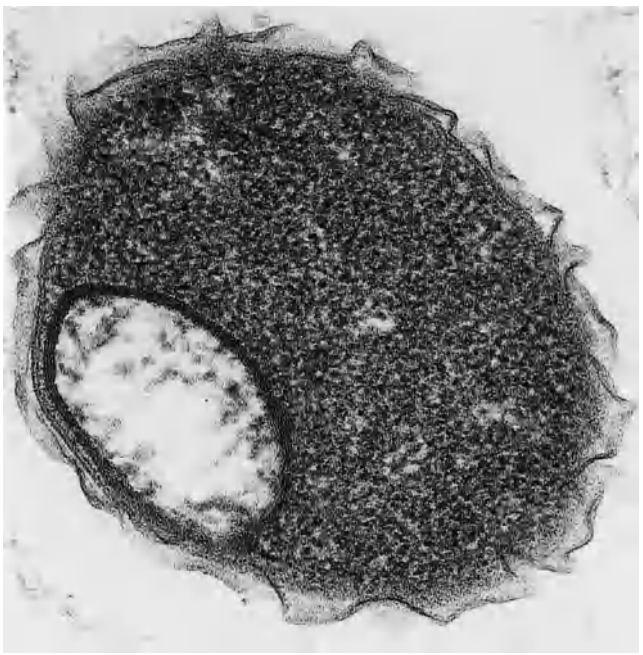


Fig. 14.5 Gram-negative bacterium with a large mesosome.

Nucleoid

Prokaryotic genomes are on a single, closed, circular chromosome and vary greatly in size. The size of *Eubacteria* genomes range from 0.6 Mbp to over 10 Mbp. The size of Archaea genomes range from 0.5 Mbp to 5.8 Mbp. Genomic DNA in bacterial cells is located in one or two compact phase-like regions near the center of the cell in a ribosome-free region referred to as the **nucleoid**. There is no nuclear membrane. In actively growing bacteria, the nucleoid is dispersed and "coralline" in appearance.[108] The nucleoid becomes confined when growth ceases. The fern-like arrangements formed by branches of mRNA and transcribing genes, which are naked in eukaryotes, are studded with ribosomes in prokaryotes. In contrast, the genome of *Borrelia* is on a linear chromosome. The genome is small (approximately 1 Mbp) and has a 30% G+C ratio. Many plasmids in *Borrelia* are also linear.

The ultrastructure of the nucleoid is dependent upon the treatment of the microbial cell and the methods of cell fixation and dehydration.[109] Earlier ultrastructural studies revealed the chromosome to contain tiny fibrils of aggregated DNA. These fibrils are 2–5 nm and are removed by digestion with DNAase; they represent DNA molecules that are artifactually condensed by osmium or glutaraldehyde fixation and are not found after freeze substitution techniques.[31,110] The chromosome is folded with marked negative supercoiling; that is, partial untwisting of the double helix, a state that is reflected in the physical properties of DNA.

Electron microscopy using the chromatin spread technique revealed sites of transcribing RNA polymerases and characteristic replication forks. Polymerase-transcript complexes appeared as electron-dense particles at the base on ribonucleoprotein fibrils being released from a central strand of chromatin. The density with which a transcription unit is loaded with RNA polymerases is a measure of the frequency with which it is transcribed.[111] Active genes such as rRNA genes (the most easily recognized in chromatin spread) have little space between RNA polymerases, whereas less active genes have more widely spaced RNA polymerases (Fig. 14.6).

A nucleoprotein structure, the **invertasome**, is formed by a regulatory recombinase protein and the DNA sequences bound by each protein. Such an example is the protein that binds to recombination sites and catalyzes a site-specific DNA inversion reaction expressing genes for flagellin in *Salmonella* species.[112] DNA resolvases and invertases are closely related, yet catalyze recombination within two distinct nucleoprotein structures termed **synaptosomes** and **invertasomes**, respectively.[113]

Vet-ebooks.com

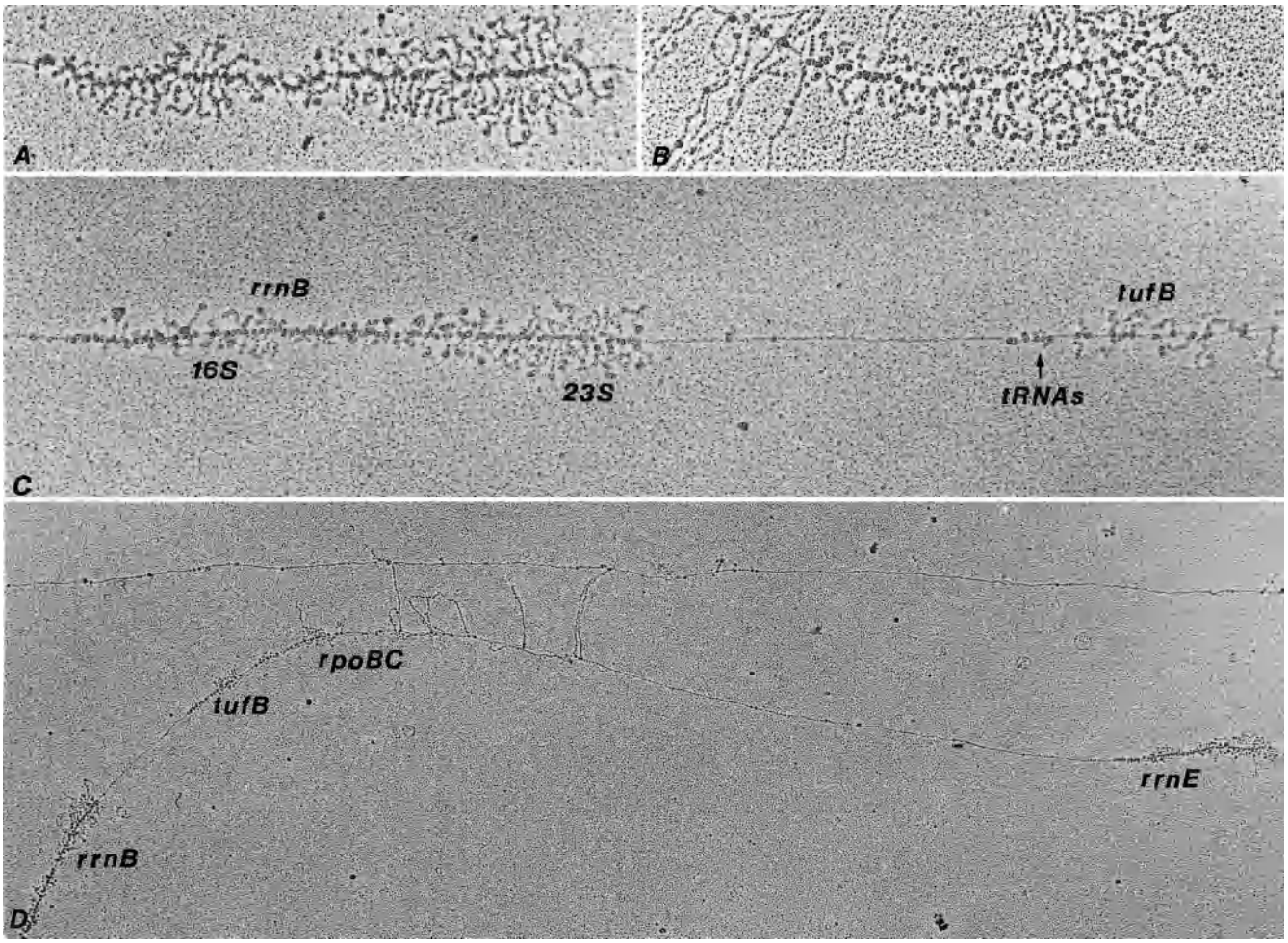


Fig. 14.6 Chromosome spreads from *E. coli*. Bacterial chromosomes are unfolded so that RNA polymerases with their transcripts remain attached to DNA templates. Transcription units (rRNA operons) are packed with RNA polymerases. **A**. **An rRNA operon**: RNAase III cleavage of transcripts between 16S and 23S cistrons gives rise to Christmas tree morphology. **B**. **An rRNA operon from an RNAase mutant strain:** operon has not been cleaved. **C** and **D**. **The *rrnB* region** on the *E. coli* genome, the most easily recognized in chromosome spreads. **C**. **The *tufB* operon**: four kilobases downstream from rrnB is the tufB operon, where four tRNAs and the gene for elongation factor are transcribed from a single promoter. **D**. **The *rpoBC* operon** (downstream of *tufB)* consists of four ribosomal protein genes followed by genes for β subunits of RNA polymerase. (Micrographs: Sarah French, *ASM News* 59:437, 1993.)

Plasmid structure has been well documented by electron microscopy and atomic force microscopy. The contour lengths of relaxed, linear plasmid strands support the helical rise (3.4 A/bp) of B-DNA in solution.[114] Plasmids can be physically cut by the scanning tip atomic force microscope and small pieces of DNA (100–150 nm in length) excised and deposited adjacent to the dissected plasmid, demonstrating that it is possible to remove and manipulate genomic DNA fragments, unresolvable by light microscopy, from defined chromosomal locations by atomic force microscopy.[115]

Pathogenicity islands contain virulence genes for hemolysins, fimbriae, hemin-binding factors and Type III secretion systems.[116] For example, *Salmonella* contains gene clusters encoding two Type III secretion systems, *sifA* (required for formation of distinctive structures associated with *Salmonella*-containing vacuoles within epithelial cells), and two groups of genes that are activated by the PhoP/PhoQ two-component regulator.[117,118] *Yersinia pestis* contains hemin storage genes, the *Yersinia* bactin receptor[119] and iron-regulated protein genes.[120] *Helicobacter pylorus* contains a pathogenicity island of approximately 40 kb of DNA that encodes Type I-specific and disease-associated factors.

Replication

Cell division in eubacteria involves the synthesis of new peptidoglycan in the cell wall during both elongation of rods (e.g., in *Bacillus subtilis, E. coli,* and *Corynebacterium diphtheriae*) and division planes (e.g., in *S.*

Vet-ebooks.com

aureus, B. subtilis, E. coli, C. diphtheriae).[11] In cocci, the peptidoglycan in the septum becomes a hemisphere in each daughter. In rods, new peptidoglycan is inserted at the division site and along the cellular sidewalls during cell elongation. No new peptidoglycan is added to the pole regions.

Z-ring formation is paramount in cell division. It marks the future division site and is controlled by Min, nucleoid occlusion, and FtsZ accessory proteins.[121,122] A Z-ring, composed of polymerized tubulin-like protein FtsZ, forms at mid-cell preceding cell division. Membrane-associated division proteins are drawn to the ring forming a complex called the divisome. The divisome induces the cell envelope invaginations to form a division septum.[123] Cell division, chromosome and plasmid segregation, maintenance of cell shape, maintenance of cell polarity, and assembly of intracellular organelle-like structures are all maintained by FtsZ in combination with MreB and Mbl that act as internal scaffolds to influence cell shape and localize synthetic enzymes.[121,124,125]

Spore Formation

Bacterial spores are metabolic dormant cells encased in a heavy covering (Fig. 14.2A). Spores are highly resistant to desiccation, heat, radiation, and chemicals. They persist in the environment for very long, extended periods.

Spores are formed by gram-positive bacteria, *Bacillus* species, and *Clostridium* species. **Sporulation** is triggered by a lack of carbon, nitrogen, or phosphorus in the immediate environment.[126] Once initiated, sporulation in *Bacillus subtilis* takes about 7 hours at 37°C. Initiation signals activate the master transcription factor Spo0A, the asymmetric sporulation division and transcription, and the developmental regulators. Activation of Spor0A and σ^H in the pre-divisional cell leads to asymmetric division and a **septum** forms toward one end of the cell. Two distinct cells then begin to form: a smaller **prespore** (forespore) and the **larger mother cell**. Each cell produces sporulation-specific RNA polymerase σ factors; σ^F becomes active in the prespore and σ^E becomes active in the mother cell. After a short period, proteins produced in the mother cell degrade the septum and trigger migration of the membrane around the prespore, thus "engulfing it." When the membranes fuse, the prespore is released as a **protoplast** in the mother cell. Additional polymerase σ factors are produced by the prespore and the mother cell that activate the transcription of genes necessary to build the protective structural **cortex** on the surface of the spore.[126] Ultrastructural changes correlate with each of these successive stages.[127,128]

The field of microbial taxonomy is rapidly evolving, first, with the discovery of new microbial species and, second, with new genomic information available on existing microbial species. Microbial taxonomy is now a multidisciplinary field involving microbiology, population genetics, microbial ecology, mathematics, and computer science for descriptions of new taxa, emendation of current taxa, and proposals of taxonomic rearrangements. Up-to-date information can be obtained from the Approved Lists of Bacterial Names (www.bacterio.cict.fr); rRNA gene, protein, and genomic sequences (GenBank-EMBL-DDBJ); Microbiological Resource Center (www.wfcc.info); and the *International Journal of Systematic Bacteriology* (http://ijs.sgmjournals.org/) from the Society for General Microbiology.

Phylum Tenericutes, Order Mycoplasmatales

Genus *Mycoplasma*

Mycoplasmas are small microorganisms varying in size from 0.2 to 0.3 μm wide for *M. hominis* to 0.1–0.2 μm wide × 1.0–2.0 μm long for *M. pneumoniae* and *M. penetrans*. Their triple-layered membrane provides structural support. They do not have cell walls, membranous organelles, fimbriae or flagella. They are gram-negative, highly pleomorphic, and appear as coccoid or filamentous forms. With *M. pneumoniae*, a spindle shape predominates because of the drag of the gliding cells pulling on the membrane and internal cytoskeleton.

Mycoplasmal cell membranes range from 7.5 to 1.0 nm thick. They are covered with a layer of a glycoprotein called variable surface antigen (Vsa) 16 nm (R3 Vsa protein) to 26 nm (R40 Vsa protein) thick. Vsa constitutes approximately 10% of the cellular protein and has a 242 amino acid constant N-terminus region and a 10–19 amino acid variable C-terminus region. Vsa undergoes high-frequency phase and size variation. Cells with long Vsa molecules do not readily adhere but are more resistant to complement-mediated killing, whereas cells with short Vsa molecules more readily adhere but are more susceptible to complement-mediated killing. Cells with long Vsa molecules form free-floating biofilms, whereas cells with short Vsa molecules more readily form attached biofilms. Vsa and lipid vesicles, 50 nm in size, bleb from the cell surface and fuse with other mycoplasma cells to transfer nutrients, DNA, and other material between cells.

Mycoplasmas contain a novel cytoskeleton and a differentiated polar structure or terminal organelle. The cytoskeleton is associated with gliding motility, shape changes, terminal organelle, and cell division.[129,130] Terminal organelles are on many mycoplasma including *M. gallisepticum* and *M. pneumoniae*.

Vet-ebooks.com

Ultrastructurally, the terminal organelle is an electron-dense core seen in ultrathin sections by electron microscopy as two parallel rods 250–300 nm long oriented along the longitudinal axis and enlarging to form a terminal bulb at the distal end.[131] The membrane around the terminal organelles is studded with a high density of protein complexes.[132] In *M. pneumoniae*, the terminal organelle has a role in gliding motility, cytoadherence, and cell division.[133] *Mycoplasma mobile* has "spikes," that protrude from the cell membrane and attach to underlying surfaces. The spikes, visualized by rapid-freeze-and-freeze-fracture rotary-shadow electron microscopy, are 50 nm in length and 4 nm in diameter. They are abundant around the neck region of the cell, contain a 349-kDa protein, and are involved in binding or gliding activities.[134] The 349-kDa protein, examined by rotary shadowing electron microscopy, forms an oval foot 14 nm long in axis with three rods extending in tandem of 43, 20, and 20 nm.[135]

There are distinctive capsular polysaccharides around *M. mycoides* and an extracellular matrix of protein, lipid, and polysaccharide on *M. pulmonis* in biofilms. The latter is likely N-acetylglucosamine and alpha-linked galactose. The central nuclear region of the mycoplasma cell is surrounded by a peripheral cytoplasmic mantle (Fig. 14.7). Ribosomes, DNA fibers, chromosomal granular material and vacuoles characterize the cytoplasm. The genome is a single chromosome, a circular DNA molecule.



Fig. 14.7 Mycoplasmal pneumonia, pig. Mycoplasmas are enmeshed with cilia at the surface of bronchiolar epithelium. There is little cellular damage except for distortion of cilia and excessive length of microvilli. (Micrograph: W. Wegmann, *Zentralbl Veterinaermed* [B] 16:428, 1969.)

Mycoplasmosis

Most mycoplasma infections occur on mucosal surfaces (Table 14.3). Respiratory mycoplasma infections are typically transmitted by the aerosol route and genital infections are typically transmitted by contact of urogenital mucosa. However, extrapulmonary infections occur in about 25% of *M. pneumoniae* infections. *M. pneumoniae* has been cultured from blood, synovial fluid, pericardial fluid, cerebrospinal fluid and skin lesions.[133] *M. pneumoniae* can invade, persist and replicate in tissue culture cells, but *M. pneumoniae* cell invasion in vivo has not been shown. Mycoplasmas are seen in deep invaginations into the cell surface, which in cross section may appear to be cytoplasmic vacuoles. Ultrastructural changes in mycoplasmosis have been documented in the joint and conjunctivae. Cytopathology results from focal damage of the host cell plasma membrane. Mycoplasmas with opportunistic roles include *Mycoplasma penetrans* and *Mycoplasma amphoriforme*. *Mycoplasma penetrans* may be an opportunistic pathogen in persons with human immunodeficiency virus infection and AIDS and associated with chronic arthritic conditions. Here it attaches to host cells and triggers a signal that recruits tubulin, α-actinin, and other cytoskeletal components.[136] *Mycoplasma amphoriforme* also may be an opportunistic pathogen in patients with chronic bronchitis.

Respiratory Mycoplasmosis In the respiratory tract, infection of the nasal cavity and trachea depends upon the capacity of the mycoplasma to attach to and colonize respiratory epithelium. The initial interaction between mycoplasma, like *M. pneumoniae*, and host cells appears to occur when it encounters the tips of the beating cilia in the mucous layer. Attachment is typically to cilia and the binding event causes membrane-associated particles to redistribute on shafts of cilia. Cilia become distorted and broken and their basal bodies degenerate, but they may remain intact despite large numbers of associated mycoplasmas. Gliding motility then allows *M. pneumoniae* to traverse the mucus to bind cilia and migrate to the base of the cilia. Gliding motility then enables the mycoplasma to spread laterally on the epithelial surface to colonize ciliated and nonciliated epithelium and then on to colonize other extrapulmonary sites. Binding to

Vet-ebooks.com

Table 14.3 Order Mycoplasmatales, family Mycoplasmataceae: pathogenic species.

Pathogen	*Disease (host) and ultrastrucural studies*	*Reference to ultrastructural pathology*
	Genus *Mycoplasma*	
M. agalactiae	Mastitis in goats	**Rodriquez**, *J Vet Med B Infect Dis Vet Public Health* 49:226, 2002
M. amphoriforme	Chronic bronchitis in immunosuppressed humans	**Hatchel**, *Microbiology* 152:2181, 2006
M. bovigenitalium	Infertility in cattle	**Bielanski**, *Theriogenology* 53:1213, 2000
M. bovoculi	Conjunctivitis	**Salih**, *Am J Vet Res* 49:1661, 1988
M. dispar	Bronchiolitis in cattle	**Almeida**, *Zentralbl Veterinarmed B* 41:473, 1994
M. felis	Conjunctivitis and respiratory diseases in cats and studies in fibroblast cell cultures	**Boatman**, *J Bacteriol* 101:262, 1970; **Larsson**, *Acta Pathol Microbiol Scand [A]* 89:9, 1981
M. gallinarum	Frequently found in poultry	**Uppal**, *Res Vet Sci* 13:200, 1972; **Shah-Majid,** *Res Vet Sci* 61:176, 1996
M. gallisepticum	Chronic respiratory disease, air sacculitis, and infectious sinusitis in poultry	**Uppal**, *Res Vet Sci* 13:200, 1972; **Shimizu**, *Curr Microbiol* 44:431, 2002; **Uppal**, *Res Vet Sci* 13:200, 1972; **Rottem**, *J Bact* 149:338, 1982
M. hyopneumoniae	Enzootic pneumonia in pigs	**Baskerville**, *Res Vet Sci* 13:570, 1972; **Baskerville**, *Res Vet Sci* 14:155, 1973; **Livingston**, *Am J Vet Res* 33:2249, 1972; **Wegmann**, *Zentralbl Veterinaermed* 16:428, 1969; **Zielinksi**, *Am J Vet Res* 53:1119, 1992
M. hyorhinis	Respiratory infections in pigs	**Duncan**, *Am J Pathol* 57:171, 1969; **Johannsen**, *J Vet Med [A]* 38:321, 1991
M. hyosynoviae	Arthritis and conjunctivitis in pigs and studies in kidney cell cultures	**Imura S**, *Kobe J Med Sci* 29:1, 1983; **Rogers**, *J Am Vet Med Ass* 198:450, 1990
M. meleagridis	*A*irsacculitis in turkeys	**Uppal**, *Res Vet Sci* 13:200, 1972
M. mycoides	Pleuropneumonia in cattle	**Gourlay**, *J Gen Microbiol* 54:155, 1968
M. neurolyticum	Conjunctivitis and encephalitis in rats and mice	**Aleu**, *J Exp Med* 124:1083, 1983; **Thomas**, *Trans Assoc Am Physicians* 79:388, 1966; **Tully**, *J Bacteriol* 88:381, 1964
M. oxoniensis	Conjunctivitis in Chinese hamsters	**Hill**, *Int J Syst Bacteriol* 41:21, 1991
M. phocidae	Epizootic pneumonia in harbor seals	**Ruhnke**, *Int J Syst Bacteriol* 42:211, 1992
M. pneumoniae	Atypical pneumonia and CNS symptoms and studies in hamsters	**Carson**, *Science* 206:349, 1970; **Collier**, *Infect Immun* 3:694, 1971; **Collier**, *Proc Soc Exp Biol Med* 136:569, 1971; **Kohn**, *Infect Immun* 46:619, 1984; **Shimizu**, *Curr Microbiol* 44:431, 2002
M. pulmonis	Pneumonia in rats and mice	**Gay**, *J Bacteriol* 94:2048, 1967; **Kohn**, *Lab Anim Sci* 21:856, 1971; **Kohn**, *Infect Immun* 35:731, 1982; **McDonald**, *J Clin Invest* 87:787, 1991; **Organick**, *J Bacteriol* 92:1164, 1966; **Pinson**, *Lab Anim Sci* 38:143, 1988
M. synoviae	Infectious synovitis in poultry	**Walker**, *Vet Pathol* 15:407, 1978
	Genus *Ureaplasma*	
U. cani-genitalium, *U. cati*, *U. diversum*, *U. felineum*, and *U. gallorale*	Urethritis in dogs, oral infections in cats, pneumonia in cattle, and pharyngitis in birds	**Harasawa**, *Int J Syst Bacteriol* 46:827, 1996
U. urealyticum	Urethritis in humans and respiratory disease in newborns	**Audring**, *Andrologia* 21:66, 1989; **Rudd**, *Infect Immun* 57:918, 1989; **Harasawa**, *Int J Syst Bacteriol* 46:827, 1996

Vet-ebooks.com

Table 14.3 *Continued*

Pathogen	*Disease (host) and ultrastrucural studies*	*Reference to ultrastructural pathology*
	Genus *Haemobartonella*	
H. blarinae and *H. muris*	Infections and anemia in shrews, mice, and rats	**Tanaka**, *J Bacteriol* 90:1735, 1965; **Rikihisa**, *J Clin Microbiol* 35:823, 1997
H. bovis	Anemia in cattle	**Simpson**, *Am J Vet Res* 31:225, 1970; **Brocklesby,** *Vet Rec* 87:761, 1970
H. canis	Anemia in immunosuppressed and splenectomized dogs	**McKee**, *Am J Vet Res* 34:1196, 1973; **Venable**, *J Parasitol* 54:259, 1968
H. felis	Feline infectious anemia with pallid mucous membranes and tongue in cats	**Demaree**, *Am J Vet Res* 33:1303, 1972; **Jain**, *Am J Vet Res* 34:697, 1973; **Maede**, *Am J Vet Res* 40:691, 1979; **Simpson**, *J Parasitol* 64:504, 1978
	Genus *Eperythrozoon*	
E. coccoides, *E. varians*, and *E. dispar*	Chronic latent infections with anemia in mice and voles	**Glasgow**, *Infect Immun* 4:425, 1971
E. ovis	Anemia and splenomegaly in sheep	**McKee**, *Am J Vet Res* 34:1196, 1973; **Nicholls**, *Aust Vet J* 63:118, 1986; **Daddow**, *Aust Vet J* 55:433, 1979
E. parvum and *E. suis*	Acute ictero-anemia in pigs	**Splitter**, *Science* 111:513, 1950; **Pospischil**, *Vet Path* 19:651, 1982; **Wu**, *Ann N Y Acad Sci* 1081:280, 2006; **Guimaraes**, *Vet Rec* 160:50, 2007
E. wenyoni	Anemia in splenectomized cattle	**Sutton**, *New Zealand Vet J* 25:8, 1977
	Order Entomoplasmatales, Genus *Spiroplasma*	
S. mirum	Cataracts in mice	**Bastian**, *Am J Pathol* 114:496, 1984; **Steiner**, *Infect Immun* 35:296, 1982; **Zeigel**, *Infect Immun* 9:430, 1974

tracheal epithelium for *M. pneumoniae* involves the receptors bearing long-chain sialo-oligosaccharides with poly-N-acetyllactosamine backbones, which can be detected by immunogold techniques.[137]

Pathogenic mycoplasmas may descend into the lungs where they localize on the surface of epithelial cells of terminal bronchioles and considerably distort the cell surface. They are seen ultrastructurally, enmeshed in remnants of degenerate cilia.[138] Ballooning and blebbing of the plasma membrane of the respiratory epithelium is common. Diffuse hyperemia and edema of alveolar walls may progress to extensive pneumonitis. Monocytes and plasmablasts line the capillary walls and become distributed throughout the lung parenchyma.

Neurotoxicity Neurological illnesses are associated with *Mycoplasma* infections. *Mycoplasma neurolyticum* infection of rats and mice produces an ataxic syndrome called rolling disease. Brains have patchy areas of vacuolation and demyelination. The basic lesion consists of enormously distended astrocytes, which encroach upon neighboring cells, myelin sheaths and axons. The toxin binds to ganglioside receptors on capillary vascular walls at the level of connections with astrocyte foot processes. A heat-labile soluble toxin has been isolated from *M. neurolyticum* that causes vascular destruction in experimental models of brain disease in mice. Striking fibrinoid necrosis of arteries in brains of *M. gallisepticum*-infected turkeys is also indicative of neurotoxicity. Experimentally, large numbers of organisms injected intravenously produce this cerebral vascular damage but organisms cannot be detected in the lesion. Neurologic manifestations are among the most common nonpulmonary manifestations of *M. pneumoniae* infection and up to 7% of humans hospitalized with *M. pneumoniae* may have central nervous system symptoms. Mechanisms behind clinical manifestations is unclear, but direct invasion, neurotoxin production, or an immune-mediated mechanism have been proposed.[139,140]

Genus *Ureaplasma*

Ureaplasma (or T-strain mycoplasmas) require urea and cholesterol for growth and are associated with urethritis and prostatitis in males, genitourinary tract infections and reproductive failure in females, and systemic and respiratory infections in neonates.[141] Ultrastructurally, *Ureaplasma* are spherical or ovoid, 0.4–0.8 μm in size with a ruthenium red stained

Vet-ebooks.com

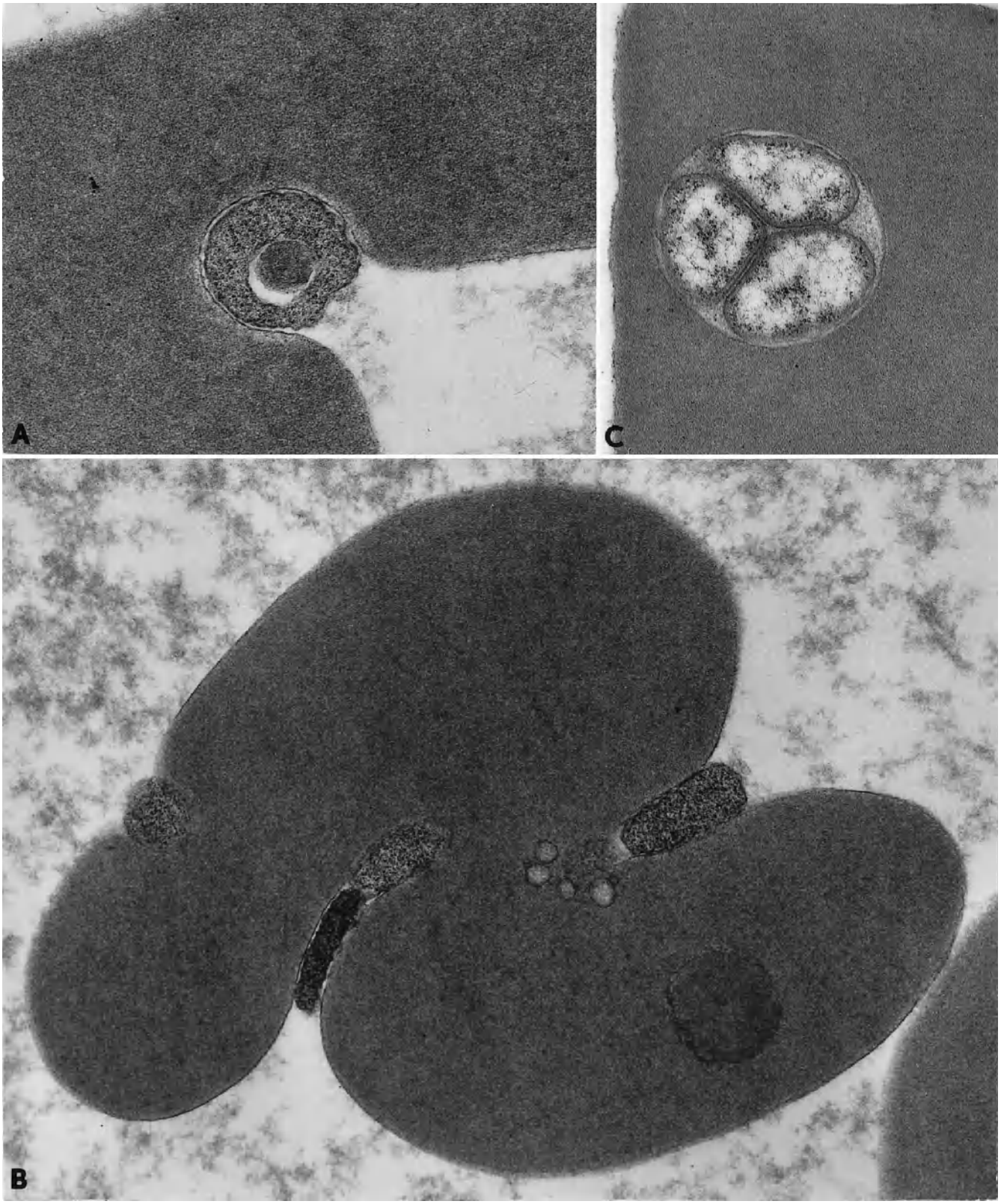


Fig. 14.8 Erythrocyte pathogens. **A** and **B**. ***Haemobartonella canis*** indented into surfaces of canine erythrocytes. (Micrographs: John W. Venable.) **C**. ***Anaplasma marginale*** within a bovine erythrocyte. (Micrograph: Charles E. Simpson.)

Vet-ebooks.com

extramembranous layer of polyanions about 15–30 nm in width composed of glucosyl-like residues.[142] Ureaplasmas are the most common microbes isolated from infected amniotic fluid, placentas, and the respiratory tracts of preterm infants. For some infants, this infection triggers a vigorous proinflammatory response by TNF-α, IL-1β, and IL-8 in the lungs and increases the risk of developing bronchopulmonary dysplasia.

Genus *Hemobartonella*

Hemobartonella species are hemotropic mycoplasmas, sometimes called hemoplasmas. They have undulant plasma membranes, are pleomorphic, and vary greatly in size from 0.2 to 1.0 μm wide × 5.0 μm long. Ring-shaped forms are due to large indentations into cytoplasmic areas of the hemoplasma. They cause infectious anemias in numerous mammalian species.[143] Interspecies transmission might play a role in the epidemiology of these microorganisms.

In this group is *Haemobartonella felis*. Hemoplasma attach to the erythrocyte surface. An attachment leads to an indentation containing the microorganisms. They exist in deep, grooved infoldings in the surface and do not enter the cell, despite the appearance of having done so when viewed in blood smears (Fig. 14.8). *H. felis* infection in kittens is typically asymptomatic. Exceptions are those in very young animals or animals with acquired immunologic or inflammatory deficits. Splenectomy will induce parasitemia and clinical disease in cats with inapparent infection. Anemia is the only known manifestation of infections and is due to increased erythrophagocytosis by splenic phagocytes, not to overt damage to the cell surface. Infected erythrocytes may be severely distorted but no defect can be shown in the plasma membrane.

Genus *Eperythrozoon*

Eperythrozoon are cell wall-less, uncultivated parasitic bacteria that attach to the surface of host erythrocytes. There are at least five species that are phylogenetically related to species in the genus *Mycoplasma.* They cause hematologic infections and anemias in mice (*E. coccoides*), sheep and goats (*E. ovis*), pigs (*E. parvum, E. suis*), and cattle (*E. wenyoni*). Disease appears as a slight or moderate normochromic, macrocytic anemia. Microscopically, *E. suis* appears alone or in groups of two or three stuck to the erythrocyte surface, often indented into erythrocyte. Ultrastructurally, *E. suis* appear as round or oval bodies, limited by a membrane containing widespread electron-dense granules and microtubule-like structures in the cytoplasm. **Porcine eperythrozoonosis** begins with mild fever, anorexia, and rapidly developing hemolytic anemia. Later, signs include icterus and bile-stained feces. Splenomegaly is marked and impression smears contain the organism.

Order Entomoplasmatales

Genus *Spiroplasma*

Spiroplasmas are 200–300 nm in size and form helical, branched, or nonhelical filaments. Using video dark-field light microscopy of live, swimming helical cells and cryoelectron microscopy, *Spiroplasma* were found to contain the subcellular structure and molecular organization of a cytoskeleton that acts as a bacterial linear motor enabling and controlling both dynamic helicity and swimming.[144]

They infect plants, arthropods and vertebrates.[145] In insects, many spiroplasmas are not pathogenic and are mutualists or incidental commensals in the gut. However, some are pathogens. *S. melliferum* and *S. apis* kill honey bees; *S. floricola* causes lethargy disease of cockchafers; and *S. poulsonii* infects *Drosophila* species. In vertebrates, *S. mirum* from rabbit ticks is pathogenic to chick embryos, newborn rodents, and adult rabbits. Strain SMCA induces high incidence of cataracts in newborn rodents. Strain GT-48 induces fatal encephalitis. Spiral membranous inclusions resembling spiroplasmas are seen in brain biopsies taken from patients with Creutzfeldt-Jakob disease. However, failure to detect spiroplasmas by serology and culture points to the absence of *Spiroplasma* involvement in spongiform encephalopathies.

Order Incertae Sedis

Genus *Erysipelothrix*

Erysipelothrix rhusiopathiae is the cause of erysipelas and economically important diseases in swine, turkeys, chickens, ducks, sheep, and humans[146] (Table 14.4). In humans, infection causes local cutaneous lesions, septicemia, and endocarditis. In swine, septicemia and cardiac valvular lesions include endothelial cell swelling, accumulation of albuminous precipitates around blood vessels, and foci of necrosis. Circulating bacteria stick to and are phagocytized by endothelial cells. Coagulopathy with fibrin deposition plays an important role. Vascular injury is widespread, even in the brain. Ultrastructurally, *E. rhusiopathia*e appears in tissue as a long rod, free in interstitial areas and within vacuoles of neutrophils and other inflammatory cells.

Vet-ebooks.com

Table 14.4 Order Incertae sedis, family Erysipelotrichaceae: pathogenic species.

Pathogen	*Disease (host) and ultrastrucural studies*	*Reference to ultrastructural pathology*
	Genus *Erysipelothrix*	
E. insidiosa	Erysipelas in a variety of avian species and studies in mice	**Petzoldt**, *Dev Biol Stand* 33:57, 1976
E. rhusiopathiae	Erysipelas in swine and penguins and studies on experimental infections	**Drommer**, *Vet Pathol* 7:455, 1970; **Gazquez**, *Rec Med Vet* 163:661, 1987; **Sakuma**, *Natl Inst Anim Health Q* 13:203, 1973; **Boerner**, *J Vet Diagn Invest* 16:145, 2004

Phylum Proteobacteriae, Order Rickettsiales

Members of the order Rickettsiales are small coccobacillary or rodlike prokaryotes. They have both DNA and RNA and contain numerous enzymes involved with energy production. Most require living cells to complete their life cycles and the host cell supplies substrates for bacteria enzymes. Organisms replicate by binary fission. They have no well-defined nucleus and no evidence of mitochondria or endoplasmic reticulum.

These bacteria are obligate intracellular small gram-negative coccobacilli that replicate directly in the host cell cytoplasm.[147] They are notoriously unstable outside of cells and use insect vectors to transmit from host to host (Table 14.5). Replication occurs in the midgut of arthropod vectors, many of which are of unknown pathogenicity. Pathogenic isolates include only a few of the many Rickettsiaceae that occur in insects. *Rickettsia*-like organisms are commonly encountered in tissues of insects, fishes, and amphibians but their associations with disease are often not established.

The Rickettsiaceae have a plasma membrane and cell wall that contains muramic acid and in thin section is undulant. The cell wall resembles that of the gram-negative bacteria and contains endotoxin of limited toxicity. In cross sections bacteria are 0.2–1.5 μm wide × up to 4 μm long. **Construction furrows**, characteristic of organisms undergoing binary fission, are common. Internally, dense aggregates of ribosomes are dispersed throughout the cell. Fine strands, probably representing DNA, are seen in open spaces in the cytosol. In some species, vacuoles of 4–10 nm are present.

Most Rickettsiaceae develop within the cytoplasm of the host cell. Closely apposed membranes may cause the appearance of being membrane-bound and some species do reside within vacuoles. *R. rickettsii* and *R. japonica* replicate within nuclei in some cell culture systems; they develop free in the nucleoplasm in central regions of the nucleus. Affected nuclei typically have large eccentric nucleoli and dispersed chromatin. The ultrastructure in tissue, insect gut epithelium, chick embryo, and cell cultures appears identical (Fig. 14.9).

Bacteria of the family Anaplasmataceae include *Anaplasma*, *Ehrlichia*, *Cowdria*, *Neorickettsia*, and *Wolbachia* species and are obligate intracellular bacteria that reside in vacuoles of eukaryotic cells. Recent genetic analyses of 16S rRNA genes, groESL, and surface protein genes now group these organisms into four distinct clades.[148] These include *Anaplasma* (including the *Ehrlichia phagocytophila* group, *Ehrlichia platys* and *Ehrlichia bovis*), *Ehrlichia* (including *Cowdria ruminantium*), *Wolbachia*, and *Neorickettsia* (including *Ehrlichia sennetsu* and *Ehrlichia risticii*).

Genus *Rickettsia*

Rickettsia species are 0.3–0.7 μm in size and of varying lengths; most are under 2 μm long, although filamentous forms of *R. prowazekii* may be as long as 4 μm. *Rickettsia* species cause febrile systemic disease in humans, usually by infecting vascular endothelium. They are unable to grow in the absence of living host cells. *Rickettsia* species cannot easily be differentiated ultrastructurally in tissue, including *R. prowazekii, R. tsutsugamushi*, and *R. quintana*. Most rickettsia pass through arthropods as an obligate part of their life cycle.

Rickettsial Fevers of Humans

R. prowazekii is the agent of classical epidemic typhus and multiplies in intestinal epithelial cells of the human body louse, *Pediculus humanus*. *R. prowazekii* in the feces of the louse is inoculated by scratching the site of the louse bite. Occasionally, in epidemics in closed communities, an aerosol of dried louse feces may be inhaled.[147] They proliferate on the endothelium of small vessels and induce the release of cytokines that damages endothelium. This leads to fluid leakage, platelet aggregation, polymorphonuclear leukocyte and monocyte proliferation, focal occlusive

Vet-ebooks.com

Table 14.5 Order Rickettsiales, family Rickettsiaceae: pathogenic species.

Pathogen	*Disease (host) and ultrastrucural studies*	*Reference to ultrastructural pathology*
	Genus *Rickettsia*	
R. australis	Queensland tick typhus	**Feng**, *Am J Pathol* 142:1471, 1993
R. canada	Structure in various organs and tissues of the hard tick, *Dermacentor andersoni Stiles*	**Brinton**, *J Bact* 105:1749, 1971
R. conorii	Boutonneuse typhus and Mediterranean spotted fever in humans	**Feng**, *Infect Immun* 55:7, 1987; **Teysseire**, *Infect Immun* 60:4388, 1992; **Teysseire**, *Infect Immun* 63:366, 1995
R. japonica	Spotted fever in humans	**Heinzen**, *Infect Immun* 61:1926, 1993
R. prowazekii	Louse-borne epidemic typhus and studies in mice	**Khavkin**, *Am J Pathol* 76:213, 1974; **Anderson**, *J Bacteriol* 90:1387, 1965; **Keysary**, *Infect Immun* 57:2390, 1989
R. quintana	Typhus	**Ito,** *J Bacteriol* 89:481, 1965
R. rickettsii	Rocky Mountain spotted fever in humans and studies in guinea pigs	**Anderson**, *J Bacteriol* 90:1387, 1965; **De Brito**, *Virch Arch A* 358:205, 1973; **Silverman**, *Infect Immun* 44:545, 1984; **Silverman**, *Infect Immun* 56:3110, 1988; **Silverman**, *Infect Immun* 59:4505,1991; **Walker**, *Lab Invest* 43:388, 1980; **Manor**, *Microb Pathogen* 17:99, 1994; **Moe**, *Lab Invest* 35:235, 1976; **Walker**, *Am J Pathol* 86:343, 1977; **Hayes**, *Infect Immun* 37:779, 1982; **Uchiyama**, *Microbiol Immunol* 32:1163, 1988
R. tsutsugamushi	Scrub typhus and fever in humans	***Rikihisa***, *Infect Immun 30:231, 1980 and 38:343, 1982*
R. typhi	Murine typhus	**Khavkin**, *Ann N Y Acad Sci* 590:85, 1990
Rickettsia-like bacteria in fish and amphibians	Diseases in fish and mussels	**Fryer**, *Emerg Infect Dis* 3:137, 1997; ***Gulka***, *J Fish Dis* 8:309, 1985; **Cvitanich**, *J Fish Dis* 14:121, 1991; **Paperna**, *J Fish Dis* 7:137, 1984; **Bradley**, *Dis Aquatic Organisms* 4:9, 1988; **Rourke**, *J. Fish Dis* 7:301, 1984
Rickettsia-like bacteria in insects	Associated with typhus-like illness in humans. From flea *Ctenocephalides felis*	**Adams**, *Am J Trop Med* 43:400, 1990

endangiitis, and microinfarctions. This process particularly affects the brain, skin, and cardiac and skeletal muscle. Capillaries are occluded by swollen endothelial cells that protrude into the lumen of the vessel and are predisposed to thrombus formation. Bacteria are found in the cytoplasm, associated with acute cell swelling and dilated rough endoplasmic reticulum, the agent of endemic typhus, multiplies in the rat flea *Xenopsylla cheopis*. Generalized lymphadenopathy is a characteristic clinical symptom.

Typhus nodules consisting of aggregates of monocytes, macrophages, and plasmacytes are important lesions, particularly in the brain. They contain large numbers of neuroglia. Death may be due predominantly to encephalitis, myocarditis, secondary bacterial pneumonia, or toxemia (with loss of blood volume, hemoconcentration and shock).

"Spotted fever" rickettsiae are transmitted by ticks from rodents, dogs, and wild animals.[147] **Rocky Mountain spotted fever** makes up 95% of human rickettsial infections in North America. **Endothelial cells** are the primary target of *R. rickettsii* and lesions are characterized by widespread vasculitis of capillaries and muscular arteries. Hematologic manifestations include thrombocytopenia, activation of coagulation, and increased concentrations of fibrinogen and von Willebrand factor in plasma.

Infected endothelial cells release cytokines, fibrinolytic factors, von Willebrand factor, and kinin-generating enzymes that combine to induce fever, increased capillary permeability, and thrombosis. Heparin protects endothelial cells infected in vitro, perhaps as a free-radical scavenger.[149] Bacteria replicate in the cytoplasm of endothelial cells; intranuclear

Vet-ebooks.com

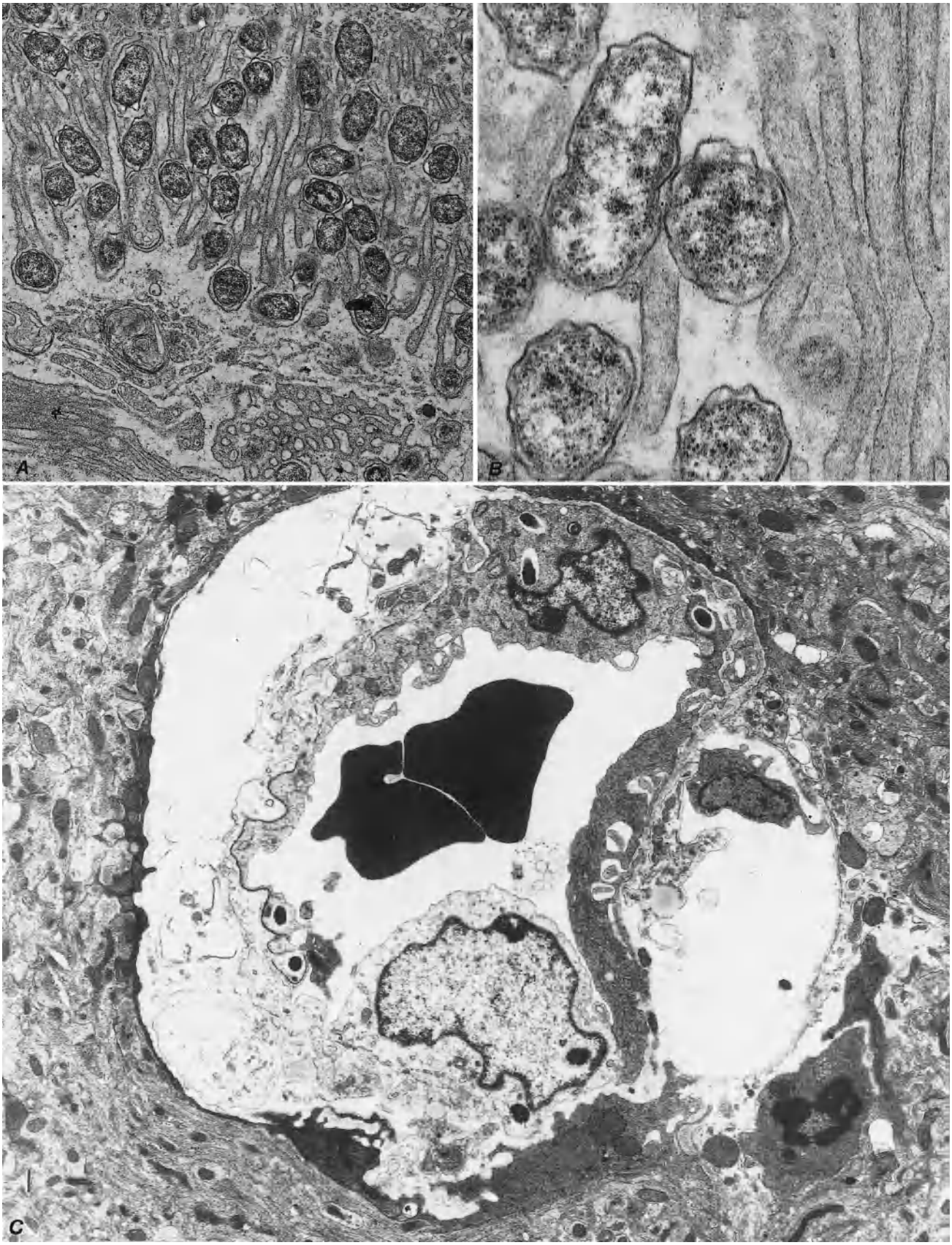


Fig. 14.9 Rickettsia. **A–B**. ***Rickettsia* sp. enmeshed in microvilli** within the gut of a tick. (Micrograph: Randall C. Cutlip.) **C**. ***R. conorii* in endothelial cells**, intramural edema in capillary of mouse brain. (Micrograph: Vsevold L. Popov, *Lab Invest* 70:358, 1994.)

Vet-ebooks.com

bacteria are reported in vitro but this has not been adequately documented ultrastructurally. Intracellular bacteria are found in many tissues but are most prominent in spleen.

In ticks, *R. rickettsii* develops in nuclei and aggregates may resemble nuclear viral inclusions. Ultrastructurally, *R. rickettsii* uses actin-based motility as a mechanism for intercellular spread.[150] It has long, >10 μm actin tails containing multiple, distinct actin bundles. They are roughly parallel to one another, and oriented with the fast-growing barbed end towards the rickettsial pole. Actin tails contain the cytoskeletal proteins vasodilator-stimulated phosphoprotein profilin, vinculin, and filamin. Tails lack ezrin, paxillin, and tropomyosin, commonly associated with actin tails induced by *Listeria* species. In contrast, *R. prowazekii* and *R. typhi* have no actin tails or only short, 1–3 μm actin tails, respectively.

Mediterranean spotted fever, caused by *R. conorii*, also involves widespread endothelial damage and deep venous thrombosis, perhaps associated with the release of von Willebrand factor and other cytoplasmic cytokines by infected endothelial cells. A mouse model of the spotted fevers, induced with *R. autralis*, demonstrates generalized vasculitis.

Genus *Ehrlichia*

Ehrlichia species replicate in leukocytes of the host and cause acute febrile disease, often involving the vascular and coagulation systems (Table 14.6). Many Ehrlichia-like agents have not been classified, nor has their ultrastructure been characterized.

Human ehrlichiosis caused by *E. chaffeensis* and *E. ewingii* are two emerging tickborne infections.[151] The disease presents as undifferentiated fever, but thrombocytopenia, leukopenia, and increased serum transaminase activities are important laboratory features.

Canine ehrlichiosis, caused by *E. canis*, is endemic in semitropical areas. Clinical signs begin as anemia, thrombocytopenia, and lymphadenopathy with petechial hemorrhages. *E. canis* replicates in monocytes and lymphocytes. Cytoplasmic inclusions develop in circulating monocytes, lymphocytes and, rarely, in neutrophils; they consist of membrane-lined vacuoles that contain elementary bodies of *E. canis*. Ultrastructurally, organisms develop in the midgut, salivary glands, and hemocytes of the tick but not in the ovary. The brown dog tick *Rhipicephalus sanguineus* transmits the *E. canis*. A second species, *E. ewingii*, replicates in neutrophils of the dog to cause the milder disease **canine granulocytic ehrlichiosis**.

Equine ehrlichiosis (Potomac fever) is caused by *E. risticii*. Clinical signs begin with a fever, anorexia, leukopenia, and diarrhea. *E. risticii* parasitizes circulating monocytes. Ultrastructurally, organisms in intestinal tissue are pleomorphic, round to bacillary, and have wavy outer membranes. Bacterial cells are found in the cytoplasm of macrophages in the lamina propria of the large colon, especially in the deep glands.

Heartwater, caused by *Ehrlichia* (*Cowdria*) *ruminantium comb. nov.*, is a vascular disease of sheep, goats, and cattle in Africa. Organisms replicate in the midgut epithelium of nymphs and are transmitted to cattle when these parasites feed. In cattle, the initial phase of heartwater occurs in regional lymph nodes where replication occurs in reticulum cells. After dissemination in the bloodstream (free in plasma and associated with leukocytes), organisms infect capillary endothelial cells throughout the animal and are best detected in renal glomeruli, cerebral cortex, and choroid plexus endothelium as they develop in membrane-bound vacuoles in the cytoplasm. Replication occurs by binary fission of small forms. In ticks, organisms replicate within intestinal epithelium.

Genus *Anaplasma*

Anaplasma are obligate intracellular gram-negative bacteria.[152] They infect a variety of wild and domestic animal species and parasitize erythrocytes of sheep, cattle, deer, and other species to cause progressive anemia (Table 14.6). Of the species in this genus, there are *Anaplasma marginale* (cattle), *A. centrale* (cattle), and *A. ovis* (sheep). The former two are distinguished structurally only by location within parasitized erythrocytes. *Anaplasma* species replicate in the midgut of *Dermacentor andersoni* and *Rhipicephalus simus*. Transmitted by ticks, other insects, and any clinical procedure that transfers blood, these organisms enter new erythrocytes becoming invaginated into the surface. Penetration occurs and the *Anaplasma* is found as a single **initial body** bound by a membrane at the periphery of the erythrocyte. Mature, juvenile, and dividing forms may be present.[153] *Anaplasma* also infects endothelial cells in vitro and in vivo.[154,155] *A. phagocytophilum* forms numerous smaller inclusions in rhesus, human, and bovine endothelial cell lines. *A. marginale* forms large intracellular inclusions in rhesus and bovine endothelial cell lines. Ultrastructurally, *A. phagocytophilum* appeared evenly spaced, whereas *A. marginale* inside large inclusions grouped tightly.[155]

Replication of the initial body by binary fission leads to two to eight bodies within the membrane-bound vacuole (Fig. 14.8C). This structure is the **marginal body** or inclusion body, the dense, Giemsa-staining body found in blood smears of

Vet-ebooks.com

Table 14.6 Order Rickettsiales, family Anaplasmataceae: pathogenic species.

Pathogen	*Disease (host) and ultrastrucural studies*	*Reference to ultrastructural pathology*
	Genus *Ehrlichia*	
E. canis	Ehrlichiosis in dogs	**Hildebrandt**, *Infect Immun* 7:265, 1973; **Simpson**, *Infect Immun* 10:590, 1974; **Smith**, *Am J Vet Res* 37:119, 1976; **Wen**, *Int J System Bacteriol* 45:250, 1995
E. chaffeensis	Human monocytic ehrlichiosis, avian ehrlichiosis, and infections in dogs	**Chen**, *J Infect Dis* 175:856, 1997; **Chen**, *Infect Immun* 63:647, 1995; **Wen**, *Int J System Bacteriol* 45:250, 1995
E. equi	Isolated from horses	**Sells**, *Infect Immun* 13:273,1976
E. ewingii	Granulocytic ehrlichiosis in dogs and infections in humans	**Hamilton**, *Modern Pathol* 17:512, 2004
E. felis	Infection in cats	**Buoro**, *Vet Rec* 125:434, 1989
E. muris	Infections in mice but grows in dog macrophage cell lines	**Wen**, *Int J System Bacteriol* 45:250, 1995
E. phagocytophila	Tick-borne fever in sheep	**Caturegli**, *Infect Immun* 68:5277, 2000
E. risticii	Potomac fever in horses and experimental infections	**Holland**, *Science* 227:522, 1985; **Rikihisa**, *Infect Immun* 49:505 and 513**,** 1985; **Wells**, *Infect Immun* 56:3209, 1988
E. sennetsu	Human ehrlichiosis	**Paddock**, *New Engl J Med* 329:1169, 1993; **Sotomayor**, *Am J Pathol* 158:757, 2001
	Genus *Neorickettsia*	
N. helminthoeca	A parasite of the fluke *Nanophyetus salmincola* and the cause of salmon poisoning disease (aka, Elokomin fluke fever) in dogs	**Frank**, *J Infect Dis* 129:257, 1954; **Wen**, *Int J System Bacteriol* 46:149, 1996
	Genus *Anaplasma*	
A. centrale	A hemolytic disease of cattle	**Waddell**, *Australian Vet J* 40:233, 1964
A. marginale	Anemia, icterus, weight loss, fever, abortion, and death. Studies in ticks	**Kocan**, *Am J Vet Res* 41:1966, 1980; **Kocan**, *Am J Vet Res* 43:586, 1983; **Kocan**, *Am J Vet Res* 45:1434 and 1800, 1984; **Kocan**, *Am J Vet Res* 49:1010, 1988; **Kocan**, *Am J Vet Res* 51:128, 1989; **Kocan**, *Am J Vet Res* 53:499, 1992; **Potgieter**, *Am J Vet Res* 44:2256, 1983; **Simpson**, *Am J Vet Res* 28:1055, 1967; **Simpson**, *J Cell Biol* 27:277, 1965; **Stiller**, *Am J Vet Res* 50:1381, 1989
A. phagocytophilum	Human granulocytic anaplasmosis, tick-borne fever of ruminants, and equine and canine granulocytic anaplasmosis	**Woldehiwet**, *J Comp Pathol* 92:649, 1982; **Dumler**, *Int J Syst Evol Microbiol* 51:2145, 2001; **Foley**, *Vector-Borne and Zoonotic Dis* 8:49, 2008
E. platys	Infections in dogs	**Arraga-Alvarado**, *Vet Pathol* 40:149, 2003
	Genus *Aegyptianella*	
A. bacterifera	Anemia in frogs	**Desser**, *J Wildlife Dis* 25:313, 1989
A. botuliformis	Anemia in birds	**Huchzermeyer**, *Onderstepoort J Vet Res* 59:97, 1992
A. pullorum	Anemia in birds	**Bird**, *Parasitology* 59:745, 1969
	Genus *Cowdria*	
C. ruminantium	Heartwater in cattle	**Pienaar**, *Onderstepoort J Vet Res* 37:67, 1970; **Prozesky**, *Onderstepoort J Vet Res* 52:71, 1985

infected animals. Elongate appendages extend from the marginal body within infected erythrocytes distinctly separating these organisms from *A. marginale*.

Replication in ixodid ticks involves transstadial transmission (larva to nymph and nymph to adult) by adults and transmission by male ticks transferred from infected to susceptible hosts occurs. In the midgut of *Dermacentor* species ticks, *A. marginale* undergo a complex developmental cycle involving several morphologically distinct stages. The final infective stage develops in the tick salivary gland.[156] Anemia begins

Vet-ebooks.com

as surfaces of large numbers of erythrocytes are damaged and cells are removed as they pass through the cords of the spleen. Bone marrow, hyperplastic in initial stages and in mild cases, becomes hypoplastic as the disease becomes severe. In late stages, an autoimmune process contributes to anemia. In chronic infection, bone marrow exhaustion contributes to severe disease and death.

Genus *Aegyptianella*

Aegyptianella species are found within vacuoles in erythrocytes of fowl: *A. pullorum* in chickens and *A. botuliformis* in guinea fowl.[157,158] In the latter, there are up to eight organisms in the mature vacuolar inclusion. Bacteria are coccobacillary and pleomorphic and up to 0.6 μm wide × 1.5–3 μm in length. There are inner and outer membranes at the cell surface, and short internal invaginations from the inner membrane are common. Bacteria divide by binary fission; webs of DNA filaments are in central areas. Intermediate forms are irregular and pleomorphic. In *A. bacterifera* and *A. ranarum* of frogs, bacteria are elongate and rod-shaped in final stages. A transfer from *"A. ranarum"* to *"Candidatus Hemobacterium ranarum" comb. nov.* has been proposed.[159]

Order Rhizobiales

Genus *Bartonella*

The genus *Bartonella* contains up to 24 human-specific, zoonotic, and animal-specific species including those previously found in the genus *Rochalimaea*.[160] The type species, *Bartonella bacilliformis*, is a small, motile, aerobic, gram-negative bacillus that infects humans in central South America. Clinical manifestations of infection may be systemic with anemia and fever (**Oroya fever**), or localized subcutaneous nodular eruptions called **verruga peruana**.[161,162] Bacteria occur in large numbers in circulating erythrocytes; they are also present in macrophages and endothelial cells of lymphatics, spleen, liver, and other lymphoid tissues. Both forms of human bartonellosis can be reproduced in monkeys. Natural infections with *B. bacilliformis* and other *Bartonellae* occur in dogs, cattle, and several species of rodents but none play a significant role in dissemination of the human disease[163] (Table 14.7).

Infections of *B. henselae* account for most cases of human bartonellosis. It is transmitted through the bite of a cat flea or a cat scratch resulting in endocarditis, angiomatosis, peliosis, neuroretinitis and fever.[160] **Bacillary angiomatosis** is a vascular proliferative lesion (distinct from Kaposi's sarcoma) first reported in the skin and lymph nodes of patients with human immunodeficiency virus infection. Lesions associated with verruga peruana are indistinguishable histologically from those of bacillary angiomatosis. Clusters of bacilli are present in lesions and the disease is presumed to be infectious, although bacteria cannot be cultured readily from the lesion in vitro. Bacilli are pleomorphic, measure 0.2–0.5 μm, and grow in clumps. Confocal microscopy localized the growth of *B. henselae* to granules around the nuclei of Vero cells and electron microscopy showed that the granules were clusters of multiple intracellular organisms.[164] Bacteria isolated from bacillary angiomatosis are causal in transient febrile episodes and bacillary peliosis hepatis of AIDS patients.

Genus *Afipia*

Afipia felis (cat scratch bacillus) is a gram-negative, pleomorphic bacillus that causes human **cat scratch fever**, a syndrome of benign lymphadenopathy and a skin or conjunctival rash. *A. felis* is associated with bacterial flora of the mouth and claws of cats and other animals, enters bite wounds, and drains to regional lymph nodes. In tissue sections, *A. felis* is identified with the Warthin-Starry or other silver impregnation techniques. It has also been identified in the feline mandibular lymph node.

Histopathologic examination of lymph nodes from 39 human patients with cat scratch disease revealed delicate pleomorphic gram-negative bacilli in 34 cases. Scratched into human skin, cat scratch bacilli cause, after an incubation of 5–50 days, dermal or conjunctival lesions associated with regional lymphadenopathy. Fever, malaise, myalgia, arthralgia, weight loss, and neuroretinitis are part of the chronic systemic reaction.

Ultrastructural examination reveals that *A. felis* is associated with collagen and necrotic debris, especially around blood vessels. Although reported within cells, intracellular replication is not a part of the life cycle. Endothelial cells are swollen and lumens are often obliterated. Neutrophils and macrophages dominant the lesion and, in late stages, there are stellate granulomas and caseation necrosis. In hyperergic or necrotizing granulomas there are few bacilli. Bacteria have thick homogenous walls resembling gram-positive bacteria (Fig. 14.10).

A. felis enters various cells and its compartmentation differs between macrophages and other phagocytic cells. In endothelial cells, invasion is dependent upon a functional cytoskeleton; bacteria are taken up via pocket-like structures and reside within membrane-surrounded phagosomes.[165] In macrophages, *A. felis* are taken up directly into a nonendocytic

Vet-ebooks.com

Table 14.7 Order Rhizobiales: pathogenic species.

Pathogen	*Disease (host) and ultrastrucural studies*	*Reference to ultrastructural pathology*
	Genus *Bartonella*	
B. bacilliformis	Bartonellosis, Carrion's disease, and Oroya fever in humans	**Benson**, *Infect Immun* 54:347, 1986; **Cuadra**, *Blood* 33:708, 1969; **Hill**, *Infect Immun* 60:4051, 1992; **Arias-Stella**, *Am J Surg Pathol* 10:595, 1986
B. bovis	Endocarditis in cattle	**Bermond,** *Inter J System Evol Microbiol* 52:383, 2002
B. henselae	Zoonotic transmission from cats to humans (cat scratch fever). Bacillary angiomatosis, a neovascular disorder of immunosuppressed patients	**Chomel**, *Emer Infect Dis* 12:389, 2006; **Perkocha**, *New Engl J Med* 323:1581, 1990
B. quintana	Zoonotic transmission from dogs to humans. Trench fever in humans	**Ito**, *J Bact* 89:481, 1965; **Chomel**, *Emer Infect Dis* 12:389, 2006
B. vinsonii	Isolated from voles	**Kordick**, *Int J Sys Bact* 46:704, 1996
	Genus *Afipia*	
A. felis	Cat scratch fever in humans	**Birkness**, *Infect Immun* 60:2281, 1992; **Hadfield**, *J Infect Dis* 152:643, 1985; **Wear**, *Science* 221:1403, 1983; **Osborne**, *Am J Clin Pathol* 87:739, 1987
	Genus *Brucella*	
B. abortus	Abortions, arthritis, and debilitating disease in ruminants and cervids and undulant fever in humans	**Hatten**, *J Bacteriol* 108:535, 1971; **Anderson**, *Am J Pathol* 124:226, 1986; **Detilleux**, *Vet Path* 27:317, 1990; **Cloeckaert**, *Infect Immun* 58: 3980, 1990; **Freer**, *Infect Immun* 67:6181, 1999
B. canis	Abortion and reproductive disease in dogs	**Detilleux,** *Vet Path* 27:317, 1990
B. melitensis	Brucellosis in humans and goats and Bang's disease in humans	**Detilleux,** *Vet Path* 27:317, 1990; **Cloeckaert**, *Infect Immun* 58: 3980, 1990
B. neotomae	Infections in rodents	**Detilleux,** *Vet Path* 27:317, 1990
B. ovis	Reproductive disease in sheep	**Detilleux,** *Vet Path* 27:317, 1990; **Freer**, *Infect Immun* 67:6181, 1999
B. suis	Abortion and reproductive disease in pigs	**Hines,** *J Bacteriol* 87:1492, 1964; **Detilleux,** *Vet Path* 27:317, 1990
Miscellaneous species (*B. maris* and *B. delphini*)	Disease in dolphins	**Ewalt**, *J Vet Diagn Investig* 6:448, 1994; **Miller**, *J Zoo Wildl Med* 30:100, 1999

compartment.[166] Within these cells, bacteria become longer and more pleomorphic.[167]

Genus *Brucella*

Brucella are small gram-negative coccobacilli that lack capsules, spores, or structures for motility. However, ultrastructural studies show that *B. melitensis* in early log phase of growth produce a flagellar structure likely involved in the persistence of a murine model of infection.[168] Also, ultrastructural studies reveal granular surface structures[169] and immunogold techniques localize proteins.[170] The carboxyl-terminal protease (CtpA) assists in maintaining the coccobacillary shape of these organisms particularly *B. suis*. Mutants of CtpA are larger and spherical with membranes partially dissociated from the cell envelope.[171]

Brucellae replicate intracellularly, largely within lysosomes in macrophages (Fig. 14.11). Human neutrophils phagocytize and degrade *Brucella* species although infection does not cause an effective level of degranulation.[172] In macrophages and dendritic cells of lymphoid tissue, *Brucella* replicate slowly and inefficiently, although protection from immune mechanisms causes infections to become chronic. Smooth and rough phenotypes of *Brucella* interact differentially with human peripheral blood monocytes. Rough

Vet-ebooks.com

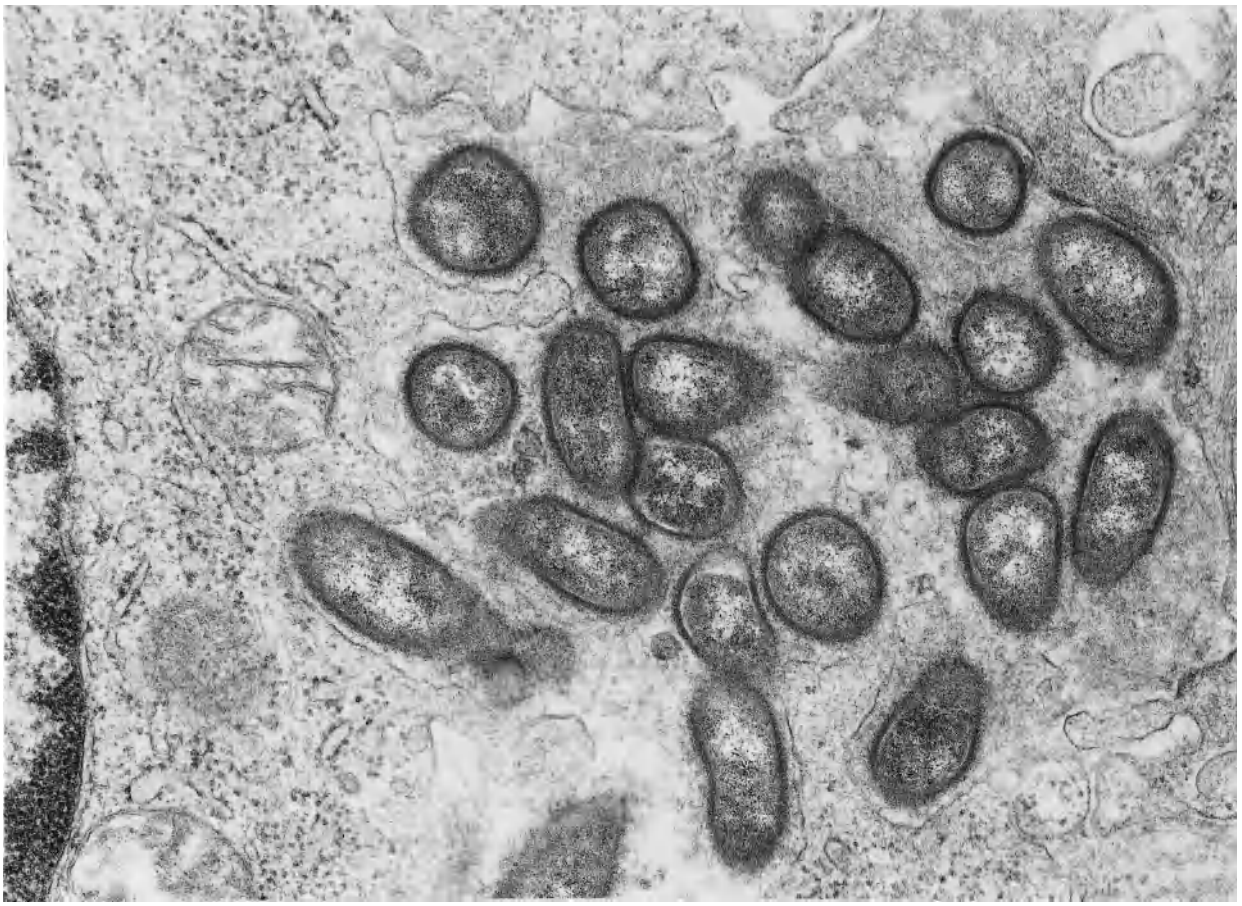


Fig. 14.10 ***Afipia* sp.**: cat scratch fever, human lymph node. Clusters of bacilli in extracellular spaces. Note association with cellular projections. (Micrograph: Barbara M. Osborne, *Am J Clin Pathol* 87:739, 1987.)

phenotypes more readily attach to and invade monocytes but only smooth phenotypes replicate in monocytes.[173]

Brucellosis

Brucellosis persists as a spectrum varying from acute infection with abortion to chronic carrier status. Chronic disease involves long lasting and intermittent bacteremia, and results in persistence of bacteria in macrophages. There is a strong tropism for the genital system and the disease centers on the placental trophoblast.[174] *B melitensis* in humans causes severe acute disease. *B. suis* and *B. canis* are only rarely associated with human disease, and infections with these tend to be localized. Human infection occurs by contact with animals with brucellosis, by aerosols from animals or animal carcasses, or via ingestion of contaminated milk and dairy products.

In **bovine brucellosis**, *B. abortus* is acquired via the alimentary canal from infected uterine or placental exudates, entering the body through lymphoid tissues. In the ileum, bacteria are taken up by specialized M cells of the Peyer's patches.[175] Acute regional lymphadenitis develops and is followed by bacteremia, which leads to infection of spleen, lymphoid tissues, mammary glands, and other organs. Chorionic epithelial cells are vacuolated and contain immense numbers of bacilli. Cells of the interplacentome are more severely affected than those covering the placentome. Tips of maternal villi are necrotic and the bases are infiltrated with leukocytes. Endometrium is not severely afflicted despite the severity of placental inflammation. *B. abortus* is first seen in phagosomes of erythrophagocytic cytotrophoblasts in the placentome and in the rough endoplasmic reticulum and nuclear envelope cisterna of periplacentomal chorioallantoic trophoblasts (Fig. 14.12).[176] Resistance of *Brucella* species to killing by host macrophages is essential for the establishment and maintenance of chronic infection and is dependent upon the RNA binding protein host factor I (HF-I) encoded by the hfq gene. Hfq translates the stationary-phase σ factor RpoS.[177]

Vet-ebooks.com

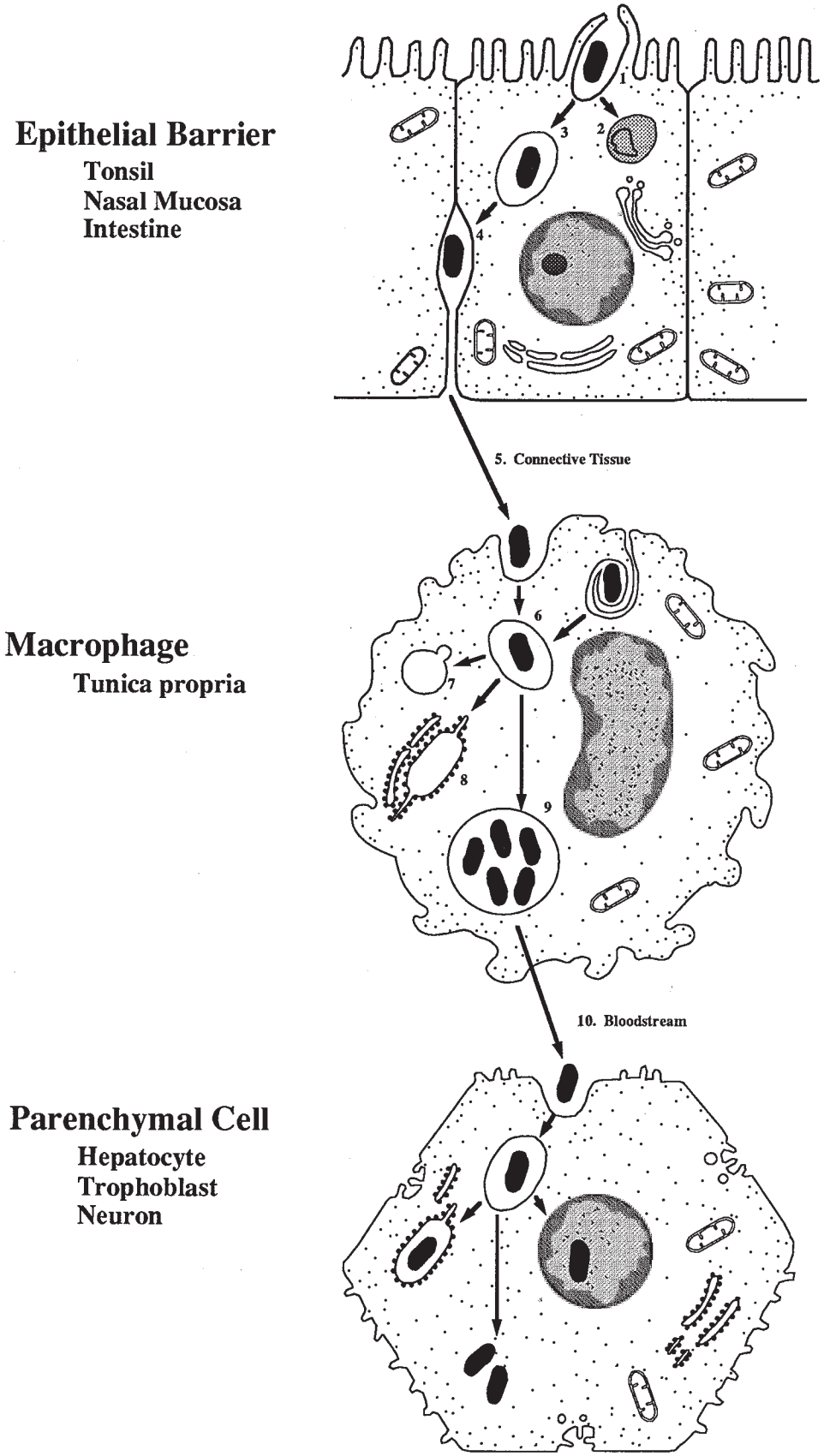


Fig. 14.11 Pathways of infection and replication of facultative intracellular bacteria. Bacteria enter epithelial cells by phagocytosis (*1*) and move to lysosomes (*2*) or phagosomes (*3*) with shunting to extracellular spaces (*4*). After passage through the interstititum, bacteria enter macrophages by direct or coiling phagocytosis to enter phagosomes (*6*); from the phagosome, bacteria move to lysosomes (*7*), cisternae of endoplasmic reticulum (*8*), or residual bodies (*9*) with exit from the cell. Bacteria enter the bloodstream (*10*) and are transported to other tissues. In parenchymal cells, bacteria are taken into phagosomes (*11*) and move to endoplasmic reticulum (*12*), cytoplasmic matrix (*13*), or nucleus (*14*).

Vet-ebooks.com

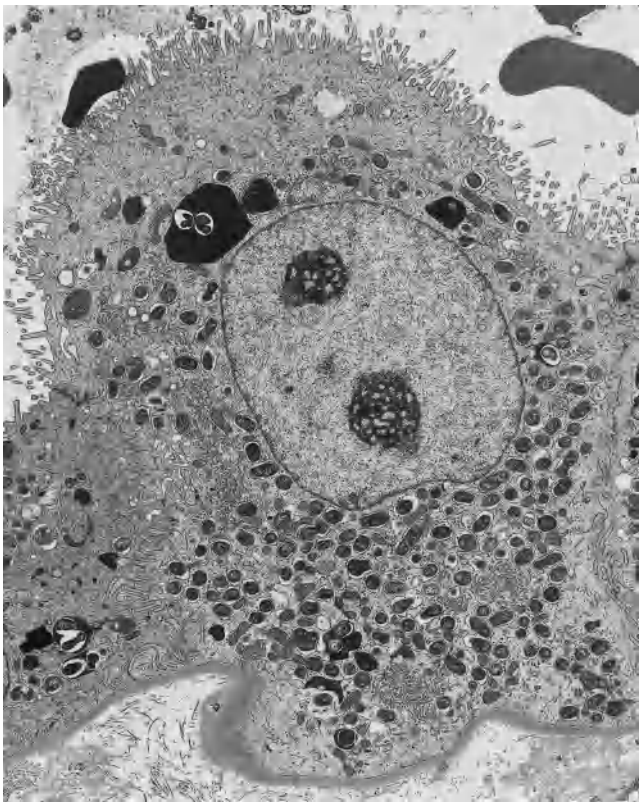


Fig. 14.12 ***Brucella abortus***: placenta, goat with brucellosis. Massive accumulation of bacilli in basal cytoplasm, trophoblast. Cytoplasm contains dense hemoglobin crystals. Microvillous surface and basement membrane appear normal. (Micrograph: Tim D. Anderson.)

Order Burkholderiales

Genus *Bordetella*

Bordetella species cause acute and chronic respiratory disease in many animal species by attaching to cilia of the upper respiratory tract and releasing factors that cause degeneration of epithelium. Pathogenic species bear fimbriae that attach to respiratory epithelial cells and secrete exotoxins (Fig. 14.13). *Bordetella* grow as biofilms and attach to nasal epithelium[178] and likely among microvilli of the trachea and major bronchioles. Ultrastructural analysis reveals close associations between bacterial surfaces and microvilli. Membranous particles are commonly found on the bacterial cell surface. Persistent colonization of ciliated epithelium leads to inflammation of the airways, loss of ciliated epithelial cells, and mucopuruent exudates. Ciliated cells are lost and replaced by immature cuboidal cells with more rough endoplasmic reticulum and small apical mucous granules.[179] The genus contains eight species, and major pathogens include *B. pertussis and B. parapertussis*, of human **whooping cough**; *B. avium*, of **turkey coryza**; and *B. bronchiseptica*, of **kennel cough** in dogs and **atrophic rhinitis** of swine (Table 14.8).

Bordetella pertussis attaches to and grows upon the ciliated mucosae of the human upper respiratory tract as a biofilm via the *bps* locus that is required for the production of poly-β-1,6-GlcNAc.[180] With scanning electron microscopy, wild type strains develop thick, uniform, multilayers of cells, whereas Δ*bps* strains do not. With Fourier transform infrared spectroscopy, virulent *B. pertussis* quickly attach and develop into minibiofilms consisting of microcolonies 299 μm in size and 24 μm deep.[181] Bacilli colonize epithelial surfaces through adhesions to host cells formed by the filamentous hemagglutinin and fimbria-like structures. Virulence factors include **filamentous hemagglutinin (FHA)**, pertactin, **pertussis toxin (PT)**, and **adenylate cyclase toxin**. FHA, PT, and other virulence factors have been localized ultrastructurally in the bacterial cell, and in other bacteria that express these antigens. Specific gold-tagged antibodies to FHA and PT identified aggregates of filamentous material on the cell surface and in the cytoplasm, but not in the nucleus, suggesting that FHA and PT occurred on the same cell structures.[182] Uptake of bacteria into cells may be mediated by interaction of the Arg-Gly-Asp sites on the pertactin molecule with eukaryotic cell surface receptors. Ultrastructurally, *B. bronchiseptica* kills human tracheal epithelial cells, which display morphological aspects of necrosis. In contrast, *B. pertussis* and *B. parapertussis* are taken up by human tracheal epithelial cells, localized in the Golgi apparatus, and degraded.[183]

Pertussis toxin (PT), a primary virulence factor, causes the local and systemic effects of disease; it is composed of two different units: an A monomer mediates ADP-ribosylation of host G proteins, and a B oligomer mediates binding of toxin to host cells.[184] The **A oligomer** ADP ribosylates the alpha subunit of heterotrimeric G_i proteins. G protein modification then leads to many different effects on signaling pathways in mammalian cells. The **B oligomer** is a lectin with carbohydrate preferences similar to those of selectins. **Tracheal cytotoxin**, a derivative of the peptidoglycan layers, causes deciliation and degeneration of respiratory epithelium.

Genus *Burkholderia*

Of the 56 species, *B. cepacia*, *B. mallei*, and *B. pseudomallei* are recognized as the prominent human or animal pathogens. *B. mallei* (**glanders**), and *B. pseudomallei* (**meliodosis**) are emerging infectious diseases as well as potential bioterrorism threats. These species are

Vet-ebooks.com

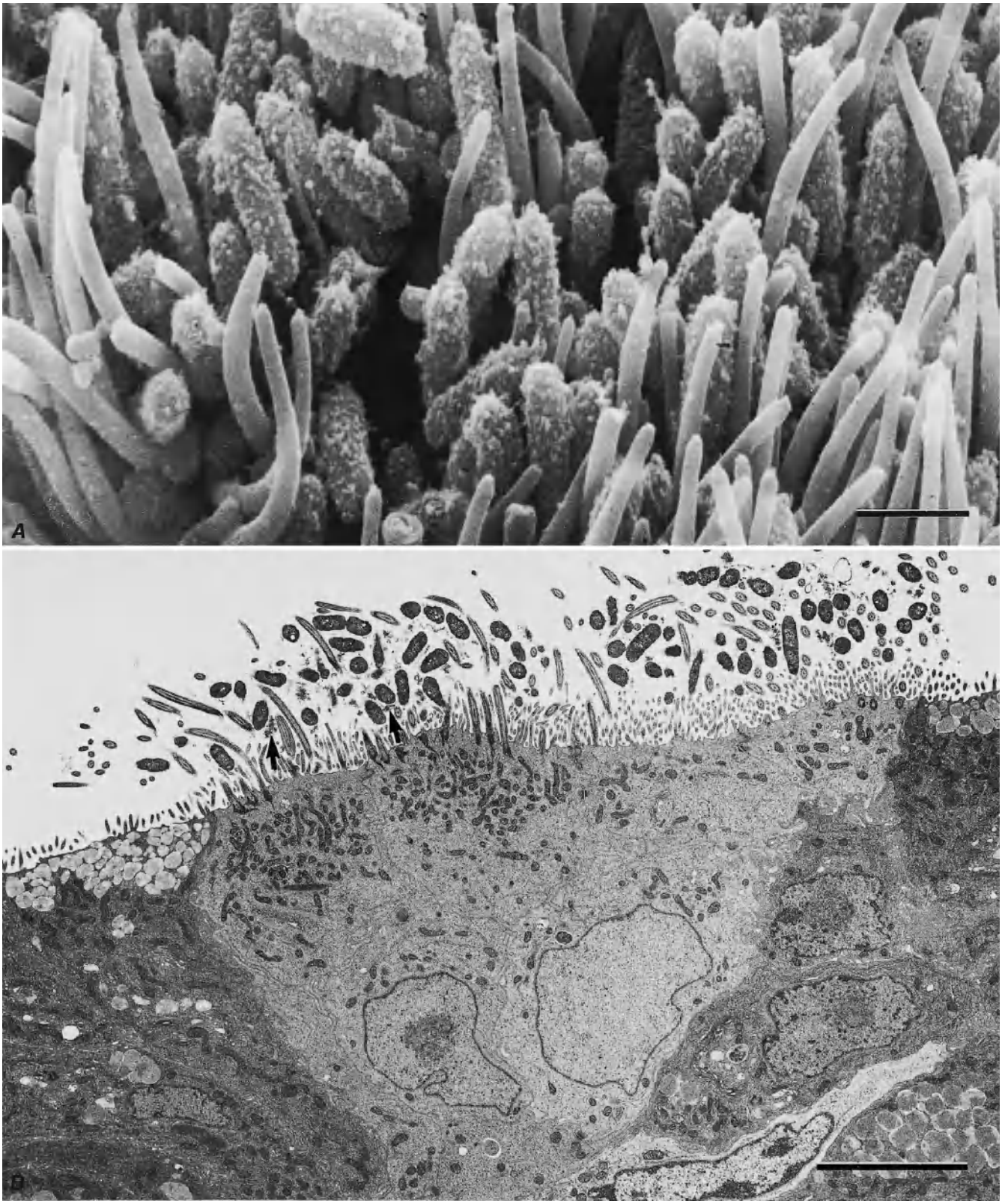


Fig. 14.13 ***Bordetella avium***: bronchiole, turkey. Bacilli are entwined among cilia. **A**. **Scanning electron micrograph**: rough-surfaced *B. avium* is closely associated with cilia. **B**. **Transmission electron micrograph**: colonization of ciliated but not nonciliated epithelial cells. (Micrographs: Lawrence H. Arp, *Vet Pathol* 24:411, 1987.)

Vet-ebooks.com

Table 14.8 Order Burkholderiales: pathogenic species.

Pathogen	*Disease (host) and ultrastrucural studies*	*Reference to ultrastructural pathology*
	Genus *Bordetella*	
B. avium	Turkey coryza	**Arp**, *Vet Pathol* 24:411, 1987
B. bronchiseptica	Atrophic rhinitis in pigs and kennel cough in dogs	**Duncan**, *Am J Pathol* 47:601, 1965; **Yokomizo**, *Res Vet Sci* 27:15, 1979; **Bemis**, *J Inf Dis* 135:153, 1977; **Fetter**, *J Am Vet Med Ass* 36:15, 1975; **Ishikawa**, *Infect Immun* 55:1607, 1987; **Zeligs**, *Infect Immun* 53:702, 1986
B. pertussis	Whooping cough in humans, studies with toxin, and studies in mice	**Black**, *Science* 240:656, 1988; **Blom**, *Infect Immun* 42:308, 1983; **Fredriksen**, *J Med Microbiol* 25:285, 1988; **Heiss**, *Infect Immun* 61:3123, 1993; **Hopewell**, *J Med Microbiol* 5:154, 1972; **Leininger**, *Infect Immun* 60:2380, 1992; **Li**, *Infect Immun* 56:3184, 1988; **Morse**, *J Exp Med* 131:1342, 1970; **Collier**, *J Infect Dis* 136:S196, 1977; **Strugnell**, *Infect Immun* 60:3994, 1992
	Genus *Burkholderia*	
B. cepacia	Respiratory disease in cystic fibrosis patients	**Kuehn**, *Infect Immun* 60:2002, 1992; **Burns**, *Infect Immun* 64:4054, 1996
B. mallei	Glanders	**Fritz**, *Vet Pathol* 36:276, 1999
B. pseudomallei	Meliodosis, a granulomatous infectious disease	**Narita,** *Natl Inst Anim Health Q (Tokyo)* 22:170, 1982; **Burns**, *Infect Immun* 64:4054, 1996
	Genus *Taylorella*	
T. equigenitalis	Metritis in horses	**Hitchcock**, *Infect Immun* 48:94, 1985; **Willems**, *Int J Syst Evol Microbiol* 52:179, 2002

aerobic, gram-negative, straight or slightly curved bacilli 0.5–1.0 μm × 1.5–5.0 μm in size. They are motile and have one or two polar flagella. *B. mallei* in not motile and not **flagellated**.

B. cepacia occurs as part of a complex of nine related bacterial species that cause life-threatening respiratory tract infections in patients with cystic fibrosis.[185] Bacteria colonize the respiratory tract, at least in part, through fimbriae. Electron micrographs reveal both polar and peritrichous fimbriae on bacterial surfaces. Virulence factors include exoenzymes (e.g., protease activity, hemolysin, phospholipase C, and lipase), repeat in toxin (RTX)-like protein determinants, and a Type IV secretion system.

Glanders and Meliodosis

Meliodosis is a granulomatous infectious disease of humans and animals in tropical Australia and Southeast Asia with a clinical spectrum that varies from acute localized suppurative lesions, acute septicemia, and acute and chronic pulmonary infections. The cause, *B. pseudomallei*, is an environmental saprophyte. These small gram-negative bacilli are found in exudates. *B. pseudomallei* is a facultative intracellular bacterial pathogen with the capacity to invade a variety of cell types including macrophages. Ultrastructurally bacteria occur in macrophages in microabscesses in liver. Escape from sequestered cellular locations is thought to explain recrudescent and delayed-onset *B. pseudomallei* infection.[186] *B. pseudomallei* entry into macrophages results in cellular effects similar to those caused by other intracellular bacteria.[187]

Glanders, caused by *P. mallei*, is a disease of equidae (with rare transmissions to humans, dogs, and ruminants) that resembles melioidosis in tissue response and clinical spectrum.

Order Neisseriales

Genus *Neisseria*

Neisseria measure 0.6–1 μm. They appear as cocci (singly or in pairs with adjacent sides flattened) or coccobacilli. *N. gonorrhoeae* infects the human genital tract causing acute diffuse purulent urethritis and cervicitis (Table 14.9). Large numbers of bacteria are found in the exudate. Peptidoglycans and other fragments liberated by gonococci during action by host hydrolases contribute to the intense inflammatory response. Significant virulence factors include pili, porin, opacity-associated outer membrane proteins, and lipooligosaccharide. *N. gonorrhoeae* is characterized by a broad ultrastructural and antigenically

Vet-ebooks.com

Table 14.9 Order Neisseriales: pathogenic species.

Pathogen	*Disease (host) and ultrastrucural studies*	*Reference to ultrastructural pathology*
	Genus *Eikenella*	
E. corrodens	Abscesses, endocarditis, meningitis, osteomyelitis, keratitis, conjunctivitis, and oral infections	**Hood**, *Infect Immun* 63:3673, 1995; **Tonjum**, *Infect Immun* 61:1993
	Genus *Kingella*	
K. kingae	Pediatric diseases including osteomyelitis, septic arthritis, bacteremia, and endocarditis	**Weir**, *Infect Immun* 60:3437, 1992; **Kehl-Fie**, *J Bacteriol* 189:430, 2007
	Genus *Neisseria*	
N. gonorrhoeae	Gonorrhea in humans and studies in urethral exudates, cervix, synovial membrane, fallopian tubes, and neutrophils	**Apicella**, *J Infect Dis* 162:506, 1990; **Apicella**, *J Infect Dis* 173:636, 1996; **Cooper**, *Infect Immun* 36:363, 1982; **Evans**, *J Infect Dis* 136:248, 1977; **Garcia-Kutzback**, *J Infect Dis* 130:183, 1974; **Robinson**, *Infect Immun* 46:361, 1984; **Robinson**, *Infect Immun* 55:1190, 1987; **Shaw**, *Infect Immun* 56:1625, 1988; **Swanson**, *Infect Immun* 10:645, 1974; **Ward**, *J Infect Dis* 129:650, 1974; **Weel**, *J Exp Med* 173:1395, 1991
N. meningitidis	Meningitis in humans and studies in the nasopharynx and skin	**Froholm**, *Acta Pathol Microbiol Scand B* 81:525, 1973; **Ross**, *J Infect Dis* 155:1266, 1987; **Virji**, *Mol Microbiol* 6:2785, 1992; **Stephens**, *Infect* Immun 51:579, 1986; **Stephens,** *Rev Infect Dis* 13:22, 1991; **Sotto**, *J Infect Dis* 133:506, 1976; **Alaaldeen**, *Infect Immun* 61:751, 1993; **Weel**, *Res Microbiol* 142:985, 1991
N. weaveri	Dog bite wounds in humans	**Holmes,** *Int J Syst Bact* 43:687, 1993
	Genus *Simonsiella*	
S. muelleri	Isolated from a gastric aspirate taken from a neonate	**Pangborn**, *Arch Microbiol* 113:197, 1977; **Whitehouse**, *J Clin Microbiol* 25:522, 1987

diverse group of surface glycoproteins.[188] Immunoelectron microscopy has been used to detect lipooligosaccharide epitope variations.[189]

Pili are also important in attachment to host cells. Type IV pili (T4P) are long, thin, flexible filaments on *N. gonorrhoeae*. GC-T4P has three-helix bundles that form the filament core, anchor the globular heads, and provide strength and flexibility.[190] Although adhesion by surface pili to host epithelium can mediate attachment, it may also be detrimental to the bacterium. Direct attachment of pili to receptors on phagocytes facilitates killing of the bacterium. Transfer of sialyl groups of cytidine 5′-monophospho-N-acetyl neuraminic acid (CMP-NANA) to surface lipopolysaccharide sites gives the appearance of a "capsule" on the cell surface.[37] Outer membrane proteins have been identified using immunogold techniques.

N. gonorrhoeae utilizes different mechanisms to infect, invade, and colonize the mucosal epithelia of the urethra and the uterine cervix.[191] In males, pilus-mediated adherence to I-domain-containing beta-1 integrins initiates infection. A lipooligosaccharide ASGP-R interaction then initiates intracellular invasion and cytokine production. In females, adherence and invasion of the cervical epithelium is mediated by the cooperative interaction of both the host and gonococcal constituents with the I-domain region CR3. CR3 then triggers membrane ruffling and internalization of gonococci within macropinosomes.[192] Here, gonococcal products modulate the ability of gonococci to survive within the host cervical cell. Ultrastructural studies of biopsies of cervical gonorrhea show that bacteria are taken into phagocytic cells by the formation of microvilli around the bacteria cells.[193]

The human nasopharynx is the natural habitat for *N. meningitidis*. Meningococci are transported across epithelial cells within vacuoles and are released by exocytosis into the submucosal space. Cytotoxicity results in breakdown of tight junctions of epithelial cells, ciliostasis, and sloughing of ciliated cells. Skin biopsy of 10 patients with *N. meningitis* and maculopurpuric lesions revealed that organisms were present in endothelial cells and neutrophils. Vascular lesions involved endothelial cell necrosis, thrombosis, and necrosis of muscle cells and pericytes.[194] Hypercoagulation occurs in some patients.

Vet-ebooks.com

Type IV pilus tip adhesins are in meningococcus attachment to epithelial cell receptors. The PilG pilus biogenesis protein is an important component of the type IV pili. It has a role in linking cytoplasmic and periplasmic protein components of the type II secretion system and type IV pilus biogenesis system.[57] A three-dimensional structure, worked out by electron microscopy, shows that PilG is a trimer with an asymmetric bi-lobed structure 125 angstroms in length and 80 angstroms in width. The PilQ complex is circular, with a donut-like appearance. The cavity is funnel-shaped in cross section, measures 6.5 nm in diameter at the top of the complex, and tapers to a closed point, effectively blocking formation of a continuous pore through the PilQ complex.[195]

Host defense against *N. meningitidis* requires a complement-dependent bactericidal activity.[196,197] Unusually severe, chronic, or recurrent infection with *Neisseria* species has been reported in association with deficiencies in the terminal complement sequences.

One family of proteins, the products of opacity (*opa*) genes, are determinants of tissue tropism. *Opa* genes are variably expressed on the bacterial surface. Most meningococcal isolates express up to four Opa protein variants (*opaA, opaB, opaD, opaJ*) and this is a factor in penetration of bacteria into host cells.[198] The use of immunogold probes on ultrathin section of infected cells in culture show that *opa* phase transitions confer a functional adaptation of the bacteria enabling penetration of host cells to occur. The *opc* gene is another virulence factor that permits pilus- and capsule-deficient strains to adhere to host cells.[199]

Order Campylobacterales

Genus *Arcobacter*

The genus *Arcobacter* comprises the former aerotolerant campylobacter species and contains six species. *Arcobacter* species have been associated with reproductive disorders, mastitis, and gastric ulcers in livestock and humans.[200] Ultrastructurally, cells are rod-shaped, slightly curved, non-spore-forming bacilli, 0.5 μm wide and 1.5 μm long with a single, unsheathed flagella at one polar end.[200,201] Isolates adhere to human and porcine intestinal epithelial cells and induce the production of IL8.

Genus *Campylobacter*

Campylobacter species are motile, non-spore-forming, comma-shaped rods. They are a leading cause of food-borne illness. Most human infections result for exposure to *C. jejuni*, although *C. coli* (from swine) and *C. fetus* subspecies *fetus* (from sheep) are also human pathogens (Table 14.10). These organisms are primarily zoonotic and a variety of animals are reservoirs of infection. *Campylobacter rectus* is a suspected periodontal pathogen.

Virulence factors include a cytolethal distending toxin, capsular polysaccharides, lipopolysaccharide, and flagella.[202,203] Biofilms and surface polysaccharides of beta 1–3 and/or beta 1–4 linkages participate in survival, transmission, and virulence of *C. jejuni*.[204]

C. jejuni is the most common species causing acute enteritis and diarrhea in humans. Rare extraintestinal infections include cholecystitis, urinary tract infection, and meningitis. Infection with *C. jejuni* is also associated with two serious sequelae; Reiter's syndrome and Guillain-Barré syndrome.[203] *C. jejuni* multiplies to greatest degree in human bile and in the bile-rich upper small intestine, although the colon is also affected. Bacteremia occurs in patients with *Campylobacter* infections, even in those without clinical signs of disease. Affected intestine has diffuse, bloody, edematous and exudative enteritis with inflammatory exudates composed of neutrophils, monocytes, and eosinophils in the lamina propria. Epithelial glands degenerate and form crypt abscesses. *C. jejuni* induces intestinal epithelial cells to produce human beta defensins 2 and 3.[202] Scanning and transmission electron studies show that these defensins damage *C. jejuni* cell walls, induce blebbing of cell wall material, and result in loss of cytoplasmic contents.

C. fetus infection is associated with reproductive failure and fetal disease in sheep and with intermittent diarrhea in humans. In pregnant sheep, *V. fetus* penetrates chorionic epithelial cells of the placenta where it replicates and forms intracellular colonies. Bacteria also develop within capillaries, and are phagocytized in large numbers by monocytes and macrophages (Fig. 14.14).

Proliferative enteropathies of swine are diseases of postweaning piglets. This is a complex of diseases that includes **intestinal adenomatosis, necrotic enteritis, regional enteritis**, and **proliferative hemorrhagic enteropathy**. The characteristic lesion is proliferation of epithelium of the ileum (and occasionally of jejunum, cecum, or colon). Slender curved intracellular bacteria can be seen in proliferative mucosal epithelial cells. *C. hyointestinalis* is found in lesions of proliferative enteropathy; *C. sputorum* subspecies *mucosalis* may also be present (but is no longer thought to be causal).

Intestinal adenomatosis affects several animal species including swine and the blue fox. In foxes,

Vet-ebooks.com

Table 14.10 Order Campylobacterales: pathogenic species.

Pathogen	*Disease (host) and ultrastrucural studies*	*Reference to ultrastructural pathology*
	Genus *Campylobacter*	
C. fetus subspecies *fetus* and *C. fetus* subspecies *venerealis*	Subspecies *fetus* infects humans and causes abortion in cattle and sheep. Subspecies *venerealis* is adapted to the genital tract of cattle	**McCoy**, *J Bacteriol* 122:307, 1975; **Ritchie**, *J Gen Microbiol* 43:427, 1966; **van Bergen,** *J Clin Micro* 43:5888, 2005
C. hyointestinalis	Enteritis in pigs	**Boosinger**, *Am J Vet Res* 46:2152, 1985
C. jejuni	Enteritis in many species including hamsters, mice, chickens, monkeys, and fox	**de Melo**, *Infect Immun* 57:2214, 1989; **Humphrey**, *Am J Pathol* 122:152, 1986; **Kiehlbauch**, *Infect Immun* 48:446, 1985; **Lee**, *Infect Immun* 51:536, 1986; **Meinersmann**, *Am J Vet Res* 52:1518, 1991; **Welkos**, *J Med Microbiol* 18:233, 1984; **Russell**, *J Infect Dis* 168:210, 1993; **Sosula**, *Am J Pathol* 131:125, 1988; **Eriksen**, *J Comp Pathol* 102, 265, 1990
C. pylori	Associated with gastritis and peptic ulcers	**Geis**, *J Clin Microbiol* 27:436, 1989; **Hazell**, *J Infect Dis* 153:658, 1986
C. pyloridis	Gastritis	**Marshall**, *J Infect Dis* 153:650, 1986
Campylobacter-like organisms	Intestinal lesions in rabbits	**Schoeb**, *Vet Pathol* 27:73, 1990
	Genus *Wolinella*	
W. recta	Necrotic root canal infections	**Borinski**, *Infect Immun* 58:2770; 1990; **Kesabalu**, *Infect Immun* 59:2806, 1991
	Genus *Helicobacter*	
H. bizzozeronii	Chronic gastritis in humans	**De Groote**, *Helicobacter* 10:398, 2005; **De Groote**, *J Clin Microbiol* 39:1197, 2001
H. heilmannii	Dyspeptic patient with gastritis	**Andersen**, *J Clin Microbiol* 37:1069, 1999; **Ierardi**, *J Clin Pathol* 54:774, 2001
H. hepaticus	Gastritis and hepatitis in mice	**Fox**, *J Clin Microbiol* 32:1238, 1995; **Ward**, *Am J Pathol* 145:959, 1994
H. muridarum	Rodents	**Lee**, *Int J Sys Bacteriol* 42:27, 1992
H. pylori	Chronic gastritis in humans, monkeys, and studies in pigs	**Blaser**, *J Infect Dis* 161:626, 1990; **Chen**, *Am J Clin Pathol* 86:575, 1986; **Dytoc**, *Infect Immun* 61:448, 1993; **Kazi**, *J Pathol* 161:65, 1990; **Lee**, *Infect Immun* 61:1601, 1993; **Tricottet**, *Ultrastr Pathol* 10:113, 1986; **Reindel**, *Vet Path* 36:1, 1999; **Rudman**, *Infect Immun* 60:2121, 1992; **Evans**, *Infect Immun* 57:2272, 1989; **Goodwin**, *Eur J Clin Microbiol Infect Dis* 155:237, 1990; **Hessey**, *Gut* 31:134, 1990
Other *Helicobacter* species including *H. salomonis* and *H. felis*	Gastric infections in humans, cheetahs, dogs, ferrets, rabbits, cats, rodents, monkeys, hamsters, and pigs	**Eaton**, *Vet Pathol* 30:55, 1993; **Henry**, *Am J Vet Res* 48:831, 1987; **Fox**, *Am J Vet Res* 43:858, 1983; **Leblanc**, *Vet Pathol* 30:391, 1993; **McNulty**, *J Clin Pathol* 2:584, 1989; **Moon**, *Vet Pathol* 11:313, 1974; **Lee**, *Infect Immun* 56:2850, 1988 (stomach); **Phillips**, *Appl Environ Microbiol* 45:675, 1983; **Sato**, *Vet Pathol* 19:17, 1982; **Schoeb**, *Vet Pathol* 27:73, 1990; **Weber**, *Am J Vet Res* 32:422, 1962 **Frisk**, *Am J Vet Res* 38:1861, 1977; **Johnson**, *Am J Pathol* 91:451, 1978; **Stills**, *Infect Immun* 55:2240, 1987; **Boosinger**, *Am J Vet Res* 46:2152, 1985; **Gebhart**, *Int J Sys Bact* 43:533, 1993; **Lomax**, *Am J Vet Res* 43:1622, 1982; **Love**, *Vet Pathol* 16:41, 1979; **McOrist**, *Infect Immun* 61:4286, 1993; **Querioz**, *Vet Microbiol* 24:199, 1991; **Rowland**, *Res Vet Sci* 17:323, 1974; **De Groote**, *Helicobacter* 10:398, 2005; **De Groote**, *J Clin Microbiol* 39:1197, 2001; **Erginsoy**, *J Wild Dis* 40:548, 2004

Vet-ebooks.com

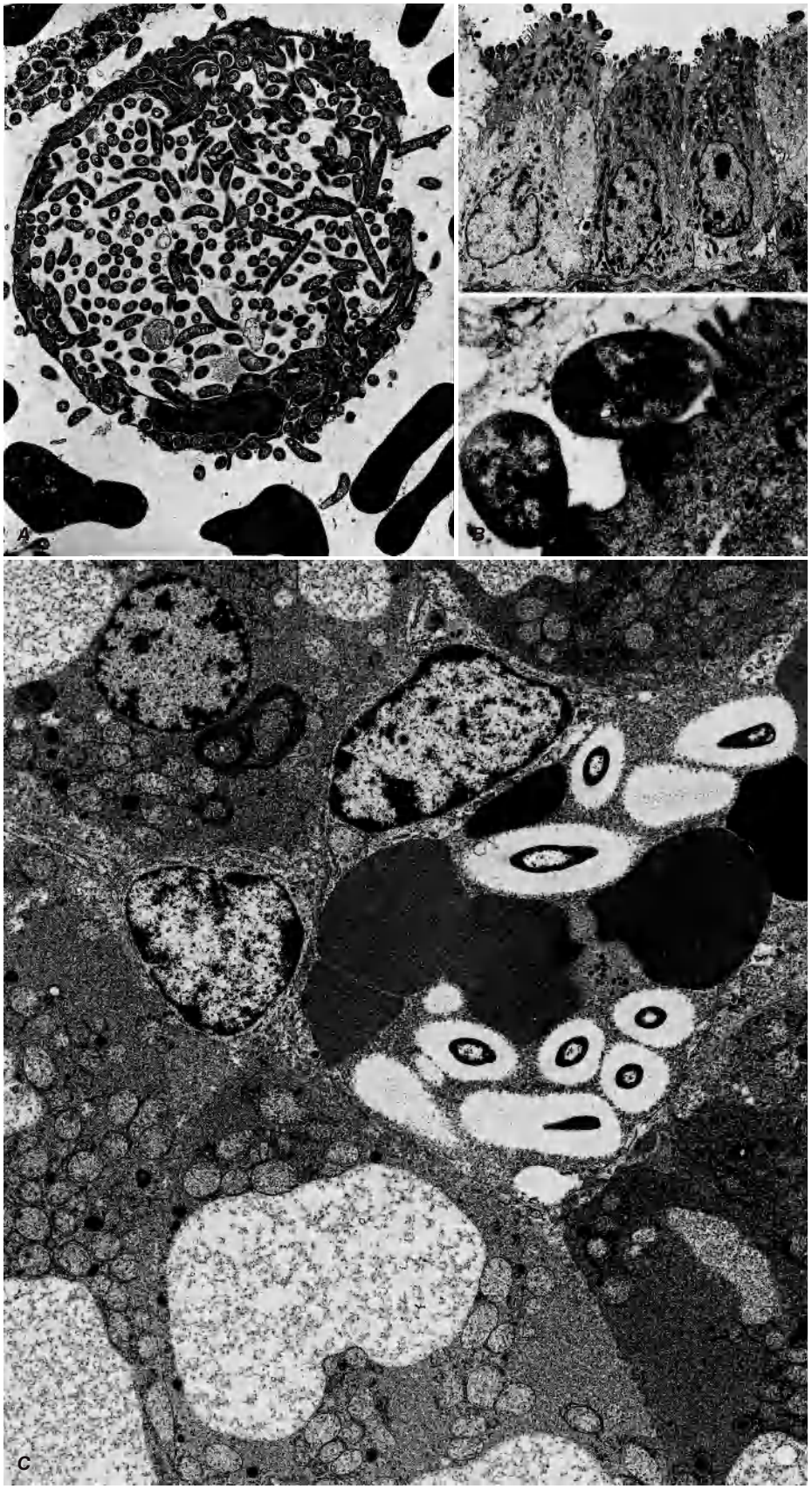


Fig. 14.14 Bacilli: **A**. ***Campylocater fetus***: masses of bacilli within a macrophage fixed in exudate from ovine campylobacteriosis. **B**. ***Citrobacter freundii***: adherence to enterocytes with effacement of microvilli. (Micrograph: S. Barthold, *Am J Pathol* 97:291, 1979.) **C**. ***Bacillus anthracis***: hepatic sinusoids, guinea pig. Bacilli are among erythrocytes and platelets. Halos around bacteria are capsules. Hepatocytes are degenerate and contain large vacuoles.

Vet-ebooks.com

intracellular bacteria of structure consistent with *Campylobacter* species are found in apical epithelial cytoplasmic of affected colonic mucosa. **Murine transmissible colonic hyperplasia** caused by *Citrobacter freundii* is not found in infected enterocytes.

Diarrheal disease caused by intraepithelial *Campylobacter*-like bacteria is common in pigs, hamsters, and has been reported in ferrets, sheep, rats, guinea pigs, dogs, horses, foxes, deer, and rabbits. The bacterium has not been identified in these species and in most, the etiologic role of the bacterium has not been confirmed.

Proliferative ileitis of hamsters involves mucosal hyperplasia and pyogranulomatous inflammation of the distal ileum. Overgrowth of normal epithelium by immature pseudostratified epithelium with high mitotic indices precedes the inflammatory phase. Curved bacilli are associated with hyperplastic ileal epithelium and ultrastructurally, the organism appears to be a *Campylobacter* species. As disease progresses, villi elongate and become leaflike and the newly formed crypts move below the underlying muscle layers. Secondary bacterial invasion leads to abscesses, peritonitis and ileal rupture.

Genus *Helicobacter*

Helicobacter species are gram-negative, microaerophilic rods. Morphologically they are spiral or curved ranging from 0.3 to 1.0 μm wide × 1.5–10.0 μm in length. *H. pylori* is short with one or two turns in its spiral body, *H. musteleae* is short, slightly curved, and rod-shaped with a unique flagellum, and *H. felis* is 5–7 μm long with a tightly spiraled body of five to six turns and distinctive periplasmic fibers. *Helicobacter* species are motile and generally have multiple bipolar-sheathed flagella. *H. pylori* have multiple monopolar-sheathed flagella and *H. pullorum* and *H. canadensis* have unsheathed flagella. *H. pylori* secretes a vacuolating toxin (VacA) that inserts into membranes to form anion-selective channels. Bilayered forms of VacA have a "flower"-like structure, consisting of a central ring surrounded by symmetrically arranged peripheral "petals." The central ring plays an important role in the process by which VacA forms membrane channels.[205]

The genus contains 30 species isolated from mammals and birds. In humans, *Helicobacter* species have preferred gastric and enterohepatic niches. *H. pylori* is associated with peptic ulcers and gastrointestinal cancers. In the stomach, it attaches to mucus overlying the gastric epithelium and survives in the acidic environment of the stomach by producing a potent urease. The urease hydrolyzes urea to carbon dioxide and ammonia, and the latter reduces the acidity immediately surrounding the bacteria. Ammonia is toxic to gastric epithelial cells and causes much of the cellular damage during infection. Analyses of gastric antral biopsies from *H. pylori*-positive patients show foci of bacterial adhesion that disappear with resolution of the gastritis.[206] *H. pylori* adheres to microvilli on cell surfaces both in vivo and in vitro.[207] Under certain circumstances, infection with *H. pylori* predisposes to gastric ulcers. Studies on the ultrastructural lesions that develop during attachment and invasion of gastric mucosa of pigs suggest that bacterial membranes fuse with epithelial cell plasma membranes. *H. pylori* was detected by transmission electron microscopic examination of endoscopic biopsy specimens. *H. pylori* was seen inside cytoplasm of epithelia cells, in intraepithelial intercellular spaces, and in underlying lamina propria, often in direct contact with immune and inflammatory cells.[208,209] A thick, very fine filamentous or reticular fringe corresponding to the bacterial glycocalyx was seen surrounding the *H. pylori* cells. *H. pylori* was connected to the epithelial cells by very fine, thickly arranged filaments and the epithelial cells showed indentations or pedestals.[210]

H. muridarum and *H. rappini* colonize the lower gastrointestinal tract of mice but cause no apparent disease. *H. hepaticus* causes chronic liver infections characterized by foci of necrosis and lymphocyte cholangitis. Ultrastructural examination reveals bacteria between hepatocytes and in bile canaliculi.

Some patients suffering from chronic gastritis have gastric *Helicobacter* species other than *Helicobacter pylori* called "*Helicobacter heilmannii*"-like organisms (HHLO) that may be transmitted through animals.[211,212] HHLO-infected patients had *Helicobacter* species that commonly colonize the stomachs of cats and dogs (Fig. 14.15).

In many animal species, *Helicobacter* species colonize the gastric mucosa where they attach either to mucous cell surfaces or to the extracellular canaliculi of gastric parietal cells. HHLO infects cynomolgus monkeys (*Macaca fascicularis*).[213] In the rhesus monkey, gastric spirilla are concentrated in gastric glands at the isthmus and are absent from the lumen. Bacteria are 8 μm long and 0.7 μm wide with bipolar flagella. They are closely associated with parietal cell surfaces and are found intracellularly lying free in the cytoplasmic matrix. Similar organisms have been seen by electron microscopy in fox[214] and detected by PCR in a variety of other species.[215] In cheetahs, HHLO may induce chronic lymphoplasmacytic gastritis, gastric hyperplasia, and vomiting. Organisms with polar flagella and helical filaments were identified ultrastructurally.

Vet-ebooks.com

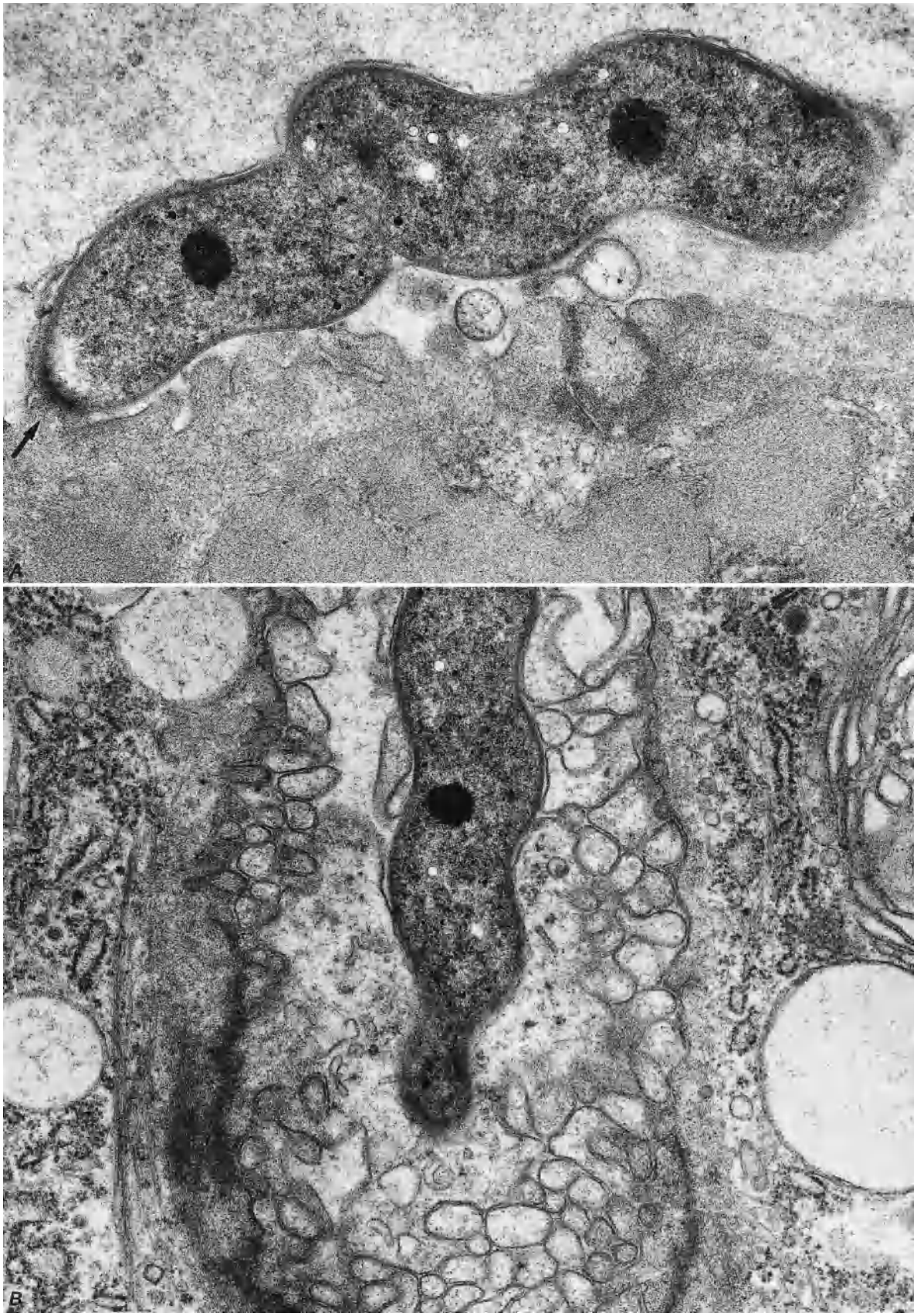


Fig. 14.15 Gastric sphirochete: stomach, dog. **A**. Spirochete attached to mucus (*arrow*). **B**. Spirochete embedded in surface microvilli of gastric parietal cell.

Vet-ebooks.com

Table 14.11 Order Aeromonadales: pathogenic species.

Pathogen	*Disease (host) and ultrastrucural studies*	*Reference to ultrastructural pathology*
	Genus *Anaerobiospirillum*	
A. succiniciproducens	Bacteremia in an HIV-infected individual	**Park**, *Am J Clin Pathol* 85:73, 1986; **Tee**, *J Clin Microbiol* 36:1209, 1998
	Genus *Aeromonas*	
A. hydrophila	Disease in aquatic animals, intestinal disease in humans, and systemic illnesses in immuno-compromised humans	**Ho**, *J Exp Med* 172:795, 1990; **Janda**, *Infect Immun* 55:3070, 1987; **Wilmsen**, *EMBO J* 11:2457, 1992; **Muller**, *Zentralbl Veterinarmed B* 27:419, 1980; **Zhang**, *Microbiology* 149:1051, 2003
A. salmonicida	Fish diseases	**Garduno**, *J Struct Biol* 109:184, 1992; **Morrison**, *J Fish Dis* 7:477, 1984

Order Aeromonadales

Genus *Aeromonas*

Aeromonas are gram-negative rods free-living in a variety of aquatic environments. They are also part of the normal intestinal flora of animals that ingest blood, for example, bats, leeches (Table 14.11). *Aeromonas* species cause epizootic infections in fish, amphibians, and reptiles. It is occasionally associated with human infections but is increasingly associated with traveler's diarrhea, septic arthritis, and necrotizing fasciitis and septicemia in immunosuppressed patients.[216,217] Ultrastructurally, *A. hydrophila* bears fimbria-like appendages and filaments.[218] In tissue, it resides in extracellular spaces and the toxin secreted is responsible for severe tissue injury. Muscle damage at local sites of infection may be severe and the skeletal myocyte develops vacuoles and proceeds through disintegration of myofilaments.

Virulence determinants include α- and β-hemolysins, extracellular proteases, and enterotoxins. *Aeromonas hydrophila* has a **Type II secretion system**–associated cytotoxic enterotoxin (Act); a **type III secretion system**–secreted AexU effector from a diarrheal isolate SSU; and a **Type VI secretion system** from isolate SSU.[219] **Aerolysin**, the cytolytic toxin secreted by *A. hydrophila*, is a channel-forming protein released as a hydrophilic, 52 kD **proaerolysin**, which is activated by proteolytic removal of a 25 amino acid C-terminal peptide. Images of aerolysin derived from electron microscopy led to a model of the membrane channel and a scheme to account for insertion of the protein into lipid bilayers to form ion channels.[75] Monomeric aerolysin has little surface activity but it can oligomerize to form stable structures that can insert into lipid bilayers to produce channels. Toxin pores have been reconstructed on the surfaces of erythrocytes.[220] *A. salmonicida*, is a pathogen of salmonids and other fish[221] and exotoxin T targets host cytoskeleton and has a Rho family GTPase-activating protein domain.[222]

Order Enterobacteriales

The family Enterobacteriaceae has at least 45 genera that form a diverse group of gram-negative, non-spore-forming bacilli, many of which are pathogenic for humans, animals, and plants.

Genus *Calymmatobacterium*

Calymmatobacterium granulomatis causes **granuloma inguinale**, a sexually transmitted veneral disease characterized by raised, beefy-red, velvety nodules of granulation tissue. *C. granulomatis* is a gram-negative bacterium measuring 1.5 × 0.7 μm with a prominent capsule. In tissue smears, *C. granulomatous* occurs in vacuoles in macrophages and in a few neutrophils. Bacteria reproduce in multiple foci in these cells until the vacuole contains 20–30 bacterial cells (which are liberated on cellular lysis). Electron microscopy reveals a sharply defined capsule and filamentous projections and pili that extend from the cell wall.[223] In tissue specimens, a typical gram-negative trilaminar cell-wall structure was seen with an outer membrane, a middle electron-opaque layer and an inner plasma membrane. Here, surface structures such as fimbriae, flagella, and bacteriophages were not seen.[224]

Genus *Escherichia*

Escherichia coli is a predominant inhabitant of the gastrointestinal tract of a variety of mammals (Table 14.12). Strains reside in the mucous layer of the

Vet-ebooks.com

Table 14.12 Order Enterobacteriales.

Pathogen	*Disease (host) and ultrastrucural studies*	*Reference to ultrastructural pathology*
	Genus *Citrobacter*	
C. freundii	Murine colonic hyperplasia	**Schauer**, *Infect Immun* 61:4654, 1993
	Genus *Edwardsiella*	
E. ictaluri	Enteric septicemia of catfish	**Miyazaki**, *J Fish Dis* 8:309, 1985
	Genus *Escherichia*	
E. coli	Septicemia in turkeys and airsacculitis in chickens. Ultrastructural studies involving hemolysin, cell walls, cell division, fimbriae, and the capsule. Ultrastructural studies on the colonization, non-invasive secretory diarrhea of enterotoxigenic disease; the attachment and effacing lesions of enteropathogenic disease; the intracellular invasion of enteroinvasive disease; the hemolytic enteritis, hemolytic/uremic syndrome of enterohemorrhagic disease; enteroaggregative disease; and septicemia, encephalitis, and urogenital disease in humans, poultry, pigs, cattle, rabbits, and other animal species	**Bhakdi**, *Infect Immun* 52:63, 1986; **Cavalier**, *Microbiol Rev* 48:326, 1984; **Conti**, *J Bact* 83:544, 1962; **Hibberd**, *J Gen Microbiol* 136:2449, 1990; **Imberechts**, *Infect Immun* 60:1963, 1992; **Kroencke**, *J Bacteriol* 172:1085 and 3469, 1990; **Ngeleka**, *Infect Immun* 61:836, 1993; **Old**, *J Med Microbiol* 23:247, 1987; **Orskov**, *Infect Immun* 47:191, 1985; **DePamphilis**, *J Bact* 105:384, 396, 1971; **De Petris**, *J Ultrastruct Res* 19:45, 1967; **Morgan**, *J Bacteriol* 93:1987, 1967; **Rafiee**, *J Cell Biol* 115:1021, 1991; **Rozenberg-Arska**, *Infect Immun* 50:852, 1985; **Sato**, *Lab Invest* 47:304, 1982; **Silverblatt**, *Infect Immun* 24:218, 1979; **Toth**, *Infect Immun* 58:1223, 1990; **Wolf**, *Infect Immun* 56:1846, 1988; **Bellamy**, *Am J Vet Res* 40:1391, 1979; **Bertschinger**, *Vet Pathol* 20:99, 1983; **Canil**, *Infect Immun* 61:2755, 1993; **Chan**, *Infect Immun* 37:1170, 1982; **Darfeuille-Michaud**, *Infect Immun* 52:468, 1986; **Fujii**, *Infect Immun* 62:3447, 1994; **Knutton**, *Infect Immun* 57:3364, 1989; **Girardeau**, *Infect Immun* 56:2180, 1988; **Nagy**, *Vet Pathol* 29:239, 1992; **Donnenberg**, *Infect Immun* 59:4310, 1991; **Helie**, *Infect Immun* 59:814, 1991; **Moon**, *Infect Immun* 41:1340, 1983; **Moxley**, *Infect Immun* 53:339, 1986; **Pedroso**, *Infect Immun* 61:1152, 1993; **Peeters**, *Infect Immun* 46:690, 1984; **Rothbaum**, *Gastroenterology* 83:441, 1982; **Schlager**, *Infect Immun* 58:1337, 1990; **Tzipori**, *Infect Immun* 57:1142, 1989; **Staley**, *Am J Dig Dis* 15:293, 1970; **Staley**, *Am J Pathol* 69:371, 1969; **Dytoc**, *Infect Immun* 61:3382, 1993; **Francis**, *Infect Immun* 51:953, 1986; **Keenan**, *Am J Pathol* 125:69, 1986; **Mainil**, *Am J Vet Res* 48:743, 1987; **Tzipori**, *Infect Immun* 55:3117, 1987; **Tzipori**, *J Infect Dis* 154:712, 1986; **Tzipori**, *Infect Immun* 63:3621, 1995; **Knutton**, *Infect Immun* 60:2083, 1992; **Nataro**, *Infect Immun* 60:2297, 1992; **Tzipori**, *Infect Immun* 60:5302, 1992; **Ackermann**, *Vet Pathol* 28:183, 1991; **Arp**, *Am J Vet Res* 42:650, 1981; **Dominick**, *Vet Pathol* 22:262, 1985; **Jones**, *Lab Invest* 54:282, 1986; **Kirtona**, *Lab Invest* 56:198, 1987; **Methiyapun**, *Vet Pathol* 21:516, 1984; **Nelson**, *J Neuropathol Exp Neurol* 21:155, 1962; **Dublin**, *Yale J Biol Med* 48:211, 1975; **Frost**, *Austr Vet J* 63:327, 1986; **Fukushi**, *Invest Urol* 17:61, 1979; **Hill**, *Res Vet Sci* 37:179, 1984; **Ivanyi**, *Virch Arch B* 59:83, 1990; **Keane**, *Am J Pathol* 126:350, 1987; **Kuriyama**, *Infect Immun* 51:193, 1986; **Johnston**, *Lab Invest* 38:439, 1978; **Matsuda**, *Infect Immun* 48:652, 1985; **Shimamura**, *Exp Mol Pathol* 29:253, 1978; **Silverblatt**, *J Exp Med* 140:1696, 1974; **Inman** *J. Infect Dis* 154:742, 1986; **Fletcher**, *Infect Immun* 60:2229, 1992
	Genus *Klebsiella*	
K. pneumoniae	Pneumonia and other infections usually in humans with underlying diseases also and studies involving fimbriae	**Di Martino**, *Infect Immun* 64:2266, 1996; **Fader**, *Infect Immun* 30:554, 1980; **Meno**, *Infect Immun* 58:1421, 1990; **Thornley**, *J Gen Microbiol* 28:51, 1962; **Zahller,** A*ntimicro Agent Chemother* 46:2679, 2002
	Genus *Plesiomonas*	
P. shigelloides	From freshwater fish and shellfish; causes diarrhea and pseudoappendicitis in humans	**Herrington**, *Infect Immun* 55:979, 1987

Vet-ebooks.com

Table 14.12 *Continued*

Pathogen	*Disease (host) and ultrastrucural studies*	*Reference to ultrastructural pathology*
	Genus *Proteus*	
P. mirabilis	Urinary tract infection and studies in kidneys	**Silverblatt**, *J Exp Med* 140:1696, 1974; **Allison**, *Infect Immun* 60:4740, 1992 (urothelium); **Chippendale**, *Infect Immun* 62:3115, 1994; **Takeuchi**, *J Urol* 132:67, 1984
P. vulgaris	Infections in humans in long-term care facilities, hospitals, or with underlying diseases and compromised immune systems. Also studies involving flagella	**Abram**, *J Bacteriol* 90:1337, 1965; **Fleck**, *J Bacteriol* 120:929, 1974; **Leene**, *J Cell Biol* 27:241, 1965; **van Iterson**, *J Cell Biol* 20:377, 1964; **Silverblatt**, *J Exp Med* 140:1696, 1974
	Genus *Salmonella*	
Salmonella species	Studies involving bacterial ultrastructure	**Ariel**, *Arch Pathol* 32:17, 1970; **Finlay**, *J Infect Dis* 162:1096, 1990; **Lin**, *Br J Exp Pathol* 68:539, 1987; **Takeuchi**, *Am J Pathol* 51:137, 1967; **Volkman**, *J Exp Med* 139:264, 1974
S. enterica subspecies *arizonae*	Chronic proliferative rhinitis in sheep	**Meehan,** *Vet Pathol* 29:556, 1992; **Brogden**, *Vet Rec* 135:410, 1994
S. enterica serovar Choleraesuis	Systemic infections in spleen, kidneys lymph nodes, and respiratory tract of pigs. Bacteremia	**Baskeville**, *J Comp Pathol* 83:207, 1973; **Baskeville**, *J Comp Pathol* 53:641, 1972; **Nnalue**, *Infect Immun* 60:2758, 1992; **Pospischil**, *Am J Vet Res* 51:619, 1990; **Reed**, *Am J Vet Res* 47:75, 1986; **Bolton**, *J Med Microbiol* 49:503, 2000
S. enterica serovar Dublin	Bacteremia	**Bolton**, *J Med Microbiol* 49:503, 2000
Salmonella enterica serovar Enteritidis	Associated with poultry	**Popiel**, *Infect Immun* 47:786, 1985; **Yamamoto**, *J Infect Dis* 116:8, 1966; **Ogunniyi**, *Infect Immun* 62:5376, 1994
S. gallinarum	Diarrhea and death in young poultry	
S. heidelberg	Experimental disease in pigs	**Reed**, *Am J Vet Res* 46:2300, 1985
S. minnesota	Experimental infection in the lung	**Ryan**, *Infect Immun* 57:1356, 1989
S. pullorum	Diarrhea and death in young poultry	**Crichton**, *J Appl Bacteriol* 67:283, 1989
S. enterica serovar Typhi	Typhoid fever in humans	**Kaiserling**, *Virch Arch* B 11:343, 1972
S. enterica serovar Typhimurium	Enterocolitis. Also persistent, asymptomic infections in pigs	**Buchmeier**, *Infect Immun* 59:2232, 1991; **Joiner**, *J Cell Biol* 109:2771, 1989; **Lin**, *Br J Exp Pathol* 68:539, 1987; **Pace**, *Cell* 72:505, 1993; **Takeuchi**, *Am J Pathol* 50:109, 1967; **Wallis**, *J Med Microbiol* 22:39, 1986; **Nnalue**, *Infect Immun* 60:2758, 1992; **Athouse**, *Infect Immun* 71:6446, 2003; **Bolton**, *J Med Microbiol* 49:503, 2000; **Meyerholz**, *Vet Path* 39:712, 2002; **Santos**, *Vet Path* 39:200, 2002
	Experimental disease models	**Gao**, *Infect Immun* 60:3780, 1992; **Guo**, *J Med Microbiol* 22:343, 1986; **Giannasca**, *Infect Immun* 64:135, 1996; **Haque**, *Gut* 53:1424, 2003
	Genus Shigella	
S. dysenteriae	Bloody diarrhea, abdominal cramps, and fever in humans and experimental studies	**Mathan**, *Am J Pathol* 123:25, 1986; **Takeuchi**, *Vet Pathol* 19 (Suppl 7):1, 1982; **Wassef**, *Infect Immun* 57:858, 1989; **Wiley**, *J Neuropathol Exp Neurol* 44:496, 1985
S. flexneri	Mild diarrhea and dehydration in humans and experimental studies with shiga toxin	**Bkernardini**, *Infect Immun* 61:3625, 1993; **Clerq**, *Infect Immun* 55:2681, 1987; **Mounier**, *Infect Immun* 60:237, 1992; **Oaks**, *Infect Immun* 48:124, 1985; **Prevost**, *Infect Immun* 60:4088, 1992; **Sandvig,** *J Cell Biol* 108:1331, 1989; **Sansonetti**, *Infect Immun* 51:461, 1986; **Takeuchi**, *Am J Pathol* 47:1011, 1965; **Takeuchi**, *Am J Pathol* 52:503, 1968; **Takeuchi**, *Am J Pathol* 81:251, 1975
	Genus *Serratia*	
S. marcescens	Urinary tract infections, occasionally wound infections, pneumonia, meningitis, septicemia, and endocarditis	**Jingushi**, *Infect Immun* 55:1600, 1987; **Johnson**, *J Clin Pathol* 51:789, 1998; **Rodriques**, *Acta Microbiol Immunol Hung* 53:89, 2006; **Moraes**, *Exp Parasitol* 115:200, 2007

Vet-ebooks.com

Table 14.12 *Continued*

Pathogen	*Disease (host) and ultrastrucural studies*	*Reference to ultrastructural pathology*
	Genus *Yersinia*	
Y. enterocolitica	Enteritis in humans and studies on bacterial ultrastructure and infection in pigs	**Kapperud**, *Infect Immun* 55:2247, 1987; **Robins-Brown**, *J Med Microbiol* 19:297, 1985; **Young**, *J Cell Biol* 116:197, 1992; **Carter**, *Am J Pathol* 81:703, 1975; **Rabson**, *J Infect Dis* 131:447, 1975
Y. pestis	Plague in humans and experimental infections in monkeys and mice	**Finegold**, *Am J Pathol* 54:167, 1969; **Straley**, *Infect Immun* 45:655, 1984
Y. pseudo tuberculosis	Gastroenteritis, diarrheal disease, and typhoid-like septicemia	**Brunius**, *J Med Microbiol* 16:245, 1983; **Isberg**, *Cell* 50:769, 1987; **Small**, *Infect Immun* 55:1674, 1987

large intestine and utilize nutrients present there for growth (Fig. 14.16).[225] The **capsule, lipopolysaccharide, fimbriae**, and **adhesins** of *E. coli* aid in the attachment and penetration of the intestinal mucous layer and consequently influence colonization of a stable microflora.

Colibacillosis and Enteritis

In humans, pathotypes of *E. coli* cause gastrointestinal tract infections, urinary tract infections, sepsis, and meningitis. At least six pathotypes alone cause gastrointestinal tract infections. **Enterotoxigenic *E. coli* (ETEC)** strains attach via fimbriae to intestinal mucosal epithelium and produce enterotoxins that induce a secretory diarrhea.[226] Occasionally they invade. *E. coli* are thought to be important in Crohn's disease pathogenesis and ultrastructural studies show that *E. coli* in these patients are found in macrophages and replicate within phagolysosomes.[227]

Enteroinvasive *E. coli* (EIEC) strains invade the epithelium, kill enterocytes, produce diarrhea and marked intestinal lesions with much inflammation. **Enteropathogenic *E. coli* (EPEC)** strains (055, 0111, 0119, 0125, et al. in humans) cause enterocyte damage by effacement of the intestinal epithelial cell brush border with pedestal and cup formation at sites of bacterial attachment to the enterocyte surface. **Enterohemorrhagic *E. coli* (EHEC)** strains (including strain 0157:H7) produce cytotoxins (vero toxins) that damage microvillous surfaces of the ileum and colon. **Enteroaggregative *E. coli* (EAEC)** strains develop an aggregative pattern of adherence to HEp-2 cells in culture. The use of cell culture adhesion assays has identified other putative classes of diarrheic *E. coli*. **Diffusely adhesive *E. coli* (DAEC)** define **diffuse** adhering bacteria versus those that are localized as microcolonies of adherent bacteria.

Strains of *E. coli* are highly adaptable and have acquired unique combinations of virulence determinants that allow them to cause disease in unique sites in a wide range of hosts. These strains are called pathotypes and have astonishing combinations of adhesins, lipopolysaccharides, flagella, and toxins; many encoded on genetic elements that are immobilized in the different strains.[228] Pathotypes that reside on mucosal surfaces produce a predominance of fimbrial and nonfimbrial adhesins whereas invasive strains produce a predominance of toxins.

Adhesins of *E. coli*

Fimbrial adhesins of *E. coli* mediate attachment of the organism to a variety of surfaces. Fimbriae of *E. coli* fall into the classes previously described. The "chaperone-usher" fimbriae pathway contains **Type 1 fimbriae** produced by all *E. coli*. These rodlike fibers have flexible tip adhesins that bind to host glycoproteins and glycolipids via a D-mannose component. Also included are the **P(pap) fimbriae** produced by UPEC. The CS1 fimbrial family contains the CFA/I fimbriae of ETEC and F17 fimbriae in *E. coli* K12. The **Type IV fimbriae** family are flexible rods and some form bundles. They bind to host CD46 receptors and glycolipid and C4BP receptors. **Bundle forming pili** produced by EPEC are members of Type IV fimbriae family and aggregate to form large rope-like structures greater than 10 μm long. The extracellular nucleator pathway family of fimbriae contains **curli fimbriae**. These fimbriae are coiled, aggregative filaments. They bind to host fibronectin, laminin, plasminogen, and plasminogen activator. Others include **long polar fimbriae** produced by EPEC and EHEC; **aggregative adherence fimbriae** encoded on the pAA virulence plasmid produced by EAEC; **Fic fimbriae** produced by UPEC; **S fimbriae** produced by UPEC and MNEC; **Dr fimbrial adhesins**; and fimbrial colonization factor antigens, **CFA/I** and **CFA/II**.[228] Type 1 fimbriae, Type IV fimbriae, and curli fimbriae are involved in host tissue-adhesion, co-aggregation, and immuno-modulation. Type 1 fimbriae and curli fimbriae are also involved in biofilm formation. Type IV fimbriae are involved in motility and uptake of DNA.

Vet-ebooks.com

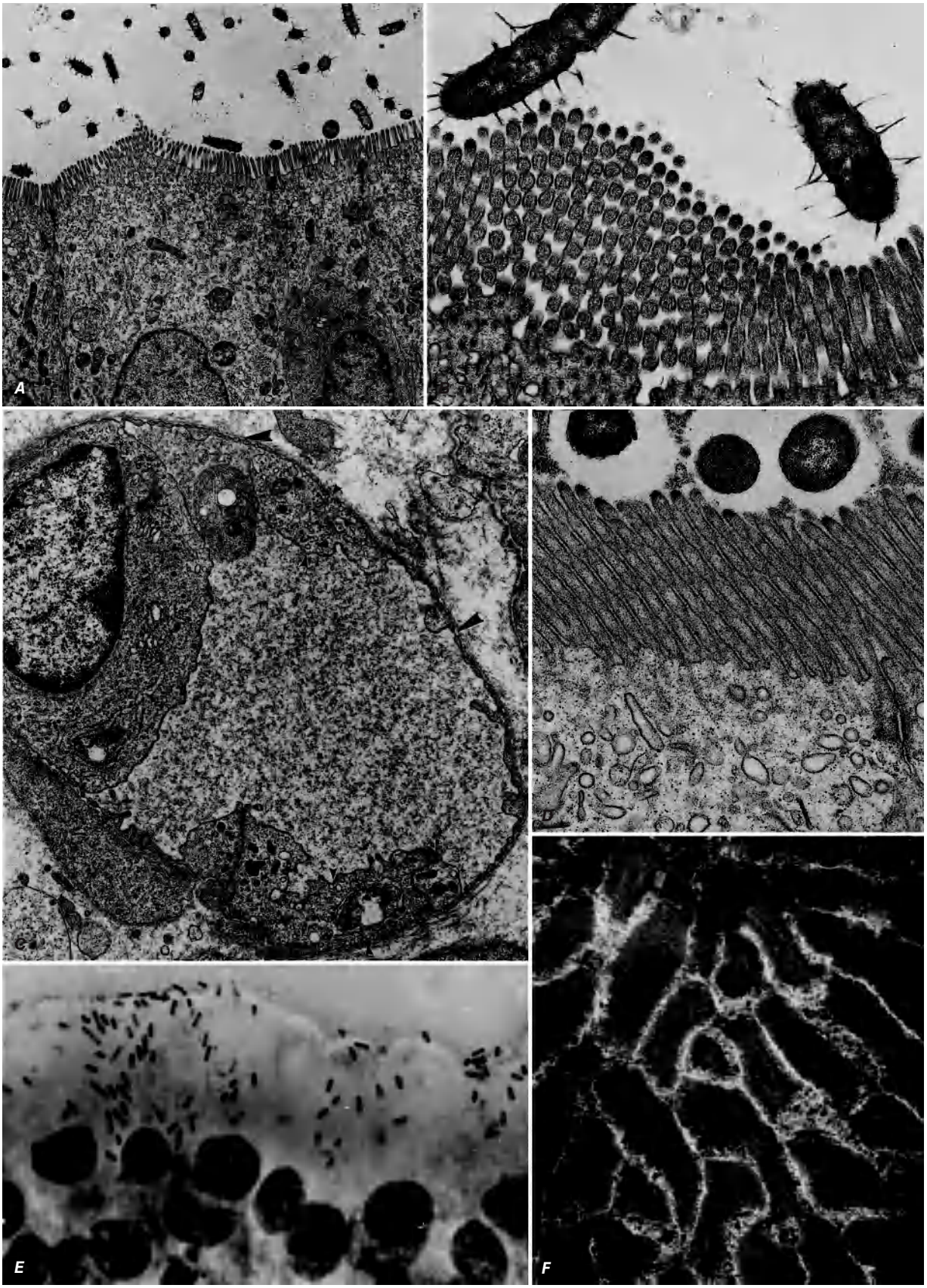


Fig. 14.16 *Escherichia coli*: intestine. **A**. **Attachment of bacilli** to enterocyte microvillous surface. **B**. **Bacterial fimbriae** attach to microvilli. Fimbriae appear thick because of fusion during processing. **C**. **Submucosal capillary** 16 hr after exposure to cholera enterotoxin: endothelium appears normal. **D**. ***E. coli* adhered to intestinal surface. E**. ***E. coli* within enterocytes. F. Heavy layer** of *E. coli* along epithelial surfaces, fluorescent antibody-stained tissue section. (Micrographs: Harley W. Moon.)

Vet-ebooks.com

Non-fimbrial adhesins of *E. coli* also mediate attachment of the organism to a variety of surfaces. Non-fimbrial surface-associated proteinaceous adhesins include adhesin porcine attaching and effacing-associated (**paa**) factor; the STEC autoagglutinating adhesin (**saa**); intimin, an outer membrane protein of EHEC O157:H7.[229] Intimin is also required for intestinal colonization in colostrum-deprived neonatal calves by *E. coli* O157:H7, for the induction of colonic edema and diarrhea, and for the formation of intestinal attaching and effacing lesions; the *E. coli* factor for adherence (**efa1**) and its nearly identical homologue (**LifA**); **AFA-I** and **AFA-III**; and nonfimbrial adhesins (**NFA-1** and **NFA-2**).

Toxins of *E. coli*

Many *E. coli* strains produce toxins in varying combinations. These include heat-labile enterotoxin (LT), shiga toxin (stx), cytolethal distending toxin (CDT), shigella enterotoxin 1 (ShET1), shigella enterotoxin 2 (ShET2), heat-stable enterotoxin a (STa), heat-stable enterotoxin b (STb), Ehx (RTX toxin); Type II secretion product (StcE); type III secretion products (including IpA, IpB, IpC, IpH, IpgD, Cif, EspF, EspH, EspK, Map, and Tir); and enzymes (SepA, Pic, EspC, urease, EspP, Pet, and hemoglobin-binding protease).

Endotoxin (e.g., **lipopolysaccharide**) of *E. coli* causes widespread damage to tissue and underlies most of the systemic effects in colisepticemia. Damage is prominent in the lungs and liver but because injury is vascular in nature, there is damage to all organ systems. Intravascular lysis of *E. coli* releases endotoxins, which absorb to surfaces of endothelial cells, platelets, leukocytes, mast cells, and other cells. Primary injury is accompanied by release of cytokines and vasoactive factors that underlie vasodilation, circulatory collapse, fever, intravascular coagulation thrombocytopenia, leukopenia, and other clinical signs of septic shock.

Enterotoxigenic *E. coli* colonize the proximal small intestine and colonization of the neonatal intestine occurs via Type 1 or CFA fimbrial adhesins.[228,230] In electron micrographs, bacteria are separated from epithelial cell microvilli and other bacteria by a space of 50–400 nm. Filamentous bacterial appendages can be seen bridging this space and forming a network among bacterial cells. As one would expect from a toxigenic pathotype, ETEC strains produce toxins that increase ion secretion resulting in noninvasive secretory diarrhea. They can produce a heat-labile enterotoxin (LT), shigella enterotoxin 2 (ShET2), heat-stable enterotoxin a (STa), and/or heat-stable enterotoxin b (STb). LT is a large immunogenic polypeptide that binds to monosialoganglioside (GM1 residues) of intestinal epithelial cells and causes ion secretion by stimulating adenyl cyclase activity. ShEt2, Sta, and STb all increase ion secretion; STa and STb activate guanylate cyclase and increase intracellular calcium, respectively.

Enteroinvasive disease strains cause disease by binding to, entering, and causing damage to intestinal absorptive cells. These strains of *E. coli* are intracellular pathogens and replicate within enterocytes causing degeneration and necrosis. Thus, disease arises from direct tissue invasion and EIEC infections with similar lesions have been reported in pigs. These strains have means to attach through Type I fimbriae and IcsA adhesins and means to kill epithelia cells. EIEC produce *Shigella* enterotoxin ShET1, ShET2, and SigA, which causes ion secretion and a variety of enzymes and factors causing actin depolymerization, apoptosis, IL-1 release, actin polymerization, microtubule destabilization, membrane ruffling, and membrane blebbing.[228]

Enteropathogenic *E. coli* strains cause acute infantile diarrhea by directly damaging enterocytes. Intestinal biopsies from infected patients show adherent bacilli to elongated and effaced microvilli of the enterocyte brush border. The term attaching-effacing is used to describe the classic EPEC strains that cause microvillus damage; for example, enteroadherent *E. coli* cause diarrhea in humans by attaching to and destroying the microvillous layer of absorptive enterocytes. EPEC strains are generally noninvasive although internalization has been documented in some studies.

In early work, an invasion determinant of EPEC has identified that conferred invasive capacity. EPEC produce Type I fimbriae, bundle forming pili, and long polar fimbriae, which allow EPEC strains to intimately associate with enterocyte plasma membranes. Fimbriae, although not essential, promotes the initial interaction with enterocyte surfaces. Although adherence to Peyer's patch lymphoid follicle epithelium (M cells) is via pili, other mechanisms appear to operate in adherence to enterocytes late in infection. EPEC strains also produce the non-fimbrial adhesins intimin and Paa. Type III secretion products (Cif, EspF, EspH, Map, and Tir), enzymes (EspC), and LifA/Efa block mitosis, open tight junctions, modulate filopodia, disrupt mitochondrial membranes, nucleate cytoskeletal proteins, and inhibit lymphocyte activation and adherence.[228] Membranes are cupped around the EPEC and raised beneath adherent bacteria in pedestal structures. Polymerized actin of microfilaments aggregates in the apical cytoplasm beneath adherent bacteria.

Enterohemorrhagic *E. coli* strains produce an impressive array of fimbriae (Type I fimbriae and long polar fimbriae); adhesins (intimin, Paa, Toxb, Efa-1/LifA, Saa, and OmpA), toxins (Shiga toxin and Ehx RTX toxin); Type II secretion products (StcE); Type III secretion products (EspF, EspH, EspK, Map, and Tir);

Vet-ebooks.com

enzymes (EspP and urease); and LifA/Efa. These block mitosis, open tight junctions, modulate filopodia, disrupt mitochondrial membranes, nucleate cytoskeletal proteins, inhibit lymphocyte activation and adherence, and cause intense vascular damage and hemorrhage.[228,231] There is petechiation in affected areas of the intestine. EHEC strains cause lesions in piglets that resemble those of humans.

Healthy dairy and beef cattle are a major reservoir of a diverse group of Shiga toxin Stx1 and Stx2-producing EHEC called O157:H7. These organisms infect humans through ingestion of contaminated food and water and direct contact. Infections result in combinations of watery diarrhea, bloody diarrhea, and hemolytic uremic syndrome.[232] Hemolytic uremic syndrome usually follows hemorrhagic colitis. The endothelial cell is a major target of injury as is the mesangial cells, renal tubular epithelial cells, and monocytes. Inflammatory cytokines are involved.[233]

Enteroaggregative *E. coli* strains cause acute and persistent diarrhea among children, adults and HIV-infected persons, in both developing and developed countries. Some EAEC infections result in diarrhea and elicit an inflammatory response, whereas other infections do not.[234] EAEC also infect humans through ingestion of contaminated food and water. EAEC strains produce fimbriae (Type I fimbriae and aggregative adherence fimbriae), toxin (ShET1), and serine proteases (Pet and Pic).[228] EAEC form unique "stacked brick" aggregates of bacterial cells on epithelial surfaces.[235] A collection of 44 EAEC strains isolated from infants with diarrhea were shown to adhere to human colonic mucosa in localized aggregates.

Diffusely adhesive *E. coli* is a new category of diarrheagenic *E. coli*. DAEC have Type 1 fimbriae, Dr fimbriae adhesin, and a vacuolating cytotoxic action in bladder and kidney tissues. A DAEC strain induced a pronounced fluid accumulation in rabbit ileum loops.[236] Villous necrosis was seen in the histopathologic examination. Morphological changes were also seen in Y1 adrenal cell cultures.

In humans, pathotypes of *E. coli* also cause urinary tract infections, sepsis, and meningitis. One pathotype, **uropathogenic *E. coli* (UPEC)**, causes urinary tract infections and one pathotype, **meningitis-associated *E. coli* (MNEC)**, causes sepsis and meningitis.

Uropathogenic *E. coli* strains induce urinary tract infections and **pyelonephritis** in humans. Renal infections commonly arise hematogenously, from lodging of bacteria circulating in the blood. Experimentally, when large numbers of *E. coli* are injected into renal arteries of rabbits, bacteria adhere to endothelium of glomerular and intertubular capillaries. Urinary glycoprotein (Tamm-Horsfall protein), secreted by the kidney, is protective since it can entrap UPEC by adhering to its fimbriae.

To efficiently attach to the luminal surfaces of transitional epithelial cells of the urinary bladder, UPEC strains produce an assortment of fimbriae and adhesins that include Type I fimbriae, P (Pap) fimbriae, F1C fimbriae, S fimbriae, and Dr fimbriae adhesin. They also produce toxins and proteases that induce leukocyte lysis (HiyA, an RTX toxin), alter cytoskeletons (CNF-1, -2), lead to vacuolation (Sat), and digest proteins and mucins (Pic). They contain siderophore receptors for iron acquisition (ChuA, IreA, and IroN).[237] Iha, IutA, and FliC are also produced. Genes encoding ChuA, IroN, hypothetical protein c2482, and IutA are more prevalent among UPEC strains than among fecal-commensal *E. coli* isolates. Pathogenic bacteria may be taken into epithelial cells by phagocytosis and most bacteria are destroyed. In ultrastructural studies of experimental rodent infections, large numbers of *E. coli* are found in some cells coincident with acute cells swelling, and eventually degeneration and desquamation into the bladder lumen. Intracellular *E. coli* colonies in exfoliated cells of women with urinary tract infections suggest that *E. coli* binds to, invades, and replicates in urothelium forming an intracellular niche.[238] Mixed infections dramatically alter the behavior of the bacteria relative to their behavior in a single infection.[239]

Meningitis-associated *E. coli* strains induce septicemia chiefly in human neonates and several animals; death is often associated with meningoencephalitis. MNEC strains produce fimbrial adhesins (Type I fimbriae and S fimbriae), non-fimbrial adhesins (OmpA), toxins, cytotoxic necrotizing factors (CNF-1, -2), and other determinants (IbdA, IbeB, IbeC, Asia, and Chu/shu). MNEC strain K1 is the most common organism causing neonatal meningitis and OmpA, IbeB, and CNF1 contribute to the invasion of strain K1 in human brain microvascular endothelial cells.[240,241] In animals, there are unique coliform infections; for example, mastitis of cattle during the neutropenic phases of midlactation; in the mammary gland, *E. coli* is present in large numbers in acinar lumens.

Avian pathogenic *E. coli* (APEC) causes respiratory infections, pericarditis, and septicemia of poultry.[242] Ultrastructural studies show that despite the absence of fimbriae, avian septicemic *E. coli* adhere but do not invade Hep-2 cells likely due to afimbrial adhesins genes on the 88 MDa plasmid.[243] However, Stg fimbriae, demonstrated on the surface of *E. coli* K-12 by immunogold electron microscopy, likely contribute to the colonization of avian respiratory tissues by APEC 078 isolates.[244]

Edema disease or *E. coli* enterotoxemia occurs in piglets at the age of weaning. Toxin (Shiga-like toxin II), produced in the digestive tract and absorbed into the circulation, causes vascular lesions in the intestine, subcutis, and brain. The causal toxigenic *E. coli* attach

Vet-ebooks.com

to epithelium of the mid-jejunum and ileum, and ultrastructural studies reveal continuous layers of bacteria and microcolonies along normal appearing brush borders of absorptive cells. An electron-lucent zone appears around adhering bacilli.[245] Tips of villi are preferentially colonized. Recent ultrastructural studies on an edema disease have shown that fimbriae develop on bacteria in the intestine and that these fimbriae adhere to isolated porcine brush border fragments. The gene cluster encoding fimbriae has been cloned and the major subunit gene defined as *fedA*, referring to fimbriae associated with edema disease.[246]

Genus *Klebsiella*

Klebsiella pneumoniae is among 12 species in the genus and is an important cause of hospital outbreaks of nosocomial infections.[247] *K. pneumoniae* develops antibiotic resistance and causes hospital-acquired urinary tract infections, pneumonia, septicemias, and soft-tissue infections. The human gastrointestinal tract may be a reservoir for *K. pneumoniae*. Adherence to gut mucosa is enhanced by pili. Three types of pili have been reported: 1, 3, and 6, and all mediate adherence.[248] The capsule is not a barrier to the penetration of antibody. Excellent electron micrographs of freeze-substitution techniques show filaments of capsules form two domains: an outer domain of interlacing filaments and an inner domain of parallel extensions.

Genus *Proteus*

P. mirabilis and *P. vulgaris* are opportunistic pathogens and cause infections in the urinary tract, respiratory tract, gastrointestinal tract, wounds, burns, skin, eyes, ears, nose, and throat of susceptible humans.[249] Urinary tract infections caused by *P. mirabilis* can be subdivided into hematogenous infections (systemic infections) and ascending infections. In the latter, bacteria colonize the urethra, bladder, ureter, and kidney, which leads to acute pyelonephritis, periurethral abscesses, and renal failure. Bacteria attach to renal pelvic epithelial cells by Type IV fimbriae (approximately 7 nm in size) and Type III fimbriae (approximately 4 nm in size). They cross epithelium by several mechanisms; for example, entry and passage through living epithelial cells, between epithelial cells, and through necrotic foci. Potential virulence factors of these bacteria include a fimbriae, flagella, enzymes (urease, proteases, and amino acid deaminases), and toxins (hemolysin and endotoxin).[249] Urease promotes alkalinization of urine by hydrolyzing urea to ammonia, and this provides a nidus for struvite stones by precipitating normally soluble polyvalent ions that crystallize around bacterial cells. The ability to invade urothelial cells is also associated with motility.[250]

Genus *Salmonella*

Salmonella causes gastrointestinal disease in a wide range of animals including humans after oral ingestion of contaminated food or water.[251–254] In mammals and birds, *Salmonella* species are associated peracute toxin-induced gastroenteritis, necrotizing enteritis, and enteric infection with septicemia and visceral involvement. In a chick model of infection, ultrastructural studies showed that bacteria are found within large phagosomes and phagolysosomes of macrophages and intestinal epithelial cells.[255] In cattle, *S. enterica* serovar Typhimurium causes a fibrinopurulent necrotizing enteritis with a diffuse neutrophilic infiltrate. In humans, *Salmonella* species are associated with bacteremia (*S. enterica* serovar Choleraesuis and *S. enterica* serovar Dublin), typhoid fever (*S. enterica* serovar Typhi), and enterocolitis (*S. enterica* serovar Typhimurium).[256] Enterocolitis is characterized by a rapidly developing neutrophilic infiltrate and necrosis of the mucosa in the terminal ileum and colon. In a human intestinal organ cultures, ultrastructural studies showed that *S. enterica* serovar Typhimurium bound predominantly to the mucous layer in the first 4 hr after inoculation.[257] At 4–8 hr, small foci of *S. enterica* serovar Typhimurium attached, induced ruffling of enterocyte membranes, and invaded enterocytes.

Salmonella are acid tolerant[258] and likely survive acidic conditions of the upper gastrointestinal tract and move into the small intestine. Depending upon the species, they can utilize multiple mechanisms for crossing the intestinal barrier.[251] Systemic infections occur with typhoidal *Salmonella* species and nontyphoidal invasive enteric species while localized intestinal infections occur with other *Salmonella* species.

To induce systemic infections, *S. enterica* serovar typhi are phagocytosed by CD18+ macrophages, which move across the intestinal epithelial barrier. Infection of macrophages by several *Salmonella* spp., including *S. enterica* serovar typhimurium and *S. enterica* serovar typhi, leads to the death of the phagocyte by apoptosis. In ultrastructural studies, Inv-Spa type III secretion apparatus targets invasin SipB induced macrophage apoptosis.

To induce intestinal infections, *Salmonella* enter the intestinal mucous layer, adhere to the apical surface of the mucosal epithelium, disrupt the brush border, induce membrane ruffling, and enter by bacterial mediated endocytosis. In cultured epithelial cells, ultrastructural studies show that *S. typhimurium* triggers host cell-signaling events forming host cell membrane ruffles and bacterial uptake.[259] Introduction of

Vet-ebooks.com

SipA into the cell induces actin polymerization, filament annealing, and bundle formation.[260] These mechanically stabilized filaments reshape the cells surface into extended ruffles.[261] Ruffles then facilitate bacterial internalization. Localized inflammation and diarrhea develop.

Salmonella also enters via microfold (M) cells and translocates through the mucosal epithelial layers.[262] In pig ileal gut-loops, ultrastructural studies show that *S. enterica* serovar *typhimurium* adhered to M cells (5 min) and invaded the apical membrane of M cells, goblet cells, and enterocytes (10 min), preferentially at sites of cell extrusion.[263] In calf ileal gut-loops, ultrastructural studies show that *S. enterica* serovar *typhimurium* adhered to M cells (15 min) and invaded the lamina propria (1 hour), preferentially at sites of cell extrusion.[264] Invasion of the Peyer's patches resulted in an acute neutrophilic inflammatory response and upregulated chemokines (IL-8, GROα, GROγ, and GCP2), IL-1β, IL-IRa, and IL-4).

Salmonella species contain a number of virulence determinants.[265] These include virulence plasmids, toxins, fimbriae, and flagella. There are five *Salmonella* pathogenicity islands and two of them, SPI-1 and SPI-2, encode Type III secretion systems.[254] SPI-1 is required for invasion of nonphagocytic cells and SPI-2 is required for intracellular survival in macrophages. In vitro, *S. enterica* serovar Typhimurium translocates Type III secreted effector proteins, SipA, SopA, SopB, SopD, and SopE2 into host cells. These proteins likely elicit infiltration of neutrophils in the calf model of enterocolitis, by inducing chemoattractant chemokines in bovine ileal tissue during infection.[256] The inflammatory response likely increases vascular permeability resulting in mucosal edema. The influx of neutrophils is associated with necrosis of the uppermost ileal mucosa. The injury to the intestinal epithelium leads to leakage of extravascular fluids and massive transmigration of neutrophils into the intestinal lumen, a process normally prevented by the epithelial permeability barrier. This data suggests that the severe fluid loss observed during *Salmonella* serovar Typhimurium-induced enterocolitis is at least in part due to an inflammatory mechanism, which causes liquid to flow from the blood to the intestinal lumen.

Adherence to epithelial cells may occur via fimbriae likely encoded via fimbrial operons in all *Salmonella* species and subspecies; for example, those in the nucleator-dependent operon, Type IV operon, and the chaperone-usher dependent operon.[265] However, the role of fimbriae in the pathogenesis is still not well understood. *Salmonella* species also produce endotoxins (e.g., containing lipopolysaccharide) and exotoxins. A heat labile, trypsin-sensitive cytotoxin is produced by Cholerasuis, Enteritidis, and Typhi serovars; a *Shigella dysenteriae*-1 like cytotoxin is produced by serovars Enteritidis, Kapemba, and Thompson; a hemolytic exotoxin called salmolysin is produced by certain strains; and a heat-labile enterotoxin is produced by serovar Typhimurium. The latter toxin exerts its effects by elevating cAMP and increasing the synthesis and release of prostaglandins.[265]

Genus *Shigella*

The genus *Shigella* only has four pathogenic species: *S. dysenteriae, S. flexneri, S. boydii,* and *S. sonnei*. They have narrow host and tissue specificities and infect colonic epithelial cells of humans and primates. *S. dysenteriae* has 15 serotypes; *S. flexneri* has 14 serotypes and subserotypes; *S. boydii* has 20 serotypes; and S. sonnei has a single serotype. *S. dysenteriae* causes bacillary dysentery or shigellosis.[266] Clinical signs vary from mild diarrhea to severe dysentery. *S. flexneri* and *S. sonnei* cause shigellosis, which is less severe than *S. sonnei* causing only mild diarrhea and dehydration.

Intestinal biopsies of rectal mucosa of patients with dysentery show that *S. flexneri* invades and replicates in the luminal third of the colonic epithelium.[267] Intact bacilli are found in phagosomes and, as cell degeneration proceeds, are free in the cytoplasmic matrix; they are also present between epithelial cells. Infected enterocytes in intact mucosa have acute cell swelling, mitochondrial swelling with cristolysis, short microvilli, and poorly formed glycocalyces. Acute cell swelling is accompanied by increased numbers of lipid globules and lysosomes, and terminates in cell shrinkage and necrosis. Degenerate bacilli are present in phagolysosomes of neutrophils. There are marked vascular lesions in the tunica propria with edema, fibrin and thrombus formation. Capillary and lymphatic endothelial cells are severely swollen.

The critical step in development of human bacillary dysentery is the invasion of the colonic mucosa. *S. flexneri*, unable to invade the apical pole of the colonic epithelial cells, invades the dome of lymphoid follicles.[268] They immediately enter or enterocytes by ruffling and macropinocytosis. *Shigella* can multiply in the epithelial-cell cytoplasm and move both intra and intercellularly.[268] Here it attracts neutrophils, which then destroy tissue barriers allowing *S. flexneri* to invade epithelial cells.[269] In cell cultures, ultrastructural studies show that when invasive and noninvasive *S. flexneri* strains are grown in HeLa cell cultures, pseudopod structures on the invasive strains facilitate bacterial cell-to-cell spread.[270]

Virulence determinants are plasmid encoded and delivered via a Type III secretion system.[271] *Shigella* enters epithelial cells by a macro-pinocytic event resulting from GTPase induced reorganization of the host cell cytoskeleton. Inside the cell, bacilli escape to the cytoplasm and move intracellularly in an actin-dependent process involving an outer membrane

Vet-ebooks.com

protein IcsA, a host cell protein N-WASP, and an actin nucleating complex Arp2/3. *Shigella* then spread from cell-to-cell following engagement of adherence junction components resulting in massive intracellular colonization of the intestinal epithelium. *Shigella* induce IL-8 resulting neutrophil recruitment and mucosal inflammation.

S. dysenteriae produces a shigatoxin. *S. flexneri* produces a **cytotoxin** that can kill the host cell (and has neurotoxic effects) and an **enterotoxin** that promotes fluid secretion by the small intestine. ***Shigella* toxin**, produced by all four *Shigella* species, is a multimeric protein made of one A subunit and five B subunits. Purified toxin binds to a membrane glycolipid receptor, globotriaosylceramide. The lessened susceptibility of human neonates is due to the absence of these receptors on the gut epithelia.

Genus *Yersinia*

Yersinia contains three human pathogens: *Y. pestis*, *Y. pseudotuberculosis*, and *Y. enterocolitica*. *Y. pestis* and *Y. pseudotuberculosis* are closely related and *Y. pestis* is considered to be a subspecies of *Y. pseudotuberculosis*. *Y. enterocolitica* and *Y. pseudotuberculosis* are transmitted via contaminated food or water and cause self-limiting infections of the intestinal tract or intestinal lymphoid system.[272] *Y. pestis* is transmitted by flea vectors or aerosols and causes bubonic, pneumonic, or septicemic plague.

Yersinia species are gram-negative, non-spore-forming bacilli or coccobacilli 0.5–0.8 μm wide × 1.0–3.0 μm long. *Y. pseudotuberculosis* and *Y. enterocolitica* are motile at 22–30°C and have **peritrichous flagella**. They are not motile at 37°C. *Y. pestis* is not motile at 22–30°C. Unlike *Y. pseudotuberculosis* and *Y. enterocolitica*, *Y. pestis* has special nutritional growth requirements, which likely limits its survival to hosts and flea vectors of transmission.

The trio of pathogens share unique virulence factors on their chromosomes and plasmids.[272] All three have a chromosomal high-pathogenicity island for a **siderophore**, *Yersinia* bactin and a 70 kb plasmid with genes for VirF protein, proteins of the Type III secretion system, and *Yersinia* outer proteins (Yops) secreted and translocated by the **Type III secretion system**. *Y. pseudotuberculosis*, and *Y. enterocolitica* have chromosomal genes for invasin and attachment-invasion-locus protein (Ali) and a 70 kb plasmid with a gene for the yadA adhesin. *Y. enterocolitica* has a chromosomal gene, *yst*, for a **heat-stable enterotoxin**. *Y. pestis* has chromosomal genes for hemin storage proteins and fimbrial components; a 9.5 kb plasmid with a gene for plasminogen activator; and a 110 kb plasmid with genes for F1 capsular protein and murine toxin protein.

The adhesins (invasin, attachment-invasion-locus protein, and yadA) confer the capacity of *Yersinia* to bind to host cells, initiate phagosomal uptake, and to translocate across the epithelia barrier via phagocytic M cells. **Invasins** are glycoproteins on the bacterial cell surface that interact with integrin molecules (especially those bearing the β1 chain) embedded within the host cell plasma membrane. **Integrins** are transmembrane proteins attached to the cytoplasmic matrix below the cell surface causing the matrix to develop and move phagosomes to and away from the cell surface. F1 capsular protein and Yops are anti-phagocytic proteins allowing survival and proliferation of *Yersinia* species within macrophages. In *Y. pestis*, murine toxin protein, a phospholipase D, and hemin storage protein are both required for its survival in the flea midgut and transmission to host tissues. Plasminogen activator, an outer surface protease, is required for rapid dissemination of *Y. pestis* from the fleabite to local lymphatic tissues.

In tissue, bacteria are attached to cell surfaces, usually at sites where filopodia have developed. Plasma membranes of filopodia are enriched in integrins and other adhesion proteins. **Adherence densities** between bacterial and cellular membranes occur at sites of contact. Aggregates of cellular proteins that bind integrins to the cytoskeleton (talin, filamin) are found in infected cells by immunogold labeling.

Y. pestis is the cause of bubonic, pneumonic, or septicemic **plague** or "black death" and is transmitted by bites from infected fleas. Rodents are natural reservoirs and more than 200 mammalian species have been reported to be naturally infected with *Y. pestis*. Transmission can occur via bites from more than 80 different flea species. Phospholipase D (*ymt* gene products) and hemin storage protein (*hms* gene products) of *Y. pestis* induce a damaged tissue and microbial cell containing bolus blocking the flea proventriculus. Fleas bite the host repeatedly directly transmitting organisms to host tissues.[273] In host tissues, *Y. pestis* disseminates rabidly and bacilli enter dermal lymphatics and drain into regional lymph nodes. They are taken up by macrophages, survive, and proliferate to high numbers due the production of anti-phagocytic and toxic Yops and F1 capsule proteins. In cell culture, ultrastructural studies clearly show that *Y. pestis* is taken up within the lysosomal compartment in phagolysosomes.[274–276] Thereafter, an acute suppurative lymphadenitis develops. Failure to stop bacterial replication results in septicemia with spread to liver, spleen, nervous system and lungs. There is extensive vascular damage including hemorrhage, necrosis, and disseminated intravascular coagulation. *Y. pestis* can invade epithelioid cells like the Pla-encoding plasmid pPCP1.[277] In HeLa cells, ultrastructural studies show that invasion was rapid, with 30–50% invasion occurring after 60 minutes.

Vet-ebooks.com

Y. enterocolitica causes gastroenteritis and leads to **diarrheal disease** with signs that vary from mild diarrhea to typhoid-like septicemia. After ingestion of bacteria with contaminated food or water, bacteria localize in ileum where they colonize epithelial lining cells. Penetration of epithelial cells by endocytosis leads to translocation of *Y. enterocolitica* to basal regions of the cell and exocytosis into the lamina propria. Growth in the terminal ileum is accompanied by mesenteric lymphadenitis. Most strains elaborate a heat-stable enterotoxin, which activates guanyl cyclase in vitro much like ST toxin of *E. coli* and seems to be responsible for diarrhea. *Y. enterocolitica* reacts with microvilli on cell surfaces. Mesenteric lymph nodes have focal areas of necrosis and are infiltrated by lymphocytes. Systemic infections may occur and secondary signs may include arthritis, erythema nodosum, and hemolytic anemia.

Y. pseudotuberculosis causes **pseudotuberculosis**; it invades enterocytes after ingestion of contaminated food. *Y. pseudotuberculosis* migrates to the lamina propria, enters the lymphatics, and is taken up by macrophages, which migrate to the mesenteric lymph node, liver, and spleen. *Y. pseudotuberculosis* produces the protein **invasin**, a glycoprotein on the bacterial cell surface that mediates both adherence and entry into cells in culture. *Y. pseudotuberculosis* surfaces attach to the target when carboxy terminal amino acids of the invasin protein bind to receptors on the host cell surface. Multiple membranes of the β1 chain integrin family of cell adhesion molecules act as invasin receptors. This transmembrane cell signal causes accumulation of actin-binding proteins and a polymerization of actin to form microfilaments, all required for the act of phagocytosis.

Order Legionellales

Genus *Coxiella*

Coxiella burnetii, the sole member of this genus, is an obligate intracellular bacterium that grows only in phagolysosomes of eukaryotic cells. *C. burnetii* is highly pleomorphic and 0.3 × 1 μm in size. Organisms replicate in phagocytic vesicles of macrophages, especially in the liver, spleen, and lung. In vitro, *C. burnetti* also survives in free-living amoeba in spore-like forms.[278] Replication is by binary fission, and leads to several developmental forms: **spore, small cell variant**, and **large cell variant**. Developmental forms of large and small-cell variants of *C. burnetii* have different phenotypes; there are unique small cell variant/large cell variant proteins and there are common small cell variant/large cell variant proteins. *C. burnetii* can undergo sporogenic differentiation, an asymmetric septational division of the cytoplasm leading to spore forms (which resemble the small cell variant after release from the mother cell). The presence of DNA is demonstrated by immunogold techniques.

Coxiella burnetii causes **Q fever**, an acute febrile illness of humans that begins with headache, fever, and myalgia.[279] After exposure via inhalation or ingestion of infectious material,[280] *C. burnetti* is taken up by macrophages. In the lung, ultrastructural studies show that it invades type I and, rarely, Type II pneumocytes as well as pulmonary fibroblasts and histiocytes,[281] resulting in a focal intra-alveolar inflammation with the macrophages prevailing in the exudate. At other sites the small-cell variant attaches to macrophages and is ingested where it develops in the phagolysosome.[282] Both virulent phase I and avirulent phase II *C. burnetii* infect human monocyte-derived macrophages and replicate with the same kinetics.[283] Cell-mediated immunity plays a decisive role in the clinical expression of *C. burnetii* infection.[284] In mice, placental tissues develop necrosis, vascular damage, and microthrombi.[285] Chronic Q fever in humans often results in osteomyelitis, hepatitis, and endocarditis.[286] Ultrastructurally, *C. burnetti* can be seen in large numbers in affected valves. Surgically removed valves, examined by transmission electron microscopy, all had endogenous spore-like *C. burnetti*.[287,288]

Genus *Legionella*

Most human infections are caused by *L. pneumophila* serogroups 1, 4, and 6. Other infections are caused by *L. micdeadei*, *L. longbeachae*, *L. dumoffii*, and *L. bozemanni*. These organisms are very versatile, naturally reside in aquatic habitats in a wide range of temperatures (0–63°C) and pH (5.0–8.5), and form biofilms. *L. pneumophila* grows in amoebae.[289]

L. pneumophila is a gram-negative rod approximately 0.3–0.9 μm wide × 2 μm long. It has polar flagella. Ultrastructurally, the organism is highly pleomorphic, suggesting that there is sporogenic differentiation associated with the existence of a developmental cycle.[290] Changes in membrane leaflet opaqueness, changes in vesiculation, and profuse invagination of the inner membrane are seen at different times in ultrathin sections and freeze fracture specimens.

Legionella species produce a range of illnesses from mild, self limiting illnesses (Pontiac fever) without pneumonia to disseminated and fatal pneumonia with extensive filtrates (Table 14.13). Pneumonia is associated with terminal bronchioles and pulmonary acini. There is acute alveolitis with marked neutrophilic exudation, fibrin, and albumin-rich fluid. Large numbers of *L. pneumophila* are present in cellular debris and in macrophages. Extra-pulmonary infections are rare.

Vet-ebooks.com

Table 14.13 Order Legionellales: pathogenic species.

Pathogen	*Disease (host) and ultrastrucural studies*	*Reference to ultrastructural pathology*
	Genus *Coxiella*	
C. burnetii	Q fever in humans, infections in seals, bacterial ultrastructure, and studies in yolk sac and chick embryo	**Anacker**, *J Bact* 88:1130, 1964; **Baumgartner**, *Infect Immun* 60:5232, 1992; **Burton**, *J Bact* 122:316, 1975; **Ciampor**, *Acta Virol* 16:503, 1972; **Haldane**, *J Infect Dis* 148:978, 1983; **Hall**, *Vet Pathol* 18:672, 1981; **Khavkin**, *Infect Immun* 56:1792, 1988; **Kraus**, *Zentralabl Veterinaermed B* 21:271, 1974; **Kruszewska**, *Infect Immun* 61:4188, 1993; **McCaul**, *J Bact* 147:1063, 1981; **McCaul**, *Ann N Y Acad Sci* 590:136, 1990; **Lapointe**, *J Vet Diagn Invest* 11:541, 1999
	Genus *Legionella*	
L. pneumophila	Legionnaires disease in humans. Studies in amoebas, macrophages, guinea pigs, and mice	**Chandler**, *Am J Clin Pathol* 71:43, 1979; **Fields**, *Infect Immun* 53:553, 1986; **Horwitz**, *J Exp Med* 158:1319 and 2108, 1983; **Katz**, *Am J Pathol* 90:701, 1978; **Baskerville**, *J Pathol* 140:77, 1983; **Brieland**, *Am J Pathol* 145:1537, 1994; **Cirillo**, *Infect Immun* 62:3254, 1994; **Fields**, *J Infect Dis* 167:1146, 1993; **Katz**, *Lab Invest* 46:24, 1982; **Swanson**, *Infect Immun* 63:3609, 1995; **Yamamoto**, *Infect Immun* 60:3231, 1992

These species produce pore forming toxins, Type IV fimbriae, flagella, and Type II and Type IV secretion systems regulated by Dot (defective for organelle trafficking), Mip (macrophage infectivity potentiator), and Icm (intracellular multiplication). Tissue destruction is associated with a bacterial protease, which is produced in large quantities in infected lung tissue. The toxin inhibits neutrophils by blocking the respiratory burst.

L. pneumophila is inhaled in small aerosols (<5 μm in size) into the distal lungs. Uptake of bacteria by macrophages is rapid and intense utilizing **coiling phagocytosis**, the extensive circumferential movement of pseudopodia around the bacterium (Table 14.13). Complement receptors CR1 and CR3 on the human monocytes (which recognize C3b and C3bi, respectively) mediate phagocytosis of *L. pneumophila*. C3 fragments bound to the bacterial surface enhance phagocytosis by C3 receptors. As monocytes transform to macrophages they become increasingly permissive to *L. pneumophila*, probably due to increasing expression of complement receptors.

Ultrastructurally, the phagosome-bearing bacilli in infected cells evade endocytic fusion with lysosomes.[291–293] Instead, *L. pneumophila* are transferred from the phagosome to cisternae of the rough endoplasmic reticulum, which then dilates as bacteria replicate. The Dot/Icm transporter is involved in maintaining the integrity of the *L. pneumophila* phagosome, independent of interception of ER to Golgi vesicle traffic, which is a function of the Type IV secretion system.[293] The Dot/Icm Type IV secretion system is thought to allow *L. pneumophila* to evade the endocytic fusion. Ultrastructural studies show that phagosomes containing Dot/Icm mutants do not fuse with lysosomes and are free in the cytoplasm.[293,294] Also, the formation of the *L. pneumophila*-containing vacuole involves the early fusion of phagosomes with vesicles derived from endoplasmic reticulum produced by the Sar1/CopII system.[295]

Order Pasteurellales

Genus *Actinobacillus*

The prominent pathogens of *Actinobacillus* include *A. pleuropneumoniae* (**pleuropneumonia of swine**) and *A. lignieresii* (pyogranulomatous lesions of ruminants) (Table 14.14). In the upper respiratory tract, ultrastructural studies show that *A. pleuropneumoniae* attaches to tonsillar epithelial cells resulting in vacuolization and desquamation of the epithelium and a strong neutrophil response in the deeper parts of the crypts.[296] In the lower respiratory tract, *A. pleuropneumoniae* associates with the epithelium of the alveoli or the cilia of the terminal bronchioli.[297] Often the bacteria associate with infiltrated cells and exudates and are often seen lying with their longest side in close opposition to the epithelial cells of alveoli and the cilia. In cell cultures, ultrastructural studies show that *A. seminis* adheres to epithelial cells,[298] *A. pleuropneumoniae* adheres to epithelial cells, [299,300] but *A. pleuropneumoniae* does not adhere to porcine brain microvascular endothelial cells.[301]

The capsule of *A. pleuropneumoniae* is a putative virulence factor and the lack of a capsule decreases the resistance of the organism to bactericidal activities of serum. RTX toxins are also important in the pathogenesis of disease. There are three types, ApxI, ApxII and

Vet-ebooks.com

Table 14.14 Order Pasteurellales: pathogenic species.

Pathogen	*Disease (host) and ultrastrucural studies*	*Reference to ultrastructural pathology*
	Genus *Actinobacillus*	
A. lignieresii	Soft tissue infections in cattle	**Rebhun**, *Cornell Vet* 78:125, 1988
A. pleuropneumoniae	Pleuropneumonia in pigs and studies in mice	**Idris**, *Vet Pathol* 30:234, 1993; **Inzana**, *Infect Immun* 56:1880, 1988; **Bog**, *Vet Microbiol* 81:51, 2001
A. seminis	Epididymal and testicular lesions in rams	**Healey,** *Can J Vet Res* 55:121, 1991; **Al-Katib**, *N Z Vet J* 55:125, 2007
	Genus *Aggregatibacter*	
A. actinomycetemcomitans	Periodontitis, gingivitis in humans	**Iacono**, *Infect Immun* 40:773, 1983; **Scannapieco**, *Infect Immun* 55:2320, 1987
	Genus *Haemophilus*	
H. ducreyi	Chancroid in humans	**Albritton**, *Microbiol Rev* 53:377, 1989; **Alfa**, *Infect Immun* 61:1735, 1991; **Marsch**, *Arch Dermatol Res* 363:153, 1978
H. gallinarum	Infectious coryza, a respiratory disease in chickens	**Iritani**, *Avian Dis* 21:39, 1977
H. influenzae	Respiratory infection, meningitis, and Brazilian purpuric fever in humans and studies in a variety of models	**Bakaletz**, *Infect Immun* 56:331, 1988; **Farley**, *J Infect Dis* 154:752, 1986; **Read**, *Infect Immun* 60:3244, 1992; **Read**, *J Infect Dis* 163:549, 1991; **Stull**, *Infect Immun* 46:787, 1984; **Peters**, *Infect Immun* 60:3423, 1990; **Deich**, *J Bacteriol* 152:855, 1982
H. parasuis	Glasser's disease consisting of polyserositis, meningitis, and pneumonia in pigs	**Vanier,** *Microbiol* 152:135, 2006
H. pleuropneumoniae	Pneumonia and ultrastructural studies	**Jensen**, *Infect Immun* 51:419, 1986; **Bertram**, *Vet Pathol* 23:681, 1985
	Genus *Histophilus*	
H. ovis	Vaginal discharge and mastitis in ewes	**Jansen**, *Onderstepoort J Vet Res* 50:125, 1983; **Beauregard**, *Can Vet J* 24:284, 1983
H. somni	Encephalitis in cattle	**Behling-Kelly**, *Infect Immun* 74:5311, 2006; **Tegtmeier**, *Zentralbl Veterinarmed B* 46:517, 1999
	Genus *Pasteurella*	
P. multocida	Pneumonia and septicemia in a variety of animals and fowl cholera in poultry and studies in a variety of models	**Ackermann**, *Vet Pathol* 28:267, 1991; **Jacques**, *Infect Immun* 61:4785, 1993; **Jacques**, *J Bacteriol* 169:3470, 1987; **Gunther**, *Acta Histochem* 33:293, 1986; **Cheville**, *Vet Pathol* 26:148, 1989; **Dominick**, *Vet Pathol* 25:30, 1987; **Dominick**, *Am J Vet Res* 47:1532, 1986; **Elling**, *Vet Pathol* 22:469, 1985; **Rutter**, *Vet Rec* 114:89, 1984
	Genus *Mannheimia*	
M. haemolytica	Pneumonia as part of the bovine respiratory disease complex and studies on the effects of RTX toxin	**Berggren**, *Am J Vet Res* 42:1383, 1981; **Morck**, *Can J Vet Res* 52:343, 1988; **Walker**, *Am J Vet Res* 45:1230, 1984; ***Whiteley***, *Vet Pathol* 28:275, 1991; **Whiteley**, *Vet Pathol* 27:150, 1990; **Breider**, *Infect Immun* 59:4570, 1991; **Clinkenbeard**, *Am J Vet Res* 50:271, 1989; **Breider**, *Vet Immunol Immunopathol* 27:337, 1991

ApxIII toxins in the 15 serotypes of *A. pleuropneumoniae*, which can occur singly, or in combinations (e.g., ApxI and ApxII or ApxII and ApxIII). Symptoms of *A. pleuropneumoniae* disease can be reproduced with the purified toxins. ApxI is hemolytic and cytotoxic, ApxII is weakly hemolytic and cytotoxic and ApxIII is cytotoxic only. Lipopolysaccharide is considered a putative virulence factor of *A. pleuropneumoniae* since lipopolysaccharide induced lesions in mice similar to whole cells but less severe and without hemolysis. Two proteins in *A. pleuropneumoniae* also facilitate the uptake of iron from porcine transferrin.

Vet-ebooks.com

Genus *Aggregatibacter*

The genus *Aggregatibacter* has three species including *A. actinomycetemcomitans*,[302] which lives in the oral cavity of healthy humans and animals. Yet, *A. actinomycetemcomitans* also is a major human oral pathogen that induces inflammation and damage to the extracellular matrices of ligament and bone.[303] One severe form of periodontitis is localized aggressive periodontitis.

A. actinomycetemcomitans is a small gram-negative coccobacillus that adheres to hydroxyapatite in vitro and ultrastructurally forms microcolonies with a fibrillar matrix.[304]

A. actinomycetemcomitans has a Type III secretion system on a 25 kb plasmid pVT745. There is a RTX toxin that kills lymphoid and myeloid cells and binds to the β2-integrin receptor LFA-1. A cytolethal distending toxin causes arrest of mammalian cell cycle in G2. Lipopolysaccharide, lipid A associated protein, capsular polysaccharide, other secreted proteins, and chaperonin 60 all stimulate bone resorption.[303]

Genus *Haemophilus*

Haemophilus species are non-motile, small gram-negative coccobacilli with variable morphologies. They are facultatively anaerobic and require hemin and NAD, supplied by erythrocytes, for growth. They reside in the nasopharynx. Some species attach to ciliated epithelium in the early phases of infection (Fig. 14.17). Most have anti-phagocytic polysaccharide capsules that contribute to pathogenicity. *H. influenzae* is a major pathogen in humans and *H. parasuis* is a major pathogen of swine. Other species can cause human disease; for example, *H. parainfluenzae* (endocarditis), *H. aegyptius* (conjunctivitis), *H. aphrophilus*, *H. paraphrophilus*, and *H. ducreyi* (chancroid).

Pneumonia and **meningitis** are caused by capsulated *H. influenzae* or noncapsulated, "non-typable" *H. influenzae.* It is a strict human pathogen and resides primarily in the upper respiratory tract, in many instances as biofilms detected by scanning electron microscopic studies of fresh isolates.[305,306] Bacteria attach to adenoid and tonsil tissue surfaces and organize as colonies. Nontypeable *H. influenzae* biofilms likely contribute to bacterial persistence and disease pathogenesis in cystic fibrosis.[306] In tissue culture, nontypable *H. influenzae* adheres to the epithelial surface, forms a biofilm, and is less susceptible to antibiotics. Airway epithelial cells remain viable throughout the 4 days of coculture and have an activated nuclear factor-κB signaling response with increased secretion of chemokines and cytokines.

Loss of control over asymptomatic nasopharyngeal colonization can result in acute (epiglottitis, pneumo-

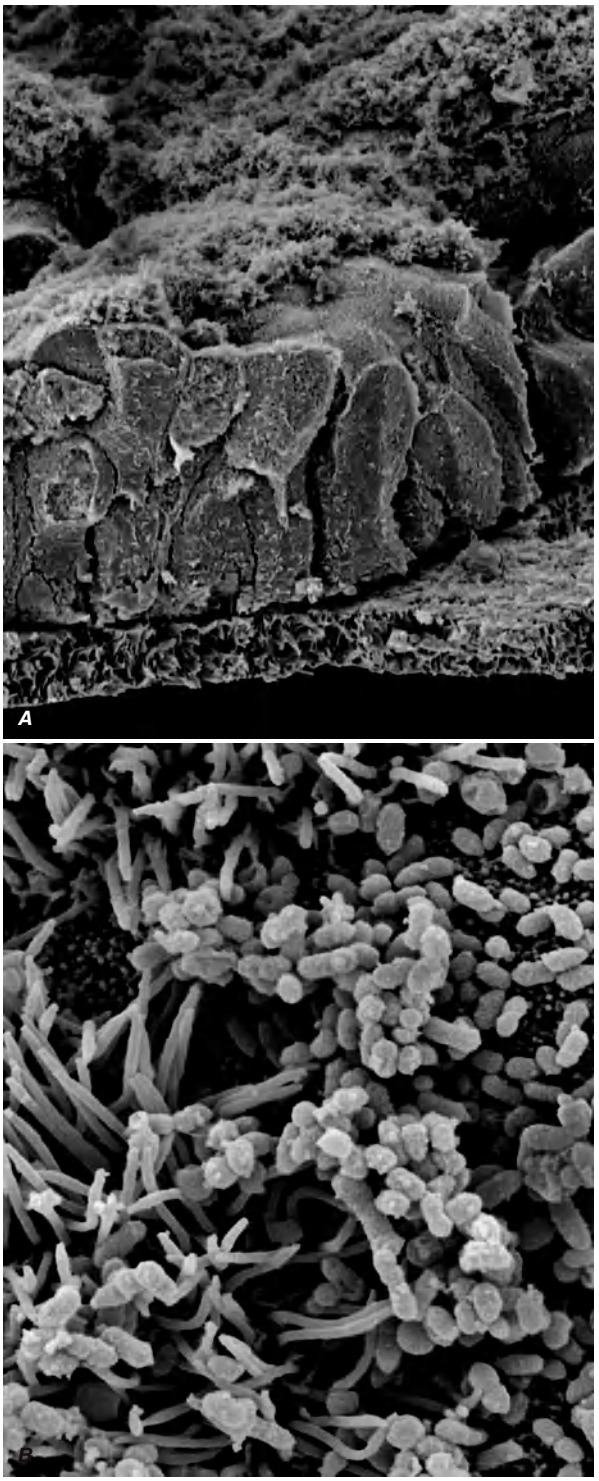


Fig. 14.17 ***Haemophilus influenzae*:** pseudocolored scanning electron micrograph, airway epithelial culture infected with nontypeable *Haemophilus influenzae* growing in a biofilm. **A**. Polarized airway epithelial culture grown at the air-liquid interface. **B**. Primary culture of polarized murine airway epithelia grown at the air-liquid interface. (Micrograph: Timothy Starner, University of Iowa.)

Vet-ebooks.com

nia, and meningitis) or chronic (adeno-tonsillitis and otitis media) infections. In young children, cellulitis and septic arthritis are rare manifestations. Nasopharyngeal epithelium is the site of primary infection and colonization begins in the mucous fluid layer. Bacteria penetrate between epithelial cells at points of cell degeneration and where intercellular junctions have separated. Pili are not required but facilitate attachment.[307] Bacterial proteases may play some role by specifically cleaving secretory IgA1. *H. influenzae* does not attach to cilia but, in the ensuing tissue destruction, is phagocytized by monocytes and macrophages infiltrating into the damaged epithelium. Vesicles bearing outer membrane proteins are released from the bacterial cell surface.

Brazilian purpuric fever is a fulminant infection affecting young children caused by *H. influenzae* biogroup *aegyptius*. Preceded by an episode of conjunctivitis, the onset is abrupt and leads rapidly to high fever, hemorrhagic lesions on the skin, septicemia, vascular collapse, shock, and death. Newborns and adults appear to be immune to this syndrome.

Chancroid (soft chancre) is a genital ulcer caused by *H. ducreyi* that leads to inguinal lymphadenopathy and soft-tissue lesions. Ultrastructurally it is a pleomorphic, gram-negative bacillus with a heavy capsule that stains deeply with ruthenium red. Bacteria bind to cells via an electron-dense granular layer but do not enter the cells.

Polyserositis is caused by *Haemophilus parasuis*.[308] Factors involved in pathogenesis of *H. parasuis* infections include transporters of iron and sugar metabolites, metabolic enzymes, DNA metabolism and hypothetical proteins with unknown functions.[308] Other factors also include homologs of fadD (a fatty acyl-CoA synthetase), apaH (diadenosine tetraphosphatase), pstI (enzyme I of the phosphoenolpyruvate-protein phosphotransferase system), cysK (cysteine synthetase), Std (Na(+)- and Cl(–)-dependent ion transporter), HSPG (a mammalian basement membrane-specific heparin sulphate core protein precursor) and PntB (pyridine nucleotide trans-hydrogenase).[309] *H. parasuis* serotype 5 adheres and invades porcine brain microvascular endothelial cells[301] via rearrangement of actin microfilaments and microtubular cytoskeletal elements but not active bacterial DNA, RNA or protein synthesis. *H. parasuis* is not toxic to these cells and viable microorganisms are found in porcine brain microvascular endothelial cells up to 6 hours after exposure.

Genus *Mannheimia*

The genus *Mannheimia* contains *M. haemolytica*, the causative agent involved in **bovine respiratory disease complex**. *M. haemolytica* is a common cause of acute and severe respiratory disease and bronchopneumonia (**shipping fever**). Neutrophils and other cells are killed by a potent leukotoxin. Once the organisms enter the lung (Fig. 14.18), early vascular lesions center on platelet and fibrin thrombi. Bacterial endotoxin (lipopolysaccharide), exotoxin (leukotoxin), capsular polysaccharide, neuraminidase, and a neutral protease are involved in initial tissue damage. Macrophage clearance is an important factor in recovery.

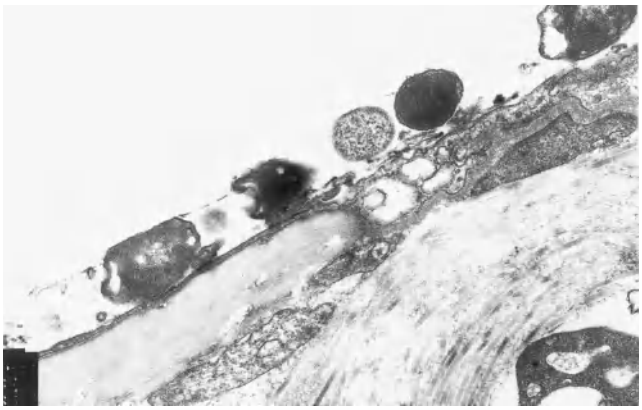


Fig. 14.18 ***Mannheimia haemolytica*:** *M. haemolytica* closely associated to pulmonary epithelia (type I) that lines the alveolar wall.

Leukotoxin has been demonstrated in pulmonary inflammatory lesions caused by *M. haemolytica*, and immunogold techniques have been used to label capsules and bacterial cell surfaces. It binds to the beta(2) integrin CD11a/CD18. Ultrastructurally the leukotoxin induces lesions in the mitochondria of leukotoxin-treated BL-3 cells. The outer mitochondrial membrane has lesions, which are larger than previous reports of the permeability transition pore through which cytochrome c is usually released.[310] The genome sequence of *M. haemolytica* A1 contains genes encoding a filamentous hemagglutinin FhaB adhesin, two trimeric autotransporter adhesins, two dual-function immunoglobulin-protease/adhesins, a third immunoglobulin protease, genes related to iron acquisition, and genes related to drug resistance.[311]

Genus *Pasteurella*

Pasteurella species are pathogens in a variety of animals including humans. There are approximately 21 species in the genus, but *P. multocida* has the most notoriety. They are gram-negative, nonmotile coccobacillary or short rods, 0.2–0.4 × 0.6–2.5 μm with ultrastructural features of bacilli. *Pasteurella* species have hydrophilic, hyaluronic acid-containing, carbohydrate capsules, multilaminar outer envelopes, and cytoplasmic membranes typical of gram-negative bacteria (Fig. 14.19).

Vet-ebooks.com

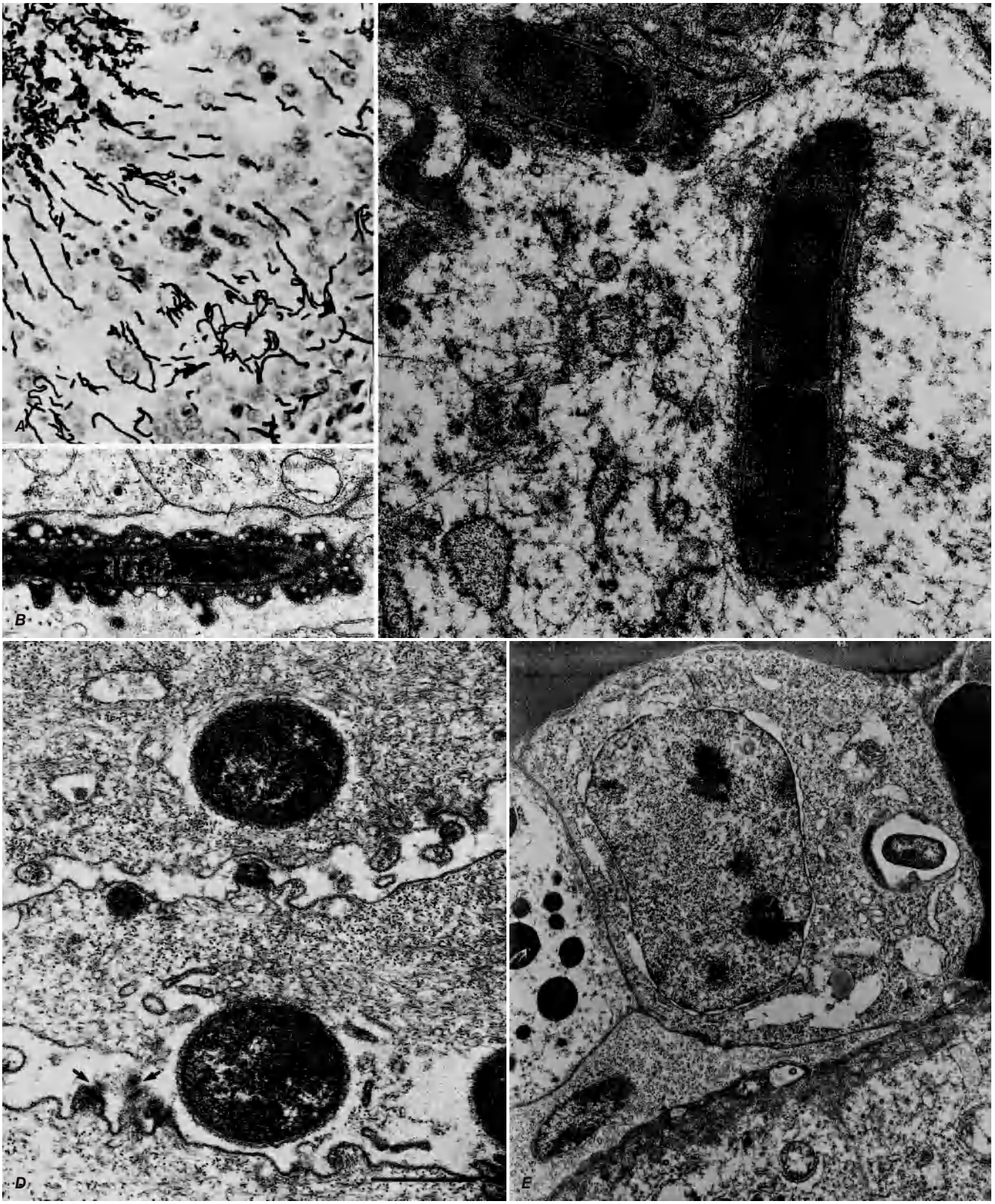


Fig. 14.19 Intracellular bacilli. A–C. *Eubacterium tortuosum*: liver, chicken (hepatic abscess). **A**. Silver impregnation stain, bacteria radiate outward from focus of infection (*top left*). **B** and **C**. Intracellular bacteria within phagolysosomes. (Micrographs: Lawrence H. Arp, *Vet Pathol* 20:80, 1983.) **D**. ***Moraxella bovis***: corneal epithelium, cow (bovine keratoconjunctivitis). Bacilli are attached to (*bottom*) and lie within (*top*) a corneal epithelial cell. (Micrograph: Douglas Rogers, *Vet Pathol* 24:287, 1987.) **E**. ***Pasteurella multocida***: monocyte, liver, turkey (acute fowl cholera). Bacterium and fibrin are in phagosome.

Vet-ebooks.com

Fowl cholera is a prototype of *Pasteurella* septicemia. Bacteria enter the bird via mucous membranes of the upper respiratory tract. Acute disease is caused by development of large numbers of bacilli within the vascular system. Lesions of hyperemia, hemorrhage, and vascular necrosis (especially in the liver) are caused by release of endotoxin, and endotoxin-induced vascular paralysis leads to capillary leakage, loss of blood volume, and shock. Capsule thickness of avian *P. multocida* type A, determined by transmission electron microscopy after labeling with polycationic ferritin, is 50.1–81.4 nm. Capsulated strains are more virulent for poultry, whereas noncapsulated strains are less virulent. *P. multocida*, isolated from turkeys with septicemia have inclusions.[101]

Hemorrhagic septicemia is caused by *P. multocida* capsular types B and E, which cause an acute and highly fatal septicemia in cattle and water buffalo in Asia, Africa, and the Middle East. Ultrastructurally, peritoneal macrophages of mice, injected intraperitoneally with serotype B:2,5, underwent cytoplasmic vacuolation, lysis, and death.[312]

Acute and chronic respiratory diseases are caused by *P. multocida* in cattle, sheep, swine, and other domestic animals. Disease is associated with environmental stress and superinfection with other respirotropic viruses. Lesions caused by *P. multocida* are acute or subacute diffuse fibrinopurulent pneumonia with the presence of large numbers of bacteria in the alveoli.

Human infections with *P. multocida* are seen in three situations: acute, focal soft-tissue purulent lesions, chronic respiratory infections, and bacteremia with or without metastatic lesions. Typically acquired from animal bites, the local lesions envelope rapidly with edema, swelling and pain. Regional lymphadenopathy often occurs. In rare cases, there is dissemination to cause osteomyelitis, tenosynovitis, or arthritis.

Atrophic rhinitis is caused by *P. multocida* type D. These serotypes colonize the nasopharynx and tonsil of young swine.[313] By electron microscopy, fimbriae with at least two distinct morphologies were seen on *P. multocida* isolated from pigs with atrophic rhinitis.[314] *P. multocida* also produces a potent necrotizing toxin that causes lesions of degeneration and disintegration of the nasal turbinates. Dermonecrotic toxin is produced in the tonsil and acts systemically; there are lesions of necrosis in the liver and other viscera in severe cases, and the toxin can be shown experimentally to cause hepatic necrosis in pigs and rats.

Order Pseudomonadales

Genus *Moraxella*

The genus *Moraxella* are gram-negative plump cocci and coccobacilli in pairs. They are normal inhabitants of the upper respiratory and genital tracts of humans and animals.

In humans, *M. catarrhalis* is an important pathogen in patients with chronic obstructive lung disease (COPD) (Table 14.15). It is internalized in respiratory epithelial cells by a trigger-like mechanism and initiates a TLR2- and partly NOD1-dependent inflammatory immune response.[315] Electron and confocal microscopy demonstrated a considerable potential of *M. catarrhalis* to invade bronchial epithelial cells, Type II pneumocytes, and primary small airway epithelial cells. *M. lacunata* is commonly associated with eye infections in humans and other *Moraxella* are associated with respiratory tract infections and septicemia in immunosuppressed humans. Ultrastructurally, *Moraxella* have typical gram-negative structure and characteristic pili.[316]

In animals, *M. bovis* is associated with eye infections in cattle. Piliated strains of *M. bovis* cause infectious bovine keratoconjunctivitis (pinkeye). The initial event in the pathogenesis of this disease is the adherence of *M. bovis* to corneal epithelium. Humoral factors produced by the bacteria cause cellular necrosis and pitting in the corneal surface. Ultrastructurally, *M. bovis* is found in these surface pits attached to surfaces of corneal epithelium.[317,318] *M. bovis* also invades and survives within corneal epithelial cells. As infection proceeds, a severe, acute inflammatory process is stimulated and neutrophils invade the tissue. Necrotic lesions in the cornea erode leaving severe ulcers in the surface of the eye.

Genus *Pseudomonas*

The genus *Pseudomonas* contains approximately 176 species. The type strain is *P. aeruginosa*. Members are gram-negative, straight or slightly curved bacilli 0.5–1.0 μm × 1.5–5.0 μm in size. They are motile and have one or two polar flagella. They are aerobic with a strict respiratory metabolism. Oxygen is the terminal electron acceptor.

In humans, *P. aeruginosa* causes a large variety of infections in physically, physiologically, and immunologically compromised patients. This includes folliculitis, corneal infections, osteomyelitis, community acquired pneumonia, and infections in individuals with underlying predisposing conditions. *P. aeruginosa* is often associated with destruction of epithelial barriers, for example, wounds, burns, and surgical incisions.

P. aeruginosa possesses a wide array of virulence determinants for adherence, colonization, invasion, dissemination, and toxinogenesis. Fimbriae, a polysaccharide capsular glycocalyx, and an alginate layer slime assist *P. aeruginosa* to adhere, colonize, and form biofilms. Severe edema, loss of ground substances and

Vet-ebooks.com

Table 14.15 Order Pseudomonadales: pathogenic species.

Pathogen	*Disease (host) and ultrastrucural studies*	*Reference to ultrastructural pathology*
	Genus *Branhamella*	
B. catarrhalis	Otitis media and respiratory tract infections in association with chronic obstructive pulmonary disease	**Catlin**, *Clin Microbiol Rev* 3:293, 1990; **Hellio**, *Ann Inst Pasteur* 139:515, 1988.
	Genus *Moraxella*	
M. bovis	Keratitis in cattle; ultrastructural and experimental studies in a variety of tissues	**Chandler**, *J Comp Pathol* 95:415, 1989; **Chandler**, *J Comp Pathol* 91:175, 1981; **Rogers**, *Vet Pathol* 24:554, 1987; **Rogers**, *Vet Pathol* 24:287, 1987; **Froholm**, *J Ultrastruct Res* 42:411, 1973
M. lacunata	Keratitis	
	Genus *Pseudomonas*	
P. aeruginosa	Infections of the urinary tract, eyes, respiratory tract, soft tissues, bone and joints, gastrointestinal tract, and skin and a variety of systemic infections in humans and animals and studies in a variety of models	**Dorff**, *Arch Intern Med* 128:591, 1971 in humans; **Hazlett**, *Infect Immun* 43:783, 1993; **Hazlett**, *Infect Immun* 34:1025, 1981; **Diedrich**, *J Bacteriol* 119:1006, 1974; **Egan**, *J Infect Dis* 130:S65, 1974; **Fuerst**, *J Gen Microbiol* 58:227, 1969; **Govan**, *J Gen Microbiol* 80:1, 1974; **Totten**, *J Bacteriol* 172:389, 1990; **Azghani**, *Infect Immun* 58:433, 1990; **Boyd**, *Infect Immun* 39:1403, 1983; **Brownstein**, *Vet Pathol* 19:169, 1982; **Cash**, *Am Rev Respir Dis* 119:453, 1979; **Chi**, *Infect Immun* 59:822, 1991; **Coalson**, *Exp Mol Pathol* 45:193, 1986; **Fleiszig**, *Infect Immun* 64:2288, 1996; **Fleiszig**, *Infect Immun* 62:3485, 1994; **Gray**, *Infect Immun* 12:419, 1975; **Hazlett**, *Infect Immun* 61:5164, 1993**;** **Hazlett**, *Infect Immun* 51:687, 1986; **Hingley**, *Infect Immun* 51:254, 1986; **Marcus**, *Infect Immun* 47:723, 1985; **Baltch**, *Infect Immun* 48:498, 1985; **Morris**, *Infect Immun* 52:445, 1986
P. pseudomallei	Granulomas and studies in human phagocytes and goats	**Narita**, *Natl Inst Anim Health Q* 22:170, 1982; **Pruksachartvuthi**, *J Med Microbiol* 31:109,1990

ulceration occur through action of these bacterial proteases. Elastase, phospholipase, and alkaline protease are also factors in local tissue necrosis. Exoenzyme S, exotoxin A, and lipopolysaccharide cause necrosis of granulocytes and tissue. **Exotoxin A** is the most toxic component of all cellular and extracellular fraction of the bacterium. Exotoxin A inhibits protein synthesis by ADP-ribosylating elongation factor 2 (EF-2). It is excreted as an enzymatically inactive proenzyme that is cytotoxic. It undergoes activation by several pathways, which may destroy toxicity. Applied to the mouse cornea, exotoxin A causes acute inflammation and necrosis. *P. aeurginosa* is susceptible to antimicrobial peptides (Fig. 14.20).

Ultrastructurally, *P. aeruginosa* has the morphology of a typical gram-negative bacillus including flagellin, pyocins, pili, cell envelope, and an exopolysaccharide layer. In adenoid organ cultures, *P. aeruginosa* adheres to areas of epithelial damage and to basement membranes. *P. aeruginosa* was seen by scanning electron

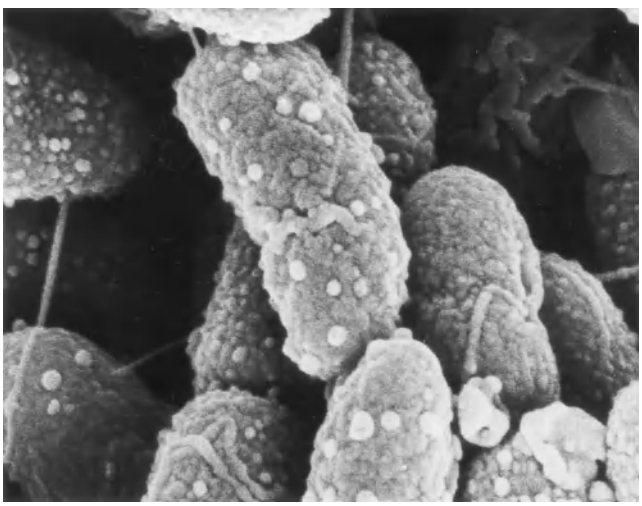


Fig. 14.20 ***Pseudomonas aeruginosa*:** *P. aeruginosa* strain PAO1 incubated with a synthetic cathelicidin showing the presence of blebs induced by the interaction of the antimicrobial peptide with the outer envelope. (Micrograph: Hong Peng Jia and Paul McCray, Jr., University of Iowa.)

Vet-ebooks.com

microscopy to associate with mucus, extruded damaged epithelial cells, occasionally with cilia, and very occasionally with unciliated cells.[319] In a corneal infection model, *P. aeruginosa* was seen by transmission electron microscopy to adhere to and inflame the stroma, causing the epithelial layer to loosen and tear away.[320]

In the respiratory tract, *P. aeruginosa* is phagocytized and killed by monocytes and other leukocytes, particularly if a host opsonin like pulmonary surfactant D is used. SP-D significantly enhanced the uptake of three of six strains of *P. aeruginosa* by rat alveolar macrophages as analyzed by both fluorescence and electron microscopy.[321] Mucoid strains, more prevalent in cystic fibrosis patients, adhere to epithelium better and resist phagocytosis more than nonmucoid strains. In immunosuppressed patients, bacteria are not killed and enter subepithelial tissues and are disseminated in the bloodstream.

Order Thiotricales

Genus *Francisella*

Francisella tularensis is among three species in this genus and is spread among rodents by blood-sucking insects. It is a tiny gram-negative coccobacillus. Ultrastructurally, the *F. tularensis* live vaccine strain has long, thin fibers, similar in appearance to Type IV pili and the highly virulent *F. tularensis*. Schu S4 strain has Type IV pilus genes.[322]

F. tularensis causes **tularemia** in humans. Organisms produce small inflammatory lesions at sites of entry, enter lymphatics, and are disseminated to tissues by circulating blood (Table 14.16). Characteristic lesions occur in liver, lung and spleen as small foci of necrosis, which progressively develop into granulomas. Bacteria enter and survive in monocytes for long periods, explaining the tendency of the disease to relapse and to remain chronic. **Respiratory tularemia** is particularly fatal. Ultrastructural examination of the liver and spleen of infected monkeys reveals that early foci of necrosis with macrophages containing phagocytized coccobacilli.

Order Vibrionales

Genus *Vibrio*

Morphologically, vibrios are gram-negative bacilli, which are short, curved or twisted, with thin, wavy cell walls. They are 0.5–8.8 μm wide × 1.4–2.6 μm in length. In liquid culture media, they are motile with monotrichous of multitrichous polar flagella surrounded by a flagellar sheath. The majority of Vibrios are pathogenic for animals and humans typically causing enteritis (Table 14.17). A few are not pathogenic or are only loosely associated with ill-defined infections. Two are important pathogens that cause enteritis by different mechanisms: *V. cholerae* is not invasive but produces enteric damage by secreting a potent toxin and *V. parahaemolyticus* invades epithelium of the colon. The *V. parahaemolyticus* thermostable hemolysin is a major virulence factor. By transmission electron microscopy, the TDH oligomer has C(4) symmetric particles with edge and diagonal lengths of 65 A and 80 A, respectively. Shape reconstruction suggests it is an oblate structure.[323]

Cholera is cause by *V. cholerae.* After ingestion, it passes the gastric acidity barrier to initiate infection in the small intestine. Biopsies of human intestine colonized by *V. cholerae* show that bacteria are trapped in mucus. Flagellar motility propels vibrios through the protective gel on epithelial surfaces. Bacteria adhere tightly to absorptive cells in the villi, in part through a toxin-coregulated pilus. They proliferate on the free surface of microvilli and elaborate a potent **enterotoxin** that causes a rapid transfer of fluid and electrolytes from the intestinal capillaries to the intestinal lumen. Intestinal structure is not markedly altered unless secondary bacterial infection ensues. Virulence of *V. cholerae* is related to the *toxR* gene, which induces the secretion of enterotoxin.

Fulminating wound infections are caused by *V. vulnificus* acquired by contact with seawater, and with septicemia, that follows ingestion of rat oysters or other shellfish. The heavy polysaccharide capsule of *V. vulnificus* is an important virulence factor via inhibition of phagocytosis. An exotoxin isolated from culture

Table 14.16 Order Thiotricales: pathogenic species.

Pathogen	*Disease (host) and ultrastrucural studies*	*Reference to ultrastructural pathology*
	Genus *Francisella*	
F. tularensis	Tularemia in humans and ultrastructural and experimental studies in models	**White**, *J Infect Dis* 114:277, 1964; **Baskerville**, *Br J Exp Pathol* 59:615, 1978; **Santic**, *Trend Microbiol* 14:37, 2006

Vet-ebooks.com

Table 14.17 Order Vibrionales: pathogenic species.

Pathogen	*Disease (host) and ultrastrucural studies*	*Reference to ultrastructural pathology*
	Genus *Vibrio*	
V. anguillarum	Hemorrhagic septicemia in fish. Ultrastructural studies with flagella	**Norqvist**, *Infect Immun* 61:2434, 1993
V. cholerae	Cholera in humans and studies in a variety of models	**Avakian**, *Arch Microbiol Epidemiol Immun* 49:86, 1972; **Chatterjee**, *J Gen Microbiol* 4:91, 1967; **Chen**, *Virch Arch B* 7:236, 1971; **Yamamoto**, *Infect Immun* 56:2753, 1988; **Yardley**, *Lab Invest* 28:482, 1973; **Guentzel**, *Scanning Electron Microsc* 22:75, 1977; **Hansson**, *Acta Pathol Microbiol Immunol Scand A* 92:15, 1984; **Jonson**, *Infect Immun* 60:4278, 1992; **Panigrahi**, *Infect Immun* 58:3415, 1990; **Yamamoto**, *J Infect Dis* 160:168, 1989; **Hashimoto**, *Am J Pathol* 74:171, 1974; **Teppema**, *Infect Immun* 55:2093, 1987; **Sharma**, *Microb Pathog* 7:437, 1989; **Sharma**, *Vaccine* 7:451, 1989
V. parahaemolyticus	Food-borne gastroenteritis	**McCarter**, *Mol Microbiol* 4:1057, 1990; **Yamamoto**, *Infect Immun* 57:2410, 1989
V. vulnificus	Infections in humans and fish and studies in mice	**Gray**, *J Infect Dis* 155:237, 1987; **Kennedy**, *Can J Microbiol* 16:1027, 1970; **Biosca**, *Infect Immun* 61:1611, 1993; **Totland**, *J Fish Dis* 11:1, 1988

fluid produced cellulitis with edema, inflammation, and necrosis of endothelial cells, myocytes, and adipocytes. *V. damsela* is a halophilic bacterium that causes wound infections and fatal disease in temperate-water damselfish, sharks and humans. Virulent isolates produce large amounts of an extracellular, heat-labile cytolysin called **damselysin**, which is a sphingomyelinase D. These are highly toxigenic vibrios reveal extensive tissue damage by the toxin.

Phylum Chlamydiae, Order Chlamydiales

Chlamydiae are gram-negative, obligate intracellular bacteria that cause a variety of diseases in human and animal species in two genus: the *Chlamydia* and *Chlamydophila*.[324] *C. pneumoniae* differs from *C. psittaci* based on the ultrastructure of elementary bodies, DNA homology values, and serologic responses in its hosts (Table 14.18). *C. pneumoniae* and *C. trachomatis* differ in inclusion body structure, glycogen content, sulfadiazine susceptibility, and natural hosts. As a whole, the family Chlamydiaceae has a large number of unique Chlamydiae-specific proteins.[325]

C. trachomatis induces venereal infections and blindness; *C. pneumoniae* induces pneumonia and respiratory tract infections; and *C. psittaci* induces atypical pneumonias. Multiple sclerosis, coronary artery disease, and atherosclerosis may be long-term sequelae of infection by members of Chlamydiaceae.[326]

Genera *Chlamydia* and *Chlamydophila*

Chlamydia species have a unique developmental cycle with two distinct forms.[327] The **elementary body** is small, 0.3 μm in size, and contains a condensed nucleoprotein core. It has no metabolic activity and does not replicate. It attaches to new cells, enters them, and initiates the replicative cycle. The **reticulate body** is larger, 1.0 μm in size, is metabolically active, and adapted for intracellular function. It has limited synthetic capacity and does not survive outside the cell nor infect new cells (Fig. 14.21). The chlamydial **nucleoid** disperses and condenses according to the replication stages. Nucleoid condensation is mediated by DNA-binding proteins of the elementary body chromosome. Doublet forms composed of two organisms with plasma membranes existing in a common cell wall have been found in ***Chlamydia*** species grown in vitro. *Chlamydia* undergo their entire intracellular developmental cycle within a vacuole termed **the chlamydial inclusion**, which is isolated from endocytic pathways but is fusogenic with exocytic vesicles that deliver sphingomyelin from the Golgi apparatus to the plasma membrane.[327]

Ultrastructurally, the chlamydial cell has a **cell wall** composed of inner and outer membranes separated by a periplasmic space but no peptidoglycan layer. The cell wall structure is novel among bacteria in that it lacks demonstrable peptidoglycan at some times in its developmental cycle. *Chlamydia* species have

Vet-ebooks.com

Table 14.18 Order Chlamydiales: pathogenic species.

Pathogen	*Disease (host) and ultrastrucural studies*	*Reference to ultrastructural pathology*
	Genus *Chlamydia*	
C. trachomatis	Eye infections, genital infections, paratrachoma, and lymphogranuloma venereum in humans; pneumonitis in mice; and conjunctivitis in guinea pigs	**Baumann**, *Infect Immun* 60:4433, 1992; **Coalson**, *Brit J Exp Pathol* 68:399, 1987; **Hearn**, *J Hist Cyt* 39:1067, 1991; **Morrison**, *J Exp Med* 169:663, 1989; **Nichols**, *J Bact* 164:344, 1985; **Phillips**, *J Ultrastruct Res* 88:244, 1984; **Quinn**, *J Infect Dis* 154:833, 1986; **Swanson**, *J Infect Dis* 131:678, 1975; **Todd**, *J Infect Dis* 151:1037, 1985; **Wenman**, *J Bact* 165:602, 1986; **Wyrick**, *Infect Immun* 57:2378, 1989; **Yong**, *Infect Immun* 53:427, 1986; **Armstrong**, *Nature* 201:371, 1964; **Williams**, *J Infect Dis* 149:630, 1984; **Barry**, *Science* 256:377, 1992; **Kaltenboeck**, *Am J Vet Res* 53:1482, 1992; **Kuo**, *Infect Immun* 55:1324, 1987
	Genus *Chlamydophila*	
C. pneumoniae	Pneumonitis in humans and studies in animal models	**Mogilevski,** *Bullet Exper Biol Med* 134:1573, 2002; **Blasi**, R*espir Res* 8:83, 2007
C. psittaci	Pneumonia, endocarditis, and urogenital disease in humans; infection in guinea pigs, ornithosis in turkeys; conjunctivitis in cats; epizootic abortion in cattle; polyarthritis, pneumonia, and abortion in sheep; enteritis in pigs; and enteritis in cattle	**Eissenberg**, *Infect Immun* 40:741, 1983; **Hiashi**, *Exp Mol Pathol* 4:24, 1965; **Hodinka**, *Infect Immun* 565:1456, 1988; **Jones**, *J Am Med Ass* 247:655, 1982; **Soloff**, *J Comp Pathol* 92:547, 1982; **Cutlip**, *Infect Immun* 1:499, 1970; **Eb**, *J Ultrastruct Res* 56:177, 1976; **Wong**, *J Clin Pathol* 38:707, 1985; **Doughri**, *Exp Mol Pathol* 18:10, 1973; **Doughri**, *Vet Pathol* 10:114, 1973; **Eugster**, *J Infect Dis* 123:41, 1971; **Goellner**, *Infect Immun* 74:4801, 2006
Other *Chlamydophila* species	Hepatitis and chlamydiosis in frogs, gill disease in fish, and epitheliocystis in fish, and gastritis in cats	**Howerth**, *Vet Pathol* 21:28, 1984; **Paperna**, *J Fish Dis* 7:37, 1984; **Desser**, *J Fish Dis* 11:453, 1988; **Hargis**, *Vet Pathol* 20:170, 1983

nearly a complete pathway for peptidoglycan synthesis, which is expressed during reticulate body development and division.[328] Extensive disulfide cross-linked outer membrane proteins also provide some structure. Surfaces of the reticulate body have spikes that extend from the cell membrane through the periplasmic space and outer membrane into the infected cell.[329]

Chlamydia use major outer membrane proteins, heat shock protein 70, OmcB, and heparan sulfate-like glycosaminoglycans as adhesins.[330] Polymorphic membrane proteins Pmps and PmpD (*C. pneumoniae*) are involved in early entry. Chlamydiae concentrate on specialized membrane microdomains, approximately 40 nm in size, at the host cell surfaces. These lipid microdomains are rich in cholesterol, glycosphingolipid, and caveolin. *C. trachomatis, C. caviae*, and *C. pneumoniae* all associate with these domains and trigger the internalization process.[330] In addition, early host signaling induces cytoskeleton rearrangements leading to bacterial uptake. Once inside, the Chlamydiae multiply with the inclusion. Clathrin-coated pits are commonly seen in membranes of the developing phagosome.[331] The inclusion then expands to accommodate the multiplying **RB**. **RB** receives components from the host cell and bacteria continue to grow within the inclusion until it occupies most of the cytoplasm. Chlamydiae use the host's glycolytic cycle and other metabolites to produce energy and are associated with glycogen in the host cell cytoplasm. *C. trachomatis* has vacuoles containing glycogen.

Chlamydia species have a Type III secretion system and secrete proteins in the inclusion membrane. Needle-like structures protrude into the membranes at the *C. caviae* attachment site to HeLa cells by both transmission and scanning microscopy.[329] This gives the inclusion its unique properties. The major **outer membrane protein**, encoded by the gene *ompA*, functions as a redox-gated porin. Specific antigens that are recognized by infected animals and that are used to differentiate species of *Chlamydia* have been localized ultrastructurally with immunogold techniques in the outer membrane.

Vet-ebooks.com

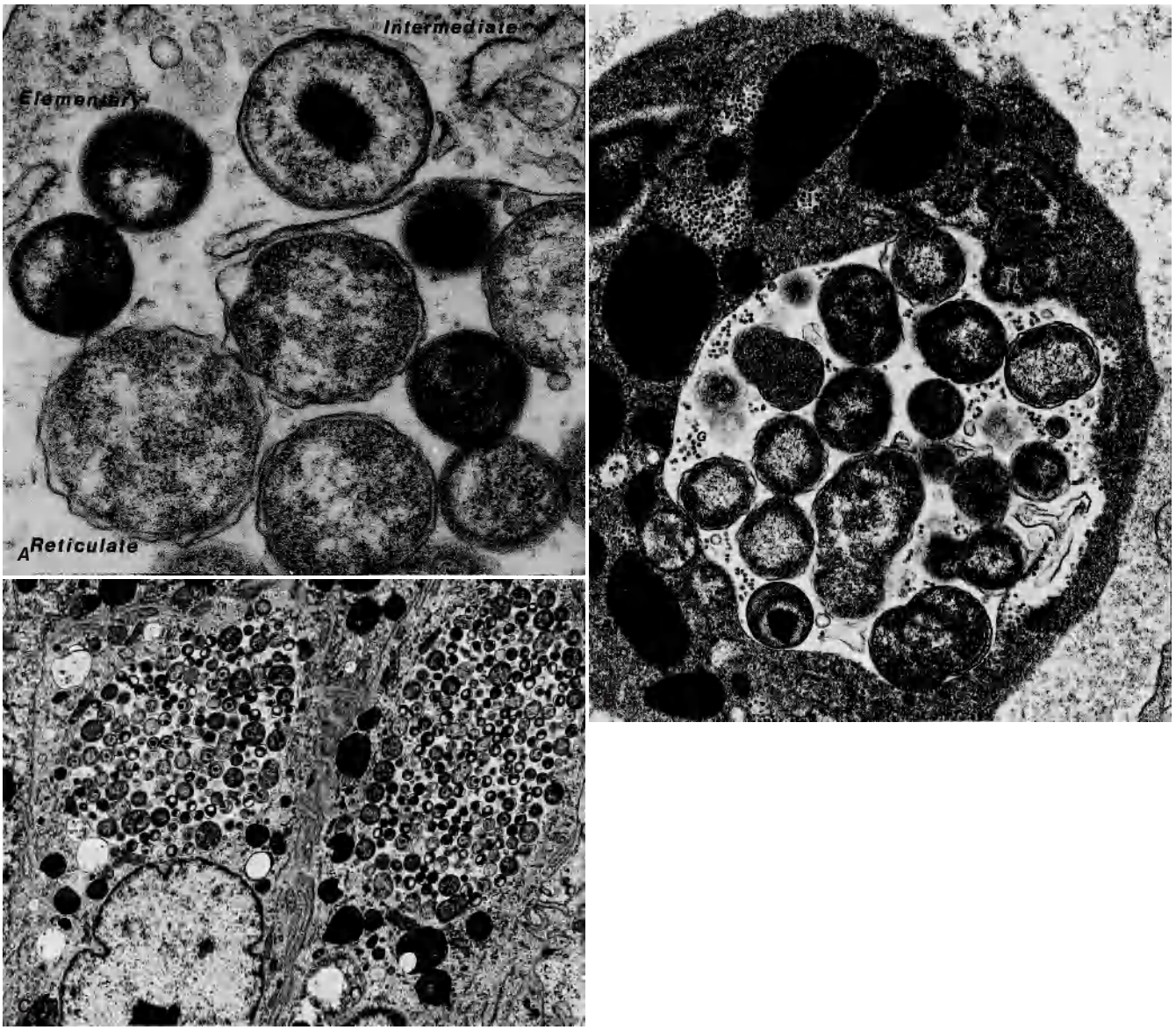


Fig. 14.21 ***Chlamydia* spp. A. Three forms of chlamydiae**: elementary, intermediate, and reticulate bodies. *Chlamydia psittaci*, the cause of lamb polyarthritis. (Micrograph: Randall C. Cutlip, *Infect Immun* 1:499, 1970.) **B**. ***Chlamydia psittaci*** within a cytoplasmic vacuole of a granulocyte. Three forms of the replicative cycle are present. Mitochondria (*M*) and glycogen (*G*) have close relationships to developing bacteria. (Micrograph: Jay Tappe.) **C**. ***Chlamydia psittaci*** in trophoblasts of the caprine placenta. Large numbers of chlamydiae fill central vacuoles; all three forms are present. Mitochondria (*M*) in host cells have close associations with the cytoplasmic vacuole. (Micrograph: Tim D. Anderson.)

Order Actinomycetales

Genera *Actinomyces* and *Arcanobacterium*

The genus *Actinomyces* are gram-positive, filamentous, branched organisms 0.4–1.0 µm wide that may be straight or curved. Shapes vary from short pleomorphic bacilli to branching filaments. They occur in tissue as a single bacterium or in groups. Filaments can be up to 50 µm long. *Actinomyces* cause chronic, focal, granulomatous lesions (**mycetomas**) in humans and animals. Lesions are massive aggregates of monocytes and macrophages, many of which contain intracellular bacteria (Fig. 14.22). During growth, lateral protrusions develop and bacteria divide to form clusters.[332] All pathogenic species cause mycetomas in humans and animals.

Actinomycosis

A. bovis causes granulomas in the tongue and mandibles of cattle, commonly called **lumpy jaw**, and

Vet-ebooks.com

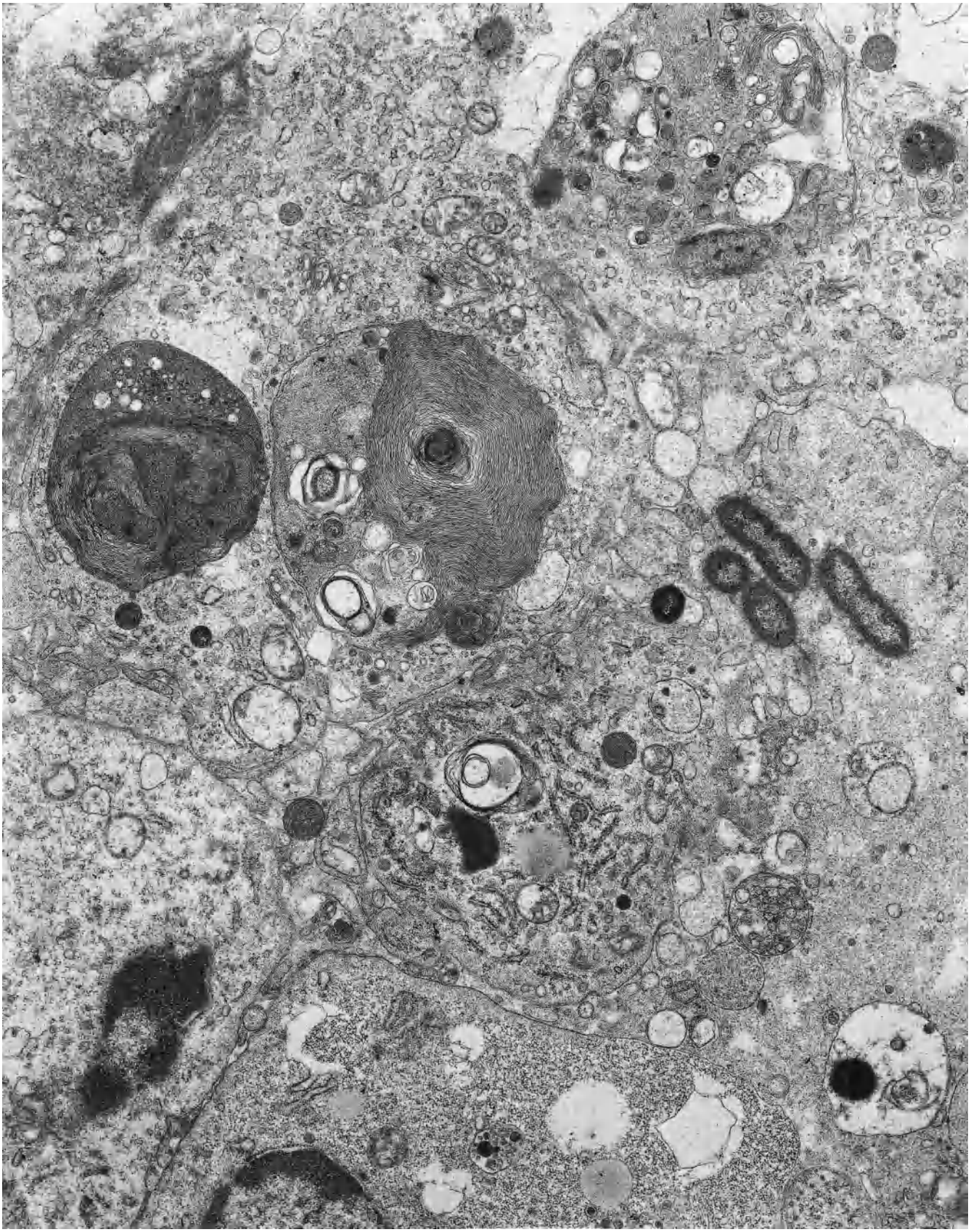


Fig. 14.22 ***Actinomyces* spp.** Granulomatous peritonitis, dog. Bacteria are largely within phagosomes inside macrophages, although extracellular bacteria are present. Macrophages are filled with large residual bodies (myeloid bodies), many of which contain whorls of membranes (myelin figures).

Vet-ebooks.com

infections in sheep, pigs, dogs, and horses (Table 14.19). The central dense nodule contains gram-positive bacteria in "sulfur granules" of purulent material. The hyalin matrix consists of bacterial polysaccharide-slime coats surrounded by antimicrobial proteins from degranulate leukocytes.

A. viscosus causes chronic pneumonia, pyothorax, and subcutaneous abscesses in dogs. It is also involved in periodontal disease and disseminated abscesses in humans.[333] In tissue, sulfur granules develop and bacteria form a spectrum from coccobacilli (in which nuclear zones dominate the cytoplasm) to fusiform or filamentous forms. In filamentous forms, the envelope is formed of an inner plasma membrane, a thick cell wall (22 nm) having a very dense internal layer, and a thick (30 nm) capsule with large numbers of pili. In tangential sections, the capsule consists of parallel segments oriented in angles to the layers of the envelope.

A. israelii is a normal inhabitant of the human mouth, grows in dental plaque, producing a factor that binds to and aggregates streptococci. *A. israelii* invades in opportunistic infections, usually in association with invasion by other bacteria. Entering a break in the

Table 14.19 Order Actinomycetales: pathogenic species.

Pathogen	*Disease (host) and ultrastrucural studies*	*Reference to ultrastructural pathology*
	Genus *Actinomyces*	
A. bovis	Actinomycosis, lumpy jaw in cattle	**Duda**, *J Gen Microbiol* 71:63, 1972
A. dentocaria (Rothia)	Dental plaque in humans	**Duda**, *J Gen Microbiol* 71:63, 1972
A. hordeovulneris	Calcification in dogs	**Buchanan**, *Am J Vet Res* 454:2552, 1984
A. israelii	Oral infection in humans	**Kolenbrander**, *Infect Immun* 40:1178, 1983
A. naeslundii	Associated with oral infections in humans	**Girard**, *Arch Oral Biol* 19:71, 1974
A. pyogenes	Abscesses in cattle and cats	**Bestetti**, *Acta Neuropathol* 39:231, 1977
A. viscosus	Dental plaque in humans	**Nesbitt**, *Oral Microbiol Immunol* 11:51, 1996
	Genus *Arcanobacterium*	
A. haemolyticum	Pharyngitis in humans	**Carlson**, *J Clin Microbiol* 32:1654, 1994
A. pyogenes	Mastitis, liver abscesses, and pneumonia in livestock	**Yanagawa,** *Infect Immun* 13:1293, 1976; **Jost**, *Antonie van Leeuwenhoek* 88:87, 2005
	Genus *Corynebacterium*	
C. bovis	Mastitis in cattle; incidental infection in humans	**Yanagawa,** *Infect Immun* 13:1293, 1976; **Sordillo**, *J Dairy Sci* 72:1045, 1989
C. diphtheriae	Diphtheria in humans and studies with diphtheria toxin	**Yanagawa,** *Infect Immun* 13:1293, 1976; **Kawata**, *Jap J Microbiol* 5:441, 1961; **Mausle**, *8th Int Congr Electron Microsc* 2:520, 1974
C. pseudotuberculosis	Caseous lymphadenitis in sheep and goats and studies on the phospholipase D	**Hard**, *Infect Immun* 12:1439, 1975; **Hard**, *J Med Microbiol* 5:483, 1972; **Yanagawa,** *Infect Immun* 13:1293, 1976; **Brogden**, *Am J Vet Res* 51:874, 1990; **Tashiian**, *Am J Vet Res* 44:690, 1983
C. renale	Pyelonephritis in cattle	**Yamagawa**, *Jap J Vet Res* 16:31, 1968; **Honda**, *Am J Vet Res* 36:1663, 1975; **Yanagawa,** *Infect Immun* 13:1293, 1976; **Honda**, *Infect Immun* 10:1426, 1974
C. xerosis	Body orifices in humans	**Yanagawa,** *Infect Immun* 13:1293, 1976
	Genus *Mycobacterium*	
M. aurum	Avian tuberculosis in birds	**Silva**, *Infect Immun* 55:2006, 1987; **Cheville**, *Am J Pathol* 64:97, 1971; **de Chastellier**, *Infect Immun* 61:3775, 1993; **Frehel**, *Infect Immun* 53:252, 1986
M. avium subspecies avium	Opportunistic pathogen of patients with chronic respiratory disease	**Rulong**, *Infect Immun* 59:3895, 1991
M. avium subspecies intracellulare	Opportunistic pathogen of patients with chronic respiratory disease. Granulomas in many species and studies in pigs	**Nakamura**, *J Comp Pathol* 94:509, 1984; **Tereletsky**, *Infect Immun* 41:1312, 1983

Vet-ebooks.com

Table 14.19 *Continued*

Pathogen	*Disease (host) and ultrastrucural studies*	*Reference to ultrastructural pathology*
M. avium subspecies *paratuberculosis*	Paratuberculosis (Johne's disease in ruminants) and ultrastructural studies in tissues	**Momotani**, *Vet Pathol* 25:131, 1988; **Bannantine**, *BMC Microbiol* 2:2, 2002
M. bovis	Tuberculosis in humans, cattle, and other species	**Leake**, *Infect Immun* 45:443, 1984
M. haemophilum	Human infection	**Fischer**, *Infect Immun* 64:269, 1996
M. leprae	Leprosy in humans and lesions and organisms in human, mouse, and armadillo nerves, bone marrow, skin, spleen, and footpads	**Adu**, *J Pathol* 139:275, 1983; **Barros**, *Acta Neuropathol* 73:387, 1987; **Brown**, *Infect Immun* 13:1199, 1976; **Allen**, *J Pathol* 89:301, 1972; **Chapman**, *J Bacteriol* 77:205, 1959; **Dastur**, *Int J Leprosy* 41:47, 1973; **Esiri**, *J Pathol* 106:73, 1972; **Evans**, *Infect Immun* 7:76, 1973; **Finlayson**, *J Neuropathol Exp Neurol* 33:446, 1974; **Job**, *Arch Pathol* 89:195, 1970; **Kaplan**, *Am J Pathol* 128:345, 1987; **Kaplan**, *J Exp Med* 158:1145, 1983; **Mor**, *Infect Immun* 42:802, 1983; **Yoshizumi**, *Acta Neureopathol* 27:1, 1987
M. tuberculosis	Tuberculosis in humans	**Armstrong**, *J Exp Med* 142:1, 1975; **D'Arcy Hart**, *J Exp Med* 166:933, 1987; **Dumont**, *Lab Invest* 14:2034, 1965; **Miller**, *Arch Pathol Lab Med* 102:360, 1978; **Arigi**, *J Electron Microsc (Tokyo)* 21:55, 1972; **Oka**, *Sci Rep Res Inst Tohoky Univ (Med)* 18:7, 1971; **Rambukkana**, *Immunology* 77:267, 1992
	Genus *Nocardia*	
N. asteroides	Nocardiosis and ultrastructural and experimental studies in mice	**Beaman**, *Infect Immun* 61:274, 1993; **Beaman**, *Infect Immun* 61:955, 1993; **Black**, *J Infect Dis* 154:952, 1986; **Farshtchi**, *J Bacteriol* 94:255, 1967; **Kawata**, *Jap J Microbiol* 9:101, 1965
N. brasiliensis	Acute or chronic pneumonitis, usually in immunocompromised individuals	**Folb**, *Infect Immun* 13:1490, 1976
	Genus *Rhodococcus*	
R. equi	Pneumonia in humans and horses	**Samies**, *Am J Med* 80:685, 1986 in humans; **Zink**, *Vet Microbiol* 14:295, 1987
	Genus *Tropheryma*	
T. whippleii	Whipple's disease (with arthralgia, fever, weight loss, diarrhea and steatorrhea) and ultrastructural and experimental studies in a variety of tissues	**Dobbins**, *Am J Pathol* 51:225, 1967; **Kent**, *Lab Invest* 12:1163, 1963; **Spapen**, *Dig Dis Sci* 34:640, 1989; **Southern**, *JAMA* 261:1467, 1989; **Watson**, *Lab Invest* 21:347, 1969; **de Groodt-Lasseel**, *Pathol Biol (Paris)* 17:121, 1969; **Wilcox**, *Am J Med* 83:165, 1987; **Jarolim**, *J Infect Dis* 163:1169, 1991; **Lie**, *Am J Clin Pathol* 66:22, 1976; **Johnson**, *Am J Clin Pathol* 74:486, 1980; **Kitamura**, *Acta Neuropathol* 19:275, 1975; **Schochet**, *Acta Neuropathol* 13:1, 1969; **Silbert**, *Acta Neuropathol* 36:31, 1976; **Ectors**, *J Pathol* 172:73, 1994
	Genus *Dermatophilus*	
D. congolensis	Dermatophilosis in cattle and horses	**Bucek**, *J Vet Med [B]* 39:495, 1992; **Richard**, *J Gen Microbiol* 49:23, 1967; **Roberts**, *J Pathol* 90:213, 1965; **Gordon**, *J Bacteriol* 88:509, 1964
D. dermatonomus	Dermatitis in sheep	**Gordon**, *J Bacteriol* 88:509, 1964
D. pedis	Footrot in sheep	**Gordon**, *J Bacteriol* 88:509, 1964
	Genus *Renibacterium*	
R. salmoninarum	Granulomatous lesions in the kidney of salmon	**Dubreuil**, *J Gen Microbiol* 136:2443, 1990
	Genus *Rothia*	
R. dentocariosa	Inhabits the oral flora and associated with endocarditis	**Gerber**, *Lancet* 1:1236, 1985; **Braden**, *South Med J* 92:815, 1999

Vet-ebooks.com

mucosal barrier it colonies fistulae and induces chronic granulomatous infections. It also has been isolated from pyogranulomatous lesions in pigs and cattle.

Actinomyces naeslundii is part of the flora in the oral cavity associated with other microorganims in subgingival plaque,[334] often ultrastructurally in biobilms.[66]

Arcanobacterium pyogenes is a commensal and an opportunistic pathogen of livestock.[335] It causes mastitis, liver abscesses, and pneumonia. *A. pyogenes* uses two neuraminidases (NanH and NanP) for adhesion to epithelial cells and several extracellular matrix-binding proteins (CbpA) for adhesion to collagen-rich tissue. It also produces a cholesterol-dependent cytolysin called pyolysin (PLO) that lyses erythrocytes and is cytolytic for leukocytes.

Genus *Corynebacterium*

The genus *Corynebacterium* contains several pathogens. Nonpathogenic diphtheroids are common commensals of the skin and mucous membranes.[336] Corynebacteria are pleomorphic rods that are difficult to locate in tissue sections. Replication is extracellular and pathogenicity often involves a toxin elaborated while bacteria are associated with epithelial surfaces. The ultrastructure of the various species from cultures is similar. Corynebacteria are commonly in macrophages in infected tissue but rarely survive within phagolysosomes.

Corynebacterium diphtheriae causes human **diphtheria**, a local and systemic toxin-induced disease manifest as acute fibrinous pharyngitis with necrosis, severe regional lymphadenitis, and widespread visceral lesions of toxemia.[337] *C. diphtheriae* localizes in the mucosal epithelium of the nasopharynx where toxin causes severe edema, fibrinopurulent exudation and necrosis that obstruct the pharynx. Respiratory failure and toxin-induced myocardiopathy progress to vascular collapse, shock and death.

C. pseudotuberculosis causes **caseous lymphadenitis** of sheep. This organism produces a potent sphingomyelin-specific phospholipase D exotoxin that is a major determinant in the pathogenesis of caseous lymphadenitis. The toxin creates spherostomatocytes that later become pitted at the cell surface[338] and plays a role in macrophage death.[339] Cell wall lipids incite inflammation.[340]

C. renale causes **pyelonephritis** in cattle. It attaches to the epithelium lining the urinary tract, ascends to the kidney, and creates a suppurative process that leads to interstitial nephritis, scarring, and dilatation of the upper nephron. Pili are important in attachment to the epithelium and can be demonstrated on the cell by immunoelectron microscopy.[341]

Diphtheria Toxin

Diphtheria toxin is a member of the ADP-ribosyl transferase toxin family.[342] It is a large, 58-kDa multidomain protein with receptor binding, transmembrane targeting, and protease resistant catalytic domains. Diphtheria toxin is a eukaryotic elongation factor 2 (eEF2) ribosylating toxin. Diphtheria toxin binds to the epidermal growth factor-like precursor on the cells surface, is cleaved, taken up via receptor-mediated endocytosis, penetrates the endosome membrane, and passes directly into the cytoplasm. In the cell, it ribosylates an exposed histidine that has been modified by the addition of a diphthamide group. Ribosylation interrupts the function of eEF2, interferes with protein synthesis, and kills the cell.[343] Diphtheria toxin is encoded by the *tox* gene, which is found, not in the bacterial chromosome, but in genomes of corynephages.[344]

Genus *Mycobacterium*

The genus *Mycobacterium* contains important human and animal pathogens. They are straight or slightly curved rods of 0.3–0.6 × 1–4 μm; coccobacillary, filamentous, and branched forms occur in some species. The **cell wall** is lipid rich and contains large amounts of C60-C90 fatty acids and mycolic acids covalently linked to arabinogalactan.[16] These lipids assemble to produce an asymmetric bilayer of unusually low permeability and exceptional thickness. During cell division of *M. tuberculosis*, the multilayered cell wall participates in septum formation while the outer layer ruptures first on one side giving the appearance of "snapping" division. Alternately, *M. tuberculosis* may form transient branching structures.[345] Surface bleb-like structures and extracellular fibrils accumulate on older cells of *M. tuberculosis*.[346]

Ultrastructurally, the mycobacterial cell contains an inner fibrillar electron-opaque nuclear region and a high-density periphery filled with ribosomes. The **cytoplasm** contains lipid storage bodies and dense granules of polyphosphates. Mycobacteria contain an electron-transparent capsule formed of fibrillar material containing arabinomannan and mannan. These polysaccharides are related to the lipoarabinomannan and lipomannan lipoglycans of the cell wall and contribute to the immunopathogenesis of mycobacterial infections.[347] The **capsule** varies in thickness and is in close contact with the cell wall. Cell wall associated proteins secreted by live mycobacteria can be seen by immunogold labeling.

In infected tissues, mycobacteria typically are found within **phagolysosomes** (Fig. 14.23) of **macrophages**. Virulent mycobacteria either replicate within these

Vet-ebooks.com

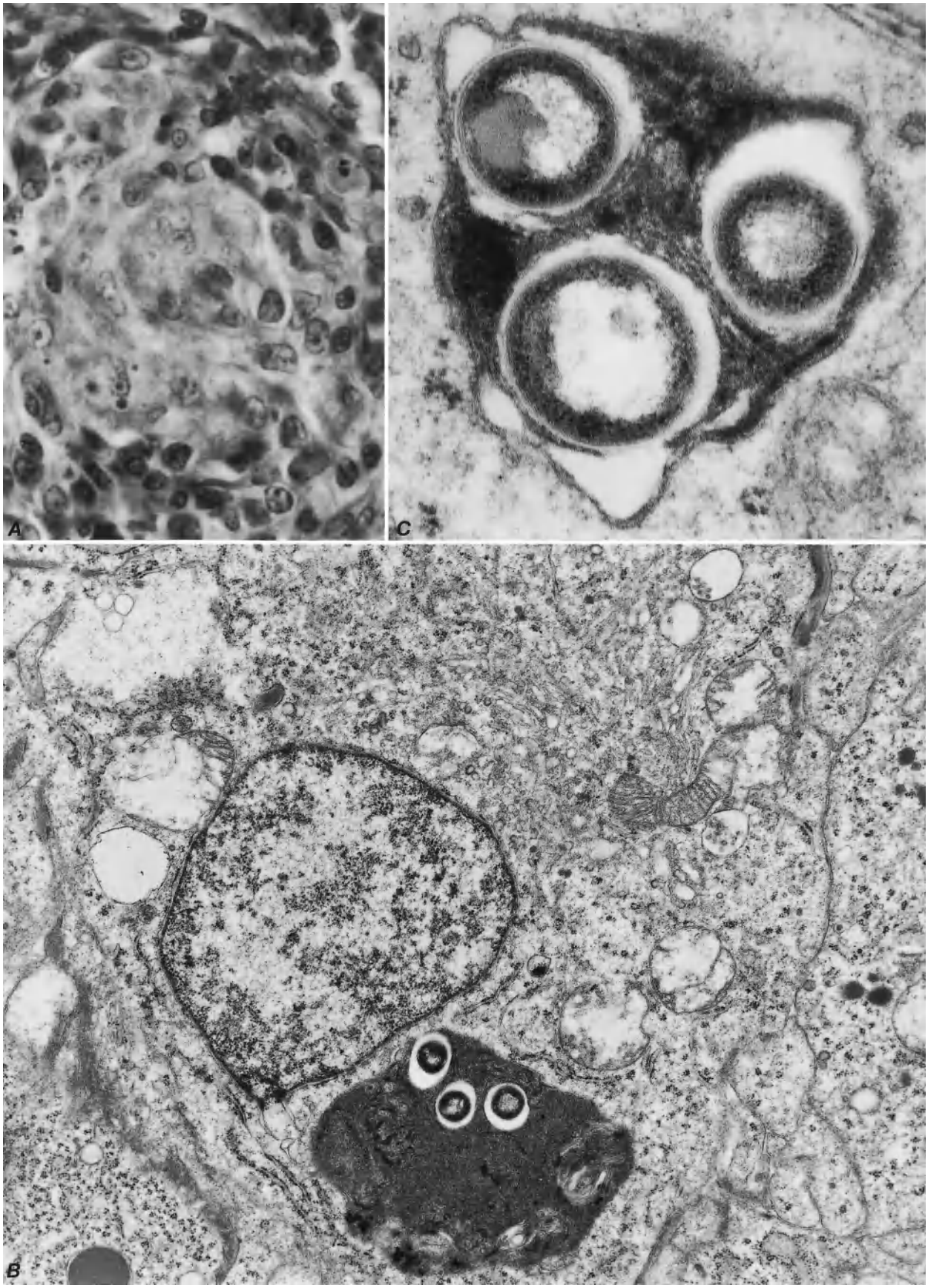


Fig. 14.23 ***Mycobacterium avium***: spleen, chicken with tuberculosis. **A**. **Granuloma**. **B** and **C**. **Bacilli** within macrophage lysosomes.

Vet-ebooks.com

macrophages because they are resistant to lysosomal hydrolases or prevent the fusion of primary lysosomes with phagosomes. Intracellular survival of mycobacteria is associated with failure of lysosomes to fuse with phagosomes. In macrophages, mycobacteria can be transported into deeper tissues.[348] Here additional macrophages gather and form **granulomas**, an organized collection of differentiated macrophages with a characteristic morphology. T cells, B cells, dendritic cells, neutrophils, fibroblasts, and extracellular matrix components may be present. There can be regions of acellular debris or caseous necrosis. Cell mediated immunity develops soon after infection. Macrophages activated by lymphocyte cytokines have enhanced mycobactericidal capacity; when infected, they more rapidly develop phagolysosomes containing degenerate bacteria. *M. tuberculosis* and *M. leprae* antigens in cultured cells, lung tissues, or skin can be seen by high-resolution immunofluorescence microscopy and cryo-immunogold electron microscopy.[349]

M. tuberculosis Complex

Five mycobacteria are closely related and make up the *M. tuberculosis* complex. *M. tuberculosis* causes **tuberculosis**; *M. africanum* causes tuberculosis in Africa; *M. canetti* causes rare mycobacterial infections; *M. bovis* causes tuberculosis in humans, cattle, and other species; and *M. microti* causes infections in voles. Although these species are closely related, they are different in morphology, biochemistry, host range of infection, and disease pathogenesis.[348]

M. tuberculosis enters the respiratory or intestinal tract to initiate primary infection.[350] Bacteria are surrounded by small foci of neutrophils and macrophages. It may be contained with small foci of infection and eliminated. If host macrophages cannot handle the primary infection, however, the lesion progressively expands due to the continuous entry of sensitized monocytes. These cells phagocytize dead macrophages containing viable bacteria and are, in turn, eliminated. At the periphery of the lesion, this activity is most intense and large plump macrophages, called epithelioid cells, are prominent. The **tubercle**, the hallmark of tuberculosis, is a nodule composed of caseous necrotic tissue surrounded by macrophages and walled off by chronic granulomatous tissue containing lymphocytes, plasmacytes, and fibroblasts. Ultrastructurally, *M. tuberculosis* releases its lipids into the vacuole where they mix with host-derived materials and accumulate in multilamellar vesicles.[350] The vesicles are released as exosomes from the infected macrophages and interact with adjacent cells.

Epithelioid cells contain markedly undulate and ruffled plasma membranes that interdigitate with neighboring cells. The endoplasmic reticulum, lysosomes, and vacuoles are abundant. Fusion of membranes results in the formation of **giant cells** in most species of animals. Dissemination occurs if the infection is not controlled. Secondary foci of infection develop by extension or, upon erosion of vascular structures, by lymphogenous or hematogenous distribution.

Leprosy

M. leprae is a non-motile, non-spore-forming, microaerophilic, acid-fast bacterium. Ultrastructurally, it is a slightly curved or straight rod with typical mycobacterial morphology.[351] *M. leprae* is smaller and has a thinner peptidoglycan layer than *M. tuberculosis.* The peptidoglycan layer of *M. leprae* is 4–5 nm, and the layer of *M. tuberculosis* is 10–15 nm. With freeze-substitution electron microscopy, both species have similarly multilayered envelope architectures composed of an electron-translucent layer, a peptidoglycan layer and the plasma membrane.[352] In infected mouse foot pads, there are only a few morphologically normal cells of *M. leprae*. The rest are degraded. In all cells, the peptidoglycan layer is intact.[353]

Human leprosy is a chronic granulomatous disease caused by *M. leprae*.[348,354] The distinctive lesions contain large lipid-laden macrophages and giant cells filled with acid-fast bacilli. **Tuberculoid-type leprosy** is characterized by an active cell mediated immune response to *M. leprae* with granuloma formation. There are predominantly T_H cells with marked activation of both T lymphocytes and macrophages.[355] Nerve damage occurs by immune-mediated killing of Schwann cells and loss of the myelin sheath. **Lepromatous-type leprosy** is characterized by a weak cell mediated immune response to *M. leprae* resulting in a heavily infected and inflamed perineurium. *M. leprae* extensively replicate in macrophages, anergy to *M. leprae* antigens and T cell unresponsiveness. The defect is associated with T cell cytokines interferon gamma and IL-2. Small amounts of interferon gamma injected into cutaneous lesions reconstitute T cell immunity and reduces lesion size by causing destruction of infected foamy macrophages.[355]

In **peripheral nerves** of patients with lepromatous leprosy, *M leprae* is present in Schwann cells, in periaxonal macrophages, and in the axoplasm of myelinated and unmyelinated nerves. In cross sections of axons, clusters of intact bacilli are found in vacuoles. In other nerves, larger vacuoles may contain degenerate bacteria and membranous debris. In rare instances, bacteria occur in the center of the nerve adjacent to the inner surface of the myelin sheath (not within the axon). Lesions also occur in the blood vessels of peripheral nerves. Intraaxonal bacteria are thought to directly cause nerve degeneration, and are responsible

Vet-ebooks.com

for spreading through the nerve. *M. leprae* has Schwann cell-specific adhesins.[356] *M. leprae* uses phenolic glycolipid-1 to bind to the α2 chain of laminin at the basal lamina of the Schwann cell-axion unit. The α2 chain of laminin is found in Schwann cells, striated muscle, and placenta, all tissues infected by *M. leprae*. *M. leprae* also uses LBP21 to bind to Schwann cells. The organism is then taken up via protein tyrosine kinase, calcium-dependent protein kinase, and phosphatidylinositol 3-kinase mediated events. Once internalized in the phagosome, *M. leprae* inhibits phagosome fusion with lysosomes, persists, and grows.[356]

In infected macrophages, *M. leprae* is found in bacteriophorous vacuoles. Phagocytosis of bacilli is mediated by complement receptors (CR1 and CCR3) in human monocytes and by C3 in serum.[357] Direct examination of biopsied human leprosy lesions and those of mice with experimental murine leprosy reveals evidence of fusion of lysosomes with phagosomes containing bacteria. Despite contact with lysosomal enzymes, bacilli continue to proliferate.

Growth of *M. leprae* in nine-banded armadillos or mouse footpads serves as experimental models of infection.[358,359] **Armadillos** are naturally infected by *M. leprae* and develop lesions resembling those of humans. Bacilli infect macrophages but also capillary endothelium. **Lepromatous placentitis** occurs in armadillos, with bacilli in trophoblasts lining chorionic villi and decidual lesions.

M. avium Complex

Environmental mycobacteria form a closely related group called the *M. avium* complex. *M. avium* subspecies avium is an opportunistic pathogen of patients with chronic respiratory disease; *M. avium* subspecies paratuberculosis causes Johne's disease; *M. avium* subspecies silvaticum is present in samples from patients with Crohn's disease, ulcerative colitis, and noninflammatory bowel disease; *M. avium* subspecies intracellulare is also an opportunistic pathogen of patients with chronic respiratory disease; and *M. avium* subspecies hominissuis is present in pigs and humans.[360,361] These mycobacteria are widespread in nature and are common in surface waters and soils. They are intrinsically drug resistant and induce disease in immunocompromised individuals.[348] Information on the relationships among these organisms is rapidly developing as their respective genomes become available.[362]

Johne's disease of cattle, sheep and goats is caused by *M. avium* subspecies paratuberculosis. Lesions of chronic granulomatous enteritis cause intermittent diarrhea and progressive emaciation.[363] After infection, bacteria colonize the mucosa-associated lymphoid tissues of the upper gastrointestinal tract.[364,365] Here they are endocytosed by M cells or phagocytosed by subepithelial or intraepithelial macrophages. Bacilli within infected cells in phagosomes and phagolysosomes multiply. Granulomas form and often involve adjacent lymph nodes.

Putative antigens and determinants of infection include lipoarabinomannan, polar glycopeptidolipid, and the proteins GroES, GroEL, alkyl hydroperoxidase proteins (AhpC and AhpD), antigens (p35 and p36), and a specific antigen, HspX.

Genus *Nocardia*

The genus *Nocardia* contains more than 50 species.[366] They are ubiquitous in the environment. Members are aerobic, catalase-positive, and non-motile. They may form rudimentary or branched hyphae. In tissues, they are typically filamentous and branched bacterial cells that fragment into short units (Fig. 14.24). They have thick cell walls and complex cytoplasmic membrane systems. Approximately half of these species are recognized as human or animal pathogens.[366] These organisms may cause cutaneous infections, pulmonary infections, or central nervous system diseases in immunocompromised individuals.

Organisms with related antimicrobial susceptibility patterns are grouped into the *N. abscessus* group (I), *N. brevicatena/paucivorans* Complex (II), *N. nova* Complex (III), *N. transvalensis* Complex (IV), *N. farcinica* group (V), and *N. asteroides* Complex (VI).[366] These organisms cause chronic suppurative cutaneous infections in humans and animals; granulomatous mastitis in cows; pneumonitis in dogs; and mycetomas in humans and other animals.

Nocardia cause pulmonary disease, purulent pericarditis, mediastinitis, skin and subcutaneous tissue infections, and **central nervous system infections** in humans and animals[366] (Table 14.19). Patients with central nervous system infections usually have one or more brain abscesses. After experimental intravenous injection, *Nocardia* lodges in the brain.[367,368] Ultrastructural analysis of mice given *Nocardia* reveals bacteria in both glia and neurons. *Nocardia* enter perivascular glia and astrocyte foot processes lying adjacent to the basement membrane beneath the capillary endothelium. Lesions are most frequent in the pons, substantia nigra, red nucleus, thalamus, and hypothalamus. Bacterial cells are located within neurons, in the cytoplasm surrounded by layers of membranes. They are also found in phagolysosomes in axons. Microglia engulf other cells containing *Nocardia* and develop large phagolysosomes but do not show evidence of structural damage. Despite this massive infection, there is little evidence of cell injury or inflammation in infected brains.

Vet-ebooks.com

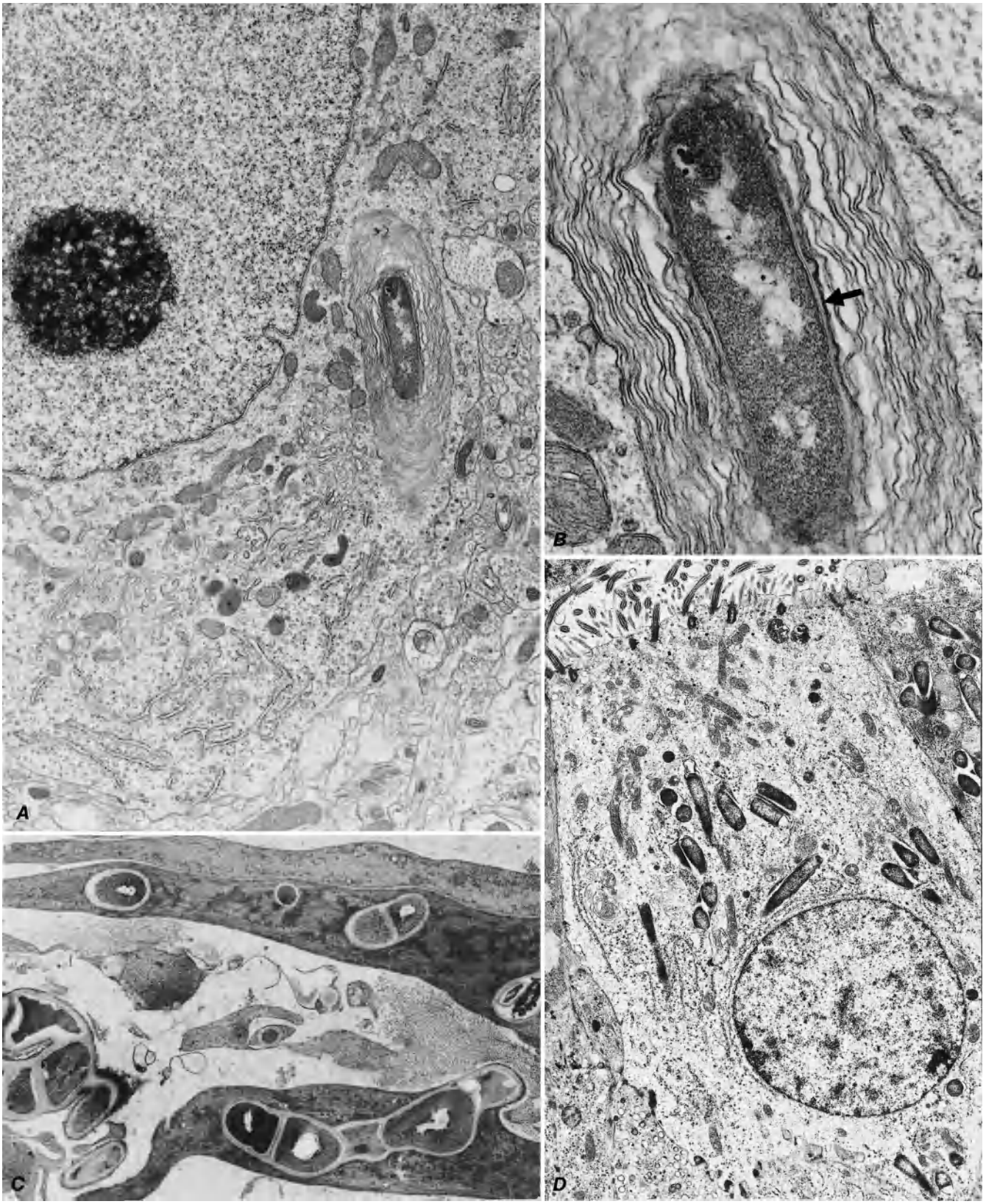


Fig. 14.24 Facultative intracellular bacteria. A. ***Nocardia asteroides*** in neuron, mouse, 24 hr after infection. No cytopathic effect is apparent. **B**. ***Nocardia asteroides*** surrounded by membranes with membrane adherent to bacterial cell wall (*arrow*). (Micrographs: Blaine L. Beaman, *Infect Immun* 61:274, 1993.) **C**. ***Dermatophilus congolensis*** in dead keratinocytes and in extracellular spaces, stratum corneum, skin, horse. **D**. ***Salmonella arizonae*** in ciliated epithelial cell of nasal cavity, sheep. (Micrograph: James Meehan, *Vet Pathol* 29:556, 1992.)

Vet-ebooks.com

Genus *Rhodococcus*

The genus *Rhodococcus* are aerobic, gram-positive, non-motile organisms widely distributed in nature. Here, most *Rhodococcus* species degrade a wide range of organic compounds, and thus play an important role in the global carbon cycle. One species, *Rhodococcus equi*, is associated with severe, usually fatal pneumonia in young horses (Table 14.19). In the respiratory tract, *R. equi* induces pulmonary abscesses and bronchitis.[369] In young horses, *R. equi* replicates in pulmonary macrophages, typically in lysosomes.[370] In foals, *R. equi* is not destroyed by the macrophage, and infection is associated with pyogranulomas and, in severe cases, with fatal necrotizing bronchopneumonia. *R. equi* also causes pneumonia and infections in severely compromised patients and persons infected with human immunodeficiency virus (HIV).[371]

Genus *Tropheryma*

Tropheryma whippleii is the sole species and type species of the genus. It is a long bacillus 1.5 × 0.2 μm in size, with slightly tapered ends. The bacterial surface is covered with a thick glycocalyx and, in extracellular sites, with cellular debris and vesicles. The matrix of bacteria-bearing lysosomes is dense and contains fibrillar material that arises from degradation of bacterial cell wall components. Bacilli have been identified ultrastructurally in a variety of tissues. Cerebral lesions involve collections of glial macrophages and subpial granulomas. Lymphatics of the intestinal wall are affected and the lymphatic outflow of chylomicrons may be obstructed. Epithelium over the lesions is normal.

Whipple's Disease

T. whippleii causes **Whipple's disease**, a progressive, multisystem granulomatous disorder that begins with arthralgia, fever, weight loss, diarrhea and steatorrhea. Focal hyperpigmentation and subtle central nervous system signs may occur. The lamina propria of the intestinal tract is heavily infiltrated with large macrophages bearing PAS-staining granules. Ultrastructurally, *T. whippleii* were found in the extracellular spaces, and remnants of *T. whippleii* were found in the phagocytic vacuoles of macrophages.[372]

Genus *Dermatophilus*

Dermatophilus chelonae and *D. congolensis* are the two species found in this genus. Microbial cells have flagella (from a few to 50 per cell) and are 8–9 μm in size. *D. congolensis* causes **cutaneous dermatophilosis**, a common exudative dermatitis in cattle, sheep, goats, horses, and deer. *D. congolensis* may be transmitted to humans by direct contact, and occasional infections occur.[373] Infection of the skin by *D. congolensis* results from lodgement of zoospores (1 μm in size) in breaks in the stratum corneum and in the protective sebaceous barrier of the epidermis. Zoospores (motile by virtue of polar flagella) are released from hyphae and are infective. They enlarge, germinate, and evolve into filaments and hyphae. Filaments penetrate living keratinocytes in the stratum spinosum, causing parakeratosis. Branching hyphae and clusters of coccoid bodies are found in the parakeratotic layers. Epidermal cells begin to cornify as soon as they are penetrated and organisms are found in cornified cells (Fig. 14.24).

Phylum Firmicutes, Order Bacillales

Genus *Bacillus*

The genus *Bacillus* contains important spore-forming pathogens (Table 14.20). **Sporulation**, which does not usually occur in vivo, involves development of spores within the vegetative form of the bacterium. DivIVA of *B. subtilis* is a protein with distinct roles in cell division and sporulation. The purified protein appears as an elongated particle with lateral expansions at both ends, producing a form that resembles a "doggy-bone." This serves as a building block giving rise to strings, wires, and, finally, two-dimensional lattices important in cell division.[374]

Anthrax

B. anthracis causes **anthrax**, a septicemic disease of cattle, sheep, horses, and humans. It can appear as a solitary local skin lesion or as a fulminating septicemia with high fever, widespread hemorrhage, subcutaneous edema and rapid progress to death. In septicemic anthrax, the blood is thick and dark, the spleen is soft, swollen and red-black; smears of both contain tangles of large, blunt-ended cylindrical rods of *B. anthracis*.

There are three clinical forms of human anthrax: **cutaneous anthrax** or **wool sorter's disease**, where bacilli penetrate the skin and bacteria multiply and produce toxin; **gastrointestinal anthrax**, in which ingested spores penetrate the mucosa, germinate, replicate, and produce toxin; and **pulmonary anthrax**, where inhaled 1 μm spores enter terminal bronchioles, are ingested by macrophages, and are carried to pulmonary lymphoid tissues where they germinate and replicate and produce toxin. Untreated pulmonary anthrax is characterized by pulmonary and mediasti-

Vet-ebooks.com

Table 14.20 Order Bacillales: pathogenic species.

Pathogen	*Disease (host) and ultrastrucural studies*	*Reference to ultrastructural pathology*
	Genus *Bacillus*	
B. anthracis	Anthrax in humans and ultrastructural and experimental studies in a variety of models	**Albrink**, *Am J Pathol* 36:457, 1960; **O'Brien**, *Infect Immun* 47:306, 1985; **Beal**, *J Infect Dis* 116:377, 1966; **Berdjis**, *Br J Exp Pathol* 44:101, 1963; **Dalldorf**, *Lab Invest* 21:42, 1969; **Roth**, *J Bacteriol* 88:523, 1964; **Dalldorf**, *Lab Invest* 21:42, 1969; **Hachisuka**, *J Bacteriol* 91:2382,1966; **Ezzell**, *J Clin Microbiol* 28:223, 1990
	Genus *Listeria*	
L. ivanovii	Animal pathogen (e.g., abortions, sepsis, and enteritis) rarely associated with human infections	**Karunasagar**, *Infect Immun* 61:162, 1993
L. monocytogenes	Human infections and ultrastructural and experimental studies in a variety of models	**Armstrong**, *J Bacteriol* 91:1346, 1966; **Cossel**, *Beitr Pathol Anat Allg Pathol* 138:65, 1991; **Deschryver-Kecskemeti**, *Lab Invest* 58:698, 1980; **Guzman**, *Infect Immun* 63:3665, 1995; **De Heer**, *Lab Invest* 43:449, 1980; **Harding**, *J Cell Biol* 119:531, 1992; **Hof**, *Med Microbiol Immunol* 173:207, 1984; **Hsu**, *Immunol Infect Dis* 1:19, 1991; **North**, *Br J Exp Pathol* 44:601, 608, 1963; **Racz**, *Lab Invest* 26:694, 1972; **Racz**, *Virch Arch* B 8:96, 1971; **Racz**, *Acta Microbiol Acad Sci Hung* 17:221, 1970; **Tenner**, *Virch Arch B* 14:35, 1973; **Tilney**, *J Cell Biol* 109:1597, 1989
	Genus *Staphylococcus*	
S. aureus	Cutaneous, respiratory tract, and systemic infections in humans, scalded skin syndrome in humans, mastitis in cattle, and ultrastructural and experimental studies in a variety of models	**Arizono**, *J Bacteriol* 173:4333, 1991; **Brewer**, *J Pathol* 86:299, 1963; **De Dobbeleer**, *J Cutaneous Pathol* 2:91, 1975; Shuter, *Infect Immun* 64:310, 1996; **Ferguson**, *Br J Exp Pathol* 69:553, 1988; **Carven**, *Br J Exp Pathol* 60:453, 1979; **Harmon**, *Am J Vet Res* 43:992, 1982; **Caputy**, *Infect Immun* 36:759, 1982; **Conti**, *J Bacteriol* 96:554, 1968; **Fussle**, *J Cell Biol* 91:83
S. saprophyticus	Studies on the hemagglutinin	**Gatermann**, *Infect Immun* 60:4127, 1992; **Gatermann**, *Infect Immun* 60:1055, 1992

nal hemorrhage and septicemia. In experimental *B. anthracis* infections, there is direct toxic injury to the pulmonary capillary bed; endothelial cells develop severe acute cell swelling leading to capillary permeability, diffuse pulmonary edema, and thrombosis.

B. anthracis has a massive homogenous **capsule** composed of a polypeptide of glutamic acids and can be identified using monoclonal antibodies to cell wall galactose-N-acetylglucosamine polysaccharides. Virulent bacilli form large capsules in tissues, which inhibit opsonization and phagocytosis. Avirulent, rough forms of *B. anthracis* lack capsules. The **toxin** produced by *B. anthracis* is lethal, affects capillary permeability, acts extracellularly, and is the basis for immunity. Like capsular material, it depresses phagocytosis.

Virulent strains of *B. anthracis* possess three plasmid-encoded virulence factors: a polyglutamic capsule that inhibits phagocytosis, and two AB toxins.[375] The two A subunits are edema factor (EF) and lethal factor (LF) and the B carrier is anthrax protective antigen (PA). This complex causes lethal edema and vascular destruction and kills the host. They enter the cell via endocytosis and affect signaling pathways. EF, a calmodulin-dependent adenylate cyclase, perturbs ion homeostasis and cell signaling by increasing the cytosolic cAMP concentration. LF, a zinc-dependent metalloprotease, cleaves the N-terminal portion of mitogen-activated protein kinases.[375]

Genus *Listeria*

The genus *Listeria* contains the pathogen *L. monocytogenes*, an aerobic, non-sporulating, motile, gram-positive bacillus that is common in soil, water, and vegetation. *L. monocytogenes* is a food-borne pathogen and infection occurs by ingesting the organism in contaminated foods; for example, dairy products (humans) and silage (ruminant species of animals). Infections can have a 30 percent mortality rate and are characterized by gastroenteritis, meningitis, encephalitis, abortion, perinatal infections, and central nervous system involvement. After ingestion, bacteria infect the intestine producing gastroenteritis. Bacteria pass the

Vet-ebooks.com

intestinal wall to become bacteremic and disseminate, infecting the brain and, in pregnant animals, the fetus. To infect the brain, *L. monocytogenes* reach dental termini of the trigeminal nerves to cause ascending **neuritis** and **meningoencephalitis**. Bacteria are found in meninges, associated with macrophages and perivascular cells.

L. monocytogenes has proteins, determinants, and mechanisms all involved in pathogenicity.[376,377] Surface proteins vary depending upon the growth of *L. monocytogenes* in environmental niches or mammalian hosts. Major surface proteins include autolysins; penicillin-binding proteins; deacetylases; enzymes involved in assembly of teichoic acids and lipoteichoic acids; and sortases. Diverse virulence factors assist the organism to adhere to cells (autolysin Ami and surface actin ActA), enter cells (internalin A, internalin B, cell wall hydrolase p60, and surface actin ActA), escape from primary and secondary vacuoles (listeriolysin O, phosphatidylinositol phospholipase C, phosphatidylcholine phospholipase C), intracellular movement and actin-based motility (ActA), nutrient procurement (sugar uptake system, Hpt), and persistence (bile salt hydrolase).

Internalin A allows *L. monocytogenes* to attach to the receptor E-cadherin on epithelial cells and macrophages.[378] **Phagocytosis** and uptake is triggered by interaction of the transmembrane adhesion molecules and the cytoskeleton.[379] In **macrophages**, the phagosomal membrane disintegrates and bacterial cells enter the cytoplasmic matrix to replicate in the cytoplasm; bacteria are found within membrane-bound phagosomes and free in the cytoplasm. Bacteria can be seen in the nucleus of the infected cell. *L monocytogenes* can spread from cell to cell without leaving the cytoplasm. Once in the cytoplasmic matrix, bacteria become coated with **actin filaments**.[380] *L. monocytogenes* cell surfaces nucleate actin filaments, which rearrange to form tails used to move the bacterium through the cytoplasm. Migration is directed into pseudopodia, facilitating spread of bacteria.[380] **ActA**, a bacterial surface protein, induces actin accumulation and has been localized by immunogold techniques to bacteria within host cells.[381] ActA is not present in *L. ivanovii*, which invades cells using actin in the same way but by another mechanism.[382]

Pathogenic strains of *L. monocytogenes* produce **listeriolysin O**, a pore-forming, cholesterol-dependent cytolysin that disrupts the membranes of the phagosome. It is active at pH 5.5 suggesting that it works in the acidic environment of endosomes or phagosomes. **β-listeriolysin** causes cell death when its components embed in the lipid bilayer to produce membrane pores.[383] Phosphatidylinositol phospholipase C, phosphatidylcholine, and phospholipase C assist listeriolysin O to escape from primary and secondary vacuoles.[384]

Genus *Staphylococcus*

The genus *Staphylococcus* are gram-positive, nonmotile, non-spore-forming cocci just under 1 μm in size. Organisms divide in several planes and the tendency for daughter cells to remain attached gives rise to large groups of bacterial cells, which often appear as microcolonies in infected tissue. They have thick cell walls. Some, but not all strains, have a capsule (Figs. 14.25 and 14.26). Capsules, when present, are anti-phagocytic.

S. aureus is an important pathogen affecting humans, livestock, and poultry.[385] While *S. epidermidis* colonizes the skin, *S. aureus* colonizes mucosal surfaces of the nose, axilla, perineum, vagina, and rectum. The carriage rate is approximately 30–40%. *S. aureus* causes a variety of infections including styes, furunculosis, paronychia, pneumonia, mastitis, urinary tract infections, osteomyelitis, endocarditis, sepsis, meningitis, food poisoning, and toxic shock syndrome.

S. aureus has a vast array of virulence factors[385,386] and even genes in some prophages contribute to virulence.[387] *S. aureus* colonizes the moist squamous epithelium of the anterior nares.[388] Here, adhering strains form biofilms and express an adhesin SasG (*S.*

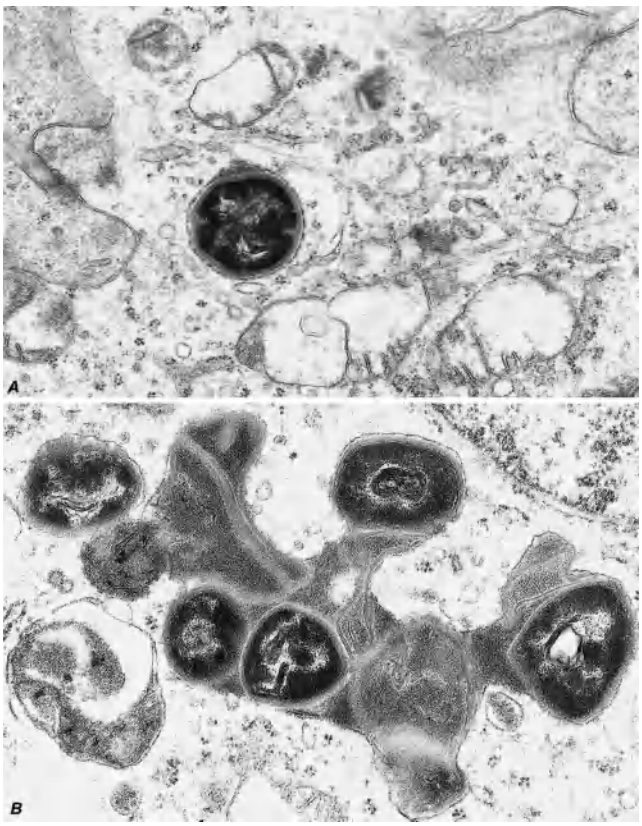


Fig. 14.25 ***Staphylococcus* sp.**: splenic reticular cell. **A**. **Intact coccus** in phagosome. **B**. **Intact and degenerate cocci** in autophagolysosome.

Vet-ebooks.com

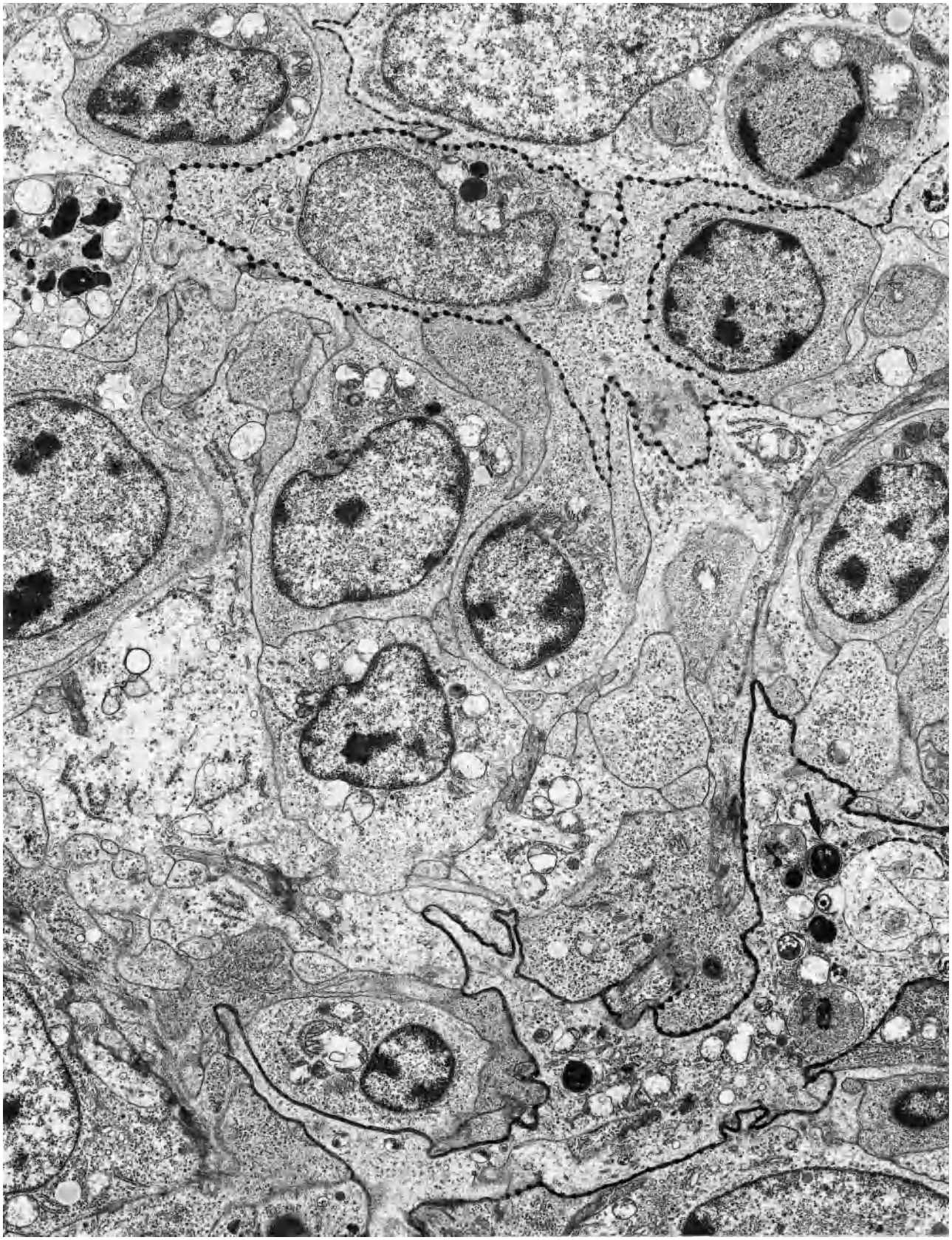


Fig. 14.26 ***Staphylococcus* sp.**: macrophages and reticular cells, splenic red pulp. Dendritic cell has close contact with lymphocyte (*dotted line*); a second dendritic cell (*solid black line*) contains *Staphylococcus* (*arrow*) within phagolysosomes.

Vet-ebooks.com

aureus surface protein G). When negative stained with immunogold and anti-SasG antibodies, SasG appear as peritrichous fibrils 53.5 nm long on the surface.[388] *S. aureus* biofilms also occur on adenoid tissues.[389] Ultrastructurally, bacterial microcolonies with glycocalyx can be seen on adenoid tissue surfaces.

S. aureus is susceptible to host defense peptides. Ultrastructurally after 30 minutes incubation with human beta defensin 3, the peripheral cell wall of *S. aureus* is perforated exposing the plasma membrane.[390] After 2 hours, cells undergo bacteriolysis and disintegration.

Staphylococcal Disease

S. aureus **pneumonia** results in mortality among healthy individuals. In these strains, alpha-hemolysin (Hla) and Panton-Valentine leukocidin (PVL) are important virulence factors.[391] Replacement of *hla*, but not *lukS-PV*, abolishes the ability of *S. aureus* isolates to cause lung infections in mice.

S. aureus **septicemia** results when bacteria circulating through the liver and spleen are entrapped and taken up by pseudopods of Kupffer cells (Fig. 14.26). Bacilli appear to adhere to their plasma membranes, finely granular aggregates develop in the cytoplasm at sites of bacterial localization, cytoplasmic tubules with a dense central matrices form, and bacteria are taken into phagosomes. Phagolysosomes containing staphylococci become denser as degradation proceeds. During septicemia, endothelial cells are damaged.[392] Staphylococci induce platelet aggregation and bacteria-platelet emboli exhibit a distinct tendency to adhere to Kupffer cells.

S. aureus **induced toxic shock syndrome** (TSS) begins with rapid onset of fever, myalgia, hypotension, hyperemia of mucous membranes, rash with desquamation, and multiorgan failure.[393] Rapid onset of hypotension leads to ischemia and multiorgan failure. TSS is mediated by direct effects of **TSST1** and secondary effects of the cytokines IL-1 and TNF that are released by macrophages. TSST1 has been identified with immunogold as it crossed endothelial cells within vesicles.[394]

S. aureus **enterotoxins** are a family of molecules, encoded by bacteriophages, that cause food poisoning. Various enterotoxin genes include sea, seg, seh, sei, sen, seo, and sem.[395] Human staphylococcal food poisoning is of rapid onset and quick recovery. Staphylococcal enterotoxins, when ingested, initiate clinical signs of food poisoning. Circulating toxin is cleared by the renal glomerulus and reabsorbed by the proximal convoluted tubule where lysosomal degradation occurs.

S. aureus **scalded skin syndrome** results from erythema and edema of the skin and progresses to end in large areas being lifted and peeled away by a layer of serous fluid.[396] Exfoliative toxin A and B cause intraepidermal separation of the granular layer.[393]

Order Lactobacillales

Genus *Streptococcus*

The genus contains small (0.6–1.0 μm in size), gram-positive, spherical or ovoid bacteria that grow in pairs or in long chains. Streptococci are common inhabitants of epithelium of the skin, oropharynx and intestine but are not saprophytic in organic material. Streptococci are pathogenic in most species of mammals and birds and cause a wide spectrum of diseases. The Lancefield system of serogrouping streptococci is useful for those isolates that express beta-hemolysis on blood agar plates but not for serogrouping non-beta-hemolytic isolates and related genera.[397] In fact, a combination of conventional tests, specific chromogenic tests, and genetic comparisons may be required. Beta-hemolytic streptococci contain important human and animal pathogens including virulent human strains (Table 14.21). Non-beta-hemolytic streptococci also contain important human and animal pathogens.[397] Ultrastructurally, these groups cannot be differentiated.

Streptococci have virulence factors for adherence, internalization, invasion, anti-phagocytic activity, systemic toxicity, and dissemination.[398–402]

Adhesins include fimbriae, lipoteichoic acid, fibronectin-binding proteins, collagen-binding proteins, capsules, and M proteins. Ultrastructurally, specific cell wall antigens of streptococci have been localized by immunoelectron microscopy.[403] **Lipoteichoic acid**, which enhances binding to epithelial cells, binds spontaneously to plasma membranes via ester-linked fatty acids. *S. salivarius* has short, thin fibrils for binding to host tissue fibronectin and *S. pyrogenes*, *S. agalactiae*, and *S. pneumoniae* have flexible pili for binding to host tissue collagen.[52] **Capsules** are composed of polysaccharide and hyaluronic acid.[402] **M protein** (major surface glycoprotein) is a virulence factor of group A streptococci. M protein is in ionic complex with **lipoteichoic acid**. This complex combines with fibronectin, the epithelial cell receptor.[404] M protein has a binding site for fibrinogen, and fibrinogen increases opsonization of streptococci via binding to M protein. The antiopsonin effect of M protein derives from binding to fibrinogen, which prevents opsonization by complement.[405] **M protein-fibrinogen complexes** impede access of C proteins to cell wall structures. Studies with colloidal gold labeling have shown that the fibrinogen-binding region in M protein is in the distal (amino-terminal) half of the molecule.[406,407]

Vet-ebooks.com

Table 14.21 Genus *Streptococcus*: pathogenic species.

Pathogen	*Disease (host) and ultrastrucural studies*	*Reference to ultrastructural pathology*
	Genus *Streptococcus*	
S. pyogenes (**Lancefield Group A**)	Mucosal infection in humans and ultrastructural and experimental studies in a variety of models	**Glick,** *Infect Immun* 4:772, 1971; **Barnett**, *Infect Immun* 60:3932, 1992; **Beachey**, *J Exp Med* 143:759, 1976; **Beachey**, *J Exp Med* 143:759, 1976; **Ayoub**, *J Bacteriol* 98:728, 1969; **Brown**, *Infect Immun* 39:403, 1983; **Voyich**, *PNAS* 100:1996, 2003; **Mater**, *Turk J Med Sci* 31:291, 2001
S. agalactiae (**Lancefield Group B**)	Mastitis in cattle, infections in humans, and ultrastructural studies	**Gibson**, *Infect Immun* 63:271, 1995; **Tyrrell**, *Microbiol* 148:3921, 2002; H**osaka**, *J Electron Microsc* 47:169, 1998; **Segura**, *Frontiers in Biosci* 9:1157, 2004
S. dysgalactiae subspecies *dysgalactiae* (**Lancefield Group C**)	Infections in animals	**Segura**, *Frontiers in Biosci* 9:1157, 2004
S. dysgalactiae subspecies *equisimilis* (**Lancefield Groups A, C, G,** and **L**)	Infections in humans and animals	**Segura**, *Frontiers in Biosci* 9:1157, 2004
S. equi subspecies *equi* (**Lancefield Group C**)	Infections in animals and equine strangles	**Segura**, *Frontiers in Biosci* 9:1157, 2004; **Timoney**, *International Congress Series* 1289:267, 2006
S. equi subspecies *zooepidemicus* (**Lancefield Group C**)	Infections in humans and animals	**Segura**, *Frontiers in Biosci* 9:1157, 2004
S. constellatus subspecies *pharyngis* (**Lancefield Group C**)	Oral infections and periodontal infections in humans	**Eick,** *J Clin Periodontol* 31:376, 2004
S. equinus (**Lancefield Group D**)	Infections in animals and occasionally in humans	**Sechi,** *Scand J Infect Dis* 31:598, 1999
S. gallolyticus (**Lancefield Group D**)	Infections in humans and cattle	**Segura**, *Frontiers in Biosci* 9:1157, 2004
S. canis (**Lancefield Group G**)	Infections in humans (IV drug users) and dogs	**Bisno**, *Infect Immun* 55:753, 1987; **Segura**, *Frontiers in Biosci* 9:1157, 2004
S. anginosus (**Lancefield Groups A, C, G,** and **F**)	Present in oral cavity but associated with thoracic and urinary tract infections and endocarditis	**Allen**, *Microb Pathog* 32:191, 2002; **Chuang**, *J Formos Med Assoc* 105:760, 2006
S. porcinus (**Lancefield Groups E, P, U,** and **V**)	Infections in humans and pigs	**Daynes**, *Infect Immun* 7:298, 1973
S. phocae (**Lancefield Groups C** and **F**)	Exophthalmia and hemorrhage with high mortality in salmonids	**Romalde,** *Vet Microbiol* Epub 2008
The Mutans group, Salivarius group, Anginosus group, Sanguinus group, and Mitis group	Pharyngeal infections, endocarditis, and nephritis in humans and ultrastructural and experimental studies in animal models	**Grenier**, *J Dent Res* 56:166, 1977; **Handley**, *Int J Syst Bacteriol* 41:543, 1991; **Albini**, *Am J Pathol* 118:408, 1985; **Ayakawa**, *Infect Immun* 55:2759, 1987; **Di Persis**, *Infect Immun* 10:597, 1974; **Dall**, *J Infect Dis* 161:1221, 1990
S. pneumoniae	Pneumonia in humans and ultrastructural and experimental studies	**Geelen**, *Infect Immun* 61:1538, 1993; **Baker**, *Lab Invest* 15:716, 1966; **Alonsodevelasco**, *Microbiol Rev* 59:591, 1995; **Segura**, *Frontiers in Biosci* 9:1157, 2004
S. suis	Meningitis in pigs	**Segura**, *Frontiers in Biosci* 9:1157, 2004

Factors for internalization include fibronectin-binding proteins, collagen-binding proteins, and M proteins. Factors for invasion of streptococci include capsules, M proteins, proteases, and DNases. Anti-phagocytic factors include capsules, M proteins, and proteases.[408]

Exotoxins, pyrogenic toxins, proteases, streptokinase, and DNase facilitate dissemination and systemic toxicity. **Streptolysin-O**, produced by β-hemolytic group A streptococci, binds to cell membranes. It is the prototype of the oxygen-labile, thiol-activated bacterial toxins, which encompass over 15 exotoxins

Vet-ebooks.com

produced by gram-positive bacteria. Membrane damage is manifest by circular, semicircular arc structures visible by electron microscopy.[409]

Streptococcal Infections

S. pyogenes infections in humans are characterized by purulent inflammation. They develop as local abscesses, cellulitis, generalized infections with septicemia, disseminated microabscesses, endocarditis, hemolytic toxemia (scarlet fever, associated with the erythrogenic toxin streptolysin O, and human erysipelas), immune-mediated diseases such as rheumatic fever, and post-streptococcal glomerulonephritis.

S. pneumoniae colonizes the upper respiratory tract in humans and infections develop as otitis media, sinusitis, pneumonia, bacteremia, and meningitis.[410]

In tissue, streptococci are rapidly phagocytized by neutrophils and macrophages. They are taken into phagosomes, which fuse with lysosomes. Ultrastructural changes during intralysosomal degradation include disorganization of the bacterial cell cytoplasm, removal of the capsule, and swelling and disintegration of the cell wall. Bacteria are quickly transformed into structureless dense granular debris. Neutrophils are killed in the process and appear dark with eccentric nuclei, large residual bodies, and many small vesicles. Bacterial cells that circulate in the bloodstream are taken up by sinusoidal phagocytic cells and by circulating leukocytes. Within the vascular system, streptococci are surrounded by aggregates of platelets, which degranulate and lyse.[411]

Order Clostridiales

Genus *Clostridium*

Clostridia are gram-positive, nonencapsulated, spore-forming rods that are ubiquitous in nature and colonize the intestinal tracts of humans and animals. Many species are motile and have peritrichous flagella. Cells vary from being coccoid to long filamentous rods with rounded, tapered, or blunted ends.

Pathogenic clostridia produce potent toxins that cause severe tissue damage[412–414] (Table 14.22). Clostridial neurotoxins are composed of botulinum (BoNT) and tetanus (TeNT), which share significant structural and functional similarity.[415] In tissue, bacterial cells are typically surrounded by an empty space or halo. *C. botulinum* does not enter the host but produces a family of potent neurotoxins (A–F).[412] *C. tetani* replicates in superficial and deep wounds in dermis and skeletal muscle and releases its toxin into the bloodstream to act on the nervous system.

Clostridial Myonecrosis

In humans, *C. perfringens* type A, *C. septicum*, *C. novyi* B, *C. sordelli*, *C. bifermentans*, and several untypable clostridia cause disease by infection of traumatic or surgical wounds. Fatal clostridial sepsis is associated with unclean abortions, perforation of the intestine, and severely contaminated deep wounds of skeletal muscle. Tissue invasion of *C. perfringens* may cause necrotizing cellulitis with little necrosis and no gas, or may cause lethal clostridial **myonecrosis** (gas gangrene), a result of locally produced alpha-toxin, a phospholipase C, and theta-toxin, a thiol-activated cytolysin. Lesions of clostridial sepsis include marked edema, lysis of myocytes, and vascular damage. Many vegetative bacilli are present and there is extensive damage to cellular membranes, particularly of erythrocytes and vascular endothelium. Erythrocyte ghosts, which are formed by loss of hemoglobin, are especially prominent surrounding bacilli.

Pseudomembranous Colitis

Clostridium difficile causes antibiotic-associated diarrhea, toxemia, and pseudomembranous colitis. The initial lesions are foci of necrosis of surface epithelium in glandular crypts with large numbers of neutrophils, capillaries in the lamina propria plugged with fibrin, and hypersecretion of mucus in adjacent crypts. Lesions arise from two potent lethal toxins: an **enterotoxin** that causes lysis of the basal part of apical epithelial cells in intestinal loops (toxin A) and a **cytotoxin** (toxin B). Both toxins interfere with the actin cytoskeletons of intestinal epithelium. Toxin production in the human intestinal tract is promoted by therapy with lincomycin, clindamycin, and other antibiotics. Normal human intestinal flora is a barrier against colonization by *C. difficile*. Human infants are refractory to infection due to colostral immunity, refractoriness of perinatal gut epithelium to toxin, and deficiency in receptors for toxin A.

Tetanus

Clostridium tetani causes **tetanus**, a toxigenic disease induced by tetanospasmin. After cleavage, the heavy chain binds to neuronal cells and the light chain binds to the neuro-exocytotic apparatus. Immuno-gold electron microscopy revealed that a fusion protein composed of green fluorescent protein and the atoxic C-terminal fragment of tetanus toxin rapidly clustered in motor nerve terminals of the neuromuscular junction.[416] Binding to the neuro-exocytotic apparatus inhibits the exocytosis of the neurotransmitter and inhibitor impulses to motor neurons are blocked

Vet-ebooks.com

Table 14.22 Order Clostridiales: pathogenic species.

Pathogen	*Disease (host) and ultrastrucural studies*	*Reference to ultrastructural pathology*
	Genus *Clostridium*	
C. botulinum	Botulism in humans and poultry and ultrastructural studies on the effects of botulinum toxin	**Black**, *J Cell Biol* 103:521; **Takumi**, *Infect Immun* 39:1346, 1983
C. butyricum	Experimental infection in gnotobiotic chick	**Popoff**, *Infect Immun* 47:697, 1985
C. colinum	Ulcerative enteritis in chickens and quail	**Kondo**, *Poult Sci* 67:1424, 1988; **Ononiwu**, *Can Vet J* 19:226, 1978
C. difficile	Intestinal infection in humans and ultrastructural studies on the effects of enterotoxin	**Borriello**, *Rev Infect Dis* 12:S185, 1990; **Duchen**, *J Neurol Sci* 14:61, 1971; **Fiorentini**, *Infect Immun* 58:2329, 1990; **Kushnaryov**, *Infect Immun* 57:3914, 1989; **Lima**, *Lab Invest* 61:419, 1989; **Mitchell**, *J Med Microbiol* 23:211, 1987
C. perfringens	Gas gangrene in humans and necrotic enteritis in poultry	**Adamson**, *Infect Immun* 73:4879, 2005; **Dang**, *J Struct Biol* 150:100, 2005; **McDonel**, *Lab Invest* 39:210, 1978; **Miyata**, *FEMS Microbiol Lett* 152:243, 1997; **Mobius**, *J Hist Cyt* 50:43, 2002
C. piliforme	Tyzzer's disease in rabbits, cats, mice, and gerbils	**Fujiwara**, *Jap J Exp Med* 48:467, 1978; **Okada**, *Jap J Vet Sci* 48:605, 1986; **Fujiwara**, *Jap J Exp Med* 33:203, 1963; **Takagaki**, *Jap J Microbiol* 12:129, 1968; **Goto**, *Jap J Exp Med* 44:373, 1974; **Port**, *Lab Invest* 25:81, 1971
C. tetani	Tetanus (skeletal muscle)	**Zacks**, *J Neuropathol Exp Neurol* 23:306, 1964 (mitochondria)
	Genus *Centipeda*	
C. periodontii	Associated with infections of endodontic origin	**Berthold**, *J Ultrastruct Res* 99:150, 1988; **Siqueira**, *J Endod* 30:135, 2004; **Berthold**, *J. Ultrastruct Mol Struct Res* 99:150, 1988; **Males**, *J Gen Microbiol* 130:185, 1984
	Genus *Eubacteria*	
E. tortuosum	Granulomas in turkeys	**Arp**, *Vet Pathol* 20:80, 1983
E. yurii subspecies *margaretiae*	Oral infection in humans and ultrastructural studies	**Margaret**, *J Med Microbiol* 31:103, 1990; **Kerosuo**, *Eur J Oral Sciences* 101:304, 1993
	Genus *Veillonella*	
V. alcalescens subspecies *dispar*	Infections in the oral cavity, intestine, and respiratory tract of humans	**Bladen**, *J Bacteriol* 88:1482, 1964; **Tortosa**, *Infect Immun* 32:1261, 1981

resulting in uninhibited firing of motor nerve transmissions and prolonged muscle spasms.

Tyzzer's Disease

Clostridium piliforme causes **Tyzzer's disease**, a chronic, wasting diarrheal disease of rabbits, mice, gerbils, primates, and other species.[417–419] Focal necrosis of the intestine and liver leads to high mortality. Bacteria are found in the cytoplasm of hepatocytes and enterocytes of the small intestine; they also are found in endothelial cells, myocardial cells, and lymphatic endothelium (Fig. 14.27). In liver, C. *piliforme* is found within hepatocytes at the periphery of foci of necrosis. Hepatocytes show disappearance of organelles with replacement by free polysomes that are interspersed by bacterial filaments. Electron microscopic examination reveals bacilli within the hepatocytes that have a characteristic vegetative form, with peritrichous flagella and spores.[420] Cytoplasmic organelles appear normal despite large numbers of bacteria. Organisms develop in nuclei and karyorhexis is common. Cellular necrosis is initiated by swelling of the mitochondria and deformation of cristae and vacuolation of endoplasmic reticulum—all causing the cell to contract into a dense coagulated mass.

Vet-ebooks.com

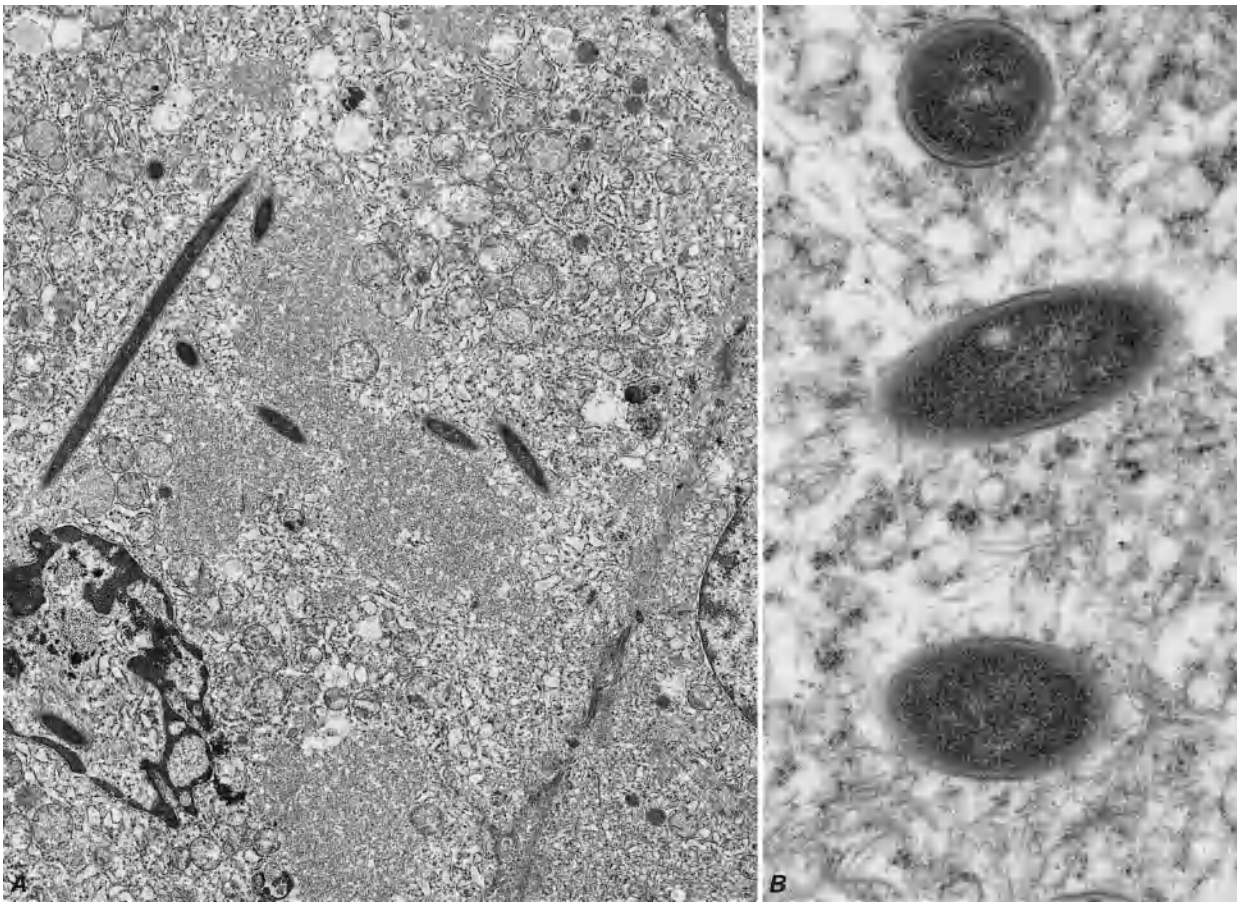


Fig. 14.27 ***Clostridium piliforme:*** hepatocyte, rabbit with Tyzzer's disease. **A. Bacilli** in cytoplasm and the nucleus is degenerate. **B. Cross section of bacilli and pili free in cytosol.** (Micrograph: Randall C. Cutlip.)

Genus *Sarcina*

The genus contains *S. maxima* and *S. ventriculi.* These organisms are gram-positive, non-motile, packet-forming cocci that are isolated from soil, cereal grains and stomachs of humans and other animal species.[421] They are implicated in gastric gas production and bloat in ruminants.[422]

Genus *Eubacterium*

Eubacteria are widely distributed in soil, water, foodstuffs, and the intestinal tracts of humans and animals.[423] They are anaerobic, gram-positive, non-sporulating, non-motile coccobacilli. Infections are often polymicrobial and involve other bacteria. *E. lentum* causes cutaneous, periodontal, abdominal, and perianal abscesses in humans.[423] *E. tortuosum* causes hepatic granulomas in turkeys. Lesions have necrotic centers with zones of heterophils, giant cells, macrophages, and lymphocytes. Bacilli form long filaments or chains that radiate outwards into the surrounding liver parenchyma. Bacteria are found extracellularly mixed with dense granular debris at the interface of heterophils with the necrotic center of the granuloma. Some bacteria appear to be in phagolysosomes, but most of these are invaginations into the surface of degranulate heterophils.

Genus *Veillonella*

The genus *Veillonella* contains 10 species and 7 subspecies. *Veillonella parvula* is an anaerobic, gram-negative coccus that is part of the normal human flora. Although associated with other oral microorganisms in polymicrobial biofilms in the oral cavity,[424] it occasionally causes osteomyelitis, and bacteremia.[425,426] Ultrastructurally, *Veillonella* has typical gram-negative morphology with an outer membrane, thin peptidoglycan layer, and a convoluted cytoplasmic membrane.[427] *Veillonella* has unusually high levels of phosphatidylserine in its membranes.[19] Freeze-fracture electron microscopy shows that the lipids in their plasma membrane go from the liquid crystalline state to the

Vet-ebooks.com

gel state when the temperature is lowered indicating that the lipids are predominantly in the fluid state.

Order Spirochaetales

Leptospira, Borrelia, Treponema, and *Brachyspira* are motile, free-living or parasitic, and grow aerobically or obligate anaerobically. They are 0.1–0.75 μm in size and 5–25 μm in length, and have periplasmic flagella (Table 14.23). Separation of the plasma membrane and glycan layers is indistinct and often called the peptidoglycan-membrane complex. **Periplasmic flagella** (also called axial filaments or endo-flagella) lie between the outer envelope and the peptidoglycan-membrane complex.

Genus *Leptospira*

In the current genotypic classification system, the genus *Leptospira* contains 14 species. Within these species are pathogenic and nonpathogenic serovars, some extensive. Serovars are defined by agglutination with antiserum, cross absorbed with homologous antigen. Leptospires are coiled, motile organisms, approximately 0.1 μm in width × 6–20 μm long, with bent or hooked ends. *Leptospira* are ubiquitous living either as free-living leptospires found in water or associate with renal infection of animals. They primarily induce a disease in domestic and wild mammals. Humans are infected via contact with animals or their excretions.

Leptospires have a number of putative virulence mechanisms that include adhesins, hemolysins, lipoproteins, and OMPA-like proteins Loa22.[428] Mutants not expressing Loa22 were attenuated in guinea pig and hamster models of infection.

Leptospires cause extensive vasculitis. After penetration of the skin and mucosal membranes, they rapidly disseminate through the blood, CSF, and tissues. In the severe leptospirosis, the biphasic course is masked by the early appearance of jaundice, renal failure, purpura and shock. Leptospires in the kidney produce an acute vasculitis in the capillaries and lymphatics of intertubular areas of the cortex causing inflammation, edema of the interstitium, and plasmacyte infiltration (Fig. 14.28). As leptospires migrate from the interstitium to the tubule lumen, they pass between epithelial cells of the proximal tubule causing necrosis of tubules with inspissation of granulocytes and cell debris. Leptospires associate intimately with microvilli of the proximal convoluted tubule, where they replicate and are shed into the urine. Plasmacytes in the interstitium bear anti-leptospiral antibody and, although leptospires are killed, massive amounts of bacterial antigens persist in macrophages of the interstitium. The resulting immunologic reactivity enhances inflammation in the kidney and the development of interstitial fibrosis.

Genus *Borrelia*

The *Borrelia* are gram-negative, microaerophilic spirochetes approximately 8–30 μm long and 0.2–0.5 μm wide. Helices are approximately 0.2–0.3 μm. Ultrastructurally, *Borrelia* species have an outer cell membrane surrounded by a mucoid layer, multiple flagella and the protoplasmic cylinder complex. The endoflagella are located beneath the outer membrane and are inserted at both ends of the protoplasmic cylinder. Antigens recognized by patients with Lyme disease have been localized ultrastructurally to the surface of the spirochete (Table 14.23). Unlike other bacterial species, the genome of *Borrelia* is on a linear chromosome.[429]

B. burgdorferi is among the *Borrelia* species that cause **Lyme disease**. Lyme disease *Borrelia* are transmitted by hard-bodied ticks of the family Ixodidae to mice, other rodents, and to humans.[430] Local infection of the skin is followed by hematogenous spread, invasion of endothelial cells, and infection of many tissues with lymphocytic and histiocytic inflammatory infiltrates. *B. burgdorferi* replicates in skin, nervous system, and joints. *B. burgdorferi* has a predilection for the extracellular matrix.[431] Infection causes a very low-density spirochetemia, erythema migrans, myalgias, arthralgias, arthritis, carditis, conjunctivitis, neurologic involvement, and acrodermatitis. Spirochetemia is short and few organisms are present in lesions, which make ultrastructural identification difficult.

B. burgdorferi attaches to αIIβ3 and αvβ3 **integrins** on the surfaces of host cells via the adhesin protein P66.[431] It also attaches to proteoglycan decorin, glycosaminoglycans, heparan sulfate, and dermatan sulfate of the **extracellular matrix** by the adhesin proteins DbpA, DbpB, Bgp, and BBK32. This likely accounts for the residence of *B. burgdorferi* in dermis, tendons, bladder, and heart. Residence in the extracellular matrix also provides a protected niche for *B. burgdorferi* against specific antibodies.

During phagocytosis, *B. burgdorferi* is taken up by "coiling phagocytosis," during which long pseudopods of macrophages and neutrophils are extended to surround the bacterial cell and then coil around it as it moves to the cell surface and is phagocytized. In coiling phagocytosis, the engulfed spirochete is surrounded by granular cytoplasm and appears to disintegrate without fusing with lysosomes. *B. burgdorferi* is taken up by neutrophils and rapidly degraded within phagolysosomes.

Vet-ebooks.com

Table 14.23 Order Spirochaetales: pathogenic species.

Pathogen	*Disease (host) and ultrastrucural studies*	*Reference to ultrastructural pathology*
	Genus *Leptospira*	
L. biflexa	None (all saprophytic)	**Sheridsan**, *Tuatara* 18:103, 1970; **Kameni**, *J Bact* 184:452, 2002
L. interrogans serogroup *Pomona*	Nephritis and hepatitis in many species and ultrastructural and experimental studies	**Cheville**, *Vet Pathol* 17:338, 1980; **McGrath**, *Pathology* 16:243, 1984
L. interrogans serogroup *Ictero-haemorrhagiae*	Infections in rodents, cows, horses, and pigs. Also experimental studies in hamsters	**Morton,** *J Bacteriol* 45:143, 1943; **Miller**, *Med Microbiol Immunol* 160:269, 1974
L. interrogans serogroup *Canicola*	Infections in dogs, cows, horses, and pigs	**Morton,** *J Bacteriol* 45:143, 1943; **Osechinsky**, *Immunol* 16:427, 1969; **Anderson**, *J Bacteriol* 95:2293, 1968
L. interrogans serogroup *hardjo*	Nephritis and studies in hamsters	**Badiola**, *Am J Vet Res* 44:91, 1983
	Genus *Borrelia*	
B recurrentis	Louse-borne epidemic relapsing fever in humans	**Cutler**, *Int J Syst Bacteriol* 47:958, 1997
B. anserina	Avian borreliosis	**Hovind-Hougen,** *Microbiology* 141:79, 1995
B. burgdorferi	Lyme disease in humans and ultrastructural and experimental studies	**Benach**, *J Infect Dis* 150:497, 1984; **Brusca**, *J Bacteriol* 173:8004, 1991; **Burgdorfer**, *Rev Infect Dis* 11:S1442, 1989; **Comstock**, *Infect Immun* 57:1626, 1989; **Luft**, *Infect Immun* 60:4309, 1992; **Peterson**, *Infect Immun* 46:608, 1984; **Ritting**, *Infect Immun* 60:4205, 1992; **Simon**, *Immunol Today* 12:11, 1991; **Szczepanski**, *Microbiol Rev* 55:21, 1991
B. coriaceae	Epizootic bovine abortion	**Lane**, *Science* 230:85, *1985;* **Osebold**, *J Am Vet Med Ass* 188:371, 1986
B. duttonii	East African tick-borne endemic relapsing fever in humans	**Kawata,** *Jpn J Microbiol* 5:203, 1961; **Cutler**, *Int J Syst Bacteriol* 49:1793, 1999
B. theileri	Bovine borreliosis	**Smith**, *J Invert Pathol* 32:182, 1978 (tick)
	Genus *Treponema*	
T. denticola	Periodontal disease in humans and ultrastructural studies	**Baehni**, *Infect Immun* 60:3360, 1992; **Egli**, *Infect Immun* 61:1694, 1993; **Haapasal**, *Infect Immun* 60:2058, 1992; **Listgarten**, *J Bacteriol* 88:1087, 1964; **Haapasalo**, *Infect Immun* 60:2058, 1992; **Baehni**, *Infect Immun* 60:3360, 1992
T. pallidum	Syphilis in humans and ultrastructural studies	**Azar**, *Arch Pathol* 90:143, 1970; **Brooks**, *Arch Pathol Lab Med* 102:502, 1978; **Konishi**, *Infect Immun* 53:32, 1986; **Musher**, *J Infect Dis* 147:77, 1986; **Radolf**, *Proc Natl Acad Sci USA* 86:2051, 1989; **Sell**, *Lab Invest* 46:355, 1982
	Genus *Brachyspira*	
B. hyodysenteriae	Dysentery in pigs, enteric spirochetosis in humans, and ultrastructural and experimental studies	**Glock**, *Infect Immun* 9:167, 1974; **Miller**, *Am J Vet Res* 49:786, 1988; **Sueyoshi**, *Infect Immun* 58:3348, 1990
B. pilosicoli	Colitis in growing pigs	**Jensen**, *Vet Pathol* 37, 22, 2000
Unclassified Spirochetes	Infections in humans and primates	**Takeuchi**, *Infect Immun* 6:1008, 1972

B. anserina causes **avian spirochetosis**. Avian spirochetes are transmitted by ticks of the *Argas* species.[432] Infection causes an enlarged and mottled spleen, listlessness, depression, and diarrhea. Ultrastructurally, they are slender and helically shaped.[433] On transmission and scanning electron microscopy, the cells have a helical shape with tapered ends. The length of these cells are variable, about 10–25 μm and 0.20–0.28 μm wide. There are five insertion points of flagella in the tapered ends and there are more than ten flagella in

Vet-ebooks.com

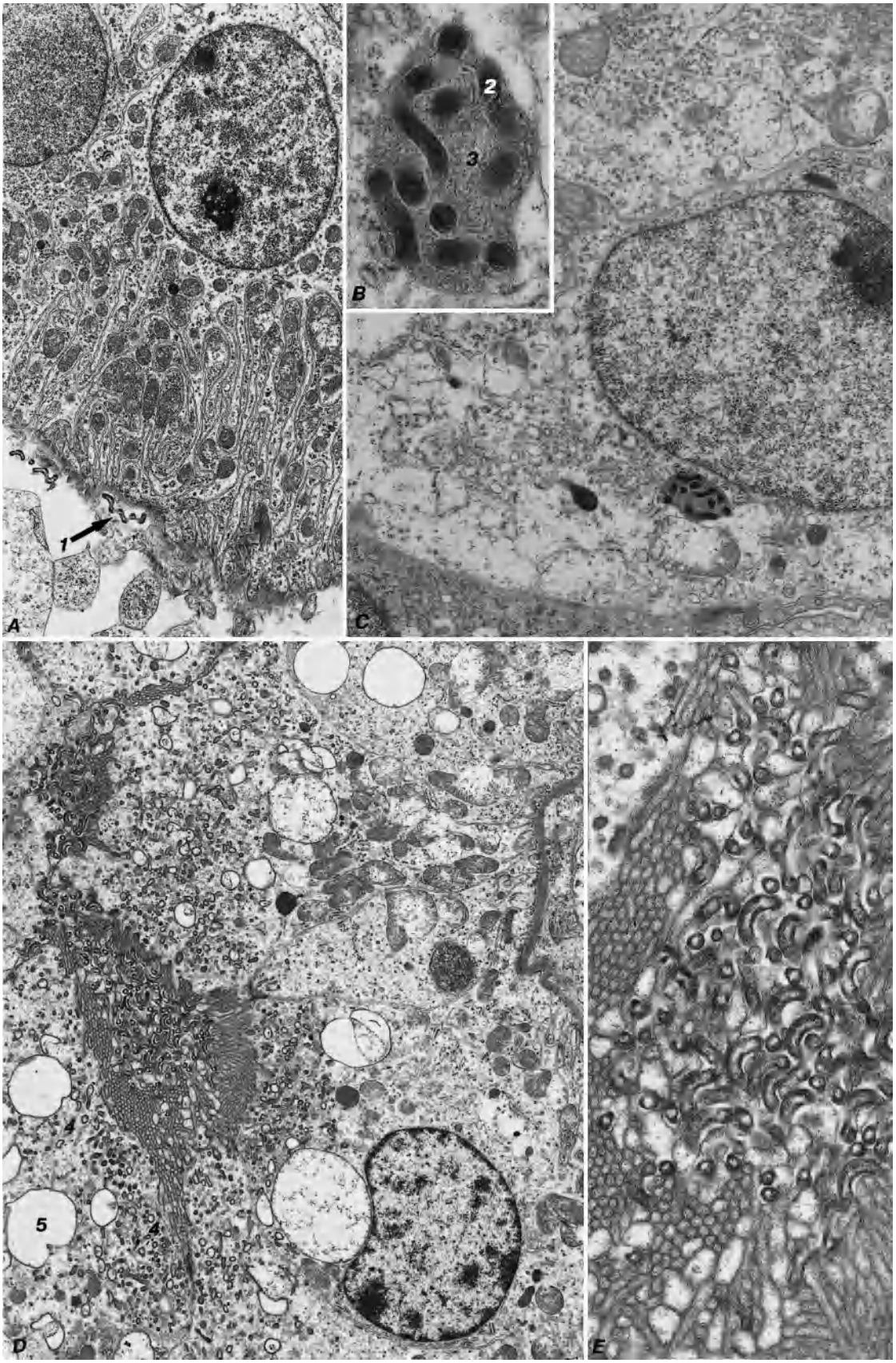


Fig. 14.28 ***Leptospira* sp.**: kidney, pig with acute leptospirosis. **A**. Spirochetes (*1*) trapped in basement membranes of proximal tubule. **B** and **C**. Spirochetes (*2*) and membrane remnants (*3*) within tubule cell phagolysosome. **D**. **Spirochetes enmeshed in microvilli:** proximal convoluted tubule cells; surface tubular system (*4*) and vacuole (*5*) of host cell. **E**. Enlargement of spirochetes in D.

Vet-ebooks.com

each end of the cell. These spirochetes divide by binary fission.

B. hermsii, *B. parkeri*, and *B. turicatae* cause **human relapsing fever**. Relapsing fever *Borrelia* are transmitted by soft-bodied ticks of the family Argasidae.[430] Infection causes a very high-density spirochetemia, no skin involvement, myalgias, arthralgias, hepatomegaly, splenomegaly, arthritis, carditis, hemorrhage, iritis, neurologic involvement, and cerebral hemorrhage. High fevers, rigors, and headache are also common. The "relapse phenomenon" in relapsing fever is an immunologic event that results from bacterial antigenic variation during the course of infection. *Borrelia* typically replicate in tick or insect vectors. During each of these cycles, the population of spirochetes changes in serotype and immunogenic lipoproteins of the outer surfaces of the bacterium. Each new population of spirochetes is associated with a single acute episode. The variable major proteins (Vmps) are composed of two multigene families, the variable large or small proteins (Vlps and Vsps).

Genus *Treponema*

The genus *Treponema* includes three invasive human host-associated pathogens: *T. pallidum* subspecies *pallidum*, *T. pallidum* subspecies *endemicum*, and *T. pallidum* subspecies *pertenue*. *T. pallidum* is a slender, tightly coiled, unicellular, helical cell 0.09–0.18 μm wide × 5–15 μm long. The cytoplasm is surrounded by the outer membrane, a peptidoglycan layer, a delicate inner mucopeptide layer (**periplast**) and an outer lipoprotein membrane containing lipopolysaccharide. The ends of the cell are tapered, and three fibrils are inserted into each end. Cytoplasmic filaments run the length of the cell in line with the endoflagella but within the cytoplasm. Filaments are connected to endoflagella basal bodies at each end of the cell. In studies using freeze fracture techniques, the outer membrane of *T. pallidum* contains important antigens and integral membrane proteins that act as targets for antibodies and can be variably expressed to avoid immune responses of the host. Ultrastructurally, human treponemal pathogens cannot be distinguished by either light or electron microscopy.

T. pallidum subspecies *pallidum* causes **syphilis**. Transmission occurs through direct contact with active lesions and *T. pallidum* penetrates the intact mucous membrane of the genital tract or through abraded epithelium. It enters lymphatics and bloodstream and is disseminated throughout the body. Lesions of syphilis evolve in three stages. In the **primary stage** (0–90 days postinfection), the chancre develops at the site of infection and is accompanied by regional lymphadenitis, and then by healing of the chancre. In the **secondary stage** (6 weeks to 6 months postinfection), there are local or generalized cutaneous eruptions, condylomata lata, alopecia, and asymptomatic central nervous system involvement. This stage has a latent period (approximately 1 year postinfection), characterized by a asymptomatic period with sero-reactivity against *T. pallidum*. In the final **tertiary stage** (months to years postinfection), there are localized **granulomatous lesions** (gummas) in liver, bone, and other organs; **cardiovascular lesions**, chiefly of the aorta (mesaortitis); and **neurosyphilis**. The hallmark of all stages of syphilis is plasmacytosis and obliterative endarteritis. Small arteries and arterioles show proliferation of endothelium and onionskin lesions that obliterate vascular lumens. Circulating immune complexes occur in lesions of secondary syphilis. Biopsies of cutaneous lesions contain neutrophilic reactions consistent with immune-mediated blood vessel damage. **Congenital syphilis** of the fetus in utero in untreated mothers may lead to abortion, stillbirth, neonatal disease, or latent infection of the fetus. Fetal lesions have a large number of spirochetes.

T. pallidum subspecies *endemicum* causes **endemic syphilis** and *T. pallidum* subspecies *pertenue* causes **yaws**. The latter disease is transmitted through body contact and cutaneous abrasions.

In addition to *T. pallidum*, there are spirochetes in the oral cavity associated with dental plaque and gingival crevices, spirochetes on the skin in sebaceous secretions in the genital region, and spirochetes in the intestinal tract associated with the colon and rectum. In periodontal tissues, spirochetes are sparse in healthy tissues, they comprise up to 30% of the flora in periodontal disease. *T. denticola*, a small spirochete cultured from periodontal pockets, attaches to epithelial cells, binds fibronectin and is cytotoxic. This bacterium possesses many putative virulence factors including motility, hydrolytic enzymes such as proteases, and factors that interfere with neutrophil function. A major 53-kD surface antigen is important in adhesion. In human gingival fibroblast cultures, *T. denticola* induces rapid cytoskeletal changes and detachment of cells, allegedly mediated by a protease. *T. denticola* has also been detected in the lesions of atherosclerosis.[434]

Genus *Brachyspira*

Brachyspira hyodysenteriae is a primary etiologic agent of **swine dysentery** and causes extensive necrosis of epithelium in the cecum and colon. Denudation of epithelium leaves villi composed only of lamina propria and a covering basement membrane. The mucosa is rugose and covered by mucus, fibrin, neutrophils, and flecks of blood. Large spirochetes are in

Vet-ebooks.com

the colonic lumen in clusters attached to and inside of epithelial cells.

Spirochetes are found in the intestinal tracts of mammals and birds. Most are incidental discoveries are not associated with disease, and have not been classified. Most appear as large clusters of spirochetes radiating into the gut lumen from attachment sites among microvilli of colonic epithelial cells. One weakly hemolytic porcine isolate has been shown to cause mucoid diarrhea, a syndrome reported as **porcine intestinal spirochetosis**, by a characteristic end-on attachment of spirochetes to colonic epithelium.[435] The day-old chick has been used as a model for pathogenicity studies for both human and porcine isolates, which attach end-on to their cecal enterocytes, induce watery diarrhea and suppress growth.[436]

Order Bacteroidales

Genus *Bacteroides*

Bacteroides species have an outer membrane that varies from 5.6–9.7 nm. The periplasmic space is relatively large (22–26 nm in width) and contains peptidoglycan layers of variable thickness (Table 14.24). The outer surface is covered with a ruthenium red-staining material that may appear fibrillar or amorphous. Membranous vesicles form at the surface of bacteria grown in vitro and are released into the medium. The cytoplasm contains ribosomes and filamentous nuclear acid. *B. melaninogenicus* and *B. asaccharolyticus* produce black hematin pigment when grown in media containing blood. *B. melaninogenicus* is commonly found in polymicrobial infections and diseases in humans and other animals.

B. fragilis causes **diarrhea** and is found in feces of diarrheic humans and animals. Ultrastructural lesions produced in rabbits colonized by *B. fragilis* include effacement of microvilli with loss of terminal microfilaments, which progress to rounding and loss of enterocytes. Porcine isolates, when given to newborn gnotobiotic piglets, colonize the intestinal tract and cause watery diarrhea, although adherence or invasion of intestinal epithelium does not occur. Enterocytes undergo acute cell swelling with vacuolation and are released prematurely into the lumen.

Genus *Porphyromonas*

Porphyromonas gingivalis is among the dominant etiologic agents of periodontal disease.[437–439] It produces a variety of determinants. Some, but not all strains of *P. gingivalis*, invade primary human coronary artery endothelial cells.[440] Scanning electron microscopy of the infected cells shows the invading organisms initially attached to the host cell surface as aggregates and by a "pedestal"-like structure (Fig. 14.29). By transmission electron microscopy internalized bacteria were present within multimembranous compartments localized with rough endoplasmic reticulum. *P. gingivalis* present within autophagosomes may use components of the autophagic pathway as a means to survive intracellularly.

Genus *Tannerella*

Tannerella forsythia is a gram-negative, anaerobic, filament-shaped, nonmotile rod found in the oral cavity. It is associated with advanced and recurrent periodontitis and is implicated as one of the three strongest etiologic agent candidates of periodontal disease. It binds to epithelial cells by virtue of a leucine-rich surface protein (BspA) that may serve as an adhesin and a surface (S–) layer.

Table 14.24 Order Bacteroidales and Order Flavobacteriales: pathogenic species.

Pathogen	*Disease (host) and ultrastrucural studies*	*Reference to ultrastructural pathology*
	Order Bacteroidales, Genus *Porphyromonas*	
P. gingivalis	Periodontal disease in humans and ultrastructural studies	**Barber**, *Microbiol Ecol Health Dis* 3:181, 1990; **Kantarci**, *J Int Acad Pediodontol* 4:119, 2002
	Order Bacteroidales, Genus *Bacteroides*	
B. fragilis	Wound infections in humans and other species	**Duimstra**, *Vet Path* 28:514, 1991; **Mayrand**, *Microbiol Rev* 52:134, 1988; **Bladen**, *J Bacteriol* 86:1339, 1963; **Stewart**, *Res Vet Sci* 23:319, 1977; **Thompson**, *Infect Immun* 59:932, 1991; **Woo**, *J Infect Dis* 139, 534, 1979; **Myers**, *Vet Pathol* 28:336, 1991
	Order Flavobacteriales, Genus *Capnocytophaga*	
C. granulosa	Associated with human dental plaque	**Wilson**, *J Infect Dis* 156:99, 1987

Vet-ebooks.com

Table 14.25 Order Fusobacteriales: pathogenic species.

Pathogen	*Disease (host) and ultrastrucural studies*	*Reference to ultrastructural pathology*
	Genus *Fusobacterium*	
F. necrophorum	Infections of deep tissues and viscera in animals and occasionally humans	**Kinder**, *Infect Immun* 57:3425, 1989; **Mangan**, *Infect Immun* 57:3601, 1989
	Genus *Streptobacillus*	
S. *moniliformis*	Human infections result from rodent bites (**rat-bite fever**) or from consumption of contaminated food or water (**Haverhill fever**)	**Gay**, *Infect Immun* 6:83, 1972

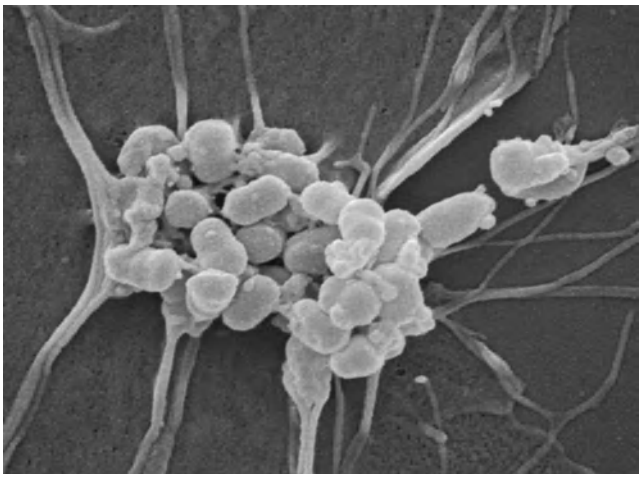


Fig. 14.29 ***Porphyromonas gingivalis*:** scanning electron micrograph of human coronary artery endothelial cells infected with *P. gingivalis* 381. (Micrograph: Myriam Bélanger and Ann Progulske-Fox.)

Order Fusobacteriales

Genus *Fusobacterium*

The genus *Fusobacterium* contains 20 species. *F. nucleatum* is the most commonly encountered species in clinical infections. It is a necrotizing bacterium that commonly colonizes body surfaces and invades deep tissues and viscera of animals (Table 14.25). It is also found in the oral cavity, upper respiratory tract, gastrointestinal tract, and the genital tract causing periodontal disease in humans.[441] *F. necrophorum* causes liver abscesses in cattle and sheep; calf diphtheria in cattle; and foot rot in sheep and cattle. The progressively expanding foci of necrosis have margins that contain masses and tangles of these long thick rods. Another species, *F. equinum*, causes necrotizing pneumonia, pleuritis, and paraoral infections in horses.[442] Leukotoxin, an important virulence factor, is produced by *F. necrophorum* and *F. equinum*.[442]

Genus *Streptobacillus*

Streptobacillus moniliformis is a facultatively anaerobic non-motile, fastidious gram-negative rod. The organism is 0.3–0.5 μm wide and 1.0–5.0 μm long but becomes pleomorphic when subcultured for extended periods. *S. moniliformis* is an inhabitant of the rat nasopharynx. Human infections result from rodent bites (**rat-bite fever**) or from consumption of contaminated food or water (**Haverhill fever**).[443] Infection is characterized by the abrupt onset of fever with rigors, myalgias, headache, polyarthritis, and rash.[444] Lesions in infected mice include abscessation of lymph nodes and chronic polyarthritis and osteomyelitis.[445] *S. moniliformis* is also implicated in infections of turkeys living in rat-infested premises. By transmission electron microscopy, *S. moniliformis*-like microorganisms in poultry have a cytoplasmic membrane, cell wall, and nucleus, but no nuclear membrane.[446] In other studies, ultrastructure among them varies. Bacterial cell walls have three layers; the innermost is most dense. Peritrichous flagella surround bacteria in the cytoplasm of the hepatocyte.

Other Bacteria

There are many species of bacteria that are pathogenic under special circumstances and that, in rare cases, cause disease of animals and humans (Tables 14.26 and 14.27). Many of these organisms are pathogens only in immunoincompetent patients, especially those that are immunosuppressed during viral infection or chemotherapy.

Cilia-associated respiratory (CAR) bacillus is a descriptive term for long, gram-negative, filamentous bacteria that colonize the ciliated epithelium of airways in mice,[447,448] rats,[449,450] pigs,[451] cattle,[452] and other species. The bacterium is unclassified and cannot be readily cultured in vitro. The **CAR bacillus** resides among cilia in airways of the rats with chronic respiratory disease. Measuring 0.2 × 6–8 μm, it lies parallel to

Vet-ebooks.com

Table 14.26 Order Nitrosomonadales: pathogenic species.

Pathogen	*Disease (host) and ultrastrucural studies*	*Reference to ultrastructural pathology*
	Order Nitrosomonadales, Genus *Spirillum*	
S. minus	Rat-bite fever, septic arthritis in humans	**Dendle,** *Eur J Clin Microbiol Infect Dis* 25:791, 2006
Other spirilliform bacteria	Ultrastructural and experimental studies in dogs, cats, pigs, and primates	**Henry**, *Am J Vet Res* 48:831, 1987; **Lee**, *Infect Immun* 56:2843, 1988; **McNulty**, *J Clin Pathol* 42:585, 1989; **Sato**, *Vet Pathol Suppl* 7:17, 1982; **Weber**, *Am J Vet Res* 23;422, 1962

Table 14.27 Miscellaneous: pathogenic species.

Pathogen	*Disease (host) and ultrastrucural studies*	*Reference to ultrastructural pathology*
	Genus *Epulopiscium*	
E. fishelsoni	Giant symbiont in surgeon fish gut	**Bresler**, *J Bacteriol* 180:5601, 1998
	Order Myxococcales, Genus *Myxococcus*	
M. xanthus	Involvement with *Streptococcus mutans* and *Fusobacterium nucleatum* in human oral infections	**Shimkets**, *Microbiol Rev* 54:473,1990; **Mueller**, *J Bact* 173:7164, 1991; **Yang**, *J Bacteriol* 182:5793, 2000

cilia throughout mucosa of the respiratory tract, eustachian tubes, and nasal cavity.[453]

Long-segmented filamentous organisms (LSFO) are in the intestine of chickens and turkeys and adhere to enterocytes. They attach in zones consisting of invaginations with a dense lamina immediately adjacent to the binding site and a zone of polymerized actin that surrounds them.[454] Similar bacteria are in lymphoid tissues of horses with neoplastic disease.[455]

Long filamentous bacteria are seen attached to enterocytes (not M cells) of the follicle-associated epithelium overlying ileal lymphoid tissues of recently weaned horses. By scanning electron microscopy these filamentous bacteria varied from 0.7 to 1.4 μm in size and in length up to 65 μm and were absent from villi surrounding the dome. They attach in shallow indentations in apical regions of enterocytes. The interface between cell and bacterium was via a specialized glycocalyx-bearing terminal segment that was apposed to a dense host cell plasma membrane lined on the cytoplasmic face by actin filaments.[456]

Segmented filamentous bacteria are nonpathogenic and colonize the intestinal epithelium and stimulate the mucosal immune system. Phagocytized by a complex process, they incorporate into host cytoplasmic components.[457]

A *Borrelia*-like spirochete is found in the soft tick *Ornithodoraus coriaceus* and appears to be a possible agent in **epizootic bovine abortion**.[458] When it is inoculated into pregnant heifers, it produces lesions in the fetus that are similar to those seen in natural disease.

Spirochetes isolated from lesions of papillomatous digital dermatitis on the feet of cattle are similar to those in the genus *Treponema*. The relationship to disease is not established nor is the location of these bacteria in tissue lesions.[459]

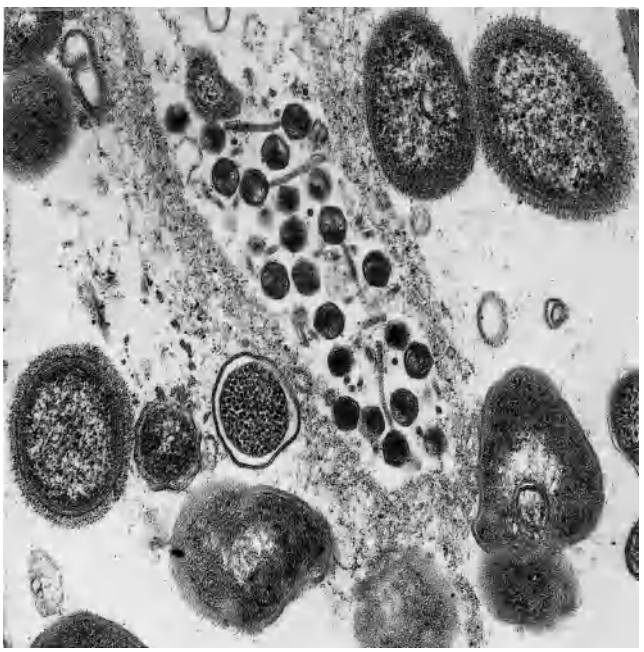


Fig. 14.30 A cluster of bacteriophages in infected tissues.

Bacteriophages

Bacteriophages are viruses that infect bacteria. They are often seen by electron microscopy in infected tissues (Fig. 14.30). Nodules in gills of sticklebacks contain colonies of actively dividing bacterial cells and

Vet-ebooks.com

many lysed bacterial cells containing bacteriophages.[460] The *P. aeruginosa* bacteriophage phiKZ has a head with icosahedral symmetry measuring 1455 A in diameter along five-fold axes. The 65 kDa capsid protein is organized into a surface lattice. It is attached to a 1,800 A-long contractile tail. The double-stranded genomic DNA is packaged into a highly condensed series of layers, separated by 24 A, that follow the contour of the inner wall of the capsid.[461] Generally, these bacteriophages are not associated with lesions, although genetic information carried by some phages plays a role in the virulence of the bacterium.[462]

References

1. Gribaldo, S, Brochier-Armanet, C. 2006. The origin and evolution of Archaea: A state of the art. *Philos Trans R Soc Lond B Biol Sci* 361:1007.
2. Lepp, PW, et al. 2004. Methanogenic Archaea and human periodontal disease. *Proc Natl Acad Sci USA* 101:6176.
3. Schloss, PD, Handelsman, J. 2004. Status of the microbial census. *Microbiol Mol Biol Rev* 68:686.
4. Gill, SR, et al. 2006. Metagenomic analysis of the human distal gut microbiome. *Science* 312:1355.
5. Hall-Stoodley, L, et al. 2004. Bacterial biofilms: From the natural environment to infectious diseases. *Nat Rev Microbiol* 2:95.
6. Brogden, KA. 2002. Polymicrobial diseases of animals and humans. In: Brogden, KA, Guthmiller, JM, eds. Polymicrobial Diseases. ASM Press, Washington, DC, p. 3.
7. Finlay, BB, Falkow, S. 1989. Common themes in microbial pathogenicity. *Microbiol Rev* 53:210.
8. Isberg, RR. 1991. Discrimination between intracellular uptake and surface adhesion of bacterial pathogens. *Science* 252:934.
9. Morioka, H, et al. 1986. Aminoglycoside binding sites in *Escherichia coli* as revealed by neomycin-gold labeling. *J Hist Cyt* 34:909.
10. Lambris, JD, et al. 2008. Complement evasion by human pathogens. *Nat Rev Microbiol* 6:132.
11. Cabeen, MT, Jacobs-Wagner C. 2005. Bacterial cell shape. *Nat Rev Microbiol* 3:601.
12. Matias VR, Beveridge, TJ. 2005. Cryo-electron microscopy reveals native polymeric cell wall structure in *Bacillus subtilis* 168 and the existence of a periplasmic space. *Mol Microbiol* 56:240.
13. Matias, VR, Beveridge, TJ. 2006. Native cell wall organization shown by cryo-electron microscopy confirms the existence of a periplasmic space in *Staphylococcus aureus*. *J Bacteriology* 188:1011.
14. Zuber, B, et al. 2006. Granular layer in the periplasmic space of gram-positive bacteria and fine structures of *Enterococcus gallinarum* and *Streptococcus gordonii* septa revealed by cryo-electron microscopy of vitreous sections. *J Bacteriology* 188:6652.
15. Whitfield, C. 2006. Biosynthesis and assembly of capsular polysaccharides in *Escherichia coli*. *Ann Rev Biochem* 75:39.
16. Brennan, PJ, Nikaido, H. 1995. The envelope of mycobacteria. *Ann Rev Biochem* 64:29.
17. Jonson, AB, et al. 2005. Fimbriae, pili, flagella and bacterial virulence. *Contrib Microbiol* 12:67.
18. Matias, VR, Beveridge, TJ. 2007. Cryo-electron microscopy of cell division in *Staphylococcus aureus* reveals a mid-zone between nascent cross walls. *Mol Microbiol* 64:195.
19. Verkley, AJ, et al. 1975. Lipid-phase transitions of the strictly anaerobic bacteria *Veillonella parvula* and *Anaerovibrio lipolytica*. *J Bacteriology* 124:1522.
20. Arteni, AA, et al. 2005. Single particle electron microscopy in combination with mass spectrometry to investigate novel complexes of membrane proteins. *J Struct Biol* 149:325.
21. Bos, MP, Tommassen, J. 2004. Biogenesis of the Gram-negative bacterial outer membrane. *Curr Opin Microbiol* 7:610.
22. Schwarz, H, Koch, AL. 1995. Phase and electron microscopic observations of osmotically induced wrinkling and the role of endocytotic vesicles in the plasmolysis of the Gram-negative cell wall. *Microbiology* 141 (Pt 12):3161.
23. Hajmeer, M, et al. 2006. Impact of sodium chloride on *Escherichia coli* O157:H7 and *Staphylococcus aureus* analysed using transmission electron microscopy. *Food Microbiol* 23:446.
24. Brogden, KA, Rimler, RB. 1983. Lysates of turkey-grown *Pasteurella multocida*: Effects of solubilizing agents on the immunologic properties of membrane vesicles. *Am J Vet Res* 44:428.
25. Rottem, S, Verkleij, AJ. 1982. Possible association of segregated lipid domains of *Mycoplasma gallisepticum* membranes with cell resistance to osmotic lysis. *J Bacteriology* 149:338.
26. Scott, JR, Barnett, TC. 2006. Surface proteins of gram-positive bacteria and how they get there. *Ann Rev Microbiol* 60:397.
27. Voss, E, et al. 2006. NOD2/CARD15 mediates induction of the antimicrobial peptide human beta-defensin-2. *J Biol Chem* 281:2005.
28. Hancock, RE, et al. 1991. Interaction of aminoglycosides with the outer membranes and purified lipopolysaccharide and OmpF porin of *Escherichia coli*. *Antimicrob Agents and Chemother* 35:1309.
29. Beveridge, TJ. 1999. Structures of gram-negative cell walls and their derived membrane vesicles. *J Bacteriology* 181:4725.
30. Kuehn, MJ, Kesty, NC. 2005. Bacterial outer membrane vesicles and the host-pathogen interaction. *Genes Dev* 19:2645.
31. Graham, LL, et al. 1991. Freeze-substitution of gram-negative eubacteria: General cell morphology and envelope profiles. *J Bacteriology* 173:1623.
32. Yamashita, Y, et al. 1990. Purification and characterization of alkaline phosphatase of *Bacteroides gingivalis* 381. *Infect Immun* 58:2882.
33. Coyne, MS, et al. 1990. Localization of the cytochrome cd1 and copper nitrite reductases in denitrifying bacteria. *J Bacteriology* 172:2558.
34. Matias, VR, et al. 2003. Cryo-transmission electron microscopy of frozen-hydrated sections of *Escherichia*

Vet-ebooks.com

coli and *Pseudomonas aeruginosa*. *J Bacteriology* 185:6112.
35. Wu, T, et al. 2006. Identification of a protein complex that assembles lipopolysaccharide in the outer membrane of *Escherichia coli*. *Proc Natl Acad Sci USA* 103:11754.
36. Parsons, NJ, et al. 1989. Sialylation of lipopolysaccharide and loss of absorption of bactericidal antibody during conversion of gonococci to serum resistance by cytidine 5′-monophospho-N-acetyl neuraminic acid. *Microb Pathog* 7:63.
37. Fox, AJ, et al. 1991. The surface structure seen on gonococci after treatment with CMP-NANA is due to sialylation of surface lipopolysaccharide previously described as a "capsule." *Microbial Pathogenesis* 11:199.
38. Brogden, KA, Phillips, M. 1988. The ultrastructural morphology of endotoxins and lipopolysaccharides. *Electron Microsc Rev* 1:261.
39. Freer, E, et al. 1995. Heterogeneity of *Brucella abortus* lipopolysaccharides. *Res Microbiol* 146:569.
40. Grenier, D, Mayrand, D. 1987. Functional characterization of extracellular vesicles produced by *Bacteroides gingivalis*. *Infect Immun* 55:111.
41. Kato, N, et al. 1990. Crystallization of R-form lipopolysaccharides from *Salmonella minnesota* and *Escherichia coli*. *J Bacteriology* 172:1516.
42. Raetz, CR, et al. 1988. Gram-negative endotoxin: A biologically active lipid. *Cold Spring Harb Symp Quant Biol* 53 Pt 2:973.
43. Howe, J, et al. 2007. Biophysical characterization of the interaction of endotoxins with hemoglobins. *Med Chem* 3:13.
44. Howe, J, et al. 2008. Structural investigations into the interaction of hemoglobin and part structures with bacterial endotoxins. *Innate Immunity* 14:39.
45. Schirmer, T. 1998. General and specific porins from bacterial outer membranes. *J Struct Biol* 121:101.
46. Schabert, FA, et al. 1995. Native *Escherichia coli* OmpF porin surfaces probed by atomic force microscopy. *Science* 268:92.
47. Piddock, LJ. 2006. Multidrug-resistance efflux pumps—not just for resistance. *Nat Rev Microbiol* 4:629.
48. Kentner, D, Sourjik, V. 2006. Spatial organization of the bacterial chemotaxis system. *Curr Opin Microbiol* 9:619.
49. Macnab, RM. 2003. How bacteria assemble flagella. *Ann Rev Microbiol* 57:77.
50. Talay, SR. 2005. Gram-positive adhesins. *Contrib Microbiol* 12:90.
51. Jones, CH, et al. 1992. Adhesin presentation in bacteria requires molecular chaperones and ushers. *Infect Immun* 60:4445.
52. Telford, JL, et al. 2006. Pili in gram-positive pathogens. *Nat Rev Microbiol* 4:509.
53. Scott, JR, Zahner, D. 2006. Pili with strong attachments: Gram-positive bacteria do it differently. *Mol Microbiol* 62:320.
54. Hultgren, SJ, et al. 1993. Pilus and nonpilus bacterial adhesins: Assembly and function in cell recognition. *Cell* 73:887.
55. Hultgren, SJ, et al. 1993. PapD and superfamily of periplasmic immunoglobulin-like pilus chaperones. *Adv Protein Chem* 44:99.
56. Giron, JA, et al. 1991. An inducible bundle-forming pilus of enteropathogenic *Escherichia coli*. *Science* 254:710.
57. Collins, RF, et al. 2007. Purification and three-dimensional electron microscopy structure of the *Neisseria meningitidis* type IV pilus biogenesis protein PilG. *J Bacteriology* 189:6389.
58. Gorby, YA, et al. 2006. Electrically conductive bacterial nanowires produced by *Shewanella oneidensis* strain MR-1 and other microorganisms. *Proc Natl Acad Sci USA* 103:11358.
59. Wilson, DR, Beveridge, TJ. 1993. Bacterial flagellar filaments and their component flagellins. *Can J Microbiol* 39:451.
60. Salazar-Gonzalez, RM, McSorley, SJ. 2005. *Salmonella* flagellin, a microbial target of the innate and adaptive immune system. *Immunol Lett* 101:117.
61. Taylor, CM, Roberts, IS. 2005. Capsular polysaccharides and their role in virulence. *Contrib Microbiol* 12:55.
62. Erlandsen, SL, et al. 2004. High-resolution visualization of the microbial glycocalyx with low-voltage scanning electron microscopy: Dependence on cationic dyes. *J Hist Cyt* 52:1427.
63. Bayer, ME. 1990. Visualization of the bacterial polysaccharide capsule. *Curr Top Microbiol Immunol* 150:129.
64. Kirby, AR, et al. 1995. Observation of the helical structure of the bacterial polysaccharide acetan by atomic force microscopy. *Biophys J* 68:360.
65. Kamper, M, et al. 2004. Methods for in situ detection and characterization of extracellular polymers in biofilms by electron microscopy. *J Microbiol Methods* 57:55.
66. Reese, S, Guggenheim, B. 2007. A novel TEM contrasting technique for extracellular polysaccharides in in vitro biofilms. *Microsc Res Tech* 70:816.
67. Stoitsova, S, et al. 2004. Lectin-binding epitopes at the surface of *Escherichia coli* K-12: Examination by electron microscopy, with special reference to the presence of a colonic acid-like polymer. *J Basic Microbiol* 44:296.
68. Candela, T, Fouet, A. 2006. Poly-gamma-glutamate in bacteria. *Mol Microbiol* 60:1091.
69. Salzano, AM, et al. 2007. A widespread picture of the *Streptococcus thermophilus* proteome by cell lysate fractionation and gel-based/gel-free approaches. *Proteomics* 7:1420.
70. Kaczanowska, M, Ryden-Aulin, M. 2007. Ribosome biogenesis and the translation process in *Escherichia coli*. *Microbiol Mol Biol Rev* 71:477.
71. Tama, F, et al. 2003. Dynamic reorganization of the functionally active ribosome explored by normal mode analysis and cryo-electron microscopy. *Proc Natl Acad Sci USA* 100:9319.
72. Mainprize, IL, et al. 2006. The structure of *Escherichia coli* signal recognition particle revealed by scanning transmission electron microscopy. *Mol Biol Cell* 17:5063.
73. Barbieri, JT, Pederson, KJ. 2000. Bacterial toxins in disease production. In: Brogden, KA, et al., eds. Virulence Mechanisms of Bacterial Pathogens, 3rd ed. ASM Press, Washington, DC, p. 163.
74. Gouaux, E. 1998. Alpha-Hemolysin from *Staphylococcus aureus*: An archetype of beta-barrel, channel-forming toxins. *J Struct Biol* 121:110.

Vet-ebooks.com

75. Parker, MW, et al. 1994. Structure of the Aeromonas toxin proaerolysin in its water-soluble and membrane-channel states. *Nature* 367:292.
76. Bauer, ME, Welch, RA. 1996. Association of RTX toxins with erythrocytes. *Infect Immun* 64:4665.
77. Kachlany, SC, et al. 2000. Secretion of RTX leukotoxin by *Actinobacillus actinomycetemcomitans*. *Infect Immun* 68:6094.
78. Lally, ET, et al. 1999. The interaction between RTX toxins and target cells. *Trends Microbiol* 7:356.
79. Henderson, IR, et al. 2004. Type V protein secretion pathway: The autotransporter story. *Microbiol Mol Biol Rev* 68:692.
80. Mota, LJ, Cornelis, GR. 2005. The bacterial injection kit: Type III secretion systems. *Ann Med* 37:234.
81. Christie, PJ, Cascales, E. 2005. Structural and dynamic properties of bacterial type IV secretion systems (review). *Mol Membr Biol* 22:51.
82. Sandkvist, M. 2001. Type II secretion and pathogenesis. *Infect Immun* 69:3523.
83. Andersen, C, et al. 2000. Chunnel vision. Export and efflux through bacterial channel-tunnels. *EMBO Rep* 1:313.
84. Pukatzki, S, et al. 2006. Identification of a conserved bacterial protein secretion system in *Vibrio cholerae* using the Dictyostelium host model system. *Proc Natl Acad Sci USA* 103:1528.
85. Abdallah, AM, et al. 2007. Type VII secretion—mycobacteria show the way. *Nat Rev Microbiol* 5:883.
86. Shively, JM. 1974. Inclusion bodies of prokaryotes. *Ann Rev Microbiol* 28:167.
87. Pallerla, SR, et al. 2005. Formation of volutin granules in *Corynebacterium glutamicum*. *FEMS Microbiol Lett* 243:133.
88. Uchino, K, et al. 2007. Isolated poly(3-hydroxybutyrate) (PHB) granules are complex bacterial organelles catalyzing formation of PHB from acetyl coenzyme A (CoA) and degradation of PHB to acetyl-CoA. *J Bacteriology* 189:8250.
89. Bobik, TA. 2006. Polyhedral organelles compartmenting bacterial metabolic processes. *Appl Microbiol Biotechnol* 70:517.
90. Kaneko, Y, et al. 2006. Intact carboxysomes in a cyanobacterial cell visualized by hilbert differential contrast transmission electron microscopy. *J Bacteriology* 188: 805.
91. Hara, F, et al. 1973. Glycogen biosynthesis in *Chromatium* strain D. I: Characterization of glucogen. *Plant and Cell Physiology* 14:737.
92. Komeili, A. 2007. Molecular mechanisms of magnetosome formation. *Ann Rev Biochem* 76:351.
93. Martins, JL, et al. 2007. Deep-etching electron microscopy of cells of *Magnetospirillum magnetotacticum*: Evidence for filamentous structures connecting the magnetosome chain to the cell surface. *Curr Microbiol* 54:1.
94. Keim, CN, et al. 2005. Intracellular inclusions of uncultured magnetotactic bacteria. *Int Microbiol* 8:111.
95. Pigott, CR, Ellar, DJ. 2007. Role of receptors in *Bacillus thuringiensis* crystal toxin activity. *Microbiol Mol Biol Rev* 71:255.
96. Aronson, A. 2002. Sporulation and delta-endotoxin synthesis by *Bacillus thuringiensis*. *Cell Mol Life Sci* 59:417.
97. Madkour, M, Mayer, F. 2003. Structural organization of the intact bacterial cellulosome as revealed by electron microscopy. *Cell Biol Int* 27:831.
98. Pond, FR, et al. 1989. R-body-producing bacteria. *Microbiol Rev* 53:25.
99. Walsby, AE. 1974. The isolation of gas vesicles from blue-green algae. *Methods Enzymol* 31:678.
100. Walsby, AE. 1972. Structure and function of gas vacuoles. *Bacteriol Rev* 36:1.
101. Brogden, KA, Rimler, RB. 1982. Lysates of turkey-grown *Pasteurella multocida*: Examination of vaccine preparations by electron microscopy. *Am J Vet Res* 43:304.
102. Miethke, M, Marahiel, MA. 2007. Siderophore-based iron acquisition and pathogen control. *Microbiol Mol Biol Rev* 71:413.
103. Frazier, BA, et al. 1993. Paracrystalline inclusions of a novel ferritin containing nonheme iron, produced by the human gastric pathogen *Helicobacter pylori*: Evidence for a third class of ferritins. *J Bacteriology* 175:966.
104. Berlutti, F, et al. 2005. Iron availability influences aggregation, biofilm, adhesion and invasion of *Pseudomonas aeruginosa* and *Burkholderia cenocepacia*. *Int J Immunopathol Pharmacol* 18:661.
105. Ala'Aldeen, DA, et al. 1993. Localization of the meningococcal receptors for human transferrin. *Infect Immun* 61:751.
106. Wai, SN, et al. 1997. Overproduction of *Campylobacter* ferritin in *Escherichia coli* and induction of paracrystalline inclusion by ferrous compound. *Microbiol Immunol* 41:461.
107. Friedrich, CL, et al. 2001. Structure and mechanism of action of an indolicidin peptide derivative with improved activity against gram-positive bacteria. *J Biol Chem* 276:24015.
108. Eltsov, M, Zuber, B. 2006. Transmission electron microscopy of the bacterial nucleoid. *J Struct Biol* 156:246.
109. Moussa, M, et al. 2007. Damage in *Escherichia coli* cells treated with a combination of high hydrostatic pressure and subzero temperature. *Appl Environ Microbiol* 73:6508.
110. Hobot, JA, et al. 1985. Shape and fine structure of nucleoids observed on sections of ultrarapidly frozen and cryosubstituted bacteria. *J Bacteriology* 162:960.
111. French, SL, Miller, OL, Jr. 1989. Transcription mapping of the *Escherichia coli* chromosome by electron microscopy. *J Bacteriology* 171:4207.
112. Heichman, KA, et al. 1991. Configuration of DNA strands and mechanism of strand exchange in the Hin invertasome as revealed by analysis of recombinant knots. *Genes Dev* 5:1622.
113. Schneider, F, et al. 2000. A DNA-binding domain swap converts the invertase gin into a resolvase. *J Mol Biol* 295:767.
114. Schaper, A, et al. 1993. Scanning force microscopy of circular and linear plasmid DNA spread on mica with a quaternary ammonium salt. *Nucleic Acids Res* 21:6004.

Vet-ebooks.com

115. Henderson, E. 1992. Imaging and nanodissection of individual supercoiled plasmids by atomic force microscopy. *Nucleic Acids Res* 20:445.
116. Hochhut, B, et al. 2005. Pathogenicity islands and their role in bacterial virulence and survival. *Contrib Microbiol* 12:234.
117. Mecsas, JJ, Strauss, EJ. 1996. Molecular mechanisms of bacterial virulence: Type III secretion and pathogenicity islands. *Emerg Infect Dis* 2:270.
118. Shea, JE, et al. 1996. Identification of a virulence locus encoding a second type III secretion system in *Salmonella typhimurium*. *Proc Natl Acad Sci USA* 93:2593.
119. Iteman, I, et al. 1993. Relationship between loss of pigmentation and deletion of the chromosomal iron-regulated irp2 gene in *Yersinia pestis*: Evidence for separate but related events. *Infect Immun* 61:2717.
120. Rakin, A, et al. 1995. Evidence for two evolutionary lineages of highly pathogenic *Yersinia* species. *J Bacteriology* 177:2292.
121. Thanbichler, M, Shapiro, L. 2008. Getting organized—how bacterial cells move proteins and DNA. *Nat Rev Microbiol* 6:28.
122. Callaway, E. 2008. Cell biology. Bacteria's new bones. *Nature* 451:124.
123. Harry, E, et al. 2006. Bacterial cell division: The mechanism and its precison. *Int Rev Cytol* 253:27.
124. Young, KD. 2003. Bacterial shape. *Mol Microbiol* 49:571.
125. Graumann, PL. 2007. Cytoskeletal elements in bacteria. *Ann Rev Microbiol* 61:589.
126. Piggot, PJ, Hilbert, DW. 2004. Sporulation of *Bacillus subtilis*. *Curr Opin Microbiol* 7:579.
127. Jonas, RM, et al. 1990. Effects of antibiotics on synthesis and persistence of sigma E in sporulating *Bacillus subtilis*. *J Bacteriology* 172:4616.
128. Santo, L, et al. 1972. Ultrastructural analysis of sporulation in a conditional serine protease mutant of *Bacillus subtilis*. *J Bacteriology* 111:248.
129. Balish, MF, Krause, DC. 2006. Mycoplasmas: A distinct cytoskeleton for wall-less bacteria. *J Mol Microbiol Biotechnol* 11:244.
130. Balish, MF. 2006. Subcellular structures of mycoplasmas. *Front Biosci* 11:2017.
131. Krause, DC, Balish, MF. 2004. Cellular engineering in a minimal microbe: Structure and assembly of the terminal organelle of *Mycoplasma pneumoniae*. *Mol Microbiol* 51:917.
132. Baseman, JB, et al. 1982. Molecular basis for cytadsorption of *Mycoplasma pneumoniae*. *J Bacteriology* 151:1514.
133. Krause, DC, et al. 2007. *Mycoplasma pneumoniae* attachment and colonization of the respiratory mucosa. In: Brogden, KA, et al., eds. Virulence Mechanisms of Bacterial Pathogens, 4th ed. ASM Press, Washington, DC, p. 135.
134. Miyata, M, Petersen, JD. 2004. Spike structure at the interface between gliding *Mycoplasma* mobile cells and glass surfaces visualized by rapid-freeze-and-fracture electron microscopy. *J Bacteriology* 186:4382.
135. Adan-Kubo, J, et al. 2006. Morphology of isolated Gli349, a leg protein responsible for Mycoplasma mobile gliding via glass binding, revealed by rotary shadowing electron microscopy. *J Bacteriology* 188: 2821.
136. Giron, JA, et al. 1996. Adherence, fibronectin binding, and induction of cytoskeleton reorganization in cultured human cells by *Mycoplasma penetrans*. *Infect Immun* 64:197.
137. Loveless, RW, et al. 1992. Immunoelectron microscopic studies reveal differences in distribution of sialo-oligosaccharide receptors for *Mycoplasma pneumoniae* on the epithelium of human and hamster bronchi. *Infect Immun* 60:4015.
138. McDonald, DM, et al. 1991. *Mycoplasma pulmonis* infections cause long-lasting potentiation of neurogenic inflammation in the respiratory tract of the rat. *J Clin Invest* 87:787.
139. Guleria, R, et al. 2005. *Mycoplasma pneumoniae* and central nervous system complications: A review. *J Lab Clin Med* 146:55.
140. Smith, R, Eviatar, L. 2000. Neurologic manifestations of *Mycoplasma pneumoniae* infections: Diverse spectrum of diseases. A report of six cases and review of the literature. *Clin Pediatr (Phila)* 39:195.
141. Waites, KB, et al. 2005. Mycoplasmas and ureaplasmas as neonatal pathogens. *Clin Microbiol Rev* 18:757.
142. Robertson, J, Smook, E. 1976. Cytochemical evidence of extramembranous carbohydrates on *Ureaplasma urealyticum* (T-strain Mycoplasma). *J Bacteriology* 128:658.
143. Willi, B, et al. 2007. From Haemobartonella to hemoplasma: Molecular methods provide new insights. *Vet Microbiol* 125:197.
144. Trachtenberg, S, et al. 2003. The bacterial linear motor of *Spiroplasma melliferum* BC3: From single molecules to swimming cells. *Mol Microbiol* 47:671.
145. Bove, JM. 1997. Spiroplasmas: Infectious agents of plants, arthropods and vertebrates. *Wien Klin Wochenschr* 109:604.
146. Brooke, CJ, Riley, TV. 1999. *Erysipelothrix rhusiopathiae*: bacteriology, epidemiology and clinical manifestations of an occupational pathogen. *J Med Microbiol* 48:789.
147. Cowan, G. 2000. Rickettsial diseases: The typhus group of fevers—a review. *Postgrad Med J* 76:269.
148. Dumler, JS, et al. 2001. Reorganization of genera in the families *Rickettsiaceae* and *Anaplasmataceae* in the order *Rickettsiales*: Unification of some species of *Ehrlichia* with *Anaplasma*, *Cowdria* with *Ehrlichia* and *Ehrlichia* with *Neorickettsia*, descriptions of six new species combinations and designation of *Ehrlichia equi* and "HGE agent" as subjective synonyms of *Ehrlichia phagocytophila*. *Int J Syst Evol Microbiol* 51:2145.
149. Silverman, DJ, et al. 1991. Heparin protects human endothelial cells infected by *Rickettsia rickettsii*. *Infect Immun* 59:4505.
150. Van Kirk, LS, et al. 2000. Ultrastructure of *Rickettsia rickettsii* actin tails and localization of cytoskeletal proteins. *Infect Immun* 68:4706.
151. Dumler, JS, et al. 2007. Ehrlichioses in humans: Epidemiology, clinical presentation, diagnosis, and treatment. *Clin Infect Dis* 45 Suppl 1:S45.
152. Rikihisa, Y. 2006. New findings on members of the family *Anaplasmataceae* of veterinary importance. *Ann N Y Acad Sci* 1078:438.

Vet-ebooks.com

153. Bretana, A, et al. 2002. Multiple infection in bovines from the tropics: Observation of blood parasites by scanning and transmission electron microscope. *Parasitologia* 44:173.
154. Carreno, AD, et al. 2007. In vivo endothelial cell infection by *Anaplasma marginale*. *Vet Pathol* 44:116.
155. Munderloh, UG, et al. 2004. Infection of endothelial cells with *Anaplasma marginale* and *A. phagocytophilum*. *Vet Microbiol* 101:53.
156. Kocan, KM, et al. 1992. Development of *Anaplasma marginale* in male *Dermacentor andersoni* transferred from parasitemic to susceptible cattle. *Am J Vet Res* 53:499.
157. Rikihisa, Y, et al. 2003. Molecular characterization of *Aegyptianella pullorum* (Rickettsiales, Anaplasmataceae). *J Clin Microbiol* 41:5294.
158. Huchzermeyer, FW, et al. 1992. Description of *Aegyptianella botuliformis* n. sp. (Rickettsiales: Anaplasmataceae) from the helmeted guineafowl, *Numida meleagris*. *Onderstepoort J Vet Res* 59:97.
159. Zhang, C, Rikihisa, Y. 2004. Proposal to transfer '*Aegyptianella ranarum*', an intracellular bacterium of frog red blood cells, to the family Flavobacteriaceae as "*Candidatus Hemobacterium ranarum*" comb. nov. *Environ Microbiol* 6:568.
160. Dehio, C. 2005. Bartonella-host-cell interactions and vascular tumour formation. *Nat Rev Microbiol* 3:621.
161. Arias-Stella, J, et al. 1986. Histology, immunohistochemistry, and ultrastructure of the verruga in Carrion's disease. *Am J Surg Pathol* 10:595.
162. Perkocha, LA, et al. 1990. Clinical and pathological features of bacillary peliosis hepatis in association with human immunodeficiency virus infection. *New Engl J Med* 323:1581.
163. Chomel, BB, et al. 2006. *Bartonella spp*. in pets and effect on human health. *Emerg Infect Dis* 12:389.
164. Zbinden, R, et al. 1995. Intracellular location of *Bartonella henselae* cocultivated with Vero cells and used for an indirect fluorescent-antibody test. *Clin Diagn Lab Immunol* 2:693.
165. Schueller, C, et al. 2007. Biogenesis of Afipia-containing phagosomes in non-professional phagocytes. *Microbes Infect* 9:355.
166. Luhrmann, A, et al. 2001. *Afipia felis* induces uptake by macrophages directly into a nonendocytic compartment. *Proc Natl Acad Sci USA* 98:7271.
167. Birkness, KA, et al. 1992. Intracellular growth of *Afipia felis*, a putative etiologic agent of cat scratch disease. *Infect Immun* 60:2281.
168. Fretin, D, et al. 2005. The sheathed flagellum of *Brucella melitensis* is involved in persistence in a murine model of infection. *Cellular Microbiology* 7:687.
169. Oberti, J, et al. 1982. Demonstration of an external layer in several species of the genus *Brucella*. *Can J Microbiol* 28:1300.
170. Raybould, TJ, et al. 1981. Ultrastructural localization of characterized antigens of *Brucella abortus* and distribution among different biotypes. *Infect Immun* 32:318.
171. Bandara, AB, et al. 2005. Carboxyl-terminal protease regulates *Brucella suis* morphology in culture and persistence in macrophages and mice. *J Bacteriology* 187:5767.
172. Riley, LK, Robertson, DC. 1984. Ingestion and intracellular survival of *Brucella abortus* in human and bovine polymorphonuclear leukocytes. *Infect Immun* 46:224.
173. Rittig, MG, et al. 2003. Smooth and rough lipopolysaccharide phenotypes of Brucella induce different intracellular trafficking and cytokine/chemokine release in human monocytes. *J Leuk Biol* 74:1045.
174. Roop, RM, 2nd, et al. 2004. Adaptation of the *Brucellae* to their intracellular niche. *Mol Microbiol* 52:621.
175. Ackermann, MR, et al. 1988. Bovine ileal dome lymphoepithelial cells: Endocytosis and transport of *Brucella abortus* strain 19. *Vet Pathol* 25:28.
176. Anderson, TD, Cheville, NF. 1986. Ultrastructural morphometric analysis of *Brucella abortus*-infected trophoblasts in experimental placentitis. Bacterial replication occurs in rough endoplasmic reticulum. *Am J Pathol* 124:226.
177. Roop, RM, 2nd, et al. 2003. *Brucella* stationary-phase gene expression and virulence. *Ann Rev Microbiol* 57:57.
178. Sloan, GP, et al. 2007. The Bordetella Bps polysaccharide is critical for biofilm development in the mouse respiratory tract. *J Bacteriology* 189:8270.
179. Arp, LH, Fagerland, JA. 1987. Ultrastructural pathology of *Bordetella avium* infection in turkeys. *Vet Pathol* 24:411.
180. Parise, G, et al. 2007. Role of a putative polysaccharide locus in Bordetella biofilm development. *J Bacteriology* 189:750.
181. Serra, D, et al. 2007. Continuous nondestructive monitoring of *Bordetella pertussis* biofilms by Fourier transform infrared spectroscopy and other corroborative techniques. *Anal Bioanal Chem* 387:1759.
182. Watanabe, H, et al. 1989. The location of filamentous hemagglutinin and pertussis toxin antigens of *Bordetella pertussis* by immunoelectron microscopy. *J Electron Microsc (Tokyo)* 38:172.
183. Gueirard, P, et al. 2005. Ultrastructural analysis of the interactions between *Bordetella pertussis*, *Bordetella parapertussis* and *Bordetella bronchiseptica* and human tracheal epithelial cells. *Microb Pathog* 38:41.
184. Carbonetti, NH, et al. 2007. Pertussis toxin targets airway macrophages to promote *Bordetella pertussis* infection of the respiratory tract. *Infect Immun* 75:1713.
185. Lipuma, JJ. 2005. Update on the *Burkholderia cepacia* complex. *Curr Opin Pulm Med* 11:528.
186. Wong, KT, et al. 1995. The histopathology of human melioidosis. *Histopathology* 26:51.
187. Kespichayawattana, W, et al. 2000. *Burkholderia pseudomallei* induces cell fusion and actin-associated membrane protrusion: A possible mechanism for cell-to-cell spreading. *Infect Immun* 68:5377.
188. Meyer, TF. 1990. Pathogenic neisseriae—a model of bacterial virulence and genetic flexibility. *Zentralbl Bakteriol* 274:135.
189. Apicella, MA, et al. 1990. Modification by sialic acid of *Neisseria gonorrhoeae* lipooligosaccharide epitope expression in human urethral exudates: An immunoelectron microscopic analysis. *J Infect Dis* 162:506.
190. Craig, L, et al. 2006. Type IV pilus structure by cryo-electron microscopy and crystallography: Implications for pilus assembly and functions. *Mol Cell* 23:651.

Vet-ebooks.com

191. Edwards, JL. 2007. Gender differences in *Neisseria gonorrhoeae* pathogenesis. In: Brogden, KA, et al., eds. Virulence Mechanisms of Bacterial Pathogens, 4th ed. ASM Press, Washington DC, 2007, p. 149.
192. Edwards, JL, et al. 2000. *Neisseria gonorrhoeae* elicits membrane ruffling and cytoskeletal rearrangements upon infection of primary human endocervical and ectocervical cells. *Infect Immun* 68:5354.
193. Evans, BA. 1977. Ultrastructural study of cervical gonorrhea. *J Infect Dis* 136:248.
194. Sotto, MN, et al. 1976. Pathogenesis of cutaneous lesions in acute meningococcemia in humans: Light, immunofluorescent, and electron microscopic studies of skin biopsy specimens. *J Infect Dis* 133:506.
195. Collins, RF, et al. 2003. Three-dimensional structure of the *Neisseria meningitidis* secretin PilQ determined from negative-stain transmission electron microscopy. *J Bacteriology* 185:2611.
196. Nicholson, A, Lepow, IH. 1979. Host defense against *Neisseria meningitidis* requires a complement-dependent bactericidal activity. *Science* 205:298.
197. Schneider, MC, et al. 2007. Interactions between *Neisseria meningitidis* and the complement system. *Trends Microbiol* 15:233.
198. Callaghan, MJ, et al. 2006. Opacity-associated adhesin repertoire in hyperinvasive *Neisseria meningitidis*. *Infect Immun* 74:5085.
199. Virji, M, et al. 1992. Expression of the Opc protein correlates with invasion of epithelial and endothelial cells by *Neisseria meningitidis*. *Mol Microbiol* 6:2785.
200. Ho, HT, et al. 2007. Interaction of *Arcobacter spp.* with human and porcine intestinal epithelial cells. *FEMS Immunol Med Microbiol* 50:51.
201. Houf, K, et al. 2005. *Arcobacter cibarius sp. nov.*, isolated from broiler carcasses. *Int J Syst Evol Microbiol* 55:713.
202. Zilbauer, M, et al. 2005. Intestinal innate immunity to *Campylobacter jejuni* results in induction of bactericidal human beta-defensins 2 and 3. *Infect Immun* 73:7281.
203. Guerry, P. 2007. The role of flagella in *Campylobacter* virulence. In: Brogden, KA, et al., eds. Virulence Mechanisms of Bacterial Pathogens, 4th ed. ASM Press, Washington, DC, p. 197.
204. McLennan, MK, et al. 2007. *Campylobacter jejuni* biofilms up-regulated in the absence of the stringent response utilize a calcofluor white-reactive surface polysaccharide. *J Bacteriology*.
205. El-Bez, C, et al. 2005. High resolution structural analysis of *Helicobacter pylori* VacA toxin oligomers by cryonegative staining electron microscopy. *J Struct Biol* 151:215.
206. Hessey, SJ, et al. 1990. Bacterial adhesion and disease activity in *Helicobacter* associated chronic gastritis. *Gut* 31:134.
207. Dytoc, M, et al. 1993. Comparison of *Helicobacter pylori* and attaching-effacing *Escherichia coli* adhesion to eukaryotic cells. *Infect Immun* 61:448.
208. Necchi, V, et al. 2007. Intracellular, intercellular, and stromal invasion of gastric mucosa, preneoplastic lesions, and cancer by *Helicobacter pylori*. *Gastroenterology* 132:1009.
209. Dubois, A, Boren, T. 2007. *Helicobacter pylori* is invasive and it may be a facultative intracellular organism. *Cell Microbiol* 9:1108.
210. Liu, Y, et al. 2006. Ultrastructure of *Helicobacter pylori* in human gastric mucosa and *H. pylori*-infected human gastric mucosa using transmission electron microscopy and the high-pressure freezing-freeze substitution technique. *J Gastroenterol* 41:569.
211. De Groote, D, et al. 2005. Detection of non-pylori *Helicobacter* species in "*Helicobacter heilmannii*" -infected humans. *Helicobacter* 10:398.
212. Ierardi, E, et al. 2001. *Helicobacter heilmannii* gastritis: A histological and immunohistochemical trait. *J Clin Pathol* 54:774.
213. Reindel, JF, et al. 1999. An epizootic of lymphoplasmacytic gastritis attributed to *Helicobacter pylori* infection in cynomolgus monkeys (*Macaca fascicularis*). *Vet Pathol* 36:1.
214. Erginsoy, SD, et al. 2004. Occurrence of *Helicobacter* infection in the gastric mucosa of free-living red foxes (*Vulpes vulpes*). *J Wildl Dis* 40:548.
215. De Groote, D, et al. 2001. Evaluation of a group-specific 16S ribosomal DNA-based PCR for detection of *Helicobacter bizzozeronii*, *Helicobacter felis*, and *Helicobacter salomonis* in fresh and paraffin-embedded gastric biopsy specimens. *J Clin Microbiol* 39:1197.
216. Von Graevenitz, A. 2007. The role of *Aeromonas* in diarrhea: A review. *Infection* 35:59.
217. Cui, H, et al. 2007. A distinct cause of necrotizing fasciitis: *Aeromonas veronii biovar sobria*. *Surg Infect (Larchmt)* 8:523.
218. Ho, AS, et al. 1990. The pili of *Aeromonas hydrophila*: identification of an environmentally regulated "mini pilin." *J Exp Med* 172:795.
219. Suarez, G, et al. 2008. Molecular characterization of a functional type VI secretion system from a clinical isolate of *Aeromonas hydrophila*. *Microb Pathog* 44:344.
220. Wilmsen, HU, et al. 1992. The aerolysin membrane channel is formed by heptamerization of the monomer. *EMBO J* 11:2457.
221. Garduno, RA, Kay, WW. 1992. Interaction of the fish pathogen *Aeromonas salmonicida* with rainbow trout macrophages. *Infect Immun* 60:4612.
222. Litvak, Y, Selinger, Z. 2007. *Aeromonas salmonicida* toxin AexT has a Rho family GTPase-activating protein domain. *J Bacteriology* 189:2558.
223. Kuberski, T, et al. 1980. Ultrastructure of *Calymmatobacterium granulomatis* in lesions of granuloma inguinale. *J Infect Dis* 142:744.
224. Kharsany, AB, et al. 1998. Ultrastructure of *Calymmatobacterium granulomatis*: Comparison of culture with tissue biopsy specimens. *J Med Microbiol* 47:1069.
225. Conway, T, Cohen, PS. 2007. *Escherichia coli* at the intestinal mucosal surface. In: Brogden, KA, et al., eds. Virulence Mechanisms of Bacterial Pathogens, 4th ed. ASM Press, Washington, DC, p. 175.
226. Ludi, S, et al. 2006. Assessing the expression of enterotoxigenic *Escherichia coli*-specific surface antigens in recombinant strains by transmission electron microscopy and immunolabeling. *J Hist Cyt* 54:473.

Vet-ebooks.com

227. Subramanian, S, et al. 2008. Replication of colonic Crohn's disease mucosal *Escherichia coli* isolates within macrophages and their susceptibility to antibiotics. *Antimicrobial Agents and Chemotherapy* 52:427.
228. Kaper, JB, et al. 2004. Pathogenic *Escherichia coli*. *Nat Rev Microbiol* 2:123.
229. Toma, C, et al. 2004. Distribution of putative adhesins in different seropathotypes of Shiga toxin-producing *Escherichia coli*. *J Clin Microbiol* 42:4937.
230. Hibberd, ML, et al. 1990. The fimbriae of human enterotoxigenic *Escherichia coli* strain 334 are related to CS5 fimbriae. *J Gen Microbiol* 136:2449.
231. Vlisidou, I, et al. 2006. Identification and characterization of EspK, a type III secreted effector protein of enterohaemorrhagic *Escherichia coli* O157:H7. *FEMS Microbiol Lett* 263:32.
232. Gyles, CL. 2007. Shiga toxin-producing *Escherichia coli*: An overview. *J Anim Sci* 85:E45.
233. Andreoli, SP. 1999. The pathophysiology of the hemolytic uremic syndrome. *Curr Opin Nephrol Hypertens* 8:459.
234. Huang, DB, et al. 2006. A review of an emerging enteric pathogen: Enteroaggregative *Escherichia coli*. *J Med Microbiol* 55:1303.
235. Knutton, S, et al. 1992. Ability of enteroaggregative *Escherichia coli* strains to adhere in vitro to human intestinal mucosa. *Infect Immun* 60:2083.
236. Taddei, CR, et al. 2005. Secreted autotransporter toxin produced by a diffusely adhering *Escherichia coli* strain causes intestinal damage in animal model assays. *FEMS Microbiol Lett* 250:263.
237. Hagan, EC, Mobley, HL. 2007. Uropathogenic *Escherichia coli* outer membrane antigens expressed during urinary tract infection. *Infect Immun* 75:3941.
238. Rosen, DA, et al. 2007. Detection of intracellular bacterial communities in human urinary tract infection. *PLoS medicine* 4:e329.
239. Garofalo, CK, et al. 2007. *Escherichia coli* from urine of female patients with urinary tract infections is competent for intracellular bacterial community formation. *Infect Immun* 75:52.
240. Wang, Y, Kim, KS. 2002. Role of OmpA and IbeB in *Escherichia coli* K1 invasion of brain microvascular endothelial cells in vitro and in vivo. *Pediatr Res* 51:559.
241. Khan, NA, et al. 2003. Outer membrane protein A and cytotoxic necrotizing factor-1 use diverse signaling mechanisms for *Escherichia coli* K1 invasion of human brain microvascular endothelial cells. *Microb Pathog* 35:35.
242. Ackermann, MR, Cheville, NF. 1991. Ultrastructural studies of the lung of turkeys (*Meleagris gallopavo*) inoculated intratracheally with *Escherichia coli*. *Vet Pathol* 28:183.
243. Stehling, EG, et al. 2008. The expression of plasmid mediated afimbrial adhesin genes in an avian septicemic *Escherichia coli* strain. *J Vet Sci (Suwon-si, Korea)* 9:75.
244. Lymberopoulos, MH, et al. 2006. Characterization of Stg fimbriae from an avian pathogenic *Escherichia coli* O78:K80 strain and assessment of their contribution to colonization of the chicken respiratory tract. *J Bacteriology* 188:6449.
245. Methiyapun, S, et al. 1984. Ultrastructure of the intestinal mucosa in pigs experimentally inoculated with an edema disease-producing strain of *Escherichia coli* (0139: K12:H1). *Vet Pathol* 21:516.
246. Imberechts, H, et al. 1992. Characterization of F107 fimbriae of *Escherichia coli* 107/86, which causes edema disease in pigs, and nucleotide sequence of the F107 major fimbrial subunit gene, fedA. *Infect Immun* 60:1963.
247. Podschun, R, Ullmann, U. 1998. *Klebsiella spp.* as nosocomial pathogens: Epidemiology, taxonomy, typing methods, and pathogenicity factors. *Clin Microbiol Rev* 11:589.
248. Darfeuille-Michaud, A, et al. 1992. R-plasmid-encoded adhesive factor in *Klebsiella pneumoniae* strains responsible for human nosocomial infections. *Infect Immun* 60:44.
249. Rozalski, A, et al. 1997. Potential virulence factors of *Proteus bacilli*. *Microbiol Mol Biol Rev* 61:65.
250. Allison, C, et al. 1992. Ability of *Proteus mirabilis* to invade human urothelial cells is coupled to motility and swarming differentiation. *Infect Immun* 60:4740.
251. Haraga, A, et al. 2008. Salmonellae interplay with host cells. *Nat Rev Microbiol* 6:53.
252. Grassl, GA, Finlay, BB. 2008. Pathogenesis of enteric Salmonella infections. *Curr Opin Gastroenterol* 24:22.
253. Coburn, B, et al. 2007. Salmonella, the host and disease: A brief review. *Immunol Cell Biol* 85:112.
254. Santos, RL, et al. 2003. Pathogenesis of *Salmonella*-induced enteritis. *Braz J Med Biol Res* 36:3.
255. Popiel, I, Turnbull, PC. 1985. Passage of *Salmonella enteritidis* and *Salmonella thompson* through chick ileocecal mucosa. *Infect Immun* 47:786.
256. Zhang, S, et al. 2003. Molecular pathogenesis of *Salmonella enterica* serotype typhimurium-induced diarrhea. *Infect Immun* 71:1.
257. Haque, A, et al. 2004. Early interactions of *Salmonella enterica* serovar typhimurium with human small intestinal epithelial explants. *Gut* 53:1424.
258. Fratamico, PM. 2003. Tolerance to stress and ability of acid-adapted and non-acid-adapted *Salmonella enterica* serovar Typhimurium DT104 to invade and survive in mammalian cells in vitro. *J Food Prot* 66:1115.
259. Ginocchio, CC, et al. 1994. Contact with epithelial cells induces the formation of surface appendages on *Salmonella typhimurium*. *Cell* 76:717.
260. Popp, D, et al. 2008. Single molecule polymerization, annealing and bundling dynamics of SipA induced actin filaments. *Cell Motil Cytoskeleton* 65:165.
261. Reed, KA, et al. 1996. Promotion of *Salmonella typhimurium* adherence and membrane ruffling in MDCK epithelia by staurosporine. *FEMS Microbiol Lett* 145:233.
262. Jang, MH, et al. 2004. Intestinal villous M cells: An antigen entry site in the mucosal epithelium. *Proc Natl Acad Sci USA* 101:6110.
263. Meyerholz, DK, et al. 2002. Early epithelial invasion by *Salmonella enterica* serovar Typhimurium DT104 in the swine ileum. *Vet Pathol* 39:712.

Vet-ebooks.com

264. Santos, RL, et al. 2002. Morphologic and molecular characterization of *Salmonella typhimurium* infection in neonatal calves. *Vet Pathol* 39:200.
265. van Asten, AJ, van Dijk, JE. 2005. Distribution of "classic" virulence factors among *Salmonella spp*. *FEMS Immunol Med Microbiol* 44:251.
266. Levine, MM, et al. 2007. Clinical trials of Shigella vaccines: Two steps forward and one step back on a long, hard road. *Nat Rev Microbiol* 5:540.
267. Mathan, MM, Mathan, VI. 1986. Ultrastructural pathology of the rectal mucosa in Shigella dysentery. *Am J Pathol* 123:25.
268. Ogawa, M, et al. 2008. The versatility of Shigella effectors. *Nat Rev Microbiol* 6:11.
269. Perdomo, OJ, et al. 1994. Acute inflammation causes epithelial invasion and mucosal destruction in experimental shigellosis. *J Exp Med* 180:1307.
270. Vala, MH, et al. 2007. Comparing invasive and non-invasive of isolated *Shigella flexneri* by electron microscopy of cell culture, SDS-PAGE and Congo red method. *Iran Biomed J* 11:47.
271. Sansonetti, PJ. 2006. The bacterial weaponry: Lessons from Shigella. *Ann N Y Acad Sci* 1072:307.
272. Viboud, GI, Bliska, JB. 2005. Yersinia outer proteins: Role in modulation of host cell signaling responses and pathogenesis. *Ann Rev Microbiol* 59:69.
273. Hinnebusch, BJ, et al. 1996. Role of the *Yersinia pestis* hemin storage (hms) locus in the transmission of plague by fleas. *Science* 273:367.
274. Straley, SC, Harmon, PA. 1984. *Yersinia pestis* grows within phagolysosomes in mouse peritoneal macrophages. *Infect Immun* 45:655.
275. Pujol, C, Bliska, JB. 2003. The ability to replicate in macrophages is conserved between *Yersinia pestis* and *Yersinia pseudotuberculosis*. *Infect Immun* 71:5892.
276. Lindler, LE, Tall, BD. 1993. *Yersinia pestis* pH 6 antigen forms fimbriae and is induced by intracellular association with macrophages. *Mol Microbiol* 8:311.
277. Cowan, C, et al. 2000. Invasion of epithelial cells by *Yersinia pestis*: Evidence for a *Y. pestis*-specific invasin. *Infect Immun* 68:4523.
278. La Scola, B, Raoult, D. 2001. Survival of *Coxiella burnetii* within free-living amoeba *Acanthamoeba castellanii*. *Clin Microbiol Infect* 7:75.
279. Cutler, SJ, et al. 2007. Q fever. *J Infect* 54:313.
280. Guatteo, R, et al. 2007. *Coxiella burnetii* shedding by dairy cows. *Vet Res* 38:849.
281. Khavkin, T, Tabibzadeh, SS. 1988. Histologic, immunofluorescence, and electron microscopic study of infectious process in mouse lung after intranasal challenge with *Coxiella burnetii*. *Infect Immun* 56:1792.
282. Zamboni, DS, et al. 2002. Mouse resident peritoneal macrophages partially control in vitro infection with *Coxiella burnetii* phase II. *Microbes Infect* 4:591.
283. Shannon, JG, Heinzen, RA. 2007. Infection of human monocyte-derived macrophages with *coxiella burnetii*. *Methods Mol Biol* 431:189.
284. Kazar, J. 2005. *Coxiella burnetii* infection. *Ann N Y Acad Sci* 1063:105.
285. Baumgartner, W, Bachmann, S. 1992. Histological and immunocytochemical characterization of *Coxiella burnetii*-associated lesions in the murine uterus and placenta. *Infect Immun* 60:5232.
286. Parker, NR, et al. 2006. Q fever. *Lancet* 367:679.
287. McCaul, TF, et al. 1994. In vivo endogenous spore formation by *Coxiella burnetii* in Q fever endocarditis. *J Clin Pathol* 47:978.
288. Brouqui, P, et al. 1994. Immunohistologic demonstration of *Coxiella burnetii* in the valves of patients with Q fever endocarditis. *Am J Med* 97:451.
289. King, CH, et al. 1991. Effects of cytochalasin D and methylamine on intracellular growth of *Legionella pneumophila* in amoebae and human monocyte-like cells. *Infect Immun* 59:758.
290. Faulkner, G, Garduno, RA. 2002. Ultrastructural analysis of differentiation in *Legionella pneumophila*. *J Bacteriology* 184:7025.
291. Yamamoto, Y, et al. 1992. Differential morphologic and metabolic alterations in permissive versus nonpermissive murine macrophages infected with *Legionella pneumophila*. *Infect Immun* 60:3231.
292. Swanson, MS, Isberg, RR. 1995. Association of *Legionella pneumophila* with the macrophage endoplasmic reticulum. *Infect Immun* 63:3609.
293. Molmeret, M, et al. 2007. Rapid escape of the dot/icm mutants of *Legionella pneumophila* into the cytosol of mammalian and protozoan cells. *Infect Immun* 75:3290.
294. Bitar, DM, et al. 2004. Molecular and cell biology of *Legionella pneumophila*. *Int J Med Microbiol* 293:519.
295. Robinson, CG, Roy, CR. 2006. Attachment and fusion of endoplasmic reticulum with vacuoles containing *Legionella pneumophila*. *Cell Microbiol* 8:793.
296. Chiers, K, et al. 1999. Early in vivo interactions of *Actinobacillus pleuropneumoniae* with tonsils of pigs. *Vet Microbiol* 68:301.
297. Dom, P, et al. 1994. In vivo association of *Actinobacillus pleuropneumoniae* serotype 2 with the respiratory epithelium of pigs. *Infect Immun* 62:1262.
298. Healey, MC, et al. 1991. A model for demonstrating the adhesion of *Actinobacillus seminis* to epithelial cells. *Can J Vet Res* 55:121.
299. Boekema, BK, et al. 2003. Adherence of *Actinobacillus pleuropneumoniae* to primary cultures of porcine lung epithelial cells. *Vet Microbiol* 93:133.
300. Van Overbeke, I, et al. 2002. Characterization of the in vitro adhesion of *Actinobacillus pleuropneumoniae* to swine alveolar epithelial cells. *Vet Microbiol* 88:59.
301. Vanier, G, et al. 2006. *Haemophilus parasuis* invades porcine brain microvascular endothelial cells. *Microbiology* 152:135.
302. Norskov-Lauritsen, N, Kilian, M. 2006. Reclassification of *Actinobacillus actinomycetemcomitans*, *Haemophilus aphrophilus*, *Haemophilus paraphrophilus* and *Haemophilus segnis* as *Aggregatibacter actinomycetemcomitans gen. nov., comb. nov.*, *Aggregatibacter aphrophilus comb. nov.* and *Aggregatibacter segnis comb. nov.*, and emended description of *Aggregatibacter aphrophilus* to include V factor-dependent and V factor-independent isolates. *Int J Syst Evol Microbiol* 56:2135.
303. Henderson, B, et al. 2003. Molecular pathogenicity of the oral opportunistic pathogen *Actinobacillus actinomycetemcomitans*. *Ann Rev Microbiol* 57:29.

Vet-ebooks.com

304. Fine, DH, et al. 1999. Tenacious adhesion of *Actinobacillus actinomycetemcomitans* strain CU1000 to salivary-coated hydroxyapatite. *Arch Oral Biol* 44:1063.
305. Galli, J, et al. 2007. Biofilm formation by *Haemophilus influenzae* isolated from adeno-tonsil tissue samples, and its role in recurrent adenotonsillitis. *Acta Otorhinolaryngol Ital* 27:134.
306. Starner, TD, et al. 2006. *Haemophilus influenzae* forms biofilms on airway epithelia: Implications in cystic fibrosis. *Am J Respir Crit Care Med* 174:213.
307. Farley, MM, et al. 1990. Pilus- and non-pilus-mediated interactions of *Haemophilus influenzae* type b with human erythrocytes and human nasopharyngeal mucosa. *J Infect Dis* 161:274.
308. Melnikow, E, et al. 2005. Microarray analysis of *Haemophilus parasuis* gene expression under in vitro growth conditions mimicking the in vivo environment. *Vet Microbiol* 110:255.
309. Hill, CE, et al. 2003. A search for virulence genes of *Haemophilus parasuis* using differential display RT-PCR. *Vet Microbiol* 96:189.
310. Atapattu, DN, Czuprynski, CJ. 2005. *Mannheimia haemolytica* leukotoxin induces apoptosis of bovine lymphoblastoid cells (BL-3) via a caspase-9-dependent mitochondrial pathway. *Infect Immun* 73:5504.
311. Gioia, J, et al. 2006. The genome sequence of *Mannheimia haemolytica* A1: Insights into virulence, natural competence, and *Pasteurellaceae* phylogeny. *J Bacteriology* 188:7257.
312. Shah, NH, et al. 1996. Vacuolating cytotoxic activity of *Pasteurella multocida* causing haemorrhagic septicaemia in buffalo and cattle. *FEMS Microbiol Lett* 143:97.
313. Ackermann, MR, et al. 1991. Colonization of the pharyngeal tonsil and respiratory tract of the gnotobiotic pig by a toxigenic strain of *Pasteurella multocida* type D. *Vet Pathol* 28:267.
314. Isaacson, RE, Trigo, E. 1995. Pili of *Pasteurella multocida* of porcine origin. *FEMS Microbiol Lett* 132:247.
315. Slevogt, H, et al. 2007. *Moraxella catarrhalis* is internalized in respiratory epithelial cells by a trigger-like mechanism and initiates a TLR2- and partly NOD1-dependent inflammatory immune response. *Cellular microbiology* 9:694.
316. Froholm, LO, et al. 1973. Electron microscopical and cultural features of *Neisseria meningitidis* competence variants. *Acta Pathol Microbiol Scand [B] Microbiol Immunol* 81:525.
317. Rogers, DG, et al. 1987. Pathogenesis of corneal lesions caused by *Moraxella bovis* in gnotobiotic calves. *Vet Pathol* 24:287.
318. Rogers, DG, et al. 1987. Conjunctival lesions caused by *Moraxella bovis* in gnotobiotic calves. *Vet Pathol* 24:554.
319. Tsang, KW, et al. 1994. Interaction of *Pseudomonas aeruginosa* with human respiratory mucosa in vitro. *Eur Respir J* 7:1746.
320. Fleiszig, SM, et al. 1996. Relationship between cytotoxicity and corneal epithelial cell invasion by clinical isolates of *Pseudomonas aeruginosa*. *Infect Immun* 64:2288.
321. Restrepo, CI, et al. 1999. Surfactant protein D stimulates phagocytosis of *Pseudomonas aeruginosa* by alveolar macrophages. *Am J Respir Cell Mol Biol* 21:576.
322. Gil, H, et al. 2004. Presence of pili on the surface of *Francisella tularensis*. *Infect Immun* 72:3042.
323. Hamada, D, et al. 2007. Tetrameric structure of thermostable direct hemolysin from *Vibrio parahaemolyticus* revealed by ultracentrifugation, small-angle x-ray scattering and electron microscopy. *J Mol Biol* 365:187.
324. Hammerschlag, MR. 2007. Chlamydia and Chlamydiales: Beyond *Chlamydia trachomatis*. *Pediatr Infect Dis J* 26:639.
325. Gupta, RS, Griffiths, E. 2006. Chlamydiae-specific proteins and indels: Novel tools for studies. *Trends Microbiol* 14:527.
326. Stratton, CW, Wheldon, DB. 2006. Multiple sclerosis: An infectious syndrome involving *Chlamydophila pneumoniae*. *Trends Microbiol* 14:474.
327. Fields, KA, Hackstadt, T. 2002. The chlamydial inclusion: Escape from the endocytic pathway. *Ann Rev Cell Dev Biol* 18:221.
328. McCoy, AJ, Maurelli, AT. 2006. Building the invisible wall: Updating the chlamydial peptidoglycan anomaly. *Trends Microbiol* 14:70.
329. Peters, J, et al. 2007. Type III secretion a la Chlamydia. *Trends Microbiol* 15:241.
330. Dautry-Varsat, A, et al. 2004. Chlamydia—host cell interactions: Recent advances on bacterial entry and intracellular development. *Traffic* 5:561.
331. Reynolds, AB, et al. 1992. p120, a novel substrate of protein tyrosine kinase receptors and of p60v-src, is related to cadherin-binding factors beta-catenin, plakoglobin and armadillo. *Oncogene* 7:2439.
332. Duda, JJ, Slack, JM. 1972. Ultrastructural studies on the genus *Actinomyces*. *J Gen Microbiol* 71:63.
333. Dahlen, G. 2002. Microbiology and treatment of dental abscesses and periodontal-endodontic lesions. *Periodontol 2000* 28:206.
334. Socransky, SS, et al. 1998. Microbial complexes in subgingival plaque. *J Clin Periodontol* 25:134.
335. Jost, BH, Billington, SJ. 2005. *Arcanobacterium pyogenes*: Molecular pathogenesis of an animal opportunist. *Antonie Van Leeuwenhoek* 88:87.
336. Lee, PL, et al. 2007. Cutaneous diphtheroid infection and review of other cutaneous Gram-positive bacillus infections. *Cutis* 79:371.
337. Vitek, CR. 2006. Diphtheria. *Curr Top Microbiol Immunol* 304:71.
338. Brogden, KA, Engen, RL. 1990. Alterations in the phospholipid composition and morphology of ovine erythrocytes after intravenous inoculation of *Corynebacterium pseudotuberculosis*. *Am J Vet Res* 51:874.
339. McKean, SC, et al. 2007. Expression of phospholipase D, the major virulence factor of *Corynebacterium pseudotuberculosis*, is regulated by multiple environmental factors and plays a role in macrophage death. *Microbiology* 153:2203.
340. Brogden, KA, et al. 1990. Effect of muramyl dipeptide on immunogenicity of *Corynebacterium pseudotuberculosis* whole-cell vaccines in mice and lambs. *Am J Vet Res* 51:200.
341. Abe, S, et al. 1990. Cloning and expression of a pili gene of *Corynebacterium renale* in *Escherichia coli*. *Nippon Juigaku Zasshi* 52:11.

Vet-ebooks.com

342. Yates, SP, et al. 2006. Stealth and mimicry by deadly bacterial toxins. *Trends Biochem Sci* 31:123.
343. Holbourn, KP, et al. 2006. A family of killer toxins. Exploring the mechanism of ADP-ribosylating toxins. *Febs J* 273:4579.
344. Oram, M, et al. 2007. Bacteriophage-based vectors for site-specific insertion of DNA in the chromosome of Corynebacteria. *Gene* 391:53.
345. Dahl, JL. 2004. Electron microscopy analysis of *Mycobacterium tuberculosis* cell division. *FEMS Microbiol Lett* 240:15.
346. Dahl, JL. 2005. Scanning electron microscopy analysis of aged *Mycobacterium tuberculosis* cells. *Can J Microbiol* 51:277.
347. Maes, E, et al. 2007. Polysaccharide structural variability in mycobacteria: Identification and characterization of phosphorylated mannan and arabinomannan. *Glycoconj J* 24:439.
348. Cosma, CL, et al. 2003. The secret lives of the pathogenic mycobacteria. *Ann Rev Microbiol* 57:641.
349. van der Wel, NN, et al. 2005. Subcellular localization of mycobacteria in tissues and detection of lipid antigens in organelles using cryo-techniques for light and electron microscopy. *Curr Opin Microbiol* 8:323.
350. Russell, DG. 2007. Who puts the tubercle in tuberculosis? *Nat Rev Microbiol* 5:39.
351. Scollard, DM, et al. 2006. The continuing challenges of leprosy. *Clin Microbiol Rev* 19:338.
352. Takade, A, et al. 2003. Comparative studies of the cell structures of *Mycobacterium leprae* and *M. tuberculosis* using the electron microscopy freeze-substitution technique. *Microbiol Immunol* 47:265.
353. Amako, K, et al. 2003. Degradation process of *Mycobacterium leprae* cells in infected tissue examined by the freeze-substitution method in electron microscopy. *Microbiol Immunol* 47:387.
354. Walker, SL, Lockwood, DN. 2007. Leprosy. *Clin Dermatol* 25:165.
355. Kaplan, G, et al. 1989. The reconstitution of cell-mediated immunity in the cutaneous lesions of lepromatous leprosy by recombinant interleukin 2. *J Exp Med* 169:893.
356. Barker, LP. 2006. *Mycobacterium leprae* interactions with the host cell: Recent advances. *Indian J Med Res* 123:748.
357. Schlesinger, LS, Horwitz, MA. 1990. Phagocytosis of leprosy bacilli is mediated by complement receptors CR1 and CR3 on human monocytes and complement component C3 in serum. *J Clin Invest* 85:1304.
358. Levy, L, Ji, B. 2006. The mouse foot-pad technique for cultivation of *Mycobacterium leprae*. *Lepr Rev* 77:5.
359. Truman, R. 2005. Leprosy in wild armadillos. *Lepr Rev* 76:198.
360. Moravkova, M, et al. 2008. Strategy for the detection and differentiation of *Mycobacterium avium* species in isolates and heavily infected tissues. *Res Vet Sci* 85:257.
361. Johansen, TB, et al. 2007. New probes used for IS1245 and IS1311 restriction fragment length polymorphism of *Mycobacterium avium* subsp. *avium* and *Mycobacterium avium* subsp. *hominissuis* isolates of human and animal origin in Norway. *BMC Microbiol* 7:14.
362. Turenne, CY, et al. 2007. *Mycobacterium avium* in the postgenomic era. *Clin Microbiol Rev* 20:205.
363. Chacon, O, et al. 2004. Johne's disease, inflammatory bowel disease, and *Mycobacterium paratuberculosis*. *Ann Rev Microbiol* 58:329.
364. Momotani, E, et al. 1988. Role of M cells and macrophages in the entrance of *Mycobacterium paratuberculosis* into domes of ileal Peyer's patches in calves. *Vet Pathol* 25:131.
365. Sigur-Dardottir, OG, et al. 2001. Uptake of *Mycobacterium avium* subsp. *paratuberculosis* through the distal small intestinal mucosa in goats: An ultrastructural study. *Vet Pathol* 38:184.
366. Brown-Elliott, BA, et al. 2006. Clinical and laboratory features of the *Nocardia spp.* based on current molecular taxonomy. *Clin Microbiol Rev* 19:259.
367. Ogata, SA, Beaman, BL. 1992. Adherence of *Nocardia asteroides* within the murine brain. *Infect Immun* 60:1800.
368. Ogata, SA, Beaman, BL. 1992. Site-specific growth of *Nocardia asteroides* in the murine brain. *Infect Immun* 60:3262.
369. Muscatello, G, et al. 2007. *Rhodococcus equi* infection in foals: The science of "rattles." *Equine Vet J* 39:470.
370. Toyooka, K, et al. 2005. *Rhodococcus equi* can survive a phagolysosomal environment in macrophages by suppressing acidification of the phagolysosome. *J Med Microbiol* 54:1007.
371. Ulivieri, S, Oliveri, G. 2006. Cerebellar abscess due to *Rhodococcus equi* in an immunocompetent patient: Case report and literature review. *J Neurosurg Sci* 50:127.
372. Finzi, G, et al. 2007. Ultrastructural evidence of *Tropheryma whippelii* in PAS-negative granulomatous lymph nodes. *Ultrastruct Pathol* 31:169.
373. Burd, EM, et al. 2007. Pustular dermatitis caused by *Dermatophilus congolensis*. *J Clin Microbiol* 45:1655.
374. Stahlberg, H, et al. 2004. Oligomeric structure of the *Bacillus subtilis* cell division protein DivIVA determined by transmission electron microscopy. *Mol Microbiol* 52:1281.
375. Puhar, A, Montecucco, C. 2007. Where and how do anthrax toxins exit endosomes to intoxicate host cells? *Trends Microbiol* 15:477.
376. Bierne, H, Cossart, P. 2007. *Listeria monocytogenes* surface proteins: From genome predictions to function. *Microbiol Mol Biol Rev* 71:377.
377. Dussurget, O, et al. 2004. Molecular determinants of *Listeria monocytogenes* virulence. *Ann Rev Microbiol* 58:587.
378. Lecuit, M, et al. 2001. A transgenic model for listeriosis: Role of internalin in crossing the intestinal barrier. *Science* 292:1722.
379. Kocks, C, et al. 1992. *L. monocytogenes*-induced actin assembly requires the actA gene product, a surface protein. *Cell* 68:521.
380. Tilney, LG, et al. 1992. How Listeria exploits host cell actin to form its own cytoskeleton. I. Formation of a tail and how that tail might be involved in movement. *J Cell Biol* 118:71.
381. Niebuhr, K, et al. 1993. Localization of the ActA polypeptide of *Listeria monocytogenes* in infected tissue culture cell lines: ActA is not associated with actin "comets". *Infect Immun* 61:2793.

Vet-ebooks.com

382. Karunasagar, I, et al. 1993. *Listeria ivanovii* is capable of cell-to-cell spread involving actin polymerization. *Infect Immun* 61:162.
383. Parrisius, J, et al. 1986. Production of listeriolysin by beta-hemolytic strains of *Listeria monocytogenes*. *Infect Immun* 51:314.
384. Vazquez-Boland, JA, et al. 1992. Nucleotide sequence of the lecithinase operon of *Listeria monocytogenes* and possible role of lecithinase in cell-to-cell spread. *Infect Immun* 60:219.
385. Sibbald, MJ, et al. 2006. Mapping the pathways to staphylococcal pathogenesis by comparative secretomics. *Microbiol Mol Biol Rev* 70:755.
386. Benton, BM, et al. 2004. Large-scale identification of genes required for full virulence of *Staphylococcus aureus*. *J Bacteriology* 186:8478.
387. Bae, T, et al. 2006. Prophages of *Staphylococcus aureus* Newman and their contribution to virulence. *Mol Microbiol* 62:1035.
388. Corrigan, RM, et al. 2007. The role of *Staphylococcus aureus* surface protein SasG in adherence and biofilm formation. *Microbiology* 153:2435.
389. Kania, RE, et al. 2008. Characterization of mucosal biofilms on human adenoid tissues. *Laryngoscope* 118:128.
390. Harder, J, et al. 2001. Isolation and characterization of human b-Defensin-3, a novel human inducible peptide antibiotic. *J Biol Chem* 276:5707.
391. Wardenburg, JB, et al. 2007. Poring over pores: Alpha-hemolysin and Panton-Valentine leukocidin in *Staphylococcus aureus* pneumonia. *Nat Med* 13:1405.
392. Lowy, FD, et al. 1988. *Staphylococcus aureus*—human endothelial cell interactions. *J Ultrastruct Mol Struct Res* 98:137.
393. Nishifuji, K, et al. 2008. Staphylococcal exfoliative toxins: "Molecular scissors" of bacteria that attack the cutaneous defense barrier in mammals. *J Dermatol Sci* 49:21.
394. Kushnaryov, VM, et al. 1988. Quantification of low numbers of immunogold label on Lowicryl K4M sections. *Cytobios* 54:167.
395. Lee, YD, et al. 2007. Expression of enterotoxin genes in *Staphylococcus aureus* isolates based on mRNA analysis. *J Microbiol Biotechnol* 17:461.
396. de Dobbeleer, G, Achten, G. 1975. Staphylococcal scalded skin syndrome. An ultrastructural study. *J Cutan Pathol* 2:91.
397. Facklam, R. 2002. What happened to the streptococci: Overview of taxonomic and nomenclature changes. *Clin Microbiol Rev* 15:613.
398. Tart, AH, et al. 2007. New understanding of the group A Streptococcus pathogenesis cycle. *Trends Microbiol* 15:318.
399. Schwarz-Linek, U, et al. 2006. Fibronectin-binding proteins of gram-positive cocci. *Microbes Infect* 8:2291.
400. Napimoga, MH, et al. 2005. Transmission, diversity and virulence factors of *Streptococcus mutans* genotypes. *J Oral Sci* 47:59.
401. Lindahl, G, et al. 2005. Surface proteins of *Streptococcus agalactiae* and related proteins in other bacterial pathogens. *Clin Microbiol Rev* 18:102.
402. Segura, M, Gottschalk, M. 2004. Extracellular virulence factors of streptococci associated with animal diseases. *Front Biosci* 9:1157.
403. Coleman, SE, et al. 1990. Colloidal gold immunolabeling of immunoglobulin-binding sites and beta antigen in group B streptococci. *Infect Immun* 58:332.
404. Beachey, EH, Courtney, HS. 1987. Bacterial adherence: The attachment of group A streptococci to mucosal surfaces. *Rev Infect Dis* 9 Suppl 5:S475.
405. Whitnack, E, Beachey, EH. 1982. Antiopsonic activity of fibrinogen bound to M protein on the surface of group A streptococci. *J Clin Invest* 69:1042.
406. Hasty, DL, et al. 1992. Multiple adhesins of streptococci. *Infect Immun* 60:2147.
407. Ryc, M, et al. 1989. Ultrastructural localization of the fibrinogen-binding domain of streptococcal M protein. *Infect Immun* 57:2397.
408. Daynes, RA, Armstrong, CH. 1973. An antiphagocytic factor associated with group E streptococcus. *Infect Immun* 7:298.
409. Bhakdi, S, et al. 1985. Mechanism of membrane damage by streptolysin-O. *Infect Immun* 47:52.
410. Jedrzejas, MJ. 2001. Pneumococcal virulence factors: Structure and function. *Microbiol Mol Biol Rev* 65:187.
411. Raskova, H, et al. 1971. Release of 5-hydroxytryptamine and morphological changes in blood platelets induced by mucopeptide of streptococcal cell walls. *J Infect Dis* 123:587.
412. Lindstrom, M, Korkeala, H. 2006. Laboratory diagnostics of botulism. *Clin Microbiol Rev* 19:298.
413. Aktories, K, Wegner, A. 1989. ADP-ribosylation of actin by clostridial toxins. *J Cell Biol* 109:1385.
414. Black, JD, Dolly, JO. 1986. Interaction of 125I-labeled botulinum neurotoxins with nerve terminals. II. Autoradiographic evidence for its uptake into motor nerves by acceptor-mediated endocytosis. *J Cell Biol* 103:535.
415. Jayaraman, S, et al. 2005. Common binding site for disialyllactose and tri-peptide in C-fragment of tetanus neurotoxin. *Proteins* 61:288.
416. Roux, S, et al. 2005. Internalization of a GFP-tetanus toxin C-terminal fragment fusion protein at mature mouse neuromuscular junctions. *Mol Cell Neurosci* 30:572.
417. Sasseville, VG, et al. 2007. Naturally occurring Tyzzer's disease in cotton-top tamarins (*Saguinus oedipus*). *Comp Med* 57:125.
418. Franklin, CL, et al. 1994. Tyzzer's infection: Host specificity of *Clostridium piliforme* isolates. *Lab Anim Sci* 44:568.
419. Feldman, SH, et al. 2006. Ribosomal RNA sequences of *Clostridium piliforme* isolated from rodent and rabbit: Re-examining the phylogeny of the Tyzzer's disease agent and development of a diagnostic polymerase chain reaction assay. *J Am Assoc Lab Anim Sci* 45:65.
420. Ikegami, T, et al. 1999. Naturally occurring Tyzzer's disease in a calf. *Vet Pathol* 36:253.
421. Lowe, SE, et al. 1989. Influence of pH extremes on sporulation and ultrastructure of *Sarcina ventriculi*. *J Bacteriology* 171:3775.
422. DeBey, BM, et al. 1996. Abomasal bloat associated with Sarcina-like bacteria in goat kids. *J Am Vet Med Assoc* 209:1468.
423. Lattuada, E, et al. 2005. Cutaneous abscess due to *Eubacterium lentum* in injection drug user: A case report and review of the literature. *J Infect* 51:E71.

Vet-ebooks.com

424. Colombo, AV, et al. 2006. Identification of oral bacteria associated with crevicular epithelial cells from chronic periodontitis lesions. *J Med Microbiol* 55:609.
425. Fisher, RG, Denison, MR. 1996. *Veillonella parvula* bacteremia without an underlying source. *J Clin Microbiol* 34:3235.
426. Marriott, D, et al. 2007. *Veillonella parvula* discitis and secondary bacteremia: A rare infection complicating endoscopy and colonoscopy? *J Clin Microbiol* 45:672.
427. Jumas-Bilak, E, et al. 2004. *Veillonella montpellierensis* sp. nov., a novel, anaerobic, Gram-negative coccus isolated from human clinical samples. *Int J Syst Evol Microbiol* 54:1311.
428. Ristow, P, et al. 2007. The OmpA-like protein Loa22 is essential for leptospiral virulence. *PLoS Pathog* 13: e97.
429. Fraser, CM, et al. 1997. Genomic sequence of a Lyme disease spirochaete, *Borrelia burgdorferi*. *Nature* 390: 580.
430. Connolly, SE, Benach, JL. 2005. The versatile roles of antibodies in Borrelia infections. *Nat Rev Microbiol* 3:411.
431. Cabello, FC, et al. 2007. Hidden in plain sight: *Borrelia burgdorferi* and the extracellular matrix. *Trends Microbiol* 15:350.
432. Ataliba, AC, et al. 2007. Isolation and molecular characterization of a Brazilian strain of *Borrelia anserina*, the agent of fowl spirochaetosis. *Res Vet Sci* 83:145.
433. Guner, ES, et al. 2003. A novel, fast-growing *Borrelia sp.* isolated from the hard tick *Hyalomma aegyptium* in Turkey. *Microbiology* 149:2539.
434. Okuda, T, et al. 2007. *Treponema denticola* induces interleukin-8 and macrophage chemoattractant protein 1 production in human umbilical vein epithelial cells. *Microbes Infect* 9:907.
435. Neef, NA, et al. 1994. Pathogenicity of porcine intestinal spirochetes in gnotobiotic pigs. *Infect Immun* 62:2395.
436. Trott, DJ, et al. 1995. Pathogenicity of human and porcine intestinal spirochetes in one-day-old specific-pathogen-free chicks: An animal model of intestinal spirochetosis. *Infect Immun* 63:3705.
437. Ledder, RG, et al. 2007. Molecular analysis of the subgingival microbiota in health and disease. *Appl Environ Microbiol* 73:516.
438. Paster, BJ, et al. 2001. Bacterial diversity in human subgingival plaque. *J Bacteriology* 183:3770.
439. Hutter, G, et al. 2003. Molecular analysis of bacteria in periodontitis: Evaluation of clone libraries, novel phylotypes and putative pathogens. *Microbiology* 149: 67.
440. Progulske-Fox, A, et al. 1999. *Porphyromonas gingivalis* virulence factors and invasion of cells of the cardiovascular system. *J Periodontal Res* 34:393.
441. Zilm, PS, Rogers, AH. 2007. Co-adhesion and biofilm formation by *Fusobacterium nucleatum* in response to growth pH. *Anaerobe* 13:146.
442. Tadepalli, S, et al. 2007. *Fusobacterium equinum* possesses a leukotoxin gene and exhibits leukotoxin activity. *Vet Microbiol*.
443. Elliott, SP. 2007. Rat bite fever and *Streptobacillus moniliformis*. *Clin Microbiol Rev* 20:13.
444. Abdulaziz, H, et al. 2006. Haverhill fever with spine involvement. *J Rheumatol* 33:1409.
445. Kaspareit-Rittinghausen, J, et al. 1990. [Pathological changes in *Streptobacillus moniliformis* infection of C57bl/6J mice]. *Berl Munch Tierarztl Wochenschr* 103: 84.
446. Yamauchi, K, et al. 1990. Scanning and transmission electron microscopic observations of bacteria adhering to ileal epithelial cells in growing broiler and White Leghorn chickens. *Br Poult Sci* 31:129.
447. Kendall, LV, et al. 2000. Antibody and cytokine responses to the cilium-associated respiratory bacillus in BALB/c and C57BL/6 mice. *Infect Immun* 68: 4961.
448. Griffith, JW, et al. 1988. Cilia-associated respiratory (CAR) bacillus infection of obese mice. *Vet Pathol* 25:72.
449. Matsushita, S. 1991. Ultrastructure of respiratory tract epithelium of rats experimentally infected with the CAR bacillus. *J Vet Med Sci* 53:361.
450. MacKenzie, WF, et al. 1981. A filamentous bacterium associated with respiratory disease in wild rats. *Veterinary Pathology* 18:836.
451. Nietfeld, JC, et al. 1995. Colonization of the tracheal epithelium of pigs by filamentous bacteria resembling cilia-associated respiratory bacillus. *J Vet Diagn Invest* 7:338.
452. Hastie, AT, et al. 1993. Two types of bacteria adherent to bovine respiratory tract ciliated epithelium. *Vet Pathol* 30:12.
453. Brogden, KA, et al. 1993. Cilia-associated respiratory bacillus in wild rats in central Iowa. *J Wildl Dis* 29:123.
454. Angel, CR, et al. 1990. Long-segmented filamentous organisms observed in poults experimentally infected with stunting syndrome agent. *Avian Dis* 34:994.
455. Detilleux, PG, et al. 1989. Ultrastructure and lectin histochemistry of equine cutaneous histiolymphocytic lymphosarcomas. *Vet Pathol* 26:409.
456. Lowden, S, Heath, T. 1995. Segmented filamentous bacteria associated with lymphoid tissues in the ileum of horses. *Res Vet Sci* 59:272.
457. Yamauchi, KE, Snel, J. 2000. Transmission electron microscopic demonstration of phagocytosis and intracellular processing of segmented filamentous bacteria by intestinal epithelial cells of the chick ileum. *Infect Immun* 68:6496.
458. Lane, RS, et al. 1985. Isolation of a spirochete from the soft tick, *Ornithodoros coriaceus*: A possible agent of epizootic bovine abortion. *Science* 230:85.
459. Walker, RL, et al. 1995. Spirochetes isolated from dairy cattle with papillomatous digital dermatitis and interdigital dermatitis. *Vet Microbiol* 47:343.
460. Valdron, KA, et al. 1994. Persistent nodular lesions of bacterial origin on the gills of gasterosteid fish inhabiting an estuarine bay in Nova Scotia. *Canada J Fish Diseases* 17:673.
461. Fokine, A, et al. 2005. A three-dimensional cryo-electron microscopy structure of the bacteriophage phiKZ head. *J Mol Biol* 352:117.
462. Brewer, GJ. 1980. Control of membrane morphogenesis in bacteriophage. *Int Rev Cytol* 68:53.

Vet-ebooks.com

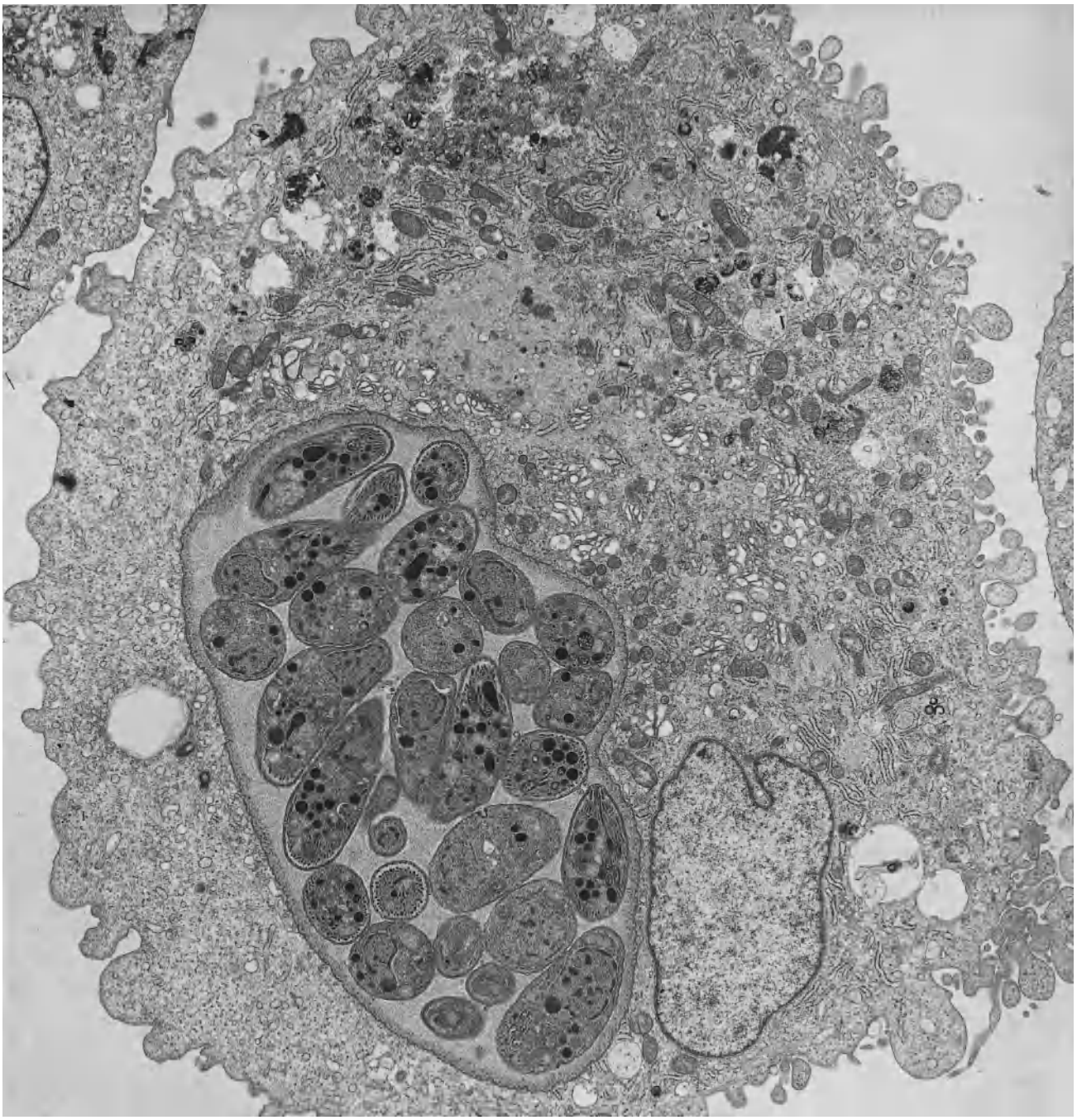


Fig. 15.1 ***Toxoplasma gondii***: parasitophorous vacuole in a macrophage with enlarged cytoplasm and many cytoplasm vesicles. Cyst wall separates parasite from cytoplasmic matrix. (Micrograph: Arliss Boothe.)

© 2009 Wiley-Blackwell. ISBN: 978-0-813-80330-2

Vet-ebooks.com

15 Pathogenic Protozoa

Protozoa are one-celled organisms. Most protozoal life cycles involve a specific mammalian host and a specific vector. Many protozoa stop the replicative cycle during adverse environmental conditions in order to survive. Many species transform into cysts that survive outside the host.

Protozoa kill host cells by a wide spectrum of virulence factors, including toxins, blockage of cell metabolism by intracellular infection, and release of pore-forming proteins secreted onto membranes of the host cells. Cell-mediated immune responses of the host can also play a role in tissue damage.[1]

The **parasite surface** is altered to reflect the needs of attachment and uptake by the host involved (Fig. 15.1).[2,3] Surfaces of protozoa have a strongly negative charge, and consist of a plasma membrane with a highly reactive **glycocalyx** of specific glycoproteins and glycolipids.[4] Immunogold labeling has permitted the identification of specific proteins on the surfaces of individual species of protozoa.[5]

The **plasma membrane** of protozoa has marked asymmetry. The outer and inner lipid layers and the proteins or glycoproteins they bear vary. In some species, the plasma membrane is underlined by one or more membranes to form a **pellicle**, typical of motile stages of the sporozoa and ciliata. Subpellicular microtubules of 15–25 nm diameter underlie the pellicle and may extend from one pole of the cell to the other, or be confined to the anterior half of the cell.

Orifices on the surface include **cytostomes** and **micropores**, which are specialized invaginations that take up nutrients. The cytoplasm of some species may be found to contain bacterial symbionts or phage particles. Cytoplasmic transport systems of the cell include phagosomes, pinocytotic vesicles, Golgi saccules and vesicles, and several types of vacuoles.

The **cytoskeleton** is composed largely of microfilaments of 4–10 nm diameter. In some protozoa these filaments resemble actin microfilaments of eukaryotic cells. Most protozoa contain filamentous actin and homologues of the fusion protein, coronin. Modifications of the cytoskeleton in individual species include: **conoid**, a hollow truncated cone produced by spirally arranged microtubules and associated rings—-during penetration, the conoid protrudes through the anterior polar ring and is used in invasion; **axostyles**, parallel rows of microtubules covered by a membrane; **subpellicular microtubules**; **kinetodesmal fibrils**; and **paraxial rods**, which form a network of microfilaments that run along the axonemal microtubules of flagella.

The **cytoplasm** is divided into the pale, peripheral **ectoplasm** and the central regions of **endoplasm**, which contain organelles. All protozoa have ribosomes, most of which are free in the cytoplasm; ribosomes of some species are associated with cisternae of a rudimentary endoplasmic reticulum, and in others with the mitochondrial matrix. **Golgi complexes** are usually present and in trichomonads are very large, being visible by light microscopy as parabasal bodies.

Secretory granules of various types fill the cytoplasm of most protozoa. Many of these are referred to as wall-forming bodies, which reflects their role in production and secretion of materials that produce cyst walls, for example, amoebae, coccidia, myxosporidia, and microsporidia. **Lipid globules** and **digestive vacuoles** are large and occur in most protozoa. The cytoplasm may also contain endosymbionts such as algae or bacteria that survive within the cell without killing it.[6,7]

Most protozoa have **mitochondria**, although the membrane infoldings may be tubular or saccular in

Vet-ebooks.com

contrast to cristae of eukaryotes. Microsporidia and trichomonads lack mitochondria and survive anaerobically. Trichomonads have microbodies called hydrogenosomes. Mitochondria of trypansosomes, called the kinetoplast, are large and contain large amounts of DNA. Mitochondria may be involved in some forms of protozoan-induced apoptosis, a mechanism of invasion in some organisms.[8] Carbohydrates are stored in the cytoplasm as **glycogen rosettes** and as **amylopectin granules**. Glycogen is found aggregated and distributed throughout the cytoplasm. Amylopectin appears as electron-lucent granules in electron micrographs.

Rhoptries, which function during penetration by releasing enzymes, lie between the nucleus and apical pole. They may be elongate or ovoid. The anterior neck of the rhoptrie is narrow and passes through the conoid at the tip of the cell. **Micronemes** are small rods with rounded ends (50–90 × 300 × 600 nm) that are in the anterior regions of motile stages.

All protozoans are motile, and the organelles that move the cell may be **flagellates** (long) or **ciliates** (short) that differ in their mechanisms of movement. Movement in both involves gliding of microtubules along each other, the linking dynein arms being sites of generation of movement. In trichomonads, the **axostyle** and **costa** are organelles of locomotion that act by flexing.

Amoebas

Amoebas are amorphous, large (15–50 μm) cells that move by the extension of pseudopodia. **Pseudopodia** use actomyosin systems of filaments for movement, and include **lobopodia** in amoebae and **filopodia** in acanthamoebae. The cytoplasm of amoebae contains ribosomes, food vacuoles, lysosomes, lipid globules and tubular bodies; neither mitochondria nor Golgi complexes are apparent. *Entamoeba histolytica* is the primary pathogen for primates. Other free-living amoebae can cause disease in immunosuppressed hosts or by gaining access to the brain and other tissues. Nonpathogenic human intestinal amoebae include *Entamoeba coli* and *E. nana* (Table 15.1).

Many species of amoebae and related protozoa cause disease in fish. Amoebae are found in most species of birds and none are implicated in significant disease. *Entamoeba gallinarum* in the cecum of chickens, for example, is not known to affect the bird; it migrates and proliferates after death and may be found in lesions of other causes.

Genus *Entamoeba*

Entamoeba histolytica is 15–40 μm in diameter and has distinctivwe central karyosomes and aggregated RNA

Table 15.1 Pathogenic amoebae.

Pathogen	*Host*	*Reference to ultrastructural pathology*
Acanthamoeba castellani		**Bowers,** *J Cell Biol* 41:786, 1969; **Chávez-Munquía**, *J Eukaryot Microbiol* 42:153, 2005 (encystation);* **Essig**, *Appl Environ Microbiol* 63:1396, 1997 (infected with Chlamydia)*
***Acanthamoeba* sp.**		**Hoffman**, *Am J Trop Med Hyg* 27:29, 1978 (human CNS); **Martinez**, *J Infect Dis* 131:692, 1975
Entamoeba histolytics	Human	**Eaton**, *Ann Trop Med Parsitol* 64:299, 1970; **Ferio-Velasco**, *J Protozool* 19:200 1972 (hamster liver); **Guerrant**, *J Inf Dis* 143:83 (in neutrophils); **Ludvik**, *Bull WHO* 43:301, 1970; **Sengupta**, *Exp Parasitol* 98:83, 2001 (surface antigens)*; **Tsutsumi**, *Am J Pathol* 130:112, 1988 (liver)
	Guinea pig	**Lushbaugh**, *J Parasitol* 60:421, 1974 (liver); **Takeuchi**, *Virch Arch [B]* 24:263, 1976 (cecum)
	Hamster	**Chávez-Munquía**, *Exp Parasitol* 107:39, 2004 (liver);* **Pérez-Tamayo**, *J Parasitol* 77:982, 1991 (liver)
E. invadens	Human	**Chávez-Munquía**, *J Submicrosc Cytol Pathol* 35:235, 2003 (encystation);* **Zaman**, *Ann Trop Med Parasitol* 67:229, 1973
***Hartmanella* sp.**		**Ito**, *J Protozool* 16:638, 1969 (in vitro)
***Naegleria* sp.**	Human	**Schuster**, *J Protozool* 10:313, 1963*; **Visvesvara**, *J Clin Microbiol* 28:2750, 1990 (brain)
	Mouse	**Martinez**, *Lab Invest* 29:121, 1973 (brain); **Schuster**, *J Protozool* 24:489, 1977 (brain); **Visvesvara**, *J Protozool* 21:239, 1974 (brain)
	Sheep	**Simpson**, *Am J Vet Res* 43:154, 1982 (brain)
***Neoparamoeba* sp.**	Salmon	**Berminhgham**, *Dis Aquat Organ* 76:231, 2007 (gill); **Lovy**, *Vet Pathol* 44:663, 2007 (gill)
***Paramoeba* sp.**		**Roubal**, *J Fish Dis* 12:481, 1987

*Studies in vitro.

Vet-ebooks.com

and DNA at the nuclear membrane. The nucleus:cytoplasmic ratio is small. The outer cytoplasmic zone is clear, glycogen rosettes are present, and there are surface pseudopodia. Mitochondria, Golgi complexes, and rough endoplasmic reticulum are absent or vestigal. The plasma membrane and cell surface bear specific transmembrane proteins, many of which are responsible for most aspects of virulence.[9] Amoebae are infected with both viral, bacterial, and protozoal parasites.[10,11]

Amoebae are actively phagocytic and *E. histolytica* in sections of intestine typically contain erythrocyte debris and remnants of neutrophilic leukocytes. Most pathogenic amoebae replicate in the gut lumen and live on digested food, erythrocytes, and other microorganisms. Amoebae maintain a digestive vacuolar compartment the volume of which expands and contracts with exposure to nutrients. They also phagocytize enterobacteria, which have been seen ultrastructurally within cytoplasmic vacuoles.[12,13] In rare cases, amoebae may contain viruses that infect specific species of organisms.[14] Within the vacuolar system, amoebae can distinguish between nutritive particles, which are retained, and undigestible material, which is exocytosed. Mixed aggregates of digestible and indigestible material are sorted as the initial large phagosome is separated into smaller vacuoles.

Amoebiasis

Entamoeba histolytica produces a clinical syndrome in humans and other primates that extends from asymptomatic carrier to severe dysentery. It invades the colonic wall, often with severe tissue destruction, and penetrates blood vessels to pass via the portal venous system to the **liver** (Fig. 15.2). Close apposition between amoeba and target cell hepatocyte is required for cytolysis. A **pore-forming polypeptide** from the outer membrane inserts into membrane bilayers of the host cell and opens acqueous pores, inducing rapid monovalent cation movement across the membrane of synthetic vesicles.[15] **Lysosomes** have been described at the surface of *E. histolytica*, each with a vermiform protrusion that may be a triggering mechanism that enhances attachment and penetration at the surface of intestinal epithelium.[16] Lysosomes from *E. histolytica* have been widely implicated in death of target host cells.[17–19]

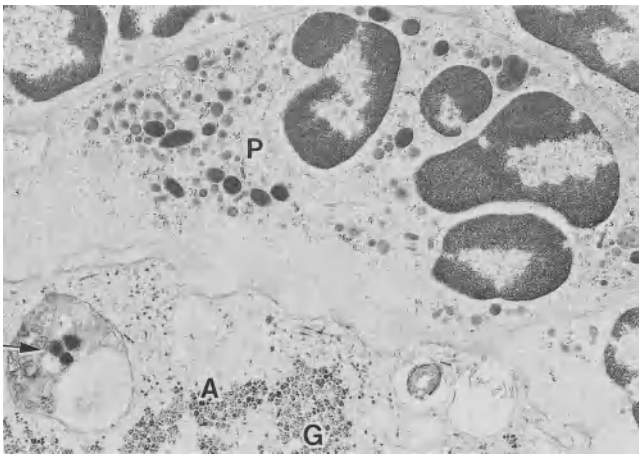


Fig. 15.2 ***Entamoeba histolytica***: hamster liver, 4 hr after intraportal inoculation of axenic amoebas. Interface between neutrophil (*P*) and amoeba (*A*). Cytoplasmic vacuoles (*arrow*) and glycogen (*G*) in the amoeba. Contact areas of neutrophil are devoid of granules. (Micrograph: Victor Tsutsumi, *Am J Pathol* 130:112, 1988.)

Genus *Naegleria*

Small free-living amoebae belonging to the genera *Naegleria* and *Acanthamoeba* cause central nervous system infections in humans known as primary amoebic meningoencephalitis and granulomatous amoebic encephalitis, respectively. Amoebas belonging to the order *Leptomyxida*, usually regarded as innocuous organisms in soil incapable of infecting mammals, have also been reported to cause amoebic meningoencpehalitis in humans and nonhuman primates.[20] *Naegleria fowleri* flagellates are widely distributed in soil, sewage, and freshwater, including thermal springs, chlorinated swimming pools, and domestic water supplies. They typically undergo transformation from amoebae to flagellates; the trophozoite is the vegetative or feeding stage. The six species described are differentiated on the basis of cyst morphology.[21–23]

N. fowleri is the cause of **primary amoebic meningoencephalitis**, a rapidly fatal disease of the CNS that is especially dangerous to immunosuppressed patients. In swimmers, amoebae enter the arachnoid space through the cribiform plate of the nose and infect meninges. *N. fowleri* has a large nucleus, small cytoplasmic mass, and is motile. Trophozoites measure 10–20 μm in diameter and are readily found in tissues of the meninges of infected patients. *N. fowleri* may have a flagellate stage, round cysts, and promitotic trophozoites, distinguishing features from *Acanthamoeba* spp.

Genus *Acanthamoeba*

Acanthamoeba are amoeboflagellates that are free-living in soil and water. Rarely parasitic in humans and animals, they cause chronic granulomatous lesions. *Acanthamoeba* enter oral or nasal cavities and invade the brain through the cribiform plate to cause chronic

Vet-ebooks.com

granulomatous amoebic encephalitis. Immunosuppression enhances infection.[24,25] Healthy individuals develop **acanthamoebic keratitis**, typically after minor trauma to the cornea involving contaminated water under contact lenses. *A. castellanii* has been reported as a cause of brain abscesses in an immunosuppressed human patient. The life cycle and encystment of *Acanthamoeba* spp. has been determined largely through studies of *A. castellanii*.[26] *Acanthamoeba* exist in cyst and trophozoite stages in the environment. The trophozoite stage is the infective and invasive form. In tissue, trophozoites measure 15–30 μm in diameter.

Genus *Neoparamoeba*

Neoparamoeba spp. are free-living amoebae that parasitize the gill to cause amoebic gill disease, a significant loss to the American salmon and turbot industries. Amoebae form pseudopods that extend deeply into invagiantions of epithelial cells.[27] They incite an eosinophilic branchiitis with fusion of secondary lamellae. Neoparamoebae must be differentiated from *Vannella* spp. and *Platyamoeba* spp., which are common amoebae isolated from fish gills.

Ciliates

Only a few ciliates are pathogenic to animals or humans. All but a few members of the phylum *Ciliophora* have cilia at some time in the life cycle. The **axoneme** (central shaft) of a cilium has microtubules that originate from the 9 microtubular triplets of the **kinetosome** (basal body). The plasma membrane surrounds the cell and its cilia. It is supported internally by membranous **alveolar sacs** (cortical alveoli) that are interconnected to form a continuous network that is interrupted only at points of emergence of cilia and at sites where secretory vesicles fuse with the surface. Alveolar sacs are a calcium compartment analagous to sarcoplasmic reticulum of muscle. Release and sequestration of calcium by this system controls the function of cilia, the cytoskeleton, and the exocytotoic membrane vesicles known as **trichocysts**.[28]

Ciliates are dikaryotic cells and the structure of nuclei, not of cilia, distinguishes ciliates from other protozoa. The large **macronucleus** (one or more) regulates cellular metabolism; the smaller **micronucleus** is involved in genetics, including sexual recombination. Nuclei divide endomitotically. The macronucleus originiates by polyploidy from micronuclei.

A **contractile vacuole** or nephridial apparatus is responsible for expelling water from the cell. The structure regulates cytoplasmic water and ion concentrations. Most ciliates have **mucocysts** that extrude materials that coat the cell, are used in trapping food, or function in formation of reproductive cysts.

The **cell cortex** is divided into two regions: the somatic region that functions in locomotion, attachment and protection, and the oral region that acquires and ingests nutrients. The cortex is underlain by the infraciliature, lattice of basal bodies and associated fibrils and cilia (Fig. 15.3).

Most ciliates are phagotrophic, ingesting nutrients through the **oral apparatus**, a cytostome-cytopharynx (mouth) that is often surrounded by rows of cilia. In the cell, nutrients are within a **food vacuole** that, after digestion, egests the residue through the **anus**, which may be a well-defined **cytoproct**, or less defined structure termed a **cytopyge**.

Genus *Balantidium*

Balantidium coli is a large parasite in the lumen of the human colon; it also occurs in nonhuman primates,

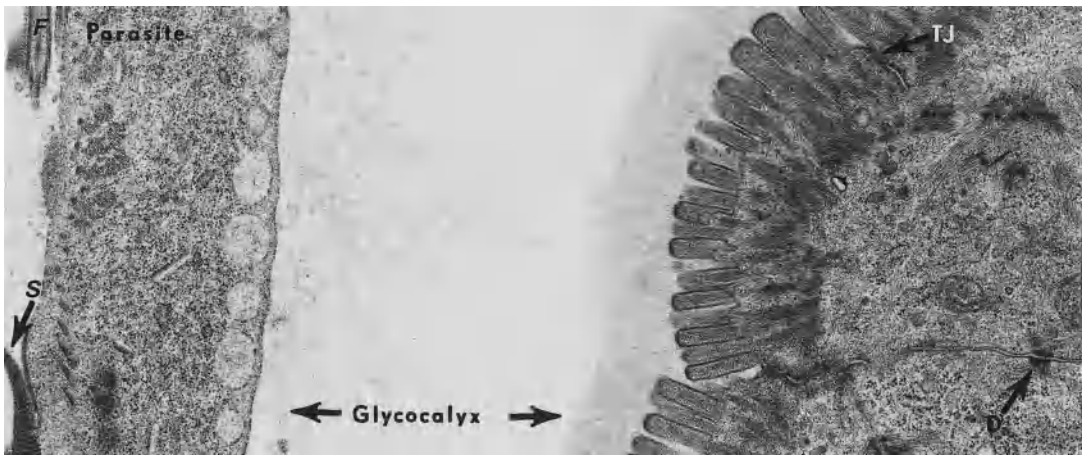


Fig. 15.3 **Cilate** (*left*) at microvillous surface (*right*) of intestine, cat. Note glycocalyx on absorptive cell microvilli. Flagellum (*F*), basal plate for suctorial disk (*S*), tight junction (*TJ*), desmosome (*D*).

Vet-ebooks.com

rats, and pigs. Other *Balantidum* species are symbionts in fish and other marine vertebrates.[29,30] In malnourished patients, *B. coli* invades the colonic wall to cause colitis. The inflammatory response is neutrophilic, perhaps more in response to bacteria that accompany penetration by the protozoa. Deep ulcers, with margins of chronic inflammatory tissue, develop, and may extend into and even through the muscle layers to penetrate the gut wall. Balantidia are found in ulcers and trophozoites are 50–100 µm in diameter.

Genus *Ichthyophthirius*

Ichthyophthirius species are parasites of the skin and gills of freshwater fishes. Life cycles include parasitic and free-living phases, and involve theront, trophont, tomont and tomite stages.

After full development in a host, the parasite leaves the fish to begin the free-living phase during which it encysts and divides. **Theronts**, the infective stage, are released from the cyst to infect new hosts. Theronts contain membrane-bounded crystalline and secretory mucocysts in the cytoplasm, which are important in invasion of host cells.[31] Free-swimming theronts seek a new fish, to attach to and penetrate epithelium, usually of the gills (Fig. 15.4). Attachment may involve the cytosome, the perfatorium (a knob-like structure at the anterior pole of the theront) and secretions of mucocysts. Contents of the mucocyst are discharged, enveloping the ciliate with a sticky surface coat that enhances attachment to the host epithelium.[32]

In trophozoite stages the ciliate lives under the epithelium of the skin or gill, feeding on host cells. Ultrastructurally, trophozoites have characteristic alveolar sacs, flattened cisternae arranged beneath the plasma membrane and pellicle.[33]

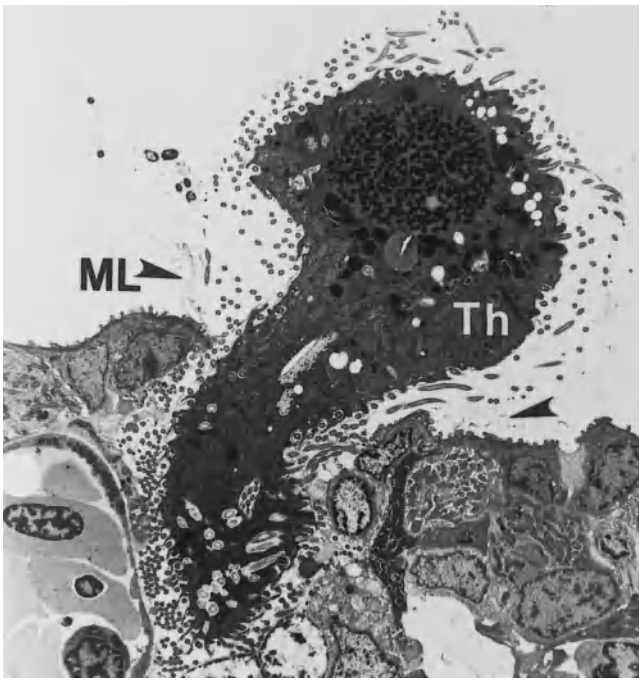


Fig. 15.4 ***Ichthyophthirius multifiliis***: theront (*Th*) penetrating gill epithelium. Amorphous mucocyst-produced layer (*ML*) remains attached to epithelial cell surface during penetration. (Micrograph: Margaret S. Ewing, *J Protozool* 32:305, 1985.)

Flagellates

All pathogenic hemoflagellates require a bloodsucking insect vector as an intermediate host. During their life cycle, these protozoa display a variety of structural manifestations typical for the growth phase in a particular host and tissue (Table 15.2). Four forms are known, based on the type and position of the flagellum: **trypanosomal, crithidial, leptomonad**, and **leishmanial**. In general, the flagellated stages inhabit body fluids in vertebrates and the alimentary canal in insects; leishmanial stages are found intracellularly. Surface characteritics of pathogenic trypanosomes determine attachment, invasion and survival in the host.[34]

Genus *Trypanosoma*

The trypanosome life cycle involves a vertebrate host (which at some stage develops a parasitemia) and a blood-sucking invertebrate. When taken into the gut of the latter, the parasite undergoes transformation through one or more stages, such as leishmanial, leptomonad, or crithidial forms, that are not infective to the vertebrate host. The final infective stage is the trypanosomal stage.

Within the mammalian host, *Trypanosoma* spp. replicate intracellularly. **Neuriaminiase** (sialidase), released by the trypanosome, is involved in attachment and invasion.[35,36] Entry into the host cell involves formation of a membrane-bound vacuole followed by escape and release of the parasite into the cytoplasm.[37] The vacuole is acidic, and agents that inhibit acidification block parasite escape into the cytoplasm. An acid-secreting, transmembrane pore-forming protein that is crossreactive with complement C9 is secreted by *T. cruzi* and has been implicated in the process of vacuole disruption. **Lysosomes** of the host cell fuse with trypanosome-containing vacuoles but in the absence of immunologic activation, do not kill the parasite. This appears to be due to the lining of the luminal parts of the lysosomal membrane by a halo of glycoconjugates composed of aggregated lysosomal glycoproteins, structures rich in sialic acid.

Trypanosomes react to the newly developing hostile environment by changing components of the glycolyx

Vet-ebooks.com

Table 15.2 Pathogenic flagellates.

Pathogen	*Host*	*Reference to ultrastructural pathology*
		Genus *Giardia*
Giardia lamblia	Human	**Al-Tukhi**, *J Exp Med* 161:437, 1985 (biopsy study); **Balazs**, *Pathol Res Pract* 163:251, 1978 (gut); **Chavez**, *J Protozool* 39:510, 1992; **Klima**, *Arch Pathol Lab Med* 101:133, 1977
	Mouse	**El-Shewy**, *Parasitology* 130:269, 2005 (Paneth cell killing); **Nemanic**, *J Infect Dis* 140:222, 1979
	Experimental	**Benchimol**, *Arch Microbiol* 183:160, 2005 (nucleus);* **Benchimol**, *J Struct Biol* 147:102, 2004 (funis); **Benchimol**, *Parsitol Res* 94:254, 2004 (nuclear envelope); **Carvalho**, *Exp Parasitol* 108:154, 2004 (caudal complex);* **Hill**, *Infect Immun* 55:3155, 19877 (phagocytosis);* **Luchtel**, *Appl Environ Microbiol* 40:821, 1980 (cyst);* **Piva**, *Biol Cell* 96:735, 2004 (median body);* **Tumová**, *Cell Motil Cytoskeleton* 64:288, 2007 (ventral disc)*
G. duodenalis	Human	**Erlandsen**, *J Parasitol* 75:787, 1989 (cyst wall)
G. microti		**Feely**, *J Protozool* 35:52, 1988 (cyst); **Hill**, *Infect Immun* 58:3202, 1990 (trophozoies, gut)
G. muris	Hamster Experimental	**Bockman**, *J Protozool* 15:26, 1968 (intestine) **Coggins**, *Exp Parasitol* 61:219, 1986 (encystation);* **Januschka**, *J Parasitol* 74:542, 1988 (cyst)
		Genus *Histomonas*
Histomonas meleagridis	Turkey	**Wilkins**, J Comp Pathol 84:589, 1974 (caecum)
		Genus *Hypotrichomonas*
Hypotrichomonas acosta		**Matern**, *J Protozool* 16:668, 1968;* **Warton**, *J Protozool* 26:56, 1979
		Genus *Leishmania*
Leishmania amazonensis	Experimental	**Antoine**, *Infect Immun* 59:764, 1991 (macrophage);* **Shepherd**, *J Exp Med* 157:1471, 1982 (parasitophorous vacuole);* **Verase**, *J Exp Med* 176:639, 1992 (parasitophorous vacuole)
Leishmania braziliensis		**Aikawa**, *Am J Pathol* 18:50, 1982 (macrophage)*
L. donovani	Dog Hamster Monkey Experimental	**Alexandre-Pires**, *Microsc Res Tech* 69:227, 2005; **Kennan**, *Vet Pathol* 21:74, 1984 **Dwyer**, *Z Parasitenkd* 43:227, 1974 (spleen); **Rudzinksa**, *J Protozool* 11:166, 1964 (spleen) **Dennis**, *J Parasitol* 71, 576, 1985 **Chang**, *J Exp Med* 147:515, 1978 (macrophage); **Chang**, *Science* 193:678, 1976 (macrophage)*
L. hertigi		**Croft**, *Ann Trop Med Parasitol* 73:213, 1979
L. mexicana		**Alexander**, *J Protozool* 22:501, 1975; **Ueda-Nakamura**, *Res Microbiol* 158:456, 2007 (megasomes)
L. panamensis	In vitro	**Eperon**, *J Protozool* 36:502, 1989
L. tropica	Human	**Langreth**, *J Protozool* 30:555, 1983 (macrophage)*
L. spp.	Fox	**Conroy**, *Vet Pathol* 7:163, 1970 (skin)
		Genus *Leptomonas*
Leptomonas samueli		**Souti-Padron**, *Z Parasitenkd* 62:127, 1980
		Genus *Pentatrichomonas*
Pentatrichomonas spp.		**Hongiberg**, *J Protozool* 15:419, 1968
		Spironucleus
Spironucleus meleagridis	Turkey	**Brugerolle**, *Protistologica* 9:495, 1973
S. elegans	Amphibians, fish	
S. muris	Vole	**Brugerolle**, *Z Parasitenkd* 62:47, 1980; **Januschka**, *J Parasitol* 74:452, 1988
S. salmonis	Fish	**Fard**, *Dis Aquat Organ* 75:37, 2007; **Ferguson**, *J Fish Dis* 2:57, 1979 (*Hexamita salmonis*); **Poynton**, *Dis Aquat Organ* 60:49, 2003
S. torosa	Fish	**Sterud**, *J Parasitol* 84:947, 1998 (turbot)
S. vortens	Ide	**Sterud**, *J Eukaryot Microbiol* 49:137, 2002

Vet-ebooks.com

Table 15.2 *Continued*

Pathogen	*Host*	*Reference to ultrastructural pathology*
		Genus *Trichomas*
Trichomonas gallinae		**Mattern**, *J Protozool* 14:320, 1967*
T. gallinarum	Chicken	**Lee**, *Parasitology* 65:71, 1972 (cecum)
	Experimental	**Mattern**, *J Protozool* 14:320, 1967 (mastigonts)
T. vaginalis	Experimental	**Bricheux**, *Eur J Cell Biol* 79:413, 2000 (coronin); **Brugerolle**, *J Protozool* 20:320, 1973;* **Brugerolle**, *Biol Cell* 88:29, 1996 (cytoskeleton); **Nielsen**, *J Microsc* 5:229, 1973
		Genus *Tritrichomas*
Tritrichomnas foetus	Cat	**Yaeger**, *Vet Pathol* 42:797, 2005 (colitis)
	Cow	**Rhyan**, *Vet Pathol* 25:350, 1988 (placenta, fetus)
	Experimental	**Benchimol**, J Protozool 30:422, 1983 (hydrogenosome);* **Honigberg**, *J Protozool* 18:183, 1971 (mastigote)
T. muris	Hamster	**Daniel**, *J Protozool* 18:575, 1971 (feces); **Mattern**, *J Protozool* 27:435, 1980 (pseudocyst)
		Genus *Trypanosoma*
Trypanosoma avium	Bird	**Baker**, *J Protozool* 15:298, 1967 (canary blood)
T. bouffardi		**Molyneux**, *An Trop Med Parasitol* 68:369, 1974
T. brucei	Mammal	**Goodwin**, *Parasitology* 67:115, 1973 (rabbit); **Hemphill**, *J Parasitol* 77:603, 1991 (cytoskeleton); **Hemphill**, *J Struct Biol* 107:211, 1991; **Soltys**, *Trans Roy Soc Trop Med Hyg* 63:490, 1969
	Insect	**Tetley**, *J Cell Sci* 87:363, 1988 (surface)
	Experimental	**Coppens**, *J Protozool* 34:465, 1987 (endocytosis); **Duszenko**, *J Cell Biol* 106:77, 1988 (surface); **Field**, *Microsc Microanal* 10:621, 2004 (review); **Olenick**, *Infect Immun* 56:92, 1988 (flagellum); **Robinson**, *J Cell Biol* 126:641, 1994 (kinetoplast)
T. congolense	Cow	**Abebe**, *Vet Pathol* 30:401, 1993 (pituitary);
	Mouse	**Vickerman**, *J Protozool* 16:54, 1969 (blood)
	Experimental	**Bayne**, *Mol Biochem Parasitol* 61:295, 1993 (surface antigens); **Frevert**, *J Ultrastruc Mol Struc Res* 99:137, 1988;
T. conorhini		**Milder**, *J Protozool* 15:65, 1967*
T. cruzi		**Brack**, *Acta Trop* 25:289, 1968; **Milder**, *J Protozool* 16:730, 1969; **Nogueira**, *J Exp Med* 143:1402, 1976 (phagocytosis)*
	Mouse	**Sanabria**, *Exp Parasitol* 23:379, 1968 (brain); **Sanabria**, *Exp Parasitol* 30:187, 1971 (liver)
T. donovani	Cow	**Muhlpfordt**, *Tropenmed Parasitol* 26:385, 1975 (blood)
	Monkey	**Dennis**, *J Parasitol* 71:576, 1985 (liver)†
T. fallisis	Toad	**Martin**, J Protozool 37:199, 1990
T. gambiense		**Lumsden**, *Exp Parasitol* 32:44, 1972
T. lewisi		**Anderson**, *J Protozool* 12:483, 1965*; **Burton**, *J Cell Biol* 39:318, 1968; **Greenblatt**, *Exp Parasitol* 34:197, 1973 (spleen); **Lee**, *Z Parasitenkd* 44:93, 1974 (rat liver)
T. lucknowi		**Weinman**, *J Protozool* 31:429, 1984 (monkey)
T. raiae	In vitro	**Preston**, *J Protozool* 16:320, 1969*
T. rhodesiense	Human	**Nagle**, *Lab Invest* 46:365, 1982 (glomerulopathy)
T. theileri	Cow	**Griebel**, *J Protozool* 36:415, 1989;* **Moulton**, *Cornell Vet* 52:124, 1972*
T. vivax	Cow	**Anosa**, *Vet Pathol* 29:33, 1992 (bone marrow)
	Fly	**Vickerman**, *J Protozool* 30:394, 1973 (eye)
T. spp.	Fish	**Gu**, *Parasitol Res* 101:723, 2007**; Karlsbakk**, *Syst Parasitol* 65:175, 2006 (cod)
		Unclassified Organisms
Dientamoeba fragilis	Human	**Windsor**, *Br J Biomed Sci* 56:293, 1999

*Studies in vitro.
†Animal model.

Vet-ebooks.com

and thereby evading host defense mechanisms.[38,39] They evade host immune responses by antigenic variation, by sequentially changing their **variant surface glycoproteins**.[40–43] Attachment of antibodies in the bloodstream to surface VSGs may lead to development of filopodia and to capping.

Subpellicular tubules interact with the plasma membrane, with the flagellum, and with each other. These interrelationships have been revealed by analysis of the cytoskeleton using high-resolution techniques of quick-freeze, deep-etch rotary-shadowing electron microscopy. At the anterior tip of the cell, subpellicular arrays of microtubules converge into a tightly closed structure while at the posterior end the microtubular array remains open.[44]

The **flagellum** is the organ of motility and excretion.[45] **Endocytosis** and **exocytosis** occur largely in the **flagellar pocket**, a deep invagination of the plasma membrane where the flagellum extends from the cell. Here is where albumin and other plasma proteins are endocytosed and chemotaxins, pyrogens and antigens are released by exocytosis.[46] Receptor molecules are retained at the flagellar pocket, and uptake involves clathrin.[47]

Trypanosomes have a single **nucleus** and several distinctive organelles (Fig. 15.5). Nuclear DNA undergoes distinct changes during antibiotic therapy and these may distort the ultrastructure of the parasite in animal tissue.[48]

The **mitochondrion** is a single tubular structure that lacks functional TCA cycle or cytochromes. During transformation, the mitochondrion develops cristae and NADH-tetrazolium reductase activity related to the ability of the stumpy form to adapt to the vector.[49]

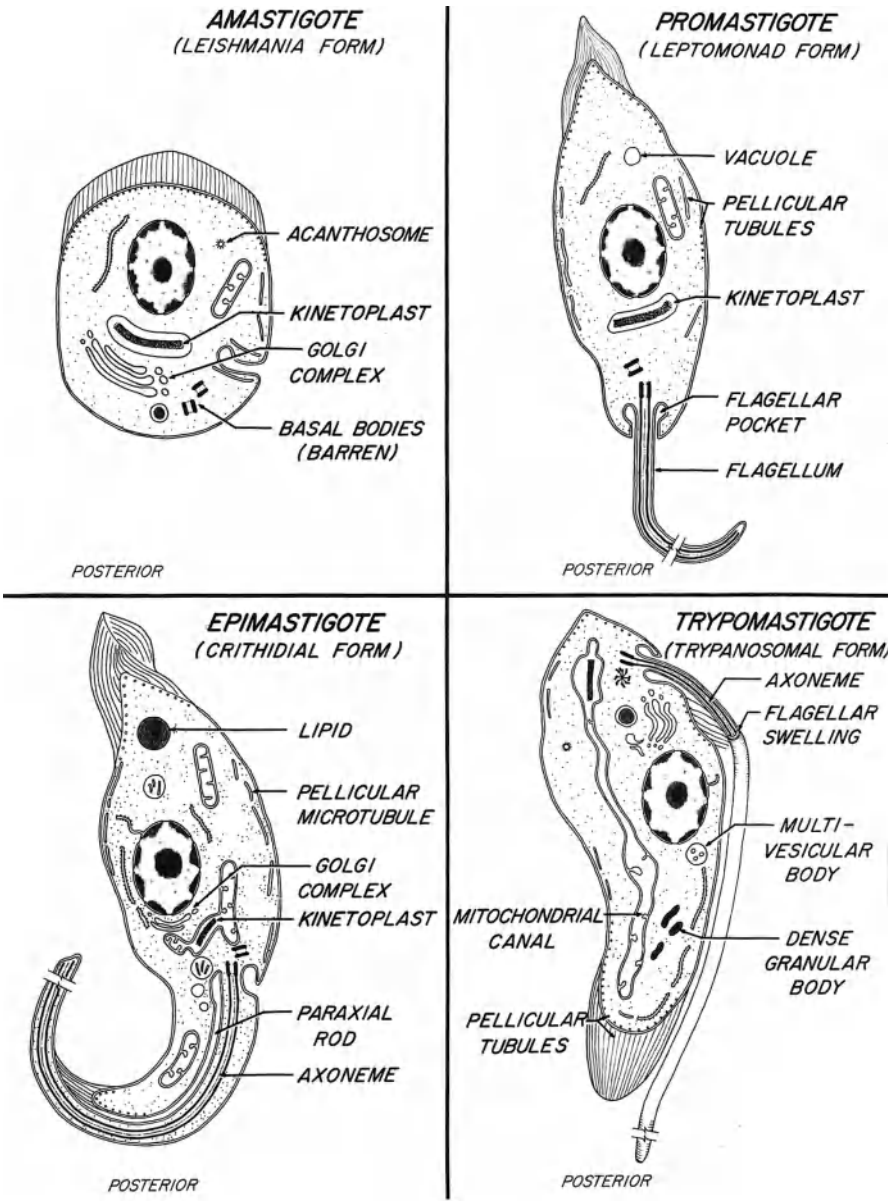


Fig. 15.5 Pathogenic flagellate forms: ultrastructural anatomy.

Vet-ebooks.com



Fig. 15.6 ***Trypanosoma fallisi***: mature bloodstream trypomastigote, longitudinal section. Bacilliform inclusion (*I*), flagellum (*F*), and undulating membrane (*U*). (Micrograph: Donald S. Martin, *J Protozool* 37:199, 1990.)

Glycosomes, a subcategory of microbody present only in kinetoplastida, contain the first nine enzymes of glycolysis and clyercol metabolisms as well as those of fatty acid β-oxidation pathways.[50,51]

The **kinetoplast** is a DNA-containing, self-duplicating cytoplasmic organelle located at the base of the flagellum adjacent to the tiny blepharoplast from which the flagellum arises (Fig. 15.6). The kinetoplast divides by binary fission prior to nuclear division of the organisms. Ultrastructurally, the kinetoplast is a mass of DNA that represents the mitochondrial genome. Organized in a complex network of circular DNA molecules it is present at a unique site in the single mitochondrion and replicates in a discrete period of the S phase of the cell cycle. Associated with and linked to the basal body, segregation of kinetoplast DNA is dependent on microtubule-mediated separation of new and old flagellar basal bodies during the cell cycle.[52]

RNA editing in mitochondria of kinetoplastic protozoa is a mechanism to alter the flow of genomic information at the RNA level. It is a processing event that results in production of an mRNA that differs in nucleotide sequence from its gene. Ultrastructural analysis of mitochondrial genomes show thousands of mini circles and up to 50 maxi circles catenated together in a single large network.[53]

Trypanosomiasis

African Trypanosomiasis Forms of African trypanosomiasis include (1) an acute febrile syndrome with purpura and disseminated intravascular coagulation, (2) chronic episodic fever with splenomegaly and lymphadenopathy, and (3) CNS infection with coma and death or "sleeping sickness". Death typically results from congestive heart failure, which is caused by a combination of myocarditis coupled with the systemic effects of anemia, loss of blood volume through edema, and increased metabolism of fever. The vector of African trypanosomiasis is *Glossina* sp., the tsetse fly.

After inoculation of salivary forms by the tsetse fly, trypomastigotes metamorphose and proliferate at the local cutaneous site prior to entry into lymphatics and blood. A large red chancre forms at the site of the bite that has marked inflammation and teems with protozoa.

Bloodstream trypanosomes (trypomastigotes) are fusiform, flagellate, and motile, having an undulating membrane that extends along the length of the cell. As parasitemia develops trypanosomes interact with circulating antibodies but because of antigen variation most are able to survive the lytic attach that follows. Within the bloodstream, trypanosomes take up plasma

Vet-ebooks.com

proteins by endocytosis. Using proteins labeled with colloidal gold, *T. brucei* has been shown to take in proteins by receptor-mediated endocytosis.[54] **Apolipoprotein L-I** is a serum trypanolytic factor that forms anion channels and is targeted to lysosomal membranes where it triggers membrane depolarization, influx of chloride, and osmotic swelling.[55] **Defensins** cause pore formation in *T. cruzi* that causes DNA fragmentation and trypanosomal lysis.[56]

During parasitemia trypanosomes localize in the brain, myocardium, subcutis, lymphoid organs and mesenchymal tissues, where they replicate extracellularly. *T. brucei* binds at intercellular junctions before crossing the blood-brain barrier.[57] *T. cruzi* migrates through extracellular matrix using a unique surface protein that promotes selective adhesion to collagen and other matrix components.[58]

In **myocardium**, amastigotes develop within mycoytes, usually free in the sarcoplasm. Cardiac myocytes undergo acute cell swelling and are lysed as new parasites appear in the sarcoplasm. Intersitital myocarditis and meningitis are the most striking lesions.[59,60] The **pancarditis** involves all cardiac layers including the cardiac conduction system. Ultrastructural analysis of biopsy tissue revealed early damage to sarcoplasmic reticulum and marked myocarditis in later stages.[61] In addition to parenchymal cell necrosis, lesions of the heart and brain contain large numbers of organisms, necrotizing vasculitis, and thrombosis.

Renal glomerular lesions are implicated in human trypanosomiasis. Experimentally, infection of *T. rhodesiense* can cause hypercellular lesions in renal glomeruli of rodents but the character of the lesions vary from one species to another.[62] In rabbits, monocytes and macrophages are present and the immunoglobulins detectable with immunolabeling techniques are associated with macrophages, not with densities in the basement membranes of the glomeruli.

American Trypanosomiasis (Chagas Disease) *T. cruzi* is transmitted by triatomidae, or kissing bugs, and causes disease in humans in Latin America; dogs, armadillos, opposums and other wild mammals are susceptible. *T. cruzi* exists in three developmental forms: **epimastigotes**, which multiply extracellularly in the midgut of reduviid bugs; **amastigotes**, which multiply inside mammalian cells, and **trypomastigotes**, which do not multiply but transmit infection from insect to mammal and back. The fusiform hemoflagellate trypomastigote circulates and invades host cells. In tissue it develops a leishmanial form that divides and reinvades the bloodstream. Entry and fate of these forms in macrophages has been documented.[63] *T. cruzi* trypomastigotes use the bloodstream only to reach target organs. In granulomatous lesions of the skin, granulocytes phagocytize and kill tissue (amastigote) and blood (trypomastigote) forms of trypanosomes. Human eosinophils degranulate and lyse *T. cruzi* amastigotes extracellular, probably via a mechanism involving eosinophil basic protein.[64]

The brain, heart, skeletal muscle, intestine and nerves are invaded and trypomastigotes cross the vascular endothelium and migrate through extracellular matrices.[65] Once inside the host cells, *T. cruzi* transforms into amastigotes, which then divide by binary fission. After several divisions, amastigotes transform back into trypomastigotes, which exit the cell, migrate through interstitium, and invade new host cells or pass into the blood to infect different organs.

In acute **myocarditis**, lesions contain swollen cardiac myocytes bearing many leishmanial forms. Experimental cardiac myocyte infection in the mouse shows that amastigotes develop within the mycardial cell, typically free in the sarcoplasm and adjacent to the sarcolemma. **Amastigotes** are 2–3.5 μm in diameter and have a short flagellum and juxtanuclear kinetoplast. Amastigotes appear to actively take up and use host cytokines to control their life cycle.[66] **Epimastigotes**, which are intermediate stages between amastigotes and trypomastigote forms, develop within nests that also contain amastigotes. The epimastigotes are elongate, often pear-shaped with anterior-posterior axes and kinetochores anterior to the central nucleus. Flagella extend beyond the body (in amastigotes, it does not). Myofibrils and mitochondria adjacent to the early amastigotes are little affected, but later as epimastigote forms appear there is acute cell swelling and lysis of the myocyte.[67]

Bovine Trypanosomiasis *Trypanosoma brucei* causes devastating loss of cattle in Africa. Flies inject trypanosomes of *T brucei* into a cow's bloodstream. Early waves of parasitemia and pancytopenia are associated with elevated reticulocyte counts in tissue-invading trypansomes. Megakaryocytes are increased, with some showing epmeripolesis of erythrocytes and leukocytes.[68]

In *Trypanosoma congolense* infection of calves, blood vessel damage is the primary lesion. There is a generalized dilatation of the microvasculature that is most prominent in the liver and mesentery. Platelets are affected and anemia is common.[69] The number of circulating erythrocytes varies directly with the degree of parasitemia. The liver is the major site of erythrocyte destruction. Lymphoid hyperplasia is a prominent lesion in infected calves.

T. theileri is ubiquitous in the blood of domestic cattle, occuring even in fetuses and newborns. Trypomastigotes are associated with lymphocytes, and growth is enhanced in immunosuppressed animals.[70] Trypomastigotes are common contaminants of cell cultures prepared with bovine sera.

Vet-ebooks.com

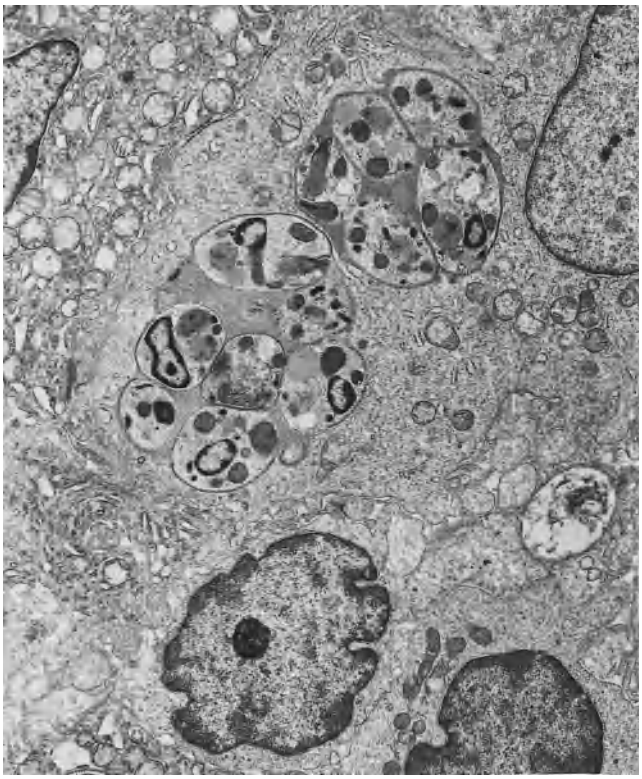


Fig. 15.7 Cutaneous leishmaniasis: activated macrophages with intact amastigotes in phagosomes; one externalized degenerate parasite. No necrosis is evident. (Micrograph: Marian J. Ridley, *Am J Pathol* 123:79, 1986.)

Genus *Leishmania*

The life cycle of *Leishmania* spp. involves two distinct stages. Flagellated **promastigotes** live extracellularly in the gut of insect phlebotomes,[71] and are transmitted to vertebrates. Within macrophages of the vertebrate host, organisms transform into nonflagellated **amastigotes** (Fig. 15.7).[72] Amastigotes are obligatory parasites of macrophages and lodge in modified phagolysosomes called **parasitophorous vacuoles**.[73] Although internalized by other phagocytes, organisms only survive and replicate in macrophages.[74] **Megasomes**, large lysosome-like structures bearing cysteine proteinases, are involved in virulence in *Leishmania*.[75]

The **invertebrate stage** is obligatory for development. *L. donovani* resides extracellularly in the gut of the sandfly vector, and intracellularly in macrophage lysosomes of its mammalian host. It replicates in an environment filled with hydrolytic enzymes. Acid phosphatase, demonstrated on surface membranes of promastigotes, may enable uptake of nutrients from organic phosphates.

When **amastigotes** are ingested by an invertebrate from an infected mammalian host, they transform into rapidly dividing extracellular **promastigotes**. Transmission occurs when metacyclic stages are regurgitated from the sandfly cardia, an event promoted by parasites attaching to and degrading the stomodeal valve of the insect.[76]

Infection of the sandfly vector depends upon attachment of the parasite to microvilli of the midgut epithelium, an event that is mediated by saccharides of lipophosphoglycan, the major surface molecule on leishmanial promastigotes. Phosphoglycans bound to epithelial cell microvilli have been localized with immunogold techniques.[77] Attachment to the midgut retains promastigotes in the gut. Parasites later detach and move anteriorly to the cuticle-lined foregut. Here they attach by forming hemidesmosomes.

The **flagellum** is a specific structure of the promastigote stage and is attached, via hemidesmosomes, to the chitinous cuticular coat. Flagella have a typical 9 + 2 microtubular axoneme and a paraxial or paraflagellar rod, a crystalline structure that abuts the axoneme. Flagellar-specific proteins have been localized by immunogold techniques.[78]

As flagellated promastigotes are transmitted to the new vertebrate host, they are taken up by macrophages. They attach using various macrophage surface receptors (including complement receptors) by means of lipophosphoglycan and a surface glycoprotein gp63. In vitro, **caveolae** are involved in uptake and target parasites to a pathway that promotes delay of lysosomal fusion and intracellular survival.[79] After opsonization by complement and phagocytic uptake into macrophages, promastigotes differentiate into amastigotes, the form that replicates in phagolysosomal compartments. During development, the parasite inhibits phagolysosomal biogenesis using surface lysophosphoglycans.[80] Parasite-bearing phagosomes develop into **parasitophorous vacuoles**, which then fuse with primary lysosomes of the host macrophage. **Acidocalcisomes**, acidic calcium storage organelles, may be involved in host resistance.[81] Within the parasitophorous vacuole, the extent to which MHC class II molecules and various cytokines are expressed determines the outcome of infection.

Leishmaniasis

Leishmaniasis is a zoonotic disease of dogs and humans worldwide. Human leishmaniasis is traditionally separated into **visceral leishmaniasis** (*L. donovani*), **mucocutaneous leishmanisis** (*L. braziliensis*), and **cutaneous leishmaniasis** (*L. major* and *L. mexicana*). Members of the *L. donovani* complex (variants: donovani, infantum, and chagasi) also cause **canine visceral leishmaniasis**. Transmitted to the dogs by sandflies of the subfamily Phleotominae, amastigotes multiply inside cells of the monocyte-macrophage

Vet-ebooks.com

system.[82] Visceral Mediterranean leishmaniasis is caused by *L. leishmania infantum*. Canidae are the reservoirs for infantile visceral leishmaniasis and offer the insect vector direct access to parasitized macrophages in skin lesions.

Cutaneous Leishmaniasis The causal organisms of human **cutaneous leishmaniasis** (tropical sore) produce lesions that consist of aggregates of infected macrophages. Large foamy macrophages contain protozoa. The tiny intracellular **amastigote** can be seen histologically as two small dots that are the deeply stained nucleus and the kinetoplast. Promastigote forms of virulent *L. donovani* and *L. tropica* are both deficient in endogenous scavengers of hydrogen peroxide (catalase, glutathione peroxidase) and are susceptible to low fluxes of this chemical. Ulcers develop as granulomatous papules surrounded by indurated areas that grow progressively to ulcerate and, after a long period, heal. *Leishmania* spp. are present in large macrophages throughout the lesions.[83,84] Neutrophils, the first cells to migrate into sites of infection, phagocytose parasites and undergo apoptosis. Ingestion of parasite-bearing apoptotic neutrophils by macrophages induces release of the anti-inflammatory cytokine TGF-β. Parasites appear to use the infected dead neutrophil as a "Trojan horse" to enter the host macrophage silently and unrecognized.[85]

Visceral Leishmaniasis **Visceral leishmaniasis** (kala azar) is an insidious febrile systemic disease characterized by pancytopenia, hepatosplenomegaly, and lymphadenopathy. Parasitized macrophages are most prominant in the liver, spleen, bone marrow, and lymph nodes. A high affinity binding site on the promastigote surface mediates rapid internalization (through a vesicular pathway) and degradation of hemoglobin. Dogs are a major reservoir, but rodents and other wild animals are reservoirs in some areas. Owl monkeys infected with *L. donovani* develop anemia, granulocytopenia, thrombocytopenia, and lymphocytosis.

Genus *Giardia*

Pathogenic giardia inhabit the gut, and are causes of malabsorption and chronic diarrhea. They are multinucleated, multiflagellar protozoa that move with a cytoskeleton made of several microtubular structures: four pairs of flagellae, an adhesive disk, a median body, and the funis. The **funis** is made of short arrays of microtubules that emanate from axonemes of caudal flagella. Funis microtubules are anchored to the epiplasm, a fibrous layer that lies below the membrane involved in flexion of the tail. During infection, the **cyst wall** acts as a barrier to movement or diffusion of environmental molecules and is involved in encystment and excystation. It consists of a **membraneous layer** of inner and outer cyst membranes separated by a thin layer of cytoplasm, and a **filamentous layer** containing filaments of 7–20 nm diameter. Filaments form a dense meshwork of branches and interconnections. They increase markedly during encystment.[86] Treatment of organisms in vitro with parasiticides and other drugs causes fragmentation of the adhesive disc and filaments.[87]

Giardia are diplomonads with two genetically identical, transcriptionally active and functional equivalent diploid nuclei. Giardia have two developmental stages: a binucleate, flagellated trophozoite that attaches to the upper small intestine, and the quadrinucleate infectious cyst, which is excreted from the body and persists in water. In encysting trophozoites, the two nuclei undergo nuclear division without subsequent cytokinesis, leading to a mature cyst with four nuclei. Karyogamy, the fusion of nuclei, and subsequent somatic homologous recombination occur in the cyst.[88]

Giardiasis

Flagellates of this group infect the intestine of humans and animals causing villous flattening and dysfunctional microvilli.[89] *G. lamblia* trophozoites live in the human duodenum and develop into infective cysts that are shed in feces. Once ingested, the low pH of gastric juice triggers excystation. In the duodenum pancreatic proteases stimulate the emergence of trophozoites, and mucus and bile provide a supportive coat for these new forms. Large numbers of organisms are present in biopsies and are easily found during ultrastructural analysis.[90] Trophozoites are pear-shaped when viewed en face but are apt to be in a sickle form in cross section. The concave surface has a brush-like sucker plate that is diagnostic (Fig. 15.8). Attachment to the intestine is mediated via parasite surface lectins and the plasma membrane over microvilli.[91,92]

Trophozoites of *Giardia* have a special organelle for attachment, the **ventral disk** (adhesive disk).[93,94] Ventral disks contain fatty acid-binding proteins. Microbial symbionts such as viruses and bacteria have been described ultrastructurally in the cytoplasm of trophozoites and cyst forms of *Giardia* spp., but have not been implicated in the infectious process in mammals.[95]

Giardiasis is less common in the young. *G. lamblia*-specific IgA antibodies occur in milk of mothers in mice, and suckling mice are protected from infection if fed milk from immune mothers. Lipases and free fatty acids in milk are giardiacidal.[96] During storage of human and bovine milk at 4°C a bile salt-independent lipolysis occurs due to lipoprotein lipase.

Vet-ebooks.com

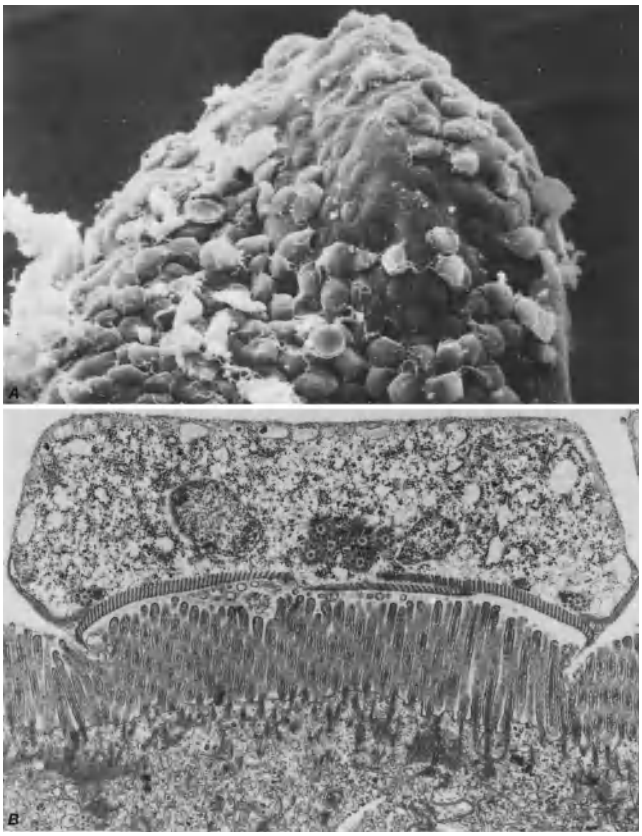


Fig. 15.8 Giardiasis: rat small intestine. **A**. **Flagellated trophozoites**: attached trophozoites cause circular, dome-shaped lesions in microvillous border, visible at sites where protozoa have been dislodged; scanning electron micrograph, apical portion of villous. **B**. **Adhesive disk of parasite at microvillous border of host**: transmission electron micrograph of A. (Micrograph: S. L. Erlandsen, *Am J Clin Nutr* 27:1277, 1974.)

Murine models of giardiasis have shown that gut-associated lymphoid tissue is the primary barrier to infection. Giardia in the gut lumen induce macrophages to pass from villous lamina propria through the basement membrane to capture organisms from epithelium. Pseudopods extend from macrophages and penetrate between columnar epithelial cells to engulf trophozoites. Lymphocytes form rosette patterns around macrophages that ingest giardia.[97] Athymic nude mice kill organisms but are unable to clear the infection until they are reconstituted with T cells.

Genus *Trichomonas*

The Trichomonadidae are anaerobic parasites, and thus lack mitochondria. They have three to five anterior flagellae, an axostyle, and an undulating membrane. The **hydrogenosome**, a membrane-bound granule, contains enzymes that participate in the metabolism of pyruvate formed in glycolysis, and is the site of hydrogen formation. Hydrogenosomes have, as do mitochondria, circular DNA, cardiolipins, and superoxide dismutase.[98–100]

Trichomoniasis

Trichomonas vaginalis causes human genital inflammation characterized by edema and erythema of the mucosa. There is a predilection for the vagina of postpubertal women and for the urethra of males. On adhesion to host cells, *T. vaginalis* switches to an amoeboid form rich in actin microfilaments, a process that involves **coronin**.[101] *T. vaginalis* is small, 15–18 μm, and organisms are difficult to find in tissue. There is a single posterior flagellum with an axostyle and an undulant membrane. Causing disease only in a small percent of infected patients, *T. vaginalis* appears to be synergistic with superinfected bacteria.

T. gallinarum parasitizes the cecum of chickens and causes enteritis with organisms in the crypt lumen. Ultrastructurally, damaged epithleial cells show loss of microvilli and glycocalyx, and increased numbers of vesicles in the cytoplasm.[102] In primates, trichomonads may cause gastritis and other lesions in animals weakened by immunosuppressive viruses.[103]

Genus *Tritrichomonas*

Tritrichomonas foetus is a pathogenic protozoan of the urogenital tract, placenta and fetus of cattle.[104] *T. foetus* also infects the colon of cats, in which it is associated with diarrheal disease (feline isolates will infect cattle). Surfaces of *T. foetus* bear special arrays of intramembranous particles localized in the the membrane of the anterior flagella that are important in attachment.[105] Freeze-fracture studies have documented the surface morphology and distribution of intramembranous particles.[106]

Genus *Spironucleus* (*Hexamita*)

Spironucleus spp. cause disease in fish, amphibians, birds, and mammals. Cysts of *Spironucleus* spp. are oval with filamentous walls 0.3–0.5 μm thick and closely resemble those of *Giardia*.[107] Trophozoite structure is distinctive. *S. meleagridis* causes catarrhal enteritis in young turkeys and has been reported in pheasants, quail, and many species of wild birds.

Genus *Histomonas*

Histomonas meleagridis is a flagellate parasite of the cecum of turkeys, wild birds, and chickens. In the former two it causes enterohepatitis (blackhead). In

Vet-ebooks.com

the cecum, trophozoites penetrate the mucosa and incite a purulent inflammatory response with erosions of the mucosa. Trophozoites enter venules of the hepatic portal vein and are transported to the liver where they enter hepatocytes and replicate. Lesions progressively expand to cause foci of necrosis with organisms at the margins.[108]

Hemosporidians

All members of the phylum **Apicomplexa** are parasitic and some have developed the capacity to invade host cells. These organisms possess an apical complex that includes rhoptries, micronemes, a conoid, and polar ring associated with microtubules.

Genus *Babesia*

Babesia spp., members of the suborder Piroplasmidea, are small (1–5 μm), elongate, tick-transmitted, intraerythrocytic protozoan parasites of animals and man. Ultrastructurally, *Babesia* spp. are limited by a plasma membrane and contain endoplasmic reticulum, Golgi complexes, and food vacuoles (Fig. 15.9). They cannot survive outside the host because feeding, development and reproduction require nutritional or environmental factors provided by the cell. Some *Babesia* spp. prefer reticulocytes for replication, reflecting a need for mitochondrial energy.[109] *B. equi* differs from other babesia in that it infects lymphocytes of its host, the horse.[110]

Erythrocyte penetration occurs by attachment and invasion into the cytoplasmic matrix.[111,112] Inside the erythrocyte, *Babesia* spp. replicate by a modified form of schizogony; the pleomorphic offspring range from round to cigar-shaped forms, with central or peripheral nuclei. Erythrocyte destruction occurs by direct action of the parasite, but anemia is often out of proportion to the number of parasitized red cells caused by a late destructive immunologic reaction. Intravascular agglutination of parasitized erythrocytes in capillaries of the myocardium may lead to severe disease and death, espeically in immunosuppressed animals.

Replication forms in ticks differ from organisms in erythrocytes (Table 15.3).[113] During feeding by ticks, the peritrophic membrane in the midgut sequesters ingested blood and organisms into the endoperitrophic space (true lumen). *Babesia* spp. are equipped with a specialized organelle, the arrowhead, pass the plasma membrane and enter the ectoperitrophic compartment by release of enzymes from the arrowhead.[114] In late stages of tick infection, sporozoites form in the salivary glands.

Merozoites of babesia are small (1–5 μm), elongate, and covered by a plasma membrane with interrupted membranes beneath it. In the anterior region, organelles that comprise the **apical complex** include polar rings, micronemes, and rhoptries. **Rhoptries** are electron-dense, teardrop-shaped structures. **Micronemes** are small, osmophilic bodies around the rhoptries. The free, extracellular merozoite is covered by a surface coat composed of fibrils that adhere to the plasma membrane. As the merozoite enters the erythrocyte, the surface coat disappears.

Babesiosis

Human babesiosis caused by *Babesia microti* appears as a subacute febrile illness ("summer flu" with headache, fever, and myalgia) along the northeastern coast of North America. An accidental host in the deermouse cycle, humans are infected when this protozoan is transmitted by nymphal stages of the bite of the tick *Ixodes damini*. Erythrophagocytosis is marked but no pigment is produced. *B. rodhaini* causes similar syndromes.

Texas cattle fever due to *Babesia bigemina* is a severe hemolytic disease with fever and hemoglobinuria. Infected female ticks feed on cattle, injecting sporozoites into the bloodstream. These enter erythrocytes and change into ring-shaped structures, then progresively transform into amoeboid trophozoites. They multiply by budding to produce two pyriform bodies that are attached at one end but later separate. Parasitemia occurs when organisms break out of red cells. They infect others to initiate succeeding asexual cycles of schizogony. Parasitemia and relapse occur at irregular intervals.

Genus *Theileria*

The *Theileria* are tick-borne, protozoan parasites that infect both wild and domestic animals throughout much of the world. Ultrastructure of developmental forms is consistent with the apicomplexan hemosporidia.[115,116]

Theileriosis

T. parva causes an acute febrile and often fatal disease of cattle in east Africa known as **East Coast fever**. The parasite causes marked alterations in the lymphoid system in which it replicates.[117] During the acute febrile stage, large numbers of parasitized lymphocytes circulate in the vascular system. Cerebral localization of parasitized leukocytes causes the nervous signs responsible for the name "turning disease". Infarction of the liver and kidney causes perivascular infiltration

Vet-ebooks.com

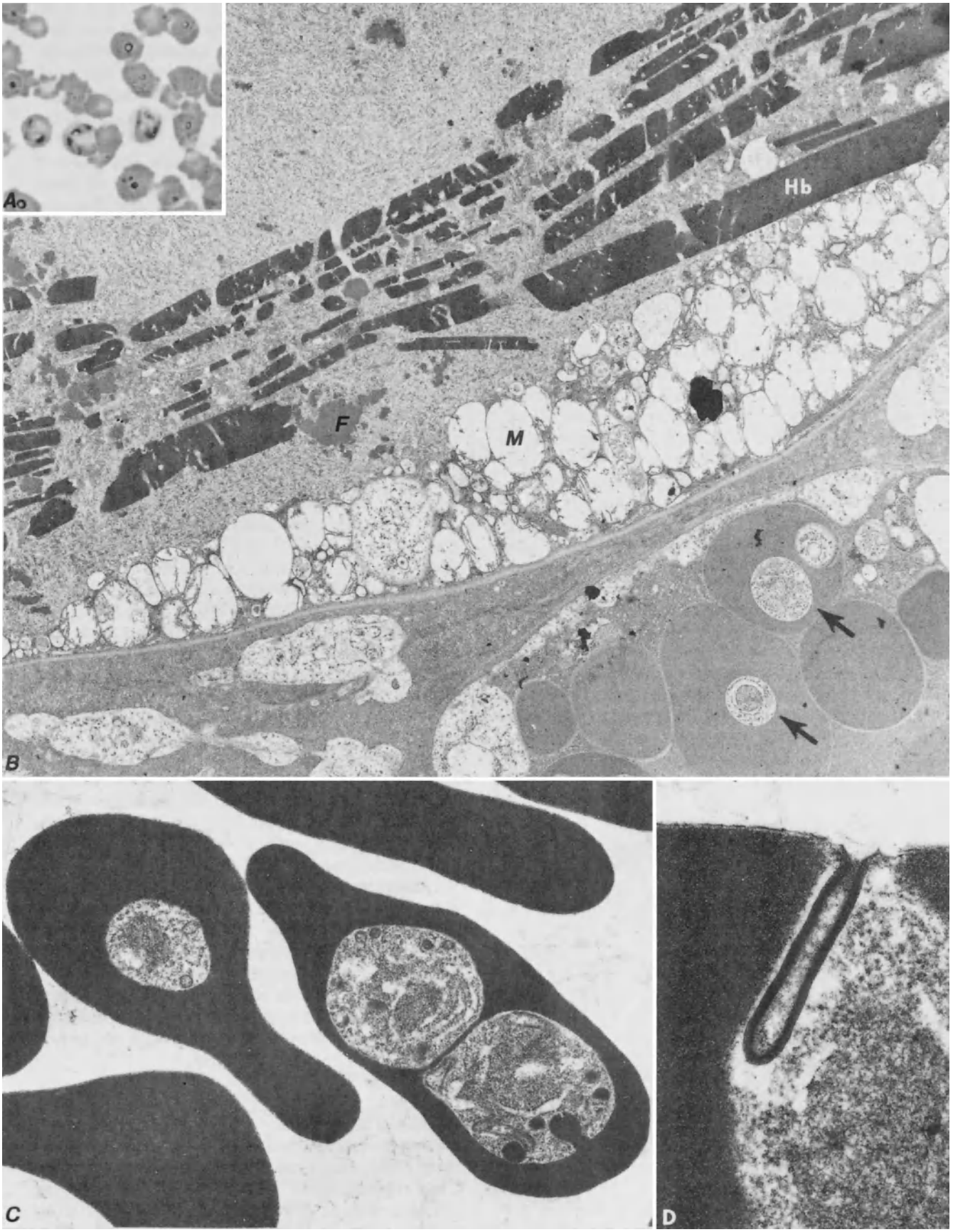


Fig. 15.9 ***Babesia equi***: erythrocytes, horse. **A**. Erythrocytes bearing protozoa. **B**. **Kidney**: renal tubular epithelium is necrotic, with vacuoles and swollen mitochondria (*M*). Hemoglobin crystals (*Hb*) and fibrin (*F*) in tubular lumen. **C**. **Intraerythrocytic *B. equi***. **D**. **Feeding tubule of *B. equi***: tubule opens to erythrocyte surface. (Micrographs B and D: James Proctor, National Animal Disease Center.)

Vet-ebooks.com

Table 15.3 Pathogenic apicomplexans.

Pathogen	*Change*	*Reference to ultrastructural pathology*
		Genus *Babesia*
Babesia argentina		**Wright**, *Int J Parasitol* 2:209, 1972 (brain)
B. bigemina	Tick	**Weber**, *Z Parasitenkd* 53:83, 1977 (gut)
B. bovis	Cow	**Potgieter**, *Onderstepoort J Vet Res* 43:1, 1976 (insect)
B. caballi	Cow	**Simpson**, *Am J Vet Res* 28:1693, 1967
	Tick	**Ribeiro**, *J Invertebr Pathol* 93:183, 2006
B canis	Dog	**Colly**, J So Afr Vet Med Ass 63:36, 1992; **Ewing**, *Am J Vet Res* 26:727, 1965; **Simpson**, *Am J Vet Res* 35:701, 1974 (neutrophil); **Buettner**, *Z Tropenmed Parasitol* 19:330, 1968
B. divergens	Cow	**Zintl**, *Clin Microbiol Rev* 16:622, 2003 (review)
	Rabbit	**Spencer**, *J Parasitol* 92:333, 2006
	Experimental	**Winger**, *Parasitol Res* 76:573, 1990
B. duncani	Human	**Conrad**, *Int J Parasitol* 36:779, 2006
B. equi	Horse	**Holbrook**, *J Am Vet Med Ass* 29:277, 1968; **Moltmann,** *J Parasitol* 69:111, 1983 (erythrocytes); **Simpson**, *Am J Vet Res* 28:1693, 1967; **Simpson**, *Am J Vet Res* 31:1763, 1971 (liver); **Simpson**, *Am J Vet Res* 41:267, 1980 (imidocarb Rx)
	Tick	**Moltmann,** *J Protozool* 30:218,1983 (salivary gland)
B. gibsoni	Coyote	**Roher**, *Am J Vet Res* 46:256, 1985 (blood)
	Dog	**Fukumoto**, *Int J Parasitol* 35:1031, 2005;† **Radi**, *J Vet Diagn Invest* 16:229, 2004
B. microti	Rodent	**Melhorn**, *Dtsch Tierarztl Wschr* 93:377, 1986; **Rudzinska**, *Cell Tissue Res* 169:323, 1976 (blood)
	Tick	**Rudzinska**, *J Protozool* 30:338, 1983 (gut epithelia)
B. ovata		**Kawai**, *Jap J Vet Sci* 48:943, 1986
B. ovis	Sheep	**Simpson**, *Am J Vet Res* 31:1763, 1971; **Simpson**, *Am J Vet Res* 35:701, 1974
	Tick	**Friedhoff**, *Z Parasitenkd* 30:347, 1968; **Friedhoff**, Z Parsitenkd 38:132, 1972 (salivary gland); **Moltmann,** *J Protozool* 29:30, 1982 (ovary)
B. rodhaini	Mouse	**Rudzinska**, *J Protozool* 9:279, 1962 (blood)
***Babesia* (unclassified)**	Dog	**Lehtinen**, *Vet Parasitol* 151:150, 2008; **Loretti**, *Vet Parasitol* 134:193, 2005 (endothelium)
	Hamster (*B. Wasington-1*)	**Braga**, J Parasitol 92:1104, 2006 (human origin)
		Genus Haemogregarina
Haemogregarina myoxocephali	Fish	**Siddall**, *J Prot* 39:545, 1992
		Genus *Hemoproteus*
Hemoproteus columbae	Pigeon	**Bradbury**, *J Protozool* 15:700, 1968 (microgametes); **Bradbury**, *J Protozool* 18:679, 1971 (merozoites); **Bradbury**, *J Protozool* 19:43, 1972 (schizonts)
	Insect	**Klei**, *J Protozool* 19:281, 1972 (sporosoites)
H. metchnikovi	Turtle	**Sterling**, *J Protozool* 19:69, 1972; **Sterling**, *J Parasitol* 58:641, 1972 (spleen)
		Genus *Hepatocystis*
***Hepatocystis* sp.**		**Garnham**, *Trans Roy Soc Trop Med Hyg* 61:58, 1967
		Genus *Hepatozoon*
Hepatozoon americanum	Dog	**Cummings**, *Vet Pathol* 42:788, 2005
		Genus *Icthyobodo*
Icthyobodo necatur		**Roubal**, *J Fish Dis* 10:181, 1987 (fish blood)
		Genus *Leucocytozoon*
Leucocytozoon caulleryi		**Morri**, *J Prot* 39:281, 1992 (chicken spleen)
L. simmondi		**Desser**, *Can J Zool* 48:641, 1970
L smithi		**Siccardi**, *Avian Dis* 18:21, 1974
L ziemanni		**Kocan**, *J Parasitol* 64:1057, 1978

Vet-ebooks.com

Table 15.3 *Continued*

Pathogen	*Change*	*Reference to ultrastructural pathology*
L. sp		**Aikawa**, *J Ultrastr Res* 32:43, 1970; **Dessar**, *J Parasitol* 65:737, 1979 (penguin); **Milhous**, *Poult Sci* 52:2138, 1973 (turkey blood); **Trefiak**, *J Protozool* 20:73, 1973 (bird blood)
		Genus *Nuttalia*
Nuttalia microti		**MacMillan**, *Res Vet Sci* 12:185, 1971
		Genus *Theileria*
Theileria annulata		**Melhorn**, *Z Parasitenkd* 48:137, 1975 (insect gut); **Schein**, *Tropenmed Parasitol* 28:349, 1977 (cow erythrocytes)
T. parva		**Jarrett**, *J Protozool* 13:301, 1966 (cow, lymph node); **Moulton**, *Lab Invest* 24:187, 1971; **Buettner**, *Z Tropenmed Parasitol* 18:245, 1967
T. mutans		**Buettner**, *Z Tropenmed Parasitol* 17:397, 1966 (erythrocyte)
T velifera		**van Vorstenbosch**, *Res Vet Sci* 24:214, 1978

†Animal model.

and proliferation of lymphocytes. Development of *Theileria* spp. in **erythrocytes** has also been documented.[118]

The infective form of *T. parva*, the sporozoite, develops within the **tick salivary gland** and is transmitted to the bovine host when the tick, *Rhipicephalus appendiculatus*, feeds. The parasite colonizes just one specific cell type in the tick salivary gland, causing the cell to expand markedly as replication occurs.[119] Replication is accompanied by massive production of glycogen, which is used by the parasite in later stages.

After infecting the cow, sporozoites enter a subpopulation of bovine **T and B lymphocytes** by a specific parasitic ligand-host cell receptor mechanism. Attachment is followed by the formation of a close continual junction between membranes of parasite and lymphocyte (Fig. 15.10). The closely apposed membranes are separated by a thin 6 nm thick dense layer of material. The movement of the sporozoite into the lymphoycte involves a progressive circumferential "zippering" of the apposed membranes and a loss of sporozoite surface coat.

The parasite, at first enclosed in a phagosomal vacuole, escapes to reside free in the cytoplasmic matrix. This process occurs concurrently with the discharge of the contents of the sporozoite rhoptries and microspheres. The intracytoplasmic parasite is covered by a layer of sporozoite-derived filamentous material to which host cell microtubules rapidly adhere. The sporozoite differentiates into the multinucleate schizont stage. In the process the schizont induces and maintains host cell blastogenesis leading to a rapid clonal expansion of parasitized cells.[120]

Infected lymph nodes develop many germinal centers, paracortical lymphocytic hyperplasia, and plasmacytosis. Large numbers of parasitized lymphoblasts occur in the paracortical zones, sinuses, medullary cords, and stroma.[121,122] Mitotic activity in host lymphoblasts, initiated by infection, is required for the development of schizonts. Infected lymphoblasts are filled with free ribosomes, parasites and few other orgnalles.

Genus *Cytauxzoon*

Diseases caused by *Cytauxzoon* spp. occur in ungulates of southern Africa and in domestic and wild cats. Intraerythrocytic forms (<5% of erythrocytes) appear in the bloodstream after development of fever. Numerous large macrophages with intracytoplasmic schizonts containing multiple small, basophilic, granular bodies are the characteristic histologic finding. The granular bodies are merozoites in various stages of development. The ultrastructure of *Cytauxzoon felis* in intraerythrocytic stages includes single and multiple organisms.[123–125] Individual parasites may be connected. Parasitized erythrocytes are deformed and may contain crytalloids of denatured hemoglobin.

In fatal cytauxzoonosis of cats, marked fever and anemia may be accompanied by icterus. Infected macrophages may be found in veins and sinusoids in lung, spleen, lymph nodes and bone marrow; they may occur in any other organ.

In the liver, schizony occurs in the cytoplasm of large macrophages lodged in sinusoids.[124] Parasitized macrophages block sinusoids and may occlude small central veins. The earliest stage of schizogony is a single, multilobed schizont that contains nonplicated mitochondria. The progressive lobulation leads to

Vet-ebooks.com

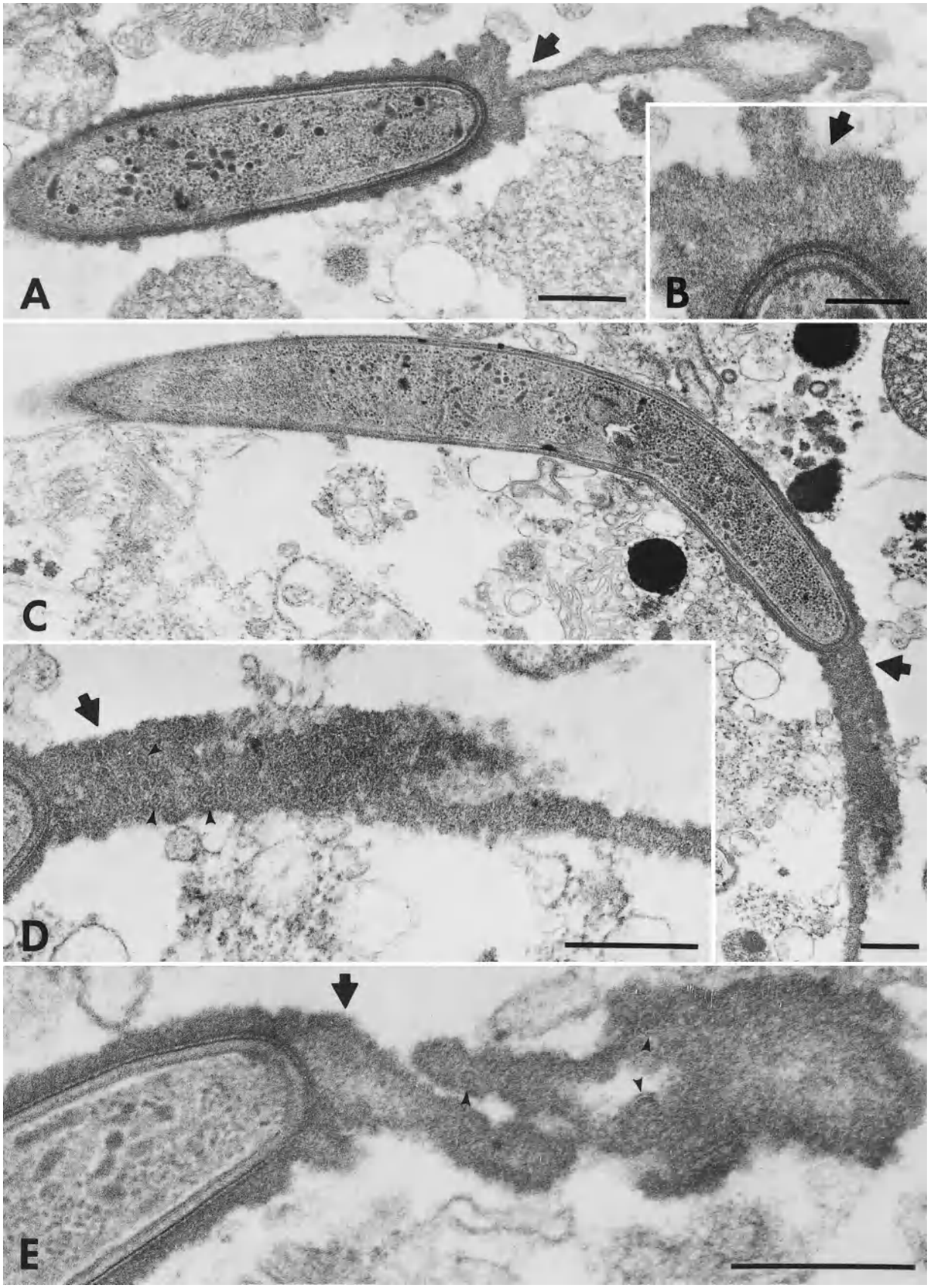


Fig. 15.10 ***Plasmodium berghei***: sporozoites form the circumsporite protein (CSP) reaction (*arrows*) that trails from the posterior end. **A–C**. **Pellicular membranes** at sporozoite's posterior end are covered with reaction product. **D–E**. **Tightly packed vesicle-like particles** form the matrix of the CSP reaction. Bars = 0.5 µm (except in B, bar = 0.2 µm). (Micrograph: Michael J. Stewart, *J Protozool* 38:411, 1991.)

Vet-ebooks.com

production of daughter cells.[126] The infected macrophage increases in size, the nucleus becomes highly irregular with large nucleoli, and the cytoplasm is devoid of organelles except for those of the parasite.

Genus *Babesiosoma*

Babesiosoma spp. (which produce four merozoites) and *Dactylosoma* spp. (which produce more than four) are intraerythrocytic apicomplexans of cold-blooded vertebrates, especially of amphibians and fish. Primary merogany of *B. stableri* begins when a merozoite enters a frog erythrocyte. It undergoes nuclear divisions to form the cruciform meronts typical of the species. Four merozoites bud from the meront surface and separate without forming a residual body. Infecting new erythrocytes, these secondary merozoites repeat the cycle or form gametes. Gamonts are ingested by leeches where they develop progressively in crop, intestine, and salivary gland. Sporozoites are injected into a new frog host. The ultrastructure of intraerythrocytic merozoites of *B. stableri* have a large nucleus and perinuclear Golgi complex, and develop within a parasitophorous vacuole.[127]

The Malarial Organisms

Genus *Plasmodium*

Plasmodium spp., the cause of malaria of reptiles, birds, and mammals, require two hosts for survival: an invertebrate, in which sexual reproduction occurs, and a vertebrate, in which they multiply asexually.[128] A bite by an infected female mosquito introduces sporozoites into the vertebrate host. Sporozoites are antigenically distinct from all subsequent development forms, and during the passage from the injection site in skin to liver they are susceptible to the host immune system (Table 15.4).

Malaria

Malaria is caused by asexual merozoites that replicate during the erythrocytic stage of the life cycle. Four species cause human malaria: *P. vivax*, *P. ovale*, *P. malariae*, and *P. falciparum*. Disease is transmitted by a dozen species of *Anopheles* mosquitos. Fever, weakness, and anemia are the clinical signs. The characteristic periodic fever results from the synchronous release of merozoites and toxic peptides produced by plasmodia. The first two species cause less serious disease with fever spikes 48 hrs apart (benign tertian malaria). In *P. malariae* infections, fever spikes occur at 72-hr intervals (benign quartan malaria). *P. falciparum*, responsible for greatest mortality, causes fevers of 48-hr periodicity (malignant tertian malaria).

Malaria begins in an **extraerythrocytic phase**, which is initiated by infection of different tissues in different species of animal. In birds, the monocyte-macrophage system is usually involved; in mammals, the liver. During this phase, the organism goes through several asexual reproductions. Sporozoites transform to trophozoites, to multinucleate schizonts, and finally to mature schizonts. The end result is an immense host cell containing unicellular merozoites. On their release, the extracellular merozoites then either invade new cells and repeat the extraerythrocytic cycle or begin the **erythrocytic phase** by infecting red blood cells.

Insect Cycles Female mosquitos are infected with *Plasmodium* spp. during feeding on parasitized hosts. Plasmodia in the blood meal pass to the posterior midgut where they are exposed to digestive enzymes. To bind to mosquite midgut epithelium, **ookinetes** use chondroitin sulfate proteoglycans.[129] Ookinetes invade epithelial cells by rupturing the cell membrane using a microneme protein with membrane-attack complex-perforin (MACPF)-related domains, the membrane-attack ookinete protein is produced in the ookinete stage and plays a critical role in midgut invasion.[130] Ookinetes possess **microneme secreteory organelles** that mediate locomotion and midgut wall egress to establish sporogonic stages and subsequent transmission. Ookinete proteins (such as chitinase, circumsporozoite, and TRAP-related proteins) are important in successful completion of midgut replication.[131]

Within the insect gut, the **peritrophic membrane** divides the gut into ecto- and endoperitrophic (lumen) spaces; that is, it forms a cylindrical sheet that separates the midgut contents from the single cell midgut epithelium, and functions to separate digestive events within the midgut. Ingested plasmodia are retained in the endoperitrophic spaces where proteases destroy some of the stages of the parasite; others survive and pass into the hemocoel. The presence or absence of the peritrophic membrane, or its thickening due to food intake, can have an enhancing or suppressing effect on the extent of infection of the mosquito.[132]

In the midgut lumen of the mosquito, plasmodial **gametocytes** are transformed to gametes, and fertilization of female by male **gametes** takes place.[133] The resulting **ookinetes** cross the midgut wall to become **oocysts**, which will eventually produce **sporozoites** in the salivary gland of the mosquito.[134]

Extraerythrocytic Phase: The Hepatocyte After inoculation by the mosquito, **sporozoites** rapidly enter the bloodstream of the new host. They release **circumsporite protein** and other proteins that move along the parasite surface and are released at the trailing or

Vet-ebooks.com

Table 15.4 Pathogenic plasmodia.

Pathogen	*Host*	*Reference to ultrastructural pathology*
		Genus *Plasmodium*
Plasmodium berghei	Mammals	**Aikawa**, *J Parasitol* 57:603, 1971; **Bodammer**, Lab Invest 28:708, 1973 (blood); **Howells**, Ann Trop Med Parasitol 64:305, 1970; **Yamada**, *Jap J Vet Sci* 34:297, 1972 (blood)
	Rodent	**Boonpucknavig**, *Am J Pathol* 70:89, 1973 (kidney); **Jap**, *Parasitology* 85:263, 1982 (rat liver); **Ladda**, *J Parasitol* 55:633, 1969 (mouse blood); **Meis**, *J Protozool* 30:361, 1983 (rat liver); **Polder**, *J Neurol Sci* 101:24, 1991 (mouse brain); **Seed**, *J Protozool* 20:603 (rat blood); **Tegoshi**, *Am J Trop Med Hyg* 47:643, 1992 (rat placenta); **Terzakis**, J Protozool 26:385, 1979 (rat Kupffer cell)
	Insect	**Davies**, *Ann Trop Med* Par 68:283, 1974
P. chabaudi	Mouse	**Kelly**, *J Protozool* 16:354, 1969 (blood); **Scalzi**, *J Ultrastruct Res* 24:116, 1968
P. coatneyi	Monkey	**Miller**, *Exp Parasitol* 32:86, 1972 (blood); **Rudzinska**, *J Protozool* 15:73, 1968 (blood)
P. cynomolgi	Monkey	**Sodeman**, *Science* 170:340, 1970 (exoerythrocytic); **Terzakis**, *J Protozool* 18:62, 1971 (mosquito)
P. elongatum		**Aikawa**, *J Cell Biol* 34:229, 1968 (asexual stages)
P falciparum	Human	**Aikawa**, *Am J Trop Med Hyg* 35:30, 1986 (erythrocyte); **Cerami**, *Cell* 70:1021, 1992 (liver); **Leech**, *J Cell Biol* 98:1256, 1984 (erythrocyte); **Luse**, *Am J Trop Med Hyg* 20:655, 1971 (heart); **Miller**, *Trans R Soc Trop Med Hyg* 66:459, 1972; **Trager**, *J Protozool* 31:562, 1984;* **Winograd**, *J Cell Biol* 108:23, 1989
	Experi-mental	**Feng**, *J Exp Med* 177:273, 1993 (genes);* **Culvenor**, *J Protozool* 37:59, 1990 (S antigen);* **Kara**, *Eur J Cell Biol* 46:9, 1988 (parasitophorous vacuole); **Yayon**, *J Protozool* 31:367, 1984 (chloroquine Rx)
	Insect	**Sinden**, *Proc R Soc Lond B* 201:375, 1978
P. fallax		**Aikawa**, *Am J Trop Med Hyg* 15:449, 1966; **Aikawa**, Am J Trop Med Hyg 17:156, 1968 (liver); **Aikawa**, *J Cell Biol* 35:103, 1967; **Hepler**, *J Cell Biol* 30:333, 1966
P. gallinaceaum	Bird	**Aikawa**, *Am J Trop Med Hyg* 17:156, 1968 (liver); **Aikawa**, *J Protozool* 31:403, 1984 (gametogenesis); **Ristic**, *J Trop Med Hyg* 67:509, 1964 (erythrocyte); **Swann**, *Exp Parasitol* 33:79, 1973 (anemia)
	Insect	**Terzakis**, *Mil Med J Cell Biol* 34:311, 1967 (mosquito); **Torii**, *J Protozool* 39:449, 1992 (midgut epithelium)
P. knowlesi	Human	**Aikawa**, *Zt Zellforsch* 100:271, 1969 (blood); **Bannister**, *J Protozool* 36:362, 1989; **Torii**, *Infect Immun* 57:3230, 1989 (erythrocyte)
P lophurae	Mouse	**Beaudoin**, *Exp Parasitol* 34:313, 1973;* **Bodammer**, *Lab Invest* 28:708, 1973 (mouse blood)
P malariae		**Atkinson**, *J Protozool* 34:267, 1987
P. ovale	Human	**Matsumoto**, *Am J Trop Med Hyg* 35:697, 1986
P. tropiduri	Lizard	**Scorza**, *Parasitology* 63:1, 1971 (blood)
	Bird	**Sterling**, *J Protozool* 20:81, 1973 (blood)
P. vinckei		**Scalzi**, *J Ultrastr Res* 24:116, 1971 (blood)
P. vivax	Human	**Djaldetti**, *Acta Haematol* 72:121, 1984 (erythrocyte)
	Monkey	**Lanners**, *Zt Parasitenkd* 77:395, 1991 (erythrocyte)
Plasmodium spp.		**Langreth**, *J Protozool* 20:606, 1973*
		Genus *Leucocytozoon*
Leucocytozoon caulleryi	Chicken	**Morii**, *J Protozool* 39:281, 1970; **Morii**, *Zentralbl Bakt Mikrobiol Hyg A* 250:198, 1981
L. dubreuili	Robin	**Wong**, *J Protozool* 25:302, 1978
L. simondi		**Desser**, *Can J Zool* 51:605, 1973 (hepatic schizogony); **Desser**, *Can J Zool* 48:417, 1970 (megaloschizogony)
L. smithi	Turkey	**Milhous**, *Poult Sci* 52:2138, 1973 (gametocytes)**; Steele**, *J Protozool* 39:530 and 690, 1992
L. ziemanni		**Kocan**, *J Parasitol* 64:1057, 1978
		Genus *Haemoproteus*
Haemoproteus columbae		**Bradbury**, *J Protozool* 17:405, 1972; **Bradbury**, *J Protozool* 18:679, 1971; **Klei**, *J Protozool* 19:281, 1972 (sporozoites)
H. meleagridis	Turkey	**Atkinson**, *J Protozool* 33:375, 1986; **Atkinson**, *J Parasitol* 75:135, 1989
H metchnikovi		**Sterling**, *J Parasitol* 58:641, 1972

*Studies in vitro.

Vet-ebooks.com

posterior end of the motile sporozoites.[135–138] Within an hour after they enter the bloodstream, sporozoites invade the liver. The circulating sporozoite is rapidly taken up by Kupffer cells and many are destroyed.[139,140] Survivors pass into the perisinusoidal spaces, and attach to and enter hepatocytes via receptors for circumsporozoite protein on the basolateral domain of the hepatocyte plasma membrane. Using immunogold techniques on human liver, binding is restricted to these sites, and is not found in other tissues or even at other locations on the hepatocyte.[141,142] Ultrastructurally, infected hepatocytes under acute cell swelling are filled with the large developing protozoal forms. Organisms are typically found in vacuoles located adjacent to the biliary canaliculi. Early in infection the cell is little altered but later the hepatocyte may undergo lysis. Merozoites are released from the liver and circulate to invade erythrocytes.

The **merozoite** is approximately 2×1.5 μm and has, at one end, an apical prominance, a pair of rhoptries, and micronemes. Proteins of the apical regions of plasmodial merozoites have been localized by immunoelectron microscopy.[143] Merozoites and sporozoites, the infective forms, possess a **conoid**, a specialized structure used for attachment. Penetration is initiated on contact of the conoid with the erythrocytic plasma membrane. A depression is created and develops into a cavity that eventually encloses the parasite without disrupting the plasma membrane.

Erythrocyte Phase During **invasion** of the erythrocyte, plasmodial **merozoites** bind to and deform the erythrocytic plasma membrane. The primary interaction site on the red cell surface is the oligosaccharide portion of the band 3 protein.[144] Ultrastructural studies reveal several distinct interactions: (1) **attachment**, mediated by erythrocyte surface band 3 protein and sialic acid, (2) **junction formation** between the anterior end of the merozoite and the plasma membrane of the erythrocyte, (3) **invagination** of erythrocyte surface by the parasite with progressive entry using a zippering mechanism, and (4) **parasitophorous vacuole** formation with sealing of the surface entry wound.[145,146]

The junctional zone, as determined by freeze-fracture studies of the erythrocyte membrane, is associated with a closely packed assembly of intramembranous particles. As invasion proceeds, the junctional zone rapidly changes from a cap on the erythrocyte surface to a constricting ring through which the merozoite enters an endocytic vacuole of the host cell (Fig. 15.11). The ring moves around the parasite as it enters the cell, forming new areas of tight junction over the entering parasite surface while deleting old tight junction areas on the membrane of the developing parasitophorous vacuole.[147]

Invasion of erythrocytes is facilitated by materials released form the parasite. Contents of **rhoptries** are injected into the erythrocytic membrane leaving foci of membranous whorls and membrane debris.[148,149] After entry, dense granules (microspheres) move to the pellicle of the parasite and release their contents into the newly formed **parasitophorous vacuole**.[150]

The erythrocytic phase is facilitated and prolonged in some species of *Plasmodium* by concentration of infected erythrocytes in the **bone marrow.** Here they attach to venular endothelium and move to have access to developing reticular cells.[151] Merozoites can thereby infected new cells without exposure to antibodies and other anti-plasmodial substances that circulate in the bloodstream. The **spleen** traps parasitized erythrocytes and, although it may be a site of intraerythrocytic replication, is more apt to function in the destruction of parasites.[152] Damaged erythrocytes and parasite pigments are removed by the spleen. Splenomegally (with congestion, reticuloendothelial hyperplasia, and pigment deposits) is a hallmark of malaria.

Parasite development within the red blood cell begins as the membrane-bound **merozoite** transforms and dedifferentiates. Erythrocytes infected with vivax-type plasmodia develop stippling (Schuffner's dots) which ultrastructurally are complexes of plasmalemmal vesicles that form at the cell surface.[153] **Maurer's clefts** are parasite-derived structures within the host cell cytoplasm that functions in protein sorting and trafficking between the parasite and host cell plasma membrane. They are flat structures with transparent lumens and electron-dense coats that extend from outside the parasite to the erythrocyte membrane.[154] They bud from the parasitophorous vacuole membrane and move to the host cell periphery.[155] Maurer's clefts are involved in transfer of proteins (as aggregates, not in vesicles) that attach to the host cell cytoskeleton and facilitate transformation of the disk-shaped erythrocyte into a rounded, rigid infected cell that is able to adhere to endothelium.[156–158]

The parasite transforms. Its pellicle loses the thick inner membrane but remnants of endoplasmic reticulum and caveolae-vesicle complexes persist. The conoid and paired organelles disappear, initiating the development of the trophozoite. **Trophozoites** that become closely associated with the erythrocyte membrane cause marked deformation of the cell surface with formation of small bullae and vesicles that protrude from the cell.[159] **Trophozoites** are capable of feeding and growth, and they begin the asexual replicative cycle. **Schizogony** occurs and ends when new merozoites bud from the mother schizont.[160,161]

As new merozoites bud from mother schizonts, the erythrocyte becomes irregular and pale. Daughter merozoites feed by lysis of the erythrocyte, probably

Vet-ebooks.com

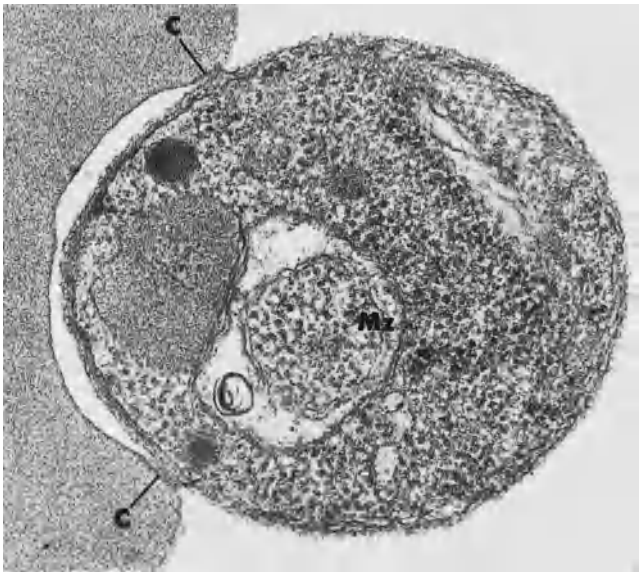


Fig. 15.11 Erythrocyte invasion by *Plasmodium*: advanced stage of erythrocyte entry by a merozoite (*Mz*). There is junctional attachment (*C*) at each side of the invasion orifice. (Micrograph: M. Aikawa, *J Cell Biol* 77:72, 1976.)

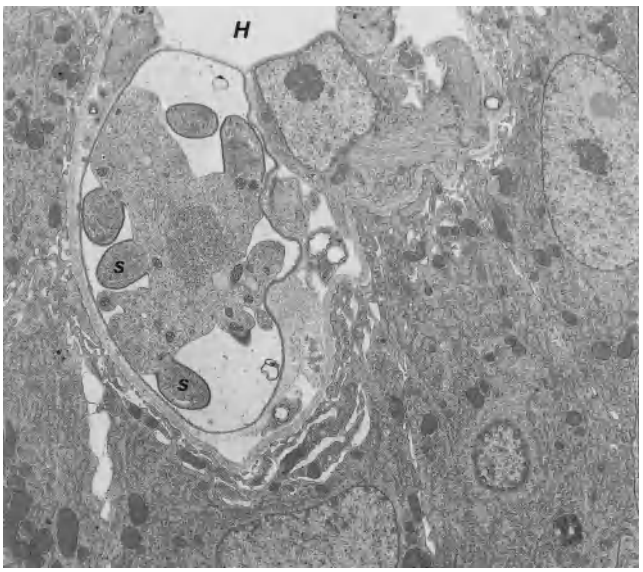


Fig. 15.12 *Leucocytozoon smithi*: sporogony in midgut epithelium of the black fly. Oocyst in hemocoel (*H*) has sporozoite buds (*S*) projecting from the sporoblastoid into the oocyst cavity. (Micrograph: Edna J. Steel, *J Protozool* 39:530, 1992.)

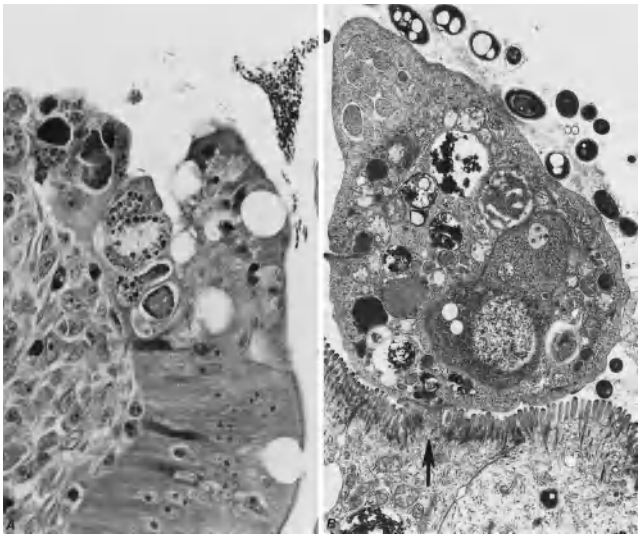


Fig. 15.13 *Eimeria* sp.: intestine. **A**. **Various forms in absorptive enterocytes** (histology). **B**. **Merozoite:** bound to epithelial cell surface.

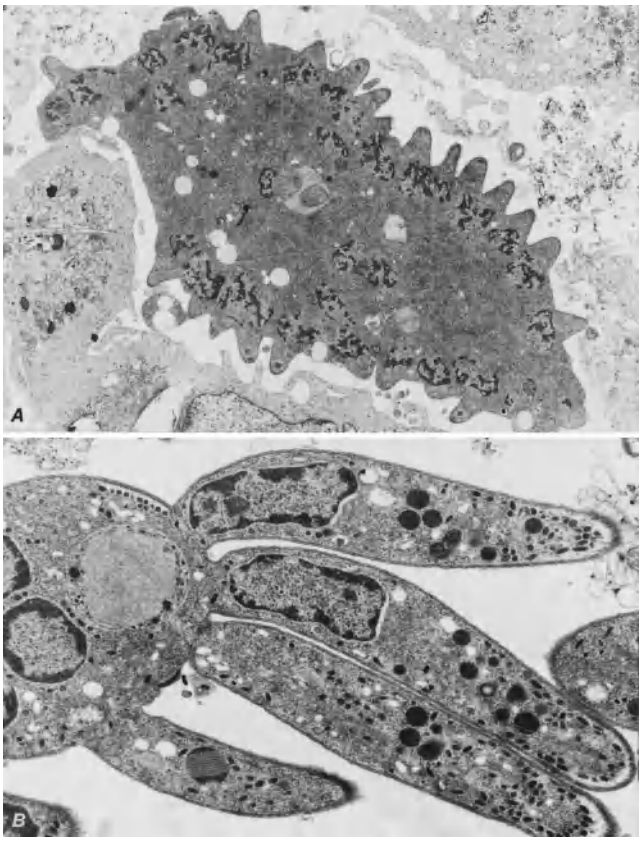


Fig. 15.14 Coccidiosis. **A**. **Trophozoite with merozoite buds**: note multiple nuclei. **B**. **Merozoites budding from mother blastophore**. (Micrographs: Gary L. Kelley, *J Parasitol* 59:1071, 1973.)

by secreting a lytic substance that disrupts the electrolyte-maintaining mechanisms of the host's plasma membrane. Merozoites, exposed to plasma of immune animals, are covered with antibodies tha prevent invasion by blocking surface receptors and by agglutinating merozoites.

Plasmodial parasites feed on **hemoglobin**. Hemoglobin is taken into the organism by two routes: pinocytosis/phagocytosis and via a cytostomal system. Phagocytosis is followed by entry of hemoglobin into a **food vacuole**. To accomplish the second route, some species have a specialized **cytostome** on the pellicular membrane that actively ingests host cell cytoplasm. **Falcilysin**, a zinc metalloprotease, degrades globin peptides in the acidic vacuole; it is also present in the apicoplast, a chloroplast-like oragnelle, where it degrades peptides.[162]

Specific peptidases and other enzymes that degrade hemoglobin have been localized in plasmodial lysosomes.[163] Endocytotic vesicles and vacuoles are surrounded by two membranes, an outer membrane derived from the plasma membrane of the parasite, and an inner membrane from the parasitophorous vacuole (formed by invagination of the erythrocyte plasma membrane during penetration of the merozoite).

As hemoglobin is degraded, the inner membrane disappears, the vacuolar matrix decreases in electron density, and malarial pigment accumulates. Dense debris, ferritin, and pigment are strewn about the host cell cytoplasm. Pigment-containing vacuoles aggregate into one large residual body. All plasmodia produce **hemozoin**, or **malarial pigment**, a brown birefringent crystal that is the residue of hemoglobin digestion. Although many parasites digest hemoglobin as an amino acid source, few produce heme polymer pigments (instead of catabolizing heme via heme oxygenase). The shape and size of hemozoin crystals distinguishes diverse *Plasmodium* species; the three-dimensional structure of each pigment is unique.[164] Feeding in erythrocytes is inhibited by treatment of the host with chloroquine. Parasites affected by this therapy show evidence of degeneration including vesiculation and accumulation of membrane debris.

There is a dependence of plasmodia on adequacy of ion transport for replication in the erythrocyte.[165] Proliferation of parasites in the erythrocytes is inhibited by depletion of glycerol facilitators from the aquaporin family. Membrane aquaporins increase the erythrocytes resistance of parasite growth.

Erythrocyte-Endothelial Interaction *Plasmodium* spp. alter erythrocyte surfaces in two ways: by shifting phospholipid molecules in the lipid bilayer so that they are more accessible to phospholipases, and by inserting new proteins and glycoproteins into the surface membrane. These surface modifications appear ultrastructurally in the formation of cytoplasmic clefts and surface knobs.[166,167] **Cytoplasmic knobs** are protuberances on the erythrocyte surface that consist of electron-dense submembrane cups and the overlying erythrocyte membrane.[168–170] **Cytoplasmic clefts** are membrane bound structures of variable shape and size. Short clefts are slit-like whereas long clefts are undulant and curved, appearing to originate from the membranes of the parasitophorous vacuole. Circular clefts may form loops that enclose cytoplasm of the host cell. Specific parasitic proteins have been localized in knobs and clefts by immunoelectron microscopy.[171–175]

The knobs attach to venular endothelial surfaces where the erythrocytes stick until the parasite matures.[176] The 88-kD leukocyte differentiation antigen CD36, present on endothelial cells, platelets and monocytes, plays a role in adherence of malaria-infected erythrocytes to these cells. Sequestration of infected erythrocytes in venules promotes the disease because parasitized cells are protected from removal during splenic circulation and because parasites appear to grow better in the hypoxic venular environment.

Infected Erythrocytes in the Brain In some infections, groups of parasites lodge in and block capillaries in specific organs. When sequestered in the brain, they can cause death. **Cerebral malaria** is a severe although infrequent complication of malaria. Adherence of plasmodia-infected erythrocytes to venous endothelial cells of the cerebral cortex is mediated by the knobs on erythrocyte surfaces. The receptor on endothelium in some infections appears to be thrombospondin.[177,178] Pathological studies of brains from patients with human malaria reveal blockage of cerebral capillaries with *P. falciparum*-infected red cells that bear knobs of 40×80 nm. Junctions between erythrocyte and endothelial cells are indicated by densities on the cytoplasmic face of the endothelial cell surface at sites where knobs have attached. Calpains, Ca^{2+}-activated cystein proteases, have been implicated in disruption of axonal transport in malaria; brain tissue from fatal falciparum malaria showed that abnormal ratios of mu- and m-calpain (the specific inhibitor of calpastatin) correlated with the extent of axonal injury.[179]

In mouse models, cerebral malaria does not develop in infected nude mice, suggesting that T cells are required for disease. Release of TNF-α by aggregates of macrophages in cerebral lesions plays a role in cerebral lesions. **Apoptosis** of endothelial cells, as well as of neurons and glia, plays a role in advanced stages of murine cerebral malaria.[180]

Because of the coincidence of geographical ranges of human malaria and sickle cell disease, the

hemoglobin S genetic mutation provides resistance to infection by plasmodia. In erythrocytes from sickle cell homozygotes (SS), plasmodia not only fail to replicate but are killed by physical disruption by the needle-like crystals of hemoglobin S.[181]

Renal Lesions The **kidneys** of human malaria patients typically contain malarial pigments. Acute tubular necrosis is caused as parasitized erythrocytes are trapped in the kidney. Ultrastructural analysis of renal tissue from 63 patients dead of malaria showed that acute tubular injury was associated with sequestration of parasitized erythrocytes and localization of host monocytes.[181] Acute malarial renal damage has been documented in a mouse model of *P. berghei* infection.[182] **Immune complex glomerulonephritis** with deposition of IgG in dense deposits in the glomerular basement membrane has been reported. *P. berghei*-infected mice have been used as a model for immune complex glomerulonephritis.[183]

Placental Lesions *P. falciparum* infection during pregnancy frequently leads to abortion and stillbirth. There is some effect of anemia on the human **placenta**, although the pathogenesis of human placentitis is not understood. Studies on placental pathology in *P. berghei*-infected pregnant rats found accumulation of parasitized erytrhocytes and mononuclear cells within maternal blood spaces. Thickening and duplication of trophoblastic basement membranes were prominent but no cytopathic changes were reported in trophoblasts.[184]

Avian Malaria

A large number of *Plasmodium* spp. infect wild birds. In general, they are less host-specific than the mammalian plasmodia. In most types of avian malaria, infective schizonts are acquired from the sucking mosquitos that harbor developing parasites in their gut. Oocytes enter the midgut epithelial cells and exit to interepithelial spaces to move to the basal lamina where ookinetes develop to oocytes.[185] In the bird, the asexual exoerythrocytic stages of *P. gallinarum* are found in sinusoidal endothelial cells of the liver.[186] Budding merozoites from the mother schizont rapidly form a cyst that displaces the nucleus and causes the cell to protrude into the sinusoidal lumen. **Endothelial cells** are filled with extraerythrocytic merozoites in large vacuoles.[187] Nutrition of the intracellular parasite depends upon intact cellular metabolism and the host endothelial cell is preserved for long periods. This differs from the erythrocytic phase wherein an actively functioning cytosome on the parasite digests host cell hemoglobin for its food and the host cell is destroyed.[188,189]

Genus *Leucocytozoon*

All species of *Leucocytozoon* are found in birds (with rare exceptions in lizards), and most are known only by their stained gametocytes in smears of peripheral blood. The life cycles and ultrastructure of *Leucocytozoon* spp., *Plasmodia* spp. and *Haemoproteus* spp. are similar and they are placed in the family Plasmodiidae. *L. simondii* (ducks and geese), *L. smithi* (turkeys), and *L. caulleryi* (chickens) are the important pathogenic species. The principal difference between the following species of the suborder Haemospororina and *Plasmodia* spp. is that the asexual schizonts occur in visceral organs instead of in erythrocytes. Infections are thus far less apt to be transmitted from bird to bird by blood transfer.

Schizogony takes place in liver, brain, spleen, and lungs, and schizonts are found in macrophages and endothelial cells of these organs. Primary (first-generation) schizonts of *L. smithi* develop in hepatocytes.[190] In **hepatic schizogony**, maturing schizonts consist of several large electron-dense multinucleate cytomeres, each bounded by a membrane and lying within a membrane-bounded vacuole. Cleavage leads to uninucleate merozoites. A second schizont type contains irregular inclusions in the hepatocyte cytoplasm. It produces the syncytia, which when released from hepatic schizonts infects macrophages and endothelial cells, which become markedly hypertrophied and give rise to megaloschizonts. Development of primary schizonts occurs in **spleen**, **kidney**, and **lungs** with *L. simondii*.[191] *L. caulleryi* replicates in endothelial cells of the **spleen** forming large aggregates of parasites.[192]

Ultrastructural changes in the hepatocyte infected with *L. smithi* include formation of young primary schizonts (pseudocytomeres) throughout the cytoplasm, each in a single parasitophorous vacuole. Many uninucleate merozoites are formed by synchronous multiple cleavage of the cytoplasm. The pear-shaped merozoites of *L. smithi* are found by a single membrane and lack a cytosome and spherical bodies; they are similar to those of *L. simondii* and others, but differ from those of *L. caulleryi*, which have a cytosome. Second-generation schizogony is initiated when merozoites enter hepatocytes. There is infiltration of the infected liver with monocyte-derived macrophages containing parasites. Megaloschizonts with massive cytoplasmic parasites and enlarged nuclei occur in most *Leucocytozoon* spp. but are variable.

Merozoites from hepatic schizonts enter mature **erythrocytes** and develop into round gametocytes. Developing merozoites are surrounded by a membrane of host origin and as they mature particulate material accumulates in the space between parasite and membrane.

Sporogony of *L. smithi* occurs in the black fly vector; ultrastructural studies show that ookinetes pass through midgut epithelium within 24 hr and pass both through and between enterocytes.[193] Gametogenesis, fertilization, and ookinete differentiation occur rapidly after ingestion by the black fly.[194] The **oocyst** wall is formed of dense granules, is of parasite origin, and can be differentiated from the basement membrane of the fly gut. The cytoplasm of the oocyte differentiates into a single dense sporoblastoid from which 30–50 sporozoites are formed (Fig. 15.12). Oocysts that develop in the insect stomach produce sporozoites that migrate to the salivary gland and are injected in the vertebrate host. Gametocytes develop in swollen monocytes and macrophages of the peripheral blood.[195]

Genus *Haemoproteus*

Haemoproteus infections, which are transmitted by biting dipterans, are characterized by schizogony in visceral endothelial cells and gametocyte development in erythrocytes. Endothelial cells are markedly distorted, especially with accumulation of hemozoin.[196] *H. columbae* of pigeons and doves produce few signs of disease other than anemia and hepatomegaly.[197,198] *H. columbae* undergoes schizogony in cells of the monocyte-macrophage system, chiefly in the lungs but also in liver and spleen.[199–201] Only gametocytes enter erythrocytes. Sporulation occurs in a fly and sporozoites are injected into the bloodstream of the avian host. Merozoites freed into blood may enter endothelial cells to complete another schizogonous cycle or enter erythrocytes to form gametocytes. In the latter they exist as small ring forms that progressively enlarge to distort the cell.

Genus *Hepatocystis*

Hepatocystis kochi is a sporozoan parasite that develops in livers of monkeys producing grossly visible cysts.[202] The life cycle begins in the hepatocyte and leads to formation of large merocysts. Cysts rupture after progressive growth to release merozoites, which then infect erythrocytes and grow into gametocytes. Other species of *Hepatocystis* found in monkeys include *H. vassali* and *H. malayensis, and H. oriheli*, which produce smaller merocysts than those of *H. kochi*.[203]

The Coccidia

All members of the class Sporozoa are parasitic. They produce spores that contain one to several sporozoites. In coccidia, whose life cycle is completed in one host, the spore membrane is thick and resistant and protects the sporozoites while they are outside the host. The **spore membrane** is thin and fragile in species that require two hosts. The organism is protected in an invertebrate host, where replication is required for it to infect the primary vertebrate host. Nearly all species of coccidia replicate in epithelial cells.[204] Binding to the host cell occurs on microvilli and attachment depends upon the formation of an adherence zone between plasma membranes of protozoa and host cell (Fig. 15.13).

In general, the three stages in the sporozoan life cycle are: **schizogony** of sporozoites to produce many merozoites; **gametogony**, or sexual reproduction; and **sporogony**, in which the zygote divides to form multiple sporozoites. Sporogony may take place within delicate oocysts in the body of invertebrates or take place outside the body of the host in protective oocysts. In either case, the sporozoites are infective when swallowed by or injected into the appropriate host (Fig. 15.14). The intestinal coccidia survive gastric acidity, pass into the appropriate segment of the intestine, and invade epithelium.[205–207]

Genus *Eimeria*

Sporozoites (10–25 × 1.53 μm) and merozoites (6–16 × 0.5 μm) of the suborder Eimeriina are fusiform and are dominated by a single nucleus and one or two large refractile bodies.[208] In the anterior part of the parasite, a large ring-shaped orifice contains a **conidium**, which gives rise to two club-shaped organelles. These extend backwards among a cluster of dense tubular **micronemes**. **Glycogen** and **amylopectin vacuoles** are prominent in dormant sporozoites but disappear during active stages.

The **pellicle** includes an outer plasma membrane and an inner membrane complex, which are closely connected to the **subpellicular microtubules**. A variety of surface glycoproteins and other antigens are released during different stages of parasite development and many of these have been localized using monoclonal antibodies and immunogold staining techniques.[209] Host cell invasion is accomplished with surface components, including flotillin-1, a component of **lipid rafts** in the plasma membrane of sporozoites.[210] *Eimeria* spp. share with *Plasmodia* spp. and *Toxoplasma gondii* the presence of an **apicoplast**, a plastid-like organelle derived from endosymbiotic enslavement of a photosynthetic alga;[211] this organelle contains the fatty acid biosynthesis protein, enoyl reductase.

A **cytostome** in the pellicle is typically near the anterior part of the cell and varies in size according to species. The pointed anterior end of the sporozoites and merozoites has electron-dense **polar rings** and a

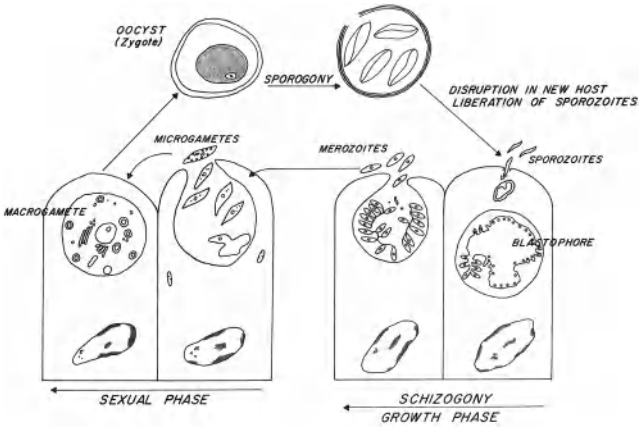


Fig. 15.15 Coccidial invasion: intestinal epithelial cells.

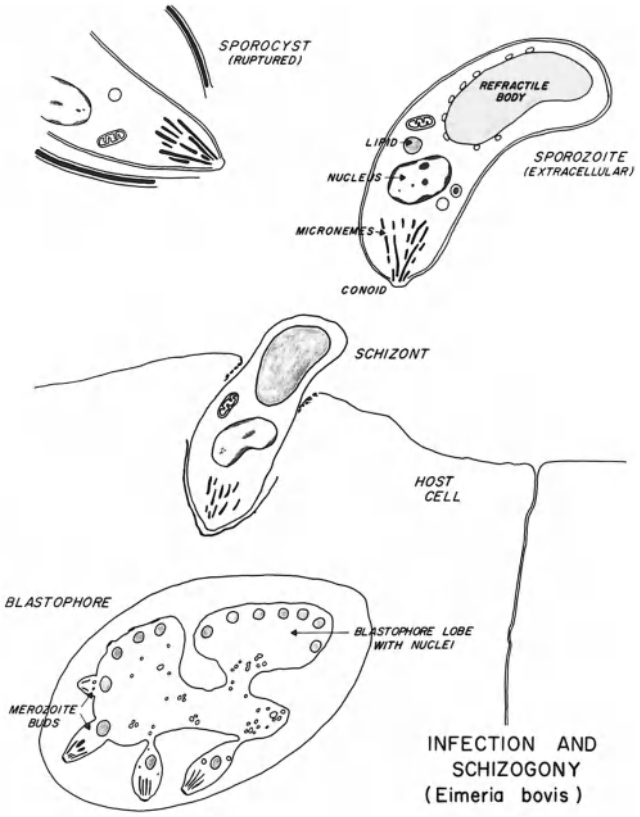


Fig. 15.16 Coccidial life cycle: replication in intestinal epithelial cells.

conoid, a hollow, truncated cone-shaped structure (80–300 μm long). **Rhoptries** and **micronemes** occur in all species. The **Golgi complex** is anterior to the nucleus. **Mitochondria**, one to several, are at random sites in the cytoplasmic matrix.[212]

After entry into host cells, sporozoites and merozites of the Eimeriina reside within **parasitophorous vacuoles**. Intracellular replication of coccidia leads to marked hyperplasia of the parasite-laden intestinal enterocyte. There is marked increase in ribosomes and RER, and later, in autophagolysosomes. During merogony, merozoite buds and multiple nuclei form in the coccidium as replication occurs (Fig. 15.15). Merozoites bud from the mother blastophore.[213–216] Ultrastructural changes in parasites during schizogony, microgametogenesis, and macrogametogenesis have been defined. Sexual forms in vertebrate hosts are highly variable. Wall-forming bodies are prevalent in macrogametocytes but not in microgametocytes (Fig. 15.16).

Merozoites break out of the infected epithelial cell and may either begin new cycles of schizogony, or initiate sexual divsion by developing into macro- or microgametocytes. Pathogenicity of individual coccidial isolates is related to their tendency to sustain asexual cycles of schizogony. It is this process that extensively destroys intestinal epithelium.

The **microgametocyte** gives rise to numerous small microgametes by a process of budding similar to that of schizogony.[217,218] During this stage the parasitized host cell undergoes marked hypertrophic changes to support the growth of the microgametocyte. The microgamete leaves its host cell and swims actively into a cell containing a macrogamete where fertilization takes place.

The **macrogamete** forms as a large inclusion in epithelium. Its cell boundary consists of a unit membrane under which lie osmiophilic masses. Numerous glycogen granules are scattered throughout the heavily granulated cytoplasm.[219,220] After fertilization, the outer and inner walls of the oocyst develop and the oocyst may be released from the cell by lysis. During transformation of macrogametes to oocysts, new organelles are formed including wall-forming, club-shaped, and residual bodies.[221]

Genus *Isospora*

The ultrastructure of many species of coccida has been reported (Table 15.5). The morphology of *Isosopora* spp. does not differ significantly from that of *Eimeria* spp.[222,223] *I. belli* parasitizes the human intestinal epithelium in which it undergoes typical coccidian cycles of schizogony and gametogony. Unsporulated oocysts are shed in the feces. Encysted zoites may be found in the lamina propria of the intestinal villi and, rarely, in the mesenteric lymph node.[224] In chronic human isosporiasis there is a lympho-plasmacytic reaction in the lamina propria and atrophy of intestinal villi.

Genus *Cyclospora*

Cyclospora spp. are coccidian parasites that infect reptiles, insectivores, mice and humans.[225] They resemble *Isospora* spp., except that *Cyclospora* have oocysts with

Table 15.5 Pathogenic coccida.

Pathogen	*Change*	*Reference to ultrastructural pathology*
		Genus *Besnoitia*
Besnoita jellisoni		**Senaud**, *Protistologica* 5:413, 1969
***B.* spp.**	Mouse	**Senaud**, *Parasitology* 40:165, 1972 (viscera); **Senaud**, *J Protozool* 21:175, 1974; **Sheffield**, *J Parasitol* 52:583, 1966 (ascites)
		Genus *Calyptospora*
Calyptospora empristica		**Fournie**, *J Protozool* 32:542, 1985
***C.* spp.**		**Overstreet**, *J Protozool* 31:332, 1984
		Genus *Cyclospora*
***Cyclospora* sp.**		**Ford**, *J Protozool* 35:223, 1988*
		Genus *Eimeria*
Eimeria acervulina	Chicken	**Fernando**, *Z Parasitenkd* 43:33, 1973; **Speer**, *J Parasitol* 75:92, 1989
E. alabamensis		**Sampson**, *J Parasitol* 57:1133, 1971 (erythrocyte)
E. auburnensis	Cow	**Hammond**, *J Protozool* 14:678, 1967; **Hammond**, *Z Parasitenkd* 33:65, 1969
E. bovis	Cow	**Speer**, *J Protozool* 35:379, 1988; **Hammond**, *J Parasitol* 53:235, 1967; **Scholtyseck**, *Z Parasitenkd* 34:310, 1970
E. brunetti	Chicken	**Ferguson**, *Acta Pathol Microbiol Scand B* 84:401, 1976
E. callospermophili		**Roberts**, *J Parasitol* 56:918, 1970
E. contorta	Mouse	**Muller**, *Z Parasitenkd* 47:91, 1975
E. falciformis	Mouse	**Melhron**, *Protistologica* 9:269, 1973 (gut)
E. ferrisi	Mouse	**Scholtyseck**, *Z Parasitol* 46:91, 1975; **Senaud**, *Z Parasitenkd* 49:217, 1976
E. intestinalis		**Peeters**, *Zbl Vet Med B* 31:9, 1984
E. labbeana	Pigeon	**Varghese**, *Z Parasitenkd* 46:43, 1975 (ileum)
E. larimerensis	In vitro	**Roberts**, *J Parasitol* 57:615, 1971*
E. magna	Rabbit	**Jensen**, *J Protozool* 22:411, 1975;* **Senaud**, *J Protozool* 16:155, 1969; **Speer**, *J Protozool* 20:274, 1973 (gut)
E. maxima	Chicken Cow	**Melhorn**, *Z Parasitenkd* 40:243, 1972 **Sheffield**, *J Parsitol* 53:831, 1967
E. meleagrimitis	Turkey	**Augustine**, *J Protozool* 31:740, 1984
E. mivati		**Wheat**, *Z Parasitenkd* 50:125, 1976
E. truncata	Goose	**Gajadhar**, *J Protozool* 33:345, 1986
E. vermiformis	Mouse	**Adams**, *J Protozool* 31:233, 1984
E. necatrix	Chicken	**Dubremetz**, *C R Soc Biol* 165:862, 1971; **Fernando**, *Z Parasitenkd* 43:105, 1974
E. neischulzi	Rat	**Colley**, *J Protozool* 15:374, 1968
E. performans	Rabbit	**Scholtyseck**, *J Protozool* 9:407, 1962
E. pragensis	Mouse	**Senaud**, *Protistologica* 6:5, 1970 (mouse gut)
E. stediae	Rabbit	**Scholtyseck**, *Z Parasitenkd* 26:91, 1965 (liver)
E. tenella	Chicken	**Doens-Juteau**, *Protistologica* 10:261, 1974; **Kefu**, *Exp Parasitol* 113:174, 2006; **McLaren**, *Parasitology* 59:563, 1969; **Scholtyseck**, *Acta Vet* 38:153, 1969
		Genus *Epieimeria*
Epieimeria anguillae		**Molnar**, *J Fish Dis* 9:99, 1986
		Genus *Frenkelia*
***Frenkelia* sp.**	Vole Mouse	**Gobel**, *Z Parasitkd* 55:29, 1978 (liver); **Scholtyseck**, *Z Parasitkd* 42:185, 1973 (brain)
		Genus *Globidium*
***Globidium* sp.**	Sheep	**Melhorn**, *Zentralbl Bakt A* 236:386, 1976 (gut)

Table 15.5 *Continued*

Pathogen	*Change*	*Reference to ultrastructural pathology*
		Genus *Goussia*
Goussia giraella	Fish	**Kent**, *J Protozool* 35:287, 1988
G. pannonica	Fish	**Lukes**, *J Protozool* 39:484, 1992
***Goussia* sp.**	Cod	**Morrison**, *J Fish Dis* 12:533, 1989 (kidney)
		Genus *Isospora*
Isosporo canaria		**Speer**, *J Protozool* 22:476, 1975*
I canis	Dog	**Roberts**, *Z Parasitenkd* 40:183, 1972 (dog feces); **Schmidt**, *J Protozool* 14:602, 1967 (gecko)
I. felis	Cat	**Melhorn**, *Z Parasitenkd* 51:15, 1976 (mouse lymph node); **Pelster**, *Z Parasitenkd* 41:29, 1973 (cat)
I. ohioensis	Dog	**Dubey**, *J Am Vet Med Assoc* 173:185, 1978 (gut)
		Genus *Haemogregarina*
H. bali		**Siddall**, *J Parasitol* 77:426, 1991
H. magna		**Paterson**, *J Protozool* 35:73, 1988
		Genus *Hammondia*
Hammondia heydorni	In vitro	**Speer**, *J Protozool* 35:352, 1988*
		Genus *Klossiella*
Kossiella helicina	Snail	**Schulte**, Z Parasitenkd 36:193, 1971 (kidney)
		Genus *Lankeseterella*
Lankesterella culicis	Mosquito	**Sheffield**, *J Protozool* 18:98, 1971
L. hylae	Frog	**Stehbens**, *J Protozool* 13:63, 1966
L. garnhami	Sparrow	**Garnham**, *J Protozool* 9:107, 1962 (spleen)
L. minima		**Dessar**, *J Parasitol* 76:97, 1990
***L.* spp.**	Various species Mosquito	**Heller**, *Acta Vet Acad Sci Hung* 24:151, 1974 (fish) **Sanders**, *J Protozool 20:594, 1973* (mosquito larvae)
		Genus *Neosporum*
Neosporum caninum	Dog	**Jardine**, *Vet Parasitol* 62:231, 1996; **Speer**, *Int J Parasitol* 29:1509, 1999; **Speer**, *J Protozool* 36:458, 1989
	Lamb	**Dubey**, *J Parasitol* 76:127, 1990 (brain)
		Genus *Tyzzeria*
Tyzzeria chalcides	Skink	**Daszak**, *J Protozool* 36:299, 1989

*Studies in vitro.

two sporocytes, each with two sporozoites. The species that causes chronic diarrhea in humans appears in feces as nonrefractile spheres 8–10 μm in diameter and containing a cluster of refractile, membrane-bound globules. There is an outer fibrillary coat of 63 nm beneath which is a 50 nm thick cell wall.[226]

Genus *Toxoplasma*

The coccidian parasite *Toxoplasma gondii* is an obligate intracellular parasite in a wide variety of birds and mamals. It has an intestinal epithelial cycle for the production of oocysts in cats and other Felidae, in which it undergoes schizogony and microgametogony in the feline ileum.[227] Oocysts are shed in the feces and are infectious after sporulation occurs. These asexual forms have distinct ultrastructural characteristics,[228,229] and surface antigens have been detected using monoclonal antibodies.[230] Organisms are enclosed by a **pellicle** consisting of an outer membrane with an underlying inner membrane and cytoskeleton.[231] The inner membrane is continuous except for slight thickenings (the polar ring) which surround the opening at the anterior end. The **conoid** is at the anterior end of the organism just inside the polar ring.

Lysosomes up to 0.3 μm in diameter are present in the cytoplasm.[232]

Asexual forms pass the intestinal wall of the cat to enter the macrophages of the new host where they encyst and propagate. On entering the secondary host, endozoites infect circulating monocytes and macrophages, and then spread to muscle, brain, spleen,[233] and other tissues.

Within the **macrophage**, *T. gondii* moves rapidly into the endosomal system.[234,235] Although a few toxoplasma may be phagocytized, active invasion with destruction of the host plasma membrane is the dominant means by which organisms enter the macrophage.[236] Within activated macrophages, *T. gondii* recruits host lysosomes,[237] and is able to suppress nitric oxide production by producing a patatin-like protein.[238]

Tachyzoites invade host cells when laminin absorbed to the tachyzoite surface binds to integrin-β1 receptors on the host cell surface. Binding to the integrin

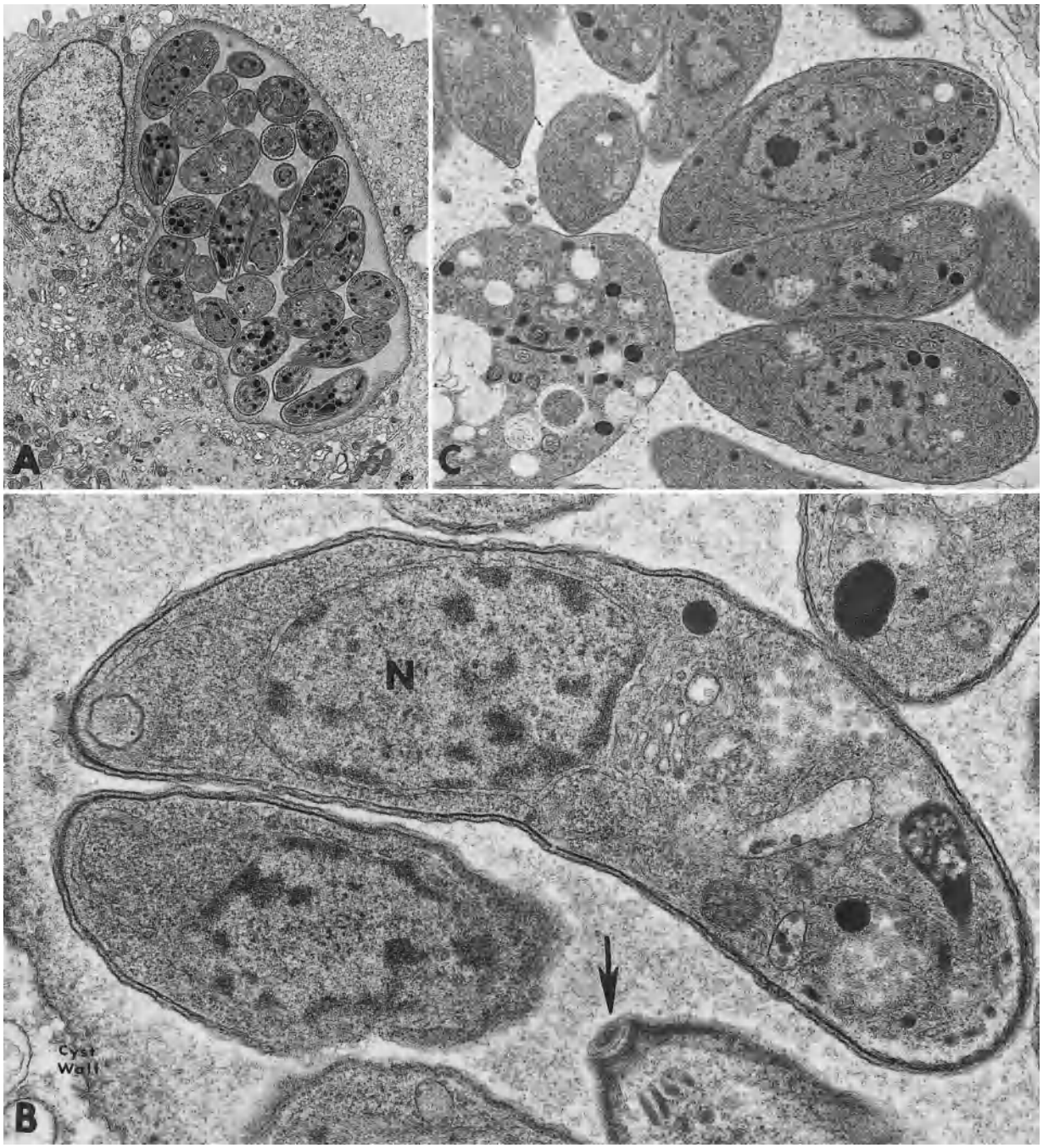


Fig. 15.17 ***Toxoplasma gondii***. **A**. **Cyst**: in macrophage. **B**. **Individual organisms**: nuleus (*N*), conoid (*arrow*). **C**. **Mother cell**: budding of daughter organisms. (Micrograph: Arliss Boothe, National Animal Disease Center.)

pathway induces parasitophorous vacuoles (Fig. 15.17) that lack host membrane glycoproteins and thus fail to fuse with acidifying endosomes and lysosomes (and thereby protect *T. gondii* from an effective host response). *T. gondii* tachyzoites use secretory organlle proteins to enhance invasion; for example, dense granules secrete **osteopontin**, a multifunctional glycophosphoprotein involved in signaling.[239]

Cellular invasion occurs via **rhoptries**, secreting organelles inside the parasite (found only in intracellular protozoa).[240] Rhoptry membranes fuse with the anterior limiting membrane to produce an opening to the parasites surface. A lytic product is then secreted that forms **fusion** rosettes on the plasma membrane of the host cell and facilitates invasion through the membrane. Masses of **tubules** (similar to those produced by the membrane lytic agent digitonin) are seen in the rhoptries 15 sec after attachment and tubules also occur in the newly formed **parasitophorous vacuoles** (PV) (Fig. 15.18).

The membrane of the **parasitophorous vacuole** is a "hybrid" membrane incorporating components of macrophage and toxoplasma membrane and thus does not fuse with lysosomes inside the macrophage. The modified phagosomal membrane suppresses acidification,[241] protects the parasite, and supports its replication. Modification of macrophage phagosomes, which occurs shortly after infection, makes the parasitophorous vacuole unable to fuse with other endocytic or lysosomal organelles. The mechanism of fusion inhibition appears to be incorporated into the vacuole membrane as it is formed (in contrast to the secretion of a soluble inhibitor by the parasite).[242]

Toxoplasmas secrete **membranous vesicles** that form a **reticulate network** within the vacuole. Normal endocytic processing is stopped as the vacuole is converted to parasite replication. The intraphagosomal membrane network is a unique structural modification of the phagosome that involves parasitic proteins.[243,244] One antigen associated with immunity has been located beneath the surface membrane in the region of the pellicle within a network of vesicles that are extruded from the surface of a *Toxoplasma* cell during entry into the host cell.

Unlike most intracellular protozoa, which are deficient in catalase, *T. gondii* is endowed with both catalase and glutathione peroxidase and is thus resistant to fluxes of hydrogen peroxide. It is killed by hydroxyl radicals and singlet oxygen, the toxic productions of oxygen-hydrogen peroxide interaction, which shows the importance of the respiratory burst in macrophage killing of *T. gondii*.[245] These radicals are dormant in the resting macrophage, but are activated when cells are infected. The cytotoxicity of neutrophils and platelets against *T. gondii* may also involve the respiratory burst.[246] Within macrophages, the rise in activity of competetive intracellular scavengers of toxic oxygen radicals (superoxide dismutase, glutathione peroxidase, and catalase) results in fewer radicals and thus less antitoxoplasma activity (acatalasemic mice have high antitoxoplasma activity).

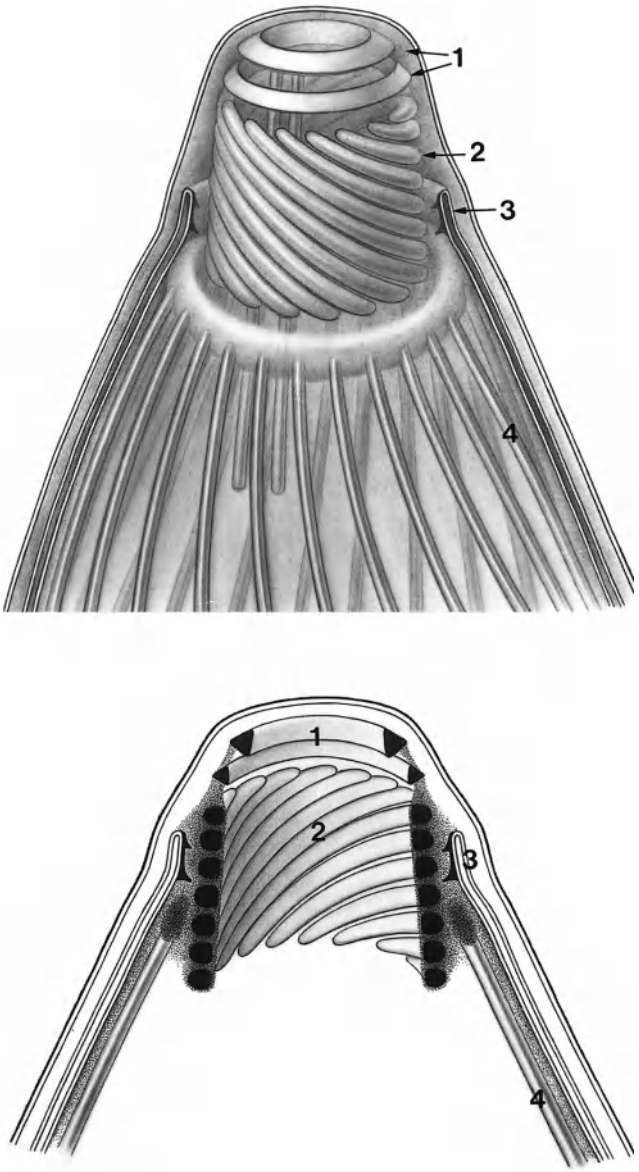


Fig. 15.18 Conoid region (anterior end): *Toxoplasma gondii*. Anterior and posterior preconoidal ring (*1*), conoid subunit (*2*), inner membrane complex (*3*), microtubule *(4)*. The polar ring complex consists of the junctional area of the conoid subunit (*3*) and inner membrane complex. (Drawing: Barbara A. Nichols, *J Protozool* 34:217, 1987.)

Inside **muscle** cells, the organism is confined to parasitophorous vacuoles. Crescent-shaped daughter parasites develop from the infecting ones. The thick wall cyst wall seen in inapparent chronic infection is a dense outer layer of host-cell origin and an inner thin membrane of parasite origin. The host reaction con-

sists of necrosis of infected cells and an attendant accumulation of macrophage and neutrophils.[247,248]

T. gondii has a predilection for brain, and is a common cause of **granulomatous encephalitis** in humans and animals that have compromised immune systems. **Chorioretinitis** is found in newborns infected in utero. In the human brain, replication occurs within parasitophorous vacuoles of glial cells; there are distinct ultrastructural features of encystation.[249,250] The ultrastructure of *T. gondii* in the spinal cord of a cat with latent infection reactivated by feline immunosuppressive virus infection has been reported.[251] Inoculation of mice reproduces the brain lesions.[252,253]

Genus *Hammondia*

Hammondia hammondi is a nonpathogenic coccidian of cats that is closely related to *T. gondii* in both structure and life cycle. It has no extraintestinal cycle in the cat however, and intermediate hosts become infected only by ingestion of oocysts. *H. heydorni* uses canids as definitive hosts and ruminants as intermediate hosts. Ultrastructural studies of in vitro grown cells reveal general coccidian features, but differences include the following: rhoptries are located both posteriorly and anteriorly, sporozoites contain a crystalloid body in the posterior cytoplasm, and during penetration the host cell plasma membrane moves to surround the sporozoite to create a cavity.[254]

Genus *Neospora*

Neospora caninum is an apicomplexan that, in dogs, causes fatal disease characterized by polyradiculoneuritis, encephalitis, and polymyositis.[255] Structurally related, but antigenically distinct from *Toxoplasma gondii*, these organisms have also been implicated in abortion and neonatal paralysis of cattle.[256,257] *N. caninum* can be differentiated from *T. gondii* ultrastructurally, on the basis of structure and numbers of rhoptries, micronemes and dense bodies.[258]

In tissue, tachyzoites, bradyzoites, and noncompartmentalized cysts of *N. caninum* are indistinguishable from *T. gondii* by light microscopy, but ultrastructurally tachyzoites differ from those of *T. gondii* by a lack of micropores, presence of numerous micronemes, more rhoptries (*N. caninum* has 12–18, *T. gondii* <10), and arrangements of micronemes perpendicular to the pellicle. *T. gondii* replicates exclusively in parasitophorous vacuoles; *N. caninum* also does, or can be free in the host cytoplasm.[259] The cyst wall of *N. caninum* is irregular and thicker than that of *T. gondi*. Microneme proteins and carbohydrate epitopes are critical for adhesion of parasite to host cell surface.[260,261]

Genus *Sarcocystis*

Sarcocystis spp. parasitize cardiac and skeletal muscles of mammals, birds, and reptiles. Ultrastructurally, intact **cysts** contain **bradyzoites** and measure up to 100 μm in diameter and 325 μm in length. Bradyzoites contain apicoplasts with four continuous membranes; the two inner membranes have a circular shape with large proteins complexes between them.[262] Typically, there is no inflammatory reaction around encysted organisms in myocytes, and cysts are found incidentally at necropsy. Visible as white dots or streaks, these intracellular organisms are surrounded by a thick cyst wall of both host and parasite origin. Rupture of cysts may be accompanied by eosinophilic myositis (Fig. 15.19). Humans are accidental intermediate hosts, mammalian, reptilian and avian carnivores being the definitive hosts (Table 15.6).

Sarcocystosis

Acute bovine sarcocystosis is a febrile disease that occurs during schizogony of *S. cruzi* within vascular endothelium.[263–265] Blood studies show anemia, decreased serum proteins, and increased tissue enzymes during acute disease; platelets and coagulation factors were abnormal just prior to death. **Abortion** in pregnant cows occurs 30–40 days after sporocysts are ingested. Edema and foci of necrosis occur in placentomes. In pregnant cattle ovarian corpora lutea are infected, and luteal regression correlates with diminished plasma progesterone and abortion.

In **equine protozoal myeloencephalitis**, *S. neurona* is found largely in pericytes of capillaries in the spinal cord although they are also found in macrophages and in myelinated fibers.[266]

Genus *Cryptosporidium*

Cryptosporium spp. are coccidian parasites, most of which attach to the surfaces of the intestine to cause diarrheal disease. *Cryptosporidium* spp. also infect a wide variety of alimentary mucosal surfaces, including epithelium of the tonsils, pharynx, salivary glands, stomach, gall bladder, pancreatic ducts, biliary tracts and, in birds, the cloacal bursae (Table 15.7). Respiratory tract infections are also reported in highly immunosuppressed humans and animals, and cryptosporidia have been reported in the nasal cavity, infraorbital sinus, trachea, and bronchi of several species. Cryptosporidial infections have also been found in the kidney, conjunctiva and reproductive tract.[267]

Monoclonal antibodies have been used as probes against *C. parvum* oocysts, sporozoites, and

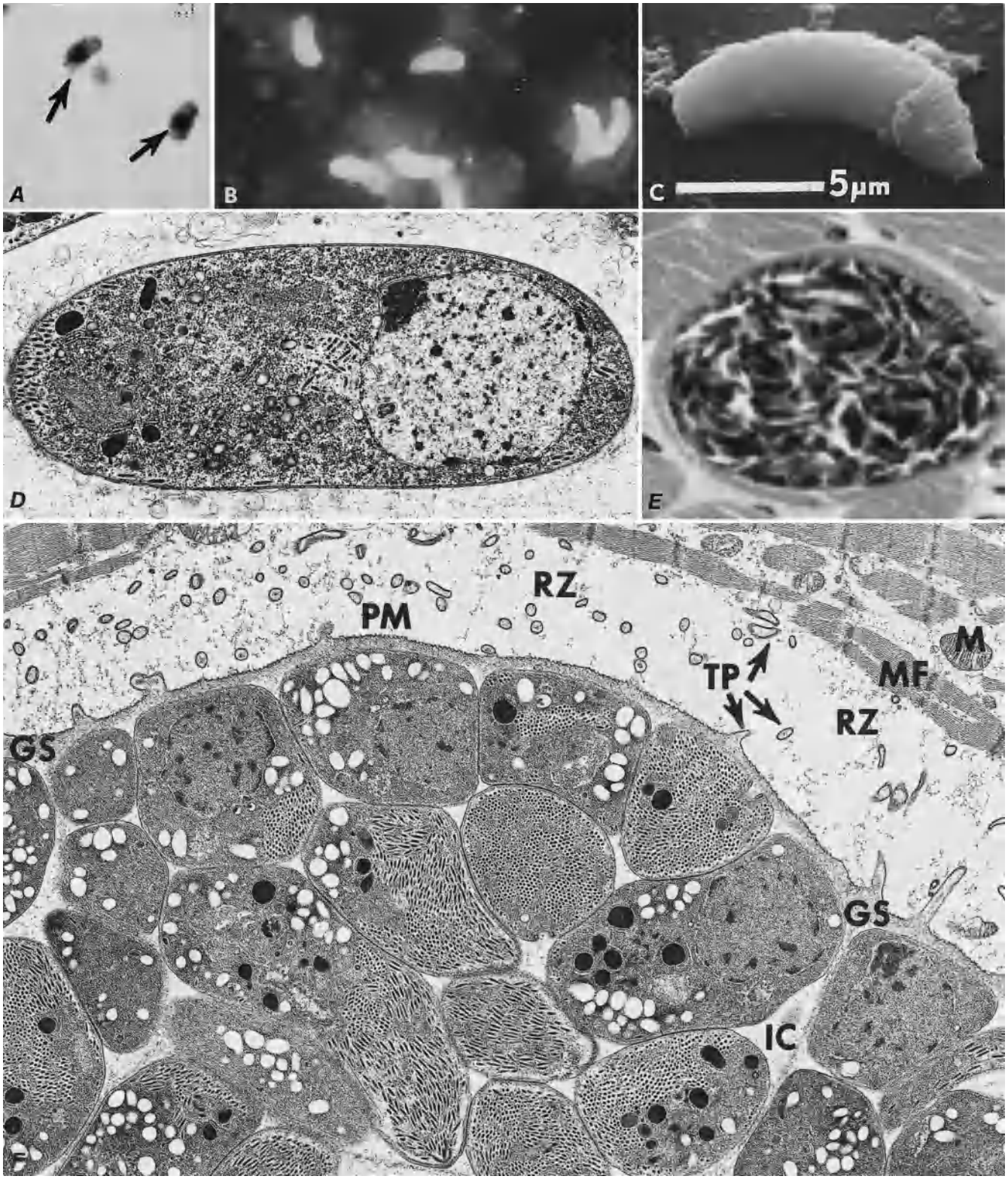


Fig. 15.19 ***Sarcocystis cruzi***: cow. **A**. **Schizonts** (*arrows*) isolated from ground tissue. **B**. **Schizonts** stained with fluorescent antibody. **C**. **Schizont** with pointed feeder end, SEM. **D**. **Schizont**: nucleus at right, tubules at left. **E**. **Cyst** in muscle, histology. **F**. **Cyst** in muscle: clear zone (*RZ*) between muscle fibers (*MF*) and parasitophorous membrane (*PM*); cyst microvilli (*TP*) extend throughout clear halo area: ground substance (*GS*) is densest immediately below parasite membrane; mitochondria (*M*); interparasite spaces (*IC*). (Micrographs: Dean Barnett, National Animal Disease Center.)

Table 15.6 Pathogenic Sarcocystis species.

Pathogen	*Host*	*Reference to ultrastructural pathology*
Sarcocystis canis	Dog	**Dubey**, *J Parasitol* 77:522, 1991; **Allison**, *Vet Clin Pathol* 335:353, 2006 (liver)
	Dolphin	**Resendes**, *J Parasitol* 88:206, 2002 (liver)
	Seal	**Yantis**, *J Parasitol* 89:1258, 2003 (liver)
S. cruzi	Cow	**Dubey**, *J Protozool* 27:380, 1980 (blood vessel); **Gajadhar**, *Can J Vet Res* 56:41, 1992 (muscle)
S. cuniculi	Rabbit	**Elwasila**, Acta Vet Hung 32:71, 1984
S. falcatula	Bird	**Smith**, *J Parasitol* 75:270, 1989 (budgerigar, liver); **Box**, *J Protozool* 31:521, 1984
S. fusiformis		**Simpson**, *J Parasitol* 52:607, 1966
S. hominis	Human	**Dubey**, *Vet Parasitol* 34:153, 1989
	Cow	***Wouda***, *J Comp Pathol* 135:249, 2006; ***Gajadhar***, *Can J Vet Res* 51:373, 1987
	Buffalo	**Chen**, *J Parasitol* 89:393, 2003
S. hirsuta	Cow	**Dubey**, *Vet Parasitol* 34:143, 1999
S. kirkpatricki	Raccoon	**Snyder**, *J Parasitol* 76:495, 1990
S. muris	In vitro	**Entzeroth**, *J Protozool* 32:446, 1985*
S. niescheriana		**Ludvik**, *J Protozool* 7:128, 1960
S. neurona	Horse	**Dubey**, *J Parasitol* 77:212, 1991 (nerve); **Bowman**, *Cornell Vet* 82:41, 1992 (nerve)
S. odoi		**Dubey**, *Am J Vet Res* 44:1738, 19 (deer)
S. tarandivulpis	Reindeer	**Gjerde**, *Acta Vet Scand* 26:91, 1985 (skin)
S. tenella		**Melhorn**, *Zt Parastiol* 41:291, 1973; **Senaud**, *Compt Rend Acad Sci* 256:1009, 1963
***Sarcocystis* spp.**	Mammals	**Davis**, *J Parasitol* 85:965, 1999 (liver); **Dubey**, *J Am Vet Med Assoc* 178:683, 1981 (goat); **Dubey**, *Am J Vet Res* 47:1052, 1986 (mule deer); **Garner**, *J Parasitol* 83:523, 1997 (polar bear liver); **Heydorn**, *Zentralbl Bakteriol A* 233:123, 1975; **Gozab**, *Vet Pathol* 44:695, 2007 (monkey); **Kan**, *Z Parasitenkd* 52:219, 1977 (rat); **Kirkpatrick**, *Vet Pathol* 23:88, 1986 (cat); **Kirkpatrick**, *J Protozool* 34:445, 1987 (raccoon); **La Perle**, *J Comp Pathol* 121:287, 1999 (alpaca); **Melhorn**, *Z Parasitenkd* 45:277, 1975 (sheep esophagus); **Melhorn**, *Z Parasitenkd* 48:83, 1975 (sheep muscle); **Melhorn**, *Z Parasitol* 51:165, 1977 (monkey); **Rzepezyk**, *Z Parasitol* 50:137, 1976 (rat); **Viles**, *Z Parasitenkd* 49:127, 1976; **Zaman**, *Z Parasitenkd* 47:69, 1975 (rat)
	Bird	**Vetterling**, *J Protozool* 20:613, 1973 (grackle

*Studies in vitro.

Table 15.7 Ultrastructure of pathogenic *Cryptosporidia* spp.

Tissue	*Host*	*Reference to ultrastructural pathology*
		Avian
Trachea	Chicken	**Fletcher**, *Avian Dis* 19:630, 1975; **Tadeja-Simborio**, *Avian Pathol* 22:113, 1993
	Goose	**Proctor**, *J Protozool* 21:664, 1974
	Turkey	**Hoerr**, *J Am Vet Med* Assoc 173:1591, 1978
		Reptilian
Stomach	Snake	***Brownstein***, *Vet Pathol* 14:606, 1977
		Mammalian
Intestine	Cat	**Iseki**, *Jap J Parasitol* 28:285, 1979
	Cow	**Meuten**, *J Am Vet Med Assoc* 165:914, 1974; **Pohlenz**, *Vet Pathol* 15:417, 1978 (intestine); **Fayer**, *J Parasitol* 91:624, 2005 (intestine)
	Guinea pig	**Vetterling**, *J Protozool* 18:248, 1971
	Human	**Bird**, *J Pathol* 132:217, 1980; **Meisel**, *Gastroenterology* 70:1156, 1976
	Monkey	**Kovatch**, *Vet Pathol* 9:426, 1972
	Mouse	**Hampton**, *J Parasitol* 52:939, 1966
	Pig	**Kennedy**, *J Am Vet Med Assoc* 170:348, 1977 (colon)
	Rabbit	**Inman**, *Vet Pathol* 16:89, 1979
	Sheep	**Berg**, *J Am Vet Med Assoc* 173:1586, 1978; **Barker**, *Z Parasitenkd* 44:289, 1974

merozoites to identify specific proteins; for example, a surface glycoprotein important in attachment had been shown with colloidal gold-labeled immunoglobulin to be around the periphery of meronts associated with the plasma membrane of the enterocyte.[268] A mitochondrial organelle, identified through use of HSP70 protein, is present in close apposition to the nucleus.[269]

Cryptosporidiosis has been documented in over 20 species of animals including mammals, birds, reptiles and fish.[270] The life cycle has been clarified in mice.[271] Transmission from host to host, as in other coccidia, occurs via oocysts. Disease occurs during active replication of the organisms and the inflammatory reaction of the intestinal wall. Several forms of the parasite are identified ultrastructurally in intestinal biopsies including trophozoites, schizonts, oocysts, and micro- and macrogametes. Cryptosporidia adhere to microvilli of enterocytes and shed cysts into the lumen of the intestine.[272]

The parasite attaches to enterocytes, displacing microvilli and establishing a characteristic complex membrane-membrane interaction with the surface of the host cell.[273] Scanning electron microscopy has shown that as excystation begins, a **suture** in the oocyst wall dissolves, leaving a slit through which sporozoites exit.[274,275]

Parasites are shed into the lumen of the gut and are phagocytized by neutrophils and other inflammatory cells. Ultrastructurally, cryptosporida attached to enterocyte surfaces are surrounded by a membrane of host origin (Fig. 15.20).[276–278] As the infection progresses, there is loss of villous epithelial cells, atrophy of villi, and hyperplasia of crypt epithelium. Microvilli of parasitized epithelial cells are short, irregular and distorted.

C. parvum causes transient diarrhea in children and protracted dysentery and malabsorption of immunosuppressed patients. **AIDS biliary cholangiopathy** arises from an enhancement of *C. parvum*–induced **apoptosis** in cholangiocytes, which is enhanced by the HIV-1 tat protein.[279] Tat does this through a paracrine-mediated, FasL-dependent mechanism.

Genus *Hepatozoon*

Hemogregarines have the ultrastrstructural characteristics that are unique to the phylum Apicomplexa: conoid, rhoptries, micronemes, micropore, pellicle with subpellicular microtubules. Unique characteristics that differ from other apicomplexans are the presence of rhoptries anterior and posterior the the nucleus and a canopy structure at the apical pole of gamonts in some species.[280]

American canine hepatozoonosis is caused by *Hepatozoon americanum*, the definitive host of which is the tick, *Amblyomma maculatum*. Infection of dogs occurs after ingestion of ticks that harbor sporulated oocysts. After penetration of the intestinal mucosa, sporozoites are disseminated systemically and enter striated muscle. Abberrant merozoites and gamonts can be found in macrophages in granulomas.[281]

Dogs are infected with *Hepatozoon canis* by ingesting an infected brown dog tick, *Rhipicephalus sanguineus*.[282] Sporozoites invade the gut wall and undergo schizogany in several tissues, especially cardiac, smooth, and skeletal muscle. Rupture of mature schizonts leads to release of merozoites into muscle with granulomatous reactions. Merozoites invade neutrophils and monocytes and develop into gametocytes. Ticks ingest blood from the dog, and gametocytes invade the gut of the tick.

Hemogregarines of snakes and other reptiles parasitize erythrocytes, in which they cause marked enlargement. The surfaces of the affected red blood cell develop marked deformation and knobs with electron-dense central masses.[283]

Genus *Goussia*

Fish coccidia differ from coccidia that parasitize warm blooded vertebrates; for example, many inhabit the microvillous regions of the enterocyte to resemble cryptosporidians. ***Goussia***, ***Eimeria***, and ***Epieimeria*** are three species in which developmental changes occur within the microvillous regions of enterocytes of the fish intestine. Most *Goussia* spp. reside in the enterotycte cytoplasm, but they remain within the microvillous environment.[284] Oocysts of *Gousia lusca* contain four ellipsoidal sporocyts that measure 13.7 × 9.2 μm. The sporocyst wall has a dense inner layer 115 nm thick, transversely striated and intercalated by thin grooves.[285]

Genus *Besnoitia*

Coccidia of the genus ***Besnoitia*** cause 100–200 μm diameter, thick-walled cysts that contain host cells and bradyzoites; bradyzoites are 6–7.5 × 1.9–2.3 μm in size and contain micronemes, rhoptries, a posterior nucleus, and amylopectin granules. When degenerate, cysts are associated with a chronic cellular response.[286,287] *Besnoitia* spp. are found in bovids (*B. besnoiti*), cats, equids (*B. bennetti*), opossums (*B. darlingi*), rabbits (*B. orycofelisi*), reindeer (*B. tarandi*), and sheep (*B. jellisoni*). Cats, which are hosts for three species, shed unsporulated oocysts in feces.[288] Oocysts sporulate and closely

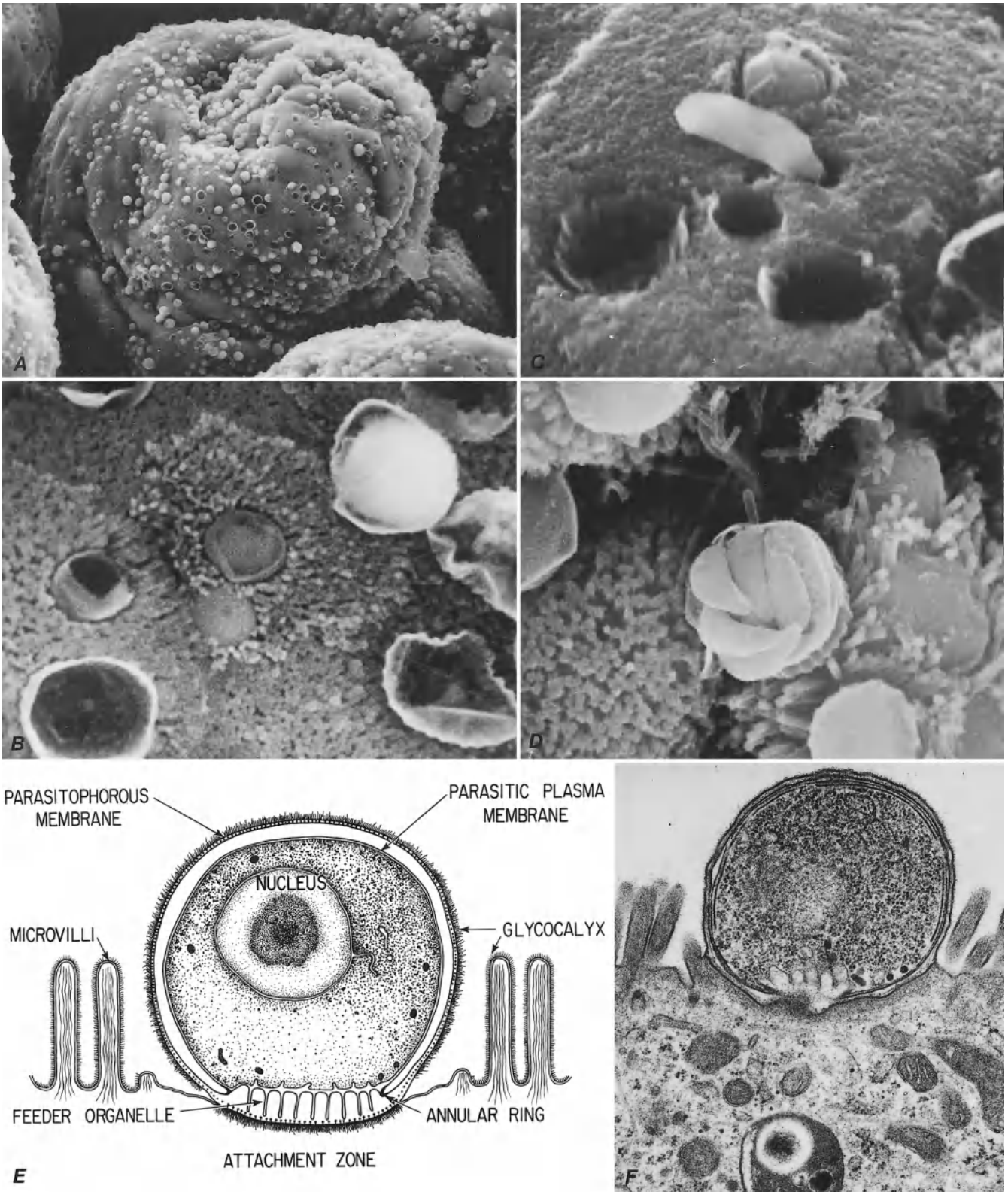


Fig. 15.20 Cryptosporidiosis. **A–D**. **Atrophic villus**: calf ileum (scanning electron micrograph). **A**. **Cryptosporidia**: white nodules on surface; black circles are craters left when parasites leave or are rinsed off. **B**. **Ruptured parasites**. **C**. **Craters**: with one merozoite. **D**. **Opened schizont with merozoites** in center; parasites in upper part are surrounded by epithelial cells. **E**. **Attachment zone:** diagram. **F**. **Epithelial cell attachment**. (Micrographs: Joachim Pohlenz, *Vet Pathol* 15:417, 1978.)

resemble those of *Isospora* spp. Severe, subacute diffuse interstitial pneumonia with syncytia and *Besnoitia* cysts has been reported in maras.[289]

Other Genera of Coccidian Parasites

Coccidia of the genus ***Frenkelia*** have an obligatory two-host life cycle that closely resemble *Sarcocystis* spp. Rodents (prey) are the intermediate hosts and raptorial birds are the predator definitive host. In tissue, organisms appear in lobulated cysts packed with bradyzoites and maturing zoites. Liver damage in the rodent host is caused by development of first-generation meronts. Lesions also occur in brain. Frenelia cysts are often incidental findings.[290]

Coccida of the genus ***Caryospora*** and ***Lankesterella***[291] are pathogenic in birds and snakes, which shed unsporulated oocysts. Life cycles center on predator-prey relations such as owl-mouse and snake-mouse cycles. Ingestion of sporulated oocyts by the prey (intermediate host) results in extraintestinal merogony, gamogony, fertilization, sporulation and formation of a caryocyst. The viperid coccidian *Caryospora bigenetica* infects rats,[292] and can be experimentally transmitted to pigs. *Lankasterella minima* parasitizes bullfrog tadpoles and adults. Oocysts develop in endothelial cells of several organs.[293]

The Microsporans

Infections by pathogens of the phylum Microspora are found in every animal group. There are dozens of genera and hundreds of species of this phylum. In humans, pathogens of five genera have been reported: *Encephalitizoon*, *Nosema*, *Pleistophora*, *Microsporidium*, and *Enterocytozoon*. The first 3 genera have been single case reports with only rare identification. Typically, human disease occurs in patients with AIDS,[294,295] or as insect-borne corneal contaminants around contact lenses (Table 15.8). *Microsporidium* is a genus created for organisms identified as microsporidia but with insufficient characteristics to place them in a specific genus.

Microspora are intracellular parasites that form spores. The three major components of the microsporidian spore are the spore wall, sporoplasm, and an extrusion apparatus. All active stages develop in the cytoplasm of the host cell. During spore germination, sporoplasm is discharged from spores into the host cell through the channel of a tubular **polar filament**.

Table 15.8 Ultrastructure of pathogenic microsporidia.

Pathogen	*Host*	*Reference to ultrastructural pathology*
Brachiola algerae	Human	**Visvesvara**, *Folia Parasitol* 52:83, 2005 (cornea)
Encephalitozoan cuniculi	Rabbit, mouse, hamster Human	**Pakes**, *J Protozool* 22:481, 1975; **Sprague**, *J Protozool* 18:560, 1971 **Orenstein**, *Ultrastruct Pathol* 29:269, 2005; **Zender**, *Am J Clin Pathol* 92:352, 1989
E. hellem	Human	**Didier**, *J Protozool* 38:502, 1991*
Enterocytozoon bieneusi	Human	**Desportes**, *J Protozool* 32:250, 1985; **Leelayoova**, *Am J Trop Med Hyg* 73:104, 2005
E. salmonica	Fish	**Baxa-Antonio**, *J Protozool* 39:699, 1992 (blood); **Chilmonczyk**, *J Protozool* 38:264, 1991;
Loma morhua	Fish	**Morrison**, *J Fish Dis* 4:15, 1981 (gill)
L. salmonae	Salmon	**Lovy**, *Dev Comp Immunol* 30:259, 2006 (gill dendritic cell)
***L.* spp.**	Fish	**Morrison**, *J Fish Dis* 4:371, 1987 (gill)
Micrifilum lutjani	Fish	**Faye**, *J Protozool* 38:30, 1991 (gill)
Microgemma hepaticus	Fish	**Ralphs**, *J Fish Dis* 9:225, 1986
Myosporidium merluccius	Fish (hake)	**Baquero**, *J Eukaryot Microbiol* 52:476, 2005
Nosema algerae	In vitro	**Undeen**, *J Protozool* 38:511, 1991*
***Nosema* spp.**	Human	**Shadduck**, *J Infect Dis* 162:773, 1990
***Pleistophora* spp.**	Human Minnow	**Chupp**, *Clin Infect Dis* 16:15, 1993 **Ruehl-Fehlert**, *J Fish Dis* 28:629, 2005
Trachipleistophora anthropopthera	Human	**Pariyakanok**, *J Infect* 51:325, 2005 (HIV patient)

*Studies in vitro.

The polar filament, coiled in an inverted position inside the spore, is formed by a special Golgi apparatus, the **posterosome**. During infection the distal end of the polar filament penetrates the host cell and injects the sporoplasm.[296]

In the life cycle, sporonts divide into two spores and sporulation occurs without formation of a sporophorous vesicle (pansporoblastic membrane).[297] During maturation, spores form 3 spore-wall layers: the **epispore** and **endospore** of plasmatic membranes, and the **exospore**, consisting of polysaccharides that do not stain in electron microscopic preprarations. The anterior pole of the spore is filled with a **polaroplast**, a lamellar structure that is inflated when the polar filament is propelled from the spore.

Genus *Encephalitozoon*

Development of members of the genus *Encephalitozoon* includes uninucleate or binucleate stages in schizogony and sporogony. Spores are approximately 2 μm in diameter. Spore walls have two layers, the exospore and endospore, each with unique spore wall proteins.[298] Developmental stages of *E. cuniculi*, the most important pathogen, is monokaryotic and sporulation occurs in large **parasitophorous vacuoles**.[299,300]

Members of the genera have meronts that are 1.3–2.7 μm in diameter, develop within a parasitophorous vacuole, divide by binary fission, and bear two nuclei. **Sporonts** are 2 × 3 μm with a thick outer membrane. **Mature spores** are 1 × 1.5 μm and more electron dense. Each spore contains a single nucleus, a polar tubule with four to nine coils, a thin electron-dense exospore and a thick electron-lucent endospore. **Sporoblasts** possess the first recognizable polar filament (Fig. 15.21).

Transmitted from host to host via urine-contaminated food, *E. cuniculi* infects the brain of rabbits, dogs, and wild carnivores. Although most infections are subclinical and have little inflammatory reaction around the parasites, *E. cuniculi* can cause encephalitis. Infected macrophages and cysts also lodge in lungs, gonads, liver, pancreatic islets, and other tissues. Parasite cysts are surrounded by lymphoplasmacytic infiltrates and form tiny granulomas.

E. cuniculi infects immunosuppressed humans. It is reported in AIDS patients with hepatic lesions,[301] peritonitis,[302] and keratoconjunctivitis.[303] *E. hellem* is a species designation for organisms isolated from microsporidian keratoconjunctivitis.[304] Although the developmental stages and ultrastructure of in vitro grown cells are indistinguishable, biochemical and antigenic analysis reveal differences in proteins.

Encephalitozoonosis of dogs is most serious in young pups, in which it causes weakness, circling, and convulsions. The kidney is the target organ and chronic interstitial nephritis is typically present in fatal cases. Transplacental transmission of encephalitozoonsis has been reported in blue foxes.

Microsporidial **keratoconjunctivitis** appears as coarse, punctate epithelial lesions. Infected epithelial cells have large vacuoles that contain organisms in various stages of development; for example, mature spores, empty spore shells, and sporoblasts, which appear as thin-walled cells with polar tubule primoridia.[305] Stromal keratitis occurs in some infections.

Genus *Pleistophora*

The genus *Pleistophora* was established in 1983 for microsporidia that produce many spores (more than 8) within a sporophorous vesicle. On the basis of ultrastructure the genus was restricted to characteristics found in protozoan parasites of vertebrate hosts.[306] *Pleistophora* spp. have been identified in tissues of human patients with AIDS.[307]

Genus *Nosema*

The genus *Nosema* contains large numbers of species that are parasites of invertebrates, particularly the honeybee.[308] Few are pathogenic for vertebrates although several are known pathogens, and other are found incidentally at autopsy. Ultrastructural pathology of human corneal nosematosis has been reported.[309] Microsporidian parasites of fish gills include *Nosema branchiale* of haddock and a closely related species that infects the gills of Atlantic cod.[309]

As in all microsporidia, spore germination, the first step for infection, involves marked changes in the spore plasma membrane,[310] including development of a highly specialized organelle, the long, hollow **extrusion apparatus**, which is everted from within the spore to allow transfer of sporoplasm to the host. Invasion begins when the sporoplast of *Nosema* is rapidly injected into the host cell. The injected sporoplasm is in direct contact with the cytoplasm of the host cell. Injection leaves behind the filaments and empty spore cases on the surface of the host cell.[311] **Cysts** (xenomas) of these parasites are similar in ultrastructure to those of *Glugea* spp.

Genus *Enterocytozoon*

Enterocytozoon bieneusi is the most commonly reported microsporidian parasite that infects humans. It was first described in the enterocytes of human AIDS patients and is practically limited to this disease.

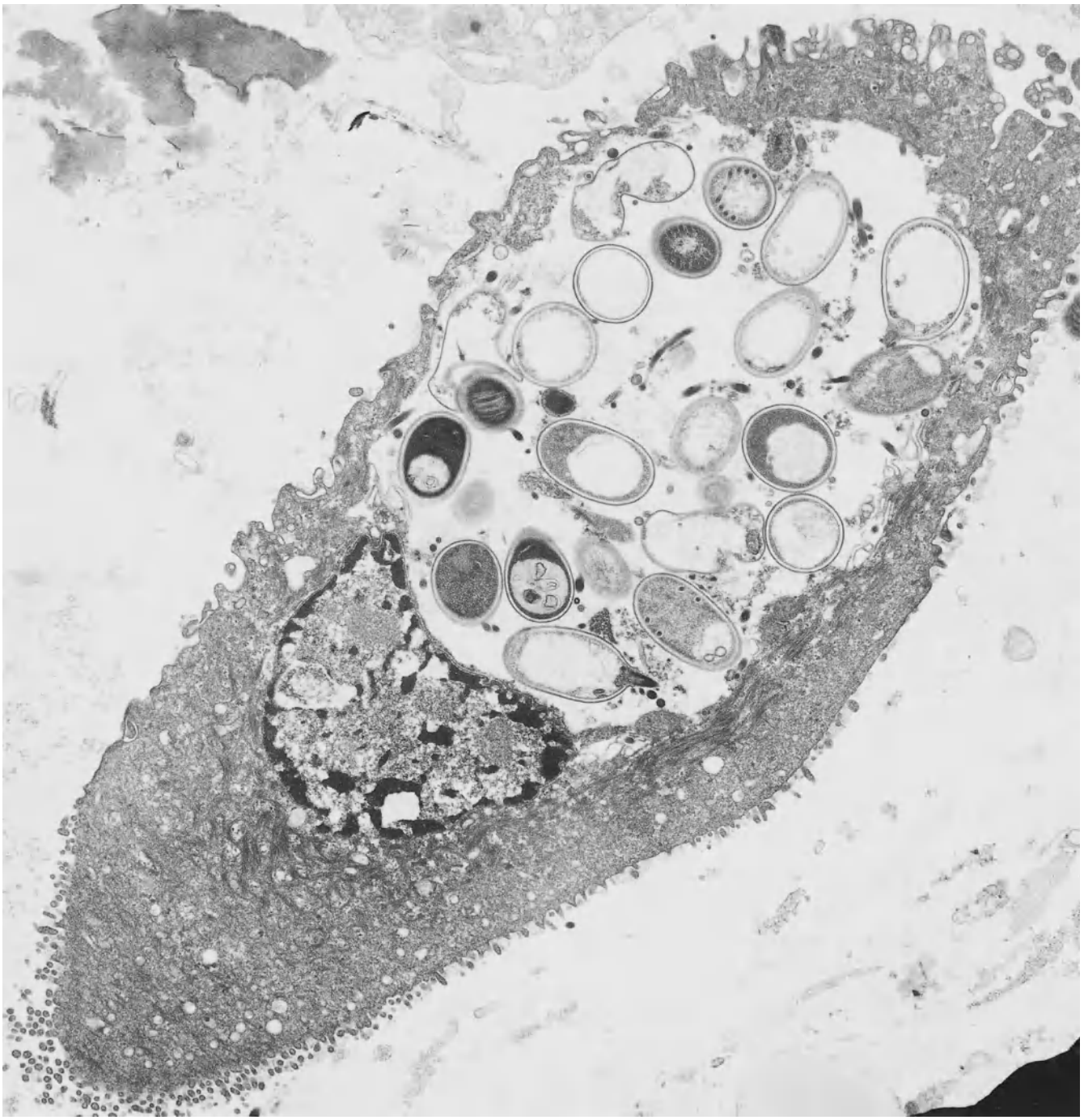


Fig. 15.21 ***Encephalitozoon hellem***: conjunctival scraping from a human patient. Mature spores in parasitophorous vacuole of infected cell. (Micrograph: Peter J. Didier and Jan M. Orenstein, *J Protozool* 38:502, 1991.)

Patients develop protracted diarrhea. *E. bieneusi* replicates by sporulation. Its distinguishing feature is premature development of polar filament precursors in the individual sporont.[312] *Enterocytozoon* is apansporoblastic, polysporous, and has characteristics not seen in other microsporidia: (1) an electron-lucent inclusion is prominent, (2) elongated sausage-shaped nuclei appear at one stage, and (3) polar tubes with electron-dense disks are present (Fig. 15.22).

Several species of *Enterocytozoon* are associated with salmonid fishes. One of these was described early as *Microsporidium rhabodphilia* in nuclei of rodlet cells of normal fish. One species that is associated with anemia, lymphoblastosis and other abnormalities of blood is *E. salmonis*, which develops within nuclei of hematopoietic cells of salmonid fish.[313,314] There is no parasitophorous vacuole and sporogony does not involve pansporoblastic membrane formation. **Spores** are

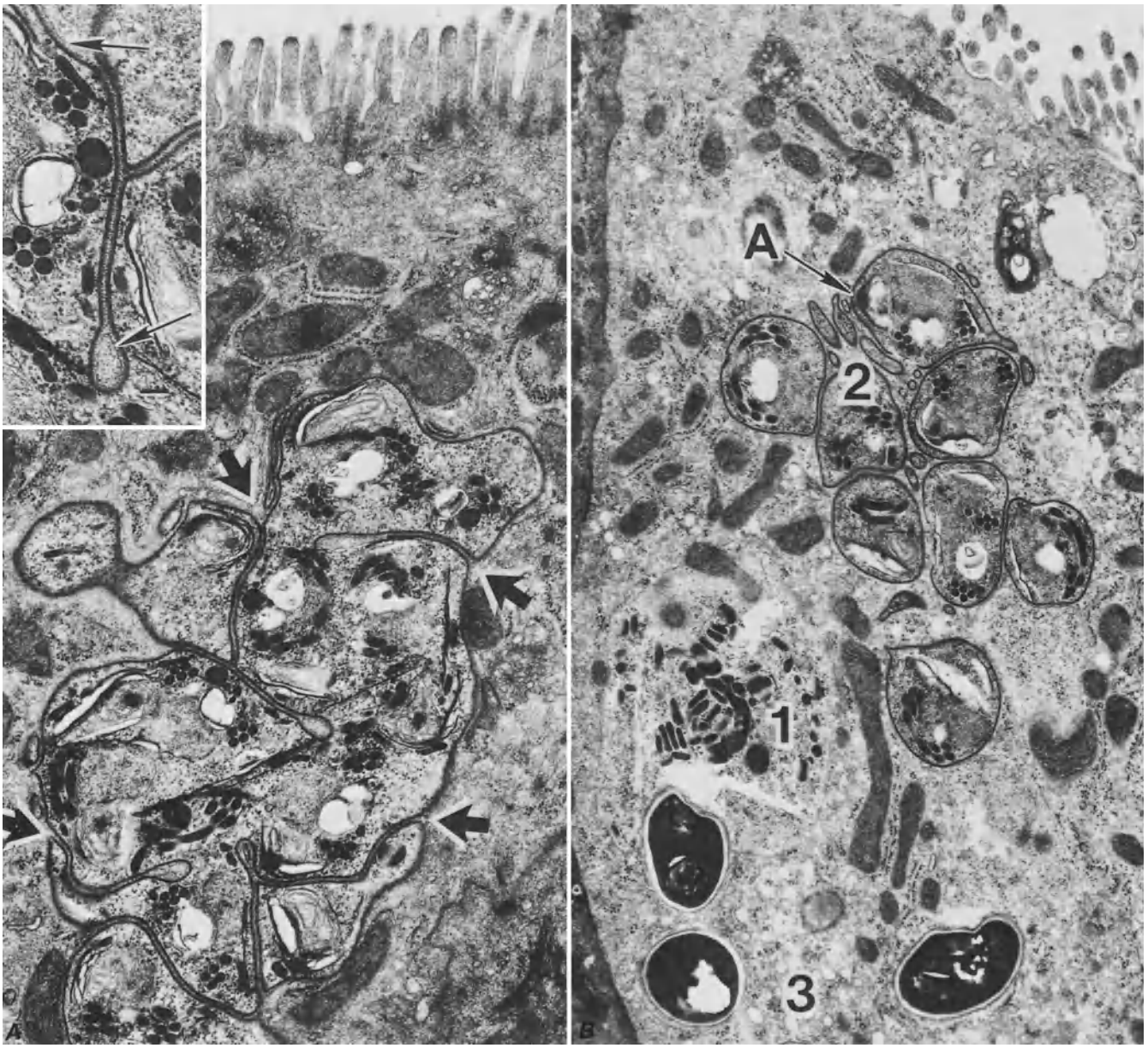


Fig. 15.22 ***Enterocytozoon bieneusi***: sporogonial division in human jejunum, 45-yr-old man with diarrhea associated with AIDS. **A**. **Thickened and invaginated plasma membrane** (*arrows*) segregates nuclei and organelles. *Inset*: invaginated membrane with outer coat formed (*arrows*). **B**. **Enterocyte**: contains sporogonial plasmodium (*1*), new sporoblasts (*2*), mature spores (*3*), and polar tube anchoring disk (*4*). (Micrograph: Ann Cali, *J Protozool* 37:145, 1990.)

ovoid (1 × 2 μm) and uninucleate with **polar tubules** coiled into 8–12 turns.

Genus *Glugea*

Glugea species infect submucosal intestinal cells of fish and induce a characteristic cytomegaly. The unique hypertrophic infected cellular mass is referred to as a **xenoma**. Xenoma cells are massively enlarged, both in nucleus and cytoplasm. The nucleus does no undergo mitosis but begins endomitotic polyploidization, and buds by amitosis.[315] The cytoplasm progressively looses its organelles as the parasite replicates. Enormous numbers of *Glugea* spp. develop in xenoma cells progressively forming a cyst in the cytoplasm.[316]

Protozoa of Uncertain Taxonomy

Blastocystis hominis

Blastocystic hominis, an organism of the human gut, was originally isolated from tropical areas and

described as a yeast. Based on ultrastructural studies, it has been classified as a protozoan parasite, although the poor quality of the micrographs indicate an uncertainty regarding the existence of this organism.[317–319]

References

1. Thorne KJI, Blackwell JM. 1983. Cell-mediated killing of protozoa. *Adv Parasitol* 22:43.
2. Paulin JJ. 1990. The dance of electrons entices protists to reveal their innermost secrets. *J Protozool* 37: 593.
3. Walzer PD. 1986. Attachment of microbes to host cells. *Lab Invest* 54:589.
4. Rudin W, et al. 1989. Binding of lectins to culture and vector forms of *Trypanosoma rangeli* Tejera, 1920 (Protozoa, Kinetoplastida) and to structures of the vector gut. *J Protozool* 36:532.
5. Aikawa M, Atkinson CT. 1990. Immunoelectron microscopy of parasites. *Adv Parasitol* 29:151.
6. Lee JJ, et al. 1985. The extent of algal and bacterial endosymbiosis in protozoa. *J Protozool* 32:391.
7. Reisser W, et al. 1985. Establishment, maintenance, and integration mechanism of endosymbionts in protozoa. *J Protozool* 32:383.
8. Bruchhaus I, et al. 2007. Protozoan parasites: Programmed cell death as a mechanism of parasitism. *Trends Parasitol* 23:376.
9. Dykstra MJ, Aldrich HC. 1978. Successful demonstration of an elusive cell coat in amebae. *J Protozool* 25:38.
10. Drozanski WJ. 1991. *Sarcobium lyticum* gen. nov., sp. nov., an obligate intracellular bacterial parasite of small free-living amoebae. *Int J Sys Bact* 41:82.
11. Scheid P, et al. 2008. An extraordinary endocytobiont in *Acanthamoeba* sp. isolated from a patient with keratitis. *Parasitol Res* 102:945.
12. Bowers B, Olsewski TE. 1983. *Acanthamoeba* discriminates internally between digestible and indigestible particles. *J Cell Biol* 97:317.
13. Mirelman D. 1987. Ameba-bacterium relationship in amebiasis. *Microbiol Rev* 51:272.
14. Mattern CFT, et al. 1972. Viruses of *Entamoeba histolytica*. *J Virol* 9:342.
15. Young J, et al. 1982. Characterization of a membrane pore-forming protein from *Entamoeba histolytica*. *J Exp Med* 156:1677.
16. Eaton RDP, et al. 1970. The functional morphology of pathogenicity of *Entamoeba histolytica*. *Ann Trop Med Parasitol* 64:299.
17. Gimenez-Scherer JA, et al. 1987. Ultrastructural changes associated with the inhibition of monocyte chemotaxis caused by products of axenically grown *Entamoeba histolytica*. *Lab Invest* 57:45.
18. Martinez-Palomo A, et al. 1985. Structural bases of the cytolytic mechanisms of *Entamoeba histolytica*. *J Protozool* 32:166.
19. Ravdin JI, et al. 1980. Cytopathogenic mechanism of *Entamoeba histolytica*. *J Exp Med* 152:377.
20. Visversa GS, et al. 1990. Leptomyxid ameba, a new agent of amebic meningoencephalitis in humans and aniimals. *J Clin Microbiol* 28:2750.
21. John DT, et al. 1985. Amebosomes of *Naegleria fowleri*. *J Protozool* 32:12.
22. Marciano-Cabral F, et al. 1990. Cytopathic action of *Naegleria fowleri* amoebae on rat neuroblastoma target cells. *J Protozool* 37:138.
23. Whiteman LY, Marciano-Cabral F. 1989. Resistance of highly pathogenic *Naegleria fowleri* amoeba to complement-mediated lysis. *Infect Immun* 57:3869.
24. Martinez AJ, et al. 1973. Acanthamoebiasis and immunosuppression. *J Neuropathol Exp Neurol* 41:548.
25. Westmoreland SV, et al. 2004. Necrotizing meningoencephalitis and pneumonitis in a simian immunodeficiency virus-infected rhesus macaque due to Acanthamoeba. *Vet Pathol* 41:398.
26. Chávez-Munquía B, et al. 2007. Ultrastructure of cyst differentiation in parasitic protozoa. *Parasitol Res* 100:1169.
27. Lovy J, et al. 2007. Ultrastructural examination of the host cellular response in the gills of the Atlantic salmon, *Salmo salar*, with amoebic gill disease. *Vet Pathol* 44:663.
28. Stelly N, et al. 1966. Cortical alveoli of *Paramecium*: A vast submembranous calcium storage compartment. *J Cell Biol* 113:103.
29. Grim JN. 2006. Food vacuole contents in the ciliate, *Balantidium jocularum* (Balantididae), symbiont in the intestine of the sturgeonfish, *Naso tonganus* (Acanthuridae). *J Eurkaryot Microbiol* 53:269.
30. Li M, et al. 2007. Light and scanning electron microscopic study of *Balantidum ctenopharyngodoni* Chen 1995 (Class: Litosomatea) from China. *Parasitol Res* 101:185.
31. Ewing MS, et al. 1991. Extracellular calcium concentration affects infectivity of Icthyophthirius (Ciliophora) theronts. *J Protozool* 38:178.
32. Lobo-da-cunha A, Azevedo C. 1990. Enzyme cytochemistry of the alveolar sacs and Golgi-like cisternae in the ciliate *Icthyophthirius multifiliis*. *J Protozool* 37:206.
33. Ewing MS, et al. 1985. *Icthyophthirius multifiliis* (Ciliophora) invasion of gill epithelium. *J Protozool* 32:305.
34. Engstler M, et al. 2007. Hydrodynamic flow-mediated protein sorting on the cell surface of trypanosomes. *Cell* 131:505.
35. Hall BF, et al. 1992. Desialylation of lysosomal membrane glycoproteins by *Trypanosoma cruzi*: A role for the surface neuraminidase in facilitating parasite entry into the host cell cytoplasm. *J Exp Med* 176:313.
36. Frevert U, et al. 1992. Stage-specific expression and intracellular shedding of the cell surface *trans*-sialidase of *Trypanosoma cruzi*. *Infect Immun* 60:2349.
37. Ley V, et al. 1990. The exit of *Trypanosoma cruzi* from the phagosome is inhibited by raising the pH or acidic compartments. *J Exp Med* 171:401.
38. Shakibael M, Frevert U. 1992. Cell surface interactions between *Trypanosoma congolense* and macrophages during phagocytosis in vitro. *J Protozool* 39:224.

39. Souto-Padron T, De Souza W. 1986. The surface charge of *Trypanosoma cruzi*: Analysis using cell eletrophoresis lectins and ultrastructural cytochemistry. *J Sub Cytol* 18:701.
40. Donelson JE. 1987. Antigenic variation in African trypanosomes. *Contr Microbiol Immunol* 8:138.
41. Duszenko M, et al. 1988. Intracellular transport of a variant surface glycoprotein in *Trypanosoma brucei*. *J Cell Biol* 106:77.
42. Frevert U, Reinwald E. 1988. Formation of filopodia in *Trypanosoma congolense* by crosslinking the variant surface antigen. *J Ult Molec Struc Res* 99:124.
43. Roditi I, et al. 1989. Procyclin gene expression and loss of the variant surface glycoprotein during differentiation of *Trypanosoma brucei*. *J Cell Biol* 108:73.
44. Hemphill A, et al. 1991. The cytoskeletal architecture of *Trypanosoma brucei*. *J Parasitol* 77:603.
45. Kohl L, Bastin P. 2005. The flagellum of trypanosomes. *Int Rev Cytol* 244:227.
46. Soares MJ, et al. 1991. Endocytosis of gold-labeled protein and LDL by *Trypanosoma cruzi*. *Zt. Parasitenkd* 77:461.
47. Hung CH, et al. 2004. Clathrin-dependent targeting of receptors to the flagellar pocket of procyclin-form *Trypanosoma brucei*. *Eukaryot Cell* 3:1004.
48. Kerschmann RL, et al. 1989. Novobiocin-induced ultrastructural changes and antagonism of DNA synthesis in *Trypanosoma cruzi* amastigotes growing in cell-free medium. *J Protozool* 36:14.
49. Giffin BF, McCann PP. 1989. Physiological activation of the mitochondrion and the transformation capacity of DFMO induced intermediate and short stumpy bloodstream form trypanosomes. *Am J Trop Hyg* 40:487.
50. Cazzulo JJ. 1992. Aerobic fermentation of glucose by trypanosomatids. *FASEB J* 6:3153.
51. Keller G-A, et al. 1991. Evolutionary conservation of a microbody targeting signal that targets proteins to peroxisomes, glyoxysomes, and glycosomes. *J Cell Biol* 114:893.
52. Robinson DR, Gull K. 1991. Basal body movements as a mechanism for mitochondrial genome segregation in the trypanosome cell cycle. *Nature* 352:731.
53. Hajduk SL, et al. 1993. RNA editing in kinetoplastid mitochondria. *FASEB J* 7:54.
54. Coppens I, et al. 1987. Receptor-mediated endocytosis in the bloodstream form of *Trypanosoma brucei*. *J Protozool* 34:465.
55. Pérez-Morga D, et al. 2005. Apolipoprotein L-I promotes trypanosome lysis by forming pores in lysosomal membranes. *Science* 309:469.
56. Madison MN, et al. 2007. Human defensin alpha-1 causes *Trypanosoma cruzi* membrane pore formation and induces DNA fragmentation, which leads to trypanosome destruction. *Infect Immun* 75:4780.
57. Grab DJ, et al. 2004. African trypanosome interactions with an in vitro model of the human blood-brain barrier. *J Parasitol* 90:970.
58. Ortega-Barria E, Pereira MEA. 1991. A novel *T. cruzi* heparin-binding protein promotes fibroblast adhension and penetration of engineered bacteria and trypanosomes into mammalian cells. *Cell* 67:411.
59. Friedman MJ. 1979. Ultrastructural damage to the malaria parasite in the sickled cell. *J Protozool* 26:195.
60. Miller LH, et al. 1979. Interaction between cytochalasin B-treated malarial parasites and erythrocytes. *J Exp Med* 149:172.
61. Palacios-Pru E, et al. 1989. Ultrastructural characteristics of different stages of human chagasic myocarditis. *Am J Trop Med Hyg* 41:29.
62. Nagle RB, et al. 1982. Glomerular accumulation of monocytes and macrophages in experimental glomerulonephritis associated with *Trypansoma rhodesiense* infection. *Lab Invest* 46:365.
63. Nogueira N, Cohn Z. 1976. *Trypanosoma cruzi*: Mechanism of entry and intracellular fate in mammalian cells. *J Exp Med* 143:1402.
64. Villalta F, et al. 1987. Extracellular killing of *Trypansoma cruzi* amastigotes by human eosinophiles. *J Protozool* 34:285.
65. Tafuri WL. 1971. Light and electron microscope studies of autonomic nervous system in experimental and human American trypanosomiasis. *Virch Arch A* 354:136.
66. Waghabi MC, et al. 2005. Uptake of host cell transforming growth factor-β by *Trypanosoma cruzi* amastigotes in cardiomyocytes. *Am J Pathol* 167:993.
67. Sanabria A. 1964. Ultrastructure of *Trypanosoma cruzi* in mouse myocardium. *Exp Parasitol* 15:125.
68. Anosa VO, et al. 1992. A light and electron microscopic study of changes in blood and bone marrow in acute hemorrhagic *Trypanosoma vivax* infection in calves. *Vet Pathol* 29:33.
69. Wellde BT, et al. 1978. *Trypanosoma congolesne*: Thrombocytopenia in experimentally infected cattle. *Exp Parasitol* 45:26.
70. Griebel PJ, et al. 1989. *Trypanosoma theileri* associated with T-lymphocytes isolated from a latently infected cow. *J Protozool* 36:415.
71. Walters LL, et al. 1987. Host-parasite relationship of *Leishmania mexicana mexicana* and *Lutaomyia abonnenci* (Diptera: Psychodidae). *Am J Trop Med* 36:294.
72. Berman JD, et al. 1981. In vivo and in vitro localization of Leishmania within macrophage phagolysosomes. *J Protozool* 28:239.
73. Castro R, et al. 2006. The ultrastructure of the parasitophorous vacuole formed by *Leishmania major*. *J Parasitol* 992:1162.
74. Alexander J. 1992. The interaction of *Leishmania* species with macrophages. *Adv Parasitol* 31:175.
75. Ueda-Nakamura T, et al. 2007. Comparative analysis of megasomes in members of the *Leishmania mexicana* complex. *Res Microbiol* 158:456.
76. Volf P, et al. 2004. Blocked stomodal valve of the insect vector. *Int J Parasitol* 34:1221.
77. Pimenta PFP, et al. 1992. Stage-specific adhesion of *Leishmania* promastigotes to the sandfly midgut. *Science* 256:1813.
78. Ismach R, et al. 1989. Flagellar membrane and paraxial rod proteins of *Leishmania* characterization employing monoclonal antibodies. *J Protozool* 36:617.
79. Rodríquez NE, et al. 2006. Role of caveolae in *Leishmania chagasi* phagocytosis and intracellular survival in macrophages. *Cell Microbiol* 8:1106.

80. Rasmusson B, Descoteaux A. 2004. Contribution of electron and confocal microscopy in the study of Leishmania-macrophage interactions. *Microsc Microanal* 10:656.
81. Miranda K, et al. 2004. Dynamics of polymorphism of acidocalcisomes in Leishmania parasites. *Histochem Cell Biol* 121:407.
82. Alexandre-Pires G, et al. 2006. Leishmaniasis—-a report about the microvascular and cellular architecture of the infected spleen in *Canis familiaris*. *Microsc Res Tech* 69:227.
83. Andrade ZA, et al. 1984. Immunopathology of experimental cutaneous leishmaniasis. *Am J Pathol* 114:137.
84. Ridley MJ, Wells CW. 1986. Macrophage-parasite interaction in the lesions of cutaneous leishmaniasis. *Am J Pathol* 123:79.
85. van Zandbergen G, et al. 2004. Cutting edge: Neutrophil granulocyte serves as a vector for Leishmania entry into macrophages. *J Immunol* 173:6521.
86. Erlandsen SL, et al. 1989. High-resolution electron microscopic evidence for the filamentous structure of the cyst wall in *Giardia muris* and *Giardia duodenalis*. *J Parasitol* 75:787.
87. Chavez B, et al. 1992. *Giardia lamblia*: Ultrastructural study of the in vitro effect of benzimidazoles. *J Prot* 39:510.
88. Poxleitner MK, et al. 2008. Evidence for karyogamy and exchange of genetic material in the binucleate intestinal parasite *Giardia intestinalis*. *Science* 319: 1520.
89. Müller N, von Allmen N. 2005. Recent insights in the mucosal reactions associated with *Giardia lamblia* infections. *Int J Parasitol* 35:1339.
90. Al-Tukhi MH, et al. 1991. Pathogenicity and antigenic components of excysted *Giarida lamblia* isolated from patients in Riyadh, Saudia Arabia. *Am J Trop Med* Hyg 45:442.
91. Lev B, et al. 1986. Lectin activation in *Giardia lamblia* by host protease: A novel host-parasite interaction. *Science* 232:71.
92. Owen RL, et al. 1979. Ultrastructural observations of giardiasis in a murine model. I. Intestinal distribution, attachment, and relation to the immune system of *Giardia muris*. *Gastroenterology* 76:757.
93. Tumová P, et al. 2007. Cell division of *Giardia intestinalis*: Assembly and disassembly of the adhesive disc, and cytokinesis. *Cell Motil Cytoskeleton* 64:288.
94. Peattie DA, et al. 1989. Ultrastructural localization of giardins to the edges of disk microribbons of *Giardia lamblia* and the nucleotide and deduced protein sequence of alpha giardin. *J Cell Biol* 109:2323.
95. Feely DE, et al. 1988. Ultrastructural evidence of the presence of bacteria, viral-like particles, and Mycoplasma-like organisms associated with *Giardia* spp. *J Protozool* 35:151.
96. Hernell O, et al. 1986. Killing of *Giardia lamblia* by human milk lipases: An effect mediated by lipolysis of milk lipids. *J Infect Dis* 153:715.
97. Owen RL, et al. 1981. Phagocytosis of Giardia muris by macrophages in Peyer's patches epithelium in mice. *Infect Immun* 33:591.
98. Brugerolle G, et al. 2000. Immunolocalization of two hydrogneosomal enzymes of *Trichomonas vaginalis*. *Parasitol Res* 86:30.
99. González-Robles A, et al. 2004. Surface properties and *in vitro* cytopathic effect of various strains of *Trichomonas vaginalis*. *J Submicr Cytol Pathol* 36:77.
100. Nielsen MH, Diemer NH. 1976. The size, density and relative area of chromatic granules "hydrogenosomes" in *Trichomas vaginalis* Donne from cultures of logarithmic and stationary growth. *Cell Tissue Res* 167:461.
101. Bricheux G, et al. 2000. Characterization, cloning and immunolocalization of a coronin homologue in *Trichomnas vaginalis*. *Eur J Cell Biol* 79:413.
102. Lee DL. 1972. Changes in the ultrastructure of the caecum of chickens caused by *Trichomonas gallinarium*, *Parasitology* 65:71.
103. Kondova I, et al. 2005. Trichomonad gastritis in rhesus macaques (*Macaca mulatta*) infected with simian immunodeficiency virus. *Vet Pathol* 42:19.
105. Rhyan JC, et al. 1988. Fetal and placental lesions in bovine abortion due to *Tritrichomonas foetus*. *Vet Pathol* 25:350.
104. Benchimol M, et al. 1992. Surface domains in the pathogenic protozoan *Tritrichomonas foetus*. *J Protrotozool* 39:480.
106. Hongiberg BM, et al. 1984. A freeze-fracture electron microscope study of *Trichomonas vaginalis* Donne and *Tritrichomas foetus* (Riedmuller). *J Protozool* 31:116.
107. Januschka MM, et al. 1988. A comparison of *Giardia microti* and *Spironucleus muris* cysts in the vole. *J Parasitol* 74:452.
108. Wilkins D, Lee DL. 1974. Scanning electron microscopy of the caecal mucosa of turkeys affected with *Histomonas meleagridis*. *J Comp Pathol* 84:589.
109. Moltmann UG, et al. 1983. Fine structure of *Babesia equi* Laveran, 1901 within lymphocytes and erythrocytes of horses. *J Parasit* 69:111.
110. Yamasaki M, et al. 2002. *Babesia gibsoni*: Preferential multiplication in reticulocytes is related to the presence of mitochondria and a high concentration of adenosine 5′-triphosphate in the cells. *Exp Parasitol* 102:164.
111. Chapman WE, Ward PA. 1977. *Babesia rodhaini*: Requirement of complement for penetration of human erythrocytes. *Science* 196:67.
112. Melhorn H. 1984. The piroplasms: Life cycle and sexual stages. *Adv Parasitol* 23:37.
113. Moltmann UG, et al. 1982. Ultrastructure of the development of *Babesia ovis* (Piroplasmia) in the ovary of the vector tick Rhipicephalus bursa. *J Protozool* 29:30.
114. Rudzinska MA, et al. 1983. Invasion of *Babesia microti* into epithelial cells of the tick gut. *J. Protozool* 30:338.
115. Schein E, et al. 1978. Electron microscopic studies on the schizogony of four *Theileria* species of cattle (*T parva*, *T lawrencei*, *T annulata* and *T mutans*). *Protistologica* 198:337.
116. Schein E, et al. 1977. Fine structural study on the erythrocytic stanges of *Theileria annulata* (Schunkowsky, Luhs, 1904). *Tropenmed Parasitol* 28:349.
117. Fawcett DW, et al. 1982. The entry of sporozoites of *Theileria parva* into bovine lymphocytes in vitro: Electron microscopic observations. *Eur J Cell Biol* 27:10.

118. van Vorstenbosch CJAH, et al. 1978. Erythrocytic forms of *Theileria velifera*. *Res Vet Sci* 24:214.
119. Melhorn H, Schein E. 1976. Elektronmikroskopische Untersuchungen und Entwicklungsstadien von *Theileria parva* (Theiler, 1904) im Darm der Uebertraegerzecke *Huyalomma anatolicum excavatum* (Koch, 1844). *Tropenmed Parasit* 27:182.
120. Shaw MK, et al. 1991. The entry of *Theileria parva* sporozoites into bovine lymphocytes: Evidence of MHC class I involvement. *J Cell Biol* 113:87.
121. Barnett SF. 1960. Connective tissue reactions in acute fatal east coast fever (*Theileria parva*) of cattle. *J Infect Dis* 107:253.
122. De Martini JC, Moulton JE. 1973. Responses of the bovine lymphatic system to infection by *Theileria parva*. *J Comp Pathol* 183:281.
123. Simpson CR, et al. 1985. Ultrastructure of the intraerythrocytic stage of *Cytauxzoon felis*. *Am J Vet Res* 46:1178.
124. Kocan AA, et al. 1992. A redescription of schizogony of Cytoauxzoon felis in the domestic cat. *Ann N Y Acad Sci* 653:161.
125. Richard MV, et al. 2005. A new species of Cytoauxzoon from Pallas' cats caught in Mongolia and comments on the systematics and taxonomy of piroplasmids. *J Parasitol* 91:420.
126. Simpson CF, et al. 1985. Ultrastructure of schizonts in the liver of cats with experimentally induced cytauxzoonosis. *Am J Vet Res* 46:384.
127. Barta JR. 1991. The Dactylosomatide. *Adv Parasitol* 30:1.
128. Sinden RE. 1983. Sexual development of malarial parasites. *Adv Parasitol* 22:153.
129. Dinglasan RR, et al. 2007. Plasmodium falciparum ookinetes require mosquito midgut chondroitin sulfate proteoglycans for cell invasion. *Proc Natl Acad Sci USA* 104:15882.
130. Kadota K, et al. 2004. Essential role of membrane-attack protein in malarial transmission to mosquito host. *Proc Natl Acad Sci USA* 101:16310.
131. Li F, et al. 2004. Plasmodium ookinete secreted proteins secreted through a common micronemal pathway are targets of blocking malarial transmission. *J Biol Chem* 279:26635.
132. Billingsley PF, Rudin W. 1992. THe role of the mosquito peritrophic membrane in bloodmeal digestion and infectivity of *Plasmodium* species. *J Parasitol* 78:430.
133. Bernier R, et al. 1983. Peritrophic membranes and protease activity in the midgut of the malaria mosquito, *Anopheles stephensi* (Liston) (Insecta: Diptera) under normal and experimental conditions. *J Ultrastr Res* 83:195.
134. Aikawa M, et al. 1984. New observations on gametogenesis, fertilization, and zygote transformation in *Plasmodium gallinaceum*. *J Protozool* 31:403.
135. Feng Z, et al. 1993. Pfs2400 can mediate antibody-dependent malaria transmission inhibition and may be the *Plasmodium falciparum* 11.1 gene product. *J Exp Med* 177:273.
136. Meis JFGM, Verhave JP. 1988. Exoerythrocytic development of malarial parasites. *Adv Parasitol* 27:1.
137. Stewart MJ, Vandenberg JP. 1991. Malaria sporozoites release circumsporite protein from their apical end and translocate it along their surface. *J Protozool* 38:411.
138. Stewart MJ, Vanderberg JP. 1992. Electron microscopic analysis of circumsporite protein trail formation by gliding malarial sporozoites. *J Protozool* 39:663.
139. Jap PHK, et al. 1982. Degenerating exoerythrocyte forms of *Plasmodium berghei* in rat liver: An ultrastructural cytochemical study. *Parasitology* 85:263.
140. Terzakis JA, et al. 1979. Exoerythrocytic merozoites of *Plasmodium berghei* in rat hepatic Kupffer cells. *J Protozool* 26:385.
141. Cerami C, et al. 1992. The basolateral domain of the hepatocyte plasma membrane bears receptors for the circumsporozoite protein of *Plasmodium falciparum* sporozoites. *Cell* 70:1021.
142. Khan ZM, et al. 1992. Early hepatic stages of *Plasmodium berghei*: Release of circumsporozoite protein and host cellular inflammatory response. *Infect Immun* 60:264.
143. Taylor D, et al. 1990. Identification of an apically-located antigen that is conserved in sporozoan parasites. *J Protozool* 37:540.
144. Ockenhouse CF, et al. 1989. Identification of platelet membrane glycoprotein as a falciparam malaria sequestration receptor. *Science* 243:1469.
145. Kara UAK, et al. 1988. The parasitophorous vacuole membrane of *Plasmodium falciparum*: Demonstration of vesicle formation using an immune probe. *Eur J Cell Biol* 46:9.
146. Cowman AF, Crabb, BS. 2006. Invasion of red blood cells by malaria parasites. *Cell* 124:755.
147. Aikawa M, et al. 1976. Erythrocyte entry by malarial parasites. *J Cell Biol* 77:72.
148. Sam-Yellowe TY, et al. 1988. Secretion of *Plasmodium falciparum* rhoptry protein into the plasma membrane of host erythrocytes. *J Cell Biol* 106:1507.
149. Stewart MJ, et al. 1985. Rhoptry secretion of membranous whorls by *Plasmodium berghei* sporozoites. *J Protozool* 32:280.
150. Torii M, et al. 1989. Release of merozoite dense granules during erythrocyte invasion by *Plasmodium knowlesi*. *Infect Immun* 57:3230.
151. Weiss L. 1983. Hematopoietic tissue in malaria: Facilitation of erythrocytic recycling by bone marrow in *Plasmodium berghei*-infected mice. *J Parasitol* 69:307.
152. Weiss L. 1989. Mechanisms of splenic control of murine malaria. *Am J Trop Med Hyg* 41:144.
153. Aikawa M, et al. 1975. Caveola-vesicle complexes in the plasmalemma of erythrocytes infected by *Plasmodium vivax* and *P. cynomolgi*. *Am J Pathol* 79:285.
154. Hanssen E, et al. 2007. Electron tomography of the Maurer's cleft organelles of *Plasmodium falciparum*-infected erythrocytes reveals novel structural features. *Mol Microbiol* 67:703.
155. Spycher C, et al. 2006. Genesis of and trafficking to the Maurer's clefts of *Plasmodium falciparum*-infected erythrocytes. *Mol Cell Biol* 26:4074.
156. Knuepfer E, et al. 2005. Trafficking determinants for PfEMP3 export and assembly under the *Plasmodium falciparum*-infected red blood cell membrane. *Mol Microbiol* 58:1039.

157. Cyrklaff M, et al. 2007. Cryoelectron tomography reveals periodic material at the inner side of subpellicular microtubules in apicomplexan parasites. *J Exp Med* 204:1281.
158. Hutchings CL, et al. 2007. New insights into the altered adhesive and mechanical properties of red blood cells parasitized by *Babesia bovis*. *Mol Microbiol* 65:1092.
159. Bodammer JE, Bahr GF. 1973. The initiation of a "metabolic window" in the surface of host erythrocytes by *Plasmodium berghei* NYU-2. *Lab Invest* 28:708.
160. Aikawa M, et al. 1986. Membrane-associated material of the asexual stages of *Plasmodium falciparum*. Evidence for movement from the intracellular parasite to the erythrocyte membrane. *Am J Trop Med Hyg* 35:30.
161. Atkinson CT, et al. 1987. Ultrastructure of the erythrocyte stages of *Plasmodium malariae*. *J Protozool* 34:267.
162. Ponpuak M, et al. 2007. A role for falcilysin in transit peptide degradation in the *Plasmodium falciparum* apicoplast. *Mol Microbiol* 63:314.
163. Slomianny C, Prensier G. 1990. A cytochemical ultrastructural study of the lysosomal system of different species of malarial parasites. *J Protozool* 37:465.
164. Noland GS, et al. 2003. The shape and size of hemozoin crystals distinguishes diverse Plasmodium species. *Mol Biochem Parasitol* 130:91.
165. Beitz E. 2007. Jammed traffic impedes parasite growth. *Proc Nat Acad Sci USA* 104:13855.
166. Gruenberg J, et al. 1983. Scanning electron microscope-analysis of the protrusion (knobs) present on the surface of *Plasmodium falciparum*-infected erythrocytes. *J Cell Biol* 97:795.
167. Luse SA, Miller LH. 1971. *Plasmodium falciparum* malaria: Ultrastructure of parasitized erythrocytes in cardiac vessels. *Am J Trop Med Hyg* 20:655.
168. Macpherson GG, et al. 1985. Human cerebral malaria. *Am J Pathol* 119:385.
169. Oo MM, et al. 1987. Human cerebral maliaria: A pathological study. *J Neuropathol Exp Neurol* 46:223.
170. White NJ, Ho M. 1992. The pathophysiology of malaria. *Adv Parasitol* 31:83.
171. Cochrane AH, et al. 1988. Membrane-associated antigens of blood stages of *Plasmodium brasilianum*, a quartan malaria parasite. *Infect Immun* 56:2080.
172. Culvenor JG, Crewther PE. 1990. S-antigen localization in the erythrocyte stages of *Plasmodium falciparum*. *J Protozool* 37:59.
173. Leech JH, et al. 1984. *Plasmodium falciparum* malaria. Association of knobs on the surface of infected erythrocytes with a histidine-rich protein and the erythrocyte skeleton. *J Cell Biol* 98:1256.
174. Matsumoto Y, et al. 1988. Immunoelectron microscopic localization of vivax malaria antigens to the clefts and caveola-vesicle complexes of infected erythrocytes. *Am J Trop Med Hyg* 39:317.
175. Winograd E, Sherman IW. 1989. Characterization of a modified red cell membrane protein expressed on erythrocytes infected with the human malaria parasite *Plasmodium falciparum. J Cell Biol* 108:23.
176. Udeinya IJ, et al. 1981. Falciparum malaria-infected erythrocytes specifically bind to cultured human endothlelial cells. *Science* 213:555.
177. Rock EP, et al. 1988. Thrombospondin mediates the cytoadherence of *Plasmodium falciparum*–infected red cells to vascular endothelium in shear flow conditions. *Blood* 71:71.
178. Lackner P, et al. 2006. Scanning electron microscopy of the neuropathology of murine cerebral malaria. *Malaria J* 5:116.
179. Medana IM, et al. 2007. Cerebral capain in fatal falciparum malaria. *Neuropathol Appl Neurobiol* 33:179.
180. Lackner P, et al. 2007. Apoptosis in experimental cerebral malaria. *Neuropathol Appl Neurobiol* 33:560.
181. Nguansangiam S, et al. 2007. A quantitative ultrastructural study of renal pathology in fatal *Plasmodium falciparum* malaria. *Trop Med Int Health* 12:1037.
182. Pulido-Méndez M, et al. 2006. Ultrastructural changes in mouse kidney caused by *Plasmodium berghei* infection. *J Submicrosc Cytol Pathol* 38:143.
183. Boonpucknavig S, et al. 1973. *Plasmodium berghei* infection in mice: An ultrastructural study of immune complex nephritis. *Am J Pathol* 70:89.
184. Tegoshi T, et al. 1992. Placental pathology in *Plasmodium berghei*-infected rats. *Am J Trop Med Hyg* 47:643.
185. Torii M, et al. 1992. Penetration of the mosquito (*Aedes aegypti*) midgut wall by the ookinetes of *Plasmodium gallinaceum*. *J Protozool* 39:449.
186. Swann AI, Kreier JP. 1973. *Plasmodium gallinaceum*: Mechanisms of anemia in infected chickens. *Exp Parasitol* 33:79.
187. Aikawa M, et al. 1968. Exoerythrocytic stages of *Plasmodium gallinaceum* in chick-embryo liver as observed electron microscopically. *Am J Trop Med Hyg* 17:156.
188. Aikawa M, et al. 1966. The feeding mechanism of avian malarial parasites. *J Cell Biol* 28:355.
189. Krizanauskiene A, et al. 2006. Variation in host specificity between species of avian hemosporidian parasites. *J Parasitol* 92:1319.
190. Steele EJ, et al. 1992 Schizogonic development of *Leucocytozoon smithi*. *J Protrozool* 39:530.
191. Dessar SS. 1973. The fine structure of *Leucocytozoon simondii*. II. Hepatic schizogony. *Can J Zool* 51:605.
192. Morii T, et al. 1992. Observations in first-generation schizogony of Leucocytozoon caulleryi in chickens. *J Protozool* 39:281.
193. Steele EJ, et al. 1992. Sporogonic development of *Leucocytozoon smithi*. *J Protozool* 39:690.
194. Steele EJ, Noblet GP. 2001. Gametogenesis, fertilization and ookinete differentiation of *Leucocytozoon smithi*. *J Eukaryot Microbiol* 48:118.
195. Aikawa M, et al. 1970. Morphological study of microgametogenesis of *Leucocytozoon simondi*. *J Ultrastr Res* 32:43.
196. Chen MM, et al. 2001. Haemoproteus and Schistosoma synthesize heme polymeres similar to *Pasmodium hemozoin* and beta-hematin. *Mol Biochem Parasitol* 113:1.
197. Atkinson CT. 1989. Ultrastructure of the ookinetes of *Haemoproteus meleagridis* (Haemosporina: Haemoproteidae). *J Parasitol* 75:135.
198. Bradbury PC, Gallucci BB. 1972. Observations on the fine structure of the schizont of *Haemoproteus columbae*. *J Protozool* 17:405.
199. Klei TR. 1972. The fine structure of *Haemoproteus columbae* sporozoites. *J Protozool* 19:281.

200. Sterling CR, DeGiusti DL. 1972. Ultrastructural aspects of schizogony, mature schizonts, and merozoites of *Haemoproteus metchnikovi*. *J Parasitol* 58:641.
201. Ailor BJ. 1972. An electron microscopic study of the microgamate of *Haemoproteus columbae* Kruse. *J Protozool* 19:458.
202. Vickers DH. 1966. *Hepatocystis kochi* in cercopithecus monkeys. *J Am Vet Med Ass* 149:906.
203. Canning EU, et al. 1976. Ultrastructural observations on the merocyst and gametocytes of *Hepatocystis* spp. from Malaysian squirrels. *Ann Parasitol Hum Comp* 51:607.
204. Ball SJ, et al. 1989. Intestinal and extraintestinal life cycles of Eimeriid coccidia. *Adv Parasitol* 28:1.
205. Andreassen J, Behnke O. 1968. Fine structure of merozoites of a rat coccidian *Eimeria miyairii*, with a comparison of fine structure of other sporozoa. *J Parasitol* 54:150.
206. Madden PA, Ruff MD. 1979. *Eimeria dispersa*, *E. adenoeides*, and *E. meleagrimitis*: Intestinal mucosal disruption in turkeys as seen with scanning electron microscopy. *J Parasitol* 65:234.
207. Riley D, Fernando MA. 1988. *Eimeria maxima* (Apicomplexa): A comparison of sporozoite transport in naive and immune chickens. *J Parasit* 74:103.
208. Roberts WL, et al. 1970. Ultrastructural study of the intra- and extracellular sporozoites of *Eimeria callospermophili*. *J Parasitol* 56:907.
209. Danforth HD, et al. 1992. Localization of a low molecular weight antigen of *Eimeria tenella* by use of hybridoma antibodies. *J Parasitol* 78:460.
210. Gallego Edel C, et al. 2007. Flotillin-1 localization on sporozoites of *Eimeria tenella*. *J Parasitol* 93:197.
211. Ferguson DJ, et al. 2007. Enzymes of type II fatty acid synthesis and apicoplast differentiation and division in *Eimeria tenella*. *Int J Parasitol* 37:33.
212. Speer CA, et al. 1989. Ultrastructural localization of antigenic sites on sporozoites, sporocysts and oocysts of *Eimeria acervulina* and *Eimeria tenella* by monoclonal IgG and IgM antibodies. *J Parasitol* 75:92.
213. Fernando MA. 1974. Fine structure of the schizonts and merozoites of *Eimeria acervulina* in the chicken. *J Parasitol* 60:149.
214. Kelley GL, Hammond DM. 1973. Fine structural aspects of nuclear division and merogany of *Eimeria ninakohlakimome*. *J Parasitol* 59:1071.
215. Melhorn H. 1972. Elektronenmikroskopische Untersuchungen an den Makrogameten von *Isospora felis* and *I. rivolta*. *Zt. Parasitol* 40:243.
216. Sheffield HG, Hammond DM. 1967. Fine structure of first generation merozoites of *Eimeria bovis*. *Parasitology* 53:831.
217. Cheissin EM. 1965. Electron microscope study of microgametogenesis in two species of coccidia from rabbit (*Eimeria magna* and *E. intestinalis*). *Acta Protozool* 3:215.
218. Hammond DM, et al. 1967. The fine structure of microgametocytes of *Eimeria perforans*, *E. stiedae*, *E. bovis* and *E. auburnensis*. *J Parasitol* 53:235.
219. Pelster B. 1973. Vergleichende elektronenmikroskopische Untersuchungen an den Makrogameten von *Isospora felis* and *I. rivolta*. *Zt Parasitol* 41:29.
220. Scholtyseck E, Hammond DM. 1970. Electron microscope studies of macrogametes and fertilization in *Eimeria bovis*. *Zt Parasitol* 34:310.
221. Kefu Z, et al. 2006. *Eimeria tenella*: Further studies on the development of the oocyst. *Exp Parasitol* 113:174.
222. Melhorn H, Marcus MB. 1976. Electron microscopy of stages of *Isospora felis* of the cat in mesenteric lymph nodes of the mouse. *Zt Parasitenkd* 51:15.
223. Roberts WL, et al. 1972. The fine structure of the sporozoites of *Isospora canis*. *Zt Parasitol* 40:183.
224. Restrep C, et al. 1987. Disseminated extraintestinal isosporiasis in a patient with acquired immune deficiency syndrome. *Am J Clin Pathol* 87:40.
225. Mohamed HA, et al. 1990. Developmental stages of *Cyclospora talpae* in the liver and bile duct of the mole (*Talpa europaea*). *Parasitology* 101:345.
226. Ortega YR, et al. 1993. Cyclospora species—-a new protozoan pathogen of humans. *New Engl J Med* 328: 1308.
227. Ferguson DJP, et al. 1974. Ultrastructural study of early stages of asexual multiplication and microgametogeny of *Toxoplasma gondii* in the small intestine of the cat. *Acta Pathol Microbiol Scand B* 82:167.
228. Cintra WM, et al. 1986. The surface charge of *Toxoplasma gondii*: A cytochemical and electrophoretic study. *J Submucrosc Cytol* 18:773.
229. Sheffield HG, Melton ML. 1968. The fine structure and reproduction of *Toxoplasma gondii*. *J Parasitol* 54:209.
230. Gross U, et al. 1991. Identification of a virulence-associated antigen of *Toxoplasma gondii* by use of a mouse monoclonal antibody. *Infect Immun* 59:4511.
231. Morrissette NS, Roos DS. 1998. *Toxoplasma gondii*: A family of apical antigen associated with the cytoskeleton. *Exp Parasitol* 89:296.
232. Hansson HA, Sourander P. 1968. Ultrastructural demonstration of lysosomes in *Toxoplasma gondii*. *Acta Pathol Microbiol Scand* 74:431.
233. Tichy J, et al. 1968. Electron microscopic findings in the spleen of mice in acute toxoplasmosis. *Pathol Microbiol* 31:307.
234. Jones TC, Hirsch JC. 1972. The interaction between *Toxoplasma gondii* and mammalian cells. *J Exp Med* 136:1173.
235. Zaman V, Colley FC. 1972. Ultrastructural study of penetration of macrophages by *Toxoplasma gondii*. *Trans Roy Soc Trop Med* 66:781.
236. Nichols BA, et al. 1983. Secretion from the rhoptries of *Toxoplasma gondii* during host-cell invasion. *J Ultrastruct Res* 83:85.
237. Coppens I, et al. 2006. *Toxoplasma gondii* sequesters lysosomes from mammalian hosts in the vacuolar space. *Cell* 125:261.
238. Mordue DG, et al. 2007. A patatin-like protein protects *Toxoplasma gondii* from degradation in activated macrophages. *Mol Microbiol* 63:482.
239. Cortez E, et al. 2008. Immunolocalization of an osteopontin-like protein in dense graules of *Toxoplasm gondii* tachyzoites and its association with the parasitophorous vacuole. *Micron* 39:25.
240. Boothroyd JC, Dubremetz JF. 2008. Kiss and spit: The dual roles of Toxoplasma rhoptries. *Nat Rev Microbiol* 6:79.

241. Sibley LD, et al. 1985. Phagosome acidification blocked by intracellular *Toxoplasma gondii*. *Nature* 315:416, 1985
242. Joiner KA, et al. 1990. *Toxoplasma gondii*: Fusion competence of parasitophorous vacuoles in Fc receptor-transfected fibroblasts. *Science* 249:641.
243. de Carvalho L, et al. 1991. Localization of lectin-binding sites and sugar-binding proteins in tachyzoites of *Toxoplasma gondii*. *J Parasitol* 77:156.
244. Sibly LD, et al. 1986. *Toxoplasma* modifies macrophages, phagosomes by secretion of a vesicular network rich in surface proteins. *J Cell Biol* 103:867.
245. Murray HW. 1981. Susceptibility of Leishmania to oxygen intermediates and killing by normal macrophages. *J Exp Med* 153:1302.
246. Yong EC, et al. 1991. Human platelet-mediated cytotoxicity against *Toxoplasma gondii*: Role of thromboxane. *J Exp Med* 173:65.
247. Melhorn H, Frenkel JK. 1980. Ultrastructural comparison of cysts and zoites of *Toxoplasma gondii*, *Sarcocystis muris*, and *Hammondia hammondi* in skeletal muscle of mice. *J Parasitol* 66:59.
248. Parker GA, et al. 1981. Pathogenesis of acute toxoplasmosis in specific-pathogen-free cats. *Vet Pathol* 18:786.
249. Powell HC, et al. 1978. Toxoplasmosis of the central nervous system in the adult. Electron microscopic observations. *Acta Neuropathol* 41:211.
250. Tang TT, et al. 1986. Cerebral toxoplasmosis in an immunocompromised host. *Am J Clin Pathol* 85:104.
251. Heidel JR, et al. 1990. Myelitis in a cat infected with *Toxoplasma gondii* and feline immunodeficiency virus. *J Am Vet Med Ass* 196:316.
252. Ferguson DJP, Hutchison WM. 1987. An ultrastructural study of the early development and tissue cyst formation of *Toxoplasma gondii* in the brains of mice. *Parasitol Res* 73:483.
253. Sims TA, et al. 1989. An electron microscope and immunohistochemical study of the intracellular location of Toxoplasma tissue cysts within the brain of mice with congenital toxoplasmosis. *Br J Exp Pathol* 70:317.
254. Speer CA, Dubey JP. 1989. Ultrastructure of sporozoites and zoites of *Hammondia heydorni*. *J Protozool* 36:488.
255. Cummings JF, et al. 1988. Canine protozoal polyradiculoneuritis. *Acta Neuropathol* 76:46.
256. Barr BC, et al. 1991. *Neospora*-like encephalomyelitis in a calf. *J Vet Diagn Invest* 3:39.
257. Dubey JP, et al. 1988. Newly recognized fatal protozoon disease of dogs. *J Am Vet Med Ass* 192:1269.
258. Lindsay DS, et al.1993. 1993. Use of infected cultured cells to compare ultrastructural features of *Neospora caninum* from dogs and *Toxoplasma gondii*. *Am J Vet Res* 54:103.
259. Speer CA, et al. 1999. Comparative ultrastructure of tachyzoites, bradyzoites, and tissue cysts of *Neospora caninum* and *Toxoplasma gondii*. *Int J Parasitol* 29:1509.
260. Srinivasan S, et al. 2006. Monoclonal antibody directed against *Neospora caninum* tachyzoite carbohydrate epitope reacts specifically with apical complex associated sialylated beta tubulin. *J Parasitol* 92:1235.
261. Keller N, et al. 2004. Identificaiton and characterization of a *Neospora caninum* microneme-associated protein (NcMIC4) that exhibits unique lactose-binding properties. *Infect Immun* 72:4791.
262. Tomova C, et al. 2006. New comprehension of the apicoplast of *Sarcocystis* by transmission electron tomography. *Biol Cell* 98:535.
263. Dubey JP, et al. 1982. Sarcocystosis in newborn calves fed *Sarcocystis cruzi* sporocysts from coyotes. *Am J Vet Res* 43:2147.
264. Frelier PF, et al. 1979. Bovine sarcocystosis. *Am J Vet Res* 40:651.
265. Nakamura K, et al. 1982. Pathology of experimental acute sarcocystosis in a cow. *Jap J Vet Sci* 44:67.
266. Bowman DD, et al. 1992. Characterization of *Sarcocystis neurona* from a thoroughbred with equine protozoal myeloencephalitis. *Cornell Vet* 82:41.
267. Liebler EM, et al. 1986. Experimental intrauterine infection of adult BALB/c mice with *Crypstosporidium* sp. *Infect Immun* 54:255.
268. Tilley M, et al. 1991. Identification of a 15-kilodalton surface glycoprotein on sporozoites of *Cryptosporidium parvum*. *Infect Immun* 59:1002.
269. Slapeta J, Keithly JS. 2004. *Cryptosporidium parvum* mitochondrial-type HSP70 targets homologous and heterologous mitochondria. *Eukaryot Cell* 3:483.
270. Tzipori S. 1988. Cryptosporidiosis in perspective. *Adv Parasitol* 27:63.
271. Current WL, Reese NC. 1986. A comparison of endogenous development of three isolates of *Cryptosporidium* in suckling mice. *J Protozool* 33:98.
272. Bird RG, Smith MD. 1980. Cryptosporidiosis in man: Parasite life cycle and fine structural pathology. *J Pathol* 132:217.
273. Marcial MA, Madara JL. 1986. *Cryptosporidium*: Cellular localization, structural analysis of absorptive parasite membrane-membrane interactions in guinea pigs, and suggestions of protozoan transport by M cells. *Gastroenterology* 90:583.
274. Reduker DW, et al. 1985. Ultrastructure of *Cryptosporidium parvum* oocysts and excysting sporozoites as revealed by high resolution scanning electron microscopy. *J Protozool* 32:708.
275. Umemiya R et al. 2005. Electron microscopic observation of the invasion process of *Cryptospordium parvum* in severe combined immunodeficiency mice. *J Parasitol* 91:1034.
276. Fayer R, Ungar BLP. 1986. *Cryptosporidium* spp. and cryptosporidiosis. *Microbiol Rev* 50:458.
277. Fayer R, et al. 1991. Immunogold labeling of stages of *Crypstosporidium parvum* recognized by immunoglobulins in hyperimmune bovine colostrum. *J Parasitol* 77:487.
278. Pohlenz J, et al. 1978. Bovine cryptosporidiosis: A transmission and scanning electron microscopic study of some stages in the life cycle and of the host-parasite relationship. *Vet Pathol* 15:417.
279. O'Hara SP, et al. 2007. The human immunodeficiency virus type 1 tat protein enhances *Cryptosporidium parvum*-induced apoptosis in cholangiocytes via a Fas ligand-dependent mechanism. *Infect Immun* 75:684.
280. Bashtar AR, et al. 1984. *Hepatozoon aegypti* nov. sp.2. Electron microscope study on the erythrocytic stages and schizogony inside the snake, *Spalorosophis diadema*. *Z Parasitenkd* 70:43.

281. Cummings CA, et al. 2005. Characterization of stages of *Hepatozoon americanum* and of parasitized canine host cells. *Vet Pathol* 42:788.
282. Baneth G, et al. 2007. Life cycle of *Hepatozoon canis* (Apicomplexa: Adeleorina: Hepatozoidae) in the tick *Rhipicephalus sanguineus* and domestic dog (*Canis familiaris*). *J Parasitol* 93:283.
283. Nadler SA, Miller JH. 1985. Fine structure of *Hepatozoon mocassini* (Apicomplexa, Eucoccidiorida) gamonts and modificiation of the infected erythrocyte plasmalemma. *J Protozool* 32:275.
284. Lukes J. 1992. Life cycles of *Goussia pannonica* (Molnar, 1989) (Apicomplexa, Eimeriorina) an extracytoplasmic coccidium from the white bream *Blicca bjoerkna*. *J Protozool* 39:484.
285. Gestal C, Azevedo C. 2006. Ultrastructural aspects of hepatic coccidiosis caused by *Goussia lusca* n. sp. (Apicomplexa: Coccidia) infecting *Trisopterus luscus* (Gadidae) from the NE Atlantic Ocean. *Dis Aquat Organ* 11:71.
286. Elsheikha HM, et al. 2005. An outbreak of besnoitiosis in miniature donkeys. *J Parasitol* 91:877.
287. Dubey JP, et al. 2003. Ultrastructure of *Besnoitia besnoiti* tissue cysts and bradyzoites. *J Eukaryot Microbiol* 50:240.
288. Sheffield HG. 1966. Electron microscope study of the proliferative form of *Besnoitia jellisoni*. *J Parasitol* 52:583.
289. Juan-Sallé C, et al. 2004. Pulmonary besnoitiasis in captive maras (*Dolichotis patagonum*) associated with interstitial pneumonia. *Vet Pathol* 41:408.
290. Laakkonen J, Henttonen H. 2000. Ultrastructure of *Frenkelia* sp. from a Norwegian lemming in Finland. *J Wildlife Dis* 36:362.
291. Dessar SS, et al. 1990. Ultrastructural observations on the developmental stages of *Lankesterella* (Apicomplexa) in experimentally infected *Rana calisis* tadpole. *J Parasitol* 76:97.
292. Sundermann CA, Lindsay DS. 1989. Ultrastructure of in vivo-produced caryocysts containing the coccidian *Caryospora bigenetica* (Apicomplexa: Eimeriidae). *J Protozool* 36:81.
293. Desser SS, et al. 1990. Ultrastructural observations on the developmental stages of *Lankesterella minima* (Apicomplexa) in experimentally infected *Rana catesbeiana* tadpoles. *J Parasitol* 76:97.
294. Shadduck J. 1989. Human microsporidosis and AIDS. *Rev Inf Dis* 2:203.
295. Satheeshkumar S, Ananthan S. 2004. Electron microscopy identification of microsporida (*Enterocytozoon bieneusi*) and *Cyclospora cayetanensis* from stool samples of HIV infected patients. *Indian J Med Microbiol* 22: 119.
296. Weidner E, Sibley LD. 1985. Phagocytized intracellular microsporidian blocks phagosome acidification and phagosome-lysosome fusion. *J Protozool* 32: 311.
297. Canning EU, et al. 1987. Microsporidia of mammals—widespread pathogens or opportunistic curiosities. *Parasitol Today* 3:267.
298. Xu Y, et al. 2006. Identification of a new spore wall protein from *Encephalitozoon cuniculi*. *Infect Immun* 74:239.
299. Pakes SP, et al. 1975. Fine structure of *Encephalitozoon cuniculi* from rabbits, mice, and hamsters. *J Protozool* 22:481.
300. Sprague V, Vernick SH. 1971. The ultrastructure of *Encephalitozoon cuniculi* (Microsporidia, Nosematidae) and its taxonomic significance. *J Protozool* 18:560.
301. Terada S, et al. 1987. Microsporidian hepatitis in the acquired immunodeficiency syndrome. *Ann Int Med* 107:61.
302. Zender HO, et al. 1989. A case of *Encephalitozoon cuniculi* peritonitis in a patient with AIDS. *Am J Clin Pathol* 92:352.
303. Friedberg DN, et al. 1990. Microsporidial keratoconjunctivitis in the acquired immunodeficiency syndrome. *Arch Ophthalmol* 108:504.
304. Didier PJ, et al. 1991. Fine structure of a new human microsporidian, *Encephalitozoon hellem*, in culture. *J Protozool* 38:502.
305. Cali A, et al. 1991. Corneal microsporidiosis in a patient with AIDS. *Am J Trop Med Hyg* 44:463.
306. Canning EU, Nicholas JP. 1980. Genus Pleistophora (Phylum Microspora). *J Fish Dis* 3:317.
307. Chupp GL, et al. 1993. Pleistophora (Microsporidia) myositis in a patient with the acquired immunodeficiency syndrome (AIDS). *Clin Infect Dis* 16:15.
308. Higes M, et al. 2007 Experimental infection of *Apis mellifera* honeybees with *Nosema ceranae* (Microsporidia). *J Invertebrate Pathol* 94:211.
309. Pinnolis M, et al. 1981. Nosematosis of the cornea. *Arch Ophthalmol* 99:1044.
310. Undeen AH, Frixione E. 1991. Structural alteration of the plasma membrane in spores of the microsporidian *Nosema algerae* on germination. *J Protozool* 38:511.
311. Weidner E. 1972. Ultrastructural study of microsporidian invasion into cells. *Z Parasitenk* 40:227.
312. Desportes I, et al. 1985. Occurrence of a new microsporidian: *Enterocytozoon bieneusi* n.g., n. sp., in the enterocytes of a human with AIDS. J Protozool 32:250.
313. Chilmonczyk S, et al. 1991. *Enterocytozoon salmis* n. sp.: An intranuclear microsporidian from salmonid fish. *J Protozool* 38:264.
314. Elston RA, et al. 1987. An intranuclear microsporidian associated with acute anemia in the chinook salmon, *Oncorhynchus tshawytscha*. *J Protozool* 34:274.
315. Weidner E. 1985. Early morphogenesis of Glugea-induced xenomas in laboratory-reared flounder. *J Protozool* 32:269.
316. Scarborough-Bull A, Weidner E. 1985. Some properties of discharged *Glugea hertwigi* (Microsporida) sporoplasms. *J Protozool* 32:284.
317. Tan HK, Zierdt CH. 1973. Ultrastructure of *Blastocystis hominis Z Parasitenkd* 42:315.
318. Yoshikawa H, et al. 1988. Freeze-fracture of *Blastocystis hominis*. *J Protozool* 35:522.
319. Zierdt CH, Tan HK. 1976. Ultrastructure and light microscope appearance of *Blastocystis hominis* in a patient with enteric disease. *Z Parasitenkd* 50:277.

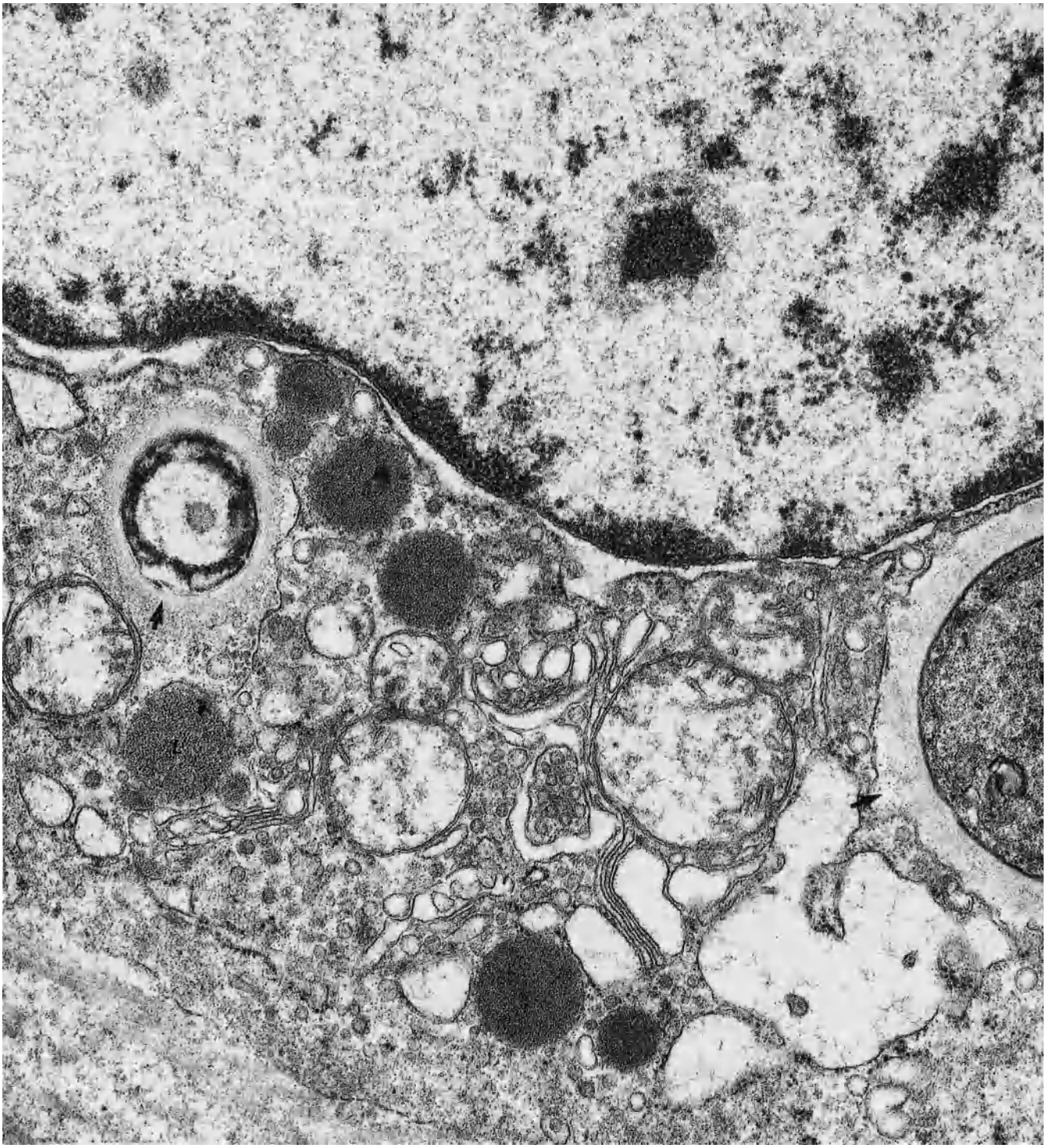


Fig. 16.1 ***Histoplasma capulatum***: cellular response to infection. Fungal cells (*arrows*) in cytoplasm of a macrophage, mesenteric lymph node, dog. Golgi complex (*center*) is vacuolated and associated with vesicles and lysosomes. Nucleus at *top*; extracellular space with collagen fibers at *bottom left*.

© 2009 Wiley-Blackwell. ISBN: 978-0-813-80330-2

16 Algae, Fungi, and Other Eukaryotes

Thousands of species of algae, fungi and other eukaryotic organisms can parasitize mammalian hosts. In this chapter, emphasis is placed on the ultrastructure of infected host cells. Many intracellular pathogenic eukaryotes are phagocytized by macrophages, endothelial cells, or other cells of the monocyte-macrophage system. How these cells react to parasitism holds the key to understanding the pathogenesis of infection (Fig. 16.1).

Algae

Algae are aquatic, nonvascular plants. *Prototheca* and *Pythium* are the only genera associated with significant disease in man and animals. Like other algae, this kind of organism is a large cell with a nucleus and cell wall.[1] **Cytoplasmic granules** in algae include lysosomes and secretory granules. Polyphosphate granules in green algae function in energy production.[2] Intracellular virions of algal viruses have been reported in algae,[3] but have never been reported in algae in tissue.

Genus *Prototheca*

Protothecae are aerobic, colorless (achlorphyllic), unicellular algae. They replicate freely in stagnant water and decaying organic matter, and are contaminants of various tissues of animals and man. Four species have been recognized: *P. stagnora*, *P. zopfii*, *P. salmonis*, and *P. wickerhamii*.[4]

Protothecae cause focal and disseminated, progressive, granulomatous lesions, especially in neutrophil-deficient or immunosuppressed hosts. They are of low pathogenecity and generally infect during wound contamination, especially of the subcutis. In vitro, the reproductive cycle of protothecae is asexual, by formation of endospores within a sporangium.[5] Two types of algae are seen. Large sporangia with organelle-rich spores are rapidly growing vegetative forms; small sporangia with starch granules, lipid globules, and few mitochondria are storage spores (hypnospores) that respond slowly to addition of nutrients. Algae in tissue resemble the latter.[6,7]

In tissue, algae are present either as single **endospores** or as large **sporangia** containing multiple sporangiospores (daughter cells). *Prototheca* spp. have been confused with the genus *Chlorella*: except for lack of green pigments, *Prototheca* resembles *Chlorella* in structure, reproductive cycle, and tissue reactivity.

Protothecal cells in **macrophages** are ovoid and contain a central nucleus with a large nucleolus. Large numbers of starch granules and dense bodies occupy the cytoplasm (Fig. 16.2). There is a thick granular cell wall, which is important in stimulating the granulomatous tissue reaction associated with this organism. The cell wall is destroyed during degradation in the host and the various stages of disintegration may lead to bizarre extracellular membranes and laminae.

Protothecosis

Protothecae are an important causes of granulomatous disease in three situations: *P. wickerhamii*-induced cutaneous protothecosis of man, *P. zopfii* mastitis in cattle, and *P. salmonis*-induced renal granulomatous disease of salmon.[8] Protothecosis also occurs sporadically in many other mammalian species including humans. These incidental infections include severe enterocolitis in dogs, in which masses of organisms

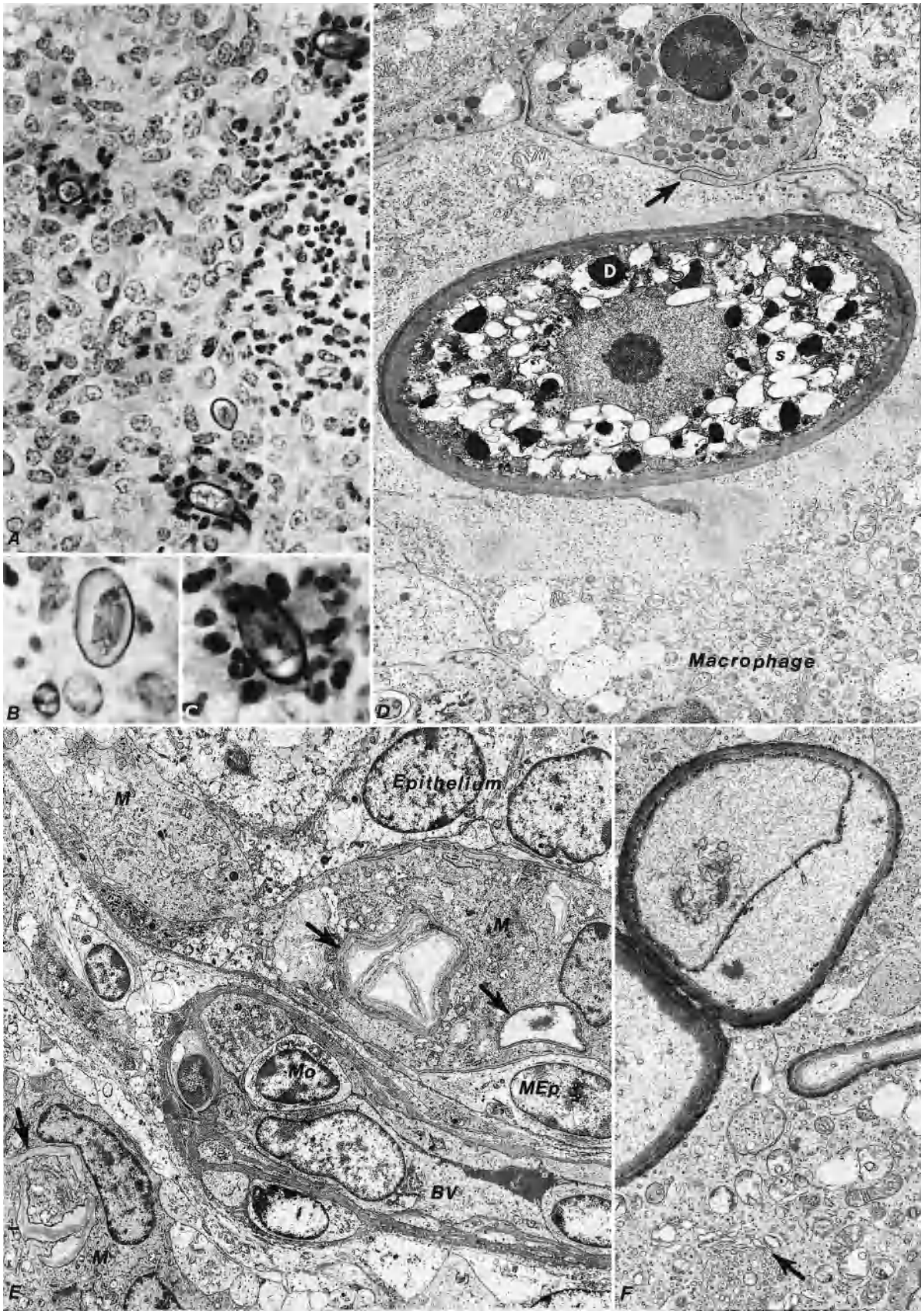


Fig. 16.2 ***Prototheca zopfii***: bovine mammary gland, chronic algal mastitis. **A**. **Histology**: degenerating algae surrounded by dense neutrophils. **B**. **Intact alga**: free of inflammatory cells. **C**. **Degenerate alga**: surrounded by neutrohils. **D**. **Intact alga**: acinar wall, mammary gland. Cytoplasm of the alga contains many vesicles, dense granules (*D*), and electron-dense starch granules (*s*). A halo of organelle-free granular material surrounds the alga. Macrophage surface interdigitates with other macrophages and one vacuolated neutrophilic leukocyte (*arrow*). The nucleus is large and has a large spherical nucleolus. **E**. **Degenerate algae**: cytoplasm of macrophage (*M*), mammary acinar wall (*arrow*). Alga lacks internal structure. Myoepithelial cell (*MEp*), monocyte (*Mo*), blood vessel (*BV*). **F**. **Structureless algal remnant**: macrophage cytoplasm. Golgi complex with associated vesicles (*arrow*).

occupied the tunica propria,[9] and severe nervous system lesions are associated with lodging and growth of protothecae in the brain.

Human Protothecosis Protothecosis in humans, although very rare, has been reported in chronic infections of the skin and olecranon bursa, and as systemic disease with visceral dissemination. Lesions appear as papules or plaques, often associated with hyperpigmentation, and consist of macrophages and multinuclear giant cells containing protothecae. Macrophages bearing algae are surrounded by infiltrates of monocytes, lymphocytes and plasma cells within the middle and upper dermis. Human neutrophils are able to kill protothecae but may be prevented from doing so by either the antiphagocytic effects of algal cell wall material or by the sequestration of algae within macrophages, away from the physical contact with neutrophils.[10] Progressive cutaneous protothecosis occurs in patients with defects in neutrophil-killing or other forms of immunosuppression and typically occurs in diabetic patients.

Bovine Mastitis Bovine mammary infections ascend from the teat, spreading into the mammary parenchyma and into supramammary lymph nodes. *P. zopfii* is found in macrophages, within the alveolus, and in the interstitium. Although organisms appear to lie in mammary acinar epithelium, they reside in macrophage trapped between mammary epithelial cells. Early in infection, macrophages bearing algae are surrounded by neutrophils, which, when algae are free in tissue, can degranulate and release enzymes that degrade the algal cell wall. In chronic infection, many algal cells are degenerate. Nuclear and cytoplasmic material disintegrates leaving amorphous debris and empty vacuoles within the confines of the cell wall that remains. Algal cellular material is digested away leaving an intact spherical **empty cell wall form**. Cell walls collapse but persist so that with time, the infected macrophage contains large profiles of hyalin laminar material (Fig. 16.3). In addition to the cell wall forms, **pseudoalgae** develop that consist of cell wall material the forms around cell cytoplasm.

Genus *Pythium*

Pythium insidiosum, the cause of **cutaneous pythiosis** in humans, horses, dogs, and other mammals, is traditionally viewed as a fungus. Based on rRNA sequences however, it is more closely related to red algae and diatoms. Mapping of hyphal antigens has been done using immunogold techniques.[11] *P. insidiosum* triggers a T_{H2} helper lymphocyte subset that recruits eosinophils and mast cells that degranulate around degenerating hyphae in a Splendore-Hoeppli reaction in the chronic lesions.

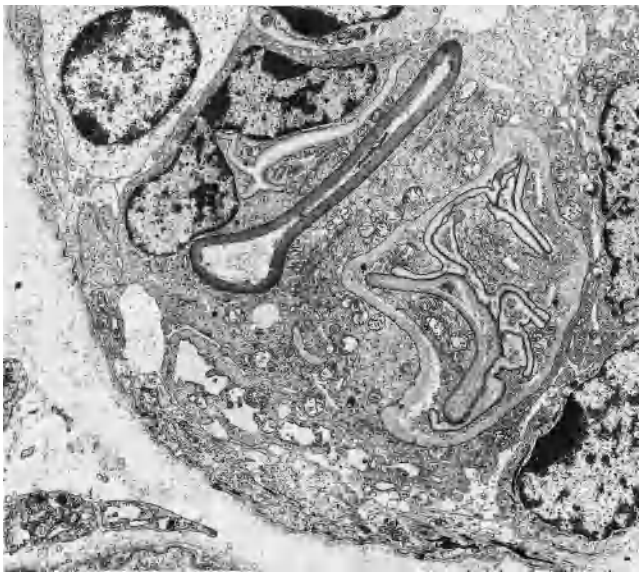


Fig. 16.3 ***Prototheca zopfii***: bovine mammary gland, chronic algal mastitis. Macrophages bearing empty algae are between acinar epithelial cells. Infected macrophage has no evidence of residual bodies or secondary lysosomes. Note absence of secondary lysosomes in the macrophage.

Blue-Green Algae

Blue-green algae, etiologic agents of red tide disease of acquatic mammals, are secreted during massive algal blooms and cause disease via algal toxins. Blue-green algae can kill animals that drink infected waters, especially in late summer and autumn. Surface blooms are concentrated into thick scums by wind and ingestion of these concentrated algae lead to signs of toxicity in 24–48 hr. Liver is the site of greatest injury. Massive hepatocyte necrosis begins in centrolobular sites.

In ruminants, ingestion of large amounts of blue-green algae can cause enteric infection, liver necrosis, and death.[12] Edema, widespread hemorrhages, and fluid in the body cavities are generally present. Inoculation of young sheep intraruminally with an algal bloom of *Microcystis aeruginosa* caused sheep to develope elevations in serum enzymes and reduced blood glucose. Sheep die 18–14 hr later with hemorrhage, and acute cell swelling and necrosis of hepatocytes.

Ultrastructurally, blue-green algae contain a nucleoid, thylakoid, and cell wall, as well as polyhedral bodies, cyanophycin granules, and membrane-lined inclusions. Using methods to detect the microcystin gene, studies suggest that the potential for toxin production occurs in members of the cyanobacteria genera *Microcystis*, *Anabaena*, *Planktothrix*, *Nostoc* and

Nodularia. Hepatotoxic **microcystins** and **nodularins** have been detected in cytoplasmic inclusions of the algal cell using immunogold techniques. Microcystins were labeled primarily in the thylakoid area and nucleoid, with smaller amounts in the cell wall and sheath.[13,14] In fish, hepatoxicity occurs during feeding in the warmest month.[15]

Fungi

Fungi are single-celled, nucleated plant eukaryotic organisms that include not only a wide variety of pathogenic species but also yeasts, molds, mushrooms, and mildews. The simplest form is the single-celled budding yeast. In culture, most fungi consist of networks of hyphae called mycelia. Individual hyphae form by elongation of the fungal cells without separation into new cells. Fungi grow by producing new hyphae at the edge of the mycelium (vegetative growth). A phylogenetic classification of the kingdom Fungi has been developed.[16]

With few exceptions, fungi pathogenic for vertebrates are classed as **Fungi Imperfecti**, and the two important groups are the pathogenic yeasts and the dermatophytes (Table 16.1). Fungi pathogenic for

Table 16.1 Pathogenic fungi that cause systemic infection.

Genus & species	*Diseases*	*Reference to ultrastructural pathology*
Absidia corymbifera	Zygomycosis,# human	**Diven**, *J Perinatol* 24:794, 2004
***Aspergillus* spp.**	Aspergillosis, human	**Denning**, *Infect Immun* 60:5153, 1992 (lung)
	Bird	**Campbell**, *Sabouraudia* 23:101, 1970 (chick)‡
	In vitro	**Merkow**, *Am J Pathol* 62:57, 1971
A. fumigatus	Aspergillosis, human	**Washburn**, *Infect Immun* 55:2088, 1987 (killing)
	In vitro	**Borgers**, *J Med Vet Mycol* 27:381, 1989 (saperconazole)*
	Mouse	**Nakai**, *Med Mycol* 43:439, 2005 (lung)‡
A. niger	Experimental	**Tanaka**, *J Gen Appl Microbiol* 9:101, 1963*
Basidiobolus ranarum	Zygomycosis,# human GI infection	**Hussein**, *Mycol Res* 111:926, 2007 (AIDS)
	In vitro	**Yangco**, *Antimicrob Agents Chemother* 25:413, 1984
Beauveria bassiana	Hyalohyphomycosis§	**Holder**, *Microbiology* 153:3448, 2007
Blastomyces dermatitidis	Blastomycosis, human	
	Mouse	**Collins**, *Sabouraudia* 7:237, 1970 (lung)‡
	In vitro	**Abou-Gabal**, *Mycoses* 24:497, 1981; **Garrison**, *Mycopathol Mycol Appl* 52:93, 1974 (microcondia)*
B. brasiliensis	In vitro	**Carbonell**, *J Bact* 96:533, 1968 (mycelia)*
Candida albicans	Candidiasis, human	**Belcher**, Lab Invest 29:620, 1973 (neutrophils); **Chow**, *Blood* 55:546, 1980 (meningitis); **Ishikawa**, *J Allergy Clin Immunol* 50:183, 1972 (eosinophils); **Maquis**, *J Leuk Biol* 50:587, 1991 (neutrophils);* **Montes**, *J Bact* 96:1349, 1968 (oral); **Muller**, *Sabouraudia* 15:87, 1977 (urine); **Myerowitz**, *Arch Pathol Lab Med* 102:506, 1978 (disseminated)
	Dog	**Chow**, *Blood* 55:546, 1980 (meningitis)‡
	Mouse	**Cole**, *J Med Vet Mycol* 27:363, 1989 (GI);‡ **Cole**, *J Med Vet Mycol* 26:173, 1988 (GI);‡ **Gargani**, *Mycoses* 32:644, 1989 (vaginitis);‡ **Kanbe**, *Infect Immun* 60:1972, 1992 (spleen);‡ **Ray**, *Infect Immun* 56:1942, 1988 (skin);‡ **De Repentigny**, *Infect Immun* 60:4907, 1992 (intestine)‡
	In vitro	**Brawner**, *Infect Immun* 51:337, 1986 (antigens);* **Edwards**, *Blood* 69:1450, 1987 (endothelial cells);* **Giordania**, *Mycoses* 34:67, 1991 (glycosidases);* **Grund**, *Mykosen* 24:349, 1981 (macrophage);* **Guarro**, *Mycoses* 32:289, 1989 (sertaconizole);* **Iwata**, *Sabouraudia* 11:205, 1973 (clotrimazole);* **Linehan**, *Infect Immun* 56:1981, 1988 (C3d receptor);* **Liss**, *Mycopathologia* 108:173, 1989 (fluconazole);* **Maquis**, *Lab Invest* 46:627, 1981 (muramidase);* **Miller**, *J Bact* 119:992, 1974 (chlamydospores);* **Montes**, *Mycoses* 34:287, 1991 (saperconazole);* **Muller**, *Mycoses* 30:528, 1987 (amorolfin);* **Scherwitz**, *Mycoses* 24:224, 1981 (econazol);* **Takamiya**, *Mycoses* 28:17, 1985 (polysaccharides);* **Tronchin**, *Infect Immun* 56:1987, 1988 (adhesins); **Wills**, *J Bact* 164:7, 1985 (mitochondria)

Table 16.1 *Continued*

Genus & species	*Diseases*	*Reference to ultrastructural pathology*
C. parapsilosis	Endocarditis, human	**Marrie**, *Infect Immun* 45:390, 1984
C. tropicalis	Oral infection, human	**Martin**, *Am J Clin Pathol* 75:671, 1981
Coccidioides immitis	Coccidioidomycosis Experimental	**Cole**, *Infect Immun* 59:2434, 1991 (antigens) **Cox**, *Infect Immun* 60:3315, 1992 (antigens);* **Frey**, *J Invest Derm* 153:933, 1986 (neutrophil);* **Gabal**, *Am J Vet Res* 46:671, 1985 (spherulogenesis);* **Galgiani**, *Infect Immun* 60:2627, 1992 (antigens);* **Sun**, *Sabouraudia* 17:265, 1979*
Conidiobolus coronatus	Zygomycosis,# Conidiobolomycosis	**Silva**, *Vet Pathol* 44:314, 2007 (sheep)
Cryptococcus neoformans	Cryptococcosis, human Experimental	**Muller**, *Acta Neurochir* 44:223, 1978 (meningitis); **Narisawa**, *Mycopathologia* 106:113, 1989 **Fiskin**, *J Med Vet Mycol* 28:197, 1990;* **Iwata**, *J Med Vet Mycol* 28:77, 1990 (ketaconazole);* **Mattia**, *Boll Soc Ital Biol Sper* 53:1817, 1977;‡ **Tani**, *J Med Vet Mycol* 25:223,1987 (mitosis)
Curvularia lunata	Human	**Tessari**, *J Eur Acad Dermatol Venereol* 17:440, 2003 (cutaneous)
Emmonsia crescens	Adiaspiromycosis, human Mammals	**Kodousek**, *Am J Clin Pathol* 556:394, 1971; **Nuorva**, *J Clin Pathol* 50:82, 1997 **Laakkonen**, *J Wildlife Dis* 34:816, 1998 (weasels); **Obayashi**, *Jap J Vet Res* 19:103, 1971
***Fusarium* spp.**	Hyalohyphomycosis§	
Geotrichum candidum	Geotrichosis	
Histoplasma capsulatum	Histoplasmosis, human Hamster In vitro	**Dumont**, *Arch Pathol* 87:168,1969; **Kirk**, *Gastroenterology* 61:46, 1971 (colitis); **Kurita**, *Mycopathologia* 115:207, 1991 (neutrophils)* **Dumont**, *Lab Invest* 23:278, 1970 (macrophage)‡ **Borgia**, *Mycoses* 32:584, 1989 (yeast form);* **Edwards**, *J Gen Microbiol* 20:469, 1959;* **Kdousek**, *Beitr Pathol* 145:83, 1972;* **Kuttin**, *Mycoses* 27:72, 1984 (kidney)
H. farciminosum	Farcy, horse Experimental	 **Garrison**, *Sabouraudia* 13:174, 1975*
Lobo loboi	Lobomycosis	**Woodward**, *Lab Invest* 27:606, 1972
***Mucor* spp.**	Mucormycosis	
Penicillium marneffei	Penicilliosis, human	**Chan**, *Ultrastruct Pathol* 14:439, 1990
***Paecilomyces* spp.**	Hyalohyphomycosis§	
Paracoccidioides brasiliensis	Paracoccidiodomycosis, human Experimental	**De Brito**, *Virch Arch A* 361:129, 1973; **Furtado**, *Sabouraudia* 5:226, 1967 **Brummer**, *Infect Immun* 58:2628, 1990 (macrophage);* **Campo-Aasen**, *Mycopathologia* 23:101, 1985 (mitochondria);* **Campo-Aasen**, *Mycopathologia* 111:169, 1990 (yeast phase);* **Edwards**, *Mycopathologia* 114:169, 1991 (conidia)*
Pseudoallescheria boydii	Pseudoallescheriasis In vitro	**Ginter**, *Mycoses* 38:369, 1995 (arthritis); **Huang**, *J Tongii Med Univ* 10:218, 1990 (meningitis) **Kiffer-Moreira**, *Arch Microbiol* 188:159, 2007
***Scedosporium* spp.**	In vitro	**Salkin**, *J Clin Microbiol* 26:498, 1988
***Scopulariopsis* spp.**	Hyalohyphomycosis§ In vitro	**Filipello**, *Mycoses* 43:281, 2000 (hair, nail) **Apprich**, *Med Mycol* 44:715, 2006 (equine hoof)*

‡Animal model.
*In vitro study.
#**Zygomycosis** is an invasive mycotic disease caused by fungi in the class Zygomycetes; the most common species associated with infection are *Absidia corymbifera*, *Apophysomyces elegans*, *Cunninghamella bertholletiae*, *Rhizomucor pusillus*, and *Rhizous* spp. *Basidiobolus ranarum* is found in dung of amphibians, reptiles, and insectivorous bats; its structural forms include both hyphae and zygospores.
§**Hyalohyphomycosis** is an opportunistic mycotic infection involving mycelial growth in tissue; species of nondematiaceous hyaline hyphomycetes include *Acremonium* (*Cephalosporium*), *Beauveria*, *Fusarium*, *Paecilomyces*, and *Scopulariopsis*. *Beauveria bassiana* is an entomopathic fungus used for biocontrol of pests and plant diseases, and human exposure occurs during field use.
ø**Adiaspiromycosis** is an opportunistic infection reported as genera (or varieties) of *Emmonsia* or *Chrysosporium*; most favor *Emmonsia*.

plants are significantly different in ultrastructure and method of parasitism from fungi pathogenic for animals.[17]

Most of the important fungal pathogens of man and animals are **dimorphic**; that is, their typical growth forms in tissue and in saprophytic stages in culture are different. For example, in histoplasmosis, the causal organism, *Histoplasma capsulatum*, is found as small, budding yeast cells within macrophages. In culture, this organism grows as septate mycelia with microconidia and tuberculate chlamydospores. The shift from mycelia in the soil to yeasts in the bloodstream or tissue of the host is triggered by changes in fungal cell temperature, and a rapid decline in intracellular ATP, respiration rate, and mitochondrial electron transport.

Fungi cause three types of disease in animals: (1) **mycosis**, the direct invasion of tissue by fungal cells; (2) **allergic disease**, the development of hypersensitivity to fungal antigens; and (3) **mycotoxicosis**, the ingestion of toxic fungal metabolites. It is not unusual for mycosis and allergic disease to occur together, especially when infection of the lung is involved.

Most fungi are omnipresent in the environment, so host resistance is a dominant factor in disease. Opportunistic fungal infections result when animals are immunosuppressed, when their mechanisms of inflammation are inhibited, and when stress is placed on their systems over long periods. Newborn and very old animals are most often affected by these factors. In immunosuppression produced by drugs, *Aspergillus* spp. and *Candida* spp. commonly produce complicating systemic infections. While aspergillosis usually occurs in the lungs, candidiasis commonly involves the kidneys. Localization in renal tissue involves attachment by specialized glycoproteins on the surface of the fungal spore, and tissue invasion occurs by specialized germ tubules that form and penetrate between and directly through surface epithelium of the renal cortex.

Inhalation by aerosol exposure is the most significant factor in enabling fungal infections to become established. The size of the fungal cell inhaled is important. In the mammalian lung, nothing over 10 μm that penetrates the nose reaches the lungs, while almost everything under 2 μm reaches the alveoli and is retained. The gastrointestinal tract, despite the ingestion of large numbers of spores, is seldom the site of primary fungal infection. One notable exception involves fungi associated with bovine mycotic placentitis and abortion, in which the disease appears to follow ingestion of spores. The urogenital tract is rarely affected because fungi are swept away by mucous secretions. The bovine teat is an important orifice for infection, and mycotic mastitis results from several species of fungi.

Mycotoxins, which are produced by several fungal genera, cause serious diseases. Animals and humans are poisoned by ingesting contaminated grain and other foodstuffs. The most important of the mycotoxins are the aflatoxins, a group of related toxins that cause necrosis of hepatocytes and are produced by *Aspergillus flavus* and *A. parasiticus*.

Fungal cells are identified in electron micrographs of infected tissue according to their size, cytoplasmic and nuclear structure, type of reproductive bodies, and distinctive cell wall. All fungal cells are nucleated and contain cytoplasmic organelles for protein synthesis. The thick **cell wall** is usually layered and may contain homogenous, fibrillar and granular components of varying electron density (Fig. 16.4).[18–22]

Fungi are eukaryotes, and thus have structurally defined nuclei. **Nuclei** are smaller and less complex than those of vertebrate animals. A defined nucleus, nucleolus, and nuclear envelope are present in all true fungi (as distinct from bacterial cells). DNA is largely located in the nucleus. Mitochondrial DNA (mtDNA) is located in the cytoplasm within the mitochondrial matrix, and is also found in unusual structures referred to as **mitochondrial nucleoid**.[23]

The cytoplasm contains vacuoles, mitochondria, and lipid (or lipoid) globules. The **fungal vacuole**, somewhat analagous to the plant vacuole and to the lysosome in mammalian cells, functions in degradation, metabolite storage and in cytosolic ion and pH homeostasis. **Ribosomes** make up much of the mass of the fungal cell. Enzymes that are produced by cytoplasmic ribosomes pass into a **Golgi complex** and are released from its maturing face as small vesicles that enlarge to form the fungal vacuole.[24] **Peroxisomes** occur in yeast cells, and peroxisome-deficient mutants have been reported in some species.[25]

Exocytosis occurs at discrete domains of the plasma membrane.[25] Vesicles are involved in both endo- and exocytosis, including transport from rough endoplasmic reticulum to Golgi complexes.[26,27] Movement is controlled by connections of the plasma membrane to an actin **cytoskeleton**.[28,29]

Appressoria are specialized invasion structures with rigid melanin-pigmented cell walls that occur in some fungal pathogens.[30] Appressoria are prominent in phytopathogens where they adhere tightly to leaf surfaces, and send a penetration peg into the host plant cell. Appressoria generate large turgor pressures on the host cell by synthesizing elevated intracellular concentration of osmotically active substances (in *M. grisea*, the osmoticum is glycerol). The plant cell is then invaded by a specialized penetration hypha that develops beneath the appressorium.

Methods for the immunogold labeling of proteins and enzymes in yeast cells have detected glycolytic enzymes and ATPase.[31,32] Fungal glycoconjugates and

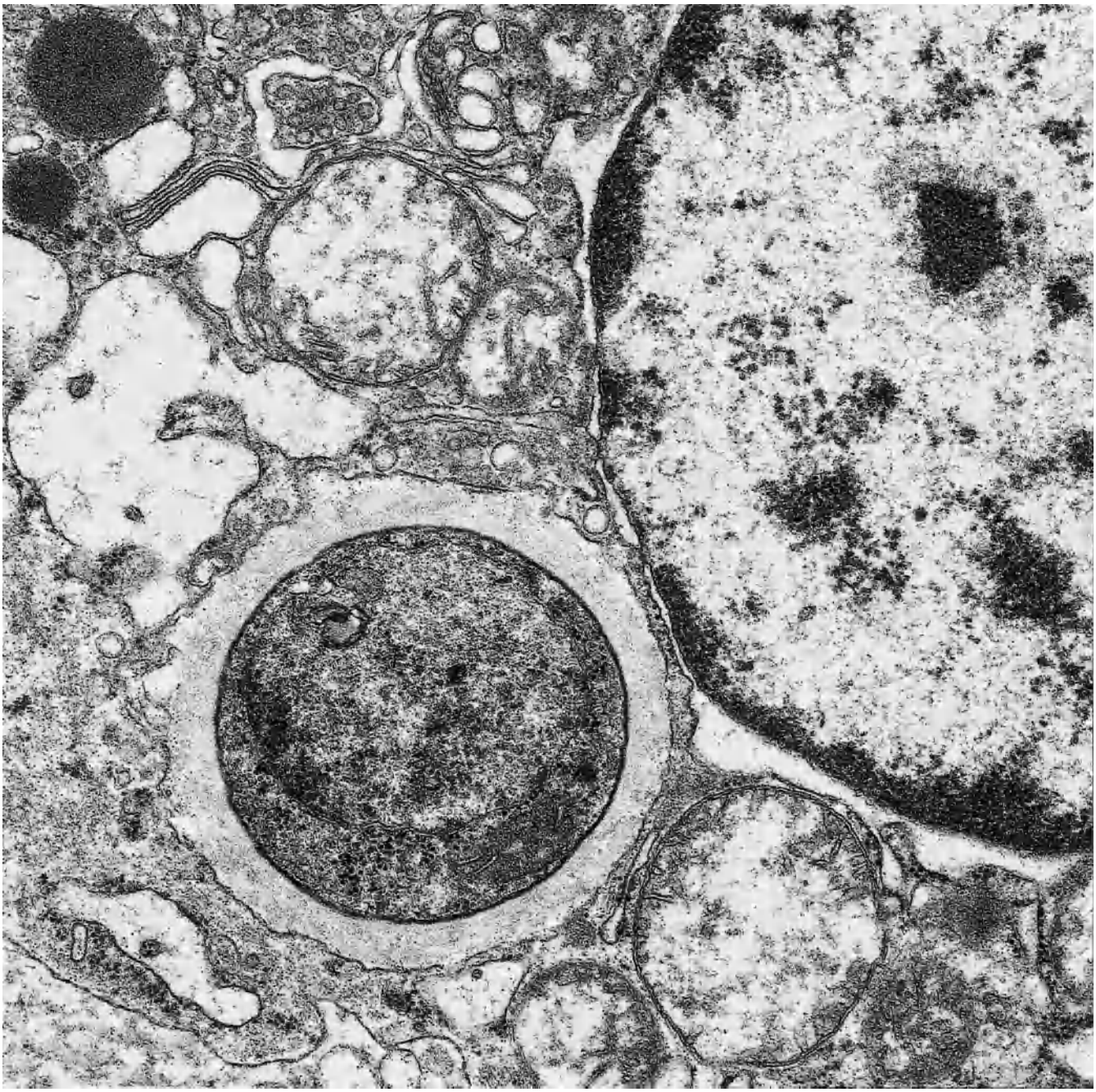


Fig. 16.4 ***Histoplasma capsulatum***: macrophage, chronic histoplasmosis, lymph node, dog.

adhesins have been localized to surfaces of **hyphae**.[33] An **adhesin** encoded by the EPA1 gene is responsible for 95% of adhesion force to host cells. The gene product is a glucan-cross-linked cell-wall protein and binds to host-cell carbohydrate, specifically recognizing asialolactosyl-containing carbohydrates.[34] A **metalloprotease** with elastinolytic activity has been characterized and shown, by immunogold techniques, to be excreted by *A. fumigatus* during infection of the mouse lung.[35]

Hyphae die as part of the normal fungal life cycle. Programmed hyphal death is an orderly process with little disruption to colony architecture. Dying hyphae exhibit progressive disorganization of nuceloid substructure, followed by degradation of DNA and cytoplasmic constituents with transient maintenance of plasma membrane integrity. In the end, hyphae collapse and appear empty of cell contents.[36] Cell death occurs in two waves—as aerial hyphae are growing, nucleoids at the level of the growth medium degenerate. **Sporulation** then starts and as a second death process starts in aerial hyphae. The first sign of degeneration is lossening of fibrilar DNA. The nucleoid and

then cytoplasm become less electron-dense, ending with a nucleoid that is translucent and has fibrillar structure. Finally, the plasma membrane retracts and the cell wall forms vesicles.

Spores are specialized reproductive bodies produced by fungi. Asexual spores arise by differentiation of cells of spore-bearing hyphae without fusion; sexual spores are produced by fusion of two cells.[37,38] Spore structure and mode of development are characteristics by which different fungi are identified and classified.

Antimycotic drugs cause lysis of the fungal cell. Ultrastructural analysis of *Candida albicans* in skin lesions of human patients treated with antimycotic drugs show marked degenerative effects.[39]

Ultrastructural studies of fungi grown in vitro and exposed to antimycotic drugs reveal a spectrum of ultrastructural change from growth suppression to inhibition of sporulation and reproduction. Individual fungal cells become vacuolated and show a variety of abnormal surface changes (disintegration of cell walls and plasma membranes) that proceed to lysis (Table 16.2).

Genus *Aspergillus*

The genus *Aspergillus* has over 900 recognized species, most of which are in soil and decaying vegetation. **Spores** are the invasive fungal cell form in tissue invasion by *Aspergillus* spp. Spore germination occurs immediately after infection. Spores swell from about 2.5 μm (typical of formancy) to over 5 μm in diameter. Protuberances, or germ tubes, bud from the surface of the swollen sore as extensions of the inner spore wall. These buds progressively elongate into true, septate hyphae. Their single nucleus divides repeatedly and vacuoles appear in the cytoplasm. Hyphal walls are single layers of electron-transparent material.[40]

Hyphae range from 2.5 to 4.5 μm.[41] Hyphae show repeated dichotomous branching, with most hyphae lying in the same direction, although some hyphae may radiate from a central point. Swollen and distorted hyphae will be present in the centers of large hyphal aggregates (Fig. 16.5), but the budding yeasts found in candidiasis are not present in aspergillous lesions. Groups of **conidiophores** and **conidia** growing as fungus balls are present when *Aspergillus* grows in a cavity within an air space. Cell wall antigens of hyphae of *Aspergillus* are important in generation of the immune response, and some of these have been localized using immunogold techinques.[42]

Cell wall material varies in thickness in the various forms of fungal cells. Galactomannan is a major cell wall component and can be excreted into the tissue environment, and into the medium of fungal cultures. In *A. fumigatus*, secreted galactomannan is composed of a branched core of α(1–2)- and α(1–6)-linked mannose, with β(1–5)galactofuranose or β(1–4)galactopyranose moieties linked linearly in side chains terminated by galactofuranose nonreducing end units.

Table 16.2 Pathologic fungi that cause subcutaneous infection.

Organism	*Disease*	*Reference to ultrastructural pathology*
Bipolaris spicifera		**Ogden**, *Clin Inf Dis* 14:596, 1992
***Chrysosporium* spp.**	Adiaspiromycosis§	
Exophiala jeanselmei	Phaeohyphomycosis#	
***Exoserohilum* spp.**		
Fonsecaea pedrosoi		**Farbiarz**, *J Med Vet Mycol* 28:373, 1990
F. compacta	Chromoblastomycosis	**Krempl-Lamprecht**, *Mycoses* 30:454, 1990
Loboa loboi	Lobomycosis	**Woodward**, *Lab Invest* 27:606, 1987
Madurella mycetomatis	Mycotic mycetoma	**Findlay**, *Mycopathologia* 67:51, 1979
Pseudoallescheria boydii	Mycotic mycetoma	
Rhinosporidium seeberi	Rhinosporidiosis, human Dog	**Lengfelder**, *Zbl Vet Med B* 27:326, 1980 **Easley**, *Vet Pathol* 23:50, 1986
Sporothrix schenckii	Sporotrichosis	**Garrison**, *Mycopathologia* 69:57, 1979
Wangiella dermatitidis	Phaeohyphomycosis#	

§ **Adiaspiromycosis** is in vivo development of adiaconidia without replication; condial enlargement is influenced by temperature.
# **Phaeohyphomycosis** is caused by dematacеous fungi that infect to cause local infection of traumatic lesions and disseminated infection in immunocompromised hosts. Melanin in cell walls of spores and hyphage causes lesions to be dark. Approximately 40 species are associated with human disease.

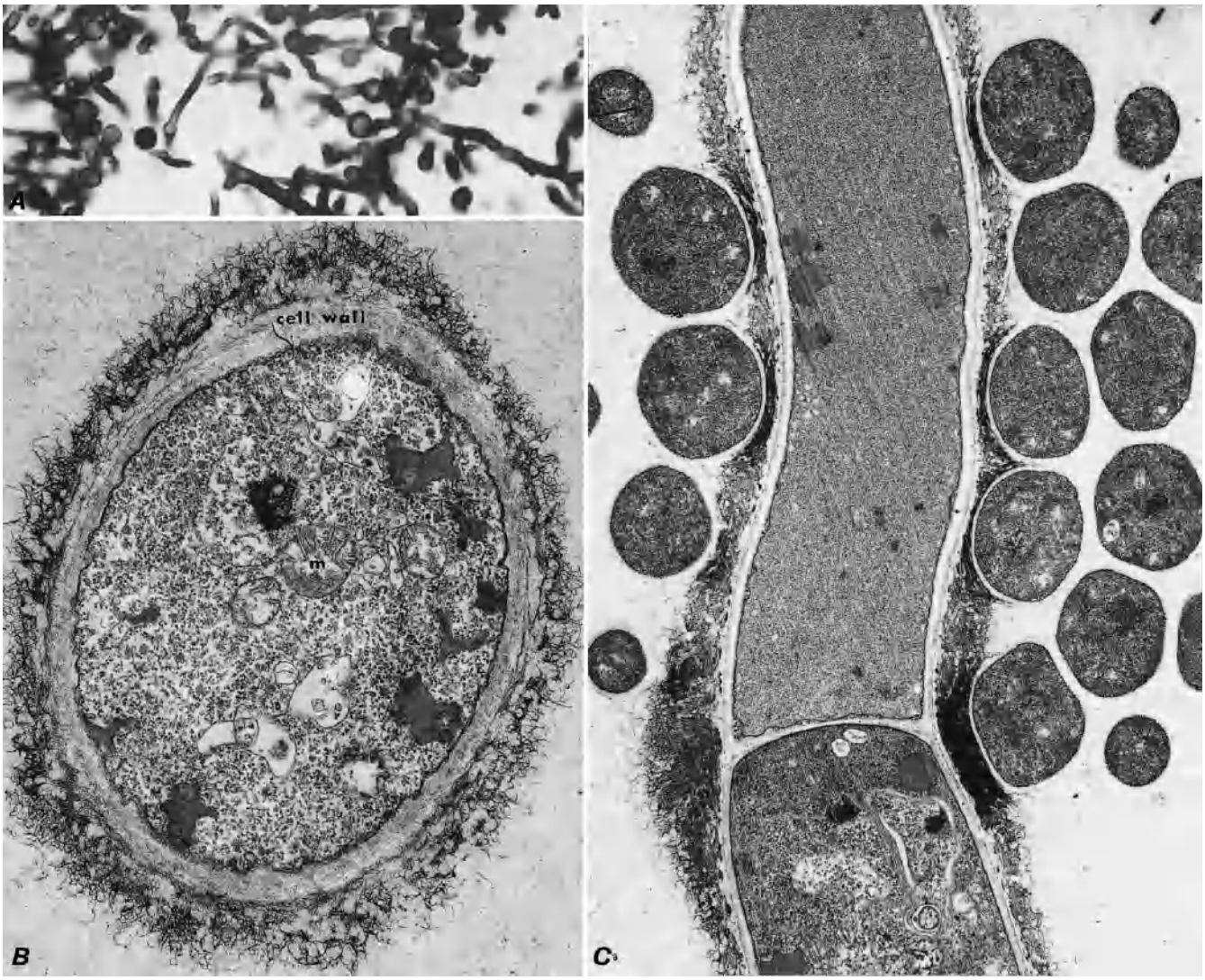


Fig. 16.5 ***Aspergillus fumigatus***: lung granuloma. **A**. **Histology**. **B**. **Spore**: fungal cytoplasm with many ribosomes, lipids, mitochondria (*m*), and a loose fibrillar structure peripheral to the cell wall. **C**. **Hyphae**: cross section and longitudinal section (with peripheral coat thickened at interhyphal junction).

The galactomannan is immunogenic, and antibodies against if have been used in antigen detection for diagnosis of invasive aspergillosis. Immunoelectron microscopy has shown that these antigens are in the fungal wall inside the cell.[43]

Aspergillosis

Aspergillus spp. cause three categories of disease, and all occur in both humans and animals: (1) **invasive aspergillosis**, with entry and growth within body organs and tissues, especially the lungs; (2) **allergic aspergillosis**, growth in tissue with superimposition of immune-mediated injury, for example, human asthmatic allergy and extrinsic allergic alveolitis; and (3) **colonizing aspergillosis**, the development of fungal balls in body orifices and airways.

Aspergillus fumigatus, a major pathogen, causes aspergillosis when the host is immunosuppressed, when there is a severe loss in epithelial barriers, or when the normal flora of body surfaces and orifices is altered. Although the newborn deprived of colostrum is at risk, the greatest danger is in patients with immunosuppression of cell-mediated immunity. The monocyte is of prime importance in resistance to aspergillosis and oxidative killing of this fungus occurs by myeloperoxidase-dependent and -independent pathways.[44]

Lung **Hyphal pneumonia** results from direct damage to lung parenchyma. When inhaled into the adult lung, spores are killed by phagocytosis and digestion in **alveolar macrophages**.[45] Factors that suppress these processes allow germination in a percent of

phagocytized spores sufficient to cause disease. During germination and growth, fungal metabolites are produced that act on cellular membranes and suppress the activity of alveolar macrophages. Fungal proteases and elastin allow fungi to breach the alveolar epithelial cell barrier. Proteases disrupt the actin cytoskeleton and focal adhesion sites of pneumocytes.[46] In human pulmonary aspergillosis, tissue elastolysis appears to play no major role in invasion of blood vessels.[47]

In **allergic pulmonary aspergillosis**, fungi grow in secretions of the respiratory tract and release fungal antigens that induce and subsequently react with host antibodies. Immunoreactivity may be of the immediate type, due to reaction of antigens with cell-bound reaginic antibody, or the immune complex type, due to deposition of antigen-antibody complexes in lung tissue. One of the other dominates in clinical infection.

Experimentally, normal mice that inhale viable spores of *A. flavus* are resistant to infection whereas mice treated with corticosteroids develop lethal hyphal bronchopneumonia. Macrophages obtained from alveolar washings of normal and immunosuppressed mice rapidly phagocytize *A. flavus* spores, but phagosomes in the later group do not fuse with lysosomes to initiate intracellular degradation.[48]

Avian Aspergillosis

A. fumigatus is highly pathogenic for newly hatched chicks and develops during the poikilothermic stages after hatching. Aspergillosis appears in several forms in domestic and wild birds. **Airsacculitis** involves superficial infections of air sac epithelium with foci of greenish-white sporulating mycelia. **Pneumonia** may be an acute inflammatory process with spore formation or, more commonly, chronic granulomas of epithelial cells, giant cells, and fungal spores. When large numbers of conidia are inhaled, an acute necrotizing vasculitis develops and leads to intense hyperemia, edema, and large areas of necrosis. **Aspergillus meningitis** develops in a significant percent of birds with respiratory aspergillosis, and is common in aggregating wild bird populations such as ducks and penguins. Phagocytosis is prominent, and both spores and hyphae are common within phagolysosomes of granulocytes and macrophages.

Genus *Blastomyces*

Blastomyces dermatitidis causes disseminated granulomatous disease in pulmonary, cutaneous, and disseminated variants. In lungs, infection is due to inhalation of conidia from saprophytic fungi growing in soil. Lesions begin as microabscesses centered on fungal cells. These foci rapidly form granulomas, the macrophage response being due to a component of the fungal cell wall.

Macrophages infected with *B. dermatitidis* show little evidence of activiation of the phagosomal-lysosomal system of intracellular microbial killing, and cytoplasmic areas have a striking lack of lysosomes and other granules; instead, there is a uniform pattern of small mitochondria in a cytoplasmic matrix of small vesicles and tiny ribosomes. As *B. dermatitidis* replicates, the macrophage progressively enlarges and nuclei become irregular (often with two or more nuclei). Giant cells occur but rarely become large multinuclear cells. Fungal cells within the lesions are budding yeast forms. The mature microconidium has a thick cell wall, an eccentric nucleus, and multiple lipid storage globules.

Systemic blastomycosis results from spread of fungi from the primary focus in the lung to other organs via lymphatics and circulating blood. Organs most frequently affected are lung, lymph node, skin, urogenital tract, eye, and meninges. In humans, leptomeningitis is the most common lesion, although pyogranulomas also occur (Fig. 16.6). Fungal cells have

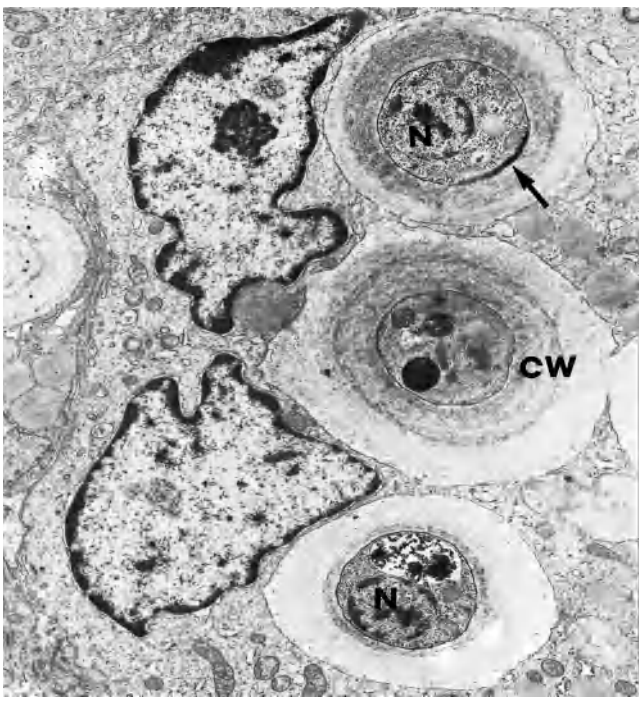


Fig. 16.6 ***Blastomyces dermatitidis***: granulomas, cerebellum, 48-year-old man. Multinucleate giant cell contains three yeasts with lamellar cell walls (*CW*), nuclei (*N*), and distinct cell membranes with focal thickening (*arrow*). Yeast cell cytoplasm contains mitochondria, glycogen, lipid droplets, dense bodies, and nuclei with peripheral chromatin and prominent nucleoli. (Micrograph: Suzanne S. Mirra, *Acta Neuropathol* 50:109, 1980.)

large nuclei with peripheral chromatin, a few have multiple nuclei, and cytoplasm that contains mitochondria, glycogen granules, lipid globulues, and dense bodies. Cell walls are lamellar and there is a wide capsule that appears to be delimited from the cytoplasm by a membrane.[49] Budding is common and often involves complex membrane profiles.

Genus *Candida*

Candida spp. are the most common opportunistic fungal pathogens and are one of the leading infectious agents that cause nosocomial infections, notably disseminated candidiasis in immunodeficient patients. *Candida albicans* and *C. tropicalis* are important opportunistic pathogens of mucosal surfaces. In all species the tissues affected are many, and the clinical signs are diverse. *C. albicans* is ubiquitous in the normal human alimentary tract, on skin, and on mucosa of genitourinary passages and body orifices. Colonization is antagonized by normal resident bacterial flora. Held in check by normal defense mechanisms, organisms invade epithelial barriers and proliferate rapidly when these are suppressed.[50] Antimicrobial peptides in saliva bind to the cell wall and damage the fungal plasma membrane.[51] Mice with a murine leukemia virus-induced immunosuppressive syndrome develop persistent coloniziation and invasive tissue infection with *Candida* spp.[52]

Candidiasis

Candidiasis may be **cutaneous** (candida granuloma, diaper disease, intertriginous candidiasis, onychomycosis), **mucocutaneous** (oral thrush, glossitis, and stomatitis, or similar infection of the respiratory, alimentary, and urogenital tracts), or **systemic** (general candidiasis that may end in meningitis, endocarditis, or disseminated disease with candidemia). The mouth of the newborn and the vagina of the gravid female are especially prone to candidiasis, perhaps because of the low pH that may permit fungal growth.

On body surfaces and in fluids, *C. albicans* occurs in the **yeast form**, which infiltrates between epithelial cells and is diagnosed on the basis of size, structure, and location (Fig. 16.7).[53] Lysozyme rapidly hydrolyzes cell wall components of *C. albicans* and these degradation reactions of the cell wall have been characterized ultrastructurally.[54]

During surface colonization, yeast forms (which are required for infection) are converted to **mycelial** forms. During germination, new **germ tubes** grow out from the yeast cell, expressing new **surface fibrillar materials** that are used to adhere to host cells and to extracellular matrix of host tissue.[55] Adherence also involves other surface glycoproteins, some of which have been localized using immunogold. The yeast-mycelial conversion is brought about by exposure to environmental factors that inhibit cell division but not growth so that elongate hyphae develop.

Penetration of *Candida* spp. through the gastrointestinal mucosa is a common mechanism leading to systemic dissemination. Autopsy studies reveal submucosal invasion by blastoconidia and pseudohyphae, preceded by a band of advancing tissue necrosis in *C. tropicalis* infections. Experimental studies in rodents reveal virulence mechanisms include lysis of mucin, adherence to mucosa, destruction of gut microvilli by candidial hydrolytic enzymes, suppression of anaerobic microflora by antibiotic therapy, and neutropenia of chemotherapy.

Invasion of epithelial barriers is enhanced by the entry of **hyphae** of *Candida* sp. into epithelial cells. Ultrastructural studies of oral epithelial plaques from human patients with candidiasis show that growth is intracellular and that the cytoplasm and nuclei of the invaded cells are not markedly changed, at least early in infection.

Once coloniziation or tissue invasion has occurred **mycelia** progressively increase with the age of the lesion. The tissue lesion is inflammatory, due either directly to invasion by neutrophils and other inflammatory cells and release of fungal toxins, or indirectly to immune phenomena.

If *C. albicans* enters the blood circulation during systemic infection, it is trapped selectively in the spleen, with uptake by macrophages in the marginal zone. Splenic zone phagocytes appear to have a unique adhesion system that differs from the known leukocyte integrins, LECAM-1, CD-44, and so on.[56]

C. albicans in skin and mucosae may be restricted to the stratum corneum or, more rarely, invade into deep layers. **Microabscesses** are the hallmark of early stages of infection, and neutrophils play an early role in destruction of fungal cells.[57,58] Some strains of *C. albicans* are relatively resistant to human neutrophils, and this causes increased virulence. Within neutrophil phagolysosomes, some blastoconidia retain their structure while others undergo degradation. Mannan-rich cell wall layers are progressively lost. **Granulomas** composed of macrophages bearing fungal cells are the tissue lesion of chronic infection. Macrophages take up *C. albicans* through receptor-mediated phagocytic events and are the important cell in elimination of subacute infection. Intracellular blastoconidia may resemble *Histoplasma* yeast forms, and thick-walled conidia may appear as blastomyces.

The **kidney** is the organ most involved in human disseminated infection. Asteroid bodies composed of fungal elements and matrix material develop in renal tissue and appear in urine. Ultrastructural studies

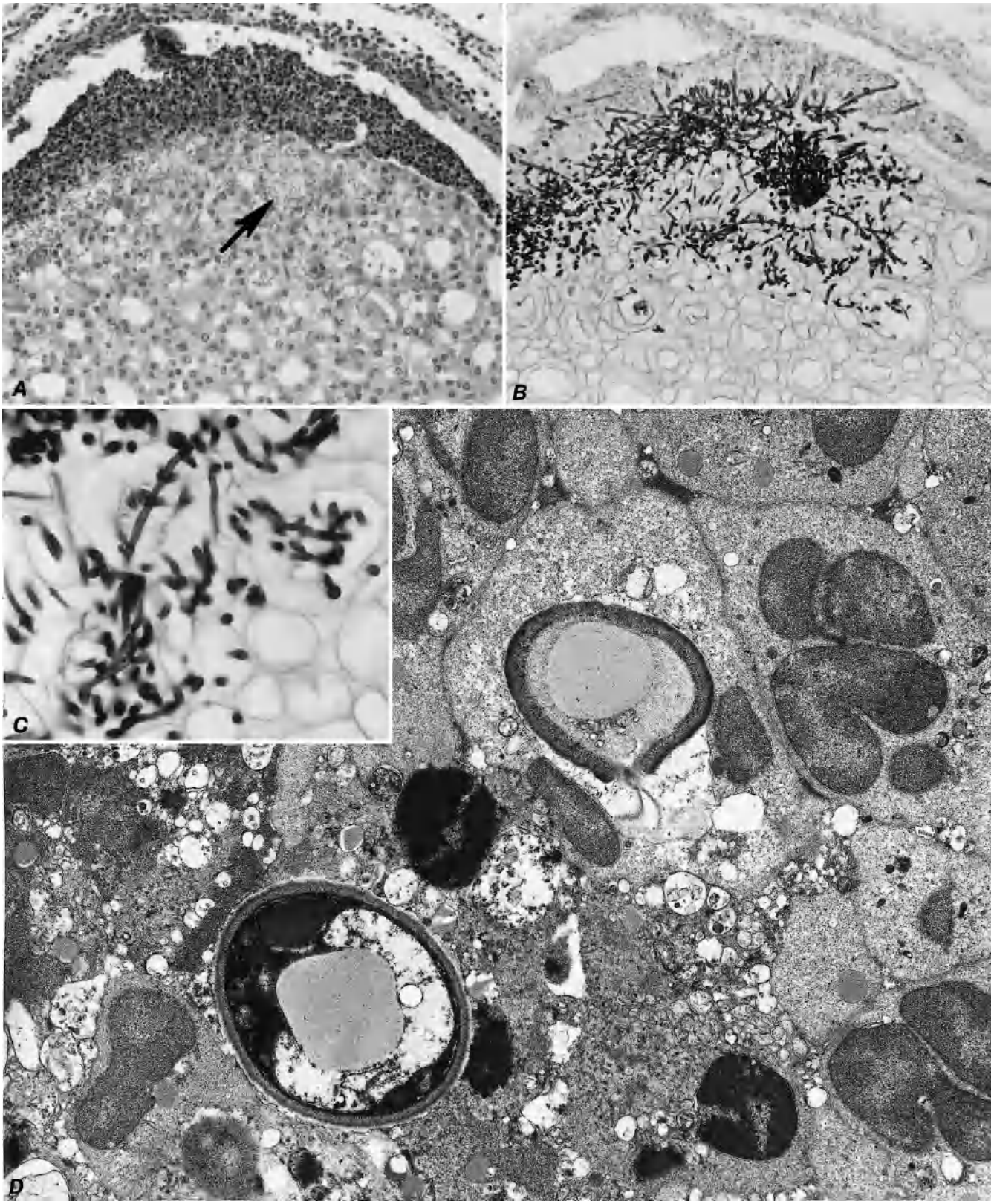


Fig. 16.7 ***Candida albicans***: experimental infection, renal papilla, mouse. **A** and **B**. **Histology**: adjacent sections stained with H&E and methenamine silver techniques. **C**. **Hyphae**: enlargement of B. **D**. **Degenerate alga**: mass of inflammatory cells. Lipid globules in fungal cells.

using ferritin-labeled IgG and IgA have shown that *C. albicans* asteroid bodies concentrated from human urine accumulate globulins on their surfaces.[59] In renal lesions of the mouse, organisms are found largely in the pelvis zones.[60,61] The liver, lungs, blood vessels, spleen, and thyroid are involved, in that order of frequency. Central nervous system invasion is rare in candidiasis but can occur.[62]

Genus *Coccidioides*

Coccidioides immitis is a respiratory fungal pathogen. Airborne **arthroconidia** of saprobic phase mycelia growing in soil are inhaled to cause pulmonary lesions. Once in the lungs, viable conidia differentiate into large **coenocytic spherules**, the contents of which convert into many **endospores**.

C. immitis has no sexual phase and is classified as a member of the Fungi Imperfecti, although it is related to the ascomycetous fungi. Ultrastructural studies of spherule-endospore formation show that spherule segmentation occurs by septal formation, and endospore formation is distinct from sporangial cleavage and sporangiospore formation of the zygomycetes.[63]

Coccidioidomycosis

Endospores are disseminated within the lungs. The most invasive forms are spherules of 10–50 μm diameter with thick walls and capsules. They become the foci of purulent and granulomatous inflammation. Typically, organisms lie in tiny microabscesses surrounded by macrophages, giant cells, and fibroblasts. Disseminated coccidiodomycosis leads to nodules in lymphoid organs, bone marrow, and meninges.

Ultrastructurally, *C. immitis* is surrounded by a cell wall and a plasma membrane that is markedly folded in young cells. These cell surface structures contain the immunoreactive glycoproteins that generate immune reponses.[64] In some organisms the capsule has club-like projections that radiate from the surface.[65] In the cysts, which are filled with endospores, individual organisms are delimited by cleavage furrows, each of which contains a distinct nucleus.

The antigenic proteins of *C. immitis* that incite antibodies in serum of the host (and react in the tube precipitin and complement fixation tests) have been localized ultrastructurally using immunogold labeling techniques. A 33 kDa spherule protein that reacts with antibodies from patients with coccidioidomycosis has been shown by immunoelectron microscopy to be present in the inner cell wall of arthroconidia and spherules and in the septa and glycocalyx surrounding the endospore.[66]

Genus *Cryptococcus*

Crytococcus neoformans occurs in yeast forms surrounded by a massive fibrillar capsule. Tiny filaments anchored in the cell wall radiate peripherally and terminate in meshes of short thick fibrils. A unique **microbody**, a modified peroxisome, is involved in xanthine and urate metabolism, and may underlie the propensity for growth of this fungus in bird feces, which are high in urates.[67]

Cryptococcosis

C. neoformans infects normal individuals, but causes serious disease in those that are immunosuppressed. It is an important fungal opportunist in AIDS, and cell-mediated immunity is required for survival.[68] Massive gelatinous lesions of the brain (torulomas) are caused by the unrestricted growth of *C. neoformans*. Ultrastructurally, brain lesions show fungal cells with characteristic filamentous capsules (Fig. 16.8). Fungi have a distinct nucleus and prominent nucleolus, as well as ribosomes and mitochondria. Other characteristics include laminated cell walls, an electron-lucent zone, and a reticulated capsule. In tissue, granulocytes and monocytes surround organisms and ring structures develop, which may destroy the yeast. Phospholipases and hydrolases are released from the phagocytes, which have pseudopodia that penetrate the polysaccharide capsule of the yeast. Macrophages containing yeasts are often surrounded by plasma cells but yeasts free in extracellular spaces are kept from phagocyte surfaces by the intact capsule.[69] Laccase, present in the cell cytoplasm, cell wall, and capsule, is a major virulence factor of *C. neoformans*.[70]

Genus *Histoplasma*

Histoplasmosis is the most common respiratory mycotic infection of humans and most mammals. The cause, *Histoplasma capsulatum*, is a dimorphic fungus with a parasitic phase consisting of yeast cells and a saprobic mycelial phase. **Yeast** cells are oval, 1–3 μm in diameter, and reproduce by budding (Fig. 16.9).[71,72] **Conidia** of *H. capsulatum* enter the animal by being inhaled or ingested along with dust, feces, or soil. Infection rates are high (organisms can be cultured from normal animals in endemic areas) but the incidence of disease is low.

Two other disease are associated with disease species of *Histoplasma*: **farcy**, a lymphatic vasculitis of horses in the Mediterranean areas is caused by *H. farciminosum*, and human **African histoplasmosis**, caused by *H. doboisii*, a much larger organism than *H. capsulatum*.

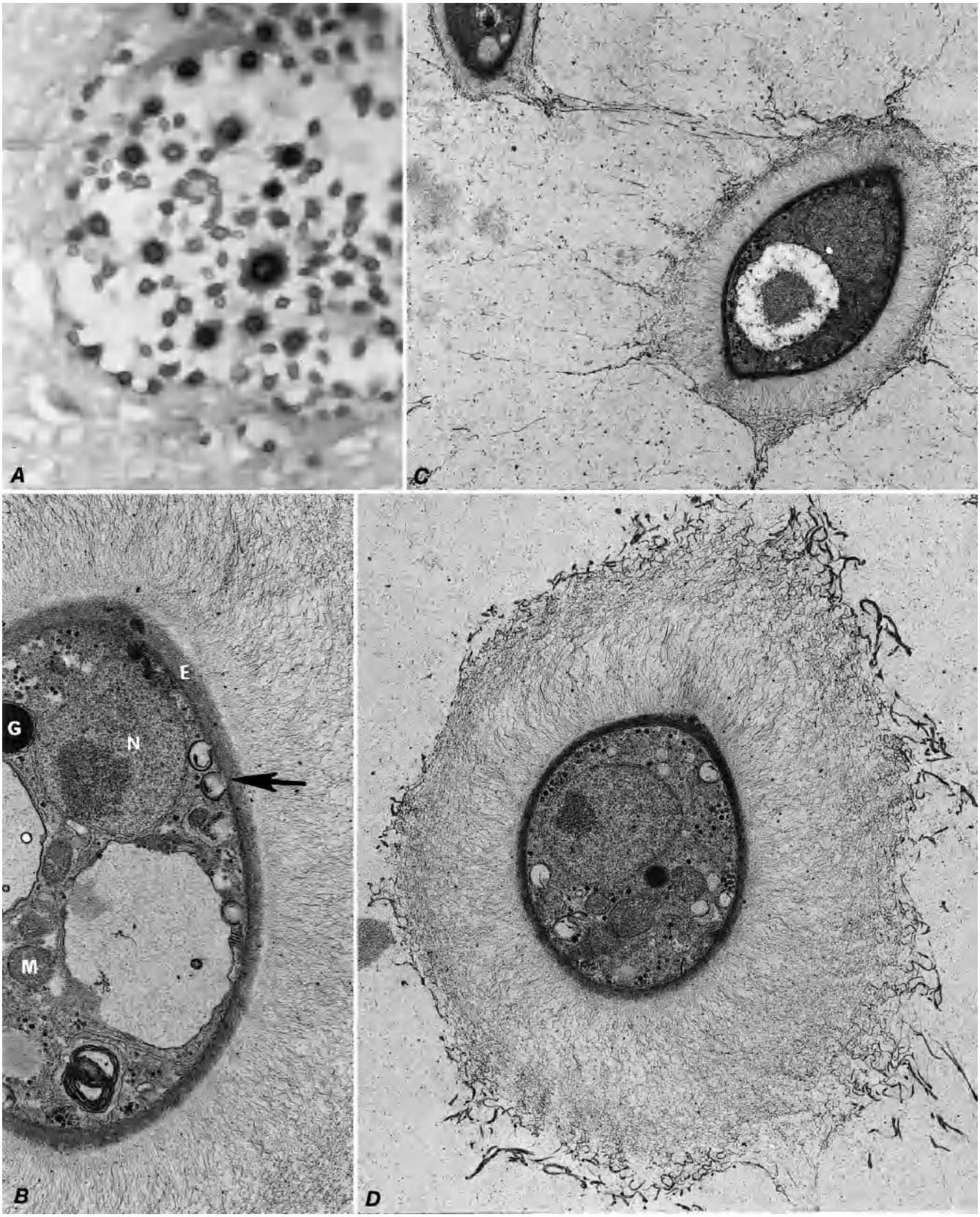


Fig. 16.8 ***Cryptococcus neoformans***: brain, mouse, experimental cryptococcosis. **A**. **Histology**: alcian blue-PAS stain. **B**. **Fungal cell**: nucleus (*N*), mitochondria (*M*), dense granule (*G*), cell envelope (*E*). Note exocytotic vesicles at the cell surface (*arrow*). **C** and **D**. *C. neoformans* cells. Thick capsule is a fibrillary layer composed of thin filaments. Outermost capsular filaments are thickened by accretion of proteins from interstitial spaces. Cell wall is a thin lamellar structure.

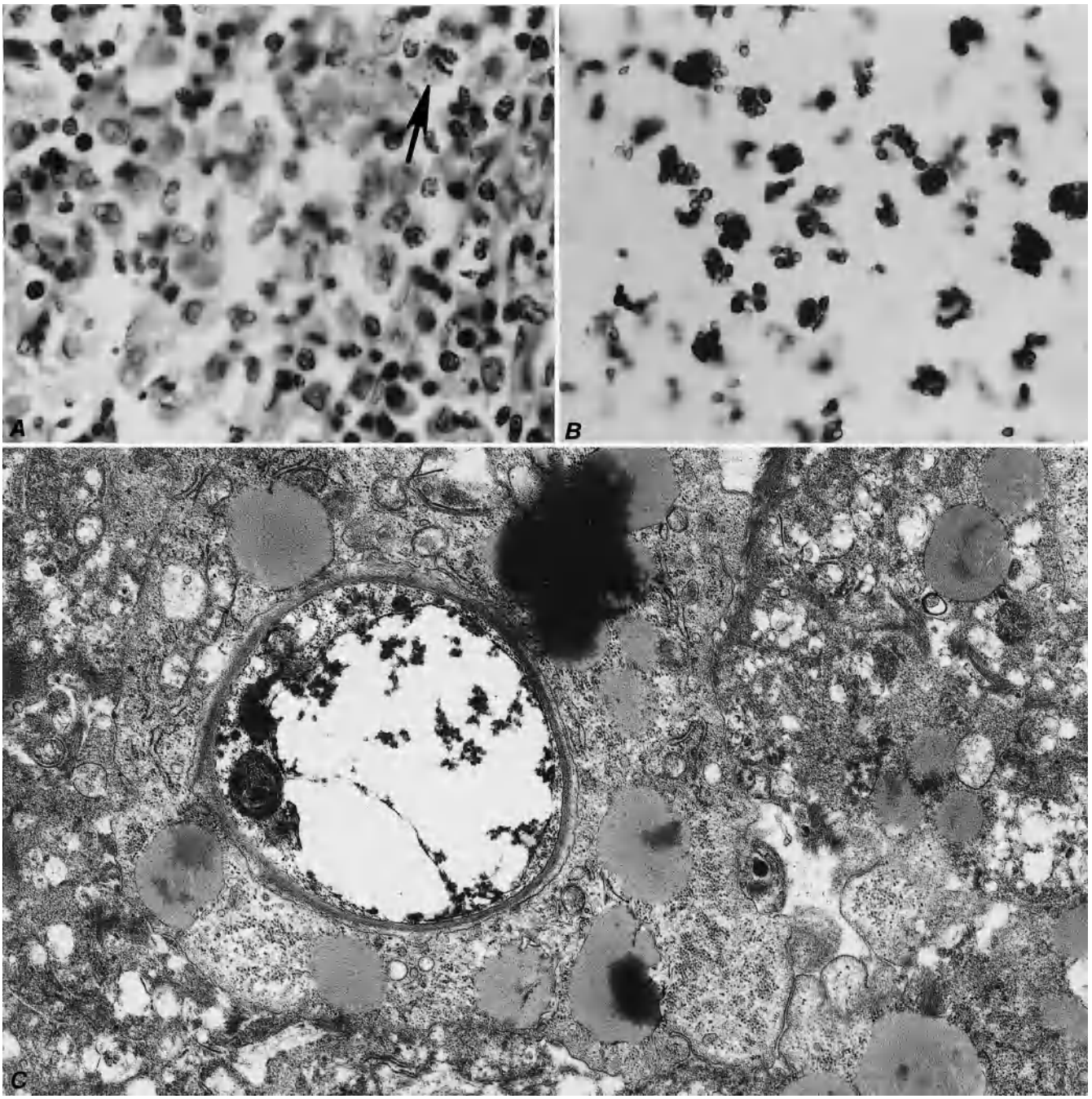


Fig. 16.9 ***Histoplasma capsulatum***: macrophages, lymph node, chronic histoplasmosis, dog. **A**. **Histology**. **B**. **Silver stain:** capsule. **C**. **Ultrastructure**: fungal cell is vacuolated. Note lipids in macrophage cytoplasm.

Histoplasmosis

Emaciation, diarrhea, and lymphadenoapthy are the signs of histoplasmosis. Fungal cells may be present in large numbers in lymphoid tissues of the intestinal tract. Enlarged lymph nodes contain intense reticuloendothelial hyperplasia. *H. capsulatum* localizes in macrophages and endothelial cells and replicates freely in the cytoplasm. It appears as small, round to oval, 2–4 μm yeast cells.

Ultrastructurally, the heavy wall of the yeast phase is electron-lucent and contains large amounts of chitin, an important virulence structure (there are no chitinases in vertebrate tissues). In chronic infection, fungal cells may be killed but although the internal structure of the cell is lysed, cell walls persist as masses of thick electron-dense material within the macrophage.

Within phagolysosomes of infected macrophages, lysosomal acid hydrolases break down cell walls.

Human neutrophils are not totally effective in killing *H. capsulatum*; fungi are phagocytized, elicit an oxidative burst, and do not significantly inhibit phagosome-lysosomal fusion.[73]

Genus *Paracoccidioides*

Human **paracoccidioidomycosis** is a pulmonary infection, often clinically silent, but with dessemination to form granulomatous lesions and ulcers of the buccal, nasal and gastrointestinal mucosa. The pathologic reaction is similar to the pyogranulomas of coccidioidomycosis and blastomycosis. Clusters of activated alveolar macrophages are surrounded by lymphocytes and plasma cells.[74] Expression of MHC-II on macrophage surfaces is related directly to the clonal recognition of antigens. Low expression of MHC-II, as detected by immunolabeling, may be related to decrease of the antigen presenting function of the alveolar macrophage.[74]

Cutaneous lesions and those of the oral mucosa have pseudoepitheliomatous hyperplasia associated with marked granulomatous responses.

P. brasiliensis is identified by its characteristic uniform budding pattern. Buds are connected by a small neck that encircles the 12–40 μm spherule ("pilot-wheel" budding). In eight cases of human paracoccidiodomycosis, fungi grew within epithelial cells of the lip mucosa, and appeared with a thick cell wall surrounding cytoplasm bearing lipid globules and other organelles (Fig. 16.10). Infected keratinocytes had evidence of cytoplasmic lysosomal activation and fluid accumulation in extracellular spaces. Intraepithelial abscesses developed as keratinocytes detached from one another.[75]

Some yeasts produce peptide hormones and hormone receptors; for example, *Saccharomyces* sp., brewer's yeast, produces the female hormone 17B-estradiol. *P. brasiliensis* has estrogen receptors and the predilection for men (75:1) may be because it has sex hormone receptors that bind and recognize specific steroids. Estrogens inhibit the conversion of the mycelial form of *P. brasiliensis* to the yeast form—the one that is inhaled. *Coccidioides immitis*, which disseminates more frequently in pregnant women, also produces sex hormone receptors.

Genus *Rhinosporidium*

Human rhinosporidiosis is a chronic, granulomatous infection of mucosal surfaces; over 70% are in the nasal cavity. The causal organism, *Rhinosporidium seeberi,* is unclassified and has not been cultured. Human infection leads to development of dense nasal polyps and pedunculated, fibromyxomatous granulomas that contain spherules and prospores. **Pseudocysts** are present and contain spores, pus and mucous debris. Giant cells, eosinophils and plasma cells are common.

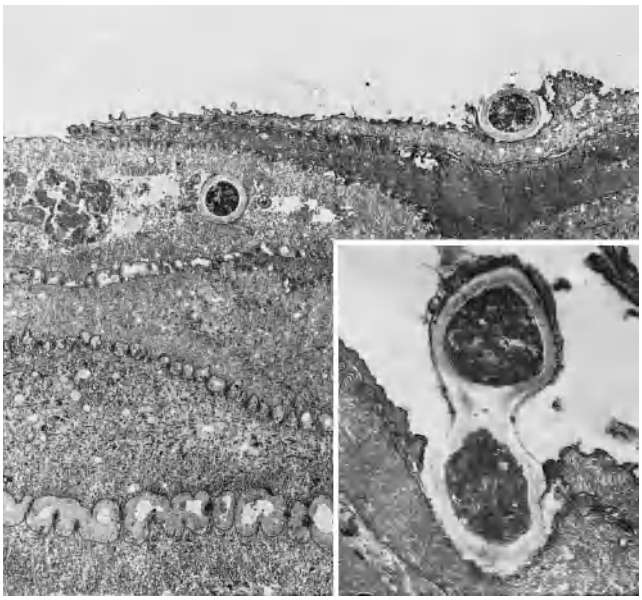


Fig. 16.10 ***Paracoccidioides brasiliensis***: epithelium, lip mucosa, human. Fungal cells are on the surface layer and inside the epithelial cell. (Micrographs: Thales de Brito, *Virch Arch A* 361:129, 1973.)

The life cycle of *R. seeberi* involves an infecting **spore** of 6–12 μm diameter that penetrates into mucosal epithelium and matures into **spherules** in the subepithelial tissues. The chitinous wall of the spherule contains granular material and lipids (Fig. 16.11). Nuclear divisions occur and at 100 μm a layer of about 3 μm of cellulose-like material is seen on the inner surface of the spherule wall. A pore develops that permits the escape of new spores.[76]

Rhinosporidiosis in animals is most commonly reported in horses, but has also been reported in cattle, dogs, and swans.[77] Fungal cells in nasal polyps of canine rhinosporidiosis vary greatly in size: immature sporangia are unilaminar and 15–75 μm in diameter; intermediate sporangia are 100–150 μm and bear immature endospores; mature sporangia are 100–400 μm and contain both immature and mature endopspores.[78]

Experimental disease in laboratory rodents has not been successful.

Genus *Sporothrix*

Sporothrix schenckii causes a chronic, nodular, pyogranulomatous infection of the cutaneous and subcu-

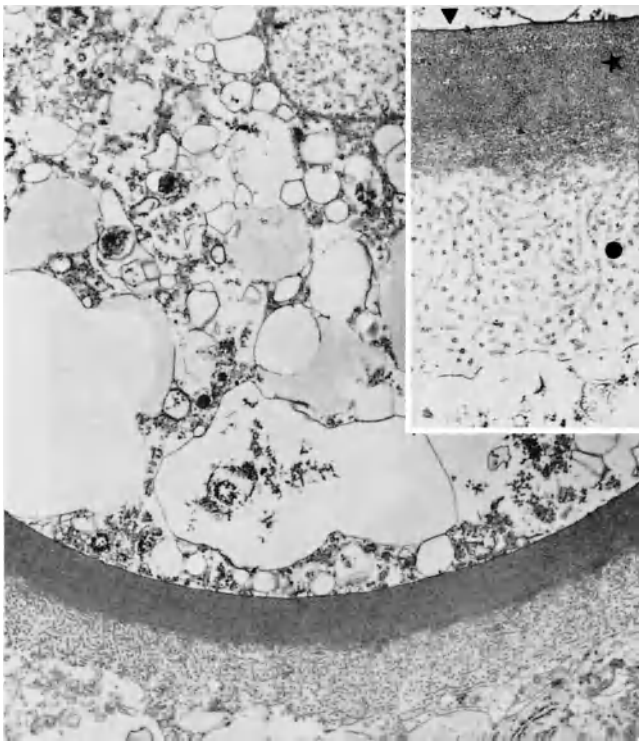


Fig. 16.11 ***Rhinosporidium seeberi***: trophozoite. *Inset*: Cell wall. (Micrograph: K. D. Lengfelder and Andreas Pospischil, *Zentralbl Veterinaermed B* 27:326, 1980.)

taneous tissues of man and horses; infections have also been reported in dogs, cats, pigs, foxes, armadillos, camels, dolphins, and birds. The primary lesions appear at a site of some previous minor injury. Human infection extends via lymphatics into the draining lymph node, but rarely beyond this point. Lesions are most common in skin and mucocutaneous sites and in systemic infection are typically found in bone, eye, sinuses and meninges.

In culture, *S. schenckii* produces mycelia with pear-shaped conidia. In infected tissue mycelia are not formed and the parasitic phase is a cigar-shaped body, 1–3 × 2–10 μm. These gram-positive bodies are present within macrophages and leukcoytes, and can be stained in smears of pus. Tissue lesions have few organisms and this makes diagnosis, especially at the ultrastructural level, difficult. Hyalin asteroid bodies, which are found in bacterial granulomas, also occur in sporotrichosis.

Ultrastructural studies of the lesions of sporotrichosis have revealed macrophages containing yeastlike cells of *S. schenckii*. The cell wall is thick and there is fibrillar material that extends outwards from the wall. Nuclei, nucleoli, mitochondria, lipid globules and dense granules are visible within the fungal cell.[79] The large budding yeast forms contain central vacuoles. **Asteroid bodies** consist of central fungal cells with peripheral rays of electron granular material arranged in layers. This material represents disintegrated host cell debris.[80]

Miscellaneous Subcutaneous Mycoses

Miscellaneous subcutaneous mycoses, although unrelated, are grouped together because they produce similar lesions in subcutaneous tissue. The fungi involved are for the most part poorly defined, most have not been cultivated in vitro, and the disease caused by each is rare. Although very rare cases of systemic spread have been reported, dissemination does not generally occur.

Phaeohyphomycosis

Phaeohyphomycosis is a heterogenous group of fungal diseases characterized by dematiaceous (darkly pigmented) hyphal to yeast forms in tissue. Lesions occur in skin and subcutis, and brain (cerebral chromomycosis, cerebral cladosporiosis). Dematiaceous fungi that cause CNS phaeohyphomycosis in humans include the genera *Wangiella*, *Fonsecaea, Dactylaria*, *Curvularia*, and *Xylohypha*. *Xylohypha bantiana* (*Cladiosporum* sp.) is responsible for most of the cases of neural phaeohyphomycosis in humans and animals.[81] **Chromoblastomycosis** cause by *Fonsecaea pedrossoi* is a subcutaneous mycosis of the tropics; lesions contain hyphal segments and dark brown, thick-walled sclerotic bodies.

Madura Mycetoma

Mycetomas are pyogranulomatous lesions of the skin, subcutis, or underlying bone that contain fistulous tracts and masses of bacteria or fungi called **grains**. The etiologic agent may be bacterial (actinomycotic mycetoma) or fungal (eumycetoma). **Eumycetomas** are caused by fungi that form either pigmented (dark) or nonpigmented (pale) fungal grains. **Dark eumycetoma** grains caused by *Madurella mycetomatis* have fungal cells encased in dense peripheral materials.[82] Causal fungi in nonpigmented **pale grain eumycetomas** include *Pseudoallescheria boydii*, *Acremonium* spp., *Fusarium* spp. *Neotestudina rosatii*, and *Aspergillus* spp. **Pythiosis** is a similar lesion of granulation tissue and fistulous tracts that contain *Pythium insidiosum*.

Mucormycosis

Mucormycosis is a rare fungal infection that occurs as a complication of debilitating disease or long-term immunosuppression. Most cases in animals are discovered incidentally during the course of meat

inspection. The identity of the causal fungi varies but in most cases the organisms involved are species of the genera *Mucor*, *Absidia*, or *Rhizopus*. These are classified in the order Mucorales, class Phycomycetes. The granulomatous lesions containing thick, non-septate, filamentous fungal cells are found in enlarged lymph nodes or in superficial ulcers on epithelial surfaces. The tissue reaction is granulomatous and fungal cells can be found in giant cells.

Penicilliosis

Of the 150 or more known species of *Penicillium* found in soil and decomposing organic debris, only *P. marneffei* is known to be dimorphic and to be pathogenic. It has been reported as a cause of tissue invasion in man, mainly as a cause of skin infection, lymphangitis, lymphadenitis, and synovial membrane infection called penicilliosis. Ultrastructural studies in infected macrophages and synovial membranes show close structural similarity to *Pencillium* spp. grown in culture.[83]

Lobomycosis

Lobomycosis is a chronic focal infection of man and dolphins characterized by nodular granulomatous lesions that bear masses of round yeastlike organisms classed as *Loboa loboi*. The subepidermal granulomas have marked fibosis with much hyalin tissue mingled with masses of macrophages and giant cells that bear the fungi (but little or no pus). Ultrastructurally, the wall of fungal cells is about 1 μm thick.[84] Radiating eosinophilic, asteroid bodies are common, and are a manifestation of the Splendore-Hoepli immunologic phenomenon. A similar, ungrouped agent causes systemic infections in owl monkey.[85]

Adiaspiromycosis

Adiaspiromycosis is a granulomatous pulmonary disease of small burrowing mammals and rarely of humans. It is a seasonal disease of wild rodents. Causal organisms have been placed in *Emmonsia* or *Chrysosporium* (they may be two species or varieties), most favor the genus *Emmonsia* (with *E. crescens* as the most significant pathogen in mammals). Disease may develop as either adiaspiromycosis or adiasporosis. The tissue form is a large, globose, thick-walled, nonproliferating **adiaspore**. Lesions develop from inhaled organisms that arise from the saprophytic mycelial phase of the fungus, which vegetates in the soil. In lung parenchyma, typical adiospores (spherules) are formed and induce a granulomatous inflammatory reaction.

Fusariomycosis

Fusarium spp. are common soil organism and plant pathogens that cause mycotic keratitis and **onychomycosis** in humans, **mycotic abortion** in cattle, and granulomas in various animal species. Lesions contain branching, septate hyphae that closely resemble hyphae of *Aspergilllus*, *Penicillium*, and *Pseudoallescheria boydii*.

Pityriasis Versicolor

Pityriasis (tinea) **versicolor**, a mild superficial infection, is caused by the lipophilic yeast *Malassezia furfur*, a saprophyte of normal human skin. *M. pachyermatis* causes otitis externa in dogs. In lesions, hyphae and budding yeasts are restricted to the stratum corneum and are found in confluent masses that extend on the surface to invade hair follicles. Abnormal melansomes are responsible for hyperpigmentation.

Dermatophytosis (Ringworm)

Dermatophytosis is the colonization by dermatophytic fungi of keratinized tissue. This is used in distinction to **dermatomycosis**, which indicates infection or contamination of tissue by soil fungi such as *Hendersonula toruloidea*, et al.

In dermatophytosis, infection is generally limited to the stratum corneum, but the inflammatory reaction may extend into deeper layers of the dermis. The major genera that cause dermatophytosis are *Trichophyton*, *Microsporum*, and *Epidermophyton* (Table 16.3). The marked variability and immense numbers of fungal species that cause ringworm are illustrated by the clinical terms applied to human ringworm: tinea capitis (scalp), tinea corporis (glabrous skin of the body), tinea cruris (groin), tinea favosa (favus due to *T. schoenleinii*), tinea imbricata (ringworm due to *T. concentricum*), onchyomycosis (nail), tinea pedis (feet), tinea barbae (beard), tinea manuum (hand).

Infection by the keratinophilic dermatophytes begins by invasion and colonization of the stratum corneum of the skin. Infection proceeds centrifugally leading to the classic ringworm pattern of growth. During the incubation period, hyphae grow in the stratum corneum and extend into orifices of hair follicles. In the epidermis, hyphae penetrate the stratum spinosum, the actively growing zone of keratinocytes. Mycelia enter the hair follicle and grow downward along the surface of the hair shaft and within the hair shaft beneath the cuticle. The hairshaft is ringed with

Table 16.3 Pathogenic fungi that cause cutaneous infection.

Organism	*Disease*	*Species*	*References to ultrastructural pathology*
***Arthrographis* sp.**	Dermatomycosis,# sinusitis, keratitis	Human	**Chin-Hong**, *J Clin Microbiol* 39:804, 2001
Candida albicans	Dermal candidiasis		
Chrysosporium tropicum	Dermatomycosis	Human	**Fusconi**, *Mycoses* 34:153, 1991 (hair)*
***Epidermophyton* spp.**	Ringworm		
Exophiala werneckii	Tinea nigra		
***Hendersonula* spp.**	Dermatomycosis		
Microsporum gypsum	Ringworm	Human	**Buchnicek**, *Mykosen* 24:472, 1981;* **Keddie**, *Sabouraudia* 6:1, 1967 (hair)
		In vitro	**Kunert**, *Mycosen* 24:485, 1981* (keratin)
M. cookei	Ringworm	In vitro	**Mares**, *Mycopathologia* 108:37, 1989
M. ferrugineum	Ringworm		**Takatori**, *Mycopathologia* 81:129, 1983
***Malassezia* spp.**	Pityriasis, tinea versicolor	Human	**Keddie**, *Sabouraudia* 5:134, 1966; **Pierard**, *Int J Dermatol* 11:116, 1972
		In vitro	**David**, *Cell Biol Int* 31:16, 2007
Piedraia hortae	Black piedra	Human	**De Almeida**, *Mycoses* 34:447, 1991
***Pityrosporum* spp.**	Pityrosporosis	Human	**Keddie**, *Int J Dermatol* 11:40, 1972
		In vitro	**Keddie**, *J Ultrastruct Res* 29:760, 1969
***Rhizopus* spp.**	Dermatomycosis	Human	**Hawker**, *Biol Rev* 40:59, 1964 (sporangiospores)*
***Scytalidium* sp.**	Dermatomycosis		
Tinea nigra	Ringworm		
***Trichophyton* spp.**	Ringworm, onychomycosis§		**Poulain**, *J Invest Dermatol* 74:205, 1980‡
T. interdigitale	Ringworm		**Rashid**, *J Med Vet Mycol* 31:305, 1993
T. mentagrophytes	Ringworm	Guinea pig	**Hutton**, *Infect Immun* 21:247, 1978‡
		In vitro	**Masperi**, *Sabouraudia* 22:27, 1984 (miconazole);* **Melchinger**, *Mycoses* 33:393, 1988 (oxiconazol)*
T. verrucosum	Ringworm	Cow	**Lepper**, *Res Vet Sci* 20:117, 1976
Trichosporon beigelii	White piedra	Human	**De Almeida**, *Mycoses* 33:491, 1990
	Trichosporonosis	Mouse	**Gokaslan**, *Infect Immun* 60:3339, 1992‡
	Experimental	Rabbit	**Walsh**, *J Infect Dis* 166:121, 1992

*In vitro study.
‡Animal model.
Dermatomycosis is infection caused by contaminants of soil fungi in tissue.
§ **Onychomycosis** is fungal infection of the nails; common causes are *Trichphyton rubrim*, *T. mentagrophytes*, and *Acremonium* spp.

a mass of hyphae. As the growing hair moves these hyphae to the surface, the specialized parasitic **conidia** (arthroconidia) are produced. The proliferative response generated by fungal products has a protective washout effect in ridding skin or organisms.

The human hair follicle is damaged by fungal cells through different mechanisms. Condia of **ectothrix** fungal species appear under the cuticle and around the hair shaft; in **endothrix** species, condia are within the hair shaft. The cuticle is spared in endothrix infections but the hair, weakened by fungal growth, breaks and disintegrates. Ultrastructural studies of parasitized hair show that dermatophytes are keratinolytic.[86] Some fungi actively invade hair and long invasive filopodia of hyphae have been seen inserted deeply into the hairshaft.

Some fungal infections involve only hair and the most superficial layers of the skin (Table 16.4). The ability of dermatophytes to invade and parasitize cornified tissue depends on their ability to colonize and catabolize keratin. The dermatophytes *Trichophyton* spp. and *Microsporum* spp. degrade keratin to cause keratolysis.[87,88] Hyphae bind to, attach, and invade the hair shaft (Fig. 16.12).

Table 16.4 Pathogenic myxozoans.

Organism	*Tissue*	*Species*	*References to ultrastructural pathology*
***Buddenbrockia allmani*§**	Body cavity	Bryozoan	**Canning**, *J Eukaryot Microbiol* 54:247, 2007
B. plumatellae	Peritoneum	Bryozoan	**McGurk**, *Dis Aquat Organ* 73:159, 2006
Ceratomyxa shasta	Intestine	Fish	**Yamamoto**, *J Fish Dis* 2:411, 1979
Henneguya adipose	Muscle	Catfish	**Current**, *J Protozool* 26:209, 1979
H. exilis	Muscle	Fish	**Current**, *Protistologica* 13:157, 1982; **Current**, *J Parsitol* 62:975, 1976
H. garavelli	Gill	Fish	**Martins**, *Vet Parasitol* 137:253, 2006
H. hamdia	Gill	Fish	**Matos**, *J Eukaryot Microbiol* 52:532, 2005
Kudoa paniformis	Muscle	Fish	**Stehr**, *J Fish Dis* 9:493, 1986
K. thyrsitis		Fish	**Harrell**, *J Fish Dis* 8:329, 1985
Myxidium hardella	Kidney	Turtle	**Garner**, *Vet Pathol* 42:589, 2005
Myxobolus hendricksoni	Brain	Fish	**Mitchell**, *J Fish Dis* 8:75, 1985
M. exiguus	Dermis	Fish	**Pulsford**, *J Fish Dis* 5:589, 1982
M. jirovecsi	Brain	Bullhead	**Lom**, *J Fish Dis* 12:15, 1989
M. lubati	Intestine	Seabream	**Ali**, *Parasitol Res* 100:819, 2007
M. maculatus	Kidney	Fish	**Casal**, *Dis Aquat Organ* 29:107, 2002
M. metynnis	Subcutis	Fish	**Casal**, *J Parasitol* 92:817, 2006
M. muellericus	Gill lamellar artery	Chub	**Molnár**, *Dis Aquat Organ* 73:49, 2006
M. stomum	Lips	Grunt	**Ali**, *Parasitol Res* 91:390, 2003
Myxosoma cerebralis	Brain	In vitro	**Lunger**, *J Parasitol* 61:476, 1975
Parvicapsula bicornis	Kidney, bladder	Fish	**Køie**, *Dis Aquat Organ* 76:123, 2007
Sphaeromyxa sabrazesi	Gill	Fish	**Grasse**, *An Sci Nat Zool* 20:193, 1978
Sphaerospora tincae	Gill	Fish	**Hermanns**, *J Fish Dis* 8:281, 1985
***S.* angulata**	Gill	Fish	**Dessar**, *J Protozool* 30:415, 1983
S. dicentrarchi		Sea bass	**Sitja-Bobadilla**, *J Protozool* 39:273, 1992
S. ectaluria	Kidney	Catfish	**Hedrick**, *J Protozool* 37:107, 1990
S. epinephali		Grouper	**Supamattaya**, *J Protozool* 38:448, 1991
Triactinomyxon legeri	Brain		**Lom**, *J Protozool* 39:16, 1992
Zschokkella russelli	Liver	Fish	**Davies**, *J Fish Dis* 11:325, 1988
Z. helmi	Gall bladder	Spinefoot	**Abdel-Ghaffar**, *Parasitol Res* 10283, 2008

§ ***Buddenbrockia*** is a parasitic cnidarian worm in the phylum Myxozoa, a group of morphologically simplified microscopic endoparasites.

Piedra

Piedra (trichosporosis) is a superficial fungal infection of hair manifest as firm, irregular nodules composed of fungal elements cemented together along the hair shaft. **Black piedra** (nodular trichomycosis) is a superficial mycosis of the hair shaft caused by *Piedraia hortae*; it is prevalent in tropical South America. Fungal cells invade keratin of the hair. Reproduction of fungal cells is both sexual (giving rise to ascospores) and asexual (giving rise to arthrospores). **Ascospores** are found in thick-walled bags called asci. **Arthrospores** undergo germination, and are eliminated through canals to disseminate the disease. Spores are prevalent and easily found ultrastructurally. They do not invade tissue, but are released on the surface of the epithelium.

White piedra, which appears as small nodules on the hair shaft, is caused by *Trichosporon beigelii* (=*T. cutaneum*), a basidiomycetic yeast possessing dolipore septa with parenthosomes. Fungal cells in skin lesions appear as hyphae and arthrospores embedded in a cementant substance. *T. beigelii* infection is uncommon, but has recently emerged as an opportunistic pathogen in immunodeficient patients. Signs of isseminated infection include fever, macronodular cutaneous lesions, chorioretinitis, and renal failure.

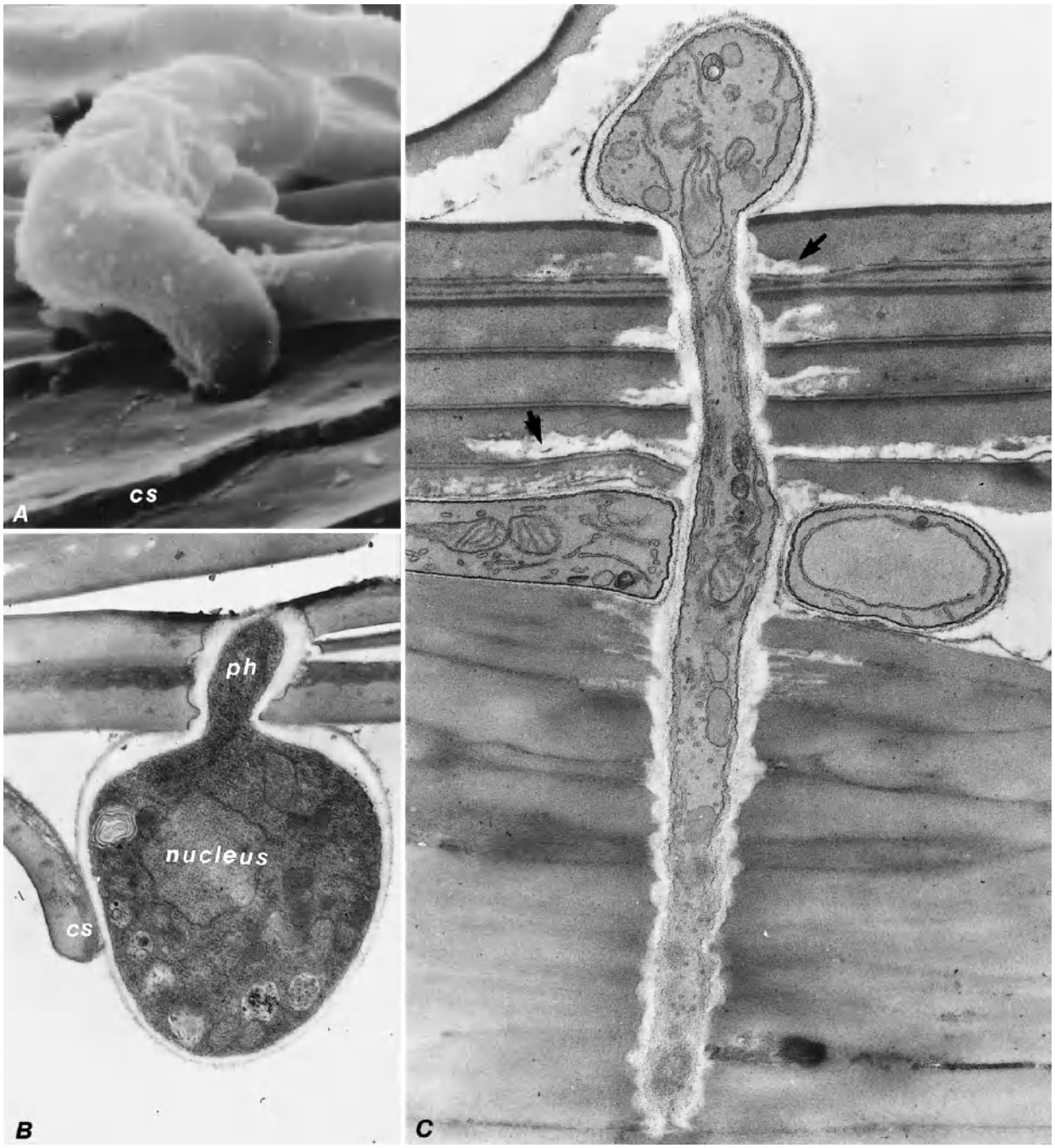


Fig. 16.12 ***Chrysosporium tropicum*:** Hyphae perforating human hair. Cuticular scales (*cs*). **A**. **Hypha**: resembles an appressorium, surface, cuticular scale (scanning electron micrograph). **B**. **Hyphae**: similar to A (transmission electron micrograph). Wall is thicker in part appressed to the hair. Perforating hypha (*ph*) penetrates to a depth of two cuticular scales. Endocuticle near the hypha is more electron dense than in the more distant area. **C**. Perforating hypha is associated with lysis (*arrows*) of endocuticle. (Micrograph: A. Fusconi, *Mycoses* 34:153, 1991.)

Chytridiomycosis

Fungi in the phylum Chytridiomycota (chytrids) are ubiquitous organisms in water and soil that parasitize amphibians. Most species are saprobic decomposers of organic matter, but others are obligate or facultative parasites of fungi, algae, plants, or invertebrate animals. Many chytrids have a simple, nonmycelial morphology and the cytoplasm of the fungal body (thallus) cleaves to form motile uniflagellate zoospores during asexual reproduction. A thallus containing zoospores is a zoosporangium. Placed in the kindom Protista, molecular sequencing data indicates that they belong in the kingdom Fungi.

Cutaneous Chytridiomycosis of Frogs

Cutaneous chytridiomycosis caused by chytrid fungi causes massive losses of riparian amphibian populations in Australia and Central America. Infection is specific for keratinized skin; although chytrids infect tadpoles, they do not kill them, probably because fungi localize in mouthparts, the only keratinized body region. After metamorphosis, when the skin becomes keratinized, the chytrid causes epidermal infection. Marked epidermal hyperplasia stimulated by chytrid infection impairs cutaneous respiration and osmoregulation. Chytrids consistently infect the pelvic patch, a major site of water absorption in anurans.[89,90]

Pneumocystis carinii

P. carinii infection is a ubiquitous pathogen for humans and animals. Long grouped with protozoa, *P. carinii* is now classed with fungi.[91] Infection, called **pneumocystosis** occurs only when latent organisms are activated in immunosuppressed patients; for example, pulmonary infection is particularly lethal in AIDS patients. Alveoli of the lung become filled with organisms that provoke a mild interstitial inflammatory reaction (Fig. 16.13).[92] Infected patients may also have organisms in lymph nodes.[93]

Surfaces of trophozoites of *P. carinii* have long surface filopodia that may be up to 6 μm in diameter.

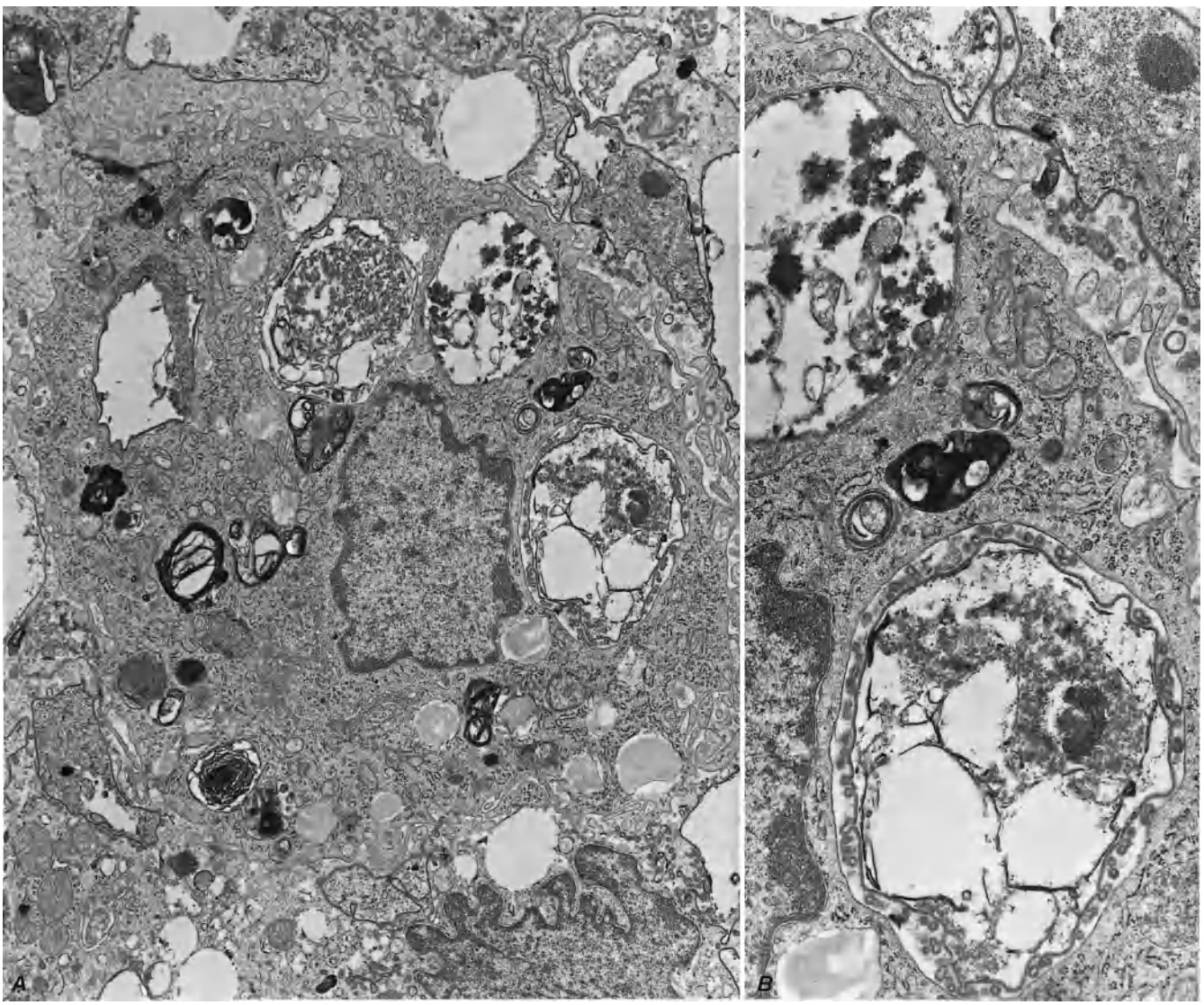


Fig. 16.13 ***Pneumocystis carinii***. **A** and **B**. Disintegrating microorganisms in alveolar macrophages; lungs of an SIV-infected monkey. (Micrograph: A. Baskerville, *J Pathol* 164:175, 1991.)

In sections of human lung with chronic disease, these appear as tubular structures. Surface components of *P. carinii* include chitin, a polysaccharide composed of repeating units of N-acetyl-D-glucosamine, a major cell wall constituent of most fungi and that is found to a lesser extent in cyst forms of several protozoa. Polyclonal antisera against chitin, when used in immunolabeling procedures, will stain *P. carinii* in human lung tissue.[94] Surfaces of organisms obtained from human tissues are also coated with host immunoglobulins, suggesting that in AIDS patients there is at least a partial host response to *P. carinii*.[95] The complex endomembrane system within the cytoplasm includes Golgi vesicles, endocytic vesicles and mitochondria.[96–100] *P. carinii* divides and forms pleomorphic cysts with heavy walls. Reproduction is completed within the cyst to form new trophozoites. In the lungs, organisms are found attached to alveolar epithelial cells by unique surface binding proteins.[101] They do not develop intracellularly (Fig. 16.14).

In rats, *P. carinii* pneumonia can be elicited by chronic cortisone treatment.[102,103] Trophozoites attach to alveolar epithelium by pinching cytoplasmic extensions of the host cell cytoplasm. Some trohozoites are attached by anchor-like extensions in invaginations of the host cell surface.[104] Ferrets are also readily infected with *P carinii*.[105]

The Myxozoans

Myxozoans (phylum Myxozoa) are metazoan parasites that use invertebrate and aquatic vertebrate hosts. Almost all are parasites of fish, annelids, and bryozoans. Myxozoa were originally placed outside the Metazoa, despite the multicellularity of their spores, and the presence of septate junctions and putative nematocysts. Myxozoan genera in the current taxonomical scheme are unsettled, and life cycles of the two classes of the phylum Myxozoa, the class Myxosporea (the best known genera that parasitize fish and annelids) and the class Malacosporea (that parasitize bryozoans), are incomplete.[106] Myxozoans form complex **spores** containing polar capsules similar to the stinging organelles, **nematocysts**, which they use to attach to a new host. **Polar capsules** of Myxozoa

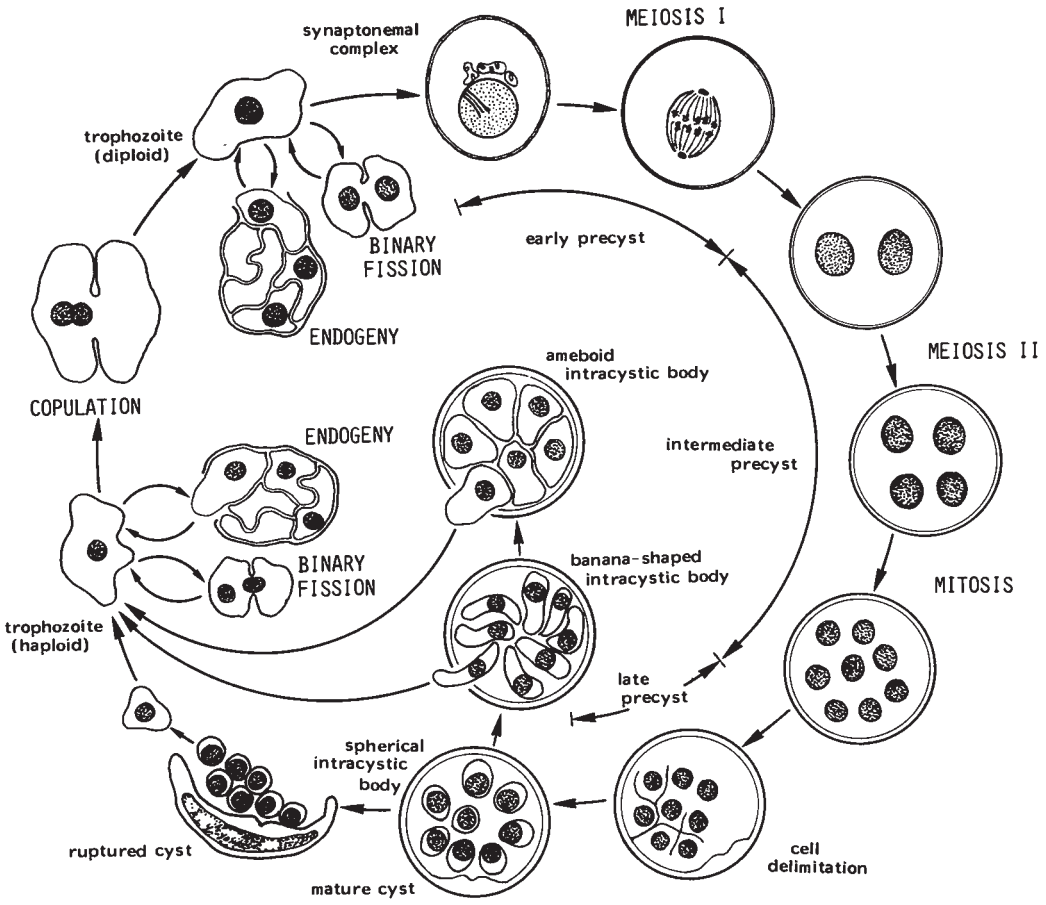


Fig. 16.14 ***Pneumocystis carinii***: hypothetical life cycle. (Drawing: Yukio Yoshida, *J Protozool* 36:53, 1989.)

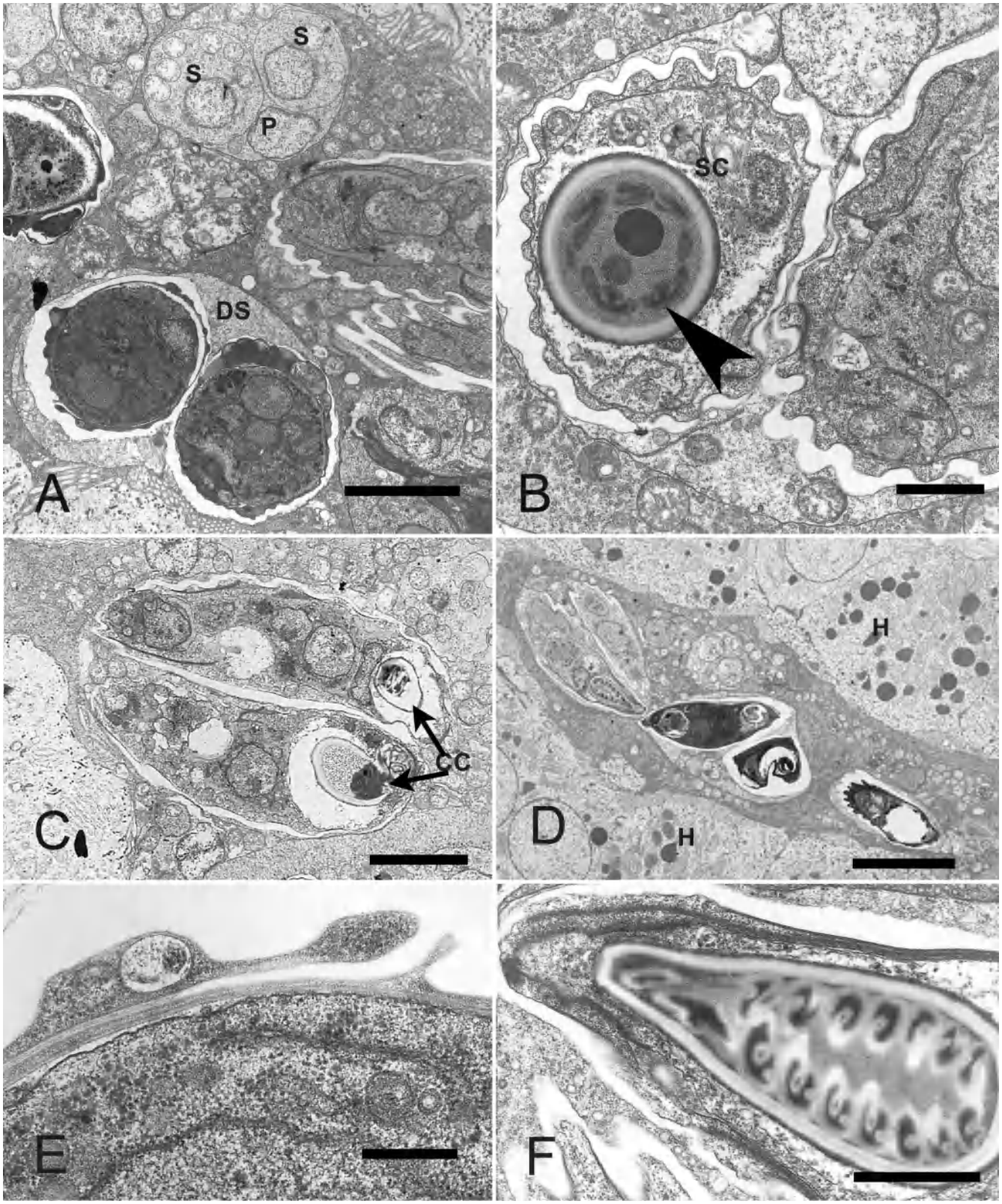


Fig. 16.15 ***Myxidium hardella***: renal myxozoonosis, turtle. **A. Developmental stages:** triplet cell with one primary cell (*P*) containing two secondary cells (*S*) and a disporoblast (*DS*) with two developing spores. Bar = 4 µm. **B**. **Late disporoblast**: capsulogenic cell (*arrowhead*), sporoplasmic cells (*SC*), the junction of the valve cells (*arrow*), and the valve cells with deep striations. Bar = 4 µm. **C**. **Disporoblast**: capulogenic cells (*CC*) and sporoplasm nuclei (*N*). **D**. **Disporoblasts and mature spores.** Bar = 10 µm. **E**. **Spore valve suture**. Bar = 1.5 µm. **F**. **Axial section** through a mature polar capsule showing the double-layered wall, coiled polar filament, and cap at tip of the capsule. Bar = 2 µm. (Micrograph: Mike Garner, *Veterinary Pathology* 42:589, 2005.)

differ from typical nematocysts of cnidarians in lacking chemo- and mechanosensory structures and neural connections that modulate discharge.[107]

Myxozoan infections of amphibians include *Dhloromyxum* sp. in Asian horned frogs and renal myxozoanosis in Crowned River turtles (Fig. 16.15).[108] Ultrastructural studies show developmental stages including primary cells harboring secondary cells, which matured into disporic pansporoblasts. A binucleate sporoplasm is located between capsulogenic cells. In mature spores, striations of spore valves and coils of polar filaments are present.

Genus *Myxosporidia*

Myxosporidia are parasitic in aquatic and amphibian poikilothermic vertebrates. Their developmental stages consist of amoeboid trophozoites of multicellular species. The motile sporoplasm (amoebula) penetrates the gut wall and enters the bloodstream. It moves into tissue where the uninucleate sporoplasm grows into a voluminous multinucleate trophozoite. In lumen-inhabiting species, the trophozoite covers the walls as a flat plasmodium that typically forms daughter plasmodia (trophozoites). Sporogenic processes occur within the trophozoites, which degenerate when the spores mature.[109]

Genus *Myxosoma*

Myxosoma cerebralis in its original host, the European brown trout, is well tolerated by the host. In contrast, in a new host such as the rainbow trout, the parasite produces the lethal whirling disease.[110] Pseudocysts form in the skeletal muscle of infected fish.[111,112] Related species include the following:

- ***Kudoa* spp**. replicate in the brain and visceral organs of fish.[113,114] *Kudao thyrsites* has caused lethal myoliquefaction in salmon.
- ***Henneguya* spp**. infect gills, appearing in interlammelar spaces as pale spherical to ellipsoidal cyst-like plasmodia. Spores have a "sperm-like" appearance with a fusiform body and two valves (with tapering tails), which surround a binucleate cell.[115,116]
- ***Myxobolus* spp**. replicate in the renal tubules of fish, forming polysporic histozoic plasmodia that contain pinocytotic channels and different life cycle stages including mature spores. Spore bodies are pyriform and have elated polar capsules.[117] *Myxobolus cerebralis* requires development of an actinosporean stage in the oligochaete, *Tubifex tubifex*.

Genus *Sphaerospora*

Sphaerospora are parasites of freshwater fish. Most sphaerosporans cause inconspicuous infection of fish, but some are serious pathogens, especially in cyprinids and salmonids.[118] Pathogenic sphaerosporans infest the kidney and urinary tract although a few parasitize the gills. At least three *Sphaerospora* spp. are associated with disease caused by prespore phases. One of the most important is **proliferative gill disease** of farm reared catfish.[119]

In the common form of **renal sphaerosporosis**, the lumen of the renal tubules is filled with disporous **pansporoblasts** of *S. angulata*. Spores are formed via paired valvogenic and capsulogenic cells, and a dikaryotic sporoplasm, all of which lie in the cytoplasm of the enveloped cell. The **polar filament** is formed through invagination of components of the elongate external tubule into the capsular primordium.[120] Renal sphaerosporosis is also caused by *S epinephali*, which has been reported in marine fish in waters of southeast Asia. Spores and monosporous or disporous pseudoplasmodia were found in lumens of renal tubules. Spores were 7.8–10.0 μm long, 12.3–14.5 μm thick, and 7.0–9.5 μm wide. There were two spherical polar capsules that were 2.9 and 4.4 μm with polar filaments of six or seven turns. Infected proximal tubular epithelial cells had markedly vacuolated cytoplasm and pyknotic nuclei.[121]

Intracellular Metazoan Parasites

Genus *Trichinella*

Trichinosis is characterized by two major biologic phases in the host: enteric and visceral. The adult nematode develops in the enteric phase, larvae are discharged into lymphatics and circulate to infect muscle. Immune mechanisms reduce the number of larvae in intestinal phases and during circulation, but have little effect on migration in muscle, encystment, or larval development. Once within the myocyte, a **nurse cell-larvae complex** protects and maintains the parasite.[122] Other *Trichinella* species that cause disease in mammals and poikilothermic vertebrates include the following:

- *T. pseudospiralis*[123]
- *T. nativa* of foxes, raccoon dogs, and bears[124]
- *T. papuae* of piranhas and other carnivorous fish[125]
- *T. zimbabwensis* of crocodiles (it infects turtles, pythons, caimans, and other animals)

Differences in tissue destruction depend on cytokines and soluble factors produced by individual

species, and how they encapsulate the developing larvae and activate peripheral satellite cells of muscle. For example, myocyte damage caused by *T. pseudospiralis* is more extensive than that of *T. spiralis* since it involves the entire length of the infected myocyte, and produces greater activation of satellite cells to proliferate. Myogenic regulatory factors (myogenin, MyoD) are activated for longer times.[126]

Ultrastructure of Parasites Electron microscopic examination of cross sections of the **adult worms** of *T. spiralis* reveals an esophagus, pseudocoelom, vagina, and developing **larvae**. There is a peripheral cord containing hypodermal glands. **Stichosomes** are exocrine organs that consist of rows of large stichocytes, heavily granulated cells that function in invasion. **Granules** occur in clusters around canalicular trees that empty into the esophageal lumen.[127] Granules vary greatly in size, the mature forms being 500 nm in diameter.

Ultrastructural analysis of *T. spiralis* **larvae** reveals **bacillary bands** (~5 μm wide) that begin at the cephalic end on each side as a row of single cells and extend with gradually increasing width to the posterior end of the worm.[128] The cuticle contains hypodermal glands and pores of 1.5–2 μm that communicate with the exterior.

Trichinosis

Enteric Phase The adult life of *Trichinella spiralis* is spent in the small intestine of many species of carnivores. All four larval stages and their molts occur in the intestine. Adult worms reside within the mucosa and developing larval stages lie within the cytoplasm of both absorptive and goblet cells.[129] Adults are threaded through rows of enterocytes and often cannot be seen on the mucosal surface. Sections of mouse intestine 24 hr after infection by *T. spiralis* reveal that parasites are enclosed within single **enterocytes**. The cytoplasm that remains of the host cell is forced to the periphery. The cuticle-host interface appears to be open but a structureless halo in electron micrographs.

The viviparous female burrows into the lamina propria of the intestinal villi and deposits her larve directly into the **intestinal lymphatics**. Larvae exit in lymph, pass through the mesenteric lymphatics and thoracic duct, and enter the **bloodstream**. During circulation through the skeletal muscle fasciculi, larvae enter the myocyte. During migration through the intestinal wall, changes in interstitial cells of Cajal at the deep muscular plexus are associated with loss of distention-induced burst-type muscle activity in mice infected by *T. spiralis*.[130]

Muscle Phase **Larvae** of *T. spiralis* enter and encyst in skeletal muscle fibers. Inside the myocyte, larvae use a stylet to suck components of the myocyte into their oral cavity. A host nurse cell system develops to nourish infective larvae.

Encystment of the larva-bearing myocyte provides a barrier to host systems of inflammation and immunity. Mild, transient inflammatory responses may surround migrating larvae in muscle. These usually are limited to edema and a few neutrophilic leukocytes. Larvae are poorly immunogenic (the cuticle and enzymic excretions of the oral orifice do not readily induce immune responses in the host), and encystment occurs before these are effective. The parasite is protected until the host is killed and its muscle eaten by a new potential carnivore host. Intestinal enzymes of the new host digest the capsule, and the liberated larvae burrow into the intestine and begin their life cycle anew.

Nurse cell development in larva-bearing myocytes leads to loss of most normal myocyte organelles and a striking transformation into a giant cell with massive amounts of smooth endoplasmic reticulum (Fig. 16.16). Myofibers become swollen and granular for a considerable distance peripheral and distal to the encysted parasite. Within 10 days after infection, larvae are well established. Ultrastructurally, myofibrils within the affected fibers become disoriented and their myofilaments are detached and frayed at the Z lines.[131] Normal myocyte organelles degenerate and disappear, especially lysosomes. **Mitochondria** of the muscle cell disappear, but new smaller mitochondria appear that produce an anti-apoptotic factor ensuring survival of the nurse cell.[132]

Larvae exist free in the cytosol of the host myofiber; they are not associated with lysosomes, intracellular debris, or pathologic membranes. At its periphery, the host myocyte is actively involved in the secretion of proteoglycans, which form the hyalin basement membrane-type material of the **capsule**. This capsule is formed exclusively by the host muscle fiber and begins about 14 days after encystation.[133] With time, capsules progressively calcify.[134]

By 2–3 mo, encapsulation is complete. The cytoplasm of the host cell becomes contracted and dense. The thick hyalin membrane of the capsule has foci of mineralization, which progressively enlarge. In protracted and severe infections, antigens may seep into the circulation of the host and antibodies against the larvae and its capsule arise. Eosinophilic and neutrophilic leukocytes surround the cyst of some larvae and can be seen within their capsules. Lymphocyte aggregates occur around cysts. Plasmacytes that contain antitrichina antibody are present in these aggregates, but their effect on encysted larvae is negligible.[135]

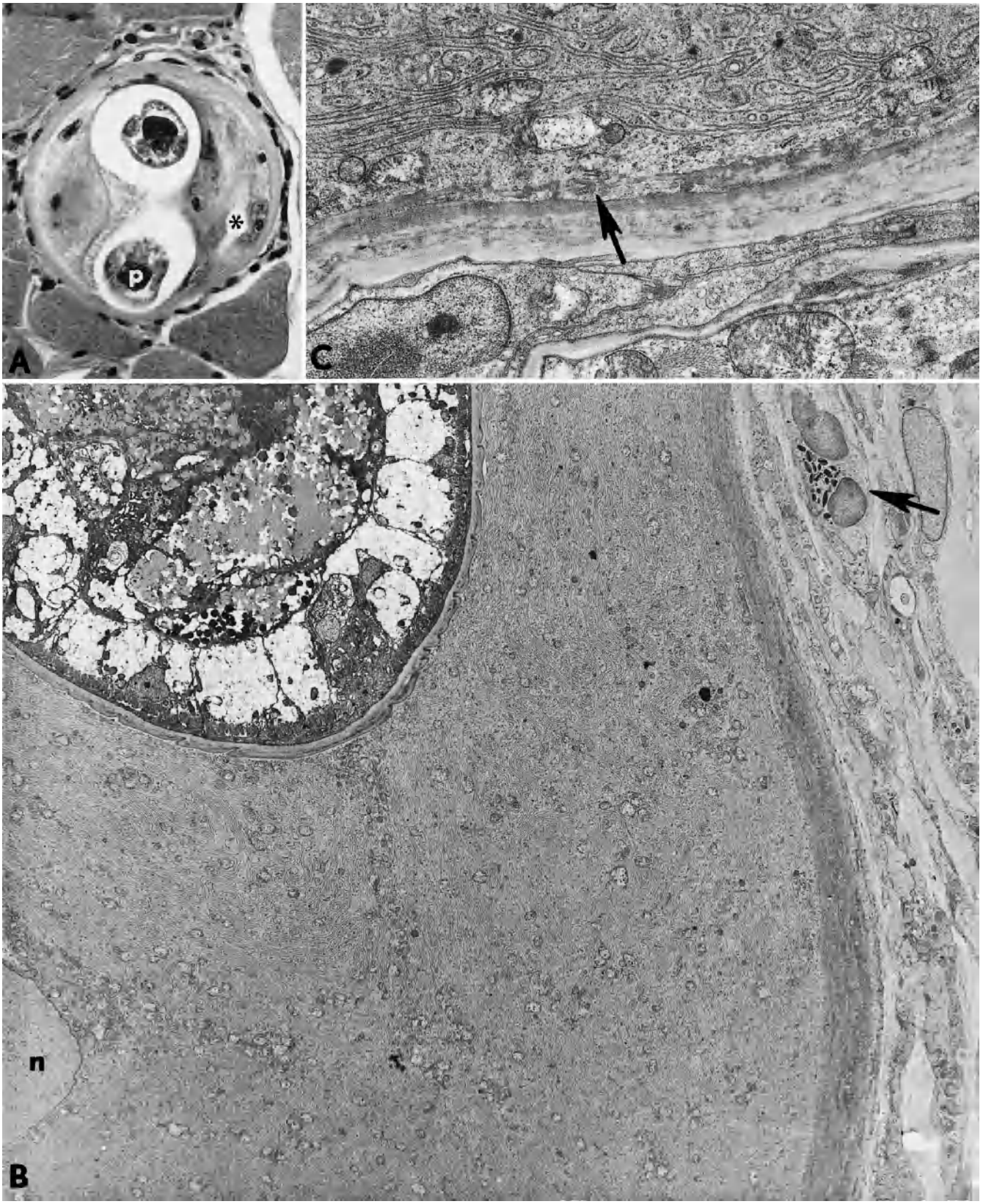


Fig. 16.16 ***Trichinella spiralis***: Encystment of larvae, skeletal myocyte. **A**. **Cyst**: includes parasite (*p*), modified host myocyte (*), and hyalin capusle. **B**. **Transformed host cell**: massive duplication of endoplasmic reticulum, with dense granular material at basal plasma membranes; host-cell nucleus (*n*), parasite (*upper left*). Note eosinophil (*arrow*) in capsule. **C**. **Basement membrane material**: deposited at periphery by altered host cell (*arrow*). There is massive development of ER in nurse cell cytoplasm.

Facultative Intracellular Nematodes

Several nematodes, especially migrating larvae, are able to penetrate, enter, and survive inside cells of their mammalian host. Larvae of *Ancyclosoma caninum* and *Trichuris muris* have been found in muscle fibers. Microfilaira of *Dipetalonema vitae* and *Litomosoides carinii* will survive within mycoytes and hepatocytes, possibly as a means to escape host defense systems or drug actions.[136]

References

1. Berliner MD. 1982. Protoplasts of eukaryotic algae. *Int Rev Cytol* 73:1.
2. Tillberg J-E, et al. 1980. X-ray microanalysis of leakage from polyphosphate granules in *Scenedesmus*. *J Ultrastruct Res* 72:316.
3. Van Etten JL, et al. 1982. Viruses of symbiotic Chlorella-like algae isolated from *Parameciumbursaria* and *Hydra viridis*. *Proc Nat Acad Sci* 79:3867.
4. Joshi KR, et al. 1975. The ultrastructure of *Prototheca wickerhamii*. *Mycopathologia* 56:9.
5. Nadakavukaren MJ, McCracken DA. 1977. An ultrastructural survey of the genus *Prototheca* with special reference to plastids. *Mycopathologia* 61:117.
6. Cheville NF, et al. 1984. Ultrastructure of *Prototheca zopfii* in bovine granulomatous mastitis. *Vet Pathol* 21:341.
7. Venezio FR, et al. 1982. Progressive cutaneous protothecosis. *Am J Clin Pathol* 77:485.
8. Smith CG. 1980. Ultrastructural studies of *Prototheca salmonis* and comparison with known isolates in Prototheca. *Mycopathologia* 71:95.
9. Font RL, Hook SR. 1984. Metastatic protothecal retinitis in a dog. Electron microscopic observations. *Vet Pathol* 21:61.
10. Phair JP, et al. 1981. Phagocytosis and algicidal activity of human polymorphonuclear neutrophils against *Prototheca wickerhamii*. *J Infect Dis* 144:72.
11. Garcia RB, et al. 2007. Mapping of *Pythium insidiosum* hyphal antigens and ultrastructural features using TEM. *Mycol Res* 111:1352.
12. Jackson ARB, et al. 1984. Clinical and pathological changes in sheep experimentally poisoned by the blue-green alga *Microcystis aeruginosa*. *Vet Pathol* 21:102.
13. Shi L, et al. 1995. Immuno-gold localization of hepatotoxins in cyanobacterial cells. *Arch Microbiol* 163:7.
14. Young FM, et al. 2005. Immunogold localization of microcystins in cryosectioned cells of Microcystis. *J Struct Biol* 15:208.
15. Li L, et al. 2007. Biochemical and ultrastructural changes of the liver and kidney of the phytoplanktivorous silver carp feeding naturally on toxic Microcystis blooms in Taihu Lake, China. *Toxicon* 49:1042.
16. Hibbett DS, et al. 2007. A higher-level phylogenetic classification of the Fungi. *Mycol Res* 111:509.
17. Mims CW. 1991. Using electron microscopy to study plant pathogenic fungi. *Mycologia* 83:1.
18. Hawker LE. 1964. Fine structure of fungi as revealed by electron microscopy. *Biol Rev* 40:59.
19. Stoian M. 1970. Aspects ultrastructuraux des dermatophytes. *Soc Suisse Derm Vener* 141:95.
20. Loewen CJR, et al. 2007. Inheritance of cortical ER in yeast is required for normal septin organization. *J Cell Biol* 179:467.
21. Momany M, et al. 2004. The Aspergillus fumigatus cell wall is organized in domains that are remodelled during polarity establishment. *Microbiology* 150:3261.
22. Dague E, et al. 2008. High-resolution cell surfaces dynamics of germinating *Aspergillus fumigatus* conidia. *Biophys J* 94:656.
23. Wills JW, et al. 1985. Circular mitochondrial genomes of *Candida albicans* contain a large inverted duplication. *J Bact* 164:7.
24. Klionsky DJ, et al. 1990. The fungal vacuole: Composition, function, and biogenesis. *Microbiol Rev* 54:266.
25. Liu H, et al. 1992. An efficient screen for peroxisome-deficient mutants of *Pichia pastoris*. *J Bact* 174:4943.
26. Shim J, et al. 1991. The BOS1 gene encodes an essential 27-Kd putative membrane protein that is required for vesicular transport from the endoplasmic reticulum to the Golgi complex in yeast. *J Cell Biol* 113:55.
27. Boyd C, et al. 2004. Vesicles carry most exocyst subunits in exocytic sites marked by the remaining two subunits, Sec3p and Exo70p. *J Cell Biol* 167:889.
28. Mulholland J, et al. 1994. Ultrastructure of the yeast actin cytoskeleton and its association with the plasma membrane. *J Cell Biol* 125:28.
29. David M, et al. 2007. Microtubular and actin cytoskeletons and ultrastructural characteristics of the potentially pathogenic basidiomycetous yeast *Malassezia pachydermatis*. *Cell Biol Int* 31:16.
30. Bechinger C, et al. 1999. Optical measurement of invasive forces exerted by appressoria of a plant pathogenic fungus. *Science* 285:1896.
31. van Tuinen E, Riezman H. 1987. Immunolocalization of glyceraldehyde-3-phosphate dehydrogenase, hexokinase, and carboxypeptidase Y in yeast cells at the ultrastructural level. *J Hist Cyt* 35:327.
32. Campo-Aasen I, Goihmon-Yarh M. 1990. Adenosine triphosphatase in yeast phase *Paracoccidioides brasiliensis*. *Mycopathologia* 111:169.
33. Benhamou N, Ouellette GB. 1986. Ultrastructural localization of glycoconjugates in the fungus *Ascocalyx abietina*, the sclerodermis canker agent of conifers, using lectin-gold complexes. *J Hist Cyt* 34:855.
34. Cormack BP, et al. 1999. An adhesin of the yeast pathogen *Candida glabrata* mediating adherence to human epithelial cells. Science 285:578.
35. Markaryan A, et al. 1994. Purification and characterization of an elastinolytic metalloprotease from *Asperillus fumigatus* and immunoelectron microscopic evidence of secretion of this enzyme by the fungus invading the murine lung. *Infect Immun* 62:2149.
36. Miguélez EM, et al. 1999. Hyphal death during colony development in *Streptomyces antibioticus*: Morphologi-

cal evidence for the existence of a process of cell deletion in a multicellular prokaryote. *J Cell Biol* 145:515.
37. Cole GT. 1986. Models of cell differentiation in conidial fungi. *Microbiol Rev* 50:95.
38. Mochizuki T, et al. 1987. Ultrastructure of the mitotic apparatus of *Cryptococcus neoformans*. *J Med Vet Mycol* 25:223.
39. Nakai T, et al. 2005. Electron microscopic findings for micafungin-treated experimental pulmonary aspergillosis in mice. *Med Mycol* 43:439.
40. Campbell CK. 1970. Electron microscopy of aspergillosis in fowl chicks. *Sabouraudia* 8:133.
41. Tanaka K, Yanagita T. 1963. Electron microscopy of ultrathin section of *Aspergillus niger*. *J Gen Appl Microbiol* 9:101.
42. Ste-Marie L, et al. 1990. Production and characterization of monoclonal antibodies to cell wall antigens of *Aspergillus fumigatus*. *Infect Immun* 58:2105.
43. Stynen D, et al. 1992. Rat monoclonal antibodies against *Aspergillus galactomannan*. *Infect Immun* 60:2237.
44. Washburn RG, et al. 1987. Oxidative killing of *Aspergillus fumigatus* proceeds by parallel myeloperoxidase-dependent and -independent pathways. *Infect Immun* 55:2088.
45. Ibrahim-Granet O, et al. 2003. Phagoctyosis and intracellular fate of Aspergillus fumigatus conidia in alveolar macrophages. *Infect Immun* 71:891.
46. Kogan TV, et al. 2004. Involvement of secreted *Aspergillus fumigatus* proteases in disruption of the actin fiber cytoskeleton and loss of focal adhesion sites in infected A549 lung pneumocytes. *J Infect Dis* 189:1965.
47. Denning DW, et al. 1992. Lack of vessel wall elastolysis in human invasive pulmonary aspergillosis. *Infect Immun* 60:5153.
48. Merkow LP, et al. 1971. The pathogenesis of experimental pulmonary aspergillosis. *Am J Pathol* 62:57.
49. Mirra SS, et al. 1980. Ultrastructural study of a cerebral toruloma. *Acta Neuropathol* 50:153.
50. Cawson RA, Rajasingham KC. 1972. Ultrastructural features of the invasive phase of *Candida albicans*. *Br J Dermatol* 87:435.
51. den Hertog AL, et al. 2005. Candidacidal effects of two antimicrobial peptides: Histatin 5 causes small membrane defects, but LL-37 causes massive disruption of the cell membrane. *Biochem J* 388:689.
52. Cole GT, et al. 1992. Retrovirus-induced immunodeficiency in mice exacerbates gastrointestinal candidiasis. *Infect Immun* 60:4168.
53. Anderson J, et al. 1990. Ultrastructure and antigenicity of the unique cell wall pimple of the *Candida* opaque phenotype. *J Bacteriol* 172:224.
54. Marquis G, et al. 1991. Histochemical and immunochemical study of the fate of *Candida albicans* inside human neutrophil phagolysosomes. *J Leuk Biol* 50:587.
55. Tokunaga M, et al. 1990. Initial attachment of *Candida albicans* cells to buccal epithelial cells. *Mycopathologia* 111:61.
56. Kanbe T, et al. 1992. Evidence that *Candida albicans* binds via a unique adhesion system on phagocytic cells in the marginal zone of the mouse spleen. *Infect Immun* 60:1972.
57. Lehrer RI, Cline MJ. 1969. Leukocyte myeloperoxidase deficiency and disseminated candidiasis. *J Clin Invest* 48:1478.
58. Sohnle PG, et al. 1976. Mechanisms involved in elimination of organisms from experimental cutaneous *Candida albicans* infection. *J Immunol* 117:523.
59. Muller J, et al. 1977. Elektronenmikroskopische darstellung von immunreaktionen an Candida-Szellen: Asteroid bodies bei Candida albicans im urin von Nephritis-patienten. *Sabouraudia* 15:87.
60. Barnes JL, et al. 1983. Host-parasite interactions in the pathogenesis of experimental renal candidiasis. *Lab Invest* 49:460.
61. Kuttin ES, et al. 1984. Electronmicroscopic study of *Candida albicans* infection kidneys in non-immunized and immunized hosts. *Mycoses* 27:72.
62. Chow HS, et al. 1980. Pathophysiology of *Candida albicans* meningitis in normal, neutropenic, and granulocyte transfused dogs. *Blood* 55:546.
63. Pan S, Cole GT. 1992. Electrophoretic karyotypes of clinical isolates of *Coccidioides immitis*. *Infect Immun* 60:4872.
64. Dugger KO, et al. 1991. An immunoreactive apoglycoprotein purified from *Coccidiodes immitis*. *Infect Immun* 59:2245.
65. Cole GT, et al. 1991. Antigen complex of *Coccidiodes immitis* which elicits a precipitin antibody response in patients. *Infect Immun* 59:2434.
66. Gargani G, et al. 1989. Scanning electron microscopic pattern of recurrent vaginitis by *Candida albicans* in the mouse. *Mycoses* 32:644.
67. Fiskin AM, et al. 1990. Electron cytochemical studies of *Cryptococcus neoformans* grown in uric acids and related sources of nitrogen. *J Med Vet Mycol* 28:197.
68. Lipscomb MF, et al. 1987. Role of natural killer cells in resistance to *Cryptococcus neoformans* infection in mice. *Am J Pathol* 128:354.
69. Mirra SS, et al. 1980. Ultrastructural study of a cerebral toruloma. *Acta Neuropathol* 50:153.
70. Garcia-Rivera J, et al. 2005. Laccase expression in murine pulmonary *Cryptococcus neoformans* infection. *Infect Immun* 73:3124.
71. Lane JW, Garrison RG. 1970. Electronmicroscopy of self-parasitism by *Histoplasma capsulatum* and *Blastomyces dermatitidis*. *Mycopathol Mycol Appl* 40:271.
72. Maresca B, Kobayashi GS. 1989. Dimorphism in *Histoplasma capsulatum*. *Microbiol Rev* 53:186.
73. Kurita N, et al. 1991. Resistance of *Histoplasma capsulatum* to killing by human neutrophils. *Mycopathologia* 115:207.
74. Bretana A, et al. 1995. Comparative ultrastructure and immunolabeling of MHC-II antigens of alveolar macrophages obtained from patients with paracoccidioidomycosis and other lung diseases. *J Leuk Biol* 57:101.
75. de Brito T, et al. 1973. Intraepithelial parasitism as an infection mechanism in human paracoccidioidomycosis (South American blastomycosis). *Virchows Arch A* 361:129.
76. Levy MG, et al. 1986. Cultivation of *Rhinosporidium seeberi* in vitro: Interaction with epithelial cells. *Science* 234:474.

77. Lengfelder KD, Pospischil A. 1980. Rhinosporidiose beim Pferd. *Zbl Vet Med B* 27:326.
78. Easley JR, et al. 1986. Nasal rhinosporidiosis in the dog. *Vet Pathol* 23:50.
79. Garrison RG, et al. 1979. Spontaneous feline sporotrichosis: A fine structural study. *Mycopathologia* 69:57.
80. Hiruma M, et al. 1991. Ultrastructure of asteroid bodies in sporotrichosis. *Mycoses* 34:103.
81. Dixon DM et al. 1989. Infections due to *Xylohypha bantiana* (*Cladosporium trichoides*). *Rev Infect Dis* 11:515.
82. Wethered DB, et al. 1986. Ultrastructural and immunogenic changes in the formation of mycetoma grains. *J Med Vet Mycol* 25:39.
83. Chan Y, Chow TC. 1990. Ultrastructural observations on *Penicillium marneffei* in natural human infection. *Ultrastruct Pathol* 14:439.
84. Woodward JC. 1972. Electron microscopic study of lobomycosis (*Loco loboi*). *Lab Invest* 27:606.
85. Miller GF, Owens JW. 1999. Ultrastructural characterization of the agent of systemic yeast infection of owl monkeys. *Med Mycol* 37:139.
86. Cario J, et al. 1991. Study of the invasion of human hair in vitro by *Aphanoascus* spp. *Mycoses* 34:145.
87. Takatori K, et al. 1983. Microscopic observation of human hairs infected with *Microsporum ferrugineum*. *Mycopathologia* 81:129.
88. Tosti A, et la. 1970. Contribution to the knowledge of dermatophytic invasion of hair. *J Invest Derm* 55:123.
89. Pessier AP, et al. 1999. Cutaneous chytridiomycosis in poison dart frogs (*Dendrobates* spp.) and White's tree frogs (*Litoria caerulea*). *J Vet Diagn Invest* 11:194.
90. Berger L, et al. 1998. Chytridiomycosis causes amphibian mortality associated with population declines in the rain forest of Australia and Central America. *Proc Nat Acad Sci USA* 95:9031.
91. Cailliez JC, et al. 1996. *Pneumocystis carinii*: An atypical fungal micro-organism. *J Med Vet Mycol* 34:227.
92. Barton EG, Jr, Campbell WG, Jr. 1967. Further observations on the ultrastructure of pneumocystis. *Arch Pathol* 83:527.
93. Matsumoto Y, et al. 1989. Proliferation of *Pneumocystis carinii* in human lymph node and in nude mice lungs. *J Protozool* 36:33S.
94. Walker AN, et al. 1990. Immunocytochemical detection of chitin in *Pneumocystis carinii*. *Infect Immun* 58:412.
95. Blumenfeld W, et al. 1990. Localization of host immunoglobulin G to the surface of *Pneumocystis carinii*. *Infect Immun* 58:456.
96. Cushion MT, et al. 1988. Analysis of the developmental stages of *Pneumocystis carinii*, in vitro. *Lab Invest* 58:324.
97. Palluault F, et al. 1991. Three-dimentional reconstruction of rabbit-derived *Pneumocystis carinii* from serial-thin sections. *J Protozool* 38:402 and 407.
98. Vavra J, Kucera K. 1970. *Pneumocystis carinii* Delanoe, its ultrastructure and ultrastructural affinities. *Protozoology* 17:463.
99. Yoshida Y. 1989. Ultrastructural studies of *Pneumocystis carinii*. *J Protozool* 36:53.
100. Yoshikawa H, et al. 1987. Freeze-fracture localization of filipin-sterol complexes in plasma- and cytomembranes of *Pneumocystis carinii*. *J Protozool* 34:131.
101. de Staffano JE, et al. 1989. Lectins as probes for *Pneumocystis carinii* surface glycocomplexes. *J Protozool* 65S.
102. Barton EG, Jr, Campbell WG, Jr. 1969. *Pneumocystis carinii* in lungs of rats treated with cortisone acetate. *Am J Pathol* 54:209.
103. Lanken PN, et al. 1980. Alveolar response to experimental *Pneumocystis carinii* pneumonia in the rat. *Am J Pathol* 99:561.
104. Long EG, et al. 1986. Attachment of *Pneumocystis carinii* to rat pneumocytes. *Lab Invest* 54:609.
105. Stokes DC, et al. 1987. Experimental *Pneumocystis carinii* pneumonia in the ferret. *Br J Exp Pathol* 68:267.
106. Lom J, Dylová I. 2006. Myxozoan genera. *Folia Parasitol* 53:1.
107. Jiménez-Guri E, et al. 2007. *Buddenbrockia* is a Cnidarian worm. *Science* 317:116.
108. Garner MM, et al. 2005. Renal myxozoanosis in Crowned River turtles *Hardella thurjii*. *Vet Pathol* 42:589.
109. Desportes-Livage I, Nicolas G. 1990. The plasma membrane of myxosporidian valve cells: Freeze fracture data. *J Protozool* 37:243.
110. Wolf K, Markiw ME. 1984. Biology contravenes taxonomy in the myxozoa. *Science* 225:1449.
111. Harrell LW, Scott TM. 1985. *Kudoa thyrsitis* (Myxosporea). *J Fish Dis* 8:329.
112. Lunger PD, et al. 1975. Thin section electron microscopy of mature *Myxosoma cerebralis* (Myxosporidea) spores. *J Parasitol* 61:476.
113. Cho JB, Kim KH. 2003. Light- and electron-microscope description of *Kudoa paralichthys* n. sp. (Myxozoa Myxosporea) from the brain of cultured olive flounder *Paralighthys olivaceus* in Korea. *Dis Aquat Organ* 20:59.
114. Wang PC, et al. 2005. Systemic infection of *Kudoa lutjanus* n. sp. (Myxozoa: Myxosporea) in red snapper *Lutjanus erythropterus* from Taiwan. *Dis Aquat Organ* 67:115.
115. Vital P, et al. 2003. Ultrastrucutral aspects of the myxosporean *Henneguya astyanax* n. sp. (Myxovoa: Myxobholidae), a parasite of the Amazonian teleost *Astyanax keithi* (Characidae). *Dis Aquat Organ* 53:55.
116. Matos E, et al. 2005. Ultrastructural studies of *Henneguya rhamdia* n. sp. (Myxozoa) a parasite from the Amazon teleost fish, *Rhamdia quelen* (Pimelodidae). *J Eukaryot Microbiol* 52:53.
117. Casal G, et al. 2002. Ultrastructural data on the spore of *Myxobolus maculattus* n. sp. (phylum Myxozoa), parasite from the Amazon fish *Metynnis maculatus* (Teoleostei). *Dis Aquat Organ* 51:107.
118. Sitja-Bobadilla A, et al. 1992. Light and electron microscopic description of *Sphaerospora dicentrarchi* N. sp. (Myxosporea: Sphaerosporidae) from wild and cultured sea bass, *Dicentrarchus labrx* L. *J Protozool* 39:273.
119. Hedrick RD, et al. 1990. *Sphaerospora ectaluri* n. sp. (Myxosporea:Sphaerosphoridae) observed in the kidney of channel catfish, *Ictalurus punctatus* Rafinesque. *J Protozool* 37:107.

120. Desser SS, et al. 1983. An ultrastructural study of the Myxosporeans, *Sphaerospora angulata* and *Sphaerospora carassii*, in the common carp, *Cyprinus carpio*. *J Protozool* 30:415.
121. Supamattaya K, et al. 1991. *Sphaerospora epinepheli* N. Sp. (Myxosporea: Sphaerosporidae) observed in grouper (*Epinephelus malabaricus*). *J Protozool* 38:448.
122. Sacchi L, et al. 2201. Ultrastructural characteristics of nurse cell-larva complexes of four species of *Trichinella* in several hosts. *Parasite* 8:S54.
123. Boonmars T, et al. 2005. *Trichinella pseudospiralis* infection is characterized by more continuous and diffuse myopathy than *T. spiralis* infection. *Parasitol Res* 97:13.
124. Hulinská D, et al. 1985. The feeding mechanism of intracellular muscle larvae, *Trichinella nativa* Britov et Boev, 1972 and *T. pseudospiralis* Garkavi, 1972. *Folia Parasitol* 32:61.
125. Pozio E, et al. 2004. *Trichinella papuae* and *Trichinella zimbabwensis* induce infection in experimentally infected arans, caimans, pythons and turtles. *Parasitology* 128:333.
126. Wu A, et al. 2001. Different response of satellite cells in the kinetics of myogenic regulatory factors and ultrastructural pathology after *Trichinella spiralis* and *T. pseudospiralis* infection. *Parasitology* 123:85.
127. Takahashi Y, et al. 1992. Ultrastructure, antigenicity, and histochemistry of stichocyte granules of adult *Trichinella spiralis*. *J Parasitol* 78:518.
128. Kozek WJ. 2005. Are bacillary bands responsible for expulsion of *Trichinella spiralis*? *Vet Parasitol* 132:69.
129. Wright KA. 1979. *Trichinella spiralis*: An intracellular parasite in the intestinal phase. *J Parasitol* 65:441.
130. Wang X-Y, et al. 2005. Changes in interstitial cells of Cajal at the deep muscular plexus are associated with loss of distention-induced burst-type muscle activity in mice infected by *Trichinella spiralis*. *Am J Pathol* 167:437.
131. Backwinkel K-P, Themann H. 1972. Elektronenmikroskopische Untersuchungen uber die Pathomorphologie der Trichinellose. *Beitr Pathol* 146:259.
132. Boonmars T, et al. 2004. Expression of apoptosis-related factors in muscles infected with *Trichinella spiralis*. *Parasitology* 128:323.
133. Teppema JS, et al. 1973. Ultrastructural aspects of capsule formation in *Trichinella spiralis* infection in the rat. *Parasitology* 66:291.
134. Machnicka B, et al. 2005. Calcification of *Trichinella spiralis* larval capsule. *Parasitol Res* 97:501.
135. Crandall RB, et al. 1967. The relative proportion of IgG-, IgA-, and IgM-containing cells in rabbit tissues during experimental trichinosis. *Immunology* 12:147.
136. Melhorn H, et al. 1980. Electron microscopic studies on microfilariae of *Dipetalonema vitae* and *Litomosoides carinii*. *Z Bakteriol [A]* 251:263.

Part V

Toxicologic Diseases

Ultrastructural Pathology The Comparative Cellular Basis of Disease
Second Edition Norman F. Cheville
© 2009 Wiley-Blackwell. ISBN: 978-0-813-80330-2

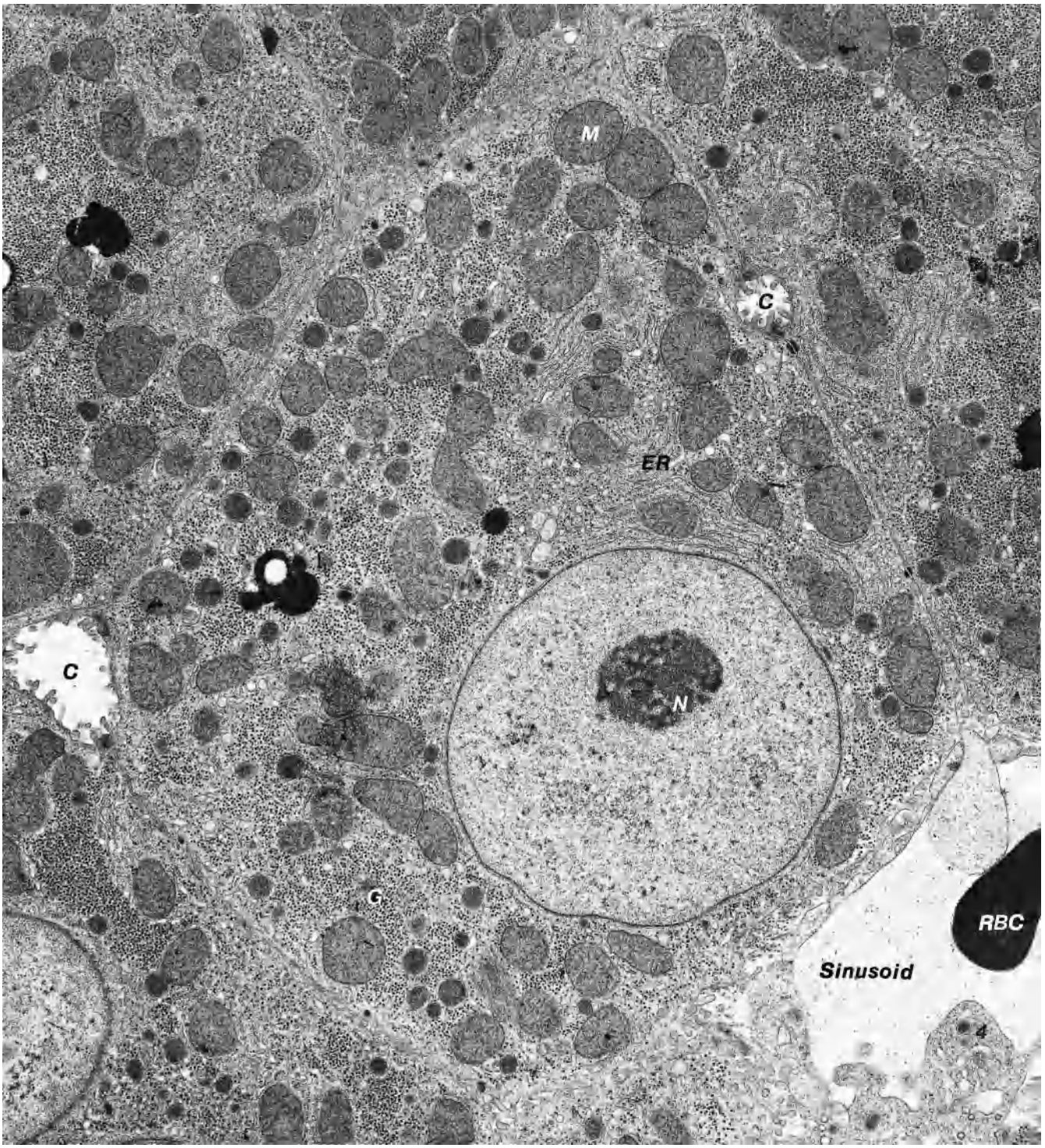


Fig. 17.1 Normal hepatocyte. Organelles: nucleolus (*N*), bile canaliculus (*C*), endoplasmic reticulum (*ER*), glycogen (*G*), erythrocyte (*RBC*), and liposfuscin (*l*). The cell has six distinct but interrelated operational systems: (1) **cell surface** controls membrane barrier functions, receipt of chemical signals, and transport of molecules into and out of the cell; (2) **cytoskeleton** provides the structural framework for the cell and acts to guide movement of organelles and inclusions. (3) **Mitochondria** (*M*) are sites of energy production; (4) **nucleolus-ribosome-rough endoplasmic reticulum–Golgi system** provides coding and production organelles for protein synthesis; (5) **cytoplasmic vacuolar system** carries out transport functions for secretion and intracellular digestion; (6) **smooth endoplasmic reticulum** is the site of synthesis of lipids and is the detoxification system for the cell.

© 2009 Wiley-Blackwell. ISBN: 978-0-813-80330-2

17 Toxicologic Pathology

Vincent P. Meador and Norman F. Cheville

The **hepatocyte** (Fig. 17.1) is the primary cell for detoxification of xenobiotics (chemicals foreign to the biologic system). Portal blood draining the gastrointestinal tract delivers toxins absorbed from the gut to the liver, where they are metabolized by oxidation, reduction, and hydrolytic and conjugation reactions for excretion into bile and urine.

In mammals, hepatocytes in portal, midzonal, and centrolobular locations have different enzymes in their cytoplasm and on their surfaces.[1,2] **Centrolobular hepatocytes** are typically the primary site of toxic injury; they have more surface receptors for toxins and larger amounts of detoxifying enzymes (but less oxygen due to the position in the hepatic sinusoid); centrolobular hepatocytes are more active in lipid, steroid, and pigment metabolism. **Portal zone hepatocyes** are most heavily oxygenated and their enzymes are designed for glycogen and protein formation.

Cyclical variances in food, water, and hormones have significant impacts on hepatocyte ultrastructure.[3–5] Hepatocytes decrease in size during **starvation.** They increase in size and weight during periods of **high food intake**. **Glucose** loading can inhibit cellular regeneration and tissue repair; it leads to accelerated progression of liver injury in thioacetamide toxicity.[6]

During feeding, the initial increase in metabolic work required to process lipids, amino acids, and glucose causes a transient and often subtle increase in **smooth endoplasmic reticulum** (SER) and in activity of its enzymes. With time, hypertrophy is associated with increased mass of all protein synthesizing organelles—nucleolus, ribosomes, RER, Golgi complexes, and vesicles of the cytoplasmic transport system. Secretions accumulate in cisternae of the endoplasmic reticulum and Golgi, and in secretory granules. **Water avoidance stress** can be associated with hepatocyte SER injury, and these lesions are reduced by melatonin, a pineal secretory product and potent scavenger of free radicals.[7]

Endothelial cells of the hepatic sinusoids are intimately associated with hepatocytes throughout sinusoidal ramifications, and markedly influence the pathogenesis of toxic disease.[8–10] Aging of the hepatic microcirculation is associated with impaired metabolism of drugs and adverse drug interactions. Studies in mice suggest that this is due to endothelial dysfunction caused by a reduced endocytic capacity, diminished sinusoidal diameters, pseudocapillarization, and accumulation of macrophages in sinusoids.[11]

Terminal aborizations of the **hepatic artery** form periductal capillaries that end by joining sinusoids (directly or by first joining portal vein branches), interlobular veins, or terminal veins (Fig. 17.2). Terminal **portal venules** (50–70 μm long; inner diameter 15–20 μm) have endothelium on a basal lamina (no smooth muscle). Large endothelial cells occur at origins of sinusoids and entry of arterial capillaries and swell or shrink to adjust blood flow

Sinusoids (250 μm long, 15–30 μm side) are fenestrated and have no basal lamina. The first part in zone 1 is narrow, nonfenestrated, and has an uninterrupted basal lamina; spaces of Disse in this areas are continuous with portal spaces. The same occurs at the terminus of the sinusoids and their association with the central vein. In chronic hepatotoxicity, collagen deposition in the sinusoids progresses to obliterate spaces and to separate hepatic acini. Myofibroblasts, present in the normal liver, expand to contribute to the fibrotic process.[12]

Kupffer cells, the resident macrophage of the liver, clear blood of foreign substances and assist in

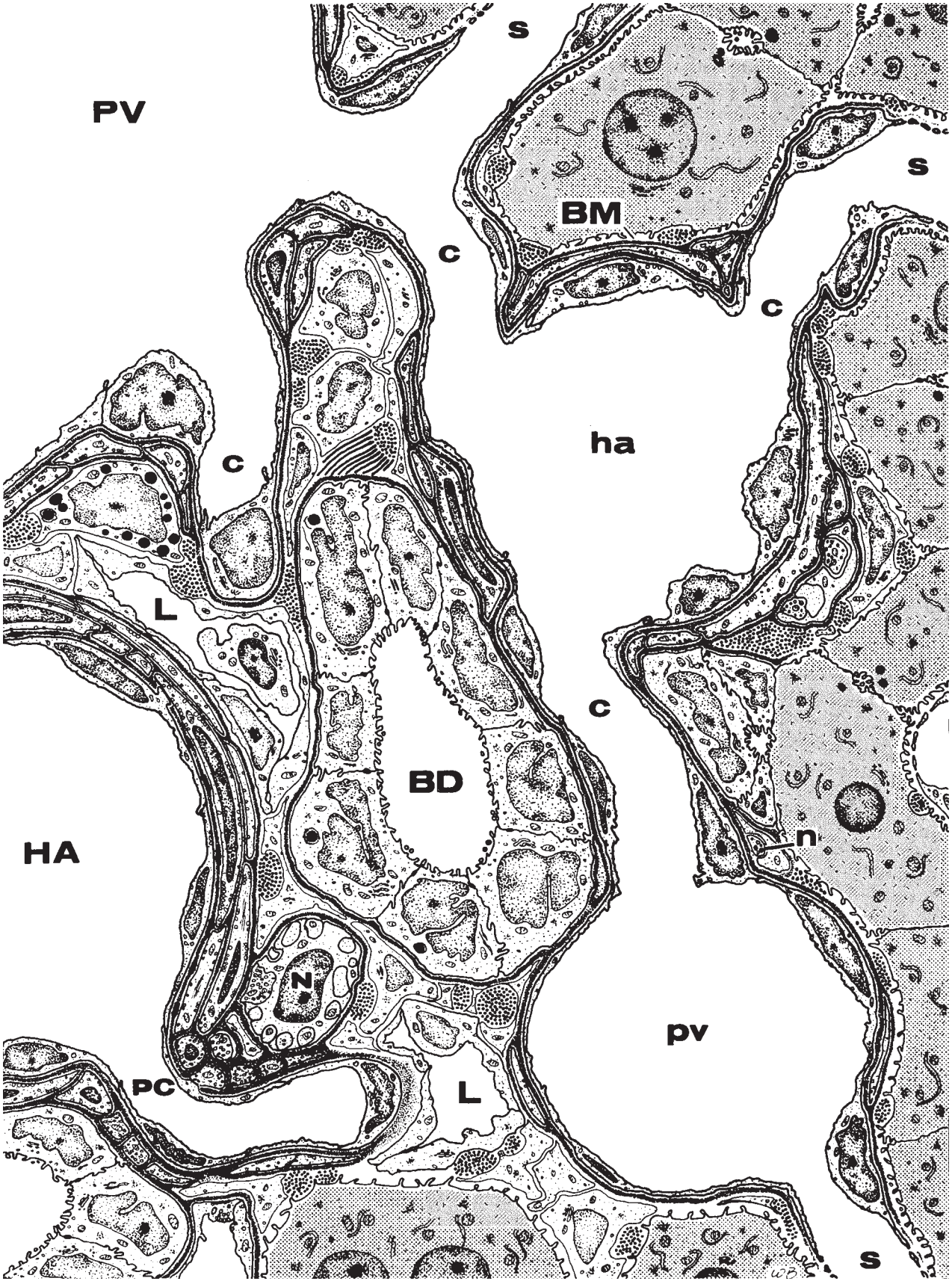


Fig. 17.2 Terminal aborization of the hepatic artery. **Arterioles** (*HA*) and terminal arterioles (*ha*) give rise to capillaries (*C*), which surround **bile ducts** (*BD*). Capillaries arising from arterioles (*PC*) have precapillary sphincters at their origins; capillaries from terminal arterioles have poorly developed sphincters. **Periductal capillaries** terminate by joining portal veins and/or sinusoids. A few capillaries join larger **interlobular veins** (*PV*), and some join terminal **distributing veins** (*pv*). Others give rise to **sinusoids** (*S*) directly (*upper right*) or to sinusoids in common with the portal vein (*upper center*). Endothelial cell nuclei are at or near junctions of capillaries with other vessels. At lobule periphery, sinusoids resemble capillaries with a complete basement membrane (*BM*). **Lymphatic vessels** (*L*); unmyelinated **nerves** (*N, n*) in portal tissue. (Drawing: William E. Burkel, *Anat Rec* 167:329, 1970.)

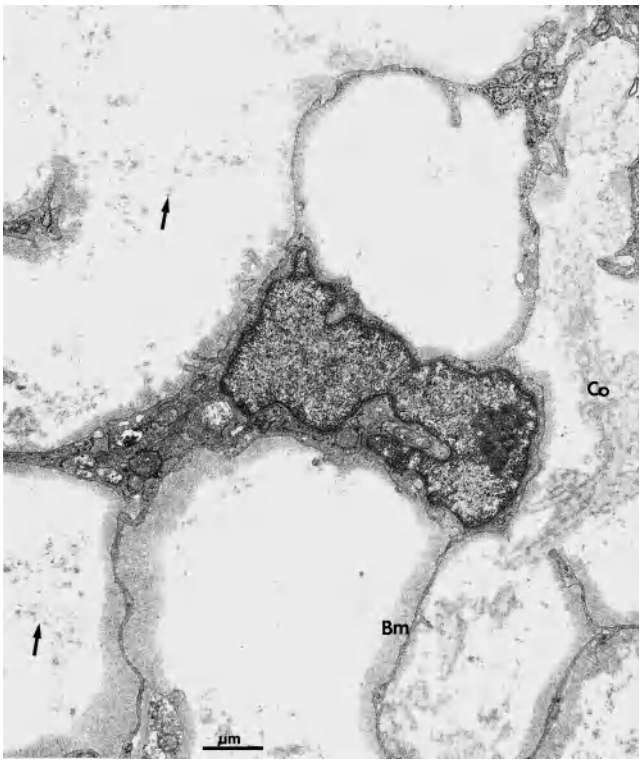


Fig. 17.3 Spongiosis hepatis: liver, rat given N-nitrosomorpholine. Fibroblast-like cell has long cytoplasmic processes coated with basement membrane-like material (*Bm*) and associated with collagen fibers (*Co*). Flocculent material (*arrows*) is in extracellular cavities. (Micrograph: P. Bannasch, *Lab Invest* 44:252, 1981.)

regulating the immune response to these substances. Liver functions include metabolism of carbohydrates, protein, fat and hormone; blood storage and filtration; metabolism and excretion of xenobiotics; bile formation; vitamin and iron storage; and production of coagulation factors—all of which can generate ROS and associated oxidative injury.[13] Kupffer cells are anchored to sinusoidal endothelium by a peculiar apposition of cellular membranes. Having an increased electron density at points of membrane apposition, they differ from typical tight junctions or desmosomes. Some Kupffer cells are also anchored to underlying endothelium by microvillar processes inserted between or through endothelial cells.

Perisinusoidal stellate cells (Ito cells, lipocytes) are large stellate cells that lie in interlobular spaces, between hepatocytes and endothelium of the sinusoids. They are fat storage cells and are important in vitamin A metabolism and toxicity. Transformation of Ito cells into fibroblasts plays a role in hepatic fibrosis. **Spongiosis hepatis** is a cystic malformation of hepatic sinusoids that involves stellate cells (Fig. 17.3); it has been produced by N-nitrosomorpholine.[14] **Spongiotic pericytoma** is a neoplasm of hepatic stellate cells that has been reported in humans.[15]

Stem cells (oval cells) are small immature epithelial cells that reside in terminal branches of the biliary tree, the canals of Hering. Stem cells have phenotypic features of both fetal hepatocytes and bile duct epithelium; they express τ-glutamyl transpeptidase and α-fetoprotein, and have the capacity to generate cells of either hepatocyte or ductal lineages. Stem cells proliferate in response to many toxins including hepatic carcinogens,[16] and are responsible for regeneration after hepatoxins suppress proliferation of existing hepatocytes. **Pit cells** are an intrasinusoidal population of large granular lymphoyctes. They were initially reported in rat livers as large lymphoid cells with dense granules, cell polarity, and pseudopods.[17]

Lysosomotropic Hepatotoxins

Many hepatotoxic drugs cause morphologic changes in the number, size and content of hepatocyte lysosomes. Affected lysosomes have variably sized intracytoplasmic vacuoles containing a variety of content types with varying combinations and concentrations of clear, granular, and pigmented material. Cellular and extracellular materials may be identifiable if degradation has not occurred. Analysis must determine if contents are exogenous, endogenous, or xenobiotic-complexed endogenous materials, and whether the material originated from intracellular and/or extracellular sources. The presence of secondary lysosomes may indicate normal function of this organelle, so that findings may be limited to morphologic appearance with no change directly attributable to other parameters.

Mechanisms of lysosomal change include: xenobiotic-endogenous substance complexes that are resistant to lysosomal enzymes; direct xenobiotic inhibition of lysosomal enzymes; change in lysosomal pH that decreases lysosomal enzyme activity; inhibition of lysosomal enzyme cofactors; increased cell metabolism causing an increase in turnover of senescent membranes and organelles; increased turnover of cell membrane secondary to injury; depletion of lysosomal enzymes; precipitation of xenobiotic components in vascular space resulting in phagocytosis of foreign material; damage to circulating blood cells causing phagocytosis by RE cells; and precipitation of xenobiotics intracellularly.[18] Accumulation of secondary lysosomes in itself is often not adverse to the cell or organism, even in the case of phospholipidosis, one of the most characterized subtypes of secondary lysosomal disorder. Adverse effects have been hypothesized to be due to physical interference with cell function or to chemical damage to cells due to release of lysosomal enzyme contents into the cytoplasm. However, conclusive evidence that injury occurs and

is directly attributable to the secondary lysosome is generally lacking.

Phospholipid formation in lysosomes leads to **concentric lamellar inclusion bodies (CLIBs)**, also referred to as lamellar membranous inclusions, myelin figures and myeloid bodies.[19] Electron microscopic identification of this characteristic structure is considered diagnostic for phospholipidosis. Since similar appearing CLIB-like structures can occur in normal tissue, caution should be taken in ensuring that CLIB is truly the predominant change in the secondary lysosomes and that its identification ultrastructurally represents the histologic change being characterized.

There is no conclusive link of lysosomal phospholipid accumulation in cells with adverse clinical outcomes. Two drugs cause phospholipidosis and severe tissue damage in humans. **Amiodarone** causes profound phospholipidosis of pulmonary macrophages and interstitial pneumonia, and **gentamycin** causes phospholipidosis of renal tubular epithelial cells and renal tubular necrosis. Both can cause phospholipidosis in liver. Direct causative effects of the phospholipid accumulation with tissue damage have not been proven. Animal models of amiodarone toxicity develop pulmonary phospholipidosis, but not the lung toxicity that occurs in humans.

Lysosomal Phospholipidosis

Many currently marketed drugs from multiple therapeutic classes are known to cause phospholipidosis in preclinical studies and sometimes in humans (e.g., amiodarone, gentamycin). One common chemical characteristic is that the majority are classified as **cationic amphiphilic drugs (CAD).** These have a hydrophobic ring structure with a hydrophilic side chain with a charged cationic amine group. The CAD is taken up into the lysosome, where the amine is protonated, being trapped by low pH and preventing efflux. Of the theoretical mechanisms for dysfunction in digestion of membranes, the two most likely are direct inhibition of enzyme activity, and binding of the xenobiotic to membrane phospholipids forming an undigestible complex.

Chronic treatment with lysomotropic drugs leads to accumulation of cytoplasmic lysosomes bearing **concentric lamellar inclusion bodies (myeloid bodies).** In advanced lesions there are giant **autophagolysosomes** filled with myelin figures. By increasing proteolysis and decreasing lipolysis these drugs cause membranes to accumulate and to form in laminar arrangements. They are tropic for lysosomes and few enter the smooth endoplasmic reticulum.

Lysosomotropic drugs that induce generalized **phospholipidosis** by complexing with polar lipids of lysosomal membranes include the depressants chloroquine, chlorpromazine, chlorphentermine, and iprindol. These are cationic amphophilic compounds containing hydrophobic and hydrophilic moieties in close proximity. Membrane damage arises from interference with enzyme substrates. Marked ultrastructural changes in lysosomes in human livers have been reported for several amphophilic compounds; for example, the coronary vasodilating agent Coralgil.

Chloroquine

Chloroquine, used for treatment of malaria and chronic immunologic disease, induces extensive lyosomal proliferation and myeloid body formation. Treatment is associated with degenerative myopathy and retinopathy. Cytoplasmic granules can also be seen in leukocytes. Development of large foamy, granular lysosomes results from markedly increased autophagy. Initial accumulation of small membranous vesicles in the lysosome lead to formation of giant autophagosomes that contain dense cellular debris and masses of membrane fragments. As the process progresses, membranes reform into laminar arrangements or **myelin figures** that develop within lysosomes as **myeloid bodies**.[20]

Tilarone

Chronic treatment of rats with the experimental immunostimulatory drug **tilarone** (and analogues of tilarone) causes lysosomal storage of sulfated glycosaminoglycans. Lesions mimic those of the inherited mucopolysaccharidoses. These drugs are dibasic amphophilic molecules that have a planary aromatic ring system and two side chains, each with a protonizable nitrogen atom. They are similar to acridine orange, which also specifically accumulates in lysosomes. Treatment of rats with tilarone is associated with a 48-fold increase in urinary excretion of sulfated glycosaminoglycans and an increase of these molecules in liver of 56-fold (especially heparan sulfate and dermatan sulfate).[21]

Peroxisomotropic Hepatotoxins

Peroxisomes contain catalase and oxidases as well as carriers. Enzymes that oxidize cholesterol intermediates to cholic acid and can convert cholesterol to proprionic acid have been localized in hepatic peroxisomes by immunolabeling. Sterol carrier protein-2, a protein molecule that carries cholesterol in its biogenesis, has been localized to peroxisomes.[22] Chronic exposure to certain hypolipidemic drugs (clofibrate), plasticizers

(di-(2-ethylhexyl)-phthalate), and herbicides (2,4,5 trichlorophenoxy acetic acid) leads to **peroxisome proliferation** and induction of endoplasmic reduplication. Striking intraperoxisomal inclusions of hollow plates arranged in layers have been reported in rats.

Hepatic peroxisomes are critical sites of **cholesterol metabolism** because they contain oxidases that affect intermediates of cholesterol metabolism, and can convert cholesterol to proprionic acids. 3-Hydroxy-3-methylglutaryl coenzyme A reductase, a rate-limiting enzyme of sterol biosynthesis, and proteins that carry cholesterol intermediates have been localized immunocytochemically to peroxisomes. Agents that inactivate **catalase** or block its synthesis produce hyperlipemia (Fig. 17.4). **Dimethrin** toxicity in rats causes prominent matrical plates and tubules in peroxisomes.[23]

Hepatic peroxisomal proliferation is caused by **clofibrate, chlorcyclizine**, and **biphenylmethylvaleric acid**, and other anti-hypercholesterolemic agents. Hepatocytes are enlarged and have marked increases in peroxisomes. Changes in other organelles include proliferation of smooth endoplasmic reticulum, vesiculation of rough endoplasmic reticulum, enlargement of the Golgi complex, and increases in lipid globules and liposomes. Loosely arranged networks of filaments accumulate around lipid globules, a process called **topolysis**. These changes are greatly influenced by other parameters of metabolism, for example, addition of sucrose markedly increases lipid globules; when clofibrate and orotic acid are used together, lipid production is reduced.

Peroxisomal Toxins

Xenobiotic-induced changes of peroxisomes are almost always confined to liver and often involve **peroxisome proliferator activated receptor (PPAR)** and hypolipidemic compounds. Stimulation of the hepatocytes with PPARα xenobiotics and induction of CYP4A cause proliferation of peroxisomes. The PPARα receptor is the transcription factor that activates CYP4A. In general, the change is quantitative, causing an increase in numbers that is appreciable in liver, but has also been reported in kidney. Microscopically, liver has centrilobular hepatocellular hypertrophy, with enlarged hepatocytes having a finely stippled eosinophilic granular appearance. Liver weight can be increased. Changes in appearance of peroxisomes have been reported, but outside of disappearance of the crystalline core, qualitative changes are seldom detected. There is species susceptibility to peroxisome proliferation: rodents are most susceptible, with dogs, nonhuman primates, humans and guinea pigs being poorly susceptible.

Compromise of hepatocellular integrity or function is generally minimal, until the magnitude of peroxisome proliferation change is marked. At this point, direct effects of peroxisome proliferation may be related to the massive cellular enlargement physically leading to compromised cellular integrity and/or pressure-induced collapse of vascular and canalicular spaces. Diagnosis of peroxisome proliferation is by electron microscopy and staining of tissues with diaminobenzidine. Acute effects on hepatocellular clinical pathology function occur with peroxisome proliferation. Plasma concentrations of albumin, synthesized by hepatocytes, increases, while concentrations of globulin decrease.[24]

The major concern with peroxisome proliferation is that it is associated with liver tumor production in the rodents.[25] Proposed mechanisms are that neoplasia is caused by alteration of fatty acid oxidation and cell cycle control, a nongenotoxic mechanism of tumor promotion. Animal species that do not have peroxisome proliferation have not been shown to develop liver tumors, thus the tumorigenic aspects of peroxisome proliferators are considered rodent-specific. A direct linkage between peroxisome proliferation and carcinogenesis is lacking.

While xenobiotic-induced decrease in peroxisome numbers or activity have not been identified, humans have a group of conditions related to genetic deficiencies in peroxisomes termed **peroxisomal biogenesis disorders**.[26] These disorders have severe hepatic dysfunction in which patients accumulate phytanic acid and very long chain fatty acids, substances that are highly toxic. Their accumulation in neurons leads to neurological dysfunction.

Clofibrate

Duplication of peroxisomes is induced by several hypolipidemic drugs; for example, **clofibrate** (ethyl chlorophenoxyisobutyrate), which is widely used for treatment of human hyperlipidemia. Drugs that induce peroxisome formation in rats include **aryloxyalkanoic acids, amide analogues**, **thiobenzimidazole, phenyl piperazine**, and **oxazole derivatives**. **Peroxisome proliferation** induced by hypolipidemic drugs is associated with increases in catalase activity and changes in peroxisome structure; that is, absence of matrix tubules or striations and elongated profiles. There are cavitations and compartmentalization with extensions of canaliculi from the peroxisome periphery.

Gemfibrozil

Gemfibrozil (Lopid) induces proliferation and marked structural alteration of hepatic peroxisomes. The peroxisomal matrix develops fibrillar inclusions as plates

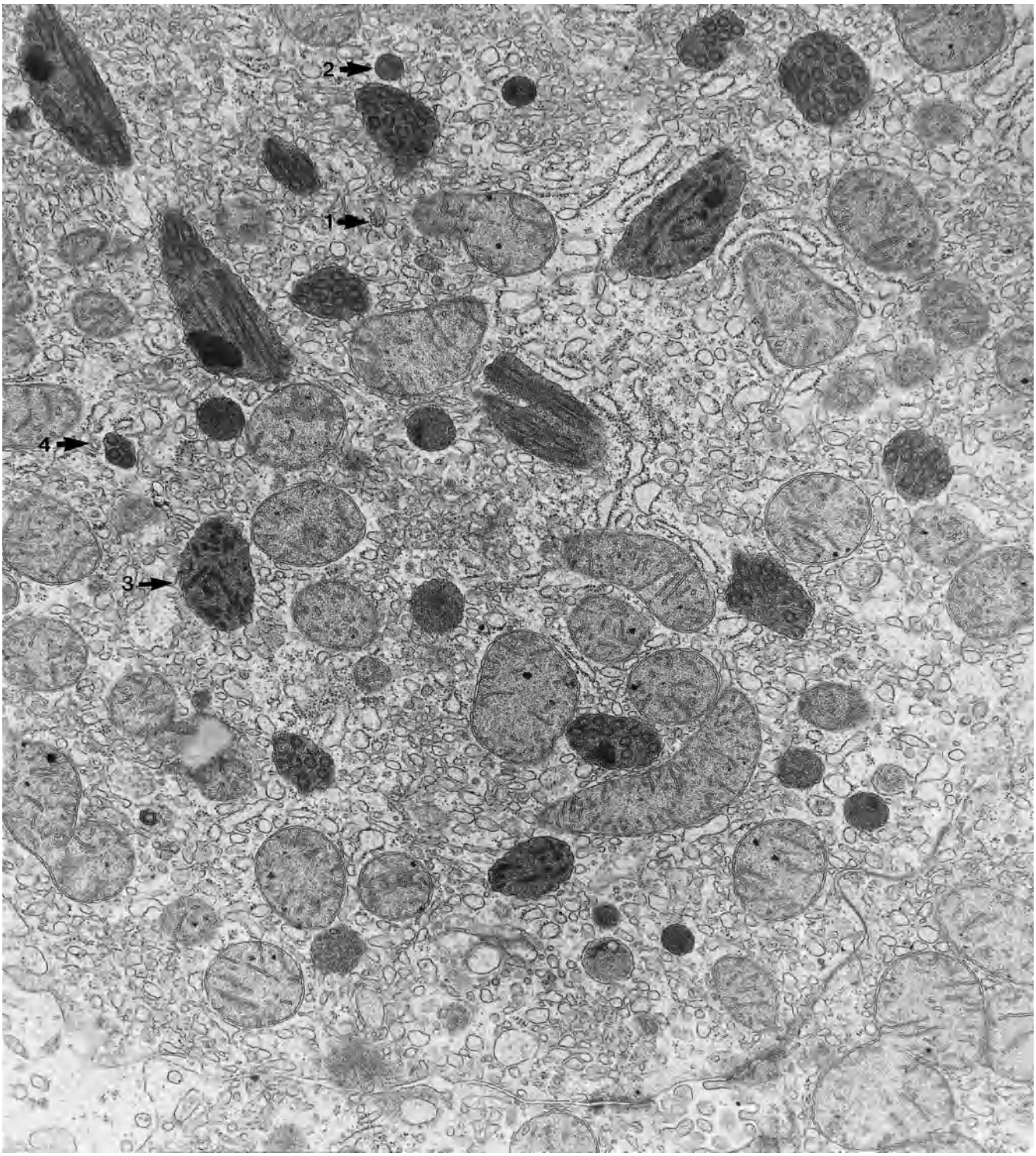


Fig. 17.4 Peroxisome injury: dimethrin toxicity, hepatocyte, rat. Most peroxisomes contain matrical tubules, but developing peroxisomes, peroxisomes without inclusions, and peroxisomes with matrical plates are also present. (Micrograph: Zdenek Hruban, *Lab Invest* 30:64, 1974.)

or tubules. Whorled configulations of smooth endoplasmic reticulum also occur. Hepatocytes in the centrolobular region are most sensitive to peroxisomal proliferation; those in periportal areas are most sensitive to matrix changes. In centrolobular areas abnormal peroxisomes are located in the cytoplasmic areas containing smooth endoplasmic reticulum and glycogen; in peripheral hepatocytes, peroxisomes are located in areas separate from endoplasmic reticulum.

Rough Endoplasmic Reticulum Hepatotoxins

In acute cell swelling of toxic injury, **rough endoplasmic reticulum (RER)** undergoes dilatation, vesiculation, and fragmentation (Fig. 17.5). These cisternal effects are accompanied by ribosomal degranulation, dispersal, redistribution, disintegration, and lack of regeneration. Carbon tetrachloride has been a model for these acute effects (see Fig. 1.2). Xenobiotics that inhibit RNA synthesis to cause RER injury include cyclohexamide, halothane, isoniazid, and ethanol.

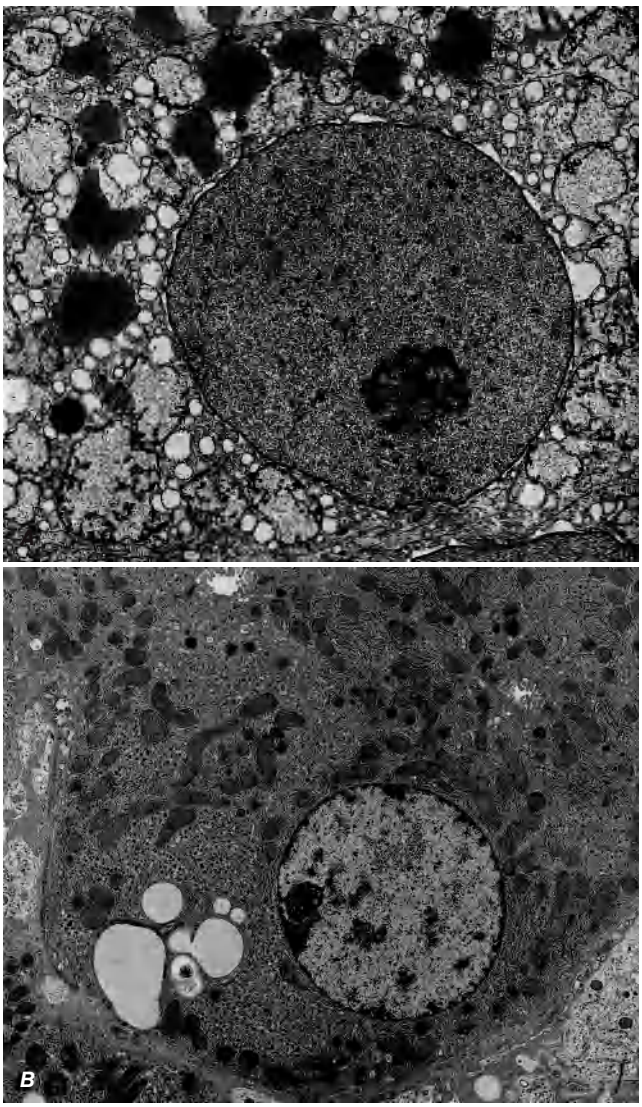


Fig. 17.5 Acute cell swelling, hepatocytes: rat. **A. Diffuse cisternal dilatation and vesiculation of rough endoplasmic reticulum**, 10 hr after *Pasteurella* type D toxin given subcutaneously: dilatation of cisternae of the nuclear envelope; and cytoplasmic lipid bodies. Mitochondria are swollen with cristolysis, matrix lysis and irregularities in the outer membrane. **B. Focal vacuolation**: cell swelling, aflatoxicosis. Nucleus appears normal except for dispersion of chromatin and eccentricity of nucleolus. Marked endothelial cell swelling (*left* and *lower right*).

Since RER is continuous with the nuclear membrane, dilatation of RER is often accompanied by dilatation of the nuclear membrane.

RER is altered by hormones and cytokines. **Estrogens**, which have a general anabolic effect on hepatocytes, increase protein synthesis and induce hypertrophy with RER proliferation. Exogenous estrogens cause both nuclear and cytoplasmic expansion; growth is prominent in nucleoli, RER, and surface microvilli. Cellular proteins that bind estrogen occur in two classes: **estrogen receptors** (estrophilin), which activate gene transcription in nuclei, and **estrogen-binding proteins** (EBP) that act in the cytoplasm. Instead of the nuclear targeting signal that is part of the ER, EBPs contain a domain that enables it to interact with the RER. Using purified anti-EPB antibodies and protein A-gold probes, activation has been shown to be associated with surfaces of the RER. The synthetic **anabolic steroids** with estrogenic activity are used as subcutaneous implants to increase cell protein synthesis and body growth of ruminant farm animals cause increases in RER and subtle mitochondrial changes in livers of cattle and sheep. Peptides produced by **estrogen**-stimulated hypertrophic hepatocytes differ among species.

- **Estrogens in mammals** cause plasma proteins and coagulation factors to increase; the latter is associated with liver disease from estrogenic contraceptives in humans.
- **Estrogenic contraceptives** in rats cause hepatocyte enlargement, nuclear volume increases, and mitosis. Microvilli and cell borders between hepatocytes are expanded.
- **Estrogens in birds** stimulate production of the egg yolk protein **vitellogenin;** hepatocytes of male frogs given estrogens also increase vitellogenin synthesis and develop large amounts of RER.

Growth hormone (somatotropin) from the pituitary directly stimulates hepatocytes to produce somatomedin, which then stimulates growth in cartilage and other support tissues. Ultrastructural changes are those of increased protein synthesis and include expansion of volume of rough endoplasmic reticulum. These changes are seen in hepatocytes of patients with growth hormone secreting tumors.

Ribosome-inactivating proteins (RIPs) are toxic to cells.[26] Type 1 RIPs consist of one peptide chain with low toxicity. They lack lectin chains, which are present in the more toxic Type 2 RIP. Examples of Type 1 RIP are trichosanthin, saporin s6 and momorchin-S. Type 2 RIPs are extremely potent toxins. Examples include abrin and ricin (the toxic component of castor beans), modeccin and volkensin. **Modeccin** and **volkensin** impair protein synthesis in hepatocytes through

damage of the 60 S ribosomal subunit. Morphologic changes occur in RER (vesiculation, degranulation, and fragmentation) and mitochondria (swelling followed by shrinkage).

Biotransformational Toxins in the RER

Phenobarbital and other barbiturates have been the classic rodent models for toxic effects on the RER (see chapter 1). Rats fed a 0.1% solution of phenobarbitone ad libitum in drinking water developed heaptomegaly with a 32% increase in liver weight (over controls) and numbers of hepatocytes. Morphometric measurements of volume of hepatocytes revealed an increase of 95% in centrolobular and 31% in periportal hepatocytes (see Table 17.1).

Ricin

Ricin, a soluble protein from castor beans, *Ricinus communis*, is readily absorbed from the gastrointesti-

Table 17.1 Ultrastructural studies in animal models of hepatotoxicity.

Toxin	*Species*	*Reference to ultrastructural pathology*
Acarbose	Rat	**Luellmann-Rauch**, *Virch Arch B* 38:89, 1981
Acetamide	Rat	**Flaks**, *Carcinogenesis* 4:1117, 1983
Acetaminophen	Hamster Mouse	**Chiu**, *Lab Invest* 39:193, 1978 **Blazka**, *Toxicol Pathol* 24:181, 1996; **Placke**, *Toxicol Pathol* 15:431, 1987; **Walker**, *Am J Pathol* 113:321, 1983
Acetylaminofluorene	Rat	**Flaks**, *J Pathol* 131:1, 1980; **Falks**, *Eur J Cancer* 4:513, 1968
Acetylsalicylic acid	Rat	**Hruban**, *Lab Invest* 30:64, 1974; **Pritchard**, *Br J Exp Pathol* 69:793, 1988
Aflatoxin	Chick Duck Frog Marmoset Monkey Rat	**Ergün**, *Dtsch Tierarztl Wochenschr* 113:363, 2006 **Theron**, *Lab Invest* 14:1586,1966 **Grassi**, *Ecotoxicol Environ Saf* 68:71, 2007 **Svoboda**, *Arch Pathol* 91:456, 1971 **Adamson**, *J Natl Cancer Inst* 50:549, 1973; **Lin**, *Lab Invest* 30:267, 1974; **Svoboda**, *Am J Pathol* 49:1023, 1966 **Bernhard**, *C R* 261:1785, 1965; **Butler**, *Cancer Res* 33:2878, 1973; **Butler**, *Am J Pathol* 49:113, 1966; **Clifford**, *Nature* 209:312, 1966; **Carnaghan**, *Nature* 200:1101, 1963; **Kim**, *Yonsei Med J* 15:17, 1974; **Monneron**, *Lab Invest* 20:178, 1969; **Pritchard**, *Br J Exp Pathol* 69:793, 1988
Allylisopropyl-acetamide	Rat	**Biempica**, *Lab Invest* 24:110, 1989; **Biempica**, *Lab Invest* 17:171, 1989; **Moses**, *Lab Invest* 22:432, 1970
Aluminum	Mouse	**Stacchiotti**, *Exp Gerontol* 43:330, 2008
α-Amanitine	Rat	**Brasch**, *Virch Arch B* 23:93, 1977; **Derenzini**, *Virch Arch B* 20:307, 1976; **Romen**, *Virch Arch B* 23:93, 1977
Amantin (mushroom)	Chicken Mouse	**Brasch**, *Virch Arch B* 27:193, 1978 **Derenzini**, *Lab Invest* 29:150, 1973
Aminoacetonitrile	Rat	**Hadjiolov**, *J Natl Cancer Inst* 50:979, 1973
Aminonucleoside	Rat	**Sturgess**, *Lab Invest* 31:6, 1974 (Puromycin)
Amiodarone	Human	**Rigas**, *Ann Intern Med* 104:348, 1986
Arsenate[#]	Rat	**Bashir**, *Toxicology* 217:63, 2006
Arsenite	Rat	**Albores**, *Toxicol Pathol* 24:172, 1996
Benthiocarb	Fish	**Kubota**, *J Fish Dis* 4:77, 1981 (carp)
Berylium	Rat	**Goldblatt**, *Arch Environ Health* 26:48, 1973
Bile salts		**Miyai**, *Lab Invest* 36:249, 1977
Bis-1-10-decase	Rat	**Feldman**, *Pathol Biol* 22:179, 1974
Bismuth	Rat	**Ghadially**, *Virch Arch B* 21:45, 1976
Calcium hopantenate	Dog	**Noda**, *Liver* 11:134, 1991
Carbon disulfide	Rat	**Torres**, *Exp Mol Pathol* 33:333, 1980

Table 17.1 *Continued*

Toxin	*Species*	*Reference to ultrastructural pathology*
Carbon tetrachloride	Dog	**Van Vleet**, *Am J Vet Res* 29:2119, 1968
	Mouse	**Leduc**, *Lab Invest* 29:186, 1973
	Rat	**Bhathal**, *Br J Exp Pathol* 64:524, 1983; **Martinez-Hernandez**, *Lab Invest* 53:166, 1985; **Takahara**, *Lab Invest* 59:509, 1988 (collagen)
Chaparral (phytotoxin)	Human	**Gordon**, *J Am Med Ass* 273:489, 1995
Chloramphenicol	Rat	**Oberholzer**, *Pathol Eur* 10:29, 1975
Chlordecone	Rat	**Lockard**, *Exp Mol Pathol* 39:230, 1983
Chlor-*m*-cresol	Rat	**Robinek**, *J Submicrosc Cytol* 12:635, 1980
4-Chloroaniline	Fish	**Braunbeck**, *Arch Environ Contam Toxic* 19:405, 1990
Chlorobiphenyl	Monkey	**Nishizumi**, *Arch Environ Health* 21:260, 1970
Chloroform	Rat	**Hewitt**, *Liver* 10:35, 1990
Chloroquine	Rat	**Abraham**, *Exp Mol Pathol* 9:212, 1968
Chlorophentermine	Guinea pig	**Lüllman-Rauch**, *Virch Arch B* 13:307, 1973
Chlorpromazine	Rat	**Balasz**, *Exp Pathol* 11:25, 1975; **Chien**, *Am J Pathol* 88:539, 1977; **Hruban**, *Virch Arch B* 26:289, 1978
Cimicifugotoxin	Rat	**Lüde**, *Cell Mol Life Sci* 64:2848, 2007
Clofibrate	Rat	**Fukuda,** *Acta Hist Cyt* 11:432, 1978; **Hruban**, *Lab Invest* 30:64, 1974; **Kolde**, *Virch Arch B* 22:73, 1976
Comfrey	Rat	**Yeong**, *Int J Exp Pathol* 1993
Copper	Mouse	**Biempica**, *Lab Invest* 59:500, 1988
	Rat	**Barka**, *Arch Pathol* 78:331, 1974
	Sheep	**Gooneratne**, *Am J Pathol* 99:429, 1980; **King**, *J Comp Pathol* 89:515, 1979
Corticosteroid	Mouse	**Kodama**, *Cancer Res* 32:208, 1972
Cocaine	Mouse	**Powell**, *Int J Exp Pathol* 75:415, 1994; **Powers**, *Toxicol Pathol* 20:61, 1992
Cyanamide	Human	**Hashimoto**, *Histopathology* 39:60, 2001; **Vazquez**, *Liver* 3:225, 1983
	Rat	**Guillen**, *Lab Invest* 50:385, 1984; **Idoate**, *Int J Exp Pathol* 73:699, 1992
Cycloheximide	Rat	**Derenzini**, *Virch Arch B* 19:115, 1975
Cytochalasin	Rat	**Oda**, *Lab Invest* 37:350, 1977
Dantrolene	Pigeon	**Silverman**, *Tissue Cell* 9:507, 1977
DDT	Rat	**Jonsson**, *Arch Environ Contam Toxicol* 10:171, 1981
Deoxycorticosterone	Rat	**Winton**, Br J Exp Pathol 68:475, 1987
Diazofluoranthen	Rat	**Thys**, *Lab Invest* 28:70, 1973
Dichloroethylene	Rat	**Reynolds**, *Am J Pathol* 101:331, 1980
Dichlorvos	Dog	**Cockrell**, *Am J Vet Res* 33:687, 1972
Diclofenac	Human	**Helfgott**, *J Am Med Ass* 264:2660, 1990
Dieldrin	Rat	**Hutterer**, *Lab Invest* 20:455, 1969; **Kimbrough**, *Arch Environ Health* 22:460, 1971
Diethylcoralgil	Human	**de La Iglesia**, *Lab Invest* 30:539, 1974
Diethyldithiocarbamate	Mouse	**Asano**, *Nagoya Med J* 19:139, 1974
Diethylnitrosamine	Fish	**Braunbeck**, *Toxicol Pathol* 20:179, 1992; **Brunton**, *Toxicol Pathol* 18:313, 1990
	Monkey	**Gyorkey**, J Natl Cancer Inst 59:1451, 1977
	Rat	**Bruni**, *J Natl Cancer Inst* 50:1513, 1973; **Scherer**, *Eur J Cancer* 11:689, 1975
Digitoxin	Rat	**Arcosoy**, *Lab Invest* 20:190, 1969
Dimethryn	Rat	**Hruban**, *Lab Invest* 30:64, 1974
Dioxin	Hamster	**Olson**, *Toxicol Appl Pharmacol* 55:67, 1980
	Rat	**Gasiewicz**, *Toxicol Appl Pharmacol* 54:469, 1980
Diphenylhydantoin	Guinea pig	**Lui**, *Toxicol Appl Pharmacol* 55:55, 1980

Table 17.1 *Continued*

Toxin	*Species*	*Reference to ultrastructural pathology*
Dipyridyl	Rat	**Rifkin**, *Lab Invest* 23:480, 1970
Endotoxin	Dog	**Boler**, *Lab Invest* 17:537, 1967
	Rat	**Ruiter**, *Lab Invest* 45:38, 1981
Estrogen	Frog	**Bergink**, *Cytobiologie* 14:362, 1977
	Mouse	**Oberly**, *Am J Pathol* 139:669, 1991
Ethanol	Baboon	**Lieber**, *Proc Natl Acad Sci* 72:437, 1982; **Nakano**, *Am J Pathol* 106:145, 1982
	Human	**Ashworth**, *Am J Pathol* 46:757, 1965; **Chedid**, *Gastroenterology* 90:1858, 1986; **French**, *Ann N Y Acad Sci* 492:262, 1987; **Nakano**, *Gastroenterology* 83:777, 1982; **Rubin**, *Fed Proc* 26:1458, 1967
	Monkey	**von Wartburg**, *Lab Invest* 50:5, 1984
	Rat	**Iseri**, *Am J Pathol* 48:535, 1966; **Koch**, *Am J Pathol* 90:325, 1978; **Rubin**, *Lab Invest* 23:620, 1970; **Rubin**, *Lab Invest* 22:569, 1970; **Tsukamoto**, *Am J Pathol* 131:246, 1988
Ethionine	Mouse	**Lombardi**, *Am J Pathol* 79:465, 1975
	Rat	**Baglio**, *J Cell Biol* 27:591, 1965; **Goldblatt**, *Lab Invest* 28:206, 1973; **Goldblatt**, *Am J Pathol* 53:1041, 1968; **Lenzi**, *Lab Invest* 66:390, 1992; **Merkow**, *Lab Invest* 26:300, 1972; **Novikoff**, *Am J Pathol* 139:1351, 1991; **Schinozuka**, *Lab Invest* 23:253, 1970; **Schlunk**, *Lab Invest* 17:30, 1975; **Steiner**, *Am J Pathol* 44:169, 1964
Ferrous sulfate	Rat	**Ganote**, *Lab Invest* 28:426, 1973
Fluorenylacetamide	Rat	**Sell**, *Am J Pathol* 114:287, 1984
Fructose	Rat	**Goldblatt**, *Lab Invest* 23:378, 1979; **Yu**, *Lab Invest* 30:85, 1974
Furan	Rat	**Sirica**, *Am J Pathol* 145:375, 1994
Furosamide	Mouse	**Walker**, *J Pathol* 135:301, 1981
Galactoflavin	Rat	**Norton**, *Virch Arch B* 23:353, 1977
Galactosamine	Rat	**Enzan**, *Virch Arch B* 26:59, 1977; **Keppler**, *Exp Mol Pathol* 9:279, 1968; **Koch**, *Virch Arch B* 26:233, 1978; **Koff**, *Exp Mol Pathol* 19:168, 1973; **Lesch**, *Virch Arch B* 21:313, 1976; **Rumpelt**, *Virch Arch B* 16:195, 1974; **Shinozuka**, *J Ultrastruct Res* 44:279, 1973
Gemfibrozil	Rat	**Fukuda**, *Acta Histochem Cytochem* 11:432, 1978
Glucan	Rat	**Deimann**, *Lab Invest* 43:172, 1980; **Deimann**, *Lab Invest* 442:217, 1980
Gold	Human	**Fleischner**, *Hepatology* 14:422, 1991
Gold thioglucose	Mouse	**Boehme**, *Virch Arch B* 15:323, 1974
Griseofulvin	Mouse	**Matilla**, *J Clin Pathol* 27:698, 1974
Halothane	Human	**Wills**, *Am J Pathol* 91:11, 1978
	Rat	**Ross**, *Am J Anat* 135:5, 1972
Heliotrine	Rat	**Kerr**, *J Pathol* 97:557, 1969
Hexachlorobenzene	Rat	**Mollenhauer**, *Am J Vet Res* 36:1777, 1972; **Mollenhauer**, *Am J Vet Res* 37:847, 1975
Hexachloraphine	Rat	**Medline**, *Arch Pathol* 96:61, 1973
	Sheep	**Reid**, *J Pathol* 115:33, 1975
Hydrazine	Mouse	**Wakabayashi**, *Exp Mol Pathol* 39:139, 1983
	Rat	**Amenta**, *Lab Invest* 11:956, 1962
Hymenoxon	Mouse	**Bowers**, *Am J Vet Res* 45:383, 1984
India ink	Mouse	**Fujita**, *Virch Arch B* 42:33, 1983
Indium	Rat	**Fowler**, *Lab Invest* 48:471, 1983
Iodoform	Rat	**Sell,** *J Cell Biol* 41:736, 1969
Iron	Rat	**Arborgh**, *Lab Invest* 30:664, 1974; **Doolittle**, *Lab Invest* 45:558, 1981; **Richter**, *Am J Pathol* 91:363, 1978
Kavain	Rat	**Fu**, *World J Gastroenterol* 14:541, 2008

Table 17.1 *Continued*

Toxin	*Species*	*Reference to ultrastructural pathology*
Kepone	Quail	**Atwal**, *J Comp Pathol* 83:115, 1973
Lead	Baboon Pig Rat	**Hoffman**, *Lab Invest* 30:311, 1974 **Watrach**, *J Ultrastruct Res* 10:177, 1964 **Hoffman**, *Exp Mol Pathol* 17:159, 1972
Levamisole	Dog	**Verheyen**, *Vet Pathol* 13:131, 1976
Lithocholic acid	Mouse	**Fickert**, *Am J Pathol* 168:410, 2006
Margosa oil	Rat	**Sinniah**, *J Pathol* 159:255, 1989
Mercury	Rat	**Desnoyers**, *Environ Res* 9:224, 1975; **Ovdea**, *Lab Invest* 12:386, 1963
Microcystin	Fish	**Li**, *Ecotoxicol Environ Saf* 67:447, 2007
Mirex	Rat	**Gaines**, *Arch Environ Health* 21:7, 1979; **Kimbrough**, *Arch Environ Health* 21:7, 1979; **Singh**, *Pathology* 13:487, 1981
Monocrotaline	Monkey Rat	**Van der Watt**, *J Pathol* 1007:279, 1972 **Afzelius**, *J Ultrastruct R*es 20:328, 1966; **Allen**, *Cancer Res* 30:1857, 1970
Nafenopin	Mouse	**Reddy**, *Cancer Res* 36:1211, 1976
Naphthoflavone	Mouse	**Oberly**, *Am J Pathol* 139:669, 1991
Naphthylisothiocyanate	Rat	**Platt**, *Acta Hepatogastroenterol* 19:356, 1972
Niacin	Review	**Etchason**, *Mayo Clin Proc* 66:23, 1991
Nickel carbonyl	Rat	**Hackett**, *Arch Environ Health* 19:337, 1969
Nitrosodiethylamine	Fish	**Couch**, *J Natl Cancer Inst* 79:297, 1987
Nitrosomorpholine	Rat	**Bannasch**, *Lab Invest* 44:252, 1981
Norethandrolone	Rat	**Phillips**, Am J Pathol 93:729, 1978
Orotic acid	Rat	**Jatlow**, *Am J Pathol* 47:125, 1965; **Novikoff**, *Lab Invest* 15:27, 1966; **Rajalakshmi**, *J Cell Biol* 41:625, 1969
Penicillin	Human	**Goldstein**, *Arch Pathol* 98:114, 1974
Pentachlorophenol	Rat	**Flesicher**, *Arch Toxicol* 44:243, 1980
Pentenoic acid	Rat	**Hidako**, *Exp Mol Pathol* 55:135, 1991
Phalloidin	Rat	**Naramoto**, *Hepatology* 13:222, 1991 (cytoskeleton); **Seiss**, *Virch Arch B* 6:151 (fetus); **Weiss**, *Beitr Pathol* 150:82, 1973
Phenethyl isothiocyanate	Rat	**Gray**, *Toxicol Pathol* 23:644, 1995
Phenobarbital	Rat	**Chiesara**, *Lab Invest* 22:329, 1970; **Herdson**, *Lab Invest* 13:1032, 1963; **Massey**, *Chem Biol Interact* 24:329, 1979
Phenethyl isothiocyanate		**Gray**, *Toxicol Pathol* 23:644, 1995
Phenytoin	Dog	**Bunch**, *Am J Vet Res* 46:105, 1985
Phosphorus	Rat	**Barker**, *Lab Invest* 12:955, 1963; **Ganote**, *Lab Invest* 21:207, 1969
Phytotoxin	Sheep	**Seawright**, *Vet Pathol* 2:175, 1965 (*Lantana* sp.)
	Mouse	**Seawright**, *J Pathol* 106:251, 1972 (*Ngaione* sp.)
Polychlorobiphenyl	Fish Monkey Rat	**Klaunig**, *J Environ Pathol Toxicol* 2:953, 1979 **Nishizumi**, *Arch Environ Health* 21:620, 1970 **Durham**, *Toxicol Pathol* 17:536, 1989; **Hiniton**, *Virch Arch B* 27:279, 1978; **Kascza**, *J Toxicol Environ Health* 1:689, 1976; **Kimbrough**, *Arch Environ Health* 25:354, 1972; **Sleight**, *J Am Vet Med Ass* 169:1231, 1976
Pregnenolone	Rat	**Garg**, *Acta Anat* 85:190, 1973; **Tuchweber**, *J Ultrastruct Res* 39:456, 1972
Promethazine	Rat	**Gallagher**, *Austr J Exp Biol* 40:241, 1991
Propiomazine	Rat	**Sarphie**, *Lab Invest* 26:648, 1972
Pyrazole	Rat	**Lieber,** *Lab Invest* 22:615, 1970
Quinacrine	In vitro	**Leduc**, *Cancer Res* 41:2832, 1981
Quinoline	Rat	**Hirao**, *Cancer Res* 36:329, 1976

Table 17.1 *Continued*

Toxin	*Species*	*Reference to ultrastructural pathology*
Retinyl acetate		**Shintaku**, *J Vet Med Sci* 60:471, 1998
Ricin	Rat	**Derenzini**, *Virch Arch B* 20:15, 1965
Rosiglitazone†	Human Mouse (ob/ob)	**Garcia-Ruiz**, *Hepatology* 46:414, 2007
Swainsonine	Rat	**Novikoff**, *J Cell Biol* 101:339, 1985
Taxol	Mouse	**Yu**, *Am J Pathol* 122:553, 1986
Thioacetamide	Rat	**Bader**, Acta Hepato-splenol 3:160, 1969; **Barker**, *Am J Pathol* 74:575, 1974; **Robenek**, *Virch Arch B* 32:57, 1979; **Thoenes**, *Virch Arch A* 335:556, 1962
Tilorone	Rat	**Lüllmann-Rauch**, *Virch Arch B* 44:355, 1983; **Rohousky**, *Toxicol Appl Pharmacol* 17:556, 1970
Toluene	Rodent	**Ungvary**, *Exp Mol Pathol* 36:347, 1982
Trichloroethane	Mouse Rat	**McNutt**, *Lab Invest* 32:642, 1975 **Ortega**, *Lab Invest* 15:657, 1966
Trifluoroethanol	Rat	**Kim**, *Toxicol Pathol* 16:35, 1988
Trimethylphenylthioethyl-4-methyl syndrome	Dog	**Stejskal**, *Virch Arch B* 18:83, 1975
Tris(hydroxymethyl)aminomethane	Rat	**Peterlik**, *Lab Invest* 40:313, 1979
Triton	Chicken Rat	**Trout**, *Virch Arch B* 38:77, 1981 **Hutterer**, *Lab Invest* 33:305, 1975; **Trout**, *Virch Arch B* 28:279, 1979
Vinblastine	Mouse Rat	**Hirsimaki**, *Virch Arch B* 41:51, 1982; **Hirsimaki**, *Virch Arch B* 22:289, 1976; **Rez**, *Virch Arch B* 58:189, 1990 **Kovacs**, *Res Exp Med* 165:245, 1975
Vincristine	Mouse	**Passat**, *J Submicrosc Cytol* 13:321, 1981
Vinyl chloride	Rat	**Szabo**, *Am J Pathol* 82:563, 1976
Vitamin A	Human Rat	**Weber**, *Gastroenterology* 82:118, 1982 **Leo**, *Gastroenterology* 82:194, 1982

Uncouples oxidative phosphorylation from the electron transport chain to generate heat.
†Thiazolidinedione peroxisome proliferator-activated receptor gamma ligand.

nal tract. Ricin is a lectin and binds to carbohydrate receptors of cell surfaces. After ricin binds to the cell, the toxin-receptor complex is taken into the cell by endocytosis. A disulfide bond between A and B chains of the ricin molecule is reduced, and the A chain translocates across the endosomal membrane to enter the cytosol. Ricin inhibits protein synthesis by inactivating a 60S ribosomal subunit, similar to diphtheria toxin. Lesions are those of toxic hepatopathy and nephropathy.

Acetaminophen

Acetaminophen (APAP, N-acetyl-p-aminophenol) is a widely used analgesic that is safe at therapeutic levels but causes fatal hepatic necrosis in large doses. Consistent dose-dependent liver lesions can be reproduced experimentally. Within the hepatocyte, acetaminophen is catabolized to highly reactive intermediates within the smooth endoplasmic reticulum. **Acute toxicity** is due to biotransformation within this organelle and to depletion of glutathione. The earliest lesion of acute toxicity is **focal vacuolation** along the sinusoidal margins of centrolobular hepatocytes. Acute cell swelling with mitochondrial disintegration and microvillous loss occur later. Acetominophen is altered in the hepatocyte by three competing pathways: glucuronidation, sulfation, and oxidation via cytochrome P-450 enzymes. The sulfate and glucuronide conjugates are nontoxic and are excreted in bile and urine. In therapeutic doses, the reactive metabolite N-acetyl-p-benzoquinoneimine (NAPQI) formed in the SER is detoxified by reaction with the cysteine-containing tripeptide glutathione (GSH) to form 3-(glutathion-S-yl)-APAP. In overdose GSH is depleted and toxicity is presumed to occur by covalent binding of NAPQI to critical cellular proteins. The histochemical demon-

stration of NAPQI reveals a progressive central-to-periheral pattern in the liver lobule.[27]

Chronic acetaminophen toxicity, like that of phenacetin (which is converted to acetaminophen in the liver), leads to hemolytic anemia, methemoglobinuria, and icterus. Erythrocyte destruction is also related to glutathione depletion, since reduced glutathione maintains hemoglobin cysteine residues in the reduced state and keeps hemoglobin in the ferrous state.

Hepatotoxins and the Golgi Complex

Brefeldin

Brefeldin A, a fungal metabolite, causes disassembly of the Golgi complex and redistribution of medial and cis-Golgi proteins to the endoplasmic reticulum. Cell cultures treated with brefeldin A show vacuolation of the Golgi saccules and abnormal tubular endosomes.[28,29] Cytochemical markers such as mannosidase II (in the medial Golgi) and galactosyl transferase (in the trans Golgi) can be shown to redistribute to the endoplasmic reticulum. The first effect of brefeldin A is an inhibition of non-clathrin-coated vesicle assembly in endoplasmic reticulum and Golgi complex an effect of inhibition of β-COP, a coated vesicle homologue of β-adaptin. Brefeldin A blocks movement of protein from the rough endoplasmic reticulum to Golgi cis areas (it does not block backwards movement). Treatment of cells blocks all forward movement including the major pathways of exocytosis (the drug acts as a specific inhibitor of exocytosis). Movement of membrane proteins from the Golgi cis to the RER continues in treated cells.

Ribosomes and Drug Injury

Toxic injury to any of the RNAs in the cell leads to failure of ribosomes to develop or, if formed, to disintegration and detachment from the membranes of the rough endoplasmic reticulum. This is the ultimate consequence of many toxic injuries, but is the specific focus of some antibiotics. **Rifampicin** and **streptomycin** are potent inhibitors of the initiation of RNA synthesis, the latter interferes with binding of formylmethionyl tRNA to ribosomes and thereby prevents protein synthesis.

Ribosomal Toxins

Cyclohexamide

Cyclohexamide interferes with translation by binding to the large 60S subunit of ribosomes. Binding excludes subsequent binding of guanosine triphosphate (GTP) and, since GTP is the energy source for translation, ribosomal protein synthesis is blocked.[30] Ultrastructurally, hepatocytes of rats given 1.5 mg/kg cyclohexamide show evidence of protein synthesis inhibition and hepatocyte degeneration within 1 hr; for example, dilatation of the rough endoplasmic reticulum and Golgi complex with degranulation of the former, and spiral aggregates of ribosomes in the cytoplasmic matrix. Lipoprotein particles develop in the Golgi saccules.

Halothane

This widely used anesthetic is hepatotoxic after prolonged use. Ultrastructural studies of liver specimens of human patients recovering from postoperative liver necrosis show the hepatocyte degeneration is centrolobular and diffuse throughout hepatic parenchyma. In rats experimentally exposed to halothane, acute cell swelling of centrolobular hepatocytes appears with in 2 hr. By 6 hr hepatocytes circumscribing the central vein are swollen and eosinophilic with finely granular cytoplasm and peripheral vacuolation. By 12 hr hydropic changes are advanced and nuclei have condensed chromatin and may be pyknotic. Necrosis appears and with time, monocytes progressively infiltrate necrotic areas. While halothane is directly hepatotoxic, it can also induce a hypersensitivity acute drug reaction, perhaps a reaction to hepatocyte antigens released by the direct toxicity.

Smooth Endoplasmic Reticulum and Hepatotoxicity

Smooth endoplasmic reticulum is the site of synthesis and metabolism of fatty acids, phospholipids and steroids. The major xenobiotic-induced change in SER are: (1) expansion of the ER internal space due to water accumulation; (2) loss of integrity due to lysis; and, (3) proliferation (also termed reduplication) secondary to endoplasmic reticulum responding to an increased functional need.

Proliferation of SER occurs secondary to administration of xenobiotics that induce cytochrome P450 enzymes. These enzymes are responsible for metabolism of a wide variety of xenobiotics and endogenous substances, and while most prominent in hepatocytes, are located in all cells.[31] Hepatocytes have a full complement of **cytochrome P450s (CYP)**, since one of the liver's main function is metabolism of foreign substances. Exposure to metabolizable xenobiotics can cause induction of CYP and proliferation of SER, which most extensively occurs in centrilobular

hepatocytes. Not all xenobiotics that induce cytochrome P450s cause proliferation of smooth endoplasmic reticulum. Proliferation is dependent on the subset of CYP that are induced, as no single agent induces all CYP. Cytochrome P450 enzymes are grouped into families CYP1, CYP2, CYP3, etc., with capital letters designating subfamilies CYP1A, CYP1B, CYP1C, etc., and numerals further identifying individual enzymes (e.g., CYP1A1). Not all CYP inducers cause SER proliferation and liver enlargement; however, SER proliferation is nearly pathognomonic for CYP induction. Species differences exist with respect to sensitivity to induction by certain xenobiotics.

Phenobarbital and its analogs are inducers of SER proliferation. Phenobarbital is metabolized by and induces cytochrome P4502B, the major membrane protein of SER. Concomitant with increased SER is a decrease in glycogen and increase in lipid. SER proliferation begins in centrilobular hepatocytes, expanding into midzonal hepatocytes with increasing magnitude of effect. Withdrawal of the inciting xenobiotic is accompanied by a rapid regression of changes. Effete SER forms aggregates and is removed from the hepatocytes by autophagocytosis. Hypertrophied hepatocytes have an increased number of autophagic vacuoles and secondary lysosomes that contain membranous material, mitochondria, glycogen, and other material. Kupffer cells appear to participate in removal of SER during recovery. Regression of hepatocellular hypertrophy is accompanied by an increase in number of heterophagic vacuoles in Kupffer cells.

Not all proliferation of SER occurs in centrilobular hepatocytes. **HMG-CoA (3-hydroxy-3-methylglutaryl coenzyme A) reductase inhibitors (statins)** cause periportal hepatocellular hypertrophy (SER proliferation) and hyperplasia. HMG-CoA reductase is bound to SER and is in highest concentrations in periportal hepatocytes. It is induced by HMG-CoA reductase inhibitors such as atorvastatin or fluvastatin.[32]

Induction of cytochrome P450 enzymes and the resulting proliferation of SER may be considered an adaptive response to a xenobiotic. Proliferation of SER to a certain magnitude in the hepatocyte is an adaptive response, and not a toxic change. At greater magnitudes of proliferation, the change is associated with alterations compatible with toxicity. These include increases in hepatobiliary clinical pathology parameters compatible with hepatocellular injury. The exact pathogenesis is not known, but it is hypothesized that cell enlargement can lead to compression and congestion of sinusoids and bile canaliculi, leading to ischemia and cholestasis.

Hepatotoxicity secondary to hepatocellular enzyme induction can occur through increased activation of xenobiotics to hepatotoxins. Subsets of CYP inactivate xenobiotics, while others activate xenobiotics to reactive electrophiles. Examples include aflatoxin B1, a mycotoxin, which is activated to a number of metabolites, including exo-8,9-epoxide, a hepatocarcinogen; acetaminophen, an analgesic, which is activated to a reactive iminoquinone; trichloroethylene (TCE), an industrial toxicant and previously used anesthetic, which is activated to TCE oxide, which forms unstable protein adducts; and troglitazone, an anti-diabetes drug, which is metabolized to electrophilic reactive metabolites.

SER is altered by cytokines and hormones. **Cortisol, corticosterone,** and other glucocorticoids stimulate target cells by inducing production of enzymes that are crucial for mitochondrial oxidation, glycogen formation, and lipogenesis. Glucocorticoids produce their effects by entering target cells and binding to cytoplasmic receptors. Ultrastructural studies using ^{3}H-dexamethasone show binding sites chiefly in smooth endoplasmic reticulum and associated areas of cytosol; binding also occurred in mitochondria.[33]

Toxins in Smooth Endoplasmic Reticulum

Cyanamide

Cyanamide and **disulfuram**, used as alcohol aversion drugs, cause hepatotoxicity at high doses; liver changes are complicated by the chronic alcohol toxicity. Ground glass inclusions are associated with cyanamide treatment in patients with alcohol dependency. The large cytoplasmic inclusions are composed of glycogen-SER complexes derived from proliferation of SER and abnormal glycogen deposits (Fig. 17.6). These complexes also result from concomitant use of other drugs, and occur in Lafora's disease, fibrinogen deposition, hepatitis B, and type IV glycogenosis. In rats, at doses of 8 or 16 mg/kg body weight, cytoplasmic inclusions in hepatocytes are round, well-demarcated, and composed of glycogen β granules, lipid droplets, and secondary lysosomes (see Table 17.1).

Carbon Tetrachloride

In the liver, enzymes of SER transform **carbon tetrachloride (CCl_4)** into highly toxic metabolites by the reaction: $CCl_4 \rightarrow CHCl_3 \rightarrow CH_2Cl_2 + Cl^+$ and further to formic acid and CO_2. Cellular damage results from toxic free radicals produced by dehalogenation and oxidation. The critical effect is on **protein synthesis**. Liver cells from rats injected with $^{14}CCl_4$ show that radiolabeling occurs first in the rough endoplasmic reticulum. The earliest structural changes occur on ribosomes (Fig. 17.7). **Polyribosomes** free in the cytosol are broken into smaller units, and ribosomes on

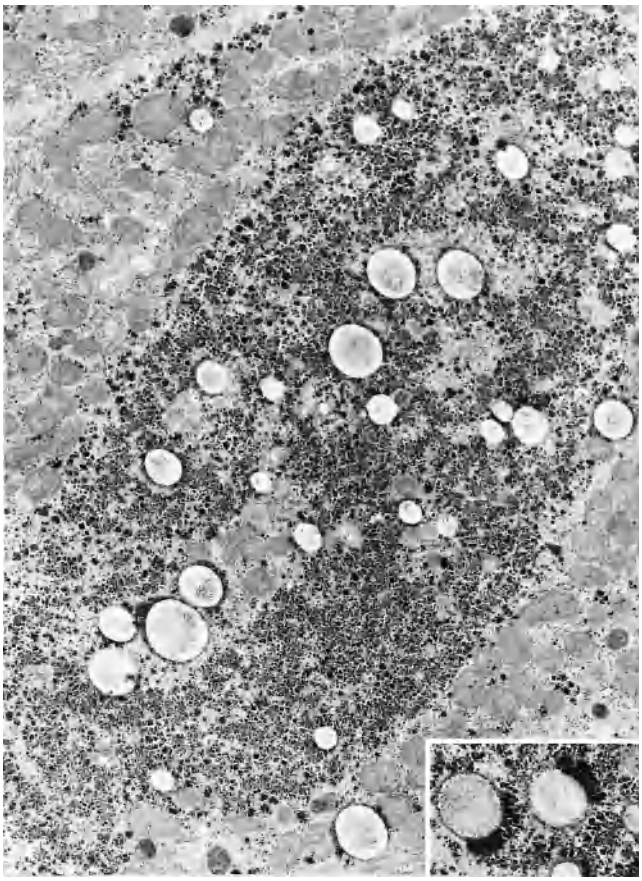


Fig. 17.6 Inclusion body, smooth endoplasmic reticulum: cyanamide toxicity, hepatocyte, rat. Inclusion contains fragmented SER. *Inset*: lipid globules and glycogen. (Micrograph: F. J. Guillen, *Lab Invest* 50:385, 1984.)

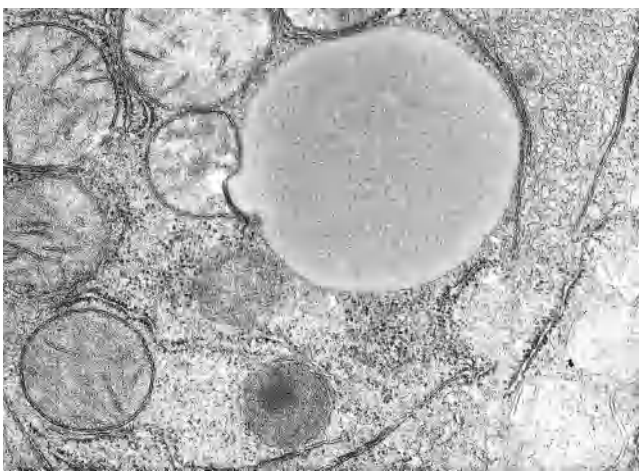


Fig. 17.7 Smooth endoplasmic reticulum duplication, acute cell swelling: carbon tetrachloride toxicity, liver, rat. Membranes of SER are irregular and collapsed into focal areas. Note dilatation, fragmentation, and vesiculation of RER.

membranes of the RER detach and are dispersed. Membranes of the RER fragment into tiny vesicles, first in focal areas and then in the entire cytoplasm. Within a few hours after injection, cisternae of the endoplasmic reticulum and nuclear envelope are markedly dilated, and irregular fragments of membrane are frayed into the adjacent cytoplasm.

Coincident with the effects on ribosomes, the **plasma membrane** becomes leaky. CCl_4 causes an increase in Ca^{++} in hepatocytes, which is maximal at 1–1.5 hr.[34] Calcium changes alter the fluidity of the membrane and cause protein segregation and aggregation in gap junctions that close. There are alterations in lipoprotein synthesis that lead to accumulation and inspissation of **liposomes** (lipoprotein droplets) within RER cisternae. A major protein suppressive effect is an inhibition of proteins that bind to triglycerides, and these accumulate early as **liposomes** and then as larger **lipid globules** free in the cytoplasmic matrix.

In CCl_4-induced **cirrhosis** collagen fibrogenesis is accompanied by progressive obliteration of blood vessels with concomitant dilatation of portal and hepatic venules. Sinusoidal changes involve obliteration of interconnecting and branching. Blood flow rates do not differ significantly from normal due to portal hypertension and an abnormally high velocity flow in the remaining direct sinusoids. TGF-β gene expression occurs similtaneous with gene expression for collagen, and this cytokine appears to have an important enhancing role in CCl_4-induced fibrosis.[35] Iodoform injury in rats resembles that of carbon tetrachloride; there is centrolobular necrosis with lesions of calcium in mitochondria of midzonal hepatocytes within 1 hr.

Ethanol

The excessive and chronic ingestion of alcohol is associated with derangements in liver structure and function. The principal manifestation of **acute toxicity** is hepatic steatosis. Hepatocytes are engorged with globules of neutral lipids. Specific damage has been reported in other organelles including mitochondria and the cytoskeleton. Membranes of smooth and rough endoplasmic reticulum and of the Golgi complex are markedly affected. In **chronic cirrhosis** from ethanol, collagen-producing cells, particularly myofibroblasts, proliferate around termini of hepatic venules, and collagen fibrils radiate into perisinusoidal spaces from centrolobular areas. Alcoholic hyalin, aggregates of fibrous material in the cytoplasm of hepatocytes, develops in chronic alcoholics (see Fig. 26.12).

Ethanol is absorbed from the anterior gastrointestinal tract by diffusion, The rate of absorption is different for stomach and duodenum so that gastric emptying rates play an important role in uptake. Blood alcohol curves after a single oral dose indicate

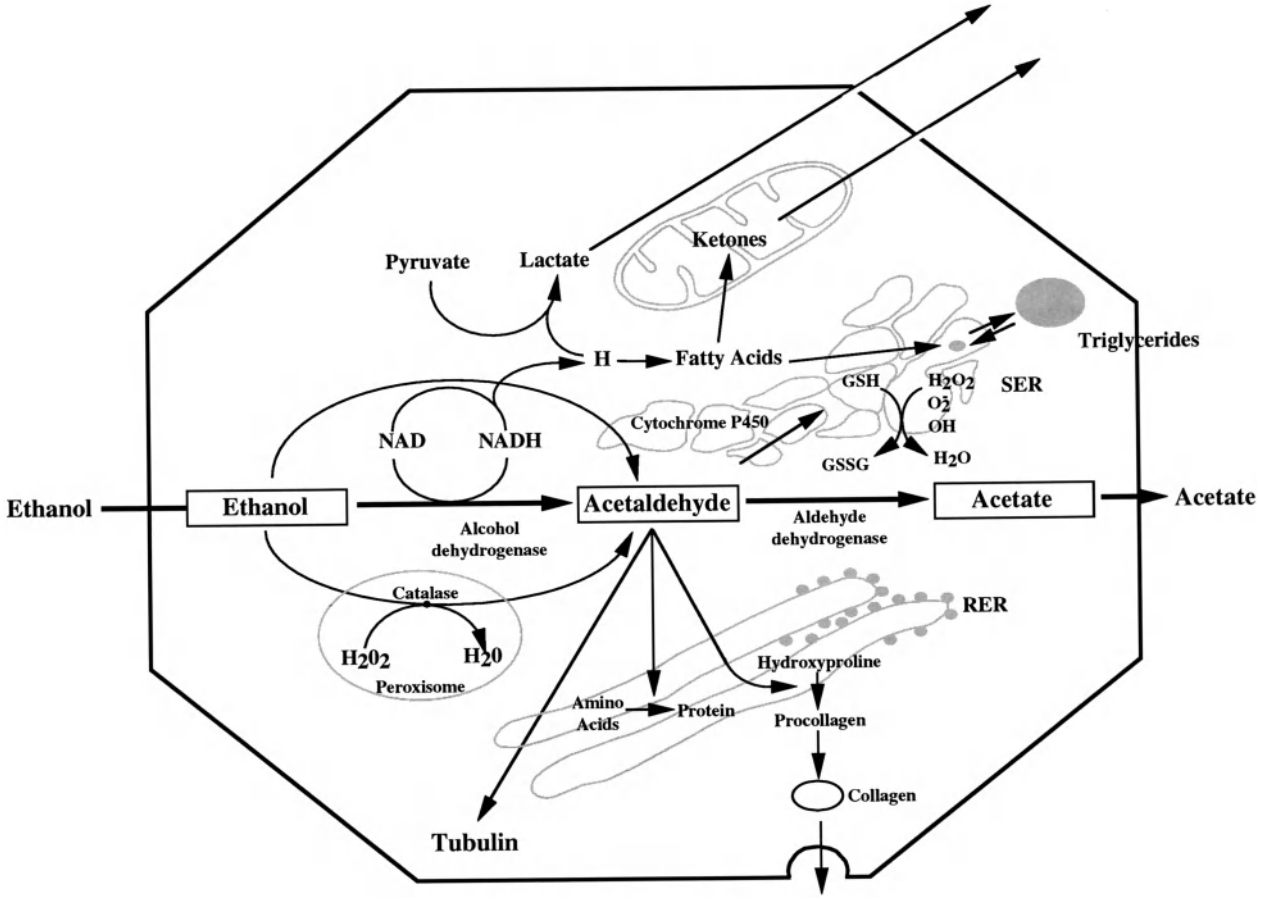


Fig. 17.8 Metabolic pathways: degradation of ethanol.

three patterns of activity: absorption, tissue distribution, and elimination. In the hepatocyte, ethanol catabolism includes three mechanisms: alcohol dehydrogenase, SER-oxidizing systems, and the catalase-hydrogen peroxidase system in peroxisomes; 90% of elimination is done by oxidation of ethanol to CO_2 and water, and 10% by SER and peroxisomes (Fig. 17.8). The conversion of alcohol to acetaldehyde, catalyzed by alcohol dehydrogenase, rapidly removes alcohol from the blood. Acetaldehyde is further oxidized to acetate and then to the key intermediate acetyl CoA.

Ethanol affects five cellular processes: (1) increased mobilization of fatty acids from peripheral adipose cells, (2) increased fatty acid synthesis by hepatocytes, (3) decreased utilization or oxidation of fatty acids, (4) increased esterification of fatty acids to triglycerides, and (5) decreased release of fat from the hepatocyte. The relative importance of these varies, but mobilization of free fatty acids from fat cells is dominant in acute toxicity. In contrast, in chronic alcohol intoxication, increased esterification and decreased release of fat are quantitatively more important. Ethanol increases **fluidity in biological membranes.** Studies with electron paramagnetic resonance and fluorescent probes detect membrane effects; for example, the initial effect is to disorder the hydrophobic core of the membrane. Membrane proteins such as critical Ca-ATPase and adenylate cyclase are sensitive to these ethanol-induced changes.

Nutritional deficiencies may complicate ethanol toxicity but are not necessary for liver lesions. In monkeys, fatty livers have been produced on a diet in which 41% of calories were derived from alcohol (control animals that had 41% contributed by sucrose did not have lesions). Addition of choline did not prevent fatty degeneration, indicating that ethanol was solely responsible.[36]

Aromatic Halogenated Hydrocarbons

Polychlorinated Biphenyls

Polychlorinated biphenyls (PCBs) are used as insulating materials in electrical transformers, in paper man-

ufacturing, and as plasticizers in waxes. Highly stable, they persist in the environment, especially in water. Because of their lipophilic nature and bioaccumulation, PCBs produce a variety of disease signs associated with enzyme induction, estrogenic activity, immunosuppression, and porphyrogenic activity. 3,4,3′,4′-**Tetrachlorobiphenyl** (TCB) impairs vitamin A metabolism in **hepatocytes.** Injected intraperitoneally (200 mg) into rats, TCB induces hepatomegaly with vesiculation of endoplasmic reticulum and megamitochondria with paracrystalline inclusions in hepatocytes. Lipid globules are markedly reduced in Ito cells. When injected, ^{3}H-TCB has been shown to accumulate in lipid globules, mitochondria, and endoplasmic reticulum.[37]

Dioxins

The family of chemicals called **dioxins**, which are byproducts of herbicide manufacture, have a basic structure: a pair of oxygen atoms joins two benzene rings, and substitution of chlorine for hydrogen on the rings produces the chlorinated dioxins; for example, 2,3,7,8-tetrachlorodibenzo-p-dioxin (TCDD) is a toxic byproduct in the synthesis of 2,4,5-T. Polychlorinated dibenzodioxins are formed during synthesis of polychlorinated phenols. They poison as contaminants of chemical products and in industrial accidents.

Dioxins bind to a cellular receptor and the dioxin-receptor complex is transported to the nucleus where it interacts with DNA. Several thousand receptors are required before a biological response occurs so that there is a dose below which the receptor does not function. In the nucleus, dioxins induce transcription of the cytochrome P450 gene; the gene product, aryl hydrocarbon hydroxylase, while it contributes to detoxification, also activates carcinogenic polycyclic aromatic hydrocarbons. The actions of dioxin are similar to those of members of the steroid receptor superfamily, especially in the manner of receptor dissociation from heat shock proteins and translocation to the nucleus. The mechanism of cell degeneration has been compared with that induced by glucocorticoids.

Tetrachlorodibenzo-p-dioxin **Tetrachlorodibenzo-p-dioxin (TCDD)** is the most potent dioxin isomer. It causes **liver damage**, porphyria, and lymphoid atrophy. Laboratory rodents vary in sensitivity to doxins. The oral LD^{50} for the guinea pig is 0.6 nm/kg body weight while that for the hamster is 2000 times greater. At very high doses over long times, dioxins are carcinogenic in rats and mice. However, rats have tolerated a daily dose of 1 mg/kg/day for 2 years without showing toxic effects. TCDD accumulates in soil.

Mitochondrial Hepatotoxins

In acute cell swelling of toxic injury, **mitochondria** undergo swelling, vesiculation of cristae, cristolysis, and fragmentation (Fig. 17.9; see Fig. 1.3). Damaged mitchondria move to and fuse with peroxisomes and lipid globules (with which mitochondria have metabolic interfaces). Mitochondrial autophagy is a common acute response (Fig. 17.10).

Mitochondrial structure in the normal hepatocyte is altered by hormones and cytokines. **Thyroid hormones** (triidothyronine, T3) and increased dietary protein increase metabolism and oxygen consumption and can augment hepatotoxicity. Thyroid hormone stimulation of cellular metabolism leads to striking changes in mitochondria and nuclei. T3 binds to intranuclear chromatin proteins associated with DNA to exert its effects on transcription. There also appears to be a mitochondria-binding protein for T3. The morphometric and stereologic ultrastructural analyses of T3 treatment on hepatocytes reveal that there are striking increases in the number of peroxisomes and mitochondria (Table 17.1). In liver, very small doses of exogenous **cortisol** will induce hypertrophy, especially in hepatocytes of the centrolobular zones within a few hours of treatment. Mitochondria are markedly increased in size but not in number.[38] Lysosomes increase, probably as a result of the stabilizing effect of cortisol on lysosomal membranes. Large doses of corticosteroids (as used in treatment of shock), or small doses given for a prolonged time, produce massive glycogen deposits in hepatocytes. Affected cells are markedly expanded by masses of glycogen, which replaces most cytoplasmic organelles. Accumulation of glycogen results from stimulation of enzymes of glycogen synthesis and of enzymes that cause amino acid degradation and gluconeogenesis.

There are multiple mechanisms that lead to dysfunction by acting on **mitochondrial DNA (mtDNa):**

- **Direct degradation** of mtDNA (ethanol, acetaminophen).
- Impairment of **mtDNA replication** by DNA intercalation or inhibition of tropoisomerases (quinolone antibiotics, tacrine, tamoxifen, pentamidine, ethidium bromide).
- Impairment of **mtDNA** by incorporation into DNA (nucleoside analogs such as fialuridine, zidovudine, stavudine).
- Decreased synthesis and stability or **mtDNA transcripts** (interferon alpha).
- Decreased translation of **mtDNA transcripts** (erythromycin, chloramphenicol)—animals deficient in mitochondrial deoxyribonucleosides

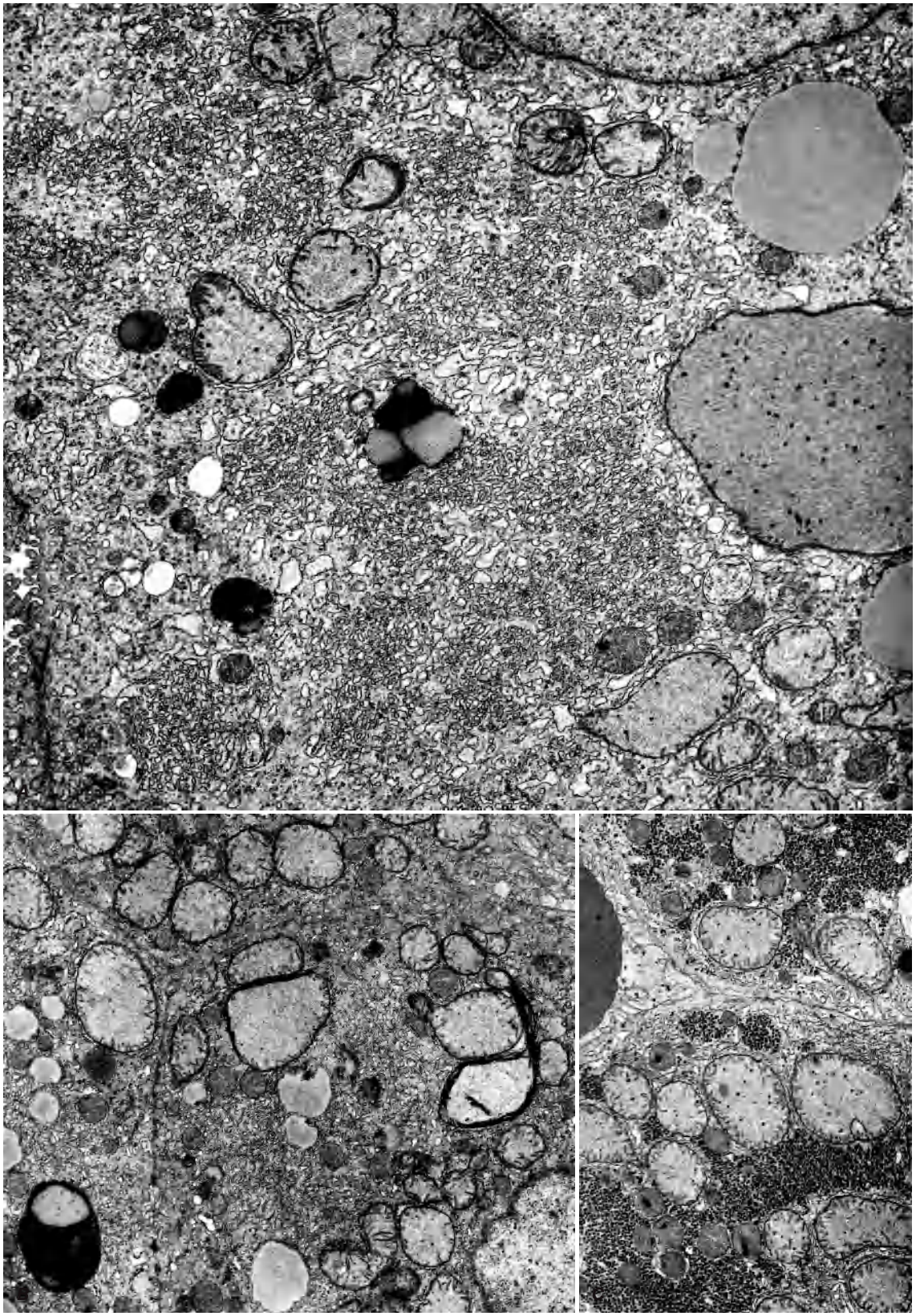


Fig. 17.9 **Mitochondriopathy**: xenobiotic drug given IM, dog. **A**. **Acute toxicity**: mitochondria are enlarged with blunted cristae and many dense granules; note the massive, degenerate mitochondrion (*center right*). Saccules of smooth endoplasmic reticulum occupy large cytoplasmic areas. Note large lipid globules, and vacuoles containing mixtures of lipids and lipofuscin. Canaliculi and associated intercellular junctions are abnormal (*lower left*). **B**. **Acute toxicity**: membrane defects in swollen mitochondria. Note absence of glycogen. **C**. **Recovery**: Peroxisomes have increased and glycogen occupies cytoplasmic areas containing SER.

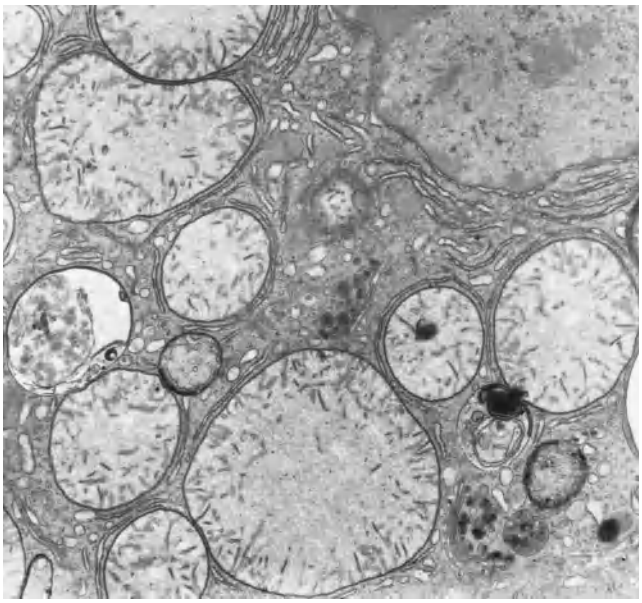


Fig. 17.10 Mitochondrial autophagy: liver, mouse, treated with emulsifier Atlox 3409 F. Mitochondrial swelling, cristolysis, dense granule depletion. Some mitochondria have dense membranous whorls that protrude into autophagolysosomes. Note dense particles in Golgi complex. (Micrograph: George Hug, *Laboratory Investigation* 45:89, 1981.)

develop mitochondriopathy and die within the first weeks of life.[39]

Mitochondrial dysfunction arising in metabolic pathways includes

- Inhibition of **beta-oxidation** (aspirin, valproic acid, tetracycline; estradiol, progesterone; glucocorticoids)
- Inhibition of **beta-oxidation** and/or **respiration** (amiodarone, tamoxifen, chloroquinone)
- **ATP synthase** inhibition
- **ANT** inhibition
- **Uncoupling of mitochondrial respiration**
- **Uncoupling protein 2** induction
- **Mitochondrial permeability transition** (e.g., salicylic acid, troglitazone)[40]

Electron transport pathways in mitochondria can be blocked at multiple sites, but whatever the site, ultimately electrons are not passed to O_2 to form water and ATP is not generated (see chapter 8). Compensation for the inefficiency of oxidative energy production by dysfunctional mitochondria results in increases in the volume of mitochondria and switching the cell to anaerobic metabolism. Common traits include enlarged mitochondria containing cristae and matrix, albeit the amounts can vary considerably. Cristae can be relatively decreased in number and size. Chloramphenicol inhibits protein synthesis leading to megamitochondria in liver. In this case, megamitochondria form from fusion, and mitochondrial numbers do not increase. Intramitochondrial filaments occur during active protein synthesis when cells are metabolically shut down, leading to inspissation of intramitochondrial proteins. These can occur secondary to other drug-induced changes.

Inhibition of liver mitochondrial β-oxidation by drugs leads to mitochondrial dysfunction, steatosis, and early necrosis. Lesions include swollen C- or O-shaped mitochondria with granular or crystalline inclusions. Drugs that inhibit mitochondrial β-oxidation do so by suppressing the enzyme carnitine palmitoyl transferase I (Etomoxir, CPI975) or others that sequester mitochondrial co-enzyme A to inhibit carnitine palmitoyl transferase II (FOX988, SD2S1–641).[41]

Free Radical Initiators

Drugs that enhance free radicals in mitochondria are potent hepatotoxins and are associated with steatosis. Reactive oxygen (ROS) and nitrogen (NOS) species damage both the respiratory chain and the mitochondrial proteome. Direct damage is especially critical at complex I of the respiratory chain. The herbicide **paraquat,** a redox cycler widely used to stimulate superoxide production in organisms, cells, and mitochondria, causes extensive mitochondrial damage at complex I.[42] When it enters the mitochondrial matrix, paraquat is reduced by complex I to form a paraquat radical cation that then reacts with oxygen to form superoxide. Many free radical initiators cause apoptosis. They generate superoxide in amounts that activate the **Trx2/Ask1 pathway**—the thioredoxin-2/apoptosis signal-regulating kinase 1 signaling pathway—that leads to mitochondrial permeabilization. **Troglitazone** produces intramitochondrial oxidant stress that actives the Trx2/Ask1 pathway to cause cell death.[43]

Nucleoside Analogues

Nucleoside analogues are associated with delayed toxicities such as peripheral neuropathy, pancreatitis and hepatitis. **Zudovidine** (AZT), **dideoxyinosine** (DDI), and **dideoxycytidine** (DDC) terminate DNA chains by inhibiting DNA polymerase τ, the enzyme for **mitochondrial DNA** synthesis. These drugs also inhibit DNA polymerase β, the enzyme involved in DNA repair, but only slightly inhibit DNA polymerases for replication of chromosomal DNA (polymerases α, δ, and ε).[44] The anti-hepatitis drug 1-(deoxyfluoroarabinofluranoxyl 5-iodo) uracil, which is incorporated into mitochondrial DNA, has caused a lethal mitochondrial hepatopathy in patients being

treated experimentally. Lesions have been reproduced in mice.[45]

Hydrazine

Hydrazine induces **megamitochondria** in hepatocytes of the rat and mouse. Ultrastructurally, affected mitochondria have short, stubby cristae and massive increases in the volume of the mitochondrial matrix. Hydrazine and its derivatives stimulate production of superoxide anions and hydroxy radicals in mitochondria and endoplasmic reticulum that lead to increased lipid peroxidation and decreased GSH. Coenzyme Q suppresses the formation of megamitochondria in rat hepatocytes by hydrazine, allegedly by scavenging free radicals.[46]

Steatosis and Hepatotoxicity

Steasosis is associated with production of reactive oxygen species (ROS) that have detrimental effects such as opening of mitochondrial permeability transition pores and release of cytochrome c into the cytosol. Steatosis occurs with metabolic perturbations such as (1) **increased uptake of lipid** mobilized from peripheral tissues; (2) **excretory defects**—the inability of cells to excrete synthesized fat; (3) **increased synthesis of fat** accompanied by decreased fatty acid oxidation; and, (4) **mitochondrial dysfunction** from uncoupling of mitochondrial respiration by free fatty acids, and impaired respiration by lipid peroxidation and TNF-α.[47–49] Representative xenobiotic-induced causes of lipid accumulation involve these multiple mechanisms: **colchicine** causes depolymerization of microtubules, leading to decreased transportation of lipoproteins from the Golgi complex to plasma membranes; **cyclohexamide** inhibits protein synthesis, leading to apolipoprotein B depletion, which interferes with formation and release of lipoproteins; **ethionine** causes decreased hepatic ATP synthesis, leading to accumulation of lipoprotein in RER and SER; **orotic acid** impairs glycoslyation of proteins; and **monensin** perturbs electrolyte ion balance.

Macrosteatosis is the accumulation of a single or few large fat droplets that displace the nucleus to the hepatocyte periphery. **Microsteatosis** is the accumulation of multiple small (generally smaller than the diameter of the hepatic nucleus) droplets of fat that do not displace the nucleus. Mixed patterns of microsteatosis and macrosteatosis can occur. In addition to xenobiotics cited previously, steatohepatitis is also associated with alcohol toxicity, certain drugs (e.g., diethylaminoethoxyhexestrol, perhexiline, tetracycline, methotrexate, amiodarone, and tamoxifen), alcohol excess, and total parenteral nutrition. Macrovesicular steatosis may be fairly benign, and can be incidental without disruption of liver function. Microvesicular steatosis potentially indicates more severe injury, and may be accompanied by hepatic dysfunction and can be an indicator of mitochondrial dysfunction. Significant hepatocellular injury and necrosis may accompany microsteatosis.[52] Ultrastructural evaluation of microsteatotic hepatocytes may identify morphologic information that can lead to identification of the mechanism of toxicity.

Hepatocyte Toxins That Act on the Nucleus

Agents that act on DNA, or on polymerases that transcribe its genetic code, produce rapid and widespread cellular change. When DNA is disrupted, structural evidence of injury occurs in **nucleoli,** ribosomes, and the Golgi complex. DNA double-strand breaks are highly cytotoxic, and affected cells are killed if they are unable to repair the injury before they enter mitosis (see chapter 6).

Nucleolar Toxins

Aflatoxins

Aflatoxins are hepatotoxic metabolites produced by certain strains of *Aspergillus flavus*. They are synthesized during growth of the fungus in feedstuffs, and poison when these feeds are ingested. The primary effect of aflatoxin is on the liver, where in most species it causes hepatocyte necrosis, fibrosis, and bile duct reduplication. Hepatomas occur in trout and hepatocarcinomas in rats.

Aflatoxins cause direct toxic effects on DNA-dependent RNA polymerase in the nucleolus, which in turn suppresses activity of RNA and protein synthesis. Ultrastructurally, studies in rats reveal that disaggregation of the nucleolus can be detected soon after treatment with aflatoxin. The appearance of numerous helical polysomes occurs within a few min of injection, and these are thought to be a special type of transient transfer RNA. Aflatoxins also affect mitochondrial DNA. They bind to liver mitochondrial DNA with preference, and may have long-lasting effects because of a lack of excision repair in the mitochondrion.[50]

DNA synthesis is affected by the affinity of aflatoxin to bind to the DNA molecule. Demonstrated in cell cultures, this inhibition allows cell survival at a nondividing stage but results in sporadic cytomegaly. Giant cells are found in livers of intoxicated animals. The inhibition of mitosis and nucleic acid synthesis is reflected in diminished incorporation of labeled precursors into cell DNA and protein.

In sublethal injury a few cells in centrolobular areas may be killed, but most hepatocytes survive with steatosis. Lesions of toxicity include reduplication of smooth endoplasmic reticulum, increases in peroxisomes, and mitochondrial swelling (Fig. 17.11). Hepatocytes in periportal areas may become hypertrophic, and cytomegaly is common in animals that survive. If aflatoxin exposure persists, the liver becomes susceptible to neoplastic change. As recovery from aflatoxin poisoning occurs, there is reduplication of bile ducts and periportal fibrosis. Collagen is deposited throughout the hepatic sinusoids, both by interstitial fibroblasts and myoepithelial cells. In some species a **venoocclusive syndrome** occurs with striking hepatomegaly, ascites, and liver changes of centrolobular congestion and fibrosis along the termini of the hepatic veins.

Hepatotoxic Drugs That Induce Cytomegaly

Hepatocytomegaly is an unusual response to toxic injury caused by some antifungal drugs. Hepatocarcinogenic drugs induce both acute liver injury and chronic neoplastic change. In rats, these toxins frequently induce cystlike lesions that lack epithelial or endothelial linings, and that histologically are multilocular cystlike complexes filled with finely granular acidophilic material.

Pyrrolizidine Alkaloids

The pyrrolizidine alkaloids are potent plant alkaloids that have been used as models for megalocytosis of the liver. After a single injection in weanling rats, marked enlargement of hepatocytes develops within 3 to 4 weeks; older rats require larger doses and repeated exposure. Rats fed a diet of 0.08% ground *Crotalaria spectablilis* seed for 8 months have small irregularly shaped livers composed of megalohepatocytes that are 2.5 times the size of normal hepatocytes. Ultrastructural changes include enlarged, irregularly shaped nuclei, organelle-filled invaginations of the nuclear membrane, and nuclear pseudoinclusions. In the cytoplasm the rough endoplasmic reticulum is decreased and there are lamellar arrays of smooth endoplasmic reticulum.

Hepatocyte Toxins That Act on the Cytoskeleton

Xenobiotic-induced disruption of the cytoskeleton interferes with normal cell function. Cytochalasins bind to actin to prevent polymerization and elongation, interfering with function. **Phalloidin** inhibits depolymerization and stabilizes actin filaments. **Colchicine** binds to a tubulin dimer to prevent depolymerization. **Vincristine** and **vinblastine** inhibit microtubule formation and induce paracrystalline aggregates of tubulin. **Taxol** promotes tubulin polymerization. **Griseofulvin** is an antimicrotubular agent that causes cholestasis but does not alter the amount and morphology of hepatic microtubules. Bile transport is integrally linked to the intracellular microfilamentous network, which is important for bile canalicular contraction and movement of bile. Disruption of the cytoskeleton can cause intracellular cholestasis.

Cytoskeletal Toxins

Microcystins

The cyanobacterium (blue-green alga, kingdom Monera) *Microcystis aeruginosa* forms surface blooms that are concentrated into thick scums by wind. Ingestion of these concentrated algae leads to signs of hepatotoxicity within 24–28 hr. Massive centrolobular hepatocyte necrosis is caused by the potent cyclic heptapeptide hepatotoxins called microcystins. Ultrastructural changes include plasma membrane invagination, loss of microvilli, and cytoplasmic vacuolation. Microcystins cause extensive surface blebbing by disrupting **microfilaments. Microcystin-LR** causes centrilobular hepatocellular apoptosis that involves hyperphosphorylation of a wide variety of cytologic proteins, resulting in cytoskeletal alterations leading to terminal cellular events.[51]

Particulate Hepatotoxins

Hepatotoxins and Microgranulomatosis

Several drugs and compounds when given intravenously accumulate in the phagocytic system of the liver, and some of these cause microgranulomas. Therapy with **iron** compounds leads to massive accumulation of iron. **Thorotrast, methyl cellulose, india ink, glucan,** and **zymosan** are known to induce foci of large granular macrophages in the liver. The macrophages contain large PAS-staining, oil red O-positive granules that ultrastructurally are shown to be phagolysosomes. Macrophages in the liver also accumulate crystalline materials (Fig. 17.12). Multinucleate giant cells derived from Kupffer cells are typical in rats poisoned by these agents. Cytochemical staining with peroxidase at the ultrastructural level show that, in glucan-induced granulomas of rats, macrophages

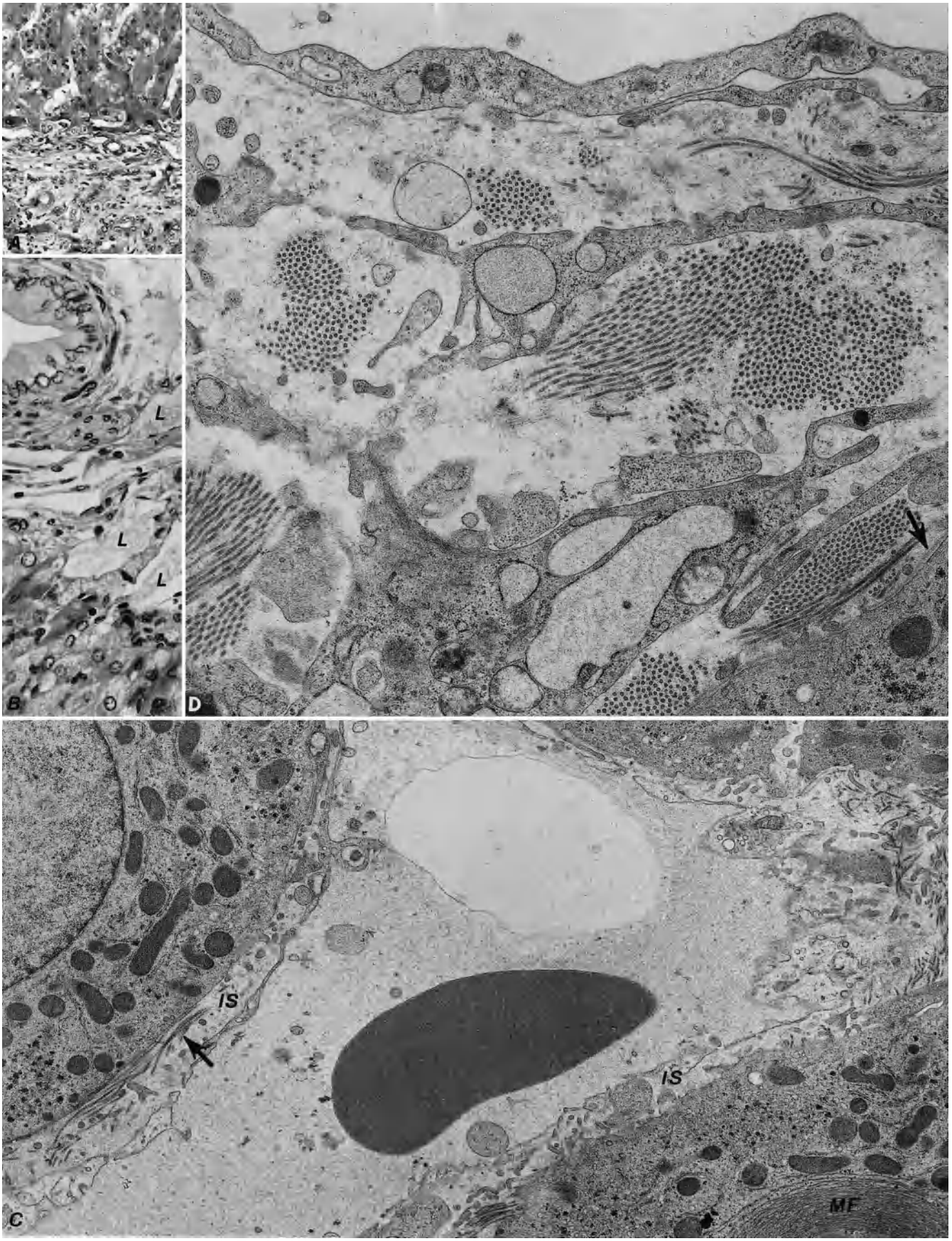


Fig. 17.11 **Periportal fibrosis**: chronic aflatoxicosis, horse. **A**. **Bile duct duplication** in area of periportal fibrosis. **B**. **Dilated lymphatics** (*L*) in portal areas. **C**. **Central vein**: expansion of intersinusoidal spaces of Disse (*IS*) and accumulation of collagen fibers (*arrow*). Myelin figures (*MF*). **D**. **Intersinusoidal spaces**: collagen fibrils cut longitudinally and in cross section. Connective tissue filaments between collagen fibrils and deposits of proteoglycans in spaces. Sinusoidal endothelium (*top*) and cytoplasmic extensions of fibroblasts (*center*). Basement membrane (*arrow*) remains apposed to hepatocyte.

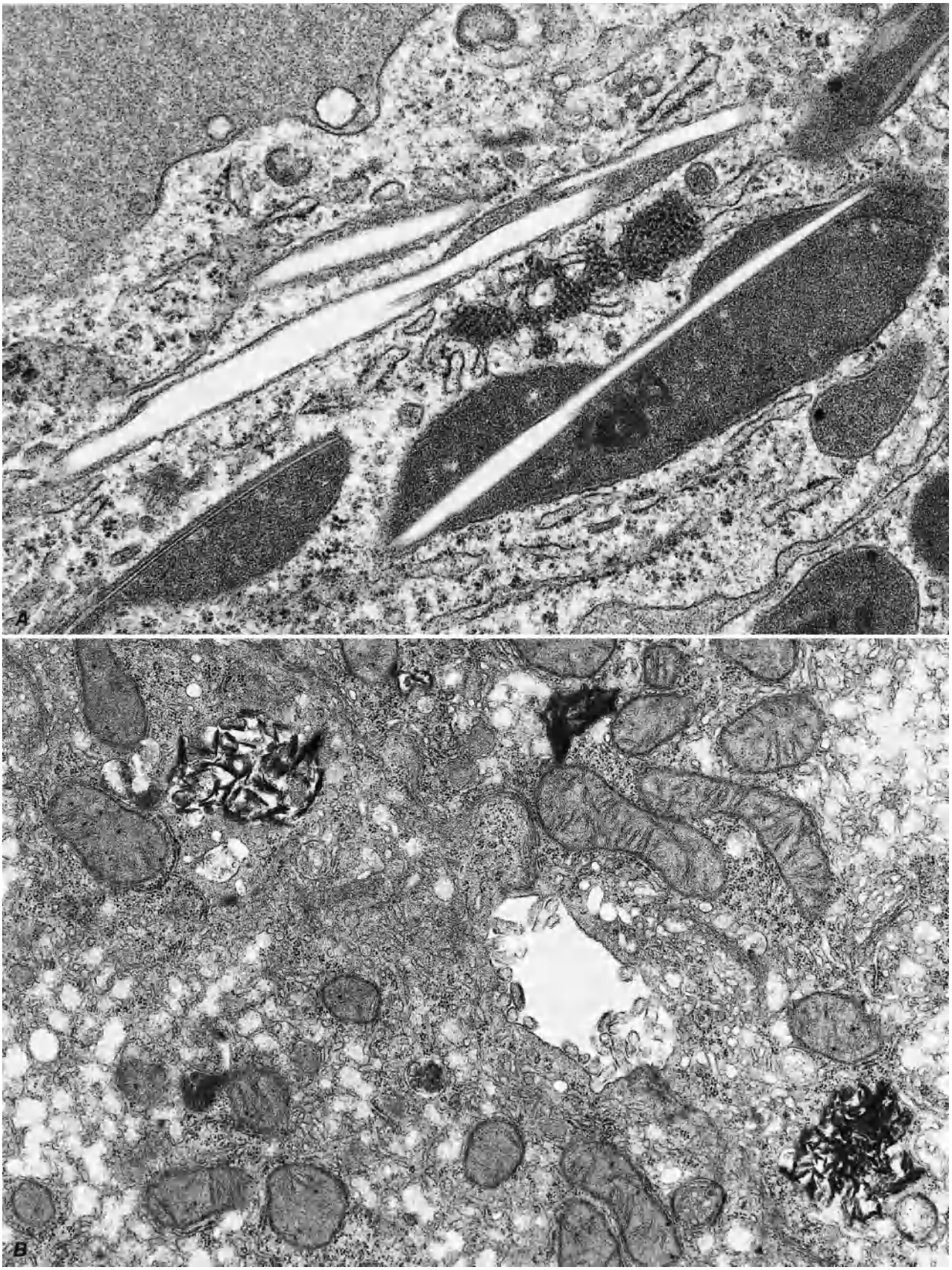


Fig. 17.12 Hepatotoxicity: **A**. **Lysosomal crystals**, dog. **B**. **Porphyrins**: small spicular aggregates. (Micrographs: Vincent Meador.)

(including giant cells) in the center of the granulomas are derived from blood monocytes.

When given orally, a potassium-sparing experimental diuretic **2,6-bis-(4-chlorophenyl)-4-pyridine carboxylic acid** has been shown to cause microgranulomatosis.[52] The drug forms complexes with cells but the exact nature of the material within the cytoplasmic phagolysosomes is not known. The catechol methyl transferase inhibitor **3-hydroxy-4-pyrone,** when fed to mice over a long period, causes periportal necrosis with lymphocytic infiltration and fibrosis in the portal tracts. Immunologic T cell cytotoxic mechanisms appear to play a role in the development of hepatic lesions, and lymphocytes are found attached to degenerate hepatocytes by gap junctions.[53]

Bile Duct Toxins and Cholestasis

Bile flows in bile canaliculi retrograde from blood flow, accumulating in bile ducts in the portal triad. In central lobular areas, bile canaliculi are small with few microvillous plasma membranes. Canaliculi diameter and the number of microvilli progressively increase the closer they are located to bile ducts. The **multidrug resistance protein 2 (Mrp2),** a conjugate export pump encoded by the Mrp2 gene, functions at the canalicular membrane surface.[54] Cholestasis commonly arises from endotoxin stimulation (Mrp2 is down-regulated by endotoxins).

Intrahepatic cholestasis can be caused by interference with microfilament-mediated canalicular motility that leads to distension of bile canaliculi, widening of the pericanalicular microfilamentous web, and loss of canalicular microvilli. Cholestasis can be caused by a number of xenobiotics: anabolic steroids, griseofulvin, chlorpromazine, and cytochalsins. The ultrastructural appearance of liver with cholestasis is rather uninformative with regards to providing additional understanding of the pathogenesis. Canaliculi are often dilated, with or without detectable contents. Microvilli may be swollen, blunted or lost. Bile canaliculi are plugged with amorphous, electron-dense material. In the periphery of the hepatocyte, a dense mat of intermediate filaments circumscribes the canaliculus as a sequelae to cholestasis. Hepatocytes may contain secondary lysosomes clustered around bile canaliculi. There can be a breakdown of the interhepatocellular junctional complexes, allowing leakage of bile into the intercellular space and into the space of Disse. This morphologic breach in the integrity of the canaliculus allows bile to leak into the blood, accounting for the increase in conjugated bilirubin seen in cholestasis.

Extrahepatic cholestasis, the accumulation of bile pigment in biliary canaliculi and bile ducts,[55] is associated with a primary hepatocellular abnormality. Drugs associated with cholestasis in humans include **chlorpromazine** and **sex steroids**, including the estrogens, methyl testosterone, and oral contraceptives. At high dose, **chlorpromazine,** the first widely used antipsychotic drug, causes hepatotoxicity with inspissated bile plugs in canaliculi between hepatocytes and in small ductules. Necrosis of bile duct epithelium is rare but has been reported to be a specific effect of some drugs; for example, **α-napthylisothiocyanate** in rats and mice. Given orally, this drug will cause necrosis of biliary epithelial cells, dilatation of ductules, and sloughing of epithelium into the biliary tree.

Porphyrin can occur in bile canaliculi and ducts. Compounds causing intrahepatic and intracanalicular porphyrin crystals are **griseofulvin** and griseofulvin analogs. These drugs cause a decrease in activity of liver porphyrin-metal chelatase, the mitochondrial enzyme that converts protophorphyrin in haem. Protoporphyrin is poorly water soluble and is secreted by hepatocytes into the bile. Aggregates of porphyrin crystals occur in bile and hepatocytes when hepatobiliary transport is overwhelmed. Crystals consist of dense aggregates of acicular crystalline structures, which can be found in hepatocellular cytosol adjacent to bile canaliculi, and in bile canaliculi, bile ducts, secondary lysosomes of Kupffer cells, and in cytosol of bile duct epithelium (Fig. 17.12).[56]

Lithocholic Acid

The monohydroxy bile acid lithocholic acid is a hepatotoxic bile acid that causes cholestatic liver injury. Feeding to rodents causes bile infarcts followed by fibrosing cholangitis. Small bile ducts are obstructed by crystals of ursodeoxycholic acid. Expression of **basolateral bile acid uptake proteins** (sodium-taurocholate cotransporter and organic anion-transporting polypeptide 1) was reduced, the **canalicular tranporters** (bile salt export pump and multidrug-related protein 2) were preserved, and the **basolateral transporters** (multidrug-related protein 3 and detoxifying enzyme sulfotransferase 2a1) were induced.[57]

Differentiation of rare bile ductule-like cells to transitional ductular cells to mature ductular hepatocytes in a model of aberrant biliary cell differentiation was demonstrated in livers of furan-treated rats. There is preferential differentiation of hyperplastic bile ductule structure along the small intestinal cell lineage in this model.[58]

References

1. Barbera-Guillem E, et al. 1990. Estimating anatomical-functional position coordinates in liver tissue. *Anat Rec* 228:267.

2. Schaff Z, Lapis K. 1990. Fine structure of hepatocytes during the etiology of several common pathologies. *J Elec Microsc Tech* 14:179.
3. Winton DJ, Flaks B. 1988. Effect of fasting on aggregation of hepatocyte rough endoplasmic reticulum in adrenalectomized and 3'MeDAB-treated rats: Quantitative electron microscope study. *Brit J Exp Pathol* 69:877.
4. Orrego H, et al. 1978. Effect of dietary proteins and amino acids on liver damage induced by hypoxia. *Lab Invest* 38:633.
5. Cardell RR, Jr. 1971. Action of metabolic hormones on the fine structure of rat liver cells. I. Effects of fasting on the ultrastructure of hepatocytes. *Am J Anat* 131:21.
6. Chanda S, Mehendale HM. 1995. Nutritional impact on the final outcome of liver injury inflicted by model hepatoxicants: Effect of glucose loading. *FASEB J* 9:240.
7. Contuk G, et al. 2005. Role of melatonin in reducing water avoidance stress-induced degeneration of the liver. *Dig Dis Sci* 50:738.
8. Oie CI, et al. 2008. Liver sinsusoidal endothelial cells are the principal site for elimination of unfractionated heparin from the circulation. *Am J Physiol Gastrointestin Liver Physiol* 294:C520.
9. Le Bail B, et al. 1990. Fine structure of hepatic sinusoids and sinusoidal cells in disease. *J Elec Micr Tech* 14:257.
10. McCuskey RS, et al. 2004. Hepatic microvascular dysfunction during evolution of dietary steatohepatotis in mice. *Hepatology* 40:386.
11. Ito Y, et al. 2007. Age-related changes in the hepatic microcirculation in mice. *Exp Gerontol* 42:789.
12. Knittel T, et al. 1999. Localization of liver myofibroblasts and hepatic stellate cells in normal and diseased rat livers: Distinct role of (myo-)fibroblast subpopulations in hepatic tissue repair. *Histochem Cell Biol* 112:387.
13. Otagawa K, et al. 2007. Erythrophagocytosis by liver macrophages (Kupffer cells) promotes oxidative stress, inflammation, and fibrosis in a rabbit model of steatohepatitis. *Am J Pathol* 170:967.
14. Bannasch P, et al. 1981. Spongiosis hepatis. *Lab Invest* 44:252.
15. Kaiserling E, Müller H. 2005. Neoplasm of hepatic stellate cells (spongiotic pericytoma). *Pathol Res Pract* 201:733.
16. Lemire JM, et al. 1991. Oval cell proliferation and the origin of small hepatocytes in liver injury induced by D-galactosamine. *Am J Pathol* 139:535.
17. Wisse E, et al. 1989. Cells of the Hepatic Sinusoids. Vol. 2. Kupffer Cell Found., Rijswijk, Netherlands.
18. Halliwell WH. 1997. Cationic amphiphilic drug-induced phospholipidosis. *Toxicol Pathol* 25:53.
19. Guiqi B, et al. 1988. Amiodarone-induced hepatic phospholipidosis. *Hepatology* 8:1063.
20. Glauman H, et al. 1992. Intracellular distribution and effect of the antimalarial drug mefloquine on lysosomes of rat liver. *Liver* 12:183.
21. Grave S, et al. 1992. Induction of mucopolysaccharidosis in rats by treatment with immunostimulatory acridine derivatives. *Toxic Appl Pharmacol* 114:215.
22. Keller GA, et al. 1989. Subcellular localization of sterol carrier protein-2 in rat hepatocytes: Its primary localization in peroxisomes. *J Cell Biol* 108:1353.
23. Hruban Z, et al. 1974. Effects of some hypocholesterolemic agents on hepatic ultrastructure and microbody enzymes. *Lab Invest* 30:474.
24. Khan KNM, Alden CL. 2002. Kidney. In: Haschek WM, et al., eds. Handbook of Toxicologic Pathology, 2nd ed. Academic Press, New York. Vol. 2:255.
25. Wanders RJA. 2004. Metabolic and molecular basis of peroxisomal disorders. *Am J Medical Genetics* 126A: 355.
26. Battelli MG. 2004. Cytotoxicity and toxicity to animals and humans of ribosome-inactivating proteins. *Mini-Reviews in Medic Chem* 4:513.
27. Roberts DW, et al. 1991. Immunohistochemical localization and quantification of the 3-(cystein-S-yl)-acetaminophen protein adduct in acetaminophen hepatotoxicity. *Am J Pathol* 138:359.
28. Prydz K, et al. 1992. Effects of brefeldin A on endocytosis, transcytosis, and transport to the Golgi complex in polarized MDCK cells. *J Cell Biol* 119:259.
29. Tooze J, Holllinshead M. 1992. In AtT20 and HeLa cells brefeldin A induces the fusion of tubular endosomes and changes their distriction and some of their endocytic properties. *J Cell Biol* 118:813.
30. Todarov IN. 1977. Control of RNA synthesis in rat liver. *Biochemistry* 1:150.
31. Guengrich FP. 2007. Cytochrome P450 activation of toxins and hepatotoxicity. In: Kaplowitz N, Deleve LD. Drug-Induced Liver Disease, 2nd ed. Informa Healthcare, New York.
32. MacDonald JS, Halleck MM. 2004. The toxicology of HMG-CoA reductase inhibitors: Prediction of human risk. *Toxicol Pathol* 32(Suppl 2):26.
33. Stalker A, et al. 1991. Subcellular distribution of [3H]-dexamethasone mesylate binding sites in Leydig cells using electron microscope radioautography. *Am J Anat* 190:19.
34. James JL, et al. 1986. Alternations in hepatocyte plasma membrane in carbon tetrachloride poisoning. *Lab Invest* 54:268.
35. Nakatsukasa H, et al. 1990. Cellular distribution of transforming growth factor-β1 and procollagen types I, III, and IV transcripts in carbon tetrachloride-induced rat liver fibrosis. *J Clin Invest* 85:1833.
36. Ruebner et al. 1972. Production of fatty liver by ethanol in rhesus monkeys. *Lab Invest* 27:71.
37. Durham SK, Brouwer A. 1989. 3,4,3',4'-tetrachlorobiphenyl-induced effects in the rat liver. II. Electron microscopic and autoradiographic localization of 3H-TCB. *Toxicol Pathol* 17:782.
38. Badylak SF, Van Vleet JF. 1982. Tissue gamma-glutamyl transpeptidase activitiy and hepatic ultrastructural alterations in dogs with experimentally induced glucocorticoid hepatopathy. *Am J Vet Res* 43:649.
39. Zhou X, et al. 2008. Progressive loss of mitochondrial DNA in thymidine kinase 2 deficient mice. *Hum Mol Genet* [E-pub].
40. Matsubuchi Y. 2006. Metabolic and non-metabolic factors determining troglitazone hepatotoxicity. *Drug Metabl Pharmacolkinet* 21:347.
41. Vickers AE, et al. 2006. Consequences of mitochondrial injury induced by pharmaceutical fatty acid oxidation

inhibitors is characteristic in human and rat liver slices. *Toxicol In Vitro* 20:1173.
42. Cochemé HM, Murphy MP. 2008. Complex I is the major site of mitochondrial superoxide production by paraquat. *J Biol Chem* 283:1786.
43. Lim PL, et al. 2008. The mitochondrial superoxide thioredoxin-2/Ask 1 signaling pathway is critically involved in troglitazone-induced cell injury to human hepatocytes. *Toxicol Sci* 101:341.
44. Parker WB, Cheng YC. 1994. Mitochondrial toxicity of antiviral nucleoside analogs. *J NIH Res* 6:57.
45. Walker DM, et al. 2004. Persistence of mitochondrial toxicity in hearts of female B6C3F1 mice exposed in utero to 3'-azido3'-deoxythymidine. *Cardiovasc Toxicol* 4:133.
46. Adachi K, et al. 1995. Suppression of the hydrazine-induced formation of megamitochondria in the rat liver by coenzyme Q_{10}. *Toxicol Pathol* 23:667.
47. Cogger VC, et al. 2004. The effects of oxidative stress on the liver sieve. *J Hepatol* 41:370.
48. Passayre D. 2007. Role of mitochondria in non-alcoholic fatty liver disease. *J Gastroenterol Hepatol* 22(Suppl 1): S20.
49. Fromenty B, et al. 1997. Microvesicular steatosis and steatohepatitis: Role of mitochondrial dysfunction and lipid peroxidation. *J Hepatol* 26:13.
50. Nirangjan BG, et al. 1981. Preferential attack of mitochondrial DNA by aflatoxin B_1 during hepatocarcinogenesis. *Science* 215:73.
51. Hooser SB. 2000. Fulminant hepatocyte apoptosis in vivo following microcystin-LR administration to rats. *Toxicol Pathol* 28:726.
52. Mesfin GM, et al. 1992. Drug-induced microgranulomatosis in cynamolgus monkeys. *Tox Pathol* 20:7.
53. Kitamura K, et al. 1992. Pathology of chemically induced chronic active hepatitis in mice. *Exp Mol Pathol* 57:153.
54. Dombrowski F, et al. 2000. Electron microscopic demonstration of multidrug resistance protein 2 (MRP2) retrieved from the canalicular membrane in response to hyperosmolality and lipopolysaccharide. *Biochem J* 348 Pt 1:183.
55. Belli DC, et al. 1991. The effect of taurine on the cholestatic potential of sulfated lithocholate and its conjugates. *Liver* 11:162.
56. Nakanuma Y, et al. 1998. An autopsy case of erythropoeitic protophyria with cholestatic jaundice and hepatic failure, and a review of the literature. *Virch Arch* 393:123.
57. Fickert P, et al. 2006. Lithocholic acid feeding induces segmental bile duct obstruction and destructive cholangitis in mice. *Am J Pathol* 168:410.
58. Sirica AE, et al. 1994. A unique rat model of bile ductular hyperplasia in which liver is almost totally replaced with well-differentiated bile ductules. *Am J Pathol* 144: 1257.

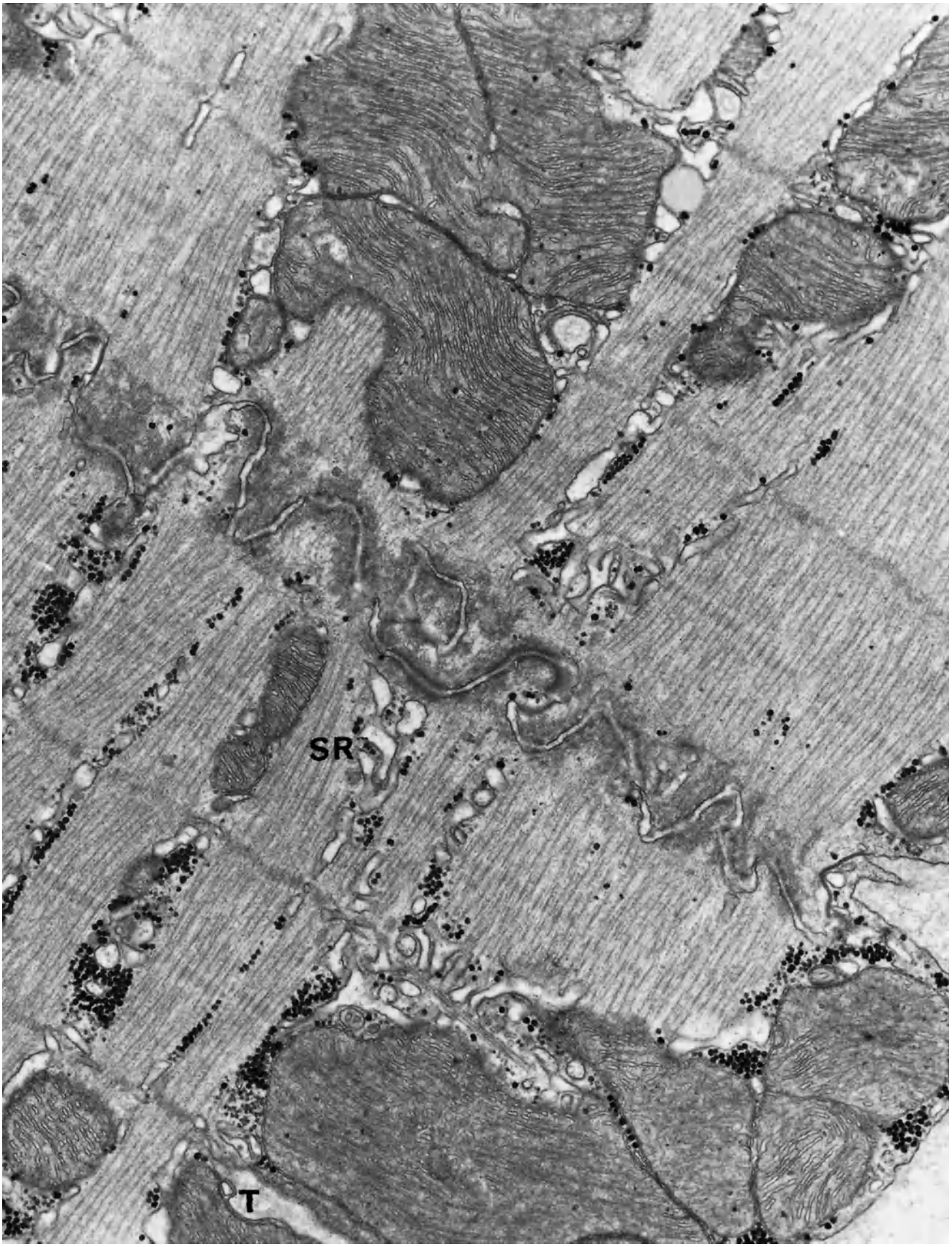


Fig. 18.1 Cardiotoxicity; reserpine-treated bat. Increase in glycogen, swollen T system (*T*) and sarcoplasmic reticulum (*SR*). (Micrograph: Hagopian M., *Lab Invest* 27:99, 1972.)

© 2009 Wiley-Blackwell. ISBN: 978-0-813-80330-2

18 Myotoxins

James T. Meehan

Cardiotoxicity

Normal Myocardium

Normal striated myofibers of the heart have several distinctive structural characters: **mitochondria** are large and have closely spaced cristae; **intercalated discs** form end-to-end connections between cells; **nuclei** are elongate and located centrally in the cell; **myofibers** bifurcate to form a complex network; **myofilaments,** thick and thin, are not organized in distinct myofibrils; and **sarcoplasmic reticulum** is arranged in rows. Myofilaments and sarcoplasmic reticulum are often the first to be altered in cardiotoxicity (Fig. 18.1).

The **sarcomere** extends from one Z line to the next. Thin actin and thick myosin filaments insert between and overlap each other. Deep-etch replica analysis after removal of actin and myosin reveals a third strand, titin (elastic filaments), that extends from M to Z lines (half a sarcomere) and connects myosin to the Z line. Desmin connects Z lines to the plasma membrane.[1,2]

During contraction, the ends of the actin filaments slide deeply into the A band between the myosin filaments. Z lines, to which the actin filaments are attached, are drawn closer together, shortening the myofibril. During relaxation, actin filaments are withdrawn from the A band and the sarcomere is lengthened. Structural analysis of the sarcomere involves examination of the integrity of the myofilaments, the apposition of Z lines, the structure of the sarcoplasmic reticulum and mitochondria, and the length of individual sarcomeres. Z-line streaming is diagnostic of myocyte degeneration (Figs. 18.2 and 18.3). Sarcomere length is a function of ventricular filling pressure, and changes in filament extension are characteristic of the failing heart.

Cardiac myofilaments are not organized into discrete myofibrils as in skeletal muscle. They exist as cylindrical bundles incompletely subdivided into irregular fascicles by deep incisures and fusiform clefts of sarcoplasm. Each myocyte is separated by an intercalated disk, the integrity of which is essential in contractility.

Intercalated disks are specialized cell-to-cell adhesion zones that are composed of unique proteins.[3] Connecting individual myofibers, these junctions facilitate and maintain tissue stability during contraction. The intercalated disk becomes detached during myocardial injury. Separation of membranes occurs when there is hypoxia or hypothermia.[4,5] During hypothermia in hibernating animals, normal structure is maintained.[6]

Myofibers are anchored at long surfaces to the basement membrane. Most attachments occur at **subsarcolemma densities,** foci of electron-dense granular material along the sarcolemma (in the cytoplasm) from which fine filaments run through the lamina rara to anchor in the lamina densa of the basement membrane. Vinculin is enriched at these sites, especially in regions of neuromuscular and myotendinous junctions. Dystrophin-glycoprotein complex connects myofibrils to the sarcolemmal and extracellular matrix, adding strength to the muscle.[2,7]

Atrial myofibers tend to be smaller than ventricular fibers and are less uniform in arrangement. They have specific secretory granules called **atrial granules,** which vary from 0.3 to 0.4 μm in diameter.[8] Located in perinuclear regions in the center of the cell, atrial granules are the source of natriuretic peptides such as atriopeptin, which is released in response to increases in vascular volume.

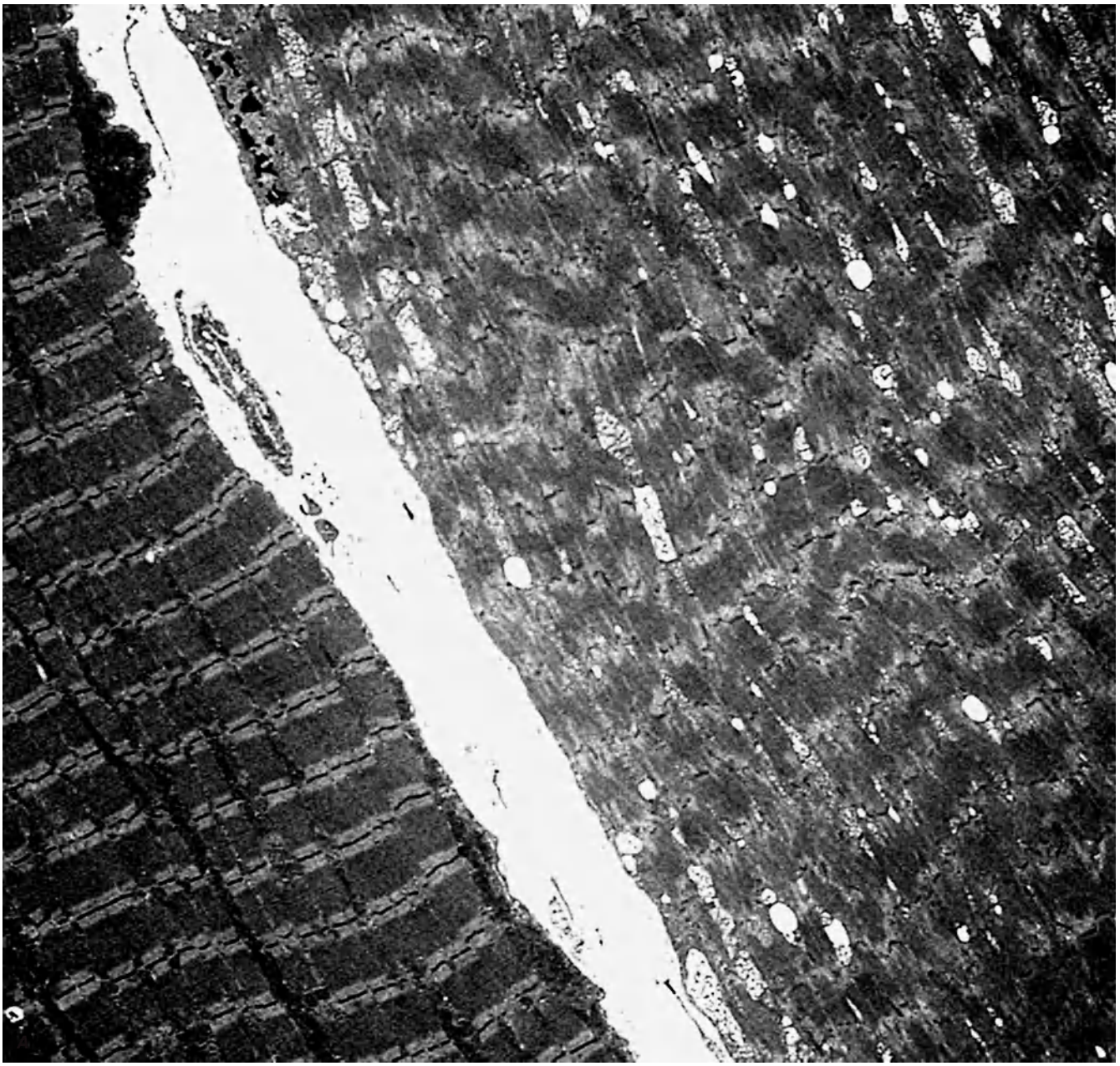


Fig. 18.2 Degenerate skeletal myofiber: rat. **A**. **Sarcomere disruption**: vacuolation is a result of mitochondrial swelling with marked cristolysis of both subsarcolemma and intermyofibril mitochondria, and dilation of sarcoplasmic reticulum. **B**. **Diffuse mitochondrial degeneration**: sarcoplasmic reticulum dilation and myofibril degeneration with segmental loss of sarcomers and multiple foci of Z line streaming (*arrows*); nucleus (*bottom*) is necrotic. **C**. **Mitochondrial swelling**: cristolysis and electron-dense inclusions (*arrow*). Dilated sarcoplasmic reticulum (*upper left*).

Organelles of the Cardiac Myocyte

Mitochondrial metabolism, number and location in the myofibers differ between muscle fiber types.[9] The differences in metabolism between myofiber types establish different levels of sensitivity to insults. This consideration is crucial for skeletal muscle so that susceptible fibers are included in the samples to be evaluated.[10,11] Mitochondria in cardiac muscle cells are distributed linearly in spaces between myofibrils and subjacent to the sarcolemma. In vitro work has shown differences in the character of these two populations of mitochondria.[12,13] **Glycogen** in the mitochondrial matrix is common in the abnormal heart, especially in hearts experiencing ischemia and vascular disease. It has been reported in dogs killed several weeks after prolonged anoxic cardiac arrest induced experimentally.[14] Mitochondria are the primary sites of injury in



Fig. 18.2 *Continued*

shock[15] and a number of myocardial toxins. In acute ischemic myocardial injury their structure may be markedly altered by drugs used to treat these conditions.[16]

Loss of the mitochondrial membrane potential and permeabilization of the mitochondrial outer membrane are the points of no return and lead to cell death if critical numbers of mitochondria are affected and the primary insult is not corrected. Where mitochondria are the primary target of the insult the degree of mitochondrial damage can determine the type of cell death (necrosis vs. apoptosis). Damage from ischemia is the result of changes that occur during the ischemia and in instances where perfusion is re-established a very significant amount of damage occurs from ischemia-reperfusion (IR). Multiple factors are involved in the damage from ischemia and IR; decreased ATP, altered pH, increased reactive oxygen

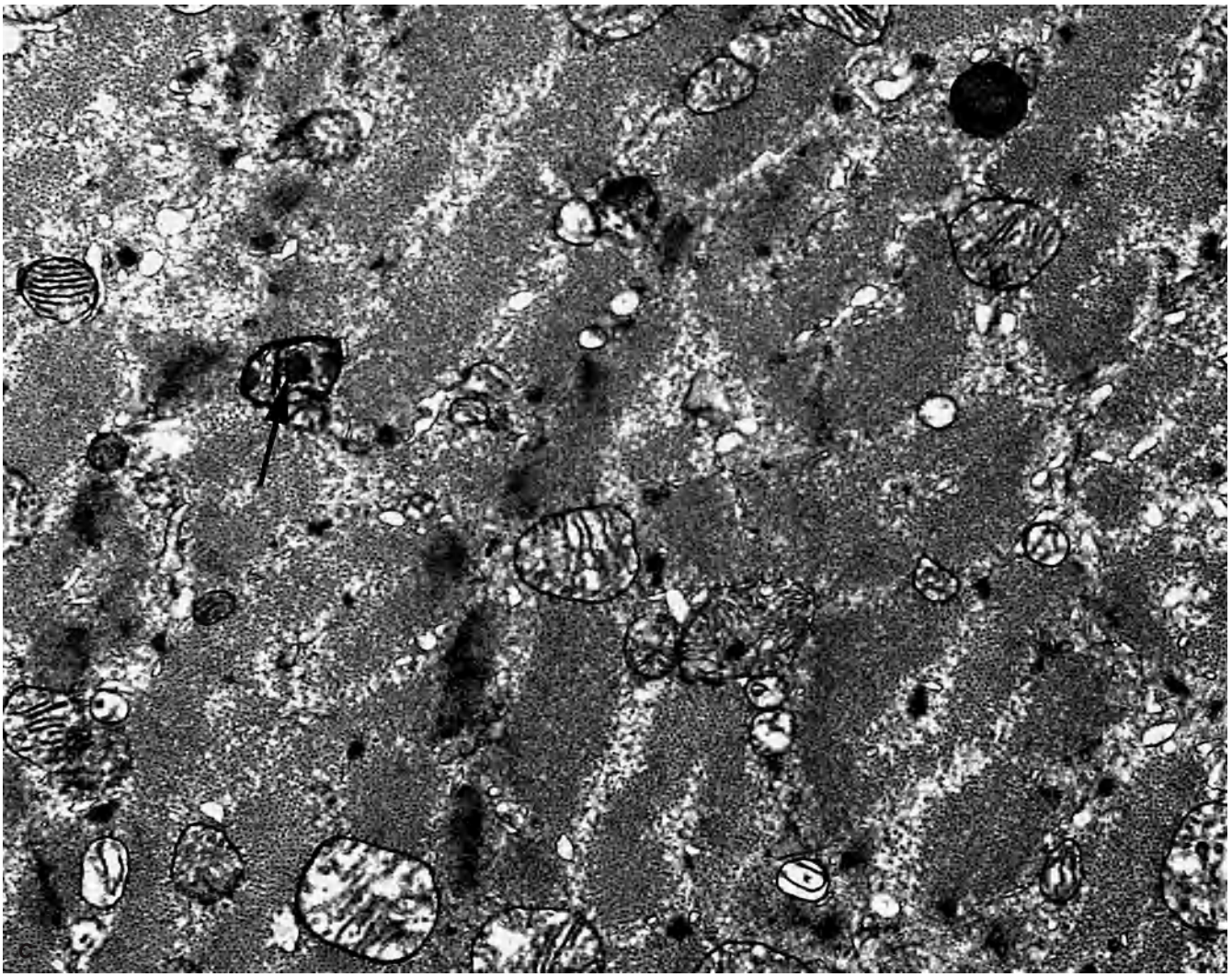


Fig. 18.2 *Continued*

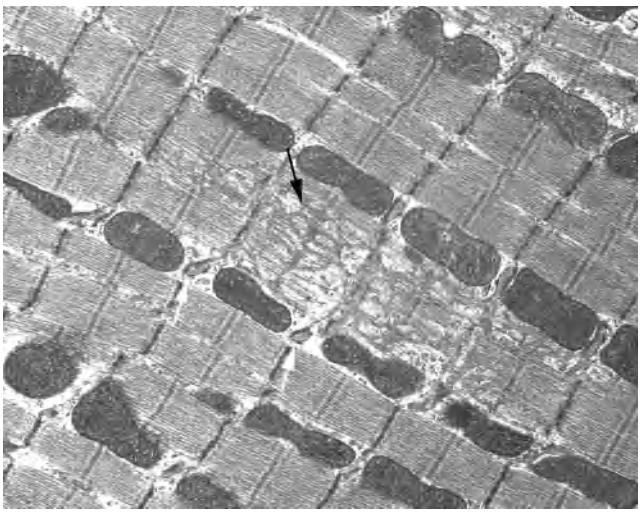


Fig. 18.3 Anastomosing sarcoplasmic reticulum (*arrow*): normal rat. Junctional triads with T tubules.

species (ROS), the positive feedback of ROS on mitochondria causing a ROS-induced ROS release (RIRR), altered sodium and calcium homeostasis and protease activation. Of these one of major concern with regards to mitochondria damage is ROS. A common mediator of the adverse effects of many of these factors is the mitochondrial permeability transition (MPT) pore.[17,18] The functional changes are reflected in the mitochondrial swelling and cristolysis seen in many different insults. Ultrastructural mitochondrial changes can be easily introduced postmortem and this must be considered during the ultrastructural interpretation.

Golgi complexes in the perinuclear region of the myocyte release primary lysosomes and other granules. Peroxisomes, although rarely encountered in ultrastructural examination, are present and smaller than peroxisomes in hepatocytes.[19] **Lysosomes,** which are involved in autophagy in toxic injury, take up and

degrade senescent cellular organelles, particularly mitochondria, lipid globules, and myofilament components. A second type of lysosome, with membranous matrices, is reported to originate from sarcoplasmic reticulum and smooth endoplasmic reticulum in the mitochondrial rows along myofilament bundles. Lysosomes are especially important in recycling membranes of the sarcoplasmic reticulum, and other membranes that require continual reformation.

Sarcoplasmic Reticulum

The sarcoplasmic reticulum (SR) of cardiac muscle is composed of three structurally distinct regions: (1) network SR, anastomosing networks of sarcotubules that surrounds myofibrils; (2) corbular SR, areas of cisternal expansion of the network SR that are not closely apposed to sarcolemma or T tubules, and (3) junctional SR, which has peripheral and interior parts. The junctional and corbular SRs are specialized domains extending from the network SR; they contain electron-dense material in spaces adjacent to the central region of the I band. Junction SR is connected either to T tubules or to sarcolemma via foot structures. Corbular SR is not, but it is the site of calcium release via ryanodine receptors during excitation-contraction coupling.[20,21]

The sarcoplasmic reticulum is the site for sequestration, storage and sudden release of Ca^{++} in response to plasma membrane excitation, calcium induced calcium release (CICR). Nonjunctional parts are involved primarily in Ca^{++} uptake; 90% of its membrane proteins are Ca^{++} ATPase. The **T system,** a tubular invagination of the sarcolemma, penetrates the center of the myofiber and is located near the Z lines. The inner surfaces of T tubules contain the same membrane proteins and glycoproteins as the sarcolemma. The T system of organelles is devoted to the distribution of calcium and other ions throughout the myofiber.

Junctional triads (Fig. 18.3) are sites of interaction of sarcoplasmic reticulum and T tubules—proteins involved in excitation-contraction coupling. On the T tubule side, release of Ca^{++} is coupled to T tubule membrane depolarization, the mechanisms of which involve voltage-sensing molecules on the T side of the junction. Junctional parts of the SR contain calcium-releasing channels, which are specialized gap junctions composed of ryanodine receptor proteins in skeletal muscle.[22]

Rapidly exchanging calcium storage sites have three components: (1) **Ca^{++}-ATPase,** the Ca^{++} uptake system, which actively transports Ca^{++} from the myofibril to the lumen of the SR during relaxation; (2) **calcium channels** that are regulated for rapid Ca^{++} release; and (3) **calsequestrin,** a low-affinity high-capacity calcium binding protein to keep free Ca^{++} relatively low, permitting calcium loading with no excess formation and thus avoiding precipitation of calcium phosphate. Ultrastructural localization of ATPase in rat cardiac muscle by immunolabeling shows that it is uniformly distributed throughout the SR membrane and is also present in foci in junctional SR near the T tubular system.[23] In cardiac muscle, calsequestrin is strategically concentrated at terminal cisternae, close to ryanodine receptors.[24,25] Calsequestrin is altered by the entry of calcium through the plasmalemmal voltage-dependent calcium channels. The calcium binding to calsequestrin alters the interaction among triadin, junctin, and ryanodine receptor (RyR) proteins, which in turn stimulates the release of calcium from the SR. As the calcium concentration in the SR lumen decreases, the calsequestrin, triadin, junctin interaction reverts to a state that is inhibitory to RyR channel complex, preventing the further release of calcium.[26,27] Obviously strict control of calcium levels is critical for effective contraction. Levels of triadin and junctin are decreased in failing humans. It is not determined if these decreased levels are a cause or a consequence of the heart failure.[28]

Following stimulation of the plasma membrane the calcium induced calcium release (CICR) from the SR causes increased intracellular calcium levels responsible for the excitation contraction coupling. The calcium interacts with troponin C, which is part of the regulatory complex on myofilaments, to produce a conformational change in this inhibitory complex that allows actin and myosin to interact, cross bridges to form, and initiate contraction. Relaxation occurs when calcium dissociates from the contractile apparatus and is resequestered by the energy-dependent calcium pump of the SR. The excitation contraction coupling is slightly different between cardiac and skeletal muscle with respect to the manner in which the initial increase in cytosol calcium leads to an RyR mediated CICR.[2]

For effective myofiber contraction there must be synchronization between the CICR and the ATP available. Demonstrating a structure function relationship this synchronizing is accomplished by the proximity of the junctional SR to the mitochondria and the presence of RyR proteins in the inner mitochondrial membrane. The RyR proteins allow the mitochondria to take up calcium during the excitation contraction event. This elevated mitochondrial calcium activates dehydrogenases, which drive the mitochondria TCA cycle increasing ATP production to power the myofiber contraction.[29–31]

Cardiac Conduction System

The **cardiac conduction system** maintains the heartbeat. Modified muscle cells function to generate the

stimulus for contraction in the heart and to carry it throughout the myocardium. The components of this system are the **sinoatrial node,** and **atrioventricular node,** and the **atrioventricular bundle** (bundle of His). **Purkinje fibers** of the atrioventricular bundle are larger than cardiac myocytes, have one or two nuclei in a clear central sarcoplasm, and are rich in glycogen and mitochondria but are poor in myofibers.

The peripheral nervous system exerts neural control of cardiac muscle. The heart is extensively innervated with extensions of the parasympathetic (vagus) and sympathetic divisions of the autonomic nervous systems. Stimulation of the vagal nerve slows the heart, and release of norepinephrine from sympathetic nerve endings accelerates it (nerve fibers do not form specialized endings resembling myoneural junctions of skeletal muscle). Large numbers of unmyelinated nerve fibers are close to the nodal and conduction tissues. Many unmyelinated fibers are also closely related to cardiac fibers in both the atrium and ventricle. Release of granulated vesicles from these sympathetic fibers exerts a direct effect upon cardiac muscle.

Purkinje cells undergo vacuolation in response to acute injury. They are affected in myocardial infarction but rarely described in studies on myocardium. Ultrastructural changes in infarction include vacuolation of the sarcoplasmic reticulum, supercontraction of myofibrils, and dissociation of intercalated disks.[32]

Myocardial Vascular System

The **myocardial vascular system** follows the planes of myofibers. The coronary artery receives fresh arterial blood as it leaves the left ventricle, therefore, toxins in portal venous and vena caval blood are exposed to the metabolic enzymes of the liver and pulmonary capillary bed before reaching the heart. This metabolism can either detoxify or generate toxic metabolites. In addition to direct effect of toxins on the myocardium, cardiac failure associated with toxicosis can occur secondary to peripheral vascular lesions, which alter vascular resistance. Additionally cardiac myocyte damage can result from excessive neuronal activity.

Capillary endothelium responds to all injuries to myocardium. Vascular cytochrome P450 enzymes are a recently recognized factor influencing the effects of stimuli on both endothelium and underlying smooth muscle.[33] Changes of acute cell swelling and of hypertrophy are common. Ultrastructural changes are especially confusing in shock[15] and metabolic disease.[34] Viruses commonly infect endothelial cells. Differentiating virions from nonviral particles is a common problem. **Tubuloreticular structures** have been reported in human myocardium, but only in endothelial and interstitial cells. These structures appear as curved or undulating tubules 20–30 nm in diameter, are branched extensively, and form net-like masses within cisterns of endoplasmic reticulum or within perinuclear cisternae.[35]

Hypertrophy of the Cardiac Myocyte

Cardiac hypertrophy, which occurs largely as ventricular hypertrophy, can be physiologic or pathologic in response to pressure or volume overload. When an increased workload is imposed on the heart, the ventricular wall enlarges, principally through myocyte hypertrophy and interstitial cell hyperplasia. Although ventricular weight and thickness increase, the number of myocytes remains the same.[36] In physiologic hypertrophy there is a proportional increase in both length and width of the cardiac myocytes. In pathologic eccentric hypertrophy with dilated cardiomyopathy the sarcomeres are added in series and there is a relatively greater increase in length than width of the myocytes. During pressure overload and concentric hypertrophy the sarcomere units are added in parallel causing a relative increase in width of the myocyte.[37] The types of hypertrophy reflect differences in the underlying gene activation such as re-expression of fetal genes including those coding for atrial natrietic peptide and brain natriuretic peptide and molecular signaling. Cytoskeletal components and their interaction with the extracellular matrix have been demonstrated to have an important role in the pathology of cardiomyopathies. In pathologic hypertrophy fibrosis occurs, as a result of the accumulation of Type I collagen.[37,38] Increased myocyte apoptosis is associated with pathologic cardiac hypertrophy and some toxicosis.[37,39]

Changes of cardiac myocyte hypertrophy occur chiefly in two organelles: **mitochondria** and **myofilaments.**[36,40] Changes in the Z band have been reported in ventricular myofibers of hypertrophied hearts in dogs. Hypertrophied myofibers of human hearts are characterized by enlargement with a progressive increase in noncontractile organelles, especially lipofuscin bearing phagosomes. Mitochondria can rapidly enlarge in response to increased workloads, and enlargement is characteristic of early hypertrophy. Larger fibers may be binucleate.[41–44] Myofibers of the left ventricle of human patients with atrial septal defects are hypertrophic. Myofibers greater than 25 μm in diameter are considered hypertrophic and characteristics of hypertrophy become greater with an increase in myofiber size.[45]

Experimentally, morphometric analysis of hypertrophic myocardium shows that the early change within the first week after application of the stimulus causes an increase in myofibrillar volume relative to mitochondrial volume.[46] This balance is restored as

hypertrophy proceeds. The ultrastructural appearance of hypertrophied myocardium varies with the stage of cardiac enlargement. In early growth or stabilized phases, cardiac myocytes are enlarged and have increases in myofilaments, mitochondria, and sarcoplasmic reticulum volumes. In contrast, in the terminal stage of dilatation and exhaustion, hypertrophic myocytes may degenerate so that these cells appear dark with loss of thick filaments, clumping and streaming of Z band material, and proliferation and dilatation of sarcoplasmic reticulum. In human cardiac hypotrophy, 38% of cases show these degenerative changes.[47]

Autophagy may accompany severe hypertrophy, but lysosomal enzymes measured in homogenates of failing dog hearts do not differ from normal.[48]

Hyperplasia of capillary endothelial cells[49,50] and hypertrophy of the cardiac conduction system[51] accompany myocardial hypertrophy.

Chronic myocardial hypertrophy is studied experimentally in animals with aortic stenosis produced by placing a band around the ascending aorta, in chronic swimming experiments in rodents, and in renal hypertension. Aortic stenosis in dogs causes the mitochondria to myofilament ratio to oscillate. Dogs (whose normal ratio is 0.42) show increased values at 3–6 days after surgery but decreased ratios develop and persist until the 25th week, when elevated values are again found.[52]

Morphometric studies of hypertrophic cat myocardium (induced by constriction of the aorta) show that mitochondrial volume is first low (relative to myofibrillar volume), then higher, and finally, in chronic hypertrophy, low again.[46] Late stages of hypertrophy are characterized by reduced surface density of the T tubular system and junctional systems.

Ultrastructural features of cardiocyte cell death in ventricular tissue of dogs with chronic heart failure induced by multiple intracoronary microemboli were intact sarcolemma, intact inner organelles, segregation of nuclear chromatin into delineated masses around the nuclear envelope, cytoplasmic shrinkage, blebbing and nuclear fragmentation, and eventual complete disorganization of inner organelles and disappearance of nucleolemma.[53]

General Responses to Toxic Injury

Most myotoxins are metabolic poisons that attack the highly specialized mechanisms for energy production, electrolyte balance, antioxidation or protein synthesis (Table 18.1 and see Table 18.3). The cardiac myocyte does not have large areas of detoxifying SER and protects itself from the constant production and release of oxygen radicals (from constantly interacting myofilaments) through mechanisms of reduced glutathione, catalase, and heme oxygenase activity.[54,55]

Myofibrillar degeneration, also referred to as myocytolysis, is a major lesion in injury to cardiac myocytes. Histologically, affected myofibers lack striations and are pale and acidophilic. Ultrastructurally, the myofibrils are detached from the insertions on the Z lines and A bands aggregate into masses in the sarcoplasm.[56] When there is limited necrosis the myofiber is affected segmentally. Condensation of the myofibrils in the degenerate portion of the fiber forms a cap acting as a barrier to excessive calcium entry into the viable remnant thus limiting the detrimental effects of the insult responsible for the lethally elevated intracellular level of calcium.[57]

Ischemia can be a complicating factor in myocardial toxicity, chiefly if the cardiac vascular system is damaged. Normal myocardium derives most of its energy from oxidation of fatty acids. This process declines rapidly in ischemia because of suppression of carnitine palmityl CoA, the mitochondrial enzyme catalyzing oxidation of fatty acids. As a result, long-chain fatty acid acyl-CoA esters accumulate and inhibit predecessor pathways in the cytosol. Free fatty acids accumulate and, if the cell survives, are shunted into triglycerides, which accumulate as **lipid globules.** This conversion increases oxygen requirements, which in turn affect the mitochondrial oxidation process. The immediate cytopathologic change in the acutely hypoxic cardiac myocyte occurs in mitochondria. The accumulation of triglycerides with cardiac myocytes may have damaging effects as demonstrated in Zucker diabetic fatty rats where the accumulation of triglycerides in cardiac myocytes, evident electron microscopically, is proposed to exert a toxicity through the induction of apoptosis and loss of cardiac function.[58]

Ischemia caused by occlusion of coronary arteries results in an injury that has a characteristic pattern of myodegeneration. The subendocardial zone is the least perfused and therefore more susceptible to ischemic episodes. The major events that occur during reflow after 40 minutes of experimental myocardial ischemia in dogs are: (1) myocardial cell swelling with separation of organelles, (2) glycogen depletion, (3) mitochondrial swelling and degeneration, and (4) interstitial edema.[59–62] Lysosomes are activated and autophagolysosomes develop as a response to infarction.[63] As discussed previously reperfusion injury accentuates the tissue damage from ischemia. Amelioration of reperfusion injury is achieved through pharmacologically induced inhibition of autophagosome and proteasome degradation[64–66] and pre- and postischemia conditioning to manipulate cell signaling pathways to favor mitochondrial-dependent cardioprotective mechanisms.[17,67]

Table 18.1 Myocardial toxins.

Drug	*Target*	*Reference to ultrastructural pathology*
Allylamine	Vascular tissue, mitochondria	**Boor**, *Lab Invest* 47:76, 1982 (rat); **Boor**, *Am J Pathol* 121:39, 1985 (rat)
Anthracyclines Doxorubicin Daunomycin Epirubicin	Mitochondria, sarcoplasmic reticulum, protein synthesis	**Lewis**, *Lab Invest* 54:416, 1986*; **MacKay**, *Ultrastruct Pathol* 18:203, 1994 (human); **Lushnikova**, *Bull Exp Biol Med* 139(4):472, 2005; **Bellini**, *Virch Arch B* 49:137, 1985 (mouse); **Fajardo**, *Lab Invest* 34:86, 1976 (rat); **Iwasaki**, *Virch Arch* 60:35, 1991 (rabbit); **Jackson**, *Am J Pathol* 117:140, 1984 (rabbit); **Merski**, *Cancer Res* 36:1580, 1976 (rat); **Olson**, *Lab Invest* 37:386, 1977 (rat); **Shirhatti**, *Toxicol Appl Pharmacol* 84:173, 1986; **Taylor**, *Lab Invest* 47:459, 1982 (rabbit); **Jaenke**, Lab Invest 30:292, 1974; **Olson**, *Lab Invest* 37:386, 1977; **Zhou**, *Cancer Res* 61:771, 2001 (rat); **Doroshow**, *Am J Pathol* 118:288, 1985; **Zanon**, *Tumori* 62:517, 1976
Anthapyrazoles Piroxantrone Losoxantrone		**Herman**, *Toxicology* 128:35, 1998 (rat)
Anthracenedione Mitoxatrone	Mitochondria	**Alderton**, *Cancer Res* 52:194, 1992 (mouse)
Bufotoxin		**Palumbo**, *J Am Vet Med Assoc* 167:1000, 1975 (dog)
Chloroquine	Lysosomes	**Hendy**, *J Ultrastruct Res* 29:485, 108–109, 1969
Cocaine		**Gradman**, *Yale J Biol Med* 61:137, 1988 (human)
Corticosteroid	Protein synthesis	**Clark**, *Lab Invest* 47:603, 1982 (rabbit)
Digitoxin	Myofibril	**Gardell**, *J Mol Cell Card* 1:175, 1970 (rat)
Diptheria toxin	Protein synthesis	**Preiss**, *Virch Arch A* 367:255, 1975 (guinea pig)
Disobutamide		**Ruben**, *Toxicol Appl Pharmacol* 97:57, 1989 (dog, rat)
Ethanol	Mitochondria, protein synthesis, myofibrils	**Hibbs**, *Am Heart J* 69:766, 1965 (human)
Furizolidone	Myofibril	**Czarnecki**, *J Comp Pathol* 96:78, 1986 (turkey)
Fusarium toxin		**Yarom**, *Br J Exp Pathol* 64:570, 1983 (rat)
Gold		**Hoke**, *Toxicol Appl Pharmacol* 100:293, 1989 (rabbit)
Halothane		**Pfaller**, *Virch Arch B* 15:224, 1974 (guinea pig)
Histamine		**Branwood**, *Lab Invest* 31:604, 1974 (mouse)
Iron		**Cox**, *Am J Pathol* 102:151, 1981*
Lactate		**Armiger**, *Lab Invest* 31:29, 1974*
Monensin	Mitochondria	**Mollenhauer**, *Am J Vet Res* 42,35, 1981; **Van Vleet**, *Am J Vet Res* 44:1629, 1983 (cow); **Van Vleet**, *Am J Pathol* 114:461, 1984 (pig)
Monocrotaline	RER	**Chesney**, *Exp Mol Pathol* 20:257, 1974 (rat); **Raczniak**, *Exp Mol Pathol* 28:107,1978 (monkey)
Propanol	Mitochondria	**Kloner**, *Am J Cardiol* 41:880, 1978 (rat)
Monocrotaline		**Chesney**, *Exp Mol Pathol* 20:257, 1974 (rat); **Raczniak**, *Exp Mol Pathol* 28:107, 1978 (monkey)
Reserpine	Mitochondria	**Hagopian**, *Lab Invest* 27:99, 1972; **Hagopian**, *Lab Invest* 29:562, 1973 (bat); **Susskand**, *Virchows Arch B* 26:73, 1977 (guinea pig)
Streptozotocin		**Seager**, *Br J Exp Pathol* 65:613, 1984 (rat)
Tellurium		**Van Vleet**, *Am J Vet Res* 43:2000, 1982 (duck)
Tyrosine kinase inhibitors Imatinib Trastuzimab	Mitochondria	**Crone**, *Nat Med* 8(5):459. 2002 (mouse, human); **Kerkela**, *Nat Med* 12(8):908, 2006 (mouse)
Venom, scorpion	Membranes	**Yarom**, *Lab Invest* 24:21, 1971 (dog)
Zidovudine	Mitochondria	**Dalakas**, *New Engl J Med* 322:1098 (human); **Lamperth**, *Lab Invest* 65:742, 1991

In experimental hyperoxia the mitochondria are spared while there is myofibrolysis comparable to that seen with catecholamine induced toxicity.[68]

Massive pulmonary embolism produced by injection of microspheres causes two types of lesions in the right ventricles: (1) local **shredding** of myofibrils (different from zonal lesions of shock), that begin as Z line lysis, and (2) necrosis associated with temporary ischemia followed by delayed reflow (perhaps with a potentiating effect of catecholamines). Most capillaries in necrotic foci remain functional for some time.[69]

Progressive leukocyte capillary plugging during myocardial ischemia contributes to preventing full restoration of capillary flow during reperfusion of recovery phases[70] and contributes to damage by generating ROS. Plasma proteins accumulate in degenerating cardiac myocytes. Biopsies from infarcted areas produced by electricity-induced thrombosis of coronary arteries in dogs show that infarcted areas have both intra- and extracellular lanthanum.[71]

Accumulation of **lactic acid** and intracellular acidosis contributes to death of cardiac myocytes, and later to necrosis of other components of tissue. Ischemic lesions in heart have been reproduced in vitro with lactic acid.[72]

Myocardial fibrosis is an expansion of the strong collagen network. This system stabilizes the myocardium and maintains cellular position despite strong contraction of the tissue.[73] Healing of cardiac tissue damage in the late stages of inflammation must occur in the presence of strong contractile forces. Myocardial scars differ from those in other tissues by the presence of many contractile cells, which appear to assist the function of the cardiac myocyte.

In experimental injury of rat hearts, pericytes and myofibroblasts predominated in early repair periods. Nonvascular smooth muscle cells appeared near the end of the first week and increased as the number of myofibroblasts decreased.[74,75] They were found first in vascular structures and were identified by residual basal lamina sheaths.

Metabolic alterations in either congenital, acquired or pharmacologically induced such as with peroxisome proliferator-activated receptor agonists or toxic levels of acetaminophen can result in the accumulation of excess lipid in nonadipose tissue. This can lead to myocyte degeneration in the heart and Type I skeletal muscle fibers. Small amounts of lipid accumulation may not be evident at the light microscopic level (Fig. 18.4). The degenerative change is proposed to result from elevated free fatty acid oxidation with increased oxidative stress or increased levels of ceramide leading to necrosis or programed cell death.[58,76–79] In diet-induced insulin resistant mice there is a mitochondrial cristae disarray and electron lucency in oxidative skeletal muscle fibers with correlating mitochondrial functional changes. These are not an early change and likely were the result of hyperglycemia and hyperlipidemia-induced reactive oxygen species production in the affected fibers.[80]

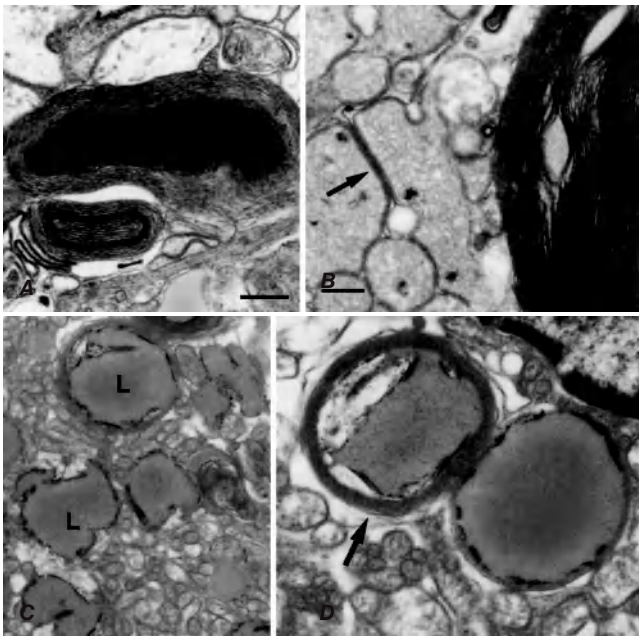


Fig. 18.4 Perturbed lipid metabolism: cardiac tissue, ventrical, end-stage MHC-ACS, 28-day-old transgenic mouse, formalin-fixed. **A**. **Complex membrane structures**: composed of multiple layers of membrane in the cytoplasm of myocytes 7500X. Bar = 1.0 µm. **B**. **Large multilamellar membrane aggregates**: membranes within the cytoplasm between mitochondria (*arrow*) 15,000X. Bar, 0.5 µm. **C–D**. Lipid globules. Bars C = 1 µm, D = 0.5 µm. (Micrograph: Hsiu-Chiang Chiu, *J Clinical Investigation* 107:813, 2001.)

Converse to adverse effects of some altered diets cardiomyopathic hamsters showed benefits from the supplementation. Diet supplementation with alpha-linoleic acid reduced the cardiopathology as judged by increased longevity, cardiac function and myocardial structural integrity as judged by less myofibril disarray, less extracellular matrix deposition and fibrosis and maintenance of plasmalemma and mitochondrial membranes.[81]

Myocardial Toxins

As with any organ system the consequences of exposure to a xenobiotic vary depending on the degree of exposure both in duration and concentration. With ultrastructural interpretation the descriptive aspect must be emphasized when evaluating individual cellular components and assessing whether changes are primary or secondary. Ultrastructural findings can provide critical information but need to be used in conjunction light microscopy, clinical pathology and

information regarding the compound's known activity to arrive at correct conclusions. Stages of myocardial cell injury have been presented.[82] Delineation of the continuum of changes into stages is artificial, but staging organizes the evaluation of cellular change.

Anthracycline Antibiotics

Cardiotoxicity is a major consideration in chemotherapy with anthracyclines such as doxorubicin (Adriamycin), daunorubicin (Daunomycin), epirubicin, and mitoxantrone (Novantrone), and anthracenedione. Anthrapyrazoles (piroxantrone and losoxantrone) were developed with the goal of minimizing cardiotoxicity by reducing the potential for generation of ROS (reactive oxygen species), while retaining antineoplastic activity. Piroxantrone and mitoxantrone cardiotoxicity in experimental studies were less than that of doxorubicin and losoxantrone. Morphologically the lesions produced by all of these compounds are similar except for the giant mitochondria reported for mitoxantrone.[83] Neuropathy can also be an issue with this class of compounds.[84] These toxic glycosidic antibiotics cause systolic and diastolic dysfunction after acute and chronic use. Cardiac output and left ventricular peak systolic pressures decrease significantly. A single dose rarely causes heart failure clinically[85] but experimentally single doses can induce myocyte degeneration. Cardiac dysfunction develops slowly and failure rarely appears until 4 wk after patients receive their last treatment.

The progressive cardiac toxicity of doxorubicin results from mitochondrial insult and alteration of proteins. These changes occur by mechanisms that are distinct from antineoplastic actions of DNA intercalation and topoisomerase inhibition. Anthracyclines cause acute cell death by disturbing mitochondrial function and calcium metabolism. Anthracyclines also suppress mRNAs that code for thin filaments of actin proteins.[86] The alteration and an inhibition of protein synthesis contribute to disruption of sarcomeres, which is an early change (Fig. 18.6). There is also evidence of an immune mediated component of doxorubicin toxicity in experimental species.[87]

Doxorubicin

The mitochondria changes, which include decreased mitochondrial biogenesis, result from increased reactive oxygen radicals generated by doxorubicin accepting unpaired electrons from complex I of the mitochondrial electron transport chain to initiate a redox cycle. This affects the electron transport chain and additionally these radicals alter the mitochondrial matrix reducing equivalents affecting protein thiol residues. One critical protein of the many affected is the regulatory domain of the mitochondrial permeability transition pore (MPT). The induction of the MPT adversely affects mitochondrial membrane potential and calcium homeostasis by irreversibly decreasing calcium-loading capacity, causes mitochondrial swelling and further impairs mitochondrial respiration with an end result of cell death at toxic levels (Fig. 18.5).

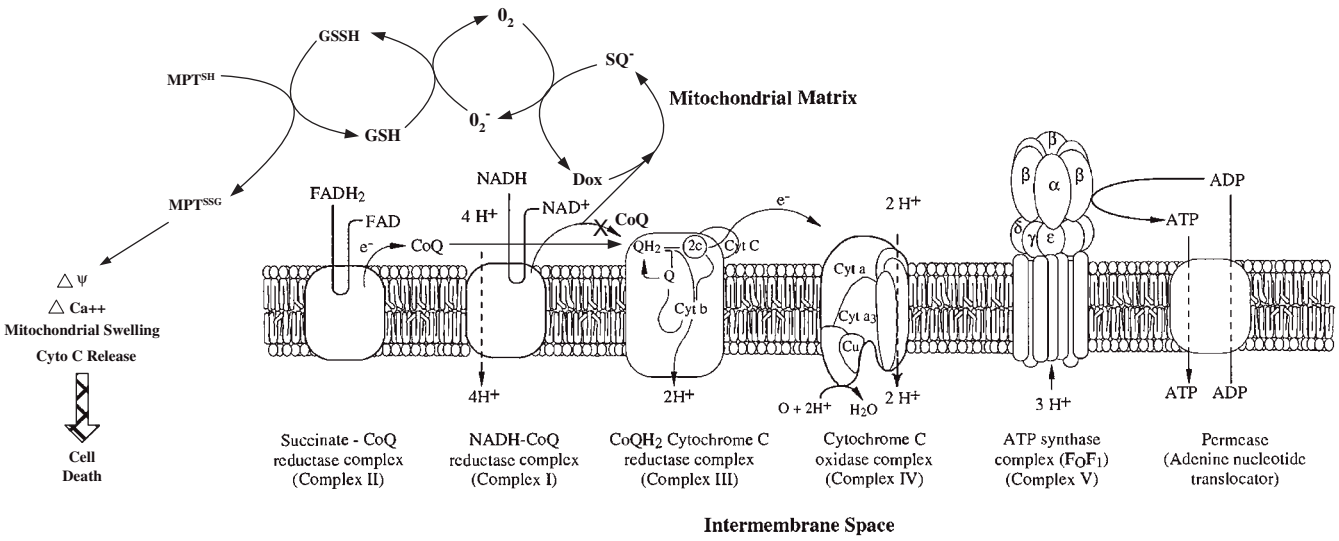


Fig. 18.5 Mechanism of doxorubicin-induced mitochondrial damage and cell death: free radical production. ATP production is decreased both by electron transport chain and mitochondrial pore transition protein (MPT) alterations, which affect chemiosmotic gradient. Doxorubicin (Dox) semi-quinone free radical of doxorubicin (SQ^-), superoxide anion free radical (0_2^-), reduced and oxidized forms respectively (GSSH & GSSG) of glutathione, mitochondrial membrane potential (ψ), cytochrome c (cyto C).

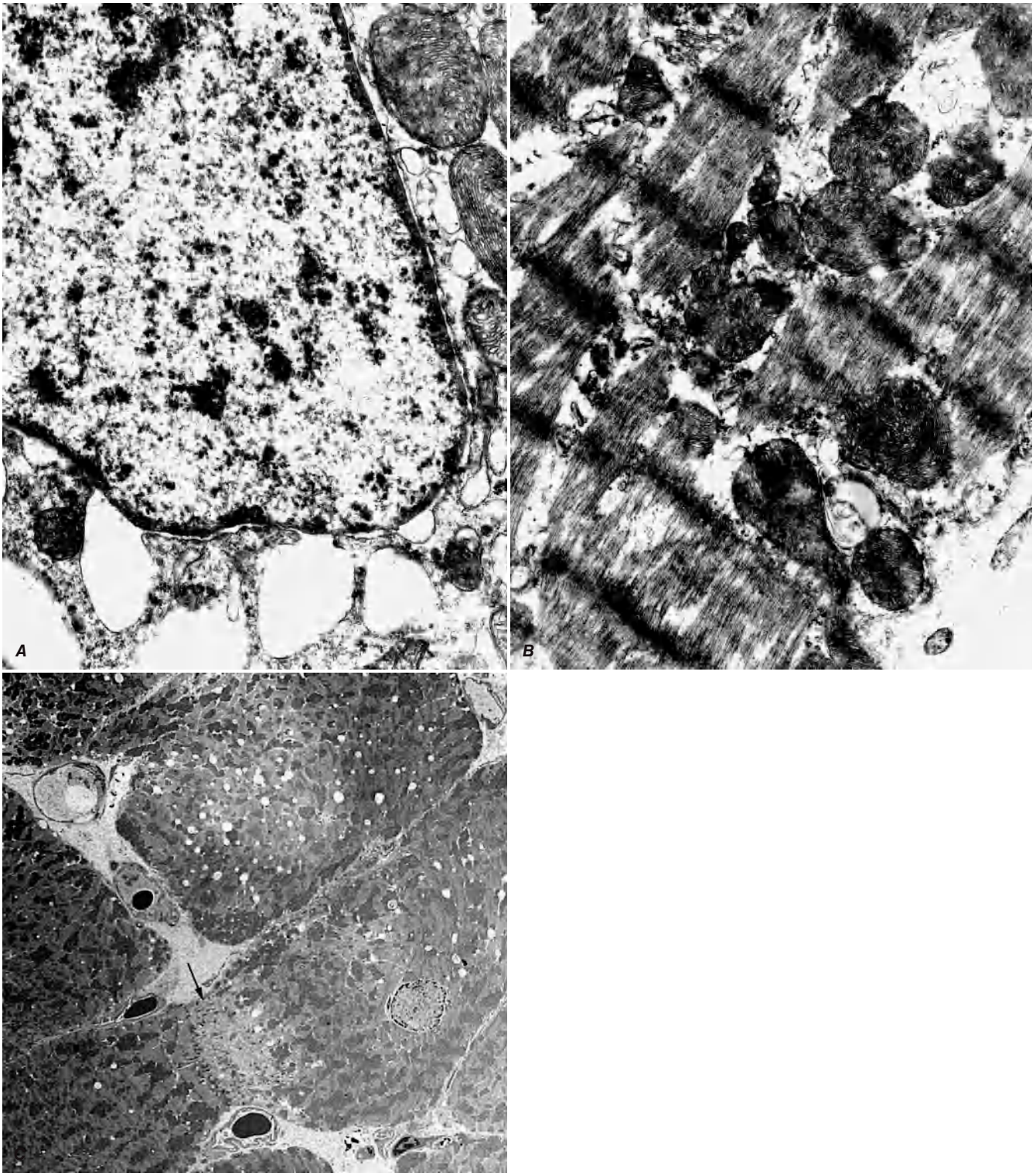


Fig. 18.6 Doxorubicin toxicity, myofibril lysis: cardiomyocytes, rat. **A–B**. **Acute toxicity**: 10 mg/kg single dose doxorubicin, rat. **A. Vacuolation**: extension of perinuclear intermembrane space and cisterns of sarcoplasmic reticulum, 15,000X. **B**. **Myofibril lysis. C**. **Chronic toxicity**: mouse (2.5 mg/kg/wk for 5 wk): vacuolation with multifocal electron-lucent areas (*arrow*) and multifocal sarcoplasmic dilation (*vacuoles*). Lowermost area of myofibrilysis is adjacent to an intercalated disc (*arrow*). (Micrographs A and B: E. Lushnikova, 2005.)

Additionally, doxorubicin binds cardiolipin on the inner mitochondrial membrane, which is involved with proper unfolding of mitochondrial proteins. Doxorubicin also interferes with the translocation of numerous nuclear-encoded proteins into the mitochondrial matrix.[88] Thus multiple factors underlie the toxicity of doxorubicin that leads to necrosis and apoptosis (intrinsic pathway).[39,55,88–90] A better understanding of the mitochondrial effects of doxorubicin has prompted experimental intervention using carbon monoxide to stimulate intrinsic anti-apoptotic pathways and promote mitochondrial biogenesis to limit the cardiomyopathy associated with doxorubicin and improve its therapeutic index.[55] Protection from the oxidate damage is also achieved by the presence of metallothionein.[91]

Doxorubinol, a metabolite of doxorubicin, is a potent inhibitor of the specific ion-dependent pumps of sarcoplasmic reticulum, mitochondria, and sarcolemma. In vitro effects have been demonstrated on Ca-Mg ATPase activity of the sarcoplasmic reticulum, proton pumps of mitochondria (MgATPase), and Na-K ATPase activity of sarcolemma. By inhibiting Ca-Mg ATPase of sarcoplasmic reticulum and ATP synthesis by mitochondria, calcium loading into the sarcoplasmic reticulum would be blocked and this would impair systolic and diastolic function.

The earliest ultrastructural change in doxorubicin toxicity in laboratory animals is transient nucleolar segregation, mitochondrial translocation to the subsarcolemma area, and mitochondrial swelling. Endoplasmic changes are evidenced as dilatation of the perinuclear space and dilation and disintegration of the sarcoplasmic reticulum (Fig. 18.7). Myofibrillar disintegration follows rapidly, and appears to be secondary to damage in the sarcoplasmic reticulum.[92] The myofibrilysis occurs initially in the actin filament of the I-band and is most pronounced in the sarcomeres near the intercalated discs. After a single large dose in mice, myofibrilysis has been reported as early as 14 hr and degenerative changes remain after 30 days.[93,94] In mice doxorubicin induced ultrastructural changes can occur before light microscopic or elevated troponin levels are evident.

Subsequent changes that develop after multiple exposures to doxorubicin include continued lysis and disappearance of myofibrils, dense bodies in mitochondria, and increase in auto phagosomes.[95] Large autophagolysosomes develop myelin figures and cellular debris. Giant lysosomes may appear histologically as inclusions or in conjunction with extensive myofibrilysis changes that will be evident as vacuoles. Marked mitochondrial changes may also be evident at the light microscopic level as a subtle vacuolar change but electron microscopy is required for definitive assessment (Fig. 18.8).

In addition to mitochondrial effects caused by doxorubicin and accompanying the structural sarcoplasmic reticulum changes the sarcoplasmic reticulum loses the ability to sequester calcium. Normally, longitudinal tubules of the sarcoplasmic reticulum sequester and transport calcium to terminal cisternae where calcium is stored for subsequent release to initiate contraction. Doxorubicin may act like caffeine, by binding to the ryanodine receptor to open calcium release channels of terminal cisternae. Calcium influx through slow channels is stimulated in perfused animals' hearts. In rat myocytes, a very low concentration of doxorubicin caused a nearly three-fold accumulation of calcium within 1 min, which is antagonized by verapamil, a slow calcium channel blocker.[96] Low doses of doxorubicin cause less severe injury to the sarcoplasmic reticulum, and small doses may cause only accumulation of lipid globules. Lesions develop at similar rates in rabbits and mice.[97–99] Skeletal muscle injury comparable to that in the heart occurs in poisoned animals.

Epirubicin, a derivative of doxorubicin and mitoxantrone (Novantrone), and anthracenedione both cause cardiac toxicity and ultrastructural changes similar to those described for doxorubicin. The mechanism of oxygen free radical production is similar between doxorubicin and epirubicin cardiac toxicity. The mechanism of mitoxantrone toxicity is unclear and cardiac toxicity is less pronounced than doxorubicin induced toxicity. Unlike doxorubicin, which is a substrate for cellular reductases, mitoxantrone is activated by peroxidases in a process that does not produce oxygen free radicals. The mitoxantrone free radical does react with hydroperoxy fatty acids inhibiting prostaglandin synthesis and altering mitochondrial and tubular calcium levels.[100]

Tyrosine Kinase Inhibitors

Both imatinib (Gleevec) and trastuzumab (Herceptin) are monoclonal antibodies that act to inhibit the activity of tyrosine kinases, Bcr-Alb and ErbB2 respectively. Imatinib is a nonreceptor tryosine kinase and trastuzumab a receptor associated tyrosine kinase. They have selective clinically effective anti-neoplastic activity. Both have an associated cardiac toxicity that ultrastructurally is similar with effacement of mitochondrial cristae and vacuolation. Additionally for imatinib dense membrane whorls within the sarcoplasmic reticulum have been described (Fig. 18.9). Imatinib induced changes involve ER stress mechanism and Jun-N terminal kinases causing alterations in the BCL-2 family of proteins and a collapse of mitochondrial membrane potential resulting in cell death. With trastuzumab, disfunction of mitochondria has also

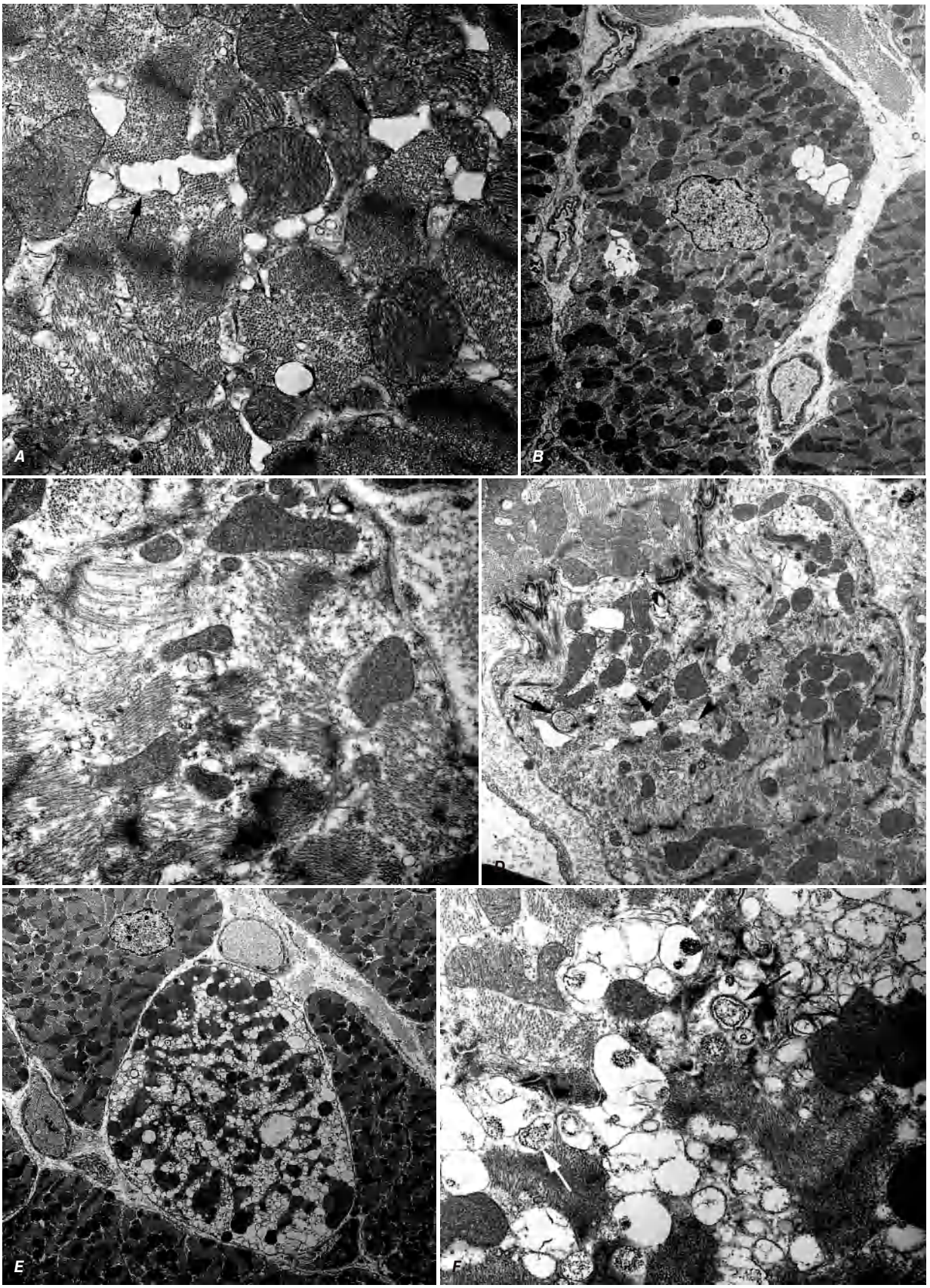


Fig. 18.7 Doxorubicin toxicity: mouse (2.5 mg/kg/wk for 5 wk). **A**. **Sarcoplasmic reticulum dilatation**. **B**. **Focal dilatation**. **C**. **Vacuolation**: marked vacuolation of dilated sarcoplasmic reticulum or autolysomes. Myofibrils are degenerate and in disarray. **D**. **Myofibrilysis** adjacent to intercalated disc dilated sarcoplasmic reticulum (*arrowheads*) and autophagocytic vacuole (*arrow*). **E. Degenerate myofibers**: scattered areas of myofibrils and mitochondria remain separated by areas of vacuolation (dilated sarcoplasmic reticulum and autolysosomes). **F**. **Vacuolated degenerate myofibers**: many autolysosomes containing cell debris (*white arrow*) with double membrane autophagosome (*black arrow*).

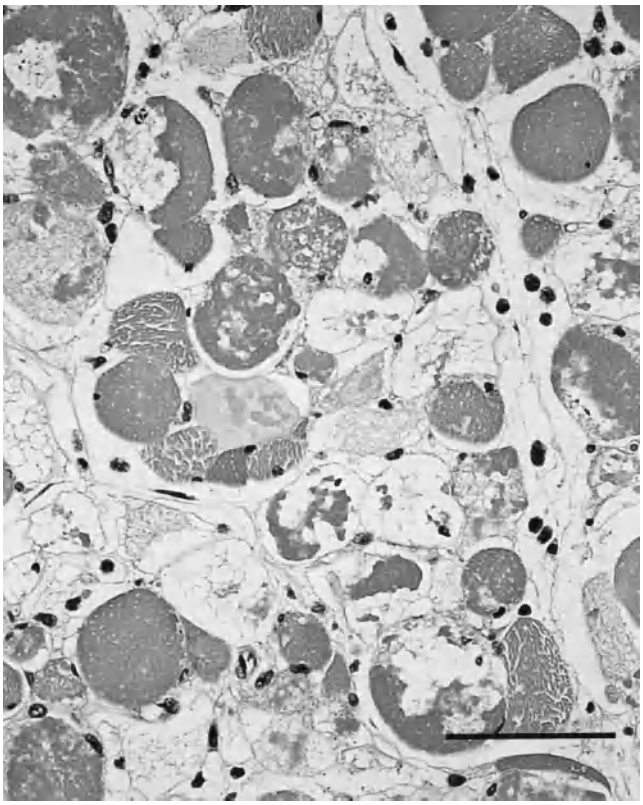


Fig. 18.8 Cardiac myocyte degeneration: rat, doxorubicin treatment. Severe myocyte degeneration (2 mg/kg/wk for 8 wk with 1 wk of recovery): vacuolation is present in greater than 30% of myocytes (histology). (Micrograph: Zhou S. et al., 2001).

been associated with altered levels of the BCL-2 family. In both situations, regulation of apoptosis contributes to the toxicity.[101–104]

Amphophile Compounds

Chloroquine

This antimalarial and anti-inflammatory drug accumulates in lysosomes altering the pH and inhibiting lysosomal enzymes. It affects lysosomes of *Plasmodium* spp., and leukocytes and other cells in multiple tissues of mammals. Chloroquine-induced changes in cardiac muscle closely resemble those in skeletal muscle.[105] Acid-phosphatase staining lysosomes develop first in perinuclear regions and disappear when the drug is discontinued. Human chloroquine-induced skeletal muscle weakness typically occurs after patients have received 500 mg per day for a year or longer. Biopsy of affected muscles of these patients reveals vacuolar myopathy. Ultrastructural examination shows that vacuoles are autophagosomes filled with varying amounts of membrane fragments and vesicles. In late stages changes consistent with phospholipidosis are evident. Large autophagosomes are filled with myelin figures (myelinoid bodies) and curvilinear bodies are characteristic.[106,107] The morphologic changes prompt congenital lysosomal storage diseases to be considered as a differential. Phospholipidosis is seen with many cationic amphophilic compounds. The toxicologic significance of phospholipidosis is uncertain. Unless there is evidence of cellular damage, drug-induced phospholipidosis, although structurally similar to storage diseases, can be considered an adaptive response.[108,109]

Experimentally in rats, chloroquine induces myopathy that is more severe in red muscles (soleus) than white (gastrocnemius, medial head). Vacuoles, autophagosomes, and split myofibers are characteristic after 5 days of treatment. The initial change is proliferation of the membranes of the sarcoplasmic reticulum and T tubule system. Specific labels for the T system (exogenous peroxidase) and for SR (adenosine triphosphatase) show that the T system is largely involved in early injury and can be seen among developing autophagosomes.[110] Ultrastructural effects of chloroquine on avian myocardium[111] and skeletal muscle,[112] and cardiac muscle of other species have shown similar changes.

Ionophores

Ionophores are drugs that act as ion channels in cell membranes. They become inserted into the cell surface and carry ions across the plasma membrane. Most of these diverse compounds have a common central ring of liganding oxygen atoms that forms a critical cavity to fit a particular ion.

Monensin

The prototype sodium ionophore, monensin, is used in food-producing animals both as a coccidiostat (it inserts into coccidial surface membranes causing ionic imbalances that cause the coccidia to swell and burst) and to enhance rumen production of protein in ruminant food-producing animals. Monensin is particularly toxic for equine species but also poisons most other species. It causes necrosis of both skeletal and cardiac muscle, and poisoned animals die in acute heart failure.

In vivo, monensin has a predilection for cardiac and skeletal muscle cells. Lesions include multifocal necrosis with type I fiber preference. Changes include vacuolation of sarcoplasmic reticulum, mitochondrial swelling, and lipid globule accumulation and, with time, formation of myeloid bodies. These changes have been documented in swine[113–115] and cattle.[116,117] In degenerating myocytes the abnormal intake of Na^+ and loss of H^+ are accompanied by entry of Ca^{++}.



Fig. 18.9 Imatinib toxicity: membrane defects, cardiac biopsies, human, Imatinib therapy. Dense membrane whorls (*arrow*). (Micrograph: R. Kerkela, 2006.)



Fig. 18.10 Simvastatin toxicity: semimembranous muscle, 80 mg/kg daily for 7 days, rat. **A–B**. Early changes: type II muscle fibers, rat. Enlarged, degenerate mitochondria in subsarcolemmal areas have aberrant myelinoid whorls and spheroids. Other components of the sarcoplasm show no abnormalities. **A**. Extensor digitorum longus muscle. **B**. Gastrocnemius muscle. Bar = 1 µm. (Micrographs: F. R. Westwood, 2005.)

Monensin impairs processing beyond the high-mannose stages, while N-linked oligosaccharides are being processed from high-mannose precursors to mature complex forms (during passage of molecules from the endoplasmic reticulum through the Golgi cis, medial, and trans areas). By this action it has widespread effects and causes defective cleavage and processing of proteins, reducing secretion, and inhibiting internalization.

Experimentally, this monovalent ionophore is used as a preferential toxin for the Golgi complex in cells in culture. It affects the post-translational glycosylation of glycoproteins by disrupting membrane permeability to protons (inducing Na^+ influx and H^+ efflux from Golgi saccules) thus making cisternae alkaline and inhibiting receptor recycling. Cells treated with monensin in vitro develop pleomorphic secretory granules and vacuolated Golgi complexes.

Catecholamines

Catecholamines are especially detrimental to myocardium under stress. They increase oxygen consumption, alter myocardial blood flow, and may have direct toxic effects on the myocyte. The major cardiac catecholamine is norepinephrine, which is located in adrenergic nerve termini. After coronary occlusion, loss of catecholamines from ischemic myocardium can be demonstrated. Norepinephrine is released from nerve terminals and retained in abnormally high concentrations in ischemic myocardium during the first few hours after coronary occlusion, during the phase of transmural spread of the wave front of necrosis.[118] Treatment to reduce catecholamines during myocardial infarction tends to limit the extent of injury. Experimentally, after ligation of the coronary artery of dogs, chronic sympathectomy and pretreatment with propranolol reduce infarct size.

Epinephrine stimulates α- and β-adrenergic receptors. Cardiovascular effects are due to stimulation of B_1 receptors of myocardium and conduction system. Effects on the human heart, although rare, have been reported in prolonged epinephrine infusions and with persistent elevations of epinephrine that occur in patients with pheochromocytoma. Acute epinephrine toxicity may be manifest as cerebrovascular hemorrhage and pulmonary edema. The effects on smooth muscle depend upon the type of receptor present on the myocytes. Experimentally, large repeated doses in rodents lead to damage to arterial walls and myocardium. Rats given epinephrine at 1 mg/kg body weight and examined at 30 min after inoculation have thickened Z lines and glycogen depletion.[119]

Isoproterenol

Administration of the synthetic catecholamine isoproterenol, as well as natural catecholamines epinephrine and norepinephrine, in toxic doses produces myocardial hypertrophy and necrosis in laboratory rodents, and marked changes in other tissues throughout the body.[120,121]

Toxic doses of isoproterenol given to humans causes necrosis of myocardium, especially in subendocardial areas of the left ventricle and interventricular septum. In experimental animals, the pathogenesis of toxicity involves ischemia, ATP depletion and intracellular accumulation of calcium. Initial damage after injection of isoproterenol is endocardial cell contraction and separation, and adherence of platelets to exposed subendocardium. Myocardial damage then occurs adjacent to endocardial defects.[122] Subcutaneous injections of isoproterenol at 40 mg/kg body weight for two days produces cardiac necrosis in rats. Lesions are prominent in the subendocardium and appear secondary to vascular changes. Affected cardiac muscle cells show rapidly developing swelling of mitochondria and tubular systems, with Z line thickening, and dilatation of sarcoplasmic reticulum to form vesicles.[123] With time there is an increase in autophagolysosomes with myelin figures, and lysis of myofibers.[124]

Antihypertensives

Reserpine

This alkaloid extracted from *Rawolfia serpentina* is used as an antihypertensive drug and tranquilizer. It causes depletion of neurotransmitters, especially norepinephrine, dopamine, and serotonin from monoaminergic neurons in the brain. Reserpine binds to the membrane of secretory granules in the presynaptic neuron to cause displacement of the catecholamines stored therein. Norepinephrine released into the cytosol is metabolized by monoamine oxidase, and none is available to cross the synaptic cleft to excite the postsynaptic membrane receptor.

Cardiac catecholamines are also depleted by reserpine treatment and this causes depression of atrial and ventricular rhythms. Although the effect is thought to be mediated by catecholamine depletion there is also evidence to support a direct effect on the myocardium (see Fig. 18.1). In rodents, reserpine induces in increase in lipid droplets and glycogen, swelling of the T system and sarcoplasmic reticulum, and abnormally shaped mitochondria. A study of chronic administration of high and low doses of reserpine to active and hibernating bats show that in active bats reserpine induced an increase in the size and number lipid globules, increased glycogen, and dilatation of the T tubules and sarcoplasmic reticulum. In contrast, treatment of hibernating bats caused little or no increase in lipids but more marked mitochondrial ultrastructural change.[125]

Inotropic agents, used in the treatment of congestive heart failure, are classified into two categories: **adrenergic receptor agonists** and **phosphodiesterase inhibitors.** High doses of either cause focal myocardial necrosis, especially in the left ventricular papillary muscles and atria.

Calcium Channel Blockers

Verapamil

Verapamil is a calcium blocking agent that reduces infarct size after experimental coronary artery

occlusion. It prevents rapid cell swelling and has a particularly protective effect on **mitochondria.** Verapamil decreases the rapid cell swelling in subendocardium after reperfusion and the sudden influx of fluid and electrolytes that leads to severe intracellular edema. It also produces beneficial effects on ischemic heart function, probably by preventing calcium influx in the damaged myocardium.[16] Biochemical studies support the hypothesis that treatment maintains normal mitochondrial oxidative phosphorylation and calcium accumulation after 60 min of hypoxia. Limiting mitochondrial calcium load provides a protective effect, however the relative importance of the mitochondrial calcium uniporter controlling influx or the Na^+/Ca^{++} exchanger controlling efflux is uncertain regarding the control of mitochondrial calcium levels in ischemia reperfusion. Also, there is not agreement between data obtained from isolated mitochondria and whole myocyte preparations as to the effect of increased mitochondrial calcium on the mitochondrial permeability transition pore, which is a major determinant in cell viability.[17]

Other Cardiotoxins

Toxic concentrations of potassium, copper, and iron are associated with naturally occurring cardiomyopathy. **Cobalt** toxicity induces a mitochondrial degeneration by depression of respiratory activity via inhibition of pyruvate and α-keroglutarate dehydrogenase. Mitochondrial lesions have also been induced with common drugs such as **digitalis, thyroxin**, **β-adrenergic blocking agents,** and the antimalarial drug **plasmoid. Venoms** of some reptiles produce foci of myocardial necrosis and are presented in subsequent sections dealing with skeletal and smooth muscle toxins.

Furazolidone

Furazolidone is a nitrofuran that is cardiotoxic to some species of birds. Ducklings develop cardiomegaly and congestive heart failure when fed 650 mg/kg feed for 28 days.[126,127] Myofibrillar lysis is the dominant lesion and leptodermic complexes (leptofibrils, leptomeres) are typical in affected myocytes.

Coffee Senna Toxicity

Among the plant toxins that cause cardiac myocyte necrosis in grazing animals, that of coffee senna (*Cassia occidentalis*) is best known. Mitochondrial damage is the primary structural lesion; there is subsequent myofibrillar degeneration, necrosis of myocytes, and congestive heart failure. In cattle and horses, myocyte destruction leads to myoglobinuria, hyperkalemia and release of muscle enzymes into the bloodstream.[128]

Pyrrolizidine Alkaloids

The pyrrolizidine alkaloids, found in several species of *Senecio*, *Crotalaria*, and *Heliotropium*, and the toxic metabolites are commonly associated with chronic liver disease in grazing livestock. Signs of wasting and icterus occur up to 2 months after ingestion. Right ventricular hypertrophy followed by heart failure develops after several months in some species. Heart lesions include focal cytolysis of myocytes, cell swelling, and fibrosis. In monkeys experimentally poisoned with the pyrrolizidine alkaloid monocrotaline, right ventricular hypertrophy and congestion developed. Heart failure occurred 7 months after subcutaneous injection. All monkeys had marked dilatation of right ventricles with focal cytolysis of myocytes, intracellular edema, and fibrosis. There was hypertrophy and hyperplasia of mitochondria and clumping of Z-band material.[129]

Ethanol Cardiomyopathy

Ethanol cardiomyopathy is characterized by hypertrophy, dilatation, and fibrosis of the heart. It appears in most alcoholic cases of greater than 10 years duration. Ultrastructural findings in the heart of six alcoholic patients included swelling of sarcoplasmic reticulum, myofiber degeneration, and an increase in lipids, lipofuscin granules, and lysosomes; mitochondrial swelling with altered cristae and matrix inclusions were common.[130]

Cocaine Cardiomyopathy

The alkaloid cocaine activates the sympathetic nervous system to cause dilated pupils, small blood vessel constriction, and cardiac dysfunction. It causes diffuse contraction bands and necrosis of cardiac myocytes by its catecholamine-like action. Diffuse myocardial damage may lead to dilated cardiomyopathy. Cocaine causes a dose-related increase in cardiovascular function in humans. It blocks the reuptake of norepinephrine back into adrenergic nerve endings, thus prolonging the neurotransmitter's activity.[131]

Skeletal Muscle

Skeletal Myotoxins

Tubular aggregates (TA) are inclusions of laminally arranged tubules, typically associated with

mitochondrial aggregates and arise from mitochondrial membranes. They are found in a wide range of neuromuscular disorders. TAs consist of densely packed tubules located between myofibrils and beneath the sarcolemma, and arranged in crystalloid patterns. Skeletal muscle TAs have been shown to involve deficits in caveolin.[132]

Ethanol

Myopathies from alcohol toxicity are divided into acute and chronic exposures. Type I fibers are more sensitive to the damage from acute toxicity and Type II fibers are more sensitive to chronic exposure. Factors underlying degenerative changes are impaired protein synthesis from decreased translation efficiency, inhibition of cytokine and growth factors such as insulin and insulin-like growth hormone factor. Metabolites of ethanol (acetaldehyde and acetate) may affect toxicity.[133,134]

Androgens and Anabolic Steroids

Muscle growth is often mediated via steroid hormones, especially anabolic hormones; for example, androgens stimulate muscle growth. Part of the body weight difference of males and females is attributed to testosterone-dependent muscle mass. Responses produced by testosterone vary widely between muscles and among species. The muscle having the greatest response is the levator ani (dorsal bulbocavernosus), which is less able to metabolize testosterone than other skeletal muscles.

Anabolic steroids are widely used in both humans and horses to promote growth of skeletal muscle, especially for the increased strength required for racing. The skeletal muscle cells respond to these androgenic steroids by developing marked hypertrophy and increased length and volume of myofibers. Treated skeletal muscle cells enlarge but do not undergo mitosis. Myocyte hyperplasia is associated with expansion of the tubular systems and with increases in length and number of myofilaments and their attachment sites at the Z lines.

The stimulus for increased protein synthesis is nonspecific because hypertrophic muscle contains extractable factors that will induce a normal heart to hypertrophy. Tissue extracts of hypertrophied canine heart and kidney, when perfused through isolated canine hearts, cause hypertrophy with increased activity of mRNA translation.[135]

Degenerative changes of high dose glucocorticoids in muscle affect preferentially Type II fibers with the thick filaments being affected first. Resembling the effects of ethanol toxicity there is decreased protein synthesis resulting from impairment of protein initiation. Also involved is the increased cytoplasmic protease activity leading to myofibrillar destruction. Glutamate synthetase activity contributes to the accelerated muscle breakdown during exposure to high level of glucocorticoids. Glutamine supplementation antagonizes the glucocorticoid induced muscle atrophy.[134]

Azidothymidine

Azidothymidine (AZT, zidovudine) is a nucleoside analogue inhibitor of reverse transcriptase, a component of human immunodeficiency virus.[136] AZT is used clinically to inhibit HIV replication, and has been implicated in toxicity for both striated and cardiac muscle.[137] Myopathy that arises after prolonged use of approximately one year has been studied in muscle biopsies of AIDS patients. The presence of degenerate myocytes called "ragged red fibers" differentiates this lesion from the myopathy caused by HIV infection. Ultrastructurally, the muscle change is characterized by abnormal mitochondria with cristolysis and intramitochondrial myelin bodies and z-discs changes. The lesions result from several mechanisms. AZT inhibits the τ-DNA polymerase of the mitochondrial matrix, impairing mtDNA replication and repair, inducing mtDNA mutations. Additionally, there is promotion of the generation of reactive oxygen species (ROS). Among the cause of ROS generation is decreased mitochondrial turnover and an associated respiratory chain dysfunction.[138–140] The damage of AZT exposure is persistent.[141] Experimental treatment of rats for 35 days led to widespread cardiac mitochondrial swelling, matrix lysis, and cristolysis that did not reverse within 14 days after treatment was stopped.[139] Ultrastructural changes correlated with reduced expression of mitochondrial mRNAs. In mice exposed to AZT in utero similar mitochondrial changes and expansion and misalignment of z-discs were demonstrated.

Vincristine

Vincristine, used previously in cancer therapy, is myotoxic. A syndrome of peripheral neuropathy was well documented in patients treated chemotherapeutically with vincristine sulfate. The earliest changes found were the aggregation of membranes into laminae and whorls in intermyofibrillar spaces that contain mitochondria and sarcoplasmic reticulum.[142] Lesions also occur in the terminal axon of the myoneural junctions. Human patients treated for cancer with high doses of vincristine and vinblastine have developed a degenerative syndrome of skeletal muscle characterized by myofibrillar and sarcoplasmic degeneration. The lesions, as reproduced experimentally in rats, suggest that whorled laminates of smooth-surfaced

membranes, vesicles and dense bodies arise from the sarcoplasmic reticulum.[142]

Colchicine

Colchicine toxicity causes a vacuolar degeneration of skeletal muscle resulting from the inhibitory effects of colchicine on tubulin, which is involved in the fusion of autophagosomes with lysosomes. This results in the accumulation of phagosomes both from impaired degradation and inhibition of exocytosis. There is a preferential effect on Type I fibers possibly because of increased levels of alpha-tubulin in these fibers.[143,144]

HMGCoA Reductase Inhibitors

Statins (HMGCoA reductase inhibitors) are a much prescribed drug. A common concern with this class of drugs is myopathy ranging from a mild myalgia to rare instances of fatal rhabdomyolysis. Type II (fast twitch) fibers are the most sensitive to statin induced damage. An early change ultrastructurally is mitochondria vacuolation and subsarcolemma accumulation of concentric multilaminated membranous whorls and spheroids (Fig. 18.10).[145] The cause of the muscle damage is uncertain with several proposed mechanisms.[146] Altered mitochondria function occurs but the literature reports differ as to the possible cause of the functional changes. Statins likely act on a number of points in mitochondrial metabolism to decrease mitochondria membrane potential resulting in altered membrane permeability contributing to apoptosis induction.[147,148] Alteration in mevalonate metabolism with subsequent effects in isoprenoid and protein synthesis likely plays a role.[134,149,150] Data implicating CoQ10 insufficiency is inconclusive.[146]

Organophosphorus Insecticides

TEPP (tetraethyl pyrophosphate), tabun, and sarin are insecticides that are highly toxic to mammals. Parathion, extensively used in agriculture, has been the pesticide most frequently involved in human fatalities. It has been replaced by other, less toxic organophosphorus compounds (Table 18.2). Focal necrosis of skeletal muscle fibers is one the lesions produced in all animals that are poisoned with acetylcholinesterase inhibitors.

Parathion

Parathion is an **acetylcholinesterase inhibitor.** It prevents inactivation of acetylcholine at neural synapses, leading to excessive stimulation of cholinergic nerves.

Table 18.2 Cytopathologic analysis of skeletal muscle.

Loss of myofilaments with relative increase in sarcoplasm and increased electron lucency, often with formation of sarcoplasmic masses at edges of myofibers that contain glycogen, degenerate myofibrils, and debris.
Streaming of Z lines (discs), irregular with extension of Z line into I band.
Wisps of electron-dense disrupted myofilaments (Carpenter and Karpati 2001).
Sarcoplasmic reticulum dilation.
Mitochondrial cristolysis, swelling, and electron-dense inclusions.
Target fibers, sarcomeres of several adjacent myofibrils, are replaced by electron-dense material (Schotland et al. 1969).
Ring fibers exhibit a peripheral ring of myofibril running obliquely or at right angles to a central longitudinal core of myofibrils (Schotland et al. 1970).
Reduplication of T systems to form honeycomb structures; in muscular dystrophy, hypokalemic paralysis, thyrotoxic hypokalemic paralysis, and chloroquine myopathy (Ishikawa et al. 1968).
Tubular aggregates, concentric arrays of tubules of caveolae origin.
Satellite cells develop along myofiber surfaces.

The immediate cause of death from this and other organophosphorus insecticides is asphyxia resulting from respiratory failure.

Myopathy is due to a combination of postsynaptic and presynaptic events: excessive release of transmitter that remains unhydrolyzed and muscle fasciculation. Like other anti-AChE reactivators, paraoxon causes antidromic firing of motor nerve action potentials.

Effects of anticholinesterase inhibitors contributing to disease and death arise from three major nerve sites: (1) **motor nerves to skeletal muscle, nicotinic** signs resulting from accumulation of acetylcholine at myoneural junctions are muscle weakness, twitching, and fasciculation; (2) **postganglionic parasympathetic nerve fibers,** muscarinic signs, which occur in cardiac and smooth muscle and exocrine glands, include bronchoconstriction, increased bronchial secretion and salivation, sweating, urination, diarrhea and defecation, and constriction of pupils; and (3) **central nervous system synapses** (accumulation of acetylcholine in brain is associated with restlessness, drowsiness, and other behavioral abnormalities).

In **muscle,**[151] the cytopathic effects of parathion arise from a combination of post- and presynaptic events; that is, the excessive release of acetylcholine plus repeated binding of unhydrolized acetylcholine to receptors. Both lead to excessive depolarization of end-plate receptors, and mitochondria and sarcoplasmic reticulum are dilated in affected muscles. The end result is myofiber degeneration and necrosis.

Structurally, within 30 min after injection of parathion, neuromuscular transmission is altered, myocyte sarcoplasm below the motor end plate is disorganized, and there is dilatation of mitochondria and sarcoplasmic reticulum. Nerve termini accumulate coated vesicles, and subsynaptic folds are widened and contain vesicles.

Other Organophosphorus Insecticides

At the ultrastructural level both reversible (neostigmine) and irreversible (soman) cholinesterase inhibitors produce subsynaptic lesions and myofiber degeneration.[152–154] At **neuromuscular junctions,** there is a decrease in the number of synaptic vesicles and mitochondria. The presynaptic membrane is often irregular and bears increased numbers of vesicles fixed in the process of exocytosis. Soman (pinacolyl methylphosphonofluoridate) induced lesions in **myocytes** are largely vacuolation of the sarcoplasmic reticulum and T tubules (Fig. 18.11). **Mitochondria** are affected and are irregular in size and contain an excess of dense granules. **Myofibril** disintegration occurs at high doses and lesions begin at the Z and I bands.[155] Vesicles in the subsynaptic cleft are most numerous in severely degenerate fibers. Analysis of **end plate morphology** such as fold width and length, interfold spacing, length of synaptic contact, and distance from folds to myoplasm showed insufficient correlation between any of these parameters and the extent of subsynaptic abnormalities.

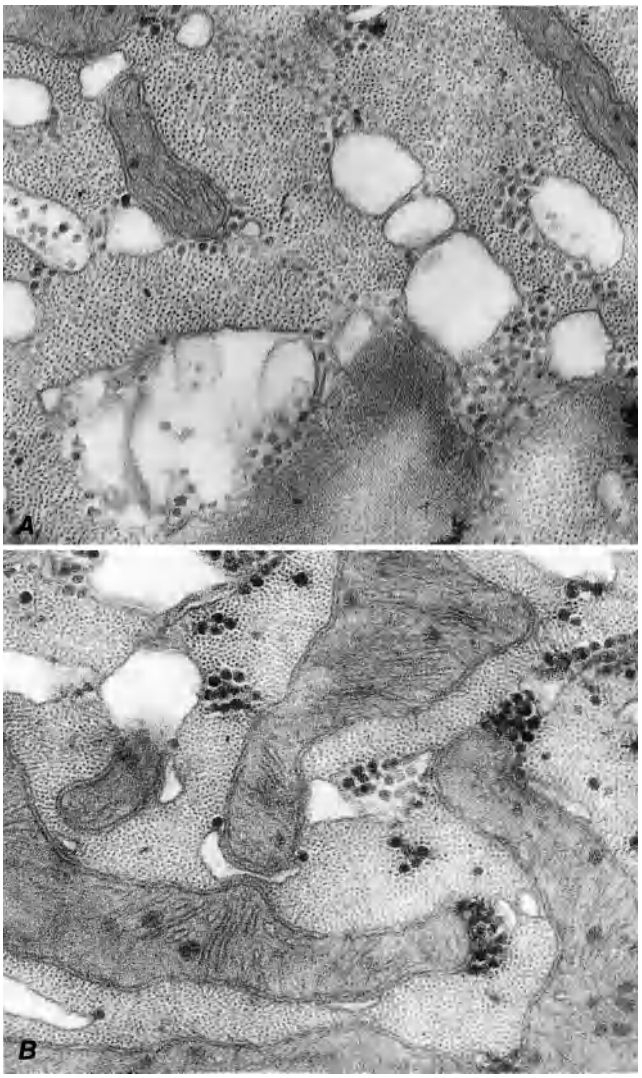


Fig. 18.11 Soman toxicity: skeletal muscle (diaphragm), rat killed 24 hr after injection of soman. Granular inclusions in mitochondrial matrix, glycogen granules between myofibrils. Vacuoles in mitochondria. (Micrograph: A. Dekleva, 1989.)

Motor End Plate Toxins

Carbamates

Carbamates inhibit the enzyme acetylcholinesterase at the muscarinic, nicotinic and neuromuscular synapses (Fig. 18.12). When mammals ingest lethal doses, respiratory failure and death occur quickly. Salivation, vomiting, and diarrhea are typical. Neuromuscular signs, which are less obvious, include ataxia, tremor, and seizures. Chronic disease may lead to degenerative myopathy. Carbamate compounds are rapidly metabolized and excreted in urine. The resulting muscle fasciculation results in increased activity in the presence of excess released and unhydrolyzed acetylcholine.

Local Anesthetics

All local anesthetics have a clinically relevant myotoxicity that is likely related to their lipophilicity and their ability to stimulate calcium release from and inhibit re-uptake of calcium by the sarcoplasmic reticulum. Ultrastructurally the less severely affected fibers have vacuoles consistent with dilation of the sarcoplasmic reticulum while the mitochondria are unchanged. In the more severe stages of degeneration there is myofibril disintegration and the mitochondria are degenerate while the sarcoplasmic reticulum remain intact until there is complete degeneration of the myofiber.[156]

Serotonin

Serotonin toxicity has become an increasingly important problem in the last decade. It occurs with the administration of compounds, that have CNS seroto-

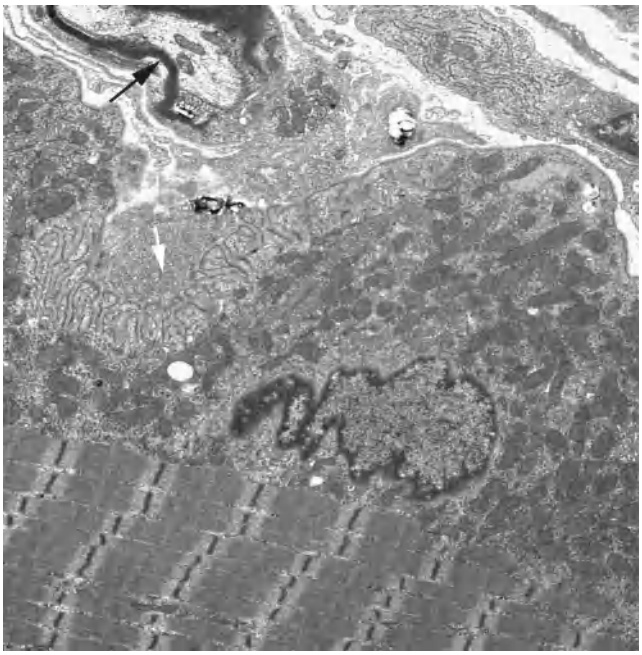


Fig. 18.12 Neuromuscular junction: normal rat skeletal muscle. Note undulating sarcoplasmic membrane, synaptic vesicles (*white arrow*) and associated myelinated nerve fiber (*black arrow*).

nergic activity such as combinations of antidepressants with and without selective serotonin re-uptake inhibitory activity and atypical antipsychotics, which act through serotoninergic pathways. The adverse effects (hyperreflexia, tremors, hypertonia, tachycardia) are likely a result of neuromuscular and autonomic effects. In humans, clinical signs and elevated creatinine are indicative of muscle damage. The more severe changes may be associated with 5HT2a activity, which is involved in transport of glucose across cell membranes. Information regarding mechanism and cellular changes is limited.[157–159]

Biological Myotoxins

Bacterial Myonecrosis

Bacterial toxins are common causes of muscle necrosis. *Clostridium* spp. cause rapidly progressive, lethal infections of skeletal muscle. Clostridial exotoxins are released and produce necrosis locally. *C. perfringens* produces α-toxin, a phospholipase C that is hemolytic, destroys platelets, and causes widespread capillary damage. Components of the lesion are (1) **lytic injury to capillary endothelium** resulting in altered permeability, edema, and hemorrhage; (2) **lysis of myocytes,** injury begins in the Z lines of the myofibrils and rapidly spreads, causing disintegration of the entire muscle fiber; and (3) **gas bubbles** produced when clostridia utilize glycogen within the myocyte. In the initial phases of muscle necrosis, lysis begins in the center of the affected fiber and spreads peripherally. As membranes are disrupted and disintegrate, precipitates of myoglobin accumulate within the dying myocyte.[160]

The lethal α-toxin of *C. novyi* types A (gas gangrene) and B (infectious necrotic hepatitis of sheep) is a phospholipase C that converts phospholipids in the plasma membrane to phosphoryl choline and a diglyceride by hydrolyzing a specific phosphorus-hydrogen bond at the C position. The discrete holes produced in the plasma membrane by α-toxin lead to widespread disintegration of endothelium and myocytes.[161] When ferritin-labeled toxin is injected intramuscularly, ferritin particles can be detected ultrastructurally in the defects of the plasma membrane.[162]

Tetanus neurotoxin may also produce direct action on skeletal muscle that, when superimposed on contracted myocytes, may enhance muscle necrosis. Degenerative changes in the affected skeletal muscle begin in the sarcoplasmic reticulum and follow the general pathway for progressive degeneration (Table 18.3). Tetanus neurotoxin-binding sites, when traced by peroxidase-labeled tetanus antitoxin, have been identified in the membranes of the T tubular system, at its junction with the sarcoplasmic reticulum, and within the sarcoplasmic reticulum cisternae.[163] Structural changes occur in myofibrils of affected muscles but are secondary to the extreme contraction and vascular pathology. Skeletal muscle degenerative lesions are not due to a direct effect of toxin on myofilaments, as are lesions produced by several other bacterial myotoxins, for example, autolysin of *Aeromonas hydrophila*, the cause of focal myositis and necrosis of frogs (red leg) and other animals (Fig. 18.13).

Venoms

Spiders are uniformly venomous but most attack only other arthropods and venom is used to paralyze their prey. When envenomated into vertebrate tissue, **muscle necrosis** may be severe, especially for venoms that act on membranes. Tarantula venom directly injures the plasma membrane of the muscle cells.[164] The **brown recluse spider** produces a hemolytic and necrotizing venom that incites a chronic ulcerating wound accompanied in early stages of systemic effects of fever, nausea, and vomiting. Venom binds to and is directly lytic for myocytes and erythrocytes.[165] Brown recluse spider venom contains a phospholipase D.

Venoms of **wasps** are often more potent locally and produce tissue necrosis with severe edema and inflammation. Venom of the **oriental hornet** produces muscle necrosis at the injection site; vacuoles in damaged myocytes arise from the initial damage by the venom to T tubules and sarcoplasmic reticulum.[166]

Table 18.3 Skeletal muscle toxins.

Drug	*Target*	*Reference to ultrastructural pathology*
A23187		**Publicover**, *J Neuropathol Exp Neurol* 37:544, 1978 (mouse); **Yoshimura**, *Acta Neuropathol* 69:184, 1986 (rat)
Bacterial toxins	Membranes	
Aerolysin		
Botulinum toxin		**Duchen**, *J Neurol Sci* 14:61, 1971 (mouse)
Clostridia		**Demello**, *Arch Pathol* 97:97:118, 1974; **Strunk**, *Am J Pathol* 50:89, 1967 (α toxin)
Diptheria toxin	Protein synthesis	
Cholchicine	Tubulin	**Fernandez**, *Acta Neuropath* 103:100, 2002.
Citral		**Aramovici**, *Virch Arch B* 14:127, 1973 (chick)
Corticosteroid	Protein synthesis, myofibrils	**Jirmanova**, *Virch Arch B* 38:323, 1982 (rabbit)
Creatine analogue		**Gori**, *Br J Exp Pathol* 69:639, 1988 (rat)
Anthracycline	Mitochondria, protein synthesis, sarcoplasmic reticulum	**Doroshow**, *Am J Pathol* 118:288, 1985 (mouse)
Germanium		**Higuchi**, *Acta Neuropathol* 79:300, 1979 (rat)
Guanidinopropionic acid		**de Tata**, *Int J Exp Pathol* 74:501, 1993 (rat)
HMGCA reductase inhibitors	Mitochondria	**Westwood**, *Toxicol Pathol* 33:246, 2005 (rat)
Marine toxins		
Centruroides toxin	Sodium channel	**Jaimovich**, *Proc Natl Acad Sci USA* 79:3896, 1982
Monensin		**Van Vleet**, *Am J Pathol* 114:461, 1984 (pig)
Neostigmine		
Phenazine methosulfate		**Duncan**, *Virch Arch B* 56:271, 1989 (frog)
Plant alkaloid	Mitochondria	**Freitas**, *Micros Res Tech* 69:108, 2006 (mouse, rat)
Veratrine		
Pyridostigmine bromide		**Schuschereba**, *Toxicol Pathol* 18:387, 1990 (rat)
Rolziracetam		**Watkins**, *Toxicol Pathol* 17:545, 1989 (dog)
Serotonin		**Narukami**, *Acta Neuropathol* 81:510, 1991 (rat)
Soman		**Dekleva**, *Acta Neuropathol* 79:183, 1989 (rat)
Strychnine		**Boyd**, *Am J Med* 74:507, 1983 (human)
Venoms		
Hornet	T tubules, sarcoplasmic reticulum	**Ishay**, *Toxicon* 13:57, 1975 (frog)
Snake	Membranes	**Dixon**, *J Neuropathol Exp Neurol* 55(12)1230, 1996; **Gutierrez**, *Exp Mol Pathol* 40:367, 1984; **Moreira**, *Exp Mol Pathol* 57:124, 1992; **Ownby**, *Am J Pathol* 85:149, 1976; **Ownby**, *Am J Pathol* 93:201, 1978; **Tu**, *Br J Exp Pathol* 64:633, 1984 (human)
Spider	Membranes	**Futrell**, *Am J Pathol* 95:675, 1979; **Kahn**, *J Mol Cell Cardiol* 41:256–264, 2006; **Ownby**, *Exp Mol Pathol* 38:283, 1983
Vincristine		**Anderson**, *J Neuropathol Exp Neurol* 26:15, 1967 (rat)
Vitamin E		**Bardosi**, *Acta Neuropathol* 75:166, 1988 (rat)
Zidovudine	Mitochondria	**de la Asuncion,** *J Clin Invest* 102(1):4, 1998 (mouse); **Lewis**, *Lab Invest* 65:228, 1991 (rat); **Shroeder**, *Acta Neuropathol* 85:39, 1992 (human); **Walker**, *Cardiovasc Toxicol* 04:133, 2004 (mouse)

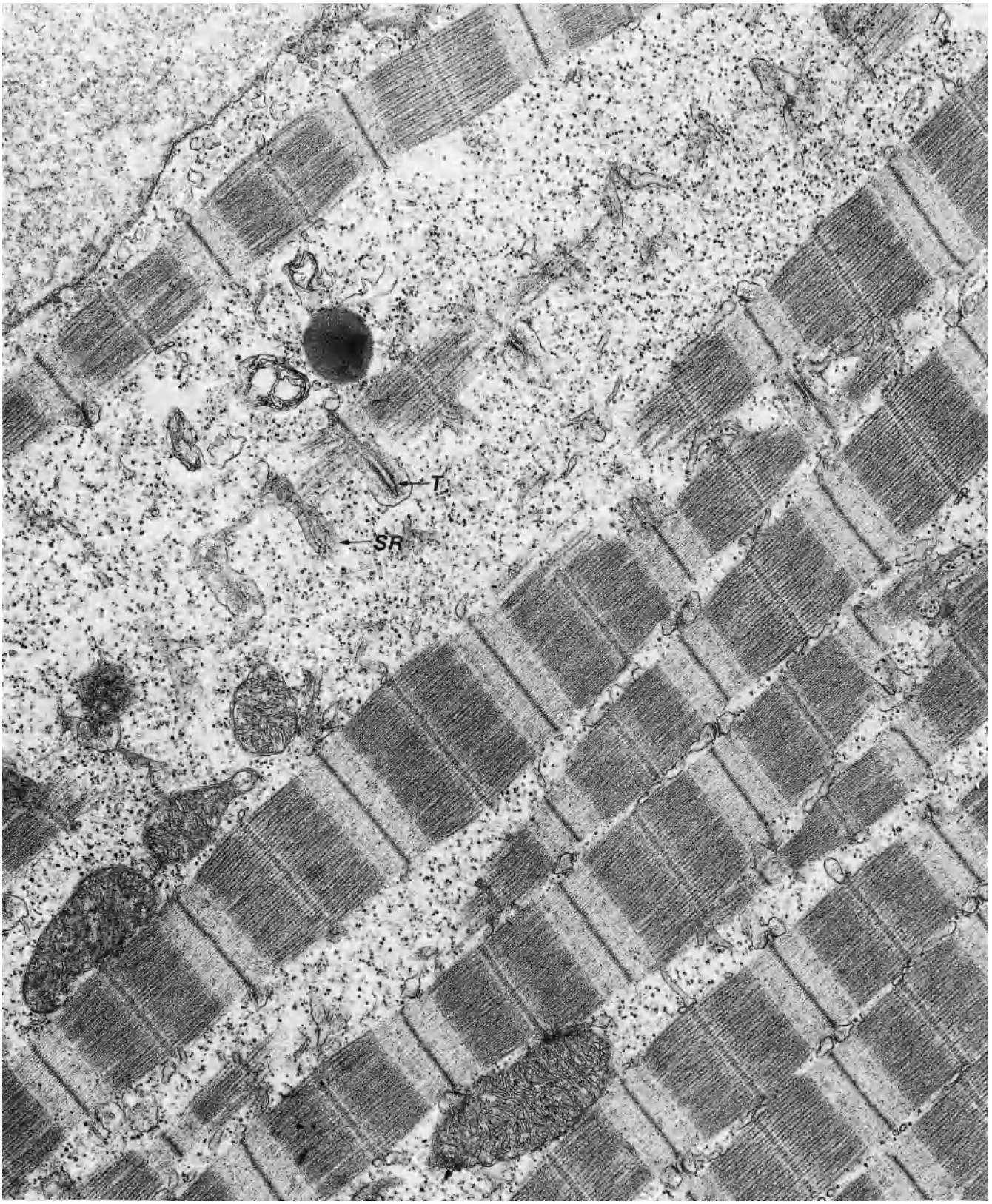


Fig. 18.13 Acute cell swelling: skeletal myocyte, aerolysin toxicity, frog. Cytoplasmic pallor, glycogen accumulation, mitochondrial swelling, and myofibrillar degeneration. Sarcoplasmic reticulum (*SR*) and T tubule system (*T*) are fragmented, and cisternae are swollen.

Snake venoms are mixtures of up to 30 different peptides, most of which are toxic either directly or through activity as enzymes. All snake venoms contain (1) phospholipase A_2, which has a direct lytic action on plasma membranes of erythrocytes, platelets, and other cells; (2) hyaluronidase, which cleaves internal glycoside bonds of acidic proteoglycans and glycosaminoglycans to facilitate diffusion of toxin into tissue; (3) phosphodiesterase; and (4) peptidases. Superimposed on these actions are different toxins in individual venoms that act specifically on neural, coagulation, and other organ systems.

Rattlesnakes and other pit vipers have fangs that reach deeply into muscle. Phospholipases and toxic peptidases in venom produce a direct lytic effect on cells of dermal connective tissue and on underlying skeletal muscle. Edema, hemorrhage, hemolysis, and muscle necrosis are produced by the combined effects of several toxins; but the phospholipases are largely responsible through their action on cell membranes.

A specific protein toxin for **skeletal myocytes** has been isolated from crude rattlesnake venom; it causes vacuolation within a few hours, progressing to loss of striation and myofiber necrosis. The primary site of action is the **sarcoplasmic reticulum,** which dilates and fragments early.[167,168] Large necrotic wounds are often complicated by infections produced by organisms introduced at the time of the bite. Ultrastructural analysis of tissue may reveal these bacteria. Rattlesnake envenomation releases nonenzyme peptides that produce increased vascular permeability, hypotension, and shock.[169]

Ultrastructural studies in skeletal muscle of mice injected with crude *Bothrops aspe* venom (or its purified phospholipase A) show widespread membrane damage, suggesting that plasma membranes of all cell types are the initial sites of injury, but that any discrete injury is soon masked by the rapidly progressive necrosis.[170] Massive capillary endothelial injury leads to hemorrhage, which is reported to occur through the endothelial cell rather than via intercellular junctions.[171]

The venom from the Australian tiger snake is a neurotoxin and myotoxin with phospholipase A_2 activity. Administration of the venom to rats causes lysis of the sarcolemma without internalization suggesting that its toxicity is not dependent on any direct effect on internal organelles or metabolism. The toxic phospholipase activity is not initiated solely by binding of the toxin to the sarcolemma as evidenced by the binding of the toxin to glycolytic muscle fibers, which are resistant to the effects of this toxin. An undetermined factor or event must take place for the phospholipase to exert its membrane destructive toxicity.[172]

Plant Alkaloids

Veratrine is an lipophilic alkaloid derived from the seed of veratrum plants of the Liliaceae family. It activates sodium channels of cell membranes. The unwanted cardiovascular effects limit its use to primarily experimental purposes. The toxicity may result from the toxins effect on the sarcolemma causing excessive early influx of sodium. Mitochondrial changes of electron lucency and cristolysis, to which oxidative fibers are more sensitive, could be secondary to the sarcolemma permeability changes. However, direct mitochondria effects should be considered because veratrine does alter mitochondrial respiration and structure both in vivo and in vitro. Since mitochondrial membranes do not possess sodium channels it may be that the toxin alters mitochondrial membranes structure creating a structural change that affects respiration.[173]

Smooth Muscle Toxicity

Vascular Toxicity

Smooth Muscle Relaxants

Various compounds have been reported to cause coronary arterial injury in dogs. These include minoxidil, digitalis, hydralazine theobromine, and phosphodiesterase III inhibitors. The mechanism of this injury may be related to the vasodilatory or to the positive inotropic properties of these compounds. Adenosine is a potent vasodilator of the coronary artery and **adenosine agonists** have been designed as potential antihypertensive drugs. Tested in dogs, these have caused electrocardiographic abnormalities and arteriopathy. The arterial lesions are characterized by vacuolation and necrosis of the media, inflammatory cell infiltrates, and transmural fibrosis. Ultrastructurally, endothelium was retracted and necrosis extended through the muscular layers. There was subendothelial accumulation of fibrin and platelets, and infiltration by granulocytes and monocytes into the arterial wall.[174]

Dopamine agonists and phosphodiesterase inhibitors, which act to elevate levels of cAMP, cause necrosis of vascular smooth muscle. Cardiac necrosis has also been noted for the phosphodiesterase inhibitors. The vascular beds affected vary with species. Lesions occur at all levels of the affected vascular bed. Loss of integrity of the internal elastic lamina was noted for the dopamine agonist **fendolapam** and hemorrhage and necrosis of the medial of larger vessels with accompanying inflammation for both classes of compounds. The most pronounced lesions are of the splanchnic vessels, which were proposed to result from excessive dilation. However mechanical changes

are not likely the only factors causing toxicity. Molecular mechanisms of endothelial cell activation, apoptosis and necrosis of the endothelium and medial smooth muscle contribute to the toxicity.[175,176]

Minoxidil (2,4-diamino-6-piperidinopyrimidine) is a potent long-acting vasodilating drug that lowers blood pressure by acting directly on arteriolar smooth muscle. The mechanism of action appears to be due to K^+ channel agonist properties; its hypotensive action is not blocked by β-adrenergic receptor antagonists or by anticholinergic or antihistaminic agents. In humans, high doses may cause signs of reflex sympathetic activation; for example, tachycardia, increased venous return, and increased cardiac output.

In preclinical tests of minoxidil in animals, hemorrhages were found in the right atrial walls in dogs, but not rodents. Left ventricular myocardial necrosis and hemorrhages in the right antrum were most common. Later studies using doses of minoxidil 3 mg/kg (twice daily) caused endothelial contraction and necrosis, basement membrane disintegration, and damage to internal elastic membranes.[177] Experiments in pigs revealed marked changes in arterioles with hemorrhages and foci of necrosis in the papillary muscles from the resulting ischemic injury.[178] Ultrastructural changes revealed vascular damage and capillaries occluded by leukocytes and platelets. In affected cardiac myocytes there were mitochondrial flocculent densities (with striking mineralization of mitochondria in late phases), myofibrillar lysis, pyknotic nuclei, and an increase in lipids in the sarcoplasm—all evidence of ischemic injury.

Immunosuppressive Agents

The calcineurin immunosuppressive agents cyclosporin and tacrolimus are associated with renal arteriolopathy and rarer thrombotic microangiography. The former causes vacuolation of the endothelium and vacuolation, apoptosis or necrosis of the vascular smooth muscle. The smooth muscle is replaced by plasma insudates, which can budge into the adventitia and subendothelial area.[179]

Allylamine Necrosis

Allylamine is an aliphatic amine used in the production of pharmaceuticals and polymers. Consumption of allylamine causes multifocal myocardial necrosis associated with severe small blood vessel and endocardial injury. Several species of animals are susceptible to allylamine. In acute injury foci of necrosis are associated with marked infiltrates of monocytes and macrophages.[180] In subacute and chronic toxicity, there is progressive fibrosis. Additional changes include vascular intimal hyperplasia in arterioles, transmural scarring, ventricular aneurysm formation, and endocardial cartilaginous metaplasia. Bizarre mitochondrial lesions, probably associated with ischemic injury, include rearrangements of cristae into plates and spiral forms.[181]

Biological Smooth Muscle Toxins

Venoms

In some snake poisoning, a direct cardiotoxic effect is responsible for death. These cases are rare but are apt to occur when envenomation occurs in blood vessels. **Sarafotoxins** are a group of cysteine-rich isocardiotoxic peptides isolated from the venom of the snake *Atractaspis engaddensis*. Some are highly lethal and cause cardiac arrest in mice within minutes of intravenous injection. Effects include a marked vasoconstriction of coronary vessels, a severe atrioventricular block, and a strong positive inotropic effect that is not blocked by α- or β-adrenergic blockers. Sarafotoxins show a high degree of amino acid sequence homology with endothelin, a natural vasoconstrictor of mammalian vascular systems.[182] Antagonist to endothelin demonstrates a vascular toxicity.[183,184]

Radiation Injury

Radiation-induced disease occurs in human patients that receive large doses of therapeutic, antineoplastic radiation. Tissue injury generally results from vascular lesions. In the **heart,** early changes of endothelial cell swelling and altered capillary permeability are followed by basement membrane reduplication, platelet aggregation, and phagocytosis.[185,186] Late phases of injury lead to myocardial fibrosis.[187]

References

1. Funatsu T, et al. 1993. Elastic filaments in situ in cardiac muscle. *J Cell Biol* 120:711.
2. Ganong WF. 2005. Exertable tissue: Muscle. In: Review of Medical Physiology, 22nd ed. McGraw-Hill, New York, pp. 65–84.
3. Laird DW, Revel J-P. 1990 Biochemical and immunologic analysis of the arrangement of connexin43 in rat heart gap junction membranes. *J Cell Sci* 97:109.
4. Abedin Z, et al. 1975. Myocardium of hypothermic rats with and without administration of dextran. *Lab Invest* 33:324.
5. Ferrans VJ, et al. 1971. Effects of hyperosmotic perfusate on ultrastructure and function of the isolated canine heart. *Lab Invest* 24:265.

6. Zimny ML, et al. 1968. Ultrastructural modifications of the intercalated disc during hypothermia in the rat and the ground squirrel. *Cryobiology* 4:317.
7. Shear CR, Block RJ. 1985. Vinculin in subsarcolemmal densities in chicken skeletal muscle. *J Cell Biol* 101:241.
8. Huet M, Cantin M. 1974. Ultrastructural cytochemistry of atrial muscle cells. Lab Invest 30:514 and 525.
9. Carpenter S, Karpati G. 2001. Normal organelles and other constituents of skeletal muscle cells. In: Pathology of Skeletal Muscle. Oxford University Press, New York, pp. 131–275.
10. Braund KG, et al. 1982. Observations on normal skeletal muscle of mature dogs: A cytochemical, histochemical and morphometric study. *Vet Pathol* 19:577.
11. Kuzon WM, et al. 1989. A comparative histochemical and morphometric study of canine skeletal muscle. *Can J Vet Res* 53:125.
12. Adhihetty PJ, et al. 2005. Differential susceptibility of subsarcolemmal and intermyofibrillar mitochondria to apoptotic stimuli. *Am J. Physiol Cell Physiol* 289: C994.
13. Riva A, et al. 2005. Structural differences in two biochemically defined populations of cardiac mitochondria. *Am J Physiol Heart Circ Physiol* 289:H868.
14. Buja LM, et al. 1972. Occurrence of intramitochondrial glycogen in canine myocardium after prolonged anoxic cardiac arrest. *J Mol Cell Cardiol* 4:237.
15. Marin AM, et al. 1969. Mechanisms in the development of myocardial lesions in hemorrhagic shock. *Ann New York Acad Sci* 156:79.
16. Kloner RA, et al. 1978. Effect of propranolol on mitochondrial morphology during acute myocardial ischemia. *Am J Cardiol* 41:880.
17. Gustafsson AB, Gottlieb RA. 2008. Heart mitochondria: Gates of life and death. *Cardiovas Res*. 77:334.
18. Powers SK, et al. 2007. Ischemia-reperfusion-induced cardiac injury: A brief review. *Med & Sci in Sports & Exer* 39(9):1529.
19. Hicks L, Fahimi HD. 1977. Peroxisomes (microbodies) in the myocardium of rodents and primates: A comparative ultrastructural cytochemical study. *Cell Tiss Res* 175:467.
20. Forbes MS, et al. 1985. The sarcoplasmic reticulum of mouse heart. *J Ultrastr Res* 93:1.
21. Jorgensen AO, et al. 1993. The Ca^{2++}-release channel/ryanodine receptor is localized in junctional and corbular sarcoplasmic reticulum in cardiac muscle. *J Cell Biol* 120:969.
22. Block BA, et al. 1988. Structural evidence for direct interaction between the molecular components of the transverse tubular/sarcoplasmic reticulum junction in skeletal muscle. *J Cell Biol* 107:2587.
23. Jorgensen AO, et al. 1985. Ultrastructural localization of calsequestrin in adult rat atrial and ventricular muscle cells. *J Cell Biol* 101:257.
24. Marks AR, et al. 1991. The ryanodine receptor/junctional channel complex is regulated by growth factors in a myogenic cell line. *J Cell Biol* 114:303.
25. Mitchell RD, et al. 1983. Morphology of isolated triads. *J Cell Biol* 96:1017.
26. Fan G-C, Yuan Q, et al. 2008. Regulatory roles of junctin in sarcoplasmic reticulum calcium cycling and myocardial function. *TCM* 18(1):1.
27. Gyorke I, Hester N. 2004. The role of calsequestrin, triadin, and junctin in conferring cardiac ryanodine receptor responsiveness to luminal calcium. *Biophys J* 86:2121.
28. Gergs U, et al. 2007. On the role of junctin in cardiac Ca^{2+} handling, contractility, and heart failure. *Am J Physiol Heart Circ Physiol* 293:H728.
29. Beuter G, et al. 2005. Type I ryanodine receptor in cardiac mitochondria: Transducer of excitation—metabolism coupling. *Biochimica et Biophysica Acta* 1717:1.
30. Csordas G, Thomas AP. 2001. Calcium signal transmission between ryanodine receptors and mitochondria in cardia muscle. *TCM* 11(7).
31. Szalai G, et al. 2000. Calcium signal transmission between ryanodine receptors and mitochondria. *Journal Biol Chem* 257(20)15305.
32. Sharov VG, et al. 1989. Ultrastructure of Purkinje cells in the subendocardium and false tendons in early experimental myocardial infarction complicated by fibrillation in the dog. *Virch Arch [B]* 27:131.
33. Fleming I. 2008. Vascular cytochrome P450 enzymes: Physiology and pathophysiology. *TCM* 18(1):20.
34. McCallister LP, Page E. 1973. Effects of thyroxin on ultrastructure of rat myocardial cells: A stereological study. *J Ultrastruct Res* 42:136.
35. Boor PJ, et al. 1979. Tubuloreticular structures in myocardium. *J. Molec Cell Cardiol* 11:967.
36. Anversa P, et al. 1979. Morphometric study of myocardial hypertrophy induced by abdominal aortic stenosis. *Lab Invest* 40:341.
37. Hunter JJ, Chien KR. 1999. Signaling pathways for cardiac hypertrophy and failure. *New Engl J Med* 341(17):1276.
38. McMullen JR, et al. 2005. Physiological versus pathological cardiac hypertrophy. In: Molecular Mechanisms of Cardiac Hypertrophy and Failure. London, Informa Healthcare, p. 117.
39. Arola OJ, et al. 2000. Acute doxorubicin cardiotoxicity involves cardiomyocyte apoptosis. *Cancer Res* 60:1789.
40. Bishop SP, Cole CR. 1969. Ultrastructural change in the canine myocardium with right ventricular hypertrophy and congestive heart failure. *Lab Invest* 20:219.
41. Fuster V, et al. 1977. Quantitation of left ventricular fibre hypertrophy and interstitial tissue in human hearts with chronically increased pressure and volume overload. *Circulation* 55:504.
42. Gregory MA, et al. 1984. Myocardial ischaemia in constrictive pericarditis—morphometric and electron microscopical study. *Br J Exp Pathol* 65:365.
43. Maron BJ, et al. 1975. Myocardial ultrastructure in patients with chronic aortic valve disease. *Am J Cardiol* 35:725.
44. Maron BJ, Ferrans VJ. 1978. Ultrastructural features of hypertrophied human ventricular myocardium. *Prog Cardiovasc Dis* 21:207.
45. Gregory MA, Whitton ID. 1990. A morphological control for ventricular pathology in man: A

morphometric and morphologic assessment of LV myofibers in secundum ASD. *Br J Exp Pathol* 71:771.
46. Breisch EA, et al. 1984. Myocardial characterization of pressure overload hypertrophy. *Lab Invest* 51:333.
47. Maron BJ, et al. 1975. Myocardial ultrastructure in patients with chronic aortic valve disease. *Am J Cardiol* 351.
48. Stoner CD, et al. 1973. Normal lysosomal enzyme levels in hypertrophied and failing dog hearts. *J Mol Cell Cardiol* 5:171.
49. Mandache E, et al. 1973. The proliferative activity of the heart tissues in various forms of experimental cardiac hypertrophy studied by electron microscope autoradiography. *Virch Arch B* 12:112.
50. Martorana PA, et al. 1984. Increased myocardial capillary density in dogs with experimental emphysema. *Lab Invest* 50:592.
51. Olivetti G, et al. 1979. Morphometric study of the atrioventricular node in normal and hypertrophic rat heart. *Lab Invest* 40:331.
52. Onishi S, et al. 1969. Das elektronenmikroskopische Bild der Herzmuskelzelle des Hundes bei experimenteller Herzhypertrophie in der Anpassungsphase. *Beitr Pathol* 139:94.
53. Sharov VG, et al. 1996. Evidence of cardiocyte apoptosis in myocardium of dogs with chronic heart failure. *Am J Pathol* 148:141.
54. Bishop SP. 1992. The myocardial cell: Normal growth, cardiac hypertrophy and response to injury. *Toxicol Pathol* 18:438.
55. Suliman HB, et al. 2007. The CO/HO system reverses inhibition of mitochondrial biogenesis and prevents murine doxorubicin cardiomyopathy. *J Clin Invest* 117(12)3730.
56. Van Vleet JF, et al. 1991. Cardiovascular and skeletal muscle system. In: Haschek, WM, Rousseaux, CG, eds. Toxicologic Pathology. Academic Press, San Diego.
57. Carpenter S, Karpati G. 2001. Major pathological reactions and their consequences for skeletal muscle. *Pathology of Skeletal Muscle* Chap 4, p. 63.
58. Zhou YT, et al. 2000. Lipotoxic heart disease in obese rats: Implications for human obesity. *Proc NAS* 97(4):1784.
59. Caulfield J, Klionsky B. 1959. Myocardial ischemia and early infarction: An electron microscopic study. *Am J Pathol* 35:489.
69. Ganote CE. 1975. Experimental myocardial ischemic injury. II. Effect of in vivo ischemia on dog heart slice function in vitro. *J Molec Cell Cardiol* 8:189.
61. Korb G, Totovic V. 1969. Electron microscopical studies on experimental ischemic lesions of the heart. *Ann New York Acad Sci* 156:48.
62. Willerson JT, et al. 1977. Abnormal myocardial fluid retention as an early manifestation of ischemic injury. *Am J Pathol* 87:159.
63. Decker RS, Wildenthal K. Lysosomal alterations in heart, skeletal muscle, and liver of hyperthyroid rabbits. *Lab Invest* 44:455, 1981.
64. Kahn S, et al. 2006. Rapamycin confers preconditioning-like protection against ischemia-reperfusion injury in isolated mouse heart and cardiomyocytes. *J Mol Cell Cardiol* 41:256.
65. Matsui Y, et al 2007. Distinct roles of autophagy in the heart during ischemia and reperfusion. *Circ Res* 100:914.
66. Stansfield W, et al. 2007. Proteasome inhibition attenuates infarct size and preserves cardiac function in a murine model of myocardial ischemia-reperfusion injury. *Ann Thorac Surg* 84:120.
67. Burwell LS, Brookes PS. 2007. Mitochondria as a target for the cardioprotective effects of nitric oxide in ischemia-reperfusion injury. *Antioxid Redox Signal* 10:579.
68. Busing CM, Kreinsen U. 1975. Light and electron microscopic examinations of experimentally produced heart muscle necroses following normobaric hyperoxia. *Vinchows Archiv A Path. Anat. Histol* 366:137.
69. Cuenoud HF, et al. 1978. Ultrastructure of the myocardium after pulmonary embolism. *Am J Pathol* 92:421.
70. Engler RL, et al. 1983. Leukocyte capillary plugging in myocardial ischemia and reperfusion in the dog. *Am J Pathol* 111:98.
71. Hoffstein S, et al. 1975. Colloidal lanthanum as a marker for impaired plasma membrane permeability in ischemic dog myocardium. *Am J Pathol* 79:207.
72. Armiger LC, et al. 1977. Fine structural changes in dog myocardium exposed to lowered pH in vivo. *Lab Invest* 37:237.
73. Caulfield JB, Borg TK. 1979. The collagen network of the heart. *Lab Invest* 40:364.
74. Vracko R, et al. 1988. Myocyte reactions at the borders of injured and healing rat myocardium. *Lab Invest* 59:104.
75. Vracko R, Thorning D. 1991. Contractile cells in rat myocardial scar tissue. *Lab Invest* 65:214.
76. Chiu HC, et al. 2001. A novel mouse model of lipotoxic cardiomyopathy. *J Clin Invest* 107(7):813.
77. Finck BN, Han X. 2003. A critical role for PPARα-mediated lipotoxicity in the pathogenesis of diabetic cardiomyopathy: Modulation by dietary fat content. *Proc NAS* 100(3):1226.
78. Pruimboom-Brees I, et al. 2006. A critical role for peroxisomal proliferator-activated receptor-α nuclear receptors in the development of cardiomyocyte degeneration and necrosis. *Am J Pathol* 169(3):750.
79. Unger RH, Zhou YT. 1999. Regulation of fatty acid homeostasis in cells: Novel role of leptin. *Proc NAS* 96:2327.
80. Bonnard C, et al. 2008. Mitochondrial dysfunction results from oxidative stress in the skeletal muscle of diet-induced insulin-resistant mice. *J Clin Invest* 118(2):789.
81. Fiaccavento R, et al. 2006. α-Linolenic acid-enriched diet prevents myocardial damage and expands longevity in cardiomyopathic hamsters. *Am J Pathol* 169(6):1913.
82. Mergner W, Jones R. 1991. Ultrastructure and histology of the heart and cardiovascular system in toxic injury. In: Baskin, S, ed. Cardiac Toxicology. CRC Press, Boca Raton, FL, pp. 167–201.

83. Herman EH, et al. 1998. Comparison of the chronic toxicity of piroxantrone, losoxantrone and doxorubicin in spontaneously hypertensive rats. *Toxicology* 128:35.
84. Zagoren JC, et al. 1984. The evolution of cellular degeneration in dorsal root ganglia exposed to doxorubicin in tissue culture. *J Neuropathol Exp Neurol* 43:384.
85. Unverferth DV, et al. 1981. Human myocardial morphologic and functional changes in the first 24 hours after doxorubicin administration. *Cancer Treat Rep* 65:1093.
86. Papoian T, Lewis W. 1992. Anthracyclines selectively decrease α cardiac actin mRNA abundance in the rat heart. *Am J Pathol* 141:1187.
87. Zhang J, et al. 1993. Dendritic cells in the hearts of spontaneously hypertensive rats treated with doxorubicin with or without ICRF-187. *Am J Pathol* 142(6):1916.
88. Wallace KB. 2003. Doxorubicin-induced cardiac mitochondrionopathy. *Pharmacol Toxicol* 93:105.
89. Childs AC, et al. 2002. Doxorubicin treatment in vivo causes cytochrome c release and cardiomyocyte apoptosis, as well as increased mitochondrial efficiency, superoxide dismutase activity and Bcl-2:Bax ratio. *Cancer Res* 62:4592.
90. Zhou S, et al. 2001. Cumulative and irreversible cardiac mitochondrial dysfunction induced by doxorubicin. *Cancer Res* 61:771.
91. Zhou Z, Kang J. 2000. Immunocytochemical localization of metallothionein and its relation to doxorubicin toxicity in transgenic mouse heart. *Am J Pathol* 156(5):1653.
92. Doroshow JH, et al. 1985. Ultrastructural features of adriamycin-induced skeletal and cardiac muscle toxicity. *Am J Pathol* 118:288.
93. Zanon PL, et al. 1976. Myocardial injury induced by a single dose of adriamycin: An electron microscopic study. *Tumori* 62:517.
94. Lushnikova EL, et al. 2005. Ultrastructural criteria of cardiomyocyte regeneratory and plastic insufficiency in anthracycline cardiomyopathy. *Bull Exp Biol Med* 139(4):472.
95. Olson HM. 1974. Electrolyte and morphological alterations of myocardium in adriamycin-treated rabbits. *Am J Path* 77:439.
96. Olson RD, Mushlin PS. 1990. Doxorubicin cardiotoxitiy: Analysis of prevailing hypotheses. *FASEB* 4:3076.
97. Jaenke RS. 974. An anthracycline antibiotic-induced cardiomyopathy in rabbits. *Lab Invest* 30:292.
98. Iwasaki T, Suzuki T. 1991. Ultrastructural alterations of the myocardium induced by doxorubicin. *Virch Arch* B 6035.
99. Payne CM. 1982. A quantitative analysis of leptomeric fibrils in an adriamycin/carnitine chronic mouse model. *J Submicrosc* Cytol 14337.
100. Alderton PM, et al. 1992. Comparative study of doxorubicin, mitoxantrone, and epirubicin in combination with ICRF-187 (ADR-529) in a chronic cardiotoxicity animal model. *Cancer Res* 52:194.
101. Crone SA, et al. 2002. ErbB2 is essential in the prevention of dilated cardiomyopathy. *Nat Med* 8(5):459.
102. Danial NN, Korsmeyer SJ. 2004. Cell death: Critical control points. *Cell* 116:205.
103. Grazette LP, Boecker W. 2004. Inhibition of ErbB2 causes mitochondrial dysfunction in cardiomyocytes. *J Am Coll Cardiol* 44(11):2231.
104. Kerkela R, et al. 2006. Cardiotoxicity of the cancer therapeutic agent imatinib mesylate. *Nat Med* 12(8):908.
105. Hendy RJ, et al. 1969. The effect of chloroquine on rat heart lysosomes. *J Ultrastruct Res* 29:485.
106. Siddiqui AK, et al. 2007. Hydroxychloroquine-induced toxic myopathy causing respiratory failure. *Chest* 131:588.
107. Albay D, Adler SG. 2005. Chloroquine-induced lipidosis mimicking Fabry disease. *Mod Pathol* 18:733.
108. Anderson N, Borlak J. 2006. Drug-induced phospholipidosis. *FEBS Letters* 580:5533.
109. Reasor MJ, et al. 2006. Drug-induced phospholipidosis: Issues and future directions. *Expert Opin Drug Saf* 5(4):567.
110. Macdonald RD, Engel AG. 1970. Experimental chloroquine myopathy. *J Neuropathol Exp Neurol* 29:479.
111. Fischer VW. 1976. Evolution of a chloroquine-induced cardiomyopathy in the chicken. *Exp Molec Pathol* 25:242.
112. Trout JJ, et al. 1981. Chloroquine-induced alterations in phasic muscles. II. Sarcoplasmic reticulum. *Exp Molec Pathol* 34:237.
113. Van Vleet JF, et al. 1983. Clinical, clinicopathologic, and pathologic alterations of monensin toxicosis in swine. *Am J Vet Res* 44:1469.
114. Van Vleet JE, Ferrans VJ. 1984. Ultrastructural alterations in skeletal muscle of pigs with acute monensin myotoxicosis. *Am J Pathol* 114:461.
115. Van Vleet JE, Ferrans VJ. 1984. Ultrastructural alterations in the atrial myocardium of pigs with acute monensin toxicosis. *Am J Pathol* 114:367.
116. Van Vleet JF, et al. 1983. Clinical, clinicopathologic, and pathologic alterations in acute monensin toxicosis in cattle. *Am J Vet Res* 44:2133.
117. Van Vleet JF, Ferrans VJ. 1983. Ultrastructural myocardial alterations in monensin toxicosis of cattle. *Am J Vet Res* 44:1629.
118. Muntz KH, et al. 1984. Redistribution of catecholamines in the ischemic zone of the dog heart. *Am J Pathol* 114:64.
119. Ferrans V, et al. 1969. Sympathomimetic agents and cardiac necrosis. *Ann N Y Acad Sci* 156:309.
120. Korb G. 1965. Elektronenmikroskopische Untersuchungen zur Aludrin (Isoproteronolsulfat)-Schadigung des Herz Muskel. *Virch Arch A* 339:136.
121. Menaker L, et la. 1974. Gel eletrophoresis of whole saliva and associated histologic changes in submandibular glands of isoproteronal-treated rats. *Lab Invest* 30:341.
122. Noronha-Dutra AA, et al. 1984. The early changes induced by isoproteronal in the endocardium and adjacent myodarium. *Am J Pathol* 114:231.
123. Ferrans V, et al. 1964. Isoproterenol-induced myocardial necrosis. *Am Heart J* 68:71.

124. Singal PK, et al. 1981. Protective effect of zinc against catecholamine-induced myocardial changes. *Lab Invest* 44:426.
125. Hagopian M, et al. 1972. An ultrastructural study of the effect of reserpine on ventricular cardiac muscle of active and hibernating bats (*Myotis lucifugus*). *Lab Invest* 27:99.
126. Van Vleet JF, Ferrans VJ. 1983. Congestive cardiomyopathy induced in ducklings fed graded amounts of furazolidone. *Am J Vet Res* 44:76.
127. Webb DM, Van Vleet JF. 1991. Early clinical and morphologic alterations in the pathogenesis of furazolidone-induced toxicosis in ducklings. *Am J Vet Res* 52:1531.
128. Barth AT, et al. 1994. Coffee senna (*Senna occidentalis*) poisoning in cattle in Brazil. *Vet Human Toxicol* 36:541.
129. Raczniak TJ, et al. 1978. Ultrastructure of the right ventricle after monocrotaline-induced cor pulmonale in the nonhuman primate (*Macaca arctoides*). *Exp Molec Pathol* 28:107.
130. Hibbs BG, et al. 1965. Alcoholic myocardiopathy. *Am Heart J* 69:766.
131. Gradman AH. 1988. Cardiac effects of cocaine. *Yale J Biol Med* 61:137.
132. Schubert W, et al. 2007. Caveolin-1(−/−) and caveolin-2(−/−)-deficient mice both display numerous skeletal muscle abnormalities, with tubular aggregate formation. *Am J Pathol* 170(1):316.
133. Lang CH, et al. 2000. Alcohol myopathy: Impairment of protein synthesis and translation initiation. *Int Journal Biochem Cell Biol* 33:457.
134. Owczarek J, et al. 2005. Drug-induced myopathies: An overview of the possible mechanisms. *Pharmacological Reports* 57:23.
135. Hammond GL, et al 1979. Molecular signals for initiating protein synthesis in organ hypertrophy. *Proc NAS* 76:2455.
136. Flexner C. 2006. Antiretroviral agents and treatment of HIV infection. In: Brunton, L, ed. Goodman & Gilman's the Pharmacological Basis of Therapeutics, 11th ed. McGraw-Hill, New York.
137. Dalakas MC, et al. 1990. Mitochondrial myopathy caused by long-term zidovudine therapy. *New Engl J Med* 322:1098.
138. De la Asuncion JG, et al. 1998. AZT treatment induces molecular and ultrastructural oxidative damage to muscle mitochondria. *J Clin Invest* 102(1):4.
139. Lamperth L, et al. 1991. Abnormal skeletal and cardiac muscle mitochondria induced by zidovudine (AZT) in human muscle *in vitro* and in an animal model. *Lab Invest* 65:742.
140. Lewis W, et al. 1991. Mitochondrial ultrastructural and molecular changes induced by zidovudine in rat hearts. *Lab Invest* 65:228.
141. Walker DM, et al. 2004. Persistence of mitochondrial toxicity in hearts of female B6C3F1 mice exposed in utero to 3″-azido-3″-deoxythymidine. *Cardiovasc Toxicol* 04:133.
142. Anderson PJ, et al. 1967. The fine structure of spheromembranous degeneration of skeletal muscle induced by vincristine. *J Neuropathol Exp Neurol* 26:15.
143. Fernandez C, et al. 2002. Colchicine myopathy: A vacuolar myopathy with selective type I muscle fiber involvement. A immunohistochemical and electron microcopic study of two cases. *Acta Neuropath* 103:100.
144. Kuncl RW, et al. 2003. Exocytic "constipation" is a mechanism of tubulin/lysosomal interaction in colchicine myopathy. *Exp Cell Res 285:196*.
145. Westwood FR, Bigley A. 2005. Statin-induced muscle necrosis in the rat: Distribution, development, and fibre selectivity. *Toxicol Pathol* 33:246.
146. Marcoff L, Thompson PD. 2007. The role of coenzyme Q10 in statin-associated myopathy. *J Am Coll Cardiol* 49(23):2231.
147. Dirks AJ, Jones KM. 2006. Statin-induced apoptosis and skeletal myopathy. *Am J Cell Physiol* 291:C1208.
148. Kaufmann P, et al. 2006. Toxicity of statins on rat skeletal muscle mitochondria. *Cell Mol Life Sci* 63:2415.
149. Baker SK. 2005. Molecular clues into the pathogenesis of statin-mediated muscle toxicity. *Muscle Nerve* 31:572.
150. Sewright KA, et al. 2007. Statin myopathy: Incidence, risk factors, and pathophysiology. *Curr Atheroscler Rep* 9:389.
151. Sevory CA. 1985. Ultrastructural changes in diseases muscle. In: Dubowitz, V, ed. Muscle Biopsy: A Practical Approach. Bailliere Tindall, London, p. 129.
152. Fischer G. 1970. Dis Azetlycholinesterase an der motorischen Endplatte des Rattenzwerchfells nach Intoxication mit Paraoxon und Soman bei Applikation von Oximen. *Experientia* 26:402.
153. Kawapuchi M, et al. 1976. Myopathic changes at the end-plate region induced by neostigmine methylsulfate. *Experientia* 32:623.
154. Preusser HJ. 1967. Die Ultrastruktur der motorischen Endplatte im Zwerchfell der Ratte und Veranderungen nach Inhibierung der Acetylcholinesterase. *Zellforsch* 80:436.
155. Dekleva A, et al. 1989. Attenuation of soman-induced lesions of skeletal muscle by acetylcholinesterase reactivating and non-reactivating antidotes. *Acta Neuropathol* 79:183.
156. Zink W, Seif C. 2003. The acute myotoxic effects of bupivacaine and ropivacaine after continuous peripheral nerve blockades. *Anesth Analg* 97:1173.
157. Boyer EW, Shannon M. 2005. The serotonin syndrome. *New Engl J Med* 352:1112.
158. Isbister GK, Buckley NA. 2005. The pathophysiology of serotonin toxicity in animals and humans. *Clin Neuropharmacol* 28(5):205.
159. Waring WS, et al. 2006. Olanzapine overdose is associated with acute muscle toxicity. *Hum Exp Toxicol* 25:735.
160. Demello FJ, et al. 1974. Ultrastructural study of clostridial myositis. *Arch Pathol* 97:118.
161. Cotran RS. 1967 Studies on inflammation. *Lab Invest* 17:39.
162. Strunk SW, et al. 1967. Ultrastructural studies on the lesions produced in skeletal muscle fiber by crude type A *Clostridium perfringens* toxin and its purified alpha fraction. *Am J Pathol* 50:89.

163. Zachs SI, Scheff MF. 1968. Tetanus toxin. *Science* 159:643.
164. Ownby CL, Odell GV. 1983. Pathogenesis of skeletal muscle necrosis induced by tarantula venom. *Exp Mol Pathol* 38:283.
165. Futrell et al. 1979. Localization of brown recluse venom attachment sites on human erythrocytes by ferritin-labeled antibody technique. *Am J Pathol* 95:675.
166. Ishay J, et al. 1975. A lesion of muscle transverse tubular system by oriental hornet (*Vespa orientalis*) venom. *Toxicon* 13:57.
167. Ownby CL, et al. 1976. Isolation of myotoxic component from rattlesnake (*Crotalis viridis viridis*) venom. *Am J Pathol* 85:149.
168. Ownby CL, et al. 1978. Hemorrhagic toxins from rattlesnake (*Crotalus atrox*) venom. *Am J Pathol* 93:201.
169. Schaeffer RC, et al. 1979. Cardiovascular failure produced by a peptide from the venom of the southern Pacific rattlesnake, *Crotalus viridis* Helleri. *Toxicon* 17:447.
170. Gutierrez JM, et al. 1984. Pathogenesis of myonecrosis induced by crude venom and a myotoxin of *Bothrops asper*. *Exp Mol Pathol* 40:367.
171. Moreira L, et al. 1992. Ultrastructural alterations in mouse capillary blood vessel after experimental injection of venom from the snake *Bothrops asper* (Terciopelo). *Exp Mol Pathol* 57:124.
172. Dixon RW, Harris JB. 1996. Myotoxic activity of the toxic phospholipase, notexin, from the venom of the Australian tiger snake. *J Neuropathol Exp Neurol* 55(12)1230.
173. Freitas EMS, et al. 2006. Effects of veratrine on skeletal muscle mitochondria: Ultrastructural, cytochemical, and morphometrical studies. *Micros Res Tech* 69:108.
174. Metz AL, et al. 1991. Acute cardiovascular toxicity induced by an adenosine agonist-antihypertensive in beagles. *Toxicol Pathol* 19:98.
175. Ikegami H, et al. 2001. Histopathological and immunohistochemical studies on arteritis induced by fenoldopam, a vasodilator, in rats. *Exp Toxic Pathol* 53:25.
176. Zhang J, et al. 2002.SK&F 95654-induced acute cardiovascular toxicity in Sprague-Dawley rats – histochemical, electron microscopic and immunohistochemical studies. *Toxicol Pathol* 30(1):28.
177. Herman EH, et al. 1989. A comparative study of minoxidil-induced myocardial lesions in beagle dogs and miniature swine. *Toxicol Pathol* 17:182.
178. Van Vleet JF, et al. 1984. Cardiac mophologic alterations in acute minoxidil cardiotoxicity in miniature swine. *Exp Molec Pathol* 41:10.
179. Liptak P, Ivanyi B. 2006. Primer: Histopathology of calcineurin-inhibitor toxicity in renal allografts. *Nat Clin Pract Nephrol* 2(7):398.
180. Boor PJ, et al. 1979. Tubuloreticular structures in myocardium. *J Molec Cell Cardiol* 11:967.
181. Boor PJ, Ferrans VJ. 1985. Ultrastructural alterations in allylamine cardiovascular toxicity. *Am J Pathol* 121:39.
182. Kloog Y, et al. 1988. Sarafotoxin, a novel phosphoinositide hydrolysis in rat heart and brain. *Science* 242:268.
183. Albassam MA, et al. 1999. Coronary arteriopathy in monkeys following administration of CI-1020, an endothelin A receptor antagonist. *Toxicol Path* 27:2:156.
184. Albassam MA, et al. 2001. Studies on coronary arteriopathy in dogs following administration of CI-1020, an endothelin A receptor antagonist. *Toxicol Path* 29(3):277.
185. Allen JR and Carstens LA. 1968. Response of *Saimir sciurers* monkeys to total body X-irradiation. *Am J Vet Res* 29:2189.
186. Khan MY and Ohanian M 1973. Radiation induced cardiomyopathy. *Am J Pathol* 74:125.
187. Fajardo LF and Stewart JR. 1973. Pathogenesis of radiation induced myocardial fibrosis. *Lab Invest* 29:244.

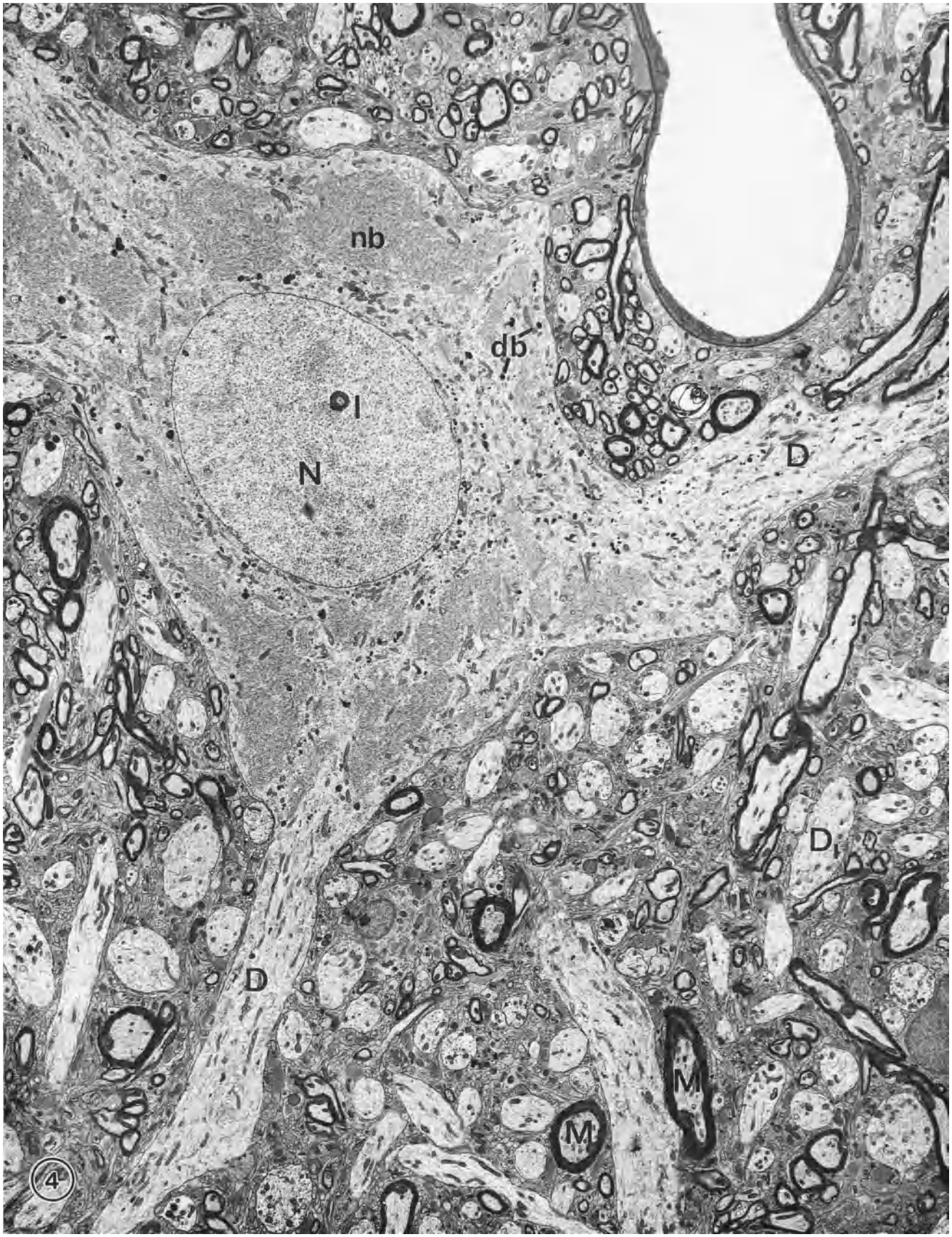


Fig. 19.1 **Neuron**: normal, aging, monkey. Large multipolar neuron. Nucleus (*N*) contains an inclusion (*I*), and large Nissl bodies (*nb*) may extend into bases of thick dendrites (*D*). Dark bodies (*db*) are of lysosomal origin. (Micrograph: Zaeem A. Siddiqi and Alan Peters, *J Neuropathol Exp Neurol* 58:903, 1999.)

© 2009 Wiley-Blackwell. ISBN: 978-0-813-80330-2

19 Neurotoxins and Neurodegeneration

Introduction

Ultrastructural analysis of toxic injury to the nervous system requires attention to neurons, glia, blood vessels, and interstitium.[1] Acute injury to the neurons is passed to support glia when etiologic agents and the cytokines they induce are transmitted from cell to cell via gap junctions. That is, the acute neuronal swelling from primary injury to neurons is rapidly reflected in swelling in oligodendrocytes and other neural connections.

Cytokines and neuronal cytokine-receptor signaling pathways play critical roles in limiting toxic injury. **Nerve growth factor (NGF)** is a neurotropic factor, and NGF signaling through the receptor TrkA enhances neuronal survival after injury. Immunogold labeling studies have shown that TrkA resides in cytoplasmic vesicles and is assembled in ring-like structures at the plasma membrane.[2] Similarly, **neuregulin** and its receptor Erb B4, expressed on somatodendrites, function in repair of the neuropil.[3]

Confounding Lesions in Neurotoxicity

Interpretation of ultrastructural lesions is complicated by natural underlying systemic disease.[4] Caution in interpretation of ultrastructural change in the brain is advisable since damage can arise from systemic disorders.

Apoptosis

Interpretation of ultrastructural change in neurotoxic injury often involves "dark neurons." **Dark neurons** are shrunken, hyperbasophilic, electron-dense neurons that are encountered in acute toxic injury (see Fig. 2.7). Dark neurons are capable of recovery, but in environments of persisting injury they most often progress to necrosis or apoptosis.[5]

Apoptosis of neurons is caused by toxins that activate specific signaling events for programmed cell death (PCD). The two main pathways of PCD, the **death receptor (extrinsic)** and the **mitochondrial (intrinsic)** pathways, are activated by caspase 8 and 9, respectively, both of which are found in the cytosol (see chapter 2). These pathways are activated when neurotoxins interact with critical death receptor molecules (either in the cytosol or embedded in the plasma membrane of the neuron). Specific death signals are then conveyed to the cytoplasm and nucleus that activate the death process. Ultrastructurally, the pathways involved in neurons have been followed by immunogold techniques.[6] The toxin lactacystin (a proteosome inhibitor that induces apoptosis by binding to caspase-3) activates the cytosolic phosphatase PTEN, which, in turn, acts at the plasma membrane to initiate PCD.[7]

Aging

Normal aging is associated with a spectrum of neuronal changes (Fig. 19.1). Many of these involve the cytoskeleton in a way that impedes fast axonal transport. In aged monkeys, abnormal microtubles extend from the main neurite axis into diverticula to form coils and provide a pathway to trap organelles. One of these is a progressive decline in cortical and striatal dopamine. In neurons of the substantia nigra pars compacta, the most consistent age-related changes are accumulation of **lipofuscin** within cell bodies and **Marinesco bodies,** granular intranuclear inclusions (Fig. 19.2).[8] Age changes in astrocytes lead to an increase in astrocytic

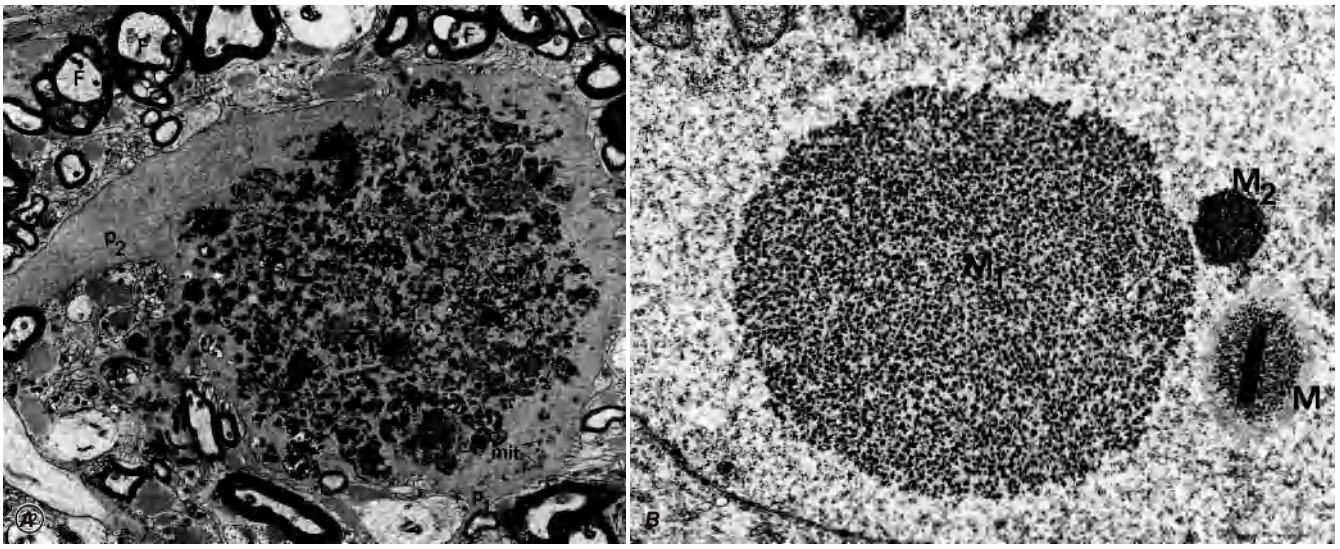


Fig. 19.2 **Age changes**: 32-year-old monkey. **A**. **Spheroid**: core of dense granular material and a periphery of filamentous cytoplasm containing mitochondria (*mit*). Processes (*P1* and *P2*) extend from the periphery of the spheroid. Surrounding myelinated nerve fibers (*F*) with split sheaths contain dark cytoplasm and vacuoles. **B**. **Marinesco body**: nucleus, large multipolar neuron (M). Two variations (M1 and M2), aged monkey. (Micrograph: Zaeem A. Siddiqi, *J Neuropathol Exp Neurol* 58:903, 1999.)

processes, and in dendrites to the loss of organelles with development of vacuoles, myelin whorls, dense bodies, and electron-dense inclusions.

Hypoglycemia

Hypoglycemia induced by large doses of insulin can lead to cerebral damage, especially of cortical neurons. Accompanying the fall in blood glucose are drowsiness, lethargy, convulsions, and stupor. The resulting nerve cell damage follows the pattern of anoxia, and when brain capillaries are examined ultrastructurally, there is a marked early disturbance of the blood-brain barrier due to endothelial damage.[9] The dentate gyrus of the hippocampus is selectively damaged in hypoglycemia, a feature distinguishing hypoglycemia from ischemic brain necrosis. The early dendritic lesions, with sparing of intermingling axons, are characteristic of excitotoxic neuronal damage caused by such drugs as kainic acid, folate and quinolinic acid.[10]

Hyperglycemia

Neurons have a constant high glucose demand and, unlike myocytes, cannot accommodate glucose uptake via insulin—glucose uptake depends on extracellular glucose. Neuronal damage can result from persistent episodes of hyperglycemia, a phenomenon referred to as **glucose neurotoxicity.** In human diabetes, this leads to a spectrum of dysfunction that ranges from cerebral neuronal hyperexcitability with epileptic seizures to loss of enteric neurons and associated gastrointestinal complication.

Ischemia

Ischemia of the central nervous system, even if transient, has major impacts on the ultrastructure of nervous tissue.[11] In neonatal hypoxia-ischemia dark neurons arise that have characteristics of both apoptosis and necrosis.[12,13] In the immature brain, apoptosis contributes to secondary neuronal loss after acute ischemia. Caspase 3 activation is the downstream event after ischemia in the immature brain. Ischemia leaves residua of injury in the brain. Hemorrhages in the neuropil may leave residues of pigment, particularly iron, which accumulate in microglia and Bergmann glia of the cerebellar cortex and in astrocytes of the piriform cortex.[14]

Neuronopathies

In neuronopathies, the **nerve cell body (perikaryon, soma)** is the site of injury. Damage to organelles of the soma is followed by degeneration of cytoplasmic processes, the axons and dendrites (see Fig. 19.1). **Axons** have a hillock region, collateral branches, varicosities, synaptic specializations, and growth cones. **Dendrites,** which provide most of the receptive surface of the neuron, possess spines, excrescences, postsynaptic specializations, and branches of different sizes, orders,

and connections. Traffic through the neuron is controlled by unique proteins. For example, the cytoplasmic protein **phocein,** localized on dendritic spines, is involved in clathrin- and dynamin-dependent pathways in neurons.[15]

Neuronophagia is the phagocytic uptake and degradation of injured neurons. Neuronophagia is a brain response to tissue damage in which **microglia** proliferate, develop elongated nuclei (rod cells), and form clusters (microglial nodules) around foci of dead neurons.

Autophagy, the regulated lysosomal degradation process in autophagosomes, is activated in acute toxic injury, and exerts a protective effect in neuronal injury. Neuronal autophagy is particularly important for maintenance of axon terminals and protection against axonal degeneration. In Purkinje cells, the specific ablation of the **autophagy gene *Atg7*** causes the axon to swell and aberrant membranes to accumulate, and progressive dystrophy to begin.[16] Autophagic pathways, the main machinery for bulk elimination of aberrant cell components, is persistently activated after toxic brain injury. The amyloid precursor protein βAPP accumulates in neurons after experimental injection of colchicine into the ventricles.[17] Accumulation of autophagolysosomes in neurons is a neuropathologic feature of Alzheimer's disease.[18,19]

Neuronopathies are arranged according to target organelle. Their mechanisms of disease induction may be classified as diffuse (methylmercury, aluminum, locoin toxicities) or selective (doxorubicin, cisplatin, MPTP).

Neuronal swelling, the initial response to most acute neuronopathies, arises from ionic imbalance, and excessive water intake and distribution (Fig. 19.3). The process is often transmitted to glia. **Neuronal chromatolysis,** the lysis of rough endoplasmic reticulum, is a prominent change in neurotoxicology; for example, chromatolysis occurs in anterior horn cells in acute toxicity. Also found are necrosis of internuncial cells, various reactions of glia, and spongy state of the neuropil. **Autophagolysosome proliferation** is a hallmark of many neuronal injuries; lysosomal production and expansion are indices of drug toxicity, particularly for lysomotropic drugs.[20] **Cytoskeleton disorganization** is a consequence of toxicity when microtubules or microfilaments are the primary site of injury; cytoplasmic aggregates and inclusions formed by the abnormal microtubules and intermediate filaments is a common manifestation of drug injury.[21] **Mitochondrial swelling** comes from any toxicity that primarily or secondarily affects the electron transport chain and oxidative phosphorylation.

Necrosis of neurons is typically a direct result of acute toxic injury (Fig. 19.4). In contrast, **apoptosis** plays major roles in chronic toxic injury and degenerative disease.

Mitochondrial Toxins

MPTP Toxicity: Mitochondrial Complex I

Methylphenyltetrahydropyridine (MPTP) is a metabolic toxin that selectively inhibits the mitochondrial complex I. MPTP has a tropism for and destroys dopamine neurons of the substantia nigra, changes that produce parkinsonism in humans. The careless and dirty production of a "synthetic heroin" by an amateur chemist in California in the early 1980s resulted in contamination of the product with MPTP, a potent neurotoxin. Since the drug reached a large number of users, patients soon appeared with tremor and muscle rigidity that closely resembled Parkinson's disease. Signs appeared only after 80–90% of the nerve cells are destroyed.

MPTP binds with high affinity to the enzyme **monoamine oxidase** (type B). The conversion by monoamine oxidase of MPTP to **methylphenylpyridine (MPP^+)** is required for neurotoxicity—prior treatment of animals with monoamine oxidase inhibitors prevents MPTP neurotoxicity. Because of the high affinity for the catecholamine uptake system, catecholamine neurons accumulate MPTP to levels many times that in extracellular fluid. In affected neurons, **mitochondrial abnormalities** are the most striking ultrastructural change in early toxicity. Inhibition of the mitochondrial complex I by MPP+ suppresses aerobic glycolysis and ATP production.

The affinity of MPP^+ for melanin and neuromelanin leads to tropism for pigmented neurons of the substantia nigra. Monkeys treated with MPTP have prominant inclusions in cells of the substantia nigra, noradrenalin neurons in the locus ceruleus, and related areas that are similar to Lewy bodies, one of the hallmarks of parkinsonism. Both humans and monkeys have a high content of neuromelanin in the substantia nigra while rodents do not; this is one explanation for the high toxicity in primates and the relative resistance in rodents. In mice, mitochondrial volume is markedly lower in dopaminergic than in nondopaminerigic neurons.[22,23] **MPP^+** (in the presence of dopamine) causes calcium release, hydrolysis of intramitochondrial nucleotides, and induction of **autophagy** via the ERK pathway.[24,25]

Annonacin Toxicity: Mitochondrial Tauopathy

Defects in microtubules and the MAPS tau are associated with neuronal mitochondriopathies.

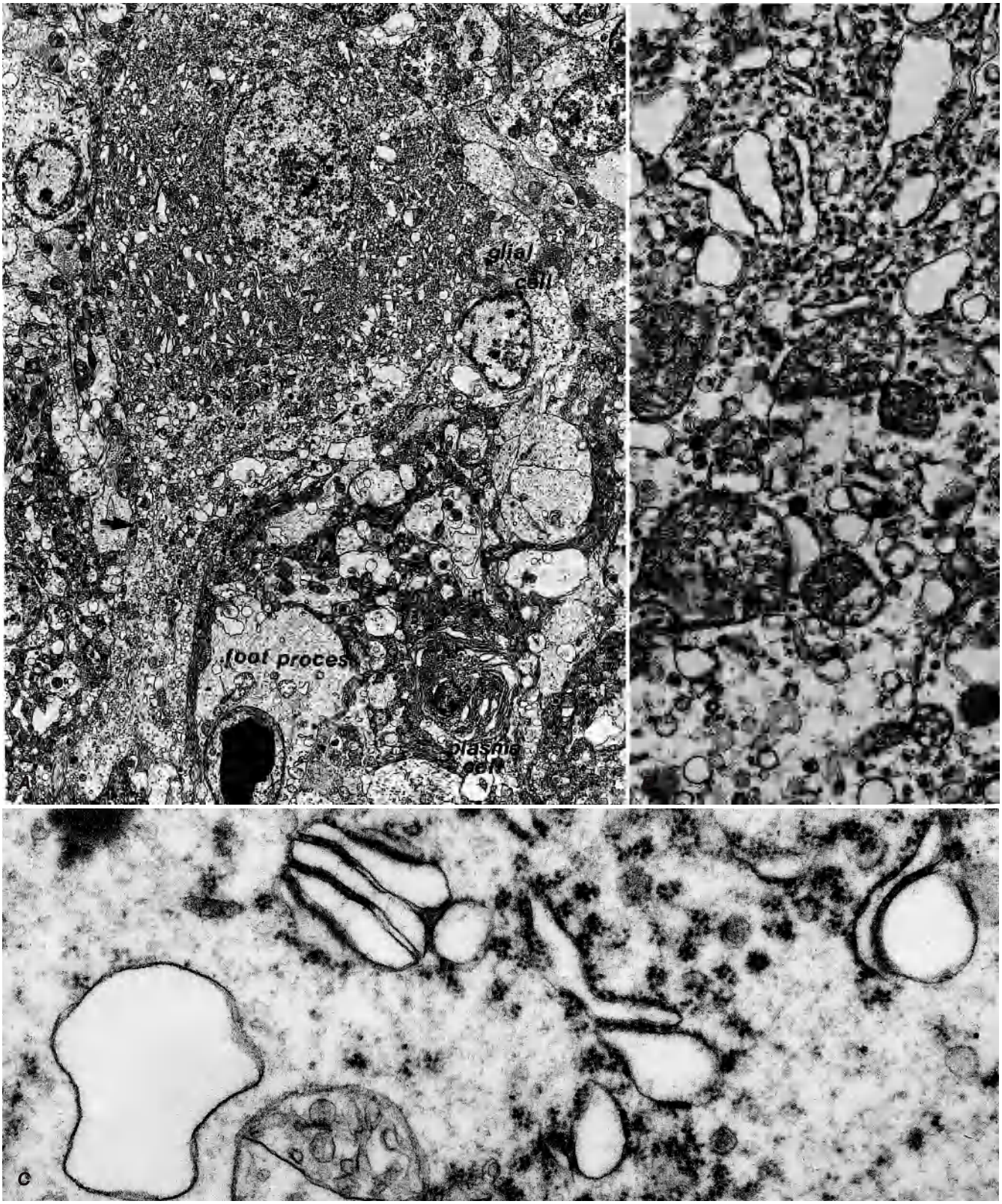


Fig. 19.3 Acute neuronal swelling and chromatolysis: Purkinje cell layer, cerebellum, chicken. **A**. **Neuronal swelling** with dilatation of RER. Proteolysis affects the entire dendrite (*arrow*) and extends into the neck of the perkaryon. **B–C. Cytoplasmic proteolysis** of RER at higher power: RER cisternae are expanded and RER membranes have lost ribosomes by degranulation and have fragmented to form vesicles and vacuoles.

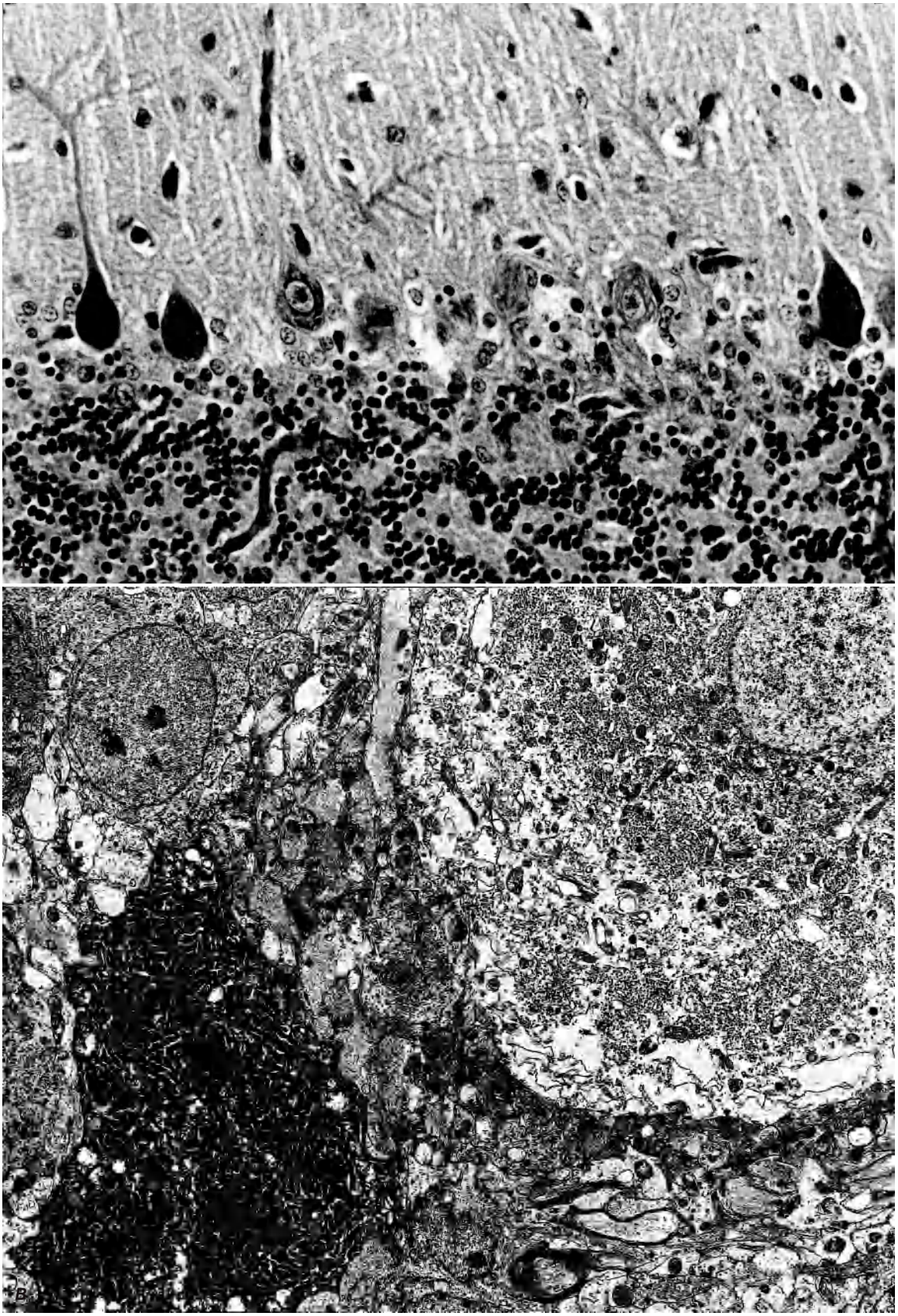


Fig. 19.4 Neuronal swelling and death: cerebellum, chicken. **A**. **Purkinje cells, histology**: various stages of degeneration and necrosis. **B**. **Purkinje cells, ultrastructure**: acute swelling (*right*) and necrosis (*left*) with oligodendrocyte (*top left*).

Neurodegenerative tauopathy endemic to the Caribbean island of Guadeloupe is associated with consumption of anonaceous plants that contain acetogenins. One of these, **annonacin**, is a potent inhibitor of mitochondrial complex I and causes neuronal mitochondriopathy. In vitro, annonacin damages complex I, and induces retrograde transport of mitochondria to the neuronal soma, some of which had tau attached to their outer membranes.[26]

Photofrin Toxicity: Reactive Oxygen Species

Photofrin and other photosensitizing agents have been used in the photodynamic therapy of malignant brain tumors. Tumor cells are killed by the liberation of free radicals in the mitochondrion. In the cerebral cortex of rats injected with photofrin II and exposed to light 48 hrs later, affected **neurons** have swollen mitochondria with increased numbers of cristae and dense matrix deposits.[27] There is early swelling and necrosis of **astrocytes** and secondary damage to the microvasculature.

Cyclosporin Toxicity: Permeability Transition Pore

Suppression by Cyclosporin

Mitochondrial permeability transition is induced by high levels of matrix calcium and results from opening of the **permeability transition pore (PTP)**, a channel consisting of the adenine nucleotide translocator, an anion channel, and cyclophilin D, a prolyl isomerase located within the mitochondrial matrix. Activation of the PTP results in loss of mitochondrial membrane potential, expansion of the matrix, and rupture of the mitochondrial outer membrane. **Cytophilin D** is a critical component of the PTP, and suppression of cytophilin D is associated with cytoprotection.[28] Cytophilin D is targeted by the immunosuppressant cyclosporin, and the cytoprotective effect of cyclosporin is well documented.

Lysosomal Neurotoxins

Chloroquine

Chloroquine is an acidotropic drug that potently perturbs membrane trafficking from endosome to lysosome. Lysosomal degradation of GM1 gangliosides in endosomes is disturbed. Endosomes bearing aggregates of gangliosides form large vacuoles with myelin figures. In neuronal cells in culture, there is accelerated release of gangliodies from the cell within exosomes.[29] In chloroquine treated birds, marked vacuolation of neuronal perikarya is found in Purkinje cells, neurons of the brainstem nuclei, and spinal cord motoneurons.[30]

Locoweed Toxin

Locoweed (*Oxytropis sericea*) contains a potent toxin that damages neuronal lysosomes. Poisoned animals develop neuronal swelling and cytoplasmic vacuolation that is prominent in Purkinje cells. Axonal swelling and dystrophy is present in white tracts, and is prominent in cerebellar peduncles.

Cytoskeletal Toxins

Neurotoxins that act primarily through suppression of the **neuronal cytoskeleton** cause defective axoplasmic transport (Table 19.1). The two important ultrastructural markers of cytoskeletal damage are

- **Axonal swelling**, with concurrent accumulation of vesicles and tubules within the axoplasm, is a general feature of this type of injury to the brain.
- **Neurofilament aggregation**: this hallmark of the axonal reaction can be assessed ultrastructurally and by the specific immunolabeling of neurofilament subunits; drugs that produce this pattern include vinblastine, vincristine, and taxol.

Toxins that specifically damage axonal transport are apt to cause accumulation of membranes and tubulovesicular structures in the axon and its terminus. **Reserpine**, which decreases norepinephrine and other catecholamine neurotransmitters, damages the transport process—large doses cause the disappearance of neurosecretory vesicles in synaptic regions and accumulation of vesicles in the nerve cell body.

Regeneration of transected nerves in the CNS is abortive. Although transected axons in the PNS form active **growth cones** after axonal transection, axons in the CNS do not regrow after injury. Attempts at regeneration of injured neurons in the brain and spinal cord lead to development of characteristic swellings called **retraction bulbs**. Disorganized microtubules are the basis for the formation of retraction bulbs and the failure of axons to regenerate.

Toxins for Serotonin-Secreting Neurons

Ecstasy

Methamphetamine is toxic to dopaminergic neurons, causing nigrostriatal denervation and striatal

Table 19.1 Ultrastructural changes in animal models of neurotoxicity.

Toxin	*Target*	*Reference to ultrastructural pathology*
Acetyl-ethyl-tetra-methyl-tetratin	Rabbit	**McManus**, *Am J Pathol* 121:55, 1985; **Sterman**, *J Neuropathol Exp Neurol* 40:112, 1981
Acrylamide	Cat	**Prineas**, *J Neuropathol Exp Neurol* 28:598, 1969
	Rat	**Cavanagh**, *J Neurocytol* 12:413, 1983; **Schmidt**, *Lab Invest* 56:505, 1987
Adriamycin (*see* Doxorubicin)		**Graeber**, *Acta Neuropathol* 78:348, 1989
Alloxan	Rat	**Powell**, *Acta Neuropathol* 65:128, 1984 (nerve)
Alkyltin		**Aleu**, *J Neuropathol Exp Neurol* 22:403, 1963
Aluminum	Rabbit	**Wisniewski**, *Acta Neuropathol* 63:190, 1984
	Rat	**Gruca**, *Acta Neuropathol* 63:2887, 1984
Aluminum phosphate	Rabbit	**Seil**, *J Neuropathol Exp Neurol* 28:74, 1969
D,L-α-Aminoadipate	Rat	**Bruni**, *Acta Neuropathol* 64:129, 1984
Aminonicotinamide	Mouse	**Aikawa**, *Acta Neuropathol* 71:243, 1986; **Aikawa**, *J Neuropathol Exp Neurol* 43:511, 1984
	Rat	**Griffiths**, *Lab Invest* 44:547, 1981; **Horita**, *Acta Neuropathol* 53:227, 1981; **Horita**, *Acta Neuropathol* 44:111, 1978
Aminodarone	Rat, mouse	**Costa-Juss**, *Brain* 108:735, 1985
Ammonia	Rat	**Diemer**, *Acta Neurol Scand* 55:425, 1977; **Laursen**, *Neuropathol Appl Neurobiol* 5:345, 1979; **Pilbeam**, *J Pathol* 140:331, 1983
	Sheep	**Hooper**, *Rev Vet Sci* 16:216, 1974
AY9944	Rat	**Suzuki**, *Lab Invest* 31:503, 1974; **Suzuki**, *Acta Neuropathol* 26:185, 1973
Bicuculline	Rabbit	**Nitsch**, *Acta Neuropathol* 69:1, 1986
	Rat	**Soderfield**, *Acta Neuropathol* 62:87, 1983
Botulinum toxin	In vitro	**Dong**, *Am J Pathol* 179:1511, 2008
Bromophenylacetylurea		**Troncoso**, *Lab Invest* 46:215, 1982 (nerve)
Bupivacaine HCl	Rat	**Nonaka**, *Acta Neuropathol* 60:167, 1983; **Wakayama**, *J Neurol Sci* 72:31, 1986
Calcium	Human	**Balantine**, *Lab Invest* 47:286, 1982; **Balantine**, *J Neuropathal Exp Neurol* 43:500, 1984
Capsicin	Mouse	**Hiura**, *Acta Neuropathol* 78:35, 1985
Carbon disulfide	Rat	**Jirmanova**, *Acta Neuropathol* 72:341, 1987 and 63:255, 1984 (nerve)
Carbon monoxide	Cat	**Horita**, *J Neuropathol* Exp *Neurol* 39:197, 1980
	Rat	**Miyagishi**, *Acta Neuropathol* 14:119, 1969
Chloroquine	Human	**Mahon**, *Curr Eye Res* 28:277, 2004 (retina); **Soong**, *Hum Pathol* 38:1858, 2007 (heart); **Tegnér**, *Acta Neuropathol* 75:253, 1988 (nerve)
	Mouse	**Gaynes**, *J Appl Toxicol* 2008 [E-pub] (retina)
	Penguin	**Wünschmann**, *Vet Pathol* 43:6, 2006 (neurons)
	Pig	**Klinghardt**, *J Hirnforsch* 37:81, 1996 (brain)
Chlorpromazine	Rat	**Seegers**, *Acta Neuropathol* 66:1999, 1985
Cisplatin	Rat	**Tomiwa**, *Acta Neuropathol* 69:295, 1986
Clioquinol	Rat	**Krinke**, *Acta Neuropathol* 47:213, 1979 (nerve); **Ozawa**, *Acta Neuropathol* 69:272, 272 (nerve)
Copper	Mouse	**Yamano**, *Acta Neuropathol* 76:574, 1988
	Sheep	**Morgan**, *Res Vet Sci* 15:88, 1973; **Howell**, *Acta Neuropathol* 29:9 1974
Cuprizone	Mouse	**Blakemore**, J Neurocytol 1:413, 1972; **Suzuki**, *Am J Pathol* 54:307, 1969
Cyanide	Rat	**Hirano**, *J Neuropathol Exp Neurol* 27:234, 1968 and 26:200, 1967; **Hirner**, *Acta Neuropathol* 13:350, 1969

Table 19.1 *Continued*

Toxin	*Target*	*Reference to ultrastructural pathology*
Cycad toxin (cycasin)	Mouse	**Hirano**, *J Neuropathol Exp Neurol* 31:113, 1972
Cyclophosphamide	Rat	***Wenk***, *J Neuropathol Exp Neurol* 38:1, 1979
***cis*-Dichlorodiamine platinum II**	Rat	***Scherini***, *Acta Neuropathol* 72:218, 1987
Dideoxycytidine	Human Rabbit	**Dalakas**, *Lab Invest* 81:1537, 2001 **Anderson**, *Lab Invest* 70:724, 1994; **Feldman**, *Lab Invest* 66:75, 1992
Dimethylhexanedione	Rat	**Anthony**, *J Neuropathol Exp Neurol* 42:548, 1983
Diisopropyl phosphofluoridate	Cat	**Boulding**, *Am J Pathol* 94:253, 1979
Disobutamide	Rat, dog, monkey	**Koizumi**, *Toxicol Appl Pharmacol* 84:125, 1986
Dithiobiuret	Rat	**Jones**, *Acta Neuropathol* 78:72, 1989
Dithiocarbamate	Sheep	**Howell**, *Acta Neuropathol* 15:197, 1970
Dizocilpine	Rat	**Fix**, *Exp Neurol* 123:204, 1993; **Olney**, *Science* 244:1360, 1989
Domoic acid	Human Rat	**Teitelbaum**, *New Engl J Med* 322:1781, 1990 **Tryponas**, *Toxicol Pathol* 18:165, 1990
Doxorubicin	Rat	**Cho**, *J Neuropathol Exp Neurol* 36:907, 1977; **Cho**, *Neurotoxicology* 1:583, 1977
Ethambutol	Monkey	**Schmidt**, *J Neuropathol Exp Neurol* 25:40, 1966
Ethanol	Rat	**Goldstein**, *J Neuropathol Exp Neurol* 42:579, 1983; **Volk**, *Acta Neuropathol* 67:179, 1985 and 63:57, 1984
Ethidium bromide	Rat	**Yajima**, *Lab Invest* 41:385, 1979
Fenfluramine		**Dastur**, *Acta Neuropathol* 67:142, 1985
Fluorothyl		**Ingvar**, *Acta Neuropathol* 75:362, 1988
Galactose		**Mizisin**, *J Neuropathol Exp Neurol* 52:78, 1993
Glutamate	Mouse	**Olney**, *J Neuropathol Exp Neurol* 30:75, 1971
Guanethidine		**Kidd**, *J Cell Biol* 116:395, 1992; **Schmidt**, *J Neuropathol Exp Neurol* 49:150, 1990
Gentamicin	Guinea pig	**Ylikoski**, *Acta Pathol Microbiol Scand B* 82 (Suppl 241):30, 1973
Hexacarboe	Rat	**Griffin**, *Lab Invest* 45:130, 1981 (nerve)
Hexachlorophene	Rat Sheep Tadpole	**Lampert**, *Acta Neuropathol* 23:326, 1973; **Towfighi**, *Lab Invest* 31:372, 1974 **Hall**, *Lancet* 2:1251, 1972 **Webster**, *J Neuropathol Exp Neurol* 33:144, 1974
Hexanedione	Rat	**Anthony**, *J Neuropathol Exp Neurol* 42:548, 1983 (nerve); **Krinke**, *Acta Neuropathol* 47:213, 1979 (nerve)
3-Hydroxy-3-methylglutarylcoenzyme A reductase	Dog	**Berry**, *Am J Pathol* 132:427, 1988
Ibotenic acid	Rat	**Nitch**, *Acta Neuropathol* 85:55, 1992
Iminodipropionitrile	Rat	**Chow**, *Acta Neuropathol* 4:590, 1965; **Hirokawa**, *J Cell Biol* 101:227, 1985
Isoniazid	Dog Rat	**Blakemore**, *J Neurocytol* 1:263, 1972 **Jacobs**, *Acta Neuropathol* 47:85, 1979 (nerve); **Ochoa**, *Brain* 93:831, 1970; **Onishi**, *Acta Neuropathol* 67:195, 1985 (nerve); **Schroder**, *Acta Neuropathol* 15:156, 1970 (nerve); **Sclaepfer**, *Am J Pathol* 45:209, 1964 (nerve)
Isonicotinic acid	Duck	**Lampert**, *J Neuropathol Exp Neurol* 27:210, 1968
Ivermectin	In vitro	**Campbell**, *Science* 221:823, 1983

Table 19.1 *Continued*

Toxin	*Target*	*Reference to ultrastructural pathology*
Kainic acid	Rat	**Herndon**, *Neuroscience* 5:1015, 1980; **Rieke**, *Acta Neuropathol* 76:185, 1988
Ketamine	Rat	**Olney**, *Science* 244:1360, 1989
Lead	Chick	**Hirano**, *Lab Invest* 29:659, 1973
	Dog	**Hamir**, *J Comp Pathol* 94:215, 1984
	Monkey	**Saver**, *Science* 169:1091, 1970 (nerve)
	Rabbit	**Hughes**, *Am J Pathol* 77:237, 1974
	Rat	**Press**, *Acta Neuropathol* 67:86, 1985; **Lampert**, *J Neuropathol Exp Neurol* 27:527, 1968 (nerve); **Powell**, *Am J Pathol* 109:193, 1982 (nerve); **Schlaepfer**, *J Neuropathol Exp Neurol* 28:401, 1969 (nerve); **Thomas**, *J Pathol* 109:45, 1973 (nerve)
Locoweed toxin	Deer	**Stegelmeier**, *Vet Pathol* 42:566, 2005 (neuron)
Lovostatin	Dog	**Berry**, *Am J Pathol* 132:427, 1988
Lysergic acid (LS)	In vitro	**Hendelman**, *J Neuropathol Exp Neurol* 31:411, 1972; **Roizin**, *J Neuropathol Exp Neurol* 33:213, 1974
Mercury	Human	**Eto**, *Virch Arch* 23:190, 1977 (nerve); **Takeuchi**, *Virch Arch* 27:137, 1978 (nerve)
	Monkey	**Shaw**, *Am J Pathol* 80:451, 1975
	Rat	**Chang**, *Acta Neuropathol* 27:171, 1974 and 20:122, 1972; **Miyakawa**, *Acta Neuropathol* 14:126, 1969 and 17:6, 1971
Methamphetamine	Guinea pig	**Miyakawa**, *Acta Neuropathol* 14:215, 1975
Methionine sulfoximine	Rat	**Rizzuto**, *J Neuropathol Exp Neurol* 33:327, 1974
Methyl-D-aspartate		**Nag**, *Acta Neuropathol* 84:471, 1992 (spinal cord)
Methylenedioxy-methamphetamine	Primates	**Ricaute**, *J Am Med Assoc* 260:51, 1988
Methylimino-bis-(N-methyl-propylamine)	Rat	**Nochlin**, *J Neuropathol Exp Neurol* 41:233, 1982
Methylphenyltetra hydropyridine (MPTP)	In vitro	**D'Amato**, *Science* 231:987, 1986
	Monkey	**Tanaka**, *Acta Neuropathol* 75:370, 1988
Monosodium glutamate	Monkey	**Olney**, *J Neuropathol Exp Neurol* 31:464, 1972
	Mouse	**Lemkey-Johnston**, *J Neuropathol Exp Neurol* 30:74, 1971; **Olney**, *J Neuropathol Exp Neurol* 30:75, 1971
		Toth, *Acta neuropathol* 75:16, 1988 (fetus)
Nicotinamide	Mouse	**Baethmann**, *J Neuropathol Exp Neurol* 32:408, 1973
	Rat	**Konig**, *Acta Neuropathol* 26:115, 1973
Nitropropionic acid	Rat	**Hamilton**, *Acta Neuropathol* 72:286, 1987
Oubain	Bowfin	**Friede**, *J Neuropathol Exp Neurol* 28:450, 1969
Oxygen	Mouse	**Bonikos**, *Lab Invest* 32:619, 1975
	Rat	**Balantine**, *Lab Invest* 31:580, 1974
Penicillin	Rat	**Okada**, *J Neuropathol Exp Neurol* 30:337, 1971
Phencyclidine	Rat	**Olney**, *Science* 244:1360, 1989
Phenylalanine	Rat	**Adelman**, *J Neuropathol Exp Neurol* 32:380, 1973
Phenytoin	Mouse	**Volk**, *Acta Neuropathol* 67:67, 1985
Plasmocid	Monkey	**Sipe**, *J Neuropathol Exp Neurol* 32:446, 1973
Pyridostigmine	Rat	**Schuschereba**, *Toxicol Pathol* 18:387, 1990
Pyridoxine		**Montpetit**, *Acta Neuropathol* 76:711, 1988
	Rat	**Krinke**, *J Neuropathol Exp Neurol* 44:117, 1985
Satratoxin	Mouse	**Islam**, *Environ Health Perspect* 114:1099, 2006 (nasal)
Sodium azide	Rat	**Shibasaki**, *Acta Neuropathol* 14:185, 1969
Solanum toxin	Cow	**Barros**, *Pesq Vet Brasil* 7:1, 1987

Table 19.1 *Continued*

Toxin	*Target*	*Reference to ultrastructural pathology*
Streptozotocin	Rat	**Schmidt**, *Lab Invest* 49:538, 1983
Styrene oxide	Rat	**Beiswanger**, *Toxicol Appl Pharmacol* 118:233, 1993
Sulfamethoxine	Rat	**Schutta**, *Lab Invest* 24:82, 1971 (mitochondria)
Taxol		**Raine**, *J Neurocytol* 16:461, 1987; **Vuorinen**, *Acta Neuropathol* 79:563, 1990 (nerve)
Tellurium	Rat	**Jackson**, *Acta Neuropathol* 78:301, 1989 (neonate); **Lampert**, *Lab Invest* 25:3880, 1971
Thalidomide	Human Rabbit	**Schröder**, *Acta Neuropathol* 39:271, 1977 (nerve) **Schröder**, *Acta Neuropathol* 65:285, 1985 (nerve); **De Iongh**, *J Neuropathol Exp Neurol* 49:564, 1990 (fetus)
Tiletamine	Rat	**Olney**, *Science* 244:1360, 1989
Tilorone	Rat	**Levine**, *Am J Pathol* 78:319, 1975
Trachyandra toxin	Sheep	**Newsholme**, *Onderstepoort J Vet Res* 52:87, 1985
Tricresylphosphate	Chick Primate	**Janzik**, *Acta Neuropathol* 6:303, 1966 **Ahmed**, *Cell Tissue Res* 175:459, 1977
Triethyltin	Rabbit Rat	**Scheinberg**, *J Neuropathol Exp Neurol* 25:202, 1966 **Aleu**, *J Neuropathol Exp Neurol* 22:403, 1963; **Graham**, *Lab Invest* 29:628, 1973; **Otani**, *Acta Neuropathol* 69:54, 1986
Trimethyltin	Rat	**Bouldin**, *Am J Pathol* 104:237, 1981; **Bouldin**, *Acta Neuropathol* 81:204, 1990
Triorthocresysl phosphate	In vitro Cat	**Bischoff**, Acta Neuropathol 9:158, 1967 **Prineas**, *J Neuropathol Exp Neurol* 28:571, 1969
Triparano	Rat	**Hruban**, *Lab Invest* 14:1652; **Suzuki**, *Lab Invest* 31:503, 1974
Tunicamycin	Rat	**Finnie**, *Acta Neuropathol* 75:411, 1988
Vacor	Human	**Watson**, *J Neuropathol Exp Neurol* 46:96, 1987
Valproate	Rat	**Sobaniec-Lotowska**, *Int J Exp Pathol* 86:91, 2005
Venom, rattlesnake	Mouse	**Hernández**, *Exp Toxicol Pathol* 59:129, 2007
Venom, scorpion	Mouse	**Love**, *Acta Neuropathol* 70:1, 1986 (nerve)
Venom, viper	Mouse	**Fertuck**, *Proc Natl Acad Sci USA* 71:1376, 1974
Vigabatrin		**Gibson**, Toxicol Pathol 18:225, 1990
Vincristine	Rabbit Rat	**Fiori**, *Tox Pathol* 23:248, 1995 (nerve); **Schochet**, *J Neuropathol Exp Neurol* 27:645, 1968 **Sato**, *Acta Neuropathol* 63:150, 1984; **Schlaepfer**, *J Neuropathol Exp Neurol* 30:488, 1971

dopamine loss. Affected neurons are vacuolated and have striking increases in autophagosomes bearing aggregates of α-synuclein. Toxicity is increased by other drugs, particularly those that suppress autophagy.[31] The amphetamine-related illegal recreational drug **3,4-methylenedioxymethamphetamine (MDMA, ecstasy)** is an analogue of the controlled drug 3,4-methylenedioxyamphetamine. In rats, MDMA produces selective dose-related depletion of serotonin and 5-hydroxyindolacetic acid. The defect was produced at doses 10 times those used in humans but were associated with selective structural damage to termini of serotoninergic nerve fibers.[32] Intrathecal infusion of MDMA into the spinal cord lumbar enlargement with horseradish peroxidase as marker reveals changes in vascular permeability. There is swelling of dendrites (which give the neuropil a vacuolated appearance) expansion of extracellular spaces, and shrunken neurons with pyknotic nuclei.[33]

Fenfluramine

Fenfluramine (Pondimin), an appetite-suppressing perscription drug, has been used for 20 years without

evidence for toxicity in humans. In rats, however, fenfluramine selectively damages terminals of nerve cells that release serotonin. Ultrastructurally, there are myelin whorls in cells of the hypothalamus.[34]

Cycasin Toxicity: Guamanian ALS-PDC

Guamanian amyotrophic lateral sclerosis-parkinsonism dementia complex (ALS-PDC), which killed over 50,000 Guamanians in the last century, was associated with cycad flour used as food during World War II. *Cycas circinalis* (sago palm) contains sterol glycosides proposed as causal. **Cycasin** and **β-N-methylamino-L-alanine (βMAA)**, an unusual non-protein amino acid (and a bicarbonate-dependent excitotoxin), have been implicated in ALS-PDC. Mice fed cycad flour develop progressive motor, cognitive and sensory behavioral deficits. Repeated oral administration of βMAA to macaques produced signs of motor-neuron, extrapyramidal, and behavioral dysfunction. Neuropathologic changes occurred in giant Betz cells in the motor cortex and in anterior horn cells of the spinal cord. Perikarya and basal apical dendrites of Betz's cells were swollen, with pale-staining areas that contained 10 nm neurofilaments. A few of these cells contained nuclear inclusions.[35] Although glutamate-mediated excitotoxicity is involved in experimental cycad exposure, the cascade of events that lead to neuronal death is uncertain.

Neurotoxins That Act on Plasma Membrane Receptors

Phencyclidine: Neuroexitatory Antagonist

Phencyclidine is a noncompetitive NMDA receptor antagonist; that is, it binds with high affinity and specificity to the membrane receptor **N-methyl-D-aspartate (NMDA)**, a subtype of glutamate receptor. It is a dissociative, nonbarbituate anesthetic that is best known as an abused street drug ("angel dust," "hog") for its potent psychotomimetic actions. It may act as a depressant, a stimulant, or a hallucinogen, and deaths are due to total loss of motor and sensory control. Phencyclidine induces **neuronal necrosis** in the brain when given subcutaneously to adult rats. Damage is selective for specific neurons in the posterior cingulate and retrosplenial cortices. Affected neurons are medium to large in size and multipolar or pyramidal in shape, and are located in cortical layers III and IV.[36] Electron microscopic evaluation of affected neurons 2–4 hr after phencyclidine treatment reveals acute cell swelling with proteolysis, disappearance of mitochondria and endoplasmic reticulum, and large cytoplasmic vacuoles. **Ketamine**, **tiletamine**, and **dizocilpine** (MK-801), compounds related to phencyclidine, also produce these vacuolar lesions in rat brains. In the prefrontal cortex, repeated treatment of monkeys and rats induces marked reductions in the parvalbumin-containing local circuit neurons, changes similar to those reported in human schizophrenia. **Dendritic spine density** is increased in the rat prefrontal cortex—a change also seen in **cocaine** and **amphetamine** toxicity.

Phencyclidine (and some of its derivatives), by antagonizing NMDA receptor-mediated neuroexcitatory and neurotoxic phenomena, protects neurons against hypoxic-ischemic, hypoglycemic, or epilepsy-related brain damage, all of which involve NMDA receptor-mediated processes. Endogenous glutamate and asparatate accumulate in high concentrations extracellularly in ischemia, and any condition that reduces energy may cause endogenous excitotoxins to leak from cells and accumulate to exert excitotoxic action at receptors on dendritic and somal surfaces of neurons. Reduced efficiency of energy-dependent reuptake mechanisms for the excitotoxins contributes to the toxic accumulation of these agents.

Guanethidine: Adrenergic Neuron Blockers

Guanethidine, an adrenergic neuron blocking agent, causes destruction of sympathetic neurons in the superior cervical ganglia of rats. Although other neurons may degenerate, the effect is relatively specific. A novel autoimmune mechanism appears to underlie cell death; that is, an exogenous chemically induced alteration of a specific subset of neurons that targets them for NK cell killing. NK cells attach to affected neurons and cause cytoplasmic degeneration and necrosis.[37]

Toxins That Bind Opioid Receptors

Narcotics have striking neurologic effects but typically do not produce overt microscopic lesions. **Tetrahydrocannabinol** (THC), a fat soluble molecule and active ingredient in marijuana, binds to the **cannabinoid receptor;** THC depresses the functions of this receptor and its endogenous ligand, named **anandamide** (from the sanskrit word meaning "internal bliss"). **Morphine** binds to **opioid receptors**, the endogenous ligands for which are a family of peptides, the enkephalins and endorphins. The three recognized types of opioid receptors (morphine-preferring μ, enkephalin-preferring δ, and benzomorphan-preferring κ) have shown distinct and different localization patterns: κ opioid receptors are involved in the presynaptic regulation of dopamine release in the neostriatum in rodents. Electron microscopic autoradiographs of

sections of guinea pig neostriatum incubated with ^{125}I-labeled dynorphin showed relatively high labeling incidence of synaptic specializations. Silver grains were over membranes of the dendritic shaft at points of contact with the axon terminal and other dendrites.[38]

Toxins of Neuronal Membrane Channels

The neuron is electrically polarized. By concentrating K^+ inside the cell and expelling Na^+, ion pumps maintain a voltage difference between inside and outside of the cell. The inside is electrically negative with respect to the outside. The event that triggers the electrical activity of the nerve impulse is a depolarization of the membrane, that is, a reduction of the voltage potential across the membrane.

In **axons**, the nerve impulse is generated solely by specific ion channels along the plasma membrane whose opening and closing are responsible for the progressing voltage difference of the nerve impulse. Depolarizaton occurs as Na^+ channels open explosively and membrane potential falls to zero. **Na^+ channels** are large proteins with central pores 0.4×0.6 nm (at least in giant invertebrate axons), a space through which Na^+ can pass. Axon membranes also have **K^+ channels** that terminate the nerve impulse by letting **K^+** flow out of the axon. Neurotoxins that disrupt these ion channels to prevent the nerve impulse include the organochlorine insecticide DDT.

Tetrodotoxin

Much of our knowledge of neuronal membrane Na^+ channels comes from studies with puffer fish nerve poison **tetrodotoxin.** This molecule firmly binds to the outer mouth of the channel to block the passage of Na^+ into the neuron. A guinidinium group on the toxin mimics Na^+ and fits into the channel, while the remainder of the toxin binds to the protein rim.

Myelin Toxins: Myelinopathies

Myelin surrounds axons as an insulating material. Composed of tightly apposed membranes, myelin contains not only basic lipid bilayer phospholipids and cholesterol but also specific myelin glycolipids, glycoproteins and long-chain unsaturated fatty acids. The glycolipid cerebroside makes up about 20% of the total dry weight of myelin. **Myelin basic protein (MBP)** is essential for maintenance of stability of the myelin sheath, and disturbances of lipid-MBP interactions lead to myelin degeneration. Citrullination of MBP destablizes myelin, and the role of peptidylarginine deiminases (which convert arginine to citrulline) is a component of multiple sclerosis.[39]

Oligodendrocytes in white matter, which produce myelin, are frequently lined up along myelinated fibers; in gray matter, they cluster around neurons as satellite cells. Ultrastructurally, oligodendrocytes have a small round nucleus, develop fewer and shorter processes than astrocytes, and contain many microtubules (making them similar to dendrites). Myelin maintenance is regulated both by diffusable axon factors and by a membrane-membrane interaction of axon and Schwann cell.

In the brain, the **myelin sheath** of the axon is part of the ensheathing oligodendrogliocyte (Fig. 19.5). The myelin sheath consists of multilayered spiral wrapping of Schwann cell membranes. At high magnification myelin is seen as a series of light and dark lines in repeating patterns of approximately 12 nm. The dark line (3 nm) is the apposition of the inner (cytoplasmic) surfaces of the membrane of the Schwann cell. Myelin with unusually large periodicities has been reported in pathologic human and animal brains.

Demyelination is the destruction, removal, or loss of the myelin sheath of an axon.[40] By some pathologists the term demyelination is reserved for acquired disorders of nervous tissue, most of which are infectious and inflammatory, and that typically spare the axon from injury; **myelin depletion** is used for the hereditary leukodystrophies, nutritional, metabolic, toxic, and traumatic disorders of myelin (the presence of marked axonal destruction distinguishes them from the demyelinating diseases). The gross term **malacia** is used as **encephalomalacia**, that is, softening of the brain. Demyelination occurs in many neurotoxic diseases, but only a few toxins primarily affect myelin or myelinogenesis (myelin formation).

Myelin striping, which characterizes most types of myelin breakdown, begins as layers of myelin peal from the main sheath by cell processes from invading monocytes (Fig. 19.6).[41] Hydration of the outer lamellae is the initial lesion, and this is followed by dissolution of myelin and vesiculation of the membranes.[42,43] Monocytes enter the tissue and phagocytize debris. This process can be completed without significant damage to the axon. Axonal dystrophy however is an effect of long-term demyelination.[44,45]

If toxins act directly on **glia**, myelin pathology develops independently from axonal degeneration. Leaves and fruits of the coyotilla shrub poison humans and animals, causing a peripheral neuropathy. The primary lesion is swelling of Schwann cells due to uncoupling of mitochondrial oxidative phosphorylation. The ultimate effect is demyelination with myelin splitting along interperiod lines, a change also seen in triethyl tin toxicity.[46]

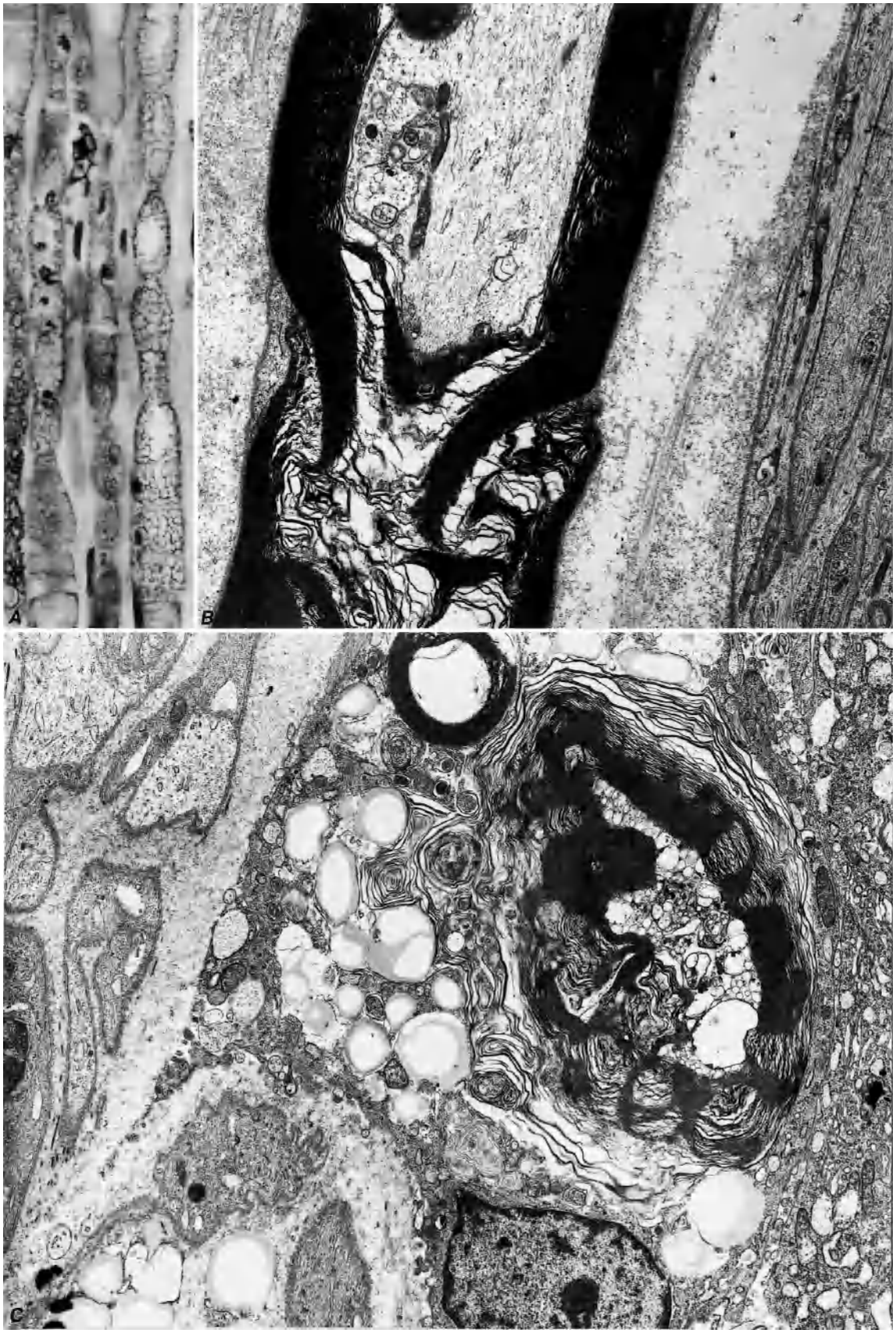


Fig. 19.5 Peripheral nerve degeneration: Wallerian degeneration, rat. Sciatic nerve distal to nerve lesion, ligation 14 days previously. Segmental swelling of axons. Dissociation of myelin sheaths surrounding the axon, vesiculation of axons, and blebbing of myelin balls into the axonal space. **A**. **Histology**: segmental swelling of axons and loss of myelin. **B**. **Myelin destruction**: nodal area of myelin sheath. **C**. **Demyelination**: advanced disruption of myelin, accumulation of myelin membranes and globules of lipid in Schwann cells. (Micrographs: Freddy Coignoul, National Animal Disease Center.)

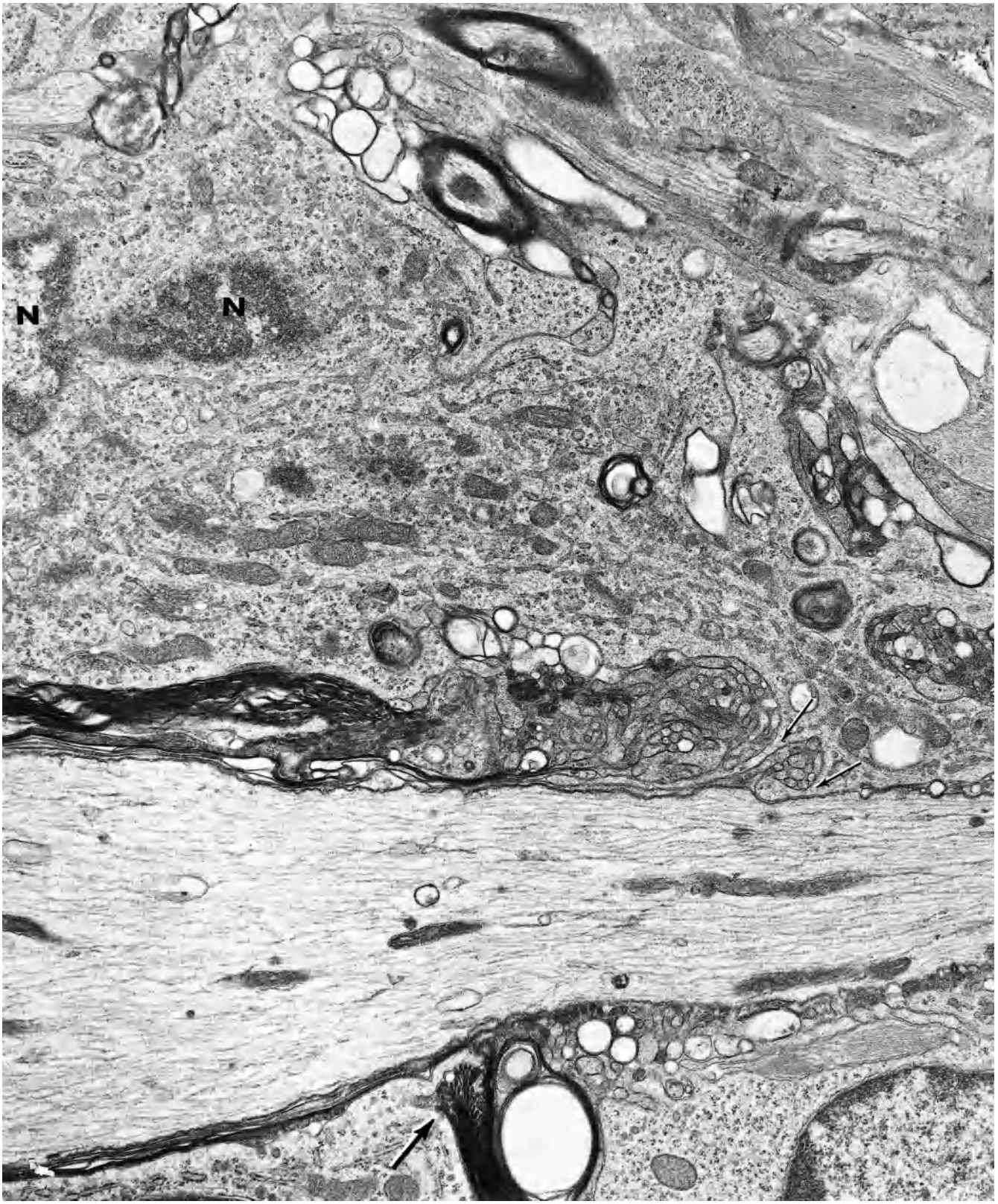


Fig. 19.6 Demyelination: acute allergic encephalomyelitis, rat. Myelin destruction by adjacent macrophages. Complex, multibranched processes emanate from cell and surround the large fiber and smaller fibers (*above*) from which myelin is dissociating as droplets or vesicular masses. Macrophage processes (*thin arrows*) extend beneath the sheath of the large fibers, the axon of which is decreased in diameter. Retracted, detached paranodal loops of myelin (*thick arrow*). (Micrograph: Cedric S. Raine, *Lab Invest* 50:608, 1984.)

Neuropathies: The Peripheral Nerves

Toxic peripheral neuropathies are usually classified as **axonopathies**, in which there is dying back of the axon and degeneration of the nerve fiber, or **myelinopathies** (demyelinating), in which there is relative preservation of the axon. Toxins associated with peripheral neuropathy include the hexacarbons, acrylamide, vincristine, isoniazid, triorthocresylphosphate, and several plant toxins.

In normal peripheral nerves, molecules move up and down the axon by two kinds of transport: **axoplasmic flow** and **axoplasmic transport**. **Axoplasmic flow** is slow and moves at a steady rate to convey materials only from nerve cell body to axon terminus. Axons contain a highly ordered cytoskeleton. Proteins of the three filament systems of the axon (actin filaments, microtubules, and intermediate neurofilaments) are synthesized in ribosomes of the nerve cell body and pass down the axon by axoplasmic flow. Movement is comparable to the protoplasmic streaming of amoebae. **Axoplasmic transport** is fast and goes in both directions. **Neurosecretory vesicles** move by this means and serve to provide neurotransmitter substances for the synapse and new membranes for repair of the axonal plasma membrane (Fig. 19.7). **Mitochondria** are transported along neuronal processes for distribution to synapses in order to meet high metabolic demand and elevated intracellular calcium.[47]

Giant proximal axonopathy, a lesion of several human toxicities, has been reproduced experimentally with the gamma-diketone 1,2-diacetylbenzene (DAB). In rats, DAB forms blue-colored polymeric protein adducts, and induces axonal swellings with formation of clumps of maloriented giant 10 nm intraspinal neurofilaments.[48]

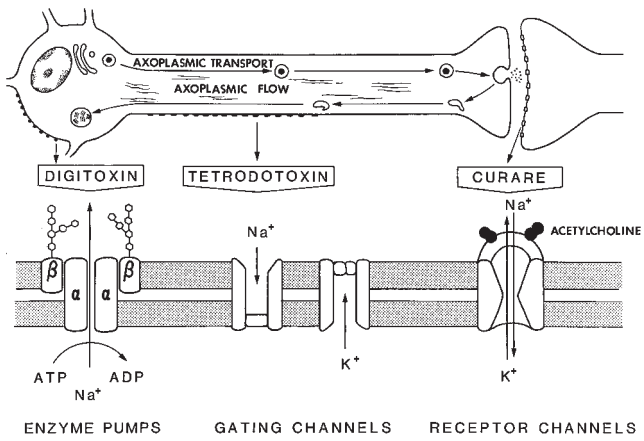


Fig. 19.7 Axoplasmic transport (*arrows in axons*) and **slow axoplasmic flow** (*center of axon*). Three types of functional proteins embedded in the plasma membrane of the neuron are shown with a prototype poison for each. Gating channels (voltage-gated) function in the nerve impulse; receptor channels (ligand-gated) function in synaptic transmission.

Proximal Axonopathy

Selective injury to the axonal hillock and the first internodes in myelinated axons, a characteristic of amyotrophic lateral sclerosis, has been reported in a few specific experimental toxicities; for example, nitriles and β,β-iminodipropionitril. Treatment of rats with the neurotoxin **β,β-iminodipropionitril** causes segregation of neurofilaments at the axon periphery and of formation of bundles of microtubules in central areas. Immunogold microscopy reveals that reagents containing anti-MAP antibodies stain tiny filaments between the microtubules, suggesting that the microtubule-associated fibrillar matrix within the axon plays a role in rapid transport.

Axonal changes in the peripheral nervous system are similar to those in the brain. The **toxic polyneuropathies** have been separated into **segmental demyelination**, which involves widespread loss of myelin with preservation of axons, and **dying-back polyneuropathies**, in which there is simultaneous degeneration of axon and its myelin but with sparing of the perkaryon. Toxicity of triorthocresyl phosphate causes accumulation of abnormal vesicles and tubules within the axoplasm of small myelinated motor nerve terminals in muscle and spinal gray matter. Perikarya are also affected and show changes in the rough endoplasmic reticulum, and increases in smooth endoplamsic reticulum, neurotubules, and neurofilaments.

Distal Axonopathy

Giant prenodal axonal swelling in distal, preterminal axons is a hallmark of neurotoxicity in the peripheral nervous system (PNS). **Hexacarbon** solvents are associated with prolonged industrial exposure or intentional inhalation of vapors for their euphoric effects; for example, 3,4-dimethyl-2,5-hexanedione. Prolonged exposure is neurotoxic to nerves.[49] Hexacarbons such as 2,5-hexanedione, methyl-*n*-butylketone and *n*-hexane have caused **multifocal distal axonopathy** in humans poisoned by inhalation of solvent fumes or glue sniffing. The progressive sensory-motor axonopathy in both central and peripheral nervous systems is characterized by neurofilament aggregations that lead to gigantic axonal swelling at the proximal side of the nodes of Ranvier.

Acrylamide

Acrylamide is an industrial polymerizing agent that produces a sensorimotor central-peripheral distal

axonopathy ("dying-back" neuropathy). Large diameter myelinated axons of the somatic nervous system have predilection for sensory axons. Ultrastructural changes are first seen in the distal axons and underlie a diminution of retrograde fast axoplasmic transport. Swollen axons contain neurofilaments and dense bodies.

Cisplatin

Cisplatin (cis-dichloro-diamine platinum II) is nephrotoxic, ototoxic, and neurotoxic. In humans, **cisplatin sensory neuropathy** is the primary manifestation of toxicity of this drug. Biopsies of nerves reveal loss of myelinated fibers, axon degeneration, and segmental demyelination. Cisplatin binds directly to DNA. Ultrastructural studies in rats show that 0.5–2 mg doses lead to nucleolar segregation of the dense fibrillar from granular component. There is also focal clearing of nucleoplasm, disorganization of ribosomes, increase in neurofilaments (often distending the initial segment of the axon) as well as hypertrophy of satellite cells and increase in perineuronal spaces.[50]

Demyelination in PNS Disease

In the **peripheral nervous system (PNS)**, myelin is produced by **Schwann cells**—myelinating Schwann cells wrap around axons, organizing the axonal membrane into distinct domains, the nodes of Ranvier. To facilitate rapid conduction, tight interaction between axons and glia occurs at regions flanking the nodes of Ranvier (axoglial paranodal junctions) and between adjacent membrane layers of glial cells. JAM-C is strongly expressed in Schwann cells, and in junctional regions of noncompact myelin. These sites are paranodal regions on either side of the node of Ranvier, from where mesaxonal bands connect internodal Schmidt-Lanterman incisures. **Junctional adhesion molecule-C** (JAM-C) is a critical component of the autotypic junctional attachment of Schwann cells where it maintains function of myelinated peripheral nerves.[51]

Intercellular traffic may traverse the periaxonal cleft that spans the internodal axon. The axonal-myelin sheath interface possesses double-walled vesicles that contain endoplasmic reticulum or ribosome-like particles, some of which are continuous with the subjacent axon through a thin stalk.[52]

Direct toxic effects on myelin or on Schwann cell myelinogenesis are ascribed to **hexachlorophene, triethyltin, lead, cyanate, tellurium, hydrazide, isoniazid**, and **ethidium bromide**. **Isoniazid** produces peripheral nerve changes that resemble Wallerian degeneration. In lower vertebrates, particularly wild species, there are myelinopathies of undetermined origin. **Avian vacuolar myelinopathy**, a neurologic disease affecting wild birds in the southeastern United States, is linked to unidentified toxins in aquatic vegetation.[53]

Toxic demyelination may also occur secondary to axonal injury. If **axonal disease** leads to demyelination, the axon lesion precedes demyelination. Chronic exposure to the neurotoxic hexacarbons or to iminodipropionitrile leads to a peripheral neuropathy in which demyelination is secondary to axon injury. Hexacarbons produce giant **myelin bulbs**, swellings of the axon near the nerve cell body. These myelin bulbs progress into "onion bulb" lesions, whorls of redundant Schwann cell processes surrounding the demyelinated axons. The swollen axon contains aggregates of neurofilaments whose accumulation is due to impairment of slow transport in the axon. After the axon change develops, secondary demyelination proceeds.

Myelin-Binding Toxins

Hexachlorophene

Hexachlorophene (2,2'-methylenebis[3,4,6-trichlorophenol]) was used as a highly effective antibacterial agent in soaps and deodorants in the 1970s. It was absorbed through the skin of newborns and produced edema in the white matter associated with intramyelinic vacuoles that arose from separation of lamellae of myelin sheaths at intraperiod lines. Intramyelinic vacuolation also occurred in peripheral nerves. Hexachlorophene binds to myelin via hydrophobic interactions. Tadpoles immersed in solutions of hexachlorophene accumulated ^{14}-labeled hexachlorophene in myelin fractions of brain.

Mitochondrial Schwannopathies

Dideoxycytidine

Dideoxycytidine (DDC), an inhibitor of HIV reverse transcriptase used in AIDS therapy, causes a painful, sensiomotor axonal peripheral neuropathy in humans. Lesions are characterized by decreases in large diameter axons, myelin splitting, intramyelin edema, demyelination, and remyelination of large axons. Schwann cells contain enlarged and abnormally shaped **mitochondria**, which are vacuolated and have electron-dense concentric inclusions.[54] Mitochondrial changes are accompanied by a decrease in mtDNA. There are vacuoles and myelin debris develop in Schwann cells, macrophages and endoneurial fibroblasts. Ultrastructural studies of nerve lesions caused by dideoxycytidine in rabbits have revealed separation of myelin

lamellae at interperiod lines, and vacuolation and fragmentation of myelin sheaths. Schwann cells contained many lipid globules. Affected myelinated nerves had pockets of degenerate myelin that aggregated within the myelin sheath and invaginated into the axon.[55] Because axonal degeneration was concurrent with myelinopathy, it is unknown if axonal change was secondary to myelin edema or a primary effect of DDC on neurons. Pain arises from upregulation of the signaling via chemokine CXCR4 in dorsal root ganglia.

Neurotoxins That Act at Nerve Termini and Synapses

Nerve cells communicate by releasing neurotransmitters at synaptic junctions. The neuron produces neurotransmitters in its endoplasmic reticulum, and packages them in the Golgi complex into neurosecretory vesicles that are moved along the axonal reticulum to the terminal synapse.[56] The **axonal reticulum** is a tubular neurosecretory system that extends from the Golgi complex in the cell soma to the nerve terminal.

At the **presynaptic membrane**, neurosecretory vesicles release their neurotransmitter cargo by exocytosis. Neurotransmitters then diffuse across the **synapse**, and bind to specific receptors embedded in the postsynaptic membrane. When **acetylcholine (ACh)** is liberated at the presynaptic membrane, it binds to its receptor proteins on the postsynaptic membrane of the adjacent nerve. The **ACh receptor complex (AChR)** opens to permit the flow of Na^+ and K^+. After the impulse is transmitted, ACh is destroyed by **acetylcholinesterase (AChE)**. The **myoneural junction** has been widely examined ultrastructurally for changes that are produced in acute and chronic (Fig. 19.8) tissue damage.

In presynaptic areas, neurosecretory vesicles are clustered close to the plasma membrane in special active zones where fusion preferentially occurs.[57]

A series of phosphoproteins are embedded in synaptic vesicles that mediate vesicle movement, fusion and exocytosis. **Synapsin I**, on the cytoplasmic surface of the synaptic vesicle, ties vesicles to the actin microments of the neuronal cytoskeleton in a way that regulates the number of vesicles available for exocytosis. **Synaptophysin** in the membrane is required for vesicle fusion and release of neurotransmitter. Synaptophysin oligmers have been shown to form channels in lipid bilayers and may function as pores. **Synaptotagmin** binds acidic phospholipids and Ca^{++}, and binds to receptors on the presynaptic plasma membrane.

Neurotransmitter receptors in the postsynaptic membrane that mediate synaptic transmission are important targets for therapeutic drugs. In the CNS, amino acids are the major excitatory and inhibitory neurotransmitters. The **glycine receptor** is the most abundant inhibitory neurotransmitter receptor in the spinal cord, whereas **$GABA_AR$** mediates inhibition in the mammalian brain.[58]

AChE inhibitors produce acute toxicity by the rapid inactivation of cholinesterases at the neuromuscular junction. Myofibers respond with spasm, hypercontraction, degeneration, and necrosis. Ultrastructurally, myopathyic lesions consist of large vacuoles in the presynaptic zone, deletion of mitochondria, Z-band dissolution, and myofilament disintegration. Damage is mediated by increased cellular Ca^{++}, especially in Type I skeletal muscle fibers. Ultrastructural studies of **pyridostigmine bromide** poisoning in rats revealed altered neuromuscular junctions. Presynaptic areas were normal but postsynaptic areas were altered.

Immunogold techniques are widely used to specifically label neurons; for example, dopaminergic neurons can be identified with gold probes using

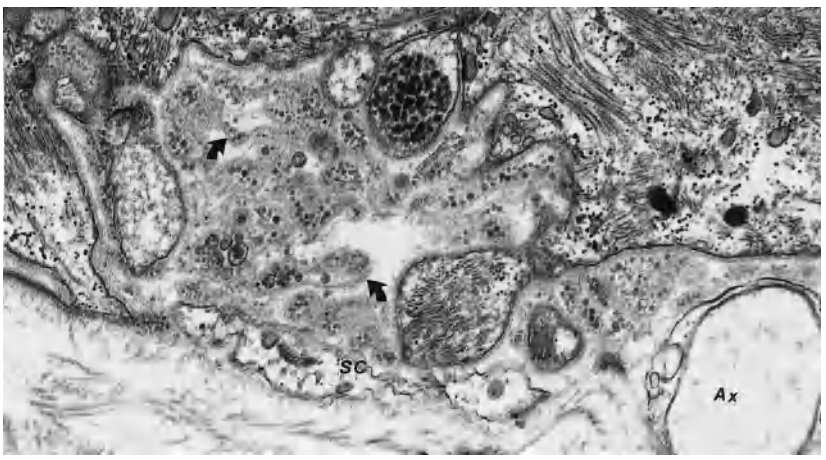


Fig. 19.8 Atrophic myoneural junction: chronic neuropathy. Basement membranes (*arrows*), axon (*Ax*). (Micrograph: B. Lach, *Acta Neuropathol* 80:611, 1990.)

antisera to tyrosine hydroxylase.[59] Serotoninergic neurons have been mapped at the ultrastructural level.[60] **Cholinergic neurons** can be identified ultrastructurally by their staining for acetylcholinesterase (AChE). **Choline acetyltransferase (ChAT)**, the synthesizing enzyme for ACh, is specific to cholinergic neurons in which it is localized throughout the axons, soma, and dendrites. The catalyzing enzyme **AChE** has a wider distribution than ChAT and is not exclusively localized in cholinergic structures. Certain noncholinergic neurons stain intensely for AChE; for example, catecholaminergic cells in the substantia nigra and locus coeruleus of the rat.

Nerve terminals have two types of vesicles that can be distinguished ultrastructurally: **large dense-cored vesicles**, which store neurotransmitters together with enzymes and peptides, and the **small dense-cored vesicles**, or translucent small synaptic vesicles, which co-store the neurotransmitter and nucleotides.

Botulinum Toxin

Botulinum toxin attaches to the synaptic vesicles of cholinergic nerves and blocks irreversibly and with high specificity the release of acetylcholine from nerve termini at the motor endplate. Toxin **blocks release of acetylcholine vesicles** at the presynaptic membrane, probably by reducing influx of Ca^{++}, preventing the action of this ion in promoting the fusion of acetylcholine vesicles with the plasma membrane at the nerve terminus.[61–64] Autoradiographic studies on the interaction of ^{125}I-labeled botulinum neurotoxins with nerve terminals (toxin was applied to the diaphragm muscle) showed that silver grains occurred over plasma membranes, synaptic boutons, and axoplasm of nerve trunks. This suggests the internalization and retrograde axonal transport of toxins and that internalization into the axon is acceptor mediated.[65]

DDT

Dichlorodiphenyltrichloroethane (DDT) has primary toxic actions on the motor cortex of the brain and on peripheral nerve fibers (both motor and sensory). DDT alters plasma membrane permeability by interfering with the stabilizing function of phospholipids in the lipid bilayer of the plasma membranes, thereby indirectly inhibiting ion-pumping ATPases located in the membrane. The manifestations of toxicity are hyperexcitability, tremor, and convulsions; they result from prolonged and repetitive action potentials in individual nerves. The normal axolemma exhibits a transient rise in permeability to Na^+ and K^+ during the action potential of its active state. The resulting ion fluxes lead to depolarization and then repolarization of the axolemma. DDT prolongs the permeability of the active state, causing increased nerve activity.

Receptor Agonists

At **synapses**, neurotoxins may interfere with impulses by preventing neurotransmitter receptor postsynaptically. Drugs called **receptor agonists**, which have configurations similar to that of the natural neurotransmitter, can bind to the membrane receptor and mimic the neurotransmitter's action. **Nicotine** is a receptor agonist for acetylcholine. Drugs with configurations similar enough to bind to the receptor but not to produce its action are called **receptor antagonists**.

A wide spectrum of antidepressant drugs act at various sites at the synapse. **Monoamine oxidase inhibitors** act presynaptically to prevent the cell from metabolizing monoamines. **Tricyclic compounds** act presynaptically to block the cells' reuptake of monoamines; for example, **imipramine** blocks reuptake of several monoamines, **fluoxetine** specifically blocks serotonin, and **buproprion** blocks dopamine. Monoamine receptor blockers act postsynaptically; the antipsychotic **haloperidol** is a dopamine receptor blocker. Other drugs, such as the antimanic agent **lithium carbonate**, act in postsynaptic membranes to inhibit synthesis of phosphotidylinositol and prevent second messenger activities.

Glutamate and Glutamate Analogue Toxicity

Amino acid neurotransmitters are ubiquitous in the mammalian CNS. **Glutamate** and **aspartate** are major excitatory neurotransmitters, and **gamma-aminobutyric acid (GABA)** is the major inhibitor neurotransmitter. **Glutamate** is released by some neurons and stimulates others to increase activity. In excess, glutamate acts as an **excitotoxin**: when it accumulates it overstimulates neurons until they die. Neuronal damaged caused by glutamate occurs in the circumventricular organ, a region that lacks a tight blood-brain barrier.

Ultrastructural analysis has revealed that after exposure to glutamate, neuronal changes involve swelling of postsynaptic elements (dendrites) and then of the entire neuronal cell body, with a general disintegration of organelles. In the acute phase, axons are not involved, and their degeneration occurs secondarily after acute neuronal swelling. Similar lesions are seen in monkeys receiving the glutamate analogue **monosodium L-glutamate (MSG)**, the flavor-enhancer

commonly added to processed foods. High dietary glutamate is associated with peripheral vascular responses but not neurotoxicity, although lesions have been reported in experimental toxicity in pregnant and fetal rats.

The mechanism for acute **excitotoxic neurodegeneration** induced by glutamate is a combination of excessive glutamate release and failure of the normal glutamate-reuptake system. The extracellular or released glutamate remains active at glutamate-sensitive receptors on postsynapatic membranes. The subsequent overactivation of these receptors induces changes in neuronal membrane permeability to ions and water that result in excitotoxic neurodegeneration.

Glutamate causes **calcium** to move into cells. Excessive glutamate stimulation leads to cell death, perhaps mediated by nitric oxide. Ca^{++}, in conjunction with calmodulin, turns on synthesis of nitric oxide, which in turn diffuses to adjacent cells to activate guanylyl cyclase, resulting in the appropriate cellular response.

Rats made thiamine deficient by treatment with **pyrithiamine** (a selective antagonist of brain thiamine pyrophosphokinase) developed symmetrical lesions of thalamic nuclei, mammillary bodies and brainstem similar to those in Wenicke's encephalopathy. Affected neurons are swollen with loss of cytoplasmic organelles and disintegration of polyribosomes, RER, and Golgi. Chromatin is clumped and marginated. Development of lesions after thiamine replacement suggests that excitotoxic and possible apoptotic mechanisms mediate neuronal degeneration in this model.[66]

Several analogues of glutamate, including **kainic acid** and **ibotenic acid**, can produce selective neuron destruction. When kainic acid is injected into rat brains, it kills neurons in the striatum. Dysfunction of complex I respiratory chain enzymes causes abnormal ultrastructural changes and epileptic seizures.[67] In 1987, about 150 Canadians were poisoned after eating mussels that contained large amounts of **domoic acid**, a potent glutamate analogue. Four died, and 12 who survived suffered memory loss similar to that in Alzheimer's disease. Postmortem analysis showed necrosis of neurons in the hippocampus. The mechanism of excitotoxic injury involves other neurotoxins.

Quinolinic acid, another glutamic acid analogue, also kills striatal neurons. Produced by astrocytes and infiltrating macrophages in a six-step pathway that begins with tryptophan, quinolinic acid increases in inflammatory lesions of the brain. Its presence is increased in CSF of HIV-infected patients up to 1,000-fold and it is hypothesized to play a role in chronic neuronal loss in the brain.

GABA Neurotransmitter Toxicity

Gamma-aminobutyric acid (GABA) is the major inhibitor neurotransmitter in the brain. **GABA transaminase** is the enzynme responsible for catabolism of GABA. GABA-containing boutons can be identified ultrastructurally.[68]

Vigabatrin, a selective inhibitor of GABA transaminase, causes increases in GABA in brain tissue. In rodents it prevents certain types of epileptic siezures. Prolonged high doses in dogs and rats are associated with intramyelin edema in the white matter of the brain.[69]

Benzodiazepines (diazepam [valium], chlordiazepoxide, flunitrazepam, clonazepan), which have a wide range of therapeutic application as anticonvulsant and muscle relaxing agents, elicit their primary therapeutic action in the CNS through GABAergic transmission; that is, they bind to specific sites on **GABA-gated chloride channels**. The receptor modulates GABA binding to the GABA-benzodiazepine chloride ionophore complex in the brain; an important role of the GABA receptor of this complex is its interaction with neurogenic steroids. Peripheral-type benzodiazepine receptors (PBR) exist in a wide variety of nonbrain tissue and differ from central type receptors in binding potency. Peripheral receptors bind to mitochondria of monocytes and to lesser degree to lymphocytes. They appear to be involved in the conversion of cytosolic cholesterol, which is delivered to the inner mitochondrial membrane, to pregnenolone. Through this pathway in lymphocytes and monocytes the PBR is involved in the control of immunity.[70]

Ivermectin

Ivermectin, a macrocyclic lactone parasiticide produced by *Streptomyces avermitilis*, is active against nematodes and arthropods, but has very low toxicity for mammals. Ivermectin inhibits transmission from interneurons to excitatory motoneurons by blocking γ-aminobutyric acid (GABA). There are different effects in different species. In mammals, GABA-mediated nerves occur only in the central nervous system; however, in invertebrates, such nerves regulate peripheral muscles. Interneuron-motoneuron junctions are blocked in nematodes. **Ivermectin** binds tightly to mammalian brain synaptosomes and stimulates presynaptic GABA release (it does not bind to GABA binding sites).

Tetanus Toxin

Tetanus is the syndrome of severe striated muscle spasm that spread progressively from muscle to

muscle from a site of wound infection with *Clostridium tetani*. *C tetani* produces several toxins at sites of tissue infection: (1) tetanospasmin, generally referred to as tetanus neurotoxin, is released on bacterial lysis, (2) tetanolysin, a hemolysin, destroys cells by acting on plasma membranes. **Tetanus neurotoxin** binds selectively to ganglioside receptors at peripheral nerve endings, is taken into the nerve, passes via retrograde transport to nerve cell bodies in the spinal cord, and diffuses back to exert its action presynaptically. Tetanus neurotoxin causes spasms by suppressing release of the inhibitory neurotransmitters GABA and glycine. It acts mainly on synaptic elements of the α and γ motoneurons or on presynaptic nerve terminals in their vicinity.[71]

Tetanus neurotoxin also produces central effects in the brain that are characterized by reflex motor convulsions. In rare cases, these effects may dominate in a syndrome of **cephalic tetanus**. Toxin may also bind to cells of the sympathetic nervous system in late stages of disease, producing hypertension, tachycardia, and peripheral vasoconstriction.

Retrograde transport of toxin was established by injected radiolabeled I^{125}-tetanospasmin into a rat leg.[72] Electron microscopic autoradiography of the ventrolateral spinal cord showed that a large part of radioactivity was in motoneurons. Dorsal root, horn, and cell bodies of spinal cord motoneurons were free of label. Morphometry of the synapse afferent to motor neuron perikarya showed decrease in total vesicle density and a shift from round to flat vesicles.[73] Toxin adsorbed onto colloidal gold as a marker has been used to demonstrate the direct effect of toxin on muscle. Injected into the anterior chamber of the eye, labeled toxin selectively associated with nerve terminals and preterminal axons. Within cells, it localized on membranes of the endoplasmic reticulum.[74]

Tetanus neurotoxin may also product direct action on **skeletal muscle**. Toxin-binding sites are in membranes of the T tubular system, at its junction with the sarcoplasmic reticulum, and within the sarcoplasmic reticulum cisternae.[75]

Arthropod Neurotoxins That Block Neuromuscular Transmission

Neurotoxins are the most potent constituents of snake venoms. They kill by blocking neuromuscular transmission at the motor end plates of skeletal muscle, blockade of the cardiac conduction system, and production of central effects that suppress both respiratory and cardiac action. Most prominent of these is **motor end plate dysfunction** and paralysis of the respiratory muscle in the diaphragm and rib cage.

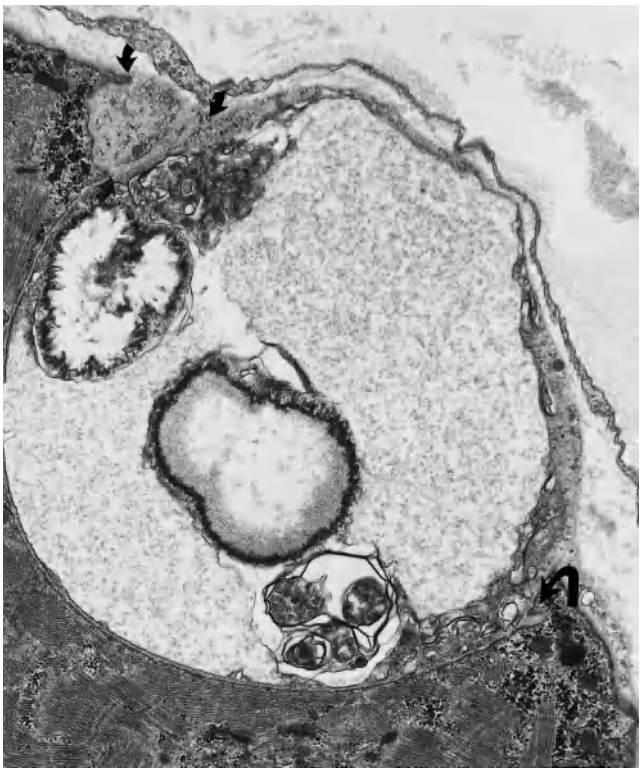


Fig. 19.9 Vacuolar neuropathy: chronic, myoneural junction, calcification. (Micrograph: B. Lach, *Acta Neuropathol* 80:611, 1990.)

Mechanistically, neurotoxin action on neuromuscular transmission is either (1) **presynaptic**, via inhibition of acetylcholine release, (2) **synaptic**, by cholinesterase acting within the synaptic cleft, or (3) **postsynaptic**, by binding to acetylcholine receptors to prevent the depolarizing action of acetylcholine (Figs. 19.9 and 19.10).[76]

Venoms of the family Elapidae (cobra, krait, tiger snake, and coral snake) kill via neurotoxins. Cobra and krait have postsynaptic toxins that bind tightly and irreversibley to **acetylcholine receptors** and act as antagonists (like curare). Injection of cobra venom into mammals produces a flaccid muscle paralysis and death occurs by respiratory failure. The lethal effect is due to the presence in the crude venom of neurotoxic proteins that bind specifically to **nicotinic acetylcholine receptors**, producing a nondepolarizin block.

Alpha-bungarotoxin of the banded krait *Bungarus multicinctus* is a specific ligand for **nicotinic acetylcholine receptors**. It causes the normal distribution of acetylcholine receptors to become nonuniformly distributed over the surfaces of the synaptic cleft. The poisoned motor end plate exhibits swollen mitochondria, decreased numbers of synaptic vesicles, and opening of synaptic clefts at the axolemma.[77]

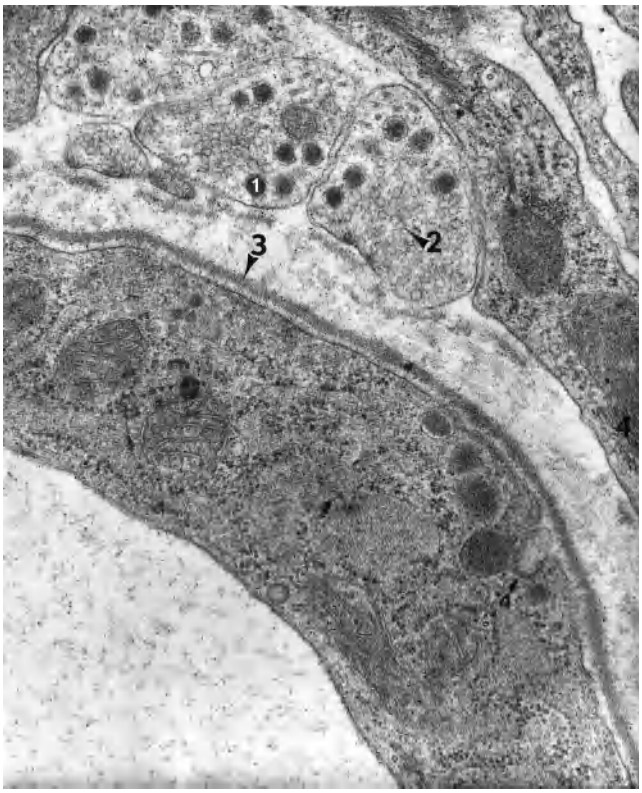


Fig. 19.10 **Synapse**: subepithelial, trachea, chicken. Dense cored vesicles (*1*), electron opaque vesicles (*2*), basement membrane of capillary (*3*). Capillary at lower left.

Antagonists of Inhibitory Neurotransmitter

Strychnine

Strychnine is in many rodenticides and several products for animal and human consumption including laxatives, sedatives, and tonics. Strychnine excites all of the central nervous system and clinically strychnine toxicity resembles tetanus. The important effects result from its anti-inhibition of spinal cord **interneurons**. Strychnine competitively antagonizes the inhibitory neurotransmitter **glycine** at the postsynaptic receptor sites of ventral horn motoneurons. In animals that survive even for a few hours, there are profound lactic acidosis, hyperthermia, and rhabomyolysis.

Uncouplers of Mitochondrial Oxidative Phosphorylation

Bromethalin

Rodenticides containing 0.01% **bromethalin** (marketed as Vengeance, Assault, and Trounce) are highly neurotoxic to rats, but also to cats and dogs. Bromethalin and its N-demethylated metabolite desmethylbromethalin cause cerebral edema and demyelination. They **uncouple oxidative phosphorylation** and causes deficits of ATP, sodium- and potassium-ATPase, and ion channel pumping. The brains develop diffuse spongy degeneration of the white matter that is characterized ultrastructurally as marked acute cell swelling of astrocytes and oligodendrogliocytes, and intramyelinic edema.[78] Myelin lamellae separate at interperiod lines forming intramyelinic vacuoles. Vacuoles rupture and coalesce into large extracellular spaces.

Glial Toxins

Astrocyte swelling is a response to many neurotoxins, and reduction of glial swelling is a critical component of the pharmacologic reduction of brain swelling. In the brain, **acquaporin-4 (AQP4)** is tied to the clearance of extracellular K^+, and loss of AQP4 from astrocytic processes results in perturbed flux of water through astrocytes and leads to impaired buffering of extracellular K^+.[79] Glia also play a critical role in acute hypoosmotic stress. Water loading leads to transient increases in glial **glutamine** and decreases in **glutamate**. Quantitative studies using immunogold labeling of these compounds reveal that the excitotoxin glutamate can also function as an organic osmolyte because it moves through the **glutamine synthetase** pathway in glia prior to an efflux into the bloodstream.[80]

Reactive glial change is a component of many toxic injuries to nervous tissue. **Fibrillary astrocytes**, acting like fibroblasts, form glial scars (gliosis) at sites of injury. Astrocyte processes contain intermediate filaments. As the damaged tissue is repaired, astrocytes lose cytoplasm, but retain processes. In long-standing gliosis, astrocytes often bear **Rosenthal fibers**, irregular, amorphous, electron-dense bodies surrounded by a feltwork of intermediate filaments. Corpora amylacia accumulate with age in astrocyte processes, especially in subependymal and subpial locations in primates (see chapter 27).

Reactive astrocytosis, a massive enlargement of astrocytes, is a common sequel to toxic injury. Reactive astrocytes, also called **gemistocytic astrocytes** have much cytoplasm and produce large amounts of intermediate filaments—detected histochemically as glial fibrillary acidic protein (GFAP). Assays for GFAP and glutamine synthetase are used as markers for toxic injury; for example, rodents exposed to methamphetamine and iminodipropionitrile have markedly increased GFAP in the brain.

Pigments are a normal component of some glia. During aging and in responses to radiation, chronic estrogenization, and other chronic processes, a subpopulation of astrocytes in periventricular and limbic

regions accumulates pigmented cytoplasmic inclusions that are distinct from lipofuscin. Granules emit orange-red autofluorescence (as does porphyrin) and stain with the peroxidase marker diaminobenzidine (DAB). The endogenous peroxidase activity appears to be due to heme (ferrous) iron or to a related metalloporphyrin.

Ammonia

Elevated blood levels of **ammonia** are toxic to astroglia, causing acute cell swelling and damage to astryocyte mitochondria. Morphometric studies of rat glial cell ultrastructure after urease-induced hyperammonemia revealed that astrocyte cytoplasmic areas increased 46% after 4 days. Oligodendroglia were unchanged.[81,82] **Valproate** (valproic acid) is an antiepileptic drug that, in some patients during long-term use, is associated with **hyperammonemic encephalopathy.** Ultrastructural studies in rats reveals dysfunctional astrocytes in the temporal lobe, and concurrent damage to the BBB.[83]

Metabolic Toxicity in Glia

Glia metabolize neurotoxins to toxic intermediates, which can cause degeneration in glia. Toxic intermediates can be transported to the neuron where it causes degeneration. Some neurotoxins show preference for glial cells over neurons. **Aminonicotinamide** produces a **glial neuropathy** in spinal cord, brainstem, and cerebellum. It affects enzymes of glycolysis and glucose utilization, particularly enzymes of the pentose phosphate shunt, which have greater impact on glia than on neurons. This is in spite of the fact that ion movement during neural transmission consumes large amounts of glucose. **Tunicamycin** is a potent inhibitor of glycosylation, and studies in rodents show that it causes vascular lesions that lead to injury of the CNS. **Adriamycin** blocks microglial transformation.

Vascular Neurotoxins and the Blood-Brain Barrier

The brain is rigorously isolated from circulating blood by anatomic structures collectively called the **blood-brain barrier (BBB)**. The BBB formed by cerebral capillary endothelium possesses unique structural and physiologic properties, including transport systems for specific families of molecules on both its luminal and abluminal parts. Inductive influences on capillary endothelium occur from astrocytes and other nonendothelial cell types (Fig. 19.11). The unique ultrastructural arrangement of endothelial cells of the BBB consists of the following structural adaptations:

- **Tight junctions** in a contiguous arrangement between endothelial cells
- Lack of **plasmalemmal vesicles** (and transendothelial channels)
- Lack of **fenestrae**
- Corona of **astrocytic foot processes** that surrounds capillaries

Exchange of substances between blood and brain must occur transcellularly, via specific carrier-mediated systems, a complex group of active transport molecules on luminal and antiluminal membranes that controls movement in and out of the neuropil.[84,85] The asymmetric distribution of the glucose transporter on lumenal and ablumenal membranes of endothelial cells of the blood-brain barrier, as detected by immunogold electron microscopy, suggests that the differential or regulated transport of molecules is probable.[86]

When the BBB is broken, tight junctions open, pinocytosis increases, and canaliculi form between capillary lumens and basal surfaces. The spectrum of neurotoxins that act on the BBB range from the vasogenic edema and extravasation of spider venoms,[87] to the fungal metaboli lovastatin. **Lovastatin** (mevinolin), a competetive inhibitor of the rate limiting enzyme of cholesterol synthesis, 3-hydoxy-3-methylglutaryl coenzyme A reductase, lowers serum cholesterol in humans without toxicity. At very high doses, lovastatin is neurotoxic in dogs, probably by virtue of endothelial damage (although direct neurotoxic action was not ruled out).[88]

Heavy Metal and Endothelial Cell Toxicity

Lead

Lead monoxide (PbO), a major biproduct of leaded gasoline and component of paint pigments, and lead tetroxide, an antirust component of paint, are major sources of environmental lead. In humans and most mammalian species, disease involves nervous, gastrointestinal, and hematologic signs. In children with marked lead poisoning, the **brain** is affected by edema with blunting and atrophy of cerebral gyri. Microscopically, there are demyelination of cerebral and cerebellar white matter, death of cortical neurons, and astrocyte proliferation. There is proliferation of

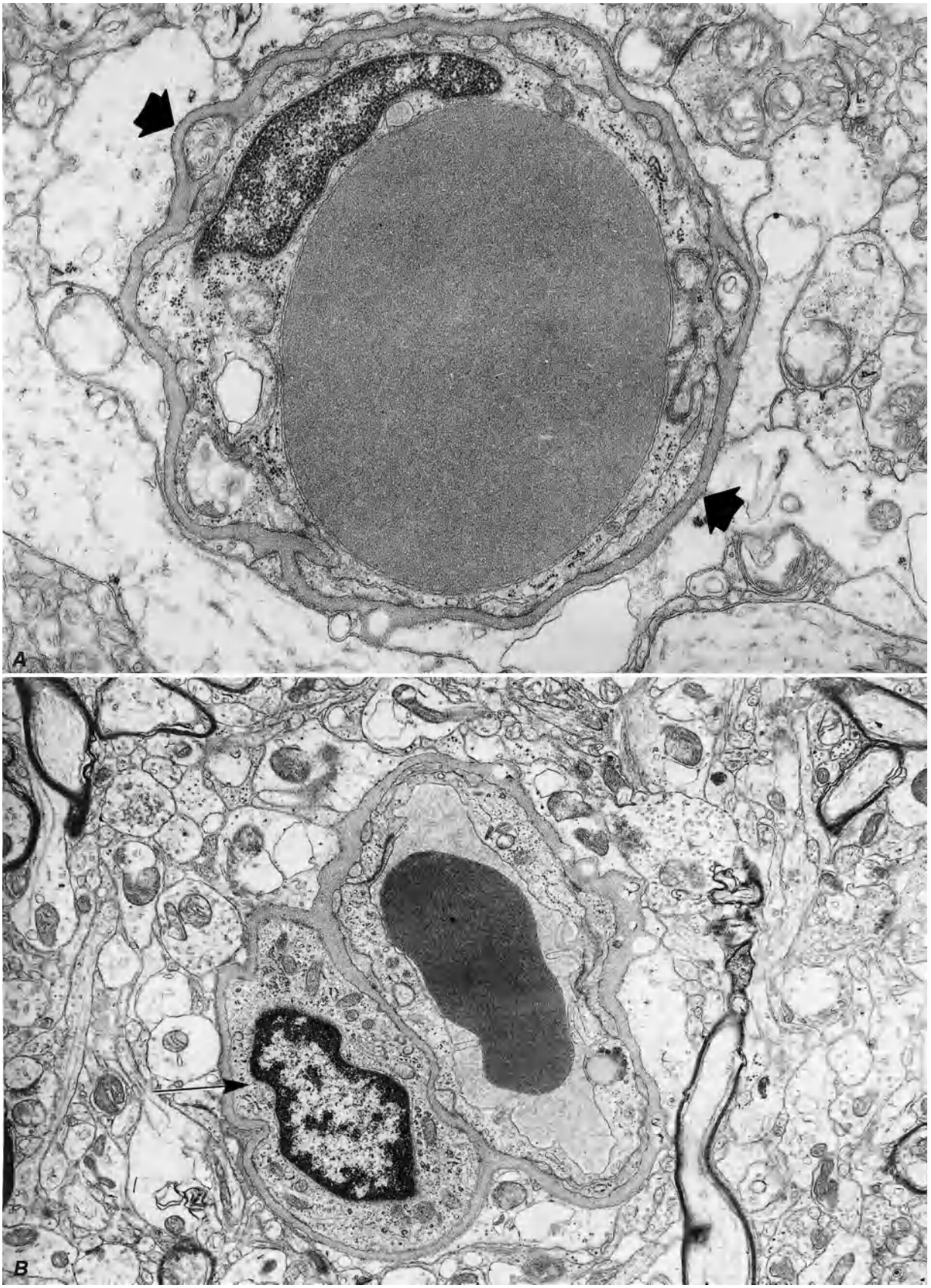


Fig. 19.11 Blood-brain barrier: Alzheimer's disease, human. **A**. **Pericyte processes** surround capillary (*arrows*). **B**. **Pericyte** (*arrow*) immediately adjacent to endothelium. (Micrographs: Patricia A. Stewart, *Lab Inv*est 67:734, 1992.)

endothelial cells in small capillaries around damaged areas of the brain.

In adults, **peripheral demyelinating neuropathy** is the lesion of lead toxicity. In all species the nervous system lesions are primarily vascular. There is **necrosis of endothelial cells** in capillaries and arterioles and damaged blood vessels are surrounded by edema and hemorrhage. Ultrastructurally, the neuropil in affected areas is vacuolated (**status spongiosis**), and there is demyelination and necrosis.[89,90] Necrotic brain tissue develops in layers, a pattern called laminar necrosis. Brain lesions in both natural and experimental lead toxicity with foci of vacuolation and demyelination were common in the cerebral cortex.

Mercury

Mercury is a potent inhibitor of sulfhydryl-rich proteins and forms cross links with plasma membrane proteins. This suppresses membrane-associated enzymes, especially ATPases of the sodium-potassium pumps. Leaky membranes lead to endothelial swelling, increased capillary permeability, and edema of the neuropil. Degenerative changes also occur in neurons of the brain and fibers in peripheral nerves and their ganglion cells. Neurons show an inhibition of protein synthesis that precedes and probably inhibits glycolysis. There are important secondary effects in the brain, and the pathogenesis of mercury neurotoxicity involves alteration of the BBB and suppression of synaptic transmission, as well as inhibition of protein synthesis in neurons. An early change in mercury-poisoned neurons is degranulation of rough endoplasmic reticulum, a reflection of altered ribosomal lipoprotein synthesis.[91] Ribosome loss is followed by progressive disorganization of Golgi membranes and neurofilaments, manifested as peripheral neuronal chromatolysis.[92] The effects of mercury toxicity are severe on the developing brain of the rat.[93] **Astrocyte foot processes** abutting capillaries are swollen in acute mercury toxicity, probably because of cell swelling of the astrocyte.[94]

Gold

Gold salts, used in the treatment of human rheumatoid arthritis may cause neurotoxicity. The neurologic complication of therapy with sodium aurothiomalate is a **sensory neuropathy** with progressive symmetrical sensorimotor polyneuropathy. Gold has been found in the cerebrospinal fluid and, through autoradiography and neutron activation analysis, in nervous tissue. Using techniques of silver enhancement (autometallography), small amounts of gold are found in dorsal root ganglia of experimentally treated rats, most in lysosomes of various cell types.[95]

References

1. Karasek M, et al. 2004. Ultrastructure of the central nervous system. *Folia Neuropathol* 42(Suppl B):1.
2. Nishida T, et al. 2007. Ultrastructural localization of the neurotrophin receptor (TrkA) in cultured rat pheochromocytoma PC12 cells: Three-dimensional analysis by high voltage electron microscopy. *Biomed Res* 28:161.
3. Mechawar N, et al. 2007. Developmental profile of neuregulin receptor ErbB4 in postnatal rat cerebral cortex and hippocampus. *Neurosceince* 148:126.
4. Hirano A, et al. 1984. Fine structural observations of neurofilamentous changes in amyotrophic lateral sclerosis. *J Neuropathol Exp Neurol* 43:461.
5. Gallyas F, et al. 2005. "Dark" (compacted) neurons may not die through the necrotic pathway. *Exp Brain Res* 160:473.
6. Barth M, et al. 2002. Pre-embedding immunogold labeling of TUNEL stain enables evaluation of DNA strand breaks and ultrastructural alterations in individual cells of neuronal tissue. *Acta Neuropathol* 104:621.
7. Choy MS, et al. 2006. PTEN is recruited to specific microdomains of the plasma membrane during lactacystin-induced neuronal apoptosis. *Neurosci Lett* 405:120.
8. Siddiqi ZA, Peters A. 1999. The effect of aging on pars compacta of the substantia nigra in rhesus monkey. *J Neuropathol Exp Neurol* 58:903.
9. Hsu DW, Hedley-Whyte EJ. 1980. Effects of insulin-induced hypoglycemia on cerebrovascular permeability to horseradish peroxidase. *J Neuropathol Exp Neurol* 39:265.
10. Auer R, et al. 1985. The dentate gyrus in hypoglycemia: Pathology implicating excitotoxin-mediated neuronal necrosis. *Acta Neuropathol* 67:279.
11. Sato M, et al. 1990. Histologic changes of neuronal damage in vegetative dogs induced by 18 minutes of complete global brain ischemia: Two phase damage of Purkinje cells and hippocampal CAI pyramidal cells. *Acta Neuropathol* 80:527.
12. Northington FJ, et al. 2007. Failure to complete apoptosis following neonatal hypoxia-ischemia manifests as "continuum" phenotype of cell death and occurs with multiple manifestations of mitochondrial dysfunction in rodent forebrain. *Neuroscience* 149:822.
13. Benjelloun N, et al. 2003. Apoptotic mitochondrial pathway in neurons and astrocytes after neonatal hypoxia-ischaemia in the rat brain. *Neuropathol Appl Neurobiol* 29:350.
14. Koeppen AH, Borke RC. 1991. Experimental superficial siderosis of the central nervous system. *J Neuropathol Exp Neurol* 50:579.
15. Liu CL, et al. 2007. Changes in autophagy after traumatic brain injury. *J Cereb Blood Flow Metab* 28: 674.

16. Komatsu M, et al. 2007. Essential role for autophagy protein Atg7 in the maintenance of axonal homeostasis and the prevention of axonal degeneration. *Proc Natl Acad Sci USA* 104:14489.
17. Haeberlé AM, et al. 2007. Immunogold localization of phocein in dendritic spines. *J Comp Neurol* 336.
18. Nixon RA, et al. 2005. Extensive involvement of autophagy in Alzheimer disease: An immuno-electron microscopy study. *J Neuropathol Exp Neurol* 64:113.
19. Yu WH, et al. 2005. Macroautophagy—a novel beta-amyloid peptide-generating pathway activated in Alzheimer's disease. *J Cell Biol* 171:15.
20. Tegner R, et al. 1988. Morphological study of peripheral nerve changes induced by chloroquine treatment. *Acta Neuropathol* 75:253.
21. Wisniewski HM, et al. 1984. Aluminum-induced neurofibrillary changes in axons and dendrites. *Acta Neuropathol* 63:190.
22. Behrouz B, et al. 2007. Unique responses to mitochondrial complex I inhibition in tuberoinfundibular dopamine neurons may impart resistance toxic insult. *Neuroscience* 13:147.
23. Liang CL, et al. 2007. Mitochondria mass is low in mouse substantia nigra dopamine neurons. *Exp Neurol* 203:370.
24. Tanaka J, et al. 1988. Neuropathological study on 1-methyl-4-phenyl-1,2,3,6-tetrahydropyridine in the crab-eating monkey. *Acta Neuropathol* 75:370.
25. Zhu JH, et al. 2007. Regulation of autophagy by extracellular signal-regulated protein kinases during 1-methyl-4-phenylpyridinium-induced cell death. *Am J Pathol* 170:75.
26. Escobar-Khondiker M, et al. 2007. Annonacin, a natural mitochondrial complex I inhibitor, causes tau pathology in cultured neurons. *J Neurosci* 27:7827.
27. Yoshida Y, et al. 1992. Neuronal injury after photoactivation of photofrin II. *Am J Pathol* 141:989.
28. Schinzel AC, et al. 2005. Cyclophilin D is a component of mitochondrial permeability transition and mediates neuronal cell death after focal cerebral ischemia. *Proc Natl Acad Sci USA* 102:12005.
29. Yuyama K, et al. 2008. Accelerated release of exosome-associated GM1 ganglioside (GM1) by endocytic pathway abnormality. *J Neurochem* 105:217.
30. Wünschmann A, et al. 2006. Neuronal storage disease in a group of captive Humboldt penguins (*Spheniscus humboldti*). *Vet Pathol* 43:1029.
31. Castino R, et al. 2008. Suppression of autophagy precipitates neuronal cell death following low doses of methamphetamine. *J Neurochem* [E-pub].
32. Ricaurte GA, et al. 1988. (+)3,4-Methylenedioxymethamphetamine selectively damages central erotonergic neurons in nonhuman primates. *J Am Med Ass* 260: 51.
33. Nag S. 1992. Vascular changes in the spinal cord in N-methyl-D-aspartate-induced excitotoxicity: Morphological and permeability studies. *Acta Neuropathol* 84:471.
34. Dastur DK, et al. 1985. Experimental neurotoxicity of the anorectic fenfluramine. *Acta Neuropathol* 67:142.
35. Spencer PS, et al. 1987. Guam amyotrophic lateral sclerosis-Parkinsonism-dementia linked to a plant excitant neurotoxin. *Science* 237:517.
36. Olney JW, et al. 1989. Pathological changes induced in cerebrocortical neurons by phencyclidine and related drugs. *Science* 244:1360.
37. Schmidt RE, et al. 1990. Ultrastructural and immunohistochemical characterization of guanethidine induced destruction of peripheral sympathetic neurons. *J Neuropathol Exp Neurol* 49:150.
38. Jomary C, et al. 1992. Synaptic localization of *k* opioid receptors in guinea pig neostriatum. *Proc Natl Acad Sci USA* 89:564.
39. Wood DD, et al. 2008. Myelin localization of peptidylarginine deiminases-2 and 4: Comparison of PAD2 and PAD4 activities. *Lab Invest* 88:354.
40. O'Hara S, et al. 1986. Ultrastructural alterations of perineural cells in the early stage of Wallerian degeneration. *Lab Invest* 54:213.
41. Raine CS. 1984. Analysis of autoimmune demyelination. *Lab Invest* 50:608.
42. Lampert PW. 1967. A comparative electron microscopic study of reactive degenerating regenerating dystrophic axons. *J Neuropathol Exp Neurol* 26:345.
43. Lampert PW, et al. 1869. An electron microscopic study of dystrophic axons in the gracile and cuneate nuclei of vitamin E-deficient rats. *J Neuropathol Exp Neurol* 23:60.
44. Raine CS, et al. 1987. Microtubule-mitochondrial associations in regeneration axons after taxol intoxication. *J Neurocytol* 16:461.
45. Raine CS, Cross AH. 1989. Axonal dystrophy as a consequence of long-term demyelination. *Lab Invest* 60:714.
46. Charlton KM, Pierce KR. 1970. A neuropathy in goats caused by experimental coyotillo (*Karwinskia humboldtiana*) poisoning. *Vet Pathol* 7:420.
47. Chang DT, Reynolds IJ. 2006. Mitochondrial trafficking and morphology in healthy and injured neurons. *Prog Neurobiol* 80:241.
48. Tshala-Katumbay DD, et al. 2005. A new murine model of giant proximal axonopathy. *Acta Neuropathol* 109:405.
49. Anthony DC, et al. 1983. The spatio-temporal pattern of the axonopathy associated with the neurotoxicity of 3,4-dimethyl-hexanedione in the rat. *J Neuropathol Exp Neurol* 42:548.
50. Tomiwa K, et al. 1986. The effect of cisplatin on rat spinal ganglia. *Acta Neuropathol* 69:295.
51. Scheiermann C, et al. 2007. Expression and function of junctional adhesion molecule-C in myelinated peripheral nerves. Science 318:1472.
52. Li YC, et al. 2005. Subsurface cisterna-lined axonal invaginations and double-walled vesicles at the axonal-myelin seath interface. *Neurosci Res* 53:298.
53. Thomas NJ, et al. 1998. Epizootic vacuolar myelinopathy of the central nervous system of bald eagles (*Haliaeetus leucocephalus*) and American coots (*Fulica americana*). *Vet Pathol* 35:479.
54. Dalakas MC, et al. 2001. Mitochondrial alterations with mitochondrial DNA-depletion in the nerves of AIDS

patients with peripheral neuropathy induced by 2′3′-dideoxycytidine (ddC0). *Lab Invest* 81:1537.
55. Feldman D, et la. 1992. Ultrastructure of peripheral neuropathy induced in rabbits by 2′,3′-dideoxycytidine. *Lab Invest* 66:75.
56. Quatacker JR, et al. 1992. Immunocytochemical demonstration of dopamine-β-hydroxylase and cytochrome B561 on the axonal reticulum in bovine sympathetic neurons. *J Hist Cyt* 40:1599.
57. Greengard P, et al. 1992. Synaptic vesicle phosphoproteins and regulation of synaptic function. *Science* 259:780.
58. Hostman SR, Ernst SA. 1987. Characterization of muscarinic acetylcholines in the avian salt gland. *J Cell Biol* 91:781.
59. Marshak DW. 1992. Localization of immunoreactive tyrosine hydroxylase in the goldfish retina with preembedding immunolabeling with one-nanometer colloidal gold particles and gold toning. *J Hist Cyt* 40:1465.
60. Chazal G, Ma W. 1989. An ultrastructural analysis of serotoninergic neurons in the nucleus raphe magnus of the rat. *Neuroscience* 33:301.
61. Duchen LW. 1971. Changes in the electron microsope structure of slow and fast skeletal muscle fibers of the mouse after the local injection of botulinum toxins. *J Neurol Sci* 14:61.
62. Hirokawa N, et al. 1979. Binding of *Clostrium botulinum* neurotoxin to the presynaptic membrane of the central nervous system. *J Cell Biol* 81:43.
63. Cross SA, et al. 2007. Acute and long-term effects of botulinum neurotoxin on the function and structure of developing extraocular muscles. *Neurobiol Dis* 25: 649.
64. Pamphlett R, Bayliss A. 1992. The effect of nerve crush and botulinum toxin on lead uptake in motor neurons. *Acta Neuropathol* 84:89.
65. Black JD, Dolly JO. 1967. Interaction of ^{125}I-labeled botulinum neurotoxins with nerve terminals. *J Cell Biol* 103:521.
66. Zhang SX, et al. 1995. Excitotoxic cytopathology, progression, and reversibility of thiamine deficiency-induced diencephalic lesions. *J Neuropathol Exp Neurol* 54:255.
67. Chuang YC, et al. 2004. Mitochondrial dysfunction and ultratructural damage in the hippocampus during kainic acid-induced status epilepticus in the rat. *Epilepsia* 45:1202.
68. Maxwell DJ, et al. 1989. Synaptic connections of GABA-containing boutons in the lateral cervical nucleus of the cat. *Neuroscience* 33:169.
69. Gibson JP, et al. 1990. Chronic toxicity studies with vigabatrin, a BABA-transaminase inhibitor. *Tox Pathol* 18:225.
70. Cahard D, et al. 1994. Subcellular localization of peripheral benzodiazepine receptors on human leukocytes. *Lab Invest* 70:23.
71. Benecke R, et al. 1977. Tetanus toxin induced actions on spinal Renshaw cells and Ia-inhibitory interneurons during development of local tetanus in the cat. *Exp Brain Res* 27:271, 1977.
72. Price DL, et al. 1975. Tetnaus toxin: Direct evidence for retrograde intraaxonal transport. *Science* 188:945.
73. Schwab. 1976. Electron microscopic evidence for a transsynaptic migration of tetanus toxin in spinal cord motoneurons. *Brain Res* 105:213.
74. Schwab ME, Thoenen H. 1978. Selective binding, uptake, and retrograde transport of tetanus toxin by nerve terminals in rat iris. *J Cell Biol* 77:1.
75. Zachs SI, Scheff MF. 1968. Tetanus toxin. *Science* 159:643.
76. Rigoni M, et al. 2005. Equivalent effects of snake PLA2 neurotoxins and lysophospholipid-fatty acid mixtures. *Science* 310:1678.
77. Chen IL, Lee CY. 1970. Ultrastructural changes in the motor nerve terminals caused by β-bungarotoxin. *Virch Arch* B 6:318.
78. Dorman DC, et al. 1992. Neuropathologic findings of bromethalin toxicosis in the cat. *Vet Pathol* 29:139.
79. Eid T, et al. 2005. Loss of perivascular aquaporin-4 may underlie deficient water and K^+ homeostasis in the human epileptogenic hippocampus. *Proc Natl Acad Sci USA* 102:1193.
80. Nagelhus EA, et al. 1996. Neuronal and glial handling of glutamate and glutamine during hypoosmotic stress. *Neuroscience* 72:743.
81. Pilbeam CM, et al. 1983. The brain in experimental portal-systemic encephalopathy. *J Pathol* 140:331.
82. Amiry-Moqhaddam M, et al. 2005. Brain mitochondria contain aquaporin water channels. *FASEB J* 19:1459.
83. Sobaniec-Lotowska ME, Lotowska JM. 2005. Ultrastructural study of cerebellar dentate nucleus astrocytes in chronic experimental model with valproate. *Folia Neuropathol* 43:166.
84. Trout JJ, et al. 1986. Blood-brain barrier breakdown by cold injury. *Lab Invest* 55:622.
85. Coomber BL, Stewart PA. 1986. Three-dimentional reconstruction of vesicles in endothelium of blood-brain barrier versus highly permeable microvessels. *Anat Rec* 215:256.
86. Farrell CL, Pardridge WM. 1991. Blood-brain barrier glucose transporter is asymmetrically distributed on brain capillary endothelial lumenal and ablumenal membranes: An electron microscopic immunogold study. *Proc Nat Acad Sci USA* 88:5779.
87. Rapôso C, et al. 2007. Acute blood-brain barrier permeabilization in rats after systemic *Phoeutria nigriventer* venom. *Brain Res* 1149:18.
88. Berry PH, et al. 1988. Brain and optic system pathology in hypocholesterolemic dogs treated with a competitive inhibitor of 3-hydroxy-3-methylglutaryl coenzyme A reductase. *Am J Pathol* 132:427.
89. Clasen AA, et al. 1974. Electron microscopic and chemical studies of lead encephalopathy. *Am J Pathol* 74:215.
90. Sundstrom R, Kalimo H. 1988. Extracellular edema and glial response to tin in the cerebellum of suckling rats with low-dose lead encephalopathy. *Acta Neuropathol* 75:116.
91. Jacobs IM, et al. 1975. Ultrastructural changes in the dorsal root ganglia of rats poisoned with methylmercury. *Neuropathol Appl Neurobiol* 1:1.

92. Herman SP, et al. 1973. An ultrastructural study of methylmercury-induced primary sensory neuropathy in the rat. *Lab Invest* 28:104.
93. Geelen JAB, et al. 1990. The early effects of methylmercury on the developing rat brain. *Acta Neuropathol* 80:432.
94. Ware RA, et al. 1974. An ultrastructural study on the blood-brain barrier dysfunction following mercury intoxication. *Acta Neuropathol* 30:211.
95. Schionning JD, et al. 1992. Autometallographic detection of gold in dorsal root ganglia of rats treated with sodium aurothiomalate. *Exp Molec Pathol* 56:239.

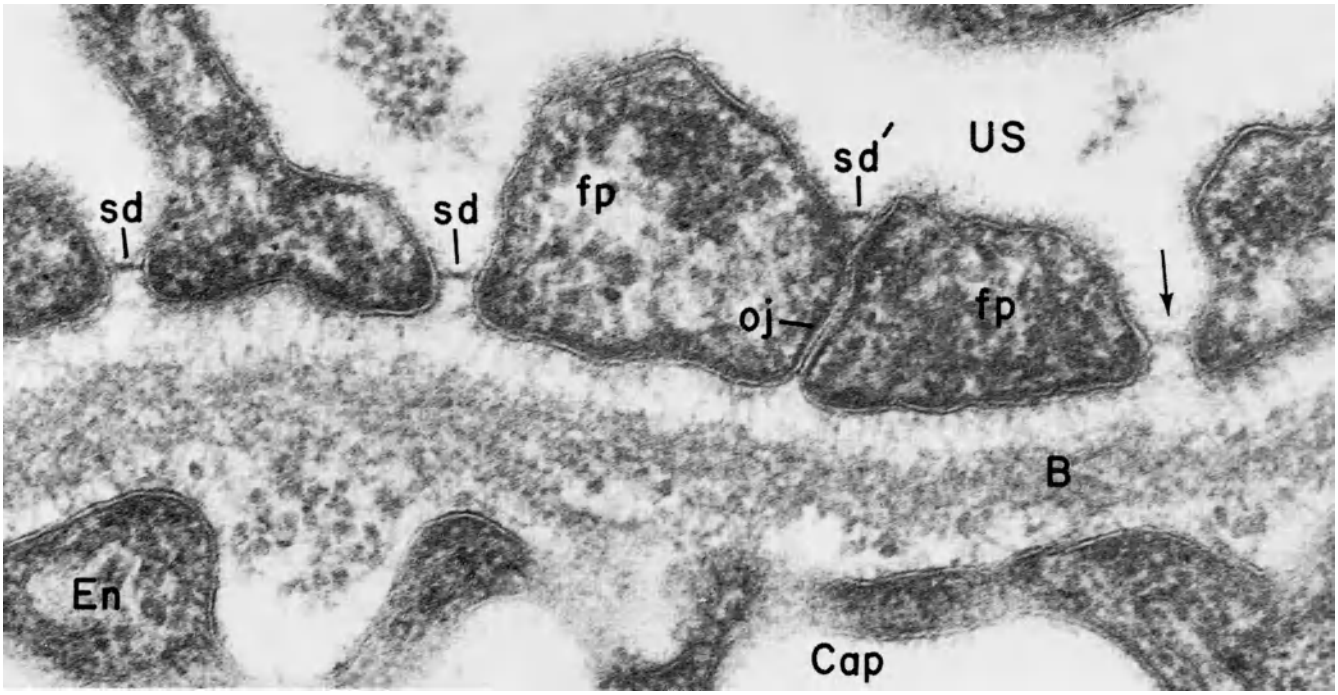


Fig. 20.1 Glomerular filtration barrier: residual filtration slits, nephrotic rat. The slit (*right*) is wider than normal (*arrow*). Foot processes (*fp*) have come together and outer leaflets have fused obliterating the intercellular space. Slit diaphragm (*sd*), urinary space (*US*), capillary (*Cap*), occluding junction (*oj*). (Micrograph: John P. Caulfield, *Laboratory Investigation* 34:43, 1976.)

© 2009 Wiley-Blackwell. ISBN: 978-0-813-80330-2

20 Nephrotoxins

Glomerular Toxins

The **glomerular filtration barrier (GFB)** regulates the passage of fluid and electrolytes and the selective retention of plasma proteins and other macromolecules from plasma to glomerular filtrate (Fig. 20.1). The GFB consists of the following structures:

- **Fenestrae** within endothelial cells of glomerular capillaries
- **Glomerular basement membrane (GBM)** between endothelium and podocyte
- **Epithelial slit pores**: gaps between podocyte foot processes that are bridged by slit diaphragms

Slit diaphragms are modified tight junctions between foot processes that contain **nephrin**, through which they are linked to the actin cytoskeleton. In the slit pores, podocytes also contain Neph-1, ZO-1, P-cadherin, and other integral proteins.[1,2] Interaction of these components with proteoglycans in the GFB is critical for regulating GFB function.[3] In immunogold stained sections, nephrin is in the slit diaphragm whereas podocyte cell bodies are unstained. The protein ZO-1, which is present only at tight junctions, is in the podocyte cytoplasm at the points of insertion of the slit diaphragm into the plasma membrane.

Visceral podocytes abut the capillary basement membrane with striking intermeshing of foot processes (Fig. 20.2). Specialized **podocyte proteins** that control foot process metabolism, position, and intracellular trafficking include podocin, podoplanin, podocalyxin, nephrin, synaptopodin, and glomerular epithelial protein-1.[4] The **α- and β-dystroglycans** maintain foot process position through connections with their ligands, the matrix proteins laminin and agrin in the glomerular basement membrane. **Dynamin**, an intracellular GTPase, is required for maintenance of podocyte morphology. Dynamin contains a cleavage site for the protease cathepsin L, and in proteinuric renal disease, cleavage of dynamin leads to rearrangement of the podocyte actin cytoskeleton and collapse of foot processes. In a mouse model of proteinuria, introduction of a protease-resistant dynamin restored podocyte function.[5] **Ras GTPase** isoforms have been identified with immunolabeling in the podocyte and other components of the kidney, but their relationship to toxic injury has not been clarified.[6]

Glomerular podocytes have a curious similarity to neurons—both have a specialized cytoskeleton that is associated with expression-restricted proteins, such as nephrin, synaptopodin, myelin protein O, and the small GTPase Rab3A and its effector rabphilin-3A.[7] **Myelin protein O** (MPZ or PO) is a transmembrane glycoprotein that, by immunogold labeling techniques, is found within the plasma membrane and internal vesicles of podocytes.[8] Mutations in the PO gene are associated with the **focal segmental glomerulosclerosis** that is a component of one form of the demyelinating peripiheral neuropathy Charcot-Marie-Tooth disease.

The glomerular filtration barrier may be damaged directly by toxic injury, with the proximal tubule nearly always being affected. Foot processes fuse, slit pores are obliterated, and intercellular junctions are narrowed and lengthened.[9] If large tracer proteins (normally stopped at the filtration barrier) are injected intravenously in animals rendered nephrotic by glomerular damage, they permeate freely into urinary spaces.



Fig. 20.2 Podocyte foot processes. Necrotic cell is dark and shrunken, and its nucleus is amorphous. Vacuoles, many with central dense material, are distributed throughout the cell. Mitochondria are markedly enlarged and relatively well preserved. Foot processes of the necrotic podocyte are intertwined with those of adjacent degenerate cells.

Although the epithelial cell with its foot processes fused provides a solid barrier at the distal side of the filter, protein molecules are transferred by **transepithelial migration.** When examined ultrastructurally, proteins are seen in conspicuous cytoplasmic vacuoles. The vacuoles begin as basal pockets in the epithelial cells adjacent to the basement membrane, become intracytoplasmic, and discharge their contents into the urinary space. The uptake of these macromolecules by the epithelial cells in toxic injury indicates their role in the conservation of protein. Although the basement membrane is not noticeably altered structurally in many acute toxic injuries, there are marked changes in permeability that indicate decreased function.

Podocytopathy

Podocytopathy, the deformation and dysfunction of foot processes is the critical consequence of toxic injury to the podocyte. The first ultrastructural evidence is **foot process fusion**. Extensive studies with the glomerular toxin aminonucleoside have shown that it causes the following lesions: (1) swelling and blunting of foot processes with narrowing of filtration slits, (2) loss of negative charges in glycocalyx carbohydrate moieties, as demonstrated by reduced staining with highly cationic alcian blue, (3) formation of cell junctions between podocyte processes, (4) displacement of slit diaphragms, (5) development of podocyte extensions into the basement membrane, and (6) excessive polymerization of actin microfilaments in foot processes.[10] Podocytes express the intermediate filaments vimentin, desmin, and nestin, which are differentially upregulated in response to injury in order to maintain stability and position in the injured cell.[11] **Foot process effacement** consists of simplification and disappearance of interdigitating foot processes. It represents an adaptive change in cell shape including hypertrophy of the contractile apparatus, in order to reinforce the supportive role of podocytes.[12]

Puromycin Aminonucleoside

Podocytopathy is the principal lesion of **puromycin aminonucleoside nephrosis** in both humans and animals. Distortion of the glomerular epithelial cell foot processes, collapse of filtration slits, and enhanced production of gap junction stress proteins are the podocyte responses. These are also the hallmark of ultrastructural change of **minimal change nephropathy** in human lipoid nephrosis, for which puromycin nephrotoxicity has served as a model. Podocyte cytoskeletal disaggregation procedes, and detachment from the GBM occurs simultaneously with the onset of massive proteinuria. In neonatal mice, puromycin aminonucleoside causes total effacement of podocyte foot processes within 2 days, and moves rapidly to mesangial damage and glomerulosclerosis, and dysfunctional capillary growth.[13]

In rats, early lesions consist of reduction of the number of foot processes, narrowing of the filtration slits, and displacement of the slit diaphragm by occluding junctions (coupled with slit diaphragm displacement), and increased endocytosis with lysosomal protein absorption droplet formation. Studies using freeze-fracture techniques reveal that the occluding junctions are composed of a few strands and contain sequestered gap junctions. The reduction in slit number and presence of occluding junctions cause

reductions in surface area of basement membrane covered by normal slits, thus reducing flow across the capillary wall. The **slit diaphragm** is effaced in acute toxicity.[14]

Late changes in experimental aminonucleoside nephrosis in rats are a reduction in protein absorption droplets and increased numbers of secondary phagosomes, detachment of the epithelium from the basement membrane, and deposition of basement membrane material in urinary spaces. Proteoglycans of the glomerulus are markedly altered.[15] These changes are part of the progressive sclerosis that affects the glomerulus in chronic toxicity.

Aminonucleoside damages blood vessels other than those of the renal glomerulus. Rats given puromycin for 10 wk develop medial necrosis of the aorta and large elastic arteries. Hypertension, hyperlipidemia, and proteinuria develop, suggesting that enhancement of atherosclerosis may be a consequence of long-term treatment.[16]

Mesangiopathy

Mesangial cells, which extend from the vascular pole of the glomerulus throughout the capillary tuft, phagocytize both endogenous and exogenous particulate material and pass it to the juxtaglomerular apparatus and lymphatic vessels. In acute toxic injury, mesangial cells may be specifically injured.[17] The nephrotoxic agent **cyclophosphamide**, although nephrotoxic by virtue of causing tubular necrosis, also is destructive to mesangial cells. In rodents, it causes acute **mesangiolysis** (swelling and lysis of mesangial cells), which is followed by **mesangiosclerosis** with deposition of mesangial fibrils.[18] Mesangiolysis is repaired by mesangial cell proliferation.[19] These new cells can be differentiated from leukocytes and endothelium by their actomyosin filaments. The mesangial reaction is conspicuous in chronic glomerular injury, in which mesangial cells proliferate and secrete basement membrane material.

Protein molecules are also taken up by mesangial cells, persisting long after removal from other sites in the glomerulus.[20] Proteins in the glomerular filtrate enter the tubules, where they attach to the microvilli of the proximal convoluted tubule cells. They are taken up at the luminal surface, concentrated into **protein absorption droplets** in the cytoplasm, and eliminated at the infoldings of the basal surface of the epithelial cell. When the absorptive capacity of the tubule mechanism is overloaded, the protein molecules pass through the nephron and appear in urine; that is, proteinuria.

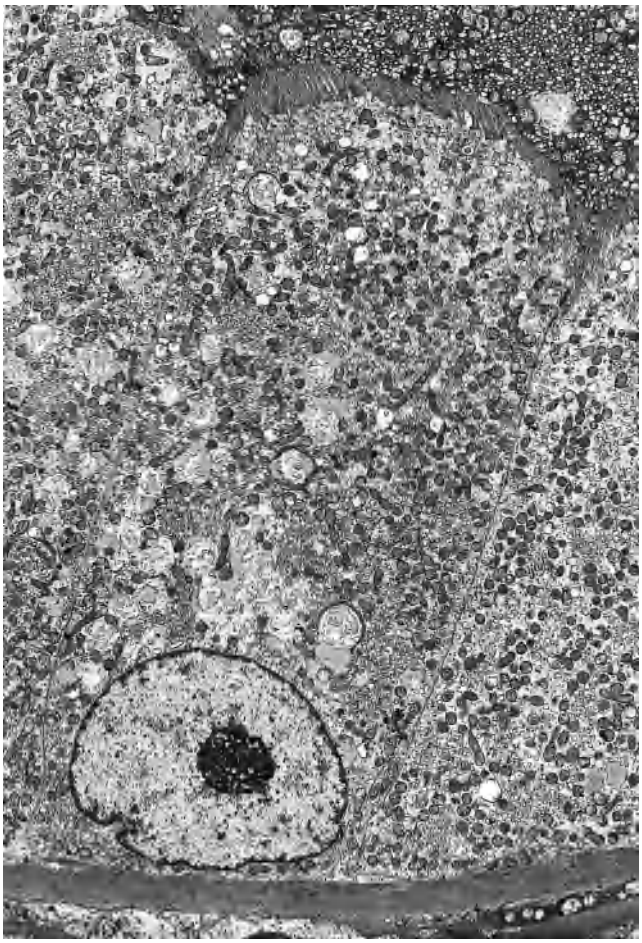


Fig. 20.3 Proximal convoluted tubule: acute cell swelling, dog. **Acute cell swelling**: massive enlargement of cytoplasm with fragmentation and vesiculation of endoplasmic reticulum. Microvilli of the brush border are distorted and there is cellular debris in the tubule lumen (*top*). Lipid globules are present throughout the cytoplasm.

Proximal Convoluted Tubule Toxins

Renal tubular epithelium is exquisitely sensitive to poisons. Acute cell swelling of PCT epithelial cells leads to striking fragmentation and vesiculation of the endoplasmic reticulum (Fig. 20.3). It is the highly metabolic **proximal convoluted tubule (PCT)** that is most seriously affected by toxins. The pars recta of the PCT is first affected, and lesions typically involve the entire proximal tubule and small patchy areas of the ascending loop of Henle.[21]

Nephrotoxicity arises from several major mechanisms (Table 20.1):

- **Direct toxic injury** to tubular epithelium by injury to specific organelles.

Table 20.1 Ultrastructural studies in animal models of nephrotoxicity.

Toxin	*Host*	*Reference to ultrastructural pathology*
		Acetaminophen
Acetylsalicylic acid	Rat	**Molland**, *J Pathol* 120:43, 1976
Actinomycin D	Mouse	**Rudofsky**, *Lab Invest* 39:441, 1980
Adenine triphosphate	Rat	**Rosen**, *Virch Arch B* 61:169, 1991
Adriamycin	Rat	**Bertani**, *Lab Invest* 46:16, 1982; **Beukers**, *Lab Invest* 59:631, 1988; **Fajardo**, *Lab Invest* 43:242, 1980; **Grond**, *Lab Invest* 51:277, 1984; **Weening**, *Lab Invest* 49:619, 1983; **Whiteside**, *Lab Invest* 61:650, 1989
Aminonucleoside	Human	**Caulfield**, *Lab Invest* 34:43, 1976; **Feldman**, *Lab Invest* 8:371, 1959
	Rat	**Abrahamson**, *Lab Invest* 49:38, 1983; **Caulfield**, *Lab Invest* 40:503, 1979; **Caulfield**, *J Exp Med* 142:61, 1975; **Ryan**, *Lab Invest* 33:461, 1975; **Schreiner**, *Lab Invest* 51:524, 1984 (Ia antigens); **Still**, *Lab Invest* 30:434, 1974 (vascular lesions); **Whiteside**, *Am J Pathol* 142:1641, 1992 (cytoskeleton)
Amphotericin	Human	**Bhathena**, *Clin Nephrol* 9:103, 1978 (biopsy)
	In vitro	**Brezis**, *Science* 224:66, 1984
Ampicillin	*	**Woodruffe**, *Med J Aust* 18:65, 1975
Aspirin	Rat	**Burrell**, *J Pathol* 164:329, 1991; **Henry**, *J Pathol* 139:57, 1983
Bromide	Rat	**Wolf**, *Tox Pathol* 26:724, 1998
Bromoethylamine	Mouse	**Wolf**, *Vet Pathol* 29:528, 1992
Carbon tetrachloride	Rat	**Striker**, *Am J Pathol* 53:769, 1968
Caffeine	Human	**Rocha**, *Proc Natl Acad Sci USA* 98:5317, 2001
Cephaloridine	Rabbit	**Rush**, *Toxicol Pathol* 20:155, 1992
Cephalosporin	Human	**Longstreth**, *Pharmacotherapy* 24:808, 2004
	Rabbit	**Rush**, *Toxicol Pathol* 20:155, 1992
Cisplatin	Rat	**Choie**, *Lab Invest* 44:397, 1981
Chromate	Human	**Orfila**, *Histochemistry* 97:293, 1992
	Rat	**Berry**, *J Hist Cyt* 26:651, 1978; **Evan**, *Lab Invest* 30:704, 1974
Cyclophosphamide	Mouse	**Hsu**, *Lab Invest* 47:281, 1983
Cyclosporin	Human	**Nacar**, *Renal Fail* 28:543, 2005 (biopsy)
	Rat	**Bertani**, *Am J Pathol* 127:569, 1987; **Blair**, *J Pathol* 138:163, 1982; **Perico**, *Am J Kidney Dis* 17:537, 1991; **Perico**, *Kidney Int* 49:1283, 1995
Codeine	Human	**Hill**, *Hum Pathol* 33:783, 2002
Copper	Fish	**Jiraungkoorskul**, *Environ Toxicol* 22:92, 2007
Daunomycin	Rat	**Sternberg**, *Lab Invest* 23:39, 1970
Dimethylnitrosamine	Rat	**Hard**, *Lab Invest* 50:569, 1984
Diphenylamine	Hamster	**Lenz**, *Exp Toxicol Pathol* 47:447, 1995
	Rat	**Evan**, *Lab Invest* 38:244, 1978
Doxorubicin	Rat	**Grond**, *Lab Invest* 51:277, 1984
Furosemide	*	
Gentamicin	Horse	**Hinchcliff**, *Am J Vet Res* 50:1848, 1989
	Human	**Houghton**, *Am J Pathol* 123:183, 1986
	Rat	**Aubert-Tulkens**, *Lab Invest* 41:481, 1978; **Giurgea-Marion**, *Toxicol Appl Pharmacol* 86:271, 1986; **Houghton**, *Am J Pathol* 82:589, 1976; **Komatsuda**, *Lab Invest* 68:687, 1993; **Kosek**, *Lab Invest* 30:48, 1974; **Wedeen**, *Lab Invest* 48:212, 1983

Table 20.1 *Continued*

Toxin	*Host*	*Reference to ultrastructural pathology*
Glucose	Rat	**Maunsbach**, *Lab Invest* 11:421, 1962
Gold	Rat	**Stuve**, *J Cell Biol* 44:667, 1970
Heroin	Human	**Grishman**, *Lab Invest* 35:415, 1976
Indomethacin	Rat	**Limas**, *Lab Invest* 34:523, 1976
Lead	Rat	**Goyer**, *Lab Invest* 32:149, 1975
Lithium	Rat	**Kling**, *Lab Invest* 50:526, 1984
Mercury	Rat	**Josepovitz**, *Lab Invest* 52:375, 1985
Methicillin	*	
Methoxyflurane	Rat	**Kosek**, *Lab Invest* 27:575, 1972
Nefiracetam		**Tsuchiya**, *Toxicol Pathol* 33:561, 2005
Norepinephrine		**Cronin**, *Kidney Int* 14:115, 1978
Ortho-phenylphenol	Rat	**Shibata**, *Cancer Lett* 48:19, 1989
Oxygen	Rat	**Greene,** *Am J Pathol* 96:737, 1979
Pamidronate	Human	**Barri**, *Kidney Int* 65:634, 2004
Paracetamol	Rat	**Burrell**, *J Pathol* 164:329, 1991
Phenacetin	Human	**Mihatsch**, *Clin Nephrol* 20:285, 1983; **Rocha**, *Proc Natl Acad Sci USA* 98:5317, 2001
Phenylbutazone	Human*	**Greenstone**, *Br Med J* 282:950, 1981
Polyene	medulla	**Brezis**, *Science* 224:66, 1984
Polyvinal alcohol	Rat	**Mauer**, *Lab Invest* 41:475, 1978; **Seiler**, *Lab Invest* 49:26, 1983
Potassisum hydrogen phosphate	Dog	**Schneider**, *Vet Pathol* 17:699, 1980
Platinate		**De Witt**, *Toxicol Appl Pharmacol* 92:157, 1988
Platinum		**Dobyan**, *Lab Invest* 45:260, 1981 (rat)
Puromycin (aminonucleoside)	Rat	**Liu**, *Kidney Int* 39:1140, 1991 (fetus); **Nagle**, *Lab Invest* 26:558, 1972; **Yaoita**, *Am J Pathol* 161:1597, 2002
Quinapril	Angiotensin-converting enzyme	**Dominick**, *Toxicol Pathol* 18:396, 1992
Quinone-thioethers	Rat	**Rivera**, *Toxicol Appl Pharmacol* 128:239, 1994
Ranitidine	Human	**Gaughan**, *Am J Kidney Dis* 22:337, 1993
Rifampin	*	
Salicylate	Renal papilla	**Harper**, *Lab Invest* 47:258, 1982 (rat); **Henry**, *J Pathol* 139:57, 1983 (rat)
Streptozotocin	Rat	**Thomson**, *Br J Exp Pathol* 70:405, 1989
Testosterone	Mouse	**Koenig**, *Lab Invest* 39:329, 1978
Thiazides	*	
Tris(2,3-dibromo-propyl)phosphate	Rat	**Reznik**, *Lab Invest* 44:74, 1981
Uranium		**Carafoli**, *Lab Invest* 25:515, 1971
Uranyl nitrate	Rabbit	**McDonald-Taylor**, *Toxicol Pathol* 25:381, 1997
	Rat	**Haley**, *Lab Invest* 46:196, 1982
Venom: rattlesnake	Mouse	**Girón**, *J Submicrosc Cytol Pathol* 334:447, 2002
Vinblastine	Rat	**Silverblatt**, *Lab Invest* 31:170, 1974
Vitamin D	Dog Rat	**Spangler**, *Am J Vet Res* 40:73, 1979 **Scarpelli**, *Am J Pathol* 36:331, 1960

*Hypersensitivity disease reactions occur in toxicity.

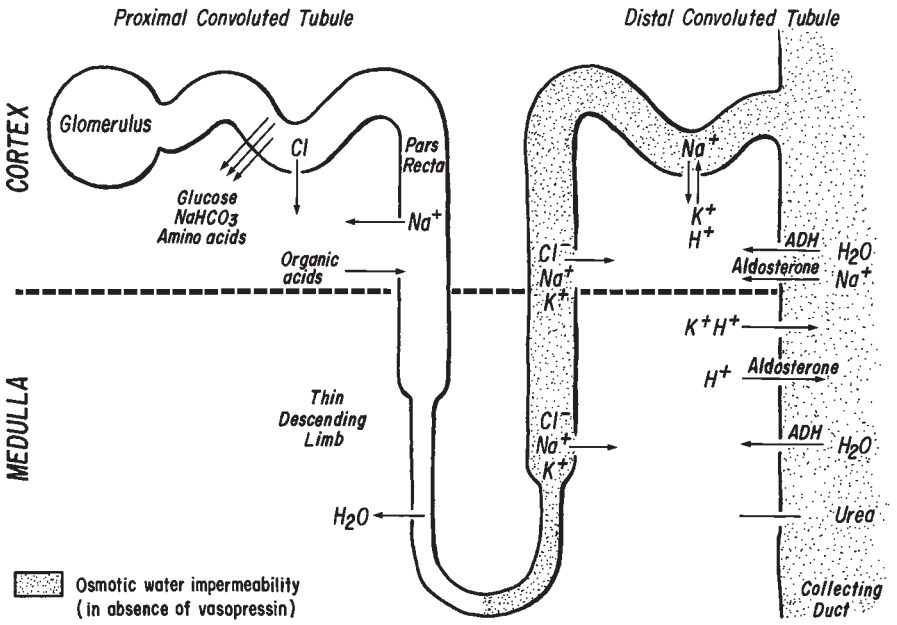


Fig. 20.4 Renal tubule function: changes in glucose, protein, potassium, and sodium as glomerular filtrate passes through the nephron. **Proximal convoluted tubules** reabsorb 50% to 65% of filtered fluid by active and passive mechanisms. **Thin descending limb** of Henle is highly permeable to water (relatively impermeable to solutes). The **thin ascending limb** is impermeable to water but highly permeable to sodium and chloride.

- **Acute hypersensitivity nephritis**: induction of immunoloigc reactions in the peritubular interstitium such as injury from ampicillin and methicillin.
- **Chronic nephrotoxicity** arising after prolonged use of toxic drugs with disease appearing years of exposure—abuse of analgesic drugs, most often phenacetin; other analgesic compounds implicated include aspirin, caffeine, codeine, and acetaminophen (a metabolite of phenacetin).

Toxic injury to proximal tubules is intimately tied to metabolic pathways in PCT epithelial cells (Fig. 20.4). Activation of the **calcium pump** of endoplasmic reticulum (arising from disrupted homeostasis of cytosolic ionized Ca^{++}) is a marker for nephrotoxicity, and can be detected before ultrastructural changes occur.[22]

Cells of the PCT epithelium differ from tubule cells in the lower nephron in having tall microvilli of the luminal plasma membrane (brush border), a vacuolar system below the plasma membrane, and prominent lysosomes in the cytoplasm. **Lysosomes** degrade macromolecules absorbed from the tubule lumen. **Peroxisomes** are in the basal part of the proximal tubule cell. They are associated with large amounts of alkaline phosphatase, which plays a role in the reabsorption process. Disaccharidases, present along the microvillous border, function in glucose transport. Cilia have been reported in epithelial cells in some types of renal disease. Destruction of the microtubules by the cytoskeletal poison vinblastine not only shortens microvilli but suppresses phagolysosome development as well.[23]

Microvilli are highly sensitive to toxic injury and anoxia. Microvilli, long and slender in epithelial cells near the glomerulus, are progressively shorter and broader on the lower part of the proximal tubule. They react by becoming ballooned and by shedding globules of various sizes into the tubule lumen. Nephrotoxins such as **mercury** and **amphotericin B** damage the tubule in this way, causing loss of the water, glucose, and sodium that are normally absorbed. Brush borders of reversibly injured tubule cells regenerate by endocytosis and recycling of damaged membranes for incorporation into new microvilli.

The **vacuolar system** below the luminal plasma membrane of PCT cells originates as invaginations in the membrane. Vacuoles reabsorb substances from glomerular filtrate. Large, round hyalin (eosinophilic) **protein absorption droplets** are dense, membrane-bound bodies. They are phagolysosomes that arise from endocytosis of protein. Vacuolar degeneration occurs in severe electrolyte imbalance, especially during marked potassium deficiency, and this must be taken into account in interpreting toxic injury to the kidney.

Mitochondria of PCT are secondarily affected by many toxins. Direct mitochondrial nephrotoxins include tenofovir, didansoine and other antiretroviral drugs used in AIDS therapy that affect mtDNA.[24]

Regeneration of tubular epithelium is evident in most cases of chronic nephrosis. Pleomorphic, deeply staining cells line the denuded tubular basement

membrane. Some cells are greatly enlarged, and others contain mitotic figures. Some tubule cells persist as thin, narrow cells that do not regain normal function. Regenerating proximal tubule epithelial cells have fewer cytoplasmic organelles, lack typical microvilli, and consist of large numbers of ribosomes.[25] The proximal convoluted tubules are the chief site of synthesis of **erythrogenin**, the precursor of erythropoietin, and the anemia that accompanies severe renal disease can be explained, in part, by a deficiency of erythrogenin production.

Lysosomal Toxins

Gentamicin

Gentamicin, like kanamycin and other non-membrane-permeative aminoglycoside antibiotics used to control gram-negative sepsis, is associated with nephrotoxicity and ototoxicity. Injury to the kidney is nearly confined to the proximal tubules, cells that transport and accumulate these drugs to attain very high intracellular concentrations. Toxicity involves dysfunctional intracellular trafficking. The vacuolar transport system of the epithelial cell is impaired, and there is inhibition of lyososome-endosomal vesicle fusion.[26]

Gentamicin and other aminoglycosides first bind to anionic receptors on the plasma membrane of PCT apical **microvilli**, and move into the PCT cell by **endocytosis**. There are marked changes to the PCT epithelial surface including **microvillous loss** and **cytoplasmic blebbing** (Fig. 20.5) Dysfunctional microvillous membranes occur early in toxicity and include decreases in transport of glucose and organic bases, and low molecular weight proteinuria. Inside the cell, gentamicin is rapid transferred to and concentrated in the Golgi complex. Within endosomes, gentamicin-containing **microvesicles** bleb into the endosomal cavity—much as treated gram-negative bacteria bleb off gentamicin-containing membrane vesicles.[27] Combined autoradiographic and ultrastructural studies show that intracellular gentamicin is predominantly unbound in the first 6 hr after injection. It accumulated in the S1 and S2 but not S3 segments of PCT, and is localized in subapical sites in the cytoplasm, a finding that is consistent with pinocytotic uptake.

Selectively accumulating in **lysosomes** in epithelial cells of the PCT, gentamicin induces formation of large **autophagolysosomes**, which accumulate lamellar material and transform into myeloid bodies. Subacute and chronic toxicity are characterized by packing of the cytoplasm of the tubule cell with large lysosomes filled with membranous whorls and myelin figures. Gentamicin causes **lysosomal phospholipidosis** via dysfunction of sphingomyelinase and probably other phospholipases. Ultrastructural changes in gentamicin nephrotoxicity are strikingly similar in different species. Aminoglycosides promote increased urinary excretion of microvillous membrane enzymes and phospholipids into urine. The **phospholipiduria** is due to shedding of massive numbers of membrane bound bodies filled with myelin figures from the damaged microvillous surfaces. Electron microscopic examination of urinary sediment reveals masses of these membranous vesicles and granules; their ultrastructural appearance differs from these vesicles found in urinary sediment of animals poisoned with mercury.[28] Desquamation of membranes into tubule lumens corresponds with excretion of transpeptidases, alkaline phosphatase, and other enzymes into urine.[29]

There are great differences in susceptibility among individuals of any species. Ultrastructural studies on localization of gentamicin in rat kidney using immunogold techniques suggest that the feeding period is critical to variations in gentamicin toxicity.[30]

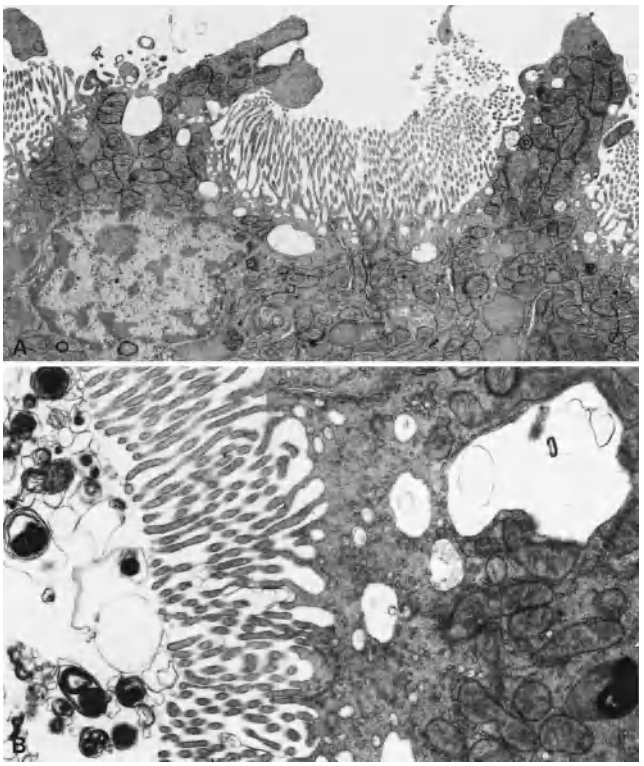


Fig. 20.5 Microvillous surface changes: proximal convoluted tubule, renal toxicity. **A**. **Myeloid bodies**: free in lumen of proximal tubule, gentamicin toxicity, rat. **B**. **Apical blebbing**: focal loss of microvilli, renal proximal tubule cell, mercuric chloride toxicity, rat. (Micrograph: Christine Josepovitz, *Lab Invest* 52:375, 1985.)

Long-term treatment of rats with gentamicin leads to acute renal tubular necrosis in 10 days. If treatment is continued however, tubular epithelium regenerates and is restored by 21 days. This "resistance phase" reflects an asynchrony of necrosis and regeneration.[31] In rats, as analyzed with immunogold labeling, tolerance to (or recovery from) long-term gentamicin treatment is associated with inhibition of endosomal uptake.[32] Ligands of the endocytic receptor megalin decrease endosomal uptake of gentamicin. **Caveolae** are prominent in recoverying cells, and production of caveolin-1, which regulates growth signaling, endocytosis, and intracellular transport, is markedly increased.[33]

Nuclear Transcriptional Injury

Cyclosporine

This cyclic unadecapeptide is the prototype of a class of cyclic peptides produced as metabolites by *Tolypocladium inflatum*. It is used specifically to inhibit activation of T helper lymphocytes in cell-mediated responses that reject tissue grafts and release of cytokines. Human patients that develop chronic cyclosporine nephrotoxicity develop vascular changes, tubular atrophy, and interstitial fibrosis. Ultrastructural studies of biopsies of renal transplants show glomerular endothelial damage in renal allografts.[34]

Cyclosporine nephrotoxicity is characterized by vascular changes in renal arterioles, foci of tubular atrophy, and interstitial fibrosis. In affected arterioles there is necrosis of smooth muscle accompanied by nodular deposits of protein, especially in the wall of the afferent glomerular arteriole. In the nephron, rats develop early changes of vacuolation and loss of microvilli of proximal tubules.[35,36] Distal tubules are less affected but appear as foci of clear cells in the renal parenchyma. This is due to massive accumulation of glycogen, perhaps due to the marked polyuria and glycosuria induced by cyclosporin (Fig. 20.6).[37]

The cephalosporine antibiotic **cephaloridine** causes acute renal injury in humans, and experimentally in rats and rabbits. The mechanism has been ascribed to peroxidative injury related to an increase in conjugated diene formation, and to specific damage to mitochondria. There is widespread necrosis of the proximal tubules, especially in the S2 segments. The earliest sign of ultrastructural damage can be seen at 4 hr after exposure, with dilatation of the apical vacuolar system and dilatation of SER, degranulation of rough endoplasmic reticulum and accumulation of granular debris.[38] **Probenecid**, which blocks renal basolateral anion transport, inhibits the toxicity of cephaloridine.

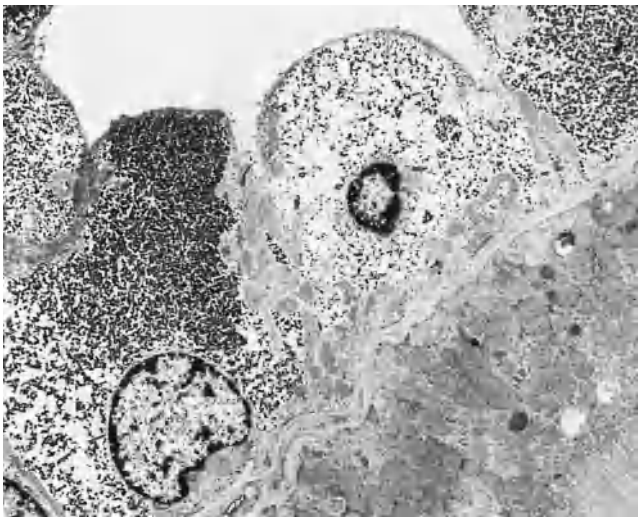


Fig. 20.6 Glycogen deposits: distal tubular epithelial cells, streptozotocin-diabetic rat treated with cyclosporin A. (Micrograph: K. J. Thomson, *Br J Exp Pathol* 70:414, 1989.)

Metallic Toxins of the Proximal Tubules

Acute tubular necrosis of the kidney is caused by several heavy metals including mercury, lead and arsenic. Lead produces its most marked effect in the nervous system, but absorbed lead is deposited in the kidney and slowly excreted in urine. In renal tissue, lead-protein complexes form in nuclei of renal tubular epithelial cells (Fig. 20.7). Because these nuclear inclusions stain with the acid-fast stain, they are diagnostic for lead toxicity.

Mercury

The capacity of mercurials to alter intracellular ion concentrations led to their use as diuretics. Toxic doses cause water and sodium to enter the renal tubule cells and to move into the cisternae of the endoplasmic reticulum, which becomes markedly dilated. The proximal convoluted tubules in affected nephrons contain large eosinophilic cytoplasmic inclusions.

Mercurials cause the inhibition of enzymes by complexing with sulfhydryl groups on the active sites of the enzyme. Lesions of mercury poisoning characteristically involve every nephron. Initially, there are loss of brush borders, dispersion of ribosomes, and duplication of smooth endoplasmic reticulum. Swelling of mitochondria and fatty degeneration are followed by necrosis.[39] Necrotic epithelial cells are sloughed into the lumen of the tubule to cause anuria. In chronic cases, necrotic cells are often calcified. If the animal survives, the tubular epithelium recovers and



Fig. 20.7 Lead inclusion: nucleus, renal proximal convoluted tubule. Lead complexes with degraded protein to form large nuclear inclusions. (Micrograph: Phillipe Detilleux, National Animal Disease Center.)

becomes lined with dense, low epithelial cells that cannot concentrate urine. An immune complex glomerulopathy has been reported in experimental mercury toxicity in rodents.[40]

Mercury in fetal rats acquired transplacentally causes impaired mitochondrial biogenesis. Crista enzymes are reduced to 75% but matrix enzymes are not affected. In the kidney, organic mercury compounds are converted to inorganic mercury, which is concentrated to high levels. Inorganic mercury selectively damages the straight portion (pars recta of the PCT). Intracellularly, mercury concentrates in the endoplasmic reticulum. Detoxifying enzymes are present at these sites, and in experimental studies on the rat kidney SER is the site of conversion of methyl to inorganic mercury.

Cadmium

Cadmium is nephrotoxic in large doses. Experimental acute cadmium nephrotoxicity in rats damages cortical proximal convoluted tubules (PCT) causing reabsorptive and secretory defects. Damage in the PCT occurs on surface microvillous borders and includes loss of **apical membrane transporters** (such as the Na^+-H^+ exchanger, water channel AQP-1, megalin, and V-ATPase) with their redistribution into cytoplasmic vesicles, degradation of **basolateral invaginations** (and loss of Na^+-K^+-ATPases), and degradation of **surface microvilli. Cytoskeletal damage** (similar to colchicine toxicity) is prominent, and includes fragmentation and depolymerization of microtubules, disrupted intracellular trafficking, and loss of clathrin followed by its relocation into vesicles throughout the cytoplasm.[41]

Long-term heavy exposure of humans leads to **cadmium nephropathy**. Cadmium continuously enters the PCT by phagocytosis from the glomerular filtrate. **Bone demineralization** and wasting has been implicated in aged Japanese women after chronic ingestion of cadmium-contaminated food. Experimentally, high levels of dietary cadmium have caused shortening and thickening of **intestinal microvilli** similar to those found in the human maladsorption syndrome.[42]

In experimental chronic cadmium intoxication in rats (after several weeks on cadmium), tubular epithelium becomes vacuolated, and there is a progressive diffuse interstitial fibrosis. In cadmium toxicity, lesions are also prominent in the **testis** and **spinal sensory ganglia**. These tissues develop edema, hemorrhage and necrosis due to damage to the vascular tissues. Affected endothelial cells are vacuolated, have increased caveolae, and widening of intercellur junctions.

Platinum

Platinum-containing antineoplastic drugs have been restricted in use because of their nephrotoxicity; for example, ***cis*-diamminedichloroplatinum** (II) (**DDP**, cis-platinum) is highly nephrotoxic despite hydration and diuretic pretreatment of treated patients. DDP is preferentially injurious to the **pars recta** (P_3) of the proximal tubule in the outer stripe of the outer medulla. Cellular changes in **platinum nephrotoxicity** include nucleolar segregation and disappearance, ribosome degranulation and dispersal, and massive aggregation of membranes of the smooth endoplasmic reticulum. Nuclear damage is accompanied by several categories of genes that are deregulated; genes that encode for cytokeratins are specifically overexpressed.[43]

Injury to the convoluted portion of the proximal tubule (P_1 and P_3) may be more important in initial damage since they correlate with functional changes in poisoned animals.[44] In segment P_3, injured epithelial cells are characteristically dome-shaped (Fig. 20.8).

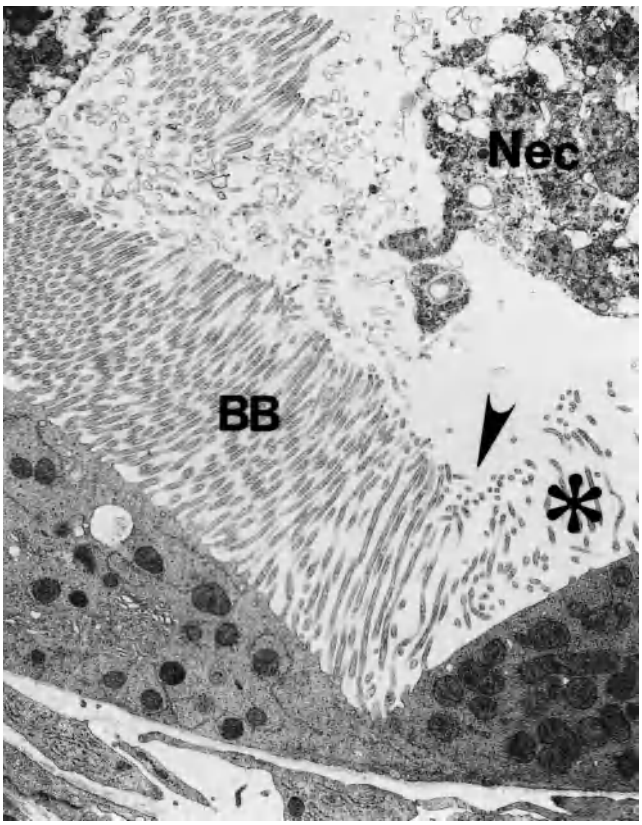


Fig. 20.8 Exfoliation: necrotic epithelial cell (*Nec*) has sloughed into the lumen of a proximal tubule, *cis*-platinum toxicity, rat. Two dome-shaped cells cover the basal lamina where a cell has detached (*arrowhead*). Brush border (*BB*) is thinned (*). (Micrograph: Thomas W. Jones, *Lab Invest* 52:363, 1985.)

This is due to the desquamation of necrotic cells into the tubule lumen and subsequent stretching of the surviving epithelial cells to cover the empty spaces along the basement membrane. In rats, renal cysts are a long-term consequence of DDP treatment.[45]

Uranium

Uranium poisoning damages the **renal tubules**. Ultrastructural stereologic and morphometric analyses of PCTs in rabbits revealed cytoplasmic vacuolation with dose-related changes in mitochondria and lysosomes.[46] The mitochondrion, through alterations of the calcium-transport mechanism, becomes a locus for calcium deposition.[47] Massive increases of mitochondrial calcium leads to mitochondrial swelling, clarification of the matrix, and death of the cell. In rats, acute tubular necrosis and proliferative glomerulonephritis have been reported. Uranium acquired naturally from well water has caused elevated β2-microglobin and creatinine (without clinical signs of renal dysfunction) in children.[48]

Lithium

Lithium is a widely used agent in management of mental disorders, has been implicated in chronic tubulointerstitial nephritis. In lithium-treated rats, proliferative tubular lesions affect the cortical collecting tubules.[49]

Distal Tubule Toxins

In the **distal tubules**, reabsorption of water is controlled by the **antidiuretic hormone** (**ADH**, vasopressin), which originates in the posterior pituitary. ADH causes the otherwise impermeable tubules to become permeable to water. Interstitial tissue must be hypertonic to provide osmotic gradients for water reabsorption. Exposure to the high osmolarity of the renal papilla causes water to be removed from the tubule. Increased permeability of the distal tubule epithelial cell is due to changes in the hormone-sensitive basolateral surface of the collecting tubule epithelial cells. When absorption occurs, the cells become swollen and have large vacuoles in the cytoplasm. Opening of the intercellular junctions (except at tight junctions) appears to facilitate reabsorption of water. ADH acts by stimulating the formation of cyclic AMP, which directly increases the permeability of the tubule membrane.

Amphotericin B

Used to combat systemic fungal infections, the polyene antibiotic **amphotericin B** combines with sterols in the plasma membrane of the fungal cell and causes leakage and lysis. The same mechanism operates on renal tubule cells of the patient being treated. In biopsies from human patients on high doses, amphotericin B caused vacuolation of medial smooth muscles in arterioles and small arteries.[50] Amphotericin B can also cause distal tubule injury and renal ischemia. Direct injury to the distal tubular epithelial cell leads to excessive potassium bicarbonate, and water loss in urine. Increased tubular epithelial cell permeability allows loss of potassium and entrance of hydrogen ions back into the cell. Hypokalemia and metabolic acidosis develop and, if renal disease is progressive, lead to death. At autopsy, kidneys show tubular degeneration and necrosis, peritubular fibrosis, nephrocalcinosis, and glomerular sclerosis. Other than cell swelling, no ultrastructural lesions have been reported in the early phases of degenerating tubule cells.

Polyene antibiotics such as amphotericin and nystatin increase membrane permeability and thus increase the amount of oxygen consumed in active electrolyte transport. In isolated perfused rat kidneys, the polyenes produce extensive injury to the medullary thick ascending limb, a segment of the nephron with limited oxygen supply.[51] Damage is prevented if reabsorptive transport is inhibited by ouabain.

Toxins in the Medulla

A portion of the nephron, **the loop of Henle**, dips deeply down into the tips of the renal papillae. It is accompanied by special capillary loops, the vasa rectae. This peritubular capillary bed is a low pressure bed, in contrast to the higher pressure of the glomerulus, and the blood is very sluggish in moving through it. There is no lymphatic drainage of the medullary area.[52] Ultrastructurally, epithelial cells of the loops are small and narrow.[53] Compared with the proximal tubules, they contain few organelles. Specialized Tamm-Horsfall glycoproteins on tubule cell surfaces of ascending loops of Henle restrict water movement.[54]

In the **medullary interstitium**, stellate mesenchymal cells play a role in blood pressure regulation and are the source of glycosaminoglycans that accumulate in the medulla and papillae in some aged animals (Fig. 20.9).[55] The size and number of their lipid inclusions are larger in water-loaded animals than in dehydrated ones.[56] These stellate, lipid-laden interstitial

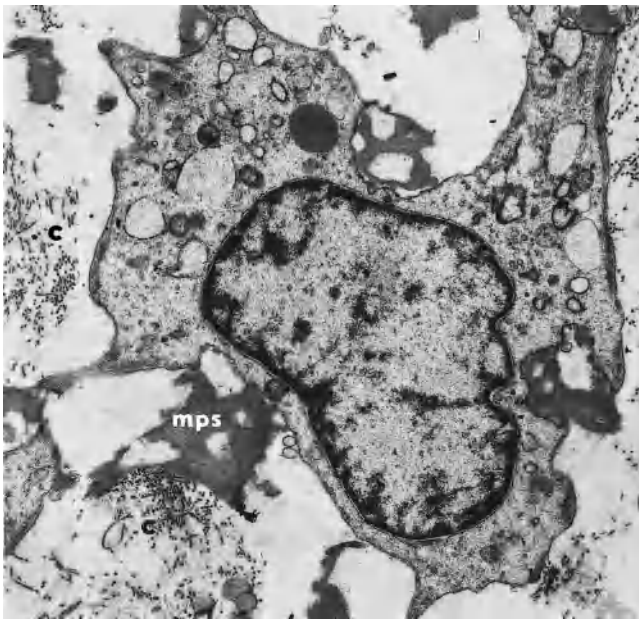


Fig. 20.9 Stellate interstitial cell: collecting tubule, renal medulla. Stellate interstitial cell with granular proteoglycan material (*mps*) and collagen (*c*).

cells are joined by slender processes to the nephron. Their cytoplasmic lipids contain prostaglandin precursors and other antihypertensive neutral lipids.[57] Treatment with the prostaglandin inhibitor indomethacin leads to disappearance of cytoplasmic granules.[58]

Interstitial tissue of the medulla is rich in albumin, which exudes through the descending limb. The release of antihypertensive factors in the renal medulla in response to increased blood pressure is associated with loss of granularity. In the spontaneous hypertensive rat, increased renal interstitial cell granularity is present, a reflection of compensation of the hypertensive vascular disease.[59]

Renal Papillary Necrosis

Renal papillary necrosis (RPN) occurs as a result of the long-term use of high doses of analgesics and nonsteroidal anti-inflammatory drugs. Lesions arise, directly or indirectly, from capillary endothelial injury. For example, the earliest lesion in RPN produced by **diphenylamine** (the parent compound of the mefenamate family of nonsteroidal anti-inflammatory drugs) is seen in the ascending vasa recta in the promial part of the renal papilla within one hour after drug treatment.[60] **Nefiracetam**, a neurotransmission enhancer, reduces renal prostaglandin synthesis and causes diminished intercellular adhesion and interdigitation of epithelial cells of the papillary ducts.[61] Analysis of toxicity in vitro of aspirin, phenacetin and caffeine and other drugs suggested that there are enhancing qualities among the group; for example, caffeine potentiated the effects of acetaminophen.[62]

Dimethylnitrosamine

The carcinogenic agent **dimethylnitrosamine** is a model of nephrotixicity. A single carcinogenic dose of 60 mg/kg in rats causes acute **peritubular capillary damage**, followed by a chronic recovery phase and then by a phase of tumor growth. In the acute stages ultrastructural changes include moderate lipid globule formation, autophagy, and proliferation of smooth endoplasmic reticulum in the P2 segment of the proximal tubule (but no cell death); changes occur within hrs of treatment (Fig. 20.10). By 18–24 hr there are cytotoxic reactions in interstitial fibroblasts and by 2–4 days, focal necrosis of vascular endothelium. Degeneration of the P_2R segment of the nephron is followed by lipid accumulation, cytoplasmic degeneration, and necrosis of single cells.[63] Infiltration of monocytes and capillary repair are complete by 7 days.

Bromoethyleneamine

Bromoethyleneamine has been used to reproduce renal papillary necrosis in rabbits and rodents. Ultrastructural changes of the **vasa recta endothelium** in the renal papillae of poisoned rats include cytoplasmic shrinkage, margination of nuclear chromatin, and necrosis. Endothelial cell loss with persistence of the basement membrane is followed by platelet aggregation and occlusion of capillaries. BEA toxicity in mice, in contrast, occurs as cortical tubular necrosis. The initial lesions appear within several minutes after poisoning as apical vacuolation and autophagy and other degenerative changes of proximal tubular epithelium, especially the S_1 segment. By several hours, mouse tubular epithelial cells are acutely swollen with breaks in microvilli and budding from the surface into the lumen. Platelet aggregates are found in renal glomerular capillaries. The mechanism of toxic action on the proximal tubule is through damage to capillary endothelium and ischemia of the renal tubule.

Phenacetin Toxicity

Phenacetin (acetaminophen) nephrotoxicity results from direct effects on the plasma membrane, endoplasmic reticulum, and mitochondria. The initial locus

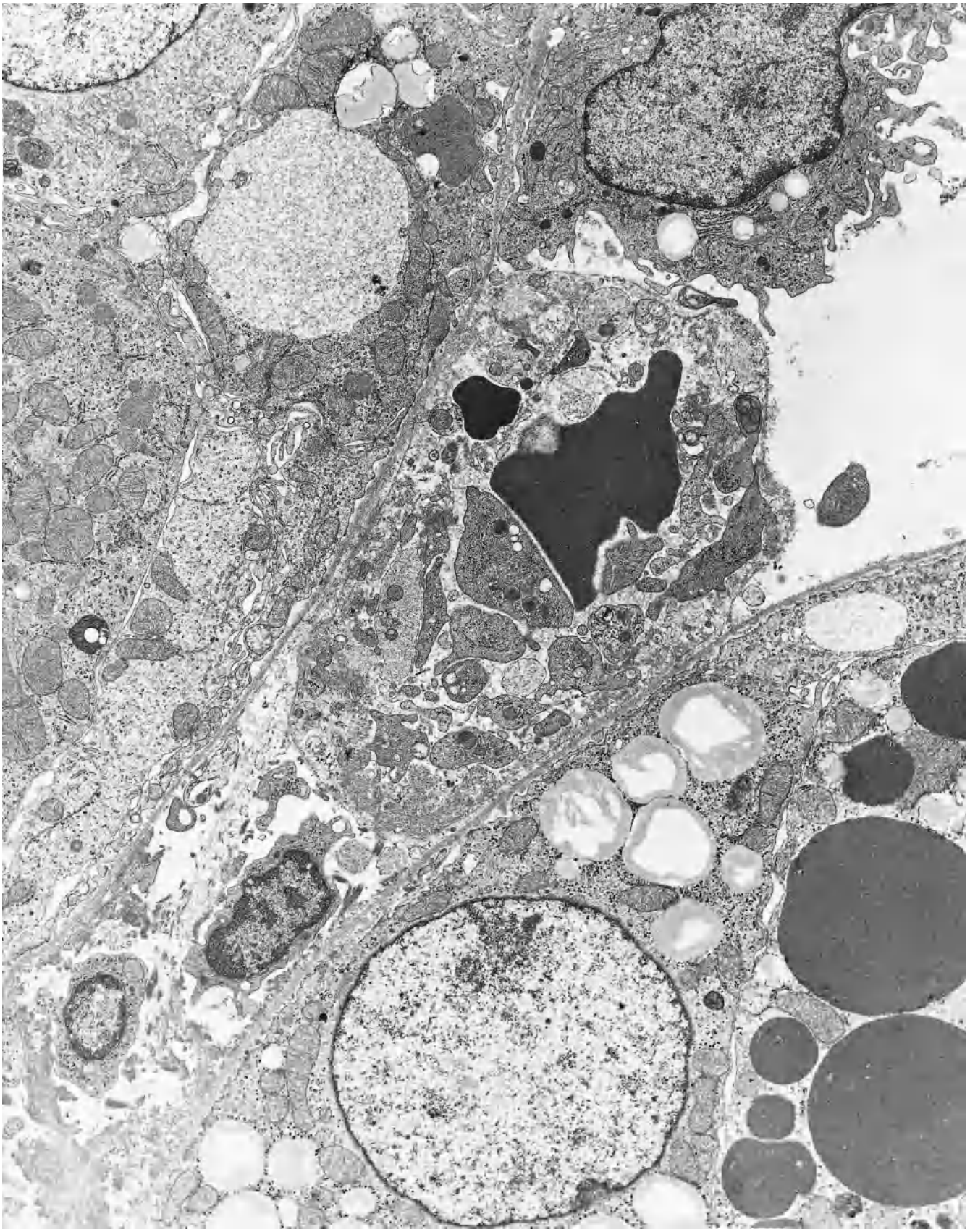


Fig. 20.10 Renal toxicity, endothelial cell necrosis: intertubular capillary, kidney, dimethylnitrosamine toxicity, rat. Basement membrane is denuded, and lumen is filled with cellular debris and degranulated platelets. (Micrograph: Gordon C. Hard, *Lab Invest* 50:659, 1985.)

of injury is often obscured, however, by secondary effects in the damaged kidney. Vascular changes, reduced blood flow, and ischemia may be superimposed upon tubule injury and exaggerate the signs of disease. Degenerating tubular cells liberate lysosome enzymes and autophagocysomal debris into the intersititum. These materials provoke a low-grade inflammatory response that leads ultimately to fibrosis and production of excess basement membrane.[64]

The Juxtaglomerular Apparatus

Ultrastructurally, the **juxtaglomerular apparatus (JGA)** consists of a tubular part, the macula densa, a vascular part, the afferent and efferent arterioles, and the extraglomerular mesangium.[65]

The JGA is a renal pressor system that is activated by lowering of blood pressure and blood sodium. Arterial pressure drop, as sensed by the arteriole, is transmitted to granular **juxtaglomerular cells** in the modified smooth muscle cells of the arteriole; action is initiated by their release of the enzyme **renin** into plasma (Fig. 20.11). Renin circulates and is taken up by a wide variety of cells that in turn have marked influences on blood pressure.

Tubuloglomerular feedback mechanisms regulate the contraction of glomerular arterioles (which in turn controls the glomerular filtration rate) in response to variation in NaCl concentration in the tubular lumen at the macula densa.

The Renin-Angiotensin System

The vasoconstrictor **angiotensin II (ANG II)** increases chloride absorption in collecting ducts by transcellular transport across intercalated cells using H^+-ATPase and pendrin, a process established by immunogold cytochemistry and morphometric analysis.[66] Vacuolar H^+-ATPase mediates acidification of urine, and its inappropriate stimulation may lead to distal renal tubular acidosis.

Hyponatremia, acting via Na^+-sensing mechanisms in the macula densea, increases renin synthesis and production of granules by the juxtaglomerular cells.[67–70] This results in increased plasma **angiotensin**, which stimulates increased blood pressure by peripheral vasoconstriction. Juxtaglomerular hyperplasia and hypersecretion of renin is associated with hypertension.[71] Angiotensin also circulates in the blood to the adrenal cortex, where it stimulates **aldosterone** secretion in the zona glomerulosa, and aldosterone, circulating back to the kidney, acts specifically on the ascending loop of Henle to increase the rate of Na^+ absorption.

Small autonomic nerves ramify through the renal cortex, and adrenergic and cholinergic termini are in close association with renal tubules. It appears that the nervous system can influence Na^+ reabsorption through these nerves.

Angiotensin II Antagonists

Angiotensin II antagonists can cause nephropathy in rats that is associated with dysfunctional juxtalomerular cells. **Angiotensin II receptor antagonists**, drugs that block angiotensin II receptors, are associated with juxtaglomerular cell hypertrophy and hyperplasia in monekys and rats. They competitively inhibit angiotensin II-mediated release of renin and cause abnormal juxtaglomerular granules, some of which develop paracrystalline or membrane laminae.[72]

Angiotensin-Converting Enzyme Inhibitors

Angiotensin-converting enzyme (ACE) is ubiquitous. ACE and ACE2 (ACE-related carboxypeptidase 2) have been localized by immunogold techiques.[73] **ACE inhibitors** are used for treatment of human hypertension. These drugs lower blood pressure by preventing angiotensin II production. Prolonged treatment of rodents with ACE inhibitors causes hypertrophy, hyperplasia, and increased granularity of juxtaglomular cells in afferent arterioles. Affected cells have prominent endoplasmic reticulum and Golgi complexes, suggesting that protein synthesis is increased. In rats, a dose-dependent increase in granule numbers and in pleomorphic or abnormal granules and vacuoles suggests that renin production is stimulated, cytoplasmic granules undergo solubilization and autophagy, and granule (renin) secretion by exocytosis is increased.[74]

FK506

FK506 is a macrolide immunosuppressant isolated from *Streptomyces tsukubaensis*. By interacting with a specific cytoplasmic immunophilin, it inhibits Ca-dependent signal transduction in T cells and modifies transcription of lymphokine genes and T cell activation. FK506 is nephrotoxic and affects renal zones with limited oxygen availability such as medullary rays and inner stripes. Injury is potentiated by salt depletion and appears to be mediated via the renin-angiotensin system.[75]

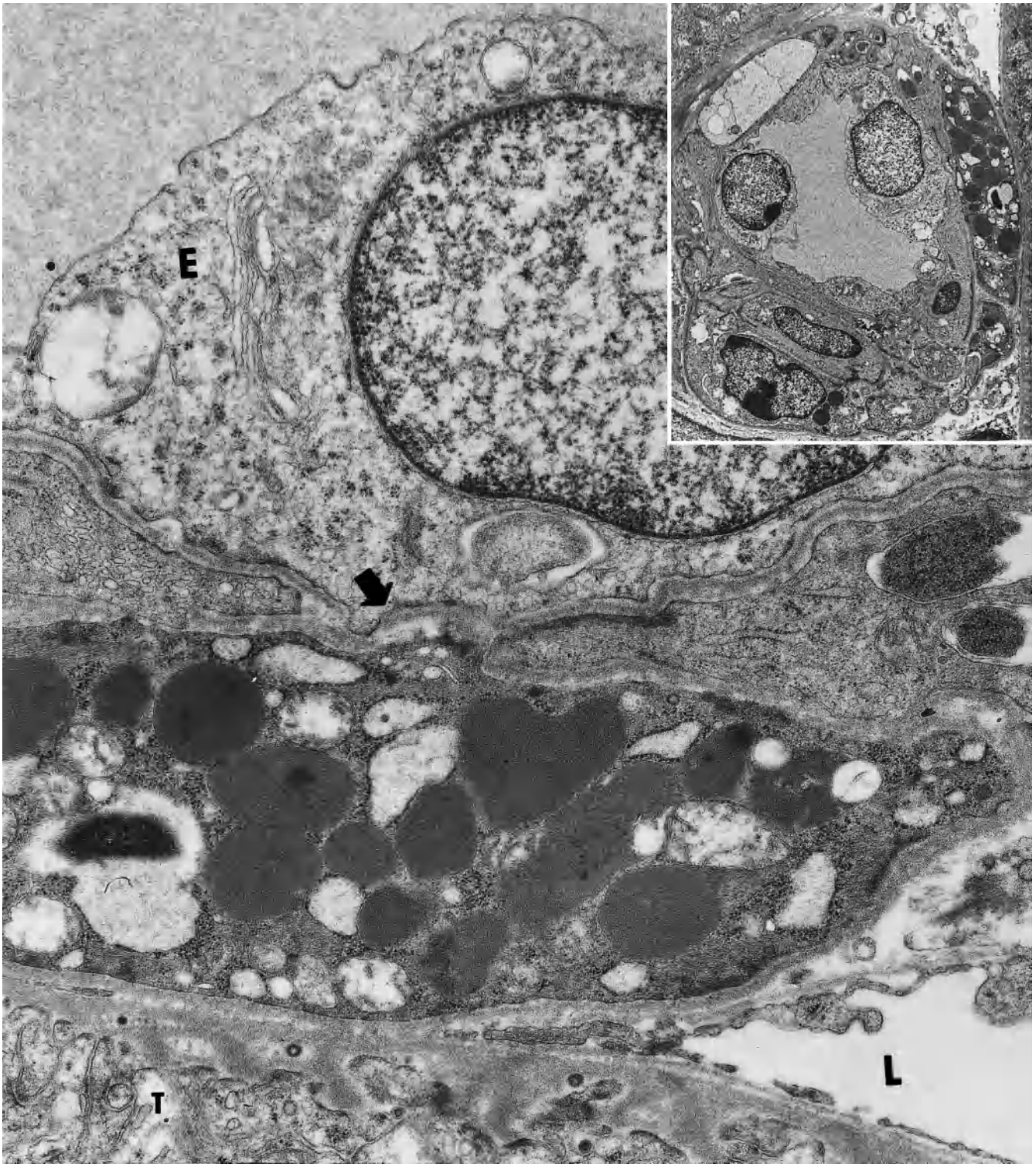


Fig. 20.11 Juxtaglomerular cells: afferent arteriole of renal glomerulus, mouse. Association of granular juxtaglomerular cell and endothlelial cell (*E*) at arrow. Lymphatic vessel (*L*) and tubule cell (*T*). *Inset*: low-power electron micrograph.

Crystal Nephropathy

The ultrastructural analysis of crystals in tissue depends upon the size and nature of the crystal, and upon data gathered from x-ray dispersal analysis on the chemical nature of the crystalline material. Scanning electron microscopy is especially useful in characterization of crystals on lumenal surfaces (Fig. 20.12).[76] Water soluble crystals are removed during aqueous fixation. Brittle crystals fracture during sectioning and drop from the section; this can be overcome by cutting thick sections. In some metabolic diseases, crystals develop so rarely that their ultrastructure is seldom reported, for example, deposition of **tyrosine crystals** in the cornea in tyrosinemia.[77,78]

Oxalate Nephropathy

Oxalate nephropathy is caused by ingestion of compounds that contain massive amounts of oxalates, the most common being the antifreeze agents ethylene glycol. Herbivorous animals are poisoned by ingestion of plants that contain large amounts of oxalic acid (halogeton, rhubarb, greasewood).



Fig. 20.12 Tyrosine crystals. (Micrograph: P. T. Valente, *Ultrastruct Pathol* 12:613, 1988.)

Calcium oxalate crystals are deposited in tissue in toxic diseases in which there is an increased amount of oxalic acid in blood and urine. In the earliest stages, **interstitial laminated oxalate plaques** first appear in the basement membranes of thin loops of Henle and then in interstitial spaces. Large oxalate crystals appear histologically as doubly refractile, translucent, yellowish crystals in the tubular lumens, interstitium, and within tubular epithelial cells. Ultrastructurally, crystals appear as electron-lucent areas with slight dense lines outlining the margins of the crystal edges. They have distinct crystalline shapes and are often contaminated with large amounts of organic material (Fig. 20.13).[79,80] Osteopontin, produced by tubular epithelium, is a major protein of the organic component. Biopsies of human renal papillae of oxalate-forming patients show that, when stained with immunogold labels, osteopontin is present on the laminar plaque surfaces during apatite crystal formation at junctions of the crystal/organic layers.[81]

At very high doses, oxalic acid produces **acute systemic toxicity** from the marked **hypocalcemia**; hypocalcemia and metabolic acidosis (caused by formation of acidic products of oxalate metabolism) combine to produce abnormalities of cardiopulmonary and CNS functions. If animals survive acute episodes, they are prone to develop **oxalate nephropathy** and **nephrolithiasis** with calcium oxalate monohydrate stones.[82,83]

Ethylene Glycol

Acute tubular necrosis caused by **ethylene glycol** toxicity in humans produces marked ballooning and hydropic or vacuolar degeneration of the proximal convoluted tubules. Calcium oxalate crystals are found in the tubular lumen. Crystals are taken up by renal



Fig. 20.13 Crystals in tissue. Oxalate crystal (*arrow*) among collagen fibrils (*C*), oxalate nephropathy, ethylene glycol toxicity, cat.

tubular epithelial cells, but the endosomal systems involved are rapidly overwhelmed by the magnitude of crystal formation. Crystal formation is inhibited by Tamm-Horsefall protein, the principal urinary protein.[84] Within the renal papillae, fibronectin and prothrombin fragment 1 are cytoprotective at PCT cell surfaces. Secreted in response to injury, these proteins inhibit oxalate crystallization and oxalate uptake. In lethal disease, crystals rapidly develop within tubular lumens and block urine formation.[85] Crystals reform within the peritubular interstitium and cause fibrosis, typically being surrounded by collagen and ground substance.

Primary Hyperoxyluria

The **primary hyperoxylurias** of humans are hereditary diseases characterized by renal excretion of oxalates. Primary hyperoxyluria type I is a rare autosomal recessive disease caused by a deficiency of the liver-specific peroxisomal enzyme alanine : glyoxylate aminotransferase, and characterized by excessive synthesis of oxalate with deposits of calcium oxalate in uroliths, nephrocalcinonosis, and systemic oxalosis. In this disease, immunoreactive aminotransferase is found between peroxisomes and mitochondria; normally it is confined to peroxisomes.[86]

Melamine Nephrosis

Melamine contaminating canned food has caused acute renal failure in pet dogs. Lesions of tubular necrosis and interstitial lymphocyte nephritis are accompanied by intratubular birefringent crystals of oxalates and of melamine. Melamine crystals are rough, pale brown, and do not stain with Alizarin Red S (as do oxalates). Crystals in these dogs have been identified by scanning electron microscopy.[87]

Sulfonamide Nephrosis

Nephrosis and uremia may result from ingestion of large doses of sulfonamides, particularly if associated with deficient fluid intake. Sulfonamide crystals are often grossly visible in the pelvis and as pale, yellowish, radial lines in the medulla. Tubular degeneration and plugging of the nephron, especially of collecting ducts, cause anuria. Sulfonamides also produce renal disease by allergic mechanisms and the ultrastructural interpretation of lesions must include the possibility of inflammatory changes of immune origin.

Calcium and Vitamin D Toxicity

Calcification of the renal parenchyma is associated chiefly with two conditions: vitamin D toxicity and uremia. Vitamin D toxicity occurs in certain species of animals and has been documented in laboratory rodents.[88] **Regeneration** of tubular epithelium is evident in most chronic cases of nephrosis. Pleomorphic, deeply staining cells line the denuded tubular basement membrane. Some cells are greatly enlarged, and mitotic figures are present. Other cells persist as thin, narrow cells that do not regain normal function. Regenerating proximal tubule epithelial cells have fewer cytoplasmic organelles, lack typical microvilli, and consist of large numbers of ribosomes.

Confounding Lesions in Nephrotoxicity

Ischemia

Ischemic injury, typically associated with shock and the resultant underperfusion of the kidney, can cause **acute tubular necrosis (ATN)**. In **ischemic ATN**, there are multiple foci of tubular necrosis at multiple sites along the nephron. Affected areas are patchy and involve short segments of proximal tubules and ascending limbs of loops of Henle. In contrast, **nephrotoxic ATN** most often involves the entire length of the proximal tubule (although with some toxins, patchy necrosis of the distal tubule occurs). In both types of ATN there are granular casts of Tamm-Horsfall and other proteins in the lumens of the nephron.

Renal ischemia is apt to be associated with severe systemic events involving clotting mechanisms, inflammation, and anemia.[89] In humans, ischemic ATN is a consequence of massive burns, crush injuries, severe tissue destruction during surgical and obstetrical treatments, and shock that follows septicemia.

Hypoxia plays a pivotal role in the reaction of the nephron to toxic injury, since the terminal patient may be hypoperfused and have lesions of ischemic ATN superimposed upon the toxic injury.

The isolated perfused rat kidney is an established model for analysis of hypoxia and the effects of acidosis and calcium levels. Extracellular calcium promotes the development of hypoxic injury and necrosis to the thick ascending limb of Henle and the cytoprotective effect of acidosis in hypoxia may be to counteract this calcium-dependent mechanism.[90] **Hyperoxia** is associated with selective mitochondrial lesions: dense matrical inclusions, which on recovery were removed by autophagocyyosis.[91]

Proteins in Blood

Hemoglobinemia

Free **hemoglobin** is normally cleared from the bloodstream by combining with circulating serum α_2-globulin (and other heme-binding proteins) to form complexes that are cleared from plasma by the monocyte-macrophage system. A portion of unbound hemoglobin dissociates into dimers, which cross the glomerular barrier.

When hemoglobin passes into the glomerular filtrate, it accumulates as reddish eosinophilic protein droplets in the proximal convoluted tubules. Hemoglobin enters the apical absorption vacuoles by endocytosis and is transferred to lysosomes where hydrolytic breakdown occurs.[92] In massive accumulation of hemoglobin associated with renal failure of hemoglobinemic nephrosis, nephrotoxicity is caused by erythrocyte stromal components.[93]

Bilirubinemia

In icterus, **bilirubin** collects in a similar manner in the proximal convoluted tubules. Swelling of affected cells occurs,[94] but there is little or no impairment of renal function. In the Gunn rat, a model for human neonatal icterus, glucuronyl transferase deficiency in hepatocytes results in unconjugated hyperbilirubinemia. Unconjugated bilirubin accumulates in the interstitium of the renal papillae, causing degeneration of interstitial cells and papillary necrosis.[95]

Homozygous Gunn rats, which have **unconjugated hyperbilirubinema** due to the deficit of the enzyme uridine diphosphate glucuronyl transferase, have a high susceptibility to nephrotoxins due to competition with bilirubin for plasma protein binding sites.[96] High concentrations of bilirubin develop in the renal papillae of affected rats, and there is a defective resorptive capacity of the ascending thick limb of Henle's loop.

Myoglobinemia

Myoglobin and hemoglobin may be part of the syndrome called **pigment-induced acute tubular necrosis. Myoglobinemia** with myoglobinuria occurs in severe alcohol toxicity and in excessive use of some drugs that cause coma. However, myoglobinemia-induced renal failure is most common after massive muscle injury of trauma, exercise rhabomyolysis, and heat stroke. In all of these cases, injury to the kidney is more dependent upon ischemia and shock, than on any effect of the pigment.

Fever and Electrolyte Imbalance

Injury to tubular epithelium, particularly fatty degeneration of the proximal convoluted tubule, accompanies any general **fever** and toxemia. Vacuolar degeneration occurs in severe **electrolyte imbalance,** especially during severe potassium deficiency, and this must be taken into account in interpreting toxic injury to the kidney.

Metabolic Acidosis

During metabolic acidosis, bicarbonate is titrated to extinction in the proximal nephron and excess acid is present in the filtrate. K^+ deficiency states are common, seen in severe diarrhea and vomiting, hyperadrenocorticoidism, and any cause of rental tubular acidosis. The tubular defects are mainfested as vacuolation of the distal tubules, diminished tubular function, accumulation of multivesicular lysosomes in the lower nephron, and mitochondrial degeneration.[97]

References

1. Routsalainen V, et al. 1999. Nephrin is specifically located at the slit diaphragm of glomerular podocytes. *Proc Natl Acad Sci USA* 96:7962.
2. Liu G, et al. 2003. Neph1 and nephrin interaction in the slit diaphragm is an important determinant of glomerular permeability. *J Clin Invest* 112:209.
3. Kanwar YS, et al. 2007. Contribution of proteoglycans towards the integrated functions of renal glomerular capillaries. *Am J Pathol* 171:9.
4. Bariety J, et al. 2006. Parietal podocytes in normal human glomeruli. *J Am Soc Nephrol* 17:2770.
5. Sever S, et al. 2007. Proteolytic processing of dynamin by cytoplasmic cathepsin L is a mechanism for proteinuric kidney disease. *J Clin Invest* 117:2095.
6. Kocher HM, et al. 2005. Subcellular distribution of Ras GTPase isoforms in normal human kidney. *Nephrol Dial Transplant* 20:886.
7. Rastaldi MP, et al. 2003. Glomerular podocytes possess the synaptic vesicle molecule Rab3A and its specific effector rabphilin-3a. *Am J Pathol* 163:889.
8. Plaisier E, et al. 2005. Glomerular permeability is altered by loss of PO, a myelin protein expressed in glomerular epithelial cells. *J Am Soc Nephrol* 16:3350.
9. Venkatachalam ME, Rennke HG. 1978. The structure and molecular basis of glomerular filtration. *Circ Res* 43:337.
10. Kerjaschki D. 1978. Polycation-induced dislocation of slit diaphragm and formation of cell junctions in rat kidney glomeruli. *Lab Invest* 39:430.
11. Zou J, et al. 2006. Upregulation of nestin, vimentin, and desmin in rat podocytes in response to injury. *Virchows Arch* 448:485.

12. Shirato I, et al. 1996. Cytoskeletal changes in podocytes associated with foot process effacement in Masugi nephritis. *Am J Pathol* 148:1283.
13. Ma J, et al. 2007. Effects of podocyte injury on glomerular development. *Pediatr Res* 62:417.
14. Kurihara H, et al. 1992. The altered glomerular filtration slits seen in puromycin aminonucleoside nephrosis and protamine sulfate-treated rats contain the tight junction protein ZO-1. *Am J Pathol* 141:805.
15. Klein DJ, et al. 1984. Alterations in proteoglycan metabolism in the nephrotic syndrome induced by the aminonucleoside of puromycin. *Lab Invest* 50:543.
16. Still WJS, et al. 1974. Vascular changes produced in the rat by aminonucleoside. *Lab Invest* 30:434.
17. Esparza AR, et al. 1981. Spectrum of acute renal failure in nephrotic syndrome with minimal (or minor) glomerular lesions. *Lab Invest* 54:510.
18. Hsu H-C, et al. 1982. Cyclophosphamide-induced glomerular injury in newborn mice. *Lab Invest* 47:281.
19. Morita T, et al. 1978. Mesangiolysis. *Lab Invest* 38:94.
20. Oliver C, Essner E. 1972. Protein transport in mouse kidney utilizing tyrosinase as an ultrastructural tracer. *J Exp Med* 136:291.
21. Evan AP, Dail WG Jr. 1974. The effects of sodium chromate on the proximal tubule of the rat kidney. *Lab Invest* 30:704.
22. De Witt LM, et al. 1988. Stimulation of the renal endoplasmic reticulum calcium pump: A possible biomarker for platinate toxicity. *Tox Appl Pharmacol* 92:157.
23. Silverblatt FJ, et al. 1974. Effect of vinblastine on the phagolysosome system of proximal convoluted tubule cells of rat kidney. *Lab Invest* 31:170.
24. Cté HC, et al. 2006. Exploring mitochondrial nephrotoxicity as a potential mechanism of kidney dysfunction among HIV-infected patients on highly active antiretroviral therapy. *Antivir Ther* 11:79.
25. Nagle RB, et al. 1972. Renal tubular effects of the aminonucleoside of puromycin. *Lab Invest* 26:558.
26. Giurgea-Marion L, et al. 1986. Impairment of lysosome-pinocytotic vesicle fusion in rat kidney proximal tubules after treatement with gentamicin at low doses. *Tox Appl Pharmacol* 86:271.
27. Kadurugamuwa JL, Beveridge TJ. 1998. Delivery of the non-membrane-permeative antibiotic gentamicin into mammalian cells by using *Shigella flexneri* membrane vesicles. *Antimicrob Agents Chemother* 42:1476.
28. Josepovitz C, et al. 1985. Contrasting effects of gentamicin and mercuric chloride on urinary excretion of enzymes and phospholipids in the rat. *Lab Invest* 52:375.
29. Rivera MI, et al. 1994. Early morphological and biochemical changes during 2-Br-(diglutathion-S-yl) hydroquinone-induced nephrotoxicity. *Toxicol Appl Pharmacol* 128:239.
30. Beauchamp D, et al. 1996. Effects of fasting on temporal variations in nephrotoxicity of gentamicin in rats. *Antimicrob Agenst Chemother* 40:670.
31. Houghton DC,et al. 1976. A light and electron microscopic analysis of gentamicin nephrotoxicity in rats. *Am J Pathol* 82:589.
32. Sundin DP, et al. 1997. Cellular mechanism of aminoglycoside tolerance in long-term gentamicin treatment. *Am J Physiol* 272:C1309.
33. Fujigaki Y, et al. 2007. Immunohistochemical study on caveolin-1alpha in regenerating process of tubular cells in gentamicin-induced acute tubular injury in rats. *Virchows Arch* 450:671.
34. Nacar A, et al. 2006. Ultrastructural examination of glomerular and tubular changes in renal allografts with cyclosporine toxicity. *Renal Fail* 28:543.
35. Bertani T, et al. 1987. Renal injury induced by long-term administration of cyclosporin A to rats. *Am J Pathol* 127:569.
36. Blair JT, et al. 1982. Toxicity of the immune suppressant cyclosporin A in the rat. *J Pathol* 138:163.
37. Thomson KJ, et al. 1989. Renal structure and function in streptozotocin-diabetes rats treated with cyclosporin A. *Br J Exp Pathol* 70:405.
38. Rush GF, et al. 1992. Cephaloridine-induced renal pathological and biochemical changes in female rabbits and isolated proximal tubules in suspension. *Tox Pathol* 20:155.
39. Ganote CE, et al. 1974. Acute mercuric chloride nephrotoxicity. An electron microscopic and metabolic study. *Lab Invest* 31:633.
40. Hinglais N, et al. 1978. Ultrastructural study of nephritis induced in brown Norway rats by mercuric chloride. *Lab Invest* 41:150.
41. Sabolic I, et al. 2006. Loss of basolateral invaginations in proximal tubules of cadmium intoxicated rats is independent of microtubules and clathrin. *Toxicology* 218:149.
42. Goyer RA, et al. 1989. Non-metallothionein-bound cadmium in the pathogenesis of cadmium nephrotoxicity in the rat. *Tox Appl Pharmacol* 101:232.
43. Uehara T, et al. 2007. Comparative analysis of gene expression between renal cortex and papilla in nedaplatin-induced nephrotoxicity in rats. *Hum Exp Toxicol* 26:767.
44. Jones TW, et al. 1985. *Cis*-Diaminedichloroplatinum (II)-induced acute renal failure in the rat. *Lab Invest* 52:363.
45. Dobyan DC, et al. 1981. Cyst formation in rat kidney induced by cis-platinum administration. *Lab Invest* 45:260.
46. McDonald-Taylor CK, et al. 1997. Uranyl nitrate-induced proximal tubule alterations in rabbits: A quantititaive analysis. *Toxicol Pathol* 25:381.
47. Carafolil E, et al. 1971. A study of Ca^{2+} metabolism in kidney mitochondria during acute uranium intoxication. *Lab Invest* 25:516.
48. Maqdo HS, et al. 2007. Nephrotoxicity in a young child exposed to uranium from contaminated well water. *Environ Health Perspect* 115:1237.
49. Kling MA, et al. 1984. Effects of long-term lithium administration on renal structure and function in rats. *Lab Invest* 50:526.
50. Bhathena DB, et al. 1978. The effects of amphotericin B therapy on the intrarenal vasculature and renal tubules in man. *Clin Nephrol* 9:103.

51. Brezis M, et al. 1984. Polyene toxicity in renal medulla. *Science* 224:66.
52. Albertine KH, O'Morchoe C. 1979. Distribution and density of the canine renal cortical lymphatic system. *Kidney Int* 16:470.
53. Bulger RE, Trump BF. 1966. Fine structure of the renal medulla. *Am J Anat* 118:685.
54. Hoyer JR, et al. 1979. Tamm-Horsfall glycoprotein. Ultrastructural immunoperoxidase localization in rat kidney. *Lab Invest* 41:168.
55. Lemley KV, Kriz W. 1991. Anatomy of the renal interstitium. *Kidney Int* 39:370.
56. Bohman S-O, Jensen PKA. 1976. Morphometric studies on the lipid droplets of the interstitial cells of the renal medulla in different states of diuresis. *J Ultrastuct Res* 55:182.
57. Majack RA, Larsen WJ. 1980. The bicellular and reflexive membrane junctions of renomedullary interstitial cells. *Am J Anat* 157:181.
58. Limas C, et al. 1976. Effects of indomethacin on renomedullary interstitial cells. *Lab Invest* 34:523.
59. Limas C, et al. 1976. Renomedullary interstitial cells in the spontaneously hypertensive rat. *Lab Invest* 34:606.
60. Lenz SD, et al. 1995. Early ultrastructural lesions of diphenylamine-induced renal papillary necrosis in Syrian hamsters. *Exp Toxicol Pathol* 47:447.
61. Tsuchiya Y, et al. 2005. Early pathophysiological features in canine renal papillary necrosis induced by nefiracetam. *Toxicol Pathol* 33:561.
62. Rocha GM, et la. 2001. Direct toxicity of nonsteroidal antiinflammatory drugs for renal medullary cells. *Proc Natl Acad Sci USA* 98:5317.
63. Hard GC, et al. 1984. Electron microscopic determination of the sequence of acute tubular and vascular injury induced in rat kidney by a carcinogenic dose of dimethylnitrosamine. *Lab Invest* 50:659.
64. Schneider P, et al. 1980. Potassium hydrogen phosphate-induced nephropathy in the dog. *Vet Pathol* 17:699 and 720.
65. Dorup J, et al. 1992. Tubule-tubule and tubule-arteriole contacts in rat kidney distal nephrons. *Lab Invest* 67:761.
66. Pech V, et al. 2008. Angiotensin II activates H^+-ATPase in type A intercalated cells. *J Am Soc Nephrol* 19:84.
67. Hackenthal E, et al. 1990. Morphology, physiology, and molecular biology or renin secretion. *Physiol Rev* 70:1067.
68. Laliberte F, et al. 1987. Cellular and subcellular immunohistochemical localization of angiotensin-converting enzyme in the rat adrenal gland. *Lab Invest* 56:364.
69. Latta H, Johnston WH. 1978. Granular and agranular cell counts in the juxtaglomerular apparatuses of rats with unilateral renovascular hypertension. *Lab Invest* 39:219.
70. Nichols J, Hennigar G. 1964. Effects of pulmonary hypertension on adrenal and kidneys of dogs infected with heart worms (*Dirofilaria immitis*). *Lab Invest* 13:800.
71. McLaren KM, MacDonald MK. 1983. Histological and ultrastructural studies of the human juxtaglomerular apparatus in benign and malignant hypertension. *J Pathol* 139:41.
72. Jackson DG, Jones HB. 1995. Histopathological and ultrastructural changes in the juxtaglomerular apparatus of the rat following administration of ZENECA ZD6888 (2-ethyl-5,6,7,8-tetrahydro-4-[(2'-(1H-tetrazol-5-yl)biphenyl-4-yl0-methoxy]quinoline), an angiotensin II antagonist. *Tox Pathol* 23:7.
73. Ye M, et al. 2004. Increased ACE-2 and decreased ACE protein in renal tubules from diabetic mice: A renoprotective combination? *Hypertension* 43:1120.
74. Dominick MA, et al. 1990. Ultrastructural juxtaglomular cell changes in normotensive rats treated with quinapril, an inhibitor of angiotensin-converting enzyme. *Tox Pathol* 18:396.
75. Stillman IE, et al. 1995. FK506 nephrotoxicity: Morphologic and physiologic characterization of a rat model. *Lab Invest* 73:794.
76. Escolar E, et al. 1990. Structure and composition of canine urinary calculi. *Res Vet Sci* 49:327.
77. Goldsmith LA. 1978. Molecular biology and molecular pathology of a newly described molecular disease—tyrosinemia II. *Exp Cell Biol* 46:96.
78. Honig S, et al. 1977. Crystal deposition disease. *Am J Med* 63:161.
79. Khan SR, Hackett RL. 1987. Crystal-matrix relationships in experimentally induced urinary calcium oxalate monohydrate crystal, an ultrastructural study. *Calcif Tiss Int* 41:157.
80. Riede UN, et al. 1973. Influence of starvation on the quantitative cytoarchitecture of the rat liver cell. *Beitr Pathol* 150:246.
81. Evan AP, et al. 2005. Apatite plaque particles in inner medulla of kidneys of calcium oxalate stone formers: Osteopontin localization. *Kidney Int* 68:145.
82. Sandersus S, Rez P. 2007. Morphology of crystals in calcium oxalate monohydrate stones. *Urol Res* 35:287.
83. Fleming DE, et al. 2003. Intracrystalline proteins and urolithiasis. *J Bone Mineral Res* 18:1282.
84. Mo L, et al. 2004. Tamm-Horsfall protein is a critical renal defense factor protecting against calcium oxalate crystal formation. *Kidney Int* 66:1159.
85. Ryall RL, et al. 2005. Intracrystalline proteins and urolithiasis. *BJU Int* 96:645.
86. Danpure CJ, et al. 1993. Enzymological and mutational analysis of a complex primary hyperoxaluria type I phenotype involving alanine : glyoxylate aminotransferase peroxisome-to-mitochondrion mistargeting and intraperoxisomal aggregation. *J Hum Genet* 53:417.
87. Thompson ME, et al. 2008. Characterization of melamine-containing calcium oxalate crystals in three dogs with suspected pet food-induced nephrotoxicosis. *Vet Pathol* 45:417.
88. Spangler WL, et al. 1979. Vitamin D intoxication and the pathogenesis of vitamin D nephropathy in the dog. *Am J Vet Res* 40:73.
89. Kaissling B, et al. 1993. Effects of anemia on morphology of rat renal cortex. Am J Physiol 264:F608.
90. Shanley PF, Johnson GC. 1991. Calcium and acidosis in renal hypoxia. *Lab Invest* 65:298.
91. Greene WB, et al. 1979. Selective mitochondrial degeneration in renal tubules following hyperbaric oxygen exposure. *Am J Pathol* 96:737.

92. Ericsson JLE, Rammer L. 1972. Renal morphology in burned rats. *Acta Pathol Microbiol Scand* 80:671.
93. Friedman H, et al. 1979. Morphologic effects following massive exchange transfusions with stroma-free hemoglobin solution. *Lab Invest* 40:655.
94. De Vos R, et al. 1972. Electron microscopy of the tubule cells of rat kidney after experimental bile duct ligation. *Exp Mol Pathol* 16:353.
95. Axelsen RA, Burry AF. 1976. Bilirubin-associated papillary necrosis in the homozygous Gunn rat. *J Pathol* 120:165.
96. Harper GS, Axelsen RA. 1982. Salicylate-induced renal papillary necrosis in the Gunn rat. *Lab Invest* 47:258.
97. Aithal HM, et al. 1977. Functional defects in mitochondria of renal inner red medulla during potassium depletion nephropathy. *Lab Invest* 37:423.

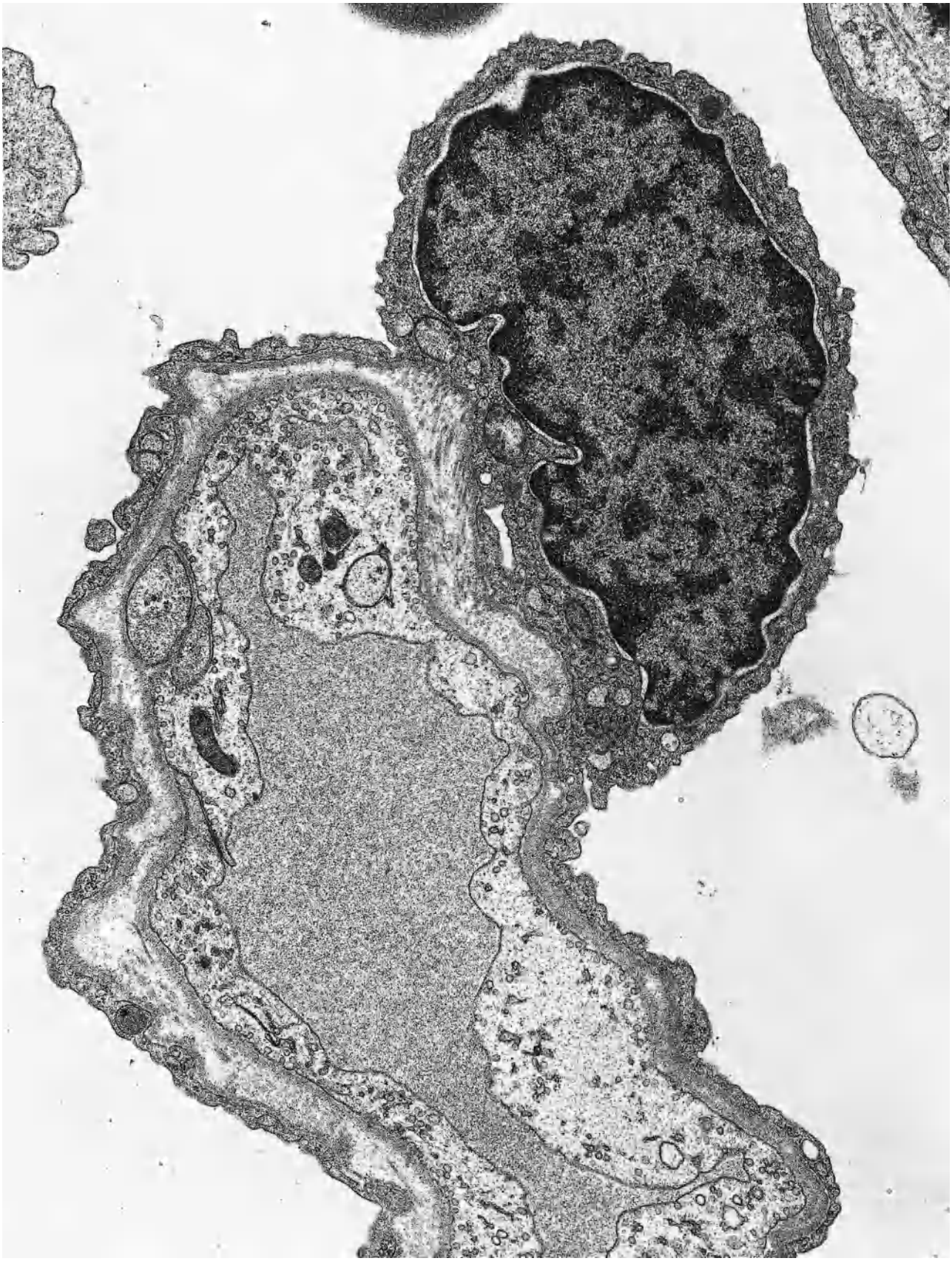


Fig. 21.1 Membranous pneumocytes: subacute pneumoconiosus, dog. The cell has a single large nucleus that projects into the alveolar space and the thin flattened cytoplasm covers the surface of the alveolar wall. The capillary of the alveolar wall has swollen endothelial cells and thickened basement membranes, and is surrounded by interstitial edema with basement membrane material and collagen.

© 2009 Wiley-Blackwell. ISBN: 978-0-813-80330-2

21 Toxicity of Respiratory Systems

Mark R. Ackermann

The Normal Mammalian Lung

The Alveolar Wall

The **alveolar wall** is a connective tissue interstitium through which capillaries ramify (Fig. 21.1). Masked by the tortuosity of the vascular bed is the pattern of connective tissue fibers that lie in a central plane and give tensile strength to the lung parenchyma.[1] The **blood-air barrier** is composed of capillary endothelium, basement membrane, and membranous pneumocyte. Its width is an indication of the capacity for gaseous interchange.[2] Movement of oxygen and CO_2 across the blood-air barrier is by passive diffusion, although the liberation of CO_2 from carbonic acid is greatly accelerated by the enzyme carbonic anhydrase. When gaseous transfer is compromised by injury to the alveolar wall, capillaries dilate (active hyperemia) and protrude into the alveolus. The exposed surface for interchange is thereby considerably enlarged.

The **endothelial cell** is commonly the first component of the alveolar wall to show change in toxic injury in the lung. Toxicity may be direct, or via the release of leukocyte cytokines.[3] Cell swelling with rarefaction of the cytoplasm progresses to blebbing of cytoplasm into the lumen of the capillary. If edema of the alveolar wall is extensive, fluid accumulation may cause focal herniation of the endothelial cell cytoplasm through the basement membrane into the pericapillary spaces. Intercellular junctions of endothelium are rarely seen open even in severe injury, although dense deposits, presumably proteoglycans, are commonly found in intercellular spaces. Normal capillary endothelial cells have no fenestrae, but in pathologic conditions such as pulmonary fibrosis, fenestrae may develop. In persistent low-level **hypoxia**, endothelial cells develop increased numbers of plasmalemmal vesicles. Vacuoles form and mitochondria degenerate.[4,5] Pulmonary capillaries have a remarkable capacity to dilate in response to hypoxia, to increased demand for oxygen, and to many vasoactive drugs.

In drug-induced **pulmonary edema**, alveolar capillaries are dilated, fluid accumulates in interstitial spaces, and endothelial cells have open intercellular junctions and subendothelial blebs. **Lymphatic vessels** flow along the lobular septa and larger veins, depending upon the species, and eventually drain into the blood.[6–8]

Pneumocytes

The thin flattened cytoplasm of the **membranous pneumocyte** (type I cell) covers the surface of the alveolar wall. Its nucleus is small and elongate. Membranous (type I) pneumonocytes express multidrug resistance (MDR) transporter P-glycoprotein and expel potential toxins into the alveolar lumen rather than the vasculature.[9] Obtaining oxygen directly from the alveolus, the membranous pneumocyte is highly susceptible to hypoxia, and lack of oxygen causes mitochondria to enlarge. In acute cell swelling, fluid distends the perinuclear cisternae and the cisternae of the endoplasmic reticulum. In some toxic reactions, membranous pneumocytes become filled with lysosomes and myeloid bodies; for example, chloroquine and amiodarone toxicity.

Granular peumocytes (type II cells) occur randomly along the alveolar wall and are of primary importance in injury to the lung (Fig. 21.2). They differ from the membranous pneumocyte by being larger and cuboidal and have dense osmiophilic lamellar inclusions. Type II pneumocytes have a high content of

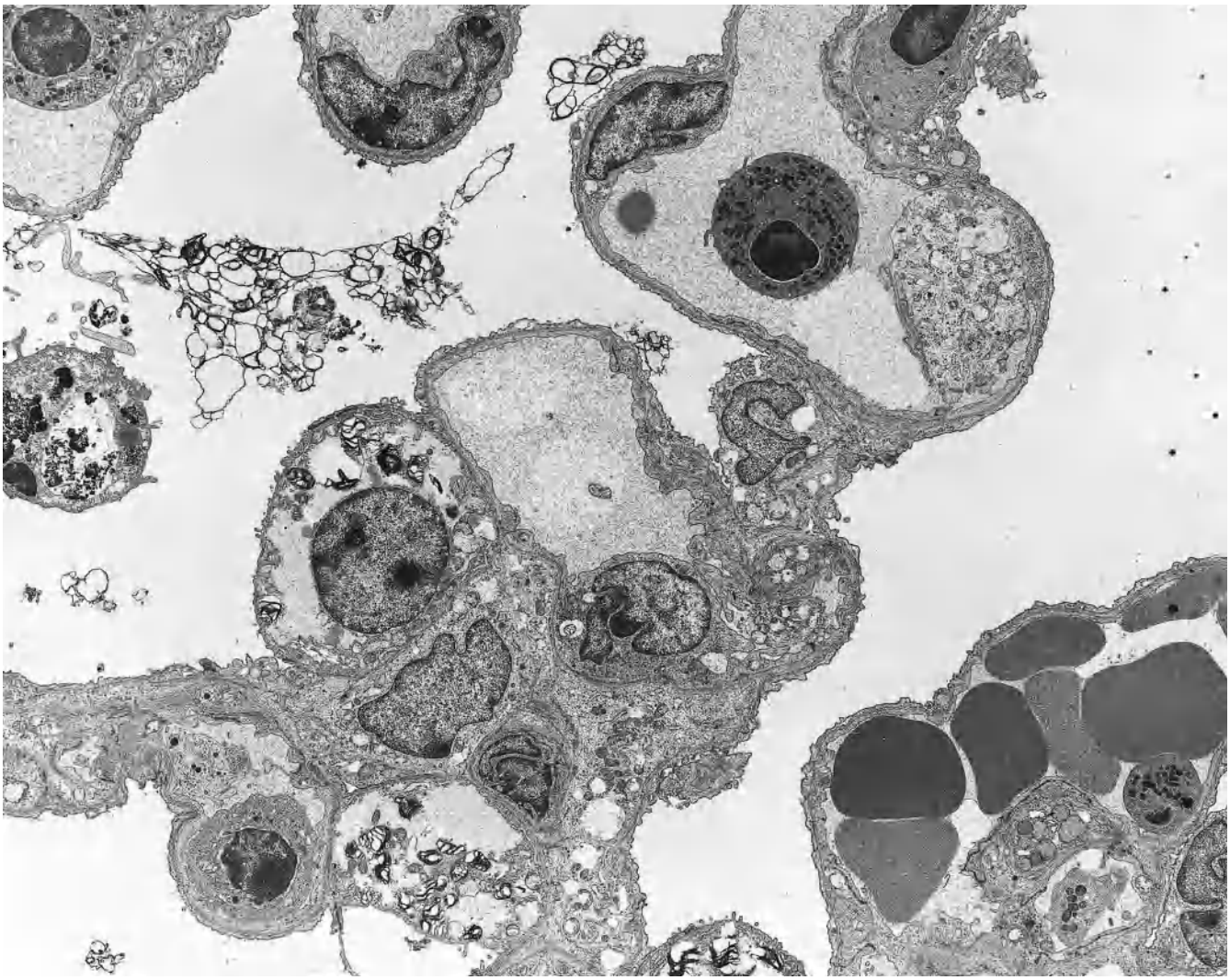


Fig. 21.2 Granular pneumocytes: hyperplasia, chronic pneumonia caused by *Bordetella bronchiseptica*, pig. Multiple swollen granular pneumocytes are present in the alveolar walls. Note pulmonary surfactant in alveolar spaces, hyperemia with many erythrocytes, neutrophils and platelets in the lumens of pulmonary capillaries.

superoxide dismutases, which are important in toxicity caused by oxygen radicles.[10] Type II pneumocytes are expelled into the alveolus by merocrine secretion, and are the source of pulmonary surfactant.[11,12] Surfactant lines the alveolar wall, stabilizing it by lowering surface tension.[13]

Pulmonary Surfactant

Pulmonary surfactant is ultrastructurally heterogeneous and contains many molecules including phosphatidylcholine and other phospholipids, cholesterol, neutral lipds, and the surfactant proteins A, B, C, and D.[14,15] When stored in lamellar bodies of type II pneumocytes, surfactant is tightly packed in multilayer arrays. After secretion and hydration in the alveolar fluid, it expands into a complex, lattice structure called tubular myelin (Fig. 21.3). Surfactant also contains small vesicles. Surfactant products then cycle back into the type II pneumocyte for reassembly and resecretion.

Surfactant protein A (SP-A) is the most abundant surfactant protein. Synthesized in both type II pneumocytes and bronchiolar Clara cells, SP-A is assembled into a large oligomer with a mass of 700 KD.[16,17] Ultrastructurally, the molecule resembles the first complement component, as a "bouquet of tulips." The collagen-like stem region is about 20 nm long. Six globular heads of the protein are held in a circular array, 20 nm in diameter. SP-A has a lectin-like binding region. SP-A and surfactant protein D (SP-D) have antimicrobial activity, which includes microbial aggregation and macrophage activation. Expression is increased physiologically when there is a demand for surfactant production and can also be increased with microbial infections and some particulates.[18]

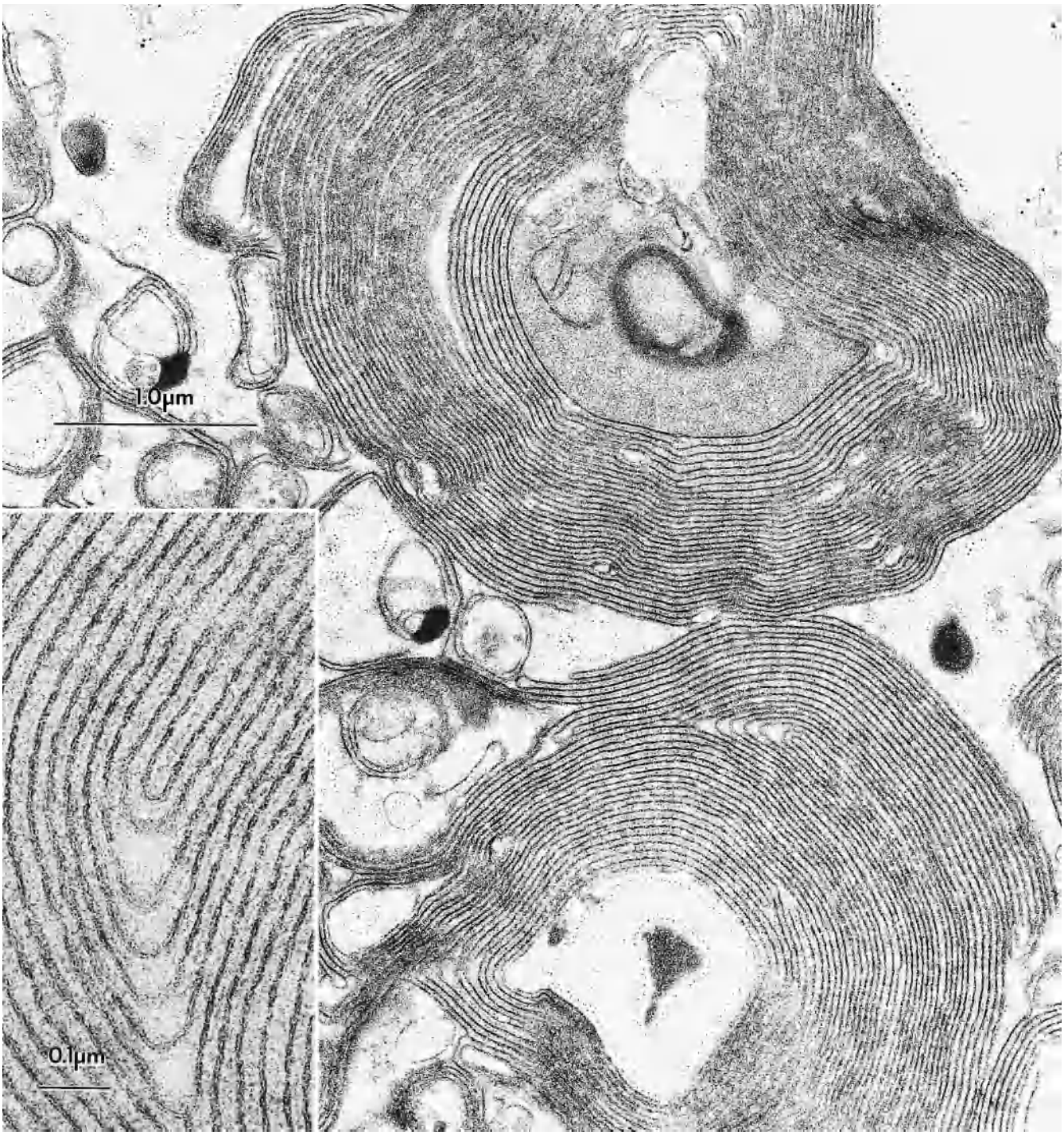


Fig. 21.3 Pulmonary surfactant: alveolar proteinosis, human lung. Multilamellated structure consists of lipid bilayers separated by amorphous material. Electron-dense bodies and vesicles are in centers of lamellated structures. (Micrograph: Gary E. R. Hook, *Lab Invest* 50:711, 1984.)

Reaction to Pulmonary Toxins

Vapors, gases, and **particulate matter** that enter the lung are dealt with in **terminal and respiratory bronchioles**. **Respiratory bronchioles** are partially alveolarized airways between the terminal bronchioles and alveolar ducts. They are the first structure to participate in gas exchange and often first to be injured airborne toxins. Ciliated bronchiolar cells, type II cells, basal cells, brush cells, and neuroendocrine (Kulchitsky) cells are relatively refractory to toxic injury, although they can be injured secondarily by toxic metabolites, inflammatory reactions or vascular damage.

Nonciliated epithelial **Clara cells** of the distal bronchioles are loaded with enzymes that catabolize inhaled pollutants; these are cytochrome P450-dependent monooxygenases, bound to smooth endoplasmic reticulum, which biotransforming toxic drugs, pesticides, and carcinogens that are often less toxic, but can be more toxic, than the parent compound. Clara cells are the principal target in the mammalian lung for many air- or blood-borne pulmonary toxins. When injured, these cells are sloughed, expelled, and replaced by their immature forms, which remain attached to the terminal bronchiolar surface. The basis for specific injury to Clara cells is the production of cytotoxic metabolites in target cells as a result of the metabolism of the parent compound by the cytochrome P450 monooxygenase system (CYP), which has many isoforms including CYP1A1 and CYP1A2. Although type II cells and macrophages have P-450 enzymes, Clara cells have up to 20-fold higher activity of P450 than is found in other cell types of the lungs. P450 enzymes generally convert the parent compound into a more polar metabolite. Differences in the susceptibility to acute Clara cell injury by toxins such as naphthalene and dichloroethylene appear to be due to isoenzyme composition that differs between individuals and from species to species; for example, the LD_{50} for naphthalene in the mouse is 380 mg/kg; in the hamster, 800 mg/kg; and in the rat, 2,200 mg/kg.[2] Differences in other cell types also affect species susceptibility. Chemicals like naphthalene induce P-450 enzymes without obvious effects but when followed by ozone (O_3), the impact is magnified over either substance alone. **Phase II** biotransformation enzymes are also present in respiratory epithelium and tend to increase water solubility of metabolites through the addition of glucuronide or other conjugates.

Alveolar Macrophages

Alveolar macrophages remove foreign substances that enter the alveolus. These cells lie free in the alveolar spaces and phagocytize and digest particular macromolecular materials (Fig. 21.4). They become engorged and in some diseases have diagnostic significance; for example, the iron-filled "heart failure cells" in chronic heart failure, and the lipid-filled "foam cells" in some toxic lesions.[19] Pneumocytes play very little role in clearance of these substances. The pulmonary clearance of low levels of inert exogenous material (such as carbon, dust, and nonpathogenic microbes) and of endogenous cell debris, surfactant, and fibrin is constant. The lungs of adults exposed to environmental contaminants contain large numbers of active macrophages. Pulmonary macrophages are markedly enlarged and filled with large pleomorphic residual bodies in lungs of smokers of tobacco and marijuana. Macrophages also internalize dusts, silicates, silica, asbestos fibers, nanoparticles, and carbonaceous material and often aggregate into **macules** (aggregates in the centers of pulmonary acini) in centriacinar areas of lung lobes or as **nodules** that form around silicates. Alveolar macrophages also produce cytochrome P450 enzymes but at a lesser level than Clara cells. **Alveolar macrophages** originate from blood monocytes. Carbon-labeled monocytes, when injected into guinea pigs, concentrate in the lungs.[20]

Intravascular Macrophages

Intravascular (IV) macrophages adhere to endothelial cells of the capillaries of alveolar septae. They have a relatively higher metabolic role than alveolar macrophages and therefore appear to internalize toxins or substances within the vasculature. The relatively low blood pressure and high blood volume within the alveolar septal capillary result in slow, perculating passage of blood and increased contact between IV macrophages and solublized material in the blood. IV macrophages increase with age and the number varies widely between species. Humans have very few IV macrophages, whereas pigs and cattle have many.

Granular Pneumocyte Hyperplasia

Type II epithelial cells are active participants in immunity and inflammation through the release of antimicrobial peptides such as defensins, cytokines, and chemokines. They also express adhesion molecule receptors such as intercellular adhesion molecule-1 (ICAM-1) and receptors for growth factors including epidermal growth factor and vascular endothelial growth factor.

Type II pneumocyte hyperplasia and release of surfactant are early responses of the alveolar wall to injury. Lamellar inclusions contain esterases that are isozymes of and act complementary to the esterases of macrophages. Secretion is stimulated by pilocarpine. It also appears that release of surfactant is partially under neural control. Degeneration of type II pneumocytes is seen when the vagus nerves are sectioned bilaterally. There is progressive decrease in osmophilia of the cytoplasmic granules. The edema and atelectasis that follow vagotomy are allegedly due to absence of surfactant, which follows a secondary atrophic reaction in membranous pneumocytes.[21]

The type II pneumocyte is the progenitor of the membranous pneumocyte because of the proliferation and repair of the damaged alveolar wall, and because of their presence and mitotic activity in the early fetal lung. Type II pneumocytes show degenerative changes, including fatty degeneration, in intoxications by



Fig. 21.4 Intravascular macrophages: erythrophagocytosis of an erythroblast (*top*) by an intravascular macrophage, cardiac failure, dog. Note inflammatory cells in lumen of pulmonary capillary. Alveolar walls are thickened. *Inset*: intravascular macrophage in pulmonary capillary and erythrocyte and granular pneumocyte in alveolar space.

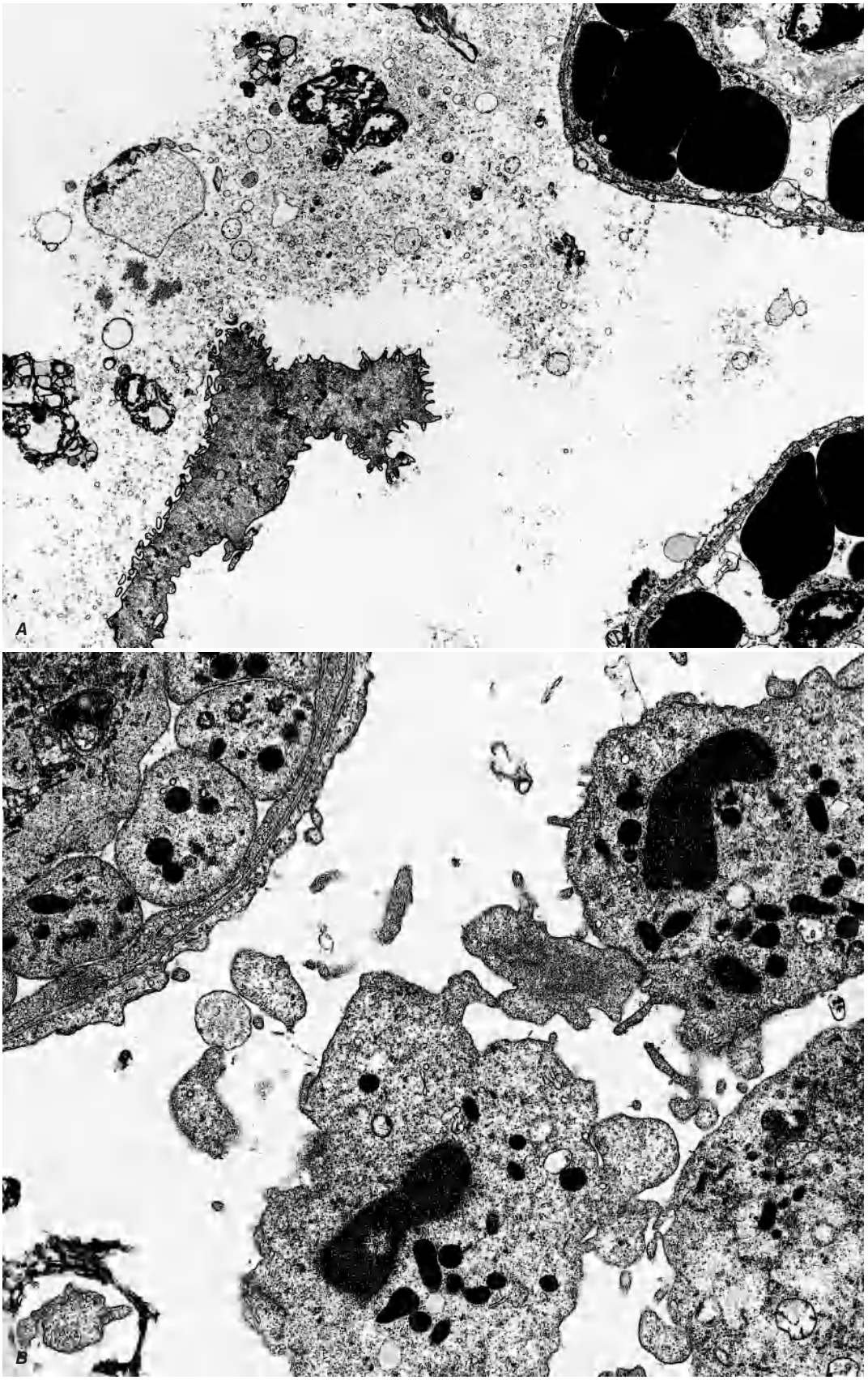


Fig. 21.5 **Fetal lung**: response to bacterial infection, *Brucella abortus*, calf. **A. Thrombosis**: capillaries in the pulmonary wall. Platelets and a macrophage obstruct capillary lumen. **B. Alveolar space**: necrotic macrophage contains debris and remnants of bacterial cells. Amnionic epithelial cell (*darker cell, upper right*) has sloughed from placenta and has been inhaled with amnionic fluids.

various causes. They contain abnormal lamellar inclusions in many toxic disease, but these inclusions have also been reported in fatty acid deficiency and in hereditary lysosomal diseases. With toxic loss of type II cells in neonates, impaired re-epithelialization persists with age.[22]

Myofibroblasts (stellate interstitial cells) in alveolar walls of mammalian lungs contain cytoplasmic actin fibrils, 3–8 nm in diameter, a fibronexus, and function as autoregulators of ventilation or blood perfusion by contracting in response to hypoxia or to substances such as epinephrine. Interstitial cells and interstitial collagen of the alveolar wall increase in most chronic toxin-induced injuries to the lungs.

The Fetal Lung

Fetal lung arises from the primitive foregut forming ducts that develop into large airways during the pseudoglandular (7–16 wk gestation) and canalicular (16–24 wk gestation) stages. Primitive alveolar ducts form during the terminal sac stage (24–36 wk) with formation of type II and I cells. During the alveolar stage (36 wk to 3 yr of age postnatally) the alveoli mature. In the early **fetal lung**, type II pneumocytes are absent but are seen with increasing frequency as birth nears.[22,23] Type II cell differentiation is associated with depletion of cellular glycogen.[24,25] Increased numbers of type II cells correlates with increasing amounts of measurable surfactant in the fetal lung. During birth, as hypoxia develops and the first breathing begins, there is rapid degranulation of granular pneumocytes with massive release of surfactant and protein A, which enters the alveolar lumen and also the blood. Surfactant not only stabilizes the lung but aids in removal of amniotic fluid and cells that lodge in the alveoli prior to birth. Neonatal Clara cells damaged by toxins such as 4-ipomeanol do not re-epithelize to the expected, proper, anatomical arrangement.[26] Fetal lung development is dependent upon the activity of vascular endothelial growth factor (VEGF) which drives vascularization and epithelial cell formation. Premature infants on ventilators can develop bronchopulmonary dysplasia and chronic lung disease characterized by altered arrangements of epithelia that can be repaired, to a certain degree, by VEGF therapy;[27] however, VEGF can invoke monocyte accumulation at high doses delivered intratracheally.[28]

In **fetal lungs**, alveolar macrophages and lung dendritic cells have important roles in removal of pulmonary debris and in the initiation of pulmonary immunity (Fig. 21.5). **Intravascular macrophages** lodge and persist in the capillaries of the pulmonary alveolar wall in neonates of several animal species.[29–31] Pulmonary intravascular macrophages have a unique surface coat,[32] and play special roles in the protection of the early developing lung. The pulmonary interstitial compartment of the newborn is increased by high levels of oxygen.[33]

When **pulmonary surfactant** is absent or inactivated in newborn animals, the resulting high surface tension at the end of respiration forces more air out of the lungs, and **atelectasis** (incomplete expansion of the lungs) results. Decreased surfactant plays a critical role in the development of **hyalin membrane disease** of premature human infants and similar syndromes in animals. **Peroxisomes** increase in type II pneumocytes as birth approaches.[34] **Corticosteroid treatment** of pregnant animals accelerates both surfactant and type II pneumocyte in the lungs of the fetus.[35] In some animals, these hormones are used to induce parturition, and the secondary effects on type II pneumocytes may mimic the natural birth process in the lung. Increased SP-A levels are also associated with birth.

Substances Damaging to Lung

Vapors and Gases

Vapors (materials that exist simultaneously as a liquid and gas at room temperature; for example, formaldehyde) and **gases** (exist as gas at room temperature and liquid when cooled or under pressure; e.g., oxygen, ozone, nitrogen dioxide or sulfur dioxide, hydrogen sulfide) are inhaled in the gaseous phase and therefore have the same absorptive principles. These include the physical/chemical characteristics of the gas, thermodynamic equilibrium, diffusion and chemical reaction and also host factors such as anatomy, strict nasal breathing, air flow rates, end-inspiratory pauses (holding breath), blood perfusion and air surface liquid levels. Once inhaled, movement of gas into the aqueous interfaces in dependent upon the concentration of the gas and solubility of the gas into the liquid or mucus, although the concentration of gas changes rapidly in the lung with entrance into the vasculature or lymphatic vessels. Some toxins, such as ethanol, can move in reverse. That is, blood ethanol can pass the alveolar wall and enter the lung airway and become exhaled/expelled.

Particulates

Particulates include organic carbon such as endotoxin, elemental carbon, and other elements. The types of particulates inhaled vary by location. Inhaled air from industrial regions have more sulfate while rural regions have more nitrate. Zinc, iron, vanadium, and nickel are more common for areas that burn oil or coal.

Dry, and desert-like areas have increased silicates. For particulates, the site and level of deposition of **particulate matter** are dependent upon particle size, shape and density, hygroscopicity, charge, breathing patterns and nose versus mouth breathing. In inhalation pulmonary injury of humans and large mammals, the most dangerous particle sizes are 1–5 μm. Most particles over 5 μm in diameter are filtered out in vibrissae of the nares or by the mucociliary clearance mechanism after they contact mucosa. Particles smaller than 1 μm may remain suspended in inspired air and be exhaled. Particulate clearance is dependent upon airway diameter, length, mucous volume, and ciliary beat frequency. Particles are cleared by either the mucociliary apparatus, lymph drainage, or vascular flow.

Fibers

Airborne, inhaled fibers include asbestos, and synthetic silicate-based vitreous fibers, refractory ceramic fibers, synthetic organic (nylon) fibers, and nanotubes. Of these, long and thin forms of both amphibole asbestos fibers and silicon carbide fibers are most pathogenic. The aerodynamic diameter (D_{ae}), not necessarily the fiber length, of the fiber determines the ability of the fiber to pass beyond the ciliated airway epithelium into the deeper lung, and those fibers <5 μm D_{ae} have optimal passage length even if the fibers are very long. Long fibers that are not easily degraded and persist cannot be adequately phagocytosed, resulting in release of inflammatory mediators, fibrosis, and genotoxicity.

Nanoparticles

Nanoparticles (ultrafine particles) are <100 nm, poorly degraded, and can be inhaled into the deep lung. They can escape macrophage detection and accumulate in the interstitium. Once within the lung, nanoparticles can incite inflammatory reactions, fibrosis and neoplastic cells, depending on the number and composition. Nanoparticles such as titanium oxide, carbon black, and diesel particulates induce great lung toxicity compared to fine-sized (between 100 nm and 3 μm) particles of the same composition. Other factors that influence nanoparticle toxicity include particle aggregation/disaggregation potential and surface coatings.

Oxidant Damage

Oxidation is a major mechanism of lung damage from gases, fibers, particulates, and nanoparticles, as well as toxins within the blood that are exhaled, such as ethanol (Table 21.1). These substances readily generate oxidative radicals that lead to membrane

Table 21.1 Pulmonary toxins.

Toxicant	*Comment*	*Reference to ultrastructural pathology*
Acetyl glyceryl ether phosphoryl choline	Acute pneumonitis	**McManus**, *Am J Pathol* 121:55, 1965 (rabbit)†
ACTH	Lung maturation	**Sundell**, *Am J Pathol* 97:393, 1979 (lamb fetus)
Amiodarone	Acute lung injury	**Costa-Jussa**, *J Pathol* 144:73, 1984 (human); **Dake**, *Am J Med* 78:506, 1985 (human); **Liu**, *Thorax* 41:100, 1986 (rat);† **Martin**, *Am J Pathol* 120:344, 1985;* **Reasor**, *Exp Mol Pathol* 53:64, 1990*
Anthrax toxin	Lung necrosis	**Beall**, *J Infect Dis* 116:377, 1966
Azothioprine	Interstitial pneumonitis	**Bedrossian**, *Am J Clin Pathol* 82:148, 1984 (human)
Azetidine-2-carboxylic acid		**Adamson**, *Lab Invest* 57:439, 1987 (rat)
Beclomethasone	Airway epithelium	**Uhlík,** *Ultrastruct Pathol* 31:221, 2007 (rabbit)
Benzylacetate	Noninhalation (Feed)	**Sells,** *Toxicol Pathol* 35:170, 2007 (mouse)
Bleomycin	Lung: alveolar type 2 cell metaplasia	**Adamson**, Am J Pathol 96:531, 1979; **Adamson**, *Libr of Cong* 90-3179:171 (mouse); **Adler**, *Am Rev Respir Dis* 133 (6):1043–1048, 1986 (rat); **Aso**, *Lab Invest* 35:558, 1976 (rat); **Bedrossian**, *Cancer* 32:44, 1973 (human); **Bedrossian**, *Arch Pathol lab Med* 101:248, 1977 (pheasant); **Daskal**, *Cancer Res* 36:1267, 1976 (human); **Phan**, *J Clin Invest* 76(1):241–247, 1985 (rat); **Singer**, *Am J Pathol* 125:258, 1986 (rodent); **Thrall**, *Am J Pathol* 95:117, 1979 (rat, fibrosis)

Table 21.1 *Continued*

Toxicant	*Comment*	*Reference to ultrastructural pathology*
Butylated hydroxytoluene	Lung	**Adamson**, *Lab Invest* 36:26, 1977 (mouse); **Haschek**, *Lab Invest* 46:438, 1982 (mouse); **Hirai**, *Exp Molec Pathol* 27:295, 1977 (mouse)
Carbon tetrachloride	Alveolar wall	**Gould**, *Arch Intern Med* 128:109, 1971
Chlorambucin	Lung	**Lane**, *Cancer* 47:32, 1981 (human)
Chlorphentermine	Lung	**Lullman**, *Virch Arch B* 12:91, 1973 (rat); **Matulionis**, *Exp Mol Pathol* 39:80, 1983 (rat)
Cobra venom		**Almeida**, *J Pathol* 121:169, 1977 (rat)
Concanavalin A	Lung	**Welsch**, *Virch Arch B* 44:45, 1983 (rat)
Copper	Gill	**Giovanett**, *Tox Path* 26:628, 1998 (mouse); **Jiraungkoorskul**, *Environ Toxicol* 22:92, 2007 (fish)
Cortiso	Lung Gill	**Wang**, *J Appl Physiol* 30:362, 1971 (fetus) **Forrest**, *Am J Physiol* 224:708, 1973
Cresylic acid		**Angus**, *J Comp Pathol* 93:33, 1983 (sheep)
Cristobalit		**Low**, *Am J Pathol* 136:923, 1990 (rat)
***Crotalaria* toxin**	Snake venom	**Dingemans**, *Lab Invest* 35:205, 1976 (rat)
Cyclosphophamide		**Gould**, *Am J Pathol* 81:513, 1975 (human)
Dexamethasone	Fetal lung	**Kauffman**, *Lab Invest* 37:497, 1977 (mouse)
Dipropylene glycol	Noninhalation (drinking water)	**Sells**, *Toxicol Pathol* 35:170, 2007 (rat)
Endosulfan	Gill	**Bernabò**, *Aquat Toxicol* 86:447, 2008 (fish)
Ethchlorvynol	Pulmonary edema	**Wysolmersk**, *Am J Pathol* 115:447, 1984
Hydrogen peroxide		**Castillo**, *Exp Cell Res* 313:2680, 2007 (human)
Hydroxytoluene	Butylated	**Hirai**, *Exp Mol Pathol* 39:129, 1983 (mouse)
4-Ipomeanol		**Doster**, *Am J Pathol* 111:56, 1983 (rat); **Durham**, *Am J Pathol* 118:66, 1985 (mouse); **Plopper**, *J Pharmacol Exp Ther* 269:867, 1994 (rabbit)
Mercuric chloride	Noninhalation (gavage)	**Sells,** *Toxicol Pathol* 35:170, 2007 (mouse)
Methimazole		**Liu**, *Virch Arch B* 60:21, 1991 (rat)
3-Methyl furan	Atmospheric contaminant	**Boyd**, *Nature* 272:270, 1978
3-Methyl indole		**Atwal**, *Am J Pathol* 114:472, 1984 (cow); **Bradley**, *Am J Pathol* 99:551, 1980 (goat); **Durham**, *Am J Pathol* 121:128, 1985 (mouse); **Woods**, *Exp Lung Res* 25(2):165–181, 1999
***Microcystis* toxin**		**Slatkin**, *Science* 220:1383, 1983 (mouse)
Monastral blue	Lysosomes in macrophages	**Attwal**, *Anat Rec* 234:223, 1992
Monochloroacetic acid	Noninhalation (gavage)	**Sells**, *Toxicol Pathol* 35:170, 2007 (mouse)
Monocrotaline pyrrole	Pyrrol carbamate	**Plestina**, *J Pathol* 121:9, 1977 (rat); **Ramos**, Vascular Pharmacology 46:439, 2007 (human); **Woods**, *Exp Lung Res* 25(2):165–181, 1999
Naphthalene		**Mahri**, *Am J Pathol* 86:559, 1977 (mouse)
Nitrogen dioxide		**Langlois**, *Am J Pathol* 89:637, 1977 (cat)
N-nitroso-N-methylurethane		**Ryan**, *Am J Pathol* 82:353, 1976 (dog)
Oxytetracycline		**Gottschall**, *Lab Invest* 41:5, 1979 (rat)
4α-Phorbol-12,13-didecanoate	Lung	**Alvarez,** *Circ Res* 99:988, 2005 (rodent)
Phorbol myristate acetate	Lung Air sac	**Johnson**, *Am J Pathol* 107:29, 1982 (rat); **McCall**, *Am J Pathol* 111:258, 1983 (rabbit); **Taylor**, *Lab Invest* 52:61, 1985 (rabbit) **Ficken**, *Am J Vet Res* 51:958, 1990 (turkey)

Table 21.1 *Continued*

Toxicant	*Comment*	*Reference to ultrastructural pathology*
Pilocarpine	Granular pneumocytes	**Goldenberg**, Lab Invest 20:147, 1969; **Smith**, *Anat Rec* 202:23, 1982 (fetal lung)
Polytetrafluoro-ethylene (teflon)		**Lee**, *Lab Invest* 35:152, 1976 (rat)
Residual oily fly ash	Lung	**Roberts**, *Toxicol Environ Health A* 70:1929, 2007 (mouse)
Trichloroethylene		**Giovanett**, *Tox Path* 26:628, 1998 (mouse)
Trimethylphosphoro-thioate		**Durham**, *J Pathol* 155:247, 1988
Streptozotocin		**Plopper**, *Lab Invest* 38:143, 1978 (rat)
Urethane		**Bocking**, *Lab Invest* 44:138, 1981; **Ryan**, *Am J Pathol* 82:353, 1976 (dog)

*In vitro study.
†Animal model.

lipoperoxidation, DNA oxidation, oxidation of cellular glycoconjugates and proteins, degradation of elastin and other extracellular matrix proteins, and generation of additional radicals that affect epithelia.[36] They deplete enzymatic antioxidants such glutathione peroxidases and nonenzymatic scavengers and can also activate sphingomyelinase.[37]

Pulmomary Vascular Toxins

The lung, in order to optimize gaseous exchange, receives a very large blood volume that percolates slowly through alveolar septal capillaries at low blood pressure. Toxins within the vasculature can linger within this location and damage endothelial cells or other portions of the alveolar septae by a variety of mechanisms. Some toxins, such as bleomycin, have been administered as a therapeutic agent. Toxins can also be absorbed from the skin or mucosal surfaces, especially the alimentary tract. There are numerous toxic plants, for example, that are ingested by herbivores. Often animals avoid these plants, but when pastures are in poor condition and when the animals are very hungry, they can ingest plants they normally would avoid.

Acute Toxic Pulmonary Injury

Ciliated cells can be altered directly by many toxins. Cigarette smoke and alcohol are two of the most common injurious agents of the human respiratory tract and both can affect ciliary activity. **Ciliary beat frequency (CBF)** is reduced by cigarette smoke and increased by acute alcohol toxicity, whereas chronic alcohol injury reduces CBF.[38] Reductions in CBF lead to impaired expulsion of entrapped particulates or toxins integrated into the air surface layer and thereby retained in the respiratory tract increasing exposure.

Terminal bronchioles are the lung sites with greatest sensitivity to most toxins, which is largely due to the presence of a large number of **Clara cells** in this region of the lung airways. Some xenobiotics may be detoxified by CYP1A1 and CYP1A2 and other cytochromes. Yet other xenobiotics are converted to highly toxic inetermediates. For example, activation of the lung edema factor (4-ipomeanol) in mold-infected sweet potatoes leads to pulmonary edema and hemorrhage. With this toxin and several other known lung contaminants, toxicity and covalent binding are both associated with the Clara cells of terminal bronchioles.

Acute Inhalant Injury

At the alveolar level, when toxic chemicals are inhaled or present in the alveolar vascular capillaries, diffuse injury to the pulmonary alveolar wall can occur and membranous pneumocytes are directly injured. Inhaled gases (oxygen, ozone, hydrogen sulfide, and sulfur dioxide) and blood borne toxins can diffuse rapidly through the lung and result in endothelial and/or epithelial damage. Regardless of exposure route or toxin, the lung response during acute injury is similar. Endothelial cells swell increasing their cytoplasmic area due to dilation of endoplasmic reticulum, nuclear membranes often associated with cristiolysis of mitochondria. Damaged endothelia allow passage of fluid into the alveolar interstitium that expands the alveolar septal interstitium separating collagen fibrils. With time, fibrin can accumulate, platelets aggregate, and neutrophils infiltrate. Alveolar epithelial damage can occur secondary to endothelial cell degeneration or as a primary response to a toxin. Degeneration and

necrosis of type I pneumocytes allows leakage of fluid into the alveolar lumen. Type I pneumocytes have increased cytoplasmic space with dilated cytocavitary networks, membrane fragmentation, and release from the basement membrane (Fig. 21.6). **Ozone**, for example, damages alveolar ducts and terminal bronchioles inducing type II cell hyperplasia and senescent rats are more susceptible to damage than adults.[39] Acute exposure to air pollutants can damage alveolar epithelium resulting in necrosis.

Acute Exhalant Injury

Substances associated with exhalation **pulmonary edema** include kerosene, turpentine, furniture polish, and lighter fluid. Their toxic components belong to the same group of aliphatic and aromatic hydrocarbons. Oral ingestion causes pulmonary edema and vascular damage during elimination via the lung (hydrocarbon pneumonitis). Pulmonary edema and pneumonitis can result from exhalation of circulating rodenticides and other chemical toxins that are eliminated in the respiratory tract. Striking and usually fatal pulmonary edema follows oral ingestion of the rodenticide **alphanaphthathioruea (ANTU)**.

Pulmonary Vascular Injury

When pulmonary capillaries are injured by toxins there is an immediate constriction of venules that initiates the process of pulmonary edema. Inhalation of fumes from host smoke and toxic chemicals is among

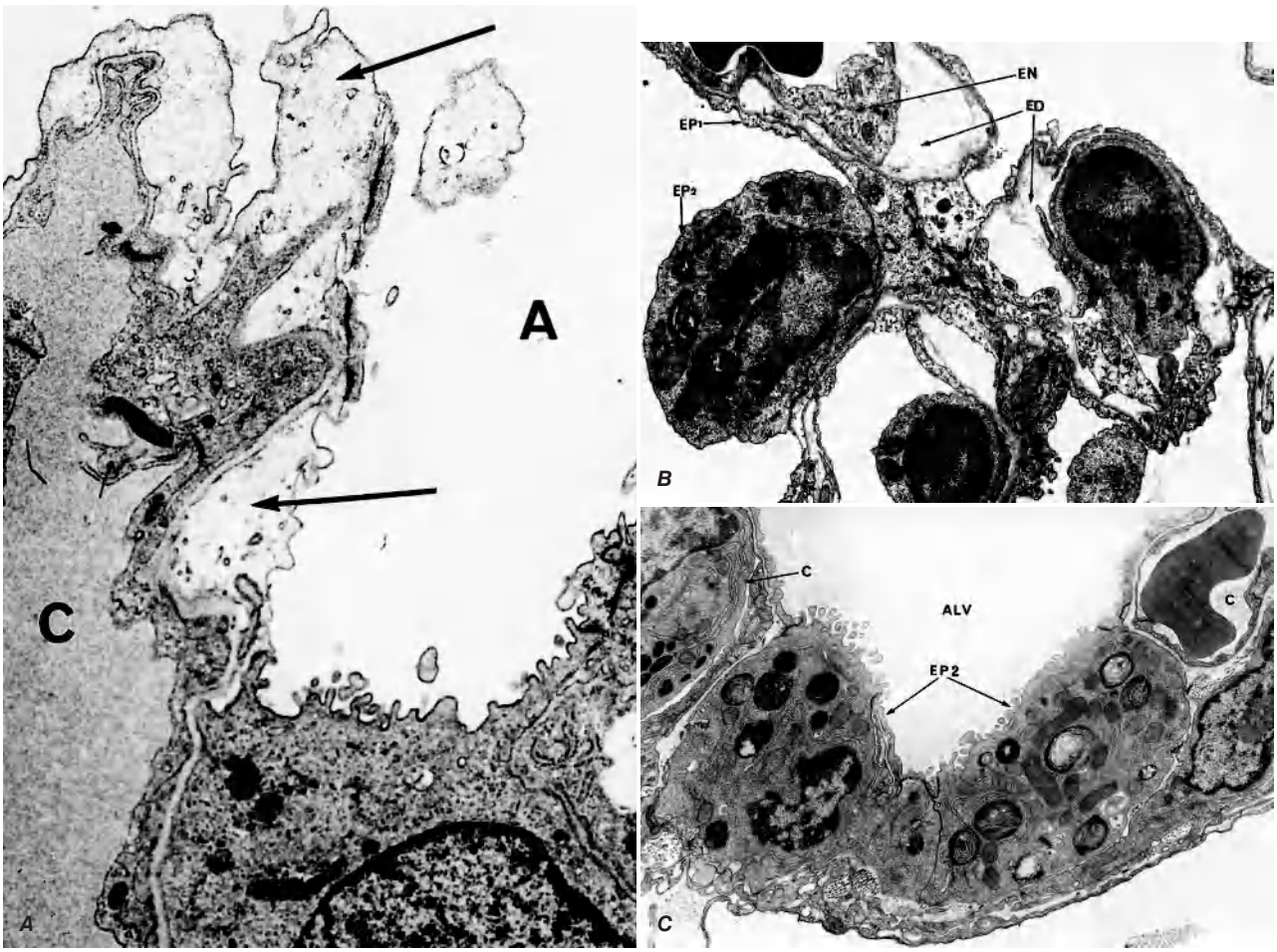


Fig. 21.6 **Oxygen toxicity**: acute (3 days at 95% oxygen), mouse. **A**. **Acute injury**: type I cell has markedly expanded cytoplasm that is pale due to cytoplasmic edema (*arrows*). Alveolar lumen (*A*), capillary lumen (*C*). **B**. **Acute injury**: endothelial cells (*EN*) with moderately expanded cytoplasm with edema (*ED*) in interstitial areas. Type I (*EP1*) and type II (*EP2*) epithelial cells are normal. **C**. **Recovery**: oxygen removal for 2 days. Hyperplastic type II cells (*EP2*) lining the alveolar septal wall of the alveolar lumen (*ALV*) and bordered by two capillaries (*C*). The capillary at left is lined by an endothelial cell (*arrow*) and the capillary at right contains an erythrocyte. (Micrograph: IYR Adamson, *Lab Invest* 30:35, 1974.)

the most common causes of injury. In the early phases of the reaction, histamine and other vasoactive substances exert a rapid but brief effect. Interendothelial gaps occur in bronchiolar venules. The pathogenesis of more severe lesions is sustained by progressive vascular injury. Fibrin polymerizes in the edema fluid, obstructs the lymphatic outflow, and seals alveolar wall pores. Fibrinolysis releases fibrin degradation products that cause increased capillary permeability and neutrophil exudation.[40] Recent work suggests that alveolar septal vascular injury differs between those endothelial cells lining vessels within alveolar septae and extra-alveolar vessels.[41] Calcium entry into endothelial cells induced by store-operated transient receptor potential channels causes gap formation in extra-alveolar vessels, whereas calcium entry mediated by transient receptor potential vanilloid (TRPV4) induces barrier disruption in the endothelial cells of the alveolar septae. Activation of extra-alveolar endothelium leads to fluid accumulation in perivascular cuffs, which has little impact on alveolar gas exchange. In contrast, disruption of the vulnerable alveolar septal barrier mediated by TRPV4, leads to alveolar flooding and would impair gas exchange as occurs in acute lung injury.

Toxins in anthrax, staphylococcal food poisoning, endotoxins, and other microbial toxic disease produce a pattern of injury that resembles the acute inhalant toxicities. Active oxygen radicals cause major damage in ischemia, radiation, cigarette smoke, and other agents. **Acute respiratory distress** is characterized by diffuse inflammation of the lung parenchyma secondary to infection, injury or acute illness. The triggering insult results in release of cytokines and other inflammatory mediators that trigger vascular leakage, neutrophil infiltration resulting in alveolar damage and hyaline cast formation (polymerized fibrin with seroproteinaceous fluid).

Furans such as **ipomeanol** in sweet potatoes (*Ipomoea* sp.) damaged by mold (*Fusarium solani*) are associated with acute interstitial pneumonitis in cattle fed moldy sweet potatoes. Pulmonary endothelium lining capillaries and small veins is the primary site of injury. Metabolism of the furans to highly reactive metabolites by the cytochrome P450 mixed function oxidase system of Clara cells and endothelial cells is responsible for toxicity.[42,43]

Administered intravenously as an anti-tumor agent, **bleomycin** produces **endothelial damage** in the alveolar wall during its passage from the bloodstream into the alveolus. Endothelial cells swelling and separation cause movement of protein-rich fluid into the interstitium and subsequent slowly progressive fibrosis of the wall of human and animal models.

Vascular leak syndrome is caused by excessive administration of **interleukin-2** and is characterized by severe pulmonary edema with endothelial cell damage, interstitial edema, alveolar septal thickening and exudation of plasma proteins into the alveolus. Extensive infiltration of lymphocytes and macrophages is associated with these changes. Cytotoxic T lymphocytes contact endothelial cells and type II epithelial cells to induce cytopathic effects.[44]

Chronic Inhalant Injury

Pulmonary Fibrosis

Diffuse pulmonary fibrosis may result from inhalation of numerous types of dusts (asbestos, silica, silicates) or expiration of toxic substances that cannot be metabolized by the lung. Prolonged low levels of noxious chemical in inspired air produce slow progressive degenerative changes accompanied by extensive diffuse fibroplasia of the alveolar wall interstitium. Electron microscopic analysis of human lung biopsy specimens from various chronic pulmonary fibrotic diseases have characterized the massive deposition of collagen, and marked deposition of basement membranes and laminin.[45,46] Pulmonary fibrosis is a general response to both vascular and epithelial toxins. It is detrimental to gaseous exchange due to the formation of a physical barrier, which widens the distance between the alveolar lumen and the vascular capillary. With epithelial injury, type II cells proliferate to covered damaged regions and fibroblasts within the alveolar septum proliferation and release extracellular matrix proteins as a protective response. With persistent injury, fibroblastic proliferation and extracellular matrix deposition also persist.

Early phases of aerogenic toxicity involve vacuolation and other degenerative changes in membranous pneumocytes and capillary endothelium. Hyperplasia of type II pneumocytes and epithelization occur as reparative processes. If toxicity continues there is progressive deposition of glycosaminoglycans, basement membranes, collagen, and, in some cases, calcium crystals.

Although chronic inhalation of environmental contaminants may produce episodes of acute pneumonitis and upper respiratory disease, the long-term problems is an increased thickness of the blood-air barrier. In photochemical smog, the principal causes are ozone and oxidant gases; in industrial smogs, sulfur compounds and particulate matter. Long-term exposure of dogs to air pollutants (auto exhaust and sulfur oxides) results in two important lesions: air space enlargement, especially in proximal acinar regions, and hyperplasia of nonciliated bronchioles.[47,48] These inhalants tend to break down the bronchiolar epithelial barrier by disrupting intercellular tight

junctions, which increases the absorption of toxins from airway to bloodstream.

Pulmonary Mineralization

Diffuse pulmonary mineralization (pulmonary microlithiasis, pumice lung) occurs, rarely, in lungs of animals that have eaten excessive vitamin D for prolonged periods in improperly formulated diets, ingested rodenticides, or calcinogenic plants. The lungs at necropsy are large, do not collapse, and have a granular, gritty feeling. Microscopically, there are innumerable calcified concretions or **calcospheres** in the alveolar wall throughout the lung. Diffuse mineralization induces a slowly progressive interstitial fibrosis and can be associated with macrophage infiltration. Mineralization is associated with expression of growth factors, matrix proteins, and bone-related proteins such as osteocalcein, osteopontin, and osteonectin.[49] Chronic renal failure (uremia) can also be associated with lung mineralization.

Inhalant Gases

High concentrations of inhaled gases such oxygen, ozone, sulfur dioxide, and hydrogen disulfide can cause acute toxicity (see acute injury), but lower concentrations inhaled over time, which are present in ambient air, smog, and polluted air, also damage lung.

Ozone

Ozone (O_3), a major oxidant of photochemical smog, can activate cytochrome P450-mediated metabolism in pulmonary epithelium. Alveoli in the proximal acinus of the lungs are primary sites of ozone injury. Slight increases in air-blood barrier thickness in rats occur after 90 days of exposure to 0.2 ppm.[50] Ozone stress initiates acute perturbations of surfactant membranes.[51]

Reactions to ozone differ among species. In the rat, 0.8 ppm causes thickening of alveolar walls and infiltration of the lung by leukocytes. The pulmonary acinus of the rat has well-developed terminal bronchioles that open directly into alveolar ducts. In contrast, the rhesus monkey has very short, poorly developed terminal bronchioles, whereas respiratory bronchioles are long and branching. The inflammatory response and hyperplastic epithelial changes in primate lungs are most severe in proximal portions of respiratory bronchioles and decrease progressively going distally.

Sulfur Dioxide

Sulfur dioxide (SO_2) is a significant air pollutant in industrial areas that causes loss of cilia on short-term experimental exposure at 100 ppm. Brief exposures of humans and dogs to such levels induce only slight increases in airway resistance. Cilia are also susceptible to low levels of ozone and nitrogen dioxide. Exposure to these gases causes bronchiolar cilia to become blunted and broken. Among rodents, mice have the lowest tolerance to SO_2, and rats the highest.[52] Exposure to 400 ppm SO_2 caused death in 6 hr of 22 of 30 rats; lesions were patchy areas of pneumonia, and there were increased numbers of pathogenic bacteria in the respiratory tract. Microscopically, changes in epithelial cells included deciliation, vacuolation, and pyknosis, and desquamation of necrotic cells into alveoli.

Hydrogen Sulfide

Hydrogen sulfide gas (H_2S) is produced in large amounts in farm slurries and pit silos, and workers may be overcome by heavy concentrations of gas in enclosed spaces. H_2S, like HCN, inhibits mitochondrial cytochrome oxidase, and death occurs suddenly without overt lesions of disease. H_2S, the dominant toxic component in natural gas emissions from petrochemical plants, can cause lethal toxicity during exposure to large concentrations. Pulmonary edema is the most common finding in humans killed in these accidents and in rats.[53]

Dibasic Ester Solvents

Dibasic ester solvent ("dibasic esters") is a solvent mixture of dimethyl adipate, dimethyl glutarate, and dimethylsuccinate that is utilized in the paint industry. Exposure to fumes from these chemicals has been implicated in human toxicity. Rats exposed to vapors for more than 90 days develop degeneration of sustentacular cells and sensory cells of the olfactory epithelium of the posterior nasal cavity (with no damage to the respiratory epithelium of the anterior region).[54]

Cigarette Smoke

Cigarette smoke damages epithelial cells of the airways to cause both acute and chronic injury (Table 21.2). Cigarette smoke induces small airway disease characterized by macules with fibrosis, muscular hyperplasia, infiltrates of lymphocytes, and mucous metaplasia.

Chronic emphysema is a permanent, abnormal enlargement of distal air spaces caused by destruction

Table 21.2 Pulmonary environmental toxins.

Toxicant	*Comment*	*Reference to ultrastructural pathology*
Alpha-naphthyl thiourea	Lung	**Cunningham**, *J Pathol* 106:25, 1972 (rat); **Fantone**, *Lab Invest* 50:703, 1984 (rat); **Meyrick**, *Br J Exp Pathol* 53:347, 1972 (rat); **Michel**, *Am J Pathol* 119:474, 1985 (dog)
Ammonia	Trachea	**Broderson**, *Am J Pathol* 85:115, 1976 (rat)
Ammonium sulfate	Pulmonary edema	**Hayes**, *J Pathol* 100:281, 1970†
Asbestos	Lung	**Adamson**, *J Pathol* 152:99, 1987 (mouse); **Adamson**, *J Pathol* 152:109, 1987 (mouse); **Bowden**, *J Pathol* 147:257, 1985 (mouse);† **Brody**, *Am J Pathol* 134:133, 1989 (rat);† **Chang**, *Am J Pathol* 131:156, 1988 (rat); **Donaldson**, *Mutat Res* 553:5, 2004; **Dodson**, *Ultrastruct Pathol* 21:321, 1997 (human); **Ghio**, *Antioxid Redox Signal* 10:371, 2008 (human); **Manning**, *Am J Respir Cell Mol Biol* Jan. 10, 2008; **Oghiso**, *Br J Exp Pathol* 65:467, 1984 (rat)
	Crysotile	**Brody**, *Lab Invest* 49:468, 1983 (membranes);* **McGavran**, *Am J Pathol* 136:695, 1990 (rat)
	Crocidolite	**Adamson**, *J Pathol* 152:99, 1987 (mouse); **Adamson**, *J Pathol* 152:109, 1987 (mouse); **Bowden**, *J Pathol* 147:257, 1985 (mouse); **Holley**, *Am J Pathol* 141:475, 1992 (rat); **Miller**, *J Pathol* 124:39, 1978 (rat)
β-Aminopropionitrile		**Das**, *Am J Pathol* 101:711, 1980 (rat); **Kida**, *Am J Pathol* 101:693, 1980 (rat)
Cadmium	Lung	**Straus**, *Am J Pathol* 84:561, 1976 (rat)
Carbon monoxide		**Brugge**, *Environ Health* 6:23, 2007; **Salvi**, *Paediatr Respir Rev* 8:275, 2007; **Zhang**, *Environ Health Perspect* 115:848, 2007
Carbon nanotubes	Lung	**Bergamaschi,** *Int J Immunopathol Pharmacol* 19:3, 2006; **Shvedova,** *Am J Physiol Lung Cell Mol Physiol* 289:698, 2005 (mouse)
Cotton smoke	Lung	**Abdi**, *Am Rev Respir Dis* 142:1436, 1990 (sheep)
Dibasic ester	Nose	**Trela**, *Exp Mol Pathol* 56:208, 1992 (nxplants)*
Diesel exhaust		**Plopper**, *Lab Invest* 49:391, 1983 (cat)
Formaldehyde		**Monticello**, *Am J Pathol* 134:515, 1989 (monkey)
Glass fibers		**Lee**, *Lab Invest* 40:123, 1979 (rat)
Hydrogen sulfide		**Lopez**, *Vet Pathol* 25:376, 1988 (rat); **Prior**, *Toxicol Pathol* 18:279, 1990 (rat)
Hydroperoxide		**Anderson**, *Arch Pathol Lab Med* 100:154, 1976 (rat)
Hydrochloric acid	Gill	**Brunelli,** *J Exp Zool* 303A:946, 2005 (fish larvae)
Lead		**DeVries**, *Lab Invest* 48:35, 1983 (rabbit)
Marijuana smoke	Lung	**Mann**, *Lab Invest* 25:111, 1971 (macrophages)*
Mercury	Fish gill	**Daoust**, *Vet Pathol* 21:93, 1989 (trout)
Nanoparticulates		**Mühlfeld**, *Part Fibre Toxicol* 4:11, 2007 (rat)
Nitric oxide		**Brugge**, *Environ Health* 6:23, 2007; **Castillo**, *Exp Cell Res* 313:2680, 2007 (human); **Mercer**, *Res Rep Health Eff Inst* 88, 1999 (rat); **Salvi**, *Paediatr Respir Rev* 8:275, 2007; **Zhang**, *Environ Health Perspect* 115:848, 2007
Nitrogen dioxide	Bronchioles	**Brugge**, *Environ Health* 6:23, 2007; **Evans**, *Am J Pathol* 123:126, 1986 (rat); **Forster**, *Br J Exp Pathol* 66:193, 1986 (rat, hamster);† **Gordon**, *Am J Pathol* 125:585, 1986 (hamster);† **Salvi**, *Paediatr Respir Rev* 8:275, 2007
Organochlorines	Gill	**Evans**, *Environ Health Perspect* 71:47, 1987 (fish)
Oxygen		**Adamson**, *Arch Pathol* 90:463, 1970 (mouse); **Adamson**, *Lab Invest* 30:35, 1974; **Adamson**, *Libr of Cong* 90-3179:163 (mouse); **Bonikos**, *Am J Pathol* 85:263, 1976 (mouse); **Crapo**, *Lab Invest* 39:640, 1978 (rat); **Jones**, *Am J Pathol* 121:212, 1985 (rat); **Ludwin**, *Lab Invest* 31:425, 1974 (mouse); **Pappas**, *Lab Invest* 48:735, 1983 (mouse); **Resnick**, Lab Invest 31:665, 1974;* **Swartz**, *Int Rev Cytol* 35:321, 1973 (review)
Ozone	Lung	**Barry**, *Lab Invest* 53:692, 1985 (rat); **Boorman**, *Lab Invest* 43:108, 1980 (rat); **Castleman**, *Lab Invest* 29:310, 1973 (rat); **Eustis**, *Am J Pathol* 105:121, 1981 (primate); **Harkema**, *Am J Pathol* 143:857, 1993 (monkey); **Salvi**, *Paediatr Respir Rev* 8:275, 2007; **Schwartz**, *Lab Invest* 34:565, 1976 (rat); **Stephens**, *Am J Pathol* 74:31, 1973; **Vincent**, *Am J Pathol* 146:1008, 1995 (rat)
	Trachea	**Nikula**, *Am J Pathol* 131:373, 1988 (rat)

Table 21.2 *Continued*

Toxicant	*Comment*	*Reference to ultrastructural pathology*
Paraquat		**Fukuda**, *Virch Arch B* 58:27, 1989 (monkey); **Hampson,** *Br J Exp Pathol* 69:57, 1988 (dog); **Nakayama**, *Virch Arch B* 61:389, 1992 (rat); **Dinis-Oliveira**, *Crit Rev Toxicol* 38:13, 2008
Particulate matter		**Adamson**, *Toxicol Appl Pharmacol* 157:43, 1999 (mouse); **Gilmour**, *Environ Health Perspect* 109:619, 2001 (mouse); **Zhang**, *FEBS Letters* 581:5315, 2007*
Silica	Pneumoconiosis	**Adamson**, *Am J Pathol* 117:37, 1984 (mouse); **Allison**, *J Exp Med* 124:141, 1966;* **Berry**, *Am J Pathol* 93:27, 1974 (guinea pig); **Brambilla**, *Am J Pathol* 96:149, 1992;† **Chong**, *Radiographics* 26:59, 2006; **Churg**, *Ultrastruct Pathol* 24:353, 2000 (human); **Dauber**, *Am J Pathol* 101:595, 1980
Solanum glaucophyllum	Toxic plant	**Barros**, *Vet Pathol* 43:494–499, 2006
Sulfur dioxide	Lung: pulmonary fibrosis	**Charan**, *Am Rev Respir Dis* 119:555, 1979 (human); **Meng**, *Inhal Toxicol* 19:543, 2007 (mouse)
	Trachea	**Asmundsson**, *Lab Invest* 29:41, 1973 (rat, hamster)
Titanium dioxide		**Baan**, *Inhal Toxicol* 19:213, 2007 (rodent); **Elo**, *Arch Pathol* 94:417, 1972 (human)
Tobacco smoke	Lungs	**Boucher**, *Lab Invest* 434:94, 1980 (guinea pig); **Hutt**, *Carcinogenesis* 26:1999, 2005 (mouse); **Oulton**, *Am J Pathol* 138:195, 1991 (mouse); **Simani**, *Lab Invest* 31:75, 1974 (guinea pig)
	Alveolar macrophages	**Mann**, *Lab Invest* 25:111, 1971;* **Pratt**, *Lab Invest* 24:331, 1971 (human)
	Tracheal explant	**Hobson**, *Am J Pathol* 139:573, 1991*

*In vitro study.
†Animal model.

of the alveolar wall. It is a consequence of chronic bronchitis from heavy cigarette smoking. As lung tissue is broken down, elastin fragments are liberated that are chemotactic for macrophages, possible via lysyl-derived cross-links. Models of chronic emphysema can be produced by injecting enzymes that destroy connective tissue collagen and elastin (papain, elastase, lathyrogens).

Carbon Monoxide

In **acute CO toxicity**, carboxyhemoglobin in the blood causes brain edema and other changes that result from systemic hypoxia; ultrastructural lesions are those of anoxia. The slowly developing hypoxia of **chronic poisoning** leads to neuronal hypoxic injury with the most severe injury in the basal ganglia and lenticular nuclei. Demyelination may develop in cerebral white matter. Renal, cardiac and hepatic injury develop from sustained hypoxia. Like NO, CO dilates blood vessels. It does so by stimulating guanylyl cyclase, the enzyme that produces cyclic GMP, in vascular smooth muscle cells. Endogenous CO is made in many tissues by the enzyme heme oxygenase, which breaks down heme. In the brain, a different hemo oxygenase produces CO that may serve as a neurotransmitter.

Exogenous Particulates

The lung can respond in limited ways to environmental factors and **particulates**, but as reviewed by Green, lesions in human lungs in response to environmental factors can be (1) agent-specific (e.g., silicotic nodules), (2) generic (small airway disease) and caused by a variety of agents (e.g., ozone, cigarette smoke, mineral dusts), and (3) site-specific (centriacinar lesions with ozone and coal mine dust).[55] The above are dependent upon lung geometry, ventilation patterns, and physicochemical properties of the inhaled material. These responses can be similar, or very different from animals, especially the rat.

Chronic inhalation of carbonaceous and mineral dust particles in the ambient air can be of little consequence but result in the aggregation of macrophages containing dust particulates in and adjacent to bronchioles and alveoli as well as the pleura. Exogenous particulate substances can lead to fibrotic or nonfibrotic lung disease known as **pneumonconiosis**. Fibrotic disease is caused by silicosis, coal worker pneumoconiosis, asbestosis, berylliosis, and talcosis; however, some forms of pneumonoconiosis are nonfibrotic, including anthracosis (caused by coal dust pigment), stannosis, and baritosis, and have little tissue reaction. Cigarette smoke, carbon, and fibrogenic dusts can induce centriacinar **macules**

(macrophages with pigment) with surrounding emphysema and, if prolonged, small airway disease.

Nodules of macrophages form around silicates and silica along with fibrosis and lymphocytes and plasma cell infiltrates. Progressive massive fibrosis, termed complicated pneumoconiosis, can occur in association with silica, coal mine dust, silicates and carbon black. Diffuse interstitial fibrosis occurs in response to asbestos, silica, silicates, and coal dust and is characterized by deposition of collagen, elastic fibers, fibroblasts, and smooth muscle cells that extend between alveolar walls; cysts can form. Idiopathic forms of pulmonary fibrosis also occur in humans as well as cats and West Highland White Terrier dogs.

Alveolar Lipoproteinosis

Alveolar lipoproteinosis is rare in humans and seen more commonly in rats. It is a diffuse lung lesion characterized by the intermittent but progressive accumulation of lipid-rich proteinaceous material within alveoli in the absence of a prominent cellular inflammatory response. It is associated with inhalation of oily mists, lipids, resins, silicates, and solvents. The pathogenesis involves edema, overproduction of phospholipids by type II pneumocytes, and desquamation of membranous pneumocytes. Damage to basement membranes and failure of lung clearance occur. Endogenous forms of lipoproteinosis can be secondary to amphophilic drugs in animals and aminodarone and chlorphentermine in humans.

The ultrastructural analyses of particles and crystals in tissue including the size and nature of the crystal, data gathered from x-ray dispersal analysis, and scanning electron microscopy are all useful in analysis of crystals on lumenal surfaces. Some crystals are water soluble and are removed during routine fixation. Often crystals are so brittle that they fracture during sectioning and drop from the section; this can be overcome by cutting very thick sections.

Silicates

Crystalline silica is a common component of the earth's crust and exists principally as silica dioxide (SiO_2). The crystalline form has four oxygen molecules forming three isoforms: quartz, tridymite, and cristobalite. Acute silicosis occurs in individuals exposed to small aerosolized silicate particles for a few months and can result in dyspnea, fever, cough, weight loss, and death. Inhalation of large amounts of silicate dust, largely complex silicates and aluminum-potassium silicates, leads to an acute inflammation. In chronic exposure to silicates, patients may have **nodules** (granulomas) composed of large foamy macrophages, often with necrotic centers and peripheral multinucleate giant cells. Macrophages contain refractile crystalline particles, usually smaller than 1 μm, both free in the cytoplasm and within lysosomes. X-ray dispersal analysis reveals the chemical nature of these silicates.[56] Silica exists in dust in amorphous and crystalline forms (Fig. 21.7). The crystalline forms of silica are particularly important in induction of fibrosing alveolitis in the the lung. Following phagocytosis by alveolar macrophages, necrosis occurs due to damage by crystals of 0.5 μm or else to lysosomal membranes. Hydrolytic enzymes leak into the interstitium of alveolar septa and produce lysis. Silica that cannot be degraded results in prolonged destruction of macrophages. Silica and necrotic debris are finally walled off by a granulomatous reaction, and collagen production throughout the lung is marked.

Glass Fibers

These include **glass wool fibers** used in manufacture of acoustic ceiling materials, air filters, thermal insulation and filter paper, and **glass textile fibers** used in fabrics, insulation tape, and plastic reinforcements. Human exposure to these has not resulted in chronic



Fig. 21.7 Crystals: silicates. Crystalline silicates from the lung of a dog with acute hemorrhagic pneumonitis.

lung disease or carcinogenesis. Aerosolized into rodent lungs, there is no significant fibrosis.[57] Large macrophage-filled deposits develop in alveoli and regional lymph nodes. In acute lesions there may be feruginous bodies mixed with membrane profiles that resemble those in alveolar proteinosis.

Asbestos

Asbestos fibers, formed from a family of **magnesium silicates**, have a spectrum of toxicity that includes **amphibolic asbestos** (crocidolite and amosite types, with great carcinogenicity and fibrosing potential) and **chrysotile asbestos**, a serpentine fiber with less fibrotic or carcinogenic activity. **Chrysotile asbestos** is the most commonly used naturally occurring fibrous mineral and accounts for 95% of asbestos present in buildings in the United States, while crocidolite asbestos is not as prevalent having been banned in the United States in the mid-1980s and in Japan in 1995.

Asbestos in humans is associated with chronic inflammatory lesions in the lungs (asbestosis), with the lethal neoplastic mesothelioma, and other cancers. Pulmonary macrophages form the initial inflammatory response. Inhaled asbestos activates complement-derived chemotactic activity on alveolar linings to attract monocytes, especially at alveolar duct bifurcations and induces fibrosis. The fibers are poorly degraded and incite a persistent inflammatory reaction with intense oxidative radical formation and lipoperoxidation, which contribute to toxicity, fibrosis, and carcinogenicity.

Asbestos fibers can enter epithelial cells and result in epithelial necrosis (Fig. 21.8) of epithelial cells. **Asbestos bodies** develop in the cytoplasm of macrophages and other cells. They are laminar, dense structures composed of asbestos particles surrounded by an iron-rich layer of ferroproteins (see Fig. 21.4). The unique layered structure involves fibrils and small tubular structures that radiate outward from the asbestos to create an organelle-free halo effect. In some studies, the membranes surrounding the asbestos body continue with the plasma membrane of the macrophage, suggesting that the membrane entwines itself around the asbestos crystal to form myelin figures.

Using electron microscopic analysis of asbestos bodies, the various elemental components have been identified. Long asbestos fibers are prone to produce asbestos bodies. Asbestos bodies usually develop in granulomas of macrophages and multinucleate giant cells with few plasma cells, lymphocytes, or monocytes. They are especially dense when iron-rich. Iron may be derived from breakdown of erythrocytes in their association with the surface of asbestos. Iron homeostasis is altered by asbestos and free radical generation along with fibrosis and cell proliferation increase with increasing concentration of iron complexed onto the surface of the fibers.[58]

The term **ferruginous body** tends to be used for spicular aggregates of complex crystals found in tissue when the exact nature of the material is not known; that is, a number of different dusts such as fibrous glass, aluminum silicate, silicon carbide, and magnesium hydroxide (brucite) can form ferruginous bodies. Most ferruginous bodies are nucleated on asbestos, almost always on amphibole asbestos and chrysotile asbestos is rarely encountered. Ferruginous bodies persist following death, embalmment, and burial.[59] In rats, both crocidolite and chrysotile asbestos fibers induce fibrosis and macrophage aggregates at alveolar duct bifurcations, while crocidolite fibers caused subpleural macrophage aggregates.[60] Ultrastructurally, crocidolite was present in alveolar macrophages, whereas chrysotile fibers were seen in the vasculature. Asbestos stimulates mitosis when inhaled, either directly or via macrophage factors.[61] Asbestos fibers also induce rapid cellular proliferation in small pulmonary blood vessels with increased DNA synthesis in endothelial cells and smooth muscle cells of arterioles and venules near bifurcations, the sites of initial fiber deposition.[62] Asbestos induces MEK1 signaling cascade, which triggers both proliferation and fibrosis.[63] Asbestos fibers have been found within endothelial cells.[64]

Atapulgite, a fibrous clay used as a substitute for asbestos in petroleum and plastic industries, and as a resorptive agent in oral antacid solutions, is a **magnesium silicate** with approximately 6% iron (as is amphibolic asbestos fibers). Asbestos markedly enhances the chronic pulmonary effects of cigarette smoke. The increase in uptake of long asbestos fibers by metaplastic squamous mucosa contributes to the synergism between asbestos and cigarette smoke as the cause of bronchiogenic neoplasms.[65]

Nanoparticles

Rodents exposed to **carbon black** and **titanium oxide** have increased risk for the development of cancer. Prolong inhalation of nanoparticles leads to chronic build-up and continual inflammation at the alveolar level. This inflammatory state is characterized by the formation of reactive oxygen species, cell injury, cell proliferation, fibrosis, DNA mutations and cancer. Ultrastructurally, nanoparticles can sometimes be difficult to distinguish from organelles or other structures. Therefore, high resolution transmission electron microscopy and immunolabeling are requirements for assessment. In mice, single-walled carbon nanotubes

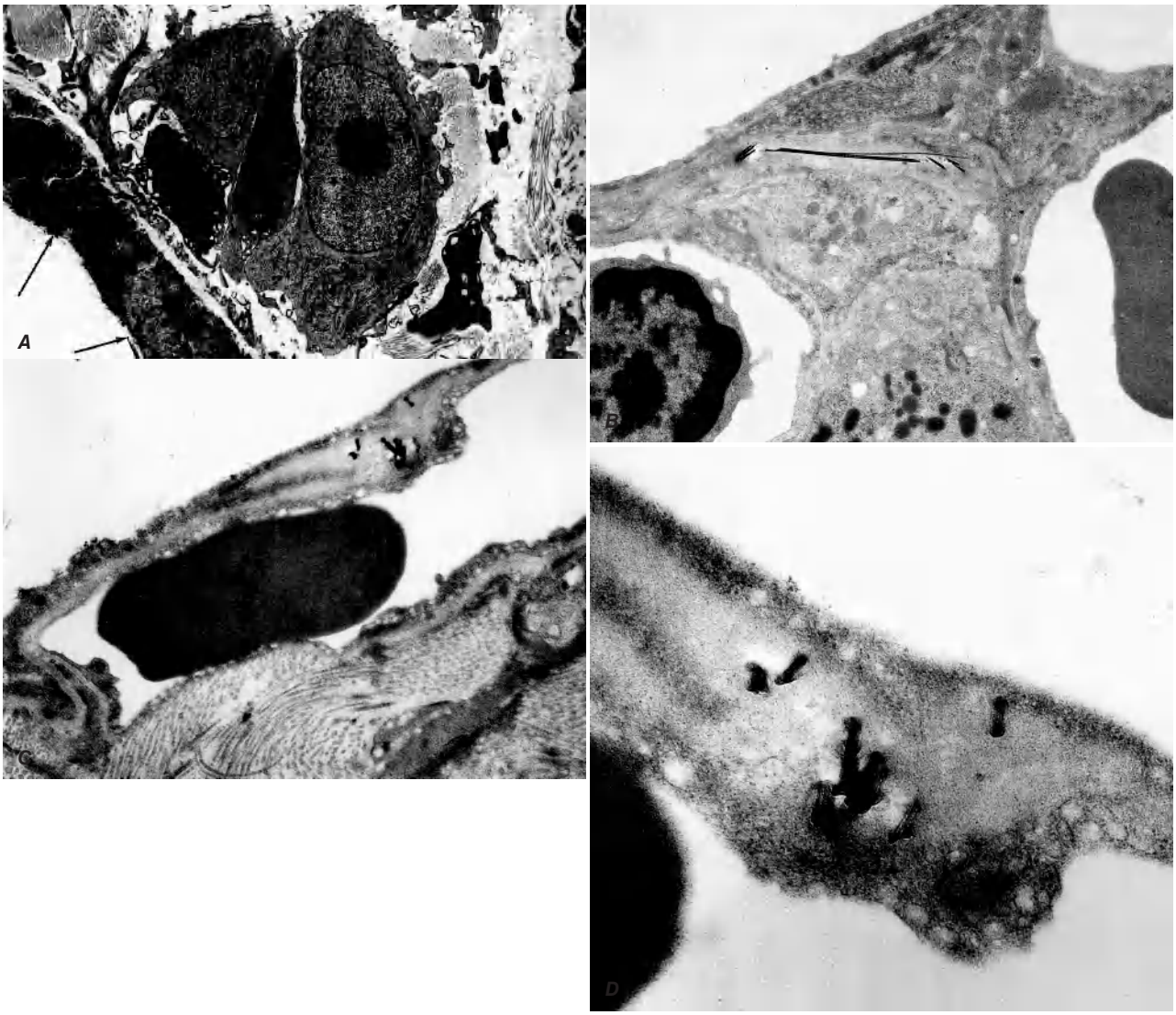


Fig. 21.8 Fibers: asbestos. A. Asbestos-induced necrosis of bronchiolar epithelium (*arrows*) in mice. Alveolar lumen contains cell debris, fibrin, asbestos, and a neutrophil. Subjacent are fibroblasts with interstitial edema expanding the area and collagen fibrils. (Micrograph: D. H. Bowden and I. Y. R. Adamson, *J Pathol* 147:257–267, 1985.) **B. Asbestos fibers**: fibers in the sub-epithelial connective tissue (*center*). Longest fibers have fragmented into shorter and thinner fibrils, which is characteristic of chrysotile. Capillary lumens: RBC (*right*) and monocyte (*left*). **C. Alveolar-capillary membrane** (ACM) at the top, an RBC in the capillary lumen and connective tissue, largely collagen, on the bottom. Chrysotile fibrils internalized by the alveolar epithelium are present in the basement membranes of the ACM. **D. Chrysotile fibers**: enlargement of C. (Micrographs B–D: A. Brody.)

induced two distinct phenotypes: (1) granulomas with hypertrophied epithelial cells, and (2) interstitial fibrosis and alveolar wall thickening. In contrast, ultrafine carbon black or crystalline silica (SiO_2) do not induce granulomas or alveolar thickening.[66]

Chronic Exhalant Toxicity

Paraquat

Of the bipyridal compound herbicides, paraquat most commonly causes toxicity; poisoning occurs by accidental ingestion or by smoking marijuana that has been sprayed to control illicit production. Acute human poisoning by a single large dose leads to **cardiomyopathy**, transient **neurologic signs**, and vague degenerative changes in the liver and kidney. Subacute injury is more common: here the target organ is the lung, regardless of route of entry. Necrosis of pneumocytes and progressively fibrosis of the alveolar wall occur during exhalation of paraquat during the process of respiratory elimination.

Paraquat evokes a slow, progressively fatal severe swelling and vacuolation of capillary endothelium and alveolar pneumocytes is followed by degenera-

tion, necrosis, and denudation, leaving foci of naked basal laminae in the alveolar wall. The wall becomes thickened with fluids with disorganization of collagen and ground substance. Type II pneumocyte hyperplasia develops as a reparative phenomenon but is inefficient in bridging damaged alveolar walls and insufficient to produce enough surfactant to maintain surface tension. Accumulation of macrophages and a few neutrophils in the wall is followed by collapse of the heavy, nonfunctional parenchyma.

In most cases the fatal outcome is **progressive pulmonary fibrosis** with extensive collagen deposition, fibroplasia, epithelization, and hyalin membrane formation. The heavy deposits of collagen and extracellular matrix in the alveolar wall are accompanied by proliferation of both type I and II pneumocytes, and often by metaplastic squamous cells. The mechanism of fibrosis is associated with secretion of proteolytic enzymes by inflammatory cells, direct actions of paraquat on fibroblasts, and delayed re-epithelialization.[67]

Chronic toxicity has been reproduced in monkeys given subcutaneous injections of 10 mg/kg body weight paraquat.[68] Paraquat is a powerful redox that fluxes from an oxidative to reduced state and oxidation of cellular NADPH with eventual depletion of NADPH. This results in the formation of superoxide anion and peroxynitrite; oxidation of cellular thiols; and damage to lipids, proteins and DNA.

Monocrotaline

Monocrotaline is a pyrrolidizine alkaloid metabolized by the liver to an active pyrrole, which can induce pulmonary hypertension characterized by hyperplasia of lung capillary endothelial cells and thickening of the tunia media. In human endothelial cells, monocrotaline pyrrole forms adducts with proteins with reactive thiols such as disulfide isomerase A(3), protein disulfide isomerase (PDI), and endothelial PDI in the plasma membrane, cytosol, endoplasmic reticulum, and mitochondria. Biochemically, the pyrrole induces Smad signaling and dysregulation of bone morphogenic protein signaling, which reduces caveoli, further affecting signaling.[42,43]

Bleomycin

Bleomycin is a chemotherapeutic drug that can damage lung endothelial and epithelial cells and cause acute injury. With time, type II cells repair areas of damage and there is increased fibronectin and collagen synthesis and deposition resulting in fibrosis (Fig. 21.9). Bleomycin hydrolase inactivates bleomycin in many tissues; however, this enzyme is present at low levels in lung and skin.

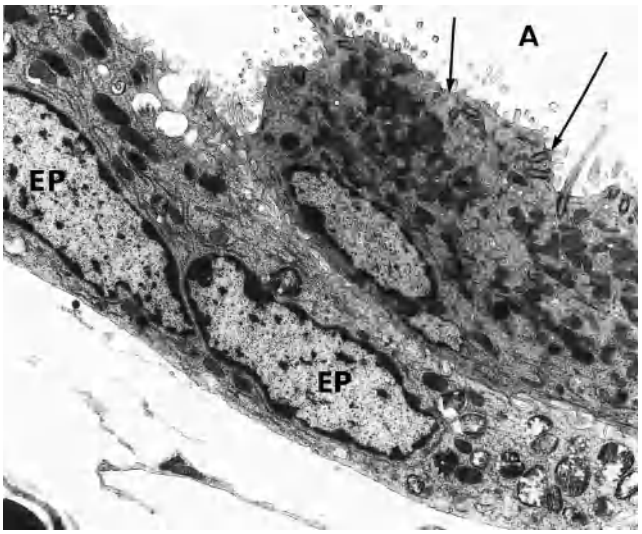


Fig. 21.9 Bleomycin. Bleomycin administration (20 mg/kg twice per week for 6 weeks) in mice induces type II epithelial cell (*EP*) hyperplasia and formation of a ciliated cell (*arrow*s) along the lumen of the alveolus (*A*). (Micrograph: I. Y. R. Adamson.)

Ethanol

Ethanol can affect ciliary beat frequency and also has numerous effects on lung epithelia, including impaired surfactant production, increased oxidant mediated necrosis of epithelial cells, increased oxidant and cytokine-mediated necrosis in alveolar epithelial cells, increased protein leakage across the alveolar barrier, increased activation of matrix metalloproteinases that degrade the septal matrix during endotoxemia, increased susceptibility to endotoxin-mediated damage, and increased transforming growth factor beta (TGF beta) within the alveolar space leading to increased permeability. Chronic alcohol exposure depletes glutathione and increases the relative expression of angiotensin II receptor expression potentiating oxidative damage, upregulates TGF beta leading to epithelial cell damage, and impairs GM-CSF signaling.[69] These alterations likely also occur in fetal lung to some degree in mothers that consume ethanol during gestation and one study has shown that lungs from lambs born from ewes receiving ethanol during gestation have reduced ciliary beat frequency and surfactant protein A production.[70]

Cationic Amphophilic Drugs

Lipoproteinosis can be secondary to cationic amphophilic drugs in animals and humans. Cationic

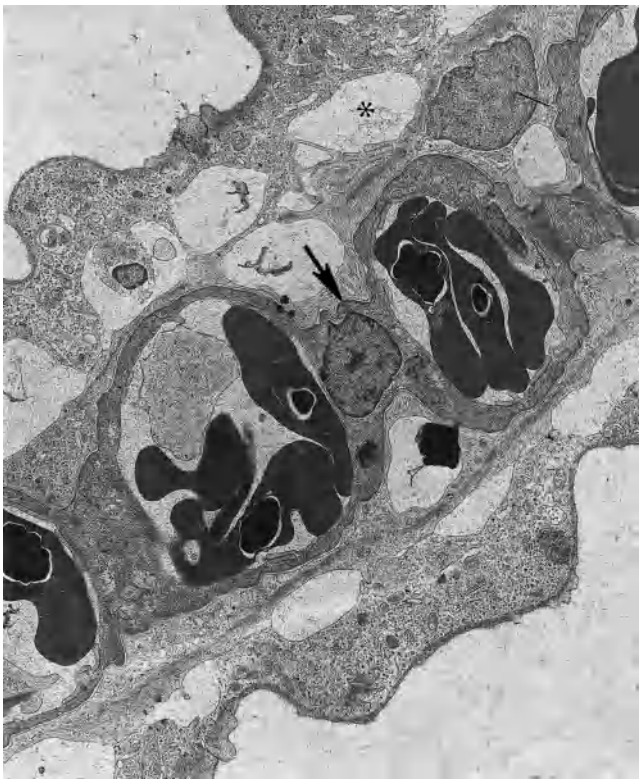


Fig. 21.10 Gill edema. (*): lamella of gill filament, fish. Capillaries are dilated. Pillar cell (*arrow*).

amphophilic drugs bind phospholipases of endothelial and epithelial cells and the complex inhibits phospholipase activity resulting in accumulation.

Comparative Respiratory Systems

The simplest lung (in the lungfish) occupies a position between fish and amphibia, and consists of two simple muscular tubes lined by capillaries. Proceeding up the phylogenetic scale there is progressive partitioning of this tube, resulting in double capillary beds. In amphibians and reptiles, the lungs are simple paired sacs, each with one major respiratory duct (bronchus). Gas exchange occurs not only through the lungs but through the skin and oral mucosa as well. In frogs, a thin continuous layer of epithelial cells overlies the heavy carpet of respiratory capillaries. These membranous pneumocytes lie between the capillaries and their thin squamous cytoplasmic extensions are stretched over the vascular walls. The avian lung contains intrapulmonary primary bronchus that subdivides into secondary bronchi that divide into the aircapillaries, which are tube-like structures and the site of gaseous exchange. The air capillaries intermingle closely with vascular capillaries and the avian lung has a very thin air-blood barrier.

Gills

Fish and larval amphibia utilize gills (branchiae) for gas exchange, ionic regulation, acid-base balance, and excretion of salt and nitrogenous wastes. Gas exchange can be accomplished through the epithelia of the pharynx, branchial cavity, and intestine of some species of stagnant swamp-dwelling fish.[71] Gills of the bony or teleost fishes consist of internal bony gill arches covered by an operculum. The respiratory unit in fish is the gill filament, attached to and projecting outward from the concave surface of the bony gill arch. Gill filaments are lancet shaped and contain a border of long respiratory (secondary) lamellae, extensions of specialized capillaries from the efferent branchial arteriole that are covered by simple, flattened, respiratory epithelium. The filament is lined by squamous pavement cells, goblet cells, neuroepithelial cells, accessory cells, and chloride cells (Fig. 21.10). Squamous pavement cells have microridges and epithelial cells contain many pinocytotic vesicles but few other organelles.[72,73] Phagocytic **pillar cells** lying between adjacent capillaries in the gill take up circulating particles.

Gills are also important in **water and electrolyte balance**.[74] Freshwater teleosts do not drink significant amounts of water but gain it by osmosis through gill lamellae. They require salts, which are actively taken in by absorptive chloride cells on the gills. Marine teleosts normally drink seawater, absorbing its salts into the blood. To maintain electrolyte levels, the gills actively transfer salt from blood to seawater via specialized excretory chloride cells on the gill lamellae. **Chloride cells** regulate water and ionic balance: α chloride cells are at the base of secondary gill lamellae in contact with basement membranes of the pillar capillary, and β chloride cells are in interlamellar regions. Ultrastructurally, chloride cells have large amounts of endoplasmic reticulum,[75,76] and repeating particles on the plasma membrane that extend into the cytoplasm. The outward transport of sodium is due to a Na^+-K^+-activated ATPase in the plasma membrane.

Fish are tolerant for long periods to **hypoxia** of low water oxygen levels due to a novel adaptive mechanism to hypoxia, the induction of genes for lysosomal lipid trafficking and degradation. Metabolic depression occurs via repression of genes in the TCA cycle, the electron transport chain, protein biosynthesis, and lysosomal lipid trafficking. There is enhanced expression of the monocarboxylate transporter and of the oxygen transporter myoglobin. **Lipoprotein lipase genes** (involved in Niemann-Pick disease and Wolman's disease), for enzymes that bind cholesterol and are involved in lysosomal lipid trafficking and degradation, are activated.[77]

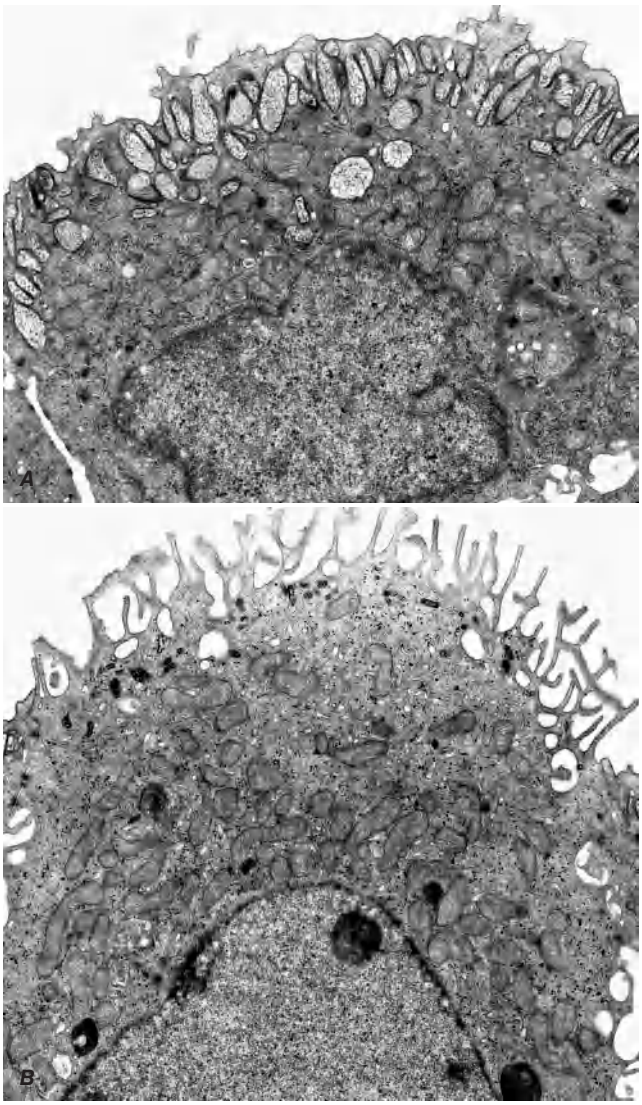


Fig. 21.11 Organochloride toxicity in gill. Organochloride after 48 hours. **A**. **Intercellular spaces** are widened with the formation of lacunae-like spaces with a pavement cell (PVC). Subjacent is a capillary with red blood cells. **B**. **Pavement cell** has numerous secretory granules (SG) in the subapical area and secretory vesicles (SV) near large lacunae-like spaces. (Micrograph: I. Bernabo, *Aquat Toxicol* 86:445, 2008.)

The **nonrespiratory gill surface** has columnar epithelium containing many goblet cells. Mucous hyperplasia with deposition of mucus on the gill follows injury. If prolonged, accumulations of **slime** may inhibit oxygen diffusion. Hyperemia, common in waters low in oxygen or excessively warm, intensifies the normal redness of gills. Fish respond to anoxia by dilation of lamellar capillaries, increased rapidity of inhalation, and wider opening of the operculae. **Infarction** of gills may be due to intravascular parasites of to gas emboli that form when fish are swimming in very warm water containing many plants. Excessive oxygen is produced and causes gas bubbles to develop and lodge in the vascular system.

Toxicity and the Gill

Branchiitis, or inflammation of the gills, is a response to some toxic injuries. Fish and amphibians are exposed to a wide variety of toxicants including organophosphates, petroleum compounds, organochlorides, carbamates, herbicides, acidification, nitrogenous compounds, heavy metal salts, and drugs present in human waste. Hyperemic and edematous lamellae are common in fish swimming in toxic water; for example, DDT toxicity. Leukocytes infiltrate the interstitial areas of the gill in DDT toxicity, causing purulent branchiitis. Ballooning of the lamellae results from accumulation of exudate.

Many environmental pollutants cause toxicity after heavy exposures. **Toxaphene** is a complex mixture of over 12 compounds formed by chlorination of camphene, a product of pine trees. In low concentrations in water, toxaphene causes stunting and skeletal deformaties in fish, the "broken back syndrome." Effects are attributed to vitamin D deficiency caused by excess utilization of vitamin C in detoxification. Metals, such as **copper**, cause filament epithelial cell damage that results in increased intercellular spaces, epithelial detachment from the basement membrane, and cell proliferation.[78] Even new generations of **organochlorines**, such as endosulfan, considered to be safer than DDT and Dieldrin, can cause damage to gill epithelium of *Bufo bufo* frog (Fig. 21.11).[79] Ultrastructural lesions include increased mucus production, formation of secretory vesicles and lamellar bodies, widening of intercellular spaces, and inflammatory cell infiltration.

Acidification of aquatic ecosystems is also damaging to gills. Low pH levels (4.5) result in keratinization of the filament of *Triturus italicus* larvae. Mitochondria-rich epithelial cells protrude and have increased microvillous length. In contrast, secondary lamellar epithelial cells are smaller and thin at low pH (Fig. 21.12).[80]

Swim Bladders

Air-filled **swim bladders**, which develop from evaginations of the foregut in teleost fishes, have a hydrostatic function. Gas enters the bladder hematogenously via a network of small arterioles and venules called the rete mirabilis (red body). Gas is reabsorbed by specialized epithelium[81] or, in fish that have a patent duct connected to the gut, is bubbled out the mouth. Toxic injury to the swim bladder results in inability to

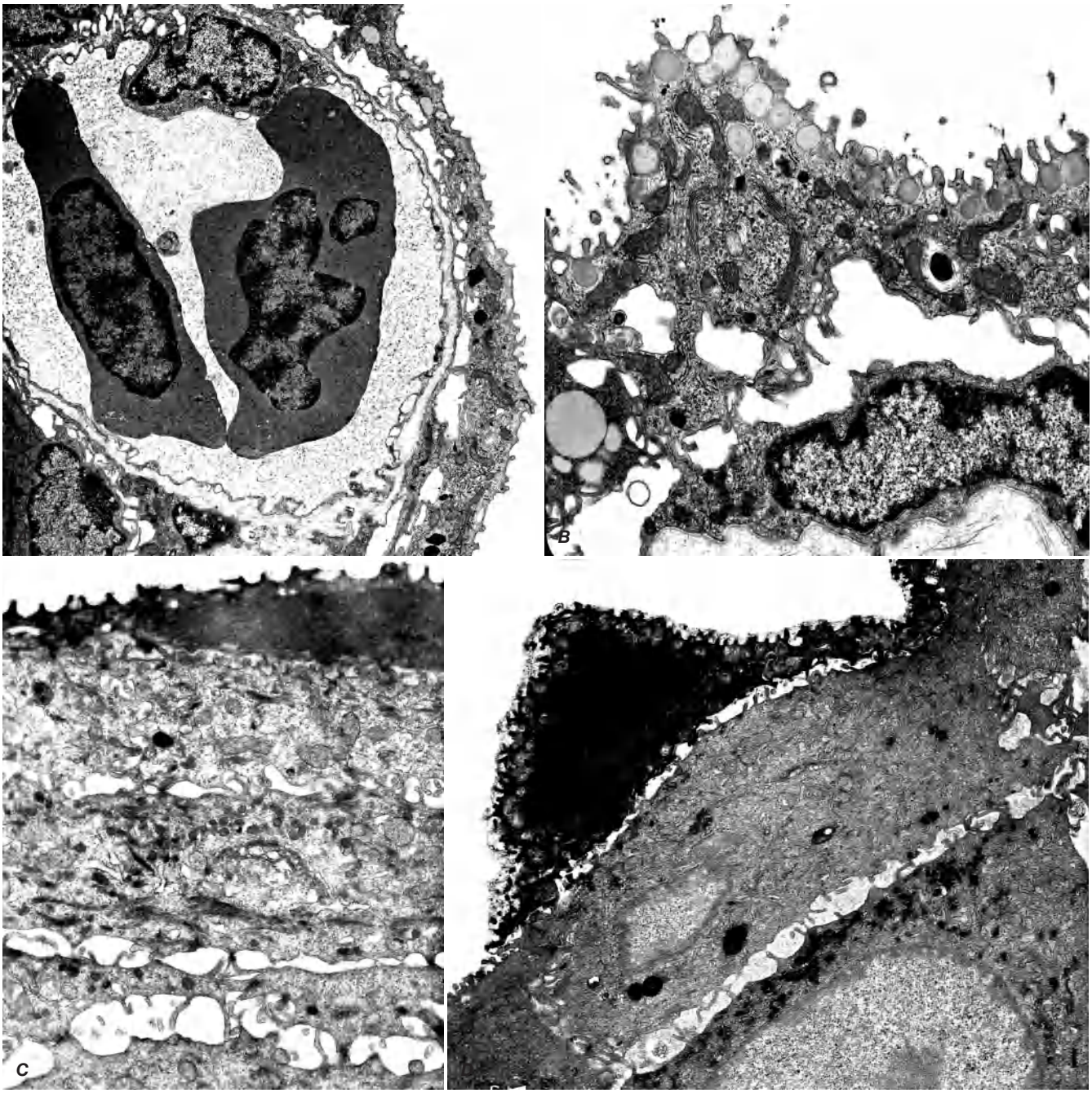


Fig. 21.12 Acid damage to gill epithelium: low pH levels (4.5) resulted in keratinization of gill filaments, *Triturus italicus* larva. **A**. **Pavement cell** (control conditions) has prominent secretory granules. **B**. **Mitochondria-rich cell** has prominent microvilli. **C–D**. Keratinization: after 48 hr of acid water, pavement cells are keratinized (**C**). There is loss of granules replaced by tonofilaments (**D**). Mitochondria-rich cells have shortened villi and reduced cytoplasmic area. (Micrograph: E. Brunelli, *J Exp Zool* 303A:946, 2005.)

maintain equilibrium causing the fish to swim to the bottom and have tumbling movement.

References

1. Ten Have-Opbroek AAW, et al. 1991. The proximal border of the human respiratory unit, as shown by scanning and transmission electron microscopy and light microscopical cytochemistry. *Anat Rec* 229:339.
2. Nickerson PA, et al. 1981. An ultrastructural study of alveolar permeability to cytochrome C in the rabbit lung. *Am J Pathol* 102:1.
3. Johnson J, et al. 1991. Morphologic changes in lungs of anesthetized sheep following intravenous infusion of recombinant tumor necrosis factor α^{1-3}. *Am Rev Resp Dis* 144:179.

4. Dingemans KP, Wagenvoort CA. 1978. Pulmonary arterieis and veins in experimental hypoxia. *Am J Pathol* 93:353.
5. Zakheim RM, et al. 1975. Prevention of pulmonary vascular changes of chronic alveolar hypoxia by inhibition of angiotensin I-converting enzyme in the rat. *Lab Invest* 33:57.
6. Aharinejad S, et al. 1992. Scanning and transmission electron microscopy of venous sphincters in the rat lung. *Anat Rec* 233:555.
7. Schraufnagel DE, et al. 1994. Lung lymphatics increase after hyperoxic injury. *Am J Pathol* 144:1393.
8. Lauweryns JM, Baert JH. 1977. Alveolar clearance and the role of pulmonary lymphatics. *Am Rev Respir Dis* 115:625.
9. Campbell L et al. 2003. Constitutive expression of P-glycoprotein in normal lung alveolar epithelium and functionality in primary alveolar epithelial cultures. *J Pharm Exp Ther* 304:441.
10. Babbs CF, et al. 1991. Endothelial superoxide production in buffer perfused rat lungs, demonstrated by a new histochemical technique. *Lab Invest* 65:484.
11. Askin FB, Kuhn C. 1971. The cellular origin of pulmonary surfactant. *Lab Invest* 25:260.
12. Crouch E et al. 2000. Collectins and pulmonary innate immunity. *Immunol Reviews* 173:52.
13. Buckingham S, et al. 1966. Phospholipid synthesis in large pulmonary alveolar cell. *Am J Pathol* 48:1027.
14. Kikkawa Y, et al. 1983. Cellular and biochemical aspects of pulmonary surfactant in health and disease. *Lab Invest* 49:122.
15. Stahlman MT, et al. 1992. The ontogeny and distribution of surfactant protein B in human fetuses and newborns. *J Hist Cyt* 40:1471.
16. Adamson IYR, Bowden DH. 1973. Intracellular site of surfactant synthesis. *Exp Mol Pathol* 18:122.
17. Chevalier G, Collet AJ. 1972. In vivo incorporation of choline-^{3}H, leucine-^{3}H and galactose-^{3}H in alveolar type II pneumocytes in relation to surfactant synthesis. *Anat Rec* 174:289.
18. Kingma PS et al. 2006. In defense of the lung: Surfactant protein A and surfactant protein D. *Curr Opin Pharmacol* 6(3):277.
19. Flodh H, Magnusson G. 1973. Genesis of foam cells. *Virchows Arch B* 12:360.
20. Adamson IYR, Bowden DH. 1980. Role of monocytes and interstitial cells in the generation of alveolar macrophages. *Lab Invest* 42:518.
21. Goldenberg et al. 1967. Pulmonary lesions in vagotomized rats. *Lab Invest* 16:693.
22. Smiley-Jewell SM et al. 2000. Acute injury to differentiating Clara cells in neonatal rabbits results in age-related failure of bronchiolar epithelial repair. *Toxcol Pathol* 28:267.
23. Meyerholz DK et al. 2006. Expression of innate immune genes (SP-AD, SBD-1, TLR4) by respiratory epithelia at preterm gestation is less than full-term. *Dev Comp Immunol* 30(11):1060.
24. Ridsdale R, Post M. 2004. Surfactant lipid synthesis and lamellar body formation in glycogen laden cells. *Am J Physiol Lung Cell Mol Physiol* 287:L743.
25. Meyerholz DK et al. 2006. Monocytic/macrophagic pneumonitis following intrabronchial deposition of vascular endothelial growth factor in neonatal lambs. *Vet Pathol* 43:689.
26. Plopper CG, et al. 1994. Elevated susceptibility to 4-ipomeanol cytotoxcity in immature Clara cells of neonatal rabbits. *J Pharmacol Exp Ther* 269:867.
27. Thebaud B, Abman SH. 2007. Bronchopulmonary dysplasia: Where have all the vessels gone? Roles of angiogenic growth factors in chronic lung disease. *Am J Resp Crit Care Med* 175:979.
28. Meyerholz DK, et al. 2006. Depletion of alveolar glycogen corresponds with immunohistochemical development of CD208 antigen expression in perinatal lamb lung. *J Hist Cyt* 54:1247.
29. Warner AE, et al. 1986. Pulmonary intravascular macrophages in sheep. *Lab Invest* 55:276.
30. Winkler GC, Cheville NF. 1985. Morphometry of postnatal development in the porcine lung. *Anat Rec* 211:427.
31. Winkler GC. 1988. Pulmonary intravascular macrophages in domestic animal species. Review of structural and functional properties. *Am J Anat* 181:217.
32. Atwal OS, et al. 1992. In vivo monastral blue-induced lamellar bodies in lysosomes of pulmonary intravascular macrophages (PIMs) of bovine lung. *Anat Rec* 234:223.
33. Adamson IYR, et al. 1988. Relationship of alveolar epithelial injury and repair to the induction of pulmonary fibrosis. *Am J Pathol* 130:377.
34. Schneeberger EE, et al. 1972. Development of peroxisomes in granular pneumocytes during pre- and postnatal growth. *Lab Invest* 27:581.
35. Mettler NR, et al. 1981. β-adrenergic induced synthesis and secretion of phosphatidylcholine by isolated pulmonary alveolar type II cells. *Lab Invest* 45:575.
36. Bils RF, Christie BR. 1980. The experimental pathology of oxidant and air pollutant inhalation. *Int Rev Exp Pathol* 21:195.
37. Castillo SS et al. 2007. Reactive nitrogen and oxygen species activate different sphingomyelinases to induce apoptosis in airway epithelial cells. *Exp Cell Res* 313:2680.
38. Wyatt TA et al. 2003. Ethanol stimulates ciliary beating by dual cyclic nucleotide kinase activation in bovine bronchial epithelial cells. *Am J Pathol* 163:1157.
39. Vincent R, Adamson IYR. 1995. Cellular kinetics in the lungs of aging Fischer 344 rats after acute exposure to ozone. *Am J Pathol* 146:1008.
40. Meyer EC, Ottaviano R. 1973. The effect of fibrin on the morphometric distribution of pulmonary exudative edema. *Lab Invest* 29:320.
41. Alvearez DF et al. 2006. Transient receptor potential vanilloid 4-mediated disruption of the alveolar septal barrier. *Circ Res* 99:988.
42. Ramos M et al. 2007. Monocrotaline pyrrole induces Smad nuclear accumulation and altered signaling expression in human pulmonary arterial endothelial cells. *Vacul Pharmacol* 46:439.
43. Woods LW et al. 1999. Manipulation of injury and repair of alveolar epithelium using two pneumotoxicants: 3-methylindol and monocrotaline. *Exp Lung Res* 25:165.

44. Zhang J, et al. 1995. Characterization of the pulmonary lesions induced in rats by human recombinant interleukin-2. *Toxicol Pathol* 23:653.
45. Basset F, et al. 1986. Intraluminal fibrosis in interstitial lung disorders. *Am J Pathol* 122:443.
46. Myers JL, Katzenstein A-L. 1988. Ultrastructural evidence of alveolar epithelial injury in idiopathic bronchiolitis obliterans-organizing pneumonia. *Am J Pathol* 132:102.
47. Hyde DM, et al. 1985. Peribronchial fibrosis in lungs of cats chronically exposed to diesel exhaust. *Lab Invest* 52:195.
48. Hyde DM, et al. 1978. Morphometric and morphologic evaluation of pulmonary lesions in beagle dogs chronically exposed to high ambient levels of air pollutants. *Lab Invest* 38:455.
49. Barros SS et al. 2006. Macrophages and giant cell proliferation associated with bone protein synthesis and calcification in the trachea and bronchi of rabbits intoxicated with *Solanum glaucophyllum*. *Vet Pathol* 43:494.
50. Castleman WL et al. 1973. Histochemically detected enzyme alterations in rat lungs exposed to ozone. *Exp Mol Pathol* 19:402.
51. Balis JU et al. 1991. Ozone stress initiates acute pertubations of secreted surfactant membranes. *Am J Pathol* 138:847.
52. Asmundsson T et al. 1973. Injury and metaplasia of airway cells due to SO_2. *Lab Invest* 29(1):41.
53. Lopez A et al. 1988. Histologic and ultrastructural alterations in lungs of rats exposed to sub-lethal concentrations of hydrogen sulfide. *Vet Pathol* 5(5):376.
54. Trela BA et al. 1992. A microscopic and ultrastructural evaluation of dibasic esters (DBE) toxicity in rat nasal explants. *Exp Mol Pathol* 56:208.
55. Green FHY et al. 2007. Comparative pathology of environmental lung disease: An overview. *Toxicol Pathol* 35:136.
56. Nugent KM, et al. 1989. The utility of bronchoalveolar lavage and transbronchial lung biopsy combined with energy-dispersive x-ray analysis in the diganosis of silicosis. *Am J Resp Dis* 140:1438.
57. Lee KP, et al. 1979. Pulmonary response to glass fiber by inhalation exposure. *Lab Invest* 40:123.
58. Ghio AJ et al. 2008. Iron homeostasis in the lung following asbestos exposure. *Antioxid Redox Signal* 10(2):371.
59. Dodson RF et al. 2005. Stability of ferruginous bodies in human lung tissue following death, embalmment and burial. *Inhal Toxicol* 17(14):789.
60. Oghiso Y et al. 1984. Intrapulmonary distribution of inhaled chrysotile and crocidolite asbestos: Ultrastructural features. *Br J Exp Pathol* 65(4):467.
61. Brody AR, et al. 1983. Interactions of chrysotile and crocidolite asbestos with red blood cell membranes. *Lab Invest* 49:468.
62. McGavran PD et al. 1990. Inhalation of chrysotile asbestos induces rapid cellular proliferation in small pulmonary vessels of mice and rats. *Am J Pathol* 136(3):695.
63. Manning CB, et al. 2008. Targeting the MEK1 cascade in lung epithelium inhibits proliferation and fibrogenesis by asbestos. *Am J Respir Cell Mol Biol* 38:618.
64. Pinkerton KE, et al. 1984. Fiber localization and its relationship to lung reaction in rats after chronic inhalation of chrysotile asbestos. *Am J Pathol* 117:454.
65. Woodworth CS, et al. 1983. Squamous metaplasia of the respiratory tract. *Lab Invest* 48:578.
66. Shvedova AA et al. 2005. Unusual inflammatory and fibrogenic pulmonary responses to single-walled carbon nanotubes in mice. *Am J Physiol Lung Cell Mol Physiol* 289:L698.
67. Dinis-Olivieira RJ, et al. 2008. Paraquat poisonings: Mechanisms of lung toxicity, clinical features and treatments. *Crit Rev Toxicol* 38:13.
68. Fukuda Y et al. 1985. Patterns of pulmonary structural remodling after experimental paraquat toxicity. The morphogenesis of intraalveolar fibrosis. *Am J Pathol* 118(3):452.
69. Guidot DM, Hart CM. 2005. Alcohol abuse and acute lung injury: Epidemiology and pathophysiology of a recently recognized association. *J Investing Med* 53:235.
70. Lazic T et al. 2007. Maternal alcohol ingestion reduces surfactant protein: An expression by preterm fetal lung epithelia. *Alcohol* 41:347.
71. Jasinksi A. 1973. Air-blood barrier in the respiratory intestine of the pond-loach *Misgurnus fossilis* L. *Acta Anat* 86:376.
72. Morgan M, Tovell PWA. 1973. The structure of the gill of the trout, *Salmo gairdneri*. *Z Zellforsch* 142:147.
73. Wright DE. 1973. The structure of the gills of the elasmobranch, *Scyliorhinus canicula* (L.). *Z Zellforsch* 144:489.
74. Evans DH. 1987. The fish gill: Site of action and model for toxic effects of environmental pollutants. *Environ Health Persp* 71:47.
75. Pisam M, et al. 1993. Effects of prolactin on α and β chloride cells in the gill epithelium of the saltwater adapted tilapia "*Oreochromis niloticus*." *Anat Rec* 235:275.
76. Threadgold LT, Houston AH. 1964. An electron microscope study of the "chloride cell" of *Salmo salar* L. *Exp Cell Res* 34:1.
77. Van der Meer DL, et al. 2005. Gene expression profiling of the long-term response to hypoxia in the gills of adult zebrafish. *Am J Physiol Regul Integr Comp Physiol* 289: R1512.
78. Jiraungkoorskul W et al. 2007. Toxicity of copper in butterfish (*Porontous triacanthus*): Tissue accumulation and ultrastructural changes. *Environ Toxicol* 22:92.
79. Bernabo I et al. 2008. Endosulfan acute toxicity in *Bufo bufo* gills: Ultrastructural changes and nitric oxide synthase localization. *Aquat Toxicol* 86:445.
80. Brunelli E, Tripepi S. 2005. Effects of low pH acute exposure on survival and gill morphology in *Triturus italicus* larvae. *J Exp Zool* 303A:946.
81. Brooks RE. 1970. Ultrastructure of the physostomatous swim bladder of rainbow trout (*Salmo gairdineri*). *Z Zellforsch* 106:473.

Part VI

Pathologic Growth

Ultrastructural Pathology The Comparative Cellular Basis of Disease
Second Edition Norman F. Cheville
© 2009 Wiley-Blackwell. ISBN: 978-0-813-80330-2

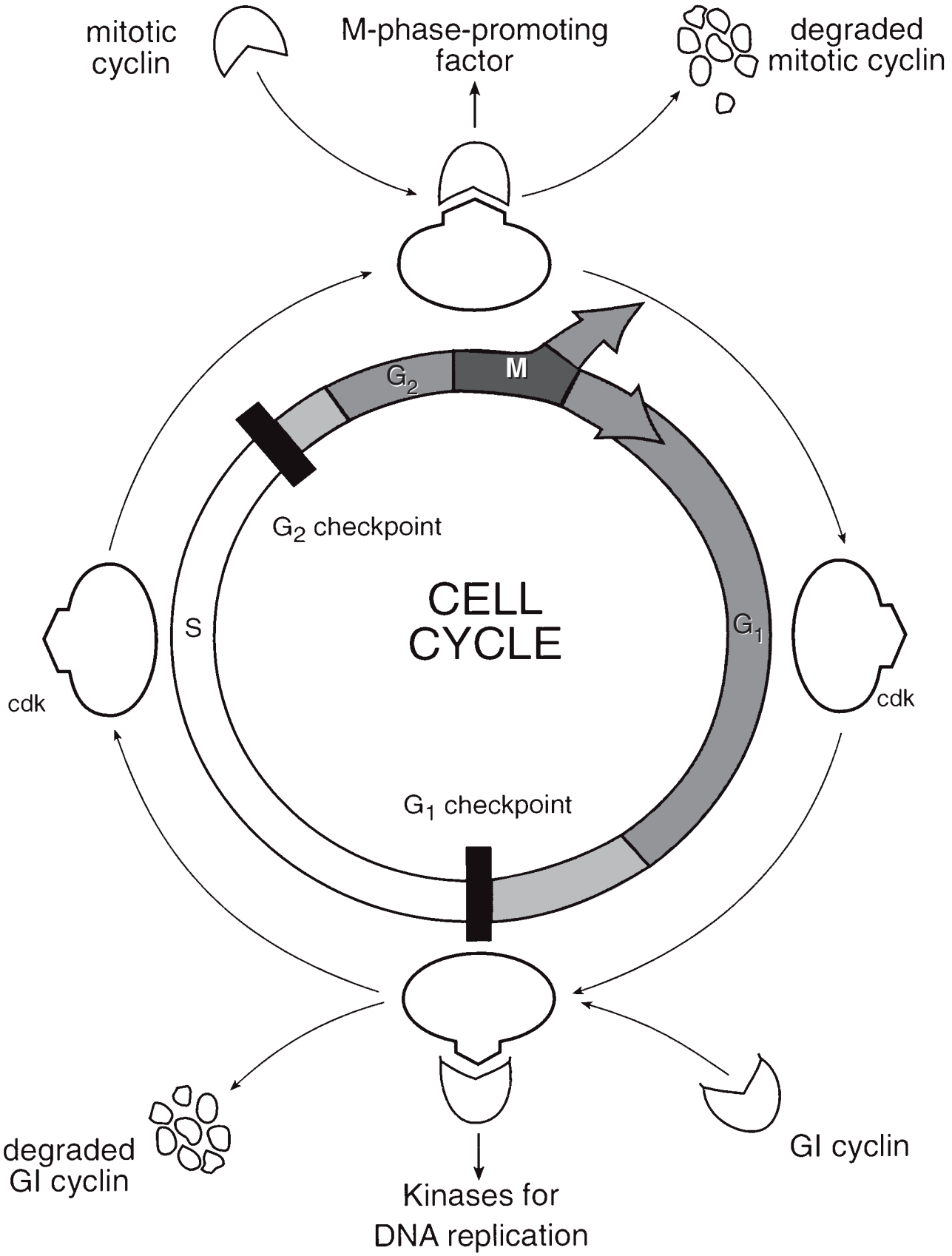


Fig. 22.1 Cell cycle model: stages of the cycle are in the outer band: gap 1 (G_1), synthesis (S), gap 2 (G_2), and mitosis (M).

© 2009 Wiley-Blackwell. ISBN: 978-0-813-80330-2

22 The Cell Cycle: Dysfunction in Aging, Senescence, and Hibernation

The Cell Cycle

The **cell cycle** is the period extending from one mitosis to the next. The cycle consists of transitions from one regulatory state to another, each change setting in motion the modifications that change the cell. Activities are geared to the nuclear cycle of chromosome replication and segregation that defines the four periods: G_1, S, G_2, and M (Fig. 22.1). During each cycle, the structural components of the cell cytoplasm and nucleus undergo doubling. Some cells—neurons and hepatocytes—remain active for long periods in a nonproliferating or quiescent state referred to as $\mathbf{G_0}$. Cells in G_0 have an unduplicated DNA content.

Each period of the cell cycle must be precisely regulated so that one is completed before the next begins. Failure to complete chromosome duplication before entering mitosis can yield cells that lack a particular chromosome. This aberration may be lethal, or may lead to growth defects or neoplasia. Regulation of the normal cell cycle is under the control of polymerases that activate DNA synthesis as well as proteins that stop and start the transitions from one phase of the cell cycle to the next.

Transition control **checkpoints** occur during G_1 and S, and at the G_2/M boundary. Checkpoints provide a stop point in the cell cycle for DNA repair, and other events driven by the ***p53* gene**. The major checkpoint regulatory kinases that drive these checkpoints are

- Checkpoint kinase 1 (Chk-1)
- Checkpoint kinase 2 (Chk-2)
- Mitogen-activated protein kinase-2 (MK2)

The G_1 Phase

In the $\mathbf{G_1}$ **phase** of the cell cycle, the nucleus is preparing for the S phase by shutting down mRNA translation and producing initiating factors for DNA synthesis. Control of this phase is regulated by multicomponent **prereplicative complexes** that are assembled at sites of replication. Within prereplicative complexes, the Cdc6 protein is critical for regulation of cell cycle phosphorylation reactions that coordinate DNA synthesis and mitosis.

The $\mathbf{G_1}$ **checkpoint** is critical because many of the etiologic agents that lead to cell death and proliferation act in G_1 phase. Acting at the G_1 checkpoint, the **nuclear phosphoprotein p53** is involved in regulation of normal cellular proliferation. The intracellular level of p53 changes in the cell cycle. It markedly increases late in the G_1 phase, but is rapidly eliminated because of its short half-life. The *p53* gene is frequently mutated in neoplastic cells of human breast, lung, and colon. Oncogene products of cancer-causing DNA viruses appear to cancel the proliferation controls in G_1. Among the regulators of the G_1 checkpoint, **Chk 1** plays a major role, and **Chk 1 inhibitors** are potential compounds that enhance antitumor drugs. Cell cycle checkpoint abrogation has been proposed as a mechanism to sensitize cancer cells to DNA-damaging agents.

The S Phase

The period of DNA replication, called the **S phase**, is the key synthetic event in the cell cycle. During the S

phase the entire DNA content of the nucleus must be replicated completely within a few hours. The cell must copy the millions of nucleotides that form its genome. It does so with precise fidelity so as to maintain genetic integrity. DNA replication begins in clusters or replication units, each activated at a different time in the S phase. The timing of replication of different genes is influenced by several factors. Genes that are transcriptionally active are replicated early in S phase; inactive genes replicate late. Members of the **NF-κB family** of transcription factors (p50, p52, p65, c-Rel, RelB) are activated by numerous endogenous and exogenous ligand stimuli and regulate large numbers of genes.

DNA Synthesis

DNA replication, demonstrated by autoradiography after injection of radiolabeled thymidine (which is incorporated into the newly formed DNA molecules), provides a striking illustration of the distribution of new DNA (Fig. 22.2). DNA replication occurs as soluble polymerases bind and then track along the template as they synthesize new DNA. Ultrastructural evidence suggests that activated polymerases are fixed to a **nucleoskeleton**, with replication occurring as DNA is reeled through the fixed complex.

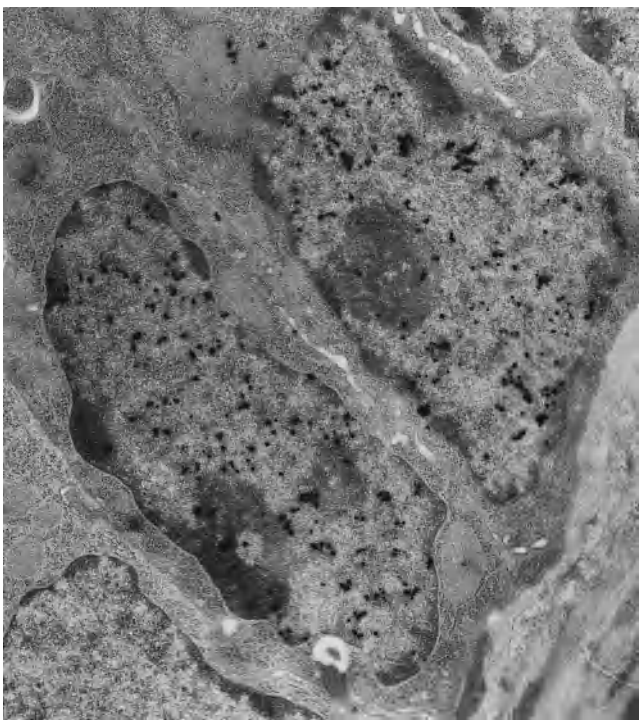


Fig. 22.2 Interphase nuclei: epithelial cells, intestinal villus, labeled with ^{3}H-thymidine for DNA. Silver grains appear over nucleoplasm associated with chromatin granules. (Micrograph: Mohamed El-Alfy and Charles Lebond, *Am J Anat* 183:45, 1988.)

Ultrastructurally, **DNA synthesis** is concentrated in discrete nuclear foci. From ultrastructural studies using biotin-dUTP and gold labeling, terminology used to distinguish two types of DNA synthetic sites are: **replication bodies**, for electron-dense structures; and **replication foci**, for focal replication sites with no distinct structure. Both structures contain proteins of DNA replication (DNA polymerase α), regulators of the cell cycle (cyclin A, cdk2), and RNA processing components (Sm and SS-B/La autoantigens, p80-coilin, hnRNPs A1 and C1/C2).[1]

As new DNA is formed, it must associate with appropriate histones for stability. Thus, there is close coupling of DNA synthesis with transcription of genes for histones. In mammalian cells, the coordinated induction of the five families of histone genes during S phase is achieved through distinct factors that interact with appropriate promoter elements.

The G_2 Phase

The G_2 phase is the preparatory time for mitosis. The G_2 checkpoint is the last chance for the cell to be blocked by unreplicated or damaged DNA. Two primary DNA damage sensors—**ATM** and **checkpoint kinase 2 (Chk 2)**—control the G_2 checkpoint. After radiation injury, cells undergo G_2-M cell cycle arrest to allow time for DNA repair. Deficits of Chk-2 or ATM will allow mitosis to occur with damaged DNA. The cyclin-Cdk complex—also termed **MPF (M-phase promoting factor)**—triggers the passage past the G_2 checkpoint into the M phase.

The M Phase: Mitosis

Mitosis, referred to as the **M phase**, is triggered by the actions of enzymes, proteins that act specifically on histones to initiate mitosis. The progression of change in mitosis has been classically, albeit arbitrarily, divided into four stages: **prophase, metaphase, anaphase**, and **telophase** (Fig. 22.3). The period between successive phases of cell division is the **interphase**. Control, regulation, and inhibition of cell reproduction are achieved by interruption of the mitotic cycle. The three major chromosomal events in cell division (reproduction, movement, and cleavage) all occur with strict continuity. If one is blocked, the others do not occur.

The Cell Cycle Clock: Cyclins and Cdks

Cyclins and **cyclin-dependent kinases (Cdks)** regulate the rhythmic fluctuations of the cell cycle. Cdks, to be active, must be attached to a cyclin, so that the

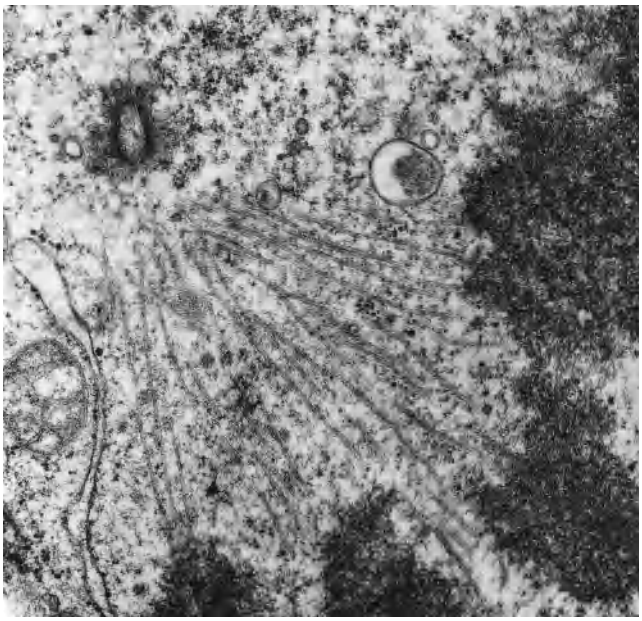


Fig. 22.3 Mitosis: long microtubules of the spindle apparatus connect the large granular chromosomes to the centriole.

activity of a Cdk rises and falls with changes in the concentration of its cyclin partner.

- **Cdc2 protein kinase** is localized to the centrosome, and is tightly bound to the nuclear matrix–intermediate filament scaffold. **Cdc2** and **pericentrin** have been labeled by imunogold techniques in the centrosome.[2,3]
- **Cyclins** accumulate in interphase and disappear (by proteolytic cleavage) at mitosis.
- The cyclin-Cdk complex triggers the passage past the G_2 checkpoint into the M phase.

These enzyme complexes composed of two subunits are regulators present in all mammalian cells. The many variants of these enzymes suggest great complexity of action.

Cyclin regulation occurs through reversible phosphorylation involving different **Cdks** and by periodic degradation of cell cycle-regulating proteins by the 26S proteosome. Proteosomal degradation is mediated by the covalent attachment of ubiquitin chain by two ubiquitin ligases, the SCF and APC complexes. The **APC complex** is active in mitosis and G_1 and degrades proteins that hold back mitotic progression. The **SCF complex** is active throughout the cycle on proteins marked by phosphorylation.

Checkpoints utilize three or more Cdk proteins and several different cyclins. For example, the **Cdk8 module** (Cdk8 along with cyclin C, Med12, and Med13) prevents RNA polymerase II interactions with the protein **Mediator**.[4] The **Cdk2 module** (Cdk2 plus cyclin A) plays important roles during S and G_2/M phases of the cell cycle; the protein SCAPER, an RER-associated regulatory protein, maintains this kinase in the cytoplasm.[5]

Cyclin destruction is required for many events that occur as cells leave mitosis—these events include chromosome decondensation, nuclear envelope reformation, and cytokinesis. Ubiquitin-mediated proteolysis destroys cyclin B when mitosis is complete. Several molecules of the small protein ubiquitin are attached to a lysine on the substrate proteins, directing it to the **proteasome**, a complex proteolytic machine that degrades the polyubiquitinated protein into small peptides.[6]

Nuclear Changes in Mitosis

Interphase nuclei have widely distributed chromatin. In addition to the chromatin spread along the nuclear envelope there are many small aggregates of 5–70 nm and a few circular or elongate packets of 70–230 nm.[7,8] In mitosis, chromatin undergoes striking changes to form the chromosomes, which move to appropriate positions relative to the mitotic spindle and centriole.[9] As the cell enter mitosis, membrane traffic ceases and fragmentation of the Golgi complex, nuclear envelope, and endoplasmic reticulum proceeds. The Golgi complex is converted into thousands of tiny vesicles that are distributed randomly in the cytoplasm.[10]

In **prophase**, the number and size of these larger aggregates increase so that at **metaphase** they have collapsed to form mature chromosomes with a diameter often greater than 800 nm. At **anaphase**, daughter chromosomes migrate to each pole where they fuse into a compact mass of chromatin. At **telophase**, nucleoplasm increases to separate the chromatin strands, which progressively become segmented.[11]

Ultrastructural analysis reveals that chromosomes consist of two parallel chromatids, each composed of two very long DNA molecules folded to form hundreds of symmetrical lateral loops that extend outward from the long axis of the chromosome. The loops are sites of active RNA synthesis. The RNAs that will direct protein synthesis are produced as large precursors called pre-mRNAs.

Centromeres The **centromere** is a constriction in the mitotic chromosome that provides attachment sites for microtubules of the spindle apparatus (Fig. 22.4). It stabilizes and provides the force for chromosomal movement along the spindle. Ultrastructural analysis of thin sections of mitotic cells reveals centromeres as dense regions of the chromosome with a single visible structural area, the **kinetochore**. The kinetochore contains four layers: an inner dense plate closely apposed to the centromere heterochromatin, an electron-lucent (clear) zone, an outer dense plate, and a peripheral fibrous corona. Special kinetochore proteins, some

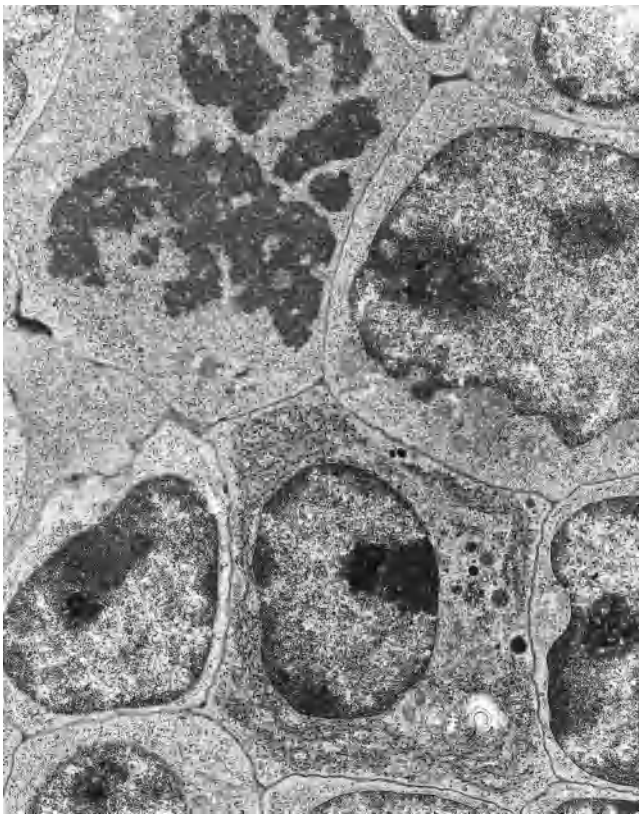


Fig. 22.4 Mitotic cell: malignant lymphoma, mouse. Mitotic figures (*upper left*); differentiated plasmacyte (*lower right*).

localized by immunogold labeling, are important in function and as antigens in autoimmune disease.[12,13]

The Centrosomes

Centrosomes are microtubule-organizing centers.[14] They are composed of complex structural proteins that are specific for the **centriole** organization and microtubule assembly.[15] The duplication cycle of the centrosome, which parallels chromosomal cycles during cell growth, has several distinct steps that occur at specific times in the cell cycle. Centrosome duplication occurs through formation of a single **procentriole** next to each centriole, once per cell cycle.[16] In G_1 a loss of orthogonal orientation is followed by procentriole budding. Procentrioles elongate in S and G_2 phases, and separation of centriole pairs characterizes the prophase of mitosis.

Pericentrin **Pericentrin** anchors tubulin complexes at centrosomes in mitotic cells, and is required for proper spindle organization. Loss of this anchoring mechanism elicits a checkpoint response that blocks mitosis and triggers programmed cell death.[17] In immunogold studies, pericentrin co-localizes with intraflagellar transport proteins (which regulate assembly of primary cilia) near basal bodies at the base of primary and motile cilia.[18]

Mitotic Spindles The **mitotic spindle**, an array of protein **spindle filaments**, separates a dividing cell's two sets of chromosomes during mitosis, ensuring that each daughter cell has the correct DNA. Mitotic spindle proteins include NuMA, a large, multifunctional, coiled-coil protein that organizes microtubule ends at spindle poles. Degradation of NuMA leads to breakdown in nuclear structure (it has been used as a marker for apoptosis).[19]

Spindle Matrix The existence of a **spindle matrix** that stabilizes the mitotic spindle was proposed in the 1960s but was discarded for lack of elements that could be observed ultrastructurally and manipulated in vitro. Recently, the concept of a spindle matrix has been revived with the isolation of several matrix proteins (named skeletor, chromator, megator, and titan) which may provide a unique meshwork for motor proteins stability and movement. In fruit flies, mutations in the genes for matrix proteins are associated with improper chromosome segregation.

Extranucleolar Regions

Structures of the **extranucleolar region**—nuclear bodies, coiled bodies, and interchromatin granules—disperse into the cytoplasm at the breakdown of the nuclear membrane.[20] **GW bodies** (mammalian P bodies) are cytoplasmic sites for storage and degradation of mRNAs that are linked to regulation of cell cycle progression (they were identified through use of a serum targeting marker protein, GW182). GW bodies vary in size and number throughout the cell cycle but are most abundant in S and G_2 phases. GW bodies are associated with small RNA functions that silence target genes; their disassembly impairs silencing activities of small interfering RNA (siRNA) and microRNA (miRNA).[21,22]

In the interphase nucleus, **snRNPs**, which are subunits of spliceosomes, are associated with specific subnuclear domains, including interchromatin granules and coiled bodies—structures that regulate snRNP storage and transport.[23] Interchromatin granules group into irregular **interchromatin granule clusters** that occupy distinct regions of the nucleoplasm and are frequently associated with coiled bodies and homogenous fibrillar bodies.

Cytoplasmic Changes in Mitosis

Cytoplasmic organelles, inactive during mitosis, reform in the new daughter cells. Conspicuous

cytoplasmic changes occur when cells change from a specific functional state to the mitotic state. Epithlelial cells, which have distinctly polar distribution or organelles and membranes, become nonpolar.[24] In most dividing cells, typical cytoplasmic changes include the following:

- **Rough endoplasmic reticulum** disappears and then reforms
- **Mitochondria** persist but enlarge and divide in the new cells
- **Nuclear pore complex** closure and dismantling with dispersal of its membranes[25]
- **Golgi complex** dissociation and reassembly occurs in late mitosis[26]

Early in mitosis the **Golgi complex** fragments, and the fragments are dispersed throughout the cytoplasm. A smaller Golgi complex is rebuilt during telophase in each daughter cell.[27]

Regeneration

Invertebrates such as hydra and other coelenterates can be cut into small pieces and each will develop into a completely new organism. Earthworms cut in half regenerate new heads and tails. When a newt's leg is amputated, the stump gives rise to pluripotential mesenchymal cells that differentiate to form a new leg, including bone and muscle. The capacity to replace lost organs and limbs is reduced as one goes up phylogenic and ontogenetic scales—frog tadpoles have powers of regeneration that are lost during metamorphosis.

Important organ models for study of regeneration include xenopus limb buds, tadpole tails, and zebrafish caudal fins.[28] When amphibian species regrow amputated limbs, new tissue arises by dedifferentiation of fibroblasts, myocytes, and oesteocytes into their earlier stem cell forms.[29] This regenerative process occurs only if there is simultaneous regeneration of the severed nerves.[30] Regeneration begins at the site of injury when a mound of stem cells, the blastema, is created under the influence of cytokines such as FGF-2, glial growth factor-2, and neurotransmitter substance P. The nerve supply cut by amputation also regenerates and regrowth is required for proliferation of the blastemal cells. Nerves are also required for most tissue regeneration in vertebrate species. A surface protein of stem cells, Prod 1 (and its ligand, nAG) are critical determinants of growth.[31]

Regeneration in Liver

The liver of mammals is capable of extensive regeneration. If large amounts of liver are removed, new hepatocytes, in most mammals, will undergo striking regeneration. The classic model of hepatic regeneration in rats involves surgical removal of entire lobes with deletion of 70% of the liver mass. The small lobes that remain regenerate by an increase in size through hypertrophy and hyperplasia. Hepatocytes that remain undergo a partially synchronous wave of **DNA synthesis** and cell division, the events of which are precisely regulated. In these experiments, at least 20% of liver mass must be removed for the growth response to be triggered, and there is a correlation between the extent of hepatic DNA synthesis and the amount of liver removed. Almost all hepatocytes replicate. Hepatocyte DNA synthesis begins at about 12 hr after hepatectomy and reaches a peak at 24 hr. Cellular proliferation begins in periportal areas and new hepatocytes move outwards to form sinusoids. Nonparenchymal cells also replicate but lag behind hepatocyte DNA synthesis by 1–3 days.

The regenerating liver doubles in size by 48–72 hr and growth ceases in 7–10 days, when the liver mass reaches the original value of the intact liver. Peak mitotoic activity occurs at 48 hr. There is no evidence of monocyte infiltration or endothelial cell mitosis.[32]

One marker of the **cyclins**, proliferating cell nuclear antigen or PCNA/cyclin, an auxiliary protein of DNA polymerase δ, is synthesized during cellular proliferation and increases from late G_1 through the S phase of the cell cycle. It is a reliable marker of proliferating hepatocytes, and antibodies against PCNA are used in immunoperoxidase techniques to demonstrate hepatic regeneration after injury.[33]

Ultrastructural analysis of regenerating hepatocytes at 5 days posthepatectomy shows moderate enlargement. The major cellular changes occur adjacent to portal triads where hepatocytes are markedly enlarged and have very large nuclei.[34,35] Changes in the hepatocyte are large increases in ribosomes and endoplasmic reticulum (Fig. 22.5, 22.6). Peroxisomes increase and remain connected to form a peroxisomal reticular arrangement.[36] At the surface of regenerating hepatocytes, microvilli are increased in length and number. Intercellular junctions are disrupted in early stages of regeneration.[37] During rapid growth, gap junctions as well as tight junctions and desmosomes are disassembled and reform as new cell-to-cell relationships are stabilized. Bile canaliculi are large with short, stubby microvilli—changes also typical of regenerative nodules in human cirrhosis (Fig. 22.6). Hepatic stellate cells are activated at day 3, and contact developing hepatocytes in the recovery process.[38]

Growth Factors in Hepatic Regeneration

Serum of hepatectomized animals contains several powerful growth factors. Early studies on dogs

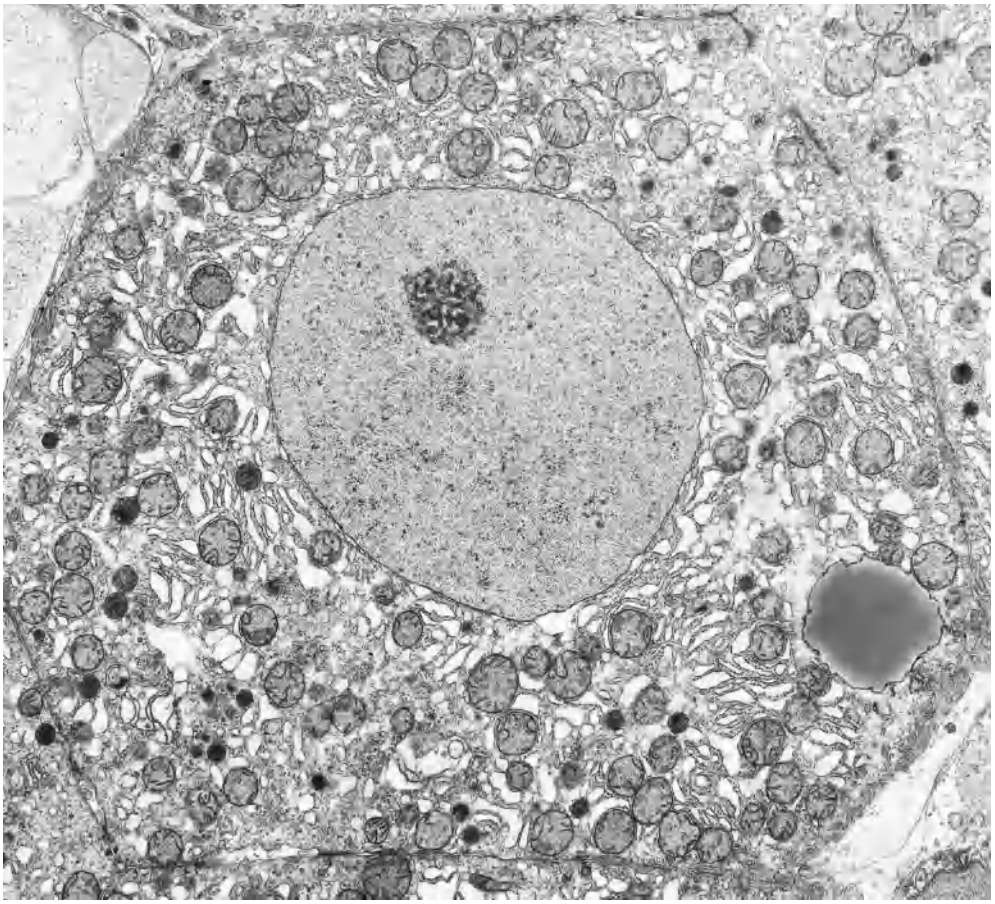


Fig. 22.5 Regeneration: regenerating hepatocytes, liver, rat (5 days after experimental partial hepatectomy). New cell has large nucleus, dilated endoplasmic reticulum cisternae, lipid globules, and absence of glycogen. Mitochondria are small. Golgi complex cannot be identified.

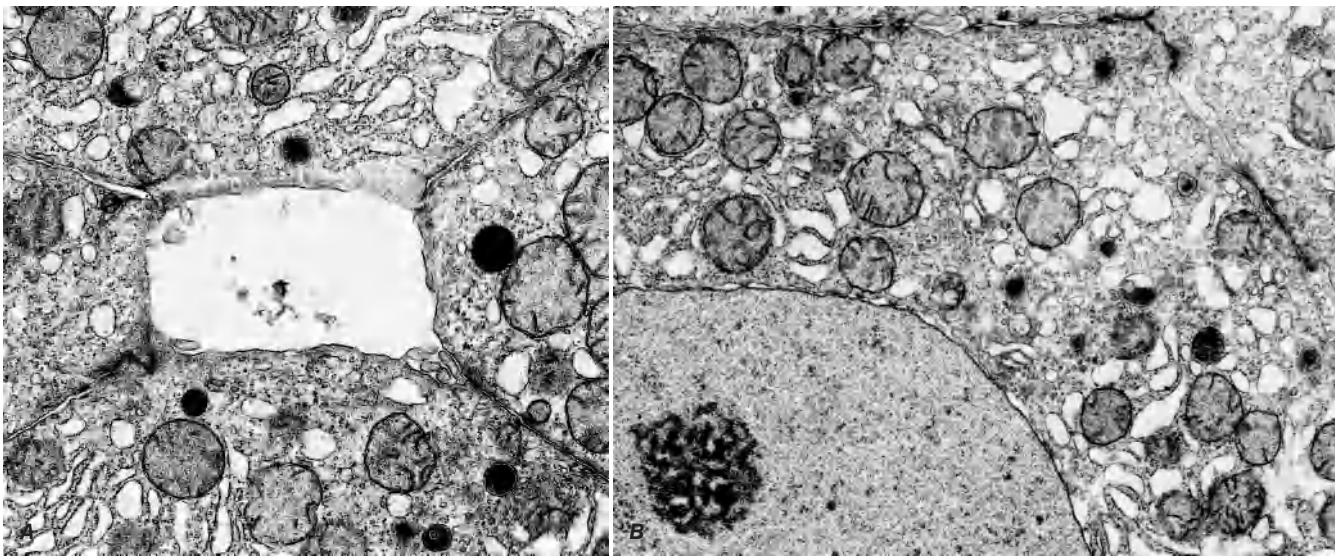


Fig. 22.6 Regeneration. A. **Bile canaliculus**: margins of four hepatocytes. Cell junctions (normally tight) are poorly formed. Microvilli are absent from plasma membranes. Many free ribosomes and peroxisomes are evident. **B**. **Cytoplasmic organelles**: diffuse dilatation of cisternae of endoplasmic reticulum and nuclear envelope. Note wide nuclear pores, long dense intercellular junctions, uniform small mitochondria, and cytoplasmic vesicles.

showed that extracts from livers (after partial hepatectomy), when injected into the portal vein, promoted growth and prevented atrophy in dogs.[39] **Transforming growth factors** (TGF-α and -β) increase in liver tissue during hepatic regeneration. **TGF-α**, produced by the hepatocyte, is an autocrine stimulatory growth factor. Its appearance correlates with the major wave of hepatocyte DNA synthesis. **TGF-β**, produced later (in endothelial cells), has an inhibitory effect, that is, it is the effector in a paracrine regulatory circuit.

Many growth factors originate outside the liver yet influence growth of regenerating hepatocytes during circulation in the bloodstream. These include **epidermal growth factor** (EGF), insulin, glucagon, vasopressin, norepinephrine, and thyroid and parathyroid hormones. The regenerating hepatocyte of rats conserves EGF; degradation of EGF is inhibited and the hepatocyte in the regenerating liver accumulates three times the amount of EGF as those in the control liver. Exogenous EGF, transported to the lysosomal pathways in normal liver, is diverted to the nucleus in regenerating hepatocytes, where it complexes with EGF-binding proteins.[40]

Gene Activation Within nuclei of regenerating hepatocytes, appropriate genes that code for growth factors are activated. Specific protooncogenes are stimulated sequentially during hepatocyte regeneration, for example, *fos*, *myc*, *p53*, and *ras*. Increase transcripts for these genes occur only transiently, for a few hours after hepatectomy levels have returned to normal. These genes are not expressed after heminephrectomy, which involves hypertrophy rather than hyperplasia.

The specific transcriptional patterns for protooncogene expression that are activated in growth and differentiation are also activated after cell injury. In the liver poisoned by carbon tetrachloride there is a complex pattern of cellular activity that leads to initial, transient expression of c-*fos* or c-*jun*, then c-*myc* and subsequently the *ras* genes. The reaction proceeds centrifugally from pericentral (zone III) to periportal (zone I) areas. Sequential expression of RNA transcripts can be detect by in situ hybridization with labeled cRNA probes.[41]

Hepatic Regeneration in Transgenic Mice

Transgenic mouse technology has provided methods to create and analyze the cell cycle. Because of its accessibility, involvement in systemic reactions, and capacity to secrete large amounts of macromolecules the liver has been a common target for gene transfer. Genes for human and bovine growth hormone, when expressed in hepatocytes of transgenic mice, cause hypertrophic and hyperplastic changes including disintegration of the rough endoplasmic reticulum and enlargement of nuclei with irregular nuclear envelopes and pseudoinclusions.[42]

Other transgenes that have caused liver lesions are those that encode growth hormone, which alters hepatocyte size and nuclear characteristics; transforming growth factor-α, which causes hyperplasia; hepatitis B virus envelope peptides, which induce hepatocellular necrosis and carcinomas; several oncogenes that induce neoplasms; and plasminogen activator, which causes hemorrhages.[43]

Other transgenic models of hepatic disease involving secretory pathways include transgenic mice expressing **α_1-antitrypsin** (*AAT*). Circulating *AAT* is synthesized primarily in the liver and secreted into the bloodstream where it serves as the major serine protease inhibitor. The human PiZ variant of the *AAT* gene is associated with decreased levels in sera as a result of its retention in the liver. In hepatocytes, the retained AAT accumulates in large cytoplasmic globules. Homozygotes for the variant allele predisposes the individual to development of pulmonary emphysema (it protects elastase fibers from hydrolytic destruction by leukocytes elastase) and to increased risk for liver disease. When the *PiZ* variant of human *AAT* gene is expressed in transgenic mice and human AAT deficiency disease, it accumulates in globules in hepatocytes. In human *AAT* there is a single amino acid substitution in *AAT* that blocks transport and leads to accumulation of unsecreted AAT in the rough endoplasmic reticulum. Ultrastructural examination of liver of AAT producing transgenic mice reportedly "accumulate in the RER" although the micrography uses to illustrate this show large globules that are clearly fat.[44]

Muscle Regeneration

Regeneration of muscle fibers after injury is sustained by the production of new myofibers. Satellite cells are important in muscle regeneration. Necdin is a protein expressed in satellite cell-derived myogenic precursors during perinatal growth and in muscle regeneration.[45] Muscle biopsies from spinal cord injured human patients show that, when lower motor neurons are destroyed, there is complete loss of myocyte internal organization. Atrophy is complicated by fibrosis and adipocyte expansion. Functional electrical stimulation (FES) (in the absence of innervation and nerve-derived trophic factors) will cause recovery of muscle ultrastructure in 90% of myofibers including both myofibrils and calcium-handling membrane systems.[46,47] Similar recovery of skeletal muscle has been confirmed in rabbits and rats.[48,49]

Regeneration in Transplanted Tissues

Tissues transplanted from donor to allogenic recipient involves delays in regeneration. If mechanisms of lymphoid and vascular rejection are sufficiently suppressed to overcome rejection, transplanted tissue undergoes cycles of proliferation and regeneration that restructure the tissue.[50] Aging impairs the responses of cells to anoxia, and the transplantation of young stem cells is more effective that cells taken from aged animals.[51]

Aging and Senescence

Increasing age is accompanied by tissue atrophy and degenerative disease even though individual cells may remain viable longer than the lifespan of the animal itself.[52,53] Relations within and between cells is reduced, destroying the feedback mechanisms that orchestrate cell functions in the efficient multicellular organism. Progressing cycles of diminished function and structural change inevitably reach a point where the tissue is more susceptible to injury. This in turn hastens the progression of tissue senescence.

Cellular Change in Aging

Cell structure and function are altered with age. Although the lack of quantitative analysis of individual cells makes general statements about aging changes unwise, there are some characteristics of senescent cells:

- **Autophagy** is less efficient: there is an increase in number, volume, and complexity of lysosomes, and in the activity of their acid hydrolases.
- **Lipofuscin** accumulates in lysosomes of highly metabolic cells such as myocytes and neurons.
- **Lipid and sterol metabolism** becomes dysfunctional and may lead to increased cytoplasmic lipid globules and cholesterol.
- **Protein synthesis** is increasingly inefficient in senescence, leaving debris and polymerized proteins in cisternae of endoplasmic reticulum.[54]

Aging cells accumulate abnormal gene products that can cause molecular mischief. Key enzymes and mechanisms for their production become increasingly sluggish. The repair mechanisms for the major macromolecules DNA, RNA, and protein are less efficient and the breaks that occur are defectively repaired. Although there are no distinct changes in nuclei, those of rodent tissues have a high incidence of polyploidy.

Aging and Growth Defects

Aging involves atrophy of most organ systems. There are striking changes that increase progressively with age—organs as diverse as the brain and hair follicles of the skin.[55] Accumulation of misfolded proteins and neuronal death are hallmarks of Alzheimer's disease (see chapter 26). In the spinal ganglia, gap junctions between perineuronal cells increase in number with age.[56]

Many aging changes are secondary to diminished function of support structures. Bone, joints, and connective tissues become increasingly rigid. Interstitial spaces are expanded by deposition of collagen and ground substance. The cardiovascular system has a diminished capacity to respond, and brain, muscle, and viscera suffer from the decreased perfusion by circulating blood.

Muscle

Muscle atrophy is closely associated with aging. In old age, it is progressive, and leads to general metabolic decline in those tissues interacting with muscle. Age-associated muscle wasting, also referred to as senescent muscle atrophy or **sarcopenia**, leads to increased density of muscle cell nuclei, aberrant myofibrils, and fibers that express embryonic myosin.[57]

Anemia: Aging of Erythrocytes

As erythrocytes age, enzymes that maintain energy production gradually wane and there is a decrease in ATP. Membrane function is affected, the normal biconcave shape become spheroidal, and cells have an increased susceptibility to osmotic lysis. In passage through the splenic filter, aged erythrocytes are removed from the circulation and the component parts are processed by splenic macrophages. Any space-occupying defect in the plasma membrane makes the erythrocyte less flexible and liable to erythrophagocytosis. **Pitting**, the removal of defective parts of the cell, may occur as it squeezes through the endothelial lining of the splenic venous sinus. The mechanical trauma of excessively fragile erythrocytes may also result in intravascular fragmentation and hemolysis.

Endocrine Dysfunction

In endocrine organs there is evidence of functional decline in aged animals, including striking changes in secretory granules, for example, great size and shape variation, crinophagy, and lipofuscin. Syndromes of premature senescence include progeria

and several variants of dwarfism. Dwarfs of the Snell-Bagg strain of mice bear a gene that limits lifespan to about 5 mo. Growth is impaired, animals never reach normal size; and in a few months cataracts develop, the skin thins, the hair grays, and the mouse dies. The pituitary fails to produce hormones that stimulate thyroid and adrenal glands and, if dwarfs are injected with pituitary hormones at weaning, life span is doubled. Effects are mediated in part through the lymphoid system; if dwarfs are injected with lymphocytes from normal littermates, life spans are similarly doubled.

Primordial Dwarfism in Humans

Mutations in the **pericentrin gene** (*PCNT*), which encodes the centrosome protein **pericentrin**, cause rare forms of human dwarfism, Seckel syndrome, and Majewski microcephalic osteodysplastic primordial dwarfism type II. These disorders share centrosomal dysfunction and small brain and body size.[58] Although the latter was originally thought to be a premature aging syndrome, there was no evidence of accelerated telomeric shortening in patient's lymphocytes, nor any predisposition to cancer—as is typical of defects in DNA repair such as the Bloom syndrome.

Progeria

Progerias (premature aging syndromes) are rare disorders caused by mutations within lamin genes and lamin assembly disruption. **Hutchinson-Gilford progeria syndrome (HGPS)** is a fatal genetic disorder characterized by segmental, accelerated aging. The major causal mutation triggers abnormal mRNA splicing of the lamin A gene. The resultant changes in nuclear architecture trigger apoptosis. Mice strains deficient in various lamins have been developed.[59,60]

Warner syndrome is a segmental aging syndrome that does not have all aspects of physiologic aging. Mutated genes have been identified and mouse models developed for the progerias.[61]

Hibernation

Torpor is a physiologic state of controlled low activity, diminished metabolism, and blocked cell cycles. Torpor is an adaptation that enables an animal to save energy while avoiding life-threatening environments. **Estivation**, or summer torpor, allows animals to survive long periods of high temperatures and scarce water. **Hibernation** is long-term torpor, and is a dormant state in which some animal species pass the winter. Hibernation is characterized by narcosis and by reduction in body temperature and metabolic activity. Some hibernating mammals cool to as low as 1–2°C. Hibernation is a cellular protective response mediated through shutdown of metabolic pathways. Cells shut down by **hibernation** are small but are not referred to as atrophic.

In medicine, hibernation is the state of reduced metabolism, muscle relaxation, and twilight sleep resembling narcosis that is produced pharmacologically by the controlled inhibition of the sympathetic nervous system that reduces homeostasis.

Development of Hibernation

A precise hypothalamic-regulated lowering of body temperature designed to conserve energy characterizes hibernation. Regulated by effects of day-length cycles on the pineal, hibernation is mediated by a protein called **thermogenen** and stimulation of heat production in mitochondria of brown fat cells in which oxidative phosphorylation and respiration are uncoupled.[62]

The **CLOCK protein**, one of a family of transcription factors, is essential for normal circadian rhythms. In hibernation, CLOCK protein is increased in hepatocytes, and is redistributed to amorphous nuclear bodies that appear to be storage sites for use during arousal when they disappear.[63]

In the **brain** of hibernating ground squirrels, there are reversible changes in the ultrastructure of asymmetric axospinous synapses in the frontal cortex, a protective mechanism against the deleterious effects of prolonged hypothermic phases of hibernation.[64]

The **cardiac conduction system** is an important tissue in hibernation. Heart rates are markedly reduced—some bats have heart rates fewer than 10 beats/min during hibernation, while in flight, they have >700 beats/min. This reduction is associated with the formation of a transmission barrier and other ultrastructural changes in the sinoatrial node; there are also secondary changes such as aggregation of acetylcholine vesicles at synaptic bulbs and loss of dense cored vesicles.[65]

Ultrastructural changes in the livers of mice under deep hibernation are marked by reduction in cell volumes due to disappearance of large parts of the endoplasmic reticulum. Total **hepatocyte** volumes are strikingly reduced, as well as total areas of Golgi complex, glycogen and residual bodies.[66] Total lipids are increased in early hibernation, reduced in deep hibernation and nearly absent during arousal. Mitochondria size increases from euthermia to hibernaton, and decreases upon arousal in all cell types. Matrix granules increase strikingly during hibernation (but do not change in brown adipocytes).[67]

Arousal

Small mammalian hibernators periodically rewarm from torpor to high, euthermic body termperatures for brief intervals throughout the long hibernating season. Rewarming is hypothesized to be related to replacement of gene products lost during torpor due to degradation of mRNA. Analyses of polyribosomes show marked reduction in torpid animals.[68]

Cell Senescence

Senescent cells live on but can never again divide. The proliferative block of senescence also safeguards against neoplastic cell division—limiting the proliferative capacity of damaged cells and thereby acting as an intrinsic mechanism of tumor suppression. In one pathway, **insulin growth factor binding protein 7 (IGFBP7)** mediates senescence induced by oncogenes in normal melanocytes.[69]

To enforce the irreversible stasis of senescence, cells switch on a self-perpetuating loop that suppresses cytokinesis. Stable cell cycle arrest is induced by activating the retinoblastoma (RB) tumor suppressor. Subsequent inactivation of RB leads to re-initiation of DNA replication but not proliferation because of a second safety mechanism that arrests senescent cells in G_2 or M phase.

Signaling Pathways in Senescence

Age-related cell signaling pathways are linked to protein aggregation processes and age-onset neurodegenerative diseases. Sirtuins are potential therapeutic targets to treat age-related diseases. There are seven mammalian **sirtuins** (SIRT1 to SIRT7). Inactivation of sirtuin genes in mice leads to premature aging, and activation of SIRT1 appears to counteract some events of aging. Natural activity of the gene encoding **SIRT1**, a sirtuin histone deacetylase, increases in restricted calorie intake and during treatment with resveratrol, both conditions that favor longevity. SIRT1 expression delays the toxic effects caused by **α-synuclein**, the protein that forms insoluble aggregates in neurons of Parkinson's disease patients, and in several other age-onset disorders.[70]

In contrast, **SIRT2** enhances toxicity of α-synuclein. **Inhibition of SIRT2** protects against α-synuclein-related lesions. In several animal models, reduced SIRT2 activity protected against α-synuclein-induced toxicity. SIRT2 inhibition led to aggregation of α-synuclein, consistent with the finding that large protein aggregates are protective, whereas small aggregates correlate with toxicity.[71] SIRT2 co-localizes with the microtubule cytoskeleton where it deacetylates lysine-40 of α-tubulin. Histone deacetylases are required for autophagy, and SIRT2 might block expression of genes that promote protection against proteotoxicity; alternatively, SIRT2 may regulate PCD—apoptosis increases when cells express less SIRT2 or are treated with sirtuin inhibitors.

Animal Models of Senescence

Genetic, metabolic and environmental factors contribute to the aging process and senescence in vertebrate species. Life cycles of some lower vertebrates are limited by adrenal cortical activity. The striking sudden senescence and death of migrating Pacific salmon is a biological model of senescence.

The Salmon Death Model

Pacific salmon undergo a rapid pattern of aging and death after their migration from the sea to freshwater rivers to spawn. After eggs are ejected and fertilized, the adults become increasingly sluggish and die within a few days. Adrenal cortical toxicosis is allegedly the cause of the rapid aging process. Changes that occur are associated with onset of sexual maturity and include atrophy of the digestive tract, muscles, and viscera. **Castration** suppresses adrenal activity and allows an increased life span.[72,73]

The salmon model may be related to mediation of aging via the hypothalamus-pituitary axis. This genetically controlled neuroendocrine clock slows with age, and the loss of its hormonal direction deprives supporting tissues of stimuli to repair and reconstruct themselves.

Aging of sockeye salmon (*Oncorhynchus nerka nerka*) is accompanied by gradual increases in dopamine and serotonin turnover and decrease of brain total protein and glutathione levels (detox of ROS is needed since activities of SOD and catalase increase with age). Studies in this species do not support an increase in apoptosis in late aging but rather an age-related downward regulation of protein and glutathione synthesis, and proteolysis that increases the need for autophagocytosis.[74]

The Klotho Mouse Model

Inactivation of the ***klotho*** gene accerates aging in mice. The gene encodes a transmembrane protein that binds to fibroblast growth factor receptors; the extracellular domain is secreted and may function as a humoral factor. **Klotho mice** (deficient in the klotho gene) have a shortened life span with early onset age-related changes such as arteriosclerosis, osteoporosis,

skin atrophy, and testicular atrophy. These mice have decreased stem cell numbers and increased progenitor cell senescence. Secreted klotho is a WNT antagonist, and appears to mediate some longevity effects. Klotho bound to Wnt family members suppresses Wnt biological activity, and continuous Wnt exposure triggered stem cell depletion and accelerated cellular senescence.[75] Klotho gene insufficiency causes dysfunction of protein sythesis in neurons, and may be related to neurodegenerative disease.[76]

Organelle Senescence

Clearance of effete organelles by an autophagy-like process is critical for cellular homeostasis, and defects in this process have been linked to aging, cancer and some degenerative diseases. Deletion of **mitochondria** in developing reticulocytes has been used for a model for which the Bcl2-related protein NIX is required (mitochondrial clearance does not require BAX, BAK, Bcl-X_L, BIM, or PUMA).[77]

References

1. Philimonenko AA, et al. 2006. The microarchitecture of DNA replication domains. *Histochem Cell Biol* 125:103.
2. Pockwinse SM, et al. 1997. Cell cycle independent interaction of CDC2 with the centrosome, which is associated with the nuclear matrix intermediate filament scaffold. *Proc Natl Acad Sci USA* 94:3022.
3. Rauch A, et al. 2008. Mutations in the pericentrin (PCNT) gene cause primordial dwarfism. *Science* 319:816.
4. Elmlund H, et al. 2006. The cyclin-dependent kinase 8 module sterically blocks Mediator interactions with RNA polymerase II. *Proc Natl Acad Sci USA* 103:15788.
5. Tsang WY, et al. 2007. SCAPER, a novel cyclin A-interacting protein that regulates cell cycle progression. *J Cell Biol* 178:621.
6. Murray A. 1995. Cyclin ubiquitination: The destructive end of mitosis. *Cell* 81:149.
7. Altmann G, Leblond CP. 1983. Changes in the size and structure of the nucleolus of columnar cells during their migration from crypt base to villus top in rat jejunum. *J Cell Sci* 56:83.
8. Robbins E, Gonatas, NG. 1964. The ultrastructure of a mammalian cell during the mitotic cycle. *J Cell Biol* 21:429.
9. Kochanski RS, Borisy GG. 1990. Mode of centriole duplication and distribution. *J Cell Biol* 110:1599.
10. Misteli T, Warren G. 1995. A role for tubular networks and a COP I-independent pathway in the mitotic fragmentation of Golgi stacks in a cell-free system. *J Cell Biol* 130:1027.
11. El-Alfy M, et al. 1989. An electron microscopic study of mitosis in mouse duodenal crypt cells confirms that the prophasic condensation of chromatin begins during the DNA-synthesizing (S) stage of the cycle. *Am J Anat* 186:69.
12. Cooke CA, et al. 1990. CENP-B: A major human centromere protein located beneath the kinetochore. *J Cell Biol* 110:1475.
13. Saitoh H, et al. 1992. CENP-C, an autoantigen in scleroderma is a component of the human inner kinetochore plate. *Cell* 70:115.
14. Ou Y, Rattner JB. 2004. The centrosome in higher organims. *Int Rev Cytol* 238:119.
15. Paintrand M, et al. 1992. Centrosome organization and centriole architecture. *J Struct Biol* 108:107.
16. Strand P, et al. 2007. Regulated HsSAS-6 levels ensure formation of a single procentriole per centriole during the centrosome duplication cycle. *Dev Cell* 13:203.
17. Zimmerman WC, et al. 2004. Mitosis-specific anchoring of gamma tubulin complexes by pericentrin controls spindle organization and mitotic entry. *Mol Biol Cell* 15:3642.
18. Jurczyk A, et al. 2004. Pericentrin forms a complex with intraflagellar transport proteins and polycistin-2 and is required for primary cilia assembly. *J Cell Biol* 166:637.
19. Sun OY, Schatten H. 2006. Role of NuMA in vertebrate cells. *Front Biosci* 11:1137.
20. Thiry M, 1995. Behavior of interchromatin granules during the cell cycle. *Eur J Cell Biol* 58:14.
21. Lian S, et al. 2006. GW bodies, microRNAs and the cell cycle. *Cell Cycle* 5:242.
22. Yan Z, et al. 2004. GW182 is critical for the stability of GW bodies expressed during the cell cycle and cell proliferation. *J Cell Sci* 117:5567.
23. Ferreira JA, et al. 1994. Differential interaction of splicing snRNPs with coiled bodies and interchromatin granules during mitosis and assembly of daughter cell nuclei. *J Cell Biol* 126:11.
24. Tamaki H, Yamashina S. 1991. Changes in cell polarity during mitosis in rat parotid acinar cells. *J Hist Cyt* 39:1077.
25. Cotter L, et al. 2007. Nuclear membrane disassembly and rupture. *J Mol Biol* 369:683.
26. Gaietta GM, et al. 2006. Golgi twins in late mitosis revealed by genetically encoded tags for live cell imaging and correlated electron microscopy. *Proc Natl Acad Sci USA* 103:17777.
27. Lucoque JM, et al. 1989. Mitotic Golgi fragments in HeLa cells and their role in the reassembly pathway. *J Cell Biol* 109:463.
28. Böckelmann PK, Bechara IJ. 2004. Effect of naproxen on tail fin regeneration in teleost. *J Submicrosc Cytol Pathol* 36:55.
29. Lin G, Slack JM. 2008. Requirement for Wnt and FGF signaling in Xenopus tadpole tail regeneration. *Dev Biol* 316:323.
30. Muneoka K, et al. 2008. Regrowing human limbs. *Sci Am* 298:56.
31. Kumar A, et al. 2007. Molecular basis for the nerve dependence of limb regeneration in an adult vertebrate. *Science* 318:772.
32. Widmann J-J, Fahimi HB. 1975. Proliferation of mononuclear phagocytes (Kupffer cells) and endothelial cells in regenerating liver. *Am J Pathol* 80:349.

33. Kawakita N, et al. 1992. Analysis of proliferating hepatocytes using a monoclonal antibody against proliferating cell nuclear antigen/cyclin in embedded tissues from various liver diseases fixed in formaldehyde. *Am J Pathol* 140:513.
34. Lane BP, Becker FF. 1967. Regeneration of the mammalian liver. *Am J Pathol* 50:435.
35. Viragh S, Bartok T. 1966. An electron microscopic study of the regeneration of the liver following partial hepatectomy. *Am J Pathol* 49:825.
36. Yamamoto K, Fahimi HD. 1987. Three-dimensional reconstruction of a peroxisomal reticulum in regenerating rat liver. *J Cell Biol* 105:713.
37. Meyer DJ, et al. 1981. Intercellular communication in normal and regenerating rat liver. *J Cell Biol* 91:505.
38. Budny T, et al. 2007. Morphologic features in the regenerating liver—a comparative interval, light microscopical and ultrastructural analysis with focus on hepatic stellate cells. *Virchows Arch* 451:781.
39. Starzl TE, et al. 1979. Growth-stimulating factor in regenerating canine liver. *Lancet* 1:127.
40. Marti U, et al. 1989. Biological effects of epidermal growth factor on the gastrointestinal tract and liver. *Hepatology* 9:126.
41. Herbst H, et al. 1991. Temporal and spatial patterns of proto-oncogene expression at early stages of toxic liver injury in the rat. *Lab Invest* 65:324.
42. Quaife CJ, et al. 1989. Histopathology associated with elevated levels of growth hormone and insulin-like growth factor I in transgenic mice. *Endocrinology* 124:40.
43. Sandgren EP, et al. 1991. Complete hepatic regeneration after somatic deletion of an albumin-plasminogen activator transgene. *Cell* 66:245, 1991.
44. Carlson JA, et al. 1989. Accumulation of PiZ α_1-antitrypsin causes liver damage in transgenic mice. *J Clin Invest* 83:1183.
45. Camargo AAP, et al. 2004. Morphological aspects of muscle regeneration in the Nile tilapia (*Oreochromis niloticus*). *J Submicr Cytol Pathol* 36:319.
46. Kern H, et al. 2004. Long-term denervation in humans causes degeneration of both contractile and excitation-contraction coupling apparatus, which is reversible by functional electrical stimulation (FES): A role for myofiber regeneration. *J Neuropathol Exp Neurol* 63:919.
47. Boncompagni S, et al. 2007. Structural differentiation of skeletal muscle fibers in absence of innervation in humans. *Proc Natl Acad Sci USA* 104:19339.
48. Ashley Z, et al. 2007. Atrophy but not necrosis, in rabbit skeletal muscle denervated for periods of up to one year. *Am J Physiol Cell Physiol* 292:C440.
49. Borisov AB, Carlson BM. 2000. Cell death in denervated skeletal muscle is distinct from classical apoptosis. *Anat Rec* 258:305.
50. Klion RM, Schaffner F. 1967. Ultrastructural features of canine hepatic auxiliary transplant rejection. *Exp Mol Pathol* 63:61.
51. Jiang S, et al. 2007. Transcriptional profiling of young and old mesenchymal stem cells in response to oxygen deprivation and reparability of the infarcted myocardium. *J Mol Cell Cardiol* 44:582.
52. Shawi M, Autexier C. 2007. Telomerase, senescence and ageing. *Mech Ageing Dev* 129:3.
53. Hulbert AJ, et al. 2007. Life and death: Metabolic rate, membrane composition, and life span of animals. *Physiol Rev* 87:1175.
54. Suzuki Y, et al. 1978. Microtubules observed within the cistern of RER in neurons of the aged dog. *Acta Neuropathol* 44:155.
55. Bodo E, et al. 2007. Dissecting the impact of chemotherapy of human hair follicle. *Am J Pathol* 171:1153.
56. Martinelli C, et al. 2004. Gap junctions between perineuronal cells increase in number with age in rabbit spinal ganglia. *J Submicr Cytol Pathol* 36:17.
57. Urso M, et al. 2005. Immunogold labeling of insulin growth factor-1 receptors in elderly human skeletal muscle. *Scanning* 27:208.
58. Rauch A, et al. 2008. Mutations in the pericentrin (PCNT) gene cause primordial dwarfism. *Science* 319:816.
59. Stewart CL, et al. 2007. Mouse models of the laminopathies. *Exp Cell Res* 313:2144.
60. Halaschek-Wiener J, Brooks-Wilson A. 2007. Progeria of stem cells. *J Gerontol A Biol Sci Med Sci* 62:3.
61. Navarro CL, et al. 2006. Molecular basis of progeroid syndromes. *Hum Mol Genet* 15 Spec No 2:R151.
62. Geuze JJ. 1970. Light and electron microscope observations on auto- and heterophagy in the exocrine pancreas of the hibernating frog (*Rana esculenta*). *J Ultrastruc Res* 32:391.
63. Malatesta M, et al. 2003. Fine distribution of CLOCK protein in hepatocytes of hibernating dormice. *Eur J Histochem* 47:233.
64. Ruediger J, et al. 2007. Dynamics in the ultrastructure of asymmetric axospinous synapses in the frontal cortex of hibernating European ground squirrels (*Spermophilus citellus*). *Synapse* 61:343.
65. Pauziene N, et al. 2000. Morphological study of the heart innervation of bats *Myotis daubentoni* and *Eptesicus serotinus* (Microchiroptera: Vespertilionidae) during hibernation. *Eur J Morphol* 38:195.
66. Malatesta M, et al. 2002. Quantitative ultrastructural changes of hepatocyte constituents in euthermic, hibernating and arousing dormice (*Muscardinus avellanarius*). *Tissue Cell* 34:397.
67. Malatesta M, et al. 2001. Fine structural modifications of liver, pancreas and brown adipose tissue mitochondria from hibernating, arousing and euthermic dormice. *Cell Biol Int* 25:131.
68. Knight JE, et al. 2000. mRNA stability and polysome loss in hibernating Arctic ground squirrels (*Spermophilus parryii*). *Mol Cell Biol* 20:637.
69. Chien Y, Lowe SW. 2008. Secreting tumor suppression. Cell 132:339.
70. Dillin A, Kelly JW. 2007. The Yin-Yang of Sirtuins. *Science* 317:461.
71. Milne JC, Denu JM. 2008. The Sirtuin family. *Curr Opin Chem Biol* 12:11.
72. Robertson OH, Wexler BC. 1962. Histologic changes in the organs and tissues of senile castrated kokanee salmon (*Oncorhynchus nerka kennerlyi*). *Gen Comp Endocrinol* 2:458.

73. Moore JF, et al. 1976. Ultrastructure of coronary arterial changes in spawning Pacific salmon (genus *Oncorhynchus*) and steelhead trout (*Salmo gairdnerii*). *J Comp Pathol* 86:259.
74. Götz ME, et al. 2005. Brain aging phenomena in migrating sockeye salmon *Oncorhyncus nerka nerka*. *J Neural Transm* 112:1177.
75. Suzuki H, et al. 2008. Histological and elemental analyses of impaired bone mineralization in klotho-deficient mice. *J Anat* 212:275.
76. Anamizu Y, et al. 2005. Klotho insufficiency causes decrease of ribosomal RNA gene transcription activity, cytoplasmic RNA and rough ER in the spinal anterior horn cells. *Acta Neuropathol* 109:457.
77. Schweers RL et al. 2007. NIX is required for programmed mitochondrial clearance during reticulocyte maturation. *Proc Natl Acad Sci USA* 104:19500.

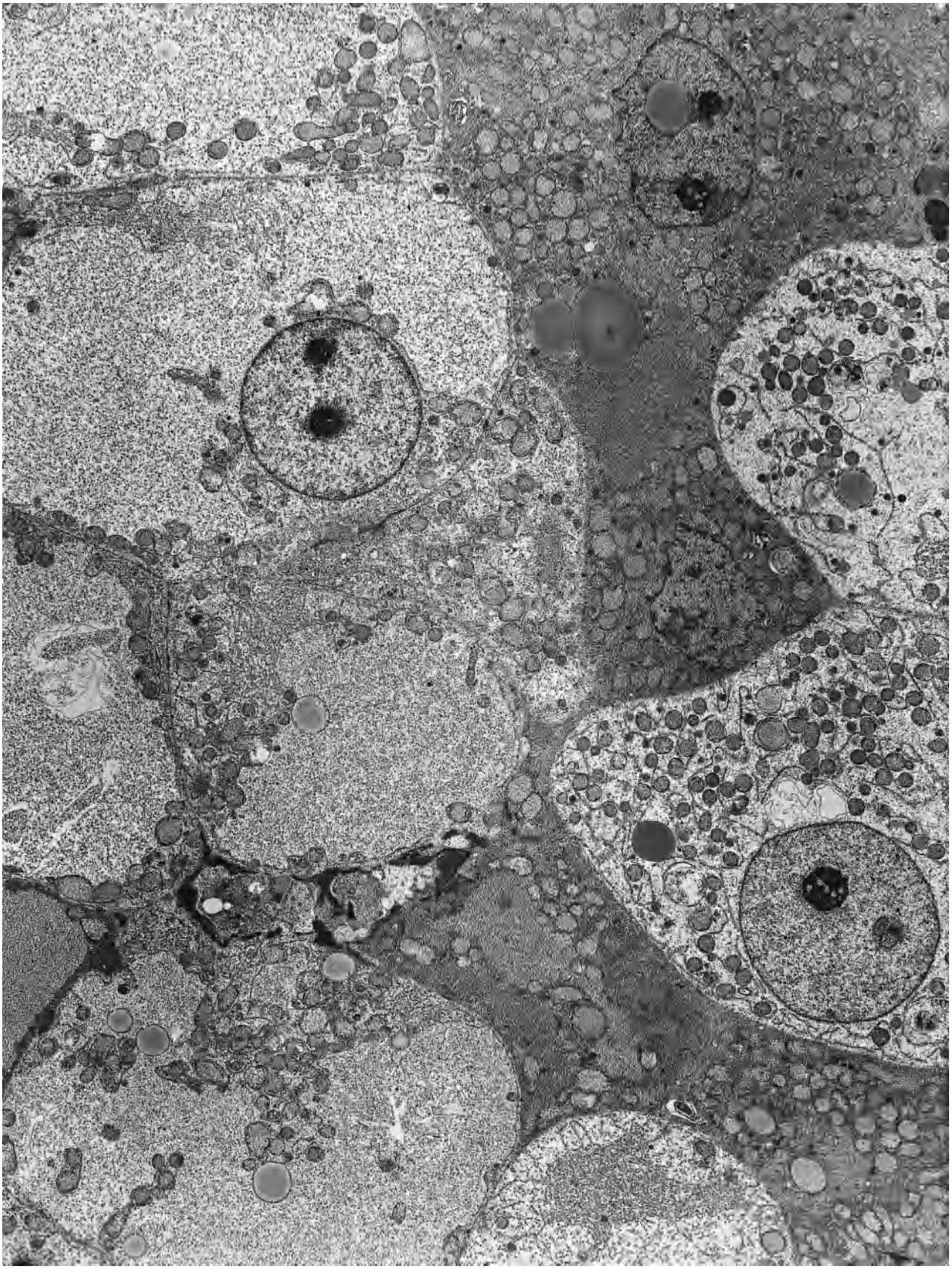


Fig. 23.1 Clear cell carcinoma: liver, dog. Different cell types: neoplastic clear cells are pale and filled with glycogen. Remnants of smooth endoplasmic reticulum and mitochondria remain at the cell periphery and around nuclei. Dark mitochondria-rich cells are variants in the tumor population.

© 2009 Wiley-Blackwell. ISBN: 978-0-813-80330-2

23 The Neoplastic Cell

The neoplastic process involves an intrinsic heritable abnormality in cells that gives rise to autonomous growth. Neoplastic cells do not behave as integrated, interdependent populations as expected in metazoan animal tissue. The regulatory mechanisms that control mitosis, differentiation, energy production, movement, and intercellular communication are defective (Fig. 23.1). Cells grow in rapidly expanding masses that ultimately compromise host structure and function.[1] Features that neoplastic cells have in common are

- **Genes**, and often chromosomes, that are abnormal, and that are expressed at inappropriate times or at unusual rates
- **Mitotic structures** that are readily activated
- **Cell surfaces** designed for movement and migration at the expense of intercellular communication
- **Cytoplasmic organelles** that resemble those of embryonic undifferentiated cells
- **Rudimentary mitochondria** and simplified energy production via fermentation of anaerobic metabolism of glucose, with less dependence upon a primitive mitochondrial respiratory chain

These are also characteristics of undifferentiated embryonic cells. Indeed, the common thread among cells of various malignant neoplasms is a failure of differentiation. What sets the neoplastic cell apart is the permanent activation of oncogenes and the inactivation of tumor suppressor and proapoptotic genes. In the end, the cancer cell is responsive to **autocrine growth stimulation;** that is, it produces growth factors to which it also responds.

Although the neoplastic cell is markedly abnormal in many ways, it is the increase in mitotic rate that sustains tumor growth. The capacity to undergo mitosis, an inherent character in all cells, is repressed or controlled in normal somatic cells. Neoplastic cells lack this repression because their mechanism of control is imperfect or because they are unresponsive to the controlling mechanism.

Genetic instability underlies the sequential acquisition of biologic characteristics of neoplasms. Human cancer-prone syndromes such as Fanconi's anemia, Werner's syndrome, Bloom's syndrome, and ataxia-telangiectasia provide striking evidence that genetic instability is heritable and predisposes to neoplastic change. Changes that arise from genetic instability may provide a selective growth advantage over adjacent cells. Neoplastic proliferation then proceeds as a result of uncontrolled mitosis in the expanding tumor population. While most variants die, due to metabolic or immunologic disadvantage, many cells survive. The surviving neoplastic population has a higher frequency of mitotic error and other genetic changes, and each cell division carries an increased risk of variation.

The **growth rate** of a tumor depends on several inherent growth characteristics: the fraction of cells in a tumor undergoing mitosis; the length of the cell cycle, that is, the interval between mitosis and completion of subsequent mitoses in daughter cells; and the number of cells lost by death, exfoliation, and metastasis. The length of the tumor cell cycle is usually (but not always) shorter than that of its normal cellular counterpart. Some of the proteins that regulate the cell cycle are used as markers for neoplastic cell proliferation; for example, cyclin (PCNA) is an auxiliary protein for DNA polymerase δ, which is used for assessing proliferative activity of nonsmall cell lung cancers.

Tumor growth also depends on the ability of the neoplastic cell to grow and move in the **tumor micro-**

environment. That is, the new cell must move within a supportive extracellular matrix, alter the connective tissue ground substance, and stimulate vascular growth. If new capillaries cannot nourish the tumor, the cancer cell will die.

The Genomic Landscape

The search for causes of neoplasia has directed attention toward two basic mechanisms: **genetic mutation** and **defective cell regulation.** These are poles in a spectrum of ways in which cells may become neoplastic and, although there is a mutational basis for neoplasia, neoplastic growth is enhanced by nonmutational means. While mutations play a prominent role in the neoplastic phenotype, neoplasia also involves aberrations at epigenetic levels in gene expression. The crucial factor is **expression** of genes for control of growth and differentiation. These genes need not be abnormal (in the sense of directing faulty protein synthesis). Instead, control of gene expression may be defective, leading to synthesis of gene products in excess or at the wrong time.

Genes, Mutations, and DNA Damage

Naturally occurring tumors show evidence of progressive changes in their **DNA.** The cells of most tumors contain multiple DNA or gene defects that combine to produce abnormal mitosis and growth. **Growth genes** (or oncogenes, their counterpart in some cancer cells) are activated to augment mitosis, cell surface changes, metabolic pathways, and other characteristics of growth. Conversely, **suppressor genes,** which function to inhibit cell growth, may be inactivated releasing the brakes on normal growth. In general, neoplastic cells that develop the most genetic mutation have the greatest capability for malignant growth. For example, in a high percentage of human malignant colon cancers, *ras* genes are activated and tumor suppressor genes are lost from chromosomes 5, 17, and 18.

DNA Damage

DNA damage and mitotic control are closely related. In normal cells, damage to DNA interrupts the cell cycle so that DNA repair mechanisms can be activated. The cell cycle is not resumed until DNA repair is complete. The G1-S and G2-M transitions of the cell cycle are halted by DNA damage and serve as checkpoints at which cells can delay the cell cycle so that abnormal DNA is not perpetuated. In neoplastic cells these checkpoints may be ineffective. The p53 gene, which is necessary for normal G_1-S checkpoint control, is implicated in early neoplastic change; for example, tumor cells that lack p53, or have mutant forms of it, lack the G_2-S delay that occurs upon exposure of cells to radiation.

Tumors do not develop from end-stage cells. For neoplasia to occur (for differentiation to fail) in adult animals, pluripotential stem cells must be present. Tumors do not arise from completely differentiated cells such as neurons or keratinized epithelial cells (Fig. 23.2). These end cells do occur in tumors but only as a result of variance in differentiation as the tumor grows. Neoplastic cells do not "dedifferentiate" but fail to respond to normal signals for differentiation.

The Genomic Landscape

The complete sequence of nucleotide bases in normal human DNA is now available, and pathologists can classify the spectrum of human genes that have a role in carcinogenesis. In the typical neoplasm, there are at least 80 DNA mutations that alter amino acids. These are composed of a few mutated genes common to most neoplasms, and a much larger number of genes that are infrequently mutated. Statistical analyses indicate that most mutations in an individual neoplasm are harmless, and that less than 15 are responsible for driving the initiation, progression and maintenance of neoplastic growth. Although many reports exist on genetic alterations in neoplasms on a genomic scale, it is difficult to clarify the role of these mutations in carcinogenesis. Human colorectal and mammary malignant neoplasms have about the same number of mutated genes, but the particular genes that are mutated in each are very different. Perhaps this reflects differences in mutagen exposure or DNA-repair processes; for example, mutations converting 5′-CpG to 5′-TpG are more frequent on colorectal than mammary neoplasms.[1]

Epigenomics

Epigenomics is defined as heritable changes in gene expression that are not due to any alteration in the DNA sequence. Epigenetic changes modify gene expression. The best known epigenetic marker is DNA methylation.

DNA Methylation

DNA methylation occurs in a complex chromatin network, and is influenced by the modifications in histone structure that are common in cancer cells.

The low level of DNA methylation in cancer cells (as compared with the level of DNA methylation in their normal-tissue counterparts) is a common attri-

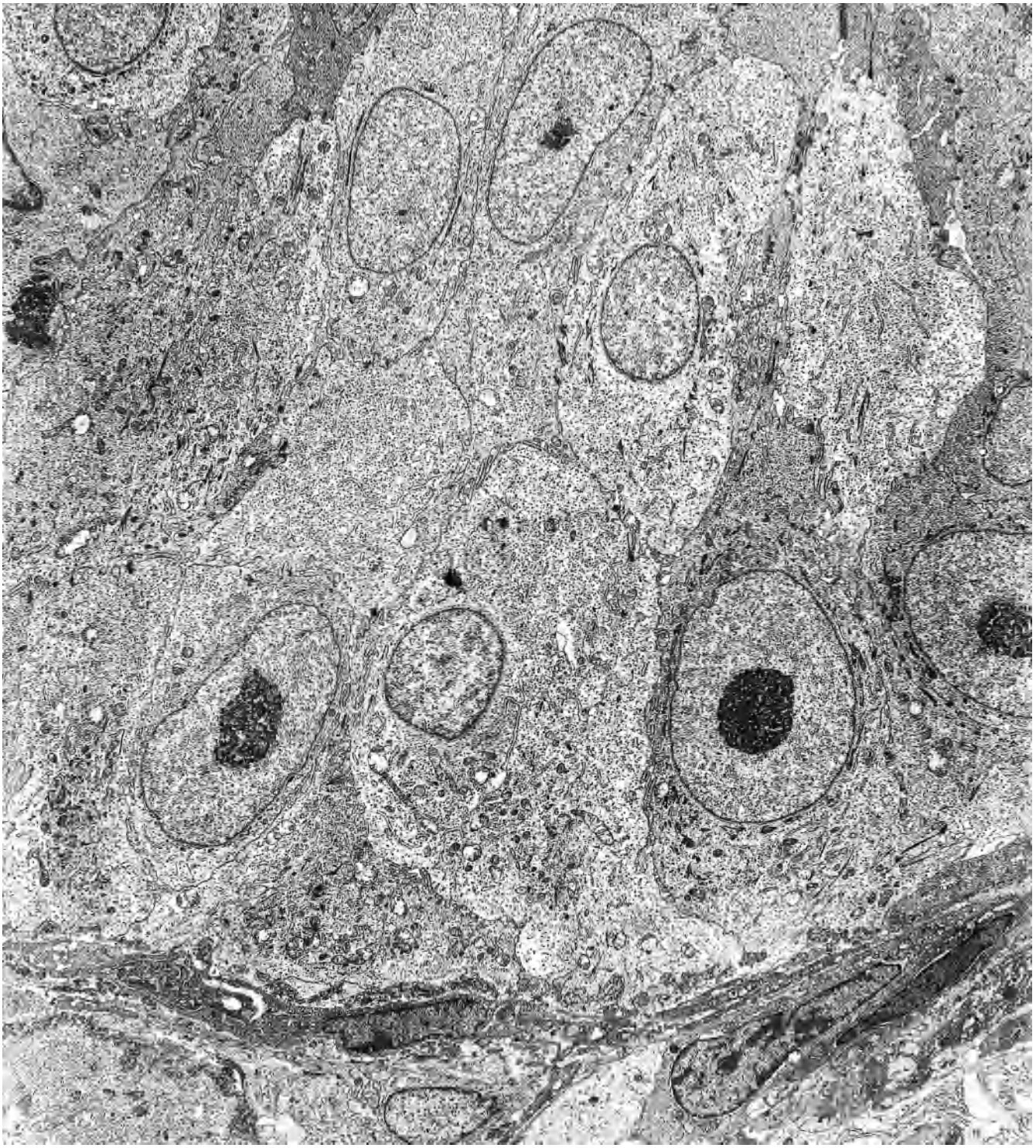


Fig. 23.2 Squamous cell carcinoma: pharynx, cat. Cells are moderately differentiated; they maintain stellate shapes, produce desmosomes and basement membranes, and progress toward keratinization. Cells are pleomorphic, are positioned vertically, lack tonofilaments, and contain large nucleoli with little visible chromatin.

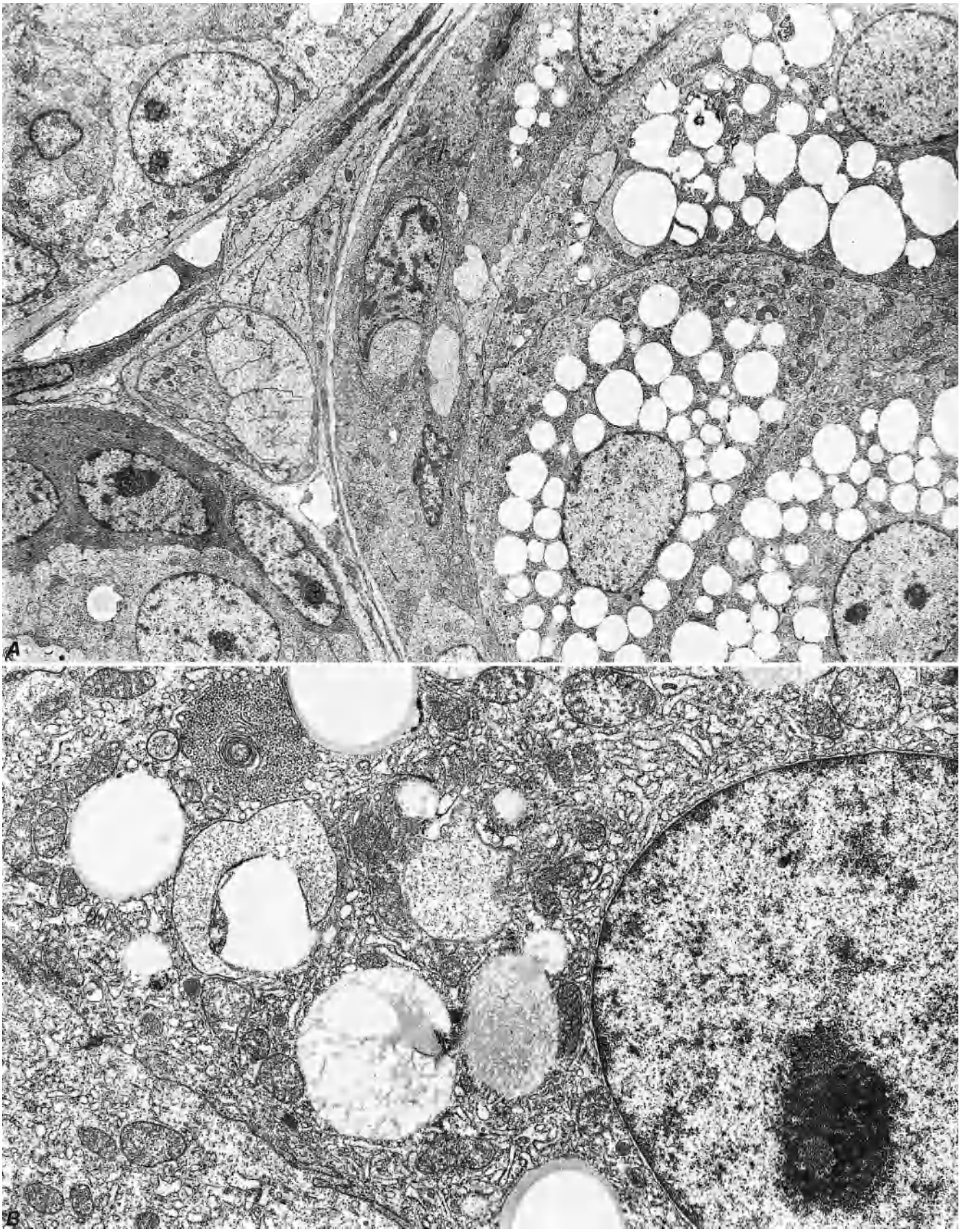


Fig. 23.3 Sebaceous gland adenoma: skin, dog. **A**. **Neoplastic sebaceous cells** (*right*) resemble their normal counterparts; they are plump with electron-lucent lipid globules. Undifferentiated basal cells also resemble normal sebaceous gland basal epithelium. **B**. **Neoplastic sebaceous cell**: much smooth endoplasmic reticulum (SER) and many lattices of SER membranes. Various distributions of clear and gray material in lipid globules are due to varying content of lipids and waxes.

bute of neoplasms. During the carcinogenesis, the degree of **hypomethylation** of genomic DNA increases as the lesion progresses from a benign to a malignant tumor. In tumors, aberrant DNA methylation leads to a spectrum of changes from hypermethylated tumor-suppressor genes to inactivation of microRNA genes. Unlike mutations, DNA methylation and histone modifications are reversible, and it is possible, at least in vitro, to awaken dormant, hypermethylated tumor-suppressor genes with drugs.[2]

Transcriptional Silencing

In neoplastic cells, aberrant gene function and abnormal patterns of gene expression are influenced by several epigenetic events. Prominent are those epigenetically mediated transcriptional silencing events associated with increased DNA methylation (particularly at promoter regions of genes). In one study of Ras epigenetic silencing effectors required for Ras-mediated epigenetic silencing of the pro-apoptotic *Fas* gene, genome-wide screens for RNA interference in K-ras-transformed cells identified 28 genes. Altered signal transduction pathways appear during early stages of neoplastic transformation. Dependency of these pathways in the transforming cancer cell predispose to new genetic mutations in the same pathways for growth.[3,4]

Benign or Malignant

Benign neoplasms are those that are well differentiated, grow slowly by expansion, and do not invade below basement membranes. Benign tumors are often **encapsulated** (but lack of a connective tissue capsule does not imply malignancy). Benign tumors can cause serious disease by exerting pressure on ducts, arteries, or the nervous system. Parathyroid adenomas may be tiny and benign yet can generate lethal disease in the animal through secretion of hormones by the neoplastic cell. Benign tumors are classified by adding, to the basic histologic stem word denoting the cell of origin, the suffix **-oma.** A benign tumor of epithelium is an **epithelioma,** of fibrocytes a **fibroma,** and of chondrocytes in cartilage a **chondroma.** In all of these, tumor cells closely resemble their normal counterpart. **Adenoma** is applied to benign epithelial tumors that produce glandular patterns. A sebaceous gland adenoma is composed of cells that closely resemble the normal sebaceous gland (Fig. 23.3). The abnormalities of secretory granules in the cytoplasm are due to enhanced crinophagy associated with failure of secretion rather than an inherent change in the formation of secretory granules.

Malignant neoplasms are composed of cells that are anaplastic and that metastasize and invade. The aggressive neoplastic cells infiltrate and, in most cases, destroy normal tissues. A "cancer" is a malignant neoplasm. Those of ectodermal derivation are called **carcinomas;** those of mesodermal origin, **sarcomas.** Features that separate malignant from benign tumors are not requisites of malignancy but are general characteristics of malignancy. **Differentiation** refers to the extent to which cells resemble the cells of their tissue of origin (in embryology, differentiation is used to indicate a change from a lower to a higher state of specialization). **Undifferentiation,** synonymous with **anaplasia,** refers to the loss of specialization and organization, with anarchic changes in cell organelles.

Preneoplastic lesions are those that are known to progress to overt malignant neoplasms after a time of dysplastic growth. Squamous carcinomas of the cervix of the human female develop within dysplastic lesions of the cervical epithelium called **carcinoma in situ.** Similar preneoplastic lesions precede squamous cell carcinomas at other sites, transitional cell carcinomas of the urinary bladder, and malignant melanomas of the skin and oral mucosa. Ultrastructural changes in intestinal lesions of familial colonic polyposis progress from local adenomas to carcinoma.

Neoplastic Cell Structure

Cellular anaplasia and invasion of tissue are the two most reliable hallmarks of malignancy (if the tumor has metastasized, there is no doubt). Characteristics of **anaplasia** are

- **Pleomorphism** (differences in cell size and shape)
- **Large irregular nuclei** with abnormal chromatin and irregular nuclear membranes
- **Nucleoli** are increased in size and number (but may be small or absent)
- **Mitotic apparatus** or centrioles are abnormal
- **Mitochondria, endoplasmic reticulum**, and other cell work-associated cytoplasmic organelles are decreased or abnormal
- **Glycocalyxes and basement membranes** are irregular and incomplete[5,6]

Structural evidence indicates that neoplastic cells are geared to function in reproduction and not in metabolic activity of other kinds. Overall, tumor cells are pleomorphic with great differences in the appearance of individual cells. The extent of pleomorphism generally correlates with the degree of malignancy (Fig. 23.4). Cells have striking increases in cell volume and, in most malignant neoplasms, are

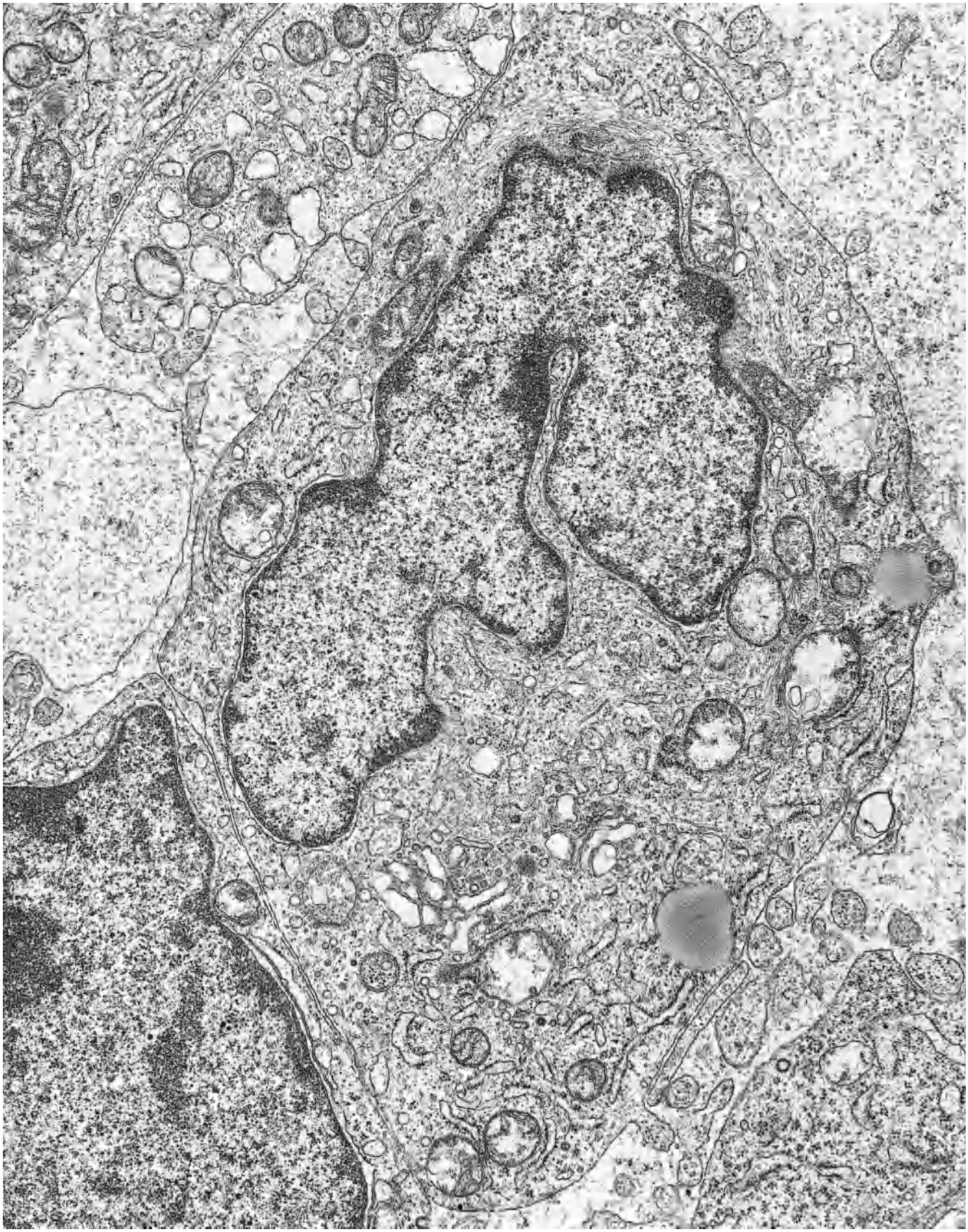


Fig. 23.4 Malignant melanoma (amelanotic): marked irregularity of nucleus, mitochondria, endoplasmic reticulum, and Golgi complex; increase in microfilaments, especially in perinucleolar areas; absence of melanin granules.

large with markedly irregular surfaces. These characteristics are the parameters for morphometric analysis of tumor cells, for example, the volume and contour of nuclei, the volume of specific cytoplasmic organelles, and other unique characteristics of neoplastic cells.[7]

Neoplastic Cell Surfaces

Loss of cohesiveness with neighboring cells is an important characteristic of malignant cells.[8] Decreased adhesiveness, a change attributed to abnormal plasma membrane glycoproteins, is manifest as the spread of cells by invasion of tissue, by implantation on new surfaces, or by metastasizing to new sites in lymphatics or blood vessels. Desmosomes are abnormal, and there is evidence of uncontrolled production of filaments and other components of the cytoskeleton. Negative surface charges reflect abnormal amounts of sialomucopeptides and this repels cells from one another.

Neoplastic cells contain highly irregular surfaces. Invaginations are common and may go so deeply into the cell that, when cut on cross section, they appear as intracellular canaliculi (Fig. 23.5). Lacking normal cell junctions, they often have **pseudopodia** and **lamellipodia** that project haphazardly into interstitial spaces.[9] Rho-like members of the Rho GTPase family and their downstream effectors are overexpressed at the advancing edge of colon cancers at filopodia, referred to as **invadopodia,** and modulate matrix metalloproteases.[10]

Marked increases in lamellipodia and surface ruffling have been produced by microinjection of the human *ras* gene into fibroblasts in vitro.[11] In some types of neoplastic leukocytes and other mobile cells long **filopodia** cover the surface. These villiform or "anemone cells" are typical of lymphomas but have also been reported in several human carcinomas.[12]

In the more dangerous leukemias such as acute lymphoblastic leukemia, **exovesicles** pinch off from surfaces and microvilli and circulate in the bloodstream. These vesicles and membrane fragments contain tumor antigens that are useful markers and can be detected by radioimmunoassay and by freeze-fracture microscopy.[13]

Plasma Membrane

Integral **membrane proteins** that function as antigens, as specific receptors, or as enzymes are defective in neoplasms. Some of the most important surface proteins on neoplastic cells are **adhesion molecules.**[14] Dysfunctional focal adhesions on the cell surface of neoplastic cells develop when **integrins** are abnormal.[15] Other important transmembrane molecules serve as **receptor molecules** and these are especially important in their interaction with cytoplasmic enzymes in the cell signaling systems. Loss of membrane proteins that function as **histocompatibility antigens** or cell markers (and thereby determine differentiation patterns) is a common defect; for example, cells of the thymoma no longer bear antigens that are present on normal thymic epithelial cells.[16]

A wide variety of other cell activities may be altered, including ionic pumping, reception of peptide hormones, and intercellular communications. Integral membrane proteins, when examined by freeze fracture of plasma membranes, are increased in both noninvasive and invasive tumors (over numbers in normal control cells).[17] Enzyme cytochemical techniques have been used to label surface proteins and to identify those that are important in invasion, metastasis, and other biological properties of neoplastic cells (Fig. 23.6).

Defective plasma membrane proteins may arise directly from abnormal genes, or as a result of a defective kinase such as the phophorylating enzymes of ATP reduction. The c-*src* gene of normal cells codes for a tyrosine-specific protein kinase that is attached to the cytoplasmic face of the plasma membrane; v-*src*, the abnormal viral version of this protein, is associated with neoplastic changes.

Virions and **virus-like particles** can be encountered in the ultrastructural analysis of neoplastic tissue. Some are causal viruses, but in naturally occurring tumors they are often passenger viruses with no causal relationship to the neoplasm. Most are retroviruses that bud from neoplastic cell surfaces (Fig. 23.7).

Cell Surface Gylcoproteins

Cell surface glycoproteins and **glycolipids** are reduced or are abnormal in some other way.[18] They may be missing, or new abnormal molecules may be incorporated due to activation of previously nonexpressed glycosyl transferases. Changes in surface glycoproteins markedly alter the capacity of the cell to bind certain critical matrix factors.[19,20] Specific sequences of oligosaccharide side chains of glycoproteins and glycolipids are considered onco-developmental antigens; that is, they are used as markers of embryonic development that reappear in neoplastic cells. The Thomsen-Friedenreich T antigen, present in fetuses but absent in adult tissue, is commonly found in carcinomas. It can be specifically labeled with immunogold techinques.[21]

Most malignant neoplasms will produce surface glycoproteins that are typical of developing embry-

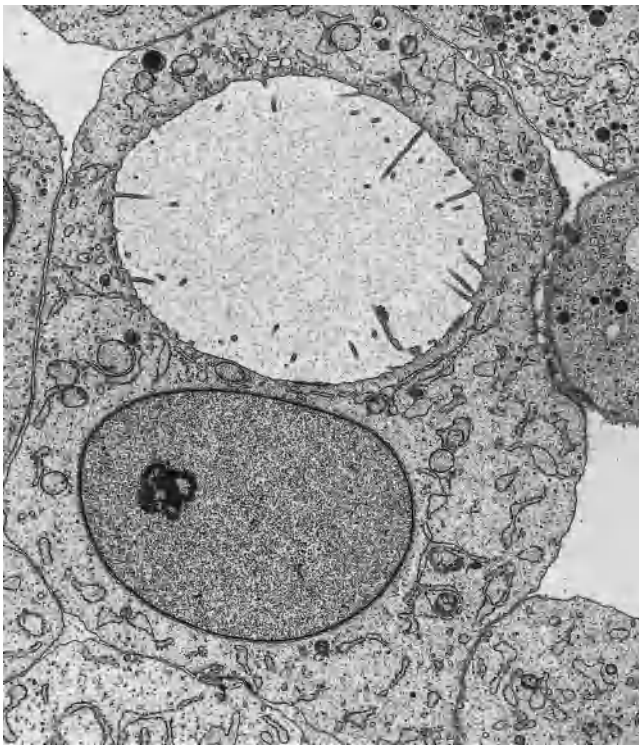


Fig. 23.5 Intracytoplasmic canaliculus: aortic body carcinoma, pleural carcinomatosis, thoracic cavity, dog. Plasma membrane invagination into the cytoplasm produces the canaliculus.

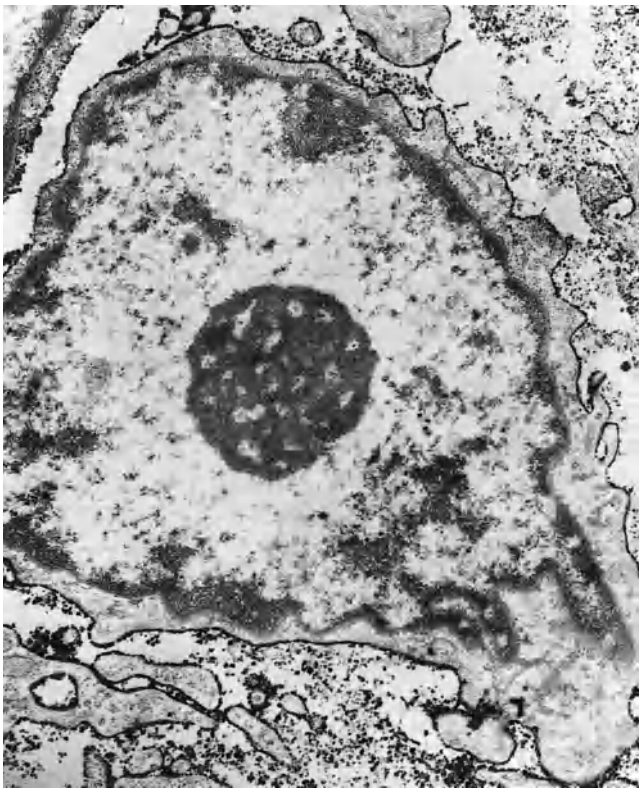


Fig. 23.6 Plasma membrane: alkaline phosphatase activity. Osteoblast-like cell with large nucleus and small cytoplasm. (Micrograph: A. Stark, *Ultrastruct Pathol* 8:143, 1985.)

onic cells; for example, the embryonal nephroma (Wilm's tumor) re-expresses polysialic acid, which is typical of embryonic cells.[22] Melanocytes express a spectrum of surface proteins that differ with the stage of differentation; so too, cells of melanomas tend to express surface antigens typical of undifferentiated melanocytes.[23]

Cytoskeleton

The cell cytoskeleton is abnormal in neoplastic cells, and cytoskeletal instability underlies many abnormal shapes and movements. Abnormal microfilament or microtubule functions are reflected in aberrant cell movement, instability in chromosome movements (via defective spindle formation),[24] and pseudopodia formation.[25]

- **Microfilaments,** normally concentrated at the cell surface, are found throughout the cytoplasm of highly malignant cells.[26]
- **Microtubules** are abnormal, causing rounding or abnormal cell shape; highly invasive carcinomas can contain many microtubules, where there are few in noninvasive counterparts,[27] and immunogold-labeled microtubule-associated proteins are used in defining neoplastic cell origins.[28]
- **Intermediate filaments** are rearranged and disconnected from their attachment sites at the cell surface.

Intermediate Filaments

Intermediate filaments (IF) commonly occur in coiled forms and whorled arrangements in the cytoplasm around the nucleus. IF, 7–11 nm in diameter, are intermediate in size between microfilaments and microtubules from which they can be distinguished by electron miscroscopy. Using specific antibodies against these proteins, one can diagnose and classify neoplasms.[29–33] Highly undifferentiated neoplasms can often be identified specifically on the basis of staining of their IF; for example, squamous cell carcinomas of the human lung have been identified by specific immunostaining of keratin proteins.[34]

Generally one type of tumor consistently produces the same polypeptide type of IF. In skin, there are different cytokeratin polypeptides for different regions. Some cells may synthesize a predominant peptide yet also produce other types, that is, vimentin is the predominant intermediate filament protein produced by human schwannomas (nerve sheath tumors), yet some of these tumors also produce glial fibrillary proteins.[35] In tumor cells, the selective production

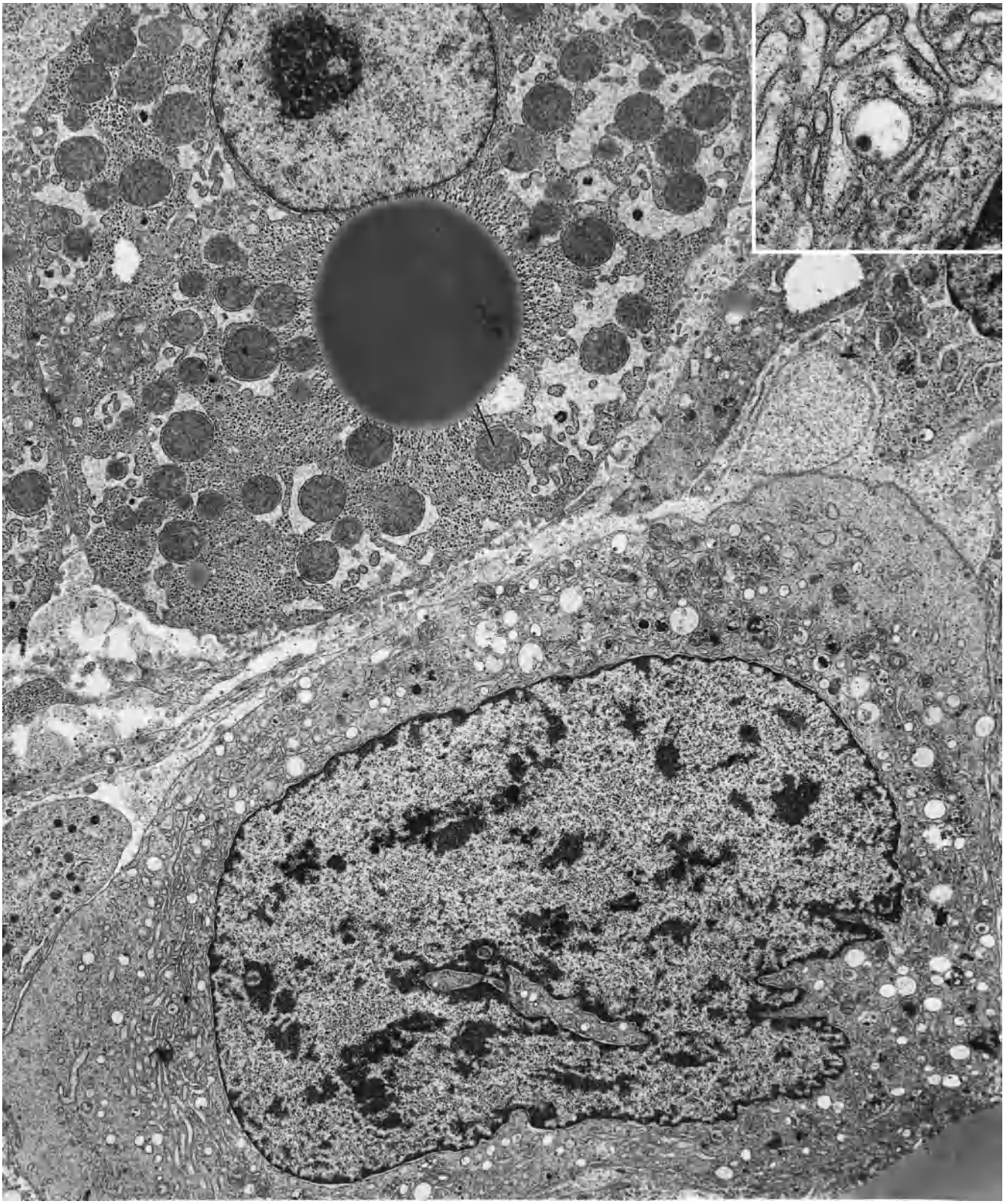


Fig. 23.7 **Retroviruses**: myeloproliferative disease, cat. Virions in the cytoplasm of a malignant hematopoietic stem cell (*bottom*). Type C virions (*inset*) are in vacuoles in the cytoplasm but are rarely found budding from the plasma membrane in natural disease.

of one type of IF may be associated with abnormal activation of genes; for example, neurofilaments accumulate in the cytoplasm of skeletal muscle and renal tubules of transgenic mice bearing genes for production of the light chain subunit of the neurofilament protein.[36]

Cilia

Cilia or remnants of cilia are common findings in mesenchymal tumors, and may occur at the cell surface or on membranes of cytoplasmic vacuoles. They typically are small, stubby with irregular connections to the basal bodies. Abnormal ciliation and ciliogenesis may result in an axial microtubular complex pattern of 9 + 0, 9 + 1, 8 + 0, 8 + 2, or 7 + 2 (in contrast to the 9 + 2 pattern of normal cilia). The presence of cilia is a confirmatory finding in ependymomas and other cilia-bearing cell derived neoplasms.[37]

Cell Junctions

Cell junction defects are typical of neoplastic cells.[38,39] **Tight junctions** are altered, usually by proliferation, fragmentation and development of discontinuities.[40] The extent of these changes correlates with the degree of tumor differentation. Changes in tight junctions are not implicated in tumor growth promotion, and they are a result (not a cause) of malignant changes.

Desmosomes are often present in fewer numbers although their numbers vary greatly in neoplasms.[41,42] In a study of bladder epithelial tumors, desmosomes were increased in noninvasive transitional cell carcinomas but were decreased in invasive tumors.[43,44] Desmosomes have been identified immunocytochemically in tumors by staining for the desmosomal protein desmoplakin.[45] In epithelial tumors that produce basement membranes, **hemidesmosomes** may develop in a vain attempt to anchor the tumor cell. Hemidesmosomes are important in determining the cytoarchitecture of the breast epithelium, and loss in carcinoma cells may be associated with loss of normal cytoarchitecture.[46]

Gap junctions in neoplastic cells may be decreased in number or qualitatively abnormal. Absence of this conduit for communication between cells has significant effects on growth. Gap junctions are freely permeable to small molecules and ions and provide a mechanism to share metabolites and control molecules so that cell systems can respond jointly to changing metabolic demands. When gap junctions are missing, the behavior of the neoplastic tissue as a homogeneous unit is changed. Abnormal phosphorylation of gap junction proteins leads to an inability to maintain gap junctions and development of malignant characteristics.[47] The loss of intercellular communication associated with this decrease correlates with the degree of malignancy in mammary adenocarcinomas; that is, less malignant more differentiated tumors are apt to have more desmosomes.

Some cancer cells have fewer gap junctions and an inability to send and receive signal molecules. This may promote uncontrolled growth, although cancer cells that have normal gap junctions may possess some internal defect in their ability to respond normally to transferred signal molecules. It has been hypothesized that vitamin A impedes development of epithelial neoplasms due to its ability to maintain epithelial differentiation and to block preneoplastic dedifferentiation by causing a significant proliferation of gap junctions.[48]

Intercellular junctions are major sites of action of protein tyrosine kinases, enzymes that are influenced by oncogenes. When cells are transformed in vitro junctions disappear, and microfilaments and some adhesion molecules move away from junction sites. Epithelial cells transformed by Rous sarcoma virus showed marked rearrangement in microfilaments and N-cadherin; immunogold labeling studies have shown that junctions were the major targets for the pp60$^{v\text{-}src}$ tyrosine-specific protein kinase.[49]

The Nucleus of the Neoplastic Cell

Nuclei of neoplastic cells are larger than those of normal cells. In benign tumors, nuclei although large tend to be similar to one another. In contrast, malignant tumors have highly variable nuclei. Some are tiny with little chromatin and no nucleolus, while others are very large with enormous nucleoli. Throughout the nucleoplasm of tumor cell nuclei there is evidence of abnormal or misdirected protein synthesis. Chromatin is dispersed throughout and tends to aggregate in irregular clumps and at unusual sites. Ribonucleoprotein and perichromatin particles may be increased or missing but these too have abnormal distributions.

Intranuclear inclusions of filaments and tubules develop in many neoplasms.[50,51] Indentations of cytoplasm into nuclei give rise to pseudoinclusions. The nuclear **helioid inclusions** of human mammary intraductal neoplasms are membrane bound bodies with radiating filaments resembling the sun (Gr. helios, "sun") and are pseudoinclusions evoked via nuclear sequestration of cytoplasm.[52]

Bizarre nuclear shapes are common in highly malignant cells (Fig. 23.8), perhaps a reflection of abnormal cytoskeletons.[53] Abnormal nuclear features are a major factor in the classification of some neoplasms, for example, the subtypes of non-Hodgkin's lymphomas.[54] The nuclear envelope of neoplastic cells often

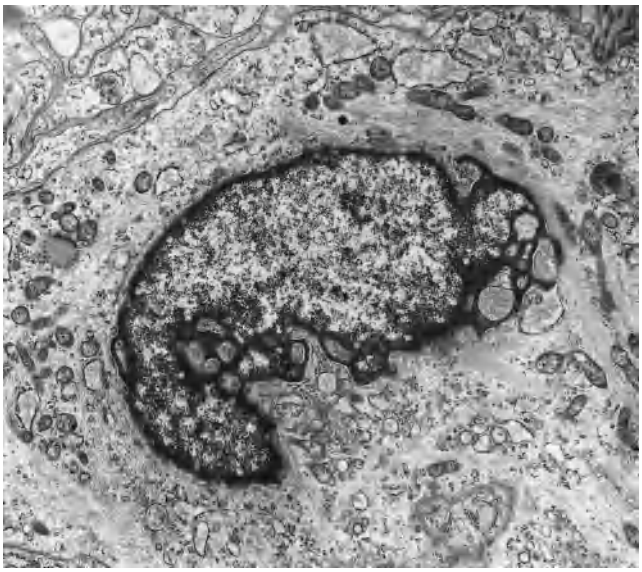


Fig. 23.8 Nucleus: marked irregularity of plasma membrane and internal structure, hemangiosarcoma, dog. Extensive deformation of the nuclear envelope, with absence of nuclear pores, and increase in perinucleolar microfilaments.

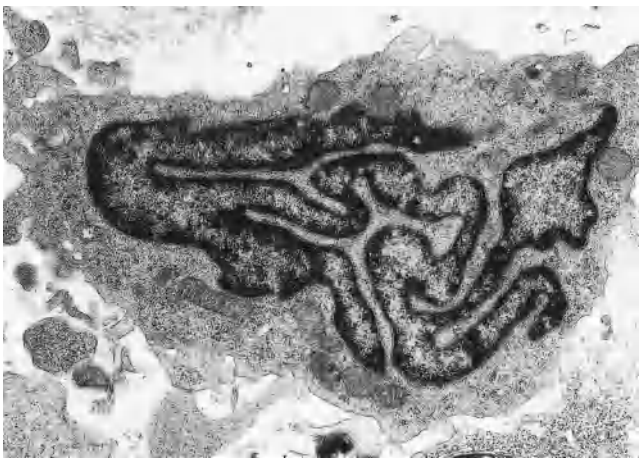


Fig. 23.9 Neoplastic lymphocyte (Sezary cell): skin biopsy, human patient with cutaneous T cell lymphoma (mycosis fungoides). (Micrograph: Claire M. Payne, *Am J Pathol* 120:263, 1985.)

contains deep indentations and invaginations. Multiple lobulation (radial segmentation, or clover-leaf nuclei) are common in some leukemias.[55]

The classic mycosis fungoides cell (Sezary cell) with its striking cerebriform or serpentine nucleus is diagnostic of human cutaneous T cell lymphomas (Fig. 23.9).[56] However, lymphocytes in most cases of mycosis fungoides lack these bizarre nuclei but have only irregular nuclei, changes that resemble lymphocytes found in chronic dermatitis. Computerized morphometric methods with image enhancement have been used to improve diagnosis. For example, a **form factor** for cell shape (defined as $4\pi\ A/P^2$ where A = area, P = perimeter) and a related **nuclear contour index** are used for diagnosis of mycosis fungoides.[57] In these studies, a contour tracing of a serpentine nucleus by computerized planimetry indicates that the nuclear shape is only 6% of a perfect circle, a value not seen in benign lymphocytes. Another shape descriptor that is more sensitive to surface roughness has been termed "perimeter ratio before and after smoothing" (PERBAS).[58] **Receptors** have been localized in the nucleus for several hormone-dependent neoplasms.

Nucleoli

Nucleoli of neoplastic cells are typically large, multiple, and irregular. These general characteristics are not reliable for distinguishing benign and malignant changes, but are useful in specific cases for defining the tumor cell population.

Increased size of nucleoli with accumulation of rRNAs and tRNAs are hallmarks of neoplasia. Nucleoli are sites of rRNA synthesis in the nucleus, and structural abnormalities in tumor cell nucleoli often correlate with the degree of change in rRNA synthesis. There is increased activity of **RNA polymerase III** (which synthesizes rRNAs, 5S rRNAs, and other RNAs that have essential roles in proteins synthesis), and this enhanced function is essential for the dysregulation of protein synthesis that characterizes malignant transformation.[59]

A **transcription initiation factor complex** (TFIIIB), which specifies the placement of RNA polymerase III for proper initation of RNA synthesis, is controlled by various oncogenic proteins, for example, the oncogenic protein c-Myc. Many **cell signaling pathways** contribute to cell transformation by modifying transcription initiation factor complexes: the extracellular signal-regulated kinase (ERK), a Ras-mitogen activated protein kinase (MAPK) pathway for EGF receptors, and the phosphatidylinositol 3-kinase (PI 3-kinase)-Akt-mammalian target the rapamycin-S6 kinase signaling pathway.

Nucleolar Ultrastructure in Cancer Cells

Ultrastructures of individual components of nucleoli of neoplastic cells resemble those in the normal eukaryotic cell except that they tend to be exaggerated in size and structure. **Fibrillar centers,** spherical structures of loosely interwoven fibrils, have greatly variable sizes and low electron opacity. **Dense fibrillar components,** which are composed of tightly packed fibrils at the periphery of the fibrillar center, are more electron

opaque and are also highly variable in shape and size. The **granular component,** an aggregate of 20 nm diameter granules that surrounds the fibrillar parts, tends to be more irregular than in normal cells. **Nucleolar chromatin** at the nucleolar periphery may be intra- or perinucleolar, the latter forming either a regular shell around the nucleolus or a rim of small clumps. Ribosomal RNA transcripts are in the dense fibrillar component, that is, the site where preribosomal RNA that has just been transcribed accumulates. Granular components contain RNA molecules re-sulting from the processing of newly synthesized pre-rRNA.

Fibrillar center size and morphology in lymphomas correlate with the grade of the tumor; that is, the size of the fibrillar center is a reflection of transcriptional activity.[60] Computerized image analysis of electron micrographs of Burkitt's lymphoma and Burkitt's-like lymphomas show that, although both lymphomas have a high nuclear to cytoplasmic ratio, prominent nucleoli, and sparse heterochromatin, they differ markedly in nucleolar and nuclear pleomorphism.[61]

Nucleolar organizer regions (NORs) in the nucleolus are fibrillar components that contain ribosomal genes and specific proteins (that stain with silver methods). During interphase, NORs are located only in the fibrillar parts of the nucleolus. In metaphase they are secondary constriction of metaphase chromosomes. NORs have been used as a criterion of high malignancy.[62–64] The mean area occupied by sliver-stained NORs has been shown to be increased in malignancy.

Nuclear Envelope

In highly anaplastic neoplasms, the nuclear envelope is often convoluted, irregular, and doubled over on itself.[65,66] Nuclear convolutions are particularly prominent in lymphomas where quantitative electron microscopy on nuclear profiles has been used to provide objective measurements of nuclear atypia. Measurement of the mean degree of nuclear convolution of lymphocytes did not adequately discriminate cutaneous lymphomas from benign dermatoses. However, better discrimination was achieved using statistical analysis of the data.[67] A gene encoding an abnormal transcription factor involved in nuclear segmentation occurs on human chromosome 1p32, a site that is involved in leukemic translocations.[68]

Nuclear pores are abnormal and the filament system of the nucleus is not properly connected to the membrane.[69] Typically malignant tumors have increased nuclear pore density.[70] In some cases the number of nuclear pores per unit of nuclear envelope may be decreased, but because nuclei are larger, the total number of pores per nucleus may resemble normal.

Annulate lamellae, arrays of double sheets of smooth-walled membranes that originate from the nuclear envelope, are common in many malignant neoplasms. They are prominent in cells that are undifferentiated and rapidly proliferating with high activity and high levels of protein synthesis. They are most common in endocrine tumors, especially those of the gonads.[71–73]

Mitotic Figures

Mitotic figures are common in malignant tumors. Microscopic examination of tumor tissue usually reveals an increase in the number of mitotic cells. The large cells with central aggregates of chromosomes are called **mitotic figures.** The mitotic process however resembles that in normal cells. Replication and migration of centrioles, appearance and disappearance of spindle tubules and kinetochores, and movement and replication of chromosomes can rarely be distinguished from normal. Nucleoli and some cytoplasmic organelles tend to persist during mitosis of neoplasms, which they do not do in normal cell cycles.

Chromatin

Abnormal patterns of chromatin vary from increased to decreased amounts. Giant **perichromatin granules** adjacent to chromatin are typical of some tumors.[74,75]

Mitotic defects involve abnormal chromatin. DNA or DNA-histone complexes isolated from neoplastic cells commonly behave abnormally when analyzed chemically. In normal cells, genetic information is transcribed from DNA to a closely related single strand of RNA and, in turn, translated from that strand into a protein constructed of amino acids. It seems that the altering of DNA molecules, either by chemical oncogenes or by insertion of viral material into the chromosome, would most readily explain the abnormal growth that occurs in neoplasms.[76]

In some cancer the DNA strand is certainly broken. Drugs such as dimethylnitrosamine break single strands of DNA, and the acetylaminofluorine compounds cause disruption of double-stranded molecules. Oncogenicity seems to be inversely related to the rapidity of strand repair in experiments in vivo.

Analysis of flow cytometric DNA histograms provides a method to determine the **S phase fraction** of a tumor. Proliferative activity can also be assessed by immunostaining with Ki-67, a monoclonal antibody that reacts with antigens expressed in actively proliferating but not in resting cells.[75] In studies of ovarian neoplasms, the % Ki-67 staining was malignant

(27.6%), borderline (12.3%) and benign (2.7%) tumors; % Ki-67 staining correlated with S phase fraction, DNA index, architectural grade, nucleolar grade, and mitotic count for malignant tumors, but not in borderline tumors. With the exception of quiescent G_0 cells, Ki-67 is expressed throughout the cell cycle. Thus, the number of Ki-67 positive cells far exceeds the mitotic index. Ki-67 expression correlates well with tumor grade and number of mitoses. Inverse correlations between high numbers of Ki-67 positive cells and survival have been found in mammary cancers, melanoma, lymphoma and multiple myeloma. **Proliferating cell nuclear antigen** (PCNA, cyclin) is also used to characterize cells that synthesize DNA; however the long half-life of PCNA means that the number of staining cells far exceeds the number of Ki-67 staining cells and that PCNA will be found in noncycling cells.

Chromosomes

Neoplastic cells are more unstable genetically and thus are more likely than normal cells to generate genetic variants. The presence of these multiple subpopulations provides the heterogeneity that is typical of highly malignant tumors.

Chromosome analysis may reveal physical abnormalities in specific chromosomes. When so examined, malignant cells are usually **aneuploid** (having more or less than the normal diploid number) and have a variety of chromosomal defects. Pathologic karyotypes may be chromosomal deletions, translocations, and other changes. Most of these tumors are associated with a heritable chromosome weakness and require some unknown predisposing event for neoplasia to occur.

Abnormal DNA Repair

Abnormalities in the functional integrity of the DNA-repair mechanism may predispose to neoplasia. Human **xeroderma pigmentosum** is characterized by extreme sensitivity to ultraviolet rays in sunlight that cause epidermal cell injury. The cellular defect is a lack of ultraviolet-sensitive endonuclease. This suppresses the normal repair of DNA molecules after ultraviolet irradiation injury and leads to multiple carcinomas. Cells taken from xeroderma patients show a higher rate of neoplastic transformation than do normal cells, when placed in culture. Tumor cells contain several oncogene alterations, for example, elevated *c-myc* transcription (not present in normal cells from the patient). The protein produced by the oncogene *myc* downregulates dozens of microRNAs, some of which contribute to neoplastic change. Other DNA-repair diseases of humans are ataxia telangiectasia and Fanconi's syndrome, both of which have a high incidence of cancer and chromosomal mutation.

Receptors of Growth in the Nucleoplasm

Receptor molecules that govern the growth of tumor cells can be located in the cytoplasm or nucleus. Involved in signals from outside the cell, these receptors increase or decrease appropriate signals for cellular change that cause a corresponding increase or decrease in function that will cause lesions. Many of these receptor-ligand reactions initiate synthesis of protein and peptides the control cell functions, including movement and mitosis. For example, the estrogen receptor estrophilin occurs in the nuclei of ovarian and endometrial cells and can be localized in endometrial and mammary carcinoma cells.

Cytoplasm

Ribosomes and Endoplasmic Reticulum

Regulation and flexibility of programmed protein synthesis is lost in neoplastic cells. Reprogramming of gene expression and messenger RNA translation in the cytoplasm is highly directed to (1) purine synthesis and utilization to supply requirement for mitosis; (2) altered mechanisms of energy production with dominance of glycolysis in the cytoplasmic matrix over mitochondrial respiration; and (3) altered plasma membrane components, especially defective sodium pumps (ATPases), skewed protein receptor molecules, and abnormal surface glycoproteins.

Much of our knowledge of metabolic shifts in neoplasia comes from studies of transplantable and carcinogen-induced liver tumors in rodents. Cells of these tumors are highly malignant and uniform in structure and metabolism. Fortunately, results from these models agree with studies on homogenates of natural hepatocellular carcinomas. Nonetheless, they do not entirely represent the spectrum of liver tumors that occur naturally in animals.

Ultrastructurally, the **ribosomes** and **rough endoplasmic reticulum** have abnormal distributions in malignant cells (Fig. 23.10). They may be lacking, present in excess, or aggregated into abnormal clumps. Similarly, the **Golgi complex** is abnormal and may have irregular, dilated saccules, and contain inspissated proteins. Morphometric analysis of human parathyroid neoplasms suggest that the Golgi complex of neoplastic cells is incapable of normal glycosylation and packaging.

Membranes of the endoplasmic reticulum are typically produced in excess in neoplastic cells with high rates of membrane metabolic activity. For example, steroid-producing tumor cells, such as those in adrenal

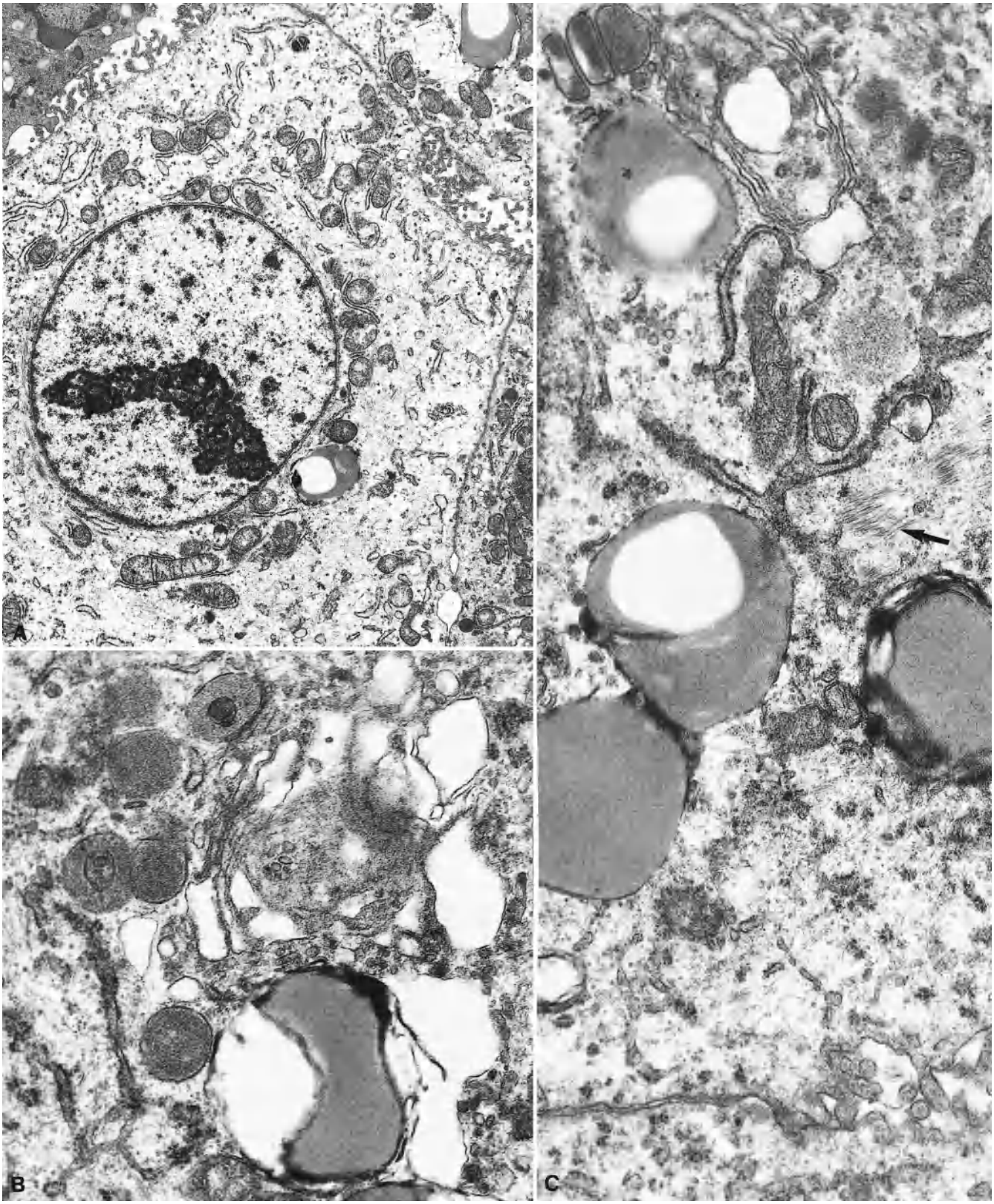


Fig. 23.10 Cytoskeleton: undifferentiated sarcoma (rhabdomyosarcoma), aged human female. **A**. **Neoplastic cell ultrastructure**: nucleus in large, surface microvilli are irregular. Cytoskeleton, Golgi complex, and secretory granules are abnormal. **B. Golgi complex**: surrounded by aggregates of mitochondria secretory granules, and lipid globules. **C**. **Lipids and endoplasmic reticulum**: microfilaments (*arrow*).

cortical carcinomas and testicular interstitial cell tumors, generally contain **membranous whorls** in lysosomes or free in the cytoplasmic matrix.[77]

The Ubiquitin-Proteosome System

Proteosome inhibitors such as bortezomib (PS-341) trigger apoptosis in some cancer cells. Affected cells form aggresomes—aggregates of ubiquitin-conjugated proteins. This process is cytoprotective. Inhibition of aggresome formation can potentiate the efficacy of proteosome inhibitors.[78]

Protein Inclusions

Secretory proteins are demonstrable in cisternae of the RER and nuclear envelope in many malignant neoplasms, especially those of endocrine tissue.[79] Inclusions arise from aberrant keratinization: labeled for keratins and actin; negative for vimentin, epithelial membrane antigen, S100, neurofilaments, GFAP. Ultrastructurally, inclusions were surrounded by a rim of tonofilaments.

These intracisternal proteins commonly precipitate in lamellar arrangements because of abnormal processing, for example, glycosylation of the protein may be abnormal, proper tertiary peptide folding may not occur, or there may be inadequate stress proteins present to stabilize the new peptides for storage. Long tortuous RER channels with serpiginous inclusions occur in some fibrous tumors.

Cytoplasmic Hyalin Bodies

Intracytoplasmic hyalin globules that are periodic acid-Schiff (PAS) staining (but diastase resistant) are found in many tissues in different pathologic conditions; for example, the α1-antitrypsin storage in hepatic cirrhosis, which is associated with the serum defect of this protease inhibitor. Protein storage globules are also commonly seen in human tumors including hepatomas, gliomas, and carcinomas of lung, intestine, and breast. Ultrastructurally, these hyalin globules are lysosomes and, like α1-antitrypsin globules of hepatomas, arise from storage of cytoplasmic proteins.[80] Globoid cytoplasmic inclusions that have α1-antitrypsin reactivity have been reported in human pancreatic islet cell tumors.[81,82]

Fibrillar Inclusions

Fibrillar inclusions, usually within cisternae of endoplasmic reticulum, are perhaps the most common cytoplasmic inclusion seen in ultrastructural studies of neoplasms. They arise from abnormal protein synthesis, particular as a result of defects during the tertiary folding and glycosylation stages. Fibrillar inclusions of secretory component (of the IgA) can be shown in the cytoplasm of glandular epithelium and in the cytoplasm of adenocarcinoma of respiratory, intestinal and biliary tracts.[83] Genes in the cancer cells that should be inactive were found to have become active.

Actin inclusions accumulate in some sarcomas; for example, in human alveolar soft part sarcomas, filaments form crystalloids. In these lesions, individual filaments are composed of two globular substances arranged in a dumbbell pattern. Similarities to actin have been shown by a three-dimensional model prepared by digital image analysis of electron micrographs.[84] Double strands cross each other at intervals of 38 nm each consisting of successive arrangements of globular substances.

Protein Lattices (Crystalloids)

Large membrane-bound cytoplasmic arregates of protein filaments arranged in lattice formations are typical of some types of sarcomas. These crystalloids have also been reported in benign and malignant salivary gland tumors,[85] and in human alveolar soft part sarcomas of the thigh and retroperitoneum. Incidence varies in these tumors; in one study, crystalloids were present in 6 of 130 pleomorphic adenomas of the minor salivary glands (Fig. 23.11).[86] Analysis of these proteins has revealed that filaments are composed of two globular substances of 6 nm diameter arranged in a dumbbell pattern. Double filament strands crossed each other at 38 nm intervals.[87] Rhomboid cytoplasmic crystals of human alveolar soft part sarcomas contain monocarboxylate transporter 1, one of a family of widely expressed proton-linked transporters for monocarbocylates such as lactate and pyruvate.[88]

Tubules

Long regular tubules that develop from infoldings of the endoplasmic reticulum are characteristic of certain tumors. In human tumors, intracisternal tubules are associated with carcinomas of endocrine glands.[89] Thyroid carcinomas of dogs invariably contain striking arrangements of tubules that invaginate into cisternae of the RER.[90]

Ribosome-lamellar complexes: these particle-filament complexes are common in tumors of lymphoid and hematopoietic tissue, especially human hairy cell leukemia, chronic lymphoid leukemia, and adrenal adenomas.[91] Composed of alternating fibrous lamellae and ribosomes, they are often associated with whorling of RER membrane. Ribosome-lamellar complexes arise from aberrant transcription. In hairy

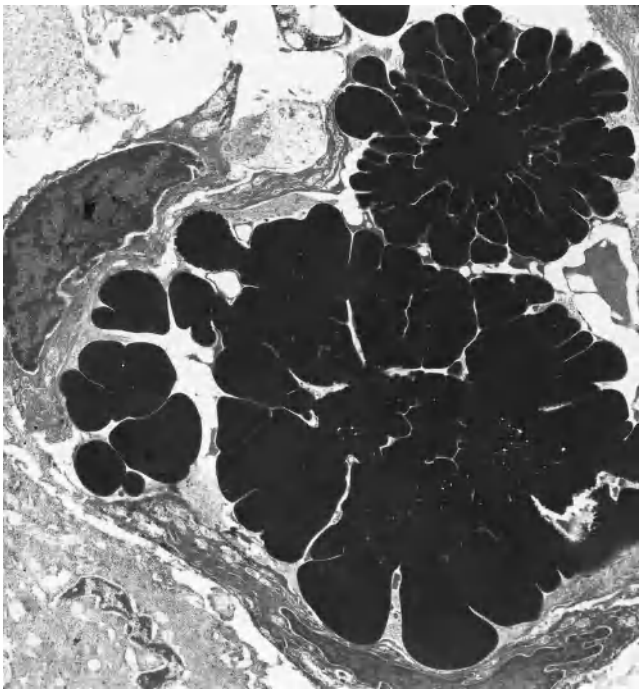


Fig. 23.11 Tyrosine-rich crystalloids: human salivary gland adenoma. Blunt-tipped, petal-shaped structures radiate from an electron-dense center. (Micrograph: Wallace G. Campbell, Jr., *Am J Pathol* 118:194, 1985.)

cell leukemia they form cylindrical double tubular structures 12.5 nm in width set in parallel arrays 12.5 apart.[92]

Confronting cisternae are dense laminae between regular arrays of rough endoplasmic reticulum saccules. In longitudinal section they appear as long tubules separated by thin dense laminae and in cross section as rosettes of vesicles.[93]

Secretory Granules

Production, storage, and exocytosis of secretory granules are abnormal in neoplasms, and granules occur in the cytoplasm of tumor cells in varying sizes, shapes, and content.[94] Neoplastic cells from tumors of exocrine and endocrine glands typically have secretory granules that are irregular, pleomorphic and fewer in number than in the corresponding normal cell type. Crinophagy (the process of secretory granule destruction wherein granules fuse with lysosomes) is increased, and large lysososomes bearing secretory granules are often prominent (Fig. 23.12).

Specific proteins within granules of neoplastic cells can be identified ultrastructurally by specific labeling using techniques of histochemistry and immunocytochemistry. Undifferentiated cells can often be classified by staining for specific secretory components (Fig. 23.13).

- **Mammary gland tumors:** techniques for casein, cytokeratins, tumor antigens, and other glycoproteins have been used in the identification of granule composition.[95–98]
- **Pituitary tumors,** including null cell adenomas, oncocytomas, and gonadotroph adenomas, have been classified based upon the ultrastructural immunolabeling of various hormones and chromogranin mRNAs;[99] annexins mediate glucocorticoid action in the anterior pituitary and have been labeled in growth hormone secretory adenomas.[100]
- **Neuroendocrine tumors** have been identified by labeling chromogranin A and neuron-specific enolase.[101,102] The neurotrophin-inducible gene ***vgf*** is expressed in human endocrine cell tumors, and immunolabeled proVGF fragments are useful diagnosis.[103]
- **Pancreatic carcinomas** labeled with immunogold techniques labeling glucagon and gastrin/cholecystokinin expression show increased secretion, co-localization, and relatedness of increased excretion with poor differentiation; in addition, **ectopic expression,** expression in normal cells surrounding neoplastic cells, was common.[104]
- **Colorectal tumors** have been labeled with immunogold for serotonin, vasoactive intestinal polypeptide, bombesin, somatostatin, and glucagon.[105]

In the leukemias and other neoplastic diseases of blood and blood-forming organs, secretory granules are particularly important, and can establish a diagnosis.[106] **Auer bodies,** a specific granule in leukemic cells of human acute granulocytic leukemia, arise from fusion of azurophile granules; they contain proteins that assemble in lattices and tubules.[107]

Neoplastic cells can secrete multiple types of hormones or growth factors, either simultaneously or in different secretory cycles. In human pituitary mammosomatotroph adenomas, cells simultaneously produce growth hormone and prolactin, which are packaged in the same granule.[108] The confusion over classification can result in double descriptive names; for example, the melanotic neuroendocrine tumor in which both melanosomes and neurosecretory granules are found (Fig. 23.14). Pituitary tumors may secrete growth hormone, which stimulates the liver to produce excess albumin, and the resulting hyperalbuminuria causes nephrosis.

Cells of the same embryologic origins may differentiate to secrete different proteins; for example, pancreatic islet cell tumors of hamsters (induced by human papova virus) secrete insulin or glucagon.[109] Secretory

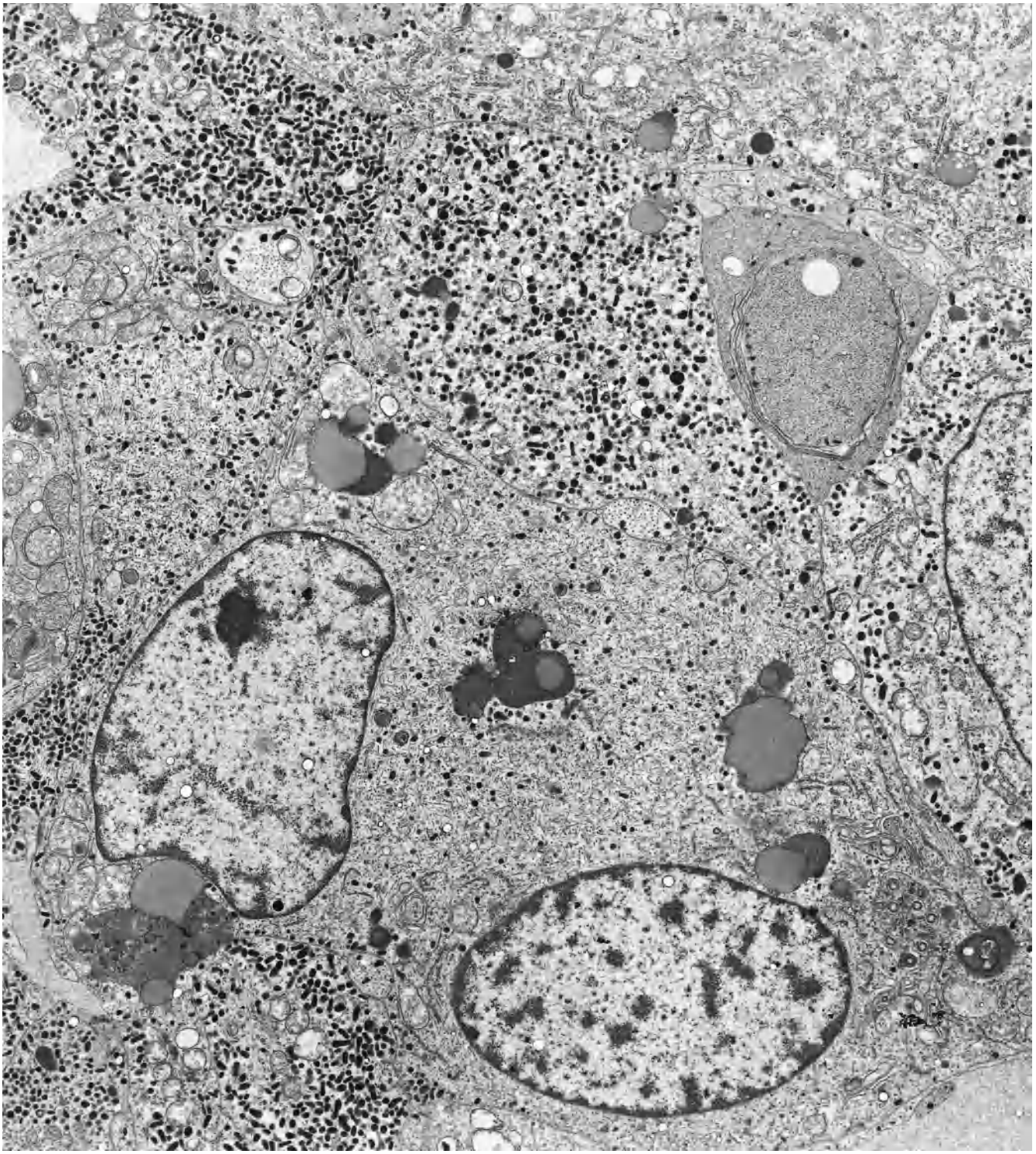


Fig. 23.12 Secretory granule crinophagy: pheochromocytoma, human female. Tumor cells produce Alzheimer's neurofibrillary tangles and paired helical filaments. Cell in center has many fibrils but few granules. (Micrograph: N. Izumiyama, *Acta Neuropathol* 81:213, 1990.)

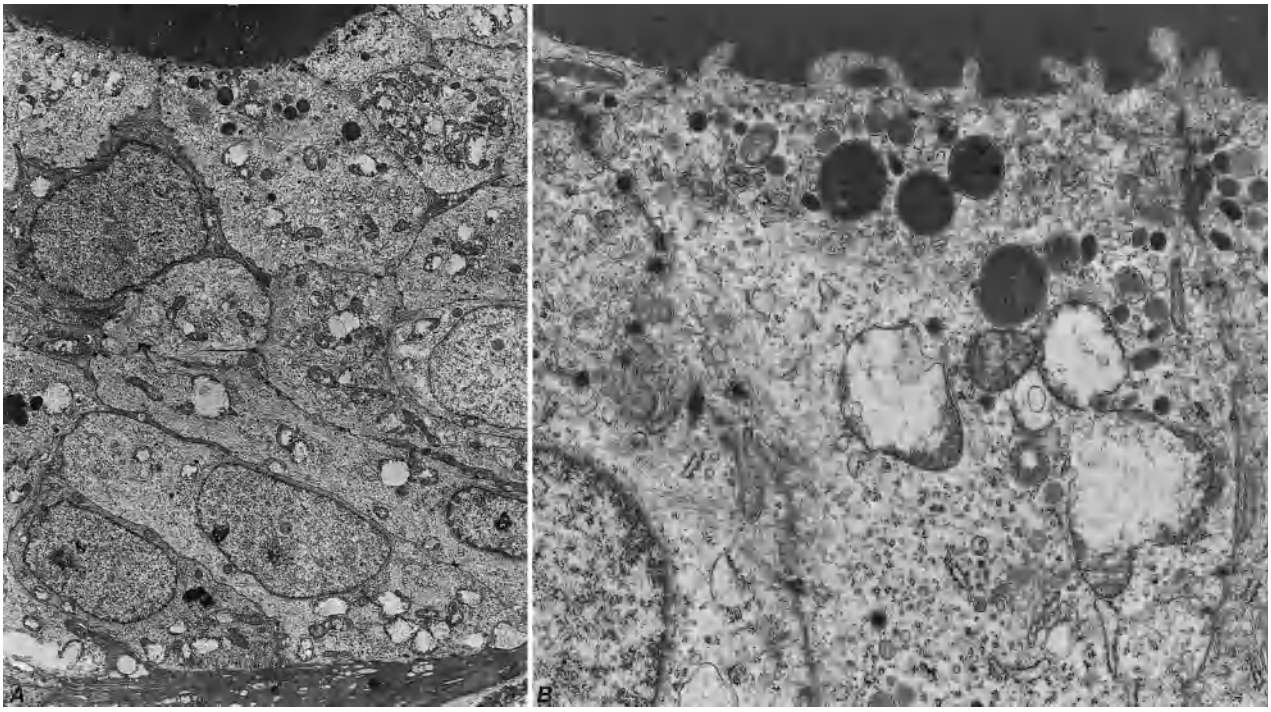


Fig. 23.13 Secretory granules: adenocarcinoma: mammary gland, dog. **A. Tumor cell acinus**: lumen at *top;* basement membrane at *bottom*. **B. Lumen surface**: differentiated neoplastic cell has irregular secretory granules and aberrant intercellular junctions with frequent desmosomes.

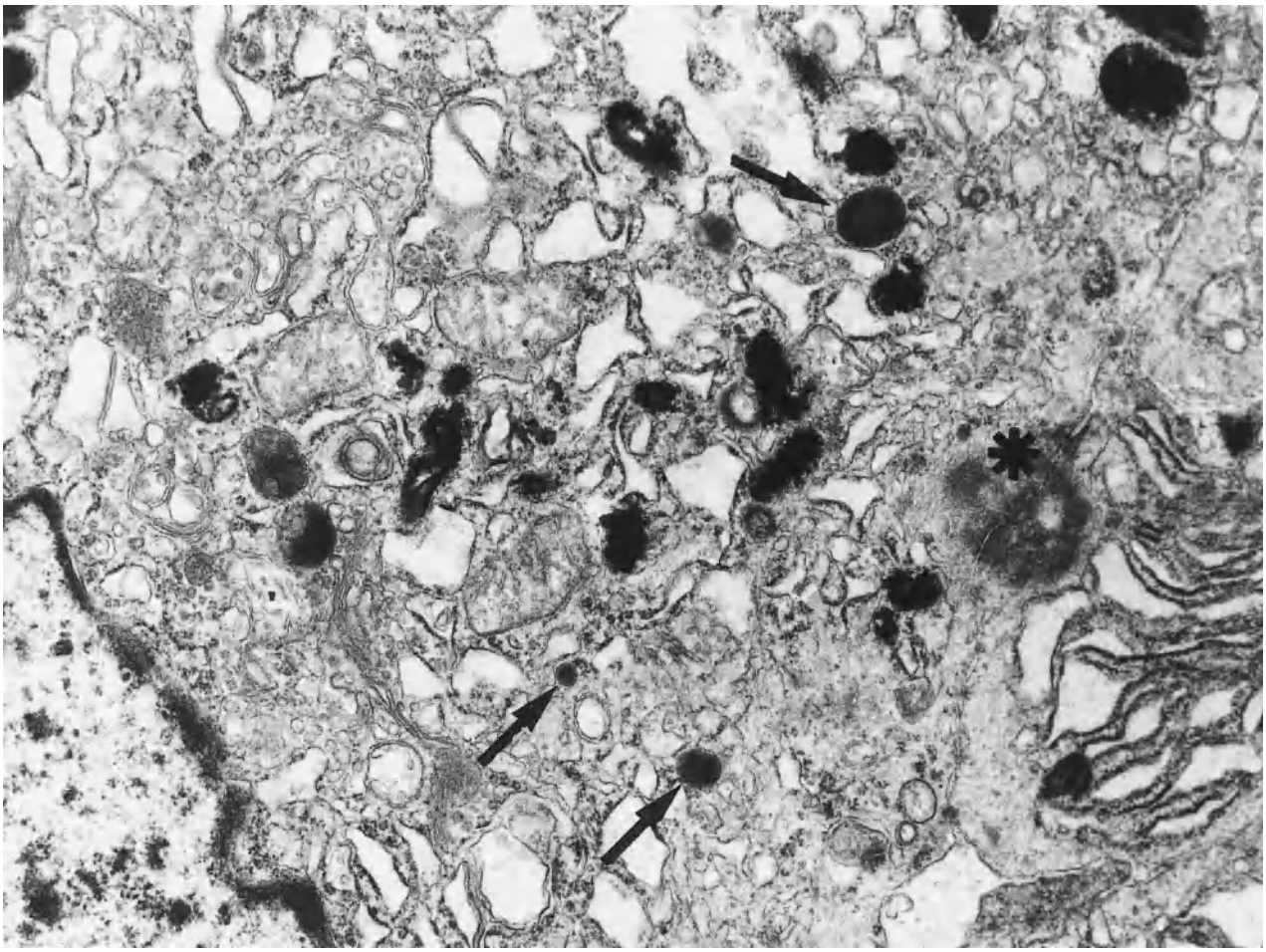


Fig. 23.14 Secretory granules: melanotic neuroectodermal tumor of human infancy. Secretory granules are small (*) and variable (*arrows*). (Micrograph: Guido Pettinato, *Am J Surg Pathol* 15:233, 1991.)

granules are different and resemble those of the parent cell type.

Melanosomes in Malignant Melanomas

Malignant melanomas are distributed throughout the phyla of the animal kingdom. The rate of growth is usually inversely related to differentiation. Malignant melanoma cells are often large, polyhedral, and black but cells show much variability in shape and pigmentation. Some are composed of elongate, stellate-shaped cells. Some contain only blastic cells, which produce little pigment. These amelanotic melanomas are detected histochemically by the content of tyrosinase present in the endoplasmic reticulum. It oxidizes dihydrophenylalanine (dopa), which is added as part of the histochemical test (the dopa reaction) to black granular foci in the tumor.

Ultrastructurally, melanomas contain varying amounts of dense melanin in melanosomes of varying size (Fig. 23.15). **Compound melanosomes,** which are membrane-bound lysosomes packed with degenerate primary melanosomes, arise by autophagy.[110] In amelanotic tumors, few melanosomes are present, but the Golgi complex is large and contains many pre-melanosomes.

Glycogen and Glycolysis

Glycogen is a common but variable component of most neoplastic cells. The immature state of differentiation causes malignant cells to resemble fetal cells, which also contain large amounts of glycogen. In contrast to the incidental finding of glycogen, the **clear cell tumors** are filled with glycogen to the exclusion of other organelles; for example, clear cell tumors of the liver and kidney have large cell volumes, much of which are composed of irregular alpha rosettes of glycogen (Fig. 23.16).

Malignant cells have a high degree of glycolytic activity (both anaerobic and aerobic). There is enhanced glycolysis and glucose utilization. Precursors are diverted into synthesis of purines, purimidines, RNA, and DNA. Neoplastic cells produce large amounts of lactic acid from glucose, and this pathway is not markedly reduced in the presence of oxygen, as it is in normal tissue. The enzymatic imbalance responsible for the shift to glycolysis involves increased key glycolytic enzymes and decreased enzymes of gluconeogenesis. Isozyme shifts replace normal enzymes with isozymes unresponsive to nutritional and hormonal regulation. This decreased dependence of the neoplastic cell on mitochondrial respiration confers a selective advantage to begin growth in the tumor mass, a poorly vascularized, oxygen-deficient environment.

Mitochondria

Although the number of mitochondria varies in individual neoplasms, malignant cells generally have diminished oxidative phosphorylation and mitochondria with short stubby cristae. Proteins, particularly the large cytochromes, may disintegrate and repolymerize to form intramitochondrial lattices.[111]

Mitochondrial respiration is disrupted in neoplasia by hypoxia or mutations in mitochondrial DNA that impede electron transport. These changes directly promote the survival of neoplastic cells by activating the **phosphatidylinositol 3-kinase-Akt survival pathway. Glucocorticoid receptors** have been localized in mitochondrial malignant neoplasms, and appear to regulate mitochondrial transcript and apoptosis in neoplastic cells.[112]

Oncocytomas are large granular tumor cells that are packed with mitochondria, for example, the oncocytomas (Hurthle cell tumor) of the thyroid gland (Fig. 23.17). Other human oncocytomas include Warthin's tumor of the parotid gland, the oxyphil cell adenoma of salivary, pituitary, and parathyroid glands, and the renal, ovarian, and bronchial oncocytomas. Abnormal mitochondria with crystalloid inclusions have been reported in the Warthin tumor. The mitochondrial defect that occurs in these tumors is not related to enzymic deficiency nor is it a compensatory mechanism.[113]

Lipids

Lipid globules accumulate in tumor cells as a results of metabolic shifts associated with very high proliferative rates. In human lymphomas, an inverse relationship between lipid globules and mitochondria has been shown[114] in studies of linear regression lines developed from mean numbers of lipid globules and mitochondria. As mitochondria increase in neoplastic cells, lipid globules decreased.

The Tumor Microenvironment

The extracellular matrix is altered by neoplastic cells to create a new **tumor microenvironment.** Host cells that populate the tumor microenvironment—tumor-associated fibroblasts, endothelial cells, macrophages, and mast cells—respond to the complex interplay of neoplastic cell **cytokines** that include TGF-β, TGF-α, VEGF (which stimulates angiogenesis), and the stroma-derived matrix metalloproteinases (MMPs). The effects of these cytokines, often working through integrins and other adhesins, can suppress or enhance neoplastic growth. **Tumor-associated fibroblasts** are,

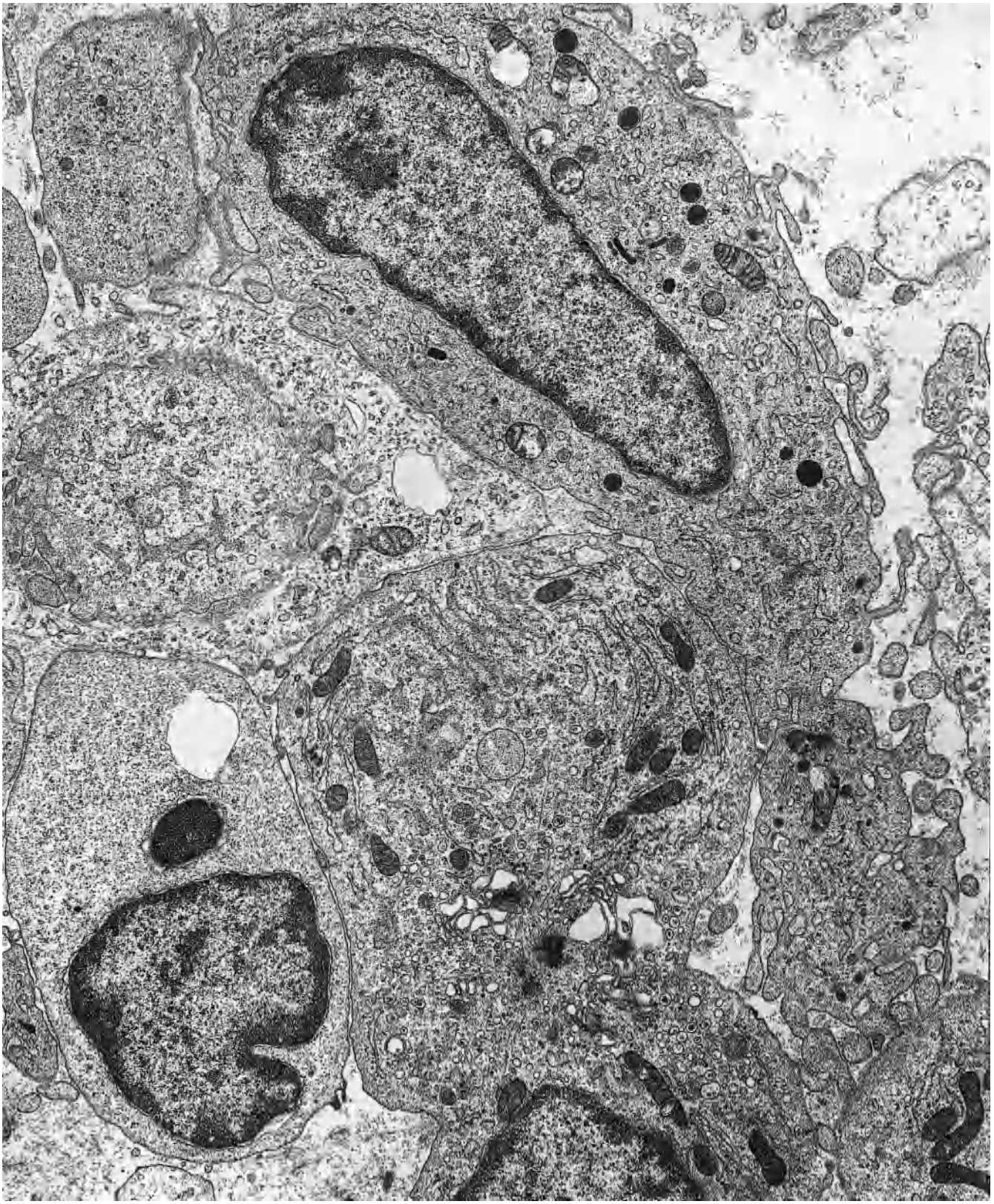


Fig. 23.15 Malignant melanoma (amelanotic type): gingiva, dog. Nuclei are large. Cell surfaces are markedly irregular and have lamellipodia, filopodia, and evidence of ruffling and endocytosis. Golgi complexes are multiple, dilated, and associated with many small Golgi vesicles. Malignant cells contain few granules; those granules that are present are abnormal. Mitochondria are small.

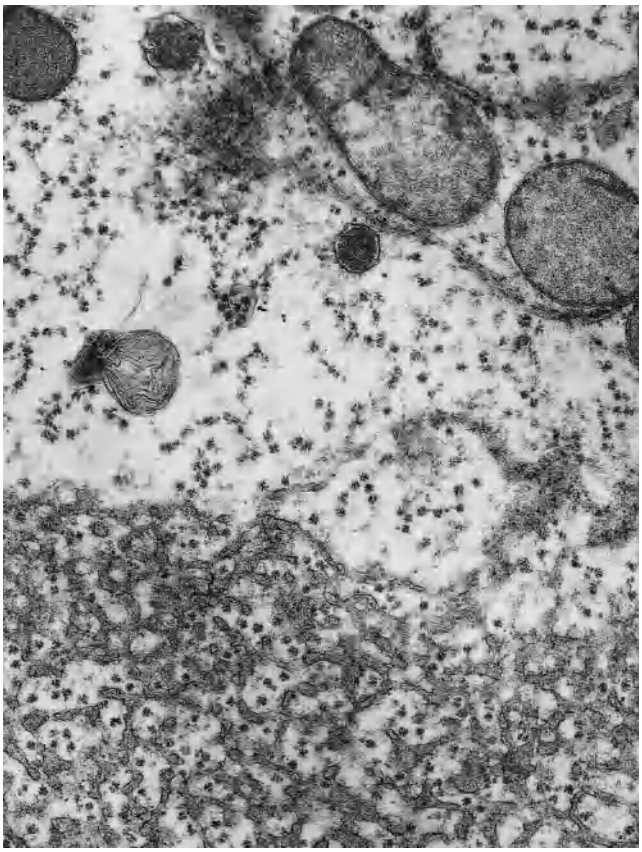


Fig. 23.16 Smooth endoplasmic reticulum (SER) proliferation: clear-cell carcinoma, liver. SER at bottom forms an interconnected tubular network. Clear areas are filled with glycogen; mitochondria lack cristae.

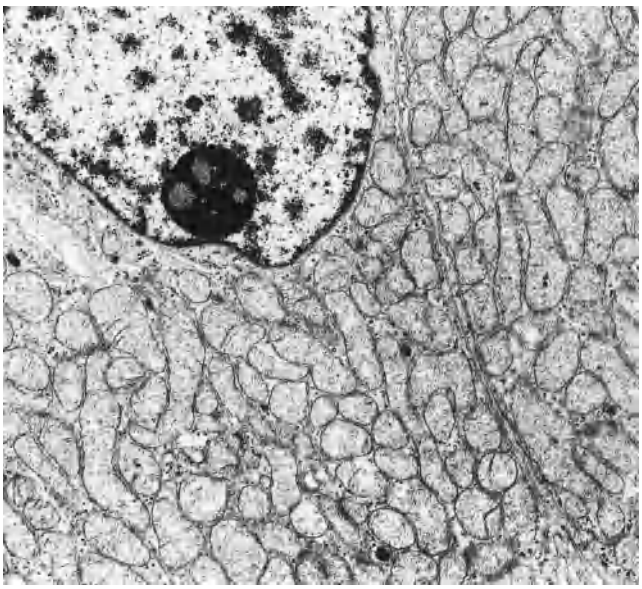


Fig. 23.17 Mitochondria-rich neoplastic cell: Hürthle cell follicular carcinoma, human. (Micrograph: Jahn M. Neslund, *Ultrastruct Pathol* 8:269, 1985.)

in some tumors, coconspirators of many solid tissue tumors.

Transforming growth factor-β (TGF-β) is produced by stromal cells of the tumor microenvironment in response to hypoxia or inflammation, or by tumor-associated fibroblasts. Cancer cells are unresponsive to the growth inhibitory effects of TGF-β and, instead, respond by increasing their growth and invasiveness, and by undergoing an **epithelial-to-mesenchyme transition**. To make matters worse, TGF-β stimulates expression of the adipokine **angiopoietin-like 4** (ANGPTL4) by activating SMAD transcription factors, and ANGPTL4 enables tumor cells to extravasate into lung tissue and to seed micrometastases.[115]

Neoplastic cells modify the tumor microenvironment in which they grow by synthesizing and releasing (1) **enzymes** that degrade the extracellular matrix, (2) **cytokines** that activate tumor-associated cells to alter the extracellular matrix, and (3) **extracellular matrix components** that facilitate invasion. In any malignant tumor, all three may take place in different regions of the tumor or one of these types may dominate.[116–119]

Complex **proteoglycans** and **mucins** are secreted by neoplastic cells derived from chondromas and chordomas and other proteoglycan-producing tissues. Adenocarcinomas of the uterus, urinary tract, and nasal cavity release elaborate mixtures of glycosaminoglycans and proteoglycans. Proteoglycans influence cytodifferentation in neoplasia by inducing cellular differentiation and can cause both proliferation and migration of cells by forming structural links between cell and interstitial components.[120] Chemical analysis of human colonic carcinomas have shown a 12-fold increase in chondroitin sulfates compared with control tissue. The source of the sulfated proteoglycan was the host fibroblast adjacent to the tumor cells.

Collagen

Collagen fibers produced by neoplastic cells typically resemble normal collagen fibers, but nodose lesions that in cross section appear as abnormally large fibers have been reported in some connective tissue tumors. In general, sarcomas produce collagens that polymerize into fibers and contribute to basement membranes. These collagens may have normal molecular structure but fail to polymerize or aggregate properly when outside the cell.

Carcinomas release **collagen IV** that combines with glycoproteins to form basement membranes (Fig. 23.18). Synthesis is variable and the excess production or loss of type IV collagen is not generally useful in classifying invasive carcinomas.[121] In situ hybridization techniques have revealed active expression of

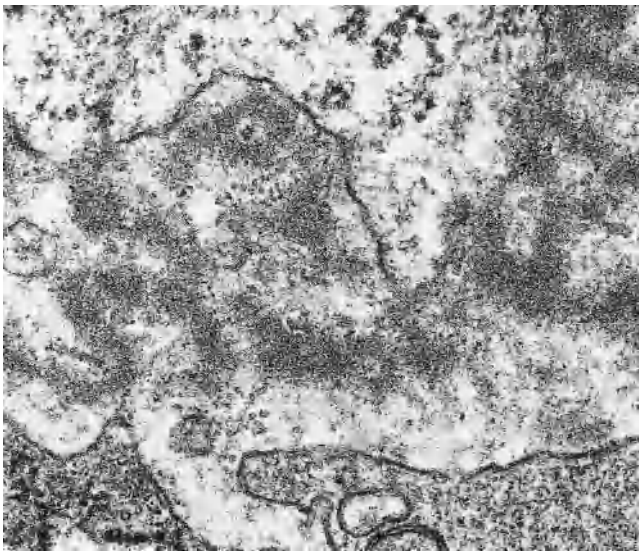


Fig. 23.18 Basement membrane material: squamous cell carcinoma; lack of linear distribution of normal membrane, and produced in excessive amounts.

type IV collagen genes in human neurofibromas, a tumor with large amounts of collagen and noncollagenous matrix.

Fibroplasia

Benign tumors often have a fibrous capsule at the periphery. Many benign tumors contain a capsule derived, in part, from the fibrous stroma of the surrounding normal connective tissue, and in part from the tumor itself (malignant tumors are almost never encapsulated). Encapsulation tends to contain the neoplasm as a discrete, palpable mass that can easily be removed by surgery. Although a capsule is a characteristic of a benign neoplasm, lack of a capsule does not make a neoplasm malignant.

Tumor-Induced Fibrous Proliferation

Fibroblast proliferation and deposition of collagen are the main components of fibromas and fibrosarcomas, and are primarily involved in some of the more rare fibrous tumors such as fibrous histiocytomas. Marked fiber deposition also occurs in some epithelial tumors. These tumors secrete factors that stimulate fibroplasia. It may be that some lack the collagenases and elastases that other tumors are known to secrete and that the scirrhous nature of the mass represents a host response that is repressed by collagenase in other tumors. **Myofibroblast** proliferation in tumor tissue has been confused with the diverse group of myofibroblastic neoplasms and neoplastic-like growths.[122]

Unique **foci of extracellular amorphous matrix (FEAM),** described in many invasive tumors, are fibronectin-rich matrix areas.[123] **Fibronectin** is absent or diminished on most neoplastic cells. The failure of the matrix formed by aggregating fibronectin destabilizes the tumor cell population. Experiments with mouse melanoma cells show that fibronectin suppresses invasiveness while laminin increases it. Cells with abnormal surfaces will be unresponsive to normal cell growth regulators. Some malignant cells secrete enzymes that degrade glycosaminoglycans of the interstitium.

During invasion, the degradation of the surrounding tissue requires action of proteolytic enzymes to eliminate fibrin. **Plasminogen activator,** which converts latent plasminogen to the active proteinase plasmin, degrades fibrin during invasion and metastasis. Plasminogen activator has been detected by electron microscopic autoradiography at the cell surface of tumor cells.[124] Plasminogen activator binds to receptors in some tumor cells, and is taken up by endocytosis and degraded.

Tumor Angiogenesis

The growth of a neoplasm is dependent on concomitant growth of a supporting vascular system—the probability of a neoplastic cell entering mitosis decreases with increasing distance of the cell from its nearest capillary.

Capillaries

Capillary growth in an expanding neoplasm is vigorous. Endothelial cells are kinky and enlarged and have extensive contortions and surface projections of the luminal plasma membrane. These changes are marked in highly malignant neoplasms (Fig. 23.19).

Tumor blood vessels are often more permeable than normal vessels. They are hyperpermeable to plasma proteins, especially the more mature veins and venules lined by continuous endothelium and having closed intercellular junctions.[125] Ultrastructural tracer studies of transplantable neoplasms in mice have shown that leakiness is associated with venules and small veins. Tracers exit venules via a system of smooth membraned vesicles and vacuoles that cluster together at intervals along the endothelium.[126] The vesicles appear to arise from caveolae.

In most neoplasms, the blood vessels are not neoplastic but a host response induced in some way by the tumor itself. Tumor vascular systems are never normal, however, and ultrastructural characteristics of tumor capillaries vary greatly. The supply of oxygen, glucose, and other nutrients to the tumor is usually less efficient than in normal tissue.

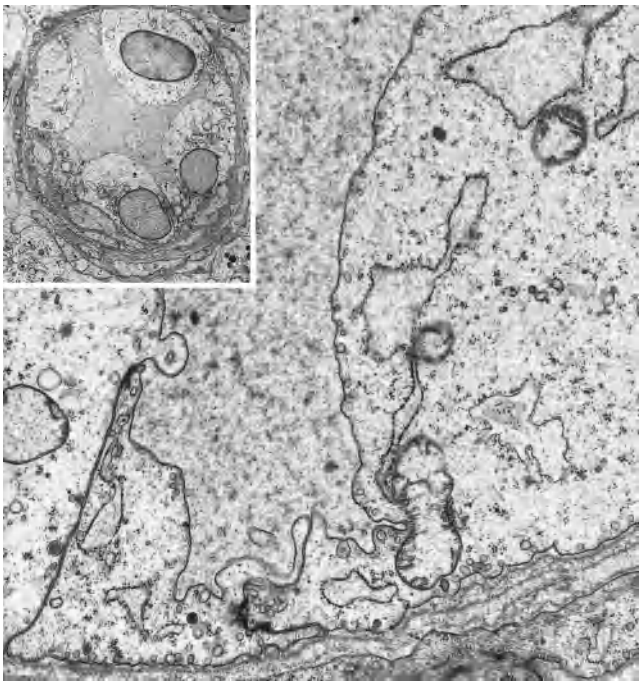


Fig. 23.19 Arteriole: aortic body carcinoma, dog. **Arteriole**: supports frond of tumor in the pleural cavity (*inset*). Intercellular junctions are irregular, endothelial cell cytoplasm is pale and relatively structureless, and there are excessive amounts of basement membrane material.

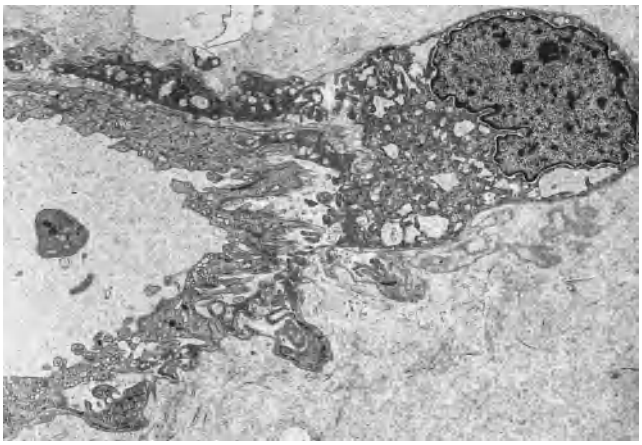


Fig. 23.20 Pericyte: adjacent to venule, mammary gland adenocarcinoma, dog. Pericyte (*top right*) is degenerate: endothelial cells are vacuolated, irregular, and thick. Basement membranes are distorted. There is an excessive amount of granular proteoglycans in the extracellular matrix.

The vascular pattern reflects tumor histology, not the tissue of origin. It can be revealed by perfusion with radio-opaque substances and radiographic examination. By this method, tumor blood vessels are shown to be haphazard networks with a predisposition to form capillaries from arterial vessels of all sizes (Fig. 23.20).

Tumor Cells and Blood Vessels Are Interdependent In many cases, populations of neoplastic cells and host endothelial cells constitute an integrated system. The mitotic indices of one population depend on the other. Tumor cells stimulate endothelial cell proliferation, and vascularizaton has an indirect effect on tumor growth.[127]

Mechanisms of Tumor Angiogenesis

Binding of **vascular endothelial growth factor A** (VEGF-A, also **VEGF**) to its **VEGF receptor (VEGFr)** (called kinase-insert domain-containing receptor in humans, and fetal liver kinase 1 in mice) is the major event that initiates **sprouting angiogenesis** in tumors. Binding of VEGF to VEGRr begins a cascade of several different signaling pathways.[128]

VEGF action arises from a paracrine mechanism: tumor cells produce VEGF but cannot response to it since they lack VEGFr (in some tumors, VEGFr are expressed not on the tumor cell surface but within the cytoplasm where they promote cell survival by an intracrine mechanism. Endothelial cells highly express VEGFr, but produce little or no VEGF. To achieve the quantity of VEGF required to drive tumor angiogenesis, other cellular sources of VEGF are required; major contributors of VEGF are platelets, myocytes, and tumor-associated fibroblasts.

Cellular Events That Drive Angiogenesis Induction of increased VEGF expression in tumors can be caused by environmental (epigenetic) factors and by genetic inductive changes. Environmental causes include hypoxia, low pH, growth factors (basic FGF), hormones (both estrogens and androgens), and IL-6 and other cytokines. Genetic inductive changes include activation of oncogenes or loss or mutational inactivation of tumor-suppressor genes. The effects of **hypoxia,** a characteristic of solid tumors, are mediated through hypoxia-inducible transcription factors 1α and 2α.

Signaling Pathways Signaling pathways in angiogenesis include Tie-2 and Notch pathways. **Tie-2,** a receptor tyrosine kinase expressed on vascular endothelium, binds to its major ligands angiopoietin-1 (ang-1) and angiopoietin-2 (ang-2) to promote angiogenesis. Ang-1 acts as an agonist, ang-2 as an antagonist—acting together to stabilize the maturing capillary. **Notch-deltalike ligand 4** is an angiogenesis signaling pathway that involves Notch cell surface receptors (1–4) expressed on endothelial cells.

Angiogenesis Factors and Cytokines in Tumor

Angiogenesis Diffusible soluble substances that are released from tumor cells to act on host endothelium include:

- **Vascular permeability factor/VEGFr complex** (VEGF-A) is a multifunction cytokine overexpressed in most malignant tumors, and is viewed as the most important angiogenic tumor cytokine.[129]
- **Vascular endothelial growth factor C** (VEGF-C) is directed to tumor lymphangiectasis.[130]
- **Vascular endothelial growth factor D** (VEGF-D) is directed to tumor lymphangiectasis.[131]
- **Tumor angiogenesis factor (TAF)** is secreted by neoplastic cells, and is mitogenic for capillary endothelium. Growth of tumors can be deliberately arrested by blockade of angiogenesis factor and prevention of vascularization.
- **Glucocorticoid hormones** interfere with vascularization of tumors, and other hormones probably delay or facilitate tumor vascularity.[132]
- **Neuropilins,** transmembrane receptors that bind semaphorin to guide axon growth, also bind VEGF to act as coreceptors for VEGFr.
- **Platelet growth factor** (PlGF) binds to VEGFr.
- **Heparin,** secreted by mast cells at sites of tumor formation, can increase migration of endothelial cells toward tumors.

Angiogenesis Inhibition

Excessive angiogenesis is inhibited by endogenous angiogenesis inhibitors such as **vasohibin,** a protein in activated endothelial cells that is induced by VEGF and other stimulators of angiogenesis. Other inhibitors include angiostatin, endostatin, thrombospondin-1, and tumstatin (see chapter 9).

As a cancerous nodule grows, the growing vascular bed recruits circulating endothelial progenitor cells from the bone marrow. These bone marrow-derived endothelial cells are pivotal for progression from a relatively avascular micrometastasis to a metastatic nodule. They have been identified by phenotypic markers including Id1, CD31, VE-cadherin, the growth factor receptor c-Kit, and VEGFr-2. In mouse models for metastatic lung and mammary tumors (in which 12% of endothelial cells within metastases were of bone marrow origin), it was shown that when expression of Id1 was reduced in these progenitors their mobilization from bone marrow was decreased by 96%, angiogenesis was blocked, and tumor formation decreased.[133]

Neoplastic Blood Vessels

Hemangioendotheliomas, hemangioendothelial sarcomas arise from endothelium. Neoplasms that arise from other parts of the vascular wall are the hemangiopericytomas and vascular leimyomas. In all of these, the neoplastic cells resemble the parent cell (Fig. 23.21).

Kaposi's sarcoma, an angioproliferative neoplasm containing several types of vascular cells, develops as multiple tumors of skin and other tissues. The proliferating tumor cells occur around small blood vessels either as fascicles of spindle cells, or individual dendritic cells interspersed among collagen fibers. The spindle cell is the primary neoplastic cell type, stains for factor XIIIa, indicating its endothelial origin. These cells closely resemble lymphatic endothelium.[134]

Metastasis

Metastasis is the hallmark of malignant neoplasms. Neoplastic cells vary in metastatic potential. Some colonize a wide variety of tissues. Others selectively colonize specific organs distant from the primary sites. Variances above are due both to blood flow within a tissue and to the degree of match between surface adhesion molecules on the neoplastic cell and liganding receptors on endothelium. An additional factor may be specific chemoattractive factors released by normal tissue; for example, bone produces a humoral factor that has been shown to attract human prostate carcinoma cells.

Invasion into Connective Tissue

The capacity to invade host tissue is an intrinsic property of the neoplastic cell. **Adhesion factors** on surfaces of neoplastic cells interact with ligands on connective tissue cell surfaces and extracellular matrix to influence the capacity to bind to tissue. Extensions of pseudopodia below basement membranes and between connective tissue planes involve other changes in the membrane such as increased negative charge, decreased calcium content, and uncontrolled cytoskeletal movements at the cell surface.

The **Wnt signaling pathway** is used by invading cancer cells to enhance cellular motility and responsiveness to chemokines. In this pathway, Wnt binds to Frizzled, its transmembrane receptor, initiating cytosolic Dishevelled proteins to prevent proteolytic destruction of β-catenin. **β-Catenin** then moves into the nucleus to convert transcriptional repressors into activators that drive the expression of target genes. In malignant melanomas, Wnt5a promotes invasiveness by recruiting actins, myosins, and adhesion molecules into intracellular complexes that trigger membrane contractility; the process involves

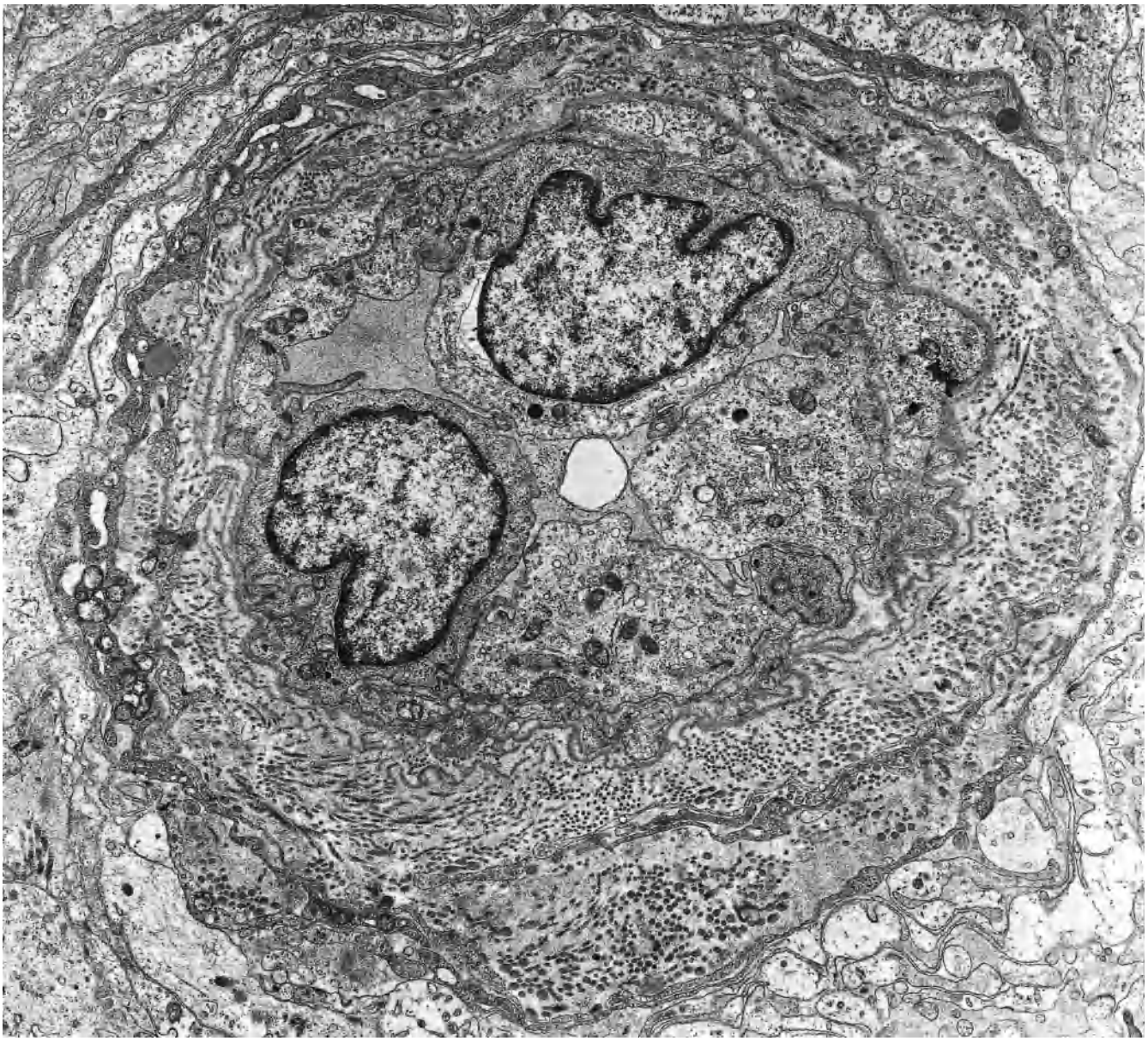


Fig. 23.21 Neoplastic capillary endothelial cells and pericytes: hemangiopericytoma, dog. The primary neoplastic cell is the pericyte, the proliferation of which is accompanied by excessive production of collagen and basement membranes.

endosomal trafficking and multivesicular bodies, and is mediated through the GTPases Rab4 and RhoB.[136]

The **cytoskeleton** of the neoplastic cell can be misdirected from participating in normal cell proliferation to enhance invasion. The ROCK-II isoform of Rho's downstream effector, Rho kinase, has been linked with greater invasion and metastasis. Rock-II is overexpressed at the advancing edge of human colon cancers, where it modulates matrix metalloproteases at the sites of **invadopodia,** finger-like projections of the cancer cell (invadopodia stain for cortactin and the matrix metalloproteases 2, 9, and 13).[135] In normal intestinal cells, ROCK-II is localized to the actin cytoskeleton; in cancer cells, it is labeled in aggregates in the cell periphery.

Degradation of Extracellular Matrix

Secretion of collagenase, elastase and some lysosomal enzymes into connective tissues by neoplastic cells may enhance invasiveness. Carcinomas elaborate enzymes that degrade connective tissues. For example,

some basal cell epitheliomas are collagenolytic, that is, they produce collagenase that degrades dermal collagen.[137] Malignant B16 melanoma cells degrade glycosaminoglycans and glycoproteins such as fibronectin by activating a surface endoglycosidase that is specific for heparin sulfate.

Some tumor cells release factors that simulate connective tissue degrading enzymes by living host cells. Experiments with a squamous cell carcinoma in rabbits indicate that cathepsin B, a cystein proteinase that degrades both collagen and proteoglycans, is stimulated in host fibroblasts and neutrophils by a humoral factor released from the neoplastic cell.[138]

The adenomatous polyposis coli gene, ***APC,*** is a tumor suppressor gene that encodes a protein that destabilizes **α-catenin**, a key effector of the Wnt signaling pathway. The gene is defective in familial adenomatous polyposis. Immunogold labeling of APC proteins and α-catenin clarifies the early events of the Wnt signaling pathway in colorectal cancer.[139] Besides its role in adhesion molecules in sarcomas, α-catenin functions as an oncoprotein in sarcomas by binding to DNA to influence proliferation.[140]

Metastasis into the Bloodstream

Highly malignant tumor cells have relatively little tendency to adhere to one another and may be washed by lymph from the tissue spaces and into **lymph vessels,** and ultimately into the thoracic duct. From the lymphatics, tumor cells enter the bloodstream by **transendothelial passage,** and travel to small blood vessels where they adhere to endothelial surfaces.[141] Injured endothelial cells have a higher rate of metastases because circulating metastatic cells adhere to extracellular matrix underlying the injured endothelium.[142]

Within a growing tumor, neoplastic cells may directly erode vascular walls and enter the bloodstream. Once the neoplastic cell has bound to endothelium, it crosses the vascular wall, usually through intercellular spaces (Fig. 23.22). The pathway across endothelium in some cases is transcellular; that is, malignant cells penetrate the intact endothelial cell and pass through in a migration channel, which is closed after the cell reaches the intravascular space.[143]

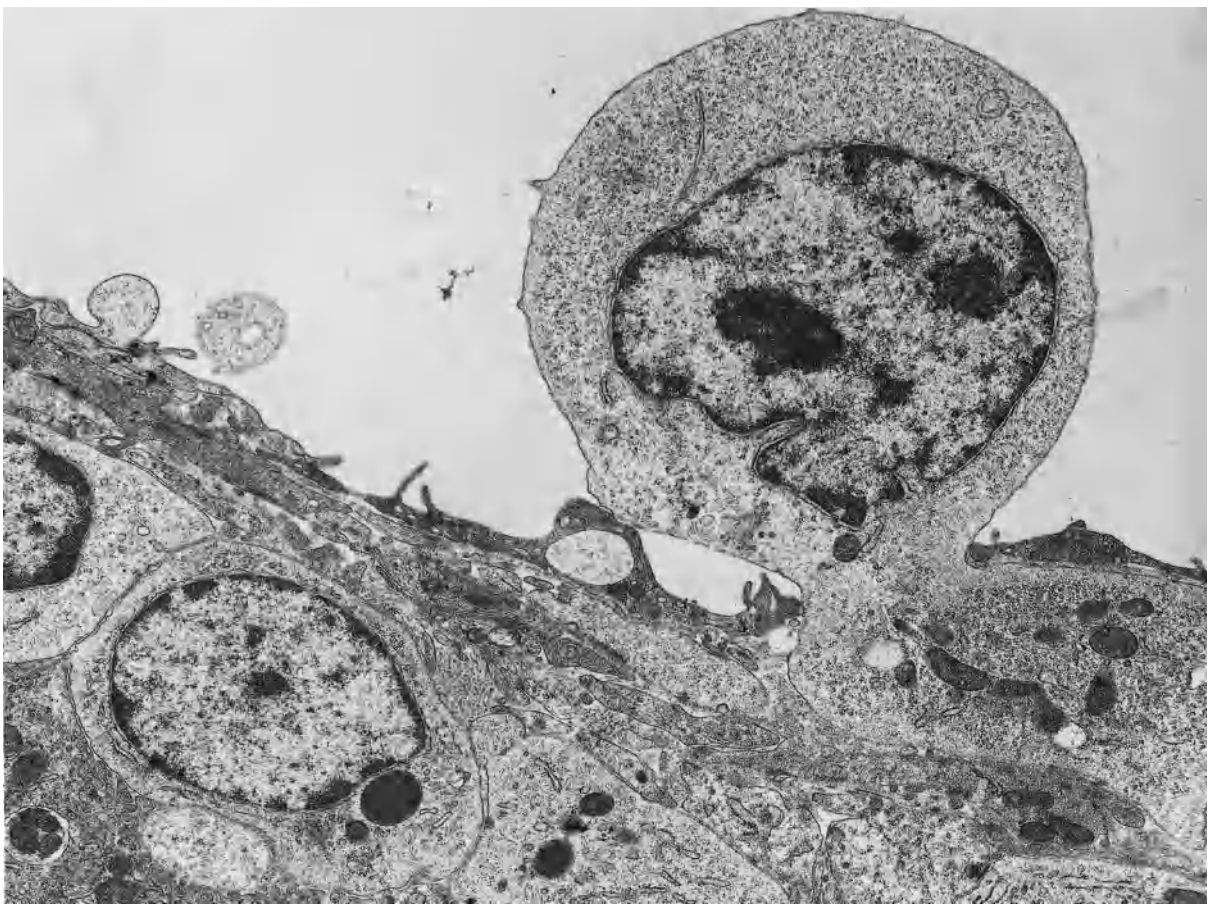


Fig. 23.22 Neoplastic lymphocyte invasion: hepatic sinusoidal endothelium, avian leukosis virus-induced lymphoid leukosis, chicken. Other neoplastic lymphocytes are in intersinusoidal spaces.

Tumor cells can cause endothelial cells to retract, exposing basement membranes, and can adhere to fibronectin, laminin, collagen IV and other components of the subendothelial matrix. These adhesive factors vary from tissue to tissue, and the specificity of some tumors may be related to the capillary endothelium and protetoglycans of that tissue and how the enzymes released by the tumor are able to enhance migration.

Intravascular arrest and proliferation characterize many metastatic foci. That is, tumors are initiated inside the capillary and grow out into tissue spaces.[144] Metastatic emboli attached to endothelium or trapped in the lumen of the blood vessels grow outward to block the lumen and inward to deface the vascular wall (Fig. 23.23).

Survival of neoplastic cells in the **bloodstream** is enhanced by several conditions. Clumps of tumor cells have a greater tendency to form metastases than single cells. The larger the tumor cell clump, the more likely it is to be trapped in capillaries to form a new colony. Some tumor cells contain surface materials that induce attachment to platelets and to cause platelet aggregation.

Once trapped in venules and capillaries, malignant cells adhere to endothelium and cause striking changes in adhesions of endothelial cells to their underlying matrix. Endothelial cells retract, leaving spaces through which the tumor cells can migrate into tissue. Once in the interstitium, the cell must induce alterations that promote further survival and replication. Again, fibrin deposited around the neoplastic cells provides a matrix for further development.[145] Within tissue tumors cells respond to chemotactic factors.[146,147]

Most cancer cells that enter the bloodstream die without initiating new metastatic foci.[148] Factors that influence whether tumor cells initiate new growths at sites distant from the primary tumor include (1) the way in which metastasis occurs (whether from single cells or from tumor emboli), (2) the intrinsic capacity of the malignant cell to lodge in and attach to host endothelial cells, and (3) the tissue environment at localization sites.

Organ-Specific Adhesion Molecules

Metastatic distribution is determined by anatomic characteristics of vascular and lymphatic vessel distribution in organs and by innate characteristics of the neoplastic cells. The spectrum of surface adhesion molecules on a neoplastic cell will determine both the survivability within the vascular system, and the capacity to metastasize to specific organs. Some adhesion molecules serve to disguise the neoplastic cell, allowing it to pass through the bloodstream as if it were a leukocyte.

The binding of neoplastic cells bearing **organ-specific adhesion molecules** will thus depend on the spectrum of counterreceptors present on endothelium in the target tissue. Expression of counterreceptors, which are also adhesion molecules, on endothelial cell surfaces can be induced by cytokines such as IL-1, TNF, and γIFN that are produced by the tumor cell.

Coagulation and Metastasis

Neoplastic cells secrete **procoagulant factors** that cause fibrinogen to polymerize on tumor cell emboli. Some cancer cells activate the clotting system by shedding plasma membrane vesicles that carry procoagulant activity.[149] The mesh of fibrin tends to protect the malignant cells from destruction, enabling them to proliferate.

Fibrin can be seen in emboli but is quickly denatured by the fibinolytic system and disappears during late stages of embolization. Some malignant cells have increased production of **plasminogen activators,** which enhance the effectiveness of the fibrinolytic system. While this would prevent the growth-promoting stabilizing effects of fibrin during metastasis and invasion, fibinolysis would enhance tumor growth in tissue once the metastatic focus was established.

Plasminogen activator inhibitor-1 (PAI-1) is a key regulator of the plasminogen activator-plasmin system, the proteolytic cascade involved in thrombosis. It is the molecular determinant of a permissive environment for tumor blood vessel growth.[150] A balance between serine proteases and their **PAI-1** is critical for pathologic angiogenesis, and **PAI-1 deficiency** is associated with tumor angiogenesis.

Platelets interact with circulating cancer cells to enhance their ability to adhere to vascular endothelium and lodge in capillaries. Use of anticoagulant and antiplatelet therapy to reduce metastases of natural tumors has given inconclusive results. However, in studies with experimental murine melanoma B16, prostacyclin remarkably decreased the number of metastases to lungs, presumably through its potent inhibiting effect on platelet aggregation.

Implantation

Because of their lack of cohesiveness, tumor cells growing on epithelial surfaces are prone to be shed into the surrounding spaces. Exfoliation of cells into fluids of the body cavities and respiratory and urogenital tracts allows for massive implantation of neoplastic cells on serosal surfaces. This pattern of growth is characteristic of some glandular tumors; for example, ovarian and pancreatic adenocarcinomas may seed throughout the peritoneal cavity. These lesions are

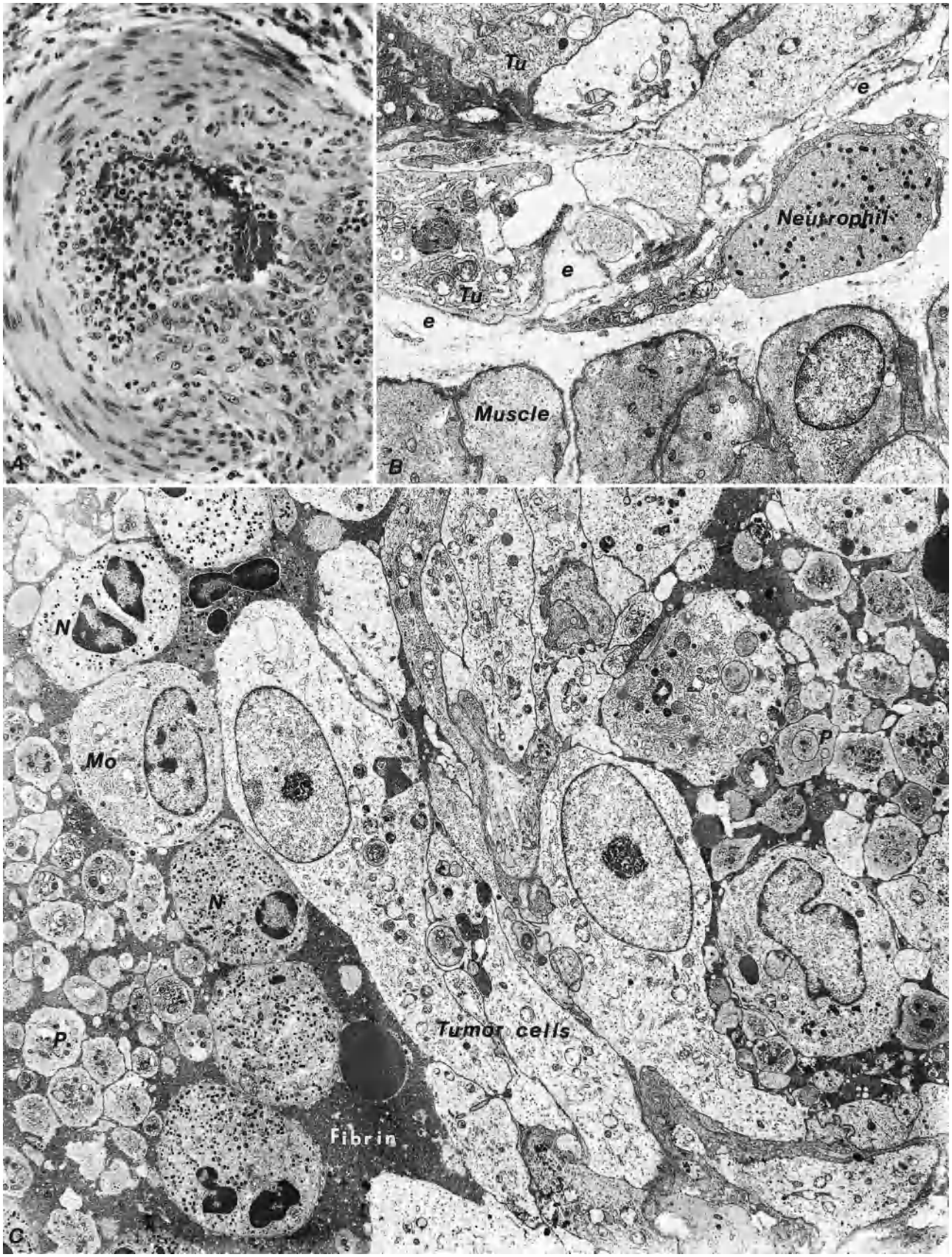


Fig. 23.23 **Tumor embolus**: squamous cell carcinoma lodged in pulmonary artery. **A**. **Tumor cells invade arterial wall** (*lower right*): lumen of artery is filled with thrombus containing many neutrophils, platelets, and monocytes. **B**. **Elastic membrane**: restricts invasion of vascular wall by tumor cells (*Tu*) and neutrophil. **C**. **Tumor cells in embolus**: tumor embolus is surrounded by platelets (*P*), neutrophils (*N*), and monocytes (*Mo*).

referred to as **peritoneal carcinomatosis.** Tumor cell localization on the peritoneal membranes is enhanced when the serosa is injured since tumor cells adhere to exposed collagen fibrils and grow more rapidly. Migration through body cavities and implantation on serosal surface allow these cells to become motile to develop striking surface changes. Filopodia and microvilli project from the cell into the cavity (Fig. 23.24). Ultrastructurally, the cell changes upon implantation to reflect its new capacity to absorb glycogen and other molecules from fluids.

Neoplastic Cell Death

Programmed Cell Death

Genetic mutation in somatic cells occurs sporadically over the life span of an animal, and these abnormal cells are removed by **programmed cell death (PCD).** The mutant gene codes for an abnormal protein that, because it is abnormal, can trigger PCD. In cellular proliferative responses, deletion of mutant cells by PCD prevents malignant cells from developing. This capacity to delete mutant cells is defective **cancer.** Suppression of PCD diminishes the ability to control cell proliferation and increases the risk for development of cancer—the failure of the developing cancer cell to trigger PCD leads to the continued replication of the mutant cell. Cancer cells promote their own survival using several strategies: increasing expression of anti-apoptotic factors (Bcl-2, X_L), activation of NFκB and PI3K-Akt pathways, and suppressing killer cell functions.

In tumors, there remain populations of abnormal cells with lethal mutations that are able to trigger PCD, and thus prevent cancer from developing. Malignant tumors that have these cells are able to initiate PCD, and have a large component of dense necrotic cells in tumor tissue.

Neoplastic Cell Caspases Trigger the Death Pathway

Caspases in neoplastic cells can trigger PCD—caspase 3 is critical for the apoptotic process (see chapter 2). Caspase, 3 localized in mitochondria using immunogold techniques, persists in the apoptotic body after PCD.[151]

Tumor Necrosis Factor-Induced Apoptosis

The potent cytokine **tumor necrosis factor-α (TNF-α)** can trigger caspase-independent PCD in neoplastic cells by binding to its specific death receptor, **TNFα-related apoptosis-inducing ligand (TRAIL).** TRAIL induces apoptosis in cancer cells but not most normal cells. The TRAIL pathway to necrosis-like cell death depends both on caspases and RIP kinase activity.[152] **Ceramide** acts as a mediator for death receptors such as TRAIL and TNF-α in the sequence: TNF-α → Bax/Bak → TRAIL → caspase 3/ceramide → apoptosis. The complex TRAIL-induced apoptosis involves the TRAIL receptors DR4 (TRAIL-R1) and DR5 (TRAIL-R2) and the **adapter protein Fas-associated death domain protein (FADD). TNF-like weak inducer of apoptosis (TWEAK)** binds to its cell surface receptor FGF-inducible 14 (**Fn14**) to regulate cell responses in apoptosis.

Anti-apoptotic Proteins in Cancer Cells

Neoplastic cells express anti-apoptotic proteins such as Bcl-2, Bcl-X(L), Mcl-1, Bcl-w, and A1/Bfl1. Therapies using small molecule inhibitors of bcl-2 family proteins are directed to the Bcl-2 binding pocket, preventing its sequestration of proapoptotic proteins such as Bid and Bim. **Bcl-2** is an anti-apoptotic member of a family of anti- and pro-apoptotic proteins that is upregulated in cancers and specifically overexpressed through chromosomal translocation in some non-Hodgkin's lymphomas. Attentuation of Bcl-2 lowers the threshhold for undergoing chemotherapy-induced apoptosis.

Other components that affect the balance of neoplastic cell survival or apoptosis include the following:

- **Akt** (protein kinase B) is a central regulator of proliferation, differentiation, and survival that is activated through growth factor receptors in PI3K-dependent mechanisms; blockade of Akt leads to apoptosis and suppressed tumor growth.
- **c-FLIP** (cellular FLICE-like inhibitory protein) is a procaspase-8-like regulator of death ligand-induced apoptosis. C-FLIP impedes TNF, Fas-L, and TRAIL-induced apoptosis by binding to FADD and/or caspase 8 or 10, which in turn prevents death-inducing signaling complex (DISC) formation and subsequent activation of the caspase cascade.
- **TGF-β,** a potent proliferation inhibitor, is ineffective in epithelial cells that lack TGF-β receptors. The TGF-β receptor-deficient cells are prone to squamous cell carcinomas; however, these cells correct this deficit by increasing apoptosis.

Shift to Senescence

Cellular senescence limits the proliferative capacity of damaged cells and thereby acts as an intrinsic mechanism of tumor suppression. In some tumors, cytokines have been shown to shift the tumor cell into senescence (rather than apoptosis). For example,

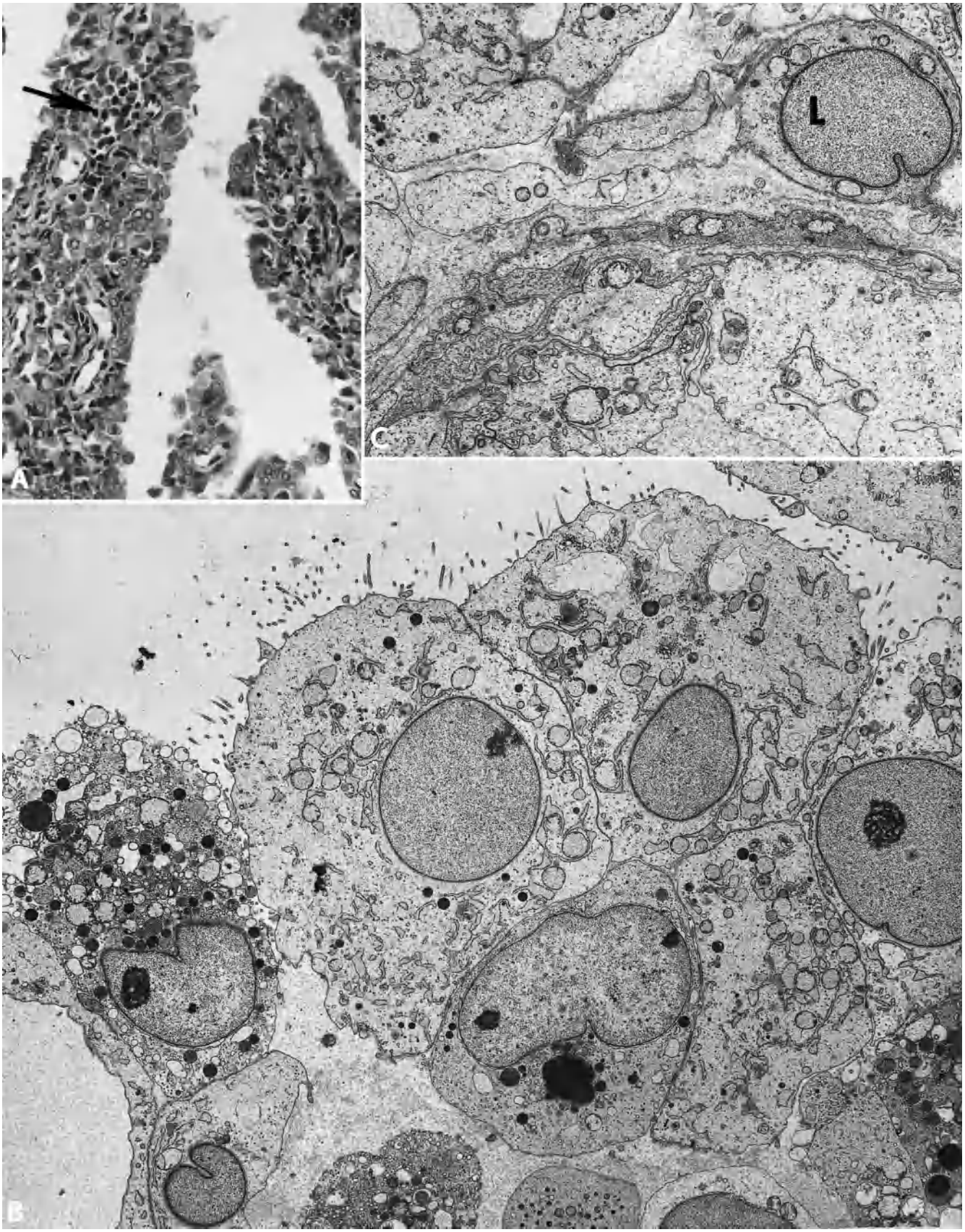


Fig. 23.24 **Implantation**: aortic body carcinoma, serosal surface of the mediatinum, dog. **A**. **Histology**: frond of tumor composed of vascular and connective tissue lined by tumor cells. Lymphoid cell infiltrates (*arrow*). **B**. **Ultrastructure**: lack of granules, lack of mitochondrial cristae, many surface microvilli, and marked pleomorphism are evident. **C**. **Tumor capillary** (*bottom*): lymphocyte (*L*) and interstitium.

insulin growth factor binding protein 7 (IGFBP7) mediates senescence induced by oncogenes in normal melanocytes.[153]

Entosis

Entosis and **empiripolesis** are names that have been applied to uptake of one cell by another. The host cell completely encloses the target cell, which is the active partner in the process. Uptake uses cadherins and requires activation of surface components. The invading cell appears to pull the host cell around itself. The invader is typically degraded in autophagolysosomes, but, at least in human breast carcinomas, can not only survive but pop out of the host cell to survive extracellularly.[154]

Lymphocyte Killing of Neoplastic Cells

Neoplasms frequently are infiltrated by lymphocytes that reside around tumor cells, and have close apposition to them.[155] Neoplastic cell surfaces bear specific proteins that act as antigens—antigens that induce a selective cell-mediated reaction that act to destroy malignant cells.

Natural Killer Cells

Natural killer (NK) cells play a central role in anticancer immunity. Ultrastructurally, NK cells attach to the target cell and cause its lysis.[156–158]

Experimentally, there is a close correlation between NK cell activity and tumor cell killing. NK cell activity is markedly increased in T cell-deficient nude mice and is diminished in some human lymphoproliferative diseases. Clinically, the lymphokine-activated killer (LAK) cell system has been used in treatment of human patients. Experiments in rodents have shown similar effects. In the murine melanoma model, LAK cells migrate to and infiltrate metastatic tumor foci.[159]

Killer Dendritic Cells

Killer dendritic cells have the capacity to both present antigens and to kill target cells. In NK cell cancer cell killing, the **interferon-γ (IFN-γ)**-induced TRAIL pathway is a vital component of cancer immunosurveillance. The main source of IFN-γ in this pathway is the subset of killer dendritic cells that act as pivotal sensors and effectors of the innate antitumor immune reponse.[160] These cells possess the lytic potential of (and are related closely to) NK cells.

Langerhans' cells are antigen-presenting cells that kill cells in epithelial tumors. Squamous carcinomas of the uterine cervix have been found to have a significant increase in the number of Langerhans' cells, many of which form specialized contacts with infiltrating lymphocytes. The Langerhans' cells within the tumor are hypertrophic and have increased amounts of rough and smooth endoplasmic reticulum and large numbers of cytoplasmic filaments.[161]

Monocytes

Activated monocytes can effectively kill neoplastic cells. When human blood monocytes are incubated with human melanoma cells, monocytes and lymphocytes attach to tumor cell within one hr. Cell surfaces of monocyte and tumor cells were markedly interdigitated, and by 4 hr up to 25% of the blood cells had been "interiorized" by tumor cells.[162] In vitro, monocytes clearly can kill transformed cells. When activated, they cluster around tumor cells, bind to them, and zones of vacuolation develop in the activated monocytes. The target cells are killed.

Human melanomas commonly contain infiltrates of monocytes.[163] Malignant melanomas are destroyed, in part, by activated killer cells. Phagocytosis of melanin granules occurs (Fig. 23.25) leading to the formation of giant melanophages in the tumor.

Enhancement of monocyte/macrophage activity in neoplastic disease has been used as a model of clinical treatment. Injection of granuloma-inciting bacteria such as *Mycobacteria* or *Corynebacterium parvum* causes phagocytosis of tumors cell.[164]

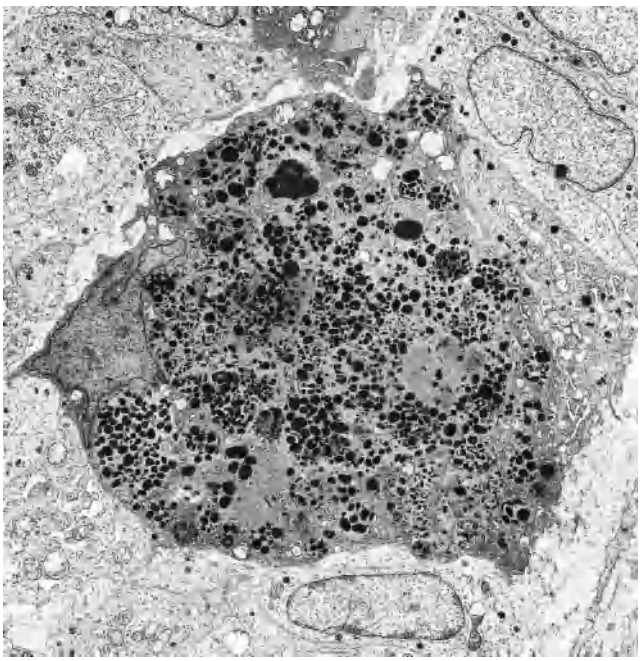


Fig. 23.25 Melanophage: contains phagocytosed melanin granules, malignant melanoma, dog.

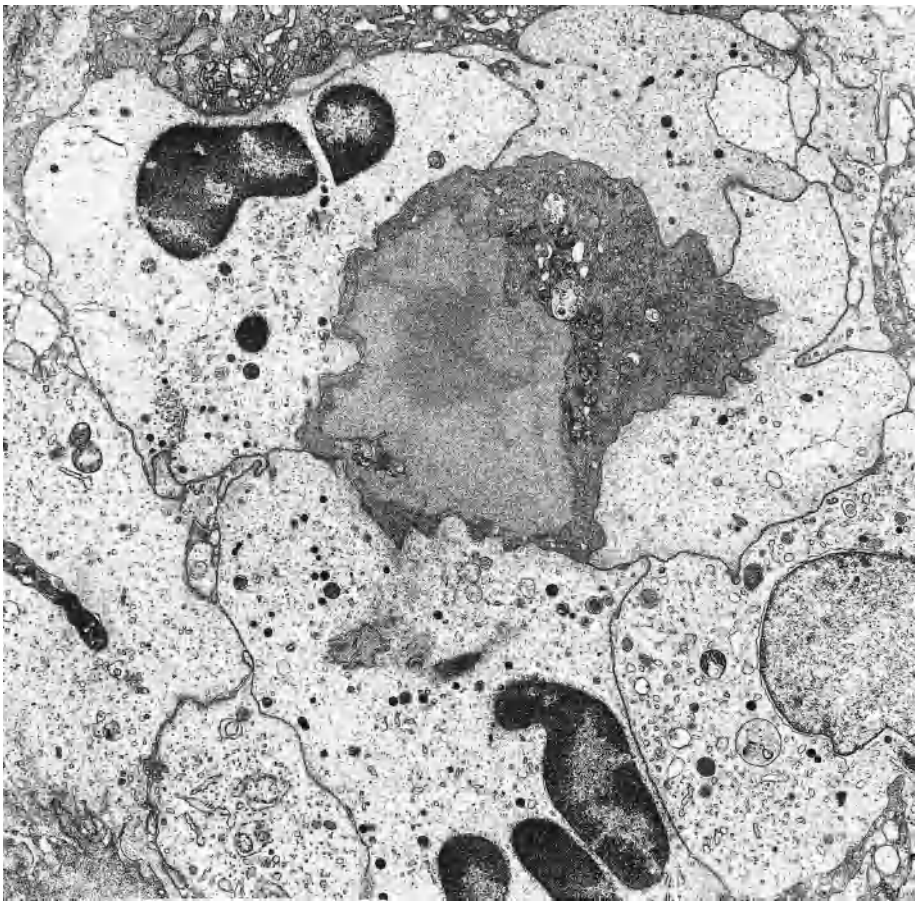


Fig. 23.26 Neutrophil phagocytosis of neoplastic cells: squamous cell carcinoma, dog. Neutrophils have expelled most of their granules.

Neutrophils

Neutrophils commonly invade neoplasms, especially those at body surfaces that are apt to become infected with bacteria and fungi. In these cases neutrophils appear ultrastructurally as highly activated and typically appear to have completed the respiratory burst and degranulation. That is, they have very few granules and those that remain are large and irregular. The neutrophils clearly phagocytize tumor cells but do so in ways that have little bearing on the growth of the neoplasm. Squamous cell carcinomas of the oral and nasal cavities commonly contain large numbers of blood neutrophils that can be seen to be in stages of phagocytosis and killing of tumor cells (Fig. 23.26). This activity is not specific and it is likely that this represents killing of necrobiotic tumor cells.

Basophils and Mast Cells

Some tumors have mast cells interspersed among the tumor cell population. No antitumor effect has been demonstrated in clinical disease but these cells may have some effect on coagulation. In vitro, mast cells can significantly enhance tumor growth. Heparin in mast cell granules is responsible.[165] Degranulation and stromal metachromasia are often reported at sites of active tumor growth. In vitro, the mast cell reaction to a tumor correlates with the tumors proliferative capacity.[166]

Platelets

Some neoplastic cells activate and aggregate platelets, and this ability correlates with their metastatic potential. Animals made thrombocytopenic prior to injection of tumor cells develop fewer lung colonies. Mechanisms involved have been hypothesized to include the following progression: (1) platelets form a protective shield around tumor cells preventing their destruction, (2) release of platelet dense granule vasoconstrictive products leads to entrapment of other platelets, (3) release of platelet alpha granules enhances tumor cell adhesion (via thrombospondin, fibronectin, and von Willebrand factor) or growth, and (4) platelets aid directly in neoplastic cell attachment to the blood vessel wall. Ultrastructural studies reveal that the platelet cytoskeleton and plasma membranes facilitate tumor attachment to endothelium.[167] In melanomas, platelet-melanoma cell intereaction is

mediated by the platelet surface receptor gpIIb-IIIa complex.[168]

References

1. Wood LD, et al. 2007. The genomic landscapes of human breast and colorectal cancers. *Science* 318: 1108.
2. Esteller M. 2008. Epigenetics in cancer. *New Engl J Med* 358:1148.
3. Jones PA, Baylin SB. 2007. The epigenomics of cancer. *Cell* 128:683.
4. Gazin C, et al. 2007. An elaborate pathway required for Ras-mediated epigenetic silencing. *Nature* 449:1073.
5. Hall TL, Fu YS. 1985. Applications of quantitative microscopy in tumor pathology. *Lab Invest* 53:5.
6. Russo J, Russo IH. 1987. Biological and molecular bases of mammary carcinogenesis. *Lab Invest* 57:112.
7. Shimazui T, et al. 1989. Evaluation of human bladder tumors by ultrastructural morphometric techniques. *Virch Arch B* 57:195.
8. Hayashi H, Ishimaru Y. 1981. Morphological and biochemical aspects of adhesiveness and dissociation of cancer cells. *Int Rev Cytol* 70:139.
9. Katayama I, et al. 1972. Ultrastructural cytochemical demonstration of tartrate-resistant acid phosphatase isoenzyme activity in "hairy cells" of leukemic reticuloendotheliosis. *Am J Pathol* 69:471.
10. Vishnubhotla R, et al. 2007. ROCK-II mediates colon cancer invasion via regulation of MMP-2 and MMP-13 at the site of invadopodia as revealed by multiphoton imaging. *Lab Invest* 87:1149.
11. Bar-Sagi D, Feramisco JR. 1986. Induction of membrane ruffling and fluid-phase pinocytosis in quiescent fibroblasts by *ras* proteins. *Science* 233:1061.
12. Deck JHN, et al. 1990. "Anemone" cell (Villiform) tumor of the brain. *Ultrastr Pathol* 14:87.
13. Losa GA, et al. 1986. Characterization of membrane vesicles circulating in the serum of patients with common acute lymphoblastic leukemia. *Lab Invest* 55:573.
14. Nickoloff BJ, et al. 1989. Markedly diminished epidermal keratinocyte expression of intercellular adhesion molecule-1 (ICAM-1) in Sezary syndrome. *J Am Med Ass* 261:2217.
15. Banai K, et al. 2004. A preliminary optical and electron microscopic study of the beta(1) integrin destruction pattern of human osteosarcoma-derived cells. *Histochem Cell Biol* 122:75.
16. Savino W, et al. 1984. Thymic epithelial antigen, acquired during ontogeny and defined by the anti-p19 monoclonal antibody, is lost in thymoma. *Lab Invest* 51:292.
17. Pauli BU, et al. 1978. Topography and numerical densities of intramembrane particles in chemical carcinogen-induced urinary bladder carcinomas in Fischer rats. *Lab Invest* 39:565.
18. Tokumitsu S, et al. 1978. Deviated formation of intestinal glycocalyx in human stomach cancer cells. *Virch Arch B* 27:217.
19. Ahnen DJ, et al. 1982. Ultrastructural localization of carcinoembryonic antigen in normal intestine and colon cancer. *Cancer* 49:2077.
20. Steck PA, Nicolson GL. 1983. Cell surface glycoproteins of 1372NF mammary adenocarcinoma clones of differing metastatic potentials. *Exp Cell Res* 147:255.
21. Sata T, et al. 1992. Studies on the Thomsen-Friedenreich antigen in human colon with the lectin *Amaranthin*. *Lab Invest* 66:175.
22. Roth J, Zuber C. 1990. Immunoelectron microscopic investigation of surface coat of Wilm's tumor cells. *Lab Invest* 62:55.
23. Houghton AN, et al. 1982. Surface antigens of melanocytes and melanomas. *J Exp Med* 156:1755.
24. Denk H, et al. 1982. Biochemical and immunocytochemical analysis of intermediate filament cytoskeleton in human hepatocellular carcinomas and in hepatic neoplastic nodules of mice. *Lab Invest* 46: 584.
25. McNutt NS, et al. 1981. Mycosis fungoides. *Lab Invest* 44:466.
26. Miettinen M. 1988. Antibody specific muscle actins in the diagnosis and classification of soft tissue tumors. *Am J Pathol* 130:205.
27. Schenk P. 1974. Microfilaments in human epithelial cancer cells. *Z Krebsforsch* 84:241.
28. Hisaoka M, et al. 2003. Microtubule-associated protein-2 and class III beta-tubulin are expressed in extraskeletal myxoid chondrosarcoma. *Mod Pathol* 16:543.
29. Erlandson RA, et al. 1989. Cytoskeletal proteins including myofilaments in human tumors. *Ultrastr Pathol* 13:155.
30. Moll R, et al. 1987. Immunocytochemical analysis of Ewing's tumors. *Am J Pathol* 127:288.
31. Schürch W, et al. 1987. Intermediate filament proteins and actin isoforms as markers for soft tissue tumor differentiation and origin. I. Smooth muscle tumors. *Am J Pathol* 128:91.
32. Skalli O, et al. 1988. Intermediate filament proteins and actin isoforms as markers for soft tissue tumor differentiation and origin. II. Rhabdomyosarcomas. *Am J Pathol* 130:515.
33. Warhol MJ. 1984. The ultratructural localization of keratin proteins and carcinoembryonic antigen in malignant mesothelioma. *Am J Pathol* 116:385.
34. Said JW, et al. 1983. Involucrin in lung tumors. *Lab Invest* 49:563.
35. Gould VE, et al. 1986. The intermediate filament complement of the spectrum of nerve sheath neoplasms. *Lab Invest* 55:463.
36. Monteirao MJ, et al. 1990. Expression of NF-L in both neuronal and nonneuronal cells of transgenic mice. *J Cell Biol* 111:1543.
37. Jeon YK, et al. 2004. Infratentorial giant cell ependymoma. *Pathol Res Pract* 200:717.
38. Nicolson G, et al. 1988. Loss of intercellular junctional communcation correlates with the metastatic potential in mammary adenocarcinoma cells. *Proc Natl Acad Sci USA* 85:473.

39. Pauli BU, et al. 1977. Ultrastructure of cell junctions in FANFT-induced urothelial tumors in urinary bladder of Fischer rats. *Lab Invest* 37:609.
40. Banner BF, et al. 1978. An ultrastructural study of acinic cell carcinoma of the canine pancreas. *Am J Pathol* 93:165.
41. Czernobilsky B, et al. 1987. Desmosomal plaque-associated vimentin filaments in the ovarian granular cell tumors of various histologic patterns. *Am J Pathol* 126:476.
42. Schwechheimer K, et al. 1984. Vimentin filament-desmosome cytoskeleton of diverse types of human meningiomas. *Lab Invest* 51:584.
43. Alroy J. 1978. Alterations of intracellular junctions in acinic cell carcinoma of the canine pancreas. *Virch Arch B* 28:21.
44. Alroy J, et al. 1981. Correlation between numbers of desmosomes and the aggressiveness of transitional cell carcinoma in human urinary bladder. *Cancer* 47:104.
45. Moll R, et al. 1986. Desmosomal proteins: New markers for identification and classification of tumors. *Lab Invest* 54:4.
46. Bergstraesser LM, et al. 1995. Expression of hemidesmosomes and component proteins is lost by invasive breast cancer cells. *Am J Pathol* 147:1823.
47. Klaunig JE, Ruch RJ. 1990. Role of inhibition of intercellular communication in carcinogenesis. *Lab Invest* 62:135.
48. Elias PM, et al. 1980. Gap junction proliferation in retinoic acid-treated human basal cell carcinoma. *Lab Invest* 42:469.
49. Volberg T, et al. 1991. Modulation of intercellular adherens-type junctions and tyrosine phosphorylation of their components in RSV-transformed cultured chick lens cells. *Cell Regulation* 2:105.
50. Djoldetti M, Kewinshi UH. 1978. Origin of intranuclear inclusions in myeloma cells. *Scand J Haematol* 20:200.
51. Torikata C, Ishiwata K. 1977. Intranuclear tubular structure observed in the cells of an alveolar cell carcinoma of the lung. *Cancer* 40:1194.
52. Tavassoli FA, et al. 1991. Intranuclear helioid inclusions in mammary intraductal hyperplasias. *Ultrastr Pathol* 15:267.
53. Tsuru A, et al. 1990. Regulation of the expression of vimentin gene during differentiation of mouse myeloid leukemia cells. *J Cell Biol* 110:1655.
54. Dardick I. 1992. Ultrastructural morphology and the control of lymphocyte nuclear size in non-Hodgkin lymphoma: A review. *Ultrastr Pathol* 16:137.
55. van der Putte SCJ, et al. 1984. Malignant lymphoma of follicle centre cells with marked nuclear lobation. *Virch Arch B* 46:93.
56. Litovitz TL, Lutzner MA. 1974. Quantitative measurement of blood lymphocytes from patients with chronic lymphocytic leukemia and the Sezary syndrome. *J Natl Cancer Inst* 53:75.
57. Payne CM. 1992. A multidisciplinary approach to diagnosis of cutaneous T-cell lymphomas. *Ultrastr Pathol* 16:99.
58. Payne CM, et al. 1989. A comparative mathematical evaluation of contour irregularity using form factor and PERBAS, a new analytical shape factor. *Anal Quant Cytol Histol* 11:341.
59. Johnson DL, Johnson SAS. 2008. RNA metabolism and ocnogenesis. *Science* 320:461.
60. Goodlad JR, et al. 1991. Nucleolar ultrastructure in low- and high-grade non-Hodgkin's lymphomas. *J Pathol* 163:233.
61. Payne CM, et al. 1987. An ultrastructural morphometric and immunophenotypic evaluation of Burkitt's and Burkitt's-like lymphoma. *Lab Invest* 57:200.
62. Derenzini M, et al. 1990. Diagnostic value of silver-stained interphasic nucleolar organizer regions in breast tumors. *Ultrastr Pathol* 14:233.
63. Derenzini M, et al. 1991. Interphase nucleolar organizer regions in cancer cells. *Int Rev Exp Pathol* 32:149.
64. Takeuchi T, et al. 1990. Nucleolar organizer regions in rat urinary bladder tumors induced by N-butyl-N-(4-hydroxy butyl)nitrosamine. *Virch Arch B* 58: 383.
65. Kaiserling E, Wolburg H. 1991. Freeze-fracture morphology of nuclear pockets. *Virch Arch B* 60:47.
66. Kaiserling E, Stein H. 1973. Atypische Kerninvaginationen bei einem lymphoblastischen Lymphosarkom. *Virch Arch B* 13:215.
67. McNutt NS, et al. 1981. Comparison of cell peripheries in the human colonic adenocarcinoma cell lines SW480 and SW620 grown in floating chamber culture, cover slip culture, athymic (nude) mice, and BALB/c mice. *Lab Invest* 44:309.
68. Goldfarb AN, et al. 1992. Expression of a chimeric helix-loop-helix gene, Id-SCL, in K562 human leukemic cells is associated with nuclear segmentation. *Am J Pathol* 141:1125.
69. Rejthar A, Blumajer J. 1974. Difference in density of nuclear pores in normal and malignant fibroblasts of Syrian hamster. *Neoplasma* 21:479.
70. Sacks-Wilner R, Freddo TF. 1990. Differences in nuclear pore density among human choroidal melanoma cell types. *Ultrastr Pathol* 14:311.
71. Boqvist L. 1970. Annulate lamellae in the parathyroid adenoma. *Virch Arch B* 6:234.
72. Biernat W, et al. 2001. Dysembryoplastic neuroectodermal tumor. *Ultrastr Pathol* 25:455.
73. Tschang T-P, et al. 1978. Annulate lamellae in human malignant tumors. *Arch Pathol Lab Med* 102:426.
74. Hill DL. 1985. Morphology of nasopharyngeal angiofibroma. *J Submicrosc Cytol* 17:443.
75. Topilko A, et al. 1984. Ultrastructural cytochemistry of intranuclear dense granules in nasopharyngeal angiofibroma. *Ultastruc Pathol* 6:221.
76. Meyer JS, Coplin MD. 1988. Thymidine labeling index, flow cytometric S-phase measurement, and DNA index in human tumors: Comparison and correlations. *Am J Clin Pathol* 89:586.
77. Kay S, et al. 1975. Interstitial-cell tumor of the testis. *Am J Clin Pathol* 63:366.
78. Nawrocki ST, et al. 2006. Aggresome disruption: A novel strategy to enhance bortezomib-induced apoptosis in pancreatic cancer cells. *Cancer Res* 66:3773.

79. Haratake J, et al. 1990. Globular cytoplasmic inclusion bodies in a metastatic hepatocellular carcinoma of the iliac bone. *Ultrastr Pathol* 14:283.
80. Muretto P, et al. 1979. Hepatocellular carcinomas with intracytoplasmic hyaline globules. *Tumori* 65:767.
81. Ordonez NG, et al. 1985. Crystals and alpha-1-antitrypsin-reactive globoid inclusions in an islet cell tumor of the pancreas. *Ultrastr Pathol* 8:319.
82. James CL. 1995. Basal cell carcinoma with hyaline inclusions. *Pathology* 27:97.
83. Harris CC, et al. 1973. Localization of benzo(a)pyrene-^{3}H and alterations in nuclear chromatin caused by benzo(a)pyrene-ferric oxide in the hamster respiratory epithelium. *Cancer Res* 33:2842.
84. Mukai M, et al. 1984. Histogenesis of clear cell sarcoma of tendons and aponeuroses. *Am J Pathol* 114:264.
85. Gould VE, et al. 1972. Ultrastructural aspects of papillary and sclerosing carcinomas of the thyroid. *Cancer* 29:1613.
86. Campbell WG, et al. 1985. Characterization of two types of crystalloids in pleomorphic adenomas of minor salivary glands. *Am J Pathol* 118:194.
87. Makio M, et al. 1984. Alveolar soft part sarcoma: An elaboration of a three-dimensional configuration of the crystalloids by digital image processing. *Am J Pathol* 116:398.
88. Ladanyi M. et al. 2002. The precrystalline cytoplasmic granules of alveolar soft part sarcoma contain monocarboxylate transporter 1 and CD147. *Am J Pathol* 160:1215.
89. Tokue A, et al. 1985. Unusual intracytoplasmic lamellar bodies in a malignant gonadal stromal tumor. *Virch Arch B* 49:261.
90. Thake DC, et al. 1971. Ectopic thyroid adenomas at the base of the heart of the dog. Ultrastructural identification of dense tubular structures in endoplasmic reticulum. *Vet Pathol* 8421.
91. Best PV. 1988. Ribosome-lamella complexes in intracranial tumors. *Acta Neuropathol* 76:265.
92. Rosner MC, Golomb HM. 1980. Ribosome-lamella complex in hairy cell leukemia. *Lab Invest* 42:236.
93. Torikata C, et al. 1991. Confronting cisternae and ciliated cells in malignant pleural mesothelioma: An ultrastructural study. *Ultrastr Pathol* 15:249.
94. Losinski NE, et al. 1989. Double labeling immunogold electron-microscopic study of hormonal colocalization in nontumorous and adenomatous rat pituitaries. *Am J Anat* 185:236.
95. Beckford U, et al. 1985. Localization of CA and HMFG-2 antigens in breast tissue by immunoperosidase, immunofluorescence, and immunoelectron microscopy. *J Clin Pathol* 38:512.
96. Foster CS, et al. 1982. Monoclonal antibodies to the human mammary gland. *Virch Arch A* 394:295.
97. Major P, et al. 1987. Ultrastructural localization of a breast tumor-associated antigen. *J Hist Cyt* 35:375.
98. Havaki S, et al. 2006. Nuclear localization of cytokeratin 8 and the O-linked N-acetylglucosamine containing epitope H in epithelial cells of infiltrating ductal breast carcinomas. *Ultrastr Pathol* 30:177.
99. Lloyd RV, et al. 1991. Analysis of pituitary hormones and chromogranin A mRNAs in null cell adenomas, oncocytomas, and gonadotroph adenomas by in situ hybridization. *Am J Pathol* 139:553.
100. Mulla A, et al. 2004. Expression, subcellular localization and phosphorylation status of annexins 1 and 5 in human pituitary adenomas and a growth hormone-secreting carcinoma. *Clin Endocrinol* 60: 107.
101. Fossmark R, et al. 2005. Ultrastructure and chromogranin A immunogold labeling of ECL cell carcinoids. *APMIS* 113:506.
102. Sørhaug S, 2007. Expression of neuroendocrine markers in non-small cell lung cancer. *APMIS* 115:152.
103. Rindi G, et al. 2007. Peptide products of the neurotrophin-inducible gene vgf are produced in human neuroendocrine cells from early development and increase in hyperplasia and neoplasia. *J Clin Endocrinol Metab* 92:2811.
104. Seretis EC, et al. 2007. Immunoelectron study of pancreatic carcinomas using antibodies to gastrointestinal hormones. *Ultrastr Pathol* 31:303.
105. Seretis EC, et al. 2004. Electron immunocytochemical demonstration of serotonin, vasoactive intestinal polypeptide, bombesin, somatostatin and glucagon in mirror biopsies from primary colorecto adenocarcinomas. *J Exp Clin Cancer Res* 23:477.
106. Peterson LA, et al. 1991. Acute basophilic leukemia. *Am J Clin Pathol* 96:161.
107. Tulliez M, Breton-Gorius J. 1979. Three types of Auer bodies in acute leukemia. *Lab Invest* 41:419.
108. Cameron S, et al. 1990. Clinical, biochemical and immunoelectron microscopical evidence of dual hormone production in a mammosomatotroph cell adenoma. *J Pathol* 161:239.
109. Bordi C, et al. 1985. Histologic, immunofluorescence, and ultrastructural study of malignant islet-cell tumors of the pancreas induced in hamsters by BK human papovavirus. *Am J Pathol* 118:256.
110. Pettinata G, et al. 1991. Melantoic neuroectodermal tumor of infancy. *Am J Surg Pathol* 15:233.
111. Seman G, Gallagher HS. 1979. Intramitochondrial rod-like inclusions in human breast tumors. *Anat Rec* 194:267.
112. Psarra AM, et al. 2005. Glucocortioid receptor isoforms in human hepatocarcinoma HepG2 and SaOS-2 osteosarcoma cells. *Int J Biochem Cell Biol* 37:2544.
113. Ebner D, et al. 1991. Functional and molecular analysis of mitochondria in thyroid oncocytomas. *Virch Arch B* 60:139.
114. Payne CM, et al. 1987. An ultrastructural morphometric and immunophenotypic evaluation of Burkitt's and Burkitt's-like lymphoma. *Lab Invest* 57:200.
115. Welm AL. 2008. TGF-β primes breast tumor cells for metastases. *Cell* 133:27.
116. Bosman FT, et al. 1985. Basement membranes in cancer. *Ultrastr Pathol* 8:291.
117. Liotta LA. 1984. Tumor invasion and metastases: Role of the basement membrane. *Am J Pathol* 117:339.
118. Paku S, Paweletz N. 1991. First steps of tumor-related angiogenesis. *Lab Invest* 65:334.

119. Yurchenco PD, et al. 1988. Type IV collagen lateral associations in the EHS tumor matrix. *Am J Pathol* 132: 278.
120. Iozzo RV. 1985. Proteoglycans: Structure, function, and role in neoplasia. *Lab Invest* 53:373.
121. Gusterson BA, et al. 1984. Invading squamous cell carcinoma can retain a basal lamina. *Lab Invest* 51: 82.
122. Eyden B. 2005. The myofibroblast. *J Submicr Cytol Pathol* 37:109 and 231.
123. Eyden B, et al. 2005. Foci of amorphous/granulofilamentous matrix in the extracellular domains of tumours. *J Submicr Cytol Pathol* 37:1.
124. Jensen PH, et al. 1990. Lysosomal degradation of receptor-bound urokinase-type plasminogen activator is enhanced by its inhibitors in human trophoblastic choriocarcioma cells. *Cell Regulation* 1:1043.
125. Dvorak HF, et al. 1988. Identification and characterization of the blood vessels of solid tumors that are leaky to circulating macromolecules. *Am J Pathol* 133:95.
126. Kohn S, et al. 1992. Pathways of macromolecular tracer transport across venules and small veins. *Lab Invest* 67:596.
127. Takeuchi H, et al. 2007. Angiogenesis in primary central nervous system lymphoma (PCNSL). *J Neurooncol* 84:141.
128. Kerbel RS. 2008. Tumor angiogenesis. *New Engl J Med* 358:2039.
129. Nagy JA, et al. 2006. Permeability properties of tumor surrogate blood vessels induced by VEGF-A. *Lab Invest* 86:767.
130. Wong SY, et al. 2005. Tumor-secreted vascular endothelial growth factor-C is necessary for prostate cancer lymphangiogenesis. Cancer Res 65:9789.
131. Kopfstein L, et al. 2007. Distinct roles of vascular endothelial growth factor-D in lymphangiognesis and metastasis. *Am J Pathol* 170:1348.
132. Miller DW, et al. 2005. Rapid vessel regression, protease inhibition, and stromal normalization upon short-term vascular endothelial growth factor receptor 2 inhibition in skin carcinoma heterotransplants. *Am J Pathol* 167:1389.
133. Gao D, et al. 2008. Endothleial progenitor cells control the angiogenic switch in mouse lung metastasis. *Science* 319:195.
134. McNutt NS, et al. 1983. Early lesions of Kaposi's sarcoma in heterosexual men. *Am J Pathol* 111:62.
135. Vishnubhotla R, et al. 2007. ROCK-II mediates colon cancer invasion via regulation of MMP-2 and MMP-13 at the site of invadopodia as revealed by multiphoton imaging. *Lab Invest* 87:1149.
136. Witze ES, et al. 2008. Wnt5a control of cell polarity and directional movement by polarized redistribution of adhesion receptors. *Science* 320:365.
137. Behrens J, et al. 1989. Dissecting tumor cell invasion: Epithelial cells acquire invasive properties after the loss of uvomorulin-mediated cell-cell adhesion. *J Cell Biol* 108:2435.
138. Graf M, et al. 1981. Histochemical localization of cathepsin B at the invasion front of the rabbit V_2 carcinoma. *Lab Invest* 45:587.
139. Sena P, et al. 2006. Subcellular localization of beta-catenin and APC proteins in colorectal preneoplastic and neoplastic lesions. *Cancer Lett* 241:203.
140. Kuhnen C, et al. 2000. Beta-catenin in soft tissue sarcomas. *Mod Pathol* 13:1005.
141. Azzali G. 2007. Tumor cell transendothelial passage in the absorbing lymphatic vessel of transgenic adenocarcinoma mouse prostate. *Am J Pathol* 170:334.
142. Adamson IYR, et al. 1987. Tumor metastasis after hyperoxic injury and repair of pulmonary endothelium. *Lab Invest* 57:71.
143. De Bryn P, Cho Y. 1982. Vascular endothelial invasion via transcellular passage by malignant cells in the primary stage of metastasis formation. *J Ultrastruct Res* 81:189.
144. Crissman JP, et al. 1985. Arrest and extravasation of B16 amelanotic melanoma in murine lungs. *Lab Invest* 53:470.
145. Chew E-C, Wallace AC. 1976. Demonstration of fibrin in early stages of experimental metasases. *Cancer Res* 36:1904.
146. Orr W, et al. 1976. Characteristics of the chemotactic response of neoplastic cells to a factor derived from the fifth component of complement. *Am J Pathol* 93: 405.
147. Lam WC, et al. 1981. The chemotactic response of tumor cells. *Am J Pathol* 104:69.
148. Weiss L. 1979. Dynamic aspects of cancer cell populations in metastasis. *Am J Pathol* 97:601.
149. Azzarelli B, et al. 1989. Leukemic cell-endothelial cell interactions in leukemic cell dissemination. *Lab Invest* 60:45.
150. Jost M, et al. 2007. Tumoral and choroidal vascularization: Differential cellular mechanisms involving plasminogen activator inhibitor type 1. *Am J Pathol* 171:1369.
151. Soini Y, et al. 2005. Activation and relocalization of caspase 3 during the apoptotic cascade of human mesothelioma cells. *APMIS* 113:426.
152. Meurette O, et al. 2007. TRAIL induces receptor-interacting protein 1-dependent and caspase-dependent necrosis-like cell death under acidic extracellular conditions. *Cancer Res* 67:218.
153. Chien Y, Lowe SW. 2008. Secreting tumor suppression. *Cell* 132:339.
154. Overholtzer M, et al. 2007. A nonapoptotic cell death process, entosis, that occurs by cell-in-cell invasion. *Cell* 131:966.
155. Dingemans KP, et al. 1978. Invasion of liver tissue by tumor cells and leukocytes: Comparative ultrastructure. *J Nat Cancer Inst* 60:583.
156. Burns ER, et al. 1982. Cytotoxicity of natural killer cells. *Lab Invest* 47:99.
157. Adelstein EH, et al. 1976. Ultrastructure of lymphocyte tumor cell interaction with localization of cell bound antibody by ferritin labelling. *Cancer Res* 36:302.
158. Bucana CD, et al. 1983. Ultrastructural studies of the interaction between liposome-activated human blood monocytes and allogeneic tumor cells in vitro. *Am J Pathol* 112:101.

159. Basse P, et al. 1991. Accumulation of adoptively transferred adherent, lymphokine-activated killer cells in murine metastases. *J Exp Med* 174:479.
160. Taieb J, et al. 2006. A novel dendritic cell subset involved in tumor immunosurveillance. *Nat Med* 12:214.
161. Caorsi I, Figueroa CD. 1984. Langerhans' cells in squamous exocervical carcinoma: A quantitative and ultrastructural study. *Ultrastr Pathol* 7:25.
162. Fujinami N, et al. 1981. Interaction of mononuclear leukocytes with malignant melanoma. *Lab Invest* 45: 28.
163. Roubin R, et al. 1975. Characterization of the mononuclear cell infiltrate in human malignant melanoma. *Int J Cancer* 16:61.
164. Snodgrass MJ, Hanna MG. 1973. Ultrastructural studies of histiocyte-tumor cell interactions during tumor regression after intralesional injection of *Mycobacterium bovis*. *Cancer Res* 33:701.
165. Roche WR. 1985. Mast cells and tumors. *Am J Pathol* 119:57.
166. Henderson WR, et al. 1981. Mast cell-mediated tumor cell cytotoxicity. *J Exp Med* 153:520.
167. Menter DG, et al. 1987. Platelet enhancement of tumor cell adhesion to subendothelial matrix. *J Nat Cancer Inst* 79:1077.
168. Bakerche H, et al. 1989. Platelet-melanoma cell interaction is mediated by the glycoprotein IIb-IIIa complex. *Blood* 74:658.

Part VII

Diagnostic Pathology

Ultrastructural Pathology The Comparative Cellular Basis of Disease
Second Edition Norman F. Cheville
© 2009 Wiley-Blackwell. ISBN: 978-0-813-80330-2

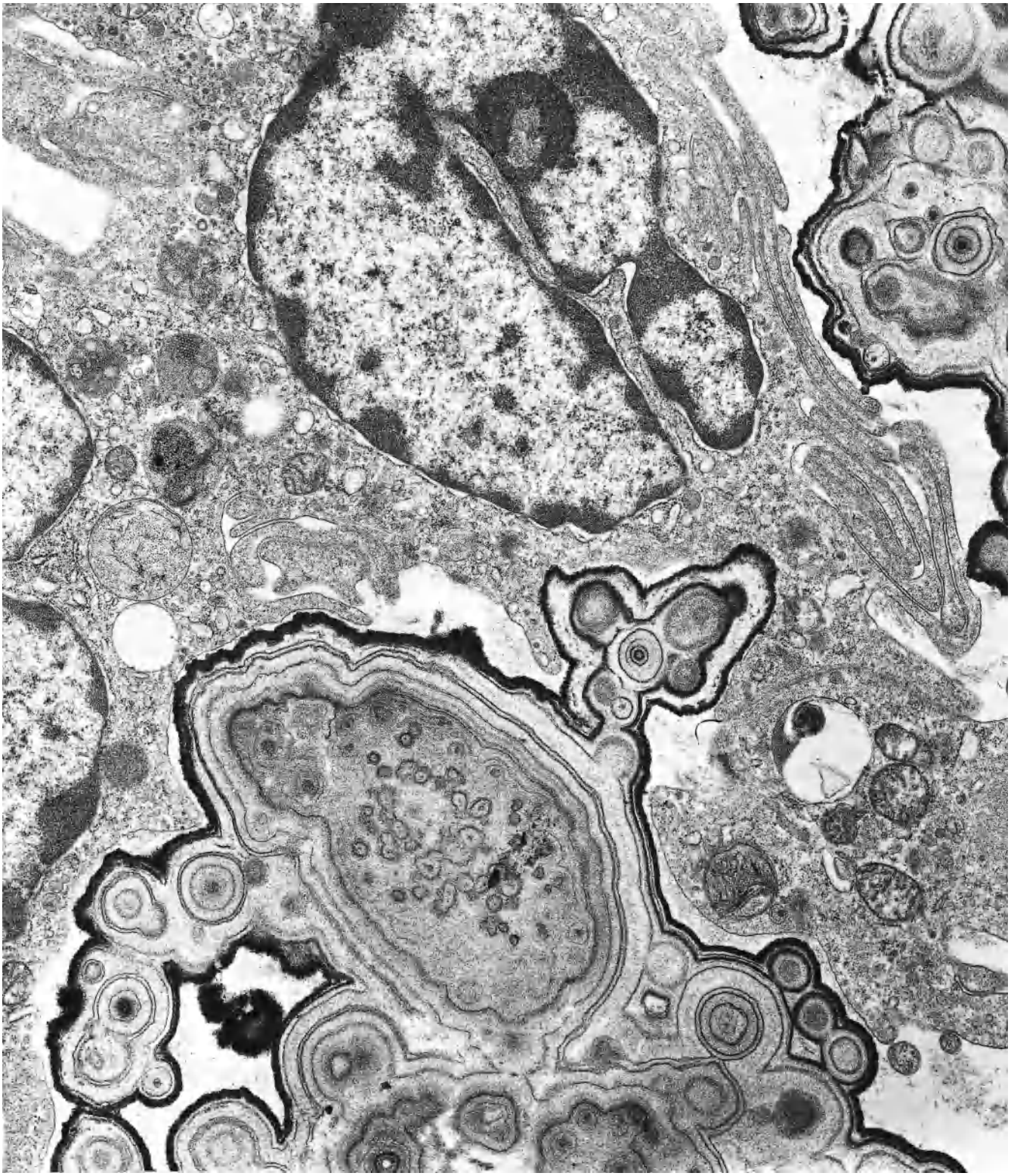


Fig. 24.1 Calcification: degeneration of interstitial extracellular matrix with calcification (*bottom*) and phagocytosis (*top*). Calcium salts are deposited in foci of proteoglycans in progressively increasing layers that first appear as small dense matrix vesicles, then as small target forms, and eventually as massive complex laminar arrangements.

© 2009 Wiley-Blackwell. ISBN: 978-0-813-80330-2

24 Calcification

Pathologic calcification (mineralization) can develop within cells or outside the cell in the extracellular matrix. Homeostatic mechanisms that regulate levels of the **calcium ion (Ca^{++})** involve (1) **passive influx** into the cytosol from three compartments (extracellular spaces, mitochondrial matrix, and cisternae of the endoplasmic reticulum); and (2) **active extrusion** of Ca^{++} from the cytosol back into these areas, driven by calcium-regulated pumps embedded in cellular membranes. Events that alter homeostasis will lead to pathologic calcification.[1,2] Once formed, deposits are degraded and removed (Fig. 24.1).

Intracellular Calcification

Calcium ions (Ca^{++}) are critical regulators of activity in the cell. Transport across plasma membranes occurs by an Na^{+}-Ca^{++} exchange transfer. Transport across membranes of mitochondria and endoplasmic reticulum is largely due to energy-requiring Ca^{++} pumps. Put another way, the Ca^{++} content of normal cells, which is low relative to that in interstitial fluid, is maintained by cyclical activity of **calcium channels** that admit Ca^{++} and **calcium pumps** that remove Ca^{++} from the cell. Because the cytosol is highly sensitive to change, the calcium-loaded cell sequesters Ca^{++} internally by moving it across membranes of mitochondria, endoplasmic reticulum, and calcisomes.

Calcisomes are calcium-pumping vesicles that regulate intracellular Ca^{++} flow. They persist in the face of acute cell swelling. In neurons, disintegration of rough endoplasmic reticulum involves loss of most cytoplasmic structures, yet the calcisomes, those parts of the endoplasmic reticulum bearing calcium pumps, remain intact (Fig. 24.2).[3]

Mitochondria do not normally sequester large amounts of calcium, so that it is the endoplasmic reticulum and its vesicles that are chiefly involved in the internal elevation of cytosolic calcium. Ca^{++} entering leaky **mitochondria** in large amounts causes lethal effects on electron transport and oxidative phosphorylation. The **mitochondrial calcium pump** is blocked when the electron transport is inhibited. Mitochondrial injury is often manifest as the accumulation of large, dense granules of calcium salts in the matrix (Fig. 24.3).

Calcium-Binding Proteins

Intracellularly, Ca^{++} is bound by one of a family of **calcium-binding proteins** that fix Ca^{++} to various parts of the cell. The diverse group of Ca^{++}-binders, most of which play critical roles in multiple events in the cell, includes the following proteins:

- **Calreticulin,** a high-affinity calcium-binding protein, functions in calcium homeostasis, in apoptosis, and as a chaperone in endoplasmic reticulum (and in sarcoplasmic reticulum of muscle).[4] Calreticulin and **calnexin,** a related protein, are intracellular chaperones critical for proper folding and transport of proteins in the ER. They have widespread impacts on cell migration, phagocytosis, wound healing, and myofibrilligenesis.[5] Calreticulin acts as a receptor complex that interacts with the collectin family of innate immune proteins (such as C1q) in the phagocytosis and removal of apoptotic cells.
- **Calpains,** neutral calcium-dependent proteases, activate several enzyme systems. They require membrane binding for activation.[6] In skeletal

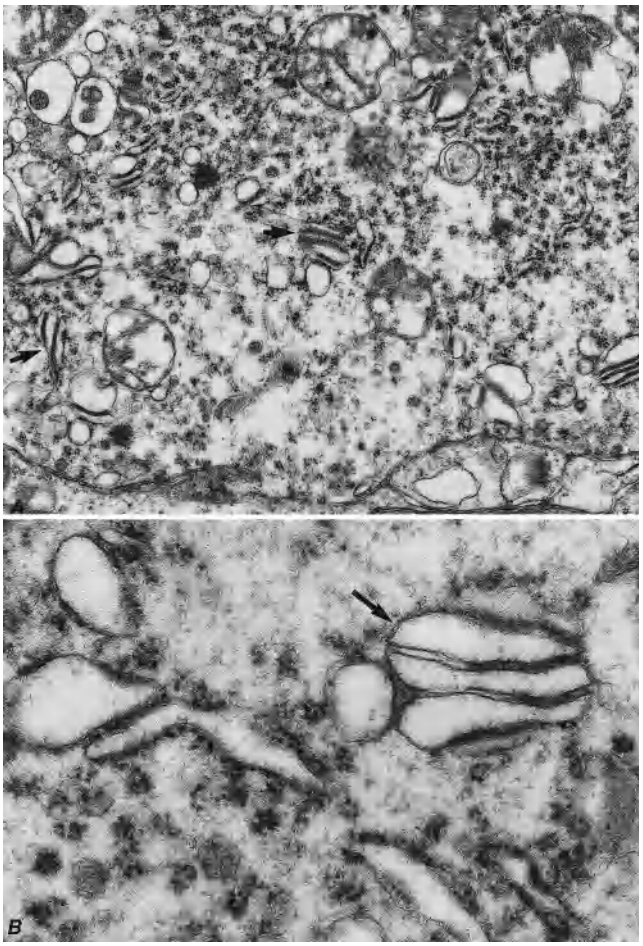


Fig. 24.2 Intracellular calcium: calcisomes. **A**. **Acute cell swelling**: neuron (Purkinje cell), cerebellum, picornavirus infection (avian encephalomyelitis), chicken. Marked cytoplasmic proteolysis and vesiculation of rough endoplasmic reticulum. Calcisomes (*arrows*) remain intact but are dilated and irregular. **B**. **Calcisomes:** high power (*arrow*).

muscle, calpains and their endogenous inhibitor, **calpastatin,** are localized by immunogold techniques to multiple membrane systems but are concentrated at the Z lines.[7] Calpain-calpastatin systems in skeletal myocytes may have different roles in various subcellular compartments.[8]

- **Calsequestrin** is the major Ca^{++}-binding protein that drives excitation-contraction in muscle. Rich in carboxylate side chains, calsequestrin is localized on the inner membrane of the sarcoplasmic reticulum, where it chelates and stores Ca^{++}. Mutation of the calsequestrin gene is associated with tachycardia.[9]
- **Calmodulin** is a ubiquitous calcium-binding protein that mediates several major cell responses to calcium. The calcium-calmodulin complex acts as a messenger and affects enzymes and nonenzyme proteins including calcium pumps, nucleotide phosphodiesterases, spectrin, histones, and tubulin. Calmodulin co-localizes with connexins and acts directly in gap junction channel gating.[10,11] It plays a crucial protective role in acute cell swelling.

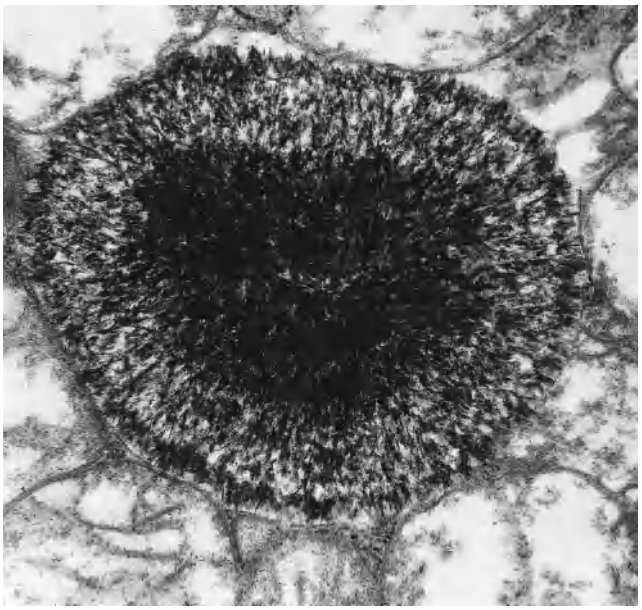


Fig. 24.3 Intracellular calcification: crystalline calcification in mitochondrion.

Extracellular Calcification

Two forms of pathologic tissue calcification are traditionally recognized: **dystrophic calcification,** in which calcium salts are deposited in degenerating cells and tissues; and **metastatic calcification,** in which they are deposited in normal tissues in the presence of hypercalcemia.

- **Dystrophic calcification** develops at sites of necrosis, hemorrhage, scarring, and chronic infections; calcium is deposited in progressively expanding laminae that are typically associated with macrophages.[12]
- **Metastatic calcification** occurs in living tissue as a result of high levels of calcium in circulating blood. The fundamental abnormality is the entry into cells of large amounts of Ca^{++}, which precipitates in organelles, chiefly in mitochondria.[13]

Calcium Deposition

Calcium deposits in connective tissue appear in electron micrographs as **apatite crystals,** as **amorphous granules** of calcium salts, or as complex **laminar arrangements** of alternating light and dense bands of

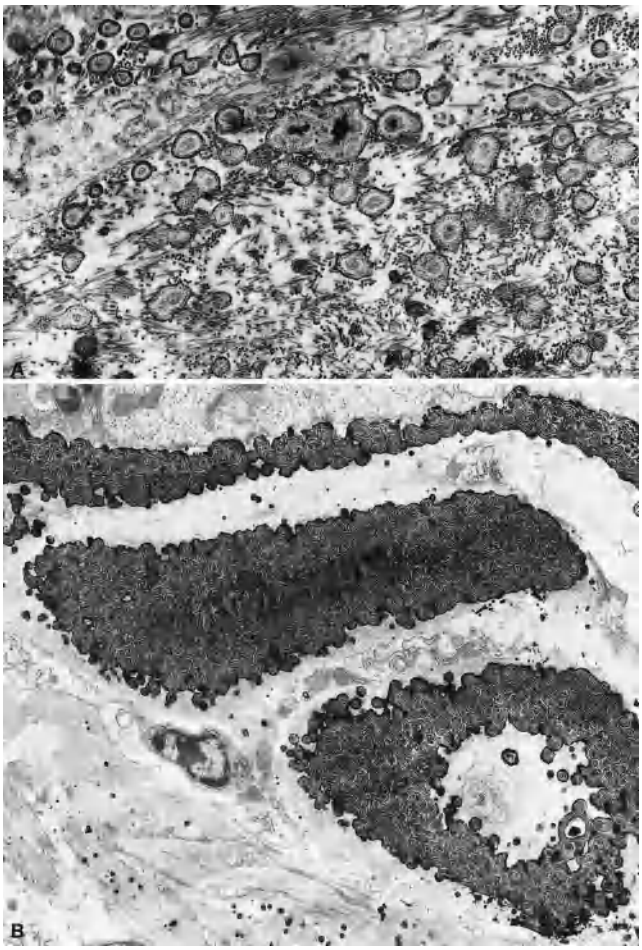


Fig. 24.4 Extracellular calcification. **A**. **Masses of coalesced multilaminar calcification centers**: calcium deposited on blood vessels, uremia, dog. **B**. **Multilaminated calcification centers**: deposited among collagen fibrils, submucosa adjacent to gastric parietal cells.



Fig. 24.5 Laminar calcification: connective tissue extracellular matrix; laminar calcification (*top*), collagen fibrils (*center*), individual calcification centers (*bottom*).

matrix and mineral (Fig. 24.4). Calcification may be initiated on granules of proteoglycans, as well as on foci of necrotic cellular debris, collagen or elastin.[14]

Amorphous apatite ($CaPO_4$) deposits are distinguished from crystalline forms by a CA:P ratio greater than 1.67, absence of sharp diffraction patterns of X-ray analysis, and formation in presence of diphosphonate compounds at concentrations that inhibit crystal formation.[16] As amorphous calcification centers form around organic material, multiple recurring episodes of hypercalcemia or hypermagnesemia lead to laminated, target-shaped spherical bodies (Fig. 24.5).

Concentrations of electrolytes in interstitial fluid determine the type of calcium phosphate compound that will be deposited. High Mg:Ca ratios favor deposition of amorphous or whitlockite compounds, whereas high Ca:Mg ratios favor deposition of **crystalline apatite** (Fig. 24.6). Variation in the organization

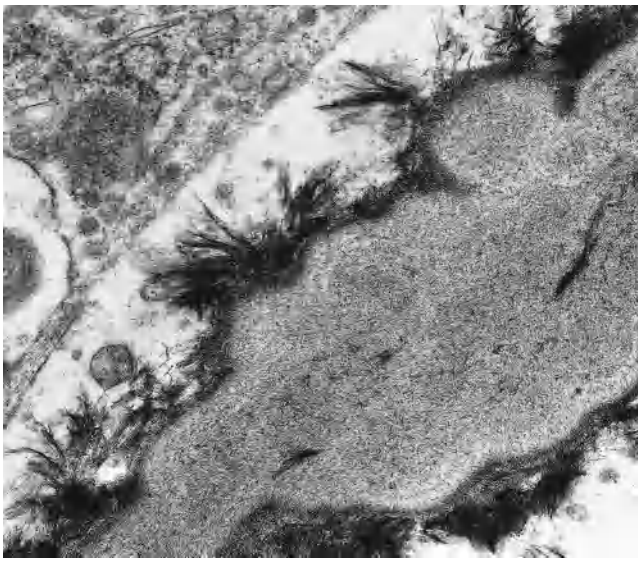


Fig. 24.6 Apatite crystals: surface of vascular smooth muscle cell; uremia, dog.

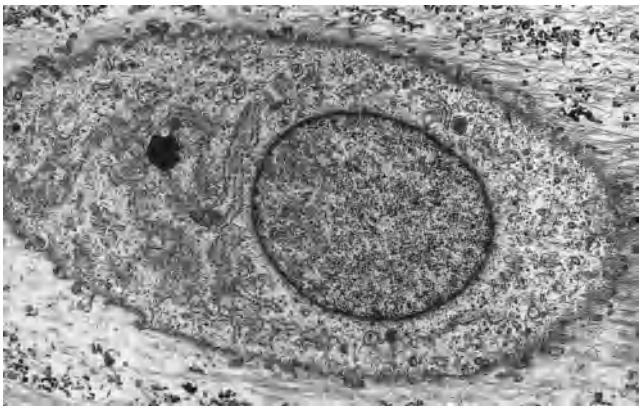


Fig. 24.7 Chondrocyte: surrounded by matrix vesicles and fibers.

of crystals is characteristic of different types of calcification.[15]

Pathologic Calcification

Three structures are involved in the formation of normal woven bone: **matrix vesicles, calcification nodules,** and **collagen fibers.** All three are mechanisms by which calcium is laid down in developing bones, tendons, and teeth.[17–21] Similar structures develop in **pathologic calcification.** Deposition of calcium salts in injured vascular and connective tissue develops in similar patterns throughout the phylogenetic scale.[22–25]

Matrix vesicles and calcification nodules appear to develop sequentially, but arise at different stages of the calcification process. **Matrix vesicles** are small membrane-bound vesicles released by osteoblasts that take up and sequester calcium salts. Within the matrix vesicle, apatite crystals form and develop to cause rupture of the vesicle membrane. The released crystals seed further crystal growth in extracellular spaces (Fig. 24.7).[26]

The deposition of calcium on **collagen fibers** in the extracellular matrix is typically initiated by a family of phosphoproteins secreted by fibroblasts (or in bone, by osteoblasts) which play important roles in the regulation of matrix calcification. Ultrastructurally, these phosphoproteins have been labeled with immunogold techniques to initial sites of calcium deposition on collagen.[27]

Studies using the model of **periosteal exostoses** induced in mice with beta-aminoproprionitrile (osteolathyrism) show that calcification begins as apatite is deposited in matrix vesicles. Vesicles evolve into larger **calcification nodules,** composed of an amorphous core surrounded by a pale zone and finally by collagen fibers. Calcification nodules enlarge, but when they reach approximately 1 μm in diameter, development is slowed or stopped by the formation of a peripheral dense zone of collagen. Although there is some coalescence of acidification nodules, further expansion of the calcified tissue develops by mineralization of **collagen fibers** that surround the calcification nodules.[28]

Calcifying Tendonitis

Calcific tendonitis is a common disorder associated with high rates of tendon rupture and persistent pain. The process is driven and sustained by excessive production of matrix vesicles, which contain enzymes responsible for mineralization. Matrix vesicles form hydroxyapatite when exposed to extracellular matrix components in vitro.[29,30]

Diffuse Pulmonary Calcification

In humans, dogs and other mammalian species, **pulmonary calcification** is commonly seen in uremia, primary hyperparathyroidism, and vitamin D toxicity. Severe cases are referred to as pulmonary microlithiasis or pumice lung. Initially, crystals of calcium are deposited in foci of proteoglycans, especially along elastic fibers. When calcium is laid down rapidly, the basement membrane between the capillary endothelium and membranous pneumocytes is also preferentially affected[31] and becomes nodular. Massive nodular deposits of concentric light and dark rings project into the alveolus. Granular pneumocyte hyperplasia accompanies the deposition and adds to the thickness of the alveolar walls, although these cells only rarely contain calcium.

Postinflammatory pulmonary microlithiasis is a consequence of acute inflammatory conditions involving acidosis and hypercalcemia. In humans, it is a sequel to viral pneumonia and may be a complication of varicella pneumonitis.[32] In severe cases, there is diffuse involvement of calcified concretions (calcospheres) in the alveolar wall.

Diffuse Vascular Calcification

Vitamin D Toxicity Maintenance of calcium and phosphorous homeostasis involves integrated actions of intestine, bone, and kidney (Fig. 24.8), and is accomplished by interaction of calcitonin and parathyroid hormone with vitamin D and its two chief biologically active metabolites, $1,25(OH)_2D_3$ and $24,25(OH)_2D_3$. The prolonged hypercalcemia of chronic **vitamin D toxicity** leads to deposition of calcium-phosphorus crystals (hydroxyapatite) in blood vessel walls, and in the parenchyma of the lungs, gastric mucosa, and kidney. Cardiac calcification occurs in uremia, in vitamin D toxicity, and as a heritable condition in mice.[33]

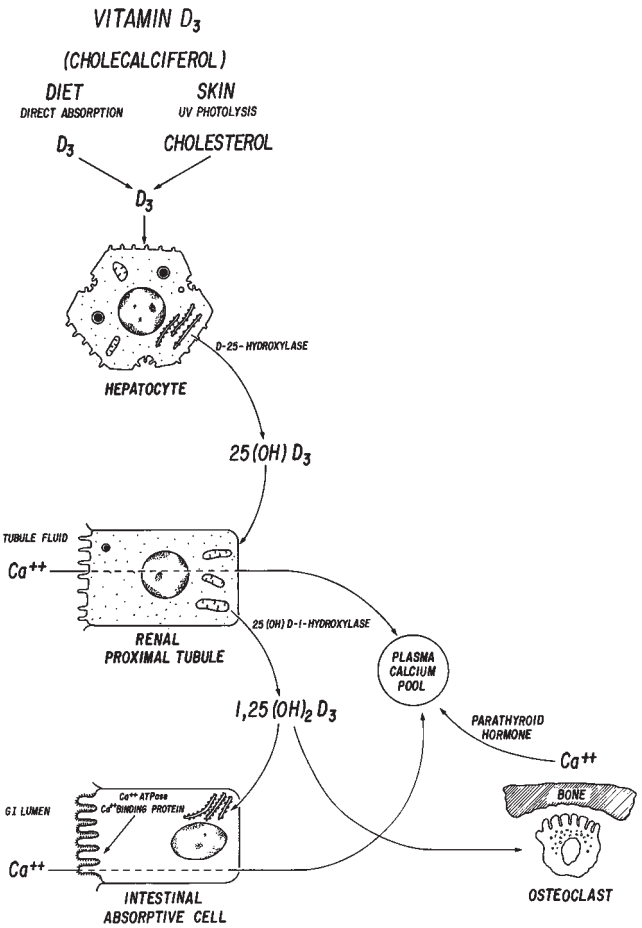


Fig. 24.8 Vitamin D pathways: paths from liver to renal tubular epithelium and bone.

Uremia In **uremia,** widespread endothelial damage leads to ischemia, degenerative lesions, edema, and infarction in several tissues. Calcification develops progressively in damaged tissues, particularly in the gastrointestinal tract.[34] Calcium metabolism is deranged in uremic animals due to acidosis, hyperphosphatemia-induced parathyroid hyperplasia with subsequent bone formation, and failure of damaged kidneys to form adequate 1,25 dihydroxycholecalciferol (required for calcium binding protein synthesis by the intestine for calcium absorption).

Calcification in the Eye

Calcific band keratopathy (CBK) arises from mineral deposits within the cornea along the epithelial basement membrane and beneath it in Bowman's membrane. It is associated with various disorders in which calcium metabolism is altered including uremia, primary hyperparathyroidism, vitamin D toxicity, and hypercalcemia of neoplastic disease. It also develops as dystrophic calcification in normocalcemic patients in areas of trauma, inflammation, dessication, and drug treatment reactions of the cornea.

Corneal calcification is a serious consequence of human **uremia.** Lesions consist of deposits of calcium and phosphorous, often in ring shapes. Ultrastructurally, they contain concentric laminar forms of mineral that shows peaks for calcium and phosphorous using X-ray dispersive anlaysis.[35,36]

CBK is also seen in aged laboratory rats and rabbits. Calcific band keratopathy in aged Fischer 344 rats appears as punctate linear superficial corneal opacities in interpalpebral fissures. Ultrastructural and x-ray dispersive analysis of the laminated and crystalline arrays reveals lesions similar to those of human keratopathy.[37]

Calcification of Foreign Materials

Materials that are not inert and not recognized as self by the host will induce mineralization. **Bioprosthetic heart valves** fabricated from glutaraldehyde-treated porcine aortic valve leaflets are used as replacements for diseased human cardiac valves; up to 20% require replacement after 10 yrs as a consequence of calcification. Calcium deposits develop as microfoci on residual porcine connective tissue, slowly and progressively evolving into nodular lesions.[38,39] Ultrastructural changes in bovine pericardial bioprostheses in use for 4–8 yr were similar.[40] Bioprosthetic tissue calcification of experimental subdermal implants are used to study mechanisms for inhibition of calcium deposition.[41]

Calcium phosphate **ceramic implants** used in surgical bone repair are composed of hydroxyapatite, biphasic calcium phosphate, or tricalcium phosphate. With time these implants degrade in vivo in much the same pattern as the natural dissolution of biological apatite that occurs in dental caries and in bone remodeling.[42,43]

Tooth implant osseointegration involves mineralization of bone extracellular matrix. Peri-implant bone calcification begins with osteoprogenitor cells secreting a mineralizable extracellular matrix. Successful bone-bonding material must have the capacity to induce matrix vesicle enzyme activity.

Calcinogenic Toxins

Livestock grazing on calcinogenic plants of the genera *Solanum*, *Cestrum*, and *Trisetum* develop hypercalcemia, hyperphosphatemia, and widespread tissue calcification. Deposits of calcium salts develop in several organs. Ultrastructurally, these appear as laminar arrangements similar to those in uremia. Soft tissue mineralization is due to a vitamin D-like action of steroid-glycoside conjugates (similar to 1,25 dihydro-

cholecalciferol, the active metabolite of vitamin D) in leaves. These toxins stimulate calcium-binding protein synthesis, enhance intestinal calcium absorption, and stimulate macrophage proliferation and fusion.[44,45]

Hypercalcemia of Cancer

Hypercalcemia in cancer arises by two mechanisms: tumor cell secretion of peptides that mimic parathyroid hormone, and osteolytic metastases of neoplasms with invasion of bone, bone resorption and Ca^{2+} release. Hypercalcemia resulting from secretion of peptides with parathyroid hormone activity causes persistent hypercalcemia and hyperphosphatemia, hyperplasia of thyroid C cells, and atrophy of parathyroids (in response to hypercalcemia), and mild skeletal demineralization. Hypercalcemia is associated with lymphomas, squamous cell carcinomas, adrenocortical carcinomas, gastric carcinomas, and multiple myeloma.[46,47] In animals, hypercalcemia of malignancy is associated with mammary gland carcinomas, fibrosarcomas, lymphosarcomas, apocrine gland adenocarcinomas, and various other adenocarcinomas. **Gastric carcinomas** in horses induce this syndrome.

Calcinogenic Bacteria

Calcium-sequestering bacteria may produce deposits of calcium salts in tissue, especially in persistent inflammation lesions. Bacteria-induced calcification provides the hardness of microbial plaque of teeth (Fig. 24.9). **Dental calculi** contain the calcite form of $CaCO_2$ mixed with small amounts of apatite ($CaPO_4$). Bacteria secrete acidic phospholipids that complex with soluble electrolytes in saliva to initiate precipitation of calcium carbonate and apatite in the calculus overlying the tooth surface. Some gram-negative bacilli produce extrabacterial debris and vesicles that become mineralized.[48] Other gram-positive bacilli sequester calcium intracellularly.[49,50] Microcalcification originates from the external surface of nanobacteria-like particles in the placental extracellular matrix.[51]

Chronic granulomatous bacterial infections frequently contain calcified extracellular amorphous bodies composed of bacterial and cellular debris (Fig. 24.10A). **Malakoplakia** is a pattern of mucosal plaques in the urogenital tract and other epithelial surfaces. Lesions are composed of large foamy macrophages interspersed with lymphocytes and giant cells. The PAS staining granularity of the macrophage cytoplasm is due to particulate and membranous debris of bacterial origin. Characteristic laminated mineralized concretions called **Michaelis-Guttmann bodies** occur within and between macrophages (Fig. 24.10B).

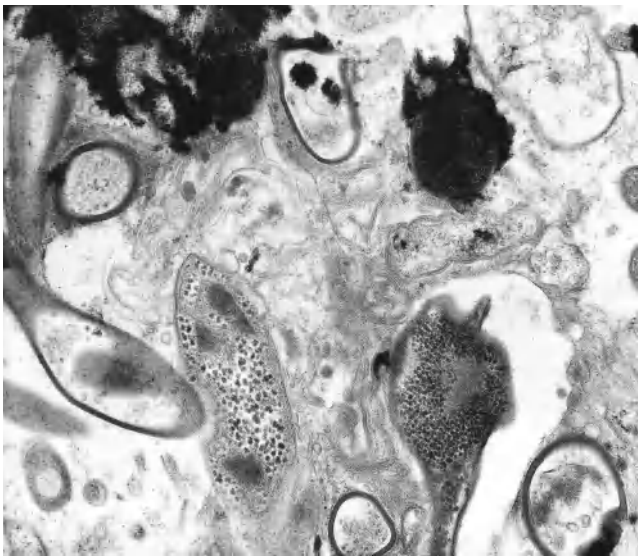


Fig. 24.9 Calcigenic bacteria: microbial plaque, tooth, dog. Dense crystals of calcium apatite have formed in bacterial cells, and have been deposited in the matrix of the dental plaque.

Lesions arise from defective phagocytosis. X-ray microanalysis reveals calcium and phosphorous.[52,53]

Microliths

Human **gallstones** form a spectrum from stones composed primarily of cholesterol to those of bilirubin.[54] About 85% are **cholesterol stones,** which in pure form are pale yellow and formed of crystalline radiating pallisades. Much less frequent are **bilirubin stones** (pigment stones) which are calcium bilirubinate with small amounts of bile acids, fatty acids and inorganic salts. The determining factor in lithogenesis is the cholesterol saturation of the bile. Supersaturation of bile by cholesterol (relative to bile salts) and an increase in unconjugated bilirubin are both lithogenic. In the former case, mucin acts as a nucleating agent in cholesterol-saturated bile. Ultrastructurally, the mixtures of gallstones underlie the lamellated appearance on cross section. (Fig. 24.11).[55–59] Ultrastructural analysis of gallstones in several animals models includes the prairie dog, which has a unique propensity to form cholesterol gallstones in response to dietary manipulation.[60,61]

Bacterial cells are present in the centers of many gallstones and may produce pigments. Bacterial factors that faciliate gallstone formation include β-glucuronidase, phospholipase, and slime.[62,63] Use of color cathodoluminescence scanning electron microscopy has been used to differentiate cholesterol, bilirubin, and other components of human gallstones.[64]

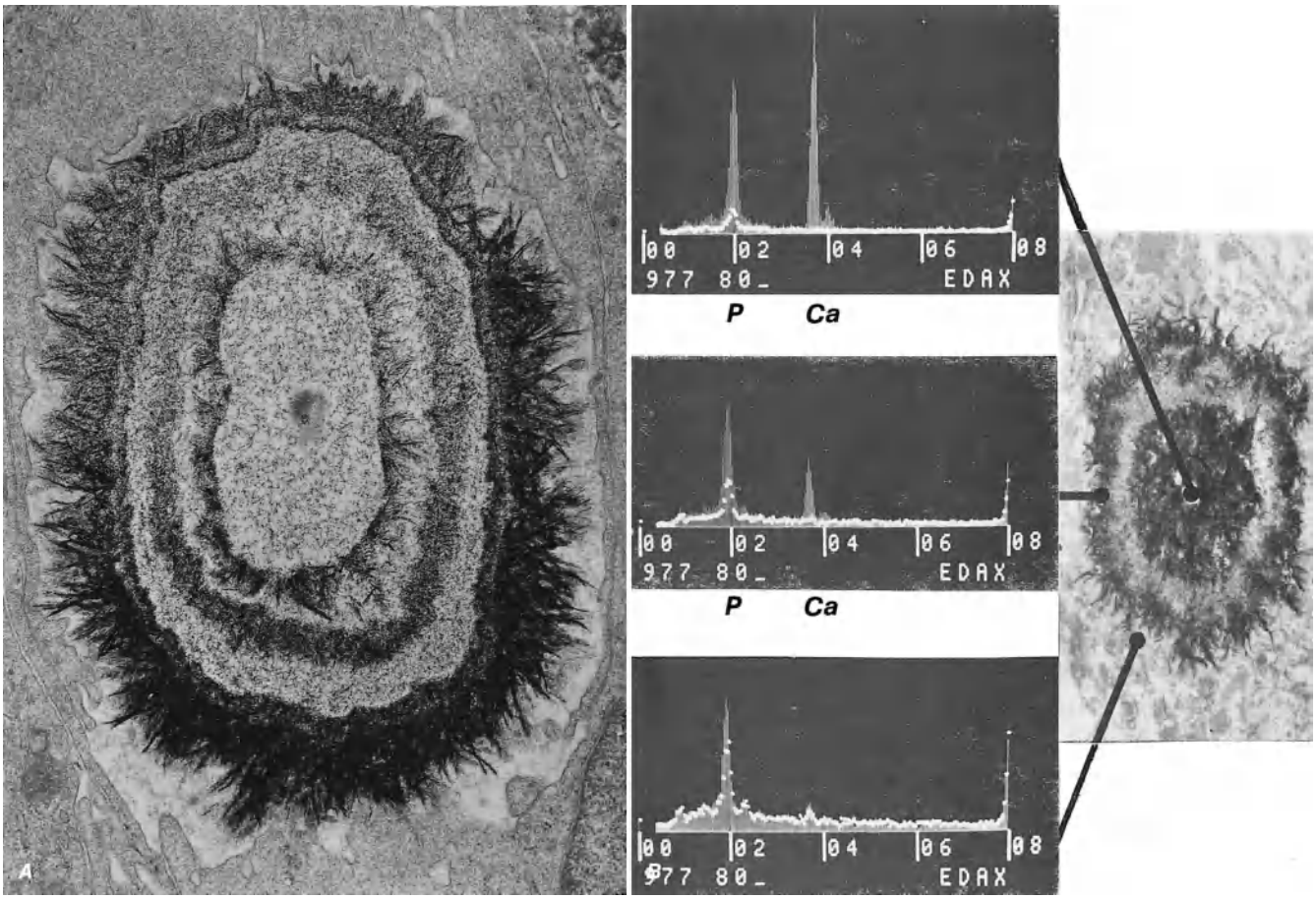


Fig. 24.10 Intracellular calcification: **A**. Schaumann's body, paratuberculosis. (Micrograph: Arliss Boothe.) **B**. **X-ray microanalysis spectra**: from core, lamina, and outer zone of Michaelis-Gutmann body of malakoplakia, human. Core and lamina give peaks for calcium and phosphorus. Outer zone gives spectrum similar to that of tissue background. (Micrograph: J. C. E. Underwood, *J Pathol* 138:41, 1982.)

Salivary gland microliths form in stagnant secretory material and cellular debris in the ductal and glandular lumens. The large laminated microliths are composed of alternating light and dense areas. Calcium deposits in phagosomes of intralobular ducts have been found in feline lithiasis induced by parasympathectomy (saliva in cats is produced by parasympathetic nerve stimuli).[65]

Calcium-Sequestering Bodies

Large laminar calcified bodies function as a normal form of calcium storage in situations that require large amounts of calcium; for example, in tissues that produce calcium-rich milk and egg yolk. In birds, yolk stores calcium absorbed from the shell and releases it from yolk-sac epithelium later as the skeleton develops. During transit from eggshell to embryo, calcium is stored in **yolk laminar spherules** (Fig. 24.12).[66] In fish, **calcospheres** function in the formation of scales.

Resorption of Calcified Tissue: The Osteoclast

Resorption of Ca^{++} from bone matrix by osteoclasts is an essential part of bone remodeling. Osteoclasts also remove calcium in bone-fracture healing, osteoporosis, periodontal disease, and in neoplasms. Giant multinucleated cells form by asynchronous fusion of precursors of the monocyte lineage; osteoclasts are located within resorptive (Howship's) lacunae along the edge of the calcified matrix at the interface of endosteum and bone marrow.[67] They seal off bone resorbing areas, secrete protons to acidify the environment (to remove calcium), and release lysosomal enzymes that digest bone matrix. In the final stages of bone resorption, as bone around osteocytes is removed, osteoclasts move to, take up, and degrade the osteocytes.[68]

Osteoclasts are polarized so that surfaces toward the bone matrix are markedly ruffled and closely

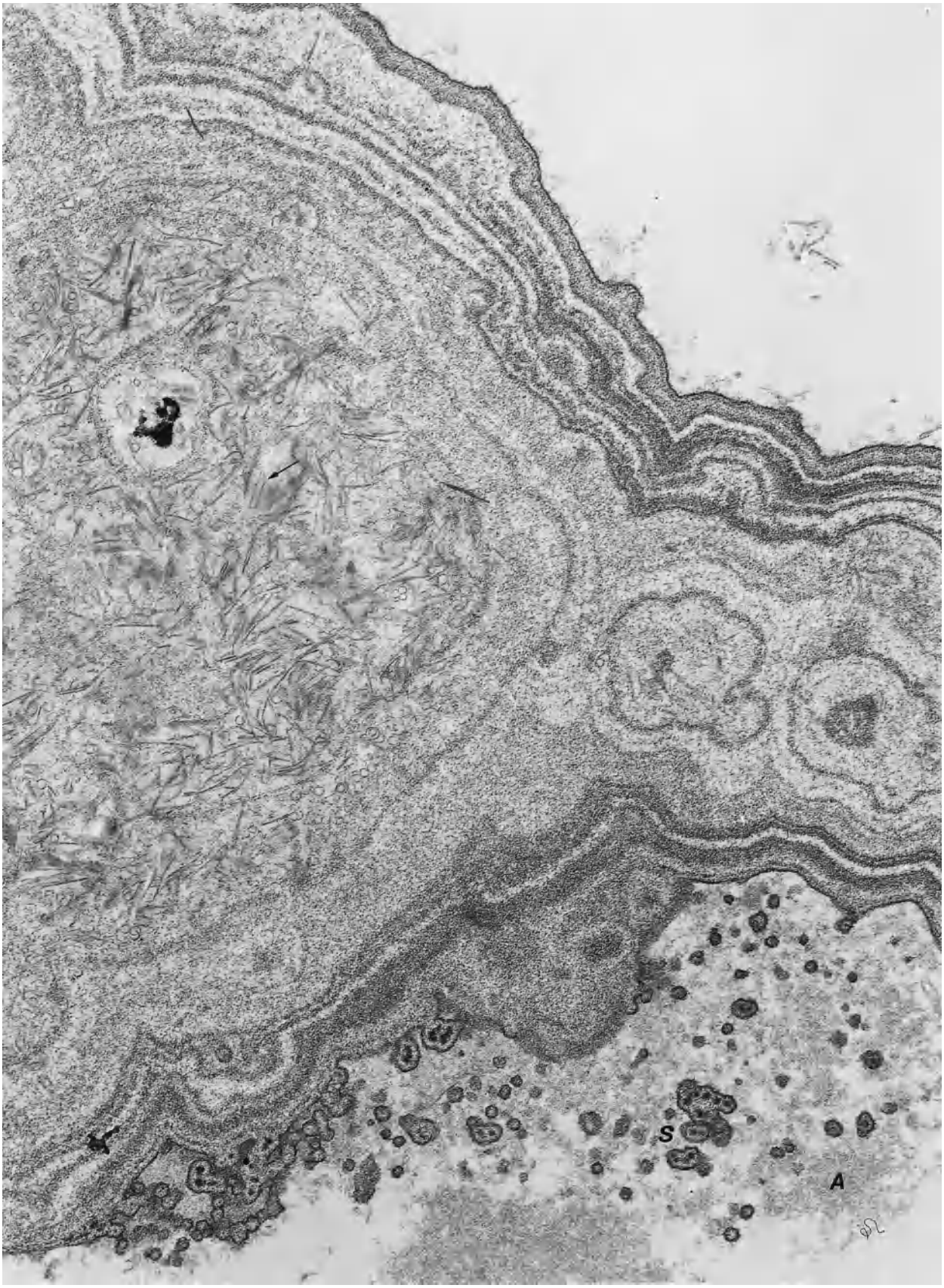


Fig. 24.11 **Gallstones**: laminar arrangement. Early foci of mineralization (*S*) and amphorous material (*A*) surround the periphery; spicules in core area (*arrow*). (Micrograph: Luida C. Saland, *Anat Rec* 187:207, 1977.)

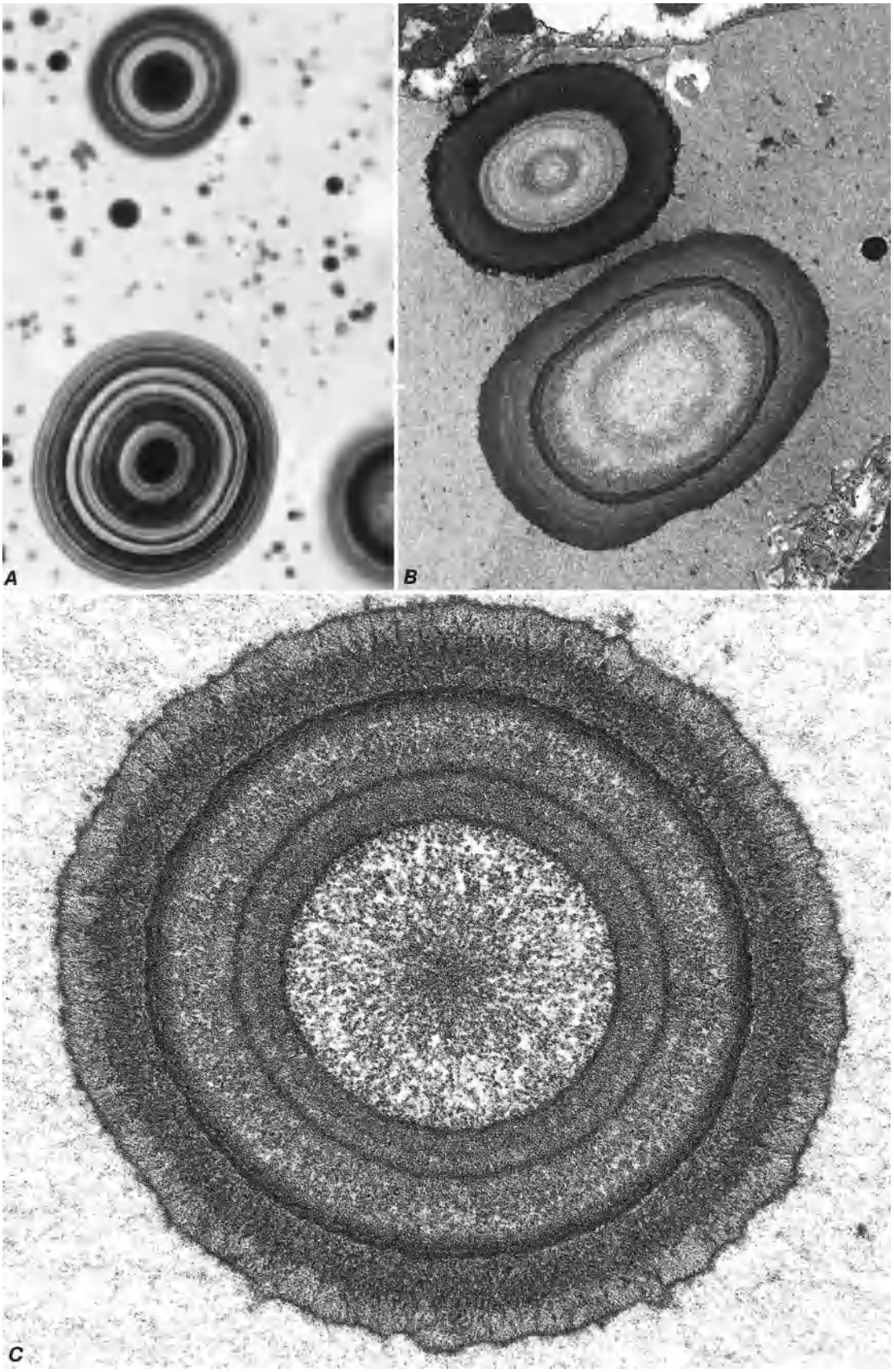


Fig. 24.12 Calcium-sequestering spherules (corpora amylacea): surface of yolk sac epithelium, developing egg, chicken. Large target forms are composed of proteoglycans complexes with calcium salts. **A**. Histology. **B** and **C**. Ultrastructure.

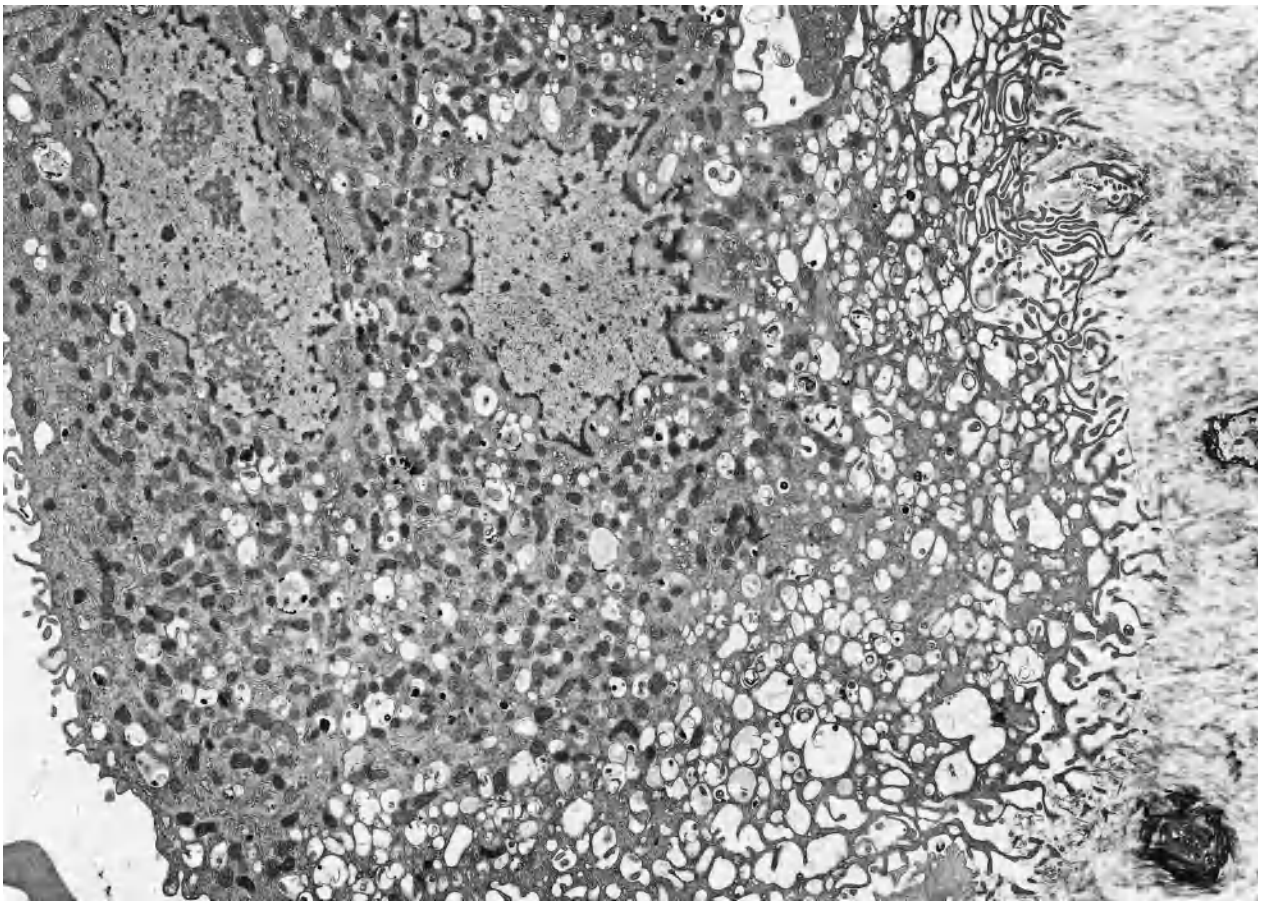


Fig. 24.13 Odontoclast-resorbing dentin: well-developed ruffled border (*right*) penetrates into dentinal tubules exposed at the resorbing surface. Many endocytic vesicles are present in the cytoplasm. (Micrograph: Takahisa Sasaki, *Am J Anat* 183:303, 1988.)

apposed to calcified bone. The plasma membrane adjacent to bone matrix forms a **ruffled border,** which has deep infoldings that may appear in cross section as vacuoles (Fig. 24.13). The plasma membrane of the ruffled border is studded with proteins, proton pumps that secrete acid. Ruffled border formation is coupled to the sequential secretion of cathepsin K and acid phospatase. The ruffled border increases in size in response to parathyroid hormone,[69,70] although this is difficult to detect in normal animals.[71] Calcitonin, which is secreted when blood Ca^{++} rises, inhibits osteoclasts.[72]

The osteoclast cytoplasm is rich in mitochondria, free polysomes and coated transport vesicles, especially in Golgi areas. Cytoplasm adjacent to this area is free of most organelles and rich in contractile proteins. Golgi complexes are large and surround the nucleus, usually with the *trans* part away from the nuclear envelope.

The apical bone-resorbing part of the cell is characterized by large numbers of cytoplasmic vacuoles bearing membrane H^+-ATPases that have been localized to the ruffled border with immunogold labeling.[73] There are also high concentrations of lysosomal enzymes and presence of substrates for these enzymes (the matrix proteins). Cytochemically, the osteoclast is enriched in acid phosphatase;[74] the enzyme is not lysosome-associated as in macrophages, but occurs in vacuoles of the exocytic pathway and is a reflection of the high metabolic activity of these cells. **Acid secretion** is important for bone resorption. Using an EM probe for pH and peroxidase-conjugated antibodies, low pH was shown in the spaces between the deep infoldings of the ruffled borders.[75] Proton pumps are important plasma membrane transport systems.

Osteoclasts in Disease

The ruffled borders of osteoclasts are abnormal in diseases such as **rickets**[76] and human **infantile osteo-**

petrosis.[77] Human **pycnodysostosis** (osteopetrosis, Toulouse-Lautrec disease) is associated with diminished activity of osteoclastic cystein-proteinase.[78] Treatment of cells in culture with leupeptin and other osteoclast inhibitors produces effects that resemble those of pycnodysostosis. The amount of demineralized matrix adjacent to osteoclasts increases markedly, evidence that demineralization had proceeded normally, but degradation of matrix was retarded.

References

1. Ghadially FN. 2001. A critique and historical review of calcification as seen with the electron microscope. *Ultrastr Pathol* 25:243.
2. Sela J, et al. 2000. Primary mineralization at the surfaces of implants. *Crit Rev Oral Biol Med* 11:423.
3. Gambetti, et al. 1975. Calcium containing structures in vertebrate glial cells. *J Cell Biol* 64:322.
4. Uehara K. 2005. Localization of TRPC1 channel in the sinus endothelial cells of rat spleen. *Histochem Cell Biol* 123:347.
5. Lozyk MD, et al. 2005. Ultrastructural analysis of development of myocardium in calreticulin-deficient mice. *BMC Dev Biol* 6:54.
6. Samis JA, Elce JS. 1989. Immunogold electron-microscopic localization of calpain 1 in human erythrocytes. *Thromb Haemost* 61:250.
7. Kumamoto T, et al. 1992. Localization of the Ca(2+)-dependent proteinases and their inhibitor in normal, fasted, and denervated rat skeletal muscle. *Anat Rec* 232:60.
8. Nori SL, et al. 1993. Immunogold ultrastructural localization of calpastatin, the calpain inhibitor, in rabbit skeletal muscle. *Cell mol Biol* 39:729.
9. Chopra N, et al. 2007. Modest reductions of cardiac calsequestrin increase sarcoplasmic reticulum Ca^{2+} leak independent of luminal Ca^{2+} and trigger ventricular arrythymias in mice. *Circ Res* 101:617.
10. Hill DJ, et al. 1984. Localization of calmodulin in differentiating pulmonary type II epithelial cells. *Lab Invest* 51:297.
11. Sotkis A, et al. 2001. Calmodulin colocalizes with connexins and plays a direct role in gap junction channel gating. *Cell Commun Adhes* 8:277.
12. Kubota T, et al. 1984. The fine structure of psammoma bodies in meningocytic whorls. *J Neuropathol Exp Neurol* 43:37.
13. Scarpelli DG, et al. 1966. Experimental pathology of vitamin-D induced nephrocalcinosis. *Methods Achiev Exp Pathol* 1:560.
14. Martinez-Hernandez A, Huffer WE. 1974. Pseudoxanthoma elasticum: Dermal polyanions and the mineralization of elastic fibers. *Lab Invest* 31181.
15. Shapiro IM, Boyde A. 1984. Microdissection—elemental analysis of the mineralizing growth cartilage of the normal and rachitic chick. *Metab Bone Dis Rel Res* 5:317.
16. Warshawsky H. 1989. Organization of crystals in enamel. *Anat Rec* 224:242.
17. Almuddaris MF, Dougherty WJ. 1979. The association of amorphous mineral deposits with the plasma membrane of pre- and young odontoblasts and their relationship to the origin of dentinal matrix vesicles in rat incisor teeth. *Am J Anat* 155:223.
18. Anderson RW, et al. 1984. Visualization of acidic organelles in intact cells by electron microscopy. *Proc Natl Acad Sci USA* 81:4838.
19. Dougherty WJ. 1983. Calcium-enriched amorphous mineral deposits as associated with the plasma membranes of chondrocytes and matrix vesicles of rat epiphyseal cartilage. *Calcif Tiss Int* 35:486.
20. Luben RA, et al. 1973. Studies of the mechanism of biological calcification. IV. Ultrastructural analysis of calcifying tendon matrix. *Calcif Tiss Res* 11:39.
21. Poole AR, et al. 1989. Cartilage macromolecules and the calcification of cartilage matrix. *Anat Rec* 224:167.
22. Daoud AS, et al. 1985. Ultrastructural and elemental analysis of calcification of advanced swine aortic atherosclerosis. *Exp Molec Pathol* 43:337.
23. Haust MD, Geer JC. 1970. Mechanism of calcification in spontaneous aortic arteriosclerotic lesions of the rabbit. *Am J Pathol* 60:329.
24. Tompa AS, Watabe N. 1976. Calcified arteries in a gastropod. *Calcif Tiss Res* 22:159.
25. Sire J-Y. 1988. Evidence that mineralized spherules are involved in the formation of the superficial layer of the elasmoid scale in cichlids *Cichlasoma octofasciatum* and *Hemichromia bimaculatus* (Pisces, Telestei). *Cell Tiss Res* 253:165.
26. Jaovisidha K, et al. 2002. Comparative calcification of native articular cartilage matrix vesicles and nitroprusside-generated vesicles. *Osteoarthritis Cartilage* 10: 646.
27. McKee MD, et al. 1990. Developmental appearance and ultrastructural immunolocalization of a major 66 kDa phosphoprotein in embryonic and post-natal chicken bone. *Anat Rec* 228:77.
28. Martino LJ, et al. 1979. An ultrastructural study of the role of calcification nodules in the mineralization of woven bone. *Calcif Tiss Int* 27:57.
29. Yu SY, Blumenthal HT. 1963. The calcification of elastic fibers. *Lab Invest* 12:1154.
30. Gohr CM, et al. 2007. Calcific tendonitis: A model. *Connect Tissue Res* 48:286.
31. Eggerman J, Kapanci Y. 1971. Experimental pulmonary calcinosis in the rat. Ultrastructural and morphometric studies. *Lab Invest* 24:469.
32. Jones EL, Cameron AH. 1969. Pulmonary calcification in viral pneumonia. *J Clin Pathol* 22:361.
33. Van Vleet JF, Ferran VJ. 1987. Ultrastructural changes in inherited cardiac calcinosis of DBA/2 mice. *Am J Vet Res* 48:255.
34. Cheville N, et al. 1979. Uremic gastropathy in the dog. *Vet Pathol* 16:292.
35. Koseki T. 1981. Ultrastructure of corneal and conjunctival calcification in renal failures. *Jap J Clin Ophthal* 35:1435.

36. van der Schaft TL, et al. 1991. Is basal laminar deposit unique for age-related macular degeneration? *Arch Ophthalmol* 109:420.
37. Losco PE, Troup CM. 1988. Corneal dystrophy in Fischer 344 rats. *Lab An Sci* 38:702.
38. Schoen FJ, et al. 1985. Onset and progression of experimental bioprosthetic heart valve calcification. *Lab Invest* 52:523.
39. Valente M, et al. 1985. Ultrastructural substrates of dystrophic calcification in porcine bioprosthetic valve failure. *Am J Pathol* 119:12.
40. Hilbert SL, et al. 1992. Ionescu-Shiley bovine pericardial bioprostheses. *Am J Pathol* 140:1195.
41. Webb CL, et al. 1992. Calcification of allograft aortic wall in a rat subdermal model. *Am J Pathol* 141487.
42. Daculsi G, et al. 1989. Crystal dissolution of biologic and ceramic apatities. *Calcif Tiss Int* 45:95.
43. Grizon F, et al. 2002. Enhanced bone integration of implants with increased surface roughness: A long term study in the sheep. *J Dent* 30:195.
44. Barros SS, et al. 2006. Macrophages and giant cell proliferation associated with bone protein synthesis and calcification in the trachea and bronchi of rabbits intoxicated with *Solanum glaucophyllum*. *Vet Pathol* 43:494.
45. Barros SS, Gimeno EJ. 2000. Cell differentiation and bone protein synthesis in the lungs of sheep with spontaneous calcinosis. *J Comp Pathol* 123:270.
46. Monma N, et al. 1987. Light and electron microscopic observation on the process of tissue calcification in a case of parathyroid adenoma. *Act Pathol Jpn* 37:1621.
47. Harrison JD. 1991. Ultrastructural observation of calcification in a pleomorphic adenoma of the parotid gland. *Ultrastr Pathol* 15:185.
48. Boyan-Salyers BD, Boskey AL. 1980. Relationship between proteolipids and calcium-phospholipid-phosphate complexes in *Bacterionema matruchotii* calcification. *Calcif Tiss Int* 30:167.
49. Legeros RZ, Shannon IL. 1979. The crystalline component of dental calculi. *J Dent Res* 58:2371.
50. Sidaway DA. 1980. A microbiological study of dental calculus. IV. An electron microscopical study of in vitro calcified microorganisms. *J Peridont Res* 15:240.
51. Agababov RM, et al. 2007. Link between the early calcium deposition in placenta and nanobacteria-like infection. *J Biosci* 32:1163.
52. Underwood JCE, et al. 1982. X-ray microanalysis of the Michaelis-Guttmann bodies of malakoplakia. *J Pathol* 138:41.
53. Kuthy E, Ormos J. 1978. X-ray microprobe analysis of Michaelis-Gutmann bodies in human and experimental malakoplakia. *Am J Pathol* 90:411.
54. Satoh H, Koga A. 1997. Fine structure of cholesterolosis in the human gallbladder and the mechanism of lipid accumulation. *Microsc Res Tech* 39:14.
55. Osuga T, et al. 1974. A morphologic study of gallstone development in the squirrel monkey. *Lab Invest* 30:486.
56. Osuga T, et al. 1974. A scanning electron microscopic study of gallstone development in man. *Lab Invest* 31:696.
57. Phillips MJ, et al. 1978. Dissolution of human cholesterol gallstones in vitro with ethanol and ether. A scanning and stereoscanning electron microscopic study. *Lab Invest* 39:497.
58. Roberts ED, et al. 1984. Calcium pyrophosphate deposition disesae (CPDD) in nonhuman primates. *Am J Pathol* 116:359.
59. Saland LC, Napolitano LM. 1976. Ultrastructure of gallstones produced in mice fed a high cholersterol diet. *Anat Rec* 187:207.
60. MacPherson BR, Pemsingh RS. 1997. Ground squirrel model for cholelithiasis. *Microsc Res Tech* 39:39.
61. Chapman WC, et al. 1998. Establishment and characterization of primary gallbladder epithelial cell cultures in the prairie dog. *J Surg Res* 80:35.
62. Stewart L, et al. 2007. Bacteria entombed in the center of cholesterol gallstones induce fewer infectious manifestations than bacteria in the matrix of pigment stones. *J Gastrointest Surg* 11:1298.
63. Stewart L, et al. 2006. Biliary bacterial factors determine the path of gallstone formation. *Am J Surg* 192: 598.
64. Loginov AS, et al. 1998. Investigation of cholesterol, bilirubin, and protein distribution in human gallstones by color cathodoluminescence scanning electron microscopy and transmission electron microscopy. *Scanning* 20:17.
65. Trianafyllo A, et al. 1993. Production of salivary microlithiasis in cats by parasympathectomy. *Int J Exp Pathol* 74:103.
66. Cheville N, Coignoul F. 1984. Calcium in the turkey yolk sac during late development and postembryonic involution. *Am J Vet Res* 45:2458.
67. Baron R. 1989. Molecular mechanisms of bone resorption by the osteoclast. *Anat Rec* 224:317.
68. Elmardi AS, et al. 1990. Electron microscopy of developing calvaria reveals images that suggest that osteoclasts engulf and destroy osteocytes during bone resorption. *Calcif Tiss Int* 46:239.
69. Holtrop ME, et al. 1979. Time-related changes in the ultrastructure of osteoclasts after injection of parathyroid hormone in young rats. *Calcif Tiss Int* 27:129.
70. Miller SC. 1978. Rapid activation of the medullary bone osteoclast cell surface by parathyroid hormone. *J Cell Biol* 76:615.
71. Weisbrode SE, et al. 1974. Effects of parathyroid hormone on bone of thyroparathyroidectomized rats. *Am J Pathol* 75:529.
72. Weisbrode SE, Capen CC. 1974. Ultrastructural evaluation of the effects of calcitonin on bone in thyroparathyroidectomized rats administered vitamin D. *Am J Pathol* 77:455.
73. Blair HC, et al. 1989. Osteoclastic resorption by a polarized vacuolar proton pump. *Science* 245:855.
74. Baron R, et al. 1985. Cell-mediated extracellular acidification and bone resorption of a 100-KD lysosomal membrane protein at the osteoclast ruffled border. *J Cell Biol* 101:2210.
75. Anderson HC. 1989. Mechanism of mineral formation in bone. *Lab Invest* 60:320.

76. Holberg K, et al. 2005. Polarization and secretion of cathepsin K precede tartrate-resistant acid phosphatase secretion to the ruffled border area during the activation of matrix-resorbing clasts. *J Bone Miner Metab* 23:441.
77. Shapiro F, et al. 1988. Variable osteoclast appearance in human infantile osteopetrosis. *Calcif Tiss Int* 43:67.
78. Everts V, et al. 1988. Effects of proteinase inhibitors leupeptin and E-64 on osteoclastic bone resorption. *Calcif Tiss Int* 43:172.

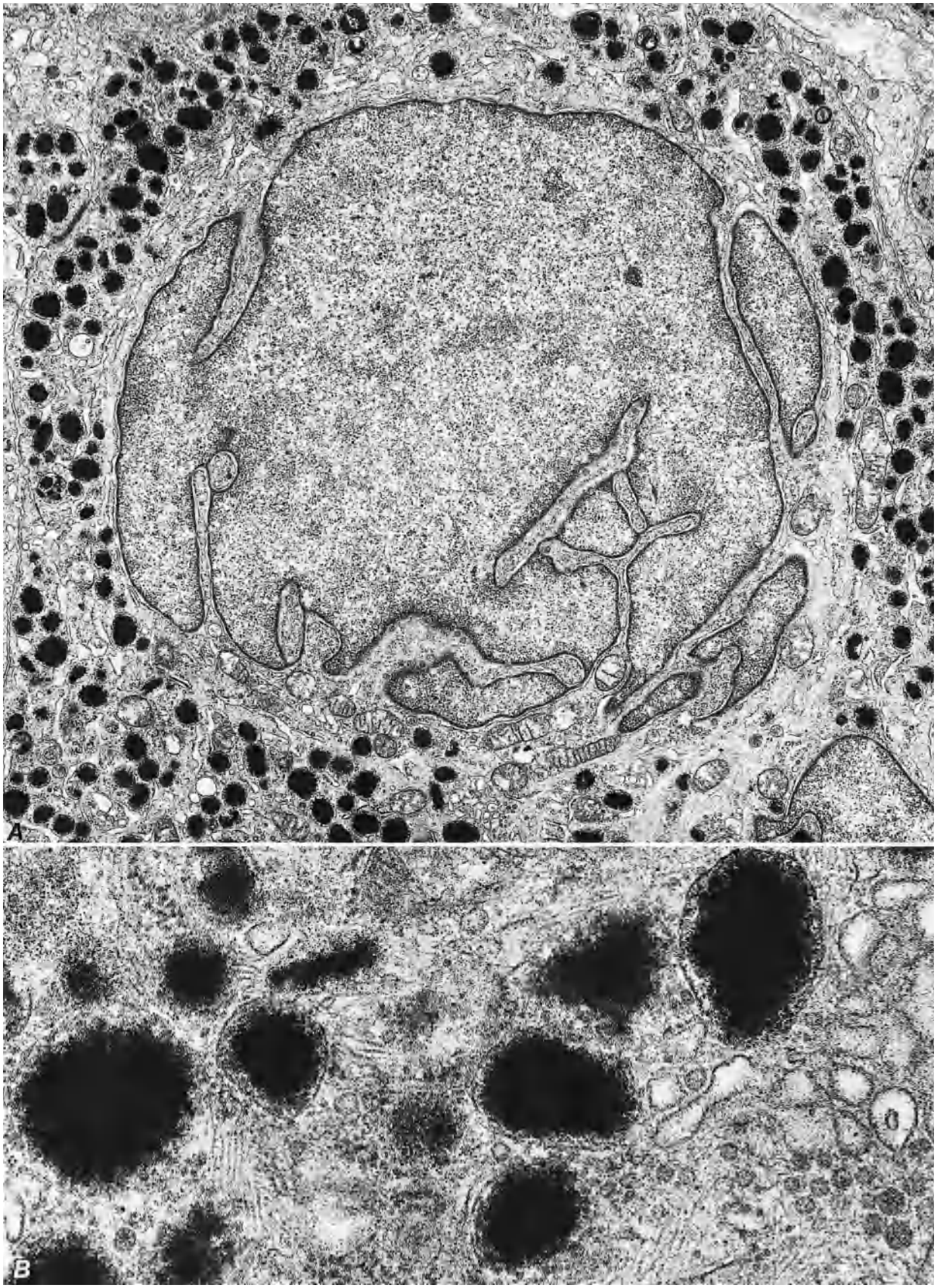


Fig. 25.1 Melanin in melanosomes: transplantable, melanotic, malignant melanoma, mouse. **A**. **Abnormal melanosomes** in the cytoplasm around a highly irregular nucleus. Organelles are in perinuclear position and granules are in the peripheral cytoplasm. **B**. **Abnormal melanosomes** adjacent to Golgi complex (*right*) contain many vesicles.

© 2009 Wiley-Blackwell. ISBN: 978-0-813-80330-2

25 Pigments

Endogenous pigments, produced within the body, involve four major types: melanins, lipfuscins, hemosiderin, and bilirubin. The last two are derived from erythrocyte breakdown. **Exogenous pigments** enter the body via skin, lung, and intestinal tract and persist, usually in macrophages.

Melanin

Melanin is the brown pigment of skin, hair, leptomeninges, and choroid of the eye. In mammals, the only known function of melanin is protection against solar ultraviolet radiation and other physical stressors.[1] It captures injurious free radicals generated in skin during injury. In lower vertebrates, melanin is widespread, occurring in the interstitium of many organs, where it has multiple protective effects in inflammation.[2]

Melanin is a high molecular weight biochrome bound to protein. Formed in **melanocytes**, melanin resides in characteristic granules called melanosomes (Fig. 25.1). Most vertebrate **melanosomes** are electron-opaque ellipsoids about 5 nm in diameter containing dense insoluble eumelanins. Some avian and mammalian epidermal melanosomes (including those in human red hair) contain phaeomelanin, a lighter-colored, sulfur-bearing melanin. In skin melanin is also transferred from melanocytes to phagocytic storage cells called **melanophages**. Melanocytes deliver pigment for secretion by transporting it along microtubules, transferring it to the actin cytoskeleton, and then delivering it to the membrane.

In the process of **cutaneous pigmentation**, melanosomes are transferred from the dendrites of the melanocytes (which lack desmosomes and tonofilaments) into keratinocytes. Increase in transfer causes increased pigmentation. Tanning of human skin by UV radiation involves an increase in the length of dendrites and increases in melanosomes and tyrosinase activity but not increased numbers of melanocytes.

The appearance of melanin varies in different tissue. In pigmented areas of the brain, melanin can arise from astrocytes, the melanosomes of which may reach 30 μm or more in diameter.[3] In pigmented retinal epithelium, melanin is in **melanophagosomes**, granules that resemble residual bodies and stain for acid phosphatase.[4]

During **melanin synthesis**, formation of melanin begins with the enzyme tyrosinase, a copper-protein compound that facilitates the oxidation of tyrosine to dioxyphenylalanine (dopa) and then to dopaquinone in the initial stages of synthesis. The detection of tyrosinase (the "dopa reaction") is the basis of the histochemical identification of melanocytes and melanoblasts.

Tyrosinase is synthesized on ribosomes and conveyed to the Golgi complex, where it accumulates in small membrane-bound vesicles called **pre-melanosomes**. In active synthesis Golgi saccules may be seen to be continuous with pre-melanosomes. During maturation of the **melanosome**, melanin develops into oriented protein strands and concentric lamellae. As melanization proceeds, melanin polymers are deposited on the protein framework of the granule, obscuring it.

The spectrum of coat coloration in mammals arises from variations in quality, quantity, and body distribution of only two pigments—black **eumelanin** and yellow **pheomelanin**. These pigments are altered in such diverse processes as hair graying, pigmentary dilution, and pigment type switching between the synthesis of eumelanin and phaeomelanin.

Pigment type switching is controlled by two genes, ***Agouti*** and ***McIr*** (melanocortin I receptor), which encode a ligand-receptor system. In dogs, a third gene is implicated, the β-defensin gene, from an additional class of ligands for signaling through melanocortin receptors.[5] The *Agouti* locus controls synthesis of eumelanin and phaeomelanin (in mice, a complex of 17 distinct alleles on chromosome 2 are active). Individual hairs of agouti animals are banded as a result of a switch from synthesis of yellow phaeomelanin to black or brown eumelanin, which occurs synchronously in every hair during the growth cycle.

Pathologic Melanization

Melanin-containing cells are impaired by a wide variety of chemical and physical agents. Melanosomes in the degenerating cells react by enlargement, by forming irregular shapes, and by increasing the homeogeneity of the granule interior.

Melanosis, the aberrant accumulation of melanin in foci, is common in young animals of several species. In ruminants melanosis of the brain, urinary bladder, and other sites is not uncommon.[6]

Hypomelaninization, a decrease in the melanin content of tissue, can be focal or multifocal. Cutaneous hypomelanization can result from hereditary disease, drug toxicity, or inflammation (Table 25.1). **Contact depigmentation** is caused by a direct effect of some chemicals, notably phenol. In chronic **dermatitis**, the skin often shows pigmented defects caused by failure of transfer to new hyperplastic keratinocytes. Keratinocytes are free of melanin, and the melanocytes are filled with melanosomes and have blunted dendrites.

Melanization Associated with Inflammation

In lower vertebrates, melanization is an integral part of the healing process and protects cutaneous wounds from solar radiation. Hyperpigmentation also occurs in mammals in chronic inflammation, although to much less extent. In the cornea, melanin accumulates in keratitis, and leukocytes and vascular invasion precede melanization.

Melanization in Toxic Injury

Hyperpigmentation associated with chemotherapeutic agents in man is common, especially involving the nails after topical application of busulfan and nitrogen mustard. Deposits of minocycline-melanin complexes cause general hyperpigmentation.[7] The drug azidothymidine, a pyrimidine analogue used in human AIDS, produces hyperpigmentation of skin and oral mucous membranes, although melanocytes are normal.[8] The syndrome has been reproduced in mice.[9]

Melanin in Tumors

Malignant melanomas and other melanin-containing neoplasms (see chapter 23) typically have aberrant and dysfunctional melanosomes (Fig. 25.2).

Vitiligo

Human vitiligo is a cutaneous depigmentation disease characterized by progressive, patchy loss of cutaneous melanocytes. Usually seen in adolescence or early adulthood, it appears as flat macules with well-demarcated zones of pigment loss. Microscopically, there is loss of melanocytes in vitiligo (in contrast to albinism, in which melanocytes are present but lack melanin pigment). At the periphery of depigmented lesions, melanocytes are vacuolated, have autophagosomes, and aggregated melanosomes.[10] Ultrastructural changes suggest that an autoimmune mechanism involving antimelanocyte antibodies is involved.[11]

Lesions similar to those of vitiligo occur in the **vitiligo mouse**[12,13] and the **Smyth chicken**. Vitiligo mice have progressive depigmentation of the skin, pelage, and ocular tissue with age. Ultrastructurally, melanocytes in regenerating hair follicles and uveal tracts are degenerate with whorled endoplasmic reticulum, vesicles with granular material, melanosome compartmentalization, and cytoplasmic rarefication. Melanocyte necrosis is accompanied by melanophages in dermal papillae of the hair follicle and in the uveal tract (clump cells of Koganei). Pathologic changes have also been reported in Langerhans' cells. In vitro, vitiligo melanocytes grow poorly and degenerate as they do in vivo.[14]

Albinism

Albinism results from a structural gene mutation at the locus that codes for tyrosinase; that is, albino animals have a genetically determined failure of tyrosine synthesis. Humans who inherit an albino gene from both parents (i.e., who are homozygous for the albino gene) are unable to make melanin because the albino gene fails to direct synthesis of the enzyme tyrosinase. Tyrosinase controls the initial step of the melanin pathway, and altered function of this enzyme is responsible for several forms of albinism.

Some albino individuals have no tyrosinase, and others form tyrosine but no melanosomes (there are at least seven variants of human albinism). In **partial**

Table 25.1 Ultrastructure of pathologic melanization.

Disorder	*Defect*	*Pathologic change*	*Reference to ultrastructural pathology*
Albinism (human)	Tyrosine synthesis	Melanocytes do not form tyrosine or melanin	**Hu**, *Am J Human Genet* 332:387, 1980; **Kikuchi**, *Arch Dermatol Res* 287:529, 1995 (fetus); **King**, *J Clin Invest* 87:1046, 1991
Albinism, ocular	Melanosome biogenesis	Macromelanosomes	**Schiaffino**, *Proc Natl Acad Sci USA* 93:9055, 1996 (OA1 gold labeling)
Albinism (human), partial	Immunodeficiency	Silver hair with large, clumped melanosomes on the hair shaft and sparse granules in keratinocytes	**Celik**, *Saudi Med J* 28:1275, 2007 (Griscelli syndrome)
Albinism (animal)	Tyrosine synthesis		**Meissner**, *Am J Pathol* 1980 (mouse)
Hypomelanosis Focal: Merle dog Piebald mouse Diffuse: White tiger Gray collie	Melanocytes absent	Inadequate differentiation or migration of melanoblasts from neural crest	**Tobin**, *J Invest Dermatol* 94:803, 1990 (alopecia); **Walsh**, *Toxicol Pathol* 17:549, 1989 (drug induced)
Chédiak-Higashi syndrome	Melanosome formation	Abnormal aggregation of melanin with bizarre shapes	**Novikoff**, *Lab Invest* 40:155, 1979; **Zelickson**, *J Invest Dermatol* 49:575, 1967
Contact depigmentation	Melanin transfer to keratinocytes	Melanocytes normal; keratinocytes lack melanosines	**Zaynoun**, *Br J Dermatol* 108:83, 1983
Melanosomopathy	Melanocyte destruction	UV radiation destroys melanocytes Lymphocytes attack melanocytes	**Murphy**, *Lab Invest* 49:680, 1983 **Rymer**, *Exp Eye Res* 85:431, 2007 (DAM chicken)
Piebald#	Melanocyte development	KIT mutation that affects tyrosine kinase	**Richards**, *J Am Acad Dermatol* 44:288, 2001
Vitiligo	Melanoblast differentiation	Autoimmune reaction causes progressive loss of melanocytes throughout life	**Bartosik**, *Eur J Dermatol* 8:95, 1998; **Galadari**, *Int J Dermatol* 32:269, 1993; **Gonvalves**, *Ann Dermatol Venereol* 105:395, 1978; **Morohashi**, *Arch Dermatol* 113:755, 1977; **Panuncio**, *Am J Dermatopathol* 25:16, 2003

Piebald in humans is an autosomal dominant disorder with hypopigmentation of skin and white forelock, and distinguished from vitiligo by the presence of lesions from birth, hyperpigmented macules of depigmented skin, and static course.

albinism, there is a general reduction in skin pigmentation but no pigments are present in the eye. Epidermal melanocytes show retarded melanogenesis; their granules are immature fibrillar pre-melanosomes. Defective receptors for melanin-stimulating hormone may be responsible for partial albinism.

Several types of autosomal recessive **oculocutaneous albinism** show diminished tyrosine and reduction or absence of melanin. Each results from a different mutant allele at the tyrosine locus, with the mutant gene producing an enzyme with little or no activity in involved tissues.[15]

A temperature-sensitive type of human oculocutaneous albinism has been reported as a result of a tyrosinease mutation produced by a temperature-sensitive enzyme. Affected individuals have no pigment in hairs of warm areas such as the scalp or axilla, but dark pigment in hair of the cooler areas such as the extremities. Melanocyte and melanosome ultrastructure are normal.[16]

Albino Mutations in Animals

Albino mutants occur in many animals.[17] **Albino cats** are homozygous for a c-locus tyrosinase-negative allele. Heterozygotes have normal pigments but abnormal vision and can be identified with a tyrosinase enzyme test. The gene *Himalayan*, a variant of albino (and at the same locus on the chromosome), codes for an enzyme that can synthesize melanin at

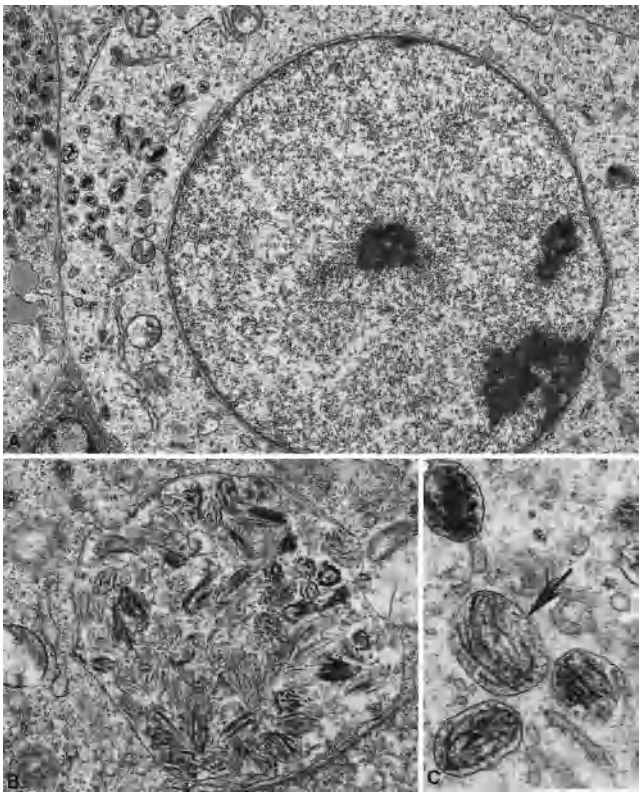


Fig. 25.2 Abnormal melanosomes: transplantable, amelanotic, malignant melanoma (tumor S91), mouse. Melanosomes are heterogeneous. **A**. Neoplastic cell: few melanosomes; tumor cell is uniform, round, and contains abnormal melanosomes and autophagosomes filled with melanin granules. **B**. **Compound melanosome**: phagosome filled with components of melanin. **C**. **Melanosome**: abnormal melanin granule (*arrow*).

relatively low temperature only, so that affected mice, **Himalayan rabbits**, and **Siamese cats** (which have this gene) have pale or white bodies with darkened extremeties.

Retinogeniculocortical pathways in the CNS are abnormal in albino mammals. Siamese cats, white tigers, albino rats, and pearl mink all have genetic mutations involving reduced pigmentation and abnormal vision with abnormal central visual pathways (some optic nerve fibers go to the wrong side of the brain). In Siamese cats, the **lateral geniculate nucleus** (LGN), the main cerebral group that relays messages from the retina to the cerebral cortex, is abnormal. These cats often have crossed eyes, since it is in the LGN that inputs from the two eyes are matched and passed to the cortex (in mammals, correct alignment of the eyes requires a normal LGN).[18,19]

Ocular albinism type 1 is an X-linked disorder characterized by retinal hypopigmentation, foveal hypoplasia, and giant melanosomes in cutaneous melanocytes and retinal pigment epithelium. The ocular albinism type 1 gene, *OA1*, controls melanosome maturation and size; its product is a pigment cell-specific membrane glycoprotein that functions in intracellular traffic of melanosomes. Mice bearing the mutated ***Ia1*** gene do not have impaired tyrosine activity, but do have dysfunctional melansomal trafficking and reduced numbers of melanosomes in melanocytes.[20] Other genetic mutations in mice include those for tyrosine and the membrane-associated transporter protein (Matp).

Other Genetic Defects in Melaninization

Genetic defects in pigmentation can result from changes anywhere in the pathway of melanin synthesis, that is, any defect from abnormal tyrosinase to defective transfer of melanosomes to keratinocytes.[21,22] Some common genetic disorders that involve defective pigmentation include the following:

- **Chediak-Higashi syndrome** (CHS), a genetically determined lysosomal disease of mink, cattle, whales, mice, and humans, is characterized by giant, bizarre melanosomes; mutations in the CHS1 (LYST) gene underlie the hypopigmentation, prolonged bleeding times, and recurrent infections of CHS patients.
- **Cyclic hematopoiesis** in humans and gray collies arises from pigment deficits due to diminished formation of melanin from tyrosine. The number of melanocytes does not differ from that in normal collies, but there are fewer melanosomes present.
- The **Hermansky-Pudlak syndrome (HPS)** is a triad of oculocutaneous albinism, bleeding diatheses, and lipofuscinosis of the lungs and intestine. Human HPS is a genetically heterogeneous disorder in which mutations in one or several genes interrupt biogenesis of melanosomes, platelet dense granules, and lysosomes. Mutations in the *HPS1* gene reduce HPS1 proteins that facilitate trafficking of melanocyte-specific gene products into pre-melanosomes; there are aberrant and giant immature melanosomes in lesions.[23,24] Melanocyte proteins tyrosinase, Tyrp1, and Dct/Tyrp2 are atypically expressed.[25] **Murine HPS** models include at least 10 strains of mutant mice, and include ashen, sandy, muted, buff, subtle gray, and others.[26]
- The **pink-eyed dilution locus** on chromosome 7 in the mouse encodes a structural protein present in melanosomes that controls the quantity of melanin produced by the melanocyte. Mutant melanosomes have a reduced capacity to bind or accumulate melanin, and affected mice are used for models of human Prader-Willi and Angelman syndromes.[27,28]

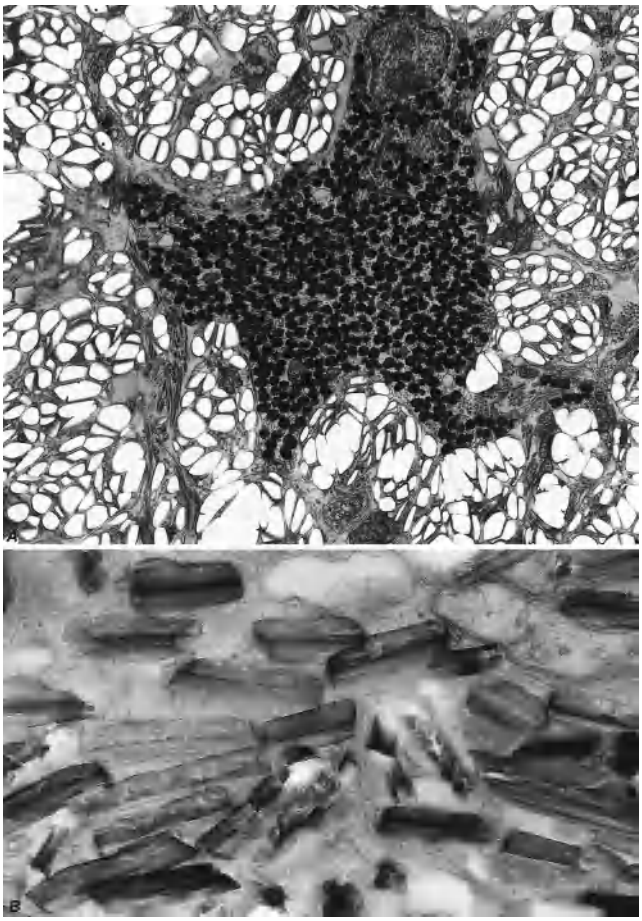


Fig. 25.3 Chromatophores: chronic inflammation, skin, butterfly fish. **A. Melanophore**: black stellate cell in a background of fibrous tissue and reflecting platelets (iridophores). **B. Crystalline reflecting platelets**: thick section.

Chromatophores

Chromatophores (contractile pigment cells) of cold-blooded vertebrates produce rapid color changes of skin by intracellular aggregation and dispersion of pigment granules. Dermal color changes are under hormonal control and are used for camouflage, sexual attraction, and protection. Granule aggregation occurs within milliseconds after hormonal stimulus and is accomplished through movement of actin microfilaments along microtubular guidelines.[29,30] Aggregation is an energy-requiring process, whereas dispersion during depigmentation is slow and does not require energy. Novel filaments with a diameter of 7 nm appear to be involved in xanthophore transport in the cytoplasm.[31,32]

Chromatophores of fish and amphibians include black **melanophores**, red **xanthopores** (that contain pteridines), and refractile **iridophores** (that contain guanine). These cells originate in embryonic neural crest cells and migrate extensively to all tissues. Mosaic pigment cells (with more than one type of granule) and mosaic pigment organelles (with more than one type of pigment) occur in some species. Like melanosomes, other chromatophore granules arise from the endoplasmic reticulum and Golgi complex.[33,34]

Pigment movement is a response to injury in lower vertebrates. Pigmentary changes protect the subcutis from ultraviolet rays of sun, allowing it to recover. Massive aggregations of chromatophores are characteristic of the responses of insects to injury and also occur as part of the chronic inflammatory response in fish (Fig. 25.3).

Hemoglobin-Derived Pigments

Hemoglobin, the oxygen-carrying pigment of erythrocytes, is a combination of **globin** and the pigment complex **heme**. During normal and pathologic breakdown, different types of pigment complexes are formed. **Ferritin** and **hemosiderin** are the principal iron storage compounds in animal tissue. Both contain trivalent iron in the form of hydrous ferric oxides $(FeOOH)_x$, and both are detected histochemically by the Prussian blue reaction.

Heme

Heme, a cyclic tetrapyrole containing a centrally chelated iron, is the prosthetic group for hemoglobin, cytochromes, and other hemoproteins. Heme initiates globin transcription by inhibiting DNA binding of the repressor, Bach1, and globin translation through inhibiting substrate phophorylation by the respressor, erythroid-specific eukaryotic initiation factor 2α kinase. Free heme is toxic (it causes defective erythropoiesis) so that cells must balance heme synthesis with utilization, a task it accomplishes via heme export protein.

Heme Export Protein

Heme export protein (HEP) maintains the free heme balance in the cell. HEP is required for erythropoiesis, erythrocyte differentiation, and iron hemostasis. It exports heme and is required by erythroid progenitors at the proerythroblast stage to complete differentiation. HEP dysfunciton leads to **heme toxicity** and defective erythropoiesis.

HEP, also identified as FLVCR (for feline leukemia virus subgroup C receptor), was discovered in retroviral studies. Cats viremic with FeLV develop severe anemia and reticulocytemeia, and red cell aplasia that

is caused by a block in erythroid differentiation at the proerythroblast stage. The FeLV-C envelope protein binds to and blocks HEP (FLVCR). *Hep* gene expression is high in yolk sac, placenta, and fetal liver—sites of erythropoisis and heme oxygenase-1 expression.

Matings to create mutant mice bearing mutations that lack the *Flvcr* gene lead to death of fetuses in utero. Dead fetuses show striking growth reduction as well as abnormal limbs, flat faces, and hypertelorism—abnormalities resembling the human congenital red cell aplasia defect known as Diamond-Blackfan anemia.[35]

Ferritin

Ferritins are iron storage proteins that sequester iron taken up by the cell and release stored iron for metabolic needs—using metallochaperones to deliver iron to appropriate transporters and enzymes. Animal ferritins are cytosolic heteropolymers consisting of 24 subunits of heavy (H) and light (L) isoforms that assemble into a hollow sphere into which iron is deposited. H chains contain the iron-binding and feroxidase proteins used in mineralization of the ferritin core. **PCBP1** (poly [rC]-binding protein 1) is a cytosolic iron chaperone that delivers iron to ferritin. **Frataxin** is a mitochondrial iron chaperone for iron-sulfur cluster and heme biopsynthesis.

Ultrastructurally, ferritin is a dense spherical morula 9.5–12.5 nm in diameter with a hydrous iron oxide core surrounded by several subunits or proteinaceous micelles of 2.7 nm diameter arranged at the apices of a regular octahedron. Ferritin is formed when iron is added to apoferritin in the cytoplasmic matrix. Intracellular transport occurs through the cytoplasmic matrix or in the cytocavitary network. These paths converge in lysosomes, where ferritin is converted to the more complex **hemosiderin** (Fig. 25.4).

Ferritin occurs in the cytoplasm of macrophages and other phagocytic cells either as free aggregates in the cytoplasmic matrix, or in membrane-bounded **siderosomes**. Free ferritin is water soluble, and because it is distributed throughout the cytoplasmic matrix, it is not easily identified. Siderosomes, in early forms, contain dispersed particles of ferritin. In **compound siderosomes**, ferritin occurs as aggregates of particles, as cores of ferritin particles, and as spicular crystals of beta-$(FeOOH)_x$ (Fig. 25.5).

Mitochondrial ferritin (mtFerritin) is a unique ferritin type found in cells with high metabolic activities, but not in hepatocytes, macrophages, or other iron-storing cells. Its role appears to be to protect mitochondria from iron-dependent oxidative damage—

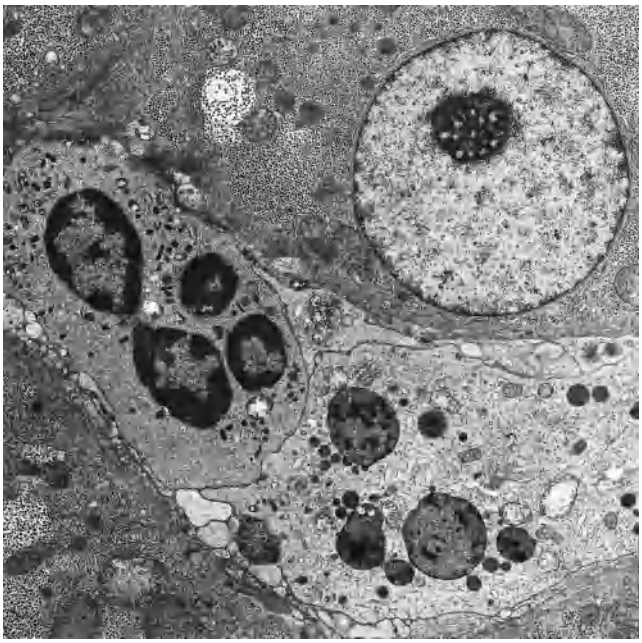


Fig. 25.4 **Ferritin**: hepatic sinusoid, liver, cardiac failure, dog; **macrophage** (lower *right*). There is accumulation of hemoglobin and erythrocytes in the macrophage cytoplasm. Hepatocyte (*top*); neutrophil (*left*).

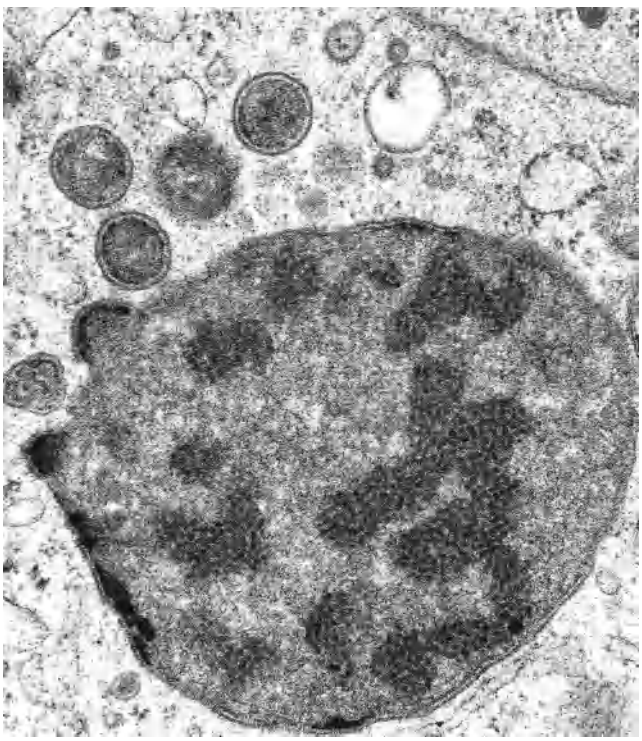


Fig. 25.5 **Siderosomes**: intrasinusoidal macrophage, liver, dog in cardiac failure. Lysosomes (*top left*) fixed in the process of moving to and fusing with a single large compound lysosome containing ferritin and ferritin aggregates.

mitochondria require iron-containing enyzmes and proteins whose biosynthesis requires a constant level of iron.

Hemosiderin

Hemosiderin is an intracellular storage form of iron in the form of yellow-brown granules consisting of complexes of ferric hydroxides, polysaccharides, and proteins. It is formed when erythrocytes are lysed. It develops within macrophages throughout the body but is especially common in the spleen and liver and in any focus of hemorrhage. Hemosiderin consists of densely packed micelles of hydrous iron oxide derived from degenerating ferritin.[36]

Hemosiderosis (siderosis), a focal or general increase in tissue iron stores, occurs in hemolytic diseases. Iron is sequestered by macrophages, and ferritin particles, formed as iron is added to apoferritin, accumulate in lattice arrays free in the cytoplasm.[37,38] Perivascular iron deposits are rare, but have been reported in diabetic neuropathy; variable sized, irregular, electron-dense pigments are present in phagocytes surrounding capillary walls.[39]

Hemochromatosis

Primary, **idiopathic hemochromatosis** is characterized by excessive deposits of ferritin and hemosiderin in the liver and other tissues. Accumulation of iron occurs first in the cytoplasm of hepatocytes. In contrast, **secondary hemochromatosis** results from systemic problems in iron associated with increased erythrocyte descruction or excess accumulation of blood transfusion or dietary iron; iron accumulates in macrophages and there is rarely associated cellular injury. In advanced disease this distinction becomes less obvious because iron moves from tissue to tissue within the body.

Animal Models of Hemochromatosis Iron loading is a widely studied model for the effects of excess iron. A wide variety of rodent models have been developed for hemochromatosis, although few actually mimic the disease. In vitro studies of iron-loaded cells have also contributed to an understanding of how iron is absorbed, reprocessed, and recycled back into the bodies iron pool.[40]

Natural occurring iron overload syndromes occur Salers cattle,[41] and in lampreys, rock hyrax, mynah birds, and birds of paradise. Lampreys feed on the blood of fishes and lack a biliary tree so that the majority of iron occurs in the hepatocyte.[42] Iron complexes with aluminum occur in the meninges of some marine animals.[43]

Iron Absorption

Atransferrinemia

In plasma, iron is complexed to the iron carrier glycoprotein **transferrin**. The iron-free form, **apotransferrin**, binds two Fe^{3+} ions to form **ferrotransferrin**. In cells that store iron, **transferrin receptors**[44] on cells bind transferrin, and the transferrin-receptor complex is taken into the cell by endocytosis. In the low pH of the endosome, Fe^{3+} dissociates from ferrotransferrin and remains in the endosome (and is later transported into the cytoplasm). Thus, iron stays in the cell, but the apotransferrin remains attached to the membrane receptor and is recycled to the cell surface, secreted into plasma, and taken to the liver or intestine, where it is reloaded with iron. **Congenital atransferrinemia** in humans (and in the hypotransferrinemia mouse model, hpx/hpx) is characterized by high levels of cytotoxic non-transferrin-bound serum iron.[45]

Erythrophagocytosis

Macrophages avidly take in senescent and damaged red blood cells (Fig. 25.6). In most mammals, erythrophagocytosis is most effective in the spleen, but in severe anemia it may occur in liver, bone marrow,

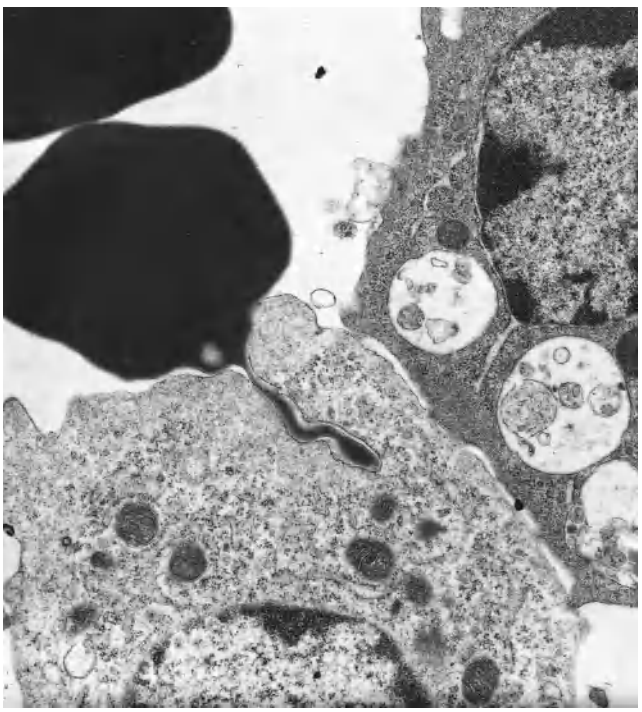


Fig. 25.6 Erythrophagocytosis. Fragmenting erythrocyte has formed a long pseudopod that has been taken into a cellular fold of a macrophage.

lung, and lymph nodes. In this function, macrophages have the major role of returning iron derived from hemoglobin catabolism to plasma for reuse in heme synthesis. Part of this iron is rapidly returned to plasma, part exchanges with storage iron in macrophages and is reutilized more slowly. Sites of iron utilization include the following:

- **Intestine**: iron is absorbed by attaching to the plasma membrane of the microvilli on enterocytes, and is transferred into the cell by receptor-mediated endocytosis via specific receptors.[46,47]
- **Bone marrow**: in stromal cells, iron is transferred through the endothelium to nurse cells that contribute iron to developing erythrocytes (Fig. 25.7); transendothelial transport (transcytosis) of iron-transferrin complexes involves a series of cytoplasmic vesicles; fenestrae, interendothelial junctions, or plasmalemmal vesicles do not transport iron.[48]
- **Placenta**: iron is transferred rapidly and unidirectionally from mother to fetus to meet high requirements of the fetus for erythropoiesis; maternal iron-transferrin complexes bind to surfaces of syncytial trophoblasts with subsequent removal of iron and release of transferrin back into maternal circulation.[49,50]
- **Mammary gland**: iron is transported from blood to milk through the mammary gland epithelial cell. The transferrin receptor level increases markedly during lactation, and transcytosis of iron occurs via a pathway that differs from that of casein.[51]

In inflamed tissue and in certain hypercoagulation states, erythrocytes pass through endothelium that is, in the normal tissue, impervious to such passage. Membrane densities at sites of contact between erythrocyte and endothelial cells indicate that a specific mechanism is involved. Experimentally, similar densities develop at sites of erythrocyte-macrophage contact. The macrophage develops dense subplasmalemmal bands of 25–35 nm thickness with periodic structure similar to clathrin.[52]

Ultrastructurally, macrophages that phagocytize erythrocytes are filled with dense bodies containing erythrocyte fragments (Fig. 25.8). Phagosomes containing this material fuse with acid phosphatase containing lysosomes that initiate enzymatic degradation.[53,54]

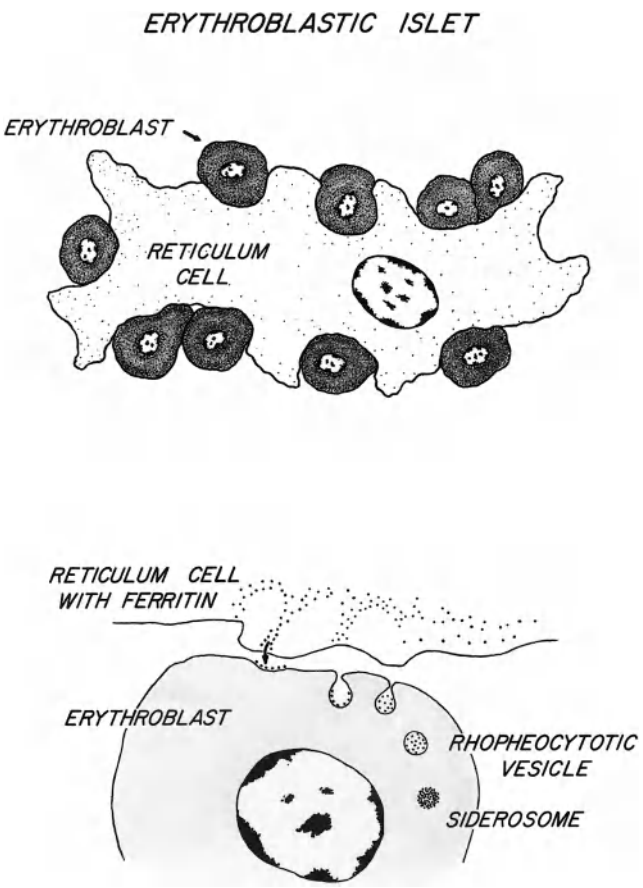


Fig. 25.7 Erythroblastic islet in bone marrow: Transfer of iron from bone marrow reticulum cell to a developing erythroblast.

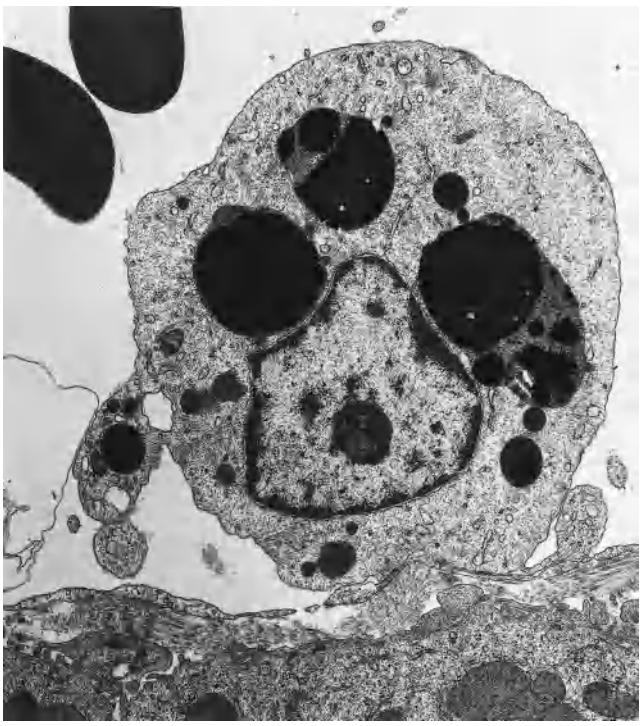


Fig. 25.8 Erythrophagocytosis: hemoglobin-filled macrophage, central vein, liver, dog. Cytoplasmic phagosomes of macrophage are filled with erythrocytes and hemoglobin.

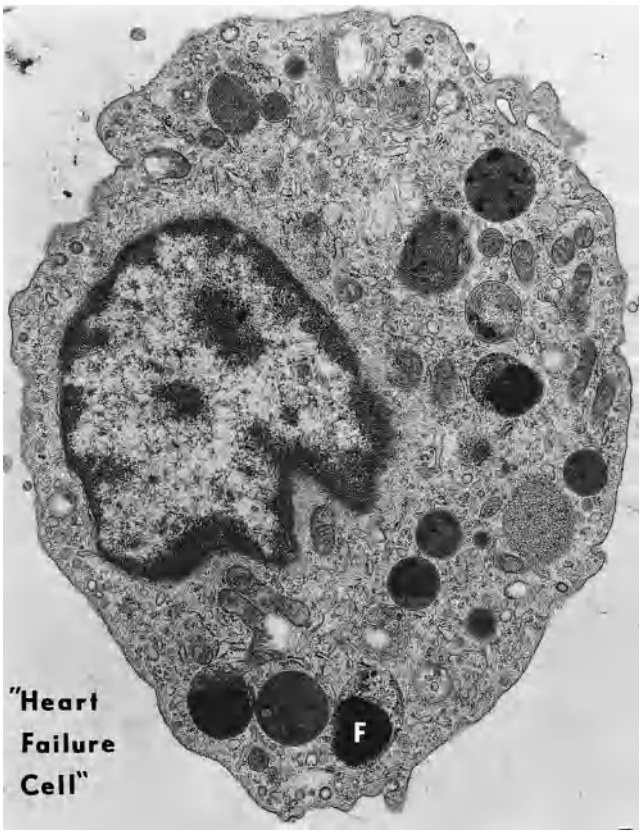


Fig. 25.9 Siderosomes: iron-filled pulmonary alveolar macrophage (heart failure cell), lung, dog. Cytoplasm contains lysosomes and phagolysosomes (siderosomes).

In the **lungs**, abnormal erythrocytes are removed from the circulation as they percolate through alveolar walls. Iron-containing macrophages are found in disease that involves circulatory stasis, and iron-laden pulmonary macrophages are referred to as "heart failure cells" (Fig. 25.9).

In the **liver**, erythrophagocytosis is seen in conditions of blood stasis in the liver vascular system, that is, the liver lesions of chronic cardiac failure. Red blood cells are also taken up within the tortuous blood vessels of hepatic neoplasms. Hypoxia and the shearing effect of fibrin combine to alter the cell surface and promote uptake intravascularly by neutrophils and monocytes (Fig. 25.10).

In the **spleen**, erthrocytes pass from the arterial to the venous system through reticular cell networks beset by macrophages and must finally squeeze through the endothelial lining cells of the venous sinuses. Phagocytosis along this route may involve pitting, fragmentation, or removal of intact erythrocytes. Nuclei of erythroblasts are also selectively removed during this passage through endothelium of the marrow sinuses.[55]

To enter venous sinuses, erythrocytes (which in most mammals measure approximately 7 μm in diameter) must pass through endothelial gaps of no more than 3 μm. To do so considerable deformation is required. Splenic blood is viscous. Its hematocrit is high; levels of oxygen and glucose are low. These factors favor spherocytosis, and these cells cannot pass the splenic filter. They are retained in the sinuses and impede circulation.

Slowing and stasis of blood in the spleen are major factors in enhancing erythrophagocytosis. Radiographic examination of the spleen after Cr^{51}-labeling of erythrocytes reveals two compartments.[56] Rapid flow of 98% of the blood goes directly to venous sinuses from the arteriole. A small percent, however, is slowed and percolates through the biliary cords. Redistribution of this flow in disease promotes splenic erythrophagocytosis.

Erythrocyte Degradation

When senescent red cells are phagocytosed and digested by macrophages, hemoglobin is degraded to heme. Heme oxygenase catalyses the initial reaction in heme catabolism, yielding equimolar amounts of biliverdin, carbon monoxide, and free divalent iron. Biliverdin is reduced to bilirubin by biliverdin reductase, while free iron is sequestered in ferritin. Divergent pathways for heme degradation products are driven in different direction by the formation of

- **Heme oxygenase-1 (HO-1)** liberates iron from heme; free iron moves to and from ferritin: $Fe^{++} \leftrightarrow$ ferritin.
- **Heme export protein** (HEP, FLVCR) exports heme iron from the macrophage.
- **Ferroportin** exports iron from the cell where it binds to plasma transferrin for delivery to the liver or bone marrow; **hepcidin** regulates this pathway by inducing the internalization and degradation of ferroportin, thereby blocking iron absorption from the gut and iron release from macrophages.

High **hepcidin** levels found in *Hep*-depleted mice contrasts with low levels in other iron-loading anemias with ineffective erythropoiesis.

Defective Heme: Porphyrias

Porphyrins are pigments normally present in hemoglobin, myoglobin and the cytochromes. **Porphyrias** include a group of hereditary or acquired diseases of porphyrin metabolism. The major types, which are based on both clinical and biochemical features, are (1) congenital erythropoietic porphyria, (2) erythrohepatic

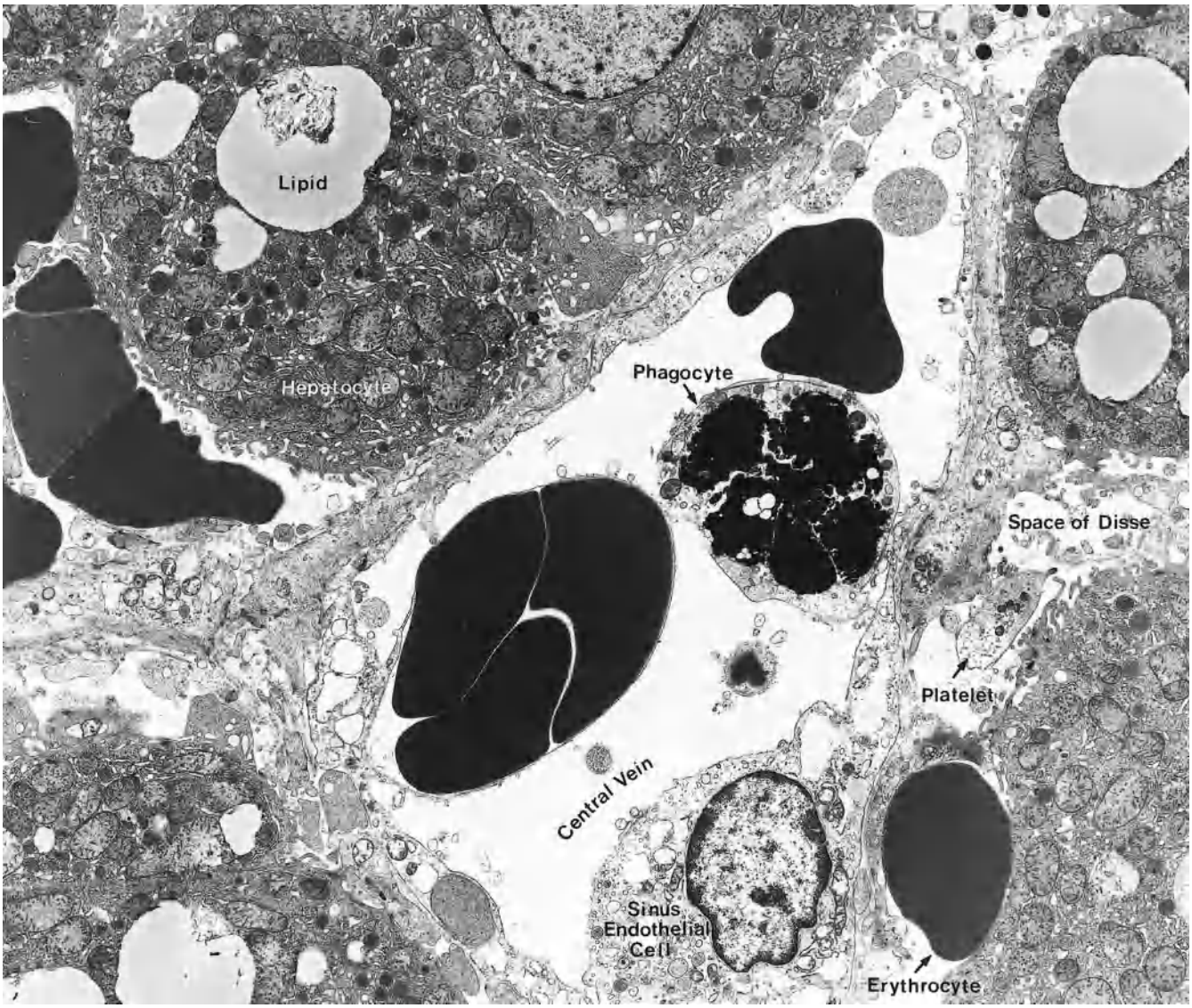


Fig. 25.10 Erythrophagocytosis: liver, blood flow stasis: stasis has caused erythrocytes to move into spaces of Disse and to be phagocytized. Macrophage in sinusoid contains large aggregates of hemoglobin.

protoporphyria, (3) acute intermittant porphyria, (4) porphyria cutanea tarda, and (5) mixed porphyria. Coproporphyria is a hereditary disorder involving excessive excretion of coproporphyrin in feces. Usually it is asymptomatic, but nerve lesions have been reported.[57]

The consequences of porphyria syndromes depend upon which porphyrins accumulate and where they are deposited. Needle-like cytoplasmic inclusions characterize deposits of porphyrins in liver and skin. The ultrastructure of crystals has been documented for most types of porphyria.[58] Analysis of liver biopsies of 16 patients with **porphyria cutanea tarda**, a syndrome of skin lesions associated with abnormal hepatic porphorin metabolism and complicated by alcohol and drug abuse, reveals electron-lucent crystals in hepatocytes.[59]

In **congenital erythropoietic porphyria**, abnormal porphyrin is formed in the developing erythrocyte. The defect of the heme molecule involves overproduction of type I porphyrins caused by an enzyme defect in the conversion of porphobilinogen to uroporphyrinogen. These porphyrins cannot be used for hemoglobin synthesis and accumulate in electron-lucent, crystal-shaped spaces in some of the human forms of porphyria.[60] This disease has been reported in pigs, cattle, cats, and fox squirrels.[61,62] Deficiency of the enzyme **uroporphyrinogen II cosynthestase** has been identified in erythrocytes of humans and cattle with

porphyria; affected animals are unable to use the pophyrin isomers to synthesize protoporphyrin and heme.

Congenital erythropoietic porphyria has been reported in cats. Elevated porphyrins (type I isomers of uroporphyrin and coproporphyrin) are present in blood, feces, teeth, bones, and most viscera. The consequences of erythropoietic porphyria depend in any species on which porphyrins accumulate and where they are deposited. Hemolytic anemia is associated with hemosiderosis of spleen, liver, and lymph nodes. Renal failure due to glomerulopathy and tubular disease occur in some forms. Photosensitivity occurs when sunlight excites the uro- and coproporphyrins in capillaries of the skin and elicits molecular changes that cause degeneration, necrosis, erythema and edema. Photosensitizing properties of these compounds increase in the order: protoporphyrin, coproporphyrin, uroporphyrin.

In **hepatogenous porphyria**, liver damage with obstruction of bile ducts leads to accumulation of phylloerythrin, a photosensitizing degradation product of chlorophyll. Models for study include damage produced by **griseofulvin**, a drug inhibiting a mitochondrial chelatase, which leads to diminished incorporation of protoporphyrin into heme and its accumulation in the erythroblasts.[63]

Bilirubin

Bilirubin, a yellow-brown or brown-green pigment, develops from breakdown of hemoglobin as macrophages process senescent erythrocytes. Porphyrin, the heme pigment, is cleaved, iron is released, and bilirubin is produced after a series of oxidation-reduction reactions within lysosomes. Although the hemoglobin-bilirubin conversions can occur in any cell of the monocyte-macrophage system, the principal organ of production is the spleen. Bilirubin enters the bloodstream, is bound to albumin, and is transported to the liver. Being insoluble in water, it is not passed through the renal glomerulus and is either processed in the liver or, if the liver is abnormal, accumulates in the bloodstream.

In the liver, bilirubin is conjugated and excreted into bile. The albumin-bilirubin complex dissociates at the plasma membrane of the hepatocyte, and bilirubin enters this cell to be conjugated, largely to glucuronide. Conjugated bilirubin, which is water soluble, is secreted into biliary canaliculi. Cholestasis and accumulation of bile within canaliculi cause degenerative changes in canaliculi with loss of microvilli and disruption of intercellular junctions.[64]

As bile reaches the duodenum the diglucuronide is cleaved and bilirubin is converted by bacteria to urobilinogen. Most urobilinogen is resorbed in the distal small intestine and transported to the liver (the "enterohepatic circulation"), some is excreted by the kidneys. Nonabsorbed urobilinogen is transformed in the gut to urobilin and excreted in the feces.

Bilirubin in Tissue

Bilirubin accumulates because of excessive production or failure of removal by damaged hepatocytes; that is, it is associated in disease with (1) excess production in hemolytic disorders, (2) impaired uptake of bilirubin by the liver, (3) impaired conjugation of bilirubin within the liver, or (4) impaired excretion of conjugated bilirubin as in cholestasis.

Bilirubin appears in cells when there is some derangement in its secretion by the liver, or when the biliary tract is obstructed.[65] Bilirubin is found within the canalicular lumen (Fig. 25.11) and in cytoplasmic granules around the canaliculus. In human cholestasis, bilirubin is also degraded in lysosomes.[66]

Kernicterus

In kernicterus, the clinical disease resulting from bilirubin deposition in the brain, bilirubin is difficult to detect on routine ultrastructural analysis. Bilirubin accumulates in vacuoles that also contain lipids and myelin figures.[67] Several rodent models have been developed to study the deposition of bilirubin in the brain.[68] In bilirubin encephalopathy of the Gunn rat, lesions are first seen in mitochondria.[69,70] Bilirubin affects membrane functions, and there are whorls of membranes and glycogen particles in neuronal cytoplasm. Bilirubin is also associated with renal papillary necrosis in the Gunn rat.[71]

Congential Hyperbilirubinemia: Dubin-Johnson Syndrome This human syndrome is a congential hepatic excretory defect in the liver involving organic anions and leads to deficient excretion of bilirubin. Livers are free of pigment at birth but become dark brown to black by a few months of age. The conjugated pigment, **bilirubin diglucuronide**, accumulates in the plasma due to the transport defect in the liver. In Corriedale sheep the defect is lethal. A rat mutant with chronic hyperbilirubinema and renal glomerular lesions has been reported that resembles the Dubin-Johnson syndrome.[72]

Congenital Hyperbilirubinemia: Gilbert's Syndrome

This sublethal trait leads to **unconjugated hyperbilirubinemia** without jaundice. An ovine model in Southdown sheep appears as a photodynamic dermatitis from retention of phylloerythrin. Clinical signs of

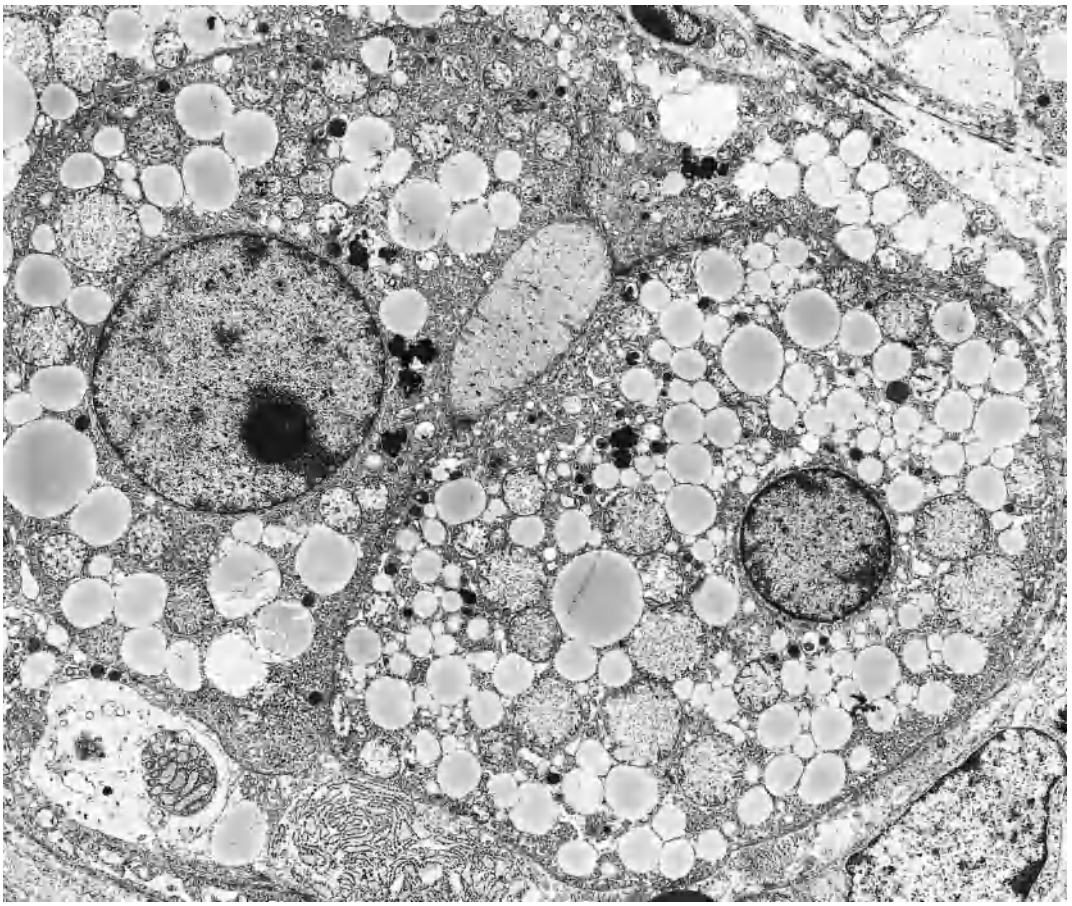


Fig. 25.11 Bilirubin: steatosis (fatty degeneration) of two hepatocytes with inspissation of bilirubin in the markedly dilated biliary canaliculus between them. Inspissated bile is composed of dense granular material with random larger dense granules. Microvilli are abnormal or missing from the canaliculus. Dense abnormal lysosomes are in hepatocyte cytoplasm surrounding the canaliculus.

acute photosensitization occurs at the time of weaning due to the ingestion of chlorophyll in green plants. Chlorophyll is converted in the rumen to phylloerythrin and inadequately excreted from the portal blood by the mutant's liver.

Malarial Pigment

Brown discoloration of the liver, spleen, and brain of patients with severe malaria is due to **hemozoin**, a crystalline malaria pigment. Malaria pigment is formed within food vacuoles of intraerythrocytic malarial parasites during catabolism of hemoglobin. Massive deposits of this pigment are found in reticuloendothleial cells of the spleen and liver of infected patients. Ultrastructural examination reveals dense, irregular granules with little characteristic structure. Analysis of malarial pigment has revealed that it represents various phases in the degradation of hemoglobin.[73,74] Soluble heme, released by proteolysis of hemoglobin, is highly toxic to membranes. Unable to cleave heme, the parasite detoxifies it by conversion to hemozoin. In hemozoin, heme molecules are linked by a bond between the ferric ion of one heme and a carboxylate side-group oxygen of another, which leads to the ordered insoluble pigment.

Copper-Containing Pigments

Menke's disease in humans arises from defective Cu absorption in the intestine and leads to Cu deficiency. Dietary copper cannot move out of the intestinal absorptive cell into the bloodstream. The gene that codes for a protein that transports copper across cell membranes is mutated. Dietary Cu is trapped and accumulated in the gut and there is excess Cu in kidney and other organs. In macular mutant mice, an animal model of Menke's disease, Cu has been localized in the gut to absorptive epithelial cells, endothelium and secretory granules of Paneth cells.[75]

Wilson's disease, a metabolic defect manifest by deposits of copper in the cornea, liver, kidney, and

brain, is caused by a variety of mutations in a single gene. Copper-bearing lysosomes accumulate in hepatocytes because of their inability to excrete copper into bile, the main route of disposal by mammals. Hepatic changes in early phases of copper toxicity involve diffusion of copper in the cytosol and degenerative changes in the hepatocyte that include lipid globules, deformation of mitochondria, and glycogen laden nuclei. In late phases of disease copper accumulates in lysosomes. Eventually there is necrosis and regeneration of hepatocytes, and collagen is deposited extracellularly, leading to nodular cirrhosis.

Bedlington terriers affected by hereditary copper storage disease begin to accumulate copper as pups, and as hepatic copper exceeds 2,000 ug/g dry liver, signs of liver failure appear. Copper localizes in centrolublar areas of the liver and also occurs in kidney, cornea, and brains. Copper may reach 10,000 ug/g liver tissue. Focal and periportal hepatitis develops, and finally cirrhosis appears.

In the **toxic milk mouse syndrome**, offspring of mutant females are born copper-deficient showing markedly reduced hepatic copper and death at 2 wk of age. The mother's milk is low in copper and does not correct the defect in the neonate. If given supplemental dietary copper, however, they rapidly sequester it in the liver, leading to ultrastructural evidence of hepatocyte degeneration. Degenerative hepatocytes show accumulation of lipid globules and striking changes in mitochondrial shape and cristae. There is marked change in the rough endoplasmic reticulum with whorling, especially around mitochondria. The nuclear membrane invaginates, forming pseudoinclusions in the nucleus.[76]

The defect in copper metabolism in Menke's kinky hair syndrome and in the brindled mouse, the murine model for this disease, leads to defective collagen, and to nervous system disease characterized by abnormal neurons with enlarged irregular mitochondria.[77,78]

Lipofuscin

Lipofuscin is a golden-brown pigment that develops within lysosomes of cells undergoing progressive and prolonged autoxoidation of unsaturated lipids. It is formed by the oxidative degradation of cell molecules by oxygen-derived free radicals and redox-active metal ions. After peroxidation of double bonds, oxidized forms are condensed into solid polymers that give the color and reactivity of lipofuscins. Deposits fluoresce brown in UV light and stain with fat-soluble dyes and the periodic acid-Schiff reaction.

Ultrastructurally, lipofuscin develops within **autophagolysosomes**.[79] Typically, residual bodies with lipofuscin are large, dense, and irregular. The heterogeneous contents contain spherical lipid droplets of variable size embedded in a granular matrix that contains spherical deposits of pigments, membrane fragments, and debris.[80–83] The mixture of lipid and protein gives a characteristic appearance (Fig. 25.12). Acid phosphatase is present in the matrix area but is not associated with lipids or pigment. Lipofuscin granules commonly contain iron since the processes that promote lipofuscin production are often involved in breakdown of iron compounds.

Lipofuscin tends to develop in actively metabolizing cells such as neurons, thyroid epithelium, muscle, renal tubules,[84] and macrophages of the spleen.[85] Lipofuscin increases with advancing age; it accrues because older cells must degrade increasing amounts of lipids and membranes at a time when their antioxidation mechanisms wane; hence the terms **aging** and **wear-and-tear pigment**.

Lipofuscins are actually a group of complex lipopigments, variants being ceroid, hemofuscin, and cytolipochrome. As oxidation proceeds in lipofusin-bearing lysosomes, cytochemical reactivity changes. Early forms, with many lipid globules and strong acid fastness, give way to dominance of membranogranular debris and weak acid-fast staining. Some lipofuscins stain for iron, which is incorporated into the lysosome during the intitial autophagocytosis.

Ceroid

Ceroid, an early variant of lipofuscin, is composed of partially oxidized and polymerized unsaturated fatty acids. It is characteristic of vitamin E deficiency in several species of animals. **Vitamin E deficiency** in animals involves lipofuscin pigment accumulation.[86] Autophagolysosomes containing liposfuscin have also been shown to contain advanced glycation end products and amyloid components.[87,88]

Ceroid devlops in macrophages, hepatocytes and other parenchymal cells and differs from classic lipofuscin in its failure to stain with the Schmorl's reaction.[89,90] The **ceroid lipofuscinoses** are a group of inherited storage diseases characterized by blindness, mental deterioration, and death (see neuronal ceroid lipofuscinoses, chapter 27).

Neuronal Ceroid and Lipofuscin

Neuronal lipofusin occurs in the aging brain. Neurons of the human cerebral cortex accumulate lipofusin peripherally. Lipofuscin granules appear ultrastructurally as a pigment matrix with lipid globules. **Neuromelanin** is a special variety of lipopigment. It is a catabolic product of catecholamines, which are incorporated into the lipopigment matrix of dopaminergic

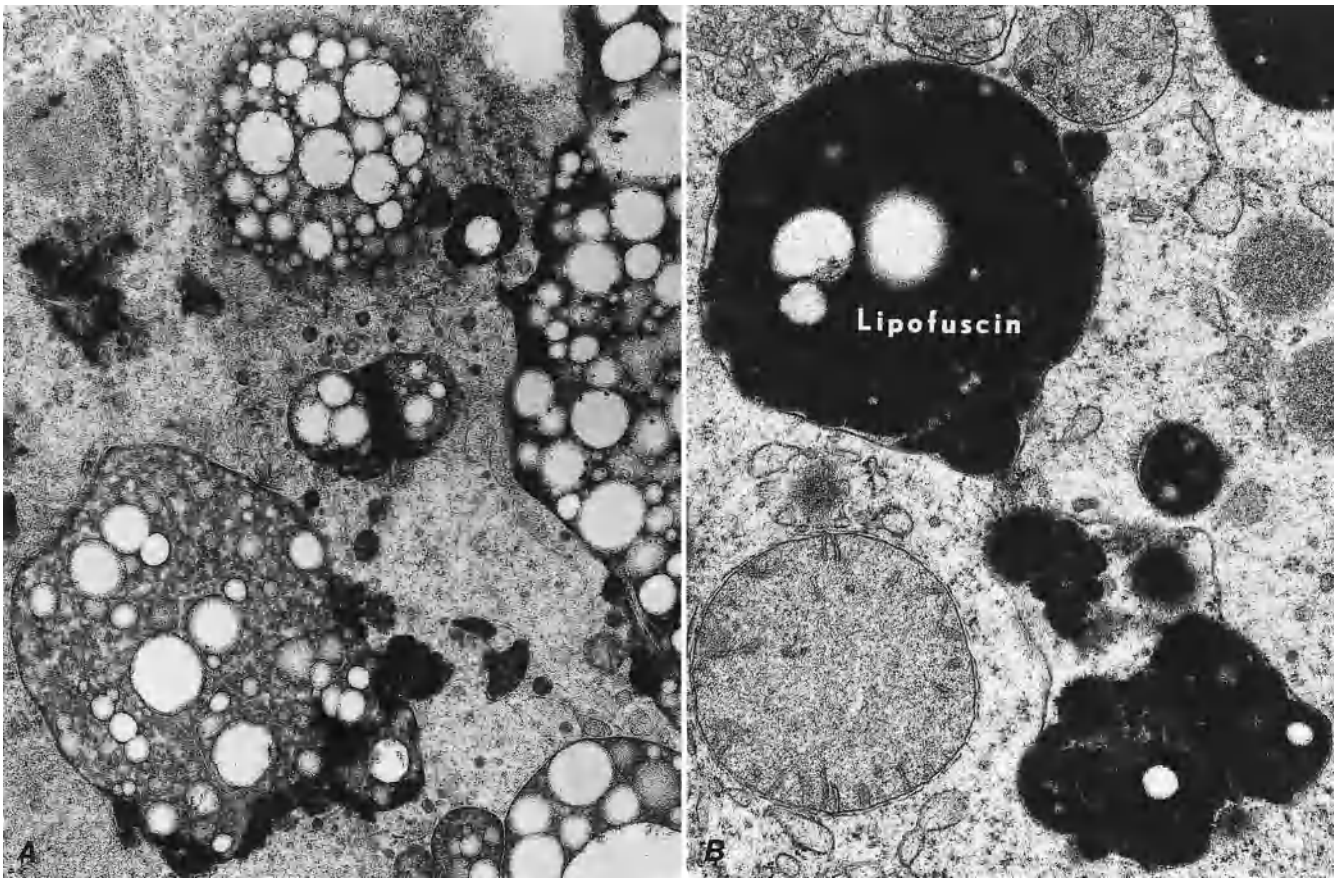


Fig. 25.12 **Lipofuscin**: dog. Membrane-bound lipofuscin granules (residual bodies). **A. Early coalescent phase of development**. Residual bodies contain many vaucoles, lipids and protein debris. **B. Dense inspissated residual bodies** of lipofuscins.

neurons to form neuromelanin. Variations occur in specific parts of the brain.[91] Anatomic sites of neuronal lipofuscin have been reported for rats.[92] **Pin1 protein**, a peptidyl-prolyl cis-trans isomerase that regulates activities of a range of proteins, is deficient in aging neurons and in neurons in Alzheimer's disease; Pin1 is present in large amounts in neuronal liposfucsin.[93]

Rett syndrome is a progressive disorder in human females characterized by autistic behavior, ataxia, seizures and growth and mental retardational lesions of diffuse cortical atrophy with increased amounts of **lipofuscin**, underpigmentation of the zona compacta nigrae, with fewer well-pigmented neurons and fewer **melanin** granules per neuron.[94]

Lipofuscin in Other Organs

- **Brown bowel syndrome** in humans and dogs is associated with chronic diarrhea, steatorrhea, pancreatic acinar deficiency, and malabsorption—aggregates of lipofuscin granules develop in smooth muscles cells, giving the intestinal serosa a brown appearance; intestinal lipofuscinosis arises from use of anthraquinone pergatives.[95]
- **Skeletal muscle lipofusin** is associated with fibromyalgia,[96] and in early stages of muscular dystrophy and in the mdx mouse model.[97]
- **Eye: melanoliposfuscin** is a complex granule with properties of both melanosomes and lipofuscin granules that accumulates in retinal pigment epithelial cells, often associated with age-related macular degeneration;[98] subretinal and perivascular microglia are the main cells that produce lipfuscin in aging mouse retinas.[99]
- **Thyroid**: minocycline therapy is associated with lipofuscin pigmentation of the thyroid glands.[100]

Exogenous Pigments

These pigments are most common and most serious in the lung, where the diseases they cause are known collectively as the **pneumoconioses**. Some of these diseases, such as anthracosis (caused by coal dust pigment), cause little tissue reaction. Others, including **silicosis** (silicon dioxide), may produce severe inflammation with extensive fibrosis. Accumulation of carbon and silica dusts is an indication of environmental

contamination. Carbon pigments in macrophages of alveoli and lining the lymphatic vessels of alveolar septae blacken the lungs. Pigments are trapped in draining lymph nodes in the hilar region of the lungs.

References

1. Costin GE, Hearing VJ. 2007. Human skin pigmentation: Melanocytes modulate skin color in response to stress. *FASEB J* 21:976.
2. Bradley TJ, Nayar JK. 1985. Intracellular melanization of the larvae of *Dirofilaria immitis* in the Malpighian tubules of the mosquito, *Aedes solicitans*. *J Invert Pathol* 45:339.
3. Ule G, Berlet H. 1979. Melanosis cerebelli. *Acta Neuropathol* 46:215.
4. Novikoff AB, et al. 1979. Retinal pigment epithelium. *Lab Invest* 40:155.
5. Candille SI, et al. 2007. A β-defensin mutation causes black coat color in domestic dogs. *Science* 318:1418.
6. Russo V, et al. 2008. Melanosis of the urinary bladder in a cow. *Vet Pathol* 45:46.
7. Simmons JJ, Morales A. 1980. Minocycline and generalized cutaneous pigmentation. *J Am Acad Dermatol* 3:244.
8. Greenberg RG, Berger TG. 1990. Nail and mucocutaneous hyperpigmentation of azidothymidine therapy. *J Am Acad Dermatol* 22:327.
9. Roth RI, et al. 1991. An animal model for the study of azidothymidine-induced hyperpigmentation. *Lab Invest* 64:437.
10. Bartosik J, et al. 1998. Melanin and melanosome complexes in long standing stable vitiligo—an ultrastructural study. *Eur J Dermatol* 8:95.
11. Panuncio AL, Vignale R. 2003. Ultrastructural studies in stable vitiligo. *Am J Dermatopathol* 25:16.
12. Boissy RE, et al. 1987. Morphology of melanocytes in hair bulbs and eyes of vitiligo mice. *Am J Pathol* 127:380.
13. Palkowski MR, et al. 1987. Langerhans cells in hair follicles of the depigmenting C57B1/Ler-vit.vit mouse. A model for human vitiligo. *Arch Dermatol* 123:1022.
14. Boissy RE, et al. 1991. Dilated rough endoplasmic reticulum and premature death in melanocytes cultured from the vitiligo mouse. *Am J Pathol* 138:1511.
15. Hu F, et al. 1980. Yellow mutant albinism: Cytochemical, ultrastructural, and genetic characterization suggesting multiple allelism. *Am J Human Genet* 32:387.
16. King RA, et al. 1991. Temperature-sensitive tyrosinase associated with peripheral pigmentation in oculocutaneous albinism. *J Clin Invest* 87:1046.
17. Meisler M, et al. 1980. Morphologic and biochemical abnormalities of kidney lysosomes in mice with an inherited albinism. *Am J Pathol* 101:581.
18. Cuillery RW. 1974. Visual pathways in albinos. *Sci Am* p 44.
19. Leventhal AG, et al. 1985. Abnormal visual pathways in normally pigmented cats that are heterozygous for albinism. *Science* 229:1395.
20. Cortese K, et al. 2005. The ocular albinism type 1 (OA1) gene controls melanosome maturation and size. *Invest Ophthalmol Vis Sci* 46:4358.
21. Ree K. 1983. Intranuclear inclusions containing melanosomes observed after PUVA therapy. *J Ultrastruct Res* 83:10.
22. Turner WA Jr, et al. 1975. Melanosome formation in the goldfish: The role of multivesicular bodies. *J Ultrastruct Res* 51:16.
23. Natsuga K, et al. 2005. Ultrastructural features of trafficking defects are pronounced in melanocytic nevus in Hermansky-Pudlak syndrome type 1. *J Invest Derm* 125:154.
24. Boissy RE, et al. 1998. Altered protein localization in melanoctes from Hermansky-Pudlak syndrome. *Lab Invest* 78:1037.
25. Richmond B, et al. 2005. Melanocytes derived from patients with Hermansky-Pudlak syndrome types 1, 2, and 3 have distinct defect in cargo trafficking. *J Invest Derm* 124:420.
26. Nguyen T, Wei ML. 2004. Characterization of melanosomes in murine Hermansky-Pudlak syndrome: Mechanisms of hypopigmentation. *J Invest Derm* 122:452.
27. Gardner JM, et al. 1992. The mouse pink-eyed dilution gene: Association with human Prader-Willi and Angelman syndromes. *Science* 257:112.
28. Orlow SJ, Brilliant MH. 1999. The pink-eyed dilution locus controls the biogenesis of melanosomes and levels of melanosomal proteins in the eye. *Exp Eye Res* 68:147.
29. Kuriyama T, et al. 2006. Ultrastructure of the dermal chromatophores in a lizard (Scincidae: *Plestiodon latiscutatus*) with conspicuous body and tail coloration. *Zool Sci* 23:793.
30. Obika M, et al. 1978. Ultrastructural demonstration of hormone-induced movement of carotenoid droplets and endoplasmic reticulum in xanthopores of the goldfish, *Carassius auratus* L. *Cell Tiss Res* 190:40.
31. Wang SM, et al. 1997. Characterization of a novel filament system in goldfish xanthopores. *Cell Motil Cytoskeleton* 36:216.
32. Kimler VA, Taylor JD. 1995. Ultrastructural immunogold localization of some organelle-transport relevant proteins in wholemounted permeablized nonextracted goldfish xanthophores. *Pigment Cell Res* 8:75.
33. Bagnara JT, et al. 1979. Common origin of pigment cells. *Science* 203:410.
34. Setoguti T. 1967. Ultrastructure of guanophores. *J Ultrastruct Res* 18:324.
35. Keel SB, et al. 2008. A heme export protein is required for red blood cell differentiation and iron homeostasis. *Science* 319:825.
36. Miyazaki E, et al. 2002. Denatured H-ferritin subunit is a major consitutent of haemosiderin in the liver of patients with iron overload. *Gut* 50:413.
37. Iancu TC, Neustein HB. 1977, Ferritin in human liver cells of homozygous beta-thalassaemia: Ultrastructural observations. *Brit J Haematol* 37:527.
38. Cooper PJ, et al. 1988. Quantitative analysis of immunogold labelling for ferritin in livers from control and iron-overloaded rats. *Histochem J* 20:499.

39. Davis DG, Markesbery WR. 1992. Perivascular siderophages in skeletal muscle from a patient with diabetic neuropathy. *Acta Neuropathol* 84:216.
40. Iancu R, et al. 1987. Ultrastructural pathology of iron-loaded rat myocardial cells in culture. *Br J Exp Pathol* 68:53.
41. O'Toole D, et al. 2001. Hepatic failure and hemochromatosis in Salers and Salers-cross cattle. *Vet Pathol* 38:371.
42. Alt ER, et al. 1990. The cytopathology of metal overload. *Int Rev Exp Pathol* 31:165.
43. Youson JH, et al. 1989. Iron and aluminum deposition in the meninges of the lamprey: Identification of an aluminum-ferritin inclusion body. *Anat Rec* 223:13.
44. Pan B-T, et al. 1985. Electron microscopic evidence for externalization of the transferrin receptor in vesicular form in sheep erythrocytes. *J Cell Biol* 101:942.
45. Iancu TC, et al. 1995. The hypotransferrinaemic mouse: Ultrastructural and laser microprobe analysis observations. *J Pathol* 177:23.
46. Humphreys J, et al. 1977. Intracellular iron transport in rat intestinal epithelium: Biochemical and ultrastructural observations. *Brit J Haematol* 36:209.
47. Parmley RT, et al. 1978. Ultrastructural cytochemistry of iron absorption. *Am J Pathol* 93:707.
48. Soda R, Tavassoli M. 1984. Transendothelial transport (transcytosis) of iron-transferrin complex in the bone marrow. *J Ultrastruct Res* 88:18.
49. King BF. 1976. Localization of transferrin on the surface of the human placenta by electron microscopic immunocytochemistry. *Anat Rec* 186:151.
50. Parmley RT, et al. 1981. Ultrastructural, cytochemical and radiographic localization of placental iron. *Am J Pathol* 105:10.
51. Seddiki T, et al. 1992. Endocytosis and intracellular transport of transferrin across the lactating rabbit mammary epithelial cell. *J Hist Cyt* 40:1501.
52. Montesano R, et al. 1983. Specialization of the macrophage plasma membrane at sites of interaction with opsonized erythrocytes. *J Cell Biol* 96:1227.
53. Schnitzer B, Smith EB. 1966. Observations of phagocytized red cells containing Heinz bodies. *Am J Clin Pathol* 46:538.
54. Collet AJ, Petrik P. 1971. Electron microscopic study of the in vivo erythrophagocytosis by alveolar macrophages of the cat. *Z Zellforsch* 116:464.
55. Tavassoli M, Crosby WH. 1973. Fate of the nucleus of the marrow erythroblast. *Science* 79:912.
56. Pictet R, et al. 1969. An electron microscope study of the perfusion-fixed spleen. *Z Zellforsch* 96:372.
57. Trapani G, et al. 1984. Peripheral nerve findings in hereditary coproporphyria. *Acta Neuropathol* 63:96.
58. Antolin I, et al. 1994. Porphyrin accumulation in the Harderian gland of female Syrian hamster results in mitochondrial damaged and cell death. *Anat Rec* 239:349.
59. Waldo ED, Tobias H. 1973. Needle-like cytoplasmic inclusions in the liver in porphyria cutanea tarda. *Arch Pathol* 96:368.
60. Bloomer JR, Enriquez R. 1982. Evidence that hepatic crystalline deposits in a patient with protoporphyria are composed of protoporphyrin. *Gastroenterology* 82:569.
61. Flyger V, Levin EY. 1977. Congenital erythropoietic porphyria. *Am J Pathol* 87:269.
62. Giddens et al. 1975. Feline congenital erythropoietic porphyria associated with severe anemia and renal disease. *Am J Pathol* 80:367.
63. Matilla A, Molland EA. 1974. A light and electron microscopic study of the liver in a case of erythropoietic protoporphyria and in griseofulvin-induced porphyria in mice. *J Clin Pathol* 27:698.
64. Loosli H, et al. 1981. Experimental intrahepatic cholestasis. *Virch Arch B* 35:213.
65. Altmann H-W. 1977. Eisenhaltige Kerneinschlusse bei menschlicher Pigmentcirrhose. *Virch Arch B* 23:277.
66. Faria V. 1977. Lysosomal degradation of bile deposits in cholestasis. *Virch Arch* 24:355.
67. Ahdab-Barmada M, Moossy J. 1984. The neuropathology of kernicterus in the premature neonate. *J Neuropathol Exp Neurol* 43:45.
68. Rose AL, Wisniewski H. 1979. Acute bilirubin encephalopathy induced with sulfadimethoxine in Gunn rats. *J Neuropathol Exp Neurol* 38:152.
69. Jew JY, Williams TH. 1977. Ultrastructural aspects of bilirubin encephalopathy in cochlear nuclei of the Gunn rat. *J Anat* 124:599.
70. Schutta HS, Johnson C. 1971. Electron microscopic observations on acute bilirubin encephalopathy in Gunn rats induced by sulfadimethoxine. *Lab Invest* 24:82.
71. Axelsen RA, Burry AF. 1975. Bilirubin-associated renal papillary necrosis in the homozygous Gunn rat: Light- and electron-microscope observations. *J Pathol* 120:165.
72. Hosokawa S, et al. 1992. A new rat mutant with chronic hyperbilirubinemia and renal glomerular lesions. *Lab An Sci* 42:27.
73. Goldie P, et al. 1990. Biochemical characterization of *Plasmodium falciparum* hemozoin. *Am J Trop Med Hyg* 43:584.
74. Morselft AFW, et al. 1973. Electron-microscopical and microphotometric studies on the breakdown of erythrocytes by macrophages. *Histochemie* 37:161.
75. Kodama H, et al. 1993. Histochemical localization of copper in the intestine and kidney of macular mice: Light and electron microscopic study. *J Hist Cyt* 41:1529.
76. Biempica L, et al. 1988. Morphologic and chemical studies on a murine mutation (toxic milk mice) resulting in hepatic copper toxicosis. *Lab Invest* 59:500.
77. Matsushima H, et al. 1985. Neuropathologic study in the heterozygotes of X-linked brindled mutant mouse. *Acta Neuropathol* 67:300.
78. Yamano T, Suzuki K. 1986. Cerebellar changes of female mice heterozygous for brindled gene. *Acta Neuropathol* 69:220.
79. Ivy GO, et al. 1984. Inhibitors of lysosomal enzymes: Accumulation of lipofuscin-like dense bodies in the brain. *Science* 226:985.
80. Brunk U, Ericsson JLE. 1972. Electron microscopical studies on rat brain neurons. Localization of acid

phosphatase and mode of formation of lipofuscin bodies. *J Ultrastruct Res* 38:1.
81. Goebel HH, Schulz F. 1979. The ultrastructural variability of non-specific lipopigments. *Acta Neuropathol* 48:227.
82. Crichton DN, et al. 1980. An ultrastructural study of murine splenic lipofuscinosis. *J Ultrastruct Res* 72:130.
83. Moore NA, Callas G. 1975. Observations on the fine structure of propylthiouracil-induced "brown degeneration" in the zona reticularis of mouse adrenal cortex. *Anat Rec* 183:293.
84. Cain H, Kraus B. 1972. Lysosomale Pigmentablagerungen in der Niere alter Wistarratten. *Virch Arch B* 10:32.
85. Frank AL, Christensen AK. 1968. Localization of acid phosphatase in lipofuscin granules and possible autophagic vacuoles in interstitial cells of guinea pig testis. *J Cell Biol* 36:1.
86. Kennedy S, Rice DA. 1988. Selective morphologic alterations of the cardiac conduction system in calves deficient in vitamin E and selenium. *Am J Pathol* 130:315.
87. Clark A, et al. 1989. Localization of islet amyloid-peptide in lipofuscin bodies and secretory granules of human B-cells and in islets of type-2 diabetic subjects. *Cel Tissue Res* 257:179.
88. Ling X, et al. 1998. Immunohistochemical distribution and subcellular localization of three distinct specific molecular structures of advanced glycation end products in human tissues. *Lab Invest* 78:1591.
89. Kajihara H, et al. 1975. Zur Ultrastruktur und Morphogenese des Ceroid Pigmentes. *Virch Arch B* 19:23.
90. Roald SO, et al. 1981. Histochemical, fluorescent, and electron microscopical appearance of hepatocellular ceroidosis in the Atlantic salmon *Salmo salar* L. *J Fish Dis* 4:1.
91. Boellaard JW, Schlote W. 1986. Ultrastructural heterogeneity of neuronal lipofuscin in the normal human cerebral cortex. *Acta Neuropathol* 71:285.
92. Brizzee KR, Johnson FA. 1970. Depth distribution of lipofuscin in cerebral cortex of albino rat. *Acta Neuropathol* 16:205.
93. Hashemzadeh-Bonehi L, et al. 2006. Pin1 protein associates with neuronal lipofuscin. *Exp Neurol* 199:328.
94. Jellinger K, et al. 1988. Neuropathology of Rett syndrome. *Acta Neuropathol* 76:142.
95. Walker NI, et al. 1988. Melanosis coli. A consequence of anthraquinone-induced apoptosis of colonic epithelial cells. *Am J Pathol* 131:465.
96. Sprott H, et al. 2004. Increase DNA fragmentation and ultrastructural changes in fibromyalgic muscle fibres. *Ann Rheum Dis* 63:245.
97. Nakae Y, et al. 2004. Early onset of lipofuscin accumulation in dystrophin-deficient skeletal muscles of DMD patients and mdx mice. *J Mol Histol* 25:489.
98. Warburton S, et al. 2007. Proteomic and phototoxic characterization of melanolipofuscin. *Mol Vis* 13:318.
99. Xu H, et al. 2008. Age-dependent accumulation of lipofuscin in perivascular and subretinal microglia in experimental mice. *Aging Cell* 7:58.
100. Gordon G, et al. 1984. Thyroid gland pigmentation and minocycline therapy. *Am J Pathol* 117:98.

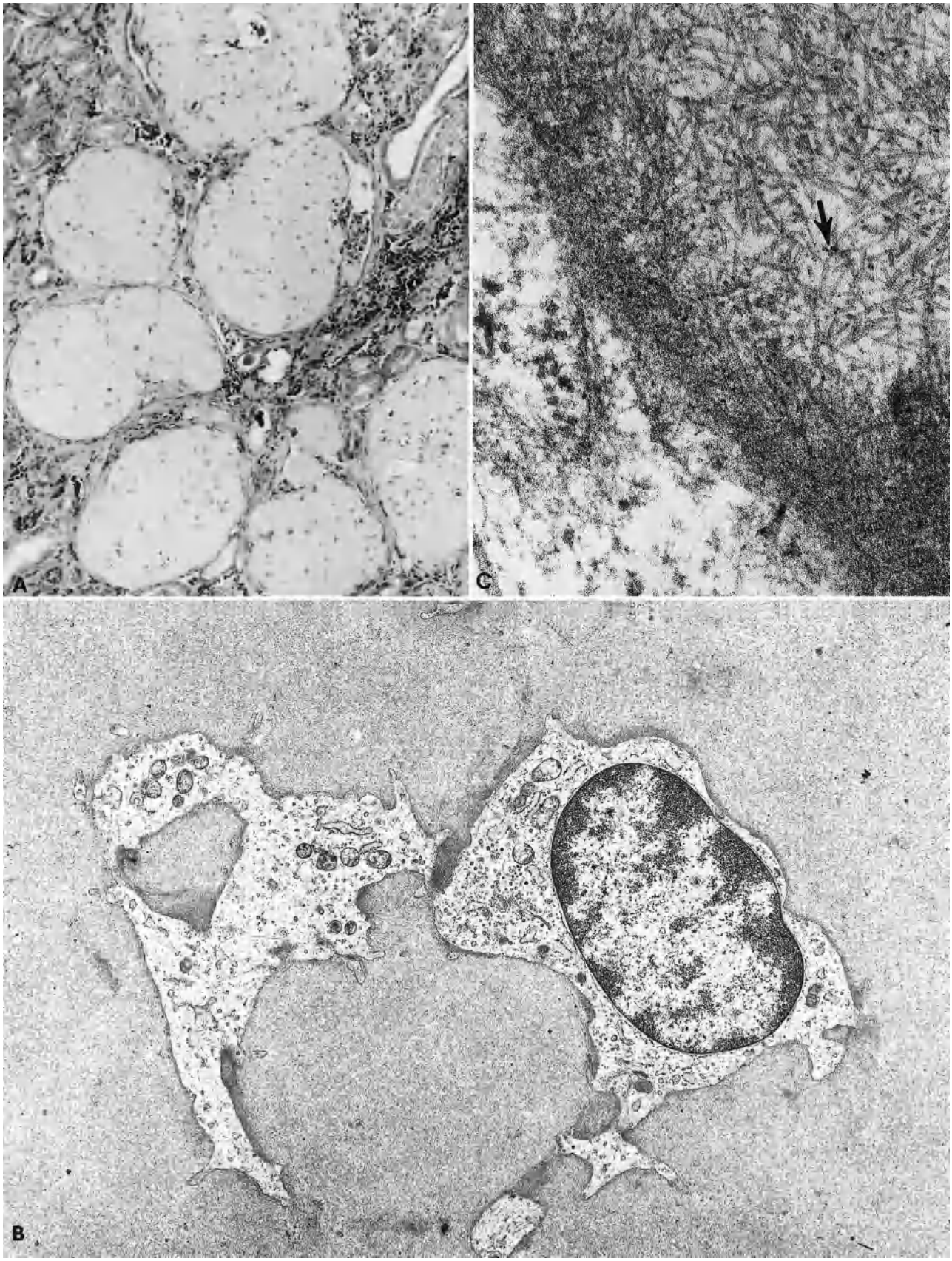


Fig. 26.1 **Amyloid**: renal glomerulus, secondary amyloidosis, dog. **A**. **Glomeruli effacement**: glomeruli are obliterated by masses of amyloid. **B**. **Amyloid-secreting reticular cell**: abnormal cells are surrounded by masses of amyloid fibrils. **C**. **Cell surface–amyloid interface of fibrillogenesis**: surface of amyloid-secreting reticular cell contains dense areas of preamyloid polymers. Amyloid fibrils in cross section and longitudinal section (*arrow*); dense granular areas at the cell surface are zones of amyloid fibrillogenesis.

© 2009 Wiley-Blackwell. ISBN: 978-0-813-80330-2

26 Amyloid, Protein Misfolding Defects, and Inclusions

Amyloid

Amyloid is a glycoproteinaceous fibrillar complex that is deposited extracellularly in tissue.[1] Histologically, a high affinity for Congo red induces green birefringence under polarized light because of the peculiar alignment of stain on parallel fibrils. Amyloid fibrils are derived from the fibrillation of **amyloid precursor proteins** that are present in normal serum or tissue. The intact amyloid precursor protein, or a degradation fragment of it, is repetitively incorporated into the developing amyloid fibril; it is formed in the cell and polymerizes into amyloid fibrils as it is released at the cell surface.

Amyloid fibrils are 7.5–10 nm in diameter (Fig. 26.1). They are rigid, nonbranching, hollow-cored tubules, and are of indeterminant length since they crisscross into and out of the plane of section. When examined by x-ray diffraction, amyloid fibrils have a characteristic β-pleated sheet configuration. This macromolecular helix of 100 nm periodicity, formed from two twisted β-pleated sheet micelles, is responsible for the resistance of amyloid fibrils to solubilization and to proteolytic digestion.[2] Thus, the implacable deposition of these inert fibrils is unlikely to be accompanied by effective degradation and removal.

P component is a pentagonal, 8 nm diameter, doughnut-like α_1-glycoprotein present in amyloid. P component (SAP, serum amyloid P component) is unrelated to amyloid protein, but is an acute phase protein of the pentraxin superfamily in normal serum, a group that includes complement component C1t, C-reactive protein, and pentraxin 3 (PTX3).[3] These substances belong to a family of pentameric proteins called pentraxins. Activated microglia accumulate at sites of amyloid in the brain, and their release of SAP may enhance amyloid fibrillogenesis.

Proteoglycans are major components of the interfibrillar matrix; heparan sulfate proteoglycan is most common.[4] In amyloidotic lesions of human brains, immunocytochemical studies of amyloid suggest that heparan sulfate-containing glycosaminoglycan chains co-localize with amyloid protein. Dermatan sulfate proteoglycan and its protein core (decorin) have been localized in amyloids of the neurofibrillary tangles found in brains of Alzheimer's disease patients.[5]

Amyloid fibrils with P component and matrix proteoglycan constitute pure amyloid. Amyloid in tissue (depending on its stage of deposition) is contaminated with varying amounts of plasma proteins and collagen. Fibrils form a sponge-like scaffold on which plasma proteins and other glycoproteins are absorbed. Variations in the density of amyloid result from differences in the nonamyloid components that have attached to the fibrillar scaffold. In blood vessels permeated by amyloid, vascular permeability is increased, and this allows for the progressive deposition of plasma proteins in the underlying fibrillar framework.[6]

Amyloidosis is the disease resulting from deposition of **amyloid fibrils** in tissue. In all types of amyloidosis there is an underlying abnormality of protein processing. Atypical reticular cells ("amyloid cells") are present in amyloid, and they are irrevocably directed toward the assembly of protein fragments into amyloid protofilaments and fibrillation into amyloid fibrils.[7,8] By redirection of protease activity, these cells produce a pre-amyloid that polymerizes into fibrils at the cell surface.[9] Amyloid is most dangerous when deposited in the renal glomerulus and other major blood vessels.

Amyloid fibrils can be formed by abnormal processing of components of such diverse proteins as acute phase proteins, immunoglobulins, and hormones (Table 26.1). Despite chemical heterogeneity, the common denominator of all amyloids is that they are aggregates of twisted, β-pleated sheet fibrils. The key is the presence of an amyloidogenic primary structure that, after proteolytic cleavage, assembles into a β-pleated sheet configuration. By this change, the amyloid fibril is resistant to further enzymatic digestion, and it accumulates in tissue. Of the known amyloid precursors, three are apolipoproteins that are associated with HDL of plasma, including the common serum protein AA (apoSAA). In experiments in mice, AA amyloidosis has been shown to be **transmissible**; that is, amyloid fibrils (when given IV or orally) will act as a template to accelerate amyloidosis in the new host (see Xing, *Lab Invest* 81:493, 2001). Fecal amyloid fibrils are reported to cause AA amyloidosis in Cheetahs (see Zhang, *Proc Nat Acad Sci* 105:7263, 2008).

AA Amyloid: Secondary Amyloidosis

Amyloidosis arising from circulating **serum amyloid A (SAA)** is common in chronic infections, sepsis, and

Table 26.1 Amyloid: ultrastructural studies.

Tissue lesion	*Change*	*Reference to ultrastructural pathology*
		AA Amyloid
Kidney	Cat	**Clark**, *Vet Pathol* 6:117, 1969
	Dog	**Slauson**, *J Comp Pathol* 80:335, 1970
	Human	**Donini**, *J Hist Cyt* 37:1101, 1989; **Shirahama**, *Am J Pathol* 51:869, 1967
	Monkey	**Walker**, *Acta Neuropathol* 80:381, 1990
	Whales	**Tajima**, *J Zoo Wildlife Med* 38:108, 2007
Joint	Chicken	**Peperkamp**, *Vet Pathol* 34:271, 1997
Liver	Avian	**Gruys**, *Amyloid* 13:13, 2006
	Marmoset	**Ludlage**, *Vet Pathol* 42:117, 2005
	Mouse	**Shirahama**, *Am J Pathol* 118:108, 1985 (hepatocyte)†
Lung	Human	**Eshun-Wilson**, *Virch Arch A* 371:89, 1976
Prosthesis-associated	Human	**Goffin**, *Am J Pathol* 114:431, 1984 (cardiac valve)
Spleen	Dog	**Cheville**, *Vet Pathol* 7:225, 1970
Experimental	Guinea pig	**Cohen**, *Arthritis Rheum* 14:429, 1971
	Mouse	**Skinner**, *Lab Invest* 36:420, 1977 (casein-induced)†
		AL Amyloid
Multiple myeloma (light chain)		
	Horse	**Kim**, *Vet Pathol* 42:81, 2005
	Human	**Kjeldsberg**, *Blood* 50:493, 1977
	Mouse	**Solomon**, *Am J Pathol* 140:629, 1992 (light chain)†
		Endocrine Amyloid
ApoA-2	Mouse	**Ge**, *Lab Invest* 57:633, 2007
Calcitonin		
	Fish	**Diociaiuti**, *Biophys J* 91:2275, 2006 (pore formation)
Glucagon	Human	**Anderson**, *Biochemistry* 46:7314, 2007*
Pancreatic islet polypeptide	Cat	**Johnson**, *Lab Invest* 66:522, 1992; **Johnson**, *Am J Pathol* 130:1, 1988; **Yano**, *Vet Pathol* 18:181, 1981; **Yano**, *Lab Invest* 45:149, 1981
	Human	**Westermark**, *Am J Pathol* 127:414, 1987
	Mouse	**Rindi**, *Am J Pathol* 138:1321, 1991
	Rat	**Hayden**, *Exp Biol Med* 232:772, 2007
Transthyretin		
	Human	**Bergström**, *J Pathol* 206:224, 2005
	Monkey	**Nakamura**, *Vet Path* 45:67, 2008

Table 26.1 *Continued*

Tissue lesion	*Change*	*Reference to ultrastructural pathology*
		Beta Amyloid
Neuritic plaques	Dog	**Cork**, *Am J Pathol* 137:1383, 1990; **Ishihara**, *Brain Res* 548:196, 1991; **Torp**, *Neuroscience* 120:291, 2003; **Wisniewski**, *Lab Invest* 23:287, 1970
	Human	**Davies**, *Am J Pathol* 143:1594, 1993; **Eriksson**, *Am J Pathol* 125:124, 1986 (choroid plexus); **Masliah**, *J Neuropathol Exp Neurol* 52:619, 1993; **Munoz**, *Am J Pathol* 140:1167, 1992; **Shirahama**, *Am J Pathol* 107:41, 1982; **Storkel**, *Virch Arch B* 44:145, 1983; **Wisniewski**, *J Neuropathol Exp Neurol* 43:643, 1984 (paired helical filaments); **Yamaguchi**, *Am J Pathol* 135:593, 1989; **Yamaguchi**, *Acta Neuropathol* 80:368, 1990; **Yamaguchi**, *Am J Pathol* 138:699, 1991
	Monkey	**Walker**, *Acta Neuropathol* 80:381, 1990; **Wisniewski**, *J Neuropathol Exp Neurol* 32:566, 1973
		Vascular Amyloid
Arteries	Human	**Miyakawa**, *Virch Arch B* 40:121, 1982; **Powers**, *Acta Neuropathol* 76:613, 1988; **Yamaguchi**, *Am J Pathol* 141:249, 1992; **Wisniewski**, *Acta Neuropathol* 84:117, 1992
Aorta	Human	**Mucchiano**, *Am J Pathol* 140:871, 1992
Lung	Dog	**Johnson**, *Am J Pathol* 141:1013, 1992
		Prion Protein Amyloid
Creutzfeldt-Jakob disease	Human	**Liberski**, *Folia Neuropathol* 42:109, 2004
Gerstmann-Sträussler-Scheinker disease	Human	**Giaccone**, *Proc Natl Acad Sci USA* 90:302, 1993
Kuru	Human	**Liberski**, *Mol Neurobiol* 8:67, 1994
Scrapie	Sheep	**Prusiner**, *Cell* 35:349, 1983
		Other Amyloids
Dialysis-related amyloidosis (β2-microglobulin)	Human	**Ohhashi**, *J Biol Chem* 280:32843, 2005
Familial amyloidotic polyneuropathy	Human	**Yi**, *Am J Pathol* 138:403, 1991 (transgenic mouse)†
Hereditary inclusion myopathy#	Human Mouse	**Malicdan**, *Hum Mol Genet* 16:115, 2006 **Miao**, *Am J Pathol* 167:505, 2005†
Hypernephroma	Human	**Dalakas**, *Am J Pathol* 116:447, 1984
Insulinoma	Human	**Yamashita**, *Cancer* 55:841, 1985
Macular amyloidosis		**Lee**, *Pathology* 23:322, 1991

*Studies in vitro.
†Animal model.
#Distal myopathy with rimmed vacuoles.

tissue destructive processes. Tissue deposits of AA amyloid are correlated with an increase in SAA, an acute phase protein produced in the liver in response to inflammation. AA amyloidosis is common in chronic immunodeficiency. Typically, amyloid is formed by **macrophages** of the spleen and lymph node that proteolytically cleave SAA to a smaller molecule that assembles into the amyloid fibril. Parenchymal cells also form amyloid A; for example, in the liver, SAA is produced by **hepatocytes**.[10–12]

Amyloid composed of SAA is most common in the spleen and liver, but is most lethal in the renal glomerulus. In the **spleen**, it develops in the white pulp around the central artery and its arterioles (Fig. 26.2). Ultrastructurally, amyloid fibrils are randomly oriented. They are extracellular although there are reports of amyloid fibrils located intracellularly.[13,14] Amyloid has been also been ultrastructurally characterized in many other organs. The ultrastructure of AA amyloid fibrils in situ resembles that of connective tissue microfibrils and contains, in addition to SAA, heparan sulfate proteoglycan, chondroitin sulfate proteoglycan, and amyloid P 3.5 nm wide pentosomal particles.[15]

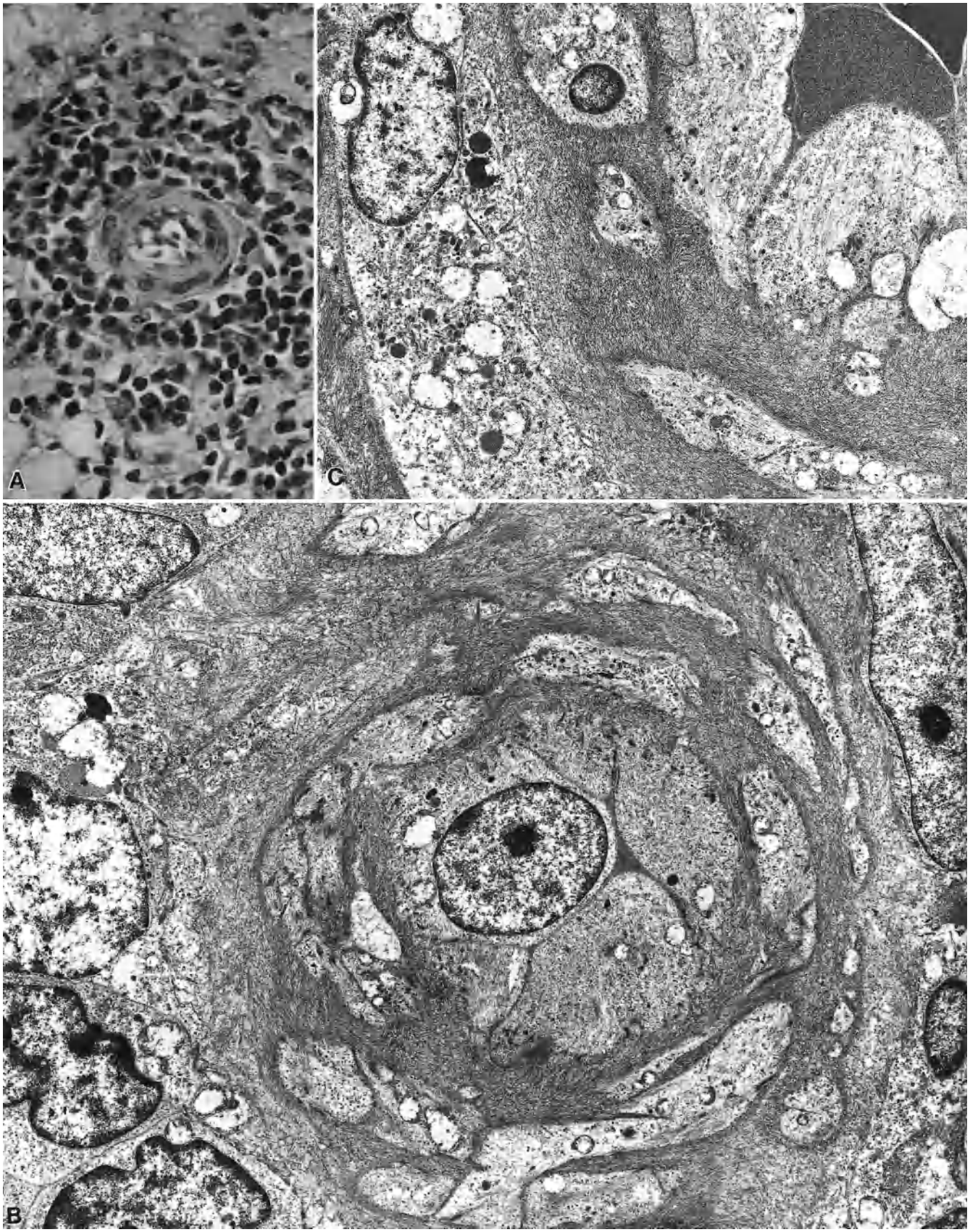


Fig. 26.2 **Amyloid**: muscular artery, spleen. **A. Histology**. **B–C**. **Amyloid fibrils**: fibrils have infiltrated vascular smooth muscle. Degeneration of surrounding vascular wall and hyperplasia of endothelial cells are evident.

SAA Amyloid Renal Disease

Deposition of SAA amyloid in the **renal glomerulus** is a common cause of renal failure. Amyloid first appears as fibrils in the mesangial matrix and in a slightly widened capillary basement membrane. These deposits progressively expand to constrict the capillary lumen and end in severe distortion of the glomerular tuft. Amyloid fibrils first accumulate on the endothelial side of the basement membrane and expand through the basement membrane to block and distort the foot processes of glomerular epithelial cells, finally obliterating the architecture of the glomerulus. Diagnostic immunolabeling of glomerular deposits in renal biopsies of 9 amyloidotic patients using protein A-gold and a panel of antibodies against amyloid proteins showed that six stained for amyloid A and 3 for amyloid light chains (Fig. 26.3).[16]

Renal **peritubular deposits** of amyloid begin in apposition to the tubular basement membrane and extend progressively to project into the tubular lumen and to move into the intertubular connective tissue.[17] Renal **blood vessels** are affected as arteriolar and arterial walls accumulate amyloid fibrils that begin in intercellular spaces of vascular smooth muscle cells. The combined effects of vascular injury and tubular atrophy lead to a shrunken, contracted kidney and death due to renal failure.

In amyloid glomerulopathy, immunohistochemical studies reveal ribbonlike immunofluorescent staining for IgG and C3 along capillary loops and in the mesangium. Electron microscopic studies using immunogold techniques on kidney biopsies of 7 patients showed staining of fibrils for IgG (both light chains), C3, and amyloid P component. Fibrils appear to be

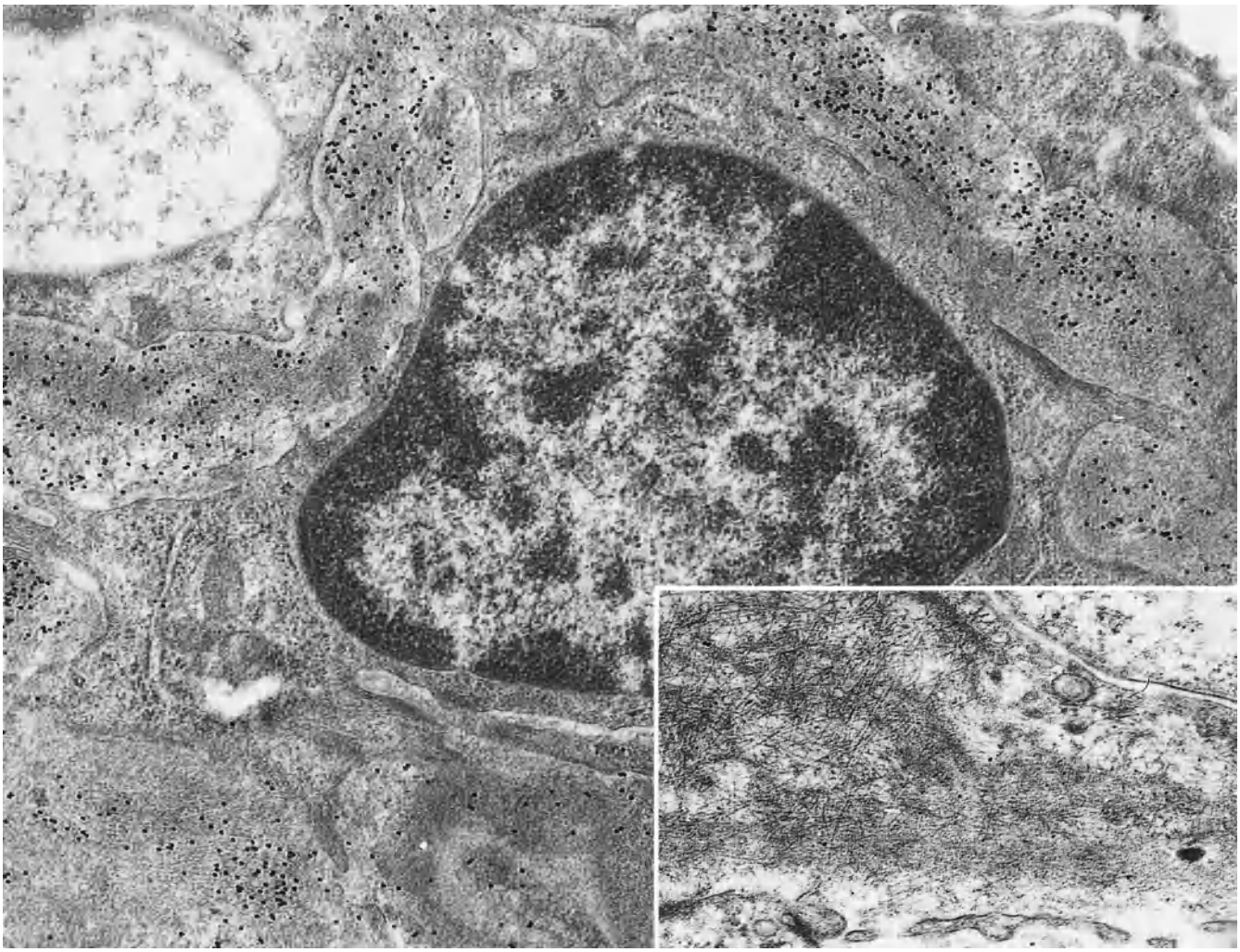


Fig. 26.3 Amyloid glomerulopathy: amyloid fibrils in the mesangial matrix labeled with immunogold using anti-A-lambda antibodies; kidney biopsy, 69-yr-old male with multiple myeloma and nephrotic syndrome. The peripheral capillary has fibrils along its inner and outer contours. *Inset*: absence of reaction on the same biopsy tissue stained with anti-AA antibodies. (Micrograph: Ugo Donini, *J Hist Cyt* 37:1101, 1989.)

formed of polyclonal IgG and C3 that binds amyloid P component.[18] This suggests that fibrils are immune deposits that have undergone fibrillogenesis, but not in a β-pleated sheet configuration that will bind Congo red. For diagnostic differentiation, note:

- **Hereditary fibrinogen amyloidosis** in humans is characterized by deposition of amyloid fibrils in renal glomeruli. The subunit of the amyloid fibrils is a proteolytic fragment of the fibrinogen α chain.[19]
- **Fibrillary glomerulopathy**, characterized by presence of amyloid-like fibrils in the glomerular basement membrane and mesangium, differs from renal amyloidosis in that fibrils are wider (mean diameter is 18–22 nm) than amyloid and do not bind Congo red.
- **Immunoglobulin light chain**-induced amyloidosis is associated with renal deposition of amyloid; it can be distinguished from SAA on the basis of ultrastructural analysis using immunogold techniques.

AL Amyloid: Plasmacytoma

AL protein is the precursor of amyloid light chains in plasmacytoma-associated amyloid, an amyloid that is predisposed to cardiac localization. It is produced by immunoglobulin-secreting cells, the prototype being the neoplastic plasmacyte found in patients with **multiple myeloma**. Amyloid fibrils composed of AL have been demonstrated ultrastructurally in lysosomes and Golgi complexes of human myeloma cells.[20] Immunolabeling of myeloma tissues shows that amyloid deposits are derived from light chains. Most AL proteins are composed of lambda light chains, but rare amyloids contain kappa chains. A model for AL amyloid has been reported wherein mice are injected with Bence-Jones proteins to induce amyloid;[21] dehydration accelerated amyloid deposition.

Myeloma light chains are released into tissues and then into lymphatics and bloodstream. They are shed in urine as Bence-Jones proteins, and fibrillar precipitates with the ultrastructure of amyloid fibrils have been produce by proteolytic digestion of Bence-Jones proteins purified from urine.

Although most AL proteins polymerize into amyloid in tissue spaces, AL chains can also polymerize within the rough endoplasmic reticulum of the neoplastic plasma cell. Fibrils are closely associated with one another and tend to be oriented parallel to the long axis of the organelle. Using immunoelectron microscopy with human AL antiserum, gold particles have been used to label these intracellular amyloid fibrils.[22]

Endocrine Polypeptide Amyloids

Islet Amyloid Polypeptide

Amyloid deposits in pancreatic islets represents a polymerized form of an islet β cell-derived protein. Called **islet amyloid polypeptide** (**IAPP**, amylin, diabetes-associated polypeptide), this peptide is cosecreted with insulin in response to glucose and other secretagogues. IAPP-induced amyloid occurs in more than 90% of humans with type 2 diabetes and in more than 80% of cats with a similar form of age-associated diabetes.[23] IAPP, a component of pancreatic islet beta-cell secretory granules, is a 37-amino-acid molecule that has been purified from islet amyloid of human insulinomas and pancreases of diabetic cats. Amyloid fibrils in this islet amyloid react strongly with reagents that immunologically label IAPP. Structurally similar to calcitonin gene-related peptide, IAPP is expressed during early development in the fetus and occurs in hyperplasia and neoplasia.[24] Extracellular IAPP oligomers are toxic to pancreatic beta-cells and may induce apoptosis. Endoplasmic reticulum stress responses are cellular signaling mechanisms that impair the ubiquitin-proteasome pathway that is associated with apoptosis.[25] In vitro, cell viability improves when a proteasome activator is added to the system. Ultrastructural changes in a rat model (transfected with the human IAPP gene) are similar to the human disease.[26]

Loss of β-cell mass and accumulation of islet amyloid are related processes. IAPP is a normal product of β-cells and is copackaged and cosecreted in a soluble form with insulin (function is not known). Intracellular amyloidogenesis occurs when normal trafficking mechanisms are impaired. Intracellular amyloid may be cytotoxic.

Transthyretin-Associated Amyloid

Senile systemic amyloidosis is caused by deposition of **transthyretin (TTR)**-containing fibrils. TTR fibrils are deposited in cardiac tissue in natural aging, and inherited mutations lead to amyloidosis by accelerating TTR deposition and disrupting its quaternary structure. The most common form of hereditary cardiac amyloidosis is associated with the Val122Ile variant of transthyretin (TTR). Amyloid deposits from apolipoprotein A have been seen in patients with TTR amyloidosis.[27] **Neuropathy** is a major manifestation of systemic amyloidosis in humans that is most often seen in patients with hereditary transthyretin amyloidosis; it also occurs in patients with systemic immunoglobulin light chain amyloidosis.

Familial amyloidotic polyneuropathy is a group of lethal heredofamilial amyloidoses of middle aged

adults transmitted by an autosomal dominant trait. Clinically, these syndromes occur in four types (I–IV). The amyloid precursor protein in types I and II is immunogically related to **transthyretin**, and the deposits of amyloid consist of variant transthyretin molecules. The N-terminus of a mutant form of **apolipoprotein AI** (apoAI) is the subunit protein of amyloid fibrils in type III, and in pulmonary vascular amyloidosis in aged dogs. Introducing the gene for the mutant transthyretin into transgenic mice causes deposition of amyloid composed of human mutant transthyretin (with mouse serum amyloid P component).[28]

Gelsolin-Associated Amyloid

The amyloid fibril protein in familial amyloidotic polyneuropathy **type IV** (Finnish) is a fragment of **gelsolin**, a cytoskeletal and plasma protein actin-binding molecule. The amyloidogenicity of gelsolin is due to a point mutation in the gelsolin gene that results in a variant gelsolin molecule with an asparagine-for-aspartic acid substitution at position 187.[29] Affected patients typically develop corneal lattice dystrophy by 20 years of age and by 40 years most have cranial neuropathy. This differs from the lower limb polyneuropathy of type I and the cardiomyopathy of type II syndromes.

Calcitonin-Associated Amyloid

Calcitonin, a polypeptide hormone of calcium metabolism in bone, has propensities for amyloid fibrillation, and has been identified as causal in human amyloidosis. In vitro, calcitonin forms annular oligomers similar to those seen for βAP and α-synuclein. Studies using immunogold labeling revealed that annular forms of calcitonin (with amyloid characteristics) embed in membranes in areas of lipid rafts and are associated with altered Ca^{++} flow.[30]

Plasma Protein-Derived Amyloidosis

The rare, non-neuropathic human amyloidoses include amyloid fibrils formed from **lysozyme**, **fibrinogen alpha-chain**, and **apolipoprotein A-I and A-II**. Human **lysozyme** variants form amyloid fibrils in patients suffering from a familial non-neuropathic systemic amyloidosis and have a highly variable clinical spectrum; the renal disease is often diagnosed as light chain amyloidosis.

The presence of the human **ApoE gene** on chromosome 19 is closely linked to the development of late-onset Alzheimer's disease, the form that begins after age 65 and makes up more than 75% of all cases. The β-amyloid gene on chromosome 21 and another unidentified gene on chromosome 14 are linked to the rare inherited, early onset forms of Alzheimer's disease. In mouse strains with the amyloidogenic apolipoprotein A-II gene (Apoa2c), the APOAIIC protein associates to form amyloid fibrils that lead to development of early onset and systemic amyloidosis.[31]

Glucagon-Associated Amyloid

The peptide hormone glucagon fibrillates to form amyloid. Some therapeutic peptides show amyloidogenic properties that lead to insolubility and cytotoxicity against neurons in vitro. For example, inappropriate preparations of therapeutic glucagon can cause undesirable products that induce amyloidosis.[32]

Beta Amyloid Protein

Amyloid in the aging brain and in neuritic plaques of Alzheimer's disease is composed of a unique protein, **beta amyloid protein (βAP)**. βAP has been localized in the neuron.[33] Neuronal toxicity of **βAP toxicity** is due both to its β-pleated sheet fibrillar structure and to its surface physicochemical composition.[34] Studies in vitro also suggest that βAP is directly toxic to neurons; that is, it causes (and is not the result of) neuronal degeneration. Some studies suggest that βAP may be indirectly toxic to neurons by making them more susceptible to **excitotoxins** (critics suggest that lesions caused by βAP injection into rat brains are injection artifacts). An alternate hypothesis is that β-amyloid deposition occurs after neuronal degeneration, and that neurons increase βAP production in an effort to compensate for neuron loss (or that neurons that fail to maintain their connections degenerate and lead to the release of the large precursor molecule). Microglia phagocytize βAP fibrils.[35]

Beta Amyloid Precursor Protein

βAP is synthesized as part of a larger precursor protein called **beta amyloid precursor protein (βAPP)**, a protein localized in senile plaques by immunolabeling techniques.[36] βAPP is an integral membrane glycoprotein with a critical function in the normal brain. It is transported down neuronal axons by fast transport and is associated with maintaining connections between nerve cells (perhaps as an adhesion molecule) at nerve termini by being inserted into plasma membranes. Several forms of βAPP have been differentiated chemically, each differentiated by the inclusion of a protease inhibitor insert.

βAPP is widely made in neurons (throughout the phylogenetic scale) and is embedded in plasma

membranes with a short segment on the carboxy end in the cytoplasm with most of the molecule protruding outside the cell. Normally, the outer part of the molecule is cleaved by an enzyme called **βAPP secretase** and is moved to the cell surface, where it is secreted from the cell. When there is a mutation in the βAPP molecule or in βAPP secretase, βAPP may be cleaved abnormally into amyloidogenic fragments. These abnormal βAPP fragments are moved to lyosomes where they either release or re-form into **β-amyloid**. Immunoelectron microscopic techniques have localized βAPP fragments and intact βAPP in lysosomes of neurons.[37] Direct sequencing of DNA from a patients with hereditary Alzheimer's disease has shown a single amino acid substitution (phenylalanine for valine) in the transmembrane domain of βAPP.

Pathogenesis of Beta Amyloidosis

Presenilins and Calcium Homeostasis Mutations in **presenilins 1** and **2** are associated with AD in which they contribute to amyloid in the brain by clipping out of the larger βAPP. In the neuronal plasma membrane, presenilins and βAP are colocalized within discrete microdomains in AD patients and in aged dogs. βAP results from misprocessing of βAPP by gamma-secretase (PS1) in these discrete plasma membrane domains. Based on immunogold labeling studies on brains of aged dogs and in humans with AD, colocalization does occur in discrete microdomains of neuronal plasma membranes.[38,39] Presenilins disrupt calcium hemeostasis in neurons. **Calcium overload** is involved in neuronal death in AD, and may underlie the toxic effects of βAP. βAP clearly causes an increase in **calcium** in neurons in vitro, and neuronal death in vivo may be caused by increased intracellular calcium, an event that causes hyperphosphorylation of tau, which, in turn, leads to formation of PHF. βAP may increase calcium entry by altering activity of receptors associated with neurotransmitters.

Mitochondriopathy in AD Mitochondrial dysfunction and autophagy are major cellular lesions of AD.[40] Ultrastructural morphometry of mitochondria in AD brains revealed decrease size and number as well as cristolysis and accumulation of osmiophilic material in the mitochondrial matrix.[41] The critical lesion appears to be the accumulation of amyloid precursor proteins across **mitochondrial import channels** that causes the hallmark mitochondrial injury in AD.[42,43] Examination of global gene expression in APP transgenic mice found elevated expression of mitochondrial genes, which suggested a compensatory response due to oxidative damage caused by overexpression of APP or βAP.[44]

βAP and Oxidative Stress βAP-induced free radical oxidative stress in **mitochondria** causes neurodegeneration in the Alzheimer's brain. Oxidative stress, manifested by protein oxidation, lipid peroxidation, DNA oxidation and nitrotyrosine formation are all observed in AD neurons. This theory implies that mitochondria generate (and are targets of) free radical damage; that is, that ROS generated in mitochondria because of βAP act as signals that trigger both mitochondrial and extra-mitochondrial signals for **apoptosis**.[45]

Loss of **neuron ionic balance** is thought to arise from βAP-mediated oxidative stress. An alternative proposal is that AD is mediated by **βAP ion channels** composed of βAP oligomers that cause neuronal leakiness by insertion as channels into the plasma membrane. Amyloid channels cause cytotoxicity by altering ion flow.[46] Put another way, there is evidence that in humans (and rat models) hypoperfusion-induced oxidative stress and mitochondrial failure initiate neuronal death in AD.[47–49]

Contaminating Proteins Aggregation of βAP leads to recruitment of other proteins into the aggregate. **Antichymotrypsin (ACT)**, a non-fibril-forming protein, is typically present in the βAP plaques of AD. In **Alzheimer's disease**, the serine protease activity of ACT may in some way enhance the local deposition of amyloid. A local excess of this enzyme might prevent a normal brain protease from clearing abnormal cleavage products of the precursors.[50] There is also evidence that antichymotrypsin interacts with a fibrillogenic apolipoprotein to accelerate amyloid fibril formation.[51]

The *βAAP* Gene

The gene for **βAAP** is on human chromosome 21, near a region that contains a gene for the hereditary form of Alzheimer's disease. The *βAAP* gene undergoes alternative splicing to generate several isoforms that are designated by the total number of amino acids in each.[52] A specific defect has been found in some cases of familial Alzheimer's disease, a mutation on chromosome 21 in the gene encoding βAPP. The mutation involves a single nucleotide change from C to T at base pair 2149 in exon 17, which results in a substitution of an isoleucine for a valine at codon 717. Similar mutations have also been identified.

Trisomy of chromosome 21, which causes **Down syndrome,** represents another route to the Alzheimer's disease phenotype. Down syndrome patients develop cerebral amyloid,[53] and have an extra copy of chromosome 21 (and thus of the β-amyloid gene). In the trisomy 16 mouse, a model for Down syndrome, βAAP gene expression varies from tissue to tissue, and as a function of development.

Amyloid in Alzheimer's Disease

Human **Alzheimer's disease (AD)** is characterized by neurofibrillary tangles and deposition of amyloid β (Aβ) in the form of neuritic plaques and congophilic angiopathy (Fig. 26.4). Three human genes have been linked to early onset AD, including the gene for **β-amyloid precursor protein** (βAPP) on chromosome 21, **presenilin** (PS)-1 on chromosome 14, and **PS-2** on chromosome 1. Most early onset AD is related to mutations in PS-1 and PS-2, and over 35 mutations have been reported in these genes in familial early onset AD. The PS-1 gene encodes a protein in normal neurons, preferentially concentrating in the cytoplasm and dendrites. PS-1 undergoes endoproteolytic cleavage to at least 2 major fragments.

Amorphous, largely nonfibrillar deposits of βAP precede the appearance of altered neurites and glia as neuritic plaques develop,[54] suggesting that the accumulation of amyloid fragments **within the neuron** initiates the process of Alzheimer's disease; that is, that the neurofibrillary tangles, neuron loss, and vascular damage are a direct result of amyloid deposition.

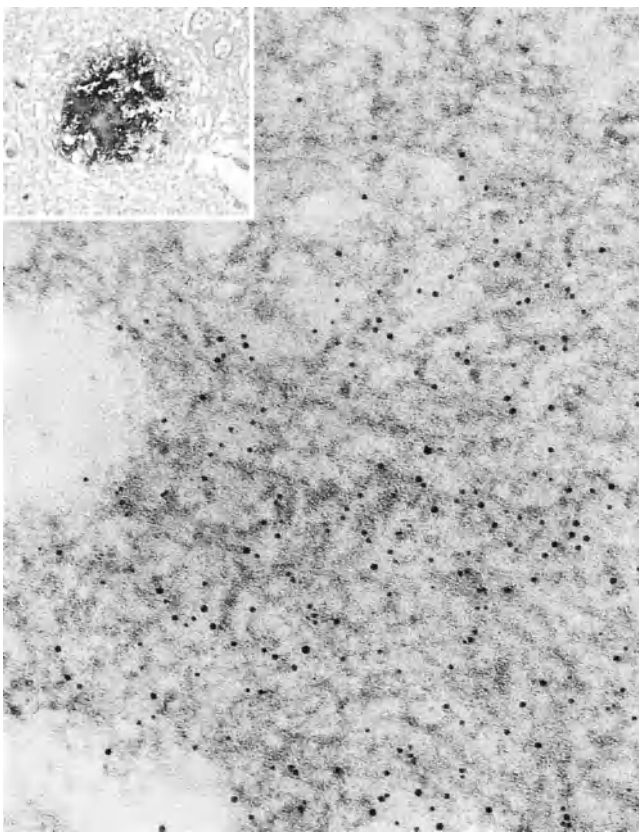


Fig. 26.4 Amyloid of Alzheimer's disease: immunogold staining of neuritic plaque amyloid. Labeling of amyloid fibrils. *Inset*: light micrograph of neuritic plaque stained with immunoperoxidase. (Micrograph: Shu-Ichi Ikeda, *Lab Invest* 57:446, 1987.)

Neuronal macroautophagy, the lysosomal pathway for turnover of organelles and long-lived proteins (and a key determinant of cell survival and longevity) is abnormal in Alzheimer's disease; it is induced early, before β-amyloid deposits appear extracellularly.[55] Immunolabeling identifies **autophagic vacuoles** in the brain as a major reservoir of intracellular β-amyloid. Autophagosomes accumulate in dystrophic dendrites, implying that there is impaired maturation of autophagosomes to lysosomes.

Amyloid Angiopathy

Cerebrovascular amyloidosis occurs as part of Alzheimer's disease; it may also arise as a sporadic idiopathic disorder, either in association with an autosomal dominant form of amyloidosis (Dutch type) or in the area of a cerebrovascular malformation. Deposition of β-amyloid fibrils in the walls of blood vessels is also found in aged monkeys and dogs,[56] and has been produced experimentally in rodents.[57]

In human **amyloid angiopathy**, amyloid fibrils form in both leptomeningeal arteries and intracortical arterioles and capillaries. Vascular amyloid first develops within the ablumenal vascular basement membrane. In the neuropil, microglia and macrophages are associated with amyloid deposits. Small focal amyloid deposits in leptomeningeal arterioles consist of clusters of small 8 nm diameter amyloid fibrils in the outer basement membrane at the media-adventitia junctions.[58] In capillaries, the fibrils are within the abnormally folded and layered basement membanes; they extend out into the neuropil and are surrounded by astrocytic foot processes.

Ultrastructural studies on the brains of Alzheimer's disease patients show that vascular amyloid production occurs adjacent to pericytes and perivascular microglia. Within the vessel wall, semicircular thickening with deposits of amyloid fibrils occurs. Tuberous amyloid deposits contain both amyloid fibrils and amorphous material, and these deposits are found in infoldings of the plasma membranes of perivascular microglia. **Amyloid stars**, composed of radially arranged bundles of amyloid fibrils, occur in human tissue (Fig. 26.5). Bundles of amyloid fibrils are found in cisternae of the endoplasmic reticulum and in channels confluent with the infoldings in the plasma membrane.[59]

Senile peripheral amyloid angiopathy of several forms has been reported, predominantly in the aorta and its branches, and in pulmonary and temporal arteries. The aortic media is a common site for senile amyloid deposition. In a study of 84 human aortas, amyloid was present in 97% of patients above 50 years of age.[60] **Medin amyloid** affects the medial layer of the

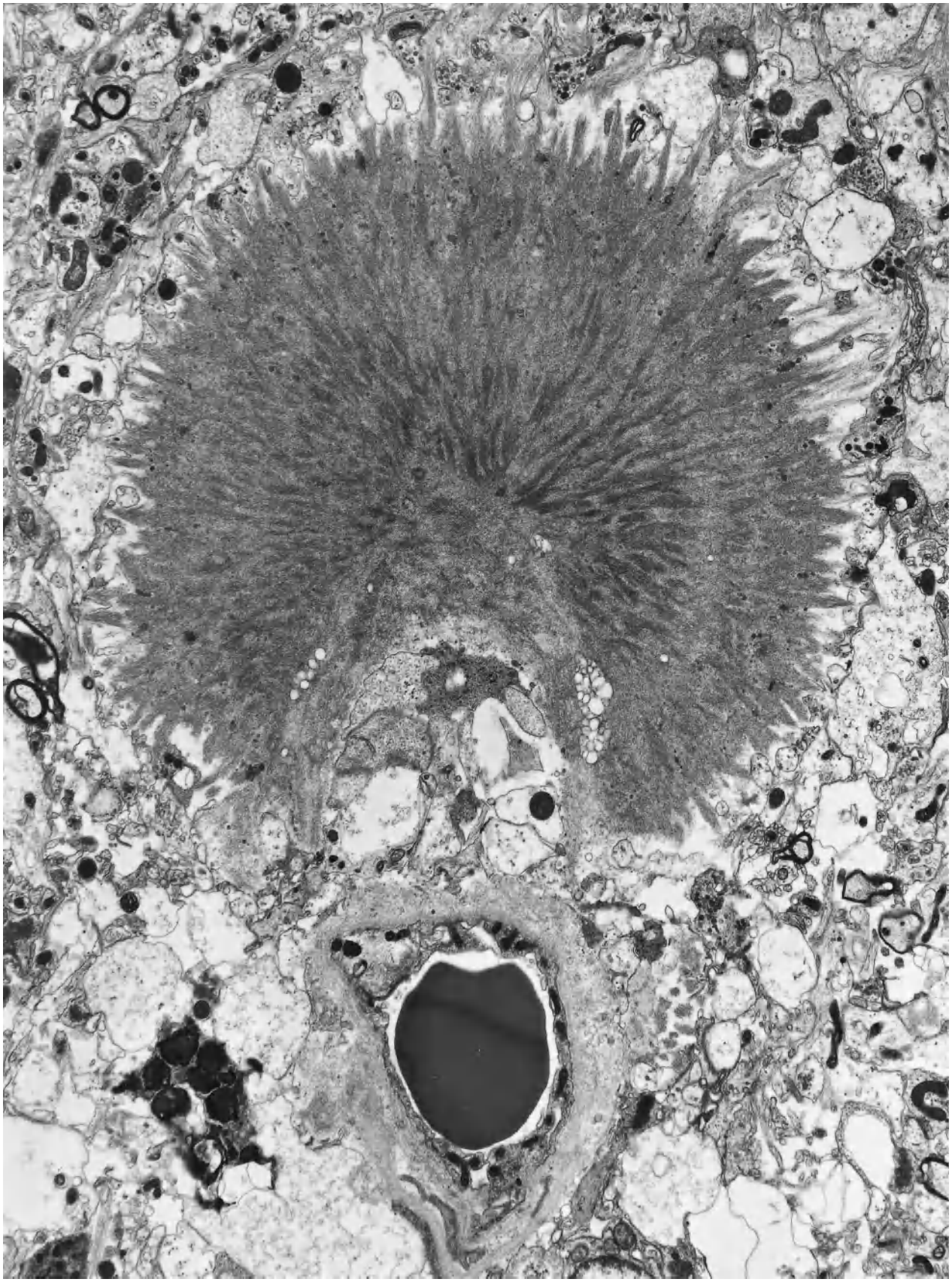


Fig. 26.5 Perivascular amyloid star: star is attached to an obliterated blood vessel. Note radial arrangement of bundles of amyloid fibrils in the star, striatal distribution of amyloid fibrils where they infiltrate basal laminae, and mantle of astrocytic processes around the star. The second blood vessel shows only minimal amyloid fibril infiltrations. (Micrograph: H. M. Wisniewski, *Acta Neuropathol* 84:117, 1992.)

thoracic aorta of humans, especially after the age of 50 years where it contributes to aneurysm development. The 50-amino acid residue peptide medin forms amyloid-like fibrils in vitro.[61]

Amyloid of Prion Diseases

Amyloid plaques are present in scrapie of sheep,[62] and in the human diseases of kuru, Gerstmann-Sträussler-Scheinker disease, and in some 10–15% of Creutzfeldt-Jakob disease patients. Conversion of the α-helical, cellular isoform of the prion protein PrP^{c} to the insoluble β-sheet-rich, disease-causing isoform PrP^{Sc} is a key event in prion disease (see chapter 30).[63] In amyloid of prion diseases, PrP-conjugated gold particles stain areas of low electron density that contain randomally oriented fibrils.[64] The florid or "daisy" plaque of variant **Creutzfeldt-Jakob disease** is seen in all cases. Unicentric **kuru** plaques consist of stars, stellate arrangement of amyloid bundles eminating from a dense interwoven center. **Gerstmann-Sträussler-Scheinker syndrome** is a familial amyloidosis with deposits in the brain that contain prion proteins. Amyloid fibrils in GSS are composed of a fragment of the prion protein PrP, and the cerebral accumulation of abnormally folded PrP fragments controls the pathogenic process of GSS.[65,66]

Tauopathies

Tauopathies are neurodegenerative diseases characterized by the presence of filamentous aggregates in neurons and glia that are composed of abnormally hyperphosphorylated forms of the microtubule-associated protein **tau**. Tau protein binds to and regulates the stability of microtubules in axoplasmic transport and axonal differentiation. Hyperphosphorylated tau is the major constituent of the **paired helical filaments (PHFs)** that surround or displace the nucleus in neurons of Alzheimer's disease patients.

The accepted model of **paired helical filament** structure is that of two 8–10 nm filaments each composed of three C-shaped protofilaments wound into a helix with a maximal diameter of ~20 nm and a half-period of 65–80 nm. Atomic force microscopy studies suggest that assembly of PHF is due to a helical winding of self-associated tau molecules arranged into a flattened structure, not to the twisting of pairwise filaments.[3]

Tau is abnormally phosphorylated, probably by the enzyme casein kinase II. Abnormal forms of **tau** have been labeled ultrastructurally by immunogold techniques.[67,68] Tauopathies include **AD**, **Pick's disease**, **progressive supranuclear palsy**, and **corticobasal degeneration**. Transgenic mice bearing mutated human tau develop aggregates tau.[69]

Alzheimer's Disease

Alzheimer's disease is a progressive dementia that arises from cortical atrophy, which is most pronounced in the frontotemporal and parietal lobes of the brain. Neuronal necrosis is prominent, but astrocyte degeneration, oligodendrocyte loss, and vascular lesions are significant changes.[70,71] The major microscopic lesions in the cerebral cortex of human Alzheimer's disease patients are

- **Neurofibrillary tangles**, collections of paired helical filaments that develop within damaged neurons
- **Neuritic (senile) plaques**, degenerate neuritic processes surrounding an amyloid core
- **Amyloidotic angiopathic lesions**, deposits of amyloid in small vessels of the brain.

All the above changes can occur to less degree in brains of aged patients that do not have Alzheimer's disease. The presence of granulovacuolar degeneration and Hirano bodies are also helpful in the microscopic diagnoses of Alzheimer's disease. **Granulovacuolar degeneration** is the formation of small 5 μm clear intraneuronal cytoplasmic vacuoles that contain argyrophilic granules. **Hirano bodies** are glassy eosinophilic inclusions in proximal dendrites that are composed of regular arrays of beaded actin filaments.

Neurofibrillary tangles are perikaryonal masses of **paired helical filaments** that surround or displace the nucleus in neurons. They are prominent in pyramidal neurons of the neocortex, hippocampus, and basal ganglia of Alzheimer's disease patients. PHFs are insoluble fibers composed of two helically wound 7–10 nm filaments with 80–100 nm half-periodicity.[72–74] Neurons containing neurofibrillary tangles degenerate and die, although they tend to persist as ghost tangles after death of the neuron.[75] Damaged **neurofilaments** are also found in neurofibrillary tangles. Moderately basophilic on hematoxylin-eosin staining, neurofibrillary tangles stain heavily with silver impregnation techniques. Although neurofibrillary tangles are not restricted to Alzheimer's disease, their number correlates with the severity of Alzheimer's dementia. PHFs also occur in neurites surrounding amyloid-rich senile plaque cores. **Beta amyloid** can be stained in neurofibrillary tangles and blood vessels by monoclonal antibodies.

Neuritic plaques are focal, 10–200 μm diameter collections of **dystrophic neurites** that surround an **amyloid core**.[76,77] In early plaques, amyloid fibrils are

first found between cell processes.[78] Altered neurites contain densely packed bundles of PHF or straight neurofilaments that accumulate progressively to expand neuronal processes. Ultrastructurally, these abnormal neurites are referred to as **neuropil threads**, or curly fibers.[79] Abnormal glial processes are a minor component of neuritic plaques. The amorphous component of amyloid in diffuse plaques, the carbohydrate-rich matrix and vesicles of 40–80 nm diameter, are thought to be derived from local neurons.[80] Perturbed vascular transport and/or perivascular enrichment of Aβ leads to formation of vasocentric dense plaques.[81]

Pick's Disease

Pick's disease is a progressive senile dementia that closely resembles Alzheimer's disease clinically. The brain has severe, asymmetric atrophy of frontal and temporal lobes. Affected neurons are distinguished by ballooned and swollen chromatolytic, irregular neurons with argentophile inclusions called **Pick bodies**. Neuronal inclusions are composed of 10–20 nm straight filaments mixed with cytoplasmic structures. Filaments contain the same neurofilament and microtubule epitopes that occur in the paired helical filaments of Alzheimer's disease neurofibrillary tangles.[82–86]

Frontotemporal Dementias

The **frontotemporal dementias** group together a clinical, genetic, and neuropathologically heterogenous group of diseases that account for nearly 20% of presenile dementia cases. **Frontotemporal lobar degeneration with ubiquitin inclusions** (ubiquitin-positive, tau-negative inclusions) is the most common underlying pathology. TAR DNA-binding protein-43 (TDP-43), a nuclear protein implicated in exon skipping and transcription regulation, is a major component of the ubiquitin immunoreactive inclusions (as well as in sporadic ALS).[87]

Synucleinopathies

The **α-synucleinopathies** are characterized by the presence of inclusions composed of fibrils of **α-synuclein (α-syn)**. The group includes **Parkinson's disease (PD)**, **dementia with Lewy bodies**, and **multiple system atrophy**. A presynaptic terminal molecule, **α-syn** has been localized by immunogold techniques.[88] Aberrent accumulation of **α-syn** into insoluble aggregates is responsible for the cellular damage and neuronal dysfunction. Truncated forms of **α-syn** enhance cytotoxicity, and proteolytic cleavage has been attributed to **calpain-1**, a member of a large family of calcium-dependent proteases. Aggresomes are associated with the neurodegenerative changes in PD.

Mutations in the de-ubiquitylating enzyme **UCH-L1** cause a rare form of parkinsonism. In response to proteasomal inhibition, overexpression of UCH-L1 forms ribbon-like aggresomes surrounded by tubulin cage-like structures.[89] UCH-L1 aggresomes co-localize with ubiquitylated proteins, Hsp70, γ-tubulin, the chaperone BiP, and proteasomal proteins. Note also that the overexpression of **Parkin**, a ubiquitin-protein ligase associated with juvenile parkinsonism, generates aggresome-like inclusions surrounded by a vimentin cage-like structure in UPS compromised cells.

Lewy Body Disease

Lewy bodies are cytoplasmic intraneuronal inclusions invariably found in the substantia nigra of **Parkinsons's disease** patients, in **Lewy body disease**, and in a variety of other dementias. The primary structural components of Lewy bodies are fibrils composed of **α-synuclein (α-syn)**. These inclusions react with antibodies against neurofilaments, ubiquitin, gelsolin, and other proteins.[90] Ultrastructurally the mass of the inclusion is composed of altered neurofilaments,[91] and contain straight 7–20 nm filaments and amorphous elements. Biochemical evidence reveals the presence not only of neurofilaments but of microtubules, ubiquitin, and proteins with epitopes for paired helical filaments, thus suggesting a close relationship to the neurofibrillary tangles of Alzheimer's disease.[92]

Polyubiquitination of Lewy body proteins can trigger ubiquitin-proteosome proteolytic pathways. The incomplete activation of these paths may play a role in formation of Lewy body neurodegenerative disease.[93] **α-Synuclein** is a constituent of filamentous Lewy bodies and Lewy neuritis, and three missense mutations in the α-*syn* gene (as well as gene duplications or triplications) have been reported in familial forms of Parkinson's disease.

Sirtuins that function in aging play a role in PD. In vitro, drugs that inhibit the human **silent information regulator 2 (SIRT2)**, a histone deacetylase involved in cell cycle regulation via α-tubulin, p53, and histones H3 and H4, can promote α-synuclein toxicity and modify aggregation and inclusion morphology.[94]

Parkinson's Disease

Parkinson's disease is a disorder of motor function caused by loss of dopaminergic neurons and development of Lewy bodies composed of filamentous α-synuclein in the substantia nigra of the brain. Abnormal iron metabolism with increased intraneuronal iron has

been found in PD,[95] and is part of the neuromelanin-iron complex in dopaminergic neurons.[96,97]

PD is the most common neurodegenerative movement disorder of humans, and the prototype neuronal synucleinopathy. Variant parkinsonian syndromes that are neurologic diseases of the nigrostriatal system include idiopathic Parkinson's disease (paraylsis agitans), striatonigral degeneration, Shy-Drager syndrome, and progressive supranuclear palsy. Postencephalitic parkinsonism, now rare, was a common sequela of encephalitis that followed influenza; lesions included neurofibrillary tangles but not Lewy bodies.

Experimental models of PD include Zitter mutant rats, which have abnormal metabolism of superoxide species and develop progressive neurodegeneration and lipofuscin accumulation of dopamine neurons in the substantia nigra.[98] Environmental factors causing nitrative damage are linked to mechanisms for synucleinopathies. Transgenic mice bearing a mutant human *a-syn* gene develop markedly increased α-synuclein pathology when treated with paraquat and maneb (chronic treatment with both, but not singly) have marked increases in neuronal α-syn pathology.[99]

Huntington's Disease

Huntington's disease is a hereditary, progressive dementia inherited through an autosomal dominant manner from a gene on chromsome 4. Neurologic signs in **Huntington's disease** arise from the preferential loss of neurons in the striatum and cortex. The genetic mutation is an unstable CAG repeat in the gene that encodes **huntingtin**, and that results in a mutation that expands the NH2-terminal polyglutamine region. Extensive polyglutamine expansions in huntingtin are associated with severe disease. Aggregation of mutant huntingtin is responsible for nuclear inclusions in the brain. The finding of ubiquitin in inclusions indicates that abnormal huntingtin is a target for proteolytic destruction by ubiquitinization, but is resistant to removal.

In Huntington's disease, **aggresomes** accumulate when the ubiquitin-proteosome system fails. In vitro, ubiquitinated huntingtin exon 1 proteins with polyglutamine repeats in the pathologic range (51 or 83 glutamates) form perinuclear aggresomes with a characteristic morphology; they develop at centrosomes and are surrounded by vimentin filaments.[100] These inclusions are immunolabeled for proteosomal components, chaperones (BiP, GRP78, Hsp 40 and 70), and alpha-synuclein. Aggresomes are accompanied by striking ultrastructural changes in the nuclear envelope, cytoplasmic vacuolation, and concentration of mitochondria at the inclusion periphery. **Mitochondriopathy** in HD is associated with calcium loading. Mutant huntingtin expression leads to cardiotoxic effects with marked changes in mitochondria in cardiac myocytes;[101] immunogold electron microscopy detected marked elevations in nuclear and mitochondrial polyglutamine. In neurons, many proteins are palmitoylated posttranslationally, a modification that increases hydrophobicity of the protein, thereby facilitating interaction with lipid bilayers. The process is deficient with huntingtin.[102]

Amyotrophic Lateral Sclerosis

Amyotrophic lateral sclerosis (ALS) is a chronic, incurable disease that is manifest as motor neuron loss and its attendent paralysis and muscular atrophy. Some classifications have included ALS, progressive bulbar palsy, progressive muscular atrophy, and primary lateral sclerosis as an ALS disease complex. Lesions in ALS are primarily necrosis of neurons; neuronophagia is prominant and remaining neurons have a shrunken appearance.

Mitochondria have an intrinsic defect in ALS. Mitochondria in 7 of 14 ALS brains examined ultrastructurally had neurons with intramitochondrial filamentous structures composed of stacks of multilayered cristae.[103] **Neuronal cytoplasmic inclusions** in ALS are immunoreactive to ubiquitin, proteasome, and ataxin, but not to tau, neurofilaments, SOD, polyglutamine, or α-synuclein.[104–106] In muscle of ALS patients, mitochondria have lower activity of complex I of the mitochondrial respiratory chain.[107]

Missense mutations in **Cu/Zn superoxide dismutase** (SOD1) are the cause of up to 20% of familial ALS cases. In transgenic mice expressing ALS-linked mutations, selective motor neuron degeneration arises from toxic properties of aggregates of the mutant enzymes. Studies here suggest that aggregates of SOD1 were common to disease caused by different mutants, implying that coaggregation of an essential component or aberrant catalysis by misfolded mutants underlies mutant-mediated toxicity.[108,109]

Fragmentation and atrophy of the **Golgi complex** of motor neurons has been reported as an early change in ALS.[110.111] The defect was not associated with abnormalities in the cytoskeleton (a common cause of primary Golgi injury) but defects in proteins involved in attachment of Golgi membranes to the cytoskeleton were not ruled out. Much of what we know of the Golgi complex comes from studies on poisons that specifically damage this structure.

Transgenic mice expressing mutant Cu,Zn SOD develop disease of motor neurons. Earliest change was vesiculation (arising from RER and mitochondria) of large neurons. Terminally, there is severe neuronal depletion and hyaline filamentous inclusions in surviving neurons.

Rosenthal Fibers

Rosenthal fibers are opaque, carrot-shaped or beaded inclusions within reactive and neoplastic astrocytes. They are present in large numbers in Alexander's disease, in the chronic stages of reactive gliosis, and in astrocytomas of the the pilocytic type.[112] Ultrastructurally, Rosenthal fibers are irregular, electron-dense and amorphous with distinct margins, and are associated with meshes of intermediate filaments and polyubiquinated **αβ-crystallin**. αβ-Crystallin, the major component, is a protein of the vertebrate eye; it appears to be stress induced.[113] Rosenthal fibers also cross-react with ubiquitin and glial fibrillar protein, but not with vimentin.[114]

Misfolded Proteins and Inspissated Inclusions

Protein Filaments of Aging

Aging is accompanied by aberrant polymerization and accumulation of proteins into inclusions. In some cases, proteins polymerize into rigid, highly insoluble filaments in which specific amino acids are cross-linked by unusual covalent bonding of glutamyl-lysine side chains (Fig. 26.6). The enzyme **transglutaminase** is activated by the rising Ca^{++} concentrations in degenerating cells and promotes polymerization of normal peptide chains. In the brain, filamentous cytoplasmic inclusions such as Lewy bodies, Pick bodies, and Rosenthal fibers develop in neurons and glia. They are composed of various filaments whose component proteins have been **ubiquitinated** during the process of denaturation; that is, the stress protein ubiquitin has bound to the abnormal protein to facilitate its sequestration in the cytoplasm.[115–118] Amyloid is an incidental finding in the brain of aged humans,[119] and in several animal species. In aged dogs, monkeys and other animals, amyloid has been defined around cortical and leptomeningeal blood vessels.[120,121]

The Ubiuitin-Proteosome System

Misfolded or denatured proteins are removed from the cell by the **ubiquitin-proteosome system** for peptide degradation. Overload, dysfunction, or failure of this system results in inclusions of aggregated, ubiquitinated proteins. Whatever the cause, most misfolded proteins aggregate into ubiquitin-rich cytoplasmic inclusions called **aggresomes**.[122] The process of protein aggregation, the hallmark of inclusion body disorders, can itself impair an overloaded ubiquitin-proteasome system, and lead secondarily to cellular damage.

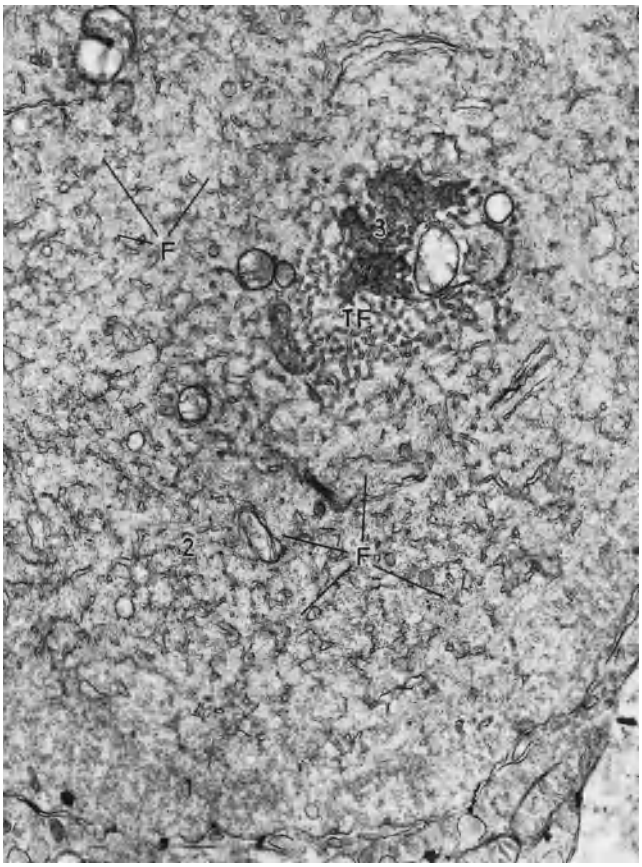


Fig. 26.6 Herring body, pituitary: Granular matrix in the outermost zone (*1*), crossing bundles of neurofilaments (*F*) in the middle zone, and dense system of tubular formations (*TF*) in the most central zone (*3*). (Micrograph: H-Dieter Dellmann, *Z Zellforsch Mikrosk Anat* 111:235, 1970.)

Misfolded proteins up-regulate **heat shock proteins (HSPs)** as a means to facilitate refolding and to prevent aggregation. HSPs help ubiquitinate and target nonrepairable proteins to the **proteasome**. Proteasome impairment is linked to formation of inclusions in neurodegenerative disorders (including Alzheimer's disease and Parkinson's disease). HSPs can also be induced by proteasome inhibitors. HSp90 is an abundant molecular chaperone that prevents protein aggregation; it can do so alone, or with other chaperones, such as Hsp70.

Aggregation and polymerization of abnormal proteins can lead to the massive accumulation of proteins in the cell. Injury to transcription in the nucleolus leads to **nuclear matrix** inclusions, and injury to ribosomal translation leads to inclusions in the **endoplasmic reticulum**. Fibrillar proteins are prone to lattice formation, but globular proteins such as hemoglobin and globulins are not. The location and character of a protein inclusion are determined by the site in the synthetic pathway that is damaged. Many proteins,

depending on peptide chain structure and folding, interact to form parallel **lamellae** or **lattice crystals**.

Inclusions in Endoplasmic Reticulum

Inspissated secretory proteins are common in **cisternae of the rough endoplasmic reticulum (RER)**. Protein producing cells, when blocked by the appropriate toxin or genetic message, develop aggregates of filamentous or granular proteins within the RER (Table 26.2). For example, **hepatocytes** when stimulated by macrophage cytokines (during inflammation) will produce large amounts of albumin or acute phase proteins. If secretion is blocked these proteins become visible as large vacuoles containing precipitates of protein (Fig. 26.7). If the block is in the **Golgi complex**, protein appears in Golgi saccules and is also apt to back up in the endoplasmic reticulum. If the block is in exocytosis, protein occurs in the Golgi complex and in its vacuoles or granules.

Premature condensation of proteins occurs in RER cisternae when the rate of export fails to keep pace with the rate of synthesis. Both endocrine and

Table 26.2 Protein intracellular inclusions.

Type (location)	*Chief component*	*Reference to ultrastructural pathology*
α1-antitrypsin	α1-antitrypsin	**Feldman**, *Gastroenterology* 67:1214, 1974 (liver)
Asteroid bodies	Vimentin	**Cain**, *Virch Arch B* 26:219, 1977; 42:213, 1983
Bunina bodies (neuron, ALS)		**Nakano**, *Acta Neuropathol* 79:689, 1990; **Tomonaga**, *Acta Neuropathol* 42:81, 1978
Corpora amylacea (astrocyte)	Glycosaminoglycan	**Auerback**, *Arch Neurol* 35:95,1978; **Ramsey**, *J Neuropath Exp Neurol* 24:29, 1965
Crooke bodies (pituicyte)	Cytokeratin	**Neuman**, *Am J Pathol* 116:214, 1984
Councilman bodies (liver)	Viral debris	
Hematoxylin bodies (kidney)	Nuclear debris	**Morita**, *Ultrastr Pathol* 7:13, 1984
Herring bodies (pitutary)	Neurosecretory granules	**Dellman**, *Z Zellforsch Mikrosk Anat* 111:293, 1970
Hirano bodies (neuron)	Actin, α-actinin	**Galloway**, *J Neuropathol Exp Neurol* 46:185, 1987; **Gibson**, *Acta Neuropatol* 42:165, 1978; **Hirano**, *J Neuropathol Exp Neurol* 327:167, 1968; **Mori**, *Acta Neuropathol* 71:32, 1986; **Schochet**, *Acta Neuropathol* 21:50, 1972; **Yamamoto**, *Acta Neuropathol* 67:167, 1985
Hyalin bodies (hepatocyte)	Fibrinogen	**Feldman**, *J Cell Biol* 67:237, 1975; **Pfeifer**, *Virch Arch* B 16:141, 1974; **Pfeifer**, *Virch Arch* B 36:247, 1981
	α1-antitrypsin	**Feldman**, *Gastroenterology* 67:1214, 1974; **Yunis**, *Am J Pathol* 82:265, 1976
	Globulin	**Stoebner**, *Am J Clin Pathol* 71:404, 1979 (human cryoglobulins); **Schweitzer**, *J Cell Biol* 114:35, 1991 (mouse)
Kurloff bodies (monocyte)	Serum proteins	
Lafora bodies (neuron)	Human	**O'Shea**, *Pediatr Dev Pathol* [E-pub], 2007; **Vanderhaeghen**, *Acta Neuropathol* 17:24, 1971 (human); **Wilson**, *Acta Neuropathol* 102:505, 2001
	Dog	**Holland**, *Am J Pathol* 58:509,1970 (dog); **Suzuki**, *Acta Neuropathol* 48:77, 1979 (dog)
Lewy bodies	Neurofilaments, MAPs	**Dickson**, *Acta Neuropathol* 78:572, 1989; **Galloway**, *Am J Pathol* 140:809, 1992; **Kosak**, *Acta Neuropathol* 42:127, 1978; **Kuzuhara**, *Acta Neuropathol* 75:348, 1988; **Murayama**, *Acta Neuropathol* 78:143, 1989 (ALS); **Wakabayashi**, *Acta Neuropathol* 76:217, 1988; **Wisniewski**, *Am J Pathol* 138:1077, 1991
Mallory bodies: alcoholic hyalin (hepatocyte)	Cytokeratin ubiquitin	**Akeda**, *Lab Invest* 54:228, 1986 (mouse);† **Denk**, *Lab Invest* 36:563, 1977 (colchicine, mouse);† **Franke**, *Biol Cellulaire* 34:99,1979 (human); **Franke**, *Lab Invest* 40:207, 1979 (mouse);† **Hazan**, *Lab Invest* 54:543, 1986; **Irie**, *Lab Invest* 50:303, 1984; **Irie**, *Lab Invest* 47:336, 1982 (mouse);† **Kachi**, Lab Invest 68:71, 1993;* **Kimoff**, *Lab Invest* 45:491, 1981; **Meierhenry**, *Lab Invest* 44:392, 1981 (mouse);† **Ohta**, *Lab Invest* 59:848, 1988; **Okanoue**, *Lab Invest* 53:534, 1985; **Rumpelt**, *Virch Arch B* 23:339, 1977; **Wiggers**, *Lab Invest* 29:652, 1973

Table 26.2 *Continued*

Type (location)	*Chief component*	*Reference to ultrastructural pathology*
Marchal bodies (skin)	Poxvirus	
Michaelis-Guttmann bodies (malakoplakia)	Calcium, phosphorus	**Underwood**, *J Pathol* 138:41, 1982 (human)
Mott bodies (plasmacyte)	Immunoglobulin	**Kodama**, *Vet Clin Pathol* 37:409, 2008 (dog)
Negri bodies (neuron)	Viral proteins	**Nietfield**, *J Vet Diag Invest* 1:333, 1989 (dog)
Nemalin bodies (myocyte)	F-actin, α-actinin	**Munnell**, *Lab Invest* 19:303, 1968 (dog)
Paschen bodies (skin)	Poxviruses (smallpox)	
Pick bodies (neuron)	Cytokeratin	**Arima**, *Acta Neuropathol* 79:629, 1990; **de Leon**, *Acta Neuropathol* 70:235, 1986; **Perry**, *Am J Pathol* 127:559, 1987; **Wisniewski**, *Arch Neurol* 26:97, 1972
Polyglucosan bodies	Human (muscle)	**Chow**, *Arch Pathol* 86:649, 1968; **Goebel**, *J Neuropathol Exp Neurol* 51:24, 1992; **Lefkowitch**, *Gastroenterology* 131:713, 2006 (liver); **Martin**, *J Pathol* 161:221, 1990; **Vucic**, *Muscle Nerve* 35:536, 2007
	Human (liver)	**Lefkowitch**, *Gastroenterology* 131:713, 2006; **O'Shea**, *Pediatr Dev Pathol* [Mar E-pub], 2007
	Dog	**Jolly**, *N Z Vet J* 50:32, 2002; **Valentine**, *Vet Pathol* 39:278, 2002
Psammoma bodies (brain)	Human	**Yamashima**, *Acta Neuropathol* 71:19, 1986
Pseudopsammoma bodies	Tubules, laminar bodies	**Berard**, *Acta Neuropathol* 42:62, 1978 (human)
Reinke crystals	Protein	**Nagano**, *J Cell Biol* 51:148, 1971
Ribosome-lamellar complexes	Ribosomes	**Rosner**, *Lab Invest* 42:236, 1980 (human, hairy cell leukemia)
Rosenthal fibers (astrocyte)	Actin-associated proteins	**Goldman**, *Am J Pathol* 130:569, 1988; **Tomokane**, *Am J Pathol* 138:875, 1991
Russell bodies (plasmacyte)	Immunoglobulins	**Schweitzer**, *J Cell Biol* 114:35, 1991 (mouse)†
Schaumann's bodies (mycobacteriosis)	Human	**Kirkpatrick**, *Ultrastr Pathol* 12:581, 1988

*In vitro study.
†Animal model.

exocrine cells condense secretory proteins in the **trans Golgi reticulum**. Hyperstimulation of endocrine cells may lead to condensation of secretion products in the **cis** and **medial** Golgi cisternae in addition to the **trans** region where it normally occurs. Condensation of protein into **intracisternal granules** may occur as far back in the pathway as the rough endoplasmic reticulum.

Abnormal proteins of various origins accumulate in the cisternae of the endoplasmic reticulum if there are defects in the primary or secondary structure of the molecule. Proteins that fail to fold or assemble correctly are not released from the endoplasmic reticulum but are retained in the cisternae and removed by degradation. A proteolytic system exists in the pre-Golgi endoplasmic reticulum that is rapid and highly selective. Several proteins have been shown to be degraded in highly regulated processes, for example, apolipoprotein B and T cell receptors. Despite these processes, crystals of proteins accumulate in otherwise normal cells of many secretory organs and endocrine tissues, for example, testicle, placenta, liver, and kidney. Appearing as dense massive crystals they generally can be seen by light microscopy (Fig. 26.8).

In diseases that involve metabolic abnormalities, large hyalin cytoplasmic inclusions are found in the liver. Ultrastructural examination typically reveals vacuolar areas that appear to develop by accumulation of tiny granular precipitates of protein that expand the cisternae of the rough endoplasmic reticulum. The specific protein that has accumulated can be identified by immunocytochemistry of these cells using a bank of reagents for individual proteins that are produced by the hepatocyte. The most common proteins found in hyalin droplet inclusions are

- **Albumin**
- **Fibrinogen**
- **α1-antitrypsin**
- **Complement components**

If the metabolic block involves secretion several different proteins may accumulate in inclusions.

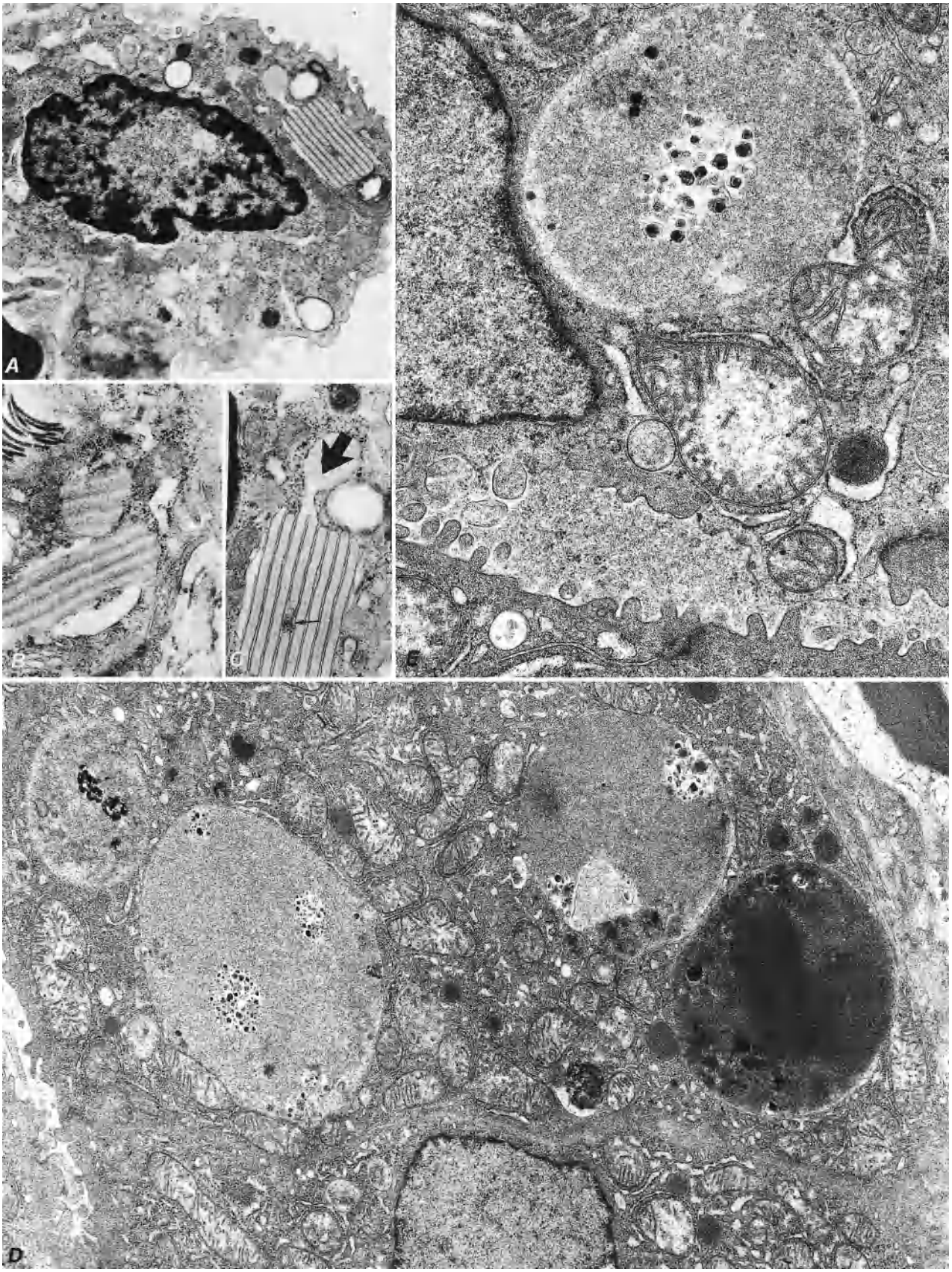


Fig. 26.7 Inclusions. A–C. **Globe-like inclusions**: inclusions develop from rough endoplasmic reticulum, alveolar type II cells, lung, normal sheep. (Micrograph: Toshishige Shibamoto, *Anat Rec* 223:49, 1989.) **D–E**. Hyalin inclusions, hepatocyte. **D**. **Granular membrane inclusions**: aggregation of proteins into vacuoles and subsequent degradation to form dense precipitates and myelin figures. **E**. Enlargement of D with membrane granules in inclusion; bile canaliculus (*bottom*).

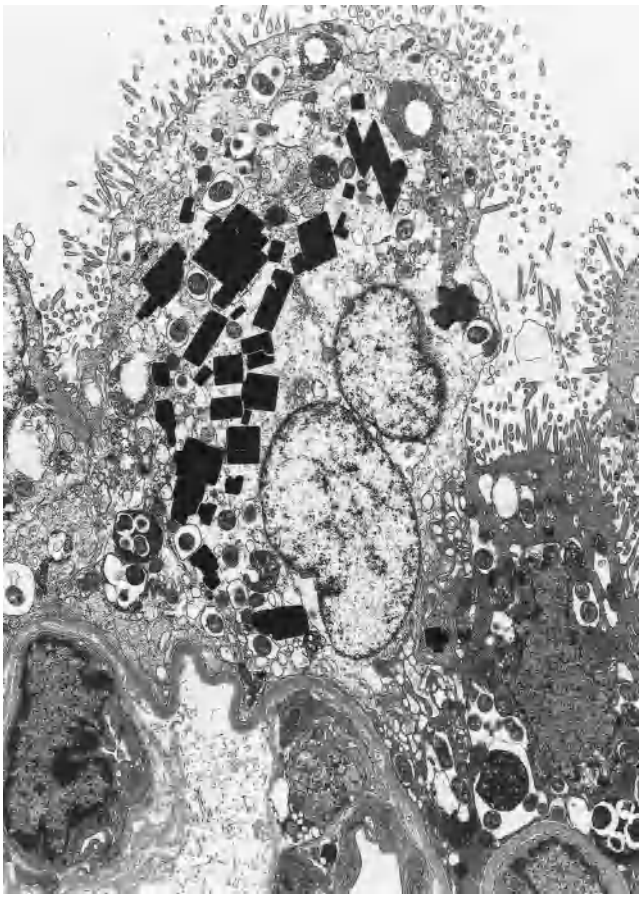


Fig. 26.8 Protein inclusion crystals: placental cell, goat. Massive amounts of protein accumulate in the cytoplasm.

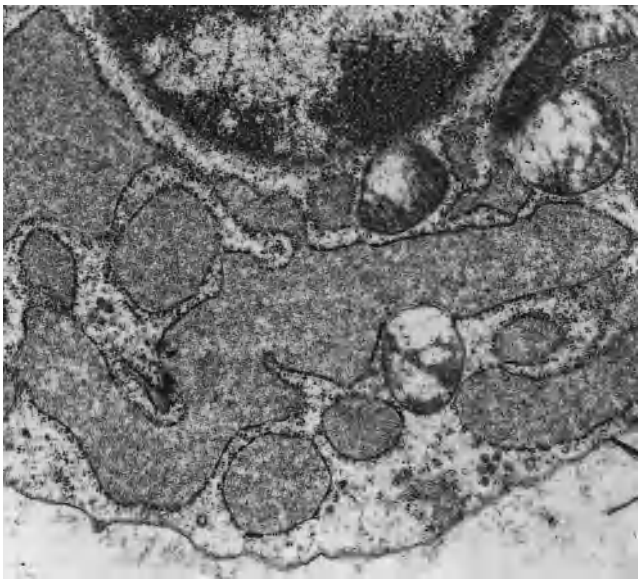


Fig. 26.9 Intracisternal protein inspissation: cisternae of rough endoplasm reticulum, plasmacyte. Large amounts of immunoglobulins have been produced but not secreted. Aggregates appear histologically as Russell body inclusion.

Russell bodies, the hyalin material in aged plasma cells (Mott's cells) are single filaments, rods, globular condensations or crystalline arrangements of inspissated immunoglobulins (Fig. 26.9). Precipitates of IgG and cryglobulins in the cisternae of the cytocavitary network form cylindrical and annular bodies with diameters of 62 nm. Similar distentions of rough endoplasmic reticulum by secretory products have been reported in congenital diseases.[123]

Ribosome-lamellar complexes, inclusions of compressed ribosomes and membrane lamellae, are characteristic of certain hypertrophic cells and some neoplasms. The lamellar components consist of tubular structures that coil around in a helical configuration to form a cylinder. Ribosome-lamellar complexes are found in various forms of leukemia, and in chronic lymphatic leukemia, vinblastine treated human leukocytes, and adrenal cortical adenoma cells.

Tubular inclusions, stacks of long, parallel tubules (that appear as regular, hexagonally arranged structures in cross section), are common in degenerate cells. They may appear as inclusions in the cytoplasm (less often in the nucleus) and are abnormal reduplications of endoplasmic reticulum and may arise when the directing influences of actin filaments and cytoplasmic microtubules are lost. Stacks of parallel tubules formed from endoplasmic reticulum may form plate-like or globe-like inclusions. Three dimentional models reconstructed from electron micrographs show extensive interconnections of these aggregates of tubules.[124] Although these inclusions can be found in normal animals, they are tpyically associated with some chronic injury to tissue.[125]

Tubular aggregates are a common nonspecific response of striated muscle to various injurious agents. Long, parallel tubules, often with dense cores or concentric inner tubules form regular hexagonally arranged aggregates. These tubular inclusions are seen in such diverse muscle diseases as hyperkalemic paralysis, myasthenia gravis, malignant hyperthermia, and chronic drug myopathy. They have been experimentally reproduced by making muscle anoxic or by treatment with cyanide.[126] In hypoxic muscle, tubular aggregation from sarcoplasmic reticulum occurs concomitantly with disappearance of Z bands, suggesting that loss of anchor effect of α-actinin in the Z line leads to tubular aggregation.

Tubular aggregates have been reported in several neoplasms. In some cases they have specific associations and are present in the same tumor from different patients (Fig. 26.10). Giant eosinophilic globular cytoplasmic inclusions in neoplastic liver cells stained immunohistochemically for **erythropoietin**. Ultrastructurally, the inclusions were granular aggregates within cisternae of the rough endoplasmic reticulum.

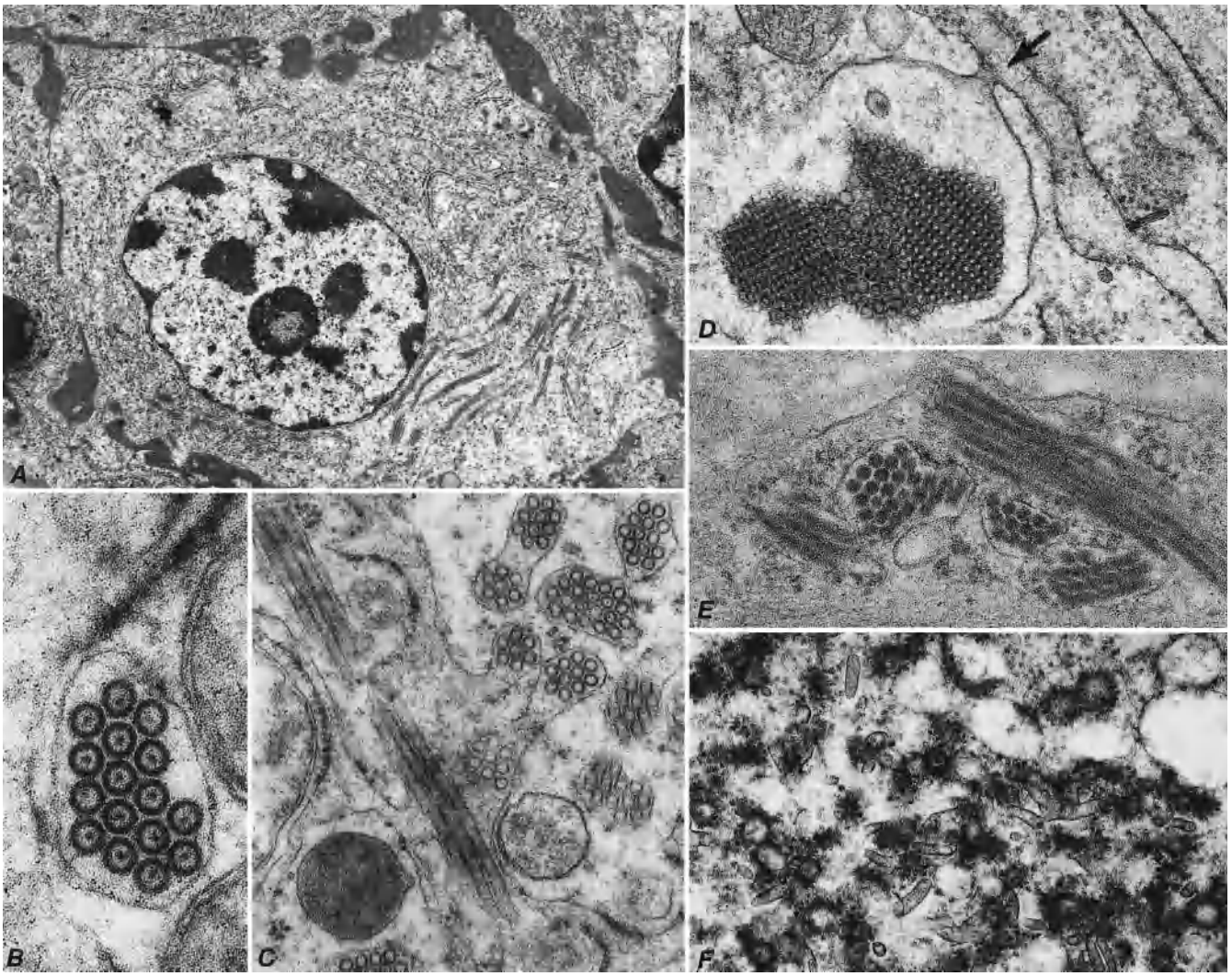


Fig. 26.10 Tubular and filamentous inclusions. A–C. Cytoplasmic intracisternal tubules: thyroid carcinoma cells, dog. Tubules contain dense outer wall and central core. Formation occurs through inversion of membranes of the rough endoplasmic reticulum. **D**. **Lattices and vesicles**: lamellar arrangements of protein polymers in cisternae of RER. **E**. Intracisternal tubules, smooth muscle cells, artery, dog. **F**. **Viral tubules**: mass of viral ribosomes and tubules, endothelial cell, arterivirus (equine arteritis virus).

Excessive production of erythropoietin was suggested as causal for the polycythemia in these mice.[127]

Tubuloreticular structures are interconnected dense tubules (20–30 nm in diameter) that lie within cisternae of the rough endoplasmic reticulum (Fig. 26.11). Structurally they appear as a reticulum since they crisscross in and out of the plane of section and their walls are ill-defined. Tubuloreticular structures are most common in abnormal lymphoid, reticular, and endothelial cells, and develop in diseases of differing and unrelated pathogenesis; that is, they are seen in neoplasms, viral disease, and autoimmune diseases.[128,129] Tubuloreticular inclusions have been found in blood monocytes of patients with chronic hepatitis that were treated with interferon; it has been suggested that viral infection has a primary role in tubuloreticular formation.[130] The significance of these tubules is unresolved, but cytochemical studies indicate that they consist of phospholipids and acidic glycoproteins.[131]

Secretory Granule Inclusions

Proteins can also accumulate in giant **secretory granules**. Bizarre nuclear inclusions originating as zymogen granules have been reported in pancreatic acinar cells of children with Reye's syndrome.[132] Experimentally, $CoCl_2$ toxicity leads to diminished export of zymogens from the rough endoplasmic reticulum of pancreatic acinar cells. The Golgi decreases in size, condensing vacuoles do not form, and intracisternal granules develop throughout the endoplasmic reticulum. Once

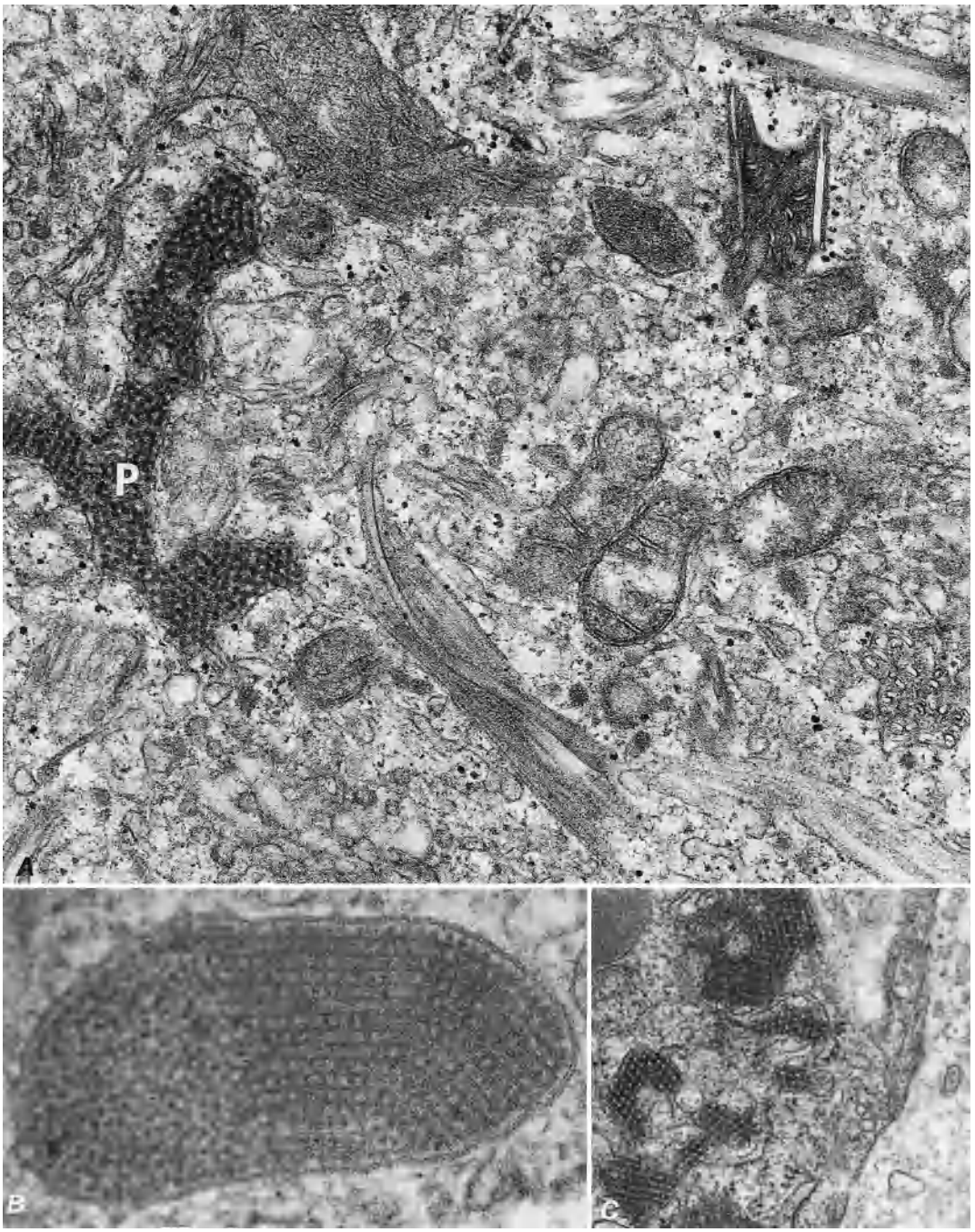


Fig. 26.11 Tubuloreticular inclusions. A. **Tubuloreticular structures**: globoid cell, canine globoid cell leukodystrophy. (Micrograph: Eduardo J. Yunis, *Am J Pathol* 85:99, 1976.) **B**. **Laminar arrangements** (crystalloids): protein filaments in inclusion granules. (Micrograph: David Steffan, Kansas State University.) **C**. **Tubuloreticular inclusion**: within cisternae of endoplasmic reticulum, endothelial cell.

regulated proteins reach a critical concentration in any component of the endoplasmic reticulum or Golgi complex they precipitate. Experimentally induced, several zymogens condense into intracisternal granules, but soluble proteins specific to the endoplasmic reticulum (such as heat shock proteins) remain in solution.[133]

Enormous, **crystalline protein-lattice inclusions** occur as large rhomboids in secretory granules of otherwise normal cells of liver, gonads, and kidneys of many species, usually as an incidental or nonspecific change. Protein is laid down in repeating units, and the inclusions have a linear structure with defined periodicity; for example, **Reinke crystals** develop in the cytoplasm of interstitial cells and spermatogonia of the human, canine, and equine testis.[134,135] Similarly, **Lubarsch crystals** occur in the cytoplasm of placenta of several species. Similar crystal occur extracellularly

in plasma; for example, cryoprecipitates in plasma sediments and blood vessel lumens contained tubular aggregates typical of mixed **cryglobulinemia**: hollow tubules surrounded by 8 lucent dots.[136]

Blocks anywhere in the pathway of protein synthesis are associated with accumulation of protein and aberrant fibrillar and tubular forms. Hepatocytes of humans and animals treated with the androgenic or estrogenic steroids will have abnormal proteins;[137] for example, fluoxymesterone induces duplication whorling of endoplasmic reticulum. Colonocytes of mice given glutamine antagonists form bundles of tubules (25–35 nm diameter with small central tubules of 5–7 nm) continuous with the RER.[138]

Autophagic Inclusions

Autophagic inclusions are common in tissues with high metabolic rates. Uncontrolled production of certain proteins in endocrine tissue commonly is associated with giant autophagosomes that sequester cellular proteins and membranes. Typically these inclusions contain lipid matrices and laminar arrangements of membranes.[139] If carbohydrate metabolism is disturbed they may contain glycogen.[140] Steroid cells and macrophages involved in degradation of membranes commonly develop myelin figure-bearing lysosomes (myeloid bodies) that may appear as inclusions.

Endocytotic and Lysosomal Inclusions

Spherical cytoplasmic hyalin droplets are common in parenchymal cells of liver, kidney, and other organs that reabsorb proteins from lumens. Ultrastructurally, most of these inclusions are large dense membrane-bound masses of granular proteins. Inclusions develop by sequestration in **lysosomes** of proteins that have been taken into the cell by endocytosis. Inclusions are thus phagolysosomes that develop from absorption of exogenous protein absorbed from lumens or interstitial spaces by phagocytosis and deposited in phagolysosomes for degradation.

In renal disease, where plasma **albumin** passes into the glomerular filtrate and out in the urine (albuminuria), proximal tubule cells reabsorb some of the protein. Albumin-bearing phagosomes form in the cytoplasm as hyalin droplets. Paraproteins of multiple myeloma (Bence-Jones proteins) are secreted into urine, then taken into lysosomes of renal tubules where they form cytoplasmic crystals.

Alcoholic Hyalin

Alcoholic hyalin (Mallory bodies) are large, eosinophilic, irregularly shaped cytoplasmic inclusions in hepatocytes consisting of aggregated filamentous material. They occur in several pathologic conditions, but their development in hepatocytes of patients with alcoholic hepatitis is most common. Ultrastructurally, Mallory bodies are composed of short, unbranched, hollow-cored filaments (14–20 nm thick) that closely resemble intermediate filaments. The filaments are covered and interconnected by a fimbriated coat of laterally projecting threads (Fig. 26.12).[141]

Mallory body filaments are composed of **prekeratin** polypeptides and stain with antibodies against epidermal prekeratin.[142,143] They are closely related to but not identical with cytokeratin and are probably prekeratin-containing intermediate filaments of the tonofilament type. Morphologically, they are shorter and thicker than actin filaments and intermediate filaments and have no antigenic relationship to actin or tubulin.

Mallory body formation involves changes in cytokeratin organization and conformation that result in

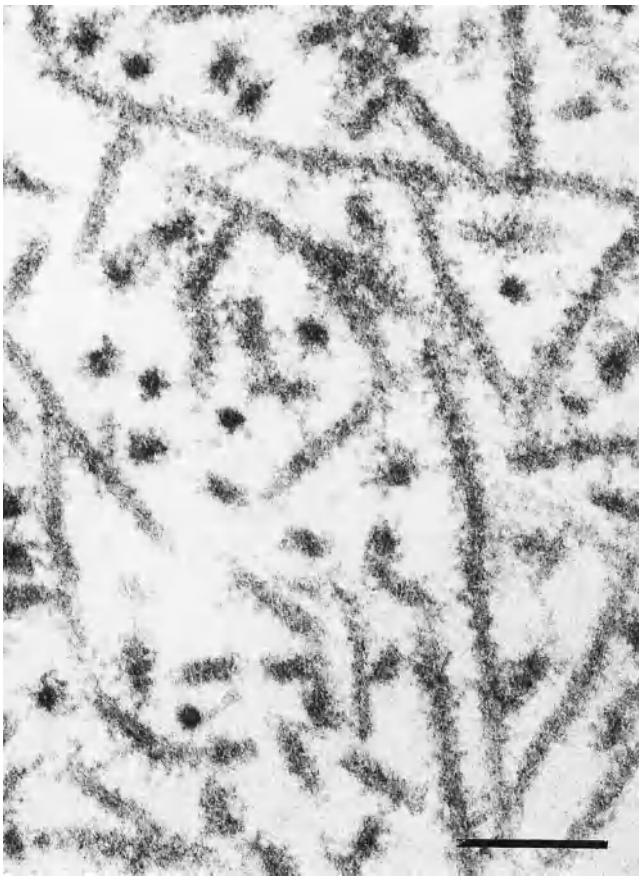


Fig. 26.12 Alcoholic hyalin: filaments of Mallory bodies induced in hepatocytes of mice by feeding griseofulvin. Filaments contain a dense core and are covered by a fimbriated coat of filaments that project outward for up to 20 nm and connect to adjacent filaments. Bar = 0.1 μm. (Micrograph: Werner W. Franke, *Lab Invest* 40:207, 1979.)

accessibility of specific antigenic determinants masked in the typical cytokeratin tetramer.[144] The insoluble material may result from liver cytokeratins that have been cross-linked by a transglutaminase enzyme in the hepatocyte. Transglutaminases catalyze cross-linking of proteins via formation of τ-glutamyl-lysine cross-links (like that of fibrin monomers in blood coagulation). Post-translational modification of cytokeratins by covalent cross-links appears to be the mechanism of development of Mallory body filaments.[145] Studies of cultures of hepatocytes isolated from greiseofulvin-fed mice suggest that newly synthesized cytokeratin monomers are incorporated into a developing polymerized filamentous network.[146]

Ethanol and other agents that damage the cytoskeleton of the hepatocyte will ultimately diminish the excretory capacity through bile canaliculi, and this effect may underlie the accumulation of precursors of cytokeratin filaments.[147,148] **Ubiquitin**, the protein that binds to denatured proteins in Mallory bodies, is involved in processing of abnormal intermediate filaments.[149]

Alcoholic hyalin filaments also occur in a variety of chronic toxic liver disease in animals and humans, including hepatomas and hepatocellular carcinomas.[150] They are also found in pulmonary alveolar cells in toxic lung disease. Experimentally, the have been produced in mice treated with griseofulvin[151]

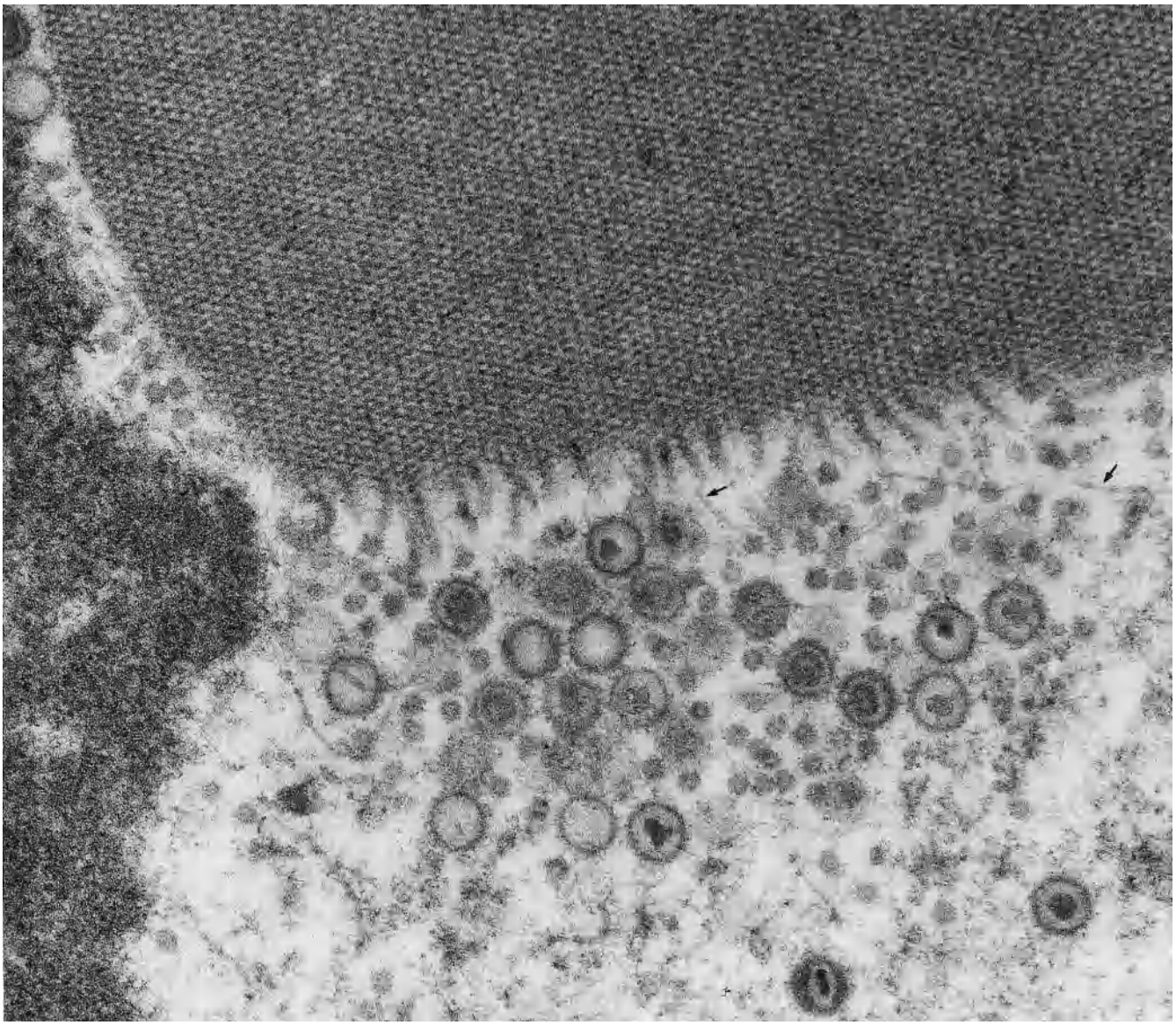


Fig. 26.13 Viral inclusion: herpesvirus. Protein crystal is formed of lattices of viral nucleoproteins. Naked virions surround periphery. DNA strands (*arrows*) are at forming edge of lattice and within immature viral particles. (Micrograph: Arlis Boothe.)

and in mice fed a vitamin A deficient diet.[152] Griseofulvin-induced Mallory bodies are made of randomly oriented unbranched rods 175–250 nm long and 14–20 nm thick, and covered by a fimbriated coat.[153]

Viral Inclusion Bodies

Viral nucleic acid templates are liberated into the host cell cytoplasm and are used as codes to create new viral genetic material, viral enzymes, and structural proteins that will become part of the external coat of the new virion. Production of proteins for new virions is unbalanced and aggegates of the various peptides and other excess components accumulate as inclusion bodies. Most viral inclusions are remnants of viral factories, and are composed of excess viral structural proteins and lipoprotein membranes with viral particles of varying maturity distributed in the periphery. In some cases viral inclusions are composed of mature viral particles (virions) arranged in lattice formations (Fig. 26.13).

Pseudoinclusions

Herniation of the nuclear envelope into the nuclear matrix carries bits of cytoplasm with it to form pseudoinclusions. The limiting membrane of the inclusion thus has two lipid bilayers and has chromatin lining the outer part and ribosomes lining the inner surface. If the membranes disintegrate, the proteins appear as a "true" inclusion. Tubular invaginations of the inner nuclear membrane may occur in nuclei of rapidly growing cells. Large inclusions of branched tubules have been reported in hypertrophic cardiac muscle, neoplastic cells, and endocrine cells.

Extracellular inclusions are the results of necrosis with inspissation of cellular debris into dense spherical masses. These typically appear as dense hyalin irregular masses. Extracellular inclusions may be composed of any component of necrotic debris. The Councilman bodies of yellow fever, burns and other severe injury are composed of dense hepatocytes that have undergone coagulation necrosis. In aged humans and animals, the endocrine and exocrine glands are prone to contain foci of extracellular protein masses (Fig. 26.14).

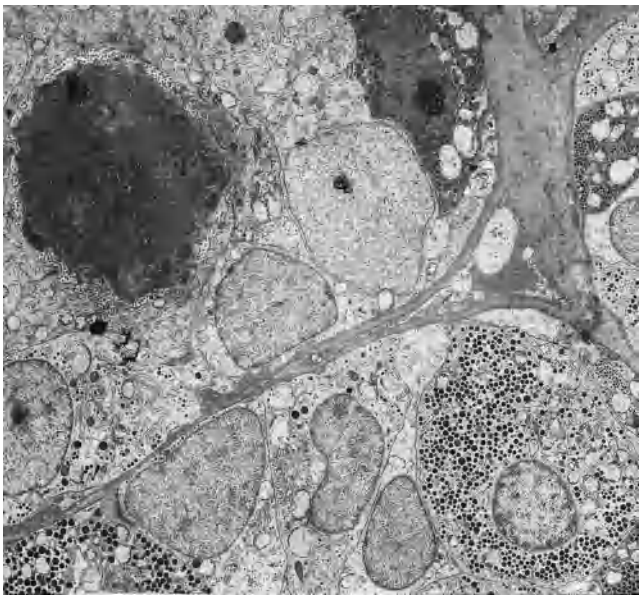


Fig. 26.14 Extracellular pseudoinclusion: large aggregate of homogenous dense material, pituitary, aged dog.

Nitrosylation

Some proteins are nitrosylated (transfer of NO to a critical thiol group), leading to protein misfolding.[154] For example, **protein disulfide isomerase (PDI)** is an enzyme responsible for normal protein folding in the ER—when PDI is nitrosylated, there is misfolding and neuron death. Another example: **E3 ubiquitin ligase** (parkin), when nitosylated, can lead to Parkinson's disease. **S-nitrosylation**, the selective modification of cysteine residues in a protein to form S-nitrosocysteine, is a major mechanism by which NO acts as a signaling molecule. High resolution immunogold electron microscopy characterizes S-nitrocysteine contained in peptides of diverse protein—cytoskeletal proteins, chaperones, translation proteins. One way to ameliorate excessive NO production and abnormal S-nitosylation is to inhibit NMDAr (N-methyl-d-aspartate)-type glutamate receptors, which leads to excessive Ca^{2+} influx through the receptors-associated ion channel and subsequent free radical production including NO and ROS.[155]

References

1. Westermark P, et al. 2007. A primer of amyloid nomenclature. *Amyloid* 14:179.
2. Inoue S, et al. 1998. Ultrastructure of familial amyloid polyneuropathy amyloid fibrils: Examination with high-resolution electron microscopy. *J Struct Biol* 124:1.
3. Urbányi Z, et al. 2003. Serum amyloid P componenent induced neuronal apoptosis and beta-amyloid immunoreactivity. *Brain Res* 988:69.
4. Inoue S, Kisilevsky R. 1996. A high resolution ultrastructural study of experimental murine AA amyloid. *Lab Invest* 74:670.
5. Snow AD, et al. 1992. Peripheral distribution of dermatan sulfate proteoglycans (decorin) in amyloid-containing plaques and their presence in neurofibrillary tangles of Alzheimer's disease. *J Hist Cyt* 40:105, 1992.

6. Schultz RT, et al. 1985. Ultrastructure of vascular lesions in experimental amyloidosis of mice. *Am J Pathol* 119:138.
7. Ferguson N, et al. 2006. General structural motifs of amyloid protofilaments. *Proc Natl Acad Sci USA* 103:16248.
8. Jaroniec CP, et al. 2004. High-resolution ultrastructure of a peptide in an amyloid fibril determined by magic angle spinning NMR spectroscopy. *Proc Natl Acad Sci USA* 101:711.
9. Yang GCH, Gallo GR. 1990. Protein A-gold immunoelectron microscopic study of amyloid fibril, granular deposits, and fibrillar luminal aggregates in renal amyloidosis. *Am J Pathol* 137:1223.
10. Miura K, et al. 1985. Immunohistochemical detection of serum amyloid A protein in the liver and the kidney after casein injection. *Lab Invest* 53:453.
11. Shirahama T, Cohen AS. 1985. Immunocytochemical study of hepatocyte synthesis of amyloid A. *Am J Pathol* 118:108.
12. Takahashi M, et al. 1985. Ultrastructural evidence for the synthesis of serum amyloid A protein by murine hepatocytes. *Lab Invest* 52:220.
13. Takahashi M, et al. 1989. Ultrastructural evidence for intracellular formation of amyloid fibrils in macrophages. *Virchows Arch A* 414:411.
14. Zucker-Franklin D, Franklin EC. 1970. Intracellular localization of amyloid by fluorescence and electron microscopy. *Am J Pathol* 59:23.
15. Inoue S, Kisilevsky R. 1996. A high ultrastructural study of experimental murine AA amyloid. *Lab Invest* 74:670.
16. Donini U, et al. 1989. Immunoelectron microscopic classification of amyloid in renal biopsies. *J Hist Cyt* 37:1101.
17. Cohen AS, Shirahama T. 1971. Ultrastructural studies of renal peritubular amyloid experimentally induced in guinea pigs. *Arthritis Rheum* 14:429.
18. Yang GCH, et al. 1992. Ultrastructural immunohistochemical localization of polyclonal IgG, C3, and amyloid P component on the congo red-negative amyloid-like fibrils of fibrillary glomerulopathy. *Am J Pathol* 141:409.
19. Serpell LC, et al. 2007. Structural analysis of fibrinogen amyloid fibrils. *Amyloid* 14:199.
20. Kjeldsberg CR, et al. 1977. Evidence for intracellular amyloid formation in myeloma. *Blood* 50:493.
21. Solomon A, et al. 1992. Induction in mice of human light-chain-associated amyloidosis. *Am J Pathol* 140:629.
22. Ishihara T, et al. 1991. Amyloid fibril formation in the rough endoplasmic reticulum of plasma cells from a patient with localized A amyloidosis. *Lab Invest* 64:265.
23. Konarkowski B, et al. 2006. The aggregation potential of human amylin determines its cytotoxicity towards islet beta-cells. *FEBS J* 273:3614.
24. Rindi G, et al. 1991. Islet amyloid polypeptide in proliferating pancreatic β cells during development, hyperplasia and neoplasia in humans and mice. *Am J Pathol* 138:1321.
25. Casas S, et al. 2007. Impairment of the ubiquitin-proteasome pathway is a downstream ER stress reponse induced by extracellular human islet amyloid polypeptides and contributes to pancreatic (beta)-cell apoptosis. *Diabetes* 56:2284.
26. Hayden MR. 2007. Longitudinal ultrastructure study of islet amyloid in the HIP rat model of type 2 diabetes mellitus. *Exp Biol Med* 232:772.
27. Bergström J, et al. 2004. Two different types of amyloid deposits. *Lab Invest* 84:981.
28. Yi S, et al. 1991. Systemic amyloidosis in transgenic mice carrying the human mutant transthyretin (Met30) gene. Pathologic similarity to human familial amyloidotic polyneuropathy, type I. *Am J Pathol* 138:403.
29. Maury CP, et al. 1994. Amyloid fibril formation in glesolin-derived amyloidosis. *Lab Invest* 70:558.
30. Diociaiuti M, et al. 2006. Calcitonin forms oligomeric pore-like structures in lipid membranes. *Biophys J* 91:2275.
31. Korenaga T, et al. 2004. Tissue distribution, biochemical properties, and transmission of mouse type A AApoAII amyloid fibrils. *Am J Pathol* 164:1597.
32. Onoue S, et al. 2004. Mishandling of the therapeutic peptide glucagon generates cytotoxic amyloidogenic fibrils. *Pharm Res* 21:1274.
33. Gomez-Ramos P, Asuncion Moran M. 2007. Ultrastructural localization of intraneuronal A beta-peptide in Alzheimer disease brains. *J Alzheimers Dis* 11:53.
34. Yoshiike Y, et al. 2007. Surface structure of amyloid-beta fibrils contributes to cytotoxicity. *Biochemistry* 46:9805.
35. Frackowiak J, et al. 1992 Ultrastructure of the microglia that phagocytose amyloid and the microglia that produce β-amyloid fibrils. *Acta Neuropathol* 84:225.
36. Joachim C, et al. 1991. Antibodies to non-beta regions of the beta-amyoid precursor protein detect a subset of senile plaques. *Am J Pathol* 138:373.
37. Kawai M, et al. 1992. Subcellular localization of amyloid precursor protein in senile plaques of Alzheimer's disease. *Am J Pathol* 140:947.
38. Wisniewski T, et al. 1997. Presenilin-1 is associated with Alzheimer's disease amyloid. *Am J Pathol* 151:601.
39. Torp R, et al. 2003. Identification of neuronal plasma membrane microdomains that colocalize beta-amyloid and presenilin; implications for beta-amyloid precursor protein processing. *Neuroscience* 120:291.
40. Moreira PI, et al. 2007. Autophagocytosis of mitochondria is prominent in Alzheimer disease. *J Neuropathol Exp Neurol* 66:525.
41. Baloyannis SJ. 2006. Mitochondrial alterations in Alzheimer's disease. *J Alzheimers Dis* 9:119.
42. Devi L, et al. 2006. Accumulation of amyloid precursor protein in the mitochondrial import channels of human Alzheimer's disease brain is associated with mitochondrial dysfunction. *J Neurosci* 26:9057.
43. Anandatheerthavarada HK, et al. 2003. Mitochondrial targeting and a novel transmembrane arrest of Alzheimer's amyloid precursor protein impairs mitochondrial function in neuronal cells. *J Cell Biol* 161:41.
44. Manczak M, et al. 2006. Mitochondria are a direct site of A beta accumulation in Alzheimer's disease neurons. *Hum Mol Genet* 15:1437.

45. Good PF, et al. 1996. Evidence for neuronal oxidative damage in Alzheimer's disease. *Am J Pathol* 149:21.
46. Lal R, et al. 2007. Amyloid beta ion channel. *Biochim Biophys Acta* 1768:1966.
47. Aliev G, et al. 2003. Mitochondria and vascular lesions as a central target for the development of Alzheimer's disease and Alzheimer disease-like pathology in transgenic mice. *Neurol Res* 25:665.
48. Aliev G, et al. 2003. Role of vascular hypoperfusion-induced oxidative stress and mitochondria failure in the pathogenesis of Alzheimer disease. *Neurotox Res* 5:491.
49. Obrenovich ME, et al. 2006. Overexpression of GRK2 in Alzheimer disease and in a chronic hypoperfusion rat model is an early marker of brain mitochondrial lesions. *Neurotox Res* 10:43.
50. Abraham CR, et al. 1988. Immunochemical identification of the serine protease inhibitor α1-antichymotrypsin in the brain amyloid deposits of Alzheimer's disease. *Cell* 52:487.
51. Powers GA, et al. 2007. Serpin acceleration of amyloid fibril formation. *J Mol Biol* 366:666.
52. Kosik KS. 1992. Alzheimer's disease: A cell biological perspective. *Science* 256:780.
53. Burger PC, Vogel FS. 1983. The development of the pathologic changes of Alzheimer's disease and senile dementia in patients with Down's syndrome. *Am J Pathol* 73:747.
54. Catteruccia N, et al. 1990. Ultrastructural localization of the putative precursors of the A4 amyloid protein associated with Alzheimer's disease. *Am J Pathol* 137:19.
55. Yu WH, et al. 2005. Macroautophagy—a novel β-amyloid peptide-generating pathway activated in Alzheimer's disease. *J Cell Biol* 171:87.
56. Ishihara T, et al. 1991. Immunohistochemical and immunoelectron microscopical characterization of cerebrovascular and senile plaque amyloid in aged dog's brains. *Brain Res* 548:196.
57. Miao J, et al. 2005. Cerebral microvascular amyloid β protein deposition induced vascular degeneration and neuroinflammation in transgenic mice expressing human vasculotropic mutant amyloid β precursor protein. *Am J Pathol* 167:505.
58. Yamaguchi H, et al. 1992. Beta amyloid is focally deposited within the outer basement membrane in the amyloid angiopathy of Alzheimer's disease. *Am J Pathol* 141:249.
59. Wisniewski HM, et al. 1992. Ultrastructural studies of the cells forming amyloid in the cortical vessel wall in Alzheimer's disease. *Acta Neuropathol* 84:117.
60. Mucchiano G, et al. 1992. Senile aortic amyloid. *Am J Pathol* 140:871.
61. Häggqvist B, et al. 1999. Medin: An integral fragment of aortic smooth muscle cell produced lactadherin forms the most common human amyloid. *Proc Natl Acad Sci USA* 96:8669.
62. Prusiner SB, et al. 1983. Scrapie prions aggregate to form amyloid-like birefringent rods. *Cell* 35:349.
63. Stöhr J, et al. 2008. Mechanisms of prion protein assembly into amyloid. *Proc Natl Acad Sci USA* 105:2409.
64. Liberski PP. 2004. Amyloid plaques in transmissible spongiform encephalopathies (prion diseases). *Folia Neuropathol* 42 (Suppl B):109.
65. Bugiani O, et al. 1993. Beta PP participates in PrP-amyloid plaques of Gerstamann-Strässler-Scheinker disease, Indiana kindred. *J Neuropathol Exp Neurol* 52:64.
66. Giaccone G, et al. 1993. Prion protein preamyloid and amyloid deposits in Gerstamnn-Sträussler-Scheinker disease, Indiana kindred. *Proc Natl Acad Sci USA* 90:302.
67. Pilanen MS, et al. 1994. Twisted ribbon structure of paired helical filaments revealed by atomic force microscopy. *Am J Pathol* 144:869.
68. Delobel P, et al. 2008. Analysis of tau phosphorylation and truncation in a mouse model of human tauopathy. Am J Pathol 172:123.
69. Leroy K, et al. 2007. Early axonopathy preceding neurofibrillary tangles in mutant tau transgenic mice. *Am J Pathol* 170:976.
70. Trojanowski JQ, Lee VMpY. 2005. The Alzheimer's brain. *Am J Pathol* 167:1183.
71. Kobayashi K, et al. 2002. Apoptosis of astrocyte with enhanced lysosomal activity and oligodendrocytes in white matter lesions in Alzheimer's disease. *Neuropathol Appl Neurobiol* 28:238.
72. Papasozomenos SC. 1989. Tau protein immunoreactivity in dementia of the Alzheimer type: II. Electron microscopy and pathogenetic implications. *Lab Invest* 60:375.
73. Perry G, et al. 1985. Paired helical filaments from Alzheimer disease patients contain cytoskeletal components. *Proc Natl Acad Sci USA* 82:3916.
74. Wrzolek MA, et al. 1992. Immune electron microscopic characterization of monoclonal antibodies to Alzheimer neurofibrillary tangles. *Am J Pathol* 141:343.
75. Tabaton M, et al. 1991. Ultrastructural localization of β-amyloid, τ and ubiquitin epitopes in extracellular neurofibrillary tangles. *Proc Natl Acad Sci USA* 88:2098.
76. Wisniewski HM, et al. 1984. Ultrastructure of paired helical filaments of Alzheimer's neurofibrillary tangles. *J Neuropathol Exp Neurol* 43:643.
77. Miyawaki K, et al. 2001. Three-dimensional structures of canine senile plaques. *Acta Neuropathol* 102:321.
78. Yamaguchi H, et al. 1991. Secondary deposition of beta amyloid witin extracellular neurofibrillary tangles in Alzheimer-type dementia. *Am J Pathol* 138:699.
79. Iwatsubo T, et al. 1992. Lack of ubiquitin immunoreactivities at both ends of neuropil threads. *Am J Pathol* 140:277.
80. Davies CA, Mann DMA. 1993. Is the "preamyloid" of diffuse plaques in Alzheimer's disease really non fibrillar? *Am J Pathol* 143:1594.
81. Kumar-Singh S, et al. 2005. Dense-core plaques in Tg2576 and PSAPP mouse models of Alzheimer's disease are centered on vessel walls. *Am J Pathol* 167:527.
82. Arima K, Akashi T. 1990. Involvement of the locus coeruleus in Pick's disease with or without Pick body formation. *Acta Neuropathol* 79:629.

83. de Leon GA, et al. 1986. Congenital Pick cell encephalopathy. *Acta Neuropathol* 70:235.
84. Murayama S, et al. 1989. Immunocytochemical and cultural study of Lewy body-like hyaline inclusions in familial amyotrophic lateral sclerosis. *Acta Neuropathol* 78:143.
85. Perry G, et al. 1987. Filaments of Pick's bodies contain altered cytoskeletal elements. *Am J Pathol* 127:559.
86. Takauchi S, et al. 1984. An ultrastructural study of Pick bodies. *Acta Neuropathol* 64:344.
87. Cairns NJ, et al. 2007. TDP-43 in familial and sporadic frontotemporal lobar degeneration with ubiquitin inclusions. *Am J Pathol* 170:227.
88. Gentile A, et al. 2008. Spontaneous aggregation and altered intracellular distribution of endogenous α-synuclein during neuronal apoptosis. *J Alzheimers Dis* 13:151.
89. Ardley HC, et al. 2004. UCH-L1 aggresome formation in respose to proteasome impairment indicates a role in inclusion formation in Parkinson's disease. *J Neurochem* 90:379.
90. Wisniewski T, et al. 1991. Lewy bodies are immunoreactive with antibodies raised to gelsolin related amyloid-Finnish type. *Am J Pathol* 138:1077.
91. Schmidt ML, et al. 1991. Epitope map of neurofilament protein domains in cortical and peripheral nervous system Lewy bodies. *Am J Pathol* 139:53.
92. Galloway PG, et al. 1992. Filaments of Lewy bodies contain insoluble cytoskeletal elements. *Am J Pathol* 140:809.
93. Iwatsubo T, et al. 1996. Purification and characterization of Lewy bodies from the brains of patients with diffuse Lewy body disease. *Am J Pathol* 148:1517.
94. Outeiro TF, et al. 2007. Sirtuin 2 inhibitors rescue α-synuclein-mediated toxicity in models of Parkinson's disease. *Science* 317:516.
95. Oakley AE, et al. 2007. Individual dopaminergic neurons show raised iron level in Parkinson disease. *Neurology* 68:1820.
96. Jellinger K, et al. 1992. Iron-melanin complex in substantia nigra of parkinsonian brains: An x-ray microanalysis. *J Neurochem* 59:1168.
97. Halliday GM, et al. 2005. Alpha synuclein redistributes to neuromelanin lipid in the substantia nigra early in Parkinson's disease. *Brain* 128:2654.
98. Natadate K, et al. 2006. Progressive dopaminergic neurodegeneration of substantia nigra in the zitter mutant rat. *Act Neuropathol* 112:64.
99. Norris EH, et al. 2007. Pesticide exposure exacerbates α-synucleinopathy in an A53T transgenic mouse model. *Am J Pathol* 170:658.
100. Waelter S, et al. 2001. Accumulation of mutant huntingtin fragments in aggresome-like inclusion bodies as a result of insufficient protein degradation. *Mol Biol Cell* 12:1393.
101. Mihm MJ, et al. 2007. Cardiac dysfunction in the R6/2 mouse model of Huntington's disease. *Neurobiol Dis* 25:297.
102. Ohyama T, et al. 2008. Huntingtin-interacting protein 14, a palmitoyl transferase required for exocytosis and targeting of CSP to synaptic vesicles. *J Cell Biol* 179:1481.
103. Sasaki S, Iwata M. 2007. Mitochondrial alterations in the spinal cord of patients with sporadic amyotrophic lateral sclerosis. *J Neuropathol Exp Neurol* 66:10.
104. Kihira, T, et al. 1991. Involvement of Onuf's nucleus in ALS. *J Neurol Sci* 104:119.
105. Seilhean D, et al. 2004. Amyotrophic lateral sclerosis with neuronal intranuclear protein inclusions. *Acta Neuropathol* 108:81.
106. Kato S, et al. 1997. Pathological characterization of astrocytic hyaline inclusions in familial amyotrophic lateral sclerosis. *Am J Pathol* 151:611.
107. Vielhaber S, et al. 1999. Visualization of defective mitochondrial function in skeletal muscle fibers of patients with sporadic amyotrophic lateral sclerosis. *J Neurol Sci* 169:133.
108. Bruijn LI, et al. 1998. Aggregation and motor neuron toxicity of an ALS-linked SOC1 mutant independent from wild-type SOD1. *Science* 281:1851.
109. Dal Canto MC, Gurney ME. 1994. Development of central nervous system pathology in a murine transgenic model of human amyotrophic lateral sclerosis. *Am J Pathol* 145:1271.
110. Gonatas KN, et al. 1992. Fragmentation of the Golgi apparatus of motor neurons in amyotrophic lateral sclerosis. *Am J Pathol* 140:731.
111. Martin LJ. 1999. Neuronal death in amyotrophic lateral sclerosis is apoptosis. *J Neuropathol Exp Neurol* 58:459.
112. Goldman JE, Corbin E. 1988. Isolation of a major protein component of Rosenthal fibers. *Am J Pathol* 130:569.
113. Iwaki T, et al. 1993. αβ-Crystallin and 27-kd heat shock protein are regulated by stress conditions in the central nervous system and accumulate in Rosenthal fibers. *Am J Pathol* 143:487.
114. Tomokane N, et al. 1991. Rosenthal fibers share epitopes with αβ-crystallin, glial fibrillary acidic protein, and ubiquitin, but not with vimentin. *Am J Pathol* 138:875.
115. Dickson DW, et al. 1989. Diffuse Lewy body disease: Light and electron microscope immunocytochemistry of senile plaques. *Acta Neuropathol* 78:572.
116. Mori H, et al. 1987. Ubiquitin is a component of paired helical filaments in Alzheimer's disease. *Science* 235:1641.
117. Askanas V, et al. 1998. Light and electron microscopic immunolocalization of presenilin 1 in abnormal muscle fibers of patients with sporadic inclusion-body myositis and autosomal-recessive inclusion-body myopathy. *Am J Pathol* 152:889.
118. Schiffer D, et al. 1991. Ubiquitin in motor neuron disease: Study at light and electron microscope. *J Neuropathol Exp Neurol* 50:463.
119. Eriksson L, Westermark P. 1986. Intracellular neurofibrillary tangle-like aggregations. A constantly present amyloid alteration in the aging choroid plexus. *Am J Pathol* 125:124.
120. Wisniewski HM, et al. 1973. Neuritic (senile) plaques and filamentous changes in aged rhesus monkeys. *J Neuropathol Exp Neurol* 32:566.
121. Walker LC, et al. 1990. Amyloid in the brains of aged squirrel monkeys. *Acta Neuropathol* 80:381.
122. Johnston JA, et al. 1999. Aggresomes: A cellular response to misfolded proteins. *J Cell Biol* 143:1883.

123. Cooper RR, et al. 1973. Metaphyseal dystosis. A rough-surfaced endoplasmic reticulum storage defect. *Lab Invest* 28:119.
124. Shibamoto T, et al. 1989. Platelike and globelike inclusion bodies associated with rough endoplasmic reticulum in alveolar type 2 cells of the sheep. *Anat Rec* 223:49.
125. Stephens RJ, et al. 1973. Cytologic changes in dog lungs induced by chronic exposure to ozone. *Am J Pathol* 73:711.
126. Schiaffino S, et al. 1977. Tubular aggregates induced by anoxia in isolated rat skeletal muscle. *Lab Invest* 37:223.
127. Horinouchi A, et al. 1997. Secondary polycythemia in male B6CSF6 mice with spontaneously occurring hepatocellular carcinoma. *Toxic Pathol* 25:511.
128. Fidzianska A, Goebel HH. 1989. Tubuloreticular structures (TRS) and cylindric confronting cisternae (CCC) in childhood dermatomyositis. *Acta Neuropathol* 79:310.
129. Schaff Z, et al. 1990. Intracytoplasmic crystalline inclusions in the hepatocytes of humans and chimpanzees. *Ultrastr Pathol* 14:303.
130. Grimely PM, et al. 1985. Tubuloreticular inclusions in peripheral blood mononuclear cells related to systemic therapy with alpha-interferon. *Lab Invest* 52:638.
131. Boor PJ, et al. 1979. Tubuloreticular structures in myocardium. *J Mol Cell Cardiol* 11:967.
132. Collins DN. 1974. Ultrastructural study of intranuclear inclusions in the exocrine pancreas in Reye's syndrome. *Lab Invest* 30:333.
133. Tooze J, et al. 1989. Condensation-sorting events in the rough endoplasmic reticulum of exocrine pancreatic cells. *J Cell Biol* 109:35.
134. Gouranton J, et al. 1979. Fine structure and nature of the crystalloid intranuclear and intracytoplasmic inclusions of dog cauda epididymidis. *J Ultrastruct Res* 69:273.
135. Nagano T, Ohtsuki I. 1971. Reinvestigation of the fine structure of Reinke's crystals in human testicular interstitial cells. *J Cell Biol* 51:148.
136. Szymanksi IO, et al. 1994. Electron microscopic and immunochemical studies in a patient with hepatitic C virus infection and mixed cyroglobulinemia type II. *Am J Clin Pathol* 102:278.
137. Roberts DK, et al. 1964. The ultrastructural response of human endometrium to medroxyprogesterone acetate. *Am J Obst Gyn* 123:811.
138. Michaels JE. 1980. The occurrence of an unusual tubular organelle in surface epithelial cells of the mouse ascending colon after injection of diazo-oxo-norleucine. *Anat Rec* 196:413.
139. Davis DA, Medline NM. 1970. Spironolactone (aldactone) bodies: Concentric lamellar formation in the adrenal corteces of patients treated with spironolactone. *Am J Clin Pathol* 54:22.
140. Lesch R, et al. 1976. The appearance and degradation of specific hepatocellular cytoplasmic inclusion bodies in rat liver due to D-galactosamine. *Virch Arch B* 21:313.
141. Rumpelt HJ, et al. 1977. Ultrastructure of alcoholic hyalin and fate of affected hepatocytes. *Virch Arch* 23:339.
142. Kimoff RJ, Huang S. 1981. Immunocytochemical and immunoelectron microscopic studies on Mallory bodies. *Lab Invest* 45:491.
143. Okanoue T, et al. 1985. Relationship of Mallory bodies to intermediate filaments in hepatocytes. A scanning electron microscopy study. *Lab Invest* 53:534.
144. Hazan R, et al. 1986. Changes of cytokeratin organization during development of Mallory bodies as revealed by a monoclonal antibody. *Lab Invest* 54:543.
145. Zatloukal K, et al. 1991. High molecular weight components are main constituents of Mallory bodies isolated with a fluorescence activated cell sorter. *Lab Invest* 64:200.
146. Kachi K, et al. 1993. Synthesis of Mallory body, intermediate filaments, and microfilaments proteins in liver cell primary cultures. *Lab Invest* 68:71.
147. Denk H, Eckerstorfer R. 1977. Colchicine-induced Mallory body formation in the mouse. *Lab Invest* 36:563.
148. Kawahara H, et al. 1989. Excretory function in cultured hepatocytes from griseofulvin-treated mice. *Lab Invest* 61:609.
149. Ohta M, et al. 1988. Ubiquitin is present on the cytokeratin intermediate filaments and Mallory bodies of hepatocytes. *Lab Invest* 59:848
150. Meierhenry EF, et al. 1981. Mallory body formation in hepatic nodules of mice ingesting dieldrin. *Lab Invest* 44:392.
151. Irie T, et al. 1984. Electron microscopic study of the *in situ* calcium-dependent degradation of Mallory bodies and intermediate filaments in hepatocytes. *Lab Invest* 50:303.
152. Akeda S, et al. 1986. Mallory body formation and amyloid deposition in the liver of aged mice fed a vitamin A deficient diet for prolonged period. *Lab Invest* 54:228.
153. Franke WW, et al. 1979. Characterization of the intermediate-sized filaments in liver cells by immunofluorescence and electron microscopy. *Biol Cellulaire* 34:99.
154. Greco TM, et al. 2006. Identification of S-nitrosylation motifs by site-specific mapping of the S-nitrosocysteine proteome in human vascular smooth muscle cells. *Proc Natl Acad Sci USA* 103:7420.
155. Lipton SA, et al. 2007. Inflammatory mediators leading to protein misfolding and noncompetitive off-rate drug therapy for neurodegenerative disorders. *Int Rev Neurobiol* 82:1.

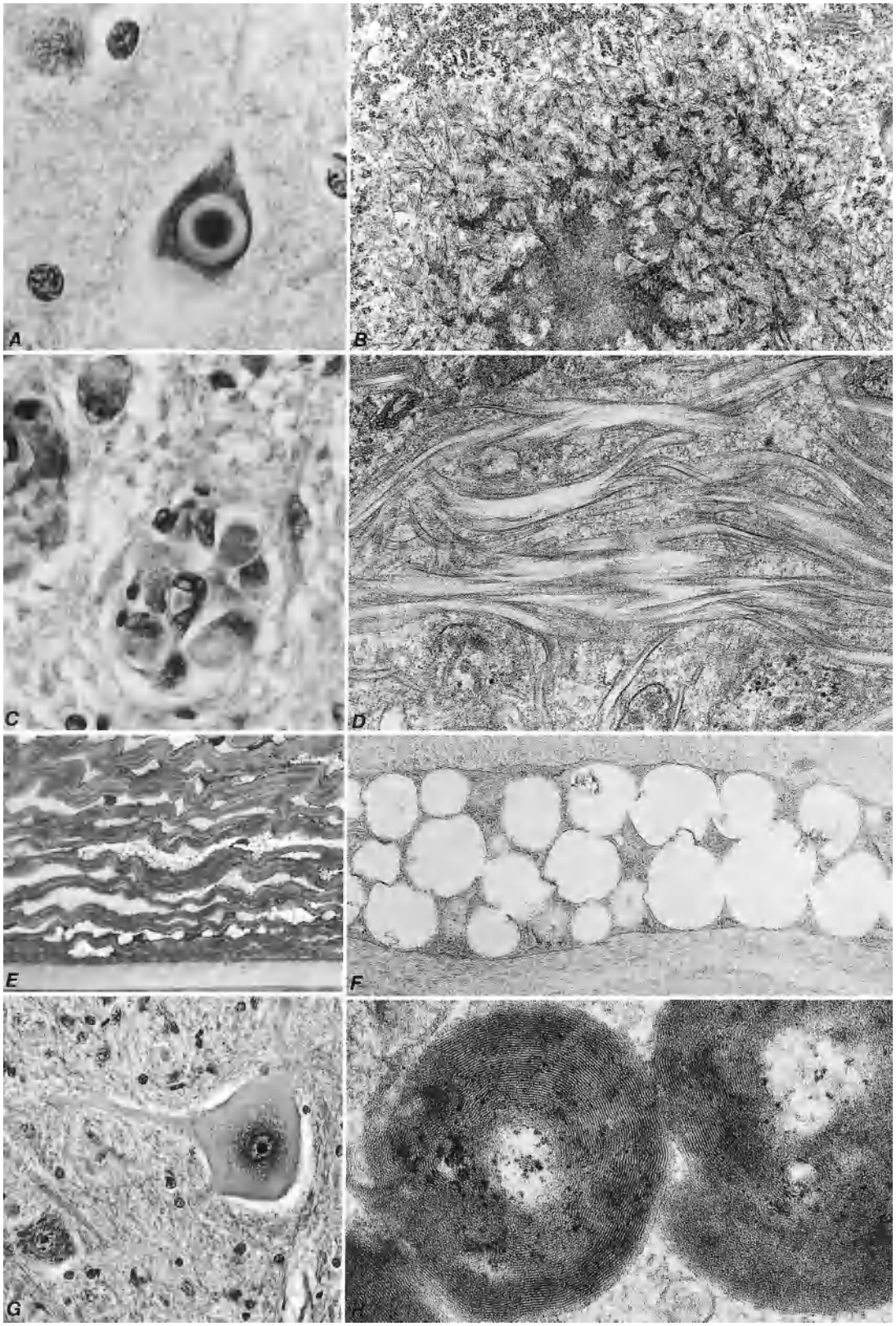


Fig. 27.1 Lysosomal storage diseases. A–B. Lafora's disease: glycoprotein cytoplasmic inclusions, neuron, dog. **B**. Core and margin of neuronal inclusion, and surrounding ribosomes of Purkinje cell. (Micrographs: J. M. Holland, *Am J Pathol* 58:509, 1970.) **C–D**. **Globoid cell leukodystrophy**: dog. Perivascular macrophages filled with cerebrosides. **D**. Arched twisted and interdigitated membrane-bound, ribbon-like structures. (Micrograph: Eduardo J. Yunis, *Am J Pathol* 85:99, 1976.) **E–F**. **Feline mucopolysaccharidosis VI**. Enlarged keratocytes are filled with aggregates of inclusions. Descemet's membrane (*bottom*) is normal. **F**. Electron-lucent vacuoles filling keratocyte cytoplasm. (Micrograph: M. E. Haskins, *Am J Pathol* 101:567, 1980.) **G**. **Gangliosidosis**: cat. Massively enlarged neuron (*right*); normal neuron (*left*). **H**. **Metachromatic leukodystrophy**: brain, human infant. Sulfatide-containing inclusions consist of myelin figures. (Micrograph: A. Gregoire, *J Pathol Exp Neurol* 25:626, 1966.)

© 2009 Wiley-Blackwell. ISBN: 978-0-813-80330-2

27 Metabolic and Storage Diseases

Lipid Storage Diseases

The **lipid storage diseases** are the most common of the lysosomal diseases. Hydrolases that degrade sphingomyelin, ceramide, and glycosphingolipids operate in a pathway that converges on ceramide. For many of the steps in this pathway, there is a specific human familial lipid storage disease and an animal model that involves the deficiency of a specific enzyme. The consequence of a missing enzyme is an accumulation of the substrate, with marked distortion of lysosomes caused by the accumulation of unused substrates. Specific ultrastructural aspects of the lysosomal inclusions are characteristic for certain syndromes: **tubules** in Gaucher's and Krabbe's diseases, **prismatic structures** in metachromatic leukodystrophy, clear **vacuolar inclusions** in the mucopolysaccharidoses, **lamellar structures** of gangliosidosis and the Niemann-Pick and Fabry's syndromes, and the **curvilinear membranes** of Farber's disease (Fig. 27.1). Electron microscopic analysis of chorionic villus biopsies is a critical tool in the diagnosis of lysosomal storage diseases.[1]

The most important lipid storage diseases involve defective or missing enzymes that degrade components of cellular membranes, particularly those of myelin. Because normal degradation occurs inside lysosomes (where terminal sugar groups are sequentially removed from these complex lipids), disease results in large abnormal lysosomes. Mechanisms of lipid synthesis are normal in most of these syndromes, that is, they are lipid catabolic defects. Rare lipid anabolic disorders have been reported in human lipid storage disease in which enzymes for formation of GM_2 from GM_3 are missing.

Lipid storage diseases result from different defects: lysosomal enzymes may be defective, enzyme activator proteins may be deficient, or newly synthesized enzymes may lack recognition markers essential for directing them to lysosomes or across the lysosomal membrane. In the first case, the defective enzyme may (1) cause the substrate of that enzyme to accumulate; or (2) lead to defective enzymatic hydrolysis, wherein substrates are hydrolyzed to nondegradable products that accumulate in the cell. Affected cells are engorged with abnormal lipid complexes.

GM_1-Gangliosidosis

GM_1-gangliosidosis is caused by deficient activity of acid β-galactosidase. Glycolipids and oligosaccharides accumulate in lysosomes in many tissues and are excreted in the urine. Human GM_1-gangliosidosis occurs in three variants: infantile (type 1), juvenile (type 2), and adult (type 3). The disease has been identified in cats, cattle, sheep, and dogs (Table 27.1).[2] Affected cells are markedly enlarged, chiefly through massive expansion of lysosomes filled with characteristic whorls and laminar arrangements of membranes. Storage materials are found in neurons, astrocytes, endothelial cells, and several retinal cell types (Fig. 27.2). They also occur in hepatocytes and Kupffer cells, and are found in renal tubular cells, pancreatic ductal epithelium, and islet β-cells. Myelin deficit is a significant part of the disease; it arises from loss of oligodendrocytes and abnormal axoplasmic transport.[3]

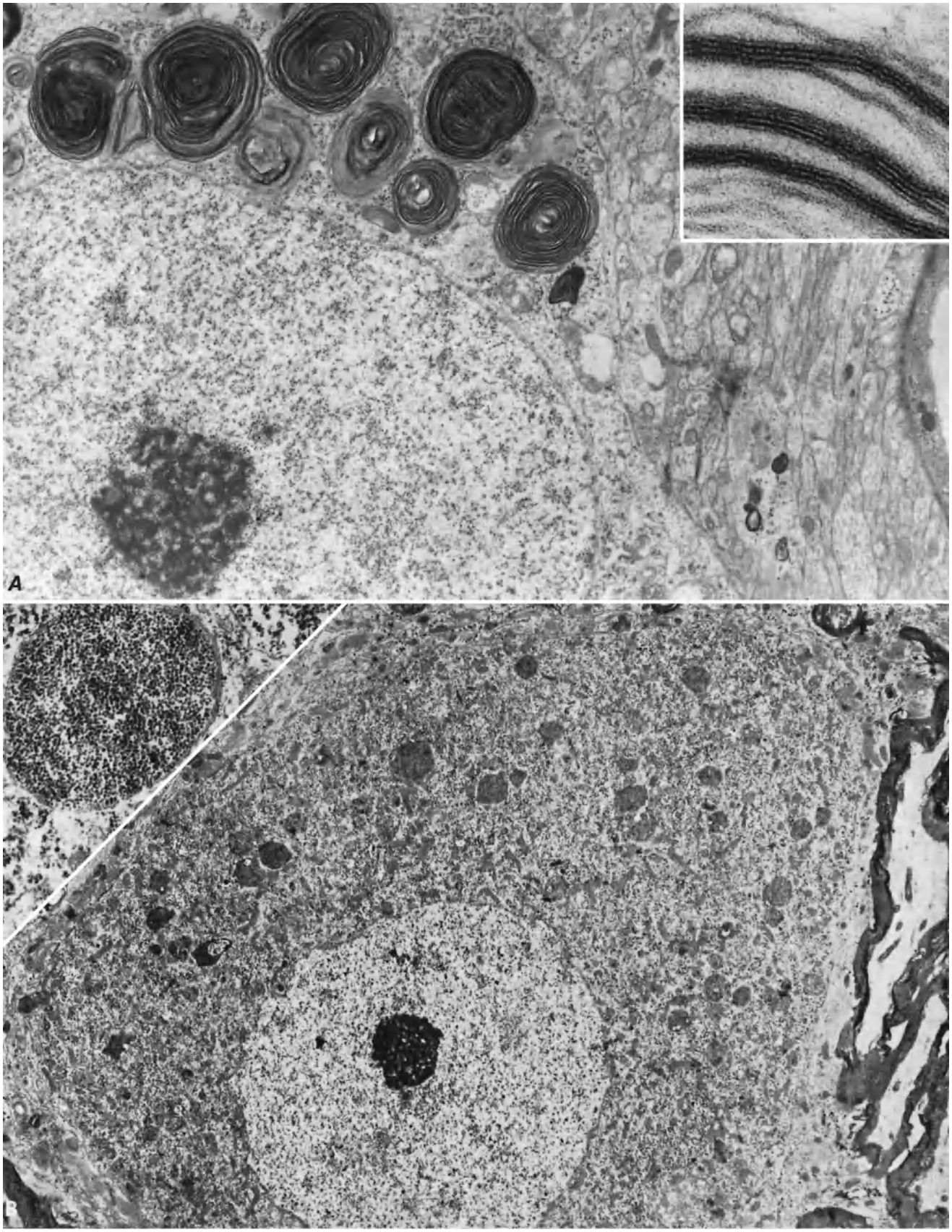


Fig. 27.2 Lysosomal storage diseases. **A**. **GM_1 gangliosidosis**: cow. Membranous cytoplasmic bodies in neuron, cerebral cortex. *Inset*: lamellae have periodicity of 5.5–6.0 nm. (Micrograph: B. Sheahan, *Acta Neuropathol* 30:73, 1974.) **B**. **Glycogen storage disease**: neuron. *Inset*: glycogenosome. (Micrograph: B. Sandström, *Acta Neuropathol* 14:194, 1969.)

Table 27.1 Naturally occurring models of sphingolipid storage diseases.

Disease	*Species*	*Reference to ultrastructural pathology*
GM_1 gangliosidosis: β-galactosidase deficiency	Cat	**Baker**, *Science* 174:838, 1971; **Blakemore**, *J Comp Pathol* 83:179, 1972; **Farrell**, *J Neuropathol Exp Neurol* 32:1, 1973; **Gonzalez-Licea**, *Am J Vet Res* 39:1342, 1978
	Cow	**Sheahan**, *Acta Neuropathol* 30:73, 1974
	Dog	**Alroy**, *Science* 229:470, 1985; **Muller**, *Vet Pathol* 38:281, 2001 (Husky); **Read**, *Science* 194:442, 1976; **Rodriguez**, *J Neuropathol Exp Neurol* 41:618, 1982; **Saunders**, *Vet Pathol* 25:265, 1988; **Whitfield**, *Acta Neuropathol* 100:409, 2000
	Human	**Folkerth**, *Pediatr Dev Pathol* 3:73, 2000; **Kasama**, *Jap J Exp Med* 56:1, 1986; **Okada**, *Science* 160:1002, 1968; **Takebayashi**, *Virch Arch* 5:301, 1970; **van der Voorn**, *Acta Neuropathol* 107:539, 2004
	Sheep	**Murnane**, *Am J Pathol* 134:263, 1989; **Ryder**, *Acta Neuropathol* 101:225, 2001 (Romney)
GM_2 gangliosidosis, Tay-Sachs disease: hexosaminidase A deficiency	Dog	**Bernheimer**, *Acta Neuropathol* 16:243, 1970; **Cummings**, *Acta Neuropathol* 67:247, 1985 (Japanese spaniel); **Karbe**, *Am J Pathol* 71:151, 1973 (German shorthair)
	Human	**Adachi**, *Lab Invest* 30:102, 1974 (fetus); **De Baecque**, *Acta Neuropathol* 33:207; **O'Brien**, *Fed Proc* 32:191, 1973
	Pig	**Kosanke**, *Vet Pathol* 16:6, 1979
GM_2 gangliosidosis, Sandhoff's disease: hexosaminidase A, B deficiencies	Human	**Blieden**, *Am J Cardiol* 34:83, 1974
GM_2 ganglioside activator deficit	Human	**Mark**, *J Mol Biol* 327:1093, 2003
Gaucher's disease: β-glucosidase deficit (glycosylceramide storage)	Dog	**Hartley**, *Vet Pathol* 10:191, 1970; **Lee**, *Proc Natl Acad Sci USA* 61:484, 1969
	Human	**Cervos-Navarro**, *Clin Neuropathol* 9:310, 1990; **Hibbs**, *Arch Pathol* 89:137, 1970
Krabbe's disease (globoid leukodystrophy): galactosylceramide deficit (galactosylsphingosine storage)	Dog	**Suzuki**, *Acta Neuropathol* 69:33, 1986 (kidney); **Yajima**, *J Neurol Sci* 33:179, 1977; **Yunis**, *Am J Pathol* 85:99, 1976
	Human	**Bischoff**, *Brain* 92:861, 1969; **Brownstein**, *Arch Ophthalmol* 96:864, 1978 (optic nerve); **Schlaepfer**, *Acta Neuropathol* 20:55, 1972; **Schochet**, *Acta Neuropathol* 36:153, 1976; **Schochet**, *Arch Pathol* 88:305, 1969; **Suzuki**, *Arch Neurol* 22:385, 1970; **Yunis**, *Lab Invest* 21:415, 1969
	Mouse	**Kobayashi**, *Am J Pathol* 131:308, 1988; **Powell**, *Lab Invest* 49:19, 1983 (galactosylceramidase); **Suzuki**, *Am J Pathol* 111:394, 1983; **Takahashi**, *Am J Pathol* 112:147, 1983 (twitcher)
	Sheep	**Pritchard**, *Vet Pathol* 17:399, 1980 (Dorset)
Fabry's disease: α-galactosidase deficit (storage of glycol-spinoglipids with terminal α-galactosyl)	Human	**Dvorak**, *Pathol Annu* 16:139, 1981; **Faraggiana**, *Am J Pathol* 103:247, 1981; **Ferrans**, *Am J Cardiol* 24:95, 1969 (heart); **Fukuhara**, *Acta Neuropathol* 33:9, 1975 (nerve); **Malmqvist**, *Lab Invest* 25:1, 1971; **Nistal**, *J Pathol* 141:113, 1983 (testes); **Tome**, *Acta Neuropathol* 38:187, 1977; **Tondeur**, *Virch Arch B* 2:239, 1969
Niemann-Pick disease: sphingomyelinase deficit (sphingomyelin storage)	Cat	**Snyder**, *Am J Pathol* 108:252, 1982; **Wenger**, *Science* 208:1471, 1980
	Dog	**Bundza**, *Vet Pathol* 16:530, 1979 (poodle)
	Human	**Ellender**, *Acta Neuropathol* 66:325, 1985; **Lazarus**, *Lab Invest* 17:155, 1967 (leukocytes); **Lynn**, *Am J Med* 37:987, 1964
	Mouse	**Adachi**, *Am J Pathol* 85:229, 1976; **Butler**, *Am J Pathol* 170:2077, 2007 (knockout mouse)
Farber's disease: acidic ceramidase deficit (ceramide storage)	Human	**Battin**, *Ann Dermatol Syphil (Paris)* 97:241, 1970; **Dustin**, *Bull Acad R Med Belg* 128:733, 1973; **Pellissier**, *Acta Neuropathol* 72:178, 1986 (nerve); **Rutsaert**, *Lab Invest* 36:474, 1977 (in vitro); **Schmoeckel**, *Arch Dermatol* 266:187, 1979
Metachromatic leukodystrophy: aryl-sulfatase A deficit (galactosylsulfatide storage)	Human	**Goebel**, *Ophthalmol Res* 24:103; **Guerra**, *J Neuropathol Exp Neurol* 49:406, 1990; **Raynaud**, *Arch Neurol* 32:834, 1975; **Resibois**, *Acta Neuropathol* 13:149, 1969
Orthochromatic leukodystrophy	Human	**Gray**, *J Neuropathol Exp Neurol* 46:585, 1987
Schindler's disease: α-*N*-acetylgalactosaminidase deficit (glycosphingolipids, oligosaccharide storage)	Human	**Bakker**, *Eur J Hum Genet* 9:91, 2001
Cerebroside-sulfate activator protein: saposin B deficit; (galactosylsulfatide storage)	Human	**Castagnaro**, *Virch Arch B Cell Pathol* 54:16, 1987
Wolman's disease (cholesterol ester storage disease): acid lipase deficit	Human	**Lough**, *Arch Pathol* 89:103, 1978
	Rat	**Kuriwaki**, *Pathol Int* 49:291. 1999

Tay-Sachs Disease (GM_2-Gangliosidosis)

The autosomal recessive **Tay-Sachs disease** is the prototype storage disease and most important gangliosidase defect. Blindness and progressive mental and motor deterioration from lesions throughout the nervous system develop in affected human infants. Lysosomal storage of GM_2-gangliosides in Tay-Sachs (and in the related disorder, **Sandhoff disease**) is caused by deficiency of β-hexosaminidase A, and is accompanied by an increase in the other isoenzyme, hexosaminidase B). Hexosaminidase A is absent from all tissues but accumulation of gangliosides in neurons and retinal ganglion cells accounts for the clinical disease. Neurons are massively enlarged and filled with cytoplasmic vacuoles, each a giant lysosome filled with myelin figures. As the disease progresses there is destruction of neurons, proliferation of microglia, and accumulation of complex lipids in phagocytes within the neuropil.

The **Korat cat** has defects in HEXB genes encoding the β subunit of the β-hexosaminidases. Two major isozymes of β-hexosaminidase in normal tissue are β-hexosaminidase A (hexA), composed of an α and β subunit, and hexB, a dimer of β subunits. Type 1 GM_2-gangliosidosis (Tay-Sachs disease) is caused by a defect in the α chain. Type II results from a defect in β subunits.[4]

Ultrastructural studies in mouse models of Sandhoff's disease inoculated intracerebrally with recombinant adeno-associated viral vectors have shown effective delivery of the missing gene.[5]

Niemann-Pick Disease

Niemann-Pick disease is characterized by accumulation of sphingomyelin and cholesterol in macrophages and parenchymal cells in many tissues. Biochemically, three groups are distinguished, each with several subgroups. Human patients with types A and B Niemann-Pick disease have an inherited deficiency of the lysosomal hydrolase, **acid sphingomyelinase (ASM). Type A** is the infantile, neurologic form; **type B** is the nonneurologic form that allows survival into adulhood. In type A, there is marked neurologic involvement, visceral accumulations of sphingomyelin, and progressive wasting. Mutations in the gene SMPD1 (encoding ASM) in types A and AB Niemann-Pick disease, and ASM knockout mice are a faithful model of the inherited human disorder.[6]

Niemann-Pick type C disease leads to the development of massive accumulations of cholesterol and other lipids in late endosomes and lysosomes. The **Niemann-Pick C protein** (NPC) binds to cholesterol from internal lysosomal membranes, and is involved in cholesterol and lipid trafficking and degradation. In about 95% of cases, disease results from mutations in the NPC1 gene; the remaining are due to mutations in the NPC2 gene. Neurodegeneration is associated with dysfunctional cholesterol metabolism, endosomal/lysosomal dysfunction, and tauopathies. Diffuse endogenous lipid pneumonia involving foamy pulmonary macrophages can be a cause of death.[7] In a mutant mouse model, cholesterol accumulation-induced changes in autophagolysosome function were a major pathogenetic factor, and involve mannose-6-phosphate receptors.[8] Affected neurons undergo apoptosis triggered by TNF-α expressing astrocytes.[9]

Gaucher's Disease

Gaucher's disease results from deficiency of β-glucocerebrosidase, the enzyme that cleaves glucose and ceramide residues from glucocerebrosides. Rare patients have been reported with normal enzyme levels but mutations in the gene for the sphingolipid activator protein C (sap-C).[10] Gaucher's disease has been divided into an adult onset form (type 1) and unlike most lysosomal proteins that are tagged with a carbohydrate modification that allows their transport to lysosomes, β-glucocerebrosidase follows a unique pathway. In lysosomal membranes, the integral membrane protein LIMP-2 is a specific binding partner of β-glucocerebrosidase. The uncleaved glucocerebroside accumulates in lysosomes, typically in foamy macrophages (Gaucher cells) in the spleen, liver, and bone marrow; lipid storage in neurons results in a neurologic form.[11] The giant pleomorphic lysosomes are filled with characteristic tubular inclusions (Fig. 27.3).

Located on human chromosome 1, the glucocerebrosidase gene is associated with a pseudogene. Alterations in the DNA sequence of the gene in patients with Gaucher's disease include point mutations in exons and in a splice site, a nucleotide insertion, crossovers between the gene and pseudogene, and gene conversions. Many mutations exist, but four account for over 97% in Ashkenazi Jews, the population group in which Gaucher's disease is most common. Within each genotype there is marked variability in severity of disease. Ultrastructural studies of children receiving enzyme replacement therapy indicate that Gaucher cells persist in the abdominal lymph nodes.[12] Ultrastructural studies of mouse models of Gaucher's disease establish the usefulness in therapeutic interventions trials.[13]

Neutral lipid storage disease with ichthyosis (NLSDI, Chanarin-Dorfman syndrome) is an ichthyosiform disorder associated with mutations in a lipid

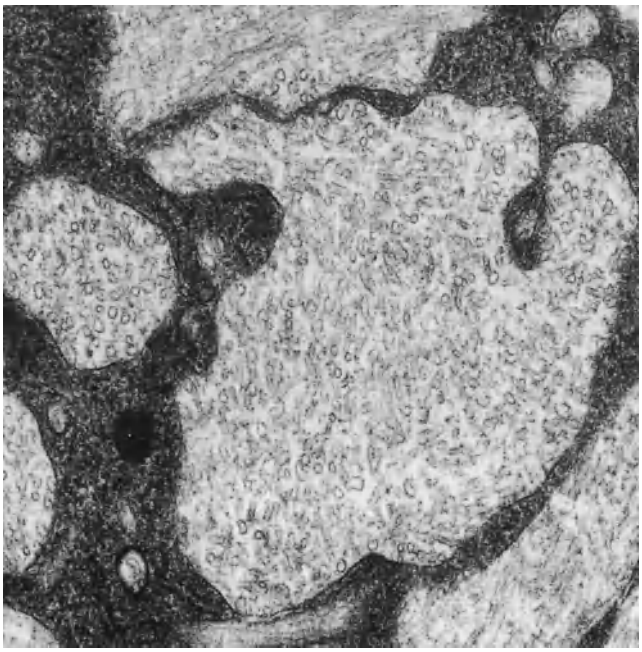


Fig. 27.3 **Lysosomal inclusions**: human infant with Gaucher's disease. (Micrograph: Theodore C. Iancu, *Ultrastruct Pathol* 16:231, 1992.)

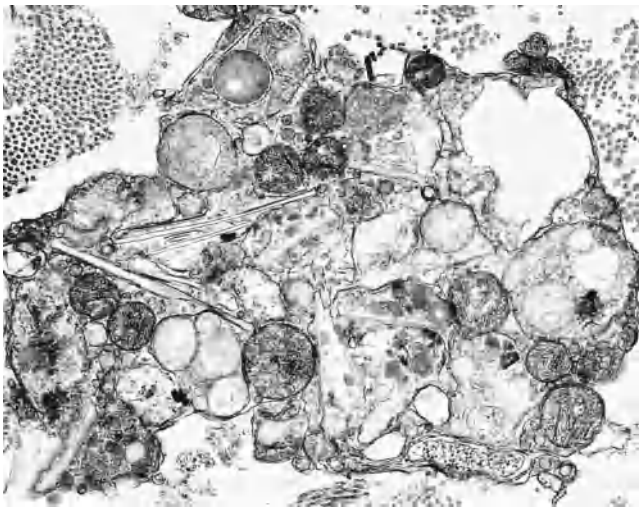


Fig. 27.4 Acid lipase deficiency: secondary lysosomes contain neutral lipids and cholesterol clefts. (Micrograph: Joseph Alroy.)

hydrolase and accumulations of neutral lipid globules in tissues in patterns that resemble type 2 Gaucher's disease; in NLSDI, the cutaneous basal permeability barrier and stratum corneum are dysfunctional.[14]

Krabbe's Disease (Globoid Cell Leukodystrophy)

Due to a deficiency of galactocerebroside-β-galactosidase, Krabbe's disease is characterized by a loss of myelin and an increased ratio of galactocerebroside to sulfatides, but not an accumulation of galactosylceramide, the deficient enzyme's substrate. The mutation involves production of normal amounts of enzyme but the activity of the mutant enzyme is low. Ultrastructurally, long tortuous and twisted tubular structures are pathognomonic for Krabbe's disease. Rhesus macaques are affected with globoid cell leukodystrophy.[15]

The **twitcher mouse** (*twi/twi*) is a model for Krabbe's disease. The marked deficit of galactosylceramidase and lactosylceramidase leads to accumulation of lysosomal phospholipids and multinucleate globoid cells in white matter. Progressive muscle weakness is associated with demyelination in central and peripheral nervous system and needle shaped cytoplasmic inclusions in Schwann cells. Demyelination is caused by metabolic disturbances of myelin-forming cells and is accompanied by massive infiltrates of macrophages into the area of demyelination.[16] There is a gradual depletion of oligodendrogliocytes by apoptosis in genetic demyelination.[17]

Globoid cell leukodystrophy has been reported in cats and in Cairn and West Highland terriers. The globoid cells, largely restricted to nervous tissue, are straight, arched, and twisted tubular inclusions having longitudinally fibrillar walls (see Fig. 27.1).

Wolman's Disease

Wolman's disease is a lethal lysosomal storage disease arising from deficiency of **lysosomal acid lipase** (LAL), a hydrolase essential for intracellular degradation of cholesteryl esters and triglycerides. Death in infancy has lesions of hepatosplenomegaly, steatorrhea, and adrenal cortical calcification. Cholesterol esters accumulate in tissues in which they are normally synthesized, for example, adrenal cortex, liver, intestine, spleen, and abdominal lymph nodes. Cholesterol clefts are common in Kupffer cells (Fig. 27.4). Gene replacement studies using a recombinant adenovirus encoding the human LAL cDNA seem promising and electron microscopy reveals lysosomal expression of recombinant LAL in vitro.[18] Wolman's disease rats (Yoshida rat) have hepatocytes with many small lipid globules and lipid crystals, and large foamy Kupffer cells with multivesicular bodies bearing curvilinear structures and crystal clefts.[19]

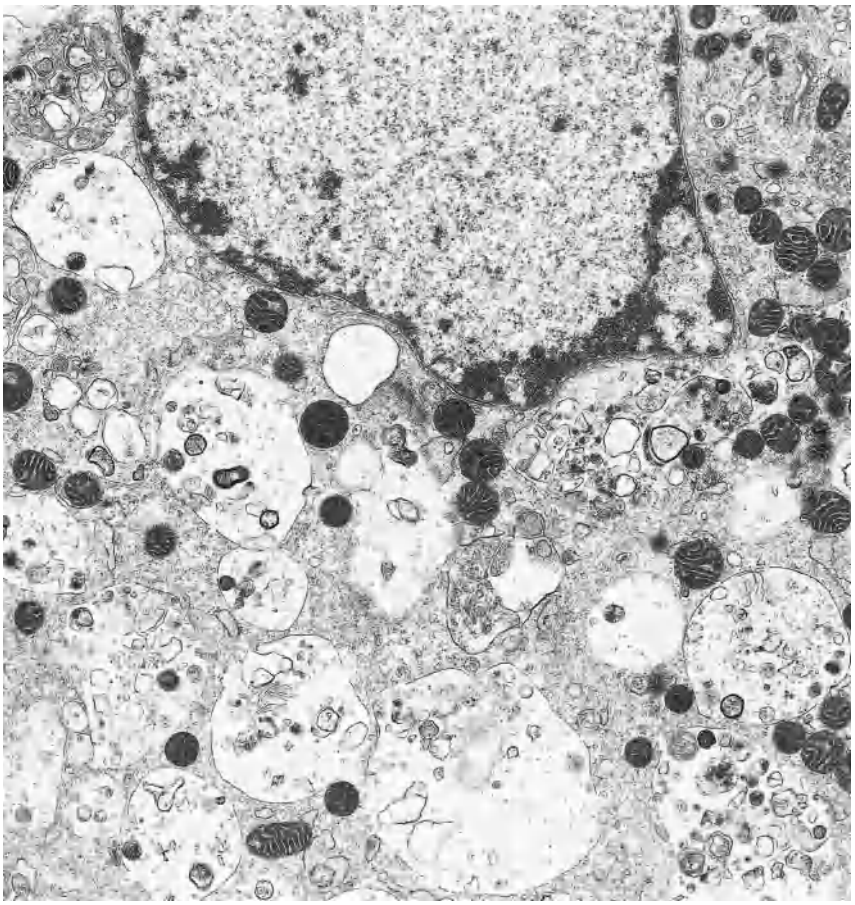


Fig. 27.5 Chloroquine toxicity: lysosomal proliferation. Large pale vacuoles containing cellular debris and myeloid bodies are autophagolysosomes. (Micrograph: James Tappe, National Animal Disease Center.)

Fabry Disease

Fabry disease is an X-linked lysosomal storage disease caused by a deficiency of alpha-galactosidase A. There are diverse mutations in the *GLA* gene. Endothelial cell accumulation of globotriaosylceramide, the main glycolipid in Fabry disease,[20] leads to progressive renal disease, cardiomyopathy, neurodegeneration, and cutaneous angiomas. Immunogold labels for globotriaosylceramide are found in the plasma membrane and cytoplasm of endothelial cells. Globotriaosylsphingosine, deacylated globotriaosylceramide, and other globotriaosylceramide metabolites are present in serum.[21]

Drug-Induced Lysosomal Lipid Storage Disease

Drugs that induce generalized lipidosis by complexing with polar lipids of lysosomal membranes are the depressants chloroquine, chlorpromazine, chlorphentermine, and iprindol (Fig. 27.5). They are amphophilic compounds containing hydrophobic and hydrophilic moieties in close proximity. **Chloroquine,** used for treatment of malaria and some chronic immunologic diseases, induces large foamy, granular lysosomes that result from markedly increased autophagy.[21] The initial accumulation of tiny membranous vesicles in the lysosome is followed by a progressive increase of membrane fragments. Failure of enzymatic digestion results in the accumulation of membrane-bound aggregates of cell membranes and myeloid bodies.[22–25]

Neuronal Ceroid Lipofuscinoses

Neuronal lipofuscinoses have in common the accumulation of autofluorescent lipopigments in neurons. Ultrastructurally, their pigment granules are massive lipofuscin bodies with lattice forms, curvilinear bodies, and fingerprint arrangements of membranes.[26,27] These bodies are **autophagolysosomes**. There is a deficit of lysosomal cathepsins that leads to neurodegeneration and neuron death. The eye is involved because of the unique metabolism of photoreceptor cells. Retinal pigment epithelium, which degrades senescent photoreceptor cells, accumulates large amounts of lipofuscin in vitamin E deficiency of dogs[28] and sheep.[29]

In children the diseases known collectively as the **neuronal lipofuscinoses** are characterized by mental retardation, blindness, and premature death. They are the most common inherited neurodegenerative diseases of childhood. Human syndromes are divided into four syndromes: infantile, late infantile, adult, and juvenile (Batten's disease). The abundance of the amino acid trimethyllysine in the pigment suggests that the disease may result from excessive methylation of the stored proteins.[30]

Studies in autophagolysosomal storage disease in cathepsin D-deficient mice suggest that these autophagolysosomes are caused by an exaggerated conversion of MAP1l-LC3 (or autophagosome formation) from the cytosolic to the membrane-bound form,[31] and that affected lysosomes contain proteolipids including subunit c of mitochondrial ATP synthase and sphingolipid activator proteins.

A group of similar diseases has been reported in monkeys, cats, South Hampshire sheep, cattle, and dogs.[32–34] In dogs, neuronal lipofuscinosis occurs as an autosomal recessive syndrome in English setters with progressive loss of cerebral function. Autofluorescent pigments consist of about 50% acidic lipid polymers. In canine neuronal lipofuscinosis there is a markedly decreased tissue level of p-phenyldiamine-linked peroxidase. Devon cattle show blindness with this syndrome associated with pigment deposits in the retina.[35] The ***mnd*** mouse is a model for neuronal ceroid lipofuscinosis. Stored material is composed of granular, multilamellar, fingerprint and curvilinear profiles.[36]

Glycoproteinoses

Degradation of oligosaccharide chains of glycoproteins, like that of sphingoglycolipids, involves the sequential action of lysosomal enzymes. Enzyme deficiencies that result in human glycoprotein lysosomal storage diseases fall into four groups: **sialidoses** (deficit of sialic acid),[37] **fucosidoses** (deficit of α-L-fucosidase), **mannosidoses,** and **aspartyl-glycosaminouria.**[38,39] There is much heterogeneity with some being lethal and others permitting survival.[40] Human disease arising from storage of glutamyl ribose-5-phosphate has been reported.[39] Certain plant toxins induce glycoprotein storage diseases that mimic the hereditary stroage diseases.[41]

Fucosidosis

Human **fucosidosis** is a rare lysosomal storage disease caused by a defect of the A-L-fucosidase gene, *FUCA1*; the spectrum of over 22 mutations detected to date include missense and nonsense mutations, deletions, duplications and one insertion. The disease presents with neurologic skeletal and cutaneous findings including angiokeratomas with characteristic electron-lucent cytoplasmic vacuolations.[106,107] **Canine fucosidosis** (in English springer spaniels) involves progressive neurologic degeneration.[108]

Sialidoses

Sialidosis (neuraminidase deficiency) is a deficit in lysosomal neuraminidase. Three different mammalian sialidoses have been described: lysosomal (Neu1, gene *NEU1*), cytoplasmic (Neu2, gene *NEU2*), plasma membrane (Neu3, gene *NEU3*), and lysosomal lumen sialidase (Neu4, gene *NEU4*). Mutations in *NEU1* and deficiency of Neu1 in humans cause the severe multisystemic disorder, **sialidosis.** Lysosomal sialidase (neurominidase-1, Neu1) is targeted to the cell surface in a multiprotein complex. Neu4 is targeted to lysosomes by a mannose 6-phosphate receptor and does not require other proteins for enzymatic activity.

Galactosialidosis, a combined deficiency of lysosomal neuraminidase and lysosomal beta-galactosidase, is a similar disorder. It is caused by a secondary Neu1 deficiency due to genetic defects in cathepsin A (cathepsin A forms a complex with Neu1 in order to activate it).

Salla Disease

Reported from Finland, this is an inherited human autosomal recessive syndrome. Patients have psychomotor retardation, spasticity, and ataxia with an early onset and slow progression. They excrete large amounts of unbound N-acetylneuraminic acid (sialic acid, NANA) and store 10–30 times the normal amounts in tissues. Characteristic vacuolated cytoplasmic inclusions are derived from swollen lysosomes with high concentrations of free NANA.[43] The amounts of NANA-containing membrane glycoproteins and gangliosides are normal in cells, and a normal amount of acid neuraminidase activity cleaves NANA from glycoconjugates in lysosomes. Fibroblasts from patients do not release sialic acids because of a defective transport of this monosaccharide across the lysosome.[44]

Mannosidosis

The various forms of mannosidosis are caused by defects in genes responsible for production of lysosomal α or β mannosidase. Disease results from the accumulation of mannose-containing oligosaccharides in tissue, especially in the central nervous system. Affected cells are large, granular, and foamy and filled with giant electron-lucent lysosomes that contain

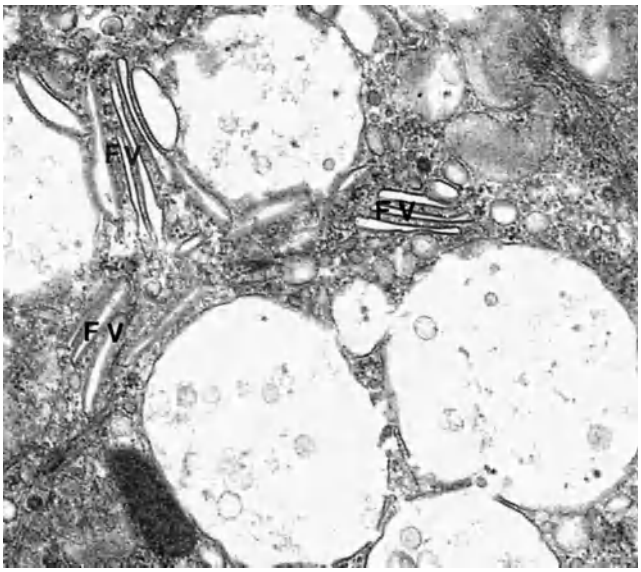


Fig. 27.6 **α-Mannosidosis**: urothelial cell, Persian kitten. Note collapsed fusiform vesicles (*FV*), fibrils, and small vesicles. Enlarged lysosomes contain oligosaccharides. (Micrograph: Joseph Alroy, *J Vet Diag Invest* 12:483, 2000.)

small amounts of granular debris and vesicles (Fig. 27.6).[45] Animal models for mannosidosis occur in cats, goats[46] and cattle.[47,48] In caprine mannosidosis, the thyroid is markedly affected and the ensuing hypothyroidism may play a role in the hypomyelination that characterizes the advanced stages of the caprine disease.[49]

Geleophysic Dysplasia

This skeletal disease has been shown to be a primary disorder of glycoprotein metabolism, and appears as a lysosomal storage disease in hepatocytes and in fibroblasts of the cardiac valve leaflets.[50] Neither the enzyme defect nor the storage material has been identified.

Mucopolysaccharidoses

The **mucopolysaccharidoses** are a group of genetic diseases characterized by storage of incompletely degraded **glycosaminoglycans (GAGs)** (Table 27.2). They result from mutations in the genes that encode different lysosomal enzymes that are required for the degradation of GAGs. GAGs are attached to protein cores to form the proteoglycans of intersitital connective tissue. Degradation of glycosaminoglycan occurs in lysosomes, where it is initiated by endoglycosidases such as hyaluronidase, which cleaves polysaccharide chains into smaller units. Storage of excessive GAGs occurs from diminished activity of specific hydrolases in lysosomes required for degradation. Massive

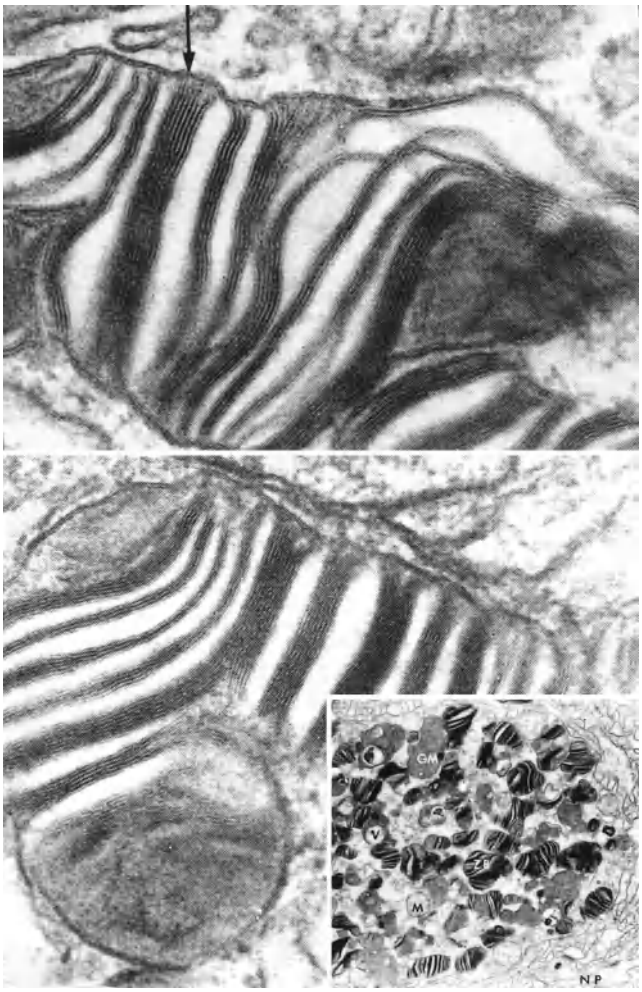


Fig. 27.7 **Gargoylism**: lysosomes, human. Cytoplasm of neuron is replaced by zebra bodies (*arrow*). *Inset*: Cytoplasm has pale mitochondria (*M*), mucopolysaccharide vacuoles (*V*), and neuropil (*NP*). (Micrograph: Fernando P. Aleu, *J Neuropath Exp Neurol* 24:304, 1965.)

accumulation of giant lysosomes bearing GAG polymers causes distortion of the affected cells (Fig. 27.7).[51,52] Each of the mucopolysaccharidoses has distinct phenotypes and urinary GAG excretion profiles.

The human **systemic mucopolysaccharidoses** are associated with syndromes of mental retardation, blindness due to corneal opacities, and cardiovascular deformities. Different lysosomal hydrolases can be demonstrated to be deficient or absent in fibroblasts cultured from skin of affected patients.[53] For example, **Sanfilippo disease** (mucopolysaccharidosis III) is a family of storage diseases caused by different enzyme defects, but all lead to accumulation of one glycosaminoglycan, heparan sulfate. Liver biopsies in types I, II, III, VI reveal inclusions not only in hepatocytes, but also in Kupffer and Ito cells: MPS type VI cases had inclusions that were fewer, smaller and contained more lipofuscin than those in other types.[54] **Localized**

Table 27.2 Ultrastructural pathology in animal models of mucopolysaccharidoses.

MPS type	*Enzyme deficiency*	*Species*	*Reference to ultrastructural pathology*
MPS I	α-L-iduronidase	Cat	**Kakkis**, *Mol Genet Metab* 72:199, 2001 (enzyme replacement therapy)
		Dog	**Shull**, *Proc Natl Acad Sci USA* 91:12937, 1994
		Human IH*: Hurler	**Huang**, *Exp Eye Res* 62:377, 1996 (eye)
		Human IS#: Scheie	**Verrips**, *Neuropediatrics* 32:93, 2001 (muscle)
		Human IH/S: Hurler-Scheie	
		Mouse	**Zheng**, *Mol Genet Metab* 79:233, 2003 (Idua knockout mouse)
MPS II*	α-L-idurono-2-sulfate sulfatase	Cat	**Hubler**, *J Small Anim Pract* 37:435, 1996
		Human (Hunter)	**Yoshimoto**, *Intern Med* 45:1133, 2006 (liver)
MPS III	Heparin N-sulfatase	Human (Sanfilippo A)	
		Dog	**Jolly**, *Vet Pathol* 44:569, 2007
		Mouse	**Bhaumik**, *Glycobiology* 9:1389, 1999
	N-acetyl-A-D-glucosaminidase	Human (Sanfilippo B)	
		Mouse	**Ohmi**, *Proc Natl Acad Sci USA* 100:1902, 2003
	α-Glucosamine-N-acetyltransferase	Human IIID (Sanfilippo C)	**Alroy**, *Acta Neuropathol* 93:210, 1997 (skin); **Kurihara**, *Pediatri Neurol* 14:317, 1996
	N-acetylglucosmamine-6-sulfatase	Goat	**Jones**, *J Neuropathol Exp Neurol* 57:148, 1998
		Human (Sanfilippo D)	
MPS IV	Arylsulfatase B	Human (Morquio A)	**Rawe**, *Cornea* 16:369, 1997 (cornea)
	Galactosamine-6-sulfatase	Mouse	**Evers**, *Proc Natl Acad Sci USA* 93:8214, 1996 (ASB gene disruption)
	β-Galactosidase	Human (Morquio B)	**Leslie**, *Br J Ophthalmol* 89:925, 2005
MPS VI	N-Acetylgalactosamine-4-sulfatase	Cat	**Abreu**, *Calcif Tissue Int* 57:185, 1995 (bone); **Crawley**, *J Clin Invest* 97:1864, 1996 (enzyme replacement therapy); **Norrdin**, *Bone* 17:485, 1995 (bone)
	Arylsulfatase B		
		Human VI: Maroteaux-Lamy	**Akhtar**, *Br J Ophthalmol* 86:147, 2002 (eye); **Walkley**, *Neuropathol Appl Neurobiol* 31:536, 2005
		Rat	**Simonaro**, *Transplantation* 63:1386, 1997
MPS VII	β-Glucuronidase	Cat	**Schultheiss**, *Vet Pathol* 37:502, 2000
		Dog	**Wolfe**, *Mol Ther* 2:552, 2000 (liver)
		Human (Sly)	**Molyneux**, *J Clin Pathol* 50:252, 1997
		Mouse	**Casal**, *Pediatr Res* 47:750, 2000 (fetus)
		Rat	**Yoshida**, *J Comp Pathol* 109:141, 1993
MPS IX	Hyaluronidase	Human	**Triggs-Raine**, *Proc Natl Acad Sci USA* 96:6296, 1999

*Both formerly gargoylism.

corneal mucopolysaccharidoses (macular corneal dystrophy), which are characterized by deposits of glycosaminoglycans in corneal stroma, occur in humans with an inability to catabolize keratin sulfate.[54]

The clinical manifestations of severe **mucopolysaccharidosis type VII** (Sly syndrome) are mental retardation, skeletal abnormalities, corneal opacity, and hepatosplenomegaly. All of these syndromes have leukocyte inclusions and excrete glycosaminoglycans in the urine. In most, the liver is enlarged and has vacuoles that contain granular material in both hepatocytes and Kupffer cells.[55] Activity of β-glucuronidase, the deficient enzyme, may be as low as 1% of normal.

Hurler's Disease

Mucopolysaccharidosis due to α-L-iduronidase (type I) is characterized by severe mental retardation, skeletal malformations, corneal opacities, abnormal facial appearance, and cardiovascular lesions including coronary arterial narrowing and cardiac valvular deformities. The activity of α-L-iduronidase, a lysosomal hydrolase, is decreased in tissue. Dermatan sulfate and heparan sulfate are present in abnormally large amounts in affected cells (and in urine). These compounds accumulate in large connective tissue cells called Hurler cells or gargoyle cells.[56,57] Hurler cells contain large lysosomes distended with storage

materials. The materials are soluble causing the cells to be clear and foamy histologically. Ultrastructurally, Hurler lysosomes, called **zebra bodies,** are filled with granular material and membranous figures. Collagen fibrils are found in lysosomes of abnormal granular cells of heart valves of Hurler patients and are thought to arise from abnormally high collagen synthesis.[58]

Animal Models of Mucopolysaccharidoses

Mucopolysaccharidoses have been reported in inbred strains of mice,[59] and in cats,[60,61] dogs,[62] and goats.[63] In **cats,** excess GAGs (dermatan sulfate and heparin sulfate) arise from deficit of the lysosomal enzyme α-L-iduronidase. Siamese cats accumulate inclusions bearing dermatan sulfate in hepatocytes, bone marrow granulocytes, vascular smooth muscle, and fibroblasts of skin, cornea, and cardiac valves (see Fig. 27.1). **Plott hounds** develop an α-L-iduronidase deficiency that serves as a model for human Hurler-Scheie syndrome. Lesions occur in cerebrocortical neurons, perithelial cells in the spinal cord white matter, chondrocytes, hepatocytes and other cells.[64] Mucopolysaccharidosis IIIA in **Huntaway dogs** is a deficit of heparan sulfate sulfamidase that results in typical lysosomal inclusions and fatal neurologic disease.[65]

Mucolipidoses

Cells from patients with mucolipidosis form large granulofibrillar vacuoles that accumulate both glycolipids and glycosaminoglcyans. Cells have characteristics of both sphingolipidoses and mucopolysaccharidoses. The mucolipidoses include **I cell disease** (mucolipidosis II),[66] **pseudo-Hurler polydystrophy** (mucolipidosis III, GlcNAc-1-phosphotransferase deficiency), and **mucolipidosis IV.** Prenatal diagnosis of type II can be done reliably by electron microscopic analysis to demonstrate vacuolated cells in chorionic villus.[67] Sialidosis, the former prototype of mucolipidosis, is now classified as a glycoproteinosis.

Mucolipidosis Type IV

Human **mucolipidosis type IV** is an autosomal recessive neurodegenerative lysosomal storage disorder characterized by corneal opacities, retinal degeneration, and psychomotor retardation. It results from mutations in the *MCOLN1* gene, which encodes the protein mucolipin-1, and a mouse model, *MCOLN1* (−/−), which develops inclusion bodies in neurons and other cells of the brain. Lysosomal storage material is seen in the cornea, in leukocytes, and in other biopsied tissues.[68] Neuronal inclusions are laminated structures in lysosomes. Lysosomal inclusions develop in gastric parietal cells in patients with hypergastrinemia.[69] Type IV was classed as a mucolipidosis after electron microscopy revealed lysosomal storage of lipids together with water-soluble granular material. The *MLIV* gene has been mapped to human chromosome 19p13.2–13.3, but the metabolic defect has not been clarified. The underlying defect, although unknown, is not thought to be a deficit of a single enzyme.

Glycogen Storage Diseases

Glycogen storage diseases (glycogenoses) are inherited syndromes caused by missing or defective enzymes of carbohydrate metabolism. Deposits of glycogen (or abnormally branched glucose polymers) accumulate to produce massive amounts of foamy cytoplasm. Although these are systemic diseases, the cells affected are largely those of tissues with high rates of metabolism. Neurons, hepatocytes, renal tubule cells, and leukocytes are especially affected, and their defectiveness is responsible for the clinical disease.

At least 10 types of glycogenoses have since been described in humans, and many of these have animal model counterparts (Table 27.3). The character of glycogen in storage cells in human patients depends on which enzyme of carbohydrate metabolism is missing. In all glycogenosis, the occurrence of multiple mutations complicates the clinical signs and lesions of disease.[70]

Type I Glycogensosis

The first glycogen storage disease to be reported was in children with hypoglycemia and massive liver enlargement due to **glucose-6-phosphatase deficiency**, an enzyme normally present in liver, kidney, and intestine. Glucose was not formed properly from glucose-6-phosphatase, and glycogen accumulated in cytoplasm and nuclei of hepatocytes and renal tubule cells. As a consequence of the block in glycogen degradation, lipids were mobilized and hyperlipidemia was common. Type I glycogenosis is the most severe hepatomegalic glycogen storage disease. In glycogenosis type 1B, a subgroup, the enzyme is normally active in frozen liver tissue but is inactive in fresh tissue and in vivo because of the lack of the translocase responsible for its transfer into the endoplasmic reticulum. Canine models for type I glycogenosis faithfully reproduce the human disease.[71]

Table 27.3 Ultrastructural pathology in models of glycogen storage diseases.*

Type	*Defect*	*Species*	*Reference to ultrastructural pathology*
I	Glucose-6-phosphatase	Human: Von Gierke's disease	**Field**, *Am J Clin Pathol* 50:20, 1968
		Dog	**Bardens**, *Vet Med* 61:1174, 1966; **Kishnani**, *Vet Pathol* 38:83, 2001
		Mouse	**Erickson**, *Proc Natl Acad Sci USA* 59:437, 1968
		Rat	**Haynes**, *Virch Arch B* 42:289, 1983
II	α-1,4-glucosidase	Human: Pompe's disease	**Baudhuin**, *Lab Invest* 13:1139, 1964; **Bruni**, *Virch Arch* B 4:196, 1970; **Fernández**, *Neuromuscul Disord* 9:136, 1999; **Griffin**, *Virch Arch B* 45:51, 1984; **Jay**, *Acta Neuropathol* 85:11a, 1992; **Byrne**, *Brain* 1986; **Nascimbeni**, *Neurology* 70:617, 2008; **Schoser**, *Neuropathol Appl Neurobiol* 33:544, 2007 (biopsy); **Thurberg**, *Lab Invest* 86:1208, 2006
		Cat	**Sandström**, *Acta Neuropathol* 14:194, 1969
		Cow	**Richards**, *Neuropathol Appl Neurol* 3:45, 1977
		Dog	**Mostafa**, *Acta Vet Scand* 11:197, 1970
		Sheep	**Manktelow**, *J Comp Pathol* 85:139, 1975
III	Amylo-1,6-glucosidase	Human: Cori's disease	**de Bruijn**, *Pathol Eur* 10:3, 1975; **Cardiff**, *Pediatrics* 37:249, 1966; **Garancis**, *Lab Invest* 22:468, 1970; **Griffin**, *Virch Arch B* 45:23, 1984; **Kretzschmar**, *J Neurol Sci* 98:169, 1990; **Witzleben**, *Lab Invest* 20:424, 1969
		Dog	**Ceh**, *Acta Vet Scand* 17:210, 1976
IV	6-glycosyltransferase (branching enzyme disease)	Human: Anderson's disease	**Konstantinidou**, *Histopathology* 48:878, 2006; **Reed**, *Lab Invest* 19:546, 1968; **Schochet**, *Acta Neuropathol* 19:137, 1971
V	Phosphorylase	Human: McArdle's disease	**Korenyi-Both**, *Acta Neuropathol* 40:11, 1977; **Byard**, *Pathology* 23:62, 1991
VI	Phosphorylase (liver)	Human: Hers' disease	**Williams**, *J Clin Invest* 40:1841, 1961
		Mouse	**Gross**, *J Biol Chem* 249:6710, 1977
VII	Phosphofructokinase	Human	**Nakajima**, *Curr Mol Med* 2:197, 2002
		Dog	**Harvey**, *Vet Pathol* 27:1, 1990
VIII	Phosphorylase (liver)	Human	**Kornfeld**, *J Neuropathol Exp Neurol* 43:568, 1984
IX	Phosphorylase kinase	Human	**Beauchamp**, *Mol Genet Metab* 92:88, 2007
		Rat (NZR/Gc)	**Haynes**, *Virch Arch B* 42:289, 1983
X	cAMP-dependent phosphorylase kinase	Human	
O#	α-Mannosidase	Human	**Kollberg**, *New Engl J Med* 357:15, 2007
		Cat	**Langohr**, *Vet Pathol* 42:502, 2005
PBD§	Polyglucosan	Human, horse	**Schroeder**, *Acta Neuropathol* 74:248, 1987

*Glycogen is deposited in all cases. In type II it is within lysosomes. Glycogen is branched in type III and unbranched in type IV. In type VIII α-rosettes accumulate in neurons.
#O = Oligosaccharide storage.
§PBD = Polyglucosan body disease.

Type II Glycogenosis

In **type II glycogenosis** (Pompe's disease), glycogen accumulates in lysosomes because the lysosomal enzyme glucosidase is missing. Accumulation of glycogen in lysosomes (**glycogenosomes**) gives affected hepatocytes, Kupffer cells and myocytes of skeletal muscle a swollen, lacy appearance.[72–74] Ultrastructurally, large glycogen-filled secondary lysosomes pack the cytoplasm. Although much of the glycogen is sequestered in these lysosomes, much is also free in the cytoplasm. Ultrastructural analysis also reveals a high incidence of autophagic vacuoles, lipofuscin debris, and Z-line disorganization. Diagnosis can be established by demonstrating a mutational defect of the *GAA* gene. Prenatal diagnosis can be established by detection of glycogen-filled vacuoles in fibrocytes of chorionic villi biopsies. Great clinical heterogeneity results from acid α-glucosidase deficiency, and a variety of mutations are associated with this disorder.

Type III Glycogenosis

In **type III glycogenosis,** the lack of a debrancher enzyme blocks degradation of glycogen beyond branching points, and stored glycogen is abnormal in structure. Only the outermost branches of the glycogen polymer can be effectively utilized. Also called limit dextrinosis, the deficiency of amylo-1,6-glucosidase causes accumulation of polysaccharides with short outer branches in many tissues including muscle, liver, leukocytes and erythrocytes. Hepatomegaly dominates in young patients while muscular and cardiac signs, limited in young, may dominate in adult patients.

Type IV Glycogenosis

Type IV glycogenosis (amylopectinosis) is unique among the glycogenoses. It causes cytoplasmic inclusions composed of glycogen rosettes, fibrils, and finely granular material.[75,76] Inclusions contain glucose polymers as polysaccharides with long outer chains. Inclusions are periodic acid-Schiff staining (diastase resistant) and contain iron. Similar inclusions that contain glucose polymers termed polyglucason are found in Lafora's disease, corpora amylacea, and basophilic degeneration of cardiac muscle.[77]

Other Glycogenosis

The remaining glycogen storage diseases are very rare. In **type V glycogenosis** (McArdle disease) there is a deficiency of muscle phosphorylase and the liver is normal. **Type VI glycogenosis** includes several enzyme deficiencies, which lead to a low activity of phosphorylase, either a deficiency of phosphorylase or of one of the four different subunits of phosphorylase kinase. **Type VII glycogenosis** is a deficiency of muscle phophofructokinase (the liver enzyme is normal, the erythrocyte enzyme is reduced); signs resemble those of type V, but this form is more rare.

Other, unclassified disorders lead to glycogenopathy. **Amylopectinosis** involves deposition of amylopectin-like material (fibrillar glycogen) in cardiac muscle.[78] Similar lesions in Quarter horses resemble GSD type IV.[79]

Polyglucosan Body Diseases

Polyglucosan body diseases are slowly progressive adult-onset glycogen storage disorders. Clinical signs are due to deposition of starch-like, long-stranded, poorly branched glycogen molecules (known as polyglucosans) which accumulate as large inclusions.

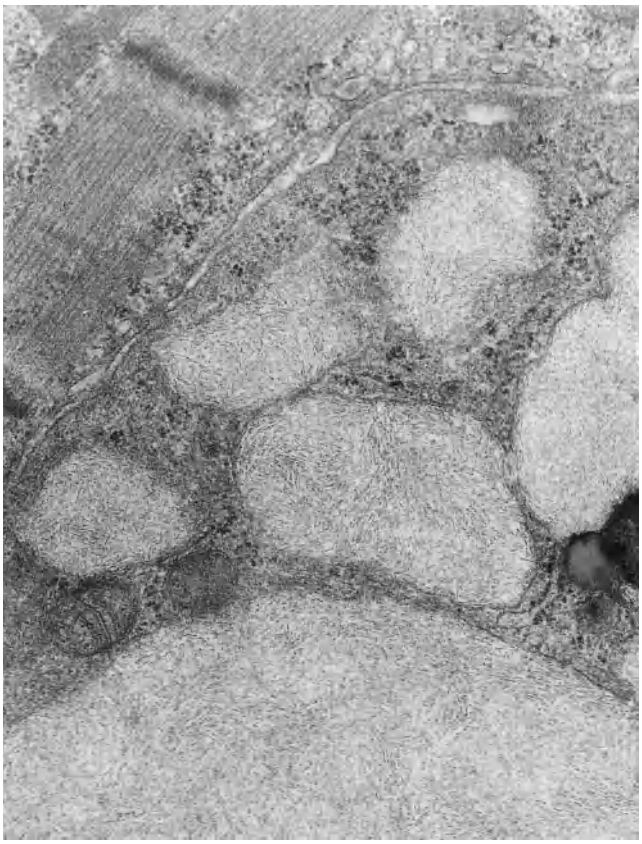


Fig. 27.8 Polyglucosan body: membrane-bound fibrillar inclusions in deltoid muscle of 46-year-old male patient with polyglucosan body myopathy. (Micrograph: Hans H. Goebel, *J Neuropathol Exp Neurol* 51:24, 1992.)

Polyglucosan inclusions are typically found in upper and lower neurons; inclusions in liver and muscle are less common.[80–82] Ultrastructurally, the enormous, round inclusions (Fig. 27.8) are composed of clusters of short, branching filaments (8–12 nm in diameter) embedded in amorphous granular material. **Polyglucason inclusions** occur in La Fora's disease, type IV glycogenosis, corpora amylacea, and basophilic degeneration of cardiac muscle. They are the hallmark of the **polyglucosan myopathies,** rare metabolic abnormalities. Affected cells are hypertrophic and vacuolated, and the cytoplasmic inclusions are pale with finely fibrillar matrices. In late-onset polyglucason myopathy, cytoplasmic inclusions are surrounded by abnormal mitochondria. Polyglucosan inclusions have been reported in dogs, cockatiels, cows, dogs, and humans, but are not always considered to be disease-specific, but as an age-related degenerative process accelerated by epilepsy.[83,84]

Lafora Disease

Lafora disease is a fatal, adolescent-onset, progressive epileptic disease due to deposition of polyglucosan

inclusions (Lafora bodies). It is an autosomal recessive neurodegenerative disorder of humans characterized by progressive epilepsy and cytoplasmic polyglucosan inclusions in neuronal bodies and dendrites (not axons), hepatocytes, and cardiac and skeletal muscle. PAS-staining inclusions in neuronal bodies and processes are diagnostic.

Disease is caused by loss of function of laforin or malin. **Laforin,** a protein phosphatase, and **malin,** a ubiquitin ligase, are defective. Malin interacts with laforin to promote polyubiquitination and degradation, and both are recruited to aggresomes in response to proteasomal impairment.[85] In early disease, laforin and malin are present in the endoplasmic reticulum and form centrosomal aggregates that are immunoreactive for tubulin, ubiquitin, ER chaperones and proteosomal subunits.[86]

Laforin is found in ribosomes adjacent to membranes of the rough endoplasmic reticulum that surround the polyglucosan deposits.

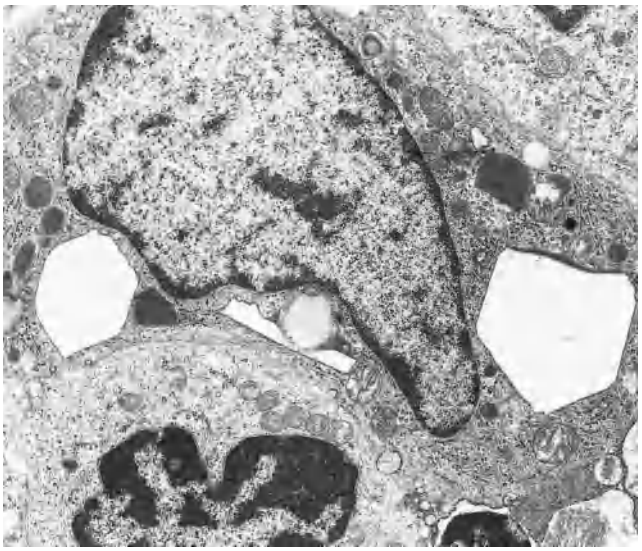


Fig. 27.9 Cystinosis: cystine crystals within lysosomes of a macrophage in the lamina propria of the intestine; rectal biopsy, human patient with nephropathic cystinosis. (Micrograph: Theodore C. Iancu, *J Pediatr Gastroenterol Nutr* 6:359, 1987.)

Oligosaccharide Storage Disease

Oligosaccharide storage diseases are less well characterized. Children with deficiency of mannosidase cannot cleave mannose from the glycoprotein heterosaccharides.[87] As a consequence, oligosaccharides containing mannose accumulate within secondary lysosomes, causing affected neurons, myocytes and hepatocytes to be vacuolated.[88]

Muscle Glycogen Storage Disease 0

Mutations in the muscle **glycogen synthase gene** are associated with severe skeletal and cardiac muscle glycogen deficiency.[89] In muscle, there is lack of glycogen, predominance of oxidative fibers, and mitochondrial reduplication with dense inclusions in intermembrane spaces.

Amino Acid Transport Storage Diseases

Cystinosis

Cystinosis in humans is an autosomal recessive disease characterized by intralysosomal accumulation of cysteine that results from defective cystine transport across the lysosomal membrane. Three forms have been described: **infantile cystinosis,** characterized by renal proximal tubulopathy and progression to end-stage renal disease; **juvenile cystinosis,**[90,91] with slower rates of progression; and **adult cystinosis,** with only ocular lesions.[92] In all cases, the defective egress of cystine leads to formation of doubly refractile cystine crystals within the lysosomal matrix, especially in macrophages. Cystine typically accumulates in the largest amounts in cornea, bone marrow, spleen, liver, kidney, thyroid, and rectal mucosa.[93] Hepatomegaly, a common feature of hereditary nephropathic cystinosis, is characterized by cystine crystal deposits in Kupffer cells, and in severe cases lipid accumulation in intrasinusoidal stellate cells and fibrosis.[94] Clinical signs are related to renal deposits of cystine crystals (Fig. 27.9). Hypothyroidism, retinopathy, and renal failure generally occur before ten years of age. Cystine crystals in affected cells, because they are removed by aqueous fixatives, typically appear as electron lucent spaces with crystalline shapes.[95–99] A mild form of cystinosis involves crystals in the cornea.

Tyrosinosis

Hereditary tyrosinemia is an autosomal recessive disorder caused by deficiency of fumaryl acetatoacetase, the last enzyme in the degradation of tyrosine. The enzyme defect results in accumulation of fumaryl- and maleyl-acetoacetate, which causes hepatocellular and renal tubular damage, often with hypophosphatemic rickets. Tyrosine catabolism is limited to liver and kidney because the enzymes involved occur exclusively in these organs. Progressive liver lesions lead to cholestatic hepatopathy, cirrhosis, and hepatocellular carcinoma. Human patients with tyrosinemia present either as neonates with acute hepatic failure or later in infancy with progressive liver dysfunction

secondary to cirrhosis. In the liver, affected hepatocytes are enlarged and show nuclear pleomorphism, hyperchromasia, and multinucleation.[100] Abnormal DNA ploidy and alpha-fetoprotein are markers of the disturbed regeneration.[101]

Amino Aciduria

In **maple urine disease,** cases commonly present as neonates with severe disease with large increase in branched chain amino acids and branched chain ketoacids. Lesions include focal and diffuse destruction of myofibrils.[102] Survivors are mentally retarded. Spongy changes in the CNS are attributed to edema and failure of myelination. In calves, ultrastructural intramyelinic vacuoles suggest edema of myelin.

Other Storage Diseases

Studies and case reports of rare storage disease have recently been identified. A neurodegenerative disease due to deficient activity of the lysosomal hydrolase **α-N-acetylgalactosaminidase** leads to tubulovesicular material accumulations in the autonomic axon of the myenteric plexus and in brain. Inclusions of lamellar, fibrillar, vesicular and granular material were also found in leukocytes, eccrine sweat glands, and cutaneous nerves.[103]

Storages Diseases of Uncertain Classification

Alexander's Disease

Alexander's disease is a progressive human degenerative neurological disorder of retardation and increasing head size that develops in early childhood and is characterized by accumulation of **Rosenthal fibers** throughout the cerebral white matter. Large numbers of round or elongate eosinophilic bodies, varying from small droplets less than one micron to elongate structures up to 30 microns, are scattered throughout the cortex.[104,105]

Infantile Osteopetrosis

Infantile osteopetrosis with neuronal storage disease is a rare autosomal recessive lysosomal storage disoder associated with mutations in the OSTM1 and chloride channel ClCN-7 genes. Skin biopsies of affected children reveal swollen unmyelinated axons containing spheroids, reduced myelinated axons, and lysosomes in Schwann cells that contain lipofuscin.[109]

References

1. Fowler DJ, et al. 2007 Electron microscopy of chorionic villus samples for prenatal diagnosis of lysosomal storage disorders. *Ultrastruct Pathol* 31:15.
2. Alroy J, et al. 1992. Canine GM_1-gangliosidosis. *Am J Pathol* 140:675.
3. Van der Voorn JP, et al. 2004. The leukoencephalopathy of infantile GM_1-gangliosidosis: Oligodendrocytic loss and axonal dysfunction. *Acta Neuropathol* 107:539.
4. Muldoon LL, et al. 1994. Characterization of the molecular defect in a feline model for the type II GM_2-gangliosidosis (Sandhoff disease). *Am J Pathol* 144:1109.
5. Cachón-González MB, et al. 2006. Effective gene therapy in an authentic model of Tay-Sachs-related diseases. *Proc Natl Acad Sci USA* 103:10373.
6. Butler A, et al. 2007. Sperm abnormalities in heterozygous acid sphingomyelinase knockout mice reveal a novel approach for the prevention of genetic diseases. *Am J Pathol* 170:2077.
7. Nicholson AG, et al. 2006. Pulmonary involvement by Niemann-Pick disease. *Histopathology* 48:596.
8. Liao G, et al. 2007. Cholesterol accumulation is associated with lysosomal dysfunction and autophagic stress in $Npc1^{-/-}$ mouse brain. *Am J Pathol* 170:962.
9. Wu YP, et al. 2005. Apoptosis accompanied by up-regulation of TNF-alpha death pathway genes in the brain of Niemann-Pick type C disease. *Mol Genet Metabol* 84:9.
10. Pàmpols T, et al. 1999. Neuronopathic juvenile glucosylceramidosis due to sap-C deficiency. *Acta Neuropathol* 97:91.
11. Naito M, et al. 1988. An ultrastructrual and experimental study on the development of tubular structures in the lysosomes of Gaucher cells. *Lab Invest* 58:590.
12. Fowler DJ, et al. 2006. Ultrastructural features of Gaucher disease treated with enzyme replacement therapy presenting as mesenteric mass lesions. *Fetal Pediatr Pathol* 25:241.
13. Sun Y, et al. 2006. Gaucher disease mouse models. *J Lipid Res* 46:2102.
14. Demerjian M, et al. 2006. Barrier dysfunction and pathogenesis of neutral lipid storage disease with ichthyosis (Chanarin-Dorfman syndrome). *J Invest Derm* 126:2032.
15. Borda JT, et al. 2008. Clinical and immunopathologic alterations in rhesus macaques affected with globoid cell leukodystrophy. *Am J Pathol* 172:88.
16. Higashi Y, et al. 1992. The twitcher mouse: Immunocytochemical study of Ia expression in macrophages. *J Neuropathol Exp Neurol* 51:47.
17. Taniike M, et al. 1999. An apoptotic depletion of oligodendrocytes in the Twitcher, a murine model of globoid cell leukodystrophy. *J Neuropathol Exp Neurol* 58:644.
18. Tietge UJ, et al. 2001. Phenotypic correction of lipid storage and growth arrest in Wolman disease fibroblasts by gene transfer of lysosomal acid lipase. *Hum Gene Ther* 12:279.

19. Kuriwaki K, Yoshida H. 1999. Morphological characteristics of lipid accumulation in liver: Constituting cells of acid lipase deficiency rats (Wolman's disease rats). *Pathol Int* 49:291.
20. Askari H, et al. 2007. Cellular and tissue localization of globotriaosylceramide in Fabry disease. *Virchows Arch* 451:823.
21. Aerts JM, et al. 2008. Elevated globotriaosylsphingosine is a hallmark of Fabry disease. *Proc Natl Acad Sci USA* 105:2812.
22. Klinghardt G. 1974. Experimental lesions of the nervous and muscular systems due to chloroquine. *Acta Neuropathol* 28:117.
23. Lullman H, et al. 1973. A comparative ultrastructural study of the effects of chlorphentermine and triparanol in rat lung and adrenal gland. *Virchows Arch B* 12:91.
24. Lullman-Rauch R. 1975. Intraalveolar foam cells associated with lipidosis-like alterations in lung and liver of rats with tricyclic psychotropic drugs. *Virchows Arch B* 19:255.
25. Lullman-Rauch R. 1983. Tilorone-induced lysosomal storage mimicking the features of mucopolysaccharidosis and of lipidosis in rat liver. *Virchows Arch B* 44:355.
26. Elleder M. 1978. A histochemical and ultrastructural study of stored material in neuronal ceroid lipofuscinosis. *Virch Arch B* 28:167.
27. Herman M, et al. 1971. Additional electron microscopic observations on two cases of Batten-Spielmeyer-Vogt disease (neuronal ceroid-lipofuscinosis). *Acta Neuropathol* 17:85.
28. Sisk DB, et al. 1990. Clinical and pathologic features of ceroid lipofuscinosis in two Australian cattle dogs. *J Am Vet Med Ass* 197:361.
29. Jolly RD, et al. 1980. Ovine ceroid-lipofuscinosis: a model of Batten's disease. *Neuropathol Appl Neurobiol* 6:195.
30. Katz ML, Rodrigues M. 1991. Juvenile ceroid lipofuscinosis. Evidence for methylated lysine in neural storage body protein. *Am J Pathol* 138:323.
31. Koike M, et al. 2005. Participation of autophagy in storage of lysosomes and neurons from mouse models of neuronal ceroid-lipofuscinoses (Batten disease). *Am J Pathol* 167:1713.
32. Taylor RM, Farrow BRH. 1988. Ceroid-lipofuscinosis in border collie dogs. *Acta Neuropathol* 75:627.
33. Cho D-Y, et al. 1986. Neuronal ceroidosis (ceroid-lipofuscinosis) in a blue heeler dog. *Acta Neuropathol* 69:161.
34. Jasty V, et al. 1984. An unusual case of generalized ceroid-lipofusinosis in a cynomolgus monkey. *Vet Pathol* 21:46.
35. Harper PAW, et al. 1988. Neurovisceral ceroid-lipofuscinosis in blind Devon cattle. *Acta Neuropathol* 75:632.
36. Pardo CA, et al. 1994. Accumulation of the adenosine triphosphate synthase subunit C in the *mnd* mutant mouse. *Am J Pathol* 144:829.
37. Yamano T, et al. 1986. Pathological study on a severe sialidosis (α-neuraminidase deficiency). *Acta Neuropathol* 71:278.
38. Arstella AV, et al. 1972. Aspartylglucosaminuria I: Fine structural studies. *Acta Neuropathol* 20:207.
39. Aula P, et al. 1975. Distribution of cytoplasmic vacuoles in blood T and B lymphocytes in two lysosomal disorders. *Virch Arch B* 18:263.
40. Freitag F, et al. 1971. Hepatic ultrastructure in chondroitin-4-sulfate mucopolysaccharidosis. *Virch Arch B* 8:1.
41. Williams JC, et al. 1984. Progressive neurologic deterioration and renal failure due to storage of glutamyl ribose-5-phosphate. *New Engl J Med* 311:152.
42. Armién AG, et al. 2007. Spontaneous and experimental glycoprotein storage disease of goats induced by *Ipomoea carnea* subsp *fisulosa* (Convolvulaceae). *Vet Pathol* 44:170.
43. Autio-Harmainen H, et al. 1988. Neuropathology of Salla disease. *Acta Neuropathol* 75:481.
44. Renlund, M., et al. 1986. Defective sialic acid egress from isolated fibroblast lysosomes of patients with Salla disease. *Science* 232:759.
45. Monus Z, et al. 1977. Histomorphologic and histochemical investigations in mannosidosis. *Virch Arch B* 26:159.
46. Jones MZ, et al. 1983. Caprine beta-mannosidosis. *J Neuropathol Exp Neurol* 42:268.
47. Jolly RD. 1974. Mannosidosis. *Am J Pathol* 74:211.
48. Patterson JS, et al. 1991. Neuropathology of bovine β-mannosidosis. *J Neuropathol Exp Neurol* 50:538.
49. Boyer PJ, et al. 1990. Caprine mannosidosis. *Lab Invest* 63:100.
50. Spranger J, et al. 1984. Geleophysic dysplasia. *Am J Med Genet* 19:487.
51. Leslie T, et al. 2005. Morquio syndrome: Electron microscopic findings. *Br J Ophthalmol* 89:925.
52. Walkley SU, et al. 2005. Abnormal neuronal metabolism and storage in mucopolysaccharidosis type VI (Maroteaux-Lamy) disease. *Neuropathol Appl Neurobiol* 31:536.
53. Alroy J, et al. 1999. Altered corneal stromal matrix organization is associated with mucopolysaccharidosis I, II and VI. *Exp Eye Res* 68:523.
54. Resnick JM, et al. 1994. Light and electron microscopic features of the liver in mucopolysaccharidosis. *Human Pathol* 25:276.
55. Haskins ME, et al. 1992. Hepatic storage of glycosaminoglycans in feline and canine models of mucopolysaccharidoses I, III, and VII. *Vet Pathol* 29:112.
56. Aleu FP, et al. 1965. Electron microscopy of two cerebral biopsies in gargolysm. *J Neuropathol Exp Neurol* 24:304.
57. Lagunoff D, Gritzka TL. 1966. The site of mucopolysaccharide accumulation in Hurler's syndome. *Lab Invest* 15:1578.
58. Renteria VG, Ferrans VJ. 1976. Intracellular collagen fibrils in cardiac valves of patients with Hurler syndrome. *Lab Invest* 34:263.
59. Vogler C, et al. 1990. A murine model of mucopolysaccharidosis VII. *Am J Pathol* 136:207.
60. Haskins ME, et al. 1980. The pathology of the feline model of mucopolysaccharidosis VI. *Am J Pathol* 101:657.

61. Schultheiss PC, et al. 2000. Mucopolysaccharidosis VII in a cat. *Vet Pathol* 37:502.
62. Haskins ME, et al. 1991. Mucopolysaccharidosis type VII (Sly syndrome): Beta-glucuronidase-deficient mucopolysaccharidosis in the dog. *Am J Pathol* 138:1553.
63. Jones MZ, et al. 1998. Caprine mucopolysaccharidosis-IIID. *J Neuropathol Exp Neurol* 57:148.
64. Shull RM, et al. 1984. Morphologic and biochemical studies of canine mucopolysaccharidoses I. *Am J Pathol* 114:487.
65. Jolly RD, et al. 2007. Pathology of mucopolysaccharidosis IIIA in Huntaway dogs. *Vet Pathol* 44:569.
66. Kitagawa H, et al. 1991. An autopsy case of I-cell disease. *Am J Clin Pathol* 96:262.
67. Carey WF, et al. 1999. Prenatal diagnosis of mucolipisosi II—electron microscopy and biochemical evaluation. *Prenat Diagn* 19:252.
68. Folkerth RD, et al. 1995. Mucolipidosis IV: Morphology and histochemistry of an autopsy case. *J Neuropathol Exp Neurol* 54:154.
69. Lubensky IA, et al. 1999. Lysosomal inclusions in gastric parietal cells in mucolipidosis type IV a novel cause of achlorhydria and hypergastrinemia. *Am J Surg Pathol* 23:1527.
70. Herrick MK, et al. 1994. Concomitant branching enzyme and phosphorylase deficiencies. *J Neuropathol Exp Neurol* 53:239.
71. Kishnani PS, et al. 2001. Canine model and genomic structural organization of glycogen storage disease type Ia (GSC Ia). *Vet Pathol* 38:83.
72. Schoser BG, et al. 2007. Adult-onset glycogen storage disease type-2. *Neuropathol Appl Neurobiol* 33:544.
73. Sharma MC, et al. 2005. Delayed or late-onset type II glycogenesosis with globular inclusions. *Acta Neuropathol* 110:151.
74. Phupong V, et al. 2005. Prenatal diagonsis of Pompe disease by electron microscopy. *Arch Gynecol Obstet* 271:259.
75. Read GB Jr, et al. 1968. Type IV glycogenosis. *Lab Invest* 19:546.
76. Schochet SS Jr, et al. 1971. Light and electron microscopy of skeletal muscle in type IV glycogenosis. *Acta Neuropathol* 19:137.
77. Martin JK, et al. 1990. Myopathy of internal anal sphincter with polyglucason inclusions. *J Pathol* 161:221.
78. Das BB, et al. 2005. Amylopectinosis disease isolated to the heart with normal glycogen branching enzymes activity and gene sequence. *Pediatr Tranplant* 9:261.
79. Render JA, et al. 1999. Amylopectinosis in fetal and neonatal Quarter horses. *Vet Pathol* 36:157.
80. Vucic S, et al. 2007. Polyglucosan body disease myopathy. *Muscle Nerve* 35:536.
81. Lefkowitch JH, et al. 2006. Ground-glass polyglucosan-like hepatocellular inclusions. *Gastroenterology* 131: 713.
82. O'Shea AM, et al. 2007. Lafora-like ground-glass inclusions in hepatocytes of pediatric patients. *Pediatr Dev Pathol* 10:351.
83. Simmons MM. 1994. Lafora disease in the cow. *J Comp Pathol* 110:401.
84. Jolly RD, et al. 2002. Polyglucosan body disease in a mixed-breed dog. *N Z Vet J* 50:32.
85. Mittal S, et al. 2007. Lafora disease proteins malin and laforin are recruited to aggresomes in response to proteasomal impairment. *Hum Mol Genet* 16: 753.
86. Chan EM, et al. 2004. Laforin preferentially binds the neurotoxic starch-like polyglucosans, which form in its absence in progressive myoconus epilepsy. *Hum Mol Genet* 13:1117.
87. Monus Z, et al. 1977. Histomorphologic and histochemical investigations in mannosidosis. *Virchws Arch B* 26:159.
88. Kawai H, et al. 1985. Skeletal muscle pathology of mannosidosis in two siblings with spastic paralysis. *Acta Neuropathol* 68:201.
89. Kollberg G, et al. 2007. Cardiomyopathy and exercise intolerance in muscle glycogen storage disease 0. *New Engl J Med* 357:15.
90. Olcay L, et al. 2005. High cystine in platelets from patients with nephropathic cystiosis. *J Clin Pathol* 58:939.
91. Mahoney CP, Striker GE. 2000. Early development of the renal lesions in infantile cystinosis. *Pediatr Nephrol* 15:50.
92. Servais A, et al. 2008. Late-onset nephropathic cystinosis. *Clin J Am Soc Nephrol* 3:27.
93. Iancu TC, et al. 1987. Intestinal mucosa in nephropathic cystinosis. *J Pediat Gastroenterol Nutr* 6:359.
94. Klenn PJ, Rubin R. 1994. Hepatic fibrosis associated with hereditary cystinosis. *Mod Pathol* 7:879.
95. Iancu TC. 1992. The ultrastructural spectrum of lysosomal storage diseases. *Ultrastr Pathol* 16:245.
96. Patrick AD, Lake BD. 1968. Cystinosis: Electron microscopic evidence of lysosomal storage of cystine in lymph node. *J Clin Pathol* 21:571.
97. Schulman JD, et al. 1969. Cystine: Compartmentalization within lysosomes in cystinotic leukocytes. *Science* 166:1152.
98. Vogel DG, et al. 1990. Central nervous system involvement in nephropathic cystinosis. *J Neuropathol Exp Neurol* 49:591.
99. Witzelben CL, et al. 1972. Electron microscopy in the diagnosis of cystinosis. *Arch Pathol* 94:362.
100. Dehner LP, et al. 1989. Hereditary tyrosinemia type I (chronic form): Pathologic findings in the liver. *Hum Pathol* 20:149.
101. Zerbini C, et al. 1992. DNA ploidy abnormalities in the liver of children with hereditary tyrosinemia type I. *Am J Pathol* 140:1111.
102. Ferriere G, et al. 1984. Abnormalities of muscle fibers in maple syrup urine disease. *Acta Neuropathol* 63: 249.
103. Schindler D, et al. 1989. Neuroaxonal dystrophy due to lysosomal α-N-acetyl-galactosaminidase deficiency. *New Engl J Med* 320:1735.
104. Townsend JJ, et al. 1985. Alexander's disease. *Acta Neuropathol* 67:163.
105. Schochet SS, et al. 1968. Alexander's disease. *Neurology* 18:543.

106. Kanitakis J, et al. 2005. Fucosidosis with angiokeratoma: Immunohistochemical and electron microscopic study of a new case and literature review. *J Cutan Pathol* 32:506.
107. Freitag F, et al. 1971. Hepatic ultrastructure in fucosidosis. *Virch Arch B* 7:99.
108. Ferrara ML, et al. 1997. Canine fucosidosis. *Neuromuscul Disord* 7:361.
109. Alroy J, et al. 2007. Electron microscopic findings in skin biopsies from patients with infantile osteopetrosis and neuronal storage disase. *Ultrastruct Pathol* 31:333.

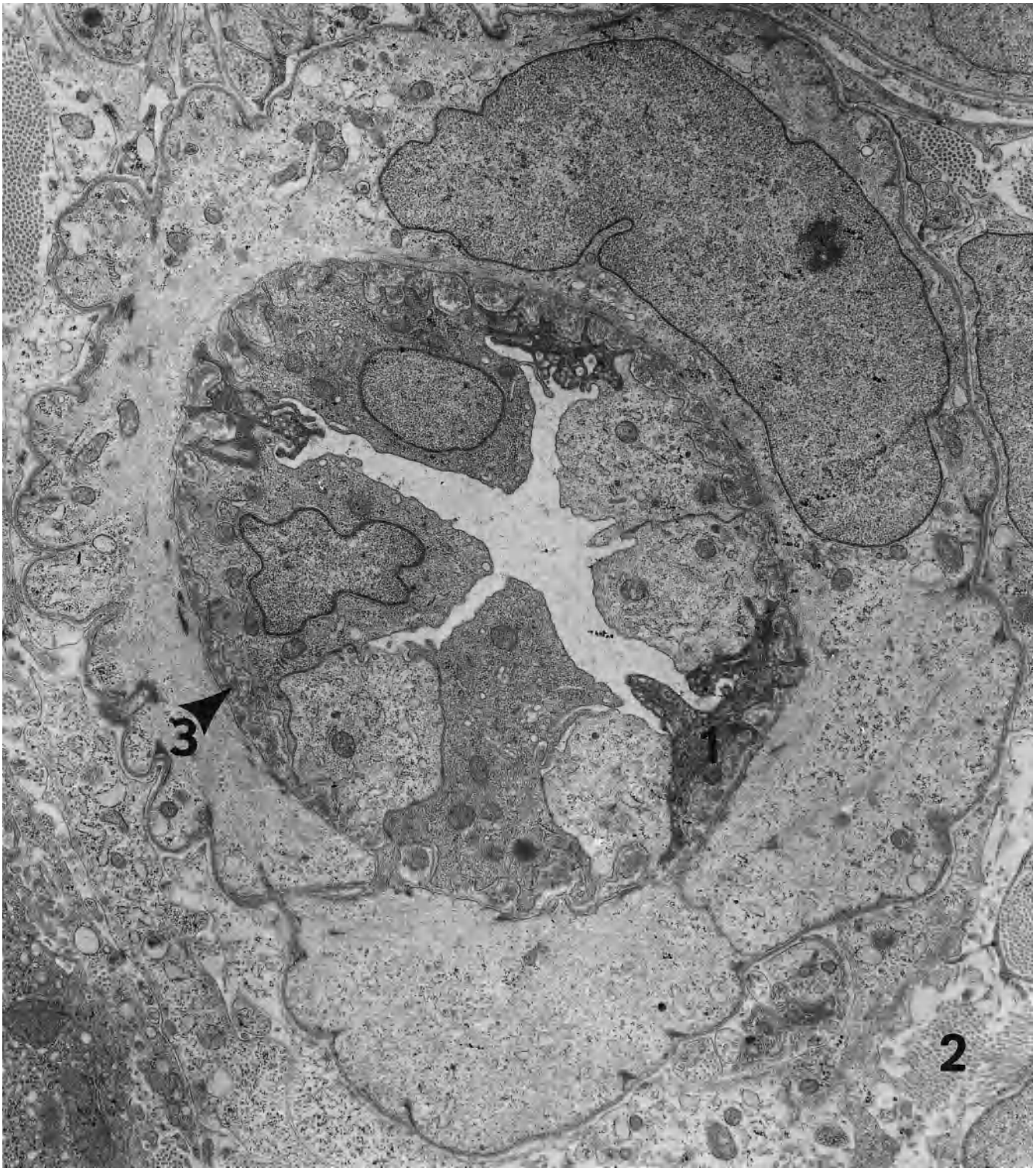


Fig. 28.1 Viral arteritis: contracted arteriole in intestinal mucosa, feline panleukopenia (parvovirus), cat. Endothelial cells are necrotic (*1*), edema fluid surrounds collagen (*2*), and basement membrane material is aggregated (*3*). Endothelial cells are swollen, intercellular junctions are thickened, and there is perivascular edema.

© 2009 Wiley-Blackwell. ISBN: 978-0-813-80330-2

28 Arteriopathy

Responses of the Artery to Injury

Injury to endothelium of arteries has four major consequences: (1) altered vascular permeability, with insudation of plasma proteins and lipids into the intima, (2) alteration of intimal glycosaminoglycans between smooth muscle cells, (3) endothelial desquamation, and (4) attachment of platelets and fibrin to exposed subendothelial surfaces (Fig. 28.1). These events trigger the migration of surrounding endothelial cells and smooth muscle cells into the wound.[1,2] Modified smooth muscle cells form a temporary luminal surface but, although relatively nonthrombogenic, the myocyte layer does not form a barrier to large molecules.[3]

The **arterial adventitia** is altered, especially when perivascular edema and inflammation are severe (Fig. 28.2). Normal constituents of the adventitia become more widely separated and precipitates of plasma proteins occupy open areas where fluid has accumulated. Basement membranes become distorted and irregular, and may be discontinuous. Pericytes that cover the smaller blood vessels are degenerate and may be necrotic (Fig. 28.3). In the diseased artery, the origin of **vasa vasorum** may shift from the adventitia to the intima.[4] Normally, the arterioles that supply blood to the media of muscular arteries break into capillary plexuses in the deep layer of the tunica adventitia and do not penetrate deeply into the media. Myocytes deeply situated thus depend for sustenance on diffusion from the arterial lumen. Hypoxia predisposes myocytes of the larger muscular arteries to injury.

Myocytes of the **arterial media** degenerate secondarily to endothelial injury, either as a direct effect of ischemia, toxic injury, or intracellular metabolic shifts.[5–9] Direct injury to endothelium causes desquamation of endothelial cells into the lumen.[10] The lost cells are rapidly replaced by proliferation of adjacent endothelial cells. Experimentally, 24 hr after giving endotoxin intravenously to rats, endothelium of the aorta contains mitotic figures.[11]

Ischemia of the arterial myocyte leads to progressive accumulation of lipid globules and autophagic vacuoles, and loss of glycogen and microfilaments. Injury may be direct, or be the result of nervous stimulation. Fenoldopam mesylate, a selective postjunctional dopaminergic vasodilator, causes severe lesions in splanchnic arteries in the rat that are characterized by necrosis of medial smooth myocytes.[12,13] Experimentally, ^{3}H-thymidine uptake and cell division in wounded arteries is first seen in the arterial media. Medial smooth muscle cells subsequently migrate through fenestrae in the internal elastic lamina to subendothelial locations.[14] Platelet factors are crucial for the stimulation of smooth muscle migration into wounded arterial intima.

Mitochondria are often one of the first organelles to be affected when smooth muscle cells are injured. This is because much of the lipid metabolism and energy production occurs in mitochondria; for example, the disturbance of arterial smooth muscle that accompanies diabetes mellitis.[15] **Intercellular junctions** between smooth muscle cells of the arterial media provide mechanical attachments and a conduit for intercellular signaling.[16] During repair, smooth muscle cells strikingly alter their cytoskeleton to a more undifferentiated states as they migrate into areas of injury. The loss and reformation of **gap junctions** between proliferating smooth muscle cells are critical to reorientation.[17]

Ultrastructural changes in the arterial wall during vasoconstriction include compression of endothelial



Fig. 28.2 Perivascular edema: acute inflammation. Note degenerate pericytes (*P*), fibroblast (*F*), and mast cells (*MC*). Mast cell granules (*G*) are free in interstitial spaces.

cells, which assume teardrop shapes as their nuclei protrude into the lumen. Smooth myocytes become short and thick with deeply indented borders. Elastic fibers develop a pleated appearance. Endothelium and muscle cells adhere tightly to the elastic membrane and their conformation follows its convolutions. Within the endothelial cell, microfilaments shorten during vascoconstriction. Ultrastructural analysis of contracting arteries must consider the postmortem and fixation artifactual contraction that occurs in immersion techniques.[18] **Spasm** can directly cause endothelial damage. When induced experimentally with norepinephrine, the tight folding of the inner elastic membrane squeezes endothelial cells, and upon relaxation, endothelium has gaps, patches of abnormal cytoplasm, and adhesions between cells.[19–21]

Myofilaments of the arterial myocyte are the target of neural and humoral factors. Adrenalin acts directly on this cell to induce vasoconstriction. Angiotensin II, a powerful vasoconstrictor, has been shown to induce widespread structural changes in both endothelium and muscle. There are increases in the number and size of pinocytotic vesicles and widening of intercellular spaces. Isotope-labeled angiotensin II localizes in the nuclear areas of affected endothelial and smooth muscle cells, probably acting on the nucleus.

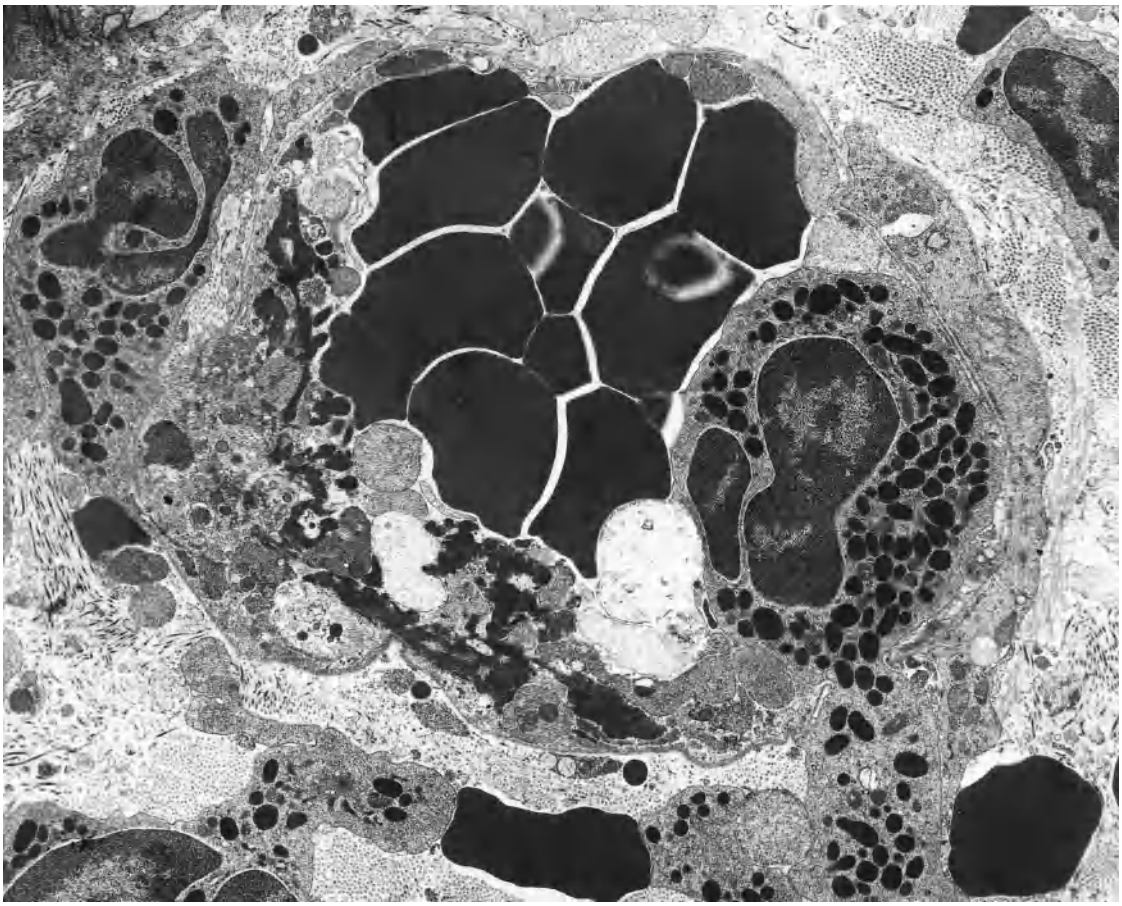


Fig. 28.3 Vasculitis, vascular necrosis, and hemorrhage: submucosal postcapillary venules, esophagus, infectious bovine rhinotracheitis (herpesvirus), cow. **Endothelial cells** are necrotic and there is disintegration of the vascular wall. **Perivascular spaces** have evidence of marked edema (separating collagen fibrils), hemorrhage, and neutrophil infiltrates. The **venule lumen** has evidence of erythrocyte stasis, deposits of dark-staining fibrin, and tissue debris including granular material and exocytotic vacuoles.

Angiotensin-induced sustained elevation in arterial pressure induces damage to arterial walls. Then endothelium, which provides a barrier protecting the media, develops focal defects. These permit the escape of plasma proteins into the wall, and amorphous dense deposits displace smooth muscle cells.

Arteries degenerate in normal processes; for example, during development of the fetus, and in involution of the uterus and other organs. Marked changes occur in **postnatal pulmonary arterial remodeling.** During and immediately after the birth of the normal infant, there are striking changes in the pulmonary arterial system. Pulmonary vascular resistance falls rapidly after birth. The high fetal pulmonary vascular resistance is reduced as small muscular arteries are reduced in diameter. A study of the pulmonary arterial tree of 12 children showed that, in the first month, arterial wall thickness decreased due to a reduction in smooth muscle diameter.[22] Similar changes were found in studies on the pig.[23]

Arteriosclerosis

Chronic arterial degenerative changes characterized by induration, loss of elasticity, and narrowing of the lumen are grouped as **arteriosclerosis.** In aging humans, these lesions develop as multiple, nodose, or focal sclerotic changes superimposed on a generalized, age-related increase in connective tissue elements of the arterial wall. In the aged arterial wall the amounts of mesenchymal matrix material increases. Random foci of dense, homogenous, alcian blue-staining ground substance, called **mucodegeneration,** precedes the deposition of fibrous materials, and is prone to calcification (Fig. 28.4) Collagen is deposited by myocytes, but fibroplasia is extensive only in species, such as birds, that have significant fibroblast population in the media (mammals do not). When the cycle of formation-degradation of collagen and elastin is disturbed, these substances accumulate. Elastolysis leaves split products of elastin in the intima that are capable of sustaining an inflammatory reaction.

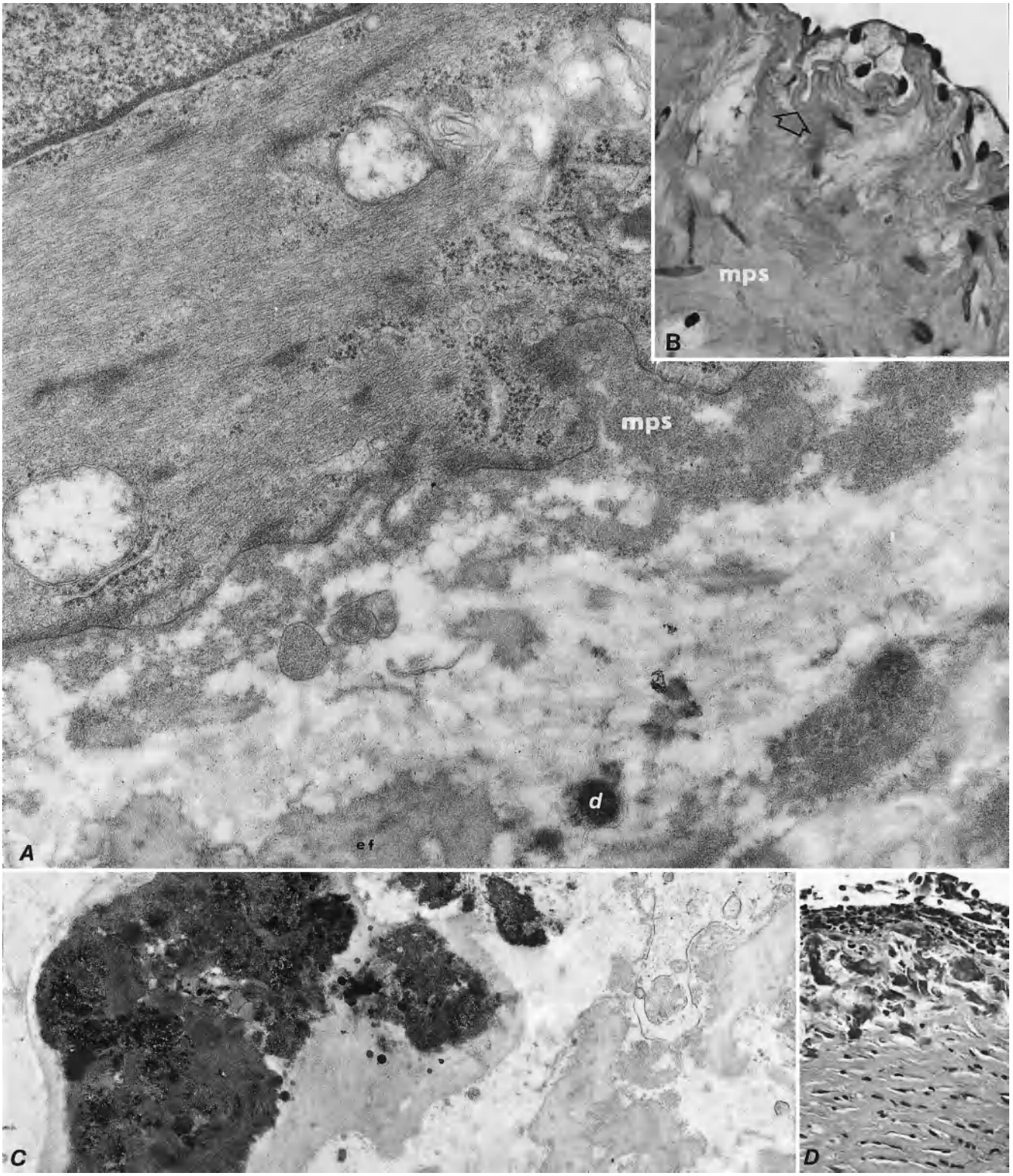


Fig. 28.4 **Arteriopathy**: mucodegeneration and calcification (mineralization), aorta, dog. **A**. **Mucopolysaccharide infiltrates**: homogenous granular mucopolysaccharides (*mps*) surround arterial smooth muscle cell; broken elastic fibers (*ef*), and calcifcation center (*d*). **B**. **Mucopolysaccharides** (*mps*) in the vascular wall (histology). **C**. **Calcium deposits** on elastic fibers are dense, granular, and irregular. **D**. **Calcification** (mineralization) of inner media (histology).

The Fibrous Plaque

Arteriosclerosis is found in all vertebrates. In most species, arteriosclerotic lesions are most apparent in the abdominal aorta and in the origins of its arterial branches. The hallmark of arteriosclerosis is the **fibrous plaque** (fibrous streak), a white, firm, glistening elevation on the otherwise smooth luminal surface of the artery. The early lesion begins as a break in the internal elastic membrane, followed by myocyte infiltration through its fenestrae and subsequent proliferation of myocytes within the intima.

The well-developed fibrous plaque consists largely of modified smooth muscle cells surrounded by increased amounts of extracellular matrix. Thickened basement membranes are present, and reduplication of and breaks in the internal elastic membrane are common. Hyperplastic smooth muscle cells in the plaque differ from the normal myocytes in the media, being smaller and lacking tight intercellular junctions.[24] In old plaques, myocytes are degenerate and contain small lipid globules, residual bodies, and disoriented organelles. Lipid deposition, hemorrhage, and calcification are secondary phenomena in most species, and the fibrous plaque may develop into a collagenous, calcified, endothelium-covered lesion.

Arteriosclerotic plaques, both fibrolipid and atheromatous, from 28 carotid endarterectomies and 15 cardiac transplant patients showed that endothelial cells had characteristics of activation, and that large (giant) endothelial cells (surface area > 800 μm^2) were frequent on the plaque surface.[25]

Hyperplastic Arteriolosclerosis

Hyperplastic arteriolosclerosis is a concentric, laminated thickening of the arteriolar wall associated with acute and severe elevations of blood pressure in man. This is the vascular lesion of malignant hypertension, where it may be complicated by deposits of fibrin and by acute necrosis (necrotizing arteriolitis). Hyperplastic arteriolosclerosis of the kidney has the most serious clinical effects, but this lesion is also found in arterioles of the intestine, gallbladder and pancreas.

Ultrastructurally, the onion skin lesions of hyperplastic arteriolosclerosis represent a vascular wall thickened by aberrant smooth muscle cells. Basement membranes are thickened and the lumen of the vessel is narrowed. In hypertension, endothelial cells develop increased surface microvilli, and have increased amounts of rough endoplasmic reticulum and microfilament bundles in the cytoplasm.[26,27] In prolonged hypertension, there are increased bundles of actin microfilaments in cells of subintimal zones.[28]

Severe hypertension is associated with several degenerative changes in the brain, and with necrotic lesions that are associated with intracerebral hemorrhage and atherosclerosis. Fibrinoid necrosis of the walls of some small arteries and arterioles are seen in hypertensive encephalopathy, a disease associated with malignant hypertension, and with the hypertension of eclampsia and acute nephritis.

Hyaline Arteriopathy

Hyaline arteriopathy is a homogenous, hyalin thickening of the arteriolar wall of the kidney, with narrowing of the lumen and loss of medial architecture.[29] It is not limited to patients with hypertension, but is more severe and generalized in this disease. Its clinical impact is benign nephrosclerosis in which lumenal obstruction causes renal ischemia.

Heritable Arteriopathies

Cerebral autosomal dominant arteriopathy with subcortical infarcts and leukoencephalopathy is an inherited systemic vascular disorder characterized by recurrrent subcortical ischemic strokes that lead to vascular dementia. The diagnosis is confirmed by identification of a mutation in the gene Notch3 that encodes a transmembrane receptor protein. Deposits of granular osmiophilic material around vascular smooth muscle cells (the pathognomonic lesion) are composed of the ectodomain of the Notch3 gene product.[30]

Vasculitides

Focal arteritis is a common finding in acute inflammatory lesions. Damage is secondary to and correlates directly with the severity of the inflammatory response. Lymphocytic arteritis involving the adventitia is common in subacute and chronic viral infections, but this lesion is apt to be periarteritis rather than arteritis.

Focal arteriolar insudation, a localized dilatation associated with endothelial damage and increased permeability, is characteristic of acute injury, especially of inflammatory lesions.[31] Cytokines released by inflammatory cells increase permeability in the large blood vessels. Arterioles become thickened as plasma proteins seep into their muscular walls. Vimentin-containing smooth muscle cells in the intima thicken after endothelium is injured.

Infectious Arteritis

Specific types of arteritis occur in a wide variety of systemic infectious diseases. Damage may be due to a direct effect of a microbial organism or its toxin on any

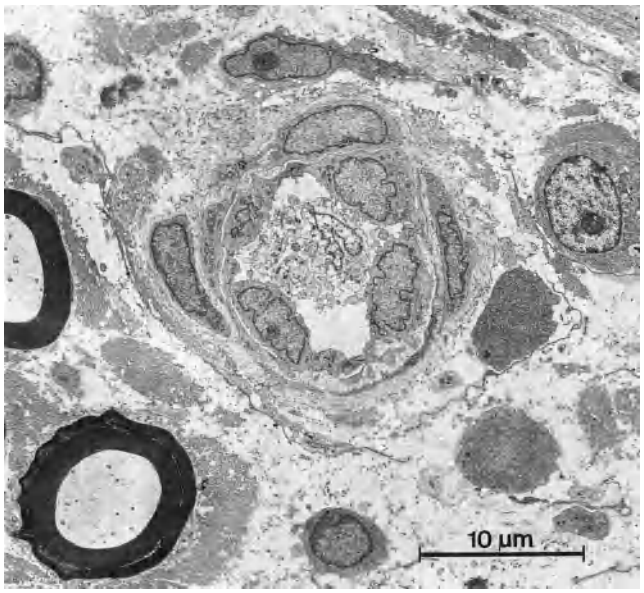


Fig. 28.5 Inflammation and edema: arteriole and surrounding nerves, biopsy of peripheral nerve of patient with Lyme disease (borreliosis). (Micrograph: C. Meier, *Acta Neuropathol* 79:271, 1989.)

component of the vascular wall. Direct invasion of the arterial wall occurs in viral, bacterial and fungal diseases. Rickettsiae, spirochetes, and bacterial toxins are known to cause specific lesions of arteritis, for example, Rocky Mountain spotted fever, leptospirosis, Q fever, heartwater, and Lyme disease (Fig. 28.5). Some bacterial toxins are associated with specific types of arteriopathy. Aspergillosis, mucormycosis, and certain other fungal diseases are apt to be associated with vasculitis and thrombosis.

In systemic viral infections, viral replication occurs in endothelium and subsequent damage leads to exudation of cells and fluids into the arterial wall (Fig. 28.6). Measles virus causes a systemic viral infection with widespread replication of virus in vascular structures. In animals, equine viral arteritis, hog cholera, and Newcastle disease are diseases in which viruses destroy endothelium and can infect myoctes of the media. As the affected myocyte degenerates, shrinks, and dies, plasma proteins exude into the empty spaces, mix with ground substance and collagen, and form an eosinophilic hyalin mass.

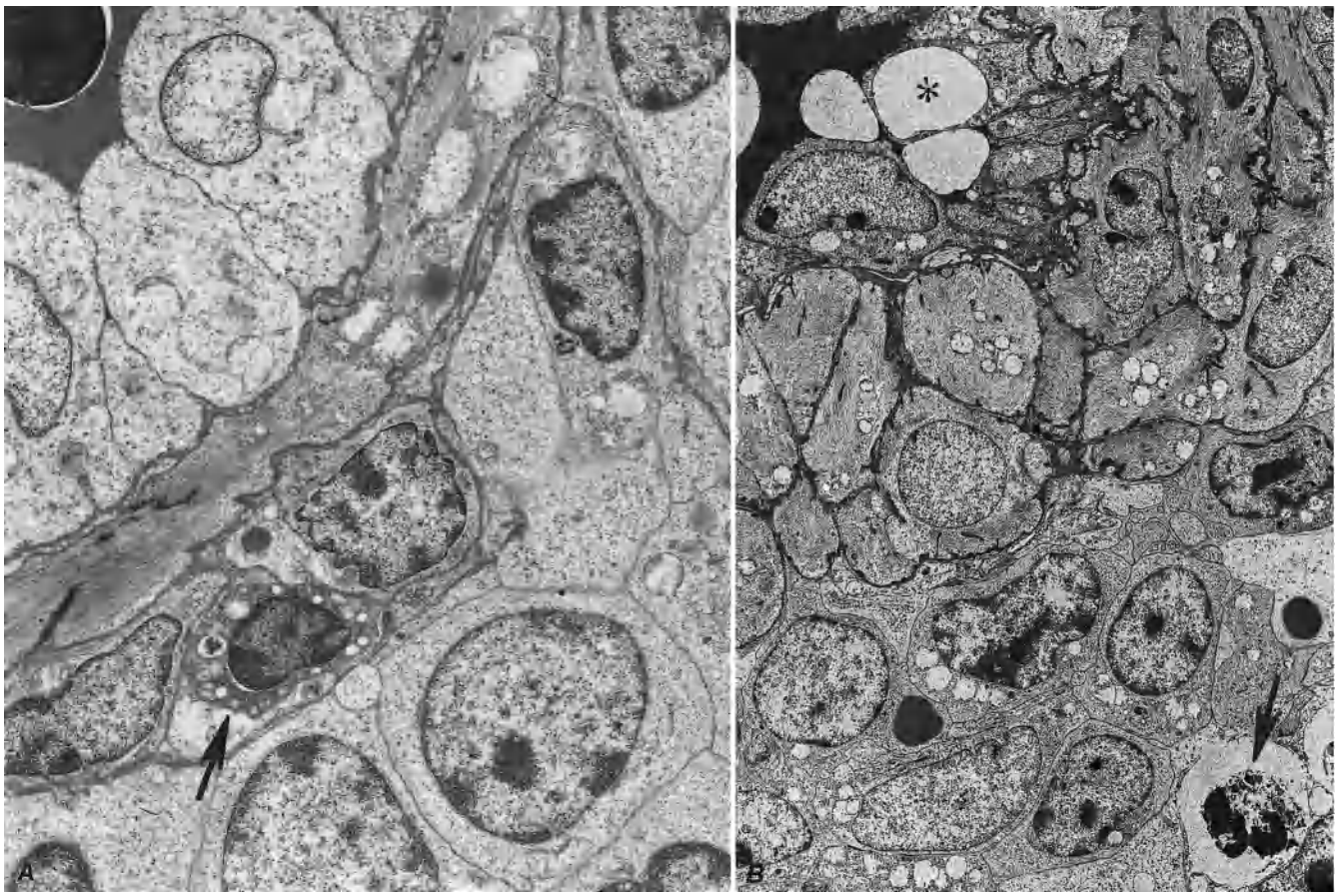


Fig. 28.6 Viral arteritis and endothelial damage. **A**. Endothelial swelling and necrosis of periarterial lymphocytes (*arrow*), Newcastle disease, chicken. **B**. Vacuolated endothelial cells (*) and necrosis of lymphocytes (*arrow*), hog cholera.

Degeneration and necrosis of the arterial wall in viral infection may be caused by replication in the vaso vasorum. Equine viral arteritis virus produces extensive necrosis of the type in arteries of the intestine, lymphoid tissue, and other viscera. Although viral antigens have been demonstrated in myocytes, it appears that the mechanism of injury involves destruction of endothelium in the vaso vasorum. Necrosis first appears in the media at the junction of the two vascular supplies, that is, at the point where the vascular wall is least oxygenated.

Noninfectious Systemic Necrotizing Vasculitides

Noninfectious systemic necrotizing vasculitides are a large, complex group of vascular disoders. Most are immune complex–mediated, and resemble the vascular lesions of the experimental local Arthus reactions and serum sickness. Ultrastructurally, the lesions closely resemble one another, and electron microscopic analysis is of little aid in the diagnosis. The clinical consequences are often thrombosis, hemorrhage, and infarction.

Calcification of the Vascular Wall

Vascular calcification is a complication of advanced atherosclerosis and occurs specifically in two syndromes: vitamin D toxicity and uremia. In both forms calcium may be present as spicules of hydroxyapatite or as laminated spherules that form complexes around the vessel wall.

Idiopathic arterial calcification of infancy is a rare, rapidly fatal process that develops in human infants before the age of 9 months. There is diffuse calcification associated with internal elastic membranes of many arteries, often with focal, obliterative fibrous proliferation. Myocytes, fibroblasts, and collagen become calcified, but calcification does not involve mitochondria.[32]

Hypervitaminosis D is characterized by elevated levels of Ca^{2+} and phosphorus in serum and urine, and by decreased amounts of parathyroid glandular parenchyma. If vitamin D-induced hypercalcemia is prolonged, calcium-phosphorus crystals (hydroxyapatite) are deposited in many tissues, particularly in blood vessels walls, gastric mucosa, lung, and kidney.

Calcification in Uremia

Chronic uremia is accompanied by marked arteriopathy and calcification of arteries in lung, kidney, and gastrointestinal tract.[32,33] This complex systemic disease syndrome is brought about by decreased glomerular filtration and failure of tubular resorption and secretion (Fig. 28.7). Dogs with prolonged uremia develop marked gastropathy. Capillaries in the lamina propria are degenerate and calcified. Muscular arteries of the submucosa have segmental lesions characterized by myocyte necrosis, clacification, and deposition of mucosubstances and fibrin. Thrombosis and obstructive arteriopathy are common, and may lead to infarction.[34] In mice, uremic vasculopathy involves degeneration of medial myocytes.[35]

Atherosclerosis

Atherosclerosis is a disease of large and medium sized arteries characterized by focal thickening of the inner arterial wall associated with lipid deposition and involving (1) smooth muscle cell proliferation in the intima, (2) release of connective tissue matrix by these cells, and (3) accumulation of lipids. Lipids aggregate in the form of elevated, lipid-filled plaques called **atheromas.** Necrosis and fibrosis follow the deposition of lipid and result in a progressively enlarging lesion that expands the arterial wall. Ischemia and infarction may develop in affected organs because of the encroachment of the vascular lumen.[36]

Lesions of human atherosclerosis are raised fatty streaks. As fatty streaks develop, smooth muscle cells accumulate lipids,[37] and represent the initial stage of atherosclerosis.[38] Small, discrete fibrolipid lesions in the human aorta have superficial layers of foam cells, cores of noncrystalline lipids and collagenous caps.[39,40] **Smooth muscle cells** arise either from existing cells, or from cells that migrate from the underlying media.[41] As they proliferate within the intima, the lesion expands to form a fibrous cap that overlies a deeper focus of macrophages, T lymphocytes and debris.

Lipids vary from small globules to locules that fill the cell. **Plasma lipoproteins** within plaques have been analyzed using immunogold techniques; in human atherosclerotic lesions, LDL and the protective HDL are present in foam cells and myocytes.[42] In rats, the protective HDLs are present in the cytoplasm of endothelial cells and myocytes.[43] Crystals of **cholesterol** are present in advanced lesions.[44] Artifactual cholesterol clefts may appear as empty spaces, as they do in histologic preparations, since they are often removed in processing. Advanced atheromas are complicated by hemorrhage, thrombosis, ulceration, and infiltration of the lesion by plasma proteins. Extracellular spaces of atheromas contain cholesterol-rich lipid particles that contain either esterified or unesterified cholesterol.[45–47] In fibrotic lesions, lipids and foam cells are interspersed with collagen fibers[48] and proteoglycans.[49]

Calcification, a major complication of atherosclerosis in humans, is first detected by the presence of

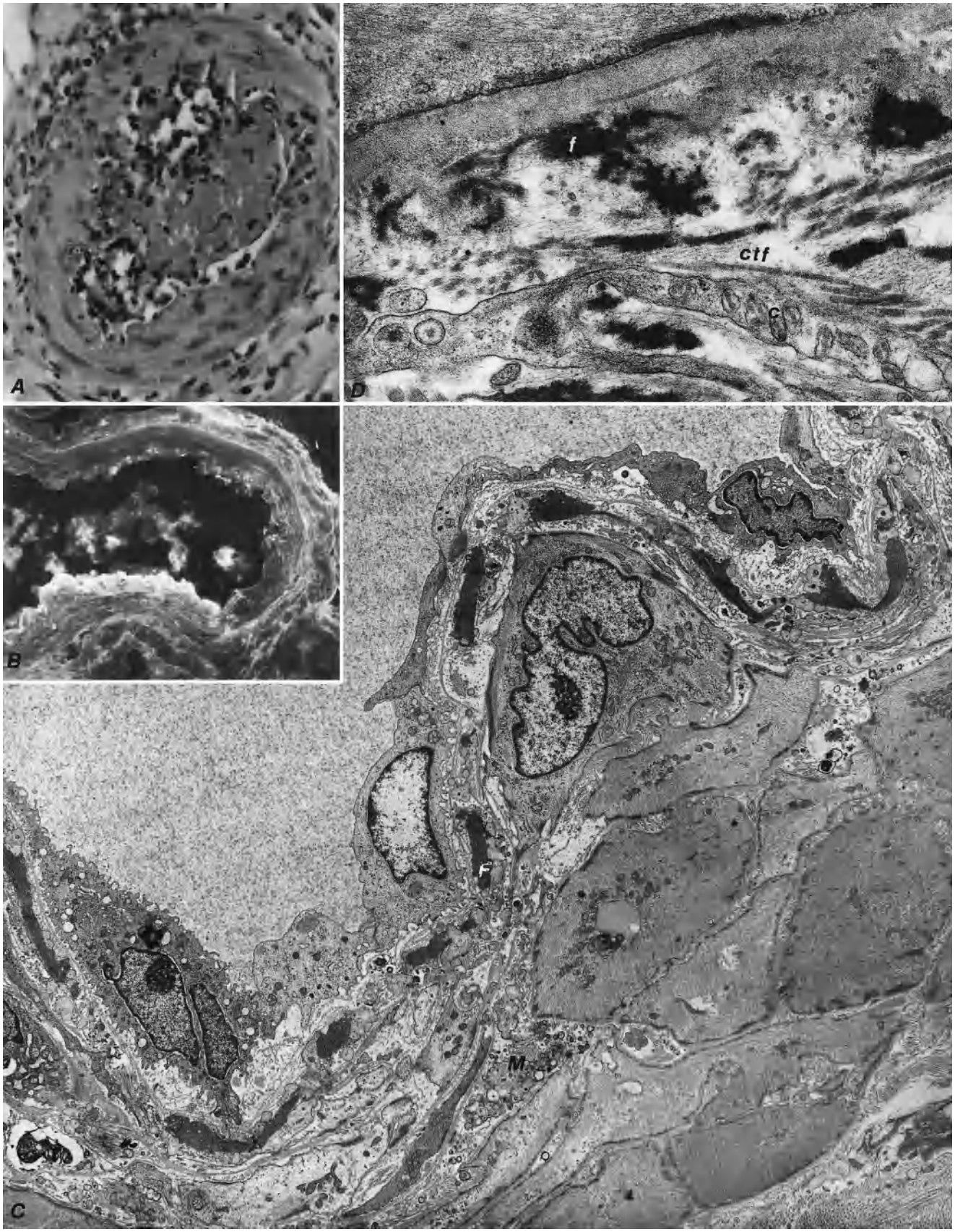


Fig. 28.7 Arterial mucodegeneration and calcification: muscular artery, stomach, uremia, dog. **A**. **Histology**: degeneration of intima and media, thrombus in the lumen. **B**. **Fibrin**: immunofluorescent label of fibrin in vascular wall. **C**. **Ultrastructure**: intima; deposits of fibrin (*F*) and mineral (*M*) below intima. Endothelial cells are swollen, pyknotic, and vacuolated. **D**. **Adventitia surrounding arteriole**: deposits of dense granular material are fibrin (*f*), irregular collagen fibrils, connective tissue filaments (*ctf*), and intracellular collagen fibrils (*c*) in fibroblast. Smooth muscle cell (*top*) with thickened basement membrane.

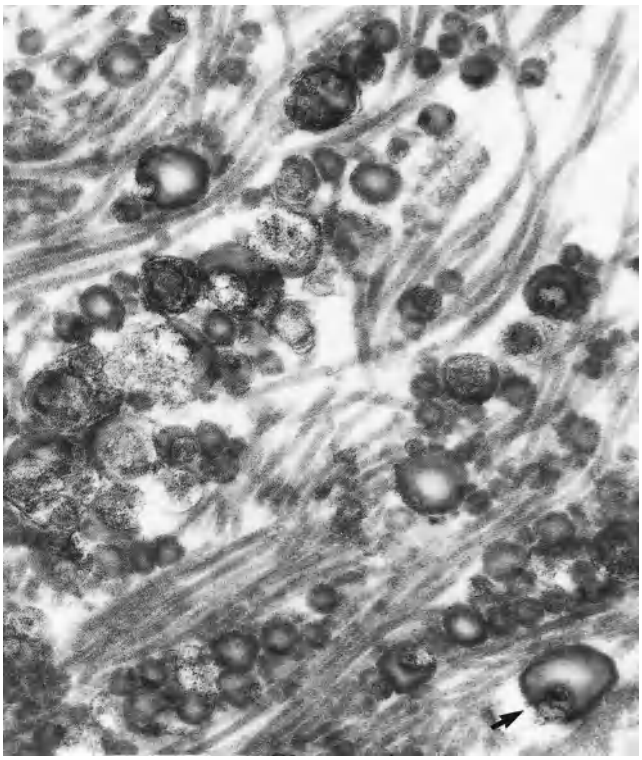


Fig. 28.8 Atherosclerosis: lipid droplets interspersed in collagen, fibrous atherosclerotic plaque, human. Pitting of droplets is found among collagen fibrils. Globular structures have thin crescents of homogeneous gray material resembling neutral lipids (*arrow*). (Micrograph: John R. Guyton, *Am J Pathol* 134:705, 1989.)

matrix vesicles. Transdifferentiation of myocytes to chondrocytes has been proposed as a contributing factor in medial calcification.

Matrix proteoglycans are present in human atherosclerotic plaques, and provide the environment for controlling the balance of coagulation and fibrinolysis. Within the atherosclerotic plaque matrix, tissue factor initiates blood coagulation. The matrix also contains **tissue factor pathway inhibitor-2 (TFPI-2),** a serine protease inhibitor of coagulation factors. TFPI-2 has been identified by immunogold techniques.[50]

Embolization

Rupture of the core region of the atherosclerotic plaque with extension to the lumen of the artery is a major cause of coronary thrombosis and subsequent myocardial infarction. Ultrastructural analysis of core lipids using special osmium-tannic acid-paraphenylenediamine stains reveals that over 90% of the core lipids are composed of small droplets (30–400 nm) of neutral lipids and lipid vesicles with aqueous centers (Fig. 28.8).[51] Cholesterol crystals inhabit regions of the plaque core that are also rich in vesicular lipid. Characteristic **pits** were detected by scanning electron microscopy in lipid droplets from fibrous plaques (but were not in lipid streaks). It has been hypothesized that pits are formed by removal of cholesteryl esters via hydrolysis.

Atheromatous emboli produce widespread damage in human atherosclerosis, especially when emboli lodge in the brain or kidney. Renal failure can results from embolization to the kidney. Atheromatous emboli found in 8 of 755 renal biopsy specimens were characterized by intimal distortion and proliferation, infiltration and growth of macrophages and giant cells, and formation of crystals in the lumen of the involved artery.[52]

Pathogenesis of Atherosclerosis

The atheroma begins as an intimal lesion that progressively extends into and affects the media.[53,54] The pathogenesis of the atheroma, as reconstructed from serial examination of naturally occurring lesions, involves most of the following: (1) endothelial injury with alterations of the underlying extracellular matrix, (2) seepage of plasma lipids and lipoproteins into the intima, (3) invasion of the intima by circulating monocytes that transform to macrophages and phagocytize lipids, (4) myocyte migration through fenestrae of the inner elastic membrane, (5) proliferation of myocytes in foci within the intima, and (6) accumulation of lipids within the cytoplasm of the myocyte. Focal clusters of myocytes become ballooned by cytoplasmic lipids, giving these cells the name **foam cells** (Fig. 28.9). Aggregates of foam cells appear grossly as small elevated fatty streaks in the arterial lumenal surfaces. Foam cells become necrotic and liberation of free lipid incites fibrosis and calcification, which in turn cause more necrosis. In progressively expanding lesions, endothelial desquamation and local release of platelet factors promote vascular matrix alterations. New intima formed during regeneration is rich in glycosaminoglycans, and these mucosubstances complex with plasma lipoproteins to predispose to atherosclerosis.[55]

Macrophages in Atherosclerosis

Macrophages accumulate and process cholesterol in atherosclerotic lesions. The two major forms of cholesterol, cholesterol crystals and LDL, induce compartmentalization of the macrophage cytoplasm. Sequestration provides a means for macrophages to remove substances from the extracellular space and later release them.[56] Macrophages use the classic complement pathway to phagocytize and remove apoptotic cells within atherosclerotic plaques, a mechanism that requires C1q.[57] Macrophages destabilize rupture-prone atherosclerotic plaques. **Mammalian target of rapamycin (mTOR)** is a ubiquitously expressed

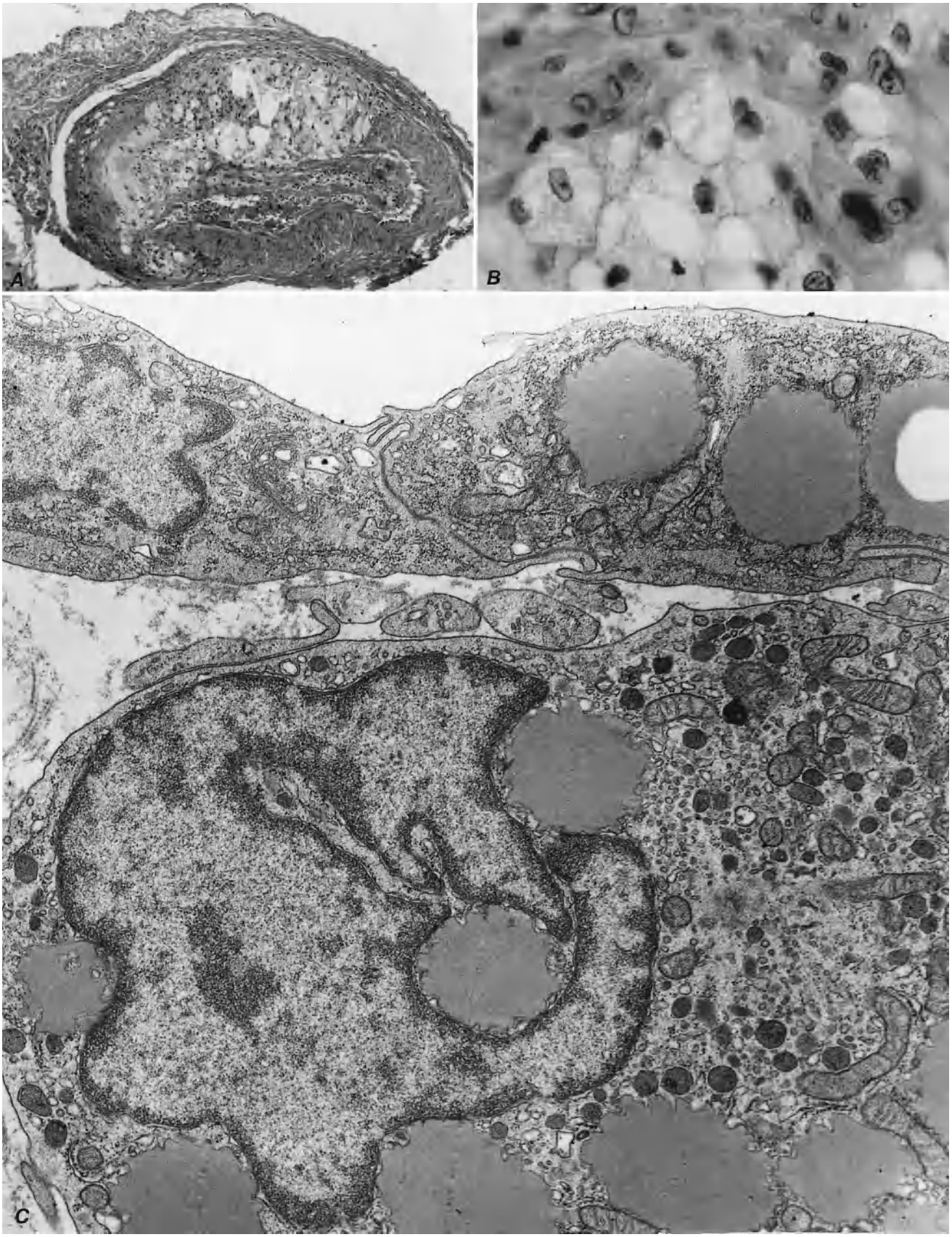


Fig. 28.9 **Atherosclerosis**: coronary artery, dog. **A** and **B**. **Histology**. **C**. **Ultrastructure**: media is distorted by fat-filled myocytes and macrophages. Endothelial cells (*top*) and subendothelial foam cells (*bottom*) are filled with lipid globules. (Micrograph C: Jack C. Geer, *Am J Pathol* 47:241, 1965.)

serine/threonine kinase that affects several key cell functions including protein synthesis and proliferation by a signal pathway that leads to translational repression; in surgery, the stent-based delivery of inhibitors of **mTOR signaling** suggests that macrophages can be cleared from these lesions by autophagic pathways.[58]

Xanthomatosis

Xanthomas are focal aggregates of foamy macrophages in the dermis that arise from both familial and acquired disorders in lipid metabolism and hyperlipidemia. Lesions may be confused with the foamy macrophages that arise in inflammatory lesions from the breakdown of fatty cells. Histologically, the finely vacuolated macrophages of xanthomas may be associated with giant cells and may have small amounts of inflammatory cells at the periphery. Ultrastructural analyses of lipidemic and normolipidemic xanthomasis has been reported.[59,60]

Experimental Atherosclerosis

In diet-induced atherosclerosis, the morphology of the atheroma is dictated by the type and degree of plasma lipid elevation and the response of the host to the lipids. In general, the high levels of plasma cholesterol and lipoproteins give rise to large, fat-laden foam cells of macrophages or myocytes that accumulate below the intima. Macrophages dominate in early phases whereas myocytes are the prominent cell in older lesions.[61,62] Myocytes have distinct myofilaments, elongate nuclei, and surface basement membrane material. Their lipid globules tend to be more electron dense and their cell surfaces do not have microvilli as do macrophages.[63]

Experimental atherosclerosis has been studied in species as diverse as pigeons, fish,[64] kangaroos,[65] and pigs.[66,67] The presence of lipid in the vascular wall of these species does not make these lesions analogous to spontaneous disease, and there is doubt that the experimental disease mimics natural human atherosclerosis. Experimental production is too drastic, for it condenses into a few weeks a condition that takes years to develop in humans.

Monkeys

A valuable model for human atherosclerosis because of its phylogenetic relationship to man, most monkeys develop atheromas on high cholesterol diets and vascular lesions resemble human antheromas.[68–70] The squirrel monkey is particularly useful because of its relatively high incidence of naturally occurring aortic lipid accumulation and the increase in atherosclerosis that can be induced by changes in diet.[71] The African green monkey is reported to more closely mimic the natural disease in humans; the early "fatty dot" lesions are reported to have marked increases in Weibel-Palade bodies, suggesting a role for these granules in early atherosclerosis.[72]

Dogs

Systemic atherosclerosis in dogs is almost always associated with hypothyroidism, and affected dogs are aged, obese, and hyperlipoproteinemic. Atheromas are prominant in the media, as well as intima of large muscular arteries and lipids are present in the cytoplasm of mycoytes and lipid-laden foam cells.[73–75] Ultrastructural examination reveals large lipid globules throughout the media of muscular arteries (Fig. 28.9).

Experimentally, a coconut oil–cholesterol diet for 1 yr will produce hypercholesterolemia (as high as 750 mg per ml) and widespread atheromas.[76] The dog is especially intolerant of circulating plasma cholesterol in the absence of dietary essential fatty acids. Dogs fed diets designed to include only trace amounts of essential fatty acids (5% cholesterol and 15% hydrogenated coconut oil) rapidly develop elevations in serum cholesterol, triglcyerides, and phospholipids. If necropsied at 1 yr, atherosclerotic plaques are present in the aorta and cerebral and coronary arteries. Addition of essential fatty acids will prevent the atherosclerosis.[77]

Rabbits

Rabbits placed on atherogenic diets rapidly develop atherosclerosis. Subendothelial accumulation of extracellular liposomes rich in unesterified cholesterol is a hallmark of this model. Large collections of foam cells in arteries are more representative of a generalized storage disease (xanthomatosis) and bear only superficial resemblance to human atherosclerosis. Macrophages are prominent in superficial areas of lesions, usually just below endothelium. Ultrastructural analysis of arteries of rabbits with various treatments designed to injure the vascular wall and thereby promote atherosclerosis reveal clearly that injury can trigger the development of lipoprotein accumulation within the vascular wall.

An ultrastructural study to identify neutral lipids in extracellular spaces of atherosclerotic lesions in rabbits used a rabbit dietary atherosclerosis model in which 0.5% cholesterol and 5% butter were added to rabbit chow; the results revealed the deposition of membranous and neutral lipid (cholesteryl ester deposits) and β-VLDL, their presumed source, in the extracellular

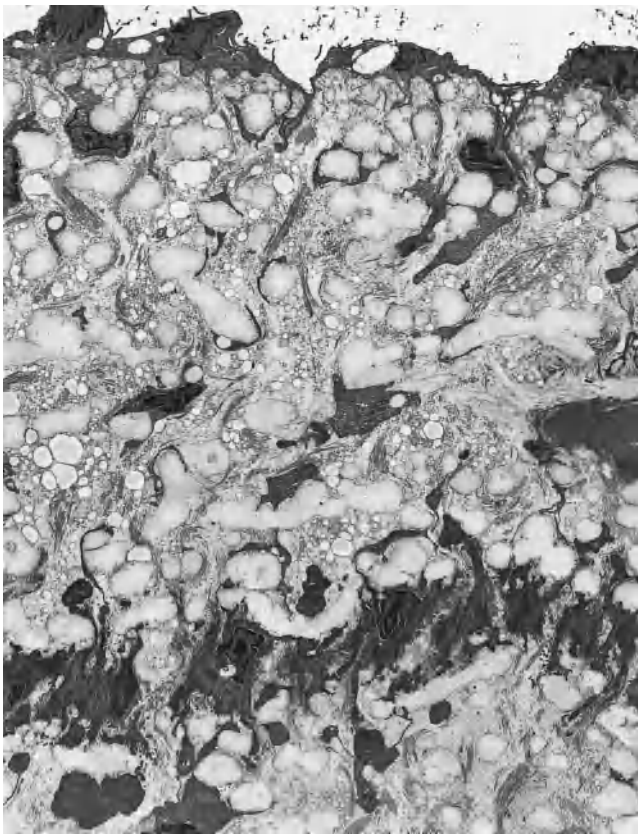


Fig. 28.10 Atherosclerosis: proximal brachiocephalic artery, pigeon. Arrangement of connective tissue collagen and elastin is disrupted, and there is random distribution of proteoglycans and extracellular lipids. (Micrograph: Deborah A. Barr, *Exp Mol Pathol* 54:99, 1991.)

spaces.[78] Neutral lipid accumulation in resident arterial cells was an early event and was viewed as an independent event, occurring before monocytic infiltration of the arterial intima. Because of the unique fixation techniques used in the above study, small (50–150 nm), round neutral lipid droplets were found (with similar frequency) associated with the luminal surface of endothelium in both control and atherosclerotic rabbits; lipid droplets were also found in the arterial intima and inner media or normal control rabbits.

The **Watanabe heritable hyperlipidemic rabbit** has a defect in LDL receptors, and develops atherosclerosis that is a model for homozygous familial hypercholesterolemia, a human genetic disorder characterized by elevated plasma low-density lipoproteins and total plasma cholesterol accompanied by xanthomas, premature atherosclerosis, and myocardial infarction at an early age. Homozygous Watanabe rabbits have plasma cholesterol levels up to 900 mg/dl, most of which is in the LDL fraction. Advanced lesions contain a necrotic cholesterol-filled core, calcification, and a fibrous cap. Smooth muscle cells and macrophages are filled with cytoplasmic lipid globules and lamellar bodies.[79,80] Circulating monocytes are the chief source of foam cells in rabbit atherogenesis.[81]

A strain of New Zealand white rabbit with genetically determined hyperlipidemia distinct from the Watanabe rabbit develops overproduction of VLDL and LDL. Lesions are elevations of the aortic intima, especially in the thoracic region. Plaques have populations of modified smooth muscle cells and lipid-laden macrophages and are similar to lesions in diet-induced hyperlipidemia.[82]

Rodents

These animals have never been popular as models of human atherosclerosis. Vascular lesions are difficult to induce and do not follow the patterns of development and regression that are seen in humans.[83,84] Several murine mutants have been described that develop widespread vascular lesions but few resemble the lesions of human atherosclerosis. Rats have been used as models to study arteriosclerosis in transplanted hearts and arteries. The transplanted abdominal aortic allografts develop intimal lesions of mononuclear inflammatory cells and progressively increasing smooth muscle cells.[85]

Pigs

Cholesterol-fed swine have served as reliable models for human atherosclerosis. Ultrastructural changes in atherosclerotic lesions follow those in simian models.[86,87] Pigs are also widely used for models of human cardiovascular diseases including studies of restinosis, cardiac valve calcification, introduction of recombinant genes into arteries, and obesity (pigs are devoid of brown fat postnatally).

Birds

The chicken has been used as a model for atherosclerosis.[88] The white Carneau pigeon is another avian model of atherosclerosis (Fig. 28.10). Smooth muscle cells of young pigeons incorporate 95% of newly synthesized fatty acids into triglycerides and phospholipids. At 12 mo (the age at which arterial walls accumulate cholesterol), there is an increase of fatty acids esterified to cholesterol. The slowed rate of cholesterol esters removed appears to be due to deficiency of lysosomal cholesterol esterase.[89] Atherosclerotic lesions in aortic and coronary arteries exhibit endothelial degeneration, migration of monocytes into subintimal areas, and development of foam cells.[90,91] Atherosclerosis also develops in other arteries by often lacks the foam cells of the more severe aortic lesions.[92]

References

1. Clark JM, Glagov S. 1979. Structural integration of the arterial wall. *Lab Invest* 40:587.
2. Reidy MA. 1985. A reassesment of endothelial injury and arterial lesion formation. *Lab Invest* 53:513.
3. Clowes AW, et al. 1978. A morphologic and permeability study of luminal smooth muscle cells after arterial injury in the rat. *Lab Invest* 39:141.
4. Heistad DD, et al. 1978. Regulation of blood flow to the aortic media in dogs. *J Clin Invest* 62:133.
5. López-Candales A, et al. 1997. Decreased vascular smooth muscle cell density in medial degeneration of human abdominal aortic aneurysms. *Am J Pathol* 150:993.
6. Kirton OC, Jones R. 1987. Rat pulmonary artery restructuring and pulmonary hypertension induced by continuous *Escherichia coli* endotoxin infusion. *Lab Invest* 56:198.
7. Kobori K, et al. 1979. Light and electron microscope studies on rat arterial lesions induced by experimental arterial contraction. *Virch Arch A* 385:29.
8. Kondo Y, et al. 1979. Accelerated serum sickness in the rabbit. IV. Characteristics endarteritis in the pulmonary artery. *Lab Invest* 41:119.
9. Naylor JR, et al. 1984. Change in the ultrastructure of the feline pulmonary artery following infection with the lung worm *Aelurostrongylus abstrussis*. *Brit Vet J* 140:108.
10. Richman AV, et al. 1980. Peritubular capillaries. A major target site of endotoxin-induced vascular injury in the primate kidney. *Lab Invest* 43:327.
11. Reidy MA, Schwartz SM. 1983. Endothelial injury and regeneration. IV. Endotoxin: A nondenuding injury to aortic endothelium. *Lab Invest* 4825.
12. Bugelski PJ, et al. 1989. Ultrastructure of an arterial lesion induced in rats by fenoldopam mesylate, a dopamine vasodilator. *Br J Exp Pathol* 70:153.
13. Kerns WD, et al. 1989. Pathogenesis of arterial lesions induced by dopaminergic compounds in the rat. *Tox Pathol* 17:203.
14. Thorgeirsson G, et al. 1979. Migration of human vascular endothelium and smooth muscle cells. *Lab Invest* 41:51.
15. Regan TJ, et al. 1974. Altered myocardial functional metabolism in chronic diabetes mellitus without ischemia in dogs. *Circ Res* 35:222.
16. Sosa-Melgarejo JA, Berry CL. 1991. Intercellular contacts in the media of the thoracic aorta of rat fetuses treated with β-aminoproprionitrile. *J Pathol* 164:159.
17. Kocher O, et al. 1991. Phenotypic features of smooth muscle cells during evolution of experimental carotid intimal thickening. *Lab Invest* 65:459.
18. Phelps PC, Luft JH. 1969. Electron microscopical study of relaxation and constriction in frog arterioles. *Am J Anat* 125:399.
19. Fein JM, et al. 1974. Sequential changes of vascular ultrastructure in experimental cerebral vasospasm. *J Neurosurg* 41:49.
20. Gordon D, et al. 1981. Intimal alterations in rat aorta induced by stressful stimuli. *Lab Invest* 45:14.
21. Joris I, Majno G. 1981. Medial changes in arterial spasm induced by L-norepinephrine. *Am J Pathol* 105:212.
22. Allen K, Haworth SG. 1988. Human postnatal pulmonary arterial remodeling. *Lab Invest* 59:702.
23. Haworth SB, et al. 1987. Thinning of fetal pulmonary arterial wall and postnatal remodelling: Ultrastructural studies on the respiratory unit arteries of the pig. *Virch Arch* 411:161.
24. Hayes JA, et al. 1978. Myointimal plaques in pulmonary vascular sclerosis associated with interstitial lung fibrosis. *Lab Invest* 41:268.
25. Burrig K-F. 1991. The endothelium of advanced arteriosclerotic plaques in humans. *Arterioscler Thromb* 11:1678.
26. Kerenyi T, et al. 1991. Changes of DNA-acridine orange binding in monocytes and endothelial cells of hypertensive arteries. *Exp Molec Pathol* 54:230.
27. Rabinovitch M, et al. 1986. Pulmonary artery endothelial abnormalities in patients with congenital heart defects and pulmonary hypertension. *Lab Invest* 55:632.
28. Gabbiani G, et al. 1982. Vimentin-containing smooth muscle cells in aortic intimal thickening after endothelial injury. *Lab Invest* 47:265.
29. Gamble CN. 1986. The pathogenesis of hyaline arteriolosclerosis. *Am J Pathol* 122:410.
30. Ishiko A, et al. 2006. Notch3 ectodomain is a major component of granular osmiophilic material (GOM) in CADASIL. *Acta Neuropathol* 112:333.
31. Cuenoud HF, et al. 1987. Focal arteriolar insudation. *Am J Pathol* 127:592.
32. Anderson KA, et al. 1985. Idiopathic arterial calcification of infancy in newborn siblings with unusual light and electron microscopic manifestations. *Arch Pathol* 109:838.
33. Legeros RZ, et al. 1973. Pathologic calcifications associated with uremia. *Calcif Tissue Res* 13:173.
34. Cheville NF. 1979. Uremic gastropathy in the dog. *Vet Pathol* 16:292.
35. Bro S, et al. 2005. Uremia specific effects in the arterial media during development of uremic atherosclerosis in apoplipoprotein E-deficient mice. *Arterioscler Thromb Vasc Biol* 26:570.
36. Ross R, et al. 1984. Human atherosclerosis. *Am J Pathol* 114:79.
37. Orekhov AN, et al. 1986. Intimal cells and atherosclerosis. *Am J Pathol* 125:40.
38. Katsuda S, et al. 1992. Human atherosclerosis. III. Immunocytochemical analysis of the cell composition of lesions of young adults. *Am J Pathol* 140:907.
39. Bocan TMA, Guyton JR. 1985. Human aortic fibrolipid lesions. *Am J Pathol* 120:193.
40. Masuda J, Ross R. 1990. Atherogenesis during low level hypercholesterolemia in the nonhuman primate. I. Fatty streak formation. *Arteriosclerosis* 10:164.
41. Babaev V, et al. 1990. Heterogeneity of smooth muscle cells in atheromatous plaques of human aorta. *Am J Pathol* 136:1031.
42. Kaesberg B, et al. 1993. In situ immunolocalization of lipoproteins in human arteriosclerotic tissue. *Arterioscler Thromb* 13:133.

43. Yang VC, et al. 1999. Immunolocalization of high-density lipoproteins in arterial walls of rats. *Atherosclerosis* 142:269.
44. Jones DB, Iannaccone PM. 1975. Atheromatous emboli in renal biopsies. An ultrastructural study. *Am J Pathol* 78:261.
45. Bobryshev YV. 2007. Intracellular localization of oxidized low-density lipoproteins in atherosclerotic plaque cells revealed by electron microscopy combined with laser capture microdissection. *J Hist Cyt* 53:793.
46. Chao F-F, et al. 1990. Characterization of two unique cholesterol-rich lipid particles isolated from human atherosclerotic lesions. *Am J Pathol* 136:169.
47. Rus HG, et al. 1986. Immunoelectron-microscopic localization of the terminal C5b-9 complement complex in human atherosclerotic, fibrous plaque. *Atherosclerosis* 61:35.
48. Bocan TMA, et al. 1986. Ultrastructure of the human aortic fibrolipid lesion: Formation of the atherosclerotic lipid-rich core. *Am J Pathol* 123:413.
49. Voelker W, et al. 1989. Cytochemical changes in a human arterial proteoglycan related to atherosclerosis. *Atherosclerosis* 77:117.
50. Crawley JT, et al. 2002. Expression and localization of tissue factor pathway inhibitor-2 in normal and atherosclerotic human vessels. *Arterioscler Thromb Vasc Biol* 22:218.
51. Guyton JR, Klemp KF. 1989. The lipid-rich core region of atherosclerotic fibrous plaques. *Am J Pathol* 134:705.
52. Jones NL, et al. 1991. Pigeon monocyte and macrophage lysosomes during βVLDL uptake. *Am J Pathol* 139:383.
53. Aleotti A, et al. 2005. The evolution of the atheromatous plaque: Ultrastructural evidence. *J Submicr Cytol Pathol* 37:53.
54. Aliev G, et al. 2004. Pathobiology of familial hypercholesterolemic atherosclerosis. *J Submicr Cytol Pathol* 36:225.
55. Richardson M, et al. 1980. Glycosaminoglycan distribution in rabbit aortic wall following balloon catheter deendothelialization. *Lab Invest* 43:509.
56. Kruth HW, et al. 1995. Sequestration of acetylated LDL and cholesterol crystals by human monocyte-derived macrophages. *J Cell Biol* 129:133. .
57. Bhatia VK, et al. 2007. Complement C1q reduces early atherosclerosis in low-density lipoprotein receptor-deficient mice. *Am J Pathol* 170:416.
58. Verheye S, et al. 2007. Selective clearance of macrophages in atherosclerotic plaques by autophagy. *J Am Coll Cardiol* 49:706.
59. Ferrando J, Bombi JA. 1979. Ultrastructural aspects of normolipidemic xanthomatosis. *Arch Dermatol Res* 266:143.
60. Schmalbruch H, et al. 1987. Abnormalities in spinal neurons and dorsal root ganglion cells in Tangier disease presenting with a syringomyelia-like defect. *J Neuropathol Exp Neurol* 46:533.
61. Gerrity RG. 1981. The role of the monocyte in atherogenesis. *Am J Pathol* 103:181.
62. Simionescu N, et al. 1986. Prelesional events in atherogenesis. *Am J Pathol* 123:109.
63. Newman H, et al. 1971. Foam cells of rabbit atheromatous lesions. *Lab Invest* 25:586.
64. House EW, Benditt EP. 1981. The ultrastructure of spontaneous coronary arterial lesions in steelhead trout (*Salmo gairdneri*). *Am J Pathol* 104:250.
65. Ward BC, et al. 1974. Atherosclerosis in rat kangaroo. *Arch Pathol Lab Med* 98:90.
66. Daoud AS, et al. 1976. Regression of advanced atherosclerosis in swine. *Arch Pathol* 100:372.
67. Reddick RL, et al. 1990. Coronary atherosclerosis in the pig. *Arterioscler Thromb* 10:541.
68. Masuda J, Ross R. 1990. Atherogenesis during low level hypercholesterolemia in the nonhuman primate. I. Fatty streak formation. *Arterioscler Thromb* 10:164.
69. Scott RF. 1967. Experimental atherosclerosis in rhesus monkeys. *Exp Molec Pathol* 7:34.
70. Trillo AA. 1981. Formation of "ghost" bodies and calcification in experimental atherosclerosis in nonhuman primates. *Virch Arch B* 38:127.
71. McCombs HL, et al. 1969. Fine structure of spontaneous atherosclerosis in the aorta in the squirrel monkey. *Am J Pathol* 55:235.
72. Trillo AA, Prichard RW. 1979. Early endothelial changes in experimental primate atherosclerosis. *Lab Invest* 41:294.
73. Geer JC. 1965. Fine structure of canine experimental atherosclerosis. *Am J Pathol* 47:241.
74. Schaub RG, et al. 1987. A study of atherosclerotic lesion development in the injured pulmonary arteries of dogs with induced hyperlipemia. *Lab Invest* 56:489.
75. Suzuki M. 1972. Experimental cerebral atherosclerosis in the dog. *Am J Pathol* 67:387.
76. Mayley RW, et al. 1977. Canine hyperlipoproteinemia and atherosclerosis. *Am J Pathol* 87:205.
77. McCullagh KG, et al. 1976. Experimental canine atherosclerosis and its prevention. *Lab Invest* 34:394.
78. Guyton JR, Klemp KF. 1992. Early extracellular and cellular lipid deposits in aorta of cholesterol-fed rabbits. *Am J Pathol* 141:925.
79. Clozel J-P, et al. 1988. Decreased coronary vascular reserve in Watanabe heritable hyperlipidemic rabbits. *Arterioscler Thromb* 8:310.
80. Rosenfeld ME, et al. 1987. Fatty streak expansion and maturation in Watanabe heritable hyperlipidemic and comparably hypercholesterolemic fat-fed rabbits. *Arterioscler Thromb* 7:24.
81. Watanabe T, et al. 1985. Role of macrophages in atherosclerosis. *Lab Invest* 53:80.
82. Seddon AM, et al. 1987. Hereditary hyperlipidemia and atherosclerosis in the rabbit due to overproduction of lipoprotein. *Arterioscler Thromb* 7:113.
83. Joris I, et al. 1983. Studies on the pathogenesis of atherosclerosis. I. Adhesion and emigration of mononuclear cells in the aorta of hypercholesteremic rats. *Am J Pathol* 113:341.
84. Melaz H, Leeson TS. 1975. Comparative electron microscope studies of the myocardium in adult rats fed on normal and cholesterol diets. *J Molec Cell* Cardiol 7:195.
85. Isik FF, et al. 1992. Transplant arteriosclerosis in a rat aortic model. *Am J Pathol* 141:1139.

86. Gutstein WH, et al. 1973. Blood flow disturbance and endothelial cell injury in preatherosclerotic swine. *Lab Invest* 29:134.
87. Imai H, et al. 1970. Ultrastructural features of aortic cells in mitosis in control and cholesterol-fed swine. *Lab Invest* 23:401.
88. Moss NS, Benditt EP. 1970. The ultrastructure of spontaneous and experimentally induced arterial lesions. *Lab Invest* 23:521.
89. Jerome WG, Lewis JG. 1987. Early atherogenesis in the white Carneau pigeon. III. Lipid accumulation in vascent foam cells. *Am J Pathol* 128:253.
90. Jerome WG, Lewis JC. 1985. Early atherogenesis in white Carneau pigeons. II. Ultrastructural and cytochemical observations. *Am J Pathol* 119:210.
91. Taylor RG, et al. 1992. Ultrastructural localization of peroxidase in atherosclerotic lesions of pigeons. *Exp Molec Pathol* 57:167.
92. Barr DA, et al. 1991. Morphologic characteristics of naturally occurring atherosclerosis in the brachiocephalic artery of the pigeon. *Exp Molec Pathol* 54:111.

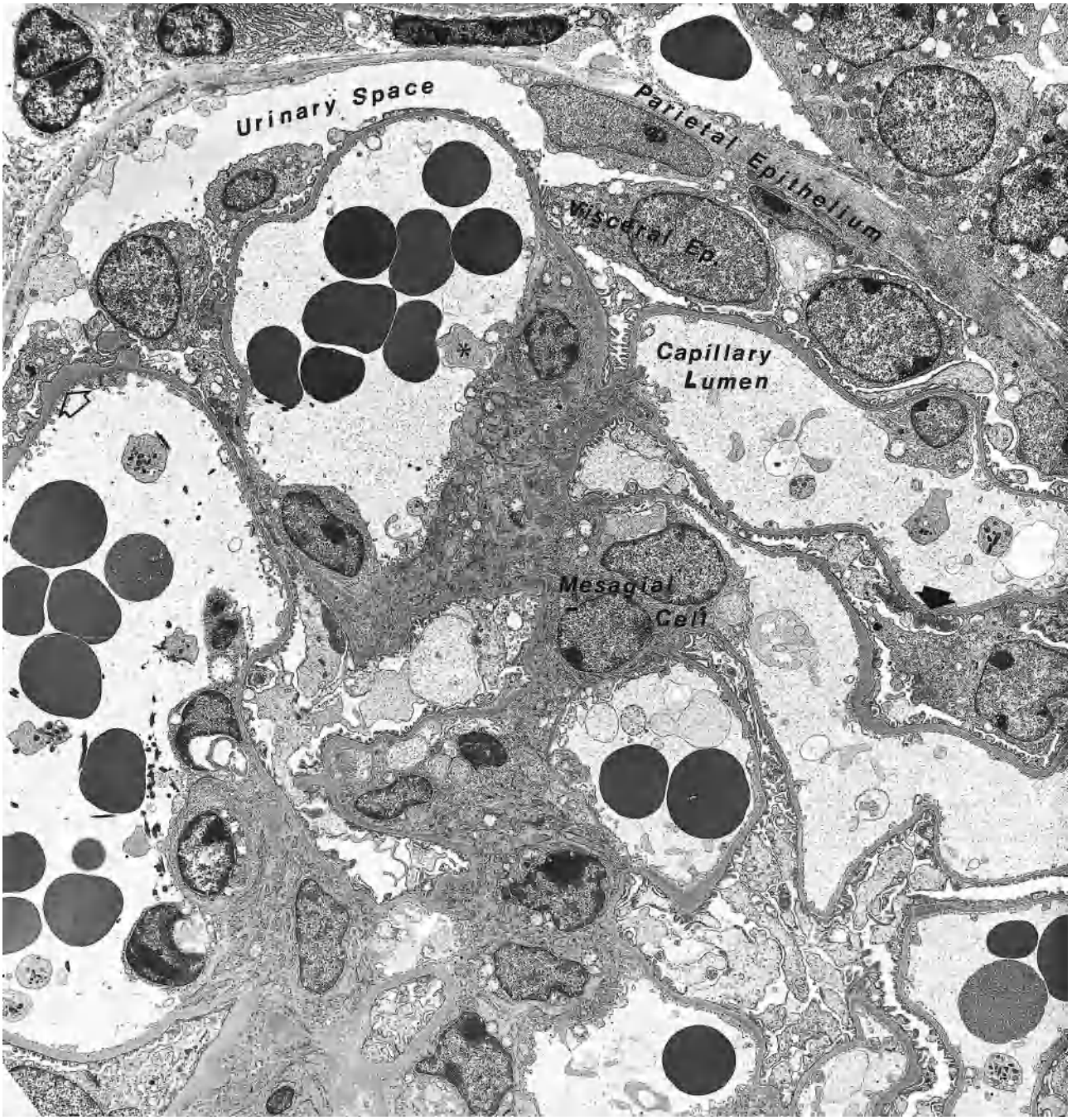


Fig. 29.1 Membranous glomerulonephritis: autoimmune type, strain NZB mouse. Early changes include granular deposits trapped beneath capillary endothelium and below capillary basement membranes (*arrow*). Dense deposits are in fused foot processes of some visceral epithelial cells.

Ultrastructural Pathology The Comparative Cellular Basis of Disease
Second Edition Norman F. Cheville
© 2009 Wiley-Blackwell. ISBN: 978-0-813-80330-2

29 The Renal Glomerulopathies

Primary glomerulonephritis, in which the kidney is the only or predominant organ involved, includes acute diffuse proliferative glomerulonephritis, membraneous glomerulonephritis, and several other types. **Secondary glomerulonephritis** arises from disease elsewhere in the body. Many of these lesions involve immunologic injury to the glomerular basement membrane (GBM) of the glomerulus, which results from deposition of circulating immune complexes, from attachment of circulating antibodies to antigens trapped in the **glomerular filtration barrier**, or from antibodies that cross-react with normal glomerular basement membrane.

Endothelial cells of glomerular capillaries have thin, fenestrated cytoplasm, and are covered by a thick, highly negatively charged (polyanionic) glycocalyx that covers fenestrae and extends into the lamina rara interna of the glomerular basement membrane. The capillary wall adjacent to the mesangium may be penetrated by the **mesangial cell**; that is, a limb of the mesangial cell extends through the endothelium into the capillary lumen (Fig. 29.1).[1–3] Molecules that penetrate beyond the lamina densa are restricted at podocyte **filtration slits** by the slit diaphragm and epithelial glycocalyx negative charges. Solutes retained at the slits are phagocytized by epithelial cells, incorporated into lysosomes, and drained away to the mesangium.[4]

The diagnosis of renal glomerular disease in biopsy specimens of the kidney is based largely upon structural changes in the capillary and GBM (Fig. 29.2).[5–7] Classification of human glomerulonephritis relies chiefly on the pattern of deposition of immune complex deposits in the GBM. Three-dimensional studies by scanning electron microscopy are useful in analysis of the podocyte and its foot processes.[8–10] Preliminary extraction of cells by digestion allows a unique view of the basement membrane surface.[11,12]

Membranous Glomerulonephritis

Membranous glomerulonephritis appears as a diffuse thickening of the glomerular capillary wall with immunoglobulin-containing, granular-dense deposits along the epithelial side of the basement membrane.[13] The electron-dense deposits in the basement membrane are typically granular and interrupted, and are referred to as "lumpy-bumpy." In early stages there may be diffuse and relative uniform thickening of the basement membrane. In late stages, except for lesions of Goodpasture's syndrome and Masugi nephritis in rats (which have linear deposits), the lesions of membranous glomerulopathy are irregular and granular. They develop progressively between the epithelial cell and its underlying basement membrane. Epithelial cells are enlarged and swollen. Epithelial foot processes are irregular and contain dense granular material, and are often fused so that the slit diaphragms disappear.

Basement membrane material is produced in excess and is deposited between foot processes. Progressive remodeling of the basement membrane occurs as the basement membrane material extends between and around the immune deposits to form characteristic spikes on the epithelial side of the basement membrane. As the spikes expand they produce dome-like protrusions, which mask the immune deposits. The expanding membrane progressively obliterates the capillary lumen, and as glomerulosclerosis proceeds, the normal glomerulus is replaced by a dense (hyalin) mass (Fig. 29.3).

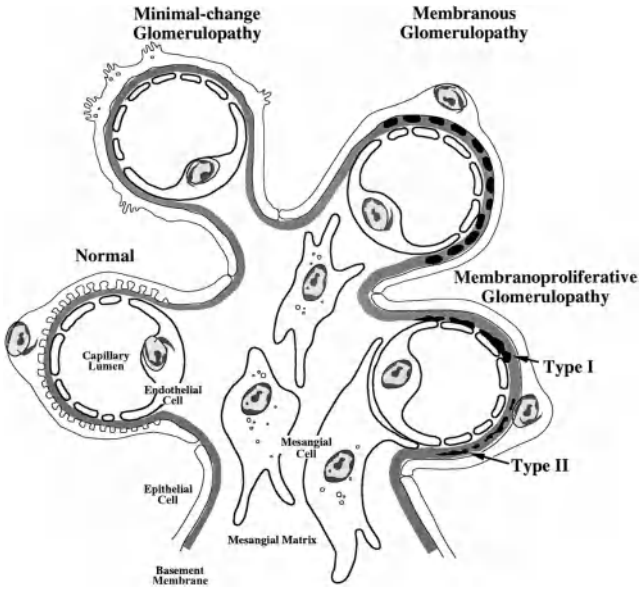


Fig. 29.2 Glomerulopathy: different patterns. Normal capillary basement membrane (*left*) is compared with changes in membranous, membranoproliferative, and minimal-change glomerulopathy.

Table 29.1 Immune mechanisms in glomerulopathies.

Antibody-mediated glomerulopathies
Immune complex deposits formed in situ
Fixed intrinsic tissue antigens (anti-tissue antibodies)
Idiopathic human membranous glomerulonephritis
Anti-GBM autoimmune glomerulonephritis: Goodpasture's syndrome
Masugi nephritis (rat)
Heymann nephritis (rat model)
Planted antigens (exogenous)
Drugs: penicillamine, captopril, gold, mercury
Bacteria: streptococcal glomerulonephritis (endostreptosin)
Viruses: measles, swine fever, bovine viral diarrhea
Planted antigens (endogenous)
DNA
Immunoglobulins
Immune complexes
Graft-versus-host reactions
Immune complexes (circulating) trapped and deposited in the GBM
Exogenous
Parasites: schistosomiasis (*Schistosoma mansoni*)
Protozoa: malaria (*Plasmodium falciparum*)
Bacteria: syphilis (*Treponema pallidum*), post-streptococcal infections
Viruses: hepatitis B antigen (HBsAg)
Endogenous
Thyroglobulin
DNA: systemic lupus erythematosus
Tumor antigens: melanoma, carcinomas of lung and colon
Cell-mediated glomerulopathies
Complement (alternate pathway) activation*

*Activation of complement pathways occurs in human membranoproliferative glomerulonephritis superimposed upon immune complex deposition.

Immune mechanisms are responsible for most types of membraneous glomerulopathy in both man and animals. Antibody-mediated mechanisms involving deposits of immune complexes in the GBM are most common. They may arise by deposition of circulating antigen-antibody complexes on a normal glomerular basement membrane (GBM), or by antibodies reacting in situ within the glomerulus, either with components of the normal glomerulus and with circulating antigens that have been fixed or "planted" on the GBM (Table 29.1).[14]

Different sizes of immune complexes formed by antibodies of different affinities have different patterns of deposition in the glomerulus. The immunoglobulin class or isotype (IgG, IgA, or IgE) are less important in defining the pattern of deposition.[15] **Microcalcification** of glomerular electron-dense deposits develops in diseases associated with hypercalcemia and systemic inflammatory disease.[16] Endothelial cell injury and **fibrinogen polymerization** is common within glomerular capillaries in acute severe glomerulonephritis, and fibrin may obscure the changes within the GBM. Increased production of thromboplastin by glomeruli with activation of the extrinsic coagulation pathway may contribute to intraglomerular fibrin.[17]

Animal Models of Membranous Glomerulopathy

In the 1960s, a wide array of animal models for human membranous glomerulonephritis were developed using injections of immune complexes prepared in vitro; for example, the serum sickness models. Ultrastructural studies of the models in rodents have elucidated many of the mechanisms of immune-mediated inflammatory disease to glomerular. Naturally occurring models of the human immune complex glomerulopathies exist in rodents and other animal species to study the pathogenesis of renal glomerular lesions.[18]

The Rat Model of Membranous Glomerulopathy

Induced by immunizing rats with preparations of proximal tubular brush borders, **passive Heymann nephritis** reproduces most features of human membranous nephropathy. Rats develop antibodies to brush border antigens, and membranous glomeru-



Fig. 29.3 Membranous glomerulopathy: Guillain-Barré syndrome, human kidney. Effacement of foot processes of podocytes with lumenal microvillous proliferation and epimembranous granular deposits. (Micrograph: Thomas S. Talamo, *Am J Clin Pathol* 78:563, 1982.)

lopathy with glomeruli being relatively evenly affected. Changes progress from small subepithelial immune deposits in the lamina rare externa of the glomerular basement membrane to large, glomerular basement membrane-matrix-encapsulated defects in the glomerular basement membrane that contain immunoglobulins and complement.[19,20] Heymann antigen, a 330 kd glycoprotein, is deposited along visceral epithelial cell surfaces and can be found in coated pits on basal surfaces.[21] Immune complexes form, and as complement is activated the complement attack sequence is inserted into the membrane.[22] This is followed by patching and capping phenomena at the visceral epithelial cell surface, and by blebbing with shedding of immune complexes into subepithelial deposits.[23] Immune deposits are subepithelial, and are granular and interrupted, not linear. Complement and monocytes are essential for inducing glomerular injury in passive Heymann nephritis.[24] Platelets are important in other types of glomerulonephritis.[25,26] There is little increase in synthesis of type IV collagen, laminin, or fibronectin.[27,28]

Nephrotoxic Nephritis

Masugi (nephrotoxic) nephritis is produced in rats by injection of anti-rat kidney antibodies produced by rabbits immunized with rat kidney tissue (the GBM antigen is a component of collagen IV). Antibodies bind diffusely and uniformly along the GBM to produce a homogeneous linear pattern of dense deposits. An early heterologous phase of glomular injury is caused directly by the anti-GBM antibodies. In a later autologous phase, glomerular damage results from reaction to immunoglobulin deposits, which, being of rabbit origin, incite the rat to produce anti-rabbit antibodies (which react with rabbit immunoglobulin within the basement membrane).[29]

Membranous Glomerulopathy of the Athymic Mouse

Glomerulopathy of the NZB mouse, a model for immune complex glomerulopathy that occurs in the autoimmune disease **lupus erythematosus**, is characterized by irregular thickening of the GBM and crescentric epithelial proliferation of the capsule. Ultrastructurally, there are mesangial and endothelial cell proliferation, fibrin thrombi, and sclerosis. Electron-dense deposits are due to trapping of specific antigen-antibody complexes. IgG, complement, and viral proteins are present in early lesions, but fibrinogen and albumin can be identified in advanced lesions.[30] Early in glomerulitis, basement membranes may be expanded by edema fluid, by the proteases released by neutrophils and other inflammatory cells, and by the retraction of epithelial and endothelial cells overlying the basement membrane.[31–35] T cells are not required for this disease.[36] Thymic deficient **nude mice** develop manifestations of autoimmunity including membraneous glomerulopathy with deposition of immunoglobulins and antinuclear antibodies.[37]

Naturally Occurring Membranous Glomerulopathies in Animals

Membranous glomerulonephropathy is the most common glomerulopathy in animals (Fig. 29.4). Characteristics are dense subepithelial immune deposits, effacement of overlying glomerular epithelial cell foot processes, and expansion of the glomerular basement membranes. Many of these cases are **postinfectious**—associated with chronic microbial infections, especially bacterial septic diseases and viral infections that depress the monocyte-macrophage system or that persist to produce immune complexes that are trapped by the renal glomerulus.

Glomerulopathy of Aging

The glomerular basement membrane thickens progressively with age in most animal species. Glomeruli of old animals have a uniformly increased width of the dense lamina and granular densities in the epithelial cell foot processes. These changes are related to pathologic turnover and synthesis of basement membrane material by the epithelial cell. Corticosteroids act on the glomerular basement membrane to increase synthesis of polysaccharides.[38]

Chronic Septic Disease

Prolonged bacterial infections accompanied by tissue necrosis and hyperproteinemia often lead to diffuse membranous glomerulonephritis. Lesions begin as thickening of capillary loops and mesangium by increased basement membrane material. The initial thickening of the dense lamina of the basement membrane and expansion of the mesangium are followed in the subacute stages by proliferation of mesangial and epithelial cells. Purulent pyometra in the bitch with cystic hyperplasia of the endometrium is characterized by nodular deposits of granular material that accumulate in the glomerulus below the endothelium, in the dense layer of the basement membrane, and adjacent to the foot processes of the epithelial cell. Swelling of endothelial cells and fusion of epithelial foot processes are accompanied by thickened basement membranes around collecting tubules.

Chronic Viral Disease

Persistant viral infections of animals are commonly associated with membranous glomerulopathy; for example, murine lymphocytic choriomeningitis, Aleutian disease of mink, equine infectious anemia, lactic dehydrogenase virus infection of mice, chronic hog cholera, and chronic bovine viral diarrhea (Fig. 29.5).[39–41] Glomerular lesions are based on the ability of these viruses to induce persistent viremia despite antibody production by the host. Natural infection of mice with Sendai virus promotes glomerular immune deposits.[42] Progressive defectiveness of the immune systems and reticuloendothelial hyperplasia occur in all these diseases.

Mink with **Aleutian disease** develop a slowly progressive systemic plasmacytosis accompanied by persistent viremia and hypergammaglobulinemia. The causal parvovirus replicates in macrophages of genetically susceptible mink and persists in high titer in blood, spleen and lymphoid tissues. Viral replication is not associated with overt tissue lesions but induces an extreme immune response that results in deposition of virus-antibody complexes and plasmacytes in tissue. Intravascular coagulation contributes to vascular and glomerular lesions. Immune complexes accumualte below the vascular endothelium. Ultrastructural analysis in early stages reveals foci of irregular, dense, granular material immediately below the capillary endothelial cells.[43] Globules are often encompassed by basal cytoplasmic folds of the endothelium. Dense deposits develop progressively throughout the glomerular filtration barrier: below the endothelium, throughout the basement membrane, and within the epithelial cell foot processes and slit pores. Proliferation of mesangial cells occurs, and dense material accumulates in the cytoplasm of these cells. Final stages of glomerular lesions are characterized by neutrophil infiltrates, fibrin deposits, necrosis, and effacement of glomerular architecture.[44]

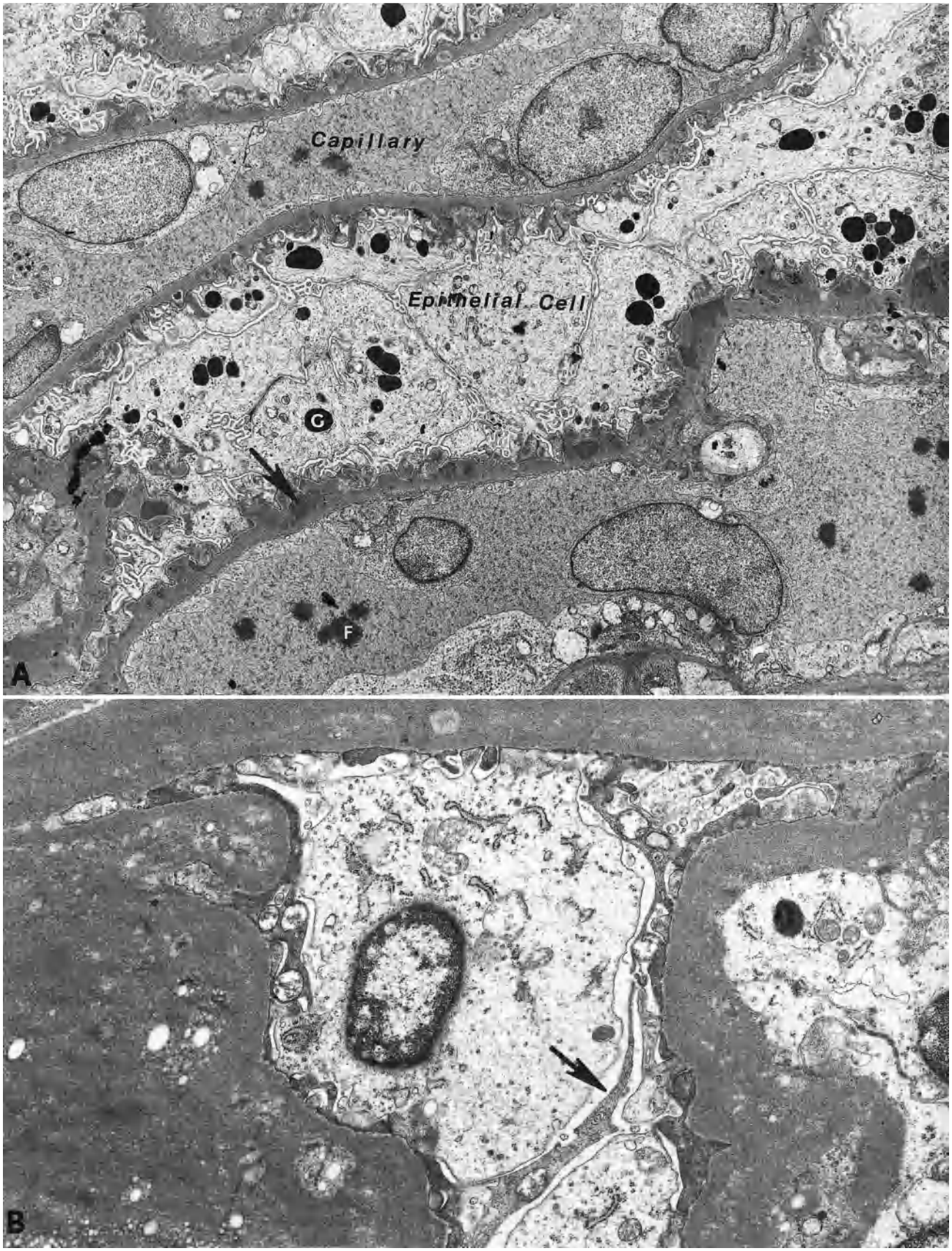


Fig. 29.4 Membranous glomerulopathy. **A**. **Feline infectious peritonitis**: thickening of capillary basement membrane with dense nodular deposits (*arrow*); aggregates of fibrin (*F*) within capillaries; dense, membrane-bound granules (*G*) in epithelial cells. **B**. **Chronic interstitial nephritis**, dog: swollen (*light*) and necrotic (*arrow*) epithelial cells; total fusion of foot processes. Note intertwined cytoplasmic processes of light and dark cells.

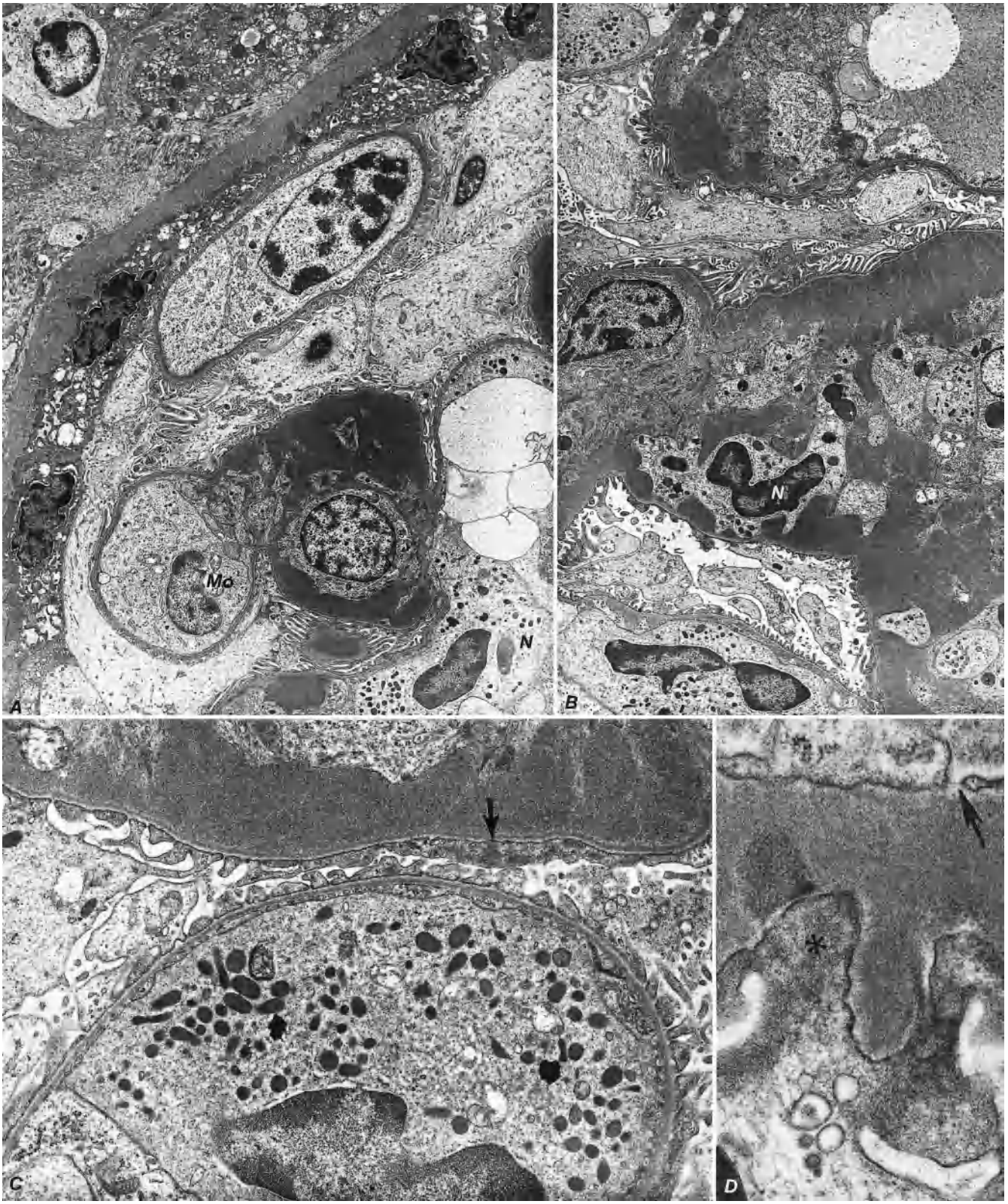


Fig. 29.5 **Glomerulonephritis**: chronic hog cholera. **A**. **Glomerular mesangium** (*right*) and capsule (*left*). Capsular parietal epithelium is necrotic; basement membrane is thick. Monocyte (*mo*) is in capillary at center, and neutrophil (*N*) is in vessel at lower right. **B**. **Neutrophils** (*N*) surround capillary and invade mesangium. **C**. **Mesangium** (*top*), urinary space with debris (*center*), and capillary with neutrophil (*bottom*). Mesangial cell filled with dense residual bodies and surrounded by electron-dense mantle. Epithelial foot processes are coalesced (*arrow*) and contain dense material, particularly at mesangial surface. **D**. **Subendothelial dense granular material**: fenestra (*arrow*); granular material in foot processes (*).

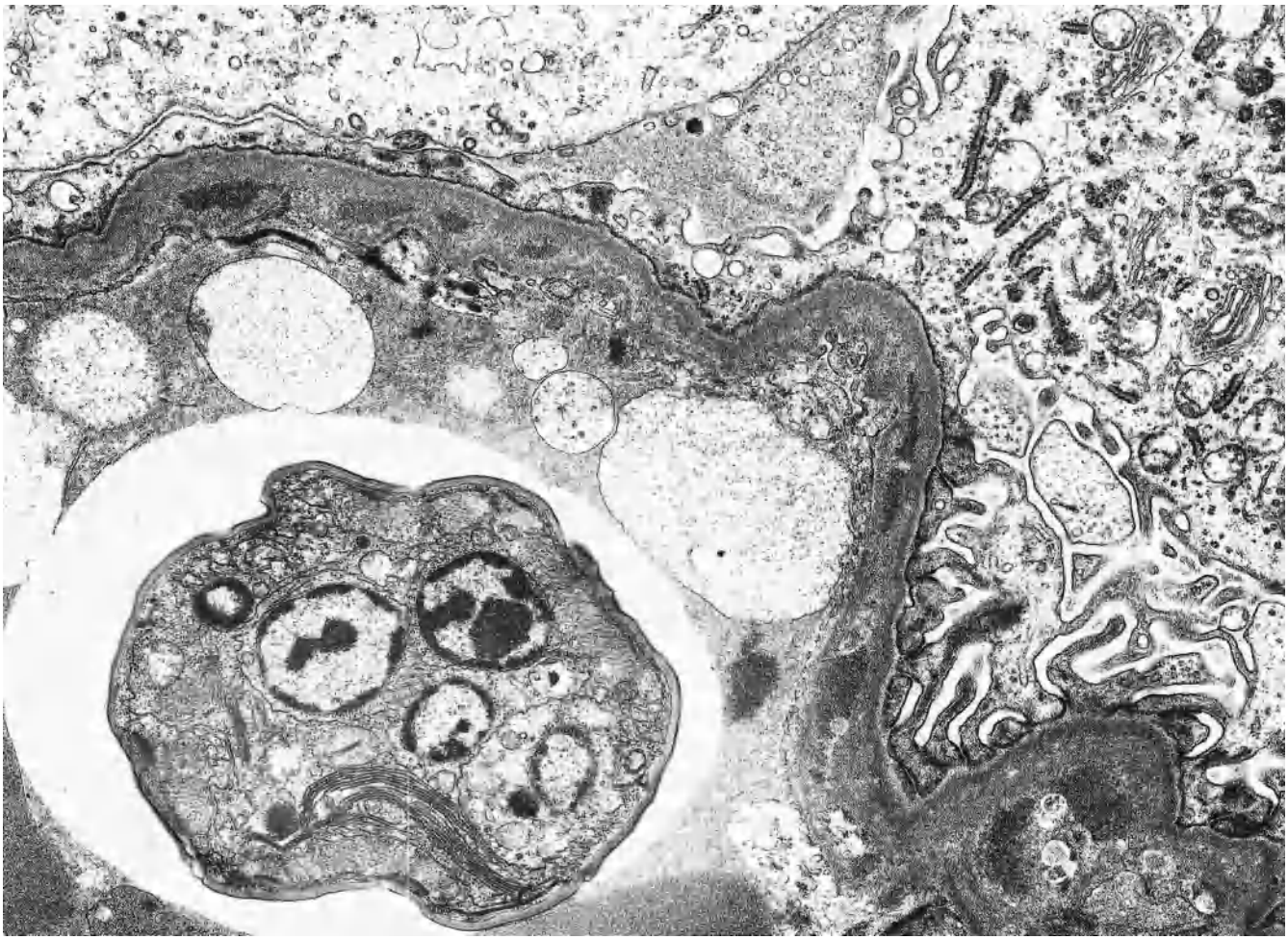


Fig. 29.6 Membranous glomerulonephritis: *Dirofilaria immitis,* dog. Larvae trapped in capillary. Glomerular basement membrane is thickened and contains dense deposits. Note fusion of glomerular foot processes.

Parasites

Chronic infection by blood-vascular parasites is often associated with membranous glomerulopathy.[45,46] Chronic malaria and schistosomiasis lead to glomerulopathy in naturally infected primates, and in experimentally infected mice. Dogs with chronic parasitism of the heartworm *Dirofilaria immitis* develop filaria-antibody immune complex glomerulopathy. Larve actually lie within the glomerular capillaries to provoke membranous deposits (Fig. 29.6). Use of the antiparasitic drug diethylcarbamazine has been implicated in enhancement of these lesions.[47,48]

Neoplasms

Chronic membranous glomerulonephritis is a common finding in terminal stages of neoplastic disease, especially in the **malignant lymphomas** of cats, mice, and humans.[49,50] One-third of cats with feline leukemia virus-related disease have membranous glomerulopathy with subendothelial, subepithelial, and mesangial deposits of immune complexes.[51] Granular material deposited along the capillary basement membranes represents antibodies against leukemia viruses and is deposited either directly as preformed antigen-antibody complexes or as the attachment of circulating antibodies to antigens localized in the glomerulus. In mice, virions have been demonstrated within the glomerular basement membrane; the antigen involved is a glycoprotein of the viral envelope.[52–54]

Other Animal Glomerulopathies

Nonhuman primates, widely used as experimental models for membranous glomerulopathy, have large numbers of complement receptors on circulating erythrocytes; rodents have large numbers on platelets, differences that may be important.[55] Renal glomerular lesions caused by trapping of antibodies against glomerular basement membrane antigens have been

reported in **horses**. Experiments in mice show that, in contrast to the irregular deposits of immune complex disease, these deposits occur in smooth linear densities along the GBM. Exfoliation of endothelial cytoplasm is an early change.[56] Anti-GBM-induced glomerulopathy occurs spontaneously in horses, although such lesions have not be established as the cause of clinical disease.[57]

X-linked renal disease in Samoyed dogs is a hereditary nephritis that appears in males by 15 months. Females are carriers and do not develop glomerulopathy. The lesion is a multilaminar capillary basement membrane with extensive reduplication and splitting that leads to separation of endothelium from the basement membrane and podocyte.[58–60]

Proliferative Glomerulonephritis

Acute Diffuse Proliferative Glomerulonephritis

Diffuse, hypercellular glomeruli in the kidneys of these patients arise from proliferation of endothelial and mesangial cells (epithelial cells are also involved but to much less extent) and by infiltrates of neutrophils and monocytes. Endothelial cell swelling, aggregates of leukocytes, and small deposits of fibrin obliterate the capillary lumen. Ultrastructurally, there are discrete, amorphous, dense granular deposits on the epithelial side of the basement membrane. By immunolabeling techniques, these focal lumps (which represent antigen-antibody complexes) are found to contain IgG, complement, and are in the mesangium and along the basement membrane.

Postinfectious Glomerulonephritis

The most common cause of this lesion is **poststreptococcal glomerulonephritis**, an immune complex disease due to inflammatory and degenerative changes induced in the renal glomerulus by antigen-antibody-complement complexes. It is not certain whether they are planted in the glomerulus or are trapped there after circulating as antigen-antibody complexes. A streptococal antigen called endostreptosin and several cationic bacterial components are present in damaged glomeruli. Complement binds to the antigen-antibody complexes in glomeruli and attracts neutrophils, which release tissue damaging enzymes. Cell-mediated reactions involving cross-reacting streptococci and glomerular basement membranes have also been implicated in poststreptococcal glomerulonephritis. Needle biopsies of nine children 5–20 days after the onset of renal signs of acute, poststreptococcal glomerulonephritis revealed enlargement of the mesangial zones with increased numbers of mesangial cells, fibrin and infiltrates of neutrophils. Capillary lumens were narrowed or obliterated by endothelial cell swelling and trapping of intravascular leukocytes.[61–63] Biopsies taken during healing stages revealed persistence of these lesions although they were much less severe.

Nonstreptococcal acute glomerulonephritis is rare but the above lesions with granular lumps in the glomerular capillary wall may be associated with **bacterial infections** (staphylococcal endocarditis, pneumonococcal pneumonia and meningococcemia) and **viral disease** (mumps, varicella, hepatitis B and infectious mononucleosis), and **parasitic diseases** (malaria, toxoplasmosis).

Membranoproliferative Glomerulonephritis

In **membranoproliferative glomerulonephritis** (mesangiocapillary glomerulonephritis), glomeruli are large and hypercellular due to proliferation of mesangial cells and thickening of the basement membrane. Infiltrates of leukocytes and crescents in Bowman's space are present but slight. Basement membrane thickening is most noticeable in the capillary loops. Although they appear similar, two distinct types of this lesion (and a variant of one) are distinguished. Glomeruli of **Type I membranoproliferative glomerulonephritis** are dominated by subendothelial electron-dense deposits of complement and IgG; a few subepithelial deposits may be found.[64] **Type II** (dense deposit disease) lesions have thick, ribbon-like deposits within the glomerular basement membranes. The lamina densa is irregular, highly electron-dense and formed in long linear arrangement.[65] C3 can be stained in irregular granular areas of the basement membrane (outside of the linear dense area). **Type III** lesions (a variant of type I) have both subendothelial and subepithelial deposits; this lesion appears to be a variant of Type I.

Proliferated of glomerular cells are increased components of most glomerular diseases. Proliferation appears to be enhanced by release of cytokines and growth factors. Increased expression of platelet-derived growth factor (PDGF) correlates with the degree of hypercellularity in mesangial proliferative IgA nephropathy models of mice produced by chronic immunization with cationic (DEAE-) or anionic (-sulfate) dextran.[66] PDGF may act in glomeruli as a paracrine growth factor from infiltrating platelets and leukocytes and as an autocrine growth factor produced by mesangial and endothelial cells.

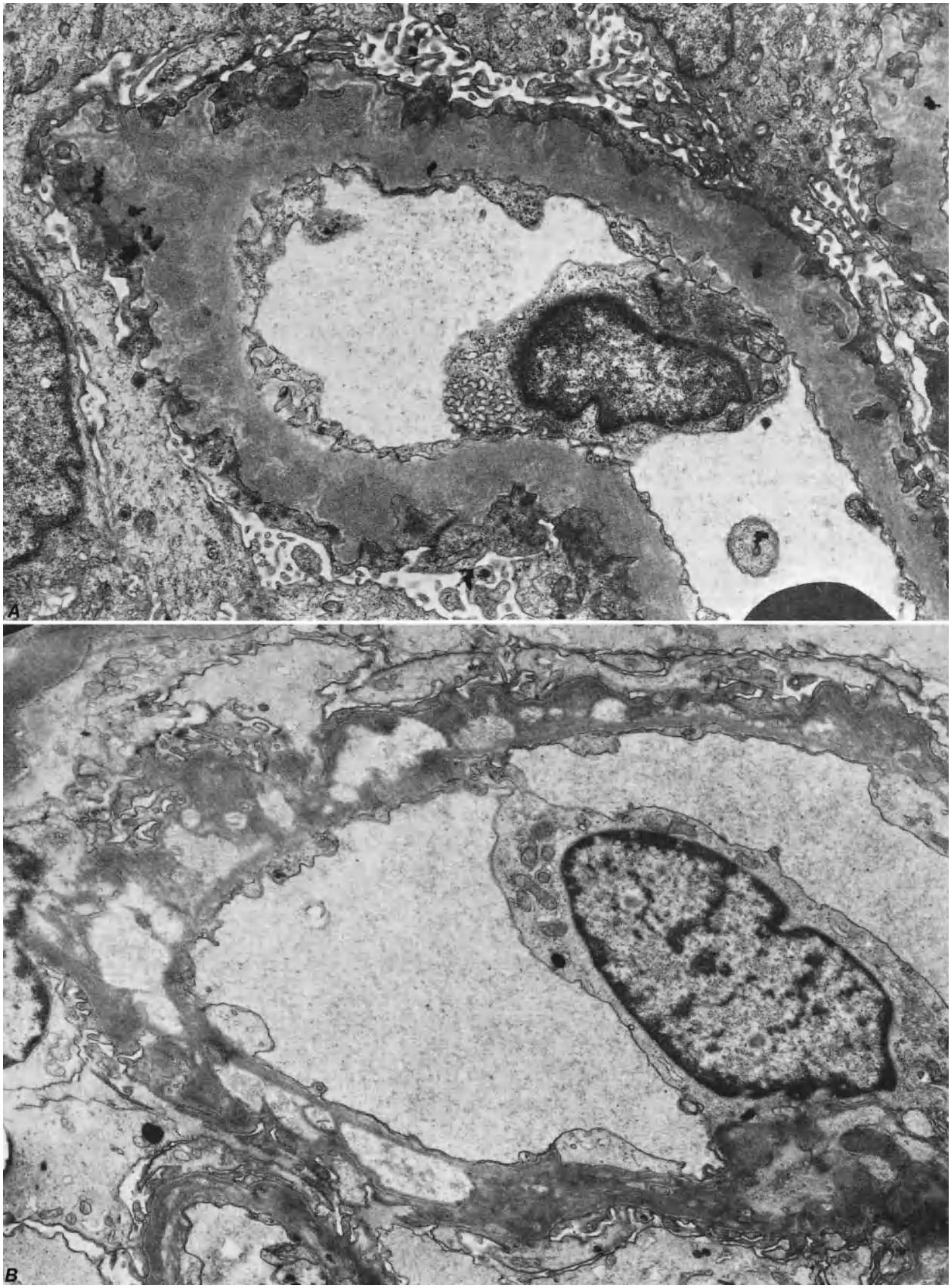


Fig. 29.7 Stages of membranous glomerulopathy: hepatitis B virus, humans. **A**. **Early stage of glomerulonephritis**: electron-dense deposits on and within basement membrane and fusion of foot processes; biopsy from 8-yr-old male human with proteinuria. **B**. **Recovered lesions**: thickened basement membrane with many electron-lucent (moth-eaten) areas indicating regression of the lesion; 13-yr-old male with no abnormalities in urine (postclinical stages of disease). (Micrographs: Hiroshi Ito and Makota Mayumi, *Lab Invest* 44:214, 1981.)

Hepatitis C Virus Glomerulopathy

Chronic **hepatitis C virus (HCV**) infection is associated with membranoproliferative glomerulonephritis and deposits of IgG, IgM, and C3 in glomeruli (but rarely with HDV antigen or RNA). Biopsy specimens have subendothelial, mesangial, and (rarely) intramembranous deposits.[67] Organized annular, finely fibrillar, cylindric, or immunotactoid structures compatible with cryoglobuins were present in 3 of 4 specimens.

Hepatitis B Virus Glomerulopathy

Chronic **hepatitis B virus (HBV)** infection is associated most commonly with membranous glomerulonephritis,[68] although associations with membranoproliferative glomerulonephritis and cryoglobulinemia have been reported. In HBV carriers, antigens and antibodies increase and decrease in the circulation depending on the phase of infection (Fig. 29.7). Both surface (HBsAg) and core (HbcAg) are components of dense deposits, and circulating HBeAg is required for induction of membranous glomerulonephropathy.[69] Recovery of HBV infection is associated with removal of immune complex deposits from the glomerular basement membrane. Biopsy of six nephrotic children with hepatitis B viral infection revealed markedly thickened basement membranes with lumpy deposits throughout the basement membrane,[70] and resolution of the viral disease led to removal of the dense material. Electron micrographs take during recovery showed electron-lucent areas that developed in the basement membrane at sites where deposits would have been. HBsAg-associated membranous glomerulonephritis in an asymptomatic child showed electron-dense deposits on the subepithelial side of the GBM.[71]

Minimal Change Disease

Minimal change disease is a diffuse effacement of foot processes of epithelial cells in glomeruli that appear normal. It is the most frequent cause of nephrotic syndrome in children, and has a striking response to corticosteroid therapy. Glomeruli may appear normal histologically, and ultrastructurally, there is no thickening of the basement membrane and no cellular proliferation. Podocyte foot processes are uniformly effaced by flattening and swelling, damage reported to be due to loss of glomerular polyanion. Podocyte cytoplasm is vacuolated and there are filopodial processes at the cell peripherally.[72–74] The term lipoid nephrosis was used for this disorder because of lipid globules in tubular epithelium and fat in the urine.

Glomerulonephritis Associated with Systemic Disease

Fibrillary Glomerulonephropathies

Amyloid Glomerulopathy

Amyloid glomerulopathy is a frequent complication of systemic amyloidosis in humans. Amyloid fibrils are 10–12 nm in diameter. The two most common renal amyloids are formed from serum amyloid A (SAA) or immunoglobulin light chains. The distinction between these has been made ultrastructurally using immunogold techniques (see chapter 26).

Fibrillary Glomerulopathy

Fibrillary glomerulopathy, characterized by presence of amyloid-like fibrils in the glomerular basement membrane and mesangium, differs from renal amyloidosis in that fibrils are wider (18–24 nm wide) than amyloid and do not bind congo red. In addition, patients lack clinical histories of disorders that are associated with renal glomerular deposits; for example, cryoglobulinemia, dysproteinemia, and systemic lupus erythematosis. The renal lesion in fibrillary glomerulopathy is heterogeneous and may be membranous, mesangiocapillary, or mesangial. Immunohistochemical studies reveal ribbon-like immunofluorescent staining for IgG and C3 along capillary loops and in the mesangium. Electron microscopic studies using immunogold techniques on kidney biopsies of 7 patients showed staining of fibrils for IgG (both light chains), C3, and amyloid P component. Fibrils appear to be formed of polyclonal IgG and C3 that bind amyloid P component.[75] This suggests that fibrils are immune deposits that have undergone fibrillogenesis, but not in a β-pleated sheet configuration that will bind congo red.

Immunotactoid Glomerulopathy

Immunotactoid glomerulopathy in humans is characterized by microfibrillar deposits 30–50 nm in width. Patients have circulating paraprotein and/or monoclonal immunoglobulin deposits in glomeruli.

IgA Glomerulopathy

IgA glomerulopathy is a nodular lesion that involves deposits of light chains in mesangial regions and along

tubular and glomerular basement membranes. Rare cases are reported in which both heavy and light chains are present. The very rare heavy chain disease is characterized by nodular glomerulopathy with linear deposits of heavy chains along glomerular, tubular and vascular basement membranes.[76] Subendothelial, intramembranous, or subepithelial deposits may be found in addition to the characteristic mesangial and paramesangial deposits.[77,78] IgA nephropathy was been reported in monkeys.[79]

Circulating IgA immune complexes are present and correlate with episodes of clinical signs of renal disease. The disorder appears to involve a genetic or acquired abnormality leading to increased mucosal IgA synthesis in response to respiratory or intestinal infections or food proteins, and is seen with increased frequency in patients with intestinal mucosal defects such as celiac disease. Young patients with terminal liver disease of any cause frequently develop glomerulopathy that resembles IgA glomerulopathy.

Glomerular lesions with immune complex deposits, especially of IgA, are commonly associated with **cirrhosis**. Mesangial deposition represent IgA-class immune complexes derived from the circulation. Studies in carbon tetrochloride-poisoned rats with cirrhosis indicate that defective hepatic sequestration of circulating IgA polymers may underlie deposition of complexes.[80]

Hereditary Nephritides

Human hereditary nephritis (HN) is a group of inherited glomerular diseases that progresses to renal failure in the third and fourth decade, and may be associated with sensorineural hearing loss. The combination of glomerulopathy and hearing loss is referred to as **Alport syndrome**. Lesions are confirmed by electron microscopy as multilaminar splitting of glomerular basement membranes, believed to be a defect in collagen IV.[81–83] The glomerular lesions include thickening of the basement membrane with splitting into thin layers that are separated by clear spaces that contain deposits of dense particles.

Alport Syndrome

Alport syndrome is a glomerular basement membrane (GBM) disease caused by mutations in type IV collagen genes with hundreds of mutations reported for the COL4A5 gene in the X-linked form. Irregular thickening, thinning, and splitting of the GBM characterize the progressive glomerular lesions. Effaced podocyte foot processes and expansion of the mesangium lead eventually to fibrotic glomeruli. Macrophage metalloelastase is markedly increased and (using immunogold-labeled collagen IV) its presence is associated with enhanced degradation of GBM.[84] The **hyaluronate receptor**, CD44, is an abundant transmembrane glycoprotein that is expressed on a wide variety of cell types and can play a role in a diverse range of important cellular processes. CD44 exists in a number of different forms due to alternative splicing of additional amino acid stretches into the extracellular domain, and these different forms can have altered functions.[85]

Light-Chain Nephropathy

Light-chain nephropathy is associated with plasma cell myeloma wherein monoclonal cryoglobulins (kappa light chains) are deposited in glomeruli in lesions resembling those of nodular diabetic glomerulosclerosis, including the development of glomerular aneurysms.[86,87] Serum proteins other than light chains are not deposited.

Glomerulopathy of Autoimmune Disease

Systemic Lupus Erythematosus

The prototype of the multisystem autoimmune diseases involves widespread deposition of antinuclear antibodies throughout the body.[88,89] All systemic lupus erythrematosus (SLE) patients have some degree of renal glomerular involvement, which may appear as mesangial, focal proliferative, diffuse proliferative, or membranous glomerulonephritis. Diffuse proliferative glomerulonephritis is the most common and serious lesion, and is characterized by dominance of proliferation of endothelial, mesangial, and even epithelial components. Membranous glomerulonephritis occurs in 10% of cases and involves diffuse thickening of capillary walls. Ultrastructurally, electron-dense deposits are found in the mesangium, subepithelial, and subendothelial locations. The latter are most characteristic of SLE,[90,91] and are rarely found in other types of human glomerulopathy. Thickening of capillary walls by subendothelial deposits gives rise to "wire-loop" lesions.

Other Glomerulopathies

The **Goodpasture syndrome** arises from anti-basement membrane antibody deposition on renal and extrarenal tissues, particularly in the renal glomerulus and alveolar wall of the lung. It first appears as **linear** deposits of anti-glomular basement membrane antibodies that outline the capillary loop of the glomerulus. The main immunoglobulin in the basement membrane is IgG; IgM and IgA are less frequent.[92]

Wegener's granulomatosis is a necrotizing or granulomatous vasculitis that involves the upper and lower pulmonary airways and the kidneys. Renal involvment, preceded by extrarenal lesions, occurs in 85% of patients during exacerbations of clinical disease. The typical glomerular lesions are segmental necrotizing glomerulonephritis with progressive crescentic proliferation of the glomerular epithelium.[93,94] Deposits in the GBM are small, pale, and limited in number. Subepithelial, mesangial, intramembranous, or subendothelial deposits have been described in a small percentage of renal biopsy specimens, but most studies have failed to find significant immune complex deposits. IgM and fibrin are present in most necrotic glomeruli. Cytotoxic therapy may alter the character of the glomerular lesions. Wegener's granulomatosis glomerulopathy may arise in previous lesions of membranous glomerulopathy.[95]

Rare **drug hypersensitivities** are associated with glomerulopathy in man. Nine of 18 patients with cystinuria were treated with D-penicillamine and developed acute hypersensitivity reactions; 3 developed proteinuria. Biopsy specimens had subepithelial deposits in the GBM, fusion of foot processes and other changes associated with membranous glomerulonephritis.[96] Mercuric chloride hypersensitivity has been used as a model for glomerulopathy.

Focal Glomerulosclerosis

Focal segmental glomerulosclerosis is associated with the nephrotic syndrome and renal failure in children and adults. It may be primary, or secondary to another renal glomerular disease, or secondary to a known systemic disorder; for example, heroin abuse, analgesic nephropathy, and AIDS. The lesions involve **sclerosis** of some, but not all glomeruli. In each glomerulus it involves part, but not all of the glomeulus. Ultrastructural changes of segmental sclerotic lesions include foot process effacement (the basement membrane is largely unaltered) and variable increase in mesangial matrix with collapse of capillaries and accumulation of monocytes. Electron microscopy of 23 biopsies revealed intracapillary monocytes and foam cells within the capillary remnant.[97]

Glomerulopathy and Thrombotic Disease

Anaphylactoid purpura (Henoch-Schoenlein syndrome) is a generalized vascularitis involving multiple organ systems, including skin, joints, gastrointestinal tract, and kidney. Acute renal disease is common. Glomerular lesions are mesangial and proliferative. In 16 renal biopsy speciments taken 4 days to 2 yr after the onset of glomerulonephritis there were early focal and late diffuse mesangial proliferation and deposits of IgG- and β1C-globulin, and fibrin.[98] GBM deposits were subendothelial (not subepithelial) and were fibrillogranular and only slightly electron-dense.

Glomerulopathy arising from **microangiopathic hemolytic anemia** is characterized by endothelial injury and intravascular coagulation in renal glomeruli; in most syndromes there is fibrin deposition in capillaries and thrombosis in the renal arterial system. Disseminated intravascular coagulation plays a dominant role in pathogenesis. In humans, this includes **thrombotic thrombocytopenia**, the childhood (most of which are infected with vero toxin producing *E. coli*) and adult **hemolytic uremic syndromes**. Glomerulopathy of this type is a rare complication of primate placentopathy and pregnancy, contraceptive agents, and infections such as shigellosis, typhoid fever, *E. coli* septicemia, and viral infections. The glomerulonephropathy of human **preeclampsia** involves deposition of fibrin in subendothelial GBM and mesangium, and a unique proliferative response of endocapillary cells.[99] Bacterial endotoxins and exotoxins that injury endothelium are widely implicated in this group of diseases.

Systemic thrombotic disease can lead to trapping of thrombi in the renal glomerulus. A biopsy specimen from one patient had membranous glomerulonephritis with subendothelial deposits of fibrin that occluded the capillary lumina.[100]

Although the occurrence of thrombotic glomerulopathy may be frequent in systemic disease, it is not commonly a significant cause of death. A potent fibrinolytic mechanism operates in the kidney,[101] suppressing developing thrombotic processes. Only when severe systemic disorders overwhelm the fibrinolytic mechanism does thrombotic glomerulopathy ensue; for example, the glomerular lesions of hemolytic uremic syndrome may be responsible for acute renal failure with uremia, but are reversible if appropriate treatment is given.[102]

Foam Cell Glomerulopathy

Foam cells in the renal glomerulus have been reported in diabetes mellitus, toxemia of pregnancy, Fabry's disease, lecithin:cholesterol acyl transferase deficiency, and the nephrotic syndrome. These lesions are mesangial. The large foamy mesangial cells and macrophages contain a wide spectrum of vacuoles from large electron-lucent vacuoles bearing tiny filaments to vacuoles with heterogeneous dense material arranged in myelin figures or membrane fragments. These cells arise from hyperlipidemia (especially with elevations in βVLDL, IDL, or LDL) that is superimposed upon glomerular malfunction such as inflammation or diabetes.

Glomeruli with mesangial cells expanded by large amounts of neutral lipid globules has been reported in dogs[103,104] and rats.[105] Similar lesions of **lipidic glomerulopathy** have been produced experimentally in rabbits by inducing hyperlipidemia.[106]

Lipid storage disease glomerulopathy is characterized by large granular cells that arise from accumulation of undegraded substrates. These lysosomal storage disoders may affect renal glomerular mesangial, endothelial and epithelial cells.[107] In Fabry's disease the cytoplasm of epithelial cells contains large lysosomes filled with myelin figures.[108] Mucopolysaccharide glomerulopathy has been reported in humans.[109]

HIV Glomerulopathy

Human immunosuppressive virus (HIV) infection is commonly associated with glomerulopathy, including various immune complex mediated variants such as postinfectious and lupuslike endocapillary proliferative glomerulonephritis. IgA nephritis (due to IgA-antiHIV antibody complex trapping, not glomerular infection with HIV), although rare, has also been reported in AIDS patients. Recently a syndrome of focal or globular glomerulosclerosis with mesangial deposits of C3, IgM and sometimes IgG (but not IgA) has been reported in HIV infection. It may occur before AIDS develops. There is tubular dilatation with lumenal casts and tubuloreticular inclusions in glomerular and peritubular capillary enthelium, a hallmark of HIV infection.[110]

Lesions in Transplanted Kidneys

Glomerular lesions in long-term human renal allografts typically involve subendothelial accumulation of electron-lucent, flocculant material.[111,112] Especially prominent in proteinuric patients, these changes result from a striking increase in glomerular basement membrane components. Ultrastructural changes center on marked thickening of the capillary basement membrane. There are varying amounts of vesicular and granular material in or near the basement membrane.[113,114] Mesangial areas also contain increased basement membrane material. Immunoglobulins and complement are demonstrable in affected kidneys. The development of the lesions involves several mechanisms as varies with the disease process underlying the original renal disease.

Diabetes

Diabetic microangiopathy, a systemic thickening of capillary endothelial basement membranes, underlies the chronic complications of human diabetes mellitus. These vascular changes lead to blindness, renal failure, and gangrene of extremities. Diabetic microangiopathy is most evident in capillaries of the kidney, retina, skin, and skeletal muscles; it also develops in tissues as diverse as placenta,[115] heart,[116] and peripheral nerves.[117,118]

Vascular lesions similar to those in diabetes develop with aging in humans but the microvascular changes that develop in aged nondiabetics are rarely as advanced as those that occur in chronic diabetes mellitus.[119]

Renal Glomerular Lesions in Diabetes

Within the kidney, vascular lesions of diabetes are most damaging in the glomerulus even though they also occur in Bowman's capsule and renal tubules.[120] The normal glomerular basement membrane is composed of a network of collagen IV and V fibrils, together with large glycoproteins and heparan sulfate proteoglycans, which are important in the charge-selective filtration process. In early diabetes mellitus basement membranes thicken; heparan sulfate proteoglycans are normal, but in late disease there is a significant reduction in their amounts.

Widespread thickening of glomerular capillary basement membranes is present in all diabetics (Fig. 29.8).[121–123] Morphometric studies of patients with juvenile or **insulin-dependent diabetes** indicate that thickening begins as early as 2 yr after the onset of the disease and continues progressively. Kidney biopsy material from seven juvenile diabetics was obtained at the onset of disease and when compared with material from those with disease for 2 and 5 yr, revealed the major changes to be widening of the basement membrane of peripheral glomerular capillaries; mesangial regions were relatively normal.[124]

Ultrastructural changes in kidneys of human diabetics with proteinuria suggest that changes in the basement membrane underlie the loss of charge and size selectivities of the diabetic glomerulus.[125] Ultrastructural analysis of kidney biopsies from 15 type-1 insulin-dependent diabetic patients with a range of albuminuria established that albuminuria is linked to progressing basement membrane thickening.[126] Scanning electron microscopy of glomeruli of rats with streptozotocin-induced diabetes using an acellular digestion technique reveals striking thickening of the GBM.[127]

The glomerular lesions in kidneys of patients with long-standing **insulin-dependent diabetes** are capillary basement membrane thickening, diffuse diabetic glomerulosclerosis, and nodular glomerulosclerosis. The latter, also known as intercapillary glomerulosclerosis or the Kimmelstiel-Wilson lesion, appears as ovoid or spherical hyalin masses in the periphery of

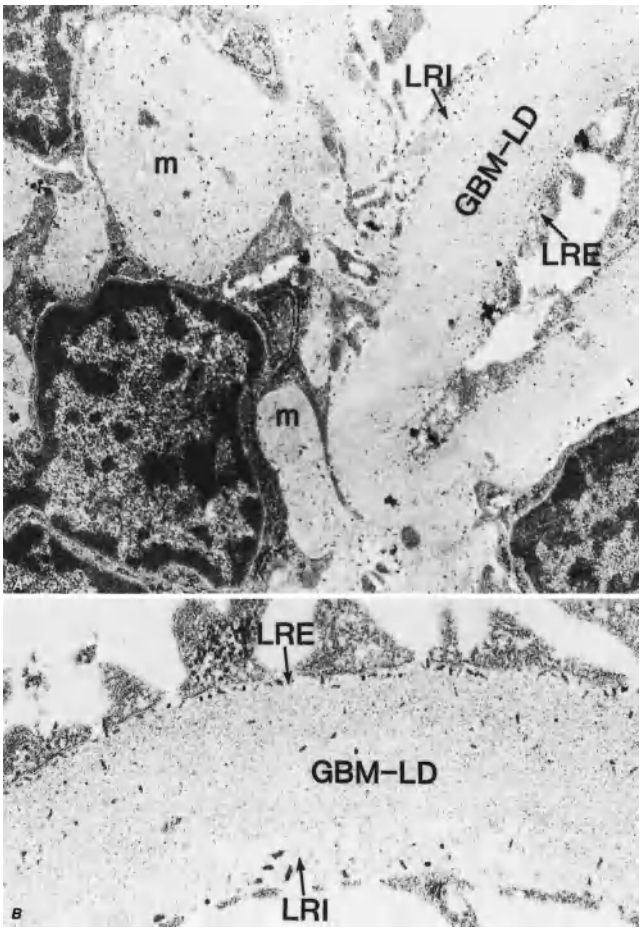


Fig. 29.8 Diabetic glomerulopathy: 31-yr-old patient with Type I diabetes mellitus, 16-yr duration. **A**. **Glomerular basement membrane** (*GBM*) is thickened and contains filaments of HSPG chiefly within the LRE and LRI. The number of HSPG filaments in the GBM-LD is increased. Numerous filaments of HSPG are distributed at the periphery of the nodular masses of mesangial matrix (*m*). **B**. Detail of GBM: increase in HSPG filaments within the GBM-LD. Most filaments in the LD lie within a zone of the epithelial half of the thickened GBM. (Micrograph: Robert L. Vernier, *Kidney Int* 41:1070, 1992.)

the glomerulus. These masses lie within the mesangial core of the glomerular lobule and are often laminated and have entrapped fibrin and lipids. These lesions expand to compress the capillaries and eventually to efface the glomerulus.

In early stages of the disease, the thickened basement membranes are homogeneous. Later, there are split basement membranes with laminar arrangements around the endothelial cells and pericytes. Within affected blood vessel walls there is an increase in the amount and synthesis of collagen type IV, and a decrease in proteoglycans.[128,129] Glomerular lesions of noninsulin-dependent diabetes are not as severe as are those of insulin-dependent disease but cannot be differentiated ultrastructurally from the latter (Fig. 29.9). Renal biopsy specimens of 29 **noninsulin-dependent diabetes** patients analyzed by ultrastructural morphometry showed that the mesangial matrix expands directly toward the capillary lumen and along the inner surface of the glomerular basement membrane.[130] In other studies a correlation between foot process width and urinary albumin excretion was clear;[131] others have not found this correlation.[132] Thin glomerular basement membranes, found in kidneys biopsied in the late phases of juvenile diabetes, have been interpreted as a result of neovascularization of capillaries.[133] A hallmark of diabetic microangiopathy is EC dysfunction characterized by loss of NO with impaired endothelium-dependent vasorelaxation and thrombosis. Dysfunctional eNOS and decreased NO availability in ECs is a major pathogenetic mechanism.[134]

Hyperglycemia, Glycosylation, and Basement Membranes

Hyperglycemia-induced glycosylation is a major pathogenic factor in basement membrane accumulation, and enzymes involved in glycosylation are increased.[135] Neural lesions are a major defect in human diabetes. In retinal capillaries, there is selective degeneration of intramural pericytes that appears to precede much of the basement membrane thickening.

Hyperglycemia also produces nonenzymatic glycolysis of basement membranes, as well as hemoglobin, collagen, and lens crystallin. In experimental diabetic glomerulopathy, renal glomeruli have been increased by nearly half after only 4 days of hyperglycemia.[136] The process is a generalized one and also affects the perineurium of peripheral nerves. Perineural cells, which surround endoneurium with its axons and Schwann cells, produce the basement membrane material.[137]

Lesions of **symmetrical peripheral neuropathy** of chronic diabetes mellitus involve Schwann cell injury, myelin degeneration, and axonal damage and are thought to be related to long-standing abnormal glucose metabolism. The more focal nervous system lesions in diabetes arise from diffuse microangiopathy. For example, the focal patchy endoneural fiber loss in human diabetics is due in part to perivascular denervation of the vasa nervorum. Ultrastructural studies have shown that abnormal innervation of the vasa nervorum leads to a reduced percentage of blood vessels with perivascular axons.[138]

The receptor tyrosine kinase **Axl** and its ligand **Gas6** (growth arrest-specific gene 6, plasma anticoagulation protein S), activated in vascular smooth muscle by reactive oxygen species, support survival (antiapoptosis) and migration of myocytes during hypoglycemia. Glucose exerts powerful effects on Gas6-Axl

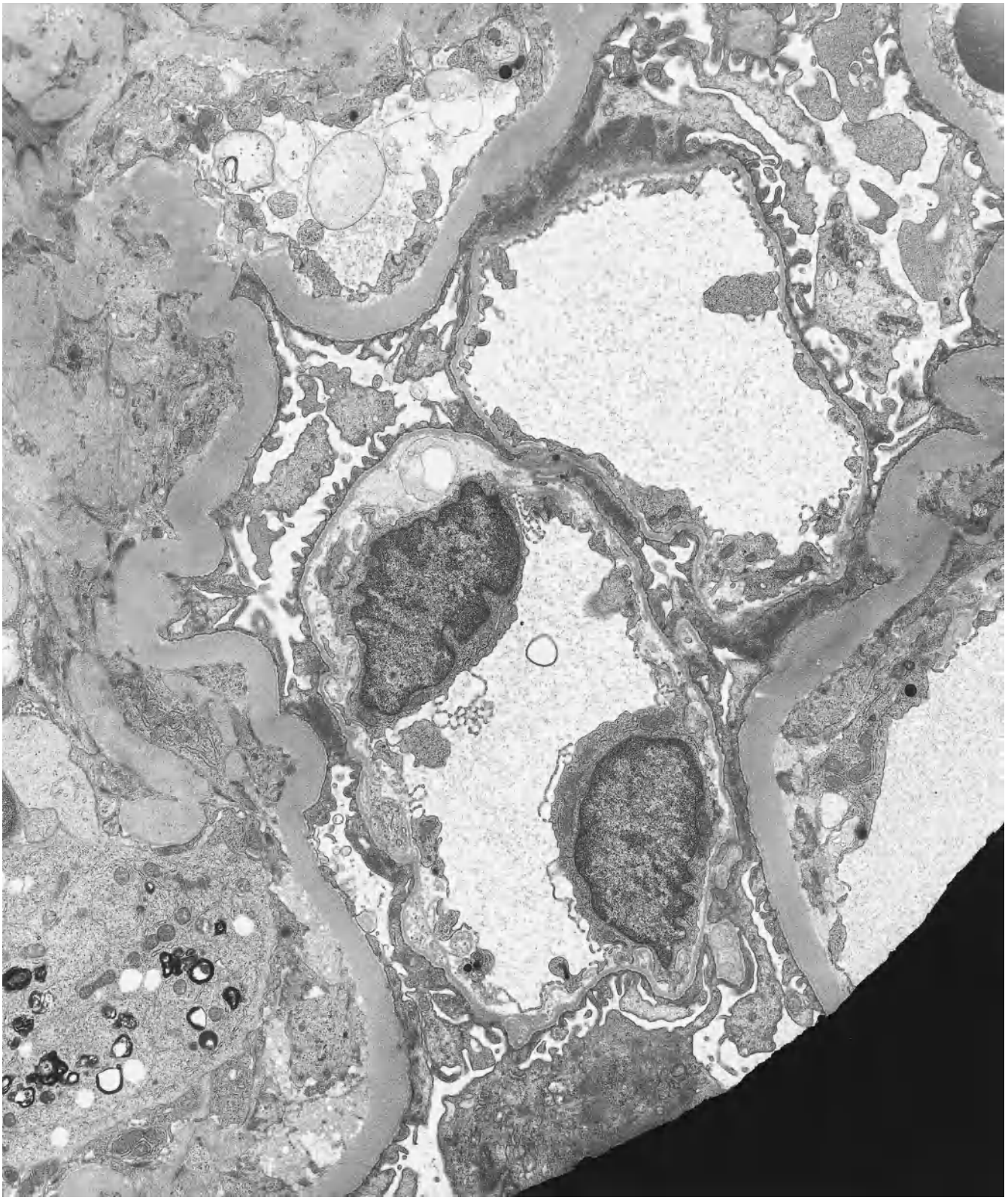


Fig. 29.9 Diabetic glomerulopathy: non-insulin-dependent (Type 2) diabetes, human. Thin and thick areas of glomerular basement membranes. (Micrograph: Hiroshi Hayashi, *Kidney Int* 41:749, 1992.)

signaling, and these events determine the severity of lesions in diabetic glomerulopathy.[139,140] The pro-survival of Gas6-Axl signaling pathway plays a pivotal role in endothelial cell responses to inflammatory stimuli and subsequent attachments to circulating leukocytes.

References

1. Ballermann BJ. 2007. Contribution of the endothelium to the glomerular permselectivity barrier in health and disease. *Nephron* 106:19.
2. Hjalmarsson C, et al. 2004. Electron microscopic evaluation of the endothelial surface layer of glomerular capillaries. *Microvasc Res* 67:9.
3. Rostgaard J, Qvortrup K. 1997. Electron microscopic demonstrations of filamentous molecular sieve plugs in capillary fenestrae. *Microsvasc Res* 53:1.
4. Kriz W. 2007. Ontogenetic development of the filtration barrier. *Nephrology* 106:e44.
5. Phillips CL, et al. 2006. Imaging glomeruli in renal biopsy specimens. *Nephron Physiol* 103:75.
6. Sato S, et al. 2005. Reduplicated basal lamina of the peritubular capillaries in renal biopsy specimens. *J Submicr Cytol Pathol* 37:305.
7. Bohman S-O, et al. 1979. Evaluation of a procedure for systematic semiquantitative analysis of glomerular ultrastructure in human renal biopsies. *Lab Invest* 40:433.
8. Andrews PM. 1975. Scanning electron microscopy of the nephrotic kidney. *Virch Arch B* 17:195.
9. Bonsib SM. 1984. Scanning electron microscopy of acellular glomeruli in human glomerulonephritis. *Ultrastr Pathol* 7:215.
10. Bonsib SM. 1985. Scanning electron microscopy of acellular glomeruli in nephrotic syndrome. *Kidney Int* 27:678.
11. Weidner N, Lorentz WB, Jr. 1986. Scanning electron microscopy of the acellular glomerular basement membranes in idiopathic membranous glomerulopathy. *Lab Invest* 54:84.
12. Carlson ED, Chatterjee SN, 1983. Ultrastructure of isolated basement membranes in the acellular human renal cortex. *Renal Physiol* 6:197.
13. Kerjaschki D. 1990. The pathogenesis of membranous glomerulonephritis from morphology to molecules. *Virchows Arch B* 58:253.
14. Fujigaki Y, et al. 1997. Glomerular handling of immune complex in the acute phase of active in situ immune complex glomerulonephritis employing cationized ferritin in rat. *Virchows Arch* 431:53.
15. Chen X-M, et al. 1987. Experimental glomerulonephritis induced by immune complexes of monoclonal antibodies produced by immunoglobulin class-switch variants. *Lab Invest* 57:665.
16. Mac-Moune Lai F, et al. 1996. Ultrastructural calcification of glomerular immune complexes. *Modern Pathol* 9:36.
17. Kanfer A, et al. 1987. Enhanced glomerular procoagulant activity and fibrin deposition in rats with mercuric chloride-induced autoimmune nephritis. *Lab Invest* 57:138.
18. Abramowsky CR, et al. 1984. Spontaneous nephrotic syndrome in a genetic rat model. *Am J Pathol* 117:400.
19. Kerjaschki D. 1992. Molecular pathogenesis of membranous nephropathy. *Kidney Int* 41:1090.
20. Salant DJ, et al. 1979. Determinants of glomerular localization of subepithelial immune deposits. *Lab Invest* 41:89.
21. Kerjaschki D, Farquhar M. 1982. The pathogenic antigen of Heymann nephritis is a membrane glycoprotein of the renal proximal tubule brush border. *Proc Natl Acad Sci USA* 79:5557.
22. Kerjaschki D, et al. 1989. Transcellular transport and membrane insertion of the C5b-9 membrane attack complex of complement by glomerular epithelial cells in experimental membranous nephropathy. *J Immunol* 143:546.
23. Andres G, et al. 1986. Formation of immune deposits and disease. *Lab Invest* 55:550.
24. Hara M, et al. 1991. Complement and monocytes are essential for provoking glomerular injury in passive Heymann nephritis in rats. *Lab Invest* 65:168.
25. Barnes JL, et al. 1990. Glomerular localization of platelet cationic proteins after immune complex-induced platelet activation. *Lab Invest* 63:755.
26. Uehara G, et al. 2004. Glomerular expression of platelet-derived growth factor (PDGF)-A, -B chain and PDGF receptor-alpha, beta in human diabetic nephropathy. *Clin Exp Nephrol* 8:36.
27. Fogel MA, et al. 1991. Glomerular basement membrane expansion in passive Heymann nephritis. *Am J Pathol* 138:465.
28. Hogendoorn PCW, et al. 1988. Antibodies to purified renal tubular epithelial antigens contain activity against laminin, fibronectin, and type IV collagen. *Lab Invest* 58:278.
29. Vassalli P, McCluskey RT. 1964. The pathogenic role of the coagulation process in rabbit Masugi nephritis. *Am J Pathol* 45:653.
30. Kashihara N, et al. 1992. Nephritogenicity of anti-proteoglycan antibodies in experimental murine lupus nephritis. *Lab Invest* 67:752.
31. Kagami S, et al. 1990. Mechanisms of formation of subepithelial electron-dense deposits in active *in situ* immune complex glomerulonephritis. *Am J Pathol* 136:631.
32. Kerjaschki D. 1990. The pathogenesis of membranous glomerulonephritis from morphology to molecules. *Virch Arch B* 58:253.
33. Kiberd BA. 1991. Murine lupus nephritis. *Lab Invest* 65:51.
34. Leardkamolkarn V, et al. 1990. Loss and rearrangement of glomerular basement membrane laminin during acute nephrotoxic hephritis in the rat. *Am J Pathol* 137:187.
35. Schneeberger EE, et al. 1983. Alterations in glomerular anionic sites in autologous immune complex nephritis. *Lab Invest* 49:445.

36. Bagheri N, et al. 2005. Development of immune-complex glomerulonephritis in athymic mice. *Lab Invest* 85:354.
37. Pelletier M, et al. 1975. Characteristic immunohistochemical and ultrastructural glomerular lesions in nude mice. *Lab Invest* 32:388.
38. Misra RP, Berman LB. 1972. Studies on glomerular basement membrane. *Lab Invest* 26:666.
39. Banks KL, et al. 1972. Immunologically mediated glomerulnephritis of horses. *Lab Invest* 26:701.
40. Cheville NF, et al. 1970. Ultrastructural and immunofluorescent studies of glomerulonephritis in chronic hog cholera. *Lab Invest* 22:458.
41. Cutlip RC, et al. 1980. Lesions in clinically healthy cattle persistently infected with the virus of bovine viral diarrhea. *Am J Vet Res* 41:1938.
42. Jessen RH, et al. 1992. Experimental IgA-IgG nephropathy induced by a viral respiratory pathogen. *Lab Invest* 67:379.
43. Henson JB, et al. 1968. The sequential development of ultrastructural lesions in the glomeruli of mink with experimental Aleutian disease. *Lab Invest* 19:153.
44. Portis JL, Coe JE. 1979. Deposition of IgA in renal glomeruli of mink affected with Aleutian disease. *Am J Pathol* 96:227.
45. George CRP, et al. 1976. Mouse malaria nephropathy. *J Pathol* 120:235.
46. Nagle RB, et al. 1982. Glomerular accumulation of monocytes and macrophages in experimental glomerulnephritis associated with *Trypanosoma rhodesiense* infection. *Lab Invest* 46:365.
47. Casey HW, Splitter GA. 1975. Membranous glomerulonephritis in dogs infected with *Dirofilaria immitis*. *Vet Pathol* 12:11.
48. Abramowsky CR, et al. 1981. *Dirofilaria immitis*. *Am J Pathol* 104:1.
49. Branca M, et al. 1971. Immune complex disease. I. Pathological changes in the kidneys of BALB/c mice neonatally infected with Moloney leukemogenic and murine sarcoma viruses. *Clin Exp Immunol* 9: 853.
50. Sutherland JC, Mardiney MR Jr. 1973. Immune complex disease in the kidneys of lymphoma-leukemia patients: The presence of oncornavirus-related antigen. *J Natl Cancer Inst* 50:633.
51. Glick AD, et al. 1978. Characterization of feline glomerulonephritis associated with viral-induced hematopoietic neoplasms. *Am J Pathol* 92:321.
52. Batzing BL, Hanna MG Jr. 1973. Localization of endogenous C-type virus in the glomerular basement membrane of aged AKR mice. *J Immunol* 110:1189.
53. Imamura M, et al. 1976. The occurrence and frequency of type C virus-like particles in placenta from patients with systemic lupus erythrematosus and from normal subjects. *Am J Pathol* 83:383.
54. Pascal RR, et al. 1973. Glomerulonephritis associated with immune complex deposits and viral particles in spontaneous murine leukemia. *Lab Invest* 29:159.
55. Hebert LA, et al. 1991. Experimental immune complex-mediated glomerulonephritis in the non-human primate. *Kidney Int* 39:44.
56. Shibatat S, et al. 1978. Exfoliation of endothelial cytoplasm in nephrotoxic serum nephritis. *Lab Invest* 38:201.
57. Banks KL, et al. 1972. Immunologically mediated glomerulonephritis of horses. *Lab Invest* 26:701.
58. Baumal R, et al. 1991. Renal disease in carrier female dogs with X-linked hereditary nephritis. *Am J Pathol* 139:751.
59. Jansen B, et al. 1986. Samoyed hereditary glomerulopathy (SHG). *Am J Pathol* 125:536.
60. Thorner P, et al. 1987. Samoyed hereditary glomerulopathy. *Lab Invest* 56:435.
61. Feldman JD, et al. 1966. Immunology and morphology of acute post-streptococcal glomerulonephritis. *Lab Invest* 15:283.
62. Jenis EH, et al. 1974. Glomerulonephritis with basement membrane deposits. *Arch Pathol* 97:84.
63. Michael AF Jr, et al. 1966. Acute poststreptococcal glomerulonephritis. *J Clin Invest* 45:237.
64. Habib R. 1973. Focal glomerular sclerosis. *Kidney Int* 4:355.
65. Kim Y, et al. 1979. Immunofluorescence studies of dense deposit disease. *Lab Invest* 40:474.
66. Gesualdo L, et al. 1991. Platelet-derived growth factor expression in mesangial proliferative glomerulonephritis. *Lab Invest* 65:160.
67. Johnson RJ, et al. 1993. Membranoproliferative glomerulonephritis associated with hepatitis C virus infection. *New Engl J Med* 328:465.
68. Johnson RJ, Couser WG. 1990. Hepatitis B infection and renal disease. *Kidney Int* 37:663.
69. Slusarczyk J, et al. 1980. Membranous glomerulopathy associated with hepatitis B core antigen immune complexes in children. *Am J Pathol* 98:29.
70. Ito H, et al. 1981. Hepatitis B antigen-mediated membranous glomerulonephritis. *Lab Invest* 44:214.
71. Hirsch HZ, et al. 1981. Membranous glomerulonephritis in a child asymptomatic for hepatitis B virus. *Am J Clin Pathol* 75:597.
72. Bohman S-O, et al. 1984. Foot process fusion and glomerular filtration rate in minimal change nephrotic syndrome. *Kidney Int* 25:696.
73. Border WA, 1988. Distinguishing minimal-change disease from mesangial disorders. *Kidney Int* 34: 419.
74. Korbet SM, et al. 1988. Minimal change glomerulopathy of adulthood. *Am J Nephrol* 8:291.
75. Yang GCH, et al. 1992. Ultrastructural immunohistochemical localization of polyclonal IgG, C3, and amyloid P component on the congo red-negative amyloid-like fibrils of fibrillary glomerulopathy. *Am J Pathol* 141:409.
76. Katz A, et al. 1994. IgG heavy-chain deposition disease. *Mod Pathol* 7:874.
77. Morita M, Sakaguchi H. 1988. A quantitative study of glomerular basement membrane changes in IgA nephropathy. *J Pathol* 154:7.
78. Woodrow DF, et al. 1989. Immunoelectronmicroscopic studies of immune complex deposits and basement membrane components in IgA nephropathy. *J Pathol* 157:47.

79. Borda JT, et al. 2004. Immunoglobin-A nephropathy with crescentic glomerulonephritis in a pigtailed macaque (*Macaca nemstrina*). *Vet Pathol* 41:44.
80. Gormly AA, et al. 1981. IgA glomerular deposits in experimental cirrhosis. *Am J Pathol* 104:50.
81. Bernstein J. 1987. The glomerular basement membrane abnormality in Alport syndrome. *Am J Kidney Dis* 10:222.
82. Spear GS, Slusser RG. 1972. Alport syndrome. *Am J Pathol* 69:213.
83. Yum M, Bergstein JM. 1983. Basement membrane nephropathy: A new classification of Alport syndrome and asymptomatic hematuria based on ultrastructural findings. *Hum Pathol* 14:996.
84. Rao VH, et al. 2006. Role for macrophage metalloelastase in glomerular basement membrane damage associated with Alport syndrome. *Am J Pathol* 169:32.
85. Gratton MA, et al. 2005. Matrix metalloproteinase dysregulation in the stria vascularis of mice with Alport syndrome. *Am J Pathol* 166:1465.
86. Sinniah R, Cohen AH. 1985. Glomerular capillary aneurysms in light-chain nephropathy. An ultrastructural proposal of pathogenesis. *Am J Pathol* 118:298.
87. Tubbs RR, et al. 1981. Light chain nephropathy. *Am J Med* 71:263.
88. Imamura M, et al. 1977. Murine type C viral envelope glycoprotein gp69/71 and lupus-like glomerulonephritis of New Zealand mice. *Am J Pathol* 86:375.
89. Norton WL. 1970. Comparison of the microangiopathy of systemic lupus erythematosus, dermatomyositis, scleroderma, and diabetes mellitus. *Lab Invest* 22:301.
90. Ben-Bassat M, et al. 1979. Lupus nephritis. Electron-dense and immunofluorescent deposits and their correlation with proteinuria and renal function. *Am J Clin Pathol* 72:186.
91. Koffler D, et al. 1969. Variable patterns of immunoglobulins and complement deposition in the kidneys of patients with systemic lupus erythematosus. *Am J Pathol* 56:305.
92. Kefalides NA. 1987. The Goodpasture antigen and basement membranes. *Lab Invest* 56:1.
93. Horn RG, et al. 1974. Renal biopsy pathology in Wegener's granulomatosis. *Am J Pathol* 74:423.
94. Weiss MA, Crissman JD. 1984. Renal biopsy findings in Wegener's granulomatosis: Segmental necrotizing glomerulonephritis with glomerular thrombosis. *Hum Pathol* 15:943.
95. Gaber LW, et al. 1993. Coexistence of anti-neutrophil cytoplasmic antibody-associated glomerulonephritis and membraneous glomerulopathy. *Am J Clin Pathol* 99:211.
96. Hayslett JP, et al. 1968. Focal glomerulonephritis due to penicillamine. *Lab Invest* 19:376.
97. Magil AB, Cohen AH. 1989. Monocytes and focal glomerulosclerosis. *Lab Invest* 61:404.
98. Urizar RE, et al. 1968. Anaphylactoid purpura. II. Immunofluorescent and electron microscopic studies of the glomerular lesions. *Lab Invest* 19:437.
99. Hill PA, et al. 1988. Morphologic changes in the renal glomerulus and the juxtaglomerular apparatus in human preeclampsia. *J Pathol* 156:291.
100. Cornog JL, et al. 1970. Immunofluorescent and ultrastructural study of the renal glomerulus in renal vein thrombosis. *Lab Invest* 22:101.
101. Myhre-Jensen O. 1971. Localization of fibrinolytic activity in the kidney and urinary tract of rats and rabbits. *Lab Invest* 25:403.
102. Courtecuise V, et al. 1967. Nonlethal hemolytic and uremic syndrome in children: An electron microscope study of renal biopsy from six cases. *Exp Mol Pathol* 7:327.
103. Weisse I, et al. 1975. "Glomerulare Lipidose" beim Hund. *Berl Muench Tieraerztl Wochenschr* 88:428.
104. Zayed I, et al. 1976. A light and electron microscopical study of glomerular lipoidosis in beagle dogs. *J Comp Pathol* 86:509.
105. Hattori M, et al. 1993. Characteristic glomerular lesions in the Ex-HC rat. *Nephron* 63:314.
106. Wellmark KF, Volk BF. 1971. Renal changes in experimental hypercholesterolemia in normal and subdiabetic rabbits. *Lab Invest* 24:144.
107. Castagnaro M, et al. 1987. Lectin histochemistry and ultrastructure of feline kidneys from six different storage diseases. *Virchows Arch B* 54:16.
108. Rodriguez FH, et al. 1985. Fabry's disease in a heterozygous woman. *Arch Pathol* 109:89.
109. Scott CR, et al. 1973. Mucopolysaccharide storage disease with involvement of the renal glomerular epithelium. *Am J Med* 54:549.
110. Van Es LA. 1992. Pathogenesis of IgA nephropathy. *Kidney Int* 41:1720.
111. Hamburger J, et al. 1968. Les lesions glomerulaires des allogreffes renales. *Adv Transplant* 1:365.
112. Hulme B, et al. 1972. Human renal transplants. IV. Glomerular ultrastructure, macromolecular permeability, and hemodynamics. *Lab Invest* 26:2.
113. Andres GA, et al. 1970. Human renal transplants. *Lab Invest* 22:588.
114. Olsen S, et al. 1974. Ultrastructure of the glomerular basement membrane in long term renal allografts with transplant glomerular disease. *Lab Invest* 30:176.
115. Okudaira Y, et al. 1966. Ultrastructure of the human placenta in maternal diabetes mellitus. *Lab Invest* 15:910.
116. Giacomelli F, Wiener J. 1979. Primary myocardial disease in the diabetic mouse. *Lab Invest* 40:460.
117. Powell HC, et al. 1985. Microangiopathy in human diabetic neuropathy. *Acta Neuropathol* 68:295.
118. Vital C, et al. 1985. Acute inflammatory demyelinating polyneuropathy in a diabetic patient. *Acta Neuropathol* 67:337.
119. Vracko R. 1982. A comparison of the microvascular lesions in diabetes mellitus with those of normal aging. *J Am Geriatr Soc* 30:201.
120. Pardo V, et al. 1966. Electron microscopic study of dermal capillaries in diabetes mellitus. *Lab Invest* 15:1994.
121. Ellis EN, et al. 1986. Glomerular filtration surface in type I diabetes mellitus. *Kidney Int* 29:889.
122. Osterby R. 1974. Early phases in the development of diabetic glomerulopathy. *Acta Med Scand* (Suppl) 574:1.

123. Osterby R, et al. 1983. Diabetic glomerulopathy. Structural characteristics of the early and advanced stages. *Diabetes* 32:79.
124. Osterby R. 1973. A quantitative electron microscopic study of mesangial regions in glomeruli from patients with short term juvenile diabetes mellitus. *Lab Invest* 29:99.
125. Makino H, et al. 1993. Ultrastructural changes of extracellular matrices in diabetic nephropathy revealed by high resolution scanning and immunoelectron microscopy. *Lab Invest* 68:45.
126. Walker JD, et al. 1992. Glomerular structure in type-1 (insulin-dependent) diabetic patients with normo- and microalbuminuria. *Kidney Int* 41:741.
127. Makino H, et al. 1992. Glomerular extracellular matrices in rat diabetic glomerulopathy by scanning electron microscopy. *Virch Arch B* 62:19.
128. Rohrbach DH, Martin GR. 1982. Structure of basement membrane in normal and diabetic tissue. *Ann N Y Acad Sci* 401:203.
129. Vernier RL, et al. 1992. Heparan sulfate proteoglycan in the glomular basement membrane in type 1 diabetes mellitus. *Kidney Int* 41:1070.
130. Hayashi H, et al. 1992. An electron microscopic study of glomeruli in Japanese patients with non-insulin dependent diabetes mellitus. *Kidney Int* 41:749.
131. Ellis EN, et al. 1987. Observations of glomerular epithelial cell structure in patients with type I diabetes mellitus. *Kidney Int* 32:736.
132. Mauer SM, et al. 1984. Structural-functional relationships in diabetes mephropathy. *J Clin Invest* 74:1143.
133. Osterby R, et al. 1987. New vessel formation in the renal corpuscles in advanced diabetic glomerulopathy. *J Diab Comp* 1:122.
134. Kanetsuna Y, et al. 2007. Deficiency of endothelial nitric-oxide synthase confers susceptibility to diabetic nephropathy in nephropathy-resistant inbred mice. *Am J Pathol* 170:1473.
135. Suganuma T, et al. 1985. Qualitative and quantitative analysis of cell surface membrane sialyl residues using affinity cytochemistry with special reference to diabetic patients. *Virch Arch B* 49:1.
136. Osterby R, Gundersen HJG. 1980. Fast accumulation of basement membrane material and the rate of morphological changes in acute experimental diabetic glomerular hypertrophy. *Diabetologia* 18:493.
137. Johnson PC, et al. 1981. Human diabetic perineural cell basement membrane thickening. L*ab Invest* 44: 265.
138. Beggs J, et al. 1992. Innervation of the vasa nervorum: Changes in human diabetics. *J Neuropathol Exp Neurol* 51:612.
139. Arai H, et al. 2008. Role of growth arrest-specific gene 6 in diabetic nephropathy. *Vitamin Horm* 78:375.
140. Cavet ME, et al. 2008. Gas6-axl receptor signaling is regulated by glucose in vascular smooth muscle cells. *Arterioscler Thromb Vasc Biol* 28:886.

30 Prions

Prions Defined

Prions are aggregated conformational isomers of host-encoded glycoproteins; that is, they are abnormal forms of neuronal proteins present in the normal animal.[1,2] Newly infecting prions change the normal prion protein, **PrP^C**, into a misfolded abnormal form, **PrP^{Sc}**, which, in turn, corrupts other normal prion proteins, self-perpetuating the molecular changes in conformation and function. Because of their unique misfolding and their lack of nucleic acid, prions are highly resistant to proteases and disinfectants.

PrP^C is a normal, α-helical, plasma membrane protein that is inserted into the neuronal synapse. It is encoded in a single exon of a single-copy gene. In normal animals, PrP^C is produced in the ribosome, translocated across the endoplasmic reticulum membrane, processed, and transported to the neuronal surface, where it is anchored to the plasma membrane by glycoinositol phospholipids. PrP^C co-localizes in synaptic terminals with synaptophysin.[3] It is required in target cells for prions to propagate and cause disease. PrP^C is also produced by **astrocytes**, **lymphocytes**, and **dendritic cells**, all of which support propagation of PrP^{Sc}.

PrP^{Sc} is a modified, protease-resistant form of the normal PrP^C. It differs from PrP^C in its resistance to proteolysis, sedimentation properties, association with infectivity, and ability to aggregate into β-pleated sheets of amyloid. PrP^{Sc} is derived from PrP^C by a post-translational process that involves a marked conformational change. PrP^{Sc} does not anchor to the plasma membrane but accumulates in the cytoplasm of the neuron. As PrP^{Sc} fibrillizes in the neuronal cytoplasm, its protease-resistant core aggregates extracellularly into amyloid fibrils.[4,5] The process is accompanied by neuronal degeneration that is associated with accumulation of PrP^{Sc} and its degradation products in neurons.[6] Loss of synapse function is a consequence of PrP^{Sc} accumulation, and leads some to refer to prion diseases as **synapsopathies**.

Prion Diseases

Prions are the etiologic agents of the **transmissible spongiform encephalopathies** (TSEs), diseases with prolonged, clinically silent incubation periods (human variant CJD may exceed 50 years). The progressive, degenerative brain diseases are characterized by neuronal vacuolation and death, accumulation of PrP, microgliosis, and reactive astrocytosis. The synaptic trait of PrP indicates that synapse loss is a key event in neuronal death.[7] Prion diseases of animals include

- **Scrapie** of sheep
- **Bovine spongiform encephalopathy (BSE)**
- **Transmissible mink encephalopathy (TME)**
- **Chronic wasting disease** of elk and deer (**CWD**)

Sporadic TSEs have been reported in cats and some other species. Human TSEs include **Creutzfeld-Jakob disease (CJD)**, **variant CJD (vCJD)**, **Gerstmann-Sträussler-Scheinker syndrome**, **fatal familial insomnia**, and a historic disease, **kuru**, that was associated with cannibalism in New Guinea.

Patterns of Transmission

Prion diseases arise by three different mechanisms:

- **Transmissible (infectious):** prions are transmitted by food or trauma

© 2009 Wiley-Blackwell. ISBN: 978-0-813-80330-2

- **Acquired (sporadic):** iatrogenic prion disease acquired from central (via brain electrodes) or peripheral (via cadaver hypophyseal hormones) pathways
- **Genetic (hereditary):** inheritance by autosomal dominant conditions caused by spontaneous mutation of a PrP gene

Once spontaneous mutation occurs, the prion can become infectious if passed from animal to animal. Different prion strains result from different conformation; each can produce a unique disease in the animal (sheep have been infected with as many as 20 different strains of scrapie prion).

Prion Disease Pathogenesis

One theory for prion disease pathogenesis is based on the kinetics of prion propagation; it proposes that $\mathbf{PrP^{Sc}}$ by itself is inert, and that toxicity resides in a smaller, labile, oligomeric PrP species, $\mathbf{PrP^{L}}$.[8] Infectivity is uncoupled from toxicity: proliferating, infectious $\mathbf{PrP^{Sc}}$ acts as a catalytic surface upon which the toxic intermediate forms before it matures into nontoxic $\mathbf{PrP^{Sc}}$. During the template-assisted progression from $\mathbf{PrP^{C}}$ to $\mathbf{PrP^{Sc}}$, the toxic intermediate $\mathbf{PrP^{L}}$ is formed:

$$\mathbf{PrP^{Sc}} + \mathbf{PrP^{C}} \rightarrow \mathbf{PrP^{Sc}}:\mathbf{PrP^{C}} \rightarrow {}^{\kappa 1}\mathbf{PrP^{Sc}}:\mathbf{PrP^{L}} \rightarrow {}^{\kappa 2}\mathbf{PrP^{Sc}}:\mathbf{PrP^{Sc}}$$

Neurotoxicity requires a critical $\mathbf{PrP^{L}}$ concentration; that is, the relative levels of infectivity and toxicity are governed by the ratio of the initial rate of conversion to toxic PrP^{L} ($\boldsymbol{\kappa 1}$) to the rate of maturation to nontoxic PrP^{Sc} ($\boldsymbol{\kappa 2}$).

The Transmissible Spongiform Encephalopathies

In the **transmissible spongiform encephalopathies**, there is a direct correlation between PrP^{Sc} concentration and pathologic changes in the brain. Prion disease is caused by release and accumulation of abnormal, mutant PrP^{Sc} in the neuron. Unable to move through the cell, PrP^{Sc} aggregates outside the cell. Prions are metabolized differently, and one mutant form becomes trapped in the membrane with its amino-terminal domain stuck in the cytosol.

A critical role is played by both agent strain and host genotype in the TSEs. The major host factor that controls the incubation period in scrapie is a gene called *Sinc* or *Prn-i*, which is closely related to the gene encoding PrP^{Sc}.[9] Studies in humans have proposed that the familial prion diseases, although transmissible, are true autosomal dominant disorders like Huntington's disease. PrP gene germline mutations in patients and at-risk individuals appear to be the cause of familial prion diseases.

An alternative to the infectious theory of prions is that prions are toxic proteins that accumulate (without replicating) by deranging the normal processing of a natural metabolite in the CNS. A post-translationally abnormal PrP interferes with breakdown of normal PrP^{c}. The native protein or an early degradative product is converted to the toxic, protease-resistant abnormal molecule intracellularly. This new abnormal PrP gradually accumulates in extracellular spaces and is highly toxic.[10]

In scrapie, there is a direct correlation between PrP^{Sc} concentration and pathologic changes in the brain. Immunogold labeling studies have shown that PrP^{Sc} accumulates in secondary lysosomes in the cytoplasm of neurons cultured in vitro.[11] The presence of acid phosphatase and myelin figures in the lysosomes indicates that the process involves **autophagy**. Vacuolation in prion diseases may be related to the **vacuolar leukoencephalopathy** that results from suppressed defenses against oxidant injury. Mice lacking the transcription factor *Nrf2*, which prevents oxidant injury to neurons, develop vacuoles and astrogliosis.[12]

Scrapie

Scrapie is a progressive, degenerative neurologic disease of sheep and goats. It begins insidiously with the animal scraping its fleece against fixed objects and progresses to tremor, ataxia, and death. Neuropathologic changes in natural scrapie of sheep include diffuse vacuolation (status spongiosus), loss of neurons, and astrogliosis of the gray matter. Vacuoles are chiefly in neurons, although some glia may be affected. Extracellular spaces are not enlarged. Typically, nerve cells degenerate but astrocytes proliferate in response to infection.

Affected **neurons** in scrapie are enlarged with chromatolysis, and large, single cytoplasmic vacuoles. Ultrastructurally, the vacuoles are membrane-bound and may contain aggregates of granular material.[13] The expanded cytoplasm of affected neurons is filled with dispersed granulofilamentous material. Scrapie-associated prion protein accumulates in astrocytes.[14] Ruptured plasma membranes and fragments of membranes are distributed throughout affected parts of the brain. Many of these occur within vacuoles. **Astrogliosis** is a constant and early response, but there is absence of an acute inflammatory component of the host's reaction.

Lymphoid tissue is the site where PrP first replicates after transmission. After inoculation or oral feeding of sheep, PrP can be demonstrated in the

spleen and lymph nodes within a few weeks, but in the brain only after 3 months. There is no evidence of humoral or cellular immunity. In lymphoid tissue, immunogold studies show that scrapie PrP accmulates in dense vesicles in hypertrophic **follicular dendritic cells**, and **macrophages** of secondary follicles. Macrophages outside the follicle accumulate PrP in pits, endosomes, lysosomes, and endoplasmic reticulum—suggesting that PrP is internalized by a caveolin-drive pathway.[15]

Rodent Scrapie

Mice and hamsters are infected by the scrapie agent and develop lymphopathic and neuropathic lesions similar to those in sheep.[16] In the **brain**, spongiform lesions in the cerebral cortex contain focally swollen perikaryal cytoplasm of nerve cells and astrocytes, and swollen neuronal and astrocytic processes, and membrane-bounded vacuoles within pre- and postsynaptic neuronal terminals. Enlarged dendrites may contain membrane fragments or small vesicles and tubular structures that are suggestive of (but are not) viral particles.

Mice PrP-associated particles from mouse brain have been identified by immunogold techniques.[17,18] Axon terminal degeneration and dendritic spine loss may be events that are due to specific PrP toxicity.[19] The neurodegenerative process in mice enhances the metallothionein expression in astrocytes and perivascular tissues.[20] In hippocampal neurons of scrapie-infected mice, **tubulovesicular particles** are a prominent finding, but they are not labeled with immunogold procedures.[21] **Scrapie-associated fibrils**, distinct particulate structures first seen in scrapie-infected mouse brain by negative staining electron microscopy, are composed of two to four twisted filaments, each 4–6 nm in diameter and of variable length (Fig. 30.1).

Hamsters Hamsters have a shorter incubation period than mice and develop larger amounts of infectious material. Immunogold techniques for prion protein label filaments of 7–17 nm diameter in subpial, subependymal, perivascular, and ventricular areas. PrP^{SC} infects ependymal cells as well as neurons and astrocytes.[22] The choroid plexus and cerebral vascular endothelial cells are not infected, and may even inhibit the passage of the scrapie agent across the blood-brain barrier. **Reactive astrocytes** are filled with glial filaments and many tortuous intercellular junctions of adhesive plaque junction type. Desmosome-like junctions connect astrocytes. **Macrophages** have many electron-lucent vacuoles with debris, and have been shown to engulf myelinated fibers.[23,24]

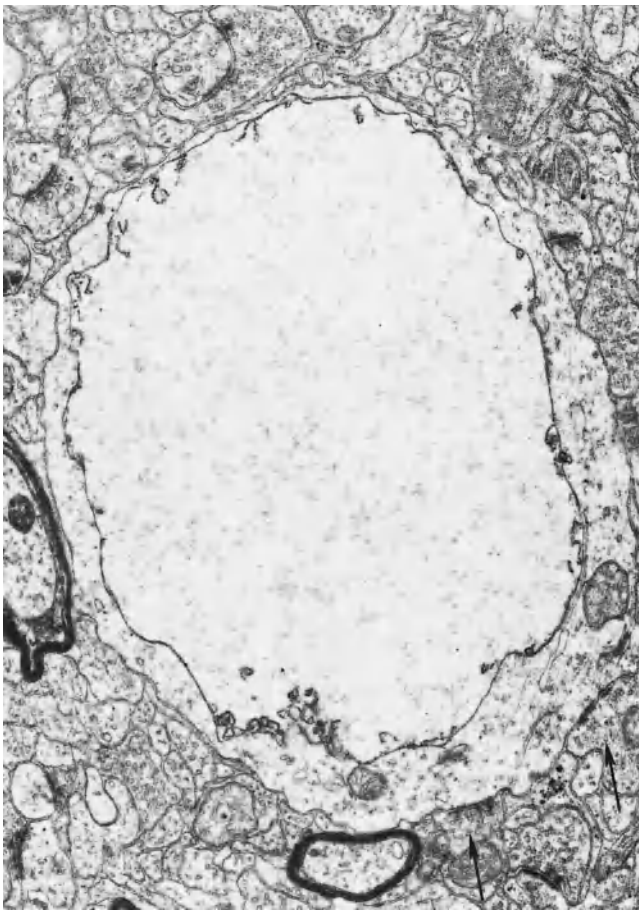


Fig. 30.1 Scrapie. Altered plasma membranes and vacuole in the neuropil. (Micrograph: Peter Lampert, *Acta Neuropathol* 19:81, 1971.)

Bovine Spongiform Encephalopathy

Lesions of **bovine spongiform encephalopathy (BSE)** closely resemble those of scrapie. The ultrastructural findings in the BSE-infected cow show quantitative differences from scrapie in hamsters and CJD in mice.[25] Membrane-bound intracellular vacuoles, predominantly in dendrites and within few myelinated axons, are reported. Vacuoles contained coiled membranes and vesicles. Masses of neurofilaments aggregated in dendrites and axons. Spheroids in the BSE-affected cow brain were larger than those in scrapie. BSE obtained from cattle and from wild bovidae produce lesions of BSE in mice.[26] BSE strains are highly promiscuous and transmit efficiently to several animal species with a distinct PRP primary structure.

Chronic Wasting Disease

Chronic wasting disease is a TSE that affects Rocky Mountain elk, and mule and white-tailed deer.[27] Like

scrapie, CWD is widely distributed to the lymphoid system early after transmission,[28] and later involves the CNS and peripheral tissues. Although cattle, sheep, and goats can be infected by intracerebral inoculation, there is no evidence they accept oral transmission.

Transmissible Mink Encephalopathy

Lesions of **transmissible mink encephalopathy** closely resemble those of scrapie.[29] TME has been transmitted to raccoons.[29]

Kuru

Kuru was a relentlessly progressive, fatal disease found among the Fore peoples in the eastern highlands of Papua, New Guinea. Kuru was transmitted by the practice of consuming dead relatives as a mark of respect. The clinical syndrome of tremor and ataxia arose from the histopathologic changes of neuronal degeneration, status spongiosis, and gliosis, which affected primarily the cerebellum, basal ganglia, and (to less extent) the cerebral cortex. Vacuoles within neurons and the neuropil are not always prominent, but astrocytic proliferation is intense. Microglial clusters develop around degenerating neurons. Mild perivascular infiltrates of lymphocytes have been reported but are rare. These changes are found throughout the gray matter and involve the cerebellum, pons, thalamus, and basal ganglia. Secondary axonal degeneration accompanied by breakdown of myelin is present in the cerebral white matter and in corticospinal and spinocerebellar tracts.[30]

Inoculation of suspensions of brain from kuru patients into chimpanzees or spider monkeys produced kuru-like signs within 1.5–3 years.[31] Ultrastructurally, the cerebral cortex of these species shows vacuolar neuronal degeneration, astrocytic proliferation, and a lack of inflammatory cells. Vacuoles develop within the neuronal perikarya, axons, and dendrites. Vacuoles are clear except for small clusters of membrane fragments and vesicles. Affected neurons have eccentric nuclei, foci of cytoplasm proteolysis (clearing), and blebbing of the cytoplasm into extracellular spaces of the neuropil. Neurotubules lack normal orientation and may aggregate in inclusions that resemble Pick's inclusions (Fig. 30.2). Astrocytes are enlarged and contain abundant glial filaments. Swelling and proliferation of astrocytes are reactive changes, secondary to the neuronal damage.[31] Experimental kuru has more severe vacuolation than occurs in the natural disease.

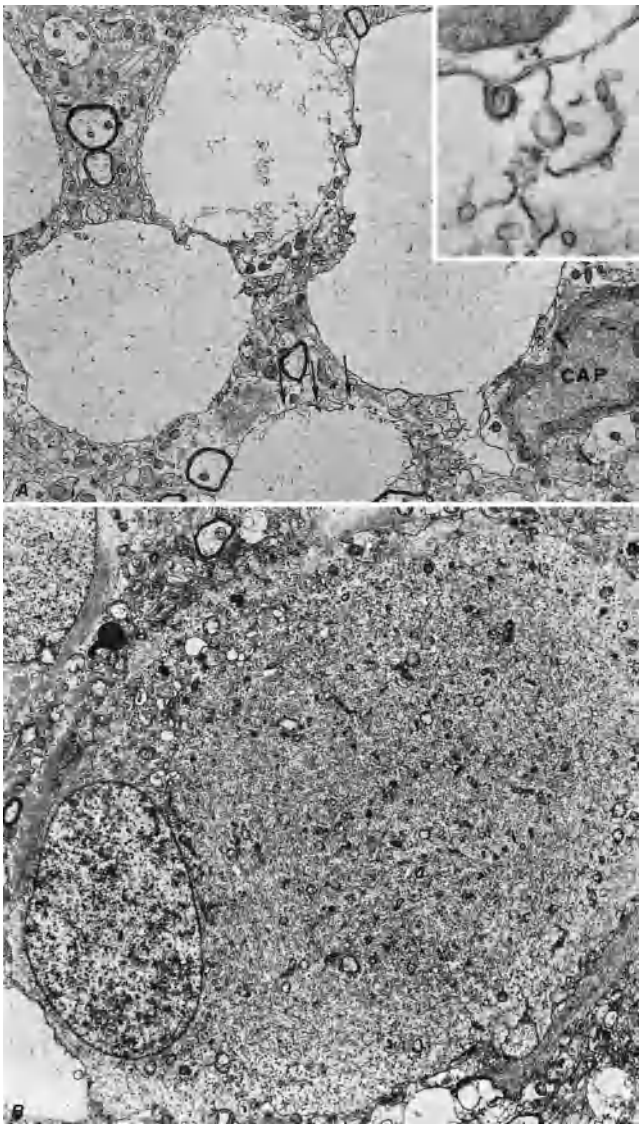


Fig. 30.2 **Kuru**, brain of chimpanzee. **A**. **Status spongiosus**, frontal cortex. Distended cytoplasmic processes distort normal processes of neurons and glia. Capillary (*CAP*) is surrounded by normal astrocytic processes. Curled processes are evident at plasma membrane (*arrows* and *inset*). **B**. **Degenerate nerve cell** with eccentric nucleus and swollen cytoplasm filled with aggregate of randomly oriented tubules. (Micrograph: Peter Lampert, *J Neuropathol Exp Neurol* 28:353, 1969.)

Creutzfeldt-Jakob Disease

Creutzfeldt-Jakob disease was reported in the 1920s in patients that developed progressive incoordination, mental disturbances, and coma. Histologic studies revealed widespread patchy degeneration of nerve cells, spongiform change, neuronophagia, and astrocytic proliferation, all without inflammation. The widespread status spongiosis of the gray matter was characterized by large (up to 50 μm) vacuoles within

and around neurons. Swollen neurons with eccentric nuclei were present but viewed as cells reacting to axonal or dendritic injury.[32,33]

The pattern of brain lesions is highly variable, and is influenced by the PrP genotype and PrP^{Sc} isotype.

Electron microscopic studies on human biopsies of CJD show that vacuoles are within swollen neurons and astrocytic processes; there is no enlargement of the extracellular spaces.[34–37] PrP immunogold labeling reveals that PrP is associated with granular and perivacuolar deposits, often with vacuoles.[37] Cytoplasmic clearings are common. **Tubulovesicular structures** (TVS), 35 nm particles regarded by some as the only disease-specific prion structures, are prominent in CJD.[36]

Human normal cellular prion protein (PrP^{c}) is encoded by a gene (PRNP) on the short arm of chromosome 20. CJD that arises from point of insertional mutations in this gene and the subsequent aberrant accumulation of PrP^{CJD}. Human CJD[38] arises by different pathways:

- **Genetic prion disease: gCJD** (also the pathways of GSS, and thalamic degenerative fatal familial insomnia)
- **Acquired prion disease:** iatrogenic CJD (**iCJD**) from central (via brain electrodes) or peripheral (via cadaver hypophyseal hormones) pathways
- **Transmissible prion disease:** variant CJD (**vCJD**) from bovine spongiform encephalopathy material

Experimental reproduction of the lesions of CJD has been attempted by inoculation of human brain suspensions into primates and guinea pigs.[39–41] Mice with experimental CJD develop progressive retinal degeneration with changes in photoreceptor cell inner and outer segment areas. Ultrastructural studies reveal a total loss of outer and most inner segment elements.[42,43]

Human Variant CJD In 1996, a new variant of CJD with distinctive clinical appearance and neuropathology was reported in adolescents and young adults, a cohort not typically affected by CJD. The appearance of vCJD coincided with the emergence of BSE in cattle. The neuropathology of vCJD shows widespread accumulation of PrP and abundant florid and cluster plaques in the cerebrum and cerebellum. Spongiform change is most marked in basal ganglia, while the thalamus has severe neuronal loss with gliosis in the posterior nuclei.[44] Unlike sCJD, PrP^{Sc} is detected in the lymphoid and peripheral nervous systems in vCJD. Western blot analyses reveal uniform isotypes with a glycoform ratio of predominating diglycosylated bands (that are distinct from sCJD).

Fatal Familial Insomnia

Human **fatal familial insomnia (FFI)** appears clinically with progressive sleeplessness and dementia. Brain lesions include spongiform change and gliosis in the thalamus and cerebral cortex, as well as in the striatum and amygdala. There are widespread perivaculolar depostis of PrP^{SC}.[45] Ultrastructural changes in FFI are indistinguishable from those of CJD.[46]

Gerstmann-Sträussler-Scheinker Syndrome

Gerstmann-Sträussler-Scheinker syndrome (GSS) is characterized by progressive adult-onset dementia with cerebellar and pyramidal signs. The mode of inheritance is autosomal dominant in many cases. Amyloid plaques are found throughout the cerebrum and cerebellum, with or without spongiform changes in the cortex. Alzheimer neurofibrillary tangles may be found in some cases,[47] although these may be due to concurrent disease processes.

A point mutation at PrP codon 102 was found to be gentically linked to the GSS syndrome; that is, the mutation may have arisen independently several different times. Studies in transgenic mice (which develop CNS lesions when the codon 102 point mutation is introduced into the mouse PrP) suggest that the PrP mutation causes GSS and familial CJD. Other mutations also segregate with inherited human prion disease. Some patients with Alzheimer's disease have a prion disease; this is based upon PrP immunostaining of amyloid plaques and the presence of PrP gene mutations.

References

1. Prusiner SB. 2004. Prion Biology and Disease, 2nd ed. Cold Spring Harbor Laboratory Press, Cold Spring, NY.
2. Fratmann R, Sivitz LB. 2004. Advancing Prion Science. National Academy Press, Washington, DC.
3. Fournier JG, et al. 1995. Ultrastructural localization of cellular prion protein (PrP^{c}) in synaptic boutons of normal hamster hippocampus. *C R Acad Sci III* 318:339.
4. Liberski M, et al. 1995. Pathology of the transmissible spongiform encephalopathies with special emphasis on ultrastructure. *Micron* 26:277.
5. Prusiner SB, et al. 1984. Scrapie prions aggregate to form amyloid-like birefringent rods. *Cell* 35:349.
6. Hegde RS, et al. 2000. Transmissible and genetic prion diseases share a common pathway of neurodegeneration. *Nature* 402:822.
7. Fournier JG. 2008. Cellular prion protein electron microscopy. *Cell Tiss Res* 332:1.

8. Collinge J, Clarke AR. 2007. A general model of prion strains and their pathogeniticty. *Science* 318:930.
9. Ersdal C, et al. 2005. Mapping PrP^{Sc} propagation in experimental and natural scrapie in sheep with different genotypes. *Vet Pathol* 42:258.
10. Pablos-Mendez A, et al. 1993. Infectious prions or cytotoxic metabolites. *Lancet* 341:159.
11. McKinley MP, et al. 1991. Ultrastructural localization of scrapie prion proteins in cytoplasmic vesicles of infected cultured cells. *Lab Invest* 65:622.
12. Hubbs AF, et al. 2007. Vacuolar leukoencephalopathy with widespread astrogliosis in mice lacking transcription factor Nrf2. *Am J Pathol* 170:2068.
13. Bignami A, Parry HB. 1972. Electron microscopic study of the brain of sheep with natural scrapie. *Brain* 95:319 and 487.
14. Detrich JF, et al. 1991. Scrapie-associated prion protein accumulations in astrocytes during scrapie infection. *Proc Natl Acad Sci USA* 88:375.
15. McGovern G, Jeffrey M. 2007. Scrapie-specific pathology of sheep lymphoid tissues. *PLoS ONE* 2:1304.
16. Lampert PW, et al. 1972. Subacute spongiform virus encephalopathies. *Am J Pathol* 68:626.
17. Kercher L, et al. 2004. Differences in scrapie-induced pathology of the retina and brain in transgenic mice that express hamster prion protein in neurons, astrocytes and multiple cell types. *Am J Pathol* 165:2055.
18. Dourmashkin RR, et al. 2004. Immunogold electron microscopy recognizes prion protein-associated particles prepared from scrapie-infected mouse brian. *J Neuropathol Exp Neurol* 63:32.
19. Jeffrey M, et al. 1997. In vivo toxicity of prion protein in murine scrapie: Ultrastructural and immunogold studies. *Neuropathol Appl Neurobiol* 23:93.
20. Vorbrodt AW, et al. 2006. Quantitative immunogold study of increased expression of metallothionein-I/II in the brain perivascular areas of diabetic scrapie-infected mice. *J Mol Histol* 37:143.
21. Jeffrey M, Fraser JR. 2000. Tubulovesicular particles occur early in the incubation period of murine scrapie. *Acta Neuropathol* 99:525.
22. Fournier JG, et al. 2008. Ultrastructural evidence that ependymal cells are infected in experimental scrapie. *Acta Neuropathol* 115:643.
23. Liberski PP, et al. 2002. Ultrastructural studies of experimental scrapie and Creutzfeldt-Jakob disease in hamsters. II: Astrocyte and macrophage reaction towards axonal destruction. *Acta Neurobiol Exp (Wars)* 62:131.
24. Fournier JG, et al. 1998. Distribution and submicroscopic immunogold localization of cellular prion protein (PrP^{c}) in extracerebral tissues. *Cell Tissue Res* 292:77.
25. Kong O, et al. 2008. Evaluation of the human transmission risk of an atypical bovine spongiform encephalopathy prion strain. *J Virol* 82:3697.
26. Bautista MJ, et al. 2006. BSE infection in bovine PrP transgenic mice leads to hyperphosphorylation of tauprotein. *Vet Microbiol* 115:293.
27. Williams ES. 2005. Chronic wasting disease. *Vet Pathol* 42:530.
28. Spraker TR, et al. 2002. Distribution of protease-resistant prion protein and spongiform encephalopathy in free-ranging mule deer (*Odocoileus hemionus*) with chronic wasting disease. *Vet Pathol* 39:549.
29. Hamir AN, et al. 2004. Transmission of transmissible mink encephalopathy to raccoons (*Procyon lotor*) by intracerebral inoculation. *J Vet Diagn Invest* 16:57.
30. Beck E, et al. 1975. Experimental kuru in the spider monkey. *Brain* 98:595.
31. Lampert PS, et al. 1969. Experimental kuru encephalopathy in chimpanzees and spider monkeys. *J Neuropathol Exp Neurol* 28:353.
32. Tyler KL. 2003. Creutzfeldt-Jakob disease. *New Engl J Med* 348:681.
33. Glatzel M, et al. 2003. Extraneural pathologic prion protein in sporadic Creutzfeldt-Jakob disease. *New Engl J Med* 349:1812.
34. Zanusso G, et al. 2007. Novel prion protein conformation and glycotype in Creutzfeldt-Jakob disease. *Arch Neurol* 64:595.
35. Kim JH, et al. 1988. Creutzfeldt-Jakob disease with intranuclear vacuolar inclusions. *Acta Neuropathol* 76:422.
36. Liberski PP, et al. 1992. Tubulovesicular structures in Creutzfeldt-Jakob disease. *Acta Neuropathol* 84:238.
37. Grigoriev V, et al. 1999. Submicroscopic immunodetection of PrP in the brain of a patient with a new variant of Creutzfeldt-Jakob disease. *Neurosci Lett* 264:57.
38. Kovacs GG, Budka H. 2008. Prion diseases. *Am J Pathol* 172:555.
39. Boellaard JW, et al. 1989. Neuronal autophagy in experimental Creutzfeldt-Jakob disease. *Acta Neuropathol* 78:410.
40. Kim JH, et al. 1988. Creutzfeldt-Jakob disease with intranuclear vacuolar inclusions. *Acta Neuropathol* 76:422.
41. Walis A, et al. 2003. Ultrastructural changes in the optic nerves of rodents with experimental Creutzfeldt-Jakob disease (CJD), Gerstmann-Sträussler-Scheinker disease (GSS) or scrapie. *J Comp Pathol* 129:213.
42. Hogan RN, et al. 1981. Progressive retinal degeneration in scrapie infected hamster. *Lab Invest* 44:34.
43. Liberski PP, et al. 1988. Tubulovesicular structures in experimental Creutzfeldt-Jakob disease and scrapie. *Intervirol* 29:115.
44. Ironside JW, Head MW. 2004. Neuropathology and molecular biology of variant Creutzfeldt-Jakob disease. *Curr Top Microbiol Immunol* 284:133.
45. Piao YS, et al. 2005. Sporadic fatal insomnia with spongiform degeneration in the thalamus and widespread PrP^{Sc} deposits in brain. *Neuropathology* 25:144.
46. Liberski PP, et al. 2005. Ultrastructural pathology of prion disease revisited: Brain biopsy studies. *Neuropathol Appl Neurobiol* 313:88.
47. Amano N, et al. 1992. Gerstmann-Sträussler syndrome—a variant type: Amyloid plaques and Alzheimer's neurofibrillary tangles in cerebral cortex. *Acta Neuropathol* 84:15.

Index

Page references followed by f denote figures; those followed by t denote tables.

A
AA amyloid, 830–834
AAT. *See* α_1-antitrypsin (AAT)
AAVs (adeno-associated viruses), 352
ABC-transporter family of proteins, 431
Abetalipoproteinemia, 169, 173
Abortion
  brucellosis, 455
  sarcocystosis, 555
Absorptive endocytosis, 109
Acanthamoeba, 527–528
Acanthamoebic keratitis, 528
Acanthosis, papillomavirus, 343
Acatalasemia, 243
Accelerated phagocytosis, 237
Acetaminophen
  hepatotoxicity, 40, 618–619
  nephrotoxicity, 706, 708
Acetylcholine (ACh), 683
Acetylcholine receptors, 686
Acetylcholinesterase (AChE), 683–684
Acetylcholinesterase inhibitor, 653–654, 683
Acetylsalicylic acid, effect on platelets, 260
ACh receptor complex (AChR), 683
Acid hydrolases, in eosinophils, 245
Acid lipase deficiency, 173, 864f
Acid secretion
  bone resorption and, 806
  by gastric parietal cells, 145
Acid sphingomyelinase (ASM), 860
Acidification
  gill damage from, 737
  in Golgi complex, 141
Acidocalcisome, 535
Acidosome, 110, 119, 119f, 145
ACP (activated protein C), 207
Acquaporin-4 (AQP4), 687
Acquired immunodeficiency syndrome (AIDS), 410–412
Acrylamide, 681–682
ActA, in listeriosis, 498
Actin
  depolymerization, 20
  filaments, 89–90, 498
  inclusions, in neoplastic cells, 771
  in listeriosis, 498
  platelet, 248
  polymerization, 89
Actin-binding proteins, 90
Actinobacillus, 477–478, 478t
Actinomyces, 487, 488f, 489t, 491
Actinomycetales (order), 487–496, 489t–490t
  Actinomyces genus, 487, 488f, 489t, 491
  Arcanobacterium genus, 489t, 491
  Corynebacterium genus, 489t, 491
  Dermatophilus genus, 490t, 495f, 496
  Mycobacterium genus, 489t–490t, 491, 492f, 493–494
  Nocardia genus, 490t, 494, 495f
  Rhodococcus genus, 490t, 496
  Tropheryma genus, 490t, 496
Actinomycin D, 135
Actinomycosis, 487
Activated protein C (ACP), 207
Activated T cells, FasL expression, 46
Actomyosin complexes, 90
Acute cell injury, programmed cell death, 49
Acute cell swelling
  aerolysin toxicity, 657f
  carbon tetrachloride toxicity, 621f
  cell-to-cell contact disruption, 17
  cytoplasmic edema, 7
  cytoplasmic shedding by exocytosis, 18–20
  cytoskeleton, disassembly of, 17–18
  defined, 5
  dilatation of cytocavitary network cisternae, 5
  endothelial cells, 213f
  fragmentation of cytocavitary network membranes, 5, 6f, 7
  glycogen-lipid droplet ratio reversal, 9
  Golgi complex vesiculation, 9
  hepatocytes, 613, 613f
  lysosome activation and autophagosome formation, 11
  membrane ion channel increase in, 62
  mitochondrial swelling, 9, 11
  neurons, 798f
  nucleus in, 13, 14f, 15
  pericellular environment, 20
  peroxisome duplication, 11, 13
  plasma membrane in, 15, 16f, 17
  proximal convoluted tubule, 697
  smooth endoplasmic reticulum proliferation and aggregation, 9
  surface structure, 18, 19f
Acute lytic infection, 319
Acute phase proteins, 215
Acute respiratory distress, 728
Acute systemic toxicity, from hypocalcemia, 710

© 2009 Wiley-Blackwell.

ISBN: 978-0-813-80330-2

Acute tubular necrosis (ATN)
  ethylene glycol, 710–711
  ischemic, 711
  metallic toxins, 702–705
  nephrotoxic, 711
  pigment-induced, 712
Acyl-CoA pools, homeostasis of, 191
Adapter protein FADD, 46
Adaptin complexes, 140
Adaptins, 140
Adaptive responses to persistent injury, 21–29
  atrophy, 26, 28f, 29
  cytomegaly, 23, 25f, 27f
  hypertrophy, 21f, 21–23, 22f, 24f
  metaplasia, 26
  multinucleate giant cells, 23, 26
Adaptor protein, 113
Addressin, neutrophil, 236
Addressins, 287
Adducin, 92, 94
Adeno-associated viruses (AAVs), 352
Adenocarcinoma, secretory granules in, 774f
Adenoma, 761
Adenomatous polyposis coli gene *(APC),* 782
Adenosine agonists, vascular toxicity of, 658
Adenoviridae family, 338–343, 339t, 340f
  Aviadenovirus genus, 343
  Mastadenovirus genus, 340–343
    canine adenoviruses 1 (CAV-1), 340–341, 343
    canine adenoviruses 2 (CAV-2), 340
    enteric adenoviruses, 340
    human adenoviruses, 340
    infectious canine hepatitis (ICH), 340–341, 341f, 343
    pulmonary adenoviruses, 340
Adenovirus
  canine adenoviruses 1 (CAV-1), 340–341, 343
  canine adenoviruses 2 (CAV-2), 340
  cytomegaly, 23, 27f
  enteric, 340
  human, 340
  pulmonary, 340
Adenylate cyclase toxin, 457
ADF ribosylation factors, 140
ADH (antidiuretic hormone), 705
Adherence densities, of *Yersinia,* 475
Adhesins, 433, 434–435, 579
Adhesion molecules, 96–97
  at endothelial surfaces, 215
  fungal, 579
  glycoproteins, 80, 84t
  neoplastic cells, 763, 780
  organ-specific, 783
Adhesion plaques, 46, 90, 96, 251
Adhesomes, 308
Adiaspiromycosis, 590
Adiaspore, 590
Adipocyte
  defects, 167
  lipogenesis, 167
  lipolysis, 167
Adipophilin, 165
Adrenal cortex, hypertrophy and hyperplasia, 22
Adrenal medulla, hyperplasia of, 24f
Adrenergic neuron blockers, 677
Adrenergic receptor agonists, cardiotoxicity of, 650
Adrenoleukodystrophy, 155
Adriamycin, 63, 688
Aegyptianella, 452t, 453
Aerolysin, 466, 655, 657f
Aeromonadales (order), 466, 466t
Aeromonas, 466, 466t
  A. hydrophila, autolysin of, 655, 657f
Afipia, 453–454, 455f
Aflatoxin
  cytomegaly, 23
  hepatotoxicity, 136, 626–627, 628f
  nuclear damage, 136
African histoplasmosis, 585
African horse sickness (AHS), 377
African swine fever (ASF), 353f, 353–354
African trypanosomiasis, 533–534
Aggregatibacter, 478t, 479
Aggregative adherence fimbriae, 469
Aggresome
  description, 67, 68f
  in Huntington's disease, 841
  misfolded proteins in, 842
  in neoplastic cells, 771
  in Parkinson's disease, 840
Aging
  cellular change in, 750
  glomerulopathy of, 894
  growth defects and, 750–751
  mitochondrial metabolism and, 195
  neuronal changes in, 667–668, 668f
  protein filaments of, 842
Aging pigment, 823
Agouti gene, 812
AHS (African horse sickness), 377
AIDS (acquired immunodeficiency syndrome), 410–412
AIDS biliary cholangiopathy, 558
AIF (apoptosis-inducing factor), 43
Air capillaries, 736
Airsacculitis, 582
Akabane virus, 392
Akt, 81, 785
AL amyloid, 834
Alaskan malamutes, dwarf, 302
Albinism, 812–814
  mutations in animals, 813–814
  oculocutaneous, 813
  partial, 812–813
Albumin
  in hyalin droplet inclusions, 844, 849
  transport function, 201–202
Alcoholic hyalin, 849f, 849–851
Aldosterone, 708
Aleutian mink disease virus, 241, 352–353, 894
Alexander's disease, 842, 870
Algae
  Prototheca, 573, 574f, 575, 575f
  Pythium, 575
Alkylation of DNA nucleotides, 135
Allergic disease, from fungi, 578, 582
Allergic pulmonary aspergillosis, 582
Allylamine necrosis, 659
Alpha granules, platelet, 251
α_1-antitrypsin (AAT), 240
  deficiency, 138
  in hepatic regeneration and, 749
  in hyalin droplet inclusions, 844
α_2-macroglobulin-TNF complexes, 270
α-actinin, 90
αβ-crystallin, 842
Alpha-bungarotoxin, 686
α-catenin, 782
αδ-storage pool disease, 256
α-hemolysin, 85
Alphaherpesvirinae subfamily, 330–335
  herpes simplex virus (HSV), 330, 332f, 332–333
  Mardivirus genus, 333, 335
  Marek's disease virus, 333, 335
  Simplexvirus genus, 330, 331f, 332f, 332–333
  Varicellovirus genus, 333
α-macroglobulin, 207, 259, 270
Alpha-methyl-acyl-CoA racemase deficiency, 156
α-N-acetylgalactosaminidase deficiency, 870
Alphanaphthathiourea (ANTU), pulmonary edema from, 727
Alpharetrovirus genus, 404
  avian leukemia virus (ALV), 404
  Rous sarcoma virus (RSV), 404
α-storage pool disease (gray platelet syndrome), 256
α-synuclein (α-syn), 195, 840–841
α-synucleinopathies. *See* Synucleinopathies
α-toxin of staphylococcal infection, 85
Alphavirus genus, 381–384
  eastern equine encephalitis (EEE), 382, 383f

Venezuelan equine encephalitis (VEE), 382, 384
western equine encephalitis (WEE), 382
Alport syndrome, 309, 901
ALS. *See* Amyotrophic lateral sclerosis (ALS)
Alveolar lipoproteinosis, 732
Alveolar macrophages, 278, 280f, 581–582, 720, 819f
Alveolar sacs, 528
Alveolar wall, 716f, 717
Alzheimer's disease
amyloid, 835, 836, 837, 837f
autophagy, 71
blood-brain barrier and, 689f
mitochondriopathy, 836
ultrastructural changes, 839–840
Amantin, 136
Amastigote, 532f, 534, 535, 535f, 536
Amdovirus genus, 352–353
Amelogenins, 303
American canine hepatozoonosis, 558
American trypanosomiasis, 534
Amianthoid fibers, 299
Amide analogues, 611
Amino acid transport storage diseases, 869–870
cystinosis, 869
maple urine disease, 870
tyrosinosis, 869–870
Aminoaciduria, 302–303, 870
Aminonicotinamide, 688
Aminonucleoside antibiotics, 135–136
Amiodarone, 610
Ammonia, as glial toxin, 688
Amoebas, 526t, 526–528, 527f
Acanthamoeba, 527–528
Entamoeba, 526–527, 527f
Naegleria, 527
Paramoeba, 528
Amoebiasis, 527
Amorphous apatite, 799
Amphetamine toxicity, 677
Amphisome, 69, 119
Amphophile compounds, cardiotoxicity of, 648
Amphotericin B, nephrotoxicity, 700, 705
Amylin, 834
Amyloid, 829–839
AA amyloid, 830–834
AL amyloid, 834
in Alzheimer's disease, 835, 836, 837f
angiopathy, 837–839, 838f
beta amyloid protein (βAP), 835–837
calcitonin-associated, 835
description, 829–830
fibrils, 828f, 829–830, 832f, 833f, 838f
gelsolin-associated, 835
glomerulopathy, 828f, 833f, 833–834, 900
glucagon-associated, 835
islet amyloid polypeptide (IAPP), 834
medin, 837, 839
plasma protein-derived, 835
of prion disease, 839
transthyretin-associated, 834–835
ultrastructural studies, 830t–831t
Amyloid fibrils, 828f, 829–830, 832f, 833f, 838f
Amyloid precursor proteins (APP), 81, 829
Amyloid stars, 837, 838f
Amyloidosis
cerebrovascular, 837
description, 829
hereditary fibrinogen, 834
immunoglobulin light-chain-induced, 834
secondary, 828f, 830–834
senile systemic, 834
Amylopectin granules, 526
Amylopectin vacuoles, coccidial, 549
Amylopectinosis, 868
Amyotrophic lateral sclerosis (ALS), 38, 92, 195, 409, 841
Anabolic steroids
hepatocyte effects, 613
skeletal muscle myopathy and, 652
Anaerobic shift to glycolysis, 63
Anandamide, 677
Anaphase, 744, 745
Anaphylactic degranulation, 222
Anaphylactoid purpura, 902
Anaplasia, characteristics of, 761, 763
Anaplasma, 451–453, 452t
A. marginale, 446f
Anchoring fibrils, 299, 307
Ancylostoma caninum, 600
Androgens, skeletal muscle myopathy and, 652
Anemia
aging of erythrocytes, 750
anaplasmosis, 451–453
Diamond-Blackfan, 816
microangiopathic hemolytic, 902
Anemone cells, 763
Aneuploid, 769
Angiogenesis, 223–225
from bone marrow stem cells, 223
extracellular regulators, 224
growth factors, 224–225
hypoxia stimulation of, 223–224
maturation of, 224
pathogenesis, 223–224
phases of development, 223, 223f
in repair of inflammation, 225
from surviving blood vessels, 223
terminating, 224–225
tumor, 778–780
capillaries, 778–779
cellular events driving, 779
factors acting on host endothelium, 779–780
inhibition, 780
interdependence of tumor cells and blood vessels, 779
mechanisms, 779
neoplastic blood vessels, 780, 781f
sprouting, 779
Angiopathy, amyloid, 837–839, 838f
Angiopoietin-like 4 (ANGPTL4), 777
Angiopoietins, 223, 224
Angiotensin, 708
Angiotensin II, 209, 708
Angiotensin II antagonists, nephrotoxicity, 708
Angiotensin-converting enzyme, 209
Angiotensin-converting enzyme inhibitors, nephrotoxicity, 708
Ankyrin, 94
Annexins, 143, 235
Annonacin, 669, 672
Annulate lamellae
description, 129
increase with colchicine, 89
neoplastic cells, 128f, 768
Anoxia. *See also* Ischemia
events in necrosis caused by, 50t
mitochondrial effects, 187
mitochondrial oxygen deficit, 11
Antagomirs, 131
Anthracycline antibiotics, cardiotoxicity of, 644f, 644–646, 645f
Anthrax, 496–497
Anti-apoptotic proteins, 785
Antichymotrypsin (ACT), 836
Antidiuretic hormone (ADH), 705
Antigen presentation, 272, 272f
Antigen-antibody complexes, immobilization by dendritic cells, 275
Antigen-presenting cells
brain, 277
cloacal bursa, 278–279, 281f
dendritic cells, 275
Langerhans' cells, 277
lung, 278, 280f
mucosal-associated lymphoid tissue, 278
skin, 277
spleen, 277–278
thymus, 279, 282f, 282–283
tonsils, 278

Antigen-retaining reticulum, 277
Antigen-transporting cells, 277
Antiglycosyl antibodies, 103
Anti-hypertensives, cardiotoxicity of, 650
Antimycotic drugs, 580
Antithrombin III, 206
Antitrypsin, 137, 138, 231
Anthracenedione, cardiotoxicity of, 644
ANTU (alphanaphthathiourea), pulmonary edema from, 727
Aortic body carcinoma, 779f, 786f
Apaf-1 (apoptosis protease-activating factor-1), 66
Apatite crystals, 798, 799, 799f
APC complex, 745
APCs. *See* Antigen-presenting cells
Aphthovirus genus, 397
  foot-and-mouth disease (FMD) virus, 397
Apical complex, babesia, 538
Apical membrane transporters, 704
Apicomplexa. *See* Hemosporidians
Apicoplast, 549
ApoE gene, 835
Apolipoprotein(a), 171
Apolipoprotein A-I, 835
Apolipoprotein A-II, 835
Apolipoprotein B (apoB), 169, 171, 173
Apolipoprotein E (apoE), 171
Apolipoprotein L-I, 534
Apoptosis. *See also* Programmed cell death
  anti-apoptotic proteins in cancer cells, 785
  autophagy role in, 71
  beta amyloid protein and, 836
  caspase-induced, 33
  Cryptosporidium parvum-induced, 558
  cytokine-induced, 47
  of endothelial cells, 547
  lesions of, 41
  of neurons, 667
  non-caspase-induced, 33
  protein-nitrosylation-initiated, 43
  radiation-induced, 188
  tumor necrosis factor-induced, 785
Apoptosis protease-activating factor-1 (Apaf-1), 66
Apoptosis signal-regulating kinase 1 (ASK1), 43
Apoptosis-inducing factor (AIF), 43
Apoptosomes, 42
Apoptotic bodies, 44
Apotransferrin, 817
Appresoria, 578
AQP4 (acquaporin-4), 687
Aquabirnavirus genus, 392–393
  infectious pancreatic necrosis (IPN), 392–393
Aquaporins, 80, 114, 143
Aquareovirus genus, 379
Arabinogalactan, 427
Arachidonic acid, 81
Arboviruses, 381
Arcanobacterium, 489t, 491
Archaea *(Archaebacteria),* 425
Arcobacter, 461
Arenaviridae family, 379–381
  Arenavirus genus, 379–381
  hemorrhagic fevers, 380–381
  lymphocytic choriomeningitis (LCM), 379–380
Arenavirus genus, 379–381
Argentine hemorrhagic fever, 380
Argosomes, 119
Armadillos, lepromatous placentitis in, 494
Aromatic halogenated hydrocarbons, hepatotoxicity of, 622–623
Arousal, 752
Arterial adventitia, 875
Arterial media, 875
Arteriopathy, 875–886
  arteriosclerosis, 877, 879
  atherosclerosis, 881, 883, 883f, 884f, 885–886, 886f
    calcification, 881, 883
    description, 881, 883, 883f
    embolization, 883
    experimental, 885
    macrophages in, 883, 885
    pathogenesis, 883
    xanthomatosis, 885
  calcification, 881, 882f, 883
  cerebral autosomal dominant, 879
  heritable, 879
  hyaline, 879
  responses to injury, 875–877
  vasculitides, 879–881
    focal arteriolar insudation, 879
    infectious arteritis, 874f, 879–881, 880f
    noninfectious systemic necrotizing, 881
Arteriosclerosis, 877, 879
  fibrous plaque, 879
  hyperplastic, 879
Arteritis, infectious, 874f, 879–881, 880f
Arteriviridae family, 384, 384t, 385f, 386
  Arterivirus genus, 384, 384t, 385f, 386
  equine arteritis virus (EAV), 384, 385f, 386
  lactate dehydrogenase-elevating (LDH) virus, 386
  porcine reproductive and respiratory syndrome (PRRS), 386
  simian hemorrhagic fever virus (SHV), 386
Arterivirus genus, 384, 384t, 385f, 386
Arthroconidia, 585, 590
Arthropod neurotoxins, 686
Arthrospore, 592
Aryloxyalkanoic acid, 611
Asbestos, pulmonary damage from, 733, 734f
Asbestos bodies, xviif, 733
Ascarids, eosinophils and, 245
Ascospore, 592
ASF (African swine fever), 353f, 353–354
Asfarviridae family, 352t, 353f, 353–354
  African swine fever (ASF), 353f, 353–354
Asialoglycoproteins (ASGPs), 113–114
ASK1 (apoptosis signal-regulating kinase 1), 43
ASM (acid sphingomyelinase), 860
Aspartate, 684
Aspartylglycosaminuria, 302, 863
Aspergillosis
  allergic, 581, 582
  avian, 582
  colonizing, 581
  invasive, 581
Asteroid bodies
  Candida infection, 583, 585
  intracellular collagen, 300
  Sporothrix, 589
Astrocytes
  antigen presentation, 277
  fibrillary, 687
  foot processes, 688, 690
  hepatic encephalopathy and, 191–192
  necrosis of, 672
  in prion diseases, 911, 913
  swelling, 687
Astrocytosis
  gemistocytic, 687
  reactive, 687
Astrogliosis, in scrapie, 912
Astroviridae family, 401
Atelectasis, 723
Ateline herpesvirus group, 337
Atheroma, 881
Atherosclerosis, 881, 883, 883f, 884f, 885–886, 886f
  calcification, 881, 883
  description, 881, 883, 883f
  embolization, 883
  experimental, 885
    birds, 886, 886f

dogs, 885
monkeys, 885
pigs, 886
rabbits, 885–886
rodents, 886
macrophages in, 883, 885
pathogenesis, 883
xanthomatosis, 885
Atherosclerotic plaques, 171
ATN. *See* Acute tubular necrosis (ATN)
ATP depletion, bleb formation and, 20
ATP synthase, 182, 185f
ATPase
Ca^{++}, 639
Ca-Mg, 646
H^{+}-K^{+}, 145
increase during injury, 80
mitochondrial complex, 182–183
Na-K, 80
Atransferrinemia, 817
Atrial granules, 635
Atrioventricular bundle, 640
Atrioventricular node, 640
Atrophic rhinitis, 457, 482
Atrophy
adaptive responses to persistent injury, 26, 28f, 29
basement membrane, 206
denervation, 29, 51–52
fat, 167, 168f, 169
gyrate, 192–193
multiple system, 840
muscle, 750
in programmed cell death, 49
prostate epithelium, 28f
of starvation and cachexia, 26, 29
thymic, 49, 53f
Attapulgite, 733
Auer bodies, 772
Autocrine growth stimulation, of cancer cells, 757
Autoimmune glomerulopathy, 901–902
drug hypersensitivities, 902
Goodpasture syndrome, 901
systemic lupus erythematosus, 901
Wegener's granulomatosis, 902
Autophagic inclusions, 849
Autophagic vacuolar myopathies, 71
Autophagic vacuoles, 26, 69, 70f, 837
Autophagocytosis, abnormal, 71
Autophagolysosome
description, 69
formation, 11
lipofuscin in, 823
lysosomal phospholipidosis, 610
neuronal lipofuscinoses and, 862
proliferation in neuronal injury, 669
proximal convoluted tubule, 701
Staphylococcus in, 498f
Autophagosome, 11, 69, 70f, 837
Autophagy
atrophy and, 26
autophagosomes, 11, 69, 70f, 837
change in aging, 750
in chronic ischemic myocardiocytes, 51
crinophagy, 11
description, 69
in development, 71
in disease, 70–71
microbial disease, 71
neuromuscular disease, 71
prion diseases, 912
toxic injury, 71
in embryogenesis, 49
functions of, 70
GAPDH and, 64
granulomatous inflammation, 273
hepatocyte, 12f
induction by methylphenylpyridine, 669
mitochondrial, 623, 625f
neuronal, 669
neuronal macroautophagy, 837
Autophagy gene *Atg7,* 669
Avermectin, 685
Aviadenovirus genus, 343
Avian aspergillosis, 582
Avian encephalomyelitis, 398f, 399, 798f
Avian influenza, 358
Avian leukemia virus (ALV), 404
Avian malaria, 548
Avian metapneumoviruses, 366
Avian pathogenic *Escherichia coli* (APEC), 472
Avian reoviruses, 376
Avian reticuloendotheliosis virus (ARV), 410
Avian spirochetosis, 506
Avian vacuolar myelinopathy, 682
Avibirnavirus genus, 393
infectious bursal disease (IBD), 393
picobirnaviruses (PBVs), 393
Avihepadnavirus genus, 355
duck hepatitis virus (DHV), 355
Avipoxvirus genus, 324, 326f
Avulavirus genus, 364
Axial zone, of arterioles, 233
Axl, 904, 906
Axon
demyelination, 678, 679f, 680f
membrane channels, 678
myelin sheath, 678
structure, 668
transport in, 681, 681f
Axonal reticulum, 683
Axonal swelling, 669
Axoneme, 528
Axonopathy
distal, 681–682
acrylamide, 681–682
cisplatin, 682
proximal, 681
Axoplasmic flow, 681, 681f
Axoplasmic transport, 681, 681f
Axostyles, 525, 526
Azidothymidine (AZT), skeletal muscle myopathy and, 652
Azurophil granules, 231, 232t, 237

B

B cells, 284, 404
Babesia, 538, 539f
B. bigemina, 538
B. equi, 538, 539f
B. microti, 538
B. rodhaini, 538
Babesiosis, 538
Babesiosoma, 543
Bacillales (order), 496–500, 497t
Bacillus genus, 496–497, 497t
Listeria, 496–497, 497t
Listeria genus, 497t, 497–498
Staphylococcus genus, 498, 498f, 499f, 500
Bacillary angiomatosis, 453
Bacillary bands, 598
Bacillary dysentery, 474
Bacillus, 496–497, 497t
B. anthracis, 463f
spore formation, 442
Bacteria. *See also* Bacterial cell structure; *specific bacterial diseases*
Actinomycetales (order), 487–496, 489t–490t
Actinomyces genus, 487, 488f, 489t, 491
Arcanobacterium genus, 489t, 491
Corynebacterium genus, 489t, 491
Dermatophilus genus, 490t, 495f, 496
Mycobacterium genus, 489t–490t, 491, 492f, 493–494
Nocardia genus, 490t, 494, 495f
Rhodococcus genus, 490t, 496
Tropheryma genus, 490t, 496
Aeromonadales (order), 466, 466t
Bacillales (order), 496–500, 497t
Bacillus genus, 496–497, 497t
Listeria, 496–497, 497t
Listeria genus, 497t, 497–498
Staphylococcus genus, 498, 498f, 499f, 500
bacteriophages of, 511f, 511–512

Bacteria (*cont'd*)
Bacteroidales (order), 509, 509t
Bacteroides genus, 509, 509t
Porphyromonas genus, 509, 509t
Tannerella genus, 509
Burkholderiales (order), 457–459, 459t
Bordetella genus, 457, 458f, 459t
Burkholderia genus, 457, 459, 459t
calcinogenic, 802, 802f
Campylobacteriales (order), 461–465, 462t
Arcobacter genus, 461
Campylobacter genus, 461, 462t, 463f, 464
Helicobacter genus, 462t, 464, 465f
Chlamydiales (order), 485–486, 486t
Chlamydia genus, 485–486, 486t, 487f
Chlamydophilia genus, 485–486, 486t
Clostridiales (order), 502–505, 503t
Clostridium genus, 502–503, 503t, 504f
Eubacterium genus, 503t, 504
Sarcina genus, 504
Veillonella, 503t, 504–505
collagen degradation by, 299
Enterobacteriales (order), 466–476, 467t–469t
Calymmatobacterium genus, 466
Escherichia genus, 466, 467t, 469, 470f, 471–473
Klebsiella genus, 467t, 473
Proteus genus, 468t, 473
Salmonella genus, 468t, 473–474
Shigella genus, 468t, 474–475
Yersinia genus, 469t, 475–476
Entomoplasmatales (order), 447
Flavobacteriales (order), 509t
Fusobacteriales (order), 510, 510t
Fusobacterium genus, 510, 510t
Streptobacillus genus, 510, 510t
giant cell formation, 23
Incertae Sedis (order), 447, 448t
Lactobacillales (order), 500–502, 501t
Streptococcus genus, 500–502, 501t
Legionellales (order), 476–477, 477t
Coxiella genus, 476, 477t
Legionella genus, 476–477, 477t
Mycoplasmatales (order), 442–447, 444t–445t
Eperythrozoon genus, 445t, 447
Hemobartonella genus, 445t, 446f, 447
Mycoplasma genus, 442–443, 444t
Ureaplasma genus, 444t, 445, 447
Myxococalles (order), 511t
Neisseriales (order), 459–461, 460t
Neisseria genus, 459–461, 460t
Nitrosomonadales (order), 511t
Pasteurellales (order), 477–482, 478t
Actinobacillus genus, 477–478, 478t
Aggregatibacter genus, 478t, 479
Haemophilus genus, 478t, 479f, 479–480
Mannheimia genus, 478t, 480, 480f
Pasteurella genus, 478t, 480, 481f, 482
phospholipases, 82
Pseudomonadales (order), 482–484, 483t
Moraxella genus, 482, 483t
Pseudomonas, 482–484, 483f, 483t
Rhizobiales (order), 453–456, 454t
Afipia genus, 453–454, 455f
Bartonella genus, 453, 454t
Brucella genus, 454t, 454–455, 457f
Rickettsiales (order), 448–453, 449t, 452t
Aegyptianella genus, 452t, 453
Anaplasma genus, 451–453, 452t
Ehrlichia genus, 451, 452t
Rickettsia genus, 448–451, 449t, 450f
Spirochaetales (order), 505–509, 506t
Borrelia genus, 505–506, 506f, 508
Brachyspira genus, 506t, 506–509
Leptospira genus, 505, 506t, 507f
Treponema genus, 506f, 508
Thiotricales (order), 484, 484t
Francisella, 484, 484t
Vibrionales (order), 484–485, 485t
Vibrio genus, 484–485, 485t
Bacterial cell structure, 425–442
adhesins, 434–435, 437t
capsules, 435–436
cell envelope, 425, 427–433, 428f, 429f
cell membrane, 429–430
cell wall, 430–433, 432f
chemoreceptors, 431, 433
membrane pumps, 431
outer membranes of gram-negative, 430–431
porins, 431
gram-negative, 427, 428f, 429f
gram-positive, 427, 428f, 429f
overview of components, 425, 427–429
cytoplasm, 436–441
inclusions and microcomponents, 438–439
iron inclusions, 439–440
mesosomes, 440, 440f
nucleoid, 440–441
protein enzymes and toxins, 436, 438
factors used by pathogenic bacteria to attach, infect, colonize, and cause disease in susceptible hosts, 426t–427t
fimbriae, 433–434
flagella, 435
size of cells, 425
spores, 442
virulence factors, 437t
Bacterial toxins, myonecrosis from, 655, 657f
Bacteriophage, 511f, 511–512
Bacteriophorous vacuoles, 71
Bacteroidales (order), 509, 509t
Bacteroides genus, 509, 509t
Porphyromonas genus, 509, 509t
Tannerella genus, 509
Bacteroides, 509, 509t
Bak, 42, 44, 66
Balantidium, 528–529
BALT (bronchus-associated lymphoid tissue), 278
Band 4.1 protein, 94
Barth syndrome, 195
Bartonella, 453, 454t
Basal body, 528
Basal lamina, 307. *See also* Basement membrane
Basal membranes, as recovery scaffolds, 54
Base excision repair (BER), 183
Basement membrane
collagen and proteoglycan relation to, 297f
components of, 307
in disease, 308–310
Alport syndrome, 309
epidermolysis bullosa, 309
immune complex trapping, 309–310, 310f, 311f
inflammation, 308–309
endothelial cell, 205–206, 206f
extracellular matrix glycoproteins, 308
glomerular, 891–892, 895f–897f, 899f, 901, 903–904, 904f
neoplasia and, 778f
thickening, 294f, 296f, 306f, 307, 311f
Basement membrane area (BMA), 205–206
Basement membrane length (BML), 206
Basolateral bile acid uptake proteins, 630
Basolateral invagination, 704
Basolateral transporter, 630

Basophil, 221f, 221–222, 222f
platelet activating factor and, 253
tumors and, 788
ultrastructure in tissue lesions, 219t
Batten's disease, 119
Bax, 42, 44, 66
Bcl-2 protein/gene, 42, 44, 65–66, 785
Bcl-xL, 42
Bedlington terriers, copper storage disease in, 823
Belt desmosome, 100
Bence-Jones proteins, 849
Benign neoplasms, 761
Benzodiazepines, 685
Bernard-Soulier syndrome, 256
Berne virus, 373
Besnoita, 558, 560
β*AAP* gene, 836
Beta amyloid precursor protein (βAPP), 835–837
Beta amyloid protein (βAP), 835–837, 839
Beta amyloid protein ion channels, 836
βAPP secretase, 835–837
β-adrenergic blocking agents, cardiotoxicity, 651
β,β-iminodipropionitril, 681
β-catenin, 780
Betaherpesvirinae subfamily, 330–335
Cytomegalovirus genus, 335, 338f
human herpesvirus 6 (HHV-6), 335
Roseolovirus genus, 335
β-listeriolysin, 498
β-N-methylamino-L-alanine (βMAA), 677
β-oxidation
of fatty acids, 181, 191, 195
inhibition by hepatotoxins, 625
Betaretrovirus genus, 404, 406
jaagsiekte sheep retrovirus (JSRV), 406
mouse mammary tumor virus (MMTV), 404, 405f, 406
β-thromboglobulin, 251
Bid, 43
Bile duct toxins, 630
Bilirubin
hyperbilirubinemia, congenital, 821–822
pigment deposits, 821–822, 822f
stones, 802
Bilirubin diglucuronide, 821
Bilirubinemia, 712
Bim (Bcl-2-interacting mediator of cell death), 44
Binding filaments, 237
Biofilms, 424f, 436
Bioprosthetic heart valves, 801
Biphenylylmethylvaleric acid, 611
Birds. *See also specific bird types*
atherosclerosis, 886, 886f
avian vacuolar myelinopathy, 682
bacterial diseases
avian pathogenic *Escherichia coli* (APEC), 472
fowl cholera, 482
spirochetosis, 506
calcium-sequestering bodies, 803, 805f
malaria, 548
viral diseases
adenovirus, 343
avian encephalomyelitis, 398f, 399
avian influenza, 358
avian leukemia virus (ALV), 404
avian metapneumoviruses, 366
avian reoviruses, 376
avian reticuloendotheliosis virus (ARV), 410
bluecomb, 373
chick anemia viruses, 356
duck hepatitis virus (DHV), 355
duck plague, 336f, 338
fowlpox, 324, 326f
infectious bronchitis virus (IBV), 373
infectious bursal disease (IBD), 393
Marek's disease virus, 333, 335
pigeon circovirus, 356
psittacine beak and feather, 356, 356f
reoviruses, 376
Rous sarcoma virus (RSV), 404
Birnaviridae family, 392–393, 393f, 393t
Aquabirnavirus genus, 392–393
infectious pancreatic necrosis (IPN), 392–393
Avibirnavirus genus, 393
infectious bursal disease (IBD), 393
picobirnaviruses (PBVs), 393
2,6-bis-(4-chlorophenyl)-4-pyridine carboxylic acid, microgranulomatosis and, 630
BK polyomavirus, 348
Black death, 475
Black piedra, 592
Blackhead, 537
BLAD, 242–243
Blastocystis hominis, 563–564
Blastomyces, 582f, 582–583
Blebbing, 19f, 20, 120–121
by bacterial cells, 431, 432f
endothelium, 211
programmed cell death, 46
Bleomycin, 728, 735, 735f
Blood vessels. *See* Angiogenesis; Vascular disease/injury
Blood-air barrier, 717
Blood-brain barrier (BBB), 217, 688, 689f, 690
Blood-retinal barrier, 217
Bloodstream, metastasis into, 782f, 782–783, 784f
Blood-testis barrier, 217
Bluecomb virus, 373
Blue-green algae, 575–576
Bluetongue virus, 377
B-lymphocyte stimulator (BLyS), 235
Bolivian hemorrhagic fever, 380
Bone demineralization, 704
Bone marrow
aplasia, human parvovirus, 350
iron utilization, 818
in malaria, 545
stem cells, angiogenesis from, 223
Border disease of sheep, 389
Bordetella, 457, 458f, 459t
Borna disease virus, 386
Bornaviridae family, 386
Borrelia, 505–506, 508
Bortezomib, 771
Botrocetin, 255
Botulinum toxin, 502, 684
Bovine brucellosis, 455
Bovine corona virus, 373
Bovine ephemeral fever, 368
Bovine herpesvirus 1, 331f
Bovine Marfan syndrome, 303
Bovine mastitis, *Prototheca* and, 573, 574f, 575
Bovine papilloma virus (BPV), 346–347
Bovine papular stomatitis, 324
Bovine respiratory disease complex, 480
Bovine rotaviruses, 378–379
Bovine spongiform encephalopathy (BSE), 913
Bovine syncytial virus, 415f
Bovine trypanosomiasis, 534
Bovine viral diarrhea (BVD) virus, 389
Brachyspira, 506t, 508–509
Bradyzoites, *Sarcocystis,* 555
Brain
antigen presentation, 277
apoptosis, 52
diseases
adenoviral infection, 341
cerebral malaria, 547–548
encephalitis
acute allergic encephalomyelitis, 680f
alphavirus, 381–384
California, 391–392
canine distemper virus, 362

Brain (*cont'd*)
eastern equine encephalitis (EEE), 382, 383f
encephalomyocarditis (EMC) viruses, 397
granulomatous amoebic, 528
herpes simplex virus, 332–333
Japanese B encephalitis virus, 388
postvaccinial, 323
Russian spring-summer encephalitis (RSSE) virus, 388
St. Louis encephalitis virus, 383f, 388
subacute sclerosing panencephalitis, 362
Venezuelan equine encephalitis (VEE), 382, 384
western equine encephalitis (WEE), 382
hepatic encephalopathy and, 191–192
HIV infection and, 412
hyperammonemia and, 192
meningitis, *Aspergillus,* 582
meningitis, *Haemophilus,* 479
meningitis-associated *Escherichia coli* (MNEC), 472
meningoencephalitis, *Listeria,* 498
meningoencephalitis, primary amoebic, 527
prion diseases, 911–915
rabies, 363f, 367–368
simian immunodeficiency virus and, 413
tumors from JC polyomavirus, 348
embryogenesis, 47, 49
intermediate filament disorders, 92
programmed cell death, 47, 48f, 49
Branchiitis, 737
Brazilian purpuric fever, 480
Breast cancer susceptibility protein (BRCA1), 64
Breda virus, 373, 374f
Brefeldin A, 141, 619
Broken back syndrome, 737
Bromethalin, 687
Bromoethyleneamine, renal papillary necrosis, 706
Bronchioles
respiratory, 719–720
terminal, 719, 726
Bronchus-associated lymphoid tissue (BALT), 278
Brown bowel syndrome, 824
Brown fat cells, 167
Brown recluse spider, 655
Brucella, 454t, 454–455, 457f
Brucellosis, 455
BSE. *See* Bovine spongiform encephalopathy (BSE)
Bullae, cytoplasmic, 19f, 20, 120
Bullous pemphigoid antigen, 100, 307, 309
Bundle-forming pili, 434, 469
Bunyaviridae family, 391t, 391–392
Hantavirus genus, 392
Nairovirus genus, 392
Crimean-Congo hemorrhagic fever, 392
Nairobi sheep disease, 392
Orthobunyavirus genus, 391–392
Akabane virus, 392
California encephalitis, 391–392
Phlebovirus genus, 392
Rift Valley fever (RVF), 392
Bupropion, 684
Burkholderia, 457, 459, 459t
Burkholderiales (order), 457–459, 459t
Bordetella genus, 457, 458f, 459t
Burkholderia genus, 457, 459, 459t
Burkitt's lymphoma, 337
Bursa of Fabricius, 278–279, 281f
Buschke-Ollendorf syndrome, 303
Bystander effect, 188

C

C1q, 52, 54
C3 receptors, 237
C4b-binding protein (C4Bb), 54
Ca^{++}-ATPase, 639
Cachexia, atrophy of, 26, 29
Cadherins, 80
Cadmium, nephrotoxicity, 704
CAG repeat, 841
Cajal body, 129, 135
Calcific band keratopathy (CBK), 801
Calcification, 797–809
arteriopathy, 881, 882f, 883
in atherosclerosis, 881, 883
bacterial ell, 432f
calcium deposition
apatite crystals, 798, 799, 799f
laminar, 798, 799, 799f
disorders
calcific band keratopathy (CBK), 801
calcifying tendonitis, 800
calcinogenic bacteria, 802, 802f
calcinogenic toxins, 801–802
diffuse pulmonary calcification, 800
diffuse vascular calcification, 800–801
hypercalcemia of cancer, 802
microliths, 802–803, 804f
dystrophic, 798
glomerular, 892
in hypervitaminosis D, 800, 881
intracellular, 797–798, 798f, 803f
metastatic, 798
mitochondrial, 39f, 39–40
pathologic, 800, 800f
in uremia, 801, 881
Calcification nodules, 800
Calcisomes, 9, 159–160, 797, 798f
Calcitonin, 835
Calcium (Ca^{++}). *See also* Calcification
altered permeability in cell death, 35
glutamate effect on, 685
homeostasis
presenilins and, 836
regulation by mitochondria, 181
homeostatic mechanisms, 797
active extrusion, 797
passive influx, 797
intracellular effects, 35
membrane repair, 61
in mitochondrial oxidative stress, 186
resorption by osteoclasts, 803, 806f, 806–807
retention defects, 160
retention in sarcoplasmic reticulum, 160–161
in secretion, 143–144
vitamin D toxicity, 711
Calcium channel blockers, 160, 650–651
Calcium channels, 35, 46, 639, 797
Calcium induced calcium release (CICR), 639
Calcium overload, 50, 836
Calcium oxalate crystals, 710f, 710–711
Calcium paradox, 50
Calcium pumps, 35, 700, 797–798
Calcium repletion, 50
Calcium-binding proteins, 35, 797–798
Calcium-sequestering bodies, in birds, 803, 805f
Calcium-sequestering granules, mitochondrial, 183
Calcosphere, 729, 803
Calf-diphtheria, 510
Caliciviridae family, 399, 401, 401t
Hepevirus genus, 399, 401
hepatitis E virus (HEV), 399, 401
Lagovirus genus, 399
Norovirus genus, 399
Norwalk virus, 399
Sapovirus genus, 399
Vesivirus genus, 399
feline calicivirus (FCV), 399
swine vesicular disease, 399
California encephalitis, 391–392
Calmodulin, 35, 143, 798

Calnexin, 797
Calpains, 61, 69, 186, 797–798, 840
Calpastatin, 186, 798
Calprotectin, 239
Calreticulin, 797
Calsequestrin, 160–161, 639, 798
CALT (conjunctiva-associated lymphoid tissue), 278
Calymmatobacterium, 466
Ca-Mg ATPase, 646
CAMP-specific phosphodiesterase, 243
Campylobacter, 461, 462t, 463f, 464
Campylobacteriales (order), 461–465, 462t
  Arcobacter genus, 461
  Campylobacter genus, 461, 462t, 463f, 464
  Helicobacter genus, 462t, 464, 465f
Canalicular transporters, 630
Canaliculus, intracytoplasmic, 763, 764f
Cancer. *See also* Neoplastic cells; *specific forms of neoplasia*
  anti-apoptotic proteins in cancer cells, 785
  autocrine growth stimulation of cancer cells, 757
  hypercalcemia of, 802
  membranous glomerulonephritis and, 897
  tumor
    angiogenesis, 778–780, 779f, 781f
    basement membrane material, 777, 778f, 781f
    benign, 761
    collagen, 777–778, 781f
    embolus, 783, 784f
    fibroplasia, 778
    growth, 757–758
    malignant, 761
    microenvironment, 775–780
Candida, 583, 584f, 585
Candidiasis, 583, 585
Canine adenoviruses 1 (CAV-1), 340–341, 343
Canine adenoviruses 2 (CAV-2), 340
Canine cyclic hematopoiesis (gray collie syndrome), 242
Canine distemper virus (CDV), 362, 363f
Canine fucosidosis, 863
Canine granulocytic ehrlichiosis, 451
Canine parvovirus, 350
Canine rotavirus, 378
Canine visceral leishmaniasis, 535
Cannabinoid receptor, 677
Cap, 5′, 131
Capillary
  basement membrane, 205–206, 206f
  endothelium, myocardial injury and, 640
  fenestrae, 204, 205, 695
  recanalization, 260
  structure, 204–205
  tumor angiogenesis, 778–779
Capping, lymphocyte, 287, 286f, 289f
Caprine encephalitis virus, 414
Capripoxvirus genus, 324
Capsules. *See also specific bacterial genera or species*
  Bacillus anthracis, 497
  description, 427, 435–436
  Mycobacterium, 491
  Streptococcus, 500
  in trichinosis, 598
CAR bacillus, 510
Carbamates, skeletal muscle toxicity of, 654
Carbon monoxide (CO) toxicity, 731
Carbon tetrachloride (CCl_4) toxicity
  acute cell swelling, 8f, 10f
  carbon-directed free radical injury, 186
  coagulation necrosis, 32f
  hepatotoxicity, 620–621, 621f
  mitochondrial degeneration, 180f
  SER degeneration, 157
  smooth endoplasmic reticulum toxicity, 620–621, 621f
  vacuolation, 6f, 8f
Carbon-directed free radical injury, 186
Carcinoma
  aortic body, 779f, 786f
  carcinoma in situ, 761
  clear-cell, 756f, 777f
  frog renal, 338
  gastric, 802
  genital carcinoma, human papilloma virus (HPV), 346
  hepatocellular, 355
  Hürthle cell follicular, 777f
  mammary gland adenocarcinoma, 779f
  nasopharyngeal, 337
  pancreatic, 772
  release of collagen IV by, 777–778
  squamous cell, 346, 759f, 778f
Cardiac conduction system, 639–640, 751
Cardiac failure, 208, 208f
Cardiac hypertrophy, 640–641
Cardiac myofilaments, 635
Cardiolipin, 43, 195
Cardiomyocytes, hypoxia and, 66
Cardiomyopathy, from paraquat, 734
Cardiotoxicity, 635–651
  normal myocardium, 635–641
  responses to toxic injury, 641, 643
  toxins, 643–651
    amphophile compounds, 648
    anthracycline antibiotics, 644f, 644–646, 645f
    anti-hypertensives, 650
    calcium channel blockers, 650–651
    catecholamines, 650
    chloroquine, 648
    cocaine, 651
    coffee senna, 651
    doxorubicin, 644f, 644–646, 645f, 647f, 648f
    ethanol, 651
    furazolidone, 651
    imatinib, 646, 649f
    ionophores, 648–649
    isoproterenol, 650
    monensin, 648–649
    pyrrolizidine alkaloids, 651
    reserpine, 634f, 650
    simvastatin, 649f
    table of toxins, 642t
    trastuzumab, 646, 648
    tyrosine kinase inhibitors, 646, 648
    verapamil, 650–651
Cardiovirus genus, 397
  encephalomyocarditis (EMC) viruses, 397
  murine polioencephalomyelitis virus (Theiler's virus), 396f, 397
Carnitine, 154
Carnitine system, 191
Carnitine transporter, 154
Caryospora, 560
Caseous lymphadenitis, 491
Caspase-independent cell death (CICD), 64
Caspases
  apoptosis induction, 33
  cascade, 41
  caspase 8 activation, 46
  executioner, 41
  initiator, 41
  lysosomal executioner, 47
  in neoplastic cells, 785
  in programmed cell death, 41, 42, 46, 47
Castration, effect on life span, 752
Cat scratch fever, 453–454, 455f
Catalase
  peroxisome, 611
  in peroxisomes, 153, 154
Catecholamines
  cardiotoxicity of, 650
  Na-K-ATPase increase and, 80
Cathepsin D, 47
Cationic amphiphilic drugs, 610, 735–736

Cats
albino, 813
mucopolysaccharidoses, 866
Siamese cat pigmentation, 814
viral diseases
feline calicivirus (FCV), 399
feline immunodeficiency virus (FIV), 410
feline infectious peritonitis (FIP), 373
feline leukemia virus (FeLV), 406–407, 408f
feline panleukopenia virus, 350, 351f
Cattle
bacterial diseases
Anaplasma, 451
anthrax, 496–497
bovine respiratory disease complex, 480
brucellosis, 455
cutaneous dermatophilosis, 496
Eperythrozoon, 445t, 447
epizootic bovine abortion, 511
Fusobacterium, 510
heartwater, 451
hemorrhagic septicemia, 482
Johne's disease, 494
lumpy jaw, 487
Pasteurella, 482
pinkeye, 482
pyelonephritis, 491
shipping fever, 480
bovine Marfan syndrome, 303
bovine spongiform encephalopathy (BSE), 913
bovine trypanosomiasis, 534
protothecosis, 573, 574f, 575
viral diseases
bovine corona virus, 373
bovine ephemeral fever, 368
bovine herpesvirus 1, 331f
bovine papilloma virus (BPV), 346–347
bovine papular stomatitis, 324
bovine rotaviruses, 378–379
bovine syncytial virus, 415f
bovine viral diarrhea (BVD) virus, 389
Breda virus, 373, 374f
foot-and-mouth disease (FMD) virus, 397
infectious bovine rhinotracheitis, 334f
malignant catarrhal fever (MCF), 338
pseudocowpox, 324
Rift Valley fever (RVF), 392
vesicular stomatitis virus (VSV), 367, 367f
Caveolae
in adipocytes, 78
description, 109, 111f, 111–112
endothelial transport, 201–202
gentamicin nephrotoxicity and, 702
Leishmania, 535
lipoprotein metabolism, 171
Caveolins, 111, 652, 702
CBK (calcific band keratopathy), 801
CC chemokines, 270
CD4, 410–411
CD11/CD18 family receptors, 270
CD14, 270
CD16, 270
CD31, 216
CD32, 270
CD44, 224
CD64, 270
Cdc2 protein kinase, 745
Cdk2 module, 745
Cdk8 module, 745
Cdks (cyclin-dependent kinases), 744–745
Cell adhesion molecules (CAMs), 96
Cell cycle
cyclins and Cdks, 744–745
description, 743
G_1 phase, 743
G_2 phase, 744
M phase, 744
model, 742f
S phase, 743–744
Cell death, 33–59
description, 33, 35
endothelial cells, 54, 55f, 56
necrosis, 35–40
chromatin aggregation, 40
coagulation, 32f
cytoskeleton depolymerization, 35, 36
endoplasmic reticulum and Golgi complex contraction, 40
ischemia and, 49–51, 50t
lytic, 33, 34f, 36, 37f
mitochondriopathy, 35, 36, 38–40
nuclear changes, 40
plasma membrane leakage, 35–36
programmed cell death, relationship to, 33, 49–52
ribosomal changes, 40
neoplastic cells, 785–789
basophils and mast cells, 788
killer dendritic cells, 787
lymphocyte killing of neoplastic cells, 787
monocytes/macrophages, 787, 787f
natural killer cells, 787
neutrophils, 788
platelet activation and aggregation, 788–789
programmed cell death, 785, 787
programmed cell death, 40–52
in acute cell injury, 49
in atrophy, 49, 51–52
caspases, role of, 41
cytoskeleton degradation, 44, 46
denervation atrophy and, 51–52
description, 40–41
in embryogenesis, 47, 49
endoplasmic reticulum, 46
examples, 41f, 45f, 48f
extrinsic pathways, 46–47
ischemia and, 49–51, 50t
in metamorphosis, 49
mitochondriopathy, 35, 42–43
necrosis, relationship to, 33, 49–52
nuclear changes, 44
removal of dead cell, 52–54
cytophagocytosis, 53f, 54
macrophage phagocytosis of cell debris, 54
phagocytosis, 52, 52f, 53f, 54
Cell envelope, bacterial, 425, 427–433, 428f, 429f
cell membrane, 429–430
cell wall, 430–433, 432f
chemoreceptors, 431, 433
membrane pumps, 431
outer membranes of gram-negative, 430–431
porins, 431
gram-negative, 427, 428f, 429f
gram-positive, 427, 428f, 429f
overview of components, 425, 427–429
Cell junctions. *See* Intercellular junctions
Cell membrane. *See* Plasma membrane
Cell senescence. *See* Senescence
Cell signaling pathways, in neoplastic cells, 767
Cell surface
cytoskeleton, 86–97
deformation in necrosis, 36
intercellular junctions, 97–101
pitting, 15
plasma membrane, 77–86
surface structures, 101–103
cilia, 101
filopodia, 102f, 103
lamellipodia, 103
microvilli, 101, 103
Cell surface death receptors, 46
Cell swelling. *See* Acute cell swelling
Cell wall, 430–433, 432f
chemoreceptors, 431, 433
chlamydial, 485

description, 427
fungal, 578, 580
membrane pumps, 431
mycobacterial, 491
outer membranes of gram-negative, 430–431
porins, 431
Cell-cell adhesion, transmembrane proteins and, 79
Cell-to-cell contact. *See also* Intercellular junctions
desmosomes, 17
disruption in acute cell swelling, 17
gap junction, 17
hemidesmosomes, 17
tight junction, 17
Cell-to-cell fusion, multinucleate giant cells formation by, 23, 26
Cellular defense and recovery
autophagy, 69–71, 70f
mitochondria, 63–64
nucleus, DNA, and genome, 64–67, 65f
plasma membrane, 61–62
proteostasis, 67–69, 68f
smooth endoplasmic reticulum and peroxisomes, 62f, 62–63
Cellular injury, response to, 5–31
acute cell swelling, 5–20
cell-to-cell contact disruption, 17
cytoplasmic edema, 7
cytoplasmic shedding by exocytosis, 18–20
cytoskeleton, disassembly of, 17–18
defined, 5
dilatation of cytocavitary network cisternae, 4f, 5
fragmentation of cytocavitary network membranes, 5, 6f, 7
glycogen-lipid droplet ratio reversal, 9
Golgi complex vesiculation, 9
lysosome activation and autophagosome formation, 11
mitochondrial swelling, 9, 11
nucleus in, 13, 14f, 15
pericellular environment, 20
peroxisome duplication, 11, 13
plasma membrane in, 15, 16f, 17
smooth endoplasmic reticulum proliferation and aggregation, 9
surface structure, 18, 19f
adaptive responses to persistent injury, 21–29
atrophy, 26, 28f, 29
cytomegaly, 23, 25f, 27f
hypertrophy, 21f, 21–23, 22f, 24f
metaplasia, 26
multinucleate giant cells, 23, 26
Cellular trafficking. *See* Intracellular trafficking
Cellulosome, 439
CEMMs (cholesterol-enriched membrane microdomains), 111
Centrioles, 88, 746
Centrolobular hepatocyte, 607
Centromere, 130, 745–746
Centromere-specific histone H3 variant (CenH3), 130
Centrosome, 88, 746
Cephalic tetanus, 686
Cephaloridine, 702
Ceramic implants, calcium phosphate, 801
Ceramide, 47, 77, 785
Cerebellar hypoplasia, feline panleukopenia virus, 350
Cerebral autosomal dominant arteriopathy, 879
Cerebral malaria, 547–548
Cerebrohepatorenal syndrome of Zellweger, 155
Cerebrovascular amyloidosis, 837
Ceroid, 823
Ceroid lipofuscinoses, 823
Cervical cancer, human papilloma virus (HPV), 346
CF transmembrane conductance regulator (CFTR), 86
CFA/I and CFA/II, 469
CFA/I fimbriae, 434
C-FLIP (cellular FLICE-like inhibitory protein), 785
Chagas disease, 534
Chanarin-Dorfman syndrome, 860–861
Chancroid, 480
Chaperone, 67, 138, 842
Chaperone-usher pathway fimbrial family, 433
Charcot-Leyden crystals, 245
Charcot-Marie-Tooth disease, 695
Checkpoint kinase 1 (Cpk-1), 743
Checkpoint kinase 2 (Cpk-2), 743, 744
Checkpoints, 743–745
Chédiak-Higashi syndrome (CHS), 241, 245, 256–257, 814
Chemoattractant receptors, 235
Chemoattractants for endothelial cells, 224
Chemokinesis, 233
Chemoreceptors, 431, 433
Chemotaxis
eosinophil, 245
neutrophil, 233–235
complement and, 234–235
cytokines, 235
cytoskeleton and, 233
leukotrienes, 234, 235
Chick anemia viruses, 356
Chickenpox, 333
Chickens
bacterial diseases
Aegyptianella, 453
Erysipelothrix, 447
viral diseases
avian leukemia virus (ALV), 404
fowlpox, 324
infectious bronchitis virus (IBV), 373
infectious bursal disease (IBD), 393
Marek's disease virus, 333, 335
Rous sarcoma virus (RSV), 404
Chimpanzee
human parainfluenza viruses, 360
kuru, 914, 914f
Chk1, 743
Chk1 inhibitors, 743
Chlamydia, 485–486, 486t, 487f
Chlamydiae, 485–496
Chlamydial inclusion, 485
Chlamydiales (order), 485–486, 486t
Chlamydia genus, 485–486, 486t, 487f
Chlamydophilia genus, 485–486, 486t
Chlamydophila, 485–486, 486t
Chlorcyclizine, 611
Chloride cells, 736
Chloride channels
cystic fibrosis and, 86
endocytosis impairment and, 114
GABA-gated, 685
Chloroquine toxicity, 610, 648, 672, 862, 862f
Chlorpromazine, 630
Cholera, 484
Cholestasis
bile duct toxins, 630
extrahepatic, 630
intrahepatic, 630
Cholesterol
atherosclerosis and, 881, 883, 886
membrane, 77
metabolism in peroxisomes, 154, 611
microliths, 802
receptor-mediated endocytosis, 171
redistribution of membrane, 141
Cholesterol ester storage disease, 173
Cholesterol-enriched membrane microdomains (CEMMs), 111
Choline acetyltransferase (ChAT), 684
Cholinergic neurons, 684
Chondrocyte calcification, 800f
Chondrodysgenesis, 302f

Chondrodysplasia, 307
Chondroitin sulfates, 304
Chondroma, 761
Chordopoxivirinae subfamily, 323–327
  Avipoxvirus genus, 324, 326f
  Capripoxvirus genus, 324
  fowlpox, 324, 326f
  Lepropoxvirus genus, 324, 327
  Molluscipoxvirus genus, 327
  mousepox, 323
  orf virus, 324, 325f
  Orthopoxvirus genus, 323
  Parapoxvirus genus, 324, 325f
  pseudocowpox, 324
  rabbitpox, 324, 327
  sheeppox, 324
  Suipoxvirus genus, 327, 327f
  swinepox, 327, 327f
  vaccinia virus, 323
  Yatapoxvirus genus, 327
Chorioretinitis, *Toxoplasma gondii,* 555
Chromatin. *See also* Chromosomes
  aggregation in programmed cell death, 44
  clamping in necrosis, 40
  clumping, 13
  condensation, 44
  condensed fibers, 130
  DNA methylation, 758, 761
  neoplastic cells, 768–769
  nucleolar, 768
  perichromatin granules, 768
  peripheralization, 15
  structure, 129–130
Chromatophores, 815, 815f
Chromoblastomycosis, 589
Chromosomal passenger complex, 66
Chromosome territories, 129
Chromosomes
  centromere, 130
  metaphase, 132f
  of neoplastic cells, 769
  spreads of bacterial, 441f
  telomeres, 130
Chronic granulomatous disease, 242
Chronic interstitial nephritis, 895f
Chronic obstructive lung disease (COPD), *Moraxella* and, 482
Chronic wasting disease (CWD), 913–914
Chrysosporium tropicum, 593f
CHS (Chédiak-Higashi syndrome), 241, 245, 256–257, 814
Chylomicron remnants, 170
Chylomicron retention disease, 173
Chylomicronemia, 170
Chylomicrons, 170
Chytridiomycosis, 593–594
CICD (caspase-independent cell death), 64
CICR (calcium induced calcium release), 639
Cigarette smoke, pulmonary damage from, 729, 731
Cilia
  damage to pulmonary, 726
  deciliation, 18
  description, 101
  immotile cilia syndrome, 89, 89f, 101
  motile, 101
  neoplastic cells, 766
  primary, 101
  protozoal cell, 526
Cilia-associated respiratory (CAR) bacillus, 510
Ciliary aplasia, 101
Ciliary beat frequency (CBF), 726
Ciliates, 528f, 528–529, 529f
  Balantidium, 528–529
  Ichthyophthirius, 529
Circoviridae family, 355–356, 356f
Circulatory failure, hypoxia and edema of, 208, 208f
Circumsporite protein, 543
Cirrhosis, 621, 901
Cis face, Golgi complex, 139–140
cis-diamminedichloroplatinum, 704–705
Cisplatin, 682
Cisplatin sensory neuropathy, 682
Citrobacter freundii, 463f
Citrullinemia, 192
CJD. *See* Creutzfeldt-Jakob disease (CJD)
c-Jun NH(2)-terminal kinase (JNK1), 43
c-Jun N-terminal kinase (JNK), 66
c-Jun/AP-1, 66
Clara cells, 720, 726
Classical swine fever. *See* Hog cholera
Clathrin-coated vesicles, 140, 171
Clathrin-mediated endocytosis, 109, 112f, 112–113
Clear-cell carcinoma, 756f, 775, 777f
CLIBs (concentric lamellar inclusion bodies), 610
Cloacal bursa of birds, 278–279, 281f
CLOCK protein, 751
Clofibrate, 611
Clostridiales (order), 502–505, 503t
  Clostridium genus, 502–503, 503t, 504f
  Eubacterium genus, 503t, 504
  Sarcina genus, 504
  Veillonella, 503t, 504–505
Clostridium
  C. botulinum, 90, 502
  C. difficile, 502
  C. novyi, 655
  C. perfringens, 82, 90, 502, 655
  C. septicum, 82f
  C. tetani, 502, 686
  myonecrosis, 502
  pseudomembranous colitis, 502
  tetanus, 502–503
  Tyzzer's disease, 503, 504f
CLP (common lymphoid progenitor), 283
CMP (common myeloid progenitor), 283
CMV. *See* Cytomegalovirus (CMV); *Cytomegalovirus* (CMV)
Coagulation, 257–260, 259t, 783
Coagulation factors, 207, 224, 259
Coagulation necrosis, 32f
Coat proteins, 139
Coatamer proteins (COP), 140
Coated pits, 171, 203
Coated vesicles, 112, 112f
Cobalt toxicity, 651
Cocaine, 651, 677
Coccidia, 546f, 549–560, 550f, 551t–552t, 553f, 554f, 556f, 557t, 559f
  Besnoita, 558, 560
  Cryptosporidium, 555, 557t, 558, 559f
  Cyclospora, 550, 552
  Eimeria, 546f, 549–550
  Goussia, 558
  Hammondia, 555
  Hepatozoon, 558
  invasion of intestinal epithelial cells, 550f
  Isospora, 550
  life cycle, 550f
  Neospora, 555
  Sarcocystis, 555, 556f, 557t
  Toxoplasma, 524f, 552–555, 553f, 554f
Coccidioidomycosis, 585
Coccidioides immitis, 585
Coenocytic spherules, 585
Coffee senna toxicity, 651
Cohesiveness, loss in malignant cells, 763
Coiled body, 135
Coilin, 135
Coiling phagocytosis, 477, 505
Colchicine
  exocytotic constipation, 119
  hepatotoxicity, 626, 627
  as microtubule poison, 89, 142
  skeletal muscle degeneration, 653
Collagen
  amianthoid fibers, 299
  in basement membranes, 307
  diseases
    Alport syndrome, 309
    aminoaciduria, 302–303
    chondrodysgenesis, 302

dermatosparaxis, 300, 302f
Ehlers-Danlos syndrome, 300–301
lathyrism, 299
progeria, 301–302
scleroderma, 301
scurvy, 303
steps in defective collagen fiber formation, 301t
fibrils, 297–298
long spacing fibers, 299
platelet aggregation, 251, 253
relation to basement membrane, 297f
Collagen fibers
deposition of calcium, 800
produced by neoplastic cells, 777–778
Collagen receptors, platelet, 248
Collagenase, 299
Colon, Na-K-ATPases of, 80
Colorado tick fever (CTF), 379
Colorectal tumors, staining for secretory components, 772
Colostrum, neutrophils in, 243
Coltivirus genus, 379
Colorado tick fever (CTF), 379
Combined lipase deficiency, 173–174
Common lymphoid progenitor (CLP), 283
Common myeloid progenitor (CMP), 283
Complement
attack sequence, 83, 85f
endothelium damage by, 215
fragment C5a, 215
in hyalin droplet inclusions, 844
neutrophil chemotaxis, 234–235
phagocytosis and, 116
Complement receptor type 2 (CR2), 337
Complex I inhibitors, 186
Concentric lamellar arrangements, 11
Concentric lamellar inclusion bodies (CLIBs), 610
Condyloma accuminatum, 346
Confronting cisternae, 772
Congenital disorders
afibrinogenemia, 254
atransferrinemia, 817
bleeding syndromes, 257
cardiolipid, 195
congenital total lipodystrophy, 155
contractural arachnodactyly, 303
ichthyosis, 92
mitochondrial mutations, 193
peroxisomal, 154–156
Conidia, 580, 585, 590
Conidiophores, 580
Conidium, 549
Conjugation of peptides, 125
Conjunctiva-associated lymphoid tissue (CALT), 278
Connective tissue
ground substance, 304–307, 305f, 306f
invasion by neoplastic cells, 780–782
Connexons, 17, 97–98
Conoid, 525, 550, 552, 554f
Construction furrows, 448
Contact depigmentation, 812
Contagious ecthyma, 324, 325f
Contractile vacuole, 528
COP (coatamer proteins), 140
COP9 signalosomes, 68
Copper, gill toxicity and, 737
Copper-containing pigments, 822–824
ceroid, 823
lipofuscin, 823–824, 824f
neuromelanin, 823–824
Coproporphyrin, 821
Corneal fibrosis, 295
Corneal mucopolysaccharidoses, 864–865
Corneocyte, 311
Cornified envelope, 311–312
Coronaviridae family, 370–373, 371t, 372f
Coronavirus genus, 370–373
bluecomb virus, 373
bovine corona virus, 373
feline infectious peritonitis (FIP), 373
hemagglutinating encephalomyelitis virus (HEV), 373
infectious bronchitis virus (IBV), 373
murine hepatitis virus (MHV), 370–372
severe acute respiratory syndrome (SARS), 370
sialodacryoadenitis virus, 372
transmissible gastroenteritis (TGE) virus, 372f, 372–373
Torovirus genus, 373, 374f
Coronavirus genus, 370–373
bluecomb virus, 373
bovine corona virus, 373
feline infectious peritonitis (FIP), 373
hemagglutinating encephalomyelitis virus (HEV), 373
infectious bronchitis virus (IBV), 373
murine hepatitis virus (MHV), 370–372
severe acute respiratory syndrome (SARS), 370
sialodacryoadenitis virus, 372
transmissible gastroenteritis (TGE) virus, 372f, 372–373
Coronin, 537
Corpora amylacea, 805f
Corticobasal degeneration, 839
Corticosteroids
effect on fetal lung, 723
glycogen overload and, 163
glycosaminoglycan accumulation in ground substance, 304
Corticosterone, smooth endoplasmic reticulum effects on, 620
Cortisol
hepatotoxicity and, 623
mitochondrial effects of, 623
smooth endoplasmic reticulum effects on, 620
Corynebacterium, 489t, 491
C. pseudotuberculosis toxin, 83f
Costa, 526
Councilman body, 388
Coxiella, 476, 477t
Coxsackieviruses, 394
Creutzfeldt-Jakob disease (CJD), 839, 914–915
variant (vCJD), 915
Crimean-Congo hemorrhagic fever, 392
Crinophagy, 11, 144, 772, 773f
CRISP-3 (cysteine-rich secretory protein 3), 243
Cristae, mitochondrial, 182f, 182–183
Cristolysis, 184, 185f
Crithidial flagellate form, 529, 532f
Crm1, 66
Crohn's disease, 494
Cryoelectron microscopy, xvi
Cryoglobulinemia, 849
Cryopyrin, 116
Cryptococcosis, 585, 586f
Cryptococcus neoformans, 585, 586f
Cryptosporidiosis, 558, 559f
Cryptosporidium, 555, 557t, 558, 559f
Crystal nephropathy, 710–711
calcium and vitamin D toxicity, 711
melamine nephrosis, 711
oxalate nephropathy, 710f, 710–711
sulfonamide nephrosis, 711
tyrosine crystals, 710, 710f
Crystalline protein inclusions, 439
Crystalline protein-lattice inclusions, 848
Crystalloid endoplasmic reticulum, 62
Crystals, apatite, 798, 799, 799f
CS1 fimbrial family, 434
Cubilin, 171
CURL (compartment of uncoupling of receptor and ligand), 113
Curli fimbriae, 434, 469

Curvilinear membranes, of Farber's disease, 857
Cutaneous anthrax, 496
Cutaneous dermatophilosis, 496
Cutaneous fibrosis, 295
Cutaneous leishmaniasis, 536
Cutaneous mastocytosis, 222, 222f
Cutaneous permeability barrier, 311–312
Cutaneous pythiosis, 575
CuZn superoxide dismutase, 841
CWD (chronic wasting disease), 913–914
CXC chemokine, 270
Cyanamide, smooth endoplasmic reticulum toxicity of, 620, 621f
Cyanate, myelinopathy from, 682
Cyanobacteria, cytoskeletal toxins of, 627
Cycasin, 677
Cyclic AMP (cAMP), 131–132
Cyclic hematopoiesis, 242, 814
Cyclin destruction, 745
Cyclin-dependent kinases (Cdks), 744–745
Cyclins, 744–745
Cycloheximide, 136–137
  hepatotoxicity, 619, 626
  ribosomal toxin, 619
Cyclophilin D, 40, 182
Cyclophosphamide, 135, 697
Cyclospora, 550, 552
Cyclosporine
  cytophilin as target of, 672
  inhibition of procaspase 8 release, 42
  nephrotoxicity, 702, 702f
  vascular toxicity, 659
Cylindrical confronting cisternae, 411
Cynomolgus polyoma virus, 348
Cyst
  Giardia, 536
  Nosema, 561
  Sarcocystis, 555
Cysteine-rich secretory protein 3 (CRISP-3), 243
Cystic fibrosis, 86, 459
Cystinosis, 869
Cytauxzoon, 541, 543
Cytocavitary network
  cisternae, dilatation of, 5
  membranes, fragmentation of, 5, 6f, 7
Cytochalasins, 23, 90, 274, 627
Cytochrome C oxidase, 39, 185f
Cytochrome P450s (CYP), 619–620
Cytokeratin, 849–850
Cytokine receptors, multivesicular bodies and, 120
Cytokines
  activation of endothelium, 214–215
  apoptosis induction, 47
  neoplastic cells, 775, 777
  neutrophil chemotaxis, 235
Cytokinesis, 274
Cytolysins, of *Listeria,* 498
Cytomegalic inclusion disease, 335
Cytomegalovirus (CMV)
  cytomegaly, 23
  description, 335
  human, 335
  pig, 338f
Cytomegaly
  adaptive responses to persistent injury, 23, 25f, 27f
  adenoviral, 27f, 340, 342f
  defined, 23
  hepatocyte, 627
  multinucleate giant spermatid, 25f
Cytonecrosis, 33. *See also* Necrosis
Cytophagocytosis, 53f, 54
Cytophilin D, 672
Cytoplasm
  bacterial cell, 436–441
    inclusions and microcomponents, 438–439
    iron inclusions, 439–440
    mesosomes, 440, 440f
    nucleoid, 440–441
    protein enzymes and toxins, 436, 438
  description, xv
  of inflamed endothelial cells, 211
  neoplastic cells, 769–775
Cytoplasmic blebs, 20, 120–121
  protozoal cell, 525
  renal proximal tubular cell, 701, 701f
Cytoplasmic clefts, 547
Cytoplasmic edema, 7
Cytoplasmic granules, 573. *See also* Granules; Inclusions
Cytoplasmic inclusion, viral. *See specific viruses*
Cytoplasmic knobs, 547
Cytoplasmic lakes, 5, 7
Cytoplasmic lipid inclusions, 165–166
Cytoplasmic membrane. *See* Plasma membrane
Cytoplasmic pallor, 7
Cytoplasmic proteolysis, 7
Cytoplasmic shedding, 18–20, 120–121
Cytoplasmic transport system, 109. *See also* Intracellular trafficking
Cytoplasmic vacuoles, 7. *See also* Vacuoles
Cytoplasmic vesiculation, 5
Cytoproct, 528
Cytoprotective enzymes, mitochondrial, 64
Cytopyge, 528
Cytoskeleton, 86–97
  activation in inflammation, 214
  in acute cell swelling, 15
  cytoplasmic blebbing, 20
  damage from cadmium, 704
  degradation in cell death
    necrosis, 35, 36
    programmed cell death, 44, 46
  disassembly in acute cell swelling, 17–18
  disruption by colchicine, 142
  endothelial transport, 201
  fungal, 578
  hepatotoxins effect on, 627
  intermediate filaments, 91–92
    hereditary disorders, 91–92
    structure and formation, 91
  microfilaments, 89–91
    linkage protein defects, 90–91
    structure and function, 89–90
    toxin/poisons, 88t, 90
  microtubules, 86–89
    centrosomes and centrioles, 88
    hereditary defects, 89, 89f
    structure and formation, 86–87, 87f
    toxins/poisons, 88t, 89
    transport, 87–88
  mycoplasma, 442
  neoplastic cells, 764, 766, 781
  neurotoxicity, 669, 672
  neutrophil chemotaxis and, 233
  plasma membrane linkage, 95–97
  platelet, 248
  protozoal cell, 525
  subsurface, 92, 94f, 94–95
  toxins, 88t
Cytosol. *See* Cytoplasm
Cytostome, 525, 547, 549
Cytotoxic T cells (CTL), 46, 83–84, 289, 289f
Cytotoxins
  Clostridium difficile, 502
  of *Shigella,* 475
  Type III secreted, 438

D

Dactylosoma, 543
DAEC (diffusely adhesive *Escherichia coli*), 469, 472
Damselysin, 485
Danon disease, 71, 116
Dark eumycetomas, 589
Dark neurons, 667
Daunorubicin, cardiotoxicity of, 644
DDC (dideoxycytidine), 625, 682–683
DDI (dideoxyinosine), 625

DDT (dichlorodiphenyltrichloroethane), 684
Death proteins, 40
Death receptor, 667
Death repressor molecule, 65–66
Death signaling, 41
Death-associated protein 3 (DAP3), 43
Deciliation, 18
Dectin 1, 235
Deer
  anaplasmosis, 451
  chronic wasting disease (CWD), 913–914
  epizootic hemorrhagic disease (EHD), 377
Defective particle, hepatitis B virus, 354
Defensins, 231, 534
Degenerate nerve cell, in kuru, 914f
Degranulation
  anaphylactic, 222
  basophil, 221–222
  eosinophil, 245
  immunologic, 221
  mast cell, 217–218, 219f, 221, 221f
  neutrophil, 239, 240f
  piece-meal, 222
Degranulation vacuoles, basophil, 222
Deltaretrovirus genus, 410
  human T-lymphotrophic virus (HTLV), 410
δ-storage pool disease, 256
Demyelination
  acute allergic encephalomyelitis, 680f
  description, 678
  in PNS disease, 682
  segmental, 681
  toxic, 682
  Wallerian degeneration, 679f
Dendrites, 668
Dendritic cells (DCs), 274–275, 276f
  activated, 276f
  as antigen-presenting cells, 275
  circulating, 275
  conventional tissue, 275
  follicular, 275, 276f
  in HIV infection, 411
  interdigitating, 275, 276f
  killer, 787
  lung, 276f
  plasmacytoid, 275
  prion protein production in, 911
Dendritic spine density, 677
Denervation atrophy, 29, 51–52
Dengue fever virus, 388
Dengue hemorrhagic fever, 388
Dengue shock syndrome, 388
Dense body, pox virion, 322
Dense fibrillar components
  in neoplastic cells, 767–768
  nucleolus, 133, 134
Dense granules
  endothelium, 207
  platelet, 248, 256–257
Dental calculi, 802, 802f
Dent's disease, 114
Depedovirus genus, 352
  adeno-associated viruses (AAVs), 352
Dermatan sulfate, 304
Dermatitis
  mast cells in, 220f
  pigmented defects, 812
Dermatomycosis, 590
Dermatophilus, 490t, 495f, 496
Dermatophytosis (ringworm), 590–591, 593f
Dermatosparaxis, 300, 302f
Desmin, 36, 91
Desmocollins, 100
Desmoglein, 100
Desmoplakins, 100
Desmosome
  acute cell swelling, 19f
  belt, 100
  description, 99–100
  disintegration of, 17
  hemidesmosomes, 100f, 100–101, 766
  neoplastic cells, 766
  spot, 100
Detoxification, role of smooth endoplasmic reticulum and peroxisomes, 62–63
Development, autophagy in, 71
DFF45 (DNA fragmentation factor of 45 kDA), 44
Diabetes mellitus
  basal membrane thickening in, 310, 311f
  glomerulopathy, 903–906, 904f, 905f
  glycogen overload, 163–164
  glycosylation of proteins in, 163
  hyperglycemia, 163–164
  insulin-dependent, 903–904, 904f
  noninsulin-dependent, 904, 905f
Diacyl glycerol, 81
Diamond-Blackfan anemia, 816
Diapedesis, 235–237, 237f
Diarrheal diseases
  Bacteroides fragilis, 509
  Campylobacter, 461, 464
  Clostridium difficile, 502
  Escherichia coli, 469
  Vibrio, 484
  Yersinia enterocolitica, 476
Dibasic ester solvent, pulmonary damage from, 729
Dichlorodiphenyltrichloroethane (DDT), 684
Dideoxycytidine (DDC), 625, 682–683
Dideoxyinosine (DDI), hepatotoxicity of, 625
Differentiation, 71, 761
Diffuse pulmonary fibrosis, 728–729
Diffuse pulmonary mineralization, 729
Diffuse vacuolar degeneration, 7
Diffusely adhesive *Escherichia coli* (DAEC), 469, 472
Diffusion
  facilitated, 79, 84t
  simple, 79
Digestive vacuoles, in protozoal cell, 525
Digitalis, cardiotoxicity, 651
Dimethrin toxicity, 611, 612f
Dimethylnitrosamine, renal papillary necrosis, 706
Dimorphic fungi, 578
Dioxins, hepatotoxicity of, 623
Dipetalonema vitae, 600
Diphenylamine, renal papillary necrosis, 706
Diphtheria, 491
Diphtheria toxin, 137, 491
Diplomonads, 536
Dirofilaria immitis, membranous glomerulonephritis and, 897, 897f
Distal tubules
  ADH effect on, 705
  amphotericin B toxicity, 705
Disulfiram, smooth endoplasmic reticulum toxicity, 620
Dizocilpine, 677
DNA
  alkylation of, 135
  intercalation of, 135
  metabolic defects, 135–136
  methylation, 758, 761
  mitochondrial DNA (mtDNA)
    description, 183
    hepatotoxin effects, 623, 625
    inhibition of synthesis, 625
    mutations, 193–195
      Barth syndrome, 195
      glutaric acidemia, 194
      Kearns-Sayre syndrome, 193
      Leber's hereditary optic neuropathy, 194
      list of, 193
      progressive ophthalmoplegia, 194
      Wilson's disease, 193–194
    toxic injury to, 193
  replication in S phase, 743–744
  structure, 130–131
  synthesis, 744, 747

DNA analogues, 135
DNA damage
  in acute cell swelling, 13
  in neoplasia, 758
  p53 and, 41–42, 44
  in programmed cell death, 42, 44
  repair
    abnormalities in neoplasia, 769
    base excision repair (BER), 183
    excision repair, 64
    in situ, 64
  response, 64
  sensors of, 136, 744
  transcription stress response, 136
DNA fragmentation factor of 45 kDA (DFF45), 44
DNA repair. *See* DNA damage, repair
DNAase, 40
Dogs
  American canine hepatozoonosis, 558
  atherosclerosis, 885
  canine cyclic hematopoiesis (gray collie syndrome), 242
  canine fucosidosis, 863
  canine granulocytic ehrlichiosis, 451
  canine visceral leishmaniasis, 535
  Huntaway dogs, mucopolysaccharidoses in, 866
  viral diseases
    canine adenoviruses 1 (CAV-1), 340–341, 343
    canine adenoviruses 2 (CAV-2), 340
    canine distemper virus (CDV), 362, 363f
    canine parvovirus, 350
    canine rotavirus, 378
    infectious canine hepatitis (ICH), 340–341, 341f, 343
  X-linked renal disease in Samoyed dogs, 898
  xmd dogs, 91
Döhle bodies, 240
Domoic acid, 685
Dopamine agonists, vascular toxicity of, 658
Dopaminergic neurons, 683–684
Down syndrome, 836
Doxorubicin, cardiotoxicity of, 644f, 644–646, 645f, 647f, 648f
Dr fimbrial adhesins, 469
Drug hypersensitivities, glomerulopathy from, 902
Drug-induced glycogen overload, 163
Drug-induced storage diseases, 862
Dubin-Johnson syndrome, 821
Duck hepatitis virus (DHV), 355
Duck plague, 336f, 338
Ducks, *Erysipelothrix* infections in, 447
Dying-back polyneuropathies, 681
Dynamin, 114, 695
Dynein, 88, 114
Dynein arm defect, 101
Dysferlin, 61
Dystroglycans, 695
Dystrophic calcification, 798
Dystrophic epidermolysis bullosa, 309
Dystrophic type EB, 92
Dystrophin, 91

E

E3 ubiquitin ligase, 851
EAEC (enteroaggregative *Escherichia coli*), 469, 472
East Coast fever, 538, 541
Eastern equine encephalitis (EEE), 382, 383f
EAV (equine arteritis virus), 384, 385f, 386, 881
EBHS (European brown hare syndrome), 399
Ebolavirus genus, 370
EBPs (estrogen-binding proteins), 613
EBV (Epstein-Barr virus), 337
Echoviruses, 394
Ecstasy, 672, 676
Ectopic expression, 772
Ectoplasm, of protozoal cell, 525
Ectothrix fungal species, 590
Ectromelia, 323
Edema
  cytoplasmic, 7
  gill, 736f
  myxedema, 304
  perivascular, 875, 876f
Edema disease, 472–473
Edema factor (EF), *Bacillus anthracis*, 497
EDIM (epizootic diarrhea of infant mice), 379
EEE (eastern equine encephalitis), 382, 383f
Efflux-pump proteins, 431
EGF (epidermal growth factor), in hepatic regeneration, 749
EGFr (epidermal growth factor receptor), 113
EGLF7 (epidermal growth factor-like domain 7), 224
EHD (epizootic hemorrhagic disease), 377
EHEC (enterohemorrhagic *Escherichia coli*), 469, 471–472
Ehlers-Danlos syndrome, 300–301
Ehrlichia, 451, 452t
Ehrlichiosis
  canine, 451
  equine, 451
  human, 451
EIA (equine infectious anemia), 414–415
Eicosanoids, 81, 254
EIEC (enteroinvasive *Escherichia coli*), 469
Eimeria, 546f, 549–550
ELAM-1 (endothelial-leukocyte adhesion molecule-1), 214, 215
Elastase, 240, 299
Elastic fibers
  description, 303
  disease, 303–304
Elastin, 303
Electrolyte imbalance, nephrotoxicity and, 712
Electron microscopic tomography
  description, xvi
  examples, xviif
Electron transport chain, 182, 183
Elementary body, of *Chlamydia*, 485
Elk, chronic wasting disease (CWD) in, 913–914
Embolization, atherosclerosis and, 883
Embolus, tumor, 783, 784f
Embryogenesis, programmed cell death in, 47, 49
Embryopathy, varicella, 333
Emphysema, chronic, 729, 731
Emperipolesis, 54, 787
Empty cell wall form, algae, 575
Encapsulation, of benign tumors, 761
Encephalitis
  acute allergic encephalomyelitis, 680f
  alphavirus, 381–384
    eastern equine encephalitis (EEE), 382, 383f
    Venezuelan equine encephalitis (VEE), 382, 384
    western equine encephalitis (WEE), 382
  California, 391–392
  canine distemper virus, 362
  encephalomyocarditis (EMC) viruses, 397
  granulomatous amoebic, 528
  herpes simplex virus, 332–333
  Japanese B encephalitis virus, 388
  postvaccinial, 323
  Russian spring-summer encephalitis (RSSE) virus, 388
  St. Louis encephalitis virus, 383f, 388
  subacute sclerosing panencephalitis, 362
Encephalitozoon, 561, 562f
Encephalomalacia, 678

Encephalomyelitis
acute allergic, 680f
avian, 398f, 399, 798f
hemagglutinating encephalomyelitis virus (HEV), 373
murine polioencephalomyelitis virus (Theiler's virus), 396f, 397
Encephalomyocarditis (EMC) viruses, 397
Encephalopathy, hepatic, 191–192
Encystment, of *Trichinella*, 598, 599f
Endocardial fibrosis, 295
Endocrine cell hyperplasia, 22–23
Endocrine dysfunction, in aging, 750–751
Endocytic compartment, macrophage, 272
Endocytic recycling compartment (ERC), 109
Endocytosis, 108f, 109–115
absorptive, 109
of aminoglycosides, 701
caveolae, 109, 111f, 111–112
clathrin-mediated, 109, 112f, 112–113
description, 109–110
endosomal pool, 113–115
endosomal receptors in tissue, 114–115
endothelium cell, 202f, 203–204
focal vacuolation, 7
inclusions, 849–851
lipid raft-mediated, 114
macroendosomes, 114
microtubule guidance, 114
pinocytic reticulum, 113–114
pinocytosis, 109, 110–111
platelet, 251
receptor-mediated, 109, 113, 171, 203–204
transcytosis, 109, 110f
trypanosome, 532
Endonuclease activation, in programmed cell death, 44
Endoplasmic reticulum (ER). *See also* Rough endoplasmic reticulum (RER); Smooth endoplasmic reticulum (SER)
calcium and, 797, 798f
concentric lamellar arrangements, 11
crystalloid, 62
inclusions, 843–849, 845f–848f
MHC class II molecules, 272, 272f
necrosis, 40
of neoplastic cells, 770f, 769–771
plasma cell, 284, 284f–285f
in programmed cell death, 46
protozoal cell, 525
tubulocisternal, 157, 159
Endosomal pool, 113–115
directing traffic in, 114–115
macroendosomes, 114
pinocytic reticulum, 113–114
Endosomal receptors in tissue, 114–115
Endosomal sorting complexes required for transport (ESCRTs), 119
Endosomal tubuloreticular compartment, 113
Endosome
description, 109
intermediate, 110, 113–115
late, 113
macroendosomes, 114
pre-endosomal vesicles, 110
smooth, 110
transport to Golgi complex, 139
Endospore
algae, 573
fungal, 585
microsporan, 561
Endostatin, 225
Endothelial cell activation, 201
cytokine, 214–215
in inflammation, 211–212, 214f, 214–215
Endothelial cells. *See also* Endothelium
alveolar, 717, 728
death, 54, 55f, 56
fluid transport, 211
hepatic sinusoids, 607
malaria and, 547, 548
murine leukemia virus replication in, 409
paramyxovirus infection, 365f
Rickettsial infection, 449, 450f
Endothelial progenitor cells, 223
Endothelial transmembrane receptors, 214
Endothelial transport, organelles of
caveolae, 201–202
coated pits and vesicles, 203–204
phagosomes, 204
transendothelial channels, 202–203, 205f
Endothelial-leukocyte adhesion molecule-1 (ELAM-1), 214, 215
Endothelin-converting enzymes, 209
Endothelins, 208–209
Endothelium, 201–228. *See also* Endothelial cells
angiogenesis, 223–225
from bone marrow stem cells, 223
extracellular regulators, 224
growth factors, 224–225
pathogenesis, 223–224
phases of development, 223, 223f
in repair of inflammation, 225
from surviving blood vessels, 223
basophil interface with, 219t, 221f, 221–222
blood-brain barrier, 688, 689f, 690
chemoattractants for, 224
endocytosis, 202f, 203–204
heavy metal toxicity, 688, 690
hypertension, 209
hypotension, 208–209
hypoxia, 208, 208f
inflammation, 209–217, 210f
blood-tissue barriers, 217
endothelial cell activation, 203f–204f, 211–212, 214f, 214–215
liver fenestrated endothelium, 216–217
lymph vessel endothelium, 215–216, 216f
perivascular changes in acute, 211t
ultrastructural evidence of, 211, 212f, 213f
vascular changes in acute, 209t
interface with blood and perivascular spaces, 201
interendothelial junctions, 204
organelles of transport, 201–204
perivascular environment, 204–206
lipoprotein metabolism, 170
lymph vessel, 215–216
mast cell interface with, 217–221, 218f–221f, 219t, 222–223
neutrophil binding to, 235, 236f
neutrophil-induced injury, 239–240
platelet attachment to, 249f
platelets and endothelial injury, 253f, 254
procoagulant activity, 206, 207–208
thromboresistance, 206, 207
Endothrix fungal species, 590
Endotoxin, 431, 432f, 471
Enlargeosomes, 120
Entactin, 307, 308
Entamoeba, 526–527, 527f
Enteric adenoviruses, 340
Enteritis, canine parvovirus, 350
Enteroaggregative *Escherichia coli* (EAEC), 469, 472
Enterobacteriales (order), 466–476, 467t–469t
Calymmatobacterium genus, 466
Escherichia genus, 466, 467t, 469, 470f, 471–473
Klebsiella genus, 467t, 473
Proteus genus, 468t, 473

Enterobacteriales (order) (*cont'd*)
Salmonella genus, 468t, 473–474
Shigella genus, 468t, 474–475
Yersinia genus, 469t, 475–476
Enterocolitis, *Salmonella,* 473
Enterocytes
lipoprotein metabolism, 170
Trichinella in, 598
Enterocytozoon, 561–563, 563f
Enterohemolysin, 85
Enterohemorrhagic *Escherichia coli* (EHEC), 469, 471–472
Enterohepatitis, 537
Enteroinvasive *Escherichia coli* (EIEC), 469, 471
Enteropathogenic *Escherichia coli* (EPEC), 469, 471
Enterotoxemia, *Escherichia coli* and, 472–473
Enterotoxigenic *Escherichia coli* (ETEC), 469, 471
Enterotoxin
Clostridium difficile, 502
cytoplasmic blebbing, 20
heat-stable of *Yersinia pestis,* 475
of *Shigella,* 475
Staphylococcus aureus, 500
Vibrio, 484–485
Enterovirus genus, 394
coxsackieviruses, 394
echoviruses, 394
poliovirus, 394
Entomoplasmatales (order), 447
Entosis, 54
Envelope, viral
herpesvirus, 327
pox virion, 322
Envoplakin, 312
Enzymes
bacterial, 436
release during necrosis, 36
secretion systems, 436–439
Eosinophil, 243–246
chemotaxis, 245
degranulation, 245
description, 243
granules, 243, 244f, 245
hypereosinophilic syndromes, 246
parasites and, 244f, 245
tissue eosinophilia, 245, 246f
Eosinophil cationic protein, 245
Eosinophil major basic protein, 243
Eosinophilic chemotactic factor, 217
EPEC (enteropathogenic *Escherichia coli*), 469, 471
Eperythrozoon, 445t, 447
Ephemerovirus genus, 368
Eph-Ephrin signals, 79
Epidemic typhus, 448–449
Epidermal eruption, from herpes simplex virus, 332
Epidermal growth factor (EGF), in hepatic regeneration, 749
Epidermal growth factor receptor (EGFr), 113
Epidermal growth factor-like domain 7 (EGLF7), 224
Epidermolytic hyperkeratosis, 92
Epidermodysplasia verruciformis, 346
Epidermolysis bullosa, 91–92, 309
Epidermophyton, 590
Epigenetics, 758, 761
Epimastigote, 532f, 534
Epinephrine
cardiotoxicity of, 650
Na-K-ATPase increase and, 80
secretion, 145–146
Epirubicin, cardiotoxicity of, 644, 646
Epispore, in microsporans, 561
Epithelial cells
collagen degradation, 299
programmed cell death, 41
thymic, 282f, 282–283
Epithelial slit pores, 695
Epithelial-to-mesenchyme transition, 777
Epithelioid cells, 272, 493
Epithelioma, 761
Epizootic bovine abortion, 511
Epizootic diarrhea of infant mice (EDIM), 379
Epizootic hemorrhagic disease (EHD), 377
Epizootic ulcerative syndrome, 379
Epstein-Barr virus (EBV), 337
Epulopiscium, 511t
Equine arteritis virus (EAV), 384, 385f, 386, 881
Equine cutaneous mastocytosis, 222–223
Equine infectious anemia (EIA), 414–415
Equine morbillivirus, 362, 364
Equine protozoal myeloencephalitis, 555
ER. *See* Endoplasmic reticulum (ER)
ER degradation-enhancing α-mannosidase-like protein-1 (EDEM 1), 139
ER stress, 46
ERK (eukaryotic protein kinase) pathway, proteostasis and, 68
Erysipelothrix, 447, 448t
Erythemic myelosis, 407
Erythrophagocytosis, 817f–820f, 817–819
Erythrocytes
aging of, 750
cell shape change, 95f
degradation, 819
Fas signaling, 47
Leucocytozoon infection, 548
malarial infection, 543, 545, 546f, 547
neutrophil erythrophagocytosis, 238f
pathogens, 446f
spectrin-actin subcortical cytoskeleton of, 94–95, 95f, 96f
surface pathology, 102f
Theileria in, 541
Erythrogenin, 701
Erythroleukemia, 407
Erythrophagocytosis, 721f
Erythropoiesis, apoptosis and, 49
Erythropoietin, tubular aggregates of, 846–847
Erythrovirus genus, 350, 352
Escherichia coli, 466, 467t, 469, 470f, 471–473
adhesins of, 469
avian pathogenic *Escherichia coli* (APEC), 472
diffusely adhesive *Escherichia coli* (DAEC), 469, 472
endotoxin release, 432f
enteroaggregative *Escherichia coli* (EAEC), 469, 472
enterohemorrhagic *Escherichia coli* (EHEC), 469, 471–472
enteroinvasive *Escherichia coli* (EIEC), 469, 471
enteropathogenic *Escherichia coli* (EPEC), 469, 471
enterotoxemia, *Escherichia coli* and, 472–473
enterotoxigenic *Escherichia coli* (ETEC), 469, 471
meningitis-associated *Escherichia coli* (MNEC), 472
pathotypes of, 469
toxins of, 471–473
uropathogenic *Escherichia coli* (UPEC), 472
Escherichia coli factor for adherence (efa1), 471
ESCRTs (endosomal sorting complexes required for transport), 119
E-selectin, 236
Esophagus, programmed cell death and, 45f
Essential menorrhagia, 259–260
Estivation, 751
Estrogen receptors, 613
Estrogen-binding proteins (EBPs), 613
Estrogens
hepatocyte effects, 613
rough endoplasmic reticulum, effects on, 613

vitellogenin production stimulation, 613
Estrophilin, 613
ETEC (enterotoxigenic *Escherichia coli*), 469, 471
Ethanol
cardiomyopathy, 651
hepatotoxicity, 621–622
metabolic degradation pathways, 622f
pulmonary toxicity, 735
skeletal muscle myopathy and, 652
toxicologic enhancement in SER, 157
Ethidium bromide, myelinopathy from, 682
Ethionine, 137, 626
Ethylene glycol toxicity, 710f, 710–711
Eubacteria, 425. *See also* Bacteria
Eubacterium, 481f, 503t, 504
Euchromatin, 130
Eukaryotic initiation factor 2 (eIF2), 51
Eukaryotic protein kinase (ERK) pathway, proteostasis and, 68
Eumelanin, 811
Eumycetomas, 589
European brown hare syndrome (EBHS), 399
Excision repair, 64
Excitotoxic neurodegeneration, acute, 685
Excitotoxin, 685–686, 835
Exfoliation, of necrotic epithelial cell, 704f
Exhalant injury, acute, 727
Exocytic vesicles, 118–119
Exocytosis
acidosomes, 119f
cytoplasmic shedding by, 18–20, 120–121
defined, 118
exosomes, 118–119
fungal, 578
microvesicular, 19
multivesicular, 118, 119–120
neutrophil degranulation, 239
secretory, 143
surface (cytoplasmic) blebbing, 19f, 20, 120–121, 121f
trypanosome, 532
vesicular, 120
Exocytotic constipation, 119
Exogenous phospholipases, 82
Exons, 132
Exosome
defects, 119
dendritic cells, 275
description, 118–119
renal excretion in urine, 119
secretory vesicles, 119, 119f
Exospore, in microsporans, 561
Exotoxins, 436
exotoxin A of *Pseudomonas,* 483
streptococcal, 501–502
Exovesicles, of neoplastic cells, 763
Expression, gene
epigenomics, 758, 761
transcriptional silencing, 761
Extracellular debris, removal of, 54
Extracellular ground substance, 304–307, 305f, 306f
Extracellular matrix, 295–315
basement membranes, 307–310, 310f, 311f
Borrelia attachment to, 505
collagen, 297–303
anchoring fibrils, 299
degradation, 299–300
diseases, 300–303, 301t, 302f
dysfunctional fibers, 299
mutations, 299
reticular fibrils, 299
synthesis, 298–299
types, 297–298, 298t
cutaneous permeability barrier, 311–312
degradation by neoplastic cells, 777
elastic fibers, 303–304
extracellular ground substance, 304–307, 305f, 306f
fibrosis, 294f, 295, 296f, 297, 300f, 306f
microfibrils, 303
mucins, 310–311
odontogenesis, 303
Extracellular nucleator pathway fimbrial family, 434
Extracellular signal-regulated kinase 1/2 (ERK 1/2), 43
Extranucleolar region, 746
Extrusion apparatus, *Nosema,* 561
Eyes
adenoviral infection, 343
calcification in, 801
melanoliposfuscin, 824

F

Fabry disease, 862
Facilitated diffusion, 79
Factor VIII complex, 257
Factor VIII-related antigen, 207
Factor XIII (fibrinoligase), 259
FADD (Fas-associated death domain), 46, 47, 785
FAK (focal adhesion kinase), 100
Falcilysis, 547
Familial acantholysis, 92
Familial amyloidotic polyneuropathy, 834–835
Familial combined hyperlipidemia, 173
Familial hypercholesterolemia, 137
Familial hyperinsulinemia hypoglycemia of infancy, 191
Familial lecithin:cholesterol acyltransferase deficiency, 173
Familial motor neuron disease, 92
Farcy, 585
Fas, 44, 52
Fas-associated death domain protein (FADD), 46, 47, 785
Fas-Fas ligand signaling, 46–47
Fat atrophy, 167, 168f, 169
Fatal familial insomnia, 915
Fatty acids
β-oxidation of, 181, 191, 195
in hepatocytes, 169
FCV (feline calicivirus), 399
FEAM (foci of extracellular amorphous matrix), 778
Fechtner's syndrome, 243, 256
Feline calicivirus (FCV), 399
Feline immunodeficiency virus (FIV), 410
Feline infectious peritonitis (FIP), 373, 895f
Feline leukemia virus (FeLV), 406–407, 408f
Feline leukemia virus subgroup C receptor (FLVCR), 815–816
Feline panleukopenia virus, 350, 351f, 874f
Fendolapam, vascular toxicity of, 658–659
Fenestrae in capillaries, 204, 205, 695
Fenfluramine, 676–677
Ferrets, respiratory syncytial virus in, 366
Ferritin, 816, 816f
Ferrotransferrin, 817
Ferruginous body, 733
Fetal lung, response to bacterial infection, 722f
Fetal vasculogenesis, 223
Fever, nephrotoxicity and, 712
FGF (fibroblast growth factor), 223
FHA (filamentous hemagglutinin), 457
Fibers, lung toxicity from, 724
Fibrillar centers, 133, 134, 767–768
Fibrillar inclusions, in neoplastic cells, 771
Fibrillarin, 133, 135
Fibrillary glomerulonephropathies
amyloid glomerulopathy, 900
fibrillary glomerulopathy, 834, 900

Fibrillary glomerulonephropathies (*cont'd*)
immunotactoid glomerulopathy, 900
Fibrillary glomerulopathy, 834, 900
Fibrillin, 303, 308
Fibrillin gene, 303
Fibrillogenesis, 297
Fibrils, of nuclear envelope lattice, 127, 129
Fibrin
coagulation and, 257, 258f, 259f, 259–260
degradation by neutrophils, 240
description, 224
hemostatic plug formation and, 247
lysis of, 206, 783
metastasis and, 783
Fibrinogen
alpha-chain, amyloid from, 835
coagulation and, 257
gold complexed with, 201
hemostatic plug formation and, 247
in hyalin droplet inclusions, 844
polymerization, 892
Fibrinogen receptor, 248, 253
Fibrinogen-GPIIb-IIIa complexes, 253
Fibrinopeptides, 234
Fibroblast
collagen degradation, 299
collagen production by, 298
description, 295
fibronectin secretion, 308
myofibroblasts, 297
tumor-associated, 775, 777, 778
Fibroblast growth factor (FGF), 223, 295
Fibroblastic reticular cells, 380
Fibroma, 761
Fibromyalgia, 824
Fibronectin, 201, 205, 205f, 253, 308, 778
Fibronectin receptor, 297
Fibronexus, 297
Fibroplasia, 778. *See also* Fibrosis
Fibrosarcoma, 407
Fibrosis
chronic, 297
cutaneous, 295
defined, 295
hepatic, 295
lung (pulmonary), 294f, 295, 296f, 306f, 728–729, 735
myocardial, 643
pathogenesis, 295, 297
skeletal muscle, 300f
Fibrous plaque (fibrous streak), 879, 883
Fibulin, 303–304
Fic fimbriae, 469
Fifth disease, 350
Filamentous bacteria
long, 511
segmented, 511
Filamentous hemagglutinin (FHA), 457
Filamentous laminae, mitochondrial, 188
Filamin, 90
Filopodia
acanthamoebae, 526
alteration in acute cell swelling, 18
description, 103
endothelial cell, 212f
erythrocyte, 96f, 102f
microfilaments and, 90
neoplastic cells, 763
platelet, 251
Filoviridae family, 369f, 369t, 369–370
Ebolavirus genus, 370
Marburgvirus genus, 369–370
Filtration slits, podocyte, 891
Fimbriae. *See also specific bacterial genera or species*
bundle-forming, 469
CS1 family, 434
curli, 434, 469
description, 427–428, 433
Escherichia coli, 432f, 469
Fic, 469
long polar, 469
P, 433, 469
S, 469
Type 1, 433, 469
Type IV, 469
FIP (feline infectious peritonitis), 373, 895f
Firmicutes, 496–510
Fish, viral diseases of
infectious pancreatic necrosis (IPN), 392–393
lymphocystic disease, 353
reovirus, 379
viral encephalopathy and retinopathy, 394
FIV (feline immunodeficiency virus), 410
5FU, 135
FK506, 708
Flagella
bacterial, 435
description, 428
Leishmania, 535
peritrichous, 475
protozoal cell, 526
Flagellar excision, 18
Flagellar pocket, 532
Flagellates, 529–538, 530t–531t, 532f, 533f, 535f, 537f
Giardia, 536–537, 537f
Histomonas, 537–538
Leishmania, 535f, 535–536
Spironucleus, 537
Trichomonas, 537
Tritrichomonas, 537
Trypanosoma, 529, 532f, 532–534
Flagellin, 435
Flavin mononucleotide (FMN), 185f
Flaviviridae family, 386–391, 387t, 390f
Flaviviris genus, 386–388
dengue fever virus, 388
Japanese B encephalitis virus, 388
Kyasanur Forest disease virus, 388
louping ill virus, 388
Russian spring-summer encephalitis (RSSE) virus, 388
St. Louis encephalitis virus, 383f, 388
yellow fever virus, 386–388
Hepaciviris genus, 389, 391
hepatitis C virus (HCV), 389, 391
Pestiviris genus, 388–389
bovine viral diarrhea (BVD) virus, 389
hog cholera, 388–389, 390f
Flaviviris genus, 386–388
dengue fever virus, 388
Japanese B encephalitis virus, 388
Kyasanur Forest disease virus, 388
louping ill virus, 388
Russian spring-summer encephalitis (RSSE) virus, 388
St. Louis encephalitis virus, 383f, 388
yellow fever virus, 386–388
Flavobacteriales (order), 509t
Flotillin, 114
Fluid phase transport, 109
Fluidity in biological membranes, 622
Fluoxetine, 684
FLVCR (feline leukemia virus subgroup C receptor), 815–816
FMD (foot-and-mouth disease) virus, 397
FMN (flavin mononucleotide), 185f
Fn14, 785
Foam cell, 902–903
atherosclerosis, 883, 884f
glomerulopathy, 902–903
in toxicity, 720
Foamy viruses, 415
Focal adhesion, 100
Focal adhesion kinase (FAK), 100
Focal adhesion plaques, 96
Focal arteriolar insudation, 879
Focal segmental glomerulosclerosis, 695, 902

Focal vacuolation, of acetaminophen toxicity, 618
Foci of extracellular amorphous matrix (FEAM), 778
Folate blockers, 135
Folate receptors, 112
Folding, protein, 125, 139
Follicular dendritic cells, in prion disease, 913
Food vacuole
  ciliate, 528
  malarial, 547
Foot process effacement, 696
Foot process fusion, 696
Foot rot, 510
Foot-and-mouth disease (FMD) virus, 397
Foreign materials, calcification of, 801
Form factor, for cell shape, 767
Formins, 90
Fowlpox, 324, 326f
Fracture face, 78
Francisella, 484, 484t
Frataxin, 195, 816
Free radical initiators, hepatotoxicity and, 625
Freeze fracture technique, 78, 78f
Frenkelia, 560
Friedreich ataxia, 195
Frog virus 3, 353
Frogs
  aerolysin toxicity, 655, 657f
  cutaneous chytridiomycosis of, 594
  renal carcinoma, 338
Frontotemporal dementias, 840
Fuchs corneal dystrophy, 299
Fucosidosis, 863
Fungal vacuole, 578
Fungi, 576–595
  adiaspiromycosis, 590
  Aspergillus, 580–582, 581f
  Blastomyces, 580–582, 582f
  Candida, 583, 584f, 585
  causes of cutaneous infection, 591t
  causes of subcutaneous infection, 580t, 589–590
  causes of systemic infection, 576t–577t
  chromoblastomycosis, 589
  chytridiomycosis, 593–594
  Coccidioides, 585
  Cryptococcus, 585, 586f
  dermatophytosis (ringworm), 590–591, 593f
  description, 576, 578–580
  dimorphic, 578
  fusariomycosis, 590
  giant cell formation, 23
  Histoplasma, 572f, 579f, 585, 587f, 587–588
  inhalation by aerosol exposure, 578
  lobomycosis, 590
  mucormycosis, 589–590
  mycetoma, 589
  mycotoxins, 578
  Paracoccidioides, 588, 588f
  penicilliosis, 590
  phaeohyphomycosis, 589
  piedra (trichosporosis), 590
  pityriasis versicolor, 590
  pneumocystosis, 594f, 594–595, 595f
  Rhinosporidium, 588, 589f
  Sporothrix, 588–589
Fungi Imperfecti, 576
Funis, 536
Furazolidone, cardiotoxicity, 651
Fursariomycosis, 590
Fusobacteriales (order), 510, 510t
  Fusobacterium genus, 510, 510t
  Streptobacillus genus, 510, 510t
Fusobacterium, 510, 510t

G

G protein-coupled receptors, 81
G_0, 743
G_1 checkpoint, 743
G_1 phase, 743
G_2 phase, 744
GABA (gamma-aminobutyric acid), 684, 685
GABA transaminase, 685
$GABA_AR$, 683
GABA-gated chloride channels, 685
GAGs. *See* Glycosaminoglycans (GAGs)
Galactogen, 161
Galactomannan, 580–581
Galactosialidosis, 863
Galactosylceramide, 861
Galectins, 235
Gallstones, 802, 804f
GALT (gut-associated lymphoid tissue), 278
Gametocytes
  Leucocytozoon, 549
  malarial, 543
Gametogony, 549
Gamma-aminobutyric acid (GABA), 684, 685
Gammaherpesvirinae subfamily, 337–338
  Epstein-Barr virus (EBV), 337
  Lymphocryptovirus genus, 337
  Rhadinovirus genus, 337–338
  saimiriine herpesvirus 2, 338
Gammaretrovirus genus, 406–410
  avian reticuloendotheliosis virus (ARV), 410
  feline leukemia virus (FeLV), 406–407, 408f
  murine leukemia viruses (MLVs), 407, 408f, 409f, 409–410
Gangliosidosis
  appearance, 856f
  GM_1, 857, 858f
  GM_2, 860
Gap junction
  arterial, 875
  closure, 17
  description, 97–99, 98f, 204
  neoplastic cells, 766
  proteins, 97
  uncoupling, 35
GAPDH (glyceraldehyde-3-phosphate dehydrogenase), 64
Gargoylism, 864f
Gas vacuole, 439
Gas6, 904, 906
Gases, lung toxicity from, 723, 729
Gastric carcinomas, 802
Gastric parietal cells, acid secretion by, 145
Gastrointestinal anthrax, 496
Gaucher's disease, 860–861, 861f
Gelatinase granules, 233
Geleophysic dysplasia, 864, 864f
Gelsolin, 90, 248, 835
Gelsolin-associated amyloid, 835
Gemfibrozil, 611–612
Gene activation, in hepatic regeneration, 749
Gene capture, 402
Gene expression, chromosome unfolding and, 130–131
Gene regulation, by transcription factors and microRNAs, 131
Generalized disseminated infection, from herpes simplex virus, 332–333
Genetic instability, of neoplasms, 757
Genetic mutation, in neoplasia, 758
Genital carcinoma, human papilloma virus (HPV), 346
Genomic landscape, neoplasia and, 758
Genotoxicity
  gene p53 activation, 41
  programmed cell death trigger, 44
  radiation, 187–188
Gentamicin
  microvesicular exocytosis, 19
  nephrotoxicity, 610, 701
German measles, 384
Germinal center
  lymph node, 275, 277
  spleen, 278
Gerstmann-Sträussler-Scheinker syndrome (GSS), 839, 915
GFAP (glial fibrillary acidic protein), 687

Giant cell pneumonia, paramyxovirus, 360, 362
Giant cells
  adaptive responses to persistent injury, 23, 26
  bacterial and fungal causes, 23, 26
  Blastomyces, 582, 582f
  formation by
    cell-to-cell fusion, 23, 26
    nuclear division, 23
  in tuberculosis, 493
  virus-induced, 26
Giant platelet syndrome, 256, 256f
Giant proximal axonopathy, 681
Giardia, 536–537, 537f
Giardiasis, 536–537
Gilbert's syndrome, 821–822
Gills, 736f, 736–737, 737f, 738f
Glanders, 457, 459
Glanzmann's thrombasthenia, 256
Glass fibers, pulmonary damage from, 732–733
Glial fibrillary acidic protein (GFAP), 687
Glial fibrillary protein, 91
Glial neuropathy, 688
Glial toxins, 687–688
Globin, 815
Globoid cell leukodystrophy, 856f, 861
Globotriaosylsphingosine, 862
Glomerular basement membrane, 695, 891–892, 895f–897f, 899f, 901, 903–904, 904f. *See also* Membranous glomerulonephritis
Glomerular filtration barrier (GFB), 694f, 695, 891
Glomerular toxins, 695–697
  mesangiopathy, 697
  podocytopathy, 696–697
Glomerulonephritis
  in hog cholera, 389
  membranous, 890f, 891–898
  primary, 891
  proliferative, 898, 900
  secondary, 891
Glomerulopathy, 891–909
  amyloid, 828f, 833f, 833–834, 900
  diabetic, 903–906, 904f, 905f
  immune mechanisms in, 892t
  lesions in transplanted kidneys, 903
  membranous glomerulonephritis, 890f, 891–898
    animal models, 892–894
      athymic mouse, 894
      rat, 892–893
    naturally occurring, 894–898
      chronic septic disease, 894
      chronic viral disease, 894, 895f, 896f
      glomerulopathy of aging, 894
      neoplasms, 897
      parasites, 897, 897f
  minimal change disease, 900
  patterns of, 892f
  primary glomerulonephritis, 891
  proliferative glomerulonephritis, 898, 900
    acute diffuse, 898
    hepatitis B virus (HBV), 900
    hepatitis C virus (HCV), 900
    membranoproliferative glomerulonephritis, 898
    poststreptococcal glomerulonephritis, 898
  secondary glomerulonephritis, 891
  systemic disease-associated
    autoimmune disease, 901–902
      drug hypersensitivities, 902
      Goodpasture syndrome, 901
      systemic lupus erythematosus, 901
      Wegener's granulomatosis, 902
    fibrillary glomerulonephropathies, 900
      amyloid glomerulopathy, 900
      fibrillary glomerulopathy, 834, 900
      immunotactoid glomerulopathy, 900
    foam cell glomerulopathy, 902–903
    focal segmental glomerulosclerosis, 902
    hereditary nephritides, 901
      Alport syndrome, 901
      light-chain nephropathy, 834, 901
    HIV glomerulopathy, 903
    IgA glomerulopathy, 900–901
    thrombotic disease, 902
Glucagon, 161
Glucagon-associated amyloid, 835
Glucan, hepatotoxicity of, 627
Glucocorticoid receptors, in neoplastic cells, 775
Glucocorticoids
  angiogenesis and, 780
  glycogen overload and, 163
  smooth endoplasmic reticulum effects on, 620
Glucose
  loading and inhibition of repair, 607
  neurotoxicity, 668
Glucose transporter, 79, 164
Glucose-6-phosphatase deficiency, 866
Glucose-regulated proteins (GRPs), 67
Glugea, 563
Glutamate, 684–685, 687
Glutamine, 687
Glutamine synthetase, 687
Glutaredoxin 2, 64
Glutaric acidemia, 194
Glutathione peroxidase, 63
Glutathione S-transferase, 64
Glutathionylation, 63–64
Glyceraldehyde-3-phosphate dehydrogenase (GAPDH), 64
Glycine, 687
Glycine receptor, 683
Glycocalyx
  in acute cell swelling, 15
  description, 77–78
  endothelial cell, 214
  protozoal cell, 525
Glycogen, 161–164. *See also* Glycogen storage diseases
  depletion in necrosis, 50–51
  deposits in distal tubule cells, 702f
  glycogenesis, 161, 162f
  glycogenolysis, 161
  granules in *Chromatium* species, 439
  inclusions, 63
  monoparticulate, 51, 161
  in myocardial mitochondria, 636
  in neoplastic cells, 775, 777f
  in neutrophils, 240, 242f
  nuclear, 163, 163f
  overload, 161–164
    diabetes mellitus, 163–164
    drug-induced, 163
  rosettes, 161, 163f, 526
  vacuoles, coccidial, 549
Glycogen bodies, 161, 162f, 163f
Glycogen storage diseases, 858f, 866–869
  Lafora disease, 856f, 868–869
  muscle glycogen storage diseases, 869
  oligosaccharide storage diseases, 869
  polyglucosan body diseases, 868f, 868–869
  type I glycogenosis, 866
  type II glycogenosis (Pompe's disease), 867
  type III glycogenosis, 868
  type IV glycogenosis (amylopectinosis), 868
  type V glycogenosis (McArdle disease), 868
  type VI glycogenosis, 868
  type VII glycogenosis, 868
  ultrastructural pathology in models of, 867t

Glycogen synthase gene, 869
Glycogenesis, 161, 162f
Glycogenesomes, 867
Glycogen-lipid droplet ratio reversal, 9
Glycogen-membrane complexes, 161
Glycogenolysis, 161
Glycogenosome, 161
Glycolipids, 77, 763
Glycolysis
  anaerobic shift to, 63
  increase with GAPDH, 64
  in neoplastic cells, 775
Glycoprotein VI, 248
Glycoproteinosis, 863–864
  fucosidosis, 863
  galactosialidosis, 863
  geleophysic dysplasia, 864, 864f
  mannosidosis, 863–864
  Salla disease, 863
  sialidosis, 863
Glycoproteins
  adhesion, 80, 84t
  asialoglycoproteins (ASGPs), 113–114
  in extracellular matrix, 308
  of neoplastic cells, 763, 765
  P, 80
  receptor, 81
  as receptors for retroviruses, 402
  variant surface, trypanosome, 532
Glycosaminoglycans (GAGs)
  cutaneous accumulation, 304
  description, 304
  mucopolysaccharidoses, 307
  storage in mucopolysaccharidoses, 864, 866
Glycosome, 154, 533
Glycosphingolipids, 77
Glycosylation, 138, 904
Glyoxysome, 154
GM_1-gangliosidosis, 857, 858f
GM_2-gangliosidosis, 860
GMP-140, 251
Goats
  bacterial diseases
    brucellosis, 457f
    cutaneous dermatophilosis, 496
    Eperythrozoon, 445t, 447
    heartwater, 451
    Johne's disease, 494
  scrapie, 912–913
  viral diseases
    Akabane virus, 392
    caprine encephalitis virus, 414
    foot-and-mouth disease (FMD) virus, 397
Gold, neurotoxicity, 690
Golgi complex
  changes in mitosis, 747
  colchicine effect on, 89
  in disease, 141–142
    amyotrophic lateral sclerosis, 841
    coccidia, 550
    drugs effects, 141–142
    viral usurpation, 142
  fungal, 578
  hepatotoxins and, 619
  hypertrophy and, 21, 22
  inclusions, 843–844
  lipoprotein metabolism, 170
  lysosome production, 116
  macrophage, 272
  in microsporans, 561
  myocardium, 638
  necrosis, 40
  of neoplastic cells, 769, 770f
  N-linked oligosaccharide construction in, 139
  protozoal cell, 525
  structure, 139, 139f
    cis face, 139–140
    medial face, 140
    saccules, 140f
    trans face, 140–141
  transport system, 139–141, 140f
    intra-Golgi vesicles, 140
    retrograde transport to RER, 139–140
    transitional vesicles from RER, 139
  tubulation, 11
  vacuolation of, 141
  very low-density lipoproteins (VLDLs), 169
  vesiculation, 9
Goodpasture syndrome, 901
Goussia, 558
GPIIb/IIIa complex, 248
GPS (gray platelet syndrome), 256
Grains, 589
Gram stain procedure, 425
Gramicidin, 84
Granular compartment, nucleolus, 133, 134
Granular matrix inclusions, mitochondrial, 39
Granular pneumocyte, 717–718, 718f
  hyperplasia, 720, 723
Granulation tissue, 295
Granules
  adhesomes, 308
  amylopectin, 526
  bacterial
    glycogen, 439
    PHB, 439
    phosphorus, 439
    volutin, 438–439
  basophil, 221f, 221–222
  calcium-sequestering granules, mitochondrial, 183
  dense, 207, 248, 256–257
  eosinophil, 243, 244f, 245
  gelatinase, 233
  glycogen, 439
  Golgi intracisternal, 9
  interchromatin clusters, 129
  intracisternal, 9, 844, 846f, 847f
  mast cells, 217–218, 221
  melanin, 787, 787f
  mitochondrial calcification, 39
  neutrophil, 231, 232t, 233
  perichromatin, 13, 134, 768
  platelet, 248, 251
  secretory
    accumulation in necrosis, 40
    autophagy, 71
    colchicine effect on, 89
    contents, 142
    crinophagy, 772, 773f
    end-stage, 144
    exocytosis, 143
    Golgi origin of, 141
    inclusions, 847–849
    increase in, 21, 22
    insulin secretion, 145
    microtubule guidance of, 88
    in neoplastic cells, 772, 773f, 774f, 775
    protozoal cell, 525
    yolk, 145, 146f
  stress, 67
  toxic, 240
  in *Trichinella,* 598
  volutin, 438–439
Granuloma inguinale, 466
Granulomas
  Candida infection, 583
  description, 273
  microgranulomas, 273f
  mycobacterial, 493
Granulomatous amoebic encephalitis, 528
Granulomatous encephalitis, *Toxoplasma gondii,* 555
Granulomatous inflammation, macrophages and, 272–273, 273f
Granulomatous lesions, syphilis, 508
Granulophysin (CD63), 231
Granulovacuolar degeneration, 11, 69, 839
Granulysin, lymphocyte, 287
Granuphilin, 143
Granzymes
  granzyme B, 83, 217
  lymphocyte, 287
Gray collies, cyclic hematopoiesis in, 814
Gray platelet syndrome (GPS), 256
Griseofulvin
  alcoholic hyalin, 849f, 850–851

hepatotoxicity, 627, 821, 849f, 850–851
porphyrin crystals and, 630
Growth cones, 669
Growth factors, in hepatic regeneration, 747, 749
Growth genes, 758
Growth hormone (somatotropin), hepatocyte effects, 613
Growth rate, tumor, 757–758
GSS (Gerstmann-Sträussler-Scheinker syndrome), 839, 915
GTPases, 115
GTP-binding proteins, 115
Guamanian amyotrophic lateral sclerosis-parkinsonism dementia complex (ALS-PDC), 677
Guanethidine, 83, 677
Guillain-Barré syndrome, 461, 893f
Gumboro disease, 393
Gummas, syphilis, 508
Gut-associated lymphoid tissue (GALT), 278
GW bodies, 746
Gyrate atrophy, 192–193

H

Haemophilus, 478t, 479f, 479–480
Haemoproteus, 549
Hairy leukoplakia, 337
Haloperidol, 684
Halothane, hepatotoxicity, 619
Hammondia, 555
Hamsters
measles in, 362
rodent scrapie, 913
Hanta pulmonary syndrome, 392
Hantavirus genus, 392
HAV (hepatitis A virus), 397, 399
Haverhill fever, 510
HBV (hepatitis B virus), 354–355, 355f, 900
HCV (hepatitis C virus), 389, 391, 900
HDL (high-density lipoprotein), 171–172, 172f
Healing, regulation by coagulation factors and platelets, 224
Heart. *See also* Myocardium
canine parvovirus enteritis, 350
cardiotoxicity, 635–651
HIV infection and, 412
Heart failure cells, 306f, 720
Heartwater, 451
Heartworm, membranous glomerulonephritis and, 897, 897f
Heat shock proteins, 66, 842
Heavy metals. *See also specific metals*
endothelial cell toxicity, 688, 690
toxicologic enhancement in SER, 157
Heinz bodies, 96f
Helicobacter, 462t, 464, 465f
Helicobacter heilmannii-like organisms (HHLO), 464
Helioid inclusions, 766
Helper T cells, 288–289
Hemagglutinating encephalomyelitis virus (HEV), 373
Hemangiopericytoma, 781f
Heme, 815–816
Heme export protein (HEP), 815–816, 819
Heme oxygenase-1 (HO-1), 64, 183, 208, 819
Hemidesmosomes
description, 100f, 100–101
detachment, 17
neoplastic cells, 766
Hemin storage, in bacterial cells, 440
Hemobartonella, 445t, 446f, 447
Hemochromatosis, 817
Hemoflagellate, 529
Hemoglobin
hemoglobin-derived pigments, 815–817
bilirubin, 821–822
erythrophagocytosis and, 817f–820f, 817–819
ferritin, 816, 816f
heme, 815–816
hemosiderin, 817
malarial pigment, 822
porphyrias, 819–821
phagocytosis by malarial parasites, 547
Hemoglobinemia, 712
Hemogregarines, 558
Hemolytic uremic syndromes, 902
Hemophore, 439
Hemoplasmas, 447
Hemopoietic stem cell, 120
Hemorrhages, in adenoviral infection, 341
Hemorrhagic fever with renal syndrome (HFRS), 392
Hemorrhagic fevers, 380–381
Hemorrhagic septicemia, 482
Hemosiderin, 816, 817
Hemosiderosis, 817
Hemosporidians, 538–543, 539f, 540t–541t, 542f
Babesia, 538, 539f
Babesiosoma, 543
Cytauxzoon, 541, 543
Theileria, 538, 541
Hemostasis, 247f
Hemoxygenase I (HO-1), 67
Hemozoin, 547, 822
Hendra virus, 362, 364
Henipavirus genus, 362, 364
Henneguya spp., 597
Henoch-Schoenlein syndrome, 902
HEP (heme export protein), 815–816, 819
Hepaciviris genus, 389, 391
hepatitis C virus (HCV), 389, 391
Hepadnaviridae family, 354t, 354–355, 355f
Avihepadnavirus genus, 355
duck hepatitis virus (DHV), 355
Orthohepadnavirus genus, 354–355, 355f
hepatitis B virus (HBV), 354–355, 355f
woodchuck hepatitis virus, 355
Heparin, 217, 224, 307, 780
Hepatic artery, 607, 608f
Hepatic encephalopathy, 191–192
Hepatic fibrosis, 295
Hepatic glycogen depletion, 161
Hepatic schizogony, 548
Hepatitis
adenoviral, 340–343, 341
herpesviral, 336f
Hepatitis A virus (HAV), 397, 399
Hepatitis B virus (HBV), 354–355, 355f, 900
Hepatitis C virus (HCV), 389, 391, 900
Hepatitis E virus (HEV), 399, 401
Hepatocellular carcinoma, 355
Hepatocystis, 549
Hepatocytes
acute cell swelling, 4f, 8f, 10f
adenoviral infection, 341
atrophy, 29
autophagy and steatosis, 12f
centrolobular, 607
coagulation necrosis, 32f
diabetes mellitus, 163
duck plague, 336f
glycogen bodies, 161, 162f
hepatitis B virus, 354–355, 355f
in hibernation, 751
hypoxia-inducible factor, 154
inclusions in endoplasmic reticulum, 843, 845f
ischemia, 51
lipids in, 169
lipoprotein metabolism, 170
malarial extraerythrocytic phase, 543, 545
mitochondria, normal, 180f
normal, xivf, 606f, 607
pinocytic reticulum, 113–114
portal zone, 607
regeneration, 747, 748f, 749
serum amyloid A production, 831
smooth endoplasmic reticulum, 156f, 157

in starvation, 607
vacuolation, 6f
water avoidance stress, 607
Hepatocytomegaly, 627
Hepatogenous porphyria, 821
Hepatotoxins/hepatoxicity, 609–630
aromatic halogenated hydrocarbons, 622–623
dioxins, 623
polychlorinated biphenyls (PCBs), 622–623
cytomegaly-inducing, 627
pyrrolizidine alkaloids, 627
cytoskeleton and, 627
microcystins, 627
Golgi complex and, 619
brefeldin A, 619
halothane, 619
lysosomotropic, 609–611
chloroquine, 610
tilarone, 610
mitochondrial, 623–626, 624f, 625f
free radical initiators, 625
hydrazine, 626
nucleoside analogues, 625–626
nuclear, 626–627
aflatoxins, 626–627, 628f
particulate, 627, 629f, 630
bile duct toxins, 630
lithocholic acid, 630
microgranulomatosis, 627, 630
peroxisomotropic, 610–612, 612f
clofibrate, 611
gemfibrozil, 611–612
ribosomes and, 619
cycloheximide, 619
rough endoplasmic reticulum (RER) and, 611–612, 613–614, 619
acetaminophen, 618–619
modeccin, 613–614
phenobarbital, 614
ribosome-inactivating proteins (RIPs), 613–614
ricin, 614, 618
volkensin, 613–614
smooth endoplasmic reticulum (SER) and, 619–622
carbon tetrachloride, 620–621, 621f
cyanamide, 620, 621f
ethanol, 621–622, 622f
steatosis and, 626
ultrastructural studies in animal models, 614t–618t
Hepatovirus genus, 397, 399
avian encephalomyelitis, 398f, 399
hepatitis A virus (HAV), 397, 399
Hepatozoon, 558
Hepcidin, 819
Hepevirus genus, 399, 401
hepatitis E virus (HEV), 399, 401
Hereditary fibrinogen amyloidosis, 834
Hereditary nephritis, 901
Hereditary tyrosinemia, 869–870
Hermansky-Pudlak syndrome (HPS), 256, 814
Herpes simplex virus (HSV), 330, 332f, 332–333
Herpes zoster, 333
Herpesviridae family, 327–338, 328t–330t, 331f
Alphaherpesvirinae subfamily, 330–335
herpes simplex virus (HSV), 330, 332f, 332–333
Mardivirus genus, 333, 335
Marek's disease virus, 333, 335
Simplexvirus genus, 330, 331f, 332f, 332–333
Varicellovirus genus, 333
Betaherpesvirinae subfamily, 330–335
Cytomegalovirus genus, 335, 338f
human herpesvirus 6 (HHV-6), 335
Roseolovirus genus, 335
duck plague, 338
frog renal carcinoma, 338
Gammaherpesvirinae subfamily, 337–338
Epstein-Barr virus (EBV), 337
Lymphocryptovirus genus, 337
Rhadinovirus genus, 337–338
saimiriine herpesvirus 2, 338
non-coding RNAs, 131
pathogenesis, 330
virion structure, 327, 330
Herring body, 842f
Heterochromatin, 130
Heterologous nuclear ribonucleoprotein (hnRNP), 129
Heterologous nuclear RNA (hnRNA), 129
Heterophagy, by Kupffer cells, 71
HEV (hemagglutinating encephalomyelitis virus), 373
HEV (hepatitis E virus), 399, 401
Hexacarbon solvents, 681
Hexachlorophene, 682
Hexamita, 537
Hexosaminidase, 860
Heymann nephritis, 892–893
HFRS (hemorrhagic fever with renal syndrome), 392
HGPS (Hutchinson-Gilford progeria syndrome), 127, 301–302, 751
HHH (hyperornithinemia-hyperammonemia-homocitrullinuria), 192
Hibernation
arousal, 752
description, 751
development of, 751
HIF-1α, 186
High endothelial venules, 287
High-density lipoprotein (HDL), 171–172, 172f
Himalayan rabbit, 814
Hirano bodies, 839
Histamine, 217
Histiocytosis X, 274, 274f
Histocompatibility antigens, 763
Histomonas, 537–538
Histone octamer, 130
Histoplasma, 572f, 579f, 585, 587f, 587–588
Histoplasmosis, 585, 587f, 587–588
HIV (human immunodeficiency virus), 410–412, 411f, 413f, 903
H^+-K^+-ATPase, 145
HMGCoA reductase, 174
HMGCoA reductase inhibitors
skeletal muscle myopathy from, 653
smooth endoplasmic reticulum proliferation, 620
hnRNA (heterologous nuclear RNA), 129
hnRNP (heterologous nuclear ribonucleoprotein), 129
Hog cholera
arteritis, 880, 880f
description, 388–389
epithelial infection, 390f
glomerulonephritis, 389, 896f
Hooded mitochondria, 188, 189
Hook2, 67
Horses
bacterial diseases
anthrax, 496–497
Dermatophilus, 496
ehrlichiosis (Potomac fever), 451
glanders, 459
Rhodococcus, 496
viral diseases
African horse sickness (AHS), 377
Berne virus, 373
Borna disease virus, 386
eastern equine encephalitis (EEE), 382, 383f
equine arteritis virus (EAV), 384, 385f, 386, 881
equine infectious anemia (EIA), 414–415
equine morbillivirus, 362, 364

Horses (*cont'd*)
Hendra virus, 362, 364
Venezuelan equine encephalitis (VEE), 382, 384
vesicular stomatitis virus (VSV), 367
western equine encephalitis (WEE), 382
HPS (Hermansky-Pudlak syndrome), 256, 814
HSV (herpes simplex virus), 330, 332f, 332–333
Human adenoviruses, 340
Human caliciviruses, 399
Human coronaviral diseases, 370
Human disease. *See also specific diseases*
prion diseases
Creutzfeldt-Jakob disease (CJD), 914–915
fatal familial insomnia (FFI), 915
Gerstmann-Sträussler-Scheinker syndrome (GSS), 915
kuru, 914, 914f
viral diseases
adenoviruses, 340
caliciviruses, 399
Colorado tick fever (CTF), 379
coronaviral diseases, 370
cytomegalovirus (CMV), 335
dengue fever virus, 388
Ebolavirus, 370
encephalomyocarditis (EMC) viruses, 397
enteroviruses, 394
Epstein-Barr virus (EBV), 337
Hantavirus, 392
hepatitis A virus (HAV), 397, 399
hepatitis B virus (HBV), 354–355, 355f
hepatitis C virus (HCV), 389, 391
hepatitis E virus (HEV), 399, 401
herpes simplex virus (HSV), 330, 332f, 332–333
human herpesvirus 3 (HHV-3), 333
human herpesvirus 4 (HHV-4), 337
human herpesvirus 6 (HHV-6), 335
human immunodeficiency virus (HIV), 410–412, 411f, 413f
human papilloma virus (HPV), 346
human T-lymphotrophic virus (HTLV), 410
influenza, 356–358
Junin virus, 380
Machupo virus, 380
measles virus, 357f, 360, 362
metapneumoviruses, 366
molluscum contagiosum, 327
parainfluenza viruses, 360
parvovirus, 350
poliovirus, 394
polyomavirus, 347–348, 348f
reovirus, 376
respiratory syncytial virus (RSV), 364, 366
rhinovirus, 394, 397
rotaviruses, 378
rubella, 384
severe acute respiratory syndrome (SARS), 370
varicella virus, 333
yellow fever virus, 386–388
Human herpesvirus 3 (HHV-3), 333
Human herpesvirus 4 (HHV-4), 337
Human herpesvirus 6 (HHV-6), 335
Human immunodeficiency virus (HIV), 410–412, 411f, 413f, 903
Human metapneumoviruses, 366
Human papilloma virus (HPV), 346
epidermodysplasia verruciformis, 346
genital carcinoma, 346
Human parainfluenza viruses, 360
Human parvovirus, 350
Human protothecosis, 575
Human relapsing fever, 508
Human reoviral disease, 376
Human rotaviruses, 378
Human T-lymphotrophic virus (HTLV), 410
Huntaway dogs, mucopolysaccharidoses in, 866
Huntingtin, 841
Huntington's disease, 841
Hurler's disease, 865–866
Hürthle cell follicular carcinoma, 777f
Hutchinson-Gilford progeria syndrome (HGPS), 127, 301–302, 751
Hyalin, alcoholic, 621, 849f, 849–851
Hyalin bodies, 771
Hyalin droplet inclusions, 844, 845f, 846
Hyalin membrane disease, 723
Hyaline arteriopathy, 879
Hyaluronic acid, 304
Hyaluronidases, 304, 658
Hydrazide, myelinopathy from, 682
Hydrazine
hepatotoxicity, 626
megamitochondria, 626
Hydrocephalus
bluetongue virus, 377
reoviral disease, 376
Hydrogen peroxide
antimicrobial action, 238, 239
increased production in ischemia, 187
in phagosome, 239
Hydrogen sulfide
protection from oxidative stress by, 186
pulmonary damage from, 729
Hydrogenosome, 154, 537
Hydropic degeneration, 5, 6f
3-hydroxy-4-pyrone, microgranulomatosis and, 630
Hydroxyapatite crystals, from ischemia, 51
12(S)-hydroxyeicosatetraenoic acid (12-HETE), 38
Hydroxyl radicals, antimicrobial action of, 238, 239
Hyaluronate receptor, 901
Hyperammonemia, 192
Hyperammonemic encephalopathy, 688
Hyperbilirubinemia, congenital, 821–822
Hypercalcemia
of cancer, 802
vitamin D-induced, 881
Hypereosinophilic syndromes, 246
Hyperglycemia
in diabetes mellitus, 163
glycosylation induced by, 904
neuronal damage from, 668
Hyperkalemia, Na-K-ATPase increase and, 80
Hyperkeratosis
epidermolytic, 92
papillomavirus, 343
Hyperlipidemia
familial combined hyperlipidemia, 173
macrophage uptake in, 174
Hyperlipidemic drugs, peroxisomal hypertrophy from, 154, 155f
Hyperornithinemia-hyperammonemia-homocitrullinuria (HHH), 192
Hyperoxaluria, 155
Hyperoxia, mitochondria lesions and, 711
Hyperoxalurias, primary, 711
Hyperpigmentation, 812
Hyperpipecolic acidemia, 155
Hyperplasia
chronic, 22, 22f
chronic active, 22f
description, 21–22
endocrine cells, 22–23

peracute, 24f
salivary gland, 26
Hypertension
endothelium and, 209
mitochondriopathy of chronic, 195–196
pulmonary, 209
Hypertrophy
adaptive responses to persistent injury, 21f, 21–23, 22f, 24f
cardiac, 640–641
defined, 21
hyperplasia, 21–23, 22f, 24f
mitochondrial, 187, 187f, 188–191, 189f, 191f
myocardial enlargement, 200f
nuclear, 126f
peroxisomal, 154, 155f
Hypervitaminosis D, calcification and, 881
Hyphae
Aspergillus, 580, 581f
Candida, 583
death of, 579
dermatophyte, 590–591, 593f
Hypocalcemia, oxalate nephropathy and, 710
Hypoglycemia, neuronal damage from, 668
Hypomelanization, 812
Hypomethylation, of genomic DNA, 761
Hyponatremia, renin-angiotensin system and, 708
Hypotension, endothelial damage from, 208–209
Hypothermia, membrane condensation in, 62
Hypothyroidism, 304
Hypoxia
alveolar wall damage, 717
anaerobic shift to glycolysis, 63
angiogenesis and, 779
angiogenesis stimulation by, 223–224
cytoplasmic blebbing, 20
endothelial damage, 208, 208f
endothelial response to, 208, 208f
fish tolerance of, 736
mitochondrial effects, 186–187
mitochondrial response to, 66–67
nephrotoxicity and, 711
peroxisomal response to, 154
as signal for energy conservation, 66–67
Hypoxia-inducible factor, 66, 67, 154

I

I cell disease, 866
Ia1 gene, 814
IAPP (islet amyloid polypeptide), 834
IBD (infectious bursal disease), 393
Ibotenic acid, 685
IBV (infectious bronchitis virus), 373
ICAM-1 (intercellular adhesion molecule-1), 214, 215, 394
Iccosome, 119, 275
ICH (infectious canine hepatitis), 340–341, 341f, 343
Ichthyophthirius, 529
Ichthyosis, 860–861
Icterus, bilirubinemia and, 712
Ichthyosis, congenital, 92
Idiopathic arterial calcification of infancy, 881
Idiopathic scoliosis, 257
IDIR (infectious diarrhea of infant rats), 379
IDL (intermediate-density lipoprotein), 170–171
IFNg-IFNg receptor complex, 269
IgA glomerulopathy, 900–901
IgG Fc receptor, 237
IL-8, 234, 270
Imatinib, cardiotoxicity of, 646, 649f
Iminodipropionitrile, 92
Imipramine, 684
Immotile cilia syndrome, 89, 89f, 101
Immune complex disease
glomerulonephritis, 548
trapping of complexes in basement membrane, 309–310
Immune system
IgA glomerulopathy, 900–901
light-chain nephropathy, 834, 901
mechanisms in glomerulopathy, 892t
Immune (idiopathic) thrombocytopenic purpura (ITP), 255
Immunoelectron microscopy, xvi
Immunoglobulin A (IgA)
endosomes and, 114
glomerulopathy, 900–901
secretory piece, 114
Immunoglobulin light-chain-induced amyloidosis, 834
Immunoglobulin superfamily adhesins, 80
Immunoglobulins, phagocytosis and, 116
Immunologic degranulation, 221
Immunosuppression, by feline leukemia virus, 406
Immunotactoid glomerulopathy, 900
Implantation, cancer cell interaction and, 783, 785, 786f
Import matrix proteins, 155
Incertae Sedis (order), 447, 448t
Inclusions
alcoholic hyalin (Mallory bodies), 849f, 849–851
autophagic, 849
bacterial, 438–439
description, xv
endocytic and lysosomal, 849–851
endoplasmic reticulum, 843–849, 845f–848f
extracellular, 851
glycogen-SER, 161
Golgi complex, 843–844
hyalin droplet, 844, 845f, 846
intracellular inclusion in *P. multocida,* 432f
intracisternal, 844, 846f, 847f
nuclear matrix, 842
protein intracellular, 843t–844t
pseudoinclusions, 15, 851, 851f
secretory granules, 847–849
tubular, 846, 847f
tubuloreticular, 847, 848f
viral, 850f, 851
India ink, hepatotoxicity of, 627
Individualization, 18
Infantile osteopetrosis, 806–807, 870
Infarction of gills, 737
Infectious bovine keratoconjunctivitis (pinkeye), 482
Infectious bovine rhinotracheitis, 334f, 877f
Infectious bronchitis virus (IBV), 373
Infectious bursal disease (IBD), 393
Infectious canine hepatitis (ICH), 340–341, 341f, 343
Infectious diarrhea of infant rats (IDIR), 379
Infectious mononucleosis, 337
Infectious myxomatosis, 324, 327
Infectious pancreatic necrosis (IPN), 392–393
Inflammasome, 116
Inflammation, 209–217, 210f
acute, 308–309
angiogenesis in repair of, 225
basement membranes in, 308–309
blood-tissue barriers, 217
chronic, 309
endothelial cell activation, 203f–204f, 211–212, 214f, 214–215
glycosaminoglycan accumulation, 304
hyperemia and edema, 212f
liver fenestrated endothelium, 216–217
lymph vessel endothelium, 215–216, 216f
macrophages in, 270–273
mast cell in early, 218f
melanization associated with, 812
perivascular changes in acute, 211t
ultrastructural evidence of, 211, 212f, 213f
vascular changes in acute, 209t

Influenza, 356–358
avian, 358
porcine, 357f
Infrared A radiation, 188
Inhalant injury, acute, 726–727, 727f
Initial body, anaplasma, 451
Initiation complex, 136
Initiation factors, 136
Injured cells, response of, xv
Injury. *See also specific agents; specific sites*
acute inhalant, 726–727, 727f
adaptive responses to persistent, 21–29
atrophy, 26, 28f, 29
cytomegaly, 23, 25f, 27f
hypertrophy, 21f, 21–23, 22f, 24f
metaplasia, 26
multinucleate giant cells, 23, 26
cellular, response to, 5–31
acute cell swelling, 5–20
adaptive responses, 21–29
responses of artery to, 875–877
Inner membrane, degradation of mitochondrial, 38
Inositol 1,4,5-triphosphate (IP3), 46
Inositol pyrophosphates, 81
Insecticides, skeletal muscle myopathy from, 653
Insertional mutagenesis, 402
Insulin
glucose transporters and, 164
secretion, 145
Insulin growth factor binding protein 7 (IGFBP7), 752, 787
Integral proteins, 78, 763
Integrin-adhesion complex, 96
Integrins
Borrelia attachment to, 505
description, 80, 96–97
hemidesmosomes, 100–101
integrin αVβ3, 223–224
integrin αVβ5, 224
leukocyte B_2, 237
neoplastic cells, 763
neutrophil chemotaxis, 234f
signal transduction, 111
of *Yersinia,* 475
Intelectin, 103
Intercalated disks, 635
Intercellular adhesion molecule-1 (ICAM-1), 214, 215, 394
Intercellular junctions
arterial, 875
description, 204
desmosomes
acute cell swelling, 19f
belt, 100
description, 98f, 99–100
disintegration of, 17
hemidesmosomes, 100f, 100–101, 766
neoplastic cells, 766
spot, 100
disruption in necrosis, 36
fluid transport, 211
gap junctions
arterial, 875
closure, 17
description, 97–99, 98f, 204
neoplastic cells, 766
proteins, 97
uncoupling, 35
neoplastic cells, 766
permeability of interepithelial spaces, 99f
tight junctions
blood-brain barrier and, 688
density, 211
description, 97, 98f, 204
disassociation, 17
neoplastic cells, 766
slit diaphragms, 695, 696, 697
Intercellular space, granulovesicular debris accumulation in, 17
Interchromatin granule clusters, 129, 746
Interchromatin regions, 129
Interdigitating cells, thymus, 282
Interendothelial junctions, 204
Interferon-γ (IFN-γ)-induced TRAIL pathway, 787
Interferon-gamma (IFN-γ)
apoptosis induction, 47
description, 269
endocytosis and, 112
IFNg-IFNg receptor complex, 269
Interleukin-1 (IL-1), 47, 116, 235, 270
Interleukin-2 (IL-2), 728
Intermediate coat, pox virion, 322
Intermediate endosome, 110, 113–115
Intermediate filaments, 17, 18, 36, 91–92
hereditary disorders, 91–92
neoplastic cells, 764, 766
structure and formation, 91
Intermediate-density lipoprotein (IDL), 170–171
Interneurons, 687
Interphase, 744
Interphase nuclei, 744f, 745
Interstitial fibrosis, 26
Interstitial laminated oxalate plaques, 710
Intestinal adenomatosis, 461
Intestine
canine parvovirus enteritis, 350
endosomal receptors, 114
intermediate filament disorders, 92
iron utilization, 818
Na-K-ATPases, 80
Intracellular alkalinization, Bax activation by, 42
Intracellular calcification, 797–798, 798f, 803f
Intracellular proteins, release during necrosis, 36
Intracellular trafficking, 108f, 109–123
endocytosis, 108f, 109–115
absorptive, 109
caveolae, 109, 111f, 111–112
clathrin-mediated, 109, 112f, 112–113
description, 109–110
endosomal pool, 113–115
endosomal receptors in tissue, 114–115
lipid raft-mediated, 114
macroendosomes, 114
microtubule guidance, 114
pinocytic reticulum, 113–114
pinocytosis, 109, 110–111
receptor-mediated, 109, 113
transcytosis, 109, 110f
exocytosis, 108f, 118–121
lysosomes, 108f, 116–118, 117f
phagocytosis, 108f, 115–116
suppression in necrosis, 40
Intracisternal granules, 9, 844, 846f, 847f
Intramembrane lysis, 81–82
Intramitochondrial tubules, 189
Intranuclear inclusions. *See also specific inclusion types*
in acute cell swelling, 13, 14f
neoplastic cells, 766
Intravascular macrophages, 720, 721f, 723
Introns, 132
Invadopodia, 763, 781
Invasins, of *Yersinia,* 475, 476
Invertasome, 440
Involucrin, 312
Involution of organs, basement membrane processing and, 307
Ion channels. *See also specific channel types*
drugs that insert as, 84–85
endocytosis regulation and, 114
transport proteins, 84t
Ion pumps, 62
Ionophores, 84–85, 648–649
IP3 receptor (IP3r), 46
IPN (infectious pancreatic necrosis), 392–393
Ipomeanol, 728
Iridophore, 815
Iridoviridae family, 352t, 353
cytomegaly, 23

Lymphocystivirus genus, 353
Ranavirus genus, 353
Iron
absorption, 817
inclusions, 439–440
oxidative, 38
Iron-sulfur clusters, 195
Ischemia
anoxic phase, 51
arterial myocyte, 875
brain injury from, 668
chronic, 187
defined, 49
events in necrosis caused by anoxia, 50t
hepatocytes in, 51
mitochondrial effects, 49, 187
myocardial, 51, 641, 643
nephrotoxicity and, 711–712
neurons in, 51
postischemic phase, 51
reperfusion injury, 641
Islet amyloid polypeptide (IAPP), 834
Isoniazid, myelinopathy from, 682
Isoproterenol, cardiotoxicity of, 650
Isospora, 550
Ivermectin, 685

J
Jaagsiekte sheep retrovirus (JSRV), 406
Japanese B encephalitis virus, 388
JC polyomavirus, 347–348
Johne's disease, 494
Junctional adhesion molecules (JAM), 204, 682
Junctional epidermolysis bullosa, 309
Junctional triads, 639
Junctions, intercellular. *See* Intercellular junctions
Junin virus, 380
Juxtaglomerular apparatus
function, 708
renin-angiotensin system, 708
toxins, 708, 709f
angiotensin II antagonists, 708
angiotensin-converting enzyme inhibitors, 708
FK506, 708
ultrastructure, 708, 709f

K
K^+ channels, 678
Kainic acid, 685
Kaposi's sarcoma, 780
Karyokinesis, 274
Karyoklasis, 15
Karyolysis, 40
Karyopherins (Kaps), 129
Karyorrhexis, 15
Kearns-Sayre syndrome, 193
Keloids, 295
Kennel cough, 457
Keratan sulphate proteoglycans, 304
Keratin, 91–92
Keratinocyte
herpesvirus, 331f, 332f
nuclear and cytoplasmic proteolysis, 14f
papillomavirus, 343–344, 345f
parapoxviruses, 325f
swinepox, 327f
Keratitis, acanthamoebic, 528
Keratoconjunctivitis, microsporidial, 561
Kernicterus, 821
Keshan disease, 190
Ketamine, 677
Ketosis, 161
Kidney. *See also* Nephrotoxins/nephrotoxicity
amyloid, 828f, 833
Candida infection, 583, 584f, 585
endosomal receptors, 114
glomerulopathy, 891–909
glomerulopathy lesions in transplanted, 903
hypertrophy, 21f
hypoxic activation of HIF-1, 67
immune complex glomerulonephritis, 548
Leucocytozoon infection, 548
malaria and, 548
Na-K-ATPases, 80
Killer dendritic cells, 787
Kimmelstiel-Wilson lesion, 903–904
Kinase signaling pathways, 43
Kinectin, 114
Kinesins, 114
Kinetochore, 130, 745–746
Kinetodesmal fibrils, 525
Kinetoplast, 533
Kinetosome, 528
Kininogen receptors, 235
Kissing bugs, American trypanosomiasis and, 534
Klebsiella, 467t, 473
Klotho mice, 752–753
Korat cat, hexosaminidase defects, 860
Krabbe's disease (globoid cell leukodystrophy), 856f, 861
Kudoa spp., 597
Kupffer cells
adenoviral infection, 341
heterophagy by, 71
role of, 607, 609
in yellow fever virus, 387
Kuru, 839, 914, 914f
Kyasanur Forest disease virus, 388

L
L forms, 430
Lactate dehydrogenase-elevating (LDH) virus, 386
Lactic acid, myocardial toxicity and, 643
Lactobacillales (order), 500–502, 501t
Streptococcus genus, 500–502, 501t
Lactoferrin deficiency, 242
LAD (leukocyte adhesion deficiency), 242–243
Lafora bodies, 67
Lafora disease, 856f, 868–869
Lagovirus genus, 399
LAL (lysosomal acid lipase), 861
Lamellipodia
description, 103
endothelial, 223
microfilaments and, 90
neoplastic cells, 763
neutrophil, 237
platelet, 251
Lamin, 127, 308
Lamina densa, 307
Lamina (pars) fibroreticularis, 307
Lamina lucida (rara), 307
Laminin, 205, 307
Laminopathy, 127
Langerhans' cell histiocytosis, 274, 274f
Langerhans' cells
antigen presentation, 277
killing of neoplastic cells, 787
skin, 277
Lankesreella, 560
Large granular lymphocyte (LGL), 287, 289f
Larvae, *Trichinella,* 598
Laryngeal papilloma, 346
Lateral bodies, pox virion, 322
Lateral geniculate nucleus, 814
Lathyrism, 299
Lattice arrangements, in autophagosomes, 11, 69
Launois-Bensaude's disease, 167
LC3, 116
LCM (lymphocytic choriomeningitis), 379–380
LDH (lactate dehydrogenase-elevating) virus, 386
LDL. *See* Low-density lipoprotein (LDL)
LDL receptor-related protein (LRP), 81
LDL receptors, 137, 171, 173
Lead
myelinopathy from, 682
nephrotoxicity, 703f
neurotoxicity, 682, 688, 690
Lead monoxide, 688

Leber's hereditary optic neuropathy, 194
Lecithin-cholesterol acyl-transferase (LCAT), 172, 173
Legionella, 476–477, 477t
Legionellales (order), 476–477, 477t
  Coxiella genus, 476, 477t
  Legionella genus, 476–477, 477t
Leishmania, 535f, 535–536
  L. braziliensis, 535
  L. donovani, 535, 536
  L. leishmani infantum, 536
  L. major, 535
  L. mexicana, 535
  L. tropica, 536
Leishmanial flagellate form, 529, 532f
Leishmaniasis, 535–536
  cutaneous, 536
  mucocutaneous, 535
  visceral, 536
Leishporin, 85
Lentivirus genus, 410–415, 411f, 413f, 414f, 415f
  equine infectious anemia (EIA), 414–415
  human immunodeficiency virus (HIV), 410–412, 411f, 413f
  simian immunodecifiency virus (SIV), 412, 414f
  visna, 412, 414
Lepromatous placentitis, 494
Lepropoxvirus genus, 324, 327
Leprosy, 493–494
Leptofibrils, 36
Leptomeres, 36
Leptomonad flagellate form, 529, 532f
Leptospira, 505, 506t, 507f
Lethal factor (LF), *Bacillus anthracis,* 497
Leucocytozoon, 546f, 548–549
Leukemia viruses
  feline leukemia virus (FeLV), 406–407, 408f
  human T-lymphotropic virus (HTLV), 410
  murine leukemia viruses (MLVs), 407, 408f, 409f, 409–410
Leukocyte adhesion deficiency (LAD), 242–243
Leukotoxin
  Fusobacterium, 510
  Mannheimia, 480
Leukotrienes
  leukotriene B, 233
  leukotriene B4, 234
  mast cells, 217
  neutrophil chemotaxis, 235
Lewy bodies, 67
Lewy body disease, 840
LGL (large granular lymphocyte), 287, 289f
Ligand, defined, 81
Ligand-receptor clustering, 253
Ligand-receptor complex, 81, 358
Light-chain nephropathy, 834, 901
Linkage protein defects, 90–91
Lipid. *See also* Lipid globules; Lipid metabolism; Lipid metabolism disorders; Lipid storage diseases
  adipocyte defects, 167
  adipocytes, 167
  in atherosclerosis, 881, 883, 883f, 884f
  atrophy of fat, 167, 168f, 169
  brown fat cells, 167
  cytoplasmic lipid inclusions, 165–166
  glycogen-lipid droplet ratio reversal, 9
  in hepatocytes, 169
  lipogenesis, 167
  lipolysis, 167
  mitochondria and metabolism of, 169
  rafts, 78, 111, 114, 549
  secretion
    mammary epithelium, 145
    yolk epithelium in birds, 145, 146f
Lipid A, 431
Lipid globule-associated proteins, 165
Lipid globules, 164–165, 165f, 169
  in bacteria, 439
  carbon tetrachloride toxicity and, 621
  in eosinophils, 245
  fowlpox and, 324
  myocardial toxicity and, 641
  in neoplastic cells, 775
  protozoal cell, 525
  Schwann cell, 683
  in toxic neutrophils, 240
Lipid locule, 167
Lipid metabolism
  cardiotoxicity and, 643, 643f
  change in aging, 750
  peroxisomes in, 154
Lipid metabolism disorders, 173–174
  macrophage uptake in hyperlipidemia, 174
  Tangier disease, 174
  transport defects, 173–174
    acid lipase deficiency, 173
    chylomicron retention disease, 173
    familial combined hyperlipidemia, 173
    familial lecithin-cholesterol acyltransferase, 173
    lipoprotein lipase deficiency, 173–174
  xanthomatosis, 174
Lipid raft-mediated endocytosis, 114
Lipid rafts, 78, 111, 549
Lipid storage diseases, 857–862
  drug-induced disease, 862
  Fabry disease, 862
  Gaucher's disease, 860–861, 861f
  glomerulopathy, 903
  GM_1-gangliosidosis, 857, 858f
  GM_2-gangliosidosis, 860
  Krabbe's disease (Globoid Cell Leukodystrophy), 856f, 861
  models of sphingolipid storage diseases, 859t
  Nieman-Pick disease, 860
  Tay-Sachs disease, 860
  Wolman's disease, 861
Lipidic glomerulopathy, 903
Lipofuscin, 118, 667, 750, 823–824, 824f
Lipogenesis, 167
Lipolysis, 167
Lipopolysaccharide (LPS), 431, 471
Lipoprotein lipase, 170
Lipoprotein lipase deficiency, 173–174
Lipoprotein lipase genes, 736
Lipoproteinosis, alveolar, 732
Lipoproteins
  atherosclerosis, 881, 883, 886
  circulation in bloodstream, 169
  high-density (HDL), 171–172, 172f, 174
  intermediate-density (IDL), 170–171
  lipoprotein(a), 171
  low-density (LDL), 113, 169, 171, 881, 883, 886
  metabolism
    chylomicron pathway, 170
    VLDL-LDL pathways, 170–172
  very low-density (VLDL), 169, 170
Liposome, 166f, 621
Lipoteichoic acid, 500
Listeria, 497t, 497–498
Listeriolysin O, 498
Lithium, nephrotoxicity, 705
Lithium carbonate, 684
Lithocholic acid, cholestasis and, 630
Litomosoides carinii, 600
Liver. *See also* Hepatocytes
  Entameba histolytica and, 527
  erythrophagocytosis, 819, 820f
  fenestrated endothelium of, 216–217
  glycogen depletion, 161
  hepatic encephalopathy, 191–192
  hepatic fibrosis, 295

hepatitis
adenoviral, 340–343, 341
hepatitis A virus (HAV), 397, 399
hepatitis B virus (HBV), 354–355, 355f, 900
hepatitis C virus (HCV), 389, 391, 900
hepatitis E virus (HEV), 399, 401
herpesviral, 336f
hepatogenous porphyria, 821
HIV infection and, 412
ischemia, 51
malarial extraerythrocytic phase, 543, 545
Na-K-ATPases, 80
peliosis hepatis, 412
pinocytic reticulum, 113–114
regeneration in, 747, 748f, 749
Reye's syndrome and, 192
Liver damage. *See* Hepatotoxins/hepatoxicity
LMNA mutations, 127
Lobomycosis, 590
Lobopodia, 526
Local anesthetics, skeletal muscle toxicity of, 654
Locoweed toxin, 672
Long spacing fibers, 299
Long-segmented filamentous organisms (LSFO), 511
Loop of Henle, 705
Losoxantrone, cardiotoxicity of, 644
Louping ill virus, 388
Lovastatin, 688
Low-density lipoprotein (LDL)
atherosclerosis, 881, 883, 886
components, 169
receptor-mediated endocytosis (RME), 113
uptake, 171
Low-density lipoprotein receptor-related protein 6 (LRP6) signalosomes, 69
LPS (lipopolysaccharide), 431, 471
L-selectin, 236
LSFO (long-segmented filamentous organisms), 511
Lubarsch crystals, 848
Luft's disease, 189
Lumpy jaw, 487
Lungfish, 736
Lungs. *See also* Respiratory system
antigen presentation, 278
erythrophagocytosis, 819, 819f
fibrosis, 294f, 295, 296f, 306f, 728–729, 735
HIV infection and, 412
Leucocytozoon infection, 548
mycoplasmosis, 443, 443f, 445
pneumonia
aspergillosis, 581–582
Haemophilus, 479
hyphal, 581
Legionella, 476–477
Mannheimia, 480
mycoplasmal, 443, 443f, 445
Rhodococcus, 496
Staphylococcus aureus, 500
Streptococcus, 502
virus of mice, 366
postinflammatory pulmonary microlithiasis, 800
pulmonary calcification, 800
surfactant, 718, 719f, 723
Lupus erythematosus, 894
Lycocalyceal bodies, 121, 121f
Lyme disease, 505
Lymph nodes
germinal center formation, 277
structure, 275
Lymphatic vessels
alveolar wall, 717
metastasis and, 782
Lymphocryptovirus genus, 337
Lymphocystic disease, 353
Lymphocystivirus genus, 353
Lymphocyte porins, 83
Lymphocytes, 283–291
antigen-specific, 273
B cells, 284
capping, 287, 286f, 289f
differentiation, 283, 283f
killing of neoplastic cells, 787
large granular (NK cells), 287, 289f
neoplastic, invasion of, 782f
plasmacytes, 284, 284f–285f
prion protein production in, 911
programmed cell death, 41f
recirculation, 288f, 287
small, 286–287
T cells, 288–291
Theileria in, 541
trafficking to lymphoid organs, 214
Lymphocyte-specific protein 1, 233
Lymphocytic choriomeningitis (LCM), 379–380
Lymphoid leukosis, 782f
Lymphoid system, in HIV infection, 411
Lymphoid tissue, in scrapie, 912–913
Lymphoma
Burkitt's, 337
feline leukemia virus, 406
Lysophosphatides, 36
Lysosomal acid lipase (LAL), 861
Lysosomal executioner caspases, 47
Lysosomal permeabilization, Bid-dependent, 47
Lysosomal phospholipidosis, 610, 701
Lysosomal storage diseases. *See* Storage diseases
Lysosome
abnormal degradation in metabolic disease, 117
activation, 11
in Alzheimer's disease, 837
autophagolysosome, 69
bacterial replication in, 454, 455
coccidial, 553
cytoplasmic trafficking, 116–118
Entamoeba histolytica, 527
glycogenesomes, 867
hepatotoxins, 609–611
chloroquine, 610
phospholipidosis, 610
tilarone, 610
inclusions, 849–851
membrane repair after infection, 61
mucopolysaccharidoses, 307
Mycobacteria in, 491, 492f, 493, 494
myeloid bodies, 118
myocardium, 638–639
neurotoxins, 672
phagolysosomes, 116–118, 117f, 118f
primary, 116
production of, 116
proximal convoluted tubule toxins and, 700, 701
Rhodococcus, 496
ROS caused membrane degradation, 47
Trypanosoma, 529
tubular, 117
Lysosome-associated membrane protein- and -2)LAMP-1 and LAMP-2), 116
Lysozyme, amyloid from, 835
Lyssavirus genus, 367–368
Lytic necrosis, 33, 34f, 36

M

M cell
description, 278, 279f
Mycobacteria in, 494
Salmonella in, 474
torovirus infection, 374f
Yersinia in, 475
M phase, 744
M protein
M protein-fibrinogen complexes, 500
streptococcal, 500–501
Mac-1-mediated phagocytosis, 47
Machupo virus, 380
Macroendosomes, 114
Macrogamete, 550
Macronucleus, 528
Macrophage
activated, 268f, 270, 271
alveolar, 278, 280f, 581–582, 720, 819f

Macrophage (*cont'd*)
amyloid formation, 831
antigen presentation, 272, 272f
in atherosclerosis, 883, 885
bacterial replication in, 454, 455
Borrelia in, 505
collagen degradation, 299
cytokine secretion, 270
description, 269–270
epithelioid cells, 272
erythrophagocytosis, 817f–820f, 817–819
hemoglobin in, 816f
HIV infection and, 411–412
in inflammation, 270–273
acute, 270–272
chronic, 272–273
granulomatous, 272–273
interaction with lymphocytes, 272f
intravascular, 280f, 720, 721f, 723
killing of neoplastic cells, 787, 787f
Legionella in, 477
Listeria in, 498
microbial killing, 271–272
Mycobacteria in, 491, 492f, 493, 494
myelin destruction by, 680f
pathologic proliferation of
giant cells, 273f, 273–274
Langerhans' cell histiocytosis, 274, 274f
sarcoidosis, 274
phagocytosis of cell debris, 54
in prion disease, 913
prothecal cells in, 573
Rhodococcus, 496
Staphylococcus in, 499f
surface receptors, 270
thymic, 282
Toxoplasma gondii in, 553
uptake in hyperlipidemia, 174
Macropinocytosis, 114
Macrothrombocytopenia, 256
Macula adherentes. *See* Desmosome
Macular degeneration, 195
Macular morneal dystrophy, 304
Macule
description, 319
pulmonary, 720, 731–732
Madura mycetoma, 589
Maedi, 414
Magnesium silicate, 733
Magnetosomes, 439
MAKAPbeta, 69
Malacia, 678
Malakoplakia, 802, 803f
Malaria
avian, 548
cerebral, 547–548
erythrocyte-endothelial interaction, 547
erythrocytic phase, 543, 545, 546f, 547
extraerythrocytic phase, 543, 545
insect cycles, 543
placental lesions, 548
renal lesions, 548
Malarial organisms, 543–549, 544t, 546f
Haemoproteus, 549
Hepatocystis, 549
Leucocytozoon, 546f, 548–549
Plasmodium, 542f, 543, 545, 546f, 547–548
Malarial pigment, 547, 822
Malassezia spp., 590
Malignant catarrhal fever (MCF), 338
Malignant hyperthermia, 191
Malignant lymphoma, 746f, 897
Malignant melanoma
amelanotic, 762f, 776f
melanophage, 787, 787f
melanosomes, 775, 776f, 810f, 812, 814f
Malignant neoplasms, 761. *See also* Cancer
Malin, 869
Mallory bodies, 67, 849f, 849–851
MALT (mucosa-associated lymphoid tissue), 278
Mammalian target of rapamycin (mTOR), 883, 885
Mammary epithelial secretion of lipids, 145
Mammary gland
adenocarcinoma, 779f
iron utilization, 818
tumor staining for secretory components, 772
Mannheimia, 478t, 480, 480f
Mannose-6-phosphate (M6P), 140–141
Mannose-6-phosphate (M6P) receptors, 140
Mannosidosis, 863–864
Maple urine disease, 870
MAPs (microtubule-associated proteins), 86–87
Marburgvirus genus, 369–370
Mardivirus genus, 333, 335
Marek's disease virus, 333, 335
Marfan syndrome, 303, 304
Marginal band, platelet, 248, 251
Marginal body, anaplasma, 451–452
Marginal ridge, 204
Marinesco bodies, 667
MARK/ERK-dependent survival pathway, 47
Mast cell
adherence to schistosome larvae, 245
degranulation, 144f, 217–218, 219f, 221, 221f
in dermatitis, 220f
granules, 217–218, 221
mastocytosis, 220f, 222f, 222–223
T cells and TC cells, 217
tumors and, 788
type I and type II, 217
ultrastructure in tissue lesions, 219t
Mastadenovirus genus, 340–343
canine adenoviruses 1 (CAV-1), 340–341, 343
canine adenoviruses 2 (CAV-2), 340
enteric adenoviruses, 340
human adenoviruses, 340
infectious canine hepatitis (ICH), 340–341, 341f, 343
Mastocytosis, 220f
Masugi nephritis, 893
Matrix, mitochondrial, 183
Matrix degrading proteases, 224
Matrix metalloproteinase-9, 243
Matrix vesicles, 800, 800f
Maurer's clefts, 545
May-Hegglin anomaly, 257
MBP (myelin basic protein), 678
M-calpain, 186
McArdle disease, 868
MCF (malignant catarrhal fever), 338
McIr gene, 812
MDC1, 64
MDMA (3,4-methylenedioxymethamphetamine), 676
Measles virus, 357f, 360, 362
Mechanical injury, to plasma membrane, 61
Mediator, 745
Medin amyloid, 837, 839
Mediterranean spotted fever, 451
Medullary interstitium, renal, 705–706, 706f
Megakaryocyte, 247
Megakaryocytic myelosis, 407
Megalin, 114–115
Megamitochondria, 189, 626
Megasome, 535
Melamine nephrosis, 711
Melanin, 811–814
albinism, 812–814
description, 811
eumelanin, 811
genetic defects in melanization, 814
melanosomes, 810f, 811, 814f
pathologic melanization, 812, 813t
pheomelanin, 811
pigment type switching, 812
synthesis, 811
vitiligo, 812
Melanocytes, 811
Melanophage, 787, 787f, 811

Melanophagosome, 811
Melanophore, 815, 815f
Melanosis, 812
Melanosome
  compound, 775
  description, 811
  in malignant melanomas, 775, 776f, 810f, 812, 814f
Melioidosis, 457, 459
Mellitin, 86
Membrane attack complex (MAC), 83
Membrane attack sequences, 83
Membrane channels, toxins of neuronal, 678
Membrane fragment accumulation, 11
Membrane fusion, in secretion, 143
Membrane internalization, 82
Membrane microdomains, 78
Membrane proteins
  integral, 78, 763
  as receptors, 763
  transmembrane, 763
Membrane pumps, 431
Membrane transport, 79–80
Membrane-acting toxins, 436, 438
Membranes, fluidity of, 622
Membranoproliferative glomerulonephritis, 898
Membranous glomerulonephritis, 890f, 891–898
  animal models, 892–894
    athymic mouse, 894
    rat, 892–893
  naturally occurring, 894–898
    chronic septic disease, 894
    chronic viral disease, 894, 895f, 896f
    glomerulopathy of aging, 894
    neoplasms, 897
    parasites, 897, 897f
Membranous pneumocyte, 716f, 717
Membranous whorls
  in autophagosomes, 11, 69
  in testicular tumors, 771
Meningitis
  Aspergillus, 582
  Haemophilus, 479
Meningitis-associated *Escherichia coli* (MNEC), 472
Meningoencephalitis
  Listeria and, 498
  primary amoebic, 527
Menkes' disease, 822
Menorrhagia, platelets in, 259–260
Mercury
  nephrotoxicity, 700, 702, 704
  neurotoxicity, 690
Merozoites
  babesia, 538
  coccidial, 549–550
  Leucocytozoon, 548
  malarial, 545, 547
Mesangial cells, 697
Mesangiocapillary glomerulonephritis, 898
Mesangiolysis, 697
Mesangiopathy, 697
Mesangiosclerosis, 697
Mesangium, 891, 896f
Mesosome, 440, 440f
Messenger RNA (mRNA), 132–133, 136
Metabolic acidosis, nephrotoxicity and, 712
Metabolic defects
  in DNA and nucleoli, 135–136
  mitochondrial, 191–192
Metabolic disease. *See also* Storage diseases
  lysosomal degradation, abnormal, 117–118
  peroxisomes in, 154
Metabolic shifts, mitochondrial sensitivity to, 184
Metachromatic leukodystrophy, 856f
Metallic toxins, of proximal tubules, 702–705
  cadmium, 704
  lead, 703f
  lithium, 705
  mercury, 702, 704
  platinum, 704f, 704–705
  uranium, 705
Metalloprotease, 579
Metallothionein (MT), 63
Metamorphosis
  autophagy role in, 71
  programmed cell death, 49
Metaphase, 132f, 744, 745
Metaplasia, 26
Metapneumovirus genus, 366
Metastasis, 780–785
  into blood stream, 782f, 782–783, 784f
  coagulation and, 783
  extracellular matrix degradation, 781
  implantation, 783, 785, 786f
  invasion into connective tissue, 780–782
  organ-specific adhesion molecules, 783
Metastatic calcification, 798
Methamphetamine, 672, 676
Methanobrevibacter oralis, 425
Methyl cellulose, hepatotoxicity of, 627
Methylenedioxymethamphetamine (MDMA), 676
Methylphenylpyridine (MPP^+), 669
Methylphenyltetrahydropyridine (MPTP), 669
MHC class II molecules, 272, 272f
MHV (murine hepatitis virus), 370–372
Mice
  Eperythrozoon infection, 445t, 447
  hepatic regeneration in transgenic mice, 749
  Hermansky-Pudlak syndrome (HPS), 814
  membranous glomerulopathy of athymic, 894
  nude, 894
  rodent scrapie, 913
  toxic milk mouse syndrome, 823
  viral diseases
    encephalomyocarditis (EMC) viruses, 397
    epizootic diarrhea of infant mice (EDIM), 379
    lactate dehydrogenase-elevating (LDH) virus, 386
    lymphocytic choriomeningitis (LCM), 379–380
    measles, 362
    mouse mammary tumor virus (MMTV), 404, 405f, 406
    mouse pneumonitis virus, 349
    mouse polyoma disease, 348
    mousepox, 323
    murine polioencephalomyelitis virus (Theiler's virus), 396f, 397
    pneumonia virus of mice, 366
    reoviral disease, 376
    Sendai virus, 360
Michaelis-Guttman bodies, 802, 803f
Microabscesses, in *Candida* infection, 583
Microangiopathic hemolytic anemia, 902
Microbeam Analysis Society, xvi
Microbial collagen degradation, 299
Microbial disease, autophagy in, 71
Microbial lysins, 82, 82f
Microbial porin-induced lysis, 85–86
Microbody, 154, 533. *See also* Peroxisome
Microcompartments, bacterial, 438–439
Microcystins, 576, 627
Microcystis aeruginosa, 575
Microfibrils
  microfibrillopathies, 303
  in scleroderma, 301
  structure of, 303
Microfilaments, 89–91
  disintegration of, 17–18
  linkage protein defects, 90–91
  neoplastic cells, 764

Microfilaments (*cont'd*)
platelet, 248
structure and function, 89–90
toxin/poisons, 88t, 90
Microgametocyte, 550
Microglial cells
antigen presentation, 277
proliferation of, 669
Microgranuloma, 273f, 627, 630
Microliths, 802–803, 804f
Microneme secretory organelles, 543
Micronemes, 526, 538, 549, 550
Micronucleus, 528
Micropinocytosis vermiformis, 113
Micropores, protozoal cell, 525
MicroRNAs, 131
Microscopical Society of America, xvi
Microspherules, 136
Microsporans, 560t, 560–563, 562f, 563f
Encephalitozoon, 561, 562f
Enterocytozoon, 561–563, 563f
Glugea, 563
Nosema, 561
Pleistophora, 561
Microsporum, 590, 591
Microsteatosis, 626
Microtubular transposition defect, 101
Microtubule-associated proteins (MAPs), 86–87
Microtubules, 86–89
centrosomes and centrioles, 88
dissociation of, 18
guidance for endocytosis, 114
hereditary defects, 89, 89f
macrophage, 274
neoplastic cells, 764
platelet, 248
structure and formation, 86–87, 87f
subpellicular, 525, 532, 549
toxins/poisons, 88t, 89
transport, 87–88
Microvesicles
description, 120–121
gentamicin-containing, 701
Microvesicular exocytosis, 19
Microvesicular rosettes, 167
Microvesicular shedding, 120
Microvillar channels, 171
Microvilli
description, 101, 103
distortion in acute cell swelling, 18
proximal convoluted tubule, 700, 701
Microvillous inclusion, 92
Mineralization, pulmonary, 729
Minimal change disease, 696, 900
Mink
Aleutian mink disease virus, 241, 352–353, 894
transmissible mink encephalopathy (TME), 914
Minoxidil, vascular toxicity, 659
Misfolded proteins, 842, 851
Mitochondria. *See also* Mitochondrial DNA (mtDNA); Mitochondrial swelling; Mitochondriopathy
arterial myocyte, 875
autophagy, 71, 623, 625f
calcium regulation by, 181
calcium within, 797, 798f
in cardiac hypertrophy, 640–641
changes in mitosis, 747
in coccidia, 550
deletion in reticulocytes, 753
doxorubicin-induced damage, 644, 644f, 646
ferritin (mtferritin), 816–817
filaments, 188
genome transmission, 183
giant, xviif, 189, 189f, 191f
hepatotoxins, 623–626, 624f, 625f
free radical initiators, 625
hydrazine, 626
nucleoside analogues, 625–626
hooded, 188, 189
hyperactive, 182f
hypertrophy, 21, 22–23, 188–191, 189f, 191f
intramitochondrial protein crystals, 188–189, 189f
megamitochondria (Macromitochondria), 189
riboflavin, 190
thiamine deficiency, 189
vitamin B12 (cobalamin), 189
vitamin E, 190–191, 191f
hypoxic stress response, 66
ischemia, 49–50
kinase signaling pathways, 43
lipid metabolism, 169
metabolic defects, 191–192
hepatic encephalopathy, 191–192
malignant hyperthermia, 191
Reye's syndrome, 192
steatosis and defects in β-oxidation of fatty acids, 191
myocardial, 636–638
of neoplastic cells, 757, 775, 777f
neurotoxicity, 669, 672
annonacin, 669, 672
photofrin, 672
normal, 181–184
calcium-sequestering granules, 183
cristae, 182f, 182–183
DNA, 183
functions, 181
hepatocyte, 180f
inner membrane, 181–183
intermembrane space, 181
matrix, 183–184
outer membrane, 181
permeability transition pores (PTP), 182
respiratory chain, 185f
ribosomes, 184
ultrastructure evaluation, 184
nucleoid, 578
oxidative stress, 836
oxygen deficit, 11
permeability transition pores (PTP), 38, 42, 49–50, 182, 644, 672
protozoal cell, 525–526
proximal convoluted tubule toxins and, 700
in recovery, 63–64
anaerobic shift to glycolysis, 63
antioxidant factors, increase in, 63
cytoprotective enzyme activation, 64
glutathionylation, 63–64
glyceraldehyde-3-phosphate dehydrogenase increase, 64
nitrosylation, 64
respiration, in neoplastic cells, 775
Schwann cell, 682
toxins that block pathways, 186
transport along neuronal processes, 681
in trichinosis, 598
trypanosome, 532–533
uncouplers of oxidative phosphorylation, 687
vacuoles, 184
verapamil effect on, 651
Mitochondrial ATPase complex, loss in necrosis, 38
Mitochondrial calcium pump, 797
Mitochondrial complex IV, 194
Mitochondrial DNA (mtDNA)
description, 183
hepatotoxin effects, 623, 625
inhibition of synthesis, 625
mutations, 193–195
Barth syndrome, 195
glutaric acidemia, 194
Kearns-Sayre syndrome, 193
Leber's hereditary optic neuropathy, 194
list of, 193
progressive ophthalmoplegia, 194
Wilson's disease, 193–194
toxic injury to, 193
Mitochondrial encephalomyopathy, 196
Mitochondrial NO synthase (mtNOS), 39

Mitochondrial permeability transition pore (MPT), 42, 644
Mitochondrial Schwannopathies, 682–683
Mitochondrial swelling
  anoxia-induced, 38
  appearance of, xviif, 184f, 185f
  description, 9, 11, 184
  hypoxia, 186–187, 187f
  myocardium, 636f–638f
  in necrosis, 38, 39f
  in neuronal injury, 669
  nitrogen gas bubble uptake, 188
  oxidative stress, 185–186
    calcium and, 186
    carbon-directed free radical injury, 186
    description, 185–186
    hydrogen sulfide protection, 186
    peroxynitrite and, 186
  radiation, 187–188
  response to acute injury, 184–188
Mitochondria-lipid globule interface, 181, 182f
Mitochondriopathy
  Alzheimer's disease, 836
  in amyotrophic lateral sclerosis (ALS), 841
  chronic hypertension, 195–196
  hepatotoxins, 623–626, 624f, 625f
  in Huntington's disease, 841
  of metabolic and chronic diseases, 188–196
    amyotrophic lateral sclerosis, 195
    defects in urea cycle enzymes, 192–193
    dysfunctional metabolic pathways, 188
    hypertrophy, 188–191, 189f, 191f
    metabolic defects, 191–192
    mitochondrial DNA-based disorders, 193–195
    neurological disease, 195–196
    Parkinson's disease, 195
    superoxide dismutase deficits, 195
    toxic injury to mitochondrial DNA, 193
  in necrosis, 35, 36, 38–40
    ATPase complex dysfunction, 38
    calcification, 39f, 39–40
    inner membrane degradation, 38
    nitrosative stress, 38–39
    oxidative stress, 38
    permeability transition pore opening, 38
  in programmed cell death, 35, 42–43
    apoptosis-inducing factor (AIF), 43
    apoptosome creation, 42
    Bid protein, 43
    death-associated protein 3 (DAP3), 43
    kinase signaling pathways, 43
    permeability transition pore opening, 42
    pro-apoptotic protein translocation, 42
    protein nitrosylation-induced apoptosis, 43
    reactive oxygen species (ROS) and, 42–43
  tauopathy, 669, 672
Mitogen-activated protein kinase (MAPK) pathway, 68, 743
Mitosis
  centromeres, 745–746
  cytoplasmic changes in, 746–747
  malignant lymphoma, 746f
  microtubules and, 88, 745f
  nuclear changes, 745–746
  stages of, 744
Mitotic figures, 768
Mitotic spindle, 746
Mitoxantrone, cardiotoxicity of, 644, 646
MLVs (murine leukemia viruses), 407, 408f, 409f, 409–410
MMTV (mouse mammary tumor virus), 404, 405f, 406
MNEC (meningitis-associated *Escherichia coli*), 472
Modeccin, hepatocyte effects of, 613–614
Mokola virus, 368f
Molluscipoxvirus genus, 327
Molluscum contagiosum, 327
Monensin, 141–142
  cardiotoxicity of, 648–649
  hepatotoxicity, 626
Monkeys
  atherosclerosis, 885
  viral diseases
    cynomolgus polyoma virus, 348
    Ebolavirus, 370
    hemorrhagic fevers, 381
    Kyasanur Forest disease virus, 388
    Marburgvirus, 369, 369f
    measles, 362
    saimiriine herpesvirus 2, 338
    simian hemorrhagic fever virus (SHV), 386
    simian immunodecifiency virus (SIV), 412, 414f
    simian rotavirus, 378
    simian varicella, 333
    simian virus 40, 348–349
    Yaba monkey tumor virus, 327
Monoamine oxidase, 669
Monoamine oxidase inhibitors, 684
Monocrotaline, pulmonary toxicity of, 735
Monocyte
  activation, 269
  attached to endothelium, 268f
  description, 269
  in HIV infection, 411
  killing of neoplastic cells, 787
  role in necrosis, 54
Monocyte-macrophage system, 269–274
Monocytosis, 269
Monomeric actin, 89
Mononuclear phagocyte system, 269
Monoparticulate glycogen, 51
Monosodium L-glutamate (MSG), 684–685
Mono-ubiquitination, 67
Moraxella, 481f, 482, 483t
Morbillivirus genus, 360, 362
Morphine, 677
Morphometric analyses, xvi, 15
Motoneuronal paralysis, MLV-induced, 407
Motor end plate dysfunction, 686
Motor end plate toxins, 654, 655f
Mott's cells, 846
Mouse mammary tumor virus (MMTV), 404, 405f, 406
Mouse pneumonitis virus, 349
Mouse polyoma disease, 348
Mousepox, 323
MPF (M-phase promoting factor), 744
MPTP (methylphenyltetrahydropyridine), 669
mRNP export complex, 129
mTOR (mammalian target of rapamycin), 883, 885
Mu-calpain, 186
Mucins, 310–311, 777, 781–782
Mucocutaneous leishmaniasis, 535
Mucocysts, 528
Mucodegeneration, 877, 878f, 882f
Mucolipidoses, 866
Mucopolysaccharidoses, 307, 864f, 864–866
  animal models, 866
  Hurler's disease, 865–866
  localized corneal, 864–865
  Sanfilippo disease, 864
  Sly syndrome, 865
  systemic, 864
  ultrastructural pathology in animal models, 865t
Mucormycosis, 589–590
Mucosa-associated lymphoid tissue (MALT), 278
Mucous metaplasia, 26

Multidrug resistance protein 2 (Mrp2), 630
Multifocal distal axonopathy, 681
Multinucleate giant cells
  adaptive responses to persistent injury, 23, 26
  Blastomyces, 582, 582f
  caused by bacteria and fungi, 23, 26
  formation by cell-to-cell fusion, 23, 26
  formation by nuclear division, 23
  virus-induced, 26
Multiple myeloma, 834, 849
Multiple systemic lipomatosis, 167
Multipotent progenitors, 283
Multivesicular bodies, 118, 119–120
  in cellular trafficking, 120
  description, 119
  enlargeosomes, 120
  excretory function, 120
Mumps virus, 364
Murine hepatitis virus (MHV), 370–372
Murine leukemia viruses (MLVs), 407, 408f, 409f, 409–410
Murine polioencephalomyelitis virus (Theiler's virus), 396f, 397
Murine rotavirus, 378
Murine transmissible colonic hyperplasia, 464
Muscle. *See also* Myotoxins; Skeletal muscle; Smooth muscle
  aging and, 750
  atrophy, 750
  glycogen storage diseases, 869
  polyglucason myopathy, 868
  regeneration, 749
  wasting syndromes, 29
Muscle cells, *Toxoplasma gondii* in, 554
Muscular dystrophy, 91
Mutagenesis, insertional, 402
MVBs. *See* Multivesicular bodies
Mycelia, 583
Mycelin protein O, 695
Mycetomas, 487, 589
Mycobacterial envelope, 427
Mycobacterium, 489t–490t, 491–494, 492f
  M. avium complex, 494
  M. tuberculosis complex, 493
Mycolic acids, 427, 491
Mycoplasma, 442–443, 444t
Mycoplasmatales (order), 442–447, 444t–445t
  Eperythrozoon genus, 445t, 447
  Hemobartonella genus, 445t, 446f, 447
  Mycoplasma genus, 442–443, 444t
  Ureaplasma genus, 444t, 445, 447
Mycoplasmosis
  description, 443
  neurological illness, 445
  respiratory, 443, 443f, 445
Mycosis, 578
Mycosis fungoides cells, 767, 767f
Mycotoxicosis, 578
Mycotoxins, 578
Myelin basic protein (MBP), 678
Myelin bodies, 11
Myelin bulbs, 682
Myelin depletion, 678
Myelin figures, 11, 118, 610
Myelin sheath, 678
Myelin striping, 678
Myelin toxins, 678
Myelin-binding toxins, 682
Myelinopathies, 678
Myeloid bodies, 69, 118, 849
  chloroquine treatment and, 610
  concentric lamellar inclusion bodies (CLIBs), 610
  proximal tubule, 701f
Myeloperoxidase deficiency, 243
Myeloproliferative disease
  feline leukemia virus, 406
  retroviral, 765f
Myocardiocyte
  death in ischemia, 51
  hypoxia, 208f
  mitochondrial hypertrophy, 187f
Myocarditis
  canine distemper, 362
  encephalomyocarditis (EMC) viruses, 397
  mast cell degranulation, 221f
  Trypanosoma, 534
Myocardium
  capillary endothelial cells, 200f
  dysfunctional β-oxidation of fatty acids, 195
  fibrosis, 295, 643
  hypertrophy, 640–641
  normal, 635–641
  responses to toxic injury, 641, 643
  toxins, 643–651
  trypanosome development in, 534
  vascular system, 640
Myocyte
  of arterial media, 875
  trichinosis, 598, 599f
Myocytolysis, 641
Myofibers, anchoring to basement membrane, 635
Myofibrillar degeneration, 641
Myofibrils
  doxorubicin-induced lysis, 645f, 646, 647f
  responses to toxic injury, 641, 643
  shredding of, 643
Myofibroblasts, 297, 778
  in alveolar walls, 723
Myofilaments
  arterial myocyte, 875
  in cardiac hypertrophy, 640–641
  increase in, 21
Myoglobin, 712
Myoglobinemia, 712
Myonecrosis, bacterial, 502, 655, 657f
Myoneural junction, 683, 683f, 686f
Myopathy, polyglucason, 868
Myosin, 90
Myotoxins, 635–664
  cardiotoxicity, 635–651
    normal myocardium, 635–641
    responses to toxic injury, 641, 643
    toxins, 643–651
      amphophile compounds, 648
      anthracycline antibiotics, 644f, 644–646, 645f
      anti-hypertensives, 650
      calcium channel blockers, 650–651
      catecholamines, 650
      chloroquine, 648
      cocaine, 651
      coffee senna, 651
      doxorubicin, 644f, 644–646, 645f, 647f, 648f
      ethanol, 651
      furazolidone, 651
      imatinib, 646, 649f
      ionophores, 648–649
      isoproterenol, 650
      monensin, 648–649
      pyrrolizidine alkaloids, 651
      reserpine, 634f, 650
      simvastatin, 649f
      table of toxins, 642t
      trastuzumab, 646, 648
      tyrosine kinase inhibitors, 646, 648
      verapamil, 650–651
  skeletal muscle, 651–658
    androgens and anabolic steroids, 652
    azidothymidine, 652
    bacterial toxins, 655, 657f
    carbamates, 654
    colchicine, 653
    ethanol, 652
    HMGCoA reductase inhibitors, 653
    local anesthetics, 654
    motor end plate toxins, 654, 655f
    organophosphorus insecticides, 653–654, 654f
    plant alkaloids, 658
    table of toxins, 656t
    venoms, 655, 658

veratrine, 658
vincristine, 652–653
smooth muscle, 658–659
allylamine necrosis, 659
immunosuppressive agents, 659
radiation injury, 659
smooth muscle relaxants, 658–659
venoms, 659
Myosin-X (myoX), 103
Myxedema, 304
Myxidium hardella, 596f
Myxobolus spp., 597
Myxococcales (order), 511t
Myxococcus, 511t
Myxosoma, 597
Myxosporidia, 597
Myxozoans, 592t, 595–597, 596f

N
Na^+ channels, 678
N-acetyl-p-benzoquinoneimine (NAPQI), 618–619
NADH, accumulation in hypoxia, 187
Nadoviridae family, 394
NADPH oxidase, 239
Naegleria, 527
Nairobi sheep disease, 392
Nairovirus genus, 392
Crimean-Congo hemorrhagic fever, 392
Nairobi sheep disease, 392
Na-K-ATPases, 80
Nalp3, 116
NALT (nasopharynx-associated lymphoid tissue), 278
Nanoparticles, pulmonary damage from, 724, 733–734
Nasopharyngeal carcinomas, 337
Nasopharynx-associated lymphoid tissue (NALT), 278
Natural killer (NK) cells, 46
in anti-cancer immunity, 787
perforin-induced cell death, 83–84
ncRNAs (non-coding RNAs), 131
NDV (Newcastle disease virus), 361f, 364, 365f, 880, 880f
Necroptosis, 49
Necrosis, 35–40
chromatin aggregation, 40
coagulation, 32f
cytoskeleton depolymerization, 35, 36
endoplasmic reticulum and Golgi complex contraction, 40
endothelial cell death, 54, 55f, 56
ischemia and, 49–51, 50t
lytic, 33, 34f, 36, 37f
mitochondriopathy, 35, 36, 38–40
of neurons, 383f, 669, 671f, 677
nuclear changes, 40
plasma membrane leakage, 35–36
primary injury and, 35
programmed cell death, relationship to, 33, 49–52
renal papillary, 706–708
ribosomal changes, 40
secondary injury and, 35
single cell, 46
Necrotic enteritis, 461
Nefiracetam, renal papillary necrosis, 706
Negri body, 363f, 368
Neisseria, 459–461, 460t
Neisseriales (order), 459–461, 460t
Neisseria genus, 459–461, 460t
Nematocysts, 595
Nematodes, facultative intracellular, 600
Neoparamoeba spp., 528
Neoplastic cells, 757–793. *See also specific cell types*
anaplasia, characteristics of, 761, 763
benign neoplasms, 761
causes, 758, 761
epigenomics, 758, 761
genetic mutation, 758
cell death, 785–789
basophils and mast cells, 788
killer dendritic cells, 787
lymphocyte killing of neoplastic cells, 787
monocytes/macrophages, 787, 787f
natural killer cells, 787
neutrophils, 788
platelet activation and aggregation, 788–789
programmed cell death, 785, 787
cell surface, 733–736
cell junctions, 766
cilia, 766
cytoskeleton, 764, 766
glycoproteins, 763–764
intracellular canaliculi, 763, 764f
plasma membrane, 763–764, 764f, 765f
common features of, 757
cytoplasm, 769–775
endoplasmic reticulum, 770f, 769–771
fibrillar inclusions, 771
glycogen and glycolysis, 775, 777f
Golgi complex, 769, 770f
hyalin bodies, 771
lipid globules, 775
melanosomes, 775, 776f
mitochondria, 775, 777f
protein inclusions, 771
protein lattices (crystalloids), 771, 772f
ribosomes, 769
secretory granules, 772, 773f, 774f, 775
tubules, 771–772
ubiquitin-proteosome system, 771–772
malignant neoplasms, 761
metastasis, 780–785
into blood stream, 782f, 782–783, 784f
coagulation and, 783
extracellular matrix degradation, 781
implantation, 783, 785, 786f
invasion into connective tissue, 780–782
organ-specific adhesion molecules, 783
nucleus, 766–769, 767f
chromatin, 768–769
chromosome analysis, 768
DNA repair abnormalities, 769
growth receptors, 769
mitotic figures, 768–769
nuclear envelope, 768
nucleoli, 767–768
preneoplastic lesions, 761
tumor microenvironment, 775–780
angiogenesis, 778–780, 779f, 781f
basement membrane material, 777, 778f, 781f
collagen, 777–778, 781f
description, 775, 777
fibroplasia, 778
Neospora, 555
Neostigmine, skeletal muscle toxicity of, 654
Neovascularization. *See* Angiogenesis
Nephrin, 695
Nephritis
acute hypersensitivity, 700
glomerulonephritis
in hog cholera, 389
membranous, 890f, 891–898
primary, 891
proliferative, 898, 900
secondary, 891
nephrotoxic, 893
Nephrolithiasis, oxalate, 710
Nephrosis
melamine, 711
sulfonamide, 711
Nephrotoxic nephritis, 893
Nephrotoxins/nephrotoxicity, 695–715
confounding lesions, 711–712
fever and electrolytic imbalance, 712
ischemia, 711–712

Nephrotoxins/nephrotoxicity (*cont'd*)
metabolic acidosis, 712
myoglobinemia, 712
crystal nephropathy, 710–711
calcium and vitamin D toxicity, 711
melamine nephrosis, 711
oxalate nephropathy, 710f, 710–711
sulfonamide nephrosis, 711
tyrosine crystals, 710, 710f
distal tubule toxins, 705
amphotericin B, 705
glomerular toxins, 695–697
mesangiopathy, 697
podocytopathy, 696–697
juxtaglomerular apparatus, 708, 709f
angiotensin II antagonists, 708
angiotensin-converting enzyme inhibitors, 708
FK506, 708
medulla toxins, 705–708, 706f
bromoethyleneamine, 706
dimethylnitrosamine, 706, 707f
diphenylamine, 706
nefiracetam, 706
phenacetin, 706, 708
proximal convoluted tubule toxins, 697, 697f, 700–705
cyclosporine, 702, 702f
gentamicin, 701–702
lysosomal toxins, 701–702
mechanisms of nephrotoxicity, 697, 700
metallic toxins, 702–705
cadmium, 704
lead, 703f
lithium, 705
mercury, 702, 704
platinum, 704f, 704–705
uranium, 705
nuclear transcription injury, 702
ultrastructural studies in animal models of, 698t–699t
Nerve cell body, 668
Nerve growth factor (NGF), 667
Nervous system. *See also* Neurotoxins/neurotoxicity
neurological disease
mitochondriopathy in, 195–196
mycoplasmosis, 445
nocardian infection, 494, 495f
peripheral nerve neuropathy, 681–683
demyelination, 682, 690
distal axonopathy, 681–682
in leprosy, 493–494
mitochondrial Schwannopathies, 682–683
myelin-binding toxins, 682
proximal axonopathy, 681
symmetrical in diabetes mellitus, 904
Wallerian degeneration, 679f
peripheral nervous system (PNS), demyelination in, 682
Nesprin-3, 127
NETs (neutrophil extracellular traps), 239
Neuregulin, 667
Neuraminidase (sialidase), 529, 863
Neuritic (senile) plaques, 839–840
Neuritis, *Listeria* and, 498
Neuroectodermal tumor, melanotic, 774f
Neuroendocrine tumors, staining for secretory components, 772
Neurofibrillary tangles, 829, 837, 839
Neurofilament aggregation, 669
Neurofilament protein, 91
Neurological disease. *See also specific diseases*
mitochondriopathy in, 195–196
mycoplasmosis, 445
nocardian infection, 494, 495f
Neuromelanin, 823–824
Neuromuscular disease, autophagy in, 71
Neuromuscular junction, 367
Neuron, 667
acute cell swelling, 798f
alphavirus infection, 382, 383f
apoptosis, 52, 667
autophagy, 71, 669, 837
ceroid lipofuscinoses, 862–863
chromatolysis, 7, 669, 670f
cytoskeleton, 669, 672
dark, 667
intermediate filament disorders, 92, 93f
ionic balance, 836
lipofuscin in, 823
macroautophagy, 837
necrosis, 383f, 669, 671f, 677
Nocardian, 494, 495f
normal, aging, 666f
rabies in, 368
swelling, 669, 670f, 671f
Neuronal cytoplasmic inclusions, in amyotrophic lateral sclerosis, 841
Neuronopathy, 668–678
diffuse *versus* selective, 669
Neuronophagia, 669
Neuropathy
amyloidosis and, 834–837
familial amyloidotic polyneuropathy, 834–835
peripheral nerve, 681–683
demyelination, 682
distal axonopathy, 681–682
mitochondrial Schwannopathies, 682–683
myelin-binding toxins, 682
proximal axonopathy, 681
Neuropil threads, 840
Neuropilins, 780
Neurosecretion
microtubules and, 88
neurosecretory vesicles, 681
Neurosyphilis, 508
Neurotoxins/neurotoxicity
confounding lesions, 667–668
aging, 667–668, 668f
apoptosis, 667
hyperglycemia, 668
hypoglycemia, 668
ischemia, 668
glial toxins, 687–688
glucose, 668
myelinopathies, 678, 679f, 680f
neurotoxins of nerve termini and synapses, 683–687
arthropod neurotoxins, 686
botulinum toxin, 684
bromethalin, 687
DDT, 684
GABA toxicity, 685–686
ivermectin, 685
receptor agonists, 684–685
strychnine, 687
tetanus toxin, 685–686
uncouplers of oxidative phosphorylation, 687
neutropathies, 668–678
cytoskeletal toxins, 672
lysosomal toxins, 672
mitochondrial toxins, 669, 672
toxins binding opioid receptors, 677–678
toxins for serotonin-secreting neurons, 672, 676–677
toxins of membrane channels, 678
toxins of plasma membrane receptors, 677
peripheral nerve neuropathies, 681–683
demyelination, 682
distal axonopathy, 681–682
mitochondrial Schwannopathies, 682–683
myelin-binding toxins, 682
proximal axonopathy, 681
ultrastructural changes in animal models, 673t–676t
vascular neurotoxins, 688–690
gold, 690
lead, 688, 690
mercury, 690
Neurotransmitter receptors, 683
Neurotransmitters, neurotoxins and, 683–687

Neutral lipid storage disease with ichthyosis (NLSDI), 860–861
Neutropathies, 668–678
  cytoskeletal toxins, 672
  lysosomal toxins, 672
  mitochondrial toxins, 669, 672
  toxins binding opioid receptors, 677–678
  toxins for serotonin-secreting neurons, 672, 676–677
  toxins of membrane channels, 678
  toxins of plasma membrane receptors, 677
Neutrophil, 231–243
  activation, 233
  in body fluids, 243
  bovine, 233
  congenital abnormalities, 241–243
    Chédiak-Higashi syndrome, 241
    chronic granulomatous disease, 242
    cyclic hematopoiesis, 242
    Fechtner's syndrome, 243
    lactoferrin deficiency, 242
    leukocyte adhesion deficiency (LAD), 242–243
    Pelger-Huet anomaly (PHA), 243
    transmembrane protein defects, 242–243
  degranulation, 239, 240f
  description, 231
  effete, 242f
  granules
    azurophil, 231
    contents of, 232t
    primary, 231
    secondary, 233
    specific, 233
    tertiary, 233
  immature, 230f
  killing of neoplastic cells, 788, 788f
  microbial killing, 238–239
  migration, 233–237, 234f
    binding to endothelium, 235, 236f
    chemotaxis, 233–235
    diapedesis, 235–237, 237f
  phagocytosis, 237–238, 238f, 240f
  pseudoplatelets, 243
  respiratory burst, 239
  role in necrosis, 54
  in thrombosis, 260
  tissue injury and repair, 239–240
  toxic, 240, 241f
Neutrophil actin dysfunction, 233
Neutrophil extracellular traps (NETs), 239
Newcastle disease virus (NDV), 361f, 364, 365f, 880, 880f
NF-κB family of transcription factors, 66, 744
NGF (nerve growth factor), 667
Nicotine, 684
Nicotinic acetylcholine receptors, 686
Nieman-Pick disease, 860
Nipah virus, 364
Nitric oxide (NO)
  binding to cytochrome C oxidase, 39
  endothelial cells and, 209
  endothelial response to hypoxia, 208
  macrophages, 271
  mitochondriopathy
    membrane injury, 186
    in necrosis, 38–39
    in programmed cell death, 43
  neutrophil production, 239
  nitrosylation, 64
Nitric oxide synthase (NOS), 64, 208, 209
  constitutive, 271
  inducible, 271
  in macrophages, 271
  mitochondrial (mtNOS), 186
Nitrogen gas, mitochondrial swelling and, 188
Nitrosative stress, 38–39
Nitrosomonadales (order), 511t
Nitrosylation
  apoptosis inhibition, 64
  of E3 ubiquitin ligase, 851
  of protein disulfide isomerase, 851
  S-nitrosylation, 851
NK cells, 46, 287–288, 289f
NLRs (NOD-like receptors), 116
NLSDI (neutral lipid storage disease with ichthyosis), 860–861
NMDA (N-methyl-D-aspartate), 677
NO. *See* Nitric oxide (NO)
Nocardia, 490f, 494, 495f
NOD-like receptors (NLRs), 116
Nodularins, 576
Nodules, pulmonary, 720, 732
Non-alcoholic steatohepatitis, 191
Nonapoptotic PCD, 49
Nonclathrin-coated vesicles, 140
Non-coding RNAs (ncRNAs), 131
Nonfibrillar collagen, 297
Noninfectious systemic necrotizing vasculitides, 881
Nopp140, 135
Norovirus genus, 399
Norwalk virus, 399
NOS. *See* Nitric oxide synthase (NOS)
Nosema, 561
Notch-deltalike ligand 4, 779
Nox1-based NADPH oxidase, 188
NRAMP1, 233
Nuclear activation
  nucleolus, xix
  perinucleolar chromatin, xix
Nuclear body, 133f, 134–135
Nuclear contour index, 767
Nuclear division, formation of multinucleate giant cells by, 23
Nuclear envelope, xviiif
  annulate lamellae, 129
  changes in programmed cell death, 44
  collapse and invagination, 15
  description, 125
  dilatation, 8f
  neoplastic cells, 766–767, 767f, 768
  nuclear lamina, 125, 127
  nuclear pores, 13, 127, 128f, 129, 747, 768
  perinuclear space, 125
Nuclear envelope lattice, 127
Nuclear export receptor Crm1, 66
Nuclear factor-κB (NK-κB), 66, 744
Nuclear glycogen, 163, 163f
Nuclear inclusion, viral. *See specific viruses*
Nuclear lamina, 125, 127
Nuclear matrix, 128f, 129
Nuclear phosphoprotein 140 (Nopp140), 134
Nuclear phosphoprotein p53. *See* p53
Nuclear pore
  description, 127, 128f, 129
  disintegration, 13
  neoplastic cells, 768
  nuclear pore complex (NPC), 127, 128f, 129, 747
Nuclear pseudoinclusions, 12
Nuclear receptors, 130f
Nuclear speckles, 129
Nuclear transcriptional injury, by nephrotoxins, 702
Nucleocapsids, herpesvirus, 327, 330
Nucleocytoplasmic transport, 129
Nucleoid, 440–441
Nucleolar channel system, 135
Nucleolar chromatin, in neoplastic cells, 768
Nucleolar organizer, 132
Nucleolar organizer regions (NORs), 768
Nucleolar segregation, 134, 134f
Nucleolin, 133
Nucleolus
  appearance, 133f
  changes in programmed cell death, 44
  margination and disintegration, 13
  metabolic defects, 135–136
  of neoplastic cells, 767–768

Nucleolus (*cont'd*)
nucleolar organizer regions (NORs), 768
in recovery, 64, 65f
structure, 133–134, 134f
Nucleoplasm
nucleoplasmic rarefaction, 15
receptors of growth in, 769
Nucleoporins (Nups), 129
Nucleoside analogues, hepatotoxicity of, 625–626
Nucleoskeleton, 744
Nucleosome, 130–131
Nucleus
in acute cell swelling, 13, 14f, 15
chromatin and protein aggregation, 13, 14f
contraction, 15
DNA damage, 13
nuclear envelope collapse and invagination, 15
nucleolar margination and disintegration, 13
nucleoplasmic rarefaction, 15
pore disintegration, 13
apoptotic bodies, 44
atrophy and, 26
Cajal body, 135
changes in programmed cell death, 44
chromatin, 129–130
chromosome territories and nuclear bodies, xviiif
compartments, 129
in cytomegaly, 23
description, 125
fungi, 578
hepatotoxins, 626–627
hyperplasia and, 22
hypertrophy, 126f
interphase, 744f, 745
in mitosis, 745–746
necrosis, 33, 40
neoplastic cells, 766–769, 767f
chromatin, 768–769
chromosome analysis, 769
DNA repair abnormalities, 769
growth receptors, 769
mitotic figures, 768
nuclear envelope, 768
nucleoli, 767–768
nuclear body, 134–135
nuclear envelope, 125–129
nucleolar channel system, 135
nucleolus, 133–134
polymorphic interphase karyosomal association (PIKA) region, 135
in recovery, 64, 65f
trypanosome, 533
Nude mice, 894
Null cell, 287
Nurse cell
thymic, 283
trichinosis and, 598
Nurse cell-larvae complex, in trichinosis, 597

O
Obesity, adipocytes in, 167
Ocular albinism type 1, 814
Oculocutaneous albinism, 813
Odontogenesis, 303
Oligodendrocyte, 678
Oligosaccharide storage diseases, 869
-oma (suffix), 761
Oncocytomas, 775
Oncogenes, 758
Oncogenic transformation, adenovirus, 339, 343
Oocyst, *Leucocytozoon,* 549
Ookinetes, 543
Open canalicular system (OCS), 248, 253
Opioid receptors, toxins that bind, 677–678
Oral apparatus, ciliate, 528
Orbivirus genus, 377
African horse sickness (AHS), 377
bluetongue virus, 377
epizootic hemorrhagic disease (EHD), 377
Orchitis, immune complex, 310, 311f
Orf virus, 324, 325f
Organelles, xv. *See also specific organelles*
Organochlorines, gill toxicity of, 737, 737f
Organophosphorus insecticides, skeletal muscle myopathy from, 653–654, 654f
Oriental hornet, venom of, 655
Orotic acid, hepatotoxicity from, 626
Oroya fever, 453
Orthobunyavirus genus, 391–392
Akabane virus, 392
California encephalitis, 391–392
Orthohepadnavirus genus, 354–355, 355f
hepatitis B virus (HBV), 354–355, 355f
woodchuck hepatitis virus, 355
Orthomyxoviridae family, 356t, 356–358, 357f
Orthopoxvirus genus, 323
Orthoreovirus genus, 376–377
Orthoretrovirinae subfamily, 404–415
Osteoclasts, 803, 806f, 806–807
Osteonectin, 251
Osteopetrosis, 806–807
Osteopontin, 145, 554
Outer membrane of gram-negative bacteria, 430–431
Outer membrane protein, *Chlamydia,* 486
Outer membrane vesicles, 430, 431
Ovarian follicles, atretic, 310
Ovine progressive pneumonia, 414
Oxalate nephropathy, 710f, 710–711
ethylene glycol, 710–711
primary hyperoxaluria, 711
Oxazole derivatives, 611
Oxidases, in peroxisomes, 153
Oxidation, lung damage from, 724, 726
Oxidative phosphorylation, 182, 183, 193
uncouplers of, 687
Oxidative stress
beta amyloid protein and, 836
mitochondria and, 38, 43, 63–64
signal transduction in, 43
Oxygen
electron transport chain requirement for, 187
toxicity, 727, 727f
Ozone, pulmonary damage, 727, 729

P
P component, 829
P fimbriae, 433
p32 protein, 184
p38 mitogen-activated protein kinase (MAPK), 43
p53 binding protein 1, 64, 188
p53 protein/gene, 41–42, 43, 44
activation by RNA polymerase II, 136
cell cycle checkpoints and, 743
DNA repair and, 64–65
mitochondrial, 183
p80 coilin, 135
PAF (platelet activating factor), 217, 224, 233, 234, 253
Paired helical filaments, 839
Pale grain eumycetomas, 589
Pancarditis, 534
Pancreas
acute cell swelling of ductule, 16f
acute necrosis, 34f, 37f
pancreatitis, 164f
Pancreatic carcinomas, staining for secretory components, 772
Pansporoblasts, 597
PapG, 433
Papilloma cells, 343
Papillomaviridae family, 343–347, 344t, 345f
bovine papilloma virus (BPV), 346–347
human papilloma virus (HPV), 346
Papule, 319

Paracellular pathway, 97
Paracoccidioidomycosis, 588, 589f
Parainfluenza viruses, 360
Parakeratosis, papillomavirus, 343
Paramoeba, 528
Paramyxoviridae family, 357f, 358–366, 359t, 361f, 363f, 365f
  Paramyxovirinae subfamily, 360–364
    Avulavirus genus, 364
    canine distemper virus (CDV), 362, 363f
    Hendra virus, 362, 364
    Henipavirus genus, 362, 364
    measles virus, 357f, 360, 362
    Morbillivirus genus, 360, 362
    mumps virus, 364
    Newcastle disease virus (NDV), 361f, 364, 365f
    Nipah virus, 364
    parainfluenza viruses, 360
    Respirovirus genus, 360
    Rubulavirus genus, 364
    Sendai virus, 360
  Pneumovirinae subfamily, 364, 366
    Metapneumovirus genus, 366
    Pneumovirus genus, 364, 366
    respiratory syncytial virus (RSV), 364, 366
Paramyxovirinae subfamily, 360–364
  Avulavirus genus, 364
  canine distemper virus (CDV), 362, 363f
  Hendra virus, 362, 364
  Henipavirus genus, 362, 364
  measles virus, 357f, 360, 362
  Morbillivirus genus, 360, 362
  mumps virus, 364
  Newcastle disease virus (NDV), 361f, 364, 365f
  Nipah virus, 364
  parainfluenza viruses, 360
  Respirovirus genus, 360
  Rubulavirus genus, 364
  Sendai virus, 360
Parapoxvirus genus, 324, 325f
Paraquat, 625, 734–735
Parasites. *See also* Protozoa; *specific organisms*
  eosinophils and, 245
  extracellular matrix degradation by, 299
  membranous glomerulonephritis and, 897, 897f
Parasitophorus vacuoles, 535, 545, 550, 554, 561
Paraspeckles, 129
Parathion, skeletal muscle myopathy from, 653–654
Parathyroid gland hyperplasia, 22f
Paratuberculosis, 803f
Paraxial rods, 525
Parkin, 840, 851
Parkinson's disease, 195, 840–841
Pars recta, damage to, 704
Particulate hepatotoxins, 627, 629f, 630
  bile duct toxins, 630
  lithocholic acid, 630
  microgranulomatosis, 627, 630
Particulates, lung toxicity from, 723–724, 731–732
Parvoviridae family, 349t, 349–353, 351f
  Amdovirus genus, 352–353
    Aleutian mink disease virus, 352–353
  Depedovirus genus, 352
    adeno-associated viruses (AAVs), 352
  Erythrovirus genus, 350, 352
  Parvovirus genus, 350
    canine parvovirus, 350
    feline panleukopenia virus, 350, 351f
Parvovirus genus, 350
  canine parvovirus, 350
  feline panleukopenia virus, 350, 351f
Passive Heymann nephritis, 892–893
Pasteurella, 478t, 480, 481f, 482
Pasteurellales (order), 477–482, 478t
  Actinobacillus genus, 477–478, 478t
  Aggregatibacter genus, 478t, 479
  Haemophilus genus, 478t, 479f, 479–480
  Mannheimia genus, 478t, 480, 480f
  Pasteurella genus, 478t, 480, 481f, 482
Pathogenicity islands, 441
Pathologic changes, factors influencing, xv
PBVs (picobirnaviruses), 393
PCBP1 (poly [rC]-binding protein 1), 816
PCBs (polychlorinated biphenyls), hepatotoxicity of, 622–623
PCD. *See* Programmed cell death (PCD)
PCNA (proliferating cell nuclear antigen), 769
PDGF (platelet-derived growth factor), 224, 251, 898
Pelger-Huet anomaly (PHA), 243
Peliosis hepatis, 412
Pellicle
  coccidial, 549, 552
  protozoal cell, 525
Pemphigus vulgaris, 92
Penicilliosis, 590
Peptidases, in snake venom, 658
Peptide fragment accumulation, 7
Peptidoglycan, 427, 430, 441–442
Peptidoglycan recognition proteins (PGRPs), 233
Perforin, 83, 85f, 287
Pericentrin, 745, 746, 751
Pericentrin gene *(PCNT),* mutations in, 751
Perichromatin fibrils, 134
Perichromatin granules, 13, 134, 768
Pericytes, 206
  blood-brain barrier, 689f
  neoplastic, 779f, 781f
Perilipins, 165
Perineural barrier, 217
Perinuclear space, 125
Perinucleolar compartment, 129
Periosteal exostoses, 800
Peripheral nerve neuropathies, 681–683
  demyelination, 682, 690
  distal axonopathy, 681–682
  in leprosy, 493–494
  mitochondrial Schwannopathies, 682–683
  myelin-binding toxins, 682
  proximal axonopathy, 681
  symmetrical in diabetes mellitus, 904
  Wallerian degeneration, 679f
Peripheral nervous system (PNS), demyelination in, 682
Peripheral proteins, 78
Periplakin, 312
Periplasmic space, 427, 430–431
Periplast, 508
Perisinusoidal stellate cells, 609
Peristomal rings, 111
Peritoneal carcinomatosis, 785
Peritonitis, *Actinomyces* spp. granulomatous, 488f
Peritrichous flagella, 475
Peritrophic membrane, 543
Peritubular capillary damage, renal, 706
Perivascular change in acute inflammation, 211t
Perivascular edema, 875, 876f
Perivascular environment, 204–206
Perlecan, 303
Permeability transition pores (PTP), 38, 42, 49–50, 182, 644, 672
Permeases, 79, 84t, 429
Peroxidase, in eosinophils, 245
Peroxisomal biogenesis disorder, 611
Peroxisomal duplication, 63
Peroxisomal proliferator-activated receptors (PPARs), 153, 611
Peroxisomal reticulum, 153
Peroxisome
  appearance, 152f
  congenital defects, 154–156
    adrenoleukodystrophy, 155

Peroxisome (*cont'd*)
alpha-methyl-acyl-CoA racemase deficiency, 156
cerebrohepatorenal syndrome of Zellweger, 155
congenital total lipodystrophy, 155
hyperoxaluria, 155
Refsum's disease, 155–156
rhizomelic chondrodysplasia, 156
description, 153–154
duplication, 11, 13
fetal lung, 723
fungal, 578
hepatotoxins, 610–612, 612f
clofibrate, 611
gemfibrozil, 611
hypertrophy from hyperlipidemic drugs, 154, 155f
hypoxia, response to, 154
in lipid metabolism, 154
microbodies, 154
myocardium, 638
proliferation, 611
proximal convoluted tubule toxins and, 700
in recovery, 63
Peroxisome proliferator activated receptor (PPAR), 611
Peroxynitrite, 39, 186
Pertactin, 457
Pertussis toxin (PT), 457
Pestiviris genus, 388–389
bovine viral diarrhea (BVD) virus, 389
hog cholera, 388–389, 390f
Peyer's patches, 278
P(pap) fimbriae, 469
P-glycoprotein, 62, 80
PGRPs (peptidoglycan recognition proteins), 233
Phaeohyphomycosis, 589
Phagocytic cup, 115, 237
Phagocytic receptors, 235
Phagocytosis, 115–116
accelerated, 237
of bacteria by M cells, 115f
of *Borrelia,* 505
coiling, 477, 505
cytophagocytosis, 54
erythrophagocytosis, 721f, 817f–820f, 817–819
of extracellular collagen, 299–300
frustrated, 116
of hemoglobin by malarial parasites, 547
inflammasomes, 116
in listeriosis, 498
macrophage, 270–272, 271f
of melanin granules, 787, 787f
melanophages, 811
neoplastic cells, neutrophil phagocytosis of, 788, 788f
neuronophagia, 669
neutrophil, 237–238, 238f, 240f, 788, 788f
phagosomes, 115
phases, 115
by pillar cells, 736
platelet, 254, 254f
removal of dead cells, 52, 52f, 53f, 54
removal of extracellular debris, 54
specificity, 116
Phagocytosis-induced cell death (PICD), 47
Phagolysosome, 116–118, 117f, 118f
Borrelia in, 505
description, 237
macrophage, 271f, 271–272
Mycobacteria in, 491, 492f, 493, 494
Nocardia in, 494
Phagophore, 69
Phagosome
description, 115, 204, 237
Legionella in, 477
Staphylococcus in, 498f
superoxide anions, 239
Phagosome-lysosome fusion, 117, 117f
Phalloidin, 90, 627
Phase II biotransformation enzymes, 720
PHB (poly (3-hydroxybutyrate) granules), 439
Phenacetin, nephrotoxicity, 706, 708
Phencyclidine, 677
Phenobarbital
RER toxicity, 614
SER proliferation and, 157, 620
toxicologic enhancement in SER, 157
Phenyl piperazine, 611
Pheochromocytoma, 773f
Pheomelanin, 811
Phlebovirus genus, 392
Rift Valley fever (RVF), 392
Phocein, 669
Phoceinpinocytotic tubules, 114
Phosphate/insulin-like growth factor II receptor, 46
Phosphatidylinositol 3-kinase-Akt survival, 775
Phosphatidylserine, 77
Phosphatidylserine scramble, 20, 54, 77
Phosphodiesterase, in snake venom, 658
Phosphodiesterase inhibitors
cardiotoxicity of, 650
vascular toxicity of, 658
Phosphoinositide 3-kinase (PI3K) signaling pathways, 81
Phospholipases
activation of endogenous cell death, 35–36
bacterial, 82
exogenous, 82
intramembrane, 82
phospholipase A, 82, 658
phospholipase D, 82
stomatocyte production, 95
Phospholipidosis, lysosomal, 610
Phospholipids
catabolites, 36
degradation, regulated intramembrane, 81
metabolism, acquired defects in, 117–118
as plasma membrane components, 77
Phospholipiduria, 701
Phosphorus-containing granules, 439
Photofrin, 672
Phylloerythrin, 821–822
PICD (phagocytosis-induced cell death), 47
Pick bodies, 840
Pick's disease, 840
Picobirnaviruses (PBVs), 393
Picornaviridae family, 394–399, 395t, 396f, 398f
Aphthovirus genus, 397
foot-and-mouth disease (FMD) virus, 397
Cardiovirus genus, 397
encephalomyocarditis (EMC) viruses, 397
murine polioencephalomyelitis virus (Theiler's virus), 396f, 397
Enterovirus genus, 394
coxsackieviruses, 394
echoviruses, 394
poliovirus, 394
Hepatovirus genus, 397, 399
avian encephalomyelitis, 398f, 399
hepatitis A virus (HAV), 397, 399
Rhinovirus genus, 394, 397
Piece-meal degranulation, 222
Piedra (trichosporosis), 592
Pigeon circovirus, 356
Pigment type switching, 812
Pigmentation, cutaneous, 811
Pigments, 811–825
chromatophores, 815, 815f
copper-containing, 822–824
ceroid, 823
lipofuscin, 823–824, 824f
neuromelanin, 823–824
endogenous, 811

exogenous, 811, 824–825
in glial cells, 687–688
hemoglobin-derived, 815–817
bilirubin, 821–822
erythrophagocytosis and, 817f–820f, 817–819
ferritin, 816, 816f
heme, 815–816
hemosiderin, 817
malarial pigment, 822
porphyrias, 819–821
melanin, 810f, 811–814, 813t, 814f
Pili. *See also specific bacterial genera or species*
bundle-forming, 434
description, 433
of *Neisseria,* 460–461
sex, 438
Type II, 434
Type IV, 434
Type VI, 460–461
Pillar cells, 736
Pin1 protein, 824
Pinkeye, 482
Pink-eyed dilution locus, 814
Pinocytic reticulum, 113–114
Pinocytosis, 109, 110–111
macropinocytosis, 114
Pinosome, 110–111
Piroxantrone, cardiotoxicity of, 644
Pit cells, 609
Pitfalls, in interpretation of electron micrographs, xv–xvi
Pitting of cell surface, 15, 82, 83f, 750
Pituitary tumors, staining for secretory components, 772
Pityriasis versicolor, 590
Placenta
iron utilization, 818
malaria and, 548
Plague, 475
Plakoglobin, 100
Plant alkaloids, skeletal muscle toxicity, 658
Plants, calcinogenic, 801–802
Plaque, 424f
Plasma cells, 284, 284f–285f
Plasma fibronectin, 308
Plasma membrane, 77–86
in acute cell swelling, 15, 16f, 17
ATPase increase during injury, 80
carbon tetrachloride toxicity and, 621
components of, 77–81
cholesterol, 77
glycolipids, 77
glycoproteins, 80–81
glycosphingolipids, 77
membrane proteins, 78–80, 79f
phospholipids, 77
cytoskeleton linkage, 95–97
defective channels, 86
focal lysis, 15
freeze fracture preparation, 78, 78f
hypertrophy and, 22
intramembrane lysis
exogenous phospholipases, 82, 82f
regulated intramembrane phospholipid degradation, 81–82
regulated intramembrane proteolysis (RIP), 81
leakage in necrosis, 35–36
Ca^{++} entry, 35
intracellular protein exit, 36
phospholipase activation, 35–36
plasma protein entry, 36
macrophage, 272
membrane internalization, 82
membrane proteins
integral, 78, 763
peripheral, 78
transmembrane, 78–80
microdomains, 78
multinucleate giant cells, 23
neoplastic cells, 763–764, 764f, 765f
neurotoxicity, 677–678
platelet, 248, 253
porin-induced damage, 83–86
complement attack sequence, 83, 85f
drugs inserting as ion channels, 84–86
microbial porins, 85
perforin-induced cell death, 83–84
protozoal cell, 525
in recovery, 61–62
lysosomal membrane repair after infection, 61
mechanical injury, response to, 61
membrane condensation in hypothermia, 62
membrane ion channels, 62
rigidity, 77
ruffled border, 806, 806f
structure of bacterial, 429–430
transport, 79–80
Plasma protein-derived amyloid, 835
Plasma protein-receptor complexes, 214
Plasma proteins
absorbed to endothelial surfaces, 207
entry into cell during necrosis, 36
overload, 309
Plasmablast, 278, 284, 284f
Plasmacyte, 284, 284f–285f
Plasmacytoma, 834
Plasmalemma. *See* Plasma membrane
Plasmalemmal microparticles, 204
Plasmalemmal vesicles, 201, 211, 688. *See also* Caveolae
Plasmatic zone, of arterioles, 233
Plasmid, 441
Plasmin, 252f
Plasminogen activator, 778, 783
Plasminogen activator inhibitor, 215, 243, 783
Plasmodium, 542f, 543, 545, 546f, 547–548
P. berghei, 542f
Plasmoid, cardiotoxicity, 651
Platelet, 246–257
activation, 251, 253
adhesion to blood vessel walls, 249f, 257
aggregation, 251, 254
cancer cell interaction, 783, 788–789
endothelial injury, 253f, 254
in menorrhagia, 259–260
normal, 247
phagocytosis, 254, 254f
phases of hemostatic plug formation, 247f
plasma membrane alterations, 253
regulation of healing, 224
release reaction, 251, 252f, 253–254
secretion, 253–254
storage pool deficiencies, 256
thrombocytopathy, 255t, 255–257, 256f
acquired, 255
hereditary, 256f, 256–257
thrombocytopenia, 254–255
thrombosis, 257–260
ultrastructure, 248–251
cytoskeleton, 248
granules, 248, 251
open canalicular system, 248
plasma membrane, 248
Platelet factor 4, 234, 251
Platelet growth factor, 780
Platelet osteonectin, 251
Platelet trapping, 250f
Platelet-activating factor (PAF), 217, 224, 233, 234, 253
Platelet-derived growth factor (PDGF), 224, 251, 898
Platinum, nephrotoxicity, 704f, 704–705
Platyamoeba spp., 528
Plectin, 91, 127
Pleistophora, 561
Pleomorphism, of neoplastic cells, 759f, 761
Pleuropneumonia of swine, 477
Plott hounds, mucopolysaccharidoses in, 866

PML (progressive multifocal leukoencephalopathy), 347–348
Pneumoconiosis, 716f
Pneumocystis carinii, 594f, 594–595, 595f
Pneumocyte
  fetal lung, 723
  granular, 717–718, 718f
  hyperplasia, 720
  membranous, 716f, 717
Pneumonoconiosis, 731, 824
Pneumonia
  aspergillosis, 581–582
  Haemophilus, 479
  Legionella, 476–477
  Mannheimia, 480
  mycoplasmal, 443, 443f, 445
  Rhodococcus, 496
  Staphylococcus aureus, 500
  Streptococcus, 502
Pneumonia virus of mice, 366
Pneumonitis, influenza, 358
Pneumovirinae subfamily, 364, 366
  Metapneumovirus genus, 366
  Pneumovirus genus, 364, 366
  respiratory syncytial virus (RSV), 364, 366
Pneumovirus genus, 364, 366
Podocyte proteins, 695
Podocytopathy, 696–697
Podophyllin, 89
Podosomes, 115
Polar capsules, 595
Polar filament, 560–561, 597
Polar rings, coccidial, 549
Polar tubules, *Enterocytozoon,* 563
Polarplast, in microsporans, 561
Poliovirus, 394
Poly (3-hydroxyalkanoates) granules, 439
Poly (3-hydroxybutyrate) granules (PHB), 439
Polyarthralgia syndrome, 350
Polychlorinated biphenyls (PCBs), hepatotoxicity of, 622–623
Polyglucosan body diseases, 868f, 868–869
Polyhedral bodies, 439
Polymicrobial infections in the oral cavity, 424f
Polymorphic interphase karyosomal association (PIKA) region, 135
Polyneuropathies, 681
Polyoma BK virus, 348
Polyoma JC virus, 347–348
Polyomaviridae family, 347t, 347–349, 348f
  cynomolgus polyoma virus, 348
  mouse pneumonitis virus, 349
  polyoma BK virus, 348
  polyoma JC virus, 347–348
  polyomavirus muris, 348
  simian virus 40, 348–349
Polyomavirus muris, 348
Polyperforin, 83, 85f
Polyphosphoinositide, 77
Polyribosomes, 64, 136, 620
Polyserositis, *Haemophilus,* 480
Polyubiquitination, 67, 840
Pompe's disease, 867
Pontiac fever, 476
Porcine attaching and effacing-associated (paa) factor, 471
Porcine eperythrozoonosis, 447
Porcine intestinal spirochetosis, 509
Porcine reproductive and respiratory syndrome (PRRS), 386
Porcine rotavirus, 378
Pore-forming polypeptide, 527
Pore-forming toxins, 438
Porin-induced damage, 83–86
  complement attack sequence, 83, 85f
  drugs inserting as ion channels, 84–86
  microbial porins, 85
  perforin-induced cell death, 83–84
Porins, 84t, 85–86, 431
Porosome, 142
Porphyria, 819–821
  congenital erythropoietic, 820, 821
  hepatogenous, 821
Porphyria cutanea tarda, 820
Porphyrins, 629f, 630
Porphyromonas gingivalis, 437t, 509, 509t, 510f
Portal venules, 607
Portal zone hepatocyte, 607
Postcapillary venules, 205
Posterosome, in microsporans, 561
Postinflammatory pulmonary microlithiasis, 800
Postnatal pulmonary arterial remodeling, 877
Poststreptococcal glomerulonephritis, 898
Post-translational modifications, 138
Postvaccinial encephalitis, 323
Postvaccinial lymphadenitis, 323
Potassium (K^+) channels, 678
Potocytosis, 112
Potomac fever, 451
Poxviridae family, 318f, 319–327, 320t–322t
  Chordopoxivirinae subfamily, 323–327
    Avipoxvirus genus, 324, 326f
    Capripoxvirus genus, 324
    fowlpox, 324, 326f
    Lepropoxvirus genus, 324, 327
    Molluscipoxvirus genus, 327
    mousepox, 323
    orf virus, 324, 325f
    Orthopoxvirus genus, 323
    Parapoxvirus genus, 324, 325f
    pseudocowpox, 324
    rabbitpox, 324, 327
    sheeppox, 324
    Suipoxvirus genus, 327, 327f
    swinepox, 327, 327f
    vaccinia virus, 323
    Yatapoxvirus genus, 327
  pathogenesis, 322–323
  virion structure, 322, 322f
PPARs (peroxisomal proliferator-activated receptors), 153, 611
Precapillary arterioles, 205
Precapillary sphincters, 205
Preeclampsia, 902
Pre-endosomal vesicles, 110
Prekeratin, 849
Prelysosomal vesicle, 116
Premelanosomes, 811
Preneoplastic lesions, 761
Prereplicative complexes, 743
Presenilins, 836
Prespore (forespore), 442
Presynaptic membrane, 683
Primary amoebic meningoencephalitis, 527
Primary cilia, 101
Primary glomerulonephritis, 891
Primary granules, neutrophil, 231, 232t
Primary hyperoxaluria, 155
Primary hyperoxaluria, 711
Primary stage, syphilis, 508
Primary transcripts, 132
Primordial dwarfism in humans, 751
Prions
  amyloid of prion disease, 839
  defined, 911
  disease pathogenesis, 912
  patterns of transmission, 911–912
  transmissible spongiform encephalopathies (TSEs)
    bovine spongiform encephalopathy (BSE), 913
    chronic wasting disease (CWD), 913–914
    Creutzfeldt-Jakob disease (CJD), 839, 914–915
    fatal familial insomnia (FFI), 915
    Gerstmann-Sträussler-Scheinker syndrome (GSS), 839, 915
    kuru, 839, 914, 914f
    rodent scrapie, 913
    scrapie, 912–913, 913f
    transmissible mink encephalopathy (TME), 914
Pro-apoptotic genes, 42

Procaspase, 41, 42, 46
Procentriole, 746
Procoagulant activity of endothelium, 206, 207–208
Procoagulant factors, secreted by neoplastic cells, 783
Procoagulant microparticles, 207–208
Procollagen, 298
Procollagen peptidase, 300
Profilin, 90, 248
Progeria, 301–302, 751
Programmed cell death (PCD), 40–52
  in acute cell injury, 49
  in atrophy, 49, 51–52
  caspases, role of, 41
  cytoskeleton degradation, 44, 46
  death proteins, 40
  denervation atrophy and, 51–52
  description, 40–41
  in embryogenesis, 47, 49
  endoplasmic reticulum, 46
  endothelial cell death, 55f, 56
  examples, 41f, 45f, 48f
  extrinsic pathways, 46–47
  ischemia and, 49–51, 50t
  lesions of apoptosis, 41
  in metamorphosis, 49
  mitochondriopathy, 35, 42–43
  necrosis, relationship to, 33, 49–52
  neoplastic cell death, 785–787
    anti-apoptotic proteins, 785
    caspases, 785
    entosis, 787
    shift to senescence, 785, 787
    tumor necrosis factor-induced apoptosis, 785
  neurons, 667
  nuclear changes, 44
Programmed cell death ligand 1 (PD-1), 380
Progressive multifocal leukoencephalopathy (PML), 347–348
Progressive ophthalmoplegia, 194
Progressive pulmonary fibrosis, 735
Progressive supranuclear palsy, 839
Prokaryotes. *See also* Bacteria
  bacterial cell structures, 425–442
  cytopathology of pathogenic, 425–523
  diversity of, 425
  factors used by pathogenic bacteria to attach, infect, colonize, and cause disease in susceptible hosts, 426t–427t
Proliferating cell nuclear antigen (PCNA), 769
Proliferative enteropathies of swine, 461
Proliferative gill disease, 597
Proliferative glomerulonephritis, 898, 900
  acute diffuse, 898
  hepatitis B virus (HBV), 900
  hepatitis C virus (HCV), 900
  membranoproliferative glomerulonephritis, 898
  poststreptococcal glomerulonephritis, 898
Proliferative hemorrhagic enteropathy, 461
Proliferative ileitis of hamsters, 464
Promastigote, 532f, 535
Promoter, 131
Prophase, 744, 745
Proplatelet fragments, 247
Proplatelet processes, 247
Prostaglandins, 207, 217
Prostate
  atrophy, 28f
  hyperplasia, 22f
Protease-activating factor-1, 42
Protein absorption droplets, 697, 700
Protein C, 207, 215
Protein clusters, 78
Protein crystalloids, 439
Protein disulfide formation, glutaredoxin 2 and, 64
Protein disulfide isomerase, 851
Protein glutathionylation, 64
Protein homeostasis. *See* Proteostasis
Protein inclusions, in neoplastic cells, 771
Protein kinase C, 81
Protein lattices (crystalloids), in neoplastic cells, 771, 772f
Protein S-nitrosylation/denitrosylation, 43
Protein tyrosine phosphatases (PTPs), 79, 79f
Proteinosis, alveolar, 719f
Proteins
  degradation in the RER, 139
  misfolded, 842, 851
  synthesis
    carbon tetrachloride toxicity, 620
    change in aging, 750
    inhibition and Golgi vacuolation, 141
    pathways, 124f
    stress proteins, 66–67
Proteobacteriae, 448–485
Proteoglycans
  amyloid and, 829
  in atherosclerotic plaques, 883
  in basement membranes, 307
  congenital disease of proteoglycan synthesis, 307
  cutaneous accumulation, 304
  embryonic development and, 307
  in ground substance, 304
  keratin sulphate, 304
  negative stain preparation, 305f
  relation to basement membrane, 297f
  secretion by neoplastic cells, 777, 781–782
Proteolysis
  cytoplasmic, 7, 14f
  nuclear, 14f
  regulated intramembrane, 81
Proteolytic complex, 67
Proteome
  aggresomes, 67, 68f
  description, 67
  proteostasis, 67–69
Proteosome
  cyclin destruction, 745
  misfolded proteins and, 139
  oxidative stress and, 186
  ubiquitin-proteosome system, 842
Proteosome inhibitors, 771
Proteostasis, 67–69
Proteus, 468t, 473
Prothrombin, 257
Protoplasts, 430, 442
Protoporphyrin, 821
Prototheca, 573, 574f, 575, 575f
Protothecosis, 573, 575
Protozoa, 525–571
  amoebas, 526t, 526–528, 527f
    Acanthamoeba, 527–528
    Entamoeba, 526–527, 527f
    Naegleria, 527
    Paramoeba, 528
  Blastocystis hominis, 563–564
  ciliates, 528f, 528–529, 529f
    Balantidium, 528–529
    Ichthyophthirius, 529
  coccidia, 546f, 549–560, 550f, 551t–552t, 553f, 554f, 556f, 557t, 559f
    Besnoita, 558, 560
    Cryptosporidium, 555, 557t, 558, 559f
    Cyclospora, 550, 552
    Eimeria, 546f, 549–550
    Goussia, 558
    Hammondia, 555
    Hepatozoon, 558
    Isospora, 550
    Neospora, 555
    Sarcocystis, 555, 556f, 557t
    Toxoplasma, 524f, 552–555, 553f, 554f
  flagellates, 529–538, 530t–531t, 532f, 533f, 535f, 537f
    Giardia, 536–537, 537f
    Histomonas, 537–538
    Leishmania, 535f, 535–536
    Spironucleus, 537
    Trichomonas, 537

Protozoa (*cont'd*)
Tritrichomonas, 537
Trypanosoma, 529, 532f, 532–534
hemosporidians, 538–543, 539f, 540t–541t, 542f
Babesia, 538, 539f
Babesiosoma, 543
Cytauxzoon, 541, 543
Theileria, 538, 541
malarial organisms, 543–549, 544t, 546f
Haemoproteus, 549
Hepatocystis, 549
Leucocytozoon, 546f, 548–549
Plasmodium, 542f, 543, 545, 546f, 547–548
microsporans, 560t, 560–563, 562f, 563f
Encephalitozoon, 561, 562f
Enterocytozoon, 561–563, 563f
Glugea, 563
Nosema, 561
Pleistophora, 561
structure, 525–526
Provirus, 402
Proximal convoluted tubule
acute cell swelling, 697
toxins, 697, 697f, 700–705
cadmium, 704
cyclosporine, 702, 702f
gentamicin, 701–702
lead, 703f
lithium, 705
lysosomal toxins, 701–702
mechanisms of nephrotoxicity, 697, 700
mercury, 702, 704
metallic toxins, 702–705
nuclear transcription injury, 702
platinum, 704f, 704–705
uranium, 705
PrP^{C}, 911, 912, 915
PrP^{L}, 912
PrP^{Sc}, 911, 912, 915
PRRS (porcine reproductive and respiratory syndrome), 386
P-selectin, 236
Pseudoalgae, 575
Pseudocowpox, 324
Pseudocysts, 588
Pseudo-Hurler polydystrophy, 866
Pseudoinclusions, 15, 851, 851f
Pseudomembranous colitis, 502
Pseudomonadales (order), 482–484, 483t
Moraxella genus, 482, 483t
Pseudomonas, 437t, 482–484, 483f, 483t
Pseudomonas, 437t, 482–484, 483f, 483t
Pseudoplatelets, neutrophil, 243
Pseudopodia
amoebas, 526
erythrocyte, 96f
filopodia
acanthamoebae, 526
alteration in acute cell swelling, 18
description, 103
endothelial cell, 212f
erythrocyte, 96f, 102f
microfilaments and, 90
neoplastic cells, 763
platelet, 251
formation, 20, 102f
lamellipodia
description, 103
endothelial, 223
microfilaments and, 90
neoplastic cells, 763
neutrophil, 237
platelet, 251
microfilament, 115
neoplastic cells, 763
phagocytic cup formation, 115
Pseudotuberculosis, 476
Pseudoxanthoma elasticum, 303
Psittacine beak and feather, 356, 356f
PTP. *See* Permeability transition pores (PTP)
PTPs (protein tyrosine phosphatases), 79, 79f
Pulmonary anthrax, 496
Pulmonary calcification, 800
Pulmonary edema, 717, 727
Pulmonary environmental toxins, 730t–731t
Pulmonary fibrosis, 294f, 295, 296f, 306f, 728–729, 735
Pulmonary hypertension, 209
Pulmonary mineralization, 729
Pulmonary surfactant, 718, 719f, 723
PUMA, 42, 66
Purkinje cells, 640, 671f
Purkinje fibers, 640
Puromycin aminonucleoside nephrosis, 696
Pustule, 319
Pycnodysostosis, 807
Pyelonephritis
in cattle, 491
Escherichia coli and, 472
Pyknosis, 40
Pyridostigmine bromide, 683
Pyrithiamine, 685
Pyrrolizidine alkaloids
cardiotoxicity, 651
hepatotoxicity, 627
Pyruvate kinase deficiency, 102f
Pythiosis, 589
Pythium, 575

Q
Q fever, 476
Quinolinic acid, 685

R
R bodies, 439
Rab GTPases, 115
Rab-5, 115, 116
Rab-7, 116
Rabbit hemorrhagic disease (RHD), 399
Rabbitpox, 324, 327
Rabbits
atherosclerosis, 885–886
Himalayan, 814
viral diseases
European brown hare syndrome (EBHS), 399
infectious myxomatosis, 324, 327
rabbit hemorrhagic disease (RHD), 399
rabbitpox, 324, 327
Rac membrane targeting, 112
Radial spoke defect, 101
Radiation
bystander effect, 188
DNA damage and, 64
mitochondrial swelling and, 187–188
smooth muscle toxicity, 659
Ranavirus genus, 353
RANTES, 243
Ras GTPase, 115, 695
Rat-bite fever, 510
Rats
infectious diarrhea of infant rats (IDIR), 379
sialodacryoadenitis virus, 372
Reactive nitrogen species (RNS), malignant hyperthermia and, 191
Reactive oxygen species (ROS)
adriamycin cardiotoxicity, 63
lysosomal membrane degradation, 47
mitochondriopathy, 638
in necrosis, 38
oxidative stress, 185–186
in programmed cell death, 42–43
oxidative stress, 38, 43, 185–186
p53 activation, 42, 43
phagocytosis and, 116
photofrin toxicity, 672
protectants of injury, 63
Recanalization, 260
Receptor molecules, transmembrane proteins as, 763
Receptor protein tyrosine phosphatases (RPTPs), 79f
Receptor tyrosine kinases (RTKs), 81

Receptor-mediated endocytosis, 109, 113, 203–204
Receptors
  agonists of, 684
  glycoproteins, 81
  nuclear, 767
Recessive cutis laxa, 303
Red blood cells. *See* Erythrocytes
Red tide, 575
Reed-Sternberg cell, 23
Refsum's disease, 155–156
Regeneration
  description, 747
  liver, 747, 748f, 749
  muscle, 749
  in transplanted tissues, 750
Regional enteritis, 461
Regulated intramembrane proteolysis (RIP), 81
Regulatory T cells, 289
Reinke crystals, 848
Reiter's syndrome, 461
Relapsing fever, human, 508
Renal excretion, of exosomes in urine, 119
Renal hypoplasia, dysfunctional programmed cell death and, 47
Renal papillary necrosis (RPN), 706–708
Renal sphaerosporosis, 597
Renal tubules
  function, 700f
  glycogen accumulation in diabetes mellitus, 163–164
  uranium poisoning, 705
Renin, 708
Renin-angiotensin system, 708
Reoviridae family, 373–379, 375t, 376f
  Aquareovirus genus, 379
  Coltivirus genus, 379
    Colorado tick fever (CTF), 379
  Orbivirus genus, 377
    African horse sickness (AHS), 377
    bluetongue virus, 377
    epizootic hemorrhagic disease (EHD), 377
  Orthoreovirus genus, 376–377
  Rotavirus genus, 377–379
    bovine rotaviruses, 378–379
    epizootic diarrhea of infant mice (EDIM), 379
    human rotaviruses, 378
    infectious diarrhea of infant rats (IDIR), 379
    porcine rotaviruses, 378
Repair in situ, DNA, 64
Reperfusion injury, 641
Replication
  bacterial, 441–442
  DNA, 743–744
Replication bodies, 744
Replication foci, 744
RER. *See* Rough endoplasmic reticulum (RER)
RER cisternae, 138
Reserpine, 634f, 650, 669
Residual bodies, 49, 69, 118, 823, 824f
Respiratory burst, 239
Respiratory chain, mitochondrial
  components, 185f
  inhibitors, 186
Respiratory syncytial virus (RSV), 364, 366
Respiratory system, 717–740. *See also* Lungs
  diseases
    adenoviral infection, 343
    Bordetella, 457, 458f
    bovine rotaviral, 379
    Hanta pulmonary syndrome, 392
    influenza, 356–358, 357f
    Pasteurella, 482
    postinflammatory pulmonary microlithiasis, 800
    pulmonary calcification, 800
    Streptococcus, 502
  fetal lung, 722f, 723
  gills, 736f, 736–737, 737f, 738f
  normal mammalian lung, 717–718
    alveolar wall, 716f, 717
    pneumocytes, 717–718, 718f
    surfactant, 718, 719f
  swim bladders, 737–738
  toxicity
    acute toxic injury, 726–728
      exhalant injury, 727
      inhalant injury, 726–727, 727f
      vascular injury, 727–728
    chronic exhalant injury, 734–736
      bleomycin, 735, 735f
      cationic amphophilic drugs, 735–736
      ethanol, 735
      monocrotaline, 735
      paraquat, 734–735
    chronic inhalant injury, 728–734
      alveolar lipoproteinosis, 732
      asbestos, 733, 734f
      carbon monoxide, 731
      cigarette smoke, 729, 731
      glass fibers, 732–733
      inhalant gases, 729
      nanoparticles, 733–734
      particulates, 731–732
      pulmonary fibrosis, 728–729
      pulmonary mineralization, 729
      silicates, 732, 732f
    environmental toxins, 730t–731t
    oxidant damage, 724
    from particulates, 723–724, 731–732
    pulmonary vascular toxins, 726, 727–728
    reaction to toxins, 719–723
    table of toxins, 724t–726t
    from vapors and gases, 723
Respirovirus genus, 360
Reticular fibrils, 299
Reticulate body, of *Chlamydia,* 485, 486
Retinogeniculocortical pathways, 814
Retraction bulbs, 669
Retrograde transport, 139–140
Retroviridae family, 401–415, 402t–403t
  Alpharetrovirus genus, 404
    avian leukemia virus (ALV), 404
    Rous sarcoma virus (RSV), 404
  Betaretrovirus genus, 404, 406
    jaagsiekte sheep retrovirus (JSRV), 406
    mouse mammary tumor virus (MMTV), 404, 405f, 406
  Deltaretrovirus genus, 410
    human T-lymphotrophic virus (HTLV), 410
  Gammaretrovirus genus, 406–410
    avian reticuloendotheliosis virus (ARV), 410
    feline leukemia virus (FeLV), 406–407, 408f
    murine leukemia viruses (MLVs), 407, 408f, 409f, 409–410
  Lentivirus genus, 410–415, 411f, 413f, 414f, 415f
    equine infectious anemia (EIA), 414–415
    human immunodecifiency virus (HIV), 410–412, 411f, 413f
    simian immunodecifiency virus (SIV), 412, 414f
    visna, 412, 414
  neoplasia and, 763, 765f
  Orthoretrovirinae subfamily, 404–415
  Spumavirinae subfamily, 415, 415f
    foamy viruses, 415
Rett syndrome, 824
Reverse transcriptase, 402
Reye's syndrome, 192
Rhabdomyosarcoma, 770f
Rhabdoviridae family, 363f, 366t, 366–368
  Ephemerovirus genus, 368
  Lyssavirus genus, 367–368
  Mokola virus, 368f
  rabies virus, 363f, 367–368
  vesicular stomatitis virus (VSV), 367, 367f
  Vesiculovirus genus, 367
Rhadinovirus genus, 337–338

Rhesus monkey
  hemorrhagic fevers, 381
  Yabapox, 327
Rhinosporidium, 588, 589f
Rhinovirus genus, 394, 397
Rhizobiales (order), 453–456, 454t
  Afipia genus, 453–454, 455f
  Bartonella genus, 453, 454t
  Brucella genus, 454t, 454–455, 457f
Rhizomelic chondrodysplasia, 156
Rho family GTPases, 214
Rhodococcus, 490t, 496
Rhoptries, 526, 538, 545, 550, 554
Rho/Rho-kinase (ROCK), 209
Riboflavin, mitochondrial hypertrophy and, 190
Ribosomal degranulation, 7
Ribosomal RNA (rRNA), 132, 133
Ribosome-inactivating proteins (RIPs), 613
Ribosome-lamellar complexes, 771–772
Ribosomes
  appearance, 137f
  autophagy, 71
  bacterial, 436
  in cytomegaly, 23
  degradation, 7
  fungal, 578
  hepatotoxins and, 619
  lamellar complexes, 846
  mitochondrial, 43, 184
  monomeric, 136
  necrosis, 40
  of neoplastic cells, 769
  polysome, 136
  rough endoplasmic reticulum, 138, 138f
  structure, 136
  toxins effect on, 136–137
  use of host by microbes, 136
Ricin, 614, 618
Ricketts, 806
Rickettsia, 448–451, 449t, 450f
Rickettsiales (order), 448–453, 449t, 452t
  Aegyptianella genus, 452t, 453
  Anaplasma genus, 451–453, 452t
  Ehrlichia genus, 451, 452t
  Rickettsia genus, 448–451, 449t, 450f
Rifampicin, 136, 619
Rift Valley fever (RVF), 392
Ringworm, 590–591, 593f
RIP (regulated intramembrane proteolysis), 81
RIRR (ROS-induced ROS release), 638
RME. *See* Receptor-mediated endocytosis
RNA editing, 133, 533
RNA polymerases, 131
  blockage of, 135–136
  RNA polymerase II, 136
  RNA polymerase III, activity in neoplastic cells, 767
RNA transcript, 131
RNS (reactive nitrogen species), malignant hyperthermia and, 191
ROCK-II, 781
Rocky Mountain spotted fever, 449, 451
Rodents
  atherosclerosis, 886
  scrapie, 913
ROS. *See* Reactive oxygen species (ROS)
Rosenthal fibers, 687, 842, 870
Roseolovirus genus, 335
ROS-induced ROS release (RIRR), 638
Rotavirus genus, 377–379
  bovine rotaviruses, 378–379
  epizootic diarrhea of infant mice (EDIM), 379
  human rotaviruses, 378
  infectious diarrhea of infant rats (IDIR), 379
  porcine rotaviruses, 378
Rough endoplasmic reticulum (RER). *See also* Endoplasmic reticulum (ER)
  autophagy, 71
  biotransformational toxins in, 614, 618–619
  changes in mitosis, 747
  chaperones, 138
  in cytomegaly, 23
  hepatotoxins and, 611–612, 613–614, 619
    acetaminophen, 618–619
    modeccin, 613–614
    phenobarbital, 614
    ribosome-inactivating proteins (RIPs), 613–614
    ricin, 614, 618
    volkensin, 613–614
  hypertrophy and, 21
  inclusions in, 843–849
  lipoprotein metabolism, 170
  of neoplastic cells, 769
  post-translational modification in the, 138
  protein degradation, 139
  retrograde transport from Golgi, 139–140
  structure, 138, 138f
  transitional vesicle movement to Golgi, 139
Rous sarcoma virus (RSV), 404
RPTPs (receptor protein tyrosine phosphatases), 79f
RSV (respiratory syncytial virus), 364, 366
RTKs (receptor tyrosine kinases), 81
Rubulavirus genus, 364
Ruffled border, 806, 806f
Russell's bodies, 284, 846
Russian spring-summer encephalitis (RSSE) virus, 388
RVF (Rift Valley fever), 392
Ryanodine receptor (RyR) proteins, 639

S
S fimbriae, 469
S phase, 743–744
S phase fraction, 768–769
SAA (serum amyloid A), 830–831, 833–834
Saimiriine herpesvirus 2, 338
Salicylate, effect on aerobic synthesis of ATP, 192
Salivary glands
  adenoma, 772f
  HIV infection and, 412
  hyperplasia, 26
  microliths, 803
  rabies in, 368
Salla disease, 863
Salmon, senescence and, 752
Salmonella, 468t, 473–474
  S. arizonae, intracellular, 495f
Samoyed dogs, X-linked renal disease in, 898
Sandhoff disease, 860
Sanfilippo disease, 864
Sapovirus genus, 399
Sarafotoxins, 659
Sarcina, 504
Sarcocystis, 555, 556f, 557t
Sarcocystosis, 555
Sarcoidosis, 274, 300
Sarcomas, 761
Sarcomere, 635
Sarcopenia, 750
Sarcoplasmic reticulum (SR)
  calcium retention in, 160–161
  doxorubicin toxicity and, 646, 647f
  myocardial, 638f, 639
  snake venom effects on, 658
Sarin, skeletal muscle myopathy from, 653
SARS (severe acute respiratory syndrome), 370
Scalded skin syndrome, 500
Scavenger receptor cysteine repeat (SRCR) domains, 270
Scavenger receptors, 270
SCF complex, 745
Schaumann's body, 803f
Schilder's disease, 155
Schistosomiasis, 245

Schizogony, 545, 548, 549, 550
Schizont, *Sarcocystis cruzi*, 556f
Schwann cells
  mitochondrial Schwannopathies, 682–683
  myelin formation, 682
Scleroderma, 301
Sclerosis
  atherosclerosis, 881, 883, 883f, 884f, 885–886, 886f
  focal segmental glomerulosclerosis, 902
Scott syndrome, 204
Scrapie, 912–913, 913f
  rodent, 913
Scrapie-associated fibrils, 913
Scurvy, 303
Sebaceous gland adenoma, 760f
Secondary glomerulonephritis, 891
Secondary granules, neutrophil, 233
Secondary stage, syphilis, 508
Secretion, 142–147
  calcium in, 143–144
  constitutive, 142
  exocytosis, 143
  membrane fusion, 143
  microtubules and, 88
  pathways
    acid secretion, 145
    epinephrine, 145, 147
    insulin, 145
    mammary epithelial secretion of lipids, 145
    yolk epithelial secretion of lipids, 145, 146f
  platelet, 253–254
  regulated, 142
  secretory canaliculi, 142–143
  transport vesicles, 142–143
Secretion exhaustion, 23
Secretion systems, 438. *See also specific bacterial genera or species*
Secretogogues, 143
Secretory canaliculi, 142–143
Secretory exhaustion, 145–146
Secretory granules
  accumulation in necrosis, 40
  autophagy, 71
  colchicine effect on, 89
  contents, 142
  crinophagy, 772, 773f
  end-stage, 144
  exocytosis, 143
  Golgi origin of, 141
  inclusions, 847–849
  increase in, 21, 22
  insulin secretion, 145
  microtubule guidance of, 88
  in neoplastic cells, 772, 773f, 774f, 775
  protozoal cell, 525
  yolk, 145, 146f
Secretory piece, immunoglobulin A (IgA), 114
Secretory vesicles, 119, 119f, 142–143
Segmental demyelination, 681
Selectins, 80, 234f, 236
Sendai virus, 360
Senescence
  animal models of, 752–753
  organelle, 753
  shift to, 785, 787
  signaling pathways in, 752
Senile peripheral amyloid angiopathy, 837
Senile systemic amyloidosis, 834
Sensory neuropathy, 690
Septic disease, membranous glomerulonephritis from chronic, 894
Septicemia, *Staphylococcus aureus*, 500
SER. *See* Smooth endoplasmic reticulum (SER)
Serotonin, 217
  skeletal muscle toxicity, 654–655
Serotoninergic neurons, 684
  toxins for, 672, 676
Serpins, 116
Serum amyloid A (SAA), 830–831, 833–834
Severe acute respiratory syndrome (SARS), 370
Sex hormones, 304
Sex pili, 438
Sex skin, 304
Sex steroids, extrahepatic, 630
Sezary cell, 767, 767f
Sheep
  bacterial diseases
    Anaplasma, 451
    anthrax, 496–497
    caseous lymphadenitis, 491
    cutaneous dermatophilosis, 496
    Eperythrozoon, 445t, 447
    Erysipelothrix, 447
    Fusobacterium, 510
    heartwater, 451
    Johne's disease, 494
  scrapie, 912–913
  viral diseases
    Akabane virus, 392
    bluetongue virus, 377
    border disease, 389
    Borna disease virus, 386
    foot-and-mouth disease (FMD) virus, 397
    jaagsiekte sheep retrovirus (JSRV), 406
    louping ill virus, 388
    Nairobi sheep disease, 392
    orf virus, 324, 325f
    ovine progressive pneumonia, 414
    Rift Valley fever (RVF), 392
    visna, 412, 414
Sheeppox, 324
Shh (sonic hedgehog), 101, 114
Shigatoxin, 475
Shigella, 468t, 474–475
Shigella toxin, 475
Shingles, 333
Shipping fever, 480
Shrinkage cytonecrosis, 33
SHV (simian hemorrhagic fever virus), 386
Sialidosis, 863
Sialodacryoadenitis virus, 372
Siamese cats
  mucopolysaccharidoses, 866
  pigmentation, 814
Siderophore, 439–440, 475
Siderosis, 817
Siderosome, 816, 816f, 819f
Signal peptide, 138
Signaling pathways
  in angiogenesis, 779
  in senescence, 752
Signalosome, 68–69
Silent information regulator 2 (SIRT2), 752, 840
Silicates, pulmonary damage from, 732, 732f
Silicosis, 824–825
Simian hemorrhagic fever virus (SHV), 386
Simian immunodecifiency virus (SIV), 412, 414f
Simian rotavirus, 378
Simian varicella, 333
Simian virus 40, 348–349
Simplex type EB, 92
Simplexvirus genus, 330, 331f, 332f, 332–333
Simvastatin, cardiotoxicity of, 649f
Single cell necrosis, 46
Singlet oxygen, antimicrobial action of, 238, 239
Sinoatrial node, 640
Sinusoids, 205, 607
SIRT1 and SIRT2, 752, 840
Sirtuins, 752, 840
Site of injury, xv, 211
Sitosterolemia, 174
Situs inversus totalis, 101
SIV (simian immunodecifiency virus), 412, 414f
Skeletal muscle
  atrophy of, 29
  cytopathologic analysis of, 653t
  denervation atrophy, 51–52
  HIV infection and, 412, 413f
  lipofuscin, 824

Skeletal muscle (*cont'd*)
lytic necrosis, 37f
mitochondria DNA congenital disorders, 193
myotoxins, 651–658
androgens and anabolic steroids, 652
azidothymidine, 652
bacterial toxins, 655, 657f
carbamates, 654
colchicine, 653
ethanol, 652
HMGCoA reductase inhibitors, 653
local anesthetics, 654
motor end plate toxins, 654, 655f
organophosphorus insecticides, 653–654, 654f
plant alkaloids, 658
table of toxins, 656t
venoms, 655, 658
veratrine, 658
vincristine, 652–653
rabies antigens in, 367
tetanus toxin effects on, 686
tubular aggregates, 651–652
Skin
antigen presentation, 277
cutaneous anthrax, 496
cutaneous leishmaniasis, 536
cutaneous mastocytosis, 222, 222f
cutaneous permeability barrier, 311–312
cutaneous pythiosis, 575
dermatitis
mast cells in, 220f
pigmented defects, 812
dermatomycosis, 590
dermatophilosis, 496
dermatophytosis (ringworm), 590–591, 593f
fibrosis, 295
SLE (systemic lupus erythematosus), 901
Sleeping sickness, 533
Slime layers, 435–436
Slit diaphragms, 695, 696, 697
Sly syndrome, 865
Small lymphocytes, 286–287
Small nuclear ribonucleoprotein particles (snRNPs), 129, 132, 135
Small nuclear RNAs (snRNAs), 132
Smooth endoplasmic reticulum (SER). *See also* Endoplasmic reticulum (ER)
aggregation, 9
appearance, 152f, 156f
autophagy, 71
in cytomegaly, 23
degradation, 63
description, 156–157
drug-induced injury, 157
degeneration, 157, 160f
proliferation, 157, 158f, 159f
glycogenesis, 161
hepatotoxicity, 619–622
carbon tetrachloride, 620–621, 621f
cyanamide, 620, 621f
ethanol, 621–622, 622f
hypertrophy, 607
lipid metabolism, 169
lipoprotein metabolism, 170
peroxisome association with, 153
proliferation, 157
aggregation, 9
as detoxification response, 62f, 62–63
in hepatotoxicity, 619–620
in neoplastic cells, 777f
reduplication, 62
structures associated with
calciosomes, 159–160
tubulocisternal endoplasmic reticulum (TER), 157, 159
toxicologic enhancement in, 157
whorling of membranes, 62, 62f
Smooth membrane vesicles, 170
Smooth muscle
atherosclerosis and, 881
myotoxins, 658–659
allylamine necrosis, 659
immunosuppressive agents, 659
radiation injury, 659
smooth muscle relaxants, 658–659
venoms, 659
Smooth muscle relaxants, 658–659
Smyth chicken, 812
Snake venoms, 82, 658, 659, 686
Snakehead reovirus, 379
SNARE proteins, 78, 115
S-nitrosylation, 851
snRNAs (small nuclear RNAs), 132
snRNPs (small nuclear ribonucleoprotein particles), 129, 132, 135, 746
SOD (superoxide dismutase), 38, 63, 66, 186, 195
Sodium (Na^+) channels, 678
Sodium-potassium pump, 80
Soman, skeletal muscle toxicity of, 654, 654f
Somatomedin, 613
Somatotropin, hepatocyte effects, 613
Sonic hedgehog (Shh), 101, 114
Spasm, arterial, 876
Specific granules, 233, 237
Spectrin, 92
Spectrin deficiency, 95
Spectrin-actin complex, 94
Spermatid, multinucleate giant, 25f
Sphaerospora, 597
Spherical microparticles, 121
Spherocyte, 94
Spherocytosis, drug-induced, 95
Spheroplast, 430
Spherules, *Rhinosporidium* and, 588
Sphingosine, 81
Spicules, in mitochondrial calcification, 39
Spiculocyte, 94, 95f
Spinal cord, intermediate filament disorders and, 92
Spinal sensory ganglia, cadmium toxicity, 704
Spindle filaments, 746
Spindle matrix, 746
Spirillum, 511t
Spirochaetales (order), 505–509, 506t
Borrelia genus, 505–506, 506f, 508
Brachyspira genus, 506t, 506–509
Leptospira genus, 505, 506t, 507f
Treponema genus, 506f, 508
Spironucleus, 537
Spiroplasma, 447
Spleen
amyloid, 831, 832f
antigen presentation, 277–278
erythrophagocytosis, 819, 820f
Leucocytozoon infection, 548
in malaria, 545
Splenic reticular cell, in adenoviral cytomegaly, 27f
Spliceosome, 133
Spongiform myeloencephalopathy, murine leukemia viruses and, 407
Spongiosis hepatis, 609, 609f
Spongiotic pericytoma, 609
Sporangia, algae, 573
Spore membrane, coccidia, 549
Spores
Aspergillus, 580, 581f
bacterial, 442
fungi, 580
myxozoan, 595, 596f
Rhinosporidium, 588
Sporoblast, in microsporans, 561
Sporogony, 549
Sporonts, 561
Sporothrix schenckii, 588–589
Sporozoite
coccidial, 549, 550
malarial, 543, 545
Sporulation, 442, 579
Spot desmosomes, 100
Spotted fever rickettsiae, 449, 451
Sprouting angiogenesis, 779
Spumavirinae subfamily, 415, 415f
foamy viruses, 415

Squamous cell carcinoma, 759f
basement membrane material, 778f
human papilloma virus (HPV), 346
Squamous metaplasia, 26
SR. *See* Sarcoplasmic reticulum (SR)
src, 46
SSPE (subacute sclerosing panencephalitis), 362
St. Louis encephalitis virus, 383f, 388
Staphylococcus, 437t, 498, 498f, 499f, 500
Starvation
atrophy of, 26, 29
basement membrane thickening in, 307
hepatocyte, 607
Statins, 209
skeletal muscle myopathy from, 653
smooth endoplasmic reticulum proliferation, 620
Status spongiosis, 690, 914, 914f
Stavudine, 183
Steatosis
hepatotoxicity, 12f, 626
lipid globules accumulation, 165, 165f
microsteatosis, 626
non-alcoholic steatohepatitis, 191
smooth endoplasmic reticulum degeneration, 160
STEC autoagglutinating adhesin (saa), 471
Stem cells
bone marrow, 223
hemopoietic, 120
liver, 609
Stereology, xvi
Sterol metabolism, change in aging, 750
Stichosomes, 598
Stomata, lymph vessel, 215
Stomatocyte, 95
Stop-transfer sequences, peptide, 138
Storage diseases, 857–870
Alexander's disease, 870
amino acid transport, 869–870
cystinosis, 869
maple urine disease, 870
tyrosinosis, 869–870
glycogen, 858f, 866–869
Lafora disease, 856f, 868–869
muscle glycogen storage diseases, 869
oligosaccharide storage diseases, 869
polyglucosan body diseases, 868f, 868–869
type I glycogenosis, 866
type II glycogenosis (Pompe's disease), 867
type III glycogenosis, 868
type IV glycogenosis (amylopectinosis), 868
type V glycogenosis (McArdle disease), 868
type VI glycogenosis, 868
type VII glycogenosis, 868
ultrastructural pathology in models of, 867t
glycoproteinosis, 863–864
fucosidosis, 863
galactosialidosis, 863
geleophysic dysplasia, 864, 864f
mannosidosis, 863–864
Salla disease, 863
sialidosis, 863
infantile osteopetrosis, 870
lipid, 857–862
drug-induced disease, 862
Fabry disease, 862
Gaucher's disease, 860–861, 861f
GM_1-gangliosidosis, 857, 858f
GM_2-gangliosidosis, 860
Krabbe's disease (globoid cell leukodystrophy), 856f, 861
models of sphingolipid storage diseases, 859t
Nieman-Pick disease, 860
Tay-Sachs disease, 860
Wolman's disease, 861
mucolipidoses, 866
mucopolysaccharidoses, 864f, 864–866
animal models, 866
Hurler's disease, 865–866
localized corneal, 864–865
Sanfilippo disease, 864
Sly syndrome, 865
systemic, 864
ultrastructural pathology in animal models, 865t
neuronal ceroid lipofuscinoses, 862–863
Stratified squamous cells, programmed cell death in, 45f
Stratum corneum permeability barrier, 311–312
Streptobacillus, 510, 510t
Streptococcus, 500–502, 501t
poststreptococcal glomerulonephritis, 898
virulence factors, 437t
Streptolysin-O, 501
Streptomycin, 619
Stress fibers, 90, 297
Stress granules, 67
Stress proteins, 66–67, 138
Stress response, endoplasmic reticulum and, 69
Strychnine, 687
Subacute encephalopathy, AIDS and, 411
Subacute sclerosing panencephalitis (SSPE), 362
Submembrane blebs, in necrosis, 36
Subpellicular microtubules, 525, 532, 549
Subsarcolemma densities, 635
Suipoxvirus genus, 327, 327f
Sulfonamide nephrosis, 711
Sulfur dioxide, pulmonary damage from, 729
Sulfur globules, 439
Summer flu, 538
Superoxide anions, 38, 39
antimicrobial action, 238, 239
in phagosome, 239
Superoxide dismutase (SOD), 38, 63, 66, 186, 195
Superoxide radical, ischemia and, 50
Suppressor genes, 758
Surface blebs, in necrosis, 36
Surface structures, 101–103. *See also specific structures*
in acute cell swelling, 18, 19f
cilia, 101
filopodia, 102f, 103
lamellipodia, 103
microvilli, 101, 103
Surfactant, 718, 719f, 723
Survivin, 66
Sweat duct, 159
Swim bladders, 737–738
Swine
atherosclerosis, 886
bacterial diseases
Brachyspira, 508–509
Eperythrozoon, 445t, 447
Erysipelothrix, 447
Leptospira, 507f
porcine eperythrozoonosis, 447
porcine intestinal spirochetosis, 509
proliferative enteropathies of, 461
viral diseases
African swine fever (ASF), 353f, 353–354
encephalomyocarditis (EMC) viruses, 397
foot-and-mouth disease (FMD) virus, 397
hemagglutinating encephalomyelitis virus (HEV), 373
hog cholera, 388–389, 390f
Nipah virus, 364
porcine reproductive and respiratory syndrome (PRRS), 386
rotavirus, 378
swine vesicular disease, 399

Swine (*cont'd*)
swinepox, 327, 327f
transmissible gastroenteritis (TGE) virus, 372f, 372–373
vesicular stomatitis virus (VSV), 367
Swine dysentery, 508–509
Swine vesicular disease, 399
Swinepox, 327, 327f
Symmetrical peripheral neuropathy, 904
Synapse
neurotoxins acting at, 683–687
vesicles, 684, 687f
Synapsin I, 683
Synapsopathy, prion diseases as, 911
Synaptophysin, 683
Synaptosome, 440
Synaptotagmin, 683
Synovial fibrosis, 295
Syntaxin clusters, 78
Syntaxins, 115
Synucleinopathies, 840–842
amyotrophic lateral sclerosis (ALS), 841
Huntington's disease, 841
Lewy body disease, 840
Parkinson's disease, 840–841
Rosenthal fibers, 842
Syphilis, 508
Systemic disease, 319
Systemic lupus erythematosus (SLE), 901
Systemic mastocytosis, 222
Systemic scleroderma, 301

T
T cell receptors (TCR), 289–291
T cells, 288–291
cytotoxic, 289, 289f
FasL expression in activated, 46
helper, 288–289
regulatory, 289
surface receptors, 289–291
T helper lymphocytes, HIV infection of, 410–411
in tissue, 291
T system, 639
Tabun, skeletal muscle myopathy from, 653
Tachyzoites, 553–554
Tacrolimus, vascular toxicity, 659
Tadpole edema virus, 353
Tadpole tail breakdown, 49
TAF (tumor angiogenesis factor), 780
Taffazzin gene, 195
Talin, 253
Tangier disease, 174
Tannerella, 509
Tau protein, 839
Tauopathies, 839–840
Alzheimer's disease, 839–840
frontotemporal dementias, 840
paired helical filaments, 839
Taxol, 89, 627
Tay-Sachs disease, 860
TCP (tetrachlorobiphenyl), hepatotoxicity, 623
TCR/CD3 complex, 291
Tegument, herpesvirus, 327
Tellurium, myelinopathy from, 682
Telomeres, 130
Telophase, 744, 745
Tenascin, 224, 308
Tendonitis, calcifying, 800
Tenericutes (phylum), 442–447
TEPP (tetraethyl pyrophosphate), skeletal muscle myopathy from, 653
TER (tubulocisternal endoplasmic reticulum), 157, 159
Tertiary granules, neutrophil, 233
Tertiary stage, syphilis, 508
Testicle
cadmium toxicity, 704
cytomegaly, 25f
Tetanus, 502–503
Tetanus toxin, 502, 655, 685–686
Tetrachlorobiphenyl (TCP), hepatotoxicity, 623
Tetrachlorodibenzo-p-dioxin (TCDD), hepatotoxicity, 623
Tetrahydrocannabinol (THC), 677
Tetrodotoxin, 678
Texas cattle fever, 538
TGE (transmissible gastroenteritis) virus, 372f, 372–373
TGF-α, 749
TGF-β (transforming growth factor-β), 234, 254, 295, 749, 777, 785
Theileria, 538, 541
Theileriosis, 538, 541
Theiler's virus, 396f, 397
Thermogenen, 751
Theronts, 529, 529f
Thiamine deficiency, mitochondrial hypertrophy and, 189
Thiamine pyrophosphate, 189
Thiobenzaimidazole, 611
Thioredoxin, 116
Thiotricales (order), 484, 484t
Francisella, 484, 484t
Thoracic duct, 287
Thorotrast, hepatotoxicity of, 627
Thrombasthenia, 256
Thrombin, 247, 257
Thrombocytopenia, 247, 254–255
Thrombomodulin, 207, 215
Thromboplastin, 259
Thrombopoietin (TPO), 247
Thromboresistance of endothelium, 206, 207
Thrombosis, 257–260, 258f
coagulation, 257, 259
pulmonary wall capillaries, 722f
variability of thrombi, 260
Thrombospondin (TSP), 224, 251, 253, 308
Thrombosthenin, 260
Thrombotic disease
glomerulopathy, 902
thrombocytopenia, 902
Thymic nurse cells, 283
Thymus
antigen presentation, 279, 282f, 282–283
atrophy, 49, 53f
Thyroid gland
lipofuscin, 824
thyroiditis, autoimmune, 309, 310f
Thyroid hormones
cardiotoxicity, 651
hepatotoxicity and, 623
mitochondrial effects of, 623
Na-K-ATPase increase and, 80
Thyroiditis, autoimmune, 309, 310f
Tie-2, 779
Tight junctions
blood-brain barrier and, 688
density, 211
description, 97, 98f, 204
disassociation, 17
neoplastic cells, 766
slit diaphragms, 695, 696, 697
Tilarone, 610
Tiletamine, 677
Tissue factor, 215, 243, 259
Tissue factor pathway inhibitor-2 (TFPI-2), 883
Tissue repair, neutrophil role in, 240
TLRs (toll-like receptors), 116, 270
TME (transmissible mink encephalopathy), 914
TNF-α-related apoptosis-inducing ligand (TRAIL), 42, 47, 785
TNF-like weak inducer of apoptosis (TWEAK), 47, 785
TNF-related apoptosis-inducing ligand (TRAIL/APO2 ligand), 235
Togaviridae family, 381t, 381–384, 383f
Alphavirus genus, 381–384
eastern equine encephalitis (EEE), 382, 383f
Venezuelan equine encephalitis (VEE), 382, 384
western equine encephalitis (WEE), 382
Rubivirus genus, 384
rubella, 384
Toll-like receptors (TLRs), 116, 270

Tonofilaments, 92
Tonsils, 278
Topolysis, 611
Torovirus genus, 373, 374f
Torpor, 751
Torres bodies, 387
Toulouse-Lautrec disease, 807
Toxaphene, gill toxicity of, 737
Toxic granules, 240
Toxic injury
  autophagy in, 71
  melanization in, 812
Toxic milk mouse syndrome, 823
Toxic milk mutant mouse, 194
Toxic neutrophils, 240, 241f
Toxic polyneuropathies, 681
Toxic shock syndrome (TSS), 500
Toxicology
  hepatotoxins, 609–630
  myotoxins, 635–664
    cardiotoxicity, 635–651
    skeletal muscle, 651–658
    smooth muscle, 658–659
  nephrotoxins, 695–715
  neurotoxicity, 667–693
  respiratory system, 717–740
Toxins. *See also specific substances*
  bacterial, 655
    Clostridium, 502–503
    Escherichia coli, 471–473
    Staphylococcus, 500
    streptococcal, 501–502
  calcinogenic, 801–802
  exotoxins, 436
  membrane-acting, 436, 438
  pore-forming, 438
  Type III secreted cytotoxins, 438
Toxoplasma, 524f, 525f, 552–555, 553f, 554f
TPO (thrombopoietin), 247
Tracheal cytotoxin, 457
Tracheobronchitis, from herpes simplex virus, 332–333
Trafficking. *See* Intracellular trafficking
TRAIL (TNF-α-related apoptosis-inducing ligand), 42, 47, 785
Trans face, Golgi complex, 140–141
Transcription
  of rRNA genes, 133
  silencing of, 761
  ultrastructure of, 132–133
Transcription factors, 131
Transcription initiation factor complex, 767
Transcription stress response, 136
Transcriptional activation, mitochondrial, 183
Transcriptional silencing, 761
Transcytosis, 109, 110f
Transdifferentiation, 26
Transendothelial channels, 202–203, 205f
Transendothelial passage, 782
Transepithelial migration, 696
Transferrin receptors, 120, 817
Transforming growth factor-β (TGF-β), 234, 254, 295, 749, 777, 785
Transglutaminase, 842, 850
Transition pores. *See* Permeability transition pores (PTP)
Transitional vesicles, 139
Translation
  genetic defects in, 137–148
  toxins affecting, 136–137
Transmembrane protein defects, 242–243
Transmembrane proteins
  detection of, 78–79
  membrane transport and, 79
  microdomains, 78
  platelet, 253
  table of functions, 84t
  water channel, 79–80
Transmissible gastroenteritis (TGE) virus, 372f, 372–373
Transmissible mink encephalopathy (TME), 914
Transmissible spongiform encephalopathies (TSEs)
  bovine spongiform encephalopathy (BSE), 913
  chronic wasting disease (CWD), 913–914
  Creutzfeldt-Jakob disease (CJD), 914–915
  description, 911, 912
  fatal familial insomnia (FFI), 915
  Gerstmann-Sträussler-Scheinker syndrome (GSS), 915
  kuru, 914, 914f
  rodent scrapie, 913
  scrapie, 912–913, 913f
  transmissible mink encephalopathy (TME), 914
Transmission electron microscopy (TEM), xvi
Transplanted tissues, regeneration in, 750
Transport, microtubular, 87–88
Transport proteins, 78
Transport vesicles, 142–143
  exocytosis, 119
  increase in, 21
Transporters, bacterial cell membrane, 429
Transthyretin-associated amyloid, 834–835
Trastuzumab, cardiotoxicity of, 646, 648
Treponema, 506t, 508
Trichinella, 597–598, 599f
Trichinosis, 597–598
Trichocysts, 528
Trichomonas, 537
Trichophyton, 590, 591
Trichosporon, 592
Trichuris muris, 600
Tricyclic compounds, 684
Triethyltin, myelinopathy from, 682
Trigeminal ganglion, HSV and, 332
Triglyceride
  globules, 169
  in smooth endoplasmic reticulum, 169
Trimetrexate, 135
Triskelion, 113
Trisomy of chromosome 21, 836
Tritrichomonas, 537
Troglitazone, 625
Tropheryma, 490t, 496
Trophozoites, malarial, 545
Tropocollagen, 298–299
Tropomyosin, 90
Trx2/Ask1 pathway, 625
Trypanosoma, 529, 532f, 532–534
  life cycle, 529, 532
  structure, 532f, 532–533, 533f
  T. brucei, 534
  T. congolense, 534
  T. cruzi, 534
  T. fallisi, 533f
  T. rhodesiense, 534
  T. theileri, 534
Trypanosomal flagellate form, 529, 532f
Trypanosomiasis
  African, 533–534
  American, 534
  bovine, 534
Trypomastigote, 532f, 533f, 533–534
TSEs. *See* Transmissible spongiform encephalopathies (TSEs)
Tsetse fly, African trypanosomiasis and, 533
TSP (thrombospondin), 224, 251, 253, 308
TSS (toxic shock syndrome), 500
Tubercle, 493
Tubular aggregates, skeletal muscle, 651–652
Tubular inclusions/aggregates, 846, 847f
Tubular lysosome, 117
Tubulation, 11
Tubules, in neoplastic cells, 771–772
Tubulin disruptors, 119
Tubulocisternal endoplasmic reticulum (TER), 157, 159
Tubuloreticular structures, 411, 640, 847, 848f

Tubulovesicular structures
in Creutzfeldt-Jakob disease (CJD), 915
in rodent scrapie, 913
Tubulovesicular system, 142
Tularemia, 484
Tumor. *See also* Neoplastic cells
angiogenesis, 778–780, 779f, 781f
benign, 761
embolus, 783, 784f
growth, 757–758
malignant, 761
Tumor angiogenesis factor (TAF), 780
Tumor microenvironment, 775–780
angiogenesis, 778–780, 779f, 781f
basement membrane material, 777, 778f, 781f
collagen, 777–778, 781f
description, 775, 777
fibroplasia, 778
Tumor necrosis factor (TNF), 215, 235
Tumor necrosis factor-α (TNF-α), 47, 217, 270, 785
Tumor-associated fibroblasts, 775, 777
Tunicamycin, 688
Turkeys, diseases of
avian reticuloendotheliosis virus (ARV), 410
bluecomb, 373
Bordetella, 458
coryza, 457
Erysipelothrix, 447
fowl cholera, 482
fowlpox, 324
Turning disease, 538
TWEAK (TNF-like weak inducer of apoptosis), 47, 785
Twitcher mouse, 861
Type 1 fimbriae, 433, 469
Type I secretion system, 438
Type II pili, 434
Type II pneumocyte hyperplasia, 720
Type II secretion system, 438, 466
Type III secretion system, 438, 466
Aggregatibacter, 479
Chlamydia, 486
Salmonella, 473, 474
Shigella, 474
Yersinia, 475
Type IV fimbriae, 469
Type IV pili, 434
Type IV secretion system, 438
Type VI secretion system, 438, 466
Type VII secretion system, 438
Typhoid fever, 473
Typhus, epidemic, 448–449
Typhus nodules, 449
Tyrosinase, 811
Tyrosine crystals, 710, 710f, 772f
Tyrosine kinase inhibitors, cardiotoxicity of, 646, 648
Tyrosinosis, 869–870
Tyzzer's disease, 502, 503f

U
Ubiquitin, 40
cyclin destruction, 745
frontotemporal dementia, 840
increase in degenerating cells, 67
Mallory bodies and, 850
Ubiquitination, 139
description, 67
polyubiquitination of Lewy body disease, 840
proteins of aging, 842
Ubiquitin-peptide complex, 67
Ubiquitin-proteosome system (UPS), 67, 69, 842
UCH-L1 enzyme, 840
Ultrastructural interpretation of pathologic change, xv
Ultraviolet (UV) radiation, apoptosis and, 188
Uncoating vesicles, 171
Unconjugated hyperbilirubinemia, 712
Uncouplers of oxidative phosphorylation, 687
Uncoupling protein 1 (UCP1), 183
Uncoupling vesicles, 171
Undifferentiation, 761
UPEC (uropathogenic *Escherichia coli*), 472
Uranium, nephrotoxicity, 705
Urea cycle enzymes, defects in, 192–193
citrullinemia, 192
hyperornithinemia, 192–193
Ureaplasma, 444t, 445, 447
Urease, 473
Uremia
calcification in, 801, 881
hemolytic uremic syndromes, 902
Uricase deficiency, 154
Urobilinogen, 821
Urokinase, 243
Uropathogenic *Escherichia coli* (UPEC), 472
Uropod, 237
Uroporphyrin, 821
Uroporphyrinogen II cosynthetase, 820
UV radiation, apoptosis and, 188

V
Vaccinia virus, 323
Vaccinia virus growth factor (VGF), 323
Vaccinial pneumonitis, 323
Vacular addressins, 287
Vacuolar leukoencephalopathy, 912
Vacuolar neuropathy, 686f
Vacuolar proton ATPases, 110
Vacuolar system, proximal convoluted tubule, 700
Vacuolation
carbon tetrachloride toxicity, 6f, 8f
diffuse vacuolar degeneration, 7
doxorubicin toxicity, 645f, 647f, 648f
focal, 7
Golgi complex, 9, 141
hepatocyte, 618
Vacuoles
amylopectin, 549
autophagic, 26, 69, 70f, 837
bacteriophorous, 71
contractile, 528
cytoplasmic, 7
food, 528, 547
fungal, 578
gas, 439
glycogen, 549
mitochondria, 184
neutrophil, 240, 242f
parasitophorus, 535, 545, 550, 554, 561
Valproate, 688
Vannella spp., 528
Vapors, lung toxicity from, 723
Varicella virus, 333
Varicellovirus genus, 333
Vasa recta endothelium, 706
Vasa vasorum, 875
Vascular change in acute inflammation, 209t
Vascular disease/injury. *See also* Vasculitides
calcification, 800–801
diabetic microangiopathy, 903
endothelial cell death, 54, 56
neurotoxins, 688–690, 690
gold, 690
lead, 688, 690
mercury, 690
pulmonary, 727–728
Vascular endothelial growth factors (VEGF), 216–217, 223–224
fetal lung development and, 723
vascular endothelial growth factor A, 779, 780
vascular endothelial growth factor C, 780
vascular endothelial growth factor D, 780
Vascular endothelial-cadherin (VE-cadherin), 204
Vascular leak syndrome, 728
Vascular systems, tumor angiogenesis and, 778–780, 779f, 781f
Vascular toxicity, 658–659, 726, 727–728

Vasculitides, 879–881
focal arteriolar insudation, 879
infectious arteritis, 874f, 879–881, 880f
noninfectious systemic necrotizing, 881
Vasculitis, herpesviral, 334f
Vasectomy, 26
Vasohibin, 780
VEGF. *See* Vascular endothelial growth factors (VEGF)
VEGF receptor (VEGFr), 223, 779, 780
Veillonella, 503t, 504–505
Venezuelan equine encephalitis (VEE), 382, 384
Venoms
cardiotoxicity of reptile, 651
myotoxicity, 655, 658
smooth muscle toxicity, 659
snake, 82, 658, 659, 686
Venoocclusive syndrome, 627
Ventral disk, giardia, 536
Verapamil, cardiotoxicity of, 650–651
Veratrine, skeletal muscle toxicity, 658
Verruga peruana, 453
Very low-density lipoprotein (VLDL), 169, 170
Vesicles, 319
Vesicular exanthema, 399
Vesicular exocytosis, 120
Vesicular stomatitis virus (VSV), 367, 367f
Vesiculotubular clusters, 138
Vesiculo-vacuolar organelle (VVO), 203
Vesiculovirus genus, 367
Vesivirus genus, 399
feline calicivirus (FCV), 399
swine vesicular disease, 399
VGF (vaccinia virus growth factor), 323
Vibrio, 484–485, 485t
Vibrionales (order), 484–485, 485t
Vibrio genus, 484–485, 485t
Vigabatrin, 685
Vimentin, 91
Vinblastine, 89, 627
Vinca alkaloids, 89
Vincristine, 89, 627, 652–653
Vinculin, 90
Viral disease. *See also* Viruses
arteritis, 874f, 880, 880f
encephalopathy and retinopathy, 394
membranous glomerulonephritis from chronic, 894, 895f, 896f
Viral FLICE-inhibitory proteins (v-FLIPs), 47
Viral inclusion bodies, 850f, 851
Viral nervous necrosis, 394
Viral RNA replication complexes, 370
Viremia, 319
Virions, 319, 763, 765f
Virulence factors, 437t. *See also specific bacterial genera or species*
Viruses, 319–423
Adenoviridae family, 338–343, 339t, 340f
Aviadenovirus genus, 343
Mastadenovirus genus, 340–343
canine adenoviruses 1 (CAV-1), 340–341, 343
canine adenoviruses 2 (CAV-2), 340
enteric adenoviruses, 340
human adenoviruses, 340
infectious canine hepatitis (ICH), 340–341, 341f, 343
Arenaviridae family, 379–381
Arenavirus genus, 379–381
hemorrhagic fevers, 380–381
lymphocytic choriomeningitis (LCM), 379–380
Arteriviridae family, 384, 384t, 385f, 386
Arterivirus genus, 384, 384t, 385f, 386
equine arteritis virus (EAV), 384, 385f, 386
lactate dehydrogenase-elevating (LDH) virus, 386
porcine reproductive and respiratory syndrome (PRRS), 386
simian hemorrhagic fever virus (SHV), 386
Asfarviridae family, 352t, 353f, 353–354
African swine fever (ASF), 353f, 353–354
Astroviridae family, 401
Birnaviridae family, 392–393, 393f, 393t
Aquabirnavirus genus, 392–393
infectious pancreatic necrosis (IPN), 392–393
Avibirnavirus genus, 393
infectious bursal disease (IBD), 393
picobirnaviruses (PBVs), 393
Bornaviridae family, 386
Bunyaviridae family, 391t, 391–392
Hantavirus genus, 392
Nairovirus genus, 392
Crimean-Congo hemorrhagic fever, 392
Nairobi sheep disease, 392
Orthobunyavirus genus, 391–392
Akabane virus, 392
California encephalitis, 391–392
Phlebovirus genus, 392
Rift Valley fever (RVF), 392
Caliciviridae family, 399, 401, 401t
Hepevirus genus, 399, 401
hepatitis E virus (HEV), 399, 401
Lagovirus genus, 399
Norovirus genus, 399
Norwalk virus, 399
Sapovirus genus, 399
Vesivirus genus, 399
feline calicivirus (FCV), 399
swine vesicular disease, 399
cell death blockage by, 47
Circoviridae family, 355–356, 356f
Coronaviridae family, 370–373, 371t, 372f
Coronavirus genus, 370–373
bluecomb virus, 373
bovine corona virus, 373
feline infectious peritonitis (FIP), 373
hemagglutinating encephalomyelitis virus (HEV), 373
infectious bronchitis virus (IBV), 373
murine hepatitis virus (MHV), 370–372
severe acute respiratory syndrome (SARS), 370
sialodacryoadenitis virus, 372
transmissible gastroenteritis (TGE) virus, 372f, 372–373
Torovirus genus, 373, 374f
families and genera, 320f
Filoviridae family, 369f, 369t, 369–370
Ebolavirus genus, 370
Marburgvirus genus, 369–370
Flaviviridae family, 386–391, 387t, 390f
Flavivirus genus, 386–388
dengue fever virus, 388
Japanese B encephalitis virus, 388
Kyasanur Forest disease virus, 388
louping ill virus, 388
Russian spring-summer encephalitis (RSSE) virus, 388
St. Louis encephalitis virus, 383f, 388
yellow fever virus, 386–388
Hepacivirus genus, 389, 391
hepatitis C virus (HCV), 389, 391
Pestivirus genus, 388–389
bovine viral diarrhea (BVD) virus, 389
hog cholera, 388–389, 390f

Viruses (*cont'd*)
Golgi complex usurpation, 142
Hepadnaviridae family, 354t, 354–355, 355f
Avihepadnavirus genus, 355
duck hepatitis virus (DHV), 355
Orthohepadnavirus genus, 354–355, 355f
hepatitis B virus (HBV), 354–355, 355f
woodchuck hepatitis virus, 355
Herpesviridae family, 327–338, 328t–330t, 331f
Alphaherpesvirinae subfamily, 330–335
herpes simplex virus (HSV), 330, 332f, 332–333
Mardivirus genus, 333, 335
Marek's disease virus, 333, 335
Simplexvirus genus, 330, 331f, 332f, 332–333
Varicellovirus genus, 333
Betaherpesvirinae subfamily, 330–335
Cytomegalovirus genus, 335, 338f
human herpesvirus 6 (HHV-6), 335
Roseolovirus genus, 335
duck plague, 338
frog, 338
Gammaherpesvirinae subfamily, 337–338
Epstein-Barr virus (EBV), 337
Lymphocryptovirus genus, 337
Rhadinovirus genus, 337–338
saimiriine herpesvirus 2, 338
in human fecal stools, 400f
Iridoviridae family, 352t, 353
Lymphocystivirus genus, 353
Ranavirus genus, 353
multinucleate giant cells, induction of, 26
Nadoviridae family, 394
Orthomyxoviridae family, 356t, 356–358, 357f
Papillomaviridae family, 343–347, 344t, 345f
bovine papilloma virus (BPV), 346–347
human papilloma virus (HPV), 346
Paramyxoviridae family, 357f, 358–366, 359t, 361f, 363f, 365f
Paramyxovirinae subfamily, 360–364
Avulavirus genus, 364
canine distemper virus (CDV), 362, 363f
Hendra virus, 362, 364
Henipavirus genus, 362, 364
measles virus, 357f, 360, 362
Morbillivirus genus, 360, 362
mumps virus, 364
Newcastle disease virus (NDV), 361f, 364, 365f
Nipah virus, 364
parainfluenza viruses, 360
Respirovirus genus, 360
Rubulavirus genus, 364
Sendai virus, 360
Pneumovirinae subfamily, 364, 366
Metapneumovirus genus, 366
Pneumovirus genus, 364, 366
respiratory syncytial virus (RSV), 364, 366
Parvoviridae family, 349t, 349–353, 351f
Amdovirus genus, 352–353
Aleutian mink disease virus, 352–353
Depedovirus genus, 352
adeno-associated viruses (AAVs), 352
Erythrovirus genus, 350, 352
Parvovirus genus, 350
canine parvovirus, 350
feline panleukopenia virus, 350, 351f
Picornaviridae family, 394–399, 395t, 396f, 398f
Aphthovirus genus, 397
foot-and-mouth disease (FMD) virus, 397
Cardiovirus genus, 397
encephalomyocarditis (EMC) viruses, 397
murine polioencephalomyelitis virus (Theiler's virus), 396f, 397
Enterovirus genus, 394
coxsackieviruses, 394
echoviruses, 394
poliovirus, 394
Hepatovirus genus, 397, 399
avian encephalomyelitis, 398f, 399
hepatitis A virus (HAV), 397, 399
Rhinovirus genus, 394, 397
Polyomaviridae family, 347t, 347–349, 348f
cynomolgus polyoma virus, 348
mouse pneumonitis virus, 349
polyoma BK virus, 348
polyoma JC virus, 347–348
polyomavirus muris, 348
simian virus 40, 348–349
Poxviridae family, 318f, 319–327, 320t–322t
Chordopoxivirinae subfamily, 323–327
Avipoxvirus genus, 324, 326f
Capripoxvirus genus, 324
fowlpox, 324, 326f
Lepropoxvirus genus, 324, 327
Molluscipoxvirus genus, 327
mousepox, 323
orf virus, 324, 325f
Orthopoxvirus genus, 323
Parapoxvirus genus, 324, 325f
pseudocowpox, 324
rabbitpox, 324, 327
sheeppox, 324
Suipoxvirus genus, 327, 327f
swinepox, 327, 327f
vaccinia virus, 323
Yatapoxvirus genus, 327
Reoviridae family, 373–379, 375t, 376f
Aquareovirus genus, 379
Coltivirus genus, 379
Colorado tick fever (CTF), 379
Orbivirus genus, 377
African horse sickness (AHS), 377
bluetongue virus, 377
epizootic hemorrhagic disease (EHD), 377
Orthoreovirus genus, 376–377
Rotavirus genus, 377–379
bovine rotaviruses, 378–379
epizootic diarrhea of infant mice (EDIM), 379
human rotaviruses, 378
infectious diarrhea of infant rats (IDIR), 379
porcine rotaviruses, 378
Retroviridae family, 401–415, 402t–403t
Alpharetrovirus genus, 404
avian leukemia virus (ALV), 404
Rous sarcoma virus (RSV), 404
Betaretrovirus genus, 404, 406
jaagsiekte sheep retrovirus (JSRV), 406
mouse mammary tumor virus (MMTV), 404, 405f, 406
Deltaretrovirus genus, 410
human T-lymphotrophic virus (HTLV), 410
Gammaretrovirus genus, 406–410
avian reticuloendotheliosis virus (ARV), 410
feline leukemia virus (FeLV), 406–407, 408f

murine leukemia viruses (MLVs), 407, 408f, 409f, 409–410
Lentivirus genus, 410–415, 411f, 413f, 414f, 415f
equine infectious anemia (EIA), 414–415
human immunodecifiency virus (HIV), 410–412, 411f, 413f
simian immunodecifiency virus (SIV), 412, 414f
visna, 412, 414
Orthoretrovirinae subfamily, 404–415
Spumavirinae subfamily, 415, 415f
foamy viruses, 415
Rhabdoviridae family, 363f, 366t, 366–368
Ephemerovirus genus, 368
Lyssavirus genus, 367–368
Mokola virus, 368f
rabies virus, 363f, 367–368
vesicular stomatitis virus (VSV), 367, 367f
Vesiculovirus genus, 367
Togaviridae family, 381t, 381–384, 383f
Alphavirus genus, 381–384
eastern equine encephalitis (EEE), 382, 383f
Venezuelan equine encephalitis (VEE), 382, 384
western equine encephalitis (WEE), 382
Rubivirus genus, 384
rubella, 384
Virus-like particles, in neoplastic tissue, 763
Visceral leishmaniasis, 536
Visna, 412, 414
Vitamin B12 mitochondrial hypertrophy, 189
Vitamin C (ascorbic acid) deficiency fibroplasia, 303
Vitamin D
hypercalcemia, 881
pathways, 801f
toxicity, 711
vascular calcification, 800
Vitamin E
deficiency, 823
mitochondrial hypertrophy, 190–191, 191f
Vitellogenin, 613
Vitiligo, 812
Vitiligo mouse, 812
VLDL (very low-density lipoprotein), 169, 170
Volkensin, hepatocyte effects of, 613–614
Voltage-dependent anion channels (VDACs), 181
Volutin granules, 438–439
Von Willebrand disease, 257
Von Willebrand factor (vWF), 207, 253, 257
VSV (vesicular stomatitis virus), 367, 367f
VVO (vesiculo-vacuolar organelle), 203

W
Waldeyer's ring, 278
Warner syndrome, 751
Warts, 346
Wasps, venoms of, 655
Watanabe heritable hyperlipidemic rabbit, 886
Water
regulation of intracellular, 79–80
transport, aquaporins and, 114
Water avoidance stress, 607
Wear-and-tear pigment, 823
Wegener's granulomatosis, 902
Weibel-Palade bodies, 207, 885
Werdnig-Hoffman disease, 92
Wernicke's encephalopathy, 189
Western equine encephalitis (WEE), 382
Whipple's disease, 496
White piedra, 592
Whooping cough, 457
Whorling of membranes, smooth endoplasmic reticulum, 62, 62f
Wilson's disease, 193–194, 822–823
Wiskott-Aldrich syndrome, 256
Wnt signaling pathways, 780
Wolman disease, 173, 861
Woodchuck hepatitis virus, 355
Wool-sorter's disease, 496
Wound infections, fulminating, 484

X
Xanthine oxidase-dependent hydrogen peroxide production, 51
Xanthomatosis, 174, 885
Xanthophores, 815
Xenoma, 563
Xerodermas pigmentosum, 769
X-linked inhibitor of apoptosis (XIAP), 42
X-linked renal disease in Samoyed dogs, 898
X-linked sparse fur mouse, 192
Xmd dogs, 91
X-radiation, mitochondrial swelling and, 187–188

Y
Yaba monkey tumor virus, 327
Yatapoxvirus genus, 327
Yaws, 508
Yeast
Candida albicans, 583
Histoplasma, 585
Yellow fever virus, 386–388
Yersinia, 469t, 475–476
Yolk epithelium secretion of lipids in birds, 145, 146f
Yolk laminar spherules, 803, 805f

Z
Zebra bodies, 866
Zellweger's syndrome, 155
Zonula adherens, 100
Zonula occludens. *See* Tight junctions
Z-ring, 442
Zudovidine (AZT), hepatotoxicity of, 625
Zymogen, 847–848
Zymosan, hepatotoxicity of, 627